सत्यमेव जयते

INDIAN AGRICULTURAL
RESEARCH INSTITUTE, NEW DELHI

24710

I.A.R.I.6.
GIP NLK—H-3 I.A.R.I.—10-5-55—15,000

Transactions of the Faraday Society

OUNDED 1903

TO PROMOTE THE STUDY OF ELECTROCHEMISTRY, ELECTROMETALLURGY,
PHYSICAL CHEMISTRY, METALLOGRAPHY, AND KINDRED SUBJECTS

VOL. XLIV, 1948

GURNEY AND JACKSON
LONDON: 98 GREAT RUSSELL STREET
EDINBURGH: TWEEDDALE COURT

PRINTED IN GREAT BRITAIN AT
THE UNIVERSITY PRESS
ABERDEEN

THE DEGREE OF DISPERSION OF THE GAS PHASE IN FOAM.

By N. O. Clark and M. B[illegible]kman.

(*Communicated by* Prof. R. P. Linstead.)

Received 28*th March*, 1946.

The degree of dispersion of the gas in a foam appears to be a property largely neglected in the literature, but of outstanding importance in influencing the properties of a foam. It has been shown to exhibit a marked effect on the resistance to radiant heat and on the critical shearing stress of such a system.[1] The property is, moreover, a fundamental one in that the maintenance of dispersion may be regarded as a measure of the stability of a foam, and as the most important property in distinguishing foam from the simple sum of its constituents.

We take *specific surface* as the unit of measurement of dispersion and define it as the total surface area in sq. cm. of the gas-liquid interface in 1 cc. of foam. (This is the definition generally applied to dispersion of solids. It is not, of course, specific as the numerical value depends on the units.)

Experimental.

The foams were prepared by the mechanical beating of suitable solutions in a brass cylinder by the vertical oscillation of a perforated disc moving with constant simple harmonic motion. Photomicrographs were taken of the plane of contact between flat glass and foam, illuminated by reflected light of a spectral range defined by passage through separate solutions of $CuSO_4$ and $K_2Cr_2O_7$. A 16 mm. apochromatic microscope objective gave an image on the screen of a reflex ¼-plate camera adapted for 2¼ in. film, permitting 12 square negatives to be taken in succession. Exposures on a fast panchromatic film were of the order of ⅛ sec. with illumination from a carbon arc lamp. The negatives were enlarged on bromide paper with a standard reference circle giving a final total enlargement of 155 diam. The bubbles in this circle were then counted and assigned to the following groups according to their diameters. These measurements were not of the true diameters of the bubbles in the internal regions of the foam, as there was some distortion due to contact with the glass plane. The camera was focussed on the maximum diameter of the front layer of bubbles.

TABLE I

Group.	Actual Diameter of Bubble (cm.).
A	0·0 -0·0025
B	0·0025-0·005
C	0·005 -0·0075
D	0·0075-0·01
E	0·01 -0·015
F	0·015 -0·02
G	0·02 -0·03
H	0·03 -0·04
J	0·04 -0·06
K	0·06 -0·08
L	0·08 -0·12
M	0·12 -0·16
N	0·16 -0·24
O	0·24 -0·32
P	0·32 -0·48

The following method was used for the calculation of specific surface from the observed group counts of the bubbles, assuming the measured dimensions to be true diameters. If d_1, d_2, etc., represent the mean diameters of the various size groups, and x_1, x_2, etc., the numbers of bubbles assigned to each, in 1 sq. cm. of the observed area, then the number of bubbles of given diameter d_n in unit depth was $1/d_n$ to a first approximation. The number of bubbles in unit volume of the foam was

---

[1] Clark, *D.S.I.R. Chem. Res. Special Rep.* No. 6 (H.M.S.O., Lond., 1947).

$$\sum\left(\frac{x_1}{d_1}+\frac{x_2}{d_2}+\ldots\right)$$

and the surface area in unit volume of foam

$$\pi\sum(x_1d_1+x_2d_2+\ldots).$$

The absolute accuracy of the method must therefore depend on the increase of maximum diameter arising from distortion of the foam by the glass plane. It must be admitted further, that an assumption is made that the layer next to the glass is a representative section. The root mean square error of 8 successive similar observations was 3 %.

Results and Discussion.

Fig. 1 gives a typical experimental curve, showing the change in specific

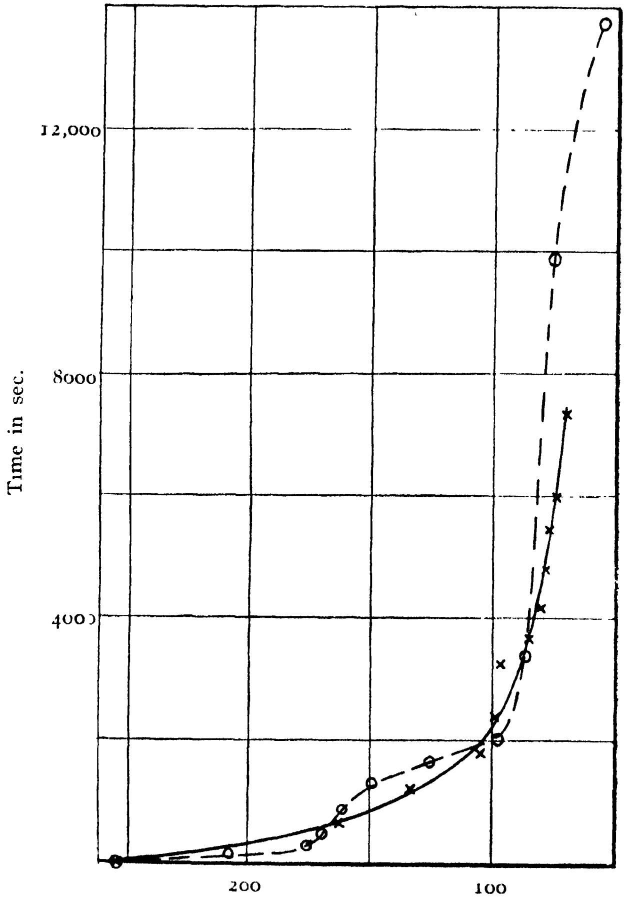

FIG. 1.—Specific Surface in sq. cm./cc.

× Expt. results from a protein hydrolysate (5 % P.W.).
○ Theor. points, $K = 4 \times 10^{-9}$.

surface with time, using a foam prepared from an aluminium protein hydrolysate solution (5 % P.W.). Let us consider the mechanism by which such changes may occur. The question of bubbles ceasing their

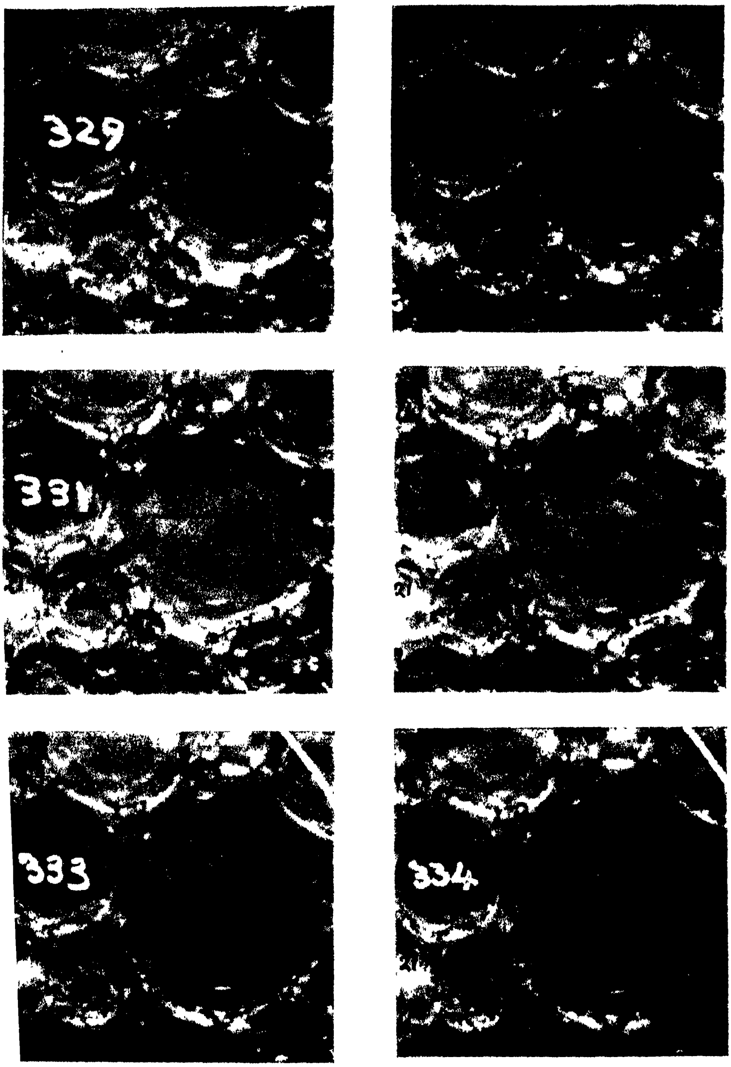

PLATE 1.

[*To face page* 3

existence by bursting does not arise in a closed system, and was certainly not observed during the period of time covered by Fig. 1. The most important change to be noted was a tendency for large bubbles to increase in size, and small ones to decrease in diameter to the point of actual disappearance. By taking a series of photographs at short time intervals this process was followed, identification of the individual bubbles being made from their geographical position. The 6 photographs on plate 1 were secured from the same foam sample at ages of 3, 4, 6, 8, 10 and 12 min. respectively. We believe that the qualitative observation of this phenomenon is not original.

The pressure of the air in relatively small bubbles is higher than that in the larger ones and the bubbles are separated by a very thin film of fluid. Diffusion of air will take place from the high pressure region (small bubbles) to the region of lower pressure (larger bubbles). The smaller bubbles will disappear and the larger will grow.

A detailed theory would have to take into account the average environment of a bubble of radius r, as well as the distribution function (the number of bubbles between radii r and $r + \mathrm{d}r$).* We suppose a bubble of radius r to be surrounded by a thin layer of liquid ; the concentration of air in the liquid is that for a pressure excess of $2Tr_m^{-1}$, where T is the surface tension of the liquid and r_m^{-1} is the average value of the inverse radius. The way in which this average is to be taken will be discussed below. The pressure difference between bubble and liquid is

$$2T\left(r^{-1} - r_m^{-1}\right).$$

The diffusion of air between bubble and liquid must be proportional to this pressure difference. The change of the number of molecules N per second in the bubble can be written as

$$\frac{\mathrm{d}N}{\mathrm{d}t} = -4\pi r^2 G \,.\, 2T(r^{-1} - r_m^{-1}) \quad . \quad . \quad . \quad (1)$$

where G is a quantity still to be determined. If V is the volume of the bubble, and P the total pressure inside the bubble,

$$PV = Nk\theta,$$

where θ = absolute temperature, k = Boltzmann's constant. If N changes at constant temperature,

$$V\Delta P + P\Delta V = k\theta\Delta N.$$

Now $P = p_0 + 2T/r$, where p_0 is the atmospheric pressure. Hence $\Delta P = -\frac{2T}{r^2}\Delta r$, where Δr is the change of radius associated with a change ΔN in N, and $\Delta V = 4\pi r^2\Delta r$. It follows that $p_0 4\pi r^2 \Delta r = \Delta N k\theta$ (if $T/r \ll p_0$), i.e.

$$\Delta r = \frac{Gk\theta}{p_0} \,.\, 2T(r_m^{-1} - r^{-1})\Delta t.$$

In the limit of small changes,

$$\frac{\mathrm{d}r}{\mathrm{d}t} = \frac{Gk\theta}{p_0} \,.\, 2T(r_m^{-1} - r^{-1}). \quad . \quad . \quad . \quad . \quad (2)$$

The calculation of G could be performed, at any rate approximately, if we were dealing with air bubbles in a normal liquid. In this case, however, an extra factor to be considered is the surface layer ; this has a marked influence or the diffusion of air and the value of G must therefore be determined from experiment. Equation (2) will be written in the form :

---

* This method of averaging the pressure excess for all the bubbles was suggested by Dr. W. G. Penney.

$$\frac{\mathrm{d}r}{\mathrm{d}t} = K(r_m^{-1} - r^{-1}). \quad . \quad . \quad . \quad . \quad (3)$$

The next point to be considered is the determination of the average r_m^{-1}. We note that the foam is at constant external pressure and (to a close approximation) at constant temperature. We would therefore expect the total volume of air to remain constant, though a redistribution takes place. Dividing the bubbles into a number of groups (N_s being the number of bubbles of radius r_s), the change in r_s, (Δr_s), in time Δt is given by (3). The condition for r_m^{-1} is, then, that

$$\Delta V = \sum_s 4\pi N_s r_s^2 \Delta r_s = 0. \quad . \quad . \quad . \quad . \quad (4)$$

This fixes r_m^{-1} at a given time, but it is clear that the value will change with time. The following procedure is therefore adopted. The initial bubble distribution is arranged in groups, as stated above (this grouping being provided by the experimental data). The number N_s in each set is fixed, but the radius r_s changes with time. Assuming that r_m^{-1} remains reasonably constant over a certain time interval, the equation (3) can be integrated. Writing $\zeta = \frac{r_s}{r_m}$, (3) becomes:

$$\frac{\mathrm{d}\zeta}{\mathrm{d}t} = \frac{K}{r_m^2}\left(1 - \frac{1}{\zeta}\right) \quad \text{or} \quad \frac{\zeta \mathrm{d}\zeta}{1 - \zeta} = -\frac{K}{r_m^2}\mathrm{d}t\,;$$

the solution is

$$\zeta_s + \log(1 - \zeta) = \frac{K}{r_m^2}t - A_s \quad (\zeta < 1). \quad . \quad . \quad . \quad (5)$$

We are concerned first with $\zeta < 1$ where the integrated form of the equation is used. The value of A_s is obtained from the initial value of ζ_s. Considering the bubbles of smallest size ($s = 0$), it will be seen that A_0 is positive and that at a certain value of t, ζ_0 will be zero, i.e., that bubbles will vanish. The equation (5) holds, it is true, only for r_m constant. The operation is performed, therefore, in several stages, at each of which the change in r_s is calculated. For all bubbles except the smallest, the differential form (3) can be used. The new value of r_m is then calculated and the operation is repeated until ζ_0 is zero. Once the smallest bubbles have disappeared, the calculation is repeated with the remaining sets until only one set remains. The number of sets should be chosen in such a way that the experimental time range is covered before only one set remains. The approximate theory would give no change in the bubble size after this stage ; this is, of course, due entirely to the sub-division into a few groups and it cannot be expected that the theory at the last stage would be in agreement with experiment. For the same reason, the theory cannot be expected to give a good representation of the distribution function. It should be able to represent the variation of the specific surface, which is less sensitive.

With a value of $K = 4 \times 10^{-9}$ c.g.s. units, the curve (for the specific surface) is shown (Fig. 1) together with the experimental points. It will be seen that the agreement obtained is reasonably good. This theory implies that resistance to the transfer of gas resides largely in the superficially absorbed film, the factor K in equation (3) being an inverse measure of this resistance, and the possible basis of an absolute definition of foam stability.

It was to be expected from equation (3) that if the reciprocal mean radius was exceeded by an individual bubble, that the rate of change of radius would be positive, while if the individual bubble radius was less than the mean, a decrease with age would follow. By following the changes of a number of bubbles, a family of curves was expected, each member diverging from a mean horizontal line (for the mean bubble) showing increasing slope (positive or negative) with increasing age. A study of a random number of bubbles in a ferrous protein hydrolysate foam (5 % NP) did not lead to the expected result but gave a series of curves (Fig. 2) with slopes, in general decreasing with age. It is believed [1] that such protein solutions exhibit a rather low rate of absorption of active material into the surfaces of their solutions, and the probable explanation of the results lies in a decrease of the constant K with age and in surface tension changes. Some confirmation of the validity of these deductions was obtained by a similar examination of foam from a material (sodium

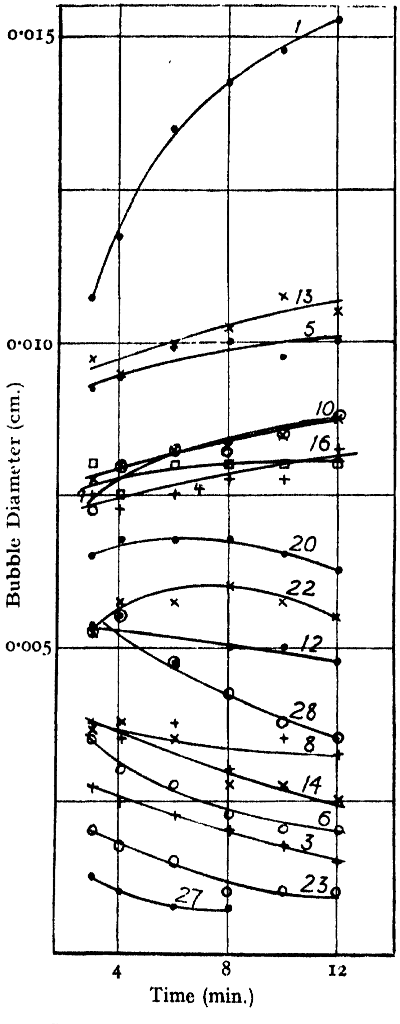

FIG. 2.—Change of individual bubble size with time. Ferrous protein hydrolysate. (5 % N.P.).

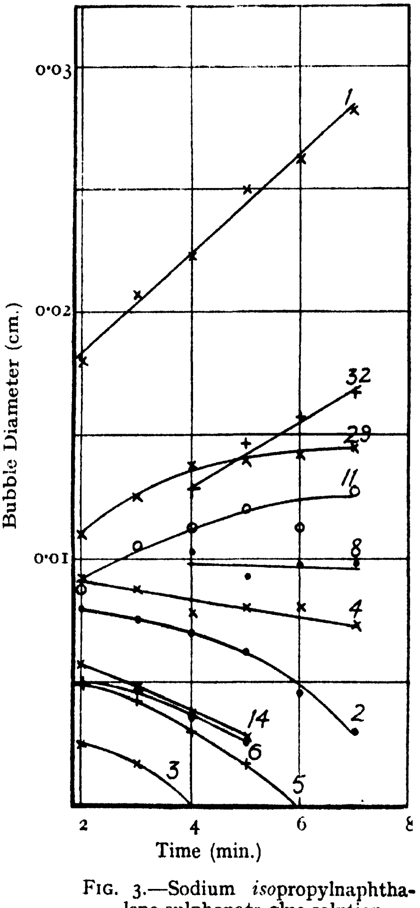

FIG. 3.—Sodium *iso*propylnaphthalene sulphonate-glue solution.

*iso*propylnaphthalene sulphonate and hydrolysed glue) known to be rapidly absorbed on the surface of its solutions, and the results confirm the theory. The curves of Fig. 2 and 3 show considerable overlapping, probably a result of local variations in the value of the reciprocal mean radius.

The reception factor G of equation (1) might be expected to be a function of the solubility of the gas, and some measurements of specific surface

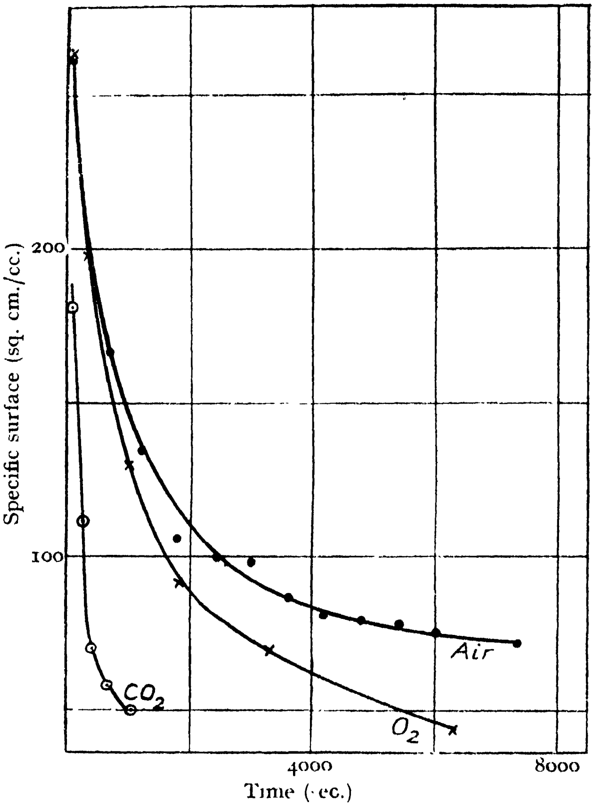

FIG. 4.

changes in a series of foams prepared from an aluminium protein hydrolysate (5 % P.W.) with a few gases, illustrate the effect to be expected from variation in the solubility of the gas phase (Fig. 4).

We have paid little attention in the above discussion to the distribution of bubble sizes. It is important to realise that the distinction between a freshly prepared and an old foam (from a structural point of view) lies in the similarity and divergence respectively of the bubble sizes in the two cases. Fig. 5 gives an indication of the change with age in the contribution to the total specific surface made by the various size groups for a ferrous protein hydrolysate solution (5 % OJ) and for a soap solution (5 % NU). New foam appears to be largely homogeneous.

Ross [2] has observed in a number of experiments on foam drainage, that a logarithmic law relating liquid content to age, was followed after a certain initial period. The failure of the law in this initial period was probably due to the change in free liquid between the bubbles resulting from changes in the relative numbers in the size groups.

---

[2] Ross, *J. Physic. Chem.*, 1943, **47**, 266.

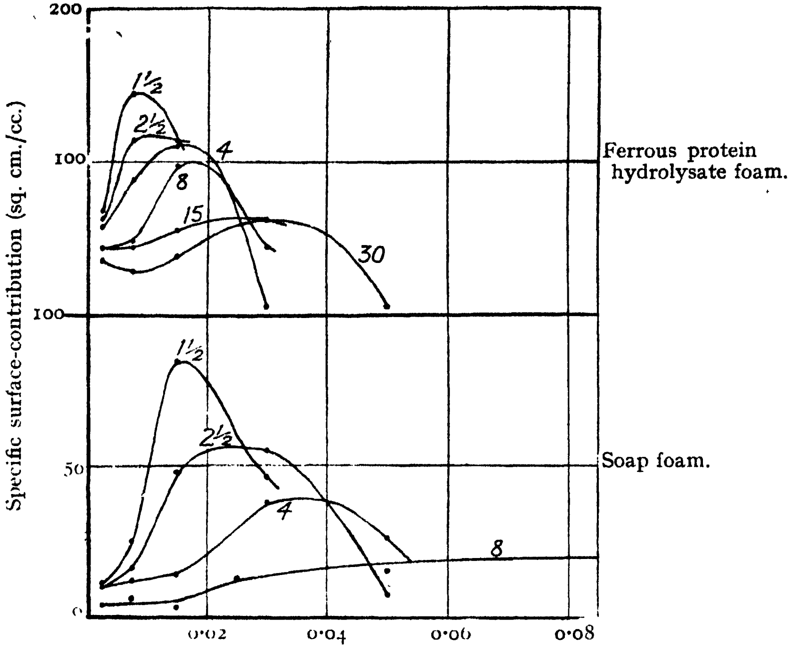

FIG. 5.—Mean diam. of bubble group C.M.
(Numbers refer to age in min.)

The authors thank the Research and Experiments Department, Home Office, and Professor R. Linstead, F.R.S., Director, C.R.L., for permission to publish, and Dr. W. G. Penney for assistance. The theory of page 3 is due to one of them (M. B.) and the other (N. O. C.) is responsible for the rest of the work.

Summary.

The specific surface of a foam is defined and its change investigated over a period of time. The mechanism of the change appears to be a transfer of gas from a high pressure small bubble to a low pressure large one. A theory of this process is presented, and confirmed by measurements of individual bubbles in a foam atmosphere and by the substitution of gases other than air.

Chemical Research Laboratory,
Teddington.

Imperial College,
London.

THE TRANSMISSION OF LIGHT THROUGH FOAM.

BY N. O. CLARK AND M. BLACKMAN.

(*Communicated by* Prof. R. P. LINSTEAD.)

Received 28*th March*, 1946.

It is well known that the comparative opacity of disperse systems is due to the scattering of incident light by multiple reflections and refractions. The loss of light on transmission through a layer of foam is explored here as a function of the degree of dispersion of air by the method described in an earlier paper.[1] The loss of light is expressed in terms of the "loss factor" which we define as the ratio of the incident to the emergent light.

Experimental

The incident light on the foam was provided by a 6 v. 6 w. bulb in a parabolic reflector with current supplied by accumulator cells through a rheostat. The foam cell, 1 cm. internal thickness and 10 cm. external diameter, rested on a horizontal platform perforated with an 8 cm. diameter hole, beneath which was supported a photo-cell of the selenium rectifying type connected to a low resistance microammeter (120 μa, 45·5 Ω). The selenium cell was circular and of 27 sq. cm. area. Standardisation of the light was achieved by continual reference to an opal glass screen placed in the position of the foam cell where the light was adjusted to give a value equivalent to a full scale deflection with the empty foam cell in position. The microammeter reading in such a system was known to be directly proportional to the light incident on the cell, so that the ratio of the full scale deflection to reading with foam in position gave directly the loss factor.

Two types of foaming agent were used in aqueous solution, the first (referred to as NU) was a solution of a potash coconut oil soap (containing glycerine) with about 30 % total fatty matter ; the second (referred to as OJ) was a solution containing about 30 % total organic matter. The first in dilute solution (5 %) showed negligible light absorption, while the second at a similar concentration appeared a deep brown colour.

Results.

Foams were prepared[1] from four solutions, and in Table I are listed the concentrations of these solutions, the expansion factor of the respective foams (i.e. the ratio of the volume of foam to that of the contained liquid) and the loss factors of layers of liquid equivalent to 1 cm. depth of foam.

Fig. 1 gives the relationship between specific surface[1] and loss factor for these foams with no correction for liquid absorption. Fig. 2 includes a direct correction for the absorption of the contained liquid.

TABLE I

Solution.	Expansion Factor.	Loss Factor of Liquid in 1 cm. Foam.
5 % NU	12·4	1·00
5 % OJ	10·9	1·35
3 % OJ	10·1	1·07
2 % OJ	9·5	1·04

Discussion.

The relation between specific surface and loss factor appears to be linear and for a non-absorbent liquid there is a proportionality between specific surface and (loss factor − 1). The method therefore provides a rapid means of measurement of specific surface.

The light entering the foam undergoes a series of refractions at the boundaries between liquid and air ; in addition to this, there is some scattering due to the liquid itself, and in most cases a true absorption of light as well. The detailed consideration is complex and to simplify the problem, approximations have to be made.

The essential part of the scattering by light of a foam seems to be total internal reflection which occurs when the light strikes the air-liquid interface at an angle greater than the critical angle ; a fair proportion (approx. 25 %) of the light striking a bubble is deviated into a direction roughly opposite to that of incidence. The effect of the air-liquid boundaries is simulated by a set of parallel planes of "liquid" per cm. of foam (which would be equal to the number of layers of bubbles were these uniform and suitably packed) and is obtained from an average diameter of the bubbles ; this is calculated from the data on specific surface.

---

[1] Clark and Blackman, *Trans. Faraday Soc.* (previous paper).

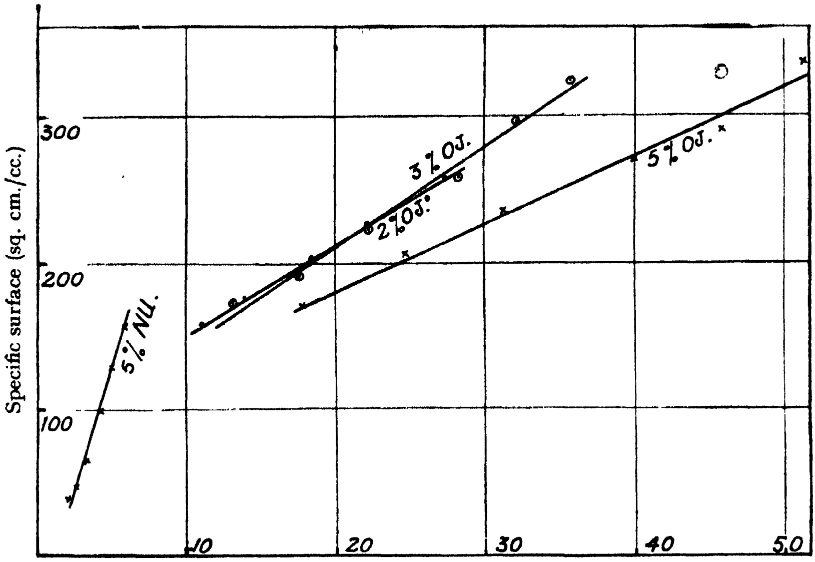

Loss factor of 1 cm. of foam.

Fig. 1.

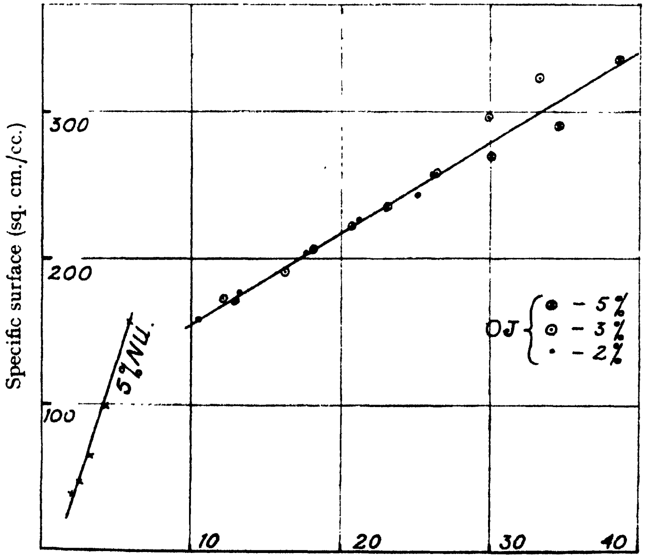

Loss factor of 1 cm. of foam.

Fig. 2.

The theory for a transparent foam is given below. The intensity of the light incident on the first layer is taken as unity.

T_n $(1-f)T_n$ $(1-f)T_n(1-T_n)$ $(1-f)^2(1-T_n)T_n$ $(1-f)^2(1-T_n)^2T_n$

$(n+1)$th layer

fT_n $f(1-f)(1-T_n)T_n$ $f(1-f)^2(1-T_n)^2T_n$.

The fraction of this, transmitted through n layers, is termed T_n; since end effects are neglected and the absorption is zero, the amount "reflected" is $1 - T_n$. Consider now what happens when the $(n+1)$th layer is added. A fraction fT_n is transmitted and $(1-f)T_n$ reflected; of this $(1-T_n)(1-f)T_n$ returns since the n layers will reflect back a fraction $(1-T_n)$. The fractions transmitted in the successive stages can now be calculated as indicated in the above diagram and the total fraction transmitted through $(n-1)$ layers, T_{n+1}, is given by the following relation

$$T_{n+1} = fT_n + f(1-f)(1-T_n)T_n + f(1-f)^2(1-T_n)^2T_n + \cdot\ \ . \quad (1)$$
$$= fT_n/[1-(1-f)(1-T_n)].$$

This gives a recurrence relation between T_n and T_{n+1}. Defining now the loss factor $L_n = T_n{}^{-1}$, equation (1) becomes

$$1-(1-f)(1-L_n{}^{1}) = fL_{n+1}/L_n \quad . \quad . \quad . \quad (2)$$

or
$$fL_n + (1-f) = fL_{n+1}$$

i.e.
$$L_{n+1} = L_n + (1-f)/f \quad . \quad . \quad (3)$$

This relation shows that a plot of L_n against n will lead to points lying on a straight line; this is in accord with the experimental results found for soap foams, with a value of $f = 0{\cdot}87$.

It should be noted that this simple form of the theory would have to be altered if very much thicker layers of the foam, than those actually used, were to be considered. Since there would be a progressive diffusion of the light towards an almost spherical distribution the value of f would be expected to alter gradually and to become larger; the L_n/n curve would then cease to be a straight line.

When the absorption of a foam is taken into account, the treatment has to be altered slightly. It is assumed that one is dealing with a fixed average absorption coefficient for white light, or with a definite absorption coefficient for monochromatic radiation. An experimental point to note in this connection is that where photocells are used, and the foam absorbs in a region of high sensitivity for the photocell, care has to be used in the interpretation of experimental results. Further, the total absorption of the foam will be appreciably larger than that of the solution from which the foam is made, because the diffusion of the light introduces longer absorbing paths in the liquid.

The same general method is used as before, and an absorbing factor per layer is introduced in the following way. The fraction of the incident light transmitted by a single layer of equivalent liquid is written as $f(1-\bar{q})$; $\bar{q}$ is termed the absorption factor; this can always be assumed to be small compared with unity. The fraction "reflected" by the layer of "liquid" is taken as $(1-f)(1-\bar{q})$ since the path will be roughly the same for "transmitted" or "reflected".

The total fraction of the incident light transmitted through n layers is again denoted by T_n; the fraction "reflected" by R_n. We can obtain T_{n+1} and R_{n+1} by considering the effect of adding an $(n+1)$th layer.

$\downarrow T_n$ $\uparrow \beta T_n$ $\downarrow \beta R_n T_n$ $\uparrow \beta^2 R_n T_n$ $\downarrow \beta^2 R_n^2 T_n$

$(n+1)$th layer

$\downarrow \alpha T_n$ $\downarrow \alpha\beta R_n T_n$ $\downarrow \alpha\beta^2 R_n^2 T_n$.

Putting $\alpha = f(1 - \bar{q})$, $\beta = (1 - f)(1 - \bar{q})$. it is seen that initially an amount αT_n is transmitted and βT_n "reflected" by the $(n + 1)$th layer; an amount $R_n \beta T_n$ of this will be "reflected" back by the n layers and this will impinge on the $(n + 1)$th layer; of this $\alpha R_n \beta T_n$ will be transmitted and $\beta^2 R_n T_n$ "reflected"; the series can now be worked out, and the total amount transmitted, can be seen to be

$$T_{n+1} = \alpha T_n/(1 - \beta R_n) \quad . \quad . \quad . \quad . \quad (4)$$

It is now necessary to find a recurrence relation for R_{n+1}. It can be seen from the above diagram that the contributions to R_{n+1}, apart from R_n are

$$\beta T_n^2 + \beta^2 R_n T_n^2 + \beta^3 R_n^2 T_n^2 + \ldots = \beta T_n^2/(1 - \beta R_n)$$

and

$$R_{n+1} = R_n + \beta T_n^2/(1 - \beta R_n) \quad . \quad . \quad . \quad (5)$$

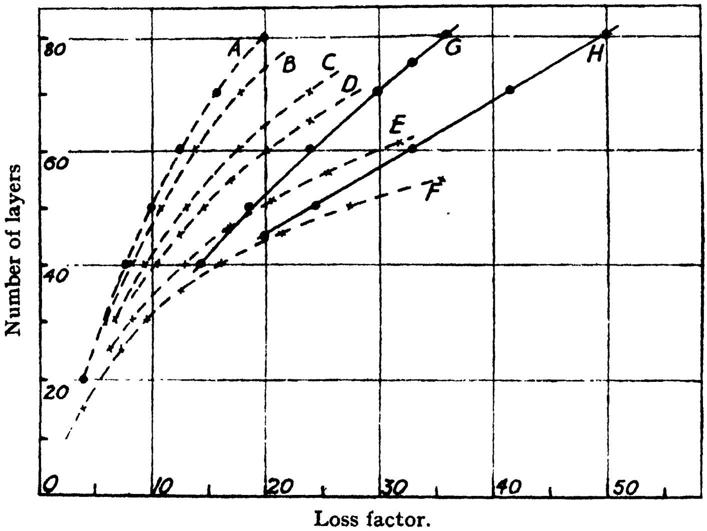

FIG. 3.—Loss of light in an absorbing foam.
A: $\bar{q} = 0{\cdot}001$; B: $\bar{q} = 0{\cdot}002$; C: $\bar{q} = 0{\cdot}003$;
D: $\bar{q} = 0{\cdot}004$; E: $\bar{q} = 0{\cdot}006$; F: $\bar{q} = 0{\cdot}010$;
G: Expt. curve for 2 and 3 % OJ foam;
H: Expt. Curve for 5 % OJ foam.

These two relations suffice to allow the loss factor $L_n = T_n^{-1}$ to be worked out, once the parameters f and $\bar{q}$ are chosen. As an example, the value of f is chosen to be the same as that for our soap solution, i.e. $f = 0{\cdot}87$ and the values of L_n are worked out for $n = 1$ to $n = 70$ for values of $\bar{q}$ ranging from 0·001 to 0·10; the results are shown on the accompanying curves (Fig. 3). The experimental results have been plotted in the same figure for 2, 3 and 5 % OJ foams. The 2 % and 3% foams seem to give points lying on the same line.

The absorption per layer for these foams was also calculated from data on the solution; taking the foams of highest specific surface, which correspond to $n = 80$, the $\bar{q}$ values from the data on solution are respectively 0·00060, 0·00088, 0·0036 if no corrections are applied. It will be seen immediately from the curves that the $\bar{q}$ values suggested by the theory are much larger, and further that one might have expected, at first sight, an appreciable difference between the 2 % and 3 % foams.

All the experimental points for a given type of foam (e.g. for the 5 % OJ foams) were obtained from one specimen which was allowed to age.

This means that the various experimental points on the 5 % line are all characterised by the fact that the total amount of absorbing material remains constant (neglecting the drainage). This means that $n\bar{q}$ should remain constant where n is the number of layers ; the decrease of specific surface with age is represented by the decrease in n, and $n\bar{q}$ is proportional to the total amount of absorbing material. The test of this relation is given below.

TABLE II.—TEST OF THE CONSTANCY $n\bar{q}$.

5 % OJ Foam.			2 and 3 % OJ Foam.		
n.	$\bar{q}$.	$n\bar{q}$.	n.	$\bar{q}$.	$n\bar{q}$.
45	0·0092	0·444	45	0·0060	0·270
50	0·0088	0·440	50	0·0057	0·285
55	0·0080	0·440	60	0·0048	0·288
60	0·0075	0·450	70	0·0040	0·280
65	0·0066	0·429	80	0·0036	0·288
70	0·0060	0·420			
80	0·0055	0·440			

The $\bar{q}$ values, it should be remembered, are taken from the theoretical curves (Fig. 3). The constancy of the $n\bar{q}$ values indicates that the value chosen for f cannot be far from the correct value. The marked difference between the $\bar{q}$ values obtained from the absorption of the solution, and those for the foams must be attributed to the increased absorption introduced by the larger paths taken by the scattered radiation in the foam. This can be investigated in the following way. Radiation downwards from the top end of one layer is assumed to have an intensity $f(\theta)$, where θ is the angle made by a ray with the vertical direction. The effective absorption $\bar{q}$ per layer then becomes

$$\bar{q} = \frac{\int_0^{\pi/2}(1 - e^{-q \sec \theta})f(\theta) \sin \theta d\theta}{\int_0^{\pi/2} f(\theta) \sin \theta d\theta}$$

where q is the absorption per layer which would be deduced from experiments on the solution ; if the radiation were mainly forward and q small, then $q = \bar{q}$.

In the extreme case of $f(\theta) = $ const., i.e., in an isotropic distribution

$$\bar{q} = \int_0^{\pi/2}(1 - e^{-q \sec \theta}) \sin \theta d\theta = \int_0^1 (1 - e^{-q/z}) dz$$

taking $q = 0·001$, the integral has a value of 0·0058, and for $q = 0·01$ of 0·0043. For $f(\theta) = \cos^2\theta$ the value of $\bar{q}$ turns out to be almost exactly $1·5q$ over the above range of q values. The relation between q and $\bar{q}$ for the actual foams is given below.

TABLE III.—EFFECTIVE ABSORPTION PER LAYER.

Solution.	$\bar{q}$.	q.	$\bar{q}/q$.
5 % OJ	0·0055	0·0036	1·5
3 % OJ	0·0036	0·00088	4·1
2 % OJ	0·0036	0·00060	6·0

The conclusion seems to be that the scattered light is (after the first few layers) almost uniformly distributed for the weakly absorbing foams but tends towards a $\cos^2\theta$ distribution when the strength of the solution increases from 2 % to 5 %.

The authors wish to thank " F " Division, Research and Experiments Department, Home Office, and Prof. R. P. Linstead, F.R.S., Director of the Chemical Research Laboratory, D.S.I.R., for permission to publish. They also wish to record that the theoretical interpretation of the results is due to one of them (M. B.) and the experimental work to the other (N. O. C.).

Summary.

The relation between specific surface and loss factor for foams prepared from a non-absorbing solution has been investigated experimentally and theoretically and found to be simple. For such solutions therefore a simple method of obtaining the specific surface of a generated foam is available. Absorbing solutions present a more complex problem, and it appears desirable to attempt the choice of a light wavelength suffering little absorption by the liquid. The method in its present form can be used as a means of specific surface measurement with suitable calibration when the foams are generated from absorbing solutions.

Imperial College,
London.

Chemical Research Laboratory,
Teddington.

THE ELECTRICAL CONDUCTIVITY OF FOAM.

BY N. O. CLARK.

(*Communicated by* Prof. R. P. LINSTEAD.)

Received 28*th March*, 1946.

In the study of foam systems, the expansion factor, i.e. the ratio of foam volume to volume of contained liquid, is a property of fundamental importance. The work described below was undertaken to provide the data necessary for its determination by the simple (and continuous) measurement of electrical conductivity. The method appears to have been used independently by Miles, Shedlovsky and Ross [1] who, however, do not seem to have investigated a range of foaming agents showing a variety of values for their specific surface, nor have they made measurements over a wide range of expansion factors.

Experimental.

Foams were prepared by mechanical beating from solutions of the following : (*a*) a mixture of acid hydrolysed glue and sodium *iso*propylnaphthalene sulphonate; (*b*) a ferrous protein hydrolysate; (*c*) a potash coconut oil soap; (*d*) sodium alginate with sodium *iso*propylnaphthalene sulphonate; (*e*) sodium alginate with saponin. The sodium alginate mixtures provided foams of sufficient stability in the low expansion factor range.

Measurement of the ratio of the resistivity of foam to that of solution, was made directly by the inclusion of two cells in the arms of a Wheatstone bridge, using current at 1000 C.P.S. with a cathode-ray tube detector. The conductivity cells were prepared in glass with bright Pt electrodes. The foam cell consisted of a ¾-in. diameter tube in which two electrodes, curved to fit the tube, were fixed opposite to one another and midway along the tube. Their dimensions (1·5 × 4 cm., and length of the tube, 18 cm.) precluded any serious dependence of cell constant on any extension of the foam column. The foam was pushed along the tube in a continuous column and removed flush with each end, while the tube remained in a horizontal position. The solution cell was a ¾-in. diameter U-tube, and in the arms were electrodes 1·5 cm. square. The specific conductivities of the solutions were in ohms^{-1} cm.$^{-1}$ approximately :

---

[1] Miles, Shedlovsky and Ross, *J. Physic. Chem.*, 1945, **49**, 93.

sodium *iso*propylnaphthalene sulphonate	0·0018
ferrous protein hydrolysate	0·0051
soap	0·0024
sodium alginate with sodium *iso*propylnaphthalene sulphonate .	0·0020
sodium alginate with saponin	0·00020.

The densities were determined by weighing a small measured sample of the foam.

Results and Discussion.

The results (Fig. 1) indicate a regular relationship between the expansion factor and the conductivity ratio of a foam. The approximate

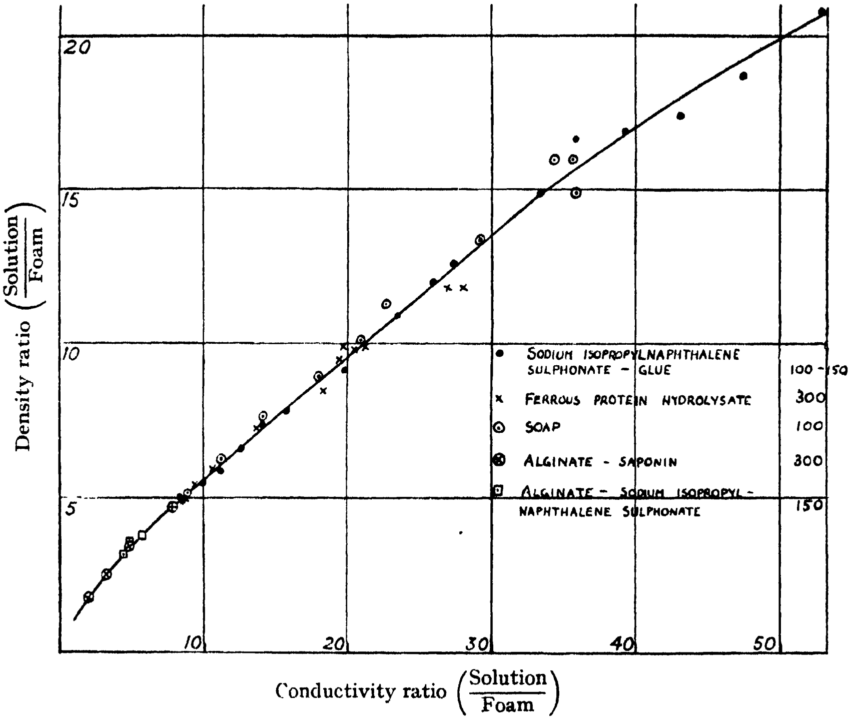

FIG. 1.

values of specific surface (sq. cm./cc.) [2] for the foams are included in the diagram, and show that the relationship is not appreciably affected by this factor, or by the nature of the solution. It is concluded that the results provide a satisfactory basis for the measurement of expansion factor by electrical conductivity ratio, within ± 4 %.

The author wishes to thank the Home Office, Research and Experiments Department, and Professor Linstead, F.R.S., Director, Chemical Research Laboratory, Department of Scientific and Industrial Research, for permission to publish.

Summary.

The electrical conductivity ratio between a foam and its generating solution has been measured for a variety of foams, and the relationship with density ratio

---

[2] Clark and Blackman, *Trans. Faraday Soc.* (in press).

determined. It appears to be independent of the nature of the foaming agent and of the specific surface of the foam and conductivity ratio may therefore be used as a measure of the density ratio.

Chemical Research Laboratory,
Teddington.

THE CONSTITUTION OF THE MAGNESIUM-INDIUM ALLOYS IN THE REGION 20 TO 50 ATOMIC PER CENT OF INDIUM.

By G. V. Raynor.

Received 23*rd July*, 1946.

The factors affecting the formation of primary solid solutions of certain elements in magnesium were discussed by Hume-Rothery and Raynor.[1] Of the elements of Group IIIB of the Periodic Table, gallium has an unfavourable size-factor with respect to magnesium, while the size-factor for aluminium is on the borderline of the favourable zone. Indium and thallium have favourable size-factors, but solid solution formation is somewhat restricted for thallium by an abnormally steep fall of the solidus curve. This abnormal depression of melting point appears to be common to solutes of the third long period of the Periodic Table.[2] Indium is therefore the only trivalent solute for which normal behaviour is expected. During an experimental study of the primary solid solutions of the elements of Group IIIB in magnesium,[3] the solid solubility curve for indium was found to show a marked change in direction at approximately 327° c., in contrast to the solubility curves for the remaining elements, which showed a regular decrease of solubility with falling temperature.

No clue to the reason for the direction change was found in the primary solid solution, and it was concluded that it was due to some transformation in the second phase with which the solid solution was in equilibrium. To obtain further information, the work was extended to cover the range 20 to 50 % indium.* Although it was originally intended to investigate the whole system, circumstances necessitated the discontinuance of the research at this point. The present paper describes the results obtained for alloys lying between 20 and 50 % indium.

The previous work of Hume-Rothery and Raynor on the system magnesium-indium is summarised in Fig. 1. The whole system was examined by X-ray methods by Werner Hancke,[4] and four intermediate phases were reported. These were said to be based on the intermetallic compounds Mg_5In_2, Mg_2In, MgIn, and either $MgIn_2$ or $MgIn_3$. The structures of the first three of these phases were found to be respectively body-centred rhombic, hexagonal, and body-centred tetragonal. The system therefore appeared to resemble the system magnesium-gallium, which was investigated by the same author,[4] and also, in some respects, the system magnesium-thallium,[5] in which there is also an intermetallic compound of composition Mg_5Tl_2.

[1] Hume-Rothery and Raynor, *J. Inst. Metals*, 1938, **63**, 227.

[2] Hume-Rothery, *The Structure of Metals and Alloys* (Inst. Metals Monograph and Report Series, No. 1, 1944).

[3] Hume-Rothery and Raynor, *J. Inst. Metals*, 1938, **63**, 201.

[4] Werner Hancke, *Naturwiss.*, 1938, **26**, (35), 577.

[5] Grube, *Z. anorg. Chem.*, 1905, **46**, 76. Grube and Hille, *Z. Elecktrochem.*, 1934, **40**, 101.

* All compositions given in the text of this paper are in atomic percentages.

From Fig. 1, the indium-rich limit of the peritectic reaction at which the primary solid solution reacts with the liquid to form the second solid phase lies at 25·7 %, whereas the composition of the reported phase Mg_5In_2 is 28·57 % indium. It is difficult, therefore, to reconcile these two researches, unless the reported phase Mg_5In_2 has a considerable range of homogeneity. The existence of Mg_5In_2 was not confirmed in the present work.

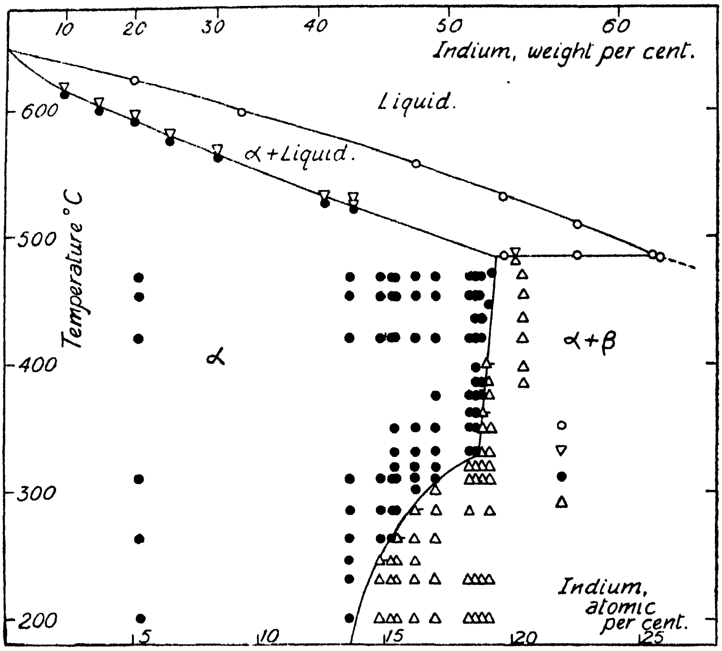

FIG. 1.

○ Points from cooling curves. ▽ Semi-liquid alloys.
● Homogeneous alloys. △ Two-phase alloys.

Experimental.

Materials.—Magnesium of purity 99·95 % was used in the preparation of the alloys; the chief impurities were iron 0·03, aluminium 0·01, and silicon 0·01 %. This material was kindly presented by the National Physical Laboratory. The indium was supplied by the Indium Corporation of America, and was specially refined before use by Messrs. Johnson, Matthey and Co., Ltd.; no impurities were detected by chemical means after this treatment.

Micrographic Work.

Alloys were prepared, in quantities of from 2 to 5 g., either by melting the pure metals together, or by remelting a previously prepared alloy of known composition with more magnesium or indium. In no case, however, was material remelted more than once. It is unlikely that any accumulation of impurities occurred during the research; no evidence of such accumulation was obtained by chemical analysis.

The alloys were melted in crucibles lined with an alumina-fluorspar mixture, well stirred under flux with a recrystallised alumina stirrer, and rapidly poured into cold block copper moulds. Some loss of magnesium occurred during the melting process; this was allowed for, to a first approximation, by weighing out a slight excess of magnesium.

For the annealing experiments, specimens were sealed *in vacuo* in hard glass tubes. Owing to the danger of volatilisation of magnesium from specimen to specimen, all alloys were sealed in separate tubes. Annealing treatments were carried out in electric tube furnaces controlled by Foster temperature regulators. The accuracy of control was ± 1° to ± 1·5° c. over periods of two to three weeks. For shorter treatments, control well within ± 1° c. was possible.

All alloys were given preliminary treatments of 7 to 18 days at temperatures lying between 430° and 350° c., according to composition. Separate specimens were then annealed at successively lower temperatures for periods of from one to three weeks. By this means all phase boundaries were determined by precipitation of a second phase from homogeneous specimens. Alloys employed for the solidus determinations were first homogenised, and small portions were then held at successively higher temperatures for periods of ½ to ¾ hour. During these experiments, temperatures were accurately controlled by hand. At the end of annealing treatments, all specimens were quenched in cold water; the glass tubes shattered and an efficient quench was obtained.

For the microscopical examination of quenched specimens, fresh surfaces were exposed by cutting the alloys with a rotary jeweller's saw, and polished in the usual manner.[3] Etching techniques are described below. All critical specimens were analysed, after a micrographic examination on both sides in order to make sure that the whole piece taken for analysis had the same microstructure. Some of the alloys were analysed by Messrs. Johnson, Matthey and Co., Ltd., to whom the author must express his thanks. The remainder were analysed by the author, using an accurate electrolytic method.

Results.

The constitutional diagram, as deduced from the results of experiments on 33 alloys, is shown in Fig. 2. In this diagram the confirmatory points are plotted in addition to the points representing critical analysed alloys, which are distinguished by full symbols.

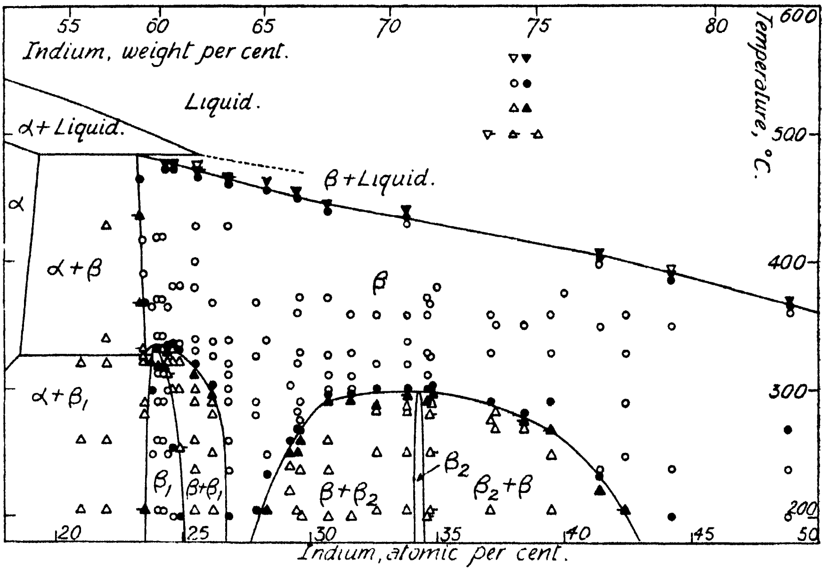

FIG. 2.

▽ ▲ Semi-liquid alloys.
△ ▲ Two-phase solid alloys.
○ ● Homogeneous alloys.
▽ △ △ Two-phase alloys with trace of one constituent.

Above 335° c., the whole composition range from approximately 23·5 to 50 % is occupied by a single homogeneous phase, which has been called β. At lower temperatures, however, two additional phases exist. The β_1-phase, with a narrow range of homogeneity, is stable up to 335° c., while the β_2-phase is stable up to 298° c.

(*a*) **The $(\alpha+\beta)/\beta$-boundary.**—Critical data for this boundary are summarised in Table I. The boundary is a straight line between the invariant point at which α and liquid react to form β (23·2 % indium at 484° c.), and that at which $\beta \rightleftharpoons \alpha + \beta_1$ (23·55 % indium at 327° c.).

TABLE I.—$(\alpha + \beta)/\beta$-BOUNDARY

Alloy No.	Analysed Composition.		Previous Annealing Treatment.	Annealing Treatment.	Microstructure.
	Wt. % In.	At. % In.			
3	58·81	23·21	None	7 days 465·4° c.	β
	58·97	23·34	7 days 465·4° c.	10 days 436° c.	β + trace α
4			10 days 367·7° c.	8 days 417·4° c.	β
			10 days 367·7° c.	12 days 390·5° c.	β
	59·01	23·36	None	10 days 367·7° c.	β + trace α
4A	59·20	23·51	None	10 days 367·7° c.	β
			10 days 367·7° c. +12 days 390·5° c.	8 days 331·1° c.	β + trace α

(*b*) **The $(\alpha + \beta_1)/\beta_1$, $\beta_1/(\beta_1 + \beta)$ and $(\beta_1 + \beta)/\beta$-boundaries.**—Table II shows the critical results for these boundaries. The boundaries of the β_1-phase are smooth curves ; the magnesium-rich boundary falls from 23·9 % indium at 335° c. to 23·5 % at 180° c., while the composition along the indium-rich boundary rises from 23·9 to 25 % indium in the same temperature interval. The $(\beta_1+\beta)/\beta$-boundary falls away from the composition 23·9 % indium at 335° c. at first gradually, and then steeply, and lies at 26·6 % indium at 180° c.

The microstructures of these alloys were not difficult to interpret since the β-phase was always more heavily tarnished than the β_1-phase on etching with alcoholic nitric acid. Confirmation was given by the fact that the β-phase showed twinning of the α-brass type, whereas no twin formation was observed in the β_1-phase.

(*c*) **Equilibrium Relations between the β- and β_1-phases.**—The $\beta/(\beta_1+\beta)$-phase boundary has a maximum, at which the homogeneous β- and β_1-phase fields meet, at 335° c. and 23·9 % indium. At 23·55 % indium the β-phase decomposes eutectoidally into the α- and β_1-phases. This transformation is responsible for the change in direction of the $\alpha/(\alpha + \beta)$-boundary observed at 327° c. in previous work.[3]

Evidence for the form of the equilibrium diagram in this region is strong :

(i) Alloys 6, 7, 8 and 9 at 329° to 331° c. contained only the β_1- and β-phases, whereas alloy 4A at 331° c. showed a typical twinned β-microstructure, with traces of the α-phase which is easily recognisable.

(ii) Alloy 4A at 331° c. showed only traces of the α-phase, whereas the specimen annealed at 326° c. contained relatively much more of this phase.

(iii) The β-phase at 331° c. was twinned, but no twins were observed in the alloy annealed at 326° c.

Similar results were obtained for other duplex alloys annealed above and below 327° c. At this temperature, the indium-rich boundary of the two-phase region steps sideways in the direction of higher indium content. Below 327° c. α is in equilibrium with β_1, but above this temperature, equilibrium involves the α- and β-phases.

(*d*) **The $\beta/(\beta + \beta_2)$ and $\beta_2/(\beta + \beta_2)$-boundaries.**—Table III contains the data from which these boundaries are established. The $\beta/(\beta + \beta_2)$-boundary rises to a maximum at 298° c. and approximately 34·3 % indium; the etching experiments indicate that the phase β_2 exists over a narrow composition range in the region of 34·3 % indium. Evidence for this is clearly illustrated by the microstructures of alloys 14 to 31 annealed at 200° to 205° c. In all cases the phase richest in indium etched dark; alloys 15 to 22 showed a mixture of light and dark phases, with the latter increasing regularly with indium content. Alloy 22 consisted mainly of the dark constituent, with a small amount of the lighter phase evenly distributed. Alloys 23 to 31, however, consisted of the dark phase together with increasing amounts of an even darker etching phase, which formed almost the whole of alloy 31.

TABLE II.—$(\alpha + \beta_1)/\beta$, $\beta_1/(\beta_1 + \beta)$, AND $(\beta_1 + \beta)/\beta$-BOUNDARIES

Alloy No.	Analysed Comp.		Previous Annealing Treatment.	Annealing Treatment.	Microstructure.
	Wt. % In.	At. % In.			
4A			10 days 367·7° C.	14 days 326° C.	$\beta_1 + \alpha$
			10 days 367·7° C. +12 days 390·5° C.	8 days 322·5° C.	$\beta_1 + \alpha$
			10 days 367·7° C.	12 days 289·4° C.	$\beta_1 + \alpha$
			,,	12 days 280·4° C.	$\beta_1 + \alpha$
	59·20	23·51	,,	14 days 205° C.	β_1 + trace α
5	59·62	23·80	11 days 365·5° C.	9 days 321° C.	β_1 + trace α
	59·80	23·90	,,	11 days 299° C.	β_1
6			9 days 419·3° C.	7 days 342° C.	β
	59·86	24·01	,,	9 days 330·7° C.	$\beta_1 + \beta$
	59·92	24·10	,,	25 days 319° C.	β_1 + trace β
			,,	16 days 311·8° C.	β_1
7			9 days 419·3° C.	7 days 342° C.	β
	60·08	24·18	,,	9 days 330·7° C.	$\beta_1 + \beta$
			,,	25 days 319·5° C.	β_1 + trace β
			,,	16 days 311·8° C.	β_1
8	60·31	24·36	11 days 365·5° C.	8 days 334·4° C.	β
	60·36	24·39	,,	10 days 329° C.	$\beta_1 + \beta$
			,,	9 days 321° C.	β_1 + little β
			,,	13 days 311·3° C.	β_1 + trace β
			,,	11 days 299° C.	β_1
9	60·69	24·65	8 days 380·7° C.	14 days 336° C.	β
			,,	7 days 331° C.	$\beta_1 + \beta$
			,,	14 days 300° C.	β_1 + little β
	60·74	24·69	,,	15 days 254° C.	β_1
10	60·98	24·88	8 days 380·7° C.	7 days 331° C.	β
			,,	6 days 321° C.	$\beta_1 + \beta$
			,,	15 days 254° C.	β_1 + trace β
	60·98	24·88	,,	12 wk. 200° C.	β_1
11	61·88	25·59	18 days 428° C.	9 days 319·8° C.	β
	61·66	25·42	,,	8 days 310·8° C.	β + little β_1
			,,	21 days 200° C.	$\beta_1 + \beta$
12	62·64	26·21	10 days 367·7° C.	14 days 303·6° C.	β
	62·63	26·20	,,	7 days 294·6° C.	β + trace β_1
			,,	14 days 205° C.	$\beta_1 + \beta$
13	63·34	26·80	18 days 428·1° C.	21 days 200° C.	β

Thus, an almost invariant intermediate phase (β_2) exists between alloys 22 and 23. Owing to the difficulty of casting small ingots to a predetermined composition, it was not practicable to place the position of this phase more accurately. The conclusions were later confirmed by X-ray examination (see page 21).

(*e*) **The Solidus.**—The solidus curve (see Table IV) falls smoothly from 484° C. at 23·2 % indium to 366° C. at 49 %. Apart from a slight inflection between 32 and 36 % indium, no evidence of any singularity was obtained. The microstructures of alloys quenched from the semi-liquid region were typical, the chilled liquid being recognisable as triangular areas at the junctions of grain boundaries.

(*f*) **The β-solid Solution.**—Throughout the whole composition range investigated, homogeneous alloys were obtained above 335° C. near 25 %, and above 298° C. in the region of 35 % indium (Fig. 2). Below 35 % indium a typical large-grained polygonal equiaxed microstructure was obtained, with twin

TABLE III.—$\beta/\beta + \beta_2$ AND $\beta_2/\beta + \beta_2$-BOUNDARIES.

Alloy No.	Analysed Comp.		Previous Annealing Treatment.	Annealing Treatment.	Microstructure.
	Wt. % In.	At. % In.			
14	64·64	27·92	10 days 367·7° c.	14 days 205° c.	β
15	65·08	28·31	14 days 338·6° c.	13 days 233·4° c.	β
	65·06	28·29	14 days 338·6° c. + 10 days 249° c.	22 days 205° c.	β + little β_2
16	66·07	29·21	14 days 303·6° c.	15 days 260·3° c.	β
	66·05	29·19	,,	8 days 250·2° c.	β + trace β_2
			,,	12 days 239·5° c.	β + little β_2
17	66·40	29·51	7 days 359° c.	7 days 268° c.	β
			,,	7 days 251·1° c.	β + little β_2
18	66·52	29·63	7 days 371·8° c.	7 days 267·9° c.	β
	66·43	29·54	,,	15 days 260° c.	$\beta + \beta_2$
19	67·71	30·76	7 days 371·8° c.	8 days 296° c.	β
	67·62	30·69	,,	16 days 290° c.	β + little β_2
20	68·51	31·56	14 days 359° c.	7 days 296° c.	β
	68·55	31·59	,,	16 days 290° c.	$\beta + \beta_2$
21	69·55	32·61	7 days 359° c.	6 days 301·3° c.	β
			,,	10 days 286° c.	$\beta + \beta_2$
22	70·70	33·83	7 days 359° c.	6 days 301·3° c.	β
			,,	8 days 296° c.	$\beta_2 + \beta$
23	71·39	34·59	14 days 359° c. + 8 days 310·8° c.	7 days 300·1° c.	β
			14 days 359° c.	16 days 290·3° c.	β_2 + trace β
24	71·47	34·68	10 days 367·7° c.	14 days 303·6° c.	β
	71·57	34·79	,,	7 days 294·6° c.	β_2 + trace β
			,,	12 days 289·4° c.	β_2 + trace β
			,,	12 days 280·4° c.	β_2 + trace β
			,,	14 days 205° c.	β_2 + trace β
25	73·60	37·14	14 days 359° c.	16 days 290·3° c.	β
			,,	8 days 275·9° c.	$\beta_2 + \beta$
27	74·60	38·36	7 days 350·1° c.	14 days 281·9° c	β
	74·68	38·46	,,	6 days 274·4° c.	β + little β_2
28	75·46	39·45	14 days 359° c.	16 days 290·3° c.	β
			,,	7 days 267·9° c.	β + trace β_2
30	76·90	41·37	7 days 350·1° c.	14 days 231·4° c.	β
	77·02	41·53	,,	6 days 220·3° c.	$\beta + \beta_2$
31	77·65	42·40	14 days 359° c.	21 days 205·2° c.	β + trace β_2

markings analogous to those observed in α-brasses. Twinning was seen after quenching from all temperatures. Above 35 %, however, although alloys quenched after long annealing below 300° to 320° c. showed the typical polygonal grain structure, alloys quenched from above this range showed characteristic parallel stripes across grains. The orientation of the stripes within any one grain was constant, but varied from grain to grain. It was concluded that the alloys were homogeneous, both above and below 300° to 320° c., but that a transformation occurred in alloys quenched from above this range, either during or shortly after quenching. Later experiments showed that the change occurred shortly after quenching; alloys containing 40 to 50 % indium were cold after quenching in water from above 320° c., but rapidly became too hot to hold in the hand. No quantitative measurements were made, but it is estimated that temperatures exceeding 100° c. were reached.

TABLE IV.—THE SOLIDUS.

Alloy No.	Analysed Composition.		Quenching Temperature °C.	Microstructure.
	Wt. % In.	At. % In.		
8	60·31	24·36	478	β + liquid
			473	β
9	60·69	24·65	478	β + liquid
			473	β
11	61·88	25·59	470·3	β + trace liquid
			466·1	β
13	63·34	26·80	466	β + trace liquid
			460·9	β
15	65·08	28·31	463	β + liquid
			457·5	β
18	66·43	29·54	454·6	β + liquid
			450	β
19	67·71	30·76	446	β + liquid
			440	β
22	70·70	33·83	440·8	β + liquid
			436	β
30	76·90	41·37	407·7	β + liquid
			403	β
32	78·91	44·22	390·5	β + liquid
			385·7	β
33	81·88	48·92	370·5	β + liquid
			366	β

X-ray Work.

The nature of the transformation observed was studied by high-temperature X-ray work, and certain conclusions from the micrographic work were verified. The technique employed in the X-ray work resembled that described in previous publications.[6, 7, 8]. Filings were prepared in an atmosphere of pure dry argon, using a fine dentist's drill (see Raynor and Hume-Rothery [8]). Devices were included for sieving the filings in argon; thus, for experiments with the high-temperature camera, alloys were filed, sieved, and sealed into evacuated thin-walled silica capillaries without exposure to air at any stage.

In some cases the filings, after suitable strain-relieving treatment, were mounted on a hair in the usual manner. Whenever heat treatments longer than those for strain-relief were required, however, the filings were sealed in silica capillaries and the complete X-ray specimen was annealed.

Copper $K\alpha$-radiation from a Metropolitan-Vickers demountable X-ray machine was used for all experiments. Exposures at room temperature were made in a 9 cm. Debye-Scherrer camera of the usual pattern, or in the 9 cm. high-temperature camera described by Hume-Rothery and Reynolds.[7] Experiments at other temperatures were all made in the high-temperature apparatus, which was fitted with two thermocouples. A ring-shaped platinum/platinum-rhodium thermocouple was used to measure the specimen temperature; the other thermocouple (alumel-chromel) was connected to a Foster potentiometric regulator. In spite of the small thermal capacity of the camera furnaces, it was possible to control the specimen temperature for periods exceeding 12 hr. to an accuracy of ± 1° c. During exposures, made after varying periods of anneal, temperatures were controlled by hand to ± 0·5° c.

---

[6] Hume-Rothery, Reynolds and Lewin, *Proc. Roy. Soc. A*, 1936, **157**, 167.

[7] Hume-Rothery and Reynolds, *ibid.*, 1938, **167**, 25.

[8] Raynor and Hume-Rothery, *J. Inst. Metals*, 1939, **65**, 379.

Before an experiment, the furnaces were adjusted to exact temperature equality to eliminate gradients along the specimen. The temperature distribution was checked at intervals, and it is estimated that the exposure temperatures quoted in subsequent sections are accurately reproducible.

(I) The Transformations.

The twinning of the β-solid solution suggested that its crystal structure was face-centred cubic. A diffraction pattern obtained at room temperature with filings from alloy 11 as quenched from 428·1° c. confirmed this. The individual lines, however, were not of high quality owing to volatilisation of magnesium during annealing. Further experiments were therefore made in the high-temperature camera. Filings from the same alloy were exposed at 361·7° c. after annealing in the camera for 5 hr. at the same temperature. The film confirmed that the structure at this temperature was face-centred cubic. A further exposure, however, taken at room temperature after quickly cooling the specimen showed that a superlattice of the Cu_3Au type had developed. All the expected superlattice lines were present and well defined (Fig. 4*a*). Thus, between 360° c. and room temperature an order-disorder transformation occurs in alloys of composition near to 25 % indium.

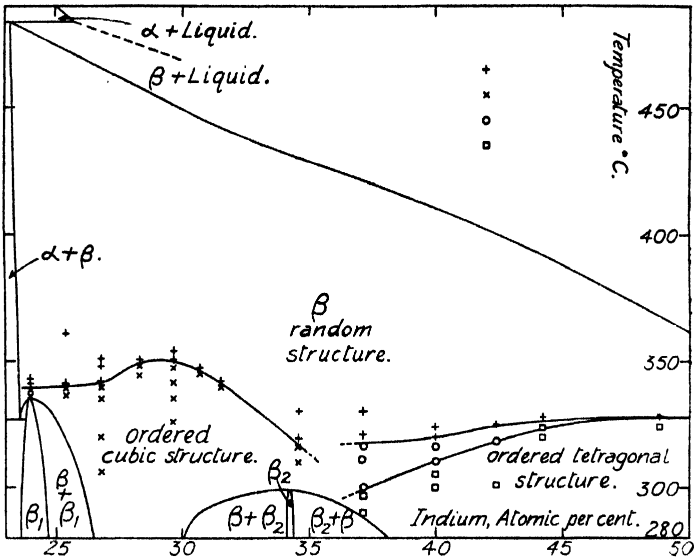

FIG. 3.

+ random face-centred cubic.
× ordered face-centred cubic.
○ ordered orthorhombic.
□ ordered tetragonal.

An exposure of alloy 31 was made at 330° c. The diffraction pattern was again face-centred cubic, and confirmed the conclusions of the micrographic work. A similar photograph, taken after cooling the specimen, showed that a superlattice of the CuAu type (ordered face-centred tetragonal) had developed (Fig. 4*b*). This change, therefore, is responsible for the thermal effects noticed in alloys containing 40 to 50 % indium. The strains involved in transition from the cubic to the tetragonal form are responsible for the micrographic effects observed.

Since only small quantities of material were available, the transformation temperatures were determined by the high-temperature X-ray method. Filings of each alloy, made after quenching the parent ingot from a temperature at which it was homogeneous, were sealed in evacuated silica tubes and annealed in the high-temperature camera for approximately 6 hr. at a given temperature; X-ray exposures were then made at the same temperature. This process was repeated until exposures at narrowly separated temperatures gave a pair of patterns, with superlattice lines present only in that obtained at the lower temperature.

TABLE V.—THE ORDER-DISORDER TRANSFORMATION TEMPERATURES FOR ALLOYS CONTAINING LESS THAN 35 ATOMIC % OF INDIUM.

Alloy No.	Composition, at % Indium.	Temperature of Exposure °c.	Condition of Alloy.
6	24·01	341·0	Random
		338·7	Ordered
11	25·42	341·4	Random
		339·5	Ordered
13	26·80	343·0	Random
		339·2	Ordered
15	28·30	350·5	Random
		348·0	Ordered
18	29·63	350·4	Random
		347·0	Ordered
19	30·70	347·5	Random
		344·9	Ordered
20	31·56	344·0	Random
		339·5	Ordered
23	34·59	319·5	Random
		316·0	Ordered

TABLE VI.—THE ORDER-DISORDER TRANSFORMATION TEMPERATURES FOR

Alloy No.	Composition, Atomic % Indium.	Temperature of Exposure °c.	Condition of Alloy.
25	37·14	321·0	Face-centred cubic random
		316·5	Orthorhombic
		300·0	,,
		296·2	Face-centred tetragonal ordered
29	40·00	320·0	Face-centred cubic random
		316·0	Orthorhombic
		310·0	,,
		305·0	Face-centred tetragonal ordered
31	42·40	325·0	Face-centred cubic random
		318·2	Orthorhombic
		301·2	Face-centred tetragonal ordered
32	44·22	328·0	Face-centred cubic random
		323·5	Face-centred tetragonal ordered
33	48·77	328·0	Face-centred cubic random
		324·0	Face-centred tetragonal ordered

In some cases only one specimen was used but in others, several. The effects were, however, accurately reproducible from specimen to specimen. For several alloys, the transformation was approached from both the high and low temperature sides. The critical temperatures obtained confirmed each other, showing that there was no hysteresis, and also that the annealing times were sufficient for equilibrium.

The results of these experiments are shown in Fig. 3, and the critical experiments are summarised in Tables V and VI. For alloys with less than 35 %

indium the maximum transformation temperature does not occur at the theoretical composition Mg_3In. The transformation curve shows an ill-defined maximum at approximately 29 %, the critical temperatures in the region of 25 % being relatively low. This may be connected with the presence of the low-temperature β_1-phase; it may also be significant that the maximum on the transformation curve corresponds with the composition range in which the β-solid solution is stable down to 200° c. The occurrence of a maximum on the transformation curve at a composition other than 25 % has been observed in the copper-palladium alloys.[9] Here the maximum occurs at 17 % Pd, but the situation is more complex than in the magnesium-indium alloys, in so far as only the alloys with less than 20 % Pd behave analogously to the Cu_3Au type of alloy. Those containing from 20 to 27 % Pd become tetragonal when ordered. The transformation temperatures for alloys with compositions between 23 and 25 % indium are slightly higher than the maximum on the $\beta_1/(\beta_1 + \beta)$-phase boundary. Equilibrium between the β_1- and β-phases therefore involves the ordered face-centred cubic structure at all temperatures.

Alloys with compositions between 36 and 50 % indium behave in some respects analogously to the CuAu type of alloy, and transform to a face-centred tetragonal lattice on ordering. Except, however, at compositions close to 50 %, the cubic and tetragonal regions in the equilibrium diagram are separated by a temperature range in which the alloys are orthorhombic. Diffraction patterns from alloys annealed in this range showed only faint superlattice lines; the extent of this range increased with increasing deviation from the equi-atomic composition. The occurrence of the orthorhombic range was unexpected under the conditions employed. Diffraction patterns obtained at room temperature from alloys 25, 29 and 31 after cooling from a temperature at which the alloys had the random cubic structure showed only the ordered face-centred tetragonal structure. The orthorhombic structure, therefore, is not stable at low temperatures; if it were an intermediate in the transformation from the cubic to the tetragonal structure the relatively rapid cooling would be expected to preserve, to a recognisable extent, the orthorhombic structure.

Since it was thought possible that the orthorhombic structure was a metastable intermediate, characteristic of the ordering process at high temperatures only, which slowly relaxed isothermally to the tetragonal form, annealing periods of 24 hr. were employed for temperatures at which the orthorhombic structure had been observed after 6 hr. In no case was any difference observed between the diffraction patterns obtained in the two series of experiments. The orthorhombic structures are therefore stable in the temperature range shown in Fig. 3. The form of the transformation curves suggests that this behaviour is connected with a deficit of indium atoms with respect to the ideal composition MgIn.

This behaviour is somewhat analogous to the mode of ordering observed for the equiatomic copper-gold alloys. In these alloys, according to Johansson and Linde,[10] an orthorhombic ordered structure is produced by quenching from temperatures near to that of the onset of order. Experiments by Källbäck, Nyström and Borelius[11] on the isothermal ordering of quenched samples of CuAu, however, indicate that the orthorhombic structure is stable above 370° c., while the tetragonal form is stable below this temperature. Support for the latter view is given by the work of Hultgren and Tarnopol,[12] who found that the orthorhombic structure was not a metastable stage in ordering, since it was obtained not only by annealing disordered alloys, but also the ordered tetragonal alloys, at 370-400° c. Further, the orthorhombic structure persisted after long annealing treatments.

A quantitative examination of the lattice spacing relationships for alloys in the range for which tetragonal structures are found has not yet been made. The axial ratio c/a of the tetragonal form, however, is approximately 0·96, while the ratio b/a for the orthorhombic form is close to unity.

II. X-ray Work carried out to confirm the Micrographic Results with regard to the β_1 and β_2-phases.

(*a*) **Alloys in the Range 23 to 26 % Indium**—Alloy 11, when cooled from 361·7° c., gave a diffraction pattern in which all lines could be accounted for

---

[9] Jones and Sykes, *ibid.*, 1939, **65**, 419.

[10] Johansson and Linde, *Ann. Physik.*, 1936 (V), **25** (1), 1.

[11] Källbäck, Nyström and Borelius, *Ing. Vetenskaps Akak.*, *Handlinger*, 1941, **157**, 21.

[12] Hultgren and Tarnopol, *Metals Tech.*, 1939, **6** (1); *A.I.M.M.E.*, *Tech. Publ.*, No. 1010, 10.

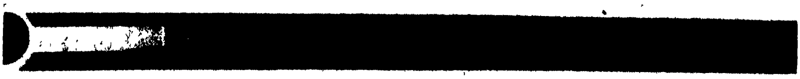

(*a*) Ordered face-centred cubic structure diffraction pattern.

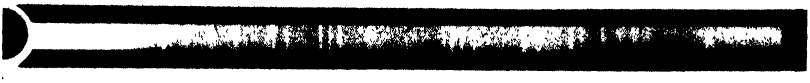

(*b*) Ordered face-centred tetragonal structure diffraction pattern.

FIG. 4.

FIG. 5.—Diffraction pattern from alloy 6 annealed at 282·6° C. β_1-phase.

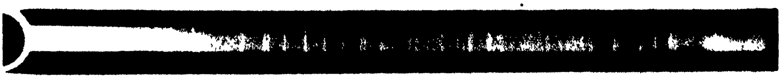

FIG. 6.—Diffraction pattern from alloy 22 annealed at 282·6° C.; mainly β_2-phase.

[*To face page* 25.

by an ordered face-centred cubic structure, in spite of its being two-phase at equilibrium below 316° c. The superlattice change therefore occurs much more easily than the phase change. Filings made from alloy 11 as quenched from the β-region were exposed at 284° c. after annealing for 5 hr. Only the face-centred cubic pattern was visible in the photograph, apart from some faint extra low-angle lines. After further annealing for 17 hr. the cubic pattern persisted, while the extra lines became rather more intense. Annealing periods of the order of 24 hr. were thus insufficient to accomplish the precipitation of β_1 from the homogeneous grains, and the specimen of filings was annealed for 6 days at 282·6° c., and exposed at room temperature. The photograph showed the ordered cubic diffraction lines, with well-marked extra lines corresponding to the β_1-phase. To confirm this, filings of alloy 6 were annealed for 6 days at 282·6° c. A complex diffraction pattern was obtained (Fig. 5), containing no face-centred cubic diffraction lines, but corresponding exactly with the extra lines in the photograph of alloy 11. Powder specimens of alloys 11 and 6, originally β, gave similar results after annealing at 263° c. for 6 days. Alloy 13 after the same treatment, however, gave a diffraction pattern showing only the ordered face-centred cubic lines.

The results of these experiments, together with others using further alloys in this region, confirm the interpretation of the micrographic work, and show that the structure of the β_1-phase, as indicated by the diffraction pattern of alloy 6 after annealing at 282·6° and 263° c., is complex.

(*b*) **Alloys in the Range 26 to 43 °/₀ Indium.**—At 200° c., two distinguishable two-phase regions should exist in the range 26 to 43 % indium (Fig. 2). From 28·1 to approximately 34 % indium, the β_2-phase and the ordered face-centred cubic β-phase are in equilibrium, while from approximately 34·5 to 42·4 % indium the β_2-phase and the ordered face-centred tetragonal β-phase rich in indium are in equilibrium.

X-ray experiments confirmed these conclusions. Alloys 18, 19, 20, 23, 25, 28, and 31 as annealed for a long period at 200° or 205° c., were filed, and the filings exposed at room temperature after a short strain relieving anneal at 200° c. In agreement with the micrographic work, a new and complex diffraction pattern appeared in the photograph from alloy 23. According to the etching experiments, this alloy consisted of the β_2-phase with a small amount of the β-phase. Alloys containing less indium (No. 18, 19 and 20) gave diffraction patterns in which the cubic β-phase lines were present in addition to the β_2-lines, while alloys richer in indium (No. 25 and 28) gave films containing the β_2- and the tetragonal β-phase lines. The film from alloy 31 (micrographically β + a trace of β_2) showed only the face-centred tetragonal pattern.

As an additional check, filings were made from specimens of alloys 17, 21 and 22 annealed at 282·6° c. After a strain relief treatment at the same temperature, diffraction patterns were obtained at room temperature. Alloy 17 showed only the ordered cubic lines, while alloy 22 showed the same complex pattern as alloy 23 annealed at 205° c., together with faint lines due to admixture with the ordered cubic phase (Fig. 6). Alloy 21 gave a diffraction pattern combining the features of those from alloys 17 and 22.

The presence of the β_2-phase is therefore confirmed; its diffraction pattern does not change between 282·6° and 200° c. It is also clear that alloy 22 lies to the magnesium-rich side of the β_2-phase, as indicated by the etching experiments. The persistence of the cubic β-phase at low temperatures between 26·6 and 27·7 % indium is also confirmed.

(*c*) **The Range 50 to 100 °/₀ Indium.**—Owing to indium shortage, it was possible to examine only one alloy, containing 92·66 % indium. It was annealed *in vacuo* for one month at 100° c. After this treatment the alloy was soft, and difficult to prepare for microscopic examination. Satisfactory results were obtained by alternate polishing and etching, and a homogeneous, equiaxed large-grained microstructure was obtained. The melting point of this alloy, from quenching experiments, lay between 180° and 175° c.; this result is consistent with a steady fall of the solidus curve from 366° c. at 49 % indium to the melting point of indium (155·4° c.), and suggests that the phase denoted β in Fig. 2 stretches continuously up to 100 % indium.

Filings were made from the annealed alloy, strain-relieved at 100° c., and exposed to X-rays. The diffraction pattern showed a face-centred tetragonal structure similar to that of indium itself. It is probable that, on further dilution with magnesium, this tetragonal structure merges into the face-centred cubic structure of the disordered alloys already described. There is no need for a two-phase region between face-centred cubic and face-centred tetragonal structures; the gradual transition, without any phase discontinuity, has already been established for solid solutions of cadmium in indium[13] and for solid solutions of copper in manganese.[14]

Discussion.

The atomic size relationships involved in the magnesium-indium alloys have been discussed in a previous paper;[1] the size-factor and other complicating effects are small, and the system is favourable for investigating the normal valency effects of a trivalent solute in magnesium. Several further points of interest arise from the present work.

(*a*) **The Transformation at 327° C.**—The change in direction of the primary solid solubility curve for indium in magnesium is due to a change in the phase with which the primary solid solution is in equilibrium. Above 327° C. the second phase has a face-centred cubic structure (ordered or disordered), while below this temperature, the β_1-phase with a complex crystal structure is stable. There is no change in the primary solid solution boundary at the temperature at which ordering occurs.

(*b*) **The β_1-phase.**—This phase has no analogy in the other binary alloys of magnesium with the elements of Group IIIB of the Periodic Table. The phases with which the primary solid solutions are in equilibrium are:

System MgAl — Mg_4Al_3
System MgGa — Mg_5Ga_2
System MgTl — Mg_5Tl_2.

The structure of the β_1-phase is complex, and not yet examined in detail. The phase does not, however, correspond with Mg_5In_2, as suggested by Hancke.[4]

(*c*) **The β_2-phase.**—This phase may correspond with the phase Mg_2In reported by Hancke.[4] The present work shows, however, that it does not occur accurately at the composition Mg_2In. The crystal structure is again complex.

(*d*) **The Superlattice Rearrangements.**—The experiments described show that the face-centred cubic β-phase orders on cooling. In alloys containing up to 35 % indium, the ordering process is the same as in Cu_3Au. For alloys containing between 36 and 50 % indium, the ordering process is analogous to that of the CuAu alloys, in so far as an ordered tetragonal structure with $c/a <$ unity is produced.

This behaviour is of interest in connection with the size-factor of indium with respect to magnesium. The variation with atomic number of the interatomic distances in the crystals of the elements suggests that metallic indium is not fully ionised. General support is given to this view by the general chemistry of indium, where the tendency towards the formation of univalent In^+ ions is well marked. According to this view, therefore, the interatomic distances in the metallic indium crystal, in which each atom has 4 neighbours at 3·241 A. and 8 neighbours at 3·368 A., correspond with the incompletely ionised state. The closest distance of approach for the fully ionised state would be expected to be of the order of 0·2 to 0·3 A. smaller, so that the interatomic distance corresponding to full ionisation may be estimated as 2·95 A. If indium when alloyed with magnesium is not fully ionised, the size-factor, expressed in the usual way as $\frac{(d_{\mathrm{In}} - d_{\mathrm{Mg}})100}{d_{\mathrm{Mg}}}$, where d represents the closest distances of approach of atoms in the respective crystal structures, is very favourable. With such a small size-factor it is improbable that such well-defined superlattices as are observed would be formed. If, however, the indium is present in the alloy in the fully ionised form, the size-factor is markedly greater, and of the order of 8 %. The formation of superlattices is much more consistent with a size-factor of this order, as illustrated by their presence in the system MgCd, where the size-factor is similar. The results of this work may be taken as evidence that, when alloyed with magnesium, indium is present in the fully ionised state. This is not unexpected, in view of the relatively high deforming power of the divalent magnesium ion.

---

[13] Betteridge, *Proc. Physic. Soc.*, 1938, **50**, 519.

[14] Dean, Long, Graham, Potter and Hayes, *Amer. Soc. Metals*, Preprint No. 9, 1944, 21.

(*e*) **The Indium-rich Alloys.**—It appears probable that indium and magnesium form an unbroken series of solid solutions between 25 and 100 % indium. This behaviour may be connected with an effect analogous to the " diagonal relationship " in the chemistry of certain elements in the periodic table. For instance, lithium tends to resemble magnesium, and beryllium tends to resemble aluminium. The effect of this on alloy formation is illustrated by the extensive solid solution of lithium in magnesium, in spite of the fact that the solubility of elements of lower valency in solvents of higher valency is usually restricted, and the very wide solid solution of magnesium in lithium. The general cause of such " diagonal relationships " is connected with the mutually compensating factors of increase in ionic charge on passing from one group to the next higher, and increase in ionic size on passing from one period to the next higher. A rough measure of the effect is given by the expression $P = \frac{\text{Ionic charge}}{(\text{Ionic radius})^2}$, which expresses the charge density round the outsides of the ions. Elements with similar values of P may be expected to show rough analogies with each other. Thus beryllium ($P = 6{\cdot}6$) resembles aluminium ($P = 4{\cdot}9$) rather than magnesium ($P = 2{\cdot}5$); similarly, lithium ($P = 2{\cdot}2$) resembles magnesium ($P = 2{\cdot}5$) rather than sodium ($P = 1{\cdot}0$). The values of P for Al, Ga, In, and Tl are respectively 4·9, 4·6, 2·7, and 2·2. Indium, therefore is the Group IIIB element, which might be expected to be most similar to magnesium in the general charge density round the ion, and it is possible that this, taken in conjunction with the favourable size-factor, is responsible for the effects observed.

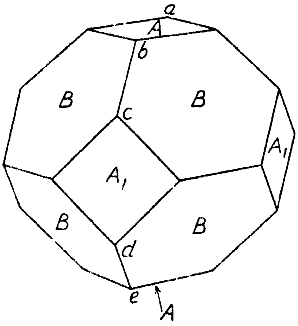

FIG. 7.

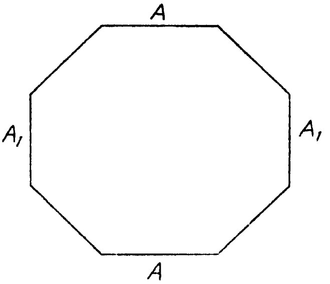

FIG. 8.

This form of equilibrium diagram implies that the tetragonal structure of indium merges into the cubic structure of the alloys less rich in indium. This phenomenon is observed in the indium-rich indium-cadmium alloys.[13] A tentative explanation may be advanced in terms of the Brillouin zone theory of metals. The Brillouin zone for the indium structure is similar to that for the face-centred cubic structure (Fig. 7), but is somewhat contracted parallel to the vertical *c*-axis of the crystal. At three electrons per atom, overlap of electrons occurs across the *B*-faces of the zone. It is possible that, for indium, overlap also occurs across the *A*-faces, which are nearer the origin of *k*-space than the side A_1-faces. According to the

Jones theory,[15] an overlap across the face of a Brillouin zone tends to compress the zone at right angles to the plane of the face. The magnitude of the effect is proportional to the number of overlapping electrons. A reduction of the overlap for a given direction thus relieves the stress, and allows expansion of the zone in this direction. Expansion of the zone corresponds with contraction of the lattice.

For convenience, we may consider a two-dimensional case obtained by taking a section of the Brillouin zone for the indium structure along the plane *abcde* (Fig. 8). The B-overlaps are symmetrical and need not be further considered. If, however, overlap does occur across the A-faces, it will be reduced by the solution in indium of a divalent metal. The zone will therefore tend to expand more in the c-direction than at right angles to it. Similar results follow from considering the vertical plane at right angles to *abcde*. Assuming overlap across the A-faces for metallic indium, therefore, the crystal lattice may be expected to contract more in the direction of the c-axis than at right angles to it, and will thus relax towards cubic symmetry, as the electron to atom ratio decreases.

Grateful acknowledgement is due to Prof. C. N. Hinshelwood, F.R.S., for laboratory accommodation and other research facilities, and to Dr. W. Hume-Rothery, F.R.S., in whose laboratory the work was carried out, for his interest and encouragement. The author also thanks the Department of Scientific and Industrial Research for a Senior Research Award, which he held while part of the work was in progress, and the Warren Committee of the Royal Society for financial assistance.

Summary.

The constitution of the magnesium-indium alloys has been examined, in the range 20 to 50 atomic % of indium, by micrographic and X-ray methods. The results show that alloys containing from 23·5 to 50 atomic % of indium, at temperatures between the solidus and 335° c. in the region of 25 atomic % of indium, or 298° c. in the region of 35 atomic % of indium, consist of a homogeneous face-centred cubic solid solution, denoted β. The solidus curve falls smoothly over this composition range, and experiment suggests that the solid solution extends to 100 % of indium. At lower temperatures, two other phases with complex structures are found. The β_1-phase (23·5 to 25 atomic % of indium at 200° c.) is stable up to 335° c., and the form of the equilibrium diagram is such that the primary solid solution of indium in magnesium is in equilibrium with β above 327° c., but with β_1 below this temperature. The β_2-phase has a limited range of homogeneity in the neighbourhood of 34·3 atomic % of indium, and is stable up to 298° c. The two-phase $\beta/(\beta + \beta_2)$ regions extend from 28·1 to 42·4 atomic % of indium at 200° c., but disappear at 298° c. Between 26·6 and 28·1 atomic % of indium, the β-phase is stable down to 200° c.

Two superlattice rearrangements are observed for the β-alloys, analogous to the ordering of Cu_3Au and CuAu alloys. Alloys in the region of 25 atomic % of indium preserve cubic symmetry on ordering, but those containing from 36 to 50 atomic % of indium become tetragonal when ordered. Between the lowest temperature at which the cubic random structure is observed, and the highest temperature at which the tetragonal ordered structure appears, there is a range of orthorhombic structures which appears to be stable. The extent of this range diminishes as the composition of the alloy approaches 50 atomic % of indium.

The bearing of some of the results on alloy theory is discussed.

Department of Metallurgy,
The University,
Edgbaston, Birmingham 15.

---

[15] Jones, *Proc. Roy. Soc. A*, 1934, **147**, 400.

EQUILIBRIUM BETWEEN $Al_2Mg_3Zn_3$ AND THE PRIMARY SOLID SOLUTION IN THE SYSTEM ALUMINIUM-MAGNESIUM-ZINC.

By G. V. Raynor and W. Hume-Rothery.

Received 7th August, 1946.

I. Introduction.

During the course of work directed towards an understanding of the equilibrium relations in the quaternary system aluminium-magnesium-manganese-zinc, the aluminium-rich corner of the ternary aluminium-magnesium-zinc system was investigated in detail.[1, 2, 3] It was found that the solid solubility isothermals, along which the primary solid solution of zinc and magnesium in aluminium is in equilibrium with a ternary compound *T*, could be represented accurately, except at high percentages of magnesium and low percentages of zinc, by the expression (Mg)(Zn) $= K$. In this expression (Mg) and (Zn) are the atomic percentages of magnesium and zinc, and *K* is a constant.

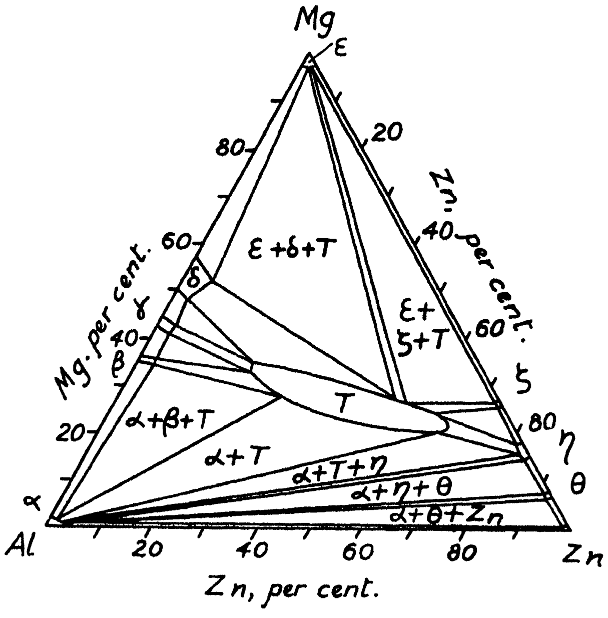

Fig. 1.

As shown by Hume-Rothery [4] this type of relation is found when a primary solid solution is in equilibrium with a compound of substantially fixed composition. The solid solubility isothermals for the equilibrium

---

[1] Butchers, Raynor and Hume-Rothery, *J. Inst. Metals*, 1943, **69**, 209.

[2] Little, Raynor and Hume-Rothery, *ibid.*, 1943, **69**, 423.

[3] Little, Raynor and Hume-Rothery, *ibid.*, 1943, **69**, 467.

[4] Hume-Rothery, *Phil. Mag.*, 1936, **22** (vii), 1013.

between the primary aluminium-rich solid solution and Mg_2Si in the system aluminium-magnesium-silicon, for example, obey the expression $(Mg)^2(Si) = K$.

According to the work of Köster and Dullenkopf,[5] however, the ternary phase T in the aluminium-magnesium-zinc system is of widely variable composition. Their results, for room temperatures, are reproduced in Fig. 1. The range of homogeneity of the T-phase includes the composition $Al_2Mg_3Zn_3$, upon which the phase is usually regarded as based.

In view of the variable composition of the ternary phase, the existence of the relation $(Mg)(Zn) = K$ was unexpected. The present paper describes work undertaken to investigate this problem.

II. Experimental.

In order to examine the equilibrium relations between the T-phase and the primary solid solution, the tie-lines connecting the compositions of the two phases in equilibrium at a given temperature must be determined. For this purpose three series of alloys were prepared.

(*a*) A series with compositions close to the aluminium-rich boundary of the T-phase, containing only very small amounts of the α-phase.

(*b*) A series with compositions close to the primary solubility limit, containing only small amounts of the T-phase.

(*c*) A series of intermediate compositions, containing the α- and T-phases in the approximate ratio 1 : 2.

The metals used for preparing the alloys were of high purity. The aluminium was of superpurity grade, supplied by the British Aluminium Company, Ltd.; the zinc was spectroscopically pure material obtained from the Zinc Development Association, and the magnesium was of 99·95 % purity, obtained from the Magnesium Metals and Alloys Company, Ltd.

Alloys were prepared by melting together the appropriate quantities of the component metals under flux in crucibles lined with an alumina-fluorspar mixture. After thorough stirring with an alumina rod, the alloys were cast into heavy copper moulds, giving ingots 5/16 in. in diameter.

Annealing treatments were carried out in sealed evacuated glass tubes. A separate tube was used for each alloy in order to avoid changes in composition by volatilisation of magnesium or zinc, and consequent distillation from one specimen to another. The furnaces in which the annealing experiments were made were controlled by Foster temperature regulators to within ± 1° C. of the required temperature.

For the X-ray experiments, the heat-treated alloys which consisted almost entirely of the α-phase were filed with a very fine steel file, and the filings annealed for a short time *in vacuo* in order to relieve stresses. The alloys which consisted mainly of the T-phase were crushed in an agate mortar until the powder produced was fine enough to pass through a 250-mesh sieve. The powder was not, however, sieved, owing to the duplex nature of the alloys. These crushed specimens were not in general re-annealed, since experiment showed that no appreciable stress remained, and annealing brought about no improvement or sharpening of the diffraction patterns obtained. The filings or powder specimens were mounted in the usual manner on hairs, using Canada Balsam dissolved in xylol as the mounting medium.

Experience showed that in the case of the alloys containing appreciable quantities of both phases, better results were obtained by using a wire-form X-ray specimen instead of filings. In spite of the brittle nature of the alloys, it was found possible to turn satisfactory rods of 0·5 mm. diam. on a small lathe, using a sharp tool.

Specimens were exposed to radiation from a Metropolitan Vickers demountable X-ray machine, in a 19 cm. Debye-Scherrer camera. In general copper K_α radiation was used, since it gave high quality photographs suitable for accurate measurements. For the purpose of indexing the complex diffraction pattern of the T-phase, however, it was necessary to use chromium K_α radiation, and for these experiments a hydrogen atmosphere was maintained inside the camera.

The films were measured on an accurately calibrated measuring microscope, each individual line being measured several times. Reproducibility was found to be good. The Debye-Scherrer camera was calibrated against quartz[6] and checked against pure vacuum-melted silver at intervals during the work. The standard angle between the knife-edges of the camera was 84·213°.

---

[5] Köster and Dullenkopf, *Z. Metallkunde*, 1936, **28**, 363.

III. The Diffraction Pattern of the *T*-phase.

According to the work of Laves, Loehberg and Witte,[7] who examined an alloy of composition close to that of $Al_2Mg_3Zn_3$, the *T*-phase is body-centred cubic with 161 atoms in the unit cell and a lattice spacing of 14·16 A. Because of the large number of diffraction lines involved, attempts to index films obtained with copper radiation led to confusion. Films obtained with chromium radiation proved more satisfactory for this purpose.

In the case of an alloy containing 20 % Mg and 65 % Zn, 32 lines were carefully measured. Assuming body-centred cubic symmetry, and a true lattice spacing of 14·1 to 14.2 A., it was possible to assign definite values $(h^2+k^2+l^2)$ for the low angle diffraction lines. Proceeding step by step to the higher angle lines, it was found that the most probable values of $(h^2 + k^2 + l^2)$ for the six outermost lines were 134, 136, 138, 140, 142 and 144. Using the $(h^2 + k^2 + l^2)$ values deduced for all the measured lines, a satisfactory extrapolation curve against $\cos^2 \theta$ was obtained, from which the extrapolated value of the lattice spacing was obtained as 14·100 to 14·102 *k*X.

Checks on this interpretation were made by recalculating the spacings assuming (*a*) that the outermost line was characterised by $(h^2 + k^2 + l^2) = 146$ and (*b*) that it corresponded to $(h^2 + k^2 + l^2) = 142$. Both these calculations led to inconsistent results. Further proof of the correctness of the indexing was given by the fact that, using the $(h^2 + k^2 + l^2)$-values which gave rise to the satisfactory extrapolation curve, reflections corresponding to even numbers which could not be represented as the sum of three squares were characteristically absent. This work therefore confirmed the body-centred cubic nature of the ternary phase.

By comparison of films obtained from the same alloy by copper and chromium radiations, the outermost six lines which were accurately measurable on the copper film were found to correspond with $(h^2 + k^2 + l^2)$ values of 302, 306, 310, 314, 318 and 326, and the extrapolated *a* value was 14·1005 ± 0·0005 *k*X, in excellent agreement with that obtained from the chromium film. It will be noted that no line corresponding to the forbidden number 316 was observed. The absence of this reflection provides a satisfactory check on the correctness of the indexing, in so far as the only alternative sequences for the outermost six lines are :

$$h^2 + k^2 + l^2 = 306, 310, 314, 318, 322, 330.$$
$$h^2 + k^2 + l^2 = 298, 302, 306, 310, 314, 322.$$

Using these values, the lattice spacings obtained are not in agreement with those obtained from the chromium film. The original indexing may therefore be taken as correct.

Since the ternary phase is of variable composition, some films, corresponding to alloys of higher lattice spacing, showed lines of higher indices than those already described. No difficulty was experienced in assigning the correct $(h^2 + k^2 + l^2)$ values to these diffraction lines.

IV. Results.

The results obtained for four duplex alloys lying just within the two-phase field close to the $\alpha/(\alpha + T)$ boundary are given in Table I. These alloys were annealed in lump form for 14 days at 500° C. and 28 days at 200° C. Filings were prepared, and internal stresses were relieved by annealing the filings for 16 hours at 200° C.

The lattice spacings of the ternary phase, obtained from duplex alloys close to the $(\alpha + T)/T$ boundary are summarised in Table II. The lump specimens were slowly heated at 10° C. per hour, in order to absorb the low melting eutectic material present in the cast ingots, to 420° C., at which temperature they were held for 10 days. After this treatment the alloys were allowed to cool slowly in the furnace, at 10° C. per hour, to 200° C., from which temperature they were rapidly cooled in air. Microscopic examination of the annealed ingots showed the presence of very small amounts of the α-solid solution in all specimens.

---

[6] Lipson and Wilson, *J. Sci. Instr.*, 1941, **18**, 144.

[7] Laves, Loehberg and Witte, *Metallwirtschaft*, 1935, **14**, 793.

TABLE I

Comp. of Alloy Wt. %			Comp. of Alloy At. %.			α-phase Lattice Spacing, *k*X, at 20° C.
Al.	Mg.	Zn.	Al.	Mg.	Zn.	
96	2	2	96·93	2·24	0·83	4·04542
94	2	4	96·05	2·27	1·68	4·04393
92	2	6	95·15	2·29	2·56	4·04322
94	4	2	94·70	4·47	0·83	4·05255

The third series of alloys, well within the two-phase $(\alpha + T)$ region, were given an annealing treatment in all respects similar to that for the alloys listed in Table II. The lattice spacing measurements are summarised in Table III.

TABLE II

Comp. of Alloy Wt. %.			Comp. of Alloy At %.			*T*-phase Lattice Spacing *k*X.
Al.	Mg.	Zn.	Al.	Mg.	Zn.	
15	20	65	23·44	34·66	41·90	14·1005
23	22	55	32·82	34·81	32·37	14·1953
30	25	45	39·33	36·34	24·33	14·2942
38	27	35	46·13	36·35	17·52	14·3588
44	31	25	49·61	38·76	11·63	14·4259

From the data in Tables I and II, the variation of lattice spacing along the two-phase boundaries may be estimated, while the data in Table III enable the appropriate tie-lines to be fixed.

TABLE III

Comp. of Alloy Wt. %.			Comp. of Alloy At. %.			Lattice α-phase *k*X.	Spacing of *T*-phase *k*X.
Al.	Mg.	Zn.	Al.	Mg.	Zn.		
42	15	43	54·99	21·78	23·23	4·0466	14·1550
46	17	37	57·42	23·53	19·05	4·0510	14·2405
48	19	33	58·05	25·48	16·47	4·0552	14·2955
52	21	27	60·17	26·94	12·89	4·0616	14·3570

V. Lattice Spacing Variations along the $\alpha/(\alpha + T)$ Phase Boundary.

The $\alpha/(\alpha + T)$ phase boundary at 200° c. is shown, plotted in atomic percentages, in Fig. 2. The compositions of the alloys examined are also plotted. These points lie on tie-lines, the intersections of which with the solubility isothermal give the saturated alloy compositions corresponding to the measured spacings. Since the compositions of the alloys examined are close to the boundary, quite large variations of the points of intersection of the tie-lines with the $(\alpha + T)/T$ phase boundary make very little difference to their points of intersection with the $\alpha/(\alpha + T)$ phase boundary. In order to obtain the lattice spacing variations along this boundary, therefore, little error is introduced by assuming the tie-lines, to a first approximation, to be evenly spaced across the two-phase region. The compositions on the phase boundary corresponding to the investigated alloys may then be written down (Table IV).

In view of the small extent of the primary solid solution area, it is justifiable to assume to a first approximation that the lattice distortions produced by magnesium and zinc in the ternary alloys are additive. The work of Schmid and Siebel [8] shows that the solution of magnesium in aluminium produces an initial expansion of 0·00412 *k*X per atomic %, while, according to Owen and Iball,[9] one atomic % Zn reduces the lattice spacing of aluminium by 0·0009 *k*X.

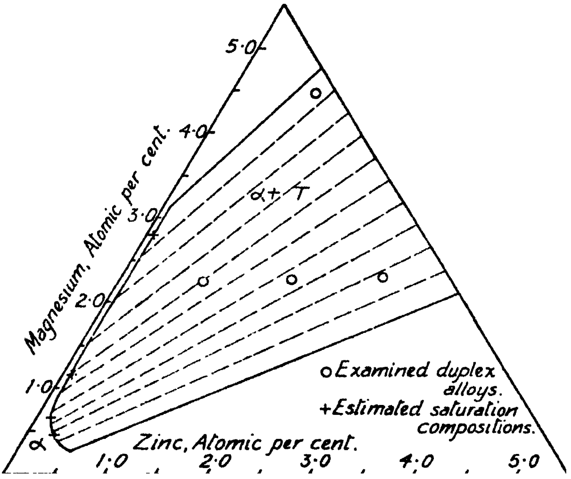
5·0
4·0
3·0
2·0
1·0
Magnesium, Atomic per cent.
α + T
α
o Examined duplex alloys.
+ Estimated saturation compositions.
Zinc, Atomic per cent.
1·0
2·0
3·0
4·0
5·0

FIG. 2.

It is of interest to note that the distortion for 1 atomic % Mg, calculated from the ternary alloys containing 1·15 and 2·80 atomic % Mg and approximately equal amounts of zinc, is very close to the value deduced from the binary alloys.

Taking the lattice spacing of pure aluminium at 20° C. as 4·0410 *k*X,[10] the observed lattice spacings may therefore be represented by the expression :

$$a = 4{\cdot}0410 + 0{\cdot}00412\,(\mathrm{Mg}) - 0{\cdot}0009\,(\mathrm{Zn}) \qquad . \quad . \quad . \quad (1)$$

where (Mg) and (Zn) are the atomic percentages of the respective solutes. It is thus possible to calculate the spacing for any alloy on the $\alpha/(\alpha + T)$ boundary, and vice versa. Values of the lattice spacing calculated from this expression are given in Table IV, together with the deviations from the observed results. These deviations are rather larger than would be expected, and are an indication that the assumption of equally spaced tie-lines is not strictly correct. In particular, the relatively large deviation of 0·00062 for the third composition in Table IV indicates that the magnesium figure of this composition is too low.

TABLE IV

Alloy Investigated, Comp. At. %.			Saturated Solid Solution Comp. At. %.			Obs. Lattice Spacing *k*X.	Calc. Lattice Spacing *k*X.	Deviation. Δ.
Al.	Mg.	Zn.	Al.	Mg.	Zn.			
96·93	2·24	0·83	98·75	1·15	0·10	4·04542	4·04565	+ 0·00023
96·05	2·27	1·68	99·20	0·65	0·15	4·04393	4·04355	− 0·00038
95·15	2·29	2.56	99·27	0·45	0·28	4·04322	4·04260	− 0·00062
94·70	4·47	0·83	97·05	2·80	0·07	4·05255	4·05248	− 0·00007

---

[8] Schmid and Siebel, *Z. Metallkunde*, 1931, **23**, 202.
[9] Owen and Iball, *Phil. Mag.*, 1934, **17**, 433.
[10] Wilson, *Proc. Physic. Soc.*, 1942, **54**, 487.

VI. Lattice Spacing Variations along the $(\alpha + T)/T$ Phase Boundary.

Since only very small amounts of the α-phase were present in the alloys listed in Table II, the compositions of these alloys may be taken to represent closely the $T/(\alpha + T)$ phase boundary. The lattice spacings given in Table II give the spacing variations along this boundary.

Fig. 3 shows the lattice spacings plotted against the atomic % Zn in the alloy.

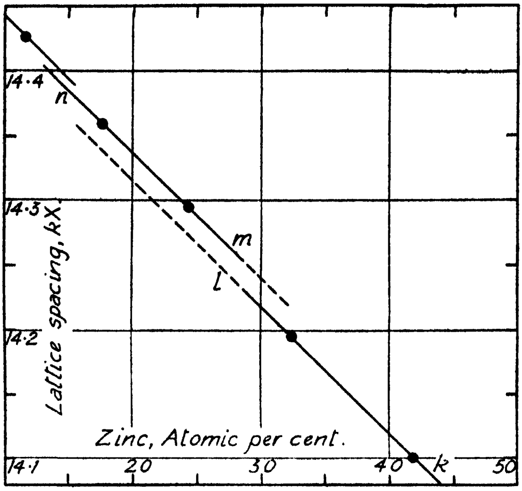

FIG. 3.

The straight line *kl*, drawn through the points for the alloys which contain 41·90 and 32·37 atomic % Zn and almost equal amounts of magnesium, is accurately parallel to the straight line *mn* drawn through the points for the alloys containing 24·33 and 17·52 atomic % Zn. The latter two alloys again have equal amounts of magnesium. The lattice spacings therefore appear to vary linearly with the zinc content; the variation, from Fig. 3, is − 0·0098 *k*X per atomic %.

The variation of the lattice spacing of the T-phase with the magnesium content cannot be directly tested with the alloys employed. Since the magnesium content does not vary greatly along the $(\alpha + T)/T$ boundary, it is justifiable to assume that the variation is linear. From the separation of the lines *kl* and *mn* in Fig. 3, an increase of one atomic % of magnesium causes a lattice spacing increase of approximately 0·0125 *k*X.

From these figures, the spacing variation along the boundary may be calculated, taking the alloy with 41·9 atomic % Zn as a basis for calculation, by means of the expression.

$$a = 14{\cdot}1005 + (41{\cdot}90 - (\mathrm{Zn})) \times 0{\cdot}0098 + ((\mathrm{Mg}) - 34{\cdot}66) \times 0{\cdot}0125 \quad . \quad (2)$$

where (Zn) and (Mg) are the atomic percentages of zinc and magnesium in the alloy whose spacing is required. Conversely, the composition corresponding to a given spacing may be approximately derived.

VII. Lattice Spacings in the Two-phase Region.

(*a*) Compositions corresponding to the measured spacings of the T-phase.

Taking the $(\alpha + T)/T$ phase boundary as represented accurately enough by the compositions given in Table II, then by the use of equation (2) the compositions along this boundary which correspond to the measured spacings given in Table III are as follows (Table V).

(*b*) Compositions corresponding to the measured spacings of the α-phase.

The lowest α-phase spacing recorded for the two-phase alloys is 4·0466 *k*X. From Table IV, this must correspond with a magnesium content greater than 1·15 atomic %, if equilibrium at 200° C. can be assumed. In this region of the 200° C. solid solubility curve, the zinc content is almost constant at 0·05 to 0·10 atomic %. The magnesium and zinc contents corresponding to the measured spacings from equation (1) are :

*k*X	At. % Zinc	At. % Magnesium
4·0466	0·1	1·38
4·0510	0·07	2·44
4·0552	0·05	3·45
4·0616	0·05	5·01

TABLE V

Spacing *kX*.	Corresponding Composition At. %.		
	Al.	Mg.	Zn.
14·1550	29·0	34·7	36·3
14·2405	35·5	35·5	29·0
14·2955	40·0	36·0	24·0
14·3570	44·0	37·0	19·0

It will be noted that the last two magnesium compositions are too high to correspond with equilibrium at 200° c. The slowly cooled two-phase alloys must therefore approximate to equilibrium at some higher temperature. Under the conditions of the experiments, it is unlikely that this temperature exceeds 300° c. The points on the 300° c. solubility isothermal which correspond with the measured spacings are :

*k*X	At. % Zinc	At. % Magnesium
4·0466	0·8	1·55
4·0510	0·53	2·55
4·0552	0·38	3·55
4·0616	0·20	5·02

Fig. 4 shows the 300° c solubility isothermal, and the tie-lines deduced from the present work. As shown in previous work,[8] at 300° c. the expression (Mg)(Zn) = K holds accurately for zinc contents greater than 0·5 to 0·6 atomic %. It is clear from Fig. 4 that the tie-lines run in such a manner that the curved portion of the $\alpha/(\alpha + T)$ boundary which obeys the expression (Mg)(Zn) = K represents equilibrium with the T-phase of a composition near to that given by the formula $Al_2Mg_3Zn_3$. The same is true if, as is probable, the slowly cooled alloys used in the present work correspond with equilibrium at some temperature between 300° and 200° c. The existence of this expression may therefore be understood from the principle of mass action, since the magnesium and zinc will be present in approximately equi-atomic proportions in the T-phase which is in equilibrium with the α-compositions involved.

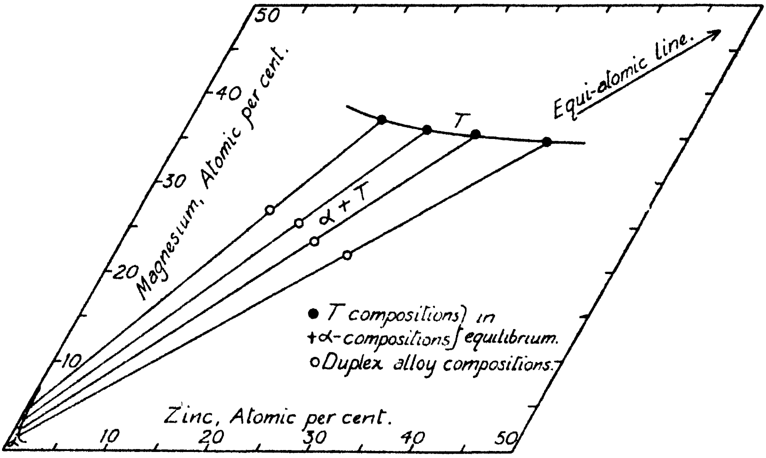

FIG. 4.

It is reasonable to conclude that the same principles apply at higher temperatures, and that this accounts for the fact that the expression (Mg)(Zn) = K applies accurately, except where the magnesium content is high and the zinc content is low. For this part of the solubility curve the composition of the T-phase does not approximate to the formula $Al_2Mg_3Zn_3$.

VIII. More Accurate Derivation of Saturated Solid Solution Compositions.

The saturated, primary, solid-solubility compositions corresponding to the measured lattice spacings of the alloys consisting mainly of the α-phase (Table IV) were derived on the assumption of equally spaced tie-lines. Fig. 4 shows that the tie-lines are not equally spaced, but, for the zinc-rich portion of the $\alpha/(\alpha + T)$ boundary, run almost parallel to the line dividing the $(\alpha + T)$ and $(\alpha + T + MgZn_2)$ phase fields. It is thus possible to revise the values of the saturated solid solution compositions given in Table IV in accordance with the new information. The revised compositions and the lattice spacings calculated from them by the use of equation (1), are given in Table VI.

TABLE VI

Alloy Invgtd. Composition.			Saturated Solid Soln.			Obs. Lattice Spacing kX	Calc. Lattice Spacing kX.	Deviation Δ.
Al.	Mg.	Zn.	Al.	Mg.	Zn.			
96·93	2·24	0·83	98·75	1·15	0·10	4·04542	4·04563	+ 0·00021
96·05	2·27	1·68	99·10	0·80	0·10	4·04393	4·04410	+ 0·00020
96·15	2·29	2·56	99·25	0·55	0·20	4·04322	4·04309	− 0·00013
94·70	4·47	0·83	97·05	2·80	0·07	4·05255	4·05248	− 0·00007

The differences between the observed and calculated lattice spacings for the second and third compositions are now much smaller. This gives confirmation to the tie-lines deduced from the present work.

This work was carried out in the Inorganic Chemistry Laboratory of the University of Oxford, and grateful acknowledgement must be made to Professor C. N. Hinshelwood, F.R.S., for providing laboratory accommodation and many other facilities which greatly aided the research.

IX. Summary and Conclusions.

(*a*) From measurements of the lattice spacings of the α-phase in duplex alloys (annealed at 200° c.) close to the solubility limit, the variation of lattice spacing along the $\alpha/(\alpha + T)$ phase boundary was established, assuming the tie-lines, as a first approximation, to be equally spaced. Within close limits, the distortions produced by magnesium and zinc in the ternary alloys are additive.

(*b*) Similar measurements of the lattice spacings of the T-phase in duplex alloys (slowly cooled to 200° c.) close to the $(\alpha + T)/T$ phase boundary allowed the spacing, and its variation with composition, along this boundary to be determined.

(*c*) Measurements of the lattice spacings of both phases in alloys (slowly cooled to 200° c.) lying well within the $(\alpha + T)$ region, combined with the determined variations of these spacings with composition, showed that the state of the alloys corresponded with equilibrium at a somewhat higher temperature than 200° c. The results were consistent with equilibrium in the region of 300° c., and tie-lines, showing the compositions of the phases in equilibrium with each other, were plotted.

(*d*) The tie-lines deduced are not evenly spaced, but indicate that the portion of the α-phase boundary for which the relation $(Mg)(Zn) = K$ is accurately obeyed involves equilibrium with the T-phase of a composition near to that given by the formula $Al_2Mg_3Zn_3$.

Dept. of Metallurgy,
The University,
Birmingham.

DISTRIBUTION FUNCTIONS AND CRYSTALLINE MATERIALS.

BY A. D. BOOTH.

Received 12*th August*, 1946.

Although the application of the idea of a distribution function to the case of X-ray diffraction from amorphous materials is well known, much less attention has been given to the case where the given information is in the form of a table of structure factors F (h, k, l). The difference is fundamentally that between a continuous and a discontinuous function and Warren and Gingrich, in their classical paper[1] derived results for the former case. It is interesting to note that historically[2] the form of the result for amorphous materials gave Patterson the basic idea for his now famous synthesis.

From the standpoint of present day technique this approach is unnecessarily complicated and it seems worth while to give an alternative derivation, applicable to single crystal data, and based directly on the Patterson synthesis.[3] In addition to this purely formal objective, the classical 3-dimensional distribution function is shown to be only one of a trilogy of results applicable to various types of summation, and furthermore, the examination of a particular case gives interesting information regarding the resolution obtainable with the normal and "sharpened" Patterson series.

The Patterson density at any point (u, v, w) is defined by the equation :

$$P(u, v, w) = \iiint \rho(x, y, z) \, . \, \rho(x + u, y + v, z + w)\mathrm{d}x \, . \, \mathrm{d}y \, . \, \mathrm{d}z \qquad (1)$$

where $\rho(x, y, z)$ is the electron density at any point (x, y, z) and the integration extends over the whole unit cell of the crystal. It is seen, on inspecting equation (1), that the Patterson distribution will have maxima whenever (x, y, z) and $(x + u, y + v, z + w)$ coincide with maxima in the original electron density distribution. Thus the maxima in P space, corresponding to atoms distant b from each other in real space, will all lie on the surface of a sphere of radius b and centred on the origin. The particular location of these maxima on the sphere will be given by the vector direction of the interatomic bond in real space. Furthermore, if the sum of all Patterson density on the surface of the sphere be taken, this will give a measure of the number of interatomic bonds of corresponding length in the original distribution. The exact interpretation is complicated by the fact that the interacting atoms may not be of equal size, and this makes the method of qualitative rather than quantitative interest. If the distribution in real space consisted of *points* having given weights, the radial distribution in P would give discrete maxima whose heights were equal to the sum of the products of all interacting weights at exactly that distance apart. This more quantitative type of distribution can be realised by the use of the sharpened Patterson synthesis, as will be shown later.

Just as equation (1) defines a Patterson function for a three-dimensional density distribution, Patterson distributions can be obtained for two- and one-dimensional cases, corresponding to electron density projections on a plane and on a line respectively. From these too, radial distributions are obtainable, the summation being over the circumference of a circle and at a point on the line.

---

[1] Warren and Gingrich, *Physic. Rev.*, 1934, **46**, 368.

[2] Warren, *A.S.X.R.E.D. Conference*, 1946.

[3] Patterson, *Physic. Rev.*, 1934, **46**, 372.

In the case of a crystal lattice, the electron density is given by:

$$\rho(x,y,z) = \frac{1}{V}\sum_h\sum_k\sum_l |\mathrm{F}(h,k,l)| \cos\left[2\pi\left(h\frac{x}{a}+k\frac{y}{b}+l\frac{z}{c}\right) - \alpha(h,k,l)\right] \quad (2)$$

and it is easily shown, using the orthogonality properties of the sine and cosine functions, that the Patterson function reduces to:

$$P(u,v,w) = \frac{1}{V}\sum_h\sum_k\sum_l \mathrm{F}^2(h,k,l)\,.\,\cos 2\pi\left(h\frac{u}{a}+k\frac{v}{b}+l\frac{w}{c}\right) \quad . \quad (3)$$

The practical importance of the series (3) lies in the fact that it does not contain the phase angles α (h, k, l), which are not at present determinable experimentally. The two- and one-dimensional versions of (3) are obtained in a like manner and are:

$$P(u,v) = \frac{1}{A}\sum_h\sum_k \mathrm{F}^2(h,k,0)\,.\,\cos 2\pi\left(h\frac{u}{a}+k\frac{v}{b}\right)lz \quad \textit{(two-dimensional)}$$

$$P(u) = \frac{1}{a}\sum_h \mathrm{F}^2(h,0,0)\,.\,\cos 2\pi\left(h\frac{u}{a}\right) \quad \textit{(one-dimensional)}.$$

Following the procedure outlined above, a distribution function $p_3(r)$ is defined by the relation:

$$4\pi r^2 p_3(r)\mathrm{d}r = \int_S P(u,v,w)\,.\,\mathrm{d}S\,.\,\mathrm{d}r \quad . \quad . \quad . \quad (4)$$

where the integration extends over the spherical surface S. Substituting from (3) in equation (4)

$$4\pi r^2\,.\,p_3(r)\,.\,\mathrm{d}r = \frac{1}{V}\sum_h\sum_k\sum_l \mathrm{F}^2(h,k,l)\int_S \cos 2\pi\left(h\frac{u}{a}+k\frac{v}{b}+l\frac{w}{c}\right)\,.\,\mathrm{d}S\,.\,\mathrm{d}r. \quad (5)$$

The integrals are best evaluated by transforming to an axis normal to the plane (h, k, l) and to two perpendicular axes in the plane. Calling the spacing of the planes $d(h, k, l)$ and the element of the normal dn, the typical integral becomes:

$$\int_S \cos 2\pi\left(h\frac{u}{a}+k\frac{v}{b}+l\frac{w}{c}\right)\,.\,\mathrm{d}S = \int_r^r \cos\frac{2\pi n}{d(hkl)}\,.\,2\pi\,.\,\mathrm{d}n \quad . \quad (6)$$

$$= 4\pi r^2\,.\,\frac{\sin 2\pi r/d(hkl)}{2\pi r/d(hkl)}$$

whence:

$$p_3(r) = \frac{1}{V}\sum_h\sum_k\sum_l \mathrm{F}^2(h,k,l)\,.\,\frac{\sin 2\pi r/d(h,k,l)}{2\pi r/d(h,k,l)}. \quad . \quad . \quad (7)$$

In a like manner the two- and one-dimensional cases can be treated. The distributions are $2\pi r\,.\,p_2(r)\,.\,\mathrm{d}r$ and $p_1(r)\,.\,\mathrm{d}r$, where:

$$p_2(r) = \frac{1}{A}\sum_h\sum_k \mathrm{F}^2(h,k,0)\,.\,J_0 2\pi r/d(h,k,0)\,^* \quad . \quad . \quad (8)$$

$$p_1(r) = \frac{1}{a}\sum_h \mathrm{F}^2(h,0,0)\,.\,\cos 2\pi r/d\,(h,0,0) \quad . \quad . \quad (9)$$

---

* $J_0(x) = \lim_{n\to\infty} P_n$ (cos x/n) where P_n is Legendre's function in view of spherical distribution of points.

J_0 is the zero-order Bessel function. It is interesting to observe that, taking account of the relation $d(h, 0, 0) = a/h$, (9) is simply the one-dimensional Patterson series.

The series (7), (8) and (9) give the qualitative type of distribution first envisaged. It is easily shown,[3] that if in equation (3) each coefficient $F^2(h, k, l)$ is divided by a quantity $f^2(h, k, l)$ to be defined later, the resulting series represents not a continuous distribution but a function which is zero except at a finite number of *points*. The magnitude at these points is simply the product of the atomic numbers of the interacting atoms in real space, and the positions of the points coincide with the maxima of the initial Patterson distribution. The function $f(h, k, l)$ is the average atomic scattering factor of the atoms comprising the distribution in real space, and is so scaled as to have the value unity at zero reciprocal spacing. This assumption, which implies a similar scattering factor curve for different atoms, has been verified in recent work.[4]

In the case of experimentally derived series the termination at a finite number of terms prevents the realisation of this ideal state of affairs, but even so the modified series is a considerable improvement on the original.

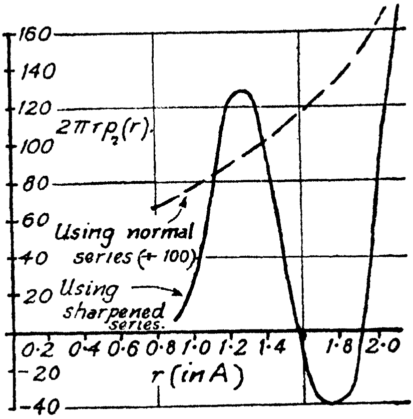

FIG. 1.—Radial distribution curves for oxalic acid projection.

From the sharpened series distribution functions ${}_s p_3$, ${}_s p_2$ and ${}_s p_1$ can be obtained by the same technique as before. They are given by:

$$ {}_s p_3(r) = \frac{1}{V}\sum_h\sum_k\sum_l \frac{F^2(h, k, l)}{f^2(h, k, l)} \cdot \frac{\sin 2\pi r/d(h, k, l)}{2\pi r/d(h, k, l)} \qquad . \quad . \quad (10) $$

$$ {}_s p_2(r) = \frac{1}{A}\sum_h\sum_k \frac{F^2(h, k, 0)}{f^2(h, k, 0)} \cdot J_0 2\pi r/d(h, k, 0) \qquad . \quad . \quad (11) $$

$$ {}_s p_1(r) = \frac{1}{a}\sum_h \frac{F^2(h, 0, 0)}{f^2(h, 0, 0)} \cdot \cos 2\pi r/d(h, 0, 0) \qquad . \quad . \quad (12) $$

The first of these series differs from that obtained by Warren in his original paper in giving a maximum at the origin. This is due to the self-interaction of atomic peaks and can be removed, if desired, by taking as coefficients the quantities:

$$ \frac{F^2(h, k, l)}{f^2(h, k, l)} - \sum_{r=1}^{n} N_r^2 \qquad . \quad . \quad . \quad . \quad . \quad (13) $$

where N_r is the atomic number of the r^{th} atom, and the summation extends over the n atoms in the unit cell. The disadvantage of this procedure lies in the fact that it requires an accurate knowledge of the absolute values of the $F(h, k, l)$. The additional maximum due to this cause is, in any case, unlikely to cause confusion as it is very close to the origin and can easily be identified. The series (11) is new and is applicable to two-dimensional data, whilst the last result is simply the one-dimensional sharpened Patterson series.

[4] Booth, *Nature*, 1945, **156**, 51; *Proc. Roy. Soc. A*, 1947, **188** 77.

Examples of the use of equation (10), modified by the introduction of the coefficients (13), have been given by Warren[1] and so it need not receive attention here; the one-dimensional Patterson series is also well known. The new series, both (8) and (11), have been applied to oxalic acid taking the F(*h*, 0, *l*) data. This affords a favourable example, since the projection is free from overlapping. In Fig. 1 is given the distribution resulting from the use of each of the two versions, and it is seen that the simple series (8) gives no indication of the presence of a minimum distance of approach, whereas the sharpened function shows it clearly. This comparison indicates the unsatisfactory nature of the ordinary Patterson synthesis and suggests the desirability of according more attention to the sharpened version.

Summary.

The application of the distribution function technique to X-ray data obtainable from amorphous substances is well known, but little use has been made of the corresponding function for the discrete observations obtained in single crystal work. The problem is approached via the Patterson series, and the classical distribution function of Warren is shown to be only one of a series of such results, applicable to observations of varying dimensions of summation.

In a particular case the method is used to demonstrate the superior resolving power of the "sharpened" version of the Patterson series.

Physics Department,
Birkbeck College,
London.

THE FORCE CONSTANTS OF SOME OH AND NH LINKS.

BY R. E. RICHARDS.

Received 12th August, 1946.

In a molecule containing a group —X—H, where X is an atom much heavier than the hydrogen atom, the frequency of the stretching vibration of the X—H link is found to be nearly independent of the mass of the grouping attached to the X-atom. To a first approximation the stretching force constant of the X—H link may therefore be written $k = 4\pi^2\nu^2\mu$, where k is the stretching force constant of the link, ν is the fundamental frequency of the valency vibration, and μ is the reduced mass of the link, the vibration being assumed harmonic. This approximation holds only if there is no other grouping in the molecule having a frequency equal to or very close to that of the X—H link. For groups with more than one hydrogen atom attached to the X-atom, appropriate expressions for the force constant must be used which take into account the interactions between the vibrations of the similar links. These have been given by Linnett.[1]

Molecules containing OH or NH links often form intermolecular hydrogen bonds in the liquid or solid state and when this occurs the valency vibration frequency of the OH or NH link is considerably affected.[2, 3] When discussing the variations of OH or NH force constants, therefore, it is most important that all the vibration frequencies used should be obtained from measurements made under comparable conditions. Since the strength of hydrogen bonding varies widely with different compounds and with the state of aggregation, comparable results can only be obtained from measurements carried out on the unassociated compounds, i.e., on the vapours or on very dilute solutions in a non-hydroxylic solvent. Discrepancies which appear between the values of the force constants listed in Tables I and II and those given by Linnett [1] are probably due to the fact that Linnett used some vibration frequencies obtained from Raman measurements on the liquid or solid substances, where association through hydrogen bonds often occurs. In particular, the values of the NH force constants of amides given by Linnett are too low, due to the very strong association which occurs in these substances.[4-6]

---

[1] Linnett, *Trans. Faraday Soc.*, 1945, **41**, 223.
[2] Pauling, *The Nature of the Chemical Bond.*
[3] Fox and Martin, *Trans. Faraday Soc.*, 1940, **36**, 897.

The stretching force constants of the OH links of a series of compounds are given in Table I. The force constant of the OH link of methyl alcohol is appreciably smaller than that of water vapour. Ethyl alcohol has a still smaller OH force constant, although further lengthening of the alkyl chain has little effect. Tertiary butyl alcohol, however, shows a further lowering of the OH force constant. The alcohols containing an aromatic ring show a steady value at about 7·25 × 10^5 dynes/cm. The force constants of the OH links of the carboxylic acids are lower than those of any of the alcohols; it is significant that the strongest acid, namely, trichloracetic acid, has the smallest force constant.

TABLE I

STRETCHING FORCE CONSTANTS OF OH LINKS

Compound.	k(OH) × 10^{-5} dynes/cm.	ν(OH) cm.$^{-1}$.	State.	Reference.
Water	7·76	3652, 3756	vapour	14
	7·44	3614, 3705	CCl_4 solution	24
Methyl alcohol . .	7·54	3683	vapour	11
	7·36	3640	CCl_4 solution	25, 10
Ethyl alcohol . .	7·36	3640	vapour	10
	7·36	3640	CCl_4 solution	25, 10
n-Butyl alcohol . .	7·35	3636	"	12
Stearyl alcohol . .	7·35	3636	"	12
Cetyl alcohol . .	7·35	3636	"	12
tert-Butyl alcohol . .	7·26	3616	"	12
Benzyl alcohol . .	7·27	3618	"	12
Diphenyl carbinol . .	7·26	3616	"	12
Triphenyl carbinol. .	7·25	3612	"	12
Phenol . . .	7·25	3612	"	12
Benzoic acid . .	7·04	3560	"	13
Acetic acid . . .	6·98	3545	"	13
Trichlor-acetic acid .	6·88	3520	"	13

These variations confirm that increasing electronegativity of the hydrogen atom relative to the oxygen atom will reduce the force constant of the OH link.[7] Thus, contributions of structures such as $H^-CH_2{=}O^{\pm}{-}H$ or $H^+CH_2 = OH^-$ explain the lowering of the force constant in methyl alcohol from the value found for water vapour, and also the further reduction observed in tertiary butyl alcohol as compared with the steady value shown by the long chain aliphatic alcohols. The low value of the

---

[4] Buswell, Rodebush, and Roy, *J. Amer. Chem. Soc.*, 1938, **60**, 2444.

[5] Buswell, Downing, and Rodebush, *ibid.*, 1940, **62**, 2759.

[6] Richards and Thompson *J. Chem. Soc.*, 1947, 1248.

[7] Longuet-Higgins, *Trans. Faraday Soc.*, 1945, **41**, 233.

stretching force constant of the OH group in the carboxylic acids is undoubtedly due to the fractional positive charge on the hydroxyl oxygen atom resulting from the contribution of the dipolar form

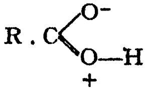

to the resonance hybrid. Trichloracetic acid, in which the strongly electrophilic —CCl_3 group causes a still further increase of the positive charge on the hydroxyl oxygen atom, shows a lower OH force constant

TABLE II

STRETCHING FORCE CONSTANTS OF NH LINKS *

Compound.	k(NH) × 10^{-5} dynes/cm.	ν(NH) cm.$^{-1}$.	State.	Reference.
Ammonia	6·38	3414, 3336	vapour	21
Methylamine	6·40	3365, 3470	,,	15, 16
Dimethylamine	6·31	3384	,,	15
Ethylene imine	6·08	3322	,,	17
Aniline	6·54	3410, 3480	CCl_4 solution	18, 19
Diphenylamine	6·55	3445	,,	18, 20
p-Toluidine	6·50	3395, 3475	,,	18
p-Anisidine	6·45	3384, 3460	,,	18
n-Methyl-*p*-toluidine	6·52	3440	,,	18
n-Ethyl aniline	6·48	3430	,,	18
Acetamide	6·66	3420, 3534	,,	4
Propionamide	6·66	3420, 3534	,,	4
Butyramide	6·66	3420, 3534	,,	18
Caproamide	6·66	3420, 3534	,,	18
Valeramide	6·66	3420, 3534	,,	4
Benzamide	6·66	3420, 3534	,,	4
n-Cyclohexyl acetamide	6·55	3448	,,	4
n-Ethyl acetamide	6·59	3460	,,	4
Acetanilide	6·55	3448	,,	4
Benzanilide	6·72	3497	,,	4

* Unfortunately it has not been possible to obtain a value for the NH stretching force constant of the NH_4^+ ion in dilute solution in carbon tetrachloride on account of the extreme insolubility of ammonium salts in this solvent.

than acetic acid. The stretching force constant of the OH link of these carboxylic acids decreases with increasing dissociation constant of the acid.

It should be noted that in the examples quoted above there is no change of bond hybridisation, and that the force constant is primarily dependent upon the fractional electric charge resident on the oxygen atom, or in other words, by the electronegativity of the hydrogen atom relative to the oxygen atom.

---

[8] Fox and Martin, *Trans. Faraday Soc.*, 1940, **36**, 897.
[9] Davies, *ibid.*, 1940, **36**, 333.
[10] Errera, *Compt. rend.*, 1937, **204**, 259.
[11] Borden, *J. Chem. Physics*, 1938, **6**, 553.
[12] Fox and Martin, *Proc. Roy. Soc. A*, 1937, **162**, 419.
[13] Buswell, Rodebush, and Roy, *J. Amer. Chem. Soc.*, 1938, **60**, 2239.
[14] Herzberg, *Infra-red and Raman Spectra*, p. 161.
[15] Kirby Smith and Bonner, *Physic. Rev.*, 1939, **55**, 1113.
[16] Cleaves, *J. Chem. Physics*, 1939, **7**, 563.

Table II shows the stretching force constants of the NH links of a series of compounds analogous to those given in Table I. The force constants of the NH links are reduced in passing along the series NH_3, CH_3NH_2, $(CH_3)_2NH$,

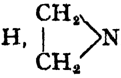

$$\begin{matrix} CH_2 \\ | \\ CH_2 \end{matrix} \!\!> NH$$

and the explanation of the change of force constant is probably similar to that applied to the aliphatic alcohols. Thus, contribution of structures such as $H^+ CH_2{=}NH\ H^-$ would account for a decreased NH force constant. The value of the force constant for methylamine does in fact appear to be higher than that of ammonia, but the accuracy of the calculations is such that no significance can be attached to this. The general trend of the figures should be considered rather than the individual values.

The NH stretching force constants of the aromatic amines, however, have slightly higher values than for ammonia, whilst in the acid amides the NH link has a still higher stretching force constant. It is evident that some other effect than that described above comes into play in these cases, particularly in view of the fact that the NH or OH stretching frequencies are often lower in solution than in the vapour.

Now it is well known that the CH stretching force constant varies considerably as the type of bond hybridisation of the carbon atom changes.[22] This is well illustrated by the series :[1]

	Ethane.	Ethylene.	Acetylene.
Force constant of CH link × 10^{-5} dynes/cm.	4·97	5·1	6·0
Type of bond hybridisation . . .	sp^3	sp^2	sp

Thus, as the proportion of the s orbital increases relative to the p orbital in the final hybrid, so the force constant of the CH link is increased.

In the simple aliphatic amines the type of bonding may be written p^3, since the nitrogen atom is using predominantly its three $2p$ orbitals. In the acid amides, however, where considerable resonance with a dipolar form occurs :[6]

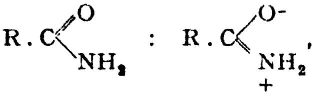

the nitrogen atom must be involved in a type of bonding having considerable sp^2 character. It seems, therefore, that as in the case of the CH bonds, a change of bond hybridisation to a type having an increased proportion of s orbital causes a rise of the NH stretching force constant, which in this case is greater than the lowering effect on the force constant due to the fractional positive charge on the nitrogen atom. In the aromatic amines, where the contribution of the form $\overset{-}{C_6H_5}{=}\overset{+}{N}H_2$ to the

---

[17] Thompson and Harris, *J. Chem. Soc.*, 1944, 301.

[18] Richards, measurements in this laboratory.

[19] Buswell, Downing and Rodebush, *J. Amer. Chem. Soc.*, 1939, **61**, 3253.

[20] Buswell, Downing and Rodebush, *ibid.*, 1940, **62**, 2760.

[21] See ref. 14, p. 177.

[22] Sidgwick, *Organic Chemistry of Nitrogen*, 1937, p. 143.

[23] Sutherland and Dennison, *Proc. Roy. Soc. A*, 1935, **148**, 250.

[24] Fox and Martin, *ibid.*, 1940, **174**, 234.

[25] Errera, *Nature*, 1936, **138**, 882 ; Errera, Gaspart and Sack, *J. Chem. Physics*, 1940, **8**, 63.

resonance hybrid is smaller than in the amides, the effect of the change of hybridisation of the bond orbitals of the nitrogen atom only just appears to outweigh the effect of the fractional electric charge on the nitrogen atom.

These results throw some light on the structure of amides in very dilute solution. It is possible [22] that these compounds could exist in an enolic form such as

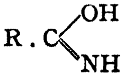

$$\mathrm{R.C}\begin{array}{l}\diagup\mathrm{OH}\\ \diagdown\mathrm{NH}\end{array} \quad . \quad . \quad . \quad . \quad . \quad . \quad (A)$$

Resonance would probably occur between this structure and the dipolar form

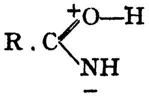

$$\mathrm{R.C}\begin{array}{l}\diagup\overset{+}{\mathrm{O}}\mathrm{-H}\\ \diagdown\underset{-}{\mathrm{N}}\mathrm{H}\end{array} \quad . \quad . \quad . \quad . \quad . \quad . \quad (B)$$

If this were so, the OH stretching force constant would be expected at a lower value than in the aliphatic alcohols (cf. the carboxylic acids) and the NH stretching force constant at a higher value than in the aliphatic amines. Using the frequencies 3420 $\mathrm{cm.}^{-1}$, 3534 $\mathrm{cm.}^{-1}$, found for acetamide in dilute solution in carbon tetrachloride, and assigning the former to the NH link and the latter to the OH link, we have $k(\mathrm{NH}) = 6{\cdot}44 \times 10^5$ dynes/cm., and $k(\mathrm{OH}) = 6{\cdot}92 \times 10^5$ dynes/cm. The force constant of the OH link is certainly much lower than in the alcohols, its value being only comparable with that of the very strongly acidic trichloracetic acid. In order to account for such a low value, the contribution of the dipolar form (B) would have to be very considerable. This in turn should cause the NH stretching force constant to be very much higher than in the aliphatic amines, but this is not the case. It is worth noting, also, that if the ketonic form is assumed for the unsubstituted amides, and the half-angle between the NH bonds taken as 60°, then the stretching force constant as calculated from the symmetrical and antisymmetrical vibration frequencies are 6·66, and $6{\cdot}66 \times 10^5$ dynes/cm. The closeness of this agreement is probably fortuitous but gives some further support for the ketonic structure of amides.

We may conclude, therefore, that in dilute solution, amides probably exist mainly in the ketonic form (see also 6).

I should like to thank the Department of Scientific and Industrial Research for a grant.

Summary.

The stretching force constants of some OH and NH links have been calculated. Interpretations are put forward for the different variations in the force constants which are observed in the two cases.

The Physical Chemistry Laboratory,
Oxford.

THE REPLACEMENT REACTIONS OF β-β'-DICHLORODIETHYL SULPHIDE AND OF SOME ANALOGUES IN AQUEOUS SOLUTION: THE ISOLATION OF β-CHLORO-β'-HYDROXY DIETHYL SULPHIDE.*

BY A. G. OGSTON, with (in part) E. R. HOLIDAY, J. ST. L. PHILPOT AND L. A. STOCKEN.

Received 20*th September*, 1946.

PART I.

THE KINETICS OF HYDROLYSIS AND REPLACEMENT REACTIONS OF β-β'-DICHLORODIETHYL SULPHIDE.

The starting point was the work of Peters and Walker.[4] They studied the rate of formation of acid by mustard gas in water and water-alcohol mixtures, in the presence and absence of salts, including chlorides; they worked at constant temperature and at approximately constant *p*H. They observed that the rate of reaction is independent of *p*H over a wide range, is strongly depressed by alcohol and is depressed by salts. The work of Ingold and his school (see Watson,[5] Hughes [6]) made it possible to interpret these results: it appeared that mustard gas must react by the SN1 mechanism and that the rate of total reaction in aqueous solutions must be unimolecular with respect to mustard gas and independent of the concentration of any substituting reagent. These results were confirmed in the present work; a very slow SN2 reaction of mustard gas with diethyldithiocarbamate was demonstrable in 95 % alcohol, still slower even than the drastically retarded SN1 reaction.

---

* This is a brief account of a part of the work undertaken as an extramural programme under the Ministry of Supply during the years 1939-1944. The programme was initiated by Prof. R. A. Peters at the outbreak of war and carried out under his direction. He has supplied the following note as to its origin and as to the part played by various members of the team.

" It was known from work in 1924/25 (Walker and Peters,[1] Walker [2]) that vesicants like dichlorodiethylsulphone (DES) and allyl *iso*thiocyanate attacked fixed —SH groups in skin, muscle, etc. Later (Peters [3]) it was found that DES had a selective action on the pyruvate oxidase system in brain. Hence, it was decided first to investigate the value of various —SH compounds in neutralising vesicants of this kind both *in vitro* on this enzyme and *in vivo*, in the hope of finding one sufficiently reactive towards mustard gas to protect the naturally occurring groups from its attack.

" This work was undertaken by a sub-group, and J. St. L. Philpot suggested the systematic examination kinetically as well as biologically of a variety of thiols. After investigation of several compounds, the valuable and wide generalisation described here and known as the "competition theory" emerged; this orientated the probable action of mustard gas towards most biochemical groupings. A major share in the kinetic work was taken by Dr. Ogston, whose work with Dr. Holiday extended over some 4 years; during the first 9 months of the war, however, before they became engaged in other work, the contributions of Mr. Philpot and Dr. Stocken were important."

The kinetics of the reaction with mustard gas of some 80 substances were examined. These were mostly suggested by J. St. L. Philpot and a number of them were made by him and by L. A. Stocken, some, it is believed, for the first time. The more promising of these were tested for protection of the pyruvate oxidate system by Prof. Peters and of animals (rats) by Philpot and Holiday. Only the kinetic work is described here. It is realised that in parts this work falls short of being a finished scientific study. Its object was primarily therapeutic. It is not being continued by any of us and is therefore reported now, as it stands. The biological bearing of this work will be discussed elsewhere.

[1] Walker and Peters, *Govt. Reports*, 1924-25.

[2] Walker, *Biochem. J.*, 1925, 19, 1085.

[3] Peters, *Nature*, 1936, 138, 327.

[4] Peters and Walker, *Biochem. J.*, 1923, 17, 260.

Experimental.

All measurements were made at 25·0° C. in 5 % ethyl alcohol v/v; the alcohol was included in order to increase the solubility of mustard gas and to provide a convenient means of adding it. One ml. of alcohol containing 10 mg. of mustard gas was added rapidly at zero time to 19 ml. of water containing the desired reagents, in a 50 ml. conical flask; the mixture was immediately shaken vigorously for a few seconds and was kept gently agitated throughout the period of observation. Two sorts of measurements were made.

(1) Acidimetric: a modification of the method of Peters and Walker[4] was used. The flask was attached flexibly to a 5 ml. burette containing N./50 NaOH. A small amount of indicator was added to the flask and the mixture was titrated with alkali in definite small amounts, each addition being sufficient to bring the contents alkaline to the chosen end-point; the times were taken at which the indicator reached the control tint. The *p*H was kept as constant as possible by making the additions of alkali small. Water and alkali free from CO_2 were used and nitrogen was passed continuously through the flask. The rate of formation of acid could thus be followed even in the presence of reagents which buffered in the neighbourhood of the end-point.

(2) Iodimetric: the reaction of thiol reagents was observed directly by withdrawing 1 ml. samples of the reaction mixture at definite times and adding them to excess of iodine in potassium iodide, buffered to a suitable *p*H (usually 4·6); back titration was performed with N./200 thiosulphate. Where the formation of acid was not suppressed by the reagent, this was kept neutralised by additions of alkali. The mustard gas was a redistilled sample, made from thiodiglycol, supplied by C.D.E.S., Porton.

A. The Complete Reaction Curve.—The essentials of this part of the work were also done independently by Mr. E. O. Powell of C.D.E.S., Porton, and it was originally reported in conjunction with him.[7] Bartlett and Swain in the U.S.A. (personal communication) reached the same conclusion simultaneously.

Each of the chlorine atoms of mustard gas reacts by the SN1 mechanism. At the very beginning of the reaction, therefore, an induction period is to be expected during which the activated form accumulates to its stationary concentration. No induction period was detectable by our methods and this means that the stationary concentration of activated mustard gas must be reached in a few seconds. This complication of the kinetics can therefore be neglected. A second complication follows from there being two replaceable chlorine atoms; after the first replacement, the second stage of the reaction is that of a substance $Y . CH_2 . CH_2—S—CH_2 . CH_2 . Cl$, where Y is the radicle that has replaced the first chlorine atom. The velocity constant of reaction of the second chlorine atom is therefore likely to differ from that of the first and to depend on the nature of Y.

Peters and Walker (1923) observed that the course of hydrolysis (Y = — OH) is not simply unimolecular but becomes relatively faster as the reaction proceeds and they interpreted this finding in the above sense. An analysis of the reaction curve enables the velocity constants of the first and second stages to be evaluated. Where X is the number of equivalents of acid liberated after time t, M is the amount of mustard gas in moles, k_0 is the velocity constant of the first stage (per mole) and ak_0 that of the second stage;

$$X = M\left(2 - \frac{2a - 1}{a - 1} . \mathrm{C}^{-k_0t} + \frac{1}{a - 1} . \mathrm{C}^{-ak_0t}\right) \quad . \quad . \quad (1)$$

k_0 having been obtained from the initial rate (see later), a was evaluated by finding what value gave the best fit of the calculated to the observed reaction curve: k_0 was $2{\cdot}90 \times 10^{-3}$ sec.$^{-1}$: $a = 1{\cdot}32$ gave the best fit, giving $ak_0 = 3{\cdot}83 \times 10^{-3}$ sec.$^{-1}$. Direct observations on the compound C (see part III) gave $ak_0 = 3{\cdot}72 \times 10^{-3}$ sec.$^{-1}$.

---

[5] Watson, *Ann. Reports*, 1938, 208.

[6] Hughes, *J. Chem. Soc.*, 1935, 255 and 1937, 1183.

[7] Ogston and Powell, 1944, *Report to Ministry of Supply* by Peters, No. 88.

Equation (1) shows, in agreement with experiment, that for $a = 1{\cdot}32$ there is a very slight inflection in the curve, which is almost linear over the first 25 % of its course: its average slope is very nearly identical with the initial slope for a truly unimolecular process of constant k_0. For values of a greater than 1·32 the inflection becomes more noticeable and the average slope over the first 25 % of reaction is sensibly greater than the initial rate. This explains the observation [8] (see later) that in the presence of certain substituents (notably monothiophosphate and thiosulphate) the total rate of reaction of mustard gas appears to be increased. This is not inconsistent with reaction by the SN1 mechanism: it means merely that the velocity constant of reaction of $Y.CH_2.CH_2.S.CH_2.CH_2.Cl$ is in these cases considerably greater than that of mustard gas itself so that, although the initial rate of the reaction is not affected, the rate is greater in the later stages.

The inhibition of the rate of hydrolysis due to chloride ion liberated in the course of hydrolysis was within the experimental error under the conditions of our experiments.

B. The Initial Rate Kinetics of the Hydrolysis and Replacement Reactions.[9] *—In order to avoid the difficulty of interpreting the two stages of replacement reactions, most of the studies were made over the first 20 % to 30 % of the reaction. This does not represent a true initial rate, since the effect of the second stage becomes appreciable after the first 5 % of the reaction. But, as has been mentioned, where a is not much greater than 1, the rate is almost constant over the first 20 % to 30 % and nearly identical with the true initial rate. This average rate was measured and the reaction was treated kinetically as if it were a one-stage process.

From acidimetric observations reagents were divisible into three classes. (1) Chloride, which slows the whole course of reaction uniformly, without reducing the total amount of acid liberated. (2) Bases (in the Brønsted-Lowry sense), such as acetate, thiocyanate, thiosulphate, and other thiols of low pK, amines of low pK and thiodiglycol, which slow the rate of liberation of acid and usually reduce the total quantity liberated. (3) Acids (in the same sense), such as phosphate, mono- and di-thiophosphates and amines and thiols of high pK, which do not themselves affect the rate or amount of acid liberation, but which increase the rate and amount in the presence of substances of class (2).

Simultaneous iodimetric and acidimetric observations with thiols of class (2) showed that the total rate of reaction was equal to that of the hydrolysis alone. In one or two cases, notably those of monothiophosphate and thiosulphate, the rate measured over the first 25 % of reaction was up to 10 % greater. This was due to the value of a being higher in these cases and not to any acceleration of the activation of mustard gas nor to a simultaneous SN$_2$ process.

These facts can be quantitatively accounted for on the hypothesis that the rate-controlling factor in all substitutions is the SN1 activation, followed by competing bimolecular reactions between the activated mustard gas and the substituting reagents; in most cases the substituent group does not itself hydrolyse at a measurable rate, exceptions being chloride and other halide ions. The reactions can be expressed thus, R . Cl representing mustard gas :

---

[8] Ogston, 1943, *Report to Ministry of Supply* by Peters, No. 66.

[9] Holiday, Ogston, Philpot and Stocken, 1940, *ibid.*, No. 7; Holiday, Ogston, Philpot and Stocken, 1940, *ibid.*, No. 15; Ogston, 1941, *ibid.*, No. 32; Ogston, 1941, *ibid.*, No. 34; Ogston, 1941, *ibid.*, No. 41.

* At a later time, work on the substitution reactions of mustard gas was started in the U.S.A. by Linstead and his collaborators (personal communication) before they had seen the reports of this work. Their conclusions were in agreement with ours. They repeated and extended the work to include other substituting reagents. Their values for some of the competition factors differed from those given here, but not seriously. They pointed out that the competition factor is often to some extent dependent on the concentration of the reagent. Later still Bartlett and Swain in the U.S.A. (personal communication) re-investigated the kinetics of replacement with mustard gas and "C" in a more refined manner. They were able to make allowance for the effect of ionic strength and showed that the competition factors might vary through this cause. The variations found were small enough (up to 50 % at moderate ionic strength) to justify our intentional neglect of this factor, our interest having been confined to the orders of magnitude of the competition factors of different reagents.

SN1 activation $\quad \mathrm{R.Cl} \xrightarrow{k_0} \mathrm{R.Cl^*}$

Hydrolysis $\quad \mathrm{R.Cl^*} + \mathrm{H_2O} \xrightarrow{k_1} \mathrm{R.OH} + \mathrm{HCl}$

Inhibition by Cl′ $\quad \mathrm{R.Cl^*} + \mathrm{Cl^-} \xrightarrow{k_{Cl}} \mathrm{R.Cl} + \mathrm{Cl^-}$

Substitution $\quad \mathrm{R.Cl^*} + B \xrightarrow{k_B} \mathrm{R.B} + \mathrm{Cl^-}$

where B is a base

Substitution $\quad \mathrm{R.Cl^*} + A \xrightarrow{k_A} \mathrm{R.B} + \mathrm{HCl}$

where A and B are conjugate acid and base.

At the beginning of the reaction the concentration of mustard gas (R . Cl) may be taken as sensibly constant so that R . Cl* reaches a stationary value after the brief induction period :

$$\frac{d(\mathrm{R.Cl^*})}{dt} = k_0\,(\mathrm{R.Cl}) - (\mathrm{R.Cl^*})\{k_1(\mathrm{H_2O}) + k_{Cl}(\mathrm{Cl^-}) + \Sigma k_B(B) + \Sigma k_A(A)\} = 0 \qquad (2)$$

The rate of liberation of acid is given by

$$\frac{dX}{dt} = (\mathrm{R.Cl^*})\{k_1(\mathrm{H_2O}) + \Sigma k_A(A)\,;$$

using equation (2)

$$= k_0\,(\mathrm{R.Cl}).\ \frac{k_A(\mathrm{H_2O}) + \Sigma k_A(A)}{k_1(\mathrm{H_2O}) + k_{Cl}(\mathrm{Cl^-}) + \Sigma k_B(B) + \Sigma k_A(A)}. \qquad (3)$$

The rate of reaction of substituent Y is, similarly,

$$-\frac{d(\mathrm{Y})}{dt} = k_0(\mathrm{R.Cl}).\ \frac{k_Y(\mathrm{Y})}{k_1(\mathrm{H_2O}) + k_{Cl}(\mathrm{Cl^-}) + \Sigma k_B(B) + \Sigma k_A(A)}. \qquad (4)$$

Now, k_0 (R . Cl) is the rate of hydrolysis, V_0, of H alone. The values of other k's cannot be determined separately and it is convenient to use instead the " competition factor," F, for each reagent, defined by:

$$F_Y = k_Y/k_1(\mathrm{H_2O}). \qquad (5)$$

If the rate of liberation of acid in the presence of reagents is written V and the rate of reaction of a given reagent V', then equations (3) and (4) become:

$$V = V_0.\ \frac{1 + \Sigma F_A(A)}{1 + F_{Cl}(\mathrm{Cl^-}) + \Sigma F_B(B) + \Sigma F_B(A)} \qquad (6)$$

and

$$V' = V_0.\ \frac{F_Y(\mathrm{Y})}{1 + F_{Cl}(\mathrm{Cl^-}) + \Sigma F_B(B) + \Sigma F_A(A)}. \qquad (7)$$

It is not proposed to give the many modifications of these equations that were used for determining the values of F. Generally the acidimetric technique was used ; the lower values of F for chloride and bases were determined from the slowing of acid liberation in water, those for acids by measuring the acceleration in the presence of chloride. Higher values of F were determined stepwise, unknown against known, acid against base or base against acid, so that the disparity between the values of F for the substances being compared was never too great.

TABLE I

Reagent.	Conc. (M).	F.
Chloride	0·005	20·9
	0·0086	19·7*
	0·01	22·7
	0·17	22·1*
	0·02	21·5
	0·04	21·9
	0·08	19·5
	0·10	19·0
Acetate	0·01	9·2
	0·02	10·8
	0·04	10·7
	0·08	9·8
Thiosulphate	0·0025	$2·64 \times 10^4$
	0·005	$2·77 \times 10^4$

* Calculated from data of Peters and Walker (1923).

The above theory is confirmed by the constancy of the values of F for a given substance measured

TABLE II

Substance.	*p*H.	*F*.
Dithiophosphate	7	$1\cdot3 \times 10^5$
Ethyl dithiophosphate	8	$6\cdot3 \times 10^4$
Butyl dithiophosphate	8	$7\cdot4 \times 10^4$
Diethyl dithiophosphate	8	$2\cdot6 \times 10^3$
Hydrogen monothiophosphate	8	$3\cdot8 \times 10^4$
Methane dithiophosphonate	8	$1\cdot1 \times 10^5$
Ethane dithiophosphonate	8	$1\cdot2 \times 10^5$
Dimethane dithiophosphonate	8	$4\cdot9 \times 10^3$
Diethane dithiophosphonate	8	$6\cdot7 \times 10^3$
Ethane monothiophosphonate	8	$3\cdot9 \times 10^4$
Butane monothiophosphonate	8	$3\cdot6 \times 10^4$
Diethane monothiophosphonate	8	$4\cdot2 \times 10^3$
Thiosulphate	8	$2\cdot7 \times 10^4$
Diethyl dithiocarbamate	8	$3\cdot4 \times 10^4$
di-*β*-Hydroxyethyl dithiocarbamate	8	$3\cdot3 \times 10^4$
Ethyl xanthate	8	$1\cdot7 \times 10^4$
n-Octyl xanthate	8	$1\cdot2 \times 10^4$
Cetyl xanthate	8	$6\cdot4 \times 10^3$
Ethyl monothiocarbonate	8	$9\cdot1 \times 10^3$
Dithiovalerate	7	$5\cdot1 \times 10^3$
Dithioacetate	7	$5\cdot2 \times 10^3$
Hydroxyl (OH^-)	—	8×10^3
Hydrosulphide (SH^-)	7	$1\cdot2 \times 10^3$
Cysteine	7	$1\cdot2 \times 10^3$
Cysteine ethyl ester	7	$1\cdot7 \times 10^3$
Thioglycollic ester	7	$1\cdot4 \times 10^3$
Mercapto-malonic ester	7	$1\cdot2 \times 10^3$
Thiomalic ester	7	$7\cdot0 \times 10^2$
Ethane dithiol	7	$8\cdot8 \times 10^2$
Thioglucose	7	$3\cdot2 \times 10^3$
2 : 3-dimercaptopropanol (BAL)	7	$7\cdot8 \times 10^2$
p-Toluene thiosulphonate	—	$5\cdot1 \times 10^2$
Thiourea	7	$1\cdot5 \times 10^2$
Phosphate	8	$7\cdot5 \times 10^1$
Pyrophosphate	7	$1\cdot6 \times 10^2$
α-Glycerol phosphate	8	$5\cdot4 \times 10^1$
Adenylate	8	$7\cdot5 \times 10^1$
Yeast nucleic acid (per 4 nucleotides)	8	$1\cdot3 \times 10^3$
Thymus nucleic acid (per 4 nucleotides)	8	$1\cdot1 \times 10^3$
Bicarbonate	8	$8\cdot3 \times 10^1$
Acetate	7	$1\cdot0 \times 10^1$
Pyruvate	7	$6\cdot4$
Oxalate	7	$4\cdot1 \times 10^1$
Fumarate	7	$1\cdot6 \times 10^1$
Ascorbic acid	7	$1\cdot9 \times 10^1$
Pyridine	7	$5\cdot4 \times 10^1$
Trimethylamine	7	$6\cdot7$
Benzamidine	8	$1\cdot4 \times 10^1$
Thiocyanate	7	$6\cdot7 \times 10^2$
Iodide	8	$6\cdot6 \times 10^2$
Chloride	7	$2\cdot1 \times 10^1$
Sulphate	7	$4\cdot9$
d-*l*-alanylalanine	7	$1\cdot8 \times 10^1$
Acetyl-*d*-*l*-alanine	7	$1\cdot1 \times 10^1$
d-*l*-leucyl-glycyl-glycine	7	$1\cdot9 \times 10^1$
Serum albumin (per mole)	8	$2\cdot3 \times 10^3$

over a range of concentration ; examples are given in Table I. Table II gives the values of *F* for a selection of the 80 substances examined; the results lay no claim to great accuracy, particularly with respect to the highest values. Table II also gives the approximate *p*H at which *F* was measured: *p*H affects the value of *F* in the range of dissociation of an acid group.

Discussion.

Differences in the rates of reaction of different ionic reagents with the activated forms of halides have been reported by Ingold and his associates[10] (see below), but the differences are of much smaller magnitude than those found for reactions with mustard gas. These differences probably show that thermal activation is necessary for the substitution process as well as for the initial activation. The fact that reagents, which react with a much higher velocity constant than that of water, do not increase the initial rate of reaction shows that the activated molecule is not subject to thermal inactivation at a rate comparable with its rate of reaction with water. It is in a relatively stable state.

Bartlett and Swain (personal communication) have put forward the view that the activated form of mustard gas is an internal sulphonium compound and that this possibly reaches, in water, a stationary concentration of about 1 % of the total. Our results throw no light on the chemical nature of the activated form ; but the establishment of a stationary concentration of 1 % of the total would occur with a time constant of about 10 sec. An induction period of such length was not observed in this work. One might assume on the contrary that dithiophosphate reacts with activated mustard gas with zero energy of activation ; on this assumption, and assuming a collision number of 10^{13}, the stationary fraction in the activated form in water alone would be about 10^{-11} and this would be established exponentially with a time constant of about 10^{-8} sec.

PART II.

THE KINETICS OF REACTION OF ANALOGUES OF DICHLORDIETHYL SULPHIDE (with E. R. Holiday).[11]

The same techniques were used to make a cursory survey of the properties of β-chlorethyl phenyl, propyl and ethyl sulphides ; of *tert.* butyl chloride ; and of *bis* (β-chloroethyl thioethyl) ether under the same conditions. All react by the SN1 mechanism. The course of reaction of the first three is truly unimolecular ; *tert.* butyl chloride was found to give an initial very rapid production of acid, followed by a truly unimolecular process (to which the results apply) ; *bis* (β-chloroethyl thioethyl) ether like mustard gas has two stages of hydrolysis, of which only the first was studied.

The solubilities of these substances in 5 % alcohol at 25° c. were obtained by measuring the rates of acid liberation in a solution kept saturated by vigorous mechanical shaking. The results are given in Table III, together with comparable data on mustard gas and on C (see below). The *tert.* butyl chloride was a commercial sample, twice redistilled : the other materials were supplied by C.D.E.S., Porton.

Discussion.

The velocity constants of hydrolysis of substances containing the group —S—CH_2—CH_2—Cl are in the order that would be expected, for the SN1 mechanism, from the electro inductive properties of the substituent groups. It is interesting that the similarity of competition factors suggests that the properties of their activated forms are closely similar ; *tert.* butyl chloride shows a much smaller range of competition factors, suggesting a smaller range of activation energies of reactions with the activated form.

---

[10] Bateman, Church, Hughes, Ingold and Tahier, *J. Chem. Soc.*, 1940, 979; Hughes, *Trans. Faraday Soc.*, 1941, **37**, 603.

[11] Holiday and Ogston, 1942, *Report to Ministry of Supply* by Peters, No. 49.

PART III.

THE PREPARATION AND PROPERTIES OF β-CHLORO-β′-HYDROXY DIETHYLSULPHIDE ("C").[12]

The conclusions of Part IA. showed that the velocity constant of hydrolysis of the second chlorine atom of mustard gas is not very much larger than that of the first, so that the product of the first stage should accumulate to an appreciable extent; this was contrary to the conclusions of Wilson, Fuller and Schur.[13] In water kept saturated with respect to mustard gas the concentration of *C* will increase exponentially to a stationary value, while the concentration of thiodiglycol will increase continuously. The stationary value of the concentration of *C* is given by

$$(C) = (\text{mustard gas})/a \qquad . \quad . \quad . \quad . \quad (8)$$

where a is the ratio of the velocity constant of the second stage of hydrolysis to that of the first (= 1·32 in 5 % alcohol at 25°); *C* was isolated from a hydrolysate of mustard gas by making use of the different partition coefficients of mustard gas, *C* and thiodiglycol between water and solvents. Simultaneously *C* was isolated at Sutton Oak by another method and on a larger scale, by treating thiodiglycol with hydrogen chloride.

Experimental.

Mustard gas (2·5 g.) was shaken vigorously with 1 l. of water containing 6 ml. of 2 N. NaOH and phenol red, at 27 to 28° C.; the amount of alkali was calculated so as to allow the concentration of *C* to come near to its maximum value by the time the alkali had been neutralised by the acid set free. As soon as the indicator changed colour (after about 12 min.), 200 ml. of cold saturated NaCl was added, to slow further hydrolysis, and a further 1 ml. of 2 N. NaOH. The solution was very rapidly extracted with four 100 ml. portions of 40-60 petrol-ether, to extract residual mustard gas; then with three 100 ml. portions of chloroform. The chloroform extracts contained the *C* with some thiodiglycol; they were pooled and dried over anhydrous sodium sulphate.

	C.	H.	Cl.	S.
Found % . . .	32·0	6·9	23·5	21·9
Theoretical C_4H_9OSCl .	34·2	6·4	25·2	22·8
Theoretical assuming 4·8 % of water .	32·5	6·6	23·8	21·7

This whole process was repeated a further 4 times; the dried pooled chloroform extract (150 ml.) was filtered. The bulk of the chloroform was removed by distillation at 250-300 mm. Hg on a water bath at 60°. The residue (100 ml.) was transferred to a beaker which was placed on a 20 w. hot plate in a vacuum desiccator and most of the remaining chloroform taken off. Finally, the residue from the beaker was transferred to a glass bottle and the last traces of chloroform were removed by thorough evacuation. The total yield of *C* (estimated by acid and chloride liberated on complete hydrolysis) was 950 mg., about 50 % of theory, with about 90 mg. of thiodiglycol.

Further purification was carried out by shaking this yield with 100 ml. of 40-60 petrol-ether; 500 mg. was dissolved, consisting of 95 % *C* and 5 % thiodiglycol. Removal of the petrol-ether by distillation and resolution in 50 ml. gave a better product. This process was repeated 4 times, the final sample being about 50 mg. of at least 99 % *C*. A sample of this product was analysed by Strauss and Weiler; unfortunately, owing to a misunderstanding, this specimen was left for a week in a loosely corked tube before being analysed and almost certainly took up some water during this period.

None of the chlorine was ionic; this was tested by means of silver nitrate in anhydrous methyl alcohol.

[12] Ogston, 1941, ***Report to Ministry of Supply*** by Peters, No. 40.

[13] Wilson, Fuller and Schur, *J. Amer. Chem. Soc.*, 1922, **44**, 2867.

Properties.—The compound *C* is a colourless oil, somewhat hygroscopic. It forms sulphonium salts[14] if left pure at room temperature; the same process appears to occur in solution in ethyl alcohol and chloroform, but very slowly; in 40-60 petrol-ether, in which it dissolves to about 5 mg./ml. at room temperature, it appears to be quite stable. It is miscible in all proportions with mustard gas and with thiodiglycol.

It is easily soluble in water. It hydrolyses unimolecularly, with a velocity constant of $3{\cdot}72 \times 10^{-3}$ sec.$^{-1}$ at 25° in 5 % alcohol ; this agrees well with the value deduced from the hydrolysis curve of mustard gas (Part IA.). Other kinetic data are given in Table III.

TABLE III

Substance.	Solubility in 5 % v/v EtOH Molar $\times 10^{-3}$.	k_0 sec^{-1} $\times 10^{-3}$.	Competition Factor.					
			Acetate.	Chloride.	Thiocyanate.	Cysteine.	Thiosulphate.	Monothiophosphate.
β-β′-Dichloride ethyl sulphide	6·4	2·90	10	21	$6{\cdot}7 \times 10^2$	$1{\cdot}2 \times 10^3$	$2{\cdot}7 \times 10^4$	$3{\cdot}8 \times 10^4$
bis (β-Chlorethyl thioethyl) ether	0·54	8·25	10	18·4	$7{\cdot}6 \times 10^2$	$1{\cdot}4 \times 10^3$	$2{\cdot}5 \times 10^4$	$3{\cdot}2 \times 10^4$
β-Chlor-β′ hydroxy diethyl sulphide " *C* "	—	3·72	5·2	24	$7{\cdot}8 \times 10^2$	$0{\cdot}9 \times 10^3$	$2{\cdot}7 \times 10^4$	$4{\cdot}2 \times 10^4$
Ethyl-β-chlor ethyl sulphide	7·2	11·0	10	20	5×10^2	$1{\cdot}8 \times 10^3$	$1{\cdot}9 \times 10^4$	$2{\cdot}9 \times 10^4$
Propyl-β-chlor ethyl sulphide	2·32	16·0	8·5	18	7×10^2	$1{\cdot}7 \times 10^3$	$2{\cdot}9 \times 10^4$	$3{\cdot}5 \times 10^4$
Phenyl-β-chlor ethyl sulphide	0·46	0·47	11	22	$6{\cdot}4 \times 10^2$	$1{\cdot}2 \times 10^3$	$3{\cdot}1 \times 10^4$	$3{\cdot}3 \times 10^4$
tert.-Butyl chloride	—	2·4	—	3·5	—	—	6·5	—

We are indebted to the Director General of Scientific Research (Defence), Ministry of Supply, for permission to publish this work.

Summary.

1. The characteristics of the reactions of hydrolysis and substitution of β-β′-dichlorodiethyl sulphide have been investigated at 25° c. in 5 % alcohol v/v. These reactions proved to be of the SN1 type. Substituting reagents showed a wide range of velocity constants of reaction with the activated halogen. The " competition factors," proportional to these velocity constants, of a wide range of reagents were measured.

2. Certain properties of some analogues of β-β′-dichlorodiethyl sulphide were determined for comparison with it.

3. The compound β-chloro-β′-hydroxydiethyl sulphide was isolated and some of its properties determined.

Department of Biochemistry,
Oxford.

---

[14] Ogston, 1943, *Report to Ministry of Supply* by Peters, No. 67.

ELECTRON DIFFRACTION AND RECTIFICATION FROM SILICON AND PYRITE SURFACES

By J. M. Cowley and J. L. Symonds.

Received 3rd October, 1946.

I. Introduction.

The work on silicon and pyrite as rectifiers was initially begun to find whether electron diffraction methods would allow the elucidation of the factors upon which the rectifying properties of metal—semi-conductor combinations depend. The characteristic of such a combination, first taken as the test for rectifying properties, is the current-voltage relation found by applying various voltages across the contact and measuring the resulting currents. A more convenient and quite satisfactory method is to measure the currents obtained by impressing one volt across the combination. The forward current is that for easy flow of electrons; the back current is that in the reverse direction. The ratio of back to forward resistance at one volt is called the B/F ratio.

In later work, the crystal was inserted in a waveguide into which was fed 600 μw. of power from a 10 cm. oscillator. The rectified current was measured by a microammeter having 400 ohms internal resistance. The electron diffraction camera used was of the Finch type.[1] The accelerating voltages (30 to 40 kv.), were measured with an electrostatic voltmeter, which was checked by the electron diffraction patterns from zinc oxide, as standard. This gave an overall accuracy of better than 1 %.

II. Silicon.

(1) Examination of Silicon Crystals by Electron Diffraction.—Surfaces which were almost single crystal faces were broken from large, coarsely crystalline lumps of silicon. The chosen faces were ground flat and etched with caustic soda solution. This gave a good matte finish to the surface which then showed distinctly the areas corresponding to individual crystals. Cross-grating patterns of spots with very little background of diffusely scattered electrons were obtained by the reflection method (Fig. 1). These patterns indicated that the larger single crystal faces were mostly parallel or almost parallel to the (111) plane of the silicon lattice. Using the reduced camera length of 25 cm., it was possible to record extensive patterns of quite sharp Kikuchi lines from such etched surfaces (Fig. 2).

The spots of these patterns show no elongation towards the " shadow edge " (the intersection of the plane of the specimen and the plate) as would be observed if a flat surface, such as a cleavage face, were used. The patterns are produced by transmission of electrons through projections from the surface, left by the etching process.

(2) Forbidden Reflections.—Silicon has a diamond-type cubic lattice. Thus reflections from planes, whose indices are all even, are forbidden by the structure factor restriction unless the sum of these indices is divisible by four. However these " forbidden " spots occurred in the cross-grating patterns, with intensity as great as those of the permitted reflections.

---

[1] Finch and Quarrell, *Proc. Physic. Soc.*, 1934, **46**, 148. Finch and Wilman, *Ergeb. exact. Naturwiss.*, 1937, **16**, 353.

For example, in Fig. 1, the forbidden reflections (222), (442), (600) and (622) are prominent. The latter pair are two of the strongest spots in the pattern. At other than the principal azimuths and by suitable inclination of the specimen, it was possible to obtain the (222) reflection as the strongest in the pattern. The forbidden (222) reflection occurs in the Kikuchi line patterns as the second order of the (111) band or pair of lines. The (222) lines have an intensity intermediate between that of the (111) and the (333) lines. In all patterns taken from silicon single crystal faces, the "forbidden" reflections occurred just as frequently as the "permitted" ones. Consequently, these patterns do not indicate whether the lattice is a diamond type or a simple face-centred cubic structure.

Beeching[2] has observed similar strong (222) reflections and sharp (222) Kikuchi lines from smooth diamond faces. He concluded from the sharpness of the lines that the production of the forbidden reflections could not be a surface effect, due to the first few atomic planes. This is confirmed by the silicon patterns produced by the transmission through projections whose thickness was probably in the region of 10^{-5} cm. A thickness of this order is indicated by the strictness with which the third Laue condition (limiting reflections to the circumference of circles) was observed on these plates. Forbidden reflections may be accounted for qualitatively on the basis of double or multiple reflections within the crystal, but the intensities observed in the case of forbidden reflections from diamond and silicon are much greater than predicted.

Ground silicon surfaces gave ring patterns. The forbidden (222) ring was present in these, in agreement with the observations of Johnsen and Grams[3] on powdered silicon. In several cases a faint ring, not observed by these authors, was found at a position corresponding to the forbidden (200) ring. However, it is possible that this may be the strongest member of a ring pattern of unknown origin. This pattern was recorded strongly, in one case, with broken rings due to large crystals. An analysis of this pattern shows correspondence with that from a hexagonal structure with $a = 5{\cdot}15$ A., and $c = 6{\cdot}55$ A.

(3) The "Blocking Layer" on Silicon.—Some of the recent theories of the rectifying action of the contact between a metal and semi-conductor have postulated a high resistance "blocking layer," physically distinct from the bulk of the semi-conductor (artificial blocking layer) of thickness 10^{-4} to 10^{-5} cm.[4, 5] Other theories have been developed on the basis of a potential barrier (natural blocking-layer) formed at the contact. In the case of cuprous oxide, measurements of the thickness of the blocking layer gave values from 10^{-3} cm.[6] to 5×10^{-6} cm.[7, 8] In point-rectifiers, the nature of the blocking layer is not definite. The electron diffraction patterns do not reveal any layer such as a layer of oxide or a layer with broken or mosaic structure.

A silica layer of thickness 10^{-6} cm. would contribute a diffuse background to the silicon spot pattern, while a layer of 10^{-4} cm. thickness would completely suppress it. Patterns from the etched silicon surfaces, which possessed quite good rectifying properties, were very clear and showed very little diffuse background. Even after prolonged exposure and heating to 400° c. in air, the pattern remained clear. Heating the specimen to a bright red produced the diffuse haloes to be expected from an amorphous layer. Thus any oxide layer on the etched surfaces, if it exists at all, cannot exceed a few molecular layers in thickness.

---

[2] Beeching, *Phil. Mag.*, 1935, **20**, 841.

[3] Johnsen and Grams, *Physic. Rev.*, 1942, **61**, 671.

[4] Mott, *Proc. Physic. Soc. A*, 1939, **171**, 27.

[5] Schottky, *Z. Physik.*, 1939, **113**, 367.

[6] Waibel, *Wiss. Veroff, Siemens Werken.*, 1938, **15**, 75.

[7] Fink and Adler, *Trans. Electrochem. Soc.*, 1941, **79**, 377.

[8] Jouse, *Physik. Z. Sowietunion.*, 1935, **7**, 1.

(4) Silicon for High Quality Rectifiers.—A sample of silicon was prepared from high purity silicon to which had been added small amounts of aluminium. Pieces from the sample were subjected to a series of treatments, a specimen from each treatment being kept in an evacuated glass tube until ready for use in the camera. The order of the treatments was as follows: (1) grinding to a plane surface; (2) heating at 1000° c. in air for about 2 hr.; (3) polishing with optical rouge; (4) heating again at 1000° c. in air for about an hour; (5) etch in commercial HF (48 %); (6) electrolytic etch in HF (a few seconds). The metal used for a contact was tungsten tapered to a point.

The silicon, after grinding (treatment (1)) was always found to be a poorer rectifier than before. The *B*/*F* ratio was in general about 5, the direction of easy flow of electrons being from crystal to metal (*N*-type). After the first heat treatment and polishing the *B*/*F* ratio was about 3, but the direction of easy flow of electrons was from metal to crystal (*P*-type). The second heat treatment gave the surface a bluish coloration which was probably due to SiO_2 with dissolved impurities, as it formed a comparatively high resistance layer. After the removal of this layer with HF, *B*/*F* ratios of about 40 were obtained and rectified currents increased from 60 to 400 μa. The rectification was of *P*-type. The short electrolytic etch in HF improved the *B*/*F* ratio to 100 or more, and rectified currents up to 700 μa. were recorded. The improvement in *B*/*F* ratio was due less to an increase in forward current than to a marked decrease in the back current. In the rectification of 10 cm. waves, the slightest grinding of the prepared surface destroyed its quality as a rectifier, reducing the rectified current to about 50 μa.

The electron diffraction by the final product (treatment (6)) gave patterns such as Fig. 3. The spots are produced by reflection from faces of several separate crystals. Their elongation indicates that the faces are very smooth. These faces are not parallel to the principal planes of the crystals, so that only isolated spots, and no regular cross-grating pattern, appear. Faint but quite sharp Kikuchi lines were visible on the plates. Rings from silicon and alumina were also present. These are due probably to random material at the crystal boundaries. The presence of the sharp Kikuchi lines indicates an almost perfect lattice structure at the crystal faces. The elongation of the spots is due to an inner potential effect, with a calculated inner potential of 6·3 v. This value decreased on exposure to air.

III. Pyrite.

Pyrite specimens used in these experiments were from natural sources among which were Leadville (Colorado) and Dial Range (Tasmania). In using such natural samples, a number of difficulties arise. Chief among these are the impurity content, surface deterioration and variation in composition (ratio, Fe/S).

(1) Effect of composition.—Smith[9] describes the effect of composition on conductivity, finding that in general a sulphur-deficient crystal has a higher conductivity. Schleede and Buggisch[10] state that the more nearly pyrite conforms to the theoretical formula FeS_2, the better the rectification (see III, (5)).

(2) Effect of the metal point used.—In general, oxidised Nichrome and silver were found to give the best characteristics with pyrite, and silver was the better of these two. Since we were seeking the properties of the crystal which influenced the characteristics, all tests were carried out with a silver point, though this metal would probably be too soft in a practical rectifier.

---

[9] Smith, *Amer. Min.*, 1942, **27**, 1.

[10] Schleede and Buggisch, *Z. anorg. Chem.*, 1927, **161**, 85.

(3) The effect of impurities.—Spectrograms * of three samples of pyrite gave some idea of the impurities likely to be present. Results indicate that natural pyrite varies too much in composition to be a useful rectifier.

Specimen 1, Colorado pyrite, showed silicon (probably as silica), lead, cobalt and a trace of copper. Rectification was excellent and very little deterioration, if any, occurred with exposure. B/F ratios had values up to 200.

Specimen 2, from the same source as specimen 1; contained nickel in addition to the elements in No. 1. Rectification was excellent on fresh surfaces but showed a marked deterioration within a few days, B/F ratios falling from about 100 to 10.

Specimen 3, from the University of Adelaide Geology Department, and contained some considerable amount of silicon, cobalt, nickel, bismuth, copper, arsenic, and a trace of lead. Rectification was poor and deterioration rapid.

(4) Crystal Size.—Investigations on several specimens of microcrystalline pyrite revealed that rectification was poor. Aggregates of small crystals also are generally poor material. Single crystals may vary remarkably from point to point both in conductivity and rectification. These differences are most likely due to changes of composition and impurity from point to point.

Electron diffraction patterns were obtained from single crystals of pyrite, ground on one face and etched in concentrated nitric acid. Fig. 4 is the cross-grating pattern obtained by reflection from a (100) face of pyrite from Dial Range. The mosaic structure of the crystal is indicated by the large numbers of spots of nearly equal intensity. The (h00) spots for which h is odd, i.e. the alternate spots on the centre line of the pattern, are forbidden by the structure factor restriction. However they occur with intensities which are of the same order as the others. Raether[11] has observed similar patterns and has attributed the presence of the forbidden spots to multiple reflections.

Fig. 5 was obtained from a well-crystallised specimen of Colorado pyrite. Its rectifying properties were excellent. The face was slightly inclined to the (100) plane. The strictness with which the spots are confined to the narrow Laue zone indicates an almost perfect crystal lattice. As was the case with silicon, there is no evidence for an insulating layer which could act as an artificial blocking-layer.

(5) Deterioration.—Some specimens of pyrite possess electrical properties which change with time. Samples differ widely in this respect, some surfaces deteriorating rapidly while others show little change in the static characteristics after months of exposure to ordinary laboratory air. When this change does occur, there is a gradual increase with time in the back current which will flow at any particular voltage. The forward current undergoes little change, usually a slight decrease. Specimens were ground with fine emery powder (600 mesh) and, after washing, the broken pieces were etched away with nitric acid. This etching process greatly improved the B/F ratios in some specimens and rendered the surface more uniform in behaviour (reduced the " spottiness ").

It was noticed after etching that in some specimens the deterioration was much slower than before. In some cases, very little deterioration occurred even after several months' exposure to air. This improvement produced by etching may be due to the removal of an impurity from the surface, or it may be due to the removal of some Fe or S from the surface layer, producing temporarily the conditions for good rectification as well as stability. It does not follow that a specimen improved by etching is stable in that condition since, even if atmospheric effects are excluded,

---

* Kindly taken by Mr. K. B. Mather.

[11] Raether, *Z. Physik.*, 1932, **78**, 527.

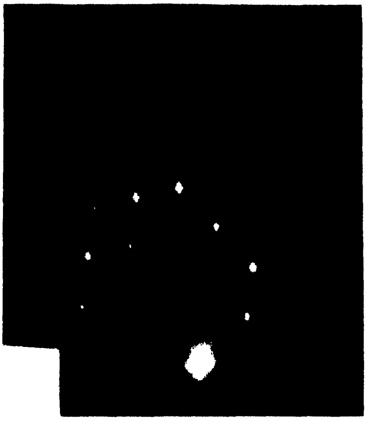

FIG. 1.—Cross grating pattern from silicon.

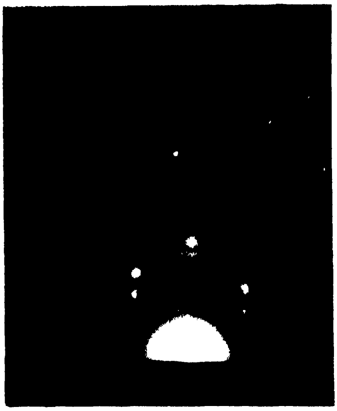

FIG. 2.—Kikuchi line pattern from silicon.

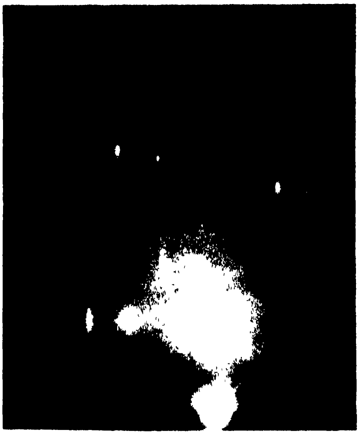

FIG. 3.—Silicon for high quality rectifiers.

FIG. 4.—Dial Range pyrite.

[*To face page* 56.

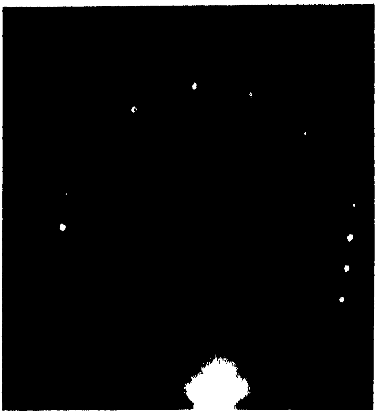

FIG. 5.—Colorado pyrite.

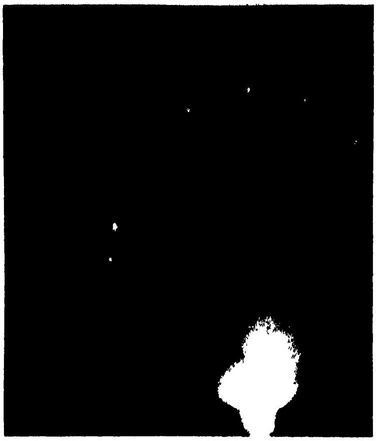

FIG. 6.—Colorado pyrite ground lightly.

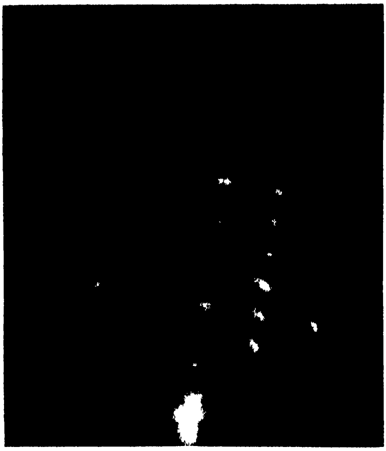

FIG. 7.—Pyrite (from Fig. 6) ground further and etched.

[*To face page* 57.

there may be a diffusion of atoms from the bulk of the crystal to the surface. This would certainly undo the effects of the etch.

Etched single crystal faces were examined by electron diffraction at intervals over a period of several months. Certain specimens of Colorado pyrite showed neither deterioration in rectification nor change in electron diffraction pattern. Crystal faces of Dial Range pyrite which did not rectify, did show weathering effects. No weathering was visible to the eye, but electron diffraction patterns indicated the formation of a thin layer of products of weathering. After six days faint rings appeared, together with a heavier diffuse background. This was in addition to the original spot pattern. No further change was observed in three months. The ring pattern gives spacings agreeing with those of $FeSO_4 . H_2O$. It is probable that other reaction products are present including some nearly amorphous material. The thickness of the layer formed cannot be much more than 10^{-6} cm.

IV. The Grinding of Surfaces of Pyrite and Silicon.

(1) The influence of surface distortion on the rectifying properties of single crystal faces of pyrite and silicon, at various stages of grinding, polishing and etching, was investigated by rectification tests combined with electron diffraction examination. In the case of pyrite, these experiments were carried further than was required for the above purpose in order to gain more complete information on the nature of the polish layer.

Well-etched pyrite crystal faces gave patterns such as Fig. 5. They showed excellent B/F ratios, some being as great as 200. Very light grinding on 303 emery paper under water (eight gentle rubs) destroyed the good rectification and reduced the B/F ratios to 2. This was due to a decrease in the back resistance, as with the silicon specimen mentioned in para II (4).

The corresponding diffraction pattern, Fig. 6, shows a spot pattern with a more even intensity distribution, with spots appearing within the Laue ring. This indicates a more mosaic structure of the surface, with crystal blocks in the surface twisted out of their previously perfect alignment. Further grinding increased this effect. The ring of strong spots faded to give an even intensity distribution while the whole spot pattern became weaker and more diffuse. Faint rings due to random powdered pyrite appeared, gradually strengthened and then became more diffuse as the grinding proceeded. There was no further change either in the contact resistances or their B/F ratio after the first light grinding.

An etch of 20 sec. in dilute nitric acid was sufficient to remove the random material from the ground surface. This revealed the layer which gave Fig. 7. The even spread of the spot pattern and the elongation of the spots into arcs indicates great distortion and mis-alignment of the crystal blocks in the surface. Further etching revealed a gradual decrease in the mis-alignment until the original perfect-crystal pattern returned. It was not until the surface had been etched down to the region of the undisturbed lattice that the rectification returned to its initial value. Only when the cat's whisker made contact with an unbroken lattice did the back resistance have a high value, giving good rectification. Conduction along the surfaces of cracks between crystal blocks may be the cause of the low value for ground surfaces. It was observed that the lattice constant calculated from spot patterns showing lattice mis-alignment was consistently low by 1 to 2 %. On the other hand, patterns from the perfect lattice and also ring patterns gave the correct value.

In the case of silicon, grinding produced a polycrystalline layer giving a ring pattern. Here the distortion of the underlying lattice was not so marked, the B/F ratios not decreasing to such low values as for pyrite. However, rectification seems to be related to the state of the surface for silicon as well as for pyrite.

(2) The Polishing of Pyrite.—Raether[12] obtained similar diffraction patterns from coarsely ground pyrite surfaces but could obtain none from finely ground surfaces. Darbyshire and Dixit[13] reported that pyrite gave very weak and diffuse rings when polished. Similar patterns were obtained by the present authors from pyrite single-crystal faces, polished either on optical rouge or on fine dry emery paper. The spot pattern remained after prolonged polishing although very faint and diffuse. Very diffuse rings, due to spacings $d = 1{\cdot}26$ A. and approximately $d = 2{\cdot}2$ A. predominated although there were a few weaker and sharper rings, probably due to pyrite.

Etching of the polished surfaces with dilute nitric acid strengthened the spots and sharpened the rings. Some of these rings were due to pyrite while the remaining rings were caused by another substance which is as yet unidentified. The strongest rings of the pattern are a pair at $d = 1{\cdot}22$ and $1{\cdot}27$ A. developing out of the outer diffuse rings of the polish pattern, and one at $d = 2{\cdot}4$ A. corresponding to the inner diffuse ring. Spacings from the pattern agree with those for a tetragonal lattice with $a = 2{\cdot}40$ A. and $c = 3{\cdot}02$ A. With an etching solution which had been used several times this ring pattern becomes stronger and more diffuse until it resembles that of the unetched polished material. Etching with concentrated nitric acid strengthens the spot patterns and gives rings attributable to Fe_2O_3, which is probably produced by the oxidation of the unidentified material mentioned above. Prolonged etching always removed the ring patterns and gradually restored the original spot patterns. The rectification remained poor during the polishing and initial etching. However, it improved as the etching revealed the undistorted lattice.

From the above, a general picture of the polish layer on pyrite can be drawn. A powdered layer of an unidentified substance and pyrite covers the crystal face. At the surface this layer is of very small crystal size but is coarser below. It is not thick enough to obscure the spot pattern from the greatly distorted pyrite crystal lattice beneath. Within the lattice itself the degree of misalignment decreased gradually until, at a considerable depth, the undisturbed lattice is reached.

V. Variation of Rectification on Single Crystals of Pyrite.

Very wide variations in rectification have been noticed between crystals which have come from the same source and even between different areas of one crystal surface. The latter is well illustrated by the following two examples :

(*a*) A single crystal of pyrite * possessed a perfect mirror-like cleavage surface about 1 cm.^{2} in area. The extensive Kikuchi line patterns from this face indicate a perfect lattice over the whole surface. However, this same surface could be mapped into sharply defined areas between which there were remarkable differences in rectification. In Fig. 8, the surface is shown divided into three sections. In section *A*, *B*/*F* ratios of 100 up to 500 were observed, the forward current being about 10 ma. Section *B* showed *B*/*F* ratios from unity up to 10, with forward currents of about 1 ma. Section *C* showed very high resistance and no rectification (*B*/*F* ratio unity). Forward currents ranged from about 10μa to 50 μa.

It is remarkable that such a surface, showing almost a perfect crystal lattice structure, should vary so widely in rectification and conductivity. Certainly no weathering had occurred on this surface. The alternative then must be a definite difference in composition (cf. (9)), with a possible difference in impurity.

---

[12] Raether, *Z. Physik.*, 1933, **86**, 82.

[13] Darbyshire and Dixit, *Phil. Mag.*, 1933, **16**, 961.

* Lent by Mr. K. L. Sutherland of the C.S.I.R. Division of Industrial Chemistry.

(*b*) The crystal surface used in the experiments described in IV, (1) and IV, (2) seemed to be a face of an unbroken single crystal of pyrite. However, there were three definite strips (*A*, *B* and *C* in Fig. 9) which showed very different rectifying properties; *A* showed excellent rectification, *B* none at all, and *C* very poor rectification. The boundaries were sharp, and were identical for two different cat's whiskers, namely silver and tungsten. After polishing on emery paper and etching in dilute nitric acid, these three strips were visibly different, *B* being lighter in colour than *A*, and *C* darker.

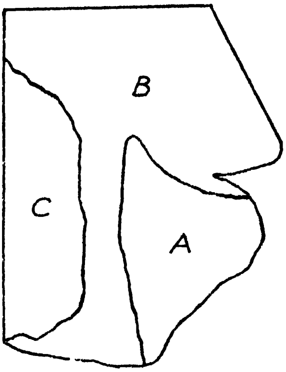

FIG. 8.—Pyrite single-crystal face (*a*).

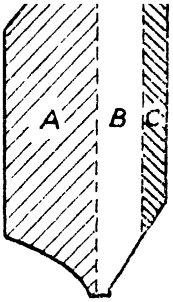

FIG. 9.—Pyrite single-crystal face (*b*).

A comparison of electron diffraction patterns from strips *A* and *B* taken under a variety of conditions revealed no very obvious difference. However, calculation of the lattice constant, or unit cube edge, *a*, revealed that, when strip *A* gave a good rectification, strip *B* had a lattice constant greater than that of *A* by 1 % on the average. This difference, although close to the limit of accuracy of the apparatus, appears to be real. It seems to indicate a variation in composition responsible for the differences in rectifying properties.

VI. Discussion.

The electron diffraction investigations have indicated throughout that the best rectification is obtained when the metal point is placed in contact with an unbroken single-crystal lattice of the semi-conductor. It is preferable, as seen in III, (4), that the crystal size should be as large as possible and that the surface should be smooth. There has been no evidence, in the electron diffraction patterns from both pyrite and silicon, that there is an " artificial " blocking layer of some other substance on the surface. The barrier must thus be a natural one due to the contact between metal and semi-conductor.

When the lattice is disrupted to give a mosaic structure, either by the action of excess impurities, or by mechanical means such as grinding, the rectification becomes very poor, (IV, (1) and (IV, 2)). Beyond this the method of electron diffraction gives no information. The rectification is highly dependent upon other factors which are probably more important. These factors are impurity content in the case of silicon, and composition in the case of pyrite. The almost perfect lattice structure is a necessary condition for good rectification after these factors have been given their correct values. The observed variation in lattice constant and coloration of the pyrite surface could be attributed to either a difference in composition or in impurity content.

The authors wish to express their thanks to Dr. R. S. Burdon for many invaluable discussions, and to the Council for Scientific and Industrial Research for research grants.

Summary.

Electron diffraction and rectification investigations have been conducted on surfaces of pyrite and silicon for different surface conditions. There is evidence that, for the best rectification, the crystal lattice should be almost perfect and free from fracture or mosaic structure. A general picture of the polish layer on pyrite is built up from electron diffraction evidence.

Physics Department,
University of Adelaide,
South Australia.

ELECTRON DIFFRACTION BY FATTY ACID LAYERS ON METAL SURFACES.

BY J. M. COWLEY.*

Received 3rd October, 1946.

The investigation of the structure of layers of long-chain fatty acids on polished metals, and the effect of heating on the structure, was undertaken in connection with work on the lubricating properties of such layers, carried out by the Tribophysics (Lubricants and Bearings) Section of the Council for Scientific and Industrial Research. A recent report [1] summarises the work of the Section in this field.

For the electron diffraction studies, palmitic acid was selected. Layers of this acid on polished platinum, silver, cadmium, steel and copper surfaces were examined by the reflection method. The orientations observed in these layers and the temperature effects were generally in accord with the indications of previous work, most of which was done with the longer-chain stearic acid. However, in the course of these observations, a new orientation was found. The unusual structure and remarkable properties of layers so orientated form the main subject of this paper.

The electron diffraction camera used was of the cold-cathode type due to Finch and collaborators.[2] An adaptation of the standard specimen holder and a special mount containing a heating coil allowed metal specimens to be heated to temperatures up to 300° c. while under observation in the camera. Purified samples of palmitic acid and cadmium palmitate, and the metal blocks employed were supplied by the Tribophysics Section, C.S.I.R. The metal surfaces were prepared by grinding on successively finer stages of emery paper under water, and polishing with rouge on a soft damp pad.

Thick Layers of Fatty Acids on Metals.

These were produced on the polished surface either by melting crystals of the palmitic acid or by evaporating a drop of a benzene solution of the acid from the surface. Several orientations were observed including, in a few cases, the pattern found by Murison.[3] This consisted of arcs near the origin due to crystallites orientated with the (110) plane of the monoclinic unit cell parallel to the surface. Diffuse bands due to molecules standing approximately normal to the surface were also present.

---

* Now with Division of Industrial Chem., Council for Scientific and Indust. Research.

[1] Bowden, Gregory and Tabor, *Nature*, 1945, **156**, 97.

[2] Finch and Quarrell, *Proc. Physic. Soc.*, 1934, **46**, 148; Finch and Wilman, *Ergeb. Exakt. Naturwiss.*, 1937, **16**, 353.

[3] Murison, *Phil. Mag.*, 1934, **17**, 201.

More common was a pattern of bands inclined to the " shadow edge " and some diffuse spots. These patterns were similar to those observed by Germer and Storks[4] from built-up multilayers, but were not so well defined owing to the poorer crystallisation of the acid. The inclination of the bands indicated that the molecular chains were tilted at an angle of about 54° to the surface, corresponding to the α-form of the acid ($a = 9{\cdot}4$, $b = 5{\cdot}0$, $c = 45{\cdot}9$ A., $\beta = 51°$). Rubbing of these thick layers in any one direction with degreased cloth produced an orientation similar to that observed by Germer and Storks[5] for rubbed stearic acid layers. The molecular chains lay inclined, against the direction of rubbing, at an angle of 5° to the surface. The acid remained crystallised in the α-form, with the b-axis parallel to the surface. Continued rubbing of the layer removed all but the first monolayer of the acid. This monolayer continued to give the characteristic diffuse-band pattern due to molecules standing normal to the surface.

On heating these thick layers, both rubbed and unrubbed, the orientations giving the spot patterns disappeared at temperatures well below the bulk melting point of the acid, 63° C. The temperature at which the spot pattern was seen to fade out ranged from 35° to 55° C. Above this latter temperature the layer gave a very diffuse band pattern, indicating that very little orientation remained.

Monolayers on Metals.

Germer and Storks[4] have shown that the molecules in the first molecular layer of long-chain fatty acid on a metal surface stand almost perpendicular to the surface, with no lateral regularity. This first layer is of particular interest from the point of view of boundary lubrication.

Fatty acid added to a paraffin oil forms such a monolayer at the oil-metal interface. The acid molecules in this layer are held strongly to the metal surface and play an important part in preventing metal-to-metal contact under the high-load conditions of boundary lubrication. Recent results[1] have shown that the lubricating action of fatty acid layers on such metals as copper and cadmium breaks down at temperatures from 30° to 60° C. above the bulk melting points of the acids, the temperature varying with experimental conditions. On such metals as platinum, silver and chromium, the fatty acids have no lubricating effect.

Electron diffraction has shown that on steel and copper surfaces, the molecules in the first monolayer lose their orientation at a temperature corresponding roughly to the temperature at which the lubricating action of the acid breaks down. The pattern of slightly curved diffuse bands given by a fatty acid monolayer becomes more diffuse on heating, and finally disappears within a temperature range of a few degrees. Beeck, Smith and Wheeler[6] found that a stearic acid layer on steel lost its orientation at 110° C., or 40° C. above the melting point. Tanaka[7] used a copper base and found that for stearic and palmitic acids, and for paraffins of similar chain-length, the orientation became random at 50° to 60° C. above the bulk melting point.

In the present investigation the temperature of transition from ordered to random array was found for monolayers of palmitic acid on platinum and cadmium. Monolayers were prepared by prolonged rubbing of thick layers with degreased cloth or by the " retracting-drop " technique. In the latter method a monolayer is formed on the metal as a drop of a solution in hexadecane spreads over the clean surface, and remains when the liquid subsequently contracts into small drops. On the two metals the behaviour of the pattern on heating was essentially the same. The bands became very diffuse and faded out completely within a few degrees of 105° C., or approximately 40° C. above the melting point of the acid. For purposes of comparison, monolayers of cadmium palmitate were formed on platinum and cadmium surfaces by prolonged rubbing of thick layers. Such soap monolayers showed band patterns similar to those from the acid, and likewise lost their orientation at 105° C.

---

[4] Germer and Storks, *Proc. Acad. Nat. Sci.*, 1937, **23**, 390 ; *J. Chem. Physics*, 1938, **6**, 280.

[5] Finch, *J. Chem. Soc.*, 1938, 1144; Germer and Storks, *Physic. Rev.*, 1939, **55**, 648.

[6] Beeck, Smith and Wheeler, *Proc. Roy. Soc. A*, 1940, **177**, 90.

[7] Tanaka, *Mem. Coll. Sci. Kyoto Imp. Uni. A*, 1938, **21**, 85 ; *ibid.*, 1939, **22**, 377 ; *ibid.*, 1941, **23**, 196.

This value of the transition temperature for palmitic acid is consistent with that given by Beeck, Smith and Wheeler for stearic acid on steel, and, to a lesser extent, with the results of Tanaka. Thus it appears that the loss of orientation in a monolayer formed from the acid occurs at a temperature which is independent of the base metal. Also the transition temperature seems to be the same whether the molecular chain is terminated by an acid group or a metal ion. In the case of a layer formed from palmitic acid on cadmium it is possible that a soap should be formed by chemi-sorption of the acid, but this seems unlikely in the case of acid layers on platinum.

A New Orientation.

In the course of the above investigations a layer of palmitic acid was prepared on a polished platinum surface by melting crystals of the acid, and smoothing the liquid over the surface with a glass rod as it solidified. The layer was then rubbed backward and forward in one direction with degreased cloth. The diffraction pattern, reproduced as Fig. 1, was obtained by reflection, with the electron beam grazing the surface in a direction perpendicular to the direction of the rubbing strokes with the cloth. The pattern is seen to consist of rather sharp spots on a number of lines perpendicular to the " shadow-edge," or the intercept of the plane of the specimen on the photographic plate. For convenience these lines will be referred to as " vertical." Faint rings pass through the spots, and the spots on those lines farthest from the centre are elongated to arcs along the rings. The spots on alternate lines form a regular cross-grating pattern. Those on intermediate lines are less numerous, more diffuse, and apparently unrelated to the cross-grating. This pattern of spots and lines will be referred to as " pattern *C*." A faint diffuse-band pattern similar to that given by a monolayer is also present.

With the specimen turned through 90°, so that the electron beam lay parallel to the rubbing direction, the pattern was very different and too weak for reproduction. There were no vertical lines, but only faint rings with one or two weak arcs along the centre line position, and a heavy diffuse background. Measurements of the cross-grating pattern on alternate lines showed that the vertical separation of the spots was due to a lattice spacing $d = 7{\cdot}4$ A. The separation of the vertical lines corresponded to $d = 5{\cdot}1$ A. Thus the horizontal spacing of the spot pattern on alternate lines was $d = 2{\cdot}55$ A.

The dimensions $a_1 = 5{\cdot}1$ and $a_2 = 7{\cdot}4$ A. are close to those of the cross-section of the monoclinic unit cell of the long-chain fatty acids. This same unit-cell cross-section is common to a large number of long-chain organic compounds, including paraffins, fatty acids, alcohols and esters. In the case of the paraffins, where the monoclinic angle becomes 90°, these are the *a* and *b* unit-cell dimensions of the ortho-rhombic cell.

Thus the cross-grating pattern was given by crystallites orientated so that the molecular chains lay approximately parallel to the surface, and perpendicular to the direction of rubbing with cloth. The planes

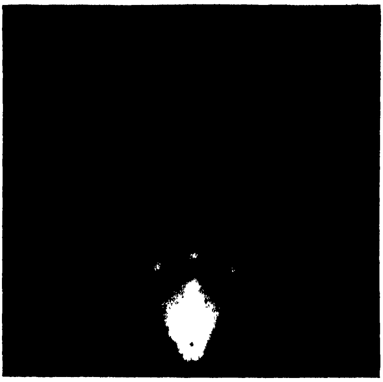

Fig. 1.—Diffraction pattern from layer formed from palmitic acid on platinum.

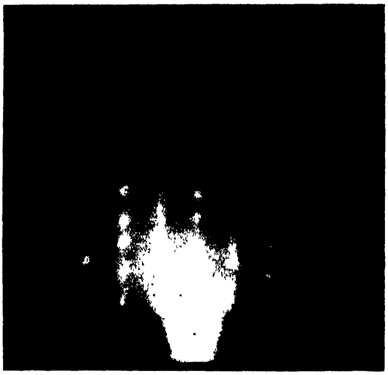

Fig. 2.—Layer soaked in benzene.

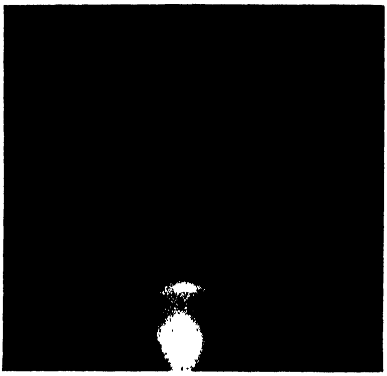

Fig. 3.—Layer after heating to 500° C.

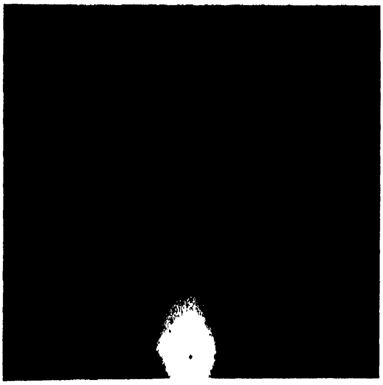

Fig. 4.—Heated to 850° C.

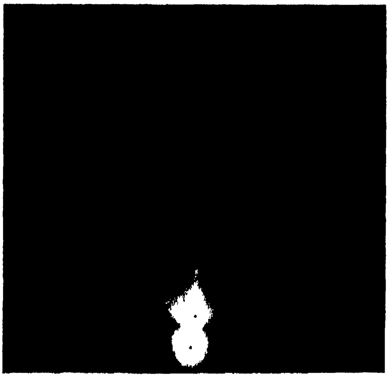

Fig. 5.—Superimposed patterns due to the two new structures.

with spacing $a_2 = 7{\cdot}4$ A. were parallel to the surface. The vertical lines corresponding to a spacing $a_1 = 5{\cdot}1$ A. are attributed to planes of discontinuity in the lattice. In the mechanically orientated and poorly crystallised material, adjacent crystallites were tilted with respect to each other, so that there was no regular arrangement of atoms in the boundary planes. Such boundary planes occurred at multiples of $5{\cdot}1$ A., and so gave rise to the observed lines.

In the cross-grating pattern the effective horizontal spacing was $d = 2{\cdot}55$ A. In this respect the pattern resembles that of the β-form of stearic acid ($a = 5{\cdot}6$, $b = 7{\cdot}5$, $\beta = 63^\circ$) for which the shorter dimension was effectively halved, rather than the α-form for which the odd orders of the $a = 9{\cdot}4$ A. dimension were suppressed.[8]

The rings are due to randomly orientated crystallites. The spots on the odd vertical lines occur where strong rings cut these lines, but not at all such intersections. The strong spots on the odd lines form a row parallel to the shadow-edge. This could possibly be the layer line for $l = 1$, where the c-spacing is taken as $c = 2{\cdot}54$ A. The strongest spots visible would then be the (101) and (301) reflections, given by strongly tilted crystallites.

The faint band pattern was given by uncrystallised molecules standing approximately normal to the surface, either in the first monolayer next to the metal, or in un-orientated parts of the layer. The pattern of faint rings appearing at the 90° azimuth was due to random crystallites. The weak arcs had a vertical spacing of $d = 7{\cdot}4$ A., and confirmed the orientation with this periodicity perpendicular to the surface. The absence of any vertical diffuse layer lines due to the spacing $d = 2{\cdot}54$ A. along the carbon chains supported the assumption that the angles of tilt of the crystallites to the surface might reach large values. The bands were spread out into the general diffuse background. Thus the crystallites seem to have been orientated with the molecular chains parallel to the vertical plane and perpendicular to the rubbing direction, but varying in tilt with respect to the surface.

The occurrence of the dimensions $a_1 = 5{\cdot}1$, $a_2 = 7{\cdot}4$ A. rather than those of either of the usual α- or β-forms of long-chain fatty acids raises the possibility that an orthorhombic form, similar to that reported by Trillat and Hirsch,[8] may have been present. These authors examined thin, well-crystallised films of stearic acid. They found that the spot pattern due to the α- or β-form of stearic acid, faded under the electron beam to give a pattern similar to that of the paraffins. This " γ-form " of stearic acid had unit-cell dimensions given as $a_1 = 7{\cdot}4$, $a_2 = 5{\cdot}1$ A. if a 2 % correction, indicated by a footnote to the above paper, is added. The writer has confirmed these results using thin films of palmitic acid, evaporated on a water surface from benzine solution.

The method first used to produce pattern *C* was rather complex and not consistent in its results. A series of experiments was undertaken to discover the essential steps of the preparation. In no case was the pattern produced without the step of smoothing the molten acid as it solidified. Rods of glass or silica, and, in one case, degreased cloth were used successfully as the smoothing implement. Rubbing of the solidified layer with degreased cloth was not essential but seemed desirable. The direction of rubbing determined the direction of orientation of the molecular chains. If a layer giving pattern *C* was rubbed at right angles to the original rubbing direction, the molecules turned round and became orientated perpendicular to the new direction of rubbing. With vigorous rubbing the pattern *C* faded until only the brightest spot, the (020) remained, together with a monolayer pattern. This last spot was very difficult to remove by rubbing. The layers produced by the above method were usually too thin to be visible, but sometimes appeared as a faint smear.

---

[8] Trillat and Hirsch, *J. Physique Rad.*, 1933, 4, 38.

In some cases, pattern *C* did not appear immediately when the specimen was examined in the electron camera. Preliminary patterns of arcs close to the central spot were first observed. These faded, and gave place to pattern *C* after a minute or two, or on heating to about 40° c. These preliminary patterns were recorded on several occasions, but were never very clear. The diffuse arcs were not due to the (110) orientation mentioned above. The arcs on the central line indicated a spacing of approximately $d = 3{\cdot}7$ A., or the second order of $d = 7{\cdot}4$ A., corresponding to an (010) orientation of the unit cells. Spots corresponding to the (110) and (130) positions for this orientation were also present.

Properties of Layers Giving Pattern C.

Layers formed from palmitic acid on a polished platinum surface and showing the new orientation, had properties differing widely from those of the bulk acid or of previously observed layers on metals. In particular the difference in behaviour on heating was very marked. Solvents which normally dissolve fatty acids, such as benzine and alcohol, did not remove the layer. Specimens giving patterns such as Fig. 1 were soaked in such solvents for 10 to 20 hr., and subsequently gave similar patterns, with an increase in clarity due to the removal of the molecules giving the diffuse band pattern, and much of the diffuse background. Fig. 2 was taken from a specimen soaked in benzine. The vertical lines and spots were much more extensive than before soaking.

The effect of heating on the orientation was first investigated by heating the specimens in the vacuum of the electron diffraction camera. At about 100° c., pattern *C* became clearer as the diffuse band pattern faded out. The pattern observed on the fluorescent screen showed no appreciable change when the temperature was raised to the limit of the heating specimen holder, viz. nearly 300° c. A pattern recorded at 260° c. was similar to those obtained at room temperature, only differing in the absence of the band pattern.

The effect of higher temperatures was investigated by heating specimens which had shown pattern *C* in an electric oven in air at atmospheric pressure, and examining them in the diffraction camera when cool. Two series of such experiments, heating to successively higher temperatures, gave similar results. After heating the specimens in air to over 300° c. the pattern showed a noticeable decrease in orientation, the spots being drawn out more into arcs, the rings becoming stronger and the vertical lines fainter. The lines were still present, although weak, after heating to 400° c. After heating to over 425° c. the vertical lines had disappeared and a pattern of rings, with stronger arcs corresponding to the brighter spots of the original spot pattern, remained. This is shown in Fig. 3, taken after heating to 500° c. Further heating of the specimens reduced the degree of orientation. After heating at 700° c. for one series, and 800° c. for the other, diffuse rings due to the platinum base appeared with the fading sharp ring pattern. Fig. 4, taken after heating to 850° c., shows diffuse platinum rings, dotted with elongated spots due to the recrystallisation of the polished surface. The inner rings of the previous pattern remain faintly, and show slight orientation.

Thus the crystallites in the layer lost most of their orientation at between 400° and 500° c., but remained on the surface after heating in air to 700° or 800° c. Below the transition temperature at about 450° c., the rings were in fair agreement with those expected from an orthorhombic lattice with $a = 5{\cdot}1$, $b = 7{\cdot}4$ and $c = 2{\cdot}54$ A. Above this temperature the ring diameters increased corresponding to a decrease in the a and b lattice dimensions of about 5 %. The spacings from patterns taken below and above the transition temperature are compared with those calculated from the appropriate lattice dimensions in Table I.

TABLE I.—SPACINGS FROM RING PATTERNS FROM LAYERS HEATED BELOW AND ABOVE 450° C.

Heated to less than 450° c.			Plane.	Heated to 700° c.		
Intensity.	*d* obs.	*d* calc.*		*d* calc.†	*d* obs.	Intensity.
M	7·4	7·40	010	—	—	—
MS	4·21	4·20	110	3·99	4·2	W
S	3·72	3·70	020	3·51	3·6	S
M	3·00	3·00	120	2·85	2·91	M
M	2·55	2·55	200	2·43	2·43	MW
M	2·48	2·47	030	—	—	—
M	2·39	2·41	210	2·29	2·25	MS
—	—	2·28	101	2·25		
W	2·17	2·18	111	2·15	2·08	W
W	2·09	2·10	220	2·00	1·94	W
W	1·97	1·94	121	1·75	1·75	MW
MW	1·86	1·85	040	1·76		
W	1·74	1·75	211	—	—	—
		1·72	230	1·69	1·66	MW
M	1·69	1·67	131	1·62		
W	1·54	1·50	041	1·45	1·50	MW
M	1·49	1·48	050	—	—	—
W	1·40	1·41	301	—	—	—
—	—	1·39	311	—	—	—
M	1·30	1·29	241	—	—	—
—	—	1·28	400	—	—	—
MW	1·25	1·23	060	—	—	—

* Values calculated for a = 5·10, b = 7·40, c = 2·54 A.
† Values calculated for a = 4·85, b = 7·03, c = 2·54 A.

On the left-hand side of the table, the spacings averaged from a number of plates taken after heating to less than 450° c. are compared with those calculated for a = 5·10, b = 7·40, c = 2·54 A. On the right-hand side, the spacings from a plate taken at 700° c. are compared with those calculated for a = 4·85, b = 7·03, c = 2·54 A., or a 5 % contraction in a and b dimensions. No great accuracy was possible in the measurements. The apparent contraction of the lattice was shown by all layers heated to more than 450° c., with the exception of one case to be mentioned later. The average linear contraction for the high temperature patterns was 5·2 (± 0·6) %.

Layers on Metals other than Platinum.

Attempts to produce the orientation giving pattern *C* on other metals met with varying success. On polished silver and steel surfaces, layers prepared by the methods outlined above gave pattern *C*, identical with that observed on platinum. On both metals the pattern was unchanged after heating the specimens to well over 100° c. in the camera. In the case of the steel, the pattern was faintly visible after heating in air to 300° c., although the surface was oxidised to a strong orange colour.

On copper surfaces, a number of patterns were observed which seemed intermediate between pattern *C* and the preliminary patterns sometimes obtained on platinum. The patterns consisted of diffuse arcs, with a spacing on the central line d = 3·7 A, or sometimes d = 7·4 A., and occasionally faint vertical lines appeared. These patterns faded out at temperatures of from 90° to 130° c., the temperature being higher in the case of layers giving patterns with more of the characteristics of pattern *C*.

Faint rings of cuprous oxide appeared when these patterns faded. Several attempts to produce pattern *C* on cadmium surfaces were unsuccessful. Pattern *C* was also given by layers prepared from stearic acid on platinum. The dimensions of the pattern and its behaviour on heating were the same as for layers prepared from palmitic acid.

A Further New Structure.—One specimen prepared from palmitic acid on platinum as previously to give pattern *C*, gave in addition a second pattern of the same form but with different dimensions. The two patterns are superimposed in Fig. 5. The second pattern has vertical lines with separation corresponding to $d = 6{\cdot}3$ A., and spots on the vertical lines indicate a spacing $d = 14$ A. of planes parallel to the surface. In this pattern the spots of the cross-grating lie on every vertical line instead of every second line as in pattern *C*.

Faint traces of this second pattern were found with pattern *C* in some layers on steel and silver. In these cases only one or two spots of the new pattern appeared. The layer on platinum was heated to increasing temperatures in air. The new pattern was almost completely removed by heating to 400° c., leaving pattern *C*. Further heating up to 700° c. gave ring patterns as previously observed at these temperatures, but with arcing indicating an orientation of the (200) plane, with $d = 2{\cdot}55$ A., parallel to the surface. For this series there was no evidence of the contraction of the lattice at temperatures above 450° c., which was observed previously.

Discussion.

There was a remarkable difference between the properties of the layers giving pattern *C* and those of layers of normal fatty acids. This difference cannot be attributed to a modification of crystal form only. The loss of solubility, and the increase in the temperature of break-down of crystal structure from 40° to 50° c. to over 800° c., represent changes of a different order of magnitude from any which could be accounted for in this way. Two alternative explanations present themselves. The pattern may have been given by an inorganic substance present as an impurity, or a reaction product or else the layer remained of a long-chain organic nature, but had undergone a change which replaced the weak van der Waals' forces between the molecular chains by stronger bonds.

The nature of the pattern supports the latter contention. The dimensions of the cross-grating are in fair agreement with those of the unit cell cross-section common to a large number of long-chain organic substances. No inorganic material which could have been present has these unit cell dimensions. The occurrence of diffuse lines is rare for inorganic materials, and for such substances a cross-grating would also have been observed at the 90° azimuth. The form and dimensions of pattern *C* were independent of the base metal, and of the material of the smoothing rod. The metal bases showed no abnormal surface structure before or after the pattern *C* was present. The possibility that the pattern *C* may have been due to metal-organic compounds seems remote in view of the poor results on the more reactive metals, cadmium and copper, as compared with platinum and silver.

The pattern *C* has no parallel in patterns from inorganic material, but shows a resemblance to some published patterns from organic substances. In particular there is a marked similarity with patterns published by Storks,[9] obtained by transmission methods from linear high polymers in stretched films. Diffuse lines in this case were given by fibre spacings. In the case of gutta percha this spacing was $d = 5{\cdot}0$ A. More recently Charlesby [10] has investigated the structure of films of polythene formed on water or rubbed on metals. The ring patterns from the polycrystalline layers agreed well with those for an orthorhombic lattice with $a = 7{\cdot}428$, $b = 4{\cdot}934$, $c = 2{\cdot}532$ A., and show a striking similarity to the ring patterns observed when pattern *C* was heated. Rubbed polythene layers were orientated with molecules lying parallel to the rubbing direction, and this orientation persisted after heating to well above the " melting point " of 90° to 100° c. Charlesby records that the orientation was weaker after heating to 180° c., and absent after heating to 300° c.

---

[9] Storks, *J. Amer. Chem. Soc.*, 1938, **60**, 1753.

[10] Charlesby, *Proc. Physic. Soc.*, 1945, **57**, 496, 510.

The comparison suggests that the change which must have occurred in the layers prepared from palmitic acid was of the nature of polymerisation, with strong lateral binding developed between molecules in small " crystallite " regions, and possibly long chains, similar to those of polythene extending through these regions. The possibility of such a change seems remote under normal conditions, but, for the conditions of low pressure, and heating and strong ionisation due to the intense electron bombardment, some such transformation may occur for molecules suitably orientated by a previous smoothing process. There is definite evidence that the change occurred under the influence of the electron beam. As recorded above, pattern *C* often appeared after a preliminary pattern, apparently due to a normal fatty acid layer, had faded. Similarly Trillat and Hirsch observed the transformation of α- and β-stearic acid crystals to a stable γ-form after a few minutes in the electron beam. Such a transformation may also explain the reference of Lark-Horovitz, Yearian and Howe [11] to organic layers of unknown composition giving rise to " extra " rings in transmission patterns from metal films. These rings were not removed by heating to 500° c.

The assumption of such a polymerisation is in agreement with the observed form of pattern *C*, and allows a qualitative explanation of the variation in pattern at high temperatures. The development of strong lateral bonds would give rise to regions of crystallisation of the chains, following the original orientation produced by the smoothing process. This orientation would be lost at a temperature lower than that at which the crystallites break up. The orientation with the molecular chains perpendicular to the smoothing, or subsequent rubbing, direction seems reasonable by analogy with the well-known effect of rubbing a damp powder under the finger. The powder forms thin filaments perpendicular to the rubbing direction, and acicular particles will lie along the filaments.

The patterns given by the layers formed on copper are interesting. These patterns were intermediate between those of the less stable layers and pattern *C*, and the layers showed intermediate properties, as if the formation of the new structure was impeded. This effect, and the absence of the new structure in layers on cadmium may have been due to a reaction between the fatty acids and these metals to give salts. These soaps do not crystallise readily and would prevent a more complete orientation of the remaining acid.

Finally, it must be stated that the technique used to obtain pattern *C* was not infallible and frequently failed to give the pattern. It is hoped that further work on the problem will be possible so that a clearer picture of the nature of the change occurring may be obtained, and such complications as the new structure with dimensions $a_1 = 14$ A. and $a_2 = 6{\cdot}3$ A. may be resolved more fully.

In conclusion, I would like to express my indebtedness to Dr. R. S. Burdon for friendly criticism and advice, to other members of the staff of the Physics Department, University of Adelaide, and to the staff of the Tribophysics Section of C.S.I.R., for their co-operation.

---

[11] Lark-Horovitz, Yearian and Howe, *Physic. Rev.*, 1935, **48**, 101.

Summary.

The structure and effect of heating of layers of palmitic acid on various metals have been investigated. The temperature at which the orientation of the molecules is lost, is below the bulk melting point for crystalline layers, and is 105° C. for monolayers, being independent of the metal used as base.

A new orientation in layers formed from fatty acids on metals is described, corresponding to an orthorhombic structure and giving a characteristic pattern. Such layers are not soluble in the usual solvents, do not lose their orientation until heated to over 400° C., and remain on the surface in crystalline form to about 800° C. It is suggested that these properties arise from a change taking place under the influence of the electron beam.

Physics Department,
University of Adelaide,
South Australia.

A REFRACTOMETRIC METHOD FOR FOLLOWING REACTIONS IN CLOSED SYSTEMS.

BY H. W. MELVILLE AND W. F. WATSON.

Received 3rd October, 1946.

Measurement of refractive index has proved one of the most generally applicable physical methods employed for following the course of chemical reactions in solution. In almost all cases, small samples of the mixture have been extracted from the system at known time-intervals and the refractive index measured usually with an Abbé or a Pulfrich refractometer. Clearly this technique cannot be extended to experiments carried out *in vacuo* or to very viscous solutions, and thus it is not surprising that little use has been made of refractometric methods in the many experimental studies of polymerisation reactions, where exact work is conducted mostly in absence of oxygen and with semi-solid solutions.

However, the laborious solution and precipitation, or " frozen benzene " technique [1] at present employed with concentrated solutions of high polymers makes any purely physical method of determining composition very desirable. In fact, the lack of rapid methods of measuring the rate of polymerisation, especially towards the end of a reaction, is a real handicap in the further study of the effects that arise when much polymer is present in the reaction system.

Dilatometry has been used to follow accurately the initial stages of polymerisation but there is no complementary method for the later viscous stages. A study of the kinetics in the transitional and solid state is becoming increasingly important since the presence of the polymer may affect the magnitude of the velocity coefficients and, in some cases, may act as an additional source of radicals for further polymerisation of the monomer. Such technique may also be used for the study of copolymerisation.

In view of the excellent optical properties of many thermoplastic materials, a new method of determining refractive index without disturbing the system has been developed using simple, and readily available, cylindrical reaction vessels. This optical device is equally applicable to fluid and very viscous solutions and is of general use outside the field of high polymers.

---

[1] Mayo and Lewis, *Ind. Eng. Chem.* (*Anal.*), 1945, **17**, 134.

Description of Refractometer.

The tube containing the mixture, the refractive index of which is changing during the course of the reaction, is considered as a cylindrical lens of varying focal length. The problem is to design suitable apparatus to measure accurately small changes in the power of this lens. The device used consists of three parts: (1) a convergent lens system composed of a simple cylindrical lens and a complex lens in media of suitable refractive indices; (2) a vertical object arranged parallel to the major axis of the cylinder to produce a real, inverted image by means of the lens system; and (3) a means of detecting the position of the image on an optical bench. The various parts are set up on a 3 m. optical bench with the optical axis of the lens combination arranged parallel to its length. Fig. 1 shows the arrangement finally employed.

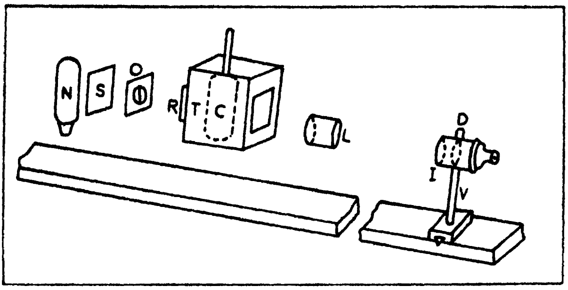

FIG. 1.—Arrangement of the refractometer for measuring image position by the focussing method.

N is a sodium lamp which, with the ground-glass screen S as diffuser, provides a uniformly luminous background for the object O. The object finally chosen was a fine Perspex fibre stretched vertically across a 1 cm. hole cut in a small brass plate, but other vertical linear objects have certain advantages in special conditions. R is a vertical slit which acts as a stop for all rays not incident on the lens system at a small angle to the optical axis. The thermostatted copper tank T contains a stand to which the reaction vessel C is firmly fixed by spring-clips. L is a complex lens producing the final inverted image, I. Stand V, which can be moved along the bench, carries a parallax pin or a powerful convex lens D to detect the position of I.

Discussion.

A system employing a specially-shaped reaction vessel, e.g. with optically flat, parallel or prismatic sides is easy to design but when one vessel may last only one run difficulties of construction and expense make this impracticable for regular use. Since this method was developed, Debye [2] has published a very accurate form of refractometer employing a prismatic vessel, but this shape is not suitable as a reaction chamber.

Optimum conditions, using a simple tubular vessel. A cylindrical lens in air has a focal length of

$$f = \frac{\mu r}{2(\mu - 1)} \quad . \quad . \quad . \quad . \quad . \quad (1)$$

With reaction vessels of a practicable size, the focal distance is thus very short. As is common with simple lenses of fairly high power, image formation is particularly poor. To obtain an image at a suitable distance from the lens, the object must be just outside the focus, in which region

---

[2] Debye, *J. Appl. Physics.*, 1946, 17, 392.

(11) is the fundamental equation relating v to the desired constants for different values of $\delta\mu$, i.e. for variable μ'. Fig. 3 and 4 are the results of experiments using values of the constants to verify (11) over a wide range. The crosses indicate experimental values, while the circles give those calculated from (11) using direct measurement of the constants. As is necessarily an accompaniment of high sensitivity, the expression is very sensitive to small errors in the direct measurements, which is unavoidable when mean values neglecting the thickness of the glass walls are chosen. It is clear that (11) is verified in practical cases.

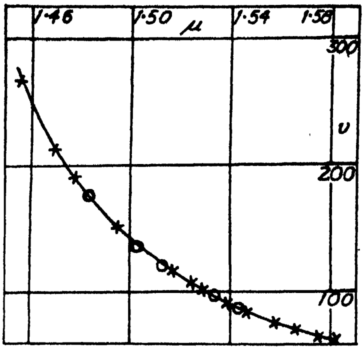

FIG. 3.—Comparison of the experimental and theoretical results for the change in image position with change in refractive index.

$r = 1{\cdot}65$ cm. ; $w_1 = 2{\cdot}7$ cm. ;
$w = 2{\cdot}5$ cm. ; $d = 11{\cdot}0$ cm.
AS $= 2{\cdot}4$ cm. ; $u = 1{\cdot}5240$.

To evolve simple relations of practical value in deciding optimum conditions for sensitivity and linearity a new constant v_0, defined as the value of v when $\mu' = \mu$, is introduced.

Let $\mu' = \mu$, then equation (10) reduces to:

$$v_0 = f \cdot \frac{[u_1 + (1 - \mu)w]/u + d}{[u_1 + (1 - \mu)w]/\mu + d + f} \quad . \quad (12)$$

Rearranging (12) gives

$$d + \frac{1}{\mu} u_1 + \frac{(1 - \mu)}{\mu} w = \frac{f v_0}{f - v_0},$$

from which $k + \mu f + u_1 = \dfrac{\mu f^2}{f - v_0}$. (13)

i.e. the implicit constants k and u_1 are replaced by the simple expression involving only v_0.

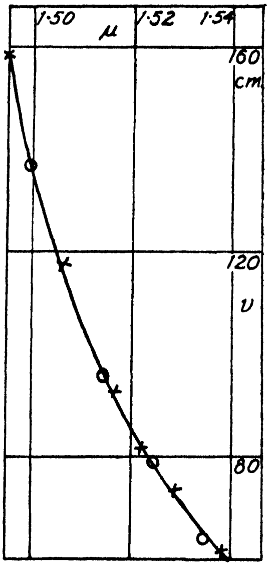

FIG. 4.—Comparison of experimental and theoretical results for a system of considerably greater sensitivity than in Fig. 3.

$r = 0{\cdot}75$ cm. ; $w_1 = 3{\cdot}2$ cm. ;
$w = 1{\cdot}5$ cm. ; $d = 10{\cdot}5$ cm.
AS $= 3{\cdot}1$ cm. ; $u = 1{\cdot}5221$.

Sensitivity.

The sensitivity of the refractometer can be found for special values of the constants by direct differentiation of (10) with respect to μ'.

Writing (10), in the form

$$v = f \cdot \frac{a\mu' + b}{c\mu' + d} \quad . \quad . \quad . \quad . \quad . \quad (14a)$$

where $a = [u_1 r + k(r - 2a_1)]$, $\quad c = u_1 r + (k + \mu f)(r - 2u_1)$,
$b = 2u_1 k\mu$, $\quad d = 2u_1\mu(k + \mu f)$,

and on differentiating, $$\frac{dv}{d\mu'} = f \cdot \frac{ad - bc}{(c\mu' + d)^2} \quad . \quad . \quad . \quad . \quad . \quad (14)$$

Substitution in (14) gives a very complex expression. However, by putting $\mu' = \mu$, we obtain a simple relation for S, which is defined as the sensitivity when $\mu' = \mu$. Thus with

$$S = \frac{dv}{d\mu'}, \text{ when } \mu' = \mu, \text{ gives from (14) and (13)}$$

$$S = \frac{2u_1^2(f - v_0)^2}{r\mu^2 f^2} \quad . \quad . \quad . \quad . \quad . \quad (15)$$

Equation (15), however, does not give information directly on the choice of the various constants for any desired sensitivity, because one of the most important parameters of the system, d, is involved in a complex manner in v_0. The influence of the independent variable, r, however, is clearly demonstrated, the sensitivity being inversely proportional to the radius of the cylindrical lens.

It is therefore preferable to introduce k into (15) since k and d are simply related by the previous expression (9), and optimum values of w are also clearly described. From (13),

$$u_1 = \frac{\mu f v_0}{f - v_0} - k.$$

Substituting in (15),

$$S = \frac{2\{\mu f v_0/(f - v_0) - k\}^2 (f - v_0)^2}{r\mu^2 f_2^2}$$

which reduces to

$$S = \frac{2v_0^2}{r}\left[1 + \frac{k(v_0 - f)}{\mu f v_0}\right]^2 \quad . \quad . \quad . \quad . \quad . \quad (16)$$

(16) is a suitable expression for the sensitivity, and we note that optimum values for high or low sensitivity can be found by inspection. $\frac{k(v_0 - f)}{\mu f v_0}$ is always negative as $-v_0 \gg -f$; k and μ are always positive, and v_0 and f are always negative, and the factor has a value between 0 and -1, as $\mu f v_0 > -k(v_0 - f)$. Hence the sensitivity depends on this term being as small as possible, and $2v_0^2/r$ as great as possible, i.e. v_0^2. For any given k, f should be as large as possible and for any given f, k should be as small as possible.

By (9), $\mu d + (1 - \mu)w$ should be as small as possible, because $\mu > -(1 - \mu)$, d is always positive, and $(1 - \mu)w$ negative, i.e. the sensitivity is a maximum when d is as small as possible, being in the limit equal to w.

Summarising, the maximum sensitivity depends on the following factors.

(1) By using a reaction tube of radius as small as possible consistent with obtaining a well-defined image (*vide infra*).

(2) By making d as small as possible even at the expense of also reducing w, since the term in d varies approximately three times as quickly as the term in w in (9). This means that the object space equivalent plane of the auxiliary lens must be as close as possible to the window of the copper tank and, further, that the cylindrical lens be brought as close as possible to the inner side of the same glass window.

(3) By having the focal length of the auxiliary lens as large as possible. This is limited by the dimensions of the apparatus as it is necessary that $v_0 \gg f$.

In Fig. 5, expression (16) is plotted against f for arbitrary values of k taking $v_0 = 100$ cm. It is seen that a high sensitivity is obtained for practical values of k by having the focal length greater than 10 cm., after which the sensitivity increases more slowly. About $f = 13$ cm. gives a useful lens.

(4) v_0 should be as large as possible. However, as is shown by all the $v - \mu$ graphs, very much greater sensitivity is gained by having $\mu' < \mu$, where v rapidly changes with $\delta\mu'$. For $v < 300$ cm., the image has considerable depth of focus and a useful value of v_0 is approximately 100 cm.

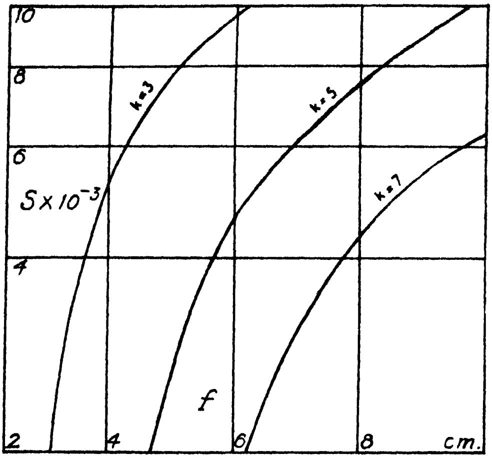

FIG. 5.—Plot of sensitivity against focal length for different values of k, showing dependence of sensitivity on k and f.

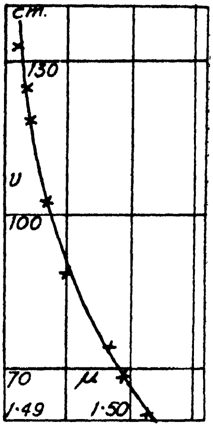

FIG. 6.—Results for a sensitive design of refractometer following the criteria of (16).

Fig. 6 shows experimental results for a fairly sensitive design. With efficient design and thermostatting, considerably greater sensitivities should be reached, making refractive index measurement more accurate than by the standard means.

Linearity.

Linear change of v with $\delta\mu$ is important in many practical cases, e.g. for following with equal sensitivity the course of a polymerisation over a range of, say, $\delta\mu = 10{\cdot}05$. The condition for linearity is that the value of the second term in the denominator of (11) should be much smaller than the first.

(11) is of the form

$$v = \frac{a + b\delta\mu}{c + d\delta\mu}, \text{ which equals } = \frac{a + b\delta\mu}{c} \text{ when } \delta\mu \text{ is small.}$$

The condition for linearity is

$$\left|\frac{\delta\mu\{u_1 r + (k + \mu f)(r - 2u_1)\}}{\mu\{r(u_1 + k + \mu f)\}}\right| \ll 1 \text{ from (11)}, \quad . \quad . \quad (17)$$

that is,

$$\left|\frac{\delta\mu}{\mu}\left\{1 - \frac{2u_1(k + \mu f)}{r(u_1 + k + \mu f)}\right\}\right| \ll 1.$$

But from (13),

$$k + \mu f = \frac{\mu f^2}{f - v_0} - u_1,$$

Therefore

$$\left|\frac{\delta\mu}{\mu}\left\{1 - \frac{2u_1}{r}\left[1 - \frac{u_1(f - v_0)}{\mu f^2}\right]\right\}\right| \ll 1 \quad . \quad . \quad . \quad (18)$$

The coefficient of $\delta\mu/\mu$ is plotted against u_1, in Fig. 7 for various f and r. The curves are in three series of three, each series with a constant, arbitrary value of f and the same three arbitrary values of r. The trends are quite clear but the curves indicate that precise formulation of the conditions is very difficult. The curves have definite trends except when the function lies between values of ± 1 where, in any case, the system is almost truly linear as the $\delta\mu/\mu$ term is small in any practical case.

From these curves we may draw the following conclusions.

(1) In all cases, increase in r increases the linearity by reducing the value of the function plotted.

(2) f has a very varied dependence on r. Generally we may say that, given any f, we can obtain a function to give linearity for all u_1 less than a certain critical value, but that the smaller f, the smaller is this critical value of u_1.

(3) In general, the smaller v_0 the greater is the linearity, as can be seen by considering v_0 as the variable and plotting as in Fig. 7 except that, say, r is now a constant.

(4) It is possible to choose values to give the function graphed a value of zero, i.e. to give perfect linearity, but this is of little practical importance in most cases as the function is changing very rapidly in this region, e.g. the point A. Small errors in the constants will greatly upset linearity. On the other hand, a case such as $f = 20$, $r = 2$ would be useful. The practical criterion for linearity is to choose constants to give a curve with a shallow trough, its minimum having a small negative value and a critical value of u_1, greater than the necessary practical value.

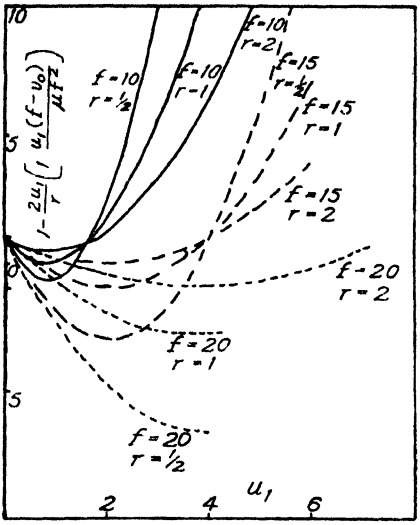

FIG. 7.—Graphical illustration of the optimum conditions for linearity.

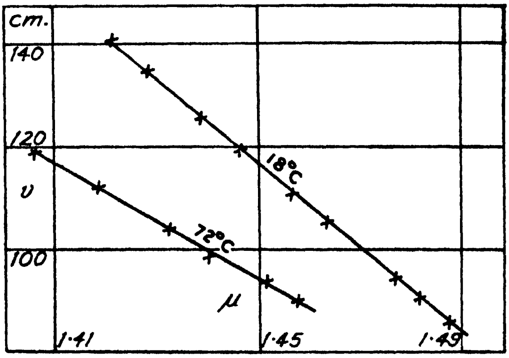

FIG. 8.—System designed for measuring the polymerisation of methyl methacrylate. The arrangement of the refractometer follows the conditions for linearity.

Two experimental curves obtained in calibrating the system for following the polymerisation of methyl methacrylate are shown in Fig. 8. The lower curve was obtained with a temperature control of 72 ± 0·2° c. Both curves are almost linear.

Experimental.

Choice of Tubing to act as the Cylindrical Lens.—The tubing must possess truly cylindrical, outer and inner surfaces, and these must be truly concentric, otherwise the glass walls will act as two lenses of power varying with the rotation of the tube. In ordinary stocks of tubing these conditions are not often found, but suitable lengths can be obtained by selection. Thick-walled tubing suffers especially from the defects considered above and also from local changes in thickness, resulting in surface distortions of the lens and consequently producing an ill-defined image.

There is also an important theoretical disadvantage of thick-walled tubing. To obtain mathematical expressions of a practical value in assessing optimum conditions, it is necessary to neglect the lens properties of the glass walls as these considerably complicate the above complex expressions. The power of each thin glass lens on opposite sides of a cylindrical tube is

$$P = \frac{1}{f} = (\mu - 1)\left(\frac{1}{r} - \frac{1}{s}\right)$$

where r and s are the radii of curvature of the incident and emergent surfaces respectively. Where r very nearly equals s, i.e. with thin-walled tubing, the lens properties of the walls are at a minimum. For these several reasons and its resistance to sudden temperature changes, thin-walled tubing is preferable.

The minimum radius of the tube necessary for accurate determination of refractive index is important. In polymerisation reactions in particular, the smaller the radius the more nearly are the conditions isothermal, for in wide tubes the heat of reaction is dissipated very slowly from the centre owing to the poor thermal conductivity of the medium. However, with narrower bore tubing the wall effects are relatively greater. Again, the optics require a narrow beam of light close to the optical axis and for a tube of small radius a wide aperture lens is obtained unless the slit S is very narrow. There is an experimental limitation to this stopping-down of illumination, and reduction in width of the slit makes the alignment of the apparatus difficult. Accurate results have been obtained using tubing down to 0·8 cm. internal diameter. There is the important compensation for image definition in that the sensitivity is inversely proportional to the radius.

The choice of the type of glass depends on two factors, the attainment of the above conditions and its durability as a reaction vessel when heated *in vacuo* and subject to the considerable internal strain imposed by the contraction of the very viscous polymer mixture tenaciously adhering to it. Both soda and heat-resistant glasses are drawn in thin-walled tubing but the commercial manufacture of resistant glasses produces many longitudinal striations which seriously affect its lens properties. On the other hand, these glasses make stronger reaction vessels.

A compromise has to be made depending on experimental requirements. For the determination of the extent of polymerisation to ± 0·5 %—usually of sufficient accuracy for single monomer polymerisations when a smoothed curve taken with observations on the same tube reduces the experimental error according to the usual mean-error law—Monax is found suitable. In certain cases, in particular in co-polymerisation, a very much greater accuracy is required and for this, soda glass would be preferable. Some runs were carried out using Veridia precision-bore tubing but the non-concentric thick walls and many striations more than nullified the advantage of the cylindrical inner surface.

The Auxiliary Lens.—This must provide a small depth of focus with a considerable magnification of image and also a very flat field. To have a focal length as small as 10-15 cm. the lens must therefore be a system of not less than two simple components. The major difficulty with such a lens is that the first (object) plane is almost at the end of the system close to the copper tank. If l is the distance from the near end to the object equivalent plane, the minimum value of d is $d = l + w$.

For sensitivity requirements, this depends largely on the smallness of l. This difficulty was encountered with the most accurate lens so far used (aperture = f 1·9, $f = -12{\cdot}7$ cm., total length = 15 cm.) giving a value to l of 8·5 cm., and thus imposing a serious limitation on sensitivity. A typical curve with almost the maximum sensitivity using this lens is shown in Fig. 3.

Choice of Object and Method of Image Detection.—This proved the most difficult practical problem. Various objects were tried as were the alternative methods of image detection, parallax and focussing.

For parallax, a very fine needle was used as object, parallax being delicately detected by having its inverted image point to point with a second pin sliding along the bench. Parallax, however, requires a fairly wide beam with an unavoidable caustic in consequence, due to the wide aperture of the simple lens. Even using a strong convex lens behind the parallax pin to widen the angle at which parallax may be detected, the image position was indefinite over a range of 1 cm. at $v = 100$ cm., and the range rapidly increased with v. The parallax method also employs a considerable area of the cylindrical lens, thus depending on true cylindrical properties to a much greater extent than focussing.

For focussing, an object of greater width than 0·1 mm. gives different parts in focus at different image distances. A Perspex fibre of diameter *ca.* 0·05 mm. stretched across a 1 cm. hole in a brass plate, which also stopped most of the unwanted illumination, proved effective. The slit was stopped down to 1 mm. in width, thus using only the central part of the lens.

To detect the image position, a powerful convex lens ($f = 4$ cm.) of very small depth of focus was used. The lens and its peephole were fixed in an adjustable mount and focussed first on fine cross-wires. The supporting stand was then moved till the cross-wires and image were in focus together. In this way a reading of ± 0·1 cm. at $v = 100$ cm. was obtained. Fig. 3 is a typical graph.

Aligning the System.—The tank is first fixed accurately perpendicular to the bench. A cylindrical lens is then introduced and arranged vertically by a spirit-level. The tube and the tank are filled with liquid of the desired refractive index for the outer medium, and the auxiliary lens set at the required distance and aligned visually. The object is then moved along the bench—after placing it approximately on the optical axis—and, without the slit, the object distance is adjusted to give the required v_0. The object and auxiliary lens are then aligned optically and the slit attached to the front window of the tank.

Thermostatting of the Tank.—For low sensitivity, e.g. the lower curve of Fig. 7, thermostatic control to ± 0·2° C. is adequate. This can be obtained by direct heating of the bottom of the tank by a mica-Nichrome element regulated by a bi-metallic spiral. For more accurate thermostatting, a specially-designed water jacket surrounds the tank. A narrow cross-section is chosen to cut down convection currents ; two optically flat microscope slides act as windows. The liquid contained in the tank must necessarily be chosen with regard to the magnitude of its refractive index, and it is preferable that it should be rather involatile at the working temperature. In the case of methyl methacrylate, decalin was found suitable for measuring polymerisation at 60-70° C.

The authors gratefully acknowledge the assistance of Mr. Ben Noble, B.Sc., of St. John's College, Cambridge, in the theoretical section of this paper, and also of Miss Sheila Thomson for assistance in experimental work.

Summary.

A refractometer has been devised for measuring continuous changes in refractive index of transparent liquid systems contained in a cylindrical vessel, without disturbing the contents. The apparatus has been found satisfactory for measuring the course of liquid-phase polymerisation reactions, particularly in the gel stage.

The geometric optics have been investigated and conditions described for obtaining a wide range of sensitivity of measurement and for designing the instrument to be equally sensitive within the desired range of refractive index. Experimental details of construction and of choice of reaction vessels have been given.

Chemistry Department,
University of Aberdeen.

SOME NOTES ON THE GILFILLAN-POLANYI MICROPYKNOMETER

By I. Lauder.

Received 7th October, 1946.

The technique of measuring concentrations of the heavy forms of water by the Gilfillan-Polanyi micropyknometer[1] is well known. Its working range is determined by several factors, mentioned below. Experimentally, if P_1 and P_2 are the pressures at which the pyknometer floats when the body contains liquids of densities d_1 and d_2 respectively, then

$$d_2 - d_1 = k(P_1 - P_2) \quad . \quad . \quad . \quad . \quad (1)$$

where k is the pyknometer constant.

Now it may be shown that, to a first approximation,

$$k = \frac{\Delta V}{V_2} d_1 - \frac{V_1}{V_2} \Delta d + \Delta d \quad . \quad . \quad . \quad . \quad (2)^*$$

where V_1 = the total volume of the pyknometer; V_2 = the internal volume of the body; ΔV = the change in volume of the head per unit pressure; Δd = the change in density of the water per unit pressure; and d_1 = the density of water at 0° c. (and 1 atm. pressure). The second term in equation (2) arises through the variation of the density with pressure of the water in which the pyknometer floats; the third term takes into account the same factor for the water in the body. V_1 and V_2 may be obtained by weighing the pyknometer with and without water in the body; Δd, assumed to be the same for the normal and test samples of water, is approximately $0{\cdot}66 \times 10^{-6}$ per cm. Hg[2] and ΔV is obtained from the measurements described below.

The Measurement of ΔV.—The change, ΔV, was determined by observing the displacement of a thread of mercury in a capillary attached to the head. For most measurements a capillary with a volume $2{\cdot}35 \times 10^{-4}$ cc./cm. was used. The open end of the stem of the pyknometer head was joined by wax or sealed directly to the top of the capillary tube. The head and the capillary were then filled with mercury by the standard vacuum procedure using the apparatus shown in Fig. 1. The capillary was then set up as in Fig. 2 and held rigidly in front of the measuring microscope. Readings were taken at intervals over the desired pressure range.

The mercury was removed from the head and, as it was very important to protect the head from heat in all subsequent operations, the head was held between two halves of a bark stopper (Fig. 3). The stem of the pyknometer head, near the point which was originally joined to the measuring capillary, was sealed off and a thin glass rod of several cm. was attached. The change in volume of the measuring capillary with pressure was negligible.

---

[1] Gilfillan and Polanyi, *Z. physik. Chem.*, *A*, 1933, **166**, 255.

[2] Tyrer, *J. Chem. Soc.*, 1913, **103**, 1675.

* Strictly speaking two further terms should be added to equation (2). Owing to the compressibility of glass, the internal volume of the body and the external volume of the body and stem vary with pressure. However, these effects are very small and do not alter k more than 0·1-0·2.

The Adjustment of the Weight of the Pyknometer.—The most satisfactory procedure for the adjustment of the weight of the pyknometer was as follows. The head was cleaned and glass removed from the end of the thin rod until the head just sank slowly in water at 0° C. As much of the glass rod as could be removed without endangering the head was then drawn off and replaced by a body of suitable capacity and of slightly greater weight (0·2-0·3 mg.).

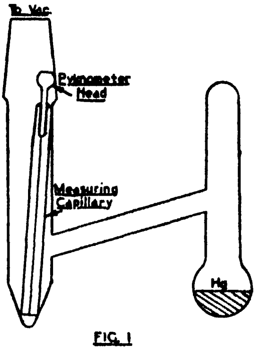

FIG. 1

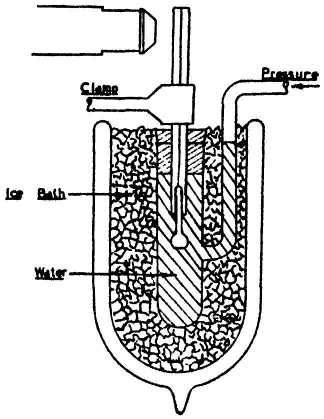

FIG. 2

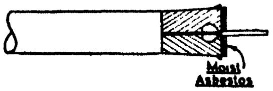

FIG. 3

The final adjustment of weight was made by dissolving glass from the body with HF. Two strengths were used, 3 N. and 0·3 N., so as to give a better control of the process. The pyknometer was cleaned and filled with normal water. After observing the rate of sinking in water at 0° C., the body of the pyknometer was dipped into the acid for a short time (2-20 sec.) and then immediately washed in water. These operations were repeated until the pyknometer floated in water at 0° C. under the desired excess pressure. From time to time during the adjustment, the pyknometer was wiped with moist filter paper and, as an added precaution when it floated at a pressure slightly less than atmospheric, it was cleaned and refilled.

The results are shown in Table I, giving the values of k calculated by equation (2) and those of k measured by the use of salt solutions of known density.

Pyknometers (4) and (5) are less compressible than water and consequently rise with increasing pressure; the others are more compressible and sink with increasing pressure. The heads of pyknometers (1)-(4) were sealed by wax to the measuring capillary; the head for (5) was sealed directly. The measurement of ΔV for the heads of pyknometers (1) and (2) was carried out (in air) at room temperature. This procedure was satisfactory when ΔV was fairly large but when small the temperature effects due to the adiabatic change in pressure of the air surrounding the head became very important. For this reason the subsequent measurements were carried out with the heads immersed in water at 0° C. Errors due to the small temperature change accompanying an adiabatic change of pressure on the water were avoided.

The discrepancy between the calculated and the measured values of k is larger than expected. It is unlikely that all the error is in the measurement of ΔV. For one head, ΔV was measured with two different capillaries; practically identical results were obtained.

TABLE I.

Pyknometer Number	ΔV cc./cm.Hg. $\times 10^{-6}$	V_1cc.	V_2cc.	k calculated $\times 10^{-6}$	k measured 10^{-6}
1	61.7	0·0772	0·0010	57·3	63.3
2	29.2	0·0820	0·0071	34·2	36.6
3	7·4	0·0670	0.0114	3·2	1.9
4	5·1	0·1310	0.0060	5·1	2·0
5	2.4	0·1260	0.0124	4·1	3·1

Some difference may be due to the "ageing" of the glass. It was found that if the whole construction and adjustment of a pyknometer was carried through in one day, the equilibrium pressure for normal water changed by 5-50 cm. Hg (depending on the sensitivity of the pyknometer). The constants given in the table were all determined 2-3 days after the pyknometer had been constructed. Subsequent calibrations showed that no appreciable changes had occurred after that period.

It is also possible that the value used for Δd ($0{\cdot}66 \times 10^{-6}$/cm. Hg) is in error. This is suggested by the fact that in four cases out of the five, better agreement would be obtained if Δd were smaller.

It is possible to cover any desired range of excess density by use of one pyknometer. The pressure P_1 at which the pyknometer floats in normal water when the body contains normal water is first measured; the pressure P_2 at which the pyknometer floats in a salt solution when the body contains the test sample is then measured. The excess density of the test sample is then given by the equation,

$$(d_2 - d_1) = k(P_1 - P_2) + V_1/V_2\,(d_3 - d_1) \quad . \quad . \quad (3)$$

in which d_3 refers to the density of the salt solution and the other terms (except P_2), have the same significance as before. The method requires careful control to avoid errors due to the possible presence of different amounts of dissolved air in the normal water and the salt solution respectively (cp. ref. [3]). Again, as a slight separation of the heavy forms of water occurs during distillation, the water in which the pyknometer is immersed for the first measurement should be from the same supply as that used for the preparation of the salt solution. The compressibility of the very dilute salt solution required for the experiment may be taken as the same as that of pure water (cf. Gilbault [4]),

The author wishes to thank Mr. E. C. M. Grigg and Mr. E. Cook for assistance with the experimental work.

Department of Chemistry,
University of Queensland,
Brisbane.

[3] Landolt-Börnstein, *Physik. Chem. Tabellen* 5. Auflage, 1, 73.
[4] Gilbault, *Z. physik. Chem.*, 1897, **24**, 385.

THE FREE RADICALS $CH_2(CH)_{2m-1}CH_2$.

By W. E. Moffitt and C. A. Coulson.

Received 21*st October,* 1946.

§ 1. Introduction.

The importance of the free radicals $CH_2(CH)_{2m-1}CH_2$ as chain carriers in the reactions of certain olefinic compounds has recently been demonstrated (see, for example, Bolland and Gee [1]). Accordingly it is of interest to know in what part of such a molecule the " free valence " is most likely to be found. In order to solve this problem using quantum mechanics it is necessary to be able to define mathematically what is meant by the free valence concept—this definition necessarily depending upon the particular approximation or picture of the chemical bond we adopt. To this end we shall be guided by the idea of free electron density.

We shall assume the electronic part of the wave equation for these radicals to have been separated in the usual way into equations containing the co-ordinates of only the σ or π electrons respectively, and seek approximate solutions of the latter using first the approximation of perfect pairing and then the molecular orbital method. In the latter (LCAO MO[2]) we construct one-electron molecular orbitals from linear combinations of atomic orbitals and allot the electrons to these, two at a time in accordance with the Pauli exclusion principle; whereas with the former (HLSP [3]) we obtain the complete wave functions for the unsaturation electrons from a linear combination of many-electron functions representing the elements of sets of independent (canonical) structures. In both we shall neglect the overlap of the atomic orbitals and the variation of the exchange and resonance integrals α and β with internuclear separation.

§ 2. The HLSP Method.

We shall illustrate this method first by treating the important case, $m = 2$, in some detail. The canonical set contains five structures $\Psi^{(\mu)} (\mu = 1, \ldots, 5)$:

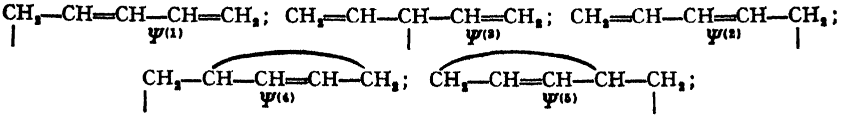

$CH_2—CH{=}CH—CH{=}CH_2$; $\Psi^{(1)}$ $CH_2{=}CH—CH—CH{=}CH_2$; $\Psi^{(3)}$ $CH_2{=}CH—CH{=}CH—CH_2$; $\Psi^{(2)}$

$CH_2—CH—CH{=}CH—CH_2$; $\Psi^{(4)}$ $CH_2—CH{=}CH—CH—CH_2$; $\Psi^{(5)}$

and, following Pauling,[3] the corresponding matrix coefficients

$$(\Psi^{(\mu)} \,|\, H - E \,|\, \Psi^{(\mu)})$$

are readily evaluated. By considering only those solutions with the symmetry of the nuclear skeleton (i.e. of the identical representation—to which the ground state is known to belong) we may factorise our secular equation at the outset by limiting the discussion to those $\Psi = \sum_{(\mu)} A^{(\mu)} \Psi^{(\mu)}$ of the form:

$$\Psi = A(\Psi^{(1)} + \Psi^{(2)}) + B\Psi^{(3)} + C(\Psi^{(4)} + \Psi^{(5)}).$$

---

[1] Bolland and Gee, *Trans. Faraday Soc.*, 1946, **42**, 236, 244.

[2] Mulliken, *J. Chem. Physics*, 1935, **3**, 375.

[3] Pauling, *ibid.*, 1933, **1**, 280.

It then becomes

$$\begin{vmatrix} 5x-8 & 2x-5 & 4x-7 \\ 2x-5 & 2x-2 & x-4 \\ 4x-7 & x-4 & 5x-2 \end{vmatrix} = 0,$$

where $x = (E - Q)/\alpha$, E is the energy and Q, α are the Coulomb and exchange integrals respectively. For the ground state, α being negative, it is found that

$$E = Q + 1{\cdot}856\alpha,$$

corresponding to the wave function

$$\Psi = (\Psi^{(1)} + \Psi^{(2)}) + 1{\cdot}080\ \Psi^{(3)} + 0{\cdot}262\ (\Psi^{(4)} + \Psi^{(5)})$$

and a resonance energy

$$E_R = 0{\cdot}856\ |\ \alpha\ |.$$

Labelling the molecule as follows

$$\begin{array}{ccccccccc} & a & & b & & b & & a & \\ CH_2 & \cdots & CH & \cdots & CH & \cdots & CH & \cdots & CH_2 \\ 1 & & 2 & & 3 & & 4 & & 5 \end{array}$$

we find the orders of the effective bonds, as defined by Penney's rule [4]

$$p_{ij} = -\tfrac{4}{3}\,\overline{s_i \, . \, s_j},$$

to be $\quad p_a = 0{\cdot}773$ and $p_b = 0{\cdot}512$

(plus one, of course, for the $\sigma\sigma$ bond contribution). This corresponds to bond lengths of

1·37 A. and 1·41 A. respectively.

This definition of bond order, referring as it does to a cosine coupling of pairs of electronic spins (the relative spin orientation of two electrons), is hardly adequate to discuss a quantity such as free valence which evidently depends upon the behaviour of an unpaired electron. Accordingly we shall take the term [5]

$$x_i = \sum_{\mu} \omega_i^{(\mu)}\ |\ A^{(\mu)}\ |^2 \Big/ \sum_{\mu}\ |\ A^{(\mu)}\ |^2$$

to define the free bond order at carbon atom i. The factor $\omega_i^{(\mu)}$ is 1 when the free valence is assigned to carbon i in the structure $\Psi^{(\mu)}$, otherwise it is 0. We notice that in this representation—i.e. with this choice of independent structures—the free bond order is necessarily zero at all even-indexed carbon atoms. (In other representations, less rationally chosen from the point of view of symmetry and chemical intuition, this would not be true and our definition of x_i would have to be considerably modified to be at all significant). For the other carbon atoms we find

$$x_1 = 0{\cdot}323 = x_5, \quad x_3 = 0{\cdot}353.$$

This leads us to the following description of the free valence : it is fairly evenly distributed between the end and middle (odd-indexed) carbon atoms with a slightly greater probability at C_3.

For the next highest member of the series, namely $CH_2(CH)_5CH_2$ with $m = 3$, the complete canonical set contains fourteen structures—four unexcited ($\Psi^{(1)}, \ldots, \Psi^{(4)}$), eight singly-excited ($\Psi^{(5)}, \ldots, \Psi^{(12)}$), and two doubly-excited (which we neglect) :

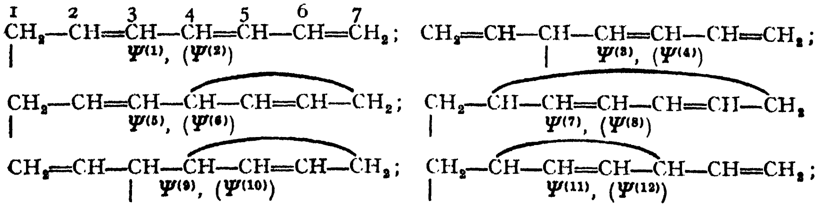

$\overset{1}{C}H_2$—$\overset{2}{C}H$=$\overset{3}{C}H$—$\overset{4}{C}H$=$\overset{5}{C}H$—$\overset{6}{C}H$=$\overset{7}{C}H_2$; $\Psi^{(1)}$, ($\Psi^{(2)}$)

CH_2=CH—CH—CH=CH—CH=CH_2 ; $\Psi^{(3)}$, ($\Psi^{(4)}$)

CH_2—CH=CH—CH—CH=CH—CH_2 ; $\Psi^{(5)}$, ($\Psi^{(6)}$)

CH_2—CH—CH=CH—CH=CH—CH_2 $\Psi^{(7)}$, ($\Psi^{(8)}$)

CH_2=CH—CH—CH—CH=CH—CH_2 ; $\Psi^{(9)}$, ($\Psi^{(10)}$)

CH_2—CH—CH=CH—CH—CH=CH_2 ; $\Psi^{(11)}$, ($\Psi^{(12)}$)

---

[4] Penney, *Proc. Roy. Soc. A*, 1937, **158**, 306.

[5] Pauling, Brockway and Beach, *J. Amer. Chem. Soc.*, 1935, **57**, 2705.

In the structures shown above, $\Psi^{(2)}$ is the mirror image of $\Psi^{(1)}$, so that the free valence is at C_7 instead of C_1, and similarly for the others. Making the approximation of giving all the singly-excited structures the same coefficient in the final Ψ, we find

$$\Psi = (\Psi^{(1)} + \Psi^{(2)}) + 1{\cdot}096\,(\Psi^{(3)} + \Psi^{(4)}) + 0{\cdot}249\,(\Psi^{(5)} + \ldots + \Psi^{(12)}),$$

so that

$$x_1 = 0{\cdot}242 = x_7,\ x_3 = 0{\cdot}258 = x_5.$$

Once more the free valence is fairly equally divided between the odd-indexed carbon atoms with a slight preference for C_3 and C_5. The actual free bond order at alternate carbon atoms of the chain is therefore predominantly determined by the "normalising" condition that the total free bond order is unity, i.e. for a chain with $2m + 1$ carbon atoms:

$$x_{2l+1} \approx \frac{1}{m+1}\ (l = 0, 1, \ldots, m), \text{ so that} \sum_l x_{2l+1} = 1.$$

§ 3. The LCAO MO Method.

The jth molecular orbital for a polyene chain of n equivalent atoms is expressed in terms of the atomic orbitals $\psi_r (r = 1, 2, \ldots, n)$ in the form

$$\phi^{(j)} = \sum_r C_r^{(j)} \psi_r$$

and it has been shown by Lennard-Jones[6] and, more particularly, by Coulson[7] that this leads to an orbital energy of

$$E^{(j)} = E_0 + 2\beta \cos \frac{j\pi}{n+1}\ (j = 1, 2, \ldots, n)$$

where E_0, β are the Coulomb and resonance integrals appropriate to this method of treatment. Since β is negative, the binding energy $\epsilon^{(j)}$ of this orbital is

$$\epsilon^{(j)} = -2\beta \cos \frac{j\pi}{n+1} = -2\beta \cos \theta^{(j)}.$$

We may say that $\phi^{(j)}$ is bonding, non-bonding, or anti-bonding according as $\epsilon^{(j)}$ is greater than, equal to, or less than 0 respectively. For the ground state, we begin by allotting to each bonding orbital its quota of two electrons. When n is even, e.g. octatetraene, we see that orbitals are all either bonding or anti-bonding, since j cannot assume the non-integral value $\frac{n+1}{2}$. For these free radicals, however, where $n (= 2m+1)$ is odd, a non-bonding orbital also arises. Thus whereas the process of assignment referred to above accounts for all the electrons of the singlet ground states for which n is even, there remains one electron which must occupy the non-bonding orbital of the (doublet) free radicals.

The normalised coefficients $C_r^{(j)}$ are given by

$$C_r^{(j)} = \sqrt{\left(\frac{2}{n+1}\right)} \sin r\theta^{(j)},$$

so that the bond orders, as defined by Coulson,[8] viz.,

$$\left(p_{rs} = \sum_{(j)} p_{rs}^{(j)} = \sum_{(j)} C_r^{(j)} C_s^{(j)}\right),$$

for our first selected example, $n = 5$, are

$$p_a = 0{\cdot}789,\ p_b = 0{\cdot}577$$

corresponding to bond lengths of

1·37 A. and $1{\cdot}40_5$ A. respectively,

almost exactly those predicted by the HLSP treatment.

---

[6] Lennard-Jones, *Proc. Roy. Soc. A*, 1937, **158**, 280.

[7] Coulson, *ibid.*, 1938, **164**, 383.

[8] Coulson, *ibid.*, 1938, **169**, 413.

We notice that in the non-bonding orbital, where $j = \frac{n+1}{2}$, $\theta^{(j)} = \frac{\pi}{2}$. This implies that the contribution of this electron to the bond orders ($s = r + 1$) is always zero, as we should expect from a truly "non-bonding" orbital. The non-bonding electron is therefore safely identified with the free valence electron and its density at C_r with the free bond order there, whose value is simply $\frac{2}{n+1}$ or 0, according as r is odd or even respectively. When $n = 5$

$$x_1 = x_3 = x_5 = 0{\cdot}333, \quad x_2 = x_4 = 0,$$

in excellent agreement with our HLSP calculations and providing a justification for the assumptions implicit in our choice of representation—namely, that $x_2 = x_4 = 0$.

Similarly for $n = 7$, $x_1 = x_3 = x_5 = x_7 = 0{\cdot}25$ and in general, completing the agreement with §2 :

$$x_{2l+1} = \frac{2}{n+1} = \frac{1}{m+1} \quad (l = 0, 1, \ldots, m).$$

§ 4. Conclusion.

We have shown that definitions of free bond order consistent with each other and the idea of free electron density may be given in both the HLSP and LCAO MO methods of treating these free radicals. The free valence may be said to spend its time almost equally among the odd-indexed carbon atoms and not at all on the even-indexed ones.

One of us (W.E.M.) would like to acknowledge the receipt of a grant from the Board of the British Rubber Producers' Research Association.

Physical Chemistry Laboratory,
Oxford.

Wheatstone Physics Laboratory,
King's College,
London.

STARCH-IODINE COMPLEXES. PART I.

By G. A. Gilbert and J. V. R. Marriott.

Received 23*rd October*, 1946.

The coloured complexes between starch and iodine continue to attract attention, due to their intrinsic interest and to the help they afford in the study of the components of starch. There seems to be as yet no certainty as to their exact nature. The very considerable body of early work, mostly carried out on whole starch or imperfectly separated components, has been surveyed by Barger.[1] Although much of it is inconclusive, it seems beyond doubt that precipitated complexes from iodine-iodide-starch solutions contain an appreciable amount of iodide in addition to iodine, and numerous investigators, among them Lottermoser[2] and Murray[3] who used potentiometric methods, have shown that iodide ions also take part in the equilibrium in solution.

An ingenious theory has been put forward for the amylose-iodine complex. Hanes[4] perceived that the linear component of starch, when coiled in the form of a helix, should be able to accommodate a core of iodine molecules, arranged end-to-end, and Freudenberg[5] in elaborating this idea, pointed out that the inside of the amylose helix was hydrocarbon in nature, and would function as an organic solvent for iodine. Further support has come from an examination of amylose-iodine precipitates with X-rays (Bear[6]), and from the dichroism of flowing amylose-iodine solutions (Rundle and Baldwin[7]). Perhaps the most important evidence comes from the potentiometric titration of amylose with iodine by Bates, French and Rundle.[8]

---

[1] Barger, *Some Applications of Organic Chemistry to Biology and Medicine* (New York, 1930).
[2] Lottermoser, *Z. angew. Chem.*, 1924, **37**, 84.
[3] Murray, *J. Chem. Soc.*, 1925, **127**, 1288.
[4] Hanes, *New Phytol.*, 1937, **36**, 189.

Using the potential between a bright platinum wire electrode and a calomel half-cell to calculate the equilibrium concentration of uncombined iodine, they showed that a sigmoid type of adsorption isotherm was followed from which it appeared that the bulk of the iodine of the complex was adsorbed at constant activity, in the manner of a heterogeneous reaction. They suggest that this activity is a function of the molecular weight of the amylose, since it appears to be lower for samples of higher molecular weight; and that the longer helices in a mixture tend to be filled before shorter ones adsorb appreciably because the stability of the iodine core increases with its length. Much of this work has been reviewed recently (Kerr[9]). A later publication by Baldwin, Bear and Rundle[10] describes the fall in maximum iodine content of the helices, from about one molecule of iodine per six glucose units to about one per eight units, when the concentration of iodide is increased through a wide range, and the conclusion of these authors is that there has been partial replacement of iodine by iodide or tri-iodide ions.

If the iodine activity of a partially filled helix or of a shorter helix is indeed greater than that of a filled helix, a ready means is available for determining the distribution of chain lengths in a sample of amylose, for the amount of iodine adsorbed over any small range of activity will then be a measure of the amount of amylose of corresponding chain length. This formed one of the reasons for undertaking the present investigation.

Experimental.

In the present kind of system, the study of the adsorption isotherm in regions of very small percentage adsorption offers most promise, because no correction need then be made for any reduction of available sites, and adsorbed molecules are less likely to interfere with one another. This requires the manipulation of concentrations of total iodine ($I_2 + I'_3$) of the order of 10^{-7} M. and the measurement of adsorption of the order of 10^{-7} mol. Differential methods are clearly necessary.

Two solutions of KI buffered to about *p*H 6, one containing amylose, were therefore joined by a salt bridge, and iodine solution added to each in such quantities that the potential between two platinum electrodes immersed in the respective solutions remained less than 0·05 mv. The amount of iodine combined with the amylose was given by difference, and losses apart from those introduced by impurities in the starch were expected to cancel. The arrangement is illustrated in Fig. 1.

The experiments were carried out in weak artificial light in a room kept at 20°, the cells being in a water thermostat at 20°. Flow between the cells was prevented by a closed ground tap rendered conducting by filling the lower part of the U-tube of the bridge with saturated KCl solution. The limbs dipping into the cells contained the same solution as the cells. The bridge was designed so that the taps projected out of the thermostat. Vessels smaller than about a litre could not be used because the loss of iodine through reaction with, or adsorption by, the walls then became an appreciable fraction of the iodine content of the solution. Rubber stoppers out of contact of the solution were not found to give trouble. The 2-inch platinum wire electrodes were sealed through soft glass, and were satisfactory after cleaning with chromic acid, washing and standing in KI_3 solution. An electrometer triode (sensitivity 1 cm. per mv.) was used either as a null instrument or for measuring small potentials. During titrations it was possible to check the concentration of the starch-free iodine solution by adding an increment of standard iodine solution to it, and measuring the change in potential produced.

---

[5] Freudenburg, *Naturwiss.*, 1939, **27**, 850.

[6] Bear, *J. Amer. Chem. Soc.*, 1942, **64**, 1388.

[7] Rundle and Baldwin, *ibid.*, 1943, **65**, 554.

[8] Bates, French and Rundle, *ibid.*, 1943, **65**, 142.

[9] Kerr, *Chemistry and Industry of Starch* (Academic Press Ind., New York, 1944).

[10] Baldwin, Bear and Rundle, *J. Amer. Chem. Soc.*, 1944, **66**, 111.

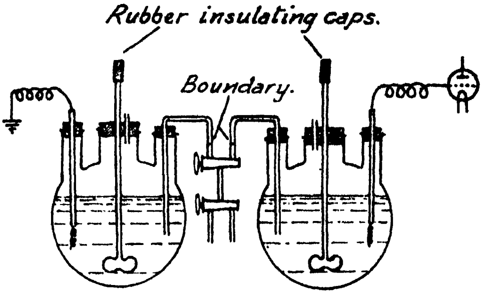

FIG. 1.—Apparatus for the differential potentiometric titration of starch with iodine.

Theoretical Outline.

It is well known[1, 3] that the development of the blue colour in starch-iodine solutions depends strongly on the presence of iodide ions, suggesting that iodide ions play more than a subsidiary role in the complex. This is confirmed in the present work where it is shown that iodide ions are an integral part of the complex as it is formed in solution, although this does not mean that iodine alone will not form a stable complex in the solid state (see Rundle and French[11]). It will therefore be supposed that helical amylose molecules adsorb iodine and iodide to form linear groups of the general type (xI_2yI'). Positive ions would not necessarily be adsorbed unless the molecule were contained in an aggregate or precipitate, but could be present as *gegen*-ions around the molecule.

For very low degrees of saturation of the amylose, the activity of any such complex is likely to be directly proportional to its amount per unit quantity of amylose, allowing its chemical potential to be written

$$\mu_{xy} = \mu^{\circ}_{xy} + RT \ln a \quad . \quad . \quad . \quad . \quad (1)$$

where a is the number of mols of complex per gram of amylose, and μ°_{xy} is independent of a but depends upon the temperature. If the chemical potentials of the iodide ions and iodine are expressed in the conventional way, and the solution is treated as ideal, the corresponding equations in terms of concentrations can be written for the ions and molecules in the solution with which the complex is in equilibrium

$$\mu_{I_1} = \mu^{\circ}_{I'} + RT \ln I' \quad . \quad . \quad . \quad . \quad . \quad (2)$$

and

$$\mu_{I_2} = \mu^{\circ}_{I_2} + RT \ln I_2 \quad . \quad . \quad . \quad . \quad (3)$$

where I_2 refers to the concentration of molecular iodine as distinct from I'_3. (If iodine in the form of I'_3 as well as the molecular form is intended, the 'total' iodine will be referred to).

Since

$$\mu_{xy} = x\mu_{I_2} + y\mu_{I'} \quad . \quad . \quad . \quad . \quad . \quad (4)$$

it follows that

$$\frac{\log (I_2)^x(I')^y}{(a)} = (1/2{\cdot}30RT)(\mu^{\circ}_{xy} - x\mu^{\circ}_{I_2} - y\mu^{\circ}_{I'}) \quad . \quad . \quad (5)$$

or that

$$(I_2)^x(I')^y = K_{xy}(a) \quad . \quad . \quad . \quad . \quad . \quad (6)$$

at a given temperature, K_{xy} being an equilibrium constant. At the low degrees of saturation for which this equation is likely to be valid, the amounts of complexes with different values of x and y would be expected to be governed by similar but independent equations, the total of iodine and iodide adsorbed being given by summation.

---

[11] Rundle and French, *J. Amer. Chem. Soc.*, 1943, **65**, 1707.

When only one kind of complex is present, x and y can be determined by varying firstly the iodine concentration at constant iodide concentration, and then the iodide concentration at constant adsorption. Under the first set of conditions,

$$\frac{\partial \log a}{\partial \log I_2} = x \quad . \quad . \quad . \quad . \quad . \quad . \quad (7)$$

from equation (6), and under the second set

$$\frac{\partial \log I_2}{\partial \log I'} = -\frac{y}{x} \quad . \quad . \quad . \quad . \quad . \quad . \quad (8)$$

or expressed in the form of finite changes in which it will be used

$$\frac{\Delta \log I_2}{\Delta \log I'} = -\frac{y}{x} \quad . \quad . \quad . \quad . \quad . \quad . \quad (9)$$

This simplicity disappears if two or more types of complex are present, but if one type is dominant an approximate value of x or y can still be found.

Determination of $\left(\frac{\partial \log a}{\partial \log I_2}\right)$.

Experiments were carried out in the first place at constant iodide concentration to enable equation (7) to be used to find x. 10^{-3} M. KI was chosen because aggregation of the amylose-iodine complex is less likely in such dilute salt solutions. It was soon found that the amylose solutions being employed were not reproducible, and that comparative measurements had therefore to be done on the same solution, and as nearly simultaneously as possible. Moreover, the reaction was slow (often being apparently complete only some 30 min. after any addition of iodine), and was succeeded by a further very slow change continuing over a period of days. A first rough survey of the whole titration curve lead to the expected sigmoid type of isotherm reproduced in Fig. 2. The lower part of the curve was then studied in detail.

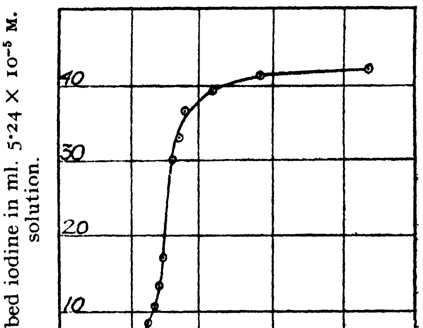

FIG. 2.—Titration of amylose (3 mg.) with $5{\cdot}24 \times 10^{-5}$ M. iodine in 10^{-3} M. potassium iodide.

Thymol-precipitated potato amylose,[12] or potato starch freed from amylopectin with $Al(NO_3)_3$ and NH_4OH[13] (120 mg.) were dispersed in 12·5 ml. 0·2 N. NaOH at 100° for 2 min., neutralised with 16 ml. 1 % by vol. H_3PO_4 and made up to 50 ml. with KI solution to give a solution 10^{-3} N. in KI. Of this solution 25 ml. were added to 800 ml. 10^{-3} N. KI in one of the cells, the final *p*H being approximately 6. An identical solution, but without amylose, was prepared for the titration solution. After bringing both cells to 20° and inserting the electrodes and salt bridge, a solution containing $1{\cdot}77 \times 10^{-6}$ mol. total iodine per litre in 10^{-3} N. KI was added in small increments to both cells. Each time, after balancing to within 0·05 mv. (constant for 5 min.), the next increment was added to the titration cell (starch-free solution) and the potential change measured to enable the absolute concentration to be calculated. Since more iodine solution had to be added to the cell containing starch, the volume in the other cell was kept equal by adding the necessary amount of 10^{-3} N. KI.

---

[12] Haworth, Peat and Sagrott, *Nature*, 1946, **157**, 19.

[13] Donnison and Peat (unpublished work).

Usually there was an initial loss of about 4 × 10^{-8} mol. of total iodine from the titration cell, and by inference from the starch solution, after which little further loss occurred during the course of an experiment (shown by the correspondence of the concentration calculated from the potential increments with the further amounts added). In addition there was usually an adsorption of about this order in the starch solution, occurring at concentrations of iodine below those required for the formation of a measurable amount of complex, and due to impurities in the amylose. This quantity could be estimated from the titration curve, and was subtracted for the calculation of the amount of adsorption due to complex formation. This is clear from Fig. 3 where such a curve is shown.

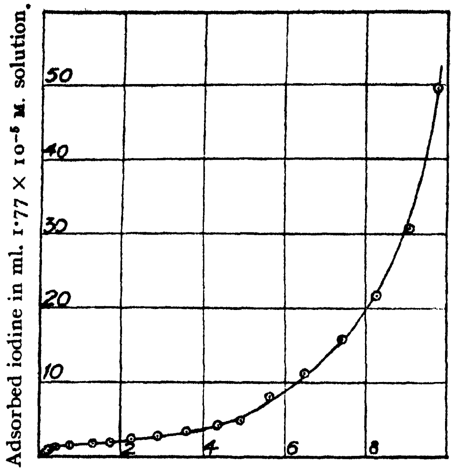

FIG. 3.—Detail of lower part of adsorption curve. Titration of amylose (60 mg.) with 1·77 × 10^{-5} M. iodine in 10^{-3} M. potassium iodide.

The plot of log (adsorbed iodine) against log (total iodine) is next drawn (Fig. 4), 1·4 ml. being subtracted from the measured adsorption to allow for impurities. According to the light absorption (Ilford Gelatine Spectrum Filter No. 608) of its solution in excess iodine and 2 % KI, compared with that of solutions of very highly purified amylose, the sample used contained about 90 % amylose and about 10 % amylopectin. It is seen that an initial slope of about 2, corresponding to $x = 2$, changes at higher activities to 3, and a few measurements at still higher activities have indicated that a further increase occurs there. Only the part drawn has yet been studied closely, and covers only the first 2 % approximately of the maximum possible adsorption. Many similar curves have been obtained, agreeing in shape, but frequently displaced vertically, the adsorption being reduced by retrogradation in the solid state or in solution, or by incomplete dispersion.

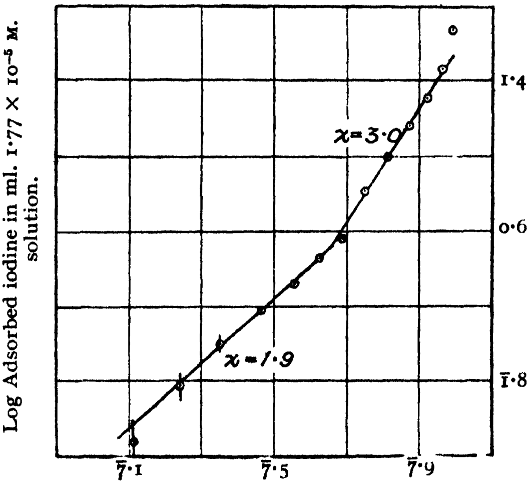

FIG. 4.—Plot of log adsorbed iodine against log concentration of total iodine. Titration in 10^{-3} M. potassium iodide.

The limits of spread of the curve through an error of ± 0·1 ml. of adsorbed iodine, i.e. of ± 1·8 × 10^{-9} mol. iodine, are shown by vertical lines drawn through the lower points of the log plot. Obviously in the region where $x = 2$ the amount of adsorption is too small in these experiments for much stress to be laid on the presence of complexes containing only two molecules of iodine. The region where $x = 3$ can be established much more exactly. The precise balance between two, three and four complexes at any point of the curve, however, which must be composite, will only be settled if a wide variation of conditions enables at least the lower ones to be separately studied.

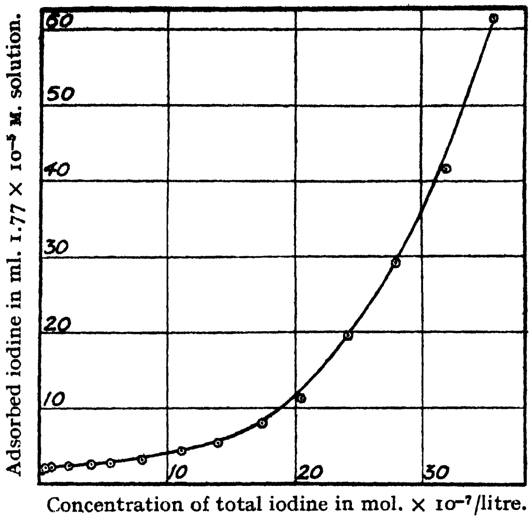

FIG. 5.—Titration of amylose (60 mg.) with 1·77 × 10^{-5} M. iodine in 10^{-4} M. potassium iodide.

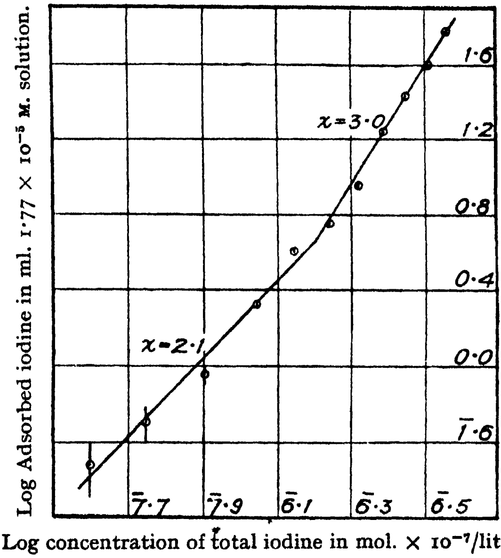

FIG. 6.—Plot of log (adsorbed iodine) against log (concentration of total iodine). Titration in 10^{-4} M. potassium iodide.

An experiment was next carried out in 10^{-4} N. KI, as shown in Fig. 5. Much higher activities of iodine were required to obtain the degree of adsorption found in 10^{-3} N. KI, providing conclusive evidence of the participation of iodide ion in the complex. The logarithmic plot in Fig. 6 would be consistent with the adsorption of a complex containing three molecules of iodine, and once again the curve suggests that initially a complex of two molecules is predominant.

Determination of y/x.

Although it is possible to increase I_2 while keeping the iodide constant in the simple way just described, the requirement for finding y/x, namely, an increase of the iodide concentration at constant adsorption, is not so easily attained. The most satisfactory method is to construct adsorption curves at chosen iodide concentrations, and from them to determine the iodine concentration required for a given adsorption. In practice, owing to the variability of the starch solutions, it is necessary to prepare a single starch solution, measure the iodine concentration required at equilibrium for an arbitrary adsorption at one strength of KI, and then without loss of time to determine the corresponding equilibrium iodine concentration for the same amount of adsorption at a second iodide concentration. When this experiment was carried out for 10^{-3} and 10^{-4} N. KI, the following result was obtained.

In 10^{-4} M. I′, 60 mg. amylose adsorbed $6{\cdot}3 \times 10^{-7}$ mol. iodine at 20° when in equilibrium with 'total' iodine of concentration $2{\cdot}84 \times 10^{-6}$ M. or molecular iodine of concentration $2{\cdot}63 \times 10^{-6}$ M. In 10^{-3} M. I′, the same adsorption occurred from a concentration of total iodine $1{\cdot}04 \times 10^{-6}$ M. or molecular iodine $5{\cdot}78 \times 10^{-7}$ M.

The concentration of molecular iodine has been calculated from the total iodine using Jones and Kaplan's[14] data for the equilibrium between I_2 and I'_3 at 25°, namely $K = (I_2)(I')/(I_3') = 1{\cdot}4 \times 10^{-3}$, together with their value for the heat of reaction of $-$ 4·22 kcal., which gives $K = 1{\cdot}24 \times 10^{-3}$ at 20°.

Applying equation (9),

$$\frac{\Delta \log I_2}{\Delta \log I'} = -y/x = \frac{(-5{\cdot}580 + 6{\cdot}238)}{(-4{\cdot}0 + 3{\cdot}0)} = -0{\cdot}658 = \frac{-2}{3{\cdot}04}.$$

Taking this in conjunction with the previous determination of x as about 3 for this degree of adsorption, the predominant complex appears to be $(3I_2 2I')$, the, the eight atoms presumably forming a linear molecule which owes its characteristic powers of light absorption, and to some extent its stability, to the presence of two unlocalised electrons.

An alternative procedure can be followed to find x/y, involving the establishment of equilibrium at one concentration of KI, and the subsequent addition of KI to both starch solution and titration solution. Since this results in an increase in the adsorption of iodine, and no more iodine is added to the solutions, a potential difference develops from which the new equilibrium adsorption and iodine activity can be calculated. This method has the disadvantage that junction potentials are introduced, and that the increase in adsorption has to be allowed for before equation (9) can be applied, but is much simpler to carry out experimentally.

It was employed with an amylose solution in 10^{-3} N. KI. The two cells were balanced at an activity that gave an adsorption of 24 ml. iodine solution, after which small quantities of strong KI solution were added equally to both cells, and the equilibrium value of the potential difference produced followed as a function of the KI concentration. After each addition there was an immediate increase in potential difference corresponding to increased adsorption, which was succeeded by a slow increase continuing for at least an hour. It was slower than would correspond to the reaction of iodine at constant iodide concentration studied previously, and is thought to be due to a considerably increased proportion of iodide being accommodated by the gradual change of the complex to one of higher iodide content.

The result of (*a*) doubling the iodide concentration, and (*b*) redoubling was as follows.

(*a*) Initial adsorption by 60 mg. amylose in 10^{-3} N. I′ = $4{\cdot}25 \times 10^{-7}$ mol. I_2.
Potential difference when I′ increased to 2×10^{-3} N. = 1·05 mv. after 90 min.
Increase in adsorption = 7×10^{-8} mol. I_2.
Initial concentration of total iodine in 10^{-3} N. I′ = $1{\cdot}02 \times 10^{-6}$ M.
Initial concentration of molecular iodine in 10^{-3} N. I′ = $5{\cdot}6 \times 10^{-7}$ M.
Final concentration of total iodine in 2×10^{-3} N. I′ = $0{\cdot}93 \times 10^{-6}$ M.
Final concentration of molecular iodine in 2×10^{-3} N. I′ = $3{\cdot}6 \times 10^{-7}$ M.
Final concentration corrected for increased adsorption assuming the latter proportional to the third power of the activity = $3{\cdot}4 \times 10^{-7}$ M.

Thus from equation (9) $$-y/x = \frac{\Delta \log I_2}{\Delta \log I'} = \frac{-6{\cdot}469 + 6{\cdot}252}{3{\cdot}301 - 3{\cdot}00} = \frac{2{\cdot}16}{3} \text{ or } \frac{2{\cdot}88}{4}.$$

---

[14] Jones and Kaplan, *J. Amer. Chem. Soc.*, 1928, **50**, 1845.

(*b*) The potential difference at equilibrium increased by a further 0·85 mv. when the iodide was increased to 4×10^{-3} N. and $\Delta \log I_2$ was found to be 0·24.

$$\text{Therefore } -y/x = \frac{\Delta \log I_2}{\Delta \log I'} = \frac{0{\cdot}24}{0{\cdot}30} = \frac{2{\cdot}4}{3} \text{ or } \frac{4}{5}.$$

A further increase of iodide concentration to 0·05 N. increased the potential difference by several millivolts.

While small increases in iodide concentration therefore confirm the type of complex proposed, they also suggest that the proportion of iodide in the complex increases as the concentration of iodide is increased in solution. While systematic experiments have not yet been done with strong iodide solutions, it has been found that the complexes become increasingly stable with increase of iodide in solution, and since the molecular iodine concentration then falls linearly with increase of iodide, it would seem at first sight that y must ultimately exceed x. Such a conclusion cannot be drawn, however, until the influence of neutral salt on the complex has been studied. The more highly charged the complex, the greater the influence to be expected from positive ions, and once aggregation has set in, the positive ions must become as important in the equilibria as the iodide ion : for example, a complex of the type $(I'I_2K^+)_n$ would then of necessity increase in stability (referred to molecular iodine) equally with increase of K^+ or of I' in solution.

The Influence of Temperature on the Equilibrium.

When a solution of amylose containing iodine and 10^{-3} N. KI was cooled below 20° and brought back to 20° the adsorption was found to have increased ; nor did it fall to its former value on standing. If, however, the solution was left some days before such treatment, or was cooled and warmed to 20° several times, the change on cooling became reversible. For the small degrees of adsorption considered in this paper, the equilibrium iodine activity required for a given adsorption was reduced in this way by about one-third. It was obviously impossible to obtain a true temperature coefficient for the system in the state in which it was originally formed, so this more stable condition was investigated.

A solution which had been standing for some days was cooled to about 0° and left to reach equilibrium. It was then titrated in the usual way by connecting it to another cell in the thermostat at 0° and adding iodine to this second cell until the potential difference was nil. This measured the concentration of free iodine in equilibrium with the starch complex at 0°. Next the temperature was raised through some five degrees, and iodine added to both cells *in equal amount* to counterbalance the tendency for a potential difference to develop through desorption of the iodine from the complex. Since equal additions of iodine were made to both solutions, and the potential difference remained zero, no change in the amount of adsorption could have occurred referred to the adsorption at 0°, for the adsorption is equal to the difference in the net amounts added to the respective cells, and this had not changed. The new value of the equilibrium iodine activity was therefore known from the iodine content of the starch-free solution, for the original amount of complex, and the information necessary for the determination of the heat of formation of the complex had been obtained. The operation was repeated at temperature intervals of a few degrees until 20° was reached. The last reading at 20° in the table below was obtained by titration after the solution had stood overnight. At each temperature the concentration of dissolved molecular iodine was calculated using the data of Jones and Kaplan for the tri-iodide equilibrium.

Temp. °c.	Total Iodine mol./litre × 10^{-7}.	Molecular Iodine mol./litre × 10^{-7}.
3·0	2·71	1·20
8·5	3·66	1·76
13·8	4·99	2·57
16·5	6·00	3·20
20·0	6·89	3·81

From equation (6) and the general thermodynamic relation between the variation of an equilibrium constant with temperature and the corresponding heat of reaction, the heat of formation of the complex is given by

$$\frac{\Delta H}{2{\cdot}30\,R} = -\left(\frac{\partial \log K_{xy}}{\partial\, 1/T}\right)_a = -x\left(\frac{\partial \log I_2}{\partial\, 1/T}\right)_a$$

since a is constant throughout, and I' is in too large an excess in solution to vary with I_2 appreciably.

According to the plot of log (molecular iodine) against the reciprocal of the absolute temperature in Fig. 7,

$$\left(\frac{\partial \log I_2}{\partial 1/T}\right)_y = 2{\cdot}45 \times 10^3$$

giving the heat of reaction per mol. of iodine adsorbed as − 11·2 kcal., i.e.,

$$yI' + xI_2 = (xI_2yI'),\ \Delta H = x\,.\,11{\cdot}2 \text{ kcal.},$$

in the presence of starch complex of the given composition (in this case about $1{\cdot}06 \times 10^{-6}$ mol. I_2 per 60 mg. amylose).

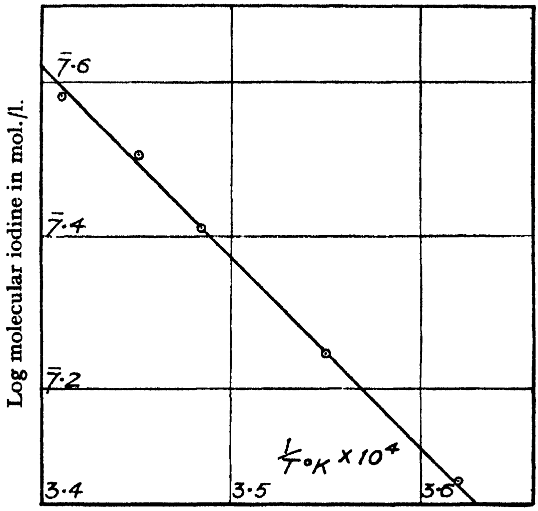

FIG. 7.—Dependence on temperature of equilibrium constant of amylose-iodine complex.

Discussion.

From the evidence found above it seems difficult to avoid the conclusion that at very low percentage adsorption and low iodide concentration, the amylose complex is composed mostly of groups of the type $(3I_22I')$, each probably a linear resonating molecule. At higher iodide concentrations the ratio of iodide ions to iodine molecules increases until it is at least equal to one. This change is accompanied by the appearance of a slightly purple tinge in the blue of the complex. Confirmation of the presence of iodide in the precipitated complex was obtained by analysing the residual solution after the precipitation of amylose from 0·02 N. KI solution with excess iodine, and in two experiments ratios of 0·97 : 1 and 1·07 : 1 were found respectively for iodine molecules to iodide ions in the complex, agreeing in general with past workers.[1]

Since the pure blue of the amylose complex was found to be well developed when the ion $(3I_22I')$ or (I_8'') was predominant, it is logical to suppose that the forms of starch or degraded starch which produce red and purple complexes are unable to stabilise a chain of iodine atoms of such length. Iodine titration by the methods described above may therefore reveal the predominance in such starches of complexes of less than eight atoms, and the determination of x and y may enable an estimate to be made of the maximum length of the sections of their molecules free to coil into helices.

Because of the extreme smallness of the quantity of complex containing only two molecules of iodine that formed at activities low enough to make the amount of the $(3I_22I')$ complex negligible, the colour of this complex has not yet been observed. Nor has its composition yet been determined, but it seems most likely to be $(2I_2I')$ or (I_5') from the very approximate data available for the shift of the log a/log I_2 curves between 10^{-3} and 10^{-4} N. I′ at the appropriate value of a.

An exact study of the higher complexes formed at higher degrees of saturation of the amylose (and also probably on long standing from the smaller complexes initially present at low saturation), is much more difficult because of the increased sensitivity to experimental error. A method which suggests itself for such determinations is the measurement of the potential between two cells containing samples of the same starch-iodine complex, to one of which a further increment of iodine has been added. The small potential change due to this increment would then be directly measured, while the absolute iodine activity could be found easily by titrating either cell. This method might also throw some light on the slow processes occurring during the ageing of the complex; thus if larger complexes were gradually forming this potential difference should decrease considerably with time.

Mention should be made of an experiment carried out in the course of the investigation above. In order to determine whether the amount of complex formed at a given iodine activity was accurately proportional to the amount of starch present (as should be the case if the helical theory is correct, and the association of two or more molecules of starch is not necessary for complex formation), a starch-iodine solution and the titration solution with which it was in equilibrium were partly exchanged. A quarter of the starch was then in one cell and three-quarters in the other, giving a concentration ratio of 1 to 3. No potential difference developed, and both solutions continued to have the same activity. This was consistent with amylose being involved only to the first power.

We are indebted to Prof. W. N. Haworth, F.R.S., for his encouragement and interest in this work, and to Dr. S. Peat and numerous colleagues for discussions and help. One of us (J. V. R. M.) wishes to acknowledge financial support from Messrs. Imperial Chemical Industries Ltd. (Dyestuffs Division).

Summary.

A method has been devised for the accurate potentiometric titration of starch with iodine, and used to investigate the nature of the complex formed between amylose and iodine in dilute potassium iodide solution. When the activities of iodine and iodide lie between certain limits and the percentage adsorption is very low, amylose is found to be associated with a molecular ion of composition (I_8'') formed by the adsorption of three iodine molecules and two iodide ions. In general, for a given iodide concentration the number of iodine molecules in the complex increases from two to three, four, etc., with increase of iodine activity; if the iodide concentration is increased the complex tends to $(I'_3)_n$. As first formed the amylose-iodine complex is metastable, a very slow change subsequently taking place to a more stable form. By measuring the dependence on temperature of the equilibrium constant of the latter, its formation from iodide ions and molecular dissolved iodine is shown to be accompanied by the emission of 11·2 kcal. per mol. of iodine. It is suggested that the complexes formed by red-staining starches contain less than eight atoms of iodine and iodide per molecule.

Department of Chemistry,
The University,
Birmingham, 15.

REVIEWS OF BOOKS.

Strategic Minerals. By J. B. De Mille. (McGraw-Hill Book Co., London, 1947.) Pp. viii + 626. Price 37s. 6d.

International economists are rightly concerned with the repercussions of the war upon the rational development of the metallurgical and mineral industries; they recognise, in principle, the normal need for equal access to the world's minerals by all peaceful nations and also the exceptional need of certain countries for maintaining supplies of strategic minerals for essential uses in a war emergency; but the immediate problem they have to face is the reconversion of these industries, which have undergone an abnormal expansion during the past ten years, to a peace-time footing, without widespread suspension of their operations and without undue dislocation of world markets.

The United States and the British Commonwealth, as the largest producers and exporters of minerals and mineral products, have a particular interest in finding a solution to this problem and in evolving a common policy which shall govern longer term developments. It is generally agreed that one of the first tasks to be undertaken should be a comprehensive survey and inventory of the world's mineral resources; for, not only is there a possibility of the imminent exhaustion of known rich deposits of certain important minerals, but recent discoveries, arising from wartime research, have created urgent demands for minerals which have hitherto been regarded as of little industrial value.

In the book under review, Mr. De Mille outlines the American point of view. The United States Government has attempted to facilitate reconversion by authorising the building up, over a period of years, from surpluses, of permanent stock piles of strategic materials, and also by sponsoring developments designed to discover new outlets for its vastly expanded metal industries. In order to illustrate the magnitude of the task involved, the author has selected some 76 metals and minerals which, during the recent war, were defined as of strategic importance, and has given a comprehensive survey of their properties, uses, sources of supply and output; he also includes statistics of the import and export markets during the period 1939-45.

The treatment of such a wide range of materials has necessarily to be brief and incomplete; and, in view of present world economic conditions, it is doubtful if the statistics on production and prices, relating to the war period, have to-day much practical significance. Nor can the results of American policy yet be assessed. The book contains, however, numerous selected references which should enable the reader adequately to revise and to supplement the information given in particular cases.

The author points out that the United States Government has, through the operation of Mineral Missions set up during the war, done much towards completing a survey and inventory of minerals at home and in the neighbouring South American countries. It is not clear that the Commonwealth Governments have been equally active. Canada certainly realises that its future prosperity is bound up with efficient and productive mining and metallurgy; and the Government is prepared to maintain mining over a period of years at war-time capacity, provided the export market can be sufficiently stimulated. In Australia and Africa, conditions are not so favourable to a rapid growth of these industries, although there is little doubt but that extensive mineral resources exist and will eventually constitute an important part of their economy.

It is to be regretted that no-one has yet thought it worth while to prepare a review similar to that of Mr. De Mille based upon Empire requirements.

D. M. N.

Advances in Enzymology and Related Subjects of Biochemistry. Vol. VII, Ed. by F. F. Nord. (Interscience Publishers, Inc., New York and London. 1947.) Pp. xi + 665. Price 52s. 6d.

This, the latest volume of a well-known series of " recent advances " books, which have been such a notable feature of scientific publishing on the other side of the Atlantic in recent years, will need little recommendation to biochemists. A glance at its list of contents shows how widely the term " enzymology " is interpreted. The subjects of the articles cover a very wide range of vital phenomena, all involving enzymes more or less intimately, as is to be expected, if, as Seifriz suggests in his article, protoplasm in the last analysis is an enzymic complex.

But this volume will also serve to illustrate the many-sided connections between physical chemistry and the biochemical field, and may perhaps encourage many more physical chemists to cast away their moorings to the friendly shores to which they have been so long accustomed, and set sail on the wide and uncharted seas of vital structures.

It begins with an article by C. S. Brooks on " Permeability and Enzyme Reactions " in which the role of diffusion in single enzyme reactions and in the working of the whole cell, are discussed. This is followed by an article by William Seifriz on the properties of protoplasm. A summary of the author's well-known point of view, it covers briefly such general properties of protoplasm as viscosity, elasticity, permeability, the origin and nature of electric potentials, effects of radiation and drugs. It is obvious that less than thirty pages are not enough to do more than skim the surface of such a formidable topic ; yet Seifriz manages to say a great many interesting and stimulating things. In most of the matters he raises, our ignorance is a great deal more conspicuous than our knowledge and the essay as a whole could well be taken as a programme for biophysical research in the immediate future. Practically every point he mentions suggests and calls for further experiment and I can only give a few quotations to illustrate the challenge. " The amount of research done on electrical forces in organisms, especially in nerve conduction, is rather great, but many questions remain, one of which is the chemical nature of the substance primarily responsible for tissue potentials." " Because we pick up some of the free energy by means of platinum electrodes and this produces an electric current which can be measured, it is not implied that an electric current is produced in the system." " I have regarded spirality as a property common to all living matter. To what extent spirality in animate nature is to be attributed to the asymmetry of crystals, the asymmetry of the carbon atom or helical organic molecules, is a matter of conjecture, but the spirality itself cannot be doubted." "The only sensible way to view Gurwitsch's hypothesis (mitogenetic rays) is to consider it as a suggestion and ignore his experiments." The writer may perhaps be permitted to wonder if there may not be danger in putting emphasis on the properties of protoplasm as a whole; possibly more progress will be made by isolating the constituents and discovering their properties separately before attempting a synthesis.

Patrick D. Ritchie gives a comprehensive discussion of the possible and realised methods of asymmetric synthesis and discusses how asymmetric compounds arose in nature. Was it due to a physical directing agency such as circularly-polarised light, or a slight statistical fluctuation which organisms made use of? G. Hevesy gives a long account of a new method, of which very much more will be heard in the near future, the application of radioactive indicators to find how quickly particular compounds are incorporated into structures present in living organisms. It is obvious that much will be learnt about metabolic routes and processes by this powerful method; but Hevesy's paper will also serve as a corrective to those who find in the tracer method a universal panacea for the solution of biochemical problems. While it exposes the great complexity of the dynamic state of the organism, its function may be more to indicate what the problems are, leaving the solution perhaps for other methods.

Frank H. Johnson summarises the Princeton work on bacterial luminescence. It has been shown that the light is produced by the action of an enzyme luciferase on a fairly simple, heat-stable substance, luciferin, which has not been identified so far. The work reported on by Johnson is mainly (1) the spectroscopic character of the emitted light, (2) the effects of temperature, pressure and certain narcotics and other enzyme-inhibiting substances on the emission. The system is peculiarly suited to physico-chemical investigation on account of the light emission in the reaction (luminescence visible to a dark-adapted eye can be obtained from luciferin at dilutions of 1 in 4×10^{10}).

Two articles follow, by H. Theorell and by S. Granick and H. Gilder on the heme proteins of which hæmoglobin is the best-known example. They all contain one or more atoms of iron per molecule, each of which is embedded in the centre of a porphyrin molecule. It is a remarkable fact that hæmoglobin can take up oxygen reversibly without effecting the oxidation of ferrous to ferric iron. Theorell shows how magnetic moments have been used to determine the state of iron in the different compounds of hæmoglobin and to interpret their dissociation constants.

The remaining articles are more biological in nature and need only a brief mention here. H. McIlwain discusses the interrelations between growth and metabolism of vitamin-like substances of micro-organisms. He adduces facts about the astonishing chemical powers of micro-organisms, which physical chemists might ponder on. Streptococci can produce their own weight of lactic acid (from glucose) in half an hour. Nevertheless it is possible that some of the enzyme systems bringing about changes are present only to the extent of a few molecules to each bacterial cell. Other articles deal with anti-biotic substances, with kidney enzymes, such as renin, which is an agent giving rise to high blood pressure, and with recent advances in industrial fermentation. The price is rather high even for a well-produced volume of over 600 pages.—J. A. V. B.

THERMODYNAMICS OF THE CONVERSION $KCl \rightarrow K_2SO_4$ WITH THE AID OF $CaSO_4$.

By E. Abel and J. M. Fanto.

Received 4th March, 1946. As amended, 13th August, 1946.

The conversion of KCl to K_2SO_4 in aqueous solutions with the aid of the intermediate formation of K_2SO_4—$CaSO_4$ double salts has attracted considerable attention from the technical point of view. As a result of some research which we carried out on behalf of Palestine Potash Ltd., the thermodynamic outlines of this process are briefly described. This description will give some idea of the theoretical extent of this conversion, its dependence on temperature and, in particular, its dependence on the choice of the form of calcium sulphate, the importance of which does not seem to have been sufficiently appreciated.

I. Theoretical Relationships.

The various kinds of conversion in its first stage,(a) namely that leading to the formation of double salts, may be expressed in the following equation :

$$2KCl + (q + 1)(CaSO_4 \,.\, pH_2O)(s) = K_2SO_4 \,.\, qCaSO_4 \,.\, H_2O(s) + CaCl_2 + (p(q + 1) - 1)H_2O;$$

($q = 1$, potassium calciumdisulphate, or syngenite (S); $q = 5$, potassium pentacalciumhexasulphate or pentasalt (P);(b) $p = 2$, gypsum (G); $p = \frac{1}{2}$, hemihydrate (H); $p = 0$, anhydrite (A)).

According to the existing literature, the two last-named forms include a range of variants which are, perhaps, entirely zeolitic and which have been critically examined and discussed from a thermodynamic point of view by Kelley, Southard and Anderson.[1] Although, quoting the authors, it is not at present possible to give " an entirely satisfactory thermodynamic portrayal of all the ramifications of the system $CaSO_4 - H_2O$ " we accept their conclusions in this paper and distinguish three hemihydrate variants (α, α^*, β) and three anhydrite variants (sol α, sol β and the insoluble form A (without further notation)). For although their thermodynamic individuality and the possibility of their exact reproducibility are not established facts, the existence of calcium sulphates of approximately the same chemical composition, though of different energy content, is hardly doubted, and methods are available for their preparation, although with no certainty of obtaining an exactly defined product. This circumstance means that the success of the KCl—K_2SO_4 conversion will to a large extend depend on the choice and treatment of the calcium sulphate. This will be shown in the following on the basis of the calculations of Kelley and his collaborators; in any case these indicate the approximate amount of free energy taken up by the solid $CaSO_4$—H_2O system under various conditions. It is, of course, important that the reacting $CaSO_4$-form does not completely lose its metastability during the conversion, and this can be attained under suitable conditions.

(a) The second stage of the decomposition of the double salt, possibly also proceeding in steps, can be conducted in such a way that it leads to quantitative splitting off of the K_2SO_4-component ; the conditions for this can be read from the well-known phase diagram.

(b) The double salt $K_2SO_4 \,.\, 2CaSO_4$ is not taken into consideration; see also Bredig.[2]

[1] Kelley, Southard and Anderson, *U.S. Dept. Interior, Bur. Mines, Tech. Paper*, 1941, 625 ; see also Southard, *Ind. Eng. Chem.*, 1940, **32**, 442.

[2] Bredig, *J. Physic. Chem.*, 1942, **46**, 747.

Let the letters p and q denote as right-hand indices the various forms of $CaSO_4$ and as left-hand indices the coexistence of the latter, singly or two together, with the respective solutions; and let a^*, m and f denote the activities, molalities and activity coefficients of the dissolved salts, and a_w the activity of the water component, then we have

$$a^*_p = {}_{p}(m^2_{\mathrm{CaSO_4}} f^2_{\mathrm{CaSO_4}} a^p_w) = {}_{p,q}(m_{\mathrm{CaSO_4}} m_{\mathrm{SO_4''}} f^2_{\mathrm{CaSO_4}} a^p_w),$$

where
$$m_{\mathrm{SO_4''}} = m_{\mathrm{CaSO_4}} + m_{\mathrm{K_2SO_4}}$$

and
$$a^*_q = {}_{q}(4m^2_{\mathrm{K_2SO_4}} m^q_{\mathrm{CaSO_4}} m^{q+1}_{\mathrm{SO_4''}} f^3_{\mathrm{K_2SO_4}} f^{2q}_{\mathrm{CaSO_4}} a_w)$$
$$= {}_{p,q}(4m^2_{\mathrm{K_2SO_4}} m_{\mathrm{SO_4''}} f^3_{\mathrm{K_2SO_4}} a_p^{*q} a_w^{1-pq}).$$

The product

$$ {}_{p,q}(4m^2_{\mathrm{K_2SO_4}} m_{\mathrm{SO_4''}} f^3_{\mathrm{K_2SO_4}}) = {}_{p,q}a^*_k = \frac{\overset{\circ}{a}_q}{a_p^{*q}}\,{}_{p,q}a_w^{pq} \quad 1$$

can be regarded as the activity of the "solid K_2SO_4 component" of the q-double salt in presence of the p-sulphate; its value is, however, variable with the water vapour pressure.

After reaction with KCl according to the above equation we have for the activities of $CaSO_4$ and K_2SO_4 in the solution (index $\overline{p,q}$):

$$ {}_{\overline{p,q}}a_{\mathrm{CaSO_4}} = {}_{\overline{p,q}}(m_{\mathrm{Ca''}} m_{\mathrm{SO_4''}} f^2_{\mathrm{CaSO_4}}) = \frac{a^*_p}{{}_{\overline{p,q}}a^p_w}$$

$$ {}_{\overline{p,q}}a_{\mathrm{K_2SO_4}} = {}_{\overline{p,q}}(m^2_{\mathrm{K'}} m_{\mathrm{SO_4''}} f^3_{\mathrm{K_2SO_4}}) = {}_{\overline{p,q}}a^*_k = \frac{a^*_q}{a_p^{*q}} \cdot {}_{\overline{p,q}}a_w^{pq} \quad 1$$

where

$$m_{\mathrm{Ca''}} = {}_{\overline{p,q}}(m_{\mathrm{CaSO_4}} + m_{\mathrm{CaCl_2}}) = \frac{n_{\mathrm{Ca''}}}{2}\,; \quad m_{\mathrm{K'}} = {}_{\overline{p,q}}(m_{\mathrm{KCl}} + 2m_{\mathrm{K_2SO_4}}) = n_{\mathrm{K'}}\,;$$

$n_{\mathrm{K'}}$ and $n_{\mathrm{Ca''}}$ are the number of g.-equ. of potassium and calcium salt in 1000 g. water after equilibrium is established:

$$\frac{n^2_{\mathrm{K'}}}{n_{\mathrm{Ca''}}} = \frac{a^*_q}{2a_p^{*\,q+1}}\,{}_{\overline{p,q}}\left(\frac{f^2_{\mathrm{CaSO_4}}}{f^3_{\mathrm{K_2SO_4}}}\right){}_{\overline{p,q}}a_w^{p(q+1)-1}.$$

Although the a_w factor can be of considerable influence under certain conditions, it may be put equal to 1 in the following; to denote this the asterisk on a will be omitted. The condition of equilibrium is then

$$\frac{n^2_{\mathrm{K'}}}{n_{\mathrm{Ca''}}} = K(p,q) \cdot \phi$$

where
$$K(p,q) = \frac{{}_{\overline{p,q}}a_k}{2a_p} = \frac{a_q}{2a_p^{q+1}}\,; \quad \phi = {}_{\overline{p,q}}\left(\frac{f^2_{\mathrm{CaSO_4}}}{f^3_{\mathrm{K_2SO_4}}}\right).$$

In a solution coexisting with p-sulphate let the initial concentration (g.-equ. in 1000 g. water) of KCl, $CaCl_2$ (e) and $CaSO_4$ be b, c and s, and let x and y (in the same units) be the amounts reacting according to the two simultaneous partial reactions

---

(e) For the sake of generality we assume the presence of the product of reaction.

$$2K^{\bullet} + p\text{-sulphate} \rightarrow q\text{-double salt} + Ca^{\bullet\bullet} \;.\;.\;.\; x$$

$$Ca^{\bullet\bullet} + SO_4'' \rightarrow p\text{-}CaSO_4 \;.\;.\;.\; y$$

then the concentrations at equilibrium will be

$$n_{K^{\bullet}} = b - x$$
$$n_{Ca^{\bullet\bullet}} = c + x + s - y$$
$$n_{SO_4''} = s - y$$

and the conditions for equilibrium (d)

$$\frac{(b-x)^2}{c+x+s-y} = K(p,q)\,.\,\phi$$

$$(c+x+s-y)(s-y) = \frac{4a_p}{f^2_{CaSO_4}}$$

at the ionic strength

$$\mu = b + \frac{3}{2}c + \frac{x}{2} + 2(s-y).$$

The evaluation of these equations is rather lengthy, especially as, in view of the dependence of f and ϕ on concentration, it can only be carried out by successive approximation. In as far as $n_{SO_4''} = s - y \lessdot x$, an easier method of calculation consists in substituting for this a value σ which can be roughly estimated. Then

$$x \doteqdot b - \frac{K(p,q)\,.\,\phi}{2}\left(\sqrt{\left(\frac{4(c+b+\sigma)}{K(p,q)\,.\,\phi} + 1\right)} - 1\right),$$

and if $c = 0$, $\sigma \sim 0$, the yield η of double salt or of potassium sulphate (e) expressed as a percentage of the KCl added

$$\eta = \frac{x}{b} \doteqdot 1 - \frac{K(p,q)\,.\,\phi}{2b}\left(\sqrt{\left(\frac{4b}{K(p,q)\cdot\phi} + 1\right)} - 1\right)$$

at the ionic strength

$$\mu \doteqdot b + \frac{x}{2} \doteqdot b\left(1 + \frac{\eta}{2}\right).$$

If at the end of the reaction the KCl content is restored to its original strength and this operation is repeated n times, then

$$\eta_n \doteqdot 1 - \frac{K(p,q)\,.\,\phi}{2b}\left(\sqrt{\left(\frac{4b}{K(p,q)\,.\,\phi}(1 + \eta_1 + \;.\;.\;.\; \eta_{n-1}) + 1\right)} - 1\right).$$

It will be seen that the yield of potassium sulphate increases as the value of $K(p,q)$ decreases, that is to say, on the whole, the more soluble the form of $CaSO_4$ and/or the more insoluble the double salt.

II. Activity Coefficients.

1. $CaSO_4$.—In as far as the surplus free energy of the various $CaSO_4$-forms, as opposed to gypsum, are expressed in Kelley's values $\Delta F(p - G)$ $\left(= RT \ln \frac{a_p}{a_G}\right)$,(f) the only knowledge required for the numerical evaluation of the p-activities is of the activity coefficients of $CaSO_4$ in the range of the solubility of gypsum, that is, between 0° and, say, 80°, in the range of about $0{\cdot}013 \leqq m_s \leqq 0{\cdot}016$. These data are not available at present, but the activity coefficients of the nearest sulphate of the same type,

---

(d) With the above-mentioned simplification.

(e) See footnote (a).

(f) See the introductory remarks.

$MgSO_4$, may be assumed to be identical with those of $CaSO_4$ in the range under consideration.(g)

With regard to the dependence on temperature $\left(\frac{\partial \ln f}{\partial T}\right) = -\frac{\overline{L}_2}{RT^2}$, the relative partial molal heat content of $MgSO_4$ ($\overline{L}_2$($MgSO_4$, m) is known,(h) but not its temperature coefficient.(i) This uncertainty is, however, as shown in Table I of little importance over a wide range of temperature.

TABLE I.—ACTIVITY COEFFICIENTS f_{MgSO_4} ($\div f_{CaSO_4}$).(j), (k)

m_{CaSO_4}	0·010	0·015	0·020	m_{CaSO_4}	0·010	0·015	0·020
$\overline{L}_2^{298}$*	+739	+817	+872	$\overline{L}_2^{298}$*	+739	+817	+872
$\Delta\overline{C}_{p_2}$** t° C.	+47·5	+54	+59	$\Delta\overline{C}_{p_2}$** t_2 C.	+47·5	+54	+59
0°	0·475 (1·00)	0·421 (1·00)	0·378[12] (1·00)	40°	0·449 (1·03)	0·396 (1·04)	0·356 (1·05)
10°	0·478 (1·03)	0·425 (1·04)	0·384 (1·05)	50°	0·431 (1·01)	0·378 (1·01)	0·338 (1·01)
20°	0·475 (1·05)	0·421 (1·05)	0·380 (1·06)	60°	0·410 (0·98)	0·357 (0·97)	0·316 (0·97)
25°	0·470 (1·05	0·417 (1·05)	0·375 (1·06)	80°	0·363 (0·89	0·312 (0·88)	0·272 (0·86)
30°	0·464 (1·95)	0·411 (1·05)	0·370 (1·06)				

* cal./mol. ** cal./mol./deg.

(g) See Lewis and Randall;[3] the calculation carried out there applies also to the more exact values of f_{MgSO_4} which have since been obtained.

[3] Lewis and Randall, *Thermodynamics* (McGraw-Hill, 1923), p. 376.

(h) That of $CaSO_4$ too.[4] The value $\Delta\overline{C}_{p_2}$($CaSO_4$, $m = 0·015$) (25°)[5] (see footnote (i)) does not seem to be fully ascertained according to more recent literature.[6]

[4] Lange and Streeck, *Z. physik. Chem. A*, 1931, **157**, 1; see also Lange and Monheim, *ibid.*, 1930, **150**, 349; Plake, *ibid.*, 1932, **162**, 257; Robinson and Wallace, *J. Amer. Chem. Soc.*, 1941, **63**, 1582.

[5] Rossini, *U.S. Bur. Stand.*, *J. Res.*, 1930, **4**, 313; R.P. 151.

[6] LaMer and Cowperthwaite, *J. Amer. Chem. Soc.*, 1933, **55**, 1004; Gucker, *Chem. Rev.*, 1933, **13**, 111; Lange and Streeck, *loc. cit.*

(i) The range in which the heat capacity of $MgSO_4$ solutions has been measured up to now,[7] is not sufficient to permit the extrapolation to $m = 0$. We believe that we shall approach the truth most closely by substituting for $\Delta\overline{C}_{p_2}$ ($MgSO_4$, m) ($= \overline{C}_{p_2}(m) - \overline{C}_{p_2}(0)$) (though to some extent by means of extrapolation) the values which are derived from the determination on $ZnSO_4$, one of the very few electrolytes of the 2—2 type of which the $\Delta\overline{C}_{p_2}$-term has been ascertained;[8] the authors point out the analogies in the thermal behaviour of $ZnSO_4$- and $CaSO_4$-solutions. See also Dunkelberger and Robinson,[8] measurements on $CaSO_4$; the values of $\Delta\overline{C}_{p_2}$ in the same range of concentration are between 31 and 36. To elucidate the uncertainty which this causes, the relationship between the values thus obtained and those which would be obtained without regard to the dependence on temperature has been added in brackets to Table I. This uncertainty vanishes, of course, in as far as the data are given relative to the activity of gypsum.

[7] Drucker, *Ark. Kem. Min. Geol. A.*, 1934, **11**, No. 12; Perreu, *Compt. rend.*, 1935, **200**, 237; D'Ans and Tollert, *Z. Elektrochem.*, 1937, **43**, 81.

[8] Dunkelberger and Robinson, *J. Amer. Chem. Soc.*, 1938, **60**, 1301.

2. $CaSO_4$ in K_2SO_4 Solutions.—As can be seen from the conditions established by Hill[18] for the coexistence of $CaSO_4 - K_2SO_4$ solutions with gypsum and anhydrite along the isotherms 100° and 60°, the expressions

$$(f_{CaSO_4})_G\, a_G^{-\frac{1}{2}} = (m_{CaSO_4} m_{SO_4''})_G^{-\frac{1}{2}} = A_G^{-\frac{1}{2}}(\mu) \quad (l)$$

$$(f_{CaSO_4})_A\, a_G^{-\frac{1}{2}} = (m_{CaSO_4} m_{SO_4''})_A^{-\frac{1}{2}} \cdot 10^{\frac{\Delta F(A-G)}{2R'T}} \quad (m)$$

TABLE II.

$m_{K_2SO_4}$.		m_{CaSO_4}.		μ.	$(f_{CaSO_4})_G$	$(f_{CaSO_4})_A$
G.	*A.*	*G.*	*A.*		$a_G^{\frac{1}{2}}$.	$a_G^{\frac{1}{2}}$.
			100°.			
—	—	0·0123	—	0·049	81·2	—
0·0150	—	0·0100	—	0·085	63·3	—
—	0·0258	—	0·00377	0·092	—	51·8
—	0·0422	—	0·00348	0·141	—	47·2
0·0456	—	0·0099	—	0·177	42·8	—
0·0633	—	0·0101	—	0·230	36·6	—
0·0881	—	0·0105	—	0·306	31·2	—
—	0·113	—	0·00382	0·354	—	25·7
0·118	—	0·0111	—	0·398	26·5	—
—	0·174	—	0·00418	0·539	—	20·2
0·175	—	0·0123	—	0·574	20·7	—
—	0·271	—	0·00460	0·831	—	15·3
0·272	—	0·0142	—	0·873	15·7	—
—	0·333	—	0·00521	1·020	—	13·1
0·322	—	0·0154	—	1·028	13·9	—
0·326	—	0·0155	—	1·040	13·8	—
0·336	—	0·0156	—	1·070	13·5	—
—	0·402	—	0·00558	1·228	—	11·5
—	0·455	—	0·00666	1·392	—	9·9
—	0·508	—	0·00689	1·552	—	9·2
—	0·529	—	0·00635	1·612	—	9·4
—	0·534	—	0·00683	1·629	—	9·1
			60°.			
—	—	0·0148	—	0·059	67·2	—
0·0299	—	0·0114	—	0·135	46·0	—
—	0·0585	—	0·00750	0·205	—	36·2
0·0722	—	0·0110	—	0·261	34·1	—
0·0960	—	0·0112	—	0·332	28·7	—
0·1082	—	0·0113	—	0·370	27·1	—
—	0·1178	—	0·00805	0·385	—	25·3
0·1438	—	0·0117	—	0·478	23·2	—
—	0·178	—	0·00840	0·568	—	20·4
—	0·212	—	0·00872	0·671	—	18·3
0·2140	—	0·0129	—	0·694	18·4	—
—	0·246	—	0·0089	0·774	—	16·9
0·267	—	0·0136	—	0·855	16·2	—
—	0·287	—	0·0092	0·898	—	15·4
—	0·324	—	0·0094	1·010	—	14·4

See following page for footnotes.

plotted against the ionic strength μ produce practically the same curve (Table II, col. 6, 7 and 13, 14) independent of the $CaSO_4$ content, although this latter varies considerably with the form of solid calcium sulphate. The activity coefficient of $CaSO_4$ in K_2SO_4 solutions is, therefore, practically a function of the ionic strength[8] only and it is not likely to be in serious error if we assume that this is generally true, that is to say, also for K_2SO_4 solutions not saturated with respect to $CaSO_4$.(n)

3. **K_2SO_4.**—The situation for K_2SO_4 is more favourable than in the case of $CaSO_4$. The heats of dilution can be obtained from the exact measurements (25°) of the heats of solution of $K_2SO_4(s)$ by Mischenko and Pronina[15] and from these the relative partial molal heat contents $\overline{L}_2^{298}(K_2SO_4, m)$ can be calculated by methods that are well known; its temperature coefficients $\Delta\overline{C}_{p_2}(K_2SO_4, m)$ (o) is available from the paper by Randall and Rossini.[16] From these data the activity coefficient of K_2SO_4 can be calculated (Table III) over a wide range of concentration

TABLE III.—ACTIVITY COEFFICIENTS $f^*_{K_2SO_4}$.[9]

$m_{K_2SO_4}$	0·10	0·20	0·30	0·40	0·50	0·60	0·70
$\overline{L}_2^{298}$ **	+ 211	+ 62	− 64	− 334	− 610	− 650	− 866
$\Delta\overline{C}_{p_2}$† / t° C.	+ 19·6	+ 28·8	+ 36·0	+ 42·0	+ 47·2	+ 52·0	+ 56·0
0°	0·441 (j)	0·353	0·307	0·275	0·247	0·225	0·209
25°	0·448	0·364	0·321	0·292	0·268	0·249	0·237
40°	0·436	0·358	0·318	0·292	0·271	0·254	0·241
60°	0·422	0·342	0·305	0·281	0·263	0·247	0·236
100°	0·381	0·305	0·266	0·241	0·223	0·207	0·200

* Some of the figures are smoothed in the third decimal.
** cal./mol.
† cal./mol./deg.

(j) Calculated from the freezing points data.[9]

[9] *Int. Crit. Tab.* IV, p. 237.

(k) See also Federoff;[10] Robinson and Jones.[11]

[10] Federoff, *Ann. Chim.*, 1941, **16**, 154.

[11] Robinson and Jones, *J. Amer. Chem. Soc.*, 1936, **58**, 959.

[12] Redlich and Rosenfeld, *Physik.-chem. Tabellen* (J. Springer, 1931), Erg. Band. II.

[13] Hill, *J. Amer. Chem. Soc.*, 1934, **56**, 1071.

(l) $\Lambda_G(\mu)$ can, though not in the classic sense, be regarded as the "solubility product" of gypsum at the ionic strength μ.

(m) $R^* = 2{\cdot}30$.

(n) Since the solubility of gypsum in K_2SO_4-solutions is also known for another range of temperature,[14] $\Lambda_g(\mu)$ can be ascertained for a given ionic strength over a considerable range.

[14] D'Ans and Schreiner, *Z. anorg. Chem.*, 1909, **62**, 129; D'Ans, *Die Lösungsgleichgewichte der Systeme der Salze ozeanischer Salzablagerungen*, Verlagsges. f. Ackerbau m.b.H., 1933; a comprehensive review of the literature is given here.

[15] Mischenko and Pronina, *J. Obschey Khmii, Khimichesky J., Seriya A*, 1936, **6** (1), 85. See also Rümelin, *Z. physik. Chem.*, 1907, **58**, 449; Plake, *loc. cit.*; Cohen and Kooy, *Z. physik. Chem. A*, 1928, **139**, 273; Shibata, Oda and Furukawa, *J. Sci. Hiroshima Univ.*, 1933, **3**, 227.

(o) See footnote (i).

and temperature,(r) starting on the one hand from $f^{(0^\circ)}_{K_2SO_4}$ obtained from freezing-point measurements,[17] on the other hand from $f^{(25^\circ)}_{K_2SO_4}$ measured by the isopiestic method.[18]

III. The Constants of the Equilibrium between the Double Sulphates and their Solutions.

Tables IV and V contain the constants of the equilibrium between the double sulphates and their saturated solutions, in the form of the activities of their "solid K_2SO_4 component" in coexistence with gypsum(s), $a_k(S,G)$ and $a_k(P,G)$:

$$\begin{aligned} a_k(S,G) &= {}_{S,G}(4m^2_{K_2SO_4}m_{SO_4''}\cdot f^3_{K_2SO_4}) \\ &= {}_{S,A}(4m^2_{K_2SO_4}m_{SO_4''}\cdot f^3_{K_2SO_4})\cdot 10^{\frac{\Delta F(A-G)}{R^{\bullet}T}} \\ &= {}_{S}(4m^2_{K_2SO_4}m_{CaSO_4}m^2_{SO_4''}\cdot f^3_{K_2SO_4})\cdot \Lambda_G{}^{1}(\mu) \\ a_k(P,G) &= {}_{P,G}(4m^2_{K_2SO_4}m_{SO_4''}\cdot f^3_{K_2SO_4}) \\ &= {}_{P,A}(4m^2_{K_2SO_4}m_{SO_4''}\cdot f^3_{K_2SO_4})\cdot 10^{\frac{5\Delta F(A-G)}{R^{\bullet}T}} \\ &= {}_{P}\text{ or }{}_{P_{P,S}}(4m^2_{K_2SO_4}m^5_{CaSO_4}m^6_{SO_4''}\cdot f^3_{K_2SO_4})\cdot \Lambda_G{}^{5}(\mu). \end{aligned}$$

Again the left-hand indices show which solid sulphates were present in the investigations [13, 14, (t)] on which these calculations are based.

$\Lambda_G(\mu)$ is the "solubility product" of gypsum in K_2SO_4 solutions of the same temperature and the same ionic strength μ as that of the coexisting solution. It will be seen from the series of the isothermal determinations that a_k shows marked constancy over a wide range of concentration, expecially if one considers the various methods of calculation.(u)

$R^{\bullet}T \log a_k(S, G\,;\ P, G)$ is the free energy of formation (v)) of the double sulphates(s) from gypsum and K_2SO_4 dissolved to its standard state (°), $R^{\bullet}T^2\,\dfrac{d\log a_k}{dT}$ is the heat of solution (heat of decomposition) of the double

---

[16] Randall and Rossini, *J. Amer. Chem. Soc.*, 1929, **51**, 323.

(p) See also Federoff [10]; Plake [4].

(q) Robinson and Wilson [18]; easily corrected, $f_{K_2SO_4}(0^\circ\,;\ m = 0{\cdot}10) = 0{\cdot}441$ instead of 0·448.

[17] Redlich and Rosenfeld, see [12], Erg. Band, II and III.

(r) According to these values we obtain (25°)

$$a(K_2SO_4(s)) = 4{\cdot}0 \times 690^3 \times 0{\cdot}237 = 1{\cdot}75 \times 10^{-2}$$

and for the free energy of formation of K_2SO_4 (s) from K_2SO_4 dissolved to its standard state, −2400 cal. This gives with

$$\Delta F^0_{298}(K^{\bullet}) = -\,67{,}630,\ \Delta F^0_{298}(SO_4'') = 176{,}500 \text{ cal.}^{3}$$

$$\Delta F^0_{298}(K_2SO_4\ (s)) = -\,314{,}160 \text{ cal.}$$

(Kelley,[19] 314,600 ; Shibata, Oda and Furukawa,[15] 313,532).

[18] Robinson and Wilson, *J. Amer. Chem. Soc.*, 1941, **63**, 1011.

[19] Kelley, *U.S. Dept. Bur. Min.*, 1937, **406**; Moore and Kelley, *J. Amer. Chem. Soc.*, 1942, **64**, 2949.

(s) The range is taken as far as $f_{K_2SO_4}$ and Λ_G are available at present. The conditions for coexistence with K_2SO_4 (s) are outside this range.

(t) See also Conley, Gabriel and Partridge [20].

[20] Conley, Gabriel and Partridge, *J. Physic. Chem.*, 1938, **42**, 587.

(u) This constancy is considerably less for pentasalt than for syngenite and this is probably due to the raising of the "$CaSO_4$ factor" to the fifth power, thus magnifying any discrepancies. In contrast to all other determinations on syngenite and pentasalt, the values given for pentasalt at 100° c. do not give constancy, without there being any obvious reasons for this.

(v) With the simplification regarding a_w, mentioned earlier.

TABLE IV.

t° C.	$m_{K_2SO_4}$.	m_{CaSO_4}.	$f_{K_2SO_4}$.	μ.	Solution in Coexistence with	$A_G(\mu)$. 10^4.	a_k (S, G) . 10^4.	
0°	0·117	0·0063	0·418	0·376	S, G	—	4·9	
11°	0·148	0·0109	0·384	0·488	S, G	—	7·9	
18°	0·165	0·0116	0·376	0·541	S, G	—	10·3	
25°	0·182	0·0112	0·365	0·591	S, G	—	12·5	12·8
	0·188	0·0118	0·362	0·611	S, G	—	13·5	
	0·205	0·0091	0·356	0·651	S	25·2	12·5	
31·8°	0·200	0·0118	0·354	0·647	S, G, P	—	15·0	15·2
	0·208	0·0128	0·351	0·675	S, G, P	—	16·5	
40°	0·221	0·0126	0·340	0·713	S, G	—	18·1	18·0
	0·226	0·0132	0·338	0·731	S, G	—	18·8	
	0·237	0·0109	0·334	0·755	S	31·8	17·7	
	0·243	0·0103	0·332	0·770	S	32·3	17·6	
	0·281	0·0078	0·321	0·874	S	38·8	17·6	
	0·289	0·0073	0·318	0·896	S	39·7	17·7	
51°	0·252	0·0134	0·310	0·810	S, G	—	20·1	
60°	0·268	0·0135	0·308	0·858	S, G	—	23·6	23·9
	0·314	0·0104	0·298	0·984	S	47·3	24·3	
	0·324	0·0094	0·296	1·010	S, A	—	23·7	
	0·327	0·0092	0·296	1·018	S	49·6	23·4	
	0·345	0·0083	0·292	1·063	S	52·4	24·3	
	0·378	0·0078	0·284	1·165	S	63·5	24·0	
75°	0·296	0·0147	0·288	0·948	S, G	—	26·2	
80°	0·303	0·0149	0·281	0·969	S, G	—	26·0	
90°	0·320	0·0152	0·266	1·021	S, G	—	25·8	
99°	0·327	0·0154	0·254	1·043	S, G	—	24·0	
100°	0·322	0·0157	0·258	0·982	S	52·4	24·6	22·6
	0·327	0·0155	0·253	1·043	S, G	—	23·7	
	0·334	0·0148	0·252	1·062	S	57·7	22·4	
	0·338	0·0145	0·251	1·072	S	59·6	22·0	
	0·350	0·0138	0·249	1·106	S	64·1	21·6	
	0·369	0·0128	0·245	1·159	S	69·0	21·8	
	0·434	0·0101	0·232	1·342	S	86·7	21·6	
	0·500	0·0082	0·220	1·532	S	112	21·6	
	0·505	0·0080	0·220	1·547	S	118	19·4	
	0·575	0·0068	0·210	1·752	S, A	—	21·6	
	0·685	0·0054	0·201	2·077	S, P	170	23·0	

TABLE V.

t° C.	$m_{K_2SO_4}$.	m_{CaSO_4}.	$f_{K_2SO_4}$.	μ.	Coexistence with	$A_G(\mu)$. 10^4.	$a_k(P,G)$. 10^4.	
31·8°	0·200	0·0118	0·354	0·647	S, G, P	—	15·0	15·2
	0·208	0·0128	0·351	0·675	S, G, P	—	16·5	
40°	0·174	0·0117	0·366	0·569	G, P	—	11·0	10·3
	0·237	0·0109	0·335	0·755	S, P	31·6	9·6	
60°	0·097	0·0112	0·408	0·336	G, P	—	2·8	2·4
	0·246	0·0089	0·316	0·774	A, P	—	2·3	
	0·345	0·0083	0·292	1·068	S, P	53·6	2·1	
80°	0·0966	0·0122	0·385	0·339	G, P	—	(2·3)	—

sulphates to infinite dilution, with the precipitation of gypsum:

$$\Delta F_{298}(S - G,\ K_2SO_4(o)) = -\ 3950 \text{ cal.};$$

$$\Delta F_{305}{}^{(w)}\ (S - G,\ K_2SO_4(o)) = \Delta F_{305}(P - G,\ K_2SO_4(o)) = -\ 3910 \text{ cal.}$$

Combining this with the activity of K_2SO_4 (*s*) (see footnote $^{(r)}$) we get for the free energies of formation of the double sulphates(*s*) from solid K_2SO_4 and gypsum:

$$\Delta F_{298}(S - G,\ K_2SO_4(s)) = -1550 \text{ cal};$$
$$\Delta F_{298}(P - G,\ K_2SO_4(s)) = -1590 \text{ cal}.$$

The heats of solution (heats of decomposition (x)) cannot be obtained with sufficient accuracy by graphical differentiation, but it can be seen from the last column of Tables IV and V and their graphical exposition that for syngenite they are at first positive (absorption of heat), decrease with increasing temperature and pass through zero between about 70° and 90°, while for pentasalt the heat of solution is negative in the range under consideration.

IV. The Equilibrium Constants of the Conversion KCl → K_2SO_4.

The activity coefficients (Table I) in combination with the molalities of saturated gypsum solutions produce the activity a_G of gypsum. From this the activities a_p of the various $CaSO_4$ forms can be calculated and from the values of a_k (Tables IV and V) the activities a_S and a_P of syngenite and pentasalt:

$$a_S = a_k(S, G) \,.\, a_G; \quad a_P = a_k(P, G) \,.\, a_G^{6}.$$

Thus we get for the equilibrium constants of the conversion KCl → K_2SO_4 with the aid of $CaSO_4$

$$K(p, S) = \left(\frac{1}{\phi}\frac{n^2_{K^\cdot}}{n_{Ca^{\cdot\cdot}}}\right) = \tfrac{1}{2} a_S\, a_p^{-2} = \tfrac{1}{2} a_k(G, S) \,.\, a_G^{-1} \,.\, 10^{\frac{2\Delta F(p - G)}{R^{\circ}T}}$$

$$K(p, P) = \left(\frac{1}{\phi}\frac{n^2_{K^\cdot}}{n_{Ca^{\cdot\cdot}}}\right) = a_P\, a_p^{-6} = a_k(G, P) \,.\, a_G^{-1} \,.\, 10^{-\frac{6\Delta F(p - G)}{R^{\circ}T}}.$$

Although, for obvious reasons, some of the equilibria contained in Table VI are far from being realisable,(y) it will be seen that in the range of temperature under consideration practically all forms of $CaSO_4$ are superior to gypsum in their ability to convert KCl to K_2SO_4, on conversion to syngenite as well as to pentasalt. The practical application of this superiority presupposes, as we have already remarked, that the selected calcium sulphate really tends to its higher solubility in comparison with gypsum and that this state of increased activity can be maintained at least for the period of coexistence between solution and double sulphate.

Furthermore, the very advantageous influence of low temperature on the position of equilibrium can be seen so that the summary given in Table VI, combined with the kinetics of the conversion, permits of an estimate of the conditions under which there is an adequate balance between the advantage of increased output and the disadvantage of a decreased rate of reaction. Fortunately the equilibrium constants decrease faster than the degree of supersaturation increases.

For $K(p, S(P)) < 1$ the theoretical yield, $\eta \doteqdot 1 - \sqrt{\frac{K \,.\, \phi}{b}}$, approaches 100 % for any considerable concentration b (aa), independent of the factor ϕ. $\phi\left(= \underset{p,s}{\overline{}}\left(\frac{f^2_{CaSO_4}}{f^8_{CaSO_4}}\right)\right)$ itself is dependent on the composition of the equilibrium solution which is in the main a solution of the respective potassium and calcium salts, at the conversion of potassium chloride.

(w) G, S and P coexist at 31·8° c.[14]. The temperature coefficient of $\Delta F_{298}(K_2SO_4\ (s) - K_2SO_3(o) \doteqdot +11$ cal./deg.

(x) See Barre[21].

[21] Barre, *Ann. Chim. Physique*, 1911, **24**, (8), 145.

(y) E.g. the solubility of $A_{sol\,\beta}$ would be about 2·5 M. at 0° c.

(aa) The limiting concentration of KCl, which has to be exceeded to give conversion, is $b_{min} = \sqrt{K(p, S(P)) \,.\, \phi \,.\, n_{Ca^{\cdot\cdot}}}$.

TABLE VI.

$CaSO_4$.	0°.		10°.		25°.		31·8°.			40°.			60°.			80°.	
		S.		S.		S.		S.	P.		S.	P.		S.	P.		S.
	$a_p \times 10^5$.	$a_S \times 10^8 = 1\cdot60$.	$a_p \times 10^5$.	$a_S \times 10^8 = 2\cdot89$.	$a_p \times 10^5$.	$a_S \times 10^8 = 5\cdot14$.	$a_p \times 10^5$.	$a_S \times 10^8 = 6\cdot00$.	$a_P \times 10^{28} = 14\cdot6$.	$a_p \times 10^5$.	$a_S \times 10^8 = 6\cdot60$.	$a_P \times 10^{28} = 6\cdot80$.	$a_p \times 10^5$.	$a_S \times 10^8 = 6\cdot76$.	$a_P \times 10^{28} = 0\cdot44$.	$a_p \times 10^5$.	$a_S \times 10^8 = 5\cdot20$.
		$K_{p,S}$.		$K_{p,S}$.		$K_{p,S}$.		$K_{p,S}$.	$K_{p,P}$.		$K_{p,S}$.	$K_{p,P}$.		$K_{p,S}$.	$K_{p,P}$.		$K_{p,S}$.
$A_{sol\,\beta}$	2550	$1\cdot2 \times 10^{-5}$	1880	$4\cdot1 \times 10^{-5}$	1060	$2\cdot3 \times 10^{-4}$	800	$4\cdot7 \times 10^{-4}$	$2\cdot8 \times 10^{-13}$	540	$1\cdot1 \times 10^{-3}$	$1\cdot3 \times 10^{-12}$	200	$8\cdot4 \times 10^{-3}$	$3\cdot4 \times 10^{-11}$	71·0	0·52
$A_{sol\,\alpha}$	362	$6\cdot1 \times 10^{-4}$	286	$1\cdot8 \times 10^{-3}$	178	$8\cdot1 \times 10^{-3}$	140	0·015	$9\cdot7 \times 10^{-9}$	98·4	0·034	$3\cdot7 \times 10^{-8}$	40·5	0·21	$5\cdot0 \times 10^{-7}$	15·6	1·07
H_β	64·6	0·019	54·8	0·048	38·8	0·17	32·0	0·29	$6\cdot8 \times 10^{-5}$	24·6	0·54	$1\cdot2 \times 10^{-4}$	11·9	2·39	$7\cdot8 \times 10^{-4}$	5·30	9·25
H_α	39·5	0·051	36·1	0·11	26·8	0·36	22·0	0·62	$6\cdot4 \times 10^{-4}$	17·6	1·06	$1\cdot1 \times 10^{-3}$	8·78	4·38	$4\cdot8 \times 10^{-3}$	4·14	15·2
H^{*}_{α}	25·4	0·12	22·9	0·28	16·8	0·91	13·2	1·72	0·014	11·0	2·66	0·019	5·58	10·9	0·073	2·64	37·3
A	8·25	1·18	7·48	2·58	5·61	8·16	4·70	13·6	6·8	3·69	24·2	13·4	1·87	96·7	51·4	0·87	343
$G^{(s)}$	3·26	7·5	3·76	10·2	4·01	16·0	3·95	19·2	19·2	3·67	24·5	13·9	2·83	42·2	4·3	(1·97)	(67·0)

We can obtain an estimate of the values of ϕ by re-calculating the experiments which were carried out by Kroll[22] on the conversion of KCl with gypsum to syngenite at 0° and 20°,(bb) keeping the reaction under observation for weeks.(cc) These give, after equilibrium has been established, the values of $\left(\frac{n^2_{K^{\cdot}}}{n_{Ca^{\cdot\cdot}}}\right)_\infty$ $(= K(G,S)(\phi)$ at the ionic strength μ_∞, given in Table VII). The resulting values of ϕ seem to be only slightly dependent on temperature and yield plotted against μ_∞ gives a smooth curve from which the values ϕ in the last row of Table VII have been read. The theoretical yields (a) on conversion of KCl (dd) to K_2SO_4 with the aid of the various forms of $CaSO_4$ are listed in Table VIII. The marked dependence on the form of $CaSO_4$ on the one hand, and on temperature on the other hand, stands out clearly.

TABLE VII.

t. °C.	0°.	20°.							
μ_∞	2·83	0·70	1·52	2·40	2·78	2·94	3·26	5·10	6·42
$\left(\frac{n^2_{K^{\cdot}}}{n_{Ca^{\cdot\cdot}}}\right)_\infty$	4·5	3·9	4·4	6·4	7·8	8·6	9·6	20·5	26·3
ϕ	0·60	0·28	0·32	0·46	0·56	0·62	0·69	1·48	1·88
μ_∞	0·5	1·0	1·5	2·0	3·0	4·0	5·0	6·0	6·5
ϕ	0·29	0·28	0·32	0·40	0·64	0·96	1·32	1·72	1·95

TABLE VIII.
$b = 4·0.$

$CaSO_4$.	η (%).		
	Conversion to		
	Syngenite.		Pentasalt.
	0°.	25°.	40°.
$A_{sol\,\beta}$ . .	~100	99	~100
$A_{sol\,\alpha}$ . .	98	94	
H_β . .	92	77	
H_α . .	87	70	96
H_α^* . .	80	58	92
A . .	54	25	19
G . .	25	17	

It will be seen from Table VIII that even calcium sulphates of moderate metastability, such as the hemihydrates,(ee) give large yields under suitable conditions, reaching three, four and even more times that of gypsum. This may also be of technical importance for the conversion of KCl to K_2SO_4 in aqueous solution, particularly as increased output is associated with *each* of the special forms of hemihydrate, so that the problem of exact reproduction to a certain extent recedes.

---

[22] Kroll, *Kali*, 1933, **27**, No. 6-7.

(a) The values are based on the following solubilities of gypsum ($m_{CaSO_4} . 10^3$) —taken from careful graphical smoothing of the numerous data—and activity coefficients (f_{CaSO_4}; see Table I) : 0° : 12·92, 0·442 ; 10° : 14·20, 0·432; 25°: 15·29, 0·414; 40°: 15·49, 0·391; 60°: 14·87, 0·358; 80°: 13·73, 0·323; 31·8: interpolated.

(bb) Experiments at other temperatures cannot be used in this connection.

(cc) A few measurements by D'Ans,[14] from which ϕ could have been calculated as well, are without doubt distorted as, apparently, the equilibrium had not yet been established.

(dd) For room temperature in nearly saturated solution; $b = 4$.

Conclusion.

The thermodynamics of the conversion of KCl to K_2SO_4 in aqueous system with the aid of $CaSO_4$ have been developed. In comparison to other forms of $CaSO_4$, conversion with gypsum is the least favourable over a wide range of temperature. Throughout the entire range the extent of conversion increases as temperature decreases.

We have great pleasure in thanking Palestine Potash Ltd., particularly their Managing Director, Mr. M. A. Novomeysky, and their Director, Mr. G. A. Stolar, for raising the problem and for their kindness in permitting publication. Our thanks are also due to Dr. Tompa for many helpful discussions, and to Mrs. B. B. Silk for her valuable assistance in translation.

(22) Compare the measurements by Jolibois and Chassevent [23] with those by Riddell [24] to see in how far these are often not exactly defined.

[23] Jolibois and Chassevent, *Compt. rend.*, 1924, **178**, 1543.

[24] Riddell, letter to Kelley, see [1].

THE IONISATION POTENTIALS OF POLYATOMIC MOLECULES. I. INTRODUCTION AND THE IONISATION POTENTIALS OF H_2O AND H_2S.

BY W. C. PRICE AND T. M. SUGDEN.

Received 23rd July, 1946.

The importance of ionisation potentials (I.P.) in the study of chemical structure and bonding has become recognised increasingly, since they give the energies required to remove the outer electrons to infinity from an atom or molecule, and it is precisely these electrons which are important in valency considerations.

During the past ten years, a number of papers have been published by Price and collaborators on the spectroscopic determinations of I.P. of a large number of simple molecules in the vacuum ultra-violet, using the convergence limits of Rydberg series. Over a longer period, scattered measurements by various electron impact methods have been made, which have not been so accurate or reproducible. The technique is, however, of wider application since it allows of determinations where no Rydberg series are obtained. This is particularly true of the higher ionisation potentials where the excitation of the more deeply seated electrons often gives rise to wide regions of continuous absorption wherein Rydberg series might be expected to occur.

Experimental.

A review of the various methods which have been employed for the measurement of I.P.'s at different times showed that the method of Mackay [1, 2] gave results which were most closely in agreement with those determined spectroscopically. The use of photo-electrons in preference to thermo-electrons was particularly advantageous in our programme of work on organic molecules since it reduced the possibility of contamination by dissociation products. The major innovation introduced in our method was the calibration of the apparatus with gases whose minimum I.P. had been determined spectroscopically, and whose " vertical " I.P.'s were known to be close to the minimum values. The vertical I.P. may be defined as the energy required to remove the electron without alteration of the interatomic distances.

[1] Mackay, *Phil. Mag.*, 1923, **46**, 828.

[2] Mackay, *Physic. Rev.*, 1924, **24**, 319.

The ionisation tube is shown schematically in Fig. 1. Light from the source S, which was an 80 w. Mercra lamp with the outer glass jacket removed, fell on the nickel target C via a quartz window in the tube. The electrons liberated from C, which was about 1 inch diam., were accelerated towards a target B by a potential, applied to B in steps of 0·05 v. up to a total of 20 v. from a potentiometer system ; B was a nickel cylinder about 3 inches long and 1 inch diam., with its upper edge bevelled to shade the collecting wire W from the reflected light at the source, and its top was covered by a fine-mesh platinum wire gauze.

Ionisation occurred beyond this gauze and the positive ions were collected on W, which was a fine platinum wire supported by a glass rod. The rate of collection of ions was measured with a Compton electrometer, which, with 50 v. on the paddle, had a sensitivity of about 3000 mm./v. The rate of deflection of the electrometer when one pair of plates was earthed and the other pair connected to the collecting wire gave a measure of the relative ion current. Absolute measurements were unnecessary, but the capacity of the charge-collecting system was estimated to be about 15 cm. A special shielded switch was designed to enable the wire W to be earthed between consecutive readings.

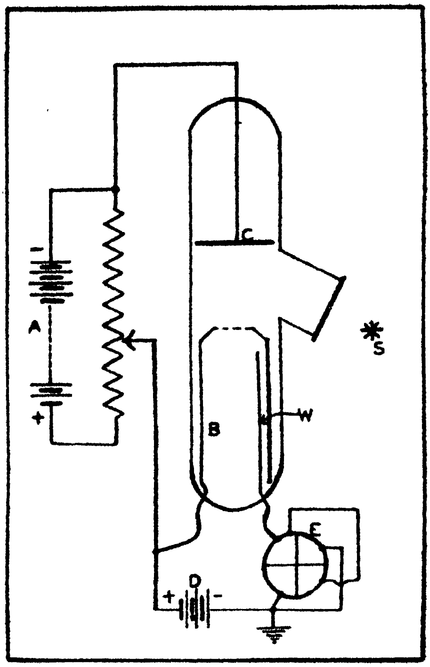

FIG. 1.

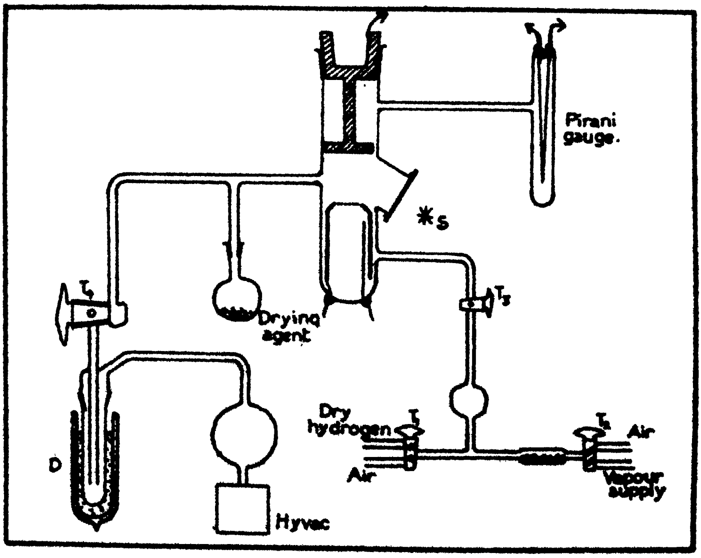

FIG. 2.

The general experimental arrangement is shown in Fig. 2. The tube could be evacuated by a Hyvac pump, vapours being condensed in the trap D. A

Pirani gauge, calibrated against a McLeod gauge for hydrogen and dry air, was attached to the apparatus to allow of rapid test of vacuum periodically, and between runs the system was cleaned out by continuous pumping with a slow steam of hydrogen. After thorough cleaning and pumping, the vapour to be studied was allowed to stream slowly through the apparatus for several minutes with the light source on. An accelerating potential of a few v. above the minimum I.P. was applied, and the vapour supply turned off ; pumping was then continued until the optimum ion current, as measured by the deflection rate, was obtained. A reading of the Pirani gauge was then taken so that the same conditions could be reproduced subsequently.

The accelerating potential was then reduced to a few v. below the minimum I.P. and readings of the positive ion current obtained as the potential was stepped by several v. by intervals of 0·1 or 0·05 v. and then stepped down again. Where a significant divergence occurred between the ion currents in the stepping-up and -down processes for a given potential the run was discarded. In no case did new breaks occur in the ion current-accelerating potential curve on lowering the potential, which would have indicated appreciable photolysis with production of new substances. A retarding potential of 6 v. was maintained between the collecting wire and the cylinder to ensure that only positive ions were collected. When the ion current became too great for accurate measurement of the deflection rate, a screen was placed so as partially to obscure the light source.

The water vapour used was obtained from conductivity water subjected to redistillation in the presence of a little $KMnO_4$. The drying tube shown in Fig. 2 was dispensed with and continuous flow of vapour through a fine capillary with constant pumping used to obtain the requisite pressure.

Hydrogen sulphide was obtained by dropping pure dil. HCl on to FeS, dried with $CaCl_2$ and traces of phosphorus and arsenic were removed by passing through a tube containing iodine. HCl was removed by distilled water and the gas stored by solution in conductivity water until required. Since the I.P.'s obtained for H_2S were below the minimum value for H_2, its presence as an impurity was of no account.

Calibration of the Ionisation Tube.—In view of the large amount of spectroscopic data available on I.P.'s, a calibration was made by obtaining results for the lowest I.P. of a number of substances for which an accurate spectroscopic value was available from Rydberg series. Results are shown in Table I.

TABLE I.

ELECTRON IMPACT AND SPECTROSCOPIC IONISATION POTENTIALS.

Substance.	Electron Impact Value (ev.)	Spectroscopic Value (ev.)	Reference.
Methyl iodide	9·5 ± 0·1	9·49	3
Acetone	10·1 ± 0·1	10·20	4
Carbon disulphide	10·3 ± 0·1	10·027	5
Hydrogen sulphide	10·5 ± 0·1	10·42	6
Methyl chloride	11·3 ± 0·1	11·17	3
Water	12·6 ± 0·1	12·56	6
Carbon dioxide	13·9 ± 0·1	13·73	7
Nitrogen	15·7 ± 0·1	15·58	8

The way in which the electron impact results were deduced from the relevant data may be seen from the accelerating potential-ion current curves for H_2O and H_2S (Fig. 3 and 4). The current below the minimum I.P. was negligible, and was a linear function of the accelerating potential above it except for a transitional region of curvature. The I.P. was obtained by linear extrapolation.

[3] Price, *J. Chem. Physics*, 1936, **4**, 539.
[4] Duncan, *ibid.*, 1934, **2**, 717.
[5] Price and Simpson, *Proc. Roy. Soc. A*, 1938, **165**, 272.
[6] Price, *J. Chem. Physics*, 1936, **4**, 147.
[7] Price and Simpson, *Proc. Roy. Soc. A*, 1939, **169**, 501.
[8] Worley and Jenkins, *Physic. Rev.*, 1938, **54**, 305.

The second two columns in Table I show good agreement and thus no significant correction for contact potentials, etc., appears to be necessary and, within the limits of error, the accelerating potential at which the break in the curve

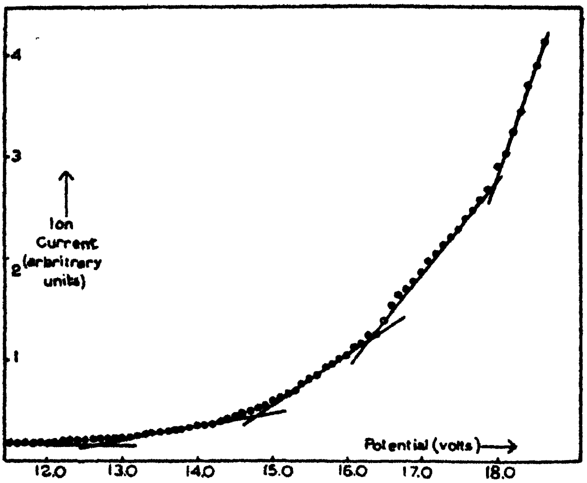

FIG. 3.—Ionisation potentials of water (H_2O).

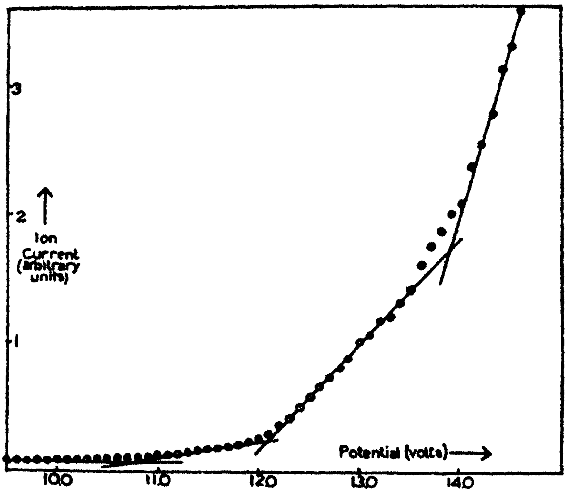

FIG. 4.—Ionisation potentials of hydrogen sulphide.

occurs may be taken as a direct measure of the ionising potential. In all the above cases the electron removed is essentially non-bonding and hence the spectroscopic result will not be very different from the "vertical" value.

Processes Leading to Positive Ion Formation.

In most of the substances examined, one or more breaks in the accelerating potential ion current curve were obtained above the lowest one, and a review of the possible types of explanation of these is now given. They may be divided into two main classes, the first arising from simple ionisation, and the second involving an additional dissociation of the molecule.

1. Production of Undissociated Positive Ions.

(i) Ordinary ionisation in which a single electron is ejected from the molecule without further excitation.

(ii) Ionisation as in (i) with excitation of another electron : very weak double excitation has been obtained by electron impact in He by Whiddington and Priestley,[9] and also in optical spectra, although very weakly. The energy required, in general, will be at least 5 ev. above the minimum I.P., unless the second electron is excited to the orbital vacated by the first. This last case has never been recorded in spectra and is considered very improbable.

(iii) Excitation by electron impact followed by ionisation at a second impact. This, although improbable, cannot be entirely ruled out on theoretical grounds, but appears not to occur in practice since no positive ions have been observed at potentials well below the established minimum values.

(iv) Ionisation by collision with an electron which has already suffered an inelastic impact with another molecule. The lowest potential corresponding with this = (first excitation potential + minimum ionisation potential).

(v) Auto-ionisation—i.e. excitation of an inner electron by impact to a state with a term value higher than that of the minimum I.P., and the possibility of radiationless transition to a positive ion and an electron. The I.P. observed in such a case should coincide with an excitation level, but a linear increase of ion current with accel. potential would be unlikely. This can be ruled out wherever sharp Rydberg series lead to the ionisation potential.

2. Production of Ions with Dissociation.

In these cases, the molecule on impact with an electron may be dissociated into two or more fragments, one of which will be ionised.

(i) The initial positive ion produced is in a repulsive state and hence dissociates into fragments, one of which will be ionised. The I.P. obtained will be equal to the sum of the dissociation energy of the unionised molecule into the same fragments, the I.P. of that fragment which is ionised, and the kinetic energy of separation of the fragments from the repulsive state. This kinetic energy will be of the order of a few ev. for the usual types of potential energy curves.

(ii) A modification occurs if the primary molecular ion (denoted AB_1^+), is itself stable, but by overlapping with a repulsive state AB_2^+ may predissociate into A and B^+. The difference is that the kinetic energy of separation will be much lower, and by assuming it to be zero, Stevenson[10] has calculated reasonable values of the C—H and C—C bond energies from electron impact data. It has been shown that, where alternative predissociation possibilities exist, that the one with the least mutual kinetic energy of separation will predominate.[11] Such an I.P., therefore, will approximate to the sum of the dissociation energy of the molecule and the I.P. of the ionised fragment.

Obvious extensions occur, e.g. predissociation of an excited molecule to give products, one of which ionises in the course of dissociation, in which case the I.P. would correspond with an excitation level of the undissociated molecule, as well as the sum of dissociation and ionisation of product energies. Wherever relevant, in this and subsequent papers, processes of the above types will be considered. The possibility of ionisation at a ternary impact of two molecules and an electron is discussed below in the case of the I.P. of H_2O at 14 v.

Results and Discussion.

I. Water.

The accelerating potential-positive ion current curve (Fig. 3) shows four distinct breaks, at 12·6 ± 0·1 v., 14·5 ± 0·3 v., 16·2 ± 0·3 v., and 18·0 ± 0·5 v. respectively. Before reviewing these in the light of the various excitation possibilities, a brief summary of the results of previous investigators is given for comparison purposes. Fig. 3 for convenience shows all the breaks on one curve. The individual I.P.'s were obtained

---

[9] Whiddington and Priestley, *Proc. Roy. Soc. A*, 1924, **145**, 462.

[10] Stevenson, *J. Chem. Physics*, 1942, **10**, 292.

[11] Rollefson and Burton, *J. Chem. Physics*, 1938, **6**, 674.

THE FARADAY SOCIETY

The following papers have been accepted for publication. (This list does not include papers presented at General Discussions.)

Author(s).	*Title.*	*Date Received.*
1. Read, J. H. and Lloyd, D. M. G.	The Thermal Conductivity of Organic Materials near the Melting Point.	21 10 46 as revised 19 9 47
2. Bolland, J. L.	Kinetic Studies in the Chemistry of Rubber and Related Materials. Part VI.	18 9 47
3. Woodward, L. A. and Glover, A. T.	Molybdenum Oxide Catalysts for the Reduction of Phenol to Benzene.	7 10 47
4. Crawford, V. A. and Tompkins, F. C.	The Adsorption of SO_2, NH_3, CO_2 and N_2O on BaF_2 Crystals.	1 10 47
5. Coulson, E. A. and Herington, E. F. G.	Fractional Distillation. I. The Selection of Test Mixtures for Estimating the Efficiency of Fractionating Columns.	14 7 47
6. Coulson, E. A., Hales, J. L. and Herington, E. F. G.	Part II: The Use of Dilute Solutions of Thiophene in Benzene as Test Mixtures and a Comparison with Mixtures of Benzene and Ethylene Dichloride.	14 7 47
7. Robertson, A. J. B.	The Thermal Decomposition of Explosives. Part I: Ethylenedinitramine and Tetryl.	26 9 47
8. Lauder, I.	Studies on Hemiacetal Formation. Part I: The System Acetaldehyde-Water.	16 12 47
9. Copp, J. L. and Ubbelohde, A. R.	Physico-Chemical Processes at High Pressures and Temperatures. Parts I and II.	11 8 47
10. Pink, R. C. and Ubbelohde, A. R.	On Some Properties of Cyclo-Octatetraene in Relation to Structure.	16 10 47
11. Pearson, J.	The Reduction of Nitrocompounds at the Dropping-Mercury Cathode. Part I: The Nitrobenzenes and Nitrotoluenes.	30 8 47
	Part II: The Nitrophenols.	30 8 47
12. Berg, W. F.	A New Cause of Low-intensity Reciprocity Failure.	24 11 47
13. Durie, R. A. and Iredale, T.	Emission Bands from the Electrodeless Discharge in Carbon Tetrabromide Vapour.	8 12 47
14. Butement, F. D. S.	Absorption and Fluorescence Spectra of Bivalent Samarium, Europium and Ytterbium.	27 6 47

Author(s).	*Title.*	*Date Received*
15. Small, P. A., Small, K. W. and Cawley, P.	The Vapour Pressures of Some High Boiling Esters.	16 12 47
16. Booth, F.	A Note on the Theory of Surface Diffusion Reactions.	24 11 47
17. Sinha, P. C. and Ray, R. C.	Pyridine Complexes of Metallic Perchlorates. Part II: Dissociation Pressures and Pressure-Composition Isothermals of Copper Pyridine Perchlorates.	20 11 47
18. Lauder, I. and Green, J. H.	The Mechanism of Formation of Diethyl Ether using the Heavy Oxygen Isotope ^{18}O as a Tracer Element.	16 12 47
19. Levine, S.	On the Interaction of Colloidal Particles. II: Discussion of Basis of Theory.	1 1 48
20. Birch, A. J. and MacDonald, D. K. C.	The Nature of Metal-Ammonia Solutions. Part II.	5 11 47
21. Flett, M. St. C.	Characteristic Infra-Red Frequencies and Chemical Properties of Molecules.	27 10 47
22. Powles, J. G.	The Effect of Molecular Inertia on Dielectric Absorption.	4 12 47
23. Everett, A. J. and Minkoff, G. J.	A Note on the Ultra-violet Absorption Spectrum of Formaldehyde.	18 12 47
24. Egerton, A., Harris, E. J. and Young, G. H. S.	Observations on the Slow Combustion of Hydrocarbons. Part I.	9 10 47
25. Egerton, A. and Young, G. H. S.	Observations on the Slow Combustion of Hydrocarbons. Parts II and III.	9 10 47
26. Harris, E. J.	A Note on the Decomposition of Hydrogen Peroxide and the Possibility of its Formation during the Slow Combustion of Hydrocarbons.	9 10 47
27. Whytlaw-Gray, R. and Teich, N.	The Mercury Meniscus in Precision Measurements on Gases.	10 11 47
28. Bannerjee, T. and Allmand, A. J.	Experiments on the Electrodeposition of Brass from Cyanide Solutions.	19 12 47
29. Melville, H. W. and Watson, W. F.	Inhibition and Retardation in Polymerisation Reactions.	8 12 47

by drawing particular parts of this with suitably chosen ordinates to give a marked change of slope; this applies particularly to the minimum value.

(*a*) **Minimum Ionising Potential** (12·6 v.).—This result is not independent in so far as water was used as one of the calibrating substances on the basis of the value of 12·56 ± 0·01 v. reported by Price,[6] but the value of 12·6 v. obtained here is highly satisfactory and shows that no appreciable correction has to be made to the values obtained in the present apparatus. Another spectroscopic result of 12·7 ± 0·2 v. had been given previously by Henning.[12] There are numerous electron impact results, ranging from 12·59 v. (Smith and Bleakney[13]) to 13·2 v. in the work of Mackay,[1] who used the present method. The most recent value is that of Mann, Hustrulid and Tate[14] who give 13·2 ± 0·2 v.

(*b*) **Second Ionising Potential** (~ 14 v.).—An I.P. at 14·4 ± 0·3 v. has been recorded by Mann *et al.* (loc. cit.) and a small subsidiary break in a mass spectrograph analysis (Smyth and Mueller[15]) in the same region. No spectroscopic value has been recorded.

(*c*) **Third Ionising Potential** (~ 16 v.).—In this case both spectroscopic and electron impact results of 16·0 ± 0·5 v. have been cited by Henning (loc. cit.) and Smyth and Mueller (loc. cit.); Mann, *et al.* do not find it.

(*d*) **Fourth Ionising Potential** (~ 18 v.).—Mann *et al.*[14] report a value at about 18 v., as do also Smyth and Mueller[15] at 18·9 v. It thus appears that there is previous evidence for the appearance of ionic species at all the values of accelerating voltage obtained here, but no investigator reports all of them, with the exception of Smyth and Mueller, who are somewhat uncertain about the 14 v. result.

It is clear that it is necessary to discuss the result in the light of the molecular orbital theory as developed principally by Mulliken and Lennard-Jones (linear combination of atomic orbitals approximation), since each I.P. may be linked with some definite molecular orbital. Mulliken[16] formulates H_2O as follows:

$$\underset{\text{O}}{[2sa_1]^2}\quad \underset{\text{H—O—H}}{[yb_2]^2}\quad \underset{\text{H—O—H}}{[za_1]^2}\quad \underset{\text{O}}{[2xb_1]^2}\,;\ {}^1A_1$$

The nuclear framework, which has symmetry C_{2v}, has the x and z planes of symmetry, and the z twofold axis. The orbitals above are linear combinations of H (1*s*) and O (2*s* and 2*p*), which are irreducible representations of C_{2v} denoted by the second letter in the brackets. They behave under the symmetry operations of C_{2v} as indicated in the comprehensive tables of Mulliken.[17] Formulation of the *s* orbitals with spherical symmetry and the *p* orbitals with axial symmetry and a node at the origin with positive and negative lobes on opposite sides of it shows that the $2xb_1$ orbital is a pure $2p_x$ of oxygen, that the orbitals of yb_2 and za_1 types overlap positively in the atomic orbitals, giving rise to bonding and that the sa_1 will not contribute much to the bonding on account of the smaller overlap of 1*s* of H and 2*s* of O, although hybridisation of $2sa_1$ and za_1 may occur. The symbols under each orbital give a rough idea of the bonding in accordance with the foregoing remarks.

It may be regarded as proved that the I.P. at 12·6 v. is due to ionisation of the non-bonding $2xb_1$ from the spectroscopic evidence of Price,[6] showing that the ionisation is the culmination of a Rydberg series, the main members of which are accompanied by very little vibrational structure. The value predicted by Mulliken[18] for this change ($O(s^2p^4, V_2) \rightarrow O(s^2p^3, V_3)$)

---

[12] Henning, *Ann. Physik.*, 1924, **13**, 599.
[13] Smith and Bleakney, *Physic. Rev.*, 1924, **24**, 319.
[14] Mann, Hustrulid and Tate, *ibid.*, 1940, **58**, 340.
[15] Smyth and Mueller, *ibid.*, 1933, **43**, 116.
[16] Mulliken, *J. Chem. Physics.*, 1935, **3**, 506.
[17] Mulliken, *Physic. Rev.*, 1933, **43**, 279.
[18] Mulliken, *J. Chem. Physics*, 1934, **2**, 782.

is 14·7 v., and the difference is set down to charge transfer effects, i.e. a drift of negative charge from the hydrogen atoms towards the more electronegative oxygen, which is also partially responsible for the dipole moment.

The positive ion resulting from this process has the structure $[2sa_1]^2 [yb_2]^2 [za_1]^2 [xb]_1$; $^2B_1$, and is probably involved in the following way with the highest I.P. obtained (18·0 v.). The results of Mann, *et al.* give a value at 18·5 v., which they showed by the mass spectrograph to be bound up with dissociation into $OH^+ + H$, or $OH + H^+$, both processes occurring with about the same energy change. If the products are in the ground state, $OH^+(^3\Sigma^-) + H(^2S)$, or $OH(^2\Pi_{inv.}) + H^+$ result, either being possible from a $^2B_1$ state of H_2O. Hence the transition,

$$OH(^2\Pi_{inv.}) \rightarrow OH^+(^3\Sigma^-)$$

requires 13·6 v. as a maximum value for the I.P. of the OH group if the change, $H_2O\ (^1A_1) \rightarrow (OH(^2\Pi_{inv.}) + H(^2S)$ occurs with absorption of 5·1 v. It is of interest that this falls approximately half-way between the predicted value of Mulliken of 14·7 v. for the valency state of O and the minimum of I.P. of H_2O (effectively two OH groups from the charge transfer aspect).

The intermediate values at ∼ 14 v. and ∼ 16 v. remain to be discussed. The potentials at which they appear are too small to allow of dissociation into an ion and an uncharged group, which requires at least 18 v. Mann *et al.* suggest that the lower value is due to the process,

$$H_2O^+ + H_2O \rightarrow H_3O^+ + OH$$

since the intensity of this ionisation in their work depended on the square of the pressure. The present work did not include systematic investigation of pressure dependence. Several comments are, however, necessary. Firstly, if the process took place in stages by ionisation followed by collision of $^2B_1$ H_2O^+ with an H_2O molecule there is no apparent reason for appearance of H_3O^+ at a given potential since it is very improbable that kinetic energy is imparted to it at the original electron impact, and further, a direct dependence on pressure would result if H_2O^+ had a long life. The appearance of H_3O^+ at a definite potential is more readily explained by ternary collision $2H_2O + e$ with direct production of H_3O^+ and OH, which would be, however, a relatively rare occurrence, or alternatively by the production of a new species of H_2O^+ capable of undergoing rapid reaction with H_2O. Such an ion could be $[2sa_1]^2 [yb_2]^2 [za_1] [2xb_1]^2$; $^2A_1$. A definite decision would necessitate the careful study of the effects of pressure and intensity of the bombarding stream. The absence of a spectroscopically determined level is explicable here if the $^2A_1$ ion is of very short life. Rydberg series do, however, lead to a value of about 16·0 v. (Henning, loc. cit.) and mass spectrography (Smyth and Mueller, loc. cit.) has shown it to be due to appearance of H_2O^+, presumably in a new electronic state. If the value of 14·5 v. is to be ascribed to the ionisation of za_1, then this obviously is connected with the other bonding orbital yb_2. Estimates of $\frac{1}{2}(I_H + I_O)$ (Mulliken [19]) gives 15·3 v. as a predicted value for an electron of this type shared between O and H, to which is to be added 1-2 v. on account of the bonding stabilisation, and from which is to be subtracted a charge transfer effect of the same order. In the absence of precise data on these effects the agreement with the experimental result is tolerably good.

As the bond angle increases from 0 to 180° in H_2O, the whole of the bonding is gradually transferred from the za_1 electrons to the yb_2, with about equal contributions at 90° (Mulliken [19]). At 105° the two orbitals would have not very different energy levels, and there is a possibility that both za_1 and yb_2 ionise at 16·0 v., this is, however, difficult to reconcile with the peculiar behaviour at about 14 v. Table II briefly summarises the evidence.

---

[19] Mulliken, *J. Chem. Physics*, 1935, **3**, 586.

TABLE II.

I.P. (v.)	Interpretation.
12·6 ± 0·1 . .	Ionisation of non-bonding $2xb_1$.
14·5 ± 0·3 . .	Uncertain : suggested ionisation of za_1 with subsequent rapid reaction, $H_2O^+ + H_2O \rightarrow H_3O^+ + OH$.
16·2 ± 0·3 . .	Ionisation of yb_2 (also of za_1 if the value at 14·3 v. is misattributed).
18·0 ± 0·5 . .	Ionisation of $2xb_1$ with dissociation into $OH^+ + H$ or $OH + H^+$.

The variation in the minimum I.P. as reported by various investigators can be ascribed, on the one hand, to experimental errors and on the other, to differences in the mode of calibration of the apparatus, bearing in mind the concept of verticality mentioned above. As far as the other I.P.'s are concerned, it is not surprising that they do not all appear as the culminations of Rydberg series in spectroscopic determinations since, apart from possible obscuring by superimposed predissociation continua, the highest value corresponds with a dissociation process, and the other two with bonding electrons. This is responsible for the wide limits of error in the result of Henning [12] at 16 ± 0·5 v. On the other hand there seems to be no apparent reason for the absence of this particular I.P. in the electron impact work of Mann *et al.*[14], it being well established both by previous electron impact work and spectroscopically. There is most doubt concerning the I.P. at 14·5 v. which it is clear from the discussion above demands further study. An extension of this type of interpretation to hydrogen sulphide will next be attempted.

II. Hydrogen Sulphide.

Three marked changes of slope in the accelerating potential ion current curve have been observed up to 15·5 v. viz. (Fig. 4), at 10·5 ± 0·1 v., 12·2 ± 0·2 v., and 14·0 ± 0·2 v. respectively. Previous results are available for the minimum I.P. only, using both types of measurement—spectroscopically by Price [8] at 10·42 v. and by electron impact by Bartlett [20] and Mackay,[9] both at 10·4 v. The minimum here, although subject to the same calibration limitations as that for water, is in good agreement.

On molecular orbital theory, the electronic formula, neglecting the inner obitals of the sulphur atom, may be written as follows :

$$\begin{array}{llllll} C_{2v}\,; & [3sa_1]^2 & [yb_2]^2 & [za_1]^2 & [3xb_1]^2\,; & {}^1A_1 \\ & \mathrm{S} & \mathrm{H{-}S{-}H} & \mathrm{H{-}S{-}H} & \mathrm{S} & \end{array}$$

The minimum value is obviously associated with removal of the $3xb_1$ electron, derived from $3p_x$ of S, as has been pointed out by Price.[8] The predicted value for such an electron is 10·8 v. (Mulliken [21]), the small difference, compared with that of ~ 2 v. in H_2O being attributed to the smaller electronegativity between H and S, and the length of the S—H bond (1·35 A.) as compared with OH (1·01 A.).

When the higher values are considered, the predicted value of $\frac{1}{2}(I_S + I_H)$ for the S—H bond is 13·4 v., using the valency state data. Both charge transfer and bonding corrections will be less than in H_2O, and the above figures therefore compares quite well with the mean of the two higher I.P.'s (13·1 v.). The obvious suggestion is that the I.P.'s of the H—S—H bonding orbitals yb_2 and za_1 are 14·2 and 12·2 v. respectively.

---

[20] Bartlett, *Physic. Rev.*, 1929, 33, 169.

[21] Mulliken, *J. Chem. Physics*, 1935, 3, 514.

Bartlett found the appearance potentials of SH^+ and S^+ to be 16·9 and 15·8 v. respectively, which are well above the values obtained here, and there is thus no evidence that dissociation processes occur in the present work, although the predicted appearance potentials of S^+ and SH^+ are 13·3 and 14·2 v. respectively, taking the values of 3·8 v. and 4·6 v. for the S—H and H—H linkages.[22] The discrepancy might be accounted for by kinetic energy of dissociation products, but in the absence of further data, these speculations will not be pursued, and the simpler ascription of the I.P.s given above adhered to. One point worth mentioning, however, is that the theory indicates that for a bond angle not far removed from 90°, as is the case in H_2S, the two pairs of bonding electrons should have equal bonding contributions, and it is therefore a little surprising that their I.P.'s are 2 v. apart.

Summary.

The paper is an introductory one in a series on the ionisation potentials of polyatomic molecules as determined by electron impact methods. The apparatus and technique which have been found to give the most reliable results are described. The I.P.'s of water and hydrogen sulphide are given and interpreted in the light of molecular orbital theory.

Laboratory of Physical Chemistry,
Cambridge.

---

[22] Pauling, *Nature of the Chemical Bond* (Cornell University Press, Ithaca, N.Y., 1939).

[23] Compton, *Physic. Rev.*, 1919, 14, 85.

THE IONISATION POTENTIALS OF POLYATOMIC MOLECULES. II. THE IONISATION OF SIMPLE ALDEHYDES AND KETONES.

BY T. M. SUGDEN AND W. C. PRICE.

Received 23*rd July*, 1946.

The experimental details of the method of electron impact measurement of ionisation potentials (I.P.'s) used in the present work has been completely described.[1] The I.P.'s of formaldehyde, acetaldehyde and acetone, being the simplest set of compounds characteristed by the grouping $>C{=}O$ have been measured. It is well known that the double bond in these compounds is associated with high polarity, and hence it is to be expected that their I.P.'s will be strongly affected by charge transfer. Previous results are available for the minimum I.P.'s in some cases and will be referred to under separate headings. The work described below also gives values for some of the more strongly bound electrons. In all cases spectroscopically pure substances were used.

---

[1] Price and Sugden (previous paper).

[2] Price and Collins, *Physical Rev.*, 1935, 48, 714.

I. The Ionisation Potentials of Formaldehyde.

The I.P.'s of this molecule, as well as its electronic structure, may be explained most clearly by considering it as intermediate between the isoelectronic molecules O_2 and C_2H_4 (using LCAO molecular orbital theory), since a direct gradation would be expected were it not for the existence of charge transfer effects which also give rise to the large dipole moment in H_2CO.

(*a*) **Oxygen.**—The structure of oxygen may be written:

$$O_2 ;\ KK(\sigma_g 2s)^2 (\sigma_u 2s)^2 (\pi_u 2p)^4 (\sigma_g 2p)^2 (\pi_g 2p)^2 ;\ {}^3\Sigma_g,$$

using standard molecular orbital notation; $\Pi_g 2p$ and $\sigma_u 2s$ are antibonding, the rest bonding orbitals. The I.P.'s of the upper three of these orbitals may be calculated using the valence state data given by Mulliken.[3] A valence state may be considered to be an electronic state of an atom which only has significance for the combined atom. A table is given below in which Mulliken's data for the term values for valence states of O and O^+ have been combined so as to give the required I.P.'s of the O_2 molecule. Each valence state is represented by a structure in terms of *s* and *p* electrons (split into σ and π) and denoted by the symbol *V* with a suffix equal to the number of unpaired electrons in the structure.

Valence State of O in O_2.	Valence State of O in O_2.	Predicted I.P. (ev.).	State of O_2 in Ion Produced.
$s^2\pi^2\pi\sigma$; V_2	$s^2\pi^2\sigma$: V_1	16·2	${}^2\Pi_g$
,,	$s^2\pi\pi\sigma$; V_3	15·2	${}^2\Pi_u$
,,	$s^2\pi^2\pi$; V_1	17·2	${}^4\Sigma_g^-$

The following results were obtained spectroscopically by Price and Collins,[2] in agreement with previous electron impact work: 12·2 ± 0·2 v., (O_2^+ as ${}^2\Pi_g$), 16·2 ± 0·1 v., (O_2^+ as ${}^2\Pi_u$), and 18·2 ± 0·1 v., (O_2^+ as ${}^4\Sigma_g^-$). Deviations from the predicted results will occur for two reasons: (i) a lowering due to antibonding or an increase due to bonding; (ii) a lowering due to charge transfer, which in this case implies interpenetration of similar electronic shells, thereby reducing the effective atomic number of the nuclei. $\pi_u 2p$ and $\pi_g 2p$ are relatively weakly bonding and antibonding respectively and to a first approximation will be similarly affected by charge transfer and also by the bonding effect, except that the latter will be in opposite senses for the two cases. If this is so, the calculated and theoretical values can be reconciled by a charge transfer reduction of 1·5 v. and a bonding effect of ± 2·5 v. A related figure is the increase in binding energy between the nuclei in passing from O_2 (${}^3\Sigma_g^-$) to O_2^+(${}^2\Pi_g$).[4] $\sigma_g 2p$ appears to show an effect very similar to that of $\pi_u 2p$.

(*b*) **Ethylene.**—This molecule is isoelectronic with O_2 when considered on molecular orbital theory, and a set of orbitals for the planar molecule has been drawn up by Mulliken[5] (see also Fig. 1).

$$\underset{H_2C—CH_2}{(s+s,\ a_{1g})^2}\ \ \underset{H_2C\longleftrightarrow CH_2}{(s-s,\ b_{1u})^2}\ \ \underset{CH_2}{(yb_3)^2}\ \ \underset{CH_2}{(yb_2)^2}\ \ \underset{H_2C—CH_2}{(\sigma+\sigma,\ a_{1g})^2}\ \ \underset{C—C}{(x+x,\ b_{2u})^2};\ {}^1A_{1g}$$

The first set of letters inside each bracket refers to the linear combination of atomic orbitals to which the molecular orbital approximates, *s*, *y*, σ, *x* refer to 2*s*, $2p_y$, ,, ,, of C respectively, σ being used to denote an orbital with axial symmetry along the C—C line. The second symbol denotes the representation of the point group (V_h) of the nuclear skeleton to which the particular orbital conforms and hence gives the symmetry properties of the orbital. The final symbol states the overall symmetry and multiplicity. In the second line the bonding is indicated qualitatively; ←→ denotes antibonding. Experimental values are available for the minimum I.P. only; Price [6] gives 10·41 v. determined spectroscopically, and Kallman and Dorsch [7] 10·0 v. by an electron impact method.

---

[3] Mulliken, *J. Chem. Physics*, 1934, **2**, 784.

[4] Herzberg, *Molecular Spectra and Molecular Structure* (Prentice-Hall, N.Y., 1939), vol. I, p. 393.

[5] Mulliken, *J. Chem. Physics*, 1935, **3**, 564.

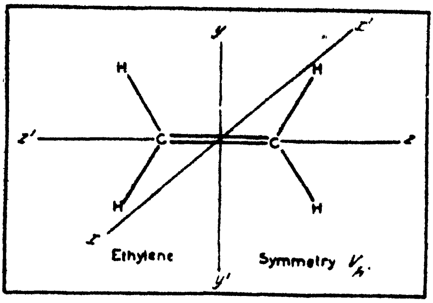

FIG. 1.

This corresponds with removal of the $x + x$ electrons, which provide the bonding of so-called π type in C=C; its predicted value from valence states is 11·2 v., i.e., the orbital is formed only from carbon $2p_x$ electrons. The lowering of the experimental below the predicted value is much less than in O_2 since here the orbital is bonding, even through the small $\overset{+}{H}$—C dipoles may exert an appreciable charge transfer effect.

Prediction for the other electrons considered in the previous case is difficult since $\sigma + \sigma$ may hybridise with $s + s$, the only experimental value available being one of ~ 12 v. for the minimum I.P. of ethane, which is for an electron of $\sigma + \sigma$ type; [8] yb_2 will be expected at about 14·5 v.—not far from the value for methane (Mulliken [5]), although here, on account of the shortness of the bond, hybridisation to $(y + y)^2 (y - y)^2$ might occur.

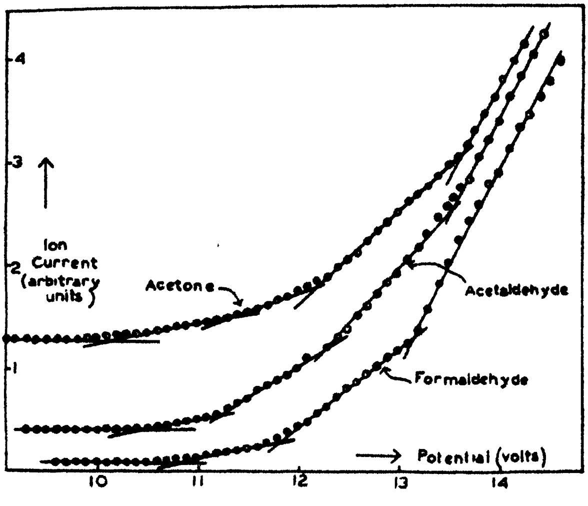

FIG. 2.—Ionisation potentials of H_2CO, CH_3CHO and $(CH_3)_2CO$.

(c) **Formaldehyde.**—The present work gives I.P.'s at 10·8 ± 0·1 v., 11·8 ± 0·2 v., and 13·1 ± 0·2 v., which are shown in Fig. 2. The lowest has been reported previously by Price[9] at 10·82 v., this value being used in calibrating the present apparatus,[1] and by Jewitt[10] at 11·3 ± 0·5 v. using a molecular beam method.

---

[6] Price, *Physical Rev.*, 1935, **47**, 444.
[7] Kallman and Dorsch, *Abh. Kaiser-Wilhelm Institut*, 1929, **12**.
[8] Mulliken, *J. Chem. Physics*, 1935, **3**, 517.

Mulliken[11] has evolved the following molecular orbital structure (see Fig. 3).

$$\begin{array}{cccccc} (2s)^2 & (sa_1)^2 & (x_0 + x_c)^2 & (yb_2)^2 & (z_0 + z_c)^2 & (2p_y b_2)^2,\ {}^1A_1 \\ \mathrm{O} & \mathrm{H_2C{-}O} & \mathrm{O{-}C} & \mathrm{CH_2} & \mathrm{O{-}CH_2} & \mathrm{O} \end{array}$$

The similarity of this structure with that for ethylene becomes apparent when it is pointed out that $2p_y b_2$, $z_0 + z_c$, $x_0 + x_c$ of formaldehyde correspond with one yb_2, $\sigma + \sigma$, and $x + x$ of ethylene respectively. Here, as was pointed out by Price,[9] the absence of much vibrational structure in the Rydberg series leading to the first I.P. implies that $2p_y b_2$, which is the most easily removed electron, is almost non-bonding, and consequently not strongly hybridised with yb_2 of CH_2. Thus all the decrease from 14·7 v. predicted for the O atom for its valence state in these conditions[11] must be attributed to charge transfer effects. The dipole moment in C—O is about 2·5 D. in the direction $\overset{+}{\mathrm{C}}$—$\overset{-}{\mathrm{O}}$.

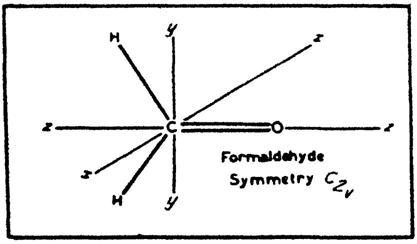

FIG. 3.

This leaves the $z_0 + z_c$ and $x_0 + x_c$ electrons which provide the σ and π bonding of the C=O group to be accounted for. The predicted I.P.'s from valence state data on the basis of the simple equation $I = \frac{1}{2}(I_c + I_0)$ are about 14 v. The charge transfer, which is largely due to these electrons, may be examined as follows. The coefficient of ψ_0 in the LCAO approximations to $z_0 + z_c$ and $x_0 + x_c$ of the form $\psi = a\psi_0 + b\psi_c$ will be much greater than that of ψ_c on account of the large electronegativity difference, and therefore the effective atomic number of the O atom will be more important than that of the C atom in determining the I.P. Consequently a reduction in I.P. is predicted which will probably have about the same value in both cases. The effect will be smaller than for the non-bonding electron on account of the stabilisation by the positive charge on the C atom. The bonding contribution of the $z_0 + z_c$ will be of the order of the 2·5 v. ascribed to the σ bond of O_2 above, and that of $x_0 + x_c$ considerably less. These qualitative arguments show that 11·9 v. and 13·1 v. are by no means unreasonable values for the I.P.'s of $x_0 + x_c$ and $z_0 + z_c$ respectively, to which they will be ascribed in the absence of evidence to the contrary. It is not likely that the I.P. at 13·1 v. is associated with C—H bonding electrons since these will have I.P.'s not far removed from that for methane (14·5 v.). It appears that extension of the readings to higher potentials with a view to finding the I.P.'s of still deeper electrons would be difficult on account of the possibility of dissociation processes occurring.

Photolysis of H_2CO by $H_2CO + h\nu \rightarrow H_2 + CO$ in ultraviolet light is known to occur but the minimum I.P.'s of H_2 and CO (16·0 v. and 14·1 v. respectively) lie well above the recorded results, and as impurities they would thus be unimportant. Since the runs on H_2CO gave the same ion currents for a given accelerating potential over the period of a run, such dissociation was considered to be negligible. All the above points have been summarised in a table.

---

[9] Price, *J. Chem. Physics*, 1935, **3**, 256.
[10] Jewitt, *Physic Rev.*, 1934, **46**, 616.
[11] Mulliken, *J. Chem. Physics*, 1935, **3**, 514.

IONISATION POTENTIALS OF O_2, H_2CO, C_2H_4

Molecule.	Corresponding Orbitals.				Corresponding Orbitals.				Corresponding Orbitals.			
	Name	I.P. obs.	I.P. pred.	Notes.	Name.	I.P. obs.	I.P. pred.	Notes.	Name.	I.P. obs.	I.P. pred.	Notes.
O_2	$(\pi_g 2p)^2$	12·2	16·2	Decrease due to C.T. and A.B.	$(\pi_u 2p)^4$	16·2	15·2	Decrease due to C.T. Increase due to B.	$(\sigma_g 2p)^2$	18·2	17·2	Decrease due to C.T. Larger increase due to B.
H_2CO	$(x_0+x_c)^2$	11·8	14·0	Decrease due to C.T. offset by B.	$(2p_y b_2)^2$	10·8	14·7	Decrease due to C.T. (N.B.)	$(z_0+z_c)^2$	13·1	14	Decrease due to C.T. largely offset by B.
					$(yb_2)^2$	—	14·5	Not Obs.				
C_2H_4	$(x_0+x_c)^2$	10·4	11·2	Decrease due to C.T. offset by B.	$(yb_2)^2$	—	14·5	Not obs.	$(\sigma+\sigma)^2$	—	~13	Not obs.
					$(yb_2)^2$							

C.T. ≡ Charge Transfer. B ≡ Bonding. A.B. ≡ Anti-Bonding. N.B. ≡ Non-Bonding.

Correlation with Long Wavelength Spectrum of Formaldehyde.—McMurry[12] has ascribed the absorption around λ 2900 A., which is very weak, to a forbidden transition from $2yb_2$ (called Y_0 in this section) to an orbital of type $(x_0 + x_c)$, which is π antibonding. This will be called X_2 and the transition $N \rightarrow E_1$.

A transition from the lowest $(x_0 + x_c)$ of H_2CO (called X_1) is denoted $N \rightarrow V_1$, using the notation of Mulliken[13] for "charge transfer spectra"; this is an allowed transition and is ascribed to the strong absorption at λ 1500 A. The fairly strong bands at λ 1750 A. are ascribed to an excited orbital of type $(z_0 + z_c)$ to which Y_0 is excited, the transition being denoted $N \rightarrow F_1$, and the upper orbital Z_2. The whole scheme is shown in Fig. 4.

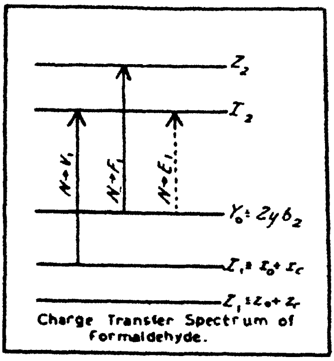

Charge Transfer Spectrum of Formaldehyde.

FIG. 4.

This suggests the I.P. of X_1 as ∼ 15 v., taking Y_0 as 10·8 v., which shows a large discrepancy with the value of 11·8 v. ascribed to it above. The discrepancy obviously arises from the interaction between the electrons, i.e. the effective nuclear charges are different for the configurations $(X_1)^2(Y_0)(X_2)$ and $(X_1)(Y_0)^2(X_2)$ by a factor of ∼ 3 v. on account of a difference in screening.

In the $N \rightarrow E_1$ change, a charge transfer takes place to the C atom, and rather the reverse in the $N \rightarrow V_1$ transition since the electronegativity difference is more pronounced for the σ than the π bonding or antibonding states. At the same time the introduction of antibonding in the two cases will result in an increase of the C—O bond length. Both these changes imply that removal of the electron in the excited orbital would require more energy in the configuration $(X_1)^2(Y_0)(X_2)$ than in $(X_1)(Y_0)^2(X_2)$ when the bonding stabilisation has been taken into account. That is, the difference between the transitions, $N \rightarrow E_1$ and $N \rightarrow V_1$, will be greater than the difference between the ionisation potentials of $Y_0(2yb_1)$ and $X_1(x_0 + x_c)$ electrons. The difference qualitatively predicted here is apparently about 3 v. in magnitude, if the I.P. interpretation is correct, but until a classification of the effects summed up under the general heading of charge transfer has been made, quantitative prediction of these apparent discrepancies is not possible. Similar disparities appear in all charge transfer spectra, giving rise to divergences in the $N \rightarrow V$ transitions, as well as in the ionisations (see Price and Walsh[14]).

II. The Ionisation Potentials of Acetaldehyde.

The experimental results obtained for acetaldehyde are shown in Fig. 2, the curve being shifted along the *y*-axis for clarity. The molecular orbital formula may be written in a similar way to that of formaldehyde,

$$\underset{\text{O}}{(2s)^2}\ \underset{\text{CH}_3}{(s)^2}\ \underset{\text{HCC—O}}{(s)^2}\ \underset{\text{C—O}}{(x+x)^2}\ \underset{\text{HCC}}{(y)^2)}\ \underset{\text{HCC—O}}{(z+z)^2}\ \underset{\text{CH}_3}{(\pi)^4}\ \underset{\text{O}}{(2p_y)^2};\ {}^1A,$$

the symmetry of H_2CO having been largely destroyed. To this is to be fitted the experimental data, i.e., breaks in the ion current curve at 10·4 ± 0·1 v., 11·3 ± 0·1 v., 12·3 ± 0·1 v., and 13·5 ± 0·2 v.

[12] McMurry, *J. Chem. Physics*, 1941, **9**, 231.
[13] Mulliken, *ibid.*, 1939, **7**, 121.
[14] Price and Walsh, *Proc. Roy. Soc. A*, 1940, **1740**, 220.

The lower three values are obviously related to those of formaldehyde. The new value at 13·5 v. obviously corresponds with the introduction of a CH_3 group, and has also been found in other series of compounds when this group is attached to a C atom in place of a hydrogen atom. It is clearly to be associated with ionisation in the C—C bond, bearing in mind the possible hybridisation between the y and s electrons bonding in this respect (i.e. ionisation to $(y)^{-1}$ occurs at 13·5 v.).

The minimum I.P. corresponds with removal of the non-bonding $2p_y$ and is known very accurately from the spectroscopic measurements by Walsh [15] to be 10·1811 ± 0·0001 v. The difference between the results of the two methods may be ascribed to lack of " verticality " in the spectroscopic case, or more likely to an error of about 0·2 v. in the calibration of the present apparatus. The decrease of 0·4 v. below the corresponding formaldehyde value is due to the extra charge transfer on substituting a CH_3 for an H atom, tending to decrease the effective nuclear charge of the O atom (cf. the " inductive " effect in the benzene nucleus in toluene). The shift may be compared with that of 0·2 v. which has been obtained in going from methyl to ethyl alcohols.[16] The greater value is possibly associated with the relatively shorter bond system in the aldehydes.

Similar shifts are found for the next two lowest I.P.'s, which on the basis of the treatment of H_2CO may reasonably be ascribed to the $(x + x)$ and $(z + z)$ electrons, forming the π and σ contributions respectively to the C=O bonding. No higher values were investigated : (π) of CH_3 is expected to appear in the region of 14·5 v., the I.P. of CH_4.

III. The Ionisation Potentials of Acetone.

The results obtained are indicated in Fig. 2, with breaks in the curve at 10·2 ± 0·1 v., 11·3 ± 0·1 v., 12·2 ± 0·1 v. and 13·6 ± 0·2 v. As expected, they fall generally into line with the results for formaldehyde and acetaldehyde.

The molecular orbital formula is :

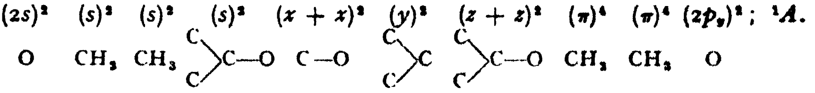

$$\underset{O}{(2s)^2}\quad \underset{CH_3}{(s)^2}\quad \underset{CH_3}{(s)^2}\quad \underset{\begin{smallmatrix}C\\ & >C\text{—}O\\ C\end{smallmatrix}}{(s)^2}\quad \underset{C\text{—}O}{(x+x)^2}\quad \underset{\begin{smallmatrix}C\\ & >C\\ C\end{smallmatrix}}{(y)^2}\quad \underset{\begin{smallmatrix}C\\ & >C\text{—}O\\ C\end{smallmatrix}}{(z+z)^2}\quad \underset{CH_3}{(\pi)^4}\quad \underset{CH_3}{(\pi)^4}\quad \underset{O}{(2p_y)^2};\ {}^1A.$$

The lowest value obviously corresponds with the non-bonding electron $2p_y$, having been observed as the culmination of a Rydberg series by Duncan [16] at 10·20 v. and by Noyes [17] at 10·1 v. using an electron impact method. The lowering given by adding the second CH_3 group to H_2CO is only half of that given by the first. This has also been observed to a more marked effect in alcohols and ethers, and mercaptans and sulphides, as compared with water and hydrogen sulphide.[18] It may be connected with (*a*) a tendency of the electronegativity of the oxygen to become saturated ; (*b*) interaction between the methyl groups, each thereby producing a smaller disturbing field, and (*c*) increased symmetry in the plane of the bonds of the C atom of C=O giving a disturbing field which is symmetrical to this plane of .

As in the case of acetaldehyde, the 13·6 v. value is probably to be associated with the ion $(y)^{-1}$, i.e. the C—C bonding electrons.

---

[15] Walsh, *Proc. Roy. Soc. A*, 1946, **185**, 176.
[16] Duncan, *J. Chem. Physics*, 1935, **3**, 131.
[17] Noyes, *ibid.*, 1935, **3**, 430.
[18] Price and Sugden (to be published).

Summary.

Three ionisation potentials of formaldehyde have been found, and four each for acetaldehyde and acetone. Their probable interpretation in terms of the electronic configuration of these molecules is given. The way in which the ionisation potentials are affected by alkyl substituents is brought out and is interpreted as being due to induction or charge transfer effects arising in the molecule.

Laboratory of Physical Chemistry,
Cambridge.

DETECTION OF CHANGES OF STATE IN FILMS ADSORBED AT THE GAS-SOLID INTERFACE.

BY S. J. GREGG AND F. A. P. MAGGS.

Received 9th September, 1946.

The possibility of the occurrence of transformations of state in adsorbed films on solids has been discussed by several workers during the last twenty years.[1] In 1932 Bangham[2] was able to demonstrate by experimental means a transformation of this kind, in adsorbed films of water and of methyl alcohol on charcoal; the work was extended by one of us, in that a considerable degree of resemblance between adsorbed films on solids and films of insoluble substances on water (" trough films ") was demonstrated.[3] Evidence was adduced for the existence of the following film states at the gas-solid interface : gaseous (G), liquid-expanded (L_1), intermediate (I), and liquid-condensed (L_2). During the past year or so, Harkins and Jura[4] have offered confirmatory evidence of the resemblance between the behaviour of certain trough films and films adsorbed on solids.

Reference to the examples quoted[3] illustrates the fact that the transformations between one state and another in gas-solid films, whilst qualitatively similar to those in trough films, are frequently much less sharp and are correspondingly more difficult to detect. Their detection, however, must enter into any general interpretation of adsorption phenomena, and is of considerable importance in relation to the determination of the internal surface of adsorbents. In the present paper we shall advance a simple method for detecting the occurrence of a transformation, based on the concept of a mobile film exerting a two-dimensional pressure analogous to that found in trough films. The method rests on the calculations from the adsorption isotherm of the two-dimensional compressibility of the film, a quantity of which the usefulness has already been emphasised by Dervichian and by Harkins[5] for trough films.

---

[1] Frenkel, *Z. Physik*, 1924, **26**, 117 ; Cassell, *Ergeb. exakt Naturewiss*, 1927, **6**, 114 ; *J. Physic. Chem.*, 1944, **48**, 195 ; Semenoff, *Z. physik. Chem. B*, 1930, **7**, 471. Langmuir, *J. Chem. Physics*, 1933, **1**, 3. Frumkin, *Acta Physicochim.* 1938, **9**, 313. Band, *J. Chem. Physics*, 1940, **8**, 178.

[2] Bangham, *Proc. Roy. Soc. A*, 1932, **138**, 162 ; *loc. cit.*, 1934, **147**, 153.

[3] Gregg, *J. Chem. Soc.*, 1942, 696.

[4] Harkins and Jura, *J. Chem. Physics*, 1944, **12**, 112.

[5] Dervichian, *ibid.*, 1939, **7**, 931 ; Harkins, *J. Physic. Chem.*, 1941, **45**, 20.

The Order of Transformation.

Phase changes in bulk matter are detected as a discontinuity * in the variation of a property of the substance under varying conditions, the variation of volume (V) with pressure (P), and that of total energy with temperature are frequently used. Ehrenfest [6] has generalised this treatment, and describing the discontinuity as a transformation of the *first order*, introduces the conception of *second order* transformations in which the first derivative (e.g. $\partial V/\partial P$) shows a discontinuity; similarly in *third-order* transformations the second derivative (e.g. $\partial^2 V/\partial P^2$) shows a discontinuity.

For our present purpose the variation of V with P will be considered. The accompanying diagram (Fig. 1) reproduced from a paper by Mayer and Streeter,[7] shows how both V and V/P vary with P when first and second order transformations occur (columns i and v). Further types of transformation of importance to this discussion are the "anomalous," "diffuse" and "lambda" first order changes (columns ii, iii and iv) where the sharpness of the transformation is blurred to various extents. Mayer and Streeter emphasise that in practice it may be very difficult to distinguish between columns ii, iii, iv because one has to rely on a finite number of experimental points; with widely spaced experimental points even i, the true first order, might be indistinguishable from ii, iii and iv. The blurring effect may be produced by certain impurities, by lack of time for equilibrium, or by absence of suitable nuclei—in fact by any of those factors which one associates with the phenomenon of suspended phase change. The discontinuities and breaks of the second and third † order changes respectively in the compressibility curve may be similarly obscured.

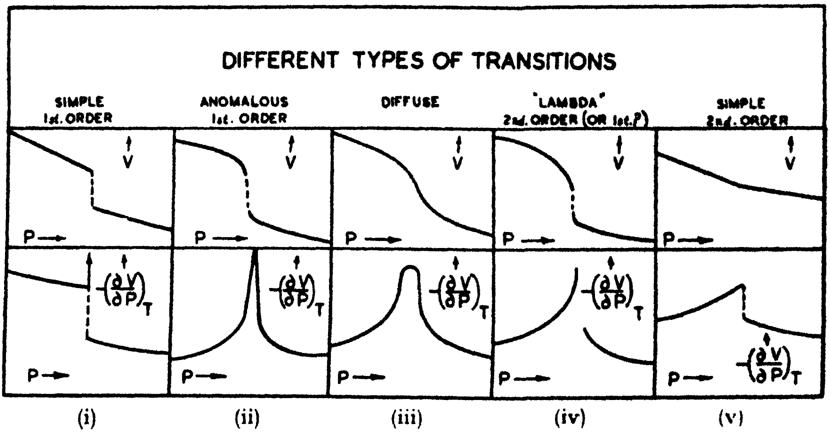

FIG. 1.—Phase changes in fluids (ref. 7).

---

* A discontinuity occurs in a curve when one variable changes value at a constant value of the other (see upper curve, I, Fig. 1). The point at which a curve changes direction abruptly will be referred to as a branch point (see upper curve, v, Fig. 1); the first derivative of this curve will show a discontinuity.

[6] Ehrenfest, *Leiden Comm. Suppl.*, 1933, **75b**.

[7] Mayer and Streeter, *J. Chem. Physics*, 1939, **7**, 1019.

† A third order transformation (not shown in Fig. 1) will give a curve of $\frac{1}{V}\frac{dV}{dP}$ against P similar in form to that of the upper curve, Fig. 1, column v.

Evaluation of Compressibility of Films Adsorbed on Solids.

As Bangham[8] has already pointed out

$$\pi S = RT\int_0^p x \, \mathrm{d} \log_e p \quad . \quad . \quad . \quad . \quad . \quad (1)$$

where S = surface area of adsorbent per g.; x = number of mole adsorbed per g. of adsorbent; π = surface free energy decrement accompanying adsorption, and is identified with the surface pressure.[8, 9]

A, the area occupied per molecule, is given by

$$A = S/xN \quad . \quad . \quad . \quad . \quad . \quad . \quad (2)$$

where N is Avogadro's Number.

Differentiation of (1) and (2) gives

$$\mathrm{d}\pi = RT\frac{x}{S}\mathrm{d} \log_e p \quad . \quad . \quad . \quad . \quad . \quad (3)$$

and

$$\mathrm{d}A = -\frac{S}{x^2N}\mathrm{d}x. \quad . \quad . \quad . \quad . \quad . \quad . \quad (4)$$

The compressibility β is therefore given by

$$\beta = \frac{1}{A}\frac{\mathrm{d}A}{\mathrm{d}\pi} = \frac{-S}{RTx^2}\frac{\mathrm{d}x}{\mathrm{d}\log_e p} = \frac{-S \, . \, p}{RTx^2}\frac{\mathrm{d}x}{\mathrm{d}p} = \frac{-S}{RTx}\frac{\mathrm{d}\log_e x}{\mathrm{d}\log_e p}.$$

The right-hand sides of these equations contain the unknown S; but writing

$$\beta' = \frac{\beta RT}{S} = \frac{-1}{x}\frac{\mathrm{d}x}{\mathrm{d}\log_e p} = \frac{-p}{x^2}\frac{\mathrm{d}x}{\mathrm{d}p} = \frac{-1}{x}\frac{\mathrm{d}\log_e x}{\mathrm{d}\log_e p}$$

we have a quantity β' proportional to the compressibility, which can be evaluated at once from the experimental data for any adsorption x; that is, from the slope of the semi-log, natural, or log-log isotherm.

Any of the transformations corresponding to columns i to v of Fig. 1 can therefore be exposed by plotting β' against πS; the true and anomalous first order are distinguished from the rest by the circumstance that β' and therefore $\mathrm{d}x/\mathrm{d}p$ become infinite; that is, the isotherm becomes actually vertical at the transformation point. In principle a third order change

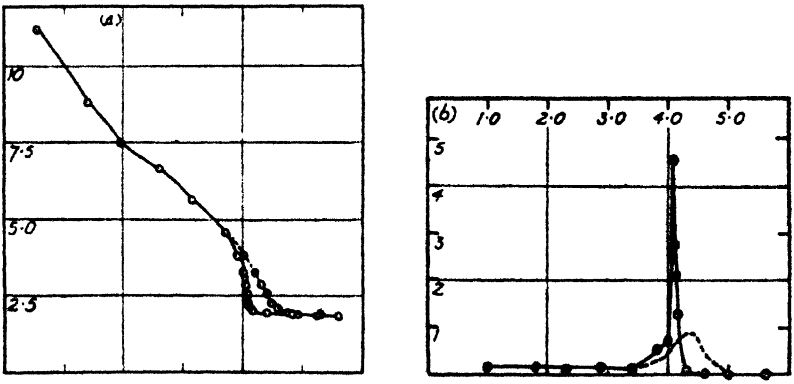

Abscissæ: (πS, 10^7 erg. g.$^{-1}$) $\propto \pi$.
Ordinates: (NA/S, 10^2 mole.$^{-1}$ g.) $\propto A$.

Abscissæ: πS, 10^7 erg. g.$^{-1}$.
Ordinate: β', 10^2 mole.$^{-1}$ g.

FIG. 2.—N_2 on porous glass at 78° K. (ref. 10).

---

[8] Bangham, *J. Chem. Soc.*, 1931, 1324; *Trans. Faraday Soc.*, 1937, 33, 804.

[9] Bangham, *Ann. Reports*, 1943.

is detectable by the same device, as a sharp change in the slope of the $\beta' - \pi S$ curve; in practice, however, the experimental points are often too widely spaced to enable this transformation to be identified with reasonable certainty. As an example, the data of Emmett and De Witt[10] for N_2 absorbed on porous glass at 78° K. have been plotted as NA/S ($= 1/x$) against πS in Fig. 2*a* and as β' against πS in Fig. 2*b*. Comparison with Fig. 1 discloses that either an anomalous or a diffuse first order transformation occurs in this film; a decision between the two possibilities turns on the question whether the isotherm ever becomes absolutely vertical or not; the experimental points are not numerous enough to provide an unambiguous answer.

In practice, a simpler procedure is available, for the general shape of the β'-πS curve is retained when β' is plotted against $\log p$; in particular, maxima in the curve will still be revealed. This is illustrated by Fig. 3*b* where the data used in Fig. 2*a* and 2*b* have been replotted in this form.

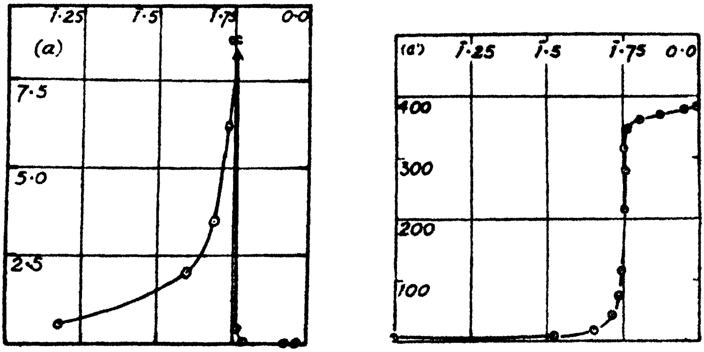

Abscissæ : $\log_{10} p/p_s = f(\pi)$.
Ordinates : β', 10^6 mole.$^{-1}$ g.

Abscissæ : $\log_{10} p/p_s$.
Ordinates : x, mm.^{3} g.$^{-1}$.

FIG. 3*a*.—D_2O on charcoal at 25° C. (ref. 11).

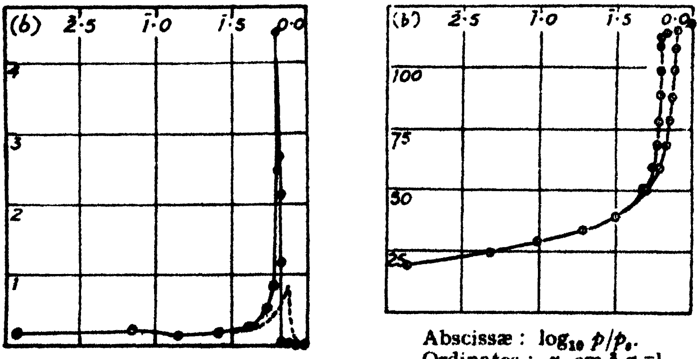

Abscissæ : $\log_{10} p/p_s = f(\pi)$.
Ordinates : β', 10^3 mole.$^{-1}$ g.

Abscissæ : $\log_{10} p/p_s$.
Ordinates : x, cm.^{3} g.$^{-1}$.

FIG. 3*b*.—N_2 on porous glass at 79° K. (ref. 10).

[10] Emmett and De Witt, *J. Amer. Chem. Soc.*, 1943, **65**, 1253.
[11] Foster and Broad, *J. Chem. Soc.*, 1945, 372.

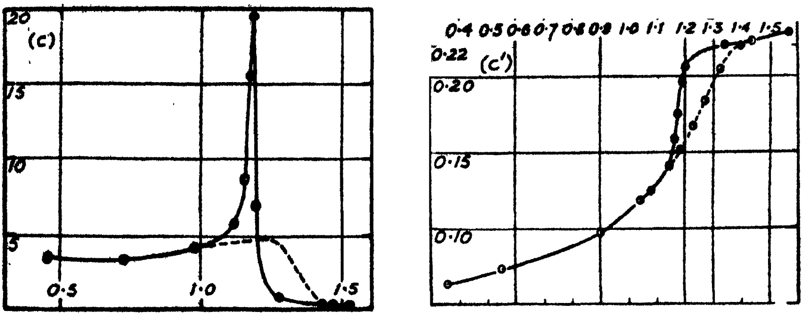

Abscissæ : log$_{10}$ $p_{cm.}$ = $f(\pi)$.
Ordinates : β', 10^3 mole.$^{-1}$ g.

Abscissæ : log$_{10}$ $p_{cm.}$
Ordinates : x, g./g.

FIG. 3*c*.—C_6H_6 on ferric oxide gel at 60° c. (ref. 12).

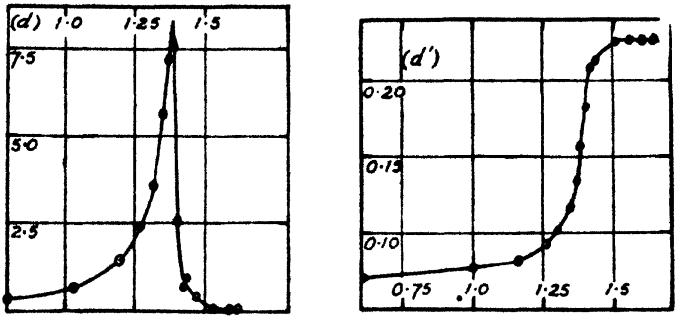

Abscissæ : log$_{10}$ $p_{cm.}$ = $f(\pi)$.
Ordinates : β', 10^3 mole.$^{-1}$ g.

Abscissæ : log$_{10}$ $p_{cm.}$
Ordinates : x, g.g.

FIG. 3*d*.—*iso*-PrOH on ferric oxide gel at 25° c. (ref. 12).

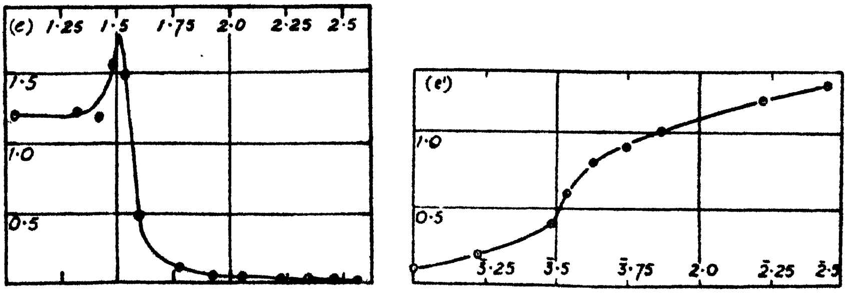

Abscissæ : log$_{10}$ $p_{cm.}$ = $f(\pi)$.
Ordinates : β', 10^6 mole.$^{-1}$ g.

Abscissæ : log$_{10}$ $p_{cm.}$
Ordinates : x, cm.^{3} g.$^{-1}$.

FIG. 3*e*.—NO on NaCl at − 90° K. c. (ref. 13).

A series of published data have been plotted as dx/d log$_e$ p against log$_{10}$ p ; the curves fall into two main groups : those showing a maximum in the values of β' (Fig. 3), and those showing no maximum (Fig. 4). The corresponding semi-log isotherms are also given for comparison (marked *a'*, *b'*, etc.). Fig. 3*a* exemplifies a true first order change, for β' rises to

---

[12] Foster, *Proc. Roy. Soc. A*, 1934, **147**, 131.
[13] Tompkins, *Trans. Faraday Soc.*, 1936, **32**, 643.

infinity; such cases are rare, other examples being the adsorption of water and methanol on charcoal, quoted as a first order change by Bangham[8]; also n-heptane on silver given as first order by Jura, Loesser,

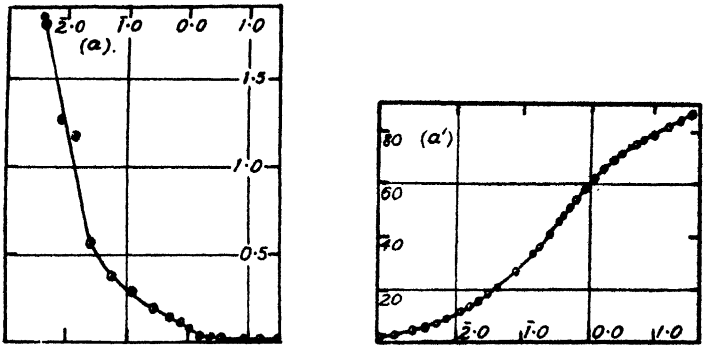

Abscissæ : $\log_{10} p_{\text{cm.}} = f(\pi)$.
Ordinates : β', 10^3 mole.$^{-1}$ g.

Abscissæ : $\log_{10} p_{\text{cm.}}$
Ordinates : x, cm.^{3} g.$^{-1}$.

FIG. 4*a*.—SO_2 on charcoal at 0° C. (ref. 14).

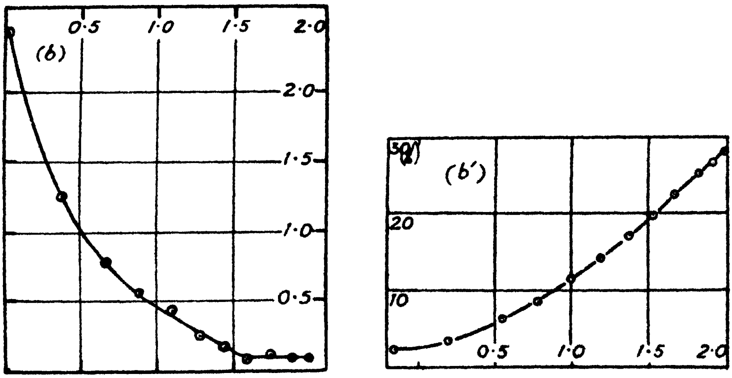

Abscissæ : $\log_{10} p_{\text{cm.}} = f(\pi)$.
Ordinates : β', 10^4 mole.$^{-1}$ g.

Abscissæ : $\log_{10} p_{\text{cm.}}$
Ordinates : x, 10^{-4} mole. g.$^{-1}$.

FIG. 4*b*.—CO_2 on charcoal at 0° C. (ref. 15).

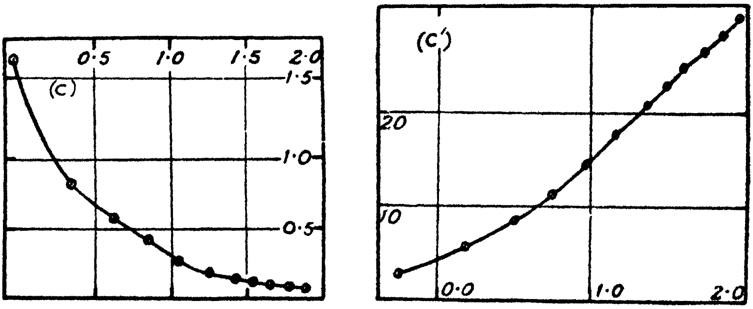

Abscissæ : $\log_{10} p_{\text{cm.}} = f(\pi)$.
Ordinates : β', 10^3 mole.$^{-1}$ g.

Abscissæ : $\log_{10} p_{\text{cm.}}$
Ordinates : x, 10^{-4} mole. g.$^{-1}$.

FIG. 4*c*.—N_2O on charcoal at 0° C. (ref. 15).

---

[14] Gregg, *J. Chem. Soc.*, 1943, 351.

[15] Gregg, *ibid.*, 1927, 1501.

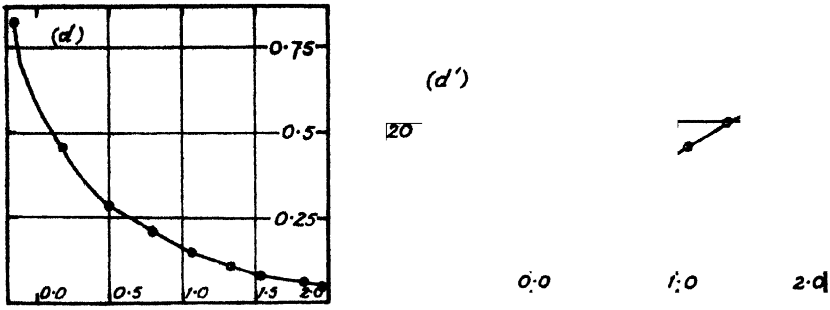

Abscissæ : $\log_{10} p_{cm.} = f(\pi)$.
Ordinates : β', 10^8 mole.$^{-1}$ g.

Abscissæ : $\log_{10} p_{cm.}$
Ordinates : x, 10^{-4} mole. g.$^{-1}$.

FIG. 4*d*.—C_2H_4 on charcoal at 0° c. (ref. 15).

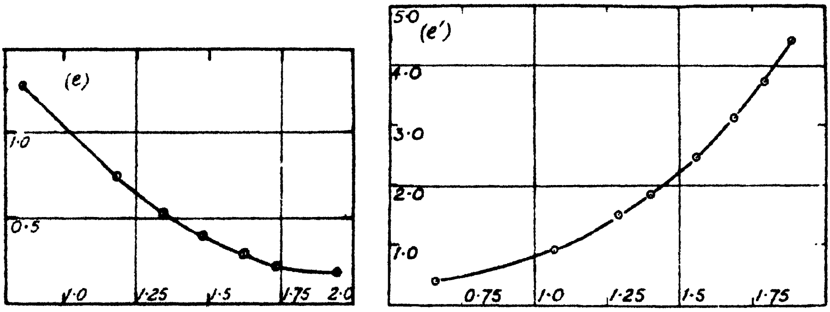

Abscissæ : $\log_{10} p_{cm.} = f(\pi)$.
Ordinates : β', 10^4 mole.$^{-1}$ g.

Abscissæ : $\log_{10} p_{cm.}$
Ordinates : x, 10^{-4} mole. g.$^{-1}$.

FIG. 4*e*.—N_2 on charcoal at 0° c. (ref. 15).

Basford and Harkins.[16] The isotherms of Fig. 3*c*, 3*d*, 3*e*, show transformations of diffuse first order, as will be seen by comparison with column iii of Fig. 1. A large number of isotherms given in the literature are of this type, showing diffuse first order transformations. The data of Fig. 2*a*, 2*b*, 3*b* and 3*c* are derived from isotherms showing a pronounced hysteresis loop ; the curves for the desorption (full lines) and the adsorption (dotted) are very different, and show that the transformation is much sharper on desorption than on adsorption.

Interpretation of Transformations.

True first order transformations in bulk matter occur when one phase (as understood by the Gibbs phase rule) converts into another under a single set of conditions ; at the transition point the two states coexist in macroscopic amounts and an infinitesimal change in conditions causes one phase to grow very rapidly at the expense of the other. Mayer and Streeter (loc. cit.) suggest that in the second order transformations, likewise, there are two phases, one growing at the expense of the other, but that the growth now occurs over a *region* of temperature at constant pressure (and therefore, presumably, over a region of pressure at constant temperature) ; the break in the $P - V$ curve marks the *completion* of the second order transition. It is to be inferred from their paper that anomalous, diffuse, and lambda first order transitions are also to be interpreted as showing the co-existence of two phases over a range of pressure; the rate of conversion of one phase into the other is a maximum at the peak of the $\mathrm{d}V/\mathrm{d}P$ against P plot, but in these cases the interconversion still proceeds on both sides of the peak.

---

[16] Harkins, Jura, Loesser and Basford, *J. Chem. Physics*, 1945, **13**, 535.

The general resemblance of behaviour between trough films and bulk matter on the one hand (Adam[17]), and between trough films and films at the gas-solid interface on the other,[8] encourages us to apply these interpretations of three-dimensional transformations to the two-dimensional state found in the field of gas-solid adsorption. The curves of Fig. 3*a* to 3*e* are therefore to be regarded as demonstrating the occurrence of transformations taking place over a greater or less range of surface pressures. To gain some insight into the nature of the phases involved, it is helpful to construct the corresponding πA—πS curves and compare them with standard πA—π curves of trough films, where π and A are measured directly and accurately. It is then found that whilst a close parallel may be drawn between certain gas-solid films and trough films, the latter usually exhibit sharper transitions, no doubt because they consist of molecules which are more anisodimensional and electrically anisotropic than those met with in gas-solid adsorption. However, the transformations in the films of Fig. 3*b* to 3*e* are found to resemble fairly closely the $L_1 \rightleftharpoons L_2$ conversion of trough films; the intermediate " phase " I seems to correspond to the transformation region itself, and so does not constitute a separate phase in the sense of this paper—it rather represents a mixture of two phases such as L_1 and L_2. It is perhaps doubtful whether at this stage one is justified in concluding that the correspondence between the L_1 and L_2 phases in trough films and the analogous phases on solids is quite complete, principally on account of the more diffuse nature of the changes in the latter films to which reference has already been made. For example, the $L_1 \rightleftharpoons L_2$ conversion in trough films commences, according to Harkins,[18] with a second order change $L_1 \rightleftharpoons I$ and finishes with a third order change $I \rightleftharpoons L_2$, so that the transformation $L_1 \rightleftharpoons L_2$ may be said to occur over a region I of (surface) pressure bounded by a second and a third order transformation; in the gas-solid films of Fig. 3*b* to 3*e* on the other hand, the interconversion occurs over a region which is not exactly defined at either end.

The transformation represented in Fig. 3*a*, when similarly examined by use of the πA—πS curve, is found to correspond to the $G \rightleftharpoons L_1$, or the $G \rightleftharpoons L_2$ conversion of trough films below the critical temperature (T_c); that is, it is analogous to a condensation in a bulk liquid.

The curves of Fig. 4*a*, 4*b* and 4*c* are important in that they are typical of a large number of isotherms, particularly of gases adsorbed on charcoal. Unfortunately they are more difficult to interpret than those of Fig. 3. They may possibly represent the right-hand branch of a peak, the left-hand branch being absent owing to lack of experimental readings at very low pressures; this, however, is unlikely, particularly in the case of Fig. 4*a* where the readings extended almost into the Henry's law range ($x \propto p$).

The curves, which essentially represent the variation of the " surface " compressibility of films with surface pressure, resemble in general form those for the variation of the bulk compressibility of bulk gases *above their critical temperature* with ordinary gas pressure; this will be seen by reference to Fig. 5 which gives the curves of $\frac{1}{V}\cdot\frac{\mathrm{d}V}{\mathrm{d}P}$ against P for (*a*) ethylene[19] at 15° above, and (*b*) nitrogen[20] at 162° above their respective critical temperatures. The curves of Fig. 4 and 5 both show the same steep gradient at the lower pressures, changing rather sharply into a small and nearly constant gradient at higher pressures; similarly, difficulty is encountered in deciding whether the change in slope at X is sharp enough to constitute a branch point or not. A branch point would signify a *third order* transformation.* It seems that there is very probably a third order transformation in Fig. 4*a*, *b*, and 5*a*, no transformation in Fig. 4*d*, *e* and 5*b*, and *possibly* a third order transformation in the intermediate case 4*c*. The state of the films is gaseous (*G*) throughout, in all these cases; but just as a highly compressed gas even *above* its critical temperature is virtually indistinguishable from a compressed liquid, so at the high pressure end of the diagrams are the films to be compared with either the L_1 or the L_2 states; reference to the corresponding πA—πS curves, which are linear in each case at the higher pressures, shows that state of the films is comparable to the L_2 rather than the L_1 state. The presence or absence of a third order transformation merely shows whether the conversion from the dilute to the compressed film produced by increasing the pressure, proceeds absolutely continuously or not.

---

[17] Adam, *Physics and Chemistry of Surfaces*, 1941, Ch. 2.

[18] Harkins, Young and Boyd, *J. Chem. Physics*, 1940, **8**, 954.

[19] Masson and Dolley, *Proc. Roy. Soc. A*, 1923, **103**, 524.

[20] Amagat, *Ann. Physique*, 1893, **29**, 68.

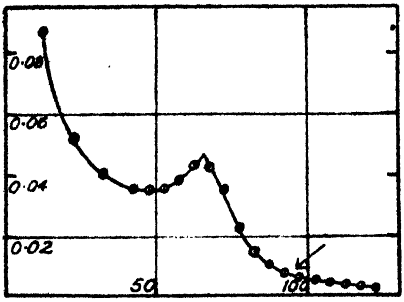

Abscissæ: pressure, atmos.
Ordinates: $\frac{1}{V}\frac{dV}{dP}$ atmos.$^{-1}$.

FIG. 5*a*.—Isothermal compression of C_2H_4 at 24·95° C. (ref. 19).

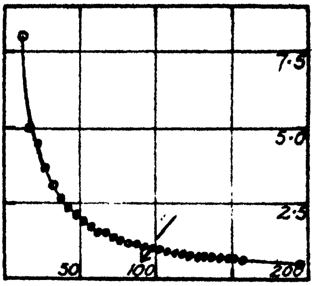

Abscissæ: pressure, atmos.
Ordinates: $\frac{1}{V}\frac{dV}{dP}$, atmos.$^{-1}$.

FIG. 5*b*.—Isothermal compression of N_2 at 16° C. (ref. 20).

It is satisfactory that in the comparable trough film curve [21] for a substance above its (film) critical temperature T_c and below the temperatures T' aud T'' (see Fig. IV of ref. [8]) the conversion from the dilute to the more highly compressed state is a third order transformation as far as one can judge.

---

* Our attention has been drawn to a recent paper by Lifshitz (*Acta Physicochim.*, 1944, **19**, 248), in which this author extends to trough films Landau's contention (*Physik. Z. Sowjetunion*, 1937, **11**, 26 and 545) that transformations of third and diffuse first order are thermodynamically impossible in bulk matter. Lifshitz is thus led to regard the *I* region as merging continuously into the L_2 state; moreover, its higher compressibility as compared with the L_1 state is taken as evidence of its higher degree of symmetry in molecular orientation—contrary to his views elsewhere in the paper and to general considerations, both of which would lead one to associate higher compressibility with lower symmetry. It is significant that Lifshitz' mathematical analysis ignores the possibility of molecular clustering, a phenomenon of great importance in transformations in bulk matter (cf. Streeter and Mayer (loc. cit.)). However, even if third and diffuse first order transformations be thermodynamically impossible, under conditions of true equilibrium, there is no doubt that *in practice* a diffuseness of first order transformations is frequently found with bulk matter; and also that the compressibility curve often shows a sudden change in slope almost impossible to distinguish from the branch point of a third order change, both in compressed films and in compressed gases above T_c. It is possible that some or all of these cases represent pseudo-equilibrium only; nevertheless, in this paper, where our main concern is to show correspondences, the terms third and diffuse first order constitute at the least, a very convenient description of the phenomena.

[21] Adam and Jessop, *Proc. Roy. Soc. A*, 1926, **112**, 377.

In view of the structural differences between molecules forming films at the surfaces of solids and those giving trough films, it is difficult at present to postulate detailed molecular models for the mechanism of gas-solid phase transitions. The term " phase " in the present connection should be interpreted widely so as to include not only clustering (see Streeter and Mayer's treatment [7]) but also to include particular states of orientation and rotation of the adsorbed molecules. A transformation then implies a change from one of these states to another.

Importance of Equilibrium.

The method given above of calculating the compressibility is based on the applicability of the Gibbs adsorption equation which relates to systems in equilibrium. The existence of hysteresis phenomena shows that the condition of reversibility is frequently unfulfilled in practice, and hence values of πS will not be calculated correctly from equation (1); if they were, an indefinite amount of work could be obtained by repeated passage round the hysteresis loop. In this connection it is significant that in his extensometric work on charcoal Bangham [22] found a lack of agreement between the value of πS calculated from (1) and that calculated from the extension of the adsorbent, *only* in those regions where phase changes were occurring and where hysteresis effects were accordingly marked. In his opinion † the anomaly is due to the absence of the correct conditions for the application of the Gibbs equation.

Nevertheless, there seems no reason to doubt that even under irreversible conditions, πS and p show a *qualitative* correspondence, in that an increase of p is related to an increase of πS even though the relation is no longer given by equation (1); whilst a change in the position and shape of the peak in the πA—πS curve is possible, the presence of a peak will still denote the occurrence of a transformation. The graphs of Fig. 3*b* and 3*d* show that the change in position associated with the hysteresis loop is often small, though the sharpness of the transformation is different for adsorption and desorption.

Monolayer ‡ ⇌ Multilayer Transformation.

The transformation which occurs when the adsorbed monolayer is completed and commences to thicken into a multilayer is of particular importance in connection with the determination of monolayer capacity from adsorption isotherms; accordingly, curves of β' against log p have been evaluated from the limited data for adsorption on surfaces of known area (Fig. 6*a*, *b* and *c*). In all these cases, the completion of the close-packed monolayer is followed by sharply increasing values of β' and in none of them does the value subsequently fall.

For example, the data of Palmer [23] for benzene adsorbed on a known area of vitreous silica show a steep rise in the curve of β' against log p, commencing where $A \stackrel{\frown}{=} 20$ A.[8] Of the experimental points given by Bosworth [24] for the adsorption of fatty acid vapours on mercury, only those for α-valeric and butyric acids are closely enough spaced at the high pressure end to permit the calculation of β'; but both of these give $\beta' - \log p$ curves, as in Fig. 6*b*, with a steep though not vertical branch commencing where $A \simeq 20$ A.[8] (the peak at lower pressures denotes a transformation within the monolayer, probably $L_1 \rightleftharpoons L_2$). Cassell's figures[25] for carbon tetrachloride vapour on mercury similarly show a

---

[22] Bangham, *Proc. Roy. Soc. A*, 1932, **138**, 162.

† Private communication.

‡ The term "monolayer" as used in this paper, implies that the surface has adsorbed on it, adsorbate units acting individually; these units are usually single molecules, but may also comprise associated molecules.

[23] Palmer, *Proc. Roy. Soc. A*, 1937, **160**, 259; *loc. cit.*, 1935, **149**, 375.

[24] Bosworth, *Trans. Faraday Soc.*, 1932, **28**, 903.

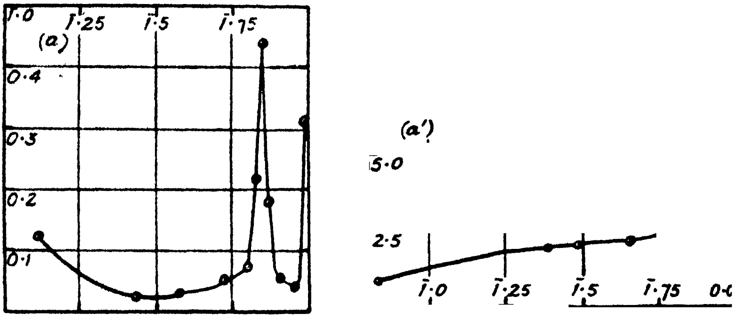

Abscissæ: $\log_{10} p/p_s = f(\pi)$.
Ordinates: β', erg.$^{-1}$ cm.^{2}.

Abscissæ: $\log_{10} p/p_s$.
Ordinates: x, 10^{14} mol. cm.$^{-2}$.

FIG. 6*a*.—α-Valeric acid on Hg at 15° C. (ref. 24).

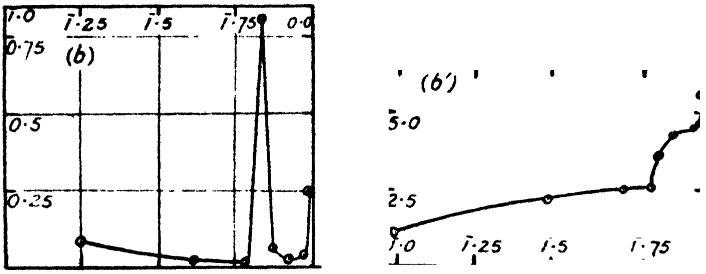

Abscissæ: $\log_{10} p/p_s = f(\pi)$.
Ordinates: β', erg.$^{-1}$ cm.^{2}.

Abscissæ: $\log_{10} p/p_s$.
Ordinates: x, 10^{14} mol. cm.$^{-2}$.

FIG. 6*b*.—*n*-Butyric acid on Hg at 15° C. (ref. 24).

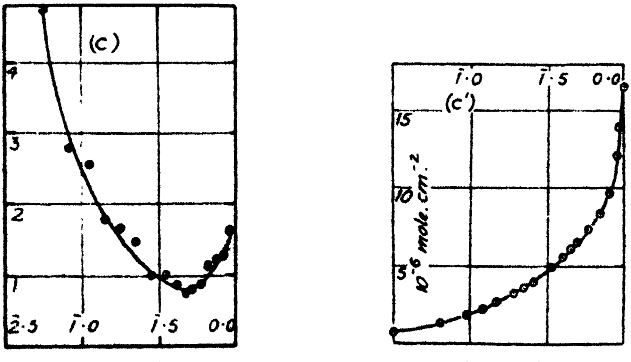

Abscissæ: $\log_{10} p/p_s = f(\pi)$.
Ordinates: β', 10^9 mole.$^{-1}$ g.

Abscissæ: $\log_{10} p/p_s$.
Ordinates: x, 10^{-6} mole. cm.$^{-2}$.

FIG. 6*c*.—C_6H_6 on vitreous silica at 25° C. (ref. 23).

---

[25] Cassell, *Trans. Faraday. Soc.*, 1932, **28**, 177.

rise commencing at $A \simeq 25$ A.[8] The results of Bangham and Mosallam,[26] though much complicated by hysteresis effects, also give a rise commencing in the region $A \simeq 20$ to 25 A.,[8] for benzene vapour on mica; whilst Armbruster and Austin's data [27] for ethyl iodide on a smooth surface of iron,

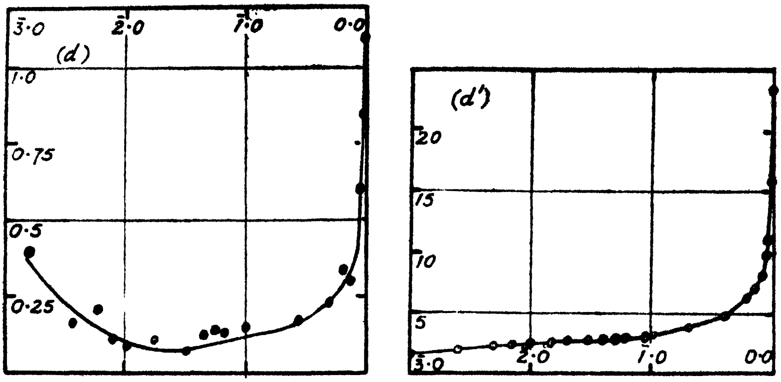

Abscissæ : $\log_{10} p/p_s = f(\pi)$.
Ordinates : β', 10^4 mole.$^{-1}$ g.

Abscissæ : $\log_{10} p/p_s$.
Ordinates : x, cm.^{3} g.$^{-1}$.

FIG. 6d.—N$_2$ on anatase at − 195·5° C. (ref. 28).

though rather widely spaced, again yield a curve for which begins to rise when A falls to about 25 A.[8] In each of these cases the areas named lie in the neighbourhood of the figure for a just complete monolayer; and the significant point is that in no case does the $\beta' - \log p$ curve fall again after the rise.

Many examples of adsorption on an unrestricted (though not plane) surface are provided by the adsorption of the inert gases on non-porous fine powders. As an example the adsorption of nitrogen on anatase is given in Fig. 6*d*, where the $\beta' - \log p$ curve is plotted. Whilst low pressure detail is absent (the data being taken from the published graph) the steep rise of the values of β' is again found.

The evidence we have presented thus suggests that a peak in the $\beta' - \pi S$ or $\beta' - \log p$ curve denotes a transformation within the monolayer (cp. Fig. 6*b*); a rising branch not followed by a falling branch is indicative of multilayer formation (provided, of course, that the isotherm has been carried to pressures close to saturation).* It must be borne in mind however, that whilst very few examples of adsorption isotherms taken to the saturated vapour pressure are cited in the literature, the conclusions we have drawn are substantiated fully by the data of all the isotherms covering the full pressure range which we have so far encountered. In cases of doubt, thermal data may be used with advantage: it is to be anticipated that the heat of adsorption would fall to a value near the latent heat when multilayer formation commences. Examples of the value of thermal data have been given by Bangham and Mosallem,[26] by Brunauer and Emmett,[29] and by Gregg.[8, 25] If the transformation

[26] Bangham and Mosallem, *Proc. Roy. Soc. A*, 1938, **166**, 558.

[27] Armbruster and Austin, *J. Amer. Chem. Soc.*, 1939, **61**, 1118.

[28] Harkins and Jura, *J. Amer. Chem. Soc.*, 1944, **66**, 1356.

* This does not *in any way* imply that multilayer formation can proceed indefinitely. Indeed, there is ample evidence to show that the adsorbed phase differs considerably from the normal bulk phase (see ref. 8, 18, also Cassel, *J. Chem. Physics*, 1945, **13**, 249; Bangham, *Nature*, 1945, **157**, 733; Bangham and Saweris, *Trans. Faraday Soc.*, 1938, **34**, 554).

[29] Brunauer and Emmett, *J. Amer. Chem. Soc.*, 1938, **60**, 309.

should prove to be a change *within* the monolayer, the multilayer transformation being absent, the monolayer capacity can still be obtained as the reciprocal of the slope of the high pressure branch of the πA against πS curve, if this branch is rectilinear (Gregg[8]).

The correctness of these tests for multilayer formation is confirmed by a consideration of the data of Lambert and Foster[30] for the adsorption of water on silica gel at 70° c. The isotherm (Fig. 7*a*′) is similar to that in Fig. 3*b*′ or 3*c*′; the point *X* has frequently been taken to denote the completion of the monolayer, and the following branch *XY* as due to multilayer formation (cf. Brunauer, Emmett and Teller[31]) or to capillary condensation (Foster[32]). On plotting the data as β' against $\log p$ (Fig. 7*a*) however, the part *XYZ* is found to include a peak, indicating a transformation *within the monolayer*; this conclusion is confirmed by the value of the differential heat of adsorption (calculated from the 60° c. and 70° c. isotherms) which remains at about 11,400 cal. mole.$^{-1}$ (the latent heat being 10,000 cal. mole.$^{-1}$) throughout the region of the transformation. There is, moreover, a further branch to the isotherm (*ZW*) which corresponds to an upward rise, but *not* a peak in the β' against $\log p$ curve; it occurs at pressures very close to saturation.* It is difficult to interpret this second rise in the isotherm if the preceding peak is ascribed to multilayer formation or capillary condensation; the suggestion that it is due to condensation of bulk liquid on the gel is discounted not only by the fact that the final pressure was below saturation, but also by the experimenters' observation that " at no time could liquid water be detected on the outside of the gel." On the views advanced in this paper, the *second* rise in the isotherm is to be ascribed to multilayer formation.

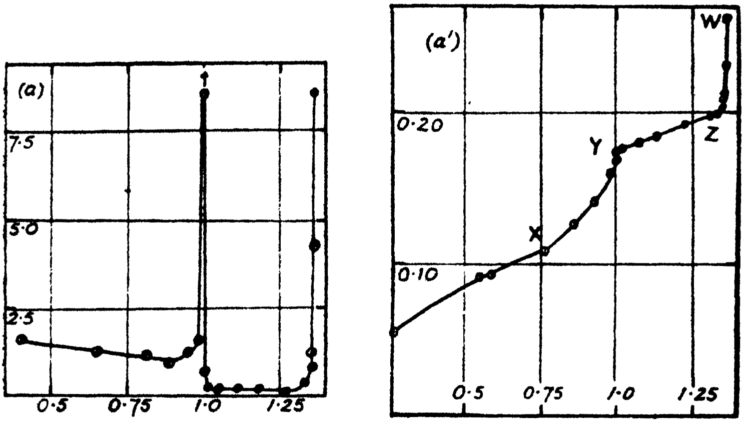

Abscissæ: $\log_{10} p_{\text{cm.}} = f(\pi)$.
Ordinates: β', 10^3 mole.$^{-1}$ g.

Abscissæ: $\log_{10} p_{\text{cm.}}$
Ordinates: x, g./g.

FIG. 7.—H_2O on silica gel at 70° c. (ref. 30).

Interpretation of Adsorption Isotherms.

The expressions we have derived relating the film compressibility to the experimental values of adsorption x and equilibrium pressure p, make it possible to offer an interpretation of the characteristics in isotherms in terms of changes of state in the adsorbed film. Thus an increase of x occurring at constant pressure in the isotherm immediately reveals the existence of a true first order transformation. Similarly a branch point in the isotherm would show the occurrence of a transformation of the second order.

---

[30] Lambert and Foster, *Proc. Roy. Soc. A*, 1932, **134**, 246.

[31] Brunauer, Emmett and Teller, *J. Amer. Chem. Soc.*, 1938, **60**, 309.

[32] Foster, *Trans. Faraday Soc.*, 1932, **28**, 652.

* This part of the isotherm (close to saturation vapour pressure) was determined in a separate experiment. Although the overlapping parts of the two experiments do not correspond exactly (due to a slight change in the adsorbent), the sharp increase in *x* is unquestionable.

We have presented evidence, however, to show that such well-defined transformations are rarely encountered in practice; instead, changes in the film are usually blurred so that assignment of the order of the transformation may be difficult in comparison with the three-dimensional state. Whilst the diffuse nature of the changes shown in Fig. 3 and in Fig. 4 may in certain cases be due to the lack of experimental detail inherent in the determination of adsorption isotherms, the widespread nature of the phenomenon, and in particular the family resemblance of the curves of Fig. 3*a* to *e*, and 4*a* to *c* strongly suggest that the diffuse nature of the change is a very general characteristic of two-dimensional transformations occurring in the pressure range normally investigated in solid-vapour adsorption.

The diffuse type of transformation leads to points of inflection in the isotherm so that the latter *appears* continuous. But the existence of transformations shows that in general adsorption cannot be represented as a *continuous* function of pressure, so that the attempts, often made, to find a single, universally applicable equation to reproduce the adsorption isotherm over the whole range from zero to the saturated vapour pressure are bound to be unsuccessful (cf. Gregg,[33] Harkins and Jura [4]).

Summary.

Published evidence for the occurrence of phase transformations in adsorbed films on solids, and for the existence of phases resembling the gaseous, liquid-expanded and liquid-condensed phases of films on water is cited. Just as in bulk fluids phase transformation may be exhibited by means of curves of compressibility against pressure, so in adsorbed films they are revealed by plotting the two-dimensional compressibility β against surface pressure.

A method for the calculation of β from the adsorption isotherm is given; it is shown, however, that a plot of $\frac{1}{x^2}\frac{\mathrm{d}x}{\mathrm{d}\log_e p}$ $\left(= \beta' = \frac{RT\beta}{S}\right.$, x = adsorption in mole., p = equilibrium pressure, and S = surface area) reproduces the general shape of the curves of β against π. Examination of the plots of β' against $\log p$ for a number of published isotherms show that: (*a*) true first order transformations are rare; (*b*) diffuse first order transformations are common; (*c*) third order transformations are sometimes found; (*d*) whilst a true or diffuse first order transformation between two phases in the monolayer (such as $L_1 \rightleftharpoons L_2$) gives rise to a maximum in the curve of β' against $\log p$, multilayer formation is exhibited as a rising branch *not* followed by a falling branch.

Since at any point in the isotherm β' is related to the gradient of the isotherm, transformations within the film are reflected in the shape of the isotherm. The significance of these results for the determination of the monolayer capacity of the adsorbent is discussed.

The authors are grateful to Dr. D. H. Bangham for the benefit of discussions with him on film behaviour.

University College,
Exeter.

56, Edge Hill Court,
Edge Hill, S.W.19.

[33] Gregg, *J. Chem. Soc.*, 1942, 704.

A THERMODYNAMIC STUDY OF BIVALENT METAL HALIDES IN AQUEOUS SOLUTION. PART XVI—COMPLEX ION FORMATION IN ZINC HALIDE SOLUTIONS.

By R. H. Stokes.*

Received 11*th November*, 1946.

In Part XV [1] data were presented for the vapour pressure lowerings of mixed solutions of 1 : 1 and 2 : 1 salts such as $2KCl \cdot MgCl_2$. It was shown that the lowerings could be calculated from those of the component salts by a simple additivity rule. The results were interpreted as meaning that complex ions, if present at all, occur only to a small extent in the solutions studied. Similar studies of mixtures of the zinc halides with other salts are now reported, and deductions are made about the nature and extent of complex ion formation in these solutions.

Experimental.

Table I gives the v.p. lowerings (Δp) of mixtures of the zinc halides with alkali halides, obtained by isopiestic measurements using NaCl or KCl or H_2SO_4 as reference substances. The molalities listed are based on the formulæ given at the head of each column : thus 0·5 M. K_3ZnCl_5 means a mixture 0·5 M. with respect to $ZnCl_2$ and 1·5 M. with respect to KCl. Table III gives the Δp's of mixtures of zinc and magnesium halides, obtained by isopiestic measurements against $CaCl_2$. This table shows the effect of a varying Zn : Mg ratio at a constant total molality. The mol fraction of zinc salt in the mixture is denoted by x. All the values refer to 25° C.

TABLE I.—Vapour Pressure Lowerings of Mixed Solutions of Zinc Halides and Alkali Halides (in mm. Hg).

M.	$KZnCl_3$.	K_2ZnCl_4.	K_3ZnCl_5.	Na_2ZnCl_4.	Li_2ZnCl_4.	K_2ZnBr_4.	K_2ZnI_4.
0·1	0·190	0·263	0·336	0·263	0·264	0·268	—
0·2	0·374	0·515	0·653	0·518	0·522	0·541	0·561
0·3	0·544	0·753	0·938	0·767	0·779	0·822	0·863
0·5	0·853	1·152	1·422	1·252	1·282	1·390	1·526
0·7	1·124	1·493	1·810	1·712	1·794	1·863	2·18
1·0	1·486	1·927	2·294	2·362	2·583	2·485	3·04
1·5	2·016	2·523	3·146	3·348	4·008	3·309	4·10
2·0	2·508	3·064	—	4·299	5·576	4·01	4·96
2·5	3·016	3·580	—	5·37	7·19	4·66	—
3·0	3·513	4·080	—	6·45	8·95	—	—
3·5	4·03	4·56	—	7·54	10·80	—	—
4·0	4·51	4·99	—	—	12·58	—	—
5·0	5·53	5·88	—	—	15·88	—	—
6·0	6·64	6·77	—	—	18·60	—	—
7·0	—	7·73	—	—	20·45	—	—

---

[1] Robinson and Stokes, *Trans. Faraday Soc.*, 1945, 41, 752.

* Present Address : Dept. of Physical Chemistry, The University, Cambridge.

Discussion.

The Variation of the Relative Molal V.P. Lowerings with Concentration.—Fig. 1, prepared from the data of Table I, compares $\Delta p/mp_0$ for mixtures of the type K_2ZnCl_4 with those of the "normal" mixtures K_2MgCl_4 and Li_2CaCl_4 studied in Part XV. The curve for K_2ZnI_4 resembles the normal type up to about 0·5 M., then turns downwards and falls rapidly. The same effect sets in at a lower concentration in K_2ZnBr_4, and in K_2ZnCl_4 the effect is so marked that there is no maximum but only a slight inflexion about 0·3 M.

The similarity of the three curves suggests that a complex of the same type is formed in each case, but most readily in the chloride mixtures and least readily in the iodides. The striking dependence of $\Delta p/mp_0$ on the nature of the alkali-metal constituent is illustrated by curves III, IV and V. An explanation of this effect is advanced later.

The Δp's of these mixtures are smaller than for normal mixtures due, in part, to the abnormally low values found for the zinc halides themselves. This can be allowed for by calculating the deviations of the mixtures from the additivity rule (cp. Table II). In each case large positive deviations appear at quite moderate concentrations, where normal mixtures show deviations of only 1-2 %. The test cannot be carried out above 1 M. except in the case of the LiCl—$ZnCl_2$ mixtures, owing to lack of knowledge of the V.P.'s of the alkali halides at the high ionic strengths involved. Table II is again consistent with a complex formation process, resulting in a diminution of the osmotic effects of the mixtures as compared with those of their constituent salts. The rapid increase of the deviations with concentration, and especially the manner in which they increase through the series $KZnCl_3$, K_2ZnCl_4, K_3ZnCl_5, suggests an equilibrium involving a fairly high power of the halide concentration, but apart from this it would be difficult to decide on any one of the following processes:

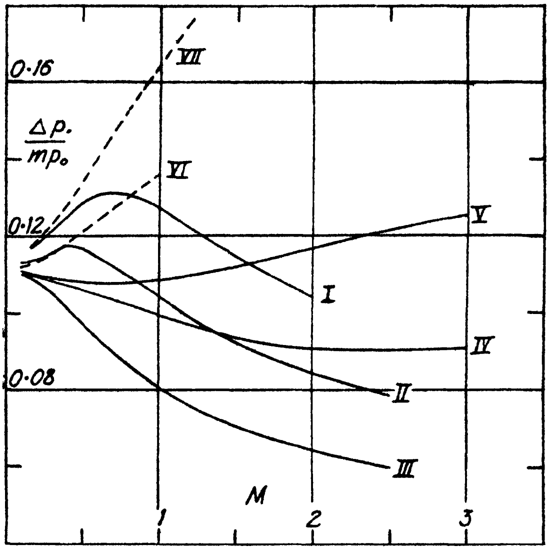

FIG. 1.—Relative molal vapour pressure lowerings in zinc halide—alkali halide mixtures.

I = K_2ZnI_4.
II = K_2ZnBr_4.
III = K_2ZnCl_4.
IV = Na_2ZnCl_4.
V = Li_2ZnCl_4.
VI = K_2MgCl_4.
VII = Li_2CaCl_4.

(a) $Zn^{++} + Cl^- \rightleftharpoons ZnCl^+$ (b) $Zn^{++} + 2Cl^- \rightleftharpoons ZnCl_2$
(c) $Zn^{++} + 3Cl^- \rightleftharpoons ZnCl_3^-$ (d) $Zn^{++} + 4Cl^- \rightleftharpoons ZnCl_4^{--}$

or even higher complexes. Fortunately there is other evidence which makes it possible to eliminate (a) and (b) as major effects: in concentrated solutions of the zinc halides the transport number of the zinc ion becomes negative,[3] passing through zero at about 2 M. in $ZnCl_2$, 2·8 M. in $ZnBr_2$, and 3·5 M. in ZnI_2. Negative transport numbers can be explained only by the formation of complex anions as (*c*) or (*d*).

The following considerations strongly suggest that the type ZnX_4^{--} is the main complex anion present. The data of Table III, obtained by interpolation at certain high total molalities in the experimental isopiestic ratio curves for mixtures of zinc and magnesium halides, have been plotted in Fig. 2. If both salts were normally dissociated the curves should be nearly straight lines, since the additivity rule [1] would result in the Δp for any mixture being a linear combination of those of its constituent salts in the ratio $x/(1 - x)$. Instead, the curves approximate towards a linear drop between the pure magnesium halide and the 1 : 1 mixture, followed by a nearly horizontal portion between this and the pure zinc halide. Assuming that the complex ion has high stability, it will in all cases be formed to the maximum possible extent. Then a solution of pure $ZnCl_2$ of molality M. contains the ions Zn^{++} at a concentration of M./2, and $ZnCl_4^{--}$ at M./2. In the mixture of $ZnCl_2$ and $MgCl_2$ in the molar ratio 2/1, ($x = 0·667$), at the same total molality M., the anion will still be entirely $ZnCl_4^{--}$, of concentration M./2; the cations

TABLE II.—PER CENT DEVIATIONS OF DATA OF TABLE I FROM THE "MIXTURE RULE."

M.	$KZnCl_3$.	K_2ZnCl_4.	K_3ZnCl_5.	Na_2ZnCl_4.	Li_2ZnCl_4.	K_2ZnBr_4.	K_2ZnI_4.
0·1	−2·3	+0·8	0·0	+0·4	+2·6	−0·7	—
0·2	−2·2	+0·2	+1·8	+2·1	+6·1	−0·2	−0·4
0·3	+0·4	+2·2	+5·8	+3·6	+8·9	+0·2	−0·3
0·5	+5·4	+9·4	+13·7	+6·7	+14·2	+1·7	+0·0
0·7	+9·6	+15·6	+21·4	+10·5	+18·3	+7·0	+1·7
1·0	+15·0	+23·7	+31·4	+15·6	+23·5	+13·3	+4·7

M.	1·5.	2·0.	2·5.	3·0.	3·5.	4·0.
Li_2ZnCl_4 devn.	+27·6	+27·6	+24·9	+20·5	+14·3	+9·0

Deviations are calculated as $(\Delta p_{calc.}-\Delta p_{obs.})100/\Delta p_{calc.}$, so that a positive sign indicates that the observed V.P. lowering is smaller than the calculated.

TABLE III.—VAPOUR PRESSURE LOWERINGS OF MIXTURES OF ZINC AND MAGNESIUM HALIDES AT CONSTANT TOTAL MOLALITIES (x = MOL. FRACTION OF ZINC SALT IN MIXTURE).

Salts.	Total M.	Δp, mm. Hg.				
		$x = 0$.	$x = 0·333$.	$x = 0·500$.	$x = 0·667$.	$x = 1$.
Chlorides . .	4	9·98	6·14	5·00	4·65	4·44
Chlorides . .	5	13·32	8·45	6·68	6·26	6·07
Chlorides . .	7	20 *	13·36	10·37	9·71	9·56
Bromides . .	5	14·54	9·36	7·63	7·15	6·80
Iodides † . .	5	15·86	10·32	8·38	7·67	7·39

* Estimated by extrapolation from saturated $MgCl_2$.

† The x values for the iodides were actually : 0, 0·339, 0·507, 0·680, and 1.

---

[3] Harris and Parton, *Trans. Faraday Soc.*, 1940, **36**, 1139; Parton and Mitchell, *ibid.*, 1930, **35**, 758; Stokes and Levien, *J. Amer. Chem. Soc.*, 1946, **68**, 1852.

will be 0·333 M. Mg^{++} and 0·167 M. Zn^{++}. Since it has been shown that the free zinc ion has very nearly the same osmotic effects as the magnesium ion,[3] this solution should show nearly the same vapour pressure lowering as pure $ZnCl_2$, i.e. we postulate an osmotic equivalence between $Zn[ZnCl_4]$ and $Mg[ZnCl_4]$. At $x = 0{\cdot}5$, in the equimolal mixture, there is still just enough zinc to bind all the chloride in the $ZnCl_4^{--}$ complex, so the solution will consist of M./2 $ZnCl_4^{--}$ and M./2 Mg^{++}. Again it should show the same Δp as the pure $ZnCl_2$. But for all mixtures with $x < 0{\cdot}5$, the position is different. There is now only enough zinc to bind part of the chloride, so, e.g. at $x = 0{\cdot}333$ the ions present are $ZnCl_4^{--}$ at 0·333 M., Cl^- at 0·667 M., and Mg^{++} at 0·667 M. Clearly such a solution will show a greater Δp than those with $x > 0{\cdot}5$, and as the zinc is progressively replaced by magnesium the Δp will rise steadily to that of pure $MgCl_2$. In this idealised case (where the process $Zn^{++} + 4Cl^- \rightleftharpoons ZnCl_4^{--}$ is assumed to have a very large equilibrium constant) the graph of Δp against x for constant total molality should be a pair of sharply intersecting straight lines, horizontal between $x = 0{\cdot}5$ and $x = 1$, and sloping down between $x = 0$ and $x = 0{\cdot}5$. The curves found approach this form; the break is definitely centred on $x = 0{\cdot}5$, but is rounded off because of a comparatively small equilibrium constant. Since the equilibrium constant involves the fourth power of the chloride activity the increasing sharpness of the break with increasing concentration is also explained.

Similarly if $ZnCl_3^-$ were the complex formed the break would set in at $x = 2/3$, while the formation of $ZnCl_5^{---}$ or $ZnCl_6^{----}$ would give breaks at $x = 2/5$ and $x = 1/3$ respectively. Fig. 2 shows that $ZnCl_4^{--}$ is the complex formed, and that if any other occurs, it is only to a very small extent and that the abnormalities of conc. $ZnBr_2$ and ZnI_2 solutions are due to the formation of the complex ions $ZnBr_4^{--}$ and ZnI_4^{--}. We see in Table II that with K_2ZnCl_4, K_2ZnBr_4 and K_2ZnI_4, the deviations appear soonest in K_2ZnCl_4, next in K_2ZnBr_4, and last in K_2ZnI_4, confirming that the order of decreasing stability of the complex ions is $ZnCl_4^{--}$— $ZnBr_4^{--}$—ZnI_4^{--}.

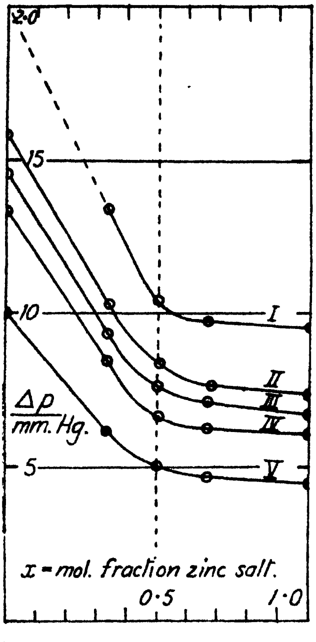

FIG. 2.—Vapour pressure lowerings of mixtures of zinc and magnesium halides at constant total molality.

I = $ZnCl_2$—$MgCl_2$ at M = 7.
II = ZnI_2—MgI_2 at M = 5.
III = $ZnBr_2$—$MgBr_2$ at M = 5.
IV = $ZnCl_2$—$MgCl_2$ at M = 5.
V = $ZnCl_2$—$MgCl_2$ at M = 4.

Sillen and Liljeqvist[4] have recently reported results of potentiometric titrations at 25°, which confirm this. They also consider that with the chloride and bromide, at least, higher complexes than ZnX^+ are formed but have not considered the possibility of ZnX_4^{--} formation specifically.

There is crystallographic evidence in favour of the existence of the $ZnCl_4^{--}$ grouping in the work of Klug and Alexander,[5] who concluded from an X-ray study of ammonium pentachlorzincate that $ZnCl_4^{--}$ forms one unit of the lattice, so that a more suitable formulation of this salt would be $NH_4Cl{\cdot}(NH_4)_2ZnCl_4$. The ion was found to be tetrahedral, with a Zn—Cl distance of 2·25 A. A number of workers have studied the Raman spectra of zinc halide solutions. Hibben[6] found for $ZnCl_2$ a shift of 275 cm.$^{-1}$ which was intensified considerably by the addition of NaCl: he attributed this to a Zn—Cl vibration in the undissociated molecule, though the possibility that it is due to a mode of the $ZnCl_4^{--}$ ion does not seem to be excluded. Da Silveira[7] found shifts of 108 and 286 cm.$^{-1}$: a value as low as 108 can scarcely correspond to a pure vibration, and is more likely to arise from one of the bending modes of the complex.

---

[3] Stokes and Levien, *J. Amer. Chem. Soc.*, 1946, **68**, 333.
[4] Sillen and Liljeqvist, *Svensk. Kem. Tid.*, 1944, **56**, 85.
[5] Klug and Alexander, *J. Amer. Chem. Soc.*, 1944, **66**, 1056.

We must next seek some explanation of the very marked dispersion shown by the $\Delta p/mp_0$ curves for K_2ZnCl_4, Na_2ZnCl_4, and Li_2ZnCl_4. At high concentrations we should expect these to behave as 1 : 2 salts like the alkali sulphates, yet the latter[8] show very little variation with the nature of the alkali ion. We can scarcely claim that the extent of the formation of $ZnCl_4^{--}$ decreases as we pass through the series, as the chloride ion activity is almost certainly greater in LiCl than in KCl, which should, if anything, increase the amount of complex formed. The explanation would seem to be rather that in the case of alkali-metal and $ZnCl_4^{--}$ ions the amount of Bjerrum ion-pair formation is very sensitive to the size of the hydrated cation. This would be expected if the sum of the ionic radii is near the critical value of 7 A. The radii of the hydrated potassium, sodium and lithium ions are respectively about 1·9, 2·1, and 2·6 A., while the $ZnCl_4^{--}$ radius may be roughly estimated as 3·2 A. The change in the radius sum brings Li_2ZnCl_4 much nearer to the critical size than K_2ZnCl_4, so that the latter should form ion-pairs to a greater extent, with a consequent diminution in its Δp, as is observed. With the substantially smaller sulphate ion, however, ion-pair formation is dominant regardless of the cation, so that little dispersion is shown.

In conclusion the author wishes to thank Dr. R. A. Robinson for many helpful discussions of the problems involved in this work.

Summary.

The anomalies found in the vapour pressure lowering of mixtures of the zinc halides with alkali-metal and magnesium halides are accounted for by the hypothesis that complex anions of the type ZnX_4^{--} are formed. This also explains the negative transport numbers of zinc in concentrated halide solutions. Other explanations such as $ZnCl_2$ or $ZnCl_3^-$ formation are shown to be inadequate. The order of decreasing stability is : $ZnCl_4^{--}$—$ZnBr_4^{--}$—ZnI_4^{--}.

Auckland University College,
New Zealand.

University of Western Australia,
Australia.

[6] Hibben, *J. Chem. Physics*, 1937, **5**, 710.
[7] da Silveira, *ibid.*, 1939, **7**, 380.
[8] Robinson, Wilson and Stokes, *J. Amer. Chem. Soc.*, 1941, **63**, 1011.

THE OXIDATION OF SULPHUR DIOXIDE IN SLOW COMBUSTION PROCESSES.

By G. Whittingham.

Received 5th December, 1946.

Many gaseous oxidations are chain reactions probably involving the participation of free atoms or radicals, such as H, O, OH and HO_2. Only by a chain mechanism is it possible to explain the existence of sharply defined explosion limits, the influence of inert gases, the inhibiting effects of surfaces, and the marked effect of small amounts of catalysts and inhibitors on reaction rates.

Whilst the kinetic evidence for chains is overwhelming there is a great need for techniques which can give independent proof of the existence and nature of the active carriers in oxidation reactions. Methods involving the introduction of externally produced atoms or radicals have been used to stimulate oxidation but these do not necessarily identify the chain carriers. There is interest in the role of O atoms, particularly in relation to the combustion of hydrocarbons, and Gaydon[1] has recently attributed the yellowish-green emission, given when small amounts of NO are added to various flames, to the association process, $NO + O = NO_2 + h\nu$ (continuous). This technique of adding NO was used to obtain a qualitative estimate of the atomic O concentration in flames.

Dooley and Whittingham[2] have studied the oxidation of SO_2 in flames, using both physical and chemical methods for the estimation of SO_3 and the results appear to indicate that SO_3 formation is brought about through reaction of SO_2 with atomic O. The amount of SO_3 produced was much higher in CO-air flames than in luminous, smoky CH_4-air flames and this was in agreement with the atomic O concentration as revealed by NO addition. Moreover, substances known from the work of Harteck and Kopsch[3] to react vigorously with atomic O brought about a reduction in the amount of SO_3 formed.

In studies of the oxidation of P carried out by Tausz and Görlacher,[4] and Melville,[5] the effect of certain substances on the upper ignition limit was greater than could be explained by the normal inert gas effect and this was attributed to direct removal of O atoms by the retarding substance X, i.e. $X + O = XO$.

For SO_2, which was a relatively weak inhibitor, Melville calculated the probability of reaction of SO_2 with O at 20° c. to be 6×10^{-6}. In a similar way Emeleus,[6] who showed that SO_2 was an inhibitor for the SiH_4—O_2 reaction, calculated the probability of reaction at 100° to be $0{\cdot}77 \times 10^{-3}$.

In contrast to the high reactivity with atomic oxygen, SO_2 is relatively inert to molecular O_2 except in the presence of a catalyst, such as platinum or iron oxide. A consideration of these facts and the results on the oxidation of SO_2 in flames indicated that the oxidation of SO_2 when added to systems undergoing slow combustion would appear to be a suitable technique for the detection of O atoms. The presence in the products of combustion of even a few parts per million of SO_3 is reflected in a marked increase in the dewpoint, for the measurement of which the electrical conductivity method[2, 7] was available.

The first part of the present paper describes some further work in which SO_2 was added to samples withdrawn from a Bunsen flame. In this way complications due to the oxidation of H_2S, CS_2 and other S compounds formed as intermediate products when SO_2 is added directly to coal gas flames were avoided. The second section deals mainly with the oxidation of SO_2 during the slow combustion of CO, a preliminary account of which has already been published;[8] some experiments on the slow combustion of CH_4, methyl alcohol, *n*-hexane and ether are also included. Oxidation of the latter two substances at temperatures of 200°-300° is characterised by " cool flame " emission and the formation of peroxides.

[1] Gaydon, *Proc. Roy. Soc. A*, 1946, **183**, 211.

[2] Dooley and Whittingham, *Trans. Faraday Soc.*, 1946, **42**, 354.

[3] Harteck and Kopsch, *Z. Elektrochem.*, 1930, **36**, 714.

[4] Tausz and Görlacher, *Z. anorg. Chem.*, 1930, **190**, 95.

[5] Melville, *Trans. Faraday Soc.*, 1934, **28**, 131.

[6] Emeleus and Stewart, *J. Chem. Soc.*, 1935, 1182.

[7] Johnstone, *Univ. Illinois Eng. Exp. Stn. Circ.* No. 20, 1929.

[8] Whittingham, *Nature*, 1946, **157**, 550.

I. The Oxidation of SO_2 in Gases Sampled from Coal Gas Flames.

Experimental.

Sulphur dioxide was used direct from a siphon and CO and CH_4 were obtained from cylinders. Nitric oxide was prepared by dropping conc. H_2SO_4 on to a mixture of KI and $NaNO_2$ and was stored over water. Lead tetraethyl and methylene chloride were A.R. products and the vapours were introduced into the system by blowing a steady stream of dry air through saturators containing the liquid and maintained at a constant temperature.

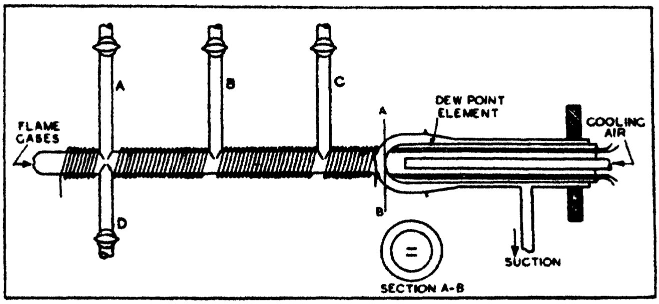

FIG. 1.—Apparatus for studying reactions of SO_2 with flame gases.

The sampling line for the withdrawal of gas from a fully aerated Bunsen flame and for examining the subsequent reactions with SO_2 is shown in Fig. 1. It consisted of a quartz tube of 1 cm. diam. and 15 cm. length narrowed down to a jet, 0·2 cm. diam. at one end. Side arms were situated at distances of 3 cm., 7 cm. and 10 cm. respectively from the jet and the other end of the tube was connected by a quartz-Pyrex ground joint to the dewpoint element. Details of the dewpoint method for estimating the SO_3 content of the gases have been described by Dooley and Whittingham,[2] who gave curves relating the dewpoint with the H_2SO_4 contents for gases containing 15 % and 10 % H_2O vapour respectively.

Sulphur dioxide was introduced through any of the side arms, A, B, or C, and other vapours and gases through D. Samples from the flame were withdrawn by means of a water pump and the volumes of all gases were measured on flow gauges containing dibutyl phthalate. When the jet was inserted into the flame there was a rapid drop in temperature over the first few cm. of the tube, but by means of a suitably wound heater it was possible to maintain the temperature of the tube from side arm A to the dewpoint element at a reasonably constant figure of 300° c.

In these and subsequent experiments in which the H_2O vapour content of the combustion gases could range from 0·1 % as in the slow combustion of CO, to 15·0 % as in a Bunsen flame, it was necessary to extend the dewpoint—H_2SO_4 measurements to include gases having a low H_2O vapour concentration. These measurements were carried out on a CO flame containing small amounts of added SO_2 and to which varying amounts of H_2 were supplied. The SO_3 content of the gases was determined by the chemical method described by Dooley and Whittingham.

As Fig. 2 shows, the dewpoint of the gases was much more dependent on the concentration of SO_3 than on that of H_2O vapour, and dewpoint changes can be attributed to changes in concentration of SO_3 and not to H_2O vapour formed in the oxidation processes. For example, in the slow combustion of methane the H_2O vapour content might increase 2- or 3-fold with a rise in furnace temperature of 50° c. ; this would only increase the dewpoint by a matter of 10°. On the other hand, the formation of only 10 parts per million of SO_3 would increase the dewpoint by 30° or 40° c.

Region of Formation of Active Centres in the Flame.—Sulphur dioxide was admitted through side arm A and samples of gas were withdrawn from various regions of the flame at a constant rate of 1·5 l./min. Fig. 3, on which the approximate dimensions of the flame zones are superimposed, gives the % conversion to SO_3 when 0·4 % SO_2 by volume was added to the products of combustion and the sampling point moved vertically upwards along the axis of the flame. The concentration of centres responsible for the oxidation of SO_2 appears to be low in the inner cone but rapidly increases towards the tip of the outer cone. Not until a region well above the flame is reached does it fall to a low value. On the addition of NO to the flame a green glow, only visible in a darkened room, extended above the flame, but it was not possible to determine whether the disappearance of this glow coincided with the rapid fall of centres to a low concentration as revealed by the oxidation of SO_2.

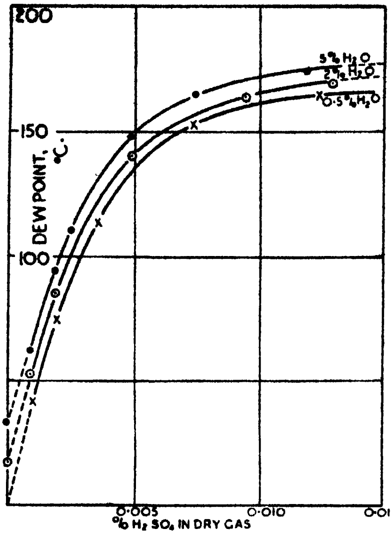

FIG. 2.—Variation of dewpoint with H_2SO_4 content for gases having different water vapour content.

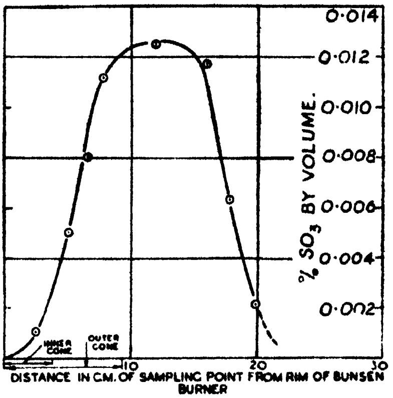

FIG. 3.—Oxidation of SO_2 when added to gases sampled from various regions of Bunsen flame (with approximate size of flame zones superimposed).

Decay of Centres in the Sampling Tube.—At a given point in the flame, the production of active centres will be governed by the various flame processes and will be sensibly constant. In the sampling tube the concentration will diminish away from the flame owing to reactions both in the gas phase and at the surface of the tube. These chain termination processes are known to depend on the presence of added gases and on the diameter and the state of surface of the tube, but a detailed investigation of the latter two factors was not carried out.

The decrease in concentration of centres under constant sampling conditions was shown by admitting SO_2 through the side arms A, B, and C in turn and measuring the SO_3 formed. To ensure that the time available for reaction should not be appreciably lessened as SO_2 was admitted successively through A, B and C, a tube was used in which the distance from side arm C to the element was 40 cm. Table I gives the % conversion to SO_3, as 0·4 % by volume of SO_2 was added through side arms A, B and C, i.e. at distances of 3 cm., 7 cm. and 10 cm. respectively from the flame. The samples were withdrawn from the central region of the outer cone. A detailed analysis of the extracted gases was not carried out but the amount of oxygen present in the samples drawn from this region was less than 0·2 %. Towards and beyond the tip of the outer cone, where secondary air was diffusing in, the amount of O_2 present rapidly increased. It is evident that the concentration of centres diminishes with the path traversed but they are still detectable in a region 10 cm. from the flame, i.e. after a time of 0·3–0·4 sec.

TABLE I.

Distance from flame in cm.	% SO_3.
3	0·008
7	0·004
10	0·002

TABLE II.

% SO_2.	% SO_3.
0·1	0·004
0·2	0·006
0·4	0·008
1·0	0·012
2·0	0·020
4·0	0·023
5·0	0·026

Variation of SO_3 formed with Concentration of SO_2.—Gas was sampled from the central region of the outer cone and SO_2 was admitted through side arm A. The amounts of SO_3 produced, expressed as % of the total gas, with varying concentrations of SO_2 are shown in Table II. For concentrations of SO_2 up to 2 % the amount of SO_3 produced appears to follow the relationship $SO_3 = K\sqrt{SO_2}$; but for higher concentrations of SO_2, the SO_3 tended to reach a limiting value.

Effect of Added Gases.—In this series of experiments various gases and vapours were introduced into the main stream through side arm A, and 2 % by volume of SO_2 was introduced through B. In this way the extent of interaction of the added agents with active centres, over the region of the tube from A to B, could be ascertained from measurement of the SO_3 content with and without the added agent.

Fig. 4 shows that the change in SO_3 content varies with the concentration and nature of the added gas, and the effect can be related to the known reactions of these substances with atomic oxygen. Methane was more effective than CO in reducing the SO_3 content of the gases. In a study of the NOCl sensitised H_2—O_2 reaction, Dainton and Norrish [9] showed that the addition of small amounts of CH_4 brought about a great increase in the length of the induction period and effectively quenched ignition. They attributed this effect to reaction with the chain species, $CH_4 + O = CH_2 + H_2O$.

Harteck and Kopsch's work showed that whilst both gases were relatively inert to O atoms at room temperature, CH_4 was more reactive than CO. Methylene chloride, on the other hand, was highly reactive to O atoms and reference to Fig. 4 shows that its presence in the gas stream reduced the amount of SO_3 formed to a greater extent.

Similarly, $Pb(C_2H_5)_4$, which Melville [8] showed to be a comparatively strong inhibitor of the phosphorus oxidation, was even more effective in bringing about a reduction in the amount of SO_3 formed. In the course of its oxidation a yellowish-white substance was deposited on the walls of the tube and, after several runs, the end of the dewpoint element became covered with a thin yellowish layer. Whilst recent work [10] has shown that the presence of certain particulate deposits on the nose of the dewpoint instrument may influence the state of condensed films and so complicate the interpretation of dewpoint data, it is considered that the effect of $Pb(C_2H_5)_4$ here can be attributed to its reactions with atomic oxygen.

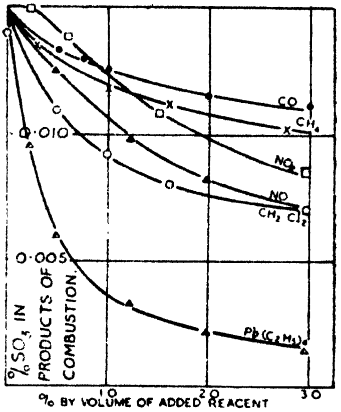

FIG. 4.—Effect of various reagents on the oxidation of SO_2 added to gases sampled from a Bunsen flame.

The results obtained with NO and NO_2 (prepared by premixing NO with O_2 and leading the mixture into the main gas stream) can also be considered in the light of their known reactions with O atoms. The addition of NO_2 has been found to reduce induction periods and promote ignition in many oxidation reactions, and this is generally attributed to its role in providing O atoms, viz. $NO_2 = NO + O - 71{\cdot}5$ cal.

However this may be, for small additions of NO_2 the amount of SO_3 produced remained almost constant, whilst larger amounts led to a reduction in SO_3 content. This is probably due to the competitive reaction by which NO_2 is known to remove O atoms, i.e. $NO_2 + O = NO + O_2$. Nitric oxide was more effective than NO_2 in its effect on the SO_3 content and this is considered to be due to the removal of O atoms by $NO + O = NO_2 + 71{\cdot}5$ kcal. This reaction is responsible for the yellow-green emission obtained when NO is added to flames containing atomic O. Under the conditions of these tests no emission was observed, probably because of the relatively low concentrations of O atoms. Any detailed interpretation of the reactions between NO, NO_2, O and SO_2 is obscured by the formation of complexes between the nitrogen oxides and SO_2 and SO_3. After a series of tests had been done involving NO_2, a whitish substance collected

[9] Dainton and Norrish, *Proc. Roy. Soc. A*, 1941, **177**, 393.

[10] Lorenz and Whittingham (unpublished work).

in the cooler regions of the sampling system beyond the element, which gave a positive test for nitrate and sulphate. The formation of such complexes has also been observed by Dainton and Reagh[11].

The Oxidation of SO_2 during the Slow Combustion of Carbon Monoxide. A flow method was adopted in which mixtures of the combustible gas and O_2 to which small amounts of SO_2 had been added, was passed at a rate of 400-500 cc. a minute through a Pyrex tube, 2·5 cm. diam. and 25 cm. long, placed in a furnace. The temperature of the furnace, measured by a chromel-alumel thermocouple inserted at the side of the reaction tube, was raised at a steady rate of 5° c./min. The SO_3 in the exit gases was estimated from a dew-point measurement, the end of the dewpoint element being inserted into the end of the tube by means of a ground glass joint. As the determination of a dewpoint is a comparatively rapid process, the SO_3 content at any time can be related directly to the conditions in the reaction tube with only a small time lag. Undried CO direct from a cylinder was used.

The oxidation of CO, in common with other chain reactions, is markedly dependent on the state of the reaction vessel, and during the first few runs, whilst reaction rates steadied down, a qualitative estimate of the SO_3 content in the exit gases was carried out in the following way. The dewpoint element was replaced by a bubbler containing water through which the gases passed, and the amount of H_2SO_4 mist formed above the liquid was observed visually. Experience has shown this to be a good qualitative indicator of SO_3 concentration, and mist production can be observed with an SO_3 concentration of 10 parts in a million.

A CO : $3O_2$ mixture to which 1 % SO_2 had been added was passed through the heated tube at 450 cc./min. No mist was observed above the bubbler until the furnace temperature was 600° c. but at about 600°-620° as the luminescent region was reached, the mist increased in density. Just prior to ignition the density of mist was extremely high and after several runs it was possible to predict when ignition was about to take place.

Although the ignition temperature fluctuated somewhat at first a steady figure of 665° c. was finally obtained under the conditions used. The results of quantitative measurements of the SO_3 content are shown in Fig. 5 and demonstrate the increase in SO_3 which takes place over a range of about 50° prior to ignition. It was not possible to maintain a steady flame in the tube after ignition but that there was a high concentration of centres in the flame was shown in the following way. The temperature of the dewpoint element was maintained about 10° c. above the dewpoint value determined just prior to ignition. As each separate flame pulse passed down the tube there was a big increase in conductivity across the element, i.e. a film of H_2SO_4 was deposited on the element, indicating a still higher dewpoint as a result of the flame reactions.

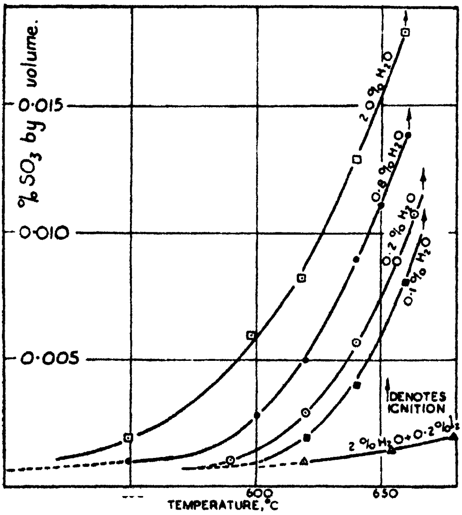

FIG. 5.—Effect of water vapour and iodine on the oxidation of SO_2 during the slow combustion of CO.

The Influence of Iodine and Water Vapour.—In view of the well-known inhibiting influence of I_2 and the catalytic influence of H_2O vapour on the CO oxidation, some experiments were carried out to determine how the growth of centres, as revealed by the SO_3 formed, was affected by each of these reagents.

The gases used in the tests already described contained small amounts (about 0·09 % by volume) of H_2O vapour. Increasing amounts of H_2O vapour were introduced into the system by passing a stream of O_2 through H_2O in a saturator maintained at 20° c. and allowing this to mix with the main stream before the reaction vessel. The volumes of O_2 used in the main stream and in the water by-pass were always adjusted so as to give the same total volume passing through the heated tube. It was soon apparent that an increase in the H_2O vapour content brought about an increase in the concentration of centres and a higher conversion to SO_3 was given, SO_3 being detected at lower temperatures than with the normal gases. The results are shown in Fig. 5.

---

[11] Dainton and Reagh, *Trans. Faraday Soc.*, 1946, **42**, 363.

Although the concentration of SO_3 at ignition was higher in the wetter mixtures the actual value of the ignition temperature was altered only slightly. This indicates that the centres responsible for the oxidation of SO_2 in the wet reaction are not directly involved in the processes leading to ignition. There remained the possibility that H_2O vapour catalyses the heterogeneous oxidation of SO_2. As the surface oxidation, as measured by passing an O_2 + 1 % SO_2 mixture through the heated tube, was extremely low a packed tube was used in order to increase the surface area/volume ratio. With a packed tube having an area/volume ratio 6 times greater than the unpacked tube, the SO_3 content of the exit gases at 600° rose to 0·1 %. When the water content was increased from 0·09 to 2·0 % the amount of SO_3 produced was 0·05 % ; H_2O vapour has then an inhibiting effect on the heterogeneous oxidation.

Small amounts of I_2 were produced in the system by passing a slow stream of O_2 through *iso*-propyl iodide maintained at a constant temperature in a saturator and allowing it to mix with the main stream. Decomposition of *iso*-propyl iodide at temperatures of 500°-600° c. is extremely rapid but it was not possible to utilise the mist technique for the qualitative estimate of SO_3 because of the formation of a cloud of iodine, some of which passed through the absorbing solution. Dewpoint measurements showed, however, that the SO_3 content of the exit gases had been greatly reduced by the I_2, even when 2 % H_2O vapour was added to the reacting gases (see Fig. 5).

During the course of these determinations a slight increase in conductivity across the element was given when the dewpoint element was cooled down, but this decreased in value with further cooling. The production of a conducting film over a definite temperature range is probably due to the deposition of I_2. Subsidiary experiments in which a film of I_2 was thermally deposited on the element and the latter inserted into a gas having a known H_2SO_4 content, showed that the detection of H_2SO_4 condensation is unaffected by the presence of a film of I_2 on the element and the reduction in SO_3 concentration in the above experiments is definite, and can be attributed to the influence of I_2 on the combustion reactions. In the presence of I_2 the ignition temperature of the CO—O_2—SO_2 mixture was raised considerably.

II. The Oxidation of Methane, Methyl Alcohol, Hexane and Ether.

Methane from a cylinder was used without further purification. Methyl alcohol, *n*-hexane and diethyl ether were all redistilled before use, and suitable mixtures of these with oxygen were obtained by bubbling O_2 through saturators containing the liquid and maintained at a constant temperature. The combustion of CH_4 and methyl alcohol was carried out in the same tube as used for CO—oxygen, and a CH_4 : $3O_2$ mixture containing 1 % SO_2 was passed through the tube at a rate of 450 cc./min.

The oxidation of CH_4 is characterised by induction periods preceding slow reaction or ignition and the duration of the induction period is known to depend on mixture composition, pressure, temperature and other factors. Around 400° c. the induction period has a duration of many minutes but this is reduced to seconds as the temperature increased to the ignition temperature. Under the conditions of the experiments described, the time of contact of the gases was of the order of 10 sec. so that the initial stages of combustion were studied. Sulphuric acid mist production in the bubblers was first observed at a temperature of about 540° and thereafter it increased in intensity up to the ignition temperature of 600° c. The density of mist just prior to ignition was not so high as in the case of CO and this is borne out by the quantitative estimate of the SO_3 formed. The variation of SO_3 content with temperature is shown in Fig. 6. Measurements of the SO_3 content during the propagation of flame were not carried out because the violence of the explosions tended to blow the dewpoint element out of the ground glass joint. With a 25 % CH_3OH mixture containing 1 % SO_2, SO_3 formation set in at still lower temperatures and ignition was observed at 560° (see Fig. 6).

For observations on the oxidation of hexane and ether an apparatus was used similar to that described by Emeleus [12] in his observations on the spectrum of the cool flame of ether, acetaldehyde and CS$_2$. This consisted of a Pyrex tube, 25 cm. in length and 1 cm. diam. through which the combustible mixture and SO$_2$ was passed at a rate of 300 cc./min. The end of the tube, prior to the dewpoint element, was electrically heated over a length of 10 cm., and the exit gases passed through the bubblers for observation of mist formation.

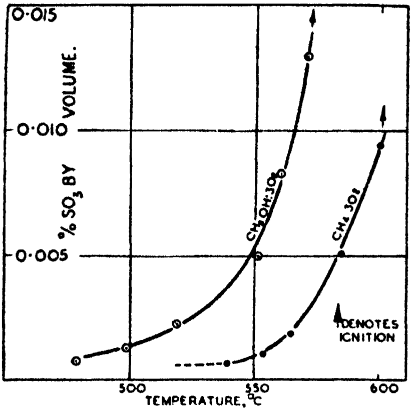

FIG. 6.—Oxidation of SO$_2$ during slow combustion of methane and methyl alcohol.

With a mixture containing 10 % ether, mist was observed even in the absence of SO$_2$. This was first detected at a gas temperature of 180° and it increased in intensity until a dense fog was obtained at 240° C.; at this temperature, marked exothermic reactions were taking place in the reaction tube. Because the tube was enclosed and end-on vision was obscured by the presence of the dewpoint element it was not possible to observe any luminescence in the reaction zone, except on isolated occasions when pale blue flashes passed down the tube. The events described were very similar to those discussed in detail by Mardles and co-workers.[13]

The formation of this mist naturally obscured the detection of H$_2$SO$_4$ when SO$_2$ was added to the system, but there was a definite increase in the intensity of mist when SO$_2$ was added. Dewpoint observations, which were obtained in spite of deposition of tarry material on the end of the element, showed that SO$_3$ formation was taking place, e.g. at 210° C. the % SO$_3$ in the exit gases was 0·004, for an SO$_2$ content of 1·0 %.

Mixtures containing 30 % hexane gave a similar behaviour over a slightly higher temperature range and in the presence of the S oxides tar production was increased. It is interesting to compare this result with the influence of SO$_2$ on C deposition from coal gas flames,[14] and the suggestion of Cloud and Blackwood [15] that the formation of SO$_3$ in the combustion of fuels in Diesel engines leads to deposit trouble due to the attack of hydrocarbons by SO$_3$.

Discussion.

The above results tend to support the conclusion drawn by Dooley and Whittingham, that oxidation of SO$_2$ in the sampling tube takes place through reaction with O atoms formed in the flame. As might be expected, the extent of oxidation is much less than that which occurs when SO$_2$ is added to the flame itself, this being due both to the rapid recombination of free atoms in the sampling tube before SO$_2$ mixes with the hot gases and to the lower prevailing temperature. As the amount of free O$_2$ in the gases sampled from the central region of the outer cone was very low, O atoms probably disappear through the three-body process, $O + O + X = O_2 + X$, rather than through the ternary collision, $O + O_2 + X = O_3 + X$. The lifetime of the free atoms was found to be of the order of 5×10^{-1} sec. corresponding to a concentration of the order of 10^{-4} mm. It is doubtful whether oxygen would act as a remover of O atoms under the experimental conditions used above as any ozone formed through $O + O_2 + X = O_3 + X$, would tend to decompose and re-generate O atoms. The influence of the various added agents on the amount of SO$_3$ formed, as indicated earlier, is in harmony with their

[12] Emeleus, *J. Chem. Soc.*, 1926, 2948.

[13] Gill, Mardles and Tett, *Trans. Faraday Soc.*, 1928, **24**, 574.

[14] Whittingham, *Nature*, 1945, **156**, 207.

[15] Cloud and Blackwood, *Soc. Automotive Engrs.*, 1943, **51**, 408.

known properties of either yielding O atoms through thermal dissociation (e.g. $NO_2 = NO + O$) or removal of O atoms through direct reaction, processes which, as Harteck and Kopsch (loc. cit.) have shown, are highly exothermic. It is not possible, however, to obtain values for the relative efficiency of collision of atomic O with the added gases because secondary reactions between the products of such collisions and SO_2 tend to obscure the issue.

Under constant sampling conditions it appears that the addition of SO_2 to gases withdrawn from flames and measurement of the SO_3 formed, would serve to give some evidence as to the region of formation and concentration of O atoms in flames. Gaydon [16] has pointed out that in addition to the direct association, $SO_2 + O = SO_3$, oxidation of SO_2 might occur through a termolecular process, viz. $SO_2+O+M=SO_3+M$, and would therefore be dependent on the nature and concentration of other constituents in the products of combustion. A study of the spectra of S oxides in flames [17] suggests that the direct association accompanied by the emission of a continuous spectrum, can take place and it is also possible that SO_3, having six vibrational degrees of freedom, can absorb the energy of reaction without requiring a three-body collision.

In order to interpret the results obtained on the oxidation of SO_2 during the slow combustion of CO it seems best to recapitulate briefly the kinetics of this reaction. Under the experimental conditions described the phenomena are those associated with the upper limit of ignition. The " wet " oxidation is known to proceed by a chain mechanism in which the rate of reaction is proportional to the H_2O vapour concentration and the CO concentration, and inversely proportional to the O_2 concentration. The development of chains is considered to take place [18] through the following sequence of reactions :

$$\left.\begin{array}{l} H_2O = H + OH \\ H_2O + M = H + OH + M \end{array}\right\} \text{Initiation}$$

$$\left.\begin{array}{l} CO + OH = CO_2 + H \\ H + O_2 + X = HO_2 + X \\ HO_2 + CO = CO_2 + OH \end{array}\right\} \text{Propagation}$$

and chains are terminated at the surface of the vessel. Oxygen atoms do not participate directly in the chains but can be formed through

$$H + O_2 = OH + O$$

a process which is fairly fast at temperatures around 600° c.

Examination of Fig. 5 and 6 show that the technique described is sensitive enough to detect the presence of O atoms below the ignition temperature where ordinary methods of analysis show that the rate of reaction is slow. As the temperature increases, the concentration of centres increases rapidly but, as the results on adding H_2O vapour show, the conditions for ignition are not directly related to the concentration of such centres. Oxygen atoms are, in fact, incidental to the main process; but any means by which the H atom concentration is affected, e.g. through dissociation of H_2O or removal by I_2, will influence the concentration of O atoms. The inhibiting effect of I_2 on the CO-oxidation is attributed to reaction with H atoms, i.e. $H + I_2 = HI + I$, and with OH, or $HI + OH = H_2O + I$.

The data for the oxidation of SO_2 during the combustion of CH_4, methyl alcohol, hexane and ether are as yet insufficient to justify very definite conclusions about the nature of the species responsible for the formation of SO_3 but the fact that oxidation of SO_2 takes place to a measurable extent even at temperatures as low as 200°-250°, is sufficiently promising to justify further work.

[16] Gaydon, *Trans. Faraday Soc.*, 1946, **42**, 362.

[17] Gaydon and Whittingham (in course of publication).

[18] Hinshelwood, *The Kinetics of Chemical Change* (O.U.P., 1940), p. 170.

The initial stages of combustion of paraffin hydrocarbons have been the subject of much discussion and two main theories have been advanced. The hydroxylation theory postulates the successive replacement of H by OH; Norrish's modification of this [19] involved a chain mechanism with atomic oxygen as the active carrier,

$$CH_4 + O = CH_2 + H_2O$$
$$CH_2 + O_2 = CH_2O + O,$$

but objection to this has been raised on the grounds that CH_4 is relatively inert to atomic O. It is interesting to note, however, that the degree of oxidation of SO_2 was highest during the slow combustion of CH_3OH and it is known that CH_3OH is extremely reactive to O atoms, the exothermicity of this reaction being sufficient to give a flame.[20]

The peroxidation theory advanced by Callendar, and supported by Egerton and others, postulates the formation of a peroxide which can set up a series of chain reactions through

$$R + O_2 = RO_2$$
$$RO_2 + RH = RO_2H + R.$$

Decomposition of the hydroperoxide can yield aldehydes and OH radicals which maintain chains through $RH + OH = R + H_2O$.

The observation therefore that SO_2 is oxidised during the combustion of hexane and ether may be of value in determining the role of peroxides in low-temperature oxidation. The work of Townend and collaborators [21] suggests that under suitable conditions the " cool flames " observed in hydrocarbon combustion (the emission from which is due to the production of excited formaldehyde molecules) can give rise to normal ignition through a two-stage process in which the decomposition of peroxides may produce centres responsible for chain branching at higher temperatures.

Hydroxyl radicals are known to play an important part in gaseous combustion and there is the possibility that SO_2 can react with OH, i.e. $SO_2 + OH = SO_3 + H$, but this reaction is endothermic and likely to be slow in comparison with $SO_2 + O = SO_3$.

Examination of the spectra of flames containing S oxides [16] shows that the normal emission from electronically excited OH is diminished but this may be due merely to de-activation and not direct chemical reaction between SO_2 and OH.

This work forms part of a programme of research on boiler deposits and corrosion sponsored by the Boiler Availability Committee and I am indebted to the Chairman of the Committee for permission to publish this work. I would like to express my thanks to Dr. D. H. Bangham and Mr. A. Dooley for their interest and many suggestions and to Prof. H. W. Melville for some constructive comments.

Summary.

The oxidation of SO_2 when added to a coal gas flame has been studied, using a dewpoint meter for the measurement of SO_3. The amount of SO_3 formed varies with (*a*) the concentration of SO_2, (*b*) the region of the flame from which the samples are withdrawn and (*c*) the presence of substances known to generate or react with atomic O.

The oxidation of SO_2 during the slow combustion of CO, CH_4, methyl alcohol, hexane and ether has also been investigated and the nature of the species responsible for the oxidation of SO_2 in each of these processes is discussed.

The British Coal Utilisation Research Association,
13 Grosvenor Gardens,
London, S.W.1.

---

[19] Norrish and Foord, *Proc. Roy. Soc. A*, 1936, **157**, 203.
[20] Geib and Vaidya, *Proc. Roy. Soc. A*., 1941, **178**, 351.
[21] e.g. Townend and Topps, *Trans. Faraday Soc.*, 1946, **42**, 345.

THE SALTING-OUT EFFECT AND DIELECTRIC CONSTANT.

By J. O'M. Bockris and Harold Egan.

Received 9th October, 1946, as revised 30th December, 1946.

Introduction.

1. Empirical Salting-out Equations.—In the following, the term " salting-out " signifies the phenomenon of change of solubility of a non-electrolyte, molecularly distributed in a solvent, as a result of the addition of a soluble electrolyte to the system. Usually, the non-electrolyte concentration is thereby decreased ; the expression " salting-in " describes the corresponding case in which the solubility increases.

Several empirical equations have been used to relate salting-out to electrolyte concentration. An appropriate equation must be primarily concerned with the solubilities of the non-electrolyte in the pure solvent (S_0) and in the electrolyte solution in that solvent (S), and the solubility ratio S_0/S, or the simply related relative solubility change $\frac{S_0 - S}{S}$, has frequently been used.

Setschenow's original empirical equation[1] for the absorption coefficient, y, of carbon dioxide in a salt solution at a given temperature, is

$$y = \alpha e^{-k'/x} \qquad . \quad . \quad . \quad . \quad . \quad (i)$$

where α is the absorption coefficient for carbon dioxide in water, x the dilution of the salt and k' a constant. This may be rewritten

$$S = S_0 e^{-kc} \qquad . \quad . \quad . \quad . \quad . \quad (ii)$$

where c is the salt concentration and k the " salting-out constant ", or as

$$\ln \frac{S_0}{S} = kc \qquad . \quad . \quad . \quad . \quad . \quad (iii)$$

(cp. Rothmund[2]) and is hereafter referred to as the Setschenow equation. As a measure of salting-out k has been widely adopted. Many other empirical relationships have been recorded,[3] most of which reduce to equation (iii) when $(S_0 - S)$, or ΔS, is small. Larsson[4] illustrated the approximately additive nature of k, showing

$$k = k_+ + k_- \qquad . \quad . \quad . \quad . \quad . \quad (iv)$$

where k_+ and k_- are cationic and anionic salting-out constants respectively. Linderstrøm-Lang[3] has obtained evidence indicating that whilst k is largely dependent on the electrolyte, it is also dependent to a lesser extent on the non-electrolyte (see also Randall and Failey[5]).

---

[1] Setschenow, *Z. physik. Chem.*, 1889, **4**, 117.

[2] Rothmund, *ibid.*, 1900, **33**, 402.

[3] See, for example, Jahn, *ibid.*, 1902, **41**, 257 ; Linderstrøm-Lang, *Compt. rend. trav. lab. Carlsberg*, 1924, **15**, No. 4, 1 ; Glasstone and Pound, *J. Chem. Soc.*, 1925, **127**, 2660 ; Chase and Kilpatrick, jnr., *J. Amer. Chem. Soc.*, 1931, **53**, 2589, 2594 ; Gross, *Chem. Rev.*, 1933, **13**, 89 ; Markham and Kobe, *J. Amer. Chem. Soc.*, 1941, **63**, 449, 1165 ; Morrison, *Trans. Faraday Soc.*, 1944, **40**, 43.

[4] Larsson, *Z. physik. Chem.*, 1931, **153**, 299.

[5] Randall and Failey, *Chem. Rev.*, 1927, **4**, 285, 291.

Some confusion has existed in the literature with regard to the names associated with ΔS and $\Delta S/S$. It appears reasonable to call ΔS the salting-out and $\Delta S/S$ the relative salting-out; this nomenclature will be used in the following.

2. Theories of Salting-out.—Explanations of the salting-out effect can be divided into two groups. On the one hand it was considered [6] that the presence of an electrolyte increased the internal pressure in the solution, and thus decreased the solubility of the non-electrolyte solute. On the other, it has been suggested that the solvation of ions forms the essential basis of the salting-out effect because concentration of the solvent molecules round the solute ions must reduce the solvent power for the non-electrolyte solute. Modern quantitative theories of the salting-out effect have been concerned only with the latter view.

Thus Debye and McAulay [7] accept as the criterion of polarity, and therefore of the degree of solvation, the change of dielectric constant of the liquid at a given temperature when a non-electrolyte is dissolved in it. They assume that

$$D = D_0(1 - \beta n - \beta' n') \quad . \quad . \quad . \quad . \quad (\text{v})$$

where D and D_0 are the dielectric constants of the solution and pure solvent, β' and β, n' and n the dielectric decrements and concentrations of the electrolyte and non-electrolyte, respectively. Using the Born solvation energy equation [8] and the Debye-Hückel limiting equation [9] the final form of the equation is

$$\ln f = \frac{\beta \Sigma n_i e_i^2 e^2}{2D_0 kTb} \quad . \quad . \quad . \quad . \quad (\text{vi})$$

where b is the mean effect ionic radius, f the activity coefficient of the non-electrolyte solute, and the other symbols bear their usual significance. Also, since the chemical potentials of the solid non-electrolyte and that in solution are equal, then

$$S_0 f_0 = Sf \quad . \quad . \quad . \quad . \quad (\text{vii})$$

f_0 being the activity coefficient of the non-electrolyte when in a saturated solution in the pure solvent. If $f_0 = 1$, then from (vi), the Debye and McAulay equation is of the same form as that of Setschenow.

Debye [10] formulated a more rigid analysis by expressing the free energy of the ions as a function involving the energy of their coulombic fields, viz.,

$$U = \frac{(DF)^2}{8\pi D} \quad . \quad . \quad . \quad . \quad . \quad (\text{viii})$$

where F is the field strength at a given point, and deduced expressions showing the distribution of the non-electrolyte in the vicinity of an ion as a function of the distance from it, and hence calculated the total amount of non-electrolyte salted out.

Butler [11] calculated the Maxwellian distribution of the solute and solvent non-electrolyte round an ion on the basis of the equation

$$W = \int_0^F P dF \delta V \quad . \quad . \quad . \quad . \quad (\text{ix})$$

where W is the work done in bringing a molecule from infinity to a point near the ion where the field is F, P the polarisation of the non-electrolyte molecule, F the field at a given point, and δV the volume of the solvent or non-electrolyte solute. As $P = \alpha F$, the distribution may be expressed in terms of the polarisabilities, α_A and α_B, of the solvent and solute. Butler obtained

---

[6] von Euler, *Z. physik. Chem.*, 1899, **31**, 360.
[7] Debye and McAulay, *ibid.*, 1925, **26**, 22.
[8] Born, *Z. Physik*, 1920, **1**, 45.
[9] Debye and Hückel, *Physik. Z.*, 1923, **24**, 185.
[10] Debye, *Z. physik. Chem.*, 1927, **130**, 56.
[11] Butler, *J. Physic. Chem.*, 1929, **33**, 1015.

$$\frac{\Delta S}{S} = \frac{(\alpha_A - \alpha_B)\Delta v_B \, . \, 4\pi N}{2D^2kT} \sum \frac{e^2c_i}{b} \quad . \quad . \quad . \quad (x)$$

where Δv_B is the volume of the non-electrolyte molecule and c_i the concentration, in g.-ions per litre, of electrolyte. Substituting $\alpha = \frac{D - 1}{4\pi}$ and $\frac{\Delta S}{S} \simeq \ln f$ shows that equation (x) is nearly equal to equation (vi) if $D \simeq D_0$.*

The three theories described involve the following assumptions.

(1) The origin of the salting-out effect is purely electrostatic; (2) the ions may be treated as solid spheres; (3) the solutions are very dilute (this assumption is involved in Debye's theory by the use, *inter alia*, of the limiting expression for the charging and discharging of an ion and the energy of a unit volume element near the ion, and in Butler's theory by the use of e^2/r^2 as the field near an ion); (4) there is an absence of dielectric saturation effects in the neighbourhood of the ions. Assumption (3) has been examined theoretically by Gross,[12] who showed that the effect of interionic attraction in less dilute solutions would be to reduce the salting-out in comparison with that obtained by Debye's equation.

3. Previous Work.—Few attempts to examine the above described electrostatic theories have been made. Gross [13] has shown that acetone is salted out from aqueous solutions by most simple electrolytes, but hydrocyanic acid is salted in as would be expected from the theory owing to the fact that the polarisability of the latter is higher than that of water. Quantitative agreement was fair but the calculated results were too low. Albright and Williams [14] showed from measurements of dielectric constants of solutions of ethyl acetate in water that the results of Glasstone and Pound [15] for salting-out in this system could be calculated well from Debye's theory.

Conversely, anomalies to Debye's and Butler's theories obtain in the existence of certain non-electrolytes which are salted out by some electrolytes and salted in by others.[16] The same non-electrolyte must have essentially the same polar properties in different electrolytic solutions at the same temperature, so that it appears that some of these anomalies originate from the electrolyte. The latter usually appear to contain large negative ions as I^-, ClO_3^-, NO_3^-, etc., and it is relevant to refer here to Sugden's report [17] of negative hydration numbers for some anions.

It is therefore seen that the scope and extent of the attempts to verify the degree of applicability of the electrostantic theories of salting-out has been very limited. It appears that the following subjects particularly require experimental examination. (1) Anomalous examples of salting-in, referred to above; (2) salting-out in dilute solutions under conditions of concentration at which the limiting laws of the theories might be expected to apply (work at concentrations of electrolyte less than about 0·25 N. involves difficulties in the accurate determination of ΔS); (3) the effect of the constitution of the non-electrolyte; (4) the effect of dielectric constant variation. The last of these four factors, i.e. the comparison between theoretical results and those of experiment for the variation of the salting-out effect with changing force of attraction between ion and solvent molecules, would seem of paramount importance in the examination of the range of applicability of the electrostatic theories. The following is a report of measurements of the salting-out effect in organic solvent-water systems of continuously varying composition.

---

* This assumption is dependent on the approximation $\frac{S_0 - S}{S} = \ln \frac{S_0}{S}$ which in many practical cases involves an error of 10-20 %.

[12] Gross, *Monatsch.*, 1929, **53-54**, 445.

[13] Gross and Iser, *Sitz. Acad. Wiss. Wien.*, 1930, **139**, 178.

[14] Albright and Williams, *Trans. Faraday Soc.*, 1937. **33**, 247.

[15] Glasstone and Pound, *J. Chem. Soc.*, 1925, 2660.

[16] Linderstrøm-Lang, ref. [8].

[17] Sugden, *J. Chem. Soc.*, 1926, 174.

Experimental.

1. The Choice of a System.—The main criteria for a suitable system in which to examine the variation of salting-out with dielectric constant are: (1) the system must allow as wide a range as possible of dielectric constant values; (2) the solubility of the added solute non-electrolyte must not vary greatly during the change of dielectric constant of the solvent medium; (3) an accurate method must be available for the estimation of the solute non-electrolyte; (4) the solubility of the latter should be comparatively small to avoid inaccuracies caused by small temperature fluctuations.

The systems chosen were benzoic acid in methanol-, ethanol- and dioxan-water mixtures. These obey the above criteria reasonably well, and the use of the two alcohols enables the salting-out to be examined under isodielectric conditions in different solvents of similar type. All solutions were 0·01 M. with respect to sodium benzoate in order to repress the ionisation of the benzoic acid; 1·025 M. NaCl (cf.[18]) was used throughout. Since dielectric constants are not available for benzoic acid-NaCl solutions, or of benzoic acid solutions, the

TABLE I.—THE SOLUBILITY OF BENZOIC ACID IN METHANOL-, ETHANOL- AND DIOXAN-WATER MIXTURES (WITH 0·01 M. SODIUM BENZOATE) AT 25° C., WITH AND WITHOUT 1·025 M. NaCl.

(*a*).	(*b*).	(*c*).
* DIOXAN		
5·132	0·0384	0·0265
9·944	0·0555	0·0394
9·979	0·0548	0·0392
15·31	0·0853	0·0625
19·99	0·1304	0·1008
24·24	0·201	0·163
* METHANOL		
5·306	0·0326	0·0227
10·08	0·0400	0·0288
15·06	0·0508	0·0383
20·51	0·0707	0·0557
24·85	0·0956	0·0773
30·44	0·1507	0·1272
35·75	0·253	0·219
40·68	0·384	0·340
46·79	0·691	0·624
52·63	1·059	0·961
58·72	1·555	1·395
61·99	1·96	1·78
WATER		
—	0·0276	0·0185
* ETHANOL		
5·54	0·0331	0·0241
9·97	0·0418	0·0315
14·99	0·0569	0·0476
15·41	0·0589	0·0495
17·84	0·0729	0·0657
20·14	0·0925	0·0886
25·08	0·171	0·183
30·64	0·350	0·390
35·21	0·585	0·642
40·16	0·919	0·976
42·34	1·051	1·105
49·74	1·698	1·672
54·58	2·135	2·090

* Solubilities are recorded in g. moles of benzoic acid per 1000 g. binary solvent in all cases.

(*a*) Weight % of non-aqueous component of binary solvent.

(*b*) Solubility in binary solvent.

(*c*) Solubility in binary solvent containing 1·025 M. NaCl.

---

[18] Morrison, ref. [8].

values of the dielectric constants of the solutions recorded in the literature for methanol[19], ethanol-[20] and dioxan-[20] water mixtures have been used.

In the case of alcohol-water systems, accurate solubility measurements were found impracticable above about 65 % w/w methanol and 55 % w/w ethanol owing to the high values attained and the relatively large effect of temperature fluctuations. For dioxan-water mixtures containing more than about 25 % w/w dioxan, two solvent phases separated out on the addition of benzoic acid when NaCl was present.

TABLE II.—DENSITIES OF BENZOIC ACID SOLUTIONS IN METHANOL-, ETHANOL- AND DIOXAN-WATER MIXTURES (WITH 0·01 M. SODIUM BENZOATE) AT 25° C. WITH AND WITHOUT 1·025 M. NaCl.

(*a*).	(*b*).	(*c*).	(*d*).	(*e*).
WATER				
—	0·9980	0·9992	1·0392	1·0395
DIOXAN				
5·132	1·0023	1·0042	1·0433	1·0441
9·944	1·0065	1·0083	1·0472	1·0481
9·979	1·0067	1·0084	1·0473	1·0482
15·31	1·0111	1·0134	1·0520	1·0539
19·99	1·0148	1·0178	1·0558	1·0572
24·24	1·0183	1·0221	1·0592	1·0612
METHANOL				
5·306	0·9897	0·9901	1·0295	1·0301
10·08	0·9808	0·9824	1·0216	1·0224
15·06	0·9732	0·9759	0·0135	1·0145
20·15	0·9654	0·9671	1·0055	1·0067
24·85	0·9584	0·9612	0·9989	1·0005
30·44	0·9496	0·9538	0·9897	0·9920
35·75	0·9404	0·9462	0·9802	0·9847
40·68	0·9314	0·9403	0·9710	0·9780
46·79	0·9188	0·9535	0·9584	0·9688
52·63	0·9072	0·9310	0·9463	0·9635
58·72	0·8962	0·9262	0·9366	
ETHANOL				
5·54	0·9882	0·9896	1·0286	1·0296
9·97	0·9815	0·9826	1·0215	1·0224
14·99	0·9746	0·9765	1·0144	1·0158
15·41	0·9739	0·9758	1·0139	1·0150
17·84	0·9705	0·9727	1·0103	1·0116
20·14	0·9672	0·9696	1·0064	1·0081
25·08	0·9596	0·9623	0·9982	1·0005
30·64	0·9506	0·9569	0·9881	0·9926
35·21	0·9420	0·9526	0·9789	0·9873
40·16	0·9315	0·9492	0·9677	0·9822
42·34	0·9277	0·9477	0·9634	0·9803
49·74	0·9109	0·9446	0·9455	0·9737
54·58	0·9000	0·9441	0·9344	0·9706

(*a*) Weight % of non-aqueous component of binary solvent.
(*b*) Density of mixed solvent.
(*c*) Density of mixed solvent saturated with BzOH.
(*d*) Density of mixed solvent containing 1·025 M. NaCl.
(*e*) Density of mixed solvent containing 1·025 M. NaCl saturated with BzOH.

[19] Åkerlöf, *J. Amer. Chem. Soc.*, 1932, **54**, 4125.
[20] Åkerlöf, and Short, *ibid.*, 1936, **58**, 1241.

2. Method.—The solvents were purified by published methods,[21] and mixtures prepared by weight. These were stirred under thermostatic conditions (25·00 ± 0·06° C.) for 72 hr. with a large excess of prepared [22] benzoic acid, samples being withdrawn and examined after 48 and 72 hr. to ascertain that measurements were made at equilibrium. All experiments were carried out in triplicate. The acid was estimated by titration with standard baryta solution, and the solubilities calculated as g. mole./1000 g. solvent (see Table I). The densities of all solvents and saturated solutions at 25° C. were determined in the normal way, using a specific gravity bottle of 50 ml. capacity (see Table II).

3. Results.—These are illustrated in Fig. 1, where the relative salting-out, $\frac{\Delta S}{S}$, is plotted against $\frac{1}{D}$. In all cases the relative salting-out initially decreases with decrease of dielectric constant, and minima occur in the alcohol-water systems at about 58 % w/w methanol ($D = 51$) and 30 % w/w ethanol ($D = 61$). In the range 27-42 % w/w ethanol, salting-in occurs. It is stressed that the relative salting-out is markedly different under isodielectric conditions in the three systems.

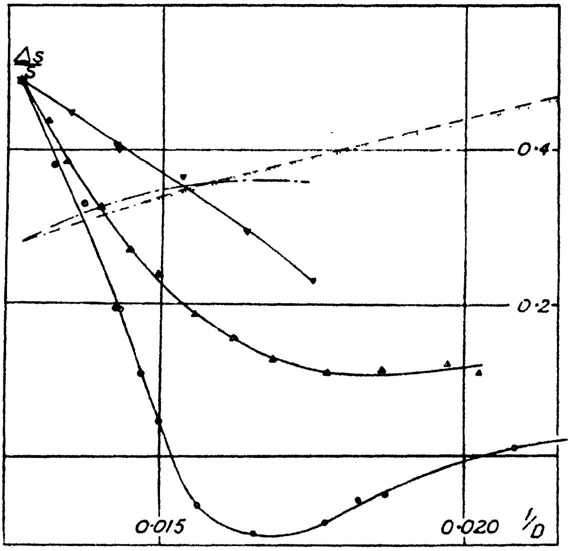

FIG. 1.—Relative salting-out and dielectric constant.

Calculated.	Observed.	
— — — —	—△—△—	Methanol-water.
—— - ——	—⊙—⊙—	Ethanol-water.
.. ..	—▽—▽—	Dioxan-water.

Discussion.

The linear section of each $\frac{\Delta S}{S} - \frac{1}{D}$ curve can be represented by an equation of the type

$$\frac{\Delta S}{S} = \frac{K}{D} + C \quad . \quad . \quad . \quad . \quad . \quad (xi)$$

where K and C are constants, K is negative and C is greater than K/D.

---

[21] Bjerrum and Zechmeister, *Ber.*, 1923, **56**, 894 (methanol); Eigenberger, *J. prakt. Chem.*, 1931, **130**, 75 (dioxan); cf. also *Organic Solvents*, Weissberger and Proskauer (Oxford, 1935).

[22] Prepared by mixing equal parts of macrocrystalline pure and finely ground pure benzoic acid, cf. Hulett and Allen, *J. Amer. Chem. Soc.*, 1902, **24**, 667.

From the equation

$$\frac{\Delta S}{S} = \frac{\beta \Sigma n_i z_i^2 e^2}{2 D_0 k T b}, \quad . \quad . \quad . \quad . \quad . \quad \text{(xii)}$$

assuming in the Debye-McAulay theory that $\frac{\Sigma n_i z_i^2 e^2}{2kTb}$ is a constant, K', for the whole range of each of the binary solvent systems studied, then

$$\frac{\Delta S}{S} = \frac{K'\beta}{D}. \quad . \quad . \quad . \quad . \quad . \quad \text{(xiii)}$$

Now β is the molecular dielectric decrement caused by the addition of the benzoic acid to the solution, which, in the present investigation, is of varying solvent composition. It is clear that β must vary with the composition of the organic solvent-water mixture used; * i.e. that β itself is a function of D. Hence a linear relationship between $\frac{\Delta S}{S}$ and $\frac{1}{D}$ would not be expected. The present results are not in accord with equation (xiii) since they indicate a negative slope of the $\frac{\Delta S}{S} \Big/ \frac{1}{D}$ relation whereas assuming b to be positive in the Debye-McAulay theory requires that β should also be positive when salting-out occurs. A negative value of β implies an increase of the dielectric constant on the addition of non-electrolyte according to this theory, and consequently is associated with salting-in. This only occurs in a small range of ethanol-water mixtures. Moreover, it appears unlikely that β can have a negative value in the present systems; it is known that each of the organic solvents brings about a decrease in the dielectric constant when added to water, and that, since it is normally salted-out, benzoic acid also causes a decrease in dielectric constant. The contributions of each of these factors to the net value of β must therefore be positive. It must therefore be concluded that the theory is not directly applicable to the results of the present investigation. Attempts to correlate the results with the equations of Debye's second theory fail similarly.

In Butler's theory of the salting-out effect the relevant variables are the dielectric constant of the solution, and the polarisabilities α_A and α_B of the solvent and solute non-electrolyte molecules. Thus Butler's equation is more easily applicable than that of Debye and McAulay, or of Debye, because the polarisabilities can be calculated by the usual equations relating them to the dielectric constant, whereas the corresponding β term in Debye and McAulay's theory and the dielectric constant terms in Debye's theory require experimental values of the dielectric constants of the non-electrolyte solutions and few of these are available.

Using the following values, $\frac{\Delta S}{S}$ has been calculated from equation (x): $\Delta v_B = 1{\cdot}61 \times 10^{-22}$ cm.^{3}, $N = 6{\cdot}02 \times 10^{23}$, $k = 1{\cdot}38 \times 10^{-16}$ erg deg.$^{-1}$, $e = 4{\cdot}80 \times 10^{-10}$ e.s.u., $\sum \frac{1}{b} = 0{\cdot}807 \times 10^8$ cm.$^{-1}$. Values of α were evaluated using $\alpha = \frac{D - 1}{4\pi}$. The calculations show that according to Butler's theory, $\frac{\Delta S}{S}$ increases regularly with decrease of D, in an approximately linear fashion with respect to $\frac{1}{D}$ (see Fig. I). The theory

---

* The equation $D = D_0 (1 - \beta n)$ is taken to be valid for a given value of D_0, so that β does not equal $(D_0 - D)/D_0 n$ if D_0 varies.

therefore does not apply at all to the results obtained in the present systems, so that factors not considered by the theories must be taken into account.

It is believed that in an electrolytic solution in organic solvent-water mixtures the solvation of the ions, and therefore presumably their powers of salting-out, is in general preferential to one of the types of solvent molecules present (in this case that of water), cf. Shaw and Butler.[23] On the addition of ethanol, for example, to the aqueous solution, it might be expected that S would increase, the solubility of benzoic acid being greater in ethanol than in water. However, ΔS would not be expected to increase in a similar manner, because although the decrease of dielectric constant increases the ability of the ions to solvate, the alcohol is probably not included in the solvation sheath [24] and its power to dissolve the benzoic acid is relatively unaffected by the presence of NaCl. Hence $\frac{\Delta S}{S}$ might be expected to decrease much more rapidly than would be expected from a simple theory which assumes a homogeneous dielectric medium. The interpretation given to the negative values of $\frac{\Delta S}{S}$ observed in the ethanol-water system may be brought out by the consideration of an extreme case. Suppose that the water content of the system in a hypothetical model is reduced to such a value that the NaCl addition results in the removal of all the water molecules into the solvation sheaths of the Na^+ and Cl' ions. Then, the effective solvent for benzoic acid would be exclusively ethanol, and the solubility in this ethanol after the addition of electrolyte would be greater than before it, i.e. ΔS would be negative. This supposes that the solubility of benzoic acid per unit volume of anhydrous ethanol is larger than in such a volume of ethanol in an ethanol-water mixture, an assumption which would seem plausible on account of the high polarity of the water, and the consequent interaction with, and reduction in solvent power of, the ethanol in the mixture. Further, at sufficiently high concentration of ethanol, the alcohol molecules will also presumably tend to enter the solvation sheath of the ions, so that since then both components are being removed by solvation, the gradient of the $\frac{\Delta S}{S}\Big/\frac{1}{D}$ should become positive. In such a case the effect of decreasing dielectric constant has become predominant over that of preferential solvation. This view is in agreement with the results obtained for the methanol- and ethanol-water mixtures, namely that $\frac{\Delta S}{S}$ decreases with $\frac{1}{D}$ to a minimum value, in the salting-in region in the latter system, and subsequently has a positive slope. In the dioxan-water system it is of interest to note that in the range examined there is no tendency for the inversion of the negative slope, and this is in accord with the relatively small dipole moment and large size of the dioxan molecule, a factor which would clearly reduce the probability of its entering the solvation sheath of Na^+ or Cl' ions at higher dioxan concentrations.

Although it would seem that preferential solvation of the ions by water accounts for the results reported in a qualitative fashion, it must be stressed that other factors may be important. Thus, decrease of dielectric constant would be expected to decrease the degree of dissociation of the NaCl, and this effect would, according to the Setschenow equation, be expected to contribute to the decrease of $\frac{\Delta S}{S}$ with decrease of D.

---

[23] Shaw and Butler, *Proc. Roy. Soc. A*, 1930, **129**, 519.
[24] Millet, *Trans. Faraday Soc.*, 1927, **23**, 515.

Calculations from the Bjerrum-Fuoss-Kraus theory of ion association[26] indicate that a decrease of D from 78 to 48 should bring about a reduction in the value of the degree of dissociation of about 70 %. Lastly, the dielectric constant in the neighbourhood of the ion is certainly different from the macroscopic value, and the variation of the microscopic value in mixed solvents may not be parallel to that of the macroscopic value as found in the usual ways. Quantitative interpretation of the results would involve a more complete knowledge of the dielectric constants of the electrolytic solutions, of the appropriate values in the vicinity of an ion, and of solvation in mixed solvents. Work on the dielectric constants of electrolyte and non-electrolyte solutions, and on solvation in mixed solvents, is in progress at Imperial College.

The authors wish to express thanks to Dr. J. A. V. Butler for helpful comments on this work.

Summary.

1. Empirical salting-out equations, and the present position of the salting-out theories are briefly discussed.

2. Results for the relative salting-out of benzoic acid in some methanol-, ethanol- and dioxan-water mixtures by NaCl at 25° c. are reported. The relative salting-out at first *decreases* with *dielectric constant decrease* for all of these systems, and for the alcohol-water systems passes through a minimum ; salting-in occurs in the range 22-47 % w/w ethanol.

3. The Debye and McAulay, Debye, and Butler theories of salting-out are quite inapplicable to the results obtained.

4. It is suggested that the inapplicability of the theories is due to the preferential solvation of the Na^+ and Cl' ions by water in all of the systems, and a qualitative account of the results can be given on this basis. Other complicating factors are discussed.

Imperial College of Science and Technology, and
Acton Technical College,
London.

---

[26] Bockris and Azzam (unpublished).

KINETIC STUDIES IN THE SOLVENTS ACETIC ACID AND ACETIC ANHYDRIDE.

PART I.—PROPERTIES OF THE SOLVO-SYSTEM.

BY H. A. E. MACKENZIE AND E. R. S. WINTER.

Received 4th March, 1947.

As a prelude to kinetic studies on reactions which take place in the solvo-system acetic acid-acetic anhydride, it is desirable to review the known properties of the system, particularly with regard to the behaviour of acids therein, and to extend the knowledge of the system in certain aspects.

Physical Properties of Acetic Acid, Acetic Anhydride and their Mixtures.

Acetic acid is a solvent of low dielectric constant (6·13 at 20° c.[1]) and displaying autoprotolysis with a constant * $K = c_{AcOH_2^+} \cdot c_{AcO^-} = 2{\cdot}5 \times 10^{-13}$ at 25° c. according to Kolthoff.[2] Although the proton in acetic acid solution is solvated, forming the $AcOH_2^+$ ion, the latter must be regarded as a strong proton donor. It has long been recognised that acetic acid is an associated liquid,[3] and much evidence has accumulated of the existence of a stable dimer both in the vapour phase and in solvents such as benzene. Independent methods leading to this conclusion include studies of infra-red spectra of the vapour,[4] of the Raman spectra of aqueous solutions,[5] of the vapour density,[6] and of the distribution of acetic acid between benzene and water.[7] The dimerisation is generally attributed to hydrogen bond formation[8] and the dimer is assigned the structure:

---

[1] Smyth and Rogers, *J. Amer. Chem. Soc.*, 1930, **52**, 1824.

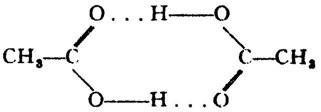

The specific conductance of acetic acid is very low, the values found by various workers showing variations with the method of purification,[2, 9–12] but found by Kolthoff[2] and Weidner, Hutchison and Chandlee[12] to be about $6{\cdot}0 \times 10^{-9}$ mho at 25° c. with highly purified specimens.

Acetic anhydride also has a low dielectric constant (20·5 at 20° c.[13]). There is no evidence of its association. Although the anhydride has a low specific conductance, viz., $1{\cdot}94 \times 10^{-7}$ mho at 25° c.[10] (but cp. [14]), this is much greater than that of acetic acid. This relatively large value suggests the presence of an equilibrium in acetic anhydride of the type: $Ac_2O = Ac^+ + AcO^-$. There are, in fact, many chemical facts which may be most simply explained by assuming the existence of such a reaction and these will be adduced below.

The liquid-liquid system, acetic acid-acetic anhydride has not been extensively studied. Pickering, however, in 1893[15] determined the freezing point of acetic acid in admixture with acetic anhydride for concentrations of acetic acid varying from 100 to about 6 % w/w. He himself was unable to explain his results, but actually they are amenable to simple

---

* Throughout this series the symbol Ac will be used to denote the group $CH_3 . CO$—.

[2] Kolthoff, *J. Amer. Chem. Soc.*, 1934, **56**, 1007.

[3] Turner, *Molecular Association*, 1915.

[4] Herman and Hofstadter, *J. Chem. Physics*, 1938, **6**, 534; *ibid.*, 1939, **7**, 460. Gilette and Daniels, *J. Amer. Chem. Soc.*, 1935, **58**, 1139. Davies, *Trans. Faraday Soc.*, 1940, **36**, 333. Buswell, Rodebush and Roy, *J. Amer. Chem. Soc.*, 1938, **60**, 2239. Davies and Sutherland, *J. Chem. Physics*, 1938, **6**, 755. Badger and Bauer, *ibid.*, 1937, **5**, 605.

[5] Leitman and Ukholin, *J. Chem. Physics*, 1934, **2**, 825.

[6] Fenton and Garner, *J. Chem. Soc.*, 1930, 694. MacDougall, *J. Amer. Chem. Soc.*, 1936, **58**, 2855.

[7] Moelwyn-Hughes, *J. Chem. Soc.*, 1940, 850.

[8] Sutherland, *Trans. Faraday Soc.*, 1940, **36**, 890. Fox and Martin, *ibid.*, 898.

[9] Creighton and Way, *J. Frank. Inst.*, 1920, **186**, 675: $0{\cdot}17 \times 10^{-6}$ mho. Hopfgartner, *Wien. Ber.*, 1911, **120**, 26, 1: 0·5 to $1{\cdot}5 \times 10^{-7}$ mho. Schall and Thieme-Wiedermarchter, *Z. Elektrochem.*, 1929, **35**, 337: $4{\cdot}9 \times 10^{-8}$ mho. Patten, *J. Physic. Chem.*, 1902, **6**, 554: $1{\cdot}05 \times 10^{-8}$ mho.

[10] Hall and Voge, *J. Amer. Chem. Soc.*, 1933, **55**, 239: $1{\cdot}05\text{-}3{\cdot}0 \times 10^{-8}$ mho.

[11] Eichelberger and La Mer, *ibid.*, 3635: $1{\cdot}4 \times 10^{-8}$ mho.

[12] Weidner, Hutchison and Chandlee, *ibid.*, 1934, **56**, 1285.

[13] Landolt-Börnstein, *Tabellen*, HwII, 1037, 1923.

[14] Walden, *Z. physik. Chem.*, 1906, **54**, 128: $4{\cdot}8 \times 10^{-7}$ mho. Schmidt, 1910 (quoted in Walden's *Elektr. Nichtwässerigen Lösungen*): $7{\cdot}5 \times 10^{-7}$ mho.

[15] Pickering, *J. Chem. Soc.*, 1893, **63**, 998.

treatment. For ideal liquid systems, the freezing point depression, θ, in °K., of a liquid A, is given by the expression:

$$-\ln x_1 = \frac{L_0\theta}{RT_0^2} + \frac{\theta^2}{T_0^2}\left(\frac{L_0}{RT_0} - \frac{C_p^L - C_p^S}{2R}\right),$$

where x_1 = mol. fraction of A present, L_0 = molar latent heat of fusion of A at its m.p., in cal./g. mol., T_0 = m.p. of A in °K., C_p^L and C_p^S are the molar specific heats of liquid and solid A respectively in the neighbourhood of the m.p., in cal./g. mol.-degree. Terms involving (θ/T_0) to powers > 2 are neglected. For acetic acid T_0 is taken as 289·6;[15] for monomeric acetic acid, $L_0 = 2785$,[16] $C_p^L = 29$[17] and $C_p^S = 37{\cdot}5$;[18] and for the dimer, $L_0 = 5570$, $C_p^L = 58$, $C_p^S = 75$.

In Fig. 1 are shown the experimental results of Pickering, together with values calculated from the thermodynamic expression. The experimental values are in excellent agreement with theory up to about 80 % w/w acetic anhydride, but only if dimeric acetic acid is assumed. At higher acetic anhydride concentrations the experimental points diverge from the theoretical curve for the dimer and approach that of the monomer, suggesting that dissociation becomes appreciable and increases with dilution of the acetic acid. The cryoscopic method affords, therefore, proof of the dimerisation of acetic acid and reveals the ideal behaviour of the system acetic acid-acetic anhydride when the concentration of the latter is less than 80 % w/w.

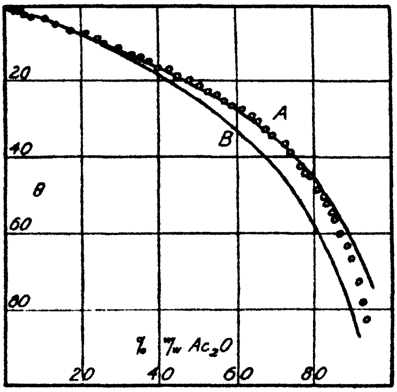

FIG. 1.

Circles—Exptl. points. (Pickering [15])
Curve A—Calcd for dimer.
Curve B—Calcd. for monomer.

Chemical Properties of Acetic Acid, Acetic Anhydride and their Mixtures.

Ruben, Allen and Nahinsky [19(a)] have recently noted an exchange reaction between sodium acetate and acetic anhydride. They found that sodium acetate ($NaOOC^*CH_3$, where C^* is a radioactive carbon isotope; C^{11} and C^{14} were both used), when shaken with pure dry acetic anhydride at room temperature, suffered rapid exchange of its radioactive atom with the acetic anhydride. After 20 min. the reaction

$$\begin{aligned}&CH_3{-}C^*O{-}ONa + (CH_3CO)_2O\\ &\quad = CH_3{-}CO{-}ONa + (CH_3{-}C^*O{-}O{-}CO{-}CH_3,\ (CH_3{-}C^*O)_2O)\end{aligned}$$

had proceeded to the right to about 55-62 %. A similar exchange occurred between sodium acetate and butyric anhydride. The latter reaction was known to early workers to occur at higher temperatures.[19(b)]

These exchanges may be explained either by the assumption that acetic anhydride is ionised according to the equation $Ac_2O \rightleftharpoons Ac^+ + AcO^-$ or as an attack by the acetate ion on the carbonyl carbon atom of the anhydride with simultaneous separation of a different acetate ion. The former assumption is favoured, since ionisation of Ac_2O is shown by its high specific conductance, and by other evidence summarised below.

---

[16] Marignac (quoted by Meyer, *Z. physik. Chem.*, 1910, **72**, 225): $L_0 = 46{\cdot}4$ cal./g.

[17] Ref. 13: 28·8 at 17° C.; 29·2 at 20° C.

[18] *ibid.*: 37·1 at 4°-8° C.; 37·6 at 1°-8° C.

[19] (*a*) Ruben, Allen and Nahinsky, *J. Amer. Chem. Soc.*, 1942, **64**, 3050. (*b*) Michael, *Ber.*, 1901, **34**, 925.

Confirmatory evidence comes from the work of Usanovitch and Yatsimirskii[20] on acid-base interaction in Ac_2O. The solvent behaves amphoterically and, in it, acetyl chloride, benzoyl chloride and trichloroacetic acid behave as acids and may be titrated with sodium acetate (which behaves as a strong base). The reactions lead the authors to postulate an Ac_2O^+ ion, presumably by analogy with H_3O^+, although the Ac^+ ion itself would be large and not necessarily solvated. It is our opinion that the acetyl ion most probably exists in the unsolvated state in this system. Many salts were found to undergo solvolysis in acetic anhydride: for example, $AlCl_3$ gave AcCl and $AlCl(OAc)_2$, HgF_2 gave AcF and $Hg(OAc)_2$ and even NaCl apparently reacted, since Ac_2O distilled from this salt gave a positive reaction for chlorine.

The acetic anhydride solvo-system is thus analogous to the water system, but is simpler in certain respects, viz., in the lack of association of Ac_2O and probably non-solvation of the acidic ion Ac^+. The postulate of the existence of stable acyl ions also facilitates the correlation of many other well-established phenomena:

(1) the electrical conductance and acidity of acetyl fluoborate in acetic anhydride;[21]

(2) exchange reactions between aliphatic acids and anhydrides, e.g.

$$2R_1\text{—COOH} + (R_2CO)_2O = 2R_2COOH + (R_1CO)_2O;$$

(3) disproportionation shown by mixed anhydrides, e.g.

$$2R_1\text{—CO—O—CO—}R_2 = (R_1\text{—CO})_2O + (R_2CO)_2O, \text{ and}$$

(4) the fact that in acid-catalysed esterifications the reaction

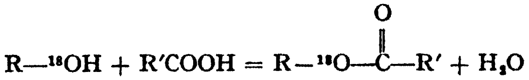

$$R\text{—}^{18}OH + R'COOH = R\text{—}^{18}O\text{—}\overset{\overset{\large O}{\|}}{C}\text{—}R' + H_2O$$

proceeds, and not the reaction

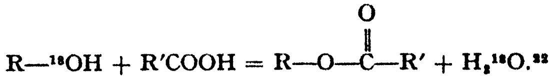

$$R\text{—}^{18}OH + R'COOH = R\text{—}O\text{—}\overset{\overset{\large O}{\|}}{C}\text{—}R' + H_2{}^{18}O.^{22}$$

The postulate would underline in general the essential difference in kind between the reactions:

$$R'\text{—COOH} + HO\text{—}R = R'COOR + H_2O$$

and

$$Cl\text{—}H + HO\text{—}R = Cl\text{—}R + H_2O.$$

It is noteworthy that Treffers and Hammett[23] have obtained direct evidence of the existence of large stable acyl ions by cryoscopic measurements in sulphuric acid. The di-*o*-substituted benzoic acids appear to ionise thus:

$$R\text{—COOH} + 2H_2SO_4 = RCO^+ + OH_3{}^+ + 2HSO_4{}^-,$$

and hydrolysis of esters of these acids (normally very slow in dilute acid or alkali) is quantitatively achieved by pouring a solution of the ester in H_2SO_4 into water.

---

[20] Usanovitch and Yatsimirskii, *J. Gen. Chem. Russ.*, 1941, **11**, 954, 959; *Abstr.*, *A*, II, 1945, 385; *A*, I, 1946, 187.

[21] Seel, *Z. anorg. Chem.*, 1943, **250**, 331.

[22] Watson, *Modern Theories of Organic Chemistry*, 2nd Ed. (Oxford, 1941), p. 126.

[23] Treffers and Hammett, *J. Amer. Chem. Soc.*, 1937, **59**, 1708.

The Behaviour of Strong Acids in Acetic Acid-Acetic Anhydride Solutions.

With the aid of the chloranil electrode and the technique developed by Conant and Hall,[24(a)] these authors and others have made an electrometric study of acids and bases in acetic acid.[24(a)-(f)] The main difficulty was the selection of an arbitrary zero for the conversion of experimental E.M.F.'s to hydrogen ion activities, but the value selected by them was substantiated by the self-consistency and applicability of their results. They defined a function, $(p\text{H})^{\text{AcOH}}$ * as a measure of hydrogen ion activity in acetic acid, in terms of the experimentally measured E.M.F. For 1·0 M. solutions of strong acids they obtained the following results:

Acid.	$(p\text{H})^{\text{AcOH}}$.	a_{H^+} (and, therefore, f_{H^+}, since $c_{\text{H}^+} = 1{\cdot}0$).
CCl_3COOH	− 0·83	6·7
H_2SO_4	− 3·23	700
$HClO_4$	− 4·4	25,000

In view of these remarkable results, the solutions were termed "super-acid." Conant and Hall[24(b)] were able to correlate the $(p\text{H})^{\text{AcOH}}$ of buffered acetic acid solutions with the indicator behaviour of arylcarbinols and unsaturated ketones in these solutions, and Rodebush and Ewart[25] have found, using a dynamic vapour pressure method, that the activities of HCl solutions in acetic acid are about 10^6 times those of equally concentrated solutions in water; so that there is evidence that the extraordinarily high activities are real and do at least parallel "acidity" as measured by indicator studies. The latter authors point out, however, that the $(p\text{H})^{\text{AcOH}}$ is not a measure of the individual activity of the hydrogen ion, but expresses the mean activity of a pair of ions, as does the $p\text{H}$ in aqueous solutions. Hence, although a correlation has been found between the $(p\text{H})^{\text{AcOH}}$ and the specific reaction rates of a restricted range of reactions (viz. the inversion of sucrose in 98 % acetic acid[24(b)] and the acetylation of β-naphthol[26]), it may be fortuitous. This is likely since the accuracy of the study of the β-naphthol acetylation was low and even in aqueous solutions of high acidity, the rate of hydrolysis of sucrose is determined more precisely by the acidity function of the solution than by the $p\text{H}$[27].

Russell and Cameron[28] have obtained values of the $(p\text{H})^{\text{AcOH}}$ of the same order as those of Conant for strong acids in acetic acid, using a hydrogen electrode coupled to a chloranil half-cell. They have shown as well that the $(p\text{H})^{\text{AcOH}}$ of acid solutions decreases still further on addition of acetic anhydride to the solution in amounts up to about 30 % v/v. The effect is large initially in the case of H_2SO_4, but becomes more gradual when about 15 % v/v acetic anhydride has been added. In the case of the other acids studied, the change is gradual throughout and of the same order as the change with H_2SO_4 for solutions containing more than 15 % v/v acetic anhydride. The authors attributed these facts to the formation of mixed anhydrides, thus: $Ac_2O + HA = AcA + AcOH$. The mixed

---

[24] (*a*) Conant and Hall, *J. Amer. Chem. Soc.*, 1927, **49**, 3047; (*b*) *ibid.*, 1927, **49**, 3062. (*c*) Hall and Werner, *ibid.*, 1928, **50**, 2367. (*d*) Conant and Werner, *ibid.*, 1930, **52**, 4436. (*e*) Hall, *ibid.*, 1930, **52**, 5115. (*f*) Hall, *Chem. Rev.*, 1931, **8**, 191.

* For the sake of consistency, the function is represented in this way, rather than by the symbol $(p\text{H})^{\text{HAc}}$ of the original authors.

[25] Rodebush and Ewart, *J. Amer. Chem. Soc.*, 1932, **54**, 419.

[26] Conant and Bramman, *ibid.*, 1928, **50**, 2305.

[27] Hammett and Deyrup, *ibid.*, 1932, **54**, 2721.

[28] Russell and Cameron, *J. Amer. Chem. Soc.*, 1938, **60**, 1345.

anhydride was assumed to be responsible for very high acidity. Neglecting the question of ionisation or dissociation of the AcA molecule, this assumption is the same as the postulate that acetyl ions of marked acidity are formed. The facts may all be accounted for in this way, except the large initial decrease in $(p\text{H})^{\text{AcOH}}$ in the case of H_2SO_4 (cp. later).

The studies on $(p\text{H})^{\text{AcOH}}$ provide no evidence of the degree of dissociation of the acids studied in acetic acid, or, in fact, what significance may be attached to the term " degree of dissociation " as applied to such solutions. This question requires reference to conductivity studies for its clarification.

Solutions of $HClO_4$ and H_2SO_4 in acetic acid have a very low molar conductance. Sulphuric acid solutions have been studied by several workers,[3, 10–12] and the results of Kolthoff,[3] Hall and Voge[10] and Eichelberger and La Mer[11] are in close accord. Kolthoff[3] has studied $HClO_4$ solutions. The molar conductances are roughly 10^{-3} of those in water Such low values may be due to two causes.

(1) Since acetic acid is strongly protogenic, solutions of $HClO_4$ and H_2SO_4 in it may be such that the undissociated molecule, or, in the case of H_2SO_4, the bisulphate ion, is present in appreciable amount.[29]

(2) The acids may ionise, but, in view of the low dielectric constant of the medium, a proportion of the ions may aggregate into pairs, triplets, etc., in which case those aggregates containing an equal number of opposite charges would have no net charge and therefore not contribute to the conductivity.[30]

Kolthoff[3] has assessed the relative applicability of the two explanations to the low conductances of H_2SO_4, $HClO_4$ and other solutes in acetic acid. The ionisation of the strong acid is determined primarily by its tendency to split off protons and by the affinity of acetic acid for protons. The equation $HA + CH_3COOH = CH_3COOH_2^+ + A^-$ will be incomplete for a weak acid and tend to go to completion in the case of a strong acid. Since water is a much stronger base than acetic acid, the addition of small amounts of water should promote the ionisation of a weak acid HA and a large increase in electrical conductance should result. If, on the other hand, the acid HA is so strong that all of it is present as ions and ion-pairs, the effect of a trace of water will be small and manifest itself only as a change in the dielectric constant. The results showed that traces of water had a negligible effect on the conductance of $HClO_4$ solutions in acetic acid, but caused large increases in the conductance of H_2SO_4 solutions. Perchloric acid is thus a strong electrolyte and H_2SO_4 a weak electrolyte in acetic acid.

In the light of Kolthoff's work, the initial large increase in the superacidity of H_2SO_4 solutions in acetic acid, on the addition of acetic anhydride may be explained by completion of the ionisation of the H_2SO_4. The way in which acetic anhydride facilitates this ionisation is not, however, readily visualised. The assumption that acetic anhydride is more protophylic than acetic acid (i.e. more basic) would afford an explanation along the lines of Kolthoff's reasoning in the case of water; but the relative basicities of acetic acid and acetic anhydride are not easy to assess *a priori*. Accepting the formulæ,

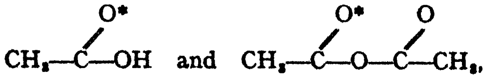

$$CH_3-\overset{O^*}{\overset{\diagup}{C}}-OH \quad \text{and} \quad CH_3-\overset{O^*}{\overset{\diagup}{C}}-O-\overset{O}{\overset{\diagup}{C}}-CH_3,$$

it might be argued that replacement of the acid hydrogen by an acetoxy group would lower the electron excess at the oxygen atom denoted by the asterisk, and that therefore the anhydride would be a weaker base than the acid; but this is doubtful since acetic acid is more correctly formulated in this case as the dimer, and acetic anhydride may well accept protons by virtue of hydrogen bond formation and chelation, thus:

---

[29] See e.g., Glasstone, *The Electrochemistry of Solutions*, 3rd Ed., (Methuen, 1945), p. 172.

[30] Ion-pair formation has been well substantiated experimentally by the work of Fuoss and his collaborators; *J. Amer. Chem. Soc.*, 1933, **55**, 1019, and succeeding papers.

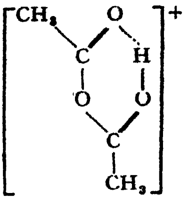

There may be some entirely different explanation, however, such as oxonium salt formation.

Murray and Kenyon[31] studied the rate of formation of sulphoacetic acid in acetic acid-acetic anhydride solutions of H_2SO_4 at 40° c. by determining the concentration of H_2SO_4 in solution after measured times, using gravimetric procedure. The rate of disappearance of H_2SO_4 obeyed a first-order law and the specific reaction rate increased 100-fold in acetic anhydride-acetic acid mixtures as the anhydride concentration was increased from 25 to 90 % v/v. They suggested the mechanism:

$$Ac_2O + H_2SO_4 \underset{k_{-1}}{\overset{k_1}{\rightleftharpoons}} AcOH + AcHSO_4$$

$$AcHSO_4 \xrightarrow{k_2} \text{Product},$$

which, by application of the method of stationary states, gives:

$$\frac{-d(H_2SO_4)}{dt} = \frac{k_1 k_2}{k_{-1}} \frac{(Ac_2O)(H_2SO_4)}{(AcOH)}, \text{ if } k_{-1} \gg k_2.$$

The mechanism can only be an approximation, since the molecules H_2SO_4 and $AcHSO_4$ are assumed to exist in solution as such with no ionisation . It is, however, in agreement with the first-order disappearance of H_2SO_4, although the authors found that a plot of specific reaction rate against the ratio $(Ac_2O)/(AcOH)$ was only approximately linear with reactant concentrations expressed as % v/v. If the concentrations are expressed as g. mol./l., approximate agreement with the equation is found only at very low or very high acetic anhydride concentrations. There is evidence of an analogous reaction between acetic anhydride and $HClO_4$, which, however, is not appreciable unless very high concentrations of acetic anhydride compared with acetic acid are present. During the work reported in the succeeding paper it was found that the catalytic activity of solutions of perchloric acid in acetic anhydride falls with time; the solution simultaneously becoming yellow and then brown, and finally depositing a large amount of tarry material. Russell and Cameron (loc. cit.) record similar observations.

The preceding remarks give some indication of the complexity of the acetic acid-acetic anhydride solvo-system, particularly in relation to the behaviour of strong acids in the system. In studying acid-catalysed reactions, the " acidity " may be defined (1) by the stoichiometric concentration of the acid, (2) by the hydrogen ion activity as measured by the $(p\text{H})^{\text{AcOH}}$, or (3) by Hammett's acidity function. The usefulness of the first definition is limited to those cases where the degree of ionisation of the catalysing acid is zero or unity, since, otherwise, alterations in medium or concentrations lead to uncertainty in interpretation. The second definition can be expected to provide at most a qualitative measure of the hydrogen ion activity. Fortunately Hammett and his collaborators[32] have provided a more precise definition of acidity which is of great value in the study of acid-catalysed reactions.

The acidity function, which was introduced by Hammett and Deyrup,[27] measures the tendency of a solution to donate a proton to a base and is therefore a logical measure of acidity in acid-catalysed reactions. It is defined by H in the equation

---

[31] Murray and Kenyon, *J. Amer. Chem. Soc.*, 1940, **62**, 1230.

[32] Hammett, *Physical Organic Chemistry* (McGraw-Hill, 1940), pp. 262 et seq.

$$H = -\log (a_{H^+} . f_B/f_{BH^+}),$$

where a_{H^+} represents the hydrogen ion activity, and f_B and f_{BH^+} are the activity coefficients of the base and its conjugate acid respectively. A subscript appended to the symbol H indicates the charge type of the base, thus: H_0, H_{++}, H_- etc. Hammett and Deyrup argued that the acidity function of a solution would not necessarily be the same for bases of different charge types, but assumed that, for bases of one charge type, the ratio f_B/f_{BH^+} would be the same and would be largely unaffected by medium composition. The latter two assumptions have been substantiated in large measure by experiment.

If the acidity constant of the conjugate acid of the base, $pK_a{}^B$ is given by

$$pK_a{}^B = -\log (a_{H^+} . a_B/a_{BH^+}),$$

then, from this and the definition of H,

$$H = pK_a{}^B + \log (c_B/c_{BH^+}).$$

The acidity function of a solution may thus be obtained by measuring the " indicator ratio " in that solution, colorimetrically, by absorption spectrophotometry, etc.

In the present studies an approach must be made which is not strictly analogous to that of Hammett. He and his co-workers were concerned chiefly with acidity functions and reactions in media composed of water and strong acids in varying proportions, where it is reasonable to assume the existence of only one acid ionic species which can function as a catalyst, viz., the proton, H_3O^+. The succeeding studies are concerned with reactions in media composed of varying proportions of the two solvents, acetic acid and acetic anhydride, containing only low concentrations of strong acid, and in which, even with constancy of acid concentration, large changes in acidity take place with changes in composition. In addition there is every reason to suspect the existence of two acid ionic species potentially capable of functioning as acid catalysts, viz., the $AcOH_2^+$ and Ac^+ ions. A base may therefore react thus:

$$B + AcOH_2^+ \rightleftharpoons BH^+ + AcOH$$
$$B + Ac^+ \rightleftharpoons BAc^+,$$

in which case, if the second reaction leads to a colour change, it would be quite wrong to interpret indicator ratios in terms of Hammett's acidity function. An examination of the literature reveals that no acidity function studies have so far been made in the acetic acid-acetic anhydride solvo-system.

The Use of 2 : 6-Dimethoxy Benzoquinone for the Measurement of Acidity Functions.

An indicator for use in an acetic acid-acetic anhydride solution of a strong acid requires the following properties.

(1) It should be a very weak base of such pK_a as to give accurately measurable ratios c_B/c_{BH^+} in the solutions under investigation.

(2) It should be stable in highly acid solutions, and, in particular, should be resistant to acetylation.

(3) The basic form of the indicator, or its conjugate acid should be coloured to permit quantitative measurement of concentrations; or, alternatively, should have an absorption band in the U.-V. region which is amenable to measurement.

(4) Ionisation of the indicator should be such that one molecule of base gives rise to one conjugate acid ion only.

Hammett and his co-workers have given a number of very weak bases fulfilling (3) and (4). Of these, only anthraquinone and *N* : *N*-dimethyl, 2 : 4 : 6-trinitroaniline seemed likely to satisfy requirement (2), but both were found to be too weak as bases to give measurable conjugate acid concentrations in the solutions investigated here.

2 : 6-dimethoxy benzoquinone is completely resistant to the Thiele acetylation,[33] and dissolves in conc. H_2SO_4 with the formation of a deep red colour. If the solution is diluted with water, the original yellow colour is restored and the quinone recovered unchanged. It does, however, char very slowly. The colour change was found to take place in H_2SO_4-H_2O mixtures with a concentration of sulphuric acid equivalent to an acidity function $H_0 = -5$. The red colour is associated with an absorption band having a maximum at about 5000 A. The absorption spectrum of an approximately 0·04 % w/v solution of the quinone in conc. H_2SO_4, determined with a Hilger spectrophotometer, is given in Fig. 2 (A). When 2 : 6-dimethoxy benzoquinone is added to an acetic acid-acetic anhydride solution of perchloric acid, a red colour is again produced, and is once more associated with an absorption band having a maximum at about 5000 A. The colour intensity increases with increasing acetic anhydride content of the solution. Specimen absorption spectra of 0·02 % w/v solutions of the quinone in different acetic acid-acetic anhydride mixtures containing 0·078 M. $HClO_4$ are given in Fig. 2. The quinone thus satisfies (1), (2) and (3).

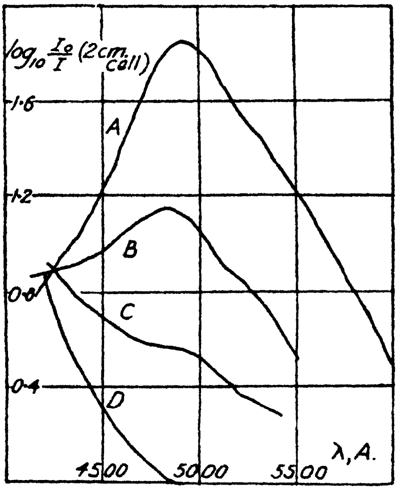

FIG. 2.

A—0·04% w/v quinone in conc. H_2SO_4.
B—0·02% w/v quinone in 9:1 v/v Ac_2O—AcOH with 0·078 M. $HClO_4$.
C—As B, but with 7:3 v/v Ac_2O—AcOH.
D—0·02% w/v quinone, 0·078 M. $HClO_4$, in AcOH.

The red form could be measured more conveniently with a Spekker photoelectric absorptiometer at those concentrations of quinone convenient for indicator-ratio studies. In view of the quantitative similarity of the absorption maxima in H_2SO_4 and acetic acid-acetic anhydride solutions, a calibration curve was constructed showing Spekker readings against quinone concentrations in standard H_2SO_4 solutions. It was assumed that the quinone was completely in the red form in conc. H_2SO_4, and that the Spekker reading gave directly, therefore, the concentration of the red form in solution. The calibration curve is shown in Fig. 3. No. 5 filters, with zero light transmission at $\lambda < 4600$ A. and at $\lambda > 7000$ A., and maximum (52 %) transmission at $\lambda = 5300$ A., were used. In all determinations the reference solution consisted of the test solution without the quinone, so that effects due to light absorption by solvents and acids were eliminated.

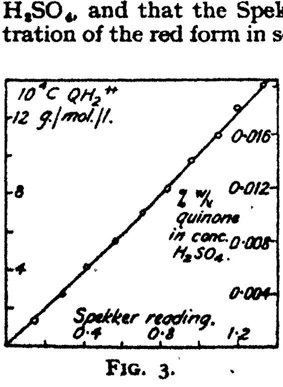

FIG. 3.

In order to study the nature of the basicity shown by the quinone, it was examined in solution in sulphuric acid-water mixtures of known acidity function. The assumption that the quinone reacts according to the equation $Q + H^+ = QH^+$ could not explain the results obtained. Two assumptions which could provide an explanation were :

---

[33] Erdtmann, *Proc. Roy. Soc. A*, 1933, **143**, 177.

(1) That 2 : 6-dimethoxy benzoquinone normally exists as a dimer, which reacts thus : $Q_2 + 2H^+ = 2QH^+$. Cryoscopic determination of the molecular weight of the quinone in acetic acid as solvent, with rigorous exclusion of atmospheric moisture, yielded a value of 172 (theor. for monomer, 168). The assumption is therefore untenable.

(2) That 2 : 6-dimethoxy quinone reacts in solutions of fairly high acidity according to $Q + H^+ = QH^+$. The QH^+ ion is then assumed to dimerise by virtue of hydrogen bond formation, giving rise to a quinhydrone-like ion, thus :

$$2QH^+ \rightleftharpoons Q_2H_2^{++}$$

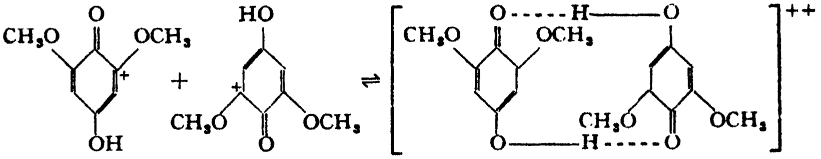

The $Q_2H_2^{++}$ ion may react further in solutions of still higher acidity, according to $Q_2H_2^{++} + 2H^+ = 2QH_2^{++}$. To the QH_2^{++} ion is attributed the red colour observed in solutions of high acidity. Attempts to demonstrate polarographically the first reaction of the quinone with a proton failed because of the high acidities necessary for the reaction to be appreciable, but some evidence of the reaction was found when it was observed that the solubility of the quinone was much greater in 10 % v/v H_2SO_4 solutions than in pure water.

The Spekker calibration curve may be adapted to give molar concentrations of the QH_2^{++} ion against Spekker readings (Fig. 3).

For a base $Q_2H_2^{++}$ which, on reaction with protons gives rise to the conjugate acid QH_2^{++} as above, it is possible, arbitrarily, to define an acidity function H by the equation :

$$H = -\log \{(a_{H^+})^2 \cdot f_{Q_2H_2^{++}}/(f_{QH_2^{++}})\}^2.$$

Then, if $$pK_a^{Q_2H_2^{++}} = -\log \{(a_{H^+})^2 \cdot a_{Q_2H_2^{++}}/(a_{QH_2^{++}})^2\},$$

$$H = pK_a^{Q_2H_2^{++}} + \log \{c_{Q_2H_2^{++}}/(c_{QH_2^{++}})^2\}.$$

H, might therefore be calculated from a knowledge of $pK_a^{Q_2H_2^{++}}$ and the indicator ratio. Alternately, if H is identical with Hammett's H_0, then

TABLE 1

% w/w H_2SO_4.	Spekker Reading.*	$10^4 . c_{QH_2^{++}}$ g.mol./l.	$10^4 . c_{Q_2H_2^{++}}$ g.mol./l.	$10^8 (c_{QH_2^{++}})^2$.	$\log \frac{c_{Q_2H_2^{++}}}{(c_{QH_2^{++}})^2}$.	H_0	$H_0 - \log \frac{c_{Q_2H_2^{++}}}{(c_{QH_2^{++}})^2}$.
58·8	0·11	1·00	6·45	1·00	4·81	−4·09	−8·90
62·8	0·19	1·79	6·00	3·20	4·28	−4·63	−8·91
66·8	0·30	2·92	5·49	8·53	3·81	−5·12	−8·93
70·6	0·48	4·69	4·60	22·0	3·32	−5·59	−8·91
74·5	0·69	6·80	3·55	46·2	2·89	−6·05	−8·94
80·4	0·93	9·36	2·27	87·6	2·41	−6·83	−9·24
84·3	1·02	10·39	1·75	108	2·21	−7·49	−9·70

* The yellow form of the quinone does not contribute to the Spekker reading, since this is zero in 10 % w/w H_2SO_4 solution.

$[H_0 - \log \{c_{Q_2H_2^{++}}/(c_{QH_2^{++}})^2\}]$ should be a constant, independent of medium composition; and the quinone, even though in this case a "complex" indicator, may be used for acidity function measurements. There is no *a priori* reason why this should be so, but experimentally it is so over a wide range.

In Table I are given the results obtained with 2 : 6-dimethoxy benzoquinone in a series of sulphuric acid-water mixtures. The H_0 values are those obtained by interpolation in the plot of H_0 against % w/w H_2SO_4 given by Hammett and Deyrup,[17] corrected according to Hammett and Paul.[24] Room temperature was approximately 20° C. The initial concentration of 2 : 6-dimethoxy benzoquinone was in all cases 0·000139 M. $c_{QH_2^{++}}$ was obtained directly from the Spekker reading and $c_{Q_2H_2^{++}}$ by difference, assuming that all the quinone was present as $Q_2H_2^{++}$ or QH_2^{++}.

$[H_0 - \log \{c_{Q_2H_2^{++}}/(c_{QH_2^{++}})^2\}]$ is constant for solutions containing up to about 75 % w/w H_2SO_4. The average value of the first five experimental results is − 8·92.

The postulate regarding the behaviour of 2 : 6-dimethoxy benzoquinone is thus supported by experiment. The departure from constancy in the last column of Table I in solutions of high H_2SO_4 content may be attributed to dissociation of $Q_2H_2^{++}$ into QH^+ ions as very high dielectric constants are reached. Irrespective of the assumptions made above, 2 : 6-dimethoxy benzoquinone may therefore be used for the determination of H_0 values in the range where $[H_0 - \log \{c_{Q_2H_2^{++}}/c_{QH_2^{++}})^2\}]$ is constant. The acidity function may be obtained from the equation:

$$H_0 = - 8{\cdot}92 + \log \{c_{Q_2H_2^{++}}/(c_{QH_2^{++}})^2\}.$$

In Table II are given the results obtained with a series of acetic acid-acetic anhydride mixtures containing $HClO_4$. The molarities of acetic acid and anhydride are corrected for the water introduced with the $HClO_4$ on the assumption * that the reaction $Ac_2O + H_2O \rightarrow (AcOH)_2$ proceeds quantitatively.

The acidity functions given in Table II are described as "apparent" H_0 values, since they will not have the same meaning as the H_0 values of Hammett if, as we believe, acetyl ions are present in the solutions in addition to protons; this question is discussed in detail later. Nevertheless, the values in Table II are of qualitative interest, since they show an increase in acidity from the point of view of indicator behaviour which parallels the increase in superacidity observed by Russell and Cameron using $(p\text{H})^{\text{AcOH}}$ measurements. The four experiments recorded in Table II, with varying quinone concentration but constant medium composition, were carried out to confirm that the mechanism proposed for the reaction of the quinone still applies in acetic acid-acetic anhydride mixtures.

The Acidity of "Acetyl Perchlorate".

When a solution of acetyl chloride in acetic anhydride was added to a solution of $AgClO_4$ in the same solvent, AgCl was immediately precipitated. The resulting solution, presumably of acetyl perchlorate initially, was very unstable, apparently decomposing in the same way as acetic anhydride solutions of $HClO_4$, but much more rapidly. No quantitative measurements of the acidity of such solutions could therefore be made with the aid of indicators. The addition of 2 : 6-dimethoxy benzoquinone did, however, result in an immediate deep red colour which faded fairly rapidly, indicating the transitory high acidity of the solution and thus affording direct evidence that the acetyl ion is a strongly acid species. Neither acetyl chloride nor $AgClO_4$ alone showed such acidic properties in acetic anhydride. The acidity of "acetyl perchlorate" and acetyl fluoborate in acetic anhydride will form the subject of later investigations.

---

[24] Hammett and Paul, *J. Amer. Chem. Soc.*, 1934, **56**, 827.

* Cp. succeeding paper.

TABLE II.

Q added, g. mol./l. . .	0·0125						$10^{-3}\times6·94$	$10^{-3}\times5·52$	$10^{-3}\times1·40$	0·0125
% v/v Ac_2O . . .	20	40	50	60	70	80				90
c_{Ac_2O}, g. mol./l. . . .	2·15	4·30	5·38	6·46	7·53	8·60				9·68
$c_{(AcOH)_2}$, g. mol./l. . .	6·94	5·20	4·34	3·47	2·60	1·74				0·87
c_{HClO_4} g. mol./l. . . .	0·0778									
Spek. reading . . .	0·311	0·424	0·500	0·604	0·738	0·918	0·681	0·610	0·296	1·143
$10^4 . c_{QH_2^{++}}$ 1st approx. .	3·00	4·16	4·89	5·94	7·28	9·20	6·71	6·00	2·86	11·8
$10^3 . c_{Q_2H_2^{++}}$ 1st approx. .	6·10	6·04	6·01	5·95	5·89	5·79	3·13	2·46	0·56	5·66
Correcn. to Spek. reading *.	0·013	0·011	0·010	0·010	0·009	0·008	0·005	0·004	0·001	0·007
Corrected Spek. reading .	0·298	0·413	0·490	0·594	0·729	0·910	0·676	0·606	0·295	1·136
$10^4 . c_{QH_2^{++}}$ 2nd approx. .	2·90	4·05	4·80	5·85	7·20	9·10	6·66	5·96	2·80	11·66
$10^3 . c_{Q_2H_2^{++}}$ 2nd approx. .	6·10	6·05	6·01	5·96	5·89	5·79	3·14	2·46	0·56	5·67
log $\frac{c_{Q_2H_2^{++}}}{(c_{QH_2^{++}})^2}$ . . .	4·86	4·57	4·42	4·24	4·05	3·85	3·85	3·84	3·85	3·62
Apparent H_0 . . .	−4·06	− 4·35	− 4·50	− 4·68	− 4·86	− 5·07	− 5·07	− 5·08	− 5·07	− 5·30

* 0·0139 M. quinone in Ac_2O (no $HClO_4$) gave a Spekker reading of 0·008, and, in acetic acid, a reading of 0·017. An approximate correction for the yellow form of the quinone has been taken as:

$$\frac{c_{Q_2H_2^{++}}}{0·0139}\left(0·017 - \frac{0·009x}{100}\right)$$

for a solution in $(100 - x) : x$ % v/v acetic acid : Ac_2O.

Summary.

The known properties of the acetic acid-acetic anhydride solvo-system are reviewed. The solvo-system is ideal with respect to the two solvents in mixtures containing up to about 80 % w/w of acetic anhydride, but acetic acid must be regarded as a dimer. The behaviour of strong acids in the system is critically discussed and it is shown that much of this behaviour may be accounted for by postulating the existence of highly acidic acetyl ions. It is found that 2 : 6-dimethoxy benzoquinone may be used to measure acidity functions in water-sulphuric acid mixtures, and its use is extended to measure apparent H_0-values of solutions of $HClO_4$ in various acetic acid-acetic anhydride mixtures. The solution which results from the reaction between acetyl chloride and $AgClO_4$ in acetic anhydride, with precipitation of AgCl, is found to be unstable, but highly acid.

Imperial College of Science and Technology,
South Kensington,
London, S.W.7.

KINETIC STUDIES IN THE SOLVENTS ACETIC ACID AND ACETIC ANHYDRIDE.

PART II. THE THIELE ACETYLATION OF BENZOQUINONE AND TOLUQUINONE (EXPERIMENTAL).

By H. A. E. Mackenzie and E. R. S. Winter.

Received 4th March, 1947.

Benzoquinone-1 : 4 reacts with acetic anhydride, even at room temperatures, in the presence of a small amount of sulphuric acid.[1] The reaction very nearly obeys the stoichiometric equation :

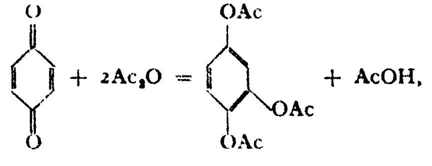

and is fairly general for quinones.[2] It is normally grouped with those reactions between quinones and substances of the general type R—H which are represented either as an addition of the reagent to one of the double bonds of the quinone with subsequent enolisation, or as a 1 : 4 addition to the conjugated system of the quinone.[3] Erdtman [4] has made a qualitative study of the Thiele acetylation of several quinones, and interpreted his results in terms of the electronic theory on the lines originally suggested by Robinson.[5] The initial step in the reaction was assumed to be the addition of acetic acid to the quinone. The present work shows that former ideas on the mechanism of the reaction have inclined to over-simplification.

---

[1] Thiele, *Ber.*, 1898, **31**, 1247.

[2] Thiele and Winter, *Annalen*, 1900, **311**, 341.

[3] E.g. Hickinbottom, *Reactions of Organic Compounds* (Longmans, 1942); and Fieser and Fieser, *Organic Chemistry* (Heath, 1944).

[4] Erdtman, *Proc. Roy. Soc. A*, 1933-4, **143**, 177.

[5] Robinson, *Outline of an Electrochemical (Electronic) Theory of the Course of Organic Reactions* (Inst. of Chem., 1932).

Experimental.

Materials.—Benzoquinone-1 : 4 of m.p. 115·5° C. was prepared by steam-distillation of the laboratory reagent, followed by two recrystallisations from 100-120° C. petroleum ether. 2-Methyl benzoquinone-1 : 4 (toluquinone) of m.p. 69° C. was obtained by recrystallisation of the laboratory reagent from water, followed by two recrystallisations from 100-120° C. petroleum ether. Acetic anhydride and acetic acid of laboratory reagent grade were distilled, with exclusion of moisture, and the middle fraction (60 %) collected in each case. Boiling ranges of the materials collected were less than 2° C. and 1° C. respectively. Although the purification was not stringent, different batches gave reproducible kinetic results. Carbon tetrachloride was dried by distillation, the first 10 % of distillate being rejected and the subsequent constant-boiling liquid collected. 60 % w/w Analar $HClO_4$ was standardised by dilution and titration with standard NaOH. A simultaneous density determination enabled the water content to be estimated accurately. Analar H_2SO_4 was taken as 98 % w/w pure. Silver perchlorate was prepared by the method of Gomberg,[7] without, however, the stringent removal of small amounts of AgCl. In order to prepare a standard solution of $AgClO_4$, the solid was dried at 140° C., transferred to a weighed dry glass-stoppered measuring flask, which was then cooled and re-weighed. The required volume of solvent was then added. All other reagents were of Analar grade.

Procedure.—The reaction mixture consisted of the solvent (acetic acid and acetic anhydride in varying proportions, together with CCl_4 in some cases) and low concentrations of quinone, acid catalyst and any other reagents. Each reaction mixture was kept in a stoppered vessel immersed in a water bath thermostatted electrically to ± 0·02° C. Benzoquinone and toluquinone have redox potentials of 0·711 and 0·656 respectively,[8] so that both are able to oxidise the iodide ion in acid solution with the liberation of iodine, and the reaction was therefore followed iodometrically. Aliquots of the reaction mixture were removed by a fast-running pipette at measured times, and run into a solution of KI in water (3 ml. 30 % w/v KI per 40 ml.). When the reaction mixture contained more than 80 % v/v acetic anhydride, the KI solution incorporated in addition 20 % v/v acetic acid, in order to facilitate mixing of the anhydride with water. The KI-quinone solution was then strongly acidified with H_2SO_4 (3 ml. 30 % v/v H_2SO_4 added per 40 ml. of solution), and the liberated iodine titrated with M./50 or M./100 sodium thiosulphate solution with starch as indicator. This procedure gave reproducible results even when the reaction mixture contained CCl_4, provided that there was rapid mixing of the aliquot sample with the aqueous medium, which, by reacting with unchanged quinone and acetic anhydride stopped the acetylation reaction.

In the work with $HClO_4$ as catalyst, the reaction was initiated by the addition of a solution of the quinone in acetic acid or acetic anhydride, previously brought to the correct temperature, to the main bulk of the mixture ; in the H_2SO_4 studies, by the addition of a solution of H_2SO_4 in acetic acid.

Absence of Uncatalysed Reaction.—Both benzoquinone and toluquinone were stable in solution in acetic acid, in acetic anhydride and in a 60 : 40 v/v mixture of acetic acid and acetic anhydride over long periods. Thus with benzoquinone, 0·54 g. was refluxed in an all-glass apparatus with 20 ml. acetic anhydride and 30 ml. acetic acid for one hour, and allowed to cool. Iodometric estimation of aliquots (*a*) before refluxing, (*b*) after one and (*c*) after two refluxing treatments gave the following titres with M./10 $Na_2S_2O_3$; (*a*) 20·0 (*b*) 19·6 and (*c*) 19·8 ml. The slightly low results are probably attributable to small and variable accumulation of the quinone in the reflux condenser.

The Nature of the Reaction Curve.—The sulphuric acid-catalysed acetylation is complicated by the simultaneous sulphonation of acetic anhydride,[9] but kinetic studies (reported later), showed that the results could be interpreted, provided that the quinone concentration was sufficiently low for the reaction to lead to negligible changes in the acetic acid-acetic anhydride content. Under such conditions, and after correcting for the gradual removal of H_2SO_4 in the sulphonation of acetic anhydride, the rates of disappearance of benzoquinone and toluquinone obeyed a first-order law.

---

[6] Mackenzie and Winter, preceding paper.

[7] Gomberg, *J. Amer. Chem. Soc.*, 1923, **45**, 398.

[8] Hammett, *Physical Organic Chemistry* (McGraw Hill, 1940), p. 392.

[9] Murray and Kenyon, *J. Amer. Chem. Soc.*, 1940, **62**, 1230.

The Thiele acetylation was also found to be catalysed by both $HClO_4$ and phosphoric acids, in which cases the reaction between the mineral acid and acetic anhydride had a negligible rate. Perchloric acid behaves, in addition, more simply in acetic acid-acetic anhydride solutions than does H_2SO_4,[6] so it has been used as the catalyst for the greater part. With $HClO_4$ and low quinone concentrations (less than about 0·2 M.) the acetylation reaction is represented accurately over 60-90 % of its course by a first-order disappearance of the quinone. Typical runs are given in Fig. 1, where $\log_{10} c_{(\text{Quinone})}$ is plotted against time. $c_{(\text{Quinone})}$ is expressed in ml. M./50 $Na_2S_2O_3$. The experimental specific reaction rate, k_e, given by the equation

FIG. 1.—(*a*) 0·1 M. benzoquinone; 0·0753 M. $HClO_4$; 2·95 M. Ac_2O; 6·35 M. $(AcOH)_2$; 30° C. (*b*) 0·1 M. benzoquinone; 0·0753 M. $HClO_4$; 6·18 M. Ac_2O; 3·75 M. $(AcOH)_2$; 30° C. (*c*) 0·1 M. benzoquinone; 0·0753 M. $HClO_4$; 9·40 M. Ac_2O; 1·15 M. $(AcOH)_2$; 30° C. (*d*) 0·05 M. toluquinone; 0·0778 M. $HClO_4$; 7·78 M. Ac_2O; 2·46 M. $(AcOH)_2$; 25° C. (*e*) 0·05 M. toluquinone; 0·0078 M. $HClO_4$; 10·7 M. Ac_2O; 0·029 M. $(AcOH)_2$; 35° C.

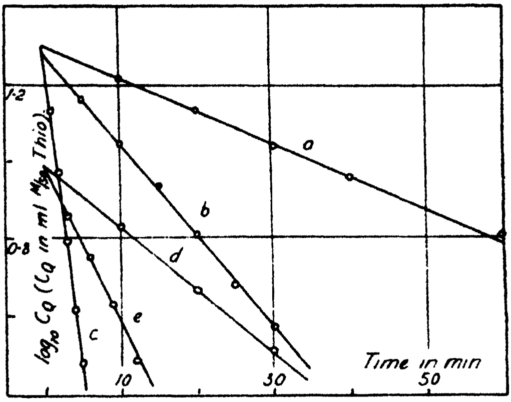

$$k_e = \frac{1}{t}\ln (c_Q)_0/(c_Q)_t,$$

where $(c_Q)_t$ is the concentration of quinone surviving after t sec. and $(c_Q)_0$ its initial concentration, has been obtained from the slopes of plots (cp. Fig. 1). From 4 to 6 points have been determined for each value of k_e. k_e is given throughout in the units sec.^{-1}.

Correction for the Water Content of the Perchloric Acid Used.—It was not clear from the literature whether the water necessarily added to the reaction mixture with the 60 % w/w perchloric acid would react immediately with the acetic anhydride to give acetic acid, under the conditions of experiment employed. Consequently, after a given acetylation reaction had proceeded for some time, a small amount of water was added. This resulted in an abrupt

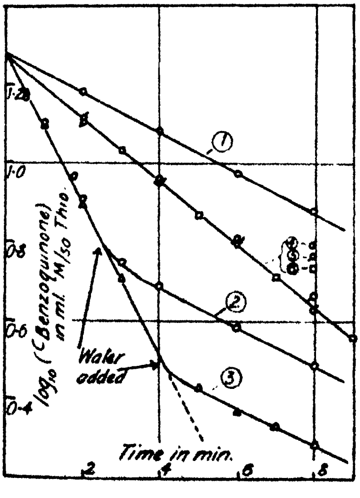

FIG. 2.—(20° C.). 0·1 M. benzoquinone; 0·0375 M. $HClO_4$: (1) 1·58 ml. $(AcOH)_2$, 18·7 ml. Ac_2O. (2) and (3) Initially 20 ml. Ac_2O; 0·15 ml. H_2O added after 2·5 and 4 min. respectively to 12 ml. reaction mixture left. (4) 0·95 ml. $(AcOH)_2$, 19·2 ml. Ac_2O. (5) 20 ml. Ac_2O. 0·15 ml. H_2O added to $HClO_4$ in Ac_2O at time = − 2 min.; benzoquinone in Ac_2O added at time = 0. (6) 20 ml. Ac_2O. 0·15 ml. H_2O added to benzoquinone in Ac_2O at time = − 2 min.; $HClO_4$ in Ac_2O added at time = 0.

change in the slope of the $\log_{10} c_Q - t$ plot. The new slope was found to be exactly that produced with a different reaction mixture to which no water was added, but in which the initial acetic acid and acetic anhydride contents had been adjusted by equivalent amounts (cp. Fig. 2, curve 1, and the latter portions of curves 2 and 3). Also, a small amount of water added initially had the same effect as an equivalent reduction in, and addition to the initial acetic anhydride and acetic acid concentrations, respectively, thus, in Fig. 2, curves 4, 5 and 6 are the same.

Thus water introduced into the reaction mixture rapidly hydrolyses acetic anhydride according to $Ac_2O + H_2O = (AcOH)_2$. It was not determined here whether this reaction occurs rapidly in the absence of strong mineral acid. In all subsequent work, therefore, the acetic acid and acetic anhydride concentrations have been corrected for the water content of the perchloric acid used and are expressed in M., taking the molecule of acetic anhydride as Ac_2O and that of acetic acid as the dimer, $(AcOH)_2$.[9] It has been assumed that the volumes of solvents are additive; a rough quantitative check showed that this would introduce negligible error ($< 0{\cdot}5$ %) in the concentration terms.

The Effect of Variation in the Acetic Acid-Acetic Anhydride Ratio—the Dependence of the Reaction on Acidity.—The results with benzoquinone and toluquinone in reaction mixtures containing different proportions of acetic anhydride and acetic acid are given in Tables I and II. The activation energies, E, were obtained in the usual way, by plotting $\log k_e$ against $1/T$; the values are considered correct to ± 0·4 kcal./g. mol.

TABLE I

$c_{\text{Benzoquinone}}$ g. mol./l.		0·10							
c_{HClO_4} g mol./l.		0·0753						0·0075	0·0025
% v/v Ac_2O		30	45	60	75	90	100	100	100
% v/v $(AcOH)_2$		70	55	40	25	10	0	0	0
Corrected c_{Ac_2O} g. mol./l.		2·95	4·56	6·18	7·79	9·40	10·48	10·70	10·74
Corrected $c_{(AcOH)_2}$ g. mol./l.		6·35	5·05	3·75	2·45	1·15	0·28	0·028	0·009
$10^4 k_e$ sec.$^{-1}$	303° K.	3·29	5·09	9·18	20·6	64·6	209	54·7	23·6
	298° K.	2·39	3·84	6·76	13·5	42·7	134	42·2	19·1
	293° K.	1·42	2·44	4·25	9·26	31·1	109	33·3	15·3
	288° K.	0·99	1·59	2·74	5·81	18·2	71·6	22·2	10·3
E, kcal./g. mol.		14·6	14·1	14·6	14·4	13·2	12·3	9·1	8·4

Determinations could not be made on solutions containing 20 % or less v/v of acetic anhydride, since in such solutions a polymerisation reaction takes place,[10] accompanied by rapid darkening of the solutions which made iodometric determinations impossible. This darkening became more marked as the acetic anhydride content was reduced.

Features of note are: (1) The constancy (within experimental error) of E, in solutions containing $<$ 80 % v/v acetic anhydride, and the marked fall of E as the amount of acetic acid is progressively reduced thereafter. (2) The large variation in k_e with variation in the acetic acid-acetic anhydride concentration ratio. The increase in k_e with increasing Ac_2O content parallels the increase in super-acidity and also the decrease in apparent acidity function of the solution.[9] The parallelism between k_e and super acidity as measured by

[10] Erdtman, *Proc. Roy. Soc. A*, 1933-4, 143, 232.

TABLE II

$c_{\text{Toluquinone}}$ g. mol./l.		0·05						
c_{HClO_4} g. mol./l.		0·0778						0·0078
% v/v Ac_2O		30	45	60	75	90	100	100
% v/v $(AcOH)_2$		70	55	40	25	10	0	0
Corrected c_{Ac_2O} g. mol./l.		2·94	4·55	6·17	7·78	9·39	10·47	10·70
Corrected $c_{(AcOH)_2}$ g. mol./l.		6·36	5·06	3·76	2·46	1·16	0·29	0·029
$10^4 k_e$ sec.$^{-1}$	308° K.	1·52	—	5·29	—	38·6	116	16·3
	303° K.	1·04	—	3·61	—	28·2	94·3	15·6
	298° K.	0·708	1·30	2·42	5·91	18·2	67·1	11·1
	293° K.	0·484	—	1·72	—	14·2	54·1	8·67
E kcal./g. mol.		13·6	—	13·6	—	11·9	9·5	8·7

$(p_H)_{AcOH}$ is not, however, general. In Table III are given the results obtained with benzoquinone in solutions of known $(p_H)_{AcOH}$ (Russell and Cameron [11]).

In Fig. 3 are shown the plots of $\log_{10} k_e$ for benzoquinone and toluquinone against the apparent acidity function, H_0, of solutions 0·0778 M. in $HClO_4$. The H_0 values are obtained from Table II of Part I [6] by interpolation. The values of k_e at 25° C. for toluquinone are taken from Table II of this paper; those of k_e at 25° C. for benzoquinone are obtained from the values in Table I by multiplying by 0·0778/0·0753, since direct proportionality between k_e and the stoichiometric concentration of perchloric acid has been established experimentally within this concentration range (cp. below). The plots are linear for solutions containing up to about 80 % v/v acetic anhydride, but not parallel The slopes are, for benzoquinone, − 0·99, and for toluquinone, − 1·20. This difference and the difference of the toluquinone value from unity are in excess of experimental error; as the acetic anhydride concentration is increased above 80 % v/v, the plots cease to be linear, and a greater difference between their slopes is apparent.

TABLE III

Benzoquinone, 0·0471 M. Ac_2O, 30 % v/v (corrected). $(AcOH)_2$, 70 % v/v (corrected).

Acid.	Molarity.	$(p_H)^{AcOH}$.	$10^4 k_e$, sec.$^{-1}$.
H_2SO_4	0·0715	− 11·45	0·77 *
	0·0357	− 10·96	0·34 *
$HClO_4$	0·083	− 5·61	2·60
	0·0083	− 4·32	0·28

* Since high accuracy was not required for this experiment, these values were obtained from initial slopes of the plot of $\log_{10}$ (titre) against time, and the correction for the simultaneous sulphonation reaction was not applied. The error incurred is likely to be considerably less than 5 %.

---

[11] Russell and Cameron, *J. Amer. Chem. Soc.*, 1938, **60**, 1345.

In Fig. 4 is shown the dependence of the k_e for benzoquinone and toluquinone on the stoichiometric concentration of $HClO_4$. The value of k_e for 0·10 M. benzoquinone solutions at 20° C., with $c_{Ac_2O} = 7{\cdot}24$ M. and $c_{(AcOH)_2} = 2{\cdot}89$ M. is given accurately by the equation

$$10^4 k_e = 84{\cdot}0 \, (c_{HClO_4}) \quad . \quad . \quad . \quad . \quad . \quad . \quad (1)$$

for values of c_{HClO_4} up to about 0·1 M. k_e for 0·05 M. toluquinone solutions at 25° C., is given by :

$$10^4 k_e = 57{\cdot}5 \, (c_{HClO_4}) \quad . \quad . \quad . \quad . \quad . \quad (2)$$

where $c_{Ac_2O} = 7{\cdot}24$ M. and $c_{(AcOH)_2} = 2{\cdot}89$ M., when c_{HClO_4} is $<$ 0·1 M. When c_{HClO_4} exceeds 0·1 M. there is a positive deviation from linearity.

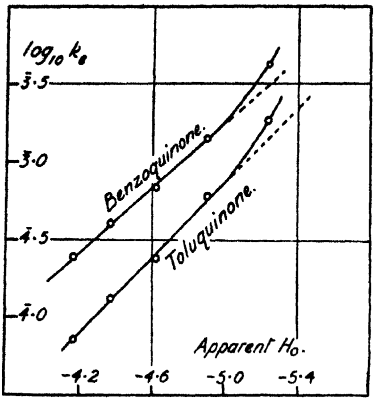

FIG. 3.

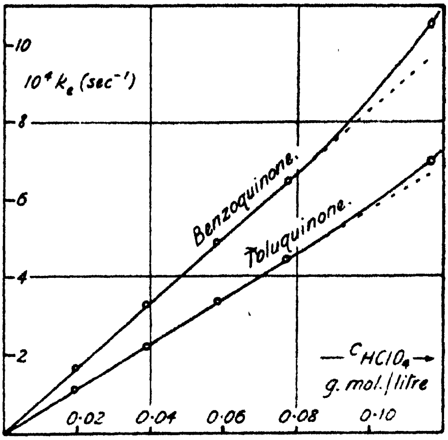

FIG. 4.

It is well known that solvent effects may be large, and in particular may be responsible for variations in the activation energy of reactions in solution. The results in Table I and II suggest, however, that the solvents acetic anhydride and acetic acid may play some direct chemical part in the reaction mechanism. An attempt has therefore been made to determine separately the effects of acetic acid and acetic anhydride by the use of a third solvent.

The Use of Carbon Tetrachloride as a Diluent.—Carbon tetrachloride was selected because it is aprotic, fairly easily purified and dried, and chemically

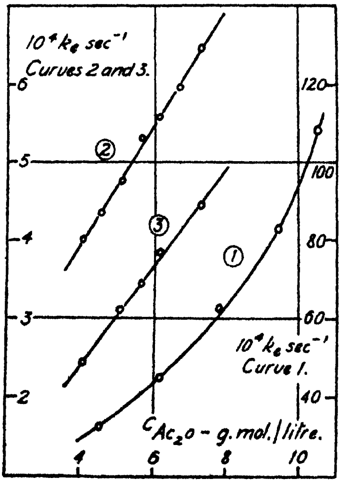

FIG. 5.—(1) Benzoquinone, 0·10 M. ; $HClO_4$, 0·0753 M. ; $(AcOH)_2$, 0·28 M., CCl_4 to maintain volume constant. 20° C. (2) Benzoquinone, 0·10 M. ; $HClO_4$; 0·0778 M. ; $(AcOH)_2$, 2·89 M. ; CCl_4 to maintain volume constant. 20° C. (3) Toluquinone, 0·05 M. ; $HClO_4$, 0·0778 M. ; $(AcOH)_2$, 2·89 M. ; CCl_4 to maintain volume constant. 25° C.

inert with respect to the reaction mixtures under investigation. In all the reaction mixtures which contained CCl_4, complete homogeneity was obtained, although the range was limited by the immiscibility of CCl_4 with mixtures of high acetic acid and low acetic anhydride content. The low dielectric constant of CCl_4 (2·2) suggests a possible " medium " effect, but, this, if present, is negligibly small, since the results correlate quantitatively with data obtained in its absence.

Using CCl_4 as diluent, the total volume of the reaction mixture, with fixed amounts of quinone and perchloric acid was maintained constant, while the concentrations of acetic anhydride and acetic acid were independently varied. In Fig. 5 are given the results obtained when the acetic anhydride content was varied. In the case of benzoquinone and in the range of lower activation energy (cf. Table I), there is no simple relationship between the k_e and $c_{\mathrm{Ac_2O}}$ (curve 1). In the range of higher activation energy, however, the plot of k_e against $c_{\mathrm{Ac_2O}}$ is linear both for benzoquinone (curve 2) and toluquinone (curve 3). With solutions in which $c_{\mathrm{HClO_4}} = 0{\cdot}0778$ M., $c_{\mathrm{(AcOH)_2}} = 2{\cdot}89$ M., k_e for benzoquinone at 20° C. is given accurately by the equation

$$10^4 k_e = 0{\cdot}778\,(c_{\mathrm{Ac_2O}}) + 0{\cdot}825 \qquad (3)$$

and k_e for toluquinone at 25° C. by the equation

$$10^4 k_e = 0{\cdot}630\,(c_{\mathrm{Ac_2O}}) - 0{\cdot}093 \qquad (4)$$

In Fig. 6 are shown the results obtained when the acetic acid content was varied. In the range of higher activation energy, the plots of k_e against $1/c_{\mathrm{(AcOH)_2}}$ are linear both for benzoquinone (curve 1) and toluquinone (curve 2). When $c_{\mathrm{HClO_4}} = 0{\cdot}0778$ M., $c_{\mathrm{Ac_2O}} = 4{\cdot}01$ M., k_e for benzoquinone at 20° C. is given accurately by the equation

$$10^4 k_e = 11{\cdot}4/c_{\mathrm{(AcOH)_2}} \qquad (5)$$

and k_e for toluquinone at 25° C. by the equation

$$10^4 k_e = 8{\cdot}70/c_{\mathrm{(AcOH)_2}} - 0{\cdot}60. \qquad (6)$$

The activation energy for the benzoquinone reaction in the presence of the maximum amount of CCl_4 used was determined. For the reaction mixture: benzoquinone, 0·10 M.; $HClO_4$, 0·0778 M.; Ac_2O, 4·01 M.; $(AcOH)_2$, 2·89 M.; CCl_4, 30 % v/v (3·14 M.), the following values of k_e were obtained:

t° C.	20	25	30	35
$10^4 k_e$	4·00	6·32	9·14	12·6

These results give a value for E of 14 kcal./g. mol., a result not significantly different from the value obtained in the absence of carbon tetrachloride.

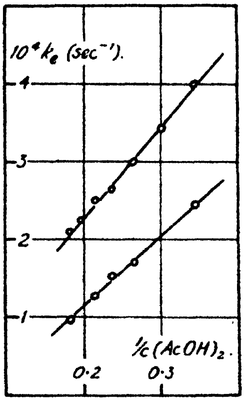

FIG. 6.

Eqn. (1), (3) and (5) for benzoquinone at 20° C. may be represented by the single equation

$$10^4 k_e = \frac{c_{\mathrm{HClO_4}}(2{\cdot}89\, c_{\mathrm{Ac_2O}} + 30{\cdot}7)}{c_{\mathrm{(AcOH)_2}}} \qquad (7)$$

which, on inserting the appropriate numerical values of the constant concentration terms, reduces to:

$$10^4 k_e = 83{\cdot}0\,(c_{\mathrm{HClO_4}}) \qquad (1')$$

$$10^4 k_e = 0{\cdot}778\,(c_{\mathrm{Ac_2O}}) + 0{\cdot}825 \qquad (3')$$

$$10^4 k_e = 11{\cdot}4/c_{\mathrm{(AcOH)_2}} \qquad (5')$$

The corresponding overall equation in the case of toluquinone at 25° C. is

$$10^4 k_e = \frac{c_{\mathrm{HClO_4}}(23{\cdot}4\, c_{\mathrm{Ac_2O}} + 18{\cdot}4 - 7{\cdot}71\, c_{\mathrm{(AcOH)_2}})}{c_{\mathrm{(AcOH)_2}}} \qquad (8)$$

which reduces to:

$$10^4 k_e = 57{\cdot}3\,(c_{\mathrm{HClO_4}}) \qquad (2')$$

$$10^4 k_e = 0{\cdot}630\,(c_{\mathrm{Ac_2O}}) - 0{\cdot}104 \qquad (4')$$

$$10^4 k_e = 8{\cdot}73/c_{\mathrm{(AcOH)_2}} - 0{\cdot}60. \qquad (6')$$

There is thus a quantitative correlation between the results obtained on the $HClO_4$ variation in the absence of CCl_4 and on the Ac_2O and $(AcOH)_2$ variations in the presence of CCl_4. Further, eqn. (7) and (8) may be used to calculate k_e for the reaction series where both Ac_2O and $(AcOH)_2$ are simultaneously varied in the absence of CCl_4. The experimental and calculated values are given together in Table IV. The agreement is good over the range of constant high activation energy, thus confirming the absence of any medium effect by CCl_4.

TABLE IV

Benzoquinone, 0·10 M. at 20° C.

c_{HClO_4} . . .		0·0753	0·0778	0·0753	0·0753	0·0778	0·0753	0·0753	0·0753
c_{Ac_2O} . . .		2·95	4·01	4·56	6·18	7·24	7·79	9·40	10·48
$c_{(AcOH)_2}$ . . .		6·35	5·49	5·05	3·75	2·89	2·45	1·15	0·28
$10^4 k_e$ sec.$^{-1}$	Found	1·42	2·10	2·44	4·25	6·46	9·26	31·1	109
	Calcd.	1·37	2·08	2·42	4·21	6·46	7·86	19·8	89·7

Toluquinone, 0·5 M. at 25° C.

c_{HClO_4} . .		0·0778							
c_{Ac_2O} . . .		2·94	4·01	4·55	6·17	7·24	7·78	9·39	10·47
$c_{(AcOH)_2}$ . .		6·36	5·49	5·06	3·76	2·89	2·46	1·16	0·29
$10^4 k_e$ sec.$^{-1}$	Found	0·70	0·97	1·30	2·42	4·44	5·91	18·2	67·1
	Calcd.	0·47	0·99	1·32	2·85	4·46	5·74	15·4	70·1

The Effect of Silver Perchlorate on the Acetylation Reaction.—In the absence of mineral acid, as much as 0·1 g. of silver perchlorate in 5 ml. 0·1 M. benzoquinone solution in acetic anhydride or in a 60 : 40 v/v acetic anhydride-acetic acid mixture, failed to catalyse the acetylation reaction after 14 days at room temperature. In the presence of perchloric acid, $AgClO_4$ had a very slight acceleratory effect, which is probably due to a primary salt effect on the reaction between an ion and a neutral molecule. For a series of solutions (in which benzoquinone was 0·10 M.; Ac_2O, 7·24 M.; $(AcOH)_2$, 2·89 M.; and $HClO_4$, 0·0389 M.) k_e was found to be $3·32 \times 10^{-4}$ sec.$^{-1}$ in the absence of $AgClO_4$, $3·39 \times 10^{-4}$ sec.$^{-1}$ in the presence of 0·1445 M. $AgClO_4$ and $3·41 \times 10^{-4}$ sec.$^{-1}$ in the presence of 0·1808 M. $AgClO_4$.

The Nature of the Acetylated Products.—Thiele and Winter[3] and Erdtman[4] state that the Thiele acetylation of toluquinone gives rise to 2 : 4 : 5 triacetoxy toluene, and no mention is made of the two other possible isomeric products (viz. 2 : 3 : 5 and 2 : 3 : 6). These authors state that the yield of the product obtained was " good ". Investigation seemed desirable, since, if only one of the isomers is produced, the proposed mechanism of the reaction should explain this feature. The results obtained with benzoquinone were so surprising that a detailed study has been made of the nature of the products when the reaction is carried out under two extreme conditions, viz. in nearly 100 % acetic anhydride and in 50 : 50 v/v acetic anhydride-acetic acid solution. Under the latter conditions the acetylation of benzoquinone gives rise to significant quantities of hydroquinone diacetate and 1 : 2 : 4 : 5-tetra-acetoxybenzene in addition to hte Thiele product, 1 : 2 : 4-triacetoxy benzene. The products obtained from toluquinone are analogous, but complicated by isomerism, and have not been fully characterised. Experimental details follow.

(*a*) 0·5 g. of benzoquinone in 10 ml. acetic anhydride was treated with 0·5 ml. of 60 % w/w $HClO_4$. The solution was allowed to stand for ½ hr. and was then poured into 100 ml. of water. Saturation of the liquid with sodium chloride permitted ether extraction of 1·08 g. of material (m.p. 92-93° c.). One recrystallisation of this product from methanol gave pure 1 : 2 : 4-triacetoxy benzene, m.p. 97·5° c. The "crude" product is thus very nearly pure, and the yield of 1 : 2 : 4-triacetoxy benzene from benzoquinone is over 90 %. A similar experiment in 50 : 50 v/v acetic anhydride-acetic acid yielded a mixture of products, so it was repeated on a larger scale.

(*b*) 27 g. of benzoquinone in a mixture of 110 ml. Ac_2O and 100 ml. $(AcOH)_2$ was treated with 10 ml. of 60 % w/w $HClO_4$, and the solution allowed to stand for 20 hr. A white crystalline solid (*A*) was deposited. This was filtered off, and the filtrate poured into 400 ml. of water which was then vigorously shaken and allowed to stand for ½ hr. The solid (*B*) was filtered off and the filtrate saturated with sodium chloride. An oil then separated, which solidified on vigorous shaking. The resultant solid (*C*) was filtered off.

When dry, (*A*) weighed 13·1 g. and had a m.p. 208-215° c. On recrystallisation from acetic acid (charcoal), the m.p. rose to 226° c. and remained unaltered on further crystallisation. Sublimation *in vacuo* did not alter the m.p. (*A*) consisted therefore of very nearly pure 1 : 2 : 4 : 5-tetra-acetoxy benzene. (Found: C, 54·6; H, 4·6 %. Calcd. for $C_{14}H_{14}O_8$: C, 54·2; H, 4·5 %.) Heilbron's Dictionary gives m.p. 226° c.

(*B*) (26·4 g.) and (*C*) (26·0 g.) were subjected to fractional crystallisation from water-methanol mixtures. Two pure materials were obtained from each: (1) hydroquinone diacetate, m.p. 120° c., characterised by hydrolysis to hydroquinone, m.p. 170° c., which in turn gave benzoquinone on treatment with acidified $K_2Cr_2O_7$ solution, and (2) 1 : 2 : 4-triacetoxy benzene, m.p. 97·5° c.; identity confirmed by a mixed m.p. determination. The fractional crystallisation was wasteful, particularly of the triacetoxy compound which was the more soluble. 8 g. of hydroquinone diacetate was obtained altogether, and therefore, by difference, the amount of triacetoxy compound in (*B*) and (*C*) was about 44 g. This experiment was repeated but with a benzoquinone concentration in the reaction mixture of one-tenth that used above, and therefore about the same as that used for kinetic determinations. The same products were obtained.

Summarising for benzoquinone, (1) acetylation in approximately 100 % acetic anhydride gives rise to more than 0·9 mole of 1 : 2 : 4-triacetoxy benzene from 1 mole of benzoquinone, and (2) acetylation in approximately 50 : 50 v/v acetic anhydride-acetic acid gives rise to 0·7 mole of 1 : 2 : 4-triacetoxy benzene, 0·17 mole of hydroquinone diacetate and 0·17 mole of 1 : 2 : 4 : 5-tetra-acetoxy benzene from 1 mole of benzoquinone.

(*c*) 5 g. of toluquinone in 40 ml. Ac_2O was treated with 2 ml. of 60 % w/w $HClO_4$. The solution was allowed to stand for 1 hr. and was poured into 150 ml. of water. The crystalline product was filtered off (6·5 g.), and the filtrate saturated with sodium chloride and extracted with ether. The oily ether extract was treated with a little methanol, when it slowly deposited a further 1·0 g. of crystalline material. The residual methanol solution was evaporated down and yielded 2·7 g. of an oil. The combined crystalline products had m.p. 104-7° c. and consisted of nearly pure 2 : 4 : 5-triacetoxy toluene; m.p. on recrystallisation from methanol, 112-114° c. The oil could be crystallised by cooling with solid CO_2, but the crystals melted below room temperature. On distillation in the vacuum of the water pump, nearly all the oil distilled between 270 and 280° c. The oil is probably a mixture of the two other isomeric triacetoxy toluenes, but it was not separated into two fractions. (Found: C, 58·8; H, 5·5 %. Calcd. for $C_{13}H_{14}O_6$: C, 58·8; H, 5·3 %.)

(*d*) 10 g. of toluquinone in a mixture of 40 ml. acetic anhydride and 35 ml. acetic acid was treated with 4 ml. 60 % w/w $HClO_4$. The solution was allowed to stand for 20 hr. and was then poured into 300 ml. of water saturated with sodium chloride. Ether extraction yielded an oily product which, on standing in ether, deposited 1 g. of crystalline product (*A*). The filtrate, on evaporation of most of the ether, gave a further 0·4 g. of (*A*). Complete removal of ether gave a further 4·5 g. of solid (*B*). Dissolution of the residual oil in ether, followed by the addition of 100-120° c. petroleum ether yielded a further 3 g. of crystalline precipitate (*C*). The residual filtrate yielded, on removal of solvents, an oil (*D*).

(*A*) was characterised as nearly pure 2 : 3 : 5 : 6-tetra-acetoxy toluene. It had m.p. 189-195° c. which, on recrystallisation from acetic acid, rose to 197-198° c. Further recrystallisation did not alter the m.p. (Found: C, 55·7; H, 5·2 %. Calcd. for $C_{15}H_{16}O_8$: C, 55·7; H, 4·9 %.) Heilbron's Dictionary gives m.p. 198° c.

(*B*) was separated by crystallisation from acetic acid-water mixtures into 1·8 g. of 2 : 3 : 5 : 6-tetra-acetoxy toluene and 2·5 g. of 2 : 4 : 5-triacetoxy toluene (m.p. 112-114° c.; mixed m.p. 112-114° c.).

(*C*) was separated by crystallisation from methanol-water mixtures into 0·2 g. of 2 : 3 : 5 : 6-tetra-acetoxy toluene and 2·3 g. of 2 : 4 : 5-triacetoxy toluene.

(*D*) slowly deposited a further 1·2 g. of 2 : 4 : 5-triacetoxy toluene from methanol solution, but the remaining oil could not be resolved. It is considered improbable that this oil contained a tetra-acetoxy compound, because of the low solubility of such compounds in methanol, but the two other isomeric triacetoxy toluenes were probably present, together with 2 : 5-diacetoxy toluene (by analogy with the benzoquinone products), and some residual 2 : 4 : 5-triacetoxy toluene. The oil contained a large amount of acetic acid, which led to decomposition on distillation, and the acetic acid could not be removed by washing an ether solution of the oil with aqueous $NaHCO_3$, since this led to serious decomposition, with the production of an intensely red colour. A similar decomposition occurred when an attempt was made to separate the constituents of the oil chromatographically on an alumina column. Further investigation was therefore not attempted.

Summarising for toluquinone, (1) acetylation in approximately 100 % acetic anhydride gives rise to about 0·7 mole of 2 : 4 : 5-triacetoxy toluene, with a further 0·3 mole of probably a mixture of the two other isomeric triacetoxy toluenes, and (2) acetylation in approximately 50 : 50 v/v acetic anhydride-acetic acid gives rise to 0·3 mole of 2 : 4 : 5-triacetoxy toluene, 0·13 mole of 2 : 3 : 5 : 6-tetra-acetoxy toluene and an oil which has not been separated, but probably contains the two other isomeric triacetoxy toluenes and 2 : 5-diacetoxy toluene.

Finally, a simple experiment showed that " acetyl perchlorate " is a very effective catalyst for the Thiele aetylation : 2·1 g. of benzoquinone was treated in 18 ml. of acetic anhydride with 2 ml. 10 % w/v $AgClO_4$ in Ac_2O, and slightly less than the theoretical quantity of acetyl chloride. Disappearance of the benzoquinone in solution was almost immediate and the liquid became hot. After the AgCl had coagulated, it was filtered off, and the solution run into a large volume of cold water. An oil separated which crystallised on shaking. The crude product (4 g.) gave, on recrystallisation from methanol, 1 : 2 : 4-triacetoxy benzene, m.p. 97·5° C. (yield over 80 %).

Several difficulties were encountered in an intended study of the acetylation of 2 : 5-dimethyl benzoquinone-1 : 4 (*p*-xyloquinone). Firstly, *p*-xyloquinone was found to undergo a rapid photochemical reaction in acetic acid or acetic anhydride solutions, giving rise to a red product, so that work had to be carried out in vessels protected from the light. Then, although the redox potential of *p*-xyloquinone is 0·597,[8] oxidation of the iodide ion by the quinone was found to be sluggish unless very high concentrations of acid and potassium iodide were used for the iodometric estimation. Under such conditions the iodometric method became inaccurate as the $HClO_4$ interfered in the determination, causing irreproducibility in the results. It should be possible, however, to study the reaction of this quinone using sulphuric acid or acetyl fluoborate as catalyst.

Summary.

A kinetic study of the acetylation of benzoquinone and toluquinone in mixtures of acetic acid and acetic anhydride has been made, using an iodometric method. The reaction does not proceed in the absence of mineral acid, and is not catalysed by $AgClO_4$. With $HClO_4$ as catalyst, the rate of disappearance of quinone obeys a first-order law, for a constant composition of medium throughout the reaction; $AgClO_4$ has a very small acceleratory effect. The reaction rate varies markedly with the $Ac_2O/(AcOH)_2$ ratio in the solvent, and this variation parallels that shown by the acidity of the medium,but there is no general relationship between the reaction rate and the $(pH)^{AcOH}$. The activation energy is constant in solvent mixtures containing up to about 80 % v/v Ac_2O, but falls off thereafter. In the range of constant high activation energy, 14·4 and 13·6 kcal./g. mol. for benzoquinone and toluquinone respectively, the rate of reaction for both quinones varies linearly with the apparent acidity function and follows the general equation :

$$k_e = \frac{c_{HClO_4}(k_1 c_{Ac_2O} + k_2 + k_3 c_{(AcOH)_2})}{c_{(AcOH)_2}} \qquad . \quad . \quad . \quad (21)$$

where $k_3 = 0$ in the case of benzoquinone.

Results obtained with and without the use of CCl_4 as a diluent are mutually and quantitatively consistent, thus demonstrating the absence of medium effect.

The product of the acetylation of benzoquinone in approximately 100 % Ac$_2$O is nearly entirely 1 : 2 : 4-triacetoxy benzene, but in 50 : 50 v/v acetic acid-acetic anhydride, the product is a mixture of 1 : 2 : 4-triacetoxy benzene, hydroquinone diacetate and 1 : 2 : 4 : 5-tetra-acetoxy benzene. Toluquinone behaves in an analogous manner. The acetylation of benzoquinone in acetic anhydride, with the solution resulting from the reaction between AcCl and AgClO$_4$ in Ac$_2$O as catalyst, yields only 1 : 2 : 4-triacetoxy benzene.

Imperial College of Science and Technology,
South Kensington,
London, S.W.7.

REVIEWS OF BOOKS

Volumetric Analysis. Vol. II. Titration Methods. By I. M. KOLTHOFF AND V. A. STENGER. (2nd Revised Ed.) Interscience Publishers, Inc., New York and London, 1947. Pp. xiii + 374. Price 36s.

In 1928 Prof. Kolthoff, in collaboration with Dr. H. Menzel of Dresden, published a monograph entitled *Die Praxis der Massanalyse*, which was translated into English by Dr. N. H. Furman and, a year later, published in two volumes by John Wiley and Sons. Possibly because of the popularity of Sutton's book on volumetric analysis and of the vogue that Treadwell and Hall's works have enjoyed in this country, this translation became less widely known and used in Britain than it deserved to be. The first two volumes of the second edition have now been published, this time with V. A. Stenger of the Dow Chemical Company at Michigan as the translator and collaborator.

Prof. Kolthoff has always been a strong supporter of the claims of volumetric over gravimetric methods of chemical analysis, and the critical and original investigations that, with a long succession of students, he has made at the University of Minnesota have done much to dispel the view that volumetric methods are necessarily less accurate than those of gravimetric analysis. His work with his students has covered such a wide range of volumetric methods that in the present volume, which deals with the practice and application of titration methods, the authors are able to present critically selected methods for determining different inorganic and organic substances. The limitations of a given method and much information concerning its precision and accuracy, often the result of first-hand acquaintance, are given frequently as notes to the procedures that are detailed for the various determinations. These notes provide much that is interesting and of value to the reader.

The subject-matter is arranged on what may be called physico-chemical lines, and in this sense the treatment is more academic than might be expected in a practical book on volumetric analysis. The procedures described are arranged according to the type of reactions involved in the titrations rather than to the field in which they are applied, but the reader who may be disappointed with this method of classification and would prefer a more utilitarian arrangement will find adequate compensation in the fullness of the subject-index.

So far as one is able to judge, the work of revision has been done well, and although in their preface the authors are careful to point out that the work does not include a complete discussion of methods published outside America since 1940, the text is quite well supported by references to papers published since that time. In a future edition, two omissions that might well be rectified, if only by references to the literature, are a later modification (Parnas, *Z. anal. Chem.*, 1938, 114, 261) of the Parnas-Wagner micro-apparatus to be used in determining macro-amounts of ammonia, and Pugh's method (*J. Chem. Soc.*, 1937, 1824) for determining chloride or bromide ions by titration with mercurous perchlorate, bromophenol blue being used as an adsorption indicator, quite one of the best examples of the use of an indicator of this type.

The authors find so much new work to have been published since the first edition of this book was written that a third volume will be needed. As this will deal with oxidation-reduction methods, the present volume has been limited to titrations involving acid-base, precipitation, and complex-formation reactions.

The early chapters of vol. ii contain much information of general interest to all who use volumetric apparatus and methods, the sections dealing with the drainage of burettes, with the requirements for primary and secondary standard substances—a matter too often neglected in this country—and particularly the two long sections that describe primary substances for standardising acids and alkalis, being of special interest and value. In fact, this volume is one of few places where there is readily to hand useful and essential information on the preparation and examination of most of the pure substances needed in this branch of analysis. Another commendable feature is the information given about indicators, especially the table on mixed and screened indicators for acid-base titrations.

The volume challenges interest from the start for on the second page of the first chapter we learn that glass vessels the surface of which is contaminated by grease " generally deliver a volume which is somewhat too large ", and on the next page there is a reference to unpublished experiments that indicate thermal hysteresis effects in glassware may be much smaller than has generally been supposed—indeed they may be negligible for the purposes of volumetric analysis. Readers may be less ready to accept the authors' statement (p. 31), concerning the preparation of standard solutions by the dissolution and accurate dilution of a weighed quantity of solid, that " it is a good practice to invert the flask from thirty to forty times ".

It is a pity that the writers of this book vacillate between expressions of the form " 25 ml. is added " and " 25 ml. are added," a fault that did not occur in the first edition where the correct form was used. There are other expressions that may grate on an English ear—the proof-reading, in fact, leaves a good deal to be desired. The printing of the book and the quality of the paper are only adequate ; they do not reach the standard set by the first edition, but it may be unfair to expect them to do so.

The appearance of vol. III, promised for late 1948, will be awaited with interest and, if its subject-matter is as good as that of vol. I and II, then any analyst who has the completed work, and " Sutton," at his disposal will have in English all that he needs on this subject for some time to come.

L. S. T.

Physikalische Chemie. By WERNER KUHN. (3rd Ed.) Wepf & Co., Verlag, Basel. Pp. xi + 374. Price 15 Swiss Francs. (In German.)

THE title of this elementary text-book is somewhat misleading as, in fact, only a few branches of physical chemistry are covered. The subject-matter included probably satisfies the requirements of some intermediate stage in a particular University curriculum, though clearly not a stage at which the student has reached the same standard all round the subject. Thus, about 300 pages of Prof. Kuhn's book are devoted to thermodynamics and electrochemistry, whereas reaction kinetics, quantum theory, spectroscopy, etc., *together* occupy about 35 pages; atomic and molecular structure, valency, etc., are completely outside the orbit of the book.

The treatment of thermodynamics itself only covers certain aspects of the subject. It is meant to help the weaker student with the unfortunate consequence of not including anything which might stimulate the good one. However, in spite of this bias, the text does not help to establish in the reader's mind the connection between laboratory measurements and the thermodynamic quantities, which to many students presents the greatest difficulty in the study of the subject. The experimental side of physical chemistry is deliberately left out of the book, and numerical examples of real merit (as distinct from numerical substitutions in formulæ) are lacking.

In short, whatever place this book may have in some particular course of instruction, where its gaps and the other sides of the subject are properly allowed for, it cannot be recommended as a general students' text-book.

V. G.

Introduction to Modern Physics. (4th Ed.) by F. K. RICHTMEYER AND E. H. KENNARD. McGraw-Hill Publishing Co., Ltd., London. Pp. xvii + 759. Price 36s.

SINCE its first appearance 20 years ago, this book has been recognised as one of the best surveys of the origin and development of some of the more important concepts of modern physics, both classical and modern. For students of chemistry and physics, it should form the basis on which more specialised courses can be built. In the first edition Richtmeyer obviously derived great pleasure and enjoyment in telling a fascinating story, rather than in providing a compendium of information which was up-to-date, rigorous and comprehensive. In the third edition, Prof. Kennard made extensive alterations; he has to a large extent modernised the viewpoint, yet has successfully retained most of the characteristic features and the spirit of the original text. It now represents an up-to-date equivalent with a newer perspective.

In this fourth edition, the main body of the text is retained. The changes in the chapter on atomic structure and optical spectra are welcomed; the discussion is now primarily in terms of quantum states rather than of wave functions. This surely is the correct approach in an introduction which has much that will appeal to those less mathematically minded. The most extensive changes are naturally in the two chapters on the nucleus and cosmic rays—these have been extended to include short sections on the induction accelerator, the synchroton, nuclear fission, the Chicago " pile," etc. The section on mesons has been rewritten and lengthened but only the more important aspects, where some definite conclusions have apparently been reached, are discussed.

This book is, as is well known, one of the International Series of Pure and Applied Physics—there is thus no need to speak highly of the printing and binding, which is of pre-war standard. We have always recommended this book without reserve—while reiterating this recommendation, we must express some regret that it has not been possible to reduce the price of this popular book in its 4th edition below 36s.

Encyclopedia of Chemical Technology. Vol. I. (A TO ANTHRIMIDES). Ed. by DR. R. KIRK and DR. D. OTHMER. Interscience Publishing Inc., New York. Pp. xxiv + 982. Price $20.

THE need of a modern, specialised encyclopedia of chemical technology in these immediate post-war years is obvious. This will be fulfilled to a large extent in the series of 10 volumes which is now promised, the first of which concludes with Anthrimides. Workers in industry, in research associations and in the universities will welcome this book, since if we may judge from this volume, they will have a comprehensive guide to the entire field with all its ramifications. It will save many hours of literature search since the material has been collected over an extensive field.

In each section, sufficient theory to bring out established principles is included and then follows a lavish display of information of the knowledge at present available on materials, methods, processes, equipment, costs, etc., including flow-sheets and well-designed diagrams. It is natural that American processes should be given preference but there are also well-balanced accounts of other recognised processes. We are informed that all the articles, although written by specialists, have been reviewed by other competent authorities before publication—it is believed that this volume shows the wisdom and advantages of such a policy.

Each section is provided with a short but well-selected bibliography and there is a system of cross-reference which assists in finding the article of interest. Since, however, one must wait quite a few years before the final volume with its index appears, it is suggested that an Abridged Index would be of great value. This could be issued as a loose inset with each fresh volume and would well serve the purpose of assisting the reader in the speedy rediscovery of some fact which he remembers to have seen. Such an index would need changes as each volume appeared but it need not be in a permanent form until the last volume appears since it could be replaced by a new index from volume to volume.

This first volume will certainly encourage the buyer to continue until he has completed the set—one recommends the purchase of the present one *now*, so that the intending owner of the set should not be dismayed by the rather costly price of the completed work.

CORRIGENDUM.

Vol. 43, 1947:

Plate facing p. 396. The three patterns shown as (*h*), (*a*) and (*b*) of Fig. 1 should be (*c*), (*f*) and (*g*) of Fig. 4, and vice versa.

G. S. W. MARLOW

Secretary and Editor, 1926–1948

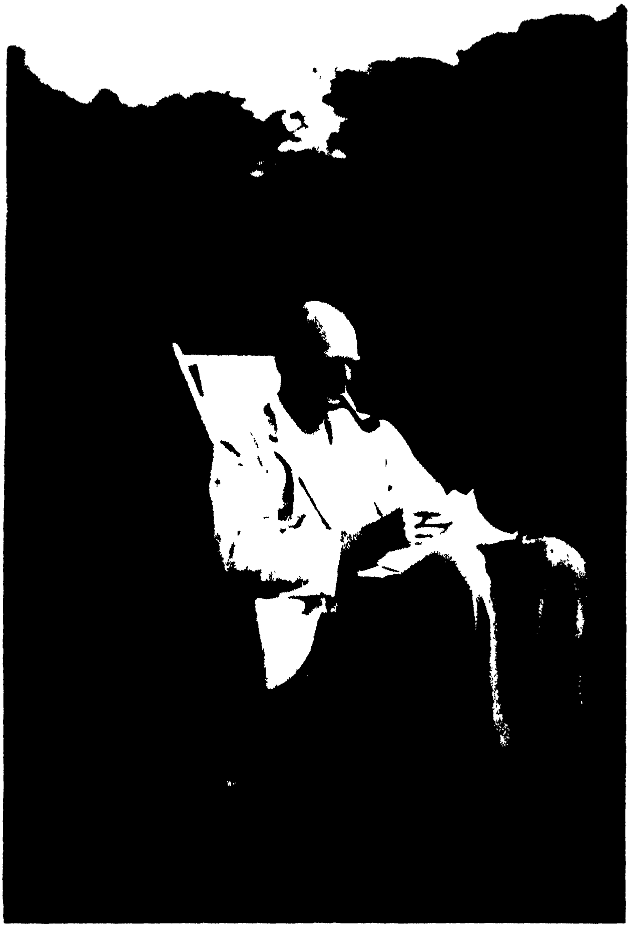

In Remembrance

THE death of our dear and highly valued friend, Mr. G. S. W. Marlow, has filled the hearts of all members of the Faraday Society with the deepest grief. Physical chemists throughout the world will share it, for Marlow had endeared himself to all who came to our meetings, or contributed to our *Transactions*, by his geniality, his kindness, and the efficiency of his work in every detail. It is no exaggeration to say that he had become an internationally known and respected personality in the world of physico-chemical science, and that his death will be felt as a great personal loss, not only by his fellow-countrymen but also by the men (and women) of many nations.

The Faraday Society has been exceptionally fortunate in the men who have acted as Secretary (and Editor). For many years Mr. F. S. Spiers, who (so far as I remember) was the first Secretary, rendered eminent services to the Society. In the year 1926 I had the honour to be President, and I remember an urgent consultation with Sir Robert Robertson as regards the appointment of a new Secretary, rendered necessary by the death of Mr. Spiers. Robertson had the brilliant idea of asking Marlow to accept the post. We telephoned to him, he came round to see us, and he agreed to act ! He had, I think, been recently called to the Bar, having prepared himself for that profession while holding a post with the Institute of Chemistry. It is to the great honour and credit of Marlow that during the next twenty-one years he devoted himself to the great development of the Society, in spite of the fact that, as time went on, he became an active and successful barrister.

Marlow was much more to us than the excellent Editor of the *Transactions* and a most efficient Secretary and arranger of the General Discussions. It was his outstanding and endearing personality as the ever-cheerful friend and counsellor of all—members and invited guests alike—that contributed so much to the success of the famous Meetings (General Discussions) of the Faraday Society. Who can forget the friendly and genial smile that accompanied his invitations to our distinguished guests to join the Society ! Many famous scientists have told me how much they appreciated Marlow's courteous way of making everybody feel happy and at home, and the efficiency of his arrangements for their comfort during their visits to this country. He did everything well.

In spite of the grievous loss of his son (who was killed in the war), many serious difficulties due to bomb damage to his house and his chambers in Gray's Inn, and much extra work in his own profession, he bravely and cheerfully kept the flag flying and the work of the Society going during the war.

The Faraday Society owes him an immense debt of gratitude for his splendid work. It is sad to think that we cannot now have the opportunity of showing him our great appreciation of his work and our personal affection for him as a man and a friend.

F. G. DONNAN.

THE QUENCHING OF FLUORESCENCE IN LIQUIDS BY COMPLEX FORMATION. DETERMINATION OF THE MEAN LIFE OF THE COMPLEX.

By G. Weber.

Received 8th July, 1946, as revised 25th April, 1947.

If a quencher is added to a solution of a fluorescent dye the ratio of the fluorescent intensities before and after quenching is[1, 2]

$$I_0/I = N_0\tau_0/N\tau \quad . \quad . \quad . \quad . \quad (1)$$

where N_0 and N are the numbers of excited molecules that may be deactivated with emission in the absence and presence of quencher respectively, and τ_0 and τ the corresponding values of the mean life of the excited state. Only in an ideally collisional quenching is $N/N_0 = 1$. In the quenching by complex formation we may assume that the molecules forming part of the complex are unable to emit. Then $N/N_0 = \alpha$, the degree of dissociation of the complex. The new mean life of the excited state of the fluorescence after addition of quencher is

$$\tau = \frac{1}{\left(\frac{1}{\sigma} + \frac{1}{\tau_0}\right)} \quad . \quad . \quad . \quad . \quad . \quad (2)$$

where σ is the mean free life of the fluorescent molecules. In general, the degree of dissociation of the complex cannot be directly determined, but α can be eliminated from eqn. (1). Calling the mean life of the complex Σ, and the total concentration of dye [F], at a definite concentration of quencher an equilibrium exists of the form

$$1/\sigma \,.\, \alpha[\mathrm{F}] = 1/\Sigma \,.\, (1 - \alpha)[\mathrm{F}] \quad . \quad . \quad . \quad (3)$$

where the left-hand side represents the number of complexes formed in unit time and the right-hand side the number broken down in the same period. Replacing $1/\sigma$ by its value given in eqn. (2), solving for $1/\alpha$ and introducing this in (1), we have

$$I_0/I = \tau_0/\tau[1 + \Sigma/\tau_0(\tau_0/\tau - 1)] \quad . \quad . \quad . \quad (4)$$

It is evident that if $\Sigma \ll \tau_0$

$$I_0/I = \tau_0/\tau \quad . \quad . \quad . \quad . \quad . \quad (5)$$

a rule proposed by Perrin[1] for the quenching by collisions. Eqn. (4) shows that Σ/τ_0 can be determined if the ratios I_0/I and τ_0/τ are known. The first can be easily obtained by photometric measurements while the second can be determined from the polarisation of the fluorescent light. According to Perrin's theory of the polarisation of the fluorescence in liquids[3, 4]

$$\frac{\tau_0}{\tau} = \frac{\frac{1}{p_t} - \frac{1}{p_0}}{\frac{1}{p} - \frac{1}{p_0}} \quad . \quad . \quad . \quad . \quad . \quad (6)$$

---

[1] Perrin, *Ann. Physique*, 1929, **12**, 169.

[2] Wawilov and Franck, *Z. Physik.*, 1931, **69**, 100.

[3] Perrin, *J. Physique*, 1926, **7**, 390.

[4] Sveshnikoff, *Acta Physicochim.*, 1936, **4**, 453.

where p_i is the polarisation of the unquenched solution, and p the polarisation after addition of the quencher, while p_0 is the limiting polarisation, i.e. that recorded in a medium where no depolarisation by molecular rotation takes place.[3]

A convenient graphical method of showing deviations from eqn. (5) is to plot the values of I/I_0 against $1/p$. This gives a straight line through $1/p_0$, if Σ is negligible compared to τ_0. Eqn. (4), however, shows that under present experimental conditions a value of $\Sigma/\tau_0 = 10^{-8}$ will give a straight line passing through $1/p_0$ within experimental error.

Experimental.

The intensity of the fluorescence was measured by means of a barrier-layer photocell using the method of complementary filters. The quenching of the fluorescence except in the quenching of riboflavine fluorescence by HCl involved no change in the absorption spectrum, as measured with a Hilger spectrophotometer. Under these conditions I/I_0 equals the ratio of the corresponding fluorescent efficiencies.[4] For the excitation of the fluorescence of riboflavine and eosin a combination of two blue filters was used (Corning Glass 5850 and 978) while observations were made through a yellow filter (C.G. 351). The fluorescence of rhodamine B was excited through a green filter (C.G. 401) and observed through a red one (C.G. 245). These combinations were perfectly complementary up to moderate light intensities.

In measuring the polarisation of the fluorescence the exciting light was polarised by a Nicol prism. The polarisation of the fluorescence was determined by means of a Savart plate and a compensator of Arago of 4 plates.[5] The Savart plate was mounted so that it could be tilted about a horizontal axis. The interference fringes could be seen moving across the field and the sensitivity considerably improved. The compensator of Arago was calibrated using the Fresnel formula.[6] In measuring low polarisations a pile of glasses inclined at an angle was introduced between the source and the compensator to increase the amount of polarised light arriving to the latter.[7] The sensitivity was thus increased enabling one to distinguish differences in polarisation of about 1/10 when the polarisation of the source was 2 %. The viscosity of the solutions was measured with an Ostwald viscometer. All measurements were carried out at room temperature.

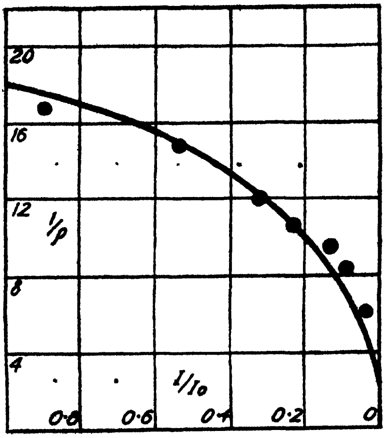

FIG. 1.

Quenching of the Fluorescence of Rhodamine B by Hydroquinone.—The average Σ/τ_0 obtained from 6 independent measurements was 1·8 ± 0·2. In Fig. 1 the curve is the theoretical one for $\Sigma/\tau_0 = 1{\cdot}8$, calculated from eqn. (4) and (6). The circles are the experimental values. The solution of rhodamine B (B.D.H.) in distilled water contained $2{\cdot}4 \times 10^{-6}$ g./ml. of the dye and 0·5 % of NaH_2PO_4.[9] The value of $1/p_0$ is 2·4. The measurements were done at 15° C. According to Gaviola[8] for rhodamine B, $\tau_0 = 2 \times 10^{-9}$ sec. The mean life of the complex would be therefore $\simeq 3{\cdot}5 \times 10^{-9}$ sec.

---

[5] Wood, *Physical Optics*, Ch. 9, 3rd Ed. (New York, 1934).

[6] Gaviola and Pringsheim, *Z. Physik.*, 1926, **24**, 24.

[7] Perrin, *Acta Physica Polonica*, 1936, **5**, 335.

[8] Gaviola, *Z. Physik.*, 1927, **42**, 853, 862.

[9] In studying the quenching effect of hydroquinone an apparent decrease in the fluorescent efficiency might result from the formation of the brown quinone which absorbs strongly the blue exciting light. Addition of an acid salt (NaH_2PO_4) was effective in preventing any appreciable formation of quinone.

Quenching of Eosine Yellow by Hydroquinone and by KI.—The solutions contained 3×10^{-5} g./ml. of eosin in water. The solution quenched by hydroquinone contained besides 0·5 % NaH_2PO_4. The addition of phosphate shortened the mean life of the fluorescence so that the polarisations of the unquenched solutions given in Table I. are somewhat different. The solutions were studied at 15° c. The following table gives the value of the ratio I/I_0 and the polarisation p together with the calculated Σ/τ_0 for different concentrations of quencher. This last value is only given for those polarisations that differ from that of the unquenched solution by an amount greater than the experimental error. Gaviola's value for the mean life of the excited state of eosin is 2×10^{-9} sec. Therefore $\Sigma \simeq 4 \times 10^{-9}$ sec.

Some static quenching seems to take place with KI, the value of Σ/τ_0 being here about 0·2. In this case, Fig. 2, where the values in the table have been plotted, shows that the upper values of I/I_0 fall approximately on a straight line which, when extrapolated to $I/I_0 = 0$ gives a $1/p$ distinctly higher than $1/p_0$. We have found this to be a regular feature of the quenching of eosin, riboflavine and acriflavine by KI. The quenching of eosin by hydroquinone showed a negative thermal coefficient while the quenching by KI had a positive one. It is remarkable that the quenching by hydroquinone was some ten times more effective than that by KI.

In Fig. 2 the curves are the theoretical ones for $\Sigma/\tau_0 = 21$ and 0·2 respectively. The open circles are experimental values for the quenching by KI, and the black circles the ones for the quenching by hydroquinone.

TABLE I

Concentration of KI in M./l. × 10^3.	I/I_0.	p.	Σ/τ_0.
Quenching by KI.			
0	1	0·070	—
3	0·90	0·077	—
15·1	0·64	0·096	0·2
30·3	0·41	0·121	0·2
45·4	0·28	0·141	0·3
60·5	0·19	0·162	0·3
90·7	0·12	0·211	0·2
120·8	0·07	0·239	0·2

Concentration of Hydroquinone in M./l. × 10^3.	I/I_0.	p.	Σ/τ_0.
Quenching by Hydroquinone.			
0	1	0·080	—
6	0·79	0·080	—
10	0·69	0·080	—
25	0·44	0·082	—
50	0·23	0·089	21
100	0·085	0·103	20
125	0·055	0·109	23
176	0·023	0·130	22

Quenching of Riboflavine Fluorescence. — The mean life of the excited state of the fluorescence of riboflavine in aqueous solution was determined by the method of Wawilov,[9] and by that of Perrin,[3] the last involving the determination of the polarisation of the fluorescence in glycerol-water mixtures of different viscosities. Both methods agreed in a value of $\tau_0 = 1 \times 10^{-8}$ sec. The limiting polarisation was 0·5.

Quenching by Caffeine and Adenosine.—The quenching of the fluorescence of riboflavine by purines[10] was not accompanied by any noticeable increase in the polarisation of the fluorescence even when the ratio I/I_0 was 0·05. According to eqn. (4) the minimum mean life of the complex would be of the order of 10^{-6} sec. The quenching had a negative temperature coefficient and its efficiency remained constant up to the highest caffeine concentrations attained (0·075 M./l.).

Quenching by Hydroquinone and by KI.—Fig. 3 shows the plotting of $1/p$ against I/I_0 for a solution of riboflavine of concentration 5×10^{-6} g./ml. in a 50 % glycerol-water mixture containing 0·5 % NaH_2PO_4, at 15° c. The upper curve is the theoretical for $\Sigma/\tau_0 = 2{\cdot}8$ and the lower one for $\Sigma/\tau_0 = 0{\cdot}2$. The open circles are the experimental values for the quenching by KI and the black ones for the quenching by hydroquinone.

---

[9] Wawilov, *Z. Physik.*, 1928, **53**, 665.
[10] Weil-Malherbe, *Biochem. J*, 1946, **40**, 363.

Quenching by Acids and Alkalies.—The fluorescence of riboflavine vanishes in strongly acid or strongly alkaline solutions, a fact that has been explained by supposing that the fluorescent form is the dipolar ion while the anionic and cationic forms are non-fluorescent.[11] The quenching by HCl was accompanied by an increase in the polarisation very much like the quenching by KI leading to a value of 10^{-9} sec. for the mean life of the anionic form in equilibrium with the dipolar ion. Quenching by HCl gives rise to a change in the absorption spectrum. The anionic form has no absorption in the visible so that I/I_0 is systematically higher than the ratio of the corresponding fluorescent efficiencies. It seems certain, however, that the figure given is accurate at least as regards the order of magnitude. Quenching by KOH, on the other hand, gives for the mean life of the cationic form 5×10^{-8} sec. The solvent was in both cases a glycerol-water mixture of viscosity 0·0658 at 20° c.

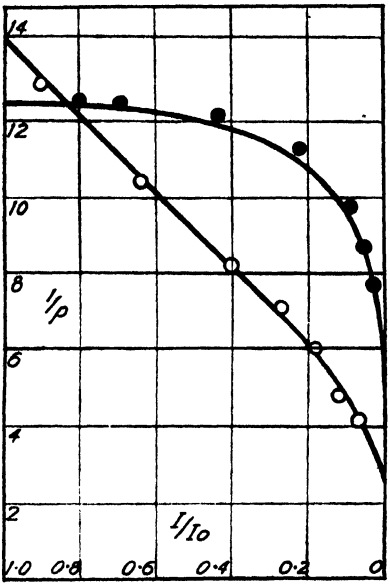

FIG. 2.

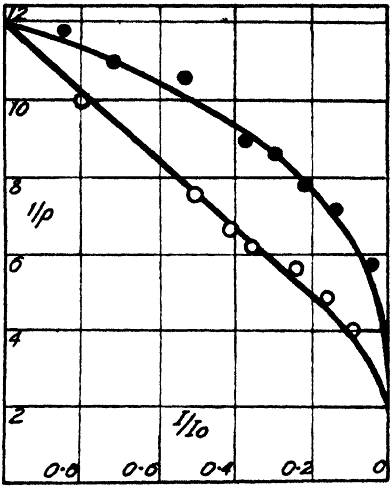

FIG. 3.

Discussion.

The values of the mean life of the complex obtained from the experimental data with the help of eqn. (4) are constant within 10 to 20 % in the different cases studied. Eqn. (4) was derived on the assumption that the complexes do not contribute appreciably to the fluorescent emission. If such were not the case the calculated mean life of the complex would show a systematic increase as I/I_0 becomes smaller. Since no significant increase took place in our experiments the assumption seems justified. The quenching processes that yielded a value of Σ/τ_0 greater than 1 showed a negative thermal coefficient and were in every case more effective than KI.

In the quenching of eosin and other dyes by KI it may be doubtful whether there is a short-lived complex or that quenching can take place when dye and quencher molecule are at non-negligible distance of each other. For the other quenchers we may rule this possibility out by the use of Einstein's equation

$$\Delta\bar{x} = (2Dt)^{\frac{1}{2}}$$

where $\Delta\bar{x}$ is the mean distance travelled by a molecule of diffusion coefficient D in time t. If t is substituted by Σ, $\Delta\bar{x}$ is now roughly the diameter of the hypothetical quenching sphere, provided Σ is not too short. In the case of the quenching of riboflavine by purines $\Delta\bar{x}$ is of the order of hundreds of A., and of about 70 A. in the quenching of eosin by hydroquinone.

---

[11] Kuhn and Moruzzi, *Ber.*, 1934, **67**, 888.

A difference of $1/p$ at vanishingly small mean life and at infinite viscosity can be explained by the existence of a " dark interval " between the excitation and the beginning of emission as well as by static quenching. There is some additional evidence for the first[3] and a combination of both factors cannot be excluded.

Eqn. (4) seems to be of possible application to the determination of the mean life of non-fluorescent, tautomeric modifications in equilibrium with the fluorescent form, as exemplified by the quenching of riboflavine by HCl and KOH. The quenching by acid could perhaps be explained as due to collisions by the H_3O^+ ions in solution : but in that case we would expect them to act in a similar way on the fluorescence of many dyes. Experiment shows, however, that HCl quenches the fluorescence of eosin without any appreciable change in the polarisation.

The author wishes to express his warmest thanks to Dr. M. Dixon, F.R.S., for much help in the experiments as well as many interesting suggestions and criticisms.

Summary.

A simple relation has been derived giving the mean life of the non-fluorescent complex as a function of the mean life of the excited state and the relative efficiency of the quenched solution. Experimental evidence is offered to show that the mean life of the complex calculated in this way is a constant for a given dye, quencher and solvent, at a fixed temperature. With the technique employed, accurate determination is only possible for complexes having mean lives within one order of magnitude of the mean life of the excited state of the unquenched fluorescence. In other cases a maximum, or a minimum value can be given. The complexes studied had mean lives ranging from 10^{-9} sec. to 10^{-6} sec. in order of magnitude.

When the non-fluorescent form is the anionic or cationic form in equilibrium with the fluorescent one, it is possible to determine its mean life in the same way. This has been done for the anionic and cationic forms of riboflavine in equilibrium with the dipolar ion.

The quenching of the fluorescence of some dyes by KI showed evidence of static quenching. The effect is small, however, and admits other alternative explanations.

Sir William Dunn Institute of Biochemistry,
Cambridge University.

AN INVESTIGATION OF THE CHEMICAL EQUILIBRIA INVOLVING THE MOLECULES ARSENIC TRICHLORIDE, MONOPHENYLCHLORARSINE, DIPHENYLCHLORARSINE AND TRIPHENYLARSINE.*

BY ALWYN G. EVANS AND ERNEST WARHURST.

Received 19*th August*, 1946.

One method of manufacture of ϕ_2AsCl consists in heating mixtures of $AsCl_3$ and ϕ_3As at about 250° C. This production of ϕ_2AsCl involves several reactions and equilibria between the four species $AsCl_3$, $\phi AsCl_2$, ϕ_2AsCl and ϕ_3As. This paper is an account of some work carried out to obtain quantitative data for these equilibria. The primary objective was to find the optimum conditions for the production of ϕ_2AsCl. Because of this the investigation was not as extensive as we should have wished, and the accuracy of the results not of an extremely high order. Nevertheless, we feel that the results as they stand are of some interest.

---

* Throughout this paper the following notation is used : $\phi AsCl_2$ = monophenylchlorarsine, ϕ_2AsCl = diphenylchlorarsine and ϕ_3As = triphenylarsine.

Of the possible equilibria involved in a mixture of the four species, only two are independent, so that the general state of equilibrium can be completely defined by two constants. We have therefore investigated the disproportionation of pure $\phi AsCl_2$ and pure ϕ_2AsCl in order to determine these equilibrium constants. We have also studied the reaction of $AsCl_3$ with ϕ_3As.

The equilibria are formulated below :—

$$2\phi AsCl_2 \underset{k_1^*}{\overset{k_1}{\rightleftharpoons}} AsCl_3 + \phi_2AsCl \quad . \quad . \quad . \quad (1)$$

$$K_1 = \frac{k_1}{k_1^*} = \frac{(AsCl_3)(\phi_2AsCl)}{(\phi AsCl_2)^2}$$

and

$$2\phi_2AsCl \underset{k_2^*}{\overset{k_2}{\rightleftharpoons}} \phi AsCl_2 + \phi_3As \quad . \quad . \quad . \quad (2)$$

$$K_2 = \frac{k_2}{k_2^*} = \frac{(\phi AsCl_2)(\phi_3As)}{(\phi_2AsCl)^2}$$

where K_1 and K_2 are equilibrium constants and k_1, k_1^*, k_2 and k_2^* are bimolecular velocity constants.

Experimental.

Method.—Samples of $\phi AsCl_2$, ϕ_2AsCl or known mixtures of $AsCl_3$ and ϕ_3As were placed in Pyrex tubes and sealed off *in vacuo*. The tubes were inserted in metal containers fitted with screw caps, and then placed in an air thermostat at the required temperature. After various time intervals, tubes were withdrawn, cooled rapidly to room temperature, and their contents analysed.

Materials.—The $AsCl_3$ was a commercial product, and was purified by two distillations. A colourless liquid was obtained, b. pt. 130·5° C. at 760 mm. The samples of purified $\phi AsCl_2$, ϕ_2AsCl and ϕ_3As were kindly provided by Prof. A. R. Todd. The degree of purity of these materials is shown by the following figures :

$\phi AsCl_2$—hydrolysable chlorine 89·2 cc. of N./10 NaOH per g. (theor. 89·7 cc.).

ϕ_2AsCl—iodine absorption 75·7 cc. N./10 iodine per g. (theor. 75·6 cc.).

ϕ_3As—m. pt. 60·5° C.; iodine absorption 65·2 cc. N./10 iodine per g. (theor. 65·4 cc.).

Analysis.*—About 0·5 g. mixture was weighed out into a 100 ml. separating funnel containing 50 ml. dil. NaOH (approx. 2N.) and vigorously agitated for a few minutes. This brings about the replacement of the Cl atoms by OH groups giving a mixture of $As(OH)_3$, $\phi As(OH)_2$, $\phi_2As(OH)$ and ϕ_3As. This mixture was extracted three times by gentle agitation with about 15 ml. of chloroform. The chloroform extracts were washed successively with 10 ml. dil. NaOH in a second separating funnel and run off into a 500 ml. iodine flask. At this stage the aqueous layer contains the $As(OH)_3$ and $\phi As(OH)_2$, while the chloroform layer contains the $\phi_2As(OH)$ and ϕ_3As.

(*a*) **Determination of the $AsCl_3$ and $\phi AsCl_2$.**—To the aqueous portions a few drops of phenolphthalein were added and then dil. HCl (approx. 2 N.) until in excess. The solution was then titrated with standard iodine (approx. N./10) with starch indicator.

This gives the reaction :

$$\phi As(OH)_2 + I_2 + H_2O \rightarrow \phi AsO\,.\,(OH)_2 + 2HI.$$

---

* Based on the methods described in the Sutton Oak Report to the Ministry of Supply, 3/12/1940, and the I.C.I. Ltd., General Chemicals Division Report to the Ministry of Supply (1/11/40).

After the addition of 2 to 3 g. $NaHCO_3$ the titration was continued to a further end point. The reaction determined in this stage is:

$$As(OH)_3 + I_2 + H_2O \rightarrow AsO(OH)_3 + 2HI.$$

(*b*) **Determination of ϕ_2AsCl and ϕ_3As.**—To the combined chloroform extracts about 50 ml. of distilled water were added, followed by a few drops of phenolphthalein and dilute HCl until just acid. About 1 g. of sodium bicarbonate was next added and the mixture was titrated with standard iodine until a faint permanent violet colour appeared in the chloroform layer. This reaction estimates the total arsenic in this layer:

$$\phi_2As(OH) + I_2 + H_2O \rightarrow \phi_2AsO\,.\,(OH) + 2HI$$
$$\phi_3As + I_2 + H_2O \rightarrow \phi_3AsO + 2HI.$$

The total hydrolysable chlorine was then determined by taking about 0·5 g of the mixture, adding 50 ml. absolute alcohol and shaking with 20 ml. N./5 NaOH in an atmosphere of nitrogen. The excess NaOH was then titrated with N./10 HCl using brom-phenol blue as indicator. The reactions involved in this stage of the estimation are:

$$AsCl_3 + 3NaOH \rightarrow As(OH)_3 + 3NaCl$$
$$\phi AsCl_2 + 2NaOH \rightarrow \phi As(OH)_2 + 2NaCl$$
$$\phi_2AsCl + NaOH \rightarrow \phi_2As(OH) + NaCl.$$

From the results the individual quantities of $AsCl_3$, $\phi AsCl_2$, ϕ_2AsCl and ϕ_3As in the mixture may be determined.

Results.

The results obtained are shown in Tables I-III, Fig. 1-4. The amounts of the four components found by analysis are shown as molar percentages of the total starting material. In the case of the more volatile components the analysis figures, which give the total amount of the component in the reaction tube, will not give the required value for the molar percentage in the liquid phase at the temperature of the experiment. They have accordingly been corrected by a simple equation based on Raoult's law and on the assumption that the vapours behave as perfect gases. It was found that the correction was very small for ϕ_2AsCl and ϕ_3As, small for $\phi AsCl_2$ and of considerable magnitude only in the case of $AsCl_3$. We have, therefore, introduced the correction only for the $\phi AsCl_2$ and $AsCl_3$ values.

TABLE I.

Equilibrium.	Temp. °c.	Equilibrium Constant ($\times 10^2$).	Velocity Constant (cc. mol.$^{-1}$ sec.$^{-1}$). ($\times 10^3$).	ΔH Heat of Reaction kcal.	E Activation Energy kcal.	B Temp. Independent Factor.
$2\phi AsCl_2 \rightleftharpoons \phi_2AsCl + AsCl_3$	256	$K_1 = 5{\cdot}7$	$k_1 = 3{\cdot}22$ $k_1^* = 56{\cdot}5$	$\Delta H_1 = +2{\cdot}6$		
	304	$K_1 = 7{\cdot}0$	— —			
$2\phi_2AsCl \rightleftharpoons \phi AsCl_2 + \phi_3As$	252	$K_2 = 5{\cdot}9$	$k_2 = 0{\cdot}89$ $k_2^* = 15{\cdot}1$	$\Delta H_2 = +3{\cdot}8$	$E_2 = 37{\cdot}6$	$B_2 = 10^{12.6}$
	304	$K_2 = \begin{cases} 8{\cdot}0 \\ 8{\cdot}4 \end{cases}$	$k_2 = 22{\cdot}7$ $k_2^* = 284$		$E_2^* = 34{\cdot}0$	$B_2^* = 10^{12.3}$

In some cases the reaction was accompanied by a certain amount of decomposition, shown by small quantities of a reddish-brown suspension, the amounts of which qualitatively increased with time. Furthermore, the hydrolysable chlorine and total arsenic were less than the corresponding theoretical values. The discrepancies increased with time and ran parallel to the amount of suspension formed. The solution was always centrifuged and the supernatant liquid used for analysis. We do not consider that this decomposition affects the accuracy of our results.

It was found that certain metals catalysed these reactions, and results of experiments in which iron was present in the reaction tube are shown in Fig. 1 and 2. The catalytic effect of various metals is shown in Table II. Their order in this table does not necessarily correspond to their catalytic efficiency, since the extent and nature of the surfaces were not known.

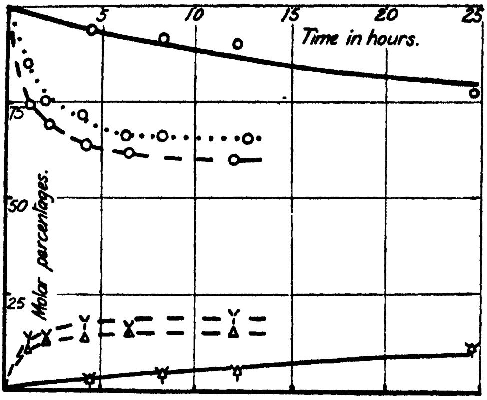

FIG. 1.—ϕ_2AsCl disproportionation at 309° C.
○ $\phi AsCl$. △ $\phi AsCl_2$. Y ϕ_3AsCl.

Discussion.

The equilibrium concentrations of the components, required for the calculation of K_1 and K_2, have been obtained by graphing the experimental data and interpolating the asymptotic values of the molar percentages. Examples of these curves are shown in Fig. 1, 2 and 3. In the case of the ϕ_2AsCl disproportionation at 252° c. equilibrium was not reached after 25 hr. (Fig. 1). We have, therefore, determined the equilibrium constant K_2, at this temperature, by catalysing the reaction with iron. In this way equilibrium was established after 6 hr., and the concentrations were unchanged, within experimental error, for a further 6 hr. The equilibrium concentrations were $\phi AsCl_2$ 14·1 %, ϕ_2AsCl 65·6 %, ϕ_3As 18·0 %, giving $K_2 = 5{\cdot}9 \times 10^{-2}$. For this experiment the fall in ϕ_2AsCl concentration is shown in Fig. 1 (dotted curve).

Iron was used as a catalyst also in one experiment on the reaction of $AsCl_3$ and ϕ_3As (Fig. 2). The value of K_2 ($8{\cdot}4 \times 10^{-2}$) obtained is in good agreement with that of $8{\cdot}0 \times 10^{-2}$ obtained from the disproportionation of ϕ_2AsCl at the same temperature (curves shown in Fig. 1). The uncatalysed reaction $AsCl_3 + \phi_3As$ was also studied. The slower rate of reaction can be seen from the plot of the ϕ_2AsCl concentration in Fig. 2 (broken curve).

TABLE II.—ϕ_2AsCl DISPROPORTIONATION IN PRESENCE OF METALS. TEMPERATURE 252 C

Metal.	State.	% Disproportionation after 1 hr.
Fe	Pig iron turnings	11·4
Fe	Pure turnings	9·2
Sn	Molten	7·8
Co	Turnings	6·2
Ni	Turnings	4·6
72 % Cr/28 % Fe alloy	Small crystals	4·4
Cr	,,	3·4
As	,,	2·8
Cu	Turnings	2·2
Glass	—	1·5

Fig. 3 shows the curves for the $\phi AsCl_2$ disproportionation at 256° c., giving $K_1 = 5{\cdot}7 \times 10^{-2}$. This reaction was also studied at 304° c., and the equilibrium concentrations were $\phi AsCl_2$ 55·0 %, ϕ_2AsCl 14·6 %, $AsCl_3$ 14·6 %, giving $K_1 = 7{\cdot}0 \times 10^{-2}$. For this latter case the fall in $\phi AsCl_2$ concentration is shown in Fig. 3 (broken curve).

Heats of Reaction.—From the values of K_1 and K_2 at two different temperatures the heats of reaction, ΔH_1 and ΔH_2, have been determined as + 2·6 and + 3·8 kcal. respectively.

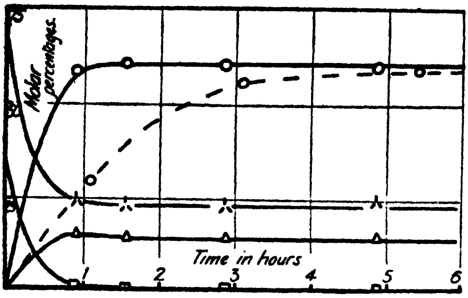

FIG. 2.—$AsCl_3$ + ϕ_3As reaction in presence of iron, at 304° C.

□ $AsCl_3$. △ $\phi AsCl_2$. ○ ϕ_2AsCl. Y ϕ_3As.

These heat content changes are small. Such a state of affairs would obtain if the strengths of all the As—Cl bonds were the same and all the As—C bonds were the same for the four molecules. Small values for ΔH_1 and ΔH_2, could also obtain, even if these bond strengths were not constant; but this would require the gradations in the As—Cl and As—C bond strengths to be related in rather a special manner.

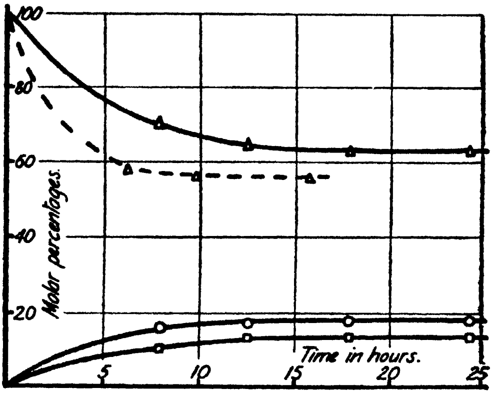

FIG. 3.

A rough calculation of the equilibrium constants for the reactions (1) and (2), based on heats of reaction of about 3 kcal. in the temperature range 250-300° C., and assuming the cancellation of the partition functions for translation, rotation and vibration (which is fairly plausible) leads to a value of about 2×10^{-2} for both K_1 and K_2. It is seen that our experimental values of K_1 and K_2 (Table I) are approximately equal and are of the same order as that given by the above calculation.

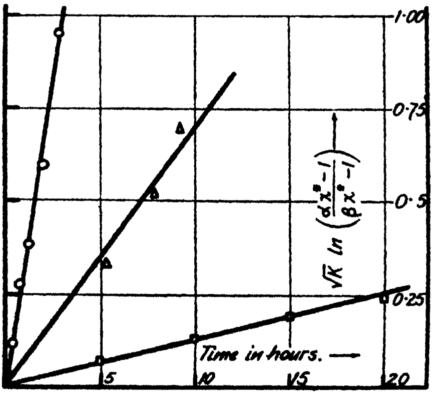

FIG. 4.

○ ϕ_2AsCl disproportionation at 304° C.
□ ϕ_2AsCl disproportionation at 252° C.
△ $\phi AsCl_2$ disproportionation at 256° C.

In the manufacture of ϕ_2AsCl from $AsCl_3$ and ϕ_3As the influence of variations in the molar ratio $\phi_3As/AsCl_3$ of the starting material is of great practical interest. Since the constants K_1 and K_2 define completely the final state of equilibrium, the values of these constants enable the equilibrium concentrations of the four components to be calculated for starting materials of any $\phi_3As/AsCl_3$ molar ratio. The method of calculation, for a starting material containing *a* moles of ϕ_3As and *b* moles of $AsCl_3$, is illustrated as follows:

$$\begin{array}{ccccccc} \phi_3As & + & AsCl_3 & \rightleftharpoons & \phi AsCl_2 & + & \phi_2AsCl \\ (a-x) & & (b-x) & & x & & x \\ \phi AsCl_2 & + & \phi_3As & \rightleftharpoons & 2\phi_2AsCl. & & \\ (x-y) & & (a-x-y) & & 2y & & \end{array}$$

The equilibrium amounts are thus : $AsCl_3 = b - x$; $\phi AsCl_2 = x - y$; $\phi_2AsCl = x + 2y$; $\phi_3As = a - x - y$; and substituting in the expressions for K_1 and K_2

$$x^2(1 + K_1) - bx - 2by + 2xy(1 - K_1) + K_1y^2 = 0$$
$$x^2(1 + K_2) - ax + ay + 4K_2xy + y^2(4K_2 - 1) = 0.$$

These can be solved to give x and y in terms of the ratio a/b. Hence the equilibrium concentrations can be evaluated in terms of the molar ratio $\phi_3As/AsCl_3$ of the starting material. Table III shows a few typical examples of results obtained by the above method.

TABLE III.

Molar Ratio $\phi_3As/AsCl_3$ of Starting Material.	Equilibrium Molar %.			
	$AsCl_3$.	$\phi AsCl_2$.	ϕ_2AsCl.	ϕ_3As.
0	100	0	0	0
0·5	17·5	65·0	17·5	0
1·0	3·5	46·5	46·5	3·5
1·5	1·0	28·5	60·0	10·5
2·0	0	18·0	63·5	18·5
4·0	0	5·0	50·0	45·0
∞	0	0	0	100

Kinetics of the Reactions.—It was found that in the disproportionation of $\phi AsCl_2$, the concentration of ϕ_3As formed during the reaction was negligible and that $AsCl_3$ and ϕ_2AsCl were produced in approximately equal concentration. Similarly, in the disproportionation of ϕ_2AsCl the concentration of $AsCl_3$ was found to be very small and the concentrations of $\phi AsCl_2$ and ϕ_3As were again approximately equal. We can, therefore, consider these disproportionation reactions to consist of two opposing bimolecular reactions, as formulated earlier.

In the general case :

$$2A \underset{k^*}{\overset{k}{\rightleftharpoons}} B + C, \text{ and } K = k/k^*,$$

let the concentration of A at zero time be a moles./cc. and the concentration at time t be $(a - x)$ moles./cc.

Then $$\frac{-\,\mathrm{d}(A)}{\mathrm{d}t} = +\frac{\mathrm{d}x}{\mathrm{d}t} = k(a - x)^2 - k^* . \frac{x^2}{4}.$$

Integrating: $$\frac{1}{a\sqrt{kk^*}} \ln \left\{ \frac{\left(\dfrac{4k - k^*}{2k + \sqrt{kk^*}}\right)\dfrac{x}{2} - a}{\left(\dfrac{4k - k^*}{2k - \sqrt{kk^*}}\right)\dfrac{x}{2} - a} \right\} = t.$$

This simplifies into :

$$\frac{\sqrt{K}}{a} \ln \left(\frac{\alpha x - a}{\beta x - a}\right) = kt$$

where $$\alpha = \frac{1}{2}\left\{\frac{4k - k^*}{2k + \sqrt{kk^*}}\right\} = 1 - \frac{1}{2\sqrt{K}}$$

and $$\beta = \frac{1}{2}\left\{\frac{4k - k^*}{2k - \sqrt{kk^*}}\right\} = 1 + \frac{1}{2\sqrt{K}}.$$

In our disproportionation experiments the starting material was pure ϕAsCl$_2$ or pure ϕ_2AsCl. In these cases, therefore, a is equal to $1/V_m$, where V_m is the molar volume at the particular temperature. We may thus write:

$$\sqrt{K} \ln \left(\frac{\alpha x^* - 1}{\beta x^* - 1}\right) = \frac{k}{V_m} \,.\, t \qquad . \quad . \quad . \quad (3)$$

where x^* is the amount per mole of A which has disappeared at time t

Although rough values of k can be obtained by estimating the slopes of the appropriate curves at zero time, the constants can be evaluated with much greater accuracy from eqn. (3). If the left-hand side of eqn. (3) is plotted against t, the result should be a straight line passing through the origin, the slope of which is k/V_m. The constant k^* can then be found from the relation $K = k/k^*$. This calculation has been carried out for the ϕAsCl$_2$ disproportionation reaction at 256° c. and for the ϕ_2AsCl disproportionation reaction at 252° c. and 304° c. These plots are given in Fig. 4 and the values of the velocity constants in Table I. The straight lines obtained from the experimental data support the view that the reactions involved in these equilibria are all bimolecular.

From the data for the ϕ_2AsCl disproportionation reaction at the two temperatures we have calculated the activation energies, E, and the temperature independent factors, B, for the forward and reverse reactions, using the expression $k = Be^{-E/RT}$. The results are given in Table I. The temperature independent factors for the forward and reverse reactions are seen to be very nearly equal, as would be expected from the similarity of the two reactions.

From these results we conclude that in these reactions states of true equilibrium are attained. The individual reactions are bimolecular, and involve small heat changes, as one would expect since they involve merely the exchange of chlorine and phenyl radicals from one arsenic centre to another.

The authors wish to express their best thanks to Prof. A. R. Todd, F.R.S., for much helpful advice and encouragement, and to the Director-General of Scientific Research (Defence), Ministry of Supply for permission to publish this work.

Summary.

We have examined the disproportionation reactions of ϕAsCl$_2$ and ϕ_2AsCl, and the reaction between AsCl$_3$ and ϕ_3As. We find that these reactions lead to states of true equilibrium by means of opposing bimolecular processes. We have determined the equilibrium constants, heats of reaction, velocity constants, activation energies and temperature independent factors involved in these reactions. From our data, the equilibrium concentrations of the four components can be calculated for starting material of any composition.

Chemistry Department,
The University,
Manchester.

REACTION KINETICS OF ADIABATIC SYSTEMS.

By M. Gordon.

Received 15*th November*, 1946.

LIST OF SYMBOLS.

T	Temperature (° K.).
k_n	Mass law constant of order n.
t	Time (min.).
n	Order of reaction.
X	Pre-exponential frequency factor in Arrhenius Law.
C	Average specific heat of system (cal. °K.$^{-1}$ kg.$^{-1}$).
c	Molality (mol. kg.$^{-1}$).
H	Heat of reaction (cal. mol.$^{-1}$).
E	Apparent energy of activation (cal. mol.$^{-1}$).
Q	$E/R\ (1/T - 1/T_f)$.
M	Maximum slope $\mathrm{d}T/\mathrm{d}t$ of heating curve.

Subscripts and Superscripts.

Subscript o	Refers to zero time.
Subscript f	Refers to final, or asymptotically approached, values.
Star (T^*)	Refers to temperature where $\mathrm{d}^2T/\mathrm{d}t^2$ vanishes.
Dash (T')	Refers to temperature where $\mathrm{d}^3T/\mathrm{d}t^3$ vanishes, (provided $T' < T^*$).
Double Dash (T'')	Refers to temperature where $\mathrm{d}^3T/\mathrm{d}t^3$ vanishes (provided $T'' > T^*$).

Kinetic measurements are conventionally carried out at constant temperature and expressed in terms of velocity constants k_n, calculated from the law of mass action. From a series of runs at different temperatures the well-known Arrhenius plot leads to the determination of E and X. According to the new method here proposed, reaction runs are carried out *adiabatically* instead of *isothermally*. There are both advantages and disadvantages attached to this change. The mathematical treatment is necessarily more complicated when an additional parameter, the temperature, is allowed to vary instead of being kept constant; on the other hand, the temperature change becomes available as a physical property for following the progress of a reaction and puts the accuracy of modern thermometric equipment at the disposal of the kineticist. Before weighing up such factors in a critical discussion, the mathematical evaluation of kinetic time-temperature data will be described.

When a reaction proceeds adiabatically, the temperature varies with time owing to the reaction heat liberated or consumed, and one obtains so-called heating or cooling curves. The differential equation appropriate to such curves will first be deduced on the basis of six assumptions; next the evaluation of the parameters n, E and X from certain *plots* based on this equation is explained. Such plots are founded on the data of a single adiabatic run, though a special technique, compounding data from a number of runs, will also be mentioned. Moreover, the differential equation may be *differentiated* in order to obtain relations involving special points which can be spotted on a heating curve, especially the inflection point; these points and relations are valuable as they give immediate estimates of n and E.

Finally the differential equation can be *solved* if n and E are known and n is integral. We thus obtain a direct and complete check by comparing experimental and theoretical time-temperature curves since the theoretical law, in its integrated form, permits the quantitative prediction of the complete heat effect of a chemical reaction carried out adiabatically.

Data are already extant on the heat effect of reactions used technologically, particularly in the polymer field, and within the limits of the listed assumptions this paper provides the mathematical theory underlying such data.

Assumptions.—(1) The law of mass action holds.

Activity coefficients are assumed to be equal to unity. Weight concentrations replace the conventional volume concentrations both for convenience and in order to make some allowance for volume changes, if any, occasioned by the reaction progress and/or the change in temperature.[1] Except where the contrary is stated, the mass concentrations of all reactants which significantly diminish (by reacting away) are taken to be molecularly equivalent.

(2) The law of Arrhenius relating velocity constants with temperature holds.

(3) The heat change is due practically exclusively to a single reaction. In particular this requires that (*a*) secondary chemical or physical changes do not contribute thermal effects to the heating or cooling curve, and (*b*) secondary changes do not enter into the kinetics of the main reaction. Thus the reacting or catalysing species of the main reaction are neither produced nor consumed significantly in secondary chemical changes, whether these be relatively slow, so as to enter the kinetic scheme as rate constants, or fast enough to enter it as equilibrium constants.

(4) The heat of reaction is independent of temperature.

(5) The specific heat of the system is independent of temperature and composition.

(6) The system is sufficiently closely adiabatic.

Mathematical Analysis of Adiabatic Heating and Cooling Curves.

The fundamental law governing the time-temperature plot of an adiabatic reaction is deduced as follows. Assumptions (4) to (6), and the last part of assumption (1), together imply that the rate of temperature change is a direct measure of the progress of an adiabatic reaction. Thus

$$|T_f - T| = cH/C \quad . \quad . \quad . \quad . \quad (1)$$

or in differential form

$$\pm\,\mathrm{d}T = (H)C\mathrm{d}c \quad . \quad . \quad . \quad . \quad (2)$$

Next, combining the mass law for a *n*th order reaction

$$k_n = -\,c^{-n}\,\mathrm{d}c/\mathrm{d}t \quad . \quad . \quad . \quad . \quad (3)$$

with the Arrhenius law

$$k_n = X\mathrm{e}^{-E/RT} \quad . \quad . \quad . \quad . \quad . \quad (4)$$

we obtain by eliminating k_n

$$\mathrm{d}c/\mathrm{d}t = -\,Xc^n\mathrm{e}^{-E/RT} \quad . \quad . \quad . \quad . \quad (5)$$

In this equation we finally eliminate the concentration c by substituting from eqn. (1) and (2):

$$\pm\,\mathrm{d}T/\mathrm{d}t = X(C/H)^{n-1}(T_f - T)^n\mathrm{e}^{-E/RT} \quad . \quad . \quad (6)$$

and thus obtain the fundamental differential equation governing the heating or cooling curves of adiabatic reactions.

A slight rearrangement gives a form convenient for plotting experimental data. For all but first-order reactions we have:

$$n \neq 1: \quad \ln[\mathrm{d}(T_f - T)^{1-n}/\mathrm{d}t] = \ln[(n-1)\,.\,X\,.\,(C/H)^{n-1}] - E/RT \quad (7)$$

while for a first-order reaction eqn. (8) holds:

$$n = 1: \quad \ln[-\,\mathrm{d}\ln(T_f - T)/\mathrm{d}t] = \ln X - E/RT \quad . \quad . \quad . \quad (8)$$

---

[1] See Bartlett and Altschul, *J. Amer. Chem. Soc.*, 1945, 67, 817.

In either case the left-hand side—obtained from experimental data—is plotted against $1/T$, and E found from the slope. If n is correctly chosen, a straight-line plot is obtained in all cases. The important first-order case is fortunately independent of H and C, and X is directly obtained from the intercept. When $n \neq 1$, the calculation of X requires an estimate of the ratio C/H which will generally be obtained by substituting the initial experimental values T_0 and c_0 in eqn. (1), though independent measurements could be used.

Turning now to the general outline of curves obeying the differential law of eqn. (6), it is clear that in endothermic reactions $T > T_f$ and dT/dt is negative, increasing steadily to zero, its asymptotic value. The much larger class of exothermic reactions now to be discussed lead to the S-shaped heating curves familiar in thermal studies of vulcanisation, polymerisation, etc. According to eqn. (6) the S-shape results from the progressive balancing and final swamping of the temperature effect (exponential term) by the mass action effect represented by the term $(T_f - T)^n$. Formally any exothermal adiabatic reaction obeying eqn. (6) belongs to an S-shaped heating curve which may be extrapolated in theory back to an asymptotic approach of the absolute zero. This feature is shown in the accompanying sketch which also illustrates results obtained by forming the first two differential coefficients of eqn. (6) with respect to time. The vanishing of the first locates the inflection point of the S-shape :

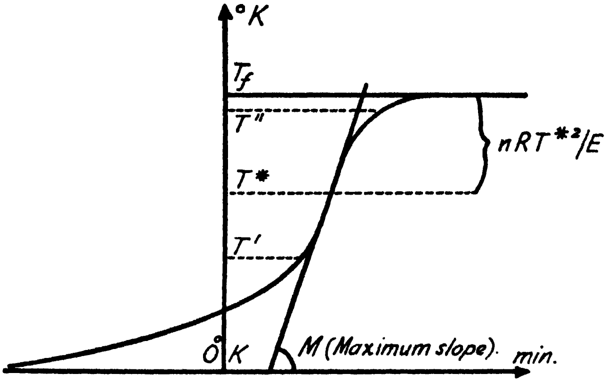

FIG. 1.—Sketch of typical heating curve.

$$T_f - T^* = nRT^{*2}/E \quad . \quad . \quad . \quad . \quad (9)$$

The vanishing of the second locates the points T' and T'' :

$$T_f - T' = G'nRT'^2/E \quad . \quad . \quad . \quad . \quad (10)$$

$$T_f - T'' = G''nRT''^2/E \quad . \quad . \quad . \quad (11)$$

where G' and G'' are easily calculated functions of n (and, formally, of the ratios E/T' and E/T'' respectively ; the slight dependence of G' and G'' on these ratios can be neglected).

A spotting of these points—particularly the easily found inflection-point—saves unnecessary graphing by suggesting the correct value of n ; thus two heating curves agreeing in all their parameters except that one belongs to a first- the other to a second-order, reaction, have in practice inflection points 15° or 20° apart. Moreover, the temperature being measured electrically, and since currents can be differentiated with respect to time quite accurately by well-known electrical circuits, direct measurement of these critical points by electrical null methods does not seem excluded ; hence E and n would be found and checked from eqn. (9) to (11).

Instead of confining attention to a single heating curve, one can combine data from a number of adiabatic runs on the same reaction. Thus a linear plot can be based on measurements of T^* and the slope M at T^* (see Fig. 1) for a number of runs according to the following equation:

$$\ln M^{1/n}/T^{*2} = -E/nRT^* + \ln(nR/E) + (1/n)\ln X + [(n-1)/n]\ln(C/H) \quad . \quad . \quad . \quad . \quad (12)$$

The left-hand side is plotted against $1/T^*$.

While a number of ways have now been presented for working up mathematically time-temperature data of adiabatic reactions, a direct comparison between theory and practice, as distinct from a mere computation of the best parameters to fit given curves, is afforded only by direct *solution* of the differential eqn. (6).

Integration of the Adiabatic Heating and Cooling Law.

For integral reaction orders n, eqn. (6) can be integrated in terms of the tabulated exponential integral:

$$E_i(y) = \int_{-\infty}^{y}(e^x/x)\,\mathrm{d}x \quad . \quad . \quad . \quad . \quad (13)$$

One uses the substitution:

$$Q = (E/R)(1/T - 1/T_f)$$

so that
$$T_f - T = RT_f^2Q/(RT_fQ + E)$$

and
$$T = ET_f/(RT_fQ + E) \quad . \quad . \quad . \quad . \quad (14)$$

in eqn. (6) and obtains:

$$\frac{\mathrm{d}t}{\mathrm{d}Q} = \frac{\mathrm{d}t}{\mathrm{d}T}\cdot\frac{\mathrm{d}T}{\mathrm{d}(1/T)}\cdot\frac{\mathrm{d}(1/T)}{\mathrm{d}Q}$$

$$= -\frac{1}{X}\left(\frac{C}{H}\right)^{1-n}\left(\frac{RT_fQ + E}{RT_f^2Q}\right)^n \mathrm{e}^{E/RT_f}\,\mathrm{e}^Q\cdot\left(\frac{ET_f}{RT_fQ + E}\right)^2\cdot\frac{R}{E} \quad . \quad (15)$$

Hence

$$t = \alpha\int\frac{(RT_fQ + E)^{n-2}}{Q^n}\,\mathrm{e}^Q\mathrm{d}Q \quad . \quad . \quad . \quad (16)$$

(with the proper limits of integration) where α is a known quantity.

The last integral is expressed in terms of the subsidiary integrals

$$J_r = \int \mathrm{e}^Q/Q^r\,\mathrm{d}Q \text{ with } 2 < r < n \quad . \quad . \quad . \quad (17)$$

J_r is itself reduced to $J_1 = E_i(Q)$ by integration by parts thus:

$$(r-1)J_r = J_{r-1} - \mathrm{e}^Q/Q^{r-1}, \text{ etc.} \quad . \quad . \quad . \quad (18)$$

The unimolecular case, $n = 1$, can be easily integrated, the solution being:

$$t = \pm\frac{1}{X}\left[E_i\left(\frac{E}{RT}\right) - E_i\left(\frac{E}{RT_0}\right) + \mathrm{e}^{E/RT_f}[E_i(Q_0) - E_i(Q)]\right] \quad . \quad (19)$$

where the positive sign on the right-hand side refers to an exothermic, the negative to an endothermic reaction.

It should be noted that X generally enters the solutions merely as a multiplier of t; variations in its value are therefore equivalent to a variation in the time unit employed. It is accordingly sufficient to know n and E in order to compare an experimental heating or cooling curve with its correct theoretical counterpart. These theoretical curves, typified by eqn. (19), form the basis of interpretation of time-temperature data collected by chemical technologists investigating the "heat-effect" of reactions carried out adiabatically.

Discussion.

We now come to a discussion—of a preliminary nature—of the possible value of the adiabatic method for making kinetic measurements. A full statement will clearly have to await the execution of planned adiabatic experiments on reactions selected from the wide range already explored by the isothermal technique.

When examining the validity of the listed assumptions on which our mathematical treatment is based, two general considerations are of importance. The first is that assumptions (4), (5) and (6), and usually (2) and (3) also, are true *limiting* conditions as the range of time-temperature measurements considered is reduced. This is also true of deviations from molecular equivalence as postulated in assumption (1). While it is obvious that in practice a reduction in the range of data employed is sooner or later checked by the attainable accuracy of thermal measurements, a brief note on modern thermometric technique will show that measurements can in fact quite accurately be made on relatively narrow ranges.

The second consideration is founded on the fact that, according to eqn. (7) and (8), the adiabatic plots are in fact analogous in form to the traditional Arrhenius plots, the expressions $\ln [\mathrm{d}(T_f - T)^{1-n}/\mathrm{d}t]$ and $\ln [- \mathrm{d} \ln (T_f - T)/\mathrm{d}t]$ taking the place of k_n and k_1 respectively. If these expressions can, therefore, be measured as accurately as the traditional mass law constants, the same temperature ranges as are normally covered by a number of isothermal runs for determining E will suffice, i.e. about 20 degrees. Such temperature changes can be obtained in numerous reactions by allowing them to proceed adiabatically to only $\frac{1}{8}$th completion. Despite the inaccuracies inherent in the graphical evaluation of the above logarithmic expressions (involving the drawing of tangents to suitable graphs), it may be possible, because of the outstanding accuracy of thermometric measurements, actually to exceed the accuracy with which the mass law constants are determinable from the conventional isothermal straight-line plot in individual cases.

Concerning the listed assumptions individually, the following remarks will suffice. *Constant* deviations of the activity coefficients from unity (as postulated in assumption (1)) only affect our mathematical treatment in a trivial manner. As regards assumption (2), it is clear that the adiabatic technique provides no separate *verification* of the Arrhenius law but has to *assume* its validity. But in cases which are found to be reasonably accurately described by our equations it is hardly conceivable that we should be misled by mutually cancelling errors into more than minor deviations in the measured reaction parameters. The Arrhenius law has almost universally been found so well obeyed over temperature ranges such as we require (in homo- and hetero-geneous, catalysed and uncatalysed reactions), that more ingenuity has had to be expended on explaining the fact of its accurate verification than departures therefrom.

Assumption (3*b*) is probably the most troublesome since it excludes from the adiabatic technique—in the simple form here given—such composite and complicated reactions as have provided the masterpieces of elucidation of isothermal kinetics. It must be admitted that if the kinetics are complicated (thus invalidating assumption (3*b*)) the mathematical inconvenience of allowing the temperature parameter to vary far outweighs any experimental advantage the adiabatic technique may provide. But though it may fail to disentangle the elementary steps of complicated reactions, it may yet serve to measure " overall " activation energies which are occasionally measured isothermally for such reactions as vinyl polymerisation. Assumptions (4) and (5) are not thermodynamically independent in the sense that if the reactant and resultant system have the same specific heat, the heat of reaction cannot vary with temperature ; both assumptions are, moreover, commonly made in physico-chemical work covering temperature ranges as limited as are here required.

Regarding assumption (6), it may be stated that with proper technique adiabatic conditions are easier to achieve than isothermal conditions. An isothermal technique requires heat exchange between the reacting system and the surroundings and this factor leads one to reduce the size of the system. Adiabatic conditions, on the contrary, are favoured by increasing the size of the reacting mass, in order to *minimise* the heat transfer. Such transfer can, moreover, be practically eliminated by jacketing, and controlling the jacket temperature electronically to correspond with that of the system.

It is true that the necessity of truly adiabatic conditions entails the need for thermometers of very low heat capacity. These are found amongst electrical instruments, both thermocouples and resistance thermometers; for accuracy and low heat-capacity the so-called " Thermistor " is outstanding. These instruments allow an accuracy to 0·0001°. It follows that in principle an adiabatic reaction covering only 10° c. should be measurable to within one part in 10^5, which compares very favourably with the accuracy of, say, chemical titration used in isothermal experiments. It is also possible to amplify accurately thermo-electric currents by a combination of photo-electric and electronic principles.[2] The relative freedom from inertia and time-lag of such systems would be valuable in relatively fast reactions; the advantages could be enhanced by replacing the galvanometer by an oscillograph. As already mentioned, the current—once amplified—can be differentiated with respect to time by suitable induction circuits.

Despite the favourable conclusions of this brief discussion, it appears as yet a matter for speculation whether an adiabatic technique can be generally developed (at least in kinetically straightforward reactions) to become a complementary tool to the conventional one. The same reservation is not made in respect of the kinetics of polymer chemistry in which the author hopes to justify the employment of his method.

Applications to the Kinetics of Polymers.

The argument for the employment of the adiabatic method in polymer chemistry rests on the following considerations.

(*a*) The isothermal technique is generally rendered difficult by the intractability of polymers (insolubility or slow rate of solution, high viscosity, etc.) and by the accumulation of the reaction heat. Thus Norrish and Brookman,[3] working on the polymerisation of styrene and methyl methacrylate, find an unavoidable S-shaped temperature rise of 20° c. in a thermostatted polymerising system of only 2 cc. in volume. Neither conduction nor convection are effective in the gelatinous polymerisate for dissipating the reaction heat; this is stated (loc. cit. p. 162) to limit the determination of E.

(*b*) As a result of these difficulties thermal studies are already used as an approach to kinetics in this field; though little attempt seems to have been made to elaborate these studies on a mathematical basis or to evaluate the reaction parameters. Bruce, Lyle and Blake[4] in a paper on vulcanisation specifically state that the " heat effect during a chemical reaction frequently assists in the understanding of its mechanism ". Brickwedde[5] investigated styrene polymerisation by its adiabatic heat effect, and thus measured its energy of activation.

(*c*) Existing data often demonstrate the *a priori* suitability of an adiabatic technique, though insufficient attention has generally been paid to strictly adiabatic conditions for a direct working up of published material.

---

[2] *J. Sci. Instr.*, 1945, **22**, 218.
[3] Norrish and Brookman, *Proc. Roy. Soc. A*, **171**, 147.
[4] Bruce, Lyle and Blake, *Ind. Eng. Chem.*, 1944, **36**, 37.
[5] Brickwedde, *India Rubber World*, 1946, 227.

In at least two fields, S-shaped heating curves with temperature rises of over 100° C. have been observed. One is the field of vinyl polymerisation already mentioned; for a graph (unfortunately insufficiently documented see[6].) The other is that of catalysed phenol- and cresol-formaldehyde resins.[7]

(*d*) In a subsequent paper an example is worked out to illustrate, on the basis of existing data, the applicability of the technique to the kinetic analysis of the vulcanisation of butadiene-styrene co-polymer with sulphur. The author is planning further experimental work in the field of the vulcanisation of rubbers. In conclusion, he would plead for the publication of relevant measurements, already in existence, on any chemical reactions.

The author desires to thank Prof. H. W. Melville, F.R.S., for his kind encouragement and helpful criticism.

Summary.

Conventional kinetic measurements, based on *isothermal* reaction runs, have hitherto been used to evaluate the reaction parameters required for the description of a chemical rate process. These parameters are the order n of the reaction, its activation energy E and its frequency factor X. A new technique is here proposed in which *adiabatic* reaction runs are employed. The temperature change is used to follow the reaction progress. The theory of the heat-effect of adiabatic reactions is deduced, and the mathematical working-up of adiabatic time-temperature data for the evaluation of n, E and X is set out on the basis of stated assumptions. A critical discussion of the method follows and shows that it is of particular value in polymer chemistry and wherever viscous rubbery or solid reaction media are encountered. The difficulties of heat exchange associated with isothermal measurements are avoided. To what extent the proposed method may be complementary to the conventional in general appears as yet a matter of speculation.

[6] *Industrie de Plastiques*, 1946, **2**, (2), 42.

[7] Unpublished observations by the author.

A SIMPLE APPARATUS FOR THE MEASUREMENT OF DIFFUSION RATES.

By A. H. W. Aten, Jun. and J. v. Dreve.

Received 27th November, 1946.

Whereas the measurement of the diffusion constant of ordinary compounds is a relatively simple matter, the problem presents many difficulties with high molecular substances. In this case accidental transport of material, due to a very slight convection of the liquid may easily cause the diffusion rate to be found unduly high. Therefore one must either use exceptional precautions against thermal fluctuations and mechanical vibrations or resort to a mechanical fixation of the liquid. It is, of course, simplest to carry out the diffusion experiment in a jelly, but this appreciably slows down the diffusion of large molecules. Northrup and Anson have developed an apparatus in which the solute diffuses through a porous glass plate.[1] It is not influenced by vibrations, but it still requires a very good temperature control and cannot be used for liquids which liberate small quantities of gases. An even simpler principle is to have the solute diffuse into a porous glass disc filled with the solvent. This can be realised in the following way.

---

[1] Northrop and Anson, *J. Gen. Physiol.*, 1929, **12**, 543.

Apparatus.—The porous glass plate of the very finest pore size (about 10μ grains, e.g. Jena G4) must be surrounded by a non-porous ring which protrudes 1 or 2 mm. above and below the disc. It can be made from a porous glass filter funnel by cutting off and grinding down the sides, or a flat porous glass disc with protruding glass rims fixed on may be used. This will cause part of the porous glass to fuse together but it will not affect the usefulness of the apparatus. Finally a small ring—either made of glass fused on to the rim or of stainless steel wire holding the disc in a loop—is needed from which the whole can be suspended.

A special glass beaker has its upper rim ground to fit the protruding rim of the porous disc and is constructed to apply suction to the disc; the air outlet is bent downwards inside the beaker to prevent loss of liquid.

Procedure.—The disc is filled with solvent by holding the beaker with the porous disc upside down and immersing the lower part in a dish filled with solvent. Gentle suction makes the liquid rise through the disc (see Fig. 1). Then the disc is covered with solvent in a beaker, heated to 40° and put inside a vacuum apparatus while covered with liquid. Evacuating removes the last traces of air.

The disc is now suspended in a vessel filled with the solvent—from now on supposed to be water—and kept in a thermostat for 2 hr. The disc is then lifted out, any drops rapidly taken off the glass rim by filter paper, and the disc immersed in a beaker containing the solution for measurement, which has been kept in the thermostat for 2 hr. If the thermostat is heated by means of an electric bulb, no direct radiation must hit the porous disc. At the end of the experiment the disc is lifted out of the solution, dipped in a beaker of dist. water and put on top of the suction vessel. Distilled water is added to the top of the disc and gentle suction is applied with the disc covered with water. After sufficient water has been passed through the disc, it is sucked dry. A chemical analysis of the liquid in the beaker now allows the calculation of the diffusion constant.

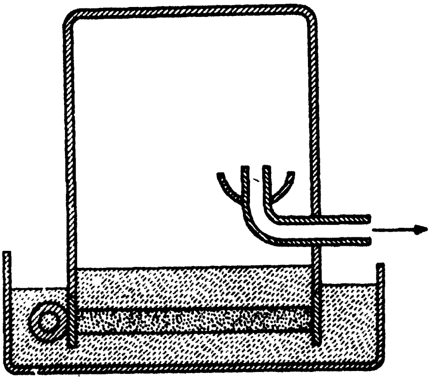

FIG. 1.—Showing the diffusion apparatus (porous disc) and beaker (suction vessel) upside down for filling the disc.

Every disc must be calibrated with a solute of known diffusion constant, e.g. KCl. For the calculation one requires the proportion between the amount of solute which diffuses into a disc during a certain time (p_t) and that which would have diffused after infinite time (p_{max}), p_{max} being calculated from the amount of liquid contained in the disc and the concentration of the solution. This proportion is determined only—apart of the characteristics of the disc—by the product of the diffusion constant (D) and the duration of the experiment (t). For each disc a calibration curve using KCl, which shows p_t/p_{max} as a function of Dt and which is valid for all solutes is constructed. (In plotting p_t/p_{max} it is desirable to take $\sqrt{Dt}$ for an abscissa (instead of Dt), because the plot initially is almost straight. In our plot it curves slightly at the start, giving a value of about 0·015 for p_t/p_{max} instead of 0, probably due to some irregular penetration through mixing while the disc is being lowered in the liquid). With the high molecular substance, p_t/p_{max} is measured after a time t and the value of Dt read from the graph. In this way each measurement provides a value of D. For the calibration the best value of D_{KCl} seems to be 1·676 × 10^{-5} cm.^{2}/sec. at 20° c.[1] It is easy to see from the calibration curve that the accuracy of the determinations decreases if the value of p_t/p_{max} rises above 0·6; values above 0·7 are practically useless. (If p_{max} has not been determined, p_t/c is plotted instead).

TABLE I.—CALIBRATION OF POROUS DISC AT 25° USING 1·5 % KCl.

t = Duration of experiment. (Min.)	p_t/p_{max} = Quantity diffused as fraction of quantity diffused after infinite time.
0	0·014
	0·015
5	0·228
	0·236
15	0·405
	0·405
30	0·580
	0·603
60	0·757
	0·765
120	0·866
	0·883

The apparatus was tested by measuring the diffusion constant of carboxyhæmoglobin. The porous disc, when filled with distilled water, contained 3·375 g. Calibration was carried out with a 1·5 % KCl solution at 25° (Table I). The CO-hæmoglobin was used in a 3·5 % solution and the protein was determined by the Kjeldahl method. In calculating the diffusion constant of hæmoglobin it was assumed that the relative change in the diffusion constants of KCl and of CO-hæmoglobin between 20° and 25° were the same.

Comparison of the figures obtained (Table II) with results of other experiments is complicated by the fact that the diffusion constant of CO-hæmoglobin is not independent of the concentration. As diffusion involves a concentration gradient it is very difficult to find an exact meaning for the experimental results. Lamm and Polson[2] found diffusion constants between 6·83 × 10^{-7} and 7·54 × 10^{-7}, Tiselius and Gross[2] give 6·3 × 10^{-7} for concentrations over 0·7 % rising with decreasing concentration to 14·9 × 10^{-7} at very low concentration. Experiments by Northrop and Anson,[1] carried out at 5° and corrected to 20° by Tiselius and Gross gave 7·35 × 10^{-7} cm.^{2}/sec. The agreement with the average of our values is satisfactory.

TABLE II.—DETERMINATION OF THE DIFFUSION CONSTANT OF CARBOXYHÆMOGLOBIN IN 3·5 % SOLUTION AT 25°.

t = Duration of experiment. (Hours).	p_t/p_{max} = Quantity diffused as fraction of quantity diffused after infinite time.	$D_{\text{CO-hæm}}$ = Diffusion coeff. of CO-hæmoglob. Calc. for 20°.
4·50	0·356	7·14 × 10^{-7} cm.^{2}/sec.
7·82	0·504	8·02
15·0	0·657	7·35
15·5	0·700	(8·40)

Natuurkundig Laboratorium der N. V. Philips' Gloeilampenfabrieken,
Eindhoven,
Netherland.

---

[1] Cohen and Bruins, *Z. physik. Chem.*, 1923, **103**, 349; 1924, **113**, 157.

[2] Lamm and Polson, *Biochem. J.*, 1936, **30**, 528. Tiselius and Gross, *Kolloid-Z.* 1934, **66**, 11.

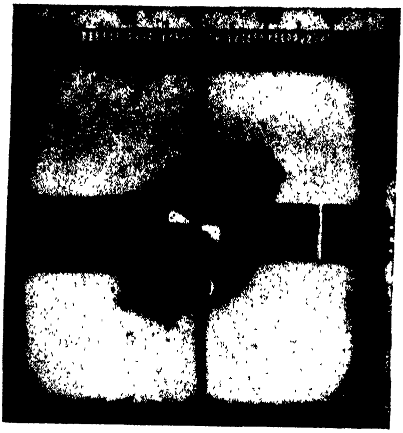

FIG. 1.

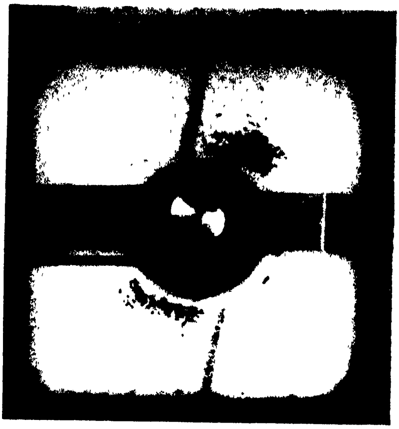

FIG. 2.

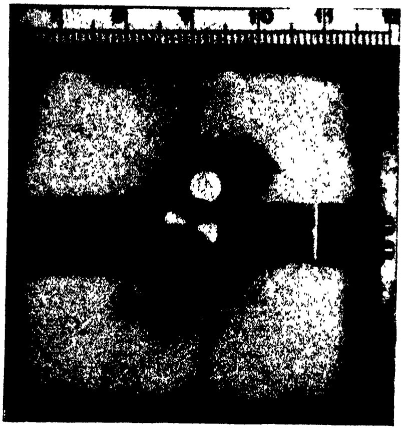

FIG. 3.

[*To face p.* 205

ON THE TRANSFORMATION OF "SOLID" FOAM TO A "FLUID" FOAM UNDER SHEAR.

BY M. BLACKMAN.

Received 31*st December*, 1946.

Most of the foams used in fire fighting are of a very viscous nature, the viscosity or apparent viscosity being of the order of 10^5-10^9 poise for certain specimens prepared by the author; these correspond fairly well with foams used in practice. It is nevertheless an empirical fact, that such foams can be squirted through a lengthy hose very much as if one were dealing with water. These two phenomena were shown in a joint investigation with Dr. W. G. Penney,[1] to be explicable on the assumption that the solid foam flowing down the pipe broke down when a critical shear stress was attained; the maximum value of this shear stress would occur at the boundary of the foam. After breakdown the foam is assumed to have a very much smaller viscosity. These assumptions could be checked qualitatively in observations on the passage of a plug of foam down a glass tube; in particular it was noticed that once the plug exceeded a critical velocity, it left layers of bubbles behind it. This theory is the same in its fundamental assumptions as that proposed by Bingham [2] in connection with the flow of paints. In the case of foams, it is novel, as far as the author is aware, and as the experimental proof of the existence of the two states is of some interest, the experiments detailed below were carried out.

A cylinder was made to rotate at a few revolutions per second in a box filled with foam. It was then seen that the foam was divided into two separate phases. It was a " fluid " foam near the cylinder, the thickness of the region varying from 2-8 mm. according to the speed of the cylinder and the nature of the foam.

This was recorded photographically in the following way. A still photograph (Fig. 1) was taken of the foam in the box. A line was drawn on the surface of the foam and a certain amount of sawdust was placed on the foam near the cylinder. A drawing pin on the cylinder indicated (for the purposes of the photographs) whether the cylinder was rotating or still.

The second photograph (Fig. 2) recorded the appearance of the surface of the foam when the cylinder was allowed to rotate. There appeared to be a clear ring round the cylinder where part of the sawdust had disappeared; the line on the foam also stopped short of the cylinder. Further, streaks could be seen in the ring where the sawdust was carried round by the highly mobile " fluid " foam. Outside the fluid region the foam was unchanged except for a deformation, as was shown by the existence of the original line on the foam, now curved over. This curving of the line was an effect of the stress applied during the break of the foam (preliminary to the formation of the " fluid " region) and during the rotation; it was due partly to elastic deformation and partly to flow of the foam under stress.

The third photograph (Fig. 3) showed the state of the foam when the rotation had been stopped. The foam was again firm, though the trace of the boundary between the "solid" and " fluid " foam remained. A comparison of Fig. 2 and 3 showed a movement in the "solid" region. The line and the boundary had rotated towards the initial position, as the stress which existed on the boundary during the rotation was removed when the rotation stopped.

---

[1] Ministry of Home Security (F Division) Report REN 282.

[2] *Fluidity and Plasticity* (New York, 1922).

The "fluid" foam state was demonstrated in sodium and ferrous protein hydrolysates derived from blood protein and keratin. The preparation of these is described by Dr. N. O. Clark[3] with the designations MW, MF, OJ. The width of the fluid region varied from 2 mm. for keratin foams to 7 mm. for blood protein foams in comparable experiments. No such region was found in a soap foam, in which the bubbles seemed to be drawn out until a film covered the cylinder or a large part of it. The film then broke and a hole was formed round the cylinder. In all other cases the "fluid" foam was perfectly stable though it probably underwent a change (in bubble-size and other properties) with time.

Measurements were made of the thickness of the "fluid" for various speeds of rotation. The viscosity was found to be $\sim$ 1 poise at the highest speeds (90 cm./sec. at the edge of the cylinder), assuming that the "fluid" foam behaved like a normal liquid for stresses exceeding the critical shear stress. It was found that the viscosity had a higher value at lower speeds. Since the theory assumed a constant viscosity (with varying velocity gradient), it will have to be modified to allow for variation of viscosity with velocity gradient.

The author is indebted to the Ministry of Home Security (F. Division) for permission to publish the above investigation, which was carried out in the Mathematics Department in 1944; thanks are due to Mr. E. V. Nehan of the Mathematics Department, Imperial College, for his assistance in carrying out the experiments, and to Prof. S. Chapman, F.R.S., for permission to use the Mathematics Laboratory.

Physics Department,
Imperial College.

[3] Clark, Chemistry Research Special Report, No. 6, D.S.I.R., H.M.S.O., 1946.

THE THERMAL DECOMPOSITION OF SILVER OXALATE.

By F. C. Tompkins.[1]

Received 14*th January,* 1947.

The rates of solid reactions in which $A_s \rightarrow B_s + C_g$ generally depend on the formation and growth of nuclei of B_s; the rates have been measured directly[2] in the BaN_6 decomposition and correlated with the p/t plots. These data, and other results obtained by irradiation with ultra-violet light,[3] have been interpreted by Mott[4] in a theory analogous to that previously proposed to explain the photo-reduction of Ag halides.[5] A latent image is produced on Ag oxalate on exposure, and its sensitivity and spectral range compare with those of the chloride[6] and on decomposition it forms metallic Ag and CO_2 only;[7] its thermal reaction might therefore be similar to that of BaN_6. A recent investigation[8] of the mercuric oxalate decomposition, however, revealed some unexpected results, which were presumed to be associated with the lack of mobility of the metal constituent and with the intermediate formation of mercurous oxalate. Previous work on Ag oxalate shows that the thermal rate is accelerated by pre-irradiation with ultra-violet light [9] and that it is sensitive to adsorbed ions and oxygen,[10] but there is doubt regarding the mechanism of decomposition. Benton and Cunningham [9] favour three-dimensional growth of nuclei, whereas Macdonald [11, 12] concludes that the reaction starts from a fixed number of centres, which grow two-dimensionally as thin plates; these latter may branch and so account for the exponential p/t plot after 5 % decomposition. Later work [13] on the conductivity of the partially decomposed salt favours the production of solid nuclei. More recently, the crystal structure of the oxalate has been elucidated [14] and X-ray photographs of the salt during decomposition have been taken.[15] Data are given here on the rate of gas evolution (1) at elevated temperatures after pre-irradiation, and (2) during irradiation at room temperature.

---

[1] I.C.I. Research Fellow (University of London).
[2] Wischin, *Proc. Roy. Soc. A*, 1939, **172**, 314.
[3] Garner and Maggs, *ibid.*, 1939, **172**, 299.
[4] Mott, *ibid.*, 1939, **172**, 325.
[5] Gurney and Mott, *ibid.*, 1938, **164**, 151.
[6] Arens and Eggert, *Phot. Korr.* 1931, Congress No. 17, **67**.
[7] Macdonald and Hinshelwood, *J. Chem. Soc.*, 1925, **127**, 2764.
[8] Prout and Tompkins, *Trans. Faraday Soc.*, 1947, **43**, 148.

Experimental.

Preparation of Oxalate.—Equal volumes (200 ml.) of N./5 A.R. $H_2C_2O_4$ and N./5 A.R. $AgNO_3$ were run into 400 ml. water at 40° C. at the same slow rate with vigorous mechanical stirring. The crystals were well washed and dried over P_2O_5 *in vacuo*, all operations being performed under dark-room conditions. Large crystals (1-2 mm. long) were obtained by crystallisation from ammoniacal solutions.[11]

Apparatus.—This comprised a pumping system (Hyvac and Hg-diffusion pump), a calibrated McLeod gauge (10^{-6} to 10^{-3} cm.), two Pirani gauges (one, as compensator) firmly clamped in a thermostat (25 ± 0·02° C.), a volume bulb for determination of the capacity of the apparatus, and a decomposition chamber. The latter was a double-walled Pyrex vessel, lagged externally and maintained at temperatures (110°-113° C.) by the vapours of boiling liquids. At the top it carried a winch for raising the quartz bucket provided with a flat base and containing the salt, and at the bottom a ground joint closed with a plane quartz plate through which the oxalate could be irradiated; a calibrated Cu-constantan thermocouple was fixed axially within the chamber. Traps, in the form of U-tubes of equal diameter limbs immersed in solid CO_2-alcohol mixtures, prevented Hg vapours from reaching the salt [16] and the Pirani gauges. The latter were calibrated both with CO_2 (liquid-air distillation from Drikold) and the decomposition gas. The temperature of the reaction vessel was varied by altering the pressure on the boiling liquid. After introducing the salt (2 mg.), it was exhausted for 18 hr. before any run.

Results.

The Thermal Reaction.—Decomposition at 125° C. on two samples of the same preparation (without pre-irradiation) are given in Fig. 1—these are indistinguishable except over the first 4 % reaction, whereas Macdonald records *ca.* 20 % divergence. The pressure measurements here are very sensitive at low pressures and it is certain (see inset of Fig. 1) that there is no slow uncatalysed emission of CO_2 at a constant rate initially as might be expected theoretically,[4] but there is, however, always a small burst of gas due to desorption as the salt is raised from room temperature to 125° C. On raising the bucket into the reaction chamber, temperature equilibrium is established within 3 min. as recorded by the thermocouple which rests on top of the salt layer. The first 5 % of the p/t plot can be expressed by $p = C(t - t_0)^{3 \cdot 90}$, where $t_0 = 3$ min. and C is a constant, and afterwards to the end of the acceleratory period by

---

[9] Benton and Cunningham, *J. Amer. Chem. Soc.*, 1935, **57**, 2227.
[10] See ref. 7, 9, 11 and 12.
[11] Macdonald, *J. Chem. Soc.*, 1936, 832.
[12] Macdonald, *ibid.*, 1936, 839.
[13] Macdonald and Sandison, *Trans. Faraday Soc.*, 1938, **34**, 589.
[14] Griffiths, *J. Chem. Physics.*, 1943, **11**, 499.
[15] Griffiths, *ibid.*, 1946, **14**, 408.
[16] Sheppard and Vanselow, *J. Amer. Chem. Soc.*, 1930, **52**, 3468.

$p = C(t - t_0)^{3.27}$; this compares well with the results of Benton and Cunningham, but not with those of Macdonald.

Microscopic Examination.—On exposure to ultra-violet light (full Hg arc, 66 v., 2·6 amp.) the crystals darken throughout their volume, i.e. the Ag is disseminated in a diffuse manner (cp. Hg fulminate,[17] KN_3 [18]), and there is no aggregation into discrete nuclei (as with BaN_6,[19] SrN_6,[20] PbN_6,[21] etc.). With large crystals, or thicker layers of micro-crystals, the darkening decreases with depth due to their high absorption coefficient but there is no indication that the reaction proceeds especially quickly at the surface, edges or imperfections. The observations with crystals undergoing thermal decomposition are similar (cp. also [11]). A small area of the surface of a single crystal was irradiated at 20° c. until it was dark brown, and then the whole maintained at 130° c. and observed under high magnification till it was opaque. The darkened area appeared as sharply defined at the end (about 10 % decomposition) as it was originally, and the reactions of the two parts seemed to proceed independently with the irradiated section decomposing at a greatly accelerated rate.

Threshold Frequency for Absorption.—A uniform film was painted on a glass slide using a water-oxalate paste and after drying used as a photographic plate in a Hilger u.-v. monochromator with the Hg arc as a source. Darkening was apparent up to 4920 A. No attempt was made to measure the extinction coefficients. Since darkening denotes decomposition (see later), this also is the threshold wave-length necessary to produce acceleration in the thermal reaction.

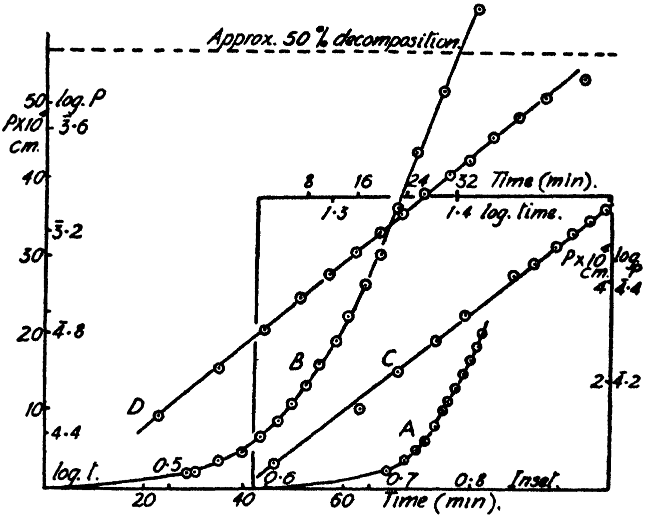

FIG. 1.—Curves C, D : log $P - t$ plot. Curves A, B : $P - t$ plot.

Measurement of Darkening.—A brass cup (1 cm. diam., 1 mm. depth) was filled with the salt which was irradiated for definite times with ultra-violet light. A brass arm, pivoted at the cup, carried a photoelectric cell at its upper end and could be rotated through 90° c. ; the brass cup itself could be turned through 360° in a horizontal plane, so that the reflected light could be explored and its intensity measured at all points on a hemisphere, using red light. The value of this (integrated) intensity was compared with that using MgO at various stages of darkening. The results are summarised in Fig. 2, where it is shown that the equation $\log (A_{max} - A_t) = kt +$ const. is obeyed, where A_{max} is the final value of the absorption intensity (extrapolated) and A_t, its value at any time t, where t is the time of irradiation.

Irradiation of O° C. and Rate of Gas Evolution.—The salt was spread in a thin uniform layer on the flat base of a 2 cm. Pyrex tube, closed at its upper end with a plane quartz plate and connected with the Pirani gauge through a side-arm. The Hg arc was focussed on the oxalate through a cell of distilled water with the tube in ice and the CO_2 pressure measured at intervals. Gas evolution commenced immediately (ct. BaN_6), initially according to $p \cong Ct^2$, but after 20 min. the rate was almost constant, although slight acceleration was always present. Gas evolution ceases immediately the light is cut off and the "constant" rate is at once reproduced on re-irradiation.

---

[17] Garner and Hailes, *Proc. Roy. Soc. A*, 1933, **139**, 576.
[18] Garner and Marke, *J. Chem. Soc.*, 1936, 657.
[19] Harvey, *Trans. Faraday Soc.*, 1933, **29**, 653.
[20] Maggs, *ibid.*, 1939, **35**, 433.
[21] Garner and Gomm, *J. Chem. Soc.*, 1931, 2123.

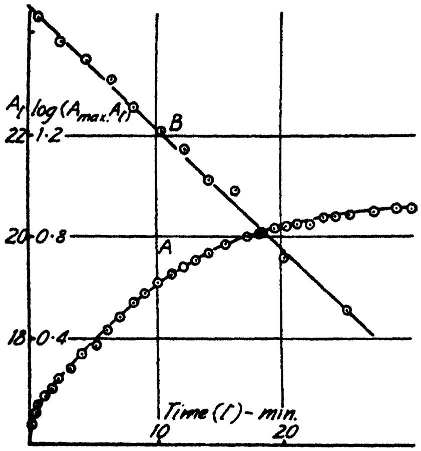

FIG. 2.

By immersing the tube in various baths the variation of rate (R) with temperature was obtained (Fig. 3). Since the difference of velocity is so small, each point was obtained as a ratio of velocities by alternation between two temperatures and extrapolating each rate to the time of temperature change. The plot approximately corresponds to $R = Ce^{-E/RT}$, where E has an average value of 850 cal. Measurement at 90° K. was impossible because of condensation of CO_2, but the velocity obtained by irradiating for short intervals at 90° K. and then raising the temperature to 195° K. in between to evaporate the gas, together with the rate of darkening, showed that no abnormally large decrease at 90° K. occurs.

The variation of light intensity on the rate at 0° C. is given in Fig. 4; metal screens placed on a quartz lens and between it and the arc were used, and the relative intensity measured by a selenium cell in place of the salt layer. The rate varies as the 1·67 power of intensity, this value being somewhat larger at higher intensities.

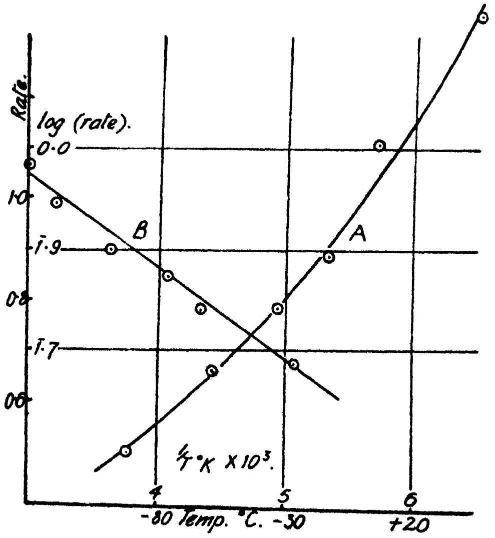

FIG. 3.

Pre-Irradiation and Thermal Decomposition.—The salt (a slightly exposed sample) was air-sprayed on the base of a Petri dish and each sample irradiated with the full arc in air for various periods of time. The powder was then stored over P_2O_5 *in vacuo* and samples (5 % of total) used for decomposition. Although the thermal rate was considerably accelerated the log p — log t plots were all linear; the results are summarised in Table I. The plots of log C and log x against log t_i (where t_i is time of pre-irradiation and x is the exponent in $p = Ct^x$) are linear, the slope of the former being 2·80. Similar experiments with constant time (10 min.) of irradiation, but with variation of intensity (I), are given in Table II; the corresponding log plots are linear, the slope of the log C — log I curve being 3·25. There was no decay of the effect of irradiation after a month.

Heat of Activation.—The values of Macdonald [12] and of Benton diverge considerably. Inaccuracies are due to (i) variation in rate from sample to sample, and (ii) self-heating of the salt, particularly when the rate of decomposition is rapid. In the present decomposition chamber, the thermo-couple which records the actual temperature of the oxalate shows a 5° increase over the temperature of the vessel. The tube used in the irradiation experiments was employed in consequence. About 1 mg. salt was spread over the base and the whole immersed in suitable temperature baths (65°-88° c.); at these temperatures the rate is very slow but accurately measurable with the sensitive Pirani gauge used, and self-heating is a minimum. The series of determinations was completed over about 1 % decomposition. The rates are not strictly constant, consequently the method of alternating temperatures and extrapolation (see above) was used, thereby referring these to the same % decomposition for each pair of temperatures. The heat of activation is found to be 24,600 cal./mole in agreement with some few results of Benton, as recalculated by Macdonald (25,400), but differing appreciably from those measured by the latter author (32,700).*

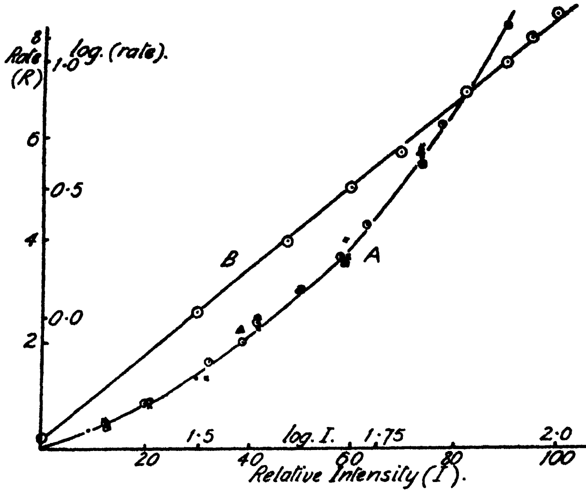

FIG. 4.—A: Rate against relative intensity. B: log R — log I.

TABLE I

Time t_t (min).	— log C.	log x.
0	4·19	0·484
2·5	3·62	0·465
5	3·00	0·431
7·5	2·43	0·400
10	2·06	0·369
12·5	1·76	0·344
15	1·56	0·318
17·5	1·36	0·295
20	1·18	0·267
25	0·87	0·212

TABLE II

Intensity (relative).	log C.	log x.
10	3·60	0·446
20	3·04	0·394
30	2·51	0·348
40	2·08	0·312
50	1·75	0·287
60	1·52	0·268
70	1·31	0·252
80	1·13	0·236
90	0·99	0·266
100	0·87	0·220

Discussion.

The p/t plots obtained in the thermal reaction by Macdonald, and by Benton and Cunningham, differ in that the results of the former can be expressed by (1) $dp/dt = kt$ over the first 5 % decomposition and

---

* In his later paper, Macdonald, using the same method as employed here, obtained a temperature coefficient of 2·48 per 10°, equivalent to an activation energy of 24·3 kcal., between 87·05° and 99·15° c. for the first 6 % reaction.

(2) $dp/dt = C(e^{k_1 t} - 1)$ over the remainder of the acceleratory period, whereas those of the latter are adequately represented over a large range by $p = Ct^n$, in agreement with the present results. It may be noted that Macdonald and Hinshelwood found Ag oxalate, prepared in presence of excess Na oxalate, to be of the "unstable accelerating" type during decomposition, in contrast with that obtained with excess silver nitrate, which was of the "stable, feebly accelerating" type. The difference above may therefore be due to preparation—the conditions used here (stoichiometrical amounts of reactants, and precipitation at a slow rate under conditions of high dilution) are similar to those of Benton and are expected to lead to minimum occlusion and adsorption of both lattice and foreign ions, and to a more homogeneous, crystalline product. This probably accounts for the present good reproducibility. Macdonald, however, used in general high excess of one reactant in fairly concentrated solutions during precipitation, both factors tending to favour ion adsorption and inhomogeneity.

In an attempt to resolve the differences it was hoped to obtain independent data on growth and formation rates, but with various optical systems and the highest magnification, no individual centres could be identified. That these are present is presumed by the darkening, and they might be as large as 1000 A. (containing 10^{16} Ag atoms, assuming spherical growth) without being distinguished; growth is therefore not excluded. With BaN_6, the rate of nucleus formation has an activation energy of 74 kcal. and is slow compared with that of growth (23·5 kcal.), whereas with Ag oxalate these energies are closer together. The threshold wavelength for BaN_6 is about 2600 A. corresponding to an energy of 108 kcal., whereas the measured energy for formation is 74 kcal.; here, the threshold is about 5000 A., or 52 kcal.—the energy of nucleus formation is therefore expected, by analogy, to be less than this. Our measured activation energy from the p/t plots over small periods of time is 24·6 kcal. Thus, with Mott, we calculate (assuming that the curve develops initially as the fourth power of time) that the activation energy of growth will be about 18 kcal.—this represents the minimum value. With a discrepancy similar to that above for BaN_6, these figures can be changed to 35 kcal. for formation and 23 kcal. for growth. Thus there is more rapid formation and slower growth which will favour the dissemination of a large number of nuclei through the crystal.

Another difference may be emphasised; with BaN_6, irradiation increases the number of potential positions at which nuclei can be formed on subsequent heating; here metallic Ag is produced during exposure, just as mercurous oxalate is when mercuric oxalate is irradiated. The decomposition of mercurous oxalate during the thermal reaction could be separated from the main decomposition and the increase in number during irradiation shown to be in accord with the equation $n_t = N(1 - e^{-kt})$, where n_t is the number formed during an exposure t, and N is the total number available for creation. This separation is not possible here since the Ag particles act as centres of growth in the thermal process and the p-t plots reflect both growth and additional thermal formation.

Some indication of the formation rate is suggested by the results on the decrease of scattered radiation with time of irradiation. Assuming that all the red light is scattered by MgO, it is found that practically all is "reflected" by unexposed Ag oxalate. Assuming, therefore, that the reduction in scattering after irradiation is due to the formation of Ag centres, and further, that no growth ensues during exposure, then the experimental relationship $(A_{max} - A_t) = Ce^{-kt}$, may be transformed to $n_t = N(1 - e^{-kt})$, as found for the corresponding mercuric salt.

Any theory of the mechanism of nucleus formation by irradiation must account for the small temperature coefficient and the dependence of rate on the intensity to a power greater than unity, but also must be consistent with the crystal structure of the salt. Silver oxalate is monoclinic, with two molecules per unit cell ($a = 3{\cdot}46$, $b = 6{\cdot}16$, $c = 9{\cdot}47$, and $\beta = 76°$), and composed of a chain of molecules parallel to the b axis; the oxalate group is non-planar, the two C-atoms being displaced to opposite sides of the plane containing the four O-atoms. The oxalate is linked with the Ag by short Ag—O bonds (2·17 and 2·30 A.); longer Ag—O bonds (2·58 and 2·61 A.) hold the chain of molecules together parallel to the 100 plane, and still longer ones (2·93 and 3·00 A.) the sheets of molecules together. The co-ordination of the Ag is 6, whereas it is 4 in the metallic state, a change involving a 6 % increase in radius of the Ag atom. The shortest Ag—Ag distances are 3·34 and 3·58 A. in the salt, and 2·88 and 4·08 A. in the metal. Considerable readjustment of these distances must therefore take place should there be any type of crystal growth.

Now with AgBr the temperature coefficient [22] of the print-out effect is large (decreased by 10^{-5} when lowered to 90° K.) and runs parallel to to the decrease of the electrolytic conductivity of the cation; [23] it is thus consistent with the fact that the bromide is an ionic conductor with a mobile cation, thereby accounting for nucleus growth. Silver oxalate, however, has a molecular layer lattice with, it is presumed, a practically immobile metallic constituent; growth by a similar process thus seems impossible. This can provide a reason for the small temperature coefficient, and is also why the product (Ag) is a pseudomorph of the original crystal.

On irradiation, an electron is presumed to be ejected from the oxalate group into the conduction band leaving a positive hole in the full band. The mobile electron is captured by a Ag atom temporarily, but for the most part it will return to a positive hole. If the Ag atom is a near neighbour of the positive hole, the process will correspond to an electronic transition (as cp. von Hippel [24]); this, however, will be relatively infrequent, since the time spent by an electron at a Ag atom near its point of ejection will be less than at those atoms some distance away because it (the electron) will lose energy by interaction with the lattice vibrations in jumping from one Ag atom to the next; with loss of energy the potential well it can create near the Ag atom by polarisation will be deeper. Thus, in crystals of high refractive index, where the potential barrier is not very steep, the electron will have a fairly long path before ultimate capture. Similarly, capture by sensitivity spots etc., will be negligible since the print-out effect is found not to be structure-sensitive here. The small number of molecules in which an electronic transition has taken place will be proportional to the light intensity (I), and if these have a short life (i.e. because of reversion back to their original state), the density of such " sites " will be proportional to I and be, to a first approximation, independent of time. Now the absorption coefficient of the salt is high so that the rate of combination of mobile electrons with positive holes will largely control their density; since the number of mobile electrons and positive holes are approximately the same, this density will be determined by $I^{\frac{1}{2}}$. The rate of combination of " sites " with mobile electrons is now presumed to measure the rate of decomposition, i.e. one of the Ag atoms in the " site " (comprising an oxalate group with its neighbouring Ag atoms) captures the electron and holds it for a sufficiently long period for the positive hole to diffuse away or to decompose by transferring its now excess electron to another neighbouring silver atom. This electron will be later rendered mobile either by thermal energy from the lattice or by light absorption. The silver now left (designated as Ag_2 for the pair of Ag atoms) will accumulate as decomposition proceeds and will provide temporary traps for mobile electrons and so influence their density; it is thus found with darkened salt that there is a dependence of rate on intensity to a power greater than 1·5, but the constant rate of CO_2 evolution is not altered with time. Since the capture of an electron does not itself lead to the production of CO_2, the above mechanism must lead to a quantum yield of considerably less than one (i.e. the value for halides) agreeing with Benton's value of 0·16 at room temperature. A difficulty arises in the escape of the CO_2 from nuclei created within the crystal because of the lack of mobility of the Ag atoms, and because the reaction has been shown not to move inwards from the surface. It is possible to suggest paths, from geometric considerations, along which the gas may escape, providing the oxalate group breaks up where it is formed, or the CO_2 may escape as a result of its production at high pressure and force its way along planes of weakness in the crystal * (cp. Ransley,[25] who has shown this effect to occur in the escape of H_2O through metallic Cu). It would provide a qualitative reason for the slow evolution initially on irradiation; when the salt is darkened there are many gaps, due to prior removal of oxalate groups, and the rate of diffusion will no longer be the slowest process. This process of diffusion will be of the activated type, but there will be sufficient energy available to the CO_2 molecules by the exothermic breakdown of the oxalate group unless there is a rapid energy interchange with the lattice. Alternatively, a method of handing-on of electrons from inner groups until they reach the surface, where they break down and escape is possible, but renders the interpretation of growth difficult if there is no, or only limited, mobility of Ag atoms (see later).

---

[22] von Hippel, *Z. Physik.*, 1936, **101**, 380.

[23] Berg, *Proc. Roy. Soc. A*, 1937, **149**, 38.

[24] Kock and Wagner, *Z. Physik. Chem. B*, 1937, **38**, 295.

In explanation of the small temperature coefficient of the print-out effect, it is assumed (cp. Hilsch and Pohl [26]) that the absorption coefficient is independent of temperature. The activation energy can then be the difference of two (larger) energies associated with opposing processes. Thus, if p_1 is the probability per unit time that redistribution of energy takes place in the " site ", possibly accompanied by a limited mobility of the Ag atoms, so that CO_2 is ultimately produced, and p_2 the probability per unit time that one of the electrons on a " site " is rendered mobile and returns to a positive hole, then the rate of CO_2 formation per quantum absorbed is given by $p_1/(p_1 + p_2)$; let each of these processes be associated with activation energies of E_1 and E_2, then

$$R = C_1 e^{-E_1/RT}/(C_1 e^{-E_1/RT} + C_2 e^{-E_2/RT})$$

where C_1 and C_2 are constants, or if $\frac{C_1}{C_2} e^{-(E_1+E_2)/RT}$ is small compared with unity and $\Delta E = E_1 - E_2$, $R \cong \frac{C_1}{C_2} e^{-\Delta E/RT}$. Here C_1 is expected to be of the order of the lattice vibration frequency, i.e. 10^{12} sec.$^{-1}$; inserting 0·16 for the quantum yield and ΔE of the order of 1 kcal. then $1/C_2$ is 3×10^{-11} sec., representing the time which an electron remains before becoming mobile; this appears short, but not unreasonably so, since a mobile electron can move from atom to atom in much less time (10^{-15} sec.) and moreover the value of C_1 above may well be too large.

Alternatively, the experimental E may be a true one, i.e. the absorbed quantum is insufficient to produce the photo-reduction without co-operation of thermal energy of the lattice in forming a stable product. Thus, the energy associated with lattice vibrations will be about 1/20 to 1/40 ev. (i.e. of the order found) and could be associated either with the escape of CO_2 from its place of formation within the lattice, or with the transmission of the positive hole to the surface, where it breaks down and escapes.

---

* I am indebted to Prof. W. E. Garner for this suggestion.

[25] Ransley, *J. Inst. Metals*, 1939, **65**, 147.

[26] Hilsch and Pohl, *Z. Physik.*, 1930, **64**, 606.

The thermal reaction after irradiation is accelerated but the power law, $p = C_t t^x$ is still valid with C_t (thermal) increasing and x decreasing with time of exposure. It is reasonable to identify C_t with the number of reaction centres, but this varies as $I^{3.35} . t^{2.8}$, whereas the dependence expected from the print-out results is as $I^{1.67} . t^{1-2}$ (the variable power of t between 1 and 2 is due to the fact that the periods of irradiation are within the acceleratory period of the print-out effect—no real comparison is possible since the conditions there and during pre-irradiation are somewhat different). It suggests that C_t (thermal) $= C_p{}^2$ (print-out), which means that not all the Ag_2 can act as growth centres, but e.g. only those which are adjacent neighbours. It may be noted that Kornfeld and Pawlow's results [27] suggest a parabolic dependence of number of centres upon the square root of deformation in the recrystallisation of metals, and it is well-known in phase transitions that centres must be greater than a critical size in order to grow. These regions of four Ag atoms form localised high stress regions which are configurationally unstable; they will provide part of the energy required to initiate further decomposition which produces additional localisation of such regions. The picture is clearer if the oxalate group decomposes within the crystal; in this circumstance, there will be a missing oxalate group between the Ag_2 pairs and a tendency for these to build up a lattice more in conformity with the metallic state by adjustment of Ag—Ag distances and so create large distortion forces. Growth is thus not by reason of mobility of Ag atoms but due to deformation; this means that there will be preferred directions of growth and, at higher temperatures, fragmentation along cleavage planes is expected as found by Griffiths from his X-ray study.

On heating unexposed salt, new centres are created when the oxalate group receives sufficient thermal energy to lose electrons to Ag atoms, as in the photo-reduction, and the measured p-t plot reflects both this and growth. The number formed in time t is given by $n_t = N_0(1 - e^{-kt})$ as before, but here N_0 is the total number of oxalate molecules; with decomposition a further term, $V_g(\tau, t)$, where V_g is the total growth volume and is a function of both time of growth (τ) and of creation (t), should be introduced since creation of new centres here is not possible. It is, however, better to use the simpler expression above giving the total number of new centres, both real and "ghosts," and then to apply a correction for overlapping of growth (cp. Avrami).[28, 29, 30] These centres are considered to be created randomly throughout the crystal (in both decomposed and undecomposed parts) at all times; a "ghost" centre is one "produced" in the decomposed volume, and thus has no physical existence. These nuclei grow three-dimensionally with velocities u, v and w in different directions, but can be replaced by $\bar{v}^3$, where $\bar{v}$ is the averaged linear growth in all directions; thus the total volume of product at time t will be

$$V_u = \int_{\tau=0}^{\tau=t} k_1\bar{v}^3(t-\tau)^3 N_0(1 - e^{-k\tau})d\tau \quad . \quad . \quad . \quad (1)$$

for all centres created at time t, which includes growth from "ghosts" and is uncorrected for overlapping. Now, if random formation within the crystal is assumed, it is possible [29] to express the actual volume produced (overlap only counted once) by $1 - V = V_n/V_u$, or for small overlap, $V/(1 - V) = V_u$, or more exactly by $V = 1 - e^{-V_u}$.

On integrating (1), we have

$$V_u = \frac{k_1 N_0 \bar{v}^3}{k^4}\left(6e^{-kt} + t^3/k\left(-\frac{3t^2}{k^2} - \frac{6t}{k^3} - \frac{6}{k}\right)\right) \quad . \quad . \quad (2)$$

---

[27] Kornfeld and Pawlow, *Physik. Z. Sowjetunion*, 1934, 6, 537.

[28] Avrami, *J. Chem. Physics*, 1939, 7, 1103.

[29] Avrami, *ibid.*, 1940, 8, 212.

[30] Avrami, *ibid.*, 1943, 11, 499.

assuming no centres are present initially, and on expanding the exponential,

$$V_u = \frac{k_1 N_0 \bar{v}^3}{4} t^4 \left(1 - \frac{kt}{5} + \frac{k^2 t^2}{6 \cdot 5} \ldots \right) \ldots \qquad (3)$$

Similarly, if there are N_t centres created in irradiation, this becomes

$$V_u = \frac{k_1 N_0 \bar{v}^3}{4} t^4 \left(1 - \frac{kt}{5} \ldots \right) + k_1 N_t \bar{v}^3 t^3. \qquad (4)$$

For small t, particularly for not too large values of k, the total volume of product V is $1 - e^{-Bt^4}$ for unexposed salt where $B = \frac{k_1 N_0 \bar{v}^3}{4}$, or more approximately Bt^4, as is found. This is true up to the time of exhaustion of the growth centres by impingement. When two growing centres touch they can coalesce to form a larger growing grain; they may continue to grow independently by pushing each other out of the way; or they may adhere such that growth ceases at their common interface. The first assumes mobility; the second, increasing deformation and thus an accelerated rate; the third, therefore, is most probable. When there are many centres and there is a rapid growth along one direction (e.g. following the sheets of Ag oxalate molecules), the three-dimensional growth will virtually become two-dimensional and p depends on t^3 approximately. Thus we replace $\bar{v}^3$ by u, v, w, in (1) and define the average duration of growth in the different directions by t_u, t_v and t_w, and then integrate between the limits of t_u, t_v, $t - t_u$, $t - t_v$ respectively (where w is the last to be affected, t_w represents the time of complete decomposition). We should therefore expect a dependence of p on t^4 in the initial stages for unexposed salt; the exponent will decrease with time due to impingement of growth and a dependence on t^2 is expected over the decay of the decomposition. With moderately exposed samples, the rate varies as t^3, since the number of initial ("light") centres growing far outweigh the effect of new creations and growth of thermal nuclei; with highly exposed samples, growth will quickly cease along one axis, and a rate determined by two-dimensional growth (or as t^2) is found.

There is one further reason for the decreasing power of t here; that is the complete decomposition of the smaller particles in the powder. Thus, in the limiting case, where growth is predominating, we may define l as an average life of a "small" particle. For times less than this,

$$V_u = 4/3 \pi \bar{v}^3 l^3 N$$

or for larger times

$$V_u = 4/3 \pi \bar{v}^3 t^3 N.$$

Where growth is not predominating, the effect is to reduce the power of t^4 to t^3. We may note, however, that a growth of planar nuclei (a possibility with the Ag oxalate layer lattice) which under certain circumstances branch at certain points in number dependent on the growth area and set up a three-dimensional growth has the form:

$$V_u = \int_{\tau_0}^{\tau = t} k_1' uv(t - \tau)^2 w(t - \tau) e^{k_1 \tau} (1 - e^{-k\tau}) d\tau$$

and if $k > k_1$ (a branching coefficient), the integration leads to a result formally similar to (2). If, however, $k_1 > k$, then the dependence of the rate is at t^x, where x will *increase* with extent of decomposition, which is contrary to our results. With highly irregular crystals, as might be expected from Macdonald's preparation, this latter case is probable and the p-t plots will be predominantly exponential in development; the difference lies thus in that $dp/dt = Ct^x$ refers to a continuous front, whereas $dP/dt = Ce^{kt}$ to a non-continuous one.

The heat of activation obtained here (24·6 kcal.) agrees with the few results of Benton (25·4 kcal.) but is much less than Macdonald's values for the later stages of decomposition. The latter's later determinations, however, show that this energy (E) increases with increasing decomposition. Now E is composed of Q, the energy for creation, and $Q'(T)$, that for growth, the latter probably being temperature dependent; we may expect Q' to be different along different crystal axes, being smallest in that of least restraint or of highest linear velocity. In the later stages of decomposition, initiation of growth will require more energy since the growth virtually becomes two-dimensional, and thus the activation energy rises continuously with increasing decomposition.

Summary.

The thermal decomposition of silver oxalate has been investigated with particular emphasis on the rate of gas evolution (1) at elevated temperatures (110°-130° C.) after pre-irradiation with ultra-violet light and (2) during irradiation at lower temperatures where the thermal rate is negligible. The latter is associated with a small temperature coefficient and this is presumed to be due to the limited mobility of the metal constituent. The rate of formation of silver nuclei has been deduced from the rate of darkening; this, when combined with three-dimensional growth of the silver centres, is shown to account adequately for the experimental results. In general, the present work is in good accord with that previously done on mercuric oxalate as might be expected from the similarity of their crystal lattices, both being of the molecular layer type, but shows in addition similarities to the decomposition of barium azide. It is, however, suggested that growth of nuclei here is associated rather with the deformation of the lattice by the product than with the process of electrolysis envisaged by Mott for the barium azide decomposition.

University of London, King's College,
Strand, W.C.2.

THE ABSOLUTE RATE OF CONVERSION OF PARAHYDROGEN BY METALLIC CATALYSTS.

BY D. D. ELEY.

Received 22nd January, 1947.

Introduction.

The parahydrogen conversion on metallic tungsten has been shown [1, 2] to proceed by an exchange of atoms between a hydrogen molecule in a van der Waals' adsorbed monolayer and a hydrogen atom in the underlying *stable* chemisorbed layer.[3] A similar mechanism holds for the $H_2 + D_2$ reaction and a general formulation is

$$\begin{array}{l} W - H \;.\;.\; pH_2 \rightarrow W - H \;.\;.\; oH_2 \\ W - H \;.\;.\; D_2 \rightarrow W - D \;.\;.\; HD \end{array}$$

in which W denotes an atom in the tungsten surface and we make no detailed assumptions about the mode of reaction between the two adsorbed layers.

The results of A. and L. Farkas [4] also establish this mechanism for the catalyst nickel, and make it very probable, in the present author's opinion, for palladium and platinum. Until we obtain contrary evidence,

---

[1] Eley and Rideal, *Proc. Roy. Soc. A*, 1941, **178**, 429.

[2] Eley, *ibid.*, 1941, **178**, 452.

[3] Roberts, *ibid.*, 1935, **152**, 445.

[4] A. and L. Farkas, *J. Amer. Chem. Soc.*, 1942, **64**, 1594.

there is no reason to doubt the general application of this mechanism, at least in the lower ranges of temperature, which are of most interest.

In this paper we shall calculate the " temperature-independent factor " for this conversion and compare our results with the available data. These data comprise fairly extensive determinations for tungsten,[1] under conditions in which the absence of surface contamination, such as oxide, was demonstrated. They also include certain data for the catalysts nickel, palladium and platinum, where the surface conditions were less rigorously defined. The agreement between theory and experiment is found to be quite satisfactory. The simplicity of the pH_2 conversion makes it a very suitable subject for quantitative study, and this paper forms part of a programme of work along this line, in which the details of the conversion on the various metals will be established. This programme includes an experimental analysis of theoretical factors which may be expected to influence the activation energy, to which reference is made in the concluding section of this paper.

Assumptions.—The experimental first-order constant, k_e, min.$^{-1}$, is expressed with the usual accuracy by

$$k_e = Be^{-E/RT}, \text{ where } E = RT^2\frac{d \ln k_e}{dT}. \qquad (1)$$

B is calculated on the following main assumptions, of which the first has been shown to be correct by experiment, and the second to be true to a first approximation.[1, 2]

(*a*) Conversion occurs through an exchange of atoms between a molecule in the van der Waals' (V.W.) layer and an atom in the chemisorbed layer.

(*b*) The surface atoms are of uniform activity.

(*c*) The V.W. layer of hydrogen molecules is a mobile (equilibrium) monolayer on localised sites, and neighbour interactions may be neglected.

(*d*) The ratio of the partition functions of the chemisorbed H atom and transition complex (" H_3 ") is unity over the temperature range concerned. This implies sufficiently strong bonding to the metal to rule out surface mobility and rotations, and also a ratio of nuclear weights of 1.

The method is to calculate the number of H_2 molecules in the V.W. layer by statistical mechanics, and to formulate their absolute rate of exchange with the atoms in the chemisorbed layer by the activated-complex method.

Potential Energy Scheme.—The lowest energy level of the H_2 molecule in the gas phase is taken as the zero of potential energy. A formal representation of the potential energy changes involved in the pH_2 conversion in the gas phase and on the surface of the metal is given in Fig. 1. χ_H denotes the potential energy change in adsorbing one H atom from the gas phase into a (nearly full) chemisorbed monolayer. χ is similarly the adsorption energy of an H_2 molecule into the V.W. layer (χ is negative for energy evolved on adsorption). Permitted rotational levels are shown as full lines. $\epsilon_g(\epsilon_s)$ denotes activation energy at 0°K. of the gas (surface) reaction, ϵ_g being 7 kcal.[5] The gas reaction goes through

$$H + pH_2 \rightarrow oH_2 + H,$$

while the surface reaction goes

$$W - H \cdot\cdot pH_2 \rightarrow W - H \cdots oH_2.$$

Therefore the two potential curves are separated by $\chi + \chi_H$.

We have assumed that χ is the same for pH_2 and oH_2 molecules, and this must be correct to a high approximation. However, for our analysis all we require is that $\chi - \epsilon_s$ is the same for $p\mathrm{H}_2$ and $o\mathrm{H}_2$, i.e. for reaction left to right and right to left over the energy hill ϵ_s. Since ϵ_s is the same for both forward and reverse reactions, this condition is seen to hold even if χ *does* differ for $p\mathrm{H}_2$ and $o\mathrm{H}_2$.

---

[5] A. Farkas, *Orthohydrogen, Parahydrogen and Heavy Hydrogen* (Cambridge, 1935), p. 68.

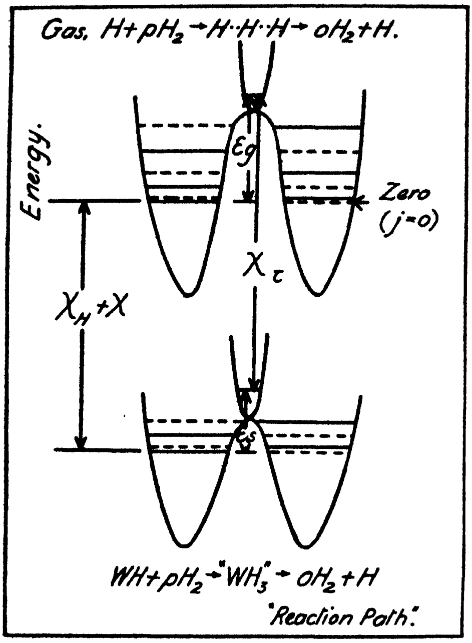

FIG. 1.—A purely formal scheme of energy changes for the exchange mechanism of the $p\mathrm{H}_2$ conversion. Permitted rotational levels are indicated by full horizontal lines, forbidden levels by dotted lines. ϵ denotes activation energy and χ adsorption energy at 0° K. Subscript g refers to gas, s to surface, τ to activated complex. χ_H refers to an H atom in the chemisorbed layer, and χ to an H_2 molecule in the van der Waals' layer.

Calculation of the Temperature-Independent Factor.

Absolute Velocity of Conversion.—The net velocity, v, of $p \rightarrow o$ conversion is the difference between the absolute velocities of $p \rightarrow o$ and $o \rightarrow p$ transitions. Since the layer of chemisorbed atoms is virtually complete over our temperature range,[8] we may write the absolute velocity for the $p \rightarrow o$ ($o \rightarrow p$) change as proportional to the surface concentration C_p (C_o) of para (ortho) molecules in the V.W. layer, in molecules/cm.^{2}. If A be the area of catalyst, and k_p and k_o the absolute rate constants in min.$^{-1}$,

$$v = A(k_pC_p - k_oC_o). \quad . \quad . \quad . \quad . \quad . \quad (2)$$

Taking f as the number of sites per cm.^{2} in the V.W. layer, and σ_p, σ_o, the fractions of this layer covered by $p\mathrm{H}_2$, $o\mathrm{H}_2$ respectively

$$v = Af(k_p\sigma_p - k_o\sigma_o). \quad . \quad . \quad . \quad . \quad . \quad (3)$$

Experimental First-Order Constant.

Consider a reaction vessel, volume V, temperature T° K., containing hydrogen gas at pressure p mm. Hg. If x be the fraction of $p\mathrm{H}_2$ at time t, and x_e the equilibrium fraction at $t = \infty$, it is found experimentally that [6, 1]

$$-\frac{dx}{dt} = k_e(x - x_e) \quad . \quad . \quad . \quad . \quad . \quad (4)$$

---

[8] A. Farkas, ref. 5, p. 98.

If n ($= NRT/pV$) be the number of hydrogen molecules present, the net velocity v in molecules min.$^{-1}$ is

$$v = -n\frac{\mathrm{d}x}{\mathrm{d}t} = nk_e(x - x_e) \quad . \quad . \quad . \quad . \quad (5)$$

To develop eqn. (3) to give a theoretical expression for k_e of eqn. (5) we require [*]

(*a*) to formulate σ_p and σ_o by statistical mechanics;
(*b*) to formulate k_p and k_o by activated-complex theory.

Calculation of σ_p and σ_o.—The V.W. layer is considered as an ideal mobile (equilibrium) monolayer of H_2 molecules, on a surface of f sites/cm.^{2}, each site being able to hold one molecule (see Fowler and Guggenheim [7]). We formulate $f_{sp}(T)$, the partition function of a parahydrogen molecule on the surface, by treating the two-dimensional vibration on the site as a translation in a free area, a_f,[8]

$$f_{sp}(T) = \frac{2\pi mkT}{h^2}a_f j_{sp}(T)e^{\chi/kT} \quad . \quad . \quad . \quad . \quad (6)$$

m is the mass of the H_2 molecule to a good approximation and $j_{sp}(T)$ includes all other degrees of freedom; $j_{sp}(T)$ is essentially the partition function for the surface rotations

$$j_{sp}(T) = \sum_{j=0,\,2,\,4,\,\text{etc.}}^{s} (2j+1)e^{\frac{-j(j+1)h^2}{8\pi^2 IkT}} \quad . \quad . \quad . \quad (7)$$

For ortho H_2, $f_{so}(T)$ is identical with (6) except that $j_{sp}(T)$ is replaced by $j_{so}(T)$.

$$j_{so}(T) = 3\sum_{j=1,\,3,\,5,\,\text{etc.}}^{s} (2j+1)e^{\frac{-j(j+1)h^2}{8\pi^2 IkT}} \quad . \quad . \quad (8)$$

The usual partition function is used for the gas phase, in which $j_{gp}(T)$ and $j_{go}(T)$ are the rotational terms identical in form with eqn. (7) and (8), the sums $\sum^{g}$ being taken over the normal rotational states of the gas phase. It then follows from Fowler's treatment [7] that

$$\frac{\sigma_p}{1-\sigma_p} = b_p p_p \text{ and } \frac{\sigma_0}{1-\sigma_0} = b_0 p_0 \quad . \quad . \quad . \quad (9)$$

the Langmuir isotherms for the para and ortho forms, with

$$b_p = \frac{h}{kT}\cdot\frac{a_f}{(2\pi mkT)^{\frac{1}{2}}}\frac{j_{sp}(T)}{j_{gp}(T)}e^{\chi/kT} \quad . \quad . \quad . \quad (10)$$

and a similar eqn. for b_0.

In our calculation we simplify (9) by assuming $\sigma < 1$ and $\sigma_p = b_p p_p$ and $\sigma_0 = b_0 p_0$ (11). In experiments where the monolayer is concentrated, this simplification leads to an error discussed later.

Absolute Rate Constants k_p and k_o.—The exchange velocity constants between an H_2 molecule in the V.W. layer and a neighbourhood chemisorbed H atom may be expressed formally by activated-complex theory,[9] as

$$k_p = \frac{kT}{h}\,\frac{\phi^{*}}{\phi_H\phi_{sp}}e^{-\varepsilon_s/kT}, \quad k_0 = \frac{kT}{h}\,\frac{\phi^{*}}{\phi_H\phi_{so}}e^{-\varepsilon_s/kT} \quad . \quad . \quad (12)$$

---

[*] For previous work along this line, see the chapter on "Heterogeneous Processes," in ref. 9.

[7] Fowler and Guggenheim, *Statistical Thermodynamics* (Cambridge, 1939), p. 426.

[8] Kimball, *J. Chem. Physics*, 1938, **6**, 447.

[9] Glasstone, Laidler and Eyring, *The Theory of Rate Processes* (McGraw Hill, 1941).

The potential energy terms have been factorised from ϕ^{+}, ϕ_{sp}, ϕ_{H} and appear in the activation energy ϵ_s; ϕ^{+} refers to the activated complex of 3H atoms on the surface, ϕ_{H} to the chemisorbed H atom, and ϕ_{sp} and ϕ_{so} to pH$_2$ and oH$_2$ molecules respectively in the V.W. layer. We now assume that ϕ^{+}/ϕ_{H} is unity for our temperature range. This is in accordance with the strong bonding to be associated with chemisorption. It also implies a ratio of nuclear weights of 1.

Since $f_{sp} = \phi_{sp}e^{\chi/kT}$ and similarly for ϕ_{so}, we may derive from eqn. (6) expressions for ϕ_{sp}, ϕ_{so}, and obtain

$$k_p = \frac{kT}{h}\,\frac{h^2}{2\pi mkTa_f j_{sp}(T)}e^{-\epsilon_s/kT}, \quad k_0 = \frac{kT}{h}\,\frac{h^2}{2\pi mkTa_f j_{sp}(T)}\cdot e^{-\epsilon_s/kT} \qquad (13)$$

Evaluation of First-Order Constant k_e.—Eqn. (3) and (11) give

$$v = Afp\{k_p b_p x - k_0 b_0(1 - x)\} \quad . \quad . \quad . \quad (14)$$

when the partial pressures of para and ortho hydrogen are expressed as fractions of the total pressure p, viz. xp and $(1 - x)p$.

Substituting for k_p and k_0 from eqn. (13), and b_p and b_0 from eqn. (10)

$$v = Af\frac{p}{(2\pi mkT)^{\frac{1}{2}}}\cdot\frac{h^2}{(2\pi mkT)}\left\{\frac{x}{j_{gp}(T)} - \frac{(1 - x)}{j_{go}(T)}\right\}e^{\frac{\chi - \epsilon_s}{kT}} \quad . \quad (15)$$

Here $p/(2\pi mkT)^{\frac{1}{2}} = Z$, the collision number per cm.^{2}, and we write the equilibrium fraction of pH$_2$ as $x_e = j_{gp}(T)/j_{gp}(T) + j_{go}(T)$

$$v = AfZ\frac{h^2}{2\pi mkT}\left\{\frac{1}{j_{gp}(T)} + \frac{1}{j_{go}(T)}\right\}e^{\frac{\chi - \epsilon_s}{kT}}(x - x_e) \quad . \quad . \quad (16)$$

Hence from eqn. (5)

$$k_e = Af\frac{Z}{h}\,\frac{h^2}{2\pi mkT}\left\{\frac{1}{j_{gp}(T)} + \frac{1}{j_{go}(T)}\right\}e^{\frac{\chi - \epsilon_s}{kT}} \quad . \quad . \quad (17)$$

Experimental Activation Energy.—From eqn. (17)

$$E = RT^2\frac{d\ln k_e}{dT} = RT^2\left[\frac{d\ln f}{dT} + \frac{d\ln Z}{dT} - \frac{1}{T} + \frac{d}{dT}\ln\left\{\frac{1}{j_{gp}(T)} + \frac{1}{j_{go}(T)}\right\}\right] - N(\chi - \epsilon_s) \quad . \quad . \quad (18)$$

For a surface of uniform sites, $\frac{d\ln f}{dT} = 0$ and we may calculate $a(T)$ in the expression

$$E = a(T) - N(\chi - \epsilon_s) \quad . \quad . \quad . \quad . \quad (19)$$

The data are collected in Table I, only the first six rotational states making any appreciable contribution.

TABLE I.—CALCULATIONS OF THE B FACTOR

T° K.	$\frac{1}{j_{gp}(T)} + \frac{1}{j_{go}(T)}$.	$\frac{Z}{n}$, min.$^{-1}$.	$-a(T)$. cal.	B min,$^{-1}$
70	2·31	4·30 × 10^3	−10	27·5 × 10^2
100	1·59	5·14 ,,	143	7·2 ,,
130	1·32	5·86 ,,	216	4·6 ,,
173	1·10	6·76 ,,	275	3·5 ,,
223	0·90	7·68 ,,	325	2·7 ,,
273	0·76	8·50 ,,	365	2·3 ,,
293	0·71	8·80 ,,	379	2·0 ,,
373	0·57	9·93 ,,	439	1·5 ,,
473	0·46	11·19 ,,	559	1·1 ,,

Calculation of the B Factor.—From eqn. (1), (17) and (19).

$$B = Af\frac{Z}{n}\cdot\frac{h^2}{2\pi mkT}\cdot\left\{\frac{1}{j_{ep}(T)}+\frac{1}{j_{eo}(T)}\right\}e^{\frac{a(T)}{RT}} \quad . \quad . \quad (20)$$

In Table I we tabulate $Z/n(=(kT/2\pi mV^2)^{\frac{1}{2}})$ for our standard reaction volume of 300 cc., together with other necessary data. A, the standard catalyst area, is 1 cm.^{2}; f is taken as $1\cdot2 \times 10^{15}$, the mean value for the two relevant planes, 110 and 100, of tungsten.[10, 11] This value is close enough to be used also for the transition elements Pt, Pd, Ni, until we possess data on known oriented lattice planes. With these values B is calculated, and the result given in units of min.$^{-1}$

Experimental Data.

In Table II we give available values of B, all corrected to the standard experimental conditions of $V = 300$ cc., $A = 1$ cm.^{2} and $p = 20$ mm. Hg. The correction for pressure is needed since, while our theory for B assumes dilute monolayers and yields B independent of pressure, this condition rarely holds in practice. In correcting $B_{\text{expt.}}$ to 20 mm. press. wherever possible the pressure dependency in the same series of experiments is used. We have taken the geometrical area as A, whereas roughness factors up to 1·5 are possible for wires, so $B_{\text{expt.}}$ is an upper value.

TABLE II.—COMPARISON OF $B_{\text{expt.}}$ WITH $B_{\text{calc.}}$

Catalyst.	T° K.	E kcal.	$B_{\text{expt.}}$ min.$^{-1}$.	$B_{\text{calc.}}$ min.$^{-1}$.
W wire [1] . .	173	1·6	27	350
Pt wire [12] . .	415	6·4	110	130
Pd disc [13] . .	297	5·8	53	200
Ni tube [14] . .	373	7·6	31	150

The data for tungsten were specifically obtained for this purpose and are the mean of five concordant values, viz. $B = 27, 33, 21, 34, 22$ min.$^{-1}$; $E = 1\cdot9$, 1·9, 1·0, 1·2, 1·8 kcal./mole, obtained with two different wires. Nevertheless, in two further cases with the same apparatus, which we have excluded, markedly larger values were obtained, $B = 143$, $E = 2\cdot1$ and $B = 5440$, $E = 3\cdot1$. The other catalysts were examined under less rigorous conditions, and B and E values depended in the case of Pt, for example, on the method of activation. The values chosen are those in the present author's opinion most likely to correspond to the least contaminated wire surface. One is further inclined to attach some weight to these values since they may be used to calculate values of k_s on films of known area, which were the subject of quite independent experiments by A. and L. Farkas.[4] The results are given as $k_{\text{calc.}}/k_{\text{obs.}}$ for the following films, Ni, 0·25; Pt, 0·5; and Pd, 10.

The calculated values of B are greater than those observed by a factor 13 for tungsten, 5 for nickel and 4 for palladium, while for platinum the values are equal. We may quite reliably attribute a large part of this discrepancy to the assumption of a *dilute* V.W. monolayer. This assumption is not fulfilled for the data given, and in the next section we shall show how to derive an approximate correction factor.

Treatment of Concentrated Monolayers.

In most cases k_s is found to depend on the pressure to some fractional power.[15] The basis for this is that the monolayer is too concentrated for the relation

---

[10] Langmuir, *Physic. Rev.*, 1923, **22**, 374.

[11] Johnson, *ibid.*, 1938, **54**, 459.

[12] A. Farkas, *Trans. Faraday Soc.*, 1936, **32**, 922.

[13] A. Farkas, *ibid.*, 1936, **32**, 1667.

[14] Fajans, *Z. physik. Chem. B*, 1935, **28**, 239.

[15] A. Farkas, *Orthohydrogen, Parahydrogen and Heavy Hydrogen* (Cambridge, 1935), p. 98 et seq.

$\sigma = bp$ to hold, and if we employ the empirical Freundlich equation $\sigma \propto p^y$, then it follows that $k_e \propto p^{y-1}$. It is well known that short ranges of the Langmuir isotherm, eqn. (9), are approximately fitted by the Freundlich equation, y varying from 1 to 0 as the monolayer becomes more concentrated. Our procedure is to calculate a number of theoretical Langmuir isotherms for the V.W. layer of hydrogen molecules, to determine the value of σ corresponding to a given experimental value of y, and hence to determine the error involved in replacing $\sigma/1 - \sigma$, by σ, i.e. in approximating eqn. (9) by eqn. (11).

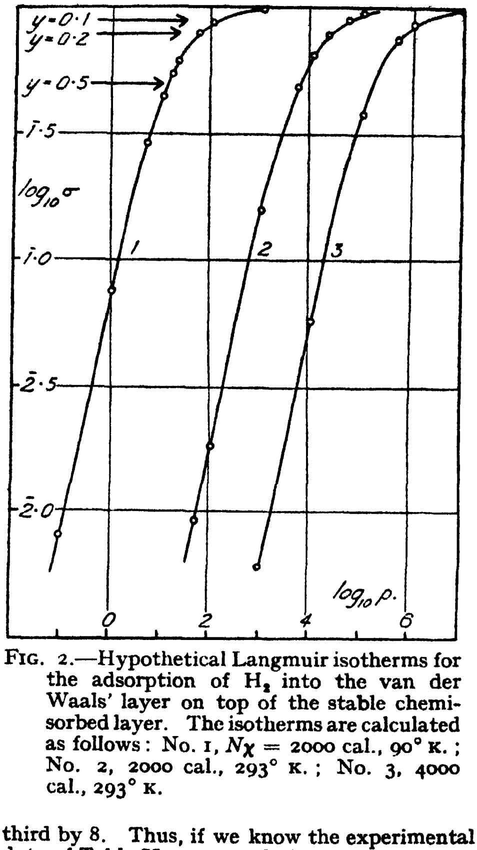

FIG. 2.—Hypothetical Langmuir isotherms for the adsorption of H_2 into the van der Waals' layer on top of the stable chemisorbed layer. The isotherms are calculated as follows: No. 1, $N\chi$ = 2000 cal., 90° K.; No. 2, 2000 cal., 293° K.; No. 3, 4000 cal., 293° K.

Fig. 2 shows three typica Langmuir isotherms, as a plot of $\log_{10} \sigma$ against $\log_{10} p$, calculated from eqn. (9) using a theoretical b value, eqn. (10), in which we assume $j_s(T) = j_g(T)$ and $a_f = 8 \times 10^{-16}$ cm.^{2}. Two values of $N\chi$ are taken, covering the values we might expect for the V.W. adsorption of hydrogen. The resultant curves thus bracket a wide range of b values. (Our argument is independent of the precise values taken of the parameters.)

y in the Freundlich isotherm is the slope, d log σ/d log p. The diagram shows that $y = 0{\cdot}5$ corresponds to $\sigma = 0{\cdot}5$, $y = 0{\cdot}2$ to $\sigma = 0{\cdot}8$, and $y = 0{\cdot}1$ to $\sigma = 0{\cdot}89$. The effect of calculating from $\sigma = bp$ in place of the proper equation $\sigma/1 - \sigma = bp$ is to give *too high* a value of σ, and hence $B_{\text{calc.}}$ in the first case by a factor 2 (0·5/0·5 instead of 0·5), in the second by 4, in the third by 8. Thus, if we know the experimental values of y corresponding to the data of Table II, we may derive a rough correction factor as above, by which we divide the value of $B_{\text{calc.}}$* The results are given in Table IV. It was necessary for the case of Pt and Pd to take data on these metals from other workers, Bonhœffer and Farkas [16] and Wagner and Hauffe,[17] respectively.

TABLE III.—CALCULATION OF THEORETICAL ISOTHERM

Curve No.	$N\chi$, cal.	T° K.	b, mm. Hg^{-1}.
1	2000	90	$8{\cdot}15 \times 10^{-2}$
2	2000	293	$6{\cdot}08 \times 10^{-6}$
3	4000	293	$1{\cdot}88 \times 10^{-4}$

The calculated values for platinum still agree well and the discrepancy for the other metals is only about a factor 3, which we may regard as a generally satisfactory result.

---

* Dr. F. C. Frank has pointed out to me that where the two isotherms approximate to each other they have the same value of d log σ/dp. Application of this condition to the equations for the two isotherms leads directly to the general result, $y = 1 - \sigma$. The correction factor, as listed in the Table, is then $1/y$.

[16] Bonhœffer and Farkas, *Z. physik. Chem. B*, 1931, **12**, 231.

[17] Wagner and Hauffe, *Z. Elektrochem.*, 1939, **45**, 409.

TABLE IV.—CORRECTION FACTOR FOR CONCENTRATED MONOLAYER

Catalyst.	y.	Correction Factor.	$B_{calc.}$	$B_{expt.}$
W wire . .	0·5-0·12 [1]	2-8	170-40	27
Pt wire . .	0·67 [16]	1·5	90	110
Pd disc . .	0·5 [17]	2	100	53
Ni tube . .	0·61 [14]	1·5	100	31

Departure from Uniformity and Ideality of the V.W. Monolayer. In spite of its success we may show that our calculation has not taken every factor into account. We may suppose that effects arise (*a*) from some variations in activity over the catalyst surface. We may expect in tungsten that both 110 and 100 planes are developed in the surface. There is reason to believe [18] that these planes may differ in catalytic activity. (*b*) A repulsive potential between hydrogen molecules in the V.W. layer.

Both these factors may be expected to make the adsorption isotherm deviate from the true Langmuir form towards a Freundlich isotherm holding over a wide pressure range with a constant value of the exponent y (in $\sigma \propto p^y$). The scanty data available show that the relation $k_e \propto p^{y-1}$, and therefore its precursor $\sigma \propto p^y$, holds over a much wider pressure range than we should expect from inspecting Fig. 2. This figure shows that $\sigma \propto p^y$ with a given y value cannot hope to approximate the Langmuir equation for a pressure alteration of more than a factor 5. For the Ni tube [14] $y = 0{\cdot}61$ held accurately for a 1200-fold change in pressure. For the W wire catalyst [1] we found in one case $y = 0{\cdot}44$ held over a 170-fold change of pressure.

While it may be supposed that non-uniformity contributes a part of this effect, it is clear that non-ideality, due to neighbour interactions, is also important. Wang [19] has shown how this kind of isotherm deviates from that of Langmuir. His curve *c*, Fig. 2, p. 137, fits $\sigma \propto p^{0.33}$ over a 40-fold range of p. Neighbour interactions in the chemisorbed layer are quite appreciable, but may be neglected since they remain unchanged during the reaction. They need consideration when a mixed chemisorbed layer of hydrogen and, say, oxygen is present.[1] Non-uniformity of surface, when marked, is shown in the next section to give abnormal values of B.

Abnormal B Factors.—Table V gives data on B factors higher and lower than those previously described.

TABLE V.—ABNORMAL B FACTORS

Catalyst.	$T°$ K.	E, kcal.	B, min.$^{-1}$	ΔE, kcal.	$RT \ln \frac{B}{B_n}$ kcal.
W wire [1] .	173	2·1	2×10^2	0·5	0·7
W wire [1] .	173	3·1	$8{\cdot}3 \times 10^3$	1·5	2·0
W wire [20] .	173	3·8	4×10^4	2·2	2·5
Pt wire [16] .	373	14·5	$1{\cdot}7 \times 10^9$	8·1	12·3
Pyrex glass [21] .	573	10·7	$2{\cdot}7 \times 10^{-3}$	—	—
Pyrex glass .	658	10·7	$1{\cdot}5 \times 10^{-3}$	—	—

The abnormally low values on Pyrex glass are obviously interpreted on the picture of a completely inactive silicate surface in which are distributed small active areas, probably small islands of metal of colloidal dimensions or even single metal ions. The right-hand side of eqn. (20) then requires multiplication by a constant factor, the ratio of active to total surface area.

---

[18] Beeck, Smith, and Wheeler, *Proc. Roy. Soc. A*, 1940, **177**, 62.

[19] Wang, *ibid.*, 1937, **161**, 127.

[20] A. Farkas, *Z. physik. Chem. B*, 1931, **14**, 371.

[21] Clough and Eley (unpublished results).

In considering the high values of B we first refer to eqn. (12). In developing this equation we assumed $\phi^{\ddagger} = \phi_H$. If, in forming the active triatomic complex, the bond to the metal surface was very much weakened, we should have $\phi^{\ddagger} > \phi_H$ and the factor $\phi^{\ddagger}/\phi_H$ would appear in the right hand side of eqn. (17) for k_s and eqn. (20) for B. But it is impossible that $\phi^{\ddagger} > \phi_H$ should reach a value of $1{\cdot}6 \times 10^7$, which is the ratio of B/B_n in the Pt case above. Here B_n is the normal value of B, and E_n is the normal value of E, as listed in Table II for the metal concerned. In such cases we must consider the effect of a surface made up of sites of varying activation energy, or more precisely, varying $\chi - \epsilon_s$.

Such a problem would be rigorously attacked by replacing the single term on the right-hand side of eqn. (17) by a sum or integral over a number of sites of different $\chi - \epsilon_s$, along lines previously laid down (cf. Constable,[22] Schwab,[23] and Eyring [24]). Referring to eqn. (18) for E, a *rough* formulation results by considering the main part of the difference ΔE between E and E_n, to be due to the term $RT^2 \mathrm{d} \ln f/\mathrm{d}T$, which gives the increase with temperature of the number of centres on which the conversion is taking place. As we see from eqn. (20) for B, this same term will give the difference $RT \ln B/B_n$, and so we should expect this term to equal ΔE. Table V shows that this is only approximately true, ΔE in all cases being rather smaller than $RT \ln B/B_n$. Other mechanisms might also lead to such an approximate compensation of E and $RT \ln B$, but we consider this the most likely one. A more rigorous treatment will be given when further data become available.

The Gap Hypothesis of Catalysis.—While the general picture of interaction between a van der Waal's layer and a chemisorbed layer seems satisfactory, the details remain to be settled. One such mechanism may be called the gap hypothesis. Roberts [3] showed that the irreversible dissociative adsorption of a diatomic gas to give an immobile atomic monolayer would necessarily result in 8 % of unoccupied sites. Rideal [25] has suggested an elegant mechanism for the parahydrogen and other hydrogen exchange reactions, in which it is supposed that a hydrogen molecule adsorbed on the gap can undergo a valency switch.

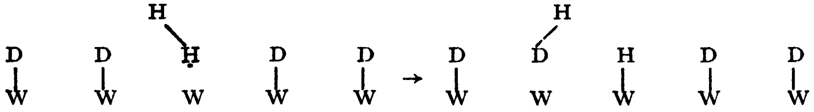

The formation of the new H—W bond may be expected to overcome the reaction inertia and result in a low activation energy. If we assume this mechanism, then we require to multiply our calculated B values by 0·08, making them now 3 to 10 times less than those observed. This difference is not sufficient to decide the mechanism on a comparison of observed and calculated B values.

At first sight a main objection to the gap mechanism, as noted by Rideal and Herington,[26] is that the conversion mechanism would cause the gaps to move about the surface, and as two became neighbours they would be immediately filled by dissociative adsorption of an H_2 molecule. In this way the gaps would disappear and the reaction become self-poisoned. However, on the simplest view the initial ratio of the conversion to the poisoning rate would be $1/(0{\cdot}08)^2$, i.e. 156. At half-activity of the surface it would be $1/(0{\cdot}04)^2 = 625$. We must further allow for a repulsive potential of 1400 cal./mole between neighbouring H atoms,[3] which will act as a repulsive potential between the gaps. The ratios are now $156e^{1400/RT}$ and $625e^{1400/RT}$, i.e. at 173° K., 8900 and 35,600. We did not detect such a self-poisoning in experiments on tungsten,[1] but the ratio is so large that the effect might escape detection in any but specially designed experiments. Some relevant data are recorded for Fe[27] and charcoal,[28] where the adsorption of H_2 at high temperatures has been stated to poison the conversion at low temperatures (80° K.). In these cases we are undecided how far the paramagnetic method of conversion enters the picture. It is unlikely for Fe (cf. results of A. Farkas [29]), and while at one time it was considered the dominant mechanism on charcoal at 80° K., recent evidence suggests an exchange mechanism may even enter here.[30]

---

[22] Constable, *Proc. Roy. Soc. A*, 1925, **108**, 355.

[23] Cremer and Schwab, *Z. physik. Chem. A*, 1929, **144**, 243.

[24] Ref. 9, p. 394.

[25] Rideal, *Proc. Camb. Phil. Soc.*, 1938, **35**, 130.

[26] Herington and Rideal, *Trans. Faraday Soc.*, 1944, **40**, 505.

[27] Emmet and Harkness, *J. Amer. Chem. Soc.*, 1935, **57**, 1624.

[28] Burstein and Kashtanov, *Trans. Faraday Soc.*, 1936, **32**, 823.

Experiments are planned in which a chemisorbed layer of hydrogen is treated with carbon monoxide, or alternatively atomic hydrogen. These gases are expected to adsorb on single sites and fill up any gaps, and so the presence or absence of poisoning by CO or H will furnish a critical test of the gap mechanism. So far the only experimental evidence in favour of the gap mechanism has been adduced by Rideal and Herington [28] on the basis of the author's poisoning curve for oxygen.[1]

A mechanism not involving gaps is that sketched below, in which a triangular activated complex of 3H atoms is formed, which may rotate to give an exchange of atoms.

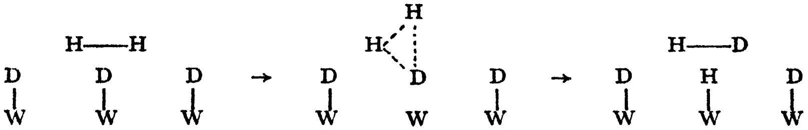

Free rotation of the complex need not be assumed, so we do not depart from the assumption $\phi^{+}/\phi_{H} = 1$. While London [31] has shown that in the gas phase exchange forces prohibit the triangular transition complex, it is possible that the metal surface might modify this condition, perhaps along lines mentioned in the concluding section.

Conclusion.

In the gas phase the conversion proceeds through

$$H + pH_2 \rightarrow oH_2 + H,$$

a reaction with an activation energy of 5-7 kcal. and a steric factor of 0·1.[32] It is now apparent that the catalysed reaction is in no wise very different, either in nature or in E and steric factor. The main inertia in the gas phase is the provision of H atoms requiring, as it does, an E of 51 kcal./g. atom and thus a temperature of 900° K. A tungsten surface will provide H atoms of similar activity at room or even liquid-air temperature. The central problem then consists in reconciling the known strength of the W—H bond of 74 kcal. with the reactivity of the hydrogen in this and other similar reactions. No hydrocarbon or non-metallic compound is definitely known at present to show such a vigorous exchange reaction, although a chance observation of Farkas and Sachsse [33] suggests a thin film of non-volatile boron hydride may have some activity. It seems, however, clear that organic or metallo-organic bodies *will* act as catalysts for hydrogen gas, since there are bacterial enzymes which are effective in this way.[34]

We may note two factors which, present at a metal surface, may be expected to lower the activation energy for the exchange of atoms below that for, say, a hydrocarbon.

(1) In the methods of London and Eyring and Polanyi, the powerful coulombic potential of the positive cores may be expected to have a general effect in lowering energy barriers.[35]

(2) The possibility of numerous resonance structures for the transition metal —H_2 complex, which by depressing the energy of the activated complex will lower the activation energy. This notion was suggested in connection with

---

[29] A. Farkas, *Trans. Faraday Soc.*, 1936, **32**, 416.

[30] Burstein, *Acta Physicochim.*, 1938, **8**, 857.

[31] London, *Probleme der modernen Physik.* (Sommerfeld Festschrift), 1928, p. 104; *Z. Elektrochem.*, 1929, **35**, 552.

[32] Ref. 15, p. 68.

[33] Farkas and Sachsse, *Trans. Faraday Soc.*, 1934, **30**, 331.

[34] Cavanagh, Horiuti and Polanyi, *Nature*, 1934, **133**, 797. A. Farkas, *Trans. Faraday Soc.*, 1936, **32**, 929.

[35] cf. Stearn, *Ergeb. Enzymforsch*, 1938, **7**, 1.

surface catalysis by Polanyi[36] and a calculation made by Evans and Warhurst[37] for the Diels reaction.

How far factors such as these are responsible for the activity of chemisorbed hydrogen remains the central problem for further investigation.

Summary.

A theoretical calculation is given of the " temperature-independent " factor for the exchange of atoms between a hydrogen molecule in a van der Waals' layer and a hydrogen atom in an adjacent position in the underlying stable chemisorbed layer on the metal, for the case of a dilute van der Waals' layer. It is shown how to apply a correction factor for the case of concentrated layers. The results so obtained agree within a factor of about 3 with data for the catalysts tungsten, nickel, platinum and palladium.

A discussion is given of the effects of non-uniformity of the surface and non-ideality of the monolayer, and also of " abnormal " values of the temperature-independent factor. Some tentative conclusions are drawn about the detailed nature of the interaction between the two adsorbed layers.

Department of Chemistry,
University of Bristol,
Bristol, 8.

[36] Polanyi, *Sci. J. Roy. Coll. of Sci.* (Lond.), 1937, **7**, 21.
[37] Evans and Warhurst, *Trans. Faraday Soc.*, 1938, **34**, 614.

A NEW METHOD FOR THE RAPID TITRIMETRIC ANALYSIS OF SODIUM ALKYL SULPHATES AND RELATED COMPOUNDS.

By S. R. Epton.

Received 29th January, 1947.

The investigation of important physico-chemical properties of dilute solutions of surface active substances such as sorption at solid interfaces, rate of migration across boundaries and diffusion phenomena would be facilitated if a rapid, accurate and flexible method of analysing these solutions were available. Although some twenty methods are to be found in the literature, no single method combines these three virtues.

The purpose of this paper is to describe a new method of analysis which possesses these desirable characteristics to a useful extent since it can be used for the titrimetric estimation of an extremely wide variety of surface active materials of organic sulphate and sulphonate classes.

Principle of the Method.—Jones[1] has shown that whereas the chloride of methylene blue is insoluble in chloroform, the alkyl sulphates and related salts are freely soluble and may be quantitatively extracted by chloroform from aqueous solution provided that the chain length of the organic part exceeds a certain value. (This fact was used as the basis of a colorimetric method of estimation.) Jones also found that extraction is inhibited if the aqueous solution contains a quantity of cation-active material more than equivalent to the anion-active material present. These observations provide a basis for determining the end-point of a titration of an anion-active material with a cation-active material.

If a dilute solution of the anion-active material containing a small quantity of acid methylene blue is shaken with chloroform, the blue colour is concentrated in the chloroform layer. If then a solution of cetyl pyridinium bromide is added slowly, the distribution of the colour is not at first altered but as the quantity nears equivalence a fairly rapid transfer of colour from the lower to the upper layer occurs. Eventually the two layers have the same colour; this is found to be the equivalence point. On further addition of cetyl pyridinium bromide the lower layer lightens in shade and finally becomes colourless. This process has been standardised in an easily usable form (see below) and applied to a wide range of materials.

---

[1] Jones, *J. Assoc. Official Agr. Chem.*, 1945, **28**, 398 ; *Chem. Abstr.*, 1945, **39**, 3951.

Experimental.

Materials

Cetyl Pyridinium Bromide.—This was obtained in a relatively pure form by recrystallising a sample of Fixanol C (*ex* Messrs. I.C.I. (Dyestuffs) Ltd.), twice from methyl ethyl ketone and once from acetone.

Methylene Blue.—A sample of B.P. quality containing about 85 % of pure dyestuff was employed.

Anion-active Materials.—The samples of pure sodium alkyl sulphates were kindly supplied by Dr. P. A. Winsor and Mr. L. N. Goldsbrough; an account of the preparation and purification of these substances is being prepared. The sodium secondary alkyl sulphates of varying chain-length range were obtained by sulphation of olefins formed by the cracking of petroleum waxes.

Procedure.—10 cc. of an approximately 0·005 M. solution of the anion-active material is pipetted into a 250 cc. stoppered reagent bottle. To this is added 25 cc. of solution containing 0·003 % Methylene Blue (B.P. quality), 1·2 % sulphuric acid, 5·0 % sodium sulphate (anhydrous), followed by 15 cc. chloroform. The bottle is shaken with just sufficient force to ensure that the phases mix thoroughly. At this stage the upper layer is a pale blue and the lower dark blue. A solution of cetyl pyridinium bromide containing about 2 g./l. of purified material is added about 2 cc. at a time with intermittent shaking. When the colour of the upper layer begins to deepen the rate of addition is reduced. The end-point is reached when both layers, viewed in reflected light, are the same colour.

The molar concentration of the cetyl pyridinium bromide solution is determined in the following manner. 50 cc. of the solution are pipetted into a beaker. 25 cc. of a 0·01 M. potassium dichromate solution is added. Insoluble cetyl pyridinium dichromate is precipitated. The beaker is heated to 90° C. to coagulate the precipitate and the liquid is then filtered through a No. 40 Whatman filter paper. The excess dichromate in the filtrate is estimated iodometrically.

Discussion.

Nature of the End-point.—The end-point was proved to be stoichiometric by the following procedure. A cetyl pyridinium bromide solution was standardised in two ways, against potassium dichromate and against a solution of pure sodium tetradecan-2-sulphate,

$$CH_3 \,.\, (CH_2)_{11} \,.\, CH(O \,.\, SO_3Na) \,.\, CH_3,$$

using the new method. By the first method its concentration was found to be 0·003845 M. by the second 0·00383 M.

Scope.—Substances with three kinds of polar group have been investigated namely sulphate, sulphonate and carboxylate. All substances of the first two classes, provided that the organic part of the molecule is sufficiently large, give satisfactory end-points, and the analyses agree well with those found by other methods. Carboxylates do not give an end-point, and their presence does not affect the titration of members of the first two classes. Satisfactory end-points can be obtained with sodium alkyl sulphates provided that the chain length is greater than six carbon atoms, but low results are obtained when it is shorter than eight (see Table I). Sodium benzene sulphonate and xylene sulphonates do not give end-points. The method has been applied with success to mixtures of sodium secondary alkyl sulphates made by sulphation of olefin mixtures of varying mean chain length. The results are shown in Table I.

The effect of the position of the polar group with respect to the hydrocarbon chain has been investigated by analysing solutions of six of the seven isomeric sodium tetradecan-sulphates and of three of the four octan-sulphates. It can be seen from Table I that the deviation of the results from those obtained by other methods is small. There is no systematic variation with change of position.

TABLE I.—PURITY OF VARIOUS ALKYL SULPHATES DETERMINED BY NEW TITRIMETRIC METHOD AND BY OTHER METHODS.

Substance	Titrimetric Method, % Purity	Independent Method, % Purity
Sodium hexan-1-sulphate	75·1	100·0 (*x*)
Sodium octan-1-sulphate	99·5	100 (*x*)
Sodium octan-2-sulphate	97·2	97·5 (*x*)
Sodium octan-4-sulphate	37·2	38·0 (*y*)
Sodium decan-2-sulphate	97·2	95·5 (*x*)
Sodium tetradecan-1-sulphate . . .	100	100·0 (*x*)
Sodium tetradecan-2-sulphate . . .	99·6	100·0 (*x*)
Sodium tetradecan-3-sulphate . . .	21·0	20·7 (*z*)
Sodium tetradecan-4-sulphate . . .	32·4	32·4 (*z*)
Sodium tetradecan-6-sulphate . . .	23·5	22·6 (*y*)
Sodium tetradecan-7-sulphate . . .	24·7	24·0 (*z*)
Sodium secondary alkyl sulphates—		
C_{10} fraction	22·0	22·9 (*y*)
C_{12}	20·45	20·0 (*y*)
C_{18}	99·1	100·0 (*x*)
C_{10}-C_{18}	96·4	96·4 (*x*)
C_{13}-C_{18}	12·4	12·7 (*y*)

x determined from sulphated ash after removal of free sodium sulphate if any.

y determined from total dry matter after removal of free sodium sulphate if any.

z determined from tensimetric or bubble-pressure method.

The concentration of the solution for most satisfactory results is found to be between 0·003 and 0·008 M. At higher concentrations the chloroform-water emulsions become too stable. The effect of continually reducing the concentration of both solutions in the titration is shown in Table II.

TABLE II.—EFFECT OF DILUTION ON THE TITRATION OF SODIUM SECONDARY ALKYL SULPHATE (C_{10}-C_{18} RANGE) SOLUTION.

Concn. of Alkyl Sulphate (M.)	Concn. of Cetyl Pyridinium Bromide (M.)	% Original Titre
0·00478	0·00464	100
0·00239	0·00232	99·1
0·001195	0·00116	98·2
0·000597	0·000580	92·4
0·000478	0·000464	90·3

Over a tenfold dilution there is a decrease of 10% in the titre. With certain exceptions the common inorganic anions and low molecular weight organic anions in reasonable concentration do not interfere. The exceptions are picrate, chromate and perchlorate.

Precision.—The behaviour of the method in the hands of relatively unskilled and inexperienced analysts has also been examined. Forty-six pairs of titrations were carried out, both titrations in each pair being performed by the same analyst. Although the average titre was about 10 cc. only seven pairs differed by more than 0·05 cc. A repeatability for the titration of about 0·5 % was, therefore, attained. The solutions analysed contained sodium secondary alkyl sulphates of mean chain length C_{14} and chain length range C_{10}-C_{18}. The reproducibility among four different analysts is epitomised in Table III.

TABLE III.—ACCURACY AND PRECISION OF ANALYSES GIVEN BY THE METHYLENE-BLUE-FIXANOL METHOD.

Maximum spread between two results for the same sample = 5·2 %
Mean deviation from the mean for all analyses = 0·87 %
" " " " Analyst A = 0·57 %
" " " " " B = 0·97 %
" " " " " C = 0·91 %
" " " " " D = 0·77 %

Analysis of Water-insoluble Surface Active Materials.—A class of surface active material known as the sodium "petroleum" sulphonates or naphtha sulphonates of high molecular weight are obtained in the sulphuric acid and oleum refining of white oils (e.g. medicinal oil). These are often insoluble in water in which case they cannot be analysed by the procedure outlined above. The method can be successfully applied to them, however, if they are dissolved in chloroform to form a solution of known weight concentration. An aliquot (10 cc.) of this solution is pipetted into the titration bottle; the titration is then proceeded with as before. The end-point is much sharper in this case than when lower molecular weight materials are analysed.

Discussion.—Three methods of rapid analysis of surface active materials described in the literature have received fairly wide attention. These are the benzidine hydrochloride method,[2] the Hartley-Runnicles method[3] and the tensimetric or bubble-pressure method.[4] The benzidine hydrochloride method depends on the insolubility in water of the benzidine salt of the alkyl sulphate. The lower limit of chain length of the organic portion of the molecule before the salt becomes too soluble has been found in this laboratory to be about 10 or 11 carbon atoms. It is claimed in the literature that analyses reproducible to ± 0·3 % are obtainable with the method.[2] This has not been realised here, difficulty having been found in obtaining reproducibility of ± 2 % without the introduction of stringent and time-consuming refinements of procedure.

The Hartley-Runnicles technique relies on the insolubility of the cetyl pyridinium or cetyl trimethyl ammonium salt of the alkyl sulphate; these are appreciably soluble up to a chain length of 10 carbon atoms. Moreover, the end-point depends upon recognising the point of most rapid colour change between a purple and blue form of the indicator. This requires the utmost skill in its detection if an accuracy of ± 1·0 % is required.

The tensimetric or bubble-pressure method gives an extremely sharp end-point but the utility of the method is restricted by its sensitivity to the presence of inorganic salts. It has also been observed in this laboratory that under these conditions the position of the end-point is affected by temperature. It appears from the results above that the new method seems to possess a wider applicability than those described above. It will operate both at chain lengths as short as eight, and at chain lengths so long that the resulting sodium salt is water-insoluble. The end-point, easily recognised by inexperienced personnel, is unaffected by the presence of large quantities of inorganic salts, or by variations in temperature. The reproducibility is of the order of 0·7 %.

---

[2] Kling and Puschel, *Melliand Textilber.*, 1934, 18, 21.

[3] Hartley and Runnicles, *Proc. Roy. Soc. A*, 1938, 168, 424.

[4] Preston, *J. Soc. Dyers Col.*, 1945, 61, 165.

The author wishes to thank Messrs. Shell Refining and Marketing Co. Ltd., for permission to publish this paper, and Dr. P. J. Garner and Mr. S. L. Levy for valable advice and suggestions.

Summary.

1. A titrimetric method for the analysis of dilute solutions of surface active materials of the organic sulphate and sulphonate class is described. The method is based on the use of a two-phase indicator for the end-point of a titration with cetyl pyridinium bromide.

2. The method determines with accuracy the concentration of alkyl sulphate solutions the chain length of which is from eight carbon atoms upwards. Water-insoluble sulphonates of very high molecular weight may also be analysed.

3. The accuracy is unaffected by the position of the polar group in the surface active anion, by the presence of common inorganic salts or by change of temperature.

4. Results are reproducible to ± 0·5 to ± 1·0 %.

5. The performance of the method is compared with that of others and is found to be superior to them in nearly all respects.

Note added in Proof.—Two methods similar in principle to the above though differing widely in practical details have recently been published by Barr, Oliver and Stubbings (*J. Soc. Chem. Ind.*, 1948, **67**, 45). One of the methods is claimed to have some advantages over that described above. Work in these laboratories has not been able to substantiate the claim. Details of these results will be published later.

THE STANDARD FREE ENERGIES OF FORMATION OF GASEOUS ORGANIC COMPOUNDS: A GROUP METHOD OF SUMMATION.

By J. G. M. Bremner and G. D. Thomas.

Received 7th February, 1947.

In catalytic work it is important to know the magnitude of the free energy changes involved in the reactions under examination so that the optimum conditions of temperature and pressure may be fixed at the beginning of the experimental work. In the past decade the Bureau of Standards in America has published comprehensive thermodynamic data for the hydrocarbon series and with this exception, reliable data on organic compounds are rare. Because of this lack of data attempts have been made to develop general equations and to define rules as a guide in deriving the standard free energies of formation of organic compounds. These attempts are intended to cover compounds for which data do not exist or to give standard free energies at temperatures not examined experimentally.

Parks and Huffman,[1] Francis,[2] and Egloff[3] have derived equations for the calculation of standard free energies but these either fail to take into account differences between isomers or refer only to one temperature, namely 298·1° K. Bruins and Czarnecki[4] assigned standard free energies of formation to various atomic linkages but found that branched chain hydrocarbons "often defy simple interpretations." Andersen, Beyer and Watson[5] have described a comprehensive group contribution method. It is, however, somewhat tedious particularly where standard free energies are required at more than one temperature.

---

[1] Parks and Huffman, *Free Energies of Some Organic Compounds* (Chemical Catalog Co., 1932).

[2] Francis, *Ind. Eng. Chem.*, 1928, **20**, 277.

[3] Egloff, *ibid.*, 1937, **29**, 1260.

To take into account the effects of chain branching and the differences between isomers we decided to assign standard free energy values to characteristic groups rather than bonds. Thus all saturated aliphatic hydrocarbons, higher than methane, may be regarded as built up from the following four groups:

$$CH_3— \qquad —CH_2— \qquad {>}CH— \qquad —\overset{|}{\underset{|}{C}}—$$

The standard free energy of formation of a compound is then obtained by summing the contributions of the characteristic groups. By assigning group values for temperatures of 300°, 600°, 800° and 1000° K. the derivation of standard free energies at other than room temperature may rapidly be carried out. The group values are given to the nearest 0·5 kcal. The standard free energies of formation given in this paper refer to the ideal gaseous state at 1 atm. pressure.

This method as applied to the aliphatic series naturally does not take directly into account the varying contributions to the entropy due to restriction in internal rotation and differences in the symmetry number of the compound concerned. For cyclic compounds it is necessary to allow for these varying contributions.

A. Aliphatic Compounds.

1. The Standard Free Energies of Formation of the Paraffins.

In the paraffin series free energy contributions were assigned to the methyl ($—CH_3$), methene ($>CH_2$) and methine ($—{>}CH$) groups and to quaternary carbon ($>C<$). The group values, derived from Rossini's[6] results, are given in Table I. The standard free energies of formation obtained by summing the group values of Table I are compared with the Rossini figures in Table II. The agreement is reasonably good.

TABLE I.—STANDARD FREE ENERGY OF FORMATION ($\Delta G°$) OF GROUPS IN THE GASEOUS PARAFFINS (kcal.)

Group	300°	600°	800°	1,000° K.
$—CH_3$	−4	2·5	7·5	12·5
$—CH_2—$	2	9·5	14·5	19·5
$—CH—$	7·5	16	21·5	27
$—\overset{|}{\underset{|}{C}}—$	13	24	30·5	37·5

2. The Standard Free Energies of Formation of the Olefins.

To calculate the standard free energies of formation of the olefins the additional group values given in Table III are required. They are derived from Rossini's[7] figures. A comparison is made between the group values and those of Rossini in Table IV.

---

[4] Bruins and Czarnecki, *Ind. Eng. Chem.*, 1941, **33**, 201.

[5] Andersen, Beyer and Watson, *Natl. Petr. News*, 1944, **36**, R. 476.

[6] Rossini, *Bur. Stand. J. Res.*, 1945, **34**, 406.

TABLE II.—COMPARISON OF GROUP WITH EXPERIMENTAL STANDARD FREE ENERGIES.

Paraffin	Source	300°	600°	800°	1000° K.
Butane	Group	−4	24	44	64
	Exptl.	−3·6	24·6	44·5	64·7
Octane	Group	4	62	102	142
	Exptl.	4·5	62·0	102·2	142·8
Eicosane . . .	Group	28	176	276	376
	Exptl.	28·7	175·2	276	377·7
2-Methyl propane . .	Group	−4·5	23·5	44	64·5
	Exptl.	−4·1	25·2	45·8	66·8
3-Methyl pentane . .	Group	−0·5	42·5	73	103·5
	Exptl.	0·0	43·5	73·9	104·5
2 : 2-Dimethyl hexane .	Group	3	62·5	104	146
	Exptl.	2·9	62·7	104·3	146·3
2-Methyl-3-ethyl pentane .	Group	3	61	102	143
	Exptl.	5·4	64·5	105·5	147·1
2 : 2 : 3-Trimethyl butane	Group	0·5	52·5	89·5	127
	Exptl.	1·1	53·9	90·7	127·7
2 : 2 : 4-Trimethyl pentane	Group	2·5	62	104	146·5
	Exptl.	3·5	63·7	105·6	147·7

3. The Standard Free Energies of Formation of the Alcohols.

In this class of compounds the lack of adequate thermodynamic data begins to make itself felt. There are, however, sufficient data to arrive at satisfactory values for the standard free energy of the hydroxyl group over the desired range of temperature.

TABLE III.—STANDARD FREE ENERGY OF FORMATION OF GROUPS IN THE OLEFIN SERIES.

Group	300°	600°	800°	1000° K.
—CH = CH_2 . .	19	23	26·5	30·5
—CH=CH— (*cis*) .	24	29·5	33	37·5
—CH=CH— (*trans*) .	23·5	28·5	32	36
>C=CH— (*cis*) .	26·5	33·5	37·5	42
>C=CH— (*trans*) .	26·5	33	37	41
>C=CH_2 . . .	22	28	31·5	35·5
>C=C< . . .	32·5	41	46·5	51·5

The standard free energy of formation of gaseous ethyl alcohol has been calculated in three ways:

(i) using the third law,
(ii) from experimental equilibrium data for the hydration of ethylene,
(iii) from calculated equilibrium data for the hydration of ethylene.

In (i) Rossini's[8] value for the heat of combustion was taken together with Parks and Huffman's[1] values for the entropy and heat capacity.

[7] Rossini, *Bur. Stand. J. Res.*, 1946, **36**, 269.
[8] Rossini, *ibid.*, 1932, **8**, 119.

From these data the formal standard free energy equation for ethyl alcohol was derived:

$$\Delta G^\circ = -51{,}220 + 21{\cdot}55\, T \ln T - 0{\cdot}0114\, T^2 - 82{\cdot}95\, T.$$

In (ii) Bliss and Dodge's [9] standard free energy values for the hydration of ethylene in conjunction with Thacker's [10] values for ethylene and water gave the standard free energy of formation of ethyl alcohol.

TABLE IV.—COMPARISON OF GROUP WITH EXPERIMENTAL STANDARD FREE ENERGIES.

Olefin.	Source.	300°.	600°.	800°.	1000° K.
Buten-1	Group	17	35	48·5	62·5
	Exptl.	17·2	35·9	49·1	62·5
Nonadecene-1 . . .	Group	47	177·5	266	355
	Exptl.	47·4	176·6	265·6	355·4
cis-Hexene-3 . . .	Group	20	53·5	77	101·5
	Exptl.	19·7	53·7	77·7	102·1
2 : 3-Dimethyl buten-1 .	Group	17·5	51·5	75·5	100
	Exptl.	17·4	52·0	76·0	100·4
3-Methyl *cis*-pentene-3 .	Group	16·5	50·5	74·5	99
	Exptl.	17	51·1	75·1	99·4
2-Methyl *trans*-pentene-3 .	Group	19	52	76	100·5
	Exptl.	17·8	52·2	76·2	100·7
2 : 3-Dimethyl buten-2 .	Group	16·5	51	76·5	101·5
	Exptl.	16·5	51·8	76·6	101·8

In (iii), Aston's [11] calculated standard free energy changes for the hydration of ethylene were used in deriving the standard free energy of formation of ethanol.

The combination of the standard free energy values of ethyl alcohol with the group values of Table I gave the standard free energies of the hydroxyl group, Table V.

TABLE V.—STANDARD FREE ENERGIES OF FORMATION OF OH GROUP FOR ALCOHOLS IN THE GASEOUS STATE (kcal.).

Source. / Temperature (°K.).	3rd Law.	Hydration of Ethylene.		Mean.
		Equil. Data.	Statistical Mechanics.	
300	− 38·5	− 37·5	− 38·0	− 38·0
600	− 34·5	− 35·0	− 34·5	− 34·5
800	− 31·5	− 33·0	− 32·5	− 32·5
1000	− 29·0	− 31·0	− 30·0	− 30·0

A comparison between experimental and empirical standard free energy values for several alcohols is given in Table VI. The experimental values given for the normal alcohols are those of Parks and Huffman.[1] Since no reliable data are available for secondary and tertiary alcohols the group values have been compared with those obtained by the Anderson, Beyer and Watson [5] group contribution method.

---

[9] Bliss and Dodge, *Ind. Eng. Chem.*, 1931, **29**, 19.

[10] Thacker, Folkins and Miller, *ibid.*, 1947, **33**, 584.

[11] Aston, Szasz and Isserow, *J. Chem. Physics*, 1943, **11**, 532.

TABLE VI.—THE STANDARD FREE ENERGIES OF FORMATION OF ALCOHOLS IN THE GASEOUS STATE.

Alcohol.	Source.	Temperature.			
		300°.	600°.	800°.	1000° K.
Ethyl alcohol	Group Ref. 1	−40 −40·6	−22·5	−10·5	2·0
n-Propyl alcohol	Group Ref. 1	−38 −38·6	−13	4	21·5
n-Butyl alcohol	Group Ref. 1	−36 −37·4	− 3·5	18·5	41
n-Amyl alcohol	Group Ref. 1	−34 −35·3	6	33	60·5
n-Hexyl alcohol	Group Ref. 1	−32 −33·7	15·5	47·5	80
iso-Propyl alcohol	Group Ref. 5	−38·5 −39·8	−14	3·5	21·5
iso-Butyl alcohol	Group Ref. 5	−36·5 −38·5	− 4·5	18	41
t-Butyl alcohol	Group Ref. 5	−37 −38·9	− 3	20·5	45
t-Amyl alcohol	Group Ref. 5	−35 −38·2	6·5	35·0	64·5
Ethylene glycol	Group Ref. 5	−72 −75·3	−50	−36	−21
Butandiol, 1 : 4	Group Ref. 5	−68·0 −71·7	−31 −36·2	− 7 −12	18 12·5

4. The Standard Free Energies of Formation of the Carboxylic Acids.

The standard free energy of formation of the carboxyl group at 300° K. was calculated from the values given by Parks and Huffman[1] for acetic and *n*-butyric acids. In order to obtain the variation of the standard free energy with temperature, the formal equation for acetic acid was calculated and gave

$$\Delta G^\circ = -101{,}700 + 16{\cdot}98\,T\ln T - 9{\cdot}835 \times 10^{-3}T^2 + 0{\cdot}99 \times 10^{-6}T^3 - 2{\cdot}108 \times 10^5\,T^{-1} - 56{\cdot}52\,T.$$

TABLE VII.—STANDARD FREE ENERGIES OF FORMATION OF THE —COOH GROUP FOR ACIDS IN THE GASEOUS STATE

Temperature (°K.).	ΔG° (kcal.).
300	−87
600	−77
800	−70
1000	−63·5

The following values of the heat[12] and entropy[5] of formation and specific heat[5] were used in deriving this equation:

$$\Delta H^\circ_{298} = -107{\cdot}3\,;$$
$$\Delta S^\circ_{298} = -54{\cdot}0\,;$$
$$\Delta C_p = 9{\cdot}88 + 0{\cdot}02678\,T - 5{\cdot}89 \times 10^{-6}\,T^2.$$

Table VII gives the values for the carboxyl group derived from the corresponding values for acetic acid and the methyl group value from Table I. In Table VIII a comparison is made between group and experimental values; the latter were taken from Parks and Huffman.[1]

---

[12] Kharasch, *Bur. Stand. J. Res.*, 1929, **2**, 359.

TABLE VIII.—THE STANDARD FREE ENERGIES OF FORMATION OF ACIDS IN THE GASEOUS STATE (kcal.).

Acid.	Source.	Temperature.			
		300°.	600°.	800°.	1000° K.
Acetic acid	Group Ref. 1	−91 −91·23	−74·5	−62·5	−51·0
n-Butyric acid	Group Ref. 1	−87 −88	−55·5	−33·5	−12
Palmitic acid	Group Ref. 1	−63 −68	58·5	140·5	222
Succinic Acid	Group Ref. 1	−170 −173	−135	−111	−88
dl-Lactic acid	Group Ref. 1	−121·5 −121	− 93	− 73·5	− 54

5. The Standard Free Energies of Formation of the Aliphatic Ethers.

Because of the lack of thermodynamic data for this class of compounds, the standard free energy values of the —O— group was calculated solely from the data available for diethyl ether. The standard free energy of formation of diethyl ether at 300° K. was taken from Parks and Huffman [1] and the heat capacity was calculated by the method of Stull and Mayfield.[13] The derived standard free energy values at 600°, 800° and 1000° K. for diethyl ether and thence for the —O— group are given in Table IX.

TABLE IX.—STANDARD FREE ENERGIES OF DIETHYL ETHER AND —O— GROUP IN THE GASEOUS STATE.

Material.	Temperature.			
	300°.	600°.	800°.	1000° K.
Diethyl ether	−27·90	+ 6·07	29·26	52·44
—O— Group	−24	−18	−14·5	−11·5

6. The Standard Free Energies of Formation of the Aldehydes.

The standard free energy of formation of the aldehyde group at the chosen temperatures, was obtained from the data for acetaldehyde by the method used in Section (5). The values are given in Table X.

TABLE X.—STANDARD FREE ENERGIES OF ACETALDEHYDE AND THE —CHO GROUP IN THE GASEOUS STATE.

Material.	Temperature.			
	300°.	600°.	800°.	1000° K.
Acetaldehyde	−33·5	−22·5	−14	− 6
—CHO Group	−29·5	−25	−21·5	−18·5

---

[13] Stull and Mayfield, *Ind. Eng. Chem.*, 1943, 35, 639.

B. Cyclic Compounds.

Entropy and standard free energy values unlike heats of formation, cannot be extended directly from the aliphatic to the cyclic series as has been fully discussed elsewhere.[14] It can be shown that the sum of the group contributions must be adjusted to allow for changes in (i) the symmetry number, (ii) the number of internal rotations, (iii) the translational entropy, (iv) the resonance energy.

Now the summing of group contributions is equivalent to writing equations as (1) in which there is an identity of groups on either side :

$3\,CH_3CH{=}CH\,.\,CH_3 =$ 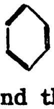 $+\ 3C_2H_4$. . . . (1)

The heat of this particular reaction and the entropy change has been shown[14] to be constant over the temperature range 300-1000° K. If the assumption is made that this constancy holds for other cyclic compounds we can correct simply for the changes (i)-(iv) enumerated above. The correction ($\Delta G'$) to be applied to the sum of the group values will be obtained by writing equations such as (1) and substituting known values for ΔG and ΔS or ΔH. Consequently from a knowledge of two of these quantities at one temperature it becomes possible to derive the standard free energy at any temperature for which group values are available.

Writing the thermodynamic changes involved for reactions such as (1) in the form

$$\Delta G' = \Delta H' - T\Delta S'$$

in which $\Delta H'$ and $\Delta S'$ are assumed constant, then the standard free energy (ΔG) of the cyclic compound is given by

$$\Delta G = \Delta G' + \Delta G^g$$

where ΔG^g represents the sum of the group values for the cyclic compounds.

The application of these equations may be illustrated by considering cyclohexane, cyclohexene, furan and tetrahydrofuran. The thermodynamic properties of these materials at 300° are summarised in Table XI.

TABLE XI.—THERMODYNAMIC PROPERTIES OF CYCLOHEXANE, CYCLOHEXENE, FURAN AND TETRAHYDROFURAN.

Cyclic Compound.	ΔG (kcal.).	ΔH (kcal.).	S (cal./degr. mol.).
Cyclohexane . . .	7·3	−29·7	71·4
Cyclohexene . . .	26·3	− 1·1	72·3
Furan	4·0	− 6·1	58·9[15]
Tetrahydrofuran . .	−14·8	−42·7[16]	61·5[15]

The entropy values for furan and tetrahydrofuran are calculated ones.[15] The heat and entropy of formation of the aliphatic compounds used in deriving the standard free energy change, $\Delta G'$, for group reactions as (1) are those given by Rossini *et al.*[6, 7]

Each of the four materials will be treated in turn.

---

[14] Bremner and Thomas, *Nature*, 1946, **158**, 592 ; *Trans. Faraday Soc.*, 1947, **43**, 779.

[15] P. G. Carter (private communication).

[16] Conant and Kistiakowsky, *Chem. Rev.*, 1937, **20**, 182.

1. The Standard Free Energy of Formation of Cyclohexane.

We may represent cyclohexane as being formed from the de-ethanation of *n*-butane as in equation (2):

$3\ CH_3CH_2CH_2CH_3 =$ 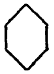 $+ 3C_2H_6$. . . . (2)

For this reaction the standard free energy change is given by:

$$\Delta G' = -0{\cdot}9 - 14{\cdot}2\ .\ 10^{-3}\ T.$$

The values derived from this equation together with the appropriate methene group values are given in Table XII.

TABLE XII.—THE STANDARD FREE ENERGY OF FORMATION OF CYCLOHEXANE

Standard Free Energy (kcal.).	300°.	600°.	800°.	1000° K.
ΔG^{g}	12	57	87	117
$\Delta G'$	−5·1	−9·4	−12·3	−15·1
ΔG° (Group Value)	6·9	47·6	74·7	101·9
ΔG° (Andersen, Beyer and Watson [5]) .	6·3	46·2	74·0	102·1

The standard free energies of formation of cyclohexane as given by the Andersen, Beyer and Watson method [5] is included in Table XII. The agreement between these and the group values is rather close.

2. The Standard Free Energy of Formation of Cyclohexene.

The formation of cyclohexene may be written as in equation (3):

$CH_3CH = CHCH_3 + 2CH_3CH_2CH_2CH_3 =$ 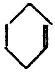 $+ 3C_2H_6$. . (3)

The standard free energy change in this reaction is given by

$$\Delta G' = -0{\cdot}7 - 17{\cdot}310^{-3}\ T$$

from which the values in Table XIII are derived. Unfortunately no experimental values are available for comparison.

TABLE XIII.—THE STANDARD FREE ENERGY OF FORMATION OF CYCLOHEXENE.

Standard Free Energy (kcal.).	300°.	600°.	800°.	1000° K.
ΔG^{g} . . .	32	67·5	91	115·5
$\Delta G'$ . . .	− 5·9	−11·1	−14·5	− 18
ΔG° . . .	26·1	56·4	76·5	97·5

3. The Standard Free Energy of Formation of Furan and Tetrahydrofuran.

The formation of furan and tetrahydrofuran from aliphatic compounds is expressed by equations (4) and (5):

$CH_3CH_2OCH_2CH_3 + 2CH_3CH = CHCH_3 =$ 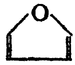 $+ 2C_2H_6 + C_4H_{10}$ (4)

$CH_3CH_2OCH_2CH_3 + CH_3CH_2CH_2CH_3 =$ 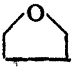 $+ 2C_2H_6$ . . (5)

The standard free energy change in these reactions is given by

$$\Delta G' = -13{\cdot}9 - 20{\cdot}1 \,.\, 10^{-3}T$$
$$\Delta G' = 6{\cdot}4 - 18{\cdot}1 \,.\, 10^{-3}T,$$

and the derived values in Table XIV.

TABLE XIV.—THE STANDARD FREE ENERGY OF FORMATION OF FURAN AND TETRAHYDROFURAN

Standard Free Energy (kcal.).	Furan.				Tetrahydrofuran.			
	300°.	600°.	800°.	1000°.	300°.	600°.	800°.	1000° K.
ΔG^g	24	41	51·5	63·5	−16	20	43·5	66·5
$\Delta G'$	−20	−26	−30	−34	1·0	−4·5	−8.1	−11·7
ΔG°	4	15	21·5	29·5	−15·0	15·5	35·4	54·8

No experimental values are available for comparison.

Summary.

The standard free energies of formation of aliphatic organic compounds may be expressed as the sum of contributions assigned to characteristic groupings. A similar summation is not valid for cyclic compounds because of the large entropy changes involved in their formation from aliphatic compounds. A simple procedure is adopted to allow of their estimation. Where possible a comparison is made between free energies calculated from group values and those determined experimentally.

Imperial Chemical Industries Ltd.,
Billingham Division,
Co. Durham.

GENERAL THEORY OF THE STATIC DIELECTRIC CONSTANT.

BY H. FRÖHLICH.

Received 14*th February,* 1947.

Introduction.

In the present paper a formula for the static dielectric constant ϵ will be derived which holds in a very general way for any type of substance. Following Lorentz [1] a spherical region is selected which is large compared with a region just large enough to have the same dielectric properties as a macroscopic specimen. This region is then treated according to the rules of classical statistical mechanics, considering the rest of the specimen as a continuous medium. The method used for this purpose is a generalised (and slightly simplified) version of the method applied by Kirkwood [2] to the case of dipolar liquids. The resulting value for ϵ in general depends on the structure of the material. Both Onsager's [3] and

---

[1] Lorentz, *Theory of Electrons* (Leipzig, 1909), p. 117.

[2] Kirkwood, *J. Chem. Physics*, 1939, **7**, 911.

[3] Onsager, *J. Amer. Chem. Soc.*, 1936, **58**, 1486.

Clausius-Mossotti's[4] formulæ are, however, contained in the general formula as limiting cases.

General Theory.

Let a homogeneous electric field $\vec{E}$ be maintained by outside sources in a dielectric medium with dielectric constant ϵ. Within this dielectric consider a spherical region of volume V which is large compared with a region just big enough to have the same dielectric properties as a macroscopic specimen. This region consists of a great number of elementary charges e_i which will be treated according to the rules of classical statistical mechanics, whereas the rest of the specimen will be treated macroscopically as a continuous medium. Let r_i be the displacement of the charge e_i from the position it holds in the lowest energy state of the whole region. Then, excluding substances with permanent polarisation,

$$\vec{M}(X) = \sum_i e_i \vec{r_i}$$

is the electric dipole moment of the region for a given set of displacements $X = (\vec{r_1}, \vec{r_2}, \ldots \vec{r_i}, \ldots)$.

In the absence of an external field the potential energy of the whole region (normalised to zero for vanishing displacements) is composed of (i) the interaction between the particles inside the region, depending on X only, and (ii) their interaction with the surroundings which depends on X as well as on the macroscopic dielectric constant ϵ which alone describes the properties of these surroundings. Let $W(X, \epsilon)$ denote the sum of both these contributions. Apply now an electric field $\vec{E}$—which is constant outside the spherical region—without altering the set of displacements,* X. Then, as has been shown by Onsager,[3] the electric field inside the spherical region is increased by a homogeneous field $\vec{G}$,

$$\vec{G} = \frac{3\epsilon}{2\epsilon + 1}\vec{E} \quad . \quad . \quad . \quad . \quad . \quad (1)$$

The total potential energy of the spherical region is thus

$$W(X, \epsilon) - \vec{M}(X)\vec{G}.$$

Therefore

$$M_E = \int M(X) \cos\theta \, e^{-[W(X,\epsilon) - \vec{M}(X)\vec{G}]/kT} dX \Big/ \int e^{-[W(X,\epsilon) - \vec{M}(X)\vec{G}]/kT} dX$$

is the average electric moment of the spherical region in the field direction, if θ is the angle between $\vec{M}$ and $\vec{E}$, and dX denotes integration over all displacements. This expression can be developed into a power series in G. The first term vanishes because it represents the average electric moment of the specimen in the absence of a field. For moderate fields, only the next term need be considered. Thus

$$M_E = J\frac{G}{kT}\int \cos^2\theta M^2(X) e^{-W(X,\epsilon)/kT} dX \quad . \quad . \quad . \quad (2)$$

where

$$1/J = \int e^{-W(X,\epsilon)/kT} dX \quad . \quad . \quad . \quad . \quad . \quad (3)$$

---

[4] cf. Debye, *Polare Molekeln* (Leipzig, 1929), p. 3.

* This does not mean, of course, that a field does not influence the average displacements; it does so by altering the probability of finding a given set of displacements.

Now average over all possible directions of the external field, i.e. replace $\cos^2\theta$ by $\frac{1}{3}$. Since ϵ is defined by

$$M_E = \frac{\epsilon - 1}{4\pi} E V,$$

a comparison with (2) using (1) then gives

$$\epsilon - 1 = \frac{4\pi}{3} \frac{3\epsilon}{2\epsilon + 1} \frac{\overline{M^2}}{VkT} \quad . \quad . \quad . \quad . \quad . \quad (4)$$

where
$$\overline{M^2} = J\int M^2(X) e^{-W(X,\epsilon)/kT} \mathrm{d}X \quad . \quad . \quad . \quad (5)$$

Assume now the spherical region to be composed of N unit cells, each of which makes the same contribution to $\overline{M^2}$. Thus if $\vec{m}(x_j)$ is the contribution of the j-th cell to $\vec{M}(X)$, and x_j represents the displacements of all elementary charges in this cell,

$$\vec{M}(X) = \sum_{j=1}^{N} \vec{m}(x_j),$$

$$M^2(X) = \sum_{j=1}^{N} \vec{m}(x_j)\vec{M}(X),$$

and, therefore, in view of (5)

$$\overline{M^2} = \sum_{j=1}^{N} \overline{\vec{m}(x)\vec{M}(X)}_j = N\overline{\vec{m}(x)\vec{M}(X)} = NJ\int \vec{m}(x)\vec{M}(X) e^{-W(X,\epsilon)/kT} \mathrm{d}X. \quad (6)$$

Here the suffix j has been dropped in $\vec{m}(x_j)$ because each unit cell makes the same contribution, so that x may represent the set of displacements of any selected unit cell.

The integration will now first be carried out over the whole region except the one selected unit cell which for convenience sake will be taken at the centre of the sphere. The volume element for this integration will be denoted by $\mathrm{d}X'$, leaving the integration $\mathrm{d}x$ over the central unit cell. Then, according to (6),

$$\overline{M^2} = N\int \vec{m}(x)\vec{m}^*(x)p(x)\mathrm{d}x = N\overline{\vec{m}(x)\vec{m}^*(x)}, \quad . \quad . \quad (7)$$

where
$$\vec{m}^*(x) = \int \vec{M}(X) e^{-W(X,\epsilon)/kT} \mathrm{d}X' \Big/ \int e^{-W(X,\epsilon)/kT} \mathrm{d}X' \quad . \quad (8)$$

and
$$p(x) = J\int e^{-W(X,\epsilon)/kT} \mathrm{d}X' \quad . \quad . \quad . \quad (9)$$

Thus inserting from (7) into (4),

$$\epsilon - 1 = \frac{4\pi}{3} \frac{3\epsilon}{2\epsilon + 1} \frac{\overline{\vec{m}(x)\vec{m}^*(x)}}{kT} N_0 \quad . \quad . \quad . \quad . \quad (10)$$

where
$$N_0 = N/V$$

is the number of unit cells per unit volume. Here $\vec{m}(x)$ is the electric moment of the unit cell for a given set (x) of displacements of its elementary charges, $\vec{m}^*(x)$ according to (8) is the average moment of a spherical region of volume V inside the macroscopic specimen if the set x of displacements of a unit cell at the centre (leading to $\vec{m}(x)$) is supposed to persist for a long time. $p(x)$ is the probability of finding the displacements x, on an average over all possible states of the surroundings, outside the unit cell, and $\overline{\vec{m}(x)\vec{m}^*(x)}$ is the average value of $\vec{m}(x)\vec{m}^*(x)$ over all possible displacements x in the unit cell.

Discussion of Special Cases.

The general expression (10) for the dielectric constant ϵ can be applied to various special cases. For crystals $\overline{\vec{m}\vec{m}^*}$, and hence ϵ, must depend on the structure, and no further general development can be given. In certain limiting cases, however, ϵ becomes independent of structure and either Onsager's [3] or Clausius-Mossotti's [4] formula may be obtained.

In the case of solids and liquids it is useful to separate off the electronic contributions n^2 to ϵ (which are known from the optical refractive index n) by treating them on a macroscopical basis. The spherical region then consists of charges e_i which follow the laws of statistical mechanics, and which are embedded in a continuous medium with dielectric constant n^2. As before, the rest of the specimen will be treated macroscopically as a continuous substance with dielectric constant ϵ. On application of an external field without changing the configuration X of the charges e_i, the field inside the sphere is now increased by [5]

$$\vec{G}' = \frac{3\epsilon}{2\epsilon + n^2}\vec{E} \quad . \quad . \quad . \quad . \quad (11)$$

instead of by $\vec{G}$ (eqn. (1)). Also, the average electric moment M_E of the charges e_i is now given by

$$M_E = \frac{\epsilon - n^2}{4\pi}VE \quad . \quad . \quad . \quad . \quad (12)$$

Eqn. (10) will, therefore, be replaced by

$$\epsilon - n^2 = \frac{3\epsilon}{2\epsilon + n^2}\frac{4\pi}{3}N_0\frac{\overline{\vec{m}(x)\vec{m}^*(x)}}{kT}. \quad . \quad . \quad . \quad (13)$$

Investigate now the assumptions that have to be made to derive from (13) either Onsager's or Clausius-Mossotti's formula. In both cases it must be assumed that

(i) there is no interaction between unit cells except the electrostatic interaction between the electric moments. This excludes, therefore, any short range force though such a force always exists. To permit this requires temperatures T for which

$$kT \gg \text{short-range interaction} \quad . \quad . \quad . \quad (14)$$

If this is fulfilled then a second assumption may be justified, namely

(ii) the spherical region can be reduced to one unit cell which will be assumed to be spherical. Actually this implies that this region has the same dielectric properties as a macroscopic specimen. Though this can hardly be accurate * the deviations of the correct interaction energy from the calculated one should be small compared to kT if T is sufficiently large. Thus from (ii),

$$\vec{m}(x) = \vec{m}^*(x) \quad . \quad . \quad . \quad . \quad (15)$$

Two cases can now be distinguished.

Case A.—The unit cell contains one molecule with a permanent dipole of moment $\vec{\mu}$ whose energy is independent of its direction. Then x represents the angles of rotation of this dipole, and

$$m(x) = \mu \quad . \quad . \quad . \quad . \quad (16)$$

---

* cf. ref. [5] for an estimate of the deviations in the case of a simple model.

is a constant. $W(x, \epsilon)$, too, is a constant, and hence with eqn. (15),

$$\overline{\vec{m}(x)m^*(x)} = \mu^2$$

which if inserted into (13) leads to Onsager's formula. It should be noted that μ is different from the dipole moment μ_0 of a molecule in the gas phase. Onsager's formula would demand

$$\mu_0 = \frac{3}{n^2 + 2}\mu$$

which is the dipole moment of a sphere of a continuous dielectric with a dielectric constant n^2, having a dipole μ at its centre.

Case B.—The unit cell contains no permanent dipole. The only displaceable charge e is bound elastically to the centre. Thus X represents the displacement $\vec{r}$ of this charge. The dipole moment is given by

$$\vec{m}(r) = e\vec{r}, \quad . \quad . \quad . \quad . \quad . \quad (17)$$

and the elastic energy by

$$c^2r^2/2 = c^2m^2/2e^2,$$

where c^2 is the force constant. The interaction energy with the surroundings (part (ii) of $W(x, \epsilon)$) is given by †

$$-\tfrac{1}{2}\vec{m}(r)\vec{R} \quad . \quad . \quad . \quad . \quad . \quad (18)$$

where [5]

$$\vec{R} = \frac{2}{n^2}\frac{\epsilon - n^2}{2\epsilon + n^2}\frac{\vec{m}(r)}{V}\frac{4\pi}{3}$$

is the reaction field, first introduced by Onsager.[3] In Case A term (18) is irrelevant because $m(X)$ is constant. Taking m as independent variable,

$$W(x, \epsilon) = \frac{c^2}{2e^2}m^2 - \tfrac{1}{2}mR = \left[\frac{c^2}{2e^2} - \frac{\epsilon - n^2}{n^2(2\epsilon + n^2)}\frac{4\pi}{3V}\right]m^2,$$

and with (15)

$$\overline{\vec{m}\vec{m}^*} = \overline{m^2} = \int m^2 e^{\,W(X,\epsilon)/kT}\, m^2 dm \Big/ \int e^{-W(X,\epsilon)/kT}\, m^2 dm$$

$$= \frac{3}{2}kT\left[\frac{c^2}{2e^2} - \frac{\epsilon - n^2}{n^2(2\epsilon + n^2)}\frac{4\pi}{3V}\right]^{-1}.$$

Introducing this expression into (13) yields

$$\epsilon - n^2 = 2\pi N_0 \frac{3\epsilon}{2\epsilon + n^2}\left[\frac{c^2}{2e^2} - \frac{\epsilon - n^2}{n^2(2\epsilon + n^2)}\frac{4\pi}{3V}\right]^{-1},$$

or using $N_0 V = 1$,

$$\frac{\epsilon - n^2}{\epsilon + 2n^2} = \frac{4\pi}{3V}\frac{e^2}{n^2c^2} \quad . \quad . \quad . \quad . \quad (19)$$

which for $n = 1$ is Clausius-Mossotti's formula.

An improved formula due to Kirkwood[2] can be obtained for Case A by dropping both assumptions (i) and (ii), but keeping eqn. (16). This implies besides $m = \mu$ that

$$m^*(x) = \mu^* \quad . \quad . \quad . \quad . \quad (20)$$

too is a constant independent of X, but in general $\mu^* \neq \mu$ in view of short-range interaction. From (16) and (20),

$$\vec{m}(x)\vec{m}^*(x) = \mu\mu^*$$

which if inserted into (13) gives Kirkwood's formula. It should hold quite generally for dipolar liquids, or even in solids in a temperature range in which there is no long-range order. In an ordered state, however, this formula is no longer valid. In this case, excluding permanent polarisation, the unit cell must contain more than one dipole because in the lowest energy state the total dipole moment of the unit cell must vanish.

---

† $-\vec{m}\vec{R}$ is the energy of a dipole m in field R ; $+\tfrac{1}{2}\vec{m}\vec{R}$ is the energy required to polarise the surroundings.

[5] Fröhlich and Sack, *Proc. Roy. Soc. A*, 1944, 182, 388.

Suppose there are $z + 1$ possible arrangements of the dipoles of the unit cell each leading to a moment m_i of the unit cell, a moment $\vec{m}_i^*$ of the spherical region, and having a probability p_i. Then from (13)

$$\epsilon - n^2 = \frac{3\epsilon}{2\epsilon + n^2} \frac{4\pi N_0}{3kT} \sum_{i=0}^{z} \vec{m}_i \, \vec{m}_i^* \, p_i . \qquad (21)$$

Let the first excited state, $i = 1$, have a finite energy difference from the ground state, if $T = 0$. Then for $T = 0$, $m_0 = 0$, and also $p_i = 0$ if $i > 0$. Thus $\epsilon - n^2 = 0$. Therefore at $T = 0$, either $\epsilon = n^2$, or the solid becomes permanently polarised.

Summary.

A general formula for the static dielectric constant is derived by an extension of the methods employed by Lorentz and by Kirkwood. This formula holds in a very general way for any substance. It contains formulæ due to Onsager, Clausius-Mossotti and others, as limiting cases, subject to certain specified conditions.

KINETIC STUDIES IN THE SOLVENTS ACETIC ACID AND ACETIC ANHYDRIDE.

PART III.—THE THIELE ACETYLATION OF BENZOQUINONE AND TOLUQUINONE (THEORETICAL).

By H. A. E. Mackenzie and E. R. S. Winter.

Received 4th March, 1947.

The Overall Rate Expressions.

The experimental study of the perchloric acid-catalysed acetylation of benzoquinone and toluquinone[1] presents certain salient features which immediately provide an insight into the mechanism of the reaction. These suggest that the rate-determining process in the acetylation involves the reaction between the neutral quinone molecule and an acidic ion, the latter being the effective catalyst for the reaction. The main problem has been to characterise the acid ion catalyst involved, or, alternately, to determine the relationship between the reaction rate and the acidity of the solution. The most useful correlation found is between the acidity function of the solution and the specific reaction rate, although even this does not account fully for the experimental facts.

It is known[2] that, over the concentration range used here, $HClO_4$ is completely ionised in acetic acid, and that the proton probably exists in the solvated form $AcOH_2^+$. If it is assumed that, in mixtures of acetic acid and acetic anhydride, the only acid ionic species is $AcOH_2^+$, then, in such solutions of perchloric acid, $c_{AcOH_2^+}$ will be equal to the stoichiometric concentration of $HClO_4$ added. The rate-determining process in the Thiele acetylation may then be postulated as

---

[1] Mackenzie and Winter, *Trans. Faraday Soc.*, 1948, **44**, p. 159.

[2] Mackenzie and Winter, *ibid.*, p. 171.

$$Q + AcOH_2^+ \xrightarrow{k} \text{products},$$

from which, the rate of reaction would be given by

$$\frac{-\,dc_Q}{dt} = k \,.\, c_Q \,.\, c_{AcOH_2^+} \,.\, \frac{f_Q \cdot f_{AcOH_2^+}}{f_{X^+}},$$

where f_{X^+} is a kinetic activity factor, or, from the viewpoint of the transition state theory, the activity coefficient of the activated complex.

But, since $c_{AcOH_2^+} \cdot f_{AcOH_2^+} = a_{H^+}$,

$$\frac{-\,dc_Q}{dt} = k \,.\, c_Q \,.\, a_{H^+} \,.\, \frac{f_Q}{f_{X^+}}.$$

Experimentally, $k_e \,.\, c_Q = \frac{-\,dc_Q}{dt}$,

and therefore $k_e = k \,.\, a_{H^+} \,.\, \frac{f_Q}{f_{X^+}}$.

Now the acidity function of the medium with respect to a neutral base is defined as

$$H_0 = -\log\left(a_{H^+}\frac{f_B}{f_{BH^+}}\right).$$

Hence, if, and only if, it is assumed that the activity coefficient of the activated complex bears a ratio to that of the quinone which is affected by the medium in the same way as the ratio f_{BH^+}/f_B for any base,

$$\log k_e = \log k - H_0.$$

Experimentally it has been shown that the plots of $\log k_e$ against H_0 for both benzoquinone and toluquinone are linear, and therefore in qualitative agreement with the above equation in solutions containing up to about 80 % v/v. acetic anhydride. But the fundamental assumption by which the relationship is deduced also implies that these plots should be parallel and of slope $-1{\cdot}0$, and differ only in their intercepts on the $\log k_e$ axis. This is contrary to the experimental facts, since the slopes are $-0{\cdot}99$ and $-1{\cdot}20$ for benzoquinone and toluquinone respectively. In addition, the above mechanism fails to account for the deviation of the plots from linearity at concentrations of acetic anhydride above 80 % v/v.

Alternative mechanisms, which postulate initially an equilibrium of the type

$$Q + AcOH_2^+ \rightleftharpoons QH^+ + AcOH,$$

or

$$Q + Ac_2OH^+ \rightleftharpoons QH^+ + Ac_2O,$$

or both, followed by a rate-determining first-order reaction of the QH^+ ion, lead again to expressions which are in disagreement with our observations, and provide no explanation of the mode of formation of the reaction products.

Evidence of the existence of the acetyl ion in solutions of $HClO_4$ in acetic acid-acetic anhydride mixtures has already been put forward,[3] and the above discrepancy is attributed to the falseness of the assumption that the $AcOH_2^+$ or Ac_2OH^+ ions are the only acid ion species in such solutions. The recognition of the acetyl ion as a distinct acidic species is necessary before a reasonable interpretation of the facts is possible.

It is known [3] that, in mixtures of acetic acid and acetic anhydride, ideal behaviour is found in solutions containing up to about 80 % w/w. acetic anhydride, provided it is accepted that acetic acid exists as the dimer. The following equilibria

$$AcOH_2^+ + AcO^- \rightleftharpoons (AcOH)_2 \rightleftharpoons 2AcOH$$

may therefore be regarded as favouring the presence of the species $(AcOH)_2$ to such an extent that the acetic acid is almost quantitatively present in this form. It may also be accepted that low concentrations of perchloric acid ionise completely in such a medium, according to the equation

$$HClO_4 + AcOH = AcOH_2^+ + ClO_4^-.$$

We propose the following additional equilibrium, whereby the acetyl ion is formed in appreciable amount when the concentration of acetic anhydride is high enough:

$$AcOH_2^+ + Ac_2O \overset{K}{\rightleftharpoons} Ac^+ + (AcOH)_2.$$

(We have as yet no means of directly investigating this equilibrium.) If x is the stoichiometric fraction of the added $HClO_4$ converted to acetyl ions, then the thermodynamic equilibrium constant, K, is given by

$$K = \frac{(1-x)\,.\,f_{AcOH_2^+}\,.\,a_{Ac_2O}}{x\,.\,f_{Ac^+}\,.\,a_{(AcOH)_2}},$$

and

$$x = \frac{a_{Ac_2O}\,.\,f_{AcOH_2^+}}{K\,.\,a_{(AcOH)_2}\,.\,f_{Ac^+} + a_{Ac_2O}\,.\,f_{AcOH_2^+}}.$$

Under those conditions where the equilibrium has not proceeded markedly to the right, i.e., where

$$K\,.\,a_{(AcOH)_2}\,.\,f_{Ac^+} \gg a_{Ac_2O}\,.\,f_{AcOH_2^+},$$

it is therefore possible to write:

$$a_{Ac^+} = \frac{a_{Ac_2O}\,.\,f_{AcOH_2^+}\,.\,c_{HClO_4}}{K\,.\,a_{(AcOH)_2}}$$

and

$$a_{(AcOH_2^+)} = f_{AcOH_2^+}\,.\,c_{HClO_4},$$

where c_{HClO_4} is the stoichiometric concentration of perchloric acid added.

The following mechanism is then proposed for the acetylation of benzoquinone and toluquinone:

(R— represents H— or CH_3—):

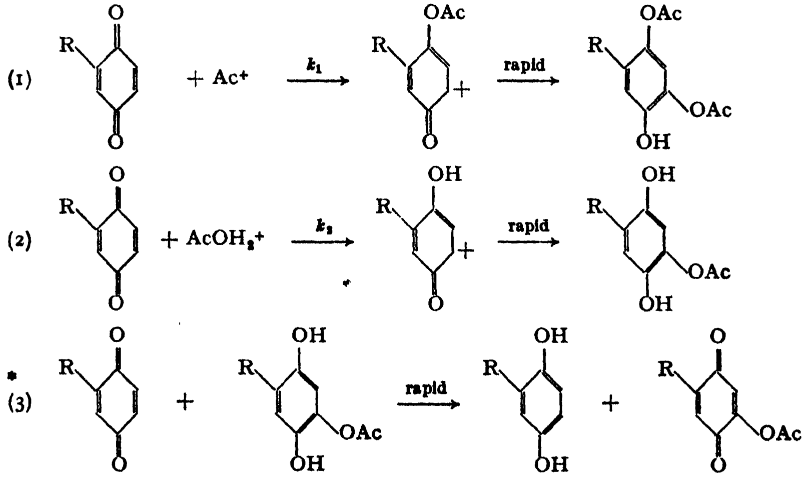

Reactions (1) and (2) are assumed to proceed simultaneously and together* to constitute the rate-determining process. Reaction (3) is introduced in order to allow for an explanation of the products formed by the reaction (cp. later).

---

* Strictly, this should probably be regarded as a redox equilibrium; the subsequent argument is not affected.

If the quinone 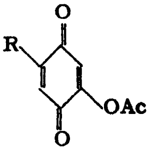 is not measured by the iodometric method used for following the reaction, then the apparent net rate of disappearance of quinone from the solution will be given by

$$\frac{-\,\mathrm{d}c_{\mathrm{Q}}}{\mathrm{d}t}=\frac{k_1\,.\,a_{\mathrm{Q}}\,.\,a_{\mathrm{Ac}^+}}{f_{x_{1+}}}+\frac{2k_2\,.\,a_{\mathrm{Q}}\,.\,a_{\mathrm{AcOH}_2{}^+}}{f_{x_{2+}}},$$

where the x's represent the activated complexes of reactions (1) and (2).

If, however, the quinone 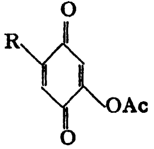 is measured by the iodometric method, an apparent first-order disappearance of the quinone would result only if the reactions

(4) 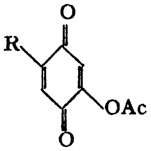 $+ \mathrm{Ac}^+ \longrightarrow$

(5) 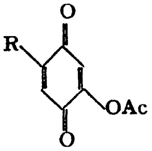 $+ \mathrm{AcOH}_2{}^+ \longrightarrow$

were of rate negligible compared with the rates of (1) and (2). In this case, the net rate of disappearance of quinone would be given approximately by

$$\frac{-\,\mathrm{d}c_{\mathrm{Q}}}{\mathrm{d}t}=\frac{k_1\,.\,a_{\mathrm{Q}}\,.\,a_{\mathrm{Ac}^+}}{f_{x_{1+}}}+\frac{k_2\,.\,a_{\mathrm{Q}}\,.\,a_{\mathrm{AcOH}_2{}^+}}{f_{x_{2+}}}$$

and appreciable concentrations of the quinone 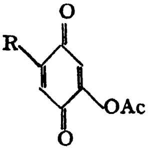 should be built up during the course of the reaction. Since this quinone could not be isolated from the reaction mixture, the former assumption is favoured, and the rate of disappearance of quinone expressed by the equation

$$\frac{-\,\mathrm{d}c_{\mathrm{Q}}}{\mathrm{d}t}=\frac{k_1\,.\,a_{\mathrm{Q}}\,.\,a_{\mathrm{Ac}^+}}{f_{x_{1+}}}+\frac{2k_2\,.\,a_{\mathrm{Q}}\,.\,a_{\mathrm{AcOH}_2{}^+}}{f_{x_{2+}}},$$

Hence,

$$\frac{-\,\mathrm{d}c_{\mathrm{Q}}}{\mathrm{d}t}=c_{\mathrm{Q}}\,.\,c_{\mathrm{HClO}_4}\left\{\frac{k_1\,.\,a_{\mathrm{Ac}_2\mathrm{O}}}{K\,.\,a_{(\mathrm{AcOH})_2}}\,.\,\frac{f_{\mathrm{Q}}}{f_{x_{1+}}}+2k_2\frac{f_{\mathrm{Q}}}{f_{x_{2+}}}\right\}f_{\mathrm{AcOH}_2{}^+}$$

Since mixtures of acetic anhydride and acetic acid behave ideally[2] when the concentration of the former is less than about 80 % w/w, it appears reasonable to assume here that $f_{\mathrm{Ac_2O}}$ and $f_{(\mathrm{AcOH})_2}$ are both equal to unity over the same concentration range, and write

$$\frac{-\,\mathrm{d}c_{\mathrm{Q}}}{\mathrm{d}t} = c_{\mathrm{Q}}\,.\,c_{\mathrm{HClO_4}}\,.\left\{\frac{k_1\,.\,c_{\mathrm{Ac_2O}}}{K\,.\,c_{(\mathrm{AcOH})_2}}\,.\,\frac{f_{\mathrm{Q}}}{f_{\mathrm{X}_1+}} + 2k_2\frac{f_{\mathrm{Q}}}{f_{\mathrm{X}_2+}}\right\}f_{\mathrm{AcOH_2^+}}\,.$$

Experimentally,

$$\frac{-\,\mathrm{d}c_{\mathrm{Q}}}{\mathrm{d}t} = k_e\,.\,c_{\mathrm{Q}},$$

and hence,

$$k_e = c_{\mathrm{HClO_4}}\left\{\frac{k_1\,.\,c_{\mathrm{Ac_2O}}}{K\,.\,c_{(\mathrm{AcOH})_2}}\,.\,\frac{f_{\mathrm{Q}}}{f_{\mathrm{X}_1+}} + \frac{2k_2\,.\,f_{\mathrm{Q}}}{f_{\mathrm{X}_2+}}\right\}f_{\mathrm{AcOH_2^+}}.$$

If it is assumed that, for the small concentrations of quinone and perchloric acid used in the experimental work, $f_{\mathrm{Q}} = 1$, and $f_{\mathrm{AcOH_2^+}}$, f_{X_1+} and f_{X_2+} are all affected by the solvent composition in the same way, so that the ratios $f_{\mathrm{AcOH_2^+}}/f_{\mathrm{X}_1+}$ and $f_{\mathrm{AcOH_2^+}}/f_{\mathrm{X}_2+}$ are constants, α and β say, then the equation reduces to the form :

$$k_e = c_{\mathrm{HClO_4}}\frac{\alpha k_1\,.\,c_{\mathrm{Ac_2O}}}{K\,.\,c_{(\mathrm{AcOH})_2}} + 2\beta\,.\,k_2.$$

This, in turn, becomes :

(1) $k_e = a\,.\,c_{\mathrm{Ac_2O}} + b$, when only the $\mathrm{Ac_2O}$ concentration is varied, (2) $k_e = a'/c_{(\mathrm{AcOH})_2} + b'$ when the $(\mathrm{AcOH})_2$ concentration only is varied, and (3) $k_e = a''\,.\,c_{\mathrm{HClO_4}}$ when only the $\mathrm{HClO_4}$ concentration is varied. a, b, a', b', and a'' are all constants ; such relationships have been found experimentally.[1] The fact that the experimental results obtained with the aid of $\mathrm{CCl_4}$ may be used to predict those obtained in its absence (ref. 1, Table IV), which indicates an absence of medium effect, lends some measure of support to the assumptions made regarding the constancy of activity coefficient ratios, over the range of experimental studies.

It is to be noted that the final form of the theoretical rate expression given above is not the same as the experimental equations ((7) and (8) of Part II). It has been found that the theoretical expression, with numerical coefficients calculated from any two sets of experimental results in Table IV of Part II will fit the observations for each quinone nearly as well as the empirical equations, and this agreement between theory and observation is satisfactory. However in the case of toluquinone the constant $2\beta k_2$ is found to be $-\,0{\cdot}45$, which implies a negative activity coefficient. The theory given above is therefore an oversimplification, but the matter cannot be pursued further until more experimental information is available.

If the above mechanism is indeed correct, and the assumption that acetyl ions are present in acetic anhydride-acetic acid solutions of perchloric acid is justified, then the interpretation of indicator ratios in such solutions is complex. A basic indicator may be expected to react thus ;

$$\begin{aligned} &\mathrm{B} + \mathrm{AcOH_2^+} \rightleftharpoons \mathrm{BH^+} + \mathrm{AcOH}\\ &\mathrm{B} + \mathrm{Ac^+} \quad\;\;\; \rightleftharpoons \mathrm{BAc^+}. \end{aligned}$$

Presumably the measured conjugate acid ion concentration will be represented by $(c_{\mathrm{BH^+}} + c_{\mathrm{BAc^+}})$, (it has been found, for example, that " acetyl perchlorate " causes 2 : 6-dimethoxy quinone to change colour in the same way as do hydrogen ions [3]), so that an experimentally determined indicator ratio will be represented by $c_{\mathrm{B}}/(c_{\mathrm{BH^+}} + c_{\mathrm{BAc^+}})$. It is then no longer possible to deduce any simple relationship between an acidity function, expressed in terms of this indicator ratio, and the specific reaction rate of an acid-catalysed reaction. The experimentally observed linear relationship between log k_e for benzoquinone and toluquinone and the apparent H_0 values is considered to be merely an approximation due to the low acetyl ion concentration in the solutions for which the relationship holds. In solutions of high c_{Ac_2O} and therefore high c_{Ac^+} the linear relationship ceases to apply.

The Nature of the Reaction Products.

In order to account for the nature of the acetylated products, it is necessary to discuss the mechanism of the reaction in some detail.

(A) **Benzoquinone.**—Benzoquinone may be regarded as a resonance hybrid of the following structures:

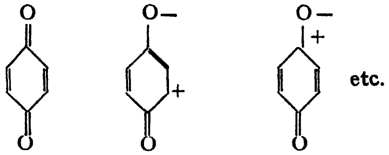

The initial and rate-determining reaction is considered as an attack by an acidic ion on the O-atom of the quinone, thus:

(1)

or

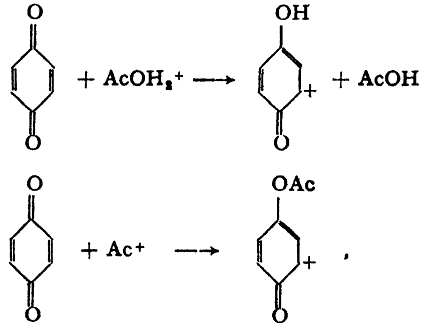

followed by rapid reaction with acetic anhydride,† thus:

(2)

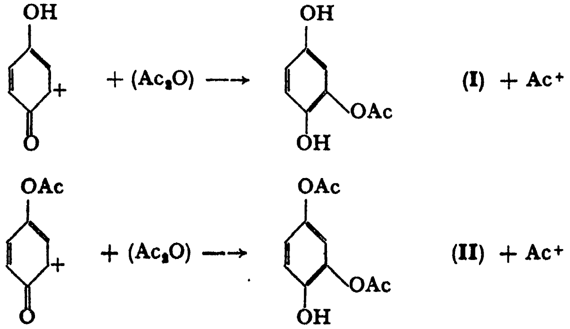

---

† Since the Thiele reaction does not occur in absence of Ac_2O. The Ac^+ ion will, of course, be subject to the equilibrium

$$Ac\,OH_2^+ + Ac_2O \overset{K}{\rightleftharpoons} Ac^+ + (Ac\,OH)_2.$$

(I) may be oxidised by unchanged quinone, thus :

(3)

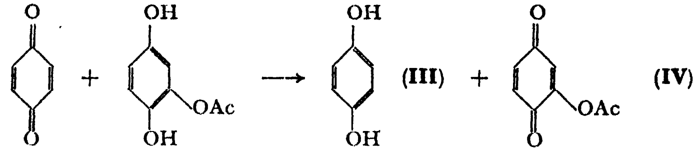

but (II) cannot undergo such a reaction.

The quinone (IV) may be represented as a hybrid of the following resonating structures :

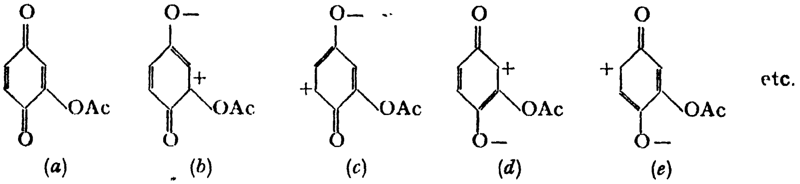

The structures (*b*) and (*c*) would be expected to constitute only a small fraction of the resonance hybrid, since the electron-attracting properties of the —OAc group would tend to oppose the accumulation of a negative charge on the oxygen at the opposite end of the conjugated system. Thus, acetylation of the quinone (IV) would proceed predominantly as follows :

(4)

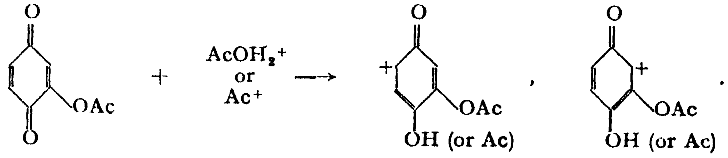

The subsequent reaction with acetic anhydride,

(5)

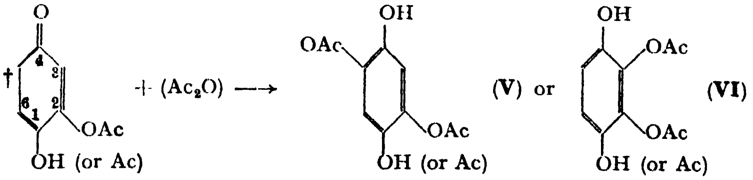

would be expected to give rise to (V) rather than (VI), since the —OAc group at position 2 would hinder sterically the reaction at position 3.

Hence, the acetylation of benzoquinone would in general, be expected to give rise to those products formed by complete acetylation of (I), (III) and (V), viz., hydroquinone diacetate, 1 : 2 : 4-triacetoxy benzene and 1 : 2 : 4 : 5-tetra-acetoxy benzene.

In a mixture of low acetic acid content, the acid would be present mainly as acetyl ions, and the amount of (I) formed would therefore be small. Hence the product would be largely 1 : 2 : 4-triacetoxy benzene. In reaction mixtures of comparable acetic acid and acetic anhydride contents, and therefore of comparable Ac^+ and $AcOH_2^+$ concentrations,* all products would be expected. The theory therefore accounts for the formation of the products obtained in practice,[1] and the agreement affords further evidence in support of the existence of acetyl ions.

(B) Toluquinone.—Here the presence of the methyl group is a complicating factor, since different isomeric products may result from the reaction. The following set of reactions may be anticipated:

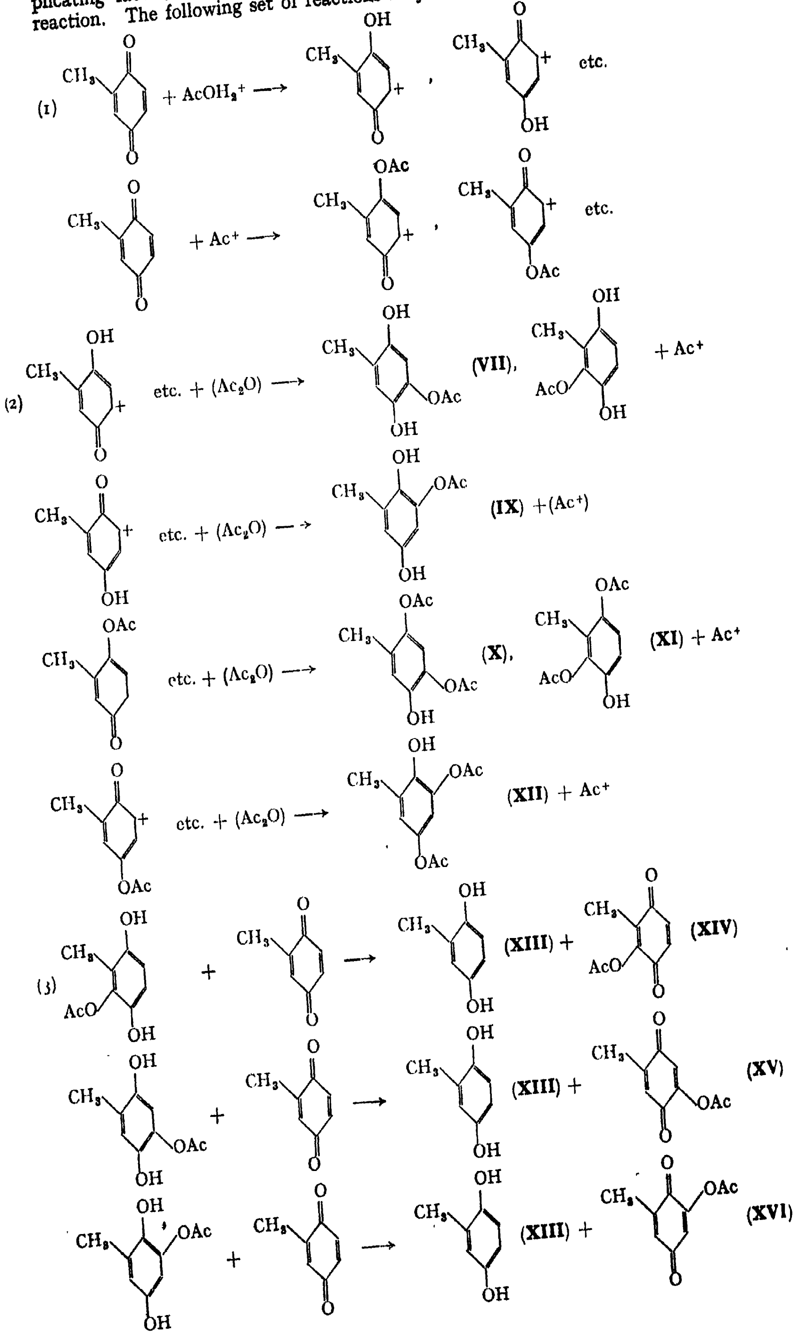

(4) (Assuming that attack takes place at the O-atom adjacent to the acetoxy group.)

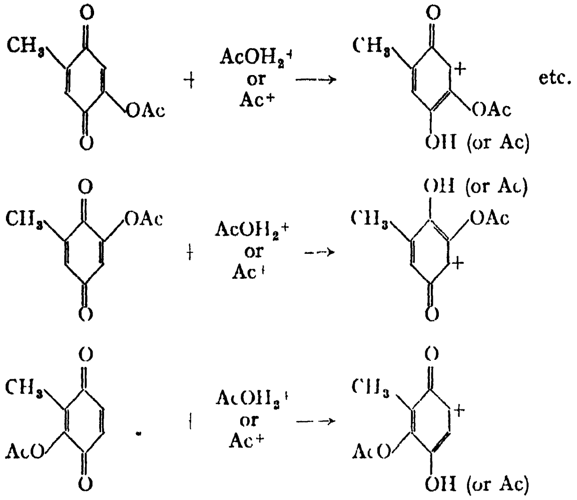

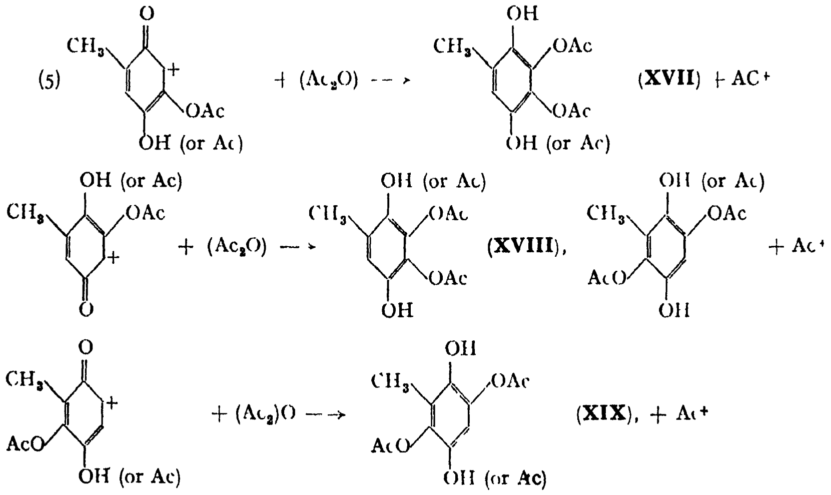

Because of steric hindrance the amounts of (**XVI**) and (**XVII**) formed would be expected to be small, so that, in general, the acetylation of toluquinone would give rise chiefly to the five products formed by complete acetylation of (**X**), (**XI**), (**XII**), (**XIII**), and (**XIX**), viz., the three isomeric triacetoxy toluenes, toluhydroquinone diacetate and 1 : 2 : 4 : 5-tetra-acetoxy toluene.

In a reaction mixture of low acetic acid content, and therefore high acetyl ion concentration, the amounts of (**VII**), (**VIII**) and (**IX**) formed would be small. Hence the products would be the three triacetoxy toluenes. In reaction media of comparable acetic acid and acetic anhydride content, all the products would be expected. Although all the products were not isolated and characterised, the results obtained [1] are in complete agreement with the theory.

Further support of the theory advanced is to be found in the qualitative work on "acetyl perchlorate". The high acidity of the solution which results from the reaction between acetyl chloride and $AgClO_4$ in acetic anhydride is direct evidence of the high acidity of the acetyl ion. The fact that the Thiele acetylation of benzoquinone proceeds in such a solution with a normal yield of the product expected from the above theory, confirms that the acetyl ion is capable of acting as a catalyst for the reaction.

The theory advanced accounts for the observed kinetics in solutions containing up to about 80 % v/v. acetic anhydride. Lack of agreement in solutions containing higher concentrations of acetic anhydride is attributed to the following causes. (1) The acetic acid dimer becomes appreciably dissociated into the monomer, and (2) hence, and because of the high Ac_2O concentration and low acetic acid content, the equilibrium,

$$AcOH_2^+ + Ac_2O \rightleftharpoons Ac^+ + (AcOH)_2,$$

is displaced to the right to such an extent that the assumption made that $K \,.\, a_{(AcOH)_2} \,.\, f_{Ac^+} \gg a_{Ac_2O} \,.\, f_{AcOH_2^+}$ is no longer valid, and the mineral acid is present nearly entirely as acetyl ions.

The Energy of Activation.

The activation energy of the acetylation reaction in solutions containing up to about 80 % v/v. acetic anhydride is constant for both benzoquinone (14·4 kcal./g. mol.) and toluquinone (13·6 kcal./g. mol.). As the acetic anhydride content is increased above 80 % v/v., the activation energy decreases rapidly. These facts may be interpreted in the following way:

If the equation

$$k_e = c_{HClO_4} \frac{k_1 \,.\, c_{Ac_2O}}{K \,.\, c_{(AcOH)_2}} \,.\, \frac{f_Q}{f_{X_1^+}} + \frac{2k_2 \,.\, f_Q}{f_{X_2^+}} f_{AcOH_2^+}$$

is taken to represent the experimental specific reaction rate in solutions containing up to 80 % v/v. acetic anhydride, it may be re-written

$$k_e = c_{HClO_4} \left\{ \frac{k'_1 \,.\, c_{Ac_2O}}{K' \,.\, c_{(AcOH)_2}} \,.\, \frac{f_Q}{f_{X_1^+}} \,.\, e^{\frac{E_1+E}{RT}} + 2k'_2 \,.\, \frac{f_Q}{f_{X_2^+}} \,.\, e^{-\frac{E_2}{RT}} \right\} \,.\, f_{AcOH_2^+}$$

where the equations,

$$k_1 = k'_1 \,.\, e^{-E_1/RT},\; k_2 = k'_2 \,.\, e^{-E_2/RT}, \text{ and } K = K' \,.\, e^{E/RT},$$

are taken to represent the effects of temperature on the specific reaction rates k_1 and k_2 and on the equilibrium constant, K. The plot of log k_e against $1/T$ would thus be linear only if $(-E_1 + E) = -E_2$, i.e. $E + E_2 = E_1$, and the fact that such plots are linear in practice suggests that this equality is closely approximated. This is not unreasonable, since E_1 is associated with the reaction between quinone and acetyl ions, and E_2 and E are associated respectively with the reaction between quinone and $AcOH_2^+$ ions and the reaction by which $AcOH_2^+$ ions are converted to acetyl ions.

In solutions containing more than 80 % v/v. of acetic anhydride, the reaction becomes largely that due to catalysis by acetyl ions, so that, in the limiting case, the specific reaction rate would be given by

$$k_e = c_{HClO_4} \,.\, k_1 \,.\, f_{Ac^+},$$

$$\text{or,}\quad k_e = c_{HClO_4} \,.\, f_{Ac^+} \,.\, k'_1 \,.\, e^{E_1/RT}.$$

Hence the change in measured activation energy as the acetic anhydride content of the solutions is increased above 80 % v/v., may be interpreted theoretically as a change from E_2 to E_1. Unfortunately the limiting case is experimentally unattainable using $HClO_4$, owing to the water which must be introduced into the system with the perchloric acid, and the value of E_1 cannot be obtained by extrapolation with any degree of accuracy. The experimental results suggest, however, that E_1 is about 8000 cal./g. mol. for both benzoquinone and toluquinone, which in turn gives a value for E of about − 6000 cal./g. mol.

One of the authors (H. A. E. M.) wishes to thank the University of South Africa for the award to him of a Croll Scholarship, and the Directorate of Demobilisation of the Union of South Africa Defence Forces for financial assistance, which has enabled him to take part in the work of Parts I, II and III of this series. Finally, the authors wish to record their gratitude to Prof. H. V. A. Briscoe for his interest and encouragement.

Summary.

The acid-catalysed acetylation of benzoquinone and toluquinoune may not be interpreted in terms of a simple theory involving the acidity function as a measure of acidity. Instead, the equilibrium, $AcOH_2^+ + Ac_2O \rightleftharpoons Ac^+ + (AcOH)_2$ is postulated to exist in solutions of perchloric acid in acetic acid-acetic anhydride mixtures, and on this assumption it is possible to account precisely for the observed kinetics of the acetylation reactions and for the nature of the products of acetylation, and to account qualitatively for the observed changes in activation energy.

Imperial College of Science and Technology,
South Kensington,
London, S.W.7.

A CELL FOR THE MEASUREMENT OF DIFFUSION IN AQUEOUS SOLUTION.

By J. C. Gage.

Received 18th April, 1947.

The sintered-glass cell of Northrop and Anson [1] is the type of apparatus most commonly used for the measurement of diffusion coefficients. The technique has been elaborated by McBain and Liu [2] and others and is stated to give results of high reproducibility, but the period is the order of 24 hr. for a molecule of the size of glucose. This length of time proved to be a serious source of error when the solutions under investigation supported microbiological growth, resulting in partial blockage of the membrane. The cell described here is simple to construct and operate and is compact and economical of material. It employs filter-paper in place of the sintered-glass disc and a diffusion period of from 2 to 3 hr. only is required for glucose.

In the figure the apparatus is shown in vertical section. It consists of a cylindrical cell turned out of a solid Perspex block; A is the cavity, approximately 7 cc. capacity, which contains the solution under investigation; B is the filter-paper membrane clamped in position by means of a Perspex ring C attached by four Tufnol studs D. E is an air-cavity which enables the cell to float when inverted in the solvent.

To operate the cell it is filled to overflowing with the solution and two layers of filter paper lowered on, care being taken to avoid the inclusion of air bubbles. After a few min., the filter-paper is clamped down by the Perspex ring and studs. It is then inverted and floated in the solution used to fill the cell; it should be properly trimmed so that it floats horizontally, and then placed in an incubator to reach the required temperature. The cell is then removed and after removal of the surplus solution, it is transferred to a 1 l. beaker containing water or the aqueous solution used as a solvent. If the density of the solution is less than that of the aqueous solvent the cell may be adapted by eliminating the air cavity and floating the cell, membrane uppermost, on mercury in a 1 l. beaker. The primary diffusion which is required for the sintered-glass cell is not necessary here, nor has it been found advantageous to remove dissolved air from the liquids before use. The cell is allowed to stand undisturbed until sufficient diffusate has left the cell to enable an accurate estimate of the decrease in concentration to be made; as the volume of liquid surrounding the cell is very much greater than that of the cell contents, the concentration of diffusate in the former does not appreciably rise above zero. The cell is removed and the surplus solvent mopped off the membrane with small pieces of filter-paper; the contents are sampled either by sliding off the filter paper or by puncturing it. The ratio of the original concentration of the solution to that obtained after diffusion is determined by a suitable analytical method.

---

[1] Northrop, and Anson, *J. Gen. Physiol*, 1928, **12**, 543.

[2] McBain and Liu, *J. Amer. Chem. Soc.*, 1931, **53**, 59. For further reference to experimental methods see Williams and Cady, *Chem. Rev.*, 1934, **14**, 171.

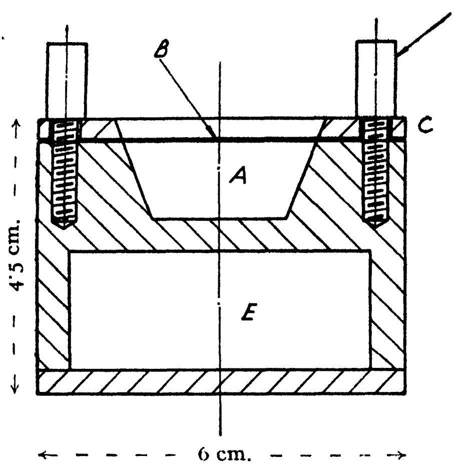

FIG. 1.

TABLE I.

Cell.	$\left(\text{Log}\,\frac{c_0}{c}\right)$ KCl.	$\left(\text{Log}\,\frac{c_0}{c}\right)$ Glucose.	Ratio.	D Glucose × 10^6.
A	0·4360	0·1602	0·367	7·05
	0·3533	0·1257	0·355	6·82
B	0·4067	0·1525	0·375	7·20
	0·3279	0·1194	0·364	6·99
C	0·3906	0·1257	0·343	6·59
	0·3054	0·1050	0·343	6·59

TABLE II.

Cell.	$\left(\text{Log}\,\frac{c_0}{c}\right)$ KCl.	$\left(\text{Log}\,\frac{c_0}{c}\right)$ Sulphaguanidine.	Ratio.	D Sulphaguanidine × 10^6.
A	0·2361	0·1057	0·444	8·53
	0·2304	0·1018	0·442	8·48
B	0·2623	0·1153	0·440	8·45
	0·2497	0·1091	0·437	8·39
C	0·2500	0·1008	0·403	7·74
	0·2469	0·1087	0·440	8·45

In this cell, as in all others of this type, the diffusion coefficients are calculated with reference to a substance whose coefficient is known. Two procedures are available here; the most convenient is to include the reference compound in the solution under investigation, and analyse the contents of the cell for both components after the diffusion period has elapsed. Thus the coefficient of glucose and sulphaguanidine have been measured using KCl as the reference diffusate. This procedure is only possible if there is no interaction between the two components; alternatively, the filter-paper membrane may be standardised with the reference compound, washed and used again for the measurement. Table III shows that two consecutive diffusion experiments using glucose with the same filter-paper membrane show good reproducibility.

Whatman 52 paper is preferred in this cell; other grades have been used with success, but the hardened paper is more robust and will resist caustic alkalis. Two layers are used to minimise the effect of any faults present; the variations of log $\frac{c_0}{c}$ in Tables I and II are in part due to the variability of filter papers from the same batch.

TABLE III.

Cell.	Concentration after Diffusion (mg. %).	
	1st Experiment.	2nd Experiment.
A	130	132
B	129	131·5
C	136	135·5

Calculation of Results.—Fick's law may be written

$$\frac{ds}{dt} = -D\frac{dc}{dx},$$

where ds/dt is the rate of passage of the diffusate per unit area and dc/dx is the concentration gradient across the membrane, assumed linear. The diffusion coefficient D may be regarded as a constant at low concentrations, hence

$$\frac{dc}{dt} = -Dk\,\Delta c$$

where c is the concentration in the cell, Δc the concentration difference across the membrane, and k is a cell constant. Since the concentration outside the cell does not appreciably rise above zero,

$$\frac{dc}{dt} = -kDc \quad \text{or} \quad \log\frac{c_0}{c} = kDt,$$

where c_0 equals the initial concentration in the cell. If two compounds with diffusion coefficients D' and D'' are initially present at concentrations c' and c''_0, and their concentrations at end of time t are c' and c'', then

$$\frac{D'}{D''} = \frac{\log\frac{c''_0}{c''}}{\log\frac{c'_0}{c'}},$$

i.e. independent of t.

Results.

(1) Glucose.—A solution containing 0·01 mole l.$^{-1}$ of glucose and 0·05 mole l.$^{-1}$ of KCl was placed in the cell and diffusion allowed to proceed for 3 hr. at 25° C. Glucose was estimated by the Hoffman colorimetric method [3] with slight modifications, and KCl by titration with N./100 $AgNO_3$ using dibromofluorescein as an absorption indicator. The mean value of the diffusion coefficient from the 6 expt. in Table I is $6{\cdot}87 \times 10^{-6}$ cm.^{2}/sec. with a standard error of $0{\cdot}1 \times 10^{-6}$. This is in good agreement with the value $6{\cdot}78 \times 10^{-6}$ cm.^{2}/sec. extrapolated to zero concentration obtained by Friedman and Carpenter[4] with the McBain cell.

---

[3] Hoffman, *J. Biol. Chem.*, 1937, **51**, 120.

(2) Sulphaguanidine.—Table II shows the results obtained with a solution of 0·00033 mole l.$^{-1}$ of sulphaguanidine and 0·05 mole l.$^{-1}$ of KCl in 0·01 M. phosphate buffer adjusted to *p*H 7·5. Diffusion was continued for 3 hr. into the same phosphate buffer at 25° C. and the sulphaguanidine was estimated colorimetrically after diazotisation and coupling with *N*-*β*-sulphato-ethyl-*m*-toluidine. The mean diffusion coefficient from 6 expt. is $8{\cdot}34 \times 10^{-6}$ cm.^{2}/sec. with a standard error of $0{\cdot}12 \times 10^{-6}$, this agrees well with the value $8{\cdot}10 \times 10^{-6}$ found in this laboratory with the McBain cell. In calculating the above results the value of $1{\cdot}92 \times 10^{-5}$ cm.^{2}/sec. at 25° C. was taken for the diffusion coefficient of KCl.[5]

Discussion.

It is evident from Tables I and II that there is an appreciable scatter in the results of individual experiments. This variation may in part be due to the lack of rigidity of the membrane, or to some extent be ascribed to errors which are inherent in the analytical methods used at these low concentrations. The precision does not compare favourably with that claimed by McBain and Liu for their technique; the simplicity and rapidity of the method, however, permit a larger number of repeat experiments to be made if a higher degree of precision is required.

Both glucose and sulphaguanidine are unionised under the experimental conditions and therefore not subject to errors arising from diffusion potentials nor from preferential adsorption of ions on the membrane. When the diffusion of ions is measured, adsorption on the membrane may be a considerable source of error; the sintered-glass cell is also subject to this criticism.

Summary.

A diffusion cell is described which is simple to construct and operate; it uses filter-paper as the diffusion membrane and yields results in less than one-tenth the time required by the sintered-glass cells of McBain and Liu. The diffusion coefficients of glucose and sulphaguanidine obtained with this cell are in good agreement with the results obtained with the sintered glass-cell. The standard error of the mean of 6 experiments is about 1·5 %.

I.C.I. Ltd.,
Research Laboratories,
Hexagon House,
Manchester.

---

[4] Friedman, and Carpenter, *J. Amer. Chem. Soc.*, 1939, **61**, 1745.
[5] McBain and Dawson, *Proc. Roy. Soc. A*, 1935, **168**, 32.

THE APPLICATION OF THE DIFFERENTIAL ANALYSER TO A PROBLEM IN CHEMICAL KINETICS.

By A. M. Wood, J. Crank and G. H. Twigg

Received 4th March, 1947

In studying the kinetics of a chemical reaction, when the differential equations expressing the rates of reaction in terms of the pressures or concentrations of the reactants have been formulated, it is usually necessary to compare solutions of these equations with experimental results, in order to verify the proposed kinetics. It frequently happens, particularly where consecutive reactions are involved, that the differential equations have no formal solution, or none convenient for numerical evaluation. It then becomes necessary to obtain graphical or numerical solutions for particular cases. A convenient way of obtaining such solutions is by means of the Bush Differential Analyser [1, 2, 3] and the present paper will describe the application of this machine to a typical problem, namely the catalytic oxidation of C_2H_4. It is thought that an account of this work may be of particular interest as this appears to be the first application of the differential analyser to a problem in chemical kinetics.

The experiments [4] were carried out in a closed reaction system, analyses were made at different times and the composition was expressed as partial pressures of the gases present. The main products of reaction between C_2H_4 and O_2 on a Ag catalyst are ethylene oxide, CO_2 and H_2O. The oxidation proceeds through the adsorption on the catalyst of oxygen as atoms, followed by reaction of the other components with this oxygen. The CO_2 and H_2O arise in part directly from C_2H_4 via short-lived intermediates, and in part from ethylene oxide which is isomerised to acetaldehyde, this in turn being rapidly oxidised. These conclusions were reached by examining separately the individual steps in the reaction, and the kinetic order of one of these steps, the production of CO_2 from C_2H_4, was determined. It remained to synthesise these conclusions and verify them by applying them to the overall reaction starting with ethylene and oxygen.

The Equations.

The equations were derived as follows. In the adsorption of oxygen, since the molecule is dissociated into atoms, the rate of adsorption is plausibly assumed proportional to the oxygen pressure p_0, and to the square of the free space on the catalyst, and the rate of desorption proportional to the square of the fraction θ of the surface covered with oxygen. This is represented by the equation

$$\frac{-\,\mathrm{d}p_0}{\mathrm{d}t} = A_0p_0(1-\theta)^2 - A'_0\theta^2 \quad . \quad . \quad . \quad (1)$$

where A_0, A'_0 are constants. Expected orders of magnitude suggest that $(A_0p_0 - A'_0)\theta^2$ will be small so that (1) may be written approximately

$$\frac{-\,\mathrm{d}p_0}{\mathrm{d}t} = A_0p_0(1-2\theta) \quad . \quad . \quad . \quad . \quad (1a)$$

In order to simplify the calculations and also because only 6 integrating units of the differential analyser were available when this work was carried out, the approximate eqn. (1*a*) was used. It is thought that while this may make some difference to the absolute values of θ found, the shape of the curves will be little affected.

The reaction of C_2H_4 can take place in two ways. A C_2H_4 molecule can react either with a single adsorbed oxygen atom to form ethylene oxide, or with a pair of oxygen atoms to form intermediate products which are rapidly oxidised to CO_2 and H_2O. Thus the rate of production of ethylene oxide should be proportional to the ethylene pressure p_1 and to the first power of adsorbed oxygen concentration θ: the rate of production of CO_2 by this route should be proportional to the C_2H_4 pressure and to the

---

[1] Bush, *J. Frank. Inst.*, 1931, **212**, 447.

[2] Hartree, *Math. Gazette*, 1938, **22**, 342.

[3] Crank, *The Differential Analyser* (Longmans, Green, in press).

[4] Twigg, *Trans. Faraday Soc.*, 1946, **42**, 284; *Proc. Roy. Soc. A*, 1946, **188**, 92, 105, 123.

square of the absorbed oxygen concentration. The net rate of reaction of C_2H_4 is thus given by

$$\frac{-\,\mathrm{d}p_1}{\mathrm{d}t} = A_1p_1\theta + B_1p_1\theta^2 \quad . \quad . \quad . \quad . \quad (2)$$

The oxidation of ethylene oxide is controlled by the rate of isomerisation to acetaldehyde, and the rate of this step should be proportional to the ethylene oxide pressure p_2 and independent of the adsorbed oxygen concentration. Thus the net rate of disappearance of ethylene oxide should be

$$\frac{-\,\mathrm{d}p_2}{\mathrm{d}t} = A_2p_2 - A_1p_1\theta \quad . \quad . \quad . \quad . \quad (3)$$

These three equations, together with the two expressing the conservation of carbon and oxygen in the system,

$$p_1 = p_1 + p_2 + \tfrac{1}{2}p_3 \quad . \quad . \quad . \quad . \quad . \quad (4)$$

$$P_0 = p_0 + \tfrac{1}{2}p_2 + \tfrac{3}{2}p_3 + R(\theta - \theta_0), \quad . \quad . \quad . \quad (5)$$

are sufficient to define the system. A_1, A_2, B_1 are constants and P_1, P_0, θ_0 are the values of p_1, p_0 θ respectively at zero time, p_3 is the partial pressure of CO_2 and R is the quantity of O_2, measured as a pressure in the reaction system, which would be adsorbed when $\theta = 1$.

Transformation of the Equations.—It is convenient to eliminate p_3 from (4) and (5) giving

$$P_0 - 3P_1 = p_0 - 3p_1 - \tfrac{5}{2}p_2 + R(\theta - \theta_0) \quad . \quad . \quad (6)$$

On dividing through each of the above equations by P_0 (the approximate eqn. 1*a* is used) and integrating formally, the equations become,

$$-\log\rho_0 = A_0(t - 2\int\theta\mathrm{d}t), \quad . \quad . \quad . \quad . \quad . \quad (7)$$

$$-\log\rho_1 = \int(A_1 + B_1\theta)\theta\mathrm{d}t, \quad . \quad . \quad . \quad . \quad (8)$$

$$-\rho_2 = A_2\int\rho_2\mathrm{d}t - A_1\int\rho_1\theta\mathrm{d}t, \quad . \quad . \quad . \quad . \quad (9)$$

$$\frac{P_0 - 3P_1}{P_0} = \rho_0 - 3\rho_1 - \tfrac{5}{2}\rho_2 + \frac{R}{P_0}(\theta - \theta_0), \quad . \quad . \quad (10)$$

where $\rho_0 = p_0/P_0$, $\rho_1 = p_1/P_0$, etc.

The eqn. (7)-(10) are in a form suitable for solution by the differential analyser.

The Differential Analyser.—Several accounts of the differential analyser have already been written.[1, 2, 3] Only a brief statement is needed here to explain the significance of the set-up diagram in Fig. 1.

A differential analyser consists of a number of units interconnected by a system of shafts and gears, which can be assembled in many different ways. A set-up diagram (e.g. Fig. 1) shows how the units are interconnected for a given equation, each unit being represented by a symbol indicating the operation performed by the unit (e.g. integration, addition). When the appropriate connections have been made the machine will draw out graphical solutions, or numerical results may be obtained from revolution counters.

The Machine Set-up.—The machine set-up for eqn. (7)-(10) is shown schematically in Fig. 1 with gears and scale factors omitted. The notation is thought to be self-explanatory. Six integrators are used and the constants A_0, A_1, etc., are introduced as gear ratios.

Initial conditions for the solution of the equations are supplied to the machine in the form of initial displacements of the integrator units;

when this has been done, the rotation by the motor, of the shaft representing t, drives the rest of the machine so as to evaluate the solution of these equations from these initial conditions. There are no data to be supplied so that no input tables are necessary and the solution proceeds automatically. In the present example initial conditions at $t = 0$ are,

$$\rho_0 = 1,\ \rho_1 = P_1/P_0 \text{ (given)},\ \rho_2 = 0.$$

The initial value of θ, i.e. θ_0 is not known however. The procedure adopted is to take a trial value of θ_0 and to run the machine solution for a few min. of experimental time. It is found that θ readily settles down to an almost constant value. Now in the experimental work subsidiary experiments were made, preceding the main one, to prepare the catalyst surface and ensure that θ should have attained this roughly constant value before the data giving the experimental $p - t$ curves were obtained. In a parallel manner, therefore, in the machine solutions the values of θ at $t = 1, 2, 3$ given by the trial solution starting from an arbitrarily chosen θ_0, are extrapolated back, assuming second-differences constant, to give a new estimate of θ at $t = 0$. This is used as the starting value of θ for the solution proper. The machine can then be made to draw out $p - t$ relations on the output tables, or tabulated results may be obtained from counter readings.

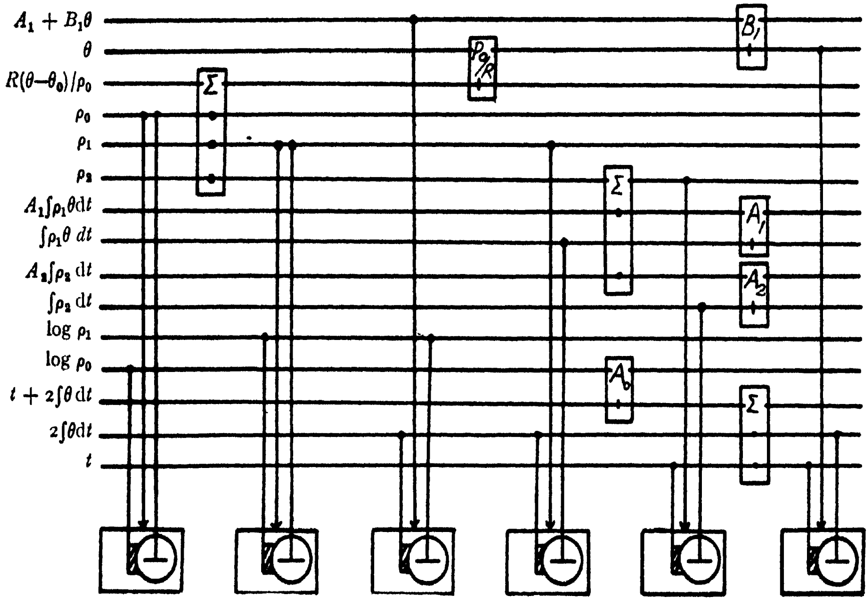

FIG. 1.—Machine set-up for equations.

Solutions.—The problem from the point of view of the differential analyser is first to choose by trial and error a set of constants A_0, A_1, etc. such that, for a chosen pair of values of P_1, P_0, the p-t curves obtained by solution of the equations agree with the corresponding experimental curves. Having successfully chosen constants which produce agreement between theory and experiment in one case, the second task for the machine is to obtain solutions for other combinations of P_1, P_0, so that the agreement between these and the experimental curves may be examined.

The constants were determined by fitting the calculated curves to the experimental data for the case of an initial mixture of 20 mm. C_2H_4 and 60 mm. O_2, i.e. $P_1 = 20$, $P_0 = 60$. Approximate values of the constants may be obtained by assuming θ to be constant throughout the reaction, in which case a formal solution of the equations is easily obtained. By comparing p-t curves from this formal solution with experimental curves, approximate values of $A_0(1 - 2\theta)$, $A_1\theta$, $B_1\theta^2$ and A_2 may be deduced. θ is not directly observable, but a reasonable estimate can be made so that estimates of A_0, A_1, B_1 and A_2 are obtained, which serve as a useful guide in starting the trial and error process of fitting by the differential analyser.

TABLE I *

	$A_1 \times 10^2$.	$B_1 \times 10^2$.	$A_2 \times 10^2$.	$A_0 \times 10^2$.	θ_0.
1	15·625	20·000	4·000	7·8125	0·316
2	15·625	21·429	4·000	4·000	0·255
3	13·333	16·667	4·000	4·000	0·273
4	15·625	20·000	5·000	4·000	0·255
5	11·667	12·500	4·000	4·000	0·299
6	11·333	8·333	4·000	4·000	0·313

The various combinations of constants tried are listed in Table I, together with the corresponding values of θ_0.

The best fit was obtained with the third set of constants and these were chosen as the best estimates of A_0, A_1, etc. The curves for this case are shown as the full lines of Fig. 2 and 3. It will be seen that in Fig. 2 the fit is very good except towards the end of the reaction, when the experiments may be at fault; in Fig. 3, for which the experimental data should be identical with that of Fig. 2, there is a better fit for the latter part of the reaction. The fact that such a good fit is obtainable is in itself considerable support for the kinetics postulated.

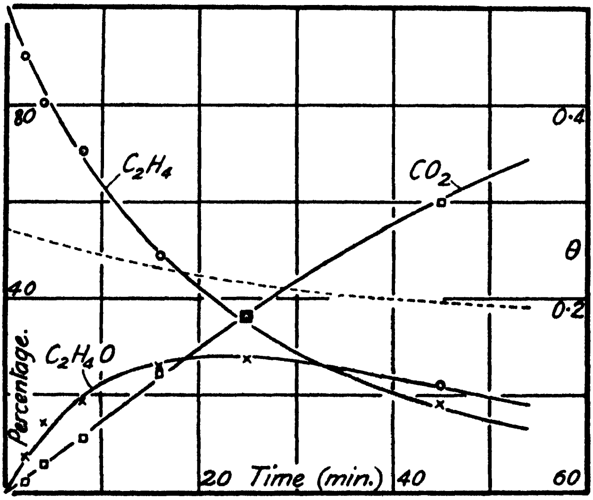

FIG. 2.†

Using the constants so determined, solutions were obtained for other

---

* The constants A_0, A_1, B_1, A_2 are obtained as gear ratios and are exact fractions, e.g. 11·667 = 35/3, 21·429 = 150/7, etc.

† FIG. 2-4.—Experimental points and machine solutions (full curves) for % C_2H_4 remaining (o), or transformed to ethylene oxide (×), or to CO_2 (□). Calculated surface oxygen concentration (dotted curves).

initial pressures of C_2H_4 and O_2. Space does not permit showing all the graphs obtained,‡ but one of these is shown in Fig. 4 where $P_1 = 40$, $P_0 = 60$. The agreement with experiment was in all cases good, and provided ample proof of the kinetics as set out in the above equations.

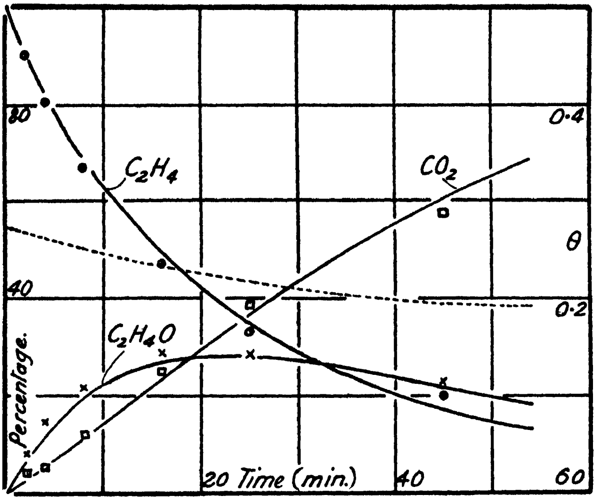

FIG. 3.†

It is probable that by taking all the series of experiments into account, a slightly better choice of velocity constants could be made, which would give an even better fit. It should be emphasised, however, that in only one case was theory fitted to experiment so that the rest of the work must

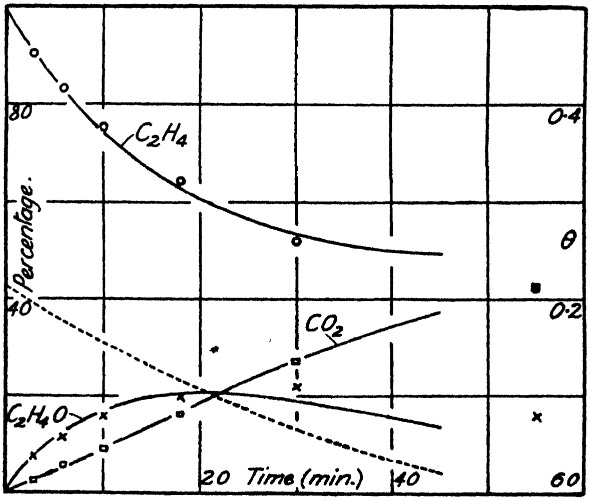

FIG. 4.†

be regarded as a prediction of the results for any desired combination of P_0 and P_1. In the figures the broken lines show the variation of θ with time.

A useful feature of the differential analyser is that once it has been set up to solve a given equation, or set of equations, a large number of solutions corresponding to different initial conditions may be readily obtained. In the present problem it was possible to evaluate machine solutions for very high and very low initial C_2H_4/O_2 ratios, which are particularly valuable as such cases cannot easily be observed experimentally.

---

‡ See, however, *Proc. Roy. Soc. A*, 1946, **188**, 123.

The authors desire to thank Professor Sir J. E. Lennard-Jones for placing the differential analyser at their disposal.

Summary.

The differential equations expressing the behaviour of chemical reactions often have solutions not expressible in terms of known functions, and this is particularly the case where simultaneous and consecutive reactions are involved. In such cases it may be possible to obtain graphical or numerical solutions by means of the Bush Differential Analyser and the application of this machine to the kinetics of the catalytic oxidation of C_2H_4 is described. The velocity constants of the reactions involved were obtained by a process of trial and error in which the machine solutions were fitted to the results of one set of experimental conditions. Using the constants so determined, machine solutions were obtained corresponding to other experimental conditions; the agreement of these predictions with the experimental results provides adequate proof of the correctness of the kinetic equations postulated.

The Distillers' Co. Ltd.,
Epsom,
Surrey.

Mathematical Laboratory,
and Dept. of Colloid Science,
Cambridge.

THE ANODIC BEHAVIOUR OF METALS. PART V.—COPPER.

By A. Hickling and D. Taylor.

Received 28th May, 1947.

In continuation of the work previously reported,[1] the anodic polarisation of copper has now been investigated by the oscillographic method which records the variation of potential with quantity of electricity passed prior to oxygen evolution. Attention has been directed primarily in the present study to the behaviour in alkaline solution where passivity sets in almost at once. No previous work on copper from the present standpoint has been published, but other methods of investigation under different conditions have yielded some relevant information. In acid solutions, copper normally dissolves on being made anodic but may become passive if conditions are such that a film of a sparingly soluble salt is formed on the surface, this being followed by the production of a more protective oxide film which in general appears to be cuprous oxide although cupric oxide is also formed under strongly oxidising conditions.[2] Müller[3] investigated the anodic behaviour of copper in very concentrated NaOH solutions, in which cupric oxide and hydroxide are appreciably soluble, and suggested that several processes occurred consecutively as follows: (*a*) dissolution to give cuprous ions, (*b*) formation of a film of cuprous oxide, (*c*) dissolution to give cupric ions, (*d*) formation of a film of cupric oxide, and (*e*) oxidation to a higher oxide (Cu_2O_3) which was unstable and decomposed to give oxygen and cupric oxide. Numerous investigations have been made on the nature of the partially protective films formed when a fresh copper surface is exposed to, or heated in, air or oxygen;[4] the bulk of the evidence seems to indicate that the film primarily formed is one of cuprous oxide, although cupric oxide may also be present particularly in films formed at high temperatures or by prolonged heating.

---

[1] Hickling, *Trans. Faraday Soc.*, 1945, **41**, 333; 1946, **42**, 518; Hickling and Spice, *ibid.*, 1947, **43**, 762; Hickling and Taylor, *ibid.* (in press).

[2] Hedges, *J. Chem. Soc.*, 1926, 1533; 1929, 1028; 1930, 566.

[3] *Z. Elektrochem.*, 1907, **13**, 133.

Experimental.

The electrical circuit and the electrolytic cell employed were fundamentally as previously described.[1] The copper electrodes used were made by plating copper from a cyanide bath under standard conditions on to a platinum wire electrode of area 0·025 sq. cm. sealed into the end of a glass tube. A fresh plating was used for each experiment. Observations have been made mainly with NaOH solutions of various concentrations as electrolytes; additional experiments have been carried out in a variety of buffer solutions. Except where otherwise stated, all experiments were made at 18° c., using air-free solutions in an atmosphere of nitrogen.

In general the results are shown as photographed oscillograms in which the ordinates represent potentials and the abscissæ are proportional to quantities of electricity passed. Suitable horizontal reference lines at intervals of 0·25 v. were photographed immediately after recording the polarisation tracks, so that significant potentials can be read directly from the oscillograms. The quantity of electricity passed at any stage in the polarisation is computed from the known capacity of the condenser used in series with the electrolytic cell and the horizontal displacement which is governed by the voltage to which the condenser is charged (on the original photographs, before reduction, 1 v. on the condenser corresponds to an average displacement of about 1 mm.). Except where otherwise stated, a 19·45 μF. condenser was used in series with the cell. All potentials quoted are on the hydrogen scale.

Results.

Behaviour in Alkaline Solution.—In Plate I A is shown the characteristic oscillogram in N. NaOH for the anodic polarisation of copper at 18° c. with a polarising current density (c.d.) of 0·04 amp./sq. cm.; the spots on the extreme left of the photograph indicate the steady hydrogen and oxygen evolution potentials at the same c.d. It is seen that a very rapid initial build-up of potential is followed by one main step or arrest during which the potential rises slowly and ultimately achieves the oxygen evolution value; this step appears to start at about $-0·35$ v. but there occurs almost at once a much more definite break at $-0·16$ v. The track was unaffected by stirring or by anodic prepolarisation and was very satisfactorily reproducible. In Plate I B. are shown the anodic tracks at three different c.d's. of 0·08, 0·04, and 0·02 amp./sq. cm. severally, the oscillograms being marked 1, 2 and 3, in order of decreasing c.d.; the polarisation track has the same characteristic form at each c.d., but the step becomes slightly extended as the c.d. decreases. In Plate I C are shown the anodic tracks with a c.d. of 0·04 amp./sq. cm. at temperatures of 18, 30 and 40° c., the tracks being marked 1, 2 and 3; it is seen that rise of temperature has a considerable effect, there being shown a definite short initial step at *ca.* $-0·32$ v. followed by a long arrest at *ca.* $-0·10$ v., and with the quantity of electricity passed in these oscillograms the potential does not rise further. Plate I D shows both the anodic and cathodic polarisation tracks for copper in N. NaOH with a c.d. of 0·04 amp./sq. cm. at 18° c.; the cathodic track shows two definite steps, the total quantity of electricity represented by these being slightly less than that passed in the arrest in the anodic track.

---

[4] Pilling and Bedworth, *J. Inst. Metals*, 1923, **29**, 529; *Ind. Eng. Chem.*, 1925, **17**, 372; Hinshelwood, *Proc. Roy. Soc.*, *A*, 1923, **102**, 318; Evans, *J. Chem. Soc.*, 1925, 2491; Vernon, *ibid.*, 1926, 2273; Constable, *Proc. Roy. Soc.*, *A*, 1927, **115**, 570; Feitknecht, *Z. Elektrochem.*, 1929, **35**, 142; Thomson, *Proc. Roy. Soc.*, *A*, 1930, **128**, 654; Darbyshire, *Trans. Faraday Soc.*, 1931, **27**, 675; Murison, *Phil. Mag.*, 1934, **17**, 96; Preston and Bircumshaw, *ibid.*, 1935, **20**, 706; Van Cleave and Rideal, *Trans. Faraday Soc.*, 1937, **33**, 635; Winterbottom, *Nature*, 1937, **140**, 364; Miley, *J. Amer. Chem. Soc.*, 1937, **59**, 2626; Campbell and Thomas, *Trans. Electrochem. Soc.*, 1939, **76**, 303.

The concentration of NaOH in the electrolyte was found to have an appreciable influence on the tracks. In Plate I E are shown the anodic and cathodic tracks in 5 N. NaOH with a c.d. of 0·04 amp./sq. cm.; it is to be noted that under the conditions of the experiment the copper never becomes completely passive on anodic polarisation but the potential remains at the value corresponding to the main break in the ordinary track; the cathodic track is fairly normal. With decreasing concentration of NaOH the step in the anodic track became shorter; this is shown in Plate I F, in which tracks obtained with a c.d. of 0·04 amp./sq. cm. using as electrolytes 1·0, 0·5 and 0·3 N. NaOH are shown, numbered 1, 2 and 3 in order of decreasing concentration. In Plate II G are shown the anodic and cathodic tracks at 0·04 amp./sq. cm. in 0·1 N. NaOH. The anodic step here begins at about −0·29 v., and is much shorter than in N. NaOH, the potential rising approximately linearly with quantity of electricity passed up to the oxygen evolution value; the track is so steep that it is difficult to distinguish any breaks subsequent to the beginning of the step, but by working with a smaller series condenser (so spreading out the track considerably) it became apparent that, as in N. NaOH, the onset of the step at −0·29 v. is followed almost at once by a break at a rather more positive potential of about −0·07 v. The cathodic track in 0·1 N. NaOH again shows two definite steps which correspond to a total quantity of electricity approximately the same as that passed during the anodic arrest. In 0·1 N. NaOH, variation of c.d. and temperature had relatively little influence on the polarisation tracks.

The influence of various anions in alkaline solution was ascertained by using N. NaOH electrolytes which had been made 0·05 M. with respect to the sodium salts of various acids. Where the anions introduced were such that their discharge was unlikely, and where they had no substantial solvent effect on oxides of copper, e.g. nitrate, no appreciable influence was apparent. The presence of NH_4OH in small amounts did not affect the tracks, but when the electrolyte was made N. with respect to NH_4OH the arrest in the anodic polarisation curve was very greatly extended.

Behaviour in Buffer Solutions.—The effect of decreasing the *p*H value on the anodic behaviour of copper was investigated using a variety of buffer and acid solutions as electrolytes. Except where otherwise stated, a c.d. of 0·04 amp./sq. cm. and standard conditions were used throughout these experiments. In Plate II H are shown the anodic and cathodic tracks in N. Na_2CO_3 (approx. *p*H 12); the anodic track shows a long and approximately linear step beginning at about −0·25 v., while the cathodic track is much less sharply defined than in the NaOH electrolytes and indicates one fairly definite step followed by a gradual decrease of potential to the hydrogen evolution value. In 0·1 N. $Na_2B_4O_7$ (approx. *p*H 9·2) the behaviour was somewhat similar as shown in Plate II I; the anodic track shows a long approximately linear step beginning at about 0 v., while the cathodic track shows two poorly defined steps and a gradual decrease of potential to the hydrogen evolution value. Plate II J shows the anodic and cathodic tracks in 0·2 M. KH_2PO_4 + 0·2 M. Na_2HPO_4 (approx. *p*H 6·8); the anodic track again shows a long approximately linear step beginning at about 0 v., while the cathodic track shows one definite step. In yet more acid solutions, the oscillograms indicated that the sole anodic process was dissolution of copper and the corresponding cathodic process the discharge of copper ions. A typical example is shown in Plate II K, which gives the anodic and cathodic tracks in N. H_2SO_4.

Measurement of the Oxide Potentials of Copper.—The electromotive behaviour of copper oxides in sodium hydroxide solutions was very thoroughly investigated by Allmand.[5] The values found in N. NaOH were:

$$Cu\text{-}Cu_2O \; -\; 0{\cdot}346, \quad Cu_2O\text{-}CuO \; -\; 0{\cdot}154, \quad Cu_2O\text{-}Cu(OH)_2 \; -\; 0{\cdot}076 \text{ v.}$$

The system Cu_2O-CuO initially gave more positive potentials, varying according to the mode of preparation and treatment of the cupric oxide, but approached the value quoted on ageing; the system Cu-CuO was found to be unstable in alkaline solution. In the present work measurements have been made to the nearest centivolt on similar relevant oxide systems in N. and 0·1 N. NaOH and in some of the buffer solutions used for the oscillographic study; a saturated calomel electrode was used as reference electrode and the values quoted may include small liquid junction potential differences which are, however, also present in the potentials read from the oscillograms. Powdered Cu was prepared by precipitation from $CuSO_4$ solution with Zn dust, Cu_2O by reduction of an alkaline tartrate solution of $CuSO_4$ with cane sugar, CuO by ignition of $Cu(NO_3)_2$, and crystalline $Cu(OH)_2$ by Becquerel's method.[6] The two components of each system were shaken up with a quantity of the boiled-out electrolyte, a short platinum wire electrode immersed in the sludge formed, and the potential set up in an atmosphere of nitrogen measured against a saturated calomel electrode using a valve potentiometer to avoid any current being taken from the system. The following steady values were obtained :

---

[5] *J. Chem. Soc.*, 1909, **95**, 2151; 1910, **97**, 603; see also Maddison, *Trans. Faraday Soc.*, 1926, **22**, 27.

Electrolyte.	Cu-Cu_2O.	Cu_2O-CuO.	Cu_2O-$Cu(OH)_2$.
N. NaOH . . .	−0·34 v.	−0·16 v.	−0·06 v.
0·1 N. NaOH . .	−0·28	−0·04	—
N. Na_2CO_3 . .	−0·14	+0·02	—
0·1 N. $Na_2B_4O_7$ . .	+0·13	+0·22	—

Measurement of the True Area of the Copper Electrode.—To obtain an idea of the ratio, accessible area/apparent area, for the copper electrode used the method of Bowden and Rideal[7] was employed in which the double layer capacity of the metal when used as a cathode in acid solution is measured and compared with that of mercury for which the accessible area may be assumed to be the same as the apparent area. Using the A.C. method previously described,[8] the minimum capacity of the copper electrode in N. H_2SO_4 immediately prior to hydrogen evolution was found to be 76·8 μF./apparent sq. cm., while that of mercury measured under the same conditions was found to be 12·0 μF./sq. cm. From these values it would appear that the true area of the copper electrode is about 6·4 times its apparent area.

Discussion.

In N. NaOH, copper gives a characteristic anodic polarisation track under standard conditions (Plate I A) which consists of (1) a very rapid rise of potential which is barely recorded by the photographic plates and which, by analogy with the previous metals studied,[1] probably corresponds to the charging of a double layer, and (2) a long step, in which the potential rises slowly, passing ultimately into oxygen evolution. This step begins at − 0·35 v., and the track almost at once undergoes an abrupt change of slope at − 0·16 v. ; the reversible potentials of the systems Cu-Cu_2O and Cu_2O-CuO in the same solution were found to be − 0·34 v. and − 0·16 v. respectively. It is difficult, therefore, to resist the conclusion that the onset of the step corresponds to the formation of cuprous oxide on the copper surface and this is almost at once oxidised to cupric oxide. The quantity of electricity passed in the step can be estimated approximately from the oscillograms and at 18° c. with a polarising c.d. of 0·04 amp./sq. cm. it is found to be about 24,900 microcoulombs per apparent sq. cm. of copper surface ; this is sufficient to liberate approximately 78×10^{15} atoms of oxygen. Taking the specific gravity of copper as 8·93, the diameter of the copper atom may be calculated to be approximately $2{\cdot}3 \times 10^{-8}$ cm., and hence there would be about $1{\cdot}9 \times 10^{15}$ atoms of metal per true sq. cm., or $12{\cdot}3 \times 10^{15}$ atoms of metal per apparent sq. cm. at a copper surface, assuming the measured value of 6·4 for the ratio accessible area/apparent area to be correct. Thus the ratio of atoms of O/atoms of Cu in the step is 6·3, which suggests that if the step corresponds to the formation of a film of CuO, as the potentials indicate, the quantity of electricity is sufficient to provide for such a film some 6-7 molecules thick. Such a considerable initial thickness would suggest that the film has only relatively poor protective powers, and this is in harmony with the well-known fact that cupric oxide is appreciably

[6] *Compt. rend.*, 1852, **34**, 573.

[7] *Proc. Roy. Soc. A*, 1928, **120**, 80.

[8] Hickling and Taylor, *loc. cit.*[1].

soluble in NaOH so that some of it is probably dissolved away as it is formed. The experiments on the influence of c.d., temperature, and alkali concentration are in conformity with this view. Decrease of c.d. (Plate I B), which diminishes the rate of oxide formation, appreciably lengthens the step in the anodic polarisation track. Increase of temperature (Plate I C) which increases the solubility of the oxide and also the diffusion away of any dissolved substance from the anode, lengthens the step tremendously; it has also the effect of demonstrating more distinctly the breaks which have been attributed to cuprous and cupric oxides respectively. Increase of alkali concentration (Plate I E), which increases the solubility of cupric oxide, also lengthens the step enormously; the presence of ammonium hydroxide, which dissolves cupric oxide, achieves the same result.

The cathodic track in N. NaOH under standard conditions (Plate I D), shows two distinct steps, and it seems reasonable to attribute these to the reduction of cupric to cuprous oxide, and to the reduction of cuprous oxide to copper respectively. The potentials corresponding to these steps are displaced to values rather more negative than the reversible values, which suggests that some polarisation is involved in the reduction processes. In agreement with this view it was found that the higher the c.d. the more negative were the reduction potentials; this is shown in Plate II L, in which are the cathodic tracks at 0·08, 0·04, and 0·02 amp./sq. cm. severally for a copper electrode in N. NaOH at 18° C. It was also noted that with the reversible electrode systems Cu-Cu_2O and Cu_2O-CuO in N. NaOH the static potentials were displaced in a negative direction by the addition of reducing agents such as hydrazine sulphate. It may be observed (Plate I D) that in passing from one step to the other, the cathodic polarisation track exhibits a characteristic valley and peak effect. If the film of cupric oxide on the electrode is several molecules thick this effect is perhaps to be expected. It may be supposed that the section of the film in contact with the metal is first reduced, the potential then dropping to the Cu-Cu_2O reduction stage; as the cuprous oxide in contact with the electrode is further reduced to copper, the freshly formed metal will come into contact with the outer layers of cupric oxide and there will be a transient tendency for the more positive Cu_2O-CuO potential to be restored, this being rapidly checked as reduction proceeds further. The total quantity of electricity passed in the cathodic steps is about 18,700 microcoulombs per apparent sq. cm. of copper surface, and on the same assumptions as above this would correspond to the reduction of a film of cupric oxide some 4-5 molecules thick. This thus supports the conclusion reached above that in N. NaOH some of the cupric oxide goes into solution, and indeed after a number of electrolyses sensitive tests showed the presence of copper in the electrolyte. In more concentrated NaOH solutions and at higher temperatures the amount of cupric oxide going into solution is greatly increased, but the amount remaining on the electrode, as shown by the cathodic tracks, seems to remain much the same.

With decreasing concentration of NaOH the step in the anodic track becomes shorter (Plate I F) as might be expected since the solubility of cupric oxide is less. In 0·1 N. NaOH at 0·04 amp./sq. cm. and 18° C. the step in the anodic track (Plate II G) begins at about − 0·29 V. and is followed by a further break at about − 0·07 V. The reversible Cu/Cu_2O and Cu_2O-CuO potentials in 0·1 N. NaOH were measured as − 0·28 V. and − 0·04 V. which are in fair agreement with the oscillogram values and suggest that the processes are the same as in N. NaOH, i.e. firstly the formation of Cu_2O followed almost at once by its oxidation to CuO. The quantity of electricity passed in the anodic step in 0·1 N. NaOH is 14,800 microcoulombs per apparent sq. cm., which is equivalent to a film of CuO slightly less than 4 molecules thick. This is less than in N. NaOH, which suggests that the film is more stable; in agreement with this, it was found

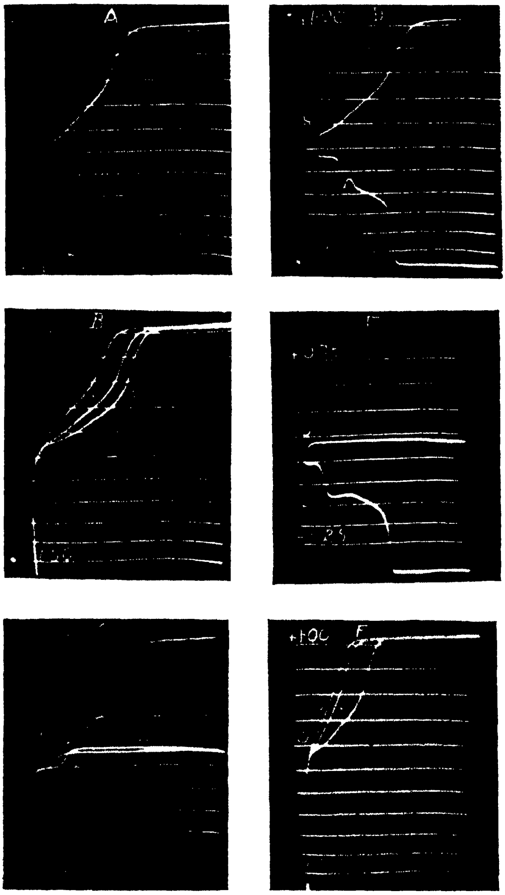

Plate I.

[*To face p.* 266

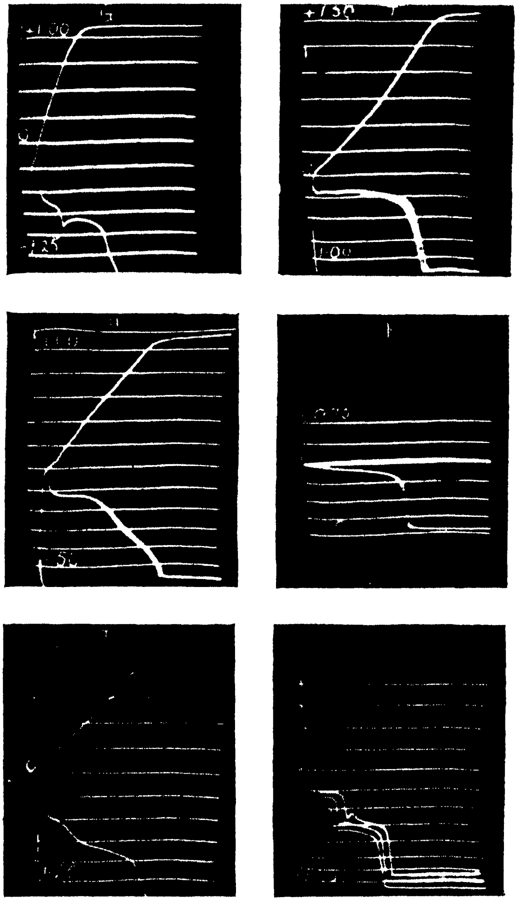

PLATE II.

[*To face p.* 267

that variation of c.d. and temperature had relatively little influence on the oscillogram. The cathodic track again shows two well-defined arrests, corresponding to the reduction of cupric to cuprous oxide and of cuprous oxide to copper. The total quantity of electricity passed in the cathodic steps is 16,300 microcoulombs per apparent sq. cm. corresponding to a film of CuO slightly greater than 4 molecules thick. It thus appears that no copper goes into solution in 0·1 N. NaOH ; the fact that the cathodic arrests indicate a very slightly thicker film than that corresponding to the anodic step is probably to be ascribed to some slight growth of the film after the oxygen evolution potential has been reached.

To summarise, therefore, the oscillograms indicate that in solutions of NaOH, following the charging-up of a double layer, cuprous oxide is first formed at a copper anode but is almost immediately oxidised to cupric oxide. When the cupric oxide film has attained sufficient thickness as substantially to protect the copper surface from further attack, oxygen is evolved at the anode. The oxide film is thinnest in 0·1 N. NaOH, and the anodic track is here not very dependent upon experimental variables ; in more concentrated solutions of NaOH the film is thicker and some copper enters the solution, and any factor influencing the solubility of cupric oxide greatly affects the anodic track. The cathodic curves indicate a successive reduction of cupric oxide first to cuprous oxide and finally to copper. It may be noted that in the present case, unlike those previously studied,[1] it is possible to say definitely from the potentials involved that it is the oxide and not the hydroxide of the metal which is formed on anodic polarisation. The oscillograms give no indication of any oxide of copper higher than cupric oxide being formed before oxygen is first evolved.

The remarks so far made apply to the behaviour of a copper anode in NaOH solutions, and the oscillograms are here very precise and definite and permit of what appears to be a quite satisfactory interpretation. In the carbonate (Plate II H), borax (Plate II I), and phosphate (Plate II J) buffer solutions the behaviour is less clearly defined. In each case there is a very long anodic step beginning at approximately − 0·29 v. in carbonate, 0 v. in borax, and 0 v. in phosphate solution. These potentials are all considerably more negative than the reversible values for the systems Cu-Cu_2O and Cu_2O-CuO in these solutions, but are of the same order as those found when a copper electrode is immersed in the solutions and a few drops of dilute copper sulphate solution added so as to give a saturated solution of the sparingly soluble copper salt. It seems likely, therefore, that following the charging-up of the double layer, the initial anodic process is the dissolution of copper to form a sparingly soluble salt. This is probably followed by oxide formation since the cathodic tracks do show some indication of oxide reduction steps, although these are in all cases shorter than the anodic steps and are not very sharply defined, as indeed might be expected if the oxide reduction is accompanied by reduction of a copper salt or by discharge of copper ions from the solution. Visual experiments on the polarisation of a large copper anode in the buffer solutions tended to confirm these conclusions. In general, with a c.d. such that oxygen was evolved, the anode became coated with a blue deposit beneath which a black film could usually be detected. In an acid electrolyte, in which any copper salt formed was reasonably soluble, the small copper anodes never became passive with the small quantity of electricity passed in the oscillographic experiments, and the anodic and cathodic tracks merely indicated dissolution and deposition of copper respectively (Plate II K).

A consideration of the results obtained in the present work on copper together with the data obtained in the previous studies on platinum, gold, nickel and silver permits some general conclusions to be drawn with regard to the anodic behaviour of metals. In all cases the oscillograms have demonstrated clearly that before the metal becomes passive and

Fifty Years of Progress. The Story of the Castner-Kellner Alkali Company told to Celebrate the Fiftieth Anniversary of its Foundation. Issued by Imperial Chemical Industries, Ltd., 1947.

The initiation of the Castner-Kellner Alkali Company, its early difficulties, and its later triumphs, are excellently told and illustrated in this interesting publication. The development of the firm represents in many ways the entry of the methods of physical chemistry into chemical industry, the old, dirty, and rather haphazard processes of the Leblanc industry giving way to the elegant and stream-lined technique of the new age. The personalities concerned are sketched and the broad principles of their achievements described. The text is essentially a history of the development of a firm, the scientific interest being slight, and almost confined to the reproduction of the original drawing of the Castner sodium process, now quite forgotten, but in its time linked up with the development of the aluminium industry. Although all the historical information contained in the book is available elsewhere, the part played by the men concerned has not, hitherto, been so clearly set out. From any point of view, this is an interesting and instructive book. The production is excellent.

J. R. P.

Journal of the Electrodepositors' Technical Society, VOL. XXI, **1945-1946.** The Society, at 27 Islington High Street, London, N.1. Pp: 297. Price to non-members, 42s.

In this volume most aspects of contemporary electrodeposition practice and related topics are represented and a fair balance is struck between the general and the specific. In the course of his Presidential Address, Dr. Wernick traces the emergence of electrodeposition as a science rather than an art. From the contents of this volume, it is to be inferred that the process is far from complete. Present-day knowledge of the mechanism of simple electrode processes is relatively scanty and consequently problems, such as the nature of the mechanism of metal deposition from complex solutions, are still unsolved. Nevertheless, it is surprising for example to find no apparent reference to a *measured* electrode potential within this volume. Fundamental aspects of the subject are not treated and it is to be hoped that the reason for this is that they are not regarded as coming under the purview of the Society.

Industrial readers will be particularly interested in the articles concerned with electro-galvanising and electro-tinning and with the requirements of the automobile industry. The general reader will be most attracted to two papers on alloy deposition, which further indicate the value of this process, two articles on electro-polishing, a review on electroplating on to aluminium, and an article on the dyeing of anodised aluminium. The excellent catalogue of "Defects in Plating Solutions and their Remedies" should prove valuable to laboratory workers as well as to the industrial platers for whom it was intended.

The Society are to be congratulated on maintaining their high standard of presentation.

J. F. H.

THE ACTION AND DESIGN OF MECHANICAL FILTERS FOR DUST AND SMOKE.

By E. A. B. Birse and (the late) J. K. Roberts.

Received 12th November, 1946.

It is well known [1] that the action of ordinary dust and smoke filters is partly due to centrifugal forces, which are set up when the stream of air carrying the dust passes round a sharp corner, and partly to the Brownian movement of the particles. These are removed when they strike against a solid wall to which they adhere. For larger and heavier particles the centrifugal action is more important and for very small particles the Brownian movement. If the filtering is in the main due to centrifugal action, the efficiency of a filter increases as the velocity of the gas passing through it increases while, if the filtering is in the main due to Brownian movement, the efficiency of filtering diminishes as the gas velocity increases.

The object of the experiments described in this paper was to attempt to throw some light on the action of filters depending on centrifugal action. With this purpose in view, model filters of geometrical construction were used so that the various factors which affected the efficiency could be accurately controlled and measured.

In order to carry out the experiments it was necessary to devise a simple, rapid and accurate method of determining the mass concentration, i.e., the mass dispersed per cm.^{3}, of the dust or smoke. The amounts so dispersed may in some cases be extremely small. The method of measurement which we shall describe in the next section can be applied to a dust or smoke of stearic acid, which was used in the experiments, or of any substance which spreads to form a monolayer on water.

Experimental.

Measurement of Mass Concentration of Dust.

A sample of the dust was drawn off by a filter pump or a Hyvac pump and sucked through a small dry filter paper clamped between two circular pieces of brass. The particles were caught on the filter paper. The volume V drawn off was measured by delivering it from the pump into a calibrated vessel. The filter paper was placed in a volume v_1 of petrol ether and a volume v_2 of the very dilute solution so formed was spread on the surface of an ordinary Langmuir trough as designed by Adam.[2] With stearic acid films the force-area curve rises rapidly when a surface concentration of $2{\cdot}02 \times 10^{-7}$ g./cm.^{2} is reached. If the film area at which this rise occurred was A, the mass concentration m of the smoke was then given by

$$m = 2{\cdot}02 \times 10^{-7} \frac{A}{V} \times \frac{v_1}{v_2}. \quad . \quad . \quad . \quad . \quad . \quad (1)$$

In the experiments described in the following sections the mass concentration of stearic acid smoke was maintained about 1×10^{-3} g./l. and about 2 l. were passed through the filter paper.

The effectiveness of the filter paper in removing the particles was tested by filling a litre flask a large number of times with air which was filtered through the paper and was originally charged with stearic acid dust. Each time the air was left in the flask for 24 hr. so that any dust in it would settle out. Finally, after 16 fillings the flask was washed out with petrol ether and the amount of stearic acid in it was measured. Knowing the initial concentration in the air each time, the fraction that passed through the filter paper could be deduced and it was found to be less than 4×10^{-4}.

---

[1] See, e.g., Freundlich, *Colloid and Capillary Chemistry* (Methuen, 1922.)

[2] Adam, *Physics and Chemistry of Surfaces* (Oxford University Press, 1930.)

Construction of the Model Filter.

The filter used is shown diagrammatically in Fig. 1*a*. It consisted of a slit S in a metal plate through which the dust laden air entered; S was 0·5 cm. long and about 0·05 cm. deep. Its width and its position relative to the base B could be varied. The jaws of the slit were carefully ground so that they were smooth and straight. Two glass microscope slides A and A′ were arranged one on either side of the slit and equidistant from it with their faces parallel to the directions of the slit length and depth. They were held parallel to each other and perpendicular to B by pressing them at the top and bottom against distance pieces held in the metal frame which supported the whole system. By using different distance pieces the distance apart of the plates could be varied.

An important feature of the model was that the stream of air passing through S did not impinge directly on the collecting plates. With the plates arranged in this way it was thought that their interference with the vortices set up by the passage of the gas through the slit would be reduced to a minimum. Vortices of this type have been investigated theoretically by von Kármán and Rubach,[3] and experimentally by Kruge and Schmidtke [4] who have discussed the application of the results to the explanation of the production of slit tones investigated by Kohlrausch.[5]

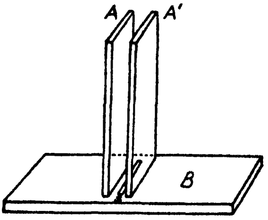

FIG. 1*a*.

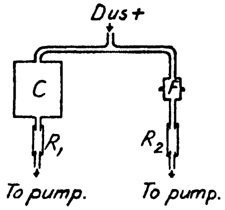

FIG. 1*b*.

The efficiency of filtering by this system was measured as follows. The rubber tube R_1 (Fig. 1*b*) was closed by a clip and a measured volume V_1 of the air containing the dust was drawn through a filter paper contained in the holder F. The rubber tube R_2 was then closed by a clip and R_1 was opened and a volume V_2 of the dust laden air was drawn in a measured time t through the container C in which the slit and plates were mounted. R_1 was then closed and R_2 opened and a volume V_3, approximately equal to V_1, of air was drawn through F. The mass concentration m of the dust was obtained from the deposit on the filter paper using equation (1) with $V = V_1 + V_3$. The amount of dust M passing into C in the second operation was given by $M = mV_2$. The amount M' removed by the filter was determined directly by dissolving the deposit on the glass plates in a volume v_1 of petrol ether, spreading a volume v_2' of the solution on the surface of the Langmuir trough, measuring the area A' at which the rapid rise in the force-area curve took place and using the equation

$$M' = 2{\cdot}02 \times 10^{-7}\frac{A'v'_1}{v'_2} \qquad . \quad . \quad . \quad . \quad . \quad (2)$$

The fraction ϕ of dust removed was given by

$$\phi = M/M'.$$

Results.

The fraction ϕ of dust removed is plotted in Fig. 2 and 3 as a function of the mean linear velocity U of the air in the slit, which was obtained by dividing the rate of flow in cc./sec. by the area of the slit. In the experiments to which Fig. 2 refers the plates were 2 mm. apart and results are included for slit widths from 0·105 mm. to 0·362 mm., while in the experiments to which Fig. 3 refers the plates were 5 mm. apart and results are included for slit widths from 0·250 to 0·362 mm. It will be seen that in neither case is there any tendency for the fraction removed to vary in a regular way with slit width.

---

[3] Von Kármán and Rubach, *Physik. Z.* (1912), **13**, 49.
[4] Kruger and Schmidtke, *Ann. Physik.* (1919), **60**, 701.
[5] Kohlrausch, *Pogg. Ann.*, 1881, **13**, 545.

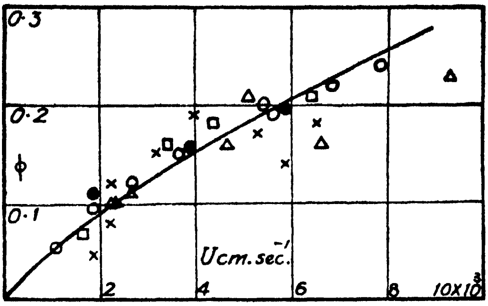

FIG. 2.

The equation of the curve drawn in each of the two figures is

$$\phi = k_1(U/10^3)^{1/1.3} \quad . \quad . \quad . \quad . \quad . \quad (3)$$

where $k_1 = 5{\cdot}20 \times 10^{-2}$ in Fig. 2 and $2{\cdot}76 \times 10^{-2}$ in Fig. 3. These curves represent the experimental results well except possibly for a tendency for the points to fall below the curves at the higher velocities.

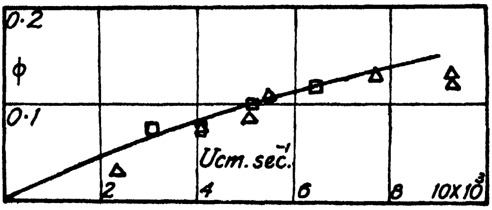

FIG. 3.

The variation of ϕ with the distance apart of the plates L is shown in Fig. 4 for four different values of U. The points plotted were taken from smooth curves like those in Fig. 2 and 3 drawn through the experimental points for $L = 2, 5, 7, 12$ mm.

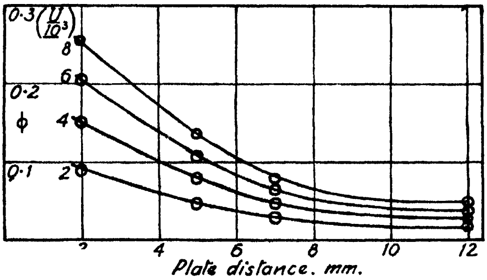

FIG. 4.

The experimental results for the range of condition tested may be summarised as follows.

(i) The fraction ϕ of dust removed by deposition on the plates at a given distance apart does not depend on the width of the slit but only on the linear velocity U of the air passing through it. ϕ is proportional to $U^{1/n}$ where n lies between 1 and 2 and is approximately 1·3.

(ii) For a given velocity, ϕ diminishes as L the distance between the plates, increases and the rate of diminution of ϕ with increase of L also diminishes a L increases.

Some preliminary experiments were made with circular holes instead of slits and a cylindrical tube instead of the two plates. A brass tube 6 mm. in diameter was closed at one end by soldering on it a thin circular brass plate of the same diameter. The circular hole was drilled in the middle of this plate. A glass tube of the same external diameter rested against the outside of the brass plate and was held in position by a piece of rubber tubing. The dust-laden air passed through the hole from the brass tube and the deposition took place inside the glass tube. The latter tube was then removed and the amount of the deposit in it measured. Holes of diameter 0·5, 1, and 2 mm. were used. It was found that here too the fraction of dust deposited depended only on the linear velocity U of the air passing through the hole and not on the diameter and it was also found to be proportional to $U^{1/n}$ with $n = 1·3$.

Discussion.

The physical factors which affect the efficiency of filtering may be discussed qualitatively in terms of the theory of vortex formation of von Kármán and Rubach [8] who show that there are two groups of vortices of opposite sign which move off from the slit in the same direction as the air issuing from it. These two groups lie on either side of a plane through the length of the slit perpendicular to the base B (Fig. 1*a*). We shall denote the distance between the two groups by h. Vortices in the two groups are detached alternately and not together.

The amount of dust removed per sec. will be given by an expression of the form

$$k_2 mNf(G, L, h) \quad . \quad . \quad . \quad . \quad . \quad . \quad (4)$$

where k_2 is a constant for a slit of fixed length, m is the mass concentration of the smoke, N is the number of vortices produced per sec. and G the strength of each vortex. The amount will depend on L, the distance between the plates A and A′ (Fig. 1*a*), and on h because these determine the distance of the vortices from the plates. The amount passing per sec. through a slit of width D is given by

$$k_3 mUD,$$

where the constant k_3 is equal to the length of the slit. The fraction ϕ removed is given by

$$\phi = k_4 \frac{Nf_1(G, L, h)}{UD} \quad . \quad . \quad . \quad . \quad . \quad (5)$$

k_4 will be constant for a given gas and a dust of given material and given particle size.

The theory of von Kármán and Rubach and an application of the theory of dimensions give the following results as a first approximation. If l is the distance between neighbouring vortices in one group, $h/l = 0·283$. This is confirmed by experiment. The other relations are

$$h \propto D, \quad . \quad . \quad . \quad . \quad . \quad . \quad . \quad (6)$$

and h is independent of U. Also

$$N \propto U/D, \quad . \quad . \quad . \quad . \quad . \quad . \quad (7)$$

and

$$G \propto UD \quad . \quad . \quad . \quad . \quad . \quad . \quad (8)$$

In using these results we shall assume as a first approximation that (5) can be written

$$\phi = k_4 \frac{N}{UD} f_2(G) f_3(L, h) \quad . \quad . \quad . \quad . \quad . \quad (9)$$

We assume further that, since $f_3(G) = 0$ when $G = 0$, we can put

$$f_3(G) \propto G^{\mu} \quad . \quad . \quad . \quad . \quad . \quad (10)$$

Using (6), (7), (8) and (10) in (9), it becomes

$$\phi = k_5 U^{\mu} D^{\mu-2} f_4(L, D) \quad . \quad . \quad . \quad . \quad (11)$$

The empirical result (1) shows that $\phi \propto U^{1/1\cdot3}$ so that $\mu = 1/1\cdot3$ or approximately 0·8.

The variation of ϕ with D is then expressed by

$$\phi \propto \frac{f_4(L, D)}{D^{1\cdot2}} \quad . \quad . \quad . \quad . \quad . \quad (12)$$

$f_4(L, D)$ will increase as D increases, because increasing D causes h, the distance apart of the two groups of vortices, to increase; this increase brings the group on the same side of the centre line as one of the plates nearer to that plate. Now the results given in Fig. 4 show that bringing the plates nearer to the vortices increases ϕ and it can be inferred that bringing the vortices nearer the plate will also increase ϕ. The general shape of the curves in Fig. 4 shows too that for a given plate the effect due to the nearer group of vortices will outweigh that due to the further group. Thus the numerator and denominator of the term expressing the variation of ϕ with D both increase as D increases and the two effects tending to cancel each other can make ϕ independent, or almost independent, of D as found in the experiments.

We cannot discuss the theory for circular holes in a similar way as the theory of the production of vortices in this case has not been examined in such detail.

Application to Design of Practical Filter.

In constructing a dust filter for practical use it is usually necessary to take into account the resistance of the filter to the flow of gas and to combine a high efficiency of dust removal with a low-pressure drop. High efficiency of dust removal can be attained by using a high velocity in the slit or hole. This, however, results in a relatively large pressure drop across the filter and the only practicable method is to use a number of larger holes in series. We shall show this by discussing the behaviour of a filter with a number of similar stages in series on the basis of the results described above.

ϕ, the fraction of dust removed at each stage of filtering, is given by

$$\phi = K' U^{1/n} \quad . \quad . \quad . \quad . \quad . \quad (13)$$

where K' is a constant and U is the linear velocity in each hole or slit. Let us compare two filters in the first of which the slits have the area A_1 and in the second the area A_2 and let us suppose that the volume of gas passing through the two filters is the same. We have then

$$\phi_1 = K A_1^{-1/n}, \quad \phi_2 = K A_2^{-1/n} \quad . \quad . \quad . \quad (14)$$

where K is constant if the volume rate of flow is constant. The fraction of dust transmitted at each stage is $1 - \phi$. For a dust in which all the particles are the same size the fraction transmitted by the whole filter of s stages is $(1 - \phi)^s$ and we shall assume this law as a working hypothesis for actual dusts.

Let us first calculate the relative number of stages required to give the same filtering efficiency in the two filters, i.e. to make

$$(1 - \phi_2)^{s_2} = (1 - \phi_1)^{s_1} \quad . \quad . \quad . \quad . \quad . \quad (15)$$

If ϕ_2, ϕ_1, $s_2\phi_2$ and $s_1\phi_1$ are small, this gives to a first approximation

$$s_2\phi_2 = s_1\phi_1$$

or

$$\frac{s_2}{s_1} = \frac{\phi_1}{\phi_2} = \left(\frac{A_2}{A_1}\right)^{1/n} \quad . \quad . \quad . \quad . \quad . \quad (16)$$

from (14). The total pressure drop in the first filter is s_1p_1 and in the second s_2p_2 where p_1 is the pressure drop per stage of the first filter and p_2 that of the second filter. Experiments with all the slit filters discussed above and with the filters considered later in this section showed that to a rough first approximation the pressure drop for a single stage depended only on the mean linear velocity of the gas in the hole or slit and not on the area. For a given hole the pressure drop was accurately proportional to U^2. Thus we can put

$$\frac{p_2}{p_1} \simeq \left(\frac{A_1}{A_2}\right)^2 \quad . \quad . \quad . \quad . \quad . \quad . \quad (17)$$

Using (16) and (17) we obtain

$$\frac{s_2p_2}{s_1p_1} \simeq \left(\frac{A_1}{A_2}\right)^{2-1/n} \quad . \quad . \quad . \quad . \quad . \quad (18)$$

Since $1/n = 0{\cdot}8$, which is less than 2, it can be seen that for a given overall efficiency of filtering the total pressure drop is diminished by increasing the area of the holes, i.e. by increasing the number of stages.

The construction of a reasonably compact filter consisting of a large number of stages in series, each stage consisting of a slit or hole with plates as in Fig. 1*a* or a tube for the gas to pass through after leaving the hole, would hardly be possible. One way of getting over this difficulty is to divert the stream of gas sideways after it has passed through the hole as shown in Fig. 5, and a model of this kind has been made. Circular plates were used packed one above the other with suitable distance pieces and the holes in alternative plates were at the centre so that the flow after the gas had passed through the central hole should be symmetrical. In this case it was found that a deposit of dust was formed at A opposite the hole and also that there were complete rings of deposit at B and B′ some distance (about 3 cm. and 2·5 cm. respectively) from the hole and a few mm. wide. The deposit at A consisted of an outer ring and a central circular spot. To investigate the behaviour quantitatively the arrangement shown in Fig. 5 was used with all the holes the same diameter and it was shown that, using the results established earlier in this paper, the effect of altering the size of the holes and the number of stages could be calculated and thus much time saved in designing filters of given performance.

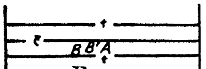

FIG. 5.

This paper was prepared in 1940 but publication was delayed by the authors since they had submitted the substance of it to a Government department as a possible contribution to the war effort. Unhappily Dr. J. K. Roberts, F.R.S. died in 1943 at an early age.

One of us (E.A.B.B.) was in receipt of research grants from the Carnegie Trust for the Universities of Scotland and expresses his indebtedness. He is grateful also to Prof. E. K. Rideal, F.R.S. for helpful criticism and advice in the final form of this paper.

Summary.

A dust filter has been constructed consisting of a slit, through which the dust-laden air passes, and of two glass plates set parallel to the direction of flow of the air after passing through. The relation between the fraction of dust removed and the linear velocity of the air in the slit is determined for slits of various widths and for plates at varying distances apart. If the distance between the plates is fixed the fraction removed depends only on the linear velocity. The results are qualitatively discussed in terms of the theory of vortex formation.

A method is described by which the mass concentration of a stearic acid dust can be easily and accurately measured. The way in which the results obtained can be applied to the design of practical filters is indicated.

Dept. of Colloid Science,
The University,
Cambridge.

ON THE CAUSE OF THE FRICTIONAL DIFFERENCE OF THE WOOL FIBRE.

By K. Rachel Makinson.

Received 16th December, 1946. As amended, 15th May, 1947.

It is well known that the wool fibre exhibits unusual frictional properties, the coefficient of friction being greater when it is rubbed towards its root than when it is rubbed towards its tip. The existence of this frictional difference is one cause of the felting of wool. The phenomenon has usually been explained as a ratchet effect produced by the overlapping scale structure of the cuticle; Martin,[1, 2] however, has suggested that it is due to an asymmetrical molecular field at the surface of the fibre. The lack of a mathematical formulation of either theory has made it difficult to design experiments to decide between them, and while the experiments of Thomson and Speakman [3] appear to provide conclusive evidence in favour of the ratchet theory, those of Martin and of Lipson and Howard[4], which appear to disprove it, remain not fully answered.

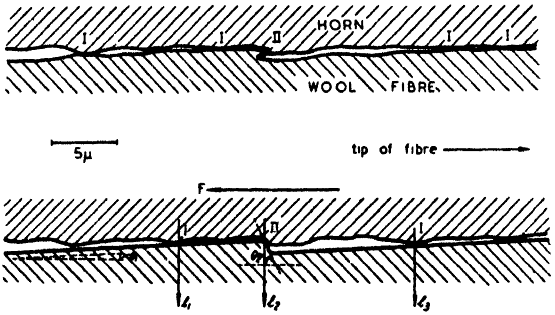

Fig. 1.—The nature of the contact between the wool fibre and the horn.

In this paper an analysis of the ratchet theory has been made for a particular, simple type of experimental arrangement. Measurements of the frictional difference with this arrangement lead to results which are all explicable by the ratchet theory, while some of them appear to be inexplicable in terms of an asymmetrical molecular field. The analysis also shows that certain other experimental observations, which have been considered by some workers to be incompatible with a ratchet mechanism, in fact, result from this mechanism.

Analysis.—Consider the initiation of sliding between a wool fibre and a second surface, e.g. polished horn, of the form shown in the upper diagram of Fig. 1, a constant load being applied between the surfaces. This arrangement is similar to that used in measuring the coefficients of static friction with a stick-slip apparatus.[5]

The lower diagram is an idealisation of the upper one. The total load L between the surfaces may be assumed to be distributed over contacts of type I on the flat face of a scale, and of type II between the steep face of a scale and an asperity (or the side of a fissure) on the horn. The average angles of inclination of the scale faces to the axis at points of type I and type II respectively are θ_1 and θ_2, the forces parallel to the axis which are required to initiate motion

---

[1] *W.I.R.A. Bull.*, 1941, **9**, 4.

[2] Martin, *J. Soc. Dyers Col.*, 1944, **60**, 325.

[3] Thomson and Speakman, *Nature*, 1946, **157**, 804.

[4] Lipson and Howard, *J. Soc. Dyers Col.*, 1946, **62**, 29.

[5] Mercer and Makinson (in preparation).

with and against the scales respectively are F_1 and F_2, and the corresponding apparent coefficients of static friction are μ_1 and μ_2. The angle of friction between the surfaces is λ ($\simeq 20°$ to $40°$); λ will be assumed to be independent of the load but the results obtained are qualitatively unchanged when this is not true.

For motion against the scales, since $\theta_2 > (\pi/2 - \lambda)$, true sliding cannot occur at contacts of type II, and rupture or deformation of the scale or of the asperity on the horn must occur; this will require a total force f for all the type II contacts; f will probably not depend much on L. In the initiation of with-scale motion, type II contacts may not be present and if they are present they contribute little to μ_1. Hence, if m is the fraction of the total load taken by all the type II contacts in against-scale motion, then

$$\mu_1 = \tan(\lambda + \theta_1) \quad . \quad . \quad . \quad . \quad . \quad . \quad . \quad (1)$$

and

$$\mu_2 = (1 - m)\tan(\lambda - \theta_1) + f/L \quad . \quad . \quad . \quad . \quad (2)$$

The frictional difference $\sigma = \mu_2 - \mu_1$ and the coefficient $\delta = (\mu_2 - \mu_1)/(\mu_2 + \mu_1)$, both of which are frequently studied in connection with felting, may be obtained from these equations.

The Relation of σ and δ to μ_1.—To a first approximation f may be expected to be independent of μ_1. Experimental confirmation of this is given below.

TABLE I.—VALUES OF f FOR $\theta_1 = 5°$.

Conditions.	pH.	Load (g. wt.).	μ_1.	μ_2.	f (g. wt.).	
					$m = 0·1$.	$m = 0·01$.
Clean . . .	7	0·15	0·53	0·95	0·099	0·095
Greasy . . .	7	0·15	0·31	0·76	0·096	0·095
Clean . . .	1	0·15	0·83	1·11	0·090	0·083
Greasy . . .	1	0·15	0·37	0·86	0·105	0·102
Clean . . .	10	0·15	0·66	1·04	0·097	0·092
Greasy . . .	10	0·15	0·35	0·72	0·087	0·084
Clean . . .	11	0·15	0·66	1·02	0·095	0·088
Greasy . . .	11	0·15	0·38	0·82	0·097	0·095
*Clean, A . .	7	0·17	0·59	0·95	0·103	0·096
*Clean, B . .	7	0·17	0·72	1·04	0·101	0·093
Mean . . .	—	—	—	—	0·098	0·092
*Benzoquinone-treated, clean .	7	0·17	0·36	0·88	0·121	0·117

Hence, if λ is changed by lubricating the surfaces, or by any other treatment which does not change θ_1, θ_2, m or f, then μ_1 and μ_2 will change in the same sense as λ, and σ and δ will change in the opposite sense, δ changing relatively more than σ. This conclusion affords an obvious explanation of the fact, reported elsewhere,[5, 6] that lubrication of the surfaces, when a wool fibre is rubbed on polished horn in the presence of a buffer solution, has been found to produce invariably a marked increase in δ and usually an increase in σ also (occasionally σ showed no significant change). This was true whether the lubricant was grease or soap. Since the lubricating layer was sometimes 0·5 microns thick, there is no obvious explanation of this result in terms of an asymmetrical molecular field. The dependence of σ and δ on μ_1 was exactly similar when μ_1 was changed by varying the pH of the buffer solution.

Magnitude of f.—The magnitude of f in eqn. (2) can be calculated from the experimental values of μ_1 and μ_2, since the result is insensitive to the assumed value of m over a reasonable range. Table I shows the result of the calculation

---

[6] Makinson and Mercer, *J. Text. Inst.*, 1946, **37**, T180.

* The wool used in these experiments differed from the other samples in showing greater variability of μ_1 and μ_2 (before treatment with benzoquinone).

for $m = 0{\cdot}1$ and $m = 0{\cdot}01$; the values of μ_1 and μ_2 were obtained in the experiments referred to above. For θ_1 the value 5° has been assumed. Except in the case of the benzoquinone-treated surfaces, it is found that f is constant within the experimental variation, which was of the order of 6 % for any one determination.

It is possible, by making reasonable assumptions as to the strength of the scales and the area which will be exposed if rupture occurs, to calculate an approximate upper limit to the value of the force required to rupture or deform one scale-edge ; such a calculation leads to the conclusion that this upper limit is of the order of one-half f, which suggests that the total number of type II contacts is small. This would be expected, since when one type II contact has been made, there is only a small probability that any other asperities will be close to a scale-tip.

To test the interpretation of f as the total force needed to deform or rupture the type II contacts, the resistance of the two surfaces to deformation was increased by treating them with boiling benzoquinone solution. The fibres were treated for 4 hr. as described by Barr and Speakman,[7] so that their resistance to extension was increased by 25 % or more ; the horn, whose surface was expected to be more reactive than the cuticle of wool, was treated for 15 min. only. Table I shows that f was increased about 20 % by this treatment.

Factors Reducing Frictional Difference.—The change in σ produced by changing μ_1 is comparatively small. If the frictional difference arises from a ratchet-effect it should be possible to reduce σ considerably by any one of three different methods. These are, firstly, by destroying the scale structure of the fibre ; secondly, by replacing the horn by a surface which is harder than the fibre and has no asperities of such a shape that they can touch the steep face of the scales ; thirdly, by weakening either surface so that f is reduced. It is shown below that the frictional difference σ has in fact been reduced by each method.

To test the first prediction, a wool fibre was set into a flat ribbon by immersion in boiling water under pressure for 30 min. and subsequent cooling under pressure. The scales on the flat surfaces were then barely visible under the microscope. While μ_1 was not significantly changed by this treatment, σ, measured under greasy conditions in water, was only about 0·05, a value which is 1/9th of the corresponding normal value. To explain this result in terms of an asymmetrical molecular field at the surface of the fibre, it would be necessary to postulate disorientation of the superficial molecules, with a consequent destruction of the asymmetrical field, in the flattening process.

To test the second prediction measurements were made of the friction of a wool fibre rubbed on a glass rod of average smoothness. Under clean conditions at *p*H 7, σ was only 0·03, or 1/14th of the corresponding value for wool on polished horn. Martin,[1] who earlier reported the existence of a frictional difference for wool on glass, regarded it as evidence against the ratchet theory. His method of detecting the frictional difference was, however, extremely sensitive ; it can easily be seen that, in theory, with his apparatus the same response would be produced by any finite frictional difference at all. Hence the method could not detect the large reduction in the frictional difference obtained by rubbing wool on glass instead of horn.

The third prediction has already been verified by several experiments which have previously been considered to disprove the ratchet theory. Treatment of wool with shrink-proofing reagents such as chlorine, reduces σ without completely destroying the scale structure.[1, 8] Reagents of this type attack the disulphide bonds in keratin, and may therefore be expected to reduce f and consequently σ. Treatment of the horn, instead of the fibre, with chlorine also reduces σ ; [4] in this case the asperities on the horn are attacked, so that the scales can plough through them and again f is reduced. That the horn surface is degraded by this treatment to a depth of about 5 microns has been confirmed by birefringence measurements.[5] The fact that a positive cast, made in gelatin, of a lock of oriented wool fibres shows no frictional difference [1] can also be attributed to the low value of f for the easily deformable gelatin.

---

[7] Barr and Speakman, *J. Soc. Dyers Col.*, 1944, **60**, 335.

[8] Mercer and Rees, *Nature*, 1946, **157**, 589.

This work was carried out as part of the programme of the Division of Physics of the Council for Scientific and Industrial Research, National Standards Laboratory, Sydney.

The author wishes to acknowledge with thanks the value of discussions of this work with Dr. G. H. Briggs, Mr. A. F. A. Harper and Mr. E. H. Mercer.

Summary.

An analysis has been made of the ratchet theory of the frictional difference of the wool fibre, and the theory developed into a semi-quantitative form. The theory has been shown to be in agreement with a number of experimental observations, some of which are not explicable in terms of an asymmetrical molecular field at the surface of the fibre, and some of which were previously regarded as disproving the ratchet theory. It therefore appears probable that the frictional difference is due to a ratchet effect.

A NEW "AVERAGING" METHOD FOR THE LOCATION OF ATOMIC POSITIONS FROM X-RAY DATA.

By A. D. Booth.

Received 11th February, 1947.

In private discussions between Cox, Crowfoot, Robertson and the writer, the suggestion emerged that the positions of atomic centres, as defined by the maxima of the *terminated* three-dimensional Fourier series :

$$\rho(x, y, z) = \frac{1}{V}\sum_{-H}^{+H}\sum_{K}^{+K}\sum_{-L}^{+L} |F(h, k, l)| \cos\left[2\pi\left(h\frac{x}{a} + k\frac{y}{b} + z\frac{z}{c}\right) - \alpha(h, k, l)\right] \quad (1)$$

might not always be the best possible. It was contended that the effect of high-order terms on the position of the maxima might be considerable, and that a better estimate of location could be formed by finding the "centre of gravity" of a spherical region of electrons in the immediate neighbourhood of the actual density maximum. Although the author did not altogether agree with this contention, and has attempted to evaluate [1] the precise bounds of any finite summation errors, it was interesting to consider the possibility of a new type of synthesis which would give, directly, the position of the mean atomic centre envisaged above.

Before giving details of the derivation of the new synthesis it is necessary to formulate the problem in a manner suitable for analysis. An equivalent statement is the following.

If a spherical surface is taken, in the unit cell of a crystal, what is the position of its centre when the total number of electrons included within that surface is a maximum ?

It is readily shown that this statement agrees with the ordinary definition of atomic position in terms of the maximum of electron density in those cases where the electron density distribution is spherically symmetrical in the region of this point.

---

[1] Booth, *Proc. Roy. Soc. A*, 1946, **188**, 77.

Notation.—As in previous papers [2, 3] the following contracted notation will be used:

$$\sum_{s} = \sum_{-H}^{H}\sum_{-K}^{K}\sum_{-L}^{L}$$
$$\mathrm{F} = \mathrm{F}(h, k, l)$$
$$\alpha = \alpha(h, k, l)$$
$$\theta = 2\pi\left(h\frac{x}{a} + k\frac{y}{b} + l\frac{z}{c}\right).$$

In accordance with the statement of the problem, given above, a function $\rho_R(x_0, y_0, z_0)$ will be defined to represent the total number of electrons included within a spherical surface of radius R and centre (x_0, y_0, z_0). Then:

$$\rho_R(x_0, y_0, z_0) = \int_S \rho(x, y, z)\mathrm{d}V \quad . \quad . \quad . \quad (2)$$

where S is the volume included within a spherical surface of radius R and centre (x_0, y_0, z_0). Using (1) this gives:

$$\rho_R(x_0, y_0, z_0) = \frac{1}{V}\sum_{s} |\mathrm{F}| \int_S \cos(\theta - \alpha)\,.\,\mathrm{d}V. \quad . \quad . \quad (3)$$

Transforming to axes (X, Y, Z) parallel to (a, b, c) and passing through (x_0, y_0, z_0) it follows that

$$\rho_R(x_0, y_0, z_0) = \frac{1}{V}\sum_{s} |\mathrm{F}| \int_S \cos(\theta_0 - \alpha + \theta)\mathrm{d}V \quad . \quad . \quad (4)$$

where $$\theta_0 = 2\pi\left(h\frac{x_0}{a} + k\frac{y_0}{b} + l\frac{z_0}{c}\right),$$

whence expanding (4)

$$\rho_R(x_0, y_0, z_0) = \frac{1}{V}\sum_{s} |\mathrm{F}| \left\{\cos(\theta_0 - \alpha)\int_S \cos\theta\mathrm{d}V - \sin(\theta_0 - \alpha)\int_S \sin\theta\mathrm{d}V\right\}. \quad (5)$$

The two volume integrals can be evaluated by making use of the relation,

$$h\frac{x}{a} + k\frac{y}{b} + l\frac{z}{c} = \frac{r}{d} \quad . \quad . \quad . \quad . \quad . \quad (6)$$

where d is the spacing of the plane (h, k, l) defined in the usual manner, and r is the perpendicular distance from (x, y, z) to the plane

$$h\frac{X}{a} + k\frac{Y}{b} + l\frac{Z}{c} = 0.$$

With this notation,

$$\int_S \cos\theta\,\mathrm{d}V = \int_{-R}^{R} \cos 2\pi\frac{r}{d}\,.\,\pi(R^2 - r^2)\mathrm{d}r$$
$$= 2\pi\int_0^R (R^2 - r^2)\cos 2\pi\frac{r}{d}\,.\,\mathrm{d}r \quad . \quad . \quad (7)$$
$$\int_S \sin\theta\,\mathrm{d}V = \int_{-R}^{R} \sin 2\pi\frac{r}{d}\,.\,\pi(R^2 - r^2)dr$$
$$= 0.$$

Thus, from (5) and (7),

$$\rho_R(x_0, y_0, z_0) = \frac{1}{V}\sum_{s} |\mathrm{F}| \cos(\theta_0 - \alpha)\,.\,2\pi\int_0^R (R^2 - r^2)\cos 2\pi\frac{r}{d}\,.\,dr. \quad (8)$$

---

[2] Booth, *Trans. Faraday Soc.*, 1946, **52**, 444.
[3] Booth, *ibid.*, 1946, **52**, 617.

The integral is easily evaluated to give :

$$2\pi\int_0^R (R^2 - r^2)\cos 2\pi\frac{r}{d}\,.\,dr = \frac{d^3}{2\pi^2}\left[\sin 2\pi\frac{R}{d} - 2\pi\frac{R}{d}\cos 2\pi\frac{R}{d}\right]. \qquad (9)$$

Whence the series for ρ_R may be written :

$$\rho_R(x_0, y_0, z_0) = \frac{1}{V}\sum_3 S\cos(\theta_0 - \alpha) \quad . \quad . \quad . \quad (10)$$

where :

$$S(= \mathrm{S}(h, k, l)) = \frac{d^3}{2\pi^2}\left[\sin 2\pi\frac{R}{d} - 2\pi\frac{R}{d}\cos 2\pi\frac{R}{d}\right].\,|\,\mathrm{F}(h, k, l)\,|\,. \quad (11)$$

The form of (10) is identical with that of the normal series (1), so that no new computational technique is needed to operate with it. The values of S(h, k, l) can be computed when F(h, k, l) (observed) are being obtained, as the spacings, $d(h, k, l)$ have in any case to be evaluated at that stage. So long as it is not wished to change the radius of the spherical region, R, one determination of the S(h, k, l) is sufficient for a complete structure analysis.

The maxima ρ_R can be found by the differential method [2] and it can be shown, as was done in a previous paper,[2] that if (x_0, y_0, z_0) is an approximate position of the maximum, a better value is $(x_0+\epsilon_x, y_0+\epsilon_y, z_0+\epsilon_z)$ where :

$$\left.\begin{aligned} B_{hh}\epsilon_x + B_{hk}\epsilon_y + B_{hl}\epsilon_z + B_h &= 0\\ B_{kh}\epsilon_x + B_{kk}\epsilon_y + B_{kl}\epsilon_z + B_k &= 0\\ B_{lh}\epsilon_x + B_{lk}\epsilon_y + B_{ll}\epsilon_z + B_l &= 0 \end{aligned}\right\} \quad . \quad . \quad . \quad . \quad (12)$$

and

$$B_{\lambda\mu} = B_{\mu\lambda}$$

$$\left.\begin{aligned} B_h &= -\frac{2\pi}{aV}\sum_3 hS\sin(\theta_0 - \alpha)\ \text{etc.}\\ B_{hh} &= -\frac{4\pi^2}{a^2V}\sum_3 h^2S\cos(\theta_0 - \alpha)\ \text{etc.}\\ B_{hk} &= -\frac{4\pi^2}{abV}\sum_3 hkS\cos(\theta_0 - \alpha)\ \text{etc.} \end{aligned}\right\} \quad . \quad . \quad (13)$$

The modification for assumed spherical symmetry should not be used, since it is contrary to the purpose of the present method.

An exactly similar treatment can be given for the two-dimensional synthesis. The interpretation is, in this case, that the projected electron density, included within a circle of radius R, and based on the point (x_0, y_0), is to be a maximum. The integral :

$$I_2 = \int_{-R}^{R} (R^2 - r^2)^{\frac{1}{2}}\cos\left(2\pi\frac{r}{d}\right)\mathrm{d}r$$

has to be evaluated, and it can be shown that

$$I_2 = \frac{R\,.\,d}{2}J_1\left(2\pi\frac{R}{d}\right),$$

where J_1 is the first-order Bessel function.

The modified two-dimensional summation is therefore :

$$\rho_R(x_0, y_0) = \frac{1}{A}\sum_2 S_2\cos(\theta_0 - \alpha) \quad . \quad . \quad . \quad (14)$$

where

$$S_2(= \mathrm{S}_2(h, k)) = \frac{R\,.\,d}{2}J_1\left(2\pi\frac{R}{d}\right).\,|\,\mathrm{F}(h, k, 0)\,|\,. \quad . \quad . \quad (15)$$

The differential synthesis can again be applied to determine the maxima. For one-dimensional summation :

$$\rho_R(x_0) = \frac{1}{a}\sum_H S(h) \cos\left(2\pi h\frac{x_0}{a} - \alpha\right) \quad . \quad . \quad . \quad (16)$$

where

$$S(h) = \frac{a}{\pi h}\sin\left(2\pi h\frac{X}{a}\right) \, |\,\mathrm{F}(h, 0, 0)\,| \quad . \quad . \quad . \quad (16)$$

X being the range of integration on either side of the central position x_0.

Physics Department,
Birkbeck College,
University of London.

THE ABSORPTION SPECTRA OF PHENYLATED ANTHRACENES.

By Y. Hirshberg.

Received 19*th February*, 1947.

In a previous paper,[1] the fluorescence spectra of 8 phenylated anthracenes were determined and compared with that of the parent substance, anthracene:

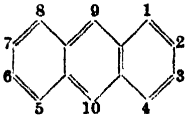

These data are supplemented in the present paper by the ultraviolet absorption spectra of these substances. The spectra of anthracene, of 9-phenyl-anthracene and of 9 : 10-diphenyl-anthracene have been determined before ; [2, 3] the present results coincide in these three cases satisfactorily with the data recorded by previous investigators. Jones [4] has already explained the close similarity in the spectra of anthracene, 9-phenyl- and 9 : 10-diphenyl-anthracene by the assumption that the *meso*-phenyl-groups are sterically prevented from becoming coplanar with the anthracene nucleus so that no resonance phenomena of the type found in the biphenyl molecule are possible. The spectrum of these phenylated anthracenes is simply the sum of the spectra of anthracene and benzene, that of the latter (2200-2650 A.) being negligible in intensity in the region in which the characteristic anthracene bands are located (2400-4000 A.).

It is interesting that 1-phenyl-anthracene and 1 : 4-diphenyl-anthracene show the same phenomenon. Here, the *meso*-methine groups and the hydrogen atoms at C_2 and C_3 interfere with a monoplanar arrangement of the molecules, in analogy with the case of 1-phenyl-naphthalene,[5] which is also similar in its spectrum to the unsubstituted naphthalene.

---

[1] Hirshberg and Haskelberg, *Trans. Faraday Soc.*, 1943, **39**, 45. The seventh curve reproduced in this paper represents 2 : 9- (and not 2 : 3-) diphenyl-anthracene, as is evident from the text.

[2] Copper and Marsh, *J. Chem. Soc.*, 1926, 724.

[3] Radulescu and Ostrogovich, *Ber.*, 1931, **64**, 2233 ; Jones, *J. Amer. Chem. Soc.*, 1941, **63**, 1658.

[4] Jones, *loc. cit.* ; *J. Amer. Chem. Soc.*, 1946, **67**, 2127 ; *Chem. Rev.*, 1943, **32**, 1.

2-Phenyl-anthracene, on the other hand, shows a spectrum different from that of anthracene: in the region 2400-3000 A., the absorption is less intense with the maximum shifted to longer wave-lengths, and the fine strucure in the second region of the spectrum (3000-4000 A.) is less pronounced. This again recalls the spectrum of 2-phenyl-naphthalene as compared with naphthalene,[6] and some other chemical observations on the peculiar character of 2-substituents in the anthracene series.[7] It is suggested that resonance forms involving the system

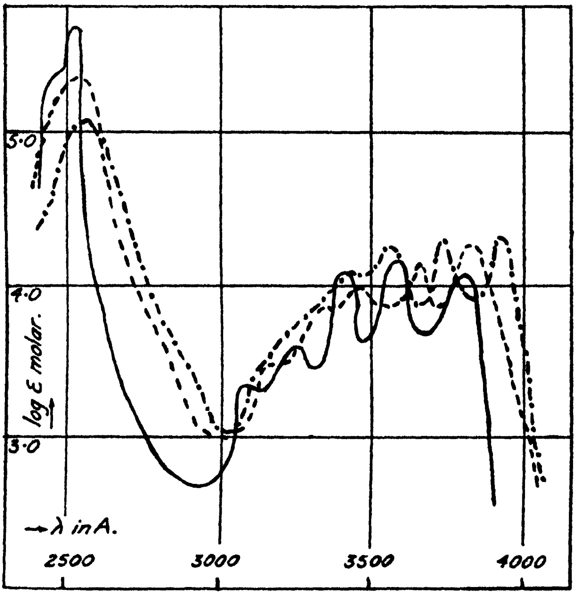

FIG. 1.
———— Anthracene.
— — — — 9-Phenyl-anthracene.
· — · — · — 9·10-Diphenyl-anthracene.

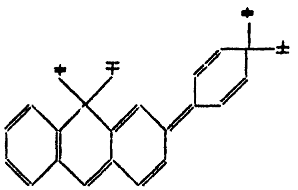

contribute markedly to the actual state of the molecule. It is consistent with this explanation that 2 : 9-diphenyl-anthracene has almost the same spectrum as 2-phenyl-anthracene; whilst the hydrogen atoms at C_1 and C_3 do not interfere with the phenyl at C_2, the methine groups C_1 and C_8 force the *meso*-phenyl out of the plane in which the remainder of the molecule is situated.

---

[5] Jacobs, Craig and Lavin, *J. Biol. Chem.*, 1941, **141**, 51.

[6] Fieser and Hershberg, *J. Amer. Chem. Soc.*, 1938, **60**, 940; Jacobs, Craig and Lavin, *loc. cit.*; Jones, *J. Amer. Chem. Soc.*, 1941, **63**, 1658.

[7] Bergmann and Blum-Bergmann, *J. Amer. Chem. Soc.*, 1937, **59**, 1239.

A rather unexpected picture is presented by the two tetra-phenylated anthracene, the 1 : 4 : 9 : 10- and the 1 : 4 : 5 : 8-compound. The former

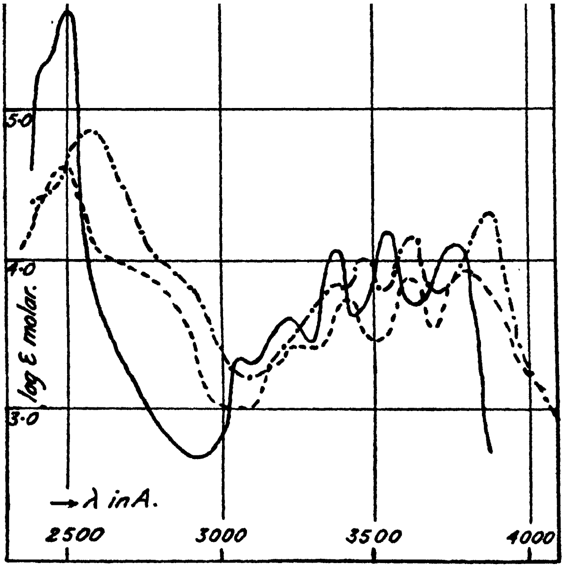

FIG. 2.

———— Anthracene.
— — — — 1-Phenyl-anthracene.
· — · — · 1·4-Diphenyl-anthracene.

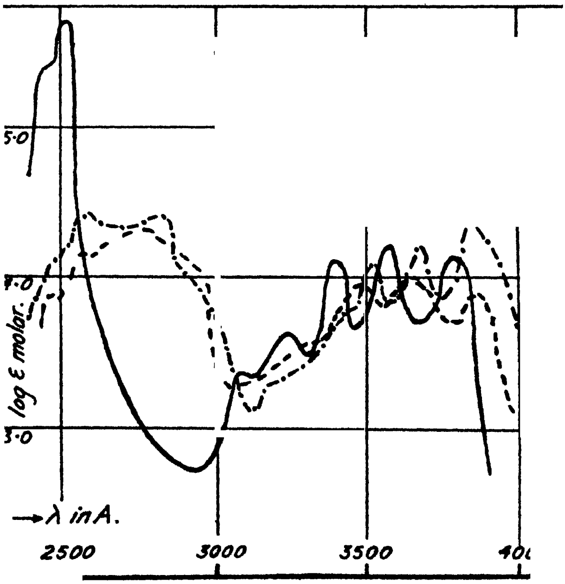

FIG. 3.

———— Anthracene.
— — — — 2-Phenyl-anthracene.
· — · — · 2·9-Diphenyl-anthracene.

shows the general bathochromic effect in the first region of the absorption spectrum and an almost complete disappearance of fine structure in the second region of absorption. Although it is not possible to make a quantitative statement, the curve shows that the accumulation of phenyl groups in the four neighbouring positions prevents the electronic transitions to which these fine bands in anthracene and its less substituted derivatives correspond. The extinction coefficients of 1 : 4 : 5 : 8-tetraphenyl-anthracene are higher for any given wave-length than for the other representatives of this series; the spectrum consists of three parts, in the first of which (2300-3000 A.) there is no bathochromic effect. The second part (3000-3600 A.) and the third part (3600-4000 A.) show no fine structure at all. One is tempted to conclude that the specific arrangements of the phenyl groups causes such a distortion of the anthracene nucleus that the molecule can be monoplanar and permit, therefore, the occurrence of resonance phenomena. This tentative hypothesis invites further investigations.

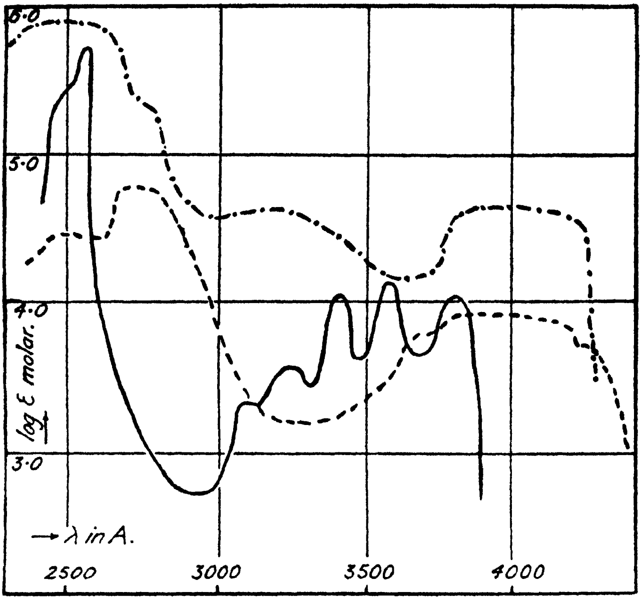

Fig. 4.

———— Anthracene.
— — — — 1 . 4 . 9 . 10-Tetraphenyl-anthracene.
· — · — · — · 1 . 4 . 5 . 8-Tetraphenyl-anthracene.

Experimental.

The preparation of the anthracene hydrocarbons has been described by Hirshberg and Haskelberg.[1] The spectra were investigated with the help of both a hydrogen discharge lamp and a steel-steel spark (15,000 v.), and of a Zeiss spectrograph characterised by the following dispersions.

A.	A. per mm.
2200-2536	17
2536-2650	31
2650-3121	40
3121-3650	66
3650-4050	100

As solvents cyclohexane and dibutyl ether were used, which proved completely transparent in the region investigated and were expected not to influence the spectrum (e.g. by solvate formation). The order of magnitude of the concentrations used was between $4 \times 10^{-}$ and 2×10^{-6} mole/l.

In the normal way, the molecular extinction coefficient was calculated from the formula

$$\epsilon = \frac{n}{c\,.\,d} \log \frac{t}{t_0}$$

in which n is 0·9 (Schwarzschild constant), c the concentration (mole/l.), d the thickness of the solution measured (in cm.), t and t_0 the times of exposure for the solution and the solvent, respectively, for the same d. The results are represented in four groups of absorption curves.

The Daniel Sieff Research Institute,
Rehovoth, Palestine.

INFRA-RED ABSORPTION SPECTRUM AND STRUCTURE OF TRIOXANE.

By D. A. Ramsay

Received 5th March, 1947

Trioxane is a cyclic trimer of formaldehyde. The physical and chemical properties of this substance have been recently reviewed by Walker and Carlisle.[1] Crystal structure[2] and dipole moment[3] investigations showed that the molecule exists in a puckered hexagonal or " chair " structure, cp. cyclohexane[4] and dioxane.[5] This conclusion may be confirmed spectroscopically as follows. Assuming a six-membered ring structure with alternate carbon and oxygen atoms, four structures are possible, viz. (i) a planar structure with symmetry D_{3h}, (ii) a " chair " form with symmetry C_{3v}, (iii) a " boat " or " cradle " form with symmetry C_s and (iv) an asymmetric ring with no symmetry elements (see Fig. 1).

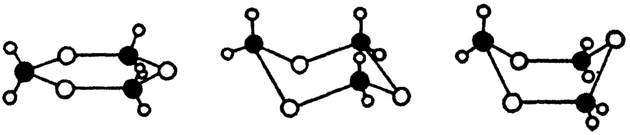

Planar (D_{3h}) Chair (C_{3v}) Boat (C_s)

●—carbon O—oxygen o—hydrogen

Fig. 1.

These structures may be distinguished on account of their different symmetries by the different numbers of fundamental vibration frequencies permitted in the infra-red and Raman spectra. The Raman data have been discussed by Kahovec and Kohlrausch[6] and shown to be consistent with the " chair " configuration. In this paper the infra-red data are discussed and shown to provide strong support for the " chair " structure.

Experimental.

The sample of trioxane was obtained from Synthite Ltd., through the Distillers Co. Ltd., and after vacuum distillation melted at 60·5° c. (literature 61-2° c.). The infra-red absorption of the vapour between 2·5 and 14μ was investigated using a Hilger D209 double beam spectrometer with a rock salt prism. The absorption was measured using a 25 cm. cell with rock salt windows; the pressure of trioxane vapour being 5 mm. Hg. and the temperature 20° c.

---

[1] Walker and Carlisle, *Chem. Eng. News*, 1943, **21**, 1250.

[2] Moermann, *Rec. Trav. Chim.*, 1937, **56**, 161.

[3] Maryott and Acree, *J. Res. Nat. Bur. Stand.*, 1944, **33**, 71.

[4] Ramsay and Sutherland, *Proc. Roy. Soc. A*, 1947, **190**, 245.

[5] Ramsay, *ibid.*, 1947, **190**, 562.

[6] Kahovec and Kohlrausch, *Z. physik. Chem. B*, 1937, **35**, 29.

The infra-red absorption of trioxane in solution was also investigated. For this purpose a 5 % solution of trioxane in CCl_4 was used and its absorption measured in a rock salt cell of thickness 0·10 mm. The absorption curves for the vapour and solution * are reproduced in Fig. 2.

The infra-red frequencies are given in Table I and compared with the Raman frequencies of Kahovec and Kohlrausch.[6]

It is seen that many Raman frequencies are in tolerable agreement with the infra-red frequencies measured in solution. The latter frequencies are also in good agreement with the infra-red frequencies observed in the vapour but are generally displaced to lower values by amounts varying from 0-20 cm.$^{-1}$. By comparing the infra-red absorption of the vapour and the solution it is seen that the sharp vapour peaks at 943 cm.$^{-1}$ and 977 cm.$^{-1}$ are probably *Q* branches of two distinct vibrational frequencies, the 934 cm.$^{-1}$ peak corresponding to the *P* branch of the former and the 990 cm.$^{-1}$ peak to the *R* branch of the latter frequency. The strong central band at 960 cm.$^{-1}$ is probably due to overlapping of the *R* branch of the 943 cm.$^{-1}$ frequency with the *P* branch of the 977 cm.$^{-1}$ frequency. The 1077 cm.$^{-1}$ vapour band and the unresolved shoulder at 1066 cm.$^{-1}$ are seen to be distinct vibrational frequencies, as also are the 1490 cm.$^{-1}$ and 1477 cm.$^{-1}$ vapour bands. The 1220 cm.$^{-1}$ and 1232 cm.$^{-1}$ vapour bands however must be ascribed to rotational contours of a single vibrational frequency. The 1175 cm.$^{-1}$, 1298 cm.$^{-1}$ and 1408 cm.$^{-1}$ vapour peaks appear to be single bands. Attempts to resolve the 1175 cm.$^{-1}$ frequency at lower vapour pressure proved unsuccessful.

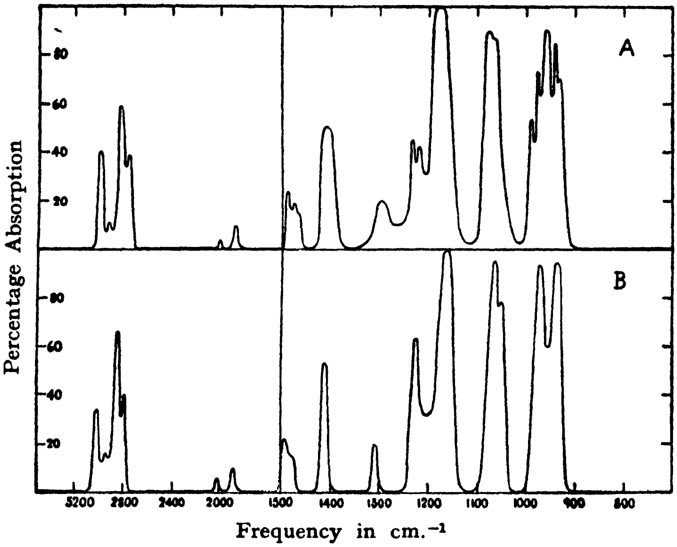

A. Trioxane vapour. B. Trioxane in carbon tetrachloride.

FIG. 2.

Symmetry Properties.

The thirty normal vibrations of the trioxane molecule may be conveniently described as 6 C—H stretching vibrations, 3 H—C—H bending vibrations, 9 $>CH_2$ rocking and twisting vibrations, 6 C—O stretching vibrations and 6 C—O—C and O—C—O bending vibrations.

---

* The infra-red spectrum of trioxane in solution had been obtained earlier in the laboratory by Mr. A. R. Philpotts in connection with a separate problem. The spectrum given here agrees completely with the earlier observations.

The frequency ranges in which each of these groups of vibrations may be expected to appear are known from earlier studies of the related molecules cyclohexane [2] and dioxane.[3] The symmetry classes of the normal vibrations for all possible symmetries of the molecule have been derived by the usual methods of group theory and are given in Table II. The infra-red and Raman selection rules are also noted.

The numbers of fundamental vibration frequencies permitted by the selection rules to appear in the various regions of the infra-red spectrum are summarised in Table III. Before using the numbers of vibrational frequencies observed in the spectrum of trioxane vapour to distinguish between the possible configurations of the molecule, the limitations of this method of structure determination will be briefly discussed.

TABLE I.—INFRA-RED AND RAMAN FREQUENCIES OF TRIOXANE.

Infra-red (cm.$^{-1}$).		Raman (cm.$^{-1}$).
Vapour.	Solution.	Solution.
		219? (0)
		520 (3)
		605? (1)
		747 (1)
P 934 (7) *Q* 943 (8)	937 (9)	930? (½)
PR 960 (9) *Q* 977 (7) *R* 990 (5)	972 (9)	958 (5)
		1025 (3)
1066 (8*S*)	1051 (8)	1047 (2)
1077 (9)	1065 (9)	
		1106 (2)
1175 (10)	1164 (10)	
1220 (4) 1232 (4)	1226 (6)	1237 (2)
1298 (2)	1305 (2)	1309 (2)
1409 (5)	1408 (5)	
1477 (2)	1475 (2*S*)	1475 (2)
1490 (2)	1488 (2)	
1894 (1)	1874 (1)	
2022 (0)	2008 (0)	
2765 (4)	2780 (4)	
2825 (6)	2840 (7)	
		2875 (2)
2925 (1)	2925 (1)	
3000 (4)	3000 (3)	3027 (3)

S denotes unresolved shoulder.

Figures in parentheses denote relative intensities of bands.

(i) The numbers of frequencies permitted by the selection rules should be compared with the numbers of frequencies observed in the vapour spectrum only, since breakdown of the selection rules is well known for the liquid and solid states.

(ii) Vibrational frequencies in the vapour spectrum should be distinguished from bands due to rotational contour by comparison with the spectrum of the liquid or solid.

(iii) Certain fundamental vibration frequencies may be extremely weak in absorption and hence escape detection except at increased pressures or longer absorption paths.

(iv) Two or more fundamental vibration frequencies may be too close together to be resolved by the spectrometer and hence appear as single bands.

(v) Some weak bands observed may be overtone or combination frequencies.

(vi) Some fundamental vibration frequencies may be split into two components by Fermi resonance with other vibrational levels in the molecule.

If, however, the difference between the numbers of active fundamentals permitted by the possible configurations of the molecule are sufficiently marked, the numbers of observed frequencies may be used to distinguish the structures

TABLE III.—SYMMETRY CLASSES OF THE NORMAL VIBRATIONS.

Type of Vibration.	Frequency Range.	Asymmetric.	Boat (C_s).		Chair (C_{3v}).			Planar (D_{3h}).					
			A^1	A^{11}	A_1	A_2	E	A_1^1	A_1^{11}	A_2^1	A_2^{11}	E^1	E^{11}
6 C—H stretching	2800-3000 cm.$^{-1}$	6	4	2	2	0	2	1	0	0	1	1	1
3 H—C—H bending	1350-1500 cm.$^{-1}$	3	2	1	1	0	1	1	0	0	0	1	0
9 >CH_2 rocking and twisting	750-1350 cm.$^{-1}$	9	4	5	1	2	3	0	1	1	1	1	2
6 C—O stretching	750-1350 cm.$^{-1}$	6	3	3	1	1	2	1	0	1	0	2	0
6 {C—O—C / O—C—O} bending	< 750 cm.$^{-1}$	6	4	2	2	0	2	1	0	0	1	1	1
Selection Rules		IR R	IR R	IR R	IR R	— —	IR R	— R	— —	— —	IR —	IR R	— R

IR—infra-red active. R—Raman active.

with reasonable certainty. This condition is satisfied by the planar, " chair " and " boat " configurations of trioxane, though it is not possible to distinguish the " boat " form from a completely asymmetric configuration.

In the region 2800-3000 cm.$^{-1}$ of the vapour spectrum, four frequencies were observed in agreement with the number allowed by the " chair " structure. In the region 1350-1500 cm.$^{-1}$, three frequencies were observed though only two fundamental frequencies are theoretically permitted by the " chair " structure. Two of the observed frequencies, however, viz., 1490 cm.$^{-1}$ and 1477 cm.$^{-1}$ lie close together and may correspond to a single frequency split by Fermi resonance. In the region 750-1350 cm.$^{-1}$ seven frequencies were observed in the vapour spectrum, providing very strong support for the " chair " structure. Lack of experimental data prevents a comparison in the region below 750 cm.$^{-1}$. The numbers of frequencies observed in the various regions of the infra-red spectrum of trioxane vapour thus provides strong evidence in favour of a " chair " configuration for the molecule. It should be pointed out, however, that the spectroscopic method does not eliminate the possibility of other structures being present in very small amounts.

TABLE III.—INFRA-RED ACTIVE FUNDAMENTALS.

Structure.	2800–3000 cm.$^{-1}$.	1350–1500 cm.$^{-1}$.	750–1350 cm.$^{-1}$.	< 750 cm.$^{-1}$.
Asymmetric .	6	3	15	6
" Boat " . .	6	3	15	6
" Chair " . .	4	2	7	4
Planar . .	2	1	4	2
Observed . .	4	3	7	—

Assignment of Frequencies.

The assignment of frequencies to the ring vibrations of trioxane is considerably aided by comparison with the corresponding assignments for cyclohexane [4] and dioxane.[5] It is also helpful to consider the Raman data of Kahovec and Kohlrausch [6] for tetrahydropyran. The approximate forms of the ring vibrations for trioxane are similar to those for cyclohexane and are given in Fig. 3.

The totally symmetric breathing frequency is readily identified as an intense polarised line in the Raman spectrum. For cyclohexane, tetrahydropyran and dioxane, intense Raman lines are found at 802, 813 and 835 cm.$^{-1}$ respectively, but for trioxane the line appears at 958 cm.$^{-1}$. The breathing frequency of trioxane is thus displaced by approximately 100 cm.$^{-1}$ from its expected value. This shift must be due either to interaction with other vibrations of the molecule or to an increase in the C—O force constant for trioxane relative to dioxane.

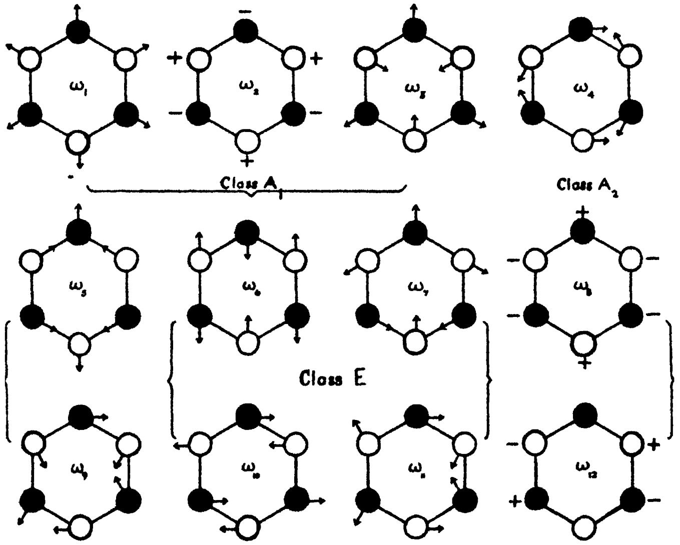

●—CH_2 group above plane of paper.
O—oxygen atom below plane of paper.

The two components of a degenerate vibration are bracketed together.

FIG. 3.

The "out-of-plane" bending frequency w_2 has probably not been observed in the case of trioxane. For cyclohexane the frequency was identified as the polarised Raman line at 384 cm.$^{-1}$. The corresponding Raman line for tetrahydropyran appears at 396 cm.$^{-1}$ while the calculated value for dioxane was 390 cm.$^{-1}$. The "in-plane" bending frequency w_3 for trioxane probably corresponds to the Raman line at 747 cm.$^{-1}$, cp. the dioxane frequency at 740 cm.$^{-1}$. The antisymmetric stretching frequency w_4 is inactive for trioxane and cyclohexane, the calculated value for the latter molecule being 1092 cm.$^{-1}$. This probably corresponds to the 1090 cm.$^{-1}$ Raman line for tetrahydropyran, while for dioxane the frequency is infra-red active and appears at 1136 cm.$^{-1}$.

The very intense infra-red absorption for trioxane at 1175 cm.$^{-1}$ is probably a C—O stretching frequency and may be assigned to the degenerate vibration $w_{5,9}$. In dioxane the degeneracy is removed and the two component frequencies appear at 1111 and 1125 cm.$^{-1}$. The corresponding assignment for cyclohexane is a degenerate C—C stretching frequency and appears at 1029 cm.$^{-1}$. The assignment for the other degenerate C—O stretching frequency $w_{7,11}$ for trioxane is uncertain. For dioxane the vibration is split into a C—O stretching frequency at 1020 cm.$^{-1}$ and a C—C stretching frequency at 889 cm.$^{-1}$, the latter corresponding to the degenerate C—C stretching frequency for cyclohexane at 903 cm.$^{-1}$.

The degenerate bending frequency $\omega_{6,10}$ appears at 426 cm.$^{-1}$ for cyclohexane. For tetrahydropyran the degeneracy is split giving two frequencies at 430 and 454 cm.$^{-1}$ while for dioxane the splitting is even greater, producing frequencies at 432 and 485 cm.$^{-1}$. In trioxane the vibration is once more degenerate and probably corresponds to the Raman line at 520 cm.$^{-1}$. The other degenerate bending frequency $\omega_{8,12}$ for trioxane will be expected to appear in the region of 200 cm.$^{-1}$. The calculated value for cyclohexane is 206 cm.$^{-1}$ while for dioxane the calculated frequencies are 205 and 233 cm.$^{-1}$. The Raman line for trioxane at 219 cm.$^{-1}$ may therefore be assigned to this vibration.

The assignments of the ring frequencies for the four molecules are summarised in Table IV.

TABLE IV.—ASSIGNMENTS OF RING FREQUENCIES.

Vibration.	Cyclohexane (cm.$^{-1}$).	Tetrahydropyran (cm.$^{-1}$).	Dioxane (cm.$^{-1}$).	Trioxane (cm.$^{-1}$).
ω_1	802	813	835	958
ω_2	384	396	(390)	?
ω_3	667 ?	756	740	747
ω_4	(1092)	1090	1136	?
$\omega_{5,9}$	1029	?	1111 1125	1175
$\omega_{6,10}$	426	430 454	432 485	520
$\omega_{7,11}$	903	?	889 1020	?
$\omega_{8,12}$	(206)	252 ?	(205) (233)	219

Figures in parentheses denote calculated frequencies.

It will now be considered whether the trioxane assignments are consistent with the contours of the infra-red bands. The "chair" configuration for trioxane is a symmetric top, hence vibrations involving a change of electric moment parallel to the symmetry axis will give bands with *P, Q, R* structures.[7] The C—O bond lengths were found from X-ray data [8] to be 1·42 ± 0·03 A. and the bond angles of the ring to be 105° ± 10°. If the C—H bond length is taken as 1·09 A. (cp. methane [8]) and all the carbon bond angles are assumed to be tetrahedral, the principal moments of inertia of the "chair" structure may be shown to be

$$I_A = I_B = 160 \times 10^{-40}\ \text{g./cm.}^2$$
$$I_C = 287 \times 10^{-40}\ \text{g./cm.}^2.$$

Substituting these values into the doublet separation formula of Gerhard and Dennison,[7] the *PR* separation for parallel bands is found to be 25 cm.$^{-1}$ at 20° C. The contours of the perpendicular bands may be obtained by reference to the curves of these authors for different values of $\beta = \frac{I_A}{I_C} - 1$. For trioxane $\beta = -0{\cdot}442$, hence the perpendicular bands will also show *P, Q, R* structures although the *PR* separation will be somewhat smaller than for the parallel bands and the *Q* branch will be less prominent. Two of the observed frequencies show a *P, Q, R* structure in the vapour, viz.,

$$\left.\begin{array}{l} P\ 934\ \text{cm.}^{-1} \\ Q\ 943\ \text{cm.}^{-1} \\ R\ 960\ \text{cm.}^{-1} \end{array}\right\} \text{ and } \left\{\begin{array}{l} P\ 960\ \text{cm.}^{-1} \\ Q\ 977\ \text{cm.}^{-1} \\ R\ 990\ \text{cm.}^{-1} \end{array}\right.$$

while one shows a doublet structure viz. $\left\{\begin{array}{l} 1220\ \text{cm.}^{-1} \\ 1232\ \text{cm.}^{-1} \end{array}\right\}$. The overlapping of the two *P, Q, R* structures makes interpretation difficult but the 977 cm.$^{-1}$ band with a *QR* separation of 13 cm.$^{-1}$ at 20° C. appears to be a parallel band while the 943 cm.$^{-1}$ band with a PQ separation of 9 cm.$^{-1}$ at 20° c. is probably a perpendicular band. Vibrations in Class A_1 produce changes in dipole moment parallel to the symmetry axis while vibrations in Class E produce changes in dipole moment perpendicular to this axis. Hence the 977 cm.$^{-1}$ frequency may be assigned to Class A_1 and probably corresponds to the 958 cm.$^{-1}$ Raman line which has been assigned to the symmetrical breathing frequency ω_1, while the 943 cm.$^{-1}$ band may be assigned to Class E and may be either a ring frequency or a CH_2 deformation frequency.

---

[7] Gerhard and Dennison, *Physic. Rev.*, 1933, **43**, 197.

[8] Ginsberg and Barker, *J. Chem. Physics*, 1935, **3**, 668.

An attempt was made to calculate the vibration frequencies of the trioxane ring by treating the molecule as a system of six mass points (= 14) and applying a simple valency force field. Similar calculations for cyclohexane [4] and dioxane [5] gave agreement between the observed and calculated frequencies to within 4 % but for trioxane, assuming the same values of the force constants as for dioxane, differences up to 10 % were obtained. This agreement could not be appreciably improved by modifying the force constants hence it appears that interaction terms are needed in the force field.

The author wishes to thank Dr. G. B. B. M. Sutherland for valuable advice and discussion, Dr. G. H. Twigg of the Distillers Co. Ltd., for vacuum-distillation of the trioxane sample, and Messrs. BX Plastics Ltd., for financial assistance.

Summary.

The infra-red absorption spectrum of trioxane between 3500 and 700 cm.$^{-1}$ has been determined under moderate resolving power using a double-beam spectrometer. The number of frequencies observed in the vapour spectrum has been compared with the numbers of frequencies permitted by the selection rules for the various possible configurations of the trioxane ring and shown to provide strong evidence for a " chair " structure for this molecule. This conclusion is in agreement with the X-ray and dipole moment evidence. Assignments for the ring vibrations of trioxane have been made and compared with the corresponding assignments for cyclohexane, tetrahydropyran and dioxane.

Department of Colloid Science,
Cambridge.

A THERMODYNAMIC STUDY OF BIVALENT METAL HALIDES IN AQUEOUS SOLUTION. PART XVII—REVISION OF DATA FOR ALL 2:1 AND 1:2 ELECTROLYTES AT 25°, AND DISCUSSION OF RESULTS.

By R. H. Stokes.

Received 10th March, 1947.

During the past seven years there has been accumulated a large amount of information about the thermodynamic properties of aqueous solutions of electrolytes of 1 : 2 and 2 : 1 valency types extending, in many cases, over a wide range of concentration. The purpose of this paper is to summarise these results and to discuss qualitatively some of their implications.

Experimental Methods.

The determination of the partial molar free energy of either solute or solvent over a range of concentration is in principle sufficient to calculate other functions e.g. activities, activity coefficients for either component. However, the direct measurement of the free energy of an involatile solute in concentrated solutions is difficult. The E.M.F. of a cell without transference is the only conveniently measurable quantity which depends directly on the free energy of the solute, and there are comparatively few cases where satisfactory reversible electrodes can be found for both anion and cation. Furthermore, many electrodes which are satisfactory in the dilute region (say $< 0·1$ M.) fail in more concentrated solutions, owing to increasing solubility of one of the components of the electrode in the solution.

In general, therefore, it is necessary to measure the partial molar free energy of the solvent. The development of the isopiestic technique[1] for vapour pressure measurements has provided a simple and accurate method for measuring the vapour pressure (and hence the free energy) of water in solutions of any concentration above 0·1 M., and this method has provided most of the data collected in this paper.

Standard Data for Isopiestic Measurements.

Recently attention has been given to the direct measurement of the vapour pressures of solutions of NaCl and KCl[2] and H_2SO_4.[3, 4] The standard values for NaCl and KCl are given by Robinson,[5] and by Stokes and Levien.[6] For more concentrated solutions ($a_w < 0·75$) H_2SO_4 is the primary standard but recently $CaCl_2$ has been used. In Table I is a set of standard values from 0·1 M. H_2SO_4 upwards, and also revised values for $CaCl_2$ solutions, the source being

TABLE I.—STANDARDS FOR ISOPIESTIC MEASUREMENTS IN CONCENTRATED SOLUTIONS: OSMOTIC AND ACTIVITY COEFFICIENTS OF CALCIUM CHLORIDE AND SULPHURIC ACID AT 25°.

M.	$CaCl_2$		H_2SO_4		M.	$CaCl_2$		H_2SO_4	
	ϕ	γ	ϕ	γ		ϕ	γ	ϕ	γ
0·1	0·854	0·518	0·680	0·2655	5·5	2·743	8·18	1·376	0·2312
0·2	0·862	0·472	0·668	0·2090	6·0	2·891	11·11	1·445	0·2567
0·3	0·876	0·455	0·668	0·1826	6·5	3·003	14·53	1·512	0·2852
0·4	0·894	0·448	0·671	0·1666	7·0	3·081	18·28	1·576	0·3166
0·5	0·917	0·448	0·676	0·1557	7·5	3·127	22·13	1·636	0·350
0·6	0·940	0·453	0·682	0·1477	8·0	3·151	26·02	1·691	0·386
0·7	0·963	0·460	0·689	0·1417	8·5	3·165	30·1	1·744	0·426
0·8	0·988	0·470	0·699	0·1374	9·0	3·171	34·2	1·793	0·467
0·9	1·017	0·484	0·710	0·1342	9·5	3·171	38·5	1·841	0·512
1·0	1·046	0·500	0·721	0·1316	10·0	3·169	43·0	1·884	0·559
1·2	1·107	0·539	0·744	0·1283	11·0	—	—	1·964	0·661
1·4	1·171	0·587	0·768	0·1266	12·0	—	—	2·030	0·770
1·6	1·237	0·644	0·793	0·1260	13·0	—	—	2·088	0·888
1·8	1·305	0·712	0·819	0·1264	14·0	—	—	2·140	1·017
2·0	1·376	0·792	0·846	0·1276	15·0	—	—	2·187	1·154
2·5	1·568	1·063	0·916	0·1331	16·0	—	—	2·228	1·300
3·0	1·779	1·483	0·991	0·1422	17·0	—	—	2·262	1·450
3·5	1·981	2·078	1·071	0·1547	18·0	—	—	2·292	1·608
4·0	2·182	2·934	1·150	0·1700	19·0	—	—	2·318	1·771
4·5	2·383	4·17	1·226	0·1875	20·0	—	—	2·341	1·940
5·0	2·574	5·89	1·303	0·2081	21·0	—	—	2·361	2·114
					22·0	—	—	2·381	2·300

---

[1] Robinson and Sinclair, *J. Amer. Chem. Soc.*, 1934, **56**, 1830.
[2] Olynyk and Gordon, *ibid.*, 1943, **65**, 224.
[3] Shankman and Gordon, *ibid.*, 1939, **61**, 2370.
[4] Stokes, *ibid.*, 1947, **69**, 1291.
[5] Robinson, *Trans. Roy. Soc. New Zealand*, 1945, **75**, 203.
[6] Stokes and Levien, *J. Amer. Chem. Soc.*, 1946, **68**, 333.

$H_2SO_4 > 3$ M.[4] and from 0·1 M. to 2·5 M.[5–8] The activity coefficient of H_2SO_4 was fixed at 0·2090 at 0·2 M.[9] and at other concentrations computed from the vapour pressure results. The revised ϕ values for $CaCl_2$ are based on previous data[10] with slight changes in the concentrated solutions resulting from the adoption of the values of Table I for H_2SO_4. The activity coefficients of $CaCl_2$, in addition, have been recomputed on the basis of $\gamma_{0\cdot1\,\text{M.}} = 0\cdot518$.[11]

The present accuracy of the standard data for the four reference electrolytes named justifies recalculation from all the existing isopiestic measurements at 25° on a uniform basis. Tables II and III and Appendix give the recalculated osmotic coefficients and activity coefficients for all the 1 : 2 and 2 : 1 electrolytes which have been studied by the isopiestic method.

The isopiestic data and Tables I, II and III all refer to 25° C. Values for other temperatures are available in certain cases from E.M.F. measurements, e.g. for the Zn and Cd halides, Na_2SO_4, H_2SO_4, and in some cases also from freezing-point measurements. The list of references in Table III, besides giving the source of the isopiestic measurements, may also be used to find results for other temperatures, but makes no claim to completeness.

The partial molar free energy of the water is conveniently expressed in terms of the osmotic coefficient defined by $\phi = -(55\cdot51/\nu m)\ln a_w$, which for 2 : 1 and 1 : 2 electrolytes becomes $\phi = -(42\cdot606/m)\log a_w$. The ϕ values of Table II are often slightly different, especially at higher concentrations, from those given originally, as a result of later changes in the values for the reference salts. For the solute the geometrical mean molal activity coefficients, γ, are tabulated in Table III.

Given ϕ values from 0·1 M. upwards as in Table I; the ratio $\gamma_m/\gamma_{0\cdot1}$ is readily computed by the equation of Randall and White :[12]

$$-\log(\gamma_m/\gamma_{0\cdot1}) = 0\cdot4343\,(h_m - h_{0\cdot1}) + \int_{0\cdot1}^{m} h\,\mathrm{d}\log m$$

where $h = 1 - \phi$.

The evaluation of $\gamma_{0\cdot1}$ in order to give absolute values of γ_m is, however, a matter of some difficulty.

(i) In a few cases, e.g. Zn and Cd halides, $CaCl_2$ and Na_2SO_4, reliable E.M.F. data for dilute solutions are available, from which Debye-Hückel extrapolations can be made with assurance.

(ii) Comparison of the $\phi - m$ curves sometimes gives a good estimate of the value of $\gamma_{0\cdot1}$ for other salts; e.g. MgI_2, $Mg(ClO_4)_2$, $Zn(ClO_4)_2$, all give ϕ curves which between 0·1 and 0·5 M. lie very close to the ϕ curve for ZnI_2. (At higher concentrations ZnI_2 shows abnormalities resulting from complex ion formation, and the similarity then disappears.) The $\gamma_{0\cdot1}$ values for these salts can therefore be estimated by comparison with ZnI_2 for which E.M.F. data are available at much lower concentrations.

(iii) Another method of fixing $\gamma_{0\cdot1}$ is to plot the isopiestic ratio, R, of a 2 : 1 salt to $CaCl_2$ and to extrapolate to unity at zero concentration. Then, since the activity coefficients of $CaCl_2$ are known down to very low concentrations from E.M.F. measurements,[11] the equation of Robinson and Sinclair :

$$\log\gamma = \log\gamma' + \log R + 0\cdot8686\int_{0}^{m} (R - 1)/\sqrt{m'\gamma'}\,\mathrm{d}\sqrt{m'\gamma'} \quad . \quad (1)$$

(where the dash refers to the reference solution) may be employed. This method was discussed in reference (29), where it was used to estimate values for $MgCl_2$. Unfortunately it appears from later work that the method is not as sound as could be wished. The redetermination by Macleod and Gordon[11] of the activity coefficients of $CaCl_2$ in very dilute solutions leads to $\gamma_{0\cdot1\,\text{M.}} = 0\cdot518$ instead of 0·524, which was the value used in reference (29). Consequently the test cases of the zinc halides there discussed will no longer give such good agreement with the E.M.F. results. A different procedure has therefore been adopted in evaluating $\gamma_{0\cdot1\,\text{M.}}$ for the majority of the 2 : 1 salts listed in Tables IIIA and IIIB. If we examine the data for the alkali-metal halides (for which both ϕ and γ at 0·1 M. are known with very fair accuracy from a variety of measurements) we

---

[7] Robinson, *Trans. Faraday Soc.*, 1939, **35**, 1229.

[8] Scatchard, Hamer and Wood, *J. Amer. Chem. Soc.*, 1938, **60**, 3061.

[9] Harned and Hamer, *ibid.*, 1935, **57**, 27.

[10] Stokes, *Trans. Faraday Soc.*, 1945, **41**, 637.

[11] McLeod and Gordon, *J. Amer. Chem. Soc.*, 1946, **68**, 58.

[12] Randall and White, *ibid.*, 1926, **48**, 2514.

TABLE IIA.—OSMOTIC COEFFICIENTS OF 2 : 1 SALTS OF ALKALINE-EARTH METALS AT 25°.

Salt.	$MgCl_2$	$MgBr_2$	MgI_2	$Mg(ClO_4)_2$	$Mg(NO_3)_2$	$CaCl_2$	$CaBr_2$	CaI_2	$Ca(NO_3)_2$	$SrCl_2$	$SrBr_2$	SrI_2	$Sr(NO_3)_2$	$BaCl_2$	$BaBr_2$	BaI_2	$Ba(NO_3)_2$
Precision.*	*a*	*b*	*c*	*a*	*b*	*a*	*b*	*c*	*b*	*a*	*b*	*c*	*b*	*a*	*b*	*c*	*b*
M.																	
0·1	0·861	0·874	0·892	0·898	0·857	0·854	0·863	0·880	0·827	0·850	0·859	0·876	0·816	0·843	0·851	0·869	0·771
0·2	0·877	0·898	0·921	0·935	0·869	0·862	0·878	0·906	0·819	0·854	0·871	0·899	0·796	0·837	0·857	0·891	0·724
0·3	0·895	0·928	0·957	0·974	0·890	0·876	0·900	0·935	0·818	0·864	0·888	0·925	0·785	0·843	0·869	0·918	0·687
0·4	0·919	0·963	0·998	1·016	0·914	0·894	0·927	0·969	0·821	0·880	0·908	0·955	0·778	0·853	0·884	0·949	0·659
0·5	0·947	1·004	1·044	1·062	0·940	0·917	0·958	1·008	0·825	0·899	0·932	0·987	0·773	0·864	0·906	0·985	—
0·6	0·976	1·042	1·090	1·108	0·967	0·940	0·990	1·044	0·831	0·918	0·957	1·021	0·769	0·877	0·926	1·017	—
0·7	1·004	1·082	1·139	1·158	0·991	0·963	1·022	1·083	0·837	0·937	0·983	1·056	0·765	0·890	0·945	1·050	—
0·8	1·036	1·127	1·192	1·211	1·017	0·988	1·057	1·128	0·843	0·959	1·011	1·095	0·762	0·904	0·965	1·085	—
0·9	1·071	1·172	1·249	1·267	1·046	1·017	1·093	1·173	0·850	0·983	1·042	1·136	0·760	0·918	0·989	1·122	—
1·0	1·108	1·218	1·306	1·323	1·074	1·046	1·131	1·217	0·859	1·009	1·074	1·177	0·757	0·934	1·013	1·159	—
1·2	1·184	1·314	1·421	1·437	1·134	1·107	1·207	1·310	0·879	1·061	1·142	1·264	0·754	0·967	1·063	1·231	—
1·4	1·264	1·410	1·537	1·558	1·192	1·171	1·286	1·407	0·898	1·116	1·210	1·352	0·754	1·002	1·112	1·308	—
1·6	1·347	1·510	1·660	1·683	1·253	1·237	1·370	1·504	0·917	1·173	1·284	1·443	0·754	1·034	1·162	1·388	—
1·8	1·434	1·610	1·784	1·815	1·315	1·305	1·455	1·605	0·934	1·232	1·360	1·540	0·755	1·065	1·212	1·470	—
2·0	1·523	1·715	1·912	1·945	1·380	1·376	1·547	1·710	0·953	1·292	1·440	1·641	0·758	—	1·263	1·599	—
2·5	1·762	1·999	2·25	2·306	—	1·568	1·790	—	1·001	1·454	—	—	0·768	—	—	—	—
3·0	2·010	2·29	2·60	2·667	—	1·779	2·048	—	1·051	1·631	—	—	0·783	—	—	—	—
3·5	2·264	2·59	2·96	3·036	—	1·981	2·297	—	1·103	1·802	—	—	0·800	—	—	—	—
4·0	2·521	2·89	3·34	3·397	—	2·182	2·584	—	1·157	1·966	—	—	0·818	—	—	—	—
4·5	2·783	3·19	3·72	(3·664 at 4·4 M.)	—	2·383	2·908	—	1·210	—	—	—	—	—	—	—	—
5·0	3·048	3·50	4·11	—	—	2·574	3·239	—	1·263	—	—	—	—	—	—	—	—
6·0	(3·513 at 5·84 M.)	(3·85 at 5·63 M.)	—	—	—	2·891	3·880	—	1·361	—	—	—	—	—	—	—	—
7·0	—	—	—	—	—	3·081	4·463	—	1·452	—	—	—	—	—	—	—	—
8·0	—	—	—	—	—	3·151	4·809	—	1·535	—	—	—	—	—	—	—	—

* (*a*) Indicates an estimated experimental accuracy of 0·2 % or better ; (*b*) 0·2 % to 0·5 % ; (*c*) about 1 %.

TABLE IIB.—OSMOTIC COEFFICIENTS OF 2 : 1 SALTS OF TRANSITION-SERIES METALS AT 25°.

Salt.	$MnCl_2$	$FeCl_2$	$CoCl_2$	$Co(NO_3)_2$	$NiCl_2$	$CuCl_2$	$Cu(NO_3)_2$	$ZnCl_2$	$ZnBr_2$	ZnI_2	$Zn(ClO_4)_2$	$Zn(NO_3)_2$	$CdCl_2$	$CdBr_2$	CdI_2	$Cd(NO_3)_2$
Precision.	*a*	*b*	*a*	*b*	*a*	*a*	*b*	*b*	*b*	*a*	*a*	*b*	*a*	*b*	*a*	*b*
M.																
0·1	0·853	0·854	0·857	0·854	0·857	0·845	0·847	0·847	0·869	0·893	0·893	0·862	0·622	0·592	0·416	0·850
0·2	0·859	0·863	0·869	0·861	0·868	0·843	0·849	0·845	0·886	0·924	0·928	0·873	0·571	0·533	0·390	0·852
0·3	0·872	0·877	0·886	0·875	0·885	0·848	0·860	0·842	0·911	0·957	0·966	0·890	0·542	0·502	0·371	0·861
0·4	0·889	0·896	0·907	0·892	0·907	0·860	0·875	0·838	0·937	0·994	1·010	0·909	0·522	0·480	0·365	0·873
0·5	0·908	0·920	0·932	0·914	0·934	0·876	0·895	0·833	0·962	1·038	1·056	0·934	0·506	0·466	0·366	0·888
0·6	0·929	0·943	0·959	0·936	0·960	0·892	0·914	0·829	0·984	1·083	1·105	0·958	0·492	0·455	0·370	0·903
0·7	0·950	0·968	0·982	0·958	0·987	0·908	0·934	0·824	1·002	1·124	1·157	0·982	0·481	0·449	0·376	0·917
0·8	0·971	0·994	1·011	0·981	1·016	0·922	0·955	0·817	1·018	1·163	1·212	1·009	0·473	0·445	0·383	0·931
0·9	0·995	1·024	1·043	1·007	1·048	0·938	0·978	0·810	1·032	1·194	1·269	1·037	0·465	0·441	0·388	0·946
1·0	1·022	1·055	1·075	1·033	1·082	0·952	1·001	0·805	1·039	1·220	1·328	1·064	0·458	0·439	0·394	0·962
1·2	1·072	1·117	1·141	1·087	1·150	0·978	1·046	0·792	1·047	1·260	1·450	1·120	0·448	0·439	0·405	0·995
1·4	1·124	1·180	1·208	1·143	1·221	1·000	1·087	0·782	1·049	1·283	1·578	1·180	0·440	0·444	0·419	1·025
1·6	1·173	1·244	1·274	1·199	1·293	1·022	1·131	0·781	1·047	1·291	1·708	1·238	0·435	0·449	0·436	1·057
1·8	1·221	1·307	1·339	1·258	1·366	1·043	1·177	0·785	1·043	1·292	1·843	1·296	0·431	0·455	0·451	1·085
2·0	1·264	1·371	1·404	1·317	1·442	1·062	1·224	0·792	1·042	1·282	1·986	1·355	0·428	0·462	0·463	1·114
2·5	1·366	—	1·564	1·468	1·633	1·100	1·339	0·820	1·048	1·262	2·358	1·510	0·430	0·483	0·507	1·182
3·0	1·454	—	1·711	1·620	1·816	1·131	1·480	0·858	1·066	1·262	2·739	1·664	0·434	0·504	—	—
3·5	1·528	—	1·821	1·769	1·969	1·160	1·610	0·903	1·100	1·278	3·117	1·814	0·442	0·527	—	—
4·0	1·584	—	1·896	1·913	2·100	1·183	1·732	0·955	1·143	1·297	3·494	1·957	0·454	0·548	—	—
4·5	1·634	—	—	2·053	2·202	1·201	1·841	1·022	1·195	1·335	(3·79 at 4·4 M.)	2·098	0·466	—	—	—
5·0	1·671	—	—	2·196	2·292	1·219	1·940	1·091	1·253	1·381	—	2·235	0·482	—	—	—
6·0	1·735	—	—	(2·323 at 5·5 M.)	(2·407 at 5·8 M.)	(1·249 at 5·8 M.)	2·125	1·229	1·379	1·487	—	2·489	0·514	—	—	—
7·0	1·798	—	—	—	—	—	2·286	1·361	1·521	1·617	—	(2·60 at 6·5 M.)	—	—	—	—
8·0	1·861	—	—	—	—	—	2·424	1·500	1·667	1·766	—	—	—	—	—	—
9·0	—	—	—	—	—	—	—	1·628	1·809	1·911	—	—	—	—	—	—
10·0	—	—	—	—	—	—	—	1·753	1·941	2·034	—	—	—	—	—	—
12·0	—	—	—	—	—	—	—	1·961	2·15	2·205	—	—	—	—	—	—
14·0	—	—	—	—	—	—	—	2·09	2·28	—	—	—	—	—	—	—
16·0	—	—	—	—	—	—	—	2·18	2·34	—	—	—	—	—	—	—
18·0	—	—	—	—	—	—	—	2·22	2·35	—	—	—	—	—	—	—
20·0	—	—	—	—	—	—	—	2·24	2·33	—	—	—	—	—	—	—
22·0	—	—	—	—	—	—	—	2·25	—	—	—	—	—	—	—	—

TABLE IIc.—Osmotic Coefficients of 1 : 2 Salts of Sodium Sulphate Type at 25°.

Salt	Li_2SO_4	Na_2SO_4	Na_2CrO_4	$Na_2S_2O_3$	Na_2 Fumarate	Na_2 Maleate	K_2SO_4	K_2CrO_4	$K_2Cr_2O_7$	Rb_2SO_4	Cs_2SO_4
Precision.	*b*	*a*	*a*	*b*	*b*	*b*	*a*	*a*	*a*	*b*	*b*
M.											
0·1	0·818	0·793	0·814	0·805	0·812	0·770	0·779	0·805	0·868	0·799	0·804
0·2	0·792	0·753	0·788	0·774	0·801	0·744	0·742	0·774	0·813	0·764	0·772
0·3	0·780	0·725	0·769	0·753	0·797	0·731	0·721	0·753	0·779	0·740	0·751
0·4	0·775	0·705	0·759	0·741	0·797	0·726	0·703	0·741	0·753	0·724	0·739
0·5	0·772	0·690	0·751	0·731	0·803	0·726	0·691	0·733	0·735	0·714	0·731
0·6	0·773	0·678	0·747	0·724	0·816	0·729	0·679	0·727	—	0·705	0·725
0·7	0·775	0·667	0·743	0·719	0·827	0·733	0·670	0·722	—	0·698	0·721
0·8	0·778	0·658	0·740	0·713	0·841	0·738	—	0·718	—	0·691	0·717
0·9	0·782	0·650	0·738	0·709	0·855	0·742	—	0·714	—	0·686	0·714
1·0	0·787	0·642	0·737	0·707	0·870	0·747	—	0·711	—	0·681	0·712
1·2	0·800	0·631	0·737	0·707	0·894	0·760	—	0·709	—	0·677	0·711
1·4	0·815	0·625	0·743	0·713	0·920	0·773	—	0·711	—	0·677	0·713
1·6	0·832	0·621	0·751	0·719	0·949	0·788	—	0·716	—	0·679	0·716
1·8	0·847	0·620	0·763	0·728	0·972	0·804	—	0·722	—	0·684	0·722
2·0	0·867	0·621	0·780	0·739	0·993	0·820	—	0·730	—	—	—
2·5	0·923	0·635	0·838	0·779	—	0·863	—	0·757	—	—	—
3·0	0·984	0·661	0·905	0·829	—	0·910	—	0·794	—	—	—
3·5	—	0·696	0·992	0·890	—	—	—	0·830	—	—	—
4·0	—	0·740	1·100	—	—	—	—	—	—	—	—

find that the graph of $\phi_{0\cdot1}$ against $\gamma_{0\cdot1}$ is linear within about 0·002 in γ for all members except LiI; and the data for LiI are of poor accuracy. We might therefore expect a similar linearity in the graph of $\phi_{0\cdot1}$ against $\gamma_{0\cdot1}$ for such 2 : 1 salts as are normally dissociated at 0·1 M. There are only two 2 : 1 salts which enable us to fix this line: $CaCl_2$ and ZnI_2. In these two cases we know $\phi_{0\cdot1}$ from isopiestic measurements and $\gamma_{0\cdot1}$ as a result of E.M.F. measurements extending down to 0·002 M. or less. Drawing the line then between $CaCl_2$ ($\phi_{0\cdot1} = 0{\cdot}854$, $\gamma_{0\cdot1} = 0{\cdot}518$) and ZnI_2 ($\phi_{0\cdot1} = 0{\cdot}893$, $\gamma_{0\cdot1} = 0{\cdot}581$), we can estimate values of $\gamma_{0\cdot1}$ for the remaining 2 : 1 salts by interpolation on this graph at the appropriate values of $\phi_{0\cdot1}$. This procedure leads at least to a consistent set of values, and it is unlikely that these are in error by as much as 1 %. In Tables IIIA and IIIB, this method has been used to fix the values of $\gamma_{0\cdot1}$ for all the alkaline-earth halides, Zn and Mg nitrates, Mn, Fe, Co and Ni chlorides, and Zn and Mg perchlorates. Those for the Zn and Cd halides are based on E.M.F. data in dilute solutions. The remainder as well as all the salts in Table IIIc, have been fixed by using the Robinson and Sinclair extrapolation discussed above, as the values of $\phi_{0\cdot1}$ in these cases lie too far below that of $CaCl_2$ to justify extrapolation of the $\phi_{0\cdot1}$—$\gamma_{0\cdot1}$ graph. In making the extrapolation the 1 : 2 salts (Table IIIc) were based on sodium sulphate as reference substance.

Accuracy of the Data.

At best, isopiestic ratios are reproducible to 0·1 % or better, giving a corresponding accuracy in ϕ provided the standard data are correct. In some cases, however, as with some of the alkaline-earth iodides, great precision was not aimed at, and accordingly the salts were not rigorously purified. The letter (*a*) is appended to the formula of the salt where the accuracy is believed to be 1 in 500 or better; (*b*) indicates an accuracy of 1 in 200 to 1 in 500; and (*c*) an accuracy of only about ± 1 %. The values of the activity coefficients, TABLE IIIA.—ACTIVITY COEFFICIENTS OF 2 : 1 SALTS OF ALKALINE-EARTH METALS AT 25°.

Salt	$MgCl_2$	$MgBr_2$	MgI_2	$Mg(ClO_4)_2$	$Mg(NO_3)_2$	$CaCl_2$	$CaBr_2$	CaI_2	$Ca(NO_3)_2$	$SrCl_2$	$SrBr_2$	SrI_2	$Sr(NO_3)_2$	$BaCl_2$	$BaBr_2$	BaI_2	$Ba(NO_3)_2$
Ref.*	28, 29	28, app.	28, app.	6	31	10	33, 59	33	34, 58	35 app.	33	33	31	35	36	33	31
M.																	
0·1	0·529	0·550	0·580	0·590	0·523	0·518	0·532	0·560	0·485	0·511	0·526	0·553	0·478	0·500	0·513	0·542	0·428
0·2	0·489	0·519	0·558	0·578	0·481	0·472	0·492	0·531	0·426	0·462	0·483	0·520	0·410	0·444	0·465	0·509	0·342
0·3	0·477	0·518	0·567	0·589	0·468	0·455	0·482	0·531	0·395	0·442	0·468	0·517	0·373	0·419	0·446	0·502	0·293
0·4	0·475	0·527	0·584	0·613	0·466	0·448	0·483	0·543	0·376	0·433	0·465	0·524	0·348	0·405	0·437	0·510	0·260
0·5	0·481	0·545	0·614	0·647	0·470	0·448	0·491	0·561	0·363	0·430	0·467	0·536	0·329	0·397	0·435	0·523	—
0·6	0·491	0·571	0·653	0·688	0·479	0·453	0·505	0·584	0·354	0·431	0·473	0·555	0·314	0·391	0·438	0·540	—
0·7	0·506	0·599	0·698	0·739	0·489	0·460	0·522	0·614	0·347	0·434	0·484	0·578	0·302	0·391	0·442	0·562	—
0·8	0·522	0·635	0·753	0·798	0·502	0·470	0·543	0·650	0·342	0·441	0·497	0·608	0·292	0·391	0·448	0·587	—
0·9	0·544	0·677	0·817	0·868	0·519	0·484	0·568	0·692	0·338	0·449	0·515	0·642	0·283	0·392	0·458	0·617	—
1·0	0·570	0·723	0·892	0·946	0·537	0·500	0·597	0·741	0·336	0·461	0·535	0·680	0·275	0·395	0·469	0·649	—
1·2	0·631	0·837	1·069	1·137	0·581	0·539	0·665	0·852	0·335	0·489	0·583	0·773	0·262	0·405	0·496	0·724	—
1·4	0·709	0·975	1·291	1·385	0·632	0·587	0·747	0·992	0·335	0·524	0·643	0·885	0·253	0·419	0·529	0·814	—
1·6	0·804	1·143	1·580	1·705	0·692	0·644	0·848	1·161	0·337	0·565	0·715	1·021	0·244	0·433	0·566	0·924	—
1·8	0·916	1·351	1·957	2·13	0·761	0·712	0·970	1·375	0·340	0·614	0·800	1·191	0·238	0·449	0·609	1·055	—
2·0	1·053	1·614	2·43	2·65	0·842	0·792	1·121	1·640	0·345	0·670	0·906	1·407	0·232	—	0·656	1·221	—
2·5	1·541	2·59	4·33	4·89	—	1·063	1·657	—	0·360	0·855	—	—	0·223	—	—	—	—
3·0	2·32	4·26	7·93	9·19	—	1·483	2·54	—	0·380	1·126	—	—	0·217	—	—	—	—
3·5	3·56	7·15	15·0	17·65	—	2·08	3·89	—	0·405	1·492	—	—	0·214	—	—	—	—
4·0	5·54	12·2	29·0	34·1	—	2·93	6·28	—	0·435	1·977	—	—	0·212	—	—	—	—
4·5	8·74	21·1	57·6	(56·6 at 4·4 M.)	—	4·17	10·66	—	0·469	—	—	—	—	—	—	—	—
5·0	13·95	36·6	115	—	—	5·89	18·47	—	0·507	—	—	—	—	—	—	—	—
6·0	31·6 at	71·2 at	—	—	—	11·11	55·8	—	0·592	—	—	—	—	—	—	—	—
7·0	5·84 M.	5·63 M.	—	—	—	18·28	163	—	0·690	—	—	—	—	—	—	—	—
8·0	—	—	—	—	—	26·0	375	—	0·801	—	—	—	—	—	—	—	—

* "App." refers to data given in Appendix.

TABLE IIIB.—ACTIVITY COEFFICIENTS OF 2 : 1 SALTS OF TRANSITION-SERIES METALS AT 25°.

Salt	$MnCl_2$	$FeCl_2$	$CoCl_2$	$Co(NO_3)_2$	$NiCl_2$	$CuCl_2$	$Cu(NO_3)_2$	$ZnCl_2$	$ZnBr_2$	ZnI_2	$Zn(ClO_4)_2$	$Zn(NO_3)_2$	$CdCl_2$	$CdBr_2$	CdI_2	$Cd(NO_3)_2$
Ref.	37, app.	38	39, 32	31, 32	37, app.	37, 24	31, 24	40, app.	41, 42	43, 44 13	6	6	45, 46	45, 47	48, 49	31
M.																
0·1	0·516	0·518	0·522	0·518	0·522	0·508	0·511	0·515	0·547	0·581	0·581	0·531	0·2280	0·1900	0·1060	0·513
0·2	0·469	0·473	0·479	0·471	0·479	0·455	0·460	0·462	0·510	0·559	0·564	0·489	0·1638	0·132	0·0685	0·464
0·3	0·450	0·454	0·463	0·452	0·463	0·429	0·439	0·432	0·502	0·564	0·573	0·474	0·1329	0·105	0·0523	0·442
0·4	0·442	0·448	0·459	0·445	0·460	0·417	0·429	0·411	0·504	0·582	0·596	0·469	0·1139	0·089	0·0433	0·430
0·5	0·440	0·450	0·462	0·445	0·464	0·411	0·426	0·394	0·511	0·610	0·629	0·473	0·1006	0·0780	0·0376	0·425
0·6	0·443	0·454	0·470	0·448	0·471	0·409	0·427	0·380	0·519	0·645	0·670	0·480	0·0905	0·0699	0·0337	0·423
0·7	0·448	0·463	0·479	0·455	0·482	0·409	0·431	0·369	0·528	0·683	0·720	0·489	0·0827	0·0638	0·0307	0·423
0·8	0·455	0·473	0·492	0·465	0·496	0·410	0·437	0·357	0·537	0·724	0·780	0·501	0·0765	0·0591	0·0285	0·425
0·9	0·466	0·488	0·511	0·477	0·515	0·413	0·445	0·348	0·547	0·762	0·850	0·518	0·0713	0·0551	0·0267	0·428
1·0	0·479	0·506	0·531	0·490	0·536	0·417	0·455	0·339	0·552	0·800	0·929	0·535	0·0669	0·0518	0·0251	0·433
1·2	0·507	0·547	0·578	0·523	0·586	0·425	0·478	0·323	0·561	0·870	1·127	0·574	0·0599	0·0468	0·0228	0·446
1·4	0·542	0·596	0·634	0·563	0·647	0·434	0·503	0·309	0·567	0·928	1·386	0·625	0·0546	0·0431	0·0214	0·460
1·6	0·581	0·653	0·699	0·609	0·720	0·444	0·533	0·300	0·569	0·972	1·719	0·680	0·0504	0·0402	0·0199	0·478
1·8	0·624	0·719	0·773	0·664	0·805	0·455	0·569	0·294	0·570	1·007	2·16	0·744	0·0469	0·0380	0·0189	0·495
2·0	0·668	0·794	0·860	0·726	0·906	0·466	0·609	0·289	·0572	1·028	2·74	0·817	0·0441	0·0361	0·0180	0·515
2·5	0·793	—	1·120	0·920	1·236	0·494	0·727	0·285	0·581	1·070	5·15	1·049	0·0389	0·0328	0·0168	0·570
3·0	0·934	—	1·458	1·182	1·692	0·520	0·903	0·287	0·598	1·123	9·99	1·363	0·0352	0·0305	—	—
3·5	1·084	—	1·832	1·526	2·26	0·547	1·118	0·295	0·626	1·188	19·60	1·773	0·0325	0·0290	—	—
4·0	1·235	—	2·22	1·972	2·96	0·573	1·381	0·307	0·664	1·259	38·8	2·31	0·0306	0·0278	—	—
4·5	1·395	—	—	2·55	3·76	0·597	1·690	0·328	0·714	1·357	(67·2 at 4·4 M.)	2·99	0·0291	—	—	—
5·0	1·55	—	—	3·31	4·69	0·621	2·05	0·354	0·774	1·476	—	3·88	0·0279	—	—	—
6·0	1·88	—	—	{4·23	{6·43	0·673	2·98	0·417	0·930	1·774	—	6·41	0·0263	—	—	—
7·0	2·25	—	—	at	at	—	4·21	0·499	1·149	2·20	—	—	—	—	—	—
8·0	2·68	—	—	5·5 M.}	5·8 M.}	—	5·79	0·607	1·439	2·80	—	—	—	—	—	—
9·0	—	—	—	—	—	—	—	0·737	1·809	3·57	—	—	—	—	—	—
10·0	—	—	—	—	—	—	—	0·898	2·26	4·47	—	—	—	—	—	—
12·0	—	—	—	—	—	—	—	1·294	3·39	6·52	—	—	—	—	—	—
14·0	—	—	—	—	—	—	—	1·73	4·63	—	—	—	—	—	—	—
16·0	—	—	—	—	—	—	—	2·18	5·90	—	—	—	—	—	—	—
18·0	—	—	—	—	—	—	—	2·63	6·92	—	—	—	—	—	—	—
20·0	—	—	—	—	—	—	—	3·06	7·86	—	—	—	—	—	—	—
22·0	—	—	—	—	—	—	—	3·46	—	—	—	—	—	—	—	—

TABLE IIIc.—Activity Coefficients of 1 : 2 Salts of Sodium Sulphate Type at 25°.

Salt	Li_2SO_4	Na_2SO_4	Na_2CrO_4	$Na_2S_2O_3$	Na_2 fumarate	Na_2 maleate	K_2SO_4	K_2CrO_4	Rb_2SO_4	Cs_2SO_4
Ref.	50	50, 51	app.	50	27	27	50	52	53	53
M.										
0·1	0·468	0·445	0·464	0·457	0·465	0·430	0·441	0·456	0·451	0·456
0·2	0·398	0·365	0·394	0·382	0·402	0·354	0·360	0·382	0·374	0·382
0·3	0·361	0·320	0·353	0·340	0·369	0·314	0·316	0·340	0·331	0·338
0·4	0·337	0·289	0·327	0·313	0·348	0·289	0·286	0·313	0·301	0·311
0·5	0·319	0·266	0·307	0·292	0·335	0·272	0·264	0·292	0·279	0·291
0·6	0·307	0·248	0·292	0·276	0·328	0·262	0·246	0·276	0·263	0·274
0·7	0·297	0·233	0·280	0·262	0·323	0·250	0·232	0·263	0·249	0·262
0·8	0·289	0.221	0·269	0·251	0.320	0·243	—	0·253	0·238	0·251
0·9	0·282	0·210	0·261	0·242	0·319	0·236	—	0·243	0·228	0·242
1·0	0·277	0·201	0·253	0·234	0·319	0·231	—	0·235	0·219	0·235
1·2	0·271	0·1860	0·241	0·222	0·320	0·224	—	0·223	0·206	0·222
1·4	0·267	0·1746	0·233	0·214	0·323	0·219	—	0·214	0·196	0·214
1·6	0·265	0·1654	0·227	0·207	0·330	0·216	—	0·207	0·189	0·207
1·8	0·264	0·1580	0·224	0·202	0·336	0·214	—	0·201	0·182	0·201
2·0	0·263	0·1520	0·222	0·198	0·343	0·213	—	0·196	—	—
2·5	0·274	0·1418	0·225	0·195	—	0·215	—	0·190	—	—
3·0	0·288	0·1365	0·236	0·199	—	0·220	—	0·190	—	—
3·5	—	0·1345	0·255	0·207	—	—	—	0·191	—	—
4·0	—	0·1354	0·285	—	—	—	—	—	—	—

relative to 0·1 M., are of accuracy comparable to that of the osmotic coefficient, but the absolute values are in some cases subject to an uncertainty of the order of 1 % owing to the necessity for extrapolations (cp. above).

Discussion.

The most striking feature of the activity coefficients in Table III is the extraordinarily wide range covered by the values for the more concentrated solutions; the low extreme occurring in the case of CdI_2 ($\gamma = 0{\cdot}0168$ at 2·5 M.) is about 1/300 of the value for $Zn(ClO_4)_2$ at the same concentration. Remarkable variations of the activity coefficient of a salt with concentration are also found, the extreme case occurring with MgI_2 where the range is from $\gamma = 0{\cdot}573$ at 0·1 M. to over 200 times this value at 5 M. These wide ranges are moreover confined to salts of the 2 : 1 type; those of the 1 : 2 type, e.g. Na_2SO_4, all have activity coefficients of 0·1 to 0·5 in the concentration range above 0·1 M.

It is best to examine the results in several groups, following the subdivisions of Tables II and III.

A. The salts formed from alkaline-earth cations and monovalent anions (Tables IIA and IIIA) from a very regular group. For a given anion, the activity coefficients descend in the order Mg > Ca > Sr > Ba with no intersections of the curves. This is the order of increasing radius of the unhydrated ion, as determined by crystallographic measurements. Pauling [14] gives $Mg^{++} = 0{\cdot}65$ A., $Ca^{++} = 0{\cdot}99$ A., $Sr^{++} = 1{\cdot}13$ A., $Ba^{++} = 1{\cdot}35$ A. The smaller the bare ion, the more intense will its surface field be, and

---

[13] Bates, *J. Amer. Chem. Soc.*, 1938, **60**, 2983.

[14] Pauling, *The Nature of the Chemical Bond* (Cornell University Press, 1944), p. 346.

therefore the greater its tendency to hydrate. Hydration increases the activity coefficient in two ways : (*a*) by increasing the " effective mean ionic diameter " of the Debye-Hückel theory, and (*b*) by removing water from the role of solvent to become, in effect, part of the solute ion[5a].

The effect of the size of the anion, however, appears to be the reverse : the order of decreasing activity coefficients for a given alkaline-earth cation is that of decreasing anion radius :

$$ClO_4^- \approx I^- > Br^- > Cl^- > NO_3^-,$$

the crystallographic radii for the three halide ions being

$$I^- = 2{\cdot}16,\ Br^- = 1{\cdot}95,\ Cl^- = 1{\cdot}81\ \text{A.};$$

the tetrahedral perchlorate ion may be estimated to have an effective radius of 2·1-2·2 A., and the planar nitrate ion, though its radius in the plane is not much different from that of Cl^-, will clearly have a smaller effective radius because of the possibility of approach by other ions normally to the plane. These anions, being only singly charged and much larger than the cations, will not be expected to hydrate as much. Bernal and Fowler [15] have shown that a negative charge is less effective in producing electrostatic hydration than a positive charge, and consider that monovalent anions, especially if large or polyatomic, may be regarded as practically unhydrated. This conclusion is consistent with the observed order of the activity coefficients, and suggests that the anion influences the activity coefficient only by its effect on the mean effective diameter of the ions.

The activity coefficient curves of the four nitrates in Table IIIA show a much greater dispersion than the corresponding halides ; e.g. while $Mg(NO_3)_2$ is only slightly below $MgCl_2$, $Sr(NO_3)_2$ is very much below $SrCl_2$. This is explicable on the grounds that the nitrate ion is small enough to permit extensive formation of Bjerrum [16] ion-pairs with the smaller hydrated cations, while the hydrated magnesium ion is so large that ion-pair formation does not become so important. All the alkaline-earth halides are probably fully dissociated in the sense that no significant number of complex ions, intermediate ions or undissociated molecules, are present, even in concentrated solutions. Not all of them have been directly tested, but those which have appear to be quite normal. Thus $MgCl_2$ and the Ca, Sr and Ba halides give no Raman spectrum [17] ; the vapour pressure lowerings of $MgCl_2$, $CaCl_2$ and $BaCl_2$ alone and in admixture with other salts obey simple additivity rules [18] ; transport numbers,[19, 20] where available, show no peculiarities, and the activity coefficient curves are free from inflexions such as are often found where complex ions are formed. The conductivity data are consistent with these conclusions.[21] It would appear therefore, that any attempt to deal theoretically with the thermodynamics of these solutions should pay attention mainly to the effects of ion size on ion-pair formation, on effective ionic diameter, and on cation hydration. Attempts to fit the Debye-Hückel and Hückel equations to the experimental activity coefficients are on the whole unprofitable ; moderate success may be obtained with $Ca(NO_3)_2$ [22] which has a fairly flat γ curve, but to obtain a fit in cases where γ rises rapidly from its minimum demands the introduction of arbitrary terms in higher powers of the concentration, and the resulting equation is of little interest except as an interpolation formula.

---

[15] Bernal and Fowler, *J. Chem. Physics*, 1933, **1**, 515.

[16] Bjerrum, *Kgl. Danske Vidensk. Selskab*, 1926, **7**, (No. 9).

[17] Hibben, *The Raman Effect and its Chemical Applications* (Reinhold Publishing Corp., New York, 1939), p. 336.

[18] Robinson and Stokes, *Trans. Faraday Soc.*, 1945, **41**, 752.

[19] *International Critical Tables*, **6**, 310.

[20] Jones and Dole, *J. Amer. Chem. Soc.*, 1929, **51**, 1073.

[21] Righellato and Davies, *Trans. Faraday Soc.*, 1930, **26**, 592.

B. Turning to the second group, the salts of the bivalent transition-series elements (Tables IIB and IIIB) we find that the nitrates and perchlorates behave like the corresponding alkaline-earth salts. Zinc nitrate and $Zn(ClO_4)_2$ give curves very close to those for $Mg(NO_3)_2$ and $Mg(ClO_4)_2$, which is consistent with the fact that the crystallographic radii of magnesium and zinc ions are close together. The other nitrates also behave in a perfectly " normal " manner, the activity coefficient showing the expected dependence on ion size. Other salts in this group which appear to behave normally are $FeCl_2$, which up to 2 M. is practically the same as $CaCl_2$, and $NiCl_2$ which is close to $SrBr_2$.

The remaining halides of this group all behave anomalously in some degree. The Cd halides are noteworthy for extremely low activity coefficients. These salts undergo extensive auto-complex formation even in dilute solutions. Similarly, the zinc halides give activity coefficients quite different from the general type. From the resemblance between $Zn(NO_3)_2$ and $Mg(NO_3)_2$, the zinc halides would be expected, if normally dissociated, to give curves close to those of the magnesium halides. However, as the concentration increases the activity coefficients of all three salts rapidly fall away from those of the corresponding magnesium salts, the divergence occurring first with the chloride and last with the iodide. This behaviour is due [22] to the formation of complex ions of the type $ZnCl_4^{--}$.

In contrast to the cadmium halides, the order of decreasing stability of the complexes is $ZnCl_4^{--} > ZnBr_4^{--} > ZnI_4^{--}$.[22] In spite of this complex formation, the activity coefficients in very concentrated zinc halide solutions exceed unity, due to hydration of free Zn ions present in solution. The Cd ion is probably too large for hydration effects to be dominant. Robinson [23] has obtained some evidence for ion-pair formation between Cd^{++} and CdX_4^{--} from unpublished measurements on $CdCl_2$-$CaCl_2$ mixtures. Again, the presence of $CdCl^+$ ions is claimed by some workers ; these provide an alternative explanation, as they " bind " the cadmium ions in a form in which little or no hydration is to be expected.

The activity coefficient curve of $MnCl_2$ lies close to that of $SrCl_2$ up to about 2 M., but thereafter does not rise as sharply as might be expected ; this possibly indicates the presence, in very concentrated solutions, of a complex ion or or undissociated molecule of very low stability.

Cobalt chloride at first gives a curve between those for $MgCl_2$ and $CaCl_2$, but at higher concentrations there is again evidence of anomalous behaviour, due to the presence of an undissociated molecule, $CoCl_2 . 4H_2O$, in concentrated solutions.

The activity coefficient of $CuCl_2$ is also much lower than would be expected. Recent work by Brown [24] has explained this anomaly as due to the formation of the intermediate ion $CuCl^+$ and the undissociated $CuCl_2$ molecule ; Bjerrum [25] on the other hand has obtained evidence for $CuCl_3^-$ and $CuCl_4^{--}$ as well.

C. It remains to consider the 1 : 2 salts formed from monovalent cations and bivalent anions (Tables IIc and IIIc). This group is characterised by much lower activity coefficients. The minimum in γ, when it occurs at all in the range studied, is at much higher concentrations than is the case with the normal 2 : 1 salts of Table IIIA. Polyatomic anions, even if doubly charged, will not be significantly hydrated,[15] and the cations of this group, though of radii comparable to the alkaline-earth cations, are only singly charged and therefore will not hydrate as readily. The comparatively slight hydration for these ions is confirmed by the fact that the " mean ionic diameter " required to produce a satisfactory fit of the Debye-Hückel formula to the activity coefficient is not much greater than the sum of the crystallographic radii: in e.g. K_2SO_4 the Debye-Hückel diameter is about 2·9 A.,[26] while the crystallographic radius sum is about 3·4 A. to 3·5 A. This strongly suggests that the K^+ ion is too large to hydrate at all firmly, an argument which applies *a fortiori* to the Rb^+ and Cs^+ ions. The small Li^+ ion, and to a less extent the Na^+ ion, will, however, be expected to hydrate to some extent. The order of decreasing activity coefficients for the alkali sulphates is

---

[22] Stokes, *Trans. Faraday Soc.*, 1948 (in press).

[23] Robinson (private communication).

[24] Brown, *Trans. Roy. Soc. New Zealand* (in press).

[25] Bjerrum, *Kgl. Danske Vidensk. Selskab*, 1946, **22**, (No. 18).

$$\begin{array}{ccccccccc} Li^+ & > & Cs^+ & > & Rb^+ & > & Na^+ & > & K^+ \\ (0{\cdot}60) & & (1{\cdot}69) & & (1{\cdot}48) & & (0{\cdot}95) & & (1{\cdot}33)\ \text{A.} \end{array}$$

the bracketed figures giving the accepted crystallographic radii. If we allow for considerable hydration of Li^+ and slight hydration of Na^+, the order of ionic radii will correspond to the order of the activity coefficients. In all the salts of this group, however, we must certainly expect a considerable amount of ion-pair formation, as the mean diameters of the ions are much below the critical distance of Bjerrum's theory[16] (7 A. for 1 : 2 salts). This factor will largely account for the lower activity coefficients. The importance of ion-pairing is well illustrated by the case of sodium fumarate and maleate. Robinson, Smith and Smith[27] have pointed out that the maleate ion, with *cis* configuration, will have a greater tendency to form ion-pairs (with sodium ion) than the fumarate which has the *trans* configuration, thus explaining the substantially higher activity coefficients of sodium fumarate.

In the case of $K_2Cr_2O_7$, only the osmotic coefficients are given, as hydrolysis of the dichromate ion precludes any extrapolation by which a reference value for the activity coefficients at 0·1 M. may be obtained.

[26] Åkerlof, *J. Amer. Chem. Soc.*, 1926, **48**, 1160.

[27] Robinson, Smith and Smith, *Trans. Faraday Soc.*, 1942, **38**, 63.

[28] Robinson and Stokes, *Trans. Faraday Soc.*, 1940, **36**, 733.

[29] Stokes, *ibid.*, 1945, **41**, 642.

[30] Stokes and Levien, *J. Amer. Chem. Soc.*, 1946, **68**, 333.

[31] Robinson, Wilson and Ayling, *ibid.*, 1942, **64**, 1469.

[32] Robinson and Brown, *Trans. Roy. Soc. New Zealand* (in press).

[33] Robinson, *Trans. Faraday Soc.*, 1942, **38**, 445.

[34] Robinson, *J. Amer. Chem. Soc.*, 1940, **62**, 3130.

[35] Robinson, *Trans. Faraday Soc.*, 1940, **36**, 737.

[36] Robinson, *ibid.*, 1941, **37**, 82.

[37] Robinson and Stokes, *ibid.*, 1940, **36**, 1137.

[38] Stokes and Robinson, *ibid.*, 1941, **37**, 419.

[39] Robinson, *ibid.*, 1938, **34**, 1142.

[40] Robinson and Stokes, *ibid.*, 1940, **36**, 740.

[41] Stokes, Stokes and Robinson, *ibid.*, 1944, **40**, 533.

[42] Stokes and Stokes, *ibid.*, 1945, **41**, 688.

[43] Stokes, *ibid.*, 1945, **41**, 12.

[44] Stokes and Levien, *J. Amer. Chem. Soc.*, 1946, **68**, 1852.

[45] Robinson, *Trans. Faraday Soc.*, 1940, **36**, 1135.

[46] Harned and Fitzgerald, *J. Amer. Chem. Soc.*, 1936, **58**, 2624.

[47] Bates, *ibid.*, 1939, **61**, 308.

[48] Robinson and Wilson, *Trans. Faraday Soc.*, 1940, **36**, 738.

[49] Bates and Vosburgh, *J. Amer. Chem. Soc.*, 1937, **59**, 1583.

[50] Robinson, Wilson and Stokes, *ibid.*, 1941, **63**, 1011.

[51] Harned and Hecker, *ibid.*, 1934, **56**, 650.

[52] Stokes, Wilson and Robinson, *Trans. Faraday Soc.*, 1941, **37**, 566.

[53] Cudd and Felsing, *J. Amer. Chem. Soc.*, 1942, **64**, 550.

[54] Stokes (not previously published).

[55] Robinson (private communication).

[56] Stokes (unpublished work).

[57] Farrelly, *Thesis* (University of New Zealand, 1945).

[58] Stokes and Robinson, *J. Amer. Chem. Soc.*, 1948 (in press), where a quantitative treatment of the hydration effect is given.

[59] Robinson and McCoach, *ibid.*, 1947, **69**, 2244.

The author wishes to express his indebtedness to Dr. R. A. Robinson, in discussion with whom many of the points made in this paper have been clarified. During the seven years in which the work has been proceeding we have been assisted by grants from the Chemical Society and from Messrs. Imperial Chemical Industries Limited, to whom thanks are due.

Summary.

Activity coefficients and osmotic coefficients at 25°, derived mainly from isopiestic vapour pressure measurements are tabulated for 45 1 : 2 and 2 : 1 electrolytes over a wide range of concentrations. All the data have been recalculated using a consistent set of values for the isopiestic standard substances. The main factor governing the behaviour of these electrolytes is ion size, through its influence on the extent of cation hydration and ion-pair formation. The anomalous behaviour of the halides of several metals of the transition series is discussed in terms of the formation of complex or intermediate ions or undissociated molecules.

Appendix.

Details of isopiestic measurements on concentrated solutions at 25°, supplementing those given in earlier papers. Each solution is isopiestic with the reference solution ($CaCl_2$, NaCl or H_2SO_4) whose molality is immediately below it The bracketed figures give reference to the source of these data.

(54)

M. $MgBr_2$	2·298	2·933	4·345	5·314	5·61 (sat.)
M. $CaCl_2$	2·650	3·400	5·137	6·508	7·023

(54)

M. MgI_2	2·081	2·233	2·501	3·314	3·402	3·970	4·616	5·009
M. $CaCl_2$	2·569	2·747	3·099	4·160	4·293	5·075	6·032	6·770

(57)

M. $ZnCl_2$	3·347	3·394	3·894	3·932	4·724	5·100	5·837	7·119	7·950
M. $CaCl_2$	2·104	2·130	2·405	2·431	2·879	3·091	3·527	4·279	4·766
M. $ZnCl_2$	9·013	9·991							
M. $CaCl_2$	5·414	6·031							

(57)

M. $ZnCl_2$	11·814	13·552	14·044	15·130	17·333	19·853	22·073	23·193
M. H_2SO_4	11·495	13·316	13·790	14·867	16·932	19·145	20·975	21·674

(56)

M. $SrCl_2$	0·07838	0·3518	0·4508	0·6067	0·6986	0·7136	0·7985	
M. $CaCl_2$	0·07810	0·3507	0·4435	0·5947	0·6820	0·6966	0·7792	
M. $SrCl_2$	0·9427	1·015	1·112	1·135	1·371	1·802	2·028	2·123
M. $CaCl_2$	0·9187	0·9859	1·078	1·102	1·325	1·731	1·948	2·034
M. $SrCl_2$	2·437	2·511	2·827	2·909	3·520 (sat.)		4·038	
M. $CaCl_2$	2·331	2·395	2·691	2·769	3·334		3·799	

(55)

M. $MnCl_2$	1·838	2·656	2·949	3·163	3·592	4·203	4·305	4·931
M. $CaCl_2$	1·754	2·413	2·628	2·780	3·066	3·499	3·507	3·861
M. $MnCl_2$	5·145	5·550	5·710	5·956	6·111	6·705	7·699	
M. $CaCl_2$	3·979	4·196	4·275	4·410	4·484	4·786	5·293	

(55)

M. $NiCl_2$	1·634	2·479	2·496	2·660	3·073	3·725	3·941
M. $CaCl_2$	1·684	2·543	2·556	2·717	3·106	3·684	3·864
M. $NiCl_2$	4·217	4·422	4·567	4·595	4·926	5·714	
M. $CaCl_2$	4·087	4·251	4·357	4·375	4·628	5·185	

M. Na_2CrO_4	0·1127	0·2158	0·5533	0·8564	1·070	1·428	2·121
M. NaCl	0·1480	0·2750	0·6725	1·016	1·249	1·653	2·490
M. Na_2CrO_4	2·357	2·462	3·118	3·489	3·866	4·363	
M. NaCl	2·815	2·951	3·922	4·475	5·150	6·105	

Chemistry Departments,
Auckland University College,
New Zealand.

University of Western Australia,
Nedlands,
Western Australia.

AN INTERPRETATION OF THE VISCOSITY OF LIQUIDS.

By R. C. L. Bosworth.

Received 14th March, 1947.

Theories of the Viscosity of Liquids.

The theories which from time to time have been proposed in an attempt to account for the property of liquid viscosity fall naturally into three classes : those which explain the phenomenon in terms of the transport of momentum, those which regard the property as one of molecular relaxation and those semi-empirical theories which relate viscosity to molecular volume.

Transport of momentum theories are essentially attempts to take over the kinetic theory which has been so successful in treating gaseous viscosity. Such attempts meet at once the difficulty that the viscosity of an ordinary mobile liquid at room temperature is some 50 times that of a typical gas and further that the viscosity of a liquid decreases with increase in temperature while that of a gas increases. Protagonists of the transport of momentum theories, such as those of van der Waals, Jr.[1] and Andrade,[2] give expressions which derive this behaviour as a consequence of the much smaller free space in the liquid state. Brillouin [3] has proposed a somewhat novel theory based on the transport of momentum from neighbouring vibrating systems, taking, as the carriers of momentum, the system of equivalent particles, or " phonons," into which the thermal motion of the molecules can be analysed. Brillouin's detailed calculation showed, however, that longitudinal waves in a liquid carried momentum in such a way as to impart a negative viscosity to the system.

Relaxation theories probably date back to Clerk Maxwell who showed that in a system of rigidity G and viscosity η an initial stress in the body will decay with a time constant (τ)

$$\tau = \eta/G \quad . \quad . \quad . \quad . \quad . \quad . \quad (1)$$

Maxwell called τ the relaxation time.

Frenkel[4] adopted a model of a liquid in which the molecules perform periodic oscillations with an occasional shift in the position of equilibrium. By considering this process as one of self-diffusion he arrives at an expression,

$$\eta = G\tau e^{U/kT} \quad . \quad . \quad . \quad . \quad . \quad . \quad (2)$$

where U is the dissociation energy for the lattice. This theory has further been developed by Prandtl.[5]

The interpretation of viscosity in terms of relaxation has been replaced by a derivation of η from the theory of absolute reaction rates by Powell, Roseveare and Eyring.[6] The expression they give reads :

$$\eta = \frac{Nh}{V} e^{\Delta G^{\ddagger}/RT}, \quad . \quad . \quad . \quad . \quad . \quad . \quad (3)$$

---

[1] van der Waals, Jr., *Proc. Acad. Amsterdam*, 1918, **21**,

[2] Andrade, *Phil. Mag.*, 1934, **17**, 497, 698.

[3] Brillouin, *Ann. Physique Rad.*, III, 1922, **6**, 326.

[4] Frenkel, *Wave Mechanics, Elementary Theory* (Clarendon Press, Oxford), 1932, pp. 266-272 ; *Z. Physik.*, 1926, **35**, 652 ; *Trans. Faraday Soc.*,1937, **33**, 58.

[5] Prandtl, *Z. angew. Math. Mech.*, 1928, **8**, 85.

[6] Powell, Roseveare, and Eyring, *Ind. Eng. Chem.*, 1941, **33**, 430.

where N is the Avogadro number, R the gas constant, h Planck's constant, T the absolute temperature, V the molecular volume and ΔG^{+} the free energy associated with the activation of a molecule to the mobile state.

Eqn. (3) makes the viscosity of a liquid inversely proportional to the molecular volume. Empirical equations expressing an approximate reciprocal relationship between viscosity and molecular volume have been proposed by a number of authors. Thus Batschinki[7] found that, approximately

$$\eta = \frac{c}{V - w} \quad . \quad . \quad . \quad . \quad . \quad (4)$$

where c and w are constant. This expression has been developed by Lederer,[8] and by Macleod[9] who gives an expression for viscosity which involves molecular weight as well as molecular volume. His expression reads,

$$\eta = \frac{KM_0\alpha}{v - b} \quad . \quad . \quad . \quad . \quad . \quad (5)$$

where K is a constant, M_0 the formula weight, α the degree of association of the liquid and $(v - b)$ is the free volume per molecule.

The Transport of Momentum.

According to the kinetic theory the force produced in a flowing mass of gas by viscosity is due to the transport of momentum across the stream lines by the moving molecules. Diffusion in such a system is due to the transport of molecular species by the same thermal motion. There is thus a close relationship between viscosity (η) and diffusivity (D) in gases. The quotient of viscosity by density η/ρ, or the so-called kinematic viscosity, has the same physical dimensions as diffusivity and for most gases:

$$\eta/\rho = Sm\,D \quad . \quad . \quad . \quad . \quad . \quad (6)$$

where Sm (a dimensionless quantity referred to as the Schmidt number) has a value between 0·66 and 0·85 depending on the nature of the forces acting between the molecules. The Schmidt number is thus a measure of the relative efficiency of the system for the transport of momentum and of mass. For liquid systems Sm, as defined by equation (6) is a large quantity of the order 10^3 to 10^6. We may accordingly describe a liquid as much less efficient at the transport of mass than at the transport of momentum, or we may conclude that there exists in liquid systems an efficient mechanism for the transport of momentum which is not simultaneously available for the transport of mass.

A possibly analogous situation occurs when considering the viscosity of gases at stellar temperatures. The thermal radiation from very hot gases carries momentum and therefore contributes to the viscosity of the gas concerned. At stellar temperature the viscosity of radiation as shown by Jeans[10] may be greater than the gas kinetic viscosity. The thermal radiation however carries no chemical species and therefore does not contribute to the diffusivity. Therefore at stellar temperature the Schmidt number must increase.

As mentioned above, the suggestion that the acoustical vibrations, into which the Einstein and the Debye theories resolve the thermal motion of the molecules of a condensed assembly, might similarly act as carriers of momentum but not of mass, was made by Brillouin in 1922. Brillouin considered only the effect of the longitudinal waves, accepting the classical argument that a liquid possesses no rigidity and therefore cannot transmit a transverse wave. The validity of this conclusion for ultra high-frequency acoustical waves has however been questioned by Burgers.[11] The complete absence of transverse waves at all Debye frequencies would lead to a value for the molecular heat of a liquid R cal./g. mol. less than that of the corresponding solid, while as a matter of experience specific heats of liquids are usually higher than those of the corresponding solids. Consequently we amend the statement that the liquid state is one which does not transmit transverse acoustical waves to read that the liquid state is one in which transverse waves are highly absorbed, or for which the transverse wave has a mean free path which is only of the order of the atomic spacing, or exists for a time of the order of the relaxation time of the molecules concerned. Indeed this short mean free path is necessary in order that the carrier of momentum should contribute to the ordinary (or Newtonian) viscosity. The author has claimed that a mean free path of the order of the dimensions of the containing vessel would produce a contribution not to true viscosity but to the so-called sigma phenomenon (Bosworth).[12]

---

[7] Batschinki, *Z. physik. Chem.*, 1913, **84**, 643.

[8] Lederer, *Kolloid Beihefte*, 1931, **34**, 270.

[9] Macleod, *Trans. Faraday Soc.*, 1923, **19**, 6; *ibid.*, 1925, **21**, 151; *ibid.*, 1936, **32**, 872.

[10] Jeans, *Roy. Astrom. Soc.*, 1926, **86**, 444.

The Viscosity of a "Phonon Gas."

In a simple derivation of the contribution to the viscosity of a liquid arising from the short lived transverse mechanical, or acoustical waves we shall use the concept proposed by Frenkel of a " phonon gas " in which a quantum of radiation of wave number k becomes replaced by a particle of momentum g given by :

$$g = hk \quad . \quad . \quad . \quad . \quad . \quad (7)$$

On the Debye theory the thermal energy associated with a vibrational frequency ν in an assembly of N atoms per unit volume at temperature T is :

$$\frac{h\nu}{e^{h\nu/kT} - 1}.$$

The number of independent modes of vibration in unit volume with frequency lying between ν and $\nu + d\nu$ is given by dz in :

$$dz = 4\pi\left(\frac{1}{c_l^3} + \frac{2}{c_t^3}\right)\nu^2\, d\nu$$

where c_l is the velocity of the longitudinal wave and c_t that of the transverse wave. The total number of modes of vibration is $3N$. We accordingly have :

$$3N = \frac{4}{3}\pi\left(\frac{1}{c_l^3} + \frac{2}{c_t^3}\right)\nu_0^3 \quad . \quad . \quad . \quad . \quad (8)$$

where ν_0 is the characteristic Debye frequency.

The energy dE associated with the transverse waves of frequency lying between ν and $\nu + d\nu$ is given by :

$$dE = 8\pi\frac{h}{c_t^3}\,\frac{\nu^3 d\nu}{e^{h\nu/kT} - 1} \quad . \quad . \quad . \quad . \quad (9)$$

The number of phonons dn_ν per unit volume derived from transverse waves in the frequency range ν to $\nu + d\nu$ (or phonons of class A) is expressed as :

$$dn_\nu = \frac{dE}{h\nu} = \frac{8\pi}{c_t^3}\,\frac{\nu^2 d\nu}{e^{h\nu/kT} - 1} \quad . \quad . \quad . \quad (10)$$

Each of these phonons carries an amount of momentum

$$g = h\nu/c_t.$$

---

[11] Burgers, *Second Report on Viscosity and Plasticity* (Amsterdam, 1938), pp. 9-10.

[12] Bosworth, *Phil. Mag.* (in press).

If we write m for the equivalent mass of a phonon of type A we have :

$$m = h\nu/c_t^2 \quad . \quad . \quad . \quad . \quad . \quad . \quad (11)$$

For the density of phonons of type A we have :

$$d\rho_\nu = m dn_\nu = \frac{h\nu}{c_t^3} \frac{8\pi}{c_t^2} \frac{\nu^2 d\nu}{e^{h\nu/kT} - 1} \quad . \quad . \quad . \quad (12)$$

Let us suppose that these phonons have a mean free path λ_t (or a mean life λ_t/c_t). It may readily be shown that in a gas of density ρ if the molecules move with a mean velocity c and mean free path λ then the viscosity is given by :

$$\eta = \frac{1}{3}\rho c \lambda.$$

Thus our phonons of class A make a contribution $d\eta$ to the viscosity of the liquid given by :

$$d\eta = \frac{8\pi}{3} \frac{h\lambda_t}{c_t^4} \frac{\nu^3 d\nu}{e^{h\nu/kT} - 1} \quad . \quad . \quad . \quad . \quad . \quad (13)$$

The total viscosity contribution arising from all the phonons present in the liquid assembly is thus,

$$\eta = \frac{8\pi}{3c_t^4} h\lambda_t \int_0^{\nu_0} \frac{\nu^3 d\nu}{e^{h\nu/kT} - 1} \quad . \quad . \quad . \quad . \quad . \quad (14)$$

where ν_0 is the Debye characteristic frequency of the assembly.

For temperatures greatly in excess of the Debye characteristic temperature $\Theta_D = \frac{h\nu_0}{k}$ we may write approximately

$$e^{h\nu/kT} - 1 = h\nu/kT \quad . \quad . \quad . \quad . \quad (15)$$

for all values of ν in excess of $T\nu_0/\Theta_D$. Since Θ_D is much less than room temperature for all except the most tightly bonded structures, which in any case would not yield fluids except at the highest temperatures, it is permissible to use approximation (15) throughout the dominant part of the integration in equation (14). Thus we have,

$$\eta = \frac{8\pi}{3c_t^4} \lambda_t kT \frac{\nu_0^3}{3} \quad . \quad . \quad . \quad . \quad . \quad (16)$$

On substitution in equation (8), remembering the $Nk = \frac{R}{V}$ (the molar gas constant divided by the molecular volume), we get finally

$$\eta = \frac{2RT}{V} \frac{\lambda_t}{c_t} \frac{c_l^3}{c_t^3 + 2c_l^3} \quad . \quad . \quad . \quad . \quad . \quad (17)$$

The Velocity of the Transverse Waves.

Eqn. 17 involves the absolute temperature T, the molecular volume V, c_l or the velocity of sound in the liquid concerned, and the quantities c_t and λ_t, an interpretation of which is necessary before the equation can be applied to observational data. Since the postulated transverse waves have but an ephemeral existence in a liquid, direct measurement is presumably out of the question and we seek some other physical property which may be related to these two quantities.

The quantity c_t depends on the magnitude of the elastic forces acting between the molecules of the assembly. For a macroscopic system we may write :

$$c_t = \sqrt{\text{Rigidity/Density}}$$

while for the longitudinal waves

$$c_l = \sqrt{\text{Bulk Modulus/Density}}.$$

On substituting this expression for λ_t in eqn. (21) we obtain

$$\eta = 0{\cdot}2068\,\frac{1}{N}\sqrt{\frac{MRT}{\gamma}}\,\frac{1}{(v-b)^{2/3}} \quad . \quad . \quad . \quad (24)$$

as the final equation for the viscosity contribution attributable to the momentum transfer produced by the phonons in a liquid. An alternative expression may be obtained by substituting for the free space $(v - b)$ its approximate value as given by eqn. (20). Thus we obtain

$$\eta = \frac{0{\cdot}2068}{N^{1/3}}\,\frac{c_l^2 M^{5/6}\rho^{2/3}}{(RT\gamma^3)^{1/2}} \quad . \quad . \quad . \quad . \quad . \quad (25)$$

or alternatively

$$\eta = \frac{0{\cdot}2095 \times 10^6}{N^{1/3}}\,\frac{M^{5/6}}{(RT\gamma^3)^{1/2}\beta_s\rho^{1/3}} \quad . \quad . \quad . \quad (26)$$

where β_s is the adiabatic compressibility of the liquid measured as the relative volume change per atmosphere pressure change.

Viscosity in Terms of the Velocity of Sound.

Eqn. (25) or the equivalent eqn. (26) gives an expression for the viscosity of a liquid in terms of a number of observable quantities. N and R are molecular constants. M, T and ρ readily available properties and β_s (or the equivalent c_l) are quantities which are known for a number of liquids at one or two temperatures. Bergmann[15] for example gives a table of the velocities of ultrasonic waves and adiabatic compressibilities of a number of organic liquids at room temperatures. A shorter list is given in the International Critical Tables, vol. 6. Data on the velocity of sound in a number of alcohols at 25° c. and at 35° c. have more recently been given by Rendell.[16] The values of γ, the ratio of specific heats are given in the International Critical Tables, vol. 5. For the various substances liquid at ordinary temperature and for which data on the adiabatic compressibilities are available, the values of γ, for the gaseous phase, vary over the comparatively narrow range from 1·08 (for hexane) to 1·29 for methyl iodide. Bergmann gives a limited number of values of γ for these same substances in the liquid state. These values are higher than those for the gaseous state and range from 1·16 (for butyl alcohol) to 1·50 (for chloroform). It is not quite clear from the deduction of Kincaid and Eyring as to what value should be taken for γ in their expression (eqn. 20), whether the low value for dispersed molecules in the gaseous phase or the somewhat higher value for the more closely packed molecules in the liquid phase. Since eqn. (20) and indeed the deduction of λ_t as given above is approximate only, it is probably sufficiently accurate to take for the value of γ for all molecules not being linear or monatomic the theoretical equipartition value for a system with no internal vibrations, viz. $\gamma = 1{\cdot}33$. From which $\gamma^{3/2} = 1{\cdot}54$. So that eqn. (26) may be rewritten

$$\eta = 1{\cdot}75 \times 10^{-7}\,\frac{M^{5/6}}{T^{1/2}\rho^{1/3}\beta_s}\ \text{poises} \quad . \quad . \quad . \quad (27)$$

Eqn. (27) may readily be tested against experimental data by plotting η for various liquids at temperatures for which the other data are available against $M^{5/6}/T^{1/2}\,\rho^{1/3}\,\beta_s$. Fig. 2 shows the result of plotting experimental data in this manner. The various points are numbered and reference to the particular liquid and temperature represented by each point is given in the attached legend. In order to produce a compact figure both coordinates of the points referring to the aliphatic alcohols have been divided

[15] Bergmann, *Ultrasonics* (Bell & Co., 1938), pp. 124 *et seq.*

[16] Rendall, *Proc. Indian. Acad. Sci.*, 1942, 16A, 369.

by 3. Similarly both co-ordinates of the point representing mercury have been divided by 4. Since we are expecting a linear relationship between

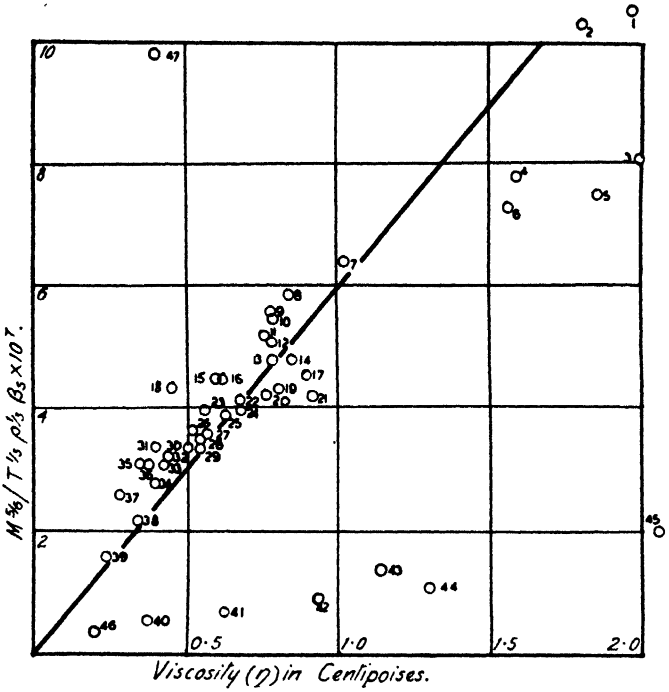

FIG. 2.

1 Bromoform at 23·5° c.
2 1 : 3-Dibrompropane at 23·5° c.
3 Diethyl malonate at 22° c.
4 Ethylene bromide at 28° c.
5 Diethyl oxalate at 22° c.
6 Tetrachlorethane at 28° c.
7 Brombenzene at 28°c.
8 Tetrachlorethylene a t 28° c.
9 Chloroform at 23·5° c.
10 Butyl iodide at 28° c.
11 Chlorbenzene at 23° c.
12 *β*-Picoline at 28° c.
13 *o*-Xylene at 22° c.
14 *α*-Picoline at 28° c.
15 *m*-Xylene at 22° c.
16 *p*-Xylene at 22° c.
17 Pyridine at 24° c.
18 Ethylene chloride at 23° c.
19 Amyl acetate at 26° c.
20 Ethyl formate at 24° c.
21 Carbon tetrachloride at 23° c.
22 Butyl bromide at 28° c.
23 Toluene at 23° c.
24 Butyl acetate at 26° c.
25 Methyl butyrate at 24·5° c.
26 Butyl formate at 24° c.
27 *n*-Octane at 19° c.
28 Propyl acetate at 26° c.
29 Methyl propionate at 24·5° c.
30 Ethyl propionate at 23·5° c.
31 Benzene at 23° c.
32 Ethyl acetate at 23·5° c.
33 Methylene chloride at 23·5° c.
34 *n*-Heptane at 23° c.
35 Ethyl formate at 24° c.
36 Methyl acetate at 24° c.
37 Ethyl bromide at 24° c.
38 *n*-Hexane at 23° c.
39 *n*-Pentane at 18° c.
40* Ethyl alcohol at 23·5° c.
41* *n*-Propyl alcohol at 24° c.
42* *n*-Butyl alcohol at 24° c.
43 Water at 15° c.
44* *Iso*amyl alcohol at 24° c.
45* *Iso*octyl alcohol at 26° c.
46* Methyl alcohol at 23·5° c.
47† Mercury at 20° c.

the co-ordinates this procedure is quite legitimate. The values of viscosities shown in the figure were taken from the International Critical Tables and the other physical properties from the sources mentioned above.

---

* Both co-ordinates of these points have been divided by 3.
† Both co-ordinates of this point have been divided by 4.

The full line drawn in Fig. 2 represents eqn. (27) and it will be noted that the data for normal liquids—hydrocarbons, halogenated hydrocarbons and esters fall within the limits of the accuracy to be expected from the calculation, or the " theoretical " line. Data for associated liquids, such as water and the alcohols fall considerably below this line but could, in principle, be made consistent with the fundamental eqn. (19) by postulating that eqn. (23) underestimates the mean free path either because the effective molecular weight is many times greater than the formula weight or else because the polar nature of these substances produce an orientation and thus an arrangement of the " holes " in a regular superlattice.

A typically dissociated liquid, mercury, gives a point which falls far above the line in Fig. 2. The data for mercury can however always be made to fit eqn. (27) by postulating an effective molecular weight less than the formula weight. As a matter of interest the effective molecular weight required to make mercury fit eqn. (27) is 35. To make water fit as an associated liquid the required effective molecular weight is 125.

The decrease with increase in temperature is a very characteristic property of the viscosity of substances in the liquid state. Unfortunately, there are not available any extensive data on the temperature variation of c_t or β_s. However the paper by Rendall[16] gives c_t for the 5 lowest saturated aliphatic alcohols at 25° c. and 35° c. and although these are "associated " liquids and do not fit eqn. (27), nevertheless the quantity $M^{5/6}/T^{1/2}\rho^{1/3}\beta_s$ plotted against η gives a smooth curve independent of the temperature. Fig. 3 shows this curve. The circles refer to data at 25° c., the crosses to data at 35° c. The numeral against each point refers to the number of carbon atoms in the alcohol. The heavy straight line represents eqn. (27). While the data plotted do not fall on any straight line they do form a single smooth curve which shows an apparent degree of association (or is it orientation of the " holes " ?) which increases with increase in molecular weight or decrease in the temperature.

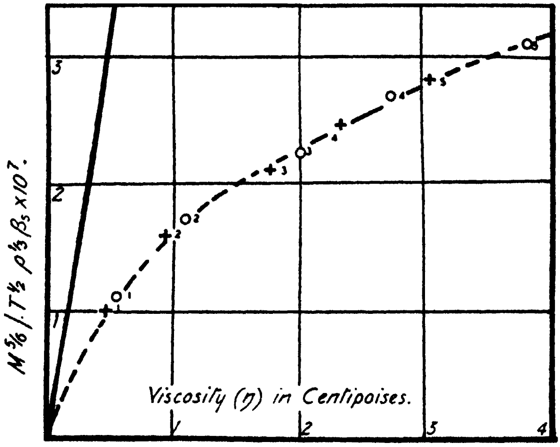

FIG. 3.

1 Methyl alcohol.
2 Ethyl alcohol.
3 *n*-Propyl alcohol.
4 *n*-Butyl alcohol.
5 *iso*Amyl alcohol.
○ Refers to 25° c.
+ Refers to 35° c.

Viscosity in Terms of Free Space.

While it is not at present possible to test eqn. (27) over a wide range of temperatures, an equation to show the variation of viscosity with temperature can be derived from the expression for η in terms of the free space (eqn. 24). This equation may be rewritten in the form

$$\eta = \text{const.} \frac{(MT)^{1/2}}{(v - b)^{2/3}} \quad . \quad . \quad . \quad . \quad (24a)$$

where the constant has, for normal liquids, the value

$$\text{const.} = 2{\cdot}56 \times 10^{-21}$$

Eqn. (24*a*) may be compared with the empirical expression of Macleod, viz.:

$$\eta = \text{const.} \frac{M}{v - b} \quad . \quad . \quad . \quad . \quad (28)$$

and may be developed in the same way as this latter expression. Jaeger [18] has written for the variation of the free space $(v - b)$ with temperature:

$$v - b = \frac{RT}{\pi_0} e^{-c'/Tv},$$

with π_0 and c' as constants. In terms of this expression eqn. (24) becomes:

$$\eta = \frac{0{\cdot}2068}{N} \pi_0^{2/3} \frac{M^{1/2}}{(\gamma)} (RT)^{-1/6} e^{2c'/3Tv} \quad . \quad . \quad . \quad (29)$$

which expresses the variation of viscosity with temperature by the familiar exponential equation (cf. eqn. 3).

Summary.

An expression is derived for the viscosity of a liquid on the assumption that the carriers of momentum are " phonons " or equivalent particles to the mechanical waves into which the Einstein and the Debye theories of the specific heat resolve the molecular motion. This expression reads:

$$\eta = 1{\cdot}047 \frac{RT}{V} \frac{\lambda_t}{c_t} \quad . \quad . \quad . \quad . \quad . \quad (19a)$$

where V is the molecular volume, λ_t is the mean free path of the phonons and c_t the velocity of sound in the liquid.

It is further assumed that λ_t is a measure of the mean distance from any arbitrary point in the liquid to a discontinuity or " hole " in the lattice as defined by the near neighbours of the arbitrary point. The expression for viscosity thus derived reads

$$\eta = 1{\cdot}75 \times 10^{-7} \frac{M^{5/6}}{T^{1/2} \rho^{1/3} \beta_s} \quad . \quad . \quad . \quad (27)$$

where M is the molecular weight, ρ the density and β_s the adiabatic compressibility. Good agreement with experimental data is recorded for normal liquids but for associated liquids eqn. (27) underestimates the viscosity and for mercury the equation overestimates the viscosity.

By using the relation between free volume and the velocity of sound as given by Kincaid and Eyring this equation may be transposed to one giving viscosity in terms of molecular weight and free volume, similar to, but not identical with, the empirical expression of Macleod.

41 *Spencer Road,*
Killara,
New South Wales.

NOTES ON THE ELECTROKINETIC POTENTIAL OF CELLULOSE AND ON ELECTROKINETIC EQUATIONS.

By A. S. Buchanan and E. Heymann.

Received 19*th March*, 1947.

Most workers in the field of the ζ-potential of cellulose calculate ζ from the streaming potential and the resistance of the cell. Neale and Peters [1] have recently made an interesting innovation by measuring the *streaming current* directly; and Neale [2] has derived an equation for this current.

It can be shown that Neale's equation is very similar to, and in the case of a non-swelling solid, identical with, the Helmholtz-Smoluchowski equation for the streaming potential, provided that, following a suggestion by Briggs [3] and the practice of several other investigators,[4, 5] one substitutes for κ the specific conductivity (κ') of the liquid whilst it is contained in the porous plug; κ' thus includes bulk-conductivity *and* surface conductivity. The equation for the ζ-potential then becomes

$$\zeta = \frac{4\pi\eta}{D} \cdot \frac{E\kappa'}{P}, \quad . \quad . \quad . \quad . \quad . \quad (1)$$

where η is the viscosity, D the dielectric constant of the liquid, E the streaming potential and P the pressure under which the liquid is forced through the plug. κ' is determined experimentally from the measured resistance (R) across the plug and its "cell constant." The latter is obtained by measuring the resistance of the plug filled with a KCl solution * of known specific conductivity. We thus have

$$\kappa' = \frac{1}{R} C, \quad . \quad . \quad . \quad . \quad . \quad (2)$$

where C is the cell constant. For the latter we may write, according to Manegold, Hofmann and Solf,[6]

$$C = \frac{l}{a(1 - F_1)\sigma}, \quad . \quad . \quad . \quad . \quad . \quad (2a)$$

where l is the length of the plug, a its cross-section, F_1 the fraction of the total plug volume that is occupied by the solid *not* including water of swelling or imbibition; $(1 - F_1)$ is thus approximately *the volume fraction that is available for ionic migration* (cf. Bikerman [7]), and σ is a term which depends on the shape and orientation of the crystals or fibres. Bjerrum, Manegold and co-workers [6] have calculated σ for a number of idealised arrangements and obtained $\sigma = 0{\cdot}33$ for a plug with cylindrical capillaries oriented at random, and $\sigma = 0{\cdot}66$ for a plug with rectangular crevices oriented at random. As a plug consisting of crystals or fibres does not correspond to either of these arrangements, it is preferable to calculate σ from an experimental determination of C by eqn. (2a). From the results of Rabinov and Heymann [5] we calculate $\sigma = 0{\cdot}64 - 0{\cdot}80$ for various celluloses (Table I).

---

[1] Neale and Peters, *Trans. Faraday Soc.*, 1946, **42**, 478.

[2] Neale, *ibid.*, 1946, **42**, 473.

[3] Briggs, *J. Physic. Chem.*, 1928, **32**, 641.

[4] Bull and Gortner, *ibid.*, 1931, **35**, 309; 1932, **36**, 111.

[5] Rabinov and Heymann, *ibid.*, 1943, **47**, 655.

[6] Bjerrum and Manegold, *Kolloid Z.*, 1927, **43**, 5; Manegold, Hofmann and Solf, *ibid.*, 1931, **55**, 273; **56**, 267; **57**, 23.

[7] Bikerman, *J. Physic. Chem.*, 1942, **46**, 724.

* The concentration of this solution must be at least 0·05 N. in order to make the surface-conductivity inappreciable compared with the bulk-conductivity.

TABLE I.

	Temp. in °C.	$A \times 10^3$.	E/P.	$R \times 10^{-5}$.	C.	F_1.	F_2.	ψ_0.	ψ'_0.	ζ.	ζ/ψ_0.	ζ/ψ'_0.	σ.	$\kappa_s \times 10^6$.
Celluloses containing Carboxyl Hydrogen														
Cotton D . .	20	4·2	86	7·70	3·12	0·148	0·22	35·3	38·7	37·3	1·06	0·96	0·72	11
Cotton B . .	21	5·6	78	7·55	3·15	0·159	0·24	32·7	35·4	33·8	1·03	0·95	0·73	11
Cotton A . .	20·5	8·3	99	8·15	2·90	0·141	0·21	37·4	38·4	37·3	1·00	0·97	0·77	10
Cotton wool . .	20	20·5	25	3·45	3·20	0·169	0·25	23·8	26·4	24·8	1·04	0·94	0·72	31
Oxycellulose E .	16·5	52	18·3	2·85	2·96	0·144	0·22	22·3	23·5	22·1	0·99	0·94	0·75	43
Oxycellulose A .	21	79	14·9	1·78	2·80	0·141	0·21	25·5	25·2	24·4	0·96	0·97	0·80	66
Oxycellulose D .	17	105	10·2	1·70	3·00	0·168	0·25	21·3	22·2	20·5	0·96	0·92	0·76	66
Oxycellulose C .	16	132	11·0	1·70	2·89	0·159	0·24	23·4	23·4	22·1	0·94	0·94	0·79	74
Calcium-containing Celluloses														
Cotton wool . .	17	8·8	33	5·00	3·15	0·162	0·24	23·2	25·1	23·7	1·02	0·94	0·73	20
Oxycellulose C .	17	34	20·0	3·00	2·84	0·137	0·21	22·5	22·8	21·6	0·96	0·95	0·78	42
Mercerised Cellulose														
Cotton wool . .	15·5	13·0	27·0	5·20	3·28	0·164	0·25	19·3	21·7	20·3	1·05	0·94	0·70	22
Regenerated Celluloses														
Viscose . . .	16	34	10·3	2·40	3·45	0·146	0·24	15·5	18·6	17·5	1·13	0·94	0·66	63
" Copper silk " .	17	19·7	10·7	2·90	3·55	0·150	0·25	13·1	16·2	14·9	1·14	0·92	0·64	48

On substituting for κ' in eqn. (1), we obtain

$$\zeta = \frac{4\pi\eta El}{DPRa(1 - F_1)\sigma}, \qquad (3)$$

or

$$I = \frac{PDa(1 - F_1)\sigma}{4\pi\eta l}\zeta \qquad (4)$$

where $I = E/R$ is the streaming current. Neale's equation is

$$I = \frac{PDa(1 - F_2)\tau}{4\pi\eta l}\psi_0, \qquad (5)$$

where ψ_0 is the surface potential, $(1 - F_2)$ *is the fraction of the plug volume that is available for flow;* hence F_2 is the fraction of the plug volume occupied by the *swollen* solid.

The terms τ and σ take into account that flow and ionic migration must follow a tortuous path through the interstices of the plug; for a plug of cylindrical fibres oriented at random, Neale has calculated that $\tau = 0{\cdot}79$. If the solid phase of the plug does not swell and possesses zero electric conductivity, $(1 - F_1) = (1 - F_2)$. Moreover, in this case, according to Manegold and co-workers, $\tau = \sigma$. *Hence for a plug of crystals embedded in an aqueous solution, eqn.* (1), (4) *and* (5) *are identical.*

However, for a plug of fibres which are swollen, the volume-fraction available for flow is smaller than that available for ionic migration, thus $(1 - F_2) < (1 - F_1)$. This point has been recognised by Bikerman,[7] who has stated an equation for the streaming current which is similar to that of Neale, though it does not contain the term τ. If the volume fractions available for ionic migration and flow are different due to swelling, the corresponding shape factors σ and τ may not be exactly equal. In this case, eqn. (4) and (5) differ by terms which are constant for the same material and the same mode of orientation.

It appears improbable that absolute values for the electrokinetic potential can be obtained by electro-osmosis or streaming potential methods when plugs of fibrous materials which undergo swelling are investigated, because flow is completely impeded in a swollen structure, whereas ionic migration is only very little impeded. If eqn. (1), (3) or (4) are used for the calculation of the surface potential, no separate determination of or theoretical assumption for F_1 and σ need be made, because these terms are contained in the cell constant C, the experimental determination of which offers no difficulty. However, an error is introduced since $(1 - F_1)$ because of swelling, is greater than the volume fraction available for flow $(1 - F_2)$. Neale's equation (5), on the other hand, gives the correct relation, but the experimental determination of F_2 is uncertain because the amount of swelling is not usually known with accuracy and the value of τ is in doubt. We consider the necessity of employing the term τ, the numerical value of which depends on the shape and orientation of the particles of the solid, as a serious disadvantage of Neale's procedure.

Caution must be exercised on comparison of various types of fibres. Differences in streaming potential may be due not only to differences in surface potential but to variations in fibre orientation, affecting σ and τ, or in the amount of swelling (affecting F_2). Neale and Peters, applying eqn. (5), have found that the most highly stretched yarns show the highest potential, and that disorientation due to swelling produces a fall. This, however, could be explained on the assumption that swelling and disorientation produce a change of F_2 and τ, rather than of the potential. Other data on textile materials (cf. Valko [8]) may require a similar reinterpretation.

When the potential ζ is customarily calculated from eqn. (1), E/P, R

---

[8] Valko, *Kolloidchemische Grundlagen der Textilveredlung* (Berlin, 1937), p. 165.

and the cell constant $C = \dfrac{l}{a(1 - F)\sigma}$ are determined experimentally. When the potential ψ_0 is calculated from eqn. (5), $I = E/R$, P and F_2 are determined experimentally, and τ is assumed to be 0·79 (Neale). We have calculated ζ and ψ_0 from data by Rabinov and Heymann[5] on celluloses and oxycelluloses of varying carboxyl group content in distilled water. For the calculation of F_1 the specific volume of cellulose is taken to be 0·65 (Ott[9]). According to Collins,[10] the amount of swelling is about 50 % of the dry volume for the native celluloses (hence $F_2 = 1{\cdot}5\ F_1$), and about 65 % for the regenerated cellulose (hence, in that case, $F_2 = 1{\cdot}65\ F_1$). The plug dimensions are $l = 3{\cdot}40$ cm. and $a = 1{\cdot}77$ cm.,^{2} A is the COOH value of the sample in m. equ./g., E/P is expressed in v./cm. Hg., C in cm.$^{-1}$ and R in ohm. ψ_0 is the surface potential (in mv.) calculated by eqn. (5), assuming $\tau = 0{\cdot}79$, and ψ'_0 is the surface potential assuming $\tau = \sigma$, σ being calculated from the experimental cell constant by eqn. (2a); κ_s is the specific surface conductivity. The latter is defined as $\dfrac{\kappa' - \kappa}{\alpha}$, where κ is the bulk conductivity and α is the weight of cellulose contained in 1 cm.^{3} of diaphragm space.[11] For methods of purification and characteristion of the samples under investigation, see Heymann and Rabinov.[11, 5]

A number of typical results are shown in Table I. The shape factor σ, calculated from eqn. (2a), varies between 0·64 and 0·80. The average is thus smaller than the value of $\tau = 0{\cdot}79$ computed by Neale. Unfortunately, experimental data for an independent determination of τ from the rate of flow according to Bjerrum and Manegold[6] are not available. A decrease of σ goes parallel with an increase of the ratio ζ/ψ_0, which varies between 0·94 and 1·14. However, if the surface potential ψ'_0 is calculated assuming that τ is equal to σ, the values of the ratio ζ/ψ'_0 show satisfactory constancy. This may be regarded as an indication that, for various kinds of cellulose and oxycellulose, τ is not constant but varies similarly to σ.

Neale states that, on applying eqn. (5), he obtains " a result independent of the ambiguous surface-conductivity." However, the customary method of calculating ζ from eqn. (1) involves no separate experimental determination of the surface-conductivity, but the latter quantity is included in the value of κ', just as it is included in the value of the streaming current (I) in Neale's equation. It is noteworthy in this respect that the ratio ζ/ψ_0 for oxycelluloses with a high COOH value (A) is little different from that for cottons A, B and D with low COOH values, although the surface-conductivity (κ_s) of the former is about ten times as great as that of the latter. This demonstrates well that the surface-conductivity is taken into account in eqn. (1), (3) and (4) as well as in eqn. (5). The results show that even with fibrous materials, such as a variety of celluloses and oxycelluloses, which exhibit swelling and show a wide variation of surface-conductivity, there is little difference between the numerical values of the electrokinetic potential calculated by Neale's equation and those calculated by the modified Helmholtz-Smoluchowski (-Briggs) equation.

In view of the close relation between these two equations, it is not surprising that ψ_0 shows variations very similar to those which previous investigators[3, 4, 5] have recorded for ζ, viz., the decrease of surface potential with increasing carboxyl group content (A in Table I) and the occurrence of a maximum in the curves showing the variation of the surface potential with the concentration of alkali metal salts (KCl, NaCl, KNO_3).

As pointed out before, swelling is neglected when ζ is calculated by eqn. (1), (3) and (4). Even on application of eqn. (5) an error may be introduced because the amount of swelling is not usually known with accuracy. These errors are comparatively small as long as the volume fraction occupied by the (swollen) solid phase is small, but will become appreciable on increase of the density of packing.* Rabinov and Heymann,[5] as well as Neale and Peters,[1] have found that the electrokinetic potential, calculated by eqn. (1), (3), (4) and (5), decreases when the density of packing is increased. They explained this on the assumption of a breakdown of the above equations when the fibres approach one another at many points within a distance of the same order of magnitude as the thickness of the diffuse double layer. Another explanation is that, owing to swelling and immobilisation of liquid, the actual volume available for flow is smaller than $(1 - F_1)$ and even $(1 - F_2)$; the values of these quantities inserted in eqn. (1), (3), (4) and (5) are therefore too great. As these terms are in the denominator, the calculated values of ζ, ψ_0 and ψ are too small. This will make itself felt more strongly with closely-packed plugs than with loosely-packed ones. Hence the apparent values of ζ and ψ_0, calculated by the above equations, will decrease with increasing density of packing.

---

[9] Ott, *Cellulose and Cellulose Derivatives* (New York, 1943), p. 419.

[10] Collins, *J. Text. Inst.*, 1930, 21 T, 311; *vide* also Hess, *Die Chemie der Cellulose* (Leipzig, 1928).

[11] Heymann and Rabinov, *J. Physic. Chem.*, 1941, **45**, 1152.

Summary.

1. A comparative discussion of Neale's equation for the streaming current and of the modified Helmholtz-Smoluchowski-Briggs equation for the streaming potential is given.

2. For non-swelling solids, Neale's equation is identical with the Helmholtz-Smoluchowski equation, provided that the specific conductivity of the liquid whilst it is contained in the porous plug (or capillary)is inserted in the latter equation (modification due to Briggs).

3. We have used the two equations for calculating the electrokinetic potential from data of the streaming potential of various samples of cellulose and oxycellulose, which show an appreciable amount of swelling and a wide variation of surface conductivity. There is little difference between the numerical values of the electrokinetic potential calculated by the two equations.

4. The influence of swelling on electrokinetic properties is discussed.

5. Results obtained by Neale and Peters are discussed and compared with those of previous investigators.

Chemistry Department,
University of Melbourne,
Melbourne, Australia.

---

* For this reason, greater errors may be expected in the calculation of ζ from measurements of streaming potential and electro-osmosis than of cataphoresis.

A CATHODE RAY POLAROGRAPH.

By J. E. B. Randles.*

Received 12th November, 1946; as revised 24th April, 1947.

In recent years a small number of papers[1] have been published describing the use of the cathode ray oscillograph for recording diffusion currents passed by a dropping mercury electrode as an alternative to the ordinary polarographic technique. However, no satisfactory analytical instrument was evolved. For the purpose of developing such an instrument the work of Matheson and Nichols[1] was regarded as the most promising starting point. Their method applies to the dropping electrode a recurrent, fairly rapid, linear potential "sweep" synchronised with drop formation and the resultant cathode ray trace is a simple current-voltage curve similar to an ordinary polarogram except that "peaks" replace the polarographic "steps."

---

* Present address: Dept. of Chemistry, University of Birmingham.

[1] Matheson and Nichols, *Trans. Amer. Electrochem. Soc.*, 1938, **73**, 193. Müller, Garman, Droz and Petras, *Ind. Eng. Chem.* (*Anal.*), 1938, **10**, 339. Boeke and van Suchtelen, *Phillips Tech. Rev.*, 1939, **4**, 213. Heyrovsky and Foretj, *Z. physik. Chem.*, 1943, **193**, 77.

Preliminary work showed that if peak height were to be reproducible, and strictly proportional to the concentration of reducible substance, there were two chief requirements. Firstly, since peak height is dependent on the rate of change of potential of the dropping electrode[2] this must be constant and independent of the current flowing. If a steadily changing potential difference (provided e.g. by the charging of a condenser) is applied to the polarographic cell and a resistance (for current measurement) in series, the rate of change of potential difference across the cell is inevitably affected by the potential drop in the resistance, i.e., by the current. To overcome this, an electronic circuit (described under (i) below) was designed, whereby the potential difference applied to the cell is effectively independent of the potential drop in the series resistance. Provided that the potential of the anode relative to the solution is constant, and that the ohmic potential drop in the electrolyte is insignificant, a constant rate of change of the potential of the dropping electrode relative to the solution is achieved. The second requirement is that the reduction process shall always occur at the same stage of drop growth (i.e., at the same drop size). This was ensured by means of a synchronising circuit giving exact control of the time-lag between the fall of a drop and the start of the next voltage sweep. Details of all circuits and general lay-out are given below.

Details of the Instrument

The essential parts of the final apparatus apart from the dropping electrode and polarographic cells are (i) the circuit for applying the potential sweep to the dropping electrode, (ii) the synchronising circuit, (iii) the amplifiers, and (iv) the cathode ray tube and the power packs. They will be described in this order.

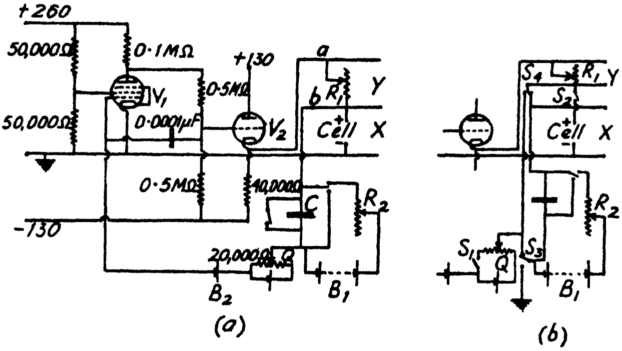

FIG. 1.

Circuit Providing the Voltage Sweep.—A diagram of the circuit is shown in Fig. 1(a). V_1 is a high gain pentode and V_2 forms a cathode follower stage; it will be seen that any small change in potential relative to earth of the grid of V_1 will result in a very much larger change in potential of point a in the opposing direction. Assuming for convenience that the ratio of the two changes is 1 : 200 then any change in the potential drop in R_1 (due to change in the cell current) necessarily results in a change of 99·5 % of this amount (relative to earth) at point (*a*) and 0·5 % (relative to earth) at point *b* (since the latter portion is transmitted directly to the grid of V_1). Thus a change in the potential drop in R_1 only alters the potential difference applied to the cell by 0·5 % of this change. In addition any direct effect on the potential at point (*b*) due to changes in the current taken from the cathode of V_2 by the cell, is entirely negligible for changes up to about 100 μa. The "sweep" of the potential applied to the dropping electrode is introduced by means of the condenser C which is charged up through R_2 by battery B_1 and across this condenser is connected the short-circuiting contact K operated by the synchronising circuit (Fig. 2). By the same argument as before it may be shown that a change in the potential across condenser C results in a change in potential relative to earth of point *b* equal to 99·5 % of that across the condenser. In short, therefore, the potential at *b* is directly dependent on the potential difference across C, but is effectively independent of that across R_1.

---

[2] Part II, p. 334.

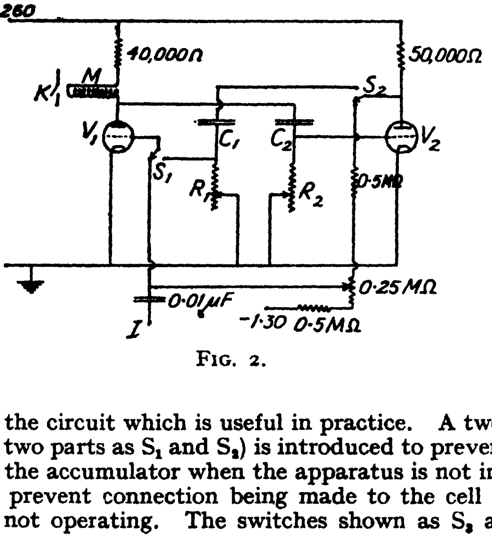

FIG. 2.

The rate of charging of the condenser depends on the value of R_2, which is variable in steps using a multiple switch. No current is taken from the condenser during the charging process, so that it may have a comparatively low capacity (8 μF.) and take only a few microamp. from the battery B_1, the life of which is therefore as long as its "shelf life." The potentiometer Q, operated by a small 2 v. accumulator, controls the starting potential of the "sweep," and the 1·5 v. dry cell B_2 provides a suitable bias for the grid of V_1. The 0·0001 μF. condenser connected between the grids of the valves serves to prevent a high frequency parasitic oscillation which otherwise may arise. Fig. 1(*b*) shows a small modification of the circuit which is useful in practice. A two pole on-off switch (shown in two parts as S_1 and S_2) is introduced to prevent the continuous discharge of the accumulator when the apparatus is not in use, and at the same time to prevent connection being made to the cell when the potentiometer Q is not operating. The switches shown as S_3 and S_4 constitute a double pole two-way switch, which in normal operation makes connections as indicated. When it is reversed a constant potential difference is applied across the cell but a horizontal sweep of the electron beam of the cathode ray tube is still obtainable by the alternate charging and short-circuiting of C. This permits the examination of the change of cell current during growth of the mercury drop, for any desired potential of the dropping electrode.

Further details of the circuit in actual use are as follows: V_1 and V_2 are Mazda S.P.41 pentodes; the screen and suppressor grids of V_2 are connected to the anode; C is an 8 μF. electrolytic condenser; R_2, 0·5 megohm to 5·0 megohms in 8 steps; and B_1, a 9 v. dry battery. R_1 is the most important resistance in the apparatus, since the normal method of operation (which is discussed in Part II), is to adjust all peaks to the same predetermined height by variation of R_1, rather than to make measurements of peak heights. R_1 is variable from 2,000 ohms to 94,000 ohms by 79 steps selected so that each setting of the resistance is 5 % greater than the one preceding it. An 80-way multiple switch specially made by Morley and Duke and Co. Ltd., of Cambridge, is used for this purpose, and the individual resistors are of the ordinary ½ w. carbon type except those below 200 ohms which are wire wound.

The Synchronising Circuit.—The circuit diagram is shown in Fig. 2. It is essentially a combined " flip-flop " and " multivibrator " circuit.[*] M is a post office type relay with a contact K which closes when current passes through the relay. K is connected across condenser C of the voltage sweep circuit (Fig. 1). The circuit operates as follows : with the double pole two-way switch (shown in two parts, S_1 and S_2) in the position shown, V_2 is normally conducting and point A is sufficiently negative for V_1 to be cut off. A positive impulse applied at I starts V_1 conducting and applies a negative impulse to the grid of V_2 (via C_2) which renders point A still more positive. This cumulative process occurs until V_1 is fully conducting and V_2 is non-conducting. As the negative charge on the side of C_2 connected to the grid of V_2 leaks away to earth through R_2, V_2 eventually becomes conducting again. A becomes more negative and the whole process is reversed as suddenly as it occurred, the original state being regained. This is stable till a new positive impulse is received at I. This impulse is derived from the output of that amplifier whose input is the potential drop across R_1 (Fig. 1), so that the sudden change of the cell current when the mercury drop falls provides the necessary impulse. Thus, on the fall of the mercury drop, V_1 becomes conducting and K closes, short circuiting the condenser C (Fig. 1). After a delay period determined by the capacity C_2 and resistance R_2, K reopens and the voltage sweep occurs again.

When the double pole switch is in the reverse position, the circuit behaves as a " multivibrator," V_1 and V_2 alternately becoming conducting and non-conducting at intervals determined by the values of C_1, C_2, R_1 and R_2. This provides a recurrent voltage sweep which is suitable for use with a stationary micro-electrode.

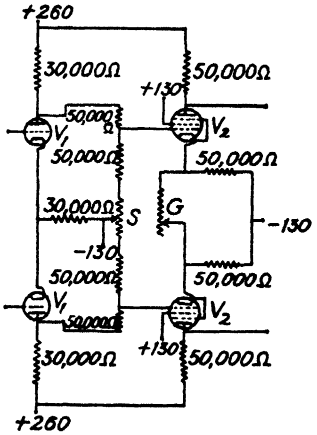

FIG. 3.

In normal operation with the double pole switch in the former position, the voltage sweep starts when contact K opens, and ends when the mercury drop falls. Its duration therefore equals the drop time of the capillary minus the delay time. The latter is proportional to the product of C_2 and R_2 and in practice is controlled by R_2, which is varied in steps by means of a multiple switch. With the values of C_2 and R_2 given below, delays from about ½ to 7 sec. are obtainable.

Details of the circuit in actual use are as follows : V_1 and V_2, a single valve, Mullard ECC31 double triode ; C_1 and C_2, 4 μF. paper dielectric condensers ; R_1, 200,000 ohms to 1 megohm ; R_2, 150,000 ohms to 750,000 ohms in 17 steps.

Amplifiers.—Since the potential changes to be amplified are slow, D.C. amplifiers of the type shown in the circuit diagram, Fig. 3 are used. These amplifiers give a very stable output if a reasonably smooth output power pack is used for the high voltage supply (see note on power packs below). The potentiometer S changes the steady output voltage for zero input voltage and is used for the purpose of shifting the whole trace on the screen of the cathode ray tube. The overall gain of the amplifier is controlled by the variable resistance G, being a maximum when G is zero.

---

[*] See, e.g., *Thermionic Valve Circuits*, E. Williams (Pitman, 1944).

The valves are Mazda S.P.41 pentodes, the first pair being connected as triodes. In the amplifier giving vertical deflection of the electron beam, S is a 5,000 ohms potentiometer and G may be 0, 500 or 2,000 ohms. In the other amplifier, S is 50,000 ohms and G may be 1,500, 3,000 or 6,000 ohms.

Cathode Ray Tube and Power Packs.—A 6″ tube N.C.18, with long afterglow screen is used. Accelerating voltage 3,000 v. is supplied by a conventional power pack. The power pack supplying the amplifiers and synchronising circuit is of conventional design with three-stage inductance capacity filtering, and the output fed to three Neon stabilisers (S.130) with the positive side of the stabiliser which is connected to the negative output, earthed. Potentials of − 130, + 130 and + 260 v. are thus available.

Batteries may be used for the high voltage supply to the circuit providing the voltage sweep since it requires no more than 5 ma. If a power pack is used, very efficient filtering is required. The A.C. ripple must be not more than 0·01 % of the D.C. output. This can be obtained, but not very easily, by feeding the output of a conventional power pack with inductance-capacity filtering, to an electronic voltage regulator.*

The interconnection between the electrical units of the apparatus are represented diagrammatically in Fig. 4. In the author's apparatus each unit is built on a tinplate chassis with controls on a front panel. The units may be built up together provided that there is efficient electrical and magnetic screening between each one.

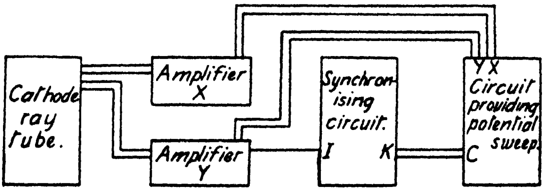

FIG. 4.

Polarographic Equipment.—Simple polarographic cells with a single side tube as a hydrogen inlet are employed, and the usual type of dropping electrode. It is necessary that the potential of the anode relative to the solution should not change appreciably when the sudden rise in the cell current occurs. A silver-silver chloride electrode is superior in this respect to a mercury pool anode. The electrode is prepared from 18 gauge silver wire by winding a helix about ½″ long and just wide enough to fit over the capillary, leaving about 4″ of straight wire to serve as a support and electrical connection. The helix is coated with AgCl by anodic treatment in dil. HCl. In use it is supported with its lower end about ⅛″ above that of the capillary. When immersed in M. KCl the A.C. resistance between the mercury reservoir and the anode was found to be less than 100 ohms, which is small enough to render the ohmic potential drop in the cell negligible.

Acknowledgment is due to the Director General, Scientific Research (Defence), Ministry of Supply for permission to publish this paper. The author is indebted to Mr. G. Bernard of the Ballistics Research Department, Royal Arsenal, Woolwich, for his assistance in the design of the electrical circuits.

---

* See, e.g., *Radio Amateur's Handbook* (American Radio League, 1945), p. 80; Müller Garman and Droz, *Experimental Electronics* (Prentice Hall, N.Y., 1944), p. 106.

Summary

The electrical circuit design and mode of operation of an instrument termed a cathode ray polarograph are described. The function of the instrument is to trace on the screen of a cathode ray tube a current-voltage curve for a dropping mercury electrode immersed in a solution containing small amounts of electro-reducible or -oxidisable substances. The current-voltage curve shows current peaks, each peak corresponding to an electro-reduction or -oxidation, and the height of a peak is accurately proportional to the concentration of the electro-reducible or -oxidisable substance.

Chemical Inspection Department,
Ministry of Supply.

A CATHODE RAY POLAROGRAPH.

PART II.—THE CURRENT-VOLTAGE CURVES.

By J. E. B. Randles.*

Received 12*th November*, 1946; *as revised* 24*th April*, 1947.

If a suitable potential is applied to a micro-electrode immersed in a solution containing a low concentration of an electro-reducible or -oxidisable substance, together with a relatively high concentration of an indifferent electrolyte, a diffusion-controlled current flows. If the application of the potential is sudden the current starts at a high value and decreases with time as the diffusion layer thickens.[1] To overcome the time dependence of diffusion currents, or, in other words, to provide what is effectively a steady state of the diffusion layer, either the rotating platinum electrode, or the dropping mercury electrode is normally used in polarography. The diffusion currents so obtained are suitable for measurement by a galvanometer or similar means. On the other hand, by means of the cathode ray oscillograph (or other instrument of sufficiently rapid response), it is possible to measure rapidly changing diffusion currents such as are obtained by the sudden changing of the potential of a micro-electrode, by the application to it of a rapid potential " sweep." Thus a voltage " sweep " covering a range of ½ to 2 v. in 1 to 2 sec. may be made to give a current-voltage curve providing as much information as the normal polarogram obtained over a period of 5 or 10 min. By means of the cathode ray polarograph described in Part I,[2] in conjunction with a stationary micro-electrode or a dropping mercury electrode, such current-voltage curves are obtainable. It is the object of the present paper to discuss the form of these curves, and their application to analytical purposes.

Theory of the Current-Voltage Curves.

The potential of the micro-electrode relative to the solution changes during a " sweep " at a rate of between 0·1 and 1·0 v./sec. This gives the best current-voltage curves in practice. As a result of the electrode reaction the concentration of the reacting substance at the electrode surface decreases and diffusion towards the electrode sets in. The relative speed of the two processes is such that both the increasing thickness of the diffusion layer and the increasing total concentration difference across it, significantly affect the diffusion current and, in fact, by their opposing influences give rise to the characteristic current peak. Therefore no simplifying assumption, such as constancy of thickness of the diffusion layer, can be made and it is necessary to solve the dynamic diffusion equation for the boundary conditions provided by the changing concentration at the electrode surface. It has only been found possible to do this by a graphical method, of which some details will be given.

---

* Present address: Dept. of Chemistry, University of Birmingham.

[1] Kolthoff and Lingane, *Polarography* (Interscience, N.Y., 1941), Chap. II.

[2] Randles, *Trans. Faraday Soc.* (preceding paper).

The Boundary Conditions.—The concentrations of reactant and product can only be easily expressed in terms of the potential of the electrode if it is assumed that (1) the reaction product is soluble either in the aqueous solution or the material of the electrode, and (2) the electrode process is rapid compared with the rate of diffusion (i.e. the electrode reaction occurs reversibly). When a mercury electrode is employed the former condition generally holds. The second is valid for the reduction of some metal ions, but is quite untrue for many electrode reactions. Nevertheless the theoretical curves derived on the basis of these two assumptions serve as a useful standard for comparison in judging the reversibility of actual electrode reactions. It will be convenient in the treatment which follows to consider a particular case, that of the reduction at a mercury electrode of the ions of a metal which is itself soluble in mercury.

The rate of change of the potential of the electrode relative to the solution is constant, so we may write

$$E = B - \alpha t,$$

where E is the potential of the electrode at time t and B and α are constants. Since the aqueous solution contains an excess of indifferent electrolyte, the activity coefficient of the reacting ions may be regarded as constant, as may that of the metal in the mercury since only dilute solutions are involved. In relating change of concentration of reactant and product to change of electrode potential we may therefore neglect activity coefficients. Thus we have

$$\frac{RT}{nF} \ln \frac{C_{AO}}{C_{SO}} = \alpha(t - t_0),$$

where n is the number of electrons involved in the reaction (the valency of the ion), C_{AO} the concentration of metal in the mercury and C_{SO} that of the ions in the solution, both adjacent to the interface, and t_0 is the time at which $C_{AO} = C_{SO}$. Inserting numerical values, for 25° C.,

$$\frac{C_{AO}}{C_{SO}} = 10^{n\alpha(t-t_0)/0{\cdot}059} \quad . \quad . \quad . \quad . \quad (1)$$

This defines a relation between the boundary conditions on the two sides of the interface to which the diffusion process in both phases must conform.

Graphical Solution of the Diffusion Equation.—The equation for linear diffusion towards a plane surface [8] is

$$\frac{\partial C}{\partial t} = D \cdot \frac{\partial^2 C}{\partial x^2}, \quad . \quad . \quad . \quad . \quad . \quad (2)$$

where C is the concentration of the diffusing substance at any point, D its diffusion coefficient, t the time and x is distance from the surface. Although diffusion to a mercury drop or similar micro-electrode is not linear, it will be shown later that this equation applies sufficiently well to such electrodes in the circumstances with which we are concerned, i.e. while the diffusion layer is thin in comparison with the diameter of the electrode. Therefore the problem is to solve eqn. (2) for the two phases using the boundary conditions at the interface defined by (1).

---

[8] Ref. [1], p. 18.

The graphical method used is based on the numerical solution of differential equations using small finite differences ; an account of this method is given in a recent article by Emmons.[4] The present equation involves only two independent variables and is therefore conveniently solved in a two-dimensional diagram. A preliminary investigation using the simplest method described by Emmons (loc. cit. pp. 174-176) and x and t as the variables brought to light an important conclusion. Taking into account the fact that the flux on the two sides of the interface must be the same, it was found that C_{A0} and C_{S0} were related to C (the concentration of reacting ions in the bulk of the solution), *at all values of t*, by

$$C_{S0} + kC_{A0} = C, \quad . \quad . \quad . \quad . \quad (3)$$

where $k = \sqrt{D_A/D_S}$, D_A and D_S being the diffusion coefficients of metal in the mercury and ions in the solution, respectively. Introducing (1) and writing R for $10^{n\alpha(t-t_0)/0{\cdot}059}$, we obtain

$$C_{S0} = \frac{C}{1 + kR}$$

and

$$C_{A0} = \frac{C}{k + R^{-1}} = \frac{Ck^{-1}}{1 + k^{-1}R^{-1}} \quad . \quad . \quad . \quad (4)$$

We now have independent boundary conditions for the two phases, which, for the purpose of the graphical procedure, are most conveniently plotted against $n\alpha(t - t_0)/0{\cdot}059$, i.e., $\log R$, as shown in Fig. 1. The mid-point of each curve corresponds to the value of $R = k^{-1}$. The C_{S0} curve approaches the limit $C_{S0} = C$ for t decreasing and $C_{S0} = 0$ for t increasing while the limits for the C_{A0} curve are 0 and C/k. The diffusion equation need only be solved for one phase, i.e., only one of the curves is required, and the C_{S0} curve has the advantage that its height is unaffected by variation in k, which merely shifts it along the $(n\alpha(t - t_0)/0{\cdot}059)$ axis. The actual value of k does not therefore affect the shape or height of the final current-voltage curve, and it may be taken as unity (which is probably near the true value in most cases). It should be noted that the C_{S0} curve is simply the curve for $C/(1 + kR)$ against $\log R$ and is therefore quite general ; C may be given the arbitrary value of 1 as is done in Fig. 1. In applying the results of the graphical solution to particular cases, the $(n\alpha(t - t_0)/0{\cdot}059)$ (i.e., $\log R$) scale is interpreted as a voltage or time scale by the insertion of appropriate values of n and α, and ordinates are multiplied by the actual value of C to give concentrations.

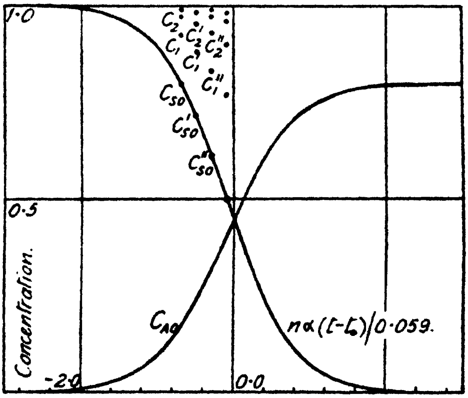

FIG. 1.

The basis of the numerical method already mentioned is as follows. To solve an equation such as (2) small finite differences in the two variables are chosen such that $(\delta x)^2 = 2D \,.\, \delta t$. Then, if C_{S0}, C_1, C_2, C_3, etc., are the concentrations at distances 0, δx, $2\delta x$, $3\delta x$, etc., from the boundary at a certain time, and if the concentrations at the same points are C'_{S0},

---

[4] Emmons, *Quart. J. Appl. Maths.*, 1944, **11**, 173.

C'_1, C'_2, C'_3, etc., after an interval δt, C''_{s0}, C''_1, C''_2, C''_3, etc., after an interval $2\delta t$, and so on, it is easily shown that

$$\left.\begin{aligned} C'_1 &= \frac{C_{s0}+C_2}{2}, \quad C'_2 = \frac{C_1+C_3}{2} \quad \text{etc.,}\\ C''_1 &= \frac{C'_{s0}+C'_2}{2}, \quad C''_2 = \frac{C'_1+C'_3}{2} \quad \text{etc.,}\end{aligned}\right\} \quad . \quad . \quad (5)$$

to a close approximation if δx and δt are small. If the boundary concentrations, C_{s0} at the electrode surface and C in the bulk of the solution, are known over a range of t and if the concentrations C_1, C_2, C_3, etc., for a series of points can be guessed or otherwise obtained for a certain value of t, then the concentrations at these points can be derived by the above method for the subsequent range of t, at intervals of δt. From the result the concentration gradient close to the electrode surface and hence the diffusion current, for this range of t, are easily deduced.

The graphical method is based on this principle but was designed to lessen the numerical work involved. Moreover, by using the ordinates and abscissae of Fig. 1 the result is quite general. The procedure was as follows. First a suitable value of δt was decided on, the controlling factor being that the change in R corresponding to δt must not be too great. Values of δt such as to make $n\alpha\delta t/0{\cdot}059 = 0{\cdot}1$ and $0{\cdot}05$ were used, the ratio of successive values of R being $10^{0\cdot1}$ and $10^{0\cdot05}$. δx is automatically determined by $(\delta x)^2 = 2D \cdot \delta t$. Next, C_{s0} values were calculated by means of (4) for a suitable range of t at intervals of δt, and plotted as in Fig. 1. Then, at a point on the C_{s0} curve where $(C - C_{s0})$ is only about 0·2 % of C, a few intermediate values, C_1, C_2, C_3, etc., were guessed and inserted between C_{s0} and C (this part of the curve being redrawn on a larger scale for convenience). The concentrations C'_1, C'_2, C'_3, etc., for the next value of $n\alpha(t - t_0)/0{\cdot}059$ were then obtained by the averaging process of eqn. (5). This was carried out by means of a straight scale graduated symmetrically about a zero at its mid-point. By applying this to the earlier set of points in such a way that, for instance, C_1 and C_3 were opposite identical scale readings, C'_2 could then be inserted opposite the zero but in the next vertical column (i.e. above C'_{s0}). Repetition of this process, with the introduction as necessary of extra points at the end of the column distant from the C_{s0} curve, provided eventually a complete set of concentration values for the range of time over which the C_{s0} curve was drawn. The first set of guessed points may, of course, be far from correct but as successive sets are derived the concentration values adjust themselves to correspond to the correct distances, δx, $2\delta x$, etc., from the boundary, and the errors are rapidly eliminated. If the start is made when $(C - C_{s0})$ is sufficiently small the errors are eliminated before an appreciable concentration gradient is reached. Actual sets of points are too close together to show in Fig. 1 but a few widely spaced points have been inserted merely to illustrate the foregoing description.

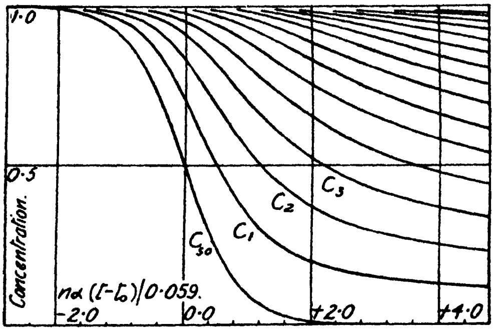

FIG. 2.

Curves showing the change of concentration with time at distances δx, $2\delta x$, etc., from the interface are obtained by joining up all C_1 points, all C_2 points, etc. These are shown in Fig. 2. It is noticeable that the change in concentration at a distance from the interface lags behind that which occurs nearer to it. Curves of concentration against x are obtained if each point in a column is shifted to the right by an amount proportional to the distance from the interface to which it refers and a curve drawn through them. These curves are shown in the upper part of Fig. 3. It is apparent that the concentration gradient close to the interface (i.e., the slope of the curves where they meet the C_{s0} curve) increases (as reduction proceeds) to a maximum and then decreases again. It is this maximum which is responsible for the peak in the current-voltage curves. The approximate scales of Fig. 2 and 3 may be indicated by a few rough figures. For $n = 2$ and $\alpha = 0{\cdot}3$ v./sec. approximately, the abscissae of both figures must be multiplied by 0·1 to give a scale in seconds, so that the whole curve in each case covers just over 0·7 sec. The concentration distance curves of Fig. 3 are drawn so that for n and α as above and $D = 1{\cdot}0 \times 10^{-5}$ cm.^{2} sec.$^{-1}$ (the value for lead), one unit of the abscissae corresponds to 0·045 cm., consequently the later curves extend over nearly 0·2 mm. from the interface.

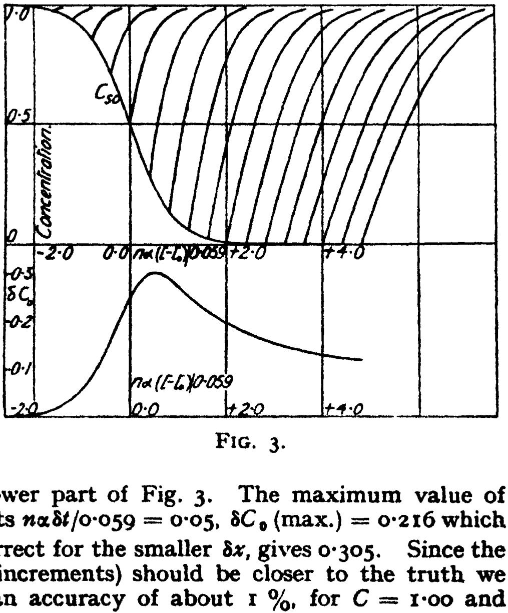

FIG. 3.

To calculate the diffusion current we require $\left(\frac{\partial C}{\partial x}\right)_{x=0}$. Denoting $(C_1 - C_{s0})$ by δC_1 and $(C_2 - C_1)$ by δC_2, it can be seen that $\delta C_1/\delta x$ gives the mean value of $\left(\frac{\partial C}{\partial x}\right)$ over the range $x = 0$ to $x = \delta x$, and a better approximation to $\left(\frac{\partial C}{\partial x}\right)_{x=0}$ is given by $\delta C_0/\delta x$ where $\delta C_0 = \delta C_1 + \frac{1}{2}(\delta C_1 - \delta C_2)$. Values of δC_0 obtained from the graphical results for increments $n\alpha\delta t/0{\cdot}059 = 0{\cdot}1$, are plotted in the lower part of Fig. 3. The maximum value of δC_0 is 0·300. For increments $n\alpha\delta t/0{\cdot}059 = 0{\cdot}05$, δC_0 (max.) $= 0{\cdot}216$ which on multiplying by $\sqrt{2}$ to correct for the smaller δx, gives 0·305. Since the latter result (using smaller increments) should be closer to the truth we may take $\delta C_0 = 0{\cdot}310$ to an accuracy of about 1 %, for $C = 1{\cdot}00$ and $n\alpha\delta t/0{\cdot}059 = 0{\cdot}1$. For δx we have

$$\delta x = (2D\,.\,\delta t)^{\frac{1}{2}} = (0{\cdot}0118\,D/n\alpha)^{\frac{1}{2}}.$$

In calculating the total flux we shall require concentrations in moles per cc., so if C_m is the molar concentration of the reacting ions,

$$\left(\frac{\partial C}{\partial x}\right)_{x=0} = \frac{C_m}{10^3}\,\delta C_0\left(\frac{n\alpha}{0{\cdot}0118D}\right)^{\frac{1}{2}} \quad . \quad . \quad . \quad (6)$$

$$\left(\frac{\partial C}{\partial x}\right)_{x=0}(\text{max.}) = \frac{C_m}{10^3}\,0{\cdot}31\,\left(\frac{n\alpha}{0{\cdot}0118D}\right)^{\frac{1}{2}}. \quad . \quad . \quad (7)$$

We have throughout been using the equation for linear diffusion (2). The results will be applicable with little error to a spherical or similar electrode of 1 mm. or greater diameter, as the thickness reached by the diffusion layer during a potential "sweep" is small compared with this. The equation for diffusion to a growing mercury drop [5, 6] is of the same form

---

[5] Ref. [1], p. 35.

[6] MacGillavry and Rideal, *Rec. Trav. Chim.*, 1937, **56**, 1013.

as (2) but with different variables. It can be treated by the same graphical method and a comparison of the results obtained from the two equations shows them to be practically identical provided that the reduction occurs at a late stage of drop growth, and occupies a small fraction of the drop life—conditions which hold in practice. Thus (6) and (7) may be taken as valid for the dropping electrode in these conditions.

When applying the results to the dropping electrode, the changing surface area must be taken into account. Since the volume of a drop increases uniformly with time we write $r^3 = \gamma t$ and hence

$$A = 4\pi r^2 = 4\pi\gamma^{2/3}t^{2/3},$$

where r is the radius of the drop, t is measured from the start of its growth, and γ is a constant depending on the rate of flow of mercury. For the diffusion current we have therefore

$$i = nFAD\left(\frac{\partial C}{\partial x}\right)_{x=0} = nF4\pi\gamma^{2/3}t^{2/3}D\left(\frac{\partial C}{\partial x}\right)_{x=0};$$

substituting for $\left(\frac{\partial C}{\partial x}\right)_{x=0}$ by (6) and (7),

$$i = \frac{4\pi FC_m}{(0{\cdot}0118)^{\frac{1}{2}}\,10^3}\,\gamma^{2/3}t^{2/3}n^{3/2}\alpha^{1/2}D^{1/2}\delta C_0 \text{ amp.} \qquad . \qquad . \qquad (8)$$

$$i_p = \frac{1{\cdot}24\pi FC_m}{(0{\cdot}0118)^{\frac{1}{2}}\,10^3}\,\gamma^{2/3}t_p{}^{2/3}n^{3/2}\alpha^{1/2}D^{1/2} \text{ amp.,} \qquad . \qquad . \qquad (9)$$

where i_p is the peak value of the current and t_p the time at which the peak occurs. The numerical value of δC_0(max.) has been used in (9).

Expression (8) permits the calculation of a theoretical current-voltage curve using the values of δC_0 obtained from the curve of Fig. 3. It will be shown in the experimental section that there is good agreement between the calculated and experimental current-voltage curves for " reversible " electrode reactions.

The Charging Current. Since the rate of change of the potential of the electrode relative to the solution is fairly high there is an appreciable charging current. However, as the rate of change of potential is constant, the current is approximately constant except for the increase due to the increasing area of the drop when a dropping electrode is used. The rate of increase of area is small in the latter stages of drop growth if the drop time is fairly long. Since an electrode of at least 7 sec. drop time is usually employed, and the potential " sweep " is applied during the last second or so of drop life, there is little interference from charging current. It has been found to be negligible when measuring diffusion currents due to ion concentrations down to 10^{-5} M.

Experimental and Discussion of Results

The apparatus used has been described in Part I.[1] For all measurements of c—v (i.e. current-voltage) curves a rectangular grid drawn on celluloid and placed in contact with the face of the cathode ray tube, was employed. Calibration of the horizontal and vertical spot deflections in terms of voltage applied to the polarographic cell, and current passing through it, respectively, were made as follows. A microammeter with a 100,000 ohm resistance in series was calibrated as a voltmeter against a standard instrument. The combination was connected in place of the polarographic cell and, with the " vertical " amplifier switched off, the applied potential was varied (by means of control Q, Part I, Fig. 1) so as to give a direct calibration of horizontal spot deflection against applied P.D. Using the " vertical " amplifier, with the " horizontal " one switched off, and reading current from the microammeter, the same method gave a calibration of vertical deflection against current.

Cambridge Instrument Co. type polarographic cells, and a polarographic thermostat bath made by the same firm, were used. All measurements were carried out on solutions at 25° c. Except where otherwise stated a silver-silver chloride anode of the type described in Part I was used. Voltage scales shown in the plates of c—v curves give the potential of the micro-electrode in volts negative to the anode.

General Form of the c—v Curves

Stationary Electrodes. Platinum and mercury stationary micro-electrodes were used. The platinum electrode was prepared by sealing a piece of platinum wire into a glass tube leaving about 3 mm. of wire projecting. This projecting piece was then fused in an oxy-coal gas flame to a sphere about 1 mm. in diameter. The mercury electrode consisted of a small hemispherical mercury meniscus about 1 mm. in diameter. It was formed at the tip of a glass tube, the lower end of which had been bent through 180° so as to be directed upwards when the tube was held vertically with its lower end in the solution. The upper end of the tube was provided with a tap and small mercury reservoir so that the electrode surface could be renewed at intervals by running through a few drops of mercury.

An automatic potential sweep (cf. Part I) is required for a stationary electrode. The interval between successive sweeps must be long enough for most of the metal deposited on the platinum, or dissolved in the mercury, to return to the solution, and for the concentration in the latter to regain uniformity by diffusion. An interval of 7 to 10 sec. is usually sufficient. With a shorter interval the peak height of successive sweeps gradually decreases owing to some exhaustion of the solution near the electrode, and accumulation of metal on the latter.

The c—v curve obtained for the reduction of cadmium ion at the platinum electrode is reproduced in Plate A. Several curves obtained with the stationary mercury electrode for the reduction of lead ion are shown in Plate N (the different curves are obtained at different rates of change of the electrode potential, and illustrate an effect to be discussed later). The c—v curves obtained with the stationary mercury electrode are similar in shape to those obtained with the dropping electrode (cp. Plate D), and exhibit the peak at the same potential as in the case of the latter. On the other hand, the peak due to the reduction of metal ions to the metal at a platinum electrode is less sharp, and occurs at a more negative potential than when a mercury electrode is used (cp. Plate A and F). This is obviously related to the solubility of the metal in the mercury. Conversely, hydrogen ion reduction occurs more readily at a platinum electrode than at a mercury electrode (due to its lower overvoltage on the former); consequently a platinum electrode is less satisfactory from an analytical point of view. Although the same objections do not apply to a stationary mercury electrode, this also has disadvantages as compared with a dropping electrode. For instance, reproducibility is not so good; but in any case, no practical method has so far been devised of renewing the mercury surface in such a way that the surface area of the new meniscus is always the same, and this has rendered it practically useless for analytical purposes.

Dropping Electrode.—Examples of the c—v curves obtained for the reduction of various metal ions are shown in Plates B-M. The reproducibility of the traces for successive potential sweeps may be judged from the fact that the exposures used for the photographs covered anything from two up to five repetitions of the trace. All the quantitative work described below was carried out with the dropping electrode.

Verification of the Theoretical Equation.

The experimental c—v curves for the reduction of thallous and lead ions shown in Plates C and D are reproduced in Fig. 4 together with a number of points calculated by means of eqn. (8). The agreement is good and shows that the assumption of reversibility of the electrode process is justified in these cases. A comparison of the experimental maximum currents (i_p) with the values calculated by means of eqn. (9) for a number of ions is made in Table I. The base solution in each case was M. KCl.

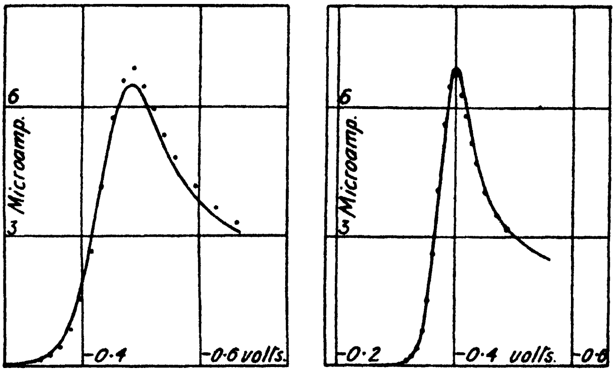

0·5 × 10^{-3} M. Tl^+ in M. KCl. 0·25 × 10^{-3} M. Pb^{++} in M. KCl.

FIG. 4.

The rate of change of potential, α, was 0·267 v. sec.$^{-1}$, and γ was calculated from the rate of flow of mercury, which was 5·80 × 10^{-4} g.sec.$^{-1}$. The time t_p at which the peak occurs is obtained by subtracting from the drop time (measured during actual operation) the period between the occurrence of the peak and the fall of the drop. The latter is obtained by dividing the potential change which occurs between the peak and the fall of the drop by α. It appears from the results that under the conditions used the reduction of thallous, lead, and cadmium ions proceeds reversibly but that there is some divergence from reversibility in the case of manganese, and still more in that of zinc. The shape of the c—v curve for zinc (Plate G), the peak of which is more rounded than in the case of reversibly reduced divalent ions, tends to confirm this.

TABLE I

Ion (C = 0·25 × 10^{-3} M.).	t_p Sec.	$t_p^{2/3}$.	D_s cm.^{2} sec.$^{-1}$.	i_p (Calcd.) μa.	i_p (Exptl.) μa.	Difference %.
Tl^+	7·41	3·80	2·0 × 10^{-5}	3·52	3·42	− 2·7
Pb^{++}	7·26	3·75	0·98 × 10^{-5}	6·88	6·93	+ 0·7
Cd^{++}	7·09	3·69	0·72 × 10^{-5}	5·80	6·14	+ 5·8
Mn^{++}	4·49	3·72	0·72 × 10^{-5}	4·27	3·61	−15
Zn^{++}	5·90	3·26	0·72 × 10^{-5}	5·12	3·70	−28

Irreversible Reduction Processes.—The c—v curves for the reduction of chromium, cobalt and nickel ions in KCl base solution and of cobalt and nickel in a KCl-KCNS base solution, are shown in Plates I-M. The concentrations of the reducible ions are all 0·25 × 10^{-3} M. (as for the reversibly reduced ions except thallous ion), so that the c—v curves are comparable among themselves and with those for reversible reductions.

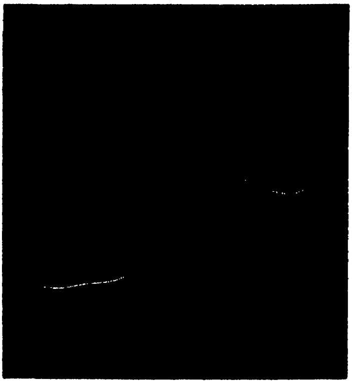

A. $\frac{1}{8} \times 10^{-3}$ M. Cd^{++} in M. KCl, stationary Pt electrode.

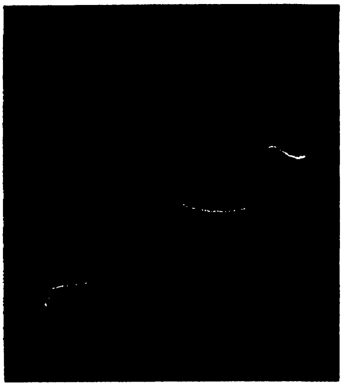

B. $\frac{1}{16} \times 10^{-3}$ M. Pb^{++}, Cd^{++}, Zn^{++} in M. KCl.

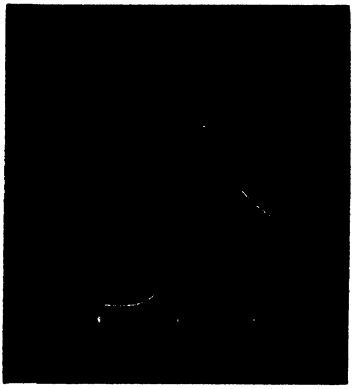

C. $\frac{1}{2} \times 10^{-3}$ M. Tl^{+} in M. KCl.

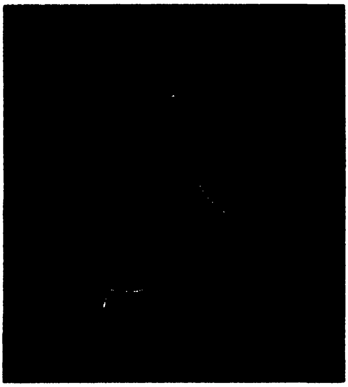

D. $\frac{1}{4} \times 10^{-3}$ M. Pb^{++} in M. KCl

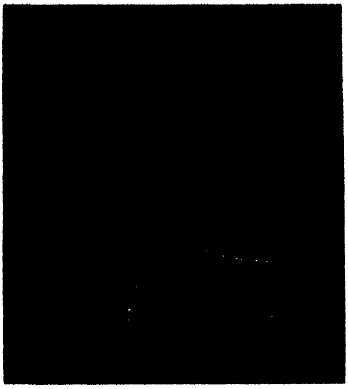

E. $\frac{1}{4} \times 10^{-3}$ M. Bi^{+++} in M. KCl.

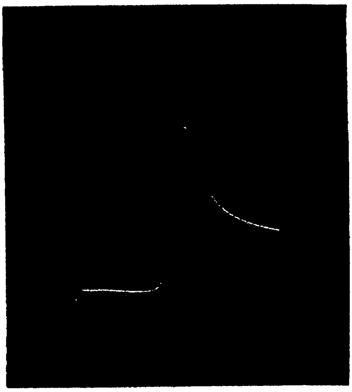

F. $\frac{1}{4} \times 10^{-3}$ M. Cd^{++} in M. KCl.

[*To face p.* 334

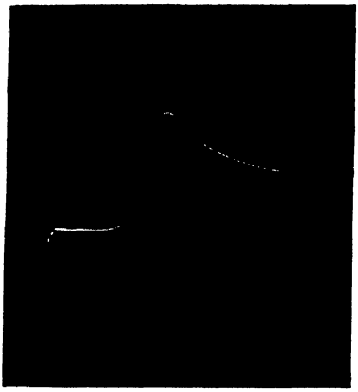

G. $\frac{1}{4} \times 10^{-3}$ M. Zn^{++} in M. KCl.

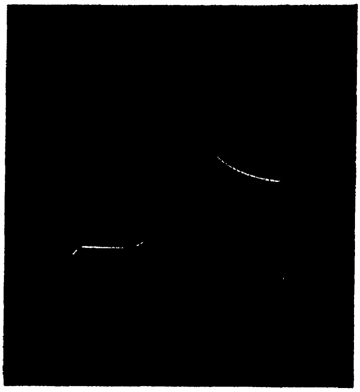

H. $\frac{1}{4} \times 10^{-3}$ M. Mn^{++} in M. KCl.

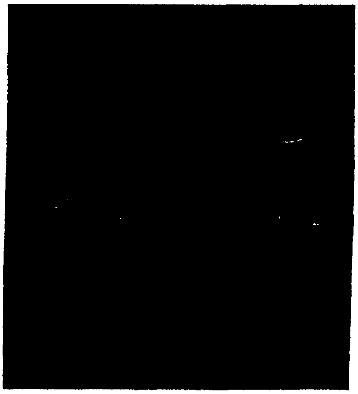

I. $\frac{1}{4} \times 10^{-3}$ M. Cr^{+++} in M. KCl.

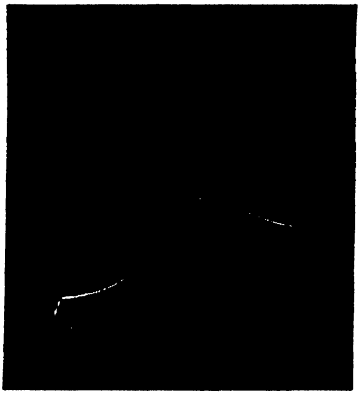

J. $\frac{1}{4} \times 10^{-3}$ M. Co^{++} in M. KCl.

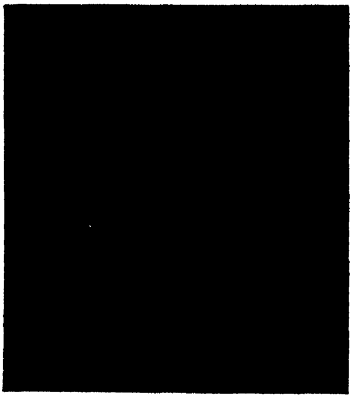

K. $\frac{1}{4} \times 10^{-3}$ M. Ni^{++} in M. KCl.

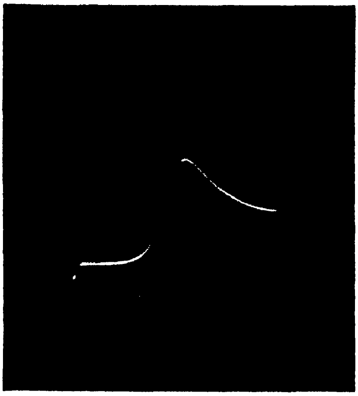

L. $\frac{1}{4} \times 10^{-3}$ M. Co^{++} in M. KCl
+ M. KCNS.

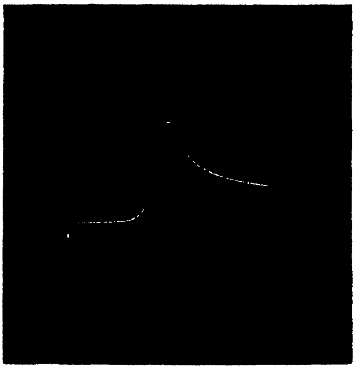

M. $\frac{1}{4} \times 10^{-3}$ M. Ni^{++} in M. KCl + M. KCNS.

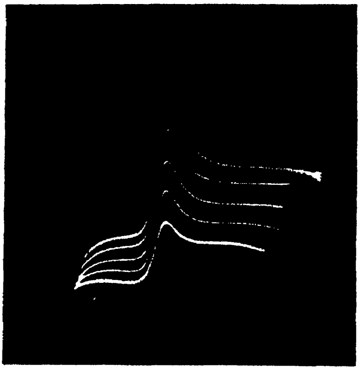

N. $\frac{1}{8} \times 10^{-3}$ M. Pb^{++} in M. KCl. Stationary Hg electrode, α = 0·144, 0·267, 0·431, 0·638, 0·882 volt sec.$^{-1}$.

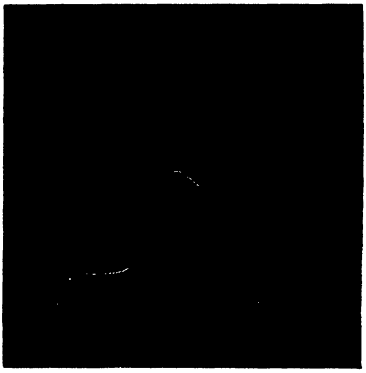

O. $\frac{1}{4} \times 10^{-3}$ M. Ni^{++} in M. KCl + 2 M. NH_4OH.

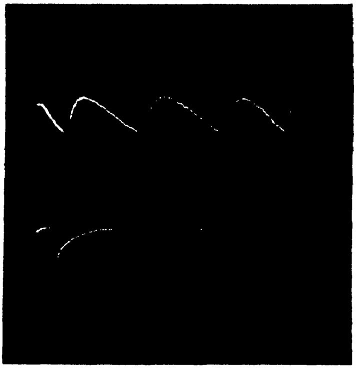

P. Current time curves corresponding to O.

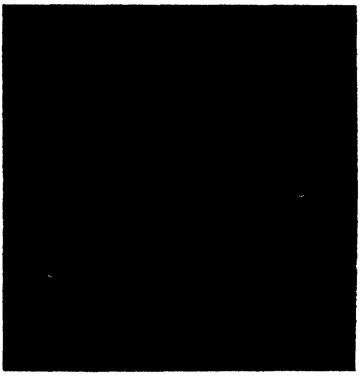

R. Mazak Alloy A, Cu, Pb, Cd.

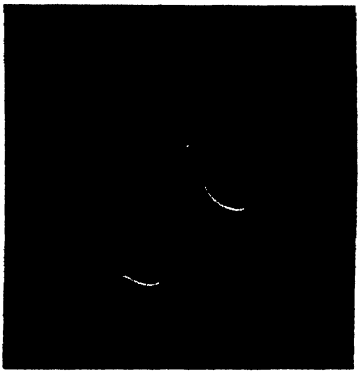

S. Pb peak of R separated and adjusted to standard height.

The most obvious feature of the c—v curves for irreversible reductions is the lower, rounded peak, becoming, in the extreme case of nickel, a mere change of slope. This is the effect to be expected from an electrode process which is itself slow enough to limit the current flowing. The acceleration of the electrode reaction resulting from the conversion of the hydrated cobalt and nickel ions into their thiocyanate complexes is illustrated by the last two of these curves.

Influence of Various Factors on the c—v Curves.—Eqn. (8) indicates that the diffusion current is dependent on the factors n, α, γ, D_s and t, apart from the concentration of the reducible ion. The nature of this dependence will be discussed briefly for each factor.

(a) Number of Electrons Involved in the Reduction.—The quantity $n\alpha(t - t_0)/0{\cdot}059$ plotted as abscissa in Fig. 3 is converted into volts by multiplying by $0{\cdot}059/n$. The scale in terms of volts is therefore inversely proportional to n, so that the width of the peak of a c—v curve is inversely proportional to n for reversible reductions. This is illustrated by the curves for thallous, lead, and bismuth ion reductions (Plates C, D, E). Since the time occupied in the completion of the peak is similarly inversely proportional to n, a higher value of n increases the speed of the whole process, and so increases the current (other things being equal). This fact emerges in the mathematical expression for the current by n appearing therein raised to the power 3/2 instead of to the first power (as in the Ilkovic equation).

TABLE II

α v. sec.$^{-1}$.	Tl^+ 0·5× 10^{-3} M.		Cd^{++} 0·25× 10^{-3} M.		Co^{++} 1× 10^{-3} M.	
	i_p(μa.).	$i_p/\alpha^{\frac{1}{2}}$.	i_p(μa.).	$i_p/\alpha^{\frac{1}{2}}$.	i_p(μa.).	$i_p/\alpha^{\frac{1}{2}}$.
0·144	4·38	11·8	4·65	12·3	6·74	17·7
0·177	4·94	11·7	5·13	12·2	7·23	17·2
0·228	5·64	11·8	5·81	12·2	8·10	17·0
0·267	6·17	11·9	6·37	12·3	8·75	16·9
0·332	6·63	11·5	7·10	12·3	9·65	16·7
0·431	7·40	11·3	7·97	12·1	10·8	16·4
0·638	8·85	11·1	9·70	12·1	12·8	16·0
0·882	10·5	11·2	11·2	11·9	14·4	15·3

(b) Rate of Change of Potential.—Eqn. (8) and (9) show that the current should be proportional to $\alpha^{\frac{1}{2}}$. This has been verified by experiment; results for the reduction of thallous, cadmium, and cobalt ions are given in Table II. Some decrease in the ratio (current)/$\alpha^{\frac{1}{2}}$ as α increases seems to occur in all cases. This is somewhat more marked for cobaltous ion than for the other two ions, but the difference was not so great as was expected from the obviously "irreversible" nature of the cobalt ion reduction (as judged from the shape of the c—v curve).

A series of c—v curves for reduction of lead ion at the stationary mercury electrode with different values of α is shown in Plate N. The actual values of α were 0·144, 0·267, 0·431, 0·638 and 0·882 v. sec.$^{-1}$.

(c) Other Factors. The factors γ and t in eqn. (8) and (9) appear as the product $\gamma^{\frac{2}{3}}t^{\frac{2}{3}}$ which is proportional to the surface area of the drop. Experiments using one capillary and varying drop rates, and using several capillaries giving different drop sizes, have proved that i_p is proportional to the surface area of the drop at the time when the peak occurs, but is independent (so far as could be detected) of the rate of growth of the drop.

The diffusion coefficient of the ions in the aqueous solution is present in (8) and (9) as $D_s^{\frac{1}{2}}$, as in the Ilkovic equation. The current is independent of the diffusion coefficient of the metal in the mercury, which influences the c—v curve only in so far as the ratio D_s/D_a influences the potential at which the peak occurs (cp. p. 331).

Occurrence of Maxima.

Maxima occur in circumstances similar to those in which they occur in ordinary polarography, but rather less readily. That is to say, solutions which give rise to a maximum when polarographed in the ordinary way frequently do not give one when the cathode ray polarograph is used. This difference probably arises from two causes: firstly, the slower rate of dropping of the electrode employed with the cathode ray polarograph, and secondly, the commencement of reduction only when each drop is almost fully grown. In ordinary polarography it is established that a more rapidly dropping electrode encourages maximum formation,[7] and this is conspicuously true under the conditions used with the cathode ray polarograph. Moreover, it has been found with the latter instrument that the earlier in the life of a drop the potential sweep is applied, the more pronounced a maximum becomes. Since the rate of increase of surface area of a drop is greatest in its earliest stages of growth, and decreases continuously, both the above facts point to the general conclusion that for a given solution the tendency to maximum formation is greater the greater is the rate of growth of drop surface. Consequently the absence of reduction during the early stages of drop growth may in part account for the relatively infrequent occurrence of maxima in cathode ray polarography.

When it occurs, the phenomenon shows itself as a sudden rise in the current either just before or just after the peak in the c—v curve. The curve for the reduction of the ammoniated nickel ion (in M. KCl containing 2M. ammonia) is shown in Plate O; and P shows the current-time curves for constant electrode potential during drop formation. The upper set of curves was obtained with the dropping electrode at the potential at which the maximum occurs, while for the lower set its potential had been made more negative. The irregular enhanced current due to a local stirring effect is apparent in the upper curves.

Analytical Applications of the c—v Curves.

The peak height is an easily measurable feature of the typical c—v curve. It corresponds to i_p, which, by eqn. (9), is proportional to the concentration of the substance undergoing reduction. Although eqn. (9) was deduced for reversible reductions, proportionality between i_p and concentration has been fully verified by experiment both for reversible and irreversible reductions. In practice, instead of measuring the peak height, the main resistance R_1 (Part I, Fig. 1) is adjusted so as to give a peak of standard height and the setting of R_1 is used as a measure of i_p (the actual value of R_1 being of course inversely proportional to i_p, so that the potential difference i_pR_1 is constant). This method has the advantage of eliminating any errors due to non-linearity of response of the amplifier or the cathode ray tube. Some of the experimental results obtained in investigations of the range over which there is proportionality between concentration and i_p are given in Table III. Allowing for deviations due to experimental error, it is clear that there is proportionality over the concentration range studied. There is little doubt that this relationship could extend over a much wider range, but measurements of lower values of i_p than the lowest in Table III were not obtainable with sufficient accuracy to be useful.

---

[7] Buckley and Taylor, *J. Res. Nat. Bur. Stand.*, 1945, **34**, 97.

As an example of the use of i_p as a measure of concentration, a calibration graph for i_p against % lead and cadmium in a zinc die-casting alloy (Mazak A) is reproduced in Fig. 5. The results were obtained on synthetic standard solutions prepared in accordance with a method for the polarographic analysis of these alloys which has been published.[8] The solutions polarographed contain 1 g. of alloy in 8 ml. of solution. The c—v curves shown in Plates R and S are for a typical Mazak A alloy (Cu = 0·0078 %, Pb = 0·0060 % and Cd = 0·0014 %). The second curve is that for lead alone, separated out and adjusted to standard size for measurements of i_p.

TABLE III

Concentration M./1000	Pb⁺⁺.		Cd⁺⁺.		Zn⁺⁺.		Co⁺⁺.	
	i_p(μa.).	Ratio.	i_p(μa.).	Ratio.	i_p(μa.).	Ratio.	i_p(μa.).	Ratio.
1	—	—	—	—	—	—	8·55	[16·0]
$\frac{1}{2}$	12·65	[32·0]	11·44	[32·0]	7·49	[32·0]	4·04	7·60
$\frac{1}{4}$	6·42	16·2	5·83	16·3	3·75	16·0	2·03	3·80
$\frac{1}{8}$	3·24	8·2	2·87	8·02	1·85	7·90	1·024	1·92
$\frac{1}{16}$	1·59	4·03	1·445	4·04	0·935	3·99	0·559	1·05
$\frac{1}{32}$	0·764	1·93	0·695	1·94	0·470	2·01	—	—
$\frac{1}{64}$	0·368	0·93	0·338	0·95	0·228	0·97	—	—

Another factor which is important from the analytical point of view is the influence, if any, which the reduction of more easily reducible ions has on the c—v curve of the ion of which the concentration is to be measured. It has been found in practice that, provided the potential sweep can be started at a potential at which all earlier reductions are occurring to completion, while that of the ion under investigation is not occurring to any appreciable extent, then the c—v curve of the latter is quite unaffected by the prior reductions. This separation can be achieved if there is about 0·2 v. at least between the half-wave potential of the ion of which the concentration is being measured and that of any other ion present. This is the same minimum difference as permits the separation of ordinary polarographic steps.

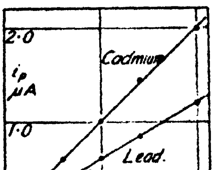

FIG. 5.

It is interesting to compare the current due to an ion which is undergoing reduction all the time with the peak current for the ion of which the concentration is being determined. At time t from the start of growth of the drop, the current due to the former is given by the Ilkovic equation for instantaneous diffusion current [1]:

$$i = 4\left(\frac{7}{3}\right)^{\frac{1}{2}} \pi^{\frac{1}{2}} nFD^{\frac{1}{2}} \gamma^{\frac{2}{3}} t^{\frac{1}{6}} C \;.\; 10^{-3} \text{ amp.}$$

where C is expressed in moles/l. By comparison with (9) for i_p, also at time t, and for equal values of C and D, we obtain

$$\frac{i_p}{i} = \left(\frac{3\pi n\alpha t}{0{\cdot}0826}\right)^{\frac{1}{2}} \times 0{\cdot}31.$$

When $n = 2$, $t = 6$ sec., and $\alpha = 0{\cdot}267$ v.sec.$^{-1}$, this ratio is about 6. Thus the current to be measured is considerably enhanced relative to that due to prior reductions. It is, of course, the change in this latter current during the rise of the peak that affects the height of the peak. Owing to the factor $t^{\frac{1}{6}}$ in the expression for this current, its rate of change, at the late stage of drop growth at which current peaks are normally obtained, is so small as to be quite innocuous. Some experimental results for i_p for $\frac{1}{16} \times 10^{-3}$ M. cadmium ($E_{\frac{1}{2}} = -$ 0·64 v. relative to saturated calomel electrode) in presence of varying concentrations of lead ($E_{\frac{1}{2}} = -$ 0·44 v. relative to saturated calomel electrode) are shown in Table IV.

---

[8] *The Polarographic and Spectrographic Analysis of High Purity Zinc and Zinc Die Casting Alloys* (H.M.S.O., 1945).

TABLE IV

Pb·· M./1000.	0.	$\frac{1}{16}$.	$\frac{1}{8}$.	$\frac{1}{4}$.	$\frac{1}{2}$.
i_p (μa.) due to $\frac{1}{16}$ millimolar Cd··	1·41	1·39	1·38	1·38	1·39

Acknowledgments are due to the Director General, Scientific Research (Defence), Ministry of Supply for permission to publish this paper. The author also wishes to express his appreciation of the encouragement given to him by Mr. S. H. Bales and Mr. A. S. Nickelson in the course of the work, to Mr. S. K. Tweedy for much helpful discussion during the preparation of the paper, and to Miss J. Strachan for her invaluable assistance with the experimental work.

Summary.

By means of an instrument previously described and termed a cathode ray polarograph, a micro-electrode immersed in a solution containing small amounts of electro-reducible or -oxidisable substances may be subjected to a fairly rapidly changing potential and the corresponding changes in the electrode current recorded on the screen of a cathode ray tube. The diffusion current-voltage curve so obtained shows a sharp maximum of the current corresponding to the onset of each individual electro-reduction or -oxidation. The theory of the diffusion process under these conditions is discussed, and a graphical solution of the diffusion equation is obtained for the case that the electrode reaction occurs reversibly, and that the reactants and products are soluble either in the aqueous medium or the electrode material (which may be mercury). Good agreement between theoretical and experimental curves is obtained. Photographs of experimental cathode ray traces show the effect on the current-voltage curves of slowness of the electrode reaction (irreversible electrode process), of variation in the rate of change of potential of the electrode, and of phenomena similar to polarographic maxima.

Experimental data are presented which indicate a strict proportionality between the concentration of a substance which reacts at the electrode, and the value of the corresponding diffusion current at its maximum. The cathode ray polarograph may therefore be used for analytical purposes.

Chemical Inspection Department,
Ministry of Supply.

THE CALCULATION OF RESONANCE ENERGIES FROM THERMAL DATA.

BY J. G. M. BREMNER AND G. D. THOMAS.

Received 13*th June*, 1947.

Dewar [1] has compared the resonance energies of aromatic compounds derived from the bond energies of Pauling with those obtained by Kistiakowsky *et al.*[2] from heats of hydrogenation. The Pauling method yields the larger values and Dewar, for example, finds that the difference for benzene is 5 kcal. and for *o*-xylene 13 kcal. To account for this difference Dewar concludes that the alicyclic compounds must possess " resonance " energy and gives values which support this conclusion. He suggests that the Pauling resonance energies of aromatic compounds be corrected by subtracting the arithmetic mean of the " resonance " energies of the corresponding alicyclic compounds. The application of this correction is shown to reduce, for example, the resonance energy of benzene from 41 to 36 kcal. given by Kistiakowsky.

---

[1] Dewar, *Trans. Faraday Soc.*, 1946, **42**, 767.

[2] Kistiakowsky, *et al.*, *J. Amer. Chem. Soc.*, 1936, **58**, 137, 146; 1937, **59**, 831.

Subsequent to Dewar's work, Rossini *et al.* have published data on aromatic [3] and alicyclic compounds [4] from which we have derived resonance energies using Pauling's bond energies and heats of atomisation.[5] Since Rossini uses graphite as standard, a correction to the experimental heats of formation of 0·45 kcal. per carbon atom [6] has been made to bring them to a diamond basis. The resonance energies of the aromatic compounds given in Table I are a few kcal. smaller than those published by Dewar but are, nevertheless, significantly higher than the Kistiakowsky values (Table III). The method of correction suggested by Dewar, originally intended to reconcile the Pauling and Kistiakowsky values, is evidently invalid as the mono-alkyl substituted cyclohexanes have, in fact, heats of formation in very close agreement with those calculated from the Pauling bond energies (Table I).

TABLE I.

Compound.	Pauling Resonance Energy (kcal).		Compound.	Pauling Resonance Energy (kcal).	
	This Paper.*	Dewar.[1]		This Paper.* †	Dewar.[1]
Benzene . .	39·28	41	Cyclohexane .	−0·87	2
Toluene . .	42·10	43	Methyl cyclohexane	+1·64	—
Ethylbenzene .	41·88	44	Ethyl ,,	+0·65	—
n-Propyl benzene .	42·08	46	*n*-Propyl ,, .	+0·75	—
n-Butyl ,, .	42·20	—	*n*-Butyl ,, .	+0·45	—
n-Hexyl ,, .	41·95	—	*n*-Hexyl ,, .	+0·20	—
n-Octyl ,, .	41·70	—	*n*-Octyl ,, .	−0·05	—
n-Decyl ,, .	41·46	—	*n*-Decyl ,, .	−0·29	—
n-Dodecyl ,, .	41·21	—	*n*-Dodecyl ,, .	−0·54	—
n-Tetradecyl ,, .	40·96	—	*n*-Tetracecyl ,, .	−0·79	—
n-Hexadecyl ,, .	40·71	—	*n*-Hexadecyl ,, .	−1·04	—
m-Xylene . .	44·88	—		—	—
Mesitylene . .	47·79	50		—	—

The relatively large " resonance " energies derived by Dewar for cyclohexane and cyclohexene are accounted for by the use of inaccurate thermal data. Thus, the heats of combustion he used imply a hydrogenation heat of only 23 kcal. against the Kistiakowsky value of 28·6 kcal.

Pauling [7] has attributed the lack of agreement between his own and

---

[3] Taylor, Wagman, Williams, Pitzer and Rossini, *Bur. Stand. J. Res.*, 1946, **37**, 95.

[4] Prosen, Johnson and Rossini, *ibid.*, 51.

[5] Pauling, *The Nature of the Chemical Bond* (Cornell, 1942), pp. 53, 54, 131.

[6] Prosen, Jessup and Rossini, *Bur. Stand. J. Res.*, 1944, **33**, 447.

[7] Pauling, *loc. cit.*, p. 134.

* The difference between the values in the two starred columns becomes constant at 41·75 kcal. from the butyl derivative onwards. Such figures represent " resonance " energies according to the Dewar method of correction.

† The negative sign implies a " strain " energy.

Kistiakowsky's values to uncertainties in his bond-energy values. This view receives emphasis from a consideration of Rossini's heats of formation both for a homologous series and for isomeric hydrocarbons. In Table II "resonance" energies for the *n*-paraffins from methane to eicosane have been calculated from Pauling's bond energies and Rossini's heats of formation. The steady drift in the values could be eliminated by only slight modifications to the Pauling bond energies but such modified values would then be less accurate in other applications. Turning to isomeric compounds, bond-energy summations make no distinction between the isomers. Such constancy is not consistent with experiment. Thus there is a variation in the experimental heats of formation amounting to 4 kcal. for the heptane and octane isomers,[8] 3 kcal. for ethyl benzene [8] and its isomers and 7 kcal. for the butyl benzene isomers.[8] In the Pauling method of calculation such differences in the heats of formation give rise to corresponding differences in resonance energies.

It is clear that in order to calculate resonance energies with an accuracy comparable with Kistiakowsky's values for benzene, a method is required that takes account of molecular structure. Such a method based on "group" rather than bond equations, has been advanced by the authors [9] and is of particular value for the treatment of isomers and compounds of high molecular weight. Both the group and the Kistiakowsky procedures make a more definite adjustment for hyperconjugation energies, common to both the aliphatic and aromatic series, than the Pauling method.[10] The application of the group method to the alkyl cyclohexanes involves the use of the paraffinic hydrocarbons in equations of the type (1) whilst the alkyl benzenes are represented by equations such as (2) involving *cis*-2-olefines.

TABLE II.

n-Paraffin.	CH_4.	C_2H_6.	C_4H_{10}.	C_6H_{14}.	C_8H_{18}.	$C_{10}H_{22}$.	$C_{12}H_{26}$.	$C_{14}H_{30}$.	$C_{16}H_{34}$.	$C_{18}H_{38}$.	$C_{20}H_{42}$.
Resonance * energy (kcal.)	0·25	−2·4	−3·0	−2·9	−3·2	−3·4	−3·7	−3·9	−4·2	−4·4	−4·7

$$2\,n\text{—}C_4H_{10} + CH_3\text{—}\overset{\overset{\textstyle R}{|}}{CH}\text{—}CH_2\text{—}CH_3 =$$

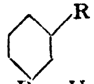

$$+\ 3C_2H_6 \quad . \quad . \quad . \quad (1)$$

where R = H, Me, Et, etc.

$$2\,CH_3\text{—}CH{=}CH\text{—}CH_3 + CH_3\text{—}C{=}\overset{\overset{\textstyle R}{|}}{CH}\text{—}CH_3 =$$

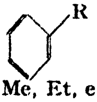

$$+\ 3\,C_2H_6 \quad (2)$$

where R = H, Me, Et, etc.

The heat change for "reactions" such as (1) and (2) gives, with a change in sign, the resonance energy of the cyclic compound involved. The resonance energies shown in Table III are obtained by substituting Rossini's heats of formation of the paraffins [8] and of the olefines [11] in such equations.

Resonance energies of the aromatic compounds calculated by the group method compare well with the recognised Kistiakowsky values.

---

[8] Prosen, Pitzer and Rossini, *Bur. Stand. J. Res.*, 1945, **34**, 403.

[9] Bremner and Thomas, *Nature*, 1946, **158**, 593; *Trans. Faraday Soc.*, 1947, **43**, 779; Pauling, ref. 5, p. 134.

[10] Cp. Mulliken, Rieke and Brown, *J. Amer. Chem. Soc.*, 1941, **63**, 41 and 1770.

[11] Kilpatrick, Prosen, Pitzer and Rossini, *Bur. Stand. J. Res.*, 1946, **36**, 559.

* The negative sign implies a "strain" energy.

It should be pointed out, however, that the latter are formally equivalent to the reaction heats of group equations such as (3):

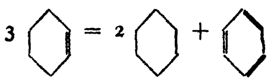
. . . . . (3)

The Kistiakowsky procedure can strictly only be applied to benzene as the hydrogenation heats of the higher mono-unsaturated alicyclic derivatives are so far undetermined. Resonance energies for aromatic compounds other than benzene are consequently bracketed in Table III.

Finally, the group method of calculation shows small " resonance " energies for the alkylcyclohexanes which may be used to correct the resonance energies of the aromatic compounds in the Dewar fashion. Such a procedure makes even closer the agreement between the resonance energies derived from the group method and those from Kistiakowsky's method. This type of correction, moreover, is implicit in the Kistiakowsky procedure as demonstrated by equation (3).

TABLE III.

Aromatic Compound.	Resonance Energy (kcal.). Group Method.	Resonance Energy (kcal.). Kistiakowsky Data.	Alicyclic Compound.	Resonance Energy (kcal.). Group Method.
Benzene . .	36·6	36	Cyclohexane . .	0·7
Toluene . .	35·9	—	Methylcyclohexane .	1·2
Ethylbenzene .	36·6	(35)	Ethylcyclohexane .	1·1
o-Xylene . .	37·6 ; 34·5*	(33)	*n*-Propylcyclohexane	1·3
n-Propylbenzene .	36·4	—	*n*-Butylcyclohexane .	1·2
Mesitylene . .	34·0	(33)		
Styrene . .	37·9	(37)		

The authors wish to thank Mr. J. A. Brayshay for assistance in some of the calculations.

Summary.

The Pauling and Kistiakowsky methods give different values for the resonance energies of aromatic compounds. This difference is ascribed to the approximate nature of the Pauling bond energies. An alternative " group " rather than bond method, is suggested for referring the aromatic to the aliphatic series. This alternative method gives resonance energies in good agreement with the Kistiakowsky values.

Imperial Chemical Industries Limited,
Billingham Division,
Billingham-on-Tees,
Co. Durham.

---

* For the two Kékulé forms 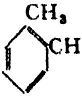 and 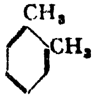 respectively.

REVIEWS OF BOOKS.

Selected Values of Properties of Hydrocarbons. Circular C 461 of National Bureau of Standards, 1947. By F. D. Rossini, K. S. Pitzer and Others. (U.S. Government Printing Office, Washington, D.C.) Pp. 483. Price $2.75.

This volume is the result of a combined effort by the National Bureau of Standards and the American Petroleum Institute, under the direction of F. D. Rossini and K. S. Pitzer, aided by some half dozen assistants. The object is to select and tabulate the " best " values of certain properties of hydrocarbons based on the available experimental evidence combined with the application of thermodynamics and statistical mechanics.

The properties listed include boiling-point, refractive index, density, freezing-point, molar volume, molar refraction, viscosity, kinematic viscosity, vapour pressure, heat of evaporation, heat of combustion, heat of formation and, last but not least, all the important thermodynamic functions for the gaseous state at a fugacity of one atmosphere. The substances listed include paraffins, olefines, acetylenes, alkyl benzenes, alkyl cyclopentanes, alkyl cyclohexanes ; also in the case of the thermodynamic functions oxygen, hydrogen, nitrogen, carbon, water, nitric oxide carbon monoxide and carbon dioxide.

The tables prepared have been and will continue to be issued in loose-leaf form monthly as compiled. The present volume is stated to be a complete collection of the tables issued between 1941 (actually since 1943) and 31st May, 1947. It is planned to publish a second volume at the end of the second 5-year period. The tables have been reproduced by a photographic process from typescript. As a result the type is not uniform, but in all other respects the appearance is good.

Needless to say the tables will be invaluable to all specialists on hydrocarbons. Those parts of the tables relating to the simpler compounds will also be of great value to a much wider class of research workers, especially those concerned with thermodynamics either classical or statistical. Even if at a later date some of the values require to be modified it is a tremendous advantage to have collected together a self-consistent set of values compiled systematically by one group of experts. The reviewer has already made considerable use of some of the tables.

The reviewer's only criticisms relate to details of presentation. The following are samples.

(*a*) The description " compound, monatomic, oxygen " seems a contradiction in terms.

(*b*) There are 17 tables of a quantity denoted by S°. The only indication of the definition of S° is in every case but one a reference to a footnote of another table, where we are told that S° is the entropy (exclusive of nuclear spin) of the given substance in the thermodynamic standard gaseous state of unit fugacity (1 atmosphere). This is an inaccurate definition. Instead of " exclusive of nuclear spin " one should say " exclusive of all nuclear contributions and of contributions from isotopic mixing." A much better description would be " taking as zero the entropy at the absolute zero of the crystal in which all molecules are orientated in a regular manner." In any case it is misleading to include, as is done, a column stating that at 0° K. the entropy of the *gas* at unit fugacity is zero.

(*c*) Since the heat of formation of an element at 25° C. is by definition zero, it is curious that for the heats of formation of oxygen, hydrogen and nitrogen at this temperature a reference is given to Wagman, Kilpatrick, Taylor, Pitzer and Rossini.

(*d*) In the tables for equilibrium constants of formation the definition given of these constants is not merely ambiguous, but nonsensical. It is only by indirect inference that one is able to find out that the equilibrium constant of formation of for example, H_2O is $p_{H_2O}/p_{H_2}\,p_{O_2}^{\frac{1}{2}}$ measured in atm.$^{-\frac{1}{2}}$, not the square of this quantity.

(*e*) There is already enough confusion in the naming of the thermodynamic functions. The compilers of these tables make confusion worse confounded by, for example, using the name " heat content function " to denote " heat content divided by temperature " and likewise " free energy function " to denote " free energy divided by temperature." Incidentally one looks in vain for any definition of the thermodynamic functions. The name free energy is used in the sense of G. N. Lewis, not of Helmholtz.

All these small defects in the presentation suggest that the actual preparation of the tables may have been left too much in the hands of mere computers rather than experienced physical chemists. However, once the user has found out the meaning of each quantity tabulated, the usefulness of the tables is nowise diminished by such minor blemishes.

The chosen unit of energy is the " thermodynamic calorie " defined as 4·1833 int. joule. The reviewer is one of many who would have preferred the choice of the joule. Alternatively it would seem preferable to tabulate molar energies divided by the gas constant R, the quotient expressed in degrees; and molar entropies divided by R the quotient being a pure number.

E. A. G.

A Text Book of Practical Organic Chemistry. BY ARTHUR I. VOGEL.
(London: Longmans, Green & Co. Ltd.) Pp. 1012. Price 42s.

Since there are already several excellent text-books on practical organic chemistry a newcomer to this field must either attain an exceptional standard of excellence, or present the subject from a new angle, in order that its publication in the present critical times can be justified. In many respects Dr. Vogel's book satisfies both these exacting requirements. In the first place it is exceptionally complete and in the second it is remarkably up to date and possesses a number of novel features not found in its contemporaries. The book is written, in the main, at the undergraduate level and amply covers all examination requirements. Indeed, it will be an unusual student who will find time to read the book from cover to cover or to accomplish more than a small proportion of the listed preparations.

The first chapter provides an elementary theoretical introduction to the subject, whilst the second deals, very fully, with experimental technique. The three succeeding chapters give details of the preparation and reactions of aliphatic, aromatic, and heterocyclic and alicyclic compounds respectively. The sixth chapter deals with a number of preparations and techniques including reactions under pressure, use of Raney nickel and copper chromite catalysts. ozonolysis, dehydrogenation, the Diels-Alder reaction and chromatography, not usually found in an undergraduate course. The four chapters which follow this possess several novel features. Chapter seven describes the preparation of organic reagents used in inorganic and organic chemistry, chapter eight gives examples of dyestuffs and indicators, chapter nine deals with synthetic compounds which show physiological activity including, for example, sulphaguanidine and D.D.T., whilst chapter ten illustrates the preparation of synthetic polymers. Chapter eleven furnishes an account of qualitative organic analysis and there is a large number of excellent and very complete tables of the physical properties of organic compounds and their derivatives scattered throughout the book. Finally, there is an appendix which provides the student with an introduction to the voluminous organic literature. A point of special interest is the frequent reference to firms which provide the apparatus illustrated in the book.

In spite of the many valuable features included in this work, some of which have been mentioned above, it is doubtful whether it will find complete favour with research workers, principally because of the total absence of references to the original literature. The author's style is, moreover, somewhat verbose and the book could probably have been condensed to three-quarters of its present length without any loss in clarity. As is to be expected in a first edition there are some small errors, which will doubtless be corrected in due course. The book does *not* treat the subject of quantitative organic analysis.

D. H. R. B.

Fundamental Principles and Applications of Induction Heating. By "HEAT-TREATER". (London: Chapman & Hall.) Pp. 147. Price 10s. 6d. net.

The title of this book is liable to be misleading to a scientific reader, for it contains very little about the fundamental principles of the subject. On the scientific side it is both rudimentary and sketchy, and it is probably intended for the man in the works rather than the man in the laboratory. The whole thing suggests a scissors and paste construction of material derived almost exclusively from American technical journals. In this respect it may give the impression that British practice is more backward than it really is, but it does give a reasonably good idea of the equipment that is commercially available in Britain as well as in America, and of the kind of production job in which it can be used to the best advantage.

L. H.

ON THE DEGRADATION OF LONG-CHAIN MOLECULES. PART II.

By H. H. G. Jellinek.

Received 28th November, 1944; as finally revised 17th March, 1947.

In Part I[1] we dealt with the degradation of chains having randomly distributed weak links. It was assumed that only the weak links were broken, the rupture of normal links being negligible. The present paper deals with degradation of chains, in which the normal as well as the weak links break, each with its own rate constant. We consider a homogeneous polymer of initial chain length P_0. Each chain has the same number, m, of weak links distributed at random over each chain. Weak and normal links are broken at the same time and the rate constants for the degradation of the weak and normal links have a definite ratio K/K'.

Distribution Functions.—It is convenient to calculate the weight distribution function instead of the number distribution. We can divide the process of degradation into two parts. Firstly, only weak links are broken, say s_1 weak links on the average per original chain. By this process a definite distribution is obtained, which is given by eqn. (2) of Part I. The resulting polymeric material having this definite distribution can now continue degradation by breaking, say s_2 normal links on the average per original chain. In reality these two processes occur simultaneously, but it is convenient to consider these two processes as successive.

By breaking the s_1 weak links per original chain, one obtains a certain distribution; e.g. one gets chains of length P from this degraded material by breaking s_2 normal links on the average per original chain. We can calculate the amount of P-chains obtained from P'-chains ($P' > P$) as follows. The weight distribution function or the amount in grams of P-chains obtained from 1 g. P'-chains is given by

$$m_P^{\mathrm{II}} = P\alpha''^2(1-\alpha'')^P\left(1+\frac{2}{\alpha''P'}-\frac{P}{P'}\right)$$

(see Schulz, Simha, etc., for reference, cp. Part I), where α'' is the degree of depolymerisation given by s_2/P_0, or more precisely $\frac{s_2}{P_0 - m}$ (i.e. the probability of breaking one normal link in the original chain). Since there are only $m_{P'}^{\mathrm{I}}$ g. ($m_{P'}^{\mathrm{I}}$ is given by the weight distribution function derived in Part I) of P'-chains present, the amount of P-chains actually obtained is given by the product $m_P^{\mathrm{II}} \times m_{P'}^{\mathrm{I}}$. Since all chains bigger than P yield P-chains during degradation, one has to sum from $P + 1$ to $P_0 - 1$. For large values of P_0 all summations can be dealt with by integration. Further, a certain amount of P-chains is already present and a definite portion of them will degrade. The amount left is then given by $m_P^{\mathrm{I}}(1-\alpha'')^P$. Lastly, there is some undegraded material left, of which a certain part will be degraded by rupturing normal links, so that the whole weight distribution function starting with 1 g. of chains of length P_0 reads as follows ($m < 6$, cp. Part I).

$$m_{P_0, s_1, s_2, m} = \left(\frac{m - s_1}{m}\right)^m\left(1 - \frac{s_2}{P_0}\right)^{P_0}$$

---

[1] Jellinek, *Trans. Faraday Soc.*, 1944, 40, 266.

$$
\begin{aligned}
m_{P,s_1,s_2,m} &= \frac{P\,.\,s_2^2}{P_0^2}\left(1-\frac{s_2}{P_0}\right)^P\left(1-\frac{P}{P_0}+\frac{2}{s_2}\right)\left(\frac{m-s_1}{m}\right)^m+\frac{Ps_2^2}{P_0^2}\\
&\times\left(1-\frac{s_2}{P_0}\right)^P\int_{P'=P}^{P_0}\left\{\left(1-\frac{P}{P'}+\frac{2P_0}{s_2P'}\right)\frac{P'}{P_0}\sum_{a=1}^{a=m}\binom{m}{a}\left(\frac{s_1}{m}\right)^a\left(\frac{m-s_1}{m}\right)^{m-a}\frac{a(a+1)}{P_0}\right.\\
&\left.\times\left(1-\frac{P'}{P_0}\right)^{a-1}\right\}dP'+\left(1-\frac{s_2}{P_0}\right)^P\frac{P}{P_0}\sum_{a=1}^{a=m}\binom{m}{a}\left(\frac{s_1}{m}\right)^a\left(\frac{m-s_1}{m}\right)^{m-a}\frac{a(a+1)}{P_0}\\
&\times\left(1-\frac{P}{P_0}\right)^{a-1}.
\end{aligned}
$$

Evaluation yields :

$$
\left.
\begin{aligned}
m_{P_0,s_1,s_2,m} &= \left(\frac{m-s_1}{m}\right)^m\left(1-\frac{s_2}{P_0}\right)^{P_0}\\
m_{P,s_1,s_2,m} &= \frac{Ps_2^2}{P_0^2}\left(1-\frac{s_2}{P_0}\right)^P\left\{\sum_{a=0}^{a=m}\frac{1}{P_0^{a+1}}\binom{m}{a}\left(\frac{s_1}{m}\right)^a\left(\frac{m-s_1}{m}\right)^{m-a}\right.\\
&\left.(P_0-P)^a\left[\frac{2P_0}{s_2}(a+1)+P_0-P\right]\right\}+\left(1-\frac{s_2}{P_0}\right)^P\frac{P}{P_0}\sum_{a=0}^{a=m}\binom{m}{a}\left(\frac{s_1}{m}\right)^a\\
&\times\left(\frac{m-s_1}{m}\right)^{m-a}\frac{a(a+1)}{P_0}\left(1-\frac{P}{P_0}\right)^{a-1}.
\end{aligned}
\right\}\qquad(1)
$$

The number distribution function is obtained by dividing by P or P_0 respectively.

Average Chain-length.—The number average chain-length is, as always, given by

$$P_n=\frac{P_0}{1+s_1+s_2}=\frac{P_0}{\beta}$$

where β is the number of fragments into which, on the average, each chain degrades.

The weight average chain-length is obtained by putting the weight distribution function into the general expression for the weight average chain-length :

$$P_w=\frac{\displaystyle\int_0^{P_0}m_{P,s_1,s_2,m}\,.\,P.dP}{\displaystyle\int_0^{P_0}m_{P,s_1,s_2,m}\,.\,dP}.$$

Evaluation leads to an expression for the weight average chain-length as follows where $(1-\alpha'')^P$ is taken $= e^{-\alpha''P}$:

$$
\left.
\begin{aligned}
\frac{P_w}{P_0}=2\Bigg\{&\left(\frac{m-s_1}{m}\right)^m\left[\frac{1}{s_2}-\frac{1}{s_2^2}(1-e^{-s_2})\right]+\binom{m}{1}\left(\frac{s_1}{m}\right)\left(\frac{m-s_1}{m}\right)^{m-1}.\,2!\left[\frac{1}{2!s_2}-\frac{1}{s_2^2}\right.\\
&\left.+\frac{1}{s_2^3}(1-e^{-s_2})\right]+\binom{m}{2}\left(\frac{s_1}{m}\right)^2\left(\frac{m-s_1}{m}\right)^{m-2}.\,3!\left[\frac{1}{3!s_2}-\frac{1}{2!s_2^2}+\frac{1}{s_2^3}-\frac{1}{s_2^4}(1-e^{-s_2})\right]\\
&\ldots+\left(\frac{s_1}{m}\right)^m(m+1)!\left[\frac{1}{m+1)!s_2}\right)-\frac{1}{m!s_2^2}+\frac{1}{(m-1)!s_2^3}\cdots\pm\frac{1}{s_2^{m+1}}\mp\frac{1}{s_2^{m+2}}\\
&\times(1-e^{-s_2})\Bigg]\Bigg\}.
\end{aligned}
\right)
$$

We can also obtain the weight average chain-length by approximate integration using Simpson's rule, which may in some cases be more convenient ; one proceeds as follows, taking, for instance, $\Delta P = 100$:

$$\int_0^{P_0} m_{P_0, s_1, s_2, m} P \cdot \mathrm{d}P \cong \tfrac{1}{3}\Delta P\{(m_{P_1} + m_{P_n} P_n)$$
$$+ 4[m_{P_{100}} \cdot 100 + m_{P_{300}} \cdot 300 + \ldots m_{P_{n-100}} \cdot (P_n - 100)]$$
$$+ 2[m_{P_{200}} \cdot 200 + m_{P_{400}} \cdot 400 + \ldots m_{P_{n-200}} \cdot (P_n - 200)].$$

In order to illustrate the above discussion a special case may be considered. The initial chain-length may be 1000, each chain having 5 weak links and the ratio of the rate constants for the weak and normal links may be $K/K' = 1000$. First one has to calculate corresponding average breaks per chain s_1 and s_2 for weak and normal links. These are obtained as follows (compare Part I) :

$$\frac{s_2}{P_0} = K't \text{ and } -\ln\left(1 - \frac{s_1}{m}\right) = K \cdot t.$$

By dividing these equations, one obtains the corresponding s_1 and s_2

$$-\frac{s_2}{P_0 \ln\left(1 - \frac{s_1}{m}\right)} = \frac{K'}{K} = \frac{1}{1000},$$

s_1 and s_2 are then inserted in the relevant distribution functions.

Fig. 1 shows the inhomogeneity U (cp. Part I) as dependent on the average total number of breaks per original chain for $m = 5$ and $K/K' = 1000$. The cases $m = 0$ and $m = 5$ (weak links only breaking) are indicated.

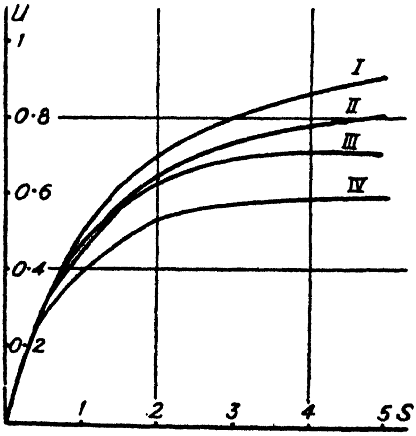

FIG. 1.—Dependence of inhomogeneity on number of average breaks per chain.

I. $m = 0$; $\gamma = 1$.

II. $m = 5$; $\gamma = 1$; weak and normal links breaking, $s = s_1 + s_2$, $K/K' = 10^3$.

III. $m = 5$; $\gamma = 1$; only weak links breaking.

IV. $m = 5$; $\gamma = 0{\cdot}6$; only weak links breaking.

It is important to note that the weight average chain-lengths in Part I and in this paper are calculated on the assumption that Staudinger's viscosity rule holds. This has, of course, to be tested experimentally in each individual case. For example Mark[3] and co-workers found that for polystyrene samples a relationship of the type $\lim_{c \to 0} \eta_{sp}/c = K \cdot P^\gamma$ holds, one has therefore in this case to evaluate the weight average chain-length according to the general formula

$$\left[\frac{\int_0^{P_0} m_P \cdot P^\gamma \cdot \mathrm{d}P}{\int_0^{P_0} m_P \cdot \mathrm{d}P}\right]^{1/\gamma}$$

---

[3] Mark, Alfrey and Bartovics, *J. Amer. Chem. Soc.*, 1943, 65, 2319.

which are such that regular (two-dimensionally crystalline) sheets are superposed without any regularity (except for a constant separation) and are held together by relatively weak forces.

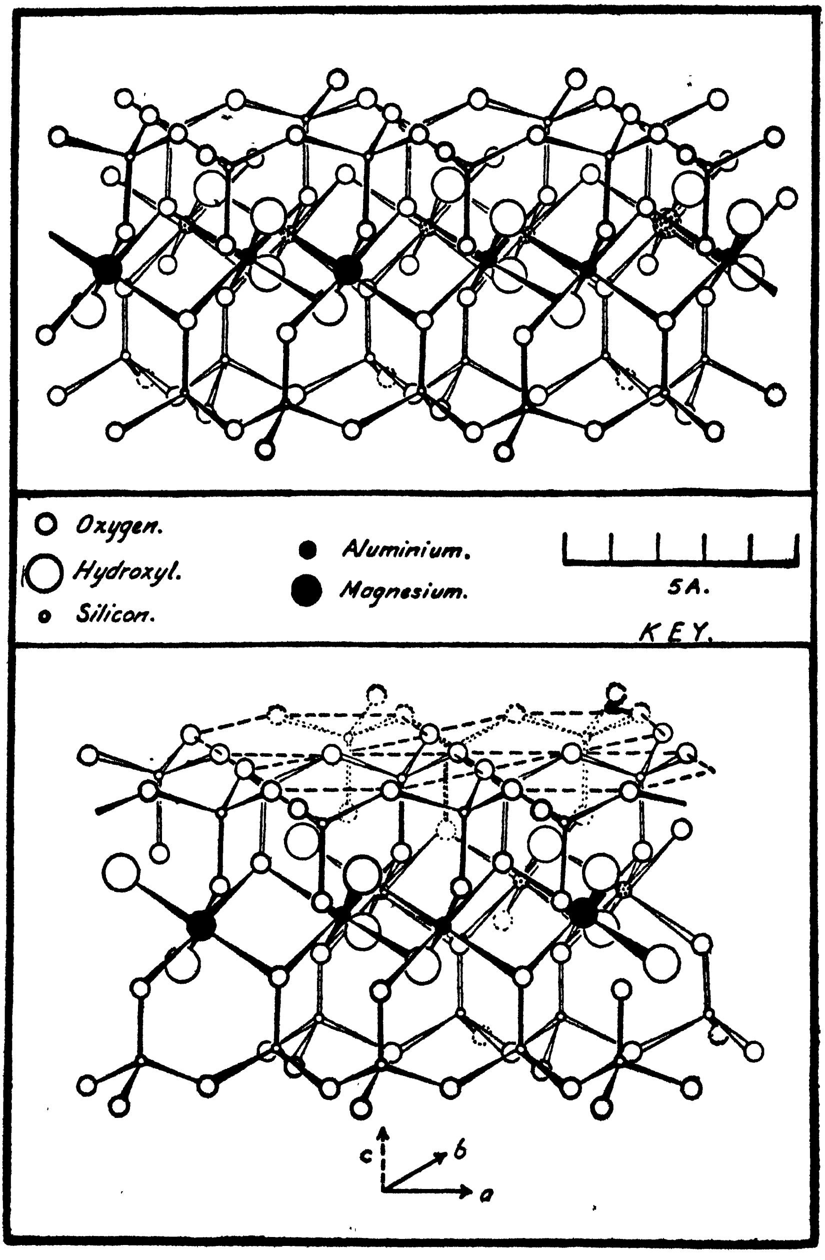

FIG. 1.—(*a*) The montmorillonite structure.

The structures which have been accepted as a basis for the interpretation of the results reported here are, for montmorillonite, the Hofmann-Endell-

Wilm-Maegdefrau structure[1] modified by the incorporation of Hendricks'[2] ideas about isomorphous replacement, and for halloysite the Hendricks-Brindley-Robinson-MacEwan[3] structure. These structures are shown in Fig. 1 (*a*) and (*b*).

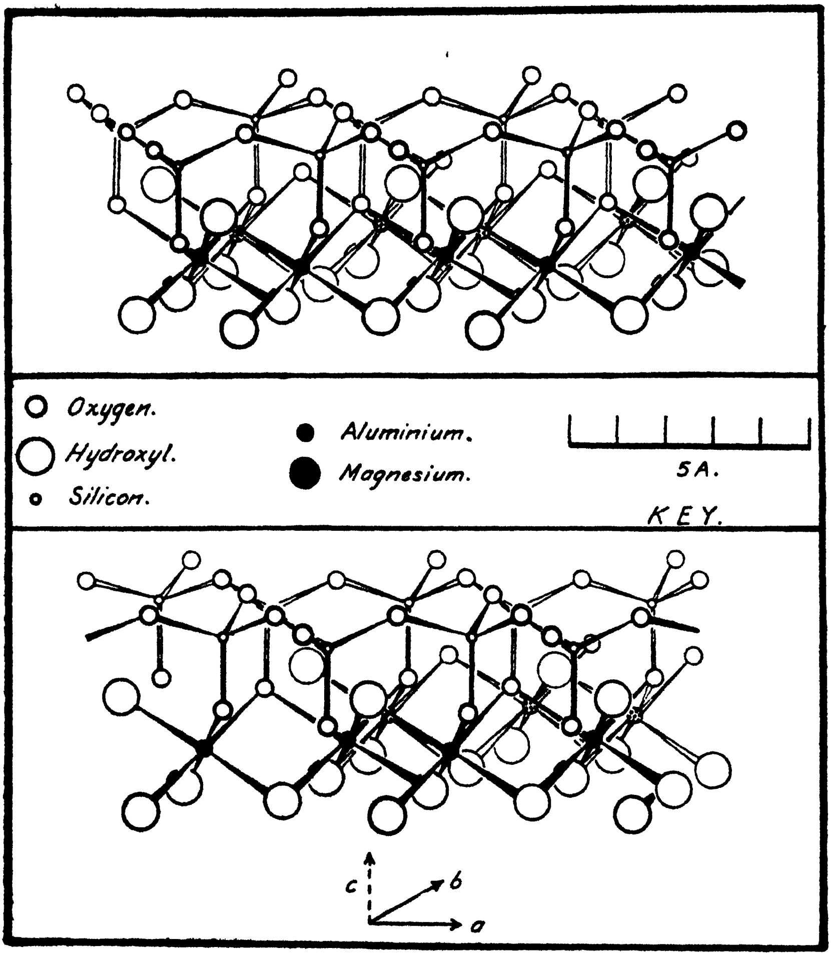

Fig. 1.—(*b*) The halloysite structures.

Two structural sheets irregularly superposed are shown.

The magnesium content of montmorillonite is from 1 to 2/3 Mg^{++} per unit cell (containing 4 six-co-ordinated ions), so the replacement rate shown here (Mg^{++} in 5 octahedral positions out of 18) is rather higher than the average.

In both structures, the octahedral positions are shown occupied in a regular way, as in pyrophillite. The actual arrangement may be less regular.

In the lower montmorillonite sheet, some of the rings of six oxygen ions are indicated by means of dotted lines (one side of each hexagon has been omitted to avoid confusion). Each ring has a hole in the centre, beneath which is an OH$^-$ ion (see Fig. 4).

---

[1] Hofmann, Endell and Wilm, *Z. Krist.*, 1933, **86**, 340; Maegdefrau and Hoffmann, *ibid.*, 1938, **98**, 299.

[2] Hendricks, *J. Geol.*, 1942, **50**, 276; cp. also Ross and Hendricks, *U.S. Geol. Survey*, 1945, No. 205-*B*.

[3] Hendricks, *Amer. Miner.*, 1938, **23**, 295; Brindley, Robinson and MacEwan *Nature*, 1946, **157**, 225.

In absorptive reactions with these minerals, molecules can penetrate between the structural sheets, thus expanding the whole crystallite structure, a change which can be followed on an X-ray powder diagram. X-ray diagrams of these materials show two separate series of lines (or bands), one due to the "two-dimensional crystallites" (indices (*hkl*), the other a single series of orders, indexed (oo*l*), due to the intersheet separation. Only the latter series changes in adsorption reactions, and from it the (oo*l*) spacing, and thus the separation of the structural sheets may readily be deduced. Hendricks[4] has pointed out that valuable information about the configuration of adsorbed molecules may be deduced from such data for montmorillonite complexes with organic cations, which may replace the mobile intersheet-cations present in natural montmorillonite. He used organic substances in water solution, in accordance with the usual base-exchange technique and found evidence for structures with one and two layers of organic groupings between the structural sheets.

The work described here is concerned with a different type of adsorption complex, in which the adsorbed molecules are not appreciably ionised. The technique used is different from Hendricks', as adsorption of the pure liquids is studied, and water is, as far as possible, eliminated. Adsorbed molecules in this type of complex are playing essentially the same role as water in the "hydrates" of montmorillonite,[5] and hydrated halloysite. This type of adsorption complex with montmorillonite has also been studied independently by Bradley.[6] In this paper attention is particularly drawn to the importance of the information on adsorption forces given by the halloysite complexes, especially in conjunction with those of montmorillonite.

Experimental.

Formation of Complex.—The montmorillonite complexes can be formed by bringing the air-dry montmorillonite into contact with the complex-forming liquid (cp. formation of complexes in some earlier experiments with the polyhydric alcohols). An oriented aggregate[7] was used as the specimen for X-ray photography; this was moistened with the liquid, and the exposure made while the montmorillonite was kept moistened with the liquid, as follows. The mineral, together with an excess of liquid, was loaded into a thin-walled soda glass capillary tube (about ½ mm. diam.) which was then sealed off in the flame at each end about 1 cm. from the specimen. With copper radiation this gave noticeable diffraction, but not enough to interfere with the measurement of the montmorillonite lines. In loading the tubes, a small mound of montmorillonite, covered with liquid, was placed on a watch glass. The tube, cut square at the end, was dabbed on to this until enough montmorillonite had collected in it; this was then pushed to the centre of the tube, excess liquid displaced from the tube and the sealing done.

With the type of complex discussed here in which adsorbed molecules are playing the same role as water in hydrated montmorillonite, all trace of water should be removed. Analyses of glycol complexes as is shown below, may well contain a mixture of water and organic liquid, and the quantities of the two are related. In order to ensure the elimination of water, the montmorillonite was covered with a large excess of liquid in a test tube and this was then boiled until about half its volume remained. The contents were then poured on to a watch-glass, and the specimen-tube loaded immediately. For some of the lower-boiling liquids the montmorillonite was dehydrated at 100° *in vacuo* over cold P_2O_5, and the liquid then run over it without breaking the vacuum.

Halloysite Complexes.—The halloysite complexes present a special problem because of the irreversible nature of the dehydration of hydrated halloysite. Halloysite from which the intersheet water has been removed (metahalloysite) even at low temperature, will not readsorb water, nor in general organic liquids.

---

[4] Hendricks, *J. Physic. Chem.*, 1941, **45**, 65.
[5] Bradley, Grim and Clark, *Z. Krist.*, 1937, **97**, 216.
[6] Bradley, *J. Amer. Chem. Soc.*, 1945, **67**, 975.
[7] Nagelschmidt, *J. Sci. Instr.*, 1941, **18**, 100.

An exception is ethylene glycol [8] which may be adsorbed incompletely by metahalloysite. In forming halloysite complexes, it is therefore essential to start with an existing complex (including in this term hydrated halloysite) and displace the intersheet molecules by others, avoiding the formation of metahalloysite.

In general, natural hydrated halloysite was used as the starting material. It was covered with a large excess of the complex-forming liquid, and left for about an hour, with frequent shaking, but without heating, except in a few cases where it was heated to 100° C.

X-Ray Photography.

A 9 cm. diam. powder camera of the type already described was used, with filtered CuK radiation and the camera was evacuated during exposure. Spacings up to 30 A. could be recorded with ease, the limit being about 35 A. Rotation of the specimens during exposure was not necessary and was seldom used. The photographs were measured visually; comparison with results obtained using a microphotometer showed this to give quite accurate results. Only the first order of the basal spacing was measured though occasionally when higher orders were visible they were measured and the mean value of $d(001)$ taken (the difference in the values never being more than a few tenths of an A.).

Materials.—Two different samples of montmorillonite were used. With alcohols, the fraction between about 0·1 and 0·05 (effective spherical diam.) of a commercial Wyoming bentonite, artificially ammonium-saturated during fractionation was used. It gave an X-ray diagram, showing only montmorillonite lines. For most of the other work, a very pure Ca^{++}-saturated montmorillonite described by Mackenzie,* was employed. With some liquids both the Ca^{++}- and NH$_4^+$-montmorillonites were tried as adsorbents. No important difference in the spacings obtained was found.

The halloysite used was a natural hydrated form from Hungary, and was kindly given by Dr. Lea, of the Building Research Station, Watford, who also supplied the following analysis, which shows it to be extremely pure: SIO$_2$, 40·3 %; Al$_2$O$_3$, 34 %; Fe$_2$O$_3$, 0·16 %; TiO$_2$, 0·00 %; CaO, 0·05 %; MgO, 0·14 %; loss on ignition, 25·3 %; total 99·95 %. The X-ray diagram also shows no extraneous lines: it was therefore used as a standard.

The organic chemicals used were Analar or pure laboratory grade. The ethylene glycol, diethylene glycol and ethanediamine were purified by redistillation before use.

Results and General Interpretation.

"**Δ-values.**"—The results are conveniently given, not in terms of the (001), spacing (which includes the space occupied by the sheets of the mineral itself), but of Δ, the "clearance space"; this is more or less equivalent to the space available for the adsorbed molecules between the structural sheets and is derived from measurements of the "basal spacing" $d_{(001)}$, in the following way. From $d_{(001)}$, we can determine the perpendicular distance between the planes containing the centres of the superficial oxygen atoms or OH groups in neighbouring surfaces of any two successive sheets. The quantity Δ is taken as this distance less twice the van der Waals radius of oxygen, according to Pauling [10] (cp. Fig. 2). It is the width of the space available for adsorbed molecules between the sheets, on the assumption that van der Waals binding is operative, and that the molecules do not pack down appreciably into the hollows of the surfaces. No deep hollows are left between neighbouring atoms or groups of the same layer, but there exist "holes" on both sides of the montmorillonite sheets, and on one side of the halloysite sheets, corresponding to the spaces where the K$^+$ ions fit in the analogous mica structures (vide Fig. 2; and Fig. 1 for structural detail).

In calculating Δ, the thickness of the montmorillonite sheets (measured perpendicularly, from one plane of oxygen ions to the other) was taken as 6·6 A., which is close to the value for muscovite [11] and rather larger than that for pyrophyllite [12] and the thickness of the halloysite sheets (O$^=$ ion plane to OH$^-$ plane) was taken as 4·4 A., which agrees with Gruner's kaolinite value. Adding twice the van der Waals radius of O to these values, we get 9·4 and 7·2 A. respectively as the quantities which must be subtracted from the measured values of $d(001)$ to give Δ.

---

[8] MacEwan, *Nature*, 1946, **157**, 159.

[9] MacEwan, *J. Soc. Chem. Ind.*, 1946, **65**, 298.

[10] Pauling, *The Nature of the Chemical Bond* (Cornell University Press).

[11] Jackson and West, *Z. Krist.*, 1930, **76**, 211.

[12] Gruner, *ibid.*, 1934, **88**, 412; *Strukturbericht*, III, p. 159.

* Mackenzie, *Trans. Faraday Soc.*, 1948, **44**, 368.

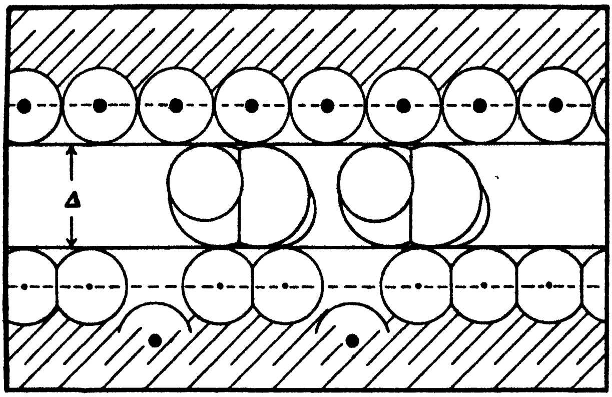

Fig. 2.—A schematic section through the halloysite structure, showing the significance of the quantity Δ. The upper layer of ions are the OH^- groups of one sheet, the lower layer are the $O^=$ ions of the next. Two glycol molecules are shown in the intersheet space. The lower $O^=$ layer has two holes, below which OH^- ions are shown at the correct depth. This arrangement is merely diagrammatic. Any *line* of $O^=$ ions on the surface of the halloysite sheets will either show no gap at all, or a gap in every alternate position (see Fig. 4). For montmorillonite, *both* surface layers would be like the lower one shown here.

Monohydric Alcohols.—The difference in properties of montmorillonite and halloysite as adsorbents is illustrated by their reactions with the monohydric alcohols. The results for the straight-chain alcohols are shown in Table I and Fig. 3, relating Δ with the number of C atoms in the alcohol molecule. No complex is formed with halloysite by alcohols higher than ethyl, since $\Delta \sim 0$. Since the starting material was hydrated halloysite in each case, this result

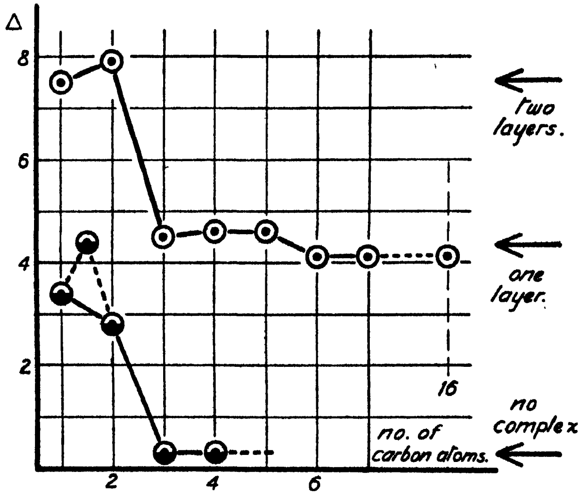

Fig. 3.—Values of Δ for the straight-chain monohydric alcohols, plotted against the number of carbon atoms in the chain. The white circles refer to montmorilonite complexes, the black and white circles to halloysite. The point at ordinate 1½ corresponds to 1 : 3-propanediol (1½ C atoms per OH group).

shows that not only is no complex formed but the existing intersheet water is extracted by the alcohol. The value of $d_{(001)}$ for the samples treated with 1-propanol and 1-butanol is larger than $d(001)$ for heat-treated metahalloysite, or kaolinite, and the basal reflection is rather diffuse. This may indicate that there are some residual adsorbed water molecules, or alcohol molecules.

In the case of methanol and ethanol, complexes are formed, as shown by the relatively high value of Δ. The $d_{(001)}$ values, however, are not very different from that of the original hydrated halloysite, i.e. 10·0 A. (owing to the irreversible nature of the dehydration process with halloysite, all complexes must be formed with hydrated halloysite—or another complex—as a starting material) so that the conclusion may appear unjustifiable. It was impossible to verify this by an analysis of the amounts of water and alcohol present since only a very limited quantity of halloysite was available. Their existence, however, is supported by the following arguments.

(1) With the methanol complex, at least the $d(_{001})$ value differs by an amount in excess of the experimental error: in the case of some other complexes (see below) the difference is much greater.

(2) 1-propanol and 1-butanol have a marked dehydrating effect on the hydrated halloysite. The dehydrating effect of methanol and ethanol must be even stronger; it is inconceivable that unaltered hydrated halloysite will remain after treatment with methanol or ethanol.

The van der Waals diameter of the CH_3-group in methanol should be[10] about 4·0 A. Actually the Δ-value for methanol is considerably lower, 3·4 A. Thus the contact between the CH_3-group in methanol and the neighbouring oxygen atoms of the halloysite sheets cannot be determined purely by van der Waals forces; an extra binding force must be operative. Its existence between CH_2- or CH_3-groups linked directly to O, and silicate oxygens has already been postulated by Bradley on the basis of one-dimensional Fourier syntheses of montmorillonite complexes, and, with little doubt, his assumption of a hydrogen bond between the C and the neighbouring oxygens is essentially correct. The C—O bond in methanol is appreciably polarised, leaving the C with a deficiency of electrons; the H atoms will therefore be left positively charged, and be atracted by the negative oxygen ions of the halloysite sheets. The alcoholic oxygen may also form hydrogen bonds either (*a*) with OH groups belonging to other alcohol molecules, or (*b*) with O^- ions and OH groups belonging to the halloysite sheets. There might also be binding between the C and the OH groups of the halloysite sheets.

The complex with ethanol should show a larger Δ-value than that with methanol, since it has a CH_3 group not linked directly to O, which therefore should be little affected by the C—O bond. The low result found is due to incomplete adsorption, as is indicated by the diffuseness of the basal spacing and occasional appearance of a line in the neighbourhood of 7 A. Similar results have been found with certain other halloysite complexes (see also Fig. 3).

With 1-propanol, and all the higher alcohols, a structure is formed in which a monomolecular layer of the alcohol goes between the montmorillonite sheets (cp. Fig. 3). The value of Δ for these complexes is almost constant, and about equal to the van der Waals diameter of a CH_2- or CH_3-group.[10] This shows, not only that van der Waals binding is an effective agent in complex formation with these alcohols, but that the alkyl residues all lie as flat as possible between the montmorillonite sheets, as is clearly brought out by the results for branched-chain and cyclic alcohols. 4-Heptanol and 2-ethyl-1-butanol show results of the same order of magnitude as those for the straight-chain alcohols. *Tert.*-amyl alcohol, and cyclohexanol, on the other hand show a markedly higher value of Δ. Clearly a secondary alcohol, or an alcohol with only one branch in the chain, can lie flat so as to take up no more room, in a direction perpendicular to its plane, than a straight-chain alcohol. A tertiary alcohol, or six-ring cyclic alcohol, on the other hand, cannot do this without severe distortion of valency angles. The fact that about the same value of Δ is obtained for cyclohexanol as for a tertiary alcohol incidentally shows that in the cyclohexanol molecule the valency angles are *not* appreciably distorted, i.e., the molecule has a puckered, and not a flat form.[14]

---

[13] Gruner, *Z. Krist.*, 1932, **83**, 75. The recent kaolinite determination of Brindley and Robinson (*Miner. Mag.*, 1946, **27**, 242), which has appeared since this paper was completed, would give 4·3 A.

[14] Hassel and Kringstad, *Tids. Kjemi Bergv.*, 1930, **10**, 128; Wierl, *Ann. Physik.*, 1931, **8**, 521.

TABLE I.—VALUES OF Δ IN A. FOR MONTMORILLONITE AND HALLOYSITE COMPLEXES.

Complex Forming Substance.	Complex with								
	Montmorillonite.					Halloysite.			
	Method of Formation.	Δ obs.	Δ calc.	No. of Layers.	Base Saturation of Clay.	Method of Formation.	Δ obs.	Δ calc.	No. of
Normal monohydric alcohols									
Methanol	*a*	7·4	6·9	2	NH_4^+	*a*	3·4	—	1
	b	7·2	—	—	Ca^{++}	—	—	—	—
Ethanol	*a*	7·9*	8·1	2	NH_4^+	*a*	2·8*d*	—	1
1-Propanol	*b*	4·5	4·5	1	NH_4^+	*a*	0·3	—	0
1-Butanol	*b*	4·6	4·5	1	NH_4^+	*a*	0·3	—	0
1-Pentanol	*b*	4·6	4·5	1	NH_4^+	—	—	—	—
1-Hexanol	*b*	4·1	4·5	1	NH_4^+	—	—	—	—
1-Heptanol	*b*	4·1	4·5	1	NH_4^+	—	—	—	—
1-Hexadecanol	*k*	4·1*d*	4·5	1	NH_4^+	—	—	—	—
Other monohydric alcohols									
4-Heptanol	*b*	3·7	4·5	1	NH_4^+	—	—	—	—
2-Octanol	*b*	4·1*d*	4·5	1	Ca^{++}	—	—	—	—
2-Ethyl-1-butanol	*b*	4·2	4·5	1	NH_4^+	—	—	—	—
2-Methyl-2-butanol	*b*	5·4	5·4	1	NH_4^+	—	—	—	—
Cyclohexanol	*b*	5·6	5·5	1	NH_4^+	—	—	—	—
Polyhydric alcohols									
Ethylene glycol	*a*	7·6*	7·3	2	NH_4^+, Ca^{++}	*a, e*	3·7	—	1
1 : 3-Propanediol	*a*	8·6*	8·6	2	NH_4^+, Ca^{++}	*a, e*	4·4	4·5	1
1 : 3-Butanediol	—	—	—	—	—	*a*	4·0*d*	4·5	1
Glycerol	*a*	8·3*	8·3	2	NH_4^+, Ca^{++}	*a, e*	3·8	3·9	1

Alcohol ethers and ethers									
1 : 4-Dioxane	*a, b*	5·6*	5·9	1	Ca++	*a*	*d*	—	—
Methyl cellosolve . . .	—	—	—	—	—	*a*	3·5	—	1
Ethyl cellosolve . . .	—	—	—	—	—	*a*	3·6*d*	—	1
Butyl cellosolve . . .	—	—	—	—	—	*a*	3·1*d*	—	1
Diethylene glycol . . .	—	—	—	—	—	*a*	3·6	—	1
Triethylene glycol . . .	—	—	—	—	—	*a*	3·5	—	1
Hydrocarbons									
n-Hexane	*b*	1·2*d*	—	0	Ca++	—	—	—	—
n-Heptane	*b*	0·6	—	0	NH_4^+	—	—	—	—
Benzene	*b, c*	4·6*d**	—	2	NH_4^+	—	—	—	—
Naphthalene	*b*	3·5*d*	—	—	NH_4^+	—	—	—	—
Tetrahydronaphthalene . .	*b*	4·6*d*	—	2	NH_4^+	—	—	—	—
Decahydronaphthalene . .	*b*	0·6	—	0	NH_4^+	—	—	—	—
Other compounds									
Chlorethanol	*b*	8·0	7·8	2	NH_4^+	*a, e*	3·6	—	1
Ethanediamine	*b*	4·3*	4·4	1	Ca++	*a*	4·5	4·4	1
1 : 2-Propanediamine . .	—	—	—	—	—	*a*	*d*	—	—
Diethylamine	—	—	—	—	—	*a*	0·3	—	0
Acetone	*a, b*	8·2	8·1	2	Ca++	*a, f*	3·9	—	1
Acetaldehyde	—	—	—	—	—	*a*	3·6	—	1
Acetonitrile	*a, b*	10·2	10·6	3	Ca++	*a*	3·4	—	1
Nitromethane	*b*	10·4	10·5	3	Ca++	*a, g, h*	3·3	—	1
Nitrobenzene	*b*	5·7	—	2	NH_4^+	*i*	*d*	—	1

a = Treated with large excess of cold liquid.
b = Boiled down to half volume with excess of liquid.
c = Dehydrated at 100° over P_2O_5 *in vacuo*, then covered with liquid.
e = Covered with excess of liquid, and heated to 100° for 1-2 hr.
f, g, h, i = As *a*, starting from complex with ethanediamine (*f*), methyl cellosolve (*g*), methanol (*h*), or chlorethanol (*i*).
d = Diffuse, or double line.

* These complexes have already been mentioned by Bradley.[6]

In the case of ethanol and methanol, the Δ-values for the montmorillonite complexes are about twice those for the corresponding halloysite complexes, and for the montmorillonite complexes with the higher alcohols. This suggests that with these *two* monomolecular layers are formed between the montmorillonite sheets. Now the surfaces of the montmorillonite sheets are each formed by a layer of negative oxygen ions and thus behave rather like sheets with a uniform diffuse negative charge. Such sheets will have an orienting effect on polar molecules in their vicinity, the positive ends being attracted, and each sheet will therefore tend to collect a layer of such molecules on both its surfaces, so that between such sheets there will be *two* layers. In the case of non-polar molecules or groups, only the van der Waals force of attraction between them and the montmorillonite sheets need be considered. Since this force is non-directional, the question of orientation does not arise, and a single monomolecular layer may be held in common by two neighbouring montmorillonite sheets.

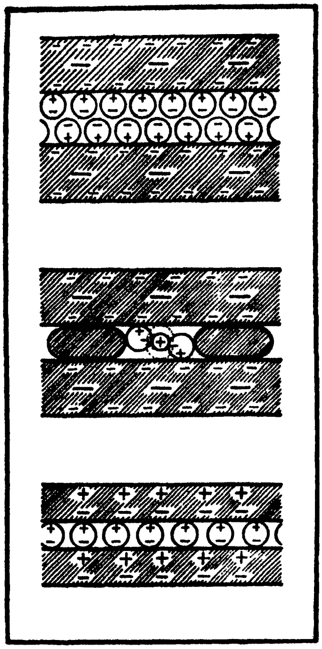

FIG. 4.—The processes of complex formation with montmorillonite and halloysite: (top) polar molecules (with montmorillonite), (middle) mainly non-polar molecules, with polar groups (with montmorillonite), (bottom) polar molecules (with halloysite). The specific role of hydrogen bond formation, which is important, has been neglected.

Thus markedly polar molecules would form a two-layer structure, and non-polar molecules a one-layer structure, as is found experimentally. Very strongly polar, highly associated liquids link on even more than two layers (e.g. acetonitrile and nitromethane). The energy involved in formation of extra layers is markedly different from that of the first layers, which are linked directly to the structural sheets of the mineral, therefore the alcohols give only the " minimum layer " structures. *Some* polar (or polarisable) groups appear to be necessary for adsorption, because saturated hydrocarbons do not form complexes (see below, and Table I). Presumably, therefore, as the hydrocarbon chain of a monohydric alcohol is made longer and longer, adsorption gradually diminishes. (Cetyl alcohol, the only alcohol above heptyl examined, shows definite adsorption.)

The necessity of polar groups for adsorption is no doubt bound up with the fact that the montmorillonite sheets are charged, and are held together by mobile positive ions in the spaces between the sheets. The energy of formation of a purely van der Waals adsorption-complex is presumably insufficient to lead to the break-up of the complex (charged sheet)-ion-(charged sheet). But if a few polar groups are present, these will tend to congregate about the charged spots on the sheets and about the positive ions. This will result in an effective increase of the radius of the ions, and a consequent diminution in electrical stress. The resulting structure may be more stable than the dehydrated montmorillonite structure, in which the " bare " cations occur between the structural sheets.

With halloysite, only highly polar molecules give complexes. Here the clay mineral sheets are themselves polar, so that there is no tendency for two layers to form with polar molecules. Fig. 4 illustrates schematically the various suggested processes of complex formation.

Polyhydric Alcohols.—The montmorillonite complexes with dihydric alcohol have been investigated by Bradley,[6] and for the monohydric alcohols he finds, in agreement with the present results, that two-layer complexes are formed with up to two carbon atoms per OH group, and single layer complexes with more.

With halloysite, single layer complexes were given by the four polyhydric alcohols used, and this is in conformity with the results for the monohydric alcohols, for they all have not more than two carbon atoms per OH group. Like ethanol, 1 : 3-butylene glycol is on the border line, and gives only an imperfect complex.

The big rise in Δ on going from ethylene glycol to 1 : 3 propanediol must be due to the extra space taken up by the central CH_2 group, which is not attached to oxygen. This dihydric alcohol has 1½ C atoms per OH group and in this respect it is intermediate between methanol and ethanol. It has been plotted in this position in Fig. 3 to show that there really is a rise from the methanol value, thus confirming that the low value for ethanol is spurious. A low value is similarly shown by 1 : 3-butanediol ; the (001) reflection is very diffuse.

The methods and results of the ethylene glycol complex are described by Mackenzie [*] but a short discussion of the relevant results is given here. The minimum amount of glycol needed in absence of water to produce a well-marked complex (i.e. with $d_{(001)} = 17{\cdot}1$ A., showing several successive orders) was 28·7 %, which corresponds to 3·3 molecules per unit cell. If glycol molecules lying flat (with both carbons and both oxygens in contact with the montmorillonite surface) are stacked as closely as possible in a monomolecular layer, there will be about 1·75 per unit cell of montmorillonite, i.e. about 3·5 per unit cell for the double layer, in close agreement with the experimental value for the minimum glycol content found by Mackenzie. The flat configuration for the glycol molecules is the one necessarily deduced from the Δ-values of the montmorillonite and halloysite complexes ; Mackenzie's results show that the whole " internal surface " of the montmorillonite crystallites is covered by a more-or-less close-packed layer of molecules. The number of molecules per unit cell does not approach an integral number but appears to be determined solely by the space required for each molecule.

Addition of extra glycol beyond the minimum necessary does not alter the complex but if some water is present, less glycol is necessary to form the complex, the water needed being proportional to the glycol deficiency in the molecular ratio of about 6 : 1. A complex with equal weights of water and glycol still showed the same regular structure and X-ray diagram (though the detailed intensities may have differed slightly) as a pure glycol complex, i.e. the glycol molecules set the pattern into which the water molecules fit. Bradley [6] has observed that characteristic complexes are formed by montmorillonite by adsorption of e.g. glycol and sucrose from water solution, and has suggested that the organic molecules are preferentially adsorbed. Our results, however, suggest that caution must be exercised in drawing this conclusion, since the complexes were unlikely to be free of water.

Maintaining the polyhydric alcohol complexes with halloysite (always kept covered with liquid) at 100° C. for 1-2 hr. was found to leave them completely unaffected. Water does not therefore appear to enter into the constitution of these complexes. Hydrated halloysite, however, loses its inter-sheet water, even when immersed in water, at 50° C., so the organic complexes evidently have a considerably higher temperature-range of stability. The extra stability of the ethylene-glycol-halloysite is also shown by the fact that metahalloysite, which will not change to hydrated halloysite on immersion in water, may give glycol-halloysite on immersion in glycol. The change, however, is seldom complete —generally, a residue of unaltered metahalloysite is left. This is true of naturally hydrated halloysite which has been dehydrated over P_2O_5 *in vacuo* at room temperature—in this case, the residue amounted to about 20 %. A Missouri halloysite, which was metahalloysite when received, gave a similar result. Dehydration at higher temperatures results, however, in a material which is less affected by glycol ; thus after heating natural hydrated halloysite to 75° for 12 hr., it was unaffected by glycol.

When halloysite is dehydrated at a low temperature, the resulting 7·2-7·5 A. reflection is diffuse, especially towards larger angles. It sharpens and moves outwards on heating to progressively higher temperatures,[15] and it is clear that at the same time the susceptibility to glycol treatment decreases. Apparently therefore, on initial low-temperature dehydration, the halloysite sheets are superposed in a non-regular fashion, and many of the O and OH ions in neighbouring sheets are too far apart to form effective hydrogen bonds. It may be also that some residual water molecules are present between some of the sheets. The glycol reaction is initiated at these " points of weakness," and goes on until complete in the region of these points. Heat treatment expels residual water,

[*] Mackenzie, *Trans. Faraday Soc.*, 1948, **44**, 368.

[15] Brindley, Robinson and MacEwan, *Nature*, 1946, **157**, 225. This observation was originally made by Brindley and Robinson.

and enables the sheets to move slightly over each other until hydrogen bonding between them becomes fully effective, thus eliminating the points of weakness.

Ethers.—Bradley[6] has pointed out that ethers and polyethers form complexes with montmorillonite of essentially the same nature as those formed by the polyhydric alcohols. The montmorillonite complexes mentioned are all of the two-layer type, so their (001) spacings did not allow any definite conclusions to be drawn as to the space requirements of their molecules. One-layer structures would be anticipated with halloysite. The polyethers used by Bradley were not available, but Table I shows results for 5 mixed ether-alcohols. The Δ-values for diethylene glycol, triethylene glycol and methyl cellosolve are essentially the same as for ethylene glycol, so that the ether linkage must have the same effect in complex formation as the alcohol linkage. This confirms Bradley's supposition of a C—H—O bond.

The Δ-values for ethyl and butyl cellosolve are certainly spuriously low due to incomplete adsorption. In fact, both show a reflection in the region of 7·5 A. as well as one in 10-11 A. region, indicating that the halloysite has been partly dehydrated. The fact that 1 : 3-propanediol which, like ethyl cellosolve, contains one C not linked to O gives a good complex suggests that the central CH_2 group in 1 : 3-propanediol may have a slight tendency to H bond formation, due to the influence of the two carbon atoms of enhanced electronegativity to which it is attached.

In 1 : 4 dioxane, all its C atoms are linked directly to O, consequently a good one-layer complex with halloysite and a two-layer complex wlth montmorillonite are expected. Actually, it does not give a true complex with halloysite although there is evidence of a tendency to be adsorbed (diffuse basal spacing) ; and the complex with montmorillonite has a Δ-value of 5·6 A., which is obviously too low for a double layer. Apparently this peculiarity must be connected with the cyclic structure of dioxane, which does not permit all the C atoms to come into the most favourable position for adsorption.

Amines.—A number of montmorillonite complexes with polyamines have been investigated by Bradley.[6] They all give a one-layer structure, with a Δ-value of about 4·3 A., i.e. about the same as for the high monohydric alcohols.

With halloysite, ethanediamine has been found here to give a good single-layer complex with a Δ-value of 4·5 A., about the same as for the montmorillonite complex. Diethylamine and 1 : 2-propane-diamine gave no definite complex. Thus, the CH_2 groups take up their full volume so there is no indication of C—H—O bond formation. The stability of the ethanediamine complex must be mainly due to N—H—O bonds. These results are linked with the much lower electronegativity of N, as compared with O. Diethylamine behaves differently from any of the alcohols in giving one-layer complexes both with montmorillonite and halloysite.

Halogenated Compounds.—2-Chlorethanol gives a halloysite complex with a Δ-value of 3·7, about the same as for ethylene glycol. This indicates that the C—Cl link has a marked effect in stabilising the complex. With montmorillonite, chlorethanol gives a two-layer structure as expected.

Two photographs of halloysite treated with bromethanol showed no trace of any 7·5 A. reflection. Probably this substance forms a complex, but the basal reflection may be diffuse, or masked by general scattering from the excess liquid.

Ketones, Aldehydes, Nitriles, Nitro-compounds.—The three simplest members of this group (excluding formaldehyde, which was not tried) all give halloysite complexes with Δ-values indicating an appreciable contraction of the C—H—O distance, the contraction being greatest for acetonitrile. This is particularly interesting because acetone, acetaldehyde and acetonitrile all contain CH_3 groups linked to C only, whereas the other substances giving low Δ-values contain only C atoms which are linked directly to a more electronegative element (compare the high Δ-value for trimethylene glycol, which contains a CH_2 group linked to C only). It appears as if the groups C=O and C=N must be regarded as being electronegative as a whole, and capable of withdrawing electrons from C atoms to which they are linked. This must be due to the high polarisation of these multiple links, giving $C^+{=}O^-$ and $C^+{\equiv}N^-$. The effects of the C≡N group is greater than that of C=O, and shows the influence of increasing multiplicity of the bond. Nitrogen is less electronegative than oxygen and this is apparent in the complexes formed by the analogous substances ethylene glycol and ethanediamine ; the C—H—O contraction is much greater for the former. Despite this, the triple-bonded nitrogen is more effective than the double-bonded oxygen in enhancing the electronegativity of an attached carbon. In contrast to the alcohols and ethers above, the C—O grouping can have only a small effect, if any, on the next C atom attached to it.

Nitromethane gives a very low Δ-value with halloysite, indicating tight bonding—compare the high value shown by ethanediamine which also contains C—N bonds. Here the influence of the partial double bonds to O in enhancing the electronegativity of the nitrogen is apparent.

With montmorillonite, acetone gives a two-layer complex; acetronitrile and nitromethane are exceptional in giving a very large spacing of about 20 A. (Δ = about 10·4). This probably corresponds to *three* layers (cp. below). It is noteworthy that the two substances which give three-layer complexes both have very high dipole moments, and are probably highly associated in the liquid state.

Hydrocarbons.—Bradley [6] has shown that benzene gives a two-layer complex with montmorillonite, in which the benzene molecules are closely bound to the montmorillonite sheets. This has been confirmed here, the complex-forming properties of a number of other hydrocarbons have been investigated. Benzene itself was found to give rather a diffuse basal spacing; on addition of a polar group (nitrobenzene), a substance is obtained which gives an excellent complex with several orders of the basal spacing. Naphthalene gives a complex, but shows signs of less complete adsorption than benzene.

Aliphatic hydrocarbons give no complex. Boiling in *n*-heptane resulted in the complete collapse of the basal spacing to 10 A. (the minimum observed in practice); boiling in *n*-hexane gave a very diffuse basal spacing varying from 11 to 12 A., evidently due to traces of adsorbed water, not completely removed by the treatment.

This result is in disagreement with Sedletskij and Jusupova [16] who suggested that aliphatic hydrocarbons are adsorbed by montmorillonite in such a way that the hydrocarbon chains are stretched between the montmorillonite sheets, thereby explaining the occurrence of high (001) spacings in montmorillonite samples found in the vicinity of natural oil, but apparently it was not confirmed by the use of pure hydrocarbons. Experiments with straight-chain alcohols here suggests that, even if complexes were formed with hydrocarbons, the chains would lie flat between the montmorillonite sheets, as they do in the alcohols. Sedletskij and Jusupova's observations may be due to adsorption of another component of the natural oils, and not of aliphatic hydrocarbons, or else that the mineral used was different from montmorillonite.

II. STRUCTURAL CONSIDERATIONS.

Interatomic Distances and Molecular Configuration.—Spacing measurements on the halloysite and montmorillonite complexes give no direct information on the location of the organic molecules. With regard to the single-layer complexes, if we assume that the carbon atoms are half-way between the structural sheets, we can calculate the distance between the plane in which they lie and the neighbouring plane of $O^{=}$ (or OH^{-}) ions. This assumption is justified for montmorillonite, where the sheets are identical on the two sides, and probably so for halloysite, on the grounds that: (*a*) to displace the C atom from the central position would shorten one of the C—O distances. They are already so short in some of the halloysite complexes that this seems ill-advised; (*b*) using the C—O distances deduced from halloysite complexes, a reasonable interpretation of the montmorillonite data is also obtained.

The quantities obtained in this way do not necessarily represent true C—O distances, since the carbons may not lie exactly above the oxygens to which they are linked, but may be displaced sideways. However, since the intersheet molecules are probably more or less irregularly disposed, it is likely that different molecules will be in different relative positions at any one time. If the molecules are able to move, the C—O distance deduced as above will be the " clearance distance " for this motion (see below). There can be no doubt that these distances have a comparative value.

Some CH—O distances deduced in this way are given in Table II. These cover nearly the whole range from the maximum possible CH—O distance (with H occupying its normal van der Waals' space) to a distance which is about equal to the sum of the C and O van der Waals' radii, i.e., in which the H appears to occupy no effective space. The gradual contraction of the CH—O distance on going up the table may be equated with increasing strength of hydrogen bonding. The strongest hydrogen bond therefore corresponds to an interatomic distance which is about equal to the sum of the van der Waals' radii of the participating atoms. This is in accord with other cases of hydrogen bonding.[10]

---

[16] Sedletskij and Jusupora, *Compt. rend., U.R.S.S.*, 1945, **46**, 27.

The van der Waals' radii used here are those given by Pauling[10] except for carbon and hydrogen. For carbon, the radius adopted is 1·7 A., which is half the C—C distance between molecules of crystalline hexamethylenetetramine. This is probably a particularly reliable value, since in this substance the H atoms are " staggered " so as to allow the closest approach of the CH_2 groups, and the structural determination is a " classical " one (cp. [17]).

Pauling gives 1·2 A. as a mean value [10] of the radius of hydrogen, but the value 1·35 A. has been used here for hydrogen contacts with the $O^=$ and OH^- ion layers of montmorillonite and halloysite, since this gives better agreement with observed values.

Data such as those of Table II are only useful if the molecule exists in such a configuration, or can readily adopt such a configuration, that effective CH—O contacts are made on both sides, i.e. for all the molecules listed there. Glycerol and 1 : 3-propanediol, however, demand special consideration for in these molecules the central groups (CHOH or CH_2) cannot rotate.

TABLE II.—C—H—O BOND DISTANCES IN HALLOYSITE COMPLEXES.

Complex-forming Substance.	C—H—O Distance (A).
Nitromethane	3·05
Methanol	3·1
Acetonitrile	3·1
Acetaldehyde	3·2
Ethylene glycol	3·25
Acetone	3·35
1 :3-Propanediol (central C)	3·6
Ethanediamine	3·65
Nitrobenzene * (in montmorillonite)	2·4
Sum of C and O (v. der Waals radii)	3·1
$-\overset{\vert}{\underset{\vert}{\mathrm{C}}}\mathrm{H}-\mathrm{O}$ distance (v. der Waals contact, linear arrangement)	3·7-3·8

* Assuming benzene rings make van der Waals contact with each other (3·7 A.)

In cases like these, an attempt was made to find configurations in which the maximum width of the molecule was as low as possible (allowing for short CH—O and OH—O contacts where necessary). It was found that the maximum width thus obtained corresponded closely with the Δ-value actually observed. Such maximum widths are given under $\Delta_{calc.}$ in Table I—they are generally obtained from scale drawings. Fig. 5 (*a*) and (*b*) show such drawings for glycerol and 1 : 3-propanediol, and Fig 5 (*c*) for ethanediamine. In this case the CH_2NH_2 groups are free to rotate ; the particular configuration illustrated enables an NH—O contact to be made ; the CH_2 hydrogens are given their full radius. The close correspondence of the maximum molecular widths with the Δ-values is striking, for it shows that no account need be taken of possible packing of the molecules into the holes in the $O^=$ ion layers (Fig. 1, 2).

Theoretical Δ-values may be obtained for the one-layer montmorillonite complexes in the same way, and are given in Table I. As expected, the ethanediamine complex with montmorillonite has about the same Δ-value as the halloysite complex, and the Δ-values for the long-chain monohydric alcohols are also about the same as for the 1 : 3-propanediol complex with halloysite. In the long-chain alcohols, the least width is taken up when the chains are stretched out as straight as possible. Fig. 5 (*d*) shows an end-on view of such a chain. Its thickness is equal to :

(covalent radius of C + covalent radius of H) × 2 cos 35° + 2 (van der Waals' radius of H) = 4·45 A.,

which is close to the observed value of Δ. The diminution in Δ for the highest alcohols is accompanied by increasing diffuseness of the basal reflection, and probably indicates that the complexes are less perfect.

[17] Dickinson and Raymond, *J. Amer. Chem. Soc.*, 1923, **45**, 22 ; Gorell and Nask, *Z. physik. Chem.*, 1923, **107**, 181 ; Bull, Grimm, Hermann and Peters, *Ann. Physik.*, 1939, **34**, 393.

Secondary and branched-chain alcohols should take up the same space as straight-chain primary alcohols. This is true of 2-ethyl-1-butanol; of the two secondary alcohols, 4-heptanol gives a markedly low spacing and 2-octanol gives a very diffuse basal reflection, no doubt due to imperfect adsorption. On the theory of the function of polar groups outlined earlier, one would expect secondary alcohols to be less readily adsorbed than corresponding primary alcohols, for active groups at the ends of the molecular chains can more easily pack themselves around charged cations than can those in the middle (note that the alkyl chains between the montmorillonite sheets must be straight, and cannot bend without distorting valency angles).

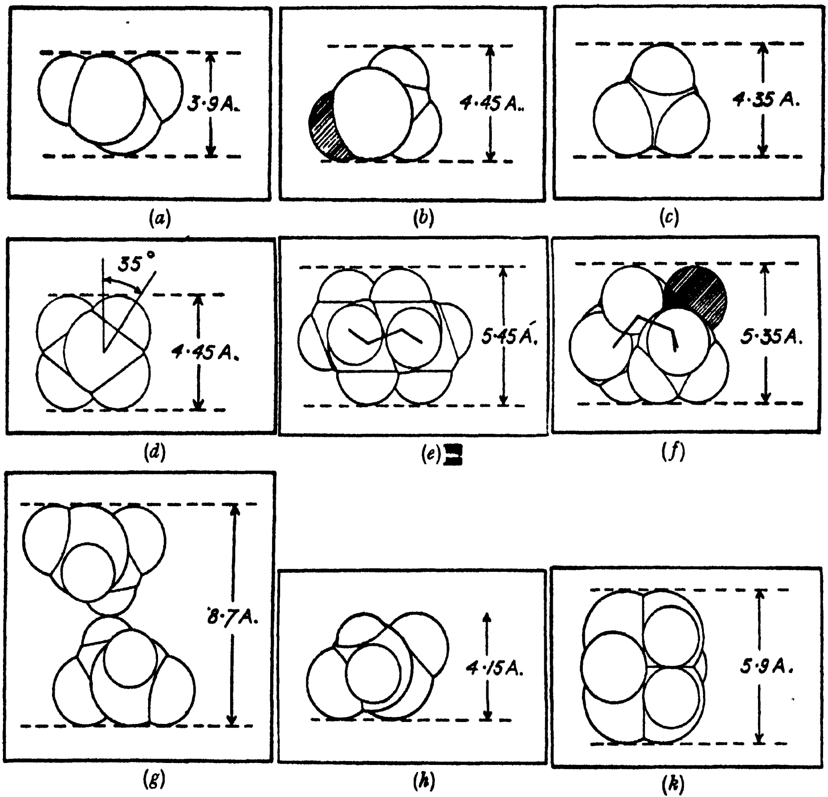

FIG. 5.—Packing diagrams of organic molecules, showing the method of deducing theoretical Δ-values. The molecules are all depicted in an end-on view. Hydrogen atoms of OH^- and NH_2^- groups, and those engaged in hydrogen bond formation, are not shown. (*a*) Glycol in halloysite. (*b*) 1 : 3 Propanediol in halloysite (OH^- group shaded). (*c*) Ethanediamine in halloysite. The largest group attached to the carbon is NH_2. (*d*) An end-on view of a long alcohol chain, showing two CH_2 units. (*e*) Cyclohexane ("chair" form)—the OH group is not shown, only the cyclohexane ring. (*f*) One way of folding up 2-methyl-2-butanol. The OH^- group is shaded, and the C to which it is attached is blackened. (*g*) A possible two-layer arrangement for glycerol. (*h*) Another two-layer arrangement for glycerol (only one molecule shown). (*k*) The suggested arrangement for 1 : 4-dioxane in montmorillonite.

Cyclohexanol and 2-methyl-2-butanol are shown in Fig. 5 (*e*) and (*f*). Of the various ways of curling up the latter molecule, that illustrated gives the smallest spacing and also the right value of Δ.

For the two-layer montmorillonite complexes the molecules are assumed to make CH—O and/or CH—O contacts with the montmorillonite sheets at the distances determined from the halloysite complexes and to make ordinary van der Waals contacts with each other. The molecules are therefore oriented so as to secure the lowest possible value of the maximum width (between parallel planes touching the molecule). Twice this maximum width is taken as the theoretical Δ-value. The radius of hydrogen for van der Waals' contacts between molecules has been assumed to be 1·2 A. (Pauling's mean value).

Fig. 5 (*g*) and (*h*) illustrate the procedure for glycerol. The former shows how the two layers are superposed in a possible arrangement: this leads to a slightly high Δ-value (8·7 A.). The second figure shows another arrangement of the molecule, which leads to the right value. It is no doubt significant that this is about the lowest value which can be reached with any orientation.

Other complexes have been treated in the same way. For acetone, the value obtained is too low (7·5 A.) if it is assumed that the CH_3 groups can rotate so as to take up the most favourable position. It has therefore been assumed they are fixed such that one of the C—H bonds is in the plane of the carbon atoms and directed away from the symmetry axis of the molecule. Such a configuration might be imposed by interaction between the CH_3 groups.

TABLE III.—OBSERVED AND CALCULATED *F* VALUES FOR NITROBENZENE AND ACETONITRILE COMPLEXES WITH MONTMORILLONITE

l.	*F* (nitromethane).	*F* (acetonitrile).	*F* (calc.)
1	50	51	+66
2	27	28	+15
3	11	14	−20
4	22	23	−20
5	0	0	+ 5
6	32	30	+28
7	20	21	+25
8	7	8	+ 3
9	12	11	−18
10	19	16	−22
11	12	8	+15
12	7	8	+ 1

For the three-layer complexes, a molecule of the middle layer is assumed to make normal van der Waals contacts with all other molecules. Otherwise the principle is the same as before—that orientation of the molecule is adopted in each layer which gives the lowest value of the maximum width. For both CH_3NO_2 and CH_3CN, only the CH_3 group need be considered, since this is the widest part of the molecule. The Δ-values obtained in this way show good agreement with the observed values.

For nitromethane, equally good agreement could be obtained by the assumption that the molecules are forming a two-layer structure by standing on end, the CH_3 groups being in contact with the montmorillonite sheets. For acetonitrile, however, this would lead to too large a value of Δ. If the molecules were assumed to lean at an angle of about 45°, Δ could be brought down to the right value but this arrangement seems unlikely, and if the CH_3 groups were close-packed, the structure as a whole would then become rigid and immobile —which would contradict the assumption that it is essentially liquid.

The observed *F* values are derived from intensities estimated visually by means of a wedge. No correction was made for the Lorentz and polarisation factors, since the effect of preferred orientation on the intensities is so uncertain. In calculating the *F* values, the organic atoms were neglected. The *f* values of James and Brindley * were used.

One-dimensional Fourier syntheses were also performed from *F* values obtained from photographs of oriented aggregates steeping in the organic liquid. Nitromethane and acetonitrile gave almost identical photographs and the syntheses obtained (Fig. 6) were definitely in favour of the three-layer structure. The signs of the terms were derived from the contribution of the clay mineral sheet alone, and as Table III shows, they could in most cases be chosen quite unambiguously. By changing the sign of the doubtful terms (8 and 12), the synthesis could be made to approach more closely to what would be expected from a two-layer structure, but not sufficiently so to make it seem very probable (note that the high contribution from the terminal oxygens in nitromethane which should be about equal to the Al^{+++} contribution, is never very evident). The sharpness of the peaks suggests that the organisation in layers is perfect even with these three-layer structures.

---

* *Z. Krist.*, 1931, **78**, 470.

A substance which offers special interest from the point of view of molecular orientation is 1 : 4 dioxane. This might occur in two forms—the *cis* (" boat ") and *trans* (" chair ") forms. The former form would be expected to give a one-layer complex with halloysite, with Δ-value of about 4·0 A. (in which the four CH_2 groups link on to the O^- ion layer, and the two oxygens to the OH^- layer), and a two-layer complex with montmorillonite with about double this spacing. In fact, no complex is obtained with halloysite, and the Δ-value of the montmorillonite complex corresponds neither to a single layer nor to a double layer, if the molecules are lying flat.

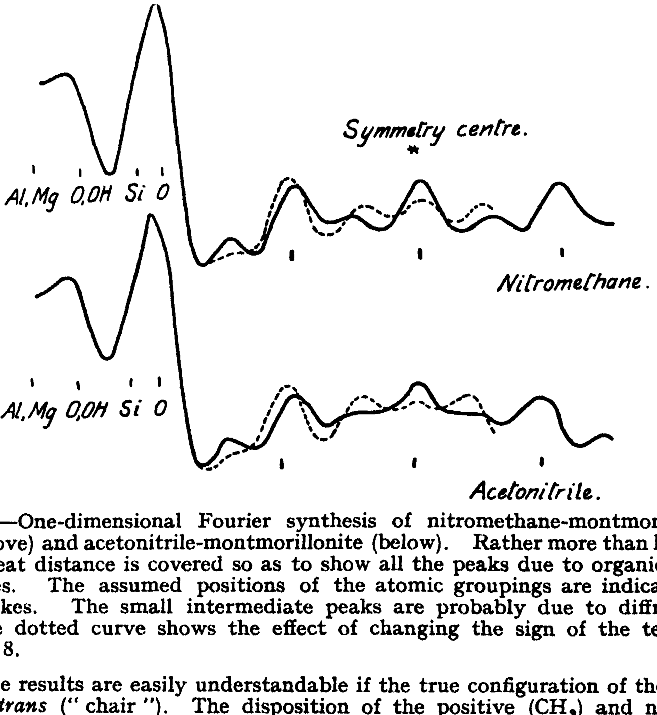

FIG. 6.—One-dimensional Fourier synthesis of nitromethane-montmorillonite (above) and acetonitrile-montmorillonite (below). Rather more than half the repeat distance is covered so as to show all the peaks due to organic molecules. The assumed positions of the atomic groupings are indicated by strokes. The small intermediate peaks are probably due to diffraction. The dotted curve shows the effect of changing the sign of the term for $l = 8$.

These results are easily understandable if the true configuration of the molecule is *trans* (" chair "). The disposition of the positive (CH_2) and negative (O) groups makes it impossible for all the former to make contact with the O^- ion layers, and the latter to point away from it. In the montmorillonite complex, there seems good reason to believe that, in contrast to all the other complexes investigated, the molecules are not lying flat. If the plane of the carbon atoms is perpendicular to the structural sheets it is possible for two carbon atoms to be bound to one sheet, and the other two to the other sheet, with the oxygen atoms in the middle. It is similar to a double layer except that, so to speak, the two layers are combined in one molecule. It leads to a Δ-value of 5·9 A., which is close to that found. The adsorption characteristics with montmorillonits and halloysite thus provide fairly strong evidence that the true configuration of the dioxane molecule is *trans*. This agrees with what Saksena found, on the basis of the Raman spectrum.[18]

The Nature of the Adsorbed Layer.—The agreement between observed and " calculated " values of Δ (Table I) is on the whole excellent even though the " calculated " values, even for multilayer complexes, have been obtained simply by summing the width between parallel planes of the molecules in each layer, after allowing for shortened contacts where necessary. It has not been necessary to take account of the numerous holes in the O^- ion layers into which molecules might pack, nor to allow for any degree of packing between the layers, even the very limited degree of packing represented by the thickest part of one molecule coming above the thinnest part of another. In the case of the 1 : 3-propanediol molecule for instance, the maximum thickness of 4·3 A. (for the two-layer complex) is shown only by the central CH_2 group ; the two end-groups are over 1 A. thinner. The assumption that the thin part of one molecule lies above the thick part of another would give a Δ-value of about 8 A., in poor agreement with the observed value.

---

[18] Saksena, *Proc. Indian Acad. Sci.*, *A*, 1940, **12**, 321.

Apparently, therefore, each layer of molecules occupies its full " clearance space " in the *c*-axial direction, i.e. the space necessary to allow its molecules to move freely over a plane parallel to the surface of the structural sheets. This would mean that the adsorbed layers are in the state of a two-dimensional liquid, firmly adhering to the clay surface, but able to move over it in a random manner.

Additional evidence for the liquid nature of the adsorbed layer are (*a*) the extremely labile nature of the complexes which is such that one complex is changed to another by washing with excess of another (miscible) liquid ; (*b*) that there is not a simple integral number of molecules per unit cell, as expected for a crystalline arrangement of the adsorbed molecules on the clay surface.

The Structure of the Water Complexes.—The water complexes are as labile as the organic complexes (cp. the stability of the vermiculites, which also contain intersheet layers of water molecules, apparently not replaceable by organic liquids [9]). This suggests that the water molecules are in a regular crystalline array, such as that suggested by Hendricks and Jefferson.[19] In the case of montmorillonite and halloysite it seems more probable that the water molecules, like the organic molecules, are in the state of a two-dimensional liquid.

The observed spacings for water complexes [5] accord with the idea of clearance space between layers, taking the diameter of a water molecule as being about 3 A., for the values of $d_{(001)}$ for the successive hydrates differ by this amount. The water complexes are unique apparently in giving up to four layers [5] (when in contact with excess liquid) due to the very high degree of association of liquid water. It is clear, however, that with water the exchangeable cations and perhaps also the base-exchange capacity have a considerable influence on the structure formed.[6] The clay used by Bradley, Grim and Clark was electro-dialysed, and so may have contained some Al^{+++} ions in exchange positions. Not all samples of montmorillonitic material give a four-layer complex with water ; e.g. octophyllite montmorillonite (unpublished results) gives a one-layer complex when NH_4^+ saturated, and a two-layer complex when Ca^{++} saturated. Redhill Fuller's earth (Ca^{++} saturated montmorillonite) also gives a two-layer complex.[20] These materials give normal results with glycerol and glycol. Since the water molecule is so much smaller and the effect of co-ordination about the cations should be very important. No influence of the cations on the number of layers has been found with the organic molecules studied.

In the halloysite-water complex, the packing of the water molecules in each layer must be fairly open, for numerous analyses have shown a water content of only about four molecules per unit cell (six would correspond to a close-packed structure). In montmorillonite, the influence of the exchangeable cations may well lead to a denser type of packing, at any rate in their neighbourhood ; this is suggested by Mackenzie's results for the replacement rate of glycol by water, and by the results of Bradley, Grim and Clark.

Relationship of the Complexes to the Clay Structure.—Glycerol and glycol complexes have been obtained with a variety of montmorillonitic minerals (montmorillonite proper, nontronite, saponite, Hector clay, but not beidellite), and with montmorillonites saturated with various cations, and no important differences have been noted. On the whole it seems likely that all the montmorillonite minerals behave in essentially the same way, but there may be differences in detail. In the case of halloysite there is not much room for variation in composition, and one would expect substantial uniformity of behaviour. Experiments with glycol, glycerol and chlorethanol have so far shown no difference between different halloysites.

It seems clear that the common structural feature of montmorillonite and halloysite which is necessary for the formation of the type of interlaced complexes discussed here is the absence of crystalling regularity in the super-position of the structural sheets. Even if crystalline regularity can be relayed over the thickness of a water layer, by means of water molecules in fixed positions, as probably occurs in vermiculite, it is difficult to see how the *same* regularity could be preserved with *all* the water replaced by any of a variety of other molecules. If an existing regularity were destroyed by complex formation, however, the energy required to do this would probably preclude the formation of a complex altogether, so that the water-structure would be stable towards potentially complex-forming substances (as that of vermiculite appears to be [9]). Alternatively, a new truly crystalline phase might be formed. Such a reaction, however, even if occurring at ordinary temperatures, would be limited to one or two favourable substances, and would not include whole groups of substances as the montmorillonite and halloysite complexes do (cp. above).

---

[19] Hendricks and Jefferson, *Amer. Miner.*, 1038, 23, 863.

[20] Emodi and MacEwan (unpublished).

Absence of crystalline regularity does not imply complete absence of regularity. The conditions of growth of halloysite and montmorillonite may be such that the structural sheets grow in a roughly parallel arrangement which will be subsequently preserved. Such approximate parallelism would not be detectable in a Debye-Sherrer diagram. The high degree of irregularity of montmorillonite and halloysite is no doubt associated with the conditions of their formation, at a low temperature, in the presence of water molecules. This will favour structures of high free energy.

Relationship to Surface Adsorption.—It seems likely the structure of the adsorbed layers discussed here is similar to that of adsorbed films on the surface of a crystal. In the three-layer complexes the conditions in the middle layer must be simulating those in the free liquid, except that the organisation in layers is preserved, and the number of layers is limited to three. It seems probable, however, that the general conclusions about orientation of molecules and type of binding would also hold for the actual surface of the crystallites.

The great value of clay minerals of this type for the study of adsorption phenomena is that phenomena which are strictly analogous to, and indeed, very nearly identical with, those of surface adsorption, may be studied with the ordinary type of X-ray technique adapted to macrocrystalline material.

I wish to thank Dr. Beevers, of the Dewar Crystallographic Laboratory, University of Edinburgh for facilities for taking some of the photographs, and to Dr. Mackenzie and Dr. Dion, Macaulay Institute, and Dr. Percival, University of Edinburgh, for helpful conversations. The experimental work (first part) was done mainly at the Macaulay Institute for Soil Research, and the second part at Rothamstead Experimental Station.

Summary.

Adsorption complexes, formed by montmorillonite and halloysite with a variety of organic liquids, have been prepared and studied. In these complexes the organic molecules enter between the structural sheets of the clay mineral, and arrange themselves in parallel layers, in the form of a two-dimensional liquid, and, with certain exceptions, to lie as flat as possible. Montmorillonite complexes with one, two and three such layers are described, but halloysite complexes have not been obtained with more than one. The relationship of this type of adsorption phenomena to surface adsorption is briefly discussed.

The results obtained with the halloysite complexes provide direct confirmation of Bradley's suggestion (based on montmorillonite complexes) of CH—O bond formation to the oxygen ion layer of the clay mineral surface. Comparative data on CH—O bond lengths, derived from measurements on the halloysite complexes, are given, which show the effect of increasing electronegativity of the attached atom, and increasing multiplicity of the bond, in enhancing the electronegativity of carbon.

These complexes are useful in determining molecular configuration, e.g. results given here support the puckered structure for the cyclohexane ring, and the *trans* structure for the 1 : 4-dioxane ring.

Macaulay Institute for Soil Research,
Aberdeen.

Pedology Department,
Rothamsted Experimental Station,
Harpenden, Herts.

COMPLEXES OF CLAYS WITH ORGANIC COMPOUNDS. PART II.

INVESTIGATION OF THE ETHYLENE GLYCOL-WATER-MONTMORILLONITE SYSTEM USING THE KARL FISCHER REAGENT.

BY R. C. MACKENZIE.

Received 14*th November*, 1946, *as revised* 18*th April*, 1947.

Recent investigations in this laboratory of the complexes formed between montmorillonite and organic compounds [1] revealed the desirability of a quantitative investigation into one of the alcohol-montmorillonite complexes. The complex with ethylene glycol, which gives a well-defined (001) spacing of 17·1 A., was chosen. So far as has been ascertained, the only data available on this complex are those given by Bradley,[2] who, using an experimental method based on the difference between the vapour pressures of glycol and water, found that 1 mol. glycol displaces 2 mol. H_2O from the two-water layer configuration and 1 mol. H_2O from the one-water layer configuration. In the present investigation, however, the glycol and water contents of specially prepared samples of montmorillonite (hereafter referred to as " treated clay," and samples with no glycol as " untreated clay ") were determined directly by means of the Karl Fischer reagent, and correlated with X-ray data for the same samples. The results obtained have added to our knowledge of the conditions which must obtain before the 17·1 A. spacing is observed.

The Karl Fischer reagent,[3, 4] which consists of a solution of I_2 and SO_2 in CH_3OH and pyridine, enables the direct and accurate titration of water in amounts as small as 2 mg. with normal titration apparatus. Much smaller amounts of water may be accurately determined by the use of a weaker reagent [3] and suitable apparatus.[5] It must be strongly emphasised, however, that on account of its extreme sensitivity to moisture every precaution must be taken to eliminate adventitious moisture.[6] In addition to water, alcohols can, *inter alia*, be conveniently and accurately assayed by the reagent, the procedure involving quantitative esterification in the presence of BF_3 as catalyst.[7] The normal procedure for alcohol determination had to be modified slightly to permit accurate results to be obtained in the presence of clays.

Although several organic [7, 8] and inorganic compounds [9] react directly with the reagent, interference by such compounds can generally be eliminated or allowed for. In clays the only interfering substances likely to be present are MnO_2 which reacts stoichiometrically and can be allowed for, and Fe_2O_3 which reacts but *not stoichiometrically*. The " free " Fe_2O_3

---

[1] MacEwan, (*a*) *Nature*, 1944, **154**, 577; (*b*) *J. Soc. Chem. Ind.*, 1946, **65**, 298; (*c*) *Trans. Faraday Soc.*, 1948, **44**, 349.

[2] Bradley, *J. Amer. Chem. Soc.*, 1945, **67**, 975.

[3] Fischer, *Angew. Chem.*, 1935, **48**, 394.

[4] Smith, Bryant and Mitchell, *J. Amer. Chem. Soc.*, 1939, **61**, 2407.

[5] Levy, Murtaugh and Rosenblatt, *Ind. Eng. Chem.* (*Anal.*), 1945, **17**, 193.

[6] Acker and Frediani, *ibid.*, 1945, **17**, 793.

[7] Bryant, Mitchell and Smith, *J. Amer. Chem. Soc.*, 1940, **62**, 1.

[8] Bryant, Mitchell and Smith, *ibid.*, 1940, **62**, 3504.

[9] Mitchell, *et al.*, *ibid.*, 1941, **63**, 2927; Zimmermann, *Fette Seifen*, 1939, **46**, 446.

content of the montmorillonite here used was very small (*vide infra*) so the Fischer reagent appeared to offer promising possibilities for the determinations involved. Fischer[9] has already employed the reagent to determine the amount of sorbed water in Fuller's earth, but his results are somewhat anomalous in that while he gets good agreement between the amounts of water determined by the reagent (15·6 %) and by heating at 120° (15·5 %), his *dry clay* gave a titre equivalent to 1·6 % water. No account was taken of possible interfering substances.

The samples of clay for X-ray examination were introduced into thin glass capillary tubes and immediately sealed to prevent alteration in moisture content by exposure to the atmosphere. The X-ray data for all samples were supplied by D. M. C. MacEwan.

Experimental.

Purity of the Montmorillonite.—The montmorillonite used was the fine fraction ($< 0{\cdot}2\mu$ equivalent spherical diam.) of an American bentonite, of unknown locality of origin, supplied by the English China Clay Sales Co., St. Austell, Cornwall. This fraction was separated by the Sharples Supercentrifuge, dried at 100° c. and ground in a mechanical agate mortar. After separation, it was predominantly Ca-saturated. Preliminary tests indicated high purity, e.g. X-ray examination showed the presence of no accessory minerals; the base exchange capacity was 102 m.equ./100 g.; the amount of Fe_2O_3 soluble in sodium hydrosulphite[10] was only 0·1 %. This amount of Fe_2O_3 should be too small to interfere appreciably with the use of the Fischer reagent.

Reagents and Apparatus.—Fischer reagent: 84·7 g. I_2 were dissolved in a mixture of 667 ml. methanol and 269 ml. pyridine and 64 g. liquid SO_2 weighed into the solution.[4] A.R. chemicals were used as far as possible. A.R. methanol was found to be sufficiently dry without any pretreatment. The pyridine was dried by treating with CaH_2 and distilling. Standardisation of the reagent was performed daily, as recommended by Smith, Bryant and Mitchell.[4]

The ethylene glycol used in preparing the complexes was distilled twice, and contained 0·13 % water, as determined by the Fischer reagent. The esterifying reagent was prepared by dissolving 100 g. boron trifluoride and 1-2 ml. water in 1 l. glacial acetic acid.[7] BF_3 was obtained by distilling, in an all-glass apparatus, 150 g. $NaBF_4$ with 50 g. B_2O_3 and 150 ml. conc. H_2SO_4, and washing the gas by bubbling through conc. H_2SO_4 saturated with B_2O_3.[11]

Since the Fischer reagent rapidly attacks rubber, the titration apparatus consisted of a gravity-filling burette with an all-glass feed system. Air entering the system was dried by $CaCl_2$ and conc. H_2SO_4. Montmorillonite did not mask the colour change at the end-point, so no electrical method for determining the end-point[12] was necessary. Esterifications were performed in 250 ml. glass-stoppered bottles immersed in a thermostat at 67° c. To prevent ejection of the stoppers or leakage of moisture into the bottles, the stopper and neck of each bottle was protected by a cellophane cover, which was tightly held in place by a rubber band and metal bar.

Procedure.

(*a*) Determination of Water in Clay Samples.—A sample which would be expected to give a titre of 10-20 ml. (about 0·2 g. at atmospheric humidity) was accurately weighed and titrated in suspension in 5 ml. methanol in a dry 250 ml. glass-stoppered bottle. A simultaneous determination was carried out on 5 ml. methanol, and from these results the water content of the montmorillonite calculated.

(*b*) Preparation of Samples of Treated Clay.—In order to obtain clay samples with different glycol contents, 3 g. samples of montmorillonite were shaken in centrifuge tubes for about 1 hr. with 45 ml. of a 50 % solution of ethylene glycol in water. After centrifuging, the centrifugate was rejected and each

[10] Galabutskaya and Govorova, *Min. Suir.*, 1934, **9**, 27.

[11] *Inorganic Syntheses*, 1939, **1**, 21.

[12] See, e.g. Carter and Williamson, *Analyst*, 1945, **70**, 369.

sample washed with a different amount of water, varying from 0-70 ml. in two washings, and in each case the clay was shaken with the water for 2 hr. before recentrifuging.

Varying water contents for a constant glycol content were obtained by dividing each of the above samples into 4 parts by quartering the deposit in the centrifuge tube and subjecting each fraction to one of the following treatments:

(*a*) drying at 100° C. in an oven,
(*b*) standing in a vacuum desiccator over P_2O_5,
(*c*) standing in a vacuum desiccator at 50 % R.H.,
(*d*) standing in a vacuum desiccator at 75 % R.H.

Since quartering was done only roughly and the clay was not sieved before use, these 4 fractions would probably not contain identical proportions of coarse and fine material (cp. later). When sufficiently dry, each fraction was finely ground in an agate mortar, then (*b*), (*c*) and (*d*) were allowed to stand for at least a further 2 days under the controlled conditions, while (*a*) was heated at 100° C. for at least a further 2 hr., before determinations of the glycol and water contents were performed.

(*c*) Determination of Glycol in the Presence of Montmorillonite.—Application of the procedure of Bryant, Mitchell and Smith,[7] using a 4 % solution of glycol in dioxan, gave apparent recovery percentages in the region of 110 % in the presence of montmorillonite, and 98 % in its absence. The exceptionally high figure of 110 % was attributed to decomposition of some of the clay by the esterifying reagent. By including a blank determination with untreated clay as well as the normal blank, a satisfactory method was evolved, the recovery percentage (using the dioxan solution) now being 99·0-100·2 %. The method as applied to the treated clay was as follows.

Two samples of 0·1 to 0·4 g. treated clay were weighed into two dry glass-stoppered bottles and two samples of oven-dry untreated clay into two similar bottles. The water contents of one sample of treated and one of untreated clay were determined as described above. To each of the remaining bottles were added 10 ml. of the esterifying reagent, another 10 ml. of which were run into another dry glass-stoppered bottle. These three bottles were then fitted with the cellophane cover and metal clasp, immersed in the thermostat at 67° C. for 2 hr., removed and allowed to cool. In order to destroy the reactivity of the esterifying reagent, 5 ml. of pyridine were added to each bottle. The mixtures were then titrated in the usual manner.

(*d*) Calculation of Results.—The titration figure for the contents of the bottle containing the treated clay is the sum of the titre for:

(1) glycol,
(2) blank,
(3) water content of the treated clay,
(4) amount of decomposition of the clay by the esterifying reagent.

Components (2), (3) and (4) can be calculated from the determinations already made, but since the correction for (4) is based on the weight of dry glycol-free clay, (1) can be got only by successive approximations. In practice, (4) being small, the second and subsequent approximations gave identical results, so the figure given by the second approximation was taken as the correct result.

For the first approximation the following equation was derived:

$$V = v_3 - \left[v_1 + \frac{(v_6 - v_4)m_1}{m_1'} + \left\{\frac{(v_2 - v_1)m_1}{m} - \frac{(v_5 - v_4)m_1}{m'}\right\}\right]$$

where V = vol. reagent for glycol present in m_1 g. treated clay; v_1 = vol. reagent for blank; v_2 = vol. reagent for blank + m g. untreated clay; v_3 = vol. reagent for blank + m_1 g. treated clay; v_4 = vol. reagent for 5 ml. MeOH; v_5 = vol. reagent for 5 ml. MeOH + m' g. untreated clay; v_6 = vol. reagent. for 5 ml. MeOH + m_1' g. treated clay. The term v_1 is the correction for the blank, $(v_6 - v_4)m_1/m_1'$ the correction for the water content of the treated clay and $\{(v_2 - v_1)m_1/m - (v_5 - v_4)m_1/m'\}$ the correction for decomposition of the clay during esterification. For the second approximation, the last term is replaced by $\{(v_2 - v_1)m_1''/m - (v_5 - v_4)m_1''/m'\}$ where $m_1'' = m_1$ less the water and glycol contents determined by the first approximation and corrected to the same water content as m and m'.

For the simultaneous measurement of the water and glycol contents of the two samples of treated clay, only two additional titration figures have to be obtained, viz., one similar to v_3 and one similar to v_6. Hence, the more samples which can be analysed simultaneously, the less the relative number of operations involved.

Results and Discussion.

Up to a certain temperature montmorillonite is reversibly dehydrated, but above this temperature irreversible dehydration sets in.[8] X-ray examination (after rehydration) showed that the montmorillonite used was reversibly dehydrated when heated at 195° c. for 5 hr., but that heating at 200° c. for the same time produced irreversibility. The transition temperature was therefore approximately 198° c., so the loss of weight on heating at 195° c. for 5 hr. was taken as the amount of reversibly removable water. As the dehydration curve shows practically no loss of weight between this transition temperature and the temperature at which structural OH-groups are removed,[13] it is generally considered that the reversibly removeable water corresponds to the total amount of sorbed water.

The agreement between the amount of reversibly removable water of several samples of montmorillonite and the amount of water determined by the Fischer reagent was excellent (Table I), i.e. the Fischer reagent determines the total amount of sorbed water, as was suggested by Fischer's results for Fuller's earth.[8]

TABLE I.—Correlation between Sorbed Water in Montmorillonite as Determined by Heating at 195° c. and by the Fischer Reagent, Expressed as Percentage Weight of Dry Clay

Determination.	1.	2.	3.	4.	5.	Mean.
% H_2O by heating	19·2	18·8	19·3	19·0	19·3	19·1
% H_2O by Fischer reagent	19·2	19·0	19·4	19·1	19·2	19·2

Although reaction with the sorbed water is complete, it is probable that the reaction does not occur in the intersheet space, but that the methanol displaces some of the water from the clay and, as this is used up during the titration, more water is displaced in an attempt to maintain the distribution coefficient. This is supported by the fact that the colour at the first end-point is stable only for about a minute, but if allowed to stand for about 5 min. and again brought to the end-point the colour is stable for at least 10 min. This is presumably due to the slow replacement of the last traces of water by methanol. Data on the removal of water from clays by alcohol [14] give added support to this conception of the mechanism.

The technique above, of determining the % recovery of glycol in the presence of clay using a dioxan solution of glycol might be objected to on the ground that glycol so added might not penetrate into the intersheet space. Hence intersheet glycol would not be quantitatively determined. However, the technique described by MacEwan [15] for preparing specimens for X-ray examination shows that if glycol alone is allowed to come into contact with dry montmorillonite, at least some of the glycol penetrates into the intersheet space. Consequently, an accurately weighed amount of glycol was allowed to drop on a weighed sample of montmorillonite (about 0·2 g.) and the % recovery of glycol determined using the technique employed for treated clays. Since the amount of dry glycol-free clay is known, the results can be calculated directly, but the method of successive approximations is also applicable. The second approximation gave the same value as the direct calculation, viz., glycol added, 0·0473 g.;

---

[13] Nagelschmidt, *Imp. Bur. Soil Sci. Tech. Comm.*, No. 42, 1944.

[14] Bouyoucos, *Soil Sci.*, 1936, **41**, 443.

[15] MacEwan, ref. [1] (*b*), (*c*).

glycol found, 0·0475 g.; recovery, 100·4 %. The method is therefore quantitatively applicable to intersheet glycol, and the results also uphold the assumption that the amount of decomposition of the treated clay by the esterifying reagent is identical with that of the untreated clay (based on similar weights of dry glycol-free clay).

The glycol and water contents of 24 samples of treated clay and the associated basal spacings are shown in Table II. The values of $d_{(001)}$, obtained by visual measurements of the X-ray photographs, are considered correct to ± 0·2 A. at the higher values and ± 0·1 A. at the lower values.

TABLE II.—VARIATION OF (001) SPACING WITH GLYCOL AND WATER CONTENTS. (PERCENTAGES EXPRESSED ON BASIS OF WEIGHT OF DRY GLYCOL-FREE CLAY.)

Sample No.	Glycol Content (%).	Water Content (%).	$d_{(001)}$ (A).
1	68·2	5·5	17·1
2	100·2	10·3	17·1
3	99·6	21·3	17·1
6	37·1	2·2	17·0
7	28·4	5·9	17·1
9	25·1	3·3	17·1
10	14·5	7·2	14·2
11	20·8	7·0	15·2
12	20·1	12·7	16·5
14	25·8	2·2	16·7
15	30·3	7·3	17·1
16	23·1	12·3	17·1
18	12·1	4·3	13·9
19	18·0	3·6	14·3
21	18·2	19·3	17·3
22	7·2	4·6	13·4
23	11·7	4·0	13·8
24	14·1	17·1	16·5
25	27·0	2·6	16·9
26	28·1	7·8	17·1
27	7·9	4·6	13·2
28	9·5	9·2	14·3
29	12·5	18·4	16·1
30	11·6	22·3	16·3

During the course of these determinations it was observed that samples obtained by quartering the deposit in the centrifuge tube (see Procedure, (*b*)) never had identical concentrations of glycol in each quarter—an effect not due to experimental inaccuracy as shown by duplicate results. The most significant variation was between samples dried at 100° C. and those dehydrated in the cold. This is probably due to volatilisation of some of the glycol during heating.

There were, however, significant differences between samples dehydrated at the various relative humidities. This might arise from the variation in the proportions of coarse and fine material in each quarter-sample (see Procedure, (*b*)) so that, while the glycol would penetrate into the intersheet space of the coarse particles,[18] more might be removed by washing from the fine than from the coarse material. However, since drying of the samples proceeded relatively slowly, it is to be expected that any slight lack of homogeneity so caused would be almost entirely removed before the sample became dry. Efficient mixing of the dry sample was ensured by grinding it finely twice—once when sufficiently dry to handle and again immediately before the determination.

This explanation might give rise to two effects.

(*a*) Since drying at 100° C. would be relatively rapid, there would be little tendency for equilibrium to be established, and the (001) reflections would be expected to be somewhat diffuse. Broad lines were, in fact, found to be associated with these samples, but since the measurements in such circumstances were made to the centre of the densest part of the lines a significant mean value of the basal spacing should result.

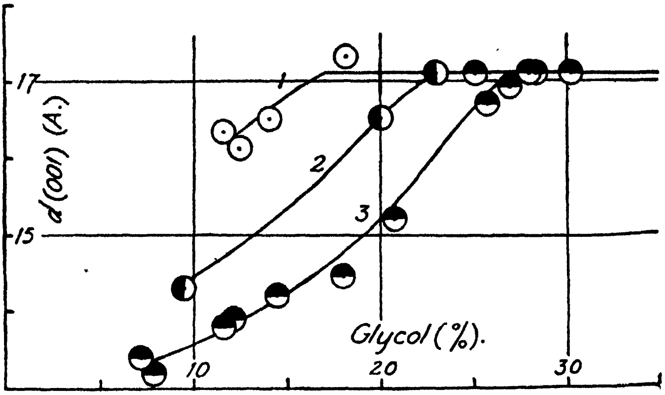

FIG. 1.—Average water contents: curve 1, 193 %; curve 2, 11·0 %; curve 3, 4·2 %.

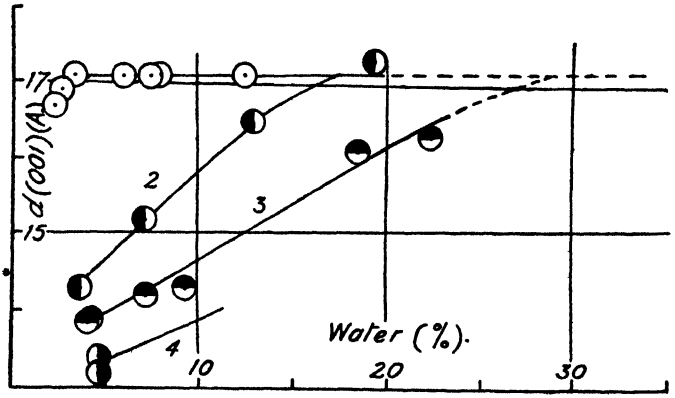

FIG. 2.—Average glycol contents: curve 1, 26·0 %; curve 2, 19·6 %; curve 3, 11·2 %; curve 4 7·5 %. Discontinuous line—extrapolated portion of curve.

(*b*) If a slight lack of homogeneity did occur, a small sample such as that used for X-ray examination might have a slightly different composition from that of the sample used for chemical analysis. This effect should be eliminated by efficient grinding, but it supplies one possible reason for the slight scattering of points from the lines in Fig. 1 and 2. The two obvious reasons for scatter are the variations in water (Fig. 1) and glycol contents (Fig. 2), and the limits of accuracy of visual measurement of the (001) reflections.

Allowing for possible slight errors, the main trends are well brought out in Fig. 1 and 2, which show, respectively, the relationship between $d_{(001)}$ and glycol content at approximately constant water contents, and the relationship between $d_{(001)}$ and water content at approximately constant glycol contents. It is concluded that :

(1) The 17·1 A. basal spacing remains constant over a wide range of glycol and water contents. Although there is no evidence that a large amount of glycol increases this spacing (e.g. samples 2 and 3, Table II), at high water contents a definite increase does occur. For instance, for two samples (not quoted in Table II), the water content of which was so high that the samples remained in a fluid state, the basal spacing was 19·5 A. It was impossible to obtain homogeneous samples of these for accurate analysis but a few rough tests on one indicated glycol and water contents in the regions of 50 % and 250 % respectively.

(2) The amounts of glycol and water required for the 17·1 A. spacing are interdependent and bear a reciprocal relationship to one another. In this connection should be mentioned a trend not observable from Table II or the graphs. On photographs showing the 17·1 A. spacing, in contradistinction to all the others, several successive orders of the basal spacing were observable, indicating a high degree of regularity in the superposition of the structural sheets. This distinction showed up even when the sample giving the 17·1 A. spacing contained a large amount of water and correspondingly less glycol. The highly ordered structure is therefore not a criterion of complexes containing glycol only in the intersheet space.

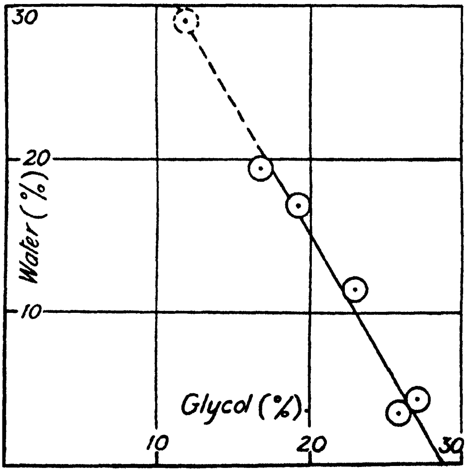

FIG. 3.—Discontinuous line—part of curve subject to some uncertainty.

(3) For very low water contents (i.e. between 2 % and 7 %) the glycol — $d_{(001)}$ curves lie very close together and are represented by one curve on Fig. 1.

(4) Even with a glycol content as high as 26 %, a decrease in $d_{(001)}$ is apparent at low water contents. When a sample containing 26 % glycol was heated at 70° C. over P_2O_5 and sealed under vacuum, $d_{(001)}$ dropped to 14·2 A. It was not possible to determine the glycol content after heating, but the water content of a similarly treated sample was 0·3 %. The 14·2 A. spacing seems somewhat low, so it is possible that some glycol was lost during the experiment, but the general trend fits in well with the results.

Taking the curves in Fig. 1 to represent those for 19·3 %, 11·0 % and 4·2 % water, and those in Fig. 2 for 26·0 %, 19·6 % and 11·2 % glycol, a graph was constructed showing the relationship between the glycol and water contents required for the 17·1 A. spacing (Fig. 3). All the points lie very close to a straight line and it appears that 28·7 % glycol is the minimum amount necessary, in the absence of water, to give the 17·1 % spacing. Taking the unit cell of montmorillonite as $Al_4Si_8O_{20}(OH)_4$, this value corresponds to 3·3 molecules glycol per unit cell, which agrees well with the theoretically expected value for an intersheet bimolecular layer of glycol (see first paper of this series).

The slope of the line in Fig. 3 indicates that approximately 6 molecules of water are necessary to replace one molecule of glycol in order to maintain a constant basal spacing. This 6/1 ratio cannot be strictly compared with Bradley's values [3] since it refers to a water layer of such thickness as to be comparable with a bimolecular layer of glycol. If the radius of the water molecule is taken as 1·5 A., the sides of the unit cell of montmorillonite as 8·9 A. and 5·15 A. and the thickness as 9·4 A., three layers of close-packed water molecules would give a spacing of 17·3 A. which is sufficiently close to the 17·1 A. spacing to permit a reasonably accurate comparison. Such a structure would also account for the 6/1 ratio. This ratio, however, is somewhat uncertain and refers only to the first stages of replacement of glycol by water. Since the clay was predominantly Ca-saturated the first amounts of sorbed water would probably be oriented around the Ca^{++} ions in a hydration shell [16] so the close packing of this water may be expected. The 6/1 ratio would, however, also depend upon the relative amounts of glycol and water sorbed on the outer surfaces of the clay micelles. Recently Mering [17] has been able to distinguish between this type of sorbed water and intersheet water, but no data on glycol are available, although the agreement between the theoretically expected number of glycol molecules per unit cell and the experimental number obtained above would seem to indicate little or no glycol sorption on the outer surfaces of the micelles. It therefore seems possible that the ratio would be considerably less than 6/1 for intersheet water at higher water contents, which would be more in accordance with the "hexagonal-net" theory of Hendricks and Jefferson.[18, 16] Possible methods which might give a direct indication of the configuration of intersheet water are at present under review in this laboratory.

The author desires to express his indebtedness to Dr. A. Muir, now at Rothamsted Experimental Station, for suggesting the use of the Fischer reagent in connection with this problem and for many helpful discussions; to Dr. D. M. C. MacEwan for the X-ray data; and to Prof. H. W. Melville, Chemistry Department, Aberdeen University for providing the facilities required for performing this work.

Summary.

The amounts of water in samples of montmorillonite as determined by the Fischer reagent correspond to the total amounts of sorbed water, i.e. the amounts of water reversibly removable by heating.

A slight modification of the method for the determination of alcohols by this reagent permits its quantitative application to the determination of intersheet ethylene glycol in montmorillonite-glycol complexes. Determination of the water and glycol contents of specially prepared samples of montmorillonite-glycol-water complexes, in conjunction with X-ray examination of the same samples, led to the following conclusions:

(*a*) the (001) spacing of the complex remained constant at 17·1 A. over a wide range of glycol and water contents;
(*b*) the minimum amounts of glycol and water necessary to give this spacing were interdependent;
(*c*) in the absence of water, 3·3 molecules of glycol per unit cell, in the form of a bimolecular layer were required for production of the 17·1 A. spacing;
(*d*) in the first stages of replacement of glycol by water one molecule of glycol has to be replaced by approximately 6 molecules of water to maintain constant basal spacing.

Macaulay Institute for Soil Research,
Craigiebuckler,
Aberdeen.

---

[16] Hendricks, Nelson and Alexander, *J. Amer. Chem. Soc.*, 1940, **62**, 1457.

[17] Mering, *Trans. Faraday Soc.*, 1946, **42B**, 205.

[18] Hendricks and Jefferson, *Amer. Miner.*, 1938, **23**, 863.

HYDROTROPY, SOLUBILISATION AND RELATED EMULSIFICATION PROCESSES.
PART I.

By P. A. Winsor.

Received 13th January, 1947 as revised 5th June, 1947.

This paper is the first in a series in which certain phenomena of hydrotropy, solubilisation and emulsification are discussed from a point of view in which emphasis is laid on the aspect of the active agent as a common solvent for the hydrophilic and lipophilic liquids present. The point of view which is extended here was earlier put forward by Lindau[1] and von Hahn[2] and has recently been further supported by the work of McKee *et al.*[3] on various cases of hydrotropic solution. This view is not in opposition to the micelle theories of solubilisation of Hartley and McBain[4] but is supplementary to them.

A qualitative classification and theory is given below which has been found useful to correlate a large number of experimental observations which will be described in detail in the later papers of this series, but which, for the sake of compactness, will to some extent be anticipated or only briefly referred to in the present introductory account.

For the purpose of the discussion in hand, the solvent affinities existing between ions and molecules in the liquid state may be grouped under two headings:

(i) H (hydrophilic) solvent affinities (A_H), e.g. affinities dependent on hydrogen bonding, and

(ii) L (lipophilic) solvent affinities (A_L), e.g. van der Waals forces.

Most molecular species (e.g. C_2H_5OH) exert both H and L affinities. The attractive forces between the molecules and ions in solution may be held to arise through the mutual satisfaction of H by H affinities and of L by L affinities. The total inter-molecular solvent attraction between any two species O and W in a single liquid phase can therefore qualitatively be represented as

$$A_{\mathrm{OW}} = A_{H\mathrm{OW}} + A_{L\mathrm{OW}}$$

and will depend in detail on the solvent affinities and concentrations of both O and W along lines such as those discussed by van Arkel.[5]

In solubilised systems all the molecular or ionic species present are here held to exist in the liquid state (cp. Bancroft[6]). On the basis of their solvent properties these species can be divided into three groups which will, of course, overlap. These are: $\overline{\mathrm{O}}$, those with predominantly lipophilic solvent affinity, e.g. most organic liquids non-miscible with water; $\overline{\mathrm{W}}$, those with predominantly hydrophilic solvent affinity, e.g. water, ethylene glycol, simple inorganic ions; $\overline{\mathrm{C}}$, those which exert simultaneously and in high degree both L and H affinities. Such species have previously been termed "amphipathic" by Hartley[7] but for consistency with the point of view now advanced will here be termed "amphiphilic." As is well known it is such species, which may conveniently be termed amphiphiles, which typically give rise to such phenomena as hydrotropy, solubilisation and emulsification.

---

[1] Lindau, *Naturwiss.*, 1932, **20**, 396.

[2] von Hahn, *Kolloid Z.*, 1932, **62**, 202.

[3] McKee, *et al.*, *Ind. Eng. Chem.*, 1946, **38**, 382.

[4] cp. McBain, *Advances in Colloid Science* (1942).

[5] van Arkel, *Trans. Faraday Soc.*, 1946, **42B**, 81.

[6] Bancroft, *Science*, 1935, **82**, 388.

[7] Hartley, *Aqueous Solutions of Paraffin Chain Salts.*

Solubilisation and Hydrotropy.

Work in these laboratories has made possible the following generalisation respecting processes of hydrotropy and solubilisation. When water (or aqueous salt solution) $\overline{W}$ and an organic liquid (a mixture or a single substance) $\overline{O}$ are mixed with a suitable quantity (say 5-25 %) of an amphiphilic compound (such as sodium phenate, cyclohexylammonium chloride, hard or soft soap, a sodium alkyl sulphate or sulphonate or a higher alkyl ether of a polyethylene glycol) C', there are four main types of equilibrium system which may result. These are indicated in Fig. 1. The phases of the heterogeneous systems, particularly when C' contains a large alkyl group, are often emulsified. In the majority of cases the equilibria are apparently rapidly established and there is little tendency to produce metastable conditions.

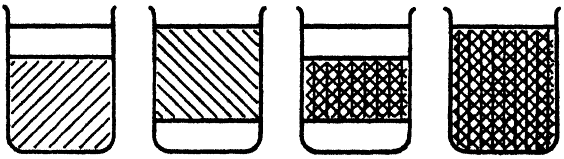

Type I. Type II. Type III. Type IV.

FIG. 1.

TYPE I SYSTEMS. An organic liquid $\overline{O}$ containing only small proportions of the other components of the system is in equilibrium with an aqueous solution of C' containing more or less solubilised $\overline{O}$. If $\overline{O}$ contains several species there is some enhancement in the proportion of the more hydrophilic species in the solubilised $\overline{O}$.

TYPE II SYSTEMS. Water or an aqueous salt solution $\overline{W}$, containing only small proportions of the other components of the system, is in equilibrium with a solution of C' in $\overline{O}$ containing more or less solubilised $\overline{W}$. If $\overline{W}$ contains several species there is some concentration in the proportion of the more lipophilic species (e.g. of water if $\overline{W}$ = water and inorganic salts) in the solubilised $\overline{W}$ (i.e. inorganic salt will be concentrated in the separated aqueous layer).

TYPE III SYSTEMS. Free $\overline{O}$ and $\overline{W}$ phases are in equilibrium with a third solubilised phase containing C', $\overline{O}$ and $\overline{W}$.

TYPE IV SYSTEMS. Type IV systems contain no free $\overline{O}$ or $\overline{W}$ layers, the $\overline{O}$, $\overline{W}$ and C' being mutually solubilised.

The foregoing classification is to some extent arbitrary. Thus a Type I system may alternatively be regarded as a Type IV system in equilibrium with excess $\overline{O}$. A Type II system is at the same time a Type IV system in equilibrium with excess $\overline{W}$, while a Type III system may be regarded as a Type IV system in equilibrium with excess of both $\overline{O}$ and $\overline{W}$.

Methods of Interconversion of Systems of Types I-IV.

TYPE I SYSTEMS. The following classification of methods which have been found applicable for increasing solubilisation of $\overline{O}$ in Type I system may be given.

Method I (*a*). A reduction in the relative proportion of $\overline{W}$.

Method I (*b*). The addition to $\overline{O}$ of an oil soluble component capable of hydrogen bonding and/or which has greater solvent attraction for C′ than $\overline{O}$ has. Such additives are fatty acids, amides, alcohols, amines, etc.

Method I (*c*). An increase in the lipophilic nature of C′—e.g. in the case of compounds of analogous structure by increase of the molecular weight of C′.

Method I (*d*). The addition to $\overline{W}$ of an inorganic salt.

If sufficient C′ is present any of the above methods applied progressively, leads first to the production of a Type IV system and ultimately, in the case of I (*b*), (*c*) and (*d*), to a Type II system.

TYPE II SYSTEMS. Solubilisation of $\overline{W}$ in Type II systems may be increased by the following methods which may to some extent be considered as respectively complementary to Method I (*a-d*) above.

Method II (*a*). A reduction in the relative proportion of $\overline{O}$.

Method II (*b*). The addition to $\overline{W}$ of a water soluble organic liquid capable of hydrogen bonding, e.g. ethylene glycol, ethanol, etc.

Method II (*c*). A reduction in the lipophilic nature of C′, e.g. in the case of compounds of analogous structure by reduction of molecular weight.

Method II (*d*). The addition to $\overline{O}$ of a less hydrophilic oil soluble component, e.g. medicinal oil.

If sufficient C′ is present, Methods II (*a*), (*b*), (*c*) and (*d*), if applied progressively, lead first to the production of Type IV systems and ultimately in the case of Methods II (*b*), (*c*) and (*d*), to Type I systems.

Effect of Temperature.—In cases where C′ is an alkali metal salt a rise of temperature usually diminishes solubilisation of $\overline{O}$ in Type I systems and increases solubilisation of $\overline{W}$ in Type II systems. There are, however, many exceptions to this behaviour, particularly in the case of Type I systems, which will be discussed in Part VI.

In Type III systems the solubilisation of $\overline{O}$ may be increased by Methods I (*a*)-(*d*) and of $\overline{W}$ by Methods II (*a*)-(*d*). Increase in the relative proportion of C′ in the system, which is equivalent to both Methods I (*a*) and II (*a*), increases the solubilisation of both $\overline{O}$ and $\overline{W}$ simultaneously. Type III systems have been described by Lester-Smith.[8]

Mechanically Reversible Homogeneity.—When a suitable Type I system is converted to a homogeneous Type IV system, e.g. by addition of cyclohexanol, at the point where excess organic liquid is just disappearing, critical solution phenomena are evident. At this point we have frequently observed both in aqueous systems and in systems containing ethylene glycol, that a mixture which is just heterogeneous becomes homogeneous on vigorous shaking and reverts to the heterogeneous condition after a few minutes resting. The agitation comminutes the organic liquid and thus extends its surface and increases its solubility. At the critical region this may cause complete solution. The same effect we have also frequently observed at the points when Type IV systems pass into Type II systems.

Discontinuities within Type IV Systems.

In Type IV systems although no free $\overline{O}$ and $\overline{W}$ phases exist, in certain cases phase changes occur. These are illustrated by the following two examples which are typical. When nonylamine or cyclohexanol is added at room temperature to a mixture of equal volumes (10 cc.) of cyclohexane and a 20 % solution of sodium tetradecan-5 sulphate in water the initial Type I system passes first into a Type IV system and finally into a Type II system. (See I (*b*) above.)

---

[8] Lester-Smith, *J. Physic. Chem.*, 1932, **36**, 1414.

Within the Type IV region the following successive stages occur (cp. Table I).

TABLE I.

Character of Mix. Temperature *ca.* 19° c.	Vol. added. Cyclohexanol.	Vol. added. *n*-nonylamine.
(1) Clear sol S_1	0·55-0·60	0·20
(2) Heterogeneous mixture of sol S_1 and gel G	intermediate volumes	intermediate volumes
(3) Homogeneous gel G	0·75	0·28
(4) Heterogeneous mixture of G and a second sol S_2	intermediate volumes	intermediate volumes
(5) Clear sol S_2	1·05-1·6	0·38-0·45

In the above case with cyclohexanol both S_1, G and S_2 disperse readily in water and do not have greatly differing electrical conductivities. With nonylamine, S_1 and G disperse in water and S_2 in cyclohexane, and there is a very great fall in electrical conductivity between G and S_2, as observed by a method similar to that described by Schulman.[8]

In some cases, particularly when C′ has a comparatively low molecular weight (e.g. sodium octyl-4 sulphate) passage of S_1 into S_2 in the above manner is continuous and no gel stage appears. In other cases, e.g. when C′ is a primary alkyl sodium sulphate and $\overline{O}$ contains a primary alcohol the gel stage is much extended and S_1, G and S_2 may not be distinguishable. More frequently, although the S_1 and gel regions merge, the S_2 sol is readily obtained as a clear solution. This is possibly true in certain of Schulman's experiments with sodium oleate.[8] In all cases yet examined S_1 and S_2 are isotropic. In all cases yet examined S_1 and S_2 are isotropic while G shows birefringence of greater or less intensity.

A diagrammatic representation of the passage from Type I to Type II system via the S_1, G and S_2 stages of a Type IV system is illustrated in Fig. 2 in which *R* has the significance explained in a later section.

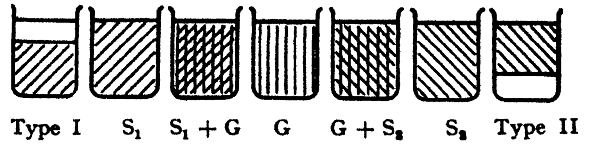

FIG. 2.

S_1, G, S_2 Changes in Aqueous Amphiphile Solutions in Absence of $\overline{O}$.—In the above two examples the effect of an amphiphile on equal volumes of water (or aqueous salt solution) and organic liquid has been described, but the same sequence of changes can be distinguished over very wide (probably all) volume ratios. In fact the whole sequence

$$S_1 \rightarrow (S_1 + G) \rightarrow G \rightarrow (G + S_2) \rightarrow S_2 \rightarrow (S_2 + Aq)$$

has been observed in the absence of any organic liquid when a 12 % aqueous solution of a mixture of C_{10}-C_{18} sodium secondary alkyl sulphates (containing 3·5 % sodium sulphate) was converted to a solution of cyclohexylammonium alkyl sulphates by gradual addition of cyclohexylammonium chloride. Also it has been found that the hydrophilic character of the molecule apparently decreases in the series sodium tetradecan -3,

---

[8] Schulman, *Trans. Faraday Soc.* 1946, 42B, 165.

-4, -5, -6 and -7 sulphates. These results will be discussed in Part VIII. In correlation with this, at room temperature 20 % aqueous solutions of sodium tetradecan sulphates are, in the case of the -3, -4 and -5 sulphates, clear sols (S_1), in the case of the -6 sulphate, a mixture of sol and gel ($S_1 + G$) and in the case of the -7 sulphate a gel. On cooling the -7 sulphate gel it gives a mobile milky emulsion (possibly a Type II system).

Solubilisation in Ethylene Glycol.

Mutual solubilisation of ethylene glycol and organic liquids immiscible with ethylene glycol by means of amphiphiles we have also found to conform to the generalisations given above. Thus, on addition of *n*-dodecanol to a mixture of equal volumes of benzene and ethylene glycol in the presence of Aerosol OT (*ca.* 14 %) the typical sequence of changes, Type I system → Type IV system (clear sol) → Type II system may be observed. Addition of water or sodium sulphate shifts this sequence of changes to the right. In this and other cases of solubilisation in ethylene glycol we have not yet observed discontinuity (S_1, G, S_2 changes) within the region of Type IV systems.

An Interpretation of the Foregoing Experimental Generalisations.

The ratio *R*.—Taking first systems containing $\overline{\mathrm{O}}$, $\overline{\mathrm{W}}$ and C′, let us consider the ratio *R* representing

$$\frac{\text{solvent attraction between C and } \overline{\mathrm{O}} \text{ in the solubilised phase}}{\text{solvent attraction between C and } \overline{\mathrm{W}} \text{ in the solubilised phase}}$$

In this expression C represents C′ solvated by chemical and van der Waals forces by both $\overline{\mathrm{O}}$ and $\overline{\mathrm{W}}$. With a semiquantitative significance we may write

$$R = \frac{A_{\mathrm{C}\overline{\mathrm{O}}}}{A_{\mathrm{C}\overline{\mathrm{W}}}} = \frac{A_{H\mathrm{C}\overline{\mathrm{O}}} + A_{L\mathrm{C}\overline{\mathrm{O}}}}{A_{H\mathrm{C}\overline{\mathrm{W}}} + A_{L\mathrm{C}\overline{\mathrm{W}}}}.$$

In Fig. 2 it is clear that $R < 1$ on the extreme left of the diagram, while $R > 1$ on the extreme right.

If Methods I (*a*)-(*d*) for passing from left to right in Fig. 2 are examined they will all be seen to be methods which would be expected to increase *R*. Conversely Methods II (*a*)-(*d*) for passing from right to left in Fig. 2 are methods which would be expected to diminish *R*. In view of the symmetrical character of Fig. 2 it may reasonably be assumed, as a working hypothesis, that the value $R = 1$ corresponds to the centre of the diagram, i.e. in cases where gels occur, to the middle of the gel region or, in the absence of gels, to the middle of the Type IV region as a whole.

Phase Structures in Fig. 2.

(1) Structures of $\overline{\mathrm{O}}$ and $\overline{\mathrm{W}}$ Phases.—Of the phases in the foregoing systems the $\overline{\mathrm{O}}$ and $\overline{\mathrm{W}}$ phases of systems of Types I, II and III are constituted similarly to the O and W phases of, e.g., a benzene-water system.

(2) Structures of S_1, G and S_2 Phases.—An attempt to elucidate the comparative structures of S_1, G and S_2 systems by X-ray methods is at present in progress. However, the following suggestion based on solubility relationships may be tentatively given here. The gradually progressive solution of $\overline{\mathrm{O}}$ and $\overline{\mathrm{W}}$ in Type I or Type II systems on gradual increase or reduction of *R* respectively, indicates strongly that Type IV systems, whether sol S_1, gel G or sol S_2, are solutions rather than emulsions of extremely small particle size. These solutions arise probably not by any increase in the solvent attraction $A_{\overline{OW}}$ due to the influence of C, but through the formation of ordered molecular assemblages within the solution in which the L affinities of $\bar{O}$ and C and the H affinities of $\bar{W}$ and C mutually satisfy each other respectively (cp. McBain[10]).

The presence of the "lamellar micelle" assembly, such as shown in Fig. 3 has now been demonstrated in solubilised systems by several investigators (cp. e.g. Harkins, Mattoon and Corrin[11]).

If the ratio R above is taken as giving a measure of the relative dispersing forces acting on the lipophilic and hydrophilic faces respectively of a C layer in such lamellæ, then when $R = 1$ there would be no tendency for the planar lamellæ to distort and their maximum extension would be expected. Any hindrance to shearing of one lamellar plane over another would have maximum opportunity to manifest itself in the appearance of gelation and a liquid crystalline structure showing birefringence.

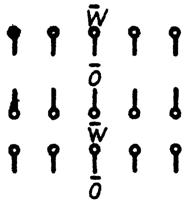

FIG. 3.

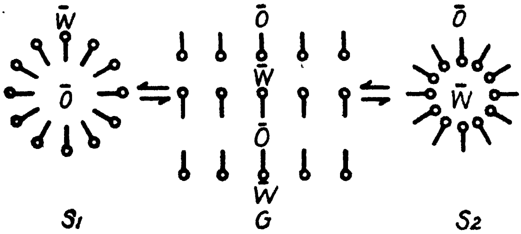

FIG. 4.

If, however, R were considerably increased or diminished one might anticipate a tendency of the planes of the lamellæ to curl and to give spheroidal lipophilic or spheroidal hydrophilic micelles respectively. If R departed too greatly from unity the curling tendency would increase sufficiently to cause breakdown of the molecular assemblages with separation of $\bar{W}$ or $\bar{O}$ respectively. It, therefore, seems possible that probable molecular arrangements, or micelles, which will occur in S_1, G and S_2 can be represented by Fig. 4 (drawn without respect to precise shapes or dimensions. The "globular" micelles need not necessarily be spherical.)

Since, however, G can co-exist with S_1 or S_2 it seems likely that the energy differences between the different micellar forms are small and that probably all three co-exist in equilibrium in the solution, their relative proportions depending both on the ratio R and the relative proportions of the components of the system. The case of sols S_2 of not very low electrical conductivity may arise from the presence of a considerable proportion of lamellar micelle in S_2.

It is likely that the globular micelles depart readily from the true spherical form. This is shown by the fact that it is possible to prepare S_1 sols of not very great viscosity that contain a very high proportion of $\bar{O}$ and to obtain S_2 sols of not very great viscosity containing a very high proportion of $\bar{W}$. The example of the S_1, G, S_2 transformation in absence of O mentioned above provides an example of such an S_2 sol.

In a case such as the latter the ratio R, still representing the relative dispersing forces acting on the lipophilic and hydrophilic radicals of the amphiphile molecules, may qualitatively be indicated by an expression such as

$$R = A_{LCO}/A_{C\bar{W}}.$$

---

[10] Palit and McBain, *Ind. Eng. Chem.*, 1946, 38, 743.

[11] Harkins, Mattoon and Corrin, *J. Colloid Sci.*, 1946, 1, 105.

Emulsification.

(1) Spontaneous Emulsification.—If known cases of spontaneous emulsification are examined (cp. e.g. Clayton [12]), it will probably be found that they fall into one or other of the following categories :

(a) emulsifier formed at interface, e.g. sodium oleate from oleic acid in oil phase and sodium hydroxide in water ; cholesterol in oil and sodium cetyl sulphate in water ;

(b) emulsifier dissolved in phase in which it is preferentially less soluble which is then added to the other phase.

In either case conditions are arranged which render possible an initial concentration and equidistribution of the emulsifier between the two phases at the interface. This is probably the condition for that extremely low *initial* interfacial tension which makes spontaneous emulsification possible. If the conditions are modified so as to make an initial concentration of the emulsifier at the interface unlikely, e.g. if the cholesterol in the case above is first dispersed in the water phase instead of in the oil, spontaneous emulsification no longer occurs.

(2) Relative Solubility of Emulsifier in the Phases and Nature of Continuous Phase of an Emulsion.—An interfacial layer of amphiphile molecules between the O and W phases of an emulsion may have different spreading pressures π_H and π_L on its hydrophilic and lipophilic faces respectively. If $R = 1$, then probably $\pi_H = \pi_L$ and the nature of the continuous phase may largely be determined by other mechanical factors. If the emulsifier is distributed in favour of the oil phase in the emulsion so that $R > 1$, then probably $\pi_H < \pi_L$ and there will be a tendency towards formation of W/O emulsions. If the emulsifier is distributed in favour of the aqueous phase so that $R < 1$ then probably $\pi_H > \pi_L$ and there will be a tendency towards formation of O/W emulsions. These conclusions are in accord with the results of many workers (cp. e.g. Wellman and Tartar [13]) and with our own experience.

The writer wishes to express his thanks to the N. V. de Bataafsche Petroleum Maatschappij and to the " Shell " Refining and Marketing Company Ltd., for permission to publish this paper.

Summary.

This paper is the first in a series in which particular aspects of hydrotropy, solubilisation and emulsification processes are discussed. The concept of the hydrotropic salt as a common solvent (cp. Lindau [1]) for water and water-insoluble organic liquids is used to interpret and systematise many phenomena in the mutual solubilisation of organic and aqueous liquids by means of 5-25 % of various hydrotropic salts and soap-like compounds. The bearing of certain of the concepts involved on related emulsification phenomena is shortly discussed.

PART II.—THE SOLUBILISATION OF PETROLEUM ETHER WITH SODIUM SECONDARY C_{10}-C_{18} ALKYL SULPHATES.

In Part I a classification of various types of completely and partially solubilised systems was given, methods of interconversion of the different types of system were described and a general theory of solubilisation correlating qualitatively the experimental facts was suggested. In the present paper an account is given in the terms of this theory of the effects of (1) cyclohexanol, (2) inorganic salts and (3) water-soluble alcohols and amines on the mutual solubilisation of petroleum ether (or petroleum ether/cyclohexanol mixtures) and water (or aqueous sodium sulphate solutions) with sodium secondary C_{10}-C_{18} alkyl sulphates.

---

[12] Clayton, *Emulsions and Their Technical Treatment* (Churchill Ltd., London, 4th ed., 1943), p. 68.

[13] Wellman and Tartar, *J. Physic. Chem.*, 1929, 33, 437.

The sodium secondary C_{10}-C_{18} alkyl sulphates used were obtained from the commercial product Teepol of Messrs. Technical Products Limited. The remaining reagents were of good commercial quality and since the experiments recorded were designed to give information of a qualitative, rather than of an exactly quantitative character, these reagents were not purified further before use. In order to prevent its crystallisation at lower room temperatures, 2 % (by vol.) of water was added to the cyclohexanol used. Although in these experiments, a mixture of sodium secondary C_{10}-C_{18} alkyl sulphates was used as solubiliser, these are regarded as operating together as a single amphiphile having approximately the mean of their individual properties. The justification for adopting this method of treatment lies in the consistent interpretation of the results thereby obtained and also in further experimental evidence which will be presented in Part IV.

Results and Discussion.

(1) The Effect of Cyclohexanol on the Mutual Solubilisation of Petroleum Ether and Water with Sodium Secondary C10-C18 Alkyl Sulphates at Room Temperature (approx. 18-20° C.)

A solution, S containing 23·9 g. sodium secondary C_{10}-C_{18} alkyl sulphates and 7·1 g. sodium sulphate per 100 cc. solution was prepared. If increasing amounts of cyclohexanol are added to mixtures of equal volumes of petroleum ether (b.p. 60-80° c.) and S and the mixtures are then allowed to settle, the following successive changes are observed.

(*a*) With no cyclohexanol most of the petroleum ether separates as an upper layer (*p*), although a small proportion is solubilised in the lower aqueous alkyl sulphate layer (*e*), i.e. a Type I system (Part I, p. 377) is produced. In terms of the theory suggested in Part I and using the symbols there employed, this indicates that in this system the ratio

$$R = \frac{A_{C\overline{O}}}{A_{C\overline{W}}}$$

is markedly less than 1.

(*b*) As the hydrophilic character of the lipophilic liquid $\overline{O}$ is further increased by addition of cyclohexanol the ratio R is increased by increase of $A_{H\overline{OO}}$. As R approaches unity the solubilisation of the excess organic layer (*p*) in the alkyl sulphate layer (*e*) increases until finally a homogeneous solution, classified as a Type IV system results (cp. Part I, Method 1(*b*)).

(*c*) Disregarding S_1, G, S_2 changes within the Type IV region (cp. Part I, p. 380) which in the systems described in this paper are in no case strongly marked, the next effect of further addition of cyclohexanol is to cause the separation of a lower aqueous salt layer (*w*) which increases as the amount of cyclohexanol is increased. Type II systems are produced, $A_{H\overline{OO}}$ having been so increased that R is sufficiently greater than 1 to cause separation of an aqueous phase.

The successive changes (*a*)-(*c*) are illustrated in Table I.

The gradual solution of (*p*) and the gradual precipitation of (*w*) and the production of Type III systems (cp. Table II below) are strong evidence against viewing the structure of (*e*) as that of an emulsion of extremely fine droplet size (cp. Schulman [1]) and indicate rather that (*e*) is a true solution of its components, although these probably have an ordered arrangement, as explained in Part I. Analysis shows that the amounts of C and $\overline{W}$ and of C and $\overline{O}$ in (*p*) and (*w*) respectively are small. (*p*) is richer in petroleum spirit than $\overline{O}$ and (*w*) contains a higher proportion of sodium sulphate than $\overline{W}$.

---

[1] Schulman, *Trans. Faraday Soc.*, 1946, 42B, 165.

Variation in the Solubilisation of Petroleum Ether and Cyclohexanol as the Concentration of Sodium Secondary C_{10}-C_{18} Alkyl Sulphate is Changed.—In Fig. 1, curves 1 and 2 illustrate the effect of added cyclohexanol on mixtures of 50 cc. petroleum ether (b.p. 60-80° c.) with 50 cc. of sodium secondary C_{10}-C_{18} alkyl sulphate solutions of various concentrations. These solutions were prepared by diluting the solution S (containing 23·9 g. RSO_4Na, 7·1 g. Na_2SO_4 per 100 cc.) with water so that amphiphile and sodium sulphate were diluted correspondingly.

TABLE I.—EFFECT OF ADDITION OF CYCLOHEXANOL TO A MIXTURE OF 50 CC. PETROLEUM ETHER (B.P. 60-80° C.) AND 50 CC. OF AN AQUEOUS SOLUTION CONTAINING 12 g. SODIUM SECONDARY C_{10}-C_{18} ALKYL SULPHATES AND 3·6 g. SODIUM SULPHATE.

Type of System.	I.				IV.	II.	
Cyclohexanol added cc.	0	1	2	3	5	8	12
Excess organic solvent layer (p) cc.	43	39	24	10	0	0	0
Solubilised layer (e) cc.	57	62	78	93	105	105	97
Separated aqueous layer (w) cc.	0	0	0	0	0	3	5

Curve 1 represents the minimum volumes of cyclohexanol required to solubilise the excess organic liquid (p) and curve 2 represents the minimum volumes of cyclohexanol required to cause separation of the aqueous layer (w). As the amount of amphiphile present is diminished curves 1 and 2 converge, i.e. the range of $\overline{O}$ compositions which, together with the $\overline{W}$ present, dissolve in the common solvent C is restricted as the amount of C is diminished. With an alkyl sulphate solution of concentration somewhat less than 10 %, precipitation of the aqueous layer (w) commences before solubilisation is complete, and three-phase, Type III systems, result. Here although R, in the solubilised phase, is in the region of 1, there is insufficient of the common solvent C present to dissolve totally both (p) and (w). An example of this is given in Table II.

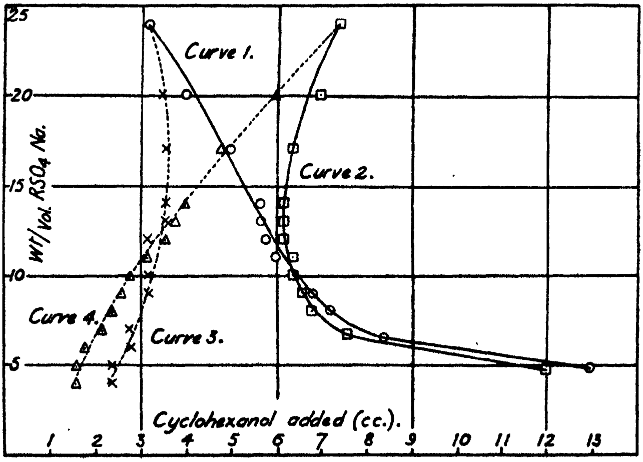

FIG. 1.—Effect of cyclohexanol on mixtures of petroleum spirit (b.p. 60-80° c.; 50 cc.) and sodium *sec.* C_{10}-C_{18}-alkyl sulphate solutions (50 cc.) of various dilutions.

—— S diluted with water. - - - S diluted with 7·1 % Na_2SO_4 soln.

Original concentration of "S" RSO_4Na 23·9 % w/v; Na_2SO_4 7·1 % w/v.

× ○ Petroleum layer just solubilised. △ □ Water layer just precipitated.

Gradual addition of cyclohexanol to a mixture of equal volumes of petroleum ether and a sodium alkyl sulphate solution containing less than 4 % RSO_4Na and 1·2 % Na_2SO_4 causes neither the formation of a Type IV nor of a Type III system. Solubilisation of petroleum ether in the alkyl sulphate solution is at first increased but on further addition of cyclohexanol the alkyl sulphate passes gradually into the organic phase. This is illustrated in Table III.

TABLE II.—EFFECT OF ADDITION OF CYCLOHEXANOL TO A MIXTURE OF 50 CC. PETROLEUM ETHER (B.P. 60-80° C.) AND 50 CC. OF AN AQUEOUS SOLUTION CONTAINING 4 g. SODIUM SECONDARY C_{10}-C_{18} ALKYL SULPHATES AND 1·2 g. SODIUM SULPHATE.

Type of System.	I.					III.	II.
Cyclohexanol added cc.	5	5·4	5·8	6·2	6·6	7·0	7·4
Excess petroleum ether (*p*) cc.	34	31·4	27·8	22·6	16·2	6·6	0
Solubilised layer (*e*) cc.	71	74	78	83·6	90·4	90·4	91
Separated aqueous layer (*w*) cc.	0	0	0	0	0	0	16·4

It is of interest that the completely settled aqueous phases of the intermediate systems show a marked opalescence. Although the interfacial tension in these intermediate systems is very low and emulsification of the phases occurs very readily, the emulsions break down quite quickly with separation of the phases and formation of a well-defined interface is soon complete. This is possibly because in these systems there is a ready passage of material from the smaller droplets (of consequently higher solubility) via the continuous phase to the larger droplets (of consequently lower solubility). The complete reaggregation of the dispersed phase may thus be brought about.

TABLE III.—EFFECT OF ADDITION OF CYCLOHEXANOL TO A MIXTURE OF 10 CC. OF PETROLEUM ETHER (B.P. 65-95° C.) AND 10 CC. OF AN AQUEOUS SOLUTION CONTAINING 0·4 g. SODIUM SECONDARY C_{10}-C_{18} ALKYL SULPHATES AND 0·12 g. SODIUM SULPHATE.

Type of System.	I.				Intermediate.				II.	
Cyclohexanol added cc.	0·5	1	2	3	4	5	6	8	10	12
Upper layer cc.	9·5	9·4	9·6	10	11·5	13·9	15·7	18·6	20	23·1
Lower layer cc.	11	11·6	12·4	13·0	12·5	11·1	10·3	9·4	9·1	8·9
RSO_4Na estd. in upper layer g.	most	most	most	0·34	0·28	0·22	0·15	0·10	0·04	most
RSO_4 Na estd. in lower layer g.	traces	traces	traces	0·05	0·11	0·20	0·25	0·29	0·39	traces

(2) The Effect of Inorganic Salts on the Mutual Solubilisation of Water and Petroleum Spirit+Cyclohexanol Mixtures with Sodium Secondary C_{10}-C_{18} Alkyl Sulphates.

(*a*) **Effect of Sodium Sulphate** (cp. Part I, Method I (*d*)).—In Fig. 1, curves 3 and 4, have the same significance as curves 1 and 2 discussed above except that the sodium alkyl sulphate solution, S, was diluted with a 7·1 % (wt./total volume) aqueous sodium sulphate solution instead of with water alone. The reversal in trend of curve 2 is thus shown to be associated with the concurrent dilution of both the sodium sulphate and the sodium alkyl sulphate.

According to the theory advanced in Part I, the effect of sodium sulphate is to increase *R* by reducing the term A_{OW}. The effects of sodium sulphate and of cyclohexanol are thus supplementary and independent increase of sodium sulphate content diminishes the volume (V_s) of cyclohexanol necessary to solubilise the petroleum ether and also that (V_w) necessary to cause separation of a free aqueous phase. V_w is reduced more rapidly than V_p and the range of completely solubilised compositions is thus diminished. This is to be expected if the origin of solubilisation phenomena is the cosolvency of the amphiphile C for both $\overline{O}$ and $\overline{W}$ and the effect of sodium sulphate is to reduce the solvent attraction between C and $\overline{W}$ rather than to increase the solvent attraction between C and $\overline{O}$. A further example of the effect of sodium sulphate is given in Table IV.

TABLE IV.—THE EFFECT OF ADDED SODIUM SULPHATE ON THE VOLUMES OF CYCLOHEXANOL REQUIRED, (V_p) JUST TO SOLUBILISE THE PETROLEUM SPIRIT AND (V_w) JUST TO PRECIPITATE AN AQUEOUS PHASE WHEN ADDED TO A MIXTURE OF 50 CC. PETROLEUM ETHER (B.P. 60-80° C.) AND 25 CC. OF AN AQUEOUS SOLUTION CONTAINING 6·0 g. SODIUM SECONDARY C_{10}-C_{18} ALKYL SULPHATES.

Added Sodium Sulphate (g.).	(V_p).	(V_w).
0	8·7	35
1·0	3·6	4·6
1·5	2·3	3·5
2·0	1·9	3·0
2·5	1·6	2·6
3·0	1·3	2·3

(*b*) Effect of other Inorganic Salts.—Other inorganic salts, e.g. NaCl, NH_4Cl, $CaCl_2$, $CuSO_4$, exert an effect on the systems which is similar in kind, though different in degree, to that of sodium sulphate.

(3) The Effect of Water Soluble Alcohols and Amines on the Mutual Solubilisation of Petroleum Ether + Cyclohexanol Mixtures with Sodium Secondary C_{10}-C_{18} Alkyl Sulphates.—The results recorded in Table V. show that the effect of water soluble alcohols is in the opposite sense to that of inorganic salts. The effects of glucose and acetone are added for comparison.

n- and *iso*-butyl alcohols behave as oil-soluble hydroxy compounds and act in the same way as cyclohexanol (Part I, Method I (*b*)). This tendency is already evident with *n*-propyl alcohol, as can be seen from Table V.

According to the view of solubilisation taken here the mode of operation of the water-soluble hydroxy and amino compounds is by diminishing *R* thereby increasing $A_{C\overline{W}}$, the total solvent attraction between C and $\overline{W}$ (cp. Part I, Method

TABLE V.—THE EFFECT OF WATER SOLUBLE HYDROXY AND AMINO COMPOUNDS ON THE VOLUMES OF CYCLOHEXANOL REQUIRED, (V_p) JUST TO SOLUBILISE THE PETROLEUM ETHER LAYER AND (V_w) JUST TO PRECIPITATE AN AQUEOUS LAYER WHEN ADDED TO MIXTURES OF 5 CC. PETROLEUM ETHER (B.P. 80-100° C.) AND 5 CC. OF AN AQUEOUS SOLUTION CONTAINING 1·2 g. SODIUM SECONDARY C_{10}-C_{18} ALKYL SULPHATES, AND 0·35 G. SODIUM SULPHATE

Volume of Water-soluble Compound Added (cc.).	0·5		1		2		3	
Compound added cc.	V_p.	V_w.	V_p.	V_w.	V_p.	V_w.	V_p.	V_w.
No additive	0·35	0·7	—	—	—	—	—	—
Water	0·40	0·75	0·45	0·80	0·55	0·85	0·60	0·90
Methyl alcohol	0·65	0·85	0·95	1·1	2·2*	2·5*	*	*
Ethyl alcohol	0·6	0·85	0·95	1·15*	1·8 *	2·7*	*	*
Propyl alcohol	0·35	0·65	0·25	0·5	0·1*	0·3*	*	*
*Iso*propyl alcohol	0·4	0·7	0·5	0·75*	0·7*	1·2*	*	*
Glycol	0·5	0·8	0·65	0·9	0·9	1·2	1·0	1·2
Glycerol	0·5	0·8	0·6	0·85	0·7	0·85	1·0	1·2
Glucose (g.)	0·3	0·65	0·3	0·6	0·25	0·55	0·25	0·55
Acetone	0·4	0·95	0·6	1·7*	*	*	*	*
Acetic acid	0·8	0·95	1·2	1·3*	*	*	*	*
1 : 2-Ethanolamine	0·55	0·85	0·75	1·15	*	*	*	*
Ethylene diamine	0·6	0·9	0·75	1·6	*	*	*	*

* Sodium sulphate precipitated.

II (*b*)). This may occur if the lipophilic solvent affinity of these organic $\overline{W}$-soluble compounds is greater than that of $\overline{W}$ originally, while their hydrophilic solvent affinity is not greatly less than that of $\overline{W}$ originally. Table V shows that mere dilution with water exerts a similar effect, though smaller in degree, to addition of these water-soluble organic liquids. In this case $A_{C\overline{W}}$ is increased mainly because $(H_2O)_n$ has a higher solvent affinity for C than has $\overline{W}$ originally, i.e. $(H_2O)_n + Na_2SO_4$). (cp. Part I, Method I (*d*)).

The writer is grateful to the N.V. de Bataafsche Petroleum Maatschappij and to " Shell " Refining and Marketing Co. Ltd., for permission to publish this work and wishes to thank Dr. P. J. Garner, Senior Chemist of these laboratories, for his encouragement and constructive criticism.

Summary.

An account is given in the terms of the theory advanced in Part I, of the effects of (1) cyclohexanol, (2) inorganic salts and (3) water-soluble alcohols and amines on the mutual solubilisation of petroleum ether (or petroleum ether-cyclohexanol mixtures) and water (or aqueous sodium sulphate solutions) by means of sodium secondary C_{10}-C_{18} alkyl sulphates.

PART III.

(*a*) The Solubilisation of Miscellaneous Organic Liquids with Sodium Secondary C_{10}-C_{18} Alkyl Sulphates.

In Part I of this series four main types of system were distinguished which may be produced from approximately equal volumes of a water insoluble organic liquid $\overline{O}$ (pure substance or mixture) and water (or an aqueous inorganic salt solution) $\overline{W}$ in the presence of from 5-50 % of an amphiphile C.

Results.

Table I records the types of system produced at room temperature (*ca* 19° C.) on mixing equal volumes of various water insoluble organic liquids and an aqueous solution S containing 23·9 g. sodium secondary C_{10}-C_{18} alkyl sulphates and 7·1 g. sodium sulphate per 100 cc. (cp. Part II, p. 383). The solvents used were of C.P. grade but without further purification except in special cases where this appeared desirable. Thus, e.g. the cyclohexanone was treated to remove cyclohexanol by shaking for 48 hr. with excess $CaCl_2$, followed by filtration and redistillation.

According to the theory of solubilisation put forward in Part I, Type I, Type IV and Type II systems are distinguished by having $R \ll 1$, R in the region of 1 and $R \gg 1$ respectively where

$$R = \frac{A_{CO}}{A_{C\overline{W}}} = \left(A_{LCO} + A_{HC\overline{O}}\right) \Big/ \left(A_{LC\overline{W}} + A_{HC\overline{W}}\right),$$

where A_{XY} signifies the solvent attraction (*L* lipophilic and *H* hydrophilic) between X and Y in the solubilised phase.

In agreement with this view, in most cases, mixtures of suitable proportions of the (heterogeneous) systems of Types I and II give (homogeneous) systems of Type IV (Part I, interconversion methods, I (*b*), II (*d*)). This phenomenon has been observed, e.g. with mixtures of (5) and (20); (10) and (4); ((1) = benzene) and (12); (3) and (9); (4) and (9); (10) and (6); (30) and (32). In the case of certain mixtures, e.g of (20) and (21); (20) and (3); or (10) and (3), passage from a Type II to a Type I system is very rapid and, with the particular concentrations used in these experiments, a homogeneous system may not be obtained. It may be noted that here at least one of the components of $\overline{O}$ would be expected to exert neither marked lipophilic nor marked hydrophilic affinity. As might be expected compounds of this type, e.g. triacetin or tributyrin, both of which form three-phase systems with excess water and higher paraffins, are not solubilised readily by sodium C_{10}-C_{18} secondary alkyl sulphates. The remaining interconversion methods given in Part I may also be used to obtain

Type IV systems from the heterogeneous systems recorded in the above table. Thus e.g. addition of ethylene glycol to (10) (Method II (*b*)) or of sodium chloride (Method I (*d*)) or cyclohexanol (Method I (*b*)) to (5) or (6) gives clear homogeneous solutions.

The relative behaviour of the isomeric octanols and tetradecanols (cp. (27)-(32)) is of particular interest and will be described in detail in a later communication.

TABLE I.

	Solvent.	Type of System Produced.
1	Hydrocarbons, chlorohydrocarbons .	I
2	Nitrobenzene	I
3	Phenyl methyl ether	I
4	Di-*iso*propyl ether	I
5	Diethyl ether	I
6	Di-*iso*butyl ketone	I
7	Methyl *iso*butyl ketone	IV (sol)
8	Octanone-2	IV (sol)
9	*n*-Heptaldehyde	II
10	Cyclohexanone	II
11	Methyl ethyl ketone	II
12	*n*-Butyraldehyde	II
13	Ethyl oleate	I
14	Ethyl nonoate	I
15	Dimethyl phthalate	I
16	*n*-Octyl acetate	IV (sol + gel)
17	Cyclohexyl acetate	IV (sol)
18	Amyl acetate (A.R. Isomer unspecified)	IV (sol)
19	*n*-Butyl acetate	Type IV (sol) at 17° C. becomes Type II on warming
20	Ethyl acetate	II
21	Ethyl butyrate	I
22	Ethyl *iso*butyrate	I
23	1-Alkanols	II
24	1-Alkanoic acids	II
25	1-Alkylamines	II
26	1-Alkanoic acid amides	II
27	Octanol-1	II
28	Octanol-4	IV below 14° C.; II above
29*	Tetradecanol-1 (m.p. 36-37° C.) . .	II
30*	Tetradecanol-2 (m.p. 32·5° C.) . .	II
31*	Tetradecanol-3 (m.p. 28-29·5° C.) . .	IV (sol + gel)
32*	Tetradecanol-7 (m.p. 41° C.) . . .	I

* Mixed just above melting point.

The less hydrophilic character of the *n*-alkanols with near medial hydroxyl groups (cp. Part I, p. 380) as compared with *n*-alkanols with near terminal hydroxyl groups, appears to be bound up with a diminished tendency to form hydrogen bonds. This is exhibited also in the relative boiling points of these alkanols (octanol-1, b.p. 196° C.; octanol-4, b.p. 173-175° C.) and in their Raman spectra (cp. Pauling[1]).

The Type IV system (16) obtained from 5 cc. *n*-octylacetate (b.p. 212-214° C.; n_D^{20} 1·4191) and 5 cc. sodium C_{10}-C_{18} secondary alkyl sulphate solution S consists of sol S_2 + gel G (cp. Part I). Addition of 0·1 cc. of hexanol-1 converts this S_2 + G mixture into a clear homogeneous sol (S_2) while 0·2 cc. hexanol-1 gives a Type II system (Method I (*b*)). Addition of 0·07 cc. ethylene glycol to the G + S_2 system gives a clear gel, 0·15 cc. gives a G + S_1 system, 0·2 cc. a clear sol S_1 and 0·4 cc. a Type I system (Method II (*b*)). If the (heterogeneous) Type I and Type II systems produced with 0·4 cc. of ethylene glycol and 0·2 cc. hexanol-1 respectively, are mixed a clear homogeneous solution (Type IV) is produced.

---

[1] Pauling, *The Nature of the Chemical Bond*, p. 304.

Although Table I records no case of a Type III system, such systems may be obtained with a single organic solvent employing suitable proportions of the components. Thus mixtures were prepared containing methyl *iso*butyl ketone (10 cc.) and aqueous solutions (10 cc.) containing various concentrations of sodium C_{10}-C_{18} secondary alkyl sulphates and 7·1 % (wt./vol.) of sodium sulphate. Type III systems were produced at room temperature (20° c.) with concentrations of RSO_4Na less than 20 %. Above this concentration clear sols were produced. This behaviour is illustrated in Table II.

TABLE II.

% RSO_4Na in Aqueous Solution.	1	2	3	5	7	10	14	20	23·9
Upper layer cc.	9·3	9·3	8·6	8·1	7·6	6·5	5	nearly clear sol †	0
Middle layer cc.	0·8	1·6	4·4	5·9	6·9	10·3	13		20
Lower layer .	9·9*	9·1*	7·0	6	5·5	3·2	2		0

* Cooling causes mutual solution of the lower and middle layers.

† Cooling causes separation of an upper ketone layer, warming causes separation of an aqueous layer, both changes being reversible with change of temperature

Temperature Effects.

It will be noted that the temperature effects recorded in Table I (19 and 26) and in Table II are the reverse of those most frequently found in these systems (Part I). This illustrates the great variability of temperature effects in solubilised systems. This subject will be discussed in a future communication.

(*b*) The Effect of Dilution on Solubilisation:

In Type I or Type II systems respectively addition of either organic liquid or aqueous solution of the same composition (apart from traces of C, etc.) as the excess phase can obviously exert little effect on *R* or on the composition of the solubilised phase. Addition of $\overline{O}$ (without alteration in composition of $\overline{O}$) to a type IV or Type II system or of $\overline{W}$ to a Type IV or Type I system will respectively increase or diminish *R* by mass action (Methods I (*a*) and II (*a*)). Addition of water to a system in which $\overline{W}$ is water + sodium sulphate will also tend to increase *R* by increasing A_{LCW} through altering the composition of $\overline{W}$ (= $(H_2O)_n$ + Na_2SO_4) in favour of the more lipophilic $(H_2O)_n$ (cp. Part II, p. 382).

TABLE III.

Volume Water Added (cc.).	Volume Cyclohexanone Added (cc.).	Type of System Produced.
<14	0	II
14	0	IV (clear sol)
14	1	II
15	1	IV
15	2	II
16	2	IV[1]
16	3	II
17	3	IV[2]
17	4	II
18	4	IV[3]

The following two experiments provide examples of certain of these principles.

(1) To 10 cc. cyclohexanone (b.p. 155-57° c. ; n_D^{20} 1·4517) and 10 cc. of S (v.s.) water and cyclohexanone were added alternately. The types of system produced are recorded in the following Table III.

The sols marked 1, 2, 3 showed increasing opalescence respectively.

(2) Cyclohexanol and water were added alternately to a mixture of 20 cc. of S (v.s.) and 20 cc. of cyclohexane. It will be seen from the following Table IV that added cyclohexanol produces changes in these systems in the direction Type I → IV → II (Method I (*b*)) while added water produces changes in the reverse direction (Method II (*b*)).

TABLE IV.

Vol. of Cyclohexanol Added (cc.).	Vol. of Water Added (cc.).	Type of System Produced.
0	0	I
2·6	0	II
2·6	10	IV (clear sol)
2·6	20	IV (clear sol)
2·6	30	IV (clear sol)
2·6	40	I
2·7	40	IV (clear sol)
4·4	40	II
4·4	50	IV (clear sol)
5·0	50	II
5·0	60	IV (clear sol)
5·0	70	IV (clear sol)
6·4	70	II
6·4	80	IV (clear sol)
7·5	80	II (20 cc. aqueous layer ; upper layer opalescent sol)

The author wishes to thank N.V. de Bataafsche Petroleum Mij., and " Shell " Refining and Marketing Co. Ltd., for permission to publish this paper, and Dr. P. J. Garner for encouragement given during its preparation.

Summary.

The classification of partly and completely solubilised systems and the theory of solubilisation advanced in Part I are used to interpret the solubilisation behaviour of 30 organic liquids and their mixtures with certain solutions of sodium C_{10}-C_{18} secondary alkyl sulphates. Dilution effects are also described in terms of the same theory.

PART IV.—SOLUBILISATION WITH MISCELLANEOUS AMPHIPHILES.

Received 11*th February*, 1947; *as revised* 5*th June*, 1947.

In Parts II and III of this series, the application of the general theory of solubilisation advanced in Part I to various systems solubilised with a mixture of sodium secondary C_{10}-C_{18} alkyl sulphates has been described. The mixed C_{10}-C_{18} alkyl sulphates were regarded as operating together as a single amphiphile. In the present paper the applicability of the theory of Part I to solubilisation with miscellaneous amphiphiles is illustrated with examples involving Aerosol OT (sodium sulpho-dioctyl succinate), sodium undecylate, mixtures of Aerosol OT and sodium undecylate, mixtures of sodium and organic ammonium secondary C_{10}-C_{18}

alkyl sulphates, sodium undecane-3 carboxylate, undecane-1 and -3 ammonium chlorides, sodium *n*-butyrate and sodium *iso*butyrate. Although differing in detail, in main outline all the amphiphiles show very closely analogous behaviour to one another and to the mixed sodium secondary C_{10}-C_{18} alkyl sulphates described in Parts II and III.

Experimental Results and Discussion.

(*a*) Solubilisation with Aerosol OT.—The Aerosol OT used was that manufactured by Cyanamide Products Ltd., London E.C. 2, and marketed as Aerosol OT 100 % Pellets. Apart from a little water it appeared to be substantially

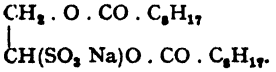
$$\begin{array}{l} CH_2\,.\,O\,.\,CO\,.\,C_8H_{17} \\ | \\ CH(SO_3\,Na)O\,.\,CO\,.\,C_8H_{17}. \end{array}$$

The relative solvent affinity of solvated Aerosol OT for organic liquids and water, is much more in favour of the organic liquids than is that of the mixture of sodium secondary C_{10}-C_{18} alkyl sulphates discussed in Parts II and III. Thus in certain cases where the latter gives Type I systems, Aerosol OT gives systems of Type IV or II.

Example I. A mixture of 10 cc. of a 20 % (wt./total vol.) solution of Aerosol OT (water content less than 1 %) in petroleum spirit (b.p. 65-95° c.) with 10 cc. of water gives a Type IV system at the stage intermediate between gel (G) and sol (S_2) (Part I, p. 377). This may be converted into a petroleum dispersible sol S_2 by addition of cyclohexanol (1·1 cc.) (Method I (*b*), Part I, p. 378). Gradual addition of ethylene glycol (Method II (*b*)) gives first a gel, then (with 3·6-4·0 cc.) a clear water-dispersible sol S_1 and finally a Type I system (with more than 4 cc.).

Example II. When a small excess of water is added to 20 cc. of a 20 % solution of the above Aerosol OT in benzene, heterogeneous Type II systems are produced. These may be converted into homogeneous benzene-dispersible S_2 sols by addition of ethylene glycol (Method II (*b*)). This effect is illustrated by Table I.

TABLE I.

Water Added (cc.).	Glycol Added (cc.).	Type of System.
>1·95	0	II
1·95	5·8	S_2
2·15	5·8	II
2·15	6·3	S_2
2·75	6·3	II
2·75	6·5	S_2
3·15	6·5	II
3·15	6·6	S_2
3·3	6·6	II

Example III. When a small amount of water (0·2 cc.) is added to 5 cc. of a 25 % (wt./total vol.) solution of Aerosol OT (water content 2 %) in highly refined mineral oil (Technical White Oil; Pool Oil Specification No. 31, S.G. 0·835-0·875, Viscosity, Redwood I, 70-80 sec. at 100° F.) an oil layer separates and a Type I system is produced which may be made homogeneous by addition of, e.g. decanol-1 (Part I, Method I (*b*)). With 5 cc. of a 25 % solution in CCl_4, a small excess of water (0·5 cc.) gives a Type II system clarifiable by addition of ethylene glycol (Method II (*b*)). As would be expected therefore, a 25 % solution of Aerosol OT in a suitable mixture of CCl_4 and mineral oil will give a homogeneous system with more water than a 25 % solution in either solvent singly (Methods I (*b*) and II (*b*)). In Figure I. and throughout this paper $R = A_{c\bar{o}}/A_{c\bar{w}}$ has the same significance as in Part I where the importance of the order of magnitude of R in solubilised systems has been discussed.

(*b*) Solubilisation with Sodium Undecylate.—A 25 % (wt./total vol.) solution of sodium undecylate containing 0·06 g. % of excess NaOH was prepared from " pure " undecylic acid (*ex* A. Boake, Roberts & Co.). This sample of undecylic acid had m.p. 25° c. (lit. 29·5-30·5° c.; equivalent, found 185·5, theory 186).

Solutions of 20, 15 and 10 % concentration were prepared by dilution of the 25 % solution. Table II illustrates the very close analogy between the solubilisation of (cyclohexane and cyclohexanol) mixtures by sodium undecylate (both in the absence and presence of added sodium sulphate) and the solubilisation of (petroleum ether and cyclohexanol) mixtures with sodium secondary C_{10}-C_{18} alkyl sulphates described in Part II.

In Table II there is no marked appearance of a gel system recorded. If, however, the *n*-alkanol, hexanol-1, is used in place of cyclohexanol, gel formation is strong as shown in Table III.

As mentioned in Part I, gel formation is especially marked in systems containing an alkanol-1 and an amphiphile with a *n*-alkane chain and its polar group in the -1 position. Thus when an alkanol-1 is added to certain Type I systems a wide range of compositions showing marked gel formation may be produced and a clear S_1 sol may not be distinguishable. The solubilised phase of the Type I system may take the gel condition before all of the excess organic phase is solubilised.

(c) Solubilisation with Mixtures of Aerosol OT and Sodium Undecylate.—A mixture of 5 cc. of water and 5 cc. of a 25 % solution of Aerosol OT (water content 2 %) in CCl_4 gives a Type II system ($R > 1$) while a mixture of 5 cc. of a 25 % aqueous solution of sodium undecylate and 5 cc. of CCl_4 give a Type I system ($R < 1$). In a system containing two or more amphiphiles these

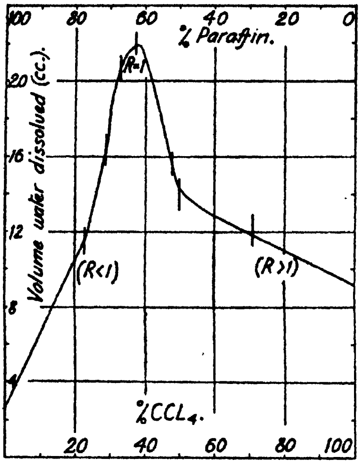

FIG. 1.—The volume of water soluble in 100 cc. of 20 % (wt./vol.) solutions of Aerosol OT ln carbon tetrachloride-paraffin mixtures.

TABLE II.—SOLUBILISATION OF MIXTURES OF SODIUM UNDECYLATE SOLUTIONS (5 CC.) AND CYCLOHEXANE (5 CC.) ON ADDITION OF CYCLOHEXANOL (CONTAINING 2 % OF WATER) AT 19° C.

Concn. of Sodium Undecylate Soln. %.	25		20		15		10	
Added Na_2SO_4 (g.)	0	0·2	0	0·2	0	0·2	0	0·2
Description of System Produced.	Volumes of Cyclohexanol (cc.) required to give Systems of Character Recorded in Left-hand Column.							
Type I . . .	<1·6	<1·2	<2·3	<1·35	<4·2	<1·55	No homogeneous systems. 1·5 cc. gives Type III system. Upper layer 1·0 cc.; middle layer 9·8 cc.; lower layer, 0·8 cc.	No homogeneous systems. Behaviour apparently as in Part II, Table III
Excess oil phase just solubilised	1·6	1·15	2·3	1·35	4·2	1·55		
Clear sols dispersible in water	1·6 mix with cyclohexanol in all proportions	1·15 (small G + S region between 1·30-1·35)	2·3 mix with cyclohexanol in all proportions	—	4·2 mix with cyclohexanol in all proportions with slight opalescence	—		
Excess aqueous phase just precipitated	—	2·80	—	2·25	—	1·85		
Type II systems	—	>2·80	—	>2·25	—	>1·85		

apparently often operate together similarly to a single amphiphile having approximately the weighted mean properties of the individual amphiphiles present (cf. Part II, p. 382). This is well illustrated by the following two examples.

TABLE III.—Effect of Addition of Hexanol-1 to a Mixture of 5 cc. Sodium Undecylate Solution (20 % wt./total Vol.) and 5 cc. Cyclohexane at 19° C.

Added Na_2SO_4 (g.).	0	0·2
Description of System Produced.	Volume of Hexanol-1 (cc.) Required to give System of Character Described in Left-hand Column.	
Type I systems (emulsions)	<1·25	<0·8
Excess oil phase just solubilised	1·25	0·8
Clear sol (S_1) (very bubbly)	1·25	0·8
Thin clear gel (S_1 + G) (apparently a homogeneous mixture)	1·40	0·95
Thick clear gel G	1·5-2·0	1·0-1·15
Hazy mix (G + S_2)	2·1	1·2
Clear sol S_2	2·75-8·1	1·35-1·65
Aqueous phase just precipitating	8·1	1·65
Type II systems	>8·1	>1·65

Example I. When the 25 % aqueous sodium undecylate solution is added to the Type II (CCl_4–Aerosol OT–water) system above, the changes recorded in Table IV are observed at room temperature (*ca.* 19°c.).

TABLE IV.

Volume of Sodium Undecylate Solution Added (cc.).	Probable Order of Magnitude of *R*.	Description of System.
<0·80	$R > 1$	Type II (excess water)
0·80		Clear sol S_2 not dispersible in water
0·85		Hazy mix (S_2 + G)
0·95		Thick slightly opalescent gel
1·00	$R \sim 1$	Clear thick gel G
1·20	$R < 1$	Thinner gel
1·25		Hazy mix (G + S_1)
1·50-1·85		Clear water-dispersible solution S_1
>1·85		Type I system (excess CCl_4)

Example II. Similarly when the 25 % solution of Aerosol OT in CCl_4 is added to the Type I CCl_4-sodium undecylate-water system, changes in the reverse order are observed as shown in Table V.

TABLE V.

Volume of Aerosol OT Solution Added.	Probable Order of Magnitude of *R*.	Description of System.
<3·5	$R < 1$	Type I system
3·5		Clear water dispersible solution S_1
3·7		S_1 + G
4·6	$R \sim 1$	Thick clear gel
6·3	$R > 1$	G + S_2

From the point of view of the theory of solubilisation advanced by Schulman[1] the last two examples and also that given under (*a*) Example III above, are noteworthy since the organic liquid solubilised contains no component of appreciable dipole moment or " surface active " character. It is also to be noted that while the S_2 sol under I contains a considerably higher W/O ratio than the S_1 sol under II, the former does not disperse in water while the latter disperses readily. The possible nature of the structural differences which may lead to these differences in dispersibility of S_1 and S_2 sols has been discussed in Part I.

(*d*) Solubilisation with Mixtures of Sodium and Organic Ammonium Secondary C_{10}-C_{18} Alkyl Sulphates.—Of the numerically classified methods of increasing *R* given in Part I, method I (*c*) involves increasing the lipophilic solvent affinity A_{L_O} of the amphiphile C. This may be done by increasing the size of the organic radical present in C, cp., e.g. the recent work of Durand[2] on the solubility of benzene in aqueous solutions of the sodium salts of the C_1-C_{11} *n*-fatty acids. Another means of increasing A_{L_O} available when C contains an inorganic ion, is to replace this ion partially or completely by a more lipophilic organic ion. In the case of the sodium secondary C_{10}-C_{18} alkyl sulphates already referred to in Parts II and III, this may be accomplished by the addition of an organic ammonium halide. The double decomposition reaction

TABLE VI.

Organic Liquid.	Diethyl-ammonium Chloride.			Cyclohexyl-ammonium Chloride.			*n*-octyl-ammonium Chloride.		
	S_1.	G.	S_2.	S_1.	G.	S_2.	S_1.	G.	S_2.
Petroleum ether (b.p. 40-60° c.)	2·3- 3·0	4·1	4·6- $5{\cdot}1_w$	0·91- 1·02	1·25	indistinct $1{\cdot}6_s$	0·76- 0·93	1·2	indistinct $1{\cdot}4_s$
Xylene (mixed isomers)	1·3- 1·5	1·8	2·1- $2{\cdot}5_w$	0·64- 0·76	0·96	1·1- 1·25	0·67- 0·72	0·96	1·15- $1{\cdot}3_s$
Carbon tetrachloride	0·72 0·92	1·1	1·3- $1{\cdot}8_w$	0·44 0·48	0·75	0·98- $1{\cdot}07_s$	0·59 0·63	0·74	0·90- $0{\cdot}97_s$

$$X^{\bullet}\,SO_4Na + AmCl \rightleftharpoons X^{\bullet}\,SO_4Am + NaCl$$

then occurs to an extent regulated by the amount of organic ammonium halide added. The sodium halide produced in this reaction is also instrumental in increasing the value of *R* since, as explained in earlier papers, an increase in the inorganic salt content of $\overline{W}$, other things remaining the same, diminishes $A_{O\overline{W}}$ and increases *R* (Method I (*d*)).

When the above reaction is incomplete the mixed amphiphiles $X \bullet SO_4Na$ and $X \bullet SO_4Am$ operate together as an amphiphile of intermediate properties in a manner similar to the sodium undecylate Aerosol OT mixtures described in the preceding section. Table VI provides examples of the solubilised systems which are produced on gradually adding diethylammonium chloride, cyclohexylammonium chloride or octylammonium chloride to the Type I systems derived from 50 cc. of petroleum ether (b.p. 40-60° c.), xylene or CCl_4 and 50 cc. of the aqueous solution of sodium secondary C_{10}-C_{18} alkyl sulphates, S, referred to in Parts II and III. The solution S contains 23·9 g. sodium alkyl sulphates and 7·1 g. sulphate per 100 cc. solution.

---

[1] Schulman, *Trans. Faraday Soc.*, 1946, **42B**, 165.
[2] Durand, *Compt. rend.*, 1946, **223**, 898.

As the organic ammonium chlorides are added to the Type I systems these pass successively into clear water-dispersible sols S_1, clear water-dispersible gels, clear sols S_2 and Type II systems. Between S_1 and G, and between G and S_2 heterogeneous mixtures of S_1 and G, and of G and S_2 respectively, are produced. The sols S_2 may be either water or solvent dispersible as indicated in Table I by the subscripts *w* or *s* respectively. In this table are given the weights of the organic ammonium chlorides which produce S_1 sols, G gels (maximum gelation point indicated) and S_2 sols when added to mixtures of 50 cc. of S and 50 cc. of the organic liquids. Judging from their differences in refractive index and density, the difference in composition of the conjugate sol and gel phases is not great. Either for this reason, or because the process is truly continuous, the point of apparent disappearance of gel in two of the cases indicated in Table I could not be at all precisely distinguished.

TABLE VII.—EFFECT OF ADDITION OF CYCLOHEXYLAMMONIUM CHLORIDE TO 100 CC. OF A SOLUTION CONTAINING 3·55 g. SODIUM SULPHATE AND 12·0 g. OF SODIUM SECONDARY C_{10}-C_{18} ALKYL SULPHATES.

Wt. of Cyclohexylammonium Chloride Added (g.).	Character of Resulting Mixtures.
0·0	Clear solution S_1
1·0	Clear solution S_1
2·0	Hazy mix (S_1 + G)
2·5	Fairly thin clear gel G
3·0	Fairly thin clear gel G
3·25	Rather thinner clear gel
3·5	Hazy mix (G + S_2)
3·6	Clear mobile solution S_2
3·8	Clear mobile solution S_2
4·0	Aqueous layer commences to separate (Type II system)

Structures of S_1, G and S_2.—A tentative suggestion as to the nature of the structural differences existing between solubilised systems in the S_1, G and S_2 conditions has been advanced in Part I. Whatever the explanation of these differences, however, it must be reconcilable with the fact that all three conditions may be obtained in aqueous amphiphile solutions in which no organic liquid is present. It is also probable that the same three conditions are also realisable in solutions of certain amphiphiles in organic solvents in absence of water. This question is now being investigated. In general it appears that the relationships of amphiphiles with water on the one hand and with organic liquid on the other, are of a very symmetrical character.

The experimental details of the case of the production of aqueous amphiphile solutions in the S_1, G and S_2 conditions in the absence of any organic liquid which was mentioned in Part I, may appropriately be recorded here. Table II shows the effect of adding successively increasing amounts of cyclohexylammonium chloride to mixtures of 50 cc. of the sodium secondary C_{10}-C_{18} alkyl sulphate solution S and 50 cc. of water. Such mixtures contain 12 g. of sodium alkyl sulphates which are approximately stoichiometrically equivalent to 5·1 g. of cyclohexylammonium chloride.

(e) Solubilisation with Sodium Undecane-3 Sulphate, Sodium Undecane-3 Carboxylate and Undecane-3 Ammonium Chloride.—In order to obtain some comparison of the hydrophilic solvent affinities of the —SO_4Na, —CO_2Na and —NH_3Cl groups the above undecane-3 derivatives were prepared by standard synthetic methods. The first two compounds were very soluble in water and were not obtained in the crystalline condition. Undecane-3 ammonium chloride (m.p. 109-110° C.; equivalent, found 207·6; theory 207·5) crystallised readily from water at room temperature, but was freely soluble at 45° C. 20 % (wt./total vol.) aqueous solutions of all three compounds, containing only traces of inorganic salts were prepared, the solutions of the sodium salts at room temperature (20° C.) and of the amine hydrochloride at 45° C. 5 cc. portions of these solutions were mixed with 5 cc. portions of cyclohexane both in absence of sodium sulphate and with 0·2 g. added. These mixtures were titrated with hexanol-1, in the case of the sodium salts at room temperature, and in the case of the amine-hydrochloride at a slightly higher temperature and before crystallisation occurred. The comparative results are recorded in Table VIII. The non-abrupt breakdown of the S_2 sol recorded in column 5 has also been observed in other S_2 systems of rather low amphiphile content and low inorganic salt content.

TABLE VIII.

Column No.	1	2	3	4	5	6
Amphiphile	$C_{11}H_{23}SO_4Na$		$C_{11}H_{23}CO_2Na$		$C_{11}H_{23}NH_3Cl$	
Na_2SO_4 added (g.)	0	0·2	0	0·2	0	0·2
Description of System Produced.	cc. hexanol-1 required to give systems described in left-hand column					
Type I	<0·90	<0·55	<1·05	<0·80	<0·60	—
Clear sols S_1	0·90	0·55	1·05	0·80	0·60	—
Sol S_1 gradually changes (S_1 + G) without heterogeneity to a thin gel G (G + S_2) (hazy) clear sol S_2	1·20 1·25 1·3	Passage from S_1 to S_2 continuous without heterogeneity or gelling	1·15 1·35 1·55	Passage from S_1 to S_2 continuous without heterogeneity or gelling	Passage from S_1 to S_2 continuous Breakdown of S_2 sol commences with gel G	0·15 cc. gives Type III system. Upper layer 2·6 cc. middle 5·2 cc. lower 2·6 cc.
Type II system	>2·0	>0·75	>2·90	>1·05	1·80 showing opalescence which gradually increases. With 2·5 cc. two opalescent phases separate on standing	

Assuming that the lipophilic character of the undecane-3 group remains the same in all three amphiphiles the above results indicate, in terms of the theory advanced in Part I, that while the hydrophilic solvent affinity of the —CO_2Na group may be slightly above that of the —SO_4Na group in this series, the —NH_3Cl group has a markedly smaller hydrophilic solvent affinity than either of the anionic groups.

(f) Solubilisation with Undecane-1 Ammonium Chloride and Undecane-3 Ammonium Chloride.—Undecane-1 ammonium chloride (m.p. 168-170° C.; equivalent: found 206·0, theory 207·5) was prepared from undecylic acid (v.s.) via the amide and nitrile. Although undecane-1 ammonium chloride has a higher m.p. (168-170° C.) than undecane-3 ammonium chloride (m.p. 109-110° C.) it is more soluble in water at room temperature and readily gives a 20 %

(wt./total vol.) solution. 5 cc. portions of this solution and 5 cc. cyclohexane were mixed both with and without 0·16 g. added sodium chloride, and the mixtures titrated with hexanol-1 at room temperature. The behaviour observed is shown in Table IX.

TABLE IX.

NaCl Added (g.)	0.	0·16.
Hexanol-1 Added cc.	Condition of System.	
0	Thin emulsion	
0·1	Thick emulsion	Thin emulsion
0·2		Thick emulsion
0·25		Clear sol S_1
0·33		Clear thin gel G
0·42		Clear sol S_2
0·50	Patches of thick white emulsion suspended in clear gel	Type II system
0·80	Clear gel G	
0·90	Hazy mix (G + S_2)	
1·20	Clear water dispersible sol S_2	
2·90	Sol begins to show opalescence	
3·02	Type II system	

Compared with the behaviour of undecane-3 ammonium chloride shown in Table VIII, there is a very much greater gelling tendency with undecane-1 ammonium chloride and the range of solubilised compositions is increased. This is especially evident in the presence of added NaCl. Under comparable conditions to those of Table IX, with 0·16 g. sodium chloride undecane-3 ammonium chloride gives a Type I system which passes into a Type III system (lower layer 0·8 cc., middle layer 6·3 cc., upper layer 3·1 cc.) on addition of 0·1 cc. hexanol-1. This system is supersaturated at room temperature and undecane-3 ammonium chloride slowly crystallises. The results apparently indicate that the ammonium chloride group exerts a greater hydrophilic solvent affinity when attached to the -1 position of the *n*-undecane chain than when it is attached to the -3 position.

(g) Solubilisation with Sodium *n*-butyrate and Sodium *Iso*butyrate.— In amphiphiles of lower molecular weight as compared with the lipophilic solvent affinity, the hydrophilic solvent affinity becomes progressively more marked and the tendency to produce Type I systems ($R < 1$) becomes greater. These amphiphiles belong to the range of the " hydrotropic salts," whose solubilising properties were first described by Neuberg.[3] There is, however, a continuous gradation in behaviour as solubilisers, between the " hydrotropic salts " or low molecular weight amphiphiles and the " detergents " of higher molecular weight.

This gradation in properties was illustrated clearly in the early work of Engler and Dieckhoff [4] who studied the solubilisation of hydrocarbons, fatty acids, phenols and mixtures of these in soap solutions. They showed the gradual increase in the effectiveness of solubilisation (in systems of the type now classified as Type I), as the series of fatty acid soaps is ascended. For a given amount of solubilisation progressively smaller quantities of soap are required in passing from the C_4 to C_{18} soaps. The same gradation has also recently been very clearly demonstrated by Durand [5] in a study of the solubility of benzene in aqueous solutions of the sodium salts of the C_1-C_{11} *n*-fatty acids. The following examples using sodium butyrate and sodium *iso*butyrate, further illustrate the very closely analogous behaviour of these typical hydrotropic salts and the amphiphiles of higher molecular weight.

---

[3] Neuberg, *Biochem. Z.*, 1916, **76**, 107.

[4] Engler and Dieckhoff, *Arch. Pharm.*, 1892, **230**, 561.

EXAMPLE 1. When octanol-1 is gradually added to 5 cc. of a 50 % (wt./total vol.) solution of sodium *n*-butyrate the following systems are successively obtained at room temperature (19° c.)

(*a*) With 0-3 cc. octanol-1 ; clear isotropic solution (S_1), (*b*) hazy mixes (S_1+G), (*c*) with 5-6 cc. octanol-1 ; a clear stiff gel (G), strongly birefringent, (*d*) with 6-10·5 cc. ; hazy mixes of gradually diminishing thickness ($G + S_2$), (*e*) with more than 11 cc. of octanol-1 ; clear isotropic solutions (S_2).

It appears that these changes (*a*)-(*e*) are the usual type of S_1, G, S_2 change which occur as R is increased. In this case the increase in R is brought about by the simple mass action effect of increase of the relative concentration of O (Part I, Method I (*a*)). With the concentrations of *n*-butyrate used, R is at no stage sufficiently small to produce a Type I system, but the completely solubilised system passes from the S_1 stage ($R < 1$) to the gel stage ($R \approx 1$) and into the S_2 stage ($R > 1$). A type II system is not produced, the S_2 sol being miscible with octanol-1. This point is further discussed below.

EXAMPLE 2. Using sodium *iso*butyrate in place of the *n*-butyrate in Example 1, the gel stage produced is much less evident, being marked only by a small haziness with from 5-6 cc. of octanol-1. Otherwise the behaviour is the same in the two cases. The relative behaviour of the *n*-butyrate and *iso*butyrate is thus another instance of the greater tendency to gelation which occurs with alkane-1 sodium salts in conjunction with 1-alkanols.

EXAMPLE 3. Addition of octanol-1 at room temperature (18° c.) to mixtures of 5 cc. of cyclohexane and 5 cc. of aqueous sodium *iso*butyrate solutions of concentration 65·5, 59·0 and 55·6 % (wt./total vol.) produces clear solutions (Type I system → S_1 sol) with 3·4, 4·7 and 6·3 cc. of octanol-1 respectively. These solutions are completely miscible with octanol-1.

A mixture of 5 cc. of a 50 % sodium *iso*butyrate solution with 5 cc. of cyclohexane gives with 5 cc. of octanol-1 a Type III system (upper layer 3·6 cc., middle layer 9·6 cc., lower layer 2·8 cc.). With 7·5 cc. of octanol-1 a Type II system is produced (lower layer 1·5 cc.) while with more than 15 cc. octanol-1, homogeneous solutions are produced.

In considering these results, the not inconsiderable solubility of water in octanol-1 or other alkanols must be borne in mind. This can prevent the breakdown of S_2 sols into Type II systems where this might otherwise be expected. It may even lead to resolution of the aqueous layer on further addition of alkanol to certain Type II systems, as in the case described here.

The writer wishes to thank the N.V. de Bataafsche Petroleum Maatschappij and " Shell " Refining and Marketing Co., Ltd., for permission to publish this paper and Dr. P. J. Garner, Senior Chemist of these Laboratories, for his encouragement during its preparation.

Summary.

Examples of the mutual solubilisation of water and various organic liquids by means of Aerosol OT, sodium undecylate, mixtures of Aerosol OT and sodium undecylate, mixtures of sodium and organic ammonium secondary C_{10}-C_{18} alkyl sulphates, sodium undecane-3 sulphate, sodium undecane-3 carboxylate, undecane-1 and -3 ammonium chlorides, sodium *n*-butyrate and sodium *iso*butyrate are described. All these examples conform in general outlines to the classification of partly and completely solubilised systems given in Part I and to the theory of solubilisation there advanced.

Thornton Research Centre,
Chemical Laboratory,
Thornton-le-Moors,
Cheshire.

A NOTE ON RATE CONSTANTS OF "UNIMOLECULAR" REACTIONS.

By R. M. Barrer.

Received 25th March, 1947.

1. Introduction.

Attention has recently been directed to two reaction schemes [1, 2] each capable, through a time lag between energisation and reaction,[3, 4] of giving first order kinetics.*

$$\text{(i) Normal molecules} \underset{\text{fast}}{\overset{\text{fast}}{\rightleftharpoons}} \text{Energised Molecules} \xrightarrow{\text{slow}} \text{Activated molecules} \xrightarrow{\text{fast}} \text{Resultants ;}$$

$$\text{(ii) Normal Molecules} \underset{\text{fast}}{\overset{\text{fast}}{\rightleftharpoons}} \text{Energised Molecules} \underset{\text{fast}}{\overset{\text{fast}}{\rightleftharpoons}} \text{Activated Molecules} \xrightarrow{\text{slow}} \text{Resultants.}$$

In scheme (i) the second step (energisation → activation) is rate-controlling (Polanyi-Hinshelwood hypothesis [5]), and in scheme (ii) the third step is rate-controlling (Kassel [6]). These schemes have led to well-known formulæ for the rate constant. When it is assumed that k_a, the rate at which energised molecules become activated, is independent of the total energy of activation the Polanyi-Hinshelwood hypothesis gives for the first order velocity constant k_{uni} † :

$$k_{\text{uni}} = k_a \sum_{s=1,2,\ldots s} \frac{1}{(s-1)!}\left(\frac{E}{RT}\right)^{s-1} e^{-E/RT} \simeq k_a \frac{1}{(s-1)!}\left(\frac{E}{RT}\right)^{s-1} e^{-E/RT} \quad (E \gg sRT). \quad . \quad . \quad . \quad . \quad . \quad (1)$$

However, it has been pointed out that the assumption that k_a is independent of the total energy of activation E is not only intrinsically unlikely, but also leads to a functional relationship between the actual velocity "constant" k, the limiting constant k_{uni} and the concentration A of the form

$$\frac{k_{\text{uni}}}{k} = 1 + \frac{\text{const.}}{A} \quad . \quad . \quad . \quad . \quad . \quad (2)$$

which is not borne out by experiment.[2]

Thus the Polanyi-Hinshelwood hypothesis, following scheme (i), needs reformulating, without assuming that k_a is independent of E. Moreover two fundamental aspects of the theory of reaction rates arise especially with scheme (i), which have remained in almost complete obscurity. Firstly, how quickly do energy distributions change in a

---

[1] Eley, *Trans. Faraday Soc.*, 1943, **39**, 168.

[2] Evans and Rushbrooke, *ibid.*, 1945, **41**, 621.

[3] Lindemann, *ibid.*, 1922, **17**, 599.

[4] Christiansen, *Reaktionskinetische Studien* (Copenhagen, 1921), pp. 50-51.

[5] e.g. Polanyi, *Z. Physik*, 1920, **1**, 337. Hinshelwood, *Kinetics of Chemical Change* (O.U.P., 1940).

[6] Kassel, *Kinetics of Homogeneous Gas Reactions* (Chemical Catalogue Co., 1932). Rice and Ramsperger, *J. Amer. Chem. Soc.*, 1927, **49**, 1617.

* By "energised" is meant containing a sufficient excess of energy for reaction, but with the energy not distributed suitably for reaction. By "activated" it is implied that this energy is so distributed that reaction can occur.

† s denotes the number of degrees of freedom containing the energy $> E$.

molecule independently of external collision or relative to the lifetime of the energised state.* Secondly, how quickly does an energised molecule become activated (determining the value of k_a). This problem will depend markedly upon the particular mechanism of reaction, because this governs in part the critical distribution of energy. The present paper is concerned with the above three aspects of the problem of " unimolecular " reactions.

2. Phenomenological Relationships.—The well-known model (cf. ref. 2) embracing schemes (i) and (ii) of section (1) must first be re-formulated, considering separately the group of molecules containing say j quanta, that containing $j + 1$ quanta, and so on. To do this, let A denote the concentration of normal molecules. Also let

A_1^* = the concentration of energised molecules with just the critical number j of energy quanta needed for reaction,
A_2^* = the concentration of energised molecules with just $j + 1$ quanta,
A_3^* = the concentration of energised molecules with just $j + 2$ quanta,

and so on. Again, let

A_1^+ = the concentration of activated molecules with just the critical number j of quanta correctly distributed for reaction,
A_2^+ = the concentration of activated molecules with $j + 1$ quanta correctly distributed for reaction,
A_3^+ = the concentration of activated molecules with $j + 2$ quanta correctly distributed for reaction,

etc. Then the model becomes :

$$\begin{array}{lllcc}
 & & & \text{Forward} & \text{Backward} \\
\text{Step (1) (energisation)} & \left\{ \begin{array}{l} \mathrm{A} + \mathrm{A} \rightleftharpoons \mathrm{A}_1^* + \mathrm{A} \\ \mathrm{A} + \mathrm{A} \rightleftharpoons \mathrm{A}_2^* + \mathrm{A} \\ \mathrm{A} + \mathrm{A} \rightleftharpoons \mathrm{A}_3^* + \mathrm{A} \\ \text{etc.} \end{array} \right. & & \begin{array}{c} {}^1k_1 \\ {}^2k_1 \\ {}^3k_1 \\ \\ \end{array} & \begin{array}{c} {}^1k_2 \\ {}^2k_2 \\ {}^3k_2 \\ \\ \end{array} \\
\text{Step (2) (activation)} & \left\{ \begin{array}{l} \mathrm{A}_1^* \rightleftarrows \mathrm{A}_1^+ \\ \mathrm{A}_2^* \rightleftarrows \mathrm{A}_2^+ \\ \mathrm{A}_3^* \rightleftarrows \mathrm{A}_3^+ \\ \text{etc.} \end{array} \right. & & \begin{array}{c} {}^1k_a \\ {}^2k_a \\ {}^3k_a \\ \\ \end{array} & \begin{array}{c} {}^1k_b \\ {}^2k_b \\ {}^3k_b \\ \\ \end{array} \\
\text{Step (3) (reaction)} & \left\{ \begin{array}{l} \mathrm{A}_1^+ \rightarrow \mathrm{B} + \mathrm{C} \\ \mathrm{A}_2^+ \rightarrow \mathrm{B} + \mathrm{C} \\ \mathrm{A}_3^+ \rightarrow \mathrm{B} + \mathrm{C} \\ \text{etc.} \end{array} \right. & & \begin{array}{c} {}^1k_3 \\ {}^2k_3 \\ {}^3k_3 \\ \\ \end{array} & \\
\end{array}$$

It can now be seen that the following equations relate in the steady state to *each group* of energised and activated molecules :

$$ {}^1k_1A^2 = {}^1k_2AA_1^* + {}^1k_aA_1^* - {}^1k_bA^+ \quad . \quad . \quad . \quad (3)$$

$$ {}^1k_aA_1 = {}^1k_bA_1^+ + {}^1k_3A_1^+. \quad . \quad . \quad . \quad (4)$$

$$\text{Rate of reaction} = \frac{\mathrm{d}B_1}{\mathrm{d}t} = {}^1k_3A_1^+ = \frac{{}^1k_1{}^1k_3{}^1k_aA^2}{{}^1k_2({}^1k_b + {}^1k_3)A + {}^1k_1{}^1k_a} \quad . \quad . \quad (5)$$

For all groups :

$$k_1 = \Sigma^1k_1 \quad . \quad . \quad . \quad . \quad . \quad (6)$$

$$k_2 = \Sigma^1k_2 \quad . \quad . \quad . \quad . \quad . \quad (7)$$

and the total reaction rate is

$$\sum \frac{\mathrm{d}B_1}{\mathrm{d}t} = {}^1k_3A_1^+ + {}^2k_3A_2^+ + \ldots = kA \quad . \quad . \quad (8)$$

---

* This information is necessary in particular if the use of statistical theorems assuming equilibrium distributions of energy quanta is to be justified. Thus in ref. 2, eqn. 6 may not be valid for scheme (i), for this theorem applies to the *equilibrium* state between energised and activated molecules, whereas in scheme (i) equilibrium, at least of concentrations, is here not established.

whence

$$k = \sum \frac{{}^1k_1{}^1k_3{}^1k_a . A}{{}^1k_b({}^1k_b + {}^1k_3)A + {}^1k_3{}^1k_a}. \quad . \quad . \quad . \quad (9)$$

These relationships generalise the usual equations so as to apply to the case in which we are interested when each group of energised or activated molecules contributes differently to the overall reaction velocity of eqn. (8), i.e. when the k_a's, k_3's, etc., vary from one group of molecules to another. The following implications from eqn. (3) to (9) may be noted.

(1) Some groups of molecules may make second-order contributions to reaction while others make first-order contributions.

(2) For an entirely second-order reaction one must have for all sets of k's throughout the summation in eqn. (9), ${}^1k_2({}^1k_b + {}^1k_3)A \ll {}^1k_3{}^1k_a$, so that

$$k = \Sigma {}^1k_1A^2 = k_1A^2. \quad . \quad . \quad . \quad . \quad (10)$$

(3) For an entirely first-order reaction one must have for all sets of k's throughout the summation in eqn. (9), ${}^1k_2({}^1k_b + {}^1k_3)A \gg {}^1k_3{}^1k_a$ so that

$$k_{\text{uni}} = \sum \frac{{}^1k_1{}^1k_3{}^1k_a}{{}^1k_2({}^1k_b + {}^1k_3)}. \quad . \quad . \quad . \quad (11)$$

(4) If step (2) is rate-controlling, ${}^1k_3 \gg {}^1k_b$, so that

$$k_{\text{uni}} = \sum {}^1k_a \frac{{}^1k_1}{{}^1k_2}. \quad . \quad . \quad . \quad . \quad (12)$$

(5) If step (2) is rate-controlling, one also has for reaction of intermediate order

$$k = \sum \frac{{}^1k_1{}^1k_aA}{{}^1k_2A + {}^1k_a} \quad . \quad . \quad . \quad . \quad (13)$$

so that the relation between k_{uni} (eqn. (12)) and k of eqn. (13) is

$$\frac{k_{\text{uni}}}{k} = \frac{\sum \frac{{}^1k_1}{{}^1k_2} . {}^1k_a}{\sum \frac{{}^1k_1{}^1k_a . A}{{}^1k_2A + {}^1k_a}} \quad . \quad . \quad . \quad . \quad (14)$$

which replaces eqn. (2), the relationship indicated by Evans and Rushbrooke,[3] and which was shown by them to be contrary to experiment. Thus the difficulty to which the Polanyi-Hinshelwood hypothesis leads if k_a is assumed to be independent of E may be removed when the model is extended in the manner indicated in this section.

(6) If step (3) is rate-controlling, ${}^1k_3 \ll {}^1k_b$ so that

$$k_{\text{uni}} = \sum {}^1k_3 . \frac{{}^1k_a}{{}^1k_b} . \frac{{}^1k_1}{{}^1k_2}. \quad . \quad . \quad . \quad . \quad (15)$$

Most of these consequences are generalisations of relationships already given. We are particularly interested in eqn. (12) corresponding to the Polanyi-Hinshelwood hypothesis, and require to evaluate the right-hand side of this equation explicitly. To do this we shall discuss a simple idealised reaction model, and subsequently (section (9)) refer to possible improvements.

3. Molecular Model for Reaction.—The case of a two-radical molecule R—R will be considered in which, when a critical amount of energy enters one radical, there occurs a reaction such as intra-molecular rearrangement or decomposition. During the period of a vibrational collision between the two radicals the chance that an energy quantum passes from one radical to the other is p, and that a quantum is not so transferred is $(1 - p)$. When the two radicals are identical, p will be the same for a quantum transference in either direction, but if the radicals are different the chance will be p_1 in one direction and p_2 in the other. While an unsymmetrical

---

[7] Glasstone, Laidler and Eyring, *Theory of Rate Processes* (McGraw Hill Book Co., 1941), p. 286.

molecule introduces no new principle into the calculations, we shall confine the present discussion to the simpler case of symmetrical molecules R—R. The chance during the interval $1/\omega$ of a vibrational collision of frequency ω that a distribution $n - m, m$ between the radicals of a total number n of similar quanta becomes another distribution can now be expressed as an algebraic function in p and $(1 - p)$. For example, the chance that the distribution $n - m, m$ becomes 0, n (or n, 0) in time $1/\omega$ is

$$P_{\substack{n,0\leftarrow n-m,m\\(\text{or } 0,\, n)}} = p^m(1 - p)^{n-m} + p^{n-m}(1 - p)^m. \qquad (16)$$

It is also assumed that when the molecule possesses a minimum of, say, j energy quanta the reaction occurs if the distribution of quanta is j, 0 (or 0, j). When the molecule possesses $j + 1$ quanta the critical distributions are $j + 1$, 0 (or 0, $j + 1$) and j, 1 (or 1, j). If there are $j + 2$ quanta the critical distributions are $j + 2$, 0 (or 0, $j + 2$); $j + 1$, 1 (or 1, $j + 1$); and j, 2 (or 2, j), and so on for still larger numbers of quanta.

4. Proportions of energised Molecules having just j, $j + 1$, etc., Quanta.—Let α_1 be the fraction of all the energised molecules in the steady state which have only j quanta, α_2 the fraction with just $j + 1$ quanta, and so on. Set *

$$\left.\begin{aligned}
\phi &= \sum_{s=1,2,..s} \frac{1}{(s-1)!}\left(\frac{E}{RT}\right)^{s-1} e^{-E/RT} \simeq \frac{1}{(s-1)!}\left(\frac{E}{RT}\right)^{s-1} e^{-E/RT}\\
\phi_1 &= \sum_{s=1,2,..s} \frac{1}{(s-1)!}\left(\frac{E_1}{RT}\right)^{s-1} e^{-E_1/RT} \simeq \frac{1}{(s-1)!}\left(\frac{E_1}{RT}\right)^{s-1} e^{-E_1/RT}\\
&\cdot\quad\cdot\quad\cdot\quad\cdot\quad\cdot\quad\cdot\\
\phi_l &= \sum_{s=1,2..s} \frac{1}{(s-1)!}\left(\frac{E_l}{RT}\right)^{s-1} e^{-E_l/RT} \simeq \frac{1}{(s-1)!}\left(\frac{E_l}{RT}\right)^{s-1} e^{-E_l/RT}
\end{aligned}\right\} \qquad (17)$$

where ϕ, ϕ_1 . . . ϕ_l are the fractions of all the molecules having total energies in their s degrees of freedom $> E$, E_1 . . . E_l. If E corresponds to j quanta, E_1 to $j + 1$ quanta, etc., one may write approximately

$$\frac{\phi - \phi_1}{\phi} = \alpha_1;\ \frac{\phi_1 - \phi_2}{\phi} = \alpha_2, \text{ etc.} \qquad (18)$$

If the unit quantum is $h\omega_1$ one has accordingly †

$$\left.\begin{aligned}
\alpha_1 &= \left[1 - \left(\frac{j+1}{j}\right)^{s-1} e^{-\frac{N_0h\omega_1}{RT}}\right]\\
\alpha_2 &= \left[\left(\frac{j+1}{j}\right)^{s-1} - \left(\frac{j+2}{j}\right)^{s-1} e^{-\frac{N_0h\omega_1}{RT}}\right] e^{-\frac{N_0h\omega_1}{RT}}\\
&\cdot\quad\cdot\quad\cdot\quad\cdot\quad\cdot\quad\cdot\\
\alpha_l &= \left[\left(\frac{j+\overline{l-1}}{j}\right)^{s-1} - \left(\frac{j+l}{j}\right)^{s-1\ -\frac{N_0h\omega_1}{RT}}\right] e^{-\frac{(l-1)N_0h\omega_1}{RT}}
\end{aligned}\right\} \qquad (19)$$

---

* $E > sRT$ for all the reactions under discussion. Accordingly the second term on the right-hand side is likely to be a reasonable approximation.

† The applicability of eqn. (19) raises a point of interest. This eqn. should hold for the Kassel hypothesis in which statistical equilibrium obtains for both steps (1) and (2). In the Polanyi-Hinshelwood hypothesis, however, one has equilibrium only up to stage (1). In this case if *all* molecules receiving the necessary energy to react initially have the energy unsuitably distributed for reaction, eqn. (19) is still valid, and reaction may be entirely of first order (eqn. (12)); but if in some molecules the energy is initially distributed suitably for reaction *these react forthwith bimolecularly*. Therefore only in the first instance is the wholly first-order reaction being discussed possible, so that it is a corollary of a wholly first-order reaction according to the Polanyi-Hinshelwood hypothesis that eqn. (19) must be applicable.

It is seen that $\Sigma\alpha = 1$, and that $\alpha_1 > \alpha_2 > \alpha_3 \ldots$. Then in eqn. (11) to (15) the quotients $\frac{{}^1k_1}{{}^1k_2}, \frac{{}^2k_1}{{}^2k_2}, \frac{{}^3k_1}{{}^3k_2} \ldots$ are given by

$$\left.\begin{aligned} \frac{{}^1k_1}{{}^1k_2} &= \alpha_1 \sum_{s=0}^{s} \frac{1}{(s-1)!}\left(\frac{E}{RT}\right)^{s-1} e^{-E/RT} \\ \frac{{}^2k_1}{{}^2k_2} &= \alpha_2 \sum_{s=0}^{s} \frac{1}{(s-1)!}\left(\frac{E_1}{RT}\right)^{s-1} e^{-E_1/RT} \end{aligned}\right\} \quad . \quad . \quad (20)$$

and so on.

5. Equilibrium Distributions of Quanta between the two Radicals.—Upon energisation and at equilibrium in absence of a reaction, the fraction of the molecules having n quanta which has the distribution $n - m, m$ between the two radicals is

$$F(n-m), m = \frac{n!}{(n-m)!\,m!}\,\frac{1}{2^n} \quad . \quad . \quad . \quad (21)$$

because the factorial quotient gives the number of ways of obtaining the distribution $n - m, m$; and $2^n = \sum_{m=0}^{n} \frac{n!}{(n-m)!\,m!}$ is the total number of ways of distributing the quanta between the two radicals.

When there are $n = j + q$ quanta and the several most unequal distributions lead to reaction (i.e. n, 0 or 0, n down to $n - q, q$ or $q, n - q$) these distributions will be missing by reaction from the final equilibrium of distributions. However, each remaining distribution, typified by $n - m, m$ can still be obtained in $\frac{n!}{(n-m)!\,m!}$ ways, and thus the fraction

$$F_{(n-m),\,m} = \frac{n!}{(n-m)!\,m!}\left[\frac{1}{2^n - \sum_{q=0}^{q=q} N_q}\right] \quad . \quad . \quad (22)$$

where $N_q = \frac{n!}{(n-q)!\,q!} + \frac{n!}{q!\,(n-q)!}$. It is seen that $\Sigma F_{(n-m),\,m} = 1$ whether there is or is not a critical distribution.

6. Rate at which non-equilibrium Distributions become equilibrium ones.—Upon energisation there may be non-equilibrium distributions of quanta. However, it will now be shown that for a range of values of p these will become equilibrium ones very rapidly. We have seen how the chance that one distribution becomes another in the time $1/\omega$ may be given as a function of p and $1 - p$, using eqn. (16) by way of illustration. A specific example of the rate of change of energy distributions of $n = 6$ quanta will now be formulated in terms of such functions. The calculation can be carried out similarly for any value of n but becomes lengthy if n is large.

(1) *Initially there are 3 quanta associated with each radical*

$$\left.\begin{aligned} P_{3,\,3 \leftarrow 3,\,3} &= F_1 = 9p^4(1-p)^2 + 9p^2(1-p)^4 + p^6 + (1-p)^6 \\ P_{4,\,2 \text{ or } 2,\,4 \leftarrow 3,\,3} &= F_2 = 18p^3(1-p)^3 + 6p(1-p)^5 + 6p^5(1-p) \\ P_{5,\,1 \text{ or } 1,\,5 \leftarrow 3,\,3} &= F_3 = 6p^2(1-p)^4 + 6p^4(1-p)^2 \\ P_{6,\,0 \text{ or } 0,\,6 \leftarrow 3,\,3} &= F_4 = 2p^3(1-p)^3. \end{aligned}\right\} (23a)$$

(2) *Initially there are 2 quanta associated with one radical and 4 with the other*

$$\left.\begin{aligned} P_{3,\,3 \leftarrow 4,\,2} &= F_5 = 12(p^3(1-p)^3 + 4p(1-p)^5 + 4p^5(1-p) \\ P_{4,\,2 \text{ or } 2,\,4 \leftarrow 4,\,2} &= F_6 = 14p^2(1-p)^4 + 14p^4(1-p)^2 + p^6 + (1-p)^6 \\ P_{5,\,1 \text{ or } 1,\,5 \leftarrow 4,\,2} &= F_7 = 8p^3(1-p)^3 + 2p(1-p)^5 + 2p^5(1-p) \\ P_{6,\,0 \text{ or } 0,\,6 \leftarrow 4,\,2} &= F_8 = p^2(1-p)^4 + p^4(1-p)^2 \end{aligned}\right\} (23b)$$

(3) *Initially there is* 1 *quantum associated with one radical and* 5 *with the other*

$$\left.\begin{aligned} P_{3,3 \leftarrow 5,1} &= F_9 = 10p^4(1-p)^2 + 10p^2(1-p)^4 \\ P_{4,2 \text{ or } 2,4 \leftarrow 5,1} &= F_{10} = 5p^5(1-p) + 5p(1-p)^5 + 20p^3(1-p)^3 \\ P_{5,1 \text{ or } 1,5 \leftarrow 5,1} &= F_{11} = 5p^2(1-p)^4 + 5p^4(1-p)^2 + p^6 + (1-p)^6 \\ P_{6,0 \text{ or } 0,6 \leftarrow 5,1} &= F_{12} = p(1-p)^5 + p^5(1-p) \end{aligned}\right\} \quad (23c)$$

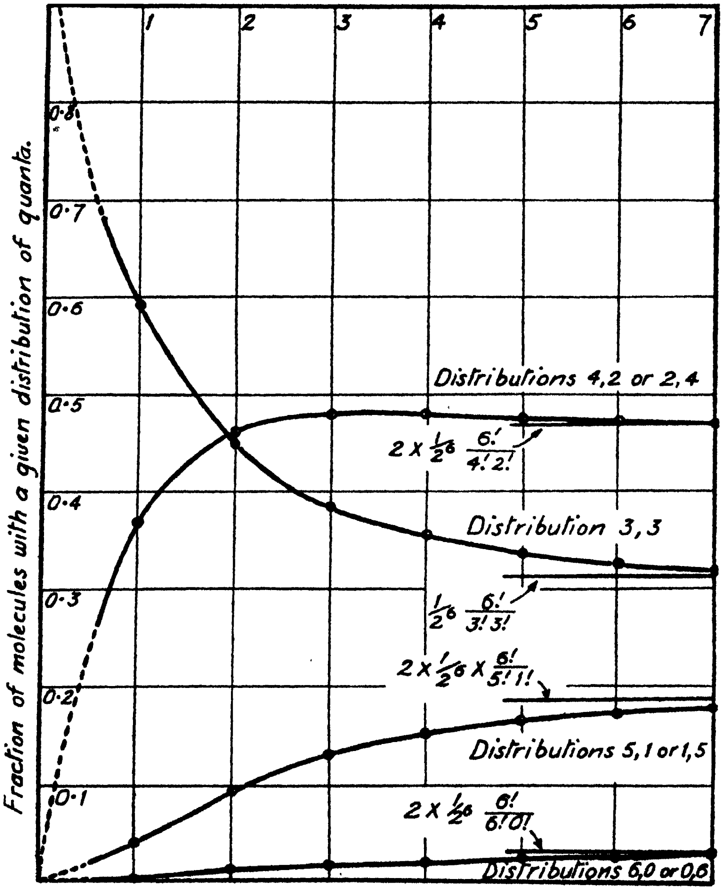

t in intervals of $1/\omega$ (ω = frequency of vibrational collision of the two radicals in a bi-radical molecule R — R).

FIG. 1.—Kinetics of transfer of six energy quanta, initially having a distribution 3 : 3 between the two radicals of a two-radical molecule R — R. The probability, p, of a quantum transfer in the interval $1/\omega$ is taken as either $p = 0{\cdot}1$ or $p = 0{\cdot}9$. If $p = 0{\cdot}5$ the equilibrium distributions of the quanta are established in the interval $1/\omega$, so that over the whole range $0{\cdot}1 < p < 0{\cdot}9$, equilibrium is rapidly set up independently of external collisions. $1/\omega$ is the interval between successive vibrational collisions of the two radicals R.

(4) *Initially there are no quanta associated with one radical and* 6 *with the other*

$$\left.\begin{aligned} P_{3,3 \leftarrow 6,0} &= F_{13} = 20p^3(1-p)^3 \\ P_{4,2 \text{ or } 2,4 \leftarrow 6,0} &= F_{14} = 15p^2(1-p)^4 + 15p^4(1-p)^2 \\ P_{5,1 \text{ or } 1,5 \leftarrow 6,0} &= F_{15} = 6p^5(1-p) + 6p(1-p)^5 \\ P_{6,0 \text{ or } 0,6 \leftarrow 6,0} &= F_{16} = p^6 + (1-p)^6 \end{aligned}\right\} \quad (23d)$$

As soon as the algebraic functions corresponding to eqn. (23*a*-*d*) are obtained for $n = 6$ or any other value, the following general procedure gives the change of distribution with time. After the first vibrational collision, assuming say an initial distribution 3, 3, one has F_1, F_2, F_3 and F_4 as the proportions with distributions 3, 3; 4, 2 or 2, 4; 5, 1 or 1, 5; and 6, 0 or 0, 6 respectively. After the second vibrational collision one has

$$\begin{aligned} F_1' &= F_1F_1 + F_2F_5 + F_3F_9 + F_4F_{13} \\ &= \text{proportion with distribution 3, 3.} \\ F_2' &= F_1F_2 + F_2F_6 + F_3F_{10} + F_4F_{14} \\ &= \text{proportion with distribution 4, 2 or 2, 4.} \\ F_3' &= F_1F_3 + F_2F_7 + F_3F_{11} + F_4F_{15} \\ &= \text{proportion with distribution 5, 1 or 1, 5.} \\ F_4' &= F_1F_4 + F_2F_8 + F_3F_{12} + F_4F_{16} \\ &= \text{proportion with distribution 6, 0 or 0, 6.} \end{aligned}$$

Similarly, after the third vibrational collision

$$\begin{aligned} F_1'' &= F_1'F_1 + F_2'F_5 + F_3'F_9 + F_4'F_{13} \\ &= \text{proportion with distribution 3, 3, etc.} \end{aligned}$$

By evaluating these functions starting from eqn. (23*a*-*d*) and plotting them as functions of the number of collisions, i.e. of the number of time intervals $1/\omega$, the approach to equilibrium was expressed graphically for different values of p (Fig. 1). When the initial distribution is 4, 2, etc., or any mixture of distributions $6 - m$, m, one proceeds in an analogous manner. It will be seen from Fig. 1 that the final proportions of the different distributions is given by eqn. (21), thus affording a check on the calculations. If critical distributions for reaction occur these must be omitted from eqn. (23 *a*-*d*), and the final equilibrium of distributions will be that expressed in eqn. (22).

Fig. 1 shows that when $0.1 < p < 0.9$ and $n = 6$ distribution equilibrium is achieved within a few vibrational collisions, and so well within the interval $\sim 10^{-10}$ sec. at N.T.P. between successive collisions of separate molecules. For larger values of n it is possible that equilibrium might be established more slowly. However, when $p = 0.5$, equilibrium was established by a single vibrational collision, i.e. within $\sim 10^{-13}$ sec., and this result is moreover true for all values of n because the fractions F_1, F_2 . . . of eqn. corresponding to (23*a*-*d*) are always those given by eqn. (21) or (22)) on setting $p = 0.5$.

7. Evaluation of the Equation $k_{\text{uni}} = \Sigma\,{}^1k_a\,\frac{{}^1k_1}{{}^1k_2}$.—The previous section indicates that equilibrium distributions of quanta are often established very speedily. In this event a complete evaluation of eqn. (12) $\left(k_{\text{uni}} = {}^1k_a\frac{{}^1k_1}{{}^1k_2}\right)$ is possible. Eqn. (19) and (20) give the ratios $\frac{{}^1k_1}{{}^1k_2}$, $\frac{{}^2k_2}{{}^2k_2}$ . . . and ${}^1k_a$ in sec.$^{-1}$ gives the number of times per sec. that the initial distributions of j quanta become the critical ones, j, 0 or 0, j leading to reaction. If there is initially distribution equilibrium then

$${}^1k_a = \omega\sum_{m=1}^{m=j-1}\left[\left(\frac{j!}{(j-m)!\,m!}\cdot\frac{1}{2^j - 2\dfrac{j!}{j!\,0!}}\right)\left\{p^{j-m}(1-p)^m + p^m(1-p)^{j-m}\right\}\right] \quad (24)$$

where ω is the number of vibrational collisions per second between the radicals R in the molecule R—R. Each term in the round bracket is the fraction of the energised molecules with the distribution $j - m$, m; while the term in the curly bracket gives the probability per vibrational collision that the distribution $j - m$, m becomes the critical ones j, 0 or 0, j. The summation outside the square bracket allows for the contributions from *all* non-critical distributions $j - m$, m. The function of p

is always symmetrical in p and $(1 - p)$ and may be written as $f_1\,(p,\ 1 - p)$ for molecules having just j quanta, $f_2\,(p,\ 1 - p)$ for molecules with $j + 1$ quanta and so on.

One may then write down the complete expression for k_{uni} in eqn. (12) as :

$$k_{\text{uni}} = \left\{\alpha_1 \sum_{m=1}^{m=j-1}\left[\frac{j!}{j - m)!\,m!}\cdot\frac{1}{2^j - 2\dfrac{j!}{j!\,0!}}\cdot f_1(p,\ 1 - p)\right]\right.$$
$$+\ \alpha_2 \sum_{m=2}^{m=j\ 1}\left[\frac{(j + 1)!}{(j + 1 - m)!\,m!}\cdot\frac{1}{2^{j+1} - 2\left(\dfrac{(j + 1)!}{(j + 1)!0!} + \dfrac{(j + 1)!}{j!\ 1!}\right)} f_2(p,\ 1 - p)\right]$$
$$+\ \alpha_3 \sum_{m=2}^{m=j-1}\left[\frac{(j + 2)!}{(j + 2 - m)!m!}\cdot\frac{1}{2^{j+2} - 2\left(\dfrac{(j + 2)!}{(j + 2)!\,0!} + \dfrac{(j + 2)!}{(j+1)!1!} + \dfrac{(j + 2)!}{j!\,2!}\right)}\right.$$
$$\left. f_3(p\,,1 - p)\right]$$
$$\left. + \ldots\ldots\right\}\omega\,.\sum_{s=1}^{s=s}\left(\frac{E}{RT}\right)^{s-1}\frac{1}{(s - 1)!}\,\mathrm{e}^{\ E/RT}. \quad . \quad . \quad . \quad . \quad (25)$$

where the α's are given by eqn. (19), and (20). It can be seen on comparing eqn. (1) and (25) that the sum of the terms in the curly bracket multiplied by ω is equal to k_a in eqn. (1) which we set out to determine. It is also seen that k_{uni} in eqn. (25) contains the term $\sum\limits_{s=1}^{s=s}\left(\frac{E}{RT}\right)^{s-1}\frac{1}{(s - 1)!}$ as in eqn. (1), but that the contribution of each group of molecules to k_a depends strongly upon the energy associated with that group.

When $p = 0{\cdot}5$ the functions $f(p,\ 1 - p)$ take very simple forms :

$$\left.\begin{aligned} f_1(p,\ 1 - p) &= 2\,\frac{j!}{j!\ 0!}\,\frac{1}{2^j} \\ f_2(p,\ 1 - p) &= 2\left[\frac{(j + 1)!}{(j + 1)!\ 0!} + \frac{(j + 1)!}{j!\ 1!}\right]\frac{1}{2^{j+1}} \\ f_3(p,\ 1 - p) &= 2\left[\frac{(j + 2)!}{(j + 2)!\ 0!} + \frac{(j + 2)!}{(j + 1)!\ 1!} + \frac{(j + 2)!}{j!\ 2!}\right]\frac{1}{2^{j+2}} \end{aligned}\right\} \qquad (26)$$

and so on. A particular $f(p,\ 1 - p)$ is therefore the same for all values of m and may accordingly be brought outside the summation sign of eqn. (25). In this event since the terms $\sum\limits_{m=1}^{m=j-1}\frac{j!}{(j - m)!\,m!}\cdot\frac{1}{2^j - 2\frac{j!}{j!\,0!}}$, etc., are all unity (eqn. 22), eqn. (25) takes the simple form :

$$k_{\text{uni}} = \left\{\alpha_1\,2\,.\,\frac{j!}{j!\,0!}\,\frac{1}{2^j} + \alpha_2\,2\left[\frac{(j + 1)!}{(j + 1)!\,0!} + \frac{(j + 1!}{j!\ 1!}\right]\frac{1}{2^{j+1}} + \alpha_3 2\left[\frac{(j + 2)!}{(j + 2)!\,0!}\right.\right.$$
$$\left.\left. + \frac{(j + 2)!}{(j + 1)!\ 1!} + \frac{(j + 2)!}{j!\ 2!}\right]\frac{1}{2^{j+2}} + \ldots\right\}$$
$$\times\ \omega\sum_{s=1}^{s=s}\frac{1}{(s - 1)!}\left(\frac{E}{RT}\right)^{s-1}\mathrm{e}^{-E/RT} \quad . \quad . \quad . \quad (27)$$

so that

$$k_a = \omega\left\{\alpha_1 2 \cdot \frac{j!}{j!\,0!}\,\frac{1}{2^j} + \alpha_2 2\left[\frac{(j+1)!}{(j+1)!\,0!} + \frac{(j+1)!}{j!\,1!}\right]\frac{1}{2^{j+1}}\right.$$
$$\left. + \alpha_3 2\left[\frac{(j+2)!}{(j+2)!\,0!} + \frac{(j+2)!}{(j+1)!\,1!} + \frac{(j+2)!}{j!\,2!}\right]\frac{1}{2^{j+2}} + \ldots\right\} \quad . \quad (28)$$

8. Numerical Evaluation of k_a.—By writing eqn. (25) as

$$k_{\text{uni}} = \left\{\alpha_1 k_1 + \alpha_2 k_2 + \alpha_3 k_3 + \ldots\right\}\sum_{s=1}^{s=s}\left(\frac{E}{RT}\right)^{s-1}\frac{1}{(s-1)!}\,e^{-E/RT} \quad (29)$$

it is seen that

$$\left.\begin{aligned} k_1 &= \omega\sum_{m=1}^{m=j-1}\frac{j!}{(j-m)!\,m!}\cdot\frac{1}{2^j - 2\dfrac{j!}{j!\,0!}}\cdot f_1(p,\,1-p) \\ k_2 &= \omega\sum_{m=1}^{m=j\ 1}\frac{(j+1)!}{(j+1-m)!\,m!}\cdot\frac{1}{2^{j+1} - 2\left(\dfrac{(j+1)!}{(j+1)!\,0!} + \dfrac{(j+1)!}{(j!\,1)!}\right)}\cdot f_2(p,\,1-p) \end{aligned}\right\} \quad (30) \text{ etc.}$$

Assuming that $\omega = 10^{13}$ sec.$^{-1}$, k_1 and k_2 were determined for all values of p in the range 0·1 to 0·9 when $j = 6$ and again when $j = 14$ (Table I).

TABLE I

k_1 and k_2 from eqn. (25) in sec.$^{-1}$.

p	0·1	0·2	0·3	0·4	0·5	0·6	0·7	0·8	0·9
(i) $j = 6$, $\omega = 10^{13}$ sec.$^{-1}$.									
$k_1 \times 10^{-11}$	1·50	2·67	2·85	3·06	3·14	3·06	2·85	2·67	1·50
$k_2 \times 10^{-11}$	5·85	8·94	11·0	12·1	12·5	12·1	11·0	8·94	5·84
(ii) $j = 14$, $\omega = 10^{13}$ sec.$^{-1}$.									
$k_1 \times 10^{-9}$	0·93	1·19	1·21	1·22	1·22	1·22	1·21	1·19	0·93
$k_2 \times 10^{-9}$	7·45	8·99	9·48	9·72	9·77	9·72	9·48	8·99	7·45

The values of k_1 and k_2 are clearly not very dependent upon p in the range noted, and what dependence there is tends to diminish as j increases. But inspection of eqn. (1) and eqn. (29) shows that $k_a = \Sigma\alpha_1 k_1$ and so it is unlikely that k_a depends significantly upon p if $0{\cdot}1 < p < 0{\cdot}9$. Thus in this range k_a may be calculated from the simpler eqn. (28) obtained from eqn. (25) by setting $p = 0{\cdot}5$.

Parameters determining k_a include j, s and $\frac{N_0 h\omega_1}{RT}$ (eqn. (25) and (28)). First the dependence on j was studied, by calculating the first 10 terms of eqn. (28) taking $s = 6$ and $\frac{N_0 h\omega_1}{RT} = 1$. The results are shown in Fig. 2 for $j = 10$, 15, 20, 25 and 50. Contributions to k_a of the sums of 1, 2, 3, . . . 10 terms are plotted against the number of terms summed. The curves flatten off, very rapidly for smaller values of j, as the number of terms summed increases. Extrapolation of the curves lead to values of k_a when an infinite number of terms is summed (Table II). For an energy quantum of 2000 cal., the total energy of activation corresponding to the curves of Fig. 2 and to the k_a's of Table II ranges from 20,000 to 100,000 cal., and the Arrhenius energy of activation from 10,000 to 90,000 cal.

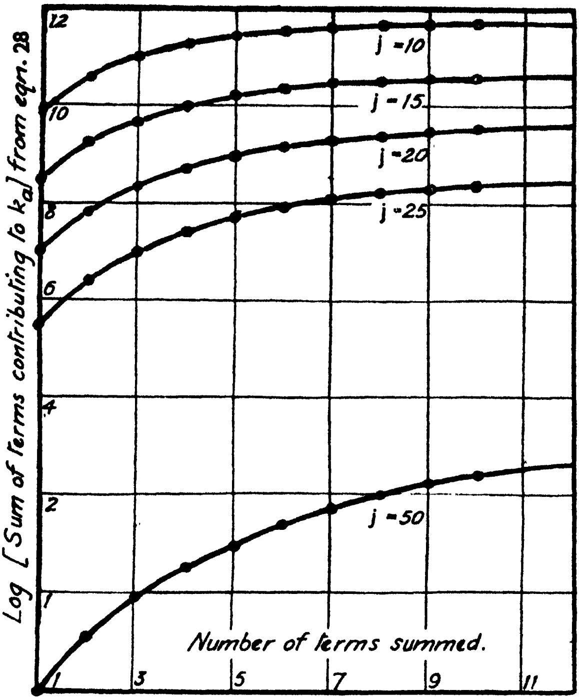

FIG. 2.—Sums of contributions of successive terms in eqn. (28) to k_a for different values of j, when $\frac{N_0 h\omega_1}{RT} = 1$; $\omega = 10^{13}$ sec.$^{-1}$; $f = 6$.

per mol. ($s = 6$, $\frac{N_0 h\omega_1}{RT} = 1$). For a reasonable value of the unit quantum and the values of j in Fig. 2 and Table II the main experimental range of the energy of activation is covered, and k_a determined from the present reaction mechanism has the right order of magnitude as illustrated by the experimental data given in Table III, although comparison should not be stressed.

While the proportion of the molecules having just the threshold energy of j quanta is larger than the proportion with $j + 1$ quanta and so on, the number of distributions leading to reaction becomes steadily larger. Therefore the contribution of each term in eqn. (25) or (28) to k_a does not necessarily decrease as the number of quanta increases, and there is in fact a maximum contribution to k_a from a term of intermediate number (Table IV). More terms had to be counted before the term of maximum contribution was included the larger j and s and the smaller

TABLE II.—VALUES OF k_a IN SEC.$^{-1}$ CALCULATED BY EXTRAPOLATION OF CURVES IN FIG 2.

Value of j.	k_a.
10	$\sim 5{\cdot}3 \times 10^{11}$
15	$\sim 4{\cdot}5 \times 10^{10}$
20	$\sim 4{\cdot}0 \times 10^{9}$
25	$\sim 3{\cdot}5 \times 10^{8}$
50	$\sim 1{\cdot}0 \times 10^{3}$

$\frac{N_0 h \omega}{RT}$. One is led to conclude that *by far the largest contribution to the reaction is made by the relatively small proportion of activated molecules having energies of activation considerably in excess of the minimum energy of activation.*

TABLE III.—EXPERIMENTAL VALUES OF k_a FOR SEVERAL REACTIONS

Reaction.	Temperature Range °K.	E_A (cal./mol.).	Experimental Value for k_a (sec.$^{-1}$).
Decomposition of $(C_2H_5)_2O$.	700-860	26,700	$6{\cdot}9 \times 10^8$ $(s = 4)$
Decomposition of $(CH_3)_2O$.	700-825	29,450	$1{\cdot}7 \times 10^9$ $(s = 5)$
Decomposition of N_2O_5 . .	273-340	12,380	$1{\cdot}8 \times 10^6$ $(s = 15)$

The value of s also influences k_a through its effect upon $\alpha_1, \alpha_2, \ldots,$ as shown in eqn. (19). Accordingly the sum of the first 10 terms in eqn. (28) was found when $s = 4, 5, 6, 7, 8, 9$ and 10, with $j = 20$, $\omega = 10^{13}$ and $\frac{N_0 h \omega_1}{RT} = 1$ (Fig. 3). It is seen that k_a increases as s increases.

TABLE IV.—CONTRIBUTIONS OF SUCCESSIVE TERMS IN EQN. (28) TO k_a WHEN $\omega = 10^{13}$ SEC.$^{-1}$, $j = 20$, $s = 6$ AND $\frac{N_0 h \omega_1}{RT} = 1$.

No. of Term.	Contribution to k_a (sec.$^{-1}$).	Sum of Contributions (sec.$^{-1}$).
1	$1{\cdot}27 \times 10^7$	$1{\cdot}27 \times 10^7$
2	$6{\cdot}68 \times 10^7$	$7{\cdot}95 \times 10^7$
3	$1{\cdot}81 \times 10^8$	$2{\cdot}07 \times 10^8$
4	$3{\cdot}36 \times 10^8$	$5{\cdot}43 \times 10^8$
5	$4{\cdot}86 \times 10^8$	$1{\cdot}03 \times 10^9$
6	$5{\cdot}96 \times 10^8$	$1{\cdot}63 \times 10^9$
7	$5{\cdot}82 \times 10^8$	$2{\cdot}21 \times 10^9$
8	$5{\cdot}59 \times 10^8$	$2{\cdot}77 \times 10^9$
9	$4{\cdot}58 \times 10^8$	$3{\cdot}23 \times 10^9$
10	$3{\cdot}50 \times 10^8$	$3{\cdot}58 \times 10^9$

TABLE V.—LIMITING VALUE OF k_a FOR DIFFERENT VALUES OF $\frac{N_0 h \omega_1}{RT}$ WHEN $\omega = 10^{13}$ SEC.$^{-1}$, $j = 20$, $s = 6$.

$\frac{N_0 h \omega_1}{RT}$.	k_a sec.$^{-1}$.
0·50	$\sim 1{\cdot}6 \times 10^{11}$
0·75	$\sim 2{\cdot}2 \times 10^{10}$
1·00	$\sim 4{\cdot}0 \times 10^9$
1·25	$\sim 1{\cdot}12 \times 10^9$
1·50	$\sim 4{\cdot}0 \times 10^8$

Finally the effect of $\frac{N_0 h \omega_1}{RT}$ on k_a was determined for the values 0·5, 0·75, 1·0, 1·25 and 1·50. The contributions to k_a of the sum of 1, 2, 3, . . . 10 terms in eqn. (28) were plotted against the number of terms summed for the different values of $\frac{N_0 h \omega_1}{RT}$ cited, when $j = 20$, $s = 6$ and $\omega = 10^{13}$. By extrapolation of these graphs the limiting value for k_a was obtained (Table V).

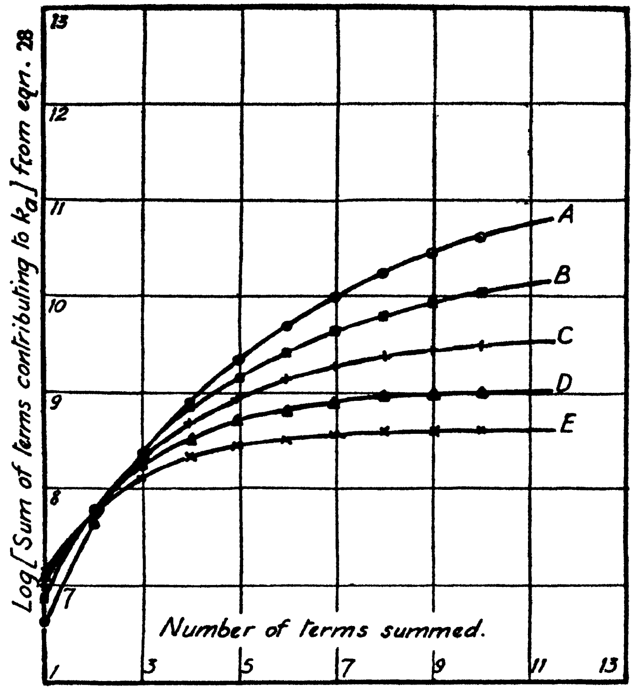

FIG. 3.—Influence of $\frac{N_0h\omega_1}{RT}$ $\left(\text{i.e. } \frac{E}{jRT}\right)$ upon k_a, according to eqn. (28), when $j = 20$; $\omega = 10^{13}$ sec.$^{-1}$; $f = 6$.

Curve A: $\frac{N_0h\omega_1}{RT} = 0{\cdot}50$

Curve B: $\frac{N_0h\omega_1}{RT} = 0{\cdot}75$

Curve C: $\frac{N_0h\omega_1}{RT} = 1{\cdot}00$

Curve D: $\frac{N_0h\omega_1}{RT} = 1{\cdot}25$

Curve E: $\frac{N_0h\omega_1}{RT} = 1{\cdot}50$.

9. Discussion.

The foregoing investigation of the Polanyi-Hinshelwood hypothesis has been based upon a very simple reaction model (section (3)). The model assumes one characteristic mean frequency ω_1 in place of the appropriate group of frequencies; and a single mean probability p of transfer, during the period of a vibrational collision between radicals, in place of a possible group of such probabilities. It thus involves idealisation, partly analogous to that in the Einstein theory of heat capacity of solids, and which may be defensible as a means of simplifying the calculation without altering the principle of the method. The energy of activation may need, moreover, to be concentrated not in a radical but in a bond, so that the critical energy distribution is more restrictive than for the model which has been discussed. The more restrictive the distribution the smaller its statistical weight in the distribution equilibrium so that other things being equal k_s would be reduced. Calculations of k_s as given in section (8) may then afford an upper limit to its value for more restrictive reaction conditions.

The Kassel hypothesis (eqn. (15)) may readily be compared with the Polanyi-Hinshelwood hypothesis (eqn. (12)). For the present reaction model, eqn. (15) becomes

$$k_{\text{uni}} = \left\{ {}^1k_s\alpha_1 \cdot 2 \cdot \frac{j!}{j!\,0!}\,\frac{1}{2^j} + {}^2k_s\alpha_2 2\left[\frac{(j+1)!}{(j+1)!\,0!} + \frac{(j+1)!}{j!\,1!}\right]\frac{1}{2^{j+1}} \right.$$
$$\left. + {}^3k_s\alpha_3 \cdot 2\left[\frac{(j+2)!}{(j+2)!\,0!} + \frac{(j+2)!}{(j+1)!\,1!} + \frac{(j+2)!}{j!\,2!}\right]\frac{1}{2^{j+2}} + \ldots \right\}$$
$$\times \sum_{s=1}^{s=s} \frac{1}{(s-1)!}\left(\frac{E}{RT}\right)^{s-1} e^{-E/RT} \quad . \quad . \quad . \quad . \quad . \quad . \quad . \quad (31)$$

where the α's are given by eqn. (19). This result may be compared with eqn. (25) and (27). The summation in the curly bracket of eqn. (31) is now to be identified with k_a of eqn. (1). For the Kassel hypothesis to be valid ${}^1k_s \ll {}^1k_b$; ${}^2k_s \ll {}^2k_b$; . . . (section (2)) ; and since k_b cannot be more than, and may approximate to, a vibration frequency ($\sim 10^{13}$ sec.$^{-1}$), ${}^1k_s$, ${}^2k_s$, . . . must be much less than this. Small values of k_s arise when the transmission coefficient, λ, of the reacting system over the energy barrier separating initial and final states is small.[7] If $\lambda \sim 1$, ${}^1k_s$, ${}^2k_s$, . . . should themselves approximate to a vibration frequency ($\sim 10^{13}$ sec.$^{-1}$), but in this case the Kassel hypothesis ($k_s \ll k_b$) cannot apply.

Eqn. (15) can also be written down in a form similar to eqn. (31) when the critical distribution for reaction is that out of a total of n quanta, j at least must be concentrated in a particular degree of freedom. At equilibrium and when there are s degrees of freedom the statistical weight of such a distribution is known to be

$$P_{n,j} = \frac{(n-j+s-1)!\,n!}{(n-j)!\,(n+s-1)!} \quad . \quad . \quad . \quad . \quad (32)$$

Therefore, considering separately groups of molecules where $n = j$, $n = j+1$ and so on, molecules of the first group may react only when all the j quanta are in a particular bond, those in the second group only when either j or $j+1$ quanta are in that bond, and so on. Accordingly

$$k_{\text{uni}} = \left\{ {}^1k_s\alpha_1\frac{(s-1)!\,j!}{(j+s-1)!\,0!} + {}^2k_s\alpha_2\left[\frac{s!(j+1)!}{1!(j+s)!} + \frac{(s-1)!(j+1)!}{0!(j+s)!}\right] \right.$$
$$+ {}^3k_s\alpha_3\left[\frac{(s+1)!(j+2)!}{2!(j+s+1)!} + \frac{s!(j+2)!}{1!(j+s+1)!} + \frac{(s-1)!(j+2)!}{0!(j+s+1)!}\right]$$
$$\left. + \ldots \right\} \sum_{s=1}^{s=s} \frac{1}{(s-1)!}\left(\frac{E}{RT}\right)^{s-1} e^{-E/RT} \quad . \quad . \quad . \quad . \quad . \quad (33)$$

Although it is difficult to evaluate the transmission coefficients λ and so to calculate k_a for the Kassel hypothesis, there may not be much difference between rate constants on the two hypotheses when the contribution to reaction of each group of molecules is considered separately.

Summary.

(1) The Polanyi-Hinshelwood hypothesis for "unimolecular" reactions has been reformulated considering separately the contribution to reaction of the group of molecules containing just the critical number j of quanta necessary for reaction, the group containing just $j + 1$ quanta, and so on. The assumption that the rate k_a at which energised molecules become activated is independent of the total energy of activation is avoided, and difficulties to which this intrinsically unlikely assumption have previously been shown to lead, no longer arise.

(2) Investigation of the velocity with which energy quanta redistribute themselves between the radicals of a two-radical molecule by intra-molecular vibrational collision shows that for a range of conditions this redistribution may occur within the period of a few vibrations, and that equilibrium may be established well within the interval between successive inter-molecular collisions.

(3) When distribution equilibrium is maintained the rate at which each group of energised molecules becomes activated was calculated using the Polanyi-Hinshelwood hypothesis and a simple molecular reaction model, and values for k_a thus obtained. For this model the contribution to k_a from each group of molecules was found to depend very much upon the energy of the group, and also the larger part of the reaction rate was due to the comparatively few molecules possessing energy considerably in excess of the minimum energy of activation.

The Chemical Laboratories,
Bedford College (University of London).
Regents Park, London.

STUDIES IN VAPOUR PRESSURE MEASUREMENT. PART IV.—THE TOTAL VAPOUR PRESSURE OF MIXTURES OF SULPHUR TRIOXIDE AND CHLORSULPHONIC ACID.

By E. W. Balson and N. K. Adam.

Received 3rd April, 1947.

The vapour pressure of mixtures of SO_3 and chlorsulphonic acid has been measured from about 0° to 40° c. using a Bourdon gauge balanced by measured pressures of air. The vapour pressure increases about threefold as the mole fraction of SO_3 increases from 0·55 to 0·7, less rapidly at other concentrations. Results were erratic above 0·7 mole fraction, where the vapour pressure was not much less than that of pure SO_3.

Experimental.

Fig. 1 shows the apparatus. The gauge E is, during the actual measurements, in contact with the de-gassed mixture in C, which has been sealed off at M. The capillary tubes (in heavy lines on the diagram) have been sealed off. The vapour pressure is balanced by dry air whose pressure is measured in the mercury manometer J.

The experimental difficulties and complication of the apparatus arise from the necessity of making up the mixtures out of contact with air, degassing them and protecting the delicate Bourdon gauge from sudden pressure differences during these operations.

Filling and de-gassing.—Chlorsulphonic acid was first distilled from A (fitted by a standard ground joint), into B, under vacuum (10^{-3} mm. or less, provided by a two-stage mercury diffusion pump backed by a glass filter pump). The receiver B and two traps G and H were cooled with liquid oxygen, to protect the greased taps and mercury from the highly corrosive vapours. After distillation of sufficient chlorsulphonic acid, dry air was admitted through T_2, and the flask A replaced by one containing pure SO_3. The ground joint at A was lubricated by a little chlorsulphonic acid. A suitable quantity of SO_3 was then distilled under vacuum into B, the tube leading to A sealed off, and the entire contents of B distilled into C. B was sealed off at M and removed.

Two troublesome difficulties occurred in the next stages, with all mixtures except those poor in SO_3; after condensation in B at the temperature of liquid oxygen, the SO_3 solidifies in a form which requires a temperature of about 75° c. to melt or dissolve in chlorsulphonic acid. This raises the vapour pressure often to much above one atmosphere, so that the re-solution must be done in a sealed vessel out of contact with the gauge. The tube from C therefore ended, at first, in a closed bulb inside D; this bulb could be broken when required by a weight of soft iron enclosed in thick glass, controlled by an electromagnet, in D. After re-solution was complete, the liquid mixture in C was cooled to about 10° c. Even at this temperature the vapour pressure was high enough to fracture the gauges when the bulb was broken and the vapour suddenly admitted to the gauge; after many accidents the small bulb K was fitted; a little SO$_2$ was allowed to distil into K, the capillary tube P being then sealed off. K was allowed to warm up until its vapour pressure nearly equalled that of the mixture, and the gauge balanced with air from the manometer J. Degassing was then completed by allowing the contents of C to warm up to about 30° c. under vacuum; C was again cooled with liquid oxygen, and the vacuum train sealed off at Q and S. The mixture in C was again liquefied, cooled to about 10°, the bulb in D broken, and K sealed off at R.

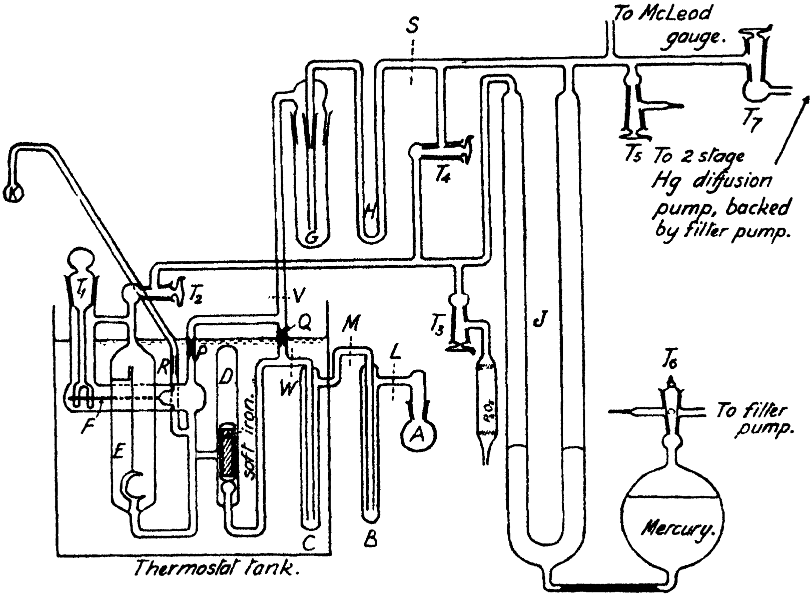

FIG. 1.

Measurement of Vapour Pressure.—The thermostat was placed round the apparatus, and readings taken both with rising and with falling temperatures, the pressure of air in J being adjusted so as to balance the vapour pressure approximately, the small difference between the air pressure (measured with a cathetometer) and the vapour pressure being read off from the movement of the gauge pointer observed with a low power microscope with eyepiece scale. Gauges of sensitivity varying from 0·2 to 1·6 mm. Hg per eyepiece division were used, the more robust gauges for the mixtures of high SO$_2$ content. Readings could be taken to about 0·2 of one eyepiece division. For each mixture at least ten readings were taken at various temperatures and all points fitted very closely to a linear plot of $\log_{10}p$ against $1/T$.

Analysis.—Before opening, the two sides of the gauge were brought to equal pressure by breaking the thin-walled tube F, by turning the stopper T$_1$. Dry air was admitted through T$_2$. The mixture was sealed off in C at W, and C was weighed. C was opened at two points convenient for emptying and placed quickly in a stoppered bottle containing a little water. The stopper being firmly tied in place, the bottle was shaken cautiously so as to introduce a drop or two of water at a time into the mixture. The reaction was very violent at first but towards the end water could be added in larger amounts. The solution was made up to a definite volume and portions taken for titration. Total acidity was determined with standard NaOH, using bromthymol blue as indicator, and chloride usually by electrometric titration with AgNO$_3$; occasionally the chloride and sulphate were determined gravimetrically as a check. To obtain the total weight of the mixture, C and the pieces of glass cut from it were collected, dried and weighed.

The above analysis gives the ratio between *total* SO_3, including the part combined as acid chlorides, and chloride. Assuming that all the chloride arises from a single compound of formula $ClSO_3H$, the amounts of SO_3 and $ClSO_3H$ can be calculated. The sum of the SO_3 and $ClSO_3H$ so calculated proved often to be slightly (about 0·6 %) greater than the weight of mixture taken. Analysis of the chlorsulphonic acid used, by the above method, gave about 0·2 mole fraction (14·5 % by weight) of SO_3. The chlorsulphonic acid was B.D.H. "redistilled," and was given one or two further distillations at 100 mm. before use. Attempts were made to reduce the apparent SO_3 content by distillation under high vacuum, but though small variations were obtained there was always a considerable quantity of SO_3 present when calculated as above from the total acidity and the chloride content. The most probable explanation of these figures is that the "chlorsulphonic acid" contained some sulphuryl chloride and pyrosulphuryl chloride or oleum. Visual evidence was sometimes obtained of the presence of a substance which reacts only slowly with water, during the decomposition of the mixtures with low SO_3 content; oily drops appeared after water had been added, which disappeared quite slowly, vanishing completely only after some hours. Sulphuryl chloride reacts slowly with water in a very similar manner.

Results.

Table I gives the composition, calculated as above, of the mixtures used, their vapour pressure at 15° c., and the constants of the equation $\log_{10} p = A - B/T$. The vapour pressures at 15° c. are plotted in Fig. 2.

TABLE I

Apparent Mole Fractions.		Vapour Pressure.	*A*.	*B*.
SO_3.	$ClSO_3H$.	mm. Hg at 15° C.		
1·000 (liquid)	0	130	10·175	2320
1·000 (solid, Smits' α form)	0	120	13·015	3150
0·955	0·045	109	10·115	2333
0·860	0·140	122	10·46	2417
0·854	0·146	117·5	10·34	2383
0·839	0·161	126	10·17	2325
0·818	0·182	119	10·26	2360
0·775	0·225	96·7	10·51	2457
0·667	0·333	77·0	9·87	2300
0·644	0·356	79·5	10·14	2377
0·625	0·375	46·8	10·04	2413
0·572	0·428	30·3	9·87	2420
0·550	0·450	26·5	10·21	2533
0·397	0·603	10·5	10·05	2620
0·367	0·633	12·8	10·16	2620
0·219	0·781	4·1	9·19	2470

In reading the curve and the table it must be remembered that the absolute quantity of *free* SO_3 is, particularly at the lower mole fractions, probably a good deal less than the amount shown as "SO_3." Nevertheless some features are of sufficient interest to place on record. Between apparent mole fractions of 0·55 and 0·70 SO_3 (45·6 to 61·5 %), the vapour pressure, which is almost entirely due to the SO_3, increases from about 30 to about 100 mm. At higher concentrations the rate of increase is much less; and perhaps because the solution has become nearly saturated with one or another of the various modifications of sulphur trioxide, which have different vapour pressures, the results were rather erratic. Pure liquid sulphur trioxide (supercooled) has a vapour pressure of about 133 mm. at 15° c. The values for *B*, which is the latent heat of evaporation per mole divided by 2·303 *R*, are probably not reliable to closer than about 4 %. There is an indication, however, that they are higher for the mixtures of low than for those of high SO_3 concentration.

The above figures for pure SO_3 are our own determinations ; the error in the case of the liquid may have been about 3 mm. ; since the value at 15° (considerably supercooled) was obtained by extrapolation from measurements on liquid, at or above 25°. A curious phenomenon was noticed ; the plots of log *p* against $1/T$ were straight for both the solid and the liquid forms and intersected at 18 ± 1°. The solid appeared, however, to have a melting point close to 32° c., the liquid being fairly easily supercooled by some 10°. Most authors give the m.p. of the *alpha*-form of solid SO_3 about 17° ; but on one occasion[1] Smits records a m.p. of 32° for a specimen which solidified from the liquid formed on melting the *beta*-form, whose m.p. is not far short of 80° and appears to be identical with the form we obtained by condensation at liquid oxygen temperatures. The reason why the break in our vapour pressure curves occurs at 18°, while the visible m.p. is at 32°, requires further investigation. There was no obvious break at 32° ; it is possible, but scarcely probable *a priori*, that two solid forms exist, with a large heat of transformation at 18°, the form stable between 18° and 32° having a very small latent heat of fusion.

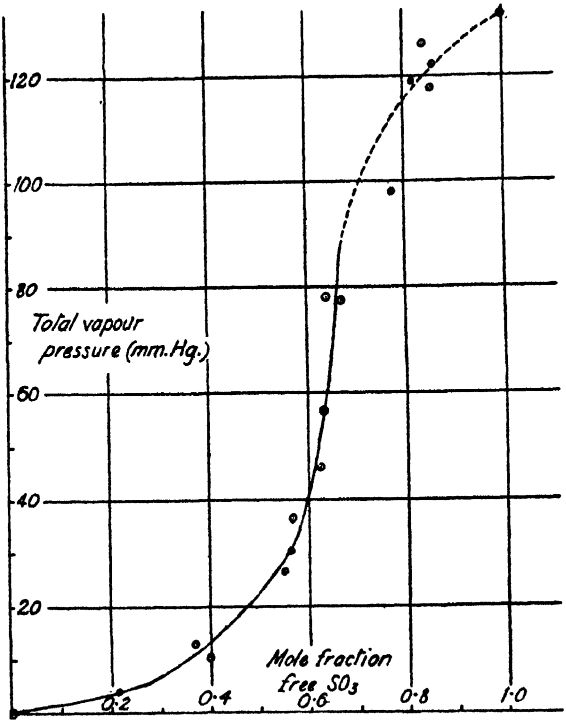

FIG. 2.

This paper is published by permission of the Chief Scientist, Ministry of Supply, and describes work carried out in 1942 and 1943.

University College,
Southampton.

[1] *J. Chem. Soc.*, 1924, 2558.

THE MECHANISM OF SPARK IGNITION. PART II.—CARBON MONOXIDE-OXYGEN MIXTURES.

By W. E. Frost and J. W. Linnett.

Received 21st April, 1947.

In Part I, Linnett, Mrs. Raynor and Frost [1] described some experiments on the spark ignition of mixtures of hydrogen and oxygen, and of mixtures of hydrogen and oxygen to which had been added the inert gases N_2, A and CO_2. They found that small amounts of the inert gases caused a lowering of the minimum ignition pressure of electrolytic gas. In the theoretical treatment of their results they assumed, as Mole had done, that the condition for ignition was that the concentration of chain-propagating radicals should increase in an uncontrolled manner in the region round the spark.[2] The authors concluded from their results that small amounts of the inert gases aided ignition by slowing up the diffusion of the chain radicals from the region of the spark (see also Thompson [3]). A quantitative explanation of the results was given based on this hypothesis. When larger amounts of inert gas were present it was found that the minimum ignition pressure of electrolytic gas was raised, and it was concluded from the relative effects of the different inert gases that this was due to the cooling effect exerted by the added gas.

In the present paper an analogous series of experiments on the ignition of carbon monoxide-oxygen mixtures will be described. It will be shown that the results can be explained, in the main, by a hypothesis similar to that advanced to explain the results in Part I.

Coward, Cooper and Jacobs [4] investigated the effect of inert gases on the minimum ignition pressure of $CO—O_2$ mixtures, using mixtures saturated with water vapour. They found a lowering of the same type as that for electrolytic gas. In addition they observed that $CO—O_2$ mixtures required a much stronger spark to ignite them than did $H_2—O_2$ mixtures.

Experimental.

The explosions were carried out in a Pyrex tube, 2·0 cm. diam. and 25 cm. long. The spark gap was placed on the axis of the tube about 1 cm. from the top of the tube. The spark was passed between two tungsten wires, 0·37 mm. diam., sealed through the walls of the tube. The points were 1·4 mm. apart.

In Part I an induction coil was used to produce the spark but, in the present series, a different spark was used. The circuit is shown in Fig. 1. The 220 A.C. mains were connected across the primary of a transformer which had a step-up ratio of 20. When igniting the mixtures used in this series of experiments the galvanometer registered about 1 ma. This was a larger current than was required for the ignition of $H_2—O_2$ mixtures (see Part III) which confirms the observation of Coward, Cooper and Jacobs. When testing a given mixture to see whether it could be ignited or not, the key in the primary circuit was closed for about 1 sec.

---

[1] Linnett, Mrs. Raynor and Frost, *Trans. Faraday Soc.*, 1945, **41**, 487.

[2] Mole, *Proc. Physic. Soc.*, 1936, **48**, 857.

[3] Thompson, *Trans. Faraday Soc.*, 1932, **28**, 299.

[4] Coward, Cooper and Jacobs, *J. Chem. Soc.*, 1914, 1069.

The oxygen and nitrogen used were obtained from cylinders and, before being admitted to the apparatus, were dried with $CaCl_2$ and P_2O_5. The carbon monoxide was prepared by allowing 98 % formic acid to drop on to conc. H_2SO_4 at 100° C. The gas produced was passed through soda-lime and then dried with $CaCl_2$ and P_2O_5. The water used was distilled into a small storage tube connected to the apparatus and any dissolved gases removed by pumping after alternate freezing and melting. Each mixture of gases which was to be tested for ignitability was made up in the explosion tube and was mixed thoroughly by withdrawing a number of times into a mercury-filled reservoir and then returning to the explosion tube. The pressures of the gases were measured on a capillary mercury manometer. The procedure for determining the limiting pressure separating ignitable from non-ignitable mixtures was the same as in Part I.

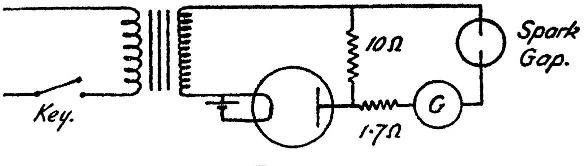

FIG. 1.

Results.

The results may be divided into three parts.

(i) The effect on the minimum ignition pressure of varying the CO/O_2 ratio in the presence of water vapour. In Table I are given the pressures of CO and O_2 at the limit between ignition and non-ignition. The pressure of water vapour was kept at 5 mm. throughout. The results are shown graphically in Fig. 2.

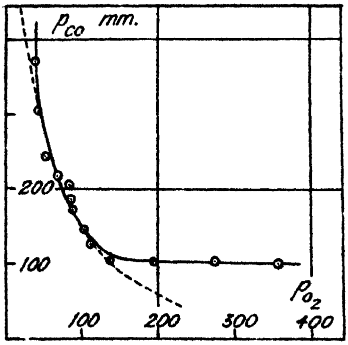

Theoretical : - - - -
Experimental : ———
FIG. 2.

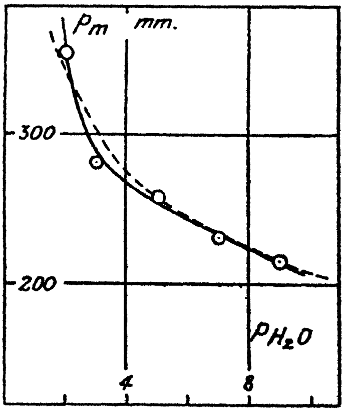

Theoretical : - - - -
Experimental : ———
FIG. 3.

(ii) The effect of the amount of added water on the limiting ignition pressure of a $2CO/O_2$ mixture. Table II gives the minimum ignition pressure of this mixture for various pressures of added water vapour. The results are plotted graphically in Fig. 3.

(iii) The effect of added N_2 on the limiting ignition pressure of a $2CO/O_2$ mixture, the water vapour pressure being kept constant at 5 mm. Table III gives the minimum ignition pressure of such a CO/O_2 mixture for various pressures of added N_2. The results are shown graphically in Fig. 4.

TABLE I.—LIMITING IGNITION PRESSURES OF CARBON MONOXIDE-OXYGEN MIXTURES WHEN p_{H_2O} IS 5 MM.

p_{CO} (mm.) .	—	101·3	104	104·3	104	125·3	146
p_{O_2} (mm.) .	—	356·7	274	194·2	135	110·7	102
p_{CO} (mm.) .	172	186	205·7	218·3	244	307·5	374·7
p_{O_2} (mm.) .	86	84	83·3	68·2	51	42	36·3

TABLE II.—THE EFFECT OF THE PRESSURE OF WATER VAPOUR ON THE LIMITING IGNITION PRESSURE OF A $2CO/O_2$ MIXTURE, p_m.

p_{H_2O} (mm.) .	1	2	3	5	7	9
p_m (mm.) .	416	355	281	258	232½	217½

TABLE III.—THE EFFECT OF ADDED NITROGEN, p_{N_2}, ON THE LIMITING IGNITION PRESSURE OF A $2CO/O_2$ MIXTURE, p_m.

p_N (mm.)	0	32	62½	139½	180	227½	270	302½
p_m (mm.)	258	248	238	211	197	186½	186	185½

Discussion.

In the following treatment the effect of changing gas composition on the electrical conditions in, and intensity of, the spark has been neglected. It is obvious that this is an over-simplification of the position. And yet it will be seen that a satisfactory account can be given of many features of the limiting spark ignition pressures of these mixtures by considering only the kinetic theory and chemical character of the gas mixtures used. It is thought, therefore, that these effects are more important and that the changing electrical properties of the spark may be neglected in such a preliminary treatment as the following.

One of the most important of the present observations is that the limiting ignition pressure is very dependent on the amount of water vapour present, and that it rises very rapidly as the amount of water is reduced below 2 mm. If we suppose that ignition results when the numbers of atoms and radicals increase without limit in the region of the spark gap (cf. Mole, and Part I) this must mean that the water is intimately connected with the chain-branching process. This is quite different from what has been observed for the reaction at *ca.* 600° c. in a heated vessel.[5] Under

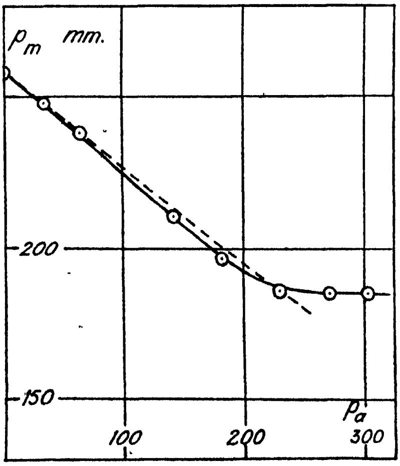

Experimental: ———
Theoretical: - - - -

FIG. 4.

---

[5] Hinshelwood, *Kinetics of Chemical Change* (O.U.P., 1940).

those conditions the explosion limits are only slightly affected by the amount of water present but the reaction outside the limits is very much accelerated by water vapour.[6] In these circumstances, therefore, the water takes part in the chain-propagating reaction but *not* in the chain-branching reaction. It is not really very surprising that there should be this fundamental difference in the spark ignition of $CO—O_2—H_2O$ mixtures because it is certain that the conditions in the spark gap are very much more violent than those represented by a temperature of 600° C. It has already been mentioned that a relatively violent spark has to be used to ignite these mixtures.

To incorporate water into the chain-branching cycle, it is suggested that the most important reactions associated with the branching that occurs in the region round the spark gap are the following :

$$\begin{aligned} &(1)\ H + O_2 = OH + O\,; \\ &(2)\ O + H_2O = 2OH\,; \\ &(3)\ OH + CO = CO_2 + H. \end{aligned}$$

It is not supposed that other reactions do not occur but it is supposed that others are less important than the above three. These reactions have been selected as the most likely bimolecular reactions involving radical-molecule collisions. Termolecular collisions are much less frequent than bimolecular ones and for this reason all termolecular processes have been ignored as being probably less important than any of the present set of bimolecular processes. It seems to us that the active particles that are likely to be present are H, O and OH, remembering that O_2, CO and H_2O are the three molecules initially present. Hydrogen atoms are more likely to react according to (1) than in any other way. Oxygen atoms would react with CO molecules but a third body would be required which would make the process termolecular. This probably makes it less likely than their reaction with a water molecule, except when the latter are present in only very small amounts. Reaction (3) is certainly the likely reaction for hydroxyl radicals and has been postulated elsewhere.[7]

In addition, we shall suppose that hydrogen atoms are lost from the region of the spark by diffusion at a rate given by $D_H[H]$, and hydroxyl radicals and oxygen atoms at rates given by $D_{OH}[OH]$ and $D_O[O]$ respectively. It may then be shown that the condition for the unlimited increase of radicals in the region of the spark is, the k's being the velocity constants of the three reactions:

$$\frac{D_{OH}}{k_3[CO]} + \frac{D_H}{k_1[O_2]} + \frac{D_{OH}D_H}{k_1k_3[O_2][CO]} - \frac{2k_2[H_2O]}{k_2[H_2O] + D_O} > 0 \quad . \quad (1)$$

The square brackets are used to represent " the concentration of." The condition for the limiting ignition pressure is that the above is equal zero.

In what follows we will make the assumption that O_2 and CO molecules interfere with the diffusion of active particles to an equal extent. This is not likely to be far from the truth because the two molecules do not differ greatly in either size or mass. Since the pressure of water vapour is always small compared with that of the other components its effect on diffusion will be supposed to be negligible. We may therefore in considering $CO—O_2—H_2O$ mixtures, substitute for D_H the expression K_H/p_t, where p_t is the sum of the pressures of CO and O_2. Similar substitutions may be made for D_{OH} and D_O. K_H is the diffusion constant for hydrogen atoms, and K_{OH} and K_O the constants for hydroxyl radicals and oxygen atoms. The equation for the limiting ignition pressures is then the following, if we use p_{O_2} and p_{CO} as a measure of the concentrations of the two gases :

$$\frac{K_H}{k_1 p_{O_2} p_t} + \frac{K_{OH}}{k_3 p_{CO} p_t} + \frac{K_{OH}K_H}{k_1 k_3 p_{O_2} p_{CO} p_t^2} = \frac{2}{1 + K_O/k_2 p_{H_2O} p_t}. \quad . \quad (2)$$

---

[6] Hadman, Thompson and Hinshelwood, *Proc. Roy. Soc. A*, 1932, **138**, 297.

[7] Hadman, Thompson and Hinshelwood, *ibid.*, 1932, **137**, 87.

When numerical constants are introduced to obtain the best approximation for the effect of water on the minimum ignition pressure and also the effect of varying the CO/O_2 ratio, the following expression results:

$$\frac{4147}{p_{O_2}p_t} + \frac{2093}{p_{CO}p_t} + \frac{8744530}{p_{O_2}p_{CO}p_t^2} = \frac{2}{1 + 9360/p_{H_2O} \cdot p_t}. \quad \quad (3)$$

That is, $$\frac{K_{OH}}{k_3} = 2095 ; \frac{K_H}{k_1} = 4174 ; \frac{K_O}{k_2} = 9360.$$

The plot of the minimum ignition pressure against the pressure of water vapour calculated from the above expression (3) is drawn in Fig. 3. It will be seen that it lies quite close to the experimental results over the whole range. The expression (3) certainly gives a satisfactory account of the effect of water on the minimum ignition pressure. This supports the inclusion of reaction (2) as an important process occurring in the region of the spark.

In Fig. 2 there is drawn the line calculated from eqn. (3) showing the effect of varying the CO/O_2 ratio on the limiting ignition pressure when p_{H_2O} is 5 mm. For the range between $p_{O_2} = 40$ and 140 mm. the calculated line follows the experimental points well. However, at high CO pressures and for O_2 pressures greater than 140 mm. the experimental points lie at higher pressures than those calculated from expression (3). That this must happen in these regions is to be expected because when one adds more and more of either component a point will be reached when the excess of either will exert a sufficient cooling effect on the gases round the spark to hinder ignition. The same effect occurred with H_2—O_2 mixtures (see Part I). However, it must be admitted that the experimental line does depart rather suddenly from the theoretical one at about $p_{O_2} = 140$ mm. It seems that there may be some specific effect of O_2 which makes itself felt when the proportion of O_2 becomes high. Nevertheless over a very considerable range the theory gives a very good account of what is observed, and some departures from the theoretical behaviour in the direction observed would be expected at high pressures of both CO and O_2.

It is interesting to consider the ratios that it is necessary to assume for K_{OH}/k_3 (2095), K_H/k_1 (4174) and K_O/k_2 (9360). The diffusion constants K_{OH} and K_O are likely to be about the same, the former being, if anything, rather smaller. This means that $k_3 > k_2$. This is not at all improbable because the reaction of OH with CO is probably quite an easy one. K_H must be bigger than both K_{OH} and K_O. This means that $k_1 > k_2$ and probably that k_1 is slightly greater than k_3.

It remains to be seen how the theory can account for the effect of N_2 on the minimum ignition pressure. The obvious course is to suppose that N_2 interferes with the diffusion of the radicals to the same extent as CO and O_2. In that case one would put $p_t = p_{CO} + p_{O_2} + p_{N_2}$. However, it is found that this does not lead to any agreement with the observed results. It is found that agreement with the experimental results is obtained if one puts $p_t = p_{CO} + p_{O_2} + 0{\cdot}54\, p_{N_2}$. The curve, obtained from expression (3) if this assumption is made, is compared with the experimental results in Fig. 4. It will be seen that the agreement is good for small additions of N_2. When larger amounts of N_2 are added the experimental points lie above the theoretical line as would be predicted, since, when larger amounts are present, the N_2 exerts a sufficiently large cooling effect to interfere with ignition in a way that is not allowed for in the present treatment. The assumption that N_2 is only about a half as efficient in preventing diffusion as are CO and O_2 is not a very satisfactory one. It would have been expected that it would have been about equally efficient. It may be that CO and O_2 are, in some way, relatively more efficient than N_2 because they are participants in the reaction. However, apart from the quantitative features, it is important to stress that the qualitative effect of added N_2 in lowering the limiting ignition pressure shows clearly the close resemblance between the ignition of this mixture and that of electrolytic gas. This is strong evidence that the nitrogen acts in the same way on this ignition as on the ignition of electrolytic gas; namely, by slowing up the diffusion of the active radicals and atoms from the region of the spark. Therefore it seems very probable that the general picture of the ignition described here is the correct one.

As regards the detailed picture, that is the sequence of three reactions used in the deduction of the formulæ, it explains the basic features and, in particular, gives a good account of the effect of water vapour on the limiting ignition pressure. It seems probable that the three reactions assumed are the most important ones in the spark ignition but it is probable that there are others occurring in the spark, and it may be they account for some of the departures from the predicted quantitative behaviour. However, considering the complexity of the system and the way in which the intensity of the spark and spark temperature have been ignored it is thought that the suggested scheme explains the results observed in a very satisfactory manner.

Summary.

The spark of ignition of CO—O_2 mixtures has been studied. It is found that the minimum ignition pressure falls very rapidly with increasing water content and that the addition of N_2 also lowers the limiting ignition pressure. A set of reactions has been suggested which accounts for the main features of the observations. It is suggested that the lowering of the minimum ignition pressure by N_2 occurs because the inert gas impedes the diffusion of chain radicals from the region of the spark. That is, it is suggested that the inert gas effect here is the same as it was for H_2—O_2 mixtures and that the concondition for ignition is, as for the H_2—O_2 ignition, the uncontrolled increase of chain-propagating radicals in the region of the spark.

Inorganic Chemistry Laboratory,
Oxford.

THE MECHANISM OF SPARK IGNITION.

PART III.—EFFECT OF ADDING ORGANIC VAPOURS TO HYDROGEN-OXYGEN MIXTURES.

By W. E. Frost and J. W. Linnett.

Received 21*st April,* 1947.

In Part I [1] the effect of added inert gases on the spark ignition of electrolytic gas ($2H_2 + O_2$) was examined. The present paper describes the effect of small amounts of some organic substances (alcohols, ethyl halides, etc.) on the minimum ignition pressure of electrolytic gas. The results obtained are such as would be expected on the basis of the hypothesis suggested in Part I. The hypothesis was that ignition occurred when there was an unlimited increase in the number of active chain-propagating radicals in the region of the spark (cf. Mole),[2] and that added inert substances affected ignition by interfering with, or aiding, the increase of these active radicals.

[1] Linnett, Mrs. Raynor and Frost, *Trans. Faraday Soc.*, 1945, 41, 487.
[2] Mole, *Proc. Physical Soc.*, 1936, 48, 857.

Experimental.

The explosion tube and spark gap, etc., have been described in Part II. The spark was produced by the electrical circuit described in Part II [3] except that a larger resistance (10 megohms) was placed in series with the spark gap. Electrolytic gas mixtures do not require such intense sparks as CO—O_2 mixtures under similar conditions (cf. Coward, Cooper and Jacobs [4]). When the key in the primary circuit was closed the current registered by the ammeter was about 0·2 ma. at pressures in the neighbourhood of the ignition limit.

The oxygen and nitrogen used were obtained from cylinders and were dried with $CaCl_2$ and P_2O_5. The hydrogen was prepared by the action of H_2SO_4 on Zn and was passed through tubes containing soda-lime, $CaCl_2$ and P_2O_5 before entering the apparatus. The organic liquids were all commercial substances. In all cases a portion was distilled into a small storage tube joined to the apparatus and then a part of this distilled away so that volatile impurities were eliminated. The mixtures to be tested were made up and mixed in the manner described in Part I, and the procedure for determining the minimum, or limiting, ignition pressure was the same. The pressures were determined on a capillary mercury manometer.

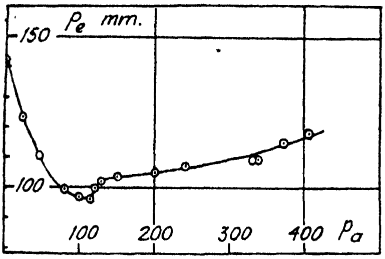

Fig. 1.

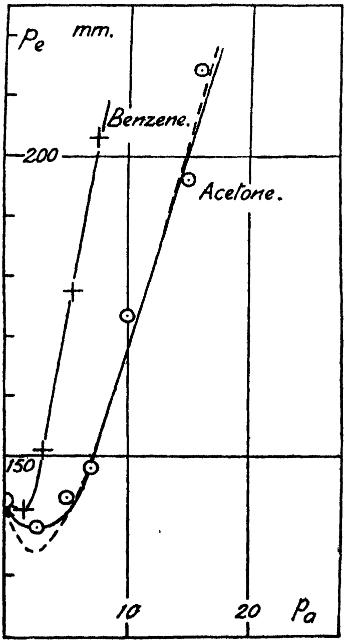

Theoretical: - - - -
Experimental: ———
Fig. 2.

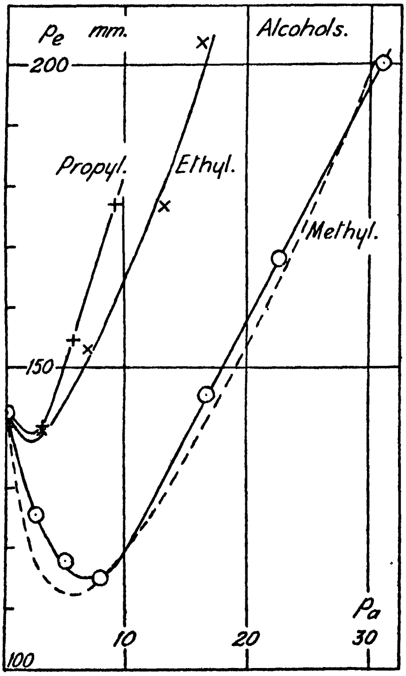

Theoretical: - - - -
Experimental: ———
Fig. 3.

The minimum ignition pressure of electrolytic gas under the conditions used here was 142½ mm. A few preliminary experiments were carried out with N_2

---

[3] Frost and Linnett, *Trans. Faraday Soc.*, 1948, **44**, 416.
[4] Coward, Cooper and Jacobs, *J. Chem. Soc.*, 1914, 1069.

added to the electrolytic gas and the results are listed in Table I. In Fig. 1 the minimum ignition pressure of electrolytic gas, p_e, is plotted against the pressure of added nitrogen, p_a. It will be seen that there is an inflection in the curve at a N_2 pressure of 115 mm. It seems probable that the condition of the spark must have changed as this pressure was passed, though there was no visible sign that this was so. However, in what follows (addition of organic vapours) we never encountered any other similar inflections. The reason for this may be that the pressure of added vapour never even approached 115 mm. We would stress that the effect of adding small amounts of N_2 which is observed here, is the same as was observed when an induction-coil spark was used (Part I)—i.e. the minimum ignition pressure of electrolytic gas is lowered by small amounts of added nitrogen.

TABLE I.—THE EFFECT OF NITROGEN (p_a) ON THE MINIMUM IGNITION PRESSURE OF ELECTROLYTIC GAS (p_e).

p_a mm. .	0	23½	46	79	100	114	120	128½
p_e mm. .	142½	123½	110½	99	97	96	100	102
p_a mm. .	150½	199½	241	330½	336½	373	402½	—
p_e mm. .	103½	105	107	109½	109½	115	118	—

TABLE II.—THE EFFECT OF ORGANIC VAPOURS (p_a) ON THE MINIMUM IGNITION PRESSURE OF ELECTROLYTIC GAS (p_e).

Benzene						
p_a mm.	1½	3	5½	7½	—	—
p_e mm.	141	151	177½	203	—	—
Methyl alcohol						
p_a mm.	2½	5	8	16½	22½	31
p_e mm.	125½	118	115	145½	168	200½
Ethyl alcohol						
p_a mm.	3	8	13	16	—	—
p_e mm.	139½	153	177	204	—	—
n-*Propyl alcohol*						
p_a mm.	3	5½	9	—	—	—
p_e mm.	140	154	177	—	—	—
Acetone						
p_a mm.	2½	5	7	10	15	16
p_e mm.	138	143	148	173½	196	214
Ethyl chloride						
p_a mm.	2½	5	8½	12	19	—
p_e mm.	126½	131	148	167	208	—
Ethyl bromide						
p_a mm.	4	6½	8	11½	—	—
p_e mm.	144	161½	189½	225	—	—
Ethyl iodide						
p_a mm.	1	2	3½	—	—	—
p_e mm.	149	185	210	—	—	—

The organic substances used were benzene, methyl alcohol, ethyl alcohol, *n*-propyl alcohol, acetone, and ethyl chloride, bromide and iodide. The results for these 8 substances are listed in Table II which gives the minimum ignition pressure of electrolytic gas, p_e, for each pressure of added vapour, p_a, for which a determination was made. The results for acetone and benzene are shown graphically in Fig. 2, those for the alcohols in Fig. 3, and those for the ethyl halides in Fig. 4.

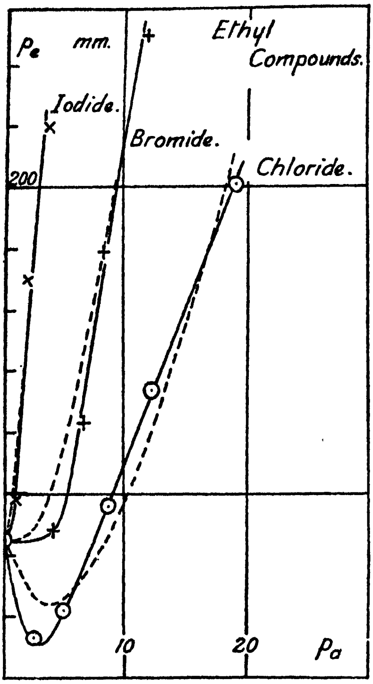

Theoretical: - - - -
Experimental: ———

FIG. 4.

Discussion.

As in Part II, it will be assumed that the effect on ignition of the changing electrical properties of the spark with changing gas composition can be neglected to a first approximation relative to effects of a kinetic theory and chemical character (cp. Part II).

We shall presume as in Part I that the important processes occurring in the electrolytic gas in the region of the spark are:

(1) $H + O_2 = OH + O$;
(2) $O + H_2 = OH + H$;
(3) $OH + H_2 = H_2O + H$.

This succession of processes constitutes a branching chain and they have all been shown to be important by investigations of the isothermal reaction at 500-600° C.[5] As in Parts I and II, it will be presumed that ignition results when there is an unlimited increase in active chain-propagating atoms and radicals in the region of the spark. Further assumptions are: (*a*) in addition to the increase in the concentration of radicals resulting from the above sequence of processes, there is a loss of radicals by diffusion from the small volume round the spark; (*b*) at the limiting pressure dividing the region of ignitable from the region of non-ignitable mixtures, the loss by diffusion just balances the increase by chain-branching, and (*c*) the loss of hydrogen atoms by diffusion is much greater than the loss of hydroxyl radicals or of oxygen atoms. This latter is not unreasonable because hydrogen atoms, being lighter than oxygen atoms or hydroxyl radicals, diffuse more quickly. Also oxygen atoms are not likely to have a long life because their rate of reaction with hydrogen molecules is likely to be high so that they will disappear by reaction (2), which is almost certainly fast, before they can diffuse out of the small spark region. The same is probably true for hydroxyl radicals under the violent conditions of the spark. Also reaction (1) probably does not occur at such a high proportion of the collisions as (2) or (3) because it is a reaction which involves the production of three free valencies from one free valency (i.e. it is the real chain-branching reaction) and it will therefore be endothermic.[6] If hydrogen atoms are able to survive a considerable number of collisions with oxygen molecules they may last long enough, on an average, to diffuse from the small region in considerable numbers. For these reasons therefore, we will neglect the loss by diffusion of oxygen atoms and hydroxyl radicals. The loss by diffusion of hydrogen atoms may be represented by $D_H[\mathrm{H}]$, where D_H is a constant for a given mixture and [H] is the concentration of hydrogen atoms. It may then be shown that the minimum ignition pressure will be given by :

---

[5] Hinshelwood and Wilbourne, *Proc. Roy. Soc. A*, 1946, 185, 353, 369, 376.

[6] Hinshelwood and Williamson, *The Reaction between Hydrogen and Oxygen* (O.U.P., 1934).

$$2k_1[\mathrm{O}_2] = D_H. \qquad (1)$$

If we are concerned with a mixture of electrolytic gas at a pressure p_e and an added inert gas at p_a then (cf. Part I) :

$$D_H = \frac{1}{K'p_e + K_s p_a} \qquad (2)$$

where K' is a constant for electrolytic gas and K_s is a constant for the added gas.[7] These constants are the reciprocals of the diffusion coefficients. This means that, for such mixtures, (1) may be transformed into

$$kp_e = \frac{1}{K'p_e + K_s p_a} \qquad (3)$$

where $k = 2/3 \,.\, k_1$.

Pressures are here used as a measure of concentration. This is identical with eqn. (6) of Part I which was deduced in a rather different way and was found to be most successful. It must be admitted, however, that the present simplification gives eqn. (4) of Part I but without the first term. The first term was, in fact, found to be considerably less important than the second term on the left-hand side of eqn. (4) of Part I (see eqn. (5) of Part I). The present more detailed, though simplified, picture does not, therefore involve any radical change from the hypothesis propounded in Part I, and it accounts equally well for the effect of added inert gases.

When acetone, benzene, or one of the alcohols is added to the gaseous mixture, the added molecules will probably exert two effects when present in small amounts. In the first place, because the molecules are both heavy and large, they may interfere considerably with the diffusion of hydrogen atoms from the spark region. In the second place, they are all oxidisable substances and they may therefore react with oxygen atoms or with hydroxyl radicals. In this way small additions of these substances may act as negative catalysts because they act as chain-breakers competing with the hydrogen for the oxygen atoms and hydroxyl radicals. The first of these two effects aids, and the second hinders, ignition. From Fig. 2 and 3 it will be seen that this dual effect is observed. For instance, on adding acetone vapour the first portions lower the minimum ignition pressure but larger quantities raise it. The same is true for benzene and the alcohols.

Let us see if we can represent this effect approximately in a quantitative form. Suppose the following reactions occur between the added organic substance, A, and oxygen atoms and hydroxyl radicals :

(4) $\mathrm{O} + \mathrm{A} = \text{products}$;
(5) $\mathrm{OH} + \mathrm{A} = \text{products}$.

It can be shown that, taking the same criterion for ignition, the equation giving the minimum ignition pressure of electrolytic gas is :

$$D_H(k_3[\mathrm{H}_2] + k_5[\mathrm{A}]) = 2k_1[\mathrm{O}_2]\left\{k_2[\mathrm{H}_2] - (k_2[\mathrm{H}_2] + \tfrac{1}{2}k_5[\mathrm{A}])\left[\frac{k_4[\mathrm{A}]}{k_3[\mathrm{H}_2] + k_4[\mathrm{A}]}\right]\right\}. \qquad (4)$$

---

[7] Melville and Ludlam, *Proc. Roy. Soc. A*, 1931, 132, 108.

With hydrogen and oxygen in the proportions in electrolytic gas, and using pressure as a measure of concentration, this may be rearranged to

$$\frac{p_e^2}{p_0^2} = \frac{1 + Mr + Nr^2}{1 + Qr - \frac{1}{2}Nr^2 - \frac{1}{2}QNr^3} \quad . \quad . \quad . \quad (5)$$

where $$r = \frac{p_a}{p_e} \quad M = \frac{3k_5}{2k_3} + \frac{3k_4}{2k_2} \quad N = \frac{9k_5k_4}{4k_3k_2} \quad Q = \frac{K_3}{K'},$$

and p_0 is the minimum ignition pressure when $p_a = 0$. The ratios k_5/k_3 and k_4/k_2 measure the ability of the added molecules to compete with hydrogen for hydroxyl radicals and oxygen atoms respectively. The ratio K_3/K' measures the relative ability of the added substance and electrolytic gas to prevent diffusion of hydrogen atoms. In Fig. 2, a theoretical curve, calculated from (5) with M, N, and Q having the values 30·74, 191·1 and 48·74 respectively, is drawn to compare with that for acetone. It will be seen that the theoretical line follows the experimental points fairly well though it is not a good fit at the minimum. Nevertheless the interpretation accounts quite well for the main features of our observations for acetone. As regards the actual values of the constants, it should be stressed that one should not deduce too much from the exact magnitudes because the fit to the experimental data is not exact. One should rather focus attention on the order of magnitude. It is found that k_4/k_2 and k_5/k_3 are of the order of ten which means that the acetone molecules react considerably more readily than hydrogen molecules with hydroxyl radicals and oxygen atoms. This would be expected. The ratio K_3/K' is *ca.* 50. This is probably rather too high because the theoretical line drops rather too sharply for small values of p_a. However, this ratio would be expected to be large because the acetone molecule is a relatively large and heavy one compare with hydrogen or oxygen, and hydrogen atoms will therefore have a low diffusion coefficient (reciprocal of K_3) through the acetone vapour. In Fig. 3 a theoretical line based on eqn. (5) is compared with the experimental line for methyl alcohol. In this case M, N and Q are taken to be 15·86, 61·6 and 47·86. The fit to the experimental points is again quite satisfactory though the theoretical line falls too sharply for small values of p_a and the value of Q (i.e. K_3/K') is probably too large. The fact that the line for ethyl alcohol rises more steeply than that for methyl alcohol means that either, or both, of the ratios k_4/k_2 and k_5/k_3 are larger. This means that ethyl alcohol competes better than methyl alcohol for oxygen atoms and hydroxyl radicals. Propyl alcohol appears to compete still better because the line rises still more steeply. The sequence would be anticipated.

The results for the ethyl halides are much the same in general form to those for the alcohols, acetone and benzene and they probably likewise remove oxygen atoms and hydroxyl radicals. However, in these cases the following reactions of the ethyl halides with hydrogen atoms may be equally or more important:

$$(6) \ \mathrm{H} + \mathrm{EtX} = \mathrm{Et} + \mathrm{HX}.$$

In the following treatment we suppose that this reaction is much more important than (4) and (5). The equations become unduly complicated if all three chain-breaking processes are included and it is our object to show that the inclusion of reaction (6) is capable of accounting for the form of the results. If, then, reaction (6) is combined with (1), (2) and (3), the condition for the minimum ignition pressure is found to be

$$2k_1[\mathrm{O_2}] = D_{\mathrm{H}} + k_6[\mathrm{A}], \quad . \quad . \quad . \quad . \quad (6)$$

and this may be rearranged for mixtures involving electrolytic gas to

$$1 + Br - Dr^2 = p_0^2/p_e^2, \quad . \quad . \quad . \quad . \quad (7)$$

where r and p_0 have the same meaning as before and

$$B = K_3/K' - 3k_6/2k_1 \quad \text{and} \quad D = 3k_6K_3/2k_1K'.$$

Fig. 4 shows theoretical lines for the three halides calculated from eqn. (7) with the following values of B and D: EtCl, 10·5 and 176; ErBr, 3·53 and 312; EtI, $-23·14$ and 832·6. The value of K_8/K' has been taken to be the same for all the halides—namely 19·5. The value of K_8 would change for the different halides but probably not largely because the three molecules are all heavy relative to the hydrogen atom and they do not differ greatly in size. Because they are heavy and large, K_8/K' is expected to be large. The values of k_8/k_1 are then 6·01, 10·66 and 28·44 for the chloride, bromide and iodide respectively. This means that the iodide reacts more readily with hydrogen atoms than do the other two halides which would be expected because the C—I link is weaker than both the C—Br and C—Cl links. The mechanism therefore gives a satisfactory account of the effect of the ethyl halides on the minimum spark ignition pressure of electrolytic gas. The removal of hydrogen atoms may, in these cases, be more important than the removal of oxygen atoms or hydroxyl radicals.

The general conclusion therefore, is that the results obtained for the effect of organic substances on the spark ignition of electrolytic gas fit into the general hypothesis that ignition results when there is an unlimited increase in the concentration of chain-propagating radicals in the region of the spark. The organic substances exert both (*a*) a pro-ignition effect which may be accounted for by supposing that, because of their weight and size, they interfere considerably with the diffusion of atoms from the spark region; and (*b*) an anti-ignition effect which may be accounted for by supposing that they behave as negative catalysts and compete with the hydrogen and oxygen for the radicals which are responsible for the chain-branching. These two effects explain the change in the minimum ignition pressure of electrolytic gas as increasing quantities of organic vapours are added.

Summary.

The effect of organic vapours on the limiting spark ignition pressure of electrolytic gas has been studied. While small amounts usually lower the ignition pressure, larger amounts exert a strong anti-ignition effect. It is suggested that this results because the organic molecules react readily with the radicals responsible for chain branching. A quantitative treatment in terms of probable elementary processes has been suggested.

Inorganic Chemistry Laboratory,
Oxford.

THE MEASUREMENT OF IONISATION IN A TRANSIENT FLAME.

BY E. R. ANDREW, D. W. E. AXFORD AND T. M. SUGDEN.

Received 12th June, 1947.

The work described below was undertaken on behalf of the Ministry of Supply during 1945, and has yielded results of some academic interest in so far as it represents the first comparison of the measurement of ionisation in a flame by the D.C. conductivity method and by measuring the attenuation of centimetric waves. The system which was investigated was essentially the bright flash obtained by firing a modified Service rifle into air. This flash is well known to be the concomitant of the combustion of the high proportion of H_2 and CO in the muzzle gases when mixed with air, and therefore it constitutes a flame which should be similar in its instantaneous properties to the more normally studied stationary flames.

Experimental.

A. The Flame System.—The flame studied was obtained by firing into air a 0·303 in. Service rifle (the barrel of which had been shortened by 5¼ in. to improve flash production). Ordinary 0·303 in. Service ammunition was used; this produces muzzle gases of the following approximate composition: CO, 45 %; H_2, 15 %; CO_2, 10 %; H_2O, 15 %; N_2, 15 %. The values of the temperature and pressure of the gases at the instant when the shot left the muzzle were 2150° K. and 560 atm., as calculated from thermochemical data.

These gases expand adiabatically, thereby cooling, and at the same time mix with air. It is considered that during the expansion a region of spontaneous ignition is entered, leading to the inception of the flash. In our experiments, the flash consisted of a yellow flame whose dimensions were obtained by taking photographs for a series of rounds using a still camera, and comparing them with a photograph of a linear scale. The general form is shown in Fig. 1 and the following mean dimensions were obtained.

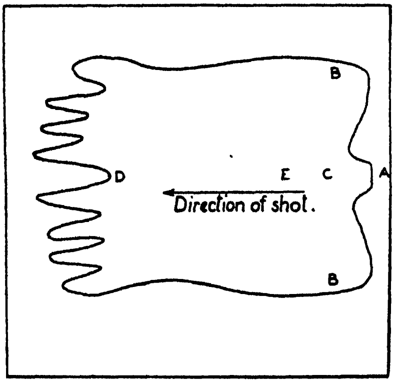

FIG. 1.—Diagram of secondary flash.

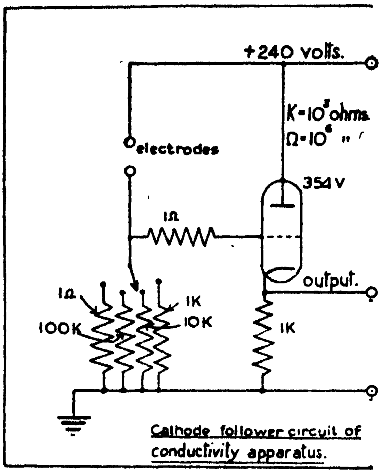

FIG. 2.

Mean distance from muzzle to commencement of flash at A = 26 cm.
,, ,, ,, ,, extremity ,, ,, ,, D = 75 cm.
,, maximum width of flash = 26 cm.
,, distance from muzzle to maximum width of flash = 42 cm.

There is a round-to-round variation in flash dimensions of the order of 10 %, with the exception that the point A remains sensibly fixed.

B. The Measurement of Electrical Conductivity.—The conductivity was measured between a pair of spherical electrodes of 0·7 cm. diam., whose centres were 3·5 cm. apart, and placed symmetrically on either side of the rifle axis at any desired distance from the muzzle. The electrodes were constructed by taking steel ball-bearings which were then electroplated first with Cu and then with Pt to resist corrosion by the gases.[1] They were supported on stout rods of reinforced Bakelite to withstand blast, and connected by about 4 yd. of shielded cable to the cathode-follower circuit shown in Fig. 2.

A potential difference of 240 v. was applied to the electrodes, and one of a set of series resistances, so that the voltage on the grid of the cathode-follower was thus a function of the conductivity of the gap. The device was calibrated by a number of known resistors, and a range of conductivities from $0·5 \times 10^{-4}$ to 1×10^{-9} mhos could be measured. The signal obtained when the flash occurred had a duration of rather less than 10^{-3} sec. This pulse was passed by the cathode-follower to an amplifier giving paraphase output to one pair of plates of an oscillograph. The cathode follower and amplifier had a flat frequency response from 5 c./sec. to 100 kc./sec. The oscillograph pulse was recorded on a drum camera rotating at 3000 R.P.M. using Ilford 5G91 recording-film. The general layout of the apparatus both for conductivity and attenuation measurements is shown in Fig. 3.

---

[1] Zvyagintsev, Amozara, Varolova and Khananov, *J. Appl. Chem., U.S.S.R.*, 1939, 10.

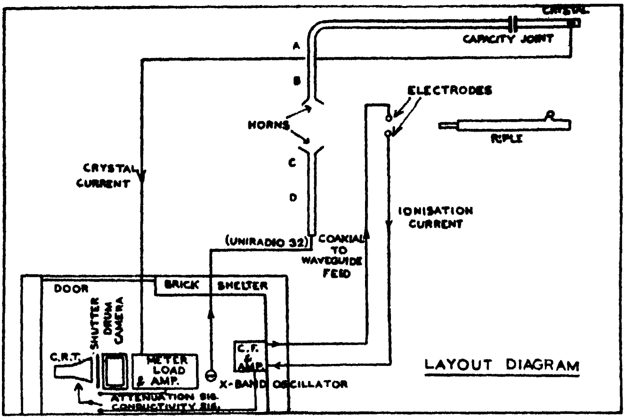

FIG. 3.

C. The Measurement of Attenuation.—3 cm. wavelength power was fed through a cable from a klystron oscillator (type CV129), which was shielded from blast, into a rectangular waveguide terminated by a 2½ in. square aperture horn (Fig. 3). Symmetrically placed with respect to the rifle axis was a similar horn, which received radiation from the first one, and guided it to the rear of the gun to a crystal rectifier. The guides were firmly clamped in wooden supports along AB and CD. A capacity joint was inserted before the crystal to prevent any mechanical shock, due to blast on the guides in front of the gun, reaching the crystal directly. The crystal and its associated waveguides were firmly clamped on a separate concrete pillar and mica discs (0·003 in. thick) were inserted at A and D to reduce the transmission of air-blasts down the guides. It was found necessary to staple the cable down firmly as it was affected by blast. This cable had an attenuation of about 10 db. and a further attenuation of about 6 db. was given by a wooden attenuator inserted in AB. These two attenuators rendered the interpretation of the results simpler by preventing the formation of standing waves.

Experiments with a 3 cm. signal generator showed that the crystal was accurately square-law in the region used, so that the crystal current was proportional to power received, and the change in power during the period of ionisation was indicated by the change of voltage developed by the crystal current in the detector load. The voltage pulse obtained during the flash was amplified and applied in paraphase to the oscillograph, the deflection being recorded on the drum camera as previously. The amplifier had a flat frequency response from 5 c./sec. to 100 kc./sec. and a gain of several values between 45 db. and 115 db. As the maximum attenuation was about ½ db./cm., the horns were placed at 12 cm. apart, since the accuracy of measurement decreases for attenuations greater than 6 db. The apparatus could be calibrated by rotating a large sector disc of brass sheet between the horns, giving alternately 0 % and 100 % attenuation at about 50 c./sec.

D. Photoelectric Measurements on the Flash.—A series of light intensity measurements along the axis of the flash was made to obtain an estimate of the variation of light intensity and duration with distance from the muzzle. The flash was observed with a photocell mounted at the end of a vertical cardboard tube (2½ in. diam. and 2½ ft. long), the other end of which was 9 in. below the rifle axis. The photocell, which had a Baird type B cathode with Ilford β and γ filters, had a response very similar to visual and was protected from blast by a thick glass plate. The photocell current was amplified and recorded as before.

E. Timing.—In order to correlate the signal obtained with the sequence of events, the following timing system was eventually found most satisfactory. The cathode-ray tube spot was triggered by a simple mechanism operated by the rifle firing-pin. A potential difference of 60 v. applied across the pair of oscillograph plates, giving a deflection normal to the pulse deflection, held the spot off the position from which it was focussed on to the film, until the breaking of a wire at the muzzle by the bullet removed this potential and caused the spot to register. A second wire placed 8 ft. from the muzzle and also broken by the shot nearly 4 millisec. later introduced a second potential of 60 v. when broken, taking the spot off again. This period was ample for the duration of the signals obtained.

In each of the above types of examination of the flash described, the mean of 3 or 4 rounds at each distance from the muzzle was taken.

Results.

A. General.—The maximum values of the conductivities and attenuation obtained at different distances in front of the muzzle are plotted in Fig. 4 and 5; a similar curve for the photo-electric experiments is given in Fig. 6. An identification between the ionisation and the flash may conveniently be made by considering the photoelectric measurements in relation to those for attenuation. The two curves show maxima at about 40 cm. from the muzzle (Fig. 5 and 6) and both die away at about the same point (~ 80 cm.). Although they both commence at rather less than 20 cm. from the muzzle, the light intensity results rise more quickly than those for attenuation. It is suggested that this is connected with the fact that the measured light intensities are to be more nearly related to the surface conditions of the flash, since the light consists in the main of resonance radiation from sodium and potassium, while the attenuation is a volume effect. In the region studied at about 20 cm. from the muzzle the flash has just been initiated and is not very wide, a fact which would tend to give the observed form of result for attenuation and conductivity if the hypothesis above is the case.

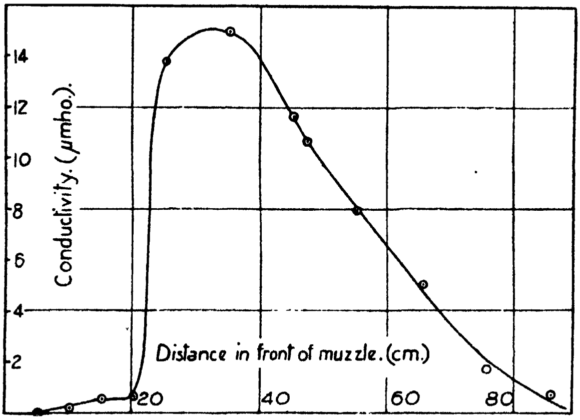

FIG. 4.

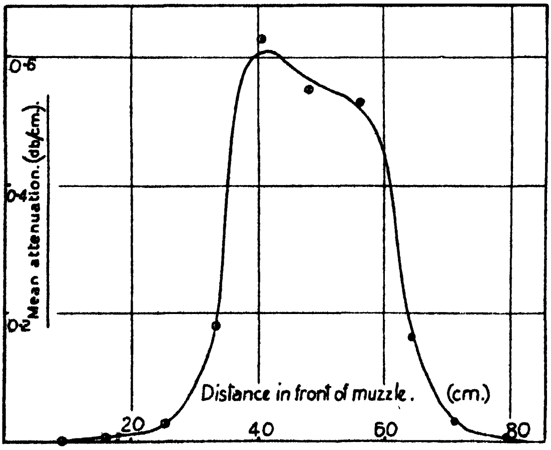

FIG. 5.

The general agreement is marked, particularly when it is considered that the time observed to develop maximum effects for attenuation and light intensity from shot emergence was the same in the two cases at a given distance from the muzzle within the limits of experimental error. The attenuation and light intensity results were chosen for correlation since the two methods sample more nearly the same amount of gases than in the case of conductivity. The general form of the results is in harmony with the known facts that the flame is initiated at the point A (Fig. 1), from which it spreads forwards and sideways. In the boundary regions rapid cooling occurs, and throughout the flash there is a general dispersal, with consequent dilution, leading to the production of a cooler flame.

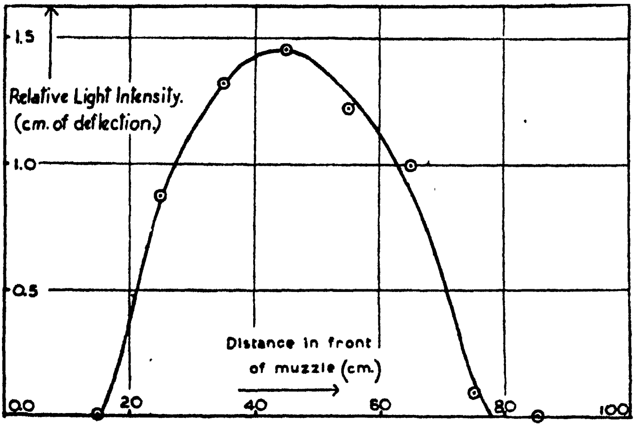

FIG. 6.—Variation of light intensity with distance from muzzle.

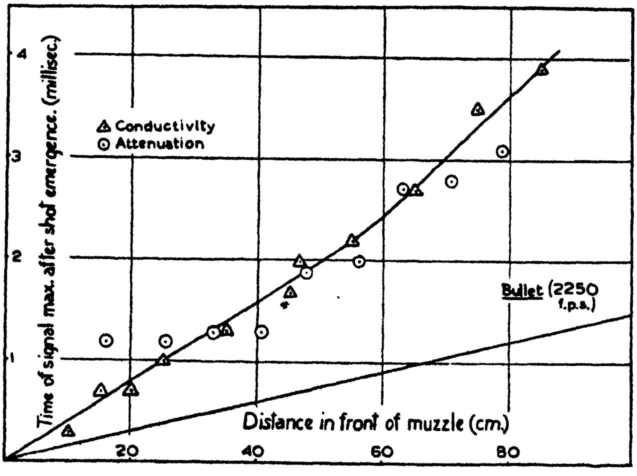

FIG. 7.

Considering the conductivity results plotted in Fig. 4, a curve of the same general form as Fig. 5 is obtained. The times of the maxima of both conductivity and attenuation signals are shown in Fig. 7 and it will be seen that they lie on a smooth curve, subject to experimental error. Since the conductivity method probes a very much smaller region of the muzzle gases, as compared with about 100 sq. cm. for the attenuation method using horns at the ends of the waveguides, more precise information may be obtained from it. The rapid increase in conductivity at 22 cm. from the muzzle is to be directly correlated with the point of initiation of the flash. The maximum of Fig. 4 is much nearer this point than that of Fig. 5, which is related to the fact that the total width of the flame, in its initial stages, although wide enough to fill the space between the electrodes, did not fill that between the horns, which were about 13 cm. apart. Both effects die out to negligible proportions at about 80 cm. from the muzzle. The rate at which the region of maximum ionisation moves forward may be estimated from Fig. 7 and is 2-2·5 × 10^4 cm./sec. in the flash. No precise conclusions can be drawn from this since two effects are involved :

(i) forward motion of the gases as a whole,
(ii) motion of the flame front.

It may be mentioned that the above velocity is high as compared with any of the flame speeds noted by Lewis and von Elbe,[2] while by no means great enough to represent a detonation wave of combustion.

The conductivity results were roughly triangular in shape and their duration became greater at increasingly distances from the muzzle as may be seen from the examples in Fig. 8. This is consistent with a relatively slow-moving zone of reaction in a cloud of gas moving forward at a higher speed, diminishing at increasing distances from the muzzle. The attenuation signals were more square in shape, and of duration not significantly dependent on distance from the muzzle. In some cases they showed two maxima with a small trough between them, which was probably caused by the motion of the flame in a sideways and even backwards direction (i.e. towards the muzzle)—a phenomenon not observed with the more centrally-situated conductivity electrodes. Qualitatively, then, the two methods are in good agreement, the differences between them being related in obvious ways to the methods of sampling the gases for the purposes of measurement.

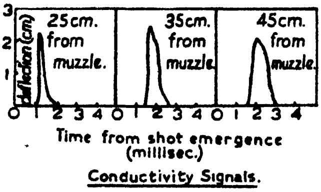

FIG. 8.

The results of both methods may now be used to derive figures for the number of electrons per cc. of gas for the maximum points of Fig. 4 and 5 respectively. The calculations involve a fair degree of approximation, but are not considered to be in error by more than a factor of 5. No further reference to the photoelectric measurements is made since their significance, apart from correlation of flash and ionisation, is small in the absence of further knowledge of the flame system.

B. Calculation of *N*, the Number of Electrons per cc.—1. FROM CONDUCTIVITY RESULTS. The muzzle gases consist mainly of N_2, CO, CO_2, H_2 and H_2O with small quantities of NH_3, CH_4 and K (from $KClO_3$ in the firing cap), Ca (from the propellant stabiliser), and unavoidable traces of Na. The principal Na and K lines and the CaO bands have been found to be the principal features of the spectrum of the flash. This spectrum is due to thermal excitation of the particular atoms or groups, and it is supposed similarly that the ionisation is of a thermal nature, such as has been detected and studied in ordinary coal-gas flames (see Wilson [3]).

The conductivity of the gases is due to the free electrons produced by the ionisation of the metallic atoms in the gases since the mobility of the metallic ions is much less, being of the order of 10^{-3} to 10^{-4} of the electron mobility, on account of their greater mass. A general expression relating the potential drop *V* between two electrodes in a flame at a distance *d* from each other, and the current *i* flowing has been found experimentally for burner flames, and has the form :

$$V = Aid + Bi^2$$

in which *A* and *B* are constants for a given flame. Wilson (loc. cit.) has deduced a theoretical expression for this, in which, if the electrodes are of unit cross-section :

$$A = \frac{1}{Ne}\left(\frac{1}{(k_1 + k_2)}\right)$$

and

$$B = \left(\frac{16}{5}\right)\left(\frac{\pi}{3k_1k_2}\right)^{\frac{1}{2}}\left(\frac{1}{qe(k_1 + k_2)}\right)^{\frac{3}{2}}(k_1^2 + k_2^2)$$

---

[2] Lewis and von Elbe, *Combustion, Flames and Explosions of Gases* (Camb. Univ. Press, 1938), Ch. IX, X and XI.

[3] Wilson, *Modern Physics* (Blackie, 1944).

where N = no. of electrons per cc. in the body of the flame, i.e. at a distance of greater than 0·5 cm. from the electrodes,
k_1 = mobility of positive ions,
k_2 = electron mobility,
e = electronic charge,
q = rate of formation of electrons = αN^2 in the body of the flame, where α = the coefficient of recombination.

The equation may therefore be written as

$$V = \frac{A'id}{N} + \frac{B'i^2}{N^3}$$

where A' and B' now contain only the constants k_1 and k_2, e and α.

We have $e = 1{\cdot}6 \times 10^{-19}$ coulomb and using the results quoted by Wilson[4] for flames, in which k_1, k_2 and α seem to be more or less independent of temperature,

$$\begin{aligned} k_2 &= 2600 \text{ cm./sec. per volt/cm.,} \\ k_1 &= 2 \quad\quad ,, \quad\quad ,, \\ \alpha &= 8{\cdot}5 \times 10^{-7} \end{aligned}$$

$$\therefore V = \frac{(2{\cdot}4 \times 10^{15})id}{N} + \frac{(4{\cdot}6 \times 10^{37})i^2}{N^3}.$$

In the present case, the area of the electrodes may be taken as 0·5 cm.,^{2} and the distance between them d as 3 cm. to the degree of accuracy possible. We have $V = 240$ v. and in the position and time of maximum conductivity the current density is $15 \times 10^{-6} \times 240 \times 2$ amp./cm.^{2} = $7{\cdot}2 \times 10^{-3}$ amp./cm.^{2} The maximum conductivity being 15×10^{-6} mhos from Fig. 4. Hence

$$240 = \frac{5{\cdot}2 \times 10^{13}}{N} + \frac{2{\cdot}4 \times 10^{33}}{N^3}.$$

This is cubic in $1/N$ which may be solved directly giving $N = 2{\cdot}2 \times 10^{11}$ electrons per cc.

Now the above equation relating V and i was derived on the assumption that the cathode would emit no electrons, resulting in an electron deficiency, with consequent high potential gradient in its neighbourhood. It is this phenomenon which is responsible for the term Bi^2 in the equation, and it does not follow that the equilibrium situation in which this holds for a burner flame is set up in the flash. It may be taken that appreciable heating of the electrodes does not occur and that emission is therefore negligible, but the velocities of the gases between the electrodes is of the order of that of sound (3×10^4 cm./sec.) and is comparable therefore with the speed with which an electron crosses the electrode gap ($\sim 2{\cdot}1 \times 10^5$ cm./sec. in uniform potential gradient of 80 v./cm.), and thus the effect which brings about the Bi^2 term may be absent, particularly in the presence of the undoubted high turbulence. In any case it is seen that the term Bi^2 has the value $(2{\cdot}40 \times 10^{33})/(2{\cdot}2^3 \times 10^{33}) = 0{\cdot}23$ which is negligible if $V = 240$, so that it is immaterial to the calculation whether the cathode phenomenon is set up or not.

2. FROM ATTENUATION RESULTS.—A calculation from the attenuation measurements leading to a value of N at maximum attenuation is now made. If the voltage attenuation of the 3 cm. radiation after penetration of s cm. of imperfect conductor is $e^{-\gamma s}$, then from classical electrodynamics :

$$\gamma = \frac{2\pi K}{\lambda} \text{ (Gaussian units)}$$

in which

$$K^2 = \frac{\mu}{2}\left[\sqrt{\left(\epsilon^2 + \frac{4\sigma^2}{f^2}\right)} - \epsilon\right] = \text{coefficient of extinction,}$$

where
λ = wavelength *in vacuo*,
f = frequency of radiation,
μ = permeability,
ϵ = dielectric constant,
σ = specific conductivity of gases at frequency f.

Here μ and ϵ do not differ appreciably from unity, and since $4\sigma^2/f^2 \ll 1$, then $K = \sigma/f$.

Therefore $\gamma = \frac{2\pi}{\lambda} \cdot \frac{\sigma}{f} = \frac{2\pi\sigma}{c}$ where c = velocity of light *in vacuo*.

---

[4] Wilson, *Rev. Mod. Physics*, 1931, **3**, 156.

But $\sigma = \frac{Ne^2}{m} \cdot \frac{v}{\omega^2 + v^2}$,

where
N = no. of electrons per cc.,
e = electronic charge,
m = electronic mass,
v = collision frequency of electrons,
ω = angular frequency of the radiation = $2\pi f$.

$$\therefore \gamma = \frac{2\pi Ne^2}{mc} \cdot \frac{v}{\omega^2 + v^2}.$$

The collision frequency v may be estimated from the kinetic theory of gases. We have

$$v = \frac{\pi}{4}\rho^2 n\bar{c} \qquad \text{(1)}$$

$$\tfrac{1}{2}mC^2 = \frac{3}{2}kT \qquad \text{(2)}$$

$$n = P/kT \qquad \text{(3)}$$

where
n = no. of molecules per cc.,
$\bar{c}$ = mean velocity of electrons,
C = r.m.s. velocity of electrons = $\sqrt{\frac{3}{8}\pi} \, . \, \bar{c}$,
ρ = molecular diameter,
T = temperature of gases (°K.),
P = gas pressure,

$$\therefore \bar{c} = \sqrt{\frac{8}{3\pi}} \, . \, C = \sqrt{\frac{8kT}{\pi m}} \text{ from (2)}$$

and $$v = \frac{\pi}{4}\rho^2 n \sqrt{\frac{8kT}{\pi m}} = \sqrt{\frac{\pi kT}{2m}} \, . \, \rho^2 n \text{ from (1) and (2),}$$

$$\therefore v = \sqrt{\frac{\pi}{2mkT}} \, . \, \rho^2 P, \text{ using (3).}$$

Taking
$K = 1{\cdot}4 \times 10^{-16}$ erg./°c.,
$m = 9 \times 10^{-28}$ g.,
$\rho = 3 \times 10^{-8}$ cm.,
$P = 10^6$ dynes/cm.^{2} ($\sim$ 1 atm.),

then $v = 7 \times 10^{10}$ impacts/sec. when $T = 2000$°K. (see later discussions of temperature).

But $\omega = 2\pi f = 6 \times 10^{10}$ sec.$^{-1}$
and $\therefore v \sim \omega$.

Now $v/(\omega^2 + v^2)$ has a maximum of ½ when $v = \omega$, falling only to ¼ as v/ω varies between ¼ and 4, and hence the error in taking $v = \omega$ will be small.

Hence $$\gamma = \frac{2\pi Ne^2}{mc} \cdot \frac{1}{2\omega} = \frac{Ne^2}{2mcf}.$$

If the attenuation is expressed as β db./cm., then $\beta = 8{\cdot}7\gamma$ and hence:

$$N = \frac{2mcf\gamma}{e^2} = \frac{2mcf\beta}{8{\cdot}7e^2} = 2{\cdot}7 \times 10^{11}\beta$$

using $e = 4{\cdot}8 \times 10^{-10}$ E.S.U.

The maximum attenuation observed is $\beta = 0{\cdot}6$ db./cm. (Fig. 5) and therefore $N = 1{\cdot}6 \times 10^{11}$ electrons/cc.

3. COMPARISON OF RESULTS.—No. of electrons/cc. by conductivity $= 2{\cdot}2 \times 10^{11}$. No of electrons/cc. by attenuation $= 1{\cdot}6 \times 10^{11}$. The agreement is therefore very satisfactory, considering the approximations involved—particularly when it is borne in mind that the conductivity method measures the electron density at the rifle axis, whereas the attenuation method measures the mean density over a much greater volume of gas and will therefore be smaller. The general form of Fig. 4 and 5 indicates that the agreement between the two methods will be good over the whole region of measurement. No previous comparison of a direct nature between these two methods for flame ionisation appears to have been made.

The agreement between the two methods will allow of a calculation of the effective temperature to be made, using the equation of Saha. This will only be equal to the true temperature if the ions and electrons are in thermodynamic equilibrium with the rest of the flame system.

Temperature Estimation for the Flash.

The degree of ionisation of any atomic or molecular species as a function of temperature under conditions of thermodynamic equilibrium has been worked out by Saha.[5]

$$\log_{10} \frac{x^2}{1 - x^2} \cdot P = - \frac{5050V}{T} + 2{\cdot}5 \log_{10}T - 6{\cdot}5$$

where
P = pressure of gases in atm.,
x = fraction of gases ionised,
V = ionisation potential (v.),
T = temperature (° K.).

This is only exact at equilibrium and when ions or electrons are not removed from the gases. It has been demonstrated to be accurate for coal-gas flames containing added alkali salts by Bennett.[6] In the range considered the temperature is a very slowly varying function of the ionisation and hence the equation may be applied with some accuracy.

A round of Service ammunition containing M.D. Cordite has the following relevant metal content:

Element.	Ionisation Potential (v.).	Amount (g.).
K . .	4·32	0·004
Na . .	5·11	a trace
Ca . .	6·12	0·004

No sodium is deliberately added but traces of it cannot be excluded although there is less of it than of the other metals. It is probably not significant, however, since 10 times as much Na and 100 times as much Ca are required to give the same number of ions as a given amount of K near the estimated temperature of ∼ 2000° K., on account of their higher ionisation potentials. Hence the electrons in such a case are derived chiefly from K atoms.

0·004 g. of K contains $(4 \times 10^{-3} \times 6 \times 10^{23})/39 = 6 \times 10^{19}$ atoms which are distributed over a volume of about 12×10^{3} cc. in the flash.

$$\therefore \text{No. of K atoms/cc.} = 5 \times 10^{15} \text{ per cc.}$$

The maximum number of ions/cc. observed in the flash by the attenuation method is $1{\cdot}6 \times 10^{11}$/cc. giving $x = 3{\cdot}2 \times 10^{-5}$, and, taking $P = 1$ atm., since the gases are about completely expanded at the time of flash occurrence:

$$\therefore - \frac{21{,}800}{T} + 2{\cdot}5 \log T - 6{\cdot}5 = - 8{\cdot}99$$

whence $T = 2000°$ K.

Using the conductivity maximum result, $T = 2050°$ K., which is quite satisfactory agreement. This also justifies the use of $T = 2000°$ K. in calculating the collision frequency, since the collision frequency is a slowly varying function of the temperature and the degree of ionisation is a rapidly varying one.

It is assumed that all the electrons produced by thermal ionisation remain free; if they combined with neutral molecules they would cease to contribute effectively to the conductivity of the gases. This combination is considered unlikely at the high temperatures dealt with here.[7a]

[5] Saha, *Phil. Mag.*, 1920, **40**, 472.

[6] Bennett, *ibid.*, 1927, **3**, 127.

[7a] Maxfield and Benedict, *The Theory of Gaseous Conduction and Electronics* (McGraw-Hill, 1942), p. 247.

Loss of electrons by recombination with positive ions takes place by two consecutive processes of which this is the first,[7b] and thus the electrons are not lost until the gases have cooled.

In the conductivity case it is assumed that secondary ionisation does not take place due to the application of an electric field, which would involve the ion falling through a potential difference of the order of V, its ionisation potential, in the course of a free path. Since the smallest value of V is about 4 v. and the field is at most 80 v./cm., this would involve a free path of about 0·05 cm. The actual mean free path is of the order of 10^{-5} cm., so that secondary ionisation is very improbable.

The possibility of selective absorption by excitation of molecular species in the attenuation case also exists, since some of the muzzle gases have absorption bands in what may be regarded as the very remote infra-red. Ammonia has a band at 1·3 cm.; O_2 at 0·5 cm.; H_2O has 17 lines at $>$ 0·05 cm., one of which is at 1·3 cm. The lines are broadened for various reasons of which the most important here is collision-damping. The oxygen and water lines are much weaker than the ammonia line, but much less ammonia is present ($<$ 0·5 %). From the known absorption coefficients of these lines the total absorption due to all these sources at 3 cm. is found to be less than 10^{-4} db./cm. and therefore not detectable in our experiments.

No other results for flash temperatures are available, although it is considered that values could be obtained by two methods:

(i) by the reversal of the Na *D* lines;
(ii) by comparison of the intensities of the first two pairs of doublets in the principal series of K.

Calculation of values is out of the question, since there is no obvious way of determination of the composition in terms of combustible/air ratio at any given place and time, but the result of 2000° K. is reasonable.

Lewis and von Elbe[8] quote values for a number of gas mixtures, the most relevant of which are given below. The determinations are by Lewis, Seaman and Jones.[9]

Combustible.	Diluent.	% Combustible.	Flame Temp. (°K.).
31·9 % CO + 22·5 % H_2 + 45·4 % N_2	Air	45·0	1991
37·0 % CO + 27·1 % H_2 + 35·9 % N_2	,,	41·7	2085
10 CO + 3 CO_2	,,	38·5	2070
H_2 + 2 N_2	,,	18·5	1748

These values show that the figure deduced above for flash temperature is of the right order of magnitude, and strengthen the supposition that the ions and electrons are in thermodynamic equilibrium.

Observations between the Flash and the Muzzle.

The observations were not entirely confined to the region of the bright yellow flame described above but were extended backwards towards the muzzle beyond the point A (Fig. 1). This region is occupied by a small dull red glow which is not a combustion, but rather a luminosity due to a pressure disturbance, which is of duration less than a millisecond and occurs before the main flame is initiated at A. The glow extended from about 10-20 cm. from the muzzle. The number of electrons/cc. in it, using the same methods of calculation as previously were $2 \cdot 4 \times 10^9$ (conductivity method), and $< 5 \times 10^9$ (attenuation method). The former corresponds with a temperature of 1300° K. The limitation of the sensitivity of the attenuation apparatus was caused by the blast waves on the horns and guides, producing an irregular output as the system was shocked into vibration. After precautions had been taken to reduce this effect, the smallest attenuation that could be measured was 0·02 db./cm., with the horns 27 cm. apart and 15 cm. in front of the muzzle. The distance between the horns was increased to this value from 12 cm. partly to increase the total attenuation but mainly to reduce the effect of the horns on the gas flow.

[7b] Maxfield and Benedict, *The Theory of Gaseous Conduction and Electronics* (McGraw-Hill, 1942), p. 246.

[8] Lewis and von Elbe (loc. cit., ref. 2), Appendix C.

[9] Lewis, Seaman and Jones, *J. Frank. Inst.* 1933, **215**, 149.

The authors wish to express their gratitude to Prof. R. G. W. Norrish, F.R.S. and C.S.R.R.D.E., who jointly sponsored this work, and to the A.R.D. for considerable assistance. They also wish to thank the Chief Scientist of the Ministry of Supply for permission to publish.

Summary.

The electrical conductivity and the attenuation of 3 cm. wavelength electromagnetic radiation in the transient flame or flash produced by firing Service ammunition from a 0·303 in. rifle into air have been measured. They show a good agreement between each other, both in time and magnitude, as well as with photoelectric measurements of light intensity. Satisfactory agreement is given by calculations of the number of electrons per cc. from the results of both methods. The application of the Saha equation leads to a value of 2000° K. for the flame temperature, which seems a reasonable value. The main conclusion is that the two methods lead to the same result.

Laboratory of Physical Chemistry,
Free School Lane, Cambridge.

REVIEWS OF BOOKS.

Chemistry of Muscular Contraction. By A. SZENT-GYÖRGYI. (Academic Press, Inc., New York, 1947.) Pp. vi + 150. Price $4.50

This book, which is based on the Cameron Lectures delivered by the author at the University of Edinburgh in 1946, is mainly an account of the work of himself and his associates on muscle proteins. Szent-Györgyi's enthusiasm is infective, but it cannot be said that he has given either a lucid or an adequately critical account of his ideas. After prolonged study the writer is unable to separate facts from suggestions and inferences, which may or may not survive critical examination. The thesis is briefly that myosin, the extractable protein of muscle, is not a simple substance. It consists of two components for one of which the name myosin is retained, and the other named actin. The latter occurs in two forms, globular and fibrous, the transformations of which can be followed by double refraction, viscosity, etc. The combination of the myosin and actin, which occurs over a range of proportions, gives rise to a substance, actomyosin, with very elongated molecules, and with the property of shrinking and dehydrating under the action of adenosine triphosphate. Szent-Györgyi sees in this the basic process of muscular contraction, but a great deal more evidence is required before this idea can be regarded as established.

Nevertheless it will be obvious to every reader that he has isolated some very interesting substances, with properties which will repay a great deal more investigation. At least it has been shown that muscular chemistry is of very great complexity, and to the first urgent need, i.e. of isolating the substances concerned, Szent-Györgyi has made a contribution which deserves serious, though not necessarily uncritical study. Physical chemists will find the third part of the book, which puts forward some ideas on the structure of proteins in general, on the basis of their quasi-crystalline phosphorescence, much less satisfactory. On the whole they may feel that something of value is being germinated, but they will not arrive at any very clear notions as to what it is.

J. A. V. B.

Statistical Methods in Research and Production. Edited by Owen L. Davies, M.Sc., Ph.D. (Edinburgh: Oliver and Boyd, 1947.) Pp. xi + 292. Price 28s.

This book is a collaborative effort by members of the staff of Imperial Chemical Industries Ltd. It is, as Lord McGowan points out in a Foreword, the first of a series of scientific and technical handbooks, published with the aim of making generally available the important body of information accumulated as a result of the Company's manufacturing experience and research.

The authors have performed their task with judgement and discretion. Their object has been to describe those statistical methods which are most applicable to the Chemical and Allied Industries and to illustrate their use by examples taken from research and process data. The book is well planned and the examples are carefully chosen from a wide range of practical problems.

In the introductory chapter, the types of problems amenable to statistical treatment are discussed; succeeding chapters deal with Frequency Distribution, Averages and Measure of Dispersion, Tests of Significance, Analyses of Variance. Regression and Correlation, Frequency Data and Contingency Tables, Sampling, Control Charts and Prediction, and Specification. Finally, there is a section devoted to such matters as Typetesting of Mathematical Expressions, Statistical and Mathematical Symbols and Tables of Statistical Functions.

To the reader new to the study of statistical methods, the importance of mastering the terminology of the subject is emphasised and, to this end, a Glossary of Statistical Terms is given. The treatment, on the whole, is clear and concise and, in particular, the chapters on Sampling and on Control Charts are of outstanding interest.

Probably no routine industrial operation causes more trouble than sampling, although the mathematical theory is now well established, and there is an extensive literature on the subject. In chapter 8, five cases are discussed in detail, namely, the Sampling of Attributes and of Variables, of Liquids and Solids, and Sampling from a Continuous Flow. The mechanical technique of sampling is not dealt with, but the examples chosen to illustrate the various methods also serve to emphasise some of the precautions which have to be observed to avoid systematic errors.

Closely related to sampling is Statistical Quality Control, which may be defined as the procedure for determining when there is a significant change in the quality of a product. The method advocated is the use of Control Charts, as part of a continuous inspection system, where readings of the quality characteristic are plotted as manufacture proceeds. The distribution of the plotted values in relation to the Control Limits then provides statistical information on the quality being studied. Although this method has been widely used in light engineering work, its application to chemical processes is relatively new; it has, nevertheless, already proved of value in a number of investigations in bringing to light significant variations, which would normally be overlooked. An instructive example is worked out in detail, in Appendix 9A, and illustrates the use of the charts in a research investigation, the setting and hardening properties of a plaster.

Probably one of the most valuable uses of the statistical method is in planning large-scale investigations, so as to obtain the maximum amount of information from a given number of experiments. This aspect of the subject, however. is not dealt with, except by implication, in the Handbook; but the authors recognise its importance in the Introduction, and hope to see it included in a subsequent volume of the series.

We cannot conclude without a word of appreciation of the enlightened policy, which has placed at the disposal of scientists generally the unique experience of a large organisation in the field of chemical technology.

D. M. N.

Theory of the Stability of Lyophobic Colloids. By E. J. W. VERWEY and J. TH. G. OVERBEEK. (Elsevier Publishing Co. Ltd., Amsterdam). Price 22s. 6d. net.

The authors of this book set out to establish the view that the force acting between two colloidal particles is the resultant of a repulsion due to electric double-layer interaction and an attraction due to van der Waals-London interaction. The reasoning follows the lines of the earlier work of Hamaker.

About the time of the outbreak of war a discussion had arisen over the way in which the force due to interaction of the diffuse parts of the double-layers of two colloidal particles should be calculated. The authors have made a very thorough examination of this matter, and confirm that, on the basis of the assumptions originally made by Gouy, this force should always be a repulsion. Numerical results are given in numerous tables and graphs both for the case of two parallel flat plates and the case of two spherical particles. The authors explain in their preface that because of the difficulty of setting out these results within the limits of articles in periodicals, they decided to present them in book form.

In their treatment of the force due to van der Waals-London interaction the authors state on pages 19 and 100 that this interaction is not greatly influenced by the presence of the liquid surrounding and separating the particles. The following point is worth considering in this connection. If, within a homogeneous mass of liquid we picture two spherical surfaces to be drawn so as to enclose two spheres of liquid in proximity, the authors' statements would lead us to conclude that these spheres would be attracted to one another. Since the condition is evidently one of equilibrium, it is clear that other forces besides the direct van der Waals-London interaction between the spheres must be taken into account. In general, we must also consider the interaction between all elements of the liquid outside the spheres which will give a further force urging the spheres together, and the interactions of the liquid inside each sphere with the outside liquid which will give rise to a repulsion. In this imaginary case the resultant force must be zero.

For hydrophobic particles it is quite possible that the balance of van der Waals-London forces is an attraction, but the foregoing considerations should make us pause before accepting the conclusion reached by Verwey and Overbeek that the attraction displayed in the flocculation of colloids is *wholly* due to these forces. The conclusion that the double-layer interaction must always cause a repulsion follows from the postulates of Gouy, but would not necessarily emerge from a theory that takes account of the magnitudes of the ions and charges. Langmuir's attempt to compute the effects of interionic forces may be proved incorrect in detail, but may yet turn out to be a pointer in the right direction.

The presentation by these authors of their conclusions will no doubt provide a stimulus to further research, both theoretical and experimental, into the complex problems presented by the behaviour of colloids. In normal times this stimulus would have been more effectively given by publication in a scientific periodical. In a book carrying the present title one would expect to find a more balanced account than the authors have achieved or even attempted. Readers who are not prepared to take a keen interest in the phases of applied mathematics which are the main concern of the authors, will derive rather meagre satisfaction from the rest of the book. It is disappointing to find tables of " flocculation values " quoted without any discussion of the part played by ionic exchange. The " classical " experiments on flocculation were made before the importance of ionic exchange was appreciated, and they need to be reconsidered and possibly re-interpreted in the light of recent knowledge. Consequently it is difficult to judge just how much importance should be attached to the agreement claimed between their theoretical results and the rule of Schulze and Hardy.

Considering that the authors were writing in a foreign language their English is astonishingly free from defects. The general style is admirable.

R. K. S.

A CONTRIBUTION TO THE THEORY OF THE STRUCTURE OF PROTEIN FIBRES WITH SPECIAL REFERENCE TO THE SO-CALLED THERMAL SHRINKAGE OF THE COLLAGEN FIBRE.

By (the late) Dorothy Jordan Lloyd and Marjorie Garrod.

Received 6*th January*, 1947; *as revised* 6*th May*, 1947.

It has previously been shown that collagen fibres, swelling under the action of aqueous solutions of acids and alkalies, pass into an axially contracted, radially swollen form, which can be extended back to its original length by loading.[1, 2, 3] Similar changes can be induced in silk, reticular and collagen fibres, by a number of organic solvents in the cold, and still others if the temperature is raised.[4] Elastin fibres show rubber-like extensibility in their natural wet condition, and continue to do so if the water which is normally present is replaced by an organic solvent.

In order to account for the change from the normal only slightly extensible form to the rubber-like form with long-range extensibility, the theory has been advanced that in these fibres the long polymeric molecules, which have been shown by X-ray analysis to be mainly in the fully extended condition, must be laterally held by two (or more) chemically distinct types of link, which may either be direct cross bonds from backbone to backbone of adjacent molecules (the carbimino link) or may be cross bonds formed through polar side chains. Moreover, that condition which leads to the opening of one type of lateral bond only will bring about overall shortening of the freed sections of the backbone (due to the gain in entropy which ensues) together with radial swelling and the development of long range elasticity, while conditions which lead to the opening of all types of lateral bond will bring about solution of the fibre.

The object of the present paper is to consider the relation between the chemical constitution of the natural protein fibres of collagen and silk fibroin and the chemical character of the solvents which induce the change, normal → rubber-like form, with the object of obtaining evidence on the chemical character of the lateral bonds in each fibre. The consideration is also extended to elastin, which normally exists in the rubber-like form. Much of the discussion in this paper is based on the experimental evidence published elsewhere.[4, 5]

The following lateral links have been suggested as occurring in protein fibres.

(1) The salt link between basic and acidic side chains—an electrovalent link, which in the presence of an ionising solvent will not be fixed in length or direction.

(2) Hydrogen bonds of several types, in which the bonds are of fixed length and direction, e.g. (*a*) the amide cross-link between an amide group and some other polar side chain; (*b*) the hydroxyl-hydroxyl link; (*c*) the direct carbimino link.

(3) Covalent links, fixed in length and direction and normally of high

---

[1] Marriott, *Biochem. J.*, 1932, **26**, 46.

[2] Jordan Lloyd, Marriott and Pleass, *Trans. Faraday Soc.*, 1933, **29**, 554.

[3] Jordan Lloyd and Marriott, *ibid.*, 1936, **32**, 932.

[4] Jordan Lloyd, Dempsey and Garrod, *ibid.*, **42B**, 1946, 228.

[5] Jordan Lloyd and Garrod, *J. Soc. Dyers Col.* (Symposium on Fibrous Proteins), 1946, p. 24.

strength, e.g., (*a*) the disulphide link —S—S— ; (*b*) a peptide link formed by condensation at a salt link.

The chemical constitution of the protein fibres under consideration in this paper so far as at present known, is shown in Table I according to the classification of their side chains. The outstanding contrast between the different fibres is brought out in the ratio of residues with no side chains, residues with non-polar side chains and residues with polar side chains, elastin having comparatively few polar side chains and collagen and silk having higher proportions. The special cases of silk, collagen and elastin may now be considered from the standpoint of their chemical constitution.

The Cross-Linkages of the Silk Fibre (silk fibroin).

The silk fibroin fibre does not swell in ethyl, propyl or butyl alcohols, propionic or butyric acids or *m*-cresol. It swells radially, 10-50 % increase without change of length, in water, methyl alcohol, formamide, acetic acid (especially at raised temperature), lactic acid, thioglycollic acid and with axial shortening with strong radial swelling in formic acid.[4] X-ray studies of silk fibroin show that in the fibre the molecule is fully extended and is built of a pair of repeating residues for the greater part of its length.[6] Reference to its chemical composition suggests :

—G—A—G—S—

where G represents glycine residues, A alanine and S hydroxyalanine (i.e., serine).

A serial arrangement of residues with glycine in every alternate position would leave one side of the extended backbone free from side chains, while on the other the non-polar side chains of alanine and the polar side chains of serine would alternate.[7] On one side, therefore, there would be scope for direct backbone linkages and on the other for hydroxyl-hydroxyl linkages across the serine residues. This structure would give two types of lateral bond of different chemical properties. X-ray studies of silk fibroin fibres show two equatorial spacings of appropriate dimensions (Astbury [8]).

The effect of formic acid in causing the contraction of silk is explicable on the assumption that this reagent breaks the backbone hydrogen bonds but not the hydroxyl-hydroxyl links, thus leaving sections of the backbone still held by one or more type of lateral link. This assumption is supported by the behaviour of Nylon and cellulose in formic acid.

The direct backbone carbimino link, $> C : O \rightarrow HNC$, is the only lateral link in the Nylon fibre, 6-6 Nylon (from hexamethylene diamine and adipic acid) having no side chains. Under X-ray analysis the extruded fibre shows a disorientated crystalline structure which becomes orientated on cold-drawing (Harris [9]). The cold drawn fibre " sets " through the parallel alignment of the long polymeric molecules which allows the formation of the direct backbone link. The presence of a 6-atom chain between each pair of lateral bonds leaves a residual elasticity in the fibre. Nylon is soluble in cold formic and thioglycollic acids and in lactic acid on warming, the warm sol setting to an opaque white gel on cooling. Hence under anhydrous conditions these organic acids (pK 3·3-3·7) must be able to break the direct lateral backbone link without attacking the backbone itself. Nylon is also soluble in *m*-cresol.

The reaction involved with *m*-cresol may be as follows :—

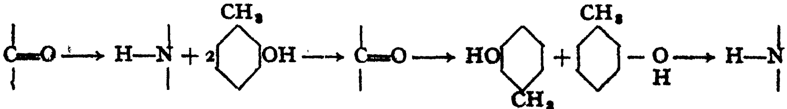

[6] Brill, *Annalen*, 1923, **434**, 204.

[7] Jordan Lloyd and Marriott, *Trans. Faraday Soc.*, 1933, **29**, 1228.

[8] Astbury, *Textile Fibres under X-rays* (I.C.I. Ltd., 1943).

[9] Harris and Sookne, *J. Nat. Bur. Stand.*, 1941, **26**, 289.

TABLE I

	g. mol. per 100 g. protein.		
	Silk Fibroin.[1]	Collagen.[3]	Elastin.[5]
Residues without side chains (*a*)			
Glycine	0·5840	0·3630	0·3822
Residues with non-polar side chains (*b*)			
Alanine	0·2966	0·0978	?
Valine	—	0·0147	0·1310
Leucines	0·0191	0·0542	0·2290
Phenylalanine	0·0091	0·0079	0·0202
Proline	0·0087	0·1644	0·1322
	0·3335	0·3390	0·5124
Residues with polar side chains (*c*)			
OH side chains—			
Serine	0·1475	0·0324	—
Threonine	0·0118	0·0118	—
Tyrosine	0·0729	0·0057	0·0100
Hydroxyproline	—	0·0825	0·0150
Total hydroxyl	0·2322	0·1324	0·0250
Methionine	0	0·0050[4]	0·0025
Basic side chains—			
Arginine	0·0055	0·0435	0·0050
Lysine	0·0017	0·0342	—
Histidine	0·0005	0·0032	—
Total basic	0·0077	0·0809	0·005
Acidic side chains—			
Aspartic acid	?	0·1300[4]	0
Glutamic acid	0·0138[2]		?
Total acidic	0·0138	0·1300	0
Tryptophan	0	0	0
Amide side chains	—	0·0470[4]	0·0029
Disulphide side chains/2	0	0	0
Total polar	0·2537	0·3953	0·0354
Total polar without amide groups c'	0·2537	0·3483	0·0325
Ratio $a : b : c'$	5 : 3 : 2	4 : 3 : 3	4 : 5 : 0·3

---

[1] Astbury, *Adv. Enz.*, 1943, 3, 74, 77.
[2] Snell, *Adv. Protein Chem.*, 2, 85.
[3] Bowes, *Ann. Reports, Appl. Chem.*, 1943, 28, 324.
[4] Bowes and Kenten (unpublished work).
[5] Stein and Millar, *J. Biol. Chem.*, 1938, 125, 612.

The action of formic acid on silk may therefore be similarly attributed to the opening of the direct backbone link, thus allowing entropy effects in the backbone to come into play. Thioglycollic acid, lactic acid and *m*-cresol do not cause silk to pass into a shortened form with rubber-like properties, but this may be due to their failure to penetrate the molecular grid, which is fine on account of the shortness of the alanine and serine side chains.

Cellulose, with its characteristic hydroxyl-hydroxyl link, is insoluble in cold formic acid : if, then, the assumption that this reagent does not attack the hydrogen bonding between hydroxyls is correct, it may explain the insolubility of silk in cold formic acid.

Both silk and cellulose are soluble in cuprammonium and cupriethylene diamine * without degradation of the long backbone of the molecule. These reagents therefore can open the hydroxyl-hydroxyl link in cellulose and silk, and on account of their character as strong bases could also be assumed to open the direct backbone carbimino link in silk.

The Cross-Linkages of the Collagen Fibre.

The collagen fibre differs from the silk fibre in its considerably greater proportion of polar side chains, particularly the basic and acidic side chains. These side chains are comparatively long and their occurrence in collagen will account for two characteristics of the fibre, namely, the open structure (the collagen fibre in its natural " wet " condition carries about 66 % of its weight as water) and the importance of the salt link.

The open nature of the structure can be demonstrated by Speakman's [10] method of judging average pore size by following the penetration of a homologous series of solvents. Collagen fibres are penetrated at 20° by methyl, ethyl, *n*-propyl and *iso*-butyl alcohols. The average pore size is, therefore, greater than that of silk and may be assumed to be of the order of 7-8 A. Collagen fibres show slight radial swelling in the alcohols but no change in length even on boiling.

X-ray studies of the collagen fibre suggest that the long polymeric molecules are normally in a position of full extension (possibly with a slight twist in the backbone), and Astbury [11] considers that the constitution of the molecule can be roughly indicated as :

—P—G—R—P—G—R

where P is proline (or hydroxyproline), G glycine and R some other residue.

Assuming, therefore, that the collagen molecules are fully extended for at least the greater part of their length, they must be held in this form by frequent lateral bonds. All the types of cross link listed above may occur in collagen except the disulphide link.

Considering the constitution of collagen (Table I), for every ten residues in the backbone there are roughly 3 with polar side chains, 3 with non-polar and 4 without projecting side chains. Two of the 3 polar side chains are basic or acidic, i.e., could take part in an electrovalent salt link ; [12] the third, terminating in a hydroxyl or amide group, could contribute to a hydrogen bond.[13, 14]

The passage of the collagen fibre from the normal form to the axially contracted form and on to the sol form can be explained on the theory already advanced, namely, that in the normal form the fully extended back-bones of the molecules are held in place by two or more chemically distinct types of lateral bond, one of which is weakened under the conditions leading to " thermal shrinkage " while the other (or others) does not give way until conditions are such that the collagen passes into solution. The more labile bond in the collagen fibre appears to be the electrovalent link formed between acidic and basic side chains ; the more stable bond appears to be a hydrogen bond between amide and possibly hydroxyl side chains or the direct carbimino backbone link or both of these.

---

* Shortened expressions used to denote aqueous solutions of the corresponding hydroxides.

[10] Speakman, *Proc. Roy. Soc. A*, 1931, **132**, 167 ; *Trans. Faraday Soc.*, 1930, **26**, 61.

[11] Astbury, *J.I.S.L.T.C.*, 1940, **24**, 69.

[12] Janakiraman and Gururajan, *Indian J. Sci. Ind. Res.*, 1945, **3**, 355.

[13] Spiers, *J.I.S.L.T.C.*, 1933, **17**, 193.

[14] Ames, *J. Soc. Chem. Ind.*, 1944, **63**, 234.

Swelling and Shrinkage Temperatures of Collagen.

The possible effects on the salt links of collagen by electrolytes, non-electrolytes, and the dielectric constant of the solvent as revealed by swelling and thermal shrinkage, have been studied.

The material was prepared from dry-salted Cape hair-sheepskin. Samples about 20 cm. by 8 cm. were selected from the best parts of the skin avoiding the neck and tail areas, and coming no nearer than 1-2 in. to the backbone. Most of the wool was removed by clipping and the skin repeatedly washed with water until all the salt had been removed. Fat was extracted by cold treatment with light petroleum ; remaining soluble proteins were removed with 5 % NaCl, and the skin then washed free from salt and dried in acetone and air. Strips were cut 0·7 × 7·0 cm. and the remaining wool, together with the upper grain layer, split off in a skiving machine. The residual material consists almost entirely of interwoven collagen fibres. The swelling of the collagen was determined in aqueous solutions of varying concentrations of NaCl, KCl, KCNS, methyl alcohol, ethyl alcohol, glucose and sucrose, and expressed as % increase in weight after 24 hr. in each solution.

For the shrinkage temperature determinations, similar strips of collagen were used, each piece being soaked for 24 hours in the various mixtures, and the shrinkage temperature then determined in these solutions, using the apparatus described by Merry.[15] The shrinkage temperature curves for KCNS, NaCl, CsF, LiI and formamide were taken from Küntzel's results.[16]

(*a*) The Effect of Electrolytes.

The inverse relation between swelling and shrinkage temperature has been pointed out by Theis and his colleagues.[17] The effects of aqueous solutions of several salts on the shrinkage temperature are given by Küntzel.

The effect of salts on both swelling and shrinkage temperature is obviously strongly influenced by the position of the salt in the Hofmeister series. Docking and Heymann [18] (confirming the work of Katz and colleagues [19]) have shown that with gelatin, salts with weakly hydrated ions, e.g., thiocyanates, are strongly adsorbed from aqueous solutions, while those with strongly hydrated ions, e.g., sulphates, show a negative adsorption. Most salts show some adsorption at low concentrations but negative adsorption as the concentration increases, the concentration at the change-over depending on the position of the salt in the Hofmeister series.

The effect of the weakly adsorbed salts, e.g., KCl, in promoting swelling and reducing the shrinkage temperature is slight. That of the strongly adsorbed salts, e.g., KCNS, is considerable. The strongly adsorbed salts reduce the strength of the salt link to such an extent that axial shrinkage may occur according to Küntzel's figures at temperatures as low as 20° (Fig. 1).

---

[15] Merry, *J.I.S.L.T.C.*, 1945, **29**, 223.

[16] Küntzel, *Stiasny-Festschrift*, 1937, p. 190.

[17] Theis and Esterley, *J. Amer. Leather Chem. Ass.*, 1940, **35**, 563.

[18] Docking and Heymann, *J. Physic. Chem.*, 1939, **43**, 513.

[19] Katz and Muschter, *Biochem. Z.*, 1933, **257**, 386. Katz and Weidinger, *ibid.*, 1933, **259**, 191.

(*b*) The Effect of Dielectric Properties of Solvent.

There is a theoretical expectation that the dielectric properties of the solvent would affect the strength of the salt link. Experimental evidence bearing on the point is confusing (see Table II). If pure solvents of a neutral character are considered there is some support to be obtained, as shown by the figures given below:

TABLE II

	Medium.	Temperature of Axial Shortening.	Temperature of Solution.	Dielectric Constant at 20° C.
1	Water	60°	120°	81
2	Aqueous solutions of acids and alkalies	< 60° temperature depending on *p*H	Owing to hydrolysis of the peptide link, the solution temperature cannot be determined	—
3	Aqueous solutions of salts	> 60° or < 60° depending on concentration and position of salt in Hofmeister series	—	—
4	Glacial formic acid (*p*K = 3·7)	< 0°	25°	47·9
5	Thioglycollic acid (*p*K = 3·3)	< 0°	20°	—
6	Lactic acid (*p*K = 3·9)	< 15°	20°	19·4-23
7	Acetic acid	20°-25°	Not dissolved on boiling	6·5
8	Propionic acid	> 40°	,, ,,	3·1
9	Butyric acid	45°	,, ,,	2·8
10	*m*-Cresol	15°	Dissolved on boiling	5·0
11	Formamide	15°	,, ,,	> 84
12	Cuprammonium	12°	Dissolved on heating	—
13	Methyl alcohol	No effect on boiling	Not dissolved on boiling	35
14	Ethyl alcohol	,, ,,	,, ,,	27

Medium.	Dielectric Constant. (E.S.U.)	Shrinkage Temperature °C.
Ethyl alcohol	27	> 78°
Methyl alcohol	35	> 65°
Glycerine	39	about 150°
Water	81	about 60°
Formamide	> 84	about 15°

Obviously further work is needed, but there is a suggestion here that raising the dielectric constant lowers the shrinkage temperature and vice versa.

Since some information is available on the dielectric constants of certain aqueous solutions, shrinkage temperatures obtained by experiment over a range of concentrations as described in the previous section were plotted against the dielectric constants calculated from the data in the literature. These are shown in Fig. 2.

At low concentration of all solutes, the fall in the dielectric constant is accompanied by a fall in the shrinkage temperature. This may be attributed to adsorption and the accompanying swelling. After this with increasing concentration of solute, in all the cases examined, a reduction in the dielectric constant of the medium was accompanied by a rise in the shrinkage temperature. It will be seen from Fig. 2 that for solutes as different in character as KCl, glucose, sucrose, methyl alcohol and ethyl alcohol over most of the range the slope of the curves is similar. Though not final proof, this suggests that the salt link is influenced by the dielectric constant.

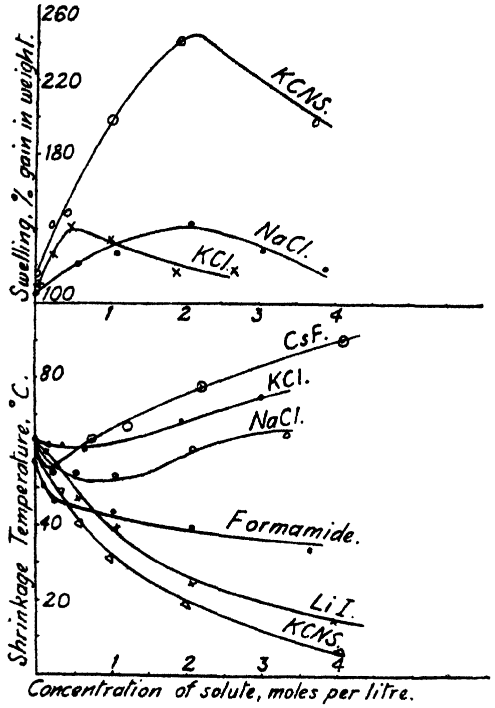

FIG. 1.—Shrinkage temperature and swelling of collagen in salt solutions and in formamide.

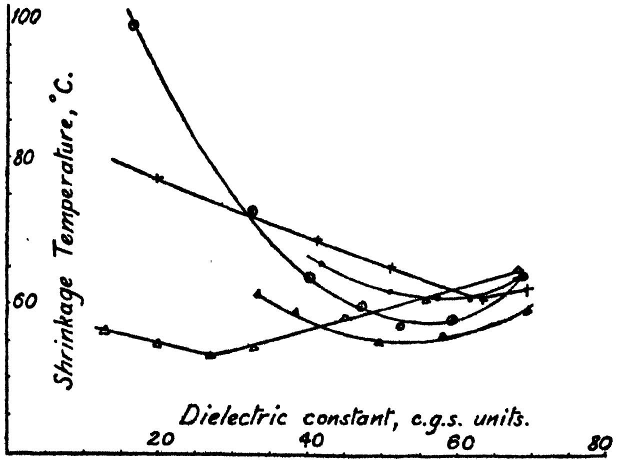

FIG. 2.—Shrinkage temperatures (from Fig. 1), plotted against dielectric constant of medium.

(c) The Effect of Non-Electrolytes.

(1) **Sugars.** — Both glucose and sucrose penetrate the fibre in aqueous solutions and cause a considerable gain in weight (Fig. 3). Over the swelling range the strength of the glucose solution which penetrated into the collagen was on average about 80 % of the initial concentration of sugar in each

solution. (The sugar was determined by washing out the collagen with water several times, after the swollen weight had been found, finally squeezing the material in a vice. Glucose in the extract was estimated by the normal reducing method.) The effect of sugar solutions on the shrinkage temperature is probably due to two opposing effects, change in dielectric constant with change in concentration and uptake of solution due to swelling. As the concentration of sugar increases, swelling increases, with a subsequent straining of the lateral links and a corresponding reduction in shrinkage temperature. A point is reached, however, when increase in concentration of the solute, causing a lowering of the dielectric constant, overcomes the swelling effect and the electrostatic forces of the salt link are strengthened by the presence of a medium of lower dielectric constant, so that the lateral salt links will become more firmly held and there is a rise in shrinkage temperature.

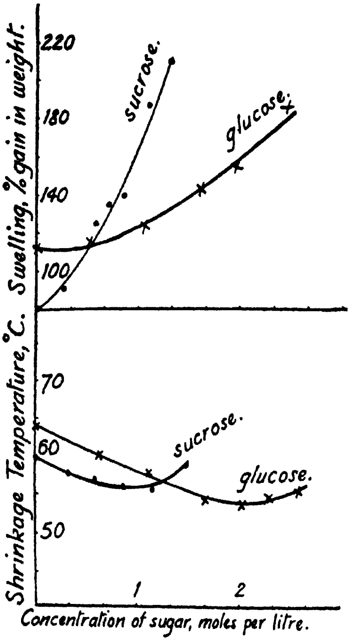

FIG. 3.—Shrinkage temperature and swelling of collagen in sucrose and glucose solutions.

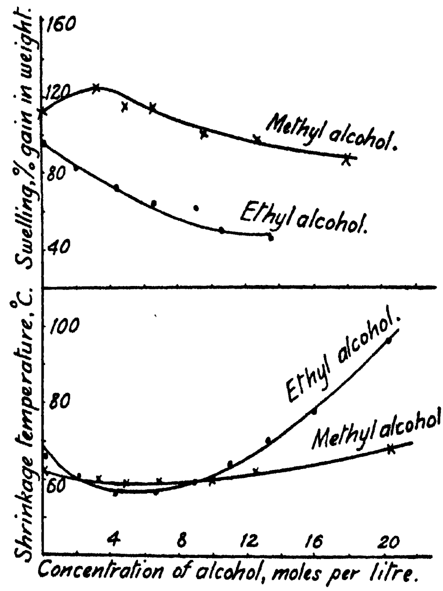

FIG. 4.—Shrinkage temperature and swelling of collagen in aqueous methyl and ethyl alcohols.

It is perhaps significant that those reagents, e.g., glucose and KCNS, which cause considerable swelling, show relatively longer descending parts of the curves—i.e., those parts which have been attributed to swelling, while a reagent such as CsF, which is only weakly adsorbed by gelatin, causes only a slight reduction in shrinkage temperature before producing the opposite effect.

(2) **Formamide.**—Formamide in aqueous solutions has considerable reducing effect on the shrinkage temperature (Fig. 1). This is attributed to the high dielectric constant of formamide, which is > 84 at 20°.

(3) **Alcohols.**—The swelling and shrinkage temperature curves for methyl and ethyl alcohol appear to be somewhat confusing (Fig. 4): in methyl alcohol, the initial fall in shrinkage temperature with increase in concentration of alcohol can be attributed to an increase in swelling. This is followed by a rise in shrinkage temperature as both the swelling

and the dielectric constant fall, although the points of maximum swelling and minimum shrinkage temperature do not coincide. However, the decrease in shrinkage temperature is comparatively small. With ethyl alcohol-water mixtures there is also an initial fall in shrinkage temperature although the swelling is decreasing in the same region. Later, as the dielectric constant decreases, the shrinkage temperature rises as predicted.

(4) **Phenols.**—Fused phenol (40°) and cold *m*-cresol, which both induce contraction in collagen fibres, may break or considerably weaken the salt link by possible hydrogen bonding between the charged carboxyl and the hydroxyl group of a phenol. *m*-Cresol is a solvent for Nylon, and therefore might be assumed to open the direct carbimino backbone link. The existence of this link is possible in collagen, but whether it is frequent is open to doubt.

Hydrogen Bonding in Collagen.—It is possible that the direct carbimino backbone link occurs in collagen, but steric considerations make its frequent occurrence unlikely. It will be influenced by the same conditions that are discussed below for the amide cross link.

There is plenty of evidence that during the conversion of collagen to gelatin by liming, ammonia is evolved and it is also established that the appearance of water-soluble gelatin coincides with the evolution of ammonia.[14] Since liming leads to a reduction in the amide nitrogen, it can be argued that in "native" collagen the amide groups are involved in a lateral link in the fibre. It is suggested here that the amide group forms a hydrogen bond with a hydroxyl group, which exists in appreciable numbers in the collagen molecule; hence it is suggested that the bond is of the amide-hydroxyl type.

Table II shows the temperatures at which collagen shrinks and temperatures at which it dissolves in various reagents. Acetic, propionic and butyric acids, even on boiling, do not dissolve collagen, though under this condition they produce axial contraction about equal to that of formic acid at low temperatures. It is to be noticed that the three organic solvents which dissolve collagen at low temperatures are not only fairly strong acids (*p*K 3·9, 3·7, 3·3 respectively) but in the cases of lactic and thioglycollic acids they also have in their molecules groups which could displace a hydrogen bond either of the amide-hydroxyl or the hydroxyl-hydroxyl type :—

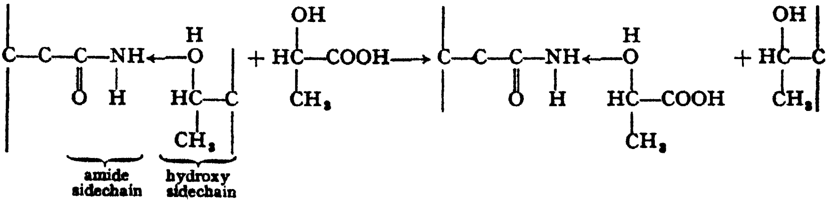

In considering the solution of collagen at low temperatures in a non-aqueous system, it is unlikely that the covalent peptide links of the main chain will be broken. With reference to cuprammonium it has been suggested by Feldman[20] that considerable degradation takes place when collagen dissolves in this reagent, breaking occurring along the main chains themselves as well as at the side chains.

The behaviour of gelatin can be considered in relation to collagen. Gelatin may be regarded as disorganised collagen with a reduced number of amide side-chain groups. Gelatin swells in aqueous acids and alkalies, but has internal cohesive forces of appreciable strength, which can be taken as evidence of cross bonds between the disorientated polymeric molecules.

---

[20] Feldman, *Legkaya Prom.*, 1943, **3** (5), 18; *Amer. Chem. Soc., Abstr.*, 1946, **40**, 1683.

Gelatin is soluble in organic reagents which cause axial shrinkage in collagen. Hence the cohesive forces of a gelatin gel may be attributed to salt links rather than hydrogen bonds, though after drying, the forces of cohesion are considerably increased.

The Cross-Linkages of Elastin.

Elastin fibres differ considerably from collagen fibres. In their natural " wet " condition they show rubber-like physical properties.[21] The fibres in the dry condition are rigid, the molecules adhering through general van der Waals forces. The dry fibres, however, swell in methyl and ethyl alcohol, showing that their average pore size is similar to the pore size of collagen.

Elastin swells considerably in formamide and in formic, acetic, thioglycollic and lactic acids and in fused phenol. The swelling occurs simultaneously in three dimensions,[4] resembling unstretched Nylon, which is indirect evidence of the absence of complete molecular orientation in the fibre.

Elastin is insoluble in the strong base cuprammonium even on boiling, and in all the other solvents examined during this work, including boiling *m*-cresol. It should be noted that the sheath of the elastin fibre is much more resistant than the core. Trypsin digests elastin—the core first breaks into short cylinders, which later contract into droplets and remain for some time held in the sheath before the whole fibre disintegrates.

An examination of the amino-acid constitution of elastin suggests that of the side chains present not more than about 1 in 30 is polar (Table I). This high proportion of non-polar side chains would account for the rubber-like properties of elastin, since the number of possible cross bonds would be too few to hold the molecule in an extended form.

As regards the cross bonds possibly present, since the proportion of glycine and proline residues in the molecule are about the same as in collagen, the formation of the direct backbone link is probably limited, as in collagen, by spatial considerations. As regards possible salt links, the chemical constitution, as far as it is known, suggests an absence of basic and acidic side chains. This absence of these groups is confirmed by the observation of Roddy and O'Flaherty [22] that chrome tanning liquors which transform collagen and reticulin fibres into leather are without effect on elastin fibres, Atkin [23] having shown that the first stage of chrome tanning is a coupling of the collagen fibre and the basic chrome tanning complex through the carboxyl groups of the collagen.

In connection with the possible cross bonds in elastin through the side chains, Roddy and O'Flaherty [22] have shown that elastin prepared from the *ligamentum nuchæ*, dried and ground in a Wiley mill, shows some swelling in acid solutions, though less than that shown by reticulin and much less than that shown by collagen, and also some swelling in alkaline solutions which is intermediate in extent between reticulin and collagen (except at *p*H 12).

The rubber-like nature of elastin is confirmed by X-ray examination. Astbury [11] reports that elastin fails to show any sign of orientation, though on stretching a few indications of such appear. Elastin may therefore be regarded as a protein fibre which normally exists in the " supercontracted " or rubber-like condition, i.e. with considerable lengths of the long molecules free from cross-bonding, hence lying in disordered configuration, but with a few cross bonds maintaining the structure as in lightly vulcanised rubber.

---

[21] Wöhlisch, Weitnauer, Grünung and Rohrbach, *Kolloid- Z.*, 1943, **104**, 14.

[22] Roddy and O'Flaherty, *J. Amer. Leather Chem. Assoc.*, 1939, **34**, 671.

[23] Atkin (private communication).

Elastin and lightly vulcanised rubber, however, differ in one important respect—the rubber molecule consists only of carbon and hydrogen, and under the forces of shear is self-lubricating. The backbone of the elastin molecule contains both oxygen and nitrogen atoms, with their potentialities for forming hydrogen bonds and with residual forces arising from the polar character of the peptide link. The elastin molecule, therefore, is not self-lubricating, but requires the presence of water or some other polar solvent for its rubber-like properties to become apparent.

Th authors are indebted to the Chairman and Council of the British Leather Manufacturers' Research Association for permission to publish this work.

Summary.

1. The relation between the chemical constitution of the protein fibres of silk fibroin, collagen and elastin and the chemical nature of the solvents which produce radial swelling, axial shrinkage and solution, is considered.

2. The fibres are held together by lateral bonds of several chemical types. The swelling of the fibres in organic solvents is due to a straining or rupture of some of the types of lateral links; the production of axial shrinkage is due to the breaking of at least one type of cross bond, thus allowing the molecules to shorten with a corresponding gain in entropy. If other kinds of lateral links are left intact, the solvent will produce only axial shrinkage, accompanied by rubber-like extensibility. Solvents which break all types of lateral bond cause solution of the protein.

3. In fibres of silk fibroin the two types of lateral bond are the direct carbimino backbone link and a hydroxyl-hydroxyl link through the serine side chains, the former being opened by formic acid and both by cuprammonium.

4. In collagen fibres there appear to be (i) a more labile salt link, (ii) one (or more) more resistant hydrogen bonds. The salt link can be broken: (*a*) by displacement of a non-diffusible ion or by a diffusible ion or a co-ordinate group; (*b*) by reagents which cause considerable swelling of the fibres; (*c*) by an increase in the dielectric constant of the medium penetrating the fibre.

The relationship between dielectric constant, shrinkage temperature and swelling of collagen in various aqueous mixtures is discussed. The hydrogen bond type can be broken by certain organic reagents such as *m*-cresol, formamide, formic acid, lactic acid and thioglycollic acid, all of which can dissolve the fibre.

5. In the elastin fibre the presence of a high proportion of long non-polar side chains limits the possibilities of the formation of lateral bonds and this fibre normally exists with the backbone in random configuration. Since elastin is insoluble in many collagen solvents it must be bonded by a few cross bonds of high resistance, the chemical nature of which is as yet unknown. The sheath of the elastin fibre is much more resistant than the core.

British Leather Manufacturers' Research Association,
London, S.E. 1.

HYDROTROPY, SOLUBILISATION AND RELATED EMULSIFICATION PROCESSES.

PART V.—SOLUBILISATION IN ETHYLENE GLYCOL.

BY P. A. WINSOR.

Received 11th February, 1947; as revised 5th June, 1947.

In earlier papers the theory and classification of solubilised systems given in Part I has been illustrated with examples of the mutual solubilisation of water and water-insoluble organic liquids by means of a variety of amphiphiles. In the present paper examples are given showing that, as already indicated in Part I, the generalisations which have been applied to water-solubilised systems are applicable, with only slight modifications, to solubilisation in ethylene glycol.

For a given amphiphile C and a given organic liquid $\overline{O}$ the ratio R (cf. Part I) appears to be probably less (because $A_{C\overline{W}}$ is greater) when $\overline{W}$ is ethylene glycol than when $\overline{W}$ is water. Corresponding to this, an amphiphile and organic liquid which under given conditions give a Type IV or Type II system with water may give a Type I system with ethylene glycol (cf. Example A (i) below).

There is an important exception to the general correspondence in behaviour between water-solubilised and glycol-solubilised systems. This is that in the glycol systems no discontinuity within the Type IV region has yet been observed and the production of a gel, even using conditions found most favourable for the production of gels in aqueous systems, has not been realised in the present work. Nor is any case of the production of such a gel recorded in the recent paper of Palit and McBain.[1]

If the production of a gel is related to the presence of the lamellar micelle (for which $R \simeq 1$) as suggested in Part I, it possibly arises through resistance to shear parallel to the planes of the layers, in both $\overline{O}$ and $\overline{W}$ layers of the " sandwich " (Part I, Fig. 3). In lamellar micelles containing water and glycol respectively the resistance to shear in the $\overline{O}$ layers might be expected to be similar in both cases. The resistance to shear in the $\overline{W}$-layers would, however, be expected to be different in the respective cases on account of differences in the strengths and directions of hydrogen bonding of water and ethylene glycol. If this were the origin of the difference in gelling tendency in water- and glycol-solubilised systems, it would indicate that the resistance to shear is greater with water than with ethylene glycol. In view of the pseudocrystalline structure with tetrahedral co-ordination which Fowler and Bernal[2] attribute to water, this would not be altogether unexpected.

In line with the above suggestion, it seems possible that the reduction in the gelling tendency in certain water-solubilised systems that is brought about by the introduction of inorganic salts (cf. Part IV, Tables VI and VII) may arise, in part at least, through a consequent reduction (or interruption) of water-to-water or water-to-amphiphile hydrogen bonding in the $\overline{W}$ layers of the lamellar micelles. Also the reduction of $A_{C\overline{W}}$ which is produced by added inorganic salts in both water- and glycol-solubilised systems (Method I (*d*)), may be due to an effect of the inorganic salt in reducing the strength of hydrogen bonding between C and $\overline{W}$. The effect of inorganic salts on hydrogen bonding in water is, however, not very clear.[3]

The particularly strong tendency to gelation which occurs in water-solubilised systems containing 1-alkanols in conjunction with alkane-1 salts (Part IV) is possibly associated with an increased resistance to shear in the $\overline{O}$-layers of the lamellar micelles. It does not seem likely that this combination could much affect the resistance to shear within the $\overline{W}$-layers of the lamellar micelles.

The very close analogy between solubilisation in water and solubilisation in ethylene glycol makes many of the conclusions reached by Palit and McBain in their recent paper[1] on the effect of soaps on the mutual solubility of organic liquids, applicable with only slight modifications to water-solubilised systems. Their conclusions are in close harmony with the more general views given in the present series of papers. In Fig. 3

---

[1] Palit and McBain, *Ind. Eng. Chem.*, 1946, **38**, 741.

[2] Fowler and Bernal, *Trans. Faraday Soc.*, 1933, **29**, 1049.

[3] Butler, *Ann. Reports*, 1937, **34**, 90.

of Palit and McBain's paper, the lower curve and tie-lines represent a case of the typical behaviour shown in Type I systems. The increase in effectiveness of the sodium soaps as mutual solvents for benzene and propylene glycol with increase in the number of carbon atoms in the soap, is a particular example of the increase in solubilisation in Type I systems ($R < 1$) brought about by increasing the lipophilic solvent affinity of the amphiphile (cf. Part I of the present series, Method I (*c*)). The analogous case for benzene and water has recently been reported by Durand.[4]

It may be emphasised here that the mutual solvent in both water- and glycol-solubilised systems, is not the solid unsolvated soap, but the liquid complex produced in the presence of the two immiscible liquids on solvation of the lipophilic and hydrophilic radicals of the soap molecule by the lipophilic and hydrophilic liquids respectively. When this point is borne in mind the apparent contradiction mentioned by Palit and McBain between the effect of soaps on benzene-propylene glycol systems and the commonly accepted point of view on mutual solvents, disappears. The aspect of the amphiphile as a mutual solvent is rather strikingly illustrated in water-solubilised systems by the production of three-phase, Type III systems (cf. Parts I and IV). Such systems may also be obtained with ethylene glycol in place of water as shown in Example C (ii) below.

Experimental.

The ethylene glycol used was a middle fraction obtained on vacuum distillation of a pure grade of ethylene glycol. Examples are given below involving solubilisation in glycol systems containing

(*a*) Aerosol OT (sodium sulpho-dioctyl succinate).
(*b*) Tetradecane-1 sodium sulphate.
(*c*) Undecane-1 ammonium chloride.

(A) Solubilisation in Ethylene Glycol with Aerosol OT.

While with excess of water a 20 % (wt./total vol.) solution of Aerosol OT (water content below 1 %) in benzene gives a Type II system, with excess ethylene glycol a Type I system is produced. Thus at room temperature (19° c.) with 20 cc. of a 20 % solution of Aerosol OT in benzene and 6 cc. of ethylene glycol a system is obtained with upper (benzene) layer (6 cc.) and lower (glycol-solubilised) layer (20 cc.). Such Type I systems may be converted into Type IV systems by the standard methods of Part I.

(i) Effect of Added Water.—Addition of water to a glycol Type I system is a case of the addition of a $\overline{W}$-soluble component which reduces $A_{O\overline{W}}$ and thus increases R. It is analogous to the addition of an inorganic salt to an aqueous Type I system (Method I (*d*)) and produces an analogous effect. This is shown in Table I.

TABLE I.—THE EFFECT OF ALTERNATE ADDITION OF GLYCOL AND WATER TO 20 CC. OF A 20 % (WT./TOTAL VOL.) SOLUTION OF AEROSOL OT IN BENZENE.

Vol. of Glycol Added (cc.).	Vol. of Water Added (cc.).	Condition of System
<5·35	0	Clear solution (S_1 sol)
5·35	0	Type I system
5·35	0·4	Clear solution
6·15	0·4	Type I system
6·15	0·5	Clear solution
6·50	0·5	Type I system
6·50	0·7	Clear solution
6·75	0·7	Type I system

---

[4] Durand, *Compt. rend.*, 1936, **223**, 898.

(ii) Effect of an Alkanol not completely Miscible with Ethylene Glycol (Method I (*b*)) and of Sodium Sulphate Method I (*d*)).—Ethylene glycol was shaken overnight with an excess of anhydrous sodium sulphate. The resulting solution was found to contain 0·44 g. sodium sulphate per 100 cc. 10 cc. portions of this solution and of pure ethylene glycol respectively were mixed with 10 cc. portions of an anhydrous solution of Aerosol OT in benzene (25·9 % wt./total vol.). The comparative behaviour of the two mixtures on gradual addition of lauryl alcohol at 20° C. is recorded in Table II.

TABLE II.

Vol. Lauryl Alcohol Added (cc.).	System without Sodium Sulphate.	System containing Sodium Sulphate.
0	Type I system (excess benzene 4·3 cc.)	Type I system (excess benzene 4·1 cc.)
0·70	Still Type I system	Clear solution
0·90	Clear solution	Clear solution
1·5	Clear solution	Solution just breaking down to Type II system. Clear on shaking, clouds on standing
3·0	Clear solution	Type II system. Two clear layers. Lower layer 3·0 cc.
4·1	Solution just changing to Type II system. Clear on shaking, clouds on standing	
4·5	Type II system. Two clear layers. Lower layer 1·0 cc.	

The results in Table II show that the effect of the sodium sulphate is here exactly analogous to its effect in water-solubilised systems. The table also provides examples of the phenomenon of mechanically reversible homogeneity in a glycol system. This phenomenon, the nature of which was discussed in Part I, is frequently observable in both water- and glycol-solubilised systems at points where two-phase systems are about to pass into systems of a single phase.

(B) Solubilisation in Ethylene Glycol with Tetradecane-1 Sodium Sulphate.

Analytically pure tetradecane-1 sodium sulphate was prepared from pure *n*-dodecyl chloride via the Grignard reaction with ethylene oxide and sulphation with chlorosulphonic acid.

It was found in Part IV that the strongest tendency to gel in water-solubilised systems occurs in those containing an alkanol-1 in conjunction with an alkane-1 salt as amphiphile. In the following experiments using tetradecane-1 sodium sulphate, and in those described in the succeeding section using undecane-1 ammonium chloride, attempts were made to obtain gels in a glycol-solubilised system.

5 cc. of ethylene glycol, 5 cc. of cyclohexane and 1 g. of tetradecane-1 sodium sulphate were mixed together. On warming, the sodium alkyl sulphate dissolved giving a Type I system from which it recrystallised on cooling. If lauryl alcohol (1.35 cc.) was added to the mixture prior to crystallisation a clear solution was obtainable at 20° C. Further addition of lauryl alcohol did not give a gel but clear solutions were produced with all proportions (cf. the cyclohexane, octanol-1, aqueous sodium *iso*butyrate systems, Part IV).

(C) Solubilisation in Ethylene Glycol with Undecane-1 Ammonium Chloride; the Effect of Calcium Chloride.

(i) To mixtures of 5 cc. cyclohexane, 5 cc. ethylene glycol and 1·5 g. undecane-1 ammonium chloride (Part IV) lauryl alcohol was gradually added. The behaviour observed in the presence of 0, 0·2 and 0·4 g. of added $CaCl_2$ is shown in Table III.

TABLE III.

Calcium Chloride Added (g.).	0	0·2	0·4
	Vol. Lauryl Alcohol (cc.) Required to give Systems Described in Left-hand Column.		
Type I	<1·6	<1·15	<0·85
Clear solution . . .	1·6	1·15	0·85
Type II	Solution miscible with lauryl alcohol	1·8	0·95

This behaviour is analogous to that recorded in Part II, Table IV, illustrating the effect of sodium sulphate on solubilisation in an aqueous system. The absence of gelation in these systems compared with the marked gelation in aqueous systems containing undecane-1 ammonium chloride and an alkanol-1 (cf. Part IV, Table IX) is noteworthy.

(ii) As suggested by the trend of the figures given in Table III, three-phase (Type III) systems can be produced in glycol-solubilised systems just as in water-solubilised systems. Thus at room temperature a mixture of 5 cc. ethylene glycol, 10 cc. cyclohexane, 1·0 g. undecane-1 ammonium chloride and 0·8 g. calcium chloride gave :

(*a*) with 0·3 cc. lauryl alcohol a Type I system (lower layer 9·0 cc.) ;
(*b*) with 0·35 cc. lauryl alcohol a Type III system (lower layer 4·4 cc., middle layer 5·6 cc., upper layer 6·8 cc.) ;
(*c*) with 0·40 cc. lauryl alcohol a Type II system (lower layer 4·5 cc.). This behaviour is analogous to that shown for an aqueous system in Table II, Part II.

If lauryl alcohol is added to a mixture of 5 cc. of ethylene glycol, 10 cc. of cyclohexane and 1 g. of undecane-1 ammonium chloride in the presence of only 0·4 g. of $CaCl_2$ neither a Type III system nor a clear solution is obtained, but the behaviour is apparently similar to that recorded in Table III, Part II. As in that case there is a gradual transition from a Type I to a Type II system and in the course of this transition the conjugate phases show opalescence and extremely low interfacial tension. Such opalescence effects in solubilised systems are probably in the nature of critical opalescence effects due to incipient separation of a single phase into two phases,[5–7], cf. however.[8]

Summary.

The analogies existing between solubilisation in ethylene glycol and solubilisation in water are discussed. The significance of the occurrence of gelation in water-solubilised systems and its absence in comparable glycol-solubilised systems, is considered.

[5] Smoluchowski, *Ann. Physik.*, 1900, **33**, 1275.
[6] Freundlich and Kruger, *Biochem. Z.*, 1929, **205**, 186.
[7] Lindau, *Naturwiss.*, 1932, **20**, 396.
[8] McBain, *et al.*, *J. Amer. Chem. Soc.*, 1941, **63**, 670.

PART VI.—EFFECT OF TEMPERATURE ON THE SOLUBILISATION OF LIQUIDS.

Received 11th February, 1947; as revised 5th June, 1947.

In earlier papers the importance of the magnitude of the expression

$$R = \frac{A_{\mathrm{C\bar{O}}}}{A_{\mathrm{C\bar{W}}}} = \left(A_{L\mathrm{C\bar{O}}} + A_{H\mathrm{C\bar{O}}}\right)\Big/\left(A_{L\mathrm{C\bar{W}}} + A_{H\mathrm{C\bar{W}}}\right)$$

in determining the condition of solubilised, or partially solubilised, systems has been described. In this expression $\overline{O}$ and $\overline{W}$ signify respectively mutually saturated non-miscible organic liquid (single compound or mixture) and aqueous liquid (water or inorganic salt solution). $A_{O\overline{O}}$ denotes the total intermolecular solvent attraction, in the solubilised phase, between the amphiphile C and $\overline{O}$ and may be considered as being made up of the sum of the lipophilic ($A_{LO\overline{O}}$) and hydrophilic ($A_{HO\overline{O}}$) solvent attractions existing between $\overline{O}$ and C. $A_{O\overline{W}}$, $A_{LO\overline{W}}$ and $A_{HO\overline{W}}$ have corresponding meanings with respect to C and $\overline{W}$.

The effect of change of temperature on solubilised systems may be regarded as operating in part through changes in the simple miscibility of $\overline{O}$ and $\overline{W}$ apart from C and also through changes in the relationships existing between the various factors in the expression for R above. The second mode of operation will clearly be partially dependent on the first since this will give rise to changes in the composition of $\overline{O}$ and $\overline{W}$.

Although precise means of measuring R are as yet not available, the correlation between the various conditions of a solubilised system and changes in R has been described in Part I. The present communication describes an attempt to determine if any generalisations concerning the effect of change of temperature on R, are possible. From the experimental results below it seems that it is not possible to say more than that in a variety of solubilised systems, rise of temperature appears to diminish R more often than to increase it. Considering the problem *a priori*, this variability of the temperature effect is not surprising in view of the variety of temperature-solubility effects observed even in binary liquid systems. It is important to note, however, that in whichever way it may operate, the effect of change of temperature on solubilisation is frequently very great indeed.

The experimental method adopted in the present work was to observe the effect of temperature change on mixtures which have been brought to the point where a Type I system has just passed into an S_1 sol or where an S_2 sol is just passing into a Type II system. Under these conditions a reduction of R produces heterogeneity through separation of a free organic phase in the first case, while an increase in R produces heterogeneity through separation of an aqueous phase in the second. A sufficient increase in R in the first case, that of the S_1 sols, may give rise to the sequences of changes, $S_1 \rightarrow G \rightarrow S_2 \rightarrow$ Type II system, described in Part I. A reduction of R in the second case, that of the S_2 sols, may lead to the reverse series of changes $S_2 \rightarrow G \rightarrow S_1 \rightarrow$ Type I system.

Some observations [1, 2] on the effect of temperature change on "saturated" solutions of organic liquids in soap solutions, have already been recorded in the literature but in these cases the distinction between saturation at the points where Type I or Type II systems are respectively produced, was not recognised. If the examples there given are re-examined in the light of the present views, it appears probable that in these cases, increase in temperature corresponded to a reduction in R. On the other hand three instances where the reverse relationship has been found, have already been recorded in Part III of the present series, the solubilising agent being a mixture of sodium secondary C_{10}-C_{18} alkyl sulphates.

Results and Discussion.

Three series of examples are given here of the effect of temperature on the solubilisation of certain organic liquids or liquid mixtures with (1) a mixture of sodium secondary C_{10}-C_{18} alkyl sulphates, (2) sodium soaps and (3) sodium

---

[1] Lester Smith, *J. Physic. Chem.*, 1932, **36**, 1401, 1672, 2455.

[2] McBain, *J. Amer. Chem. Soc.*, 1944, **66**, 13.

phenate. The organic liquids used were of "pure" grade and, since the experiments were designed to be of a qualitative rather than an exactly quantitative character, these were not purified further.

As already stated, rise of temperature most frequently produces a reduction of *R*. The results for which the opposite relationship holds are indicated by an asterisk. It will be noticed that these are mainly among the results obtained using the more concentrated sodium alkyl sulphate solution S. It was with this solution that the temperature effects recorded in Part III,[3] on the solubilisation of octanol-4, *n*-butyl acetate and methyl *iso*butyl ketone and which also indicated an increase of *R* with rising temperature, were obtained.

(1) Effect of Temperature on Solubilisation with Sodium Secondary C_{10}-C_{18} Alkyl Sulphates.—To mixtures of equal volumes of organic liquid and an aqueous solution of a mixture of sodium secondary C_{10}-C_{18} alkyl sulphates of various concentrations, cyclohexanol or *n*-octylamine were added until the system was at the stage of (*a*) a clear sol S_1, organic liquid just solubilised, (*b*) an S_2 sol just clouding and commencing to precipitate an aqueous phase. The effects of warming and cooling on mixtures at these points were then noted and are recorded in Tables I, II and III.

TABLE I.—AMPHIPHILE SOLUTION CONTAINS 23·9 g. SODIUM SECONDARY C_{10}-C_{18} ALKYL SULPHATES AND 7·1 g. SODIUM SULPHATE PER 100 CC. (SOLUTION S, PARTS II AND III.)

Initial State of System.	Organic Liquid.	Petroleum Ether (b.p. 65-95 °c.).		Xylene.		Carbon Tetrachloride.	
	Additive	Cyclo-hexanol	*n*-Octyl-amine	Cyclo-hexanol	*n*-Octyl amine	Cyclo-hexanol	*n*-Octyl-amine
Organic liquid just solubilised (*a*)	Cooling	Clouds *	Clouds *	Clouds *	Clouds *	Clouds *	Clouds *
	Warming	Gels *	Clear *	Clouds	Clouds	Clear *	Clear *
Aqueous phase just precipitating (*b*)	Cooling	Clears *	Cloudy	Clears *	Cloudy	Clears *	Cloudy
	Warming	Cloudy *	Clears	Clears	Clears	Cloudy *	Clears

TABLE II.—AMPHIPHILE SOLUTION CONTAINS 14·0 g. SODIUM SECONDARY C_{10}-C_{18} ALKYL SULPHATES AND 4·2 g. SODIUM SULPHATE PER 100 CC.

Initial State of System.	Organic Liquid.	Petroleum Ether (b.p. 65-95° c.).		Xylene.		Carbon Tetrachloride.	
	Additive	Cyclo-hexanol	*n*-Octyl-amine	Cyclo-hexanol	*n*-Octyl-amine	Cyclo-hexanol	*n*-Octyl-amine
Organic liquid just solubilised (*a*)	Cooling	Clear	Clouds *	Clear	Clouds *	Clear	Clouds *
	Warming	Pet. ether separates	Clouds near b.p.	Xylene separates	Clouds	CCl_4 separates	Clouds *
Aqueous phase just precipitating (*b*)	Cooling	Cloudy	Cloudy	Cloudy	Cloudy	Cloudy	Cloudy
	Warming	Clears ; then pet. ether separates	Clears ; then gels	Clears ; then xylene separates	Clears ; re-clouds at b.p.	Clears	Clears ; gels nr. b.p.

TABLE III.—AMPHIPHILE SOLUTION CONTAINS 14·0 g. SODIUM SECONDARY C_{10}-C_{18} ALKYL SULPHATES AND 7·1 g. SODIUM SULPHATE PER 100 CC.

Initial State of System.	Organic Liquid.	Petroleum Ether (b.p. 65-95° c.).		Xylene.		Carbon Tetrachloride.	
	Additive	Cyclohexanol	*n*-Octylamine	Cyclohexanol	*n*-Octylamine	Cyclohexanol	*n*-Octylamine
Organic liquid just solubilised (*a*)	Cooling	Clear	Clouds *	Clouds *	Clouds *	Clouds *	Clouds *
	Warming	Pet. ether separates	Clouds	Xylene separates	Clouds	Clouds at b.p.	Clouds
Aqueous phase just precipitating (*b*)	Cooling	Clears at 0° c.*	Cloudy	Cloudy	Cloudy	Cloudy	Cloudy
	Warming	Clears then pet. ether separates	Clears then gels and finally re-thins	clears then xylene separates	Clears	Clears	Clears

(2) Effect of Temperature on Solubilisation with Sodium Pelargonate, Sodium Laurate and Sodium Oleate.—Solutions of sodium pelargonate, sodium laurate and sodium oleate (all 10 % wt./total vol.) gave Type I systems with excess cyclohexanone and Type II systems with excess cyclohexanol. The maximum volumes of cyclohexanone and cyclohexanol which 10 cc. of these 10 % solutions would dissolve at room temperature (18° c.) were found, a slight excess was added and the effect of temperature on these mixtures was noted. The results are recorded in Table IV.

TABLE IV.

10 % Sodium Soap Solution.	Pelargonate.	Laurate.	Oleate.
Cyclohexanone dissolved (cc.) .	4·2^{Q}	3·9^{Q}	3·6^{Q}
Cyclohexanol dissolved (cc.) .	15·0^{PR}	9·8^{PQ*}	4·2^{PQ*}

P, clarifies on warming ; Q, clarifies on cooling ; R, temperature effect small.

On warming the mixtures containing cyclohexanone and 10 % pelargonate or laurate, ketone separated. The sodium oleate solution became slightly more heterogeneous at first but redissolved the ketone near the boiling point. The mixtures containing cyclohexanol solubilised with sodium laurate cleared both on cooling or warming. In these cases therefore, which are Type II systems, there must be a minimum solubility and maximum R at about 18° c.

It will be noted that at room temperature the amount of organic liquid solubilised per mol soap increases with the molecular weight of the soap in the Type I systems (cyclohexanone) and diminishes in the Type II systems (cyclohexanol). This is in agreement with Methods I (*c*) and II (*c*) of the classification given in Part I.

(3) Effect of Temperature on Solubilisation with Sodium Phenate.—With excess cyclohexanol or cyclohexanone a 14·5 % (wt./total vol.) sodium phenate solution gave Type II and Type I systems respectively. At 20° c., 40 cc. of the sodium phenate solution became cloudy with 1·5 cc. cyclohexanol or 7·5 cc. cyclohexanone but, as would be expected, dissolved much more of suitable mixtures of these two, e.g. 10 cc. cyclohexanol, 29 cc. cyclohexanone. The Type II system with 1·5 cc. of cyclohexanol became homogeneous on warming and at 85° c. a clear solution could be obtained with 3 cc. of cyclohexanol. The Type I system, with 7·5 cc. cyclohexanone, separated cyclohexanone on warming but clarified on cooling and at 1·5° c. a clear solution was obtained with 15 cc. of cyclohexanone.

Summary.

The significance of temperature effects on solubilised systems in relation to the ratio R is discussed, and examples are given illustrating the large effect of temperature on certain of these systems.

PART VII.—SOLUBILISATION OF SOLIDS, FREEZING POINT DEPRESSION EFFECTS IN SOLUBILISED SYSTEMS.

Received 12*th March*, 1947; *as revised* 5*th June*, 1947.

On solubilisation of a solid compound O the change of state

$$\underset{\text{(crystalline O)}}{\text{solid}} \rightarrow \underset{\text{(solubilised or dissolved O)}}{\text{liquid}}$$

occurs, the latent heat of fusion opposing the change. The ease of solubilisation of a solid compound would therefore, other things being equal, be expected to be considerably less than that of the same compound existing as a super-cooled liquid in the absence of crystal nuclei, or than that of a closely related liquid compound. A gradual increase in the ease of solubilisation of a solid as its melting-point is approached followed by a greater increase near its melting-point, would be expected. Also, since the mutually solubilised species are such as show high positive deviations from Raoult's law, relatively high temperature coefficients of solubility might be anticipated.[1]

In earlier papers the factor $R = A_{\text{OO}}/A_{\text{CW}}$ has been shown to exert a large effect on the solubilisation of liquids. In the case of the solubilisation of a solid, R will still affect the capacity of the solubilised phase to take up liquid O without appearance of a second liquid phase but, due to the counter tendency of O to be redeposited on its crystal lattice, the amphiphile solution will not dissolve O to the limit of its capacity to take up liquid O.

These considerations are important in discussing the variation in the solubility of solid bodies, e.g. dyes, in amphiphile solutions with temperature, salt content, etc. The solubilisation of solid, coloured bodies has already been extensively studied by Hartley[2] and by McBain and co-workers.

Experimental Results and Discussion.

(*a*) Effect of Temperature on the Solubility of Solid Organic Compounds in Aqueous Amphiphile Solutions.

The following two examples illustrate certain of the principles regulating the effect of temperature on the solubilisation of solid organic compounds in aqueous amphiphile solutions.

(1) Solubility of Thymol in a 7·5 % Sodium Pelargonate Solution.—With 5 g. of thymol (freezing point when saturated with water (about 2·5 %) 39·7° c.) 60 cc. of a 7·5 % solution of sodium pelargonate gave a clear solution at 40° c. More thymol gave a Type I system. On heating the clear solution, liquid thymol separated at 50° c., the solution becoming clear again on cooling. This is in accordance with the fairly general phenomenon of reduction of solubilisation in Type I systems on heating (cf. Part VI). On cooling to room temperature in the absence of crystals, the solution remained clear indefinitely but on seeding with thymol, 2·9 g. of thymol slowly crystallised out. On cooling the mother liquor to 0° c. additional thymol crystallised but this slowly redissolved on warming the mixture to room temperature.

---

[1] Hildebrand, *Solubility* (2nd Ed., 1936), p. 55.

[2] Hartley, *J. Chem. Soc.*, 1938, 1968; for further references and discussion see McBain, *Advances in Colloid Science*, Vol. I (Interscience Publishers, Inc., New York, 1942), p. 127.

In this example we have a system which dissolves increasing quantities of liquid thymol with falling temperature, but below the freezing point of thymol saturated with water, crystallisation occurs on seeding and the solubility of the solid diminishes with fall of temperature. The type of behaviour shown here is illustrated in Fig. 1.

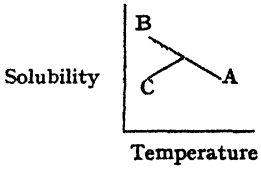

A, solubility of liquid O in amphiphile solution.
B, solubility of super-cooled liquid O.
C, solubility of solid O.

FIG. 1.

(2) Solubility of Thymol in Sodium Thymate Solution.—A homogeneous solution was prepared (at about 40° c.) containing 10·9 g. thymol, 4·6 g. sodium thymate and 8·0 g. water. Further addition of water gave a Type II system. The original solution remained clear on warming. On cooling in the absence of thymol crystals, it became cloudy at 5° c., clearing again above this temperature and remaining clear indefinitely at room temperature. This is in accordance with the fairly general phenomenon of increase in solubilisation in Type II systems with rise of temperature (Part VI). On seeding this solution at room temperature, the bulk of the thymol slowly crystallised out as very large crystals. On warming to 40° c. these crystals redissolved. On seeding, crystals tended to separate from the solution at 39° c., i.e. at a temperature about 1° below that of the freezing point of thymol directly saturated with water. This example and the foregoing both indicate the low solubility of solid as compared with supercooled liquid thymol in "solubilised" preparations.

The results illustrate the point that the solubility of a solid compound in an amphiphile solution is limited not so much by the capacity of the solution to accommodate the (liquid) compound as by the tendency of the dissolved compound to redeposit on its crystal lattice. This tendency diminishes with rise of temperature, and it may be this effect rather than any significant change in the solvent properties of the amphiphile solution, which occasions the increase in solubilisation of many dyes with rise of temperature recorded by McBain.[3] Concerning the direct effect of change of temperature on the inherent capacity of the amphiphile solution to accommodate (liquid) dye, this would be expected to be increased or diminished according to whether the effect of the temperature change were to bring the ratio R nearer to or further from unity.

(b) Effect of added Salts on the Solubilisation of Solids.

The free energy decrease on adding a small definite additional quantity of super-cooled O to a series of aqueous amphiphile C solutions of fixed amphiphile concentration, but of various inorganic salt contents, will probably be a maximum for that salt concentration which leads to a value of $R = 1$, because it is under this condition that C produces the maximum increase in mutual solubility of O and $\overline{W}$ (cp. Part I; also e.g. Part IV, Fig. 1).

If the transfer of the same definite quantity of crystalline O to these amphiphile solutions is considered, the free energy decrease will be made up of the free energy of solution of liquid O as before, minus the free energy of lattice formation (a constant). The total free energy decrease will be less than in the case of the solution of super-cooled liquid O, but will still be maximum when $R = 1$. This argument is over-simplified but it indicates that in cases where R is initially less than 1, the addition of an inorganic salt to an amphiphile solution should at first increase and then diminish its power of solubilising a solid. This behaviour has been found by McBain *et al.* in the case of the solubilisation of certain dyes.[4, 5, 6]

In cases where R is initially more than 1, added salt would be expected only to decrease the solubilisation of the solid. This may be the case in McBain's

[3] McBain, *Ind. Eng. Chem.*, 1942, **34**, 919.
[4] McBain, *ibid.*, p. 915.
[5] McBain, *et al.*, *J. Physic. Chem.*, 1942, **46**, 10.
[6] *idem.*, *J. Amer. Chem. Soc.*, 1944, **66**, 9.

experiments on the solubilisation of Yellow AB in 0·1 N. sodium deoxycholate solutions.[4] It may be noted that if the lipophilic character of sodium cholate is sufficiently increased by its conversion to sodium dehydrocholate, it loses its solubilising power for this dye.[7] On the basis of these views, addition of ethylene glycol or of ethyl alcohol (which exerts the reverse effect to the addition of inorganic salts on the ratio *R*) might be expected to increase the solubilisation of Yellow AB with sodium deoxycholate or sodium dehydrocholate and also possibly that of azobenzene with potassium dioctyl oxybenzene sulphonate.[8] These would be interesting experiments to make.

(*c*) Freezing Point Depression Effects in Solubilised Systems.

Work on the depression of the freezing point of water by *iso*octane solubilised with sodium oleate has already been carried out by Johnston and McBain who obtained very small depressions [9] and Palit has shown that the freezing point of benzene is not appreciably lowered by water solubilised with electrolytic detergents.[10] Certain additional aspects of the typical behaviour shown are illustrated by the following examples.

(3) Depression of the Freezing Point of Cyclohexanol by Water.—The sample of cyclohexanol used in the following experiments was of " pure " grade, but was not further specially purified. On cooling it commenced to crystallise at 19° c.

To 10 cc. of this cyclohexanol, water was added up to saturation (1·2 cc.). The mixture obtained crystallised on cooling to − 7° c. and remelted on warming to − 5° c. To cyclohexanol (10 cc.) was added a solid fraction (1 g.) of a mixture of sodium C_{10}-C_{18} secondary alkyl sulphates (isolated from the commercial product Teepol of Messrs. Technical Products Ltd.), followed by water (2 cc.). A clear solution resulted. On cooling to − 8·5° c. crystallisation occurred, the crystals remelting on warming to − 5° c.

These results indicate that the effect on the depression of the melting point of cyclohexanol produced by water dissolved directly in the cyclohexanol is markedly greater than the effect produced by additional water solubilised in the cyclohexanol with an amphiphile. This may be understood in terms of Fig. 4, Part I, by the assumption that the water dissolved directly in the cyclohexanol must be considered as being actually included in that part of the micelle structure indicated by $\overline{O}$ while the additional solubilised water is included in $\overline{W}$. Further analogous results recorded below may be similarly interpreted and the rise in melting point on addition of the amphiphile recorded in Tables II and III is also understandable along these lines.

(4) Depression of the Freezing Point of Water by Cyclohexanol.—Some freezing points of water in the presence of cyclohexanol and a mixture of sodium secondary C_{10}-C_{18} alkyl sulphates are recorded in Table I. These results are exactly complementary to those in (3), and show the marked difference in the effect on the freezing point of water of cyclohexanol dissolved directly and of cyclohexanol solubilised in water with an amphiphile.

TABLE I.

Water (cc.)	10	10	10	10	10	10
RSO_4Na (g.)	0	0	1	1	1	1
Cyclohexanol (cc.)	0	1	1	3	4	5
Character of mixture at f.p.		Excess cyclohexanol	Clear sol	Clear sol	Clear sol	Type II system
Freezing point (° c.)	0	−1·0	−1·0	−1·0	−1·0	−1·0

(5) Depression of the Freezing Point of Water with Cyclohexanone.—Some freezing points of water in the presence of cyclehexanone and a mixture of sodium secondary C_{10}-C_{18} alkyl sulphates are recorded in Table II. From these results it is clear that cyclohexanone dissolved directly in water has a much greater effect in depressing its freezing point than has solubilised cyclohexanone.

---

[7] *idem. J. Amer. Chem. Soc.*, 1941, **63**, 674.

[8] Hartley, *Trans. Faraday Soc.*, 1940, **37**, 130.

[9] Johnston and McBain, *Proc. Roy. Soc. A*, 1942, **181**, 123.

[10] cp. Gonick, *J. Colloid Sci.*, 1946, **1**, 394.

TABLE II.

Water (cc.)	10	10	10	10	10	10	10
RSO_4Na (g.) . .	0	0	1	1	1	1	1
Cyclohexanone (cc.) .	0	1	1	2	3	5	7
Character of mixture at f.p.		Excess cyclohexanone	Clear sol	Clear sol	Clear sol	Clear sol	Clear sol
Freezing point (° c.) .	0	−2·5	−1·0	−2·0	−2·5	−2·6	−2·6

(6) Depression of the Freezing Point of Thymol by Solubilised Water.—The thymol used had a freezing point of 49·3° c. Freezing points obtained in the presence of water and a mixture of sodium secondary C_{10}-C_{18} alkyl sulphates are given in Table III.

TABLE III.

Thymol (g.) .	10	10	10	10	10	10	10	10	10
RSO_4Na (g.) .	0	0	1·0	1·0	1·0	1·0	2·0	2·0	2·0
Water (cc.) .	0	0·25	0	0·5	1·0	1·5	1·5	2·0	2·5
Character of mixture at f.p. .		satd. soln. of water in thymol	RSO_4Na mainly in soln.	Clear soln.	Clear soln.	Cloud near f.p.	Clear soln.	Clear soln.	Clouds near f.p.
Freezing point (° c.)	49·3	39·7	48·8	41·7	40·0	39·7	40·3	39·9	39·7

These results and (2) above, describing the solubilisation of thymol with sodium thymate, show that water dissolved directly in thymol exerts a far greater effect in depressing the freezing point than does the water solubilised by the amphiphile. Examples 5 and 6 further show that addition of an amphiphile to a saturated solution of cyclohexanone in water or of water in thymol may even bring about a rise in the freezing point of the saturated liquid.

From the measurements of McBain and Johnston[9] and of Palit,[10] and from the foregoing results it is clear that the additional mutual freezing point depression effects produced by O and $\overline{W}$ on solubilisation by an amphiphile C are, on a per molecule basis, small, but of a symmetrical character. Likewise the depression of the freezing point of both O and $\overline{W}$ by C is per molecule small, except at high dilution.

The characteristic smallness of freezing point depression effects and of other colligative effects is implicit in the phase compositions of partially solubilised systems. Thus Type I systems typically show a solubilised phase, which may contain considerable proportions of both O and $\overline{W}$, in equilibrium with an O phase containing very little C or $\overline{W}$. Since the chemical potentials of all components must be the same in both phases in equilibrium, the chemical potential of O in the solubilised phase, must be the same as that in the excess phase consisting very largely of O. Hence in the solubilised layer the dissolved water and amphiphile must produce only a very small reduction in the various colligative properties of the organic liquid. Similarly it follows from the phase compositions of Type II and Type III systems that the dissolved organic solvent and amphiphile produce only a very small reduction in the chemical potential of the water.

Attempts have been made to deduce information about the degrees of molecular association in solubilised systems from measurement of freezing point depression effects and other colligative properties. It has, however, been emphasised by Hildebrand[11] that simple relationships between mol fractions and colligative properties are approached only when the molecular species present are such as might be expected to obey Raoult's law fairly closely. This condition is very far from realised in the case of solubilised systems, where O and $\overline{W}$ show the very large positive deviations from Raoult's law that are expressed in their immiscibility. It does not, therefore, appear that measurements of freezing point depression or other colligative properties can give much precise information concerning molecular association in solubilised systems.

Summary.

The solubilisation of solids and freezing point depression effects in solubilised systems are discussed, more particularly in relation to the work described in earlier papers of this series on the solubilisation of liquids.

---

[11] Ref. 1, p. 130.

PART VIII.—EFFECT OF CONSTITUTION ON AMPHIPHILIC PROPERTIES.

Received 12*th May*, 1947; *as revised* 5*th June*, 1947.

Certain of the effects of constitution on amphiphilic properties have already been mentioned in earlier papers of this series. In Part IV comparison of Tables III and IX provides information on the effect of conversion of $C_{10}H_{21}.CO_2Na$ to $C_{10}H_{21}.CH_2NH_2$ on the solubilising properties of the molecule. Table VIII compares the solubilising properties of undecane-3 sodium sulphate, undecane-3 sodium carboxylate and undecane-3 ammonium chloride, while Tables VIII and IX provide an example of the comparative behaviour of undecane-3 and -1 ammonium chlorides respectively. Table IV illustrates the effect of gradual substitution of organic ammonium radicals in place of sodium on the solubilising properties of a mixture of secondary C_{10}-C_{18} alkyl sodium sulphates.

The present paper describes certain of the comparative solubilising properties of tetradecane-1 to -7 sodium sulphates, octane-1 sodium sulphate and octane-4 sodium sulphate. The determination of the critical concentrations for micelle formation of the isomeric tetradecane sodium sulphates and of undecane-3 sodium carboxylate and of undecane-3 sodium sulphate by means of Harkins pinacyanol method[1] is described. Results illustrating the effect of the point of attachment of the —OH group to the *n*-alkane chain on the solubilising properties of tetradecanols (-1 to -7) and octanols (-1 to -4) are given.

Experimental.

Materials.

Alkanols.—The tetradecanols and tetradecane sodium sulphates were prepared by methods which were briefly as follows. Tetradecanols -1, -2, -3, -4, and -7 were prepared by the action of the Grignard reagents from *n*-dodecyl, *n*-undecyl, *n*-decyl and *n*-heptyl chlorides on the appropriate oxygenated intermediates. The chlorides and other intermediates used were carefully fractionated at ordinary pressures to ensure their homogeneity of molecular weight. Tetradecanols-6 and -5 were prepared by reduction of the ketones obtained from nonanonic and decanoic acid chlorides and zinc *n*-amyl iodide and zinc *n*-butyl iodides respectively. The physical properties found for the tetradecanols are recorded in Table I. Octanol-1, b.p. 196-197° c., n_D^{20} 1·4300, was redistilled from a commercial sample and octanol-4, b.p. 174-176° c., n_D^{20} 1·4230, was prepared by the action of *n*-butyl magnesium chloride on *n*-butyraldehyde.

---

[1] Corrin, Klevens and Harkins, *J. Chem. Physics*, 1946, **14**, 480

TABLE I.

Tetradecanol . .	7*	2	3†	4	5‡	6	7
Melting point (°c.) .	35-36	32·5-33	28-29·5	26-27	28-29	28-29	41-42
B.p. at *ca.* 14 mm. (°c.) . . .	168	170	157	152	154	156	156
n_D^{45} . . .	1·4368	1·4342	1·4340	1·4329	1·4332	1·4335	1·4330

Alkane Sodium Sulphates.—The alkane sodium sulphates were prepared by sulphation of the corresponding alkanols with chlorsulphonic acid following substantially the methods described by Miles *et al.*[5]

Tetradecane-1 and -2 sodium sulphates were recrystallised both from methyl ethyl ketone containing a little water and from water. Octane-1 sodium sulphate was recrystallised from aqueous acetone, strong cooling being necessary. The remaining alkane sodium sulphates were not obtained crystalline (cf. [5]). The crude sulphates were almost completely freed from inorganic salts by evaporation to dryness, digestion with acetone (with addition of a little water) which dissolved the alkane sodium sulphates leaving the inorganic salts. The acetone was removed *in vacuo* and the residue dissolved in water to an approximately 12 % solution which was repeatedly extracted with its own volume of ether till free from unsulphated organic matter. The extracted solutions were freed from ether by evaporation *in vacuo* and their concentration adjusted with water to about 20 %. To prevent autocatalytic acid hydrolysis, the solutions were maintained just alkaline to phenolphthalein during the above operations.

Analysis of Alkane Sodium Sulphates.

The compositions of the tetradecane sodium sulphate preparations, were determined by the two independent methods below, which gave closely concordant results. Reliable analyses of the octane sodium sulphates could be obtained by the first method only.

Method (1)—Gravimetric.—The samples analysed were first evaporated almost to dryness in a platinum crucible in an air current, the sample being manipulated to coat as large a surface of the crucible as possible. The residue (0·5-1·0 g.) was finally dried completely by evaporating 4 times with 10 cc. portions of acetone in an air current and drying in an oven at 80° c. for 2 hr. Dry weight and total ash as sodium sulphate were determined. Assuming practically complete removal of unsulphated organic matter by the ether extractions, for the low inorganic salt (NaCl, CH_3CO_2Na, Na_2SO_4) contents present, as a close approximation :

$$\text{Weight of } RSO_4Na \text{ in sample} = (\text{Dry wt.} - \text{total ash}) \times \frac{316}{245}.$$

$$\text{Weight of inorganic salt in sample (as } Na_2SO_4) = (\text{Dry weight} - \text{weight of } RSO_4Na).$$

Method (2)—Volumetric.—The following method, which is similar to that recently described by Marron and Schifferli,[6] has been found satisfactory for univalent anionic detergents above C_{10}. About 0·5 g. of sample (or a suitable volume in the case of a solution) was introduced into a 50 cc. burette, expanded at its upper end into a 150 cc. glass bulb having a ground glass stopper, containing 20 cc. of a 6 % cyclohexanammonium chloride solution and 30 cc. of methyl *iso*butyl ketone (M.I.B.K.). The mixture was well shaken, and allowed

* *Organic Syntheses* [2]: m.p. 39-39·5° c., b.p. 170-173° c./20 mm.
† Pickard and Kenyon [3]: m.p. 25° c., b.p. 173° c./25 mm.
‡ Komarewsky and Coley [4]: m.p. 28·5° c.

[2] *Organic Syntheses*, Vol. II, p. 374.

[3] Pickard and Kenyon, *J. Chem. Soc.*, 1913, **103**, 1950.

[4] Komarewsky and Coley, *J. Amer. Chem. Soc.*, 1941, **63**, 3269.

[5] Miles, *et al.*, *Ind. Eng. Chem.*, 1944, **36**, 610.

[6] Marron and Schifferli, *Ind. Eng. Chem.* (*Anal.*), 1946, **18**, 49.

to settle overnight and the volume of the clear M.I.B.K. layer noted. 20 cc. of the M.I.B.K. layer, which contains all the alkyl sulphate as cyclohexylammonium salt, were diluted with 40 cc. acetone and titrated with standard alcoholic KOH using phenolphthalein as indicator. A blank run was made concurrently.

If V is the volume of the M.I.B.K. layer, v is the titration of 20 cc. of the M.I.B.K. layer and b is the blank titration of 20 cc. of blank M.I.B.K. layer, then weight of tetradecane sulphate in sample $= \frac{V}{20} \times \frac{(v - b)}{1000} \times n \times 316$ where n is the normality of the alcoholic KOH.

Comparative results by the two methods are given in Table II. The volumetric figures for the octane sodium sulphates are not reliable, since quantitative extraction of the cyclohexylammonium alkane sulphates is not obtained below about C_{10}.

TABLE II.

Position of $-SO_4Na$.	Gravimetric Analysis.		Volumetric Analysis.
	$C_{14}H_{29}SO_4Na$.	Na_2SO_4.	$C_{14}H_{29}SO_4Na$.
−1	99·5 % (wt./wt.)	(taken nil)	99·3 % (wt./wt.)
−2	99·7 ,,	0·3	100·0 ,,
−3	20·8 (wt./tot. vol.)	0·5	21·1 (wt./tot. vol.)
−4	33·8 ,,	0·4	33·6 ,,
−5	30·2 ,,	0·4	30·6 ,,
−6	22·2 ,,	0·55	22·6 ,,
−7	24·4 ,,	0·55	24·8 ,,
	$C_8H_{17}SO_4Na$.		$C_8H_{17}SO_4Na$.
−1	99·9 ,,	(taken nil)	96·5 ,,
−4	38·0 ,,	0·45	34·2 ,,

Effect of the Point of Attachment of the —SO_4Na Group on the Solubilising Properties of the *n*-alkane Sodium Sulphates.

(*a*) **Tetradecane Series.**—The effect of the point of attachment of the —SO_4Na group on the solubilising properties of the *n*-alkane sodium sulphates accords with the interpretation, in terms of the theory given in the earlier papers of this series, that while the lipophilic solvent affinity of the *n*-alkyl group is substantially the same throughout the series, the hydrophilic solvent affinity of the —SO_4Na group diminishes markedly as its point of attachment to the *n*-alkane chain recedes from terminal. The effect is thus analogous to that found with undecane-1 and -3 ammonium chlorides (cf. Part IV). On account also of the high degree of molecular order in solubilised systems, steric factors would be expected to be strongly influential in producing the above results though it is difficult to envisage the precise mode of their operation.

In its practical result then the effect of stepwise removal of the —SO_4Na group from terminal to medial positions in the alkane chain on the solubilising properties of an alkane sodium sulphate solution of given concentration, is similar to the effect of gradual addition of inorganic salt (cf. Part II). Thus in both cases, considering the effect of addition of cyclohexanol to a mixture of equal volumes of a 20 % solution of tetradecane sodium sulphate and of cyclohexane, there is a reduction in the amount of cyclohexanol required to reach each of the successive stages in the sequence S_1, G, S_2, Type II system, and the range of compositions falling within the Type IV region is diminished.

The effects, both of constitutional change and of addition of sodium sulphate, are shown in Table III. In this and later experiments the cyclohexanol contained 2 % by vol. of water, added to avoid crystallisation at lower room temperatures. The volume of cyclohexanol given under G is that estimated to correspond to the middle of the gel region. Similar comparative results were obtained using 15 % tetradecane sulphate solutions. It will be noted that the change in solubilising properties in passing from the -1 to the -2 sulphate is much less marked than that between other consecutive members of the series.

TABLE III.—VOLUME (CC. OF CYCLOHEXANOL REQUIRED TO GIVE S_1, G, AND S_2 SYSTEMS WHEN ADDED TO MIXTURES OF 10 CC. OF CYCLOHEXANE AND 10 CC. OF 20 % (WT./VOL.) SOLUTIONS OF TETRADECANE SODIUM SULPHATES (-1 TO -7) AT 18-20° C.

Position of —SO_4Na.	-1.			-2.			-3.		
Wt. of Added Sodium Sulphate (g.).	S_1.	G.	S_2.	S_1.	G.	S_2.	S_1.	G.	S_2.
0	2·0-2·3	3·1	4·8-10	2·0 S_1 to G continuous	3·3	4·7-10	1·3-1·5	1·7	2·0-4·0
0·25	1·1-1·2	1·5	2·0-2·7	1·3	1·7	2·0-2·7	0·7-0·9	1·0	1·1-1·4
0·5	0·8-0·9	1·1	1·4-1·8	0·9-1·0	1·1	1·45-1·8	0·5-0·6	0·7	0·8-1·0

Position of —SO_4Na.	-4.			-5.			-6.			-7.		
Wt. of Added Sodium Sulphate (g.).	S_1.	G.	S_2.	S_1.	G.	S_1.	S_1.	G.	S_1.	S_1.	G.	S_1.
0	0·84-1·0	1·1	1·3-2·0	0·55-0·6	0·75	1·05-1·6	0·25-0·30	0·40	0·50-0·70	0·025-0·075	0·175	0·275-0·45
0·25	0·43-0·5	0·6	0·7-0·85	0·15-0·20	0·25	0·35-0·40	0-0·5	0·05	0·15-0·20	Type II systems without cyclohexanol		
0·5	0·30-0·35	0·4	0·47 0·6	—	0·1	0·15-0·25	Type II systems without cyclohexanol			,, ,,		

The solutions of the -1, -2, -6 and -7 sulphates were measured at the minimum temperatures at which they were homogeneous. All solubilisation experiments refer to room temperature, the solubilities of tetradecane -1 and -2 sodium sulphates being greater in the mixtures of aqueous and organic liquids than in either singly.

The solubility relationships of the tetradecane sodium sulphates towards water alone are interesting. The -1 and -2 compounds crystallise readily from water or organic solvents and have a solubility in water of less than 0·5 % at room temperature, but show fairly low Krafft points above which they are readily soluble giving solutions which probably correspond to the S_1 condition. The -3, -4 and -5 compounds at room temperature form clear mobile 20 % solutions, again probably corresponding to the S_1 condition. At 21 % overall concentration at 18° C. the -6 compound forms a mixture of mobile isotropic solution (S_1) and birefringent gel (G) in the approximate proportions of 1 : 3. The sol contains 12·3 % RSO_4Na, the gel being correspondingly enriched. On slight warming, the (S_1 + G) mixture becomes homogeneous, being converted wholly to the isotropic S_1 condition. A 20 % solution of sodium tetradecane-7 sulphate forms an almost clear birefringent gel at 18° c. which on cooling to 0° c. gives a mobile milky emulsion and on warming to about 90° c. gradually melts to a homogeneous isotropic solution S_1. Such anisotropy is of quite common occurrence in gel systems. Thus for example, the gels produced from a 50 % aqueous solution of sodium *n*-butyrate on addition of octanol-1 (cf. Part IV) are strongly birefringent, while both the S_1 and S_2 sols are isotropic.

(*b*) **Octane Series.**—The relationships between the solubilising properties of octane-1 and -4 sodium sulphates are analogous to those between the solubilising properties of tetradecane-1 sodium sulphate and tetradecane-3, -4, -5, -6 or -7 sodium sulphates. This is shown in Tables IV and V. No gels were produced in the experiments recorded in Table IV. Table V provides a further example of the very marked tendency to gelation in systems containing both -1 alkanols and -1 alkane salts (cf. Parts IV and VI).

TABLE IV.—EFFECT OF CYCLOHEXANOL (+ 2 % WATER) ON MIXTURES OF 20 % (WT./VOL.) AQUEOUS OCTANE SODIUM SULPHATE SOLUTIONS (10 CC.) CYCLOHEXANE (10 CC.) AND SODIUM SULPHATE (0·2 g.).

Character of Systems Obtained.	Position of – SO_4Na.	
	1	4
	Volume of Cyclohexanol Added (cc.).	
Type I	7·6	4·2
Sol (S_1 and S_2 continuous) . .	7·6-11·0	4·2-4·4
Type II	11·0	4·4

TABLE V.—EFFECT OF OCTANOL-1 ON MIXTURES OF 20 % (WT./VOL.) AQUEOUS OCTANE SODIUM SULPHATE SOLUTION (10 CC.), CYCLOHEXANE (10 CC.) AND SODIUM SULPHATE (0·2 g.)

Character of Systems Obtained.	Position of – SO_4Na.	
	-1	-4
	Volume of Octanol-1 Added (cc.).	
Type I .	Only thick emulsions and partly gelled systems obtained	2·8
Type IV .		2·8-3·3
Type II .		3·3

Effects of Structure on Critical Concentration for the Formation of Micelles.

The critical concentrations for micelle formation for the sodium tetradecane sulphates and for undecane-3 sodium sulphate and undecane-3 sodium carboxylate have been determined using Harkins pinacyanol method and noting the colour change, blue to violet, visually. The dye concentration employed was 0·04 g./l. It was found necessary to make up a series of solutions of the detergents at different concentrations and allow these to stand in the dark for about ½ hr. in order for the equilibrium colours to be reached. The concentrations corresponding to a stable colour change, blue (micellar) → violet, were noted. It was also found desirable to allow the solutions to equilibrate in the dark, since illumination by bright sunlight quite rapidly produced an irreversible colour change violet → blue in the region of the end point. The results obtained are given in Table VI. Lottermoser and Puschels'[7] conductivity measurements indicate a value of 2·5 × 10^{-3} M. for the critical concentration of tetradecane-1 sodium sulphate at 60° C., and the value of 1·6 × 10^{-3} M. at 40° C.

TABLE VI.

Compound.	Concentrations × 10^{-3} M.	
	Final Blue.	First Violet.
Tetradecane-1 sodium sulphate	1·69	1·62
,, -2 ,, ,,	3·40	3·12
,, -3 ,, ,,	4·62	4·43
,, -4 ,, ,,	5·89	5·63
,, -5 ,, ,,	8·1	7·79
,, -6 ,, ,,	12·7	11·9
,, -7 ,, ,,	16·5	15·1
Undecane-3 sodium sulphate	38·2	39·4
,, -3 ,, carboxylate	76	80

It will be noted that the critical concentrations in the tetradecane sodium sulphate series follow the reverse order to that which might have been expected from a comparison of the properties of the more concentrated solutions and from the comparative solubilisation results.* However, the state of a sodium alkyl sulphate solution at the critical concentration will correspond to the extreme left of Fig. 2, Part I, and it might be expected that the micelles tend strongly to be spherical. Thus in the case of the tetradecane sodium sulphates above, the main factor affecting the critical concentration for micelle formation may therefore well be of the steric type suggested by Hartley.[8] With undecane-3 sodium sulphate and undecane-3 sodium carboxylate, where steric considerations might be expected to be similar in both cases, the critical concentration is higher with the sodium carboxylate which is also indicated as the more hydrophilic compound by the solubilisation results given in Table VIII, Part IV. Similarly the critical concentrations for the alkane-1 sodium carboxylates are higher than those of the corresponding alkane-1 sodium sulphates (cf. Hess, Phillipoff and Keissig[9]).

---

* *Note added in Press :*

Di-*n*-hexyl ethanol and di-*n*-hexyl ethyl sodium sulphate, prepared via di-*n*-hexyl acetic acid, closely resemble the corresponding tetradecane -5 and -6 derivatives in solubilising properties. The 20 % aqueous solution of di-*n*-hexyl ethyl sodium sulphate is a birefringent gel. The critical concentration is (8·30-8·45) × 10^{-3} M. As with solutions of the sodium tetradecane sulphates with near medial sulphate groups, the foam stability of a 0·25 % aqueous solution of di-*n*-hexyl ethyl sodium sulphate is greatly reduced by small amounts of sodium stearate (cf. Winsor, *Nature*, 1946, **157**, 660) ; 1 molecule sodium stearate to 125 molecules di-*n*-hexyl ethyl sodium sulphate shows about the maximum effect.

[7] Lottermoser and Puschel, *Kolloid Z.*, 1933, **63**, 175.

[8] Hartley, *Trans. Faraday Soc.*, 1941, **37**, 130.

[9] Hess, Philipoff, and Keissig, *Kolloid Z.*, 1939, **88**, 50 (Fig. 9).

Effect of Point of Attachment of the —OH Group on the Solubilising Properties of the *n*-Alkanols.

In terms of the theory of solubilisation used in the present series, the effect of the point of attachment of the —OH group to the *n*-alkane chain on the solubilising properties of the alkanols, is analogous to that found with the alkane sodium sulphates. In both cases the hydrophilic solvent affinity of the hydrophilic group diminishes as the group recedes from the end of the hydrocarbon chain. The effect is very marked in both cases.

(*a*) **Tetradecane Series.**—Some examples illustrating these effects in the case of the tetradecanols are given in Tables VII and VIII. For ease of manipulation the tetradecanols were first dissolved as their 33 % (wt./total vol.) solutions in cyclohexane.

TABLE VII.—EFFECT OF ADDITIONS (CC.) OF CYCLOHEXANOL TO MIXTURES OF 10 CC. OF 33·3 % (WT./TOTAL VOL.) SOLUTIONS OF TETRADECANOLS-1 TO -7 IN CYCLOHEXANE WITH 10 CC. OF A 20 % SOLUTION (WT./TOTAL VOL.) OF TETRADECANE-5 SODIUM SULPHATE

Character of System Produced.	Type I.	S_1.	Gel or Mixtures of Sol and Gel.	S_2.	Type II
Position of —OH					
1					initially
2					,,
3			initially	0·20-0·30	>0·30
4	initially		transitions not clearly defined	0·98-1·74	>1·74
5	,,		,, ,,	1·36-2·6	>2·6
6	<0·62	0·62-0·64	0·64-1·34	1·34-3·0	>3·0
7	<0·77	0·77-0·86	0·86-1·42	1·42-3·3	>3·3
10 cc. cyclohexane alone	<0·55	0·55-0·62	0·62-1·06	1·06-1·6	>1·6

TABLE VIII.—EFFECT OF ADDITIONS (CC.) OF 33·3 % SOLUTIONS OF TETRADECANOLS-1 TO -7 ON MIXTURES OF 10 CC. OF CYCLOHEXANE AND 10 CC. OF A 20 % (WT./TOTAL VOL.) SOLUTION OF TETRADECANE-5 SODIUM SULPHATE

Character of System Obtained.	Type I.	S_1 (Water Dispersible).	Gel or Gel and Sol.	S_2 (Cyclohexane Dispersible).	Type II.
Position of —OH					
1	<1	1·0	1·1-2·1	2·1-*ca.* 3	>3
2	<1·5	1·5	1·7-2·75	2·75-*ca.* 3·7	>4
3	<4·2	4·2	4·9->10	—	—
4, 5, 6, 7	all mix.	—	—	—	—

The breakdown of the S_2 sols recorded in Table VIII did not proceed abruptly. An opalescence first appeared and was followed by increased turbidity and ultimately by separation of an aqueous layer.

(*b*) **Octane Series.**—The differences in solubilising properties between octanol-1 and octanol-4 are very marked and in the same sense as in the tetradecanol series. The apparent reduction in the hydrophilic solvent affinity of the *n*-alkanols as the hydroxyl group recedes from terminal, as indicated in Part I, very probably parallels a concurrent reduction in the intramolecular hydrogen bonding capacity of the alkanols. This is also indicated by a marked reduction in boiling point. Thus octanol-1 boils at 196-197° C., octanol-2 at 179·5° C., octanol-3 at 178·5-179·5° C., and octanol-4 at 174-176° C. Infra-red spectra give supporting evidence (cp. Badger and Bauer [10]).

The difference in the hydrophilic solvent affinity of octanol-1 and -4 is shown very clearly by the following examples.

Mixtures of octanol-1 and octanol-4 containing respectively 0, 25, 33·3 and 50 % by vol. of the latter were added gradually to mixtures of 10 cc. of cyclohexane and 10 cc. of a solution containing 24·7 % (wt./total vol.) of a mixture of secondary C_8-C_{12} alkyl sodium sulphates and 5·9 % sodium sulphate. The volumes of the octanol mixtures required at 20° C.:

(a) just to solubilise the cyclohexane, and

(b) just to cause separation of an aqueous layer

were noted and are plotted in Fig. 1. At constant temperature these points are easily and precisely determined visually with good reproducibility. Obviously Fig. 1 contains curves of two characteristics both of which can be used for the analysis of octanol-1 and octanol-4 mixtures. Use was made of this to see what degree of partial separation of octanol-1 and octanol-4 could be obtained on partial solubilisation of a mixture of the two.

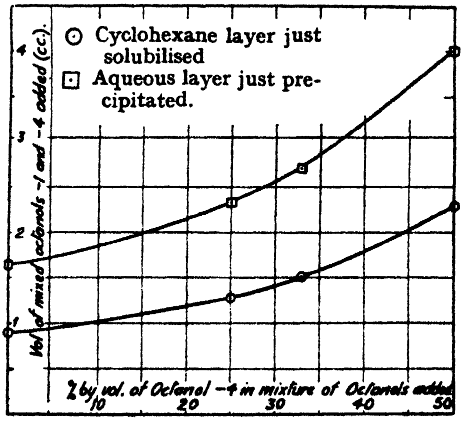

FIG. 1.—Effect of mixtures of octanol-1 and -4 on mixtures of 10 c.c. of sodium secondary C_8—C_{12} alkyl sulphate solution (RSO_4Na 24·7 %; Na_2SO_4 6·4 % (wt/total vol.)) with 10 cc. of cyclohexane.

25 cc. of octanol-1 and 25 cc. of octanol-4 were added to 100 cc. of a 19 % (wt./total vol.) solution of octane-4 sodium sulphate. 26 cc. of octanol remained undissolved and 23 cc. were recovered from the solution by steam distillation. The two mixtures were analysed by placing them on the two curves in Fig. 1.

In the case of the undissolved octanol, to obtain points on the curve it was necessary first to dilute 2 vol. of the undissolved octanol with 1 vol. octanol-1. 1·65 cc. of this mixture was required to solubilise the cyclohexane (corresponding to 37·6 % octanol-4 in the mixture) and 2·90 cc. were needed to precipitate an aqueous phase (corresponding to 36·5 % octanol-4). The percentage of octanol-4 in the undissolved octanol was therefore 37·1 × 3/2 = 55·6 %.

In the case of the octanol recovered from solution, 1·95 cc. were required to solubilise the cyclohexane (corresponding to 44·5 % octanol-4) and 3·52 cc. were required to precipitate an aqueous phase (corresponding to 44·7 % octanol-4). The percentage of octanol-4 in the dissolved octanol was therefore 44·6 %.

The method of analysis of (octanol-1 + octanol-4) mixtures described above is generally applicable, with small modifications to suit individual cases, to the analysis of binary mixtures of any two organic liquids which show differing solubilisation characteristics. The amphiphile solution used must be chosen suitable for the particular case in hand. For high accuracy careful thermostatic control is necessary.

---

[10] Badger and Bauer, *J. Amer. Chem. Soc.*, 1940, **62**, 305.

The writer wishes to thank N.V. de Bataafsche Petroleum Maatschappij and Shell Refining and Marketing Co., for permission to publish Parts V–VIII of this series of papers, and Dr. P. J. Garner, Senior Chemist of these laboratories, for his encouragement during their preparation.

Summary.

(1) The comparative solubilising properties of isomeric *n*-alkyl sulphates accord with the interpretation that while $A_{H_{RSO_4Na}}$ diminishes as the point of attachment of the $-SO_4Na$ group recedes from the end of the hydrocarbon chain, $A_{L_{RSO_4Na}}$ is proportionately much less affected.

(2) In isomeric *n*-alkanols the solvent affinity for amphiphiles diminishes steeply as the point of attachment of the $-OH$ group recedes from the end of the *n*-alkane chain. This effect is paralleled by a reduction in the intramolecular hydrogen bonding capacity of the alkanols.

(3) The critical concentrations of the isomeric *n*-tetradecane sodium sulphates have been determined and are found to increase progressively as the $-SO_4Na$ group recedes from the end of the hydrocarbon chain. The critical concentration of undecane-3 sodium carboxylate is significantly higher than that of undecane-3 sodium sulphate.

(4) A method which may be termed "solubilisation titration" is described which may be adapted to the analysis of any binary mixture of organic liquids having sufficiently different solubilisation characteristics.

Thornton Research Centre,
Chemical Laboratory,
Thornton-le-Moors,
Cheshire.

THE PHOTO-REACTION BETWEEN IODINE AND HYDROGEN PEROXIDE IN AQUEOUS SOLUTION.

BY J. G. BENNETT AND R. O. GRIFFITH

Received 11*th March*, 1947

Though the thermal behaviour of aqueous solutions containing H_2O_2, I_2 and I^- has been much studied over a period of more than 50 yr., there does not appear to have been any work carried out with the aim of testing the possible action of light Actually we find that these systems can be moderately photosensitive, but owing to circumstances to be mentioned later, it is not possible to evaluate in a quantitative manner the effect of light except under somewhat extreme conditions, well outside the range employed by investigators of the thermal reaction. Our work was carried out in 1938-1940; it is in some respects incomplete, but as it is not possible for us to pursue the subject further at present, it appears expedient to publish now the results which have been established.

Experimental.

The thermal reactions which occur in systems containing H_2O_2, I_2 and I^- have been established by the work of Magnanini,[1] Noyes,[2] Brode,[3] Walton,[4] and particularly by Abel [5] and by Liebhafsky and his co-workers.[6] It has been shown that in solutions of *p*H greater than 4, the reactions which occur are:

---

[1] Magnanini, *Gazz. chim. Ital.*, 1891, **21**, 476.
[2] Noyes, *Z. physik. Chem.*, 1895, **18**, 119; 1896, **19**, 599.
[3] Brode, *ibid.*, 1904, **49**, 208.
[4] Walton, *ibid.*, 1904, **47**, 185.

$$H_2O_2 + I^- \rightarrow H_2O + IO^- \quad \text{(1)}$$
$$H_2O_2 + IO^- \rightarrow H_2O + O_2 + I^- \quad \text{(2)}$$
$$H_2O_2 + HIO \rightarrow H_2O + O_2 + H^+ + I^- \quad \text{(2')}$$

and that, after a time, a stationary state is reached in which by the rate of reaction (1) becoming equal to the sum of the rates of reactions (2) and (2′), stationary concentrations of I_2 and I^- are attained. It follows then that

$$k_1[H_2O_2][I^-]_0 = k_2[H_2O_2][IO^-]_0 + k_2'[H_2O_2][HIO]_0$$

and

$$k_1[I^-]_0 = \frac{k_2K_{HIO}K_H[I_2]_0}{[H^+]^2[I^-]_0} + \frac{k_2'K_H[I_2]_0}{[H^+][I^-]_0} \quad . \quad . \quad . \quad (3)$$

where the suffix denotes conditions at the (thermal) stationary state, K_H is the hydrolytic constant of iodine and K_{HIO} the ionisation constant of HIO. The value of $[H^+]$ may be fixed by the use of a suitable buffer; we may then write for the thermal stationary state:

$$k_1[I^-]_0 = K\frac{[I_2]_0}{[I^-]_0} \text{ or } K = k_1\frac{[I^-]_0^2}{[I_2]_0},$$

where K is a constant for a given buffer and given temperature.

On illuminating such a system at the thermal stationary state there is superimposed on these three thermal reactions a photo-reaction involving consumption of iodine with production of iodide. The extent of such photo-reaction we have determined by two methods; in the first the system at the stationary state is illuminated by light of constant intensity and the (initial) rate of disappearance of iodine is measured, while in the second method the illumination is continued until the system attains a photo-stationary state, in which $[\Sigma I_2]$ becomes constant, and the value of this $[\Sigma I_2]$ is determined.

In the first method, at any time after the start of illumination

$$-\frac{d[\Sigma I_2]}{dt} = -k_1[H_2O_2][I^-] + \frac{K[I_2][H_2O_2]}{[I^-]} + P,$$

where P is the rate of the photo-reaction, and the absence of the suffix denotes conditions prevailing under illumination. Substitution of the value of K obtained above in terms of thermal stationary conditions yields

$$-\frac{d[\Sigma I_2]}{dt} = -k_1[H_2O_2]\left\{[I^-] - \frac{[I^-]_0^2}{[I_2]_0}\frac{[I_2]}{[I^-]}\right\} + P.$$

This differential equation cannot be solved explicitly, but sufficiently accurate for the purpose in view is the approximation

$$\frac{[\Sigma I_2]_1 - [\Sigma I_2]_2}{t_2 - t_1} = -k_1[H_2O_2]\left[[I^-]_m - \frac{[I^-]_0^2}{[I_2]_0}\left\{\frac{[I_2]}{[I^-]}\right\}_m\right] + P \quad . \quad (4)$$

where $[\Sigma I_2]_1$ and $[\Sigma I_2]_2$ are the concentrations of iodine at times t_1 and t_2 after illumination, and

$$[I^-]_m = \tfrac{1}{2}\{[I^-]_1 + [I^-]_2\} \text{ and } \left\{\frac{[I_2]}{[I^-]}\right\}_m = \frac{1}{2}\left\{\frac{[I_2]_1}{[I^-]_1} + \frac{[I_2]_2}{[I^-]_2}\right\}.$$

Eqn. (4) may be written in an alternative form. At the thermal stationary state the catalytic decomposition of H_2O_2 proceeds according to the equation

$$\frac{-d[H_2O_2]}{dt} = k_{uni}[H_2O_2],$$

and, moreover, since for every mole of H_2O_2 reduced by reaction (1), one mole of H_2O_2 is oxidised by the compensating reactions (2) and (2′), the rate of disappearance of H_2O_2 at the thermal stationary state is equal to twice the rate of reaction (1). Hence we have

$$\frac{-d[H_2O_2]}{dt} = k_{uni}[H_2O_2] = 2k_1[I^-]_0[H_2O_2]$$

and thus

$$k_1 = \frac{k_{uni}}{2[I^-]_0}.$$

---

[5] Abel, *Z. Elektrochem.*, 1908, **14**, 598; *Z. physik. Chem.*, 1920, **96**, 1; 1928, **136**, 161.

[6] Liebhafsky, *et al.*, *J. Amer. Chem. Soc.*, 1932, **54**, 1792, 3499; 1933, **55**, 3977; 1934, **56**, 2369.

Substituting this relationship in eqn. (4) we obtain

$$P = \frac{[\Sigma I_2]_1 - [\Sigma I_2]_2}{t_2 - t_1} + \tfrac{1}{2}k_{\text{uni}}[H_2O_2]\left[\frac{[I^-]_m}{[I^-]_0} - \frac{[I^-]_0}{[I_2]_0}\left\{\frac{[I_2]}{[I^-]}\right\}_m\right] \quad . \quad (5)$$

Thus the rate P of photo-reaction in the initial stages of illumination may be obtained from a knowledge of k_{uni} and of the values of $[I_2]$ and $[I^-]$ at the thermal stationary state and at two times during illumination. A knowledge of the mean energy absorbed during this time interval leads to an evaluation of the quantum yield.

In the second method illumination is continued until the rate of disappearance of iodine becomes zero, i.e. until a photo-stationary state is attained in which the sum of the rates of the photo-reaction and reactions (2) and (2′) is exactly counterbalanced by the rate of reaction (1). Hence equating $\frac{[\Sigma I_2]_1 - [\Sigma I_2]_2}{t_2 - t_1}$ to zero in eqn. (4) and (5) we obtain

$$P = k_1[H_2O_2]\left\{[I^-]_l - \frac{[I^-]^2_0}{[I_2]_0}\cdot\frac{[I_2]_l}{[I^-]_l}\right\} \quad . \quad . \quad . \quad (6)$$

and the alternative

$$P = \tfrac{1}{2}k_{\text{uni}}[H_2O_2]\left\{\frac{[I^-]_l}{[I^-]_0} - \frac{[I^-]_0}{[I^-]_l}\cdot\frac{[I_2]_l}{[I_2]_0}\right\} \quad . \quad . \quad . \quad (7)$$

where the suffix l denotes conditions at the photo-stationary state.

The experimental conditions which we were forced to employ in the study of the photo-reaction derive from the following considerations. Since in all systems both thermal and photo-reactions occur, the accuracy of any estimate of photo-rate depends in the first instance upon making conditions such that the ratio $\frac{\text{photo-rate}}{\text{thermal rate}}$ is as high as possible. High light intensity and low temperature are obviously favourable factors; accordingly most of the experiments have been carried out at 10° C. Even at this temperature, however, the thermal reactions are much too fast for the employment of any analytical method for determining $[\Sigma I_2]$, and the only feasible method of analysis of the reaction mixture is the relatively insensitive spectrophotometric determination of $[\Sigma I_2]$. Unfortunately this method imposes severe restrictions on the range of conditions which can be investigated. The values of the extinction coefficients of I_2 and I^-_3 for blue light are such that using reaction cells of reasonable length it is not possible, in view of the fact that moderate absorption of the incident light must prevail, to work accurately with solutions in which $[\Sigma I_2]$ is greater than about 5×10^{-4}. As regards the lower limits of $[\Sigma I_2]$ which might be employed, one is restricted by the length of the cell it is possible to employ to obtain reasonable absorption and by the fact that with very low concentrations of iodine accidental impurities decrease the possible accuracy very greatly. For these reasons, and using a 2 cm. cell, the concentration $[\Sigma I_2]$ of iodine has had to be maintained between about $0{\cdot}5 \times 10^{-4}$ to 5×10^{-4}. Further, the choice of this concentration of iodine imposes limits to the range of iodide concentrations it is possible to employ. Since all systems are initially at the steady state, there is a relation between $[I^-]$, $[I_2]$ and $[H^+]$ imposed by the steady state function F (easily derivable from equation (3)) namely:

$$F = A + B[H^+] = \frac{[H^+]^2[I^-]^2}{[I_2]}, \text{ where } A \text{ and } B \text{ are constants.}$$

Since also we have $[\Sigma I_2] = [I_2] + [I^-_3]$; $[\Sigma I^-] = [I^-] + [I^-_3]$; and $K_3 = \frac{[I_2][I^-]}{[I^-_3]}$, there exists a relation between $[\Sigma I_2]$, $[\Sigma I^-]$ and $[H^+]$. Now it is inadvisable to work with $[H^+]$ much greater than 10^{-4}, owing to the fact that under such conditions the reaction

$$H_2O_2 + H^+ + I^- \rightarrow HIO + H_2O \quad . \quad . \quad . \quad (1')$$

becomes of importance and increases the thermal rate of reaction. Furthermore if $[H^+]$ is made too small, then with $[\Sigma I_2]$ kept constant in the above-mentioned range, $[I^-]$ and thus $[\Sigma I^-]$ must increase in order to keep $F = A + B[H^+]$. But an increase in $[I^-]$ results in an increased rate of thermal reaction. Therefore in order to keep the thermal rate as low as possible the photo-experiments have been carried out with $[H^+]$ in the range $1{\cdot}2 \times 10^{-4}$ to $0{\cdot}2 \times 10^{-4}$, and this range together with the range of iodine concentrations used fixes the possible range of concentration of iodide. The latter has been from about 7 × 10^{-4} to about 1·0 × 10^{-2}.

With minor differences the apparatus used was similar to that of Callow, Griffith and McKeown [7] in their study of the photo-reaction between Br_2 and H_2O_2 in aqueous solution. The same light was employed both for insolation and for the photometric estimation of iodine; it was of importance, that, in addition to its being strong, it should be of constant intensity. Two light sources have been used. One was a 1000 w. tungsten filament lamp run off a 110 v. storage battery; a filter consisting of 2 cm. of 5 % $CuCl_2$ solution + 1 cm. of a 2 % solution of quinine acid sulphate + a Schott glass filter B.G. 12 (1 mm.) transmitted light in the wave-length range 420 mμ-480 mμ (mean 450 mμ). The other light source was a quartz-mercury lamp of vacuum type and end-on pattern, burning at 150 v. and 3·0 amp., and run off a 3 kw. D.C. generator, whose dynamo was driven by a synchronous motor and whose generator field was excited from a 72 v. storage battery of large capacity. With the same filter reasonably monochromatic light of wavelength 436 mμ was transmitted. The thermopile-galvanometer system employed was calibrated for light from both sources by means of a uranyl oxalate actinometer, using the data of Leighton and Forbes.[8]

Reaction mixtures were made up from H_2O_2, KI and the buffer constituents. The hydrogen peroxide used throughout was Merck's Perhydrol. Acetic acid and sodium acetate were purified by recrystallisation, and glycollic acid (and its sodium salt) by the method of Pedersen [9] through barium glycollate. Analar samples of KI, phosphoric acid and KH_2PO_4 were used without further purification.

The procedure which was adopted in order to determine from the measured values of incident (I_0) and transmitted (I) light intensities in the photochemical experiments the concentrations of I^- and I_2 was as follows. All reaction mixtures were made up so that initially they contained no iodine but with [iodide] equal to either 0·00078 or 0·0014 M. Subsequently part of the iodide is converted by reaction with H_2O_2 into iodine, so that at any time $[I]_{tot}$ = 0·00078 or 0·0014 $= [\Sigma I^-] + 2[\Sigma I_2]$, where $[\Sigma I^-] = [I^-] + [I^-_3]$ and $[\Sigma I_2] = [I_2] + [I^-_3]$. As a preliminary, therefore, to the photochemical experiments with H_2O_2 present, values of $\log I_0/I$ were determined for a series of solutions in which $[\Sigma I_2]$ and $[\Sigma I^-]$ were known and varied, but in which $[I]_{tot} = 2[\Sigma I_2] + [\Sigma I^-]$ was maintained constant and equal to 0·00078 or 0·0014. These determinations were made in absence of H_2O_2 but in the presence of [HAc] = 0·5, [NaAc] = 0·1, and with both sources of light, with a 2 cm. cell at 10° C. It was verified that variations in the concentrations of the buffer constituents did not affect to any appreciable extent the absorption of light by the iodine. Application of these data to measurements of light absorption in the photochemical experiments thus gave the corresponding values of $[\Sigma I_2]$ and $[\Sigma I^-]$; using for the tri-iodide equilibrium constant K_3 a value of 1·00 × 10^{-3} at 10° C. the corresponding values of $[I_2]$ and $[I^-]$ were then calculated.

The values of k_{ual} required (see eqn. (5) and (7)) were obtained by determining the rate of decomposition of H_2O_2 at the thermal stationary state for many of the reaction mixtures used in the photo-experiments; the remainder were obtained by interpolation of these results. Two methods giving results in good agreement were used; in one the rate of evolution of O_2 was measured with a modified Warburg apparatus, while in the other method the reaction was followed by determining H_2O_2 analytically. We may refrain from publishing these data, as the results in general confirm the expectation of Abel's [5] theory, though the concentrations of the reactants in the systems now studied were widely different from those in previous investigations; the additional data which we have obtained relate only to slight medium effects of the buffer salt and of hydrogen peroxide.

Results and Discussion.

Tables I and II show how the quantum yield varies with energy absorbed and with concentration of H_2O_2. In the tables, E = quanta absorbed per minute, P = molecules I_2 disappearing per minute by photoreaction, and γ = quantum yield (molecules I_2 reacting per quantum absorbed). Concentrations are expressed in M. and k_{ual} in $min.^{-1}$.

---

[7] Callow, Griffith and McKeown, *Trans. Faraday Soc.*, 1939, 35, 412.
[8] Leighton and Forbes, *J. Amer. Chem. Soc.*, 1930, 52, 3139.
[9] Pedersen, *ibid.*, 1931, 53, 23.

By comparing experiments in which $[I^-]$ has much the same value, the data of these tables show, within the somewhat large experimental error, that γ is proportional to $[H_2O_2]$ and inversely proportional to $\sqrt{E}$. The accuracy with which γ can be determined in such experiments is not high, owing to the relatively high velocities of the thermal reactions, to the small concentrations of I_2 and I^-, and to the insensitive photometric method of analysis. It is considered, however, that the γ values should be reliable to the extent of ± 10 %.

TABLE I.

$[I]_{tot} = 7{\cdot}8 \times 10^{-4}$; Temp. = 10°.

λ(mμ).	$[H_2O_2]$.	$[I^-] \times 10^4$.	$P \times 10^{-16}$.	$E \times 10^{-17}$.	γ.	$\gamma\sqrt{E} \times 10^{-8}$.
$[HAc] = 0{\cdot}4$; $[NaAc] = 0{\cdot}4$; $k_{uni} = 1{\cdot}361 \times 10^{-4}$						
436	0·149	3·82	7·29	1·56	0·466	1·84
436	0·149	3·50	3·27	0·279	1·17	1·95
450	0·141	4·17	8·93	2·85	0·313	1·67
450	0·141	3·79	3·92	0·593	0·662	1·61
$[HAc] = 1{\cdot}0$; $[NaAc] = 0{\cdot}2$; $k_{uni} = 3{\cdot}912 \times 10^{-5}$						
450	0·150	1·81	12·60	4·09	0·308	1·97
450	0·150	1·58	5·35	0·80	0·668	1·89
$[H_3PO_4] = 0{\cdot}0102$; $[KH_2PO_4] = 1{\cdot}00$; $k_{uni} = 3{\cdot}57 \times 10^{-5}$						
450	0·160	1·04	6·17	4·29	0·144	0·94
450	0·160	0·97	2·38	0·858	0·277	0·81

TABLE II

$\lambda = 450$ mμ ; $[I]_{tot} = 7{\cdot}8 \times 10^{-4}$; Temp = 10°

$[H_2O_2]$.	$[I^-] \times 10^4$.	$P \times 10^{-16}$.	$E \times 10^{-17}$.	γ.	$\frac{\gamma\sqrt{E}}{[H_2O_2]} \times 10^{-8}$.
$[HAc] = 1{\cdot}5$; $[NaAc] = 0{\cdot}3$, $k_{uni} = 3{\cdot}975 \times 10^{-5}$					
0·307	1·95	11·1	0·768	1·46	1·32
0·193	1·89	18·8	0·392	0·479	1·55
0·079	2·11	6·87	0·394	0·174	1·39
0·306	4·05	9·63	3·08	0·312	0·565
0·193	4·09	6·45	2·90	0·223	0·622
0·079	4·13	2·43	2·99	0·081	0·561
$[HAc] = 0{\cdot}5$; $[NaAc] = 0{\cdot}1$; $k_{uni} = 3{\cdot}835 \times 10^{-5}$					
0·311	1·253	5·60	0·754	0·743	0·656
0·196	1·393	8·89	3·68	0·241	0·747
0·078	1·325	1·62	0·826	0·198	0·727
0·311	2·778	7·25	3·21	0·226	0·408
0·196	2·805	4·89	3·15	0·155	0·444
0·078	2·900	1·83	3·66	0·050	0·389

The effect on the quantum yield of other variables, such as $[\Sigma I_3]$, $[H^+]$, concentrations of buffer constituents and particularly of [I⁻] cannot be obtained in a quantitative manner, since, for the reasons given above, the variation in $[\Sigma I^-]$ has been too small. An indication of the effects of $[I^-]$ and of buffer constituents is, however, given by the data of Table III.

TABLE III

Temp. = 10° ; $[I^-]_{tot} = 7{\cdot}8 \times 10^{-4}$; $\lambda = 450$ mμ ; $[HAc]/[Ac^-] = 5$

$[HAc]$ . .	0·1	0·1	0·1	0·1	0·2	0·2	0·2	0·2	0·5	0.5	0·5
$[Ac^-]$ . .	0·02	0·02	0·02	0·02	0·04	0·04	0·04	0·04	0·1	0·1	0·1
$[I^-] \times 10^4$.	1·06	1·21	1·265	1·66	1·14	1·37	1·515	2·065	1·275	1·97	2·83
$\frac{\gamma\sqrt{E}}{[H_2O_2]} \times 10^{-8}$	2·93	2·38	2·28	1·91	4·81	3·79	3·59	2·67	7·53	5·46	4·13

It will be seen that increase in $[I^-]$ brings about a decrease in $\gamma\sqrt{E}/[H_2O_2]$, while the effect of proportionally increasing the concentration of the buffer constituents (pH = constant) is to increase the value of $\gamma\sqrt{E}/[H_2O_2]$. Comparison of these data with the results of further experiments in which $[HAc]/[Ac^-] = 1$ shows that it is the acetate ion and not the acetic acid molecule which exerts a catalytic effect on the photo-reaction.

In order to proceed further with the analysis of the experimental results it is necessary to make some assumption in respect of the effect of iodide ion on the quantum yield. We shall assume that the mechanism of the photo-reaction is analogous to that of the photochemical H_2O_2—Br_2 reaction,[7] and that the effect of $[I^-]$ on the iodine reaction is the same as that of $[Br^-]$ on the bromine reaction, i.e. we shall assume that $\gamma\sqrt{E}/[H_2O_2]$ is inversely proportional to $\sqrt{[I^-]\{K_2\alpha_1/\alpha_2 + [I^-]\}}$, where α_1 is the molecular extinction coefficient of the halogen and α_2 that of the tri-halide ion. The latter assumption for the iodine reaction is probably not entirely correct, since for the bromine reaction the analogous dependence of rate on concentration of halide ion is an approximation only valid for a particular range of $[Br^-]$, the postulated reaction mechanism leading to a more complicated functional dependence of rate on $[Br^-]$. However, since the range of $[I^-]$ covered in our experiments is small, and since further as shown in Table III retardation by I^- lies in the range between rate $\propto \frac{1}{\sqrt{[I^-]}}$ and rate $\propto \frac{1}{[I^-]}$, a postulated dependence of rate inversely proportional to $\sqrt{[I^-]\{K_2\alpha_1/\alpha_2 + [I^-]\}}$ does not appear to be seriously in error for the experimental conditions we have employed. It is further to be noted that, whatever is the true functional dependence of $\gamma\sqrt{E}/[H_2O_2]$ on $[I^-]$, the main conclusion we derive from this work can hardly be invalidated by the specific assumption we make in respect of dependence of rate on $[I^-]$.

Seven series of experiments have been carried out, five with acetic acid-sodium acetate buffers, one with a glycollic acid-sodium glycollate buffer and one with a H_3PO_4—KH_2PO_4 buffer. In each series the ratio [acid]/[base] of the buffer constituents was maintained constant. Table IV gives the experimental conditions of these runs and summarises the results. In this table r and s signify the method used to determine γ (r = rate method, s = stationary state method), while

$$F = \gamma\sqrt{E}\sqrt{\{K_2\ \alpha_1/\alpha_2 + [I^-]\}[I^-]}/[H_2O_2]$$

K_2 was taken to be 0·0010, and α_1/α_2 determined to be 0·325 for λ = 436 mμ and 0·62 for λ = 450 mμ.

In general the values of F obtained by the "rate" method agree fairly well with those from the "stationary state" method; in presence of concentrations of acetic acid greater than about 0·6 M., however, the values of F given by the photostationary state method are lower than those from the "rate" method, particularly when the ratio [HAc]/[Ac⁻] is high. The cause of this discrepancy was not established, but in only one series of experiments, that with [HAc]/[Ac⁻] = 5, was the effect at all pronounced, and in this series the results of the "rate" experiments were taken as the more reliable.

The main conclusion from these experiments is that there exists in each series an approximately linear relation between F and the concentration of the basic constituent of the buffer. The last column of the table gives the numerical relationships. For acetate buffers the slopes of the plots of F against [Ac⁻] are reasonably constant, with a mean value of $16{\cdot}1 \times 10^5$. The intercepts on the F axis are also in moderate agreement, except that for the second series, and give a mean intercept of $0{\cdot}42 \times 10^5$. The slopes of the plots for glycollate and phosphate are, however, less, viz. $2{\cdot}36 \times 10^5$ and $1{\cdot}30 \times 10^5$ respectively, but the intercepts are much the same as with acetate. These results point strongly to a general base catalysis of some rate-determining step in the photo-reaction, the values of the catalytic coefficients, $16{\cdot}1 \times 10^5$, $2{\cdot}36 \times 10^5$ and $1{\cdot}30 \times 10^5$ being in the order of decreasing basic strength of the bases CH_3COO^-, $CH_2(OH)COO^-$ and $H_2PO_4^-$. Further, the mean intercept from all the series with a value of $0{\cdot}39 \times 10^5$ should be ascribable to the catalytic effect of H_2O as a base, and hence on this basis the catalytic coefficient of water is $0{\cdot}39 \times 10^5/55 = 0{\cdot}007 \times 10^5$. Compared with the catalytic coefficients of CH_3COO^-, $CH_2(OH)COO^-$ and $H_2PO_4^-$ this value is a reasonable one in terms of the Brønsted relation between catalytic coefficient and ionisation constant of the base.

TABLE IV

Temp. = 10°

$[I]_{tot} \times 10^4$.	[Acid]/[Base].	Range of [Base].	Range of $[I^-] \times 10^4$.	Method.	Relation between F and [Base].
$\lambda = 436$ mμ; Acetate buffers					
7·8	1	0·1-0·4	3·4-5·0	*r*, *s*	$F \times 10^{-5} = 0{\cdot}28 + 15{\cdot}7\,[Ac^-]$
14·0	1	0·2-0·6	4·5-5·7	*r*	$F \times 10^{-5} = 0{\cdot}80 + 15{\cdot}9\,[Ac^-]$
14·0	0·5	0·2-0·6	6·8-8·3	*r*, *s*	$F \times 10^{-5} = 0{\cdot}28 + 13{\cdot}2\,[Ac^-]$
$\lambda = 450$ mμ; Acetate buffers					
7·8	1	0·05-0·5	3·3-5·7	*r*, *s*	$F \times 10^{-5} = 0{\cdot}43 + 17{\cdot}8\,[Ac^-]$
7·8	5	0·004-0·4	1·0-2·3	*r*	$F \times 10^{-5} = 0{\cdot}30 + 18{\cdot}0\,[Ac^-]$
$\lambda = 450$ mμ; Glycollate buffers					
7·8	0·61	0·125-0·7	1·2-2·8	*r*, *s*	$F \times 10^{-5} = 0{\cdot}28 + 2{\cdot}36\,[Gly^-]$
$\lambda = 450$ mμ; Phosphate buffers					
7·8	0·01	0·25-1·0	1·0-2·3	*r*, *s*	$F \times 10^{-5} = 0{\cdot}39 + 1{\cdot}30\,[H_2PO_4^-]$

In the absence of a satisfactory determination of the retardation by iodide of the photo-reaction, the nature of the reaction mechanism and of the part-process which is subject to general base catalysis can only be subjects of speculation. It seems not unlikely, however—and none of the results obtained is inconsistent with the view—that the reaction mechanism is analogous to that of the H_2O_2—Br_2 reaction, except for the occurrence of base catalysis. If this view is correct, the probable mechanism is:

$$\begin{array}{ll} \text{Primary processes} \quad . & \left\{\begin{array}{l} I_2 + h\nu \rightarrow I + I \\ I_3^- + h\nu \rightarrow I_2^- + I \end{array}\right. \\ \text{Maintained equilibrium} & I_2^- \rightleftharpoons I^- + I \\ \text{Chain reactions} \quad . \quad . & \left\{\begin{array}{ll} I + H_2O_2 \rightarrow HO_2 + H^+ + I^- & . \quad (a) \\ HO_2 + I_2 \rightarrow O_2 + H^+ + I^- + I & . \quad (b) \end{array}\right. \\ \text{Chain-breaking reactions} & \left\{\begin{array}{l} I + I_2^- \rightarrow I_3^- \\ I_2^- + I_2^- \rightarrow I_3^- + I^- \end{array}\right. \end{array}$$

The analogous mechanism for the bromine reaction has already been discussed; it is now only necessary to add that while for bromine both chain reactions (*a*) and (*b*) are exothermic, in the iodine reaction (*a*) is endothermic to the extent of about 13·6 kcal., while (7) is about thermoneutral. These estimates are arrived at on the basis that the heat evolved in the reaction $H + O_2 \rightarrow HO_2$ is 45 kcal., a value based on the estimates of Bray [10] (50 kcal.), Bodenstein and Schenk [11] (not greater than 44 kcal.) and Griffith, Callow and McKeown [7] (not greater than 50 kcal.). Reaction (*b*) could thus have a low critical increment and be sufficiently fast to maintain a chain.

The novel feature of the photo-reaction between H_2O_2 and I_2 is the catalysis by bases, and it is clear that in terms of the mechanism suggested it must be reaction (*a*) which is catalysed. Instead of (*a*) we must therefore write:

$$I + H_2O_2 + B \rightarrow HB^+ + I^- + HO_2 \quad . \quad . \quad (a')$$

where HB^+ is the conjugate acid of the base B. This appears to be the first instance of general acid or base catalysis to be observed in a photochemical reaction.

Summary.

The photochemical reaction between H_2O_2 and I_2 in aqueous solution has been investigated by spectrophotometric methods at 10° C. using blue light under conditions of low concentrations of iodine and iodide in the presence of buffered solutions of *p*H about 4. The reaction occurring on illumination is

$$h\nu + I_2 + H_2O_2 \rightarrow 2HI + O_2,$$

and, depending on conditions, quantum yields varying between 0·03 and 1·5 were obtained. Quantum yields were found to be proportional to $[H_2O_2]$, inversely proportional to the absorbed energy, to be diminished by increase of $[I^-]$, and increased by increase in the concentration of the basic constituent of the buffer. The catalysis by bases is in the order of basic strength indicating that a rate-determining step in the reaction is subject to general base catalysis. The results have been discussed on the basis of a mechanism involving primary production of iodine atoms, together with the chain reactions

$$(a) \; H_2O_2 + I \rightarrow HO_2 + H^+ + I^-$$

and

$$(b) \; HO_2 + I_2 \rightarrow O_2 + H^+ + I + I,$$

and the chain-breaking reactions $I + I^-_2 \rightarrow I_3^-$ and $I_2^- + I^-_2 \rightarrow I^-_3 + I^-$. It is suggested that it is process (*a*) which is catalysed by bases.

Muspratt Laboratory of Physical and Electrochemistry,
Department of Inorganic and Physical Chemistry,
University of Liverpool.

---

[10] Bray, *J. Amer. Chem. Soc.*, 1938, **60**, 82.

[11] Bodenstein and Schenk, *Z. physik. Chem.*, *B*, 1933, **20**, 420.

THE KINETICS OF OPEN REACTION SYSTEMS.

By K. G. Denbigh, Margaret Hicks and F. M. Page.

Received 13*th March*, 1947.

Reactions are usually studied in the laboratory under the conditions of a more or less isolated system. In nature, on the other hand, the most commonly occurring reaction systems are those through which there is a continuous flow of matter and radiation. The distinction is similar to that between " closed " and " open " systems in thermodynamics.

A reaction process in a closed system is limited by the amount of reactant which is present and equilibrium is attained when the capacity for reaction is exhausted. In the open system, supply and removal of material take place indefinitely and it becomes possible for a stationary state to develop, which however is not a true equilibrium. The living cell, for example, is a permeable reaction chamber, containing all its necessary catalysts, and which operates continuously due to the flow of metabolites. The conditions of reaction in nature are thus in some respects comparable to those of a continuous reaction process in chemical industry.

The concept of the steady state in biology was discussed by Hill [1] and Straub [2] and originated from their observations that organisms are able to maintain themselves in a state which is displaced from true equilibrium. More recently the work of Schoenheimer [3] on the passage through living creatures of tracer elements has confirmed the existence throughout the body of a more or less stationary state of rapid reaction. The steady state is very well exemplified by the constancy of the sugar content of the blood. The concentration of other substances in the blood, such as lactic acid, varies between different levels according to the rate at which the subject performs work. In vital processes we are thus concerned both with steady states and with the kinetics of transitions between such states.

The importance to biology of a theory of such changes has been emphasised by Ancel Keys.[4] A very interesting discussion, in relation to physiology, of the steady state of a single first-order reaction has been given by Burton.[5] A number of special cases have also been discussed by Spiegelman and Reiner [6] and by Hinshelwood.[7] Steady state systems have also been described in connection with economics and the study of biological populations.

In previous papers, I and II, by one of the authors [8] certain aspects of continuous reaction were discussed, with special reference to the chemical industry. Our object below is to attempt a rather more general survey of reactions in " open " systems, in particular: (1) the conditions which make possible a time-independent state, (2) its properties, (3) the nature of transitions between such states, (4) the anomalous behaviour of autocatalytic reactions.

I. Conditions which make Possible a Steady State.—The majority of reaction systems, when operated continuously, gradually approach a stable time-independent state. However, in one or two chemical examples (and many physical ones) this does not occur and instead the system gives rise to a steady oscillation. In view of these exceptions the general conditions must be determined which give rise to time invariance.

---

[1] Hill, *Trans. Faraday Soc.*, 1930, **26**, 667; *Adventures in Biophysics* (Oxford, 1931).

[2] Straub, *Rec. trav. chim.*, 1929, **48**, 59.

[3] Schoenheimer, *The Dynamic State of the Body Constituents* (Harvard, 1942).

[4] Ancel Keys, *Trans. Faraday Soc.*, 1937, **33**, 942.

[5] Burton, *J. Cell Comp. Physiol.*, 1939, **14**, 327.

[6] Spiegelman and Reiner, *J. Gen. Physiol.*, 1945, **28**, 385.

[7] Hinshelwood, *Chemical Kinetics of the Bacterial Cell* (Oxford, 1946).

[8] Denbigh, (I), *Trans. Faraday Soc.*, 1944, **40**, 352; (II), *ibid.* 1947, **43**, 648.

Consider any region of space which is "open" to its environment. We define the steady state as that condition in which it is impossible to detect any macroscopic change inside the system with respect to time. This is not necessarily an equilibrium, as dissipative processes may be taking place within the region at constant speed. The steady state is essentially the time-independent condition of an open system; equilibrium is the time-independent state of a closed one.

A familiar example of the establishment of a steady state is that which is obtained when water flows into an open tank and at the same time passes out through a hole in the bottom. If, at a particular moment, the outflow is either greater or less than the inflow, the level of water in the tank will change until the two flows become equal. The tank is thus a system which has a certain capacity of self-maintenance (between the limits of the top and bottom) and this capacity depends entirely on the fact that the outflow rate is controlled by the hydrostatic head of the water.

This simple example has been mentioned because it illustrates an important principle, namely that the stability, and the capacity for self-adjustment in an open system, is obtained only when there is a mechanism whereby the rate of removal of the various species is dependent on their internal concentrations or potentials. Consider now the behaviour of a system which contains a number of substances or species, A, B, C . . . N, between which there is the possibility of transformation, $A \rightleftharpoons B \rightleftharpoons C \rightleftharpoons \dots N$. It is convenient to use the term flux rate, F, for the rate of each elementary process which can give rise to a change of internal concentration. These elementary processes consist in the first place of the processes of inflow and outflow across the boundaries of the system and, secondly, of the internal processes of transformation between the species. Thus, for a particular member, A, the rate of change, $\mathrm{d}a/\mathrm{d}t$, of its concentration within the system is determined by the algebraic sum of a number of terms, F_{a1}, F_{a2} etc., each of which corresponds either to a process of flow across the boundaries or to a process of change, such as $A \rightarrow B$. The change of the whole system in the course of time can then be expressed by the family of differential equations:

$$\left.\begin{aligned} \frac{\mathrm{d}a}{\mathrm{d}t} &= \sum_i F_{ai}, \\ \frac{\mathrm{d}b}{\mathrm{d}t} &= \sum_i F_{bi}, \text{ etc.} \end{aligned}\right\} \quad . \quad . \quad . \quad . \quad . \quad . \quad (1)$$

where a, b, etc., are the internal concentrations and the summation is carried out in each case over all the rate terms which affect the particular species. The state in which the system becomes time independent is then determined by

$$\frac{\mathrm{d}a}{\mathrm{d}t} = \frac{\mathrm{d}b}{\mathrm{d}t} = \dots \frac{\mathrm{d}n}{\mathrm{d}t} = 0, \quad . \quad . \quad . \quad . \quad . \quad (2)$$

i.e. the steady state is obtained when the flux rates adjust themselves in such a way that

$$\sum_i F_{ai} = \sum_i F_{bi} = \dots \sum_i F_{ni} = 0, \quad . \quad . \quad . \quad . \quad (3)$$

The condition of time independence thus requires that, for each species, the *algebraic sum* of the rates of all those processes which affect its concentration, shall be equal to zero. There is no necessity for the individual rates themselves to be zero. A system for which eqn. (3) is satisfied is a steady-state system and is to be distinguished from an equilibrium system by the fact that it allows of irreversible processes of flow and reaction. An equilibrium state is only obtained if additional restraints are imposed. In particular it requires that the rate of each individual process of transfer across the boundary of the system shall be separately equal to zero. Steady states may thus be regarded as displacements from static equilibrium due to a flow between the system and its environment.

Now the rate, F, of each elementary process of transfer or of internal change is, in general, dependent on the concentrations of some or all of the various species:

$$F_a = F_a(a, b, c \dots n). \quad . \quad . \quad . \quad . \quad . \quad (4)$$

Explicit expressions of this function will be considered in the next section. For the present it is sufficient to mention that only certain special values of the concentrations will allow of the conditions (2) or (3) being satisfied. These are the stationary or steady state concentrations and will be denoted $\bar{a}$, $\bar{b}$, etc.

Although there may exist a set of such concentrations $\bar{a}$, $\bar{b}$, etc., which satisfy the conditions of the steady state, it is possible that the system may not approach this state, due to its instability. Cases of this kind are very rare when we are concerned with chemical reactions, but an example of a permanent oscillation about a steady state will be discussed in section IV. In almost all other chemical examples, the system, if left to itself, will gradually approach the stationary concentrations and then become constant. This is the same behaviour as in the case of the level of water in a tank, as discussed above, and the causes of stability are also very similar. For example, if the concentration of a particular species, J, exceeds its stable level, there will be an increased tendency both for it to be transformed into some other species and for it to flow out of the system. Both of these processes will reduce its concentration towards the stationary level $\bar{j}$. On the other hand, stability would not be obtained if one of the species underwent only zero-order processes, i.e. changes at rates independent of the concentration. In this case there would be no self-regulating mechanism. A very general condition of stability is therefore that the rates of the various elementary processes shall increase or decrease according to whether there is a rise or a fall in the concentration of the species which undergoes the change.

These considerations are necessarily somewhat qualitative. The question whether a steady state exists, or whether the system tends to approach it, can only be answered by solution of the differential equations (1). The properties of such equations have been discussed by Poincaré and Picard [9] and their application to the stability of biological population has been made by Lotka [10] and Volterra.[11]

The general form of the solution is that of a sum of exponential terms. We consider only the special case in which each of the flux rates, F, is a concentration term of the first degree, as in first-order reactions or transport processes. The solution of eqn. (1) is then

$$\left.\begin{aligned} a &= \bar{a} + \mu_{1a}e^{-\lambda_1 t} + \mu_{2a}e^{-\lambda_2 t} + \ldots \mu_{na}e^{-\lambda_n t} \\ b &= \bar{b} + \mu_{1b}e^{-\lambda_1 t} + \mu_{2b}e^{-\lambda_2 t} + \ldots \mu_{nb}e^{-\lambda_n t} \end{aligned}\right\} \quad . \quad . \quad (5)$$

etc., for all n components.

In these equations the λ's are determined only by the parameters of the system, but the μ's depend also on the values of a, b, etc., at $t = 0$.

The solution (5) gives the progress of the system in time from any particular starting point. It is evident that if the λ's are all real and positive the exponential terms become infinitesimally small as $t \to \infty$ and the concentrations a, b, etc., approach asymptotically the values $\bar{a}$, $\bar{b}$, etc. The steady state which is attained is thus a stable one. On the other hand, if any of the λ's is real and negative, the concentrations a, b, etc., *diverge* from the values $\bar{a}$, $\bar{b}$, etc., and the latter thus represent an unstable state *. If all the λ's are imaginary the system oscillates permanently about the point $\bar{a}, \bar{b}, \ldots \bar{n}$. On the other hand, complex λ's give rise to damped oscillations which converge towards the steady state if all the real parts are positive and diverge from it if any one of the real parts is negative.

Apart from the exponents λ, the coefficients μ in eqn. (5) can also give rise to a type of oscillation, if their signs are not all the same. This is, in fact, the origin of the " overshoot " and " false start " phenomena discussed in a later section.

II. Properties of the Steady State in a Chemical System.

(a) Equations of the Steady State.—We begin by setting up the differential equations (1) for chemical reaction in an open system. It is necessary to assume that the system is uniform throughout its spatial extent. In the case of a large reaction vessel this condition is normally satisfied by the provision of efficient mixing. On the other hand, an assumption of this kind is obviously not applicable to a living cell. It may be supposed, however, that the reaction space under consideration is a small element of the whole cell within which is achieved a fair approximation to uniformity.

---

[9] Picard, *Traité d'Analyse* (Paris, 1928), vol. III.

[10] Lotka, *Elements of Physical Biology* (Williams and Wilkins Co., Baltimore, 1925) ; *Proc. Amer. Acad. Sci.*, 1920, **55**, 137.

[11] Volterra, *Théorie Mathématique de la Lutte pour la Vie* (Paris, 1931).

* In regard to the determination of stability, the exponents λ are somewhat analogous to the thermodynamic functions of a static system. It is hoped to discuss this point more completely in a subsequent publication.

The setting up of the equations requires a knowledge of the functions F in eqn. (4). In the case of a chemical reaction the function is simply the normal mass action expression for the reaction velocity. In the case of a transfer process. a very general expression for F, for the species J, is :

$$F_j = r_j(j^\circ - j), \quad . \quad . \quad . \quad . \quad . \quad . \quad (6)$$

where j is the concentration of J within the system, j° is a constant concentration, r_j is a coefficient. This expression is valid for several types of transfer process. In many examples we are concerned with transfer by diffusion and in this case eqn. (6) is based on Fick's law. The quantity j° is the concentration of J in a source external to our system, j is the internal concentration and r_j is a coefficient which depends on the volume of the system, on the area of the boundary across which diffusion takes place and on the nature of J. The rates of other kinds of diffusional transfer, such as the growth or dissolution of solid material within the system itself, are also described by eqn. (6). (2) The equation also describes the case of transfer by mass transport, as in the type of industrial reaction vessel discussed in I and II. Let V be the volume of the reaction space and let u be the volumetric rate of flow, which is taken as constant. Let j° be the concentration of reactant in the inflow and let j be the corresponding concentration in the outflow. The latter is also the concentration within the reaction space, on account of the assumption of uniformity. The net amount of J which accumulates in the system in unit time, due to the flow, is thus $u(j^\circ - j)$ and the rate of increase of concentration is $u(j^\circ - j)/V$. This expression is of the same form as (6), with r identified as u/V. The only distinction from the case of diffusion is that $r(= u/V)$ is the same for all substances which are carried by the mass flow of solution.

Consider a reversible first-order reaction. This may be represented as $\underset{r_a}{\longleftrightarrow} \mathrm{A} \underset{k'}{\overset{k}{\rightleftharpoons}} \mathrm{B} \underset{r_b}{\longleftrightarrow}$, where the first and last arrows denote the flows of A and B across the boundary of the system. Any other substances, such as water, which may participate in this reaction are assumed to be present in great excess. The differential equations (1) now take the particular form :

$$\left.\begin{aligned} \frac{\mathrm{d}a}{\mathrm{d}t} &= r_a(a^\circ - a) - ka + k'b \\ \frac{\mathrm{d}b}{\mathrm{d}t} &= r_b(b^\circ - b) + ka - k'b \end{aligned}\right\} \quad . \quad . \quad . \quad . \quad . \quad (7)$$

At the steady state $\mathrm{d}a/\mathrm{d}t = \mathrm{d}b/\mathrm{d}t = 0$, and hence solving the equations we obtain the steady state concentrations, $\bar{a}$ and $\bar{b}$:

$$\left.\begin{aligned} \bar{a} &= \frac{k'(r_a a^\circ + r_b b^\circ) + r_a r_b a^\circ}{r_a r_b + r_a k' + r_b k} \\ \bar{b} &= \frac{k(r_a a^\circ + r_b b^\circ) + r_a r_b b^\circ}{r_a r_b + r_a k' + r_b k} \end{aligned}\right\} \quad . \quad . \quad . \quad . \quad . \quad (8)$$

The setting-up of the equations for a second-order reaction can be carried out in the same way. The only additional point of interest is that the equation is in the form of a quadratic. It might be expected that two steady states would be possible, corresponding to the two roots. However, it is found that one of these corresponds to a negative concentration, which has no meaning. The same state of affairs is found for an enzyme reaction when for the reaction rate, F, we use either the equation of Michaelis and Menten,[12] or the corresponding equation of Haldane [13] for a reversible enzyme process. In each case only one of the roots of the quadratic is positive, so that there is only the one steady state.

(b) Adaptability of the Steady State.—The steady state concentrations $\bar{a}$ and $\bar{b}$, of eqn. (8), are determined entirely by the parameters r, k, a° and b°, and do not depend on the concentrations a and b which prevailed in any earlier state of the system. Burton[5] refers to this property of the steady state as "equifinality" and suggests that it may be the reason why biological form is relatively unchanging.

---

[12] Michaelis and Menten, *Biochem. Z.*, 1913, 49, 333.

[13] Haldane, *Enzymes* (Longmans, Green and Co., 1930).

There are moreover an infinite number of possible stationary states and a change in any of the parameters will cause the system to move towards a new level. The possibility that physiological stimulus and response may be associated with the change of a velocity constant has been suggested by Gerard.[14] In accordance with this view Burton,[5] and more recently Spiegelman and Reiner[15] have examined the steady state eqn. (8), in relation to the effect of changes in k and k' on the stationary concentrations $\bar{a}$ and $\bar{b}$. It was thus shown that the relationship between $\bar{b}$ and log k, or between $\bar{a}$ and log k', is a sigmoid one, closely similar to the relationship between a physiological response and the logarithm of a stimulus intensity. (It is to be noted, however, that Hecht[16] had shown previously that a second-order reaction at equilibrium gives a similar relation.) The effect on dynamic systems of changes of velocity constants has also been discussed by Hinshelwood[7] in relation to the adaptation of bacteria to the action of drugs. Hinshelwood's use of the term steady state is rather different from that adopted above, in that he uses it as applying to two species whose ratios of concentrations are constant, although the actual values may be changing. In the simplest form of his theory it is supposed that the effect of the drug is to reduce a velocity constant in a sequence of enzyme reactions. Prior to its addition the various enzymes were present in the system in constant proportions. The effect of the drug is to destroy temporarily this constancy. The result is a change of the system in such a way that an increased mass action effect is able to counterbalance the effect of the reduced velocity constant. The overall rate of chemical change and of growth is then the same as before, and the bacteria is said to have become trained to the drug. Hinshelwood's mechanism of adaptation is a particular aspect of the stability of a dynamic system, as discussed above.

Another aspect of adaptability is shown by the way in which the open reaction system responds to changes of its environment, as characterised by changes of the external concentrations—a°, b°, etc. Consider a sequence of reactions involving n species :

$$\mathrm{A} \underset{k_1'}{\overset{k_1}{\rightleftharpoons}} \mathrm{B} \underset{k_2'}{\overset{k_2}{\rightleftharpoons}} \mathrm{C} \rightleftharpoons \ldots \rightleftharpoons \mathrm{N}.$$

The rates of the transfer processes are given by eqn. (6). For simplicity, suppose that each of the reaction rates is first order. Then at the steady state, the differential equations (1) reduce to :

$$r_a(a^\circ - \bar{a}) - k_1\bar{a} + k_1'\bar{b} = 0$$

$$r_b(b^\circ - \bar{b}) + k_1\bar{a} - k_1'\bar{b} - k_2\bar{b} + k_2'\bar{c} = 0, \text{ etc.}$$

Summing these equations over all the n species :

$$\sum_{i=a}^{n} r_i(i^\circ - \bar{i}) = 0, \text{ or } \sum r_i i^\circ = \sum r_i \bar{i}. \quad . \quad . \quad . \quad (9)$$

The expressions for the rates of the chemical changes have thus disappeared in the summation, and the same would clearly have been true whatever the order of the reactions. Suppose now that the external concentration of one of the species, J, changes by an amount δj°. From eqn. (9) we obtain :

$$r_j \delta j^\circ = \sum r_i \delta \bar{i}. \quad . \quad . \quad . \quad . \quad . \quad . \quad (10)$$

For simplicity suppose that all the r's are identical, so that $\delta j^\circ = \Sigma \delta \bar{i}$.

The external change thus causes an equal change of the internal composition, but this internal change is distributed to varying degrees over *all the* n *components*. It tends to be largest for the species, J, which is directly affected,* but for long chains the ratio, $\delta \bar{j}/\delta j^{\circ}$, of the internal and external changes of J, may be shown numerically to be quite small. The system has thus a kind of buffer capacity and its ability to maintain approximate constancy, in the face of changes in the environment, is higher the greater the number of interlinked reactions.

---

[14] Gerard, *Cold Springs Harbor Symposia on Quant. Biology*, 1936, **4**, 194.

[15] Spiegelman and Reiner, *Psychometrika*, 1945, **10**, 27.

[16] Hecht, *J. Gen. Physiol.*, 1924, **7**, 235 ; 1927, **11**, 255.

* There is also a tendency for the disturbance to accumulate at any point of the chain at which a low velocity constant causes a resistance, or at one end of the chain if the velocity constants are all much greater in the one direction than in the other.

(c) **Other Properties of the Steady State.**—In Part I it was shown that the continuous process can sometimes be used to give a higher yield than can be achieved in a static system. This occurs with those types of reaction, for example, nitration, which give an optimum yield at one particular condition of the medium. A flow process, of the type discussed above, can be adjusted so that this optimum condition can be maintained as a steady state.

Enzyme reactions are of the same type and usually require a closely controlled value of the *p*H. In the enzymatic hydrolysis of an ester, acid is released and, in a static system, the *p*H tends to change. In a continuous reaction system, on the other hand, the *p*H can be permanently maintained at its optimum value if the rate of outflow of hydrogen ion is properly adjusted to its rate of production. It seems probable that an important aspect of *flow* in living systems is its ability to give rise to a steady state of optimum efficiency, despite the occurrence of reactions which, in the absence of flow, would tend to reduce the efficiency. Factors of this kind may contribute to the ability of cells to synthesise substances of low stability.

Another important property of a continuous reaction system is that it is an *energy transformer* and may be compared to a continuously operating machine, such as a heat engine. Energy can be withdrawn from the system at a steady rate, at the expense of the inflowing reactant but without change of the system itself.

In chemical industry the energy liberated in a continuous reaction process is normally obtained as heat. Under favourable conditions a part of the chemical energy may be obtained in a more useful form. For example, Teorell [17] and Meyer [18] have shown how the continuous flow, across a membrane, of ions of unequal mobility, can give rise to a steadily maintained E.M.F. Straub [19] and Brooks [20] have suggested that it is the continuous production inside the cell of hydrogen and bicarbonate ions, and their subsequent diffusion across a membrane, which is the cause of bioelectric potentials.

For biological purposes the continuous reaction system is superior to a machine in that it possesses also an internal capacity, due to the buffer action discussed in the previous section. For example, consider a long sequence of reversible reactions involving, say, glucose residues or amino acids, taking place in a cell which is normally at a steady state of continuous reaction. Any sudden change of respiratory activity may cause greatly accelerated addition or withdrawal of material at *either end* of the chain. Large amounts of energy can thus be absorbed or released, but without appreciable change in the concentrations of any of the species. The steady state system may thus be compared to an accumulator which is capable of charge or discharge with little change of voltage.

III. Transitions between Steady States.

(a) **Theory.**—During a process of change in a continuous reaction system the steady state condition (3) does not hold and the progress of the system can only be determined by solution of the basic differential equations. This solution has been carried out by Burton [5] for the case of a single first-order reaction, $A \rightleftharpoons B$. The present authors have extended Burton's treatment of this case and have made some progress towards a rather more general solution. The mathematical work is presented in the Appendix.

Consider a sequence of $n - 1$ first-order reactions involving n species, as discussed in the previous section. The expressions for the time dependence of the concentrations are the eqn. (5), n in number and each of which contains n exponential terms. The exponents λ are always real and positive, indicating eventual approach to a stable state. On the other hand, there is no such limitation on the signs of the coefficients μ. If, for one of the species, J, the signs of the terms in eqn. (5) are alternatively positive and negative when the terms are placed in the order of increasing numerical magnitude of λ, then the particular concentration may pass through $n - 1$ maxima and minima before the steady state is attained.

---

[17] Teorell, *Proc. Nat. Acad. Sci.*, 1935, **21**, 152 ; *J. Gen. Physiol.*, 1937, **21**, 107.
[18] Meyer, *Helv. Chim. Acta.*, 1937, **20**, 634.
[19] Straub, *Trans. Faraday Soc.*, 1930, **26**, 673.
[20] Brooks, *The Permeability of Living Cells* (Berlin, 1941).

The cause of these maxima and minima may be appreciated as follows. The steady state requires that for every species in the system the algebraic sum of its flux rates is equal to zero, as in eqn. (3). However, during a process of change in the system it may occur at a particular moment, that the sum of the flux rates is zero for one of the species J, but not for the others. When this takes place dj/dt becomes momentarily equal to zero and the particular concentration j passes through a maximum or a minimum.

If the various parameters of the system are known, the differential equations can be solved numerically and the concentrations of the species plotted as a function of time. Fig. 1 and 2 show curves of this type for the first-order reactions $A \rightleftharpoons B$ and $A \rightleftharpoons B \rightleftharpoons C$ respectively, using arbitrarily chosen values of the coefficients k and r and of the " external " concentrations, a°, b° and c°. In these curves the ordinates represent the difference between the concentration of one of the species at time t and its concentration at $t = \infty$, i.e. at the steady state. The latter is therefore represented by zero ordinate. The curves as shown are for the final state being at a lower concentration than the initial state. In the reverse case the corresponding curves are obtained by rotation of the figures through 180° about the time axis.

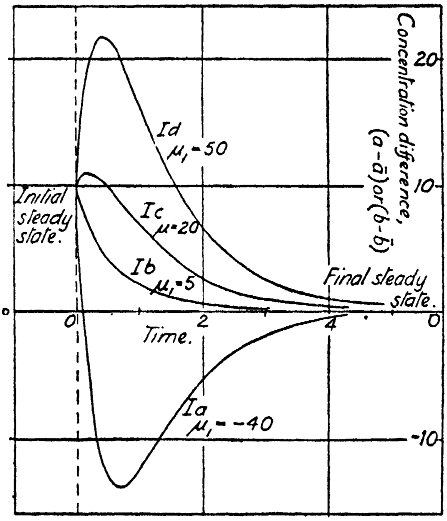

FIG. 1.—Transitions between steady states of the reaction $A \rightleftharpoons B$.
($\lambda_1 = 1$, $\lambda_2 = 3$, μ_1 as shown, $\mu_2 = 10 - \mu_1$.)

The curve (*a*) of Fig. 1 is the type discussed in Burton's paper and is described as showing " overshoot " since, during the course of the transition, the concentration passes beyond its final steady level. The curves (*c*) and (*d*) of Fig. 1 do not emerge from Burton's analysis. They may be described as showing " false start," because the initial change of concentration is in a direction opposite to that of the final steady state.

The same phenomena are evident in the curves of Fig. 2, for the case of two consecutive first-order reactions. In addition there is the possibility that the concentrations of one of the reacting substances may show both a maximum and a minimum in the same transition, as in curves 2*a* and 2*c*.

The curves may apply to any of the reactants, but it is to be noted that all the reactants do not follow similar curves in the same transition. For example, in the case of the single reaction, if one of the reactants follows curves such as 1*a*, 1*c* or 1*d*, which have maxima and minima, then the other reactant follows the simpler type of curve 1*b*. Similarly, in the case of the double reaction, in any transition only one of the reactants is able to follow curves such as 2*a* or 2*c*, which have both a maximum and a minimum.

In accordance with the view that physiological response may be related to the transitions between steady states in living cells, Burton has compared his overshoot curve with a variety of vital phenomena in which the same effect is observed experimentally.* Curves of the types 2*a* and 2*c* seem also to be obtained occasionally in the study of physiological phenomena.† The mechanism of the observed effects may, of course, be quite different from that which is considered here. It is useful to show, however, that the maxima and minima of the theoretical curves may be obtained at periods of time, as reckoned from the initial disturbance, which are of the right order of magnitude for application to physiological response. For example, if we consider the case of the irreversible reaction, A → B, it follows from the treatment given in the Appendix that the time t at which the concentration of B reaches a maximum or minimum, in a transition due to a change in k, is given by :

$$t = \frac{l_n k - l_n(r_b - r_a)}{r_a + k - r_b} . \quad . \quad . \quad . \quad . \quad (11)$$

The value of r, for the case of transport by diffusion, is usually quite small and of the order 10^{-4}. The k's may be large, however. For example, in the study of the reaction $H_2CO_3 \rightarrow CO_2 + H_2O$, Roughton [21] obtained $k = 11{\cdot}1$, at 18° c. Substituting $k = 11{\cdot}1$ and $r_b - r_a = 10^{-4}$ in the above expression, $t = 1{\cdot}05$ sec.

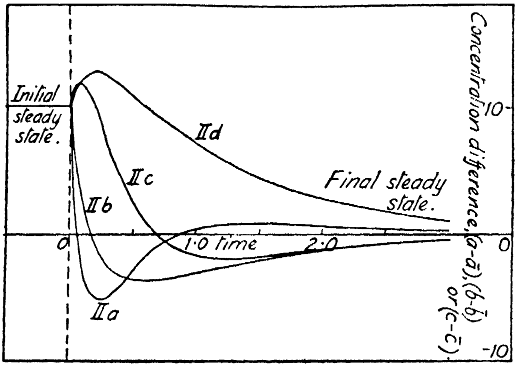

FIG. 2.—Transitions between steady states of the reaction A ⇌ B ⇌ C.

$(\lambda_1 = 1, \lambda_2 = 3, \lambda_3 = 8)$.

II*a* $\mu_1 = 5, \quad \mu_2 = -30, \quad \mu_3 = 35.$
II*b* $\mu_1 = -10, \quad \mu_2 = 10, \quad \mu_3 = 10.$
II*c* $\mu_1 = -10, \quad \mu_2 = 40, \quad \mu_3 = -20.$
II*d* $\mu_1 = 20, \quad \mu_2 = -5, \quad \mu_3 = -5.$

The physical causes of the various types of transition may be understood by considering the change in the flux rates during the course of the transition. The following example refers to a particular case of "false start." Consider a change from one steady state to another in the system A ⇌ B, caused by an increase of a° and a decrease of b°. Before the transition we have

$$r_a(a^\circ - a) = ka - k'b = r_b(b - b^\circ)$$

where $a^\circ > a$ and $b > b^\circ$, corresponding to flow and reaction in the direction $a^\circ \rightarrow a \rightarrow b \rightarrow b^\circ$. The three flux rates of the above equation may be denoted F_1, F_2 and F_3 respectively. As soon as a° is increased and b° is decreased we have $F_1 > F_2$, $F_3 > F_2$. The internal concentration of A rises and that of B falls. However, the reaction rate, F_2, quickly accelerates and at a particular moment it can occur that $F_1 = F_2$, $F_3 > F_2$. Hence $da/dt = 0$ and the concentration of A is at a maximum. The internal concentration of B is still falling and this causes subsequent fall in the concentration of A. If the decrease in b° is considerably greater than the increase in a°, the final steady level, $\bar{a}$ may be appreciably lower than its original one. The curve of the change of concentration of A is then as shown in Fig. 1*d*. The concentration of B has, at the same time, passed along a curve of the type 1*b*.

---

* Curves showing overshoot have also been obtained by Bosworth in an experimental study of "thermal inductance." *Nature*, 1946, **158**, 309.

† See, for example, Lovatt Evans, *Principles of Human Physiology*, 9th ed., p. 919.

[21] Brinkman, Margaria and Roughton, *Phil. Trans.*, 1934, **232**, 65.

During transitions of this kind it is also possible for the overall direction of reaction to reverse itself. This occurs, for example, in the transition between steady states of the system A $\rightleftharpoons$ B which is described by the following parameters: $r_a = 1$, $r_b = 3$, $k = 4$, $k' = 3$, a° (initial) $= 9$, a° (final) $= 6$, b° (initial) $= 0$, b° (final) $= 6$. The direction of reaction is A $\rightarrow$ B in both the initial and final states but for a short period, between $t = 0{\cdot}25$ and $t = 0{\cdot}5$, it is the reverse. This is a mass action effect, not in any way contrary to thermodynamics, and is due to a temporary state of *inward* flow of B, with resultant excess of this component. The main point of interest in this example is that it shows the possibility of anomalous thermal effects during transitions in steady-state systems, e.g. of a normally exothermic process giving rise to a short period of heat absorption.

The various conditions which must be satisfied for the occurrence of false start or overshoot are discussed in the Appendix. For the present it is sufficient to say that transitions due to a change in k and k', in the system A $\rightleftharpoons$ B, do not give rise to false start, but do give overshoot if the transfer coefficients, r_a and r_b of the two species are unequal. (This condition would not be satisfied if the transfer process were by mass flow, for in this case, as shown previously, the coefficients r are the same for all species.) On the other hand, a transition due to simultaneous changes in a° and b° can give rise to either overshoot or false start and without the necessity for inequality in the r's. These phenomena are thus able to occur in an industrial reaction system and may be related to what is known as "hunting."

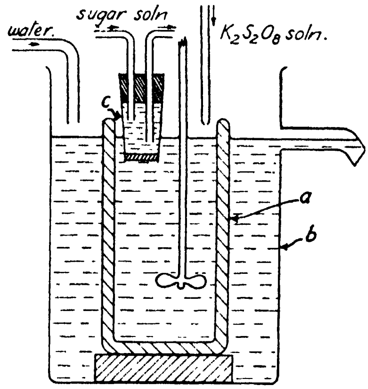

FIG. 3.

(*b*) Experimental Study of some Transitions. — Experimental demonstration of the curves showing overshoot and false start has been obtained in a simple chemical system. The reaction which was used for this purpose was one in which potassium persulphate acts as an oxidising agent:

$$K_2S_2O_8 + H_2O \rightarrow K_2SO_4 + H_2SO_4 + O.$$

The oxygen acceptor which was found most convenient was glucose. The reason for choosing this reaction was twofold: (1) the reaction is catalysed by silver ion, so that change from one steady state to another could be caused by addition or precipitation of the catalyst, (2) the reaction could be followed conveniently by titration of the sulphuric acid which is liberated. The reaction system, when set up continuously, may be represented as follows:

$$\text{Source} \underset{1}{\rightarrow} \text{Reactants} \underset{2}{\rightarrow} \text{Products} \underset{3}{\rightarrow} \text{Sink.}$$

Now for demonstration of overshoot by change of velocity constant it is necessary that the transfer coefficients, r, for processes 1 and 3, shall differ appreciably. It was at first hoped that this might be achieved by choosing reactants and products having a large difference of diffusivity. Finally, however, the reaction system described above was chosen and the difference of the coefficients was obtained by passing the inflow and outflow through porous barriers of greatly different *area*. The reaction vessel consisted of a porous pot, A (Fig. 3), standing in a tank B through which there was a steady flow of water. Supported in the neck of the pot was a grade 3 sintered-glass filter, C, closed at its upper end by a bung which carried inlet and outlet tubes. An M./4 solution of glucose was supplied to C at a constant rate from a Mariotte bottle. A saturated solution of potassium persulphate was simultaneously supplied at a slow constant rate direct into the porous pot from a second Mariotte bottle. The two diffusional autocatalytic reaction A → B, taking place in a system in which there is a steady supply and removal of A and B. The differential equations are

$$\left.\begin{aligned} \frac{da}{dt} &= r_a(a^\circ - a) - kab, \\ \frac{db}{dt} &= r_b(b^\circ - b) + kab \end{aligned}\right\} \qquad . \quad . \quad . \quad . \quad . \quad (16)$$

The steady state concentrations $\bar{a}$ and $\bar{b}$ are obtained by setting the differential coefficients equal to zero. Solving for $\bar{b}$ between these equations we obtain the quadratic :

$$r_b k\bar{b}^2 + \bar{b}(r_a r_b - r_a k a^\circ - r_b k b^\circ) - r_a r_b b^\circ = 0. \quad . \quad . \quad (17a)$$

There are thus two possible values for $\bar{b}$ and to each of these there is a corresponding value of $\bar{a}$, as given by :

$$r_a(a^\circ - \bar{a}) + r_b(b^\circ - \bar{b}) = 0. \quad . \quad . \quad . \quad . \quad (17b)$$

Now the only concentrations which have physical meaning are those which are real and positive. We can therefore apply to the quadratic the familiar condition for real, positive roots. When this is done it is evident that three physically distinct cases can arise :

(1) If b° is greater than zero the equations have a single solution. This solution corresponds to finite values of both $\bar{a}$ and $\bar{b}$. By graphical integration of the original differential equations it can be shown that the system does, in fact, tend to approach these values which therefore correspond to a stable state.

(2) If b° is zero and $ka^\circ < r_b$, the only solution is $\bar{b} = 0$, $\bar{a} = a^\circ$. This corresponds to a stable state of zero reaction.

(3) If b° is zero and $ka^\circ > r_b$, the equations have two solutions. The first is $\bar{b} = 0$, $\bar{a} = a^\circ$, as in case (2) above. The second is $\bar{b} = r_a(ka^\circ - r_b)/kr_b$ and $\bar{a} = r_b/k$.

The physical significance of these three cases is quite clear. The first corresponds to an ordinary steady state, such as has been discussed previously, and which is gradually approached as the system settles down. The second also corresponds to a stable state, but is one of zero reaction. Thus, if any of the autocatalyst B is injected into the system, reaction will occur for a short period but will slowly die out due to B passing out of the system more rapidly than it can be formed. (In the absence of B no reaction can take place.) The third case is the most interesting for it shows the possibility of two alternative steady states of the system. Of these the one corresponding to $\bar{a} = a^\circ$, $\bar{b} = 0$ is unstable. For, inserting $a = a^\circ$ and $b^\circ = 0$ into the original differential equations, we obtain $db/dt = b(ka^\circ - r_b)$; thus, since $ka^\circ > r_b$, the least amount of the substance B in the system will cause db/dt to be positive, so that the concentration of B will increase. The solution corresponding to $\bar{b} = 0$ can thus be maintained only for as long as there is no accidental entry of the substance B into the system.

As a possible application of these results consider the autocatalytic reaction A → B as occurring at the point of branching of a metabolic process :

$$\begin{tikzcd} & & B \arrow[r] & C \\ {} \arrow[r] & A \arrow[ur] \arrow[dr] & & \\ & & P \arrow[r] & Q \end{tikzcd}\;.$$

For the sake of the illustration the process A → Q may be regarded as the normal route and the process A → C as a route deleterious to the organism. The autocatalyst B is thus a poison.

If the conditions of case (3) above are satisfied, the reaction A → B → C may occur either at a finite rate or not at all, according to whether or not the substance B is present in the system or its environment. The least trace of the poison is thus able to cause a switching of the metabolic process to the route A → C and once it has occurred it continues indefinitely. On the other hand, if the conditions of case (2) are satisfied, the entry of a quantity of B causes only momentary reaction in the direction A → C. The system in this state has thus tolerated the poison, a condition only made possible by the state of flow.

V. Discussion.

Our purpose above has been to survey those properties of open reaction systems which are consequences of the simple laws of chemical kinetics. It is for the biologist to consider whether these properties have a bearing on vital phenomena and to indicate the directions in which the simple models which have been discussed need greater elaboration. We conclude by summarising the very general properties of an open reaction system which seem to make it at least a necessary part of the mechanism of living things.

Chemical reaction can take place only for as long as there are differences of chemical potentials. In the closed system the effect of reaction taking place is continually to reduce these potentials and thus to exhaust the system. The output of chemical energy therefore falls practically to zero after a certain period of time. Moreover, the only stationary state which is possible is that which occurs when reaction has ceased, i.e. when the system is " dead." In biological terms the closed system would thus allow neither of development during youth nor of approximate constancy during maturity.

In the open reaction system, on the other hand, the effect of the transfer processes is to replenish continually the reactant material. The time scale of an energy-yielding process is thus extended indefinitely, or at least for as long as the differential transfer across the boundaries is able to take place. The open system also allows of the possibility of a stationary state whilst the output of energy *continues to take place*, due to the balance of the transport processes and of the internal reactions. In this respect it is like a machine and is able to perform energy transformation at the expense of the environment, but without departing from its own internal constancy.

Summarising :

(*a*) The properties of the open reaction system provide the organism with a greatly extended time scale, with the possibilities of development and of approximate constancy during maturity.

(*b*) From a thermodynamic point of view the continuous reaction system is not isolated. It is therefore not prevented from increasing its degree of organisation at the expense of a degradation of substances which flow through it from the environment.[26] As pointed out by Reiner and Spiegelman,[27] the increase of entropy due to the diffusional flow alone may be sufficient to compensate the entropy decrease of synthetic reactions.

(*c*) The open reaction system is able to adapt itself to changes of its surroundings. Quite large changes of environment may take place without the need for more than a small internal readjustment.

(*d*) Although the general behaviour of the open reaction system is that of a maintained steady state, there is also a mechanism which allows of *variety* in its behaviour under stimulus. This variety consists in the complex changes which are able to take place during the transition of the system between one steady level and another.

In conclusion we wish to express our thanks to many of our colleagues at this laboratory for the benefit of stimulating discussion.

Summary.

Earlier studies on continuous reaction have been extended, and a general survey is made of the properties of reactions in " open " systems, with possible application to the living cell. Conditions for the establishment of a steady state are discussed and also some of its characteristic properties. The form of transitions between steady states is evaluated for certain cases and the phenomena of " overshoot " and " false start " have been demonstrated experimentally. The anomalous behaviour of autocatalytic processes is also considered. The paper concludes with a brief discussion on the possible significance of open reaction systems in living creatures.

I. C. I. Ltd.,
Butterwick Research Laboratories,
Welwyn,
Herts.

---

[26] In this connection, see Butler, *Nature*, 1946, 158, 153.

[27] Reiner and Spiegelman, *J. Physic. Chem.*, 1945, 49, 81.

Appendix.

II. Transitions between Steady Stages of a Single First-order Reaction.

The appropriate differential equations are eqn. (7) above. At the steady state these reduce to

$$r_a a^{\circ} - (r_a + k)\bar{a} + k'\bar{b} = 0, \text{ etc.}$$

Putting $\alpha = a - \bar{a}$, $\beta = b - \bar{b}$, the differential equations can be expressed more conveniently as :

$$\left.\begin{aligned} \frac{d\alpha}{dt} &= -(r_a + k)\alpha + k'\beta \\ \frac{d\beta}{dt} &= k\alpha - (r_b + k')\beta \end{aligned}\right\} \quad . \quad . \quad . \quad . \quad . \quad (18)$$

Integrating, we get

$$\left.\begin{aligned} \alpha &= \mu_{1a} e^{-\lambda_1 t} + \mu_{2a} e^{-\lambda_2 t} \\ \beta &= \mu_{1b} e^{-\lambda_1 t} + \mu_{2b} e^{-\lambda_2 t} \end{aligned}\right\} \quad . \quad . \quad . \quad . \quad . \quad (19)$$

where the μ's are constants of integration and λ_1, λ_2 are the roots of

$$\lambda^2 - (r_a + k + r_b + k')\lambda + (r_a r_b + r_b k + r_a k') = 0. \quad . \quad . \quad (20)$$

By inspection, and comparison with the equation

$$\lambda^2 - (r_a + k + r_b + k')\lambda + (r_a + k)(r_b + k') = 0,$$

λ_1 and λ_2 are both real and also

$$0 < \lambda_1 < \left\{\begin{matrix} r_a + k \\ r_b + k' \end{matrix}\right\} < \lambda_2, \quad . \quad . \quad . \quad . \quad (21)$$

where λ_1 is taken as the smaller of the two roots.

The constants of integration, μ, are obtained from (18) and (19) as follows

$$\frac{d\alpha}{dt} = \{-(r_a + k)\mu_{1a} + k'\mu_{1b}\} e^{-\lambda_1 t} + \{-(r_a + k)\mu_{2a} + k'\mu_{2b}\} e^{-\lambda_2 t}$$

$$= -\lambda_1 \mu_{1a} e^{-\lambda_1 t} - \lambda_2 \mu_{2a} e^{-\lambda_2 t}$$

$$\left.\begin{aligned} \therefore\ k'\mu_{1b} &= (r_a + k - \lambda_1)\mu_{1a}, \\ k'\mu_{2b} &= -(\lambda_2 - r_a - k)\mu_{2a} \end{aligned}\right\} \quad . \quad . \quad . \quad . \quad . \quad (22)$$

At $t = 0$ put $\alpha = \alpha_0$ and $\beta = \beta_0$. Hence from (19) :

$$\alpha_0 = \mu_{1a} + \mu_{2a}, \ \beta_0 = \mu_{1b} + \mu_{2b} \quad . \quad . \quad . \quad . \quad . \quad (23)$$

$$\left.\begin{aligned} \therefore\ \mu_{1a} &= \frac{(\lambda_2 - r_a - k)\alpha_0 + k'\beta_0}{\lambda_2 - \lambda_1} \\ \mu_{2a} &= \frac{(r_a + k - \lambda_1)\alpha_0 - k'\beta_0}{\lambda_2 - \lambda_1} \end{aligned}\right\} \quad . \quad . \quad . \quad . \quad (24a)$$

And similarly :

$$\left.\begin{aligned} \mu_{b1} &= \frac{k\alpha_0 + (\lambda_2 - r_b - k')\beta_0}{\lambda_2 - \lambda_1} \\ \mu_{2b} &= \frac{k\alpha_0 + (r_b + k' - \lambda_1)\beta_0}{\lambda_2 - \lambda_1} \end{aligned}\right\} \quad . \quad . \quad . \quad . \quad (24b)$$

It is to be noted that all the bracketed terms of equations (22), (24a) and (24b) are positive.

Condition for Overshoot.

For overshoot in a, α must change sign during the transition, as may be seen from Fig. 1. This means that for large values of t, α has the opposite sign from α_0. When t is large, $e^{-\lambda_2 t}$ is small compared with $e^{-\lambda_1 t}$ (since $\lambda_1 < \lambda_2$), so that the sign of α, after a certain time, is the same as that of μ_{1a}. Therefore there is overshoot in a if μ_{1a} and α_0 have opposite signs, or similarly in b if μ_{1b} and β_0 have opposite signs.

If α_0, β_0 have the same sign, (24a) and (24b) show that μ_{1a} and μ_{1b} have that sign also, and there is no overshoot.

If α_0, β_0 have opposite signs, since (22) shows μ_{1a} and μ_{1b} to have the same sign, there should be overshoot in either a or b. The overshoot is in a if μ_{1a} takes the sign of β_0, i.e., if

$$(\lambda_2 - r_a - k)\,|\,\alpha_0\,| < k'\,|\,\beta_0\,|. \qquad (25a)$$

The overshoot is in b if

$$(\lambda_2 - r_a - k)\,|\,\alpha_0\,| > k'\,|\,\beta_0\,|. \qquad (25b)$$

There is no overshoot if

$$(\lambda_2 - r_a - k)\,|\,\alpha_0\,| = k'\,|\,\beta_0\,| \qquad (25c)$$

as this causes μ_{1a} and μ_{1b} to disappear, leaving α and β as single exponential terms.

Condition for False Start.

A false start in the concentration of A means that initially the absolute value, $|\,\alpha_0\,|$, increases—i.e. α_0 and $\left(\frac{d\alpha}{dt}\right)_0$ have the same sign (see Fig. 1). Then $-(r_a + k)\alpha_0 + k'\beta_0$ has the same sign as α_0. This can only occur if α_0 and β_0 have the same sign and

$$\frac{\alpha_0}{\beta_0} < \frac{k'}{r_a + k}. \qquad (26a)$$

Similarly, there is false start in b if

$$\frac{\alpha_0}{\beta_0} > \frac{r_b + k'}{k}. \qquad (26b)$$

These two conditions are incompatible, so that there can never be false starts in both a and b.

If

$$\frac{r_b + k'}{k} > \frac{\alpha_0}{\beta_0} > \frac{k'}{r_a + k} \qquad (26c)$$

neither a nor b shows false start.

Transition from One Steady State to Another.

Change in k's.—Suppose k, k', were initially K, K'. Then using eqn. (8), α_0 is the value of $\bar{a}$ obtained using K, K', minus the value obtained using the final values k, k' and similarly for β_0. It is found that $r_a\alpha_0 = -r_b\beta_0$.

Thus α_0, β_0 have opposite signs and there is overshoot in a or b unless eqn. (25c) holds.

If $r_a\alpha_0 = -r_b\beta_0$, $r_a\,|\,\alpha_0\,| = r_b\,|\,\beta_0\,|$ and

$$(\lambda_2 - r_a - k)\,|\,\alpha_0\,| - k'\,|\,\beta_0\,| = \lambda_2\,|\,\alpha_0\,| - (r_b + k')\,|\,\beta_0\,| - k\,|\,\alpha_0\,|$$

$$\therefore\ (\lambda_2 - r_a - k)\,|\,\alpha_0\,| - k'\,|\,\beta_0\,| \overset{<}{\underset{>}{=}} (\lambda_2 - r_b - k')\,|\,\beta_0\,| - k\,|\,\alpha_0\,| \qquad (27)$$

according as $|\,\alpha_0\,| \overset{<}{\underset{>}{=}} |\,\beta_0\,|$, i.e. $r_a \overset{>}{\underset{<}{=}} r_b$.

From (20), $\lambda_2^2 - \lambda_2(r_a + k + r_b + k') + (r_a + k)(r_b + k') = kk'$,

$\therefore\ (\lambda_2 - r_a - k) : k' = k : (\lambda_2 - r_b - k')$, so that $\{(\lambda_2 - r_a - k)\,|\,\alpha_0\,| - k'\,|\,\beta_0\,|\}$ is a negative multiple of $\{(\lambda_2 - r_b - k')\,|\,\beta_0\,| - k\,|\,\alpha_0\,|\}$. The two quantities of inequality (27) are therefore of opposite sign, so that o lies between them. Therefore $(\lambda_2 - r_a - k)\,|\,\alpha_0\,| - k'\,|\,\beta_0\,| \overset{<}{\underset{>}{=}} 0$ according as $r_a \overset{>}{\underset{<}{=}} r_b$, i.e., from conditions (25a, b, c), there is overshoot in a, no overshoot, or overshoot in b according as $r_a > r_b$, $r_a = r_b$, $r_a < r_b$.

Thus the existence of overshoot is independent of the type of the changes in k's.

Changes in r's, or External Concentrations.

By similar calculations, it is found that if r_a, r_b are changed simultaneously in opposite directions, *or* if $a°$, $b°$ are changed in the same direction, a and b both show simple curves (type 1b).

Like changes in r_a, r_b, *or* unlike changes in $a°$, $b°$ give: (i) false start in a if r_a (or $a°$) changes considerably less than r_b (or $b°$); (ii) false start in b if r_b (or $b°$) changes considerably less than r_a (or $a°$); (iii) overshoot in either a or b if the two changes are more nearly of the same absolute magnitude. Roughly speaking, the overshoot is in a if r_a (or $a°$) changes rather less than r_b (or $b°$), but the boundary point is defined by a fairly complicated relation which includes the parameters which do not change as well as those which do.

II. The Transitions of Two Successive First-Order Reactions.

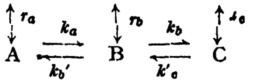

$$\frac{\mathrm{d}a}{\mathrm{d}t} = r_a a^\circ - (r_a + k_a)a + k_b'b$$

$$\frac{\mathrm{d}b}{\mathrm{d}t} = r_b b^\circ + k_a a - (r_b + k_b + k_b')b + k_c'c$$

$$\frac{\mathrm{d}c}{\mathrm{d}t} = r_c c^\circ + k_b b - (r_c + k_c')c.$$

As in the single reaction, these give

$$\bar{a} = \frac{\{(r_b + k_b + k_b')(r_c + k_c') - k_b k_c'\}r_a a^\circ + k_b'(r_c + k_c')r_b b^\circ + k_b' k_c' r_c c^\circ}{(r_a + k_a)(r_b + k_b + k_b')(r_c + k_c') - k_b k_c'(r_a + k_a) - k_a k_b'(r_c + k_c')},$$

$$\bar{b} = \frac{k_a(r_c + k_c')r_a a^\circ + (r_a + k_a)(r_c + k_c')r_b b^\circ + k_c'(r_a + k_a)r_c c^\circ}{(r_a + k_a)(r_b+k_b+k_b')(r_c+k_c') - k_b k_c'(r_a+k_a) - k_a k_b'(r_c+k_c')},$$

$$\bar{c} = \frac{k_a k_b r_a a^\circ + k_b(r_a + k_a)r_b b^\circ + \{(r_a + k_a)(r_b + k_b + k_b') - k_a k_b'\}r_c c^\circ}{(r_a + k_a)(r_b+k_b + k_b')(r_c + k_c') - k_b k_c'(r_a + k_a) - k_a k_b'(r_c + k_c')}.$$

Also, putting $a = \bar{a} + \alpha$, $b = \bar{b} + \beta$, $c = c + \gamma$ as before, differential equations in α, β, γ are obtained which may be integrated to give :

$$\alpha = \mu_{1a}\mathrm{e}^{-\lambda_1 t} + \mu_{2a}\mathrm{e}^{-\lambda_2 t} + \mu_{3a}\mathrm{e}^{-\lambda_3 t}$$

and similar expressions for β and γ, where λ_1, λ_2, λ_3 are the roots of the equation :

$$\begin{aligned}\lambda^3 - (r_a+k_a+r_b+k_b+k_b'+r_c+k_c')\lambda^2 + \{(r_b + k_b+k_b')(r_c+k_c') + (r_c+k_c')(r_a+k_a)\\ +(r_a+k_a)(r_b+k_b+k_b') - k_a k_b' - k_b k_c'\}\lambda - \{(r_a+k_a)(r_b+k_b+k_b')(r_c+k_c')\\ - k_a k_b'(r_c+k_c') - k_b k_c'(r_a+k_a)\} = 0.\end{aligned}$$

It may be shown that this equation has three positive real roots, and if $\lambda_1 < \lambda_2 < \lambda_3$,

$$0 < \lambda_1 < \left\{\begin{matrix} r_a + k_a \\ r_b + k_b + k_b' \\ r_c + k_c' \end{matrix}\right\} < \lambda_3$$

and λ_2 lies between $(r_a + k_a)$ and $(r_c + k_c')$.

Each of α, β, γ is the sum of three negative exponential terms. Each may show a maximum and a minimum, or one of these only, or neither, according to the magnitudes and signs of the coefficients (the μ's). A necessary, but not sufficient, condition for a maximum or minimum is a change of sign in adjacent coefficients (e.g. there may be maximum *and* minimum in a if μ_{1a} is − ve, μ_{2a} + ve, μ_{3a} − ve, whereas only a minimum may occur if μ_{1a} is − ve, μ_{2a} + ve, μ_{3a} + ve, and there can only be a simple curve if μ_{1a}, μ_{2a}, μ_{3a} have the same sign). This may be seen by considering the comparative sizes of $\mathrm{e}^{-\lambda_1 t}$, $\mathrm{e}^{-\lambda_2 t}$, $\mathrm{e}^{-\lambda_3 t}$ as t increases, or may be proved (rather arduously) by finding conditions for the sums of the exponentials to be zero.

It is found that μ_{1a}, μ_{1b}, μ_{1c} always have the same sign, μ_{2a}, μ_{2c} always have opposite signs, while μ_{3a} is like μ_{3c} and unlike μ_{3b}. This means that the signs of the μ's always follow one of three definite patterns.

		μ_1	μ_2	μ_3			
I.	α	+	−	+	2 changes of sign	or	0 change of sign
	β	+	±	−	1 change ,,		1 change ,,
	γ	+	+	+	0 change ,,		2 changes ,,
II.	α	+	±	−	1 change ,,		
	β	+	+	+	0 change ,,		
	γ	+	∓	−	1 change ,,		
III.	α	+	±	−	1 change of sign		
	β	+	−	+	2 changes ,,		
	γ	+	∓	−	1 change ,,		

(These patterns are held to be the same as those where + and − are interchanged throughout.)

Thus only one at the most of α, β, γ can show maximum and minimum, which, as has been stated, is due to two changes of sign of the corresponding μ's.

THE ABSORPTION OF ORGANIC VAPOURS BY THIN FILMS OF POLYSTYRENE.

By E. C. Baughan.

Received 28th March, 1947. As amended 18th June, 1947.

This paper presents measurements of the vapour-pressure equilibrium of organic vapours absorbed by thin films of polystyrene. The technique consisted of weighing thin films of the polymer, on suitable supports, at measured vapour pressures of the low molecular component; these were obtained by solution of the non-volatile compound butyl sebacate. The apparatus could not give temperature coefficients sufficiently precisely; results are therefore confined to free-energy data at one temperature (20° c.), but cover several vapours ranging from those of liquids (benzene, toluene, *m*-xylene, CCl_4, butyl acetate, dioxane, diethylketone) in which polystyrene dissolves (at 20°) to those of liquids (cyclohexane, propyl ether, nitromethane) in which it will only swell. The experiments were done in the Physical-Chemistry Institute of Copenhagen University during 1937-38; at that time similar data were available for the systems nitrocellulose-acetone [2] and nitrocellulose-cyclohexanone [3] also at one temperature. Such systems are, from their polar nature, difficult to interpret; this earlier work showed, however, that hysteresis could be made negligible by using thin films, and this conclusion is verified in this present paper. Since that date, comprehensive data on free energy, heat content, and entropy over wide concentration ranges have been published only for the single system rubber-benzene.[4] The theory of such solutions, however, has been greatly advanced in terms of the entropy effects possible for a flexible molecule occupying points in a fixed lattice. In this paper, therefore, the experimental results are first presented, and then discussed in the light of these modern theories.

Experimental.

Apparatus.—A bulb X, placed in a thermostat at 20°, contained solvent plus butyl sebacate. This could be connected by mercury cut-offs to an electromagnetic balance, a manometer system, and a mercury pump. In the manometer system there were two instruments (*a*) a simple U-tube mercury manometer for higher pressures, (*b*) a Bodenstein spoon gauge coupled to a butyl-sebacate manometer for the air side; this was used for lower pressures. For both instruments the vacuum side was exhausted anew before each run.

Fig. 1 shows the balance. The knife-edges were of hard steel, the beam A of aluminium, C is a piece of soft iron screwed on to the beam; underneath it, clamped to the glass tube, was an electromagnet. Current through this at balance was read on a galvanometer. At the other end of the beam was a hook H. Below this dipped into the thermostat a long side tube in which the polystyrene films were hung from H by a platinum wire. The balance also was fitted with an adjustable screw lock-nut rough compensator (B, D), and a brass plate with stops (E) to restrict swing. The knife-edge support was fixed by an expanding collar in the glass side-arm under F; this was then sealed off and fixed rigidly by plaster (G) as a support for the whole balance-case. Access to the balance

---

[1] A preliminary summary of this work has been presented to the Faraday Society's Discussion on Swelling and Shrinking in 1946 (*Trans. Faraday Soc.*, 1946, **42B**, 49) as a comment on a paper by Gee (*ibid.*, p. 33). The discussion on Gee's paper (*ibid.*, pp. 44-50) is relevant to several points in this present paper.

[2] Schulz, *Naturwiss.*, 1937, **22**, 346.

[3] Boissonnas and Meyer, *Helv. Chim. Acta*, 1937, **20**, 783.

[4] Gee and Treloar, *Trans. Faraday Soc.*, 1942, **38**, 147; Gee and Orr, *ibid.*, 1946, **42**, 507.

is possible through the grinds K, I; to get at K the thermostat must be moved, so a special small tank was necessary.

The point of balance was obtained as the limit between those currents for which the beam came to rest at the upper stop and those for which it came to rest at the lower stop; the beam could easily be made to swing by gently tapping the balance case. The calibration was done by hanging a small pan and weights from the hook H; some 30-40 points were taken for each calibration. It was found that the square of the balance current was a linear function of the weights added; the slope of this graph being constant to within 1 % for successive calibrations of which four were done at roughly two-month intervals. The lock-nuts D were always so adjusted that zero of a run corresponded to about one-third of the full current; under these circumstances no trouble could be detected from *magnetic* hysteresis, which would, of course, show itself as a shifted zero for each fresh *up* point, and for each fresh solvent. Magnetic weighing had not, as far as I am aware, been used before for this type of work. I am indebted to one of the Referees of this paper for pointing out that Blewitt [5] has since used magnetic technique for other high-vacuum work. By using light balances of quartz rod, he was able to obtain higher accuracy (± 0·05 mg. or so) at the cost of very greatly increased difficulty in determining the point of balance. He also found, for a balance where the force is applied by an electromagnet acting on an iron rod, a linearity between weight and *square* of current applied in agreement with the present results.

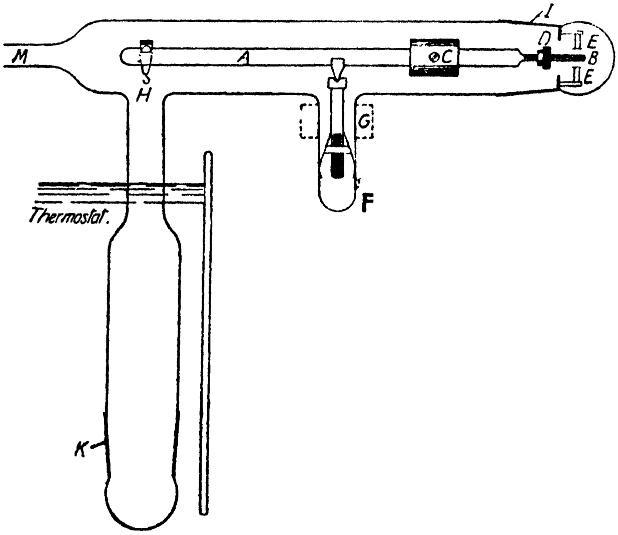

FIG. 1.

The whole apparatus contains no taps on the vapour side and only three grinds. One, connecting the solvent bulb X, was not greased but protected by a mercury seal. The other two (K, I) need greasing, and considerable trouble was experienced. Phosphoric acid greases and mixed phosphoric-boric greases [6] stuck very badly. Finally the outside halves of the grinds were greased with ordinary tap grease, and the inside halves with a 25 % w/w lithium chloride in glycerol previously fractionated *in vacuo*. This was very satisfactory as a grease, and could be completely softened in a few hours by letting water vapour into the balance-case. It is extremely hygroscopic and so was kept over P_2O_5, and all air entering the apparatus was also dried.

Polystyrene.

Kahlbaum *reinst* styrene was polymerised under various conditions, and fractionated by adding alcohol to benzene solutions so as to split the liquid into two phases of nearly equal volume. Films I and III were then made on the outside of glass cylinders (surface about 30 cm.^{2}) by rotating them slowly in a trough containing the polystyrene dissolved in benzene. It was found that 3 % w/v, 2-5 R.P.M. were about the best concentration and rotation speed, and that it was essential to blow warm dry air over the still rotating film for an hour or so to avoid blisters on evacuation.

---

[5] *Rev. Sci. Inst.*, 1939, **10**, 231.

[6] Boughton, *J. Amer. Chem. Soc.*, 1930, **52**, 2813.

In making Film II this method failed owing to the lower viscosity of the solutions ; a more or less even film was obtained by allowing a dilute benzene solution to evaporate in a set of little brass trays fixed round a central rod.

Molecular weights for these fractions were estimated by measuring their specific viscosity in benzene solutions at several concentrations and extrapolating to infinite dilution (Staudinger's rule). These measurements agreed well, in general functional form, with those of Staudinger and Heuer[7] from whose comparison with osmotic data one can estimate the molecular weight of the films used to be : Film I, 500,000 ; Film II, 20,000 ; Film III, 200,000.

Solvents.

All solvents were commercial *reinst* or *zur analyse* specimens except *n*-dipropyl ether, made from the alcohol using benzene-sulphonic acid as catalyst, and *n*-octane and toluene, which were synthetic samples prepared some years previously in the Institute (a commercial A.R. specimen of toluene gave irregular and irreproducible results). They were washed, dried with appropriate agents (P_2O_5, Na, $CaCl_2$, anhydrous K_2CO_3), fractionated, and middle-fractions boiling over less than half a degree collected ; the boiling points and freezing points (benzene, cyclohexane, dioxane) agreed well with the values in the literature.

One minor point is worth mentioning here : an experiment was started using ethylene dibromide. After a few hours it was observed that a fine white deposit, showing marked Liesegang rings, had formed up the glass walls above the mercury in the cut-offs. This product darkened in the light but could be completely removed by evacuation and warming. This reaction does not seem to have been observed before. No further attempts were made, therefore, to measure the adsorption isotherm with this solvent.

Procedure.—The film was hung from hook H, the thermostat lifted into position and the apparatus evacuated by a water-pump until the vapour pressure of the solvent was almost reached. The bulb cut-off was then shut and the rest thoroughly evacuated with the mercury pump. The balance was then shut off, and the bulb cut-off opened ; solvent then distils into a CO_2 trap and the residual air coming through can be seen in a Geissler tube. Evacuation was continued for 5 min. after this discharge had once more disappeared.

Experiments were then begun : by evacuating the bulb alone the butyl sebacate can be made more concentrated, and so points for diminishing vapour pressure obtained (*down* points). For *up* points the film was re-exhausted to its original weight ; this usually required its removal and evacuation at 80-90°. By adding *more* solvent to the bulb and repeating the procedure a second up-point can be obtained. That this procedure does not affect the film was checked at the end with Film I (used for 11 solvents in all) by (*a*) repeating a few points on the benzene isotherm—the first done, (*b*) cutting it off with a razor-blade, and checking that its specific viscosity had not changed. Before each new solvent was used the weight of a film was checked to 0·1 mg. on an ordinary balance.

In this technique the ascertainable errors of measurement are in the manometer readings and in the weighings. The first are only serious when the vapour pressure is near saturation ; the Hg manometer was read to 0·1 mm., and the butyl sebacate to 0·5 mm. The standard weighing error was estimated, from internal consistency of calibrations, to be 0·9 mg. The thermostat was set by a thermometer calibrated at the Physikalische Reichsanstalt in Berlin.

Results.

Table I gives the properties of the three films used and Table II shows, for the solvents, their vapour pressure as measured at 20°, their density (from Beilstein) at 20°, their boiling point, and the value adopted for their "energy density" at 20° (calculated as explained later). The vapour pressure for ethylbenzene at 20° was taken from the data of Guttman, Westrum, and

---

[7] *Z. physik. Chem. A*, 1934, **171**, 129.

Pitzer.[8] Measurements were not actually made with ethylbenzene ; the data are quoted only as giving its " energy density ".

TABLE I.

	Support.	Weight of Film. mg.	Approx. M. Wt.	Mean Thickness. mm.
Film I . .	Glass cylinder	61·2	500,000	0·02
Film II . .	Brass trays	75·7	20,000	uneven
Film III . .	Glass cylinder	109·9	200,000	0·04

TABLE II.

PROPERTIES OF LOW-MOLECULAR COMPOUNDS USED.

Compound.	Vapour Pressure at 20° (cm. Hg).	Density at 20°.	Boiling-point °C.	" Energy Density."
Benzene	7·46	0·878	80·1	9·28
Toluene	2·18	0·866	110·8	8·98
m-Xylene . . .	0·63	0·865	138·8	8·90
CCl_4	9·12	1·595	76·8	8·69
Di *n*-propyl ether . .	5·15	0·736	91·0	7·50
n-Butyl acetate . .	0·84	0·882	126·5	8·60
Dioxane	2·77	1·033	101·5	10·10
Diethylketone . . .	2·75	0·814	102·7	9·02
Cyclohexane . . .	7·75	0·779	81·4	8·26
Nitromethane . . .	2·78	1·139	101·0	12·80
n-Octane . . .	1·09	0·704	—	—
(Ethyl benzene . .	0·718	0·867	136·2	8·83

The results are given in Table III, showing the weight of solvent (column 2) taken up by the films at measured vapour pressures (column 1) of the low-molecular compound. Column 3 shows the volume-fraction V_1 of solvent in the film, calculated on the assumption of additivity of volume, and column 4 gives the value of V_1 calculated from Huggins' equation (see later).

TABLE III.

BENZENE (p_0 = 7·46 cm. Hg).

Film I (Wt. 61·2 mg.)

p_1 Solvent Vapour Pressure. cm. Hg.	W Wt. of Solvent in Film. mg.	V_1 Vol. Fraction of Solvent in Film.	V_1 (calc.).	p_1 Solvent Vapour Pressure. cm. Hg.	W Wt. of Solvent in Film. mg.	V_1 Vol. Fraction of Solvent in Film.	V_1 (calc.).
Up Points				*Down* Points			
7·35	88·9	0·57	0·68	6·69	44·0	0·46	0·47
6·91	56·4	0·46	0·50	6·55	41·0	0·44	0·44
6·30	34·5	0·34	0·39	5·96	27·0	0·34	0·35
5·48	19·4	0·23	0·29	5·80	24·9	0·33	0·33
3·73	7·9	0·11	0·16	5·08	14·8	0·22	0·25
1·96	4·8	0·07	0·07	4·53	12·0	0·19	0·21
				3·95	10·3	0·17	3·17
				2·51	6·6	0·11	0·09
				1·65	3·7	0·07	0·06

---

[8] *J. Amer. Chem. Soc.*, 1943, **65**, 1246.

TABLE III (*cont.*).

Film II (Wt. 75·7 mg. ; M.Wt. about 25 times smaller than Film I).

p_1.	W.	V_1.	V_1 (calc.).	p_1.	W.	V_1.	V_1 (calc.).
Up points				*Down* points			
7·21	94·8	0·60	0·63	6·83	61·9	0·50	0·49
6·28	41·3	0·40	0·39	6·55	55·8	0·47	0·43
4·03	11·6	0·16	0·17	6·02	37·9	0·38	0·36
2·95	7·5	0·11	0·11	5·78	32·0	0·34	0·33
1·83	5·4	0·08	0·06	5·17	22·2	0·26	0·26
				4·42	18·5	0·23	0·20
				3·47	13·4	0·18	0·14
				2·27	11·4	0·15	0·08

(Note slight hysteresis.)

TOLUENE.

Film I (p_0 = 2·18 cm. Hg).

p_1.	W.	V_1.	V_1 (calc.).	p_1.	W.	V_1.	V_1 (calc.).
Up points				*Down* points			
2·02	45·4	0·47	0·50	1·93	37·8	0·43	0·43
1·39	13·9	0·22	0·22	1·83	31·5	0·38	0·37
0·53	4·3	0·07	0·08	1·75	24·6	0·33	0·34
				1·58	18·8	0·27	0·27
				1·45	18·1	0·26	0·23
				1·17	7·7	0·13	0·17
				0·98	5·6	0·10	0·13
				0·74	4·8	0·09	0·09
				0·37	3·2	0·06	0·04

Film III (Wt. 109·9 mg.).

p_1.	W.	V_1.	V_1 (calc.).	p_1.	W.	V_1.	V_1 (calc.).
Up points				*Down* points			
2·08	107·7	0·54	0·59	1·86	62·6	0·41	0·39
1·97	75·2	0·45	0·46	1·70	47·1	0·34	0·32
1·52	34·6	0·28	0·25	1·57	37·0	0·29	0·27
0·57	1·6	0·02	0·07	1·39	28·5	0·24	0·22
				1·06	18·0	0·17	0·15
				0·66	13·6	0·13	0·08
				0·36	10·3	0·10	0·04

m-XYLENE.

Film I (N.B. pressures in cm. butyl phthalate ; p_0 = 8·75 cm.).

p_1.	W.	V_1.	V_1 (calc.).	p_1.	W.	V_1.	V_1 (calc.).
Up points				*Down* points			
8·55	70·5	0·58	0·63	8·00	54·6	0·52	0·50
8·40	66·0	0·56	0·59	7·40	39·9	0·44	0·40
7·90	41·7	0·45	0·48	7·30	31·7	0·38	0·38
6·20	20·5	0·29	0·28	7·00	28·3	0·36	0·35
				6·50	23·4	0·31	0·30
				5·60	15·2	0·23	0·23
				4·70	12·4	0·20	0·18
				3·00	8·7	0·15	0·10
				1·90	7·9	0·13	0·06

TABLE III (*cont.*).

CARBON TETRACHLORIDE.

Film I (Pressures in cm. Hg ; $p_0 = 9·12$ cm.).

p_1.	W.	V_1.	V_1 (calc.).	p_1.	W.	V_1.	V_1 (calc.).
Up points				*Down* points			
8·50	125·3	0·57	0·55	7·93	75·3	0·44	0·44
8·11	85·4	0·47	0·47	7·51	58·4	0·38	0·38
7·20	50·7	0·35	0·34	6·89	45·9	0·33	0·32
				6·36	37·6	0·29	0·28
				5·95	33·6	0·26	0·25
				5·70	29·8	0·24	0·23
				5·50	25·7	0·22	0·22
				5·40	25·8	0·22	0·21
				5·08	22·3	0·19	0·19
				4·95	21·2	0·18	0·18
				4·83	20·7	0·18	0·18

(Below this pressure, hysteresis.)

DIOXANE.

Film I ($p_0 = 2·77$ cm. Hg).

p_1.	W.	V_1.	V_1 (calc.).	p_1.	W.	V_1.	V_1 (calc.).
Up points				*Down* points			
2·37	38·5	0·39	0·36	2·20	27·8	0·31	0·30
1·90	17·9	0·23	0·23	2·10	24·8	0·29	0·27
1·44	9·9	0·14	0·15	1·70	13·2	0·18	0·19
				0·99	8·3	0·12	0·09
				0·52	5·6	0·08	0·03

Film III.

p_1.	W.	V_1.	V_1 (calc.).	p_1.	W.	V_1.	V_1 (calc.).
Up points				*Down* points			
2·56	82·9	0·43	0·45	1·99	34·9	0·24	0·25
2·50	68·8	0·39	0·41	1·68	25·9	0·19	0·19
2·30	55·5	0·34	0·33	1·25	20·9	0·16	0·12
2·29	54·9	0·34	0·33	0·91	20·5	0·16	0·08
1·87	7·5	0·06	0·22				
1·03	3·9	0·04	0·09				
0·48	3·2	0·03	0·03				

(Note : bad hysteresis on thicker film, both on *up* and *down* points.)

n-BUTYL ACETATE.

Film I (N.B. pressures in cm. butyl phthalate ; $p_0 = 11·9$ cm.).

p_1.	W.	V_1.	V_1 (calc.).	p_1.	W.	V_1.	V_1 (calc.).
Up points				*Down* points			
11·35	27·3	0·35	0·36	11·0	23·7	0·31	0·33
9·4	15·8	0·23	0·22	10·85	21·4	0·29	0·32
				10·2	19·1	0·27	0·26
				8·7	12·4	0·19	0·19
				7·85	9·5	0·16	0·16
				7·0	7·1	0·12	0·13
				5·4	5·4	0·09	0·09

TABLE III (*cont.*).

Diethyl Ketone.

Film I (Pressures in cm. Hg ; p_0 = 2·75 cm.).

p_1.	W.	V_1.	V_1 (calc.).	p_1.	W.	V_1.	V_1 (calc.).
Up points				*Down* points			
2·70	56·7	0·54	0·52	2·49	28·1	0·37	0·37
2·65	43·8	0·48	0·47	2·42	18·5	0·28	0·34
2·59	33·3	0·41	0·43	2·29	14·3	0·23	0·29
1·71	4·5	0·09	0·17	2·26	13·7	0·22	0·28
				2·12	10·6	0·18	0·25
				1·94	7·8	0·14	0·21
				1·44	2·6	0·05	0·13

Film III.

p_1.	W.	V_1.	V_1 (calc.).	p_1.	W.	V_1.	V_1 (calc.).
Up points				*Down* points			
2·66	81·4	0·49	0·48	2·59	71·6	0·46	0·43
2·47	41·2	0·32	0·36	2·49	52·1	0·38	0·37
2·05	17·6	0·17	0·23	2·35	36·9	0·30	0·32
1·30	3·1	0·04	0·12	2·05	24·1	0·22	0·23
0·63	1·3	0·02	0·04	1·78	16·5	0·16	0·18
				1·22	13·6	0·14	0·11
				0·79	8·3	0·09	0·05

(Slight hysteresis.)

The preceding solvents have all been those in which, as liquids, polystyrene will dissolve. There now follow some results for solvents in which it will only *swell* at room temperature.

Di *n*-Propyl Ether.

Film I (p_0 = 5·15 cm. Hg).

p_1.	W.	V_1.	V_1 (calc.).	p_1.	W.	V_1.	V_1 (calc.).
Up points				*Down* points			
$p_{sat.}$	56·6	0·56	0·40	4·97	26·6	0·38	0·34
5·08	32·9	0·43	0·36	4·83	21·9	0·33	0·31
4·42	13·6	0·24	0·25	4·76	19·9	0·31	0·30
3·84	10·1	0·19	0·18	4·60	17·0	0·28	0·27
				4·28	11·6	0·21	0·23
				3·13	5·7	0·11	0·13
				2·10	3·6	0·08	0·08

Cyclohexane.

Film I (p_0 = 7·75 cm. Hg).

p_1.	W.	V_1.	V_1 (calc.).	p_1.	W.	V_1.	V_1 (calc.).
Up points				*Down* points			
$p_{sat.}$	71·4	0·61	0·40	7·50	39·0	0·39	0·34
7·13	24·2	0·28	0·29	7·32	28·5	0·32	0·32
6·20	14·4	0·19	0·20	7·02	23·2	0·28	0·28
				6·65	17·4	0·22	0·24
				5·89	12·8	0·17	0·18
				5·18	11·8	0·15	0·15
				3·54	9·3	0·13	0·09

TABLE III (*cont.*).

NITROMETHANE.

Film I (p_0 = 2·78 cm. Hg).

p_1.	W.	V_1.	V_1 (calc.).	p_1.	W.	V_1.	V_1 (calc.).
Up points				*Down* points			
$p_{sat.}$	8·2	0·109	0·092	2·66	6·2	0·084	0·085
2·70	6·7	0·091	0·083	2·48	6·0	0·082	0·078
1·61	3·3	0·047	0·045				

n-OCTANE.

Film I.

At $p = p_0$, W = 6·5, V_1 = 0·135.

No other points taken.

As can be seen from Table III and Fig. 2, hysteresis effects were, in general, insignificant. The following general remarks may be made on this phenomenon as observed in these experiments. At *low* solvent concentrations, equilibrium was often impossible to reach on *down* points over several hours, though at *high* concentrations 10 min. was often sufficient. With those solvents for which two films were used there is a noticeable tendency for hysteresis to be worse for

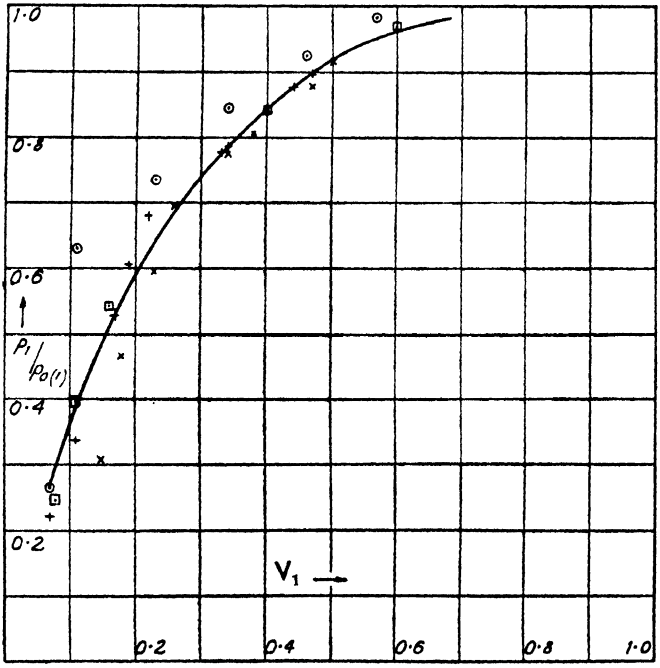

FIG. 2.

Illustrates for benzene : (*a*) Effect of hysteresis.
(*b*) Effect of molecular weight of polymer.
(*c*) Accuracy of Huggins' equation.

M.Wt. ~ 500,000 *Up* points ⊙ M.Wt. ~ 20,000 *Up* points ⊡
Down points + *Down* points ×

The curve drawn is a Huggins curve with μ = 0·43.

the thicker film; one may venture the estimate that equilibrium could not be reached at all with a film 0·2 mm. thick. In most cases constant weight was reached within an hour (to check this about $\frac{1}{4}$ of the points were left overnight, and a few for yet longer). The only exceptions were *n*-octane, requiring several days for the single point measured, and CCl_4, for which with vapour pressure less than about 50 % of saturation *no* absorption could be detected on the *up* points; even at 70 %, no change was observed for 6 hr. after which the weight changed rapidly, becoming constant after 10 min. This peculiar phenomenon was not further studied.

Discussion.

It has been shown that polystyrene is a true "molecular-colloid" (mainly by the work of Staudinger and Schulz), and the remarkable deviations from Raoult's law in such solutions have been analysed in terms of (*a*) the entropy contributions arising from the great molecular weight and the flexibility of the polymer (Flory, Huggins, Miller, Guggenheim [9, 10, 2]) together with (*b*) the usual heat of mixing effects well known in low-molecular solutions. The past history of this development has been well summarised by Gee [10] and will be omitted here.

For systems of this kind, Huggins [11] derived the equation

$$\ln p_1/p_{1(0)} = \ln V_1 + V_2(1 - y) + \mu V_2^2 \quad . \quad . \quad (1)$$

where $p_{1(0)}$ is the saturation vapour pressure of the low-molecular component (1) over its pure liquid, p_1, that over a solution of the polymer (2) containing a volume fraction V_2 of polymer, V_1 of low-molecular component; y is the ratio of molar volume of 1 divided by molar volume of 2; μ is a constant for any given 1-2 pair at a given temperature. In the present work, the approximation $1 - y \simeq 1$ can be safely made, so that

$$\ln p_1/p_{1(0)} = \ln V_1 + V_2 + \mu V_2^2. \quad . \quad . \quad . \quad (2)$$

The simplicity of this equation, involving only one adjustable constant, has led to its being very widely used for the analysis of such systems; the discussion in this paper therefore has the two-fold aim of testing the Huggins equation on the experimental results just quoted, and of attempting to interpret the constant μ. It will be noticed that the equation implies that for strong solutions the depression of vapour pressure should be independent of the molecular weight of the polystyrene; this can be seen from Fig. 2, which gives the results for benzene for two polymers differing by a factor of about 25 in molecular weight, and Table III which includes data for toluene, dioxane, and diethylketone for polymers differing in molecular weight by about a factor of 2.

The experimental results were therefore fitted graphically to equations of this form, particular attention being paid to points at higher V_1, for which hysteresis and weighing errors are least. Table III shows that the values calculated from these equations, with the μ values chosen for each solvent listed in Table IV (second column), agree with the experimental data; where hysteresis is significant the Huggins curve passes between the *up* and *down* points. The fit of the equation may also be judged from Fig. 2 showing the results for benzene. Table III shows one significant exception; the vapours (*n*-propyl ether, and cyclohexane) in which polystyrene only *swells* but does *not dissolve*, show more low molecular component in the neighbourhood of $p_1/p_{1(0)} = 1$ than Huggins' equation would predict; the values for the third swelling vapour, nitromethane, are too scanty to illuminate this point one way or the other. This effect has also been observed by Gee [12] for rubbers, and may well therefore be a general phenomenon.

---

[9] *Ann. Reports*, 1942, **39**, 7.

[10] *J. Chem. Soc.*, 1947, 280; *Quart. Rev. Chem. Soc.*, 1947, **1**, 265.

[11] (*a*) *J. Amer. Chem. Soc.*, 1942, 1712; (*b*) *Ind. Eng. Chem.*, 1943, **35**, 217.

[12] *Trans. Faraday Soc.*, 1946, **42B**, 33.

Table II summarises the values adopted for μ; they cover ranges in V_1 from 0·1-0·2 up to 0·4-0·6 and in $p_1/p_{1(0)}$ from 0·35-0·50 up to 0·93-0·97. The probable errors in μ vary from about 0·03 for a good series (e.g. toluene) to 0·05 where hysteresis is appreciable (e.g. diethylketone), and 0·08 for the swelling-vapours where deviations from Huggins' equation occur.

When V_1 is close to unity, μ can be derived from the deviations from ideal behaviour shown by osmotic pressure data.[12] For polystyrene there are such data for solutions in toluene,[13] benzene, CCl_4, and dioxane.[14]

Table IV shows in the first two columns the values of μ calculated from these osmotic data, and from the vapour-phase absorption data of the present work. It will be seen that the values for benzene and toluene are practically unchanged over the whole concentration range, while the differences for dioxane and CCl_4 are probably significant. Although we have no osmotic data for dioxane, diethylketone and butyl acetate, it is clear that a constant μ cannot characterise the whole isotherm. For, from eqn. (2), it can easily be shown that, if $\mu > \frac{1}{2}$, then there will be a value of V_2, other than the trivial case $V_2 = 0$, which satisfies the conditions $p_1 = p_{1(0)}$. In other words, pure liquid 1 will be in thermodynamic equilibrium with a system of 1 and 2; or, the polymer will have a definite solubility (" limited swelling ") instead of being miscible in all proportions. But dioxane, diethylketone, and butyl acetate do not show " limited swelling "; hence for these solvents also a single μ value cannot characterise the whole isotherm. Such simple behaviour must be the exception rather than the rule.[15]

TABLE IV.

Values of the μ-Parameter in Huggins' Equation.

	μ from Osmotic Data.	μ (obs.) (μ from these Experiments.	μ (calc.).	μ (obs.)-μ (calc.).
(*a*) *Solvents*—				
Benzene	0·45	0·43	0·33	+0·10
Toluene	0·44	0·47	0·46	+0·01
m-Xylene	—	0·41	0·52	−0·11
CCl_4	0·46	0·38	0·56	−0·18
Dioxane	0·47	0·56	0·23	+0·33
Diethylketone	—	0·67	0·45	+0·22
Butyl acetate	—	0·82	0·75	+0·07
(*b*) *Swelling Vapours*—				
Propyl ether	—	0·89	1·84	−0·95
Cyclohexane	—	0·89	0·86	+0·03
Nitromethane	—	1·75	0·91	+0·84

It is fairly generally agreed that the Huggins equation over-estimates the number of polymer-polymer contacts in dilute solution (osmotic pressure); this error should not affect so much the concentrated solutions studied in this paper.

In a theoretical discussion of the μ values it may be pointed out that Huggins' equation may remain formally valid provided it accounts correctly for the form of the entropy contributions and provided also that the heat content of mixing, if not negligible, is proportional to the square of the volume fraction of component 2. Such a proportionality is common for low-molecular solutions [16] and has been shown by Orr [17] for the heat of solution of squalene ($C_{30}H_{50}$) in benzene.

---

[13] Schulz, *Z. physik. Chem. A*, 1937, **176**, 317.

[14] Dobry and Schwob, *Bull. Soc. Chim. France*, 1936, *T* **2**, 1790.

[15] cp. also Gee, ref. [10].

Moreover, Brønsted and Koefoed [18] have shown that the activity coefficient of one hydrocarbon (A) in a solution of a higher hydrocarbon (B) depends on two terms, one due to the " imperfection " of the vapour of A, the other implying that the remaining free energy difference ΔG is proportional to the square of the *mole-fraction* of B ; in fact their extremely accurate data are fitted equally well if ΔG is proportional to the square of the *volume-fraction* of B ; moreover, the constant of proportionality then becomes the same for the three hydrocarbon-pairs they studied.

We may, therefore, following Gee, extend the analysis by supposing that μ is a function of an entropy effect (probably roughly the same for all the solvents here used) and an energy term which should be calculable from the " energy-density " theory which has been successfully applied to low-molecular solutions by van Laar [19] and by Hildebrand.[16] The way in which this has been tested is explained in the Appendix to this paper ; the values of μ so predicted are shown in the third column of Table IV. It can be seen that the agreement is fairly satisfactory for benzene, toluene, xylene, CCl_4, cyclohexane ; for the polar solvents the deviations are very large, though they seem to swing about zero. This, however, is what would be expected, for Hildebrand's formulæ will only be valid for molecules with symmetrical fields of force. The conclusion may therefore be drawn that further explanation of these experimental data must await further development of the theory of heats of mixing of polar molecules of normal low molecular weights.

The work described in this paper was done in the Physical Chemistry Institute of Copenhagen University. The author wishes to acknowledge his indebtedness to Prof. J. N. Brønsted, who suggested this problem and designed the apparatus, for his invaluable advice throughout the work, to the Goldsmiths' Company of London for a Senior Research Studentship which enabled the author to work in Copenhagen, and to Dr. G. Gee for helpful discussion.

Appendix.

Test of the Hildebrand Equation.[20]

(*a*) The problem is : given $\mu = A + B/T$, where the A is an entropy and the B an energy term, to see if the data in Table IV can be explained by a constant A and B given from Hildebrand's theory by

$$B = V_1/R \,.\, (X_1 - X_2)^2$$

(where V_1 = molar volume of the low-molecular component 1 ; $X_1 \equiv \sqrt{\Delta E_1/V_1}$, where ΔE_1 is the energy of vaporisation of pure component 1 from its liquid, X_2 is the same function for polystyrene).

(*b*) $\Delta E_1 = \Delta H_1 - RT$, where ΔH_1 is the heat of vaporisation at constant pressure. For this, few calorimetric data are available, and for small differences in X it is better to use the *same* method for all, even if this is not the best for some liquids. The Clausius-Clapeyron equation has therefore been integrated between the two temperatures : 20° C., to which refer the vapour pressures in Table II and the boiling points, for which $p = 760$ mm. This gives an average ΔH, as a further refinement this has been corrected to 20° by assuming a constant specific heat difference of 10 cal./degree/mole between liquid and vapour. The requisite data, including the densities used for V, are all given in Table II with niuts of (cal./cc./mole)$^{\frac{1}{2}}$ for X_1.

(*c*) This leaves A and X_2 adjustable constants, whose values are, however, not entirely arbitrary. For A is the limit of μ as $B \rightarrow 0$, or $T \rightarrow \infty$, and there are data by Walling, Briggs, and Mayo [21] on the depression of vapour-pressure of styrene by polystyrene at 127° C. (400° K.) for which $\mu = 0{\cdot}33$. The results of this present paper apply to the lower temperature 293° K.; moreover, the heat of mixing of even styrene and polystyrene cannot be zero (double bond), and hence A at 293° must be considerably less than 0·33. Again, the nearest low-molecular analogue of polystyrene is not styrene, but ethylbenzene. For this $X = 8{\cdot}78$ (Table II). One could assume *either* simply that X for polystyrene $= X$ for ethylbenzene *or* that the energy of vaporisation of a polystyrene of degree of polymerisation N is N times that of ethylbenzene, and correct for the difference in density. The second approximation is likely to be nearer the truth, whence $X_2 \simeq 9{\cdot}7$ (very roughly).

---

[16] Hildebrand, *Solubility* (Reinhold Publishing Co., N. York, 1936).

[17] *Trans. Faraday Soc.*, 1944, **40**, 320.

[18] *Kgl. Danske. Videnskab. Sels*, 1946, Medd. XXII, No. 17.

[19] *Z. physik. Chem. A*, 1928, **137**, 421.

[20] Gee, *Trans. Inst. Rubber Ind.*, 1943, **18**.

(*d*) Using these rough indications " best " values of A and X_2 have been obtained in the following way: $\mu = A + B/T$; B is known if X_2 is known. Plotting A as a function of X_2 (X_1 and μ being taken as known) gives a family of parabolas, one for each low-molecular compound. Looking at this diagram one finds the value of X_2 giving (i) the A values of the non-polar vapours closest together, with (ii) their mean value between 0 and 0·25, (iii) X_2 as approximately 9·7. Evidently there is some freedom of choice, but the best value of X_2 appears to be 10·1 (± 0·2 perhaps).

(*e*) Taking X_2 as 10·1, A as 0·23, from the X_1 values in Table II, the $\mu_{\text{calc.}}$ values in Table IV have been obtained.

University of Copenhagen,
Copenhagen.

The Military College of Science,
Shrivenham,
Nr. Swindon, Wilts.

[21] *J. Amer. Chem. Soc.*, 1946, **68**, 1145.

THE HYDROLYSIS OF ACETIC ANHYDRIDE.

BY V. GOLD.

Received 19*th June*, 1947.

The kinetics of the hydrolysis of acetic anhydride in aqueous or near-aqueous media has been the subject of a number of investigations [1a–n] of which the most notable are those of Sidgwick and co-workers,[1c, 1e] and of Kilpatrick.[1l] It is known from the earlier work that the reaction is catalysed by both OH^- and H^+ ions, the former being very much more effective, but that it will proceed at a measurable rate without these catalysts. Under these conditions the reaction is a strictly first-order one; the molecularity with respect to water does not appear in the kinetic equation owing to its constant concentration. The constancy of the velocity coefficients demonstrates that, with the concentrations of OH^- and H^+ ions present in dilute solutions of acetic acid, catalysis by these ions can be neglected (see also [1l]), so that the observed velocity really corresponds to the purely spontaneous hydrolysis.* Similar arguments

[1] (*a*) Menschutkin and Vasilieff, *J. Physic. Chem.* (*Russ.*), 1889, **21**, 192; (*b*) Lumière and Barbier, *Bull. Soc. Chim.*, 1906, **35** (3), 625; (*c*) Rivett and Sidgwick, *J. Chem. Soc.*, 1910, 732; (*d*) Orton and Jones, *ibid.*, 1912, 1708; (*e*) Wilsdon and Sidgwick, *ibid.*, 1913, 1959; (*f*) Verkade, *Rec. trav. chim.*, 1915, **35**, 79; (*g*) Connolly, *Carnegie Inst. Publ.*, 1915, **230**, 112; 1918, **260**, 131; (*h*) Skrabal, *Monatsh.*, 1922, **43**, 493; (*i*) Jowett, *Ph.D. Thesis* (Liverpool 1923); Moelwyn-Hughes, *Kinetics of Reactions in Solution* (Oxford 1933); (*j*) Szabo, *Z. physik. Chem.*, 1926, **122**, 405; (*k*) Olivier and Berger, *Rec. trav. chim.*, 1927, **46**, 614; (*l*) Kilpatrick, *J. Amer. Chem. Soc.*, 1928, **50**, 2891; (*m*) Caudri, *Rec. trav. chim.*, 1930, **49**, 1; (*n*) Vles, *ibid.*, 1933, **52**, 809.

* It is probably safe to disregard the mechanism in which simultaneous attack by OH^- and H^+ ions is taking place. When allowance is made for the temperature variation of the ionic product for water this mechanism would lead to a negative heat of activation for the hydrolysis of acetic anhydride.

can be applied to the interpretation of the analogous reaction between Ac_2O and EtOH (as solvent) where the constancy of the first-order rate coefficients rules out the proposed mechanism :

$$Ac_2O + OEt^- \rightarrow EtOAc + OAc^- \text{ (cf.}^2\text{)}.$$

The present paper deals with the following aspects of the spontaneous hydrolysis; (*a*) the solvent effect (*b*) the temperature coefficient and (*c*) the interpretation of new and old kinetic data with reference to the theory of solution kinetics and the mechanism of aliphatic substitution reactions.

Experimental.

Materials. WATER : Conductivity water ($\kappa = 1{\cdot}0 - 1{\cdot}5 \times 10^{-6}$ mhos at 25° c.) was used.

ACETONE : Analar acetone was dried over $CaCl_2$ and K_2CO_3 and then fractionally distilled, as recommended for conductivity measurements.[3] ($\kappa < 1 \times 10^{-7}$ mhos at 25° c.)

SOLVENT MIXTURES : Made up by weight, a good stock serving for a block of experiments.

ACETIC ANHYDRIDE (B.D.H.) was refluxed over magnesium turnings for several days and carefully fractionated, and a small middle fraction only used for kinetic experiments.

ACETIC ACID : The Analar product was purified by the method of Orton and Bradfield.[4]

Conductivity Apparatus.—This was of usual design, embodying a screened 6-dial Cambridge low inductance resistance box, a Cambridge non-inductive ratio box, balancing condensers across the cell and the resistance box. Audio-frequency A.C. was provided by a simple 3-frequency valve oscillator (Hartley circuit). A single-stage amplifier used in conjunction with headphones served as detector. The bridge circuit embodied a modified Wagner earth.[5]

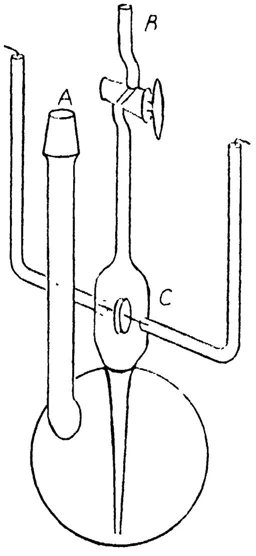

FIG. 1.

The design of the conductivity cell (Fig. 1) proved useful both for ordinary conductivity measurements and in kinetic runs because of the ease of filling and mixing solutes in it rapidly. It was constructed in Pyrex ; the electrode surfaces were platinum-grey. Addition of reagent and solvent was effected by means of weight pipettes through A. The measuring cell C, was filled and emptied by pressure, using N_2 after bubbling it through a sufficient number of bubblers containing the solvent at the thermostat temperature. A or B could alternately be connected to N_2 by turning a single 4-way tap. The thermostat tank for use at 5° was a well-lagged large accumulator jar with steady cooling provided by the immersion to a fixed depth of a tube containing powdered solid CO_2, with the temperature control provided by an intermittent low-power immersion heater operated by a relay and toluene-mercury regulator. During experiments the regulation was constant to ± 0·001° at the higher temperatures and ± 0·003° in the 5° tank, as measured on a Beckman thermometer. The actual temperatures of the baths were measured on a N.P.L. calibrated thermometer (± 0·02° c.) graduated in $\frac{1}{10}$ degree and read by means of a cathetometer.

Method for Conductivity Measurements.—The main purpose of the conductivity measurements was to provide an accurate calibration for the kinetic experiments, and not an absolute determination. For this reason good reproducibility, rather than absolute accuracy, was aimed at, and not very much attention paid to the elimination of small systematic errors, e.g. by a " Parker

---

[2] Moelwyn-Hughes and Rolfe, *J. Chem. Soc.*, 1932, 241.
[3] Dippy, Jenkins and Page, *ibid.*, 1939, 1391.
[4] Orton and Bradfield, *ibid.*, 1927, 983.
[5] Jones and Josephs, *J. Amer. Chem. Soc.*, 1928, **50**, 1049.

effect" caused by the employment of water as thermostat liquid.[6] Similarly, the solvent conductivities were not reduced to the lowest possible values as it was more desirable to use a solvent of reasonably low and constant conductivity which could be used for a group of experiments rather than one of very low, but sensitive and variable, conductivity. Blocks of conductivity measurements were carried out by weighing into the cell a certain amount of solvent, measuring its conductivity, and then introducing successive small amounts of a solution of acetic acid, made up by weight, from a weight pipette and measuring the conductivity after each addition. The same cell was employed for all measurements, the values of the resistances measured (apart from solvent resistances) ranging for the most part between 1,000ω and 10,000ω. The cell constant was determined directly by means of a KCl solution (0·0631, but this value may be in error by as much as 0·0003).

Procedure for Kinetic Measurements.—These were carried out conductometrically employing the apparatus and cell described above. After measurement of the solvent resistance a small amount (1 or 2 drops) of acetic anhydride was added to the cell, the liquid mixed, and C filled and emptied with the reaction mixture several times, after which the cell was left filled and conductance measurements recorded at short intervals. It was found preferable to observe the time at which the resistance of the cell reached a certain setting of the bridge rather than the reverse procedure, and this permitted accurate timing of the kinetic progress of fast reactions. An " infinity " reading was taken after approx. 12 half-lives. A calibrated stop-watch was used for timing.

The admissibility of the conductometric technique for following the rate of this reaction has been demonstrated by Rivett and Sidgwick. These authors showed that the concentration of acetic acid produced at the end of the reaction —as indicated conductometrically—was exactly twice the concentration of acetic anhydride initially weighed out and their rate constants have been accurately confirmed by different independent chemical methods. It is therefore certain that the conductivity change in the course of the reaction is wholly dependent on the generation of acetic acid. In the present investigation the concentration of the non-electrolyte reactant was so low that it can also be shown by consideration of the influence of non-electrolytes on conductivities that no analytical error could arise out of its presence. Internal evidence for this is provided by the good constancy of the first-order rate coefficients found under all conditions (cf. Table III).

It is one of the chief advantages of the conductometric technique that it is probably the only one by which precision measurements are possible at the very low concentrations desirable for accurate kinetic work and, unlike most other physical measurements used in reaction kinetics, does in itself provide good evidence concerning the chemical nature of the process observed.

Evaluation of Concentrations from Conductance Measurements.

Unfortunately, the concentration of acetic acid cannot be expressed as a simple function of the resistance. Plotting $1/r$ or r (resistance) against C (concentration) a curved plot is obtained from which interpolations are not easy, though this appears to have been the method used by Sidgwick,[1c, 1e] etc. The computation procedure adopted here is considerably more cumbersome and only practicable with the aid of a mechanical calculating machine. However, it achieves a much more satisfactory conversion and requires much less extensive conductivity measurements than the direct procedure. It was found empirically that over the rather limited concentration range employed the product Cr is a linear function of $1/r$ to a considerable degree of accuracy (where r is the resistance of the cell after making allowance for the conductance of the solvent, though naturally it is not suggested that this solvent correction should be applied in general for acid solutions). Such a linearity could be expected if Ostwald's dilution law were applicable and the solvent correction employed justifiable, as it follows from

$$K = \frac{\Lambda^2 C}{\Lambda_0(\Lambda_0 - \Lambda)}$$

that

$$Cr = \frac{B^2}{K\Lambda_0^2} \cdot \frac{1}{r} + \frac{B}{\Lambda_0},$$

where B is the cell constant.

---

[6] Jones and Bollinger, *J. Amer. Chem. Soc.*, 1931, **53**, 411.

The procedure adopted was therefore to fit the experimental data to an equation of the form :

$$Cr = \frac{m}{r} + a \qquad . \quad . \quad . \quad . \quad . \quad . \quad (1)$$

using the method of least squares and then applying this equation to the values of $1/r$ obtained during a kinetic run and thus obtain the concentration value. The empirical success of eqn. (1) may be judged from the following typical data, which illustrate the accuracy attainable.

TABLE I.—" OSTWALD PLOT " CALCULATION FOR 10 % ACETONE AT 15° C.

$C \times 10^4$	2·70	6·95	11·38	16·51	22·54	29·39	36·93	45·78
$1/r$ (corr.*) $\times 10^4$	1·844	3·195	4·197	5·143	6·081	7·002	7·897	8·837
Cr (corr.*) $\times 10$	14·66	21·74	27·11	32·11	37·06	41·97	46·77	51·80
Cr (calc.†) $\times 10$	14·60	21·78	27·10	32·13	37·11	42·00	46·76	51·73
C (calc.‡) $\times 10^4$	2·69	6·96	11·37	16·52	22·57	29·41	36·93	45·75

As even approximate values of the conductivities of acetic acid in acetone-water mixtures do not seem to have been previously recorded, a short summary of some of the measurements is given in Table II, expressing the data in terms of the constants of eqn. (1).

TABLE II

Solvent (% Me_2CO).	t° C.	Range of Measurements ($C \times 10^4$).	Solvent Resistance (ohms).	m.	a.
10	5	3-64	53,900	$8·49 \times 10^3$	0·561
10	15	3-46	61,200	$5·31 \times 10^3$	0·480
10	25	5-48	44,000	$3·47 \times 10^3$	0·308
14·45	15	3-40	51,100	$8·47 \times 10^3$	0·574
14·45	25	3-50	57,700	$5·94 \times 10^3$	0·398
20	5	2-43	115,000	$2·618 \times 10^4$	0·803
20	25	3-35	43,000	$1·055 \times 10^4$	0·576
30	5	4-32	157,000	$8·61 \times 10^4$	1·47
30	25	8-44	88,000	$3·327 \times 10^4$	1·021

Results.

(a) Kinetic Order and Accuracy.—In order to illustrate the accuracy with which the first-order law is applicable the method of least squares has been applied to the calculation of the rate constant of a randomly-selected run. (As a rule, rate constants were obtained graphically. In neither method is the time of starting the reaction involved in the calculation.) The rate coefficients calculated for every point of the example were obtained by taking as " starting-point " the point

$$\left(t = \frac{\Sigma t}{n} = 793·28 \text{ sec.}, \log_{10}(c_\infty - c) = \frac{\Sigma \log_{10}(c_\infty - c)}{n} = 1·23575\right),$$

where n is the number of observations. This point must lie on the best straight line through the data. In appraising the constancy of the rate coefficients it should be noted that by this procedure the least accuracy (owing to relatively larger timing errors) will occur round this " starting-point," and departure from a good first-order law would appear particularly through divergence of

---

* Denotes that solvent correction has been applied to the experimental resistance values.

† Values calculated from $Cr = \left(\frac{5·313}{r \times 10^{-4}} + 4·80\right) \times 10^{-1}$.

‡ From rows 2 and 4.

the constants in opposite directions near the beginning and the end of the observations.

For each temperature and solvent several (3 to 6) experiments were carried out which usually gave mean rate constants concordant within 0·5 % or better. The result for water at 25° may be slightly outside this experimental accuracy, as under these conditions accurate timing is difficult.

It is therefore estimated that the mean value given for each solvent and temperature is significant to about ± 0·3 % and the apparent activation energies to about 0·5 %, i.e. approximately ± 50 cal. When it was impossible to carry out all experiments with the same batch of a particular solvent mixture,

TABLE III.

ILLUSTRATION OF FIRST-ORDER LAW FOR EXPT. 91 (10 % ACETONE, 15° C.).

Time (sec.).	$\frac{1}{r}$(corr.) × 10^4 (mhos.).	$C \times 10^4$ AcOH.	$\log_{10} (C_\infty - C)$.	$0{\cdot}4343k_1 \times 10^4$ (sec.$^{-1}$).
84	2·068	3·27	1·4961	3·671
126	2·445	4·35	1·4809	3·674
176	2·800	5·51	1·4639	3·696
226	3·155	6·80	1·4442	3·675
276	3·446	7·96	1·4257	3·672
324	3·695	9·03	1·4079	3·668
370	3·909	10·00	1·3911	3·670
417	4·109	10·94	1·3741	3·677
479	4·350	12·14	1·3516	3·686
601	4·767	14·36	1·3065	3·680
653	4·923	15·24	1·2872	3·668
714	5·090	16·21	1·2684	3·664
784	5·267	17·27	1·2391	(3·61)
837	5·392	18·04	1·2193	(3·76)
897	5·522	18·85	1·1976	3·678
965	5·659	19·73	1·1726	3·677
1085	5·877	21·17	1·1284	3·680
1132	5·953	21·69	1·1113	3·674
1208	6·071	22·50	1·0832	3·678
1264	6·152	23·06	1·0626	3·678
1327	6·236	23·65	1·0399	3·670
1393	6·321	24·26	1·0150	3·681
1431	6·365	24·58	1·0013	3·676
1510	6·453	25·22	0·9727	3·670
1553	6·499	25·56	0·9567	3·673
10200(∞)	7·632	34·61	—	—

Mean $0.4343k_1$ by complete least-squares calculation = 0·0003674 sec

key runs were dupicated with the different batches of solvent in order to eliminate spurious results due to the employment of slightly different solvents, but no significant differences were detected between different batches.

(*b*) Rate Constants and Analysis of Data.—The new data presented refer to measurements in water and five acetone-water mixtures at 5°, 15° and 25° C., and a summary of these is given in Table IV. As it had been found by Sidgwick [1c, 1e] and partially confirmed by other workers (cf. Verkade[1f]) that the first-order rate constants of different runs depend on the initial concentration of acetic anhydride in a peculiar manner, all measurements were performed in extremely dilute solution (initial concentration of $Ac_2O = 1 - 3{\cdot}5 \times 10^{-4}$ g. mol./l.). Over this small range the rate constants showed no trend so that it may be assumed that temperature coefficients and solvent effects are free from spurious deviations due to this cause. In all cases the first-order law was obeyed accurately (cf. Jowett [1f]).

In addition to the directly-measured first-order constants (k_1), second-order rate coefficients have been calculated on the assumption that the reaction is a bimolecular one and that the hidden molecularity with respect to water is unity. Two sets of these were computed, the first by dividing k_1 by the molarity of water

(k_2^c) and the second by dividing by the mole fraction of water in the acetone water mixture (k_2^N) (Table V). (This should not be taken to mean that such a step has been theoretically justified.)

In both these sets the second-order rate coefficients decrease rapidly with increasing proportion of acetone in the medium. The order of magnitude of

TABLE IV.

FIRST-ORDER RATE CONSTANTS FOR THE SPONTANEOUS HYDROLYSIS OF Ac_2O (SEC.$^{-1}$).

Solvent.	5° C.	15° C.	25° C.
Water . . .	$69{\cdot}6 \times 10^{-5}$	$141{\cdot}8 \times 10^{-5}$	$262{\cdot}5 \times 10^{-5}$
10 % Acetone . .	$42{\cdot}1 \times 10^{-5}$	$84{\cdot}7 \times 10^{-5}$	$154{\cdot}5 \times 10^{-5}$
14·45 % ,, . .	—	$66{\cdot}3 \times 10^{-5}$	$120{\cdot}9 \times 10^{-5}$
20 % ,, . .	$23{\cdot}7 \times 10^{-5}$	$47{\cdot}5 \times 10^{-5}$	$86{\cdot}6 \times 10^{-5}$
30 % ,, . .	$11{\cdot}8_8 \times 10^{-5}$	$23{\cdot}9_5 \times 10^{-5}$	$44{\cdot}2 \times 10^{-5}$
50 % ,, . .	$2{\cdot}51 \times 10^{-5}$	$5{\cdot}16 \times 10^{-5}$	$9{\cdot}79 \times 10^{-5}$

the solvent effect near the water-end of the scale is very approximately given by

$$k_1 = k_0 \times N_{H_2O}^{14} \quad \text{or} \quad k_1 = k_0' \times C_{H_2O}^{4\cdot5}.$$

The rate constants have been analysed in the conventional manner in terms of the parameters of the Arrhenius equation (Table V). In each solvent the temperature coefficient of the reaction varies in a way which is inconsistent with the equation

$$\ln k_1 = \ln B - \frac{E}{RT}.$$

Both B and E are temperature-dependent and the variation is more marked the richer the water content of the medium. In addition to its dependence on temperature E changes slightly with the solvent composition, but this is less important than the temperature variation of this parameter and it is therefore the variation in the factor B which is almost exclusively responsible for the rate reduction accompanying acetone addition.

TABLE V.—ARRHENIUS PARAMETERS FOR FIRST-ORDER CONSTANTS k_1.

Solvent.	$E_{5/15}$ (kcal.).	$E_{15/25}$ (kcal.).	$-\frac{\Delta E}{\Delta T}$ cal. °c^{-1}.	$\log_{10} B_{5/15}$ sec.$^{-1}$.	$\log_{10} B_{15/25}$ sec.$^{-1}$.	$-\frac{\Delta E}{\Delta T}$ (for k_2^c)
Water . .	11·34	10·51	83	5·75	5·11	80
10 % Acetone .	11·12	10·26	86	5·36	4·71	86
14·45 % ,, .	—	10·25	—	—	4·70	—
20 % ,, .	11·04	10·27	77	5·05	4·47	82
30 % ,, .	11·16	10·47	69	4·85	4·32	68
50 % ,, .	11·47	10·93	54	4·41	4·00	35

This analysis has also been carried out for the second-order rate coefficients k_2^N and k_2^c. In the former case the E-values are of course identical with those given in Table V and in the latter case they differ only slightly (up to 0·2 kcal.). The conclusions regarding the temperature variation of E remain therefore qualitatively unchanged and, for comparison, the last column in Table V gives the temperature variation of E as calculated from k_2^c.

Discussion.

(a) Reaction Mechanism.

Before proceeding to a consideration of the meaning of these observations to the theory of reaction kinetics, we must consider the molecular mechanism of the reaction, in particular the probable molecularity with respect to water which, of course, is not revealed by the kinetic order of the observed reaction as the concentration of water remains virtually constant throughout any one run.

The hydrolysis of acetic anhydride may be classified as a nucleophilic substitution reaction; the nucleophilic substituting reagent is either the water molecule (for neutral or acid solutions) or the hydroxyl ion (for alkaline solutions). Looked at from this point of view, the hydrolysis of acetic anhydride shares certain features of the non-acid catalysed ester hydrolysis by " alkyl-oxy " (B'') and " acyl-oxy " (B') mechanisms [7a] and of the hydrolysis of acyl halides.

$$\mathrm{R|{-}O\,.\,CO\,.\,CH_3 + H_2O \rightarrow ROH + HOAc} \quad . \quad . \quad . \quad (\mathrm{B}'')$$

$$\mathrm{CH_3\,.\,CO|{-}OR + H_2O \rightarrow AcOH + HOR} \quad . \quad . \quad . \quad (B')$$

$$\mathrm{CH_3\,.\,CO|{-}Cl + H_2O \rightarrow AcOH + HCl} \quad . \quad . \quad . \quad (S_N)$$

$$\mathrm{CH_3\,.\,CO|{-}O\,.\,CO\,.\,CH_3 + H_2O \rightarrow AcOH + HOAc}$$

In each case the vertical line represents the position of bond fission. It has been established by Hughes, Ingold and co-workers that reaction of this type may be either unimolecular (S_N1) or bimolecular (S_N2) apart from special mechanism operating under certain conditions, and they have developed experimental criteria for distinguishing between the two types.* A large number of organic compounds have been studied under different conditions and classified in this manner, and the logical generalisations permit the prediction of probable reaction mechanism in other cases.

In the neutral hydrolysis of acetic anhydride the possibility of the two mechanisms arises in the following manner.

S_N1

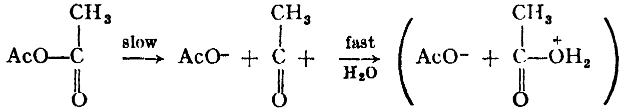

$$\mathrm{AcO{-}C(=O)CH_3 \xrightarrow{slow} AcO^- + \overset{+}{C}(=O)CH_3 \xrightarrow[H_2O]{fast} \left(AcO^- + CH_3C(=O){-}\overset{+}{O}H_2\right)}$$

S_N2

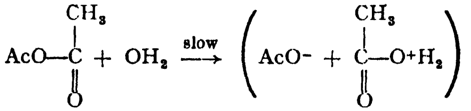

$$\mathrm{AcO{-}C(=O)CH_3 + OH_2 \xrightarrow{slow} \left(AcO^- + CH_3C(=O){-}O^+H_2\right)}$$

The subsequent fast proton-transfer equilibria have no bearing on the kinetics.

The theory of aliphatic substitution rules out S_N1 as a very unlikely mechanism in the present case. On passing from an aliphatic halide to an acetate, S_N2 becomes very much more important relative to S_N1, and as acyl halides are known to react by the S_N2 mechanism, acyl acetates (e.g. acetic anhydride) would be even more inclined towards this mechanism. Actually the acyl halides for which this mechanism has been confirmed were benzoyl halides,[8] but the change from benzoyl to acetyl would favour S_N2 relative to S_N1 (cf. the effect of allyl groups [7b]). A further argument for an S_N2 mechanism is the high value for the ratio of the reaction with OH^- ions and with H_2O [1h, 4] $\left(\frac{k_{2(\mathrm{OH^-})}}{k_{2(\mathrm{H_2O})}} \approx 10^4\right)$ which renders it improbable that there is a slow ionisation stage not involving the nucleophilic reagent.[7b]

One of the criteria for an ionisation reaction is the prediction of a

---

[7] (*a*) Day and Ingold, *Trans. Faraday Soc.*, 1941, **37**, 686; (*b*) Hughes, *ibid.*, 1941, **37**, 603.

* These investigations have been summarised by Hughes,[7] and frequent reference will be made to his review where particulars of the original papers will be found.

[8] E. R. A. Peeling, quoted by Hughes.[7b]

large positive salt effect arising out of the influence of ionic strength upon the activity coefficient of the zwitterion-like structure which must be expected to constitute the transition state leading to ionisation.[9b] This activity coefficient can be derived by a modification of the interionic attraction theory and is given by [9a, b]

$$-\ln f = \frac{4\pi N e^2}{1000 k^2} \cdot \frac{\mu^2}{l} \cdot \frac{I}{(DT)^2} \quad . \quad . \quad . \quad . \quad (2)$$

where N is Avogadro's number, k Boltzmann's constant, e the electronic charge, D the dielectric constant, I the ionic strength of the solution, l the radius and μ the dipole moment of the dipole molecule. According to the Brönsted-Bjerrum equation :

$$k = k_0 \frac{\prod^r f_r}{f_x},$$

or

$$\ln k = \ln k_0 + \sum^r \ln f_r - \ln f_x \quad . \quad . \quad . \quad (3)$$

where the symbols $\prod^r$ and $\sum^r$ signify product and sum respectively over all reactant molecules. Therefore, if all molecular species are dipoles and all effects other than electrostatic ones may be neglected, combination of (2) and (3) leads to

$$\ln k = \ln k_0 - B\left(\sum^r \frac{\mu_r^2}{l_r} - \frac{\mu_x^2}{l_x}\right) I \quad . \quad . \quad . \quad (4)$$

where

$$B = \frac{4\pi N e^2}{1000 k^2} \cdot \frac{1}{(DT)^2},$$

the suffixes r and x referring to reactants and transition state respectively. Therefore, if the transition state is considerably more polar than the reactants, as is to be expected for an ionisation reaction, an increase in ionic strength should lead to an increase in reaction velocity. The general correctness of this theory has been confirmed in cases where there is strong other evidence for an ionisation mechanism.[7b]

For the hydrolysis of acetic anhydride the relevant measurements have been performed by Kilpatrick.[11] The effect of added neutral salts is small and decelerating (the bracketed quantity in eqn. (4) is positive), i.e. in the opposite direction to that expected on an ionisation mechanism. Because of the smallness of the effect the exact relationship between $\ln k$ and I is not established with certainty, but it does not appear to agree with eqn. (4). These salt-effect measurements will be referred to again in the discussion of the solvent effect below.

It has been shown that it is possible under certain conditions to verify an ionisation mechanism by the detection of a depression of reaction velocity by a common-ion mass law effect.[7b] The rather curious effect of added acetate ions on the hydrolysis of acetic anhydride is accelerating and therefore does not admit such an explanation. It does not support —though not necessarily disprove—the S_N1 mechanism.

Taking all these arguments in conjunction it is concluded that the hydrolysis of acetic anhydride in water is a bimolecular reaction. This does not exclude the possibility of some other reactions of acetic anhydride and even of the hydrolysis under very different conditions proceeding through the intermediate acetylium ion CH_3CO^+, in particular in cases of catalysis by strong acids or Group III trihalides.

In arriving at this conclusion no use has been made of the erroneous arguments previously given to prove the bimolecular nature of the reaction [11]

---

[9] (*a*) Kirkwood, *Chem. Rev.*, 1939, **24**, 233 ; (*b*) Bateman, Church, Hughes, Ingold and Taher, *J. Chem. Soc.*, 1940, 983.

from the apparent order with respect to water as these were based on an inadequate appreciation of the medium effect.[14, 10]

(*b*) The Solvent Effect.

A bimolecular reaction between water and acetic anhydride belongs to the class of dipole-dipole reactions and, provided non-electrostatic effects are small compared with the electrostatic effect and the transition state is dipolar in character, the influence of solvent variation on the reaction velocity should conform with the equation [11]

$$\ln k = \ln k_0 - \frac{1}{kT}\frac{D-1}{2D+1}\left(\sum^{r}\frac{\mu_r^2}{l_r^3} - \frac{\mu_x^2}{l_x^3}\right) \quad . \quad . \quad (5)$$

In the present case it is indeed found that ln k is a linear function of $\frac{D-1}{2D+1}$ (Fig. 2) whence it is possible to evaluate the quantity in brackets which, as the sign of the slope shows, is negative. It is of interest to compare this result concerning the electrical nature of the reaction with the previously-quoted measurements of the salt effect. The following two relations now exist:

$$\left(\sum^{r}\frac{\mu_r^2}{l_r^3} - \frac{\mu_x^2}{l_x^3}\right) < 0$$

$$\left(\sum^{r}\frac{\mu_r^2}{l_r} - \frac{\mu_x^2}{l_x}\right) > 0$$

and it follows algebraically that they are not mutually compatible in the case where the dipole radius of the transition state is greater than that of every one of the reactants, as it would be natural to expect on chemical grounds.

An explanation of these conflicting effects does not seem possible at present. Of course, it is realised that in reactions of this type non-electrostatic effects often overshadow the electrostatic ones (cf. [12-14]) and the question arising here is whether the solvent or the salt effect is less subject to non-electrostatic effects and more reliable as evidence concerning the electrical nature of a reaction.

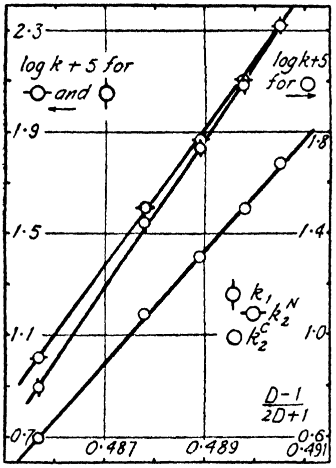

FIG. 2.

In the present case it is possible to invert the argument as not only a direct ionisation mechanism (S_N1) but also the more probable bimolecular mechanism (S_N2) is attended by an intermediate formation of ions. In the S_N2 mechanism the final process is a rapid proton transfer, so that the transition state for the whole reaction must be that for the first stage, i.e. the dipolar complex preceding a separation into ions.

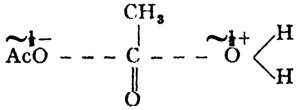

$$\overset{\sim\frac{1}{2}-}{\text{AcO}} - - - \underset{\underset{\text{O}}{\|}}{\overset{\overset{\text{CH}_3}{|}}{\text{C}}} - - - \overset{\sim\frac{1}{2}+}{\text{O}}\begin{matrix}\diagup\text{H}\\ \diagdown\text{H}\end{matrix}$$

---

[10] (*a*) Philip, *Proc. Chem. Soc.*, **28**, 259; (*b*) Benrath, *Z. physik. Chem.*, 1909, **67**, 508; (*c*) cf. Dunstan and Mussell, *J. Chem. Soc.*, 1911, 570.

[11] Glasstone, Laidler and Eyring, *The Theory of Rate Processes* (McGraw Hill, 1941), Chap. VIII.

[12] Amis, Jaffé and Overman, *J. Amer. Chem. Soc.*, 1944, **66**, 1823.

[13] Amis and Jaffé, *J. Chem. Physics*, 1942, **10**, 598.

[14] Akerlöf, *J. Amer. Chem. Soc.*, 1928, **50**, 1272.

This transition state would be more polar than the reactants and the mechanism in agreement with the solvent effect. It would be possible to devise termolecular or even more complex transition states. These may have advantages energetically, but have a much lower probability or entropy of activation. But whatever mechanism is involved, as long as the substituting reagent is a neutral water molecule a heterolytic substitution must produce a separation of charges and hence a polar transition state. Naturally, all polar transition states will be polymolecular in the sense that they owe their stability to solvation forces,[16] but as solvation forces may be explained without any molecular model,[17] it is probably wrong to treat the solvating molecules on the same basis as the actually reacting molecules in a kinetic mechanism. It has been shown in certain cases that the solvent effect is smaller for S_N2 than for S_N1 reactions,[7] which can be explained on electrostatic grounds, as it will depend on the extent of charge transfer which has taken place when the most energised configuration is reached.

Some of the qualitative arguments which can be advanced relating to the explanation of the salt effect which in the present reaction conflicts with this picture are analogous to those met in discussions of the behaviour of electrolytes in concentrated solutions or in non-aqueous and mixed solvents. It is probable that the interpretation of the salt effect depends on the specific reaction studied.*

From the magnitude of the effect of acetone addition it is concluded that the main variation of the rate constant accompanying the change of initial concentration of acetic anhydride [1c, 1e] may be interpreted as a solvent effect. A more detailed electrostatic analysis is not possible, as dielectric-constant measurements for mixtures of acetic acid and anhydride with water are hardly feasible.

A very different interpretation of solvent effects in solvolytic reactions has been given in which electrostatic effects are not considered specifically.[18] It was pointed out by Olson and Halford [18a] that the rate of a reaction with a solvent species in a mixed solvent could be represented by

$$v = k\prod^{r} p_r \quad . \quad . \quad . \quad . \quad . \quad (6)$$

where the p_r terms are the partial vapour pressures of the reactants. Since the partial vapour pressures are proportional to the activities of the reactants, this equation is equivalent to the old activity rate theory,[19] another form of which is Dimroth's solubility rule.[20] The original tests of eqn. (6) were actually rather irrelevant, but it has since been demonstrated that the agreement is excellent for the bimolecular solvolysis

---

[15] Dobson, *J. Chem. Soc.*, 1925, 2866.

[16] (*a*) cf. Steigmann and Hammett, *J. Amer. Chem. Soc.*, 1937, **59**, 2536; (*b*) Hughes, ref. [7], p. 607.

[17] Gurney, *Ions in Solution* (Cambridge 1936), Chap. I.

* It has been privately pointed out to the author by Prof. Ingold that in the heterolysis of the acetic anhydride molecule there is a considerable distribution of both the positive and negative charges of the transition state and, as ion atmospheres are not very local, this might cancel out most of the positive salt effect predicted by simple theory. On the other hand the distribution of dipolar solvent molecules is a very local affair and more influenced by the dipoles in the individual bonds than by the overall dipole moment, so that the electrostatic solvent effect would be roughly correct as long as the multipole transition complex involves a larger separation of charges.

[18] (*a*) Olson and Halford, *J. Amer. Chem. Soc.*, 1937, **59**, 2644; (*b*) Bartlett, *ibid.*, 1939, **61**, 1630; (*c*) Bateman, Hughes and Ingold, *J. Chem. Soc.*, 1938, 881; *J. Amer. Chem. Soc.*, 1938, **60**, 3080; (*d*) Bateman, Church, Hughes, Ingold and Taher, *J. Chem. Soc.*, 1940, 1008; (*e*) Bird, Hughes and Ingold, *ibid.*, 1943, 255; (*f*) cf. Winstein, *J. Amer. Chem. Soc.*, 1939, **61**, 1635.

[19] cf. Bell, *Acid-Base Catalysis* (Oxford 1941), Chap. I.

[20] Dimroth, *Annalen*, 1910, **377**, 127.

of *n*-BuBr in alcohol-water mixtures.[18a] It was pointed out by Bartlett [18b] that this ought not to necessitate an overthrow of the otherwise well-established Brönsted-Bjerrum equation, but should be interpreted as meaning that the activity coefficients of the transition states involved were not much affected by the solvent variation. But this can only be so if the transition state is non-polar—which by the previous arguments it is not—or if the theory of the electrostatic effects is inadequate.

It is, therefore, contended that this fugacity rate equation is not compatible with the electrostatic theory for the solvent effect and that both cannot be valid for the same reaction as they are based on mutually contradictory postulates. A study of range of validity of each theory and the region of overlap in which both represent fair approximations may provide useful data for a comparative assessment of electrostatic and non-electrostatic interactions in solution but the above considerations indicate that the Olson-Halford equation should only be applied with great caution as a diagnostic tool in studies of reaction mechanisms.

It can be shown that the solvolysis of acetic anhydride does not obey the Olson-Halford equation and that therefore the correctness of the electrostatic solvent effect theory is not contradicted.

This test follows from Caudri's data on the kinetics of the simultaneous hydrolysis and esterification of acetic anhydride in water-ethyl alcohol mixtures [1m] and Dobson's measurements of the partial vapour pressures of these solvent mixtures [15] and assuming that, over the concentration range considered, Henry's law is obeyed by acetic anhydride in every case. According to eqn. (6) :

with H_2O : $v_w = k_w{}^\circ p_w p_{\mathrm{Ac_2O}} \equiv k_w\,[\mathrm{Ac_2O}]$

with EtOH : $v_A = k_A{}^\circ p_A p_{\mathrm{Ac_2O}} \equiv k_A\,[\mathrm{Ac_2O}]$

where v_w is the instantaneous velocity of hydrolysis and v_A that of esterification. k_w and k_A are the conventional first-order constants for these reactions, $k_w{}^\circ$ and $k_A{}^\circ$ the " fugacity rate constants " which, according to Olson and Halford, are independent of the medium (*w* refers to water and *A* to ethyl alcohol). Therefore, the ratio $k_w{}^\circ/k_A{}^\circ = p_A k_w / p_w k_A$ should be constant for all solvent compositions. An alternative approximation due to Bartlett[18b] leads to the conclusion that the ratio $k_w N_A / k_A N_w$ should be such a constant, whereas the application of the Brönsted-Bjerrum equation to non-ionic reactions would require $k_w p_A f_x / k_A p_w f_y$ = constant, where f_x and f_y are the activity coefficients of the transition state for hydrolysis and esterification respectively. Table VI gives a summary of these tests ; the vapour pressures used are approximate interpolations only.

TABLE VI.

TESTS OF ACTIVITY RATE THEORY FOR THE REACTION OF $\mathrm{Ac_2O}$ WITH EtOH—H_2O MIXTURES AT 25°.

Vol. % EtOH.	k_w (min.$^{-1}$).	k_A (min.$^{-1}$).	$p_A k_w / p_w k_A$.	$N_A k_w\ N_w k_A$.
0	0·1544	0	—	—
20	0·0887	0·0068	8·2	0·99
40	0·0399	0·0097	4·9	0·80
60	0·0171	0·0085	3·2	0·85
80	0·00582	0·00516	2·5	1·23
95	0·00184	0·00196	2·4	2·04
100	0	0·00060	—	—

The test shows that, if the bimolecular mechanism is accepted for these reactions, the fugacity rate equation is not valid in the present case. As we might expect the transition states for the two reactions to be rather similar, also as far as the charge distribution is concerned, and therefore to exhibit a roughly parallel variation of their activity coefficients it would not have been surprising to find fair constancy in the fourth column of Table VI but this is not confirmed.

(*c*) The Temperature Effect.

It has been mentioned that one of the features of the reaction observed in all solvent compositions studied is the distinct departure from the Arrhenius law. The effect is in the opposite direction to that which would take place if it were caused by the incursion of a side reaction or second mechanism, so that this most frequent cause of breakdowns of the Arrhenius law can be ruled out as an explanation.

According to Svirbely, Warner *et al.*,[22, 21] the conventional method of determining activation energies for reactions whose rates depend on the dielectric constant of the solvent leads to a wrong answer, as the temperature variation of the dielectric constant is not taken account of. More correctly

$$\mathrm{d}\ln k = \left(\frac{\partial \ln k}{\partial(1/T)}\right)_D . \mathrm{d}\left(\frac{1}{T}\right) + \left(\frac{\partial \ln k}{\partial D}\right)_T . \mathrm{d}D$$

whence
$$E_D = E_{\mathrm{app.}} + R\left(\frac{\partial \ln k}{\partial D}\right)_T . \frac{\mathrm{d}D}{\mathrm{d}(1/T)}$$

where E_D (isodielectric activation energy) $= - R\left(\frac{\partial \ln k}{\partial(1/T)}\right)_D$

and
$$E_{\mathrm{app.}} = - R\,\frac{\mathrm{d}\ln k}{\mathrm{d}(1/T)}.$$

It is stated that these isodielectric activation energies conform with the Arrhenius law. Applying this formula to the present data, using Wyman's measurements for the dielectric constant of water,[23] the following results are obtained for water (the dielectric constants of the acetone water mixtures have not been measured below 20°).

TABLE VII.

	$E_{\mathrm{app.}}$ (k_1) (kcal.).	E_D (kcal.).	$R\left(\frac{\partial \ln k}{\partial D}\right)_T . \frac{\mathrm{d}D}{\mathrm{d}(1/T)}$ (kcal.).
For 15-25°	10·51	16·50	5·99
For 5-15° .	11·34	17·14	5·80

This effect may therefore explain roughly 25 % of the deviation from the Arrhenius law, but cannot be the major effect. Its consideration also brings about a very substantial change in the value of the heat of activation of the reaction. The calculation of these effects is probably not as accurate as the experimental data, owing to the interpolations

---

[21] La Mer and Kamner, *J. Amer. Chem. Soc.*, 1935, **57**, 2662.

[22] Svirbely and Warner, *J. Amer. Chem. Soc.*, 1935, **57**, 1883 ; La Mer and Kamner, *ibid.*, 1935, **57**, 2267 ; Eagle and Warner, *ibid.*, 1936, **58**, 2335 ; Svirbely and Schramm, *ibid.*, 1938, **60**, 330 ; Lander and Svirbely, *ibid.*, 1938, **60**, 1613 ; Amis, *ibid.*, 1941, **63**, 1606 ; Amis and Holmes, *ibid.*, 1941, **63**, 2231 ; Amis and Cook, *ibid.*, 1941, **63**, 2621 ; Amis and Potts, *ibid.*, 1941, **63**, 2883 ; Amis and Price, *J. Physic. Chem.*, 1943, **47**, 338 : Braude, *J. Chem. Soc.*, 1944, 443.

[23] Wyman, *Physic. Rev.*, 1930, **35**, 623.

involved, but is certainly correct as far as these conclusions are concerned. A much more extensive test would, of course, be possible on the present data with the knowledge of temperature variation of the dielectric constants of acetone-water mixtures down to 0° c.

Apart from the ionic reactions for which the departure from the Arrhenius law may with some confidence be attributed to the neglect of the temperature variation of the dielectric constant, a number of other reactions with variable activation energies have been reported, and some of them re-investigated with care.

It is noteworthy that nearly all the well-established cases are very similar in type to the present one, viz. : reactions of a solute molecule with the solvent or an ion produced from the solvent which is, in most cases, water. All known cases are found in two complementary summaries by La Mer and Moelwyn-Hughes.[24] For this reason the effect probably calls for a more specific explanation than the general arguments of La Mer,[25] which must be fundamentally correct but equally applicable to all types of reactions.

The chief difference between the mechanism of a solvolytic reaction and a non-solvolytic one appears to be not so much in the process of forming and decomposing the critical complex and in its structure, as in the *a priori* probability of activation taking place, and it is tentatively suggested that the explanation of the effect is to be sought in a larger temperature dependence of the frequency factor than is deduced in the conventional collision theory, or the application of transition state theory for simple gas phase reactions. This point will be treated more fully in another communication.

The author wishes to express his gratitude to Prof. C. K. Ingold, F.R.S., for encouragement given at various times and also for a most helpful discussion during the preparation of this paper. His thanks are also due to Dr. H. C. Bolton, Department of Physics, University College, Nottingham, for advice on A.C. measurements.

Summary.

The first-order rate constants for the " spontaneous " hydrolysis of acetic anhydride in water and five acetone-water mixtures have been determined conductometrically at 5°, 15° and 25°, and the data analysed in terms of the parameters of the Arrhenius equation. A review of miscellaneous evidence shows that the reaction belongs to the class of nucleophilic bimolecular (S_N2) [7b] solvolytic substitution reactions. The solvent effect on the rate constants can be explained on the basis of the electrostatic theory for a dipole-dipole reaction involving a more strongly polar transition state, though on this basis the simple electrostatic theory does not agree with previous measurements of the neutral salt effect. It is shown that the fugacity theory of the solvent effect [18] which has been applied to other reactions of this class is incompatible with the electrostatic theory of the solvent effect. The temperature dependence of the rate-constants does not agree with the Arrhenius law, and the departure cannot in the main be due to the effect of the temperature variation of the bulk dielectric constant.

Department of Chemistry,
King's College, London.

---

[24] La Mer and Miller, *J. Amer. Chem. Soc.*, 1935, **57**, 2674 ; Moelwyn-Hughes, *Proc. Roy. Soc. A*, 1938, **164**, 295 ; cf. Bell, *Ann. Reports*, 1939, 82.

[25] La Mer, *J. Chem. Physics*, 1933, **1**, 289.

[26] Akerlöf, *J. Amer. Chem. Soc.*, 1932, **54**, 4132.

STUDIES IN ELECTROLYTIC POLARISATION (IV). THE EFFECT OF THE SOLVENT ON THE HYDROGEN OVERPOTENTIAL (ii).

By J. O'M. Bockris and S. Ignatowicz.

Received 2nd July, 1947.

It has been shown in a previous publication [1] (i) that the properties of the solvent have a considerable effect on the hydrogen overpotential at high current densities. In the systems examined previously, particular attention was paid to the effect of the solvent on the relation between overpotential and c.d. in a number of anhydrous and mixed aqueous-non-aqueous systems, containing N. HCl. In the present communication, these results have been extended by determinations of overpotential at tin and copper cathodes, both metals of fairly high hydrogen overpotential, in systems containing methyl alcohol, ethyl alcohol and 1 : 2 dioxane, and their mixtures with water. A report is also given of the long time-variation of overpotential in various mixed and anhydrous systems, to which, as Hickling and Salt [2] have stressed, few authors [3] have paid sufficient attention, and a model is suggested upon the basis of which the results of this and a previous paper can be interpreted.

Experimental.

Purification of Solvents. (i) Methyl Alcohol.—For mixtures with water, technically pure methyl alcohol was refluxed with lime for several hours and distilled. For anhydrous solutions, the alcohol was further treated by the method of Bjerrum and Zechmeister [4] (use of magnesium and iodine). It was finally distilled into the solution-preparation vessel as described in (i).

(ii) Ethyl Alcohol.—Technically pure ethyl alcohol was distilled and the constant boiling mixture collected. This was used without further treatment for the aqueous-non-aqueous mixtures. For anhydrous solutions, the alcohol was dehydrated by the method of Walden, Ulich and Laun [5] (use of amalgamated aluminium). The solvent collected boiled at 77-78°.

(iii) Dioxan.—Technical dioxan was refluxed for several hours with NaOH and then distilled. The portion boiling at 100-101° was collected and stored over barium oxide in a closed vessel. Portions were removed as desired, distilled over sodium and immediately used for the preparation of the solution.

Water used in these experiments was twice re-distilled in an all-glass apparatus.

Apparatus.—No essential changes were made from that described in (i).

Reference Electrodes.—Two hydrogen electrodes of different areas were used and the potential of the working electrode measured against each. Differences of up to 2 mv. were found between the potentials of the reversible electrodes. The value of the potential of the hydrogen electrodes in aqueous N. HCl was examined before each experiment as also was the E.M.F. of the cell formed by the hydrogen electrodes in the non-aqueous test solution and the normal calomel electrode with a sat. KCl bridge.

Cathodes.—For tin, molten Analar tin was poured into a glass tube of L-shape, the end of which was kept closed by means of a porcelain plate to prevent leakage of the metal. The surface of the solid tin filling the end of the tube was then removed and the new surface scraped with a sharp knife, washed with distilled water and wiped with a filter paper. The average apparent area of cathodes thus prepared was about 0·2 sq. cm. Copper cathodes were of electrolytic copper wire, and were sealed into Pyrex. Treatment of the surface was analogous to that for tin.

---

[1] Bockris, *Faraday Soc. Discussions*, 1947, **1**, 95.

[2] Hickling and Salt, *Trans. Faraday Soc.*, 1940, **36**, 1226.

[3] cf. e.g. Baars, *Sit. Ges. Naturwiss. Marburg*, 1928, **63**, 213.

[4] Bjerrum and Zechmeister, *Ber.*, 1923, **56**, 894.

[5] Walden, Ulick and Laun, *Z. physik. Chem.*, 1925, **114**, 275.

PREPARATION OF SOLUTIONS.—Aqueous-non-aqueous mixtures were prepared by the introduction of the appropriate quantity of the non-aqueous solvent into a corresponding amount of water, both components having been raised to the boiling temperature and cooled during passage of a stream of oxygen-free hydrogen. Dry HCl gas (produced by H_2SO_4 on NH_4Cl) was then passed into the mixture together with a stream of hydrogen to facilitate stirring of the solution, the concentration being estimated by removal at intervals of a few cc. of the solution by means of hydrogen pressure and titration. Solutions thus prepared were 1 ± 0·05 N. with respect to HCl. For the anhydrous solution the solvent from the last stage of its dehydration was distilled in a hydrogen atmosphere into the solution vessel (cf. (**i**)) and the HCl solution prepared as described previously. The solution was in contact only with glass and hydrogen during preparation, transfer to the electrolytic cell and measurement, the apparatus being filled with hydrogen before introduction of the solution. For further experimental details, and a discussion of the choice of solvent, see (**i**).

Results.

Results from the effects of the solvent composition on overpotential, and on the Tafel lines in various solvents, are given in Fig. 1-6. Results for the variation with time are given in Fig. 7. Potentials are on the hydrogen scale.

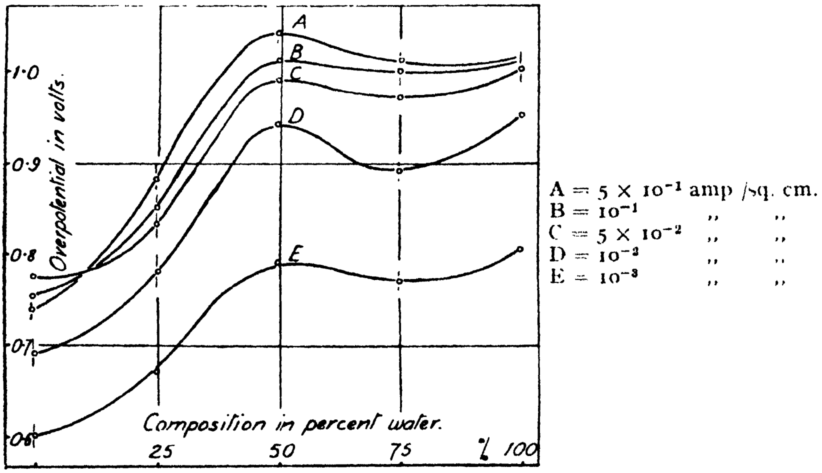

FIG. 1.—Hydrogen overpotential on tin in ethyl alcohol-water mixtures. Variations with solution composition.

It is seen from Fig. 7 that the increase of overpotential with time after switching on the current is by no means negligible and that it is therefore of importance to make allowance for this variation in the method used for measuring overpotential. This important fact was made clear by Hickling and Salt [2] whose method of allowing for the time variation has been utilised (as described in (**i**)). Recent work by the present authors and A. Azzam [6] shows that an increase of overpotential with time occurs at high c.d.'s in solutions distilled in hydrogen and through which a rapid stream of hydrogen has been passed for at least 12 hr. in an all-glass apparatus protected from oxygen, so that an explanation of the variation with time as being connected with the presence of oxygen does not appear probable. The degree of variation with time depends on the electrode material and the state of its surface. A large amount of the more reliable and recent work on hydrogen overpotential has been carried out on mercury where the variation with time is very small so that the importance of the time factor has not been realised by most authors.

[6] Unpublished.

From Fig. 7 it is also seen that overpotential on Sn and Cu decays almost instantaneously on cessation of the polarising current to a small fraction of its value during polarisation and then changes slowly towards the original rest potential. The proportion of the total overpotential represented by this slow change is generally smaller at tin, lead and copper than at nickel cathodes.

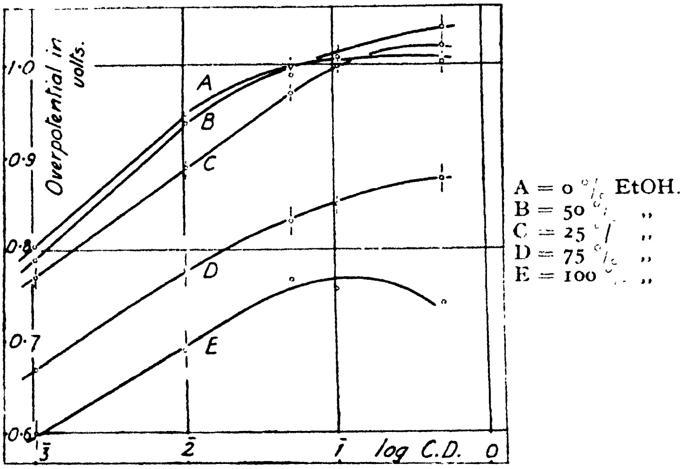

FIG. 2.—Hydrogen overpotential on tin in ethyl-alcohol-water mixtures. Variations with current density.

It is seen from Fig. 1 that for a tin cathode in ethyl alcoholic solution the hydrogen overpotential is lower than in aqeuous solution at ordinary temperatures at all the c.d.'s examined. In aqueous ethyl alcoholic solution, the overpotential passes through a minimum at about 75 % aqueous content and a maximum at approximately 50 % aqueous content. In aqueous dioxan solution (Fig. 3), the behaviour is essentially similar in that a maximum is attained at about a 25 % dioxan content. The overpotential then decreases with increasing dioxan content towards a value somewhat lower than than in aqueous solutions. On copper (Fig. 5), there is a gradual decrease upon increase of methyl alcohol content to values considerably lower than those in aqueous solution.

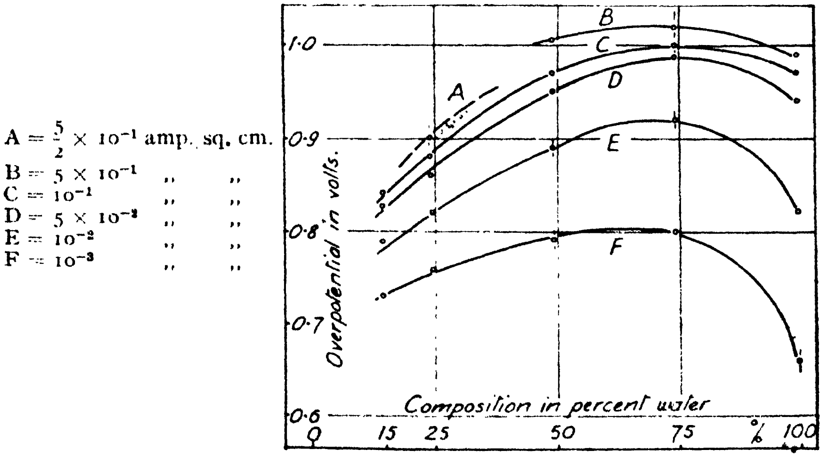

FIG. 3.—Hydrogen overpotential on tin in dioxan-water mixtures. Variations with solution composition.

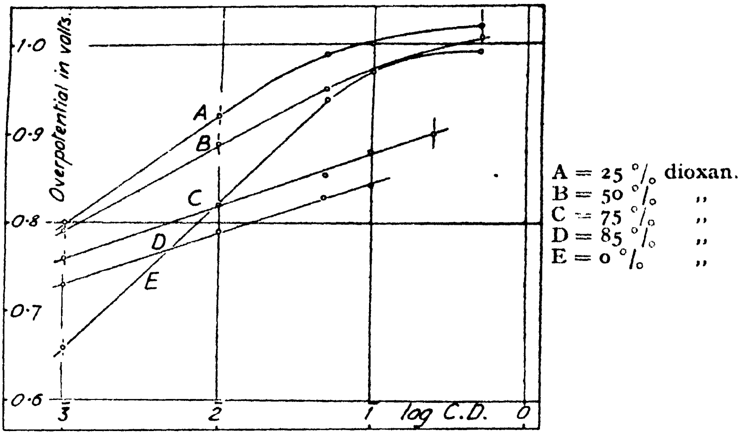

A = 25 % dioxan.
B = 50 % ,,
C = 75 % ,,
D = 85 % ,,
E = 0 % ,,

FIG. 4.—Hydrogen overpotential on tin in dioxan-water mixtures. Variations with current density.

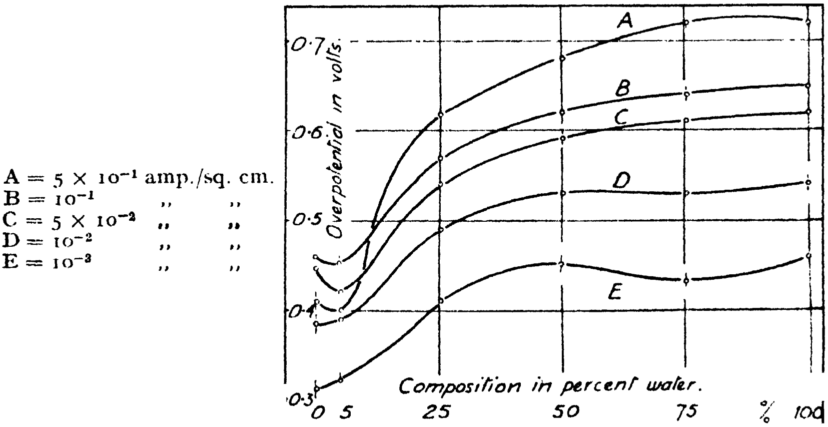

A = 5×10^{-1} amp./sq. cm.
B = 10^{-1} ,, ,,
C = 5×10^{-2} ,, ,,
D = 10^{-2} ,, ,,
E = 10^{-3} ,, ,,

FIG. 5.—Hydrogen overpotential on copper in methyl-alcohol-water mixtures. Variations with solution composition.

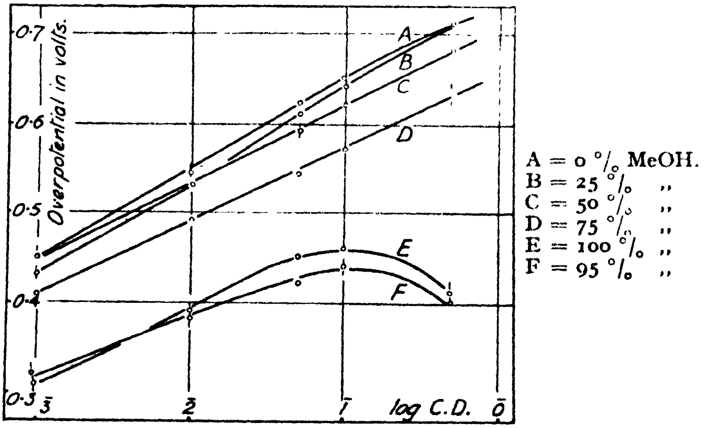

A = 0 % MeOH.
B = 25 % ,,
C = 50 % ,,
D = 75 % ,,
E = 100 % ,,
F = 95 % ,,

FIG. 6.—Hydrogen overpotential on copper in methyl-alcohol-water mixtures. Variations with current density.

On tin cathodes in ethyl alcohol solutions (Fig. 2) there is little effect of the solvent upon the slope of the overpotential-log c.d. relation and this tends to depart from linearity to the greatest extent in the anhydrous solutions where, at the highest c.d. a slight decrease in overpotential was observed. In dioxan solutions (Fig. 4) the slopes of the Tafel lines are generally less than those in aqueous solutions and they tend to be more linear. On copper (Fig. 6), the approximate linearity of the results for most aqueous and mixed solutions is changed at non-aqueous contents of 95 and 100 % methyl alcohol to lines showing considerable departures from linearity and at the highest c.d. some decrease of overpotential with increasing c.d. is observed (cf. Hickling and Salt[3]). It cannot yet be definitely stated whether this behaviour at high c.d.'s depends on the presence of trace impurities in solution or a change in mechanism at the higher c.d.'s.

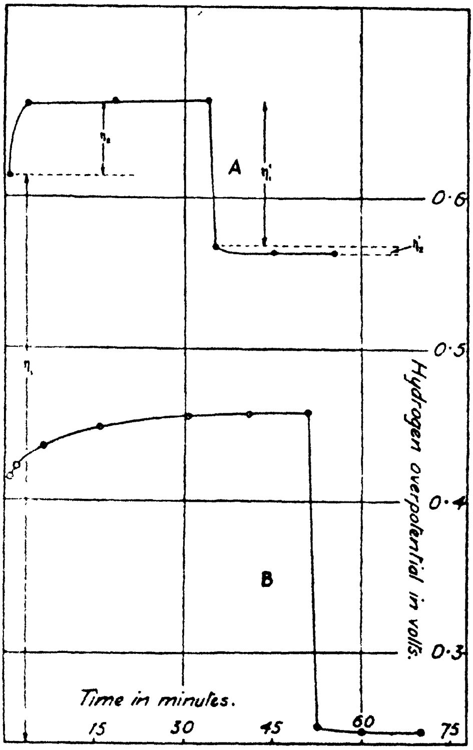

FIG. 7.—Variations of overpotential with time. Growth and decay curves.
A. For tin in 100 % EtOH at 10^{-1} amp./cm.^{2}
B. For copper in 100 % MeOH at 10^{-1} amp./cm.^{2}

Discussion.

(i) General.—The changes of overpotential with time are not clearly interpreted upon the slow discharge theories[7] although they become a consequence of the slow approach to equilibrium which would be expected if a chemical combination reaction governs the value of the final overpotential obtained.[8] No direct relation appears to exist between the type of variation with time and the solvent system. The slow decrease of overpotential with time which follows the initial rapid decrease suggests that at least *some* part of the overpotential at the electrode depends upon the presence of electromotive adsorbed material at the electrode. It may be noted that these results are not similar quantitatively to those of Frumkin[9] on the highly active metal palladium where this author found that, approximately (see Fig. 7):

$$\eta_2 = \eta'_2.$$

The solvent effects reported here may be compared with those of Lewina and Silberfarb[10] who obtained at a mercury cathode in a N. HCl solution in anhydrous ethyl alcohol an analogous lowering of the overpotential compared with that in aqueous solution, deviations from linearity in the overpotential-log c.d. relation in the same sense as that observed here being observed at about 10^{-3} amp./sq. cm. Results reported here at tin and copper cathodes in alcoholic solutions are similar to those of Part I for the analogous systems, lead in methyl and ethyl and copper in methyl alcoholic solutions. The minimum shown in Fig. 5 at 95 % methyl alcohol content can be compared with that reported in

---

[7] Gurney, *Trans. Faraday Soc.*, 1932, **82**, 447; *Proc. Roy. Soc. A*, 1932, **134** 137; Erdy, Gruz and Wick, *Z. physik. Chem. A*, 1932, **162**, 53; Frumkin, *ibid.*, 1933, **164**, 121; *Acta Physicochim.*, 1943, **18**, 23.

[8] Von Naray Szabo, *Z. physik. Chem., B*, 1937, **137**, 355; Massing and Laue, *ibid., A*, 1936, **178**, 1.

[9] Frumkin and Aladjalowa, *Acta Physicochim.*, 1944, **19**, 1.

[10] Lewina and Silberfarb, *Acta Physicochim.*, 1936, **4**, 282.

Part I where an analogous minimum was observed at 90 % methyl alcohol content at a nickel cathode for all c.d.'s.

These results do not seem to be easily interpretable according to the slow discharge theories of overpotential. This is most clearly borne out by the variations of overpotential at tin in the ethyl alcoholic system where the dependence of the overpotential on the solvent in no way corresponds to Goldschmidt's [11] curves for the variation of concentration of the hydroxonium ion with the proportion of water present in this system which would seem to be the approximate behaviour expected were the theory applicable. Hence a further discussion of the solvation possibilities of the proton appears unnecessary. The increase of overpotential at a tin cathode observed at all c.d.'s upon addition of methyl alcohol or dioxan to the solution is in contradiction to the prediction of the effect of the addition of similar substances made by Eyring, Glasstone and Laidler [12] on the basis of their reaction-rate theory of overpotential.

General conclusions which can be drawn from the results of (**i**) and (**ii**) on the solvent effect on overpotential may be summarised thus :

(*a*) the solvent effect on hydrogen overpotential depends both on the properties of the cathode and of the solvent ;

(*b*) the effect is generally greatest for cathodes of lead and tin (low adsorptive metals) where in anhydrous non-aqueous solvents, the overpotential is generally lowered ;

(*c*) at nickel (high adsorptive power) the overpotential is either little changed or somewhat increased by the presence of substances capable of forming hydrogen bonds with the metal (e.g. alcohols). In other solutions, it is lowered similarly to the behaviour of lead, tin and copper ;

(*d*) the effect of the solvent on copper cathodes, which are intermediate with regard to power of adsorption for hydrogen, resembles that on lead and tin more than on nickel ;

(*e*) in mixed solvents, complex variations of overpotential tend to occur with varying composition. For lead and tin there is often a tendency to pass through a maximum at intermediate compositions;

(*f*) the solvent may either increase or decrease the value of b in the Tafel equation. There is some tendency at tin and lead cathodes for the b-value to pass through a maximum at intermediate compositions.

The most notable conclusion which may be drawn from the results hitherto obtained is that the solvent effect is dependent on the cathode material and therefore does not seem to depend principally upon the environment of the hydrogen ion, which would seem to follow according to the slow discharge theories. This latter conclusion supports a similar one, made upon a quite different basis, by Hickling and Salt.[13] It seems that an attempted explanation of the results of (**i**) and (**ii**) must assume a model in which the properties of the metal surface are essential factors determining the hydrogen overpotential.

(ii) Solvent Layer Theory.—In recent years it seems that there has been some tendency again to regard the slow combination of some entities on a cathode surface as the limiting reaction governing overpotential. Thus Frumkin and Aladjalowa,[9] commenting on their results for the hydrogen overpotential at a palladium cathode, state that " in the most general case the rate of combination of atoms must be rate-determining." Evidence for the cathode materials examined here is insufficient to indicate finally the mechanism involved. The present theory is given to indicate that an interpretation of the solvent effect on overpotential is possible according to a slow combination mechanism also.

In the model tentatively proposed here it is postulated that a layer of solvent molecules is situated at the cathode surface, held by coulombic and/or van der Waals adsorption forces, i.e. by the interaction of the solvent molecules with the long-range electric and adsorptive forces respectively at the cathode-solution interface. Thus, the solvent molecules are regarded as being held electrostatically to the surface of the cathode, the negative ends of their dipoles being oriented towards the bulk of the solution ; for some systems, where adsorption forces are strong, these may predominate over the coulombic forces and thus change the principal mode of attachment, the solvent molecules then being held to the cathode by some particular group attached to an appropriate centre on the cathode.

---

[11] Goldschmidt, *Z. physik. Chem.*, 1914, **89**, 129.

[12] Eyring, Glasstone and Laidler, *Trans. Electrochem. Soc.*, 1939, **76**, 331 ; Frumkin, *Acta Physicochim.*, 1940, **12**, 481.

[13] Hickling and Salt, *Trans. Faraday Soc.*, 1941, **37**, 224.

Approach of an ion brings about neutralisation near the electrode and it is assumed that this is not generally the rate-determining step. The hydrogen atom formed from the neutralised ion is then adsorbed on to the electrode and this is followed by catalytic combination and evolution of hydrogen. The details of the mechanism of the slow catalytic combination need not be discussed for the present purposes but it may be supposed to be predominantly that of Tafel [14] at low and intermediate c.d. with a probable component from the electrochemical mechanism [16] at higher c.d. The hydrogen overpotential, established at the cathode when a steady state is reached, is then a function of several factors. Energetically, the essential cause would be said to be in the difference in activity between the adsorbed hydrogen atoms and the hydrogen particles just outside the cathode-solvent layer, this difference being caused by the fact that the slow rate of formation of hydrogen molecules from entities at the cathode surface constitutes a block preventing the immediate removal of hydrogen atoms formed on the negative side of the solvent layer. This mechanism implies that overpotential is affected by the nature of the solvent layer for the latter obviously governs the fraction of the cathode available for catalysis. Thus hydrogen overpotential in a given solvent must be affected by the following factors.

(i) The adsorptive properties of the cathode for solvent molecules : If the capacity of the electrode for chemisorption is low, the mode of attachment of the solvent dipoles is likely to be predominantly electrostatic. Conversely for metals generally considered to have good adsorbent power, this property may govern the attachment of solvent molecules to the cathode, so that the solvent layer does not depend primarily upon the polar properties of the solvent molecule.

(ii) The dipole moment and chemical structure of the solvent molecule : For cathodes at which attachment of the solvent layer is predominantly electrostatic, lowering of the solvent dipole moment should bring about a less intense attachment to the cathode. Correspondingly, where the metal has a capacity for adsorption, molecules possessing groups such as $-OH$, which may take part in a hydrogen-bond attachment to the cathode, seem more likely to be strongly adsorbed on the cathode than molecules lacking these groups.

(iii) The dimensions of the solvent molecule : For a given degree of attachment to the cathode, this factor clearly affects the fraction of the surface occupied.

Application of the above model to the results reported in **(I)** and the present paper can be briefly outlined as follows. For lead and tin cathodes it seems reasonable to assume that the solvent layer is attached to the cathode by predominantly coulombic means. Substitution of water by methyl alcohol would then bring about a less intense attachment of the dipoles to the cathode than in aqueous solution because the dipole moment of methyl alcohol is less than that of water.* A greater cathode area is thus available for combination of atomic hydrogen so that in methyl and ethyl alcoholic solution at tin and lead cathodes, the overpotential might be expected to decrease as actually found. A similar reasoning may be applied to the results reported for copper in methyl and ethyl alcohols and also to acetic acid and dioxan solutions, where similar decrease of overpotential are indicated by extrapolation from measurements made at high non-aqueous contents. No strict parallelism between the decrease of overpotential and the dipole moment of the solvent would be expected because other factors, such as molecular size, may vitiate any simple relation. Thus, as acetic acid and dioxan have notably smaller dipole moments, than water, the corresponding decrease in the number of molecules attached to the cathode surface is compensated by the relatively large size of these, so that the overpotential at a lead cathode in acetic acid and dioxan solutions may be reasonably expected to be intermediate between that in water and methyl alcoholic solvents, is so.

For nickel cathodes, a greater tendency to form hydrogen bonds is expected and hence if the structure of the solvent be appropriate, e.g. for alcohols, the mode of attachment to the cathode is entirely by means of hydrogen bonds. If, now, a non-aqueous additive such as methyl alcohol is introduced into the solution, the centres formerly occupied by water will be partially replaced by methanol and the net number of spaces occupied should then be of the same order. Thus the overpotential might be assumed to remain approximately the same or to undergo some increase owing to the larger cross-sectional area of the organic molecule. The same reasoning renders clear the results reported on nickel in alcoholic, glycollic and formic acid solutions (see (i)). In dioxan solution where the tendency for chemisorption on the cathode is small, predominantly electrostatic attachment must occur, so that, similarly to the reasoning adduced for tin and lead cathodes, the overpotential tends to decrease when the dioxan content increases.

---

[14] Tafel, *Z. physik. Chem.*, 1905, **50**, 641.

[15] Butler and Ockrent, *J. Physic. Chem.*, 1930, **34**, 2286. Ockrent, *J. Physic. Chem.*, 1931, **35**, 3354.

[16] Okomoto, Horiuti and Hitora, *Sci. Papers Inst. Phys. Chem. Res., Tokyo*, 1936, **29**, 223.

* The quantitative relation between the probability of adsorption of methyl alcohol and water molecules involves an exponential term containing the polarisability of the molecules concerned. Relatively small differences in dipole moments and polarisabilities therefore cause relatively large differences in probabilities of attachment to the cathode.

In mixed solvents the variations of overpotential shown are complex and the attempted interpretation is difficult. In systems similar to that of a copper cathode in methyl alcoholic solution, the essential explanation may be similar to that advanced in the limiting case of anhydrous solutions. In attempting to interpret the behaviour of systems such as that of tin in aqueous ethyl alcoholic HCl solution, and aqueous dioxane HCl solution where there is a maximum of the overpotential for all c.d.'s, it may be observed that in a mixed solution on cathodes having a low power of adsorption, solvent molecules of the two components are probably held electrostatically in a proportion depending on their dipole moments. Electrostatic interaction would then be expected in that the +ve poles of the smaller molecule attached to the cathode, tends to attract the negative poles of the larger, which was originally oriented towards the solution. The configuration of the solvent layer therefore tends to increase the area of the cathode which it effectively poisoned for the combination of hydrogen atoms, so that the overpotential should be increased. When a sufficient quantity of the non-aqueous component is present on the cathode, the lowering of overpotential brought about in the way suggested above for anhydrous systems, predominates, so that a maximum is found on the overpotential-solvent composition relation. The interaction between the dipoles would presumably take place irrespective of the mode of attachment for the high and medium overpotential metals discussed.

It should be stressed that the experimental knowledge of adsorption on the systems discussed above is very limited. Some information exists [16] for the adsorption of alcohols, etc., on mercury, however, and experiments on the solvent effect on the hydrogen overpotential at this substance are therefore in progress.

Finally, it can be shown that a quantitative development of the above model, utilising a suitable isotherm such as that of Freundlich, yields equations for the relation of overpotential and log c.d. of the same form as those given by most recent theories. It seems of little advantage to present here a quantitative description of the model until data have been obtained which will allow the order of the main parameters involved to become known. Experiments with the aim of determining such parameters are in progress in the present department.

One of us (J. O'M. B.) wishes to give sincere thanks to Dr. H. J. T. Ellingham for his interest in a part of the above work. Thanks are also due to the Polish Board of Technical Studies, London, for financial assistance to S. I.

Summary.

The hydrogen overpotential in mixed aqueous-non-aqueous and anhydrous solutions of HCl containing methyl alcohol (copper cathode), ethyl alcohol (tin cathode) and dioxan (tin cathode) has been measured over a complete range of solvent compositions in the c.d. range $10^{-8} - 5 \times 10^{-1}$ amp./sq. cm.

In all systems examined, hydrogen overpotential tends to be lowered in the anhydrous solutions. On tin cathodes, maxima are reached at intermediate compositions.

The long time-variations of overpotential both after commencement and cessation of the polarising current are described.

The time-variation of overpotential supports the view that at least a part of the total overpotential is not concerned with the slow discharge mechanism generally described. The solvent effect is discussed according to a model of the working electrode in which the essential feature consists in the assumption that

a solvent layer, held on the surface of the electrode, affects the velocity of the rate-determining combination reaction occurring at the cathode during the electrolytic evolution of hydrogen molecules. The mode of attachment of the solvent layer is postulated as being either predominantly by coulombic or van der Waals forces according to the nature of the cathode surface, and the electrical and chemical properties of the solvent molecules. The qualitative version of the theory described accounts for the main features of the results reported in this and a previous paper.

Department of Inorganic and Physical Chemistry,
Imperial College of Science,
South Kensington,
London, S.W.7.

PENETRATION OF PROFLAVINE INTO BACTERIAL CELLS.

BY S. JACKSON AND C. N. HINSHELWOOD.

Received 25th June, 1947.

One of the suggestions made in connection with the inhibitory action of drugs on the growth of bacteria is that the effect depends to an important extent upon the ease of penetration of the cell. In particular, adaptation to resist the action of drugs is sometimes assumed to be due to an alteration in the permeability of the cell to them, or to the selection of strains less permeable than the average.

One example of drug adaptation which has been extensively studied is that observed with *Bact. lactis aerogenes* and proflavine, and some success has been achieved in accounting for the observations in terms of a theory which takes no account of permeability as a possible limiting factor.[1]

The experiments to be described were made to throw some light upon the problem of the importance of permeability. The most obvious way of determining the rate at which inhibition by proflavine occurs was to find the effect of adding it to a culture already in the phase of logarithmic growth. Such cultures were accordingly prepared, the phosphate-ammonium sulphate-glucose medium, previously described, being employed. In this the bacteria grow well, and have a mean generation time of 33 min. at 40° C. A number of tubes of medium were inoculated in parallel from the same parent culture. One was allowed to grow normally and served as a control. To the others, as soon as logarithmic growth was well established, suitable small volumes of concentrated proflavine solution were added, so as to establish concentrations ranging from 10 to 200 mg./l.

The growth of all the cultures was followed by sampling and counting at suitable times—5 min. intervals after the drug additions. The counts are recorded as average numbers in a haemacytometer field, the actual number of cells per ml. being $1{\cdot}25 \times 10^6 \times$ count.

The controls grew quite normally in respect of rate and total population. When proflavine was added at a count of about 100, growth continued for about 20 min., during which time the number of cells increased by about 20 %. After this, growth was sharply arrested for a period of hours (this period being comparable with the lag which would have been shown had the cells been inoculated directly into medium containing proflavine). The results are shown in the table, from which it is seen the extra growth occurring after the addition of the drug is not only slight, but is practically independent of the drug concentration.

---

[1] Davies, Hinshelwood and Pryce, *Trans. Faraday Soc.*, 1944, 40, 397; 1945, 41, 163; 1945, 41, 778; Pryce, Davies and Hinshelwood, *ibid.*, 1945, 41, 465.

TABLE I.

Concentration of Added Drug mg./l.	Count at Addition.	Count at Arrest.	Ratio.	Mean.
10	110	138	1·25	1·20
	116	132	1·14	
20	93	115	1·24	1·28
	100	140	1·40	
	118	144	1·22	
40	98	123	1·26	1·26
100	89	103	1·16	1·21
	76	95	1·25	
200	95	112	1·18	1·14
	107	118	1·10	

This fact seems to be of some significance. Suppose that for effective inhibition of division a concentration x of proflavine must be attained inside the cell. The average concentration during the time between the addition of the drug and the cessation of growth will be approximately $x/2$. During this time the average rate of penetration will be $(c - x/2)/d$, where c is the external proflavine concentration and d is a factor depending upon the permeability. Even 10 mg./l. of the drug produces inhibition, so that in most of the experiments, c must be very much greater than x. Hence the rate of attainment of the inhibitory concentration in the cell should be nearly proportional to c. Since, however, the time required for the onset of the inhibition and the extra growth occurring are practically constant over the range of proflavine concentrations 10-200 mg./l., it would seem that the rate of penetration is not of great importance in the mechanism of the inhibition.

What appears to happen is that about one cell in five suffers division once more after the addition of the drug, and, since the penetration factor seems not to be a limiting one, it is probable that those cells which are far enough advanced towards division when the drug is added complete the process, while the others divide no more.

Summary.

When proflavine is added to a culture of *Bact. lactis aerogenes* in logarithmic growth about one cell in five undergoes one further division before the inhibitory action of the drug is complete. Since the proportion is independent of the proflavine concentration over a wide range, it is argued that the rate of penetration of the drug into the cell is not a significant controlling factor.

Physical Chemistry Laboratory,
South Parks Road,
Oxford.

MOLECULAR DISTILLATION AND SUBLIMATION.

By P. C. Carman.

Received 24th January, 1947; as revised, 23rd July, 1947.

In comparatively recent years, the process of molecular distillation has been developed to the status of a large-scale, chemical engineering unit operation; but there has been little discussion of its general limitations, or of its relationship to other modes of distillation. Articles on molecular distillation leave the general impression that it becomes operative only at pressures of the order of 10^{-4} mm. and that the distance of the condensing surface from the evaporating surface must be less than one mean free path of the vapour molecules.[1, 2] It is proposed to show here that molecular distillation has a much wider scope than would be suggested by these limitations.

Distillation implies a combination of the following stages: (i) transfer of heat to an evaporating liquid to provide latent heat of vaporisation and to maintain the liquid at absolute temperature, T, (ii) formation of vapour at the liquid-vapour interface, (iii) transfer of vapour and (iv) condensation of vapour at a condenser surface maintained at a relatively low temperature, T_c. In text-books on distillation, little attention is devoted to the fact that formation and transfer of vapour is achieved by three distinct mechanisms, which may be described as (*a*) ebullition, (*b*) normal evaporative distillation and (*c*) molecular evaporative distillation or molecular distillation. The relationship between these can be explained by considering a liquid maintained at constant temperature, while the pressure, P, in the space above it is gradually decreased. Initially, P is much greater than the saturation vapour pressure, Π, of the liquid at temperature, T, so that an inert gas, such as air, is present, through which vapour produced at the liquid surface is transferred by diffusion and/or convection to the condensing surface. Under these conditions of *normal evaporative distillation*, the rate of distillation is controlled by the rate of mass transfer between evaporating and condensing surfaces, not by the rate of heat transfer. If the rate of heat transfer is increased, the liquid rises in temperature till the increase in Π produces a corresponding increase in rate of mass transfer.

If P is decreased till it is equal to Π, bubbles can form and grow in the liquid, so that distillation normally takes place by *ebullition*. The rate of distillation is here controlled by the rate of heat transfer, since the temperature of the liquid remains constant, while the liquid-vapour interface can be increased to an unlimited extent by formation of bubbles. Above the liquid, vapour is not transferred by diffusion or convection, but by bodily movement, and, as the condenser must usually be well separated from the boiling liquid to avoid splashing, there can be a distinct difference in total pressure between boiler and condenser, owing to frictional losses.

For most common liquids, there is thus an abrupt change in the mode of distillation when P is decreased to Π, and P cannot be decreased below Π. In the case of many oily liquids with very high boiling points, Π is very small up to the highest temperatures to which it is safe to heat them, and, under these conditions, bubbles do not form readily. It is then possible to decrease P below Π, and there is a more-or-less gradual change

---

[1] *J. Soc. Chem. Ind.*, 1939, **58**, 39 and 43.

[2] Hickman, *Chem. Rev.*, 1944, **34**, 51.

from normal evaporative distillation, controlled by rate of transfer of vapour, to *molecular distillation*, in which the rate of distillation is controlled by the absolute rate of evaporation, i.e. the rate at which molecules escape from the free surface of the liquid.

It is important to note here that *sublimation* of solids can be treated in exactly the same way as distillation of liquids; and that, as ebullition is impossible, sublimation can only show the change from the normal evaporative to the molecular evaporative process as P is decreased.

Equations for Evaporative Distillation.

The transition from normal evaporative to molecular distillation or sublimation may now be discussed quantitatively. It is not easy to express rates of distillation quantitatively if convection is involved, but the essential points can be made clear by assuming that transfer of vapour takes place only by true diffusion to a parallel condenser, at a distance, x, from the evaporating surface and equal to it in area. Then, if

w = rate of distillation in g./cm.^{2} of liquid-vapour interface/sec.
M = molecular weight of vapour relative to O = 16.
D = coefficient of diffusion in cm.^{2}/sec.
P_i = partial pressure of vapour in dynes/cm.^{2} at liquid-vapour interface.
Π_c = saturation vapour pressure at T_c in dynes/cm.^{2}.
R = gas constant in c.g.s. units = $8{\cdot}3 \times 10^7$.

$$w = \frac{MDP}{RTx} \ln \left(\frac{P - \Pi_c}{P - P_i}\right). \qquad (1)$$

In this, DP is independent of P and proportional to $T^{3/2}$ so that

$$w = \frac{k}{x} \ln \left(\frac{P - \Pi_c}{P - P_i}\right) = \frac{k_1}{x} \log \left(\frac{P - \Pi_c}{P - P_i}\right) \qquad (2)$$

where $k_1 = 2{\cdot}3k = \frac{2{\cdot}3MDP}{RT}$ and is proportional to $\sqrt{T}$, but is otherwise constant.

The usual practice in chemical engineering calculations is to assume equilibrium at the liquid-vapour interface, i.e. $P_i = \Pi$, whence

$$w = \frac{k_1}{x} \log \frac{P - \Pi_c}{P - \Pi} \qquad (3)$$

and, if Π is small compared with P, this becomes

$$w = \frac{k}{x} \cdot \frac{\Pi - \Pi_c}{P}. \qquad (4)$$

The equation generally employed for the absolute rate of evaporation, w_0, in molecular distillation is

$$w_0 = \Pi \sqrt{\frac{M}{2\pi RT}}. \qquad (5)$$

Now, the right-hand side of this equation represents a calculation of the rate of collision of vapour molecules with the liquid surface in a saturated vapour. If no colliding molecules rebound, this equals the rate of condensation and hence the rate of evaporation, w_0. It follows that, if the partial vapour pressure at the liquid-vapour interface is P_i, the rate of collision and hence the rate of condensation will be $w_0 \,.\, P_i/\Pi$, while the absolute rate of evaporation is unchanged. Then,

rate of distillation = absolute rate of evaporation − rate of condensation

or

$$w = w_0\left(1 - \frac{P_i}{\Pi}\right). \qquad (6)$$

Eqn. (7) would still be obtained if the accommodation coefficient, α, is less than unity, i.e. if part of the colliding molecules rebound; provided that α is the same at vapour pressure, P_t, as at Π. In the following treatment, it will be assumed that this is true and that eqn. (6) is therefore valid. In the curves calculated for water in the next section, it is assumed that $\alpha = 1$, but they would be little affected if α had smaller values.

Putting (2) and (6) together,

$$w = w_0\left(1 - \frac{P_t}{\Pi}\right) = \frac{k_1}{x} \cdot \log\left(\frac{P - \Pi_c}{P - P_t}\right) \quad . \quad . \quad . \quad (7)$$

emerge as the fundamental equations defining rates of evaporative distillation, i.e. by eliminating P_t, w can be calculated under any given set of conditions, P, x, T and T_c, the latter two quantities giving k_1, w_0, Π and Π_c.

Eqn. (7) lead to two important limiting approximations. First, solving for P_t in eqn. (6),

$$P_t = \Pi\left(1 - \frac{w}{w_0}\right) \quad . \quad . \quad . \quad . \quad (6a)$$

whence, if w/w_0 is very small, $P_t \simeq \Pi$, i.e. eqn. (3) is obtained for normal evaporative distillation. As eqn. (3) only gives real values of w when $P > \Pi$, normal evaporative distillation is similarly limited.

Second, solving for P_t in eqn. (2)

$$P_t = P - (P - \Pi_c) \times 10^{-\frac{wx}{k_1}} \quad . \quad . \quad . \quad (2a)$$

so that, when $\frac{wx}{k_1} > 1$, or $\frac{w}{w_0} > \frac{k_1}{w_0 x}$, the second term rapidly becomes very small, giving $P_t \simeq P$. It follows that the equation typifying molecular distillation is

$$w = w_0\left(1 - \frac{P}{\Pi}\right). \quad . \quad . \quad . \quad . \quad (8)$$

This gives positive values of w only if $P < \Pi$. Clearly, over a more-or-less limited range of P near $P = \Pi$, a distillation is neither normal evaporative nor molecular, but a combination of the two as described by eqn. (7). Eqn. (2a) also apparently shows that P_t should be greater than P, if $P < \Pi_c$, so that molecular distillation is limited to $\Pi_c < P < \Pi$. The meaning of this is that, when $P = \Pi_c$, the vapour has this pressure at both the evaporating and the condensing surfaces, so that much or most of it is removed uncondensed by the vacuum pump. Actually, P can be reduced below Π_c, but the condenser then ceases to function, all vapour being removed by the pump, and the process ceases to be distillation.

Evaporative Distillation of Water.

Further discussion of eqn. (7) in terms of mathematical symbols would not be very fruitful, so that the essential points are illustrated by plotting curves for water. Rates are plotted as ratios, w/w_0, against the variable of chief interest, P, using logarithmic scales in both cases. Curves in Fig. 1 and 2 are for 20° c., −20° c., −50° c. and −80° c. when $x = 1$ cm., and in Fig. 3 for $x = 1$ mm., 1 cm., and 1 m., respectively, when the temperature is −20° c. It is assumed that the condenser temperature is always so low that Π_c can be neglected. Thus, eqn. (7) become

$$\frac{w}{w_0} = \left(1 - \frac{P_t}{\Pi}\right) = \frac{k_1}{w_0 x} \cdot \log \frac{P}{P - P_t} \quad . \quad . \quad . \quad (7a)$$

and eqn. (3) becomes

$$\frac{w}{w_0} = \frac{k_1}{w_0 x} \cdot \log \frac{P}{P - \Pi} \quad . \quad . \quad . \quad . \quad (3a)$$

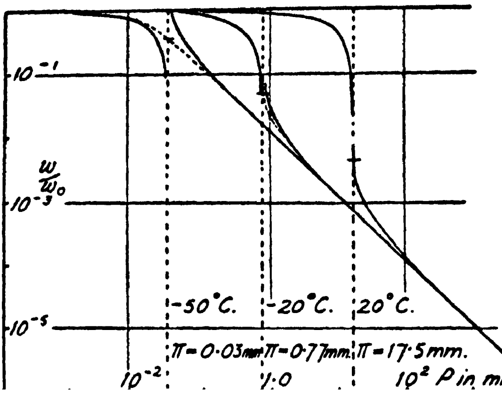

FIG. 1.—w/w_0 against P at three different temperatures, $x = 1$ cm. Full curves for equations (3*a*) and (8), broken curves for equation (7*a*).

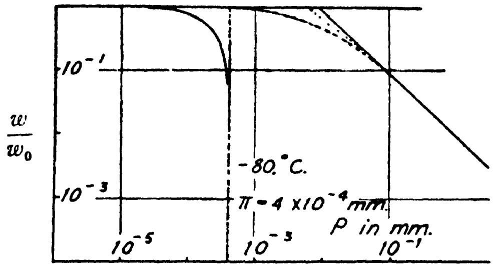

FIG. 2.—w/w_0 against P at $-80°$ C., $x = 1$ cm. Full curves for equations (3*a*) and (8), broken curve for equation (9), dotted curve for mean free path correction, equation (10).

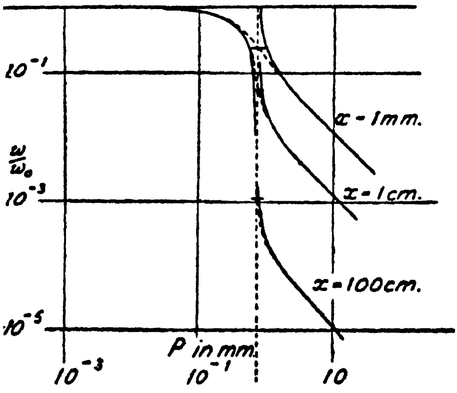

FIG. 3.—w/w_0 against P at $-20°$ C. for three values of x. Full curves for equations (3*a*) and (8), broken curves for equation (7*a*).

Experimentally, for water vapour-air at 0° c. and 1 atm., D is 0·22 cm.^{2}/sec., from which it can be calculated that

$$k_1 = 4 \times 10^{-4}, \text{ in consistent c.g.s. units.}$$

Other essential data are as follows :

Temperature.	Π in mm.	w_0.	w_0/k_1.
20° c. (water) . .	17·5	0·25	600
−20° c. (ice) . .	0·77	$1{\cdot}2 \times 10^{-2}$	30·4
−50° c. (ice) . .	0·03	$4{\cdot}9 \times 10^{-4}$	1·34
−80° c. (ice) . . .	4×10^{-4}	$7{\cdot}1 \times 10^{-6}$	$2{\cdot}1 \times 10^{-2}$

In Fig. 1-3, the true curves given by eqn. 7(a) are plotted as broken curves for each set of conditions, and it can be seen how these merge into the limiting eqn. (3a) and (8) which are plotted as full curves. The value of w/w_0 for $P = \Pi$ is also clearly marked. The fact that the curve at 20° c. refers to liquid water and the others to ice is immaterial, since almost exactly the same curves will be given for liquid and solid, provided they are compared, not at the same temperature, but at the same values of Π and of x. The curves for ice at −20° c. have recently become of great importance, since it is the temperature employed for removal of water from aqueous penicillin solutions.

First consider water at 20° c., this being characteristic also of higher vapour pressures. Even when P is decreased to Π, w/w_0 is extremely small, so that eqn. (3a) for normal evaporative distillation applies with great accuracy down to $P = \Pi$, at which water boils. If, however, boiling could be prevented, or if ice could exist with the same vapour pressure, the curve in Fig. 1 shows an abrupt transition to molecular distillation as given by eqn. (8) when $P = \Pi$, accompanied by a great increase in rate of distillation.

The behaviour of ice at − 50° c. in Fig. 1 typifies evaporative distillation of substances with low vapour pressures. Here $w/w_0 = 0{\cdot}35$, when $P = \Pi$, with the result that there is no sharp change from normal evaporative to molecular distillation, and there is a considerable range on either side of $P = \Pi$ for which eqn. (3a) and (8) are not applicable.

The curve for ice at − 20° c. in Fig. 1 when $x = 1$ cm. is intermediate, as would be expected, but it will be noted that, when x is varied, as in Fig. 3, the curve for $x = 1$ mm. is similar in character to that for − 50° c. and $x = 1$ cm., while the curve for $x = 1$ m. is similar in character to that at 20° c. for $x = 1$ cm. This is solely because of the influence of x on rates of diffusion, as given in eqn. (3a). Rates of molecular distillation are independent of x, as shown by eqn. (8) and illustrated by the curves for − 20° c.

For ice at −80° c. as in Fig. 2, with a vapour pressure of the order of 10^{-4} mm., the limiting eqn. (3a) and (8) are clearly not of much use, and w remains nearly equal to w_0 up to values of P which are considerably greater than Π. It is not difficult to show that, when $\dfrac{k_1}{w_0 x} \gg 1$, as is the case here, P_i is always much less than P, whence

$$\frac{k_1}{x} \cdot \log\left(\frac{P}{P - P_i}\right) \simeq \frac{k}{x} \cdot \frac{P_i}{P}$$

and eqn. (7a) then reduce to

$$\frac{w_0}{w} = 1 + \frac{w_0 x}{k} \cdot \frac{P}{\Pi}. \quad . \quad . \quad . \quad . \quad . \quad (9)$$

Influence of Free Mean Paths.

In the case of ice at − 80° c., the mean free path, λ, of the water vapour molecules in air becomes greater than x while P is still much greater than Π. Thus, at 0° c. and 1 atm.

$$\lambda \simeq 1 \times 10^{-5} \text{ cm},.$$

whence
$$\lambda \simeq 1 \times 10^{-5} \times \frac{T}{273} \times \frac{760}{P} \quad (P \text{ in mm.})$$

and therefore, at − 80° c.,

$$\lambda \simeq \frac{5{\cdot}4 \times 10^{-3}}{P},$$

i.e. $\lambda = 1$ cm. when $P = 5{\cdot}4 \times 10^{-3}$ mm. This introduces a fundamental point which has thus far been ignored, since, if x is of the same order as λ, evaporating vapour molecules can reach the condensing surface before colliding with an air molecule. Under such conditions, the diffusion coefficient, D, used in calculating k_1 of eqn. (7*a*) and k of eqn. (9), loses its meaning. The form of the correction to be adopted would be difficult to obtain on purely theoretical grounds, but an approximate method has been suggested by Fuchs.[3] A concentration gradient of vapour through the surrounding air or other permanent gas cannot be set up by the processes of diffusion until evaporating vapour molecules collide with air molecules. One can therefore postulate that the average effect is the same as if P_t were constant over a finite thickness, Δ, which is equal to, or of similar magnitude to λ, and that a normal diffusion gradient is established beyond this point. In brief, eqn. (7*a*) and (9) can be corrected by replacing x with $(x - \Delta)$. The effect of this correction, assuming $\Delta = \lambda$, is shown in Fig. 2 by a dotted curve, the main point being that $w/w_0 = 1$ when $\lambda = x$.

Evaporation of Droplets.—Some experimental data which afford at least a partial confirmation for Fuch's theory have been provided by Bradley, Evans and Whytelaw-Gray,[4] measuring rates of distillation of liquid droplets in an enclosure lined with adsorbent charcoal (i.e., $\Pi_c = 0$). According to Langmuir,[5] if evaporation is governed by diffusion, the rate of evaporation from a droplet of mass m, and radius a, into an infinite enclosure is given by

$$-\frac{dm}{dt} = 4\pi a^2 w = 4\pi a \, . \frac{MD\Pi}{RT}$$

i.e.
$$w = \frac{MD\Pi}{RTa} = \frac{k\Pi}{aP}.$$

This assumes $P \gg \Pi$, as was always the case in Bradley's experiments and is analogous to eqn. (4). Similarly, if w approaches w_0, Π must be replaced by P_t, and we derive an equation analogous to eqn. (9)

$$\frac{w_0}{w} = 1 + \frac{w_0 a P}{k\Pi}.$$

Suppose now that correction be made for the Fuchs layer, Δ. Then diffusion takes place from a sphere of radius, $(a + \Delta)$, whence

$$-\frac{dm}{dt} = 4\pi a^2 w = 4\pi(a + \Delta) \, . \frac{MDP_t}{RT}$$

i.e.
$$w = \frac{(a + \Delta)kP_t}{a^2 P}$$

---

[3] Fuchs, *Physik. Z. Sowjet.*, 1934 **6**, 224.

[4] Bradley, Evans and Whytelaw-Gray, *Proc. Roy. Soc. A*, 1946, **186**, 368.

[5] Langmuir, *Physic. Rev.*, 1918, **12**, 368.

and
$$\frac{w_0}{w} = 1 + \frac{w_0 a^2 P}{(a + \Delta)k\Pi}.$$

Bradley has shown that an equation of this type accords with his results.

Influence of Correction.—The correction for λ cannot become appreciable till λ becomes comparable with x. Now, in general, even for larger molecules, λ at 760 mm. and the distillation temperature is of the order of 10^{-5} to 10^{-6} cm., while x is of the order of cm., whence λ cannot become comparable to x until P is less than 10^{-3} to 10^{-4} mm. On the whole, therefore, we can distinguish two cases.

(i) If Π is well above 10^{-4} mm., diffusion no longer controls when the correction becomes effective, so that corrections of x are immaterial. Eqn. (7*a*) can then be applied as they stand.

(ii) If Π is of the order of 10^{-4} mm. or less, $\lambda = x$ when $P < \Pi$, so that the correction must be applied. As eqn. (7*a*) reduce to eqn. (9) under these conditions, the equation to be applied is

$$\frac{w_0}{w} = 1 + \frac{w_0(x - \Delta)P}{k\Pi}. \quad . \quad . \quad . \quad (10)$$

Discussion.

In general, distillation or sublimation will be carried out at the highest practicable temperature, since the increase in vapour pressure favours rapid distillation; but temperatures are often limited in practice by danger of decomposition. The usual procedure for liquids has been, and will continue to be, to reduce pressure till boiling takes place at a safe temperature, since this only requires simple apparatus and gives high rates of distillation. Ebullition, however, possesses some distinct limitations. To avoid splashing, the condenser must be at some distance from the boiling liquid and, since vapour is transferred by flow instead of by diffusion, the condenser must be placed between boiler and vacuum pump. Now, at very low pressures, the volume of vapour produced is so great that (i) frothing and splashing tend to be excessive, (ii) the frictional losses between boiler and condenser are very appreciable, compared with the pressure maintained in the receiver by the vacuum pump. This is recognised in modern apparatus by use of wide passages for flow of vapour, but, even so, it is found that, no matter how small the pressure maintained by the vacuum pump, the pressure in the boiler might remain as high as 5 mm. Thus, if the liquid cannot safely be heated until its vapour pressure exceeds 5 mm., it cannot be boiled. In addition to this, nucleation and growth of vapour bubbles does not take place easily at very low pressures, and boiling may not occur at all, particularly in liquids with high viscosities.

It is in such cases that evaporative distillation is employed. The condensing surface is brought into the same space as the evaporating surface, and the whole space is evacuated to a uniform, small pressure, generally small enough to bring about the change from normal to molecular evaporative distillation. With this arrangement, boiling must clearly be avoided. Rates obtainable by this method may be compared with ebullition. A good overall heat-transfer coefficient to boiling water is 700 B.t.u./ft.^{2}/hr./°F., which, even at a temperature difference of 100° F., corresponds only to a distillation rate of about 1×10^{-2} g./sec./cm.^{2} of heating surface, i.e. it is similar to w_0, per cm.^{2} of evaporating surface, for ice at $-20°$ C.

It can be seen that the most important quantity in distillation at a given temperature, T, is the saturation vapour pressure, Π, and three cases will be considered, namely, (i) Π is of the order of 10^{-4} mm. or less, (ii) Π is of the order of 10^{-2} mm. or more, (iii) Π is greater than 1 mm.

(i) Molecular distillation first proved a useful technique for oily liquids of very low volatility, which could not be distilled by boiling. The considerations of the previous section show that a maximum rate of distillation is achieved by decreasing P until λ is of the same order as the distance between the evaporating and condensing surfaces, i.e. it is desirable to decrease pressures to 10^{-3} to 10^{-4} mm. If this is done, no matter how small the value of Π, distillation rates should not be very sensitive to variations in either P or x.

These factors are familiar in design of large-scale molecular distillation for non-volatile oils. It is necessary now to stress that quite other considerations apply for more volatile substances.

(ii) In the first place, when Π is greater than 10^{-2} mm., mean free paths can play no part in the character of the distillation or upon design. Again, if w is to approach w_0, P must be reduced well below Π, and, in fact, conditions must be reached where eqn. (8) can be used. Consideration of this equation shows that, if $w = 0{\cdot}8\ w_0$ can be accepted as a reasonably high value for w, it is only necessary to decrease P to $0{\cdot}2\,\Pi$, and that there is little point in proceeding to lower values, e.g. a decrease to $0{\cdot}1\ \Pi$ would only increase w to $0{\cdot}9w_0$. Further, when eqn. (8) is obeyed, distillation rates are quite unaffected by x.

(iii) When Π is greater than 1 mm., the same considerations apply as in (ii), but values of w_0 are so great that it is not necessary for w to approach equality with w_0. It would be desirable to utilise the rapid increase in w when $P = \Pi$, but there is little point in using much lower values of P. It is true that the actual values of w when $P = \Pi$ are sensitive to changes in x, as shown in Fig. 3, but the differences are greatly reduced if P is made a little less than Π.

In brief, molecular distillation is not necessarily limited to liquids of extremely low volatility. For substances with vapour pressures over 10^{-2} mm., it offers a possibility of very rapid distillation without use of very low pressures, and is more or less independent of the space between evaporating and condensing surfaces; though, of course, the design must ensure that evaporating molecules can be effectively removed by collision with the condensing surface. The main practical limitation is that P must be decreased somewhat below Π, and, in the case of most liquids, this would at once cause boiling to take place.

This limitation does not apply to sublimation of solids. In fact, the only limitations in this case seem to be the design problems involved in rapid transfer of heat into the solid being sublimed and in scraping the solid sublimate from the condenser surface. The outstanding application is "freeze-drying," as in sublimation of ice from penicillin preparations at −20° c. to −30° c.; and here, as to be expected, the gap between evaporating and condensing surfaces does not appear to be critical, and it is not necessary to use particularly low pressures. From Fig. 3, it should not be necessary to go below 0·1 mm., and it would appear that the vacuum pump used is designed to give 0·01 mm. without load.[6]

[6] *Ind. Chem.*, 1945, 663.

C.S.I.R.,
Pretoria,
S. Africa.

MEASUREMENT OF ABSORPTION IN LIQUIDS AT 1·2 cm. AND 0·8 cm. WAVELENGTH USING A WAVE-GUIDE ABSORPTION CELL OPERATING IN THE $H_{01}^{\sqcap}$ MODE.

By J. G. Powles.

Received 27*th March*, 1947.

PART I.

Measurements at 1·2 cm.

Recent reports [1, 2, 3] of measurements of the energy absorption of solutions of polar substances in non-polar solvents at approximately 1 cm. wavelength have shown considerable variations among the values obtained by the different methods employed. The present work was undertaken in an attempt to resolve these differences. A waveguide absorption cell, similar to that used by Whiffen and Thompson,[2] has been employed, though the technique of measurement is different from the one described by these authors. The possible sources of error are analysed and the final results are compared with the previously-published ones.

Experimental Arrangement and Theoretical Treatment.

The experimental arrangement is shown diagrammatically in Fig. 1. The absorption cell consisted of rectangular-section, extruded copper tube provided with flanges at each end. Brass tubes for admitting and draining the liquid under test were attached at the flanges in the centre of the broad side of the guide. Beyond the ends of the cell were attached standing wave detectors, S.W.D. 1 and 2. These were separated from the cell by short lengths of guide to avoid detection of any evanescent modes [*] which might be associated with the discontinuity. The cell was closed by either mica or polythene sheets (see later) held by the clamping screws of the waveguide flanges. The output end of the waveguide system was completed by an oak-wedge termination in front of which the power standing wave ratio was 1·03. The input end was attached to a klystron oscillator through a 10 db. attenuation pad, and was provided with a T-junction and detector so that any variation of power, or impedance as seen from the input end, could be detected. The standing wave detectors, used for power measurement, were of standard pattern provided with tuned crystal

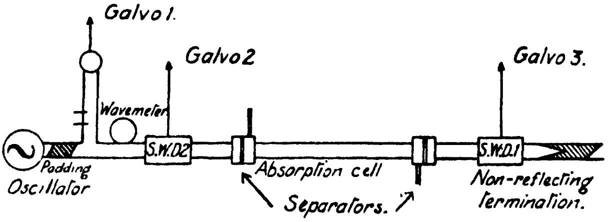

Fig. 1.

---

[1] Jackson and Powles, *Trans. Faraday Soc.*, 1946, **42A**, 101.

[2] Whiffen and Thompson, *ibid.*, 1946, **42A**, 114.

[3] Sutherland and Cripwell, *ibid.*, 1946, **42A**, 149.

[*] In fact, in view of the transverse form of the cell ends, it was not expected that any such modes would be of significant amplitude.

detectors leading to sensitive galvanometers. From the measured values of the resultant power flow at each end of the cell the absorption may be calculated as shown below.

With reference to Fig. 2, let Z_0 and Z_ε be the characteristic impedances

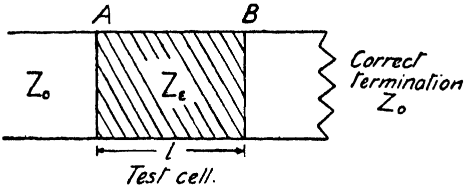

FIG. 2.

of the air- and liquid-filled sections of the waveguide system respectively and let it be supposed that the waveguide is correctly terminated. Then the impedance at the front end A of the liquid section, the test cell, is

$$Z_A = Z_\varepsilon \frac{1 - r\,e^{-2Pl}}{1 + r\,e^{-2Pl}}$$

where $P = \alpha + j\beta$ is the propagation constant in the liquid-filled section and $r = \dfrac{Z_\varepsilon - Z_0}{Z_\varepsilon + Z_0}$ is the voltage reflection coefficient at A.

If an alternating voltage $\sqrt{2}V_A e^{j\omega t}$ is supposed established at A, then the power flowing past A is

$$W_A = \frac{V_A{}^2 \mathscr{R}(Z_A)\,\dagger}{|Z_A|^2}.$$

The corresponding voltage at B is

$$V_B = \frac{V_A(1 - r)\,e^{-Pl}}{1 - r\,e^{-2Pl}}$$

and

$$W_B = |V_B|^2/Z_0.$$

Hence

$$\frac{W_A}{W_B} = \frac{V_A{}^2}{|V_B|^2} \cdot \frac{Z_0 \mathscr{R}(Z_A)}{|Z_A|^2}$$

which leads on substitution to

$$\frac{W_A}{W_B} = \frac{e^{2\alpha l}(1 - r^2 e^{-4\alpha l})}{\dfrac{Z_\varepsilon}{Z_0}(1 - r)^2}, \text{ } \beta \text{ disappearing.}$$

Since

$$\frac{Z_\varepsilon}{Z_0} = \frac{1 + r}{1 - r}$$

$$\frac{W_A}{W_B} = e^{2\alpha l}\,\frac{(1 - r^2 e^{-4\alpha l})}{1 - r^2}. \quad . \quad . \quad . \quad . \quad . \quad (1)$$

In this expression the factor $(1 - r^2 e^{-4\alpha l})$ represents the effect of internal reflection at the two ends of the cell.

For large values of α

$$\frac{W_A}{W_B} \to \frac{e^{2\alpha l}}{1 - r^2}.$$

In practice it was required to determine the difference in absorption coefficient of a pure solvent and the solvent containing a known, small concentration of a polar substance. The effect of the latter on the permittivity was sufficiently small not to affect the value of r significantly, so

---

† $\mathscr{R}$ denotes the " real part of."

that if α_1 and α_2 are the absorption coefficients of the two liquids it follows from (1) that

$$\alpha_2 - \alpha_1 = \frac{1}{2l}\left[\log_e \frac{(W_A/W_B)_2}{(W_A/W_B)_1} + \log_e \frac{1 - r^2 e^{-4\alpha_1 l}}{1 - r^2 e^{-4\alpha_2 l}}\right]. \quad . \quad (2)$$

in nepers/metre, where l is in metres.

The second term is small compared with the first so that an initial value of $(\alpha_2 - \alpha_1)$, may be obtained by ignoring it. The second term may then be taken into account by use of the value of α_1 derived from a comparison of the cell when filled with pure solvent and with air. Since α_1 only occurs explicitly in the correction term its value need not be determined accurately.

The effect of internal reflections is smaller the larger the value of α_1, and in fact for the benzene solvent used, for which $\tan \delta = 0{\cdot}0011$ at 1·22 cm., and for the range of $\tan \delta$ values measured, the correction term affected the incremental $\tan \delta$ (ref.[1]) to the extent of less than $2\frac{1}{2}$ % for the 30 cm. cell and $1\frac{1}{2}$ % for the 60 cm. cell.

It will be noted from eqn. (2) that the relative sensitivity of the two standing-wave detectors need not be known, though it is necessary that it should remain constant during a series of measurements. Eqn. (2) automatically allows for the copper loss in the waveguide walls although this is small in any event. The effect of a slightly imperfect termination may be shown to give a small apparent modification in r but since this quantity only occurs in the correction term the effect on the derived $(\alpha_2 - \alpha_1)$ value is negligible. $(\alpha_2 - \alpha_1)$ having been determined, the corresponding incremental loss angle ($\tan \delta$) value is obtained from the relation

$$\tan \delta = (\alpha_2 - \alpha_1)\frac{\lambda}{\pi}\frac{[1 - (\lambda/\lambda_{\epsilon_0})^2]^{\frac{1}{2}}}{\sqrt{\epsilon/\epsilon_0}}$$

where λ is the free space wavelength and λ_{ϵ_0} is the cut-off wavelength in the liquid-filled cell.

Experimental.

The whole system was held in a sloping position to ensure that the cell was filled completely and occluded air-bubbles avoided. The sensitivity of the standing-wave detectors was adjusted to give convenient galvanometer deflections for the range of power levels occurring in the series of measurements, and the sensitivity of the detectors was such that with the cell empty, and the termination replaced by a short circuit, movement of either detector from the maximum to the minimum of the standing wave, showed no effect on the other, or on the input detector, indicating that the power taken by them was of negligible magnitude.

Standing-wave observations were made with the cell filled first with solvent, then with solutions of increasing concentration of solute and finally, in order to check that the relative sensitivity of the detectors had not changed during the measurements, with the solvent again. During the process the reading of galvanometer 3 changed considerably but the power flow as measured by S.W.D. 2 was substantially constant. It should be noted that by use of two standing-wave detectors any change in power output of the oscillator during the period in which the liquid was changed, or due to the difference in input impedance of the solvent and solution-filled cell, was automatically accounted for. The value of $(\alpha_2 - \alpha_1)$ as a function of concentration was then determined by eqn. (2) and a typical result is shown in Fig. 5.

The standing-wave detectors were tested by observing the standing-wave pattern in front of a short-circuited termination. It was found that the curves were somewhat flatter than the ideal sinusoidal shape and that the shape was independent of the probe penetration used provided this was less than 5 % of the guide width. This indicated either that the crystal did not have a square-law characteristic, that the galvanometer deflection was not linear or that there was appreciable third harmonic content in the power obtained from the oscillator. The latter possibility is unlikely and was shown not to be the reason by measurements taken with and without the insertion of a frequency selective filter. The relation of power level to galvanometer deflection was calculated from the standing-wave pattern observed in front of the short circuit and is shown in Fig. 3, from which it is seen that the law of the detector system has an average exponent of rather less than 2. This method is considered better than the calibration of the crystal separately since the galvanometer deflection is related directly to the power level in the guide.

As previously mentioned, the test cell was formed between thin sheets of mica or polythene tightly held between flanges attached to the ends of the cell section and the adjacent standing-wave detector sections of waveguide. The presence of the separating sheets and the discontinuity in the metal of the waveguide wall means an imperfect transition from air- to liquid-filled guide. The degree of the imperfection was investigated by studying the variation of the standing-wave ratio in front of the liquid-filled cell as a function of cell

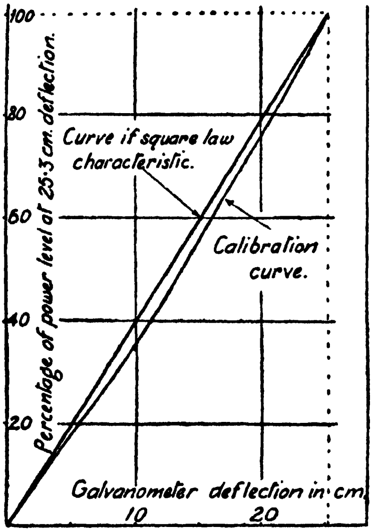

FIG. 3.

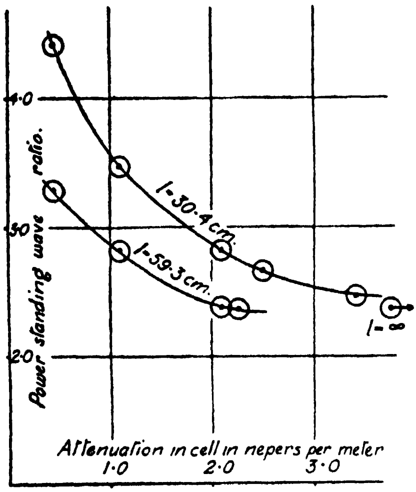

FIG. 4.—Standing wave in front of cell against attenuation.

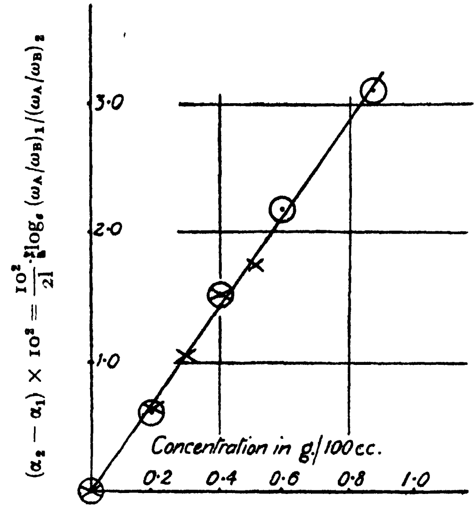

FIG. 5.—Relation of attenuaion in cell to concentration of solution.

attenuation. Fig. 4 shows this relation for two cell lengths. In both cases the standing-wave ratio approaches the value of approximately $2{\cdot}3_5$ as the attenuation is increased. This value was confirmed by measuring the standing-wave ratio when the separator at the output end of the cell was replaced by an oak wedge which formed a correct termination to the cell. The standing-wave ratio can be easily calculated for a perfect transition from air- to liquid-filled guide followed by a correct termination and for benzene as the dielectric is found to have the value 2·9. This differs from the measured value, $2{\cdot}3_5$ by much more than the experimental error and the difference must be ascribed to the imperfect nature of the air-liquid transition. It may be noted, however, that the difference in power standing-wave ratios observed can be caused by a change in reflected power of only 2½ %.

The possible effects of this imperfection on the results was investigated by varying the cell length and the material and thickness of the separators. Fig. 5 gives the results obtained with two cells of lengths 30·4 and 59·3 cm. closed by mica sheets of thickness 0·003 cm. The relation between attenuation coefficient and concentration is linear and identical for the two lengths, suggesting that the end-effect was not important.

Polythene should be more satisfactory than mica since its permittivity is approximately equal to that of benzene, the solvent employed in the present investigation. No effect on the measured $(\alpha_2 - \alpha_1)$ was observed for thicknesses of polythene as large as 0·5 mm. It is likely that a small leakage of energy occurred at the cell ends and that the amount of this varied with the material and thickness of the separators, but it may be shown mathematically that, to a first approximation, the effect of this on $(\alpha_2 - \alpha_1)$ is insignificant and the experimental results mentioned confirm this.

Although with the waveguide employed in the preceding measurements (cross-section 10·7 × 4·3 mm.) only the H_{01} mode is freely propagated in the air-filled portions, propagation of the H_{02} mode is possible in the cell when filled with benzene. The occurrence of this mode will change the energy absorption in the cell but it may be shown theoretically that the derived value of $(\alpha_2 - \alpha_1)$ is unaffected to a first approximation. Nevertheless, and notwithstanding the improbability of the introduction of this mode in significant amplitude at the separators, it seemed desirable to carry out measurements with a cell in which propagation of the H_{02} mode was impossible.

The results of measurements using a cell of dimensions 6·36 × 4·3 mm. are given in Table I alongside those obtained with the 10·7 × 4·3 mm. guide. It will be seen that the difference between corresponding results is not significant.

TABLE I.—SOLUTIONS IN BENZENE AT 19 ± 1° C.

Solute.	Benzophenone.	Nitrobenzene.	Bromobenzene.	Chloroform.	Acetone.
Tan δ for * guide 10·7 × 4·30 mm.	1·55	3·52	$0{\cdot}60_0$	$0{\cdot}32_2$	1·55
Tan δ for guide 6·36 × 4·30 mm.	1·48	3·56	$0{\cdot}59_7$	$0{\cdot}33_1$	1.53
% difference . . .	4½	− 1	½	3½	1½

* These tan δ values, and the others given in the paper, are extrapolated values for a concentration of 1 g. mol. per 100 cc.

Results.

The results given in Table II for solutions of five polar substances in benzene are the average values obtained from several runs, analogous to the one illustrated

TABLE II.—SOLUTIONS IN BENZENE AT 19 ± 1° C. AND 1·22 CM. WAVELENGTH.

Solute.	Benzophenone.	Nitrobenzene.	Bromobenzene.	Chloroform.	Acetone.
Tan δ	1·51	3·54	$0{\cdot}59_9$	$0{\cdot}32_6$	1·54

in Fig. 5, with both the large and small section waveguides. The figures were obtained from the slope of the best-fitting straight line through the points corresponding to a range of concentrations. The standard deviation of the individual points from this line was about ± 3 % for all the solutions investigated.

Consideration of the Results in Relation to other Values.

Measurements of the absorption of liquid solutions at a wavelength of 1·23 cm. using a H_{01} resonator carried out by the author have already been reported.[1] The results obtained by this method and the one just described are compared in Table III where the resonator values have been reduced by 5 % compared with the values previously reported to allow for the presence of the cup, as was then suggested (ref.[1], p. 103).

TABLE III.

Solute.	Benzophenone.	Nitrobenzene.	Bromobenzene.	Chloroform.	Acetone.
Tan δ by resonator at 1·23 cm.	1·67	3·49	0·628	$0{\cdot}33_9$	1·61
Tan δ by waveguide cell at 1·22 cm.	1·51	3·54	$0{\cdot}59_9$	0·326	1·54
% difference . . .	10	−1	5	4	4½

It will be seen that except in the case of the benzophenone solution the difference between the waveguide and resonator results lies within the ± 5 % limit given previously [1] as the estimated observational accuracy of the latter, outside the cup correction mentioned above. It may be justifiable to suspect that the 5 % cup correction applied to the resonator results is too low. However, no evidence in support of this can be drawn from the resonator work, and unfortunately it has not proved possible to resolve the discrepancy further.

Taking these waveguide results as the basis of comparison, Table IV shows the % differences among all the recorded tan δ values at about 1·22 cm. for the range of solutions referred to in Table III.

TABLE IV.

Solute.	Benzophenone.	Nitrobenzene.	Bromobenzene.	Chloroform.	Acetone.
(1) Cell method at 1·22 cm. : present paper* . . .	0	0	0	0	0
(2) Resonator method at 1·23 cm. : Willis Jackson and Powles [1]	+10	−1	+5	+4	+4½
(3) Cell method at 1·27 cm. : Whiffen and Thompson [2] .	−14½	−6	−3	—	−7
(4) Cell method at 1·25 cm. : Sutherland and Cripwell [3] .	−5½	−2	—	+5	+9
(5) Cell method at 1·23 cm. : Hall, Halliday, etc.[4] . .	−4	—	0	—	+2½

* Reference values.

The effect which possible inaccuracies in individual results of the order shown may exercise on values of dipole moment and relaxation

[4] Hall, Halliday, Johnson and Walker, *Trans. Faraday Soc.*, 1946, **42A**, 158.

time derived from measurements at a limited number of wavelengths, possibly involving two or more different experimental assemblies, depends on the proximity of the points of measurement to the absorption maximum and their location relative to this maximum. It is evident that if reliable values of dipole moment and relaxation time are to be obtained the range of wavelength covered must be sufficiently extensive to embrace both sides of the peak of absorption and to permit a substantial plot of the absorption curve. This is emphasised in the succeeding section of the paper.

PART II.

Measurements at 8 mm. Wavelength.

Experimental.

An exactly similar arrangement to that employed at 1·22 cm. was used at 8 mm. wavelength. It would have been preferable to use special components of smaller size than those used at 1·22 cm.‡ but unfortunately these were not available. The oscillator power available in this case was considerably smaller so that it was not possible to use the apparatus under such ideal conditions. It was found, however, that approximately 5 db. of padding could be retained at the oscillator, although this involved a larger probe penetration in S.W.D. 1 (approximately 25 % of the guide width) than was desirable.

Standing-wave patterns taken looking into a short circuit were found to be flatter than the theoretical sinusoidal shape and to have the maxima a little displaced from the mid-point between the adjacent minima. It was possible to obtain an estimate of the probe admittance from this measurement and from a measurement of the observed standing wave in a correctly terminated guide following a similar method to that used by Altar, Marshall and Hunter.[5] Allowance for this was somewhat simplified here since the measurement of relative power levels only is involved. An analysis was carried out showing that this can be done to a sufficient degree of accuracy for the large probe penetration used in the experiments.

It was found in addition that the amplitude of successive maxima of the standing wave in front of a short circuit decreased slowly indicating a certain amount of radiation from the slot, but this was not sufficient to affect seriously the measurement of relative power level.

Results.

A typical experimental relation of $(\alpha_2 - \alpha_1)$ to concentration of solution is shown in Fig. 6, and the derived tan δ values for the range of solutions covered by the preceding measurements are given in Table V.

TABLE V.—SOLUTION IN BENZENE AT 19 ± 1° C. AND 8·0 MM. WAVELENGTH.

Solute.	Benzophenone.	Nitrobenzene.	Bromobenzene.	Chloroform.	Acetone.
Tan δ	$0{\cdot}98_3$	2·43	$0{\cdot}40_8$	$0{\cdot}25_6$	2·16

The loss factor of the benzene used was measured as approximately 0·0015 which is in keeping with the trend of values at longer wavelengths.

Relation to Longer Wavelength Values.

These 8 mm. results may be combined with the ones previously reported[1] over the wavelength range 1·2-50 cm. In the case of the solution of benzophenone in benzene, Fig. 7, the 8 mm. measurement is well down the high frequency side of the absorption curve. The Debye curve shown has been drawn as the best fit of the experimental points while giving weight to each point according to its estimated accuracy of measurement, and is slightly different from the one drawn in the preceding paper.[1]

---

‡ It is possible to propagate 8 mm. waves in the H_{02} mode in the air-filled 1·2 cm. guide, but this mode is not recorded by the standing-wave detectors.

[5] Altar, Marshall and Hunter, *Proc. Inst. Radio Eng.*, vol. 34, Jan. 1946.

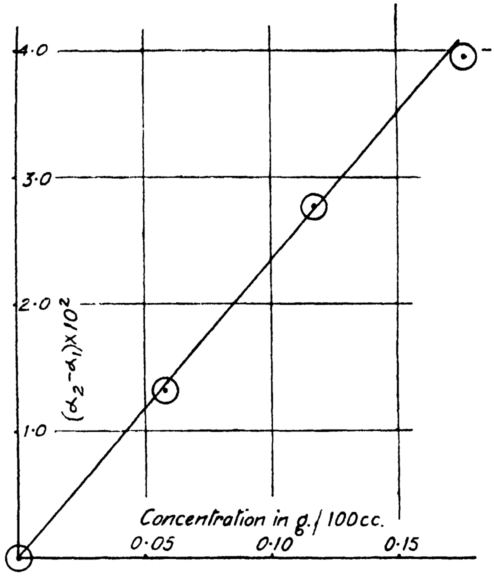

FIG. 6.—Relation of attenuation in cell to concentration of solution.

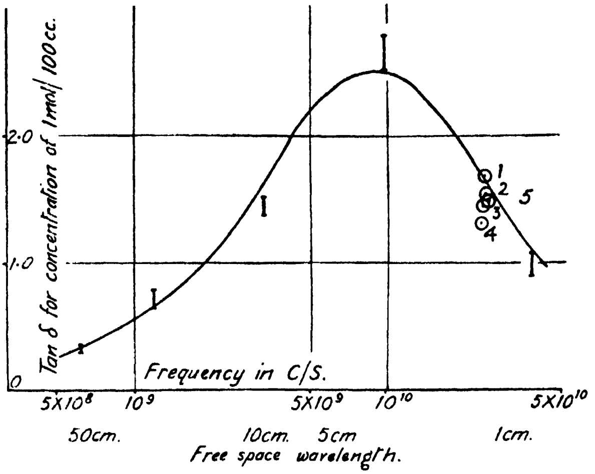

FIG. 7.—Loss in benzophenone in benzene. $\tau = 17{\cdot}8 \times 10^{12}$ sec. (The points 1, 2, 3, 4, 5 refer to the results given in Table IV.)

A smooth curve through the experimental points would indicate a variation of absorption with a rather sharper dependence on frequency than that corresponding to the Debye curve. This was also the case for solutions of the other polar substances studied. To establish the observation beyond doubt would, however, require experimental points at much closer intervals in wavelength and of considerably improved individual accuracy. Since there is no theoretical evidence to suggest the possibility of an absorption curve sharper than that given by the Debye relation, and in view of the experimental error this observation tends to strengthen the conclusion drawn in the preceding paper that the behaviour of the solutions referred to conforms to the simple Debye theory.

It may be mentioned that the acceptance of the Onsager, rather than the Debye, concept of the internal field leads to a change in the height of the absorption curves for the solutions studied of less than ½ %.[6]

We have also estimated the possible effect of molecular inertia under these conditions and find that the absorption is unlikely to be affected by more than 1½ % (calculations in preparation for publication).

This work was carried out with the assistance of a research grant from the Department of Scientific and Industrial Research, and the author wishes to express his appreciation of this support.

Summary.

A method for the measurement of energy absorption in low-loss liquids at 1·2 cm. (Part I) and 0·8 cm. (Part II) wavelength by measuring the absorption of energy passing through a waveguide cell containing the test material is described. Results are given for the absorption of solutions of a number of polar substances in benzene. The results at 1·2 cm. are compared with those obtained by previous workers using alternative methods. Finally the results of the present paper are related to values at longer wavelengths.

[6] Calculated from equations given by Cole, *J. Chem. Physics*, 1938, **6**, 385.

Electrical Engineering Department,
Imperial College,
London.

THE THERMAL DECOMPOSITION OF DISILANE AND TRISILANE.

BY K. STOKLAND.

Received 3rd April, 1947.

In a paper on the thermal decomposition of ordinary disilane and trisilane Emeléus and Reid [1] have reported that these reactions proceed in a relatively simple manner, at any rate when compared with the results of the decomposition of the analogous hydrocarbons. (For information regarding the latter reactions see, for example, the monographs of Steacie [2] and Schumacher.[3]) Thus, in the decomposition of both the silicon hydrides mentioned above the only reaction products found at any stage were hydrogen, monosilane and silicon. This latter substance contained in the case of disilane a considerable amount of hydrogen, corresponding to an average composition $SiH_{0\cdot7}$, whilst in the decomposition of trisilane the deposited silicon was almost free from hydrogen. The experimental procedure was still further simplified by their discovery that the pressure change was very nearly proportional to the amount of decomposition for both silanes. This enabled the course of the reaction to be followed by pressure measurements, and series of experiments at different temperatures have been performed according to this method by the above-mentioned investigators.

---

[1] Emeléus and Reid, *J. Chem. Soc.*, 1939, 1021.

[2] Steacie, *Atomic and Free Radical Reactions* (New York, 1946).

[3] Schumacher, *Chemische Gasreaktionen* (Dresden and Leipzig, 1938).

The statement concerning the composition of the reaction mixture in the decomposition of disilane is not in agreement with the results of Stock and Somieski.[4] These investigators found that at not too high temperatures higher silanes also were formed in fairly large amounts.

The results obtained by Stock and Somieski, however, are not quite comparable with those obtained by Emeléus and Reid, since the former investigators used a dynamical method in decomposing the disilane, whilst the latter carried out their experiments under static conditions. In general, dynamical methods may often be assumed to give mixtures of reaction products somewhat different in composition from those obtained by statical methods. In this instance it seems reasonable to believe that the dynamical method used by Stock and Somieski favoured the formation of the higher silanes. In the earlier stages of the reaction there is a large probability of collision between the unchanged disilane molecules and the radicals which are presumably the first product of decomposition, and although the thermal stability of the silanes decreases with increasing molecular weight, the result of such collisions might be a certain amount of trisilane. This latter substance may then further react in a similar way to form tetrasilane and so on. By rapid cooling of the reaction mixture down to temperatures where the higher silanes are stable, larger amounts of these substances should be expected.

For the same reason it might have been expected that such compounds should also have been found, though to a lesser extent, when analysing the reaction mixture from the statical experiments. It is, of course, possible that the stationary concentration of such radicals was too small to produce higher silanes in sufficient quantity to be detectable by fractionation after quenching. However, the results from the analogous decomposition experiments with ethane make it probable that higher silanes would actually be formed in the reaction vessel.

In a series of investigations [*] on some properties of the lower silanes with light and heavy hydrogen, carried out by the present author, their thermal stability has been studied. Owing to the uncertainties referred to above, it was necessary to re-examine the course of the decomposition by analyses of the reaction mixture.

Experimental.

The construction of the apparatus for pyrolysis of the silanes was similar to that employed by Hogness, Wilson and Johnson [5] in research on the decomposition of monosilane, the most important difference being that in the present investigations a spherical reaction vessel was used instead of a cylindrical one as in the experiments of the authors just mentioned. The vessel had a capacity of about 250 ml. In order to obtain information as to a possible influence of the surface on the rate of decomposition two pieces of apparatus of this kind were used. In one of them (called A in the following) the reaction vessel was unpacked, whilst in the other (B) the vessel was filled with small Raschig rings, thus producing a variation in the surface-volume ratio of about 1 : 20. Both the apparatus and the Raschig rings were made of Duran glass, but before use the inner surfaces were completely covered by silicon, deposited from decomposition of some samples of monosilane.

Each apparatus was supported on the top of a large electric furnace, the reaction bulb hanging freely in the middle of it. The temperatures were measured by means of nickel-nichrome thermocouples, the electromotive force being determined potentiometrically. The thermocouples were calibrated at the melting points of tin, lead, zinc and aluminium. The samples of the three latter metals had been furnished, together with certificates, by the National Bureau of Standards, U.S.A., whilst the sample of tin was a *pro analysi* preparation from Merck. The potentiometer, the sensitive galvanometer and the certificated standard cells used were all manufactured by Tinsley and Co.

---

[4] Stock and Somieski, *Ber.*, 1923, **56**, 247.

[*] To be published shortly.

[5] Hogness, Wilson and Johnson, *J. Amer. Chem. Soc.*, 1936, **58**, 108.

Since the room temperature was maintained fairly constant, temperature variations were due almost entirely to variations of the voltage in the network. No automatic device was employed to compensate this effect. Instead, the current was kept as constant as possible by manual operation of a resistance in series with the furnace. As the furnace had a very large heat capacity and the experimental temperatures were comparatively low, this procedure required little experience in order to maintain the temperature within the limits of variation of ±0·1°c. Further, in order to smooth out possible temperature gradients, a thick-walled cylindrical aluminium box was inserted, the lid of which was divided into two parts and provided with holes for the thermocouple and the capillary of the reaction bulb. The preparation of the crude mixture of silanes and the separation of the individual components from it by fractionation were very carefully performed in a manner similar to that described by Stock and Somieski.[6]

Each sample of a pure substance was accurately measured in one of the calibrated sections of the large vacuum apparatus and transferred by means of liquid nitrogen into an auxiliary cylindrical vessel fitted with a tap and attached to the apparatus with a ground joint. Then the vessel was detached and connected to the decomposition apparatus. This latter was now thoroughly evacuated, and in the meantime the sample was allowed to evaporate and attain room temperature. Just before starting an experiment the manometer of the apparatus was read and simultaneously the atmospheric pressure. This was necessary because in these experiments an open manometer was used. Then the tap between the pump and the apparatus was closed and the silane allowed to stream into the apparatus until the pressures were equalised. The time necessary for this operation was 2-4 sec., and the moment of opening of the tap was taken as zero time. Immediately after closing the tap of the decomposition apparatus the pressure was read. This was always possible in these experiments on account of the apparent induction periods.

The amount of silane remaining in the auxiliary vessel and the external part of the apparatus was frozen in liquid nitrogen, transferred back into the vacuum apparatus and the volume measured. The difference between the two volume determinations was the amount taken for the decomposition.

The decomposition was now allowed to proceed for a length of time decided on beforehand. The manometer and the atmospheric pressure were again read, and immediately afterwards the reaction mixture was pumped off through a long U-tube of about 10 mm. diam. immersed in liquid nitrogen in order to condense the reaction products for analysis. This operation was carried out as rapidly as possible in order to prevent further decomposition, but not so rapidly as to pull condensable gases through the trap. The hydrogen formed was not collected, but was drawn off through the pump. This procedure was considered to be the best one since the collection of hydrogen would have required a Töpler-pump or some other slowly working device. Instead the amount of hydrogen was indirectly determined. However, even though the results so obtained seem to be very reasonable, as will appear from the following tables, it must be admitted that direct checks upon the amounts so found would have been of great value.

The condensate was brought into the large vacuum apparatus and analysed by means of fractionation at low pressures. Thus, monosilane was distilled off at about −160° c., disilane at about −105° c., trisilane at −70° c. and tetrasilane at −30° c. When a residue still remained after these distillations it was always very small in amount, and it has therefore been combined with and recorded as tetrasilane. This should cause only very small errors in the subsequent calculations. Of course, objections may be made to the method of separation of the components of the mixture ; but at the present time no better method is available for this purpose. Repeated fractionations of the same mixture in most cases showed good agreement, and the vapour pressures of the single components generally did not differ appreciably from those determined on very pure samples of the same substances.

---

[6] Stock and Somieski, *Ber.*, 1916, **49**, 111.

Results.

The results of the experimental investigations are shown in Tables I and II. Owing to difficulties caused by the war situation, rather limited series of experiments have been carried out. The decomposition of disilane has been studied at five different temperatures but at one pressure only, viz. about 10 cm., whilst in the case of trisilane a single series of experiments at about 592° K. and about 8 cm. pressure has been performed.

The two tables have been arranged as follows. The first four columns show the absolute temperatures, times, reaction vessels used and apparent induction periods of the experiments. In columns 5 and 6 are listed the figures of the initial pressures and changes of pressure. The next three columns show the amounts of silane employed, recovered and decomposed given in ml. N.T.P., and the next column gives the % amounts decomposed. Then follow the relative changes of pressure expressed for convenience as $100\frac{\Delta p}{p_0}$. The amounts of hydrogen given have been calculated from the changes of pressure and the amounts of the other volatile components of the reaction mixture. The columns 13, 14 and 15 show the amounts of these latter substances, also referred to N.T.P. Finally, the last two columns give the amounts of the hydrogen-containing deposits of silicon given as ml. of the hypothetical gaseous compound SiH_x, and the value of x. These two quantities have been calculated from the differences between the amounts of silicon and hydrogen in the original sample of silane and those of the gaseous reaction products. The tables give strong evidence that in the decomposition of disilane and trisilane, higher silanes are really among the products formed.

In trying to find the correct order of reaction in the two cases the data obtained at each temperature have been plotted appropriately for different orders. The temperature variations within each series of experiments are only small and most probably cause less error than some other factors. Further, since it is a somewhat difficult matter to correct the results to a common temperature, no such corrections have been applied.

From the plots it was found that the rate of decomposition could be represented approximately only by a first-order relationship. The first-order graphs for the decomposition of disilane at about 584, 611 and 633° K. are shown in Fig. 1, 2 and 3, respectively, and for the single series of trisilane in Fig. 4. In the early stages of the decomposition there was an almost linear dependence of $\log \frac{p_0}{p_t}$ with time (p_0 = initial pressure, p_t = pressure at a time t). In the later stages, however, considerable deviations from the unimolecular course were found as is shown by the graphs. This result is quite similar to that found in the pyrolysis of the monosilane, carried out by Hogness, Wilson and Johnson and later confirmed by the present author.

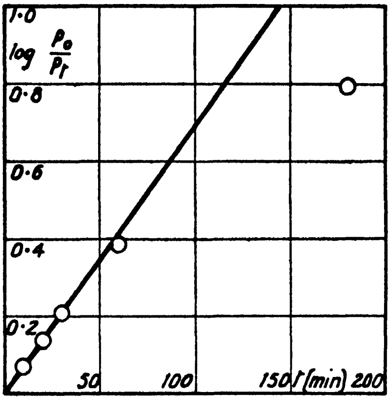

FIG. 1.

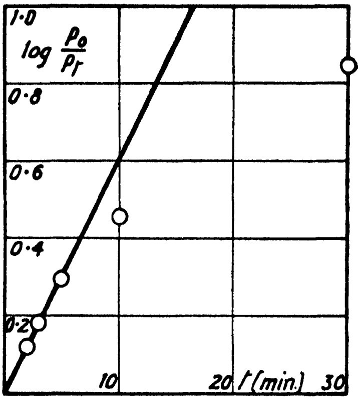

FIG. 2.

The curves seem in all cases to pass through the origin, and in the graphs only the limiting straight lines corresponding to an ideal unimolecular course

TABLE I.—THERMAL DECOMPOSITION OF Si_2H_6.

Temp.	Time.	Re-action vessel.	Apparent Induction Period.	p_0.	Δp.	Si_2H_6.				$100\frac{\Delta p}{p_0}$.	Reaction Products.					x in $(SiH_x)_n$.
						Empl.	Rec.	Dec.			H_2.	SiH_4.	Si_3H_8.	Si_4H_{10}.	SiH_x.	
°K.	min.		min.	mm.	mm.	ml.	ml.	ml.	%.		ml.	ml.	ml.	ml.	ml.	
584·6	10	A	10-15	90·5	0·1	16·30	13·86	2·44	15·0	0·1	0	1·55	1·05	0·05	0	—
584·9	20	A	—	88·0	0·7	15·78	11·47	4·31	27·3	0·8	0	2·80	1·77	0·13	0	—
584·6	30	A	—	88·3	1·2	16·19	10·00	6·19	38·2	1·4	0·22	3·86	1·93	0·39	1·17	1·64
584·5	60	A	—	88·7	7·2	15·99	6·54	9·45	59·1	8·1	0·72	7·69	1·78	0·56	3·63	1·28
584·2	180	A	—	89·8	32·5	16·06	2·58	13·48	83·9	36·2	2·31	15·93	0·78	0·27	7·61	0·47
583·7	24 hr.	A	—	90·5	61·0	16·45	0·79	15·66	95·2	67·4	6·66	19·95	0·14	0	10·95	0
597·5	3	B	5	110·0	0	14·51	12·64	1·87	12·9	0	0	1·14	0·82	0·09	0	—
597·3	5	B	—	108·8	0·4	14·32	11·43	2·89	20·2	0·4	0	2·02	1·07	0·14	0	—
611·2	2	B	3	109·7	0·7	13·93	10·57	3·36	24·1	0·6	0	2·28	1·29	0·11	0	—
611·9	3	B	—	110·8	0·6	14·14	9·33	4·81	34·0	0·5	0	3·00	1·54	0·40	0·40	1·35
611·4	5	B	—	106·9	2·1	13·70	6·96	6·74	49·2	2·0	0·21	4·67	1·62	0·51	1·91	1·72
611·5	10	B	—	108·1	10·1	13·85	4·88	8·97	64·8	9·3	0·76	7·83	1·22	0·45	4·65	1·45
611·9	30	B	—	107·4	47·8	13·63	1·95	11·68	85·7	44·5	2·95	14·08	0·54	0·18	6·94	0·25
613·1	24 hr.	B	—	107·0	108·7	13·63	0·23	13·40	98·3	101·6	14·48	12·73	0·04	0	13·95	0·01
621·2	1	A	1·5	92·3	0·5	15·63	12·44	3·19	20·4	0·5	0	2·03	1·27	0·06	0·30	0·87
621·0	2	A	—	92·0	0·9	15·69	9·92	5·77	36·8	1·0	0·43	3·43	1·89	0·18	1·72	1·81
633·4	1	A	1	93·6	0·5	15·51	10·38	5·13	33·1	0·5	0	3·56	1·68	0·13	1·14	1·58
632·7	2	A	—	93·0	6·8	15·54	6·96	8·58	55·2	7·3	0·71	6·90	1·72	0·38	3·58	1·37
633·2	3	A	—	92·4	12·2	15·46	4·70	10·76	69·6	13·2	0·67	10·43	1·27	0·43	5·56	1·27
632·7	5	A	—	92·8	24·0	15·51	3·15	12·36	79·7	25·9	1·53	13·74	0·86	0·25	7·40	0·91
632·5	24 hr.	A	—	93·0	154·2	15·64	0·01	15·63	99·9	165·8	37·38	4·14	0·04	0	27·00	0·08

TABLE II.—THERMAL DECOMPOSITION OF Si_2H_8.

Temp.	Time.	Re-action Vessel.	Apparent Induction Period.	p_0.	Δp.	Si_3H_8.				$100\frac{\Delta p}{p_0}$.	Reaction Products.					x in $(SiH_x)_n$.
						Empl.	Rec.	Dec.			H_2.	SiH_4.	Si_2H_6.	Si_4H_{10}.	SiH_x.	
°K.	min.		min.	mm.	mm.	ml.	ml.	ml.	%.		ml.	ml.	ml.	ml.	ml.	
591·5	5	A	2	74·8	1·7	13·48	10·36	3·12	23·1	2·3	1·00	2·02	0·35	0·05	6·44	1·91
591·7	10	A	—	75·0	5·3	13·57	8·43	5·14	37·9	7·1	1·28	4·08	0·57	0·16	9·56	1·80
591·8	15	A	—	75·3	10·7	13·61	6·84	6·77	49·7	14·2	2·34	5·43	0·71	0·22	12·58	1·69
591·3	30	A	—	75·0	23·3	13·43	4·98	8·45	62·9	31·1	1·82	9·30	0·82	0·69	11·65	1·28
592·0	45	A	—	74·7	38·3	13·46	3·41	10·05	74·7	51·3	2·34	13·27	0·91	0·43	13·34	0·97
591·6	60	A	—	75·0	50·1	13·48	2·18	11·30	83·8	66·8	3·37	15·16	1·37	0·40	14·40	0·75
590·8	120	A	—	73·6	69·2	13·27	1·27	12·00	90·4	94·0	5·31	17·16	1·74	0·26	14·32	0·26
592·3	41 hr.	A	—	75·1	112·3	13·45	0·06	13·39	99·6	149·5	13·75	19·63	0·12	0	20·30	0·02
592·7	100 hr.	B	—	87·7	140·6	11·49	0·10	11·39	99·1	160·3	14·51	15·14	0·16	0	18·71	0·03

have been drawn. The result is remarkable since at the temperatures in question there should be no induction periods or, at most, only very short ones. The observed apparent induction periods are most probably due to the circumstance that in the initial part of the decomposition the gaseous reaction products have the same volume as the decomposed part of the reactant.

Making use of the linearity of $\log \frac{p_0}{p_t}$ with time in the early stages of decomposition, the rate constants at different temperatures have been calculated from the first figure of each series of measurements. The results in the case of disilane are evident from Table III, which for comparison also includes the rate constants found by Emeléus and Reid. Although this is not expressly stated, it must be assumed that their figures are given in min.$^{-1}$ units, and they have, therefore, here been converted to sec.$^{-1}$. As it will be seen the rate constants found by the present author are considerably higher than those of Emeléus and Reid, which result is easily understood from what has already been said.

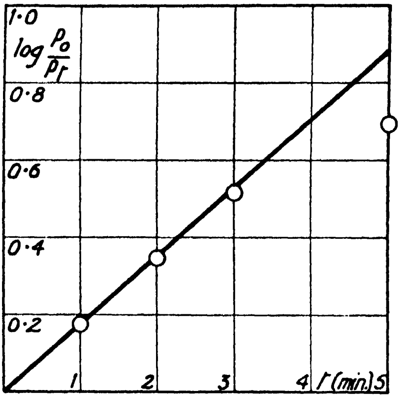

FIG. 3.

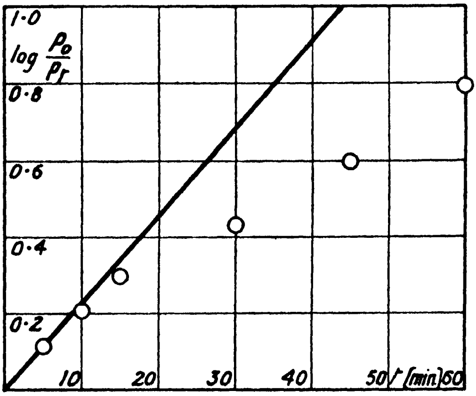

FIG. 4.

On the basis of the data of this table the following expression for the specific rate of decomposition as a function of the temperature has been obtained by the method of least squares: $k = 5{\cdot}8 \times 10^{14}\, e^{-\frac{48900}{RT}}$. The result has been plotted in Fig. 5.

TABLE III.—RATE CONSTANTS OF THE DECOMPOSITION OF Si_2H_6.

Temp. °K.	$\frac{1}{T} \times 10^3$.	k sec.$^{-1}$.	log k.	Experiments by E. & R.	
				Temp. °K.	k sec.$^{-1}$.
584·6	1·711	$2{\cdot}71 \times 10^{-4}$	$-3{\cdot}567$	587	$1{\cdot}0 \times 10^{-4}$
597·5	1·674	$7{\cdot}68 \times 10^{-4}$	$-3{\cdot}115$	605	$4{\cdot}2 \times 10^{-4}$
611·2	1·636	$2{\cdot}30 \times 10^{-3}$	$-2{\cdot}638$	622	$1{\cdot}1 \times 10^{-3}$
621·2	1·610	$3{\cdot}80 \times 10^{-3}$	$-2{\cdot}420$	633	$2{\cdot}8 \times 10^{-3}$
633·4	1·579	$6{\cdot}70 \times 10^{-3}$	$-2{\cdot}174$	—	—

The above equation indicates that the activation energy of decomposition of disilane should be 48·9 kcal., whilst Emeléus and Reid found 51·3 kcal. In spite of the differences in the rates of decomposition the agreement between the activation energies is good. It may be assumed, however, that this agreement is largely accidental.

For the single series of experiments with trisilane the rate constant in the early stage of decomposition has been calculated to be $8{\cdot}76 \times 10^{-4}$ sec.$^{-1}$ at 591·5° K., whilst Emeléus and Reid obtained $2{\cdot}57 \times 10^{-4}$ sec.$^{-1}$ at 589° K. and $4{\cdot}95 \times 10^{-4}$ at 600° K. Thus, for trisilane also, the rate of decomposition has been found to be higher than that reported by the above-mentioned investigators.

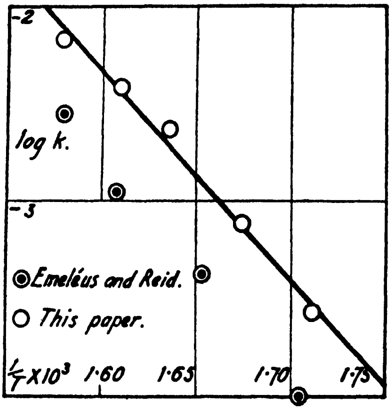

Fig. 5.

Discussion.

Disilane.—Since the decomposition of the disilane follows a unimolecular course, the primary step must be a splitting of the molecule. The most probable alternatives then seem to be:

$$Si_2H_6 \rightarrow 2SiH_3 \quad . \quad . \quad . \quad . \quad . \quad (1)$$

or

$$Si_2H_6 \rightarrow SiH_4 + SiH_2. \quad . \quad . \quad . \quad . \quad (2)$$

However, other initial reactions such as

$$Si_2H_6 \rightarrow Si_2H_5 + H$$

and

$$Si_2H_6 \rightarrow Si_2H_4 + H_2$$

are possible.

The two former reactions are entirely analogous to the initial steps proposed by Rice [7] and Rice and Herzfeld [8] and by Storch and Kassel [9] in the pyrolysis of ethane. A comparison between the decomposition mechanisms of disilane and ethane seems to be justified to a certain degree, while the reaction products show great analogies in the two cases. In the decomposition of ethane the products are chiefly ethylene and H_2 and small amounts of CH_4, C and higher hydrocarbons, whilst in the case of Si_2H_6 they are monosilane, H_2 and solid polymerised silicon hydrides and smaller amounts of higher silanes. As to the composition of the latter substance Table I shows that at the beginning of its formation the formula is near $(SiH_2)_n$, whilst in the later stages it is becoming, on the average, poorer in hydrogen. This result is in accordance with the investigations of Schwarz and Heinrich,[10] who found that polysilene decomposes at the temperatures in question.

It seems very reasonable to assume that the polysilene has been formed by polymerisation of silico-olefines. This assumption seems to be supported by the fact that in the initial stage of decomposition no polysilene is present. Since during this period there is no change of volume, there may at first be a conversion of disilane into monosilane and higher silanes. Because of the large concentration of disilane compared with the concentrations of radicals and silico-olefines, these latter substances may react with disilane to form higher silanes rather than polymerise. The higher silanes, however, are less stable than disilane and decompose more rapidly, giving rise to new radicals and olefines. With decreasing amount of disilane collisions between unsaturated molecules become more frequent, leading finally to the formation of polysilene.

---

[7] Rice, *J. Amer. Chem. Soc.*, 1931, **53**, 1959.
[8] Rice and Herzfeld, *ibid.*, 1934, **56**, 284.
[9] Storch and Kassel, *ibid.*, 1937, **59**, 1240.
[10] Schwarz and Heinrich, *Z. anorg. Chem.*, 1935, **221**, 277.

The decomposition of this latter substance is a heterogeneous process. Therefore, only the initial part of the decomposition of disilane can be treated as a purely homogeneous reaction. The study of the decomposition of ethane is a more easy one, since, with the exception of elementary carbon, only gaseous reaction products are formed. But although in this case a large amount of work in different directions has been done to discover the reaction mechanism, there still prevails considerable doubt about it. Even more difficult is the interpretation of the decomposition mechanism of disilane, since here the tendency of the unsaturated hydrides to polymerise eliminates characteristic features which would otherwise appear from the nature and amounts of the individual compounds. It seems, therefore, to be of little use to try to suggest a complete scheme for the decomposition mechanism, and in the present paper only a more limited discussion concerning the information to be derived from some experimental facts will be given.

It was suggested by Emeléus and Reid, by analogy with the then most widely accepted interpretation of the decomposition of ethane, that the decomposition of disilane is mainly a chain reaction of the Rice type, the initial step of which is the reaction (1). In support of this theory they stated that an increase of the surface-volume ratio decreased the rate of decomposition. However, since this result was probably obtained from determinations of pressure changes alone, further experiments with analysis of the reaction products ought to be performed before drawing a definite conclusion. Experiments with different surface-volume ratios at the same temperature have not been carried out by the present author, but Table I and Fig. 5 indicate that the influences of chain reactions would be small.

This result is in accordance with the view now commonly held in the case of ethane. Though it has been certainly found that chain reactions actually do take place in the decomposition of this substance, a large part of it proceeds by a chain-free mechanism. There exists at the present time very little knowledge about this part of the reaction. There appears, however, to be much to be said in favour of the mechanism suggested by Storch and Kassel. Their scheme involves the methylene instead of the methyl radical, and although there is still no certain experimental evidence as to the existence of methylene radicals in this case, the assumption of its participation explains the formation of the main reaction products in the simplest and most natural manner.

In addition to the decomposition experiments with pure disilane Emeléus and Reid also carried out investigations on the effects of added hydrogen and ethylene. The effect of hydrogen was to remove the induction period, and analyses of the reaction products showed that considerably more monosilane had been formed. This result they thought to give support to a mechanism of the Rice type. It will, however, at once be seen that both silyl and silene radicals may well account for the increased amount of monosilane.

The experiments quoted in the present paper show that at the temperatures in question there are most probably no induction periods at all. The induction periods found by the investigators mentioned above have been obtained from pressure readings and are only apparent. The disappearance of the induction periods when hydrogen is added is due to the change in the relative amounts of the different reaction products.

In the decomposition experiments on mixtures of disilane and ethylene there was a certain polymerisation of the latter compound. This result is quite analogous to that found when decomposing lead tetramethyl in the presence of ethylene as reported by Taylor and Jones.[11] However, whilst in the latter case each methyl radical produced caused on the average a polymerisation of 6-7 molecules of ethylene, the amount of this substance polymerised by the decomposition of disilane was only approximately equal to the amount of disilane decomposed. It may be that the polymerising effect of methyl radicals is greater than that of the silyl radicals. It seems, however, that the results in the two cases are too different to support the theory of a mechanism in which silyl radicals play the most important part.

A comparison of the rates of decomposition of the disilanes with light and heavy hydrogen shows that the deuterium disilane decomposes at a considerably lower rate than the ordinary compound. In a relatively narrow temperature range around 600° K. the average ratio of the decomposition rates, k_D/k_H, was 0·71. Although it was expected that the deuterium compound would be the more stable one, the difference seems to be too large if the rate-determining step in both cases is the split of the Si—Si bond. It is hardly reasonable to assume that the deuterium atoms attached to the silicon atoms should influence the strength of the Si—Si bond to such a high degree.

This difficulty does not arise if (2) is assumed to be the primary step. Here a rearrangement of the atoms within the molecules may be assumed to precede decomposition, and this process almost certainly requires a different activation energy in the two cases.

Considering the diamond arrangement of the atoms in the silicon crystal, the strength of the Si—Si bond should be simply one-half of the heat of sublimation of silicon. Unfortunately, the figures for this latter quantity obtained by different investigators from vapour pressure determinations show very large inconsistency, covering a range from 44 kcal. as previously found by von Wartenberg[12] up to 102-105·5 kcal. more recently obtained by Ruff.[13] It seems very reasonable to consider the latter figure as the most reliable one, and this would give a bond strength of 51-53 kcal., which is within the limits of error equal to the activation energy derived by Emeléus and Reid. (Pauling[14] gives 42·5 kcal. for the strength of the Si—Si bond.) In the opinion of the present author, however, the heat of sublimation of silicon is far too uncertain to give any valuable support to the assumed strength of the Si—Si bond. It seems on the contrary that the activation energy obtained for the decomposition of disilane should rather be used to choose the most reliable figure for the heat of sublimation, since the bond strength can hardly be assumed to be less than that of the activation energy.

However, owing to the complex nature of the decomposition, it seems doubtful whether the overall activation energy can be used as a measure of the rate of the initial reaction. The participation of the original disilane molecules in reactions with radicals and other molecules formed and the re-formation of disilane molecules in different ways make the whole problem very obscure. The activation energy seems to be rather high as it is only slightly smaller than that of the decomposition of the monosilane, viz., 51·7 kcal., found by Hogness, Wilson and Johnson[6] and confirmed by the present author. Finally, it may be mentioned that the decomposition of the analogous substance digermane, examined by Emeléus and Jellinek,[15] most probably is also more complex than reported by these investigators.

Trisilane.—In the decomposition of trisilane, the mechanism certainly is even more complex, more modes of decomposition being possible here. Emeléus and Reid suggested that the first step might be

---

[11] Taylor and Jones, *J. Amer. Chem. Soc.*, 1931, **52**, 1111.

[12] von Wartenberg, *Z. anorg. Chem.*, 1913, **79**, 71.

[13] Ruff, *Trans. Electrochem. Soc.*, 1935, **68**, 87.

[14] Pauling, *The Nature of the Chemical Bond* (New York, 1944).

[15] Emeléus and Jellineke, *Trans. Faraday Soc.*, 1944, **40**, 93.

$$Si_3H_8 \rightarrow 2SiH_3 + SiH_2.$$

However, such a simultaneous split of two Si—Si bonds must be rare, as it would most probably imply the accumulation within the molecule of a larger amount of energy than is required for the break of only one bond.

Decomposition experiments with trisilane mixed with an excess of hydrogen, carried out by the authors just mentioned, gave the result that almost exactly two moles of monosilane were formed per mole of trisilane decomposed. They explained this fact by assuming that the silyl radicals were hydrogenated to monosilane, whilst the silene radicals were dehydrogenated. However, if this assumption is correct, it would be expected that the decomposition of disilane in presence of an excess of hydrogen would also give two moles of monosilane per mole of disilane decomposed, since a simple splitting of a disilane molecule also gives two silyl radicals. But the experimental results [1] show that the maximum amount of monosilane obtained in this case is only 1·5 moles per mole of disilane.

Experiments with added ethylene gave an amount of polymerisation of ethylene of 1·33 moles per mole of trisilane decomposed. This result presumably indicates a somewhat larger concentration of silyl radicals than in the case of disilane.

The author is much indebted to Norsk Hydro-Elektrisk Kvælstof A/S for financial aid and supply of liquid nitrogen. He also wishes to express his thanks to Mr. J. B. M. Herbert, University of Manchester, for valuable help and advice in correcting the manuscript.

Summary.

The thermal decomposition of disilane in the temperature range 584-633° K. and of trisilane at 592° K. has been studied by a static method and with analyses of the reaction mixture. It has been found that there is no exact proportionality between the amount of silane decomposed and the observed change of pressure.

For both substances the rates of reaction at given temperatures have been found to be larger than those previously obtained. The induction periods reported by other investigators from observations of pressure changes have been shown to be only apparent.

The activation energy of the decomposition of disilane has been found to be 48·9 kcal., which is not much below the figure given previously, viz. 51·3 kcal.

Some arguments have been advanced that chain reactions involving silyl radicals may not be the most important process in the decomposition of the two compounds.

Institute of Applied Inorganic Chemistry,
The Technical University of Norway,
Trondheim.

MOLECULAR FORCE FIELDS. I.
THE STRUCTURE OF THE WATER MOLECULE.

By D. F. Heath and J. W. Linnett.

Received 11*th April*, 1947.

Darling and Dennison [1] have deduced from the spectrum of water and heavy water the vibration frequencies of these molecules for infinitesimal vibrations. They have also obtained the third and some of the fourth power anharmonic terms in the potential energy (P.E.) function. These have been given in terms of special co-ordinates proportional to the normal co-ordinates. It is the first object of the calculations presented here to express the P.E. function in terms of the distortions of the bond lengths and angle between the bonds. The second object is to see whether the " cross quadratic terms " and the cubic and quartic terms in the P.E. function, which is now expressed in co-ordinates related to the structure, can be accounted for in terms of any reasonable forces which are likely to exist in the water molecule.

Calculations.

In the following calculations the atomic masses of hydrogen and deuterium have been taken to be 1·00813 and 2·01473, the velocity of light as $2·99776 \times 10^{10}$ cm./sec., Avogadro's number as $6·023 \times 10^{23}$, Planck's constant as $6·624 \times 10^{-27}$ erg-sec., and $4\pi^2c^2/N$ as $5·890342 \times 10^{-2}$ in c.g.s. units.[2] The values of the frequencies for infinitesimal amplitude are: H_2O: symmetric, 3825·32 and 1653·91; antisymmetric, 3935·59; D_2O: symmetric, 2758·06 and 1210·25; antisymmetric, 2883·79 cm.$^{-1}$. The inter-bond angle is 104° 31′ and the OH equilibrium length is $r = 0·9580$ A.[1]

The potential energy function, omitting all terms other than quadratic ones, is written as

$$2V = k_1 . \Delta r_1^2 + k_1 . \Delta r_2^2 + k_\theta . \Delta\theta^2 + k_{11}\Delta r_1 . \Delta r_2 + k_{1\theta}(\Delta r_1 + \Delta r_2) . \Delta\theta \quad (1)$$

where Δr_1, Δr_2 and $\Delta\theta$ represent the changes in the two bond lengths and in the interbond angle from the values they have in the equilibrium configuration. From the frequencies of the vibrations of infinitesimal amplitude we can calculate the force constants. We find that they are

$$\begin{aligned} k_1 &= 8·42541 \times 10^5 \text{ dynes per cm.} \\ k_\theta/r^2 &= 0·768l4 \times 10^5 \text{ dynes per cm.} \\ k_{11} &= -\ 0·20084 \times 10^5 \text{ dynes per cm.} \\ k_{1\theta}/r &= 0·50469 \times 10^5 \text{ dynes per cm.} \quad . \quad . \quad . \quad (2) \end{aligned}$$

We will see if we can account for these values of the cross-term constants. They are small showing that the molecular force field is not very different from the simple valency force field (S.V.F.F.) but they are by no means negligible. In the main we shall consider the signs of the cross-term constants.

Let us first consider the possibility of these cross-term constants being explained in terms of repulsion between the hydrogen atoms. Let the P.E. of the interaction of the two hydrogen atoms is

$$V = V_0 + A(\Delta R) + \tfrac{1}{2}B(\Delta R)^2 \quad . \quad . \quad . \quad (3)$$

---

[1] Darling and Dennison, *Physic. Rev.*, 1940, **57**, 128.

[2] Birge, *Reports Prog. Physics*, 1941, **8**, 90.

where V_0 is the value of V when ΔR is zero, and ΔR is the change from the distance separating the hydrogen atoms when the water molecule is in its equilibrium configuration. The function need only be taken as far as the quadratic term in ΔR at the present stage. If the ΔR is transformed into Δr_1, Δr_2 and $\Delta\theta$ it may be shown that

$$\begin{aligned} V = V_0 + A \times 10^8\{0{\cdot}124(\Delta r_1 - \Delta r_2)^2 - 0{\cdot}103\,.\,r^2\Delta\theta^2 \\ + 0{\cdot}319\,.\,r\Delta\theta(\Delta r_1 + \Delta r_2)\} \\ + \tfrac{1}{2}B\{0{\cdot}625(\Delta r_1 + \Delta r_2)^2 + 0{\cdot}375\,.\,r^2\Delta\theta^2 \\ + 0{\cdot}968\,.\,r\,.\,\Delta\theta(\Delta r_1 + \Delta r_2)\} \quad (4) \end{aligned}$$

This means that, if k_{11} and $k_{1\theta}$ are to be explained by interaction between the hydrogen atoms, we must then have

$$\begin{aligned} 0{\cdot}625B - 0{\cdot}248A' &= k_{11} = -0{\cdot}201 \times 10^5 \\ 0{\cdot}484B + 0{\cdot}319A' &= k_{1\theta}/r = 0{\cdot}505 \times 10^5 \quad . \quad . \quad (5) \\ \text{where} \qquad A' &= A \times 10^8. \end{aligned}$$

If the repulsion between the hydrogen atoms is of the van der Waals type, A' must be negative since $A = \mathrm{d}V/\mathrm{d}R$ which is negative for a repulsion. B will be expected to be positive since at separations less than that corresponding to the minimum the van der Waals P.E. curve has a positive curvature—B is $\mathrm{d}^2V/\mathrm{d}R^2$. This means that, if repulsion between the hydrogen atoms were the major factor in causing the presence of cross-terms in the P.E. function of the water molecule, we would expect k_{11} to be positive. It is, in fact, negative and this implies that there is some other more important factor which results in the presence of cross-terms in the P.E. function.

The inter-bond angle in water is 104° 31′. It has been suggested that the ideal inter-bond angle is 90° because the unpaired electrons in the oxygen atom are 2*p* electrons, but that the angle is greater than this ideal value because of repulsion between the hydrogen atoms.[3] An alternative explanation of why the valency angle is greater than 90° is the following. Two *p*-orbitals are directed at right-angles to one another and, on Pauling's theory of directed valency, two bonds which use *p*-orbitals should ideally be at 90° to one another. However, in the oxygen atom, there are a pair of 2*s* electrons and the *s*-orbitals may contribute to the bond forming orbitals. If there is complete hybridisation of the *s*- and three *p*-orbitals the angle between the valency bonds will be 109° 48′ (tetrahedral angle).[4] If there is partial hybridisation with the *s*-orbital then the inter-bond angle will lie between 90° and 109° 48′. It may be that this is the main reason why the bond angle in water is 104° 31′. We will see how we would expect partial hybridisation to contribute to the cross-terms in the P.E. function of water.

The reason why this effect may contribute to the cross-terms is that the alteration of one part of the molecule may affect the equilibrium configuration of another part. For instance, the alteration of the length of one of the bonds may change the equilibrium configuration of the other.[5] In what follows it is presumed that at each stage of the vibration the electronic configuration takes up instantaneously the arrangement of minimum energy for each particular nuclear configuration.[6] This is equivalent to saying that the electron movements are very much more rapid than the nuclear movements.

From the available evidence it seems reasonable to take the tetrahedral covalent radius of the oxygen atom to be 0·66 A.[7] and the divalent

[3] Pauling, *Nature of the Chemical Bond* (Cornell), III, Sect. 13.
[4] Pauling, *J. Amer. Chem. Soc.*, 1931, **53**, 1367.
[5] Linnett, *Quart. Review*, 1947, **1**, 73.
[6] Born and Oppenheimer, *Ann. Physik*, 1927, **84**, 457.
[7] Pauling, *Nature of the Chemical Bond*, V, Sect. 21 ; V, Sect. 23*a*.

radius to be 0·74 A.[8] This is in agreement with the view that sp^3 hybridised bonds are stronger than p-bonds.[9] This means that the lengthening of either of the OH bonds will favour an electronic configuration involving more p-bond and less sp^3 bond than in the equilibrium configuration. This increase in the p-bond contribution will mean that the whole structure will become more p-bonded, which will mean that the equilibrium length of the other bond will increase and the equilibrium angle will decrease. Similarly a decrease in the angle towards 90° will favour a greater contribution from the p-bonded structure and hence an increase in the length of both bonds. Let us represent the equilibrium length of bond No. 1 when the whole molecule is in its equilibrium configuration as r°_1 and as r_1^e when bond No. 2 is lengthened by Δr_2 and the angle increased by $\Delta\theta$. Similarly for bond No. 2 and for the angle θ. Then, taking into account what has been said above, we may write

$$\begin{aligned} r_1^e &= r_1^\circ + c_1 \,.\, \Delta r_2 - c_2\Delta\theta. \\ r_2^e &= r_2^\circ + c_1 \,.\, \Delta r_1 - c_2\Delta\theta. \\ \theta^e &= \theta^\circ - c_3 \,.\, \Delta r_1 - c_3\Delta r_2. \end{aligned} \qquad . \quad . \quad . \quad (6)$$

where $\Delta r_1 = r_1 - r_1^\circ$, $\Delta r_2 = r_2 - r_2^\circ$ and $\Delta\theta = \theta - \theta^\circ$. The constants c_1, c_2 and c_3 in (6) are all positive on the basis of the arguments used. Now let us suppose that the P.E. for very small displacements is given by

$$2V = k_1(r_1 - r_1^e)^2 + k_1(r_2 - r_2^e)^2 + k_\theta(\theta - \theta^e)^2. \qquad . \quad (7)$$

Substitution of (6) in (7) gives

$$2V = k_1(\Delta r_1^2 + \Delta r_2^2) + k_\theta\Delta\theta^2 - 4k_1c_1\Delta r_1\Delta r_2 + (2k_1c_2 + 2k_\theta c_3)\Delta\theta(\Delta r_1 + \Delta r_2) \quad (8)$$

Terms involving c_1^2, c_2^2, c_3^2 and c_1c_2 are ignored since it is presumed that c_1, c_2 and c_3 are all small. It will be seen at once that this accounts for the sign of the cross-term constants k_{11} and $k_{1\theta}$. If c_2/r is put equal to c_3r, we obtain $c_1 = 0{\cdot}007 \times 10^5$ and $c_2/r = c_3r = 0{\cdot}03 \times 10^5$ dynes per cm. Because these are small it was justifiable to neglect their squares and products. The general conclusion we make, therefore, is that changes in the extent to which the s-orbital is hybridised with the p-orbitals during a vibration are able to explain satisfactorily the signs of the cross-term constants in the P.E. function of the water molecule. That is, these changes account for the deviations from the S.V.F.F.

Before concluding this section we will consider briefly the electrostatic repulsion between the hydrogen atoms. Pauling gives the bond moment of the OH link in water as $1{\cdot}51 \times 10^{-18}$ E.S.U.[10] It is presumed, as a simple picture, that the charges are located on the nuclei, which means that each hydrogen carries $1{\cdot}58 \times 10^{-10}$ E.S.U. Repulsion between these charges gives a resolved force, normal to the bond, of $6{\cdot}7 \times 10^{-5}$ dynes. The restoring force when the inter-bond angle is opened through θ radians is $k_\theta \,.\, \theta/r$. With $k_\theta/r^2 = 0{\cdot}77 \times 10^5$, a restoring force of $6{\cdot}7 \times 10^{-5}$ dynes would be given with θ equal to about 5°. So electrostatic repulsion seems to be inadequate to explain the opening up of the bonds from 90° to 104½°. Of course, the calculation is very much simplified but it appears to indicate that other factors are required to explain why the inter-bond angle in the water molecule is so much greater than 90°.

Therefore, taking into consideration what we have said before, we suggest that probably the most important reason why the HOH angle is greater than 90° is because hybridisation of the s-orbital with the p-orbitals occurs to a considerable extent when the oxygen forms its two bonds in water. Repulsion between the hydrogen atoms appears, on the present evidence, to be less important than the hybridisation of the orbitals.

---

[8] Palmer, *Valency* (C.U.P.), pp. 45 and 82.

[9] Pauling and Sherman, *J. Amer. Chem. Soc.* 1937, **59**, 1450.

[10] Pauling, *Nature of the Chemical Bond*, II, Sect. *11d.*

Cubic and Quartic Terms.

Darling and Dennison used co-ordinates X_1, X_2 and X_3 which were proportional to the normal co-ordinates. They wrote the P.E. function of the water molecule in the form :

$$\begin{aligned} V/hc = {} & \tfrac{1}{2}(n_1X_1^2 + n_2X_2^2 + n_3X_3^2) + (\alpha_1X_1^3 + \alpha_2X_2^3 + \alpha_3X_1^2X_2 \\ & + \alpha_4X_1X_2^2 + \alpha_5X_1X_3^2 + \alpha_6X_2X_3^2) + (\beta_1X_1^4 + \beta_2X_2^4 \\ & + \beta_3X_3^4 + \beta_4X_1^2X_2^2 + \beta_5X_1^2X_3^2 + \beta_6X_2^2X_3^2 + \beta_7X_1X_2^3 \\ & + \beta_8X_1^3X_2 + \beta_9X_1X_2X_3^2) \qquad (9) \end{aligned}$$

where n_1, n_2 and n_3 are the vibration frequencies for infinitesimal displacements in wave-numbers. They were unable to determine β_7, β_8 and β_9.[11] From the determination of the force constants k_1, k_θ, k_{11} and $k_{1\theta}$ it is possible to express X_1, X_2, and X_3 in terms of Δr_1, Δr_2 and $\Delta\theta$. It is found that

$$\begin{aligned} X_1 \times 10^{-8} &= \pm\,(7{\cdot}40256\,.\,\Delta S + 0{\cdot}455730\,r\Delta\theta) \\ X_2 \times 10^{-8} &= \pm\,(4{\cdot}78628\,r\Delta\theta - 0{\cdot}0248547\,\Delta S) \\ X_3 \times 10^{-8} &= \pm\,(7{\cdot}38567\,\Delta D) \quad . \quad . \quad . \quad . \quad (10) \end{aligned}$$

where $\Delta S = \Delta r_1 + \Delta r_2$ and $\Delta D = \Delta r_1 - \Delta r_2$. The alternative signs do not matter in the quadratic terms but they do in the cubic.

These expressions (10) are now substituted in the cubic part of (9) together with the $\alpha_1-\alpha_6$ values found by Darling and Dennison to give the cubic part in terms of ΔS, ΔD and $\Delta\theta$. The positive sign in the expression for X_1 is used because it is found that if the expression with the negative sign is used a most improbable expression is obtained (see later). There are now two possibilities according to whether the positive or negative sign in the expression for X_2 is used. We will not at the moment select one rather than the other. The two possibilities are :

$$\begin{aligned} V' \times 10^{-8} = {} & -2{\cdot}594 \times 10^5\,\Delta S^3 - 0{\cdot}481 \times 10^5\,r\Delta S^2\Delta\theta \\ & + 0{\cdot}700 \times 10^5\,r^2\Delta S\Delta\theta^2 - 0{\cdot}057 \times 10^5\,r^3\Delta\theta^3 \\ & - 7{\cdot}293 \times 10^5\,\Delta S\Delta D^2 + 0{\cdot}381 \times 10^5\,r\Delta\theta\,.\,\Delta D^2 \quad (11a) \end{aligned}$$

or

$$\begin{aligned} V' \times 10^{-8} = {} & -2{\cdot}594 \times 10^5\,\Delta S^3 - 0{\cdot}492 \times 10^5\,r\Delta S^2\Delta\theta \\ & + 0{\cdot}697 \times 10^5\,r^2\Delta S\Delta\theta^2 + 0{\cdot}146 \times 10^5\,r^3\Delta\theta^3 \\ & - 7{\cdot}284 \times 10^5\,\Delta S\Delta D^2 - 1{\cdot}278 \times 10^5\,r\Delta\theta\,.\,\Delta D^2 \quad (11b) \end{aligned}$$

where V' is the cubic part of V.

The first thing that stands out, whichever of these two is correct, is that the two biggest terms are those involving ΔS^3 and $\Delta S\Delta D^2$ and that the ratio of the coefficients of these two terms is quite close to 1 : 3. If we take the coefficients of these two terms as 2·59 and $7{\cdot}29 \times 10^5$ respectively and replace ΔS and ΔD by Δr_1 and Δr_2 we obtain as far as these two terms are concerned :

$$V \times 10^{-8} = -9{\cdot}88 \times 10^5(\Delta r_1^3 + \Delta r_2^3) - 0{\cdot}48 \times 10^5(\Delta r_1^2\Delta r_2 + \Delta r_1\Delta r_2^2) \quad (12)$$

That is, the terms which do not involve the mixing of Δr_1 and Δr_2 are far more important than the $\Delta r_1^2\Delta r_2$ and $\Delta r_1\Delta r_2^2$ terms (coefficients in the ratio of 20 : 1). Therefore the most important cubic terms are those which represent the departure of the OH bond P.E. function from the parabolic form.

We will compare the above coefficient of the Δr_1^3 term with the similar term for the ground state of the OH radical. For the OH radical: $\nu_e = 3727{\cdot}95$ cm.$^{-1}$; $\nu_e x_e = 78{\cdot}15$ cm.$^{-1}$; and $r_e = 0{\cdot}9710$ A.[12] Substituting these into the Morse function we get $a = 2{\cdot}21106 \times 10^8$ and $D = 8{\cdot}8282 \times 10^{-12}$, and when the Morse function is expanded we get $-9{\cdot}54 \times 10^{13}$ for the coefficient of the cubic term in the expression for V.

---

[11] Dennison, *Rev. Mod. Physics*, 1940, **12**, 175.

[12] Tanaka and Koana, *Proc. Phys. Math. Soc. Japan*, 1934, **16**, 365; Herzberg, *Molecular Spectra and Molecular Structure of Diatomic Molecules* (Prentice-Hall), p. 491.

This is the same order of magnitude as that obtained above and the agreement is quite as good as would be expected for the presence of the second hydrogen atom is bound to affect the electron distribution in the other OH link. This comparison with the OH diatomic molecule therefore confirms the above finding.

It may be pointed out at this stage that, had the negative sign been taken in the expression (10) for X_1, the coefficient of Δr_1^3 and Δr_2^3 would have been positive which is not at all likely.

Before considering the remainder of the cubic terms in the potential energy expression we will take a look at the quartic terms which involve only Δr_1 and Δr_2. Since the coefficient of ΔS in X_2 is so small this means that we need consider, for quite an accurate result, only the terms involving X_1^4, X_3^4 and $X_1^2X_2^3$. Darling and Dennison give the coefficients of these terms as $\beta_1 = 39$, $\beta_3 = 35$, and $\beta_5 = 212$. Now, to a close approximation $X_1 \times 10^{-8} = 7{\cdot}4\Delta S$ and $X_3 \times 10^{-8} = 7{\cdot}4\Delta D$. It will also be seen that β_1 and β_3 are about equal and a sixth of β_5. Since

$$\Delta S^4 + \Delta D^4 + 6\Delta S^2\Delta D^2 = 8\Delta r_1^4 + 8\Delta r_2^4,$$

this means that the main quartic terms involving Δr_1 and Δr_2 are those which do not involve any mixing and that the coefficients of the $\Delta r_1^3\Delta r_2$, $\Delta r_1^2\Delta r_2^2$ and $\Delta r_1\Delta r_2^3$ are relatively small. The coefficient of the quartic terms Δr_1^4 and Δr_2^4 is approximately 17×10^{21} in the expression for V. The quartic term in the expanded Morse function of the OH radical is *ca.* 12×10^{21} which is of the same order of magnitude. It is interesting that in the quartic terms as in the cubic terms, the terms which are associated with each OH link taken separately are the most important.

In (11) we gave the two possible expressions for the cubic terms in the P.E. function. Let us now see if it is possible to decide which is more likely to be the correct one. A marked difference between them is that in (11*a*) the coefficient of the $\Delta\theta^3$ term is negative, while in (11*b*) it is positive. Since it is very probable that the P.E. increases more rapidly as the angle decreases than as it increases because of the crowding together of the orbitals, it seems to us that it is probable that the coefficient of $\Delta\theta^3$ has a negative sign (cf. that of Δr^3). This means that the correct set of cubic terms is probably (11*a*). It remains to be seen whether it is possible to offer any reasonable explanation of the coefficients of $\Delta r_1\Delta r_2(\Delta r_1 + \Delta r_2)$, $r\Delta S^2\Delta\theta$, $r^2\Delta S\Delta\theta^2$ and $r\Delta D^2\Delta\theta$ which are $-0{\cdot}48$, $-0{\cdot}48$, $+0{\cdot}70$ and $+0{\cdot}38 \times 10^5$ respectively in the expression for $V \times 10^{-8}$. We will see whether repulsion between the hydrogen atoms can account at all for these coefficients. Let the repulsion potential energy function be taken as

$$V = V_0 + A(\Delta R) + \tfrac{1}{2}B(\Delta R)^2 + \tfrac{1}{6}C(\Delta R)^3 + \dots \qquad (13)$$

It may be shown that the above coefficients are:

$$\begin{aligned} \Delta S\Delta r_1\Delta r_2 &= -0{\cdot}0645A'' + 0{\cdot}0978B' + 0{\cdot}2472C = -0{\cdot}48 \times 10^{13}, \\ r\Delta S^2\Delta\theta &= 0{\cdot}2526B' + 0{\cdot}1787C = -0{\cdot}48 \times 10^{13}, \\ r^2\Delta S\Delta\theta^2 &= -0{\cdot}1941A'' + 0{\cdot}0324B' + 0{\cdot}1481C = +0{\cdot}70 \times 10^{13}, \\ r\Delta D^2\Delta\theta &= -0{\cdot}2167A'' + 0{\cdot}0757B' = 0{\cdot}38 \times 10^{13} \qquad (14) \end{aligned}$$

where $A'' = A \times 10^{16}$ and $B' = B \times 10^8$.

As was stated earlier, for a van der Waals repulsion between the hydrogen atoms, we would expect A to be negative and B to be positive. We would, moreover, on the basis of a P.E. function of the type used by Lennard-Jones,[13] expect C to be negative. If we use the last three equations of (14) to solve for A, B and C we obtain $C = 1{\cdot}7 \times 10^{13}$, $B = -3{\cdot}0 \times 10^5$ and $A = -2{\cdot}8 \times 10^{-3}$. Thus, of these, only A has the correct sign. Further tests show that the equations under (14) cannot be explained by any likely set of values for A, B and C. We conclude, therefore, that repulsion between the hydrogen atoms cannot explain the cubic cross-terms.

[13] Lennard-Jones, *Proc. Physic. Soc.*, 1931, **43**, 461.

Of course the sign of certain of the cubic cross-terms could be accounted for by such a repulsion but this is probably of no significance and would be anticipated on chance alone. We are therefore brought to the same conclusion as we reached when considering the quadratic terms. That is, that there are factors other than repulsion between the hydrogen atoms which are important in causing departures from the P.E. function based on the simple valency force field. At the moment we are not able to offer any satisfactory explanation of the cubic cross-terms in the P.E. function and, because of this, it seems pointless to consider the cubic terms further than we have done already. Suggestions might be made to explain these cubic cross-terms but they would be valueless as they could not be tested.

Our two main conclusions are: (i) Repulsion between the hydrogen atoms does not seem to be of major importance in the water molecule and the reason that the HOH angle is greater than 90° appears to be that there is considerable hybridisation of the *s*-orbital with the *p*-orbitals of the oxygen atom in bond formation. On this supposition we can account for the quadratic cross-terms in the P.E. function. (ii) The most important cubic and quartic terms in the P.E. function are those involving Δr_1^3, Δr_2^3, Δr_1^4 and Δr_2^4 and they have coefficients very close to those of similar terms in the P.E. function of the OH radical. The most important cubic and quartic terms are therefore those which measure the departure of the bond P.E. functions from the simple parabolic form and not those which measure interactions between the two bonds or the bonds and the angle. The cubic cross-terms cannot be accounted for satisfactorily by repulsion between the hydrogen atoms.

In conclusion we wish to thank the Hope Department and the Christopher Welch Trust for allowing us the use of a calculating machine and Mr. R. P. Bell for his advice.

Summary.

Darling and Dennison's P.E. function for the water molecule has been transformed into a function involving as variables the changes in the bond lengths and inter-bond angle. The form of this function is discussed in relation to various structural factors in the water molecule. It is concluded that the most important reason why the HOH angle in water is greater than 90° is because there is hybridisation of the 2*s*-orbital of the oxygen atom with the 2*p*-orbitals in the formation of the O—H bonds.

Inorganic Chemistry Laboratory,
Oxford University.

MOLECULAR FORCE FIELDS. II.

THE FORCE FIELD OF THE TETRAHALIDES OF THE GROUP IV ELEMENTS.

BY D. F. HEATH AND J. W. LINNETT.

Received 11th April, 1947.

Urey and Bradley[1] accounted for the vibration frequencies of the tetrahedral molecules XY_4 by supposing that the inter-atomic forces in the molecule could be divided into two types: (*a*) valency forces tending to restore valency bonds to their equilibrium lengths and valency angles to their equilibrium angles; (*b*) repulsion forces between non-bonded atoms. Type (*a*) in the tetrahedral molecules necessitates the use of two valency force field (V.F.F.) constants which are (i) the force constant of the XY bond; (ii) the constant of the YXY angle. Urey and Bradley supposed that the repulsion between the non-bonded Y atoms could be represented by a/R^7, where R is the distance between the Y atoms and a is a constant. With this type of force field, Urey and Bradley calculated the four frequencies of the XY_4 molecules from three constants, the two V.F.F. constants and a. Using a completely new set of constants for each molecule they obtained satisfactory results for the molecules CCl_4, $SiCl_4$, $TiCl_4$, $SnCl_4$, CBr_4 and $SnBr_4$. It appears from their results that this type of force field is satisfactory. However, it does seem likely that, if a repulsion exists between the non-bonded Y atoms, it should be possible to discover a function relating the potential energy (P.E.) and the distance between the Y atoms which may be used in all the XY_4 molecules whatever the nature of X provided that Y remains the same (e.g. in the series of tetrachlorides). This will, of course, only be possible if the electronic structure of the bonded Y atoms does not change greatly from molecule to molecule. The present paper is concerned with showing that it is possible to find such a function for the tetrachlorides and tetrabromides. Unfortunately the vibration frequencies of only two tetrafluorides are known.

---

[1] Urey and Bradley, *Physic. Rev.*, 1931, **38**, 1969.

That repulsion between the non-bonded atoms is an important factor in the tetrahedral molecules is indicated by the following considerations. If the P.E. function of the molecule XY_4 could be represented entirely in terms of the two V.F.F. constants, it may be shown that the following relation between the frequencies would hold [2]

$$\lambda_3 + \lambda_4 = \lambda_1\left(1 + \frac{4m_Y}{3m_X}\right) + \frac{2}{3}\lambda_2\left(1 + \frac{8m_Y}{3m_X}\right) \quad . \quad . \quad (1)$$

where $\lambda_i = 4\pi^2c^2\nu_i$, where ν_i is the frequency of the *i*th vibration frequency expressed in wave-numbers. The vibrations are numbered as follows: (1) the totally symmetric vibration; (2) the doubly-degenerate vibration; and (3) and (4) the two triply-degenerate vibrations. Table I gives

TABLE I.—COMPARISON OF DEPARTURES FROM THE SIMPLE VALENCY FORCE FIELD WITH THE SIZES OF THE ATOMS FOR THE TETRAHEDRAL GROUP IV TETRAHALIDES.[2]

Molecule.	$\lambda_3 + \lambda_4$ obs.	$\lambda_3 + \lambda_4$. calc.	Percentage Diff.	Radius of X.	Radius of Y.	$\frac{\text{Radius X.}}{\text{Radius Y}}$
SiH_4 . .	3·29	3·36	2·1	1·17	0·30	3·9
CD_4 . .	3·59	3·76	4·7	0·77	0·30	2·6
CH_4 . .	6·38	6·69	4·9	0·77	0·30	2·6
NH_4^+ .	6·93	7·27	4·9	0·70	0·30	2·3
SiF_4 . .	0·72	0·79	9·7	1·17	0·64	1·8
$SnCl_4$ . .	0·106	0·118	11·3	1·40	0·99	1·41
$SnBr_4$.	0·050	0·059	18·0	1·40	1·14	1·23
$TiCl_4$ . .	0·156	0·191	22·4	1·31	0·99	1·32
$GeCl_4$ . .	0·138	0·169	22·5	1·22	0·99	1·23
$GeBr_4$. .	0·071	0·089	25·3	1·22	1·14	1·07
$SiCl_4$ . .	0·25	0·32	28·0	1·17	0·99	1·19
$SiBr_4$ . .	0·151	0·20	32·5	1·17	1·14	1·03
CF_4 . .	1·18	1·89	60·2	0·77	0·64	1·2
CBr_4 . .	0·29	0·53	83·0	0·77	1·14	0·68
CCl_4 . .	0·41	0·78	90·2	0·77	0·99	0·78

---

[2] Herzberg, *Infra-red and Raman Spectra of Polyatomic Molecules* (van Nostrand), p. 182.

($\lambda_3 + \lambda_4$) observed, and the same calculated using (1) from λ_1 and λ_2 for fifteen molecules. It will be seen that for all, the former is less than the latter, and the fourth column gives the percentage difference between these. The molecules have been arranged in the table in the order of this percentage difference. In the fifth and sixth columns are given the tetrahedral radii of the central X atoms and the outer Y atoms, and in the last column the ratios of these radii are listed. It will be seen that, in the main, the figures in the last column decrease on passing down the table. That is, as Y increases in size relative to X (the ratio becomes smaller) the departure from the simple V.F.F. becomes greater. This is precisely what would be expected if repulsion between the non-bonded atoms is the cause of the departure from the simple V.F.F. So this evidence supports the view that the forces between the non-bonded atoms are important in the vibrations of these molecules.

Vibration Frequency Calculations.

In the following treatment it is supposed that the variation of P.E. with change of the XY_i distance (represented by r_i) is given by $f(r_i)$; that the variation of P.E. with change of the Y_iY_j distance (represented by R_{ij}) is given by $\mathrm{F}(R_{ij})$; and that the variation of P.E. with changes in the Y_iXY_j angle (represented by $\Delta\alpha_{ij}$) is given by $V = \frac{1}{2}k_\alpha \,.\, \Delta\alpha_{ij}^2$. The total P.E. is therefore :

$$V = \sum_i f(r_i) + \sum_{ij} \mathrm{F}(R_{ij}) + \sum_{ij} \tfrac{1}{2}k_\alpha \,.\, \Delta\alpha_{ij}^2. \qquad . \quad . \quad (2)$$

For calculating the vibration frequencies for vibrations of infinitesimal amplitude we shall expand $f(r)$ and $\mathrm{F}(R)$ in powers of Δr and ΔR up to the second where these measure the changes in r and R from the values they have at equilibrium ($r_i{}^\circ$ and $R_{ij}{}^\circ$). Then

$$\begin{aligned} V = {} & \sum_i \mathrm{f}(r_i{}^\circ) + \sum_i \mathrm{f}'(r_i{}^\circ)\Delta r_i + \sum_i \tfrac{1}{2}f''(r_i{}^\circ)(\Delta r_i)^2 \\ & + \sum_{ij} \mathrm{F}(R_{ij}{}^\circ) + \sum_{ij} \mathrm{F}'(R_{ij}{}^\circ)\Delta R_{ij} + \sum_{ij} \tfrac{1}{2}\mathrm{F}''(R_{ij}{}^\circ)(\Delta R_{ij})^2 \\ & + \sum_{ij} \tfrac{1}{2}k_\alpha \,.\, \Delta\alpha_{ij}^2. \quad . \quad . \quad . \quad . \quad . \quad . \quad . \quad (3) \end{aligned}$$

We will represent the above differentials as follows :

$$f'(r_i{}^\circ) = C \,;\; f''(r_i{}^\circ) = k \,;\; \mathrm{F}'(R_{ij}{}^\circ) = -B \,;\; \tfrac{1}{2}\mathrm{F}''(R_{ij}{}^\circ) = A. \quad . \quad (4)$$

k is the force constant of the XY link. The expressions for the vibration frequencies are then : [3-5]

$$\lambda_1 = (k + 8A)/m_Y \quad . \quad . \quad . \quad . \quad . \quad . \quad . \quad (5)$$

$$\lambda_2 = (3k_\alpha/(r^\circ)^2 + 2A + B/R^\circ)m_Y \quad . \quad . \quad . \quad . \quad . \quad (6)$$

$$\begin{aligned} \lambda_3 + \lambda_4 = {} & (k + 8A/3 - 4B/3R^\circ)(1/m_Y + 4/3m_X) \\ & + (2k_\alpha/(r^\circ)^2 + 4A/3 + 10B/3R^\circ)(1/m_Y + 8/3m_X) \\ & - (8A/3 - 4B/3R^\circ)(8/3m_X) \quad . \quad . \quad . \quad . \quad . \quad (7) \end{aligned}$$

$$\begin{aligned} \lambda_3\lambda_4 = {} & (k + 8A/3 - 4B/3R^\circ)(2k_\alpha/(r^\circ)^2 + 4A/3 + 10B/3R^\circ) \\ & - [\tfrac{1}{2}(8A/3 - 4B/3R^\circ)^2][1/m_Y{}^2 + 4/m_X \,.\, m_Y]. \quad . \quad . \quad (8) \end{aligned}$$

The first stage in our calculations was to use the four observed frequencies of each of the molecules (see Table IV) to calculate k, $k_\alpha/(r^\circ)^2$, A and B/R° for all the molecules. That is the four constants are determined from the four vibration frequencies. The results are shown in

---

[3] Dennison, *Astrophys. J.*, 1925, **62,** 84.

[4] Scaeffer, *Z. physik.*, 1930, **60,** 586.

[5] Trumpy, *ibid.*, 790.

Table II. If we now assume that the P.E. function, F(R), may be represented by $V = a/R^n$, then $B/R^\circ = na/(R^\circ)^{n+2}$ and $A = n(n + 1)a/2(R^\circ)^{n+2}$; and $\frac{A}{B/R^\circ} = (n + 1)/2$. The values of n given in the last column of Table II were obtained using the values of A and B/R° in the fourth and

TABLE II.—CALCULATION OF THE FOUR CONSTANTS k, $k_\alpha/(r^\circ)^2$, A and B/R° FROM THE FOUR VIBRATION FREQUENCIES OF THE TETRAHALIDE MOLECULES.

CF_4 . .	4·32	0·240	0·603	0·211	4·7
SiF_4 . .	5·7	0·5	0·198	0·213	0·9
CCl_4 . .	1·79	0·0797	0·318	0·094	5·9
$SiCl_4$ . .	2·55	0·0408	0·146	0·056	4·3
$GeCl_4$ . .	2·40	0·0369	0·106	0·037	4·7
$TiCl_4$ . .	2·46	0·0460	0·076	0·0069	21
$SnCl_4$ . .	2·34	0·0279	0·053	0·033	2·2
CBr_4 . .	1·38	0·0482	0·241	0·086	4·6
$SiBr_4$ . .	2·01	0·0366	0·115	0·042	4·5
$GeBr_4$ . .	1·90	0·0290	0·085	0·030	4·7
$SnBr_4$ . .	1·84	0·0204	0·055	0·0225	3·9

TABLE III.—CALCULATION OF THE CONSTANT, a, IN THE SUGGESTED REPULSION P.E. FUNCTION.

Molecule.	r° in A.[1]	R° in A.	a in ergs. (A.)$^{-4·5}$
CF_4	1·36	2·22	10·0 × 10^{-11}
CCl_4	1·755	2·87	24·4
$SiCl_4$	2·00	3·27	26·1
$GeCl_4$	2·08	3·40	24·3
$TiCl_4$	2·18	3·56	28
$SnCl_4$	2·30	3·76	22
CBr_4	1·94	3·17	35·1
$SiBr_4$	2·14	3·49	31·4
$GeBr_4$	2·29	3·74	37·2
$SnBr_4$	2·44	3·98	35·0

TABLE IV.—CALCULATED AND OBSERVED VIBRATION FREQUENCIES USING CALCULATED VALUES OF A AND B/R° AND ADJUSTED VALUES OF k AND k_α. THE OBSERVED VIBRATION FREQUENCIES ARE GIVEN IN BRACKETS.

Mol.	A × 10^{-5}.	B/R° × 10^{-5}.	k × 10^{-5}.	k_α × 10^{11}.	ν_1 calc. (obs.).	ν_3 calc. (obs.).	ν_4 calc. (obs.).	ν_2 calc. (obs.).
CF_4 .	0·603	0·219	4·23	0·370	899 (904)	1272 (1265)	624 (613)	433 (437)
SiF_4 .	0·214	0·078	5·7	0·207	814 (800)	1007 (1022)	354 (420)	260 (260)
CCl_4 .	0·326	0·119	1·71	0·213	459 (459)	787 (790)	315 (313)	216 (217)
$SiCl_4$.	0·140	0·051	2·59	0·186	424 (425)	608 (607)	218 (221)	151 (151)
$GeCl_4$	0·109	0·040	2·39	0·147	398 (397)	450 (451)	172 (171)	132 (132)
$TiCl_4$.	0·081	0·029	2·42	0·119	386 (386)	496 (497)	156 (144)	114 (120)
$SnCl_4$.	0·056	0·021	2·31	0·196	366 (366)	402 (404)	129 (134)	109 (104)
CBr_4 .	0·240	0·087	1·37	0·181	264 (265)	669 (667)	183 (183)	123 (123)
$SiBr_4$.	0·128	0·047	1·95	0·119	252 (249)	482 (487)	139 (137)	90 (90)
$GeBr_4$.	0·080	0·029	1·91	0·153	233 (234)	329 (328)	111 (111)	78 (78)
$SnBr_4$	0·055	0·020	1·84	0·126	220 (220)	279 (279)	87 (88)	64 (64)

---

[1] Pauling, *Nature of the Chemical Bond* (Cornell).

fifth columns and the above relation. It will be seen that, for a high proportion of the molecules, the value of n is close to 4·5. We will take this to be the value of n. The constant a can now be calculated from the values of A listed in Table II using the relation already given with $n = 4{\cdot}5$, and the values of R° which have been determined by electron diffraction and other methods. The results of this are shown in Table III. As a result of the figures obtained in Table III we will assume for the fluorides that $a = 10 \times 10^{-11}$, for the chlorides that $a = 25 \times 10^{-11}$, for the bromides that $a = 35 \times 10^{-11}$. Using these we can calculate the values of A and B/R° for each of the molecules, the values of R^0 that are used being those in Table III. In Table IV are given the observed and calculated vibration frequencies for the eleven molecules considered together with the values of k and k_α that have been used. The calculated values of A and B/R^0 that were used for each molecule have also been included.

Discussion.

In the first place it will be seen that for the four tetrabromides the observed frequencies are accounted for very well. The average % error over all the sixteen frequencies is 0·4 and the maximum errors occur in $SiBr_4$. The sixteen vibration frequencies have been explained using eight separately-adjusted valency force field constants, and the two constants a and n, i.e. ten in all. For the chlorides the vibration frequencies of CCl_4, $SiCl_4$ and $GeCl_4$ are accounted for very well but the frequencies of the bending vibrations of $SnCl_4$ are not determined so closely and those of $TiCl_4$ still less closely. For these five molecules the average % errors in the frequencies are 0·4, 0·5, 0·3, 2·5 and 3·5 respectively. However, taken as a whole, the results for the chlorides are quite good. As regards the fluorides the results for carbon tetrafluoride are quite good (average % error = 0·9) but those for the bending frequencies of SiF_4 are very poor. It seems that the frequencies of the other tetrafluorides need to be known before the problem of the fluorides can be settled.

However, the general conclusion for the tetrachlorides and tetrabromides must be that the vibration frequencies can be explained by a simple valency force field together with a repulsion between the non-bonded halogen atoms. Also the results in Table IV show that the same function may be used for the forces between the chlorine atoms in all the tetrachlorides—and similarly for the forces between the bromine atoms in all the tetrabromides. The actual result is that the P.E. in ergs between two non-bonded chlorine atoms separated by R A. is

$$V = 25 \times 10^{-11}/R^{4\cdot5} + \text{const.}$$

between 2·8 and 3·8 A. That between two non-bonded bromine atoms is

$$V = 35 \times 10^{-11}/R^{4\cdot5} + \text{const.}$$

between 3·1 and 4·0 A. That between two non-bonded fluorine atoms is

$$\mathrm{V} = 10 \times 10^{-11}/R^{4\cdot5} + \text{const.}$$

at about 2·2 A. The forces in the three cases are given by

(*a*) fluorine atoms : $F = -\,\mathrm{d}V/\mathrm{d}R = 45 \times 10^{-3}/R^{5\cdot5}$ dynes ;

(*b*) chlorine atoms : $F = -\,\mathrm{d}V/\mathrm{d}R = 112{\cdot}5 \times 10^{-3}/R^{5\cdot5}$ dynes ;

(*c*) bromine atoms : $F = -\,\mathrm{d}V/\mathrm{d}R = 157{\cdot}5 \times 10^{-3}/R^{5\cdot5}$ dynes.

The second differentials which give the curvatures of the P.E. curves are in the three cases :

(*a*) fluorine atoms : $\mathrm{d}^2V/\mathrm{d}R^2 = 247{\cdot}5 \times 10^5/R^{6\cdot5}$ dynes per cm. ;

(*b*) chlorine atoms : $\mathrm{d}^2V/\mathrm{d}R^2 = 618{\cdot}75 \times 10^5/\mathrm{R}^{6\cdot5}$ dynes per cm. ;

(*c*) bromine atoms : $\mathrm{d}^2V/\mathrm{d}R^2 = 866{\cdot}25 \times 10^5/R^{6\cdot5}$ dynes per cm.

These forces between non-bonded atoms in molecules might be expected to show some resemblance to the forces between iso-electronic inert gas atoms in the gaseous state. Lennard-Jones[7] used the (p, v, T) relationships of the inert gases helium, neon and argon to determine these forces.[8, 9] We would expect bonded fluorine to resemble neon and bonded chlorine to resemble argon. Table V gives the comparison of dV/dR and d^2V/dR^2 at $R = 2{\cdot}2$ *A*. for bonded fluorine and neon, and at $R = 3$ A. for bonded chlorine and argon. For bonded chlorine and argon both dV/dR and d^2V/dR^2 are of the same order of magnitude and it appears to us that the agreement is as good as could be expected. For bonded fluorine and neon the agreement is not as good but it must be remembered that the repulsion formula for bonded fluorine was based on one molecule only—namely CF_4. It is a pity that bonded bromine cannot be compared with krypton, since the results for the tetrabromides were the best, but no figures for the latter are available. It must be remembered, of course, when considering the comparisons in Table V that the variation with R of the function used here is very different from that of the Lennard-Jones function, so that agreement between the figures compared will vary with varying R. However, the comparisons in Table V have been made in the ranges for which our function has been used. The agreement in order of magnitude that is observed in Table V does encourage one to believe that the van der Waals repulsions that have been included in the present treatment do have a very real effect on the molecular vibration frequencies.

TABLE V.—COMPARISON OF REPULSION REQUIRED FOR BONDED HALOGEN ATOMS IN THE TETRAHALIDES WITH THAT REQUIRED FOR INERT GAS ATOMS.

Case Considered.	$-dV/dR$.	d^2V/dR^2.
Bonded fluorine at 2·2 A.	$5{\cdot}89 \times 10^{-4}$	$1{\cdot}47 \times 10^5$
Neon atoms at 2·2 A.	1·31 ,,	0·83 ,,
Bonded chlorine at 3 A.	2·67 ,,	0·49 ,,
Argon atoms at 3 A.	0·94 ,,	0·46 ,,

As regards the magnitudes of the V.F.F. constants that it has been found necessary to assume, it seems that the bending constants are much smaller than would have been expected. In all cases except CF_4, k_α is of the order of 0·1 to $0{\cdot}2 \times 10^{-11}$ dyne cm. per radian, whereas the bending constants in other cases, where van der Waals repulsions are not likely to be important (e.g. CH_4 and NH_3), have been found to be bigger than this ($0{\cdot}4$-$0{\cdot}8 \times 10^{-11}$). On the other hand, our knowledge of bending constants is very meagre[10] and we cannot say that the values it has been necessary to assume for k_α are impossibly small.

The bond force constants of the CF, CCl and CBr linkages are lower than would have been expected from the results that have been obtained for these linkages in the methyl halides, where the constants are 5·6, 3·4 and $2{\cdot}9 \times 10^5$ dynes per cm. respectively.[10] This will be considered further later in this paper. The force constants of the linkages from the other central atoms to the halogens are all quite reasonable in magnitude.

In the series CCl, SiCl, GeCl, SnCl the bond force constant increases considerably from CCl to SiCl and then decreases steadily, though slowly, from SiCl to SnCl. The same variation is observed in the similar bromide series and the beginnings of it in the fluoride series. It would perhaps have been expected that there would have been a steady decrease in force constant right through from carbon to tin. However it is possible that the increase on passing from CCl to SiCl is due to the fact that in silicon (and Ge and Sn) the covalency maximum is greater than four whereas in carbon it is four because there are no *d*-orbitals with a principal quantum number of two. This would mean that non-ionic structures involving Si=Cl would be possible but that non-ionic structures involving C=Cl would not be possible. An alternative explanation is that in the carbon halides the repulsion between the halogen atoms is so great that the carbon halogen bond is distorted and weakened to a much greater extent than in the non-carbon tetrahalides where the central atom is larger. The variation in bending constant with position in the Periodic Table is less well marked though it may be noted that throughout there is a drop on passing from the carbon to the silicon compound.

---

[7] Lennard-Jones, *Proc. Roy. Soc. A*, 1931, **43**, 461.
[8] Buckingham, *ibid.*, 1938, **168**, 264.
[9] Fowler and Guggenheim, *Statistical Thermodynamics* (C.U.P.), p. 285.
[10] Linnett, *Quart. Reviews*, 1947, **1**, 73.

The repulsion between the halogen atoms must mean that the distances between the central atoms and the halogen atoms in the tetrahalides are greater than they would be if there were no repulsion between the non-bonded atoms. It is a matter of considerable interest to know the probable extent of this stretching. In the first place let us make the simple assumption that r^e is the unstretched equilibrium length of the XY link and that the P.E. of the link is of the simple form $V = \frac{1}{2}k(r - r^e)^2$. This means that $f'(r^\circ) = k(r^\circ - r^e)$ and $f''(r^\circ) = k$. Now it is necessary for equilibrium that, at the position of minimum potential energy, $\sqrt{6}F'(R^\circ) = -f'(r^\circ)$. Or, using the results above, that $\sqrt{6}B = k(r^\circ - r^e)$. Since B and k are known for each molecule, $r^\circ - r^e$, which is the stretching of the XY link resulting from the repulsion between the Y atoms, may be calculated. The results of these calculations for CF_4, the five chlorides and the four bromides are shown in Table VI. The interesting result of these calculations is the surprisingly large stretching that these linkages seem to have experienced. This is particularly true for the carbon tetrahalides. Admittedly, there may be considerable error in this estimate of the stretching for we have made several assumptions which may not be justifiable (e.g. that the parabolic form of the XY P.E. function is satisfied over a considerable range of r), and also the value of B may be somewhat in error. The results given in Table V indicated that the first differential of the repulsion P.E. function may have been taken to be bigger than is actually the case. However, the present results do support strongly the conclusion of Badger [11] that the elongation of the bonds in these molecules is considerable. We agree with him that it seems very surprising that the determination by electron diffraction of the C—Cl bond lengths in CH_3Cl and CCl_4 yields virtually the same value. We are therefore inclined to agree with the conclusion of Sutherland [12] that the C—Cl link in CH_3Cl is, in fact, shorter than in CCl_4, rather than with the recent suggestions of Börge Bak [13] for explaining the apparent lack of agreement between the spectroscopic and electron diffraction observations. However,

TABLE VI.—STRETCHING OF XY LINKS CAUSED BY REPULSION BETWEEN Y ATOMS.

Molecule .	CF_4	CCl_4	$SiCl_4$	$GeCl_4$	$TiCl_4$
Stretching .	0·28	0·49	0·16	0·14	0·11 A.
Molecule .	$SnCl_4$	CBr_4	$SiBr_4$	$GeBr_4$	$SnBr_4$
Stretching .	0·08	0·49	0·20	0·14	0·10 A.

---

[11] Badger, *J. Chem. Physics*, 1935, **3**, 710.
[12] Sutherland, *Trans. Faraday Soc.*, 1938, **34**, 325.
[13] Börge Bak, *J. Chem. Physics*., 1946, **14**, 698.

whatever the final decision regarding the size and shape of these molecules, it is certain that no consideration of the carbon-halogen links in the carbon tetrahalides should ignore the distorting effect of the repulsion between the halogen atoms, as so many have done in the past. The same is true to a lesser degree for the other tetrahalides.

Summary.

It has been shown that the vibration frequencies of the tetrahalides of the Group IV elements can be explained using a S.V.F.F. combined with repulsion between the non-bonded halogen atoms. It is found that the same repulsion P.E. function can be used for all five tetrachlorides—and similarly for the four tetrabromides. The magnitudes found for the first and second differentials of the repulsion P.E. function are found to be reasonable if the repulsion is of a van der Waals type. The effect on the molecular structure of these repulsions between the non-bonded atoms is discussed.

Inorganic Chemistry Laboratory,
Oxford.

THE TRAINING OF BACTERIA TO NEW CARBON SOURCES. *BACT. LACTIS AEROGENES* AND *d*-ARABINOSE.

By S. Jackson and C. N. Hinshelwood.

Received 18th June, 1947.

One of the properties of bacteria which most challenges physicochemical interpretation is the power of adaptation. The phenomena of response to changed environment, for example where one carbohydrate is replaced by another as a source of carbon for growth, follow what appear at first sight to be two main patterns. According to one, what is usually called training occurs. Cells able to utilise A but not B are grown in serial subculture in a mixture of A and B, the proportion of A being gradually reduced to zero, and at the end of this process they are able to utilise B alone. According to the other, what is usually referred to as the production of variants occurs. This is illustrated by the example of *Bact. coli mutabile* and lactose. With this sugar as carbon source no growth occurs for some days, after which a multiplication of " lactose variants " is observed.[1]

The nature of these phenomena seems to be worthy of further detailed study. In those of the first type, if the cells acquire the property of utilising B while growing in A, it would imply that some intermediate substance formed during growth in A modifies the cells in such a way that they can incorporate B. The dependence of the effect upon the nature of A and B assumes considerable interest. On the other hand, the problem arises whether " variant " production is merely a question of time, or whether it is likely to be helped by serial subculture in suitable mixed media. The answer will have some bearing on the nature of variants, and will in any event help to systematise our knowledge about changes in bacterial character.

The experiments described in this paper deal with the second of the problems mentioned. The example chosen for study was that of *Bact. lactis aerogenes* which under suitable conditions grows with optimum efficiency in an artificial medium containing glucose or *l*-arabinose as carbon source, but under corresponding conditions refuses to utilise *d*-arabinose except after a lag period of the order of days.[2] It was proposed to determine whether some process of subculture in mixed media would encourage the emergence of the *d*-arabinose "variants." These experiments led to others designed to throw light on the nature of the *d*-arabinose utilising cells.

---

[1] Massini, *Archiv. Hyg.*, 1907, **61**, 250. Postgate and Hinshelwood, *Trans. Faraday Soc.*, 1946, **42**, 45.

In the first series of experiments a strain of *Bact. lactis aerogenes* was serially subcultured in a medium containing as carbon source a mixture of *d*- and *l*-arabinose, the other constituents of the medium being as described in previous papers from this laboratory on carbohydrate adaptation.[1, 2] At various stages tests were made of the lag shown on transfer to a medium with *d*-arabinose as sole carbon source and, as control, into *l*-arabinose. These test transfers were all made at the moment when the lag in the new medium would be minimal, that is, when the lag in the *l*-sugar would be nearly zero. A standard inoculum size of 0·2 cc. (into 26 cc. fresh medium) was employed. The value of the quantity (lag in *d*-arabinose minus lag in *l*-arabinose) plotted against the serial subculture number gave smooth curves, and decreased from an initial value of 160 hr. almost to zero in the course of about 50 subcultures. (This same result would have been achieved by leaving the first inoculum into *d*-arabinose for the 160 hr. necessary for growth and then subculturing instead of subculturing daily as was done in the actual series.) This series, which is illustrated in Fig. 1, shows that adaptation does occur in the course of subculture in the *d*-*l* mixture, but only slowly.

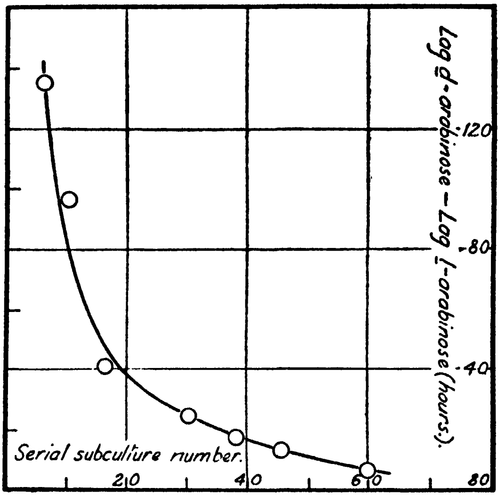

FIG. 1.

In the next group of experiments three series of subcultures were carried out in parallel, each in a *d*-*l*-arabinose mixture, transfers being made at intervals of 12, 24 and 48 hr. respectively. In a similar group the corresponding transfers were made in a medium with a mixture of *d*-arabinose and glucose. As before, the progress of the adaptation was measured by the value of (lag in *d*-arabinose—lag in *l*-arabinose) in a series of parallel tests. With the strain of cells used in these experiments the initial lag in the *d*-arabinose was 60 hr. The results showed that the power to utilise the *d*-compound was acquired much more slowly when the transfers were made at the shorter intervals. In other words the important factor appeared to be the periods of rest in contact with the

---

[2] Cooke and Hinshelwood, *Trans. Faraday Soc.* (in press).

d-arabinose. Separate experiments having shown that the logarithmic growth phase occupied approximately 3½ hr. for each subculture, the total resting time could be computed. In Fig. 2 the measure of the lag difference is plotted against the total length of the resting time. The results strongly suggest that no progress at all is made during the actual growth in the mixed sugars but that before growth can occur in *d*-arabinose a period of contact without growth must elapse, irrespective of interruptions by growth phases in other sugars.

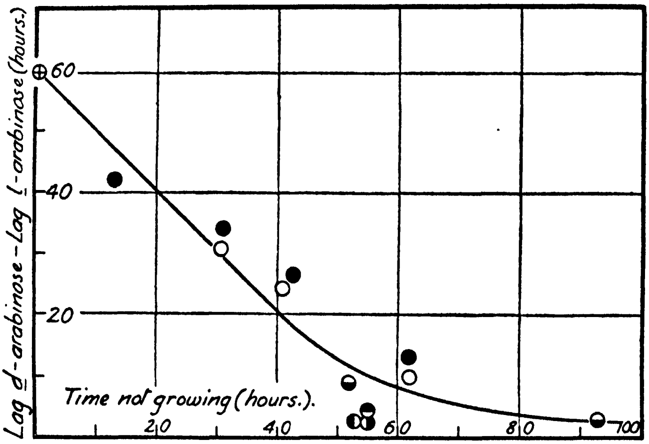

FIG. 2.—Open circles and horizontally divided circles, subcultures in *d*-*l*-arabinose mixtures, 12, 24 and 48 hr. series. Blacked-in circles and vertically divided circles, subcultures in glucose-*d*-arabinose mixtures, 12, 24 and 48 hr. series.

To test this conclusion more rigidly the following experiments were made. A number of inocula were made in parallel into *d*-arabinose. Some were left until growth occurred, the observations giving the initial lag, L_0. To others, after given times, T, was added 0·5 g. glucose or *l*-arabinose and full growth was allowed to take place. When it was just complete, that is, when the condition for minimal lag was reached, inocula were re-transferred to *d*-arabinose and the lags, L, were determined. Within the range of the experimental error it proved that $L = L_0 - T$. The total lag may thus be divided into parts by the interruption of a growth period in another sugar, but its total value remains constant.

Strain.	L_0.	T.	L.	$L+T$.
I . . .	45 hr.	24	15	39
II . . .	69	11	54	65
III . .	*ca.* 190	3	186	189
		20	165	185
		27	150	177
		45	137	182
		97	103	200
		115	92	207
IV . .	94	16	89	105
		38	51	89
		24	74	98
V . .	113	16	89	105
		24	76	100
		37	70	107

These results show that most of the cell modification must occur during the resting period, and suggest that none takes place during growth in the foreign sugar. To decide this matter an apparatus was constructed in which continuous logarithmic growth could be maintained. The population of a growing culture was maintained approximately constant by running out some of the culture and at the same time introducing new medium at an equal rate, a process achieved by a suitable device of inlet tubes and siphons. The initial inoculum was untrained to *d*-arabinose and was grown in glucose, to which in due course *d*-arabinose was added in the flow system. At intervals samples were removed from the apparatus and tested in *d*-arabinose in the usual way. The results showed that no power to use the latter sugar was acquired during the time of continuous growth in the mixed sugar.

Time of Continuous Logarithmic Growth in Presence of *d*-arabinose (hr.).	Lag of Test Sample in *d*-arabinose alone. (hr.).
0	44
3	44
25	38
48	39
53	32
56	36
72	48
78	44
96	33
100	32
120	30
144	41

Another approach to the problem was made by determining whether any of the *d*-arabinose in a mixture was used by cells which had not yet been adapted to use it alone. Cells were grown in media containing respectively (1) 30 mg. *l*-arabinose, (2) 30 mg. *l*-arabinose and 30 mg. *d*-arabinose, (3) 30 mg. *d*-arabinose. With these concentrations the total supportable bacterial population is directly proportional to the amount of utilisable carbohydrate (the total supply being much smaller than that normally used in the growth experiments, namely, 500 mg.). The total bacterial population, n_s, of the culture tubes was determined 24 hr. after the logarithmic growth phase had come to its end. For cells which had not been grown previously in *d*-arabinose the value of n_s was approximately 1000 (arbitrary units) for glucose, *l*-arabinose and for the *d*-*l*-arabinose mixture, showing that none of the *d*-arabinose had been used in these conditions. In a corresponding time the *d*-arabinose culture showed no growth. After a long waiting period this culture, as well as those in the mixed sugars, showed a further burst of growth.

All the observations which have been described show that for the growth of the cells in *d*-arabinose the essential requirement is a sufficient time of contact between the sugar and the non-growing culture, that is, that the phenomenon is primarily one of lag. What emerges clearly is that training does not depend upon the incorporation into the molecular structure of the cell of fragments derived from the attack on the new sugar of active intermediates in the normal growth process. Properly speaking the initial reluctance to utilise *d*-arabinose depends simply upon the existence of an abnormally long lag which must be traversed in presence of the *d*-arabinose itself and cannot be short-circuited. The true adaptation then occurs by the multiplication of the cells in the *d*-arabinose, as a result of which they never again need to pass through the long lag. Second subcultures in the sugar always show normal lags.[2]

Three interpretations of the results seem possible.

(1) In a given culture of the bacteria there exist a few cells of a special strain inherently capable of growing in *d*-arabinose—which the majority are not. The lag period is simply the time required for these to multiply up to the threshold of detectable growth.

(2) Whenever growth occurs, whether in presence of *d*-arabinose or not, a few cells are thrown off which have become endowed by chance with

the power of utilising *d*-arabinose. Even if once eliminated, they are reformed in small proportions by fresh divisions. As in (1) the lag is the time required for these special cells to attain a number comparable with the normal cells.

(3) The cells in general are inherently capable of growth in *d*-arabinose, but the requisite enzyme mechanisms are in a dormant state corresponding precisely to that of aged cells in their normal medium (i.e. the necessary intermediates, growth factors and so on are not present). During the lag the necessary changes occur in the cells by reactions between their enzymes and the medium, including the *d*-arabinose itself.

The first of these alternatives was eliminated in the following manner. Since the initial lag in *d*-arabinose is very long, the number of special cells present must, according to the terms of the hypothesis, be very small.* If, therefore, the parent culture is plated out on agar, most of the colonies formed would grow from inactive cells and only very rare ones from cells of the active type. (Even the chance that a colony grows from two or three adhering cells would not affect this argument.) The experiment was made and ten colonies were taken off agar and transferred to bouillon, subcultured once in glucose after one day (at low concentrations, so that little glucose would be carried over with inocula), and then tested in the usual way. The various sub-strains derived in this way showed little spread, as the results in the following table reveal.

TABLE

Parent culture gave initial lag in *d*-arabinose of 44 hr. Colonies removed after plating on agar and treated as described. Lags in *d*-arabinose (duplicate determinations).

Colony.	1	2	3	4	5	6	7	8
Lag (hr.)	69, 59	74, 95	73, 95	87, 87	35	33, 48	62, 178	161, 161

From this may be concluded that each of the individual colonies, probably derived from single cells, or at most from a few cells, was more or less representative of the entire population in respect of its behaviour towards arabinose. According to alternative (1) most of the sub-strains should have refused to grow at all in *d*-arabinose, and very occasional ones should have grown with no more lag than they showed in glucose, i.e. practically none.†

The decision between alternatives (2) and (3) is more difficult. Considering the problem as a whole and taking into account all the phenomena

---

[*] The quantitative aspect of the theory of special cells has some points of interest. The inoculum contains about 2×10^8 cells, and the number of *d*-arabinose-utilising cells would have, in the time of the apparent lag, L, to grow from an initial value n_0 to something of this order for growth to be recognised. Thus $2 \times 10^8 \sim n_0 e^{kL}$, where $k = 0{\cdot}693/\tau$, and τ is the mean generation time. There is no means of measuring the τ in the "lag" period, but if the value of 75 min. corresponding to normal logarithmic growth is assumed, then to account for a lag of 100 hr., n_0 would work out at far less than one cell per culture tube, an impossible result. To make the theory of special cells fit the observed lags, a mean generation time of the order of 400 min. would have to be assumed.

[†] The plating-out operations caused a general lengthening of the lag, and this result must be regarded as an influence of the cultural history on the behaviour in *d*-arabinose—a matter worthy of further study. The effect was shown to be due to the solid agar medium, passage through bouillon having no effect on the lag. Thus a parent culture showed a lag in *d*-arabinose of 44 hr., and after passage through bouillon followed by dilute glucose, various derivative strains gave lags of 42, 42, 39, 39, 36 and 42 hr. respectively. Thus the bouillon passage by itself had little effect.

of training and adaptation, a good case can be made out for (3) rather than (2).[3] The general problem will not be debated here and the discussion will be confined to the particular example with which the experiments deal. The present results alone do not in themselves lead to an unambiguous choice.

If variants were continuously thrown off independently of the *d*-arabinose, according to (2) one might have supposed that in the mixed medium they would have had a better chance of attaining a high proportion than in glucose alone. But in fact the growth rate of the " variants " in *d*-arabinose is initially quite low ($\tau = 75$ min.), so that, on this ground, enrichment in the mixed medium would not occur. (The " variants " grow in glucose at the same rate as normal cells, $\tau = 33$ min.). On the other hand, the assumption that during growth in any medium the proportion of the variants remains constant is a special one, which certainly does not help, even if it does not oppose the variant theory.

On general grounds (3) is the most likely, and, if true, has several interesting consequences, relating to the general character of cell mechanisms. In the first place, we may consider the lag phase in general. During this time the cells are in contact with the growth medium without apparent change. Actually, however, there must be important changes involving (*a*) the accumulation of necessary intermediates and (*b*) repair or modification of the enzymes structures of the cell. Cells which are ready for immediate growth in glucose (the condition provided for in most of these experiments) are still unable to grow in *d*-arabinose until they have been in contact with it for a long additional period. During this, special changes of the types (*a*) and (*b*) must occur to prepare the cell for the sequence of reactions involved in the growth in *d*-arabinose. Now the experimental results show two things. First, since intervening periods of growth in glucose do not affect the total *d*-arabinose lag, whereas diffusible intermediates would be lost and diluted in the subculturing process, it seems that the most important changes are those of type (*b*), that is, preparatory modifications of the cell enzymes by contact with the new sugar. Secondly, since growth in glucose does not reverse the partial preparation achieved during an interrupted lag period, it follows that once the cell pattern has been modified, that modified structure is reproduced by growth even in a medium not containing *d*-arabinose. Thirdly, since the periods of active growth in other sugars do not count towards the *d*-arabinose " apprenticeship," even when the latter sugar is present throughout, it follows that the preparatory reactions of the lag are in abeyance during the period of active growth.

This latter point is of some general interest, and has parallels of a rather important kind. There are clearly two sets of cell reactions, those of the lag phase and those of the logarithmic phase. The latter appear to inhibit the former. The state of affairs is expressed diagrammatically as follows :

$$\begin{tikzcd} \text{Sugar} \arrow[r] & \text{intermediate} \arrow[r, "(1)\ (\text{lag})"] \arrow[d, "(2)\ (\text{growth})"] & \text{enzymes modified in preparation for growth} \\ & \text{consumption of intermediate in growth reactions.} & \end{tikzcd}$$

If the intermediate has two possible fates (1) and (2), then it is clear that the vigorous operation of (2) will keep its concentration very low and thereby inhibit (1). If, further, the arabinose intermediate is consumable in glucose-growth, then the observed facts are accounted for.

Three important parallels may be adduced : (i) the Pasteur effect, whereby oxidation reactions inhibit fermentation; (ii) the inhibition of nitrate reduction by *Bact. lactis aerogenes* when ammonium salts are provided as alternative sources of nitrogen; and (iii) the inhibition of nitrate reduction by the same organism under certain conditions of aeration.[4]

---

[3] Hinshelwood, *Chemical Kinetics of the Bacterial Cell* (Oxford, 1946), cites references.

All these phenomena probably have the common explanation that they depend upon the changes in concentration of an intermediate which is itself involved in more than one sequence of reactions.

Summary.

Bact. lactis aerogenes utilises *d*-arabinose only after a lag of the order of days. Once growth has occurred the cells are adapted and subsequent lags are normal. It has been shown in several different ways that the essential condition for utilisation is that the *resting cells* should remain in contact with the new sugar for a given *total time*, irrespective of interruptions by phases of growth in other media. Continuous growth in a mixture of *d*-arabinose and another sugar prevents any utilisation of the former. Individual cells appear not to show much difference in their response to *d*-arabinose.

The results are discussed in relation to the problem of the nature of variants, and also in relation to some general aspects of the kinetics of cell reactions.

[4] Lewis and Hinshelwood (in press).

Physical Chemistry Laboratory,
Oxford.

AN EXAMINATION OF THE ADSORPTION THEORY OF BRUNAUER, EMMETT, AND TELLER,[*] AND BRUNAUER, DEMING, DEMING AND TELLER.[†]

By S. J. Gregg and J. Jacobs.

Received 19*th February*, 1947. *As revised*, 9*th July*, 1947.

The problem of formulating an equation for the adsorption isotherm has attracted a great deal of attention during the last 30 years. Almost invariably, however, the proposed solutions have been restricted in application to one type of isotherm in each case, and even then their success in reproducing experimental results has been but limited for the most part.[1] Consequently, the combined theory of Brunauer, Emmett and Teller [2] and of Brunauer, Deming, Deming and Teller,[3] has excited much interest recently inasmuch as, on the basis of a single mechanism, it claims to derive equations representing 5 at least of the types of isotherm encountered in practice. This interest is enhanced by the further claim that the differential heat of adsorption can be calculated from the isotherm at a single temperature, for it is well known that the accurate determination of this quantity, either calorimetrically or by application

[*] Abbreviated to BET.

[†] Abbreviated to BDDT.

[1] For a description of the various hypotheses, see (*a*) McBain, *The Sorption of Gases by Solids* (1932), p. 247 *seq.*; (*b*) Brunauer, *Physical Adsorption of Gases and Vapours* (1944), pp. 53-179.

[2] Brunauer, Emmett and Teller, *J. Amer. Chem. Soc.*, 1938, **60**, 309.

[2a] Brunauer, Emmett and Teller, *ibid.*, 1938, **60**, 315.

[3] Brunauer, Deming, Deming and Teller, *ibid.*, 1940, **62**, 1723.

[3a] Brunauer, Deming, Deming and Teller, *ibid.*, 1940, **62**, 1727.

of the Clausius-Clapeyron equation to isotherms at neighbouring temperatures, is beset by many difficulties. However, the theory is based on the fundamental, though tacit, assumption that interaction between adsorbate molecules in the adsorbed film is negligible in directions parallel to the adsorbent surface. This assumption has already been criticised by Cassell,[4] on the grounds that it requires the completely built-up film to have a negative surface tension ; and since in any case the neglect of lateral interation would appear to be contradictory to accepted views on the nature of molecular forces, it is proposed to examine the theory both theoretically and by reference to experimental data to find how far its claims can be substantiated.

The Basic Assumptions of the Theory.—Like Langmuir's theory,[5] the BET-BDDT theory assumes that adsorption occurs on fixed adsorption sites ; it no longer restricts adsorption to a monolayer, however, but postulates that the film may, on an open surface, extend to an indefinite number of molecular layers. The mathematical treatment is based on the principle of microscopic reversibility : when a steady state has been reached, the rate of condensation of molecules from the gas space on to the empty sites is equated to the rate of evaporation from the first layer, so that

$$a_1 p s_0 = b_1 s_1 e^{-E_1/RT} \quad . \quad . \quad . \quad . \quad . \quad (1)$$

Here s_0 and s_1 are the surface areas (per unit quantity of adsorbent) covered with 0 and with 1 molecular layers respectively ; E_1 is the molar heat of adsorption for molecules in the first layer ; a_1 is a condensation constant and b_1 an evaporation constant ; p is the pressure in the gas space.

Similar equations can be written for the other layers :

$$a_2 p s_1 = b_2 s_2 e^{-E_2/RT} \quad . \quad . \quad . \quad . \quad . \quad . \quad (2)$$

$$a_3 p s_2 = b_3 s_3 e^{-E_3/RT} \quad . \quad . \quad . \quad . \quad . \quad . \quad (3)$$

$$a_i p s_{i-1} = b_i s_i e^{-E_i/RT} \quad . \quad . \quad . \quad . \quad . \quad . \quad (4)$$

By a summation process the total adsorption for the pressure p can be obtained. To carry out this summation, it is assumed (i) that the number of layers becomes infinite when p reaches p_0, the saturated vapour pressure of the pure liquid adsorbate ; (ii) that the heat of adsorption for all layers after the first is the same, and equal to λ, the ordinary latent heat of condensation, so that $E_2 = E_3 = E_i = \lambda$; this has the consequence that $\frac{a_2}{b_2} = \frac{a_3}{b_3} = \frac{a_i}{b_i}$ and is equivalent to assuming that the evaporation-condensation conditions in the second and subsequent layers are identical, and the same as those of the bulk liquid.‡

In this way, Brunauer, Emmett and Teller arrive at equation (A)

$$\frac{p}{x(p_0 - p)} = \frac{1}{x_0 c} + \frac{(c-1)}{x_0 c}\frac{p}{p_0} \quad . \quad . \quad . \quad . \quad . \quad (A)$$

where x is the adsorption per unit quantity of adsorbent at the pressure p ; x_0 is the monolayer capacity, i.e. the amount of adsorbate (in the units of x) which can be taken up in a completed monolayer ; c is, strictly, given by

$$c = \frac{a_1}{b_1} \cdot \frac{b_i}{a_i} e^{(E_1 - \lambda)/RT} \quad . \quad . \quad . \quad . \quad . \quad . \quad (5)$$

but for working purposes this is replaced by

$$c = e^{(E_1 - \lambda)/RT} \quad . \quad . \quad . \quad . \quad . \quad . \quad . \quad (6)$$

by introducing the simplifying assumption that

$$\frac{a_1}{b_1} \cdot \frac{b_i}{a_i} = 1 \quad . \quad . \quad . \quad . \quad . \quad . \quad . \quad (7)$$

If now we put

$$\frac{x}{x_0} = X, \text{ and } \frac{p}{p_0} = P$$

---

[4] Cassell, *J. Chem. Physics*, 1944, **12**, 115.

[5] Langmuir, *J. Amer. Chem. Soc.*, 1918, **40**, 1361.

‡ A similar treatment had been proposed by Baly, *Proc. Roy. Soc. A*, 1937, **260**, 465.

equation (A) becomes

$$X = \frac{cp}{1 - P} \cdot \frac{1}{1 + (c - 1)P} \quad . \quad . \quad . \quad . \quad . \quad (A')$$

a form which is sometimes more convenient.

The special case where adsorption is restricted to n molecular layers (e.g. by the pore diameter of the adsorbent) is also considered; the summation process is now carried to n terms only, the film reaching the finite thickness of n molecular diameters when $p = p_0$. Equation (B) is thus obtained:

$$X = \frac{cP}{1 - P} \cdot \frac{1 - (n + 1)P^n + nP^{n+1}}{1 + (c - 1)P - cP^{n+1}} \quad . \quad . \quad . \quad (B)$$

Equations (A) and (B) include isotherms of Types I, II and III of Fig. 4. Equation (A) corresponds to Type III if $c = 1$, and to the portion of Type II lying between $P = 0{\cdot}05$ and $P = 0{\cdot}35$ if $c > 1$; equation (B), with $n = 1$, corresponds to Type I, and with $n >$ *ca.* 2 to the high pressure end of Type II. Brunauer, Deming, Deming and Teller[8] have put forward a modification of the theory, enabling it to embrace Type IV and V isotherms; they thus arrive at rather complicated equations (D) and (E) which, however, both reduce to (A) at the low pressure end.

Mathematical Properties of Equations (A) and (B).—Equation (A) or (A′) may be transformed into

$$X = \frac{1}{1 - P} - \frac{1}{1 + (c - 1)P} \quad . \quad . \quad . \quad . \quad . \quad (8)$$

so that the graph of X against P consists of the difference of the upper branches

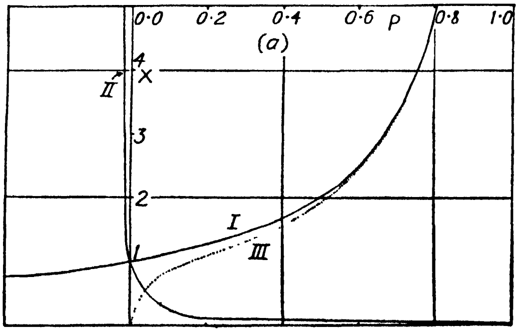

FIG. 1*a*. I. Graph of equation, $X = 1/(1 - P)$.
II. Graph of equation, $X = 1/\{1 + (c - 1)P\}$ for $c = 30$.
III. Graph of equation (8) for $c = 30$.

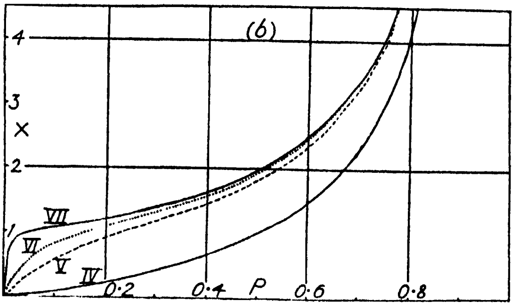

FIG. 1*b*. Graphs of equation (8):
IV. $c = 1$. V. $c = 11$. VI. $c = 101$. VII. $c = 10001$.

FIG. 1.—Graphs relevant to equation (8). Ordinates, X; abscissæ, P.

of two rectangular hyperbolæ; the first, (I), is independent of c, has asymptotes $X = 0$ and $P = 1$, and cuts the X axis at $X = 1$; the second, (II), has asymptotes

$X = 0$ and $P = -1/(c - 1)$, and also cuts the X axis at $X = 1$ (see Fig. 1*a*). Since the parameter c plays such an important part in the theory, it is necessary to examine the dependence on c of the graph of (8); and to do this it is sufficient to examine the dependence on c of hyperbola (II) only, for hyperbola (I) is independent of c.

The graphs of (I) and (II) for a typical value of c ($= 30$) are shown in Fig. 1*a* (full lines) together with the resultant graph of equation (8) (dotted line). The effect of increasing c is to cause the knee of the curve to become more and more sharp (Fig. 1*b*), pushing it into the range of lower pressure; it should be noted that the graphs of (8) are practically indistinguishable for values of c in excess of 10000 for $P > 0{\cdot}05$.

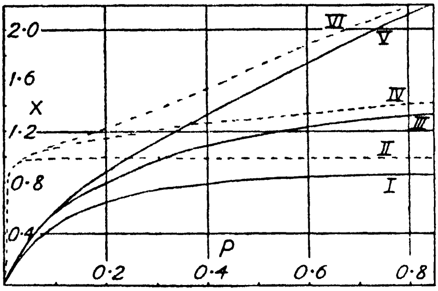

FIG. 2.—Graphs of X against P from equation (8). Ordinates, X; abscissæ, P.

I. $c = 10$, $n = 1$.
II. $c = 1000$, $n = 1$.
III. $c = 10$, $n = 2$.
IV. $c = 1000$, $n = 2$.
V. $c = 10$, $n = 4$.
VI. $c = 1000$, $n = 4$.

Curves of equation (B) have been plotted in Fig. 2, both for fixed c at a low value of n, and for two values of c with fixed n. Increase in c at constant n again tends to draw the curves towards the X axis—leading as with (A) to a sharp bend in the curve—and again there is little variation for $c > 1000$. Rather similarly, an increase in n for constant c also draws the curves up so that they tend towards the form of (A). The agreement with the general form of (A) is particularly close at the lower values of P, where P^n is negligible, as indeed the authors themselves have already pointed out. Thus for the two cases P small or n large, equation (B) approaches equation (A); for the range $P = 0{\cdot}05$ to $0{\cdot}35$, indeed, the curves for the two equations do not differ appreciably.

Examination of the Theory.

The validity of the assumptions of the theory will now be examined in a number of different ways: (i) by application of the Clausius-Clapeyron equation to equation (A); (ii) by testing equation (6) against experimental data; (iii) by calculation of the integration constants for vapour pressure and for adsorption respectively; (iv) by general considerations. In (i), (ii) and (iii), equation (A) only will be subjected to the direct examination; but since the range studied is restricted to low pressures where (A), (B) and also (D) and (E) are nearly identical, the conclusions will apply equally to these last three equations.

Calculation of the Heat of Adsorption by the Clausius-Clapeyron Equation.—A simple thermodynamic test of the internal consistency of the theory is provided by comparing the heat of adsorption (ΔH) calculated by application of the Clausius-Clapeyron equation, with the value calculated from the constant c by means of equation (6). In so doing, it must be borne in mind that the BET-BDDT model expressly lays it down that adsorption shall occur in the first and in higher layers at the same time: when the total adsorption increases from x to $(x + \delta x)$, only a fraction, say r, of the increment δx goes into the first layer with heat of adsorption

E_1 cal. mole.$^{-1}$, the remainder $(1 - r)$ going into higher layers with heat of adsorption λ cal. mole.$^{-1}$. Thus the " BET " heat of adsorption E' corresponding to the adsorption x is $E' = rE_1 + (1 - r)\lambda$,

i.e.
$$E' - \lambda = r(E_1 - \lambda) \quad . \quad . \quad . \quad . \quad (9)$$

and E' should be equal to value ΔH calculated from the Clausius-Clapeyron equation. The theoretical value of r can be calculated from the BET model : let f be the ratio of the number of empty sites to the total number of sites when the relative pressure is P ; then fx_0 is the adsorption capacity still vacant in the monolayer, and the increase in monolayer adsorption when P increases by dP is equal to the *decrease* $-\,\mathrm{d}f\,.\,x_0$ in fx_0.

But
$$f = \frac{s_0}{\sum\limits_{i=0}^{\infty} . \, s_i} = \frac{s_0}{s_0\left\{1 + c\sum\limits_{i=1}^{\infty} P^i\right\}}$$

i.e.
$$f = \frac{1}{1 + cP/(1 - P)} \quad . \quad . \quad . \quad . \quad . \quad . \quad (10)$$

as will readily be seen by reference to the BET analysis (ref.[2], p. 312).

Differentiating (10) we have
$$-\,\mathrm{d}f = \frac{c\mathrm{d}P}{\{1 + (c - 1)P\}^2} \quad . \quad . \quad . \quad . \quad . \quad (11)$$

so that the *increase* in monolayer adsorption resulting from the increase dP is
$$x_0\,.\,\mathrm{d}f = x_0\,.\,\frac{cP}{\{1 + (c - 1)P\}^2} \quad . \quad . \quad . \quad . \quad (12)$$

The corresponding increase dx in total adsorption is found by differentiating equation (A) and is :
$$\mathrm{d}x = x_0\left[\frac{1}{(1 - P)^2} + \frac{(c - 1)}{\{1 + (c - 1)P\}^2}\right]\mathrm{d}P \quad . \quad . \quad . \quad (13)$$

Since
$$r = \frac{x_0\,.\,\mathrm{d}f}{\mathrm{d}x}$$

we have, on dividing (12) by (13),
$$r = \frac{x_0\,.\,c\mathrm{d}P}{\{1 + (c - 1)P\}^2}\Big/x_0\left[\frac{1}{(1 - P)^2} + \frac{(c - 1)}{\{1 + (c - 1)P\}^2}\right]\mathrm{d}P$$

i.e.
$$r = \frac{(1 - P)^2}{\{1 + (c - 1)P^2\}} \quad . \quad . \quad . \quad . \quad . \quad . \quad . \quad . \quad . \quad . \quad (14)$$

Turning now to the Clausius-Clapeyron equation, assuming that the vapour obeys the perfect gas laws, and that the volume of the liquid is negligible compared with that of the vapour, we have
$$\frac{\mathrm{d}\ln p_0}{\mathrm{d}T} = \frac{\lambda}{RT^2} \quad . \quad . \quad . \quad . \quad . \quad (15)$$

and
$$\left(\frac{\partial \ln p}{\partial T}\right)_x = \frac{\Delta H}{RT^2} \quad . \quad . \quad . \quad . \quad . \quad (16)$$

where ΔH is the differential heat of adsorption at constant x, viz. the " isoteric " heat of adsorption for an adsorption x. By subtraction
$$\left(\frac{\partial \ln p/p_0}{\partial T}\right)_x = \frac{\Delta H - \lambda}{RT^2} \quad . \quad . \quad . \quad . \quad (17)$$

i.e.
$$\left(\frac{\partial \ln P}{\partial T}\right)_x = \frac{\Delta H - \lambda}{RT^2} \quad . \quad . \quad . \quad . \quad (18)$$

Now from equation (8) we have by simple differentiation

$$\left(\frac{\partial \ln P}{\partial T}\right)_x = -\left(\frac{\partial \ln c}{\partial T}\right)_x \cdot \frac{(1 - P)^2}{\{1 + (c - 1)P^2\}} \quad . \quad . \quad (19)$$

By equation (6)

$$c = e^{(E_1 - \lambda)/RT} \quad . \quad . \quad . \quad . \quad . \quad (6)$$

whence by differentiation we have

$$\frac{\partial \ln c}{\partial T} = \frac{E_1 - \lambda}{RT^2} \quad . \quad . \quad . \quad . \quad . \quad (20)$$

because E_1 and λ vary so slightly with temperature that they may be taken as constants for small ranges of temperature.

Substituting (20) into (19) we obtain

$$\left(\frac{\partial \ln P}{\partial T}\right)_x = \frac{E_1 - \lambda}{RT^2} \cdot \frac{(1 - P)^2}{\{1 + (c - 1)P^2\}} \quad . \quad (21)$$

and by equating the right-hand sides of (18) and (21) :

$$\frac{\Delta H - \lambda}{RT^2} = \frac{E_1 - \lambda}{RT^2} \cdot \frac{(1 - P)^2}{\{1 + (c - 1)P^2\}}$$

or

$$\frac{\Delta H - \lambda}{E_1 - \lambda} = \frac{(1 - P)^2}{\{1 + (c - 1)P^2\}} \quad . \quad . \quad . \quad . \quad (22)$$

By comparing (22) and (9) it is seen that $E' = \Delta H$, i.e. the heat of adsorption calculated by the BET method fulfils thermodynamic requirements as expressed in the Clausius-Clapeyron equation. Referring to equation (20) it will be seen, however, that exactly the same results would be obtained if c were defined as

$$c = C e^{(E_1 - \lambda)/RT} \quad . \quad . \quad . \quad . \quad (23)$$

where C is a constant independent of temperature, for C disappears on differentiating to obtain equation (20). Hence, assuming the BET model, the heat of adsorption could be given by

$$(E_1 - \lambda) = RT \ln c - RT \ln C \, ; \quad . \quad . \quad . \quad (24)$$

and whilst the value given by

$$(E_1 - \lambda) = RT \ln c \text{ (i.e. } C = 1),$$

is not excluded, the thermodynamic argument does not support it as against the more general expression (24).

Comparison of the Heat of Adsorption calculated from *c* with the Experimental Value.

A useful test of the BET-BDDT theory is furnished by comparing the values of the heat of adsorption calculated from the adsorption isotherm by means of the theory, with the experimental value ΔH. Such a comparison has been carried out in Table I, which is based on the examination of a large number of published data. The value of ΔH has been taken wherever possible from the workers' own calorimetric measurements, otherwise it has been calculated by application of the Clausius-Clapeyron equation to the recorded isotherms at neighbouring temperatures. Actually, the number of suitable data is disappointingly small. On the calorimetric side the number of recorded determinations is not very large, and of those extant several have had to be rejected because the corresponding isotherm fails to give a reasonably linear plot of equation (A). And of the isosteric heats of adsorption many have also had to be rejected because they are so erratic ; for example, the value of ΔH calculated from the 25° and 35°, and the 35° and 45°, pairs of isotherms respectively have been found to differ by 50 % or more in several cases—a variation no doubt due to the presence of irreversible conditions, such as a change in the adsorbent itself during the progress of the experiment, or hysteresis effects, or both.

The first step in calculating the heat of adsorption from the experimental isotherm is to plot $p/x(p_0 - p)$ against p/p_0 (cf. equation (A)) ; the slope of the linear portion is then $1/x_0$ and the intercept is $1/x_0c$, so that the value of c

TABLE I.

System.	Temp. °c.	$x_0 \times 10^3$ mole. g.$^{-1}$	c.	$E_1-\lambda$ cal. mole.$^{-1}$	$x' \times 10^3$ mole. g.$^{-1}$	P at x'.	r.	λ cal. mole.$^{-1}$	ΔH at x' C=Calorimetric I=Isosteric.	(Differential Heat of Adsorption) −(Latent Heat) cal. mole.$^{-1}$ From BET: $r(E_1-\lambda)$.	From Experiment $(\Delta H-\lambda)$.	Difference BET−Expt. $r(E_1-\lambda)-(\Delta H-\lambda)$.	Reference.
Charcoal—													
C_2H_6	0	2·9	620	3470	1·8	0·012	1	2250	8200 (C)	3470	5950	−2480	14
CO_2	0	3·5	110	2540	2·3	0·018	1	2420	7000 (C)	2540	4580	−2040	14
C_2H_2	0	3·3	180	2800	2·5	0·02	1	3900	6900 (C)	2800	3000	−200	14
C_2H_4	0	2·7	370	3200	2·25	0·016	1	3350	6400 (C)	3200	3050	+150	14
CO_2	0	3·7	130	2600	2·42	0·016	1	2420	6400 (C)	2600	3980	−1380	13
SO_2	0	3·2	10000	5000	2·85	0·012	1	5850	8600 (C)	5000	2750	+2250	22
CCl_4	25	2·5	350	3450	1·42	0·06	1	7730	1400 (C)	3450	6720	−3270	24
									$\Delta H-\lambda$				
CS_2	0	9·4	29	1820	7·1	0·105	1	—	2200 (I)	1820	2200	−380	23
C_2H_5Cl	0	7·9	26	1760	6·7	0·20	1	—	2800 (I)	1760	2800	−1040	23
$(C_2H_5)_2O$	0	5·4	68	2280	4·6	0·089	1	—	3400 (I)	2280	3400	−1120	23
Silica gel—													
C_4H_{10}	30	2·1	5	980	1·22	0·168	0·62	5100	6000 (I)	610	900	−290	26
CH_3NH_2	0	5·7	310	3100	5·5	0·039	0·63	6350	1600 (C)	1950	9650	−7700	27
SO_2	0	4·1	50	2100	3·5	0·076	0·66	5850	8200 (C)	1380	2350	−970	28
H_2O	60	7·8	9	1450	6·4	0·20	0·48	10100	11000 (I)	700	900	−200	9
Chabasite—													
NH_3	0	1·1	260	3000	1·05	0·056	1	5140	8400 (C)	3000	3260	−260	29
Activated alumina—													
H_2O	25	2·5	19	2030	2·1	0·10	0·69	10550	10700 (C)	1400	150	+1250	11
CCl_4	25	0·63	53	2370	0·40	0·23	0·16	7730	11200 (C)	380	3470	−3090	11
Ferric oxide gel—													
C_6H_6	40	1·28	20	1850	1·15	0·166	0·46	7790	9400 (I)	850	1610	−760	25

can be calculated the value of E_1 then follows from equation (6). Ideally, the curve should be straight over the whole of its course, but in practice the linear portion is usually restricted to the range approximately $0{\cdot}05 < p/p_0 < 0{\cdot}35$, as Brunauer, Emmett and Teller themselves point out.[2]

These workers ascribe this failure of equation (A) at low pressures to the non-uniformity of the adsorption potential over the surface of the adsorbent; the derivation of the equation utilises the idealisation that the heat of adsorption is constant for all adsorption sites. If the surface is non-uniform, however, adsorption must occur preferentially on sites of high potential, so that in the region of low pressures E_1 and c have higher values than elsewhere, and are moreover functions of x. According to this picture, the linear portion of the plot of equation (A) (and of (B)) corresponds to a condition where the more active parts of the surface are nearly all occupied, and the recruitment of molecules into the first layer is largely confined to the more uniform, though less active, parts of the surface.

Strictly, of course, a linear plot demands an *absolutely* constant value of c and therefore of E_1; but in practice, as can be shown by simple approximate calculation, if E_1 varies by an amount not exceeding some ± 250 cal. mole.$^{-1}$ from one part of the surface to another, the resultant plot of $p/x(p_0 - p)$ against p/p_0 will appear nearly straight. Within the limits of their model, Brunauer, Emmett and Teller [2a] are therefore justified in regarding E_1 as " the average heat of adsorption over the less active parts of the adsorbing surface."

To carry out correctly the comparison of the BET heat of adsorption with the experimental value, ΔH, it is essential, then, that the latter shall have been measured at an x-value lying within the linear range of the plot of equation (A). In Table I the value of x actually chosen is $x' = (x_1 + x_2)/2$, where x_1 and x_2 are the adsorptions at the beginning and the end respectively, of this linear range. Moreover, the effect of the simultaneous adsorption into the first and into higher layers has been taken into account by use of the factor r as in equation 9). The quantities to be compared are therefore $(\Delta H - \lambda)$ and $r(E_1 - \lambda)$. In those cases where a better straight line is obtained when p/xp_0, instead of $p/x(p_0 - p)$, is plotted against p/p_0 the value $r = 1$ has been used : this plot corresponds to equation (B) with $n = 1$ and implies that adsorption is here restricted to the first layer.

Examination of Table I shows that there is a moderately good qualitative agreement between the theory and experiment : a high value of c, say > 250, usually corresponds to a large value of $(\Delta H - \lambda)$, and a small c, say $c = 5$ to $c = 20$, to a small value of $(\Delta H - \lambda)$. But the quantitative agreement is very variable; in some cases the difference between the observed and calculated values (column 13) is no more than 300-400 cal./mole. and therefore lies within probable experimental error; but in more than half the cases this difference exceeds 1000 cal./mole and

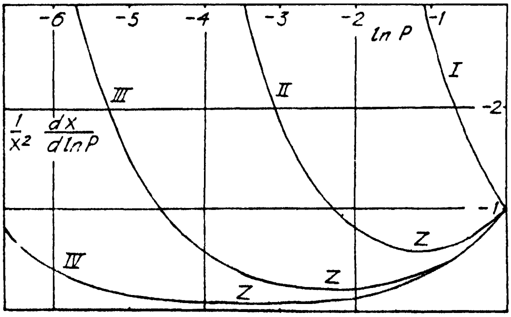

FIG. 3.—Graphs of $\frac{1}{X^2}\cdot\frac{dX}{d\ln P}$ against ln P, from equation (A).

Ordinates, $\frac{1}{X^2}\cdot\frac{dX}{d\ln P}$; abscissæ, ln P.

I. $c = 1$; II. $c = 11$; III. $c = 101$; IV. $c = 1001$; V. $c = 10001$.

so is too large to be accounted for by experimental error. Furthermore, the difference is too irregular to be corrected by the inclusion of the $RT \ln C$ term of equation (24) unless C be assumed to vary in an unpredictable manner from one case to another.

The qualitative correspondence between c and $(\Delta H - \lambda)$, already noted, is to be expected on general grounds: equation (A) can reproduce the general shape of any experimental isotherm having the form of Types I and II (Fig. 4); and in order to fit the equation to experimental curves showing high adsorptions at low pressures, a high value of c has to be used (cf. Fig. 1*b*). Now an essential part of any adsorption mechanism is the process of exchange of molecules between the adsorbed film and the outside gas; and this process, together with its resultant equilibrium, must be controlled by the heat of adsorption. The latter is involved,[6] in the expression for any kinetic mechanism, in the form $e^{-\Delta H/RT}$. Consequently, there must be a degree of correspondence between the heat of adsorption and any parameter which can express the dependence of adsorption on the relative pressure P. It is to the credit of the authors of the BET theory that they have succeeded in expressing this qualitative correspondence between the general shape of the isotherm and the heat of adsorption in so simple a mathematical manner, in terms of the parameter c; but in view of the results of Table I it is doubtful whether c can be used for the accurate *quantitative* determination of the heat of adsorption.

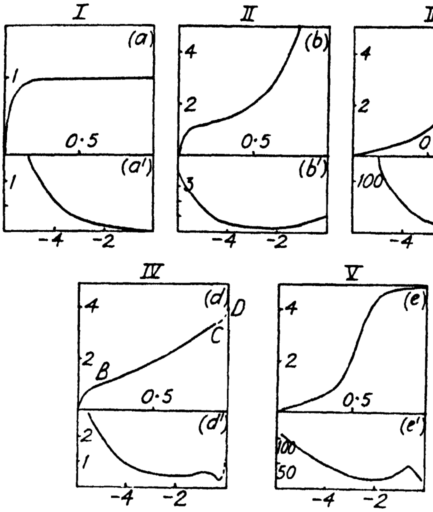

FIG. 4.—Isotherms of types I-V, and corresponding compressibility curves. (*a*), (*b*), (*c*), (*d*) and (*e*), isotherms. Ordinates, X; abscissæ, P. (*a'*), (*b'*), (*c'*), (*d'*) and (*e'*), compressibility curves. Ordinates $\beta' = (1/X^2)(dX/d \ln P)$; abscissæ, $\ln P$.

The Integration Constants of the Vapour Pressure Equation and of the Adsorption Isostere.

The validity of the BET assumption as to the near-identity of the multilayer and the bulk liquid will now be tested by consideration of the relation which it tacitly assumes between the integration constants of the vapour pressure equation and of the adsorption isotere respectively.

---

[6] E.g. Frenkel, *Z. Physik*, 1924, **26**, 117; Hückel, *Adsorption und Kapillarkondensation* (1928), p. 159; Polanyi, *Z. physik. Chem. A*, 1928, **138**, 460; Kar and Ganguli, *Physik. Z.*, 1929, **30**, 918; Fowler, *Proc. Camb. Phil. Soc.*, 1935, **31**, 260; Henry, *Phil. Mag.*, 1938 (6), **44**, 689.

By integrating the Clausius-Clapeyron equation applied to vapour pressure, viz.:

$$\frac{\partial \ln p_0}{\partial T} = \frac{\lambda}{RT^2} \quad . \quad . \quad . \quad . \quad . \quad . \quad . \qquad (15)$$

we obtain

$$\ln p_0 = -\frac{\lambda}{RT} + I_L \quad . \quad . \quad . \quad . \quad . \quad . \qquad (25)$$

where I_L is an integration " constant " which remains constant in value for ranges of temperature small enough for λ to be assumed constant; the vapour is assumed to obey the perfect gas laws and the volume of liquid is taken as negligible compared with that of the vapour.

Similarly, application of the Clausius-Clapeyron equation to adsorption, as already mentioned, gives

$$\left(\frac{\partial \ln p}{\partial T}\right)_x = \frac{\Delta H}{RT^2} \quad . \quad . \quad . \quad . \quad . \quad . \qquad (16)$$

where p is the equilibrium pressure for the adsorption x; by integration we have

$$(\ln p)_x = -\frac{\Delta H}{RT} + I_x \quad . \quad . \quad . \quad . \quad . \qquad (26)$$

I_x is also an integration " constant " which for a given x remains constant over small ranges of temperature, but is a function of x; the equation is subject to limitations similar to those explained for (25).

Subtracting (25) from (27) we obtain

$$\left(\ln \frac{p}{p_0}\right)_x = -\frac{(\Delta H - \lambda)}{RT} + (I_x - I_L) \quad . \quad . \quad . \qquad (27)$$

Now, according to equation (9) we can put

$$(\Delta H - \lambda) = r(E_1 - \lambda),$$

so that

$$\left(\ln \frac{p}{p_0}\right)_x = -\frac{r(E_1 - \lambda)}{RT} + (I_x - I_L)\,; \quad . \quad . \quad . \quad . \qquad (28)$$

and since from equation (6)

$$\ln c = \frac{(E_1 - \lambda)}{RT} \quad . \quad . \quad . \quad . \quad . \quad . \quad . \quad . \qquad (29)$$

equation (28) becomes

$$(\ln P)_x = -r \ln c + (I_x - I_L) \quad . \quad . \quad . \quad . \qquad (30)$$

where P is written for p/p_0, as usual.

By transforming equation (A′) it is readily shown that

$$(\ln P)_x = -\ln c + \ln \left\{\frac{x_0/(1 - P) - x}{x}\right\} \quad . \quad . \quad . \quad . \qquad (31)$$

if $c \gg 1$.

On comparing (30) and (31) it is seen that the BET assumptions are equivalent to the assertion that

$$(I_x - I_L) = -(1 - r)\ln c - \ln \left\{\frac{x_0/(1 - P) - x}{x}\right\}$$
$$= y, \text{ say.} \quad . \quad . \quad . \quad . \quad . \quad . \quad . \quad . \quad . \qquad (32)$$

The validity of this assertion is tested in Table II, which is based on the same collection of isotherms as Table I. I_L has been obtained from the vapour pressure data for the liquid in question (the International Critical Tables often give data in the form $\log_{10} p = A + B/T$, so that $I_L = 2{\cdot}303A$); I_x has been calculated by equation (26) for the same value of x, viz. x', as that used in Table I; and for ΔH and x_0 the same values have been used as those quoted in Table I.

The number of suitable data is again small; not only are the adsorption data scanty, as already explained, but it is frequently impossible to arrive at a reliable value of I_L. For example, if, as sometimes happens, the value of λ calculated from the slope of the curve of $\log_{10}p_0$ against $1/T$ differs markedly from the calorimetric latent heat, the corresponding value of I_L is too uncertain to use. However, as far as they go the figures of Table II fail to support the theory; as is seen from column 9, the disagreement between $(I_x - I_L)$ and y is considerable in several cases, and moreover shows no obvious regularity which would suggest some relationship other than equality, between the two quantities.

TABLE II.

System.	Temp. °C.	I_x.	I_L.	$(1-r)\ln c$.	$-\ln\left\{\frac{\frac{x_0}{1-P}-x}{x}\right\}$.	y (See equation (32))	(I_x-I_L).	$(I_x-I_L)-y$.	Ref.
Charcoal—C_2H_4 .	0	15·74	16·88	0	+1·58	+1·61	−1·14	−2·73	14
Charcoal—SO_2. .	0	16·98	17·98	0	+1·84	+2·05	−1·00	−3·05	22
Charcoal—$(C_2H_5)_2O$.	0	21·80	18·00	0	+1·23	+1·23	+3·80	−2·57	23
Silica gel—SO_2 .	0	19·07	17·98	1·33	+1·52	+0·19	+1·09	+0·90	28
Activated alumina—CCl_4	25	24·97	18·70	−3·36	−0·04	−3·40	+6·27	+9·67	11
Chabasite—NH_3 .	0	20·73	17·90	0	+2·21	+2·21	+2·83	+0·62	29

N.B.—For the values of x_0, $x(= x')$, ΔH, P, c and r used in compiling this Table, see Table I.

The failure of I_x and I_L to show the inter-relationship demanded by the BET theory, must result from the incorrectness of the assumption that the multilayer differs inappreciably from the bulk liquid state; for, as Le Chatelier pointed out, the integration constants for similar processes should lie close to one another.

The Assumed Similarity of the Multilayer and of the Bulk Liquid. The assumption that the state of the multilayer differs inappreciably from that of the bulk liquid is open to criticism on a number of other grounds. In the first place it is incompatible with the BET-BDDT molecular model for adsorption itself, according to which the adsorbed material is in a highly patterned condition; not only are the molecules in the first layer adsorbed on fixed sites, but those in subsequent layers are attached on top of them.[3a] All interaction in directions parallel to the surface is ignored, the only attraction taken into account being that normal to the adsorbent surface.[*] This state of affairs is in marked contrast with that in the interior of a liquid, where patterning, though not entirely absent, is extremely rudimentary (Bernal and Fowler,[7] Stewart [8]), and where forces of attraction act symmetrically on any one molecule.

In the second place, there is experimental evidence. It is known, for example, that an adsorbate vapour frequently fails to condense as a bulk liquid on to a solid surface when the vapour is saturated[9] or even supersaturated.

---

[*] Since writing this paper there have come to our notice two papers by Hill (*J. Chem. Physics*, 1946, **14**, 263, 441) in which attention is drawn to this limitation in the BET-BDDT theory. In the second of these papers, Hill has put forward a modified model in which the molecular interactions are taken into account in the first layer only, the higher layers being regarded as liquid-like. By statistical-mechanical reasoning he derives a more general isotherm which includes the BET isotherm as a special case on neglecting the term taking care of the interactions.

[7] Bernal and Fowler, *J. Chem. Physics*, 1933, **1**, 515.

[8] Stewart, *Trans. Faraday Soc.*, 1933, **29**, 982.

[9] Lambert and Foster, *Proc. Roy. Soc. A*, 1932, **134**, 246.

Thus, outgassed alumina gel, exposed for 24 hr. to saturated CCl_4 vapour, adsorbs only a finite amount of CCl_4, whereas if the multilayer were, at $p = p_0$, identical with the bulk liquid, the vapour should distil on to it to an indefinitely large uptake.[11] The course of the isotherm in the neighbourhood of p_0 points to the same conclusion : the experimental investigation of this region is extremely difficult and is rarely attempted, but in certain cases at least, the isotherm does not approach p_0 asymptotically, but runs into the line $p = p_0$ at a finite angle.[11, 12]

At first sight, the presence of the parameter p_0 in the BET and BDDT equations, which are able to reproduce the general shape of certain types of isotherm over a reasonable range, lends support to the view that the adsorbed state is closely allied to that of the bulk liquid. It should be realised, however—as indeed pointed out by the authors themselves—that the validity of equation (A) is restricted to the approximate range $p/p_0 = 0{\cdot}05$ to $0{\cdot}35$. In practice, the range of validity varies somewhat from case to case. Consequently, the replacement of p_0 in the equation by an empirical quantity (constant), say q, differing from p_0 by 50 % or less, still gives a linear range for equation (A) ; the only difference is that this range now lies between different fractions of p_0. True, the new constant q will still be closely related to p_0, and so will suggest some correspondence between adsorption and ordinary condensation ; but a loose correspondence of this kind is only to be expected, and in itself signifies no more than the fact that both processes involve the same kind of forces —van der Waals forces.

It is to be doubted, therefore, whether p_0 plays the fundamental part in the adsorption equation claimed by the authors, and the underlying hypothesis that the evaporation-condensation properties of the multilayer and of the bulk liquid are nearly identical seems improbable.

The Role of the Critical Temperature in Adsorption.—Owing to the presence of p_0 in the fundamental equations (A) and (B) the application of the BET-BDDT theory is restricted to temperatures below the critical temperature T_c of the adsorbate ; adsorption at temperatures above T_c would require either quite a different, at least a modified, formula, so that the isotherms for a given adsorbent-adsorbate would be expected to show some obvious difference above and below T_c respectively. This point is not easy to test for isotherms of Types II, III, IV and V of the BDDT classification [3] (Fig. 4), as the great majority of experiments in the literature for these types have been carried out at temperatures below T_c ; but for Type I isotherms there are several instances in which measurements have been done on the same system at temperatures both above and below T_c, and these quite definitely fail to show any obvious change at T_c. For example, Titoff's isotherms [13] for CO_2 on charcoal at 0°, 30°, and 80° c. belong to one family and there is no break in the family relationship at $T_c (= 32{\cdot}1°)$. N_2O at 0° and 40·3° ($T_c = 38{\cdot}8°$) similarly showed no obvious difference in type up to 1 atm. pressure ; [14] McBain [15] states that " no special difference is noted when studying N_2O and C_2H_4 above and below their critical temperatures," yet both were studied up to pressures of 40-50 atm. where the isotherms become almost flat ; the nitrous oxide isotherms of McBain and Britton [16] at 20°, 45° and 67° c., for example, form a family with no noticeable difference above and below T_c ; in general shape they do not differ from that of nitrogen at −77°, i.e. well above its critical temperature ($T_c = -146°$).

---

[10] Bangham and Saweris, *Trans. Faraday Soc.*, 1938, **34**, 554 ; Bangham and Mosallam, *Proc. Roy. Soc. A*, 1938, **165**, 554.

[11] Gregg and Sing (unpublished work).

[12] e.g. Palmer, *Proc. Roy. Soc. A*, 1937, **160**, 250 ; Whipp, *ibid.*, 1933, **141**, 228.

[13] Titoff, *Z. physik. Chem.*, 1910, **74**, 641.

[14] Gregg, *J. Chem. Soc.*, 1927, 1494.

[15] McBain, ref. 1*a*, p. 111.

[16] McBain and Britton, *J. Amer. Chem. Soc.*, 1930, **52**, 2214.

Now the BET equation for Type I isotherms is

$$\frac{p}{x} = \frac{p_0}{cx_0} + \frac{p}{x_0} \quad . \quad . \quad . \quad . \quad . \quad (33)$$

if $c \gg 1$; it represents a modification of the Langmuir isotherm:

$$\frac{p}{x} = \frac{1}{bx_0} + \frac{p}{x_0} \quad . \quad . \quad . \quad . \quad . \quad . \quad (34)$$

wherein the parameter c/p_0 replaces b. But in view of the considerations just put forward it would seem that the original Langmuir equation (34) is preferable, for its applicability is not restricted to temperatures below T_c. An additional weakness of equation (33) is that it arises in two quite different ways from the BET-BDDT mechanism, (*a*) as a limiting case of equation (A) when $p \ll p_0$ and $c \gg 1$, in which case it should be valid only for the low pressure region; (*b*) as a special case of (B) where n is limited to unity, e.g. by the width of the pores. In this case, it should remain valid over the whole range of the isotherm, from $p = 0$ to $p = \infty$. Yet in cases where the experimental results are available for the low pressure range only, there seems no way of deciding whether one is dealing with case (*a*) or case (*b*); though Brunauer [17] seems to suggest that with charcoal, case (*b*) is common.

The Effect of Phase Change in the Adsorbed Layer on Determination of Monolayer Capacity.—As already pointed out, the BET-BDDT theory ignores all interaction between the adsorbed molecules in directions parallel to the surface of the adsorbent; according to many workers, however, not only is such interaction appreciable, but it may under appropriate conditions actually bring about "two-dimensional" phase transformations in the adsorbed layer.[18] In a recent paper [19] it has been shown that transformations of this kind can be detected by plotting $\frac{1}{x^2}\frac{dx}{d \ln p}$ $(= \beta')$ against $\ln p$ or $\log_{10} p$; the shape of the resulting curve is similar to that of the two-dimensional compressibility of the film plotted against its surface pressure π. A first-order transformation within the film reveals itself as a peak in this curve, which becomes less and less sharp as the transformation becomes more and more diffuse; and the inception of a multilayer is reflected as a rise in the curve of β' against $\ln p$, not followed by a falling branch.

This method will now be applied to isotherms following equation (A) (Types II and III, Fig. 4). In Fig. 3 there are plotted the values of β' (obtained by transformation and differentiation of equation (A)) against $\ln p/p_0$, for a series of values of c, viz.: 1, 11, 101, 1001 and 10001. In each case (except $c = 1$, which is Type III) the curve rises from a minimum very close to point Z, corresponding to $X = 1$ $(x = x_0)$ indicating that at that point the monolayer is completed and the multilayer begins to form; the form of the initial branch is typical of a monolayer "gaseous" (G) film which becomes increasingly compressed as p, and therefore π, increases, up to a maximum compression at Z; but with no transformation in the monolayer region. Thus, for isotherms of Type II, the "phase transformation" method leads to the same value for the monolayer capacity as does the BET method.

For isotherms of Type IV, on the other hand, the two methods disagree. According to the BET-BDDT theory the monolayer is completed near B; but the form of the β'—$\ln p$ curve, Fig. (4*d*) now signifies that the bend towards the p axis at B is due to a transformation (of diffuse first-order) within the monolayer, and that the monolayer is only completed near to point C. This interpretation is supported by the fact that in some, at least, of the very few cases of Type IV that have been experimentally extended to pressures near p_0, the isotherm again turns upwards (see dotted lines, Fig. (4*d*)); this last rise would appear to denote the beginning of the multilayer for it corresponds to a characteristic rise, with no falling branch, in the β'—ln p curve. If, as in the BET-BDDT interpretation, the earlier upward sweep BC is ascribed to the building-up of the multilayer, it is difficult to see how this second rise, CD, is to be explained. Somewhat similarly for the Type V isotherm, the form of the β'—ln p curve suggests that the branch YD is due to a transformation within the monolayer, not to the formation of a multilayer; the monolayer is still incomplete at D, so that the monolayer capacity is somewhat in excess of the adsorption at D; the BDDT treatment, on the other hand, gives a value in the region of Y. (For type V, $c \sim 1$, so that x_0 must lie near the adsorption corresponding to $p/p_0 = 0{\cdot}5$).

---

[17] Brunauer, ref. 1*b*, p. 166.

[18] Frenkel, *Z. Physik*, 1924, **26**, 117; Cassell, *Ergeb. exakt. Naturwiss.*, 1927, **6**, 114; *J. Physic. Chem.*, 1944, **48**, 195; Semenoff, *Z. physik. Chem. B*, 1930, **7**, 471; Bangham, *Proc. Roy. Soc. A*, 1932, **138**, 162; 1934, **147**, 153; Band, *J. Chem. Physics*, 1940, **8**, 178; Langmuir, *ibid.*, 1933, **1**, 3; Gregg, *J. Chem. Soc.*, 1942, 696; Frumkin, *Acta Physicochim.*, 1938, **9**, 313; Harkins and Jura, *J. Chem. Physics*, 1944, **12**, 112.

[19] Gregg and Maggs, *Trans. Faraday Soc.*, 1948, **44**, 123.

Isotherms of Type I when plotted as β' against ln p show the possible occurrence of a third-order transformation (sudden change in slope) near Z, but no multilayer formation—also found absent by the BET method. Actually both methods derive values of x_0 by what is essentially extrapolation, and these agree reasonably.

Type III isotherms, according to the BET-BDDT treatment, obey equation (A) with $c \sim 1$, and monolayer completion occurs at $p/p_0 = 0{\cdot}5$, i.e. in the region of Z. The form of the compressibility curve indicates (Fig. 3*a*, 4*b*), however, that neither monolayer completion—nor indeed any transformation at all—occurs in isotherms which strictly obey this equation.

It is thus seen that the BET-BDDT and the phase-change methods lead to values of the monolayer capacity in reasonable agreement for isotherms of Types I and II, but which differ for Types III, IV and V. In applying the phase-change method to isotherms believed to be Type II, it is essential to have measurements carried up to high pressures to ensure that they are not Type IV.

Interpretation of the Adsorption Isotherm.—The BET-BDDT and phase-change methods lead to fundamentally different views of the isotherm. According to the former, every isotherm is in principle capable of representation by a single equation covering the whole range from zero pressure up to the saturated vapour pressure; whereas according to the latter, if transformations occur in the film the adsorption isotherm is virtually split up into a number of separate parts, one for each film state; in such cases it is impossible to represent the whole isotherm by a single equation, but each part must be represented by its own distinct equation. Harkins and Jura have also emphasised this point.

A rather strong argument for the phase-change theory as against that of BET-BDDT is the existence of adsorption hysteresis. The BET-BDDT theory in its original form is unable to account for the effect at all; it is true that Dietz [20] has put forward a modification of the theory which attempts to account for the effect by assuming (somewhat arbitrarily) that the heat of adsorption is smaller during adsorption than during desorption; even so, the theory fails to reproduce the desorption branch even approximately. Once the possibility of phase changes in the adsorbed film is conceded, however, we have a natural explanation of hysteresis; for, by analogy with the behaviour of bulk matter and of trough films,[21] a time lag—suspended phase-transformation—is only to be expected as a frequent, though not inevitable, accompaniment of it. This lag would make itself manifest as a slow drift in the surface pressure and therefore in p, the gas pressure.

[20] Dietz, *J. Res. Nat. Bur. Stand.*, 1945, **35**, 303.

[21] Adam, *Physics and Chemistry of Surfaces* (1941), 56.

Summary.

The theory of Brunauer, Emmett and Teller (BET) and Brunauer, Deming, Deming and Teller (BDDT) has been examined.

(1) The heat of adsorption E_1 calculated via the parameter c of the theory, is shown to be compatible with thermodynamic requirements as expressed in the Clausius-Clapeyron equation ; but the latter are equally compatible with a value $E_1 + RT \ln C$ (C = any constant).

(2) E_1 shows a moderate qualitative correspondence with the calorimetric or isosteric value, but close quantitative agreement is lacking.

(3) The relationship which the theory implies between I_L and I_x, the integration constants of the vapour equation and the adsorption isostere respectively is not found to hold in practice.

(4) Arguments are adduced against the assumption made by the theory that the evaporation-condensation conditions of the adsorbed multilayer differ inappreciably from those of the bulk liquid.

(5) The implicit assumption that the adsorption isotherms above and below the critical temperature of the adsorbate are markedly different, is shown to be improbable.

(6) The values of the monolayer capacity derived from the theory and from the " phase-change " method of Gregg and Maggs are compared. Only for isotherms of Type I and II of the BDDT classification, is agreement to be found.

(7) According to the phase-change method, the adsorption isotherm cannot invariably be represented by a single equation as assumed by the BET-BDDT theory ; where phase changes occur, the isotherm is split up into separate parts, each following its own equation.

(8) The BET-BDDT theory does not account for hysteresis, but the phase-change conception includes it as a natural consequence.

[22] Gregg, *J. Chem. Soc.*, 1943, 351.
[23] Goldmann and Polanyi, *Z. physik. Chem.*, 1928, **131**, 333.
[24] Pearce and Reed, *J. Physic. Chem.*, 1931, **35**, 908.
[25] Lambert and Clark, *Proc. Roy. Soc. A*, 1929, **122**, 497.
[26] Patrick and Long, *J. Physic. Chem.*, 1925, **29**, 339.
[27] Felsing and Ashby, *J. Amer. Chem. Soc.*, 1934, **56**, 2226.
[28] Patrick and Greider, *J. Physic. Chem.*, 1925, **29**, 1038.
[29] Evans, *J. Chem. Soc.*, 1931, 1556.

Washington Singer Laboratories,
Prince of Wales Rd.,
Exeter.

A FEEDBACK POTENTIOMETER FOR THE MEASUREMENT OF *p*H VALUES AND OXIDATION-REDUCTION POTENTIALS.

By C. Morton.

Received 18*th August*, 1947.

The use of the thermionic valve in the determination of electrode potentials is due to Goode.[1] The method consists essentially in applying the E.M.F. to be measured to the input terminals of a thermionic valve D.C. amplifier and reading the output voltage, which is assumed to be proportional to the applied voltage, on a suitably calibrated voltmeter connected in the output circuit. In its original form, Goode's valve voltmeter suffered from the drawback that the calibration was dependent on the varying characteristics of the amplifier but, as a result of the introduction of negative feedback, errors due to this cause can now be greatly reduced. The overall accuracy of a deflection instrument, however, cannot exceed that of the voltmeter which serves to indicate the output voltage ; this is of the order of ± 1 % of full-scale deflection for high-grade pointer instruments.

---

[1] Goode, *J. Amer. Chem. Soc.*, 1922, **44**, 26 : 1925, **47**, 2483.

In 1928 the author[2] introduced the thermionic valve potentiometer, the readings of which are independent of the characteristics of the amplifier. In common with other null devices, the method has the advantages that the instrument can be calibrated with any desired degree of accuracy and, unlike the valve voltmeter, retains its calibration unimpaired by age or overload. Unfortunately, as each measurement entails three adjustments, accuracy is gained at the expense of convenience ; nevertheless, the majority of the instruments described in recent years[3] have been of the potentiometric type.

1. Basic Design of the Feedback Potentiometer.

Hitherto, negative feedback appears to have been applied only to deflection instruments, although the writer[4] has made use of positive feedback to enhance the sensitivity of a potentiometric recorder. The basic design of the feedback potentiometer[5] now described is illustrated in Fig. 1.

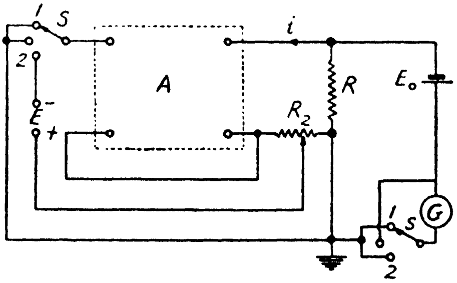

FIG. 1.

The calibrated potentiometer R_2 and standardising resistance R are connected in series across the output terminals of an amplifier A, and a Weston cell E_0 and galvanometer G are similarly connected in series across R. When released, the double-pole, three-position switch SS rests in the mid-position, in which it disconnects the Weston cell from the circuit and short-circuits the galvanometer. In order to measure a potential E, (1) the switch is thrown to position 1, and the gain control of the amplifier (not shown in the diagram) is adjusted until the galvanometer is undeflected, (2) the switch is thrown to position 2, and the movable contact on the potentiometer R_2 is adjusted until the galvanometer is again undeflected. The reading of the potentiometer scale then gives the voltage E of the source of E.M.F. The measurement entails only two adjustments, the first of which requires repetition only at infrequent intervals, since the potentiometer and galvanometer currents are stabilised (as explained in section 5) to an extent depending upon the gain of the amplifier.

2. Modifications Required for the Measurement of *p*H Values and Oxidation-reduction Potentials.

In order to eliminate the tedious calculations entailed in the translation of electrode potentials into *p*H units, it is convenient to modify the basic circuit of Fig. 1 in such a manner that the reading of the instrument gives directly the

---

[2] Morton, *Trans. Faraday Soc.*, 1928, **24**, 5 ; *J. Sci. Instr.*, 1932, **9**, 289.

[3] Britton, *J. Sci. Instr.*, 1946, **23**, 89 ; Britton, *Hydrogen Ions*, (Chapman and Hall, Ltd., 1942) ; Dole, *The Glass Electrode* (Chapman and Hall, Ltd., 1941).

[4] Morton, *J. Chem. Soc.*, 1932, 2469.

[5] B.P. Application, No. 14889/45.

*p*H value of the solution in contact with the electrodes. This may be accomplished (Fig. 2) by the addition of temperature-compensating and electrode-standardising networks; it is also necessary to replace the double-pole switch

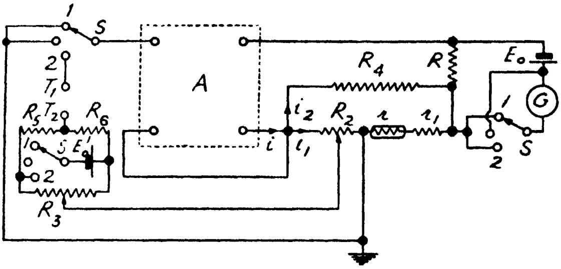

FIG. 2.

of Fig. 1, by a triple-pole three-position switch which, when released, returns automatically to the mid-position.

The temperature-compensating network, the purpose of which is to provide automatic compensation for variations in the E.M.F. of the electrodes due to changes in the temperature of the solution in which they are immersed, comprises the ohmic resistances r_1 and R_4 and the temperature-sensitive element r. The latter, which is immersed in the solution under investigation, consists of a thermistor, i.e. a bead of oxides approximately 0·05 in. in diameter, sealed in the drawn-out tip of a glass tube. The advantage of this form of resistance thermometer, which has a high negative temperature coefficient of resistance, over the more familiar type lies in its small dimensions and consequent low heat capacity, by virtue of which it responds almost instantaneously to temperature changes. The fact that it functions satisfactorily when only a few drops of solution are available makes it especially suitable for use in the investigation of biological fluids. The manner in which automatic temperature-compensation is effected is described more fully in section 5.

The electrode-standardising network consists of the resistances R_5 and R_6 and the uncalibrated potential divider R_3, current being supplied to the network by a Weston cell E_0'. As the ohmic value of each of the resistances R_3, R_5, R_6, is at least 1 MΩ the load imposed upon the cell is negligible. Within reasonable limits the E.M.F. of the cell is immaterial, and it may be inexpensively constructed from unpurified commercial materials.

The purpose of the network is to permit of the superimposition of a positive or negative potential of approximately 500 mv. on the E.M.F. of the hydrogen-ion cell in order to compensate for changes in the potential of the latter due, e.g., to contamination of the electrode materials or to variations in the asymmetry potential when the glass electrode is employed.

The indicator electrode, which may be a hydrogen, quinhydrone, or glass electrode, and the reference electrode (usually a calomel, or silver chloride, electrode) are connected to the terminals T_1 and T_2 respectively. The subsequent adjustments are identical with those described in the preceding section, i.e. (1) the switch is thrown to position 1, and the gain control of the amplifier is adjusted until the galvanometer is undeflected, (2) the switch is thrown to position 2, and the contact on R_2 is adjusted until the galvanometer is again undeflected. Assuming that the electrode-standardising control R_3 has been correctly pre-set and that the potentiometer R_2 is suitably calibrated as described in sections 4 and 5, the potentiometer reading then gives directly the *p*H value of the solution in contact with the indicator electrode.

It is advisable to check the adjustment of the electrode-standardising control R_3 occasionally in order to ensure that no change has taken place in the normal potentials of the electrodes. For this purpose the indicator electrode is put into contact with a buffer solution of known *p*H value. If, on completing adjustment (2) above, an incorrect reading is obtained, R_2 is set to the correct *p*H value and R_3 is adjusted until the galvanometer is undeflected. Subsequent readings will in general be correct for at least 24 hr. when the glass electrode is employed, or for longer periods if the indicator electrode is a hydrogen or quinhydrone electrode.

In the investigation of oxidation-reduction intensity, it is in general preferable to express the state of oxidation-reduction balance in terms of the potential

E_H (on the so-called hydrogen scale) which is assumed by an unattackable electrode immersed in the solution, and the method by which such a measurement may be made with the aid of the apparatus illustrated schematically in Fig. 1 will be apparent from the preceding description. Clarke suggested that the unattackable electrode should be regarded as a hydrogen electrode in equilibrium with hydrogen gas at a hypothetical pressure P, and that the properties of the solution should be expressed in terms of $r\text{H} = \log 1/P$, the common logarithm of the reciprocal of the pressure of hydrogen gas at the electrode. The abuse of the symbol *r*H consequent upon a misunderstanding of its true meaning led him subsequently to recommend its discontinuance; however, provided that discretion is exercised, definition of the state of oxidation-reduction balance in terms of a unit which is independent of the *p*H value of the solution has considerable advantages. In order to measure the *r*H value of a solution, a glass electrode and an unattackable electrode, such as an unplatinised gold or platinum electrode, may be immersed in the solution and connections taken to the terminals T_1 and T_2 respectively (Fig. 2). The electrode system is standardised as described above, but with the aid of a solution of known *r*H value instead of one of known *p*H value. For this purpose a freshly prepared solution made by shaking an acid buffer solution (such as a dilute solution of potassium hydrogen phthalate) for a few minutes with a little solid quinhydrone is suitable; such a solution has $r\text{H} = 24{\cdot}2$ at 18° C. or $r\text{H} = \dfrac{717{\cdot}5 - 0{\cdot}74t}{0{\cdot}099\,(273 + t)}$ at t° C. On replacing the solution of known *r*H value by the solution under investigation and carrying out the measurement as described above, the scale reading of the potentiometer R_2, when multiplied by a scale factor of 2, gives directly the *r*H value of the solution.

3. Amplifier.

Multi-stage amplifiers based on the ballistic or impulse type suggested by the author[6] have been used by workers in America and elsewhere;[3] in this country, however, single-valve amplifiers appear to be preferred on account of their greater reliability and stability. The choice of a suitable valve for use in the circuits of Fig. 1 and 2 presents some difficulty.

From the instrument maker's point of view it is undesirable that the resistance of the potentiometer slidewire should exceed 200 Ω; assuming that the customary voltage drop of 100 mv. along the slidewire is required, it follows that the minimum value of the potentiometer current is 500 μa. Comparatively few valves, even those of the electrometer type, are capable of delivering an anode current of this order whilst maintaining an adequate input resistance and low grid current. As Mulder and Razek[7] have pointed out, when the control grid is appreciably negative and the anode potential is raised sufficiently to produce an anode current in excess of about 100 μa., grid current is due mainly to positive ions collected by the negative grid, and is sensibly proportional to the anode current; in view of the fact that the positive ions attracted to the grid arise from collisions between the stream of electrons which constitutes the anode current and the neutral molecules present within the envelope, such a proportionality is to be expected. Tetrodes of the type in which the inner grid functions as a space-charge grid were found to give the most satisfactory results in the circuit of Fig. 2; examples of such valves are the recently-developed electrometer tetrode E1892, the Mullard PM1DG, and the Cossor 210DG. The space-charge grid has the property of reducing the internal resistance of the valve, thus making it possible to obtain adequate emission without raising the anode voltage appreciably above the ionisation potential of the residual gas in the envelope and also, by virtue of its positive charge, repels positive ions which would otherwise be attracted to the negative control grid.

If grid current of the order of 10^{-11} amp. can be tolerated, an indirectly-heated valve of the radio-frequency pentode or beam tetrode type, such as the KTW61M is satisfactory; the positively-charged screen, which in this type of valve is usually more or less closely interwoven with the control grid, appears to play the same role in the repulsion of positive ions as does the space charge grid in the E1892. When using an indirectly-heated valve as an electrometer valve it is essential to reduce the filament current to about 70 % of the maker's rated value in order to reduce grid emission and the emission of photo-electrons which otherwise cause a very large increase in grid current; as the anode current under operating conditions is only about 5 % of the maker's rating, operation at a low cathode temperature is permissible. The valve may be triode-connected in order to reduce its internal resistance, or the screen grid may be used as the anode and the suppressor grid (if any) and normal anode connected to earth.

---

[6] Morton, *J. Chem. Soc.*, 1931, 2977.

[7] Mulder and Razek, *Rev. Sci. Instr.*, 1929, **18**, 466.

4. Description of the Completed Instrument.

By the incorporation of a simple switching device the circuits of Fig. 1 and 2 may be combined in one instrument (Fig. 3). When the plug P, to which the resistance thermometer *r* is connected, is inserted in the jack J, the circuit is transformed into that of Fig. 2 and may be used for the measurement of *p*H or *r*H as previously described. On removing the plug the temperature-compensating network is disconnected from the circuit; simultaneously, the electrode-standardising network becomes currentless and may be disregarded. The circuit thus becomes in effect identical with that of Fig. 1, and may be used for the measurement of an E.M.F. in millivolts as described in section 1.

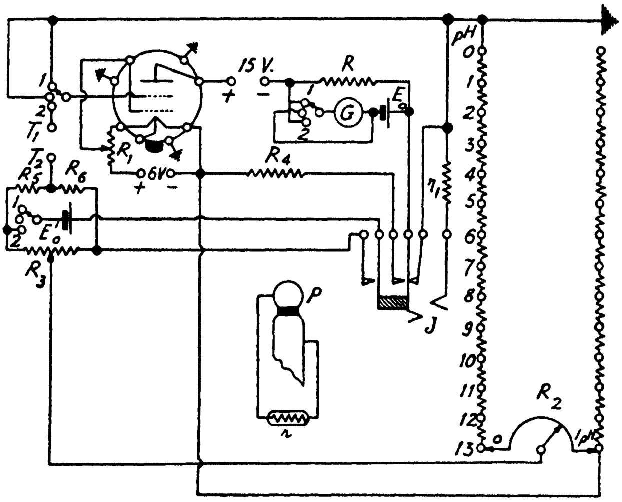

FIG. 3.

For reasons which are discussed in section 3, it was decided to use a single-stage amplifier in the instrument as finally constructed. Through the courtesy of the General Electric Company, the author was able to make use of prototypes of a new electrometer tetrode, the E1892. In this valve the control grid is connected to a cap at the upper end of the glass envelope, thus obviating the necessity for removing the valve base to improve the insulation resistance; the remaining electrodes are joined to an international octal base, the connections to which (viewed from above) are shown in the figure. It was found essential to earth valve pins to which there are no internal connections, and also to shield the valve from light, since otherwise there was an appreciable increase in grid current. It was found convenient to supply the series-connected half-filaments with 50 ma. from a 6-volt source, the excess voltage being absorbed by the uncalibrated potential divider R_1, the resistance of which is 64 Ω. With an anode potential of 15 v., and control grid bias of − 1·4 v., the space charge or inner grid requires a positive potential of approximately 3·5 v. in order that an anode current of 500 μa. may be maintained. This space-charge grid voltage is conveniently obtained, by means of a movable contact on R_1, from the source of filament supply; R_1 then constitutes a satisfactory gain control. The power consumption is only about 310 mw., permitting of the use of dry batteries of moderate capacity as the source of power; if it is preferred to supply power from A.C. mains by means of rectifying and smoothing equipment, it is desirable that the transformer used should have constant-voltage characteristics.

The potentiometer R_2 consists of 26 coils of 200 Ω each and a slidewire, also of 200 Ω resistance, bearing 100 subdivisions. As the standardising resistance $R = 2036{\cdot}6\ \Omega$, the potentiometer current is 500 μa. and the potentiometer covers a range of 1400 mv. with subdivisions to 1 mv.; when the plug is inserted in the jack, the corresponding ranges are 14 *p*H or 28 *r*H units, subdivided to 0·01 *p*H or 0·02 *r*H respectively.

The instrument is operated as previously described, R_1 being used as the gain control. Under the operating conditions described above, the sensitivity is approximately 65 μa./v., input resistance $10^{12}\ \Omega$, grid current 10^{-13} amp., permitting of the measurement of an E.M.F. through an external circuit resistance of 10,000 MΩ with an accuracy of ± 1 mv. If the power is supplied from A.C. mains by means of a constant-voltage transformer and suitable rectifying and smoothing equipment, a change of ± 10 % in mains voltage during the period occupied by the measurement introduces an error of less than ± 1 mv. or ± 0·01 *p*H.

5. Theory.

(1) Fundamental Theory of the Feedback Potentiometer.—The theory underlying the feedback potentiometer is readily understood from a consideration of the equivalent electrical circuit (Fig. 4), in which R_a represents the internal resistance of the output stage, r_0 is the sum of the resistances of the Weston cell E_0 and the galvanometer G, and i_0 is the galvanometer current. The output current i which is utilised as the potentiometer current, is the algebraic sum of (a) a constant component independent of the E.M.F. applied to the input circuit, (b) a variable component proportional to the input potential e; these components are attributed in the diagram to the inclusion of a generator V of constant voltage and a source μe of variable potential respectively, μ being the gain of the amplifier. The application of Kirchhoft's laws to the two networks gives

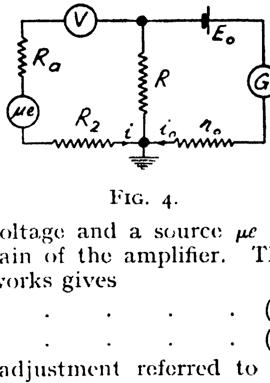

FIG. 4.

$$V - \mu e = ir_2 + i_0R \quad . \quad . \quad . \quad . \quad (1)$$

and

$$E_0 = i_0(r_0 + R) + iR \quad . \quad . \quad . \quad . \quad (2)$$

where $r_2 = R_a + R_2 + R$. During the first adjustment referred to in sections 1 and 2, the voltage drop across R_2 is fed back to the input circuit; hence eqn. (1) may be written

$$V - \mu iR_2 = ir_2 + i_0R. \quad . \quad . \quad . \quad (1a)$$

The elimination of i from eqn. (1a) and (2) leads to an expression for the galvanometer current:

$$i_0 = [(r_2 + \mu R_2)E_0 - RV]/[(r_2 + \mu R_2)(r_0 + R) - R^2]. \quad . \quad (3)$$

The adjustment will be completed ($i_0 = 0$) when $E_0/V = R/(r_2 + \mu R_2)$, that is, when the gain μ of the amplifier has been adjusted to the value $\mu = (RV - r_2E_0)/R_2E_0$.

During the second adjustment referred to in sections 1 and 2 the voltage E to be measured is connected, in series with the feedback potential derived from R_2, across the input terminals of the instrument, and the sliding contact on the potentiometer is adjusted until the potentiometer current is restored to its former value, as evidenced by the fact that the galvanometer is again undeflected. If the resistance of that portion of R_2 which is now included in the feedback circuit is R_2', when this adjustment is completed

$$V - \mu(iR'_2 + E) = ir_2 + i_0R. \quad . \quad . \quad (4)$$

From (1a) and (4) it follows that

$$E = i(R_2 - R'_2) = i \, . \, \mathrm{d}R_2 ; \quad . \quad . \quad . \quad (5)$$

that is, the increment in feedback voltage, which can be read on the scale of the potentiometer, is equal to the applied voltage E.

(2) Sensitivity.—If, on the completion of the first adjustment referred to above, a voltage dE is applied to the input terminals of the instrument, the potentiometer and galvanometer currents will assume new values i' and i'_0 respectively such that

$$V - \mu i'R_2 + \mu \, . \, \mathrm{d}E = i'r_2 + i'_0R \quad . \quad . \quad . \quad (6)$$

and

$$E_0 = i'_0(r_0 + R) + i'R \quad . \quad . \quad . \quad . \quad (7)$$

whence

$$i'_0 = [(r_2 + \mu R_2)E_0 - R(V + \mu \, . \, \mathrm{d}E)]/[(r_2 + \mu R_2)(r_0 + R) - R^2] \quad (8)$$

From (8) and (3)

$$\mathrm{d}i_0 = i_0 - i'_0 = \mu \, . \, \mathrm{d}E \Big/ \left[\left(r_2 + \mu R_2\right)\left(\frac{r_0}{R} + 1\right) - R\right]$$

or

$$\mathrm{d}i_0/\mathrm{d}E = 1 \Big/ \left[R_2\left(\frac{r_0}{R} + 1\right) + \frac{1}{\mu}\left\{r_2\left(\frac{r_0}{R} + 1\right) - R\right\}\right]. \quad . \quad (9)$$

Eqn. (9) defines the voltage sensitivity $\mathrm{d}i_0/\mathrm{d}E$ of the instrument, that is, the change in galvanometer current for unit change in applied potential. If the amplifier has an even number of stages the feedback is positive, resulting in increased gain but decreased stability; as $\left(\frac{r_0}{R} + 1\right)(r_2 - \mu R_2)$ approaches R in magnitude the sensitivity increases very greatly. Using a two-stage amplifier, a voltage sensitivity of 40 ma./v. is readily obtained. Due to the increased dependence of the amplification upon the supply voltages, however, full advantage cannot be taken of the high degree of sensitivity thus obtainable unless all supply voltages are maintained constant within close limits. On the other hand, assuming that the amplifier comprises a single valve, or consists of an odd number of stages, the feedback is negative, leading to decreased sensitivity but increased stability; when μ is sufficiently great, equation (9) becomes

$$\mathrm{d}i_0/\mathrm{d}E = 1/R_2\left(\frac{r_0}{R} + 1\right) \quad . \quad . \quad . \quad (10)$$

the galvanometer current i_0 and also the potentiometer current i being then independent of μ and thus of the valve characteristics and supply voltages. If in addition $r_0 \ll R$ (a condition which may be satisfied by using a low-resistance galvanometer and an unsaturated Weston cell of low internal resistance) the equation reduces further to

$$\mathrm{d}i_0/\mathrm{d}E = 1/R_2. \quad . \quad . \quad . \quad . \quad (11)$$

(3) Extension of the Theory to the Measurement *p*H Values and Oxidation-reduction Potentials.—The E.M.F. of a hydrogen-ion cell composed of an indicator electrode (a hydrogen, quinhydrone or glass electrode) of normal potential e_0 and a reference electrode of constant potential E_r, such as a calomel or silver chloride electrode, is

$$E = K - 0{\cdot}000198T \, . \, p\text{H}, \quad . \quad . \quad . \quad (12)$$

where T is the absolute temperature of the solution in contact with the indicator electrode and $K = e_0 - E_r$ is a constant for a given electrode system. The value of K may differ both in magnitude and sign for different combinations of electrodes, and is also affected, when the glass electrode is employed, by variations in the so-called asymmetry potential. From the form of eqn. (12) it is clear that, in order to adapt the instrument for use as a direct-reading *p*H meter, temperature-compensating and electrode standardising networks must be incorporated in the circuit.

The former network (Fig. 2) consists of the series combination of the temperature-sensitive element r (immersed in the solution under investigation) the ohmic resistance r_1 and the potentiometer R_2, shunted by the ohmic resistance R_4. The potentiometer R_2 is subdivided into b main sections, each representing one *p*H unit and having a resistance of R_2/b ohms; these main sections may be further subdivided, by means of a slidewire, to any desired degree. The output current i on entering the network divides into currents i_1 and i_2 flowing through the series combination R_2, r, r_1 and the shunt R_4 respectively. As the temperature of the solution rises the resistance of the thermistor r decreases, with the result that i_1 increases at the expense of i_2, causing the voltage drop across the potentiometer R_2 to increase. The values of the resistances in the network are so proportioned that the voltage drop across each main section of the potentiometer, representing one *p*H unit, is $0{\cdot}000198T$ volt within the range throughout which the resistance of the thermistor is a linear function of its temperature. If, at a solution temperature T', the values of r, i_1 and i_2 become r', i_1' and i_2' respectively, the ohmic values of r_1 and R_4 required to satisfy this condition may be deduced from the relationships :

$$i_1 = 0{\cdot}000198Tb/R_2 \qquad . \quad . \quad . \quad . \quad (13)$$

$$i'_1 = 0{\cdot}000198T'b/R_2 \qquad . \quad . \quad . \quad . \quad (14)$$

$$i'_2 = i - i'_1 \qquad . \quad . \quad . \quad . \quad . \quad . \quad (15)$$

$$i'_2 = i - i'_1 \qquad . \quad . \quad . \quad . \quad . \quad . \quad (16)$$

$$i_1(R_2 + r + r_1) = i_2R_4 \qquad . \quad . \quad . \quad . \quad (17)$$

$$i'_1(R_2 + r' + r_1) = i'_2R_4 \qquad . \quad . \quad . \quad (18)$$

From these equations we obtain :

$$r_1 = [i_2i'_1(R_2 + r') - i'_2i_1(R_2 + r)]/(i'_2i_1 - i_2i'_1) \qquad . \quad (19)$$

$$R_4 = i_1(r + r_1 + R_2)/i_2 \qquad . \quad . \quad . \quad . \quad . \quad . \quad (20)$$

where i_1, i'_1, i_2, i'_2 are defined by eqn. (13), (14), (15) and (16) respectively. When $R_2 = 2800\Omega$, $b = 14$, $i = 500\ \mu$a., $T = 20°$ C. $= 293°$ K., $T' = 30°$ C. $= 303°$ K., eqn. (19) and (20) reduce to

$$r_1 = 11{\cdot}59r - 12{\cdot}59r' - 2800 \qquad . \quad . \quad . \quad (19a)$$

and

$$R_4 = 3882{\cdot}5 + 1{\cdot}387\ (r + r_1) \qquad . \quad . \quad . \quad (20a)$$

respectively. For example, if the resistance of the thermistor is $r = 2000\ \Omega$ at 20° C. and $r' = 1500\ \Omega$ at 30° C., the appropriate values of r_1 and R_4, as calculated by means of eqn. (19*a*) and (20*a*), are 1495 and 8730 Ω respectively.

At the completion of either of the adjustments referred to in section 2, the potential of the terminal T_1 (Fig. 2) with respect to earth is zero. By eqn. (12) the hydrogen-ion cell impresses an E.M.F. of $K - 0{\cdot}000198T\,.\,p$H volt upon this terminal and an additional potential of $- K$ volts is superimposed upon this by the electrode-standardising network ; it follows that the P.D. between the contact on R_2 and earth is $+\ 0{\cdot}000198T\,.\,p$H volt. In other words, the reading of the potentiometer scale gives directly the *p*H value of the solution.

The E.M.F. of an oxidation-reduction cell composed of a glass electrode and an unattackable electrode is

$$E = (e_0 - 0{\cdot}000198T\,.\,p\text{H}) - 0{\cdot}000198T(0{\cdot}5r\text{H} - p\text{H}) = e_0 - 0{\cdot}000099Tr\text{H} \qquad (21)$$

and is independent of the *p*H value of the solution. From a comparison of eqn. (21) and (12) it is clear that, on the completion of the adjustments described in section 2, the reading of R_2, when multiplied by a scale factor of 2, gives directly the *r*H value of the solution under examination.

The author is indebted to the Royal Society for a Government Grant.

Summary.

A description is given of a thermionic valve feedback potentiometer for the determination of *p*H values and oxidation-reduction potentials. The instrument has the advantage over *p*H meters of the deflection type that it may be calibrated in *p*H units or in millivolts with any desired degree of accuracy, the calibration being permanent and independent of the characteristics of the amplifier. The feedback potentiometer differs from the potentiometric *p*H meters previously described in the following respects. (1) The measurement entails only two

adjustments. (2) If the feedback from the potentiometer is negative, these adjustments are stabilised to such a degree that a variation of ± 10 % in the supply voltage during the time occupied by the measurement introduces an error of less than ± 1 mv. or ± 0·01 *p*H ; on the other hand, when positive feedback is employed, high voltage sensitivity (of the order of 40 ma./v.) is obtained at the cost of decreased stability. (3) Automatic compensation for variations in the E.M.F. of the electrodes due to changes in the temperature of the solution is provided by means of a thermistor (a bead of oxides 0·05 in. in diam.) immersed in the solution ; due to its small dimensions and low heat capacity, this element responds almost instantaneously to temperature changes and is capable of use when only a few drops of solution are available.

Chelsea Polytechnic,
London, S.W.3.

THE DETERMINATION OF FLAME SPEEDS IN GASEOUS MIXTURES.

By S. Sherratt and J. W. Linnett.

Received 21st August, 1947.

The majority of the determinations of the movement of flame have been carried out under conditions where it has not been possible to assess the movement of the gases. These results are of little academic value. For academic considerations we wish to know the movement of the flame relative to the unburnt gas (often called the burning velocity), and not relative to an object external to the gaseous system. Measurements of such burning velocities are of three types : (1) measurement of flame movement in a spherical bomb as carried out by Fiock and others ; [1] (2) measurement of flame movement in an explosive mixture originally contained in a soap bubble—cf. Stevens ; [2] (3) measurement of the shape of the luminous inner cone of the flame on a Bunsen type burner. The last method is our subject for study in the present paper. It will be found that, from our investigations, we are also able to make certain conclusions regarding the flame region, or flame front, that is observed on the Bunsen burner.

The use of Bunsen flames in the measurement of burning velocities depends on the assumption that the flame is stationary in space because the burning velocity is exactly balanced by the movement of the gas. This means that the gas velocity resolved along a direction normal to the flame front must equal the burning velocity. If the angle between the Bunsen cone and the flow lines is θ then, at any point, we have

$$B = L \sin \theta \qquad . \quad . \quad . \quad . \quad . \quad (1)$$

where B and L are the burning velocity and the velocity of gas movement respectively at that point.

Calculations of the shape of the flame cone were made by Michelson [3] who made the following simplifying assumptions :

(i) the gas velocity varies in a parabolic manner across the tube (stream-lined flow) ;

---

[1] Fiock, Marvin, Caldwell and Roeder, *Nat. Adv. Comm. Aero. Tech. Report*, No. 682, 1939.

[2] Stevens, *J. Amer. Chem. Soc.*, 1926, 48, 1896 ; 1928, **50**, 3244.

[3] Michelson, Wiedemanns *Annalen*, 1889, **37**. See also Mache, *Die Physik der Verbrennungserscheinungen* (Leipzig, 1918).

(ii) the boundary between burned and unburned gas is a surface, the change being instantaneous ;
(iii) the burning velocity is constant over the whole surface ;
(iv) the movement of the gas is parallel to the axis of the tube right up to the flame surface.

The observed shape differed radically from that calculated by Michelson in two particulars. In the first place the cone of the Bunsen flame is rounded at the tip whereas the Michelson hypotheses predicted that it should be pointed. In the second, the visible flame has a greater diameter at the base than the diameter of the orifice. The Michelson hypotheses were really unable to predict the form of the base of the flame. The first difference between theory and experiment is due mainly to the failure of (iii) because the rounding at the tip proves that the burning velocity there is greater than that over the rest of the cone. This increase in velocity towards the apex has been demonstrated by Lewis and von Elbe. The second difference between theory and experiment is due to the failure of (iv) for Lewis and von Elbe have shown that the gas-flow lines bend away from the axis before the flame cone is reached.[4] Besides these two departures, (ii) cannot be regarded as a satisfactory assumption because the flame zone certainly has a definite thickness and consists of a succession of different zones which merge into and overlap one another. We will discuss this later. The only assumption of Michelson that can be accepted with only very minor reservations (providing that the conditions are such as to avoid turbulence) is (i).

Before describing our experimental method we will summarise briefly the ways in which other workers have used observations on Bunsen cones to determine burning velocities. Gouy,[5] finding that the Bunsen cone differed from the geometric cone, projected the image of the flame on to a screen and estimated the area of the flame cone. He divided this into the volume flow rate and so obtained the *average* burning velocity. Such a measurement would have given the required velocity if there had been no expansion of the gases before the luminous flame front was reached. That is, however, an unjustifiable assumption since Lewis and von Elbe have shown that there is expansion before this flame front is reached. Garside, Forsyth and Townend[6] used a somewhat similar method to that of Gouy taking great care over the measurement of the flame area.

Stevens[7] determined the slope of the cone at $0{\cdot}707R$ from the axis (R is the internal radius of the burner tube) because, if the gas flow is streamlined, it is at this distance from the axis that the gas velocity is the same as the mean velocity of flow. He then constructed a geometric cone which had sides parallel to the tangent to the flame cone at $0{\cdot}707R$ and having as its circular base the cross-section of the burner tube. To obtain the burning velocity he divided the area of this cone into the volume-flow rate of the gas. However, Stevens, like Gouy, omitted to make any allowance for lateral expansion of the gases before they reach the luminous cone. A number of other workers have expressed burning velocity as volume-flow rate divided by the area of the flame cone. Of these, some use the actual integrated area while some use a hypothetical cone as Stevens did. Smith and Pickering[8] measured the angle the flame cone made with the axis at $0{\cdot}707R$ from the axis and expressed the burning velocity as

$$B = L_a \sin \alpha \quad . \quad . \quad . \quad . \quad . \quad (2)^*$$

where L_a is the average linear flow rate and α is the angle the cone makes with the axis at $0{\cdot}707R$ from the axis. This method fails to allow for the fact that the flow lines of the gas cease to be parallel to the axis of the tube before the flame cone is reached.

---

[4] Lewis and von Elbe, *J. Chem. Physics*, 1943, **11**, 75.
[5] Gouy, *Ann. Chim. phys.*, 1879, **18**, 27.
[6] Garside, Forsyth and Townend, *J. Inst. Fuel*, 1945, **18**, 175.
[7] Stevens, *Nat. Adv. Comm. Aero. Tech. Report*, No. 305, 1929.
[8] Smith and Pickering, *J. Res. Nat. Bur. Stand.*, 1936, **17**, 7.

Lewis and von Elbe,[4] by putting light magnesium oxide powder into the flame and photographing it with transverse illumination, were able to trace the gas-flow lines through the flame. A rectangular burner tube was used. From the photographs they constructed diagrams such as Fig. 1. The cone used is the inner border of the luminous zone of 0·2-0·3 mm. thickness. It will be seen that the flow lines depart from the vertical—presumably because the gases have expanded as a result of a rise in temperature. From such a diagram, the length a of the cone from the tip to the intersection of any registered flow line originating at radius r at the orifice was determined. From the plot of a against r, the gradient da/dr was obtained for any value of r. The burning velocity was then found at various parts of the cone using the equation of continuity :

$$B da = L_r dr$$

where L_r is the velocity of the unburned gas in a filament of width dr at r from the centre of the orifice and da is the width of the same filament as it enters the luminous zone. The merits of this procedure will be discussed later along with our own results. But we must stress at this stage that Lewis and von Elbe found that their method showed that the burning velocity over the majority of the cone was a constant for a given mixture, but that it was greater at the centre and less near the base and walls of the tube. So that their experiments showed that assumptions (iii) and (iv) of Michelson were unsatisfactory.

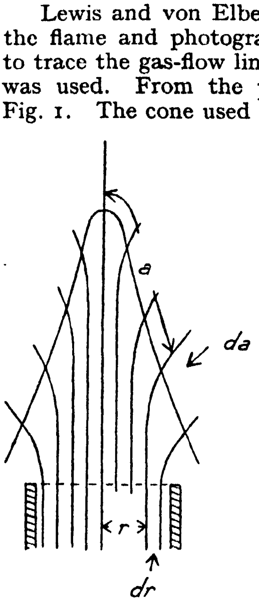

FIG. 1.—A diagram showing the flow-lines and luminous cone obtained by Lewis and von Elbe together with the measurements that they made.

The present paper describes some experiments that have been carried out on the flame at the top of a cylindrical burner. The cones were studied by using a bright source of light to throw a shadow of the flame on to light-sensitive paper. This shadow cone has been used for the determination of burning velocities.

Experimental.

(*a*) **Direct and Shadow Photographs of Flames.**—In our experiments a coal gas-air mixture was used. The flow rates of both gases were measured by passing through previously calibrated flow-meters which measured the pressure drop across a capillary tube. The gas pressures on the high-pressure side of the flow-meters were maintained by " blow-offs " and pressure fluctuations were evened out by having several large bottles between the blow-offs and the flow-meters. The gases were brought together at a smoothly blown Y-tube and mixed in a mixer through which the gases had to flow in a turbulent manner. From this they passed to a litre bottle so that any pressure fluctuations were evened out, and from there, by wide bore tubing, to the bottom of the burner tube. This was a straight smooth iron cylindrical tube, 110 cm. long and 1·05 cm. internal diam., which was fitted with a metal water-jacket. This extended to 2 mm. from the top of the tube so that it would not be heated by the flame. The temperature of the water leaving the top of the jacket was measured. It is essential to use a burner tube at least 1 m. long so that the gas flow will be streamlined by the time it issues into the flame (cf. Lewis and von Elbe). The burner tube was set vertical by using a plumb line. The flame was enclosed in a glass-sided rectangular chimney to protect it from draughts.

Arrangements were made for taking both direct and shadow photographs of the flame. For direct photographs the image of the flame was thrown on to

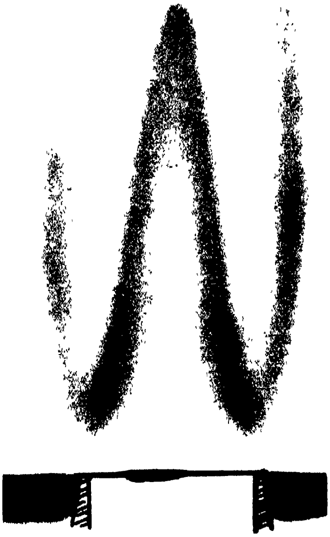

FIG. 2.—A direct photograph of the flame on the top of a cylindrical burner tube.

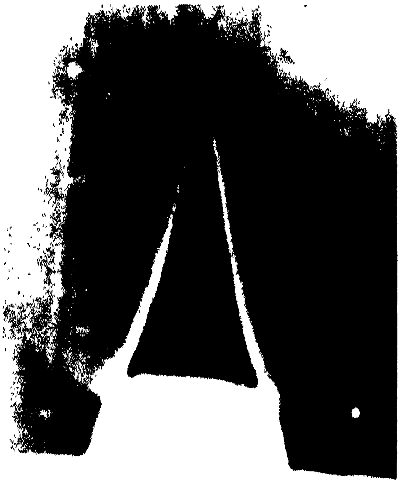

FIG. 3.—A shadow photograph of the flame on the top of a cylindrical burner tube.

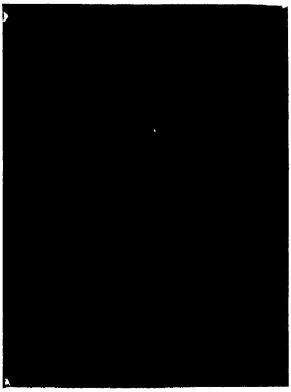

FIG. 5.—Photograph of the flame taken when the gas is carrying a light powder which is illuminated from the side.

[*To face p. 598.*

a piece of photographic paper by a lens of focal length 17·5 cm. for about 15 min. A two-fold magnification was used. When such a photograph was taken there was no means of deciding the position of the burner relative to the flame. Therefore, immediately the photograph had been taken (without moving the paper) the flame was extinguished and a metal sheet was placed with its straight edge resting firmly on top of the burner and a light was placed on the opposite side of the burner from the photographic paper. The same paper on which the flame had been photographed was then exposed again. This meant that the shadows of the sides of the burner tube were thrown on the paper and the top was defined by the shadow of the metal edge which was resting on the top of the burner. The magnification was calculated from these photographs and the external diameter of the tube. By this procedure the burner tube could be drawn on to the picture in the correct position relative to the flame. An example of a photograph taken in this way is shown in Fig. 2.

For shadow photographs, a pin-hole in a copper sheet was illuminated by the light from a 500 C.P. Pointolite lamp. The flame was placed about 70-80 cm. from the pin-hole and the photographic paper about 80 cm. beyond, so that the magnification was about two-fold. The exposures required were 30-60 sec. A photograph obtained by this means is shown in Fig. 3. Because of the deflection of the light by the hot gases round the top of the burner, the shadow of the very top of the burner tube cannot be seen. Therefore, in order to locate the burner on the shadow photograph a separate picture was taken with the same arrangement but with the flame extinguished. Moreover from the size of the shadow of the burner in this photograph and the known external diameter of the burner tube, the magnification was calculated.

(*b*) **Photographs of Flames Carrying Powder.**—Before considering the results obtained using the above types of photographs another set of experiments will be described. These resemble closely the experiments of Lewis and von Elbe in which they used a light powder for tracing the flow-lines in the gases. In our experiments we illuminated a region above the top of the burner from both sides with the light from two Pointolite lamps (one each side) focused by two lenses. The light was restricted by two vertical slits (width *ca.* 1 mm.) placed diagonally on opposite sides of the burner. A plan of the arrangement is shown in Fig. 4. The region above the top of the burner was photographed from a direction at right-angles to the line joining the two Pointolite lamps by a Kodak f/6·3 camera combined with a second lens. The powder consisted of MgO which was placed at the bottom of the U-tube joined to the burner tube. By tapping this U-tube, which was joined flexibly to the burner tube by rubber tubing, the powder was introduced into the gas stream without disturbing the flow. The magnesium oxide, which had to contain very little sodium, was prepared in the following way. An ammoniacal aqueous-alcoholic solution of $(NH_4)_2CO_3$ was added to an aqueous-alcoholic solution of $MgSO_4$. The crystalline precipitate of the double carbonate of magnesium and ammonium was filtered off and washed with $(NH_4)_2CO_3$ solution until a sample of the solid on a Ni wire gave only a faint yellow colour to a flame in which it was placed. The precipitate was then dried, ignited to MgO and stored in a desiccator. The powder was sieved before use to remove coarse particles. A photograph of the flame in which this powder was being carried was made with an exposure of 1/25 sec.

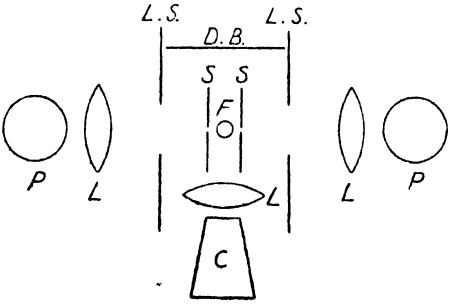

FIG. 4.—The experimental arrangement for taking a powder photograph. P = Pointolite lamp; L = lens; C = camera; S = slit; D.B. = dark background; L.S. = light shield; F = flame.

(c) Gases at Different Initial Temperatures.—Shadow photographs of flames were taken using a gas mixture of one composition but with the water-jacket at different temperatures. The experiments were carried out in the same way as in series (*a*) but the water that was passed through the jacket of the burner tube was pre-heated to *ca.* 50° and *ca.* 90° c. The temperature of the water was measured as it left the top of the jacket. A thermometer placed in the air leaving the burner tube in a blank experiment showed that the water jacket was long enough to set up temperature equilibrium between the air and the jacket.

Results.

In the first place a comparison of the direct and shadow photographs of a Bunsen flame was made. To do this, direct and shadow photographs of the same flame were taken with the same magnification. However, before making this comparison we must consider how the shadow photograph is produced and the reason for the light and dark regions on it. The diagram in Fig. 6 is a horizontal section of the arrangement drawn very diagrammatically. The two circles in Fig. 6 represent the inner and outer edges of the flame region. Between these the gases are at high pressure and temperature, have a different composition, and have a different refractive index from the rest of the air and gases. The result of this different refractive index is that rays of light entering and leaving this region are bent. For instance, a ray of light *ff* is first bent inwards and then back to its original direction. A ray *gg* which does not pass into the inner region of unburnt gas emerges from the flame in a direction different from its original one. The ray *hh* is not bent at all. The result is that a shadow of the flame zone is cast on to the photographic paper since all the light that would have reached that part is refracted away. On the photograph, Fig. 3, this appears white. Also because the rays *ff* and *gg* fall on the same area the region inside receives double the amount of light and appears black on the photograph. The line separating the white and doubly-intense black regions of the photograph in Fig. 3 is surprisingly sharp and this line may be considered to indicate the place where there is a sudden rise in temperature and pressure. It is the beginning of the first of the succession of zones that constitute the flame.

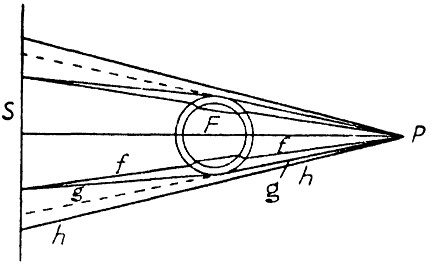

FIG. 6.—A diagram showing how the shadow photograph is produced. P = point source of light; F = flame; S = screen or film.

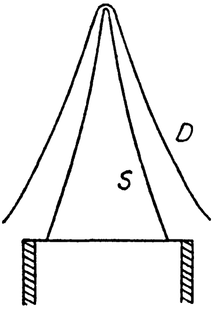

FIG. 7.—Diagram showing the relative positions of the cones seen on the direct (D) and shadow (S) photographs.

Now we will compare the direct and shadow photographs of the flame. Fig. 7 makes the comparison, showing the line separating the dark and light regions on the shadow photograph and the edge of the luminous region on the direct photograph. The former is much more sharply defined than the latter. It may be noted that the line used in Fig. 7 to represent the flame cone on our direct photographs is the outer border of the luminous zone, whereas Lewis and von Elbe investigated the inner border. The luminous zone is *ca.* ¼ mm. thick. It will be seen that the shadow-photograph line is well within the luminous region of the flame which is consistent with the view that the shadow-photograph line marks the beginning of the flame region. We conclude that the emission of light occurs at a late stage in the sequence of events. The distance between the lines on the direct and shadow photographs is *ca.* 1 mm. (allowing for magnification). This corresponds to a time of the order of 10^{-3} sec. That the emission of light is separated by a distance of the order of 1 mm. from the start of the flame zone is perhaps surprising as several workers have concluded that the reaction zone of the flame is *ca.* 0·1 mm. thick. It is possible that the " reaction " zone is as narrow as that, but that the chemiluminescence is delayed.

Having come to these conclusions regarding the direct and shadow photographs, it is now important to know how the gases flow up and through the reaction zone. To discover this the powder photographs (cf. Fig. 4) were taken. It is found that the powder tracks bend away from the vertical before the luminous cone is reached. This confirms the result already obtained by Lewis and von Elbe. However, if a shadow photograph of the same flame is taken and the line on this photograph drawn on to the powder photograph, it is found that the flow-lines depart from the vertical when they are past this line. That is, the flow-lines are still parallel to the axis of the burner tube when they enter the reaction zone, as defined by this line on the shadow photograph. They begin to depart noticeably from the vertical when they are about a third of the distance between the beginning of the reaction zone and the luminous zone. The state of affairs is shown diagrammatically in Fig. 8. This is an extremely important observation from the point of view of using the shadow photographs for the determination of burning velocities because it means that, if we measure the angle which the shadow cone makes with the vertical, we are measuring the angle which the line marking the start of the flame region makes with the direction in which the unburned gases are flowing. Also, the fact that the lines have not so far deviated from their original direction makes it certain that no lateral expansion has occurred. On the basis of the above arguments we therefore concluded that determining the shape of the shadow cone (as defined by the line separating the dark and light regions on the shadow photograph) provided a satisfactory means of determining burning velocities. This method is much simpler and less laborious than the method of Lewis and von Elbe since it is not necessary to take and measure the illuminated powder photograph each time—an experimental procedure which is difficult to carry out. The taking of the shadow photograph, on the other hand, proves to be relatively straightforward.

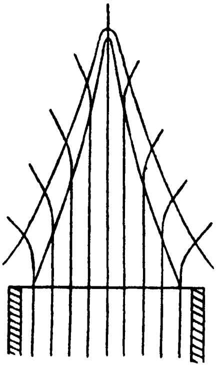

FIG. 8.—Diagram showing the flow-lines indicated by the powder photograph together with the positions of the cones seen on the direct and shadow photographs—see Fig. 7.

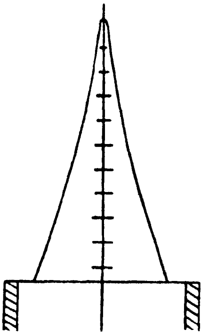

FIG. 9.—A diagram showing how the shadow photograph was marked to enable the *h* and *d* measurements to be made.

Our procedure in measuring the cones on the shadow photographs was the following. The photograph was marked out in Indian ink in the manner shown diagrammatically in Fig. 9. The distance between the cross lines (using one side) marked up the axial line were then measured with a travelling microscope. After this the picture was rotated through 90° and the width of the cone at each cross-line was measured. These measurements of the width of the cone could be made to ± 0·0005 cm. Let the width of the cone at the ith cross line be d_i and the distance between the ith and the $(i + 1)$th cross line be h_i. Then, to a first approximation, the tangent of the angle the cone makes with the axis

(α_i) when the distance across the cone is $(d_i + d_{i+1})/2$ is $(d_i - d_{i+1})/2h_i$. Tests have shown that the first approximation is perfectly satisfactory if the difference between α_i and α_{i+1} is less than 2°. If not, a small correction has to be applied because the mean slope between the ith cross line and the $(i + 1)$th cross-line is not the slope at the place where the distance across the cone is the mean of that at the ith and $(i + 1)$th cross-lines. The correction is that $\tan \alpha_i$ is $(d_i - d_{i+1})/2h_i$ when the distance across the cone on the shadow photograph is

$$\left(\frac{d_i + d_{i+1}}{2}\right) - \frac{h_i}{2}\left[\tan \alpha_i - \tan\left(\frac{\alpha_i + \alpha_{i+1}}{2}\right)\right].$$

The calculation was then carried through with the corrected value of $(d_i + d_{i+1})/2$. The correction is negligible when α_i is not very different from α_{i+1}. In fact it is negligible over most of the cone and is only appreciable near the base where the curvature of the shadow line is considerable. It was found necessary to apply the correction in the last one or two angle measurements near the base of the cone.

To test this suggested method of measuring burning velocity we measured the shadow photographs of five cones, all obtained with the same coal gas-air mixture, the flow rate having different values for the five cones. Table I shows the flow-rates used for these together with the approximate unmagnified heights

TABLE I.—TABLE OF FLOW-RATES USED FOR FIVE CONES.

External diam. of burner tube = 1·13 cm. Magnified external diam. on shadow photo = 2·489 cm. Magnification = 2·203. Internal diam. of burner tube = 1·05 cm. ($2R$).

Number of Photo.	Flow-rate in cc./sec.			Percentage Comp. by Volume of Gas.	Approx. Height of Cone.
	Gas.	Air.	Total (V).		
1	32·7	70·3	103·0	31·7	2·5
2	25·3	54·2	79·5	31·7	2·0
3	19·8	42·5	62·3	31·7	1·5
4	18·3	39·2	57·5	31·7	1·3
5	14·7	31·7	46·4	31·7	0·9

TABLE II.—DETAILED MEASUREMENT OF d_i, h_i AND α_i FOR THE LARGEST CONE (NO. 1).

d_i (cm.).	$d_i - d_{i+1}$ (cm.).	h_i (cm.).	α_i.
1·9047			
	0·1816	0·3025	16° 43′
1·7231			
	0·2030	0·3989	14° 16′
1·5201			
	0·1565	0·3929	11° 16′
1·3636			
	0·1500	0·4279	9° 57′
1·2136			
	0·1123	0·3514	9° 5′
1·1013			
	0·2336	0·8423	7° 54′
0·8677			
	0·2218	0·8009	7° 53′
0·6459			
	0·1897	0·7963	6° 48′
0·4562			
	0·1857	0·7302	7° 15′
0·2705			

of the cones. Table II shows the detailed measurements for the tallest of the five cones (No. 1).
values of α. Table III gives the values obtained for the burning velocity of

TABLE III.—SUMMARY OF RESULTS FOR FIVE CONES BURNING A 31·7 % COAL GAS-AIR MIXTURE.

$\frac{d_i + d_{i+1}}{2}$ (corr.) cm.	Radius of Cone (r) cm.	Linear Gas Velocity (L_r) cm./sec.	Angle α_i.	Burning Velocity B cm./sec.
CONE NUMBER 1				
1·8104	0·411	92·24	16° 43′	26·5
1·6161	0·367	121·8	14° 16′	30·0
1·4418	0·327	145·5	11° 16′	28·4
1·2886	0·292	164·1	9° 57′	28·4
1·1574	0·263	178·3	9° 5′	28·2
0·9845	0·223	194·8	7° 54′	26·8
0·7568	0·172	212·5	7° 53′	29·1
0·5510	0·125	224·4	6° 48′	26·6
0·3633	0·083	232·0	7° 15′	29·3
CONE NUMBER 2				
1·8219	0·413	69·67	19° 54′	23·7
1·5844	0·360	97·41	17° 44′	29·7
1·3801	0·313	118·2	14° 46′	30·1
1·2005	0·272	134·1	12° 36′	29·3
1·0323	0·234	147·0	11° 41′	29·8
0·8633	0·196	158·0	11° 19′	31·0
0·6835	0·144	169·7	10° 39′	31·4
0·4032	0·091	177·9	10° 26′	32·2
CONE NUMBER 3				
1·6442	0·373	71·23	21° 48′	26·5
1·2656	0·287	100·9	17° 8′	29·7
1·0157	0·231	116·1	14° 55′	29·9
0·8605	0·195	124·0	13° 46′	29·5
0·7173	0·163	130·1	13° 12′	29·7
0·5772	0·131	135·0	13° 4′	30·5
0·4234	0·097	139·0	14° 50′	35·6
0·2697	0·061	142·0	16° 5′	39·4
CONE NUMBER 4				
1·7498	0·397	56·78	24° 12′	23·3
1·4505	0·329	80·52	19° 48′	27·3
1·1804	0·268	98·14	16° 21′	27·6
0·9349	0·212	111·0	14° 15′	27·3
0·6279	0·142	122·9	13° 29′	28·6
0·3303	0·075	130·0	16° 12′	36·3
CONE NUMBER 5				
1·6383	0·372	53·43	28° 39′	25·6
1·3259	0·301	71·99	23° 30′	28·7
1·0662	0·242	84·42	20° 5′	29·0
0·8319	0·189	93·34	17° 20′	27·8
0·5969	0·136	100·1	18° 6′	31·1
0·3682	0·084	104·5	19° 19′	34·6

this 31·7 % coal gas–air mixture using the five different cones. In this table the first column gives $(d_i + d_{i+1})/2$ on the shadow photograph, corrected if necessary. The second column gives the radius of the actual cone (r) at the various points at which angle measurements have been made ($(d_i+d_{i+1})/2 = 2rM$, where M is the magnification factor). The third column gives the linear gas velocity, L_r, at this distance, r, from the axis assuming that the flow is streamlined. This is given by

$$L_r = \frac{2V}{\pi R^2}\left[1 - \left(\frac{r}{R}\right)^2\right].$$

The fourth column gives the cone angle and the fifth the burning velocity as deduced from

$$B = L_r \,.\, \sin \alpha_t.$$

Let us consider the results obtained from the third cone (No. 3). These results are the most satisfactory because the tall cones give small values of α which are more susceptible to error, while the short cones give fewer measurements of the burning velocity. The accuracy of the distance measurements would suffer if the usual number of B-values were obtained on the short cones. It will be seen that between $r = 0{\cdot}131$ and $0{\cdot}287$ cm. the burning velocity is constant being 29·8 cm./sec. (the root-mean-square deviation from this is 0·35 cm./sec.—i.e. about 1 %, but this is admittedly a good set). Nearer the axis of the tube at $r = 0{\cdot}097$ and $0{\cdot}061$ cm. the burning velocity is greater than this, being 35·6 and 39·4 cm./sec. respectively. Nearer the walls at $r = 0{\cdot}373$ it is less than 29·8 being 26·5 cm./sec. Therefore our results show the same feature as those of Lewis and von Elbe, namely that the burning velocity is constant over quite a large part of the cone but increases near the axis and decreases near the walls. This will also be observed clearly for cones 2, 4 and 5, but it is less noticeable in cone 1.

From this we may conclude that the burning velocity of the mixture used is that constant value it has over the greater part of the cone. Near the walls it is reduced by the cooling effect of the walls and near the axis it is increased by self-heating. This will be discussed later. In Table IV we compare the mean burning velocities obtained from the five cones. We have taken the means of the values over the range where the burning velocities are constant within our error of measurement. The mean of the five figures obtained is 28·9 cm./sec. and the root-mean-square deviation is 0·85—i.e. about 3 %. We think that these results confirm our view that by determining burning velocities in this way we are measuring a true burning velocity which is characteristic of the particular combustible mixture.

TABLE IV.—MEAN BURNING VELOCITIES OBTAINED FROM THE FIVE CONES STUDIED.

Cone number . . .	1	2	3	4	5
Mean burning velocity B, in cm./sec.	28·1	29·7	29·8	27·7	29·2

Lastly we made measurements of burning velocities when heated water was passed through the water jacket. We did this, with the same burner tube, using a coal gas-air mixture containing 30·8 % of the former. Measurements were made at 16°, 52° and 88° C. The weight of gas flowing into the apparatus per unit time was kept constant, the volume-flow rates being 76·3 at 16°, 85·8 at 52° and 95·4 cc. per sec. at 88° C. Pictures were taken in the following sequence: (A) 16°; (B) 52°; (C) 88°; (D) 16°; (E) 52°; (F) 88° C. This was to ensure that there had been no change during the course of the experiment. The results are shown in Table V. In this table we give the linear gas velocities, cone angles and burning velocities at various points on the cone designated by the distance, r cm., from the axis of the burner. As before, in all the cones there is a range where the burning velocity is constant. Also, when the measurements are extended far enough, there is an increase in the burning velocity near the axis and a decrease near the walls. The mean values for the burning velocity over the constant range for the six cones are shown in Table VI. It will be seen that for all three pairs the agreement is good. The final mean is shown in the same table. The burning velocity is seen to increase rapidly as the temperature rises, which results in the cones becoming smaller as the temperature rises.

Discussion.

The discussion will be divided into three parts: (*a*) a comparison of our method of obtaining burning velocities with other methods that have been used; (*b*) a consideration of the shape of the shadow cone; (*c*) a discussion of the effect of temperature on the burning velocity.

(*a*) In the introduction it was pointed out that the methods of Gouy, Stevens, Smith and Pickering, etc., all suffered from certain objections as ways of determining flame velocities from Bunsen cones. The only method that allowed for the deviation of the gas flow from the axial direction before reaching the luminous flame cone was that of Lewis and von Elbe.[4] However, it seems to us that this method suffers from the objection that, at the luminous flame cone, the gases have suffered expansion both lateral and longitudinal though the extent is not known. If the expansion on passing from the beginning of the reaction zone to the luminous region were only parallel to the flow lines, then the measurement of burning velocity by the method of Lewis and von Elbe would give a correct value for the burning velocity relative to the unburned gas. However, if there is longitudinal expansion there must be lateral expansion perpendicular to the flow lines between the beginning of the reaction zone and the luminous region. Moreover, the flow lines show that this has happened. Lewis and von Elbe's results do not take account of this and will therefore be in error.

By burning velocity we mean the speed of movement of some particular part of the flame with reference to unburned gas. In our method of measurement using the shadow cast by the flame we have employed the point which marks the very beginning of the sucesssion of zones which constitute the flame. By doing this we have avoided any difficulty of gaseous expansion or departure of the flow lines from the axial direction. This is shown by the flow-line photographs. We therefore believe that the method we suggest will give more reliable results for the burning velocity than others that have been tested. In addition because, for a large part of the cone, the burning velocity is constant, it is possible to make several measurements on one cone and so obtain a check. Moreover our method is very much simpler to carry out than that of Lewis and von Elbe because we do not have to measure and plot the flow–lines for each zone.

(*b*) As regards the shape of the shadow cone, the main points are (i) that it seems to be decided, over the majority of its area, by a constant burning velocity, and (ii) that there is an increase in burning velocity near the centre and a decrease near the walls of the tube. The decrease near the walls is to be expected, as pointed out by Garside, Forsyth and Townend [6] and by Lewis and von Elbe [4] because the walls will cool the gases ahead of the flame and they will therefore be heated less rapidly and so the flame will proceed more slowly. The increase in burning velocity near the centre is also to be expected because the gases approaching points near the apex of the cone are pre-heated not only by heat from the flame zone they are about to enter but also, to an appreciable extent, by heat from the flame on the other side of the cone. This will not be appreciable farther down the cone where the other side of the cone is so much more distant. Our experiments on the effect of temperature on flame-speed have shown that pre-heating the gas by only 36° c. causes the burning velocity to increase relative to the unheated gas (i.e. allowing for the expansion on raising the temperature 36°) by nearly 30 %. A rough calculation shows that we may expect the gas on the axis at a point where the diameter of the cone is about 2 mm. to have its temperature raised of the order of 50° c. It would therefore be expected that there would be an increase in burning velocity near the apex of the cone. Moreover it is not unreasonable that the burning velocity appears to start increasing at about $r = 0{\cdot}1$ cm.—cf. Table II. The change in burning velocity at the top of the cone is therefore quite consistent with our measurements of the effect of temperature on the burning velocity.

In Fig. 3, which shows the shadow cone, it will be seen that the

TABLE V.—Effect of Initial Temperature on Burning Velocity.

Radius of Cone, *r*, cm.	Linear Gas Velocity L_r, cm./sec.	Cone Angle, α_r.	Burning Velocity *B*, cm./sec.
Cone A. Initial temperature of unburned gases = 16° c.			
0·392	78·65	19° 38′	26·4
0·340	103·0	16° 4′	28·5
0·280	126·8	12° 59′	28·5
0·227	144·3	11° 24′	28·5
0·190	154·0	10° 8′	27·1
0·157	161·4	9° 38′	27·0
0·123	167·6	9° 23′	27·3
0·087	172·5	9° 20′	28·0
Cone D. Initial temperature of unburned gases = 16° c.			
0·388	80·56	19° 10′	26·4
0·338	103·6	16° 3′	28·6
0·298	120·3	13° 53′	28·9
0·261	133·6	12° 10′	28·1
0·225	144·6	11° 4′	27·7
0·178	156·9	10° 4′	27·4
0·134	165·8	9° 52′	28·4
0·104	170·3	10° 36′	30·5
Cone B. Initial temperature of unburned gases = 52° c.			
0·387	91·04	21° 55′	34·0
0·331	119·9	17° 55′	36·9
0·283	141·3	15° 12′	37·0
0·241	157·3	13° 50′	37·6
0·202	169·9	12° 50′	37·7
0·147	183·8	11° 35′	36·9
0·087	193·9	12° 12′	41·0
Cone E. Initial temperature of unburned gases = 52° c.			
0·401	83·06	22° 19′	31·5
0·344	113·9	19° 5′	37·2
0·294	136·8	16° 40′	39·2
0·248	155·0	14° 33′	38·9
0·203	169·6	12° 57′	38·0
0·164	180·0	12° 5′	37·7
0·113	190·1	11° 28′	37·8
Cone C. Initial temperature of unburned gases = 88° c.			
0·395	96·16	25° 3′	40·7
0·329	134·3	22° 6′	50·5
0·271	162·6	18° 20′	51·1
0·222	181·9	15° 31′	48·6
0·161	200·6	14° 17′	49·5
0·104	212·7	13° 47′	50·7
0·068	217·8	16° 37′	62·3
Cone F. Initial temperature of unburned gases = 88° c.			
0·396	95·27	26° 15′	42·1
0·325	136·8	22° 46′	52·9
0·267	164·0	18° 8′	51·0
0·218	183·4	16° 28′	52·0
0·174	197·2	14° 57′	50·9
0·133	207·3	14° 26′	51·7
0·095	214·3	15° 13′	56·2
0·060	218·6	15° 57′	60·1

diameter of this cone at the top of the burner is less than the internal diameter of the burner. It may be supposed that the shadow cone really continues down inside the burner tube until it meets the wall normally. This is to be expected for the line that marks the start of the flame zone in the region where it meets the wall and so our consideration of the line on the shadow photograph removes the difficulties that appear in the use of direct photographs of the luminous cone because of the way in which that cone overhangs the burner.

TABLE VI.—SUMMARY OF RESULTS ON EFFECT OF TEMERATURE ON BURNING-VELOCITIES.

Temp. of Unburned Gases.	Cone.	Mean Burning Velocity cm./sec	Cone.	Mean Burning Velocity cm./sec.	Final Mean Burning Velocity.
16° c.	A	27·8	D	28·2	28·0
52° c.	B	37·2	E	38·1	37·6
88° c.	C	50·1	F	51·7	50·9

(*c*) Table VI summarises our measurements of the effect of initial temperature on burning velocity. It will be seen that the rate of increase with temperature is quite large.

We shall see how far this change can be explained. A modified form of the Mallard–Le Chatelier equation [9] (see Lewis and von Elbe [10]) is

$$B = \frac{L}{\rho_u x_b c_p} \frac{T_b - T_{ig}}{T_{ig} - T_u}$$

where B is the burning velocity, T_b, T_u and T_{ig} are the temperature of the burned gas, the temperature of the unburned gas and the ignition temperature respectively, ρ_u is the density, x_b is the thickness of the reaction zone and c_p is the mean specific heat at constant pressure. With $B = 30$ cm./sec.; $L = 10^{-4}$ cal./sq. cm./sec. for unit temperature gradient; $T_b = 1750°$ c.; $T_{ig} = 650°$ (a not-unreasonable figure); $\rho_u c_p = 10/22400$ cal. per cc., we find that x has to be of the order of $\frac{1}{10}$ mm. which is not unreasonable.

We will now compare the observed % change in the burning velocity with the % changes in the terms on the right-hand side of the above equation:

$$\frac{B_{52}}{B_{16}} = \frac{37·6}{28·0} = 1·34.$$

Taking $T_{ig} = 650°$ c., $T_b = 1750°$ when $T_u = 16°$ and $T_b = 1786°$ for $T_u = 52°$; L to be proportional to $\sqrt{T}$ and using mean temperatures; ρ_u as proportional to T and c_p as independent of T since the initial temperature has only changed 36°, we have from $B_{52} = 1·34\ B_{16}$ that $x_{52} = 0·93\ x_{16}$. This is not unreasonable since the thickness of the reaction zone is expected to decrease as the temperature rises. Let us suppose, quite arbitrarily, that x is a linear function of the initial temperature. Then, $x_{88} = 0·86\, x_{16}$ and the formula predicts that $B_{88} = 1·80\ B_{16}$, and since $B_{16} = 28·0$ we get $B_{88} = 50·4$. The observed value is 50·9. It seems that the simple thermal picture of Mallard and Le Chatelier does, in this case, account for the effect of temperature quite well. It is not useful for absolute predictions of the burning velocity because some of the terms are extremely uncertain, in particular, the thickness of the reaction zone, x, and the ignition temperature, T_{ig}. Also, it should be stressed that the results for this combustible mixture may not be a general result as other flames may depend much more on radical diffusion for their propagation (cf. Lewis and von Elbe).

---

[9] Mallard and Le Chatelier, *Ann. Mines*, 1875, **7**, 355.

[10] Lewis and von Elbe, *Combustion, Flame and Explosions in Gases* (C.U.P., 1938).

Summary.

We have taken shadow and direct photographs of the flame cones on a cylindrical burner burning a coal gas–air mixture. A new procedure for using the cones on the shadow photographs to determine burning velocities is described and its merits considered. Certain conclusions regarding the form of the flame region are also made. Lastly, the effect of temperature on the burning velocity of a coal gas–air mixture was measured and the results considered in the light of a formula that has been suggested for calculating burning velocity in terms of other properties of the combustible mixture.

Inorganic Chemistry Laboratory,
Oxford.

MOLYBDENUM OXIDE CATALYSTS FOR THE REDUCTION OF PHENOL TO BENZENE.

BY L. A. WOODWARD AND A. T. GLOVER.

Received 7th October, 1947.

It is known [1] that phenols may be reduced to the corresponding aromatic hydrocarbons by hydrogen at atmospheric pressure in the presence of suitable catalysts, including compounds of molybdenum. The behaviour of molybdenum oxide catalysts has been investigated more particularly by Bahr and Petrick [2,3] and by Kingman.[4] The former workers explained the deterioration of the catalysts during use as due principally to the progressive reduction of the trioxide MoO_3, which they supposed to be the active species, to form the dioxide MoO_2, which they supposed to be inactive. In support of this view they found that a specimen of the dioxide, prepared by reduction of the trioxide, showed hardly any activity. On the other hand Kingman, by X-ray examination of active catalysts with and without promoters, found that they all possessed the MoO_2 structure. The present work was undertaken in the hope of throwing light on the apparent incompatibility of these earlier results and upon the general behaviour of molybdenum oxide catalysts in the reduction of phenol to benzene by hydrogen at atmospheric pressure.

Determination of Catalyst Activities.

Experimental.

A flow method similar to that of Kingman [4] was used, in which phenol vapour was entrained by passing a steady stream of hydrogen through molten phenol at constant temperature, the mixture was passed over a weighed quantity of catalyst at known temperature, and the reaction products were collected and analysed. The constancy of the rate of passage of hydrogen (approx. 10 l. per hr.) was indicated by a capillary flow-meter and the stream of gas passed through P_2O_5 drying-tubes and also a liquid-air trap (to remove traces of condensible matter) before entering an oil thermostat containing two spiral phenol saturators in series. The thermostat temperature was regulated to $75 \pm 0{\cdot}1°$ C. By a suitable arrangement of mercury seals, also immersed in the thermostat, the hydrogen stream could be made to pass either directly into the reaction vessel without phenol entrainment, or alternatively through the phenol saturators. The glass reaction vessel was vertical, the catalyst sample being supported near the middle on an asbestos plug resting on a suitable constriction. The vessel was heated by an electric furnace and the reaction temperature measured to ± 2° c. by a fine-gauge thermocouple situated within a thin glass sheath at the centre of the catalyst bed. The hydrogen entered at the top through a ground glass joint, the purpose of which will be explained below in the section dealing with the X-ray investigation of the catalysts. For the whole of its passage from thermostat to reaction vessel, the reaction mixture was electrically heated to 100° c. to prevent condensation of phenol vapour. The products issuing from the bottom of the reaction vessel were collected by passage for a measured time through two weighed receivers immersed in liquid air, condensation before reaching the receivers being prevented by electrical heating. The receivers were then re-weighed, the condensate washed out with NaOH solution and the amount of phenol present determined with standard bromate-bromide solution in the usual way.

---

[1] Fischer, Bahr and Petrick, *Brennstoff-Chemie*, 1932, **13**, 45.
[2] *ibid.*, 1933, **14**, 161.
[3] *ibid.*, 1933, **14**, 187.
[4] *Trans. Faraday Soc.*, 1937, **33**, 784.

Before undertaking activity determinations, hydrogen was passed through the phenol saturators for 24 hr., after which the condensate collected in absence of catalyst was found to be 100 % phenol. Collection was always complete in the first of the two receivers. The rate of input of phenol was about 0·38 g./hr., the variations being so small as not seriously to affect the observed values of catalyst activity.

From the equation :

$$C_6H_5OH + H_2 \rightarrow C_6H_6 + H_2O$$

it follows that, if W is the weight of condensate and w the weight of phenol it contains, the % conversion of phenol to benzene is given by $\frac{\frac{94}{96}(W - w) \times 100}{w + \frac{94}{96}(W - w)}$. The value of this expression was taken as a measure of the mean catalyst activity over the period of collection. No account was taken of the very small quantities of water that may be formed by reduction of the catalyst.

Activities of Catalysts without Preliminary Reduction.—The starting material, as for all catalysts used in the present work, was Analar molybdenum trioxide previously dried at 100° c. Preliminary experiments showed that 0·35 g. was a suitable amount for test and, except where otherwise stated, this was the weight taken. In each run the catalyst was raised to the reaction temperature

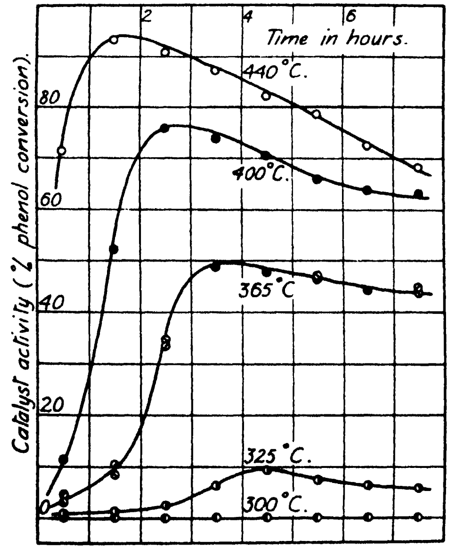

FIG. 1.—Effect of reaction temperature on the variation of activity of MoO_3 catalyst with time.

in half an hour with pure hydrogen passing. Then phenol entrainment was started and condensates collected over successive 1 hr. periods.

A series of runs was carried out with reaction temperatures of 300, 325, 365, 400 and 440° c. The results are shown graphically in Fig. 1, in which activities are plotted at the middle of the corresponding 1 hr. periods. To illustrate the degree of reproducibility of the determinations, the points for duplicate runs are included for one reaction temperature (365° c.). Results at other temperatures showed similar agreement. Some differences between duplicate runs are to be expected, owing principally to non-reproducibility of catalyst packing and slight variations of phenol input rate. They are seen, however, to be too small to cast doubt on the general shapes and relative positions of the curves.

Discussion.

The activity-time curves show an initial rise (probably from zero) to a maximum. This effect was not present in the work of Kingman[4] whose catalysts were subjected to preliminary reduction before test; and it received only brief mention from Bahr and Petrick.[2, 3] The time required to attain the maximum activity is seen to diminish regularly with increase of reaction temperature. These phenomena can best be accounted for on the view that the original molybdenum trioxide is inactive and that the activity is developed as the result of reduction, the rate of which increases with increase of temperature. The attainment of a maximum followed by a slow fall indicates that the generation of activity by reduction is opposed by a process of deterioration, probably due to thermal sintering of the active surface and cloaking by deposit of small quantities of products of high molecular weight from side-reactions. That such deposits play a part in the deterioration is shown by the observation of Bahr and Petrick that CO_2 was evolved when a spent catalyst was heated in air, and that a revivification of activity resulted. Our observations, however, are not in harmony with the view of these workers that the active species is the trioxide and that the reduced catalyst is inactive. The principal evidence adduced in support of their theory was that a specimen of molybdenum dioxide, prepared by complete reduction of the trioxide, was found to have hardly any activity. The significance of this evidence was further investigated by the following experiments on pre-reduction of molybdenum trioxide.

Reduction of Molybdenum Trioxide by Hydrogen.

Reduction in absence of phenol was studied at 300, 350 and 450° c. The weight of trioxide taken for each run was 5 g., which was the largest amount that could be accommodated in the reaction vessel so as to lie wholly within the range of constant temperature of the furnace. In order to remove adsorbed water, each sample was first kept for several hours in a stream of hydrogen at 150° c., at which temperature reduction is negligible. Reduction was then allowed to proceed at the desired temperature until the rate of collection of water in the liquid-air traps became inappreciable. The times required at 300, 350 and 450° c. were respectively 120, 90 and 60 hr. The total weights of water collected were the same within 3 %, showing that practically the same stage of reduction had been attained in all three cases. All the products had the dark colour of molybdenum dioxide. The trioxide is white.

The products were cooled to room temperature and removed from the reaction vessel for analysis. In the case of the product of reduction at 450° c., exposure to the air produced no observable effect. The molybdenum content, determined gravimetrically as lead molybdate,[5] was found to correspond within the limits of experimental error to MoO_2 (theoretical, 75·0 %; observed 74·65 %). This result is in agreement with that of Herington and Rideal[6] who found that the loss of weight on reduction at 475° c. corresponds to formation of molybdenum dioxide only, though at 550 and 575° c. appreciable further reduction (presumably to molybdenum metal) occurs. It also confirms the observation of Bahr and Petrick[3] that reduction at 450° c. gives the dioxide quantitatively.

---

[5] See Treadwell and Hall, *Analytical Chemistry* (1935), Vol. II, p. 277.

[6] *Proc. Roy. Soc. A*, 1945, **184**, 434.

As shown by the equality of the amounts of water formed, the product of reduction at 300° c. and 350° c. is likewise molybdenum dioxide ; but when the samples were exposed to the air (after cooling to room temperature) they were found to be pyrophoric and glowed brightly. The percentages of molybdenum by weight in the resulting powders were found to be 69·6 for the sample reduced at 300° c. and 72·6 for that reduced at 350° c. These correspond roughly to 35 % MoO_2 + 65 % MoO_3 and 70 % MoO_2 + 30 % MoO_3 by weight respectively. After exposure to air the powders retained the dark colour of the dioxide unchanged.

Activities of Pre-reduced Catalysts.—Activity-time curves for the phenol-hydrogen reaction at 350° c. were determined for catalysts which had been pre-reduced to molybdenum dioxide at temperatures of 300, 350 and 450° c. For each run the standard weight (0·35 g.) of the trioxide was taken and the times of pre-reduction (120, 90 and 60 hr. respectively) were chosen in the light of the above results so as to ensure complete formation of molybdenum dioxide in all cases. After pre-reduction the temperature was adjusted as rapidly as possible to 350° c., whereupon phenol entrainment and hourly activity determinations were begun. The results obtained are shown in Fig. 2. A similar sample of trioxide reduced for 60 hr. at 550° c. was found to be completely inactive.

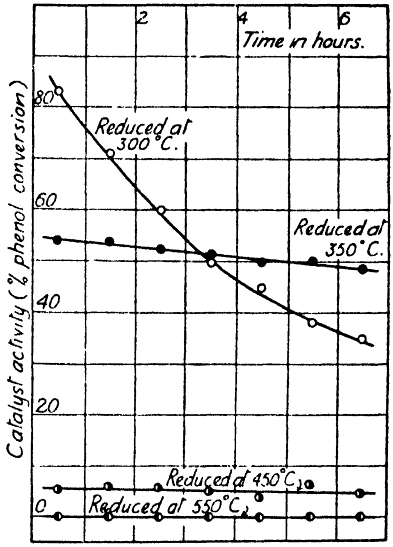

Fig. 2.—Effect of pre-reduction temperature on activity of MoO_3 at 350° c.

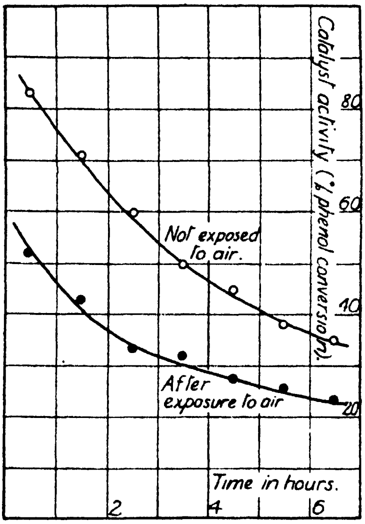

Fig. 3.—Activity at 350° c. of catalyst pre-reduced at 300° c.

The curves of Fig. 2 are essentially different in form from those of Fig. 1. The initial rise of activity from zero to a maximum, observed for the trioxide without pre-reduction, is absent. This provides strong evidence for the view expressed above that this initial rise is due to reduction of the inactive trioxide, and shows the incorrectness of the view of Bahr and Petrick that the trioxide is the active species. Furthermore, it is seen from Fig. 2 that, although all the catalysts tested had been reduced completely to molybdenum dioxide, their initial activities decrease sharply with increase of reduction temperature. Now it appears from their account that the specimen of dioxide which Bahr and Petrick found to be nearly inactive had been prepared by reduction of the trioxide at 450° c. Their observation as to its very low activity is thus in agreement with ours ; but their deduction that molybdenum dioxide is always inactive is seen to be inadmissible, and the apparent inconsistency with the results of Kingman's X-ray examination of active catalysts is resolved.

Evidence is given below that the active dioxide formed at the lower temperatures differs in particle size from the almost inactive dioxide formed at 450° c.

Reference to Fig. 2 shows that, although the catalyst reduced at 300° c. has a considerably higher initial activity than that reduced at 350° c., the rate of deterioration of the former is much greater. In consequence, the activity-time curves cross after about 3 hr. working. From a practical point of view, therefore, there is clearly an optimum temperature of pre-reduction for the best overall catalyst performance. This can be explained on the view that the initially more active catalyst surface is either more susceptible to thermal sintering or that it enhances the small amount of side reaction and so becomes more rapidly cloaked with products of high molecular weight.

Activity of Pre-reduced Catalysts after Exposure to Air.—0·35 g. of molybdenum trioxide was reduced for 120 hr. at 300° c. and cooled to room temperature. Air was then passed through the reaction vessel and a sharp rise of temperature was observed. When this pyrophoric effect had subsided, the air stream was replaced by hydrogen, the temperature raised to 350° c. and activity determinations at once started. The activity-time curve for this catalyst is shown in Fig. 3, which for comparison also shows the curve from Fig. 2 for the corresponding catalyst pre-reduced at the same temperature but not exposed to air. An exactly analogous pair of curves was obtained for catalyst pre-reduced at 350° c.

Exposure to air is seen to cause an appreciable reduction of activity, but it is notable that the two curves of Fig. 3 are of similar form. Although by analysis the composition after exposure to air corresponded roughly to 35 % MoO_2 + 65 % MoO_3 instead of pure MoO_2, there is no sign of an initial rise of activity of the kind observed with molybdenum trioxide. The diminution of activity caused by exposure to air may be due to sintering of the active surface at the high temperatures of the pyrophoric effect ; but apart from this it appears that the active structure, when once developed, survives the oxidation by air and does not have to be produced afresh by re-reduction of trioxide. Further light on this interesting point is provided by the X-ray investigation of these catalysts described below.

Reaction of Catalysts with Phenol in Absence of Hydrogen.

It has been shown by Woodward and McKee [7] that active catalysts will react with phenol at 350° c. in absence of hydrogen and that benzene is produced. The evidence was as follows. A sample of active molybdenum oxide catalyst was thoroughly de-gassed by evacuation at 420° c., after which the temperature was lowered to 350° c. and phenol vapour admitted up to a pressure of approximately 0·1 mm. Hg. The pressure was unchanged after 6 hr., showing that in any reaction that might have been occurring each molecule of phenol had been replaced by one molecule of product in the gas phase. That benzene had in fact been formed was proved by determination of the pressure-volume curve of the resulting vapour at room temperature. The curve obtained was quite different from that of phenol vapour and showed a distinct break at the saturated vapour pressure of benzene.

In the present work this reaction of catalysts with phenol in absence of hydrogen was investigated by the flow method in a manner similar to that for the activity determinations described above. A sample of catalyst that had been completely reduced at 300° c. cooled and exposed to air (pyrophoric) was raised to 350° c. in a stream of nitrogen, whereupon phenol entrainment and activity determinations were started. Reaction with phenol took place, but in order to obtain an initial activity of a suitable magnitude for measurement it was found convenient to use a larger weight of catalyst (3 g.) than in the activity determinations for the phenol-hydrogen reaction. The phenol input rate was also slightly lower (approx. 0·32 g./hr.). The results obtained are shown in Fig. 4.

---

[7] Unpublished work.

In calculating the activities it was assumed that the oxygen of the phenol is taken up by the catalyst with production of benzene. As far as condensation of products is concerned, therefore, the reaction is $C_6H_5OH \rightarrow C_6H_6$ and the activities (i.e. % conversions) are accordingly obtained from the expression :

$$\frac{\frac{94}{78}(W - w) \times 100}{w + \frac{94}{78}(W - w)}.$$

Owing to the different catalyst weight the scale of activities is of course different from that for the previous experiments with phenol and hydrogen.

A similar curve to that of Fig. 4 was obtained for the catalyst reduced at 350° c. and exposed to air, the initial activity being lower and the rate of fall slightly less. A catalyst reduced at 450° c. showed no measureable reaction with phenol at 350° c. in absence of hydrogen. Unreduced molybdenum trioxide was likewise without activity.

Although in the experiments of Woodward and McKee, quoted above, the catalyst was thoroughly pumped out before admission of phenol vapour, it might possibly be objected that adsorbed hydrogen from the original reduction may not have been completely removed and that the formation of benzene may have been by the ordinary reaction,

$$C_6H_5OH + H_2 \rightarrow C_6H_6 + H_2O.$$

To account for the constancy of the pressure it would then be necessary to assume that the water remained strongly adsorbed. Such an objection appears to be inadmissible in relation to the present work, however, since the catalyst in question had been exposed to air before use, and it is most unlikely that any hydrogen remained associated with it after the consequent pyrophoric oxidation.

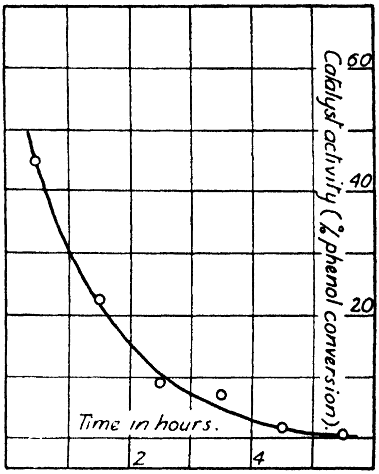

FIG. 4.—Reaction of catalyst with phenol at 350° c. in absence of hydrogen.

As stated above, the activities of Fig. 4 were calculated on the assumption that the catalyst takes up the oxygen from the phenol molecule with formation of benzene. This finds support in the fact that the weights of the successive hourly condensates were all the same within a few per cent., although their phenol contents were so markedly different. The reaction cannot therefore have involved any serious breakdown of the phenol to gaseous products or polymerisation to involatile material remaining on the catalyst surface. It is thus reasonable to suppose that the reaction is simply : phenol + active catalyst → benzene + " oxidised catalyst." The active catalyst on the left-hand side of this equation had taken up oxygen, on exposure to air, so as to attain a composition corresponding approximately to 35 % MoO_2 + 65 % MoO_3 (see above). From the weight of catalyst used and the total amount of phenol converted a rough calculation shows that the uptake of oxygen from phenol was sufficient to make the final composition correspond to about 25 % MoO_2 + 75 % MoO_3. It is remarkable that after its pyrophoric reaction with air the catalyst should still be able thus to take up oxygen from phenol at 350° c. The amounts concerned indicate that in both cases the reaction is not confined to the surface of the catalyst, but involves penetration of oxygen into the interior of the particles. Possibly the rapid fall of activity in Fig. 4 is due to the increasing slowness of this penetration with increase of the amount of oxygen taken up at the catalyst surface.

It is interesting to note that, since the " oxidised catalyst " may be reduced with hydrogen, it is possible to effect the overall reaction, $C_6H_5OH + H_2 \rightarrow C_6H_6 + H_2O$, in two separate stages: (i) phenol + active catalyst → benzene + " oxidised catalyst," followed by (ii) " oxidised catalyst " + hydrogen → water + active catalyst. It is not suggested that the catalytic reduction of phenol in presence of hydrogen necessarily proceeds by such stages, but it appears probable that the affinity of the catalyst for oxygen is intimately concerned; for the experiments show that catalysts that are active for the reduction of phenol by hydrogen will also react with phenol alone, whereas catalysts that are inactive for the phenol-hydrogen will not react with phenol.

This striking parallelism is also of interest in relation to the view of Herington and Rideal [6] that the active species in the reduction of phenol by hydrogen is not molybdenum dioxide but a thin surface layer of molybdenum metal, the presence of which they infer from the fact that appreciable reduction beyond the stage of MoO_2 is possible at higher temperatures. The work of these authors is concerned principally with catalysis of a quite different reaction, the aromatisation of paraffins. By comparing their results with those of Kingman [4] they find, for molybdenum oxide catalysts containing different promoters, that in general greater ease of reduction beyond MoO_2 at high temperatures is associated with lower activity for aromatisation and higher activity for phenol reduction. This they take as evidence that the catalytically active species for the two reactions are respectively molybdenum dioxide and molybdenum metal. The possibility that molybdenum dioxide is the active catalyst for phenol reduction cannot, however, be ruled out on this evidence; for if one property of this species (namely, ease of high-temperature reduction to metal) is affected by the presence of promoters, it is not unreasonable to suppose that other properties (for instance, catalytic activity for phenol reduction or aromatisation) will also be affected. The present work indeed provides evidence in support of the view that it is the dioxide that is active in the reduction of phenol by hydrogen; for it is improbable that any surface molybdenum metal would survive pyrophoric oxidation, and yet the catalytic activity is not thereby destroyed. Were it only a question of the survival of activity for the phenol-hydrogen reaction, it could be objected that the excess hydrogen might be able rapidly to reduce the oxidised molybdenum to metal again: but after the pyrophoric effect the catalyst is still active for reaction with phenol in absence of hydrogen, where such re-reduction is out of the question. Hence, if we admit the parallelism between the activities of catalysts for the reaction with phenol in absence of hydrogen and for the catalytic reduction of phenol by hydrogen, it becomes difficult to maintain the view that the active species is molybdenum metal.

X-Ray Examination of Catalysts.

Samples were examined by the X-ray powder method in the hope of throwing light upon the structure of the " oxidised catalyst," referred to in the preceding discussion. It should of course be borne in mind that this method gives information about the bulk structure of the catalyst particles, whereas their catalytic activity is a property of the surface. However, the quantities of oxygen taken up when active molybdenum dioxide samples are exposed to air indicate that this reaction is not confined to the surface. As capacity to take up oxygen in this manner is associated with catalytic activity, it was thought to be of interest to use the X-ray powder method of investigation.

Experimental.

Owing to the pyrophoric character of some of the powders, specimens to be photographed were not mounted in the customary manner upon a hair, but were enclosed in thin-walled capillary tubes filled with hydrogen. The capillaries (diam. 0·5 mm. ; wall thickness $<$ 0·02 mm.) were made of boro-silicate glass having a high permeability to X-rays. Capillaries of Lindemann glass proved to be too fragile and collapsed on evacuation.

The following technique was adopted for transferring catalyst from reaction vessel to capillary without contact with air. A current of hydrogen was passed upwards through the reaction vessel (i.e. in the reverse direction from that during catalyst reduction or activity determination), the ground-glass joint at the top was then opened and the phenol lead-in tube replaced by a vertical tube blown out a few inches above the joint into a thin-walled bulb with a hydrogen exit at the top. After allowing sufficient time for the hydrogen stream to replace all the air, the tube above the bulb was drawn off. The reaction vessel and attached bulb-tube, filled with hydrogen, were then withdrawn from the reaction furnace and inverted, whereupon the catalyst fell into the bulb, which was drawn off. The bulb containing the catalyst was then transferred to a specially constructed vessel fitted with an internal 100-mesh sieve and tapering below to a narrow neck to which the boro-silicate capillary was attached. This vessel was evacuated and hydrogen let in to 1 atm. pressure, after which the bulb containing the catalyst was broken by a suitable device operated from outside without admission of air. By tapping, a sample of the catalyst powder was made to pass through the sieve and so into the capillary, which was then drawn off for mounting in the X-ray camera.

The copper *K*-lines were used, and for purposes of comparison photographs were first taken with specimens of pure molybdenum dioxide (prepared by complete reduction of the trioxide at 450° C.) and of pure re-sublimed trioxide. Both specimens gave well-defined diagrams. Owing to the finite sizes of specimen and source, the values of the interplanar spacings *d*, deduced in the usual way from the measured positions of the lines, are subject to systematic corrections known from previous work with comparable samples to range from − 0·15 A. at small angles to − 0·01 A. at angles near 90°. Taking these corrections into account, the *d*-values and relative intensities of all the lines measured (11 for the dioxide and 23 for the trioxide) agreed well with the values calculated from the recorded crystal structure data for the respective compounds.[8]

Samples of dioxide prepared by the complete reduction of the trioxide at 300° C. and 350° C. and transferred to the capillaries without contact with air were next examined. The diagrams corresponded to the MoO_2 structure, but with the same exposure time as before, were less well-defined and showed only the strongest lines. This indicates that the particle size is smaller than for the inactive dioxide produced at 450° C.

Diagrams were also obtained for samples of the catalysts reduced at 300° C. and 350° C. and then exposed to air. Although by analysis these had compositions corresponding to about 65 % and 30 % molybdenum trioxide by weight respectively, both had the dark colour of the dioxide and gave diagrams showing only the strongest lines of the MoO_2 structure with no trace of the MoO_3 structure. The observed *d*-values for these samples, as deduced from the measured positions of the lines without the corrections referred to above, are given in Table I, together with the corresponding values observed for MoO_2.

TABLE I.—UNCORRECTED LATTICE SPACINGS OF ACTIVE CATALYSTS AFTER EXPOSURE TO AIR.

MoO_2.			" 65 % MoO_3."		"30 % MoO_3."	
h. k. l.	*d* (A.).	Intensity.	*d* (A.).	Δ*d* (A.).	*d* (A.).	Δ*d* (A.).
1 1 0	3·31	strong	3·35	+ 0·04	3·34	+0·03
2 0 0 1 0 1	2·35	strong	2·39	+0·04	2·37	+0·02
2 2 0 2 1 1	1·68	strong	1·74	+0·06	1·72	+0·04
3 1 0	1·50	medium	—	—	1·53	+0·03

---

[8] Wyckoff, *The Structure of Crystals* (2nd. Edn., 1931), p. 238 ; *ibid.* (2nd Edn. Suppl., 1935), p. 38.

Although the values of *d* in Table I require correction to convert them to true lattice spacings, the values for each (*h k l*) are comparable with one another. It is seen that the spacings for the active catalysts after exposure to air are all greater than those for pure MoO_2. The differences shown in the table in the columns headed Δd are small, but outside the estimated limits of experimental error (± 0·01 A.) of the uncorrected *d*-values.

X-ray powder photographs were also taken for samples of trioxide catalyst after use for different times in the phenol-hydrogen reaction at 350° c. The same procedure was followed as in the determination of the activity curves of Fig. 1, the reaction being started without pre-reduction of the catalyst. After the desired time the catalyst was allowed to cool and was then transferred to the capillary without contact with air. Samples that had been working for 5 hr. (corresponding roughly to attainment of maximum activity) and 10 hr. both showed the black colour of molybdenum dioxide, but gave normal X-ray diagrams of MoO_3 only. A sample after 10 hr. working at 440° c. again gave the normal MoO_3 diagram strongly, but the most intense lines of MoO_2 also appeared faintly. The *d*-values of these lines were all greater by 0·03 A. than the corresponding lines for ordinary MoO_2 (cf. Table I).

The X-ray diagrams show that samples of molybdenum dioxide formed by reduction at 300 and 350° c. have the same structure as the product of reduction at 450° c., but a smaller particle size. This may well be connected with the fact that the dioxide formed at the lower temperatures shows high catalytic activity, whereas that formed at 450° c. is almost inactive. Kingman [4] found that a large surface area is necessary in order that a catalyst shall be highly active.

Associated with the catalytic activity is the pyrophoric oxidation on exposure to air. Despite the large amounts of oxygen taken up, the X-ray diagrams show that the dioxide structure persists, but with an expansion of the lattice spacings. It seems probable that when the active catalyst reacts with phenol in absence of hydrogen the oxygen of the molecule is taken up by the dioxide lattice in this way.

After use for 5 or 10 hr. in the phenol-hydrogen reaction at 350° c., samples of molybdenum trioxide (not pre-reduced) showed high activities and the dark colour of the dioxide, but gave X-ray diagrams of MoO_3 only. The amounts of dioxide present were evidently too small to be recorded in the X-ray photographs, and the result shows that the activity is developed as soon as a thin surface layer has been reduced.

Our thanks are due to Mr. J. L. Copp for carrying out preliminary experiments, to Dr. W. Hume-Rothery for facilities and advice in connection with the X-ray investigations and to Dr. E. F. G. Herington for helpful discussion.

Summary.

1. When molybdenum trioxide is used as catalyst for the reduction of phenol to benzene at atmospheric pressure, the activity-time curves for temperatures from 325° to 440° c. show an initial rise from zero to a maximum, indicating that the effective catalyst is formed from the trioxide by reduction.

2. Samples of molybdenum dioxide prepared by complete reduction of the trioxide at 300° c. or 350° c. are active when tested at 350° c. Dioxide similarly prepared by reduction at 450° c. is almost inactive at 350° c. X-ray examination shows that the active samples have the smaller particle size.

3. Active dioxide is pyrophoric, inactive dioxide is not. Considerable quantities of oxygen are taken up by active dioxide on exposure to air, but the X-ray diagram is still that of MoO_2 without any MoO_3 and the material remains catalytically active.

4. Active dioxide after exposure to air reacts with phenol at 350° c. in absence of hydrogen. Molybdenum trioxide and inactive dioxide do not. The reaction is apparently a removal of oxygen from the phenol molecule by the catalyst with formation of benzene. The evidence is discussed and shown to favour the view that the catalytically active species in the reduction of phenol by hydrogen is molybdenum dioxide rather than molybdenum metal possibly present on the surface.

Jesus College,
Oxford.

ABSORPTION AND FLUORESCENCE SPECTRA OF BIVALENT SAMARIUM, EUROPIUM AND YTTERBIUM.

By F. D. S. Butement.

Received 27*th June*, 1947.

The absorption and fluorescence of the tervalent rare earths have been extensively studied, and correlated with their electronic configurations. Three rare earths, samarium, europium and ytterbium can also be bivalent, but the corresponding spectra have not been much studied.

Absorption.—Butement and Terrey[1] measured the positions of the absorption maxima for aqueous samarous chloride solution, in the visible and ultra-violet. McCoy[2] found that a high concentration of europous chloride in water showed diffuse absorption at wave-lengths below about 4480 A., and Ball and Yntema[3] found that aqueous ytterbous sulphate solution showed diffuse general absorption in the red. The ultra-violet absorption of these last two substances has not been studied.

Fluorescence. Samarium and Europium.—The published data are somewhat conflicting and uncertain. The spectra have been studied by Przibram,[4, 5, 6, 7] Karlik and Przibram,[8] Gobrecht,[9] and Eckstein.[10, 11] Przibram's final conclusions[7] were that bivalent europium on irradiation with ultra-violet light gave a violet fluorescence with a diffuse band, maximum about 4000 A., and bivalent samarium a diffuse red band, maximum 6300 A., a line spectrum with a red line at 6900 A. and others in the near infra-red.

A similar fluorescence attributed by Gobrecht (loc. cit.) to $EuCl_2$ was explained as being due to contamination with $SmCl_2$, and a similar cathodic phosphorescence spectrum, observed by Tomaschek and Deutschbein[12] with calcium sulphate containing samarium (and attributed by them to Sm^{+++}) was explained as being due to Sm^{++} formed during the electron bombardment. There is no *direct* evidence of the valency state of the samarium responsible for this fluorescence.

Ytterbium.—Karlik and Przibram (loc. cit.) found that calcium fluoride containing bivalent ytterbium fluoresced in ultra-violet light, at − 180°, with a band maximum at 5700 A.

Experimental.

The absorption spectra were photographed from 9000-2000 A. on a Hilger medium spectrograph on the same plate as a series of calibration spectra, and the values of the molar extinction coefficient ϵ in aqueous solution deduced by the usual technique of photometric comparisons of plate blackenings.

The ϵ-values were plotted against wave number, $\tilde{\nu}$, in cm.$^{-1}$, and the resultant curves analysed into component bands, for each of which the value of the absorption probability P, or number of " classical oscillators " per rare earth ion, was calculated from

$$P = \frac{1000}{N} \cdot \frac{mc^2}{\pi e^2} \int \epsilon(\tilde{\nu}) d\tilde{\nu}$$

---

[1] *J. Chem. Soc.*, 1937, 1112.

[2] *J. Amer. Chem. Soc.*, 1936, **58**, 1577.

[3] *ibid.*, 1930, **52**, 4264.

[4] *Z. Physik.*, 1936, **102**, 348; *Nature*, 1935, **135**, 100.

[5] *Akad. Wiss. Wien.* II*a*, 1935, **144**, 141.

[6] *Nature*, 1937, **139**, 329.

[7] *Z. Physik.*, 1937, **107**, 709.

[8] *Akad. Wiss. Wien*, II*a*, 1937, **146**, 208.

[9] *Ann. Physik.*, 1937, **28**, 673.

[10] *Nature*, 1938, **142**, 256.

[11] *ibid.*, 1939, **143**, 1067.

[12] *Z. Physik.*, 1933, **82**, 309.

where N = Avogadro's number, m = electronic mass, e = electronic charge, c = velocity of light.

The aqueous solutions were used in a 1 cm.-thick quartz cell. Samarous chloride solution decomposes completely in a few min. according to the equation :

$$6SmCl_2 + 6H_2O \rightarrow 4SmCl_3 + 2Sm(OH)_3 + 3H_2.$$

In order therefore to determine the actual concentration of solution when the spectra were photographed, a solution of known initial concentration was made by dissolving powdered samarous chloride in water and a series of spectra photographed at known time-intervals after the preparation of the solution, while decomposition proceeded.

By determining the absorption at a suitable wavelength, and assuming the validity of Beer's law, a graph of the change of relative concentration with time was obtained, whence, by extrapolation to zero time at which the initial concentration was known, the concentration at each exposure could be calculated. The small amount of samaric hydroxide formed caused no appreciable absorption. Aqueous europous and ytterbous chloride solutions decompose fairly slowly so that the spectra could be photographed before any appreciable fall in initial concentration occurred.

The europous chloride solution was prepared directly from a known weight of powdered material, the ytterbous chloride by electrolytic reduction of ytterbic chloride solution in 0·1 N. HCl, at a mercury cathode in the base of the absorption cell. The concentration of ytterbous ion produced was calculated by allowing the solution to stand 1 hr., until the reaction :

$$6YbCl_2 + 6H_2O \rightarrow 4YbCl_3 + 2Yb(OH)_3 + 3H_2,$$

was complete, and determining the volume of H_2 evolved by means of a micro-gas burette. The concentrations of the above three chlorides used were of the order of 0·01 M.

Owing to the instability of aqueous bivalent rare earth chloride solutions, it was desirable to have a stable, solid material suitable for absorption-spectra measurements, such as a crystalline isomorphous chloride containing a small known amount of the rare earth uniformly dispersed in it.

The following data given by Doll and Klemm [13] and by Pauling and McCoy [14] are relevant.

	Ba^{++}	Sr^{++}	Sm^{++}	Eu^{++}	Yb^{++}
Ionic radii, A. .	1·35	1·13	~1·17	1·17	1·10

Such materials were also desirable for fluorescence studies.

Preparation.—A known weight of sodium, barium, or strontium chloride was fused in a platinum boat. Sufficient of the appropriate rare earth oxide was spread along the surface to yield a product containing 0·5 % of bivalent chloride. The boat was heated at 1000° in HCl for 1 hr., and then in H_2 for 4 hr. The temperature was then lowered to just above the melting point of the chloride used, and then reduced 50° per hour until well below the melting point, in order to allow growth of single crystals.

$NaCl + SmCl_2$:

There was evidently no isomorphism, since the product was not homogeneous. The greater part of the material, crystallising first, contained little Sm, and was greenish-blue, suggesting that there was a slight excess of sodium in the NaCl, as in the similar well-known case of " colour centres " in NaCl crystals. Adjacent to this material was a small zone of light pink material containing more Sm^{++}. A few small, irregular-shaped, but clear pieces were extracted for use. The last zone to solidify was deep red, contained most of the Sm, and was too opaque for use.

$BaCl_2 + SmCl_2$:

Unfortunately $BaCl_2$ is dimorphous with a transition point a little below the melting point. The product consequently was micro-crystalline, but of a uniform, deep pink colour, indicating uniform dispersion of the Sm^{++}.

$SrCl_2 + SmCl_2$:

This product crystallised excellently, and optically-clear cleavage blocks several mm. across were easily obtained. The colour was purplish-red, suggesting that it is due to the red Sm^{++} colour plus a blue due to " colour centres " caused by Sr (cp. NaCl + $SmCl_2$). Barium, being more electro-positive than strontium, is evidently not reduced by the bivalent samarium.

---

[13] *Z. anorg. Chem.*, 1939, **241**, 239. [14] *J. Amer. Chem. Soc.*, 1937, **59**, 1131.

$BaCl_2 + EuCl_2$:
Colourless, micro-crystalline.
$SrCl_2 + EuCl_2$:
Colourless, optically-clear crystals.
$BaCl_2 + YbCl_2$:
Colourless, micro-crystalline.
$SrCl_2 + YbCl_2$:
Colourless, not of good optical quality.

For the excitation of fluorescence a 120-watt high-pressure mercury-vapour lamp with filter transmitting from 2500-3700 A. was used.

Results.

Many of the spectra show both diffuse bands and narrow lines, superimposed in the same spectral region. For clarity these two types are drawn and tabulated separately.

$SmCl_2$ in Water ; absorption.—The results are plotted in Fig. 1. There are heavy diffuse bands in the visible and ultra-violet. The heavy curve gives the observed absorption, the light curves the resolution of this into separate bands whose sum almost exactly reproduces the observed absorption. There are also four weak narrow peaks superimposed. These are plotted separately on a larger scale in Fig. 2 E.

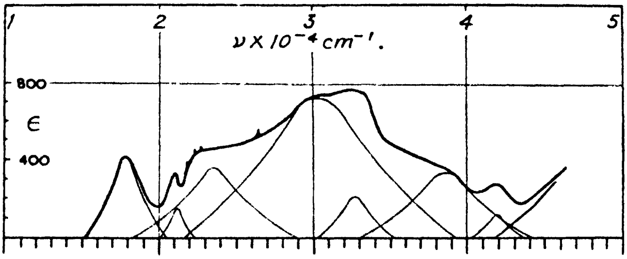

FIG. 1.

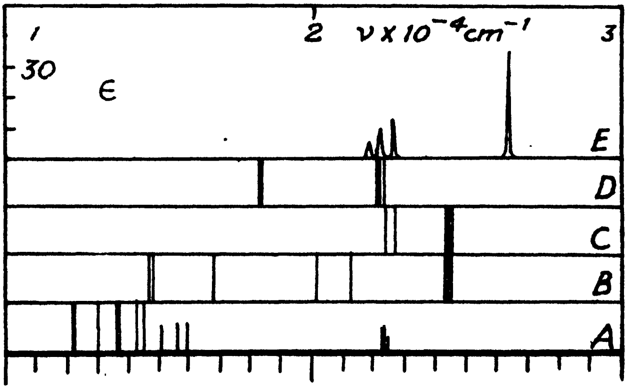

FIG. 2.

$SmCl_2$ in NaCl ; absorption.—Owing to the irregularity of the crystal fragments, only the relative values of the extinction coefficient on an arbitrary scale could be plotted. There were diffuse bands (Fig. 3 and Table II) and some weak lines or very narrow bands (Fig. 2 C and Table III). The light source also excited some weak fluorescence lines simultaneously (Fig. 2 D and Table IV).

TABLE I.—$SmCl_3$ IN WATER.

Absorption maxima, diffuse bands.			Narrow weak bands.		
λ. A.	$\bar{\nu}$. cm.$^{-1}$	$P \times 10^8$.	λ. A.	$\bar{\nu}$. cm.$^{-1}$	$P \times 10^8$.
5587	17,900	1·80	4590	21,790	0·69
4739	21,100	0·34	4490	22,270	1·4
4274	23,400	2·78	4415	22,650	1·2
3311	30,200	11·00	3781	26,450	3·4
3068	32,600	0·94			
2597	38,500	3·23			
2387	41,900	0·34			

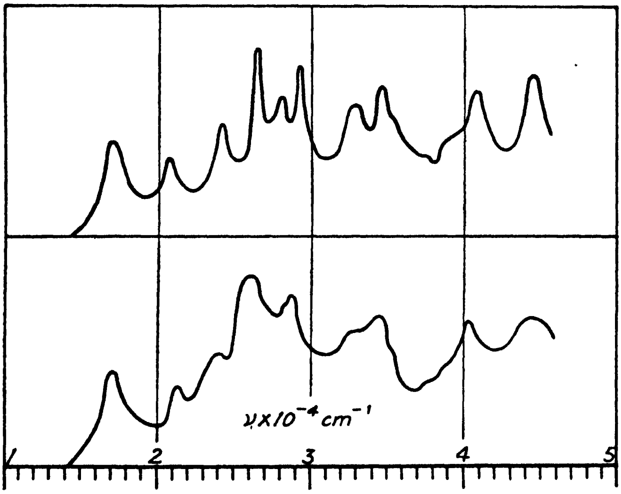

FIG. 4.

FIG. 3.

TABLE II.—ABSORPTION MAXIMA; DIFFUSE BANDS.

$SmCl_2$ in NaCl.		$SmCl_2$ in $SrCl_2$.	
λ. A.	$\bar{\nu}$. cm.$^{-1}$.	λ. A.	$\bar{\nu}$. cm.$^{-1}$
2260	44,250	2240	44,640
2470	40,490	2450	40,820
2590	38,610	2580	38,760
2670	37,450	2650	37,740
2830	35,340	2830	35,340
2910	34,360	2880	34,720
3030	33,000	3030	33,000
3500	28,570	3430	29,150
3570	28,010	3560	28,090
3800	26,320	3770	26,530
4100	24,390	4120	24,270
4700	21,280	4800	20,830
5870	17,040	5860	17,060

$SmCl_2$ in $SrCl_2$; absorption.—The diffuse bands were similar to $SmCl_2$ in NaCl. The relative values of the extinction coefficient are plotted in Fig. 4, and the maxima tabulated in Table II. No weak narrow bands could be observed. A calculation of the approximate absolute value of the band strengths gave results of the same order of magnitude as for the aqueous solution. Visual observation showed no change in the width or intensity on cooling to liquid-air temperature.

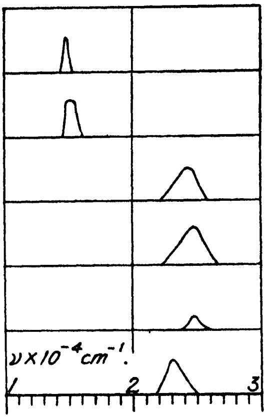

FIG. 5.

FIG. 6.

FIG. 7.

FIG. 8.

FIG. 9.

FIG. 10.

$SmCl_2$ in $BaCl_2$; absorption.—Owing to heavy scattering by the micro-crystalline material, only the visible region could be studied. The diffuse bands were almost identical with those in NaCl. The weak very narrow lines or bands are given in Fig. 2 B and Table III.

$SmCl_2$ in $SrCl_2$; fluorescence.—A brilliant diffuse band was present in the red, the range being about 6550-6900 A. with a maximum 6760 A. (14,790 cm.$^{-1}$) (Fig. 5) and no narrow bands.

$SmCl_2$ in $BaCl_2$; fluorescence.—A brilliant red fluorescence was observed. The spectrum showed :

(i) weak blue lines ;
(ii) strong orange lines ;
(iii) a very strong red line and four groups in the infra-red (Fig. 2 A and Table IV) ;
(iv) diffuse orange fluorescence, in the same region as the lines, ranging from 6200-6850 A. with a flat maximum at 6400-6700 A. (15,600-14,900 cm.$^{-1}$) (Fig. 6.)

TABLE III.—LINES, OR VERY NARROW BANDS.

$SmCl_2$ in $BaCl_2$; absorption.		$SmCl_2$ in NaCl; absorption.	
λ. A.	$\bar{\nu}$. cm.$^{-1}$	λ. A.	$\bar{\nu}$ cm.$^{-1}$
6800	14,706	—	—
6755	14,804	—	—
5990	16,694	—	—
4975	20,101	—	—
4695	21,299	—	—
—	—	4452	22,462
—	—	4400	22,727
4120	24,272	4115	24,301
4098	24,402	4095	24,420
4075	24,540	4070	24,570

$EuCl_2$ in water ; absorption.—No infra-red or visible absorption was found. There are only two diffuse ultra-violet maxima, and a group of four evenly-spaced narrow bands superimposed (Fig. 11 and Table V.) The solution was not fluorescent in ultra-violet light.

$EuCl_2$ in $SrCl_2$; fluorescence.—A brilliant violet fluorescence, showing a smooth peak, maximum 4090 A. (24,450 cm.$^{-1}$) was observed. Limits on long exposure were 3850-4400 A. (Fig. 7). No lines or infra-red fluorescence was found.

$EuCl_2$ in $BaCl_2$; fluorescence.—Simlar to above, with maximum 4000 A, (25,000 cm.$^{-1}$) and limits 3750-4450 A. (Fig. 8). No lines or infra-red fluorescence was found.

$YbCl_2$ in Water ; absorption.—There was no infra-red absorption. Two heavy diffuse maxima were observed in the ultra-violet (Fig. 12) very similar to europium, but no narrow bands were present. The solution showed no fluorescence in ultra-violet light.

TABLE IV.—LINES, OR VERY NARROW BANDS.

$SmCl_3$ in $BaCl_2$; fluorescence.			$SmCl_3$ in NaCl ; fluorescence.	
λ . A.	$\bar{\nu}$. cm.$^{-1}$	Intensity.	λ . A.	$\bar{\nu}$. cm.$^{-1}$
8205	12,188	strong	—	—
8165	12,247	medium	—	—
7680	13,021	medium	—	—
7330	13,643	strong	—	—
7290	13,717	medium	—	—
7020	14,245	medium	—	—
6890	14,514	very strong	—	—
6625	15,094	medium	—	—
6390	15,649	medium	—	—
6275	15,936	medium	—	—
—	—	—	5460	18,315
—	—	—	5440	18,382
4505	22,198	weak	4530	22,075
4480	22,321	medium	4500	22,222
4454	22,452	medium	4470	22,371

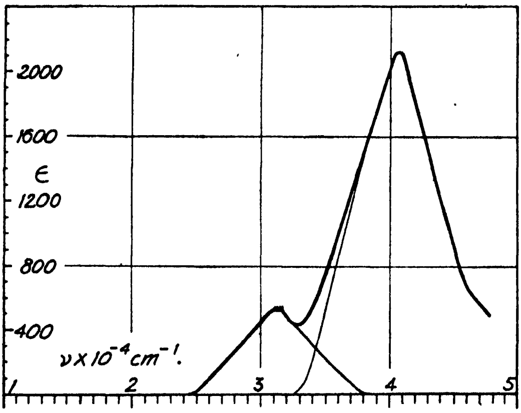

FIG. 11.

TABLE V.—$EuCl_3$ IN WATER.

Absorption maxima ; diffuse bands.			Narrow bands.		
λ . A.	$\bar{\nu}$. cm.$^{-1}$	$P \times 10^3$.	λ . A.	$\bar{\nu}$ cm.$^{-1}$	$P \times 10^6$.
3205	31,200	6·2	3230	30,960	0·56
2480	40,320	31·2	3205	31,200	0·76
			3180	31,450	2·1
			3155	31,700	2·7

$YbCl_2$ in $SrCl_2$; fluorescence.—Very weak, smooth-peak maximum was obtained at 4020 A. (24,880 cm.$^{-1}$) (Fig. 9).

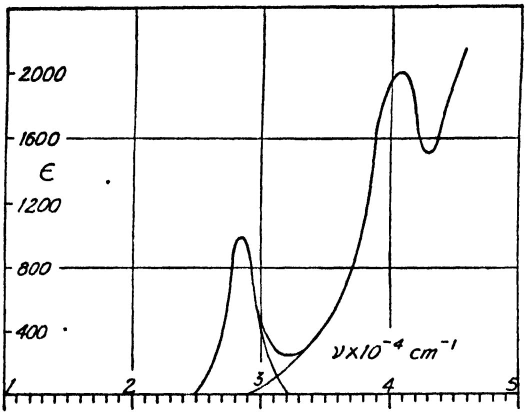

FIG. 12.

$YbCl_2$ in $BaCl_2$; fluorescence.—A bright smooth peak in the violet, maximum 4310 A. (23,200 cm.$^{-1}$) with limits on long exposure of 4000-4600 A. (Fig. 10) but no lines or infra-red fluorescence were found.

TABLE VI.—$YbCl_2$ IN WATER.

Absorption maxima, diffuse bands.

λ. A.	ν. cm.$^{-1}$	$P \times 10^3$.
3520	28,410	5·1
2460	40,650	27·5

Discussion.

All the results given may be attributed to the bivalent ions. The characteristic bands all disappear as the aqueous solutions are kept long enough for oxidation to occur, or the solid materials are fused under oxidising conditions. None can be correlated with any known tervalent bands. Two types of transitions may be expected for these ions:

(i) $4f \rightarrow 5d$, or $4f \rightarrow 6s$, etc.
(ii) Internal $4f$.

TYPE (i) should be diffuse, owing to the large perturbation of the external level by its environment, should remain diffuse at liquid-air temperature, and should have a P-value of 10^{-2} to 10^{-3}. The heavy diffuse bands of Sm^{++}, Eu^{++}, and Yb^{++} are obviously of this type. In the tervalent rare earths, such bands are usually in the extreme ultraviolet (e.g. Ce and Yb), or else beyond 50,000 cm.$^{-1}$. Bivalent Sm, Eu, and Yb are all very readily oxidised to the tervalent state. This means that the binding energy of the $4f$ electrons is abnormally low until one of them has been raised to a higher level or removed. When this has occurred the nuclear charge is sufficient to hold the remaining $4f$ electrons firmly enough to prevent the exhibition of definite quadrivalence by any rare earth except cerium.

Polarographic study by Noddack and Brukl[15] has shown that Sm, Eu and Yb differ from the other rare earths in showing two well-separated reduction-potentials, corresponding to $M^{+++} \rightarrow M^{++}$ and $M^{+++} \rightarrow M$.

Sm : — 1·720 and — 2·010 v.
Eu : — 0·710 and — 2·510 v.
Yb : — 1·430 and — 2·005 v.

---

[15] *Angew. Chem.*, 1937, **50**, 362.

Qualitatively it is found that the temperature necessary to reduce the trichlorides to dichlorides increases in the order Eu, Yb, Sm, and that the rate of reaction of the dichlorides with water increases in the order Eu, Yb, Sm. The above facts mean that the type (i) absorption for Sm^{++}, Eu^{++} and Yb^{++} should set in at a lower frequency than for tervalent rare earths, and that the frequency at which absorption begins should be lowest for Sm. This is precisely what is found.

Until an analysis of the line spectra of these ions has been made, any correlation of individual bands with particular transitions must be very conjectural. The simplest case is Yb. The ground state of Yb^{++}, $4f^{14}$ is $^1S_0$, and the excited states with one electron in $5d$ or $6s$ will give $^1(PDFGH)$ and $^3(PDFGH)$. If the transition (of high intensity) is to be "permitted" then $\Delta L = 0$ or 1, which would allow $^1S_0 \rightarrow {}^1P$ and $^1S_0 \rightarrow {}^3P$. This may be the explanation of the two observed maxima. Eu^{++} is somewhat analogous. The ground state of Eu^{++}, $4f^7$ is $^8S_{\frac{7}{2}}$. The excited states are formed by the addition of one $5d$ or $6s$ electron to the system $4f^6$, and the lower terms of the resultant will be $^8(PDFGH)$ and $^6(PDFGH)$. The permitted transitions for the lower frequency part of the absorption should therefore be somewhat similar to Yb^{++}, and this may explain the close similarity of the spectra. For Sm^{++} the configurations are more numerous. The ground state is $^7F_0$, and the lower excited states could be formed by addition of one $5d$ or $6s$ electron to the three low-lying states $4f^5$, $^6(HFP)$, which would give $^7(SPDFGHIK)$ and $^5(SPDFGHIK)$ so that possible permitted transitions are ^7F to $^8(DFG)$ and to $^5(DFG)$ The spectrum should therefore be more complicated than for Eu^{++} or Yb^{++}, as is the case. It will be noticed that the Sm^{++} bands become narrower as the "solvent" is changed in the order water, NaCl, $SrCl_2$ (Fig. 1, 3, 4). This may be ascribed to the rather random perturbations due to water molecules, the somewhat more uniform environment of Sm^{++} in the NaCl lattice (which must however be distorted) and the very uniform environment of Sm^{++} in the isomorphous $SrCl_2$. The general similarity of the three spectra show that any absorption due to Na or Sr "colour centres" in the crystals must be small. The fluorescences are always at lower frequencies than the corresponding absorptions (Gurney and Mott).[16]

Type (ii), internal $4f$ transitions, should give narrow line-like bands, and being "forbidden" will be of low intensity ($P \sim 10^{-6}$) in an asymmetric field.

Ytterbium.—For Yb^{++}, the $4f$ shell is full, and Pauli's principle excludes internal transitions. Accordingly there should be no type (ii) bands and none could be observed.

Europium.—Eu^{++} should be isoelectronic with Gd^{+++}. The narrow bands could only be observed under the conditions of greatest asymmetry (water), and not in $EuCl_2$ in $SrCl_2$. Compared with Gd^{+++} the frequencies for corresponding transitions should be, in general but not invariably, decreased. The most probable frequency shift should be,

$$\frac{\bar{\nu}(Eu^{++})}{\bar{\nu}(Gd^{+++})} = \left(\frac{Z\mathrm{Eu} - \sigma\mathrm{Gd}}{Z\mathrm{Gd} - \sigma\mathrm{Gd}}\right)^2 = 0{\cdot}934$$

where Z = atomic number, the screening constant for Gd, $\sigma = 34{\cdot}2$, being used for Eu^{++} also.

The Eu^{++} absorption group around 31,200 cm.$^{-1}$ may be the analogue of the strongest Gd^{+++} group around 36,500 cm.$^{-1}$. The symmetrical pattern of the band is probably due to splitting by the external field, a partial symmetry being provided by co-ordination of water molecules round the Eu^{++} ions. The splitting of several hundred cm.$^{-1}$ is the correct order of magnitude.

---

[16] *Trans. Faraday Soc.*, 1939, **35**, 71.

Samarium.—Sm^{++} should be isoelectronic with Eu^{+++}. The fluorescence in $BaCl_2$ does show a striking resemblance to that of Eu^{+++} given by Gobrecht.[9] The red and infra-red spectrum falls clearly into five groups of lines, of which the one at 14,514 cm.$^{-1}$ may be regarded as a transition from a 14,514 cm.$^{-1}$ level to the ground state $^7F_0$, and the others as transitions from the same level terminating in the next four levels of the basic multiplet, viz. $^7F_1$, $^7F_2$, $^7F_3$, $^7F_4$. Using a screening constant equal to that for Eu, $\sigma = 33{\cdot}8$, the theoretical separation of the ^7F levels may be calculated from Goudsmidt's formula[17] and compared with the observed values obtained by subtracting the mean wave numbers of each group from 14,514 cm^{-1}.

Mean $\bar{\nu}$. cm.$^{-1}$	$\Delta\bar{\nu}$. obs.	$\Delta\bar{\nu}$. calc.	Lower Level.
14,514	—	—	$^7F_0$
14,245	269	228	$^7F_1$
13,680	834	682	$^7F_2$
13,021	1493	1365	$^7F_3$
12,218	2296	2280	$^7F_4$

The three orange lines may be similarly attributed to a transition from a level at 15,936 cm.$^{-1}$ to the first three terms of the basic multiplet.

$\bar{\nu}$. cm.$^{-1}$	$\Delta\bar{\nu}$ obs.	Lower Level.
15,936	—	$^7F_0$
15,649	287	$^7F_1$
15,095	841	$^7F_2$

A similar group of lines is also shown by Eu^{+++}. The agreement in $\Delta\bar{\nu}$ values between the two lots of observations is within the limits of experimental error. The above fluorescence is only shown in $BaCl_2$ where there is some asymmetry owing to lack of good isomorphism. As is to be expected, Sm^{++} in $SrCl_2$ shows no line fluorescence, and Sm^{++} in NaCl (which consists mostly of separate $SmCl_2$ crystals dispersed in the NaCl) shows only some weak lines.

Any detailed comparison of the absorption of Sm^{++} with Eu^{+++} is difficult since probably only a few of the stronger Sm^{++} lines have been observed. It is impossible to look for weaker lines by increasing the concentration of material, since the superimposed diffuse absorption is so much stronger than the lines that to increase the absorption due to the latter 10 times would reduce the transmitted light perhaps 1000 times, requiring exposures beyond practicable limits. In addition most of the Eu^{+++} lines are so faint that probably not all have been recorded as yet. The strong group around 22,000 cm.$^{-1}$ in aqueous solution may however be the analogue of the very strong Eu^{+++} group at 25,380 cm.$^{-1}$. The triplet structure of this Sm^{++} band is too wide to be attributed to Stark splitting of the levels, but may be explained if the 22,650 cm.$^{-1}$ band is a transition from the ground state $^7F_0$, to a level at 22,650 cm.$^{-1}$ and the other two bands are transitions from the $^7F_1$ and $^7F_2$ levels to the same upper level.

The bands are too diffuse for accurate location of maxima so that the agreement with the other observed values is reasonable. Both the $^7F_1$ and $^7F_2$ levels can have a considerable population at room temperature, for which $kT \sim 205$ cm.$^{-1}$. The first two bands also appear as lines in Sm^{++} in NaCl, at 22,727 and 22,462 cm.$^{-1}$, $\Delta\tilde{\nu} = 265$ cm.$^{-1}$, in good agreement with the values deduced from fluorescence. As with fluorescence, the strongest lines or narrow bands occur under conditions of greatest asymmetry (water), and Sm^{++} in $SrCl_2$ shows no lines. The fluorescence around 22,200 cm.$^{-1}$ in both $BaCl_2$ and NaCl appears to be the converse of the above process, complicated by level-splitting in the crystal field.

---

[17] *Physic. Rev.*, 1928, **31**, 946.

$\tilde{\nu}$. cm.$^{-1}$	$\Delta\tilde{\nu}$. obs.	Lower Level.
22,650	—	$^7F_0$
22,270	380	$^7F_1$
21,790	860	$^7F_2$

Summary.

The absorption and fluorescence spectra of aqueous solutions of samarous, europous and ytterbous chloride, and some solids containing the bivalent ions have been measured, and the absorption probabilities for the bands calculated. The assignment of bands to possible electronic transitions is discussed. All three ions show heavy diffuse bands due to $4f \rightarrow 5d$, or $6s$ transitions, and Sm^{++} and Eu^{++} show narrow, weak bands which can be correlated with those of the isoelectronic Eu^{+++} and Gd^{+++} respectively.

Chemistry Department,
University of Aberdeen.

SURFACE TENSION OF A REGULAR SOLUTION.

By I. Prigogine.

Received 11*th July*, 1947.

In a recent paper,[1] Guggenheim has calculated the surface tension of a regular solution. He obtained [2]

$$\gamma = \gamma_A + \frac{kT}{a}\log\frac{x'_A}{x_A} + \frac{w}{a}l(x'^2_B - x_B^2) - \frac{w}{a}mx_B^2$$

$$= \gamma_B + \frac{kT}{a}\log\frac{x'_B}{x_B} + \frac{w}{a}l(x'^2_A - x_A^2) - \frac{w}{a}mx_A^2 \quad . \quad . \quad (1)$$

Eqn. (1) together with

$$x'_A + x'_B = 1 \text{ and } x_A + x_B = 1 \quad . \quad . \quad . \quad (2)$$

permit the calculation of γ, x'_A, x'_B in terms of x_A, x_B, γ_A and γ_B. We can compare eqn. (1) with the experimental data for the system ether-acetone.

As is evident from vapour-pressure data (Porter [3]) and the boiling-point curve (Prigogine [4]), this system is a regular one. On the other hand, the surface tension of this system has been studied by Sutherland [5] at 288° K.

---

[1] Guggenheim, *Trans. Faraday Soc.*, 1945, **41**, 150.

[2] For the notation, see Guggenheim's paper.

[3] Porter, *Trans. Faraday Soc.*, 1920, **16**, 339.

[4] Prigogine and Defay, *Thermodynamique Chimique*, Vol. II (Liège, 1946), p. 260.

[5] Sutherland, *Phil. Mag.*, 1894, **38**, 188.

The values of the parameters for this system are :

$w = 450$ cal./mole $a = 30$ A.^{2}

$\gamma_A = 19{\cdot}1$ dyne/cm. (ether) $\gamma_B = 25$ dyne/cm. (acetone).

The numerical evaluations have been carried out assuming either a simple cubic lattice ($l = \frac{2}{3}$, $m = \frac{1}{6}$) or a close-packed lattice ($l = \frac{1}{2}$, $m = \frac{1}{4}$).

Fig. 1 gives the values of x'_B as a function of x_B. As expected, there is in the surface layer an excess of ether, due to its lower surface tension. The simple cubic lattice and close-packed lattice give quite similar results. Fig. 2 and 3 give the surface tension of the system assuming a simple cubic lattice and a close-packed lattice respectively.

The close correspondence between calculated and observed data gives strong support for Guggenheim's statistical theory of surface tension.

Summary.

Guggenheim's formulæ giving the surface tension of a regular solution are compared with the experimental data for the system ether-acetone. The agreement is good.

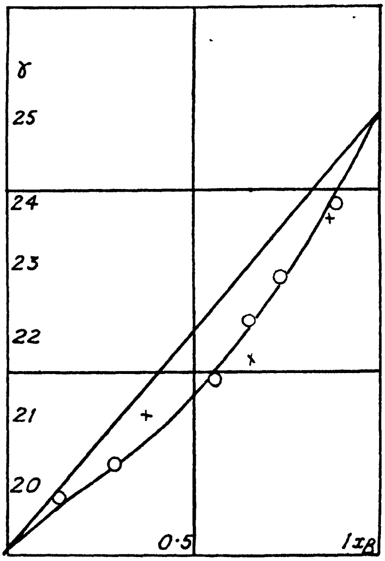

FIG. 1.—Composition of surface layer (x'_B) as function of composition of bulk phase (x_B) for the system ether-acetone.

{O—calculated points with $l = \frac{1}{2}$, $m = \frac{1}{4}$.
{X—calculated points with $l = \frac{2}{3}$, $m = \frac{1}{6}$.

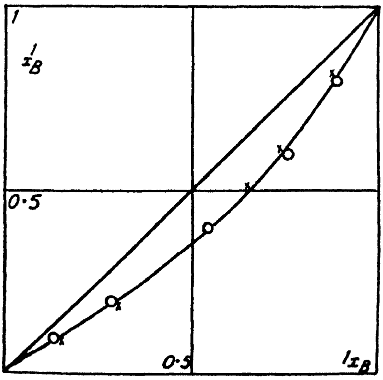

FIG. 2.—Surface tension of the system ether-acetone. O—calculated points ($l = \frac{2}{3}$, $m = \frac{1}{6}$), X—observed points.

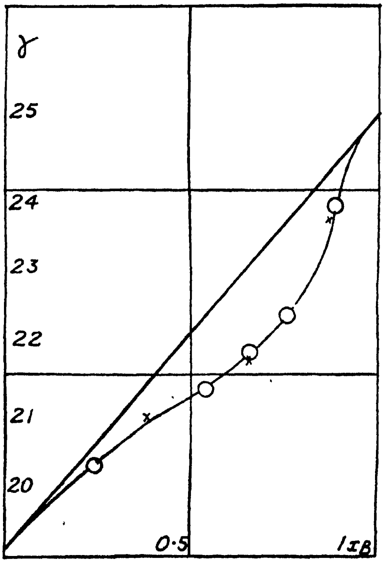

FIG. 3.—Surface tension of the system ether-acetone. O—calculated points ($l = \frac{1}{2}$, $m = \frac{1}{4}$), X—observed points.

ADDENDUM.

BY I. PRIGOGINE AND J. NARBOND.

Received 13*th July,* 1948.

Sutherland's values for the system ether-acetone used in the preceding paper are rather ancient (1894) and fragmentary. So we have taken new measurements at 288° K. and 303° K. The pure substances have been supplied by the *Bureau des Etalons physico-chimiques de Bruxelles.* The method used is the capillary-rise method and the details have been described elsewhere.* Our results are given in the Tables I and II and are compared with Guggenheim's formula for the surface tension of a regular solution.

TABLE I.—SURFACE TENSION OF THE SYSTEM ETHER-ACETONE AT 288° K.

x_B. Mole fract. acetone.	γ (Expt. values dynes/cm.).	γ (Calc. simple cubic lattice).	Deviation.	γ (Calc. close-packed lattice).	Deviation.
0	17·66 ± 0·15	—	—	—	—
0·217	18·64	18·57	+ 0·07	18·55	+ 0·09
0·263	18·78	18·72	+ 0·06	18·70	+ 0·08
0·470	19·30	19·36	− 0·06	19·56	− 0·26
0·580	20·02	20·07	− 0·05	20·21	− 0·19
0·669	20·76	20·63	+ 0·13	20·84	− 0·08
0·799	21·57	21·64	− 0·07	21·80	− 0·23
0·912	22·60	22·56	+ 0·04	22·88	− 0·28
1	23·72	—	—	—	—

TABLE II.—SURFACE TENSION OF THE SYSTEM ETHER-ACETONE AT 303° K.

x_B. Mole fract. acetone.	γ (Expt. values dynes/cm.).	γ (Calc. simple cubic lattice).	Deviation.	γ (Calc. close-packed lattice).	Deviation.
0	15·78 ± 0·15	—	—	—	—
0·217	16·75	16·75	0·00	16·74	+ 0·01
0·263	17·02	16·90	+ 0·12	16·95	+ 0·07
0·470	17·49	17·65	− 0·16	17·80	− 0·31
0·580	18·26	18·25	+ 0·01	18·42	− 0·16
0·669	19·15	18·90	+ 0·25	19·05	+ 0·10
0·799	19·80	19·90	− 0·10	20·02	− 0·20
0·912	21·06	21·00	+ 0·06	21·15	− 0·09
1	22·01	—	—	—	—

The agreement with Guggenheim's formulæ is surprisingly good, specially with a simple cubic lattice.

We are indebted to Prof. Timmermans for his permission to publish these measurements which have been made in his laboratory.

Université Libre de Bruxelles,
Faculté des Sciences,
Bruxelles.

---

* Mme. Hennaut and L. Lek, *Bull. Soc. Chim. Belg.*, 1931, **40**, 177.

FRACTIONAL DISTILLATION. I. THE SELECTION OF TEST MIXTURES FOR ESTIMATING THE EFFICIENCY OF FRACTIONATING COLUMNS.

By E. A. Coulson and E. F. G. Herington.

Received 14*th July*, 1947.

The method which has come into universal use for assessing the performance of laboratory fractional distillation equipment consists in the application of the Fenske equation to the results of test distillations performed, at total reflux, upon a suitable binary mixture.[1] In the theoretical derivation of Fenske's expression a number of assumptions regarding the test mixture, the fractionating equipment and the mode of operation must be made [2] but as usually applied the expression takes the form :

$$\frac{x_t}{1 - x_t} = \alpha^n \frac{x_b}{1 - x_b} \quad . \quad . \quad . \quad . \quad (1)$$

where x_t is the mol fraction of the more volatile component in the liquid flowing back from a total condenser into the top of the fractionating column, and x_b is the mol fraction of the same component in the contents of the still when a stationary condition has been established ; n is the efficiency expressed as the number of theoretical plates to which the column and boiler are equivalent and α is the volatility ratio, which is usually taken as a constant and independent of x. The volatility ratio as defined by eqn. (1) when $n = 1$ is seen to be the ratio of the molar fractions of the components in the vapour divided by their ratio in the liquid when the two phases are in equilibrium.

The test mixture must conform very closely to the requirements of ideality in both the liquid and vapour phases. For an ideal mixture at a given temperature

$$\alpha = \frac{p_1^\circ}{p_2^\circ} \quad . \quad . \quad . \quad . \quad . \quad (2)$$

where p_1° and p_2° are the vapour pressures of the more and less volatile components respectively in the pure states. But α as defined by eqn. (2) is in general a function of temperature, i.e. of x, the liquid composition, when a distillation is carried out at constant pressure, unless the molar latent heats of vaporisation of the pure components are identical. Hence the arithmetical or geometrical mean value of the vapour pressure ratio is commonly employed although a further and greater perturbation in α is often introduced by departures from strict ideality in the text mixture. In practice therefore it has often been customary to use experimentally determined values for α.

The magnitude of the error in the estimated number of plates which may result in realisable cases, if n is great, from small uncertainties in the value of α is not always appreciated. From eqn. (1) by differentiation and rearrangement :

$$\mathrm{d}n = \frac{1}{\log_e \alpha}\left[\frac{\mathrm{d}x_t}{x_t(1 - x_t)} - \frac{\mathrm{d}x_b}{x_b(1 - x_b)} - \frac{n}{\alpha}\mathrm{d}\alpha\right] \quad . \quad . \quad (3)$$

and considering errors in n arising solely from errors in α it is clear that

$$\frac{\mathrm{d}n}{n} = -\frac{\mathrm{d}\alpha}{\alpha \log_e \alpha}. \quad . \quad . \quad . \quad . \quad (4).$$

Test mixtures are usually chosen to have α close to, or less than, 1·10 in order that the values of x_t and x_b which result when n is between 20 and 100 will be suitable for analytical determination. Computations made from (4) show that if α is 1·10 an error of 0·01 in the value of α will introduce an error of 10 % in the values of n calculated from Fenske's equation, while if α is 1·20 the error is still 5 %.

---

[1] Fay, *Ann. Reports*, 1944, 40, 219.

[2] See, for example, Robinson and Gilliland, *Elements of Fractional Distillation* (McGraw Hill, 1939), pp. 85-6.

It appears that to reduce the uncertainty in values for α found experimentally to ± 0·01 has, in the past, been extremely difficult. Thus the values of α determined by Bragg and Richards[3] for the system ethylene dichloride-benzene showed a variation of 0·06 about a mean value 1·07 at 760 mm. and in consequence Carlson and Colburn[4] suggested that an α value derived from eqn. (2) above should be used by preference and until any observed variations from this value could be shown to be consistent with the thermodynamical requirements of the system.

Test Fractional Distillations.

Considerations such as these seemed to make it very desirable to devise a fresh technique for test fractionations and one which would permit the use of the Fenske equation in conditions where α is very nearly constant and its value determinable with the high accuracy appropriate to the purpose.

A general expression for α in terms of thermodynamic quantities, deduced with the assumption that the vapours obey the ideal gas laws and that the volumes of the liquids are negligible compared with those of the vapours, is the following :

$$\log_e \alpha = \log_e \frac{p_1^{\circ}}{p_2^{\circ}} - \frac{1}{RT}\left(\frac{\partial \Delta G^E}{\partial N_2}\right)_T \quad . \quad . \quad . \quad (5)$$

which is a simple rearrangement of an equation given by us in a previous paper.[5] Since test mixtures are chosen to approximate closely to ideality in the liquid state their vapours will in general be even more closely ideal in behaviour and the expression given above, when restricted to test mixtures, requires little or no further justification. It may be mentioned here that Carlson and Colburn[4] have calculated that in the particular case of benzene-ethylene dichloride, deviations of the vapours from ideal gas behaviour cause the relative volatility to be only 0·3 % lower than the ratio p_1°/p_2°, which is equivalent to a deviation in α of 0·003.

In eqn. (5), ΔG^E is the difference between the free energy of formation of an ideal solution and that of the actual solution (the "excess free energy") and N_2 is the mol fraction of the component which has vapour pressure p_2° in the pure state. A number of conclusions may be drawn from this equation.

(*a*) If ΔG^E plotted against N_2 exhibits a maximum, a minimum, or a point of inflexion, then at the corresponding value of N_2, eqn. (5) reduces to eqn. (2) and $\alpha = p_1^{\circ}/p_2^{\circ}$

(*b*) If $\Delta G^E \neq 0$, then at one concentration at least $\left(\frac{\partial \Delta G^E}{\partial N_2}\right)_T$ will be zero, whereupon α will again $= p_1^{\circ}/p_2^{\circ}$.

(*c*) An interesting test to decide whether experimentally determined α values are consistent with the thermodynamic requirements can be derived from eqn. (5). Rearrangement, substitution of $-\partial N_1$, in place of ∂N_2 followed by integration with respect to N_1 between the limits $N_1 = 0$ and $N_1 = N_1^1$ yields

$$\int_0^{N_1^1}\left(\log_e \alpha - \log_e \frac{p_1^{\circ}}{p_2^{\circ}}\right) dN_1 = \frac{1}{RT}\Big[\Delta G^E\Big]_{N_1=0}^{N_1=N_1^1}$$

$$. \quad = \frac{1}{RT}\Delta G^E_{N_1^1} \quad . \quad . \quad . \quad (6)$$

---

[3] Bragg and Richards, *Ind. Eng. Chem.*, 1942, **34**, 1088.

[4] Carlson and Colburn, *ibid.*, 1942, **34**, 1553.

[5] Coulson and Herington, *J. Chem. Soc.*, 1947, 597.

where $\Delta G^{\mathrm{E}}_{N_1^1}$ is the value of ΔG^{E} for the solution containing N_1^1 moles of N_1, and $\alpha = \dfrac{p_1 N_2}{p_2 N_1}$. Clearly eqn. (6) can be used to calculate $\Delta G^{\mathrm{E}}_{N_1^1}$ if the plots of $\log_e p_1^\circ/p_2^\circ$ and of $\log_e \alpha$ each against N_1 are available. If $N_1^1 = 1$, then the right-hand side of eqn. (6) is equal to zero and the left-hand side of eqn. (6) is then represented graphically by the total area between the $\log_e \alpha$ against N_1 and $\log_e p_1^\circ/p_2^\circ$ against N_1 curves. If this area be reckoned positive when $\log_e \alpha > \log_e p_1^\circ/p_2^\circ$ and negative when $\log_e p_1^\circ/p_2^\circ < \log_e \alpha$, then the positive and negative areas must be equal. For example in Fig. 1 if the data plotted are self-consistent thermodynamically the area ABC plus the area EGH should equal the area CDEF. This is a test which can be readily applied planimetrically or otherwise. The essential assumption involved in the derivation of eqn. (6) is that the vapours obey the ideal gas laws but it is only strictly applicable to an isothermal system. However, if the components boil at nearly the same temperature then this test for self-consistency of experimental results may be applied to isobaric data as will now be shown.

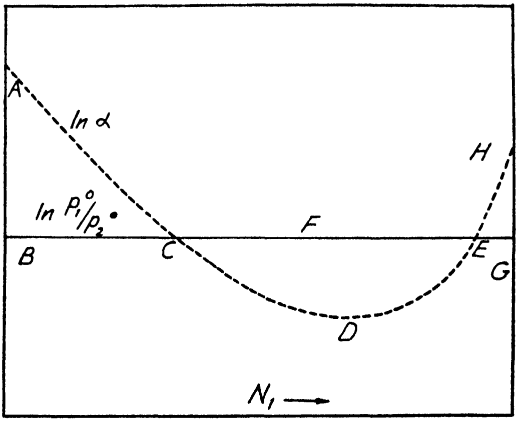

FIG. 1.

The most general form of eqn. (6), which can be applied to isobaric data, may be derived from eqn. (5) by writing it in the form

$$RT\,[\log_e \alpha - \log_e p_1^\circ/p_2^\circ] = \left(\frac{\partial \Delta G^{\mathrm{E}}}{\partial N_1}\right)_T = \left(\frac{\mathrm{d}\Delta H}{\mathrm{d}N_1}\right) - T\left(\frac{\mathrm{d}\Delta S^{\mathrm{E}}}{\mathrm{d}N_1}\right) \quad (7)$$

where ΔH is the heat absorbed in the formation of one mole of mixture and ΔS is the excess entropy of mixing corresponding to the excess free energy ΔG^{E}. Eqn. (7) is true for any temperature T. Integrating between the limits $N_1 = 0$ and $N_1 = N_1^1$ remembering T is a function of N_1 yields

$$\begin{aligned}\int_0^{N_1^1} RT\left[\log_e \alpha - \log_e \frac{p_1^\circ}{p_2^\circ}\right]\mathrm{d}N_1 &= \int_0^{N_1^1}\left[\left(\frac{\mathrm{d}\Delta H}{\mathrm{d}N_1}\right) - T\left(\frac{\mathrm{d}\Delta S^{\mathrm{E}}}{\mathrm{d}N_1}\right)\right]\mathrm{d}N_1 \\ &= \Big[\Delta H - T\Delta S^{\mathrm{E}}\Big]_{N_1=0}^{N_1=N_1^1} + \int_{T_2}^{T_1^1} \Delta S^{\mathrm{E}}\mathrm{d}T \\ &= \Delta G^{\mathrm{E}}_{N_1^1} + I \quad . \quad . \quad . \quad . \quad . \quad . \quad . \quad . \quad . \quad . \quad . \quad (8)\end{aligned}$$

where $I = \int_{T_2}^{T_1^1} \Delta S^{\mathrm{E}}\mathrm{d}T$. . .

In the case of isobaric data, T_2 is the boiling point of the pure component 2 at the given pressure p while the boiling point of the solution containing N_1^1 moles of component 1 is T_1^1 at the same pressure. In the left-hand side of eqn. (8), $\log_e \alpha$ and $\log_e p_1^\circ/p_2^\circ$ are the values of these quantities at the temperature T which is the boiling point of the solution containing N_1 moles of component 1.

Eqn. (6) and (8) differ by the term I. If $N_1^1 = 1$, the limits of integration for I are the boiling points of the pure components and the left-hand side of eqn. (8) is then equal to I.

Some special cases may be considered. If the data are isothermal then $I = 0$ for all values of N_1^1 and eqn. (8) reduces to eqn. (6). If $\Delta G^E = \Delta H$ (see eqn. (14)), then $\Delta S^E = 0$ for all values of N_1, and the left-hand side of eqn. (8) is equal to $\Delta G^E_{N_1^1}$, which is zero when $N_1^1 = 1$. Finally if the boiling points of the mixtures and components at constant pressure are all nearly the same, I will be small and eqn. (8) will approximate to eqn. (6). It is under these conditions that eqn. (6) is applied in Part II.

While the plot of ΔG^E against N_2 may take various forms and may resemble actual heat of mixing curves (see Fig. 2), nevertheless $\left(\frac{\partial \Delta G^E}{\partial N_2}\right)_T \rightarrow$ constant, when $N_2 \rightarrow 0$ or 1 and provided the solutions are not extremely non-ideal $\left(\frac{\partial \Delta G^E}{\partial N_2}\right)_T$ will not change very rapidly in the neighbourhood of $N_2 \rightarrow 0$ or 1 and furthermore, if the concentration range is restricted to a low value for either component, the variation of the first term on the right-hand side of eqn. (5), namely p_1°/p_2°, will also be negligible because at constant pressure the boiling point will be sensibly that of the component in excess. Hence α should be nearly constant at a low concentration of one of the components even though the mixture may not be ideal and $\alpha \neq p_1^\circ/p_2^\circ$.

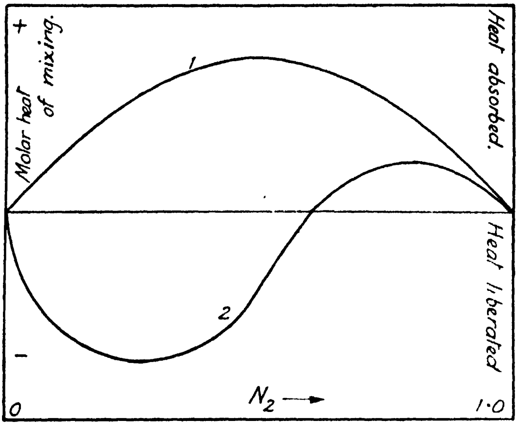

FIG. 2.

If a test mixture is to be used at one end of its concentration range, as is suggested by the foregoing analysis, it is necessary next to consider the effect of errors likely to arise from the experimental determination of working compositions. When a physical measurement such as density or refractive index is employed for analytical purposes, there is an approximately constant error in x_t and x_b not dependent on actual values, i.e. dx_t and dx_b are constant and eqn. (3) shows that dn is minimised when x_b is as much below 0·5 as x_t is above. This is the condition sought in the orthodox procedure. If, however, a colorimetric method of analysing the test solution is used then in general $\frac{dx}{x}$ = constant = $\pm K$ and from eqn. (3) it follows that

$$dn = \frac{1}{\log_e \alpha}\left[\frac{K}{1 - x_t} + \frac{K}{1 - x_b} - \frac{n}{\alpha}d\alpha\right] \qquad . \quad . \quad (9)$$

and clearly dn is minimised when x_t and x_b are both small. Here indeed it is advantageous to work at one end of the concentration range, and a similar argument applies if small quantities of the less volatile component are estimated colorimetrically.

When that constituent of the binary test mixture present at low concentration which is estimated by a colorimetric method (e.g. thiophene in benzene-thiophene mixtures—see Part II) is the less volatile then the Fenske equation simplifies to

$$n = \frac{\log_e R}{\log_e \alpha} \quad . \quad . \quad . \quad . \quad . \quad (10)$$

where R is now the thiophene concentration ratio which is found directly by colour matching. By differentiation of (10)

$$dn = \frac{dR}{R \log_e \alpha} - \frac{n d\alpha}{\alpha \log_e \alpha}. \quad . \quad . \quad . \quad (11)$$

By way of example, suppose $\alpha = 1{\cdot}10$ and dR = 0·05R (i.e. the colorimetric estimation is accurate to 5 %) then the uncertainty in the number of theoretical plates amounts only to 0·5 plate (and is the same for all values of n).

The positive advantages in using a test mixture at one end of its concentration range are: first, $\log_e \alpha$ will remain sensibly constant and, secondly, the suitably modified Fenske equation yields an accurate value for n, provided R, the ratio of the concentration of the constituent in low concentration above and below the column, can be determined with reasonable precision by a suitable method.

There remains to be considered the choice of component which shall be in excess. If a mixture shows the more usual deviation from ideality it will tend to form a minimum b.p. azeotrope rich in the lower-boiling component, so that it would seem to be preferable to use a test solution containing excess of the higher-boiling component. However, if the deviations are much too small to provoke azeotrope formation it is a matter of indifference which component preponderates. The use of a test mixture containing a small proportion of the higher-boiling component is illustrated in Part II where the technique of using a dilute solution of thiophene in benzene as a test mixture is studied in detail.

Relative Volatility and Heat of Mixing.

It will be of interest to consider the thermodynamic properties of solutions in relation to slight deviations from ideality and with particular reference to those binary liquid mixtures which have been used to measure theoretical plate equivalence and to express in some cases the divergencies of α from ideal values quantitatively in terms of measurable heats of mixing.

That small deviations from ideality were of material consequence in this connection was appreciated by Beatty and Calingaert,[6] who proposed experimental methods of testing for ideality based on the application of the Duhem-Margules equation. Griswold,[7] however, has criticised these methods on the ground of their lack of sensitivity.

---

[6] Beatty and Calingaert, *Ind. Eng. Chem.*, 1934, **26**, 504, 904.

[7] Griswold, *Ind. Eng. Chem.*, 1943, **35**, 247.

As is well known, two conditions which must be satisfied simultaneously before a solution can be ideal at all temperatures and pressures are

$$\Delta \bar{H}_1 = 0 \quad . \quad . \quad . \quad . \quad . \quad . \quad (12)$$

that is, there is no heat of mixing; and

$$\bar{v} = v \quad . \quad . \quad . \quad . \quad . \quad . \quad (13)$$

that is, there is no volume change on mixing at any constant temperature or pressure. Here $\bar{v}$ is the partial molar volume of a component in solution and v is the molar volume in the pure state.

In general, for many close-boiling pairs chosen as test mixtures the molar volumes of the components will be nearly equal and eqn. (13) approximately satisfied. In these circumstances (12) should provide a useful criterion of ideality. Nevertheless, heats of mixing seem rarely to have been studied in connection with test mixtures. Complete data for the commonly used mixtures, benzene-ethylene dichloride and *n*-heptane-methylcyclohexane do not seem to have been determined, although in the case of the last mentioned Lecat[8] claims that there is a heat of mixing and formation of an azeotrope and some departure from ideality is shown in the values of α given by Griswold[7] which do not accord with eqn. (12). Baud[9] has published a value for the heat of mixing of benzene-ethylene dichloride at one concentration which indicates that this system is far from ideal.

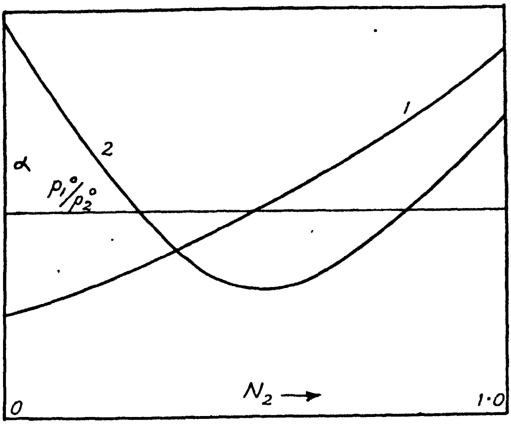

FIG. 3.

In those cases where eqn. (13) is obeyed but not eqn. (12), it follows that the conclusions reached earlier will generally be approximately true if ΔG^E is replaced by ΔH and α can then be calculated from the vapour pressures of the pure components and the heat of mixing, since eqn. (5) now becomes:

$$\log_e \alpha = \log_e p_1/p_2 \,.\, N_2/N_1 = \log_e p_2^\circ/p_1^\circ - \frac{1}{RT}\left(\frac{\mathrm{d}\Delta H}{\mathrm{d}N_2}\right). \quad . \quad (14)$$

Baud[9] has published a series of ΔH against N_2 curves, for mixtures of normal liquids, and some are of the types shown in Fig. 2. These will give rise to α against N_2 curves of the forms shown in Fig. 3 if the conditions under which eqn. (14) is valid are satisfied.

An interesting system which has been studied in more detail is that of benzene-carbon tetrachloride. Although it has frequently been used in the testing of fractionating equipment it is indeed so far from being ideal as to form an azeotrope containing 0·918 mol. fraction of carbon tetrachloride and boiling at 76·75° c.[10, 11] As the volume change on mixing has been found to be small [12] and since also the molecular volumes of the components are not very different, it might be expected that eqn. (13) is nearly satisfied. Hence, experimental data for the system may be used to test the applicability of eqn. (14). It is obviously convenient in this instance to use the heat measurements and the vapour pressures of the pure components to calculate α for the azeotropic composition as determined experimentally, which should, of course, equal unity.

---

[8] Lecat, *Rec. trav. chim.*, 1926, **45**, 620.

[9] Baud, *Bull. Soc. Chim.*, 1915, **17**, 329.

Taking the boiling point of carbon tetrachloride as 76·75° c. at 760 mm. (Young [11]) the vapour pressure of benzene at this temperature was calculated from the data of Willingham, Taylor, Pignocco and Rossini.[13] Using these vapour pressures, p_1°/p_2° was found to be 1·1095.

ΔH for use in eqn. (14) should strictly be measured at the boiling temperature. The available measurements, which were made at room temperature, are those of Baud,[9] Hirobe,[14], Schmidt [15] and Vold,[16] and are plotted in Fig. 4 on such a scale that the geometric tangent at the carbon tetrachloride concentration 0·918 mole is inclined at an angle of approximately 45° to the axis. This permits the slopes to be found graphically with most exactness. The values of Boissonas and Cruchard [17] are not included as they do not appear to possess greater accuracy than earlier determinations.

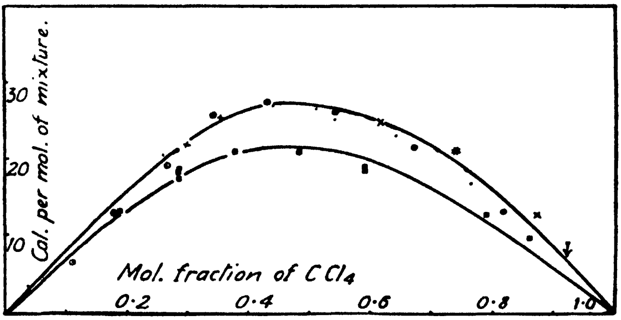

Fig. 4.

● Baud, *Bull. Soc. Chim.*, 1915, **17**, 329 (Temp. ~ 18° c.).
× Hirobe, *J. Sci. Tokyo*, 1926, **1**, 155.
* Recalculation from Hirobe's experimental values.
○ Schmidt, *Z. physik. Chem.*, 1926, **121**, 221.
☐ Vold, *J. Amer. Chem. Soc.*, 1937, **59**, 1515.

If the heat of mixing values of Baud and Schmidt, which agree well with each other in this range of concentration, are used to determine $\mathrm{d}\Delta H/\mathrm{d}N_2$ at the azeotropic composition and the result is then used to calculate α by means of eqn. (14) the value of α so obtained is 1·001. The upper curve of Fig. 4 is approximately the mean of Hirobe's, Baud's, and Schmidt's measurement and yields by the same process a value for α of 0·9996. Vold's values, being less throughout, yield α = 1·02.

---

[10] Fenske, Quiggle and Tongberg, *Ind. Eng. Chem.*, 1932, **24**, 408.

[11] Young, *Distillation, Principles and Processes* (Macmillan, 1922), p. 52.

[12] Scatchard, Wood and Mochel, *J. Amer. Chem. Soc.*, 1940, **62**, 712.

[13] Willingham, Taylor, Pignocco and Rossini, *J. Res. Nat. Bur. Stand.*, 1945, **35**, 219.

[14] Hirobe, *J. Sci. Tokyo*, 1926, **1**, 155.

[15] Schmidt, *Z. physik. Chem.*, 1926, **2**, 221.

[16] Vold, *J. Amer. Chem. Soc.*, 1937, **59**, 1515.

[17] Boissonas and Cruchard, *Helv. Chim. Acta*, 1944, **27**, 994.

Summary.

The Fenske equation as used for measuriug the plate equivalence of fractionating equipment is discussed. Sources of variation in α (the volatility ratio) are considered and the errors which result in the estimation of n (the plate equivalence of a column) from a lack of knowledge of the true value of α are estimated.

Assuming the vapours behave as ideal gases, a general equation connecting $\log_e \alpha$ with $p_1°$, $p_2°$ and ΔG^E and N_2 is discussed where $p_1°$, $p_2°$ are the vapour pressures of the pure compounds at the temperature considered, ΔG^E is the difference between the free energy of mixing of an ideal solution and that of the actual solution, and N_2 is the mol. fraction in the liquid of the component with vapour pressure $p_2°$ in the pure state.

A test for the self-consistency of $\log_e \alpha$ against N_1 data based on a thermodynamic argument has been developed, which shows that the algebraic area between the $\log_e \alpha$ and $\log_e p_1°/p_2°$ curves taken over the whole range $N_1 = 0$ to $N_1 = 1$ should be zero. This test, which assumes only that the vapours obey the ideal gas laws and that the volumes of the liquids are negligible compared with those of the vapours, is strictly applicable only to isothermal data but may be used for testing values obtained under isobaric conditions provided the components and mixtures boil at nearly the same temperatures.

Departures from ideality of test mixtures are considered and it is shown that by using solutions with a low concentration of one component the variation of $\log_e \alpha$ over the concentration range used should be small. It is recommended that in general the component in excess should have the higher boiling point, but in the absence of an azeotrope it is immaterial which is in excess.

An expression is given for the accuracy with which the ratio of concentrations of the dilute component must be determined in order to estimate to any accuracy the plate efficiency. It is shown that colorimetric methods of analysis should readily yield an accuracy of at least 0·5 plate and that with such a method of analysis it is beneficial to work at one end of the concentration range.

The systems n-heptane-methylcyclohexane, ethylene dichloride-benzene and carbon tetrachloride-benzene are discussed briefly in terms of the general thermodynamic equation. An approximate equation applicable in certain cases to the calculation of $\log_e \alpha$ from the heat of mixing is presented.

FRACTIONAL DISTILLATION. II. THE USE OF DILUTE SOLUTIONS OF THIOPHENE IN BENZENE AS TEST MIXTURES AND A COMPARISON WITH MIXTURES OF BENZENE AND ETHYLENE DICHLORIDE.

By E. A. Coulson, J. L. Hales and E. F. G. Herington.

Received 14th July, 1947.

A suggestion that benzene containing a small percentage of thiophene would offer attractions as a test mixture was made to us in the first place by Mr. H. M. Lowe (of Dorman, Long and Co.). Such mixtures are available in any quantity and might therefore be used to test equipment of any size; and the determination of small thiophene contents has already received much attention and can be done very easily. That the use of such mixtures for the purpose suggested is feasible follows from a clarification already made of the problems raised by test-distillation procedure (see Part I) and the work now described was undertaken to secure necessary data and to provide detailed experimental methods.

No examination of vapour-liquid equilibria in benzene-thiophene mixtures has been reported, although quantitative data derived from such a study would have an obvious bearing on the question whether the thiophene content of crude or of refined benzene can be economically reduced by efficient fractional distillation. A parallel re-examination of the benzene-ethylene dichloride system has supplied evidence that the new vapour-liquid data are trustworthy, and that efficiency tests of one and the same equipment with the two mixtures give similar results.

Experimental.

Purification of Materials.

Benzene.—A sample of benzene was prepared by fractional freezing from Analar benzene $n_D^{20} = 1{\cdot}4987$, which contained paraffins. It was cooled at $-18°$ c. until all but approximately 5 % by volume had solidified and the liquid remaining was decanted. The crystalline benzene was melted and re-frozen in this way 7 times successively, whereby the volume of liquid originally taken was reduced by $\frac{1}{8}$ and its refractive index had reached 1·5011, asymptotically. The purified material was then fractionally distilled in a 25-plate column and the middle fraction [b.p. = 80·1° c., $n_D^{20} = 1{\cdot}5011$, $d_4^{20} = 0{\cdot}8790(4)$] was employed in the present investigation. Its thiophene content was approximately the same as that of the benzene employed as diluent in the colorimetric estimation of thiophene (see below).

Benzene Used as Diluent in the Colorimetric Estimation of Thiophene.—Benzene for this purpose must contain the minimum of thiophene but need not be free from paraffins and was prepared by boiling Analar benzene with half its volume of a 20 % w./w. aqueous mercuric acetate solution. It then contained less than the maximum permissible thiophene concentration, i.e., less than 0·000075 % S, as tested by French's colorimetric method.[1]

Thiophene.—A commercial specimen was washed 3 times with 10 % aq. HCl ; then with 10 % NaOH solution and lastly with water prior to fractional distillation through a 50-plate column. The middle fraction (75 %, b.p. = 84·0° c.), used in the present work, had $d_4^{20} = 1{\cdot}0647(0)$ and $n_D^{20} = 1{\cdot}5286(5)$, values in good accord with those reported by Fawcett and Rasmussen.[2]

Ethylene Dichloride.—The commercial material was fractionally distilled in a 25-plate column and after rejection of the first 20 % of distillate the remainder (b.p. = 83·5° c.) had constant n_D^{20} (1·4449(5)) and d_4^{20}(1·2529(7)).

Analytical Methods.

Colorimetric Determination of Small Amounts of Thiophene in Benzene.—A discussion of the colorimetric methods available has recently been given by French [1] and the method employed in the present work was based on one he described. The colour-developing reagent consisted of a solution of 0·01 % w./v. of alloxan in 90·5 ± 0·5 % w./w. H_2SO_4. The optimum colour is produced in benzene containing 0·001 % by volume of thiophene and the estimation of an unknown concentration is carried out in trial dilutions and by direct comparison with a made-up standard of this strength.

The accuracy of comparison was increased approximately 5-fold with the aid of a Duboscq tintometer. To compare the thiophene concentrations of two unknown solutions, they were first diluted, by trial, until after reaction with the alloxan reagent for 30 min. both developed colours matching visually that of the standard containing 0·001 % thiophene. Fresh samples of the unknowns at these dilutions were prepared, shaken and allowed to stand with the reagent as before in stoppered tubes, and then poured into the tintometer vessels. The relationship between depth of colour and concentration was sufficiently linear for Beer's law to apply so long as the thiophene concentrations did not differ by more than 10 %. Outside this range there are changes in hu, and the accuracy of matching is lessened.

Analysis of Benzene-Thiophene and Benzene-Ethylene Dichloride Mixtures by Density Measurement.—In Part I it was shown that a colorimetric method of comparing the thiophene contents of test-distillation samples would entail an uncertainty of 0·2 plates in the value calculated for the equivalence of the column if the thiophene estimations were subject to errors of 2 %. While such an accuracy is adequate for most purposes connected with the use or testing of fractionating columns equivalent to 20-60 theoretical plates, it is clearly insufficient in the examination of samples from an equilibrium still, i.e., a one-plate apparatus. Analysis by density measurement has therefore been used in the determination of α (the volatility ratio) for the systems benzene-thiophene and benzene-ethylene dichloride over the full ranges of composition.

---

[1] French, *J. Soc. Chem. Ind.*, 1946, **65**, 15-23.

[2] Fawcett and Rasmussen, *J. Amer. Chem. Soc.*, 1945, **67**, 1705.

The technique of density measurement was briefly as follows. A 6 ml. stoppered weighing-bottle with a 3 mm. diam. capillary neck carrying an etched mark was always weighed with the usual precautions (e.g. similar wiping of the bottles, application of buoyancy corrections, etc.), against an empty " tare " consisting of a similar bottle to secure reproducibility. The weighing-bottle was filled and emptied by the use of a glass tube fitted with a rubber bulb at one end and drawn out at the other into a filament. It was cleaned before use with pure acetone and blown out with dry air.

The filled bottle was supported in a thermostat bath maintained at 20·00° ± 0·002° C. After 15 min. the liquid meniscus was brought approximately to the mark ; the fine adjustment was made by drawing a little liquid up the side of the capillary with a thin wire until the meniscus was slightly below the mark, the liquid was then allowed to flow slowly back and when the mark was reached excess liquid was removed from the capillary. The efficacy of the manipulative technique is illustrated by a comparison of two separate determinations of the weight of the standard volume of water, 6·02225 and 6·02217 g. made at the beginning and at the end of the work. Two density estimations were made on each sample and the mean value used in subsequent calculations.

TABLE I.—BENZENE-THIOPHENE.

Mol. Fn., Benzene $= x$.	d_4^{20}.	Vol. Fn., Benzene $= \dfrac{1}{1 + \dfrac{1-x}{x} \cdot \dfrac{M_T^*}{M_B}}$.	$\dfrac{d_4^{20}\text{ Thiophene} - d_4^{20}\text{ Mixture}}{d_4^{20}\text{ Thiophene} - d_4^{20}\text{ Benzene}}$.
0·00000	1·06470	0·00000	0·00000
0·10036	1·04392	0·11147	0·11193
0·19712	1·02440	0·21635	0·21706
0·29807	1·00453	0·32320	0·32409
0·38928	0·98703	0·41753	0·41835
0·50335	0·96562	0·53264	0·53366
0·62002	0·94432	0·64726	0·64839
0·70462	0·92928	0·72845	0·72940
0·80397	0·91199	0·82181	0·82253
0·89681	0·89619	0·90717	0·90765
1·00000	0·87904	1·00000	1·00000

Measurements of density at different liquid compositions for both systems, and of refractive index, n_D^{20}, in addition in the case of benzene-ethylene dichloride mixtures, were made. The samples were prepared in glass-stoppered tubes and, in weighing, a similar tube was used as tare. Buoyancy corrections were applied to the weights and the liquid. The results for the benzene-thiophene mixtures are shown in Table I.

The values in the first column were calculated from weights of components and the molecular weights of benzene, 78·11, and thiophene, 84·13. The numerical values set out in the fourth column would be volume fractions if there were no volume changes on mixing. Comparison of columns 3 and 4 shows that deviations from strict volume additivity are but small. A plot of the values in column 4 against the corresponding differences between the values in columns 3 and 4 finds convenient use in the calculation of the molar fraction of benzene in a mixture of unknown composition from the measured density. The method consists in first calculating the value of the expression (d_4^{20} thiophene $- d_4^{20}$ mixture) / (d_4^{20} thiophene $- d_4^{20}$ benzene), then finding with the aid of the plot the true volume fraction. The mol. fraction is then readily calculated. In Table II data for the benzene-ethylene dichloride system are assembled, based on a molar weight for ethylene dichloride of 98·965.

---

* M_T = mol. vol. of thiophene, M_B = mol. vol. of benzene.

Calculations from the data reveal that volume changes on mixing are considerable. The values in columns 1 and 2 were fitted by the empirical expression

$$x = 5{\cdot}09754 - 6{\cdot}57779\,(d_4^{20}) + 2{\cdot}59659\,(d_4^{20})^2 - 0{\cdot}474\,(d_4^{20})^3 \quad . \quad . \quad (1)$$

which was used for the calculation of molar fractions of benzene in mixtures of unknown composition.

Fractionation of Dilute Solutions of Thiophene in Benzene.—From the theoretical discussion in Part I it was concluded that the ratio (R) of the thiophene concentration in the still contents to that in the liquid condensate flowing back into the top of the column, at total reflux, should be constant, provided the former concentration did not exceed 1 %. Experiments were made in order to test this conclusion.

The fractionating column was 1 in. diam. and 2 ft. long containing 72 stainless steel gauze Stedman lenticular elements. It was jacketed with an electrical heater, and further protected against draughts by an outer glass tube. The boiler had a capacity of 300 ml. Mixtures of benzene and thiophene (0·075 to 1 % by vol.) were placed in the boiler. After flooding the column in the usual way, heat to the jacket and boiler was regulated so that an equal drip rate was maintained above and below the packing at a boil-up rate from the still of 400 ml./hr. These conditions were adhered to throughout. After 5 hr. of total reflux the taps at the column head and on the boiler were momentarily opened to flush out dead spaces and, after 2 hr., samples were drawn off into tubes cooled in ice. In an experiment in which, after taking samples at 7 hr., the refluxing was continued during a further 16 hr. and further samples were then taken, no significant difference was found between R for the two sets of samples. It was concluded that 7 hr. was long enough to ensure equilibrium with these dilute solutions. The results set out in Table III are for total reflux at barometric pressure.

TABLE II.—BENZENE-ETHYLENE DICHLORIDE.

Mol. Fn., Benzene $= x$.	d_4^{20}.	n_D^{20}.
0·00000	1·25297	1·4449 (5)
0·09768	1·21103	1·4500
0·19347	1·17135	1·4550 (5)
0·29815	1·12927	1·4607
0·39690	1·09081	1·4661 (5)
0·50399	1·05039	1·4721 (5)
0·61957	1·00813	1·4786 (5)
0·70389	0·97829	1·4835
0·80099	0·94471	1·4890 (5)
0·89672	0·91263	1·4948
1·00000	0·87904	1·5011

Clearly $\log_{10} R$ is constant and when the volatility ratio (α) is known the plate equivalence of the still and column (n) can be found from any of the values of $\log_{10} R$ set out above, since $n = \log_{10} R/\log_{10} \alpha$ (eqn. 10, Part I).

Determination of the Volatility Ratio (α) for Benzene-Thiophene Solutions weak in Thiophene.—The most direct method of obtaining this ratio is to examine the liquid-vapour system by means of an equilibrium still over as wide a composition range as possible and obtain α, at the extreme compositions required, by extrapolation of the experimental results. In preliminary work various types of equilibrium still were tried and found to suffer from the well-recognised failings which lead to non-reproducibility and lack of agreement, namely, fractionation of the vapours, entrainment of liquid, etc.[3, 4] The still designed by Gillespie [5] was much superior to others.

---

[3] Othmer, *Ind. Eng. Chem.*, 1943, **35**, 615.

[4] Scatchard, Raymond, and Gilmann, *J. Amer. Chem. Soc.*, 1938, **60**, 1274.

[5] Gillespie, *Ind. Eng. Chem.* (*Anal.*), 1946, **18**, 575.

The boiler was filled with benzene-thiophene solutions of suitably-chosen compositions. The immersion heater was regulated so that a boil-up rate of about 20 drops/min. was maintained but the first few drops of condensate were rejected since in most cases they contained a trace of moisture. Samples from the boiler and the condensate receiver were taken with the usual precautions, density, and hence mol fraction, was determined, and α was then calculated from the expression

TABLE III.

Vol. % Thiophene in Still Contents.	Ratio of Thiophene Conc. = R.	$\log_{10} R$.
0·075	12·27	1·089
0·082	12·42	1·094
0·158	12·21	1·087
0·173	12·31	1·090
0·243	12·50	1·097
0·282	12·50	1·097
0·382	12·76	1·106
0·416	11·98	1·079
0·545	12·04	1·081
0·607	11·79	1·072
0·776	12·79	1·107
0·793	12·31	1·090
0·955	12·04	1·081
1·100	12·12	1·084
		Mean = 1·0894 Stand. Dev. of mean = 0·0027

$$\alpha = \frac{x_t}{1 - x_t} \bigg/ \frac{x_b}{1 - x_b} \quad . \quad . \quad . \quad . \quad . \quad (2)$$

Here x_t is the composition of condensate in mol fraction of benzene and x_b that of the liquid in the boiler—see eqn. (1), Part I.

The experimental values of $\log_{10} \alpha$ plotted against x_b are shown in Fig. 1.

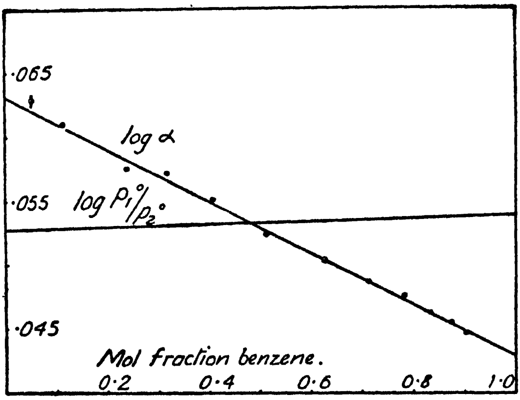

FIG. 1.—Volatility ratios for system benzene-thiophene.

The standard deviation in x_b was computed from that of the density determination (0·000006 unit) to be 0·000032 mol fraction and independent of x_b. Since x_t and x_b are nearly equal, the standard deviation in $\log_{10} \alpha$ can be taken as

$$\frac{\sqrt{2}}{2{\cdot}303} \cdot \frac{\text{Standard deviation in } x_b}{x_b(1 - x_b)} \quad . \quad . \quad . \quad . \quad (3)$$

and increases rapidly when x_b tends to 0 or 1.

Values of $\log_{10} p_1^\circ/p_2^\circ$ at the b.p. of the components (p_1° and p_2° being the vapour pressures of the pure components) derived from the data of Fawcett and Rasmussen [8] are also shown in Fig. 1 connected by a straight line.

Clearly, $\log_{10} \alpha$ is linear with mol fraction. It has already been seen (Table I) that the volume change on mixing is very small, while the molar volumes of the components at 20° c. (benzene, 88·858 ; thiophene, 79·018) are not very different. It is probable therefore that this system will show the properties of a strictly regular solution and that

$$\Delta H = kN_1 \,.\, N_2 \qquad . \quad . \quad . \quad . \quad . \quad . \quad (4)$$

where ΔH, the molar heat of mixing, $= \Delta G^E$, the excess free energy. Hence from eqn. (5), Part I,

$$\log_e \alpha = \log_e p_1^\circ/p_2^\circ - \frac{k}{RT}(1 - 2N_2) \qquad . \quad . \quad . \quad . \quad (5)$$

and $\log_e \alpha$ should equal $\log_e p_1^\circ/p_2^\circ$ at $N_2 = 0{\cdot}5$. The two curves plotted in Fig. 1 cross at a point corresponding to a mol fraction of benzene = 0·485, so that the condition is nearly satisfied by the experimental values ; although the latter are not strictly isothermal as required by (5) above.

The experimental values of $\log_{10} \alpha$ and x_b were fitted to the straight line,

$$\log_{10} \alpha = 0{\cdot}063141 - 0{\cdot}020013\, x_b \qquad . \quad . \quad . \quad . \quad (6)$$

by the method of least squares, individual experimental values being weighted according to 1/(standard deviation)^2 ; and the value of $\log_{10} \alpha$ extrapolated to

TABLE IV.

Nominal Efficiency in Theoretical Plates, n.	Standard Deviation in n.	
	For $\Delta \log_e R = 0{\cdot}02$.	For $\Delta \log_e R = 0{\cdot}10$.
10	0·21	1·01
20	0·23	1·01
30	0·27	1·02
40	0·31	1·04
50	0·36	1·05
60	0·41	1·07

$x_b = 1$ using Birge's method [6] is 0·04313, with a standard deviation of 0·00026. Since $\log_{10} \alpha$ varies by only 0·00020 between thiophene contents of 0 and 1 %, it may be taken as constant over this range, as was indicated by the values of R in Table III. The corresponding value for α is 1·1045.

Accuracy of Plate Equivalence Determinations with Dilute Solutions of Thiophene in Benzene.—Taking $\log_{10} \alpha = 0{\cdot}04313$ and from Table III, the mean value of $\log_{10} R = 1{\cdot}0894$, the plate efficiency of the still and fractionating column used, $n = \dfrac{\log_{10} R}{\log_{10} \alpha} = 25{\cdot}3$ plates (standard deviation 0·15).

It may be shown that the standard deviation in n, under the limitations considered, is given by $\sqrt{101{\cdot}35(\Delta \log_e R)^2 + 3{\cdot}63 \times 10^{-5} \,.\, n^2}$ and in Table IV are set out computed values of deviations to be expected in practical cases, taking $\Delta \log_e R = \dfrac{\Delta R}{R} = 0{\cdot}02$ (the accuracy to be expected in a single determination of $\log_{10} R$ with colorimetric comparison) or $\Delta \log_e R = 0{\cdot}10$ (for visual comparison).

Volatility Ratio and Heat of Mixing in Thiophene-Benzene System.—As shown in Part I the areas intercepted between the lines plotted in Fig. 1 should be approximately equal since the data are substantially isothermal and it can be seen at once since the lines are straight and cross at a mol fraction (benzene = 0·485) that this is the case—the difference being 7 % of the total. Moreover, using the data plotted in Fig. 1 and eqn. (6) in Part I, with $\Delta G^E \sim \Delta H$, the calculated heat of mixing for a solution containing 0·47 mol. fraction of benzene is 4·0 cal./g. mol. (compared with 5·0 cal./g. mol. found experimentally). The experimental $\log_{10} \alpha$ curve is thus not inconsistent with thermodynamic requirements.

---

[6] Birge, *Physic. Rev.*, 1942, **40**, 207.

Volatility Ratios for the Ethylene Dichloride-Benzene System.—Mixtures of ethylene dichloride and benzene have been extensively used in testing laboratory fractionating columns although doubts regarding the accuracy or self-consistency of published volatility ratios have not been resolved.[7, 8] Casual inspection of the most recent data [8] shows that they do not pass the test for thermodynamic consistency developed in Part I.

In our re-examination of this system the experimental technique was the same as with benzene-thiophene mixtures and the results are plotted in Fig. 2 ($\log_{10} \alpha$ against x_b). The standard deviation of $\log_{10} \alpha$ may be obtained from eqn. (3) by insertion of 0·000045 for the standard deviation of x_b and is indicated at extreme points on the curve. While the $\log_{10} \alpha$-x_b curve has the same general form as that recorded previously,[8] application of the area-intercept test shows a difference amounting to only 4 % of total area, which may be taken as satisfactory.

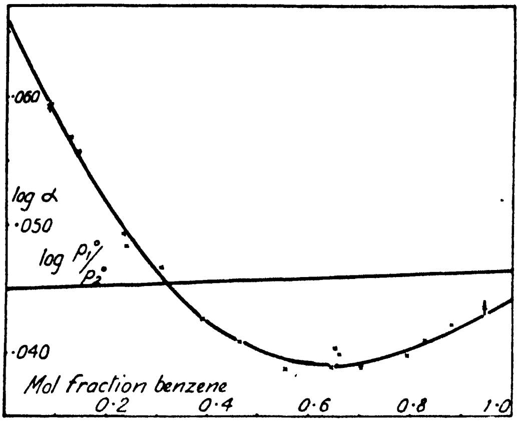

FIG. 2.—Volatility ratios for system benzene-ethylene dichloride. Standard deviation shown by the length of the vertical line.

The Supposed Ideality of the Ethylene Dichloride-Benzene System.—It has been suggested [9] that this system, frequently quoted as an ideal one,[10] actually owes its properties to opposing heat and entropy effects. There is strong evidence that this is the case. The volume change on forming an equimolar mixture is approximately 15 times that observed with a mixture of benzene and thiophene ; i.e., $\frac{V_m}{V_0} \times 100$ is 0·30 against 0·0195 for benzene-thiophene, where V_m is vol. change per mol of mixture and V_0 the volume of unmixed components. It is to be expected, therefore, that the entropy change on mixing may not be equal to that for an ideal solution, i.e. $\Delta G^E \neq \Delta H$. The molar heat of mixing, at 0·26 mol fraction of benzene, has been reported [11] as 17·5 cal./g. mol. at 15-20° C. and a redetermination gave a value of 13 cal./g. mol., which confirms the magnitude of the heat effect. However, ΔG^E obtained by calculation from eqn. (6) Part I, is only 4·9 cal./g. mol. so that $T\Delta S^E = 12{\cdot}6$ cal./g. mol. In short, $|\Delta G^E| < |\Delta H|$ and $|\Delta G^E| < |T\Delta S^E|$, and the behaviour of the system is more nearly ideal than would be expected from considering the magnitudes of the excess heat or excess entropy of mixing separately.

Determination of Plate Equivalence of the Column and Still with an Ethylene Dichloride-Benzene Mixture.—As the use of a benzene-thiophene mixture for measuring fractionating efficiency has novel features, a direct com-

---

[7] Carlson and Colburn, *Ind. Eng. Chem.*, 1942, **34**, 1533.

[8] Bragg and Richards, *ibid.*, 1942, **34**, 1088, 1533.

[9] Glasstone, *Text-book of Physical Chemistry* (Macmillan & Co. Ltd.), 1947, 711.

[10] Guggenheim, *Trans. Faraday Soc.*, 1937, **33**, 151.

[11] Baud, *Bull. Soc. Chim.*, 1915, **17**, 329.

parison of the method against the orthodox procedure with ethylene dichloride-benzene mixtures was desirable. By employing one and the same fractionating equipment the comparison is limited strictly to the behaviour of the two mixtures.

The test distillations were carried out in the usual way but analysis of the samples was by refractive index (the still-head sample was too small for analysis by density) the mol fraction being determined from a plot of the refractive index-mol fraction data assembled in Table II.

Calculation of the plate efficiency was made algebraically from the Fenske equation by a stepwise procedure, the appropriate value for $\log_{10} \alpha$ at each step being taken from Fig. 2. The results for four separate determinations are set out in Table V.

TABLE V.

x_b.	x_t.	n.
0·1385	0·725	27·51
0·2595	0·8226	27·21
0·3985	0·8925	27·28
0·3433	0·868	27·20
		Mean = 27·30 Stand. Dev. of mean = 0·07

The agreement of these values among themselves, embracing as they do a good range of concentrations, is satisfactory support for the α values obtained with the equilibrium still. The difference in the rating of the still and column, 27·3 plates with ethylene dichloride-benzene against 25·26 with benzene-thiophene, is significant and is inherent in the theoretical plate concept.

Scope of Benzene-Thiophene Test Mixtures.—Working between concentrations of 1 % and 0·001 % thiophene, in the boiler and at the still head, the maximum fractionating efficiency which it is convenient to estimate by the technique outlined is clearly the equivalent of $\dfrac{\log_{10} 10^3}{0{\cdot}04313}$ (= 69·5) theoretical plates.

Preparation of a Test Mixture from Crude Benzole.—A commercial sample of No. 1 benzole of n_D^{20} 1·4995, and containing 0·17 % by vol. of thiophene gave a normal colour test with the alloxan reagent. When, however, it was placed in the 25-plate fractionating equipment the colour reaction of a sample taken from the still head after a period of total reflux was abnormally yellow and clearly the No. 1 benzole contained some light component which interfered with the alloxan-thiophene estimation. This contaminant was removed by first fractionating the benzole with the column and rejecting the first 20 % and the last 10 %; the middle fraction was refractionated and the first 50 % of distillate rejected again. The residue in the still now contained 0·18 % of thiophene and, after allowing a period of total reflux, samples were taken from the still head and the boiler and the ratio of thiophene contents was determined colorimetrically, as in previous test distillations. From this ratio the efficiency of the still and column was calculated to be equivalent to 24·8 theoretical plates—agreeing well with the results of tests made with mixtures of pure benzene and thiophene.

Purification of Benzene from Thiophene by Fractional Distillation.—To reduce substantially the thiophene content of an impure thiophene-containing benzene, by fractional distillation alone, would require equipment of considerable effectiveness. An approximate calculation on the basis of the volatility ratio as now determined, i.e., $\log_{10} \alpha = 0{\cdot}04313$, indicates that a stripping column equivalent to 70 theoretical plates run at a very high reflux ratio would furnish from 100 parts of benzene containing 0·1 % thiophene, 90 parts of benzene with a thiophene content reduced to 0·001 %. In practice, many more plates would be necessary to get this result.

Thanks are due to Mathematics Division, National Physical Laboratory, for derivation of eqn. (1), giving mol fraction in terms of density for benzene-ethylene dichloride mixtures and for preparing an interpolation table.

The work described in Parts I and II forms part of the programme of the Chemistry Research Board and is published by permission of the Director, Chemical Research Laboratory. A preliminary report on the test for consistency of data on the volatility ratio (Part I, Fig. 1) has appeared elsewhere.[12]

Summary.

The volatility ratios of the components in binary mixtures of benzene with thiophene and with ethylene dichloride have been measured through the entire concentration ranges and the results have been expressed graphically. The measured volatility ratios are shown to be consistent with thermodynamic requirements. The benzene-thiophene solutions are not ideal, but approximate to " strict regularity " as defined by Guggenheim and Fowler.

If a colorimetric method of analysis is adopted solutions containing less than 1 % of thiophene in benzene can be used to determine the plate equivalence of fractionating columns with efficiencies up to 65 plates (probable error less than 0·3 plate). The method may be used for both laboratory and large scale fractionating equipment since a fraction from No. 1 benzole can be employed as the thiophene-containing benzene solution.

The data for the thiophene-benzene system can be used to estimate the plate efficiency required to prepare a benzole fraction of any chosen thiophene content from a crude benzole.

Chemical Research Laboratory,
D.S.I.R.,
Teddington,
Middlesex.

---

[12] Herington, *Nature*, 1947, **160**, 329.

AN AMPLIFIER FOR USE WITH CONDUCTANCE BRIDGES.

BY D. J. G. IVES AND R. W. PITTMAN.

Received 23rd July, 1947.

The use of high-gain audio-frequency amplifiers with null-point detectors for conductance measurements is attended by difficulties which limit sensitivity, so that increase of amplification beyond a certain point may defeat its own object. Interference is outstanding as such a difficulty. It mainly occurs because of the interception of stray fields by the bridge network but may also arise in the amplifier itself. The effects of such interference are commonly reduced by screening, earthing and the use of discriminating detectors, such as the ear or the cathode ray oscillograph. The use of frequency discriminating networks of the type recommended by Jones and Bollinger [1] has been considered and found to be unsatisfactory in many respects. In particular, such networks should be in a part of the circuit where the power-handling requirements are small, and will not therefore deal with interference arising in following amplification stages. If, contrary to this, the network is placed in the output stage of a high-gain amplifier, very grave deterioration of stability will occur. The construction of non-standard components of rigid specification is, perhaps, the decisive disadvantage.

Earthing requires particular care, since it may well aggravate the trouble by conveying interference to the amplifier by cathode, as well as grid, swing. Large differences and fluctuations of potential may occur between various connections commonly used for earthing, and it is therefore essential to use only one " earth " for all sections of the bridge and its ancillary equipment. Even when all these precautions have been taken as far as possible, interference still remains as a standing obstruction to the achievement of high sensitivity.

---

[1] *J. Amer. Chem. Soc*, 1929, **51**, 5413.

An alternative method of attack on the problem was suggested by the balanced valve voltmeter described by Hartshorn.[3] It consists of the duplication of part, or all, of the amplifying equipment, so that two amplifying channels become available. One of these channels, the signal amplifier, is supplied with the required signal from the bridge, together with its inseparable interference. The other channel, the balancing circuit, is fed with interference alone, deliberately collected by an aerial system in the close vicinity of the bridge. At some stage in the amplifier before the final output, these two channels are mixed in such a way that self-cancellation of the interference occurs, leaving the signal unobscured. The full circuit diagram of an amplifier incorporating this device is shown in Fig. 1, which requires no detailed explanation. The aerial, W, consists of a few feet of insulated wire hung above the bridge. The controls X, Y and Z of the balancing circuit are mutually dependent in adjustment, so that any one of them may be used to tune the interference noise to a minimum, which, under favourable conditions, may be quite sharp. The control of the magnitude and phase of the interference input is critical; quite different settings of the controls X and Y are required according to whether adjustments of the bridge itself, or of the associated Wagner earthing circuit is being made. As shown, the amplifier feeding a small loudspeaker appears to be sensitive to a few microvolts at 1200 to 5000 cycles and allows a bridge-setting to be made with a precision of the order of two parts per million, a limit which was found to be unapproachable, under the local conditions, with a " straight " high-gain amplifier.

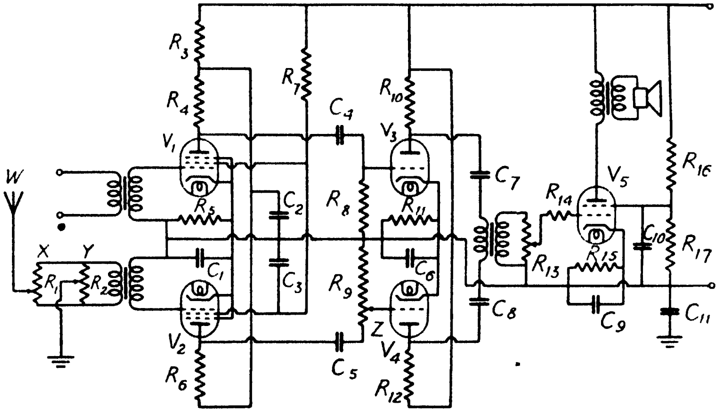

FIG. 1.

Schedule of Components.

R_1	2,000 Ω	C_1	25 μF.	R_{10}	20,000 Ω	C_{10}	8 μF.
R_2	1,000 Ω	C_2	8 μF.	R_{11}	500 Ω	C_{11}	2 μF.
R_3	20,000 Ω	C_3	8 μF.	R_{12}	20,000 Ω		
R_4	200,000 Ω	C_4	0·05 μF.	R_{13}	0·5 M Ω	V_1	6J7
R_5	1,000 Ω	C_5	0·05 μF.	R_{14}	100,000 Ω	V_2	
R_6	200,000 Ω	C_6	25 μF.	R_{15}	200 Ω	V_3	6C5
R_7	0·5 MΩ	C_7	0·05 μF.	R_{16}	20,000 Ω	V_4	
R_8	0·5 MΩ	C_8	0·05 μF.	R_{17}	20,000 Ω	V_5	KT33C.
R_9	1·0 MΩ	C_9	25 μF.				

---

[3] *Radio-frequency Measurements*, 1941, 90.

It is probable that improvements in the circuit could readily be made in fairly obvious ways, but in its present form the amplifier has been found an indispensable component of a sensitive bridge, and may possibly have other applications.

Summary.

An amplifier for use in conjunction with conductance bridges is described, sensitive to a few microvolts of audio-frequency potential. It incorporates a device for suppressing interference and is particularly suitable for measurements of high precision under unfavourable local conditions.

Birkbeck College,
*E.C.*4.

PHYSICO-CHEMICAL PROCESSES OCCURRING AT HIGH PRESSURES AND TEMPERATURES. PART I. INTERACTION BETWEEN TRINITROTOLUENE AND AMMONIUM NITRATE.

BY JOHN L. COPP AND A. R. UBBELOHDE.

Received 11*th August*, 1947.

When a shock wave passes through a system, there is a local rise of pressure and temperature at the front of the shock wave. If a system is composed of molecules which decompose on heating, with liberation of energy, a shock wave which is sufficiently intense can lead to extensive thermal decomposition, and the energy liberated can maintain detonation. A detonating system is characterised as a chemical reaction, that results in the rapid release of energy in a form capable of doing work on its surroundings. For detonation to be set up in an aggregate of complex molecules, such as organic nitro-compounds, it is essential that in consequence of a suitable applied stimulus, the molecular units undergo a rapid, exothermic, self-propagating reaction. The conditions for detonation to be stable will not be discussed here, except to point out that the release of energy in such a reaction must be so rapid that the product gases, as formed, are driven in the direction of propagation with adequate mass-flow velocity, and that detonation is then manifest as a sharp increase in pressure and temperature at the boundary between the unexploded and exploded material, which moves through the mass of the explosive with a velocity of the order of several km./sec.

Stable detonation was first treated theoretically as a problem in hydrodynamics, by assuming that an actual discontinuity of temperature and pressure occurred at the head of the detonation wave. By solution of the equations of conservation of mass, energy and momentum across the discontinuity with respect to pressure and temperature, together with the Hugoniot equation, Chapman[1] and Jouguet[2] provided an adequate treatment of an infinite plane wave of detonation in a perfect gas, in which the detonation velocity was determined solely by the initial and final states of the molecules reacting, and was independent of the rate of chemical decomposition. This treatment proved inadequate when applied to velocity data for detonation in solid and liquid systems, for two reasons.

---

[1] Chapman, *Phil. Mag.*, 1899, **47**, 90.

[2] Jouguet, *J. Math.*, 1905, **1**, 347. *Mecanique des Explosifs*, Doin (Paris, 1917).

(i) It did not account for the very general linear relation which is found to hold between detonation velocity D and the loading density d of such systems. Becker,[3] Schmidt [4] and other workers have shown that the hydrodynamic treatment of detonation accounts for this linear dependence, when it is assumed that the gaseous products of detonation conform to the Abel equation of state, $p(V - b) = RT$, where b is a covolume term, i.e. when allowance is made for the finite volume occupied by the molecules. Abel's equation in essence corresponds with van der Waals' equation at high temperatures.

(ii) Experimental velocities of detonation are not in general determined solely by the nature of the explosive and its loading density, but are dependent for example on factors such as the radius, material, and thickness of cylindrical tubes surrounding the explosive charge. This fact indicates that the energy release, which accompanies thermal decomposition of explosive molecules in the front of a plane detonation wave, does not occur instantaneously.

To account for the effects observed, various physico-chemical conditions may be investigated which control the thermal decomposition and rate of energy release from molecules of explosive. In fact, the experimental study of velocities of detonation, and their dependence on the above factors, can be used to investigate the physical chemistry of reactions at high temperatures and pressures, provided the data are sufficiently refined to permit calculations of the deviations from the simple theories of Chapman, Jouguet, Becker, and Schmidt.

The experimental methods and calculations described in this paper involve systematic measurements of the influence of the boundary conditions on the detonation velocity of charges of finite radius. They were evolved concurrently with theoretical considerations due to Sir Geoffrey Taylor, Dr. H. Jones,[5] Dr. Devonshire, and others, during the period 1942-1945. A brief and rather simplified review of the formulæ used is as follows.

The Effect of Boundary Conditions on the Detonation Velocity of Charges of Finite Radius.

Behind the very steep pressure-temperature gradient at the front of a detonation wave, the molecules of explosive are activated by random collisions, by the collisions due to mass flow in the hydrodynamic shock wave, and possibly by radiation. As a result, they decompose exothermically during a small but finite time interval $\bar{t}$, after which the reaction products may be considered as in thermodynamic equilibrium. A " reaction-zone thickness " X may be defined by the relation $X = D\bar{t}$.

The essential feature of any theory which discusses the relation between an observed detonation velocity D and the boundary conditions of the charge is that owing to the high pressures behind the detonation front, the products of detonation will expand laterally.

If this expansion is at all appreciable during the reaction time $\bar{t}$, it will modify the detonation velocity, because (1) part of the energy released is used up in producing the lateral expansion, and does not therefore contribute to propagation of the detonation wave, and (2) the peak temperature and pressure are lower than when lateral expansion can be neglected.

Dimensional considerations indicate that the ratio D/D_0, where D_0 is the detonation velocity when lateral expansion is negligible, will be a function of R_t/R, where R_t is the expanded charge radius at the end of the time $\bar{t}$, and R is the initial charge radius.

---

[3] Becker, *Z. Schiess. Spreng.*, 1932, **27**, 226.

[4] Schmidt, *ibid.*, 1935, **30**, 364; 1936, **31**, 8, 37, 80, 114.

[5] Jones and co-workers, Ministry of Supply Reports, 1941, 1943, 1944. (Since writing this paper part of the theoretical work has been published, *Proc. Roy. Soc. A*, 1947, **189**, 415).

The rate at which the lateral expansion can occur will depend on the nature of the confinement at the surface of the charge. The actual relationship between the observed detonation velocity and the confinement at the surface is rather complex, owing to the complex factors which control the rate of expansion of a charge of explosive after detonation. The problem can be simplified in three cases.

(i) " BARE CHARGES," for which the rate of lateral expansion of the products of detonation is determined merely by the movement of the shock waves in the hot gases, and in the atmosphere surrounding the charge.

In this case it has been shown [5] that

$$(D_0/D)^2 = 1 + 9/4[\phi^4(X/R) - 1].$$

The function ϕ takes the form

$$\phi(X/R) = 37/20[1 - X/R \cot \theta]$$

with θ given by

$$X/R = 34/37 \, [\sin \theta/(1 + \cos \sqrt{2}\theta)].$$

When X/R is small, as in the practical applications below, the plot of $(D_0/D)^2$ or $(1/D)^2$ against $1/R$ gives a straight line, from which X is evaluated by numerical solution of the above equations.

(ii) CHARGES WITH " LAMINAR " CASES.—When the casing of a charge is sufficiently thin, and is of comparatively high density, the rate of lateral expansion of the products of detonation is determined by the rate at which this thin (laminar) casing can be pushed outwards. In practice, this refers to thin casings of metals such as steel. If S is the mass of the case forming the boundary, per unit surface area of the charge, it has been shown [5] $(D_0/D)^2 = 1 + 9/8 \, X^2d/RS$ where d is the density of the charge.

Here again a linear plot should be obtained between $1/D^2$ and $1/R$, but the constants of the linear equation involve X in a different way, and furthermore they depend upon the experimentally accessible variable S. Qualitative confirmation of this dependence was obtained (Fig. 2) but the data have not been used for quantitative computation of X, since it is difficult to obtain precise experimental criteria to show that the casing behaves as a true " lamina."

It was however possible to test experimentally how thick the casing had to be to attain limiting condition (iii).

(iii) THICK CASES.—These are taken as being so thick that the shock wave, which is set up in the casing material owing to the compression of its internal wall by the expanding gases, does not reach the outside of the case within the time $\bar{t}$. A satisfactory experimental test is that further increase in the thickness of casing material makes no further difference to the relation between D and R. In this instance the internal wall of the case merely bulges outwards by compressing the casing material. There is no mass motion of the case as a whole during the reaction time $\bar{t}$. As a first approximation, where X/R is small, and B the angle between the expanded inner wall and its original direction is small (cf. Fig. 1 (*b*)).

$$\left(\frac{D_0}{D}\right)^2 = 1 + 9X \, (\tan B)/R$$

or

$$1/D^2 = 1/D_0^2 + 9D\bar{t} \, (\tan B)/RD_0^2. \quad . \quad . \quad (3)$$

Values of the expansion angle B have been calculated for various metals from Bridgman's compressibility data [6] (which however refer to static pressures), assuming expansion pressure of the order of 10^6 kg./cm.^{2}. For purposes of extrapolation the coefficients, determined by Bridgman for the equation for solid substances

$$(V_0 - V)/V_0 = ap - bp^2 \quad . \quad . \quad . \quad . \quad (4)$$

[6] Bridgman, *The Physics of High Pressures* (Bell & Sons, London, 1931).

were substituted in the equation of state obtained by Bridgman for liquids

$$(V_0 - V)/V_0 = \{a^2 \log_e (1 + 2bp/a)\}/2b. \quad . \quad . \quad (5)$$

Eqn. (5) is equivalent to eqn. (4) over the range of data obtained by Bridgman, but is more satisfactory for extrapolation.

The extrapolation from 12,000 kg./sq. cm. (the maximum pressure recorded by Bridgman) to 100,000 kg./sq. cm. (the approximate pressure set up by shock waves in the charge casings) involves a compression which is about 200 % of that from 0 to 12,000 kg./sq. cm. Possible differences between static compressibilities obtained by Bridgman, and the dynamic compressibilities involved in the compression of the inside of thick metal casings during detonation are ignored, since no experimental values of dynamic compressibilities are yet available. The important point to notice about this expression is that the relationship between D/R and $1/D^2$ is of the same form for all metals: only the constants vary. A similar relationship between D/R and $1/D^2$ (or between $1/R$ and $1/D^2$, since in the cases investigated $D \simeq D_0$) had in fact been obtained by us by a semi-empirical argument, and had been confirmed experimentally, before the detailed theory was available.

For evaluating experimental data (i) the fact that a linear relationship between $1/R$ and $1/D^2$ is predicted for bare charges, and for heavily confined charges a linear relationship between D/R and $1/D^2$, is of great convenience in permitting linear extrapolation to $R = \infty$, so as to evaluate D_0. This linear relationship is however so general that it cannot be regarded as a complete test of any detailed theory of the effects of boundary conditions on observed detonation velocities. On the other hand, if the values of $\bar{t}$, calculated by a particular theory from the appropriate constants for very different boundary conditions, are in reasonable agreement, this may be regarded as strong support for such a theory. (ii) To obtain the maximum spread of experimental data from which to establish the line of closest fit, for the plot of $1/D^2$ against $1/R$ for bare charges, or of $1/D^2$ against D/R for heavily confined charges, rather small values of R (below 1 cm.) would be preferable. On the other hand with many explosive mixtures, for which the reaction time $\bar{t}$ is of greatest interest, cast charges of uniform composition, and stable detonation can only be obtained under a wide range of boundary conditions, for rather large values of R (above 3 cm.).

Since it is essential to make measurements under stable conditions of detonation, large charge radii have been used in much of the work described below. Although space restricts a discussion of the experimental tests used, a "stable detonation wave" is one which continues to travel over any length of a uniform charge without acceleration or "fading." Experimental tests have been made to verify that this condition holds for all the detonating systems described below, for lengths of charge up to 20 charge diameters or more.

The use of charges of large radii limited the methods of timing the velocity of the detonation wave. With the charges of from 2 to 7 lb. of explosive which were used, only the Dautriche method was applicable at the time the experiments were carried out. The resulting limitation on the accuracy of the individual data is discussed below.

Experimental.

Detonation velocities of cast explosive charges were determined by the method first described by Dautriche.[7] In the technique adopted in our experiments, the mid-point of a length of cordeau detonant, of known detonation velocity V in m./sec. is placed over a fiducial line scribed on a lead strip 30 × 10 × 0·75 cm., and about 25 cm. of the fuse is fixed along the axis of the lead strip by adhesive tape. The free ends of the fuse are inserted in two holes drilled in the charge

[7] Dautriche, *Compt. rend.*, 1906, **143**, 641.

to a depth equal to the charge radius, and any convenient distance L cm. apart. A special cordeau containing P.E.T.N. manufactured by Messrs I.C.I. was used in many firings. It was found to be preferable to cordeau containing powdered T.N.T. for "picking-up" from feeble detonation waves, e.g. in the mixtures of T.N.T. with inert fillers. On firing the cylindrical charge from one end, a detonation wave is set up in the explosive column, and after travelling a short distance determined by trial, it proceeds down the column with a constant velocity of D m./sec., the detonation velocity. Detonation is set up in the two ends of the fuse with a time interval between the events of $L/D \times 10^{-2}$ sec., provided the wave remains uniform so that the "pick-up" times are the same at the two ends of the cordeau.

The plane of impact of the detonation waves travelling in the two branches of the fuse which is recorded as a sharp line on the lead strip, is displaced a distance m cm. from the fiducial line, such that $2m = VL/D$; i.e. $D = LV/2m$ The distances L and m can normally be measured to within ± 0·025 cm. : V, the detonation velocity of the fuse is calibrated independently to an accuracy of ± 20 m./sec. by means of an Argon Chronoscope. D, the average detonation velocity of the explosive filling over the distance between the two fuse inserts, is calculated from the above expression. Implicit in this calculation is the assumption that the difference in "pick-up" times for the two ends of the fuse is zero, which is true if the wave travels under uniform conditions between these points.

Statistical analysis of the large number of values of detonation velocity reported in this paper showed that this method is capable of providing a *mean* velocity of detonation for 10 or more individual shots within limits of about ± 50 m./sec. These limits are taken as twice the standard error, $\sigma/\sqrt{n}$, in the sample mean $\bar{D}$ of n determinations, and there is a 19 to 1 chance that these limits will include the "true" detonation velocity. The standard deviation σ of the normal population from which the experimental sample of n values is drawn, is estimated by means of the expression :

$$\sigma^2 = \Sigma(\bar{D} - D)^2/n(n - 1).$$

Detonation velocities discussed in these papers refer to *mean* values for about 10 individual records, for charges of cast trinitrotoluene (T.N.T.), and for charges of cast T.N.T. mixed with various inorganic materials. Part I of this paper deals with a mixture (60/40 ammonium nitrate/T.N.T.) in which the inorganic material may participate in energy release in the detonation zone. Part II deals with the effect on the detonation properties of cast T.N.T. of admixture with various substances which are chemically inert.

Results.

60/40 Amatol Containing "Coarse Grist" Ammonium Nitrate.

Approximately 1000 lb. of 60/40 Amatol, supplied from Service stocks, were used in these experiments. The explosive mixture had an average composition by weight of 60·0 % ammonium nitrate and 40·0 % of T.N.T. (setting point > 80·4° c.). The average sieve analysis of the ammonium nitrate incorporated in molten T.N.T. in the production of the Amatols is given above in Table I.

TABLE I.—SHOWING THE WEIGHT PERCENTAGE OF AMMONIUM NITRATE RETAINED ON B.S. SIEVES.

Sieve No.	25.	52.	72.	100.	200.
Sieve aperture in mm.	0·599	0·295	0·211	0·152	0·076
% Retained "Coarse Grist" NH_4NO_3.	4	26	50	69	95
% retained "Fine Grist" NH_4NO_3 (see below)	0	0	7	26	89

Assuming that the individual grains of ammonium nitrate are cubical, an estimate of the surface area of 1 g. "coarse" ammonium nitrate was calculated to be 195 sq. cm.

In the fabrication of experimental charges, lump Amatol as supplied in Service was heated in a steam-jacketed stainless steel pan to obtain a suspension of ammonium nitrate in molten T.N.T. This material was stirred continuously to prevent segregation, and the viscous suspension was loaded into the appropriate cylindrical tubes of seamless steel, seamless lead, or light cardboard impregnated with Bakelite, and allowed to solidify. The finished cast charge was weighed, its dimensions recorded, and the charge density calculated. The mean charge density recorded for cast 60/40 Amatol (coarse) was 1·50 g./cc. Samples taken from different points in a cast charge show a fluctuation in composition not exceeding ± 1 % axially, and not exceeding ± 2 % radially.

The charge was then primed with 30 g. of a sensitive plastic explosive at one end, and the holes to receive the ends of the fuse drilled to a depth equal to the charge radius. The experimental lay-out prior to detonation is illustrated in Fig. 1 (*a*). Fig. 1 (*b*) gives a conventional representation of the conditions behind a detonation wave front in a heavily confined system.

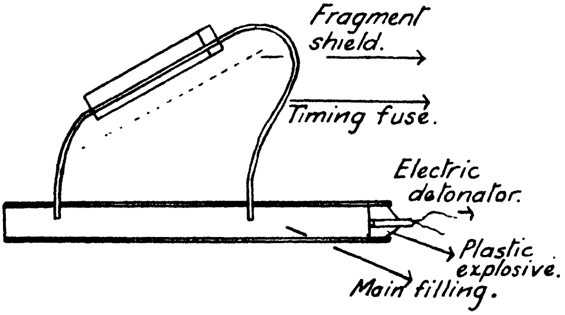

FIG. 1 (*a*).—Experimental lay-out for measuring detonation velocities by the Dautriche method.

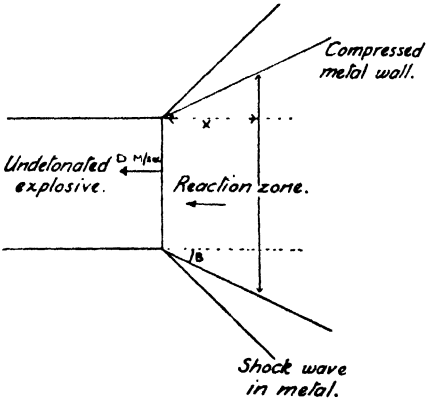

FIG. 1 (*b*).—A representation of the reaction zone for a charge confined in a thick-walled metal tube.

A summary of the mean detonation velocities recorded for cast 60/40 Amatol confined in cylindrical tubes of steel, lead, and cardboard (the last approximating to an unconfined or bare charge) together with other relevant information is given in Table II.

Data are plotted in Fig. 2, to illustrate the dependence of D on wall-thickness of steel tubes surrounding the explosive, for three different radii. The data for cardboard confinement are conveniently taken as giving the origin (for steel of zero thickness). It will be seen that at constant radius, the measured detonation velocity increases with wall thickness up to about 0·3 cm. Thereafter further increase in wall thickness up to a value of 1·3 cm. results in no significant change

TABLE II.—THE DETONATION VELOCITY IN m./SEC. OF 60/40 AMATOL FOR VARIOUS BOUNDARY CONDITIONS.

Average charge density 1·50 g./cc.
Calculated surface area of ammonium nitrate :—

(*a*). 195 sq. cm./g. for coarse grist.
(*b*) 310 sq. cm./g. for fine grist.

Charge Radius R(cm.)	Case Thickness Z(cm.)	Case Inertia S(g./sq. cm.)	No. of Independent Results n.	Mean V of D m./sec.	Confidence Limits. $\pm 2\frac{\sigma}{\sqrt{n}}$.
"Coarse grist" ammonium nitrate.					
(1) *Seamless Steel Tubing.*					
1·27	0·64	5·55	8	5730	± 50
1·59	1·30	14·00	5	5900	± 80
1·70	0·55	4·70	11	5860	± 70
1·70	0·47	3·82	29	5920	± 50
1·63	0·28	2·30	7	5800	±100
1·71	0·17	1·46	10	5780	± 70
1·87	0·13	1·15	7	5750	±100
1·54	0·05	0·41	6	5610	±100
2·54	1·27	12·50	9	6080	± 90
2·52	0·50	4·15	24	6010	± 60
2·54	0·13	1·10	13	5930	± 90
2·52	0·05	0·43	14	5750	± 50
3·78	1·30	11·90	4	6140	± 70
3·92	0·51	4·72	7	6210	± 80
3·83	0·23	1·88	7	6140	±110
(2) *Seamless Lead Tubing*					
1·25	0·62	8·80	6	5460	± 80
1·60	1·25	19·20	6	5510	±100
1·62	0·62	8·90	6	5540	± 60
2·54	1·26	17·70	18	5790	± 70
2·52	0·82	11·20	10	5880	± 40
2·52	0·25	3·15	4	5810	±180
(3) *Thin Cardboard Tubing*					
1·90	0·1	0 approx.	8	5110	± 90
2·52	0·1	0	15	5570	± 90
*2·52	0·1	0	9	5570	±120
3·56	0·1	0	11	5680	±110
"Fine grist" ammonium nitrate.					
(4) *Seamless Steel Tubing*					
1·70	0·45	3·76	13	6060	± 40
2·60	0·42	3·74	8	6210	± 70
(5) *Thin Cardboard Tubing*					
1·62	0·1	0 approx.	5	5380	± 90
2·22	0·1	0 approx.	8	5680	± 80

* Timing points at the surface of the charge.

in detonation velocity. For each value of wall-thickness, the detonation velocity is the greater, the larger the charge radius.

The less extensive results in Table II for charges confined with lead tubes (not plotted) again show that the detonation velocity of cast 60/40 Amatol increases to a limiting value, characteristic of the charge radius, as the wall-thickness is increased to a value intermediate between zero and 0·3 cm. It is further noteworthy that this limiting velocity at constant radius observed for charges confined by lead is less than for steel-confined charges, despite the much greater inertia of the lead walls. As explained above, this is because the compressibility of the metal controls the effective confinement. These experimental data show quite definitely that the detonation velocity of 60/40 Amatol is not a unique value (as the classical hydrodynamic theory of detonation in solid and liquid explosives demands) but that it varies in a characteristic manner with changes in the charge radius, wall-thickness, and material of the charge envelope.

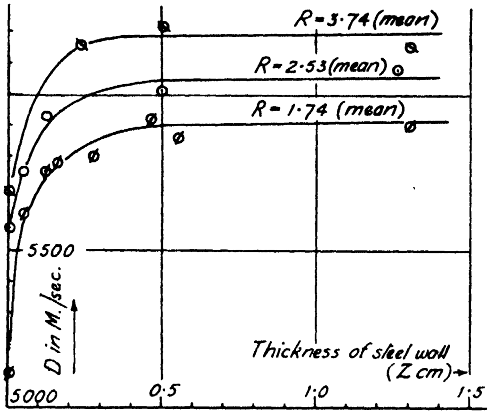

FIG. 2.—The effect of thickness of steel wall on D for 60/40 Amatol (coarse NH_4NO_3), at three charge radii.

60/40 Amatol Containing "Fine Grist" Ammonium Nitrate.

A short series of experiments was also carried out to determine what effects changes in the grist of the ammonium nitrate have on the detonation velocity of 60/40 Amatol. Commercial ammonium nitrate (Billingham) was dried at 100° C., ground in a Kek-mill and incorporated in molten T.N.T. in the proportion by weight of 60 parts ammonium nitrate to 40 T.N.T. (cp. Table I for grist sizes). This mixture was cast into cardboard tubes, and also into thick-walled steel tubes, and the detonation velocities were measured by the Dautriche method. The details of these measurements are set out in Table II.

Discussion.

(i) Effect of Boundary Conditions on *D* (cp. results in Table II).

Bare Charges (coarse grist 60/40 Amatol.)—The detonation velocities of 60/40 Amatol in bare charges may for practical purposes be equated to the experimental values of D recorded for cardboard-confined charges of three radii, since increasing the thickness of the cardboard does not affect D appreciably. The experimental values of D can be related with the charge radius R according to the line

$$1/D^2 = 10^{-12}(2{\cdot}36 + 2{\cdot}66/R) \qquad . \quad . \quad . \quad (6)$$

D being expressed in cm./sec.

Light Confinement.—Inspection of the curves in Fig. 2 shows that in the region where dD/dZ is changing rapidly, the value of D is a function of both R and S. as is required by the theoretical equation (2). The number of experimental points in this region is however insufficient to test this relationship in quantitative detail.

Heavy Confinement. (Coarse grist 60/40 Amatol).—For wall thicknesses of steel or lead greater than 0·3 cm., D is substantially a function of R only, and is independent of S. The experimental data for steel walls fit the calculated line of closest fit:

$$1/D^2 = 10^{-12}\,(2{\cdot}40 + 0{\cdot}15D \times 10^{-5}/R) \qquad . \quad . \quad (7)$$

and for lead walls, the line

$$1/D^2 = 10^{-12}\,(2{\cdot}44 + 0{\cdot}24D \times 10^{-5}/R) \qquad . \quad . \quad (8)$$

where D is expressed in cm./sec.

These equations, of the same form as the theoretical equation (3), are plotted in Fig. 3.

For the fine grist Amatol, the straight lines joining the experimental points are for bare charges

$$1/D^2 = 10^{-12}(2{\cdot}37 + 1{\cdot}80/R) \qquad . \quad . \quad . \quad (9)$$

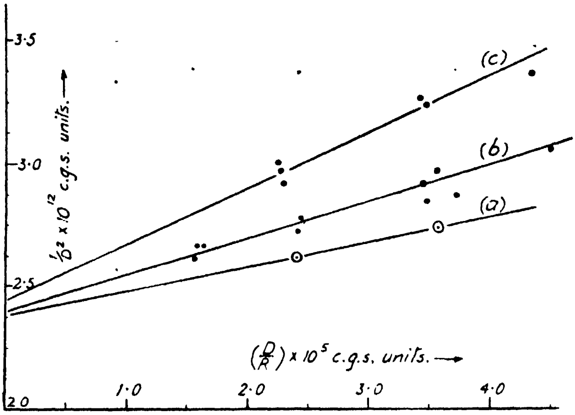

FIG. 3.—The linear relationships between $\frac{1}{D^2}$ and $\frac{D}{R}$ for:

(a) Fine grist 60/40 Amatol in thick-walled steel tubes.
(b) Coarse grist 60/40 Amatol in thick-walled steel tubes.
(c) Coarse grist 60/40 Amatol in thick-walled lead tubes.

and for charges confined in thick steel walls,

$$1/D^2 = 10^{-12}(2{\cdot}38 + 0{\cdot}10D \times 10^{-5}/R) \qquad . \quad . \quad (10)$$

It is important to note that all five empirical equations (6), (7), (8), (9), and (10) calculated to give the lines of closest fit have very approximately the same origin, which corresponds to a value of $D_0 = 6500$ m./sec.

These results show that the grist size of the ammonium nitrate, and the boundary conditions, have a marked influence on the values of D at a given radius of charge, but not on the value of D_0. In other words, the boundary conditions control the rate of physico-chemical processes in the detonation wave, but have no longer any major effect on the detonation velocity at infinite charge radius. The reaction times for 60/40 Amatol, calculated from the experimental data and the appropriate theoretical equation are set out in Table III.

Having regard to the nature of the assumptions which must be made to obtain numerical values for the constants in the theoretical equations, the good agreement between the values of $\bar{t}$ for bare and steel-cased charges, lends considerable support to the analysis and calculations involved.

A very wide range of variables is in fact controlled by a single value of $\bar{t}_1$. This may be taken to have a value of about 3·1 microsec. for 60/40 Amatol containing coarse grist ammonium nitrate, and a value of 2·1 microsec. for 60/40 Amatol containing fine grist ammonium nitrate. It seems likely that the result for lead-cased charges is less trustworthy than the others, owing to the nature of the assumptions involved in evaluating the angle B in eqn. (3) from compressibilities of lead under static pressures (ref. 5).

TABLE III.—THE CALCULATION OF REACTION TIMES FROM THE EXPERIMENTAL DATA.

Grain Size of NH_4NO_3.	Basis of Calculation.	Mean Reaction Time $\bar{t}$.
Coarse grist $(NH_4)NO_3$	Experimental data on charges confined by cardboard and eqn. (1). Bare charges	2·82 microsec.
ditto	Experimental data on charges confined by thick steel and eqn. (3).	3·31 microsec.
ditto	Experimental data on charges confined by thick lead, and eqn. (3)	2·17 microsec. (see below)
Fine grist NH_4NO_3	Bare charges (as above)	2·08 microsec.
ditto	Thick steel (as above)	2·09 microsec.

Interpretation of the Significance of the Mean Reaction Time $\bar{t}$ in 60/40 Amatol.—Two aspects of the above results may be used to examine the physico-chemical significance of $\bar{t}$, the reaction time of the heterogeneous system 60/40 Amatol. (1) Firstly, the value of the limiting detonation velocity for infinite charge radius, $D_0 = 6500$ m./sec. for 60/40 Amatol of charge density 1·50 g./cc. (2) Secondly, the observation that $\bar{t}$ is a function of the grist size of the ammonium nitrate in the explosive.

The Chemical Contribution of the Ammonium Nitrate to the Energy available for Detonation.—With regard to the limiting detonation velocity, various semi-empirical methods have been proposed for calculating D_0 from a knowledge of the chemical processes occurring in the reaction zone, which control the energy available for the propagation of detonation.

A simple treatment [8] gives the expression

$$D_0 = 430\sqrt{NT/M} + 3500\,(d - 1)$$

where $$T = 300 + H_R/\{\Sigma(cv_i) - 0{\cdot}8N\}$$

is the detonation temperature in °K., H_R the heat of reaction at constant volume, N the number of g.mol. gaseous products formed on decomposition of M g. of explosive, and C_{v_i} is the mean specific heat of the ith gaseous species over the temperature range 300° K. to T° K. Self-consistent values of T and $\Sigma(C_{v_i})$ are calculated making use of known heats of formation to estimate values of H_R.

If only the T.N.T. decomposed in the reaction zone of 60/40 Amatol, the energy available for propagating detonation would derive from the decomposition

$$C_7H_5N_3O_6 \rightarrow 6CO + 2{\cdot}5\,H_2 + 1{\cdot}5\,N_2 + C,$$

the ammonium nitrate being chemically inert. The effective heat of reaction, H_E per mole of T.N.T. for this system will be given by the expression

---

[8] Marshall, Ministry of Supply Report, 1944.

$$H_E = H_R - H_C$$

where H_C is the energy imparted to the chemically inert ammonium nitrate during its passage through the reaction zone, by the process of compression (see Part II). By the methods developed in Part II it is found that $H_C = 32{\cdot}1$ kcal., $H_R = 148{\cdot}3$ kcal., and $H_E = 116{\cdot}2$ kcal. Thus $T = 2400°$ K. and $D_0 = 4640$ m./sec.

If, on the other hand, the ammonium nitrate participates completely in the reactions contributing to the energy of detonation, this energy is given by $C_7H_5N_3O_6 + 4{\cdot}26\,NH_4NO_3 \rightarrow 6{\cdot}24\,CO + 0{\cdot}76\,CO_2 + 11{\cdot}02\,H_2O + 5{\cdot}76\,N_2$, making $H_R = 503$ kcal., $T = 3280°$ K., and $D_0 = 6790$ m./sec.

From a comparison of these two calculated values of D_0 with the observed result, $D_0 = 6500$ m./sec., it appears probable that the ammonium nitrate does in fact contribute to the energy available for maintaining detonation in 60/40 Amatol. The total time required for its energy contribution, of the order of 3 microsec. decreases with decreasing size of its grains. Experiments on the detonation of pure T.N.T. (see Part II) show that $\bar{t}$ for this explosive in its normal cast form is about 0·5 microsec., and is not altered appreciably by addition of chemically inert salts.

In the light of the information so far obtained, the sequence of physico-chemical processes in the detonation of Amatols appears to be roughly as follows. The T.N.T. first detonates, giving rise to hot detonation products which reach thermodynamic equilibrium in about 0·25 microsec. During this time, the ammonium nitrate grains have been compressed somewhat, which raises their temperature some few hundred degrees (see Part II). Their surface is however exposed to the much higher temperature of the hot gaseous products of detonation of T.N.T. Surface erosion of the ammonium nitrate grains results, and is completed in about 3 microsec.

The Effect of Grist Size of Ammonium Nitrate on the Reaction Time of Amatol.

A simple treatment of this erosion of ammonium nitrate grains is as follows. If we consider a spherical grain of radius r, and mass m, surrounded by hot gases at a temperature T, the rate of loss of mass by surface erosion may be assumed to be proportional to the instantaneous grain surface a. That is

$$-\frac{dm}{dt} = k.a. \qquad . \quad . \quad . \quad . \quad . \quad (11)$$

The precise nature of erosion at the very high pressures and temperatures prevailing need not be specified. Simple evaporation would be hindered in a static gas at these pressures by molecular collisions, but in detonation the grains are swept by the stream of gas molecules taking part in the mass motion of the detonation wave, and this would favour erosion. In general K will depend on the properties of the ammonium nitrate, and on the temperature of the detonation products.

If ρ is the crystal density of ammonium nitrate,

$$dm = a\,.\,\rho\,.\,dr \qquad . \quad . \quad . \quad . \quad . \quad (12)$$

so that from (11)

$$-\frac{dr}{dt} = \frac{K}{\rho}.$$

Noting that when $r = r_0$, $t = 0$, the time required for complete erosion is

$$t_0 = r_0\rho/K.$$

Since chemical interaction of the ammonium nitrate follows erosion, the reaction time of Amatol will be a little longer than the time at which erosion is just completed, say $\bar{t} = \frac{r_0\rho}{K} + \delta\bar{t}$. If A is the surface area of 1 g. ammonium nitrate crystals of uniform radius, r_0, $r_0 = 3/A\rho$ and $\bar{t} = \frac{3}{KA} + \delta\bar{t}$, so that a linear relationship would be anticipated for the plot of $\bar{t}$ for Amatol against the grist size of the ammonium nitrate, expressed as $1/A$.

Our data are too few in number to test this relationship fully. We are permitted to use data, as yet unpublished, to which we had access in 1943. Payman, Masson and co-workers,[9] related the velocity of detonation of carefully standardised 50/50 and 60/40 Amatol in bare cylinders with the grain size and area of the nitrate component. Using their figures for D and A, we find that the reaction time is a linear function of $1/A$, such that for 60/40 Amatol

$$\bar{t} = 3{\cdot}7 \times 10^{-4}/A + 9 \times 10^{-7} \quad . \quad . \quad . \quad (13)$$

and for 50/50 Amatol

$$\bar{t} = 3{\cdot}3 \times 10^{-4}/A + 7 \times 10^{-7}. \quad . \quad . \quad . \quad (14)$$

The two values of $\bar{t}$ and A calculated from our quite independent data on coarse and fine grist 60/40 Amatol, $A = 195$ sq. cm./g., $\bar{t} = 3{\cdot}1$ microsec., and $A = 310$ sq. cm./g., $\bar{t} = 2{\cdot}1$ microsec., lie on the above line for 60/40 Amatol, in excellent agreement, so that eqn. (13) has a firm experimental foundation.

The extrapolated values of $\delta\bar{t}$ are equivalent to the times of complete interaction of vaporised ammonium nitrate with detonation products of T.N.T. at the pressures and temperatures that exist at the end of the reaction zones of 60/40 and 50/50 Amatol. These temperatures are calculated to be 3280° K. for 60/40 Amatol, and 3320° K. for 50/50 Amatol. The corresponding values of $\delta\bar{t}$ are 0·9 microsec., and 0·7 microsec., respectively. The pressure obtaining is of the order of 10^5 atm.

It is of some interest as a guide to further experiments to pursue the problem of reaction kinetics of gaseous ammonium nitrate at high temperatures and pressures a little further, though the discussion is at present necessarily speculative. The object is to attempt to evaluate the temperature coefficient for the chemical interaction of ammonium nitrate after vaporisation.

We have as guide the following values of $\delta\bar{t}$.

Explosive.	$T°$ K	$\delta\bar{t}$ microsec.
50/50 Amatol	3320	0·7
60/40 Amatol	3280	0·9
Ammonium nitrate ($d = 1{\cdot}0$ g./cc.)	1640	3·0 (see below)

The third line in the above table is derived from experimental data on the detonation velocity of ammonium nitrate obtained by Parisot and Laffitte[10] for charges confined by glass tubing. From their experimental results, values of $1/D^2$ and D/R are calculated exactly as above.

R cm.	D m./sec.	D/R.	$1/D^2$.
0·325	1300	$4{\cdot}0 \times 10^5$	$5{\cdot}91 \times 10^{-11}$
0·380	1450	$3{\cdot}82 \times 10^5$	$4{\cdot}77 \times 10^{-11}$

---

[9] Gwylim, Cybulski, Payman, Masson, Ministry of Supply Report, 1943.

[10] Parisot and Laffitte, *Compt. rend.*, 1936, **203**, 1516.

The line joining the two points ($1/D^2$, D/R) extrapolates to a value of $1/D_0^2$ at $D/R = 0$, from which a value D_0 identical with the calculated hydrodynamic velocity of detonation of ammonium nitrate, 3640 m./sec., is derived. The slope of this line is equated to $9\bar{t}\,(\tan B)/D_0^2$ where B is taken equal to 3° 48′ from the compressibility of glass,[6] and $\bar{t}$ calculated to be about 9 microsec. Parisot and Laffitte do not record the size of the ammonium nitrate used in their experiments but on the basis of our results for 60/40 Amatol, a value of $\delta\bar{t} = 3$ microsec. is not likely to be much in error.

The important point is that however gross the assumptions may be, the temperature coefficient of values of $\delta\bar{t}$ must be very small, so that the rate-controlling process in the decomposition of gaseous ammonium nitrate is not likely to be one of chemical activation at all. This conclusion is of general application to processes of energy release in detonation, since there is a superabundance of activated molecules and radicals available as a result of mass-motion effects, and the high temperatures in the detonation products of the explosive. The rate-controlling process is probably a physical process with low temperature coefficient, such as diffusion.

In view of the high densities hindering diffusion in the explosion products, it seems plausible that the rate of energy release from the oxidising action of ammonium nitrate is determined not by the difficulty of finding active molecules, but of getting them at the incompletely oxidised products of the T.N.T.

Further experiments on detonation are necessary before a more precise analysis of chemical kinetics in detonation processes, i.e. at high pressures and temperatures, will be possible. The above tentative analysis is presented as an indication to what problems can be attacked by a detailed study of detonation processes, and to summarise the extent of present knowledge on these extremely rapid chemical reactions.

Summary.

When detonation is set up in a system, the molecules undergo rapid exothermic chemical decomposition, and simpler molecules are produced, at pressures which may be initially of the order of 10^5 atm. and at temperatures which may be of the order of 5000° K. Reaction rates controlling various processes at these high temperatures and pressures are estimated from experimental values of the detonation velocity, which have been determined under various conditions for mixtures containing trinitrotoluene and ammonium nitrate. Fair agreement is obtained for the reaction rate determined under very different conditions of confinement, and the rate is found to depend to some extent on the grist size of the ammonium nitrate. The temperature coefficient of the controlling reaction rate is found to be small.

PHYSICO-CHEMICAL PROCESSES OCCURRING AT HIGH PRESSURES AND TEMPERATURES.

PART II. THE EFFECT OF "INERT" COMPONENTS ON DETONATION.

By John L. Copp and A. R. Ubbelohde.

Received 11*th August*, 1947.

Data on the velocity of detonation for 60/40 Amatol, presented in Part I, illustrated the use of a theory of the effect of boundary conditions on the rate of propagation of a detonation wave in a charge of finite cross-section. By means of this theory, the time of decomposition of an explosive to give gaseous products in thermodynamic equilibrium at high pressures and temperatures was determined. When an explosive consists of more than one component, as in Amatol, the time of release of the energy available for the propagation of detonation depends on a sequence of physico-chemical events, and is controlled by the behaviour of the least reactive component. As a limiting case, it is of interest to determine what happens when one of the components is chemically inert.

In the present paper, data are presented on the detonation velocity of cast trinitrotoluene, and of mixtures of this explosive with chemically inert materials. These data have been obtained for " heavy confinement " i.e., for charge-boundary conditions, such that the lateral expansion of the zone in which primary explosive decomposition occurs, is controlled by the compressibility of the boundary medium. In these experiments the explosives were cast into steel tubes of wall thickness greater than about 0·3 cm., so that as with the results for 60/40 Amatol (see Part I),

$$1/D^2 = 1/D_0^2 + 9\bar{t}\,(\tan B)\, D/D_0^2R \quad . \quad . \quad . \quad (1)$$

where D is the observed detonation velocity, D_0 is the hydrodynamic detonation velocity, in charges of infinite cross-section, R is the experimental charge radius, and B is the angle of case expansion after a time $\bar{t}$, where $\bar{t}$ is the time to equilibrium of the primary processes of explosive decomposition.

In general terms, the results of these experiments can be summarised in the two following statements.

(1) The addition of chemically inert solids to cast trinitrotoluene decreases its hydrodynamic detonation velocity D_0, progressively, without substantially modifying the rate of its primary decomposition (the reaction time $\bar{t}$).

(2) The decrease in detonation velocity, resulting from additions of chemically inert solids to cast trinitrotoluene, can be attributed to an energy transfer from the gaseous detonation products to the chemically inert filler, by means of physical processes of heat conduction and compression. In the reaction zone of the explosive, these processes result in a decrease in the energy available for raising the temperature of the gaseous products of detonation, and in an increase in their specific volume. Thus for such mixtures the effective detonation temperature T, and the effective density of the explosive d, are smaller than the values that would obtain, ignoring these physical processes. In consequence, the value of D_0, observed for such mixtures, will be lower than the value calculated by hydrodynamic theory when these processes are neglected, as is clear for example, from the simplified equation of Marshall[1]

$$D_0 = 430\sqrt{NT/M} + 3500(d - 1) \quad . \quad . \quad (2)$$

where N is the number of gas moles produced on decomposition of M. g. of explosive.

In the analysis of the experimental data given below, the hydrodynamic theory of detonation has been modified in a simple manner to allow for the physical processes of energy transfer, outlined above. The most important fundamental aspect of this line of inquiry is that such experiments maybe used to evaluate the compressibility of materials at pressures up to 10^5 atm., and for high rates of stress. A practical application of the methods employed is in the field of safe mining explosives. The role of flash suppressants in such explosives may be analysed in a semi-quantitative manner, and the subject developed along systematic lines rather than by trial and error.

Experimental and Results.

Detonation velocities have been recorded for charges of pure trinitrotoluene, and of various mixtures of this explosive with sodium chloride, barium sulphate, and aluminium, cast into thick-walled steel tubes of various internal radii. Full details of experimental conditions are summarised in Tables I, II, III and in the following text.

---

[1] Marshall, Ministry of Supply Report, 1944.

Trinitrotoluene.—Trinitrotoluene (setting point not less than 80·4° c.) was melted in a steam-jacketed stainless steel pan, and the melt maintained at 100° c. for 30 min. The melt was cooled to its setting point and vigorously stirred to induce formation of a large number of small crystals. When the mixture of solid and liquid explosive was just sufficiently viscous to permit of successful casting, it was loaded into steel tubing, and allowed to set. This type of casting, designated as " cast cloudy T.N.T.," consists of an aggregate of small crystals of the explosive, the smallest crystals being at the charge periphery, the largest growing into the charge axis.

TABLE I.

DETONATION VELOCITIES FOR CAST CLOUDY T.N.T. IN STEEL TUBINGS.

Internal Radius *R* (cm.).	Wall Thickness *Z* (cm.).	No. of Results.	Mean Charge Density. (g. cc.).	Mean *V* of Det. (m./sec.)	St. Error in Mean *V* of Det.
0·74	0·31	5	1·61	6850	±30
1·30	0·60	14	1·60	6790	±30
1·28	0·40	11	1·60	6850	±40
1·70	0·48	13	1·59	6790	±30
1·63	0·28	11	1·60	6730	±40
2·54	0·51	7	1·61	6860	±30
3·85	0·63	5	1·60	6850	±40

Trinitrotoluene.—Salt Mixture.—Common salt was dried at 100° c., and milled in a Kek mill. The dry, milled salt, or a sieved fraction of it, was incorporated in molten trinitrotoluene in the proportions of 50/50 or 60/40 NaCl/T.N.T. The mixture was maintained at 100° c. for 30 min., cooled to the setting point of the T.N.T. and the viscous suspension loaded into steel tubes. Throughout the casting procedure, the bulk of the mixture was stirred vigorously to ensure that its composition did not change, and to minimise segregation of the salt particles. A check was kept on the uniformity of the castings by analysis of various segments of sample charges, and of samples drawn from the bulk of the mixture during casting. In no instance did the salt percentage at any part of the charges differ from that of the bulk mixture by more than 2 %.

The same technique was adopted in the casting of mixtures of trinitrotoluene with various percentages of barium sulphate, and with aluminium powder. Detonation velocities recorded for these cast charges by the Dautriche method (see Part I) are summarised below in Table II. (Stable detonation was verified as in Part I.)

TABLE II.—DETONATION VELOCITY RESULTS FOR VARIOUS MIXTURES OF T.N.T. AND INERT FILLERS, CAST IN THICK-WALLED STEEL TUBING.

Composition of ot Mixture.	Charge Radius *R* (cm.).	Wall Thickness *Z* (cm.).	No. of Results *n*.	Mean Charge Density g./cc.	Mean *V* of Det. *D* (m./sec.).	Standard Error in Mean *V* of Det.
T.N.T./NaCl 50/50	1·67	0·50	13	1·85	5990	±25
	2·50	0·45	13	1·85	6030	±25
T.N.T./NaCl 40/60	1·65	0·50	9	1·84	5440	±40
	2·60	0·45	6	1·84	5450	±20
T.N.T./BaSO$_4$ 75/25	1·02	0·32	5	1·90	6420	±35
	1·32	0·35	7	1·90	6450	±25
	1·65	0·50	7	2·02	6540	±25
T.N.T./BaSO$_4$ 85/15	0·78	0·28	5	1·78	6570	±35
	1·02	0·32	5	1·78	6620	±30
	1·67	0·48	7	1·82	6690	±25
T.N.T./Al 74/26	0·76	0·30	8	1·80	6500	±20
	1·30	0·38	23	1·80	6560	±15
	1·67	0·48	15	1·79	6520	±20
	2·50	0·51	22	1·79	6700	±20

The particle size distribution for the sodium chloride, aluminium, and barium sulphate, used in these experiments were determined for the first two materials by sieve analysis, and for the barium sulphate by sedimentation analysis in water. The barium sulphate was shown to be equivalent to an aggregate of dispersed spheres of sedimentation radius 0·0005 cm. In Table III is shown the sieve-analysis data obtained for the salt and the aluminium.

TABLE III.—SHOWING THE WEIGHT PERCENTAGE THAT FAILS TO PASS A SPECIFIC SIEVE-MESH.

B.S. sieve no.	44	72	100	200	300
Sieve aperture mm.	0·353	0·211	0·152	0·076	0·053
% NaCl retained	0	8·2	28·0	73·6	100
% Al retained	10·7	32·2	44·6	78·5	100

From the plot of weight-percentage retained against sieve apertures it is inferred that the aggregates of salt and aluminium particles can, to a first approximation, be regarded as made up of uniform spheres of various average radii in the percentage by weight shown in Table IV. This approximation is adopted to facilitate the final analysis of the detonation velocity results.

TABLE IV.—EQUIVALENT SIZE DISTRIBUTION OF SALT AND ALUMINIUM WHEN TREATED AS SPHERICAL PARTICLES.

Average equivalent particle radii in microns	25	50	100	170
Wt.-% of salt particles	26	33	39	2
Wt.-% of aluminium particles	12	37	26	21

Exploratory experiments with other sieve ranges of NaCl showed that the observed detonation velocities of NaCl/T.N.T. mixtures were insensitive to the exact size range of the inert filler. For very coarse salt particles it was difficult to obtain stable detonation. Salt particles finer than 300 B.S. sieve were not available; they would be expected to affect the energy transfer of heat by conduction, especially when the size falls below 1 μ.

Discussion.

Tables I and II give detonation velocities for T.N.T., cast cloudy, and for cast T.N.T. with various solids. In these experiments, the effect of charge radius on detonation velocity is rather small, and graphical evaluation of the mean reaction time $\bar{t}$, according to eqn. (1) above, is unprofitable.

Calculation of the coefficients in eqn. (1) from the data in Table I, by the method of least squares, leads to the best values, $D_0 = 6970$ m./sec., and $\bar{t} = 5{\cdot}2 \times 10^{-7}$ sec. The above value of D_0 agrees well with the value calculated by Marshall's simple hydrodynamic theory, $D_0 = 6960$ m./sec. for T.N.T. at a density of 1·60 g./cc., thereby confirming that the present values of D_0 agree with those previously determined for T.N.T. by other workers. Payman, Cybulski and Woodhead[8] have obtained a mean value of 6950 m./sec. for the maximum velocity of detonation of a T.N.T. of set point 80·86° c. (corresponding with a purity of 99·8 %).

Estimation of D_0 for Mixtures of T.N.T. with Inert Components. Inspection of Table II shows that for these mixtures, as for pure T.N.T., the effect of charge radius on detonation velocity is only small. The data are insufficient to calculate $\bar{t}$ and D_0 for each mixture from a linear plot of $1/D^2$ against $1/R$. However, since it is convenient to eliminate the effect of the boundary conditions in investigating the role of inert admixtures on detonation processes, values of D_0 (and of $\bar{t}$) have been calculated by the following method of approximation.

---

[8] Payman, Cybulski and Woodhead, Ministry of Supply Reports, 1944-45.

(i) Using eqn. (1), and assuming a value for the reaction time of a mixture equal to that of pure T N.T., values of D_0 are calculated from the experimental D and R data.

(ii) With the mean of these values of D_0, values of $\bar{t}$ are calculated from the same D and R data and eqn. (1). The operation (i) is then repeated with this value of $\bar{t}$, and so on.

A method of trial and error results in the consistent values of D_0 and $\bar{t}$ shown in Table V.

From the fourth column of Table V it is clear that the addition of up to 60 % by weight of an inorganic material to cast T.N.T. has no large influence on its reaction time. This fact substantiates the view that the added inorganic materials are chemically inert in the reaction zone of the explosive component of these mixtures. The third column shows that the addition of chemically inert materials to cast cloudy T.N.T. progressively decreases the values of D_0 estimated for these mixtures from the experimental values of D.

TABLE V.—CONSISTENT VALUES OF D_0 AND $\bar{t}$ FOR VARIOUS MIXTURES OF T.N.T. AND INERT MATERIALS.

Composition of Mixture.	Cast Density (g./cc.)	Estimated Value of D_0 (m./sec.).	Estimated Value of $\bar{t}$ (sec.).	Crystal Density of Filler. (g./cc.).	Nominal T.N.T. Density. (g./cc.).	Nominal Value of D_0 (m./sec.).
NaCl/T.N.T. 60/40 . .	1·85	5520	$4{\cdot}5 \times 10^{-7}$	2·16	1·50	6610
NaCl/T.N.T. 50/50 .	1·84	6100	$4{\cdot}5 \times 10^{-7}$	2·16	1·62	7030
T.N.T./BaSO$_4$ 75/25 . .	1·94	6640	$5{\cdot}0 \times 10^{-7}$	4·50	1.63	7060
T.N.T./BaSO$_4$ 85/15 . .	1·80	6830	$5{\cdot}0 \times 10^{-7}$	4·50	1·62	7030
T.N.T./Al 76/24 . .	1·80	6740	$5{\cdot}0 \times 10^{-7}$	2·70	1·62	7030
T.N.T. . .	1·60	6970	5.2×10^{-7}	0·0	1·60	6960

An Interpretation of the Effect of Chemically Inert Materials on the Detonation Velocity of T.N.T.—In column 6 of Table V, values of the "nominal density" of T.N.T. are given for each mixture. These correspond with the ratio (weight of T.N.T.)/(the volume available to the explosive reaction products), assuming the inert admixture is incompressible :

$$\text{i.e.} \qquad \text{nominal density of T.N.T.} = \frac{\text{Wt. of T.N.T. per cc. cast}}{\left(1 - \dfrac{\text{Wt. of filler}}{\text{density of filler}}\right)}.$$

With one exception, in the case of the cast mixtures used, the nominal density of T.N.T. lies between 1·60 and 1·63 g./cc., the upper limit being slightly less than the density of T.N.T. single crystals.

If the filler were chemically and physically inert, i.e. in no way affected the energy available for propagating detonation, either by undergoing chemical interaction with the gaseous products of detonation of T.N.T., or by absorbing heat by processes such as conduction and compression, then the detonation velocity D_0 of a mixture might be expected to be determined solely by the nominal density of the T.N.T., apart from possible effects of viscous drag of the large surface of the particles on the detonation wave, which must for the present be neglected. The nominal values of D_0 shown in Table V have been calculated on this basis from eqn. (2) above. This equation is known to hold for a wide range of experimental variables.

It is assumed that in all the experimental mixtures the primary processes of decomposition of T.N.T., that liberate the energy available for propagating detonation can be represented by the equation:

$$C_7H_5N_3O_6 \rightarrow 6CO + 2{\cdot}5\,H_2 + 1{\cdot}5\,N_2 + C. \qquad . \quad . \quad (3)$$

In eqn. (2), N is the number of gas molecules formed in this process from M g. T.N.T. and T is the temperature to which they are raised in virtue of the liberation of the heat of reaction H_R. The method of calculating D_0 is illustrated below.

H_R the heat of reaction at 18° c., and a constant volume can be calculated from the equation :

$$H_R = \Sigma H_{f\text{products}} - \Sigma H_{f\text{reactants}},$$

or $$H = 6H_{f\text{CO}} - H_{f\text{T.N.T.}}$$

Now $$H_{f\text{CO}} = 26{\cdot}43 \text{ kcal. } (C_{\text{graphite}}),$$

and $$H_{f\text{T.N.T.}} = 10{\cdot}3 \text{ kcal., so that } H_R = 148{\cdot}3 \text{ kcal.}$$

This heat evolution raises the temperature of the reaction products from 291° K. to T° K., where

$$(T - 291) = H_R/[\Sigma(C_{v_i}) - 0{\cdot}8\,N]. \qquad . \quad . \quad . \quad (4)$$

In eqn. (4), C_{v_i} is the mean specific heat at constant volume of the i^{th} product species between 291° K. and T° K., and $0{\cdot}8\,N$ is a term correcting for the adiabatic compression of the gaseous detonation products from 1 atm. to the detonation pressure (see ref. [1]).

From tables of specific heats [1] a method of successive approximations results in a value for the detonation temperature, $T = 2900$° K., which is a constant for each mixture, provided the fillers are both chemically and physically inert. Substituting in eqn. (2), $T = 2900$° K., $N = 10$, $M = 227$ g., and the appropriate values for the nominal density of T.N.T., the nominal values of D_0 shown in Table V were obtained for each mixture. It has been verified that these values of D_0 are not sensitive to the eqn. (3) assumed for the decomposition, owing to compensation in the ratio T/N if the assumed decomposition is varied. Comparison of the experimental estimates of D_0 (column 3, Table V) with the nominal values calculated as above (column 7, Table V) shows that the experimental values lie uniformly below the nominal values, and that the differences become larger as the amount of admixed filler increases.

Various considerations indicate that chemical effects due to the fillers used will not be important in determining D_0. Two physical effects which calculations show to be important are:

(i) the compression of the filler in the reaction zone of the explosive,

(ii) abstraction of heat by the filler from the hot detonation products of the explosive.

The following analysis shows that for the fillers selected these two effects can account for the difference between the experimental and nominal values of D_0 in Table V.

Compression and Heat Conduction of Inert Fillers in the Rection Zone of T.N.T.—In the zone of high pressure and temperature behind a detonation wave-front, a chemically inert material can abstract energy from the gaseous products of detonation. Abstraction of heat from the hot detonation products of T.N.T., takes place by conduction to the interior of the particles. Furthermore, the pressure exerted on the particles by the gaseous products of detonation compresses them; the work of compression ultimately appears as heat in the particles, and a corresponding cooling of the gaseous detonation products occurs. The energy abstracted from the gaseous detonation products by such processes during the time of energy release from the primary explosive decomposition, reduces the effective detonation temperature, whilst the volume available to the product gases is increased by the compression of the inert material. It is these effects that reduce the detonation velocities of the experimental mixtures below the nominal values calculated in Table V.

The object of this discussion is to modify simple hydrodynamic theory (cp. [1]) to allow for the effects of compression of inert materials, and heat conduction, in the reaction zone of T.N.T. It is required to calculate values for these two energy terms. More refined theories of detonation would give no advantage at the present stage of the investigation. The results of this rather tentative analysis of chemical and physical processes in the detonation zone are sufficiently consistent with the independent estimates of these energy terms to justify the claim that further development of these experimental and theoretical techniques should lead to a simple method of determining equations of state for solids up to pressures of the order of 10^5 atm., especially if explosives are used with different densities and different maximum pressures and temperatures.

General Equations used in the Analysis.—It is assumed that Marshall's equation, which applies to a wide range of pure explosives, can also be used to express the detonation velocity of an explosive mixed with inert components, provided the appropriate temperature and density of the product gases of detonation at the end of the reaction zone are inserted. This assumption implies in effect, that the values of T and d substituted in the equation :

$$D_0 = 430\sqrt{NT/M} + 3500\,(d - 1)$$

include corrections to allow for the energy abstracted by the inert material in the explosive reaction zone, and that the grains of the inert material acquire no appreciable momentum during their passage through this zone. Viscous drag by the surface of the inert filler is neglected.

Consider a mixture containing x g. of T.N.T. and y g. of an inert filler in 1 cc. Then yM/x g. of inert material are associated with 1 mole of explosive. If in the reaction zone of this mixture H_A is the heat of compression of yM/X g. of filler, and H_B is the heat abstracted by conduction by this amount of filler, then the effective temperature T of the products of detonation is given by the equation :

$$(T - 290) = [H_R - (H_A + H_B)]/]\Sigma C_{v_i}) - 0{\cdot}8N] \qquad . \quad (5)$$

where H_R is the heat evolved in the primary processes of explosive decomposition, which is assumed to follow the course,

$$C_7H_5N_3O_6 \rightarrow 6CO + 2{\cdot}5\,H_2 + 1{\cdot}5\,N_2 + C,$$

and the other symbols are used as previously.

Allowing for the effect of compression of the inert filler on the volume available to the reaction products at the end of the reaction zone of the explosive, the effective volume available to the product gases per cc. of mixture is $(1 - yV_p)$ and the effective density of the detonation products is

$$d = x/(1 - yV_p) \quad . \quad . \quad . \quad . \quad . \quad (6)$$

where $(V_0 - V_p)$ represents the degree of compression of the inert filler at the detonation pressure p. The compressibility of the inert filler is given by

$$Q_p = 1 - V_p/V_0$$

H_A, the heat abstracted from the gaseous detonation products owing to compression of the amount of filler associated with M g. of explosive, can be equated to the work done by the gases in compressing the filler. That is

$$H_A = p(V_0 - V_p)yM/x. \qquad (7)$$

The pressure p decreases somewhat during this compression. An average value of p, the detonation pressure, is calculated from the expression

$$P = D.W.d. \qquad (8)$$

where W, the gas-flow velocity in the direction of detonation, is given by

$$W = \sqrt{8310 \, . \, T/KM_2}, \qquad (9)$$

M_2 is the mean molecular weight per gas molecule, and $K = \bar{C}_p/\bar{C}_v$ (cp. [3]).

Eqn. (2) to (9) are soluble by a method of successive approximations, provided the conditions are such that independent values of either H_A or H_B can be calculated. For this purpose estimates of H_B, the heat transferred by conduction to the interior of the grains of the inert filler during their stay in the reaction zone of the explosive may be evaluated by the method of Williamson and Adams.[4] For calculating the heat conducted into small spheres of a solid from a hot gas, the temperature T_a, attained by a spherical shell of radius a in a sphere of radius r, a time t, after its surface has been raised instantaneously to a temperature T, may be related to the expression Kt/r^2, where K, the diffusivity constant of the material of the sphere, is equal to CV_0/c. C is the thermal conductivity of the material, of density $1/V_0$, and specific heat c.

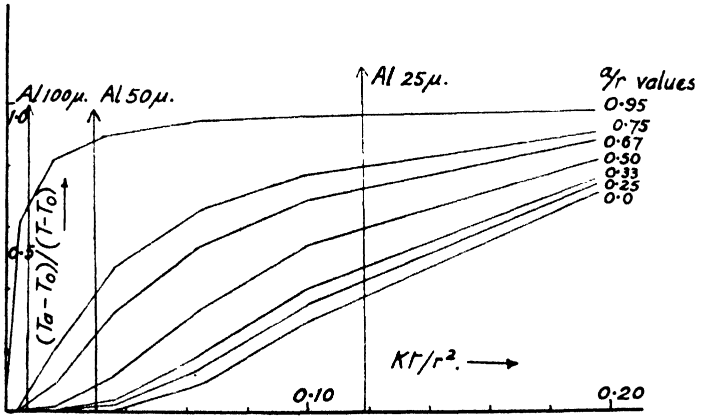

FIG. 1.—Temperature distributions in spherical grains for various values of Kt/r^2 (see ref.[4]).

In Fig. 1 we have plotted values of $(T_a - T_0)/(T - T_0)$ against Kt/r^2 for various values of a/r. By using a radius giving a surface equivalent to that of the non-spherical inert fillers used in our experiments, values of Kt/r^2 are calculated for a heating time of 5×10^{-7} sec., and the temperature distribution in such grains is determined from Fig. 1. The amount of heat absorbed by 1 g. of the material in the attainment of the calculated temperature distribution can be obtained from the relationship

$$h = c\int_0^1 (T_a - T_0)\mathrm{d}(a/r)^3 \qquad (10)$$

by graphical integration, as in Fig. 2.

Then $$H_B = yMh/x. \qquad (11)$$

---

[3] Schmidt, *Z. Schiess. Spreng*, 1936, **31**, 8, 37, 80 and 114.

[4] Adams and Williamson, *Physic. Rev.*, 1919, **14**, 99.

The method of calculation of self-consistent values of Q and H_A will be appreciated from a specimen set out in detail.

For cast 75/25 T.N.T./$BaSO_4$ (cp. Table V) the extrapolated value of D_0 is 6640 m./sec. at a density of 1·94 and $y = 1{\cdot}94 \times 0{\cdot}25 = 0{\cdot}485$ g. By sedimentation analysis, the barium sulphate was shown to consist, almost entirely, of particles of sedimentation radius equal to 5×10^{-4} cm. To begin the series of successive approximations it is assumed that the compressibility Q of barium sulphate at the detonation pressure of the above mixture has a value of 0·32. Then d = weight of explosive/volume available to the explosive products i.e.

$$d = 1{\cdot}455/(1 - 0{\cdot}485 \times 0{\cdot}68/4{\cdot}50) = 1{\cdot}57 \text{ g./cc.}$$

Substituting $D_0 = 6640$ m./sec., and $d = 1{\cdot}57$ g./cc. in eqn. (2), the effective detonation temperature T on this basis would be 2600° K., if the primary process of detonation is represented by

$$C_7H_5N_3O_6 \rightarrow 6\,CO + 2{\cdot}5\,H_2 + 1{\cdot}5\,N_2 + C.$$

The temperature distribution in uniform spheres of barium sulphate of radius 5×10^{-4} cm., 5×10^{-7} sec. after their surface has been raised from 290° K. to 2600° K. can be read off in terms of $(T_a - T_0)/(T - T_0)$ from the intersection of a vertical line drawn through the appropriate value of Kt/r^2 with the curves in Fig. 1.

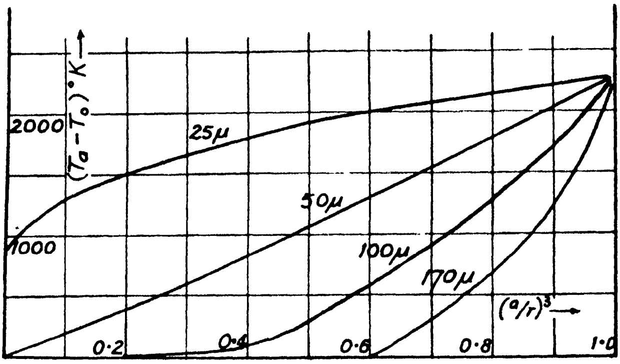

FIG. 2.—Curves for evaluating H_B for aluminium by graphical integration of eqn. (10) taken with size distribution in Table IV.

The values adopted for the terms necessary to evaluate Kt/r^2 are: $C = 0{\cdot}002$ cal./sec., $c = 0{\cdot}17$ cal./g., $1/V_0 = 4{\cdot}5$ g./cc., $t = 5 \times 10^{-7}$ sec., and $r = 5 \times 10^{-4}$ cm. The values adopted for both C and c are estimates, since no direct measurement of these terms have been made at the high temperatures and pressures obtaining in detonation processes. The derived value of Kt/r^2 for barium sulphate grains is 0·005 c.g.s. units. From the values of $T_a - T_0$ for various values of a/r that are obtained from Fig. 1 for $Kt/r^2 = 0{\cdot}005$, and graphical integration of eqn. (10), $h = 105$ cal./g., when $T = 2600°$ K.

Eqn. (11) gives

$$H_B = 227 \times 105 \times 10^{-3}/3 \text{ kcal.} = 7{\cdot}95 \text{ kcal.}$$

Substituting in eqn. (4), the following numerical values: $T = 2600°$ K., $H_R = 148{\cdot}3$ kcal. (cp. previously), $H_B = 7{\cdot}9$ kcal., $N = 10$, and

$$\Sigma(C_{v_i}) - 0{\cdot}8\,N = 56{\cdot}54.$$

H_A is calculated to be 10·3 kcal. on this basis.

From the hydrodynamic eqn. (8) and (9), the detonation pressure is calculated to be $p = (6640 \times 1{\cdot}57 \times W)/101{\cdot}3$ atm., and since $W = \sqrt{(8310 \times 2600)/(1{\cdot}33 \times 21{\cdot}5)} = 870$ m./sec., $p = 8{\cdot}9 \times 10^4$ atm. From eqn. (7), Using consistent values

$$(V_0 - V_s) = 10{,}300 \times 3/8{\cdot}9 \times 227 \times 0{\cdot}0242 \times 10^4 = 0{\cdot}063 \text{ cc.}$$

and $Q = 0{\cdot}063 \times 4{\cdot}50 = 0{\cdot}28$.

In this calculation the initial value assumed for the compressibility of barium sulphate was 0·32. The next approximation should proceed from a value of $Q = 0{\cdot}28$, but as a short cut it is found by trial that the mean of the first and second approximations, viz. $Q = 0{\cdot}30$ gives values of H_A, Q, and H_B consistent with the experimental data on this mixture, and with the assumptions involved in the analysis. Table VI summarises the results of similar calculations carried out on the data available for the various mixtures used in our experiments.

In the last two columns of Table VI are shown values of the detonation pressures and resultant compressibilities of the chemically inert materials present in the reaction zone of cast trinitrotoluene. The compressibilities are rather sensitive to the value assigned to D_0 which is, itself, subject to some experimental uncertainty. On these grounds the inversion of values of the compressibility of NaCl and of barium sulphate, with increase in the magnitude of p, is not considered to be significant, in view of the rather complex analysis by which the values were obtained. More refined calculations would have to allow for the thermal expansion, in cases where H_B is appreciable.

TABLE VI.—A SUMMARY OF SELF-CONSISTENT VALUES OF CHARACTERISTICS REACTION ZONES OF T.N.T.—INERT MATERIAL MIXTURES.

Composition of Mixture.	Equivalent Radius of Fillers cm.	D_0 m/sec.	Mixture Density.	Kt/r^2.	H_B kcal.	H_A kcal.	T° K.	P in Units of 10^4 Atm.	$\frac{V_0 - V_p}{V_0}$ Q.
T.N.T./NaCl 50/50 .	> 0·005	6100	1·85	0	0	24·3	2500	7·50	0·13
T.N.T./NaCl 40/60 .	> 0·005	5520	1·84	0	0	34·8	2370	5·85	0·15
T.N.T./BaSO$_4$ 75/25 .	5×10^{-4}	6640	1·94	0·005	7·95	70·3	2600	8·90	0·30
T.N.T./BaSO$_4$ 85/15 .	5×10^{-4}	6830	1·80	0·005	4·50	4·40	2740	9·60	0·24
T.N.T./Al 76/24 .	See Table IV	6740	1·80	See Fig. 2	15·5	3·60	2580	8·60	0·07

The orders of the compressibilities determined for NaCl and for aluminium by our experiments—which refer to high rates of stress—may be compared with values determined at comparable static pressures by Bridgman, i.e. by a completely independent method. For NaCl, Bridgman [5] quotes values of Q at intervals of 10^4 kg./sq. cm. up to a pressure of 5×10^4 kg./sq. cm. A short extrapolation of his data to pressures of $7{\cdot}5 \times 10^4$ and $5{\cdot}85 \times 10^4$ atm. leads to values of Q of about 0·17 and 0·15 respectively. The extrapolation formula used, is

$$= (a^2/2b) \ln (1 + 2\,bp/a),$$

where a and b are the coefficients of the equation $= ap - bp^2$, chosen to fit Bridgman's experimental data (cp. Part I). The values calculated from detonation velocity data on T.N.T./salt mixtures are in good agreement with the static compressibilities for salt.

---

[5] Bridgman, *Physic. Rev.*, 1940, **57**, 237.

For aluminium the compressibility under dynamic loading up to a pressure of $8{\cdot}6 \times 10^4$ atm., calculated by the above hydrodynamic theory applied to detonation velocities recorded for T.N.T./Al mixtures, is necessarily more unreliable than the values recorded for salt. For in this instance the effect of aluminium on the detonation velocity of T.N.T. is largely associated with its high, though quantitatively uncertain, thermal conductivity, which swamps the effect of compressibility (from Table VI, $H_B \sim 5H_A$). In the calculation of the magnitude of H_B, possible melting of the aluminium in the explosive reaction zone (estimated m.p. of aluminium at 10^5 atm. is about 1500° K.) has been neglected, and an average value of its thermal conductivity, in the temperature range 290° K. to 2600° K., assumed to be 1·00 c.g.s. units. Nevertheless the order of magnitude for Q_p obtained in our analysis compares remarkably well with the compressibility of aluminium at a static pressure of 86,000 atm. recorded by Bridgman, viz. $(V_0 - V_p)/V_0 = 0{\cdot}09$. For barium sulphate no static compressibility data are available up to pressures greater than about 10,000 atm., so that no reliable comparison with our values can be given. On the grounds that we are dealing with a lattice of doubly-charged ions it is considered that the values given in the table are too large, probably as a result of under-estimating the heat conductivity term H_B for T.N.T./$BaSO_4$ mixtures. More reliable values of the thermal conductivity are required.

In view of the fact that our analysis deals with the properties of matter in a region of high pressure and temperature, and under conditions of extremely high rates of loading, the above comparisons between the results of two very different experimental techniques give good promise that more refined experimental and theoretical methods of treating detonation phenomena will result in an extension of our knowledge of the behaviour of materials in a new region of pressure and temperature. It may be pointed out that so far the work has been restricted to cast explosives; by using pressed explosives the range of densities and detonation pressures available can be greatly extended, so that a complete equation of state could be plotted. With more refined determinations of D, it would be possible to use a smaller proportion of filler, and thus to lessen the possibility that viscous drag affects the results.

One feature of our results has not as yet been commented on. The fact that the reaction time of cast T.N.T. is only little affected by addition of inert diluents implies that the reaction time of this explosive is not markedly dependent on the temperature of the gaseous products of its primary decomposition, at least between 2,900° K. and 2,400° K. Hence, as in the case of the reaction of ammonium nitrate in the detonation of 60/40 Amatols (see Part I) the rate-controlling process in the primary rearrangement of trinitrotoluene to give simple gaseous products has a small temperature coefficient. Probably it involves a physical process of low activation energy, such as the rate of vaporisation of the explosive at high pressures, for which the latent heat would be only small owing to the small density change.

Conclusions.

(1) In general terms the effect of chemically inert materials in reducing the velocity of detonation of trinitrotoluene can be attributed to the energy they abstract from the product gases during their passage through the reaction zone of the explosive, by physical processes of heat conduction, and dynamic compression.

(2) A method of analysing such effects in a quantitative manner results in values for the dynamic compressibilities of the inert fillers, which are in reasonable agreement with the corresponding static values.

(3) The primary processes of chemical decomposition in the detonation zone of an explosive have only small temperature coefficients.

The authors are indebted to the Director General of Scientific Research (Defence), Ministry of Supply, for permission to publish this paper (Parts I and II), and to Sir R. Robertson for his continued interest.

Summary.

In this paper more detailed measurements and calculations are made of the energy transferred to chemically inert " fillers " by physical processes such as heat conduction, and compression, during the detonation of trinitrotoluene. Further evidence is obtained that the temperature coefficient of the processes controlling reaction rates in the detonation zone is small. It is suggested that the methods described may be developed to determine experimentally the equation of state of various substances to much higher pressures than have hitherto been studied.

University College, Dundee.

Queen's University, Belfast.

KINETIC STUDIES IN THE CHEMISTRY OF RUBBER AND RELATED MATERIALS.

VI. THE BENZOYL PEROXIDE-CATALYSED OXIDATION OF ETHYL LINOLEATE.

BY J. L. BOLLAND.

Received 18th September, 1947.

A kinetic analysis of the autocatalysed oxidation of ethyl linoleate given in an earlier paper [1] of this series suggested a chain-reaction mechanism, the initiation step of which was the formation of free radicals by the thermal decomposition of ethyl linoleate hydroperoxide. A critical test of the correctness of the proposed mechanism can obviously be provided by detailed comparison of the autocatalysed oxidation with that initiated by catalysts known to produce free radicals under the conditions of experiment. Benzoyl peroxide is a particularly valuable source of free radicals in this connection since firstly, the kinetics of thermal dissociation have been worked out in detail and secondly, the ease of thermal dissociation is such as to promote conveniently measurable rates of oxidation of many olefins in a temperature range in which the oxidation chains are long and secondary reactions of the initial oxidation products are unimportant.

The rates of oxidation can be measured rather more precisely in the benzoyl peroxide-initiated oxidation than in the autocatalysed oxidation of ethyl linoleate. It has therefore been possible to submit the former system to a more searching kinetic examination than was possible with the latter, and it is gratifying that the results obtained fully substantiate the reaction mechanism previously advanced.[1]

Some of the general conclusions arrived at in this paper have already been published,[2] without, however, their detailed experimental justification being given.

Experimental.

The rates of oxidation were measured in the manner already described.[1] More accurate results and more convenient operation were obtained by substituting a Pyrex spiral made from 1-2 mm. quill tubing for the neoprene connection between the reaction vessel and the gas-burette system. In the present experiments, initial rates of oxidation were invariably required. The increase in rate of oxidation as oxidation proceeded was always sufficiently gradual, for extrapolation of rate measurements to zero extent of oxidation to be made with precision : it is estimated that the error in determining the initial rate of oxidation was in general not more than 1 %.

---

[1] Bolland, *Proc. Roy. Soc. A*, 1946, **186**, 218.

[2] Bolland and Gee, *Trans. Faraday Soc.*, 1946, **42**, 236 and 244.

Materials.—Ethyl linoleate and ethyl stearate were prepared as already described.[1] Methyl oleate prepared from olive oil was kindly supplied by Dr. D. A. Sutton ; it was refractionated on a molecular still. All three esters were finally purified by careful chromatographing on an alumina column.

The Experimental Rate Equation.

The parameters which can be varied experimentally in the benzoyl peroxide-catalysed oxidation of ethyl linoleate are (i) benzoyl peroxide and (ii) ethyl linoleate concentrations, (iii) the oxygen pressure and (iv) the temperature. These factors were systematically varied and the results are dealt with in order below.

(i) Benzoyl Peroxide Concentration [Bz_2O_2].—The effect of [Bz_2O_2] on the initial rate of oxidation (R_0) of ethyl linoleate was determined carefully at 35, 45 and 55° c. at an oxygen pressure of 100 mm. Hg. The experimental results at 45° c., are presented in Fig. 1. It is apparent that the data agree either with the relationship R_0 = constant × $[Bz_2O_2]^{\frac{1}{2}}$, or with R_0^2 = constant × $[Bz_2O_2]$, the intercept at $[Bz_2O_2] = 0$ being too small to permit any definite choice between these two forms. Similar relationships are obeyed accurately at 35 and 55° c.

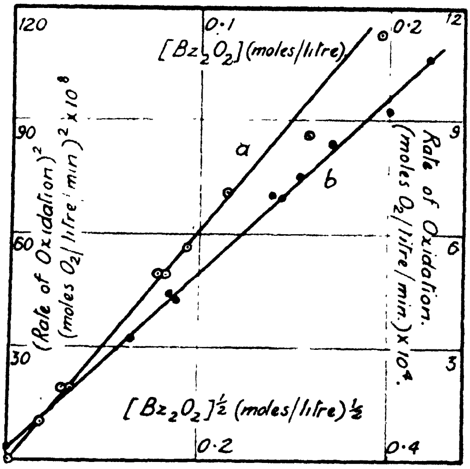

FIG. 1.—Influence of benzoyl peroxide concentration on rate of oxidation (R_0) of ethyl linoleate at 45° c. :

(a) relation between R_0^2 and $[Bz_2O_2]$;
(b) relation between R_0 and $[Bz_2O_2]^{\frac{1}{2}}$.

(ii) Olefin Concentration, [RH].—Ethyl stearate and methyl oleate were used as diluents in determining the influence of olefin concentration on the initial rate of oxidation. By plotting the ratio of initial rates of oxidation in diluted and undiluted samples of olefin against ethyl linoleate concentration, a direct proportionality is found between initial rate of oxidation and [RH] (Fig. 2). The straight lines (*a*) and (*b*) in Fig. 2 join the points representing the relative rates of oxidation of pure ethyl linoleate (1·00) and pure methyl oleate ($0{\cdot}08_5$) and pure linoleate (1·00) and pure ethyl stearate (*ca.* $0{\cdot}00_5$) respectively. The rates recorded in Fig. 2 refer to infinite oxygen pressure, extrapolations being carried out by means of eqn. (1).

(iii) Oxygen Pressure.—The influence of variation of oxygen pressure was followed by carrying out a series of short oxidation runs at different oxygen pressures on a sample of ethyl linoleate containing benzoyl peroxide. Any rate increase throughout the series arising from autocatalysis was allowed for by interspersing the runs with measurements at a convenient standard pressure.

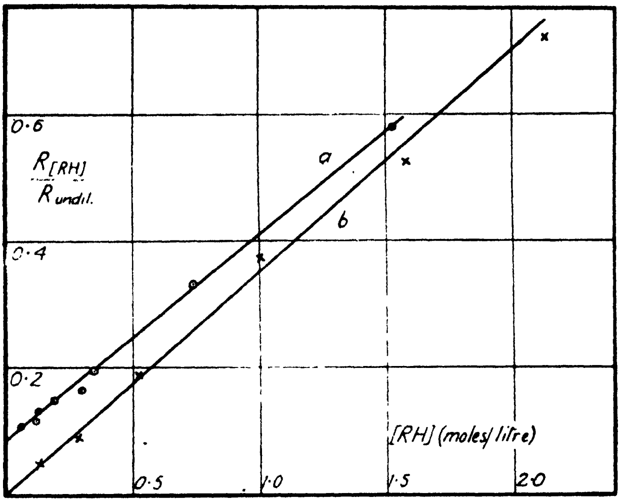

FIG. 2.—Influence of ethyl linoleate concentration, [RH], on rate of oxidation at 55° C. in ethyl linoleate-methyl oleate (curve *a*) and ethyl linoleate-ethyl stearate (curve *b*) mixtures. Curves *a* and *b* are drawn to pass through the point for pure ethyl linoleate.

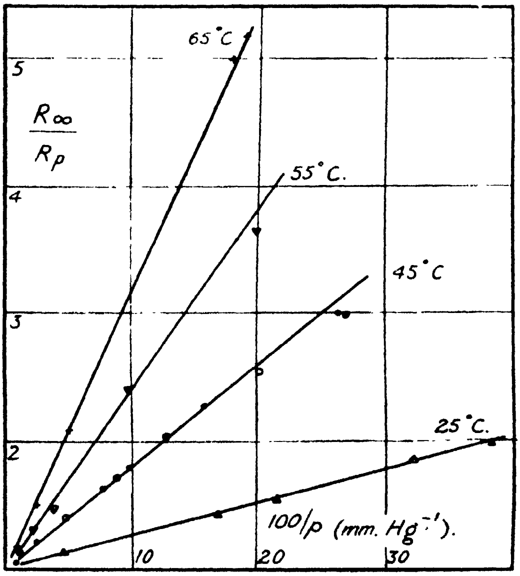

FIG. 3.—Influence of oxygen pressure (p) on rate of oxidation of ethyl linoleate. [Bz_2O_2] at 45° C. is 0·026 and 0·160 moles/l. for full and open circles respectively.

The rate of oxidation and oxygen pressure (p) were found to be accurately related by the equation

$$R_\infty/R_p = 1 + \lambda_c/p \quad . \quad . \quad . \quad . \quad . \quad (1)$$

where R_p and R_∞ are the rates of oxidation when the oxygen pressure is p mm.

Hg and infinite respectively. Fig. 3 gives typical sets of experimental data of this kind, for the four temperatures 25, 45, 55 and 65° c.

Before the precise form of the experimental rate equation can be defined, the dependence of λ_e on the concentration variables $[\mathrm{Bz_2O_2}]$ and [RH] must be known. From the 45° c. curve, Fig. 3, it appears that a six-fold variation in $[\mathrm{Bz_2O_2}]$ has no appreciable effect on the form of the R_∞/R_p against $1/p$ curve : λ_e is therefore apparently independent of $[\mathrm{Bz_2O_2}]$. The influence of [RH] on λ_e was determined from measurements of the dependence of rate of oxidation on oxygen pressure in series of (*a*) ethyl linoleate—ethyl stearate and (*b*) ethyl linoleate—methyl oleate mixtures. In the first case, linear R_∞/R_p against $1/p$ plots were obtained down to ethyl linoleate contents of 8·9 % (curve *c*, Fig. 4), but at lower linoleate concentrations distinct deviations from linearity appeared at very low oxygen pressures (curve *d*, Fig. 4). When, however, the diluent was methyl oleate the R_∞/R_p against $1/p$ plot was linear at linoleate concentrations as low as 4·1 % (curve *e*, Fig. 4). Values of λ_e are plotted against [RH] in Fig. 5. A linear relation between λ_e and [RH] appears to exist for linoleate-oleate mixtures over the entire composition range ; for linoleate-stearate mixtures the same relation is approximately obeyed, though there are undoubted deviations at low linoleate concentrations.

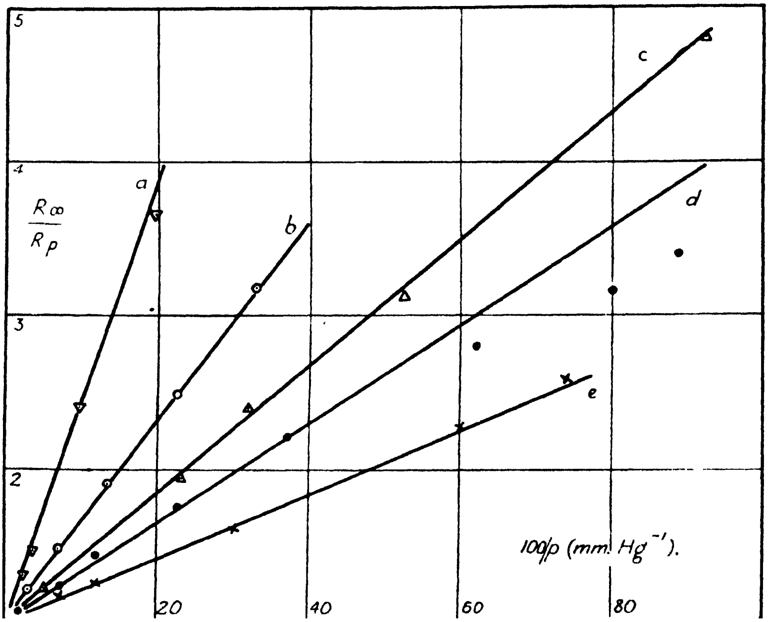

FIG. 4.—Influence of oxygen pressure on rate of oxidation at 55° c. of ethyl linoleate (curve *a*) and ethyl linoleate diluted with (*b*) 65·3 %, (*c*) 91·1 % and (*d*) 95·3 % ethyl stearate and (*e*) 95·9 % methyl oleate.

(iv) Influence of Temperature.—The temperature dependence of (*a*) the rate of oxidation and (*b*) λ_e were determined. In theory (see below) the overall energy of activation of oxidation is best deduced from the variation of the square root of the slope of the $(\text{rate})^2$ against $[\mathrm{Bz_2O_2}]$ relation (as in Fig. 1) with temperature. Provided chromatographed samples of ethyl linoleate were used, the rate of oxidation at zero $[\mathrm{Bz_2O_2}]$ was sufficiently low for this characteristic to be almost undistinguishable from the slope of the linear R_0 against $[\mathrm{Bz_2O_2}]^{\frac{1}{2}}$ curves. Values of this slope determined at an oxygen pressure of 100 mm. are collected in column 2, Table I. The corresponding slopes at infinite oxygen pressures (column 3) were calculated from a relation analogous to eqn. (1). They give an accurately linear log (slope) against $1/T$ curve, the slope of which corresponds to an overall energy of activation (E_0) of $20{\cdot}_5$ kcal./mole. The experimental values of λ_e quoted in the same table also give a linear log λ_e against $1/T$ curve, the apparent energy of activation (E_e) being 9·8 kcal./mole. See p. 676.

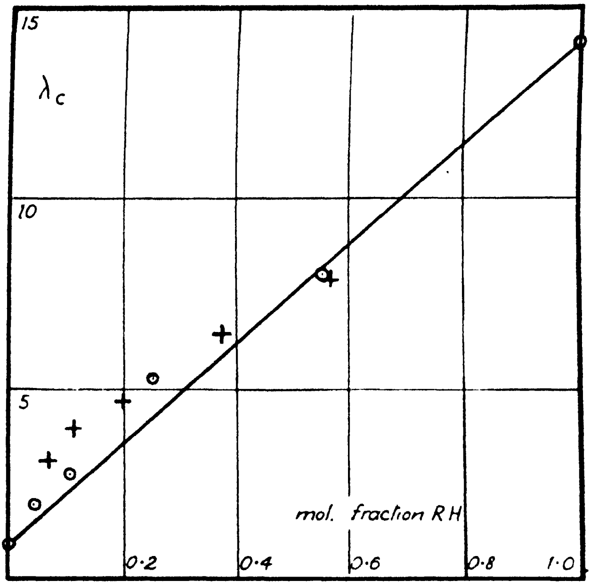

FIG. 5.—Dependence of λ_c on [RH], with ethyl stearate (+) and methyl oleate (○) as diluents.

TABLE I

Temp. °C.	Slope × 10^3. (moles./litre)$^{\frac{1}{2}}$/min.		λ_c (mm. Hg).	λ_a (mm. Hg).
	100 mm.	$p \to \infty$.		
25	0·36	0·37	2·7	2·6
35	0·93	0·97	—	—
45	2·35	2·54	8·1	7·7
55	6·3	7·2	14·0	—
65	14·0	17·0	21	18

The values of λ previously obtained for the autocatalytic oxidation of ethyl linoleate[1] are included in Table I under the column heading λ_a.

Kinetic Analysis.

Investigation of the kinetics of the autocatalysed oxidation of ethyl linoleate[1] showed that the experimental oxidation rates obeyed the relationship

$$-\frac{d(O_2)}{dt} = k_a[RO_2H][RH]\frac{p}{\lambda_a + p} \quad . \quad . \quad . \quad (2)$$

where RO_2H represents the α-methylenic hydroperoxide of ethyl linoleate and k_a and λ_a are constants. This relation was then shown to be consistent with the chain reaction scheme, (R1)-(R6) :

$$
\begin{array}{lrcll}
\text{Initiation:} & 2RO_2H & \rightarrow & R- \text{ or } RO_2- \quad k_1 & \ldots (R1) \\
\text{Propagation:} & R- + O_2 & \rightarrow & RO_2 \quad k_2 & \ldots (R2) \\
 & RO_2- + RH & \rightarrow & RO_2H + R- \quad k_3 & \ldots (R3) \\
\text{Termination:} & R- + R- & \rightarrow & \multirow{3}{*}{} & \\
 & R- + RO_2- & \rightarrow & \left.\begin{matrix}\\ \\ \\ \end{matrix}\right\} \text{Stable products} \left\{\begin{matrix} k_4 \\ k_5 \\ k_6 \end{matrix}\right. & \begin{matrix} \ldots (R4) \\ \ldots (R5) \\ \ldots (R6) \end{matrix} \\
 & RO_2- + RO_2- & \rightarrow & &
\end{array}
$$

where R— represents the hydrocarbon radical obtained by extraction of an α-methylenic hydrogen atom from ethyl linoleate, and RO_2— the corresponding peroxidic free radical; $k_1 \ldots k_6$ are the respective velocity coefficients of the reactions (R1) . . . (R6).

If now the initiation reaction (R1) is written in the generalised form:

$$\text{production of } R- \text{ or } RO_2- \text{ radicals} \quad R_i$$

where R_i represents the rate of chain initiation, stationary-state methods readily yield the following tractable expression for the rate of oxidation.

$$\frac{d(O_2)}{dt} = \frac{R_i^{\frac{1}{2}} . k_3 . [RH]}{\sqrt{k_6}} . \frac{k_2\sqrt{k_6}[O_2]}{(k_2\sqrt{k_6}[O_2] + k_3\sqrt{k_4}[RH] + \sqrt{k_1k_4k_6}[RO_2H])} \quad . \quad (3)$$

the term $\sqrt{k_1k_4k_6}[RO_2H]$ being negligible at all but very short chain lengths.*

The several effects of the systematic variation of $[Bz_2O_2]$, [RH] and oxygen pressure on the rate of the benzoyl peroxide-catalysed oxidation, and the influence of $[Bz_2O_2]$ and [RH] on the factor λ_c lead to a rate equation of the form:

$$-\frac{d(O_2)}{dt} = k_c[Bz_2O_2]^{\frac{1}{2}}[RH] . \frac{p}{k'_c[RH] + p} \quad . \quad . \quad . \quad (4)$$

where k_c is a constant at any given temperature and $k_c' = \lambda_c/[RH]$.

Eqn. (4) is clearly equivalent to the theoretical expression, (3), provided $R_i = k_7[Bz_2O_2]$. It has on several occasions [3-8] been demonstrated that the thermal decomposition of benzoyl peroxide is to a close approximation a first-order reaction. Recent detailed kinetic investigations [6, 7, 9] of the decomposition have stressed the occurrence of secondary reactions which give rise to small deviations from first-order kinetics. Cass, and Nozaki and Bartlett account satisfactorily for the deviation from first-order kinetics in terms of a chain decomposition initiated by radical fragments arising from unimolecular peroxide breakdown. While the precise reaction sequence involved in this chain type of decomposition has not as yet been elucidated in general, the experiments of Cass on the identity of the decomposition products of benzoyl peroxide when certain ethers are used as solvents strongly suggests that here at least the chains are propagated by the reaction cycle:

$$
\begin{array}{ll}
C_6H_5 . COO- + RH \rightarrow C_6H_5 . COOH + R- & \quad . \quad . \quad (P2) \\
R- + (C_6H_5 . COO)_2 \rightarrow C_6H_5 . COOR + C_6H_5 . COO- & \quad . \quad (P3)
\end{array}
$$

---

* This equation requires the simplifying assumption that $k_4k_6 = k_5^2$. It is, however, possible to derive a rate equation without introducing this condition. The resulting relation differs from (3) only in predicting a rather more complex connection between rate of oxidation and oxygen pressure. We have preferred to use the less rigorous but more easily tested eqn. (3), because the wide range of conditions over which it accounts satisfactorily for the effect of oxygen pressure on the rate of benzoyl peroxide-catalysed oxidation makes it evident that the underlying assumption is at least a good approximation to the truth.

[3] McClure, Robertson and Cuthbertson, *Can. J. Res.*, *B.*, 1942, **20**, 103.

[4] Kamenskaya and Medvedev, *Acta Physicochim.*, 1941, **13**, 565.

[5] Brown, *J. Amer. Chem. Soc.*, 1940, **62**, 2657.

[6] Cass, *ibid.*, 1946, **68**, 1976.

[7] Nozaki and Bartlett, *ibid.*, 1946, **68**, 1686.

[8] Barnett and Vaughan, *J. Physic. Chem.*, 1947, **51**, 926.

[9] Cass *J. Amer. Chem. Soc.*, 1947, **69**, 50c.

If this mechanism is applicable to olefins the reaction (P3) would certainly be suppressed completely in presence of oxygen by the reaction,

$$R- + O_2 \rightarrow RO_2-$$

which would at the same time commence the propagation phase of an oxidation chain. In this way the reaction which forms the rate determining step in the initiation process (i.e. R1) would remain unimolecular even in the concentration range in which the overall order of the benzoyl peroxide decomposition, measured *in vacuo*, departs appreciably from unity.

In the derivation of eqn. (4) results obtained with methyl oleate as diluent were adduced as evidence that both the rate of oxidation (at given $[Bz_2O_2]$, oxygen pressure and temperature) and λ_c were proportional to [RH]. In justification of this we must anticipate the conclusion, contained in a following paper, that the mechanism of the benzoyl peroxide-initiated oxidation of methyl oleate is precisely analogous to that for ethyl linoleate. For the present purpose it is sufficient to state that a detailed consideration of the kinetics of the simultaneous oxidation of two olefins according to the above mechanism, (R2)-(R7), leads to the conclusion that both the rate of oxidation and the factor, λ_c, should be linear functions of the concentration of either component—and this in fact was found (cp. Fig. 2 and 5).

A rigorous kinetic analysis of either the autocatalytic or benzoyl peroxide catalysed-oxidation of ethyl linoleate should take into account the small but finite rate of oxidation at zero $[RO_2H]$ or $[Bz_2O_2]$. Experimental examination [2, 10] of this initial uncatalysed rate of oxidation indicates that it occurs by a chain mechanism, the propagation and termination steps of which are represented by (R2)-(R6), while the chain-initiation step involves bimolecular interaction between oxygen and the olefin. The generalised form in which (3) is written thus requires no amendment on this account; but since R_i now becomes, in the case of the benzoyl peroxide-initiated reaction, $k_7[Bz_2O_2] + k_8[O_2][RH]$, it follows that the exact relation between rate and $[Bz_2O_2]$ (at any given oxygen pressure, [RH] and temperature) should not be:

$$\text{rate} \propto [Bz_2O_2]^{\frac{1}{2}}, \text{ but } (\text{rate})^2 \propto [Bz_2O_2] + \text{constant}.$$

Reference to Fig. 1 makes it apparent that this latter law is in fact obeyed (curve *a*), and also that the rate of oxidation at zero $[Bz_2O_2]$ is here so small that the approximation involved in our comparison of the experimental and theoretical expressions for the rate of oxidation (i.e. eqn. (4) and (3)) is fully justified. It should be stressed that this holds true only for carefully chromatographed samples of ethyl linoleate: the presence of polar impurities, presumably mainly free linoleic acid, increases the intercept at zero $[Bz_2O_2]$ to appreciable proportions.

Comparison of the Autocatalytic and Benzoyl Peroxide Catalysed Oxidations.

The conclusion that the mechanisms operating in these two oxidation systems differ only in the manner of chain initiation is so far supported by three experimental findings.

(i) The similarity of the eqn. (2) and (4) above, governing the overall rates of oxidation of the two systems; (ii) the similarity of the rate equations for the two oxidation systems in presence of the chain terminator, hydroquinone; [11] (iii) the fact that the rate equations for both systems conform to a single generalised equation, both when hydroquinone is absent (cp. eqn. (3) above) and present (eqn. (1), Part IV) [11] provided

---

[10] A detailed account of these experiments is now in preparation.

[11] Bolland and ten Have, *Trans. Faraday Soc.*, 1947, **43**, 201.

expressions for the rate of chain initiation are introduced which agree with the observed order of the thermal decomposition of the peroxides concerned, bimolecular decomposition of ethyl linoleate hydroperoxide, and unimolecular decomposition of benzoyl peroxide.

These arguments, which are based on experimentally-determined reaction orders, may be supplemented by comparison of certain quantitative characteristics of the autocatalysed and benzoyl peroxide-catalysed oxidation systems. Three such factors are :

(*a*) the chain length of oxidation,
(*b*) the term λ_c,
(*c*) the energies of activation of the elementary reactions.

(*a*) This comparison has already been made,[1] and shows that if the rate of chain initiation is taken as equal to the rate of peroxide decomposition and if conditions are chosen so that R_i is the same then the chain length in the benzoyl peroxide-initiated oxidation is 2·2 times that for the autoxidation.

(*b*) The values of λ_a and λ_c included in Table I make it obvious that over the temperature range 25°-65° c. the value of λ is the same whether the chain initiatior is linoleate hydroperoxide or benzoyl peroxide.

(*c*) At high oxygen pressures, when the eqn. (4) simplifies to

$$-\frac{d(O_2)}{dt} = \frac{R_i^{\frac{1}{2}} k_3[RH]}{\sqrt{k_6}}$$

the overall energy of activation for the autoxidation and benzoyl peroxide-catalysed oxidation (E_a and E_c respectively) may be written in terms of the energies of activation of the elementary reactions (R1)-(R7) as $\frac{1}{2}E_1 + E_3 - \frac{1}{2}E_6$ and $\frac{1}{2}E_7 + E_3 - \frac{1}{2}E_6$. Taking E_a and E_1 as 17·2 and 26 kcal./mole[1] respectively, $E_3 - \frac{1}{2}E_6$ for the autoxidation becomes 4·2 kcal./mole ; the best available values for E_c and E_7 are 20·5 and 31 kcal./mole, giving a second estimate of $E_3 - \frac{1}{2}E_6$ based on the benzoyl peroxide catalysed oxidation of 5·0 kcal./mole.

It is further found that values of E_λ are very similar for the two oxidation systems. For the autoxidation [1] the determined value of E_λ was 8·7 kcal./mole, compared with the figure of 9·5 kcal./mole for the benzoyl peroxide-catalysed reaction (p. 673). In terms of the activation energies of the elementary reactions this means that for the two oxidation systems, very similar estimates of $E_2 - E_3 - \frac{1}{2}(E_4 - E_6)$ and (since $E_3 - \frac{1}{2}E_6$ is the same for both systems) $E_2 - \frac{1}{2}E_4$ are obtained.

These various correlations between the two types of oxidation system are sufficiently exact to provide very strong confirmatory evidence for the correctness of the mechanisms of oxidation, deduced for each system when considered independently.

The author is indebted to Dr. G. Gee and Dr. L. Bateman for valuable advice and criticism. This work forms part of the programme of fundamental research undertaken by the Board of the British Rubber Producers' Research Association.

Summary.

Kinetic investigation of the interaction of oxygen and ethyl linoleate in presence of benzoyl peroxide leads to the conclusion that oxidation chains are initiated by the unimolecular dissociation of benzoyl peroxide into radicals, which in turn lead to the production of R-radicals. The propagation reactions are

$$\mathbf{R- + O_2 \rightarrow RO_2 -}$$
$$\mathbf{RO_2 - + RH \rightarrow RO_2H + R -}$$

and termination occurs through mutual interaction of pairs of the chain carriers, $R -$ or $RO_2 -$. (RH represents ethyl linoleate, $R -$ the radical produced by removal therefrom of an α-methylene hydrogen atom, and $RO_2 -$ the corresponding peroxide radical.)

Comparison of various kinetic features of the oxidation of ethyl linoleate initiated by benzoyl peroxide, and the autoxidation of the same olefin indicate that the chain-propagation and chain-termination steps of these two systems are identical.

The British Rubber Producers, Research Association,
48-52 Tewin Road,
Welwyn Garden City,
Herts.

THE THERMAL DECOMPOSITION OF EXPLOSIVES. PART I. ETHYLENEDINITRAMINE AND TETRYL.

BY A. J. B. ROBERTSON.

*Received 26th September, 1947.**

It has been shown by many investigations, notably those of Will,[1] Robertson,[2] Farmer,[3, 4] and Hinshelwood,[5] that all explosives undergo a thermal decomposition at temperatures far below those at which spontaneous explosion may occur. The decomposition reaction is of considerable importance in determining the stability of the explosive and has consequently received much attention, especially of a somewhat empirical kind. Roginsky[6] has represented some of the reported results for decomposition rates by assuming the applicability of the unimolecular equation and then evaluating the constants in the Arrhenius expression for the unimolecular constant, $k = Ae^{-E/RT}$. He concludes from this treatment that the frequency factor A varies from 10^{19} to 10^{25} sec.$^{-1}$ and E is of the order 50,000 cal./mole for many of the high explosives. The extremely large value of the term A as compared with the normal value of about 10^{13} for unimolecular reactions is considered by Semenoff[7] to indicate the formation of long and stable chains in these decompositions, although an alternative explanation in terms of the activated-complex theory of reaction rates can be advanced. It seems desirable, however, that the experimental facts should be established more securely in view of the divergency in activation energies for the decomposition of explosives found in the literature. Kinetic data for various explosives are also of interest in the fundamental study of the sensitiveness of explosives to external stimuli, and they may have some interest in connection with condensed liquid-phase reactions.

Here we describe an experimental investigation of the two nitroamines, *N*, *N′*-dinitroethylenediamine and 2 : 4 : 6-trinitrophenylmethylnitramine (tetryl). In investigating these decompositions it was thought desirable to follow the reaction over its whole course, and to work under conditions enabling the transformation of thermal decomposition into explosion to be examined; hence the range of enquiry was extended to relatively high temperatures. Thermal decompositions of explosives are usually highly exothermic, and since the conditions should be as nearly isothermal as possible in determining decomposition rates, it is necessary to use apparatus which allows the heat evolved to be readily conducted away from the explosive, and to use rather small quantities of material. The reactions may then be very rapid although they are not explosive so that special recording methods must be used. Apparatus was developed for heating samples of explosives to a given temperature within a small fraction of a second, the resulting liberation of gaseous decomposition products being followed by automatic recording. With this method reactions taking less than a second were investigated using quantities down to 1 mg.

---

[1] Will, *Z. angew. Chem.*, 1901, **14**, 743, 774.

[2] Robertson, *J. Soc. Chem. Ind.*, 1902, **21**, 819 ; *J. Chem. Soc.*, 1909, **95**, 1241 ; 1921, **119**, 1.

[3] Farmer, *J. Chem. Soc.*, 1920, **117**, 1432 ; 1922, **121**, 174.

[4] Farmer, *ibid.*, 1920, **117**, 1603.

[5] Hinshelwood, *ibid.*, 1921, **119**, 721.

[6] Roginsky, *Physik. Z. Sowjet.*, 1932, **1**, 640 ; *Z. physik. Chem.*, *B*, 1932, **18**, 364.

[7] Semenoff, *Chemical Kinetics and Chain Reactions*, Chap. 17 (Oxford Univ. Press, 1935).

Experimental.

For rapid heating of the sample of explosive in a closed system two forms of apparatus were used. In the first, the material was introduced into a hot glass bulb. In the second, the sample was suddenly enclosed between two hot parallel surfaces. The first apparatus had the advantages of simplicity and cleanliness, and the second the advantage of a more precise definition of the heating conditions since the thin liquid explosive layer was maintained by surface tension at a constant thickness equal to the distance between the two hot surfaces. This was of some utility in investigating the transformation of thermal decomposition into explosion, since the arrangement could be regarded as practically a reaction vessel with plane parallel walls, which is a specially simple shape for mathematical treatment. The conditions for the initiation of explosion could also be examined in general features in the glass bulb apparatus.

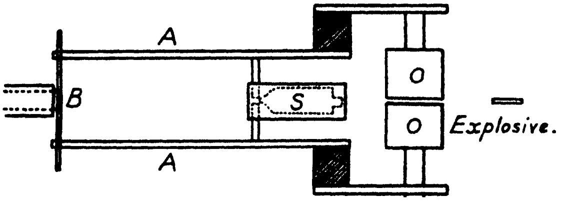

FIG. 1.—Ovens Apparatus.

GLASS APPARATUS.—In the glass apparatus the sample of explosive was placed in a small glass spoon rotating on a horizontal ground joint so that the sample could be dropped into the heated bulb. The bulb, of Pyrex glass about 2 cm. diam., was directly immersed in a bath of transparent heating liquid (the eutectic mixture of sodium, potassium and calcium nitrates) so that the reaction could be observed visually. With vigorous stirring of the liquid, heat removal from the reaction zone was facilitated and very rapid reactions could be brought about without explosion. The bath temperature was kept constant to within ½° c. Mercury thermometers calibrated at frequent intervals were employed, corrections for the emergent stem being made. The reaction bulb was removed by means of a ground-glass joint for cleaning in hot nitric and chromic acids after each experiment.

OVENS APPARATUS.—In the alternative apparatus the explosive under investigation, supported on a mica slide about 10^{-3} cm. thick, was suddenly enclosed between two parallel horizontal copper surfaces a known distance apart and maintained at the required temperature, the apparatus being adjusted so that the mica slide was resting on the lower hot surface. A diagrammatic representation of the essential mechanism used is shown in Fig. 1. The apparatus is shown in the original position before the experiment is started. The heating ovens (O), consisting of hot copper bobbins, were carried on two arms (A) hinged to a back strip (B) fastened to a spindle sliding in a bearing. When the experiment started the spindle was pulled forward by springs (not shown) on being released by a catch operated by the movement of a Tombac bellows. The ovens then moved forward and opened at the same time under the influence of the springs and the shell-shaped device (S) shown in the diagram. When the ovens were above and below the explosive they automatically closed upon it. The distance between the ovens was set prior to the experiment at the desired value. Both ovens could be moved up and down with respect to the arms holding them. The oven temperature was measured with a copper-constantan thermocouple, hard-soldered into the face of each bobbin. Frequent calibrations of the thermocouple readings were made with substances of known melting point. The entire apparatus could be enclosed by a vacuum-tight cylindrical brass cylinder containing two Perspex observation windows. The cover was clamped to a base plate through which the various leads passed.

When the apparatus was used in the presence of an inert gas, as was usually required to prevent complete and rapid vaporisation of the explosive from the hot zone, the movement of the hot ovens through the cooler gas produced a rapid expansion and contraction of gas lasting about 4 sec.; this effect was imposed upon the records of pressure against time, the magnitude of the pressure fluctuation at atmospheric pressure being about the same as the pressure change produced by a few mg. explosive. For examining the rate of rapid reactions by pressure changes in the presence of inert gas the copper ovens apparatus was not, therefore, so convenient or so accurate as the glass bulb apparatus, which was quite free from this effect.

Measurement of Reaction.—Both the bulb apparatus and the ovens apparatus formed part of a closed system in which the decompositions were followed by the pressure increase. For slow reactions the pressure change was read on an Apiezon oil manometer connected to the reaction vessel by several feet of thin tubing to minimise errors from possible solution of gaseous products in the oil. Rapid reactions were followed with a manometer of the membrane type, the small displacement of a thin horizontal brass membrane being magnified with a pivoted mirror and light beam and registered on photographic paper moving with a suitable steady velocity. This device gave a linear relation between pressure change and the displacement of the light spot, since only a small fraction of the possible displacement of the membrane was used. The whole membrane manometer was enclosed in a larger vacuum-tight vessel with glass windows. A small mercury seal was provided between the two sides of the membrane as a protection against explosion.

Analysis of Gaseous Products.—A separate apparatus was used for the formation and analysis of the gaseous decomposition products. The explosive was again decomposed in a Pyrex bulb of about 2 cm. diam. which could be removed at a ground joint for cleaning. The bulb was heated after the explosive had been weighed into it by immersion in a heating bath, and visual observations of the progress of the decomposition were made. A known quantity of N_2 was added to reduce vaporisation of the explosive to negligible proportions. Cylinder N_2 was purified by passage over red-hot copper, a sodium hydroxide preparation (Carbosorb) and P_2O_5. The gases were first divided into two fractions by pumping off separately those volatile at liquid air temperatures and at −80° c. The gases were dried by passing over P_2O_5 and collected over mercury with a Toepler pump. The liquid-air fraction was analysed for NO by absorption in chromous chloride, CO and H_2 by a copper oxide combustion, the final residue being N_2. Dissolved gases in the chromous chloride were first pumped off with a rotary pump. Nitric oxide was determined again in the −80° c. fraction with chromous chloride as this gas could only be removed at liquid-air temperatures by very prolonged pumping. Carbon dioxide both from oxidation of CO and as such was absorbed with solid Carbosorb; and the residual gas was N_2O. The use of a solid reagent for CO_2 was found advantageous in eliminating the corrosive effect of the usual potash reagent which may be inconvenient in a vacuum apparatus. Any NO_2 remained behind at −80° c., but only traces were encountered during experiments with nitroamines. The gas samples could be manipulated and measured quite readily to an accuracy of 0·01 ml.

The Decomposition of Ethylenedinitramine.

The thermal decomposition was examined in the glass bulb apparatus. In a vacuum (about 10^{-3} mm. Hg) the substance vaporised and distilled on to the cooler parts of the apparatus before undergoing appreciable decomposition. On preventing this by having an inert gas (usually N_2) present at 10 cm. pressure the liquid explosive was found to decompose under suitable conditions according to the equation for a first-order reaction over the whole temperature range 184-254° c. The unimolecular constant k was evaluated from the usual equation, $\log_e p_\infty/(p_\infty - p) = kt$, where p_∞ is the final pressure increase and p is the pressure increase after time t, or from an equation given by Guggenheim,[8] which does not require a value for p_∞, $kt + \log_e (p_\tau - p) =$ constant, where p is the pressure at time t and p_τ is the pressure at time $t + \tau$, τ being some arbitrary constant time-interval of convenient magnitude: for accuracy it should be greater than the half-life of the reaction.

The half-life for the decomposition of ethylenedinitramine was 43 sec. at 184° c. and ½ sec. at 254° c. The observed rate constant was independent of mass at the lower temperatures using quantities varying from 5 to 30 mg. and an inert gas pressure of 10 cm. The larger quantities at the higher temperatures underwent an explosive decomposition. The decomposition rate was the same in the presence of air and N_2 and was not altered by further recrystallisation of the sample of explosive from acetone. At the higher temperatures it was found necessary to use only a few mg. of the explosive in the form of very small particles in order to make the attainment of thermal equilibrium a sufficiently rapid process for the determination of the decomposition rate. On deriving unimolecular constants and plotting $\log_{10} (k \times 10^2)$ against $1/T$ the points shown in Fig. 2 were obtained. A straight line to fit the points was determined by the method of least squares and gave for the unimolecular constant the expression k (sec.$^{-1}$) $= 10^{12.8} e^{-30,500/RT}$. The experimental error in activation energy was estimated to be less than 1,500 cal./mole. This expression for the decomposition rate does not hold for solid ethylenedinitramine. Although appreciable decomposition occurred below the melting point the rate was very much less than that given by the equation above.

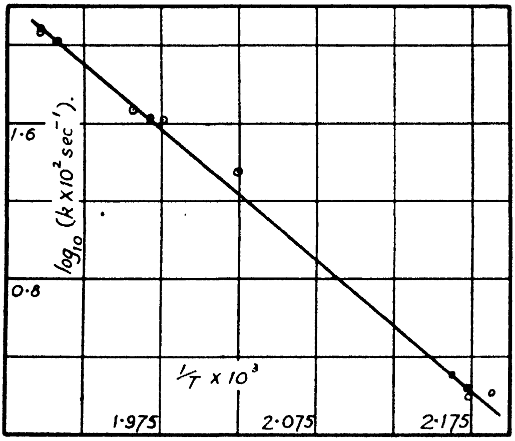

FIG. 2.—Ethylenedinitramine.

Analyses were made of the gaseous products from ethylenedinitramine heated at 195° c. for 3·5 min. (giving practically complete decomposition), N_2 being initially present at 5 cm. pressure. From 1 mole of the explosive the following quantities in moles of gaseous products were obtained: NO, 0·10; N_2O, 1·4; N_2, 0·39; CO, 0·028; CO_2, 0·065. Water was also formed and acetaldehyde was detected by carrying out the decomposition in a stream of hot air passed subsequently through aqueous dimedone solution, the derivative separating after a few hours. The decomposition in part can therefore be represented by the equation, $C_2H_6N_4O_4 = 2N_2O + CH_3CHO + H_2O$, but it is clear from the considerable quantities of N_2 formed that some other mode of decomposition is also operative.

---

[8] Guggenheim, *Phil. Mag.*, 1926, 2, (7), 538.

The Decomposition of Tetryl.

The thermal decomposition in the liquid phase was examined over the temperature-range 211-260° c. The copper ovens apparatus was used with air present, usually at atmospheric pressure, to prevent vaporisation without decomposition as far as possible. A quantity of 20-30 mg. was taken for each experiment. The separation between the two hot surfaces was 0·2 mm. The pressure-time curves showed the occurrence of some acceleration of reaction rate during the decomposition, which was considered to be due to autocatalysis in general agreement with the findings of Farmer[4] and Hinshelwood.[5] At 217° c. the rate of gas evolution remained constant for nearly half the decomposition, corresponding to an accelerative reaction; the subsequent falling-off in rate was slightly greater than that for a first-order decomposition. At increasing temperatures the period of constant rate of gas evolution increased somewhat relative to that of the rest of the decomposition, and in the region of 250° c. and above, a rapid evolution of gas at an almost linear rate was followed by a small diminution in pressure; this was thought to be due to the cooling of hot gaseous products of reaction. On diminishing the air pressure to 10 cm. the initial decomposition rate was unchanged, but slightly less autocatalysis was noted. In vacuum the tetryl vaporised without appreciable decomposition. The initial linear rate of pressure increase divided by the total or maximum pressure increase in the same experiment gives a quantity which can be regarded as a unimolecular constant for the decomposition before it is appreciably influenced by accumulation of the autocatalyst. On determining the initial rate in this way and plotting $\log_{10} (k \times 10^2)$ against $1/T$ the points shown in Fig. 3 were obtained, the straight line shown giving for the unimolecular constant of the initial decomposition the expression

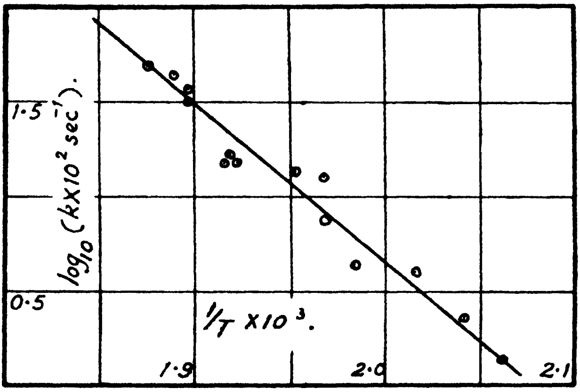

FIG. 3—Tetryl.

$$k \ (\text{sec.}^{-1}) = 10^{15 \cdot 4} \, e^{-38,400/RT}$$

The experimental error in E was estimated to be 2,500 cal./mole.

The initial decomposition of tetryl has also been investigated by Farmer.[4] He found at 129·9° c. a gas evolution of 1·5 cc./g./hr. Utilising his observation that 5 g. tetryl (in the solid state) gave 500 cc. on decomposing completely and assuming this would also be the case for the liquid, the unimolecular constant for the initial decomposition at 129·9° c. is $4 \cdot 2 \times 10^{-6}$ sec.$^{-1}$. The value calculated from the equation given above is $4 \cdot 0 \times 10^{-6}$. The agreement is satisfactory as far as the absolute rate is concerned. From Farmer's results on the temperature variation of the rate over the small temperature range 129·9-138·6° c. the initial rate can be represented by $k = 10^{27} e^{-60,000/RT}$ as Roginsky[6] has pointed out, and he has attached some significance to this result. This expression, however, gives for the initial rate at 260° c. a value some 500 times greater than the experimental one given here. It seems clear, therefore, that in this particular case the Arrhenius frequency factor has a value which is not very much greater than the normal one for unimolecular decompositions.

Discussion.

The simplest behaviour which an explosive under effectively isothermal conditions can exhibit is to break down into gases by a homogeneous reaction of constant velocity. This behaviour is shown by ethylenedinitramine. The homogeneous nature of the decomposition was deduced from the non-variation of rate with quantity of explosive. The fact that the first-order equation is applicable does not necessarily imply that the decomposition is unimolecular, since it is occurring in the condensed liquid phase. Experiments in dilute solution are required to elucidate this point. For both ethylenedinitramine and tetryl the temperature variation of the decomposition rate can be represented by an equation of the Arrhenius type, and in the case of ethylenedinitramine the frequency factor has the normal value found for unimolecular decompositions in the gas phase.

A number of factors may complicate the later stages of the decomposition of explosives and cause deviations from the unimolecular equation. In general these factors produce an acceleration of the reaction, such as that observed in the tetryl decomposition. Intermediate or final products may be formed which exert a catalytic effect on the primary decomposition or which by their own decomposition contribute appreciably to the observed rate of gas evolution. Catalysis by gaseous or volatile products may make the interface between liquid and gas of importance. It is probable that factors of this kind explain the very high frequency factor computed by Roginsky for tetryl. Self-heating of the explosive may also be of importance in many cases. This, however, is favoured by larger quantities of explosive and by higher gas pressures. At higher pressures the bubbles of gaseous decomposition products are smaller and the agitation of the liquid caused by them is less. Studies of the initiation of explosion in liquids have shown that heat loss by convection is of primary importance, and the part played by bubbling in causing this seems to be very significant. Self-heating is thus diminished by working at lower gas pressures. Hence it is possible by varying the quantity of explosive or the inert gas pressure to verify that observed decomposition rates are not seriously in error on account of self-heating. As judged by these tests the data given here should not be seriously complicated by this factor.

This work forms part of a programme carried out jointly with the Department of Chemistry, Bristol University. The author has much pleasure in thanking Dr. C. E. H. Bawn for information on the decomposition of tetryl and on the method of gas analysis employed, Prof. E. K. Rideal for his constant advice and encouragement, and Mr. W. N. Dear for his help in constructing the analytical apparatus. This paper is published by permission of the Chief Scientist, Ministry of Supply.

Summary.

Two methods for studying the thermal decomposition of explosives are described. The rate of decomposition of ethylenedinitramine and tetryl has been studied and Arrhenius expressions are given. The decomposition of ethylenedinitramine follows the unimolecular equation and the frequency factor is normal. With tetryl, catalytic effects are encountered and the frequency factor is somewhat large. Analyses of the gaseous products from ethylenedinitramine have been made.

Department of Colloid Science,
The University,
Cambridge.

THE REDUCTION OF NITROCOMPOUNDS AT THE DROPPING-MERCURY CATHODE.

PART I.—THE NITROBENZENES AND NITROTOLUENES.*

By J. Pearson.

Received 30th September, 1947.

Although a considerable amount of work has been carried out, mainly by Shikata and his collaborators [1, 2, 3] on the reduction of nitro-compounds at the dropping-mercury cathode, the published results do not contain any explicit statement as to the nature of the electrode reactions. Moreover, the method employed in these previous investigations for the reporting of reduction-potentials has now been superseded because of ambiguity.[4] The electrode reactions occurring during "polarographic reduction" have therefore been studied more fully and particular attention paid to the influence of the nature of the medium in which the compounds were dissolved upon the reduction-potentials and the mechanism of reduction.

Experimental.

The polarograph employed was of the conventional, photographically recording type, constructed in the laboratory. It incorporated condenser galvanometer-damping and diffusion-current compensation as recommended by Lingane and Kerlinger [5] and a modification of the Ilkovic and Semerano [6] counter-current control. The electrolysis-cells were immersed in a thermostat, maintained at 25 ± 0·25° C. and a separate saturated calomel electrode was used as anode. The illustrations are drawn (without showing galvanometer oscillations) from the photographically-recorded originals.

Solutions were made by dissolving the requisite weight of purified compound in 98 % ethyl alcohol, diluting five-fold with distilled water, and then diluting two volumes of the aqueous-alcoholic solutions to five volumes with an aqueous buffer solution. The buffer solutions employed were those recommended in standard works, except that they were made up to a concentration two and a half times the normal. They contained in addition sufficient gelatine, as maximum suppressor, to render the final solutions 0·01 % with respect to this substance. The *p*H of all solutions was determined with a Cambridge *p*H-meter before polarographing. The buffer solutions used were :

*p*H	Buffer
0·5	potassium chloride-hydrochloric acid.
1·7	sodium acetate-hydrochloric acid.
2·5 3·0 3·8	potassium hydrogen phthalate-hydrochloric acid.
4·1 5·7 7·4	potassium hydrogen phthalate-sodium hydroxide.
9·2	borax.

Dissolved O_2 was removed by passing N_2 for 5 min. ; the gas was previously passed through a bottle containing a portion of the solution under test. After a polarogram had been recorded, the potentials at which diffusion-current plateaux were well developed were noted, and the drop-time of the cathode determined at these potentials. The cell leads were then disconnected and with the electrodes still in position, the cell-resistance was measured. To the value so obtained was added the resistance of the rest of the cell-galvanometer circuit and the result employed to evaluate the iR term for the correction of the applied voltage to obtain true cathode potentials. The rate of flow of mercury from the cathode-capillary was determined at frequent intervals by allowing it to discharge into water at 25° c. as suggested by Kolthoff and Lingane.[7]

---

* This communication forms part of a thesis submitted in January, 1946 to the University of London in partial fulfilment of the requirements for the Degree of Ph.D.

[1] Shikata, *Trans. Faraday Soc.*, 1925, **21**, 42, 53.

[2] Shikata and Hozaki, *Mem. Coll. Agr. Kyoto Imp. Univ.*, 1931, **17**, 1, 21.

[3] Shikata and Watanabe, *J. Agr. Chem. Soc., Japan*, 1928, **4**, 924.

[4] Müller, *Chem. Rev.*, 1939, **24**, 95.

[5] Lingane and Kerlinger, *Ind. Eng. Chem.* (*Anal.*), 1940, **12**, 750.

[6] Ilkovic and Semerano, *Coll. Czech. Chem. Comm.*, 1932, **4**, 176.

Results.

(a) The Nitrobenzenes.—Solutions of nitrobenzene made up in the manner described above, over the concentration-range 0·04-0·6 millimolar, were polarographed in media of pH 2·5, 5·7 and 9·2, i.e. in acid, approximately neutral, and alkaline conditions. A pH higher than 9·2 was not employed, lest alkaline decomposition of the nitrocompound should occur. The solutions of lower concentration were polarographed at higher galvanometer sensitivities to record convenient wave-heights. Typical results are shown in Fig. 1.

The number of electrons involved in the reduction of 1 molecule of substance may be derived, from the Ilkovic equation,[8] as $n = i_d/605 \,.\, D^{1/2} \,.\, C \,.\, m^{2/3} \,.\, t^{1/6}$. Lingane and Loveridge[9] have proposed the term " diffusion-current constant " for the value of $i_d/C \,.\, m^{2/3} \,.\, t^{1/6}$. In the polarogram shown, at pH 9·2 (Fig. 1 (c)) i_d and C were 7·56 μa. and 0·60 millimolar, respectively, and at a cathode potential of $-1·1$ v., at which the diffusion-current was well established, the value of $m^{2/3} \,.\, t^{1/6}$ was 1·846. The diffusion-current constant (K) for nitrobenzene is therefore $7·56/(0·60 \times 1·846) = 6·82$. The diffusion-coefficient of nitrobenzene may be taken to be the same as that of the benzoate ion,[10] which is calculable from conductivity data as $8·28 \times 10^{-6}$ cm.^{2} sec.$^{-1}$ at 25° c. The value for n for the reduction of nitrobenzene is therefore $6·82/605 \times (8·28 \times 10^{-6})^{1/2} = 3·92$. Since the reduction process must involve a whole number of electrons, it follows that the number concerned in this reaction is four. The molecular sizes, and presumably also the diffusion-coefficients, of all the nitrobenzenes are of the same order, and it is therefore logical to assume for all of them that a diffusion-current constant of 6·8 corresponds to a four-electron reduction, i.e. $n = K/1·7$.

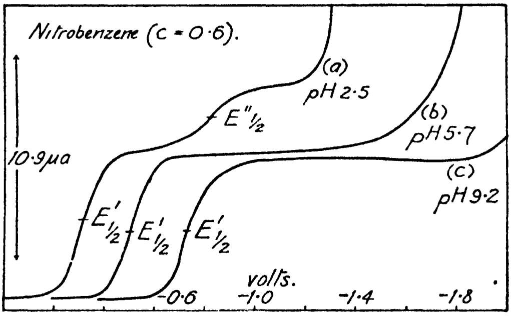

FIG. 1.

The value for K for nitrobenzene at pH 5·7 was 6·88 and it therefore follows that here also a four-electron reduction occurs. At pH 2·5, there are two waves, K-values being 6·77 and 9·8 respectively. The number of electrons concerned in the two stages of reduction are therefore four and six, or if we think of them as consecutive reactions, four and two.

A reduction of nitrobenzene involving four electrons implies production of phenylhydroxylamine or azobenzene ; the latter requires eight electrons for each two molecules of nitrobenzene. It is known, however, that azobenzene is reducible to hydrazobenzene at *p*H values from 1·2 to 13·0.[11] Moreover, the reduction potential of azobenzene is more positive than that of nitrobenzene at the same *p*H.[11] If, therefore, nitrobenzene were reduced to azobenzene it is to be expected that this would immediately be further reduced to hydrazobenzene. This would involve a total of five electrons per molecule of nitrobenzene. Since the number actually involved is only four, the reduction-product must be phenylhydroxylamine. Although at *p*H 2·5 the initial reduction-product is further reducible, it proceeds to aniline, i.e. a total of six electrons is involved. This again implies that the four-electron reduction of nitrobenzene is to the hydroxylamine state.

---

[7] Kolthoff and Lingane, *J. Amer. Chem. Soc.*, 1939, **61**, 825 ; *Chem. Rev.*, 1939, **24**, 1.

[8] Ilkovic, *Coll. Czech. Chem. Comm.*, 1934, **6**, 498 ; MacGillavry and Rideal, *Rec. trav. chim.*, 1937, **56**, 1013.

[9] Lingane and Loveridge, *J. Amer. Chem. Soc.*, 1944, **66**, 1425.

[10] Kolthoff and Lingane, *Polarography* (Interscience Pub. Inc., New York, 1941), 51.

Since the reduction process at *p*H 2·5 is different from that at *p*H 5·7 and 9·2, it was decided to investigate other media to ascertain at what *p*H the change occurs. Accordingly, similar experiments were performed at *p*H 0·5, 1·7, 3·0, 3·8, 4·1 and 7·4. At the four lower values it was found that the reduction process is the same as that at *p*H 2·5, but at *p*H 4·1 and 7·4 polarograms similar to those at *p*H 5·7 and 9·2 were obtained. This indicates that there is a fairly sharp division between complete and partial reduction of nitrobenzene. From results to be described later, it is not considered that this division occurs at a definite *p*H, but over a range which may be narrow, as with nitrobenzene, or fairly wide with other substances. It should be noted that the second wave in Fig. 1 (*a*) is not particularly well defined, and at other low *p*H values it is even less so. In tabulating results, therefore, the half-wave potentials of these second waves are not given.

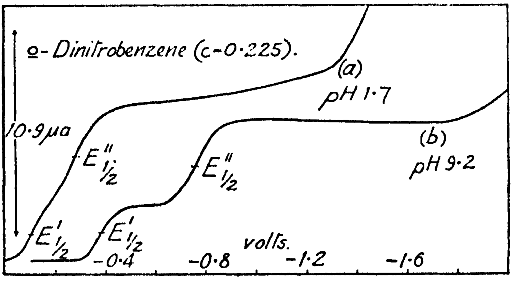

FIG. 2.

The polarographic half-wave potentials of nitrobenzene at all the above hydrogen-ion concentrations are given in Table I. Over the range of concentration and *p*H studied, diffusion-currents are directly proportional to, and half-wave potentials are constant and independent of, concentration.

The other compounds listed in Table I were polarographed at all *p*H values mentioned above; their solutions were made up in the same manner as for nitrobenzene, except that on account of lower solubility in aqueous alcohol the maximum concentrations (indicated on the accompanying figures) were somewhat lower. In each instance it was found that reduction in acid was different from that in alkaline media. Fig. 2, 3, 4 and 5 depict typical polarograms and Table I gives half-wave potentials and numbers of electrons concerned in the various reductions, calculated from the diffusion-current constants.

It is to be noted that *o*-dinitrobenzene (at *p*H 3·8), *m*-dinitrobenzene (*p*H 3·0 and 3·8) and trinitrobenzene (*p*H 3·8 and 4·1) exhibit stages of reduction intermediate between that occurring in acid and that in alkaline media. This is presumably because some proportion of the molecules are reduced in one way and the remainder in the other. Attention is also called to the fact *p*-dinitrobenzene suffers complete reduction at *p*H 9·2; formation of *aci*-salts may be responsible, as the third step in the current-voltage curve is only just discernible at *p*H 8·6, but quite distinct at *p*H 9·0 and fully developed at *p*H 9·2. As with nitrobenzene, at all *p*H values, half-wave potentials are independent of, and diffusion currents directly proportional to, concentration.

[11] Shikata and Tachi, *Mem. Coll. Agr. Kyoto Imp. Univ.*, 1931, **17**, 45; 1937, **40**, 1, 11; 1938, **71**, 1785.

Where an apparently single wave is known to be due to the merging of two or more waves, half-wave potentials for the components have been inserted in the figures. Reductions involving four electrons are assumed to produce the corresponding hydroxylamine ; those involving an extra two electrons to produce the amine.

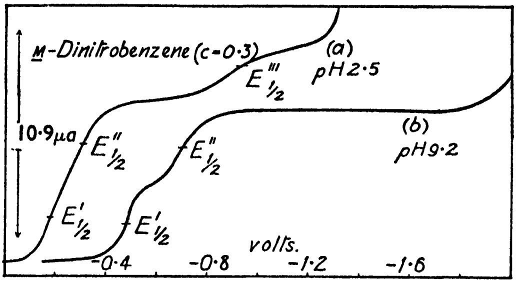

FIG. 3.

(b) The Nitrotoluenes.—Apart from slight differences in half-wave potentials, the behaviour of the nitrotoluenes investigated is essentially similar to that of the analogous nitrobenzenes. The change from " acid " to " alkaline " type of reduction covers a wider *p*H range for the mono-nitrotoluenes than for nitrobenzene. The half-wave potentials and *n*-values for the nitrotoluenes are given in Table II. The ranges of concentration studied were the same as for the mono-, the di- and the tri-nitrobenzenes and as with these, the half-wave potentials are independent of, and diffusion-currents proportional to, concentration.

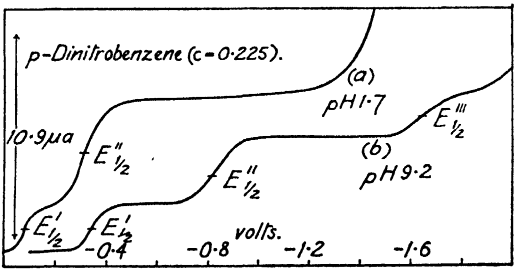

FIG. 4.

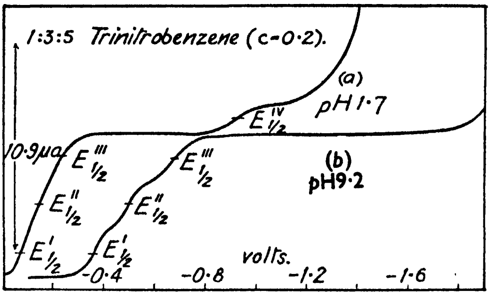

FIG. 5.

Discussion.

(i) Influence of Hydrogen-ion Concentration on Reduction Process and on Half-wave Potential.—One feature is immediately obvious from an inspection of Tables I and II, namely the marked change in the reduction process as the hydrogen-ion concentration changes. This appears not to have been previously reported. Reduction in acid media leads in general to the formation of the polyamino-compounds, through the intermediary of the hydroxylamines. In alkaline media, reduction is not complete; the polyhydroxylamines are generally produced. The change from " acid " to " alkaline " reduction occurs apparently abruptly with some compounds and over a range of *p*H with others.

It is also of interest to observe that the effect of *p*H on half-wave potential is different in acid and alkaline conditions (see Fig. 6), and that the intersections of the branches of the curves occur in the *p*H range where reduction-process changes. This behaviour appears to be connected with the fact that the initial reduction-product is basic and can form salts in acid media, by combining with a hydrogen-ion. The " phenylhydroxylammonium-ion " is capable of further reduction if the cathode potential is sufficiently low, whereas the hydroxylamine base is resistant to further reduction, at least before electrolysis of the supporting electrolyte intervenes. In the range between acid and alkaline conditions, some of the reduced material will undergo salt-formation and will thus be further reducible. The result will be current-voltage curves intermediate between those occurring in acid and those in alkaline media. The variation in base-strength of the hydroxylamines derived from the different nitro-compounds would account for the fact that the range where change from acid to alkaline reduction occurs differs for each compound. Since the reduction product in acid media combines with a hydrogen ion, it is to be expected that the effect of *p*H on half-wave potential will be different from that in alkaline solutions.

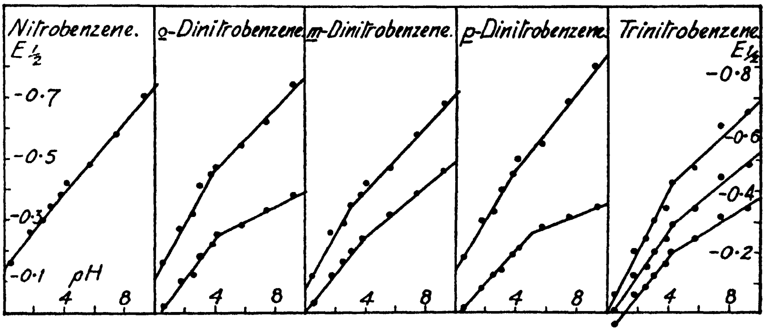

FIG. 6.

(ii) The Reduction of Nitrocompounds.—It is customary [12] to express the reversible reduction of an organic compound as

$$A + ne + nH^+ = B.$$

For irreversible reductions which involve apparently as many as four or more electrons and hydrogen-ions, this simple picture is very unlikely. The following process which is analogous to that proposed by Heyrovsky [13] to account for the relation between the potential, the current, and the hydrogen-ion concentration in the discharge of hydrogen at the dropping electrode, appears to be more feasible. The primary electrode reaction consists of the reversible deposition of hydrogen ions at the cathode:

$$H^+ + e = H. \quad . \quad . \quad . \quad . \quad . \quad (1)$$

---

[12] ref. [10], p. 184.

[13] Heyrovsky, *Coll. Czech. Chem. Comm.*, 1937, 9, 273.

TABLE I.—POLAROGRAPHIC CONSTANTS OF THE NITROBENZENES.

*p*H.	0·5		1·7		2·5		3·0		3·8		4·1		5·7		7·4		9·2	
Constant.	$E_{\frac{1}{2}}$.	*n*.	$E_{\frac{1}{2}}$.	*n*.	$E_{\frac{1}{2}}$.	*n*.	$E_{\frac{1}{2}}$.	*n*.	$E_{\frac{1}{2}}$.	*n*.	$E_{\frac{1}{2}}$.	*n*.	$E_{\frac{1}{2}}$.	*n*.	$E_{\frac{1}{2}}$.	*n*.	$E_{\frac{1}{2}}$.	*n*.
Nitrobenzene	−0·16 ?	4 6	−0·26 ?	4 6	−0·30 ?	4 6	−0·34 ?	4 6	−0·38 ?	4 6	−0·42 —	4 —	−0·48 —	4 —	−0·58 —	4 —	−0·70 —	4 —
o-Dinitrobenzene	−0·01 −0·16	4 12	−0·10 −0·27	4 12	−0·12 −0·32	4 12	−0·18 −0·41	4 12	−0·22 −0·45	4 (11)	−0·25 −0·47	4 10	−0·28 −0·54	4 10	−0·33 −0·62	4 10	−0·38 −0·74	4 10
m-Dinitrobenzene	−0·03 −0·12 ?	4 8 12	−0·12 −0·26 ?	4 8 12	−0·17 −0·29 ?	4 8 12	−0·20 −0·35 ?	4 8 (10)	−0·23 −0·38 ?	4 8 (9)	−0·25 −0·42 —	4 8 —	−0·31 −0·47 —	4 8 —	−0·39 −0·58 —	4 8 —	−0·46 −0·68 —	4 8 —
p-Dinitrobenzene	−0·01 −0·18 —	4 12 —	−0·08 −0·30 —	4 12 —	−0·12 −0·33 —	4 12 —	−0·14 −0·40 —	4 12 —	−0·19 −0·45 —	4 12 —	−0·21 −0·50 —	4 12 —	−0·28 −0·55 —	4 10 —	−0·31 −0·69 —	4 10 —	−0·34 −0·80 ?	4 8 12
1 : 3 : 5-Trinitrobenzene	+0·04 −0·01 −0·06 ?	4 8 12 14	−0·06 −0·12 −0·20 ?	4 8 12 14	−0·08 −0·15 −0·24 ?	4 8 12 14	−0·12 −0·20 −0·30 ?	4 8 12 14	−0·16 −0·24 −0·34 ?	4 8 12 (?)	−0·20 −0·29 −0·42 ?	4 8 12 (?)	−0·24 −0·34 −0·47 —	4 8 12 —	−0·31 −0·44 −0·61 —	4 8 12 —	−0·34 −0·48 −0·65 —	4 8 12 —

The values of $E_{\frac{1}{2}}$ (corrected for *iR* drop) are in v. against a saturated calomel electrode, and those of *n* are the total number of electrons involved in the reduction producing the diffusion-current. The values in parenthesis are somewhat uncertain because the waves are not well defined, or because they correspond to stages intermediate between two reduction processes. An interrogation mark indicates that the wave is too indefinite to assign constants with any degree of certainty.

TABLE II.—POLAROGRAPHIC CONSTANTS OF THE NITROTOLUENES.

*p*H.	0·5		1·7		2·5		3·0		3·8		4·1		5·7		7·4		9·2	
Constant.	$E_{\frac{1}{2}}$.	*n*.	$E_{\frac{1}{2}}$.	*n*.	$E_{\frac{1}{2}}$.	*n*.	$E_{\frac{1}{2}}$.	*n*.	$E_{\frac{1}{2}}$.	*n*.	$E_{\frac{1}{2}}$.	*n*.	$E_{\frac{1}{2}}$.	*n*.	$E_{\frac{1}{2}}$.	*n*.	$E_{\frac{1}{2}}$.	*n*.
o-Nitrotoluene	−0·20 ?	4 6	−0·32 ?	4 6	−0·35 ?	4 6	−0·44 ?	4 6	−0·45 ?	4 6	−0·50 ?	4 (5)	−0·55 —	4 —	−0·62 —	4 —	−0·75 —	4 —
m-Nitrotoluene	−0·15 ?	4 6	−0·25 ?	4 6	−0·30 ?	4 6	−0·37 ?	4 6	−0·41 ?	4 (5)	−0·46 ?	4 (?)	−0·51 —	4 —	−0·59 —	4 —	−0·71 —	4 —
p-Nitrotoluene	−0·10 ?	4 6	−0·22 ?	4 6	−0·30 ?	4 6	−0·35 ?	4 6	−0·43 ?	4 6	−0·48 ?	4 (?)	−0·50 —	4 —	−0·58 —	4 —	−0·69 —	4 —
2 : 4-Dinitrotoluene	−0·05 −0·14 ?	4 8 12	−0·13 −0·25 ?	4 8 12	−0·18 −0·30 ?	4 8 12	−0·22 −0·36 ?	4 8 12	−0·26 −0·40 ?	4 8 (?)	−0·29 −0·43 ?	4 8 (?)	−0·35 −0·48 —	4 8 —	−0·40 −0·58 —	4 8 —	−0·50 −0·70 —	4 8 —
2 : 6-Dinitrotoluene	−0·10 −0·19 ?	4 8 12	−0·19 −0·34 ?	4 8 12	−0·24 −0·40 ?	4 8 12	−0·29 −0·44 ?	4 8 12	−0·32 −0·48 ?	4 8 12	−0·37 −0·54 —	4 8 —	−0·41 −0·57 —	4 8 —	−0·46 −0·64 —	4 8 —	−0·55 −0·74 —	4 8 —
2 : 3-Dinitrotoluene	−0·03 −0·22	4 12	−0·13 −0·34	4 12	−0·16 −0·41	4 12	−0·23 −0·50	4 12	−0·28 −0·56	4 (11)	−0·30 −0·58	4 10	−0·34 −0·63	4 10	−0·40 −0·69	4 10	−0·45 −0·81	4 10
3 : 4-Dinitrotoluene	−0·03 −0·21	4 12	−0·13 −0·32	4 12	−0·16 −0·37	4 12	−0·22 −0·46	4 12	−0·26 −0·50	4 (11)	−0·28 −0·53	4 10	−0·31 −0·60	4 10	−0·36 −0·69	4 10	−0·42 −0·79	4 10
Trinitrotoluene	−0·01 −0·08 −0·14 ?	4 8 12 (?)	−0·07 −0·16 −0·24 ?	4 8 12 (?)	−0·10 −0·20 −0·31 ?	4 8 12 (?)	−0·14 −0·24 −0·36 ?	4 8 12 (?)	−0·17 −0·28 −0·41 ?	4 8 12 (?)	−0·19 −0·31 −0·45 —	4 8 12 —	−0·25 −0·38 −0·53 —	4 8 12 —	−0·31 −0·48 −0·62 —	4 8 12 —	−0·40 −0·55 −0·73 —	4 8 12 —

This is the reaction which determines the potential of the cathode, and which actually produces the observed current. The hydrogen atoms remain on the electrode surface, for they are not capable of combining together to form hydrogen molecules. The speed at which this reaction proceeds is dependent upon the diffusion of organic molecules to the cathode, for fresh hydrogen ions can be deposited only when some of the hydrogen atoms have been removed by interaction with the reducible molecules. Thus the current will be a function of the rate at which reducible material diffuses to the cathode, but independent of the rate at which hydrogen ions diffuse, since the *p*H is maintained constant in the cathode surface-layer by the buffering action of the supporting electrolyte. The overall reduction reaction may thus be written:

$$H^+ + e = H,$$

followed by

$$A + nH = B$$

or

$$A + nH + H^+ = C^+.$$

The potential of the dropping electrode is therefore dependent upon eqn. (1), i.e.

$$E = E_0 - 0{\cdot}0591 \,.\, \log C_H{}^0/C_{H^+}^0 \text{ (at } 25° \text{ c.)} \qquad (2)$$

where $C_H{}^0$ and $C_{H^+}^0$ are the concentrations of hydrogen atoms and hydrogen ions in the layer of solution in contact with the mercury drop.

The current at any moment will be proportional to the rate at which hydrogen ions replace the hydrogen atoms removed by reaction with reducible material, i.e. the current will be proportional to the speed of reaction between hydrogen atoms and reducible material, in alkaline media, or proportional to the speed of reaction between hydrogen ions, hydrogen atoms and reducible material in acid media. Dealing first with alkaline conditions, we may write

$$i = K \,.\, C_A{}^0 \,.\, C_H{}^0 \qquad (3)$$

where $C_A{}^0$ is the concentration of the reducible material in the layer of solution immediately in contact with the electrode. Therefore

$$C_H{}^0 = i/KC_A{}^0. \qquad (4)$$

Now $C_A{}^0 = (i_d - i)/k_A$, where i_d is the diffusion current and k_A is a constant depending upon the diffusion coefficient of the reducible material,[12] and thus

$$C_H{}^0 = k_A \,.\, i/K(i_d - i). \qquad (5)$$

Combining eqn. (2) and (5) :

$$E = E_0 - 0{\cdot}0591 \,.\, \log \left[\frac{k_A}{K} \cdot \frac{i}{i_d - i} \cdot \frac{i}{C_H{}^0}\right]. \qquad (6)$$

The strongly buffered solutions maintain the hydrogen-ion concentration constant and equal to that of the bulk of the solution, and we may therefore rewrite eqn. (6) :

$$E = E_0 - 0{\cdot}0591 \,.\, \log (k_A/K) - 0{\cdot}0591 \,.\, \log [i/(i_d - i)] - 0{\cdot}0591 \,.\, p\text{H} \qquad (7)$$

Since in acid solutions, hydrogen ions are also involved, we may write :

$$i = K'C_H{}^0 \,.\, C_{H^+}^0 C_A{}^0. \qquad (8)$$

By the arguments as given above :

$$C_H{}^0 = k_A \,.\, i/K' (i_d - i)C_{H^+}^0 \qquad (9)$$

and therefore :

$$E = E_0 - 0{\cdot}0591 \,.\, \log (k_A/K') - 0{\cdot}0591 \,.\, \log [i/(i_d - i)] - 0{\cdot}1182 \,.\, p\text{H} \qquad (10)$$

Eqn. (7) and (10) are of the same form as that for reversible reactions, but the potential is dependent upon log (k_A/K) or log (k_A/K'), i.e. upon the diffusion coefficient of the reducible material and upon its reaction rate with hydrogen atoms. Since the electrode potential is independent of the concentration of reduced material, the half-wave potential will not coincide with the hypothetical oxidation-reduction potential of the system.

Eqn. (7) and (10) predict that the plots of half-wave potential against *p*H should be straight lines, with slopes of 0·0591 and 0·1182 v. per *p*H unit in alkaline and acid media, respectively. It is seen from Fig. 6 that the slopes in acid are in general about twice those in alkali, as predicted ; the divergence from the theoretical values may be connected with the fact that K and K' may be dependent upon *p*H.

It is also seen from the above that at a given *p*H, plots of electrode potential against log $[i/(i_d - i)]$ should be straight lines with slopes of 0·0591. Thermodynamic treatment of reversible systems[12] gives an essentially similar result, except that the slope of the plot of E against log $[i/(i_d - i)]$ has a slope given by $0{\cdot}0591/n$, where n is the number of electrons concerned in the overall reduction giving rise to the polarographic wave. Table III gives the slopes of these plots for several of the compounds studied, the number of electrons involved in the overall reaction, and the slope to be expected if the reactions were reversible.

TABLE III.

Compound.	*p*H.	*n*.	Slope.	Expected Slope.
Nitrobenzene . .	2·5	4	0·075	0·015
	9·2	4	0·088	0·015
o-Dinitrobenzene . .	9·2	4	0·060	0·015
		6	0·088	0·010
m-Dinitrobenzene .	2·5	8	0·093	0·007
Trinitrobenzene . .	1·7	12	0·090	0·005

It is seen that although the slopes found are not those to be expected they are essentially independent of the number of electrons concerned in the reductions, as predicted.

It can thus be stated that thermodynamic arguments will predict, at least qualitatively, the phenomena observed in the reduction of the nitrobenzenes and nitrotoluenes at the dropping mercury cathode, that is, (i) diffusion-currents are directly proportional to concentration, (ii) half-wave potentials are independent of concentration, (iii) half-wave potentials are linear functions of *p*H, with slopes greater in acid than in alkaline media, and (iv) plots of electrode potential at any point on the polarographic waves against log $[i/(i_d - i)]$ are straight lines, with slopes independent of the number of electrons taking part in the overall reaction.

(iii) The Activating Influence of the Nitro-group.—It is seen from Table I and II that introduction of a nitro-group raises the reduction potential of a nitro-group already in the aromatic nucleus, and that the raising of the reduction potential of the first group is greater in the case of *o*- and *p*-dinitrobenzenes than in that of *m*-dinitrobenzene. The effect of the nitro-group is thus an inductive one through the carbon chain of the benzene ring. Since the nitro-group attracts electrons, its action would appear to be that of weakening the binding of the oxygen atom, or atoms, attached to the other nitrogens, so making these easier of removal by atomic hydrogen in the reduction process. It will be seen that the introduction of a methyl group into a nitrobenzene molecule makes no marked change in the reduction-potentials of the nitro-groups, though *o*-nitrotoluene is more difficultly reduced than nitrobenzene.

(iv) Step-wise Reduction of Symmetrical Polynitro-compounds.—The reduction of the various nitro-groups of polynitro-compounds gives rise to polarographic waves consisting of a series of steps. It is, however, to be expected that the nitro-groups in the symmetrical compounds (di- and tri-nitro-benzenes and 2 : 6-dinitrotoluene) would have identical reduction potentials. Presumably they have, but as the molecules approach the cathode one nitro-group will be nearer than another. Due to the dipole nature of the group it will be attracted electrically and reduced before the other group can approach sufficiently closely to the cathode. The other group, or groups, are then no longer subject to the activating influence of a nitro-group and so will have lower reduction potentials.

(v) Wave Separation.—An interesting feature of the polarographic behaviour of the polynitro-benzenes and -toluenes is seen from an inspection of Fig. 2-6 and Tables I and II. This is that as hydrogen ion concentration decreases, the separation between the component parts of a multiple wave increases, i.e. $(E_{\frac{1}{2}}' - E_{\frac{1}{2}}'')$ increases, as *p*H increases. It has been indicated above that the half-wave potential of a nitro-group depends upon the activating influence of other substituents. After a first nitro-group has been reduced its effect upon a second or third will be that of a hydroxylamine group. As *p*H increases the electronegativity of this group will increase as it is involved less and less in salt formation. Its electron-attraction, and thereby its activating influence on other nitro-groups, will decrease progressively, and the rate of change of $E_{\frac{1}{2}}''$ with *p*H will be greater than that of $E_{\frac{1}{2}}'$.

Acknowledgement is made to the Chief Scientist, Ministry of Supply, for permission to publish this paper which describes work carried out in a branch formerly of the Armament Research Department, but now of the Chemical Research and Development Department.

Summary.

The behaviour of the nitro-benzenes and -toluenes at the dropping-mercury cathode has been studied to ascertain the effect of the solvent upon reduction processes and reduction potentials. The extent of reduction undergone by the nitro-groups depends upon the acidity of the solvent. In neutral to alkaline conditions, reduction generally proceeds to the polyhydroxylamine state, whereas in acid conditions stepwise reduction occurs through the hydroxylamines to the polyamines. In the region between acid and neutral conditions (*p*H about 3-6), a proportion of the molecules are reduced completely and the remainder only partially, even at the lowest possible cathode potentials. It is found that half-wave potentials are linear functions of *p*H but that the slope of the connecting line changes in the same *p*H-range as that in which reduction process changes. A possible explanation for these changes has been advanced.

Assuming the reduction to take place through the intermediary of cathodically, and reversibly, deposited hydrogen atoms, an argument has been developed which accounts, at least qualitatively, for the fact that the plots of half-wave potentials against log $[i/(i_d - i)]$ are straight lines with slopes independent of the number of electrons concerned in the overall reaction. As predicted by the Ilkovic equation, diffusion-currents produced by a given reduction process are directly proportional to the concentration of the compound undergoing reduction.

PART II.—THE NITROPHENOLS.*

The behaviour of certain nitrobenzenes and nitrotoluenes at the polarised dropping-mercury cathode has been reported previously;[1] the investigation has now been extended to the nitrophenols. Although

* This communication forms part of a thesis submitted in January 1946 to the University of London in partial fulfilment of the requirements for the Degree of Ph.D.

[1] Pearson, *Trans. Faraday Soc.*, 1948, 44, 683.

Shikata and his collaborators[2, 3] have studied the polarography of *o*-, *m*-, and *p*-mono-, and 2 : 4- and 2 : 6-di-nitrophenols and reported single reduction potentials for the mono- and two potentials for the di-nitro-compounds, it was suspected that the complex behaviour of the nitrobenzenes and -toluenes might be repeated with the hydroxy-compounds.

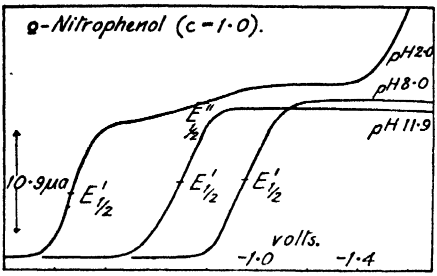

FIG. 1.

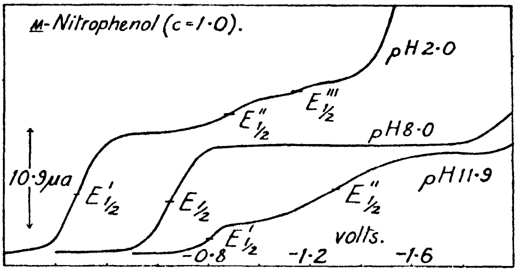

FIG. 2.

Experimental.

The apparatus employed was that previously described[1] and the method of making solutions was the same except that a universal buffer solution containing trisodium phosphate, sodium acetate, sodium metaborate, and hydrochloric acid, as recommended by Newbery,[4] was used. Measurements were made in media of *p*H 2·0, 4·0, 6·0, 8·0, 10·0 and 11·9, and, as before, the numbers of "electrons" participating in the reductions have been calculated from the diffusion-current constants. The mono- and di-nitrophenols were studied over a concentration-range of 0·1-1·0 millimolar, and picric acid over a range 0·05 to 0·5 millimolar and typical records are depicted in Fig. 1-4.

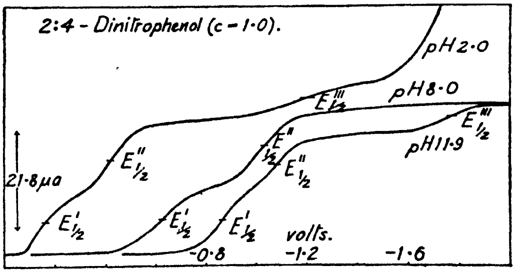

FIG. 3.

---

[2] Shikata and Watanabe, *J. Agr. Chem. Soc. Japan*, 1928, **4**, 924.
[3] Shikata and Hozaki, *Mem. Coll. Agr. Kyoto Imp. Univ.*, 1931, **17**, 1, 21.
[4] Newbery, *Trans. Roy. Soc. S. Africa*, 1944, **30**, 175.

Results.

Half-wave potentials and *n*-values are given in Table I. It is seen that at low *p*H, *o*-nitrophenol is reduced in two stages, as is nitrobenzene, whereas at high *p*H reduction occurs in one stage only. At intermediate *p*H (5-8), some of the molecules are reduced to the hydroxylamine state only, and the remainder completely to the amine. Supplementary experiments showed that the change from a two-stage to a one-stage reduction occurs at about *p*H 5.

m-Nitrophenol differs from *o*-nitrophenol in that it is only at low *p*H that it is reducible to the amine, and even then there appears to be some phase intermediate between the reduction to the hydroxylamine and that to amine. At high *p*H (11·9 and more) there is evidence of a one-electron reduction ; the significance of this is not clear. *p*-Nitrophenol behaves much like *o*-nitrophenol, except that in alkaline solutions reduction is a two-stage process, involving apparently nitrosophenol as an intermediary. At *p*H 8·0, it appears that about 25 % only of the molecules reaching the cathode are reduced to the nitroso-state at the higher potential. 2 : 4- and 2 : 6-Dinitrophenols behave in a manner somewhat similar to the analogous nitrobenzenes, in that complete reduction occurs at low *p*H and partial reduction only at high. One nitro-group in these compounds is reduced to the amine at all hydrogen-ion concentrations ; this takes place in two stages at high *p*H with the 2 : 4-isomer.

No half-wave potentials are given for picric acid, as the component waves of the polarograms are not sufficiently well defined. The final diffusion-currents are in all instances approximately equivalent to that required for a total of 16 electrons, though, since the diffusion-coefficient of picric acid may be somewhat lower than that of the benzoate-ion upon which the calculations have been based, the total involved may well be greater. It is not clear by what stages the reduction proceeds, though three reductions involving approximately equal numbers of electrons are indicated.

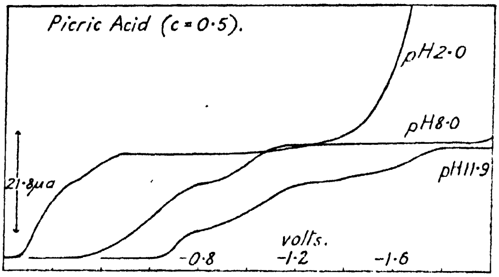

FIG. 4.

For all the above nitrophenols, it has been established that where a diffusion-current is sufficiently well defined to permit accurate measurement, it is directly proportional to concentration, and that where a half-wave potential can be estimated, it is independent of concentration.

Discussion.

While the work described above was being carried out, Astle and McConnell[5] published the results of their investigations of the polarography of *o*- and *p*-nitrophenols. They found that in strongly alkaline media *o*-nitrophenol is reduced in one stage to the amine and in acid media to the hydroxylamine only. At intermediate hydrogen-ion concentrations, the diffusion-current of the single wave increases gradually, with *p*H, from a value equivalent to a four-electron to one equivalent to a six-electron reduction. This they explain as being due to the fact that, in acid media, *o*-nitrophenol has a hydrogen-bonded structure and that this bonding interferes with the normal resonance of the nitro-group, rendering it more easily reduced than a non-bonded group. It also

---

[5] Astle and McConnell, *J. Amer. Chem. Soc.*, 1943, **65**, 35.

TABLE I.

*p*H.	2·0		4·0		6·0		8·0		10·0		11·9	
Constant.	$E_{\frac{1}{2}}$.	*n*.	$E_{\frac{1}{2}}$.	*n*.	$E_{\frac{1}{2}}$.	*n*.	$E_{\frac{1}{2}}$.	*n*.	$E_{\frac{1}{2}}$.	*n*.	$E_{\frac{1}{2}}$.	*n*.
o-Nitrophenol . .	−0·23	4	−0·37	4	−0·50	(5·2)	−0·65	(5·5)	−0·80	6	−0·91	6
	?	6	?	6	—	—	—	—	—	—	—	—
m-Nitrophenol . .	−0·25	4	−0·37	4	−0·53	4	−0·62	4	−0·76	4	−0·80	(1)
	(−0·84)	(5·5)	—	—	—	—	—	—	—	—	−1·27	4
	(−1·10)	6	—	—	—	—	—	—	—	—	—	—
p-Nitrophenol . .	−0·35	4	−0·46	4	−0·64	6	−0·82	(5)	−0·92	2	−0·96	2
	?	6	?	6	—	—	−1·28	6	−1·33	6	−1·67	6
2 : 4-Dinitrophenol .	−0·14	4	−0·25	4	−0·42	4	−0·59	4	−0·66	4	−0·83	4
	−0·32	8	−0·48	(9)	−0·69	10	−0·91	10	−0·96	8	−0·99	8
	?	12	?	(11)	—	—	—	—	?	10	−1·63	10
2 : 6-Dinitrophenol .	−0·09	4	−0·23	4	−0·40	4	−0·51	4	−0·62	4	−0·83	4
	−0·24	10	−0·36	10	−0·54	10	−0·69	10	−0·80	10	−0·97	10
	?	12	—	—	—	—	—	—	—	—	—	—

stabilises the hydroxylamine formed, so that reduction beyond this stage is not possible. In alkaline solutions, there is no hydrogen-bonding and reduction is "normal," i.e. direct to the amine. At intermediate *p*H, some of the molecules are in the bonded and some in the non-bonded state; the proportion of the latter, and therefore the diffusion-current, increases with *p*H. The results quoted in Table I are broadly in agreement with this, but it is not possible to agree that the hydrogen-bonded form is not reducible beyond the hydroxylamine. *o*-Nitrophenol behaves much like nitrobenzene, except that the anionic or quinoid form present in alkaline solutions permits reduction direct to the amine. The results reported are thus explicable on the assumption that a neutral molecule is reducible in two stages to the amine up to about *p*H 5, but beyond this value reduction is possible only to the hydroxylamine, as with nitrobenzene. The quinoid form is reducible to the amine; the total amount of reduction will therefore increase as the hydrogen-ion concentration decreases. Thus we observe diffusion-current constants (which are equivalent to the diffusion-currents in microamperes yielded by a millimolar solution at a dropping electrode whose $m^{2/3}t^{1/6}$ value is 1·0) of 6·9, 8·2, 8·7 and 9·4 at *p*H 4·9, 6·0, 8·0, and 10·0, respectively.

Taking account only of the results from *p*H 2·0 to 10·0, *m*-nitrophenol behaves in much the same manner as nitrobenzene. Since hydrogen-bonding is not possible, there is no equilibrium between chelated and unchelated molecules. This result is in substantial agreement with that reported by Astle and Cropper[6] for certain nitrocresols.

p-Nitrophenol is found to be reducible at all *p*H values completely to the amine, though in media of low *p*H the reduction proceeds as for nitrobenzene, and not in a single stage. The occurrence of a nitroso- intermediate stage at high *p*H may be connected with the stabilisation of the reduction-product by isomerisation to the quinone monoxime. 2 : 4- and 2 : 6-Dinitrophenols behave essentially like the dinitrobenzenes; the complete reduction of one nitro-group at high *p*H is probably an effect of the adjacent hydroxyl. It should be noted that 2 : 4-dinitrophenol exhibits a phase intermediate between "acid" and "alkaline" reduction at *p*H 4·0.

No clear interpretation can be given to the behaviour of picric acid, though it appears that reduction proceeds in three stages at all *p*H values. It should be noted at this juncture that Lingane[7] has shown by coulometry at controlled potentials that reduction of picric acid in acid medium involves seventeen electrons per molecule, the reduction product thus being di-(hydroxydiaminophenyl)-hydrazine.

In those instances where a given reduction process (e.g. reduction of one nitro-group to hydroxylamine) persists over a fair range of *p*H, the lines connecting half-wave potential with *p*H are practically straight, slopes about 0·06-0·07 v. per *p*H unit, and show no break at *p*H 4-5 as do the nitro-benzenes and -toluenes. It thus appears that the hydroxyl-group precludes the formation of "phenylhydroxyl-ammonium-ion"[1] in acid solution. In line with this, it is found that the slopes of the plots of $E_{\frac{1}{2}}$ against *p*H for the two persistent waves of 2 : 6-dinitrophenol are the same (0·07), i.e. wave-separation does not increase with *p*H. If "ammonium ions" are not formed, increasing *p*H cannot influence their electronegativity.

In Table II are listed the characteristics of some plots of cathode potential against log $[i/(i_d - i)]$ and for comparison the values of the slope to be expected if the reductions were reversible, i.e. $0{\cdot}0591/n$, where n is the number of electrons involved in the reduction of 1 molecule of substance. It is seen that the slopes are much the same as for the nitrobenzenes,[1] and it is therefore assumed that reduction also occurs through the intermediary of cathodically deposited hydrogen atoms, followed by interaction between these and reducible material.

---

[6] Astle and Cropper, *J. Amer. Chem. Soc.*, 1943, **65**, 2395.

[7] Lingane, *ibid.*, 1945, **67**, 1916.

It was observed previously[1] that the introduction of a further nitro-group into a nitrobenzene or nitrotoluene molecule had the effect of raising the first reduction potential, i.e. of making the first nitro-group more easily reducible than that in the mono-nitrocompounds. The hydroxyl-group, contrary to the nitro-group, favours *o*-*p*-substitution by electrophilic reagents, and must therefore be regarded as essentially electron-donating (+ *T* effect). This will stabilise the bonding of the oxygen atoms in the nitro-group, and make them more difficult to remove. In line with this concept, it is found that the lowering of half-wave potential, as compared with nitrobenzene, is less with *m*-nitrophenol than with *p*-nitrophenol. The lowering effect of the hydroxyl-group in *o*-nitrophenol is counteracted, as Astle and McConnell[5] point out, by hydrogen-bonding between the two groups. When further nitro-groups are introduced into the nitrophenol molecule these raise the reduction potentials of the nitro-group already present, as with the poly-nitro-benzenes and -toluenes, the electron-donating + *T* effect of the hydroxyl-group being opposed by the electron-attraction (— *I* effect) of the nitro-group.

TABLE II.

Compound.	*p*H.	*n*.	Slope.	Expected Slope.
o-Nitrophenol . .	2·0	4	0·055	0·015
	8·0	(5)	0·092	0·012
m-Nitrophenol . .	2·0	4	0·082	0·015
	8·0	4	0·092	0·015
p-Nitrophenol . .	2·0	4	0·080	0·015
	8·0	(5)	0·130	0·012
2 : 4-Dinitrophenol .	2·0	4	0·070	0·015
		4	0·075	0·015
2 : 6-Dinitrophenol .	6·0	4	0·064	0·015
		6	0·097	0·010

Acknowledgement is made to the Chief Scientist, Ministry of Supply, for permission to publish this work, which was carried out in a branch, formerly of the Armament Research Department, but now of the Chemical Research and Development Department.

Summary.

The introduction of a hydroxyl-group into a nitrated aromatic nucleus has the following effects upon mode of reduction and reduction potentials. The + *T* influence lowers half-wave potentials as compared with the analogous nitrobenzene, though hydrogen-bonding when the nitro- and hydroxyl-groups are adjacent reduces this lowering. Though the mode of reduction of the nitrophenols in " acid " media is essentially the same as that of the nitrobenzenes, the presence of the hydroxyl-group appears to prevent the formation of phenylhydroxylammonium ions as the initial reduction product and the plot of half-wave potential against *p*H is a straight line without a change of slope at about *p*H 4 as with the nitrobenzenes and nitrotoluenes. It appears also that the anionic or quinoid forms facilitate, in general, reduction to the amine instead of to the hydroxylamine as with the nitro-benzenes and -toluenes. Reduction of *p*-nitrophenol in alkaline media proceeds through the nitroso-state. This is the only instance so far encountered of the production of such an intermediary.

British Iron and Steel Research Association,
Sketty Hall,
Swansea.

THE ADSORPTION OF GASES SO_2, NH_3, CO_2 AND N_2O ON BaF_2 CRYSTALS.

By V. A. Crawford and F. C. Tompkins.

Received 1*st October*, 1947.

Reliable data on the adsorption of gases on ionic crystals are few, although for certain systems, viz. the inert gases on KCl, NaCl and CsI for which it has been possible to calculate the adsorption potential and its variation over the surface of the adsorbent,[1-4] experimental results are available showing that some confidence may be placed in the theoretical computations. The same theoretical treatment has been applied here, admittedly crudely, to the present systems and the purpose was to provide experimental data with which to test these approximate calculations. These latter showed that the adsorption of SO_2, NH_3, CO_2 and N_2O on BaF_2 provides good examples of localized physical adsorption in the first layer by reason of the lattice structure of the adsorbent and the molecular diameters of the adsorbate molecules. Certain consequences of this, e.g. the constant volume of adsorbates, independent of their molecular diameters, in the completed monolayer, the variation of the heat of adsorption with amount adsorbed, and the difference of this heat, as derived from the multilayer theory and from purely thermodynamic considerations have therefore been examined experimentally.

Experimental.

Materials.—Barium fluoride was obtained by dropwise addition of calculated volumes of M./6 HF to hot M./63 $Ba(OH)_2$ with vigorous stirring. The product contained irregularly-shaped micro-crystals and amorphous agglomerates which, however, were transformed into well-developed cubes of side about 0·01 mm. by ageing for two weeks in the mother liquors at 100° C. in the presence of dil. HNO_3. After filtering, the crystals were thoroughly washed with boiling water, dried over solid KOH *in vacuo*, later evacuated at 130° C., and after lightly pressing the aggregates between glass plates, stored over solid P_2O_5 in a vacuum desiccator for one month.

The four adsorbates were subjected, where possible, to repeated fractional distillations from solid CO_2-alcohol baths at low pressure and stored at − 78° C. over previously outgassed P_2O_5. Ammonia was prepared by Barrer's [5] method, CO_2 obtained from Drikold, and SO_2 and N_2O from cylinders.

Apparatus.—This was of the usual volume type and contained a blank system so that the adsorption of gas by the glass walls could be measured simultaneously. Evacuation to 10^{-6} mm. Hg was affected with a single-stage Hg-diffusion and Hyvac pump. Volume calibrations at various temperatures of adsorbent was accomplished with hydrogen, the adsorption of which had been proved negligible even at −78° C. The temperature range, − 78° to 119° C., was covered by use of (*a*) low m. p. solids, (*b*) water circulated from thermostats at suitable temperatures and (*c*) liquids refluxing at their b. p. under atmospheric pressure ; these were contained in Dewar vessels which surrounded the adsorbent bulb, containing 35·9 g. BaF_2 crystals.

Procedure.—After a preliminary outgassing at 300° C. for 72 hr., the adsorbent was always evacuated at 200° C. for 12 hr., then allowed to cool for 1 hr., after which 1 cm. pressure of hydrogen was admitted to hasten attainment of thermal equilibrium [6] with the isothermal bath which was placed around

---

[1] Orr, *Trans. Faraday Soc.*, 1939, **35**, 1247 ; *Proc. Roy. Soc. A*, 1939, **173**, 349.

[2] Lenel, *Z. physik. Chem. B*, 1933, **23**, 379.

[3] Roberts and Orr, *Trans. Faraday Soc.*, 1933, **34**, 1346.

[4] Lennard-Jones and Dent, *ibid.*, 1928, **24**, 92.

[5] Barrer, *ibid.*, 1943, **39**, 237.

[6] Tompkins, *ibid.*, 1936, **32**, 643.

the adsorbent vessel at this stage. After a further 1 hr., the hydrogen was evacuated and successive small increments of adsorbate admitted. The amount adsorbed after each admission was calculated from the theoretical pressure assuming no adsorption, and that obtained experimentally.

Results.

Fig. 1-4 summarize the amounts *v* of the various gases adsorbed at different temperatures. These have been corrected for adsorption on the glass walls; they are expressed in cc. N.T.P. and the equilibrium pressures (*p*) in cm. Hg; the values of *v* have an accuracy of better than 1 % at the lower *p*, and 2 % at the highest equilibrium pressure, the increase being due to the cumulative errors with increasing number of increments; this was restricted to six, and other intermediate *v*-values obtained after a further outgassing. The amounts adsorbed were independent of the number of increments by which any *p*-value was obtained (with the restriction above) and of whether the fluoride had been exposed to the same or a different adsorbate providing that it was outgassed between such experiments; the outgassing procedure was therefore effective. The adsorption of the four gases was reversible and complete within 5 min. of their admission at all temperatures. No correction was necessary for deviations from the perfect gas equation in the pressure range used since these were less than the experimental error.

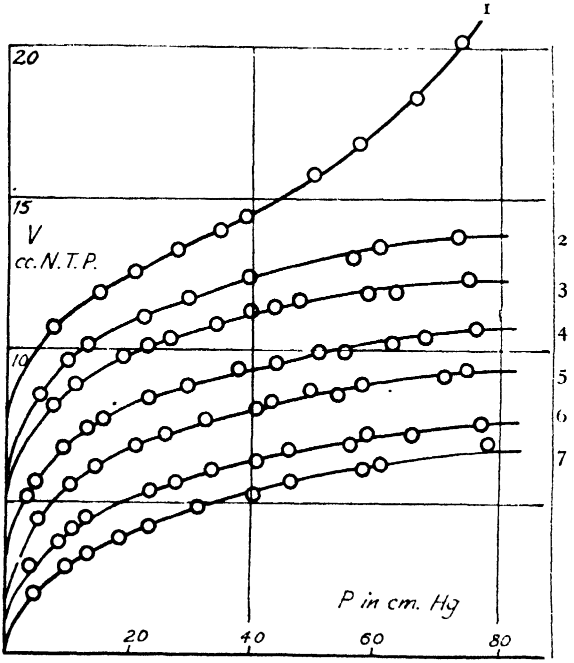

FIG. 1.—Adsorption of SO_2.

Curve No.	1	2	3	4	5	6	7
Temp. °c.	0·0	18·3	31·8	55·9	74·9	98·5	119·6

Heats of adsorption (ΔH_e) expressed in cal./g. mol. adsorbate in the various temperature intervals and for different values of *v* were calculated from the Clausius-Clapeyron equation. The variation of ΔH_e with temperature showed no constant trend, but it decreased with increase of *v* for all gases. Since the variation was sensibly independent of temperature the ΔH_e-v plots given in Fig. 5 are composite ones for the whole temperature range. They show that ΔH_e falls considerably with *v* in an approximately linear manner.

Discussion.

A preliminary analysis was made using the Langmuir equation[7] in the form :

$$\frac{p}{v} = \frac{p}{v_m} + \frac{1}{bv_m} \quad . \quad . \quad . \quad . \quad . \quad . \quad (1)$$

where v_m is the amount adsorbed in the completed monolayer and b is a function mainly of ΔH_c and assumed independent of v. The plot of p/v against p was satisfactorily linear over the middle pressure range, particularly for the non-polar gases, but at both high and low p, $v_{\text{expt.}}$ was greater than that required by (1). The discordance at low p is largely explained by high adsorption at re-entrant angles and cracks, the area of these constituting at least 15 % of the total surface. Their presence renders speculative any deductions about the variation of heats of adsorption at sparse coverage. The divergences at high p are not due to the decrease of ΔH_c with increasing v since this would cause the values of $v_{\text{expt.}}$ to be still smaller : it suggests an explanation in terms of multilayers (Brunauer, Emmett and Teller[8] (B.E.T.)).

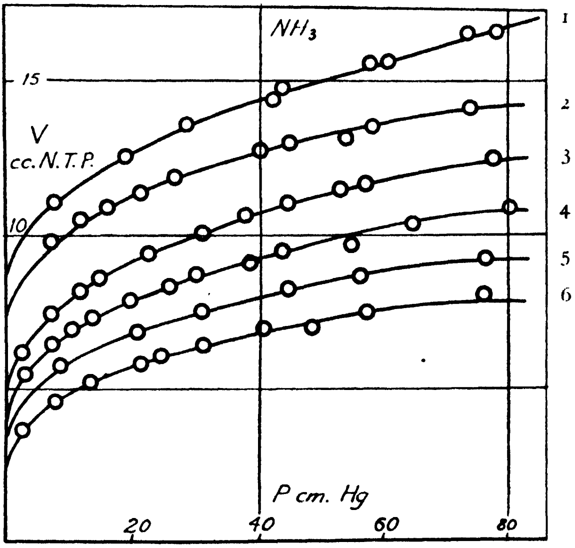

FIG. 2.—Adsorption of NH_3.

Curve No. .	1	2	3	4	5	6
Temp. °c. .	0·0	18·6	36·0	54·9	73·9	98·4

Their equation may be written in the form :

$$\frac{pv}{(p_0 - p)} = \frac{1}{cv_m} + \frac{p(c-1)}{cv_m p_0} \quad . \quad . \quad . \quad . \quad (2)$$

where p_0 is the vapour pressure of the liquid adsorbate at $T°$ K., $c \sim e^{-\Delta H_n/RT}$ and ΔH_n is the net heat of adsorption and equals $(\Delta H_1 - \Delta H_2)$; ΔH_1 refers to the first layer and ΔH_2 to the second and is assumed to be equal to the heat of liquefaction (ΔH_L). It is implied that c (not necessarily ΔH_1) is independent of v. Fig. 6 shows the plot of $\frac{pv}{(p_0 - p)}$ against

---

[7] Langmuir, *J. Amer. Chem. Soc.*, 1918, **40**, 136.

[8] Brunauer, Emmett and Teller, *ibid.*, 1938, **60**, 309

p/p_0 for the four gases at different temperatures selected at random. The plots are linear except at low p where departures were anticipated (cp. above). In general $v_{\text{expt.}}$ tends to be too small at high p in keeping

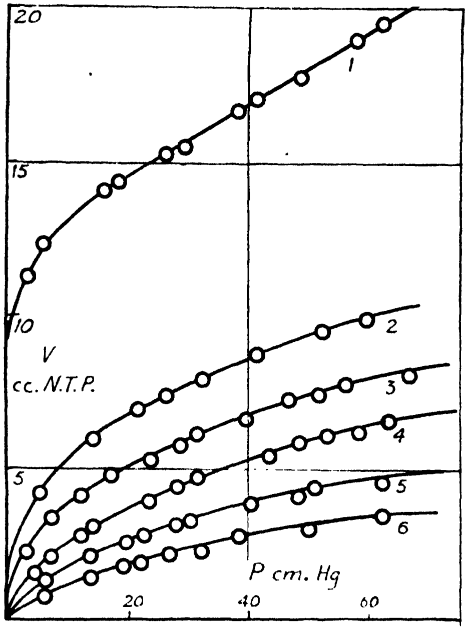

FIG. 3.—Adsorption of CO_2.

Curve No.	1	2	3	4	5	6
Temp. °c.	−78·5	−17·0	0·0	18·6	36·0	55·0

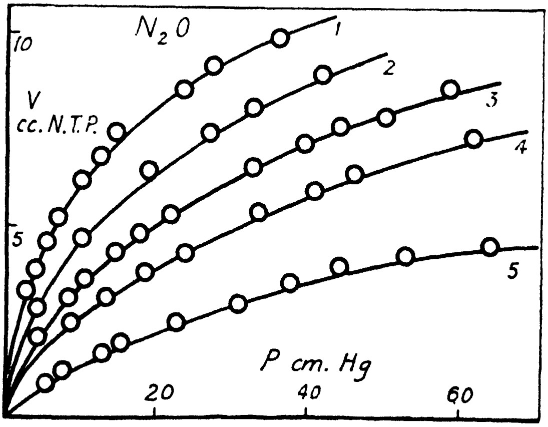

FIG. 4.—Adsorption of N_2O.

Curve No.	1	2	3	4	5
Temp. °c.	−40·0	−22·8	−13·0	0·0	23·7

with the decrease of ΔH_e and therefore of c (ΔH_L = constant for any isotherm) with increasing v.

However, since c and v_m of eqn. (2) have physical significance they should be of the correct magnitude. Now because $c = K e^{-\Delta H_n/RT}$, ΔH_n

can be evaluated from a single isotherm assuming $K = 1$; the heat of adsorption is then $\Delta H_n + \Delta H_L = \Delta H_B$. By reference to (2)

$$\Delta H_B = \Delta H_L + RT \log_e p_0 + RT \log_e v_m I$$

where I is the intercept on the $\dfrac{pv}{(p_0 - p)}$ axis; thus a twofold error in $v_m I$ at 300° K. corresponds to 300 cal. showing that the method is capable of considerable accuracy. Similarly from the work of Coolidge,[9] ΔH_e (except at high p where the p-values are not well defined for a particular v-value) is a reliable estimate of the calorimetrically-determined heat. Nevertheless where direct comparison of ΔH_B and ΔH_e have been made,[10] the agreement is 10-20 % or worse, and there is, moreover, no consistent divergence of the two heats.

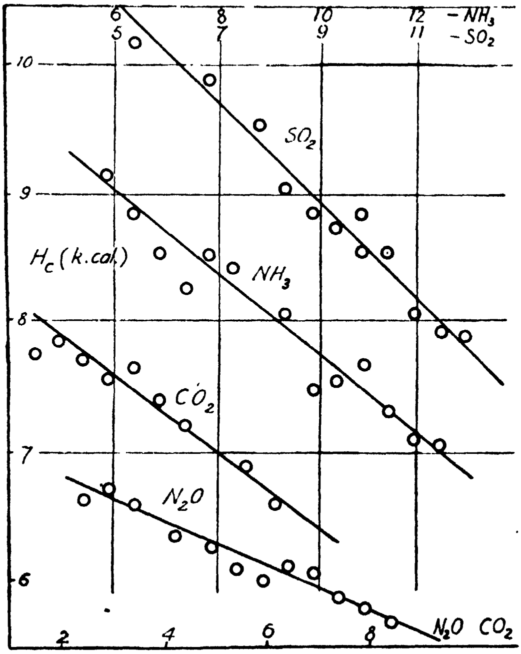

FIG. 5.—Variations of heats of adsorption of SO_2, NH_3, CO_2 and N_2O with increasing v, averaged over the whole temperature range.

Now K is the ratio of the partition functions of the adsorbed molecule in the first and second layer, i.e. j_1/j_2, or

$$(j_1'/j_2')(\nu_2)^3/(\nu_1)^3$$

if harmonic oscillator models are assumed and j_1', j_2' refer to the partition functions of all other degrees of freedom. These latter may be approximated to $j_1'/j_2' = \dfrac{1}{e}$ to account for the randomness of molecules in the second or liquid layer, but ν_2 and ν_1 will differ since ν_1 refers to vibrations of the adsorbed molecule with respect to a plane array of doubly-charged ions and ν_2 to an array of dipoles. It follows that $K < 1$ and that $\Delta H_B < \Delta H_e$; Cassie[11] has likewise shown by some approximate calculations that this should be of general occurrence.

[9] Coolidge, *J. Amer. Chem. Soc.*, 1926, **48**, 1795.
[10] e.g. Foster, *J. Chem. Soc.*, 1945, 360.
[11] Cassie, *Trans. Faraday Soc.*, 1945, **41**, 450.

An experimental estimate of K may be made in the following way. From the B.E.T. model

$$c = \frac{K_1}{K_2} = \frac{k_1/k_1'}{k_2/k_2'},$$

where K_1, K_2, are equilibrium constants and k_1, k_1', and k_2, k_2' are velocity constants referring to condensation and evaporation phenomena at the first and second layer respectively. Hence

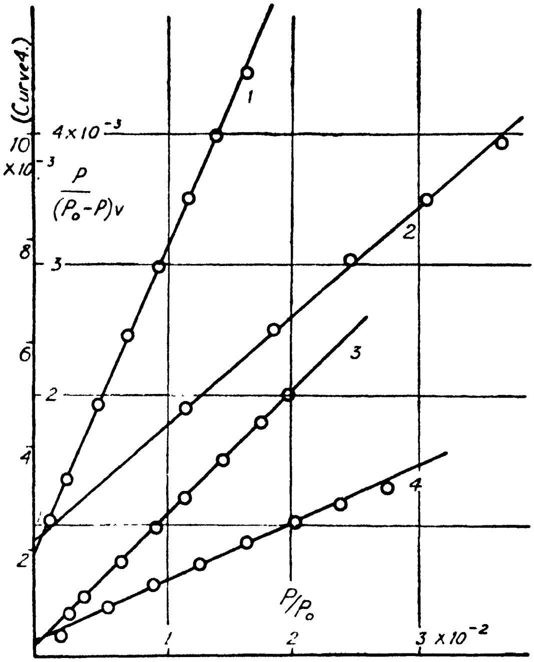

Fig. 6.—Test of the B.E.T. equation.

Curve No. (1) N_2O at −40·0° c. Curve No. (3) SO_2 at 31·8° c.
(2) CO_2 at −17·0° c. (4) NH_3 at 73·9° c.
The scale for SO_2 is ten times larger than that indicated in the figure.

$$RT \log_e c = RT \log_e \frac{K_1}{K_2} = -\Delta G_1 + \Delta G_2$$
$$= -\Delta H_1 + \Delta H_2 + (\Delta S_1 - \Delta S_2)T$$

or
$$\delta(\Delta S) = R \log_e c + (\Delta H_1 - \Delta H_2)/T \qquad . \quad . \quad (3)$$
and since
$$c = K\,e^{-(\Delta H_1 - \Delta H_2)/RT}$$
then
$$R \log_e K = \delta(\Delta S).$$

Here $\Delta H_1 - \Delta H_2$ must be obtained independently of c i.e. from the Clausius-Clapeyron equation and the heat of liquefaction. Unfortunately ΔH_e is not a true measure of ΔH_1 since

$$\Delta H_e = x\Delta H_1 + (1 - x)\Delta H_2$$

where x is the fraction of v in the first layer; the correction is large when $\Delta H_1 \gg \Delta H_L$ and p is commensurate with p_0. The experimental fall of ΔH_e with v is due not only to this, but to (a) the increasing repulsive forces between similarly oriented dipoles and (*b*) the higher adsorption potential existing at the 100 plane as compared with the 111 plane, etc. These two factors are estimated (see later) and ΔH_1 found by extrapolation to $v = 0$. Values of ΔH_1 at intermediate v-values can then be calculated; in Table I are collected values of $\Delta \bar{H}_1$ and $\Delta \bar{H}_e$, i.e. averaged values of ΔH_1 and ΔH_e over all v-values. Similarly, Anderson[12] in an analysis of the region of validity of the B.E.T. equation shows that the range may be extended to higher pressures if p_0 is replaced by kp_0; k for most systems examined is 0·6 to 0·7. This corresponds to a reduction of 50 cal. at 78° K. or 500 cal. at room temperature in ΔH_2. Consequently, in Table I, ΔH_2 values are corrected ΔH_L values. As with previous workers, $\Delta \bar{H}_e$ and ΔH_B agree within 10-20 % but there is no consistent divergence whereas $\Delta \bar{H}_1$ values are always greater than ΔH_B. Values of $\delta(\Delta S)$ in cal./degree and therefore of K can be calculated from eqn. (3) and are given in Table II. The negative entropy value implies that the molecules are more ordered in the first layer than in the second layer—the increasing (negative) magnitude with increasing T suggests that the disorder is more pronounced at higher temperatures. Similarly the ratio j_1/j_2 is of the order of 1/30 if it is assumed that the second layer corresponds to a two-dimensional liquid layer in which molecules have lateral mobility.

TABLE I.

	SO_2.	NH_3.	N_2O.	CO_2.
ΔH_1	9000	8100	5450	6750 cal.
ΔH_e	8200	7050	5220	5270 ,,
$\Delta \bar{H}_1$	7310	7770	5040	4990 ,,

TABLE II.—VALUES OF $\delta(\Delta S)$ AT VARIOUS TEMPERATURES.

SO_2.		NH_3.		N_2O.	
Temp. °c.	$-\delta(\Delta S)$.	Temp. °c.	$-\delta(\Delta S)$.	Temp. °c.	$-\delta(\Delta S)$.
53·9	3·90	36·0	2·89	−40·0	3·70
74·9	5·03	54·9	3·35	−22·8	1·71
99·5	5·29	73·9	3·82	−13·0	3·32
119·0	7·46	119·0	3·90	0·0	3·60

Values for CO_2 are not given here since they appear to be very high (of the order of 10 cal./degree) due to the high value of ΔH (Table I).

The decreasing heat ΔH_e with increasing v is due to three causes: (*a*) the inhomogeneity of the surface in as much as the 100 plane has a higher adsorption potential than the 111, etc., (*b*) the increasing repulsive field in the first layer with increasing coverage and (*c*) the filling-up of higher layers. These are all inter-related so that it is only possible to indicate the order of magnitude of each contribution. The difference in ΔH_e for the 100 and 111 plane is, according to the calculations here, about 1000 cal. The effect of (*b*) as the first layer is completed is estimated by making use of Roberts' formula, viz.,

$$\Delta\phi_e(\theta) = \tfrac{1}{2}\alpha_r F^2 \Big/ \left(1 + \frac{9}{a^3}\alpha\theta\right)$$

---

[12] Anderson, *J. Amer. Chem. Soc.*, 1946, **68**, 686.

where ${}_rF$ is the resultant field from the crystal, α the polarisability, a the distance apart of the dipoles in square array. With ${}_rF = 3{\cdot}2 \times 10^5$ E.S.U., $\alpha = 3{\cdot}77 \times 10^{-24}$ and $a = 4{\cdot}37$ A., $\Delta\phi_e(\theta)$ is 810 cal. A similar calculation for the permanent moment gives 1100 cal. or a total of 1900. This is a maximum value since the van der Waals attractive forces are neglected—these however will be small when a is as large as 4·37 A. Finally, the ΔH_e value is given by $x\Delta H_1 + (1 - x)\Delta H_2$, where x is the fraction of the total in the first layer—since it follows from Hill's treatment of the B.E.T. equation that

$$p/p_0 = v_2/(v_1 + v_2), \text{ then } \Delta H_c = p/p_0 \,.\, (\Delta H_2 - \Delta H_1) + \Delta H_1\,;$$

for SO_2 at 0° C. with $\Delta H_L = 5000$ cal., or $\Delta H_2 = 4300$ cal., ΔH_e (corrected) = 9000 cal. and $k = 0{\cdot}3$, the fall is 1500 cal. as p is increased from 0-40 cm. The total fall in heat in this range should therefore be about 4400 cal. as compared with the experimental value of 4000 cal. The agreement is not stressed, but it is felt that the fall is adequately accounted for in general by these three factors.

The constant v_m in eqn. (2) is related to the surface area A, but some confusion is found. The adsorbed molecules can theoretically (a) assume the close-packing arrangement of the liquid state when A = no. of molecules in the completed monolayer (N_1) × their cross-sectional area as derived from the liquid (or solid) density, or (b) be constrained to occupy definite sites on the surface, when $A = N_1 \times$ (an area determined by the lattice parameters of the adsorbent) and v_m is independent of the dimensions of the adsorbate molecule. The test is the magnitude of the variations of the heat of adsorption $\delta(\Delta H)$ which arises from the periodic nature of the ionic surface at various points on the surface; when $kT < (\Delta H)$, there is no lateral mobility and localised physical adsorption results, i.e. (b) above, but if $kT > \delta(\Delta H)$, the layer is mobile and close packing may be assumed. In this latter case (a), it is permissible to regard the layer as a two-dimensional gas under high pressure (at low v) which approaches the two-dimensional liquid state with increasing v; to transform by the Gibbs relation to force-area concepts; to speak of phase transitions and to anticipate a decrease in v_m with increase of temperature in terms of the two-dimensional expansion of the surface phase. In case (b) however, force-area diagrams have little meaning and v_m should be temperature independent; the layer here will correspond more nearly to a solid under a high negative pressure and it can undergo phase transitions involving only configurational changes (cp. later).

Eqn. (2) is valid only if case (b) holds; this is emphasised in the statistical treatments of Cassie [11] and later of Hill [13] in a more correct form. Even a change from a square array to a hexagonal close-packing, as occurs in the A—KCl system at low temperatures must necessarily invalidate the statistical reasoning. Now in general, except at liquid-air temperatures, localised van der Waals adsorption is rare; thus with inert gases on NaCl lattices $\delta(\Delta H)$ is about 500 cal., i.e. a mobile layer is formed at room temperatures and eqn. (2) is not applicable. Nevertheless, it has been used quite generally without regard to this. In certain systems, however, immobile layers at room temperatures are possible.

Thus for A on CsI, which has a body-centred lattice (lattice constant = 4·56 A.) and the planes of which contain either all Cs^+ or all I^- ions, Orr [1] has calculated that $\delta(\Delta H)$ is 2068 cal. on the Cs^+ faces, and 1321 cal. on the I^- planes; thus most of the adsorbed molecules are immobile at 0° C. The first value is particularly high because the A atom ($r = 1{\cdot}98$ A) can penetrate into the surface layer of Cs^+ ions and make contact with the underlying I^- ions. Now the present adsorbent, BaF_2, which is of the face-centred cubic group, (lattice constant 6·18 A.) has two planes

---

[13] Hill, *J. Chem. Physics*, 1946, **14**, 263, 268, 441.

(100 and 111) containing all Ba ions and the adsorbate molecules, the largest of which is SO_2 ($r = 2·47$ A.), may again penetrate the surface Ba layer. Unfortunately it is only possible to calculate in an approximate manner because of our lack of knowledge of the repulsive forces operating between SO_2 molecules which makes the value of the equilibrium distance (r_e) of the adsorbed molecule from the surface uncertain, and also because of the marked asymmetry of the molecule. We have, however, taken r_e to be the sum of the radii of the SO_2 molecule, assumed spherical, and the Ba^{++} ion ($r = 1·30$)—cp. A on CsI where a similar assumption was necessary; details for SO_2 on the 100 plane only are given here. The 100 plane may be regarded as a square array of Ba^{++} ions of side 4·37 A. with an underlying square of F^- ions of 1·30 A. radius, 1·54 A. below the Ba^{++} plane, and of side 3·09 A., the square being rotated through 45° in a horizontal plane. The difference in adsorption heat of the adsorbed molecule over the centre of a lattice square of side 4·37 A. (I), and directly over a Ba^{++} ion (II), will give $\delta(\Delta H_{\text{max.}})$. From Fig. 7, $r_2 = 2·16$ A. from the plane of the Ba^{++} ions and 3·70 A. from the underlying F ions in (I), and 3·77 A. and 5·31 A. respectively in (II). In (I), penetration of the surface layer occurs although not sufficiently for contact with the F^- ions. The van der Waals contribution has been calculated from the polarisabilities (3·77 and $1·6 \times 10^{-24}$ cc. respectively for SO_2 and Ba^{++}) and the ionisation potentials (12·05 and 10·0 e.v. respectively for SO_2 and Ba^{++}) making use of the summations given by Orr. Full details are given in his paper and it is only necessary to note (using his nomenclature) that $\Sigma_1 \rho$ must be used for the Ba^{++} and F^- layers in (I); and $\Sigma_3 \rho$ for the Ba^{++} layer, and $\Sigma_1 \rho$ for the F^- layer in (II), as may be seen from Fig. 7. The difference of the van der Waals contribution to $\delta(\Delta H)$ is found to be 3000 cal., the heat being larger for (I).

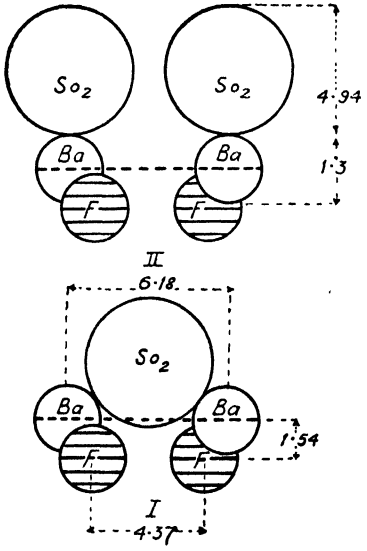

FIG. 7.

A similar calculation (cp. Orr) is performed for the electrostatic forces where in case (I):

$$_rF_1(\rho) = f_1(\rho) - f_1(\rho + 0·71)$$

and in case (II):

$$_rF_3(\rho) = f_3(\rho) - f_1(\rho + 0·71).$$

After subtraction and introducing the values of the dipole moment (1·60 D.) and the polarisability of the SO_2 molecule into the expressions, $\delta(\Delta H)$ (electrostatic) is found to be 3500 cal. and is a maximum over the centre of the lattice square (cp. a NaCl lattice where $\delta(\Delta H)_{\text{electr.}} = 0$); the total difference is thus 6500 cal. This value appears on first considerations to be very large but penetration of the surface layer allows the adsorbate molecule in (I) to be at a distance 1·5 A. nearer the plane of the Ba^{++} ions than is possible in (II). Furthermore, the electrostatic contribution is high on account of the permanent dipole associated with, and the high polarisability of, the SO_2 molecule and also because the surface ions (Ba^{++}) carry double charges. It may well be that the values of r_e taken are too small and therefore the value of $\delta(\Delta H)$ is too large, but by comparison with the A—CsI system (in which the theoretical requirements are more completely satisfied) where $\delta(\Delta H)$ is 2000 cal., we may place some confidence in the order of magnitude of this value. Similarly, on the 111 face a value of 5500 cal. is obtained assuming that r_e (Case I) is 2·55 A. Comparable magnitudes are obtained for NH_3; for CO_2 and N_2O, $\delta(\Delta H)$ is 2500 cal. less, or about 4000 cal. on the 100 plane. Such values necessitate the formation of immobile layers, i.e. the motion of the adsorbed molecule is primarily vibrational and it can jump only very infrequently from one potential minimum to another except via the processes of evaporation and condensation. There is the possibility of a phase transition in the first layer; the most likely is from the square array to a close-packed structure as indicated in Fig. 8. Proceeding on the lines indicated above, the difference in energy between these two arrangements is found to be about 4000 cal. Again, although very approximate in nature, the order of magnitude precludes any configurational change (as is found with A on KCl) which would again lessen the validity of eqn. (2). Values of v_m may thus be correctly evaluated from eqn. (2), and are collected in Table III. For each gas there is a fall of about 14 % for a temperature rise of 120° C.; the mean over this temperature range differs by 6 % from the average for all four gases although there are considerable differences in the cross-sectional areas as derived from the liquid state (SO_2, 19·2; NH_3, 12·9; N_2O, 16·8; and CO_2, 17·0 A.^{1}). The constant v_m value is good evidence that the layer is immobile and that the area of adsorbent is determined by the lattice parameters. The small variation of v_m with temperature is due to the assumption that $\Delta H_s = \Delta H_L$ since there are good reasons for believing that $\Delta H_s < H_L$, the values of p_0 used to obtain the linear plots of eqn. (2) and so to evaluate v_m are too large and lead to a spurious change of v_m with T. The small change of v_m with T is to be compared with the large temperature coefficients

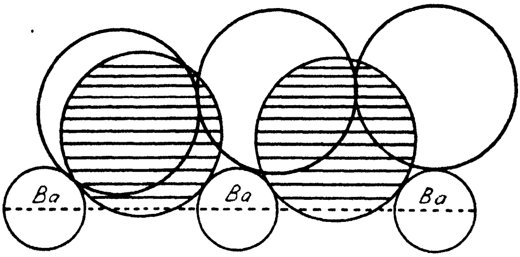

FIG. 8.

The large circles represent the SO_2 molecules : ●, position as in Case (I) (Fig. 7) ○, close-packing.

TABLE III.—VALUES OF v_m AT DIFFERENT TEMPERATURES.

SO_2.		NH_3.		N_2O.		CO_2.	
Temp. °C.	v_m (cc. N.T.P.).	Temp. °C.	v_m (cc.).	Temp. °C.	v_m (cc.).	Temp. °C.	v_m (cc.).
31·8	10·19	18·6	12·41	−40·0	11·80	−17·0	10·53
55·9	10·36	36·0	10·48	−22·8	10·72	0·0	10·46
74·9	10·19	54·9	10·06	−13·0	11·08	18·6	10·04
98·5	8·92	73·9	10·33	0·0	10·72	36·0	9·93
119·6	8·89	98·4	8·73	23·7	8·73	55·0	9·68

obtained by Ausin and Armbruster,[14] and by Wilkins,[15] using the Langmuir equation. Such a variation is obtained here using this equation and moreover their empirical relationship (log v_m is a linear function of $1/T$) is also valid. It seems that the reason is the restriction to the formation of a single monolayer; this may in fact be proved and the log $v_m - 1/T$ relationship follows from the multilayer theory if we assume that the free energy of mixing is negligible.

In the second layer, the molecules are absorbed on a regular square array of dipoles in the first layer. Since the second layer of molecules cannot be closer than 4·94 A. to the adsorbent surface, the direct effect of the adsorbent field, and in particular the variation of it over the surface, is very small. The method of B.E.T.[8] may therefore be used and the adsorption potential due to the first layer of (enhanced) dipoles may be calculated together with its variation over the surface. This latter is found to be less than 600 cal. so that most molecules will here have lateral mobility corresponding to a two-dimensional liquid. Moreover, more molecules can be packed into the second layer than in the first layer. However, on average, the dipoles in this second layer will be oriented parallelwise so that the repulsive field will prevent a packing as close as that in the three-dimensional liquid state. This, in part, may account for ΔH_2 being less than ΔH_L here.

One of the authors (V. A. C.) wishes to express thanks to the National Research Council and Board of S. Africa for a Research Scholarship held during this investigation.

Summary.

The adsorption of SO_2, NH_3, CO_2 and N_2O on BaF_2 crystals has been measured at various temperatures between − 78 and 119° c.; from these isotherms heats of adsorption have been obtained using the Clausius-Clapeyron equation and the B.E.T. equation. The decrease of heats with coverage found experimentally is discussed and compared with those expected theoretically. Variation in adsorption potential over the crystal surfaces have been calculated in an approximate manner and the significance of these discussed from the viewpoint of the applicability of the B.E.T. multilayer theory.

Natal University College,
University of S. Africa,
Natal,
S. Africa.

Royal College of Science,
Imperial College of
Science and Technology,
London, S.W.7.

---

[14] Armbruster and Austin, *J. Amer. Chem. Soc.*, 1939, **61**, 1117; 1938, **60**, 467; 1944, **66**, 159, etc.

[15] Wilkins, *Proc. Roy. Soc. A*, 1938, **164**, 496.

ON SOME PROPERTIES OF CYCLO-OCTATETRAENE IN RELATION TO STRUCTURE.

BY R. C. PINK AND A. R. UBBELOHDE.

Received 16*th October*, 1947.

In spite of their limitations, the thermal data reported on cyclooctatetraene[1] are of considerable interest in relation to the structure of this compound.

(1) Approximate Vaporisation Constants.—With quoted b.p. of 142-143° c. at 760 mm., and 42-42·5° c. at 17 mm. Hg, the mean latent heat of vaporisation over this temperature interval, calculated from the equation, $\log p = \Delta H/4{\cdot}57T + \text{const.}$, is 9·86 kcal./mole. and the entropy of vaporisation at the boiling point is 23·7 cal./deg. These values compare with $\Delta H = 7{\cdot}0$ kcal. and $\Delta S = 19{\cdot}73$ cal./deg./mole. for benzene.

---

[1] Reppe, B.I.O.S. Final Report, No. 137, Item No. 22, 1945.

(2) Heat of Formation and Resonance Energy.—The heat of formation of the liquid[2] is 40 kcal./mole and of the gas (adding the result from (1) above) 49·9 kcal./mole.,

$$\begin{array}{llr}
\text{i.e.} & 4H_{2\,\text{gas}} + 8C_{\text{solid}} \rightarrow C_8H_{8\,\text{gas}} + & 49{\cdot}9\,; \\
\text{adding} & 8H_{\text{gas}} \rightarrow 4H_{2\,\text{gas}} & -\ 413{\cdot}6, \\
 & 8C_{\text{gas}} \rightarrow 8C_{\text{solid}} & -\ 994{\cdot}4, \\
\hline
 & 8H_{\text{gas}} + 8C_{\text{gas}} \rightarrow C_8H_{8\,\text{gas}} & -\ 1358{\cdot}1.
\end{array}$$

Whereas the bond energies $8D(\text{C—H}) + 4D(\text{C—C}) + 4D(\text{C=C})$

$$= 698{\cdot}4 + 234{\cdot}4 + 400{\cdot}0 = 1332{\cdot}8.$$

Values are taken throughout from Pauling[3] so as to base them on a consistent heat of vaporisation of carbon. On this basis the resonance energy of the cyclo-octatetraene molecule is 25·3 kcal. compared with 39 for benzene. (Much lower resonance energies for C_8H_8 were reported verbally at the XIth International Congress of Pure and Applied Chemistry.)

While this resonance energy is less than that of benzene and not unexpectedly high for an aliphatic type of structure, it suggests the possibility that C_8H_8 may have some aromatic character. The reactivity of C_8H_8 does not necessarily rule out this possibility completely, since differences of reaction rate of 1000 : 1 at, say, 100° c., correspond with differences in activation energy of only 5 kcal./mole. Again, phenanthrene is much more reactive than anthracene though the resonance energy is actually higher, and the aromatic character is quite definite.

(3) Diamagnetic "Structure Constants" as a Test of Aromatic Character.—For both theoretical and empirical reasons, the diamagnetic susceptibility should provide a much more definite test for the presence of "aromatic" character than either chemical reactivity or resonance energy. Theoretically, aromatic character implies the presence of a "pool" of electrons with orbits with radius extending over the whole of the "aromatic" region.[4] In the summation of. contributions to the diamagnetic susceptibility from individual orbits, of the form

$$\sum n_a \bar{r}_a^2,$$

the presence of giant or "aromatic" orbits involves a substantially larger value of "radius" for the aromatic electrons, and consequently substantially higher diamagnetism per electron, than in the case of orbits bound to single atoms. The only complication in using this enhanced diamagnetism as a simple test of aromatic character is the possibility of superposed paramagnetic effects. Especially in the polynuclear aromatic hydrocarbons, such paramagnetic contributions may mask the giant diamagnetic orbits. This is referred to again in the discussion below.

Empirically, Pascal's data give $\chi_m = \sum n_a C_a + \lambda$ where the atomic constants C_a and numbers of atoms of one kind n_a are inserted from data established for a large range of compounds, and the structure constant λ allows for double bonds, ring formation, etc.[5] For our particular problem, which is to distinguish between "aromatic" rings of carbon atoms and cyclic systems of conjugated double and single bonds (c.d.s.b.), the *empirical* distinction on the basis of Pascal's data is particularly clear cut. Thus:

---

[2] Reppe, B.I.O.S. Final Report, No. 137, Item No. 28, 1945, p. 3.

[3] Pauling, *Nature of the Chemical Bond* (Cornell University Press, 1940).

[4] Coulson, *Quart. Rev.*, 1947, **1**, 144 ; cp. Ubbelohde, *Nature*, 1933, **132**, 1002.

[5] cp. Selwood, *Magnetochemistry* (Interscience Press, 1943), p. 51, who also gives full references to the literature.

BENZENE	c.g.s. units × 10^{-6}
$\chi_{\text{mol.}}$ (aromatic ring)	$= -55{\cdot}02$
$\chi_{\text{mol.}}$ (cyclic system c.d.s.b.)	$= -37{\cdot}08$
$\chi_{\text{mol.}}$ Direct observation	$= -55{\cdot}58$
CYCLO-OCTATETRAENE	
$\chi_{\text{mol.}}$ (aromatic ring)	$= -73{\cdot}36$
$\chi_{\text{mol.}}$ (cyclic system c.d.s.b.)	$= -50{\cdot}24$
$\chi_{\text{mol.}}$ Direct observations (see below)	$= -51{\cdot}9$

The most direct conclusion from our experiments would appear to be that cyclo-octatetraene C_8H_8 behaves like a cyclic system of conjugated double bonds, and does not give any evidence of an aromatic pool of electrons. More subtle possibilities are discussed below.

(4) Thermal Changes in Solid Cyclo-octatetraene at Low Temperatures.—On condensing C_8H_8 *in vacuo*, using liquid oxygen (cp. later) it was observed that the yellow colour exhibited by both liquid and solid C_8H_8 changed more or less completely to white in the neighbourhood of the boiling point of oxygen, but reappeared well below the melting point, on warming solid C_8H_8. In view of the possible presence of small amounts of a "diradical" such as 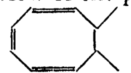 in C_8H_8 (see discussion, below) this colour change was of particular interest. However, for various reasons the change of colour was not very satisfactory evidence of a change in the solid (cp. later). Experiments were therefore carried out to test for a possible thermal transition in the solid on cooling, and also to test for a possible change in magnetic susceptibility at low temperatures.

Low-temperature magnetic measurements have not so far been successful, on account of the difficulties of technique. Measurements of the apparent specific heat of C_8H_8 have, however, indicated a transition in the solid in the neighbourhood of 98° K. The technique used did not make it quite definite whether the transition was discontinuous or continuous,[6] but probably the effect occurs over a range of a few degrees. The heat change was estimated to be about 0·4 kcal./mole. and the entropy change about 4 cal./deg./mole. The possible significance of this transition is discussed below.

Experimental.

Samples of liquids were used as follows.

Cyclo-octatetraene :	M.p. −4·85° c., b.p. 30·0° c. at 13 mm.
Cyclo-octane :	B.p. 148-149° c. at 760 mm.
Cyclo-octene :	B.p. 142-144° c. at 760 mm.
Benzene (Analar, B.D.H.) :	B.p. 80·1 ± 0·05° c. at 758 mm.
n-Hexane (B.D.H., spectroscopically pure) :	B.p. 68·5 ± 0·05° c. at 755 mm.
Cyclohexene (stood over solid KOH and distilled) :	B.p. 83·2 ± 0·1° C. at 760 mm.

As a general rule, the sample of liquid was transferred to one limb of a high-vacuum distillation apparatus, using an atmosphere of nitrogen to avoid introducing oxygen and water vapour in the case of the unsaturated substances. The substance was then frozen using liquid air, and after reducing the pressure to about 10^{-4} mm. by means of a mercury diffusion pump, it was allowed to warm up, and a middle fraction was distilled into a Pyrex pyknometer (Fig. 1 *a*) which was again frozen, and sealed off *in vacuo* when sufficiently full.

---

[6] Ubbelohde and Woodward, *Proc. Roy. Soc. A*, 1947, **188**, 358, which gives other references.

Before filling the pyknometer in this way, its volume was previously calibrated up to various marks, by weighings with distilled water at a known temperature, so that the volume of liquid used could be determined by interpolation. The pyknometer was also calibrated for measurements of magnetic susceptibility by suspending it by means of a Nylon filament (2x Nylon gut) from one arm of an Oertling " chainomatic " balance, weighing down to 0·0001 g., in such a position that the flat bottom of the pyknometer was situated on the axis of the pole pieces of an electromagnet.[7] A typical series of calibrations and measurements may be given for benzene. Weighings are in each case the mean of several observations.

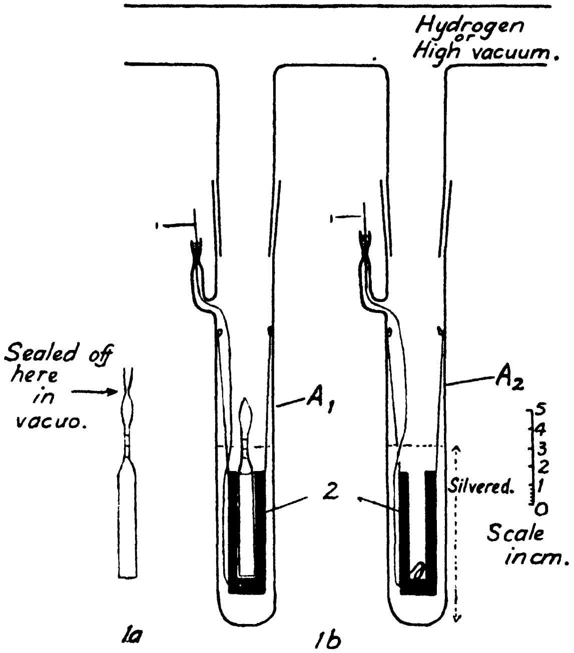

FIG. 1.
1. Thermocouple wires. 2. Polished copper cylinders.
Differential calorimeter.

Weight of tube empty	7·6943
Weight of tube with 4·30 amp. in electromagnet	7·6918
Pull due to glass tube	– 2·5 mg.
Weight of tube filled with boiled distilled water up to Mark 1	11·0525 at 15·5° C.
Ditto with 4·30 amp.	11·0402
	– 12·3 mg.
Up to Mark 2	11·1785
Ditto with 4·30 amp.	11·1663
	– 12·2 mg.
Up to Mark 3	11·2729
Ditto with 4.30 amp.	11·2607
	– 12·2 mg.

---

[7] cp. Selwood, *ibid.*, p. 3.

From these calibrations it was clear that the diamagnetic repulsion was substantially independent of the exact level of liquid between the three volume-calibration marks.

The tube was emptied, dried, filled with Analar benzene by distillation, and sealed off.

Weight of tube filled with benzene	9·8112 at 14·0° c.
Ditto with 4·30 amp.	9·8002
	— 11·0 mg.

Taking a value of $-0{\cdot}720 \times 10^{-6}$ for the volume susceptibility of water, the mass susceptibility of benzene calculated from these data by the method described by Michaelis[8] is $-0{\cdot}713 \pm 0{\cdot}007 \times 10^{-6}$ which agrees very well with the value quoted by *International Critical Tables*[9] ($-0{\cdot}712 \times 10^{-6}$ c.g.s. units). The various mass and molecular susceptibilities determined in this way are given in Table I. The probable error in all cases is 1 %.

TABLE I.

Magnetic susceptibilities $x(-1 \times 10^{-6})$ at 20° c.

Substance.	χ Found.	$\chi_{\text{calc.}}$ (Pascal/Selwood).	χ (mol.) Found.
Benzene	0·713	0·706	55·6
Cyclohexane . . .	0·805	0·847	67·7
n-Hexane . . .	0·878	0·897	75·6
Cyclohexene . . .	0·701	0·728	57·5
Cyclo-octene . . .	0·768	0·759	84·6
Cyclo-octane . . .	0·815	0·846	91·4
Cyclo-octatetraene . .	0·499	0·483 (dbcs) 0·705 (ar)	51·9

In the table, some of the experimental values may be compared with the data in *International Critical Tables*,[10] e.g. benzene 0·712, cyclohexane 0·810, *n*-hexane 0·888 and cyclohexene 0·711. In general the agreement is within the probable error.

In the column for $\chi_{\text{calc.}}$, the susceptibility of cyclo-octatetraene is calculated both for the cyclic system of 4 double and 4 single bonds and for the aromatic " pool " of 8 carbon atoms. As is discussed below, the result found experimentally agrees much more closely with the first of these structures.

Thermal Transformations in Cyclo-octatetraene.—As explained above, when solid C_8H_8 is cooled in liquid oxygen it becomes almost colourless, compared with the yellow colour of the solid near its melting point. The amount of C_8H_8 available was not sufficient to permit exhaustive purification, and it was thought possible, though not likely, that the change coloured ⇌ colourless was due to the freezing-out of impurities which remain in solid solution at higher temperatures. Such a freezing out might lead to a break up of the (soft) crystals and consequently an increase in apparent whiteness. On the other hand, the change might be due to the self-combination of a yellow diradical at low temperatures, to a structure which is probably colourless (cp. [18], which does not, however, decide this finally).

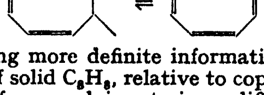

In the hopes of obtaining more definite information on this point, measurements of the heat content of solid C_8H_8, relative to copper, were made by plotting rates of temperature rise for equal input, in a differential calorimeter. The apparatus as finally used is illustrated in Fig. 1*b*. Here A1 and A2 are two glass vessels silvered on the outside to minimize radiation, and as nearly similar as possible. A polished copper cylinder hangs by thin copper wires centrally inside A1. The Pyrex tube filled with C_8H_8 (Fig. 1*a*) slips inside this, and good thermal contact is ensured by a thin layer of " J " Apiezon oil. A copper cylinder of the same outer dimensions hangs inside A2. The mass of copper in this cylinder is adjusted by adding a piece of copper wire, by trial, so that the two cylinders are as nearly as possible of equal heat capacity when empty. Two thermocouples are inserted into the cylinder A1. One of these has the other junction in ice, and serves to measure its temperature. This couple is calibrated at the boiling point of liquid oxygen and the freezing point of mercury. The second couple has its second junction in A2 so as to measure the difference in temperature between the copper cylinders in A1 and A2. Dummy wires similar to the thermocouple in A1 are also inserted into the appropriate hole in A2, so that any heat conducted to the two copper cylinders is as nearly as possible equal.

---

[8] Michaelis, *Physical Methods of Organic Chemistry* (ed. Weissberger), (Interscience Press), Vol. 2.

[9] *Int. Crit. Tables*, Vol. VI, p. 354.

[10] *ibid.*, p. 362.

It was found desirable to start at the lowest available temperature, so that the outer Dewar flask (not shown) was fitted with a vacuum-tight lid. By rapid pumping off, the liquid oxygen in the Dewar could be partially frozen. At the beginning of each experiment, the apparatus was filled with hydrogen whilst the temperature of the outer bath was reduced to the freezing point of oxygen. When both blocks had attained the bath temperature the hydrogen was pumped out, and after a vacuum of 10^{-3} mm. or lower had been attained the bath was removed. The blocks slowly gain heat by conduction and to some extent by radiation, at closely similar rates. The temperature θ_1 of A1 and the temperature difference $\Delta\theta$ between the blocks are plotted as a function of time.

Assuming Newton's law of cooling, the rate of gain of heat of the blocks in A1 and A2 is

$$C_1 \mathrm{d}\theta_1/\mathrm{d}t = k_1(\theta_1 - \theta_r)$$
$$C_2 \mathrm{d}\theta_2/\mathrm{d}t = k_1(\theta_2 - \theta_r)$$

where the constant k_1 is assumed the same owing to the similarity of external conditions, and C_1 is the total heat capacity of the block and its contents in A1, C_2 of the block in A_2 and θ_r the effective temperatures of the surroundings. Writing $C_1 = C_2 + \Delta C$ where ΔC, the difference in heat capacity, may include heats of transition, and subtracting,

$$C_2 \mathrm{d}\Delta\theta/\mathrm{d}t + \Delta C \mathrm{d}\theta_1/\mathrm{d}t = k_1\Delta\theta = \frac{C_2\Delta\theta \mathrm{d}\theta_2/\mathrm{d}t}{(\theta_2 - \theta_r)}.$$

Since the weight of copper is known, all the quantities in this expression can be calculated. Any large heats of transition are marked by pronounced changes of slope in the plot of $\Delta\theta$ against t.

The curves showed evidence in the case of C_8H_8 that there was a transition which appeared to occur over several degrees with a maximum around −175° C. It was not possible to evaluate the heat of transition at all accurately. Approximate estimates are

$$\Delta H = 400 \text{ cal. mole.}$$
$$\Delta S = 4 \text{ cal./degree/mole.}$$

There was some evidence that it was necessary to cool the solid for some time well below the transition point in order to complete the change to the low temperature structure.

Discussion.

Structure and Diamagnetism.

The probable error in our susceptibility measurements is ± 1 %, which appears to be usual in this type of measurement.[11] Definite significance may thus be attached to differences in molecular susceptibility exceeding this probable error. The purity of some of the cyclic compounds used could not be assessed very closely, owing to the relatively small quantities available, but since the likely impurities such as water or organic compounds in the C_8H_8 would not have widely different susceptibilities, this uncertainty is unlikely to affect the data by more than a few figures in the third place in Table I. The main conclusion seems to be quite definitely that the diamagnetic susceptibility of cyclooctatetraene accords with a cyclic system of conjugated double bonds.

[11] cp. Michaelis, *ibid.*, p. 1226.

This agrees with recent observations on the infra-red and Raman spectra [12] and would explain the chemical reactivity.

Table I gives the values of χ_m calculated by means of Pascal's constants.[13] Our data also permit certain calculations independent of these constants as follows—

$$\text{(i)} \qquad \chi_m \text{ (cyclo-octane—cyclo-octatetraene)} = 39{\cdot}5$$
$$\chi_m \text{ (cyclohexane-benzene)} = 12{\cdot}1$$

It is evident that the difference in diamagnetism between benzene and cyclohexane is markedly less than the difference between C_8H_8 and cyclo-octane. This is most simply explained, as above, if C_8H_8 does not exhibit "aromatic" diamagnetism.

(ii) Pascal's data show that the constitutive correction for double bonds is almost the same whether these are conjugated, or in isolation.[14] From the data in Table I, χ_m (cyclohexane-cyclohexene) = 10·2 units. Using Pascal's nomenclature, this gives a direct experimental value for $2(H) - \lambda(C{=}C) = 10{\cdot}2$ units. If C_8H_8 behaves as a cyclic system of conjugated double and single bonds with no aromatic character, the value of χ_m (cyclo-octane—cyclo-octatetraene) should be 4 times this quantity, i.e. 40·8 units, in good agreement with the experimental value of 39·5. Thus, these calculations support the interpretation of C_8H_8 as "aliphatic."

An alternative hypothesis may however be considered, viz. that C_8H_8 consists mainly of an "aromatic hydrocarbon" with mass susceptibility about $-0{\cdot}705 \times 10^{-6}$, as calculated from Pascal's constants, together with a very small amount of paramagnetic diradical, for example with a structural formula :

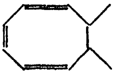

This would have two unpaired electrons and from Paulings' formula the magnetic moment would be $\mu = \sqrt{n(n+2)} = \sqrt{8} = 2{\cdot}83$ Bohr magnetons.[15] Neglecting the diamagnetic contribution, the molecular susceptibility $\chi_m = (\mu/2{\cdot}83)^2/T$ magnetons for the diradical. The molar susceptibility at 292° K. for 100 % of the diradical would be 3413×10^{-6} c.g.s. units.

The mol. fraction x of diradical required to raise the mass susceptibility of C_8H_8 from the value for an aromatic hydrocarbon C_8H_8 ($-0{\cdot}705 \times 10^{-6}$) to the observed value of $-0{\cdot}499 \times 10^{-6}$ can be calculated from the equation :

$$3413x + 73{\cdot}3\,(1 - x) = 51{\cdot}9$$

$$\text{i.e.} \qquad x = \frac{21{\cdot}4}{3412{\cdot}3} = 6{\cdot}27 \times 10^{-3}.$$

This amount of diradical might be expected to decrease with fall in temperature, if the tautomeric equilibrium

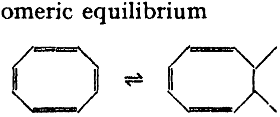

---

[12] Flett, Cave, Vago and Thompson, *Nature*, 1947, **159**, 739 ; Lippincott, *J. Amer. Chem. Soc.*, 1946, **68**, 1868. See also Bastiansen, Hassel and Langseth, *Nature*, 1947, **160**, 128.

[13] Selwood, *ibid.*, p. 52.

[14] cp. Selwood, *ibid.*, p. 52.

[15] Michaelis, *ibid.*, p. 1237.

shifts in the direction of the structure of the lower energy with fall in temperature. At 292° K. the free energy change cyclic (aromatic) → diradical with the above concentration would be, on this basis :

$$\begin{aligned}\Delta G &= -\,RT \ln K \\ &= -\,4{\cdot}57T \log (6{\cdot}27 \times 10^{-3}) = 2{\cdot}9 \text{ kcal./mole.}\end{aligned}$$

It is not possible to assess the heat change and thus to calculate the temperature coefficient. But any decrease in % of diradical with falling temperature would to some extent mask the increase in effective magnetic moment with falling temperature.

Following this hypothesis, if it is supposed that the yellow colour and unduly low diamagnetism of C_8H_8 are due to a small % of a diradical, the change from yellow ⇌ white which is observed on cooling should be accompanied by a substantial increase in diamagnetism. The temperature at which the transition is observed in the solid is around −175° C. and up to the present it has not been possible to carry out magnetic measurements below the transition point. Thus this possibility must be left for further experimental work to decide.

The calculations given above refer to small amounts of one particular " tautomeric form " of C_8H_8. From the chemical reactions described by Reppe, two other tautomeric forms might be present in small amounts, viz.,

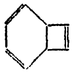

χ_m according to Pascal
8C = − 48·00
8H = − 23·44
Three C=C = + 16·50
4-membered ring = + 3·05
− 51·89

and $\chi_{spec} = -\,0{\cdot}499 \times 10^{-6}$ c.g.s. units.

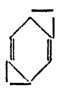

8C = − 48·00
8H = − 23·44
Two C=C = + 11·00
Two 3-membered rings = + 8·2
− 52·24

$\chi_{spec} = -\,0{\cdot}502 \times 10^{-6}$.

Although one or both of these tautomers may be present in small amounts, their presence in such amounts would not help to explain why the observed diamagnetism at 20° C. falls so far *below* that of an " aromatic " structure.

In the above calculations, it should be noted that no allowance has been made for possible temperature-independent paramagnetic contributions to the susceptibility. Any evidence for such contributions in aromatic compounds is very limited,[16] and they are not likely to be important except in systems with several fused rings.

For example, the experimental average susceptibilities collected by Krishnan and Banerjee[17] (see Table II) agree within a few % with the calculated values according to Pascal, which do not allow for such paramagnetic contributions.

Thanks are due to Messrs. I.C.I. (Dyestuffs Division) for the gift of samples of cyclo-octatetraene, cyclo-octane and cyclo-octene.

[16] cp. perhaps, Enderlin, *Ann. Chim.*, 1938, **10**, 5.

[17] Krishnan and Banerjee, *Phil. Trans. Roy. Soc. A*, 1935, **234**, 278.

[18] Maccoll, *Nature*, 1946, **157**, 695.

TABLE II.—TESTS OF PASCAL'S CONSTANTS FOR AROMATIC HYDROCARBONS, USING DATA FROM KRISHNAN AND BANERJEE.

(Mean molar susceptibilities × 10^{-6}.)

Hydrocarbons.	χ_m Found.	χ_m Calc.	χ_m (Found-calc.).
Hexamethyl benzene	− 122·5	− 126·2	+ 3·7
Durene (tetramethyl benzene)	− 101·2	− 102·5	+ 1·3
Terphenyl	− 152	− 153·3	+ 1·3
Triphenylbenzene	− 203	− 202·5	− 0·5
Dimesityl	− 171·6	− 169·5	− 2·1
Fluorene	− 99·5	− 110·2	− 10·7
Phenanthrene	− 129	− 128·1	− 0·9
Chrysene	− 160·7	− 164·2	+ 3·5
Pyrene	− 154·9	− 146·3	− 8·6
Pluoranthene	− 138·4	− 146·3	+ 7·9

Summary.

Calculations from published data show that the latent heat of vaporisation of liquid cyclo-octatetraene is comparable with that of benzene. The Trouton constant is 23·7 cal./degree/mole. Measurements have been made of the diamagnetism of the liquid. The values have been compared with cyclo-octane, cyclo-octene, cyclo-hexene, and benzene to test whether the rather large resonance energy of C_8H_8 might be ascribed to aromatic character. It has been found that the diamagnetism of C_8H_8 agrees with a cyclic system of conjugated double bonds with no evidence of an aromatic pool of electrons. However, the presence of as little as 0·6 mole. % of a diradical may upset this interpretation of the experimental data. Thermal measurements on solid C_8H_8 indicate a transition in the solid state at about 98° K. An observed colour change from yellow to (almost) white appears to be associated with this transition.

Chemistry Laboratories,
Queen's University,
Belfast.

THERMODYNAMIC FUNCTIONS OF THE QUARTIC OSCILLATOR: APPLICATION TO CYCLOBUTANE.

BY T. L. COTTRELL.

Received 16*th October*, 1947.

Bell[1] has shown that in certain modes of vibration of plane rings the potential energy for small displacements is proportional to the fourth power of the displacement. This type of vibration is likely to occur in cyclobutane and its derivatives, in a number of halides having the formula X_2Y_6, and in the hydrides of the group III elements. Since one of the possible methods of confirming the existence of such vibrations is the calculation of the thermodynamic properties of suitable molecules, and comparison of these with experiment, it seemed desirable to make available a sufficiently accurate calculation of the thermodynamic properties of the quartic oscillator.

[1] Bell, *Proc. Roy. Soc. A*, 1945, **183**, 328.

For a potential function $V(x) = ax^4$, the wave equation is

$$\frac{d^2\psi}{d\xi^2} + (\lambda - \xi^4)\psi = 0$$

$$\xi = \left\{\frac{8\pi^2 ma}{h^2}\right\}^{\frac{1}{6}} x\,; \quad \lambda = 4W\left\{\frac{\pi^4 m^2}{h^4 a}\right\}^{\frac{1}{3}} \quad . \quad . \quad . \quad (1)$$

and W is the total energy.

Bell,[1] using the numerical difference equation method of Kimball and Shortley,[2] obtained the eigenvalues of λ for the first 4 levels to an estimated accuracy of about 2 %. Accurate values for the first 5 levels have now been obtained by the linear variation method by Coulson and McWeeny[3] and it is, therefore, now possible to calculate the thermodynamic functions fairly accurately.

In column (*a*) of Table I are quoted Coulson and McWeeny's results, which are accurate to the number of figures given, and have in fact been obtained to several more significant figures, which have not been quoted because they are not required for the present work. Bell's results are quoted in column (*b*) and in column (*c*) are given results obtained using the first term of the Brillouin-Wentzel-Kramers (B.W.K.) expression for the eigenvalues (cp. eqn. 4-7 of Bell's paper). Inserting numerical values in the B.W.K. expression we have

TABLE I.—EIGENVALUES OF EQN. (1).

	(*a*).	(*b*).	(*c*).
λ_0	1·06036	1·09	0·87
λ_1	3·7997	3·81	3·75
λ_2	7·4557	7·36	7·41
λ_3	11·645	11·40	11·61
λ_4	16·262	—	16·24

$$\lambda_n = 2{\cdot}186(n + \tfrac{1}{2})^{4/3} \quad . \quad . \quad . \quad . \quad (2)$$

which seems to give fairly accurate results. In the following calculations the eigenvalues in column (*a*) of Table I have been used for the first 5 levels, and those obtained using eqn. (2) have been used for the higher levels.

The lowest spectrum frequency is given by

$$\nu_0 = \tfrac{1}{4}(\lambda_1 - \lambda_0)\left\{\frac{ha}{\pi^4 m^2}\right\}^{\frac{1}{3}}. \quad . \quad . \quad . \quad . \quad (3)$$

Thus W_n/kT, where W_n is the energy of the nth level, is given by

$$W_n/kT = z\lambda_n'$$

$$z = \frac{h\nu_0}{kT}\,; \quad \lambda_n' = \frac{\lambda_n}{\lambda_1 - \lambda_0}. \quad . \quad . \quad . \quad . \quad (4)$$

If the usual thermodynamic convention is adopted that the lowest energy level has the value zero, i.e. the energy zero is the energy possessed by the oscillator in the lowest vibrational state, λ_0 is put equal to zero, and the values of λ_n given in Table I are replaced by $\lambda_n - 1{\cdot}06036$. Thus the values of λ_n' used in the calculations are given by

$$\lambda_n' = \frac{\lambda_n - 1{\cdot}06036}{2{\cdot}7393}. \quad . \quad . \quad . \quad . \quad . \quad (5)$$

---

[2] Kimball and Shortley, *Physic. Rev.*, 1934, **45**, 815.

[3] Coulson and McWeeny, *Proc. Camb. Phil. Soc.* (in press).

The zero-point vibrational energy of the oscillator is given by

$$W_0 = h\nu_0 \frac{\lambda_0}{\lambda_1 - \lambda_0} = 0{\cdot}3871\ h\nu_0 \quad . \quad . \quad . \quad (6)$$

which is to be compared with the familiar $\frac{1}{2}h\nu_0$ for the harmonic oscillator.

By the usual formulæ,[4] considering N oscillators, we have for the vibrational partition function, Q_v, the free energy, G_v, the entropy S_v, the heat content H_v, and the specific heat C_v :

$$\begin{aligned} Q_v &= \sum_n \exp(-z\lambda_n') \\ G_v &= -RT \ln Q_v \\ S_v &= R\Big[\ln Q_v + \frac{1}{Q_v}\sum_n z\lambda_n' \exp(-z\lambda_n')\Big] \quad . \quad . \quad . \quad . \quad . \quad (7) \\ H_v &= E_v = RT\frac{1}{Q_v}\sum_n z\lambda_n' \exp(-z\lambda_n') \\ C_v &= R\Big[\frac{1}{Q_v}\sum_n (z\lambda_n')^2 \exp(-z\lambda_n') - \Big\{\frac{1}{Q_v}\sum_n z\lambda_v' \exp(-z\lambda_n')\Big\}^2\Big]. \end{aligned}$$

TABLE II.—THERMODYNAMIC FUNCTIONS OF THE QUARTIC OSCILLATOR.

z.	Q.	$-(G^0-E_0{}^0)/RT$.	$(H^0-E_0{}^0)/RT$.	S/R.	C/R.
0·30	2·9806	1·0921	0·6522	1·7443	0·7409
0·35	2·6984	0·9927	0·6376	1·6303	0·7388
0·40	2·4806	0·9085	0·6233	1·5318	0·7365
0·45	2·3069	0·8359	0·6092	1·4451	0·7340
0·50	2·1650	0·7724	0·5955	1·3679	0·7314
0·55	2·0468	0·7163	0·5821	1·2984	0·7287
0·60	1·9468	0·6662	0·5689	1·2351	0·7259
0·65	1·8612	0·6212	0·5559	1·1771	0·7229
0·70	1·7869	0·5805	0·5432	1·1237	0·7198
0·75	1·7219	0·5434	0·5307	1·0741	0·7166
0·80	1·6645	0·5095	0·5184	1·0279	0·7133
0·85	1·6136	0·4785	0·5063	0·9848	0·7100
0·90	1·5681	0·4499	0·4944	0·9443	0·7065
0·95	1·5272	0·4234	0·4827	0·9061	0·7030
1·00	1·4903	0·3990	0·4713	0·8703	0·6993
1·2	1·3730	0·3170	0·4271	0·7441	0·6834
1·4	1·2896	0·2544	0·3858	0·6402	0·6656
1·6	1·2280	0·2054	0·3471	0·5525	0·6457
1·8	1·1813	0·1666	0·3111	0·4777	0·6235
2·0	1·1452	0·1356	0·2777	0·4133	0·5988
2·5	1·0851	0·0817	0·2054	0·2871	0·5279
3·0	1·0507	0·0495	0·1483	0·1978	0·4481
4·0	1·0184	0·0183	0·0728	0·0911	0·2901
5·0	1·0068	0·0067	0·0336	0·0403	0·1673
6·0	1·0025	0·0025	0·0148	0·0173	0·0890

The functions actually tabulated are Q, $-(G^0 - E_0{}^0)/RT$, $(H^0 - E_0{}^0)/RT$, S/R and C/R, which are dimensionless quantities. These are given in Table II. They were obtained by direct summation, there being no satisfactory approximation method which would have involved much less labour. The values of C/R and $(H^0 - E_0{}^0)/RT$ for values of z from 0·30 to 1·00 were calculated at intervals of 0·10, and the 0·05 intervals were obtained by interpolation. The $\dot{Q}$ and $-(G^{\circ} - E_0^{\circ})/RT$ values, however, were calculated separately for each interval. In the range $z = 0{\cdot}30$ to $1{\cdot}00$, at intervals of $0{\cdot}10$ the values of C/R and S/R were checked by repeating the calculations with $\lambda_0 = 1{\cdot}06036$, instead of setting the first level equal to zero. This should give the same result, since these quantities are independent of the energy zero chosen; in no case did any of the values differ from those previously obtained by more than one in the fourth place of decimals, showing that the calculations are consistent to this standard. The results for higher values of z are probably equally accurate.

---

[4] Mayer and Mayer, *Statistical Mechanics*, p. 128.

In the range $z = 0{\cdot}3$ to $z = 1{\cdot}0$ the intervals are sufficiently close for adequate accuracy to be obtained by graphical interpolation for the heat-content function and the heat capacity, but the use of an interpolation formula is necessary for the free-energy function or the partition function. Since in general the fourth-power vibration would be expected to have a fairly low frequency, the functions have only been calculated for fairly wide intervals of the argument from $z = 2$. The chief interest of the complete range of values calculated is in comparing the functions for the quartic oscillator with those of the harmonic oscillator. In Fig. 1, $(H^{\circ} - E_0^{\circ})/RT$ and C/R are plotted against z for the two types of oscillator. The values for the harmonic oscillator are from tables given by Sherman and Ewell.[5] Qualitatively the results are as might be expected, but it is of interest to note that C/R for the quartic oscillator does not, as Bell indicated, exceed the high-temperature classical value of $0{\cdot}75$.

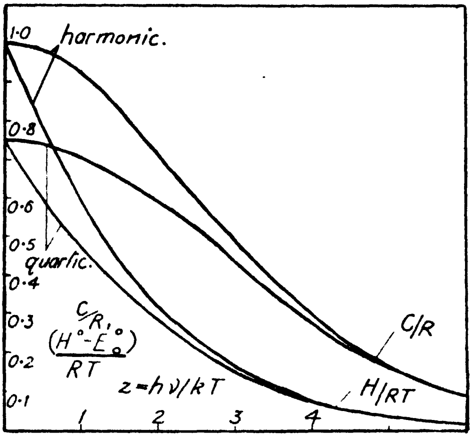

FIG. 1.—Graph of C/R and $(H^{\circ} - E^{\circ}_0)/RT$ against $z = h\nu/kT$ for the harmonic oscillator and the quartic oscillator.

Application to Cyclobutane.

The thermodynamic functions for cyclobutane in the ideal gas state have been calculated in the usual manner,[6] using the harmonic oscillator approximation. The vibrational frequency assignment is due to Wilson[7] and, with him, the following molecular dimensions are assumed: C—C, 1·53 A; C—H, 1·09 A; $\widehat{CCC}$, 90°; $\widehat{HCH}$, 109° 28′. These lead to moments of inertia of 132·56 and 76·89 × 10^{-40} g. cm.^{2}. Cyclobutane belongs to the point group D_{4h}, and the symmetry number $\sigma = 8$.

[5] Sherman and Ewell, *J. Physic. Chem.*, 1942, **46**, 641.
[6] cp. Herzberg, *Infra Red and Raman Spectra.*
[7] Wilson, *J. Chem. Physics*, 1943, **11**, 369.

In the calculations the values of the fundamental constants quoted by Wagman, Kilpatrick, Taylor, Pitzer and Rossini,[8] have been used. These differ slightly from those given by Herzberg[4] in the value of R, which, because of the use of the thermochemical calorie, is 1·98718 cal./deg. mole.

TABLE III.—THERMODYNAMIC FUNCTIONS OF CYCLOBUTANE

(Units : Calories per degree, except for $(H^0 - E_0^0)$ which is in kcal.)

T° K.	S_{total}.		$-(G^0-E_0^0)/T$.		$(H^0-E_0^0)/T$.		$(H^0-E_0^0)$.		C_p.	
	a.*	b.	a.	b.	a.	b.	a.	b.	a.	b.
289·16	62·49	61·99	51·34	51·13	11·15	10·86	3·325	3·238	17·35	16·87
300	62·60	62·09	51·41	51·20	11·19	10·90	3·357	3·269	17·46	16·99
400	68·50	67·86	54·94	54·64	13·56	13·22	5·426	5·289	23·84	23·35
500	74·49	73·73	58·25	57·87	16·23	15·86	8·117	7·931	29·76	29·26
600	80·36	79·51	61·45	60·99	18·91	18·52	11·35	11·11	34·70	34·20
700	86·03	—	64·56	—	21·47	—	14·84	—	38·83	—
800	91·45	—	67·58	—	23·86	—	19·09	—	42·32	—
900	96·61	—	70·52	—	26·09	—	23·48	—	45·30	—
1000	101·51	—	73·38	—	28·14	—	28·14	—	47·85	—

* (*a*) Values—harmonic oscillator.
(*b*) Values—ring-bending vibration quartic.

The harmonic vibrational contributions were calculated from Sherman and Ewell's tables.[5]

The thermodynamic functions have also been calculated on the assumption that the out-of-plane ring-bending frequency makes the vibrational contribution of the quartic oscillator. Following Bell in the assumption that the quartic vibration can be treated independently of the other modes of vibration of the molecule, its contributions to the thermodynamic functions may be estimated from the results given in Table II. Wilson[7] has assigned a frequency of 145 cm.$^{-1}$ to the ring-bending vibration. In Table III the total thermodynamic functions for cyclobutane obtained on the two assumptions are tabulated, and in Table IV the effect on the vibrational contributions is shown. From

TABLE IV.—THERMODYNAMIC FUNCTIONS OF CYCLOBUTANE

VIBRATIONAL CONTRIBUTIONS

(Units : calories per degree.).

T° K.	S_{vib}.		$-(G^0-E_0^0)/T$.		$(H^0-E_0^0)/T$.		C.	
	a.	b.	a.	b.	a.	b.	a.	b.
298·16	5·056	4·553	1·852	1·642	3·204	2·911	9·398	8·920
300	5·115	4·610	1·874	1·662	3·242	2·948	9·515	9·037
400	8·732	8·086	3·117	2·813	5·615	5·273	15·886	15·405
500	12·941	12·185	4·657	4·273	8·284	7·912	21·810	21·313
600	17·362	16·515	6·402	5·949	10·960	10·566	26·748	26·249

---

[8] Wagman, Kilpatrick, Taylor, Pitzer and Rossini, *J. Res. Nat. Bur. Stand.*, 1945, **34**, 143.

Table III it is obvious that the effect should be detectable experimentally, both in the specific heat and in the entropy.

The author wishes to express thanks to Mr. McWeeny and Prof. C. A. Coulson for allowing him to use the energy levels from their paper before publication, to Mr. R. P. Bell, F.R.S., for helpful discussion, and to the Explosives Division of I.C.I. Ltd., for enabling him to carry out the work.

Summary.

The partition function, the heat capacity, the heat-content function, the free-energy function and the entropy have been calculated for the oscillator with potential function $V(x) = ax^4$, and are tabulated for values of $z = h\nu/kT$ of 0·30—(0·05)—1·00—(0·2)—2·0—(0·5)—3·0—(1·0)—6·0. Using these tables, the thermodynamic functions of cyclobutane have been calculated, on the assumption that the out-of-plane bending vibration of the ring obeys a quartic potential function. The results are compared with those obtained assuming all vibrations to be harmonic, and it is suggested that the difference in specific heat and entropy should be detectable experimentally.

Physical Chemistry Laboratory,
Oxford.

THE THERMAL CONDUCTIVITY OF ORGANIC MATERIALS NEAR THE MELTING POINT.

By J. H. Read and D. M. G. Lloyd.

(*Communicated by* Prof. W. E. Garner.)

Received 21*st October,* 1946, *as revised* 19*th October,* 1947.

Though there have been numerous measurements of the thermal conductivity of liquids and of solids and of the dependence of thermal conductivity on temperature, few measurements have been carried out at, or near, the melting point. The behaviour of solid and liquid sulphur has been investigated with the aid of a special apparatus,[1] but even in this case it proved impracticable to take measurements at the melting point. Measurements of specific heat near the melting points of organic materials, such as those of Ubbelohde on long-chain paraffins,[2] have been of value in interpreting the phenomenon of melting and for the theory of liquid structure, so that it seemed likely that measurements of thermal conductivity should provide additional information. The difficulty of constructing an apparatus suitable both for solids and for liquids and capable of operation during the very considerable volume changes near the melting point has been overcome, and this paper is mainly devoted to the experimental technique involved, though some interesting results are described.

Experimental.

It was clear that most of the thermal conductivity apparatuses previously described[3] were quite unsuited to the present investigation. With solids, the main difficulty is the elimination of air-gaps and temperature discontinuities between the sample and the surfaces across which the temperature gradient is applied. It is important that the structure of a polycrystalline, anisotropic specimen should be capable of examination and specification.

---

[1] Kaye and Higgins, *Proc. Roy. Soc. A*, 1929, **122**, 633.

[2] Ubbelohde, *Trans. Faraday Soc.*, 1938, **34**, 282.

[3] See the useful summaries in *Archiv. Technisches Messen,* May 1943, V9213-3, and Hutchinson, *Trans. Faraday Soc.*, 1945, **41**, 87.

For liquids, the " hot-wire " method of Goldschmidt,[4] of which a convenient modification has recently been described,[5] is one of the most reliable, and it was therefore adapted to measurements on solids. In principle, a very thin platinum wire is embedded axially in a cylinder of the material under test, which is immersed in a thermostat. Passage of an electric current through the wire raises its temperature, setting up a temperature gradient through the sample. The heat supplied by the wire is readily calculated from the resistance and current; the resistance also gives the temperature of the wire, provided that the temperature coefficient of resistance is known. Hence the thermal conductivity of the sample may be calculated.

Preparation of Test Pieces.—Initially, cylinders of the material under test were cast with the platinum wire embedded axially, and immersed directly in the thermostat; but by this means measurements could only be carried out at temperatures below the melting point.

The apparatus employed for obtaining readings over the melting-point is shown in Fig. 1. A length of platinum wire (A) of 0·05 mm. diam. (only the best quality, such as Johnson, Matthey's " thermo-pure " variety, is suitable) was soldered between two brass end-pieces, the lower of which (B) was ground to fit a hole in the bakelite plug (C), which was tightly held in the thin-walled cylindrical brass container (D), of 1 cm. internal diam. The upper end-piece (E) was held by a set-screw (not shown in Fig. 1) in a brass collar (F) itself screwed to the flange (G) which was soldered to the outside of the tube. The collar, and so the end-piece, was insulated from the flange and tube by Bakelite washers (H) of such design as to eliminate as far as possible, the distortion and splitting that so readily occur with an apparatus intended for use over a wide temperature range, and to make possible their easy replacement. The flange was threaded on the outside, and a wide brass funnel (I) could be screwed to it. The apparatus was filled, after heating in the oven, by pouring the molten material into the funnel, whence it ran by feeding holes into the tube. Cooling began near the bottom so any cavities were filled up by liquid flowing downwards from the reservoir, which cooled last. In practice, two cylinders were cast separately, one containing a wire 11 cm. long, and the other a wire 3 cm. long. These were then inserted into opposite arms of the measuring bridge, so as to eliminate end-effects. The thermal conductivity of the brass sheath was so great that the temperature gradient across its walls could be neglected.

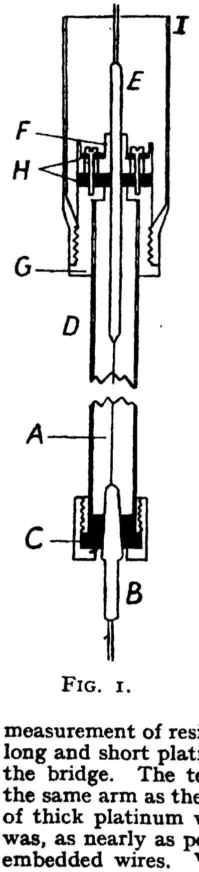

FIG. 1.

This apparatus is, of course, suitable for liquids in general, but, for ordinary purposes, simpler and better modifications of Goldschmidt's original apparatus have been described.[5]

The Measuring Bridge.—The modified Wheatstone bridge shown in Fig. 2 was employed. The same current, supplied from accumulators in series with a rheostat, was used both for heating the platinum wire and for making the measurement of resistance. The ratio arms (A and B) were made equal, and the long and short platinum wires (C and D) were inserted in the other two arms of the bridge. The temperature gradient was measured directly by including in the same arm as the shorter embedded wire, a resistance thermometer (E) wound of thick platinum wire and immersed in the thermostat liquid. Its resistance was, as nearly as possible, equal to the difference in resistance between the two embedded wires. When current was passed, thus heating the thin embedded wires but not appreciably raising the temperature of the thick wire in the bath, the circuit was balanced with the aid of a calibrated rheostat (F), adjustable to 0·001 ohm, and a galvanometer (G) connected through a reversing switch. The current was measured with a calibrated ammeter (H) included in the bridge circuit, the resistance of the ammeter and also that of all lead-wires being permanently balanced by a constant compensating resistance (N) in the opposite arm of the bridge.

---

[4] Goldschmidt, *Physik. Z.*, 1911, **12**, 417.

[5] Hutchinson, *loc. cit.*

The accuracy of the method depends upon the sensitivity of the rheostat, and the precision with which the temperature is controlled in the thermostat bath. Fluctuations of more than 0·05° c. in the bath made it impossible to obtain a sharp balance point. An adjustable Sun-Vic thermoregulator was used in conjunction with a hot-wire vacuum switch. With careful setting the bath temperature could be controlled to 0·05°-0·01° c., but more rigid control is desirable. Considerable difficulty was encountered over the variable contact resistance of the slider of the rheostat, and the circuit could be improved by inserting the rheostat (F) between (C) and (D), increasing its sensitivity by the use of a much longer and thicker slide wire and by connecting the slider to the galvanometer.

It is, of course, desirable, especially in the neighbourhood of the melting point, that the whole sample should be as nearly as possible at the same temperature; it is therefore preferable to obtain increased sensitivity by improving the measuring apparatus rather than by imposing large temperature gradients.

If T is the temperature of the bath corresponding to a steady temperature T' at the centre of the cylinder, $R_1{}^0$ and $R_1{}^{T'}$, and $R_2{}^0$ and $R_2{}^T$ the resistances respectively of the embedded wire at 0° c. and T' °c., and of the immersed resistance thermometer at 0° c. and T° c., and α the temperature coefficient of resistance of pure platinum, it follows from definition that:

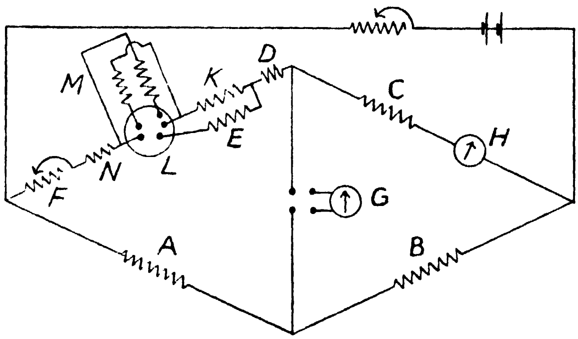

FIG. 2.

$$T' = \frac{R_1{}^{T'} - R_1{}^0}{\alpha R_1{}^0} \text{ and } T = \frac{R_2{}^T - R_2{}^0}{\alpha R_2{}^0}$$

whence, if

$$R_2/R_1 = k$$

$$\Delta T = T' - T = \frac{\Delta R - R_1{}^{T'}(1 - k)}{\alpha R_2{}^0} \quad . \quad . \quad . \quad . \quad (1)$$

where $\Delta R = R_1{}^{T'} - R_2{}^T$, i.e. the reading of the sensitive rheostat. It will be noted that $\alpha R_2{}^0$ is a constant, and that the second term of (1) disappears if $R_1 = R_2$ (when $k = 1$). In practice, it was not possible to solder the platinum wires with an accuracy of more than 0·5 mm., so that the second term of eqn. (1) remained as a correction, and it was necessary to measure directly $R_1{}^{T'}$, the absolute resistance of the hot wire, a figure which was also required for the calculation of the input of heat.

When steady conditions have been established, the thermal conductivity is given by the formula: [6]

$$K = \frac{0{\cdot}239\, I^2 \,.\, R_1{}^{T'} \log_e \frac{r_2}{r_1}}{2\pi l \,.\, \Delta T} \quad . \quad . \quad . \quad . \quad . \quad (2)$$

where r_1 and r_2 are the respective radii of the platinum wire and of the specimen, and l the difference in length of the two embedded wires, and I the current.

Measuring Procedure.—It was found that when the sample and its embedded wire were heated, the resistance of the wire increased but not exactly in the manner to be expected. If, from the measured values of the resistance at increasing temperatures, the resistance of the wire was calculated for a fixed temperature (e.g. 0° c.) by means of the temperature coefficient of resistance, α, values were obtained which were not quite constant. Though this deviation was very small, it was thought better not to rely on a single reading and a simple substitution in eqn. (2), a procedure which demands that the resistance of the embedded wire at 0° c. remain constant (quite small deviations lead to appreciable errors in the calculated value of K), but to eliminate error in the following manner.

---

[6] Carslaw, *The Mathematical Theory of the Conduction of Heat in Solids* (London, 1921), 114.

Eqn. (1) and (2) were combined and written in the form :

$$\frac{\Delta R}{R_1{}^{T'}} = \alpha R_2{}^0\left(\frac{0{\cdot}239 \log_e \frac{r_2}{r_1}}{2\pi l K}\right)I^2 + (1 - k). \quad . \quad . \quad . \quad (3)$$

Hence when readings were taken for different values of the current, a plot of $\frac{\Delta R}{R_1{}^{T'}}$ against I^2 gave a straight line, from the slope of which K could readily be calculated. Currents of 50-150 ma. were usually employed, corresponding to temperature gradients of 1·5°-8·5° c. for a typical sample of liquid TNT and to gradients of about half these values for solid TNT.

Values of K calculated in the fashion described were independent of slight fluctuations in $R_1{}^0$, and the extent of such small variations could be checked by reading off the intercepts, $1 - k$, from the graphs. The extent of the variations over typical runs is shown in Table I.

TABLE I.

TNT (S.P. = 80·4° c.).		Palmitic Acid (M.P. ~ 58° c.).	
Temp. °c.	$k(= R_2/R_1)$.	Temp. °c.	$k(= R_2/R_1)$.
25	0·9760	18	0·9789
35	0·9758	25	0·9795
45	0·9757	35	0·9791
55	0·9754	45	0·9785
65	0·9745	55	0·9783
75	0·9724	60	0·9787
110	0·9737	65	0·9789
90	0·9750	75	0·9787
80	0·9757	85	0·9784

It is significant that the only measurable change in the value of k occurred near the melting point, where there is a large change in the volume of the sample. It is also noteworthy that the change in k was greater with TNT, which gives a dense casting with hard well-formed crystals, than with palmitic acid with its soft ill-defined crystals, which would tend to adhere to the wire less firmly. Indeed with palmitic acid, the trend of the results is hardly significant.

The specially-purified platinum employed for the experiment behaved very nearly as a perfectly elastic solid up to a linear extension of 0·23 %. Over a temperature range of 80° c., the linear expansion of the brass case, relative to that of the wire, was 0·08 %, i.e. well within the elastic limit of the platinum. The change in resistance that might be ascribed to alteration in geometrical dimensions was negligible.

The expansion of the solid TNT over the range 20°-80° c. might be enough to deform the wire, but because of the confinement of the TNT to the case and the radial arrangement of the crystals, the main result of the expansion must have been, apart from local effects, an increased pressure on the wire. Owing to the temperature gradient across the sample, the wire at the centre was sheathed with a liquid cushion during the melting of the great bulk of the solid. Though the pressure was probably not relieved immediately melting started because of the blockage of the feeder holes by solid TNT, such a cushion would tend to transmit the pressure evenly to the wire.

An estimate of the upper limit of the pressure in the cylinder may be made from the pressure necessary to disrupt the cylinder; since the cylinder did not disrupt, and was probably not even stretched beyond the elastic limit, this figure obviously cannot have been reached.

Different types of brass have tensile strengths varying between 22 and 50 kg./mm.^{2}. Using these values it may be calculated that the critical bursting pressure for the cylinders lay between 400 and 1000 atm. Consequently 1000 atm. may be taken as an upper limit to the pressure and it is improbable that it at any time exceeded 500 atm., this being the pressure required to stretch the brass beyond an elastic limit of 25 kg./mm.^{2}.

Bridgman [7] found that the resistance of pure platinum decreased with increase in pressure, a pressure of 500 atm. corresponding approximately to a drop in resistance of 0·1 %. However, a drop in the value of k, representing an *increase* in the resistance of the embedded wires, was observed, so that it appears that the pressure at the centre was quickly released, or was not excessive. Bridgman also found that there was little variation of the pressure coefficient of resistance with temperature, and concludes that the temperature coefficient of resistance is nearly independent of pressure.

The very slight rise in resistance may have been caused by local straining of the wire. The results in Table I are recorded in the order of measurement, which took place at intervals of about ½ hr., and it will be seen that with TNT, even after liquefaction and the complete release of pressure and local tension, total recovery of the wire was slow.

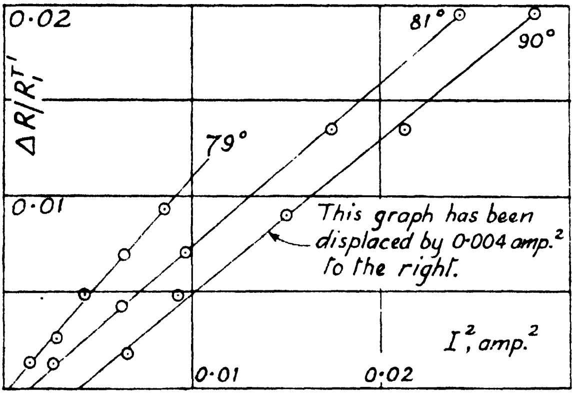

FIG. 3.

This discussion has been given, because, although the experimental technique eliminated errors arising from *slight* changes in k, it is clearly of importance to understand what happened to the embedded platinum wire during temperature change.

When measuring the change of thermal conductivity with temperature, measurements on solids were always carried out during rise of temperature to avoid the possible splitting away of the sample from the wire that might occur during cooling and contraction. Measurements on liquids could clearly be carried out during either rise or fall of temperature. The apparatus came to equilibrium within a few minutes after the setting of the bath temperature, and measurements with different currents were made at 5 min. intervals, 20 min. being allowed between changes in the temperature of the bath. Thermoelectric effects were avoided by eliminating, as far as possible, bimetallic junctions, and their effect was nullified by reversing the connections when balancing the circuit, and averaging the two settings of the sensitive rheostat. The curves of Fig. 3 obtained for TNT at different temperatures by the procedure described, show how accurately eqn. (3) is obeyed. It should, however, be mentioned that for currents below 25-50 ma. the straight line relationship appeared to hold no longer and that very erratic results were obtained. It was thought that this effect was caused by imperfections in the measuring apparatus.

Calibration of Apparatus.—It was possible, by measuring the dimensions of the test pieces and platinum wires with a travelling microscope, to calculate absolute values for the thermal conductivity. Absolute measurements of TNT cylinders immersed directly in a water-bath, and determinations on castings encased in our apparatus with the brass sheaths, as described above, were sufficiently close in view of the differing structures of the polycrystalline blocks.

---

[7] Bridgman, *The Physics of High Pressure* (London, 1931), 268.

It was found, however, when the thermal conductivities of a series of liquids was measured in our apparatus, that, although the relative values agreed sufficiently well with the results of previous workers, the absolute values were somewhat high; the results which follow were calculated on the basis of Bates' figure of 3·10 × 10⁻⁴ cal./sec. cm. °c. for chloroform at 20° c.[8]

Distilled water and carefully dried B.D.H. Analar materials were used. In view of the difficulty of measuring the thermal conductivities of liquids and of the uncertainty of published results, it is considered that agreement was sufficiently good to justify the use of the instrument for determining changes with temperature in the conductivity of the same sample, though the apparatus, in its present form, is not suited to exact determination of the absolute conductivities of different liquids. Chloroform was used as standard as it was the liquid studied most in our apparatus, and gave most reproducible results.

That the curves of $\Delta R/R_1^{T'} - I^2$ (Fig. 3) were straight lines is a demonstration that the method is fundamentally sound, for, if convection currents had been set up, eqn. (3) would no longer have held, and the plots would have been curvilinear (as actually happened when large temperature gradients were deliberately imposed). The calibration constant obtained from the measurements on chloroform was applied in calculating the results that follow.

TABLE II.—K IN CAL./SEC. CM. °C.; TEMP., 20° C.

Material.	K Observed $\times 10^{-4}$.	K Literature. $\times 10^{-4}$.
Chloroform	3·10	3·10 Bates
Carbon disulphide	3·77	3·85 I.C.T.
Ether	3·23	3·30 ,,
Ethyl alcohol	3·81	4·35 ,,
Ethyl iodide	2·37	2·65 ,,
Water	13·1	14·0 ,,

Results.

The variation with temperature of the thermal conductivity of TNT is shown in Fig. 4. The TNT was of the quality known as Grade I, of setting-point 80·4° c., and consisting almost entirely of 2 : 4 : 6-trinitro-toluene.

Owing to the decision to use at least 5 different heating currents for each determination, the experiments were long drawn-out and it was impossible to obtain all the data during one run, so that the results of Fig. 4 were drawn from several experiments, as shown by the circles, triangles, etc. It has already been explained that the measurements on solid samples were always carried out during rise of temperature. The use of different currents was also a safeguard against the occurrence of convection, as revealed by curvature of the $\Delta R/R_1^{T'} - I^2$ plots. For solid TNT, the numerical results of different determinations varied by some 15 %, as was not surprising in view of variations in crystal structure of successive castings.

The striking feature of all the curves for solid TNT was the sharp drop in thermal conductivity near the melting point. It is not known just how low the conductivity fell, because the readings were taken discontinuously at arbitrary temperatures, but values were obtained below those subsequently recorded for liquid TNT. The temperatures plotted as abscissæ are those of the thermostat bath, as measured to the nearest 1/10° with a mercury-in-glass thermometer calibrated at the N.P.L.; the temperatures at the centre of the cylinders were from 1°-4° c. higher, depending upon the heating current, and fell away exponentially towards the perimeter. In view of the large expansion of TNT during heating and of the resulting increased pressure inside the cylinders, the melting point may have been raised. It is, however, clear that the drop occurred substantially at the melting point itself. Owing to the temperature gradient across the cylinders and to the slowness with which a mass of solid melts when heated only slightly above its melting point, it is probable that the condition of the sample at bath temperatures just below the melting-point was that of a liquid surrounded by a solid annulus. Even if the liquid sheath were very thin, such a sample would behave more like a liquid than a solid, because the fall in temperature across the samples takes place very largely in the region nearest the heating wire.

---

[8] Bates, *Ind. Eng. Chem.*, 1941, **33**, 375.

Measurements carried out during the cooling of liquid TNT revealed little variation of thermal conductivity with temperature in the region more than 5° c. bath temperature above the melting point ; below this temperature there was evidence of a downward trend in thermal conductivity, but it did not prove possible to establish any sudden drop at the melting point, possibly because the TNT at the outside began to solidify before the material round the wire, in which practically the entire temperature drop occurs, was sufficiently near the melting point. (Once solidification was observed, the experiment was discontinued because of the possibility of entrapping air bubbles in the sample during the marked contraction associated with solidification, which would vitiate any results obtained then.) It should be added that the incipient fall in conductivity shown in the figure depended to a marked extent on the previous history of the sample and was probably related to the number of crystal nuclei present in the liquid. Experiments on pure specimens of α-nitro-naphthalene and vanillin gave very similar results.

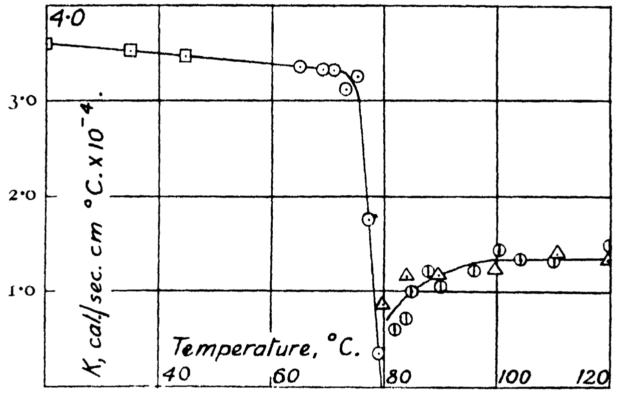

FIG. 4.

Experiments were also carried out on a sample of palmitic acid. B.D.H. material was used and not specially purified ; it did not melt sharply, but became " mushy " at about 55° c. In this case a maximum in thermal conductivity was obtained near the melting point. Further experiments on a purified sample are required in this case ; the present result is quoted to show that the results obtained with the other materials were not simply conditioned by the apparatus and method of measurement.

Discussion.

The occurrence of abnormally low values of thermal conductivity near the melting point of cast samples of TNT prompts the question as to whether the effect was a gross one, conditioned perhaps by convection currents within the partially melted block or by cracks in a solid annulus, or whether it was conditional upon changes in the lattice or in the internal state of the molecules. Convection was unlikely, both because straight lines were obtained for the plot of $\Delta R/R_1T' - I^2$ and because convection currents should help to dissipate heat and therefore to *increase* the apparent conductivity. A more probable explanation is that the pressure set up by the expansion of the melting TNT fractured the crystalline part of the block, thus multiplying areas of temperature discontinuity. Neither of these explanations is altogether convincing; moreover, it remains to account for the incipient fall in conductivity observable after complete liquefaction and subsequent cooling to a temperature *above* the set point. In the case of palmitic acid, which melted indefinitely, it is possible that fragments of solid material dropped through the liquid, setting up currents and thus accounting for the apparent maximum in thermal conductivity.

The persistence of some form of solid structure into the liquid state has been widely discussed, among others by Stewart,[9] Frenkel,[10] and Malkin,[11] who have brought forward interesting X-ray and thermal evidence. The downward turn of the thermal conductivity-temperature curve at temperatures just above the melting point would seem to provide new evidence for a structure in that region markedly different from that of the liquid at higher temperatures.

It is possible that the decrease in conductivity observed both just below and just above the melting point is due to the material behaving neither as a true solid nor as a true liquid in the respective cases, but that in one case premelting and in the other case presetting might be occurring locally at numerous points giving rise to a mosaic-like structure with very frequent interfaces separating regions differing in local degrees of order. The presence of such interfaces and consequent discontinuities might well be a contributing factor to the decrease in thermal conductivity observed here.

Ubbelohde has shown that paraffins and various other long-chain compounds, even when very highly purified, are subject to a sharp rise in specific heat before the melting point is reached and that the enhanced specific heat most probably persists for some degrees above the melting point. The general relation between thermal conductivity and specific heat is that

$$K = c\rho\lambda\mu \quad . \quad . \quad . \quad . \quad . \quad (5)$$

where c is the specific heat, ρ the density, and λ and μ are the wavelength and mean free path of the elastic heat waves. It is tempting to compare the maximum in the thermal conductivity curve for palmitic acid with Ubbelohde's specific heat data, but such correlation is not straightforward, and must, in any case, await conductivity data for purer material.

It is realised that the data put forward are incomplete, but, as the apparatus has been dismantled for the present, it seemed appropriate to publish an account of the work which had been carried out. Further experiments, preferably with more than one type of apparatus, are required to establish finally that the thermal conductivity-temperature plot cannot be represented by a step-shaped curve and that the minimum suggested by the present experiments is generally characteristic.

We are grateful to Miss Mary L. Woods for carrying out much of the experimental work during the latter stages of the research, to Mr. E. Hutchinson for advice as to apparatus, and to Prof. R. Peierls for valuable consultation. Thanks are also due to Messrs. Imperial Chemical Industries for the award to one of us (J. H. R.) of a Research Fellowship at the University of Birmingham, which made possible the continuance of the experiments.

The work, which formed part of a programme of fundamental research sponsored by the Ministry of Supply at the Universities of Sheffield and of Birmingham, was completed in July 1946; approval for publication has been granted by the Director General of Scientific Research (Defence), Ministry of Supply.

[9] Stewart, *Rev. Mod. Physics*, 1930, **2**, 116.

[10] Frenkel, *Trans. Faraday Soc.*, 1937, **33**, 58.

[11] Malkin, *J. Chem. Soc.*, 1939, 1141; 1939, 103; 1937, 1409; 1936, 1628; 1934, 666.

Summary.

An apparatus has been constructed for the measurement of thermal conductivity near the melting point of organic solids, and has been calibrated with liquids for which data are already available. Repeated measurements have revealed an abrupt discontinuity in the thermal conductivity of TNT at the melting point and suggest that a minimum in conductivity exists under the conditions of experiment. The interpretation of these results is briefly discussed.

Department of Chemistry,
The University,
Sheffield, 10.

Department of Chemistry,
The University,
Birmingham, 15.

STUDIES ON HEMIACETAL FORMATION.

PART I.—THE SYSTEM ACETALDEHYDE-WATER.

By I. Lauder.

Received 16th December, 1946, *as revised 21st October,* 1947.

The physico-chemical properties of acetaldehyde-water mixtures have been the subject of several investigations.[1] The deviation of the measured property from the value given by the ordinary mixture law has usually been taken as an indication of the formation of hydrates or ethylidene glycol. Although this latter compound has never been isolated, its existence in aqueous solution has been fairly definitely established by the investigation of the interchange of oxygen between acetaldehyde and water.[2] This interchange reaction was found to have a half-life period of approximately 2 hr. at room temperature and so it appeared that it should be possible to measure a time-variation of the physical properties of the reaction mixture corresponding to the establishment of the equilibrium,

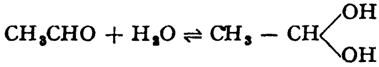

$$CH_3CHO + H_2O \rightleftharpoons CH_3 - CH(OH)_2 \quad . \quad . \quad . \quad (1)$$

No previous investigation has shown any such variation. Perkin,[3] however, found that heat was evolved for 2-3 hr. after mixing the reagents but did not study the reaction quantitatively.

Ethylidene glycol may be regarded as the first member of the homologous series of hemiacetals derived from acetaldehyde and, in an earlier paper,[4] it was predicted that, under similar conditions, the rate of formation of a hemiacetal should run roughly parallel to the rate of the corresponding oxygen exchange reaction.

The work described in this paper, on the change of refractive index (and of volume) with time for acetaldehyde-water mixtures and for acetaldehyde-methyl alcohol mixtures respectively, was begun to find out how far the above predictions would hold true.*

---

[1] Ramsay and Young, *Phil. Trans.*, 1886, **174**, (1), 117; Homfray, *J. Chem. Soc.*, 1905, **87**, 1435; Schou, *Compt. rend.*, 1926, **182**, 965.

[2] Herbert and Lauder, *Trans. Faraday Soc.*, 1938, **34**, 432.

[3] Perkin, *Trans. Chem. Soc.*, 1887, **51**, 813.

[4] Herbert and Lauder, *Trans. Faraday Soc.*, 1938, **34**, 1219.

* The experimental work was carried out at the University of Manchester during the session 1938-39 and was interrupted by the outbreak of war. Although the work was not completed, the results are presented for publication to avoid their loss.

Experimental.

ACETALDEHYDE.—Commercial acetaldehyde was fractionated and the middle fraction, boiling at 21° C. (76 cm. Hg), was collected. This material was outgassed and, before use, it was subjected to two further fractionations *in vacuo* from room temperature to 0° C.

WATER.—Distilled water of high purity, free from air, was used.

The Change of Refractive Index with Time.—The Pyrex glass reaction vessel in which the mixing of the acetaldehyde and the water took place, is shown on the right of Fig. 1. The approximate amounts of reagents required for any desired mixture were distilled *in vacuo* into the storage vessels S_1 and S_2 respectively. The bulb of the reaction vessel was cooled to − 80° C. and the water was distilled over. The ice was warmed to − 5° C. and the acetaldehyde was distilled over as rapidly as possible. The vapour left in the dead-space of the apparatus was condensed back into the storage vessel by use of liquid air. The decrease in weights of the two storage vessels gave the actual amounts

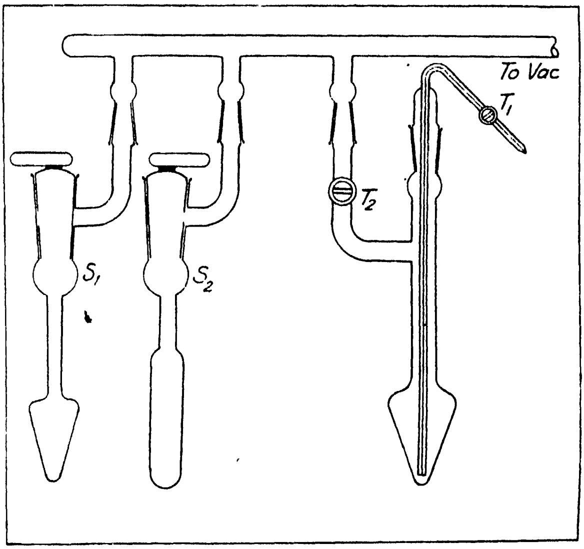

FIG. 1.

Results.

TABLE I.—TEMPERATURE 0° C.

Mol. Fraction Aldehyde.	R.I. Initial.	R.I. Final.	Half-life Period (Min.).
0·00	1·33440	—	—
0·115	1·35700	1·36087	20
0·322	1·37268	1·38327	58
0·392	1·36796	1·38637	40
0·455	1·36536	1·38674	40
0·55	1·35977	1·37637	60
0·63	1·35721	1·37583	66
0·72	1·35113	1·35744	43
0·826	1·34626	1·35015	32
0·833	1·34540	1·34868	40
1·0	1·33673	—	—

of reagents present in the reaction mixture. The reaction vessel was removed from the system and it was then shaken in an ice-bath. The zero time was taken as that at which all the ice had disappeared from the mixture. Hydrogen was passed into the reaction vessel through tap T_1 to a pressure slightly above atmospheric. This served to displace any solution in the capillary tube and, subsequently, it served to blow the solution from the reaction vessel into the refractometer cell.

The refractive index (R.I) was measured with respect to the sodium *D*-line by use of a Pulfrich refractometer. Most measurements were made at 0° c.; a few were made at 13·5° c. Each measurement was made on a fresh sample from the reaction vessel and, after the sampling process, the liquid remaining in the delivery tube was displaced by H_2.

TABLE II.—TEMPERATURE 13·5° C.

Mol. Fraction Aldehyde.	R.I. Initial.	R.I. Final.	Half-life Period (Min.).
0·455	1·35481	1·36761	112
0·622	1·35123	1·36243	120

The Change of Volume with Time.—The apparatus used for this investigation is shown in Fig. 2. The dilatometer was cooled to 0° c., and the reaction mixture was prepared in the tube A by the same procedure as is described in the previous section. The portion A-B-C of the apparatus was shaken in an ice bath for a few min. and then the reaction mixture was tipped into the tube C. With tap T_2 open, the mixture was forced into the vacuous dilatometer by opening tap T_1 to the atmosphere. The capillary was cut at D and the distance between

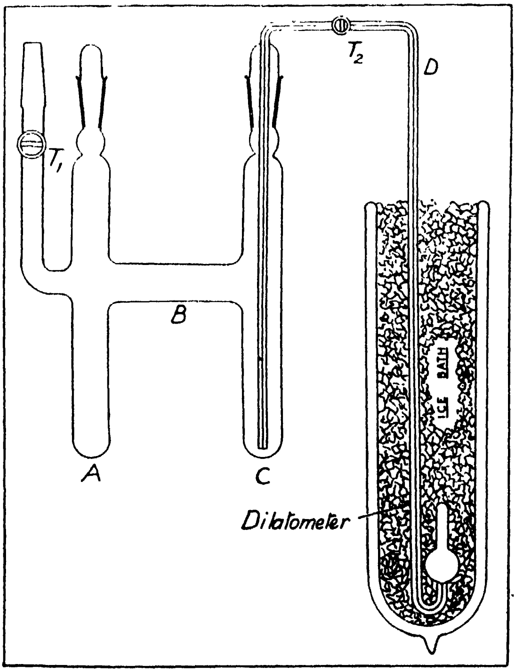

FIG. 2.

the meniscus and a fixed mark on the tube was determined from time to time. The end of the capillary was blocked to prevent loss by evaporation.

The results obtained by the use of the refractometer are shown in Tables I and II; those by the use of the dilatometer in Table III. Good end-points for the refractometer readings were obtained over the whole range of composition. This, however, was not the case for the dilatometer readings; the "final values" were usually good up to about 0·6 mol. fraction of aldehyde but, at higher concentrations, the volume gradually decreased over a period of days suggesting that polymerisation of the aldehyde was occurring. In a few cases, the % volume-contractions were measured and these are given in column 2 of Table III.

Results.

TABLE III.—TEMPERATURE 0° C.

Mol. Fraction Aldehyde.	% Volume Contraction.	Half-life Period (Min.).
0·06	1·1	9
0·11	—	11
0·256	5·5	26
0·329	—	44
0·331	7·2	40
0·488	8·2	44
0·53	—	13
0·60	—	4
0·605	8·8	70
0·642	—	70

From a kinetic point of view, the results indicate that a reversible reaction, first-order in each direction, occurs on mixing the reagents. The plot of log $(X_e - x)$ against time is a straight line. (X_e stands for the final value and x for the value of any time t.) Typical graphs for $(X_e - x)$ and $\log_{10} (X_e - x)$ against time are shown in Fig. 3 and 4 respectively. Graphs of the initial and final refractive indices against mol fraction are shown in Fig. 5.

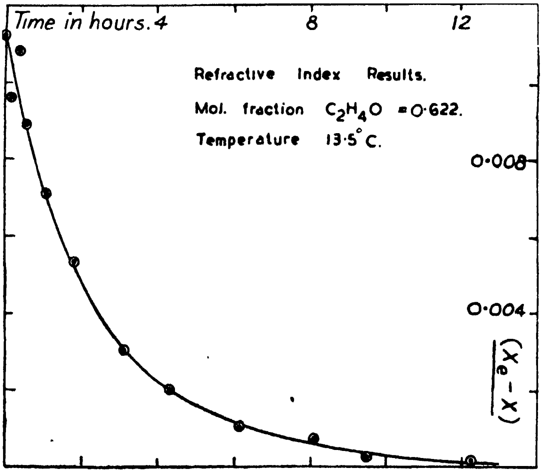

FIG. 3.

The reaction which occurs cannot follow the stoichiometric equation (1) because this is second-order in the forward direction. In the absence of more definite information it is suggested that some type of loose complex or hydrate, such as $C_2H_4O . H_2O$, is formed almost instantaneously when acetaldehyde and water are mixed, and that the equilibrium,

$$CH_3CHO + H_2O \rightleftharpoons CH_3CHO . H_2O \quad . \quad . \quad . \quad (2)$$

lies well over to the right. The change which is measured would then be due to the establishment of the equilibrium,

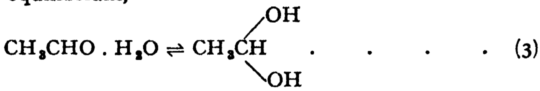

$$CH_3CHO . H_2O \rightleftharpoons CH_3CH\begin{matrix}\diagup OH \\ \diagdown OH\end{matrix} \quad . \quad . \quad . \quad . \quad . \quad (3)$$

If reaction (3) proceeded to completion when equivalent quantities of acetaldehyde and water were mixed, it is probable that the " final " refractive index would be near that for ethylene glycol, namely, 1·438. The fact that for the above mixture a change from 1·363 to 1·385 (at 0° c.) was observed, suggests that only a small proportion of glycol was present at equilibrium.

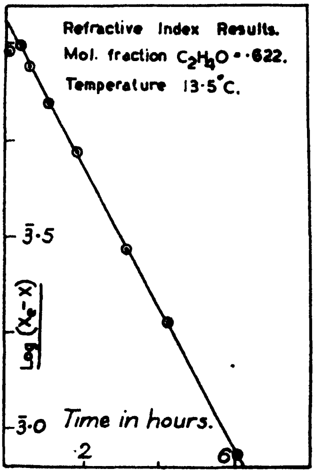

FIG. 4.

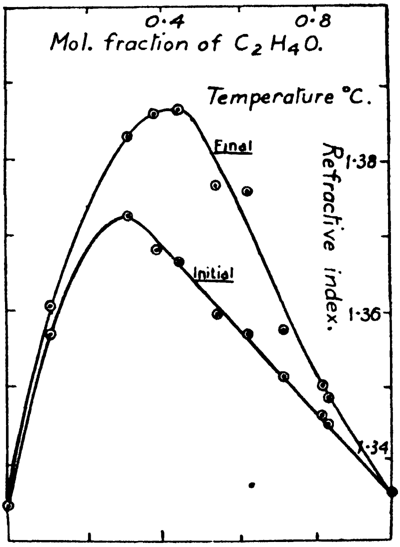

FIG. 5.

For a first-order equilibrium reaction the time of half-life should be a constant ($t_{\frac{1}{2}} = 0{\cdot}693/k_1 + k_{-1}$). Possibly more consistent results would have been obtained if the reaction mixtures had been buffered. From this aspect, it is worth mentioning, perhaps, that Cohn and Urey [5] found that for the exchange of oxygen between acetone and water, reproducible results could only be obtained in buffered solutions.

TABLE IV.

Time (Hr.).	% Equilibrium R.I.	% Equilibrium Exchange.
3	74	75
6	94	84
24	100	95

It is of interest to compare the refractive-index results with the oxygen-exchange results. The exchange was found to have a half-life period of 2 hr. at room temperature ; almost the same value was found for the change of refractive index at 13·5° c. Figures for the approach to equilibrium are given in Table IV.

---

[5] Cohn and Urey, *J. Amer. Chem. Soc.*, 1938, **60**, 679.

The values in column 2 were obtained from the curve shown in Fig. 3; those in column 3 from the earlier paper.[3] The agreement is fairly good considering that for each exchange result a fresh reaction mixture had to be prepared.

Summary.

The reaction between acetaldehyde and water has been studied by use of a refractometer and a dilatometer. The results indicate that a reversible reaction, first-order in each direction, occurs on mixing the reagents. It is suggested that immediately on mixing the reagents a complex $C_2H_4O\,.\,H_2O$ is formed which subsequently changes over to ethylidene glycol.

It was found that the rate of change of refractive index runs roughly parallel to the rate of interchange of oxygen between acetaldehyde and water.

PART II.—THE SYSTEM ACETALDEHYDE-METHYL ALCOHOL.

Little information on the physico-chemical properties of the system acetaldehyde-methyl alcohol could be found in the literature. Herold and Wolf[6] measured the rate of hemiacetal formation in several aldehyde-alcohol systems by ultra-violet absorption experiments, but, in the case of the present system, it was concluded the reaction proceeded too rapidly for exact measurement.

Experimental.

Methyl alcohol (A.R.) was fractionated in the presence of Ca turnings and the middle fraction, B.P. 64·6° C. (76 cm. Hg) was collected. This was outgassed and, before use, it was subjected to two further distillations *in vacuo* from room temperature to 0° C. The mixtures were made up and the change of refractive index with time was measured, at 0° C., as is described in the previous section.

Results.

The results are shown in Table I. Graphs of the initial and final refractive indices against mol. fraction are shown in Fig. 6. As for the acetaldehyde-water system, it was found that a reversible reaction, first-order in each direction, occurred on mixing the reagents and, therefore, the same type of process may be postulated—the establishment of equilibrium between an alcoholate and the hemiacetal,

TABLE I.

Mol. Fractson Aldehyde.	R.I. Initial.	R.I. Final.	Half-life Period (Min.).
0·00	1·33174	—	—
0·16	1·33787	1·35266	90
0·25	1·34140	1·36229	156
0·34	1·34213	1·37375	186
0·46	1·34376	1·38178	460
0·62	1·34179	1·37435	110
0·81	1·34039	1·35661	75
1·00	1·33673	—	—

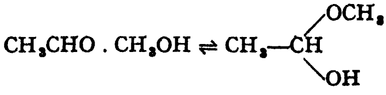

$$CH_3CHO\,.\,CH_3OH \rightleftharpoons CH_3{-}CH\begin{matrix}\diagup OCH_3\\ \diagdown OH\end{matrix}$$

---

[6] Herold and Wolf, *Z. physik. Chem. B*, 1931, **12**, 165.

If the above reaction proceeded to completion when equivalent quantities of the reagents were mixed it is probable that the "final" refractive index would be near that for 2-methoxyethanol, namely, 1·404. For the above mixture an initial value of 1·344 and a final value of 1·383 respectively was found. These figures suggest that a fair proportion of hemiacetal was present at equilibrium —greater than in the corresponding case for the acetaldehyde-water system.

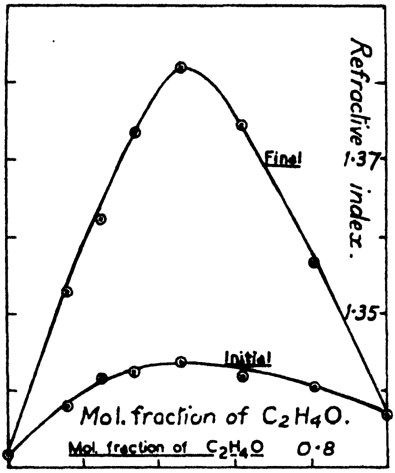

FIG. 6.

In conclusion the author wishes to thank Prof. M. Polanyi and Mr. J. B. M. Herbert for much helpful advice and criticism and Mr. A. S. Wilson for his help with the experimental work.

Summary.

The reaction between acetaldehyde and methyl alcohol has been investigated by use of a refractometer. The results indicate that a reversible reaction, first-order in each direction, occurs on mixing the reagents. It is suggested that an equilibrium is set up between an alcoholate and the hemiacetal.

Department of Chemistry,
University of Queensland,
Brisbane.

THE NATURE OF METAL-AMMONIA SOLUTIONS. PART II.

BY A. J. BIRCH AND D. K. C. MACDONALD.

Received 5th November, 1947.

Re-awakened interest in the problem of the constitution of metal-ammonia solutions, due to the claim by Ogg[1] to have demonstrated super-conductivity in solidified sodium-ammonia solutions over the range −95° C. to −183° C., has led us to make a more detailed examination of other metals. The outstanding properties of such solutions are: that the alkali and alkaline earth metals dissolve in liquid ammonia without reacting with it; that these solutions may show separation into two immiscible liquid phases; and that some of the metals form solid "ammoniates" which are definite crystalline substances with a dissociation pressure depending on the temperature. Of the metals, sodium is the only one hitherto examined in any detail and we report here an examination of other metals of these groups, undertaken in the hope of attaining a further understanding of their nature by correlation of the different metals.

The ability to dissolve in ammonia is confined to the metals of groups I and II excepting only beryllium, which does not dissolve at all, and magnesium which is said to be slightly soluble.[2] These are all metals of low work function, and since the solutions are highly conducting and metallic in character—the concentrated ones have a characteristic metallic lustre —it seems likely that solution is brought about by the ready formation of metal cations and electrons, both of which are solvated by the ammonia. The deep blue colour by transmitted light of the solutions is almost certainly due to solvated electrons [3] formed through the ability of the hydrogen atoms to act as electron acceptors (compare their role in the association of water or ammonia). Solvation of the cations would appear to depend on the donor properties of the unshared electrons of nitrogen.

---

[1] Ogg, *Physic. Rev.*, 1946, **69**, 243; 1946, **69**, 544; 1946, **70**, 93.

[2] Johnson and Meyer, *Chem. Rev.*, 1931, **8**, 295.

Other substances capable of dissolving the metals (e.g. methylamine, ethylenediamine) are all amines, and their solvent power runs roughly parallel to their NH_3-content. The fact that such solvents do not react with the metals is due to their low acidity. It is probable that substances containing OH groups would similarly act as solvents but for their high acidity, and it is noteworthy that reaction of potassium with the comparatively inert *tert.*-butyl alcohol is accompanied by the formation of a deep indigo-blue surface-film.

On freezing the metal-ammonia solutions, eutectics are formed. With sodium and potassium, these undoubtedly contain mixtures of ammonia crystals and silvery metal crystals, but in other cases—calcium, strontium, barium and lithium—the solvation is carried over into the solid state with the production of ammoniates mixed with solid ammonia. In the case of caesium, on which only a few experiments could be performed owing to scarcity of material, the deep bronze colour of the solid eutectic would appear to indicate the formation of an " ammoniate."

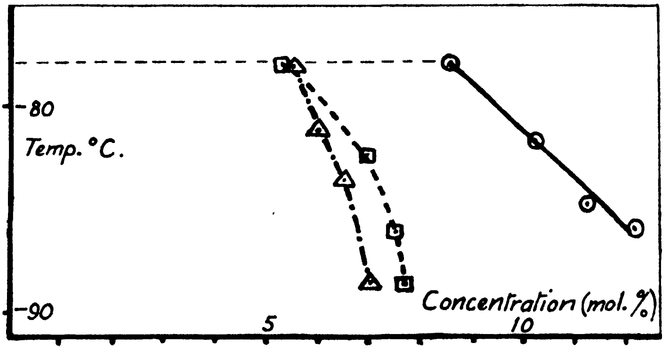

FIG. 1.—Liquid-solid phase curves.

○—○ Ca   △——△ Sr   □- - - -□ Ba

These ammoniates are metallic (either brass, or bronze-like) solids of high electrical conductivity. Their non-formation with sodium and potassium is presumably due to the inability to form a suitable lattice. With the alkaline earth metals the hexammoniates are known to be fairly stable even at room temperature; it has been denied that lithium forms an ammoniate at all,[4] but our work shows that it probably does so, at least at the eutectic temperature (−185° c.). If so, the ammoniate must contain four, or less, ammonia molecules for each lithium atom. The metal ammoniates in thin layers, by transmitted light, show the blue colour of the solutions.

Reasonably accurate phase curves for the region below the melting-point of ammonia (−78° c.) have been constructed (Fig. 1 and 2) for all the metals except examined caesium due to small amount available, and

[3] Gibson and Argo, *J. Amer. Chem. Soc.*, 1918, **40**, 1327.
[4] Kraus and Johnson, *ibid.*, 1925, **47**, 725.

sodium, which has already been estimated, although with no great accuracy, by Ruff and Zedner.[5] It can be concluded from these that liquid-liquid phase separation above about − 78°c. is exhibited by all except lithium, although a slight doubt exists in the case of potassium. Thermal measurements, confirmed by conductivity measurements, also showed the existence of specific heat anomalies in the solidified solutions of the alkaline earth metals. These anomalies did not appear in magnetic susceptibility, or dielectric constant measurements.

Previous work on sodium-ammonia solutions has been published[6] and a preliminary report of the present work has appeared elsewhere.[7] *

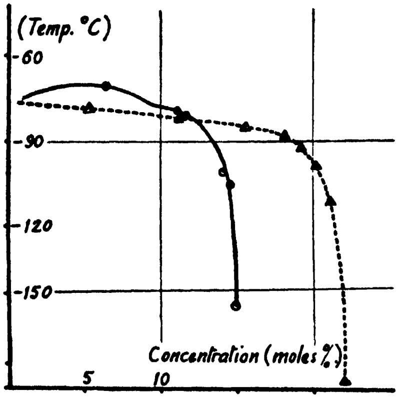

FIG. 2.—Phase curves.
Potassium ○——○ Lithium △----△

Experimental.

The metals used were the purest commercial samples available. Owing to the possibility of the anomaly in the alkaline earth warming-curves being due to impurity, barium and strontium from two sources were used, the purity in one case being quoted as at least 99 %. The solutions were made up, as a rule, in the vessel in which measurements were to be taken, the ammonia being stirred and kept below its boiling-point by appropriate cooling. The solution of the alkali metals takes place readily with little heat evolution; the alkaline earth metals produce considerable heat and tend to form solid lumps of ammoniate.

Thermal Measurements.—Copper-constantan thermocouples were used, the cold junction generally being immersed in liquid oxygen; the leads up to the actual junction were enclosed in glass. For most measurements a galvanometer, providing an average reading accuracy $\sim$0·3° c., was employed; for particularly sensitive measurements (such as those directed towards investigation of the solid-state anomalies with the alkaline earth metals), this accuracy was increased by a factor greater than 10, and a limited range of temperature was covered by immersing the cold junction in subliming carbon dioxide. For slow heating or cooling rates (about 2°/min.) the solution was made up in a small Dewar flask, which could be evacuated or filled with a small pressure of exchange gas at will. A heating coil of constantan wire enclosed in a glass capillary spiral was used to provide a controlled heat influx when necessary.

Electrical Conductivity.—In some preliminary measurements the glass T-piece described in Part I was used, but for later work a glass tube with current and potential electrodes of platinum and an inner close-fitting tube was employed (Fig. 9). The top was loosely plugged with cotton-wool or with a divided cork. The inner tube contained a small quantity of mercury to provide for good thermal contact with the thermocouple junction which was immersed in it. The whole could be immersed in the Dewar vessel described above in order to provide any desired heating or cooling rate. Measurements were mostly carried out with direct current, but in order to eliminate the possibility of polarisation effects, these were also checked with 50 c./sec. alternating current using a vibration galvanometer.

Magnetic Susceptibility.—The method used was identical with that described in Part I. Smaller quantities of solution had to be used owing to the smaller amounts of the alkaline earth metals available; the accuracy obtainable

[5] Ruff and Zedner, *Ber.*, 1908, **41**, 1948.

[6] Birch and MacDonald, *Trans. Faraday Soc.*, 1947, **43**, 792.

[7] Birch and MacDonald, *Nature*, 1947, **159**, 811.

* Our paper "Some Physical Properties of Solidified Sodium-Ammonia Solutions" (*Trans. Faraday Soc.*, 1947, **43**, 792) is to be regarded as Part I.

measurements by a method similar to that used by Kraus[8] for sodium solutions showed for a concentration of 5·9 mol. % a marked resistance change in the expected direction on warming or cooling through − 74° c., but nowhere else up to the boiling-point of ammonia. It may be noted that no such change could be observed with lithium. A slight increase in the slope of the warming curves is also observable about this temperature. We therefore venture to propose the separation curve shown for potassium in Fig. 2. This curve, and much more markedly the ones for Ca, Sr and Ba must have a discontinuity of slope at the liquidus-solidus junction since otherwise the upper consolute point (above the boiling-point of ammonia for the alkaline earth metals) cannot easily be accommodated on the curve. That such a discontinuity is to be expected can be seen from the following considerations. Above the freezing-point of ammonia the concentrated phase must have the same vapour pressure as the dilute phase, and since the freezing-point of the solutions differs but slightly from that of ammonia the vapour pressure at this temperature must be almost identical with that of pure ammonia. If solidification did not occur the curve would proceed smoothly, but since solid ammonia necessarily has a considerably lower vapour pressure than (supercooled) liquid ammonia at the same temperature, in its presence the metal solution must have a higher concentration to depress its vapour pressure to this lower value. The curve is therefore bent towards higher concentrations at the point where freezing occurs. A discontinuity of slope of this type is not immediately evident in the curve for sodium,[8] but the curve is in any case practically vertical in this region, and only a small alteration in slope would suffice to provide the necessary vapour-pressure modification.

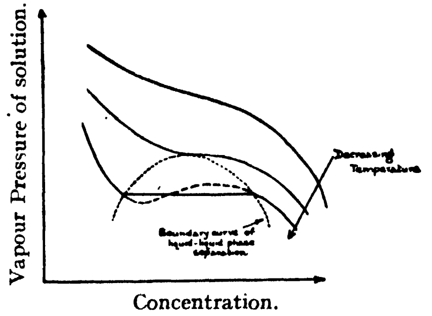

FIG. 7.

Hildebrand's theory of partial miscibility[9] illustrates the type of anomalous vapour-pressure phenomena which must lead to the formation of two liquid phases (Fig. 5). In the case of metal-ammonia solutions the deviations from Raoult's law must clearly arise from two sources. The first (positive) departure with increasing concentration (neglecting very dilute solutions) arises presumably from association of the solute. For strong solutions the deviation becomes rapidly negative, presumably indicating strong association of the solvent and solute molecules reaching its limit in the formation of lattice compounds in suitable cases.[*] This behaviour is shown in the work of Kraus[10] on the apparent molecular weight of sodium in ammonia at the boiling-point (−33° c.), although the slope of the vapour-pressure curve is nowhere horizontal as it would be if phase separation occurred at this temperature. In fact, it occurs only below −42° c. Kraus has stated that the vapour-pressure deviations arise as a result of phase separation, and not as the result of aggregation of the solute. It seems clear, however, that the phase separation is to be regarded as a direct consequence of the aggregation vapour-pressure phenomenon. Bowden[11] has pointed out that the shape of the vapour-pressure curves is reminiscent of van der Waals' $p-v$ curves when phase separation takes place. We find, in fact, that a semi-quantitative approximation for the phase separation curve may be derived by direct use of the van der Waals' modification of Boyle's law in van't Hoff's law of osmotic pressure. The requisite constants would be most appropriately derived from data at the upper consolute point, but since these have not been determined, we have used data from the eutectic point (−110° c.) in the case of sodium. The concentration is known, and the assumption was made that the vapour-pressure curve there is practically vertical. The resulting theoretical curve of vapour pressure for the temperature of the freezing-point of ammonia (−78° c.) gives concentrations of the right order for the two phases.

---

[8] Kraus and Lucasse, *J. Amer. Chem. Soc.*, 1922, **44**, 1949.

[9] Hildebrand, *Solubility* (Reinhold Publ. Corp., 1936).

[*] Note added in proof: For more detailed considerations leading to a modified viewpoint, see Birch and MacDonald, *Oxford Science*, 1948, p. 1.

[10] Franklin and Kraus, *Amer. Chem. J.*, 1898, **20**, 850.

A new phenomenon was revealed in the warming curves for the alkaline earth metals (see Fig. 3). A point of arrest was clearly visible in the case of Sr (−98° c.) and Ba (−109° c.) and a careful examination indicated the probability of a similar effect just below the eutectic temperature (−89° c.) for calcium. Clear confirmation for the anomalies were found for Sr and Ba in measurements of the variation of electrical conductivity with temperature of concentrations of 3·9 mol. % for Sr (Fig. 7) and 4·0 mol. % for Ba. It must be remarked, however, that no sign of an anomaly in electrical resistivity was found with a solution of Sr at the concentration 2·5 mol. % (Fig. 7). No anomaly could be found in a measurement of magnetic susceptibility. In view of recent interest in the ferro-electric properties of $BaTiO_3$ and $SrTiO_3$, a qualitative examination of the variation of dielectric constant was also made, but there was no noticeable anomaly.

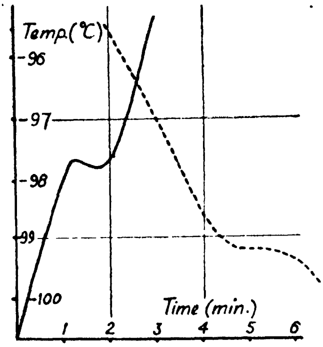

FIG. 8.—Strontium-ammonia anomaly point. Temperature intervals are accurate, but absolute values may be in error by about 1° c.

—— warming, ----- cooling.

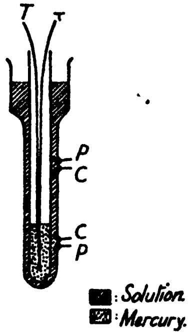

FIG. 9.—Apparatus for measuring electrical resistivity.

PP Potential electrodes.
CC Current electrodes.
TT Thermocouple leads.

Two possible explanations of the anomalies suggest themselves to us. There may be some type of order-disorder transformation within the lattice, or alternatively a solid-solid phase transformation between different crystalline forms or compounds. Neither the presence of a latent heat nor hysteresis rules out the first hypothesis.[12] Careful examination with a sensitive thermocouple has shown the presence of both (Fig. 8). On the other hand, the onset of the rapid increase of electrical resistance somewhat *before* the transformation temperature (Fig. 7), does not militate against the second explanation since, for example, similar changes accompanied by a fading-out of the X-ray pattern have been observed with the alkali metals before the melting-point, which is itself quite sharp.[13] This indicates a preliminary loosening of the lattice. The anomaly was not visible in the curves for solid Ca, Sr or Ba hexammoniate, so the most likely chemical explanation of the anomaly—by analogy with salt hydrates—is the conversion from a higher to a lower ammoniate, the transition point marking the intersection of their vapour-pressure curves. Physical methods such as X-ray crystallography or absorption spectra might shed further light on the problem.

---

[11] Bowden, *The Phase Rule and Phase Reactions* (Macmillan, London, 1945), 132.

Conclusion.—The ultimate constitution of metal-ammonia solutions has not yet been resolved, but the foregoing investigation should assist in furthering an understanding of the phenomena encountered. Some remaining problems of interest comprise the examination of ternary solutions, the determination of phase curves for caesium and rubidium, completion of a systematic examination of the temperature and concentration variation of electrical conductivity, the relation of atomic species to the phase curves—for example, why the eutectic temperatures of the alkaline earth metals, unlike those of the alkali metals, lie so close together, and an examination of heats of solution at varying concentration.

This work was carried out during the tenure of an I.C.I. Research Fellowship (A. J. B.) and a Nuffield Research Fellowship (D. K. C. McD.).

The Dyson Perrins Laboratory,
The Clarendon Laboratory,
Oxford University.

---

[12] Mott and Jones, *Theory of Properties of Metals and Alloys* (Clarendon Press, Oxford, 1936), 28-40.

[13] Hume-Rothery, *The Metallic State* (Clarendon Press, Oxford, 1931), 100, 101.

CORRIGENDA.

P. 192, Fig. 1. *The legend should read* Disproportionation of ϕ_2AsCl.
At 252° c. —○— ϕ_2AsCl_2 —△— $\phi AsCl_2$ —Y— ϕ_3As.
At 304° c. --⊙-- ϕ_2AsCl_2 --△-- $\phi AsCl_2$ --Y-- ϕ_3As.

P. 193, Fig. 2. *Add to legend* --⊙-- ϕ_2AsCl_2 uncatalysed reaction.
Fig. 3. *The legend should read* Disproportionation of $\phi AsCl_2$.
At 256° c. —△— $\phi AsCl_2$ —○— ϕ_2AsCl —□— $AsCl_3$.
At 304° c. --△-- $\phi AsCl_2$.

P. 345, l. 4. *Delete* as finally revised 17th March, 1947.

P. 346, eqn. (1). *For* $\left(\frac{m}{a}\right)$ *read* $\binom{m}{a}$.

P. 396, Table VIII, columns 1 and 3. The numbers within chain brackets refer to G, G + S_2 and S_2 respectively in vertically descending order. Column 5. *Delete* gel G.

P. 397, Table IX, column 3. Type to be moved one line up.

P. 403, eqn. (20). *For* E_1 *read* E.

REVIEWS OF BOOKS.

Synthetic Methods of Organic Chemistry. A Thesaurus by W. THEILHEIMER. Vol. I, 1942-1944. Translated from the German by HANS WYNBERG. (New York: Interscience Publishers Inc. 1948.) Pp. 254. Price 30s. net.

This volume is a translation into English of the original *Synthetische Methoden der Organischen Chemie, Repertorium I*, published in Basel in 1946. It is intended to be the first of a series of volumes in which are recorded " new methods for the synthesis of organic compounds, improvements of known methods, and also old proved methods that are now scattered about in the specialised journals and in the original published work." Although the precise meaning of the foregoing quotation is far from clear, it is obvious that the publication of this work is a courageous and welcome venture. In the Foreword by Prof. Reichstein it is pointed out that whereas a well-organised system is already in operation for the systematic recording of all new organic compounds, little has been done to place on record the actual *methods* of organic chemistry. It is noted that his references to existing works which attempt to cover some part of this field make no mention of Hickinbottom's *Reactions of Organic Compounds*, a work of proved merit which has now, after twelve years, reached its second edition. The reason for this gap in the literature of organic chemistry is to be found mainly in the difficulties inherent in the systematic classification of methods or reactions, which do not arise in the classification of compounds. Dr. Theilheimer has attempted to overcome these by the introduction of a number of reaction symbols representing addition, elimination, rearrangement, exchange, ring opening, ring closure and electrolysis, which are used in conjunction with a few empirical rules. When this relatively simple system has been mastered it is then possible to find one's way about the pages of this volume with comparative ease, but for those who fight shy of new hieroglyphs and unaccustomed conventions there is an adequate alphabetical subject index arranged on a bilateral system which relates an individual item both to a starting material from which it can be synthesised, and to compounds for which the entry itself is a starting material. Each entry contains what is considered to be the minimum necessary for an appraisal of the applicability of a synthesis, and references are given both to the original work and to *Chemical Abstracts*. This volume in no sense relieves the worker from consulting the original literature; it is merely a useful guide to enable him to find what he wants more readily.

It is obvious, both to the author and to the reader, that the compilation of a lexicon of new organic reactions presents yet another problem which does not arise in the case of new organic compounds. With the latter the material for inclusion selects itself, but with organic reactions the determination of what should be considered new is often a matter of personal experience and opinion. It is, therefore, almost certain that many chemists will not agree entirely with the author's selection of material. In spite of these difficulties and limitations, which incidentally are fully appreciated by the author, there can be no doubt that all workers engaged, for one reason or another, in preparative organic chemistry will find this volume useful and it may aptly be termed a Thesaurus, since it is a storehouse within which the research worker will often find an unexpected stimulus or a new suggestion to help him on his way. The further volumes in this series will be looked forward to with interest.

It is unfortunate that the first volume shows some signs of carelessness in presentation and perhaps in proof reading. The authors " Gorvin and Hinkel " appear on different pages as " Gorving and Hinkel," " Corvin and Hinkel," and " Gorvin and Henkel," abbreviations used for journals are not always consistent, angular methyl groups are missing in some formulæ, authors' initials are not used consistently and nomenclature is sometimes faulty. In a book which contains so much detailed information it is perhaps inevitable that small inaccuracies should occur, but if this series of volumes is to find a permanent place among the universally accepted reference works of the organic chemist only the highest standards of accuracy can be permitted.

D. H. H.

Tables of Physical and Chemical Constants, 10th Edn. By G. W. C. KAYE AND T. H. LABY. (Longmans, Green & Co., 1948.) Pp. viii + 194. Price 21s.

In October, 1911, the first edition of Kaye and Laby (as it is known to everyone) was published; 37 years later we now welcome the 10th edition of this popular and useful compilation, and realise, with regret, that neither of the two original authors are still with us. Throughout these many years, it has fulfilled the need of a set of physical and chemical tables for use during teaching and in the laboratory. It has grown larger, a little dearer and better with each edition and still remains a valued friend. Few libraries or laboratories will not have at least one copy and that well-thumbed and somewhat soiled by constant reference to it. As with each new edition, the constants, both astronomical and physical, have been thoroughly revised and reasons given for the adoption of a particular value wherever controversy or ambiguity exists; in this last edition, the valuable chapter on optical glass has also been expanded and largely re-written. We do not believe that Kaye and Laby requires further recommendation except to urge the individual to buy a copy for himself so that he need not depend on its ready availability in the library nor be at a loss for the value of a constant when away from his laboratory.

OBSERVATIONS ON THE SLOW COMBUSTION OF HYDROCARBONS.

PART I.—THE ABSORPTION SPECTRA OF PEROXIDES.

BY SIR ALFRED EGERTON, E. J. HARRIS AND G. H. S. YOUNG.

Received 9th October, 1947.

During investigations into the cause of knock (Egerton and Gates [1]) the importance of peroxides in the slow combustion of hydrocarbons became evident, but purely chemical methods of identifying the various peroxides were not very satisfactory, not only because of the difficulty of finding suitable reagents to differentiate between them (Egerton, Smith and Ubbelohde [2]), but also because of the unstable nature of some of the peroxides which may be present during combustion and may not exist long enough to be found in the products. For these reasons the study of the absorption spectra of hydrocarbons during combustion was commenced (Egerton and Pidgeon [3], Ubbelohde [4]). General absorption in the region below 2700 A. was found to be associated with peroxide formation and for hydrocarbons with four or more atoms a diffuse band in the region 2750-2550 A. was observed, but there was no certainty as to the identity of the substances responsible for this band. Experiments on the behaviour of alkyl peroxides (Harris and Egerton [5], Harris [6]) and of their influence on hydrocarbon combustion (cp. Neumann and Aivazov [7]) made it worth while to extend the former spectroscopic investigation, in order to find out at what stage peroxides make their appearance during slow combustion. The experiments were made during 1939. Part I of the paper deals with the absorption spectra of various peroxides and this information is applied in helping to interpret the observed absorption spectra of butane undergoing slow combustion (Part II).

Experimental.

The apparatus used consisted of a quartz spectrograph, either the Hilger E. 31 (small) or E. 2 (medium), a hydrogen power discharge tube to provide a continuous source in the U.-V., and a cylindrical quartz vessel with plane ends, 25 cm. long and 4 cm. diam , which could be heated electrically. In some experiments this quartz cell was replaced by a Pyrex tube, 100 cm. long and 4 mm. diam., which had quartz windows cemented on the ends. In most cases the peroxide was admitted as vapour to the evacuated vessel, from a small bulb containing the liquid peroxide, and the pressure was measured by an amyl phthalate manometer, or by a frequently-calibrated spoon gauge, to indicate any pressure changes occurring during the decomposition of the peroxides. The temperature of the quartz vessel was kept constant throughout any single set of measurements. Accurate determinations of extinction coefficients by measurement of light intensity before and after absorption were not attempted ; but the pressure of the vapour, giving a figure proportional to the number of molecules in the light path, was used to correlate the observations, and the other conditions were kept as constant as possible : blank exposures were taken on each plate ; Ilford Zenith (H. and D. 700) plates were used and a standard development procedure was followed. A small cell consisting of two plane quartz plates at ½ mm. separation was used for tests of the absorption of the liquids.

---

[1] Egerton and Gates, *J. Inst. Petr. Tech.*, 1927, **13**, 281.
[2] Egerton, Smith and Ubbelohde, *Phil. Trans. Roy. Soc.*, 1935, **234**, 133.
[3] Egerton and Pidgeon, *Proc. Roy. Soc. A*, 1933, **142**, 26.
[4] Ubbelohde, *ibid.*, 1935, **152**, 354.
[5] Harris and Egerton, *ibid.*, 1938, **168**, 1.
[6] Harris, *ibid.*, 1939, **173**, 126.
[7] Aivazov and Neumann, *Acta Physicochim.*, 1937, **6**, 57.

The absorption spectra of the vapours of the following classes of peroxide have been investigated : alkyl hydrogen, dialkyl, oxyalkyl hydrogen, oxydialkyl, dioxyalkyl peroxides ; but only a few observations were made with other peroxides such as peracids, alkylene and alkylidene peroxides.

Alkyl Peroxides.—Methyl Hydrogen Peroxide was prepared by the action of hydrogen peroxide and potassium hydroxide on dimethyl sulphate. The purity (by KI method) was 90 %.[*] The pressure limit at which absorption was detected was 1·8 cm. Hg in the 25 cm. cell ; the limit of the photographed spectrum, or " cut-off," was then at about 2150 A. Without peroxide but with the same conditions, the transmission extended to 2100 A. With increasing pressure the " cut-off " moved towards the visible, e.g. at 2·8 cm. Hg the " cut-off " was at 2300 A. There was no trace of a banded structure. The spectroscopic evidence only indicated the formation of formaldehyde on decomposition.

Ethyl Hydrogen Peroxide (92 % pure) was prepared similarly. The absorption was slightly less than with the methyl compound ; a pressure of 2·0 cm. Hg was required to give a " cut-off " at 2150° A. (cp. Table I).

TABLE I.

Pressure (cm. Hg).	Complete Absorption (A).	60 % Absorption (A).	30 % Absorption (A).
2·0	2150	2180	2200
3·0	2250	2300	2480
3·5	2400	2450	2570
4·5	2550	2600	2690
5·5	2650	2700	2780

The peroxide decomposed on heating above 150° C. and the absorption then steadily diminished ; as decomposition proceeded, formaldehyde bands gradually appeared and became progressively stronger. Acids or peracids, which absorb in the same region as the peroxide, were not formed in amounts which might have been sufficient to detect spectroscopically. No bands other than known formalehyde bands were noted ; acetaldehyde, which analysis had shown to be present in earlier work (Harris [6]), would have not been detected spectroscopically other than as a background of general absorption in the presence of the formaldehyde.

Propyl Hydrogen Peroxide was prepared in a similar manner (purity 80 % by KI method, but 95 % by direct C and H determinations) showed similar, but slightly less, absorption than ethyl hydrogen peroxide. The behaviour on decomposition at 160° C. was also similar (cp. Table II).

TABLE II.

Pressure (cm. Hg).	Complete Absorption (A).	60 % Absorption (A).	30 % Absorption (A).
2·2	2150	2180	2200
3·6	2250	2300	2350
4·5	2320	2360	2460
6·2	2390	2480	2540

Diethyl Peroxide was prepared by Baeyer's method by action of hydrogen peroxide and potassium hydroxide on diethyl sulphate (cp. Harris and Egerton [6]). The sample had the same b.p. and refractive index as given by Harris.[6] The absorption was similar to that of the alkyl hydrogen peroxides, with an extinction coefficient evidently less than that of ethyl hydrogen peroxide, but slightly greater than that of propyl hydrogen peroxide (cp. Table III). The decomposition above 180° C. was accompanied by diminution of the " cut-off " i.e. increased transmission of the shorter waves, as the strength of formaldehyde bands increased. No other bands were detected : acetaldehyde, which was found along with formaldehyde in the slow decomposition of diethyl peroxide (Harris and Egerton [5]) was presumably also present.

---

[*] The reaction of KI with the various peroxides is not a sufficient measure of their purity, as the reaction is incomplete.

TABLE III.

Pressure (cm. Hg).	Complete Absorption (A).	60 % Absorption (A).	30 % Absorption (A).
2·0	2150	2180	2200
3·4	2250	2300	2350
4·2	2320	2370	2450
6·2	2400	2470	2540

Dipropyl Peroxide of purity 90 % (by KI method), behaved similarly but absorbed slightly less strongly.

The absorption of equal numbers of moles of these peroxides is in the following order :

$$\begin{array}{l} H_2O_2 > CH_3\,.\,OOH > C_2H_5\,.\,OOH > C_3H_7\,.\,OOH \\ \qquad\qquad\qquad\qquad\qquad\quad \vee \\ \qquad\qquad\qquad C_2H_5\,.\,OO\,.\,C_2H_5 > C_3H_7\,.\,OO\,.\,C_3H_7. \end{array}$$

This order is in agreement with the experiments of Rieche on the liquid peroxides, and their solutions in hexane ; for the measurements on hydrogen peroxide see page 749.

Oxyalkyl Peroxides.—Dioxydialkyl Peroxides $R'\,.\,(OH)\,.\,OO\,.\,(OH)\,.\,R''$. These peroxides were prepared by methods due to Rieche,[8] namely by the action of a dry solution of hydrogen peroxide (3 %) in ether on the theoretical amount of the requisite aldehyde. The ether was removed by distillation under reduced pressure, and the crude product recrystallised from ether, usually at low temperatures. Only one of the peroxides, $CH_2\,.\,OH\,.\,OO\,.\,CH_2OH$, could be obtained crystalline at ordinary temperatures ; the other peroxides were viscous liquids which solidified to glassy solids at about − 50° C. The purity was estimated by KI, and checked by converting the peroxide to acid by heating with water at 100° C., according to $CH_2\,.\,OH\,.\,OO\,.\,CH_2\,.\,OH \rightarrow 2HCOOH + H_2$. Both methods give low results because of secondary reactions. Difficulties due to condensation arose when the pressure was made high enough to obtain absorption in the 25 cm. tube, so that the longer tube was used for the experiments with the oxyalkyl peroxides.

(i) Dioxydimethyl Peroxide, $CH_2\,.\,OH\,.\,OO\,.\,CH_2OH$ (Wieland and Sutter [9]). The vapour of this peroxide (at 105° C.) gave a general " cut-off " extending to 2600 A. at 1·5 cm. Hg pressure in the long Pyrex tube. No formaldehyde bands were visible which indicates that the compound is not much dissociated at this temperature. When the temperature of the tube was raised, the " cut-off " diminished somewhat, and formaldehyde bands appeared and became strong at 190° C. This diminution in the " cut-off " indicates that the H_2O_2 formed by dissociation is decomposing. At 170° C. (1 cm. Hg pressure) in addition to faint formaldehyde bands, the quite distinct additional system of bands in the far U.-V. was observed (Table IV).

TABLE IV.

λ (A.).	1/λ.	Difference (A.$^{-1}$).
2463	40600	—
2445	40900	300
2427	41205	305
2420	41322	117
2396	41750	428
2375	42100	350
2350	42220	120

In general, bands in the region 2450-2200 A. are indicative of ring formation so that it can be suggested that a peroxide of the type, 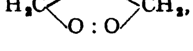 has been formed by the elimination of water; Neumann[10] has supposed that such peroxides may be formed but no direct evidence of their existence is available.

---

[8] Rieche and Meister, *Ber. B*, 1933, **66**, 718.

[9] Wieland and Sutter, *ibid.*, 1930, **63**, 66.

(ii) Dioxydiethyl Peroxide $CH_3 . CH(OH) . OO . CH(OH) . CH_3$ was obtained in a similar manner from acetaldehyde and H_2O_2 (Wieland and Wingler[11]).

The vapour gave a "cut-off" extending to 2350 A. at 1·2 cm. pressure in the Pyrex tube at 110° C. This "cut-off" *increased* with rise in temperature and acetaldehyde bands 3050-2650 A. appeared. No other bands, as found with dioxydimethyl peroxide, were noted. Some absorption in the region 2700-2500 A. occurred when this peroxide was heated at 118° C.

(iii) Dioxydipropyl Peroxide $C_2H_5 . CH(OH) . OO . CH(OH) . C_2H_5$ prepared from propaldehyde and H_2O_2, was very similar in properties and in its absorption. The dissociation which seemed to commence at 160° C. was accompanied by an increasing "cut-off," and propaldehyde bands (3150-2700 A.) appeared. The aldehyde bands disappeared again at higher temperatures (190-220° C.), indicating further reactions, but the "cut-off" still increased. Finally, at 230°, ignition occurred. The combustion of pure propaldehyde in air at 150° C. led to similar behaviour as regards the character of the absorption spectra. The increased "cut-off" was shown not to be due to the formation of unsaturated hydrocarbons, and was therefore due to either acids or peroxides (which were both shown to be present by analysis).

Amongst these dioxyperoxides, dioxymethyl peroxide appears to behave in an exceptional way in giving the special bands, and in the diminution of the "cut-off" on rise of temperature: for the other peroxides, the decomposition has as its first stage the formation of free aldehyde, and possibly hydrogen peroxide, or other peroxides formed by the oxidation of the aldehyde by the hydrogen peroxide. Further reactions subsequently occur, with the formation of peracids, acids and similar products, which absorb in the region 3000-2000 A. Since the aldehyde bands only appear on rise of the temperature, dissociation can be by no means complete at 100° C., and the compounds may exist at considerably higher temperatures in the absence of surfaces.

Newitt and Baxt[12] observed bands in the region 2450-2300 A. in the combustion of propane-air mixtures under pressure. The bands were very diffuse in character, and were provisionally ascribed to propaldehyde; however, there are no bands of the latter in this region recorded in the literature, and it is likely that they are similar to the bands obtained with dioxydimethyl peroxide and are due to a similar peroxide produced during combustion.

There is difficulty in identifying these bands with any known compound and they are apt to disappear on slight changes of procedure. As an example of this, some dioxydimethyl peroxide was prepared from hydrogen peroxide (3 % in ether) and formaldehyde in ether, which was obtained not in the usual way by extracting aqueous formaldehyde from ether, but by dissolving liquid formaldehyde (obtained from paraformaldehyde by heating) in ether at − 50° C. The peroxide so prepared, although apparently identical with that obtained by the other methods, did not give the bands described. The reason is obscure but the original dioxydimethyl peroxide possibly contained $CH_2 . (OH) . OOH$, which might influence the character of the substances formed from it.

Monoxydialkyl Peroxides.—These peroxides are prepared by the action of the theoretical amounts of alkyl hydrogen peroxide on an aldehyde in solution. All the peroxides studied were oily liquids; and there were the same difficulties in determining the purity of the samples examined.

(i) Monoxymethyl Ethyl Peroxide $CH_3 . CH(OH) . OO . CH_3$ was prepared by the action of methyl hydrogen peroxide on acetaldehyde. The vapour gave general absorption extending from the U.-V. to 2500 A. at 2 cm. pressure in the Pyrex tube.

(ii) Monoxydiethyl Peroxide $CH_3 . CH(OH) . OO . C_2H_5$ was prepared by action of ethyl hydrogen peroxide on acetaldehyde. The vapour (at 2 cm.) gave similar absorption in the Pyrex tube. At lower pressures (1-2 cm.), a very weak absorption band in the region 2700-2500 A. was noted on one plate. in addition to the "cut-off" at 2200-2300 A. * It was in this region that the pronounced band occurs in hydrocarbon combustion (for C_4H_{10} and above).

---

[10] Neumann, *Acta Physicochim.*, 1938, **9**, 527.

[11] Wieland and Wingler, *Annalen*, 1923, **431**, 301.

[12] Newitt and Baxt, *J. Chem. Soc.*, 1939, 1703.

* The observations on the vapour of monoxydiethyl peroxide have been confirmed in this laboratory by Minkoff and Everett; the peroxide gradually decomposes above 140° C. and formaldehyde bands appear. The weak absorption band in the region 2700-2500 A. was not observed.

(iii) Monoxydipropyl Peroxide, ($C_2H_5 . CH(OH) . OO . C_3H_7$), gave absorption in the region 2500-2000 A. only. All the oxyperoxides seemed to absorb rather more strongly than the alkyl peroxides but not so strongly as hydrogen peroxide.

Hydrogen Peroxide.—The peroxide used was 60-70 % aqueous solution prepared by repeated distillation of 30 % peroxide under reduced pressure. The vapour pressure at room temperature is less than that of water (the ratio of the vapour pressure of water to that of H_2O_2 is 1·138). The small amounts vaporised at normal temperature in the long Pyrex absorption tube were rapidly decomposed. For this reason the experiments were carried out in the short quartz tube, heated electrically, the peroxide being admitted from a small bulb through a heated side-arm. After the exposure had been made the vapour was pumped through a trap cooled with solid CO_2-alcohol mixture, and condensed. The peroxide content was determined with N./100 $KMnO_4$ (in presence of H_2SO_4). The results are summarised in Table V. The absorption of solutions of H_2O_2 in water was compared using the same 25 cm. quartz cell. The limit of detection was 0·007 % which gave a " cut-off " to 2100 A. (The limit of transmission for the spectroscope was 2000 A. with Ilford special Q plates.) Table VI gives the vapour pressure which the H_2O_2 would exert if present as such in the tube. In this way the results can be compared with those obtained for the vapour.

TABLE V.

Pressure H_2O_2 (cm. Hg).	Complete Absorption (A).
0·5	2150
1·04	2190
1·48	2230
2·06	2260

TABLE VI.

Concn. H_2O_2 %.	Vapour Press. cm. Hg.	Cut Off A.	Concn. H_2O_2 %.	Vapour Press cm. Hg.	Cut Off A.
0·0007	0·34	2100	0·10	49·0	2770
0·001	0·49	2150	0·25	122·5	2950
0·0025	1·22	2200	1·00	490·0	3100
0·005	2·45	2320	—	—	—
0·01	4·90	2500	—	—	—

By using the relationship, $I = I_0 e^{-Kl}$, at the chosen wavelength, an approximate measure of the extinction coefficient was obtained, which showed no maxima in the region studied. The results are in good agreement with those obtained by Rieche,[13] Henri and Wurmser,[14] and Urey, Dawsey and Rice.[15] The absorption of the vapour does not differ appreciably from that of the liquid.

Formaldehyde.—The absorption spectra of formaldehyde vapour between 50° and 300° C. was studied in the long Pyrex tube (110 cm.), the vapour being admitted from a small heated bulb containing paraformaldehyde and a spoon gauge being used to measure the pressure.

The formaldehyde bands first became noticeable at a pressure of 0·6 cm. Hg, with the tube at 180° C. As the pressure was increased, the bands became wider and more pronounced and extended towards the far U.-V. At 1·74 cm., bands in the region 2700-2600 A. became pronounced. In no case, however, were bands detected in the region 2500-2200 A., although there was some general absorption (about 10 %) in this region for higher pressures of formaldehyde. This was largely due to a film of paraformaldehyde being deposited on the quartz windows, as shown by purposely depositing such a film. A general reduction in intensity of about 5 % for the whole region 4500-2100 A. was obtained. The intensity maxima of the formaldehyde bands as measured by the microphotometer are given in Table VII and are in good agreement with previous results (cp. Henri and Schou [16]).

---

[13] Rieche, *Alkyl Peroxyd* (Leipzig, 1931).

[14] Henri and Wurmser, *Compt. rend.*, 1913, **126**, 157, 284.

[15] Dawsey, Rice and Urey, *J. Amer. Chem. Soc.*, 1929, **51**, 1371.

[16] Henri and Schou, *Z. Physik.*, 1928, **49**, 774.

The absorption spectra of acetic acid, peracetic acid, acetaldehyde and propionaldehyde were also photographed, but it would be superfluous to quote results as they were in complete agreement with known data. The absorption coefficient of the acids which absorb in the same region were found to be rather less than those of the peroxides: peracetic acid (75 %) was found to absorb to about the same extent as acetic acid.

TABLE VII.

λ(A.).	$1/\lambda$(cm.$^{-1}$).	λ(A.).	$1/\lambda$(cm.$^{-1}$).	λ(A.).	$1/\lambda$(cm.$^{-1}$).	λ(A.).	$1/\lambda$(cm.$^{-1}$).
3706	26984	3170	31546	2935	34072	2732	36604
3530	28329	3143	31817	2906	34414	2680	37313
3430	29155	3089	32373	2884	34673	2630	38023
3389	29506	3054	32744	2844	35162	2617	38214
3294	30327	3036	32938	2807	35624	2592	38579
3260	30675	2979	33569	2792	35816	—	—
3203	31223	2952	33875	2756	36285	—	—

Summary.

The absorption spectra of the vapours of hydrogen peroxide, alkyl hydrogen, dialkyl, oxydialkyl and dioxyalkyl peroxides were investigated. The extent of the extinction in the U.-V. end of the spectrum at different pressures was determined. All the following vapours cut off similarly, but in the following order of decreasing extinction:

$H_2O_2 > CH_3OOH > C_2H_5OOH > C_3H_7OOH, >$ and $C_2H_5OOH > C_2H_5OOC_2H_5 > C_3H_7OOC_3H_7$.

The spectroscopic evidence indicated that the oxydialkyl and dioxyalkyl peroxides could exist undissociated even above 100° C. Their decomposition into formaldehyde and other peroxides and acids was investigated spectroscopically. Dioxydimethyl peroxide at 170° C. provided a band system between 2460 and 2350 A. which indicated possibly polymerisation and ring formation. The higher oxyperoxides did not give rise to similar bands. With increase in temperature, extinction decreased with dioxydimethyl peroxide but increased with other dioxydialkyl peroxides owing to the formation of other peroxides and acids. The absorptions of the vapours of hydrogen peroxide, formaldehyde and formic and acetic acids were measured under similar conditions.

Department of Chemical Technology,
Imperial College,
S.W.7.

OBSERVATIONS ON THE SLOW COMBUSTION OF HYDROCARBONS.

PART II.—THE ABSORPTION SPECTRA OF BUTANE UNDERGOING SLOW COMBUSTION.

BY SIR ALFRED EGERTON AND G. H. S. YOUNG.

Received 9th October, 1947.

Former work (Egerton and Pidgeon[1]) has been extended in order to determine at what stage in hydrocarbon combustion the various absorption bands make their appearance.

Experimental.

Reactions between various mixtures of *n*-butane and oxygen were carried out in the same quartz reaction vessel 25 cm. long and 4 cm. diam., under

---

[1] Egerton and Pidgeon, *Proc. Roy. Soc. A*, 1933, **142**, 26.

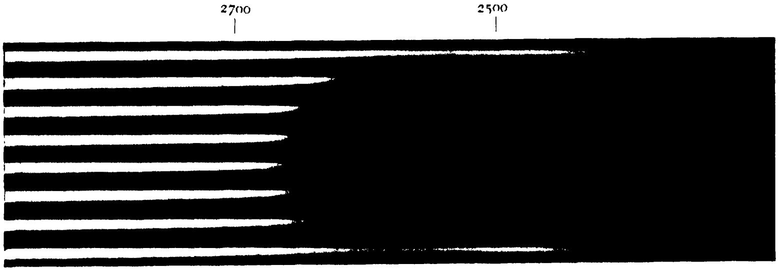

PLATE I.—1/1 Butane-oxygen. Static conditions, 275° C. and 730 mm. initial pressure. Showing change of the absorption band, and the "cut-off" with time: exposures at 1 min. intervals approximately, after the first 5 min.

[*To face page* 751.

flow and static conditions. Particular attention was paid to the early stages of the reaction between butane and oxygen, and to the conditions for the formation of the absorption band in the region 2750-2550 A. found in the earlier work. Propane in slow combustion at atmospheric pressure gives no such band. Tables I and II give the experimental conditions for obtaining this band, and for reaching complete reaction with no further light absorption for various mixtures.

(i) Slow Flow Conditions.

TABLE I

Mixture C_4H_{10}–O_2.	Temp. (°c.).	Maximum Rate of Flow for Band (cc./min.).	Approx. Time for Band to Appear (min.).	Rate of Flow for Complete Reaction (cc./min.).	Approx. Time for Complete Reaction (min.).
2/1	290	40	6·2	20	6·2
3/2	290	35	7·1	18	14
1/1	290	27	9·2	16	15·6
1/2	290	18	14	14	16·4

Since these experiments were carried out under flow conditions, the apparent contact time in columns 4 and 6 has, of course, little significance, since the point at which the butane commenced to react is unknown.

(ii) Static Conditions.

TABLE II

Mixture C_4H_{10}–O_2.	Temp. °c.	Time for Band to Appear (min.).	Complete Reaction (min.).
2/1	270	5-6	$>$11
3/2	270	5-6	$>$10
1/1	270	4-5	$>$ 8
1/2	270	5-6	$>$11

Under flow conditions, the 2/1 mixture appeared to react faster, whilst under static conditions the 1/1 mixture reacted most rapidly. In both cases, however, the times for appearance of the band were related to the times for complete reaction. The actual time of appearance obviously depends on the concentration which is needed to give detectable absorption. In the flow experiments, the destruction of intermediate peroxides at the walls would be greater; that the 2/1 mixture is more reactive is probably due to the buffering effect of the excess butane. The influence of the walls in destruction of chain-carriers was shown by the temperature required, being about 30° higher in a narrower tube for a similar rate. From the evidence afforded by the absorption spectra, the reaction passed through the following stages, the one merging into the next:

(i) No detectable absorption (to 2050 A.).
(ii) Slight absorption to 2100 A.; no detectable aldehyde bands.
(iii) Appearance of the band 2750-2550 A., gradually increasing in intensity, the " cut-off " remaining practically unaltered; no aldehyde bands yet visible.
(iv) Decrease in intensity of the 2750-2550 A. band, accompanied by the appearance of formaldehyde bands; the " cut-off " also increasing.
(v) Final disappearance of the 2750-2550 A. band; formaldehyde bands become strong; " cut-off " extended to 2600 A.
(vi) Complete reaction, accompanied by slight diminution in intensity of the formaldehyde bands, and in the extent of the " cut-off."

The appearance and disappearance of the 2750-2550 A. band and the change of the " cut-off " is shown in the Plate.

Propylene alone in the long tube at atmospheric pressure " cut-off " at 2430 A. and gave a slightly diffuse band from 2470-2430 A. The addition of

5 % propylene to a 1/1 butane-oxygen mixture in the tube at 260° did not produce any visible difference from the photograph obtained with the 1/1 mixture without addition of propylene. The extinction coefficient of the unsaturated hydrocarbons and the percentage of these found in the butane oxidation products is insufficient to change appreciably the character of the absorption. Propylene oxygen mixtures themselves gave rise to formaldehyde bands on combustion.

Experiments were also carried out in which a pressure gauge of the aneroid type (which Dr. E. J. Harris had devised) was attached to the reaction vessel, and analyses were made before, and immediately after, an exposure. The methods of analysis were similar to those employed by Harris and Egerton [3] in the slow combustion of propane, the reaction being stopped at the appropriate instant by plunging the reaction vessel into water at 0° C. Table III gives the partial pressures of the various constituents capable of absorption during the time-intervals stated. Unsaturated hydrocarbons were less than 1·5 %; no acid other than formic was found.

TABLE III.—1/1 MIXTURE AT 275° C.; 73 CM. INITIAL TOTAL PRESSURE.

Time (min.).	Press. (mm. Hg).	Absorption (see Schedule of Stages).	C_4H_{10} (mm.).	O_2 (mm.).	Peroxide (total) (mm.).	Acid (total) (mm.).	Aldehyde (total) (mm.).
0	730	None	365	360	—	—	—
6- 6½	730	(i)	321	300	14	4	—
8- 8½	733	(ii)	270	232	30	7	7
9- 9½	736	(iii)	228	175	44	10	14
10-10½	742	(iv)	175	117	44	13	22
11-11½	751	(iv)	140	73	36	16	42

Fig. 1 illustrates the changes in absorption with time for a 1/1 mixture at 73 cm. pressure. The dashed line indicates approximately the extent of absorption which would be expected from the quantity of peroxide determined by analysis (all assumed to be ethyl hydrogen peroxide). The dotted line indicates the absorption by the formic acid as determined by analysis. The full line indicates the extent of the observed " cut-off ", which was definitely rather greater after 5 min. than that estimated from the peroxide found by analysis.

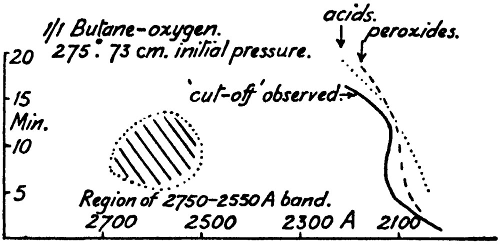

FIG. 1.

Discussion.

It seems quite clear that the initial cut-off which occurs before there is any appreciable pressure rise, can only be attributed to an alkyl peroxide or to hydrogen peroxide, whilst the diffuse band (2750-2550 A.) is due to a more complicated peroxide, probably possessing a ring structure which may be due to polymerisation or condensation reactions between aldehydes and alkyl peroxides or hydrogen peroxide. Four-membered ring structures, formed from ketene, and other such ring compounds tend to give an absorption band in this region: so that there is good reason to consider that the substance responsible for the band is both a ring compound and a peroxide (Ubbelohde[3]). The peroxide found by analysis in the later stages of the reaction appears to consist chiefly of hydrogen peroxide in co-existence with formaldehyde, so that alkoxy-peroxides may be present after condensation of the reaction products, if water and other substances are not in too great concentration to prevent this. Harris has shown that hydrogen peroxide vapour can be led through a silica tube at quite high temperature (500° C.) without being completely decomposed, and at temperatures (200-300° C.) important in hydrocarbon slow combustion, the chance of survival is quite long ; part of the "cut-off" observed in hydrocarbon combustion may therefore be due to H_2O_2. Similarly, provided the pressure is below a critical value, alkyl peroxides can survive (Harris[4]). The results quoted in Part I show that oxyperoxides may also exist in the vapour state at temperatures up to about 150° C., and possibly some may survive in absence of surfaces at still higher temperatures, but the quantity so existing in hydrocarbon combustion is probably very much less than corresponds to the amount which appears to be present in the condensed products, which are formed after condensation from aldehydes and other more stable peroxides. It is doubtful whether any oxyperoxide would be formed, and remain as such, by direct reaction of aldehyde and hydrogen peroxide vapours at the temperature of the combustion.

---

[3] Harris and Egerton, *Chem. Rev.*, 1937, **21**, 287.

The evidence in the case of propane was that whether or not peroxides are detected in the condensate, the percentage of the other products, aldehydes, etc., in the vapour remains the same (Harris and Egerton[2]), indicating that hydrogen peroxide was the main peroxide present in the vapour. With propane, special bands have been observed (see previous paper, p. 747), which seem also connected with peroxide formation.

In the butane oxidation, the measurements of the extent of " cut-off " and the analyses of the products indicated that the initial " cut-off " was not sufficiently great to be explained by absorption by hydrogen peroxide only, but is more likely to be due to alkyl (and possibly oxyalkyl) peroxides, which absorb less strongly. Analyses showed a total concentration of peroxides at the end of the induction period of 6 %, and the assumption that 3 % of this was alkyl hydrogen peroxide and 3 % oxyalkyl peroxide would account for the experimentally determined absorption (both band and " cut-off ").

In the case of propane, very little reaction occurs before the pressure rise begins, but for butane an appreciable amount of butane and oxygen is consumed in equivalent amounts before any pressure rise occurs, and there is a noticeable " cut-off " and band appearance before this rise. This would be consistent with the view that an alkyl hydrogen peroxide and an oxyalkyl peroxide were formed during the induction period.

Another difference is observed between the combustion of propane and butane in the amount of unsaturated hydrocarbons formed. Not only were unsaturated products formed in much smaller amount with butane, but propylene had no effect on its combustion. This is probably due to the lower temperature at which combustion occurs.

The absorption spectra of formic and acetic acids were investigated at various pressures and temperatures and were found to be similar to those of the alkyl peroxides, the absorption of the acids per mole, however, being considerably less than that of the peroxides. The absorption could not be distinguished from that due to the peroxides, unless, after analysis for acid and peroxide, allowance was made for their respective extinctive effect. The analytical evidence definitely shows that the initial " cut-off " cannot be attributed to acid formation. The amount of acid becomes appreciable only in the later stages of the reaction, and during that period the absorption is actually decreasing, which can be attributed to the decrease in the amount of peroxide present being more than sufficient to compensate for the increase in the amount of acid.

---

[3] Ubbelohde, *Proc. Roy. Soc. A*, 1935, **152**, 354.
[4] Harris, *ibid.*, 1939, **173**, 141.

The absorption by various other hydrocarbon vapours undergoing combustion was determined in the same apparatus during the course of the work and are summarised in Table IV.

TABLE IV.

Propane.	No absorption band (2750-2550 A.); two narrow bands in region 2300-2250 A. (1/1 mixture at 300° C. in long tube); there are the usual " cut-off " and formaldehyde bands; the initial " cut-off " being rather greater for propane than for butane.
Pentane.	The absorption band 2750-2550 A. is rather more pronounced than that with butane (e.g. for 3/1 mixtures at 314° C., rate of flow 30 cc./min. in long tube); rather more acid formed and therefore greater " cut-off " at the completion of the reaction.
Hexane.	Similar results.
Propylene.	Already cited.
Butylene-1.	No band in region 2700-2600 A. detected on combustion; only formaldehyde bands; the " cut-off " to 2590 A. by the hydrocarbon itself prevented observation of any bands further in the U.-V.
*Iso*butane.	Did not show any band in the region 2700-2550 A., though the usual " cut-off " was observed.

The absorption given by formaldehyde, acetaldehyde, propionaldehyde, butyraldehyde, was also re-investigated; the temperature had no effect on the absorption, unless oxygen was present, when the " cut-off " was observed.

On the spectroscopic evidence the combustion of *n*-butane is accompanied by formation of peroxides, chiefly hydroperoxides amongst the initial products. These peroxides may decompose into simpler products, or may condense along with aldehydes, giving oxyperoxides and then polymerising to give one or other cyclic peroxides. These peroxides apparently decompose into formaldehyde, water and other products. If any appreciable quantity of higher aldehydes (e.g. butyraldehyde and propionaldehyde) is formed, it has not been detected spectroscopically, although it has already been pointed out that neither this nor the analytical method are satisfactory for small quantities of the higher aldehydes.

This investigation had to be closed down early in 1940. Though not carried as far as it was intended, the results seem worth recording in furtherance of the study of hydrocarbon combustion. Further work is now in hand.

Summary.

The absorption spectrum in the U.-V. of *n*-butane undergoing slow combustion was photographed in flow and static conditions, and at various temperatures and for different initial proportions of butane and oxygen. The former observations by Egerton and Pidgeon [1] on absorption of the shorter waves and on the band between 2750 and 2550 A. were extended by photographing the spectrum and analysing the products as the combustion proceeds.

It is shown that two absorption bands appear during the induction period, i.e. before pressure-rise occurs, and that peroxides are then present. The absorption in the early stages is mainly due to peroxides, whereas part of the absorption is due to formic acid in later stages. The band (2550-2750 A.) is only given by hydrocarbons with four or more carbon atoms. It is not found during the combustion of butyraldehyde or *iso*butane, or of butylene.

The presence of 5 % propylene did not alter appreciably the character of the absorption spectra of *n*-butane undergoing combustion; the amount of unsaturateds formed in the combustion of *n*-butane is insufficient to account for the

absorption. Attention is drawn to the differences between the behaviour on combustion of propane and that of *n*-butane, and between the absorption spectra obtained.

Department of Chemical Technology,
Imperial College,
S.W.7.

PART III.—THE EFFECT OF DILUENTS AND OTHER SUBSTANCES ON THE SLOW COMBUSTION OF BUTANE.

Simultaneously with the investigations of the absorption spectra of butane in slow combustion (see Part II), other experiments were carried out in 1939 on the slow combustion of this hydrocarbon with the analytical technique used by Harris[1] for the study of the propane combustion. Preliminary experiments were made using a flow method, followed by static experiments on a 1/1 mixture of butane and oxygen in which the effects of diluents were particularly studied.

The slow combustion of butane has been investigated by Pease[2] by a flow method, and this was followed by a later communication[3] in which he concluded that since KCl was active in destroying the peroxides without otherwise influencing the combustion, the latter were not essential to the combustion process. He considered the combustion to be initiated by thermal decomposition. Briner and Carceller[4] studied the action of ozone in lowering the temperature at which slow combustion of butane occurs and Neumann and Tutakin[5] the effect of diethyl peroxide on its ignition.

Experimental.

Preliminary Experiments by Flow Method.

In studying the combustion using a flow method, the rate of flow determines the times of contact of the gas mixture with the walls of the tube and so affects the extent of chain-initiating and -breaking.

In the following experiments, a measured volume of butane and oxygen (400 cc.) was passed through the reaction tube at a rate of 10 to 20 cc./min. giving a contact-time for the butane of about 1 min. A quartz reaction tube, 10 cm. long and 1 cm. diam. was employed in a vertical furnace arranged for very even heating over the length of the tube. Products were condensed at − 5° c.; the formaldehyde was scrubbed out in a spiral washer: the butane was not condensed. The ratio of butane to oxygen was varied from 2/1 to 2/3. About 25 to 30 % of the butane was burnt, and the ratio of the percentage of butane entering to that in the gases leaving after condensation of products was unity, generally within about 10 %. The ratio of oxygen to butane burnt for a 1/1 mixture was about 3/1 as compared with about 2/1 for a 1/1 propane mixture, the butane, of course, requiring more oxygen per mole burnt.

Table I shows that:

(*a*) the total amounts of final products—aldehydes, alcohols, acids—did not vary much;
(*b*) total peroxides varied greatly with the condition of the surface;
(*c*) total carbon monoxide was higher for higher proportions of oxygen;
(*d*) total unsaturated products were greater the higher the temperature.

The aldehydes were about 60 % formaldehyde, the alcohols mainly ethyl alcohol, and the acids almost entirely formic acid.

---

[1] Harris, *Analyst*, 1937, **62**, 729.
[2] Pease, *J. Amer. Chem. Soc.*, 1929, **51**, 1839.
[3] Pease and Munro, *ibid.*, 1934, **56**, 2034.
[4] Briner and Carceller, *Helv. Chim. Acta.*, 1935, **18**, 973.
[5] Neumann and Tutakin, *Bull. Acad. Sci. U.R.S.S.*, 1938, 329.

The constancy of the proportion of butane in the gas entering to that in the gas leaving seems to follow from the fact that the quantity of total liquid product was more or less independent of the quantity of butane entering and from the adjustment between the proportion of CO_2 and CO in the exit gas, the CO being higher when the butane proportion was low.

TABLE I.

Temp. °c.	Rate cc./min.	C_4H_{10}.	O_2. in.	O_2 used.	CO_2.	CO.	C_nH_m.	Total Acid.	Total Aldehyde.	Total Alcohol.	Peroxide (as H_2O_2).	Approx. Initial Composition C_4H_{10}/O_2.
	g. mol. $\times 10^{-4}$ per g. mol. of Butane Consumed.											
325	5	328	335	330	25·4	170·0	25·9	7·7	63·0	38·2	4·7	1/1
325	11	354	261	212	7·0	103·0	16·1	2·0	63·0	56·0	3·4	4/3
325	4	438	199	162	11·6	76·0	16·2	2·0	60·0	46·7	Nil	2/1
335	7	321	480	467	26·9	287·0	22·2	8·8	97·1	66·0	24·3*	2/3
340	12	305	340	293	8·1	128·0	12·7	10·0	92·0	32·0	1·5	1/1
345	8	437	362	312	23·8	143	35·6	7·2	78·0	40·0	12·2*	6/5
355	6	331	254	220	11·5	110	36·2	3·2	73·8	60·4	0·9	4/4
355	7	350	268	231	20·9	131	44·1	3·7	65·0	69·5	1·0	4/4

* Tube cleaned with hydrofluoric acid.

The carbon balance shows a deficiency of about 20 % and the hydrogen considerably more. This is probably accounted for by a polymer being formed. In experiments in longer soda-glass tubes in a horizontal furnace, solid products appeared at a definite distance from the point of entry of the gases into the heated tube. The solid product was shown to contain paraformaldehyde. Peroxides were not found when soda-glass tubes were used.

Under the above conditions, butyraldehyde oxidised at a much lower temperature (230° c.) giving chiefly CO, formaldehyde and water. No unsaturated hydrocarbons were found but a considerable amount of peroxide (H_2O_2 and $CH_2(OH)OOCH_2(OH)$) were identified in the products.

Propionaldehyde oxidised rapidly at 250° and a small amount of propionaldehyde added to the 1/1 butane-oxygen mixture caused violent ignition at 310° c., while with 20 % the reaction proceeded at the same rate as without the addition, but at about 70° lower.

Static Experiments.

Pressure Change.—The investigation of the combustion of butane under static conditions was confined mainly to the 1/1 butane-oxygen mixture to which diluent gases had been added. The mixtures could be passed from a large storage vessel into the reaction vessels evacuated by a high-vacuum system. Three reaction vessels were in use :

(i) a spherical soda-glass vessel, 120 cc. (surface to volume, 0·17) ;
(ii) a spherical quartz vessel, 120 cc. ;
(iii) a cylindrical quartz vessel, 600 cc. (27 × 5·4 cm. ; surface to volume, 0·79) ;

(i) and (ii) were heated electrically, and the temperature controlled to about ± 1° c. ; (iii) was heated by diphenylmethane vapour and was constant to about ± 0·5° c.

Pressure was measured on a diaphragm gauge (an altimeter modified by Dr. E. J. Harris for such purposes). An angular deflection of 1° per mm. change of pressure was obtained between 50 and 80 cm. ; a pointer could be used to indicate pressure, or when the rate of change was rapid, a beam of light was projected from a mirror on the instrument on a photographic film. Mercury manometers were ruled out—except for calibration purposes because mercury vapour was found to affect the reactions.

After introduction of the mixture into the reaction vessel, the change of pressure (Δp) in cm. with time (t) in min. was observed. It was first necessary to " stabilise " the surface of the vessel : however much the surface was cleaned by reagents, reproducible results were not obtained unless at least one ignition had been permitted to occur, thereafter results could be repeated quite satisfactorily (to within about 15 sec.). The surface thereby got an invisible coating which was uninfluenced by the reaction products.

From the curves obtained under various conditions, values of ϕ and A in the equation

$$\int_0^t w\,dt = \frac{A}{\phi}(e^{\phi t} - 1 - \phi t)$$

were obtained for the initial portion of the curve, where w = reaction rate. It was necessary to use

$$\phi = \left(\frac{\log \Delta p_1 - \log \Delta p_2}{t_1 - t_2}\right)$$

derived from the more approximate expression $\int_0^t w\,dt = Ae^{\phi t}$, to get the first estimate of the rate of reaction and then to obtain the value of $\int_0^t w\,dt$ by successive approximation.

On the following graphs (Fig. 1 and 2) the effect of pressure and of temperature on the values of A and ϕ are given for a 1/1 butane-oxygen mixture. Other

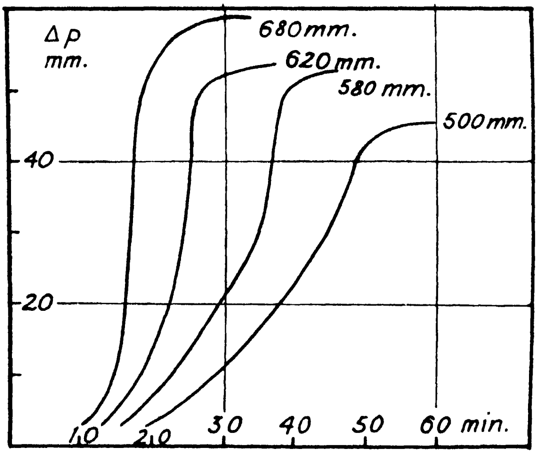

FIG. 1.

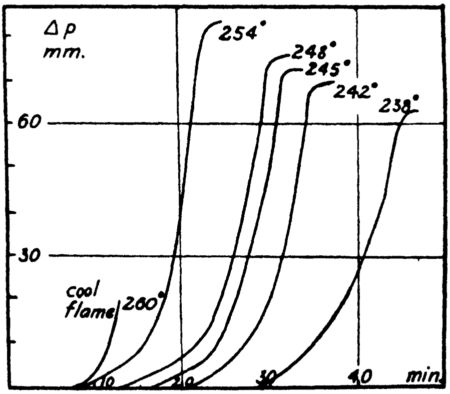

FIG. 2.

results are given in Tables II and III where τ indicates the length of the induction period. It was found that :

(i) the values of A and ϕ for a 1/2 butane-oxygen mixture are higher than for a 1/1 mixture ;

(ii) in the large quartz vessel, the value of ϕ changed only slightly, but A increased considerably with temperature ; in the small quartz vessel both values increased with temperature ;

(iii) the effect of pressure varied with the composition of the mixture.

TABLE II.—1/2 BUTANE-OXYGEN.
TEMP. 255° C. SMALL QUARTZ BULB.

P (mm.).	τ_5 (min.).	τ_c (min.).	ϕ.	log A.
400	17·5	45	0·20	— 2·8
470	14·0	30	0·20	— 2·1
600	11·0	26	0·20	— 1·5
708	11·0	25	0·23	— 1·6
743	8·7	25	0·25	— 1·5

TABLE III.—1/1 BUTANE-OXYGEN AT 740 MM.
SMALL QUARTZ BULB.

Temp. °c.	τ_5 (min.).	τ_c (min.).	ϕ.	log A.
235	75	—	0·075	— ·49
240	46	75	0·081	— 3·0
245	28	45	0·100	— 2·1
250	20	30	0·120	— 1·7
254	13	22	0·136	— 1·1

When an attempt was made to use a similar equation as Prettre applied to interpret the combustion of propane, viz.,

$$\phi = K p_b p^2_t \left(1 + \frac{a p_i}{p_t}\right),$$

in which p_b represents the partial pressure of butane, p_t the total pressure of butane and oxygen, and p_i the partial pressure of the inert gases,

$$\phi' = \frac{p'_b p'^2_t \left\{1 + a\frac{p'_i}{p'_t}\right\}}{p_b p_t \left\{1 + a\frac{p_i}{p_t}\right\}} \phi_0$$

was found to vary with Δp.

Prettre had obtained a constant value for ϕ' for propane with $a = 1·5$. No value of a was found to give a constant ϕ' with butane ; $a = 3$ gave constancy up to $\Delta p = 40$ mm., but above this the agreement was poor. The pressure rise was not a measure of the oyxgen consumed, as it appeared to be with propane : even before any rise of pressure occurs, some oxygen is consumed. The rate of consumption depends on the concentration of intermediate products and at $\Delta p = 30$ mm. a change in the nature of the reaction occurs resulting in increased rate of oxygen consumption. The pressure-rise is a composite curve which is not easy to interpret ; as the results of analyses at various stages of the reaction subsequently showed, only the initial part of the pressure-rise is proportional to the oxygen consumption.

Result of Analyses of the Products at Various Stages of the Reaction.— The gas mixture was admitted to the reaction vessel and when a certain pressure-rise had occurred the reaction vessel was withdrawn and quenched at 0° c. The residual gas pressure was measured, a sample of the gas analysed and the liquid products were dissolved in water and also analysed. Both the small quartz and the large quartz reaction vessels were used, with a mixture of 1/1 butane-oxygen, at a temperature of 242° c. and an initial pressure 700 mm. Hg. The results were similar for both vessels, except the maximum percentage of aldehyde found was 10 % in the smaller, instead of 7·9 % as found in the larger vessel.

The final products were practically identical. The results are given in percentages actually present in the gas-phase at the temperature of the reaction. (See Table IV (*a*) and (*b*) and Fig. 1.)

In Table IV (*b*), the effect of temperature on the final products for a 6/5 butane-oxygen mixture is recorded. The figures in (*a*) and (*b*) are not comparable because of the change in initial concentration.

If the values in Table IV (*a*) are plotted, the curves show that (*a*) the aldehydes and peroxides increase rapidly over the first 30 mm. pressure rise and then fall off, the peroxides more rapidly than the aldehydes, (*b*) the CO_2 commences to increase after 20 mm. pressure rise, whereas CO commences earlier and gives a slightly more S-shaped curve, (*c*) the alcohols increase regularly up to 40 mm. and then rather more slowly, the acids quite regularly throughout, and also the water. The consumption of oxygen and butane is regular over the first 20 cm. and then the consumption of oxygen becomes more rapid up to 50 cm.-rise. The unsaturated products remain at about the same small concentration at this temperature (240° c.).

Analytical Methods.

Gaseous Products : A Bone-Newitt apparatus was employed using palladium for hydrogen and copper oxide for hydrocarbons. The *n*-value (column 12, Table IV), if lower than 4, indicates the proportion of hydrocarbons lighter than butane.

TABLE IV.—Quartz Vessel 600 cc. Initial Pressure 70 cm.
$T = 242°$ c.

(*a*)

Pressure Rise (mm.).	C_4H_{10}.	O_2.	CO_2.	CO.	C_nH_m.	HCOOH.	Total Aldehyde.	Total Alcohol.	Peroxide.	H_2O (Diff.).	*n*-Value of Gas.
2	50·0	45·0	—	—	0·8	—	—	—	1·0	3·2	4·0
10	44·0	40·0	—	1·0	0·8	1·2	1·0	2·0	1·5	4·0	3·9
15	40·8	39·6	—	1·0	0·5	2·6	3·8	5·9	6·6	6·0	3·9
20	38·0	34·8	—	1·5	0·5	3·0	4·2	5·9	6·6	8·0	3·9
30	34·0	25·0	1·0	2·5	0·5	3·0	7·8	5·9	6·4	15·5	3·7
40	31·0	13·0	6·0	6·0	0·7	3·0	7·0	6·1	4·0	22·0	3·7
50	27·2	2·8	7·7	11·0	0·9	5·5	6·0	7·0	2·2	31·0	3·6
60	26·8	2·4	8·2	11·3	0·8	5·2	5·2	8·7	2·0	31·0	3·8
End of reaction	25·0	0·8	10·9	11·3	1·0	6·5	4·8	15·0	1·0	30·0	3·7

(*b*)

Temp. °c.	C_4H_{10}.	O_2.	CO_2.	CO.	C_nH_m.	HCOOH.	Total Aldehyde.	Total Alcohol.	Peroxide.	H_2O (Diff.).	*n*-Value of Gas.
238	30·0	0·1	10·9	10·9	—	7·2	6·3	17·8	1·6	15·5	3·9
242	32·1	0·1	11·1	11·1	—	7·0	5·8	17·0	1·4	14·5	3·7
247	34·2	0·2	8·0	13·5	—	7·0	5·5	15·6	1·1	16·0	3·6

Acids : by titration using bromphenol blue ; free formic acid by mercuric chloride method. The latter method was used to determine the formic acid obtained after decomposing oxyperoxides by refluxing with water at 100° c.

Peroxides : by KI in presence of ammonium molybdate. All peroxide determinations were low ; the method gave results 95 % correct with H_2O_2, but only about 60 % for most organic peroxides. No correction was applied on this account. The ammonium thiocyanate method also gave low results and was not therefore used. The behaviour with Methylene Blue helped to distinguish oxyperoxides from H_2O_2 and alkyl hydrogen peroxides.

Aldehydes : the *total aldehyde* by Blank and Finkenbeiner's method with H_2O_2 and caustic soda ; the *free aldehyde* by the hydroxylamine method. The difference indicates the amount of oxyalkylperoxides, which do not liberate

HCl immediately from a neutral solution of hydroxylamine hydrochloride. The *formaldehyde* was determined by Romijn's cyanide method and by the mercuric chloride method.

ALCOHOLS : by a modification of Washburn and Osbourn's method, after removal of aldehydes, using phosphoric acid and N./5 dichromate. (In Table IV, the alcohol is assumed to be ethyl alcohol ; the quantity of methyl alcohol was determined occasionally and, from the results obtained, the figures given may be 5 % low for total alcohol.)

The initial portion of the curve (up to 10 mm.) represents approximately the rate of combustion of the butane and oxygen. Above about 30 mm., the pressure-rise is affected by the rate of combustion and decomposition of aldehydes and peroxides. The A and ϕ values have no simple interpretation in such a complicated reaction except in the initial stages.

It was found that addition of carbon dioxide to the butane-oxygen mixture gave a greater final pressure-rise than would be expected, considering that carbon dioxide had replaced some of the butane-oxygen mixture.

The analyses of the final gases for varying additions of carbon dioxide (Table V) shows the effect of the diluent CO_2 in increasing the percentage of butane relative to the oxygen consumed and correspondingly increasing the percentage of aldehyde formed.

TABLE V.—INITIAL PRESSURE 700 MM. $T = 242°$ C.

C_4H_{10}.	O_2.	CO_2.	CO.	Total Aldehyde.	Total Alcohol.	H_2O_2.	Acid.	H_2O.	n-Value.	% CO_2 added.
32·1	0·1	11·1	11·1	5·8	17·0	1·4	7·0	14·5	3·7	—
25·9	1·2	21·2	10·7	6·2	11·0	0·9	2·7	19·0	3·6	11·4
24·9	1·2	24·9	10·2	8·3	12·6	0·5	1·9	16·0	4·0	14·3
21·0	1·2	37·5	8·6	11·4	12·2	1·0	2·3	5·1	4·6	28·6
11·3	2·5	47·0	6·4	18·8	12·8	0·5	2·3	1·2	5·2	35·0

The carbon dioxide presumably prevents aldehydes reacting with oxygen at the walls of the vessel and the aldehydes tend then to increase the rate of the reaction by supplying active centres. It is important to determine the proportion and nature of the higher aldehydes in relation to the formaldehyde and it is intended to resume the experiments with this object.

Measurement of Pressure Change in Presence of Inert Gases.—The effect of additions of CO_2, H_2, helium and argon on the rate of rise of pressure is given in Table VI.

TABLE VI.

A. EFFECT OT INITIAL PRESSURE OF CO_2 AT 256° C. 70 CM. TOTAL INITIAL PRESSURE.

Pressure CO_2 (cm.).	τ_5 (min.).	ϕ.	log A.
—	8·0	0·301	−1·7
2	7·5	0·301	−1·6
4	8·2	0·301	−1·7
6	10·5	0·270	−2·1
15	13·0	0·198	−1·9
18	15·0	0·178	−2·0
28	18·5	0·150	−2·1
38	20·5	0·125	−1·9

B. EFFECT OF PARTIAL PRESSURE OF CO_2. AT 244° C.

Pressure CO_2 (cm.).	Total Pressure (cm.).	τ_5 (min.).	Final Pressure.	ϕ.	log A.
8	70	16	10·7	0·300	−4·1
10	71	21	8·6	0·300	−5·5
20	72	26	7·0	0·170	−3·7
24	73	34	5·5	0·100	−2·7

TABLE VI.—(*continued*).

C. Effect of Addition of Hydrogen; 256° c.; 70 cm.

Pressure H_2 (cm.).	τ_5 (min.).	$\Delta p/\Delta t$.	ϕ.	log A.
—	9·0	10·0	0·301	−2·0
1·9	6·5	Expl.	0·400	−1·9
3·8	8·0	,,	0·400	−1·9
7·6	9·0	40·0	0·301	−2·0
11·4	11·0	25·0	0·286	−2·4
15·2	11·0	20·0	0·301	−2·5
19·0	12·5	13·3	0·250	−2·4
23·8	19·2	10·0	0·286	−4·8

D. Effect of Addition of Helium; 248° c.; 70 cm.

Pressure He (cm.).	τ_5 (min.).	$\Delta p/\Delta t$.	ϕ.	log A.
—	20·0	7·2	0·150	−2·3
9	18·5	11·0	0·202	−3·0
5	18·2	11·0	0·190	−2·8
2·5	16·0	12·5	0·170	−2·0
1·2	16·0	12·5	0·165	−1·9

E. Effect of Addition of Argon; 256° c.; 72 cm.

Pressure A. (cm.).	τ_5 (min.).	$\Delta p/\Delta t$.	ϕ.	log A.
—	10·8	12·0	0·301	−2·4
0·6	10·0	Expl.	0·325	−2·5
2·7	10·5	,,	0·310	−2·4
3·6	10·5	25·0	0·200	−1·3
5·4	10·5	20·0	0·150	−0·5
13·4	11·0	20·0	0·090	−0·3
8·0	11·0	10·0	0·075	−0·1

The following may be noted—

(i) Addition of CO_2.—The values of A were unaffected, as were values of ϕ for small amounts of CO_2 but the ϕ-values fall off for larger additions. The final pressure is greater than for the mixture alone at the same total pressure of butane-oxygen mixture.

(ii) Addition of Hydrogen.—Although the values of A and ϕ (for 7·6 cm. addition, for instance) were similar to the undiluted mixture, the reaction was four times as fast. This acceleration was not due to the participation of the hydrogen in the oxidation.

(iii) Addition of Helium.—The accelerating effect was even greater than for hydrogen. At 256°, below 11 cm. addition, the mixture exploded.

(iv) Addition of Argon.—The acceleration was greater than provided by CO_2, but less than that by H_2 or He.

Further evidence (see Table VI **B**), that the value of ϕ may be maintained apparently constant owing to the decomposition of intermediate products, was afforded by some experiments in which CO_2 was added to the undiluted mixture in such amount that the total pressure was equal to that of the undiluted mixture for a given pressure increment. The values for the total pressure of butane and oxygen for the undiluted mixture were obtained from the pressure-time curves and corresponding analyses.

ϕ fell off considerably in spite of the pressure increase. From the values of τ_5 at 244° c. and 70 cm. pressure, it would be expected that the time for the pressure to increase from 10 to 30 mm. would be 13 min., but actually it was only 3 min., which indicated that secondary reactions were occurring.

The general inference from all the static experiments is that the sigmoid pressure-rise curves for the butane oxidation cannot be interpreted in terms of a simple chain reaction, but that the chain reactions are complex and influenced by the various products formed during the reaction. The accelerating influence of the diluents is probably due to their action as buffers preventing oxidation of the aldehydes or other intermediates in the chain process at the walls.

There appears to be an additional accelerating effect with the monatomic gases, due perhaps to the easier transference of energy. This is suggested because the effect of helium is even greater than that of hydrogen, although the effect of conductivity would be much the same as for hydrogen.

Effect of Addition of Aldehydes and of Hydrogen Peroxide.—The effect of addition of aldehydes was also investigated (see Table VII).

TABLE VII.—INITIAL PRESSURE 700 MM. TEMPERATURE 242° C.

Pressure Propionaldehyde. (mm.).	τ_5 (min.).	ϕ.	log A.
—	30·5	0·120	−3·0
1·8	21·0	0·150	−2·5
3·6	15·0	0·120	−1·1
4·5	14·0	0·120	−1·0
5·5	11·0	0·135	−0·8
7·3	9·0	0·150	−0·65
10·4	6·0	0·150	−0·20
16·3	3·0	0·200	0·10
18·2	2·0	0·200	0·30

The chief effect of the addition of propionaldehyde was to decrease the induction period; the value of ϕ was little altered until the proportion of aldehyde was high. Butyraldehyde had more effect than furfuraldehyde, the latter more than acetaldehyde, while furfuradelhyde had a small effect. Formaldehyde also had quite small effect.

If P is the partial pressure of the aldehyde and τ is the induction period in min., $\tau = \text{const.} - \log (P + X)$, X depending on the particular aldehyde used. When carbon dioxide and propionaldehyde were both added, the values of ϕ and A were identical in spite of differences in the amount of aldehyde and carbon dioxide (and hence also the butane and oxygen) which were initially present. The value of ϕ was increased as compared with the value for butane and oxygen alone. Since both carbon dioxide and aldehyde are formed in the reaction, it is probable that the increase in ϕ is due to their combined effect. Mixtures with a high butane content (66 % and over) exhibit a sharp break in the slope of the curve at 40 mm. Similar breaks were noted when propionaldehyde was added, and the oxidation of the aldehydes is presumably the reason for this sudden change in the shape of the curve.

TABLE VIII.—EFFECT OF PROPIONALDEHYDE AND CARBON DIOXIDE. INITIAL PRESSURE (TOTAL) 70 CM. TEMPERATURE 242° C.

No.	Press. CO_2 (cm.).	Press. C_2H_5CHO (cm.).	τ_5 (min.).	ϕ.	log A.
Blank	—	—	30·5	0·120	− 3·0
P1	32·0	0·90	8·0	0·115	− 0·23
P2	23·0	1·35	5·0	0·195	− 0·28
P3	32·0	1·63	5·5	0·195	− 0·35
P4	16·3	1·63	5·0	0·195	− 0·28
P5	12·0	1·70	4·0	0·301	− 0·50
P6	26·4	1·70	5·0	0·195	− 0·28
P7	9·0	2·60	4·0	0·301	− 0·50

Addition of hydrogen peroxide to the 1/1 butane-oxygen mixture at 244° C. and 70 cm. initial pressure had no appreciable effect in small quantity (8 mm.); a larger amount (15 mm.) caused a slow pressure rise amounting to about 5 mm. at the end of the normal induction period; thereafter the pressure-time curve was unaffected except that the final pressure was 8 mm. higher than usual. Analyses showed a higher peroxide content than usual, but the other products were not appreciably changed. Assuming that the additional 8 mm. was due to the dissociation of the peroxide, the amount decomposed was equivalent to 6 mm. of the original peroxide pressure and 9 mm. being the excess peroxide found on analysis, the total 15 mm. was accounted for, so that the hydrogen peroxide does not appear to have played a part in the reaction.

Conclusion.

Investigations carried out on the oxidation of propane (Harris,[6] Newitt and Thornes [7]) show that very little reaction occurred before pressure change commenced and that after the induction period, the pressure-time curve was proportional to the propane consumed. The present studies show that butane behaves rather differently; not only is there a measurable quantity of butane consumed before the pressure-rise commences, but the shape of the pressure-time curve is not simply related to the oxygen or butane consumed. The analytical evidence is supported by the evidence from the absorption spectra given in Part II, a noticeable "cut-off" band being obtained before any pressure-rise occurs.

The analyses showed that butane and oxygen were consumed in equivalent amounts during the induction period and as no change of pressure occurred, the reactions must provide two molecules of product. The spectroscopic evidence suggested that an alkyl hydrogen peroxide and an oxyalkyl peroxide were both present, the latter being formed from the alkyl hydrogen peroxide and the aldehydes also produced at this stage. Even if these peroxides are only formed momentarily in the vapour state and then either decompose, or polymerise, or reform on cooling (for they are found in the liquid products), the radicals giving rise to them must be present in the gas-phase.

There seems to be an underlying similarity of behaviour in all gaseous oxidation processes. The hydrogen-oxygen reaction is the reaction about which most is known and assuming that the underlying process is akin to that reaction, then it follows that where RH is a hydrocarbon, $RH \rightarrow R' + H$; $R' + O_2 \rightarrow RO'_2 \rightarrow RO'_2 + RH \rightarrow R' + ROOH$. This peroxide ROOH immediately breaks down into aldehydes, alcohol, formaldehyde, CO, H_2O, etc. It may not even be formed; if it is found to be present, it is indicative of the general character of these initial reactions, but does not necessarily affect their course. Aldehydes probably react according to a similar mechanism through the radical RCO′, producing the peroxides RCO . OOH, which also may not be actually formed as a stable product. Radicals such as C_2H_5O, formed by decomposition of organic nitrates and the like, which like aldehydes shorten the induction period, probably oxidise similarly to aldehydes.

On this basis, a mechanism of reaction could be built up to fit the observations which have been here recorded. The peroxides found are indicative of the mechanism but are not controlling the reaction; aldehydes play an essential role, particularly in initiating the reaction and controlling the rate. The course of the oxidation of the aldehydes at the walls is probably not the same as in the body of the gas and if the aldehydes formed are prevented from reaching the walls, the reaction proceeds at a different rate.

It is not intended to draw conclusions or to discuss more fully the observations made in this communication until the experimental results have been extended using improved analytical methods.

Summary.

Mixtures of butane and oxygen varying from 2/1 to 2/3 were oxidised at 325° C. to 355° C. under flow conditions in a quartz tube, and the products analysed. The total condensate and the proportion of aldehyde, alcohols and acids did not vary much. The amount of peroxides varied considerably; the proportion of CO increased with the oxygen and unsaturated products increased with temperature. Similar experiments were made at lower temperatures on

---

[6] Egerton and Harris, *Chem. Rev.*, 1937, **21**, 287.
[7] Newitt and Thornes, *J. Chem. Soc.*, 1937, 1656.

butyraldehyde and on propionaldehyde, and on a mixture of 20 % propionaldehyde and 1/1 butane-oxygen which caused the butane oxidation to proceed at a temperature about 70° lower.

Experiments in quartz and in glass vessels were done under static conditions on the 1/1 butane-oxygen mixture by measurement of the pressure-rise under different conditions of temperature and pressure. The results were not susceptible of interpretation in terms of a simple chain mechanism.

The influence of carbon dioxide, hydrogen, argon and helium on the pressure-rise was determined. The diluent gases increased the rate of rise of pressure, argon more than carbon dioxide; hydrogen, and particularly helium, were still more effective.

Analyses of the products at various stages of the reaction were made for a 1/1 butane-oxygen mixture at 242°. During the induction period and the first part of the pressure-rise, the rate of butane and oxygen consumption is equal and peroxides and aldehydes, etc., are formed; when the pressure rises by 20 or 30 mm., the peroxides and aldehydes commence to be consumed, and oxygen to be used up faster, CO being formed in corresponding amounts.

The effect of addition of CO_2 is to increase the percentage of butane consumed and the aldehydes produced. The main effect of the addition of aldehydes was to shorten the induction period. Addition of hydrogen peroxide did not greatly affect the reaction. Provisional conclusions are discussed.

Department of Chemical Technology,
Imperial College,
S.W.7.

NOTE ON THE DECOMPOSITION OF HYDROGEN PEROXIDE AND ITS FORMATION DURING THE SLOW COMBUSTION OF HYDROCARBONS.

BY E. J. HARRIS.

(*Communicated by* SIR ALFRED EGERTON.)

Received 9*th October*, 1947.

The study of the products of the slow oxidation of hydrocarbons has shown that under favourable conditions peroxides can be obtained which have the properties of compounds of aldehydes with hydrogen peroxide.[1, 2, 3] The possibility of isolation of such peroxides depends to the greatest extent on the nature and condition of the surface: silica and Pyrex favour their isolation, whereas alkali-washed surfaces and soda-glass reduce the quantity found to very small amounts.[4, 5]

The properties of some alkyl peroxides have been investigated[6] and it has been shown that the alkyl hydrogen peroxides decompose heterogeneously. It has been of interest therefore to compare the behaviour of hydrogen peroxide under comparable conditions. If hydrogen peroxide can exist in quantity at temperatures of 300-350° C., its direct formation during slow combustion is possible, and in order to explain its presence in the reaction products, it is unnecessary to postulate the conversion of radicals, such as HO_2, to H_2O_2 at a cool part of the reaction tube. Hinshelwood[7] has shown that the decomposition of hydrogen

---

[1] Lenher, *J. Amer. Chem. Soc.*, 1931, **53**, 3737.
[2] Ubbelohde, *Proc. Roy. Soc. A*, 1935, **152**, 354.
[3] Egerton and Harris, *Chem. Rev.*, 1937, **21**, 287.
[4] Harris and Egerton, *Proc. Roy. Soc. A*, 1938, **168**, 1.
[5] Pease and Munro, *J. Amer. Chem. Soc.*, 1934, **56**, 2034.
[6] Harris, *Proc. Roy. Soc. A*, 1939, **173**, 126.
[7] Hinshelwood and Prichard, *J. Chem. Soc.*, 1923, 2725.

peroxide is heterogeneous at lower temperatures. In an empty vessel the half-life was about 160 sec. at 76° c, while in a vessel containing glass wool the decomposition was so rapid that no peroxide survived after only an " exceedingly short heating ".

Experimental.

A flow system similar to that used for hydrocarbon oxidation was employed, consisting of two traps, one at each end of a quartz reaction tube which was 0·35 cm. diam. and 3 cm. in length. A quantity of peroxide of known strength (about 65 % H_2O_2) was weighed from a small pipette into the inlet trap and the outlet trap was cooled in solid CO_2 to − 60° c. The peroxide was vaporised in a stream of nitrogen, the inlet trap being kept at 52° c. to provide a suitable vapour pressure. The gas flow was kept steady at 1-2 cc./sec. When 4-5 l. of gas had been used, the experiment was stopped and the residual peroxide in the vaporiser was washed out and titrated, and the condensate at the outlet was similarly analysed. The efficacy of the collecting trap was checked by passing the exit gas through a bubbler containing acid permanganate.

The amount of peroxide distilled during the experiment was deduced by subtracting the amount remaining unvaporised in the inlet trap from the original amount used, and since the amount which survived distillation is known, the quantity decomposed is found.

It was necessary to check the amount of peroxide which decomposed in the vaporiser itself during the run. This was done by parallel experiments in which a quantity of peroxide was stored at 52° c. in a tube fitted with a reflux condenser. The amount of peroxide used was then corrected for the decomposition which had been found to take place in the liquid-phase ; this was not more than 5 % of the total amount which was vaporised.

Results and Discussion.

The fraction of the peroxide distilled which survived exposure to high temperature in the reaction tube was very variable and it is not useful to set out the full results. They may be summarised as follows. At 251°, with a contact time of 0·5-1 sec. between 15 % and 47 % was decomposed when the tube was " clean ". At 305° with a clean tube, a contact time of 1 sec. led to 15 % decomposition. At 505-525° c. with contact time 0·4-0·5 sec., the figure was 55 % decomposed, which increased to 80-100 % at 550° c.

The rate of gas flow did not affect the fraction decomposed in a regular way, and had only a subordinate influence. The state of the surface of the tube has a considerable influence and varied in an irregular manner during the course of the work. Putting a few crystals of KCl in the tube increased the decomposition from 18 % to 36 %, whereas washing the tube with a solution of the salt increased the decomposition to 80-90 %. This indicates that the chloride is catalytically active, but is nevertheless not strikingly efficient. A trace of mercury put in the tube at the inlet end completely led to destruction of all the peroxide, some mercuric oxide being deposited along the tube. The use of mercury manometers in systems designed for the examination of the products of slow combustion reactions which may contain peroxides appears inadvisable in this respect; the vapour pressure of the mercury may be sufficient to lead to complete decomposition of the peroxides. The increase of the surface brought about by packing the tube also increased the decomposition (to 96 % at 251° c.). This result would be anticipated for a surface reaction.

From these results it is clear that hydrogen peroxide can exist at temperatures up to 525°, and at that temperature has a half-life of about 0·5 sec. in the experimental vessel. At 204°, only a quarter was decomposed in 2 to 1·5 sec. This may be compared with a 5 % decomposition of ethyl hydrogen peroxide at 180° for a contact time of 4 sec. The surface, however, is capable of so much change that in another run the hydrogen peroxide was only 4 % decomposed at 231° after 0·8 sec.

The effect of adding aldehyde vapour carried in nitrogen to the peroxide-nitrogen mixture inside the reaction tube was investigated. In slow combustion reactions, aldehydes are always present and it is therefore important to know whether their presence greatly modifies the rate of decomposition of hydrogen peroxide; propaldehyde was employed in the tests as it had a convenient vapour pressure. The number of moles of aldehyde used was approximately twice the number of moles of hydrogen peroxide distilled during the experiment (2 millimoles). It was found that, under otherwise comparable conditions, the fraction of peroxide decomposed was about 40 %, as against 25 % in absence of aldehyde (temperature 325°, contact time 0·5 sec.). This difference was, however, within the limits of variation of the experiments and it may be due entirely to a change in the nature of the surface. Analyses were carried out on the material collected from the aldehyde + peroxide runs. The amount of acid formed did not exceed 0·1 m.-equiv. The peroxide in the product was determined either by titration with permanganate at 0° c., or by the titration of the iodine liberated from acid KI in the presence of a trace of ammonium molybdate. The aldehyde in the condensate was determined by hydroxylamine hydrochloride as it was found that the presence of peroxide did not interfere. It appears, therefore, that the combination between hydrogen peroxide and propaldehyde is very loose in solution.

The small quantity of acid in the condensate indicates that under the conditions of these experiments in which rather narrow tubes were used, the second of the reactions, $R.CHO \xrightarrow{H_2O_2} R.CHOH.OOH \longrightarrow R.COOH + H_2O$, does not take place in the gas-phase. With formaldehyde, hydrogen peroxide in solution forms the fairly stable dioxymethyl peroxide: this compound is known to decompose at temperatures as low as 65° in the solid state to form hydrogen and formic acid.[8] If its formation and subsequent decomposition by the same course had proceeded in the gas-phase in the propane oxidation,[4] the hydrogen content of the gas should have been 2-3 times as great as they found; however, it is possible that the decomposition in the gas-phase does not lead to hydrogen, so an examination of its decomposition in the vapour-phase is required.

Such hydrogen peroxide as is found in slow combustion experiments (combined with aldehyde or not) may only be a fraction of that which has been formed during the reaction. If the surface is not alkaline and mercury is absent, it may represent some 70 % of the true figure; on the other hand, if traces of catalytically-active substance are present, the apparent yield is reduced to zero in just the same way as all the hydrogen peroxide is destroyed by similar treatment of the tube in these experiments. As the quantity of the other products formed in slow combustion of propane were not affected by salt-washing,[4] the main reaction does not appear to be influenced by the possibility of survival of hydrogen peroxide, i.e. the hydrogen peroxide represents the termination of a series of reactions, so its own fate does not determine that of any other molecule.

Summary.

Hydrogen peroxide can exist for an appreciable time (*ca.* 0·5 sec.) in the vapour state at 500° c. in a quartz tube. Its formation and temporary accumulation during slow combustion of hydrocarbons can therefore occur, but its own fate does not alter the nature of the other end-products.

Admixture of proprionic aldehyde did not greatly increase the decomposition of hydrogen peroxide at 325° c. Coating the surface of the tube with KCl increased the decomposition and the presence of mercury, or use of a packed tube, led to complete decomposition.

Department of Chemical Technology,
Imperial College,
S.W. 7.

---

[8] Wieland and Wingler, *Annalen*, 1923, **431**, 301.

CHARACTERISTIC INFRA-RED FREQUENCIES AND CHEMICAL PROPERTIES OF MOLECULES.

By M. St. C. Flett.

Received 27th October, 1947.

It is well known that certain atomic groupings give rise to infra-red bands at characteristic frequencies even when they occur in complicated molecules. These frequencies correspond to modes of vibration of the molecule, which are primarily controlled by the motions of atoms within the group in question. It has been shown mathematically that such characteristic frequencies are to be expected when the force constant of some bond is much greater than the other force constants of the molecule. The C═C, C═O and C═N— bonds provide examples of this. The presence of atoms, such as hydrogen, of mass quite different from that of other atoms present, causes bonds such as C—H, N—H, O—H to have characteristic frequencies. Small variations are observed in the value of any characteristic frequency in a series of molecules, and it was decided to examine these variations in some detail. The variations are attributable partly to the fact that all frequencies are properties of the molecule as a whole, and partly to variations of force constants within the atomic group in question. In many cases the latter effect seems to predominate.

In general, force constants can be calculated from vibration frequencies only by a normal co-ordinate treatment, which is practicable only for molecules with few atoms or high symmetry. Accordingly calculation of force constants has not been attempted in most of the work described below. It has however been shown[1] that in the case of X—H bonds, force constants can be calculated fairly successfully from characteristic frequencies. Results described below also indicate that in a series of related molecules, changes in characteristic frequency run parallel to force constant changes.

One of the factors in determining reaction velocities is the ease with which the bonds of the reacting groups can be stretched so as to form the transition-state complex. Hinshelwood, Laidler and Timm[2] consider the formation of the activated complex in a reaction of the type

$$A + B—C \longrightarrow A \ldots B \ldots C$$

to involve two processes, the approach of A against the repulsion of B—C, and the stretching of B—C. The activation energy is regarded as made up of repulsion energy and bond-stretching energy, either of which may in suitable circumstances be the more important factor. Accordingly, it was thought that the characteristic frequencies, being determined, in part at least, by the force constants of the bond in question, might in some cases parallel reaction rates.

It therefore appeared that two types of information might be obtained by studying the characteristic frequencies of a group in a series of related molecules in which the reactivity of the group in question in each member had been determined by reaction-rate measurements. Firstly, empirical relationships might be obtained between reaction rates and frequencies, which would be of value in predicting unknown rates, since, owing to recent advances in the technique of infra-red spectroscopy, measurement of spectra is easier than rate measurements, particularly with very slow or very fast reactions. The problem of correlating structure and reactivity of organic compounds is complicated by the presence of both kinetic and potential energy terms in the rate equation.[3] It may however be shown that for a series of reactions of similar molecules, where the entropies of activation of the reactions are approximately equal, the differences in the kinetic energy terms are small. It is in such cases that correlations between characteristic frequencies and reaction rates might be expected. Hammett[3] summarises evidence showing that in certain series of reactions, particularly side-chain reactions of *m*- and *p*-disubstituted benzenes, the observed rates provide a good measure of the electronic shifts occurring in the molecule. This leads to the second possible application. If relations could be established between frequencies and rates in such cases, it would become possible, in suitable cases to use infra-red frequencies to gain information about electronic distribution in molecules where rate data are not obtainable. Small variations in characteristic frequencies will clearly be useful in structural investigations if they can be definitely connected with the electronic nature and strength of the bond in question.

---

[1] Linnett, *Trans. Faraday Soc.*, 1945, **41**, 223.

[2] Hinshelwood, Laidler and Timm, *J. Chem. Soc.*, 1938, 851.

To test the above suggestions correlations have been sought: (*a*) between the C═O, —OH and C—O frequencies in various *m*- and *p*-substituted benzoic acids and their rates of esterification; (*b*) between the N—H frequencies in substituted anilines, the C═O frequencies in acid chlorides, and rates of benzoylation; (*c*) between C═O frequencies of aldehydes and ketones and rates of semi-carbazone formation, and (*d*) between the —C≡N frequency in substituted benzonitriles and rates of H_2S addition.

Experimental.

(*a*) MATERIALS.—The acids, anilines, aldehydes and ketones were mostly commercial materials, purified by distillation or recrystallisation till their boiling points or melting points showed them to be sufficiently pure. The acid chlorides were prepared from pure acids and thionyl chloride: *p*-chloro and *p*-nitro benzonitrile were prepared by the Sandmeyer reaction, and *p*-aminobenzonitrile by reduction of the nitro nitrile. The solvents used were of Analar quality.

(*b*) SPECTRAL MEASUREMENTS.—Most measurements were made with a Hilger D209 Infra-red Spectrometer, using a rock-salt prism. The resolution was adequate, except for the measurement of the monomer —OH frequency in the acids. Single-beam photographic recording was used. All the frequencies reported were measured with reference to some band or bands of accurately known wavelength which appeared on the same record. To provide this calibration and ensure that the cell was clean a spectrum of the solvent was always measured in the same cell immediately before the sample. There are, for example, water vapour bands which serve to locate C═O frequencies. The $—NH_2$ frequencies were determined by interpolation between one of the peaks in the 2·7μ water band, and a band in the spectrum of liquid carbon tetrachloride at about 3070 cm.$^{-1}$, the frequencies of which were in turn obtained by interpolation between the bands of liquid benzene which were accurately measured by Ingold *et al.*[10] —C≡N frequencies were obtained by interpolation between bands in the spectrum of chloroform at 2425 and 1963 cm.$^{-1}$ whose frequencies were in turn obtained by interpolation from the well-known peaks of the 6μ water-vapour band and the carbon dioxide band at 2363 cm.$^{-1}$. In this region it was found necessary to use the rock-salt prism in conjunction with the cam designed for the quartz prism so as to obtain adequate dispersion of the records. Where necessary the interpolation was made more precise by using a travelling microscope. Dr. H. W. Thompson of Oxford University very kindly had the —OH frequencies of the monomeric acids in carbon tetrachloride measured on his double-beam recorder, with a fluorite prism.

Results and Discussion.

(*a*) SUBSTITUTED BENZOIC ACIDS.—Since the rates of esterification were measured in methanol[4] the C=O frequencies were first measured in this solvent. The acids are believed to be monomeric in methanol. The C=O frequencies lie between 1695 and 1720 cm.$^{-1}$ in methanol, as compared with 1735-1750 cm.$^{-1}$ for the acid monomers in carbon tetrachloride. This is a larger shift than we have observed for most aldehydes and ketones in passing from carbon tetrachloride to methanol. With benzaldehyde, acetone and acetophenone e.g. the shift is only about 10 cm.$^{-1}$. It presumably indicates strong hydrogen-bonding to the solvent molecules. Unfortunately the C=O bands in methanol were so broad that in most cases it was possible to determine their frequency only with an accuracy of ± 5 cm.$^{-1}$. Accordingly the measurements were repeated in carbon tetrachloride, where two bands are observed in the carbonyl region. Of these, one has been attributed by Davies and Sutherland [5] to monomers and the other to dimers. 0·05 mm. layers of 2 % methanol solutions and 0·5 cm. layers of 0·05 % carbon tetrachloride solutions were used. Table I summarises measurements on the acids. The velocity constants are those determined in ref. 4. The carbonyl frequencies were also plotted against Hammett's σ factor.[3] By examining the effect of various substituents on a series of side-chain reactions of benzene derivatives such as esterifications of acids, hydrolyses, and benzoylations of amines, Hammett found it possible to assign to each substituent a σ value which is defined by the equation :

---

[3] Hammett, *Physical Organic Chemistry*, p. 186.

[4] Hartmann and Borders, *J. Amer. Chem. Soc.*, 1937, **59**, 2107.

$$\log_{10} k = \log_{10} k_0 + \sigma\rho$$

where k is the rate constant of the substituted compound and k that for the unsubstituted compound, and ρ a constant of the reaction. The σ factor therefore gives an overall measure of the effect of the substituent on a series of reactions. For example, a large σ indicates that the substituent in question markedly slows reactions, whereas a substituent with negative σ has the reverse effect.

TABLE I.—DATA ON SUBSTITUTED BENZOIC ACIDS.

Substituent.	Monomer C=O Frequency in Methanol (cm.$^{-1}$).	Monomer C=O Frequency in CCl$_4$ (cm.$^{-1}$).	Dimer C=O Frequency in CCl$_4$ (cm.$^{-1}$).	OH Frequency in CCl$_4$ (cm.$^{-1}$).	Velocity Constant × 10^5.	σ.
p—NO$_2$	1720±3	—	—	3541	—	0·778
m—NO$_2$	1723±3	1750±1	1705±1	3548	7·25	0·710
m—Cl	1715±5	1746±2	1701±1	—	12·4	0·373
p—Cl	1713±5	1746±2	1699±1	3551	11·4	0·227
p—Br	1710±5	—	—	—	12·3	0·232
—H	1705±5	1743±2	1696±1	3551	19·2	0·0
p—CH$_3$	1700±2	1739±2	1693±1	3556	19·7	−0·170
p—OCH$_3$	1695±2	1737±2	1691±1	3560	—	−0·268
p—NH$_2$	1690±2	—	—	—	—	−0·660

It will be observed that there is a parallel trend in the rates, and the carbonyl frequencies and the hydroxyl frequencies. In Fig. 1 and 2 the dimer C=O frequencies (which were the most accurately measurable) are plotted respectively against the rates of esterification and σ. Electron-attracting substituents, such as the nitro group, increase the carbonyl frequency, presumably strengthening the bond. It may be supposed that this results from pulling of the oxygen atom and the surrounding electrons closer to the carbon atom. The OH frequency on the contrary is lowered, and the bond probably weakened by electron-attracting substituents. All the acids showed, in carbon tetrachloride solution, a band at about 1450 cm.$^{-1}$ which is probably connected with carbon-oxygen single bond. Shifts in its frequency were too small to be measured with certainty but seemed to be in the same direction as the OH frequencies. Thus the overall effect of an electron-attracting group is probably to strengthen the carbon-oxygen double bond and weaken the O—H and carbon-oxygen single bonds. The reason why this should slow the esterification is not clear, since the rate-determining step in this reaction is not known for certain.

---

[5] Davies and Sutherland, *J. Chem. Physics*, 1938, **6**, 755.

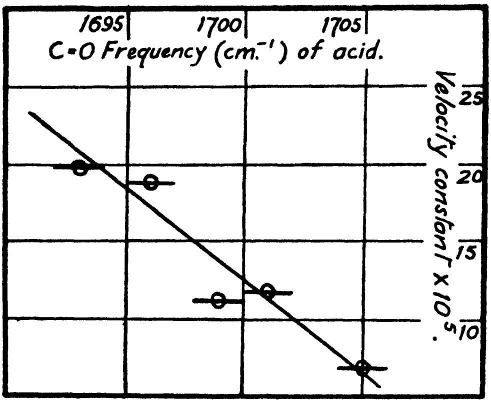

Fig. 1.

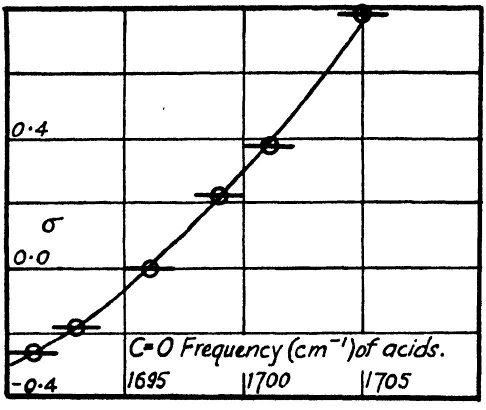

Fig. 2.

(*b*) Anilines and Acid Chlorides.—The rates of benzoylation of substituted anilines by substituted benzoyl chlorides have been carefully determined.[6] The NH frequencies of a number of substituted anilines were measured, using 0·05 % solution in carbon tetrachloride, in a 3·3 cm. cell. In each case 2 N—H bands were observed, corresponding to the

symmetrical 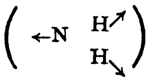 $\left(\leftarrow\mathrm{N}\begin{matrix}\mathrm{H}\nearrow\\ \mathrm{H}\searrow\end{matrix}\right)$

and antisymmetrical 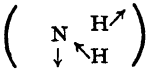 $\left(\begin{matrix}\mathrm{N}\\ \downarrow\end{matrix}\begin{matrix}\mathrm{H}\nearrow\\ \nwarrow\mathrm{H}\end{matrix}\right)$ stretching modes.

The frequencies are shown in Table II, together with approximate N—H force constants and inter-bond angles (2θ), calculated by Linnett's method, assuming that only the nitrogen and hydrogen atoms move during the vibration.

---

[6] Williams and Hinshelwood, *J. Chem. Soc.*, 1934, 1079.

TABLE II.—DATA ON SUBSTITUTED ANILINES.

Substituent.	Sym. (cm.$^{-1}$).	Anti. (cm.$^{-1}$).	NH Force Constant × 10^5.	θ.	Rate of Benzoylation.	σ.
p—NO_2	3436	3535	6·729	57° 29′	0·0042	1·27
m—NO_2	3420	3510	6·650	56° 22′	0·0444	0·710
p—CN	3427	3518	6·679	56° 28′	—	1·00
p—Cl	3415	3501	6·623	55° 52′	1·63	0·227
—H	3410	3489	6·591	54° 58′	7·55	0·0
p—CH_3	3405	3487	6·577	55° 22′	29·8	—0·170
p—OCH_3	3400	3473	6·541	54° 12′	—	—0·268
p—$N(CH_3)_2$	3398	3464	6·520	53° 18′	—	—0·205

The frequencies are probably accurate to about ± 2 cm.$^{-1}$.

The values of the angles should be regarded with caution in view of the general failure of spectroscopic methods to give angles very accurately. In Fig. 3 the force constants are plotted against σ. With the exception of the p—NMe_2 point, the points lie fairly close to a straight line. This exception is probably due in part to error in the σ value, which is based on comparatively little experimental data. It is clear that as the substituent becomes more electron-attracting, the NH bonds are strengthened, probably as a result of pulling the hydrogen atoms closer to the nitrogen atoms with development of positive charge on it, and the angle between them increases. The force-constant changes (like σ) measure the sum of the inductive and electromeric effects. Thus p-nitro produces a larger effect than m-nitro, presumably because in the p-case the inductive effect

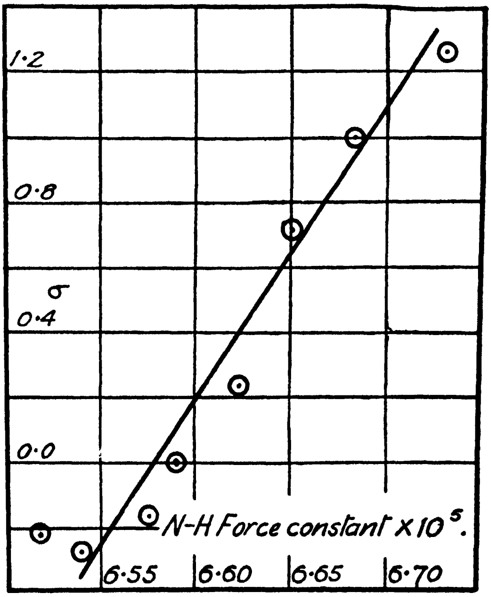

FIG. 3.

is augmented by the electromeric effect involving resonance with the form:

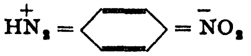

A complicating factor was encountered in investigating the acid chlorides. All those studied showed in dilute carbon tetrachloride solution two bands in the C=O frequency region as shown in Table III, together with rate of benzoylation of aniline and σ.

TABLE III.—DATA ON SUBSTITUTED BENZOYL CHLORIDE.

Substituent.	Band 1 (cm.$^{-1}$).	Strength.	Band 2 (cm.$^{-1}$).	Strength.	Rate of Benzoylation.	σ.
p—NO_2	1785±2	weak	1767±1	strong	38·1	0·778
m—NO_2	1784±2	weak	1764±1	strong	—	0·710
p—Cl	1779±1	medium	1746±2	medium	10·4	0·227
—H	1778±1	strong	1744±2	weak	7·55	0·00
p—CH_3	1777±1	strong	1748±2	weak	3·91	−0·170
p—OCH_3	1775±1	strong	1747±2	medium	—	−0·268

The cause of the double band is not understood. It was thought that it might be caused by dimerisation by dipole interaction, but measurements on the effect of dilution on the relative intensities of the two bands in p-nitro benzoyl chloride did not support this view. Fermi degeneracy is another possible cause. The trend in band 1 (but not in band 2) parallels the rate data. No definite conclusions can be drawn in this case but electron-attracting substituents again appear to shift the bands toward higher frequencies.

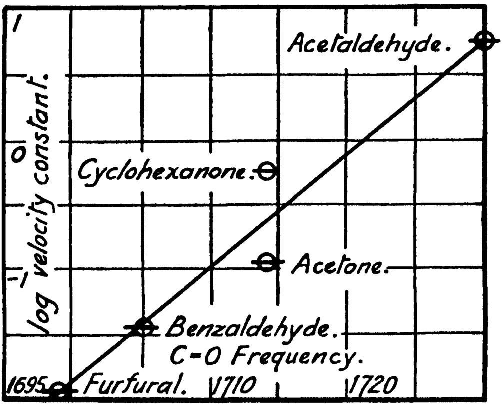

FIG. 4.

The driving force in this reaction is probably the tendency for the lone pair on the nitrogen atom to attach itself to the carbon atom of the —COCl group. An electron-attracting group draws electrons from the nitrogen atom in the anilines, making its lone pair less readily available and slowing the reaction. Similarly it draws electrons from the —COCl group in the acid chlorides, stiffening the C=O bond, and facilitating the reaction by increasing the positive charge in the vicinty of the carbon atom.

(c) C=O FREQUENCY IN ALDEHYDES AND KETONES AND RATES OF SEMICARBAZONE FORMATION.—The kinetic measurements were made in aqueous alcohol.[7] The C═O frequencies could not, of course, be measured in this solvent owing to its intense absorption, but it was thought that measurements in carbon tetrachloride might be of interest, in view of the parallelism between carbonyl frequencies in methanol and carbon tetrachloride in the case of acids. Results are given in Fig. 4. Furfural also showed a shoulder at about 1685 cm.$^{-1}$. The trends of velocity constant and frequency are again parallel, although in this case the structures differ widely. In this case strengthening of the C=O bond increases the rate of reaction. Kinetic measurements have shown [3] that the rate-determining step in this reaction is, in the case of a ketone $R_2C{=}O$,

$$[R_2C(OH)—NH_2—NH—CONH_2]^+ + A^- \rightarrow R_2C(OH)—NH.NHCONH_2 + HA.$$

It may be supposed that electron-attracting R groups which stiffen the C═O bond also tend to remove electrons from the nitrogen atom, facilitating release of the proton.

(*d*) ADDITION OF H_2S TO NITRILES.—Kindler [8] has studied the addition of H_2S to aromatic nitriles.

$$X.C_6H_4.CN + H_2S \rightarrow X.C_6H_4.CS.NH_2$$

in alkaline alcohol solution. The —CN frequencies in a series of such nitriles were measured, 2 % solutions in chloroform being used since this solvent readily dissolves all the nitriles used, and is spectroscopically suitable. The results are displayed in Fig. 5. As in other cases electron-attracting groups increase the frequency presumably strengthening the bond. This stiffening probably results from a drawing of the nitrogen atoms and the surrounding electrons closer to the carbon atoms.

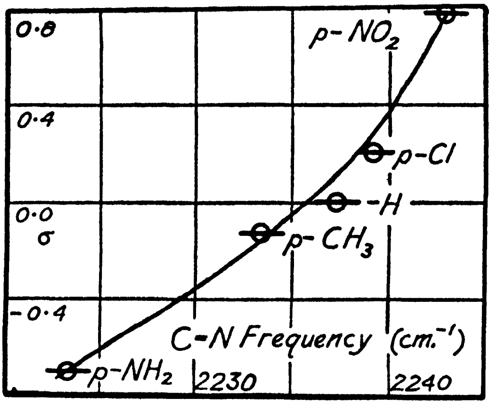

FIG. 5.

As seen from the figures, there is in each of the cases studied a reasonably close relationship between frequency shifts, reaction rates, and the σ factor in the case of benzene derivatives. No attempts will be made to account for the precise shape of the curves obtained. The calculation of rates is so difficult even for the simplest reactions that it is doubtful whether any very detailed interpretation of the results is possible. It seems clear that empirical curves can be used in suitable cases to predict approximate reaction rates from characteristic frequencies. Such methods could for example, be applied in the reactions of benzene derivatives to poly-substituted derivatives for which σ values are not known. It is likely that the effect of substituents on reactions of naphthalene, anthracene, etc., and heterocyclic systems could be predicted similarly by measuring frequency shifts in a suitable series of derivatives. Studies of the above kind might also throw light on reaction mechanisms in suitable cases. This would, however, usually be difficult since in general rate-determining steps do not involve directly species on which measurements can be made.

---

[7] (*a*) Conant and Bartlett, *J. Amer. Chem. Soc.*, 1932, **54**, 2881; (*b*) Westheimer, *ibid.*, 1934, **56**, 1962.

[8] Kindler, *Annalen*, 1926, **450**, 1.

Since the σ factor provides a measure of electronic shifts occurring in aromatic molecules, the observed correlations with σ indicates that in suitable cases frequency shifts can be used as a means of detecting electronic shifts in molecules. It might therefore be possible, for example, in the case of carbonyl bonds, to correlate their infra-red frequencies with ultra-violet absorption maxima and ionisation potentials.[9] It seems that, provided due caution is exercised in not considering cases where the variations in structure are very large, the characteristic frequency of a bond can be used with some confidence in predicting variations in its properties. This might, for example, be useful in ring systems other than benzene, where the directions and magnitude of the shifts produced are less well understood.

I am grateful to Dr. H. W. Thompson, Oxford University, and to various colleagues for helpful discussions.

Summary.

It is known that many atomic groupings give rise to characteristic frequencies in the infra-red spectral region, even when they occur in complex molecules. The variation of the $C=O$, NH_2 and $C\equiv N$ frequencies within series of structurally similar compounds has been investigated, and the shifts interpreted in terms of the reactivities and electronic natures of the bonds involved. A sufficient degree of correlation is observed between frequency shifts and reactivities to suggest the application of similar methods for the prediction of electronic structures and reaction rates in suitable cases from infra-red measurements.

Research Laboratories,
Imperial Chemical Industries Ltd.,
Hexagon House,
Blackley,
Manchester 9.

[9] Walsh, *Trans. Faraday Soc.*, 1945, **41**, 498.
[10] Ingold *et al.*, *J. Chem. Soc.*, 1936, 934.

THE MERCURY MENISCUS IN PRECISION MEASUREMENTS ON GASES.

BY R. WHYTLAW-GRAY AND N. TEICH.

Received 10*th November*, 1947.

In the measurements of the compressibilities of gases at pressures below 1 atmosphere, and indeed in many other gasometric operations in which mercury is used, the form of the mercury meniscus should be taken into account if results of high accuracy are to be attained.

In manometry a varying capillary depression may introduce appreciable errors which only become negligible in wide tubes. In volumetric measurements where mercury is used in a dead space to define a constant gas-volume, errors may be caused by a variation in the volume of the meniscus itself and to reduce these, narrow tubing is desirable. Hence in compressibility measurements, and also in the determination of the coefficients of expansion of gases, a compromise has to be made between the accurate measurement of pressure and of dead-space volume and the apparatus constructed of tubing of such a diameter that both errors are minimised.

Probably many of the published values of the compressibilities of gases at low pressure are affected by this error, for few of the workers in this field record meniscus heights and they usually assume that capillary errors are avoided when pressure readings are made with a rising meniscus, and that this procedure also ensures constancy of volume in the dead space in successive settings of the mercury to the fixed point. As far back as 1905, Rayleigh [1] in discussing the results obtained in his work on *The Compressibilities of Gases between One Atmosphere and Half an Atmosphere of Pressure*, attributed the unexpected deviations he found to " a variable contact between mercury and glass in the lower chamber of the first manometer " and later Porter [2] worked out the variation to be expected from this cause and showed that it would explain the discordance.

Guye [3] and his co-workers, it is true, took account of the varying shape of the meniscus in estimating the dead space volume but they did not give details of what corrections they applied.

Heuse and Otto [4] in more recent work, which is admirable in many respects, adjust the meniscus in the dead space by tapping, to a height of about 1·6 mm. and make a correction which they say is small for any departure from this height. The correction never exceeded 5 c. mm. They do not state the diameter of the tubing used for the dead space but if it was round about 14 mm. it is difficult to understand how the correction could be so small.

Cragoe [5] in a recent review of the precision attained by various workers on high and low pressure compressibilities emphasised the relatively wide scatter of the points on low pressure *PV-P* isothermals when compared with high pressure results, and comes to the conclusion that these divergences are most likely due to differences in meniscus heights. It is clear that in the past insufficient attention has been paid to meniscus errors when determining the low pressure isothermals of gases.

Many workers in this field have used manometric tubes of about 14 mm. diam. In such tubes the height of the mercury meniscus can vary from 1 to 1·8 mm. From Palacios's [6] figures the volumes corresponding to these meniscus heights are 101 and 193 c. mm., a change in dead space volume of 92 c. mm. For the same difference in height the capillary depression would alter by 0·1 mm.

This, of course, is an extreme case, for with careful setting it is always possible to ensure a much closer equality in height between the meniscus in the dead space and that *in vacuo* in the upper chamber of the manometer. If the setting can be made so that the meniscus height difference does not exceed 0·1 mm., the uncertainty in the dead-space volume can be reduced to 11 c. mm. and the capillary depression variation to 0·011 mm. Actually it is difficult in practice to be sure of such a close equality and a better plan is to measure the heights of the two meniscuses each time the pressure is read after a point setting has been made. The appropriate correction can then be obtained from published tables of capillary depression and meniscus volume. The actual error involved in making a point setting is very small. A point can be set to a mercury surface to within ± 0·001 mm. so that errors in dead space volume on account of inaccuracies in setting are insignificant compared with errors caused by volume changes in the meniscus itself.

---

[1] Rayleigh, *Collected Papers* (V), 1905, p. 230.

[2] Porter. *Phil. Mag.*, 1934, **17**, 517.

[3] Guye, Jacquerod and Scheuer, *Mém. Soc. Phys. Hist. Nat. Genève*, 1908, **35**, 81.

[4] Heuse and Otto, *Ann. Physik.*, 1930, **6**, 778; **8**, 1012.

[5] Cragoe, *J. Res. Nat. Bur. Stand.*, 1941, **26**, 495.

[6] Palacios, *Physik. Z.*, 1923, **24**, 151.

If then a dead space and manometer are constructed from 14 mm. diam. tubing and a practice is made of measuring meniscus heights, the error due to capillary depression need not exceed 0·01 mm. in the pressure whilst that due to the meniscus volume may be as large as 11 c. mm.

A precision of ± 0·01 mm. in the pressure reading is about the limit of accuracy that can be reached with a good cathetometer and scale, and at low pressures, say of 100 mm., would allow an overall accuracy of 1 part in 10,000 to be approached; for greater accuracy than this a multiple-point gauge of the Rayleigh type would have to be employed which would entail wider diameter tubing in order to avoid capillary errors. To reach the same accuracy in the volume measurement at a pressure of 1 atmosphere, where this error is the greatest, the total volume of dead space and volumeter must not be less than 100 cc. An initial volume much larger than this would involve cumbrous apparatus at low pressure and be difficult to deal with experimentally. From these considerations, it is evident that apart from other errors inherent in work of this type, those due to the behaviour of the mercury meniscus set a limit to the precision attainable when low pressure compressibility determinations are carried out in apparatus of the usual design.

This estimate of the errors in volume and pressure presupposes (*a*) that the meniscus heights can be determined to within 0·1 mm. and (*b*) that these heights can be correlated accurately with meniscus volume and capillary depression.

(*a*) In practice, it is difficult to be sure that the meniscus height measured in one direction with the cathetometer telescope is the true mean height; for even although the procedure of always reading with a rising meniscus is followed, irregularities in the line of contact between mercury and the walls of the tube are often noticeable. Further it has frequently been observed that in a cylindrical tube the line of contact may not be truly circular, the mercury rising more readily on one side of the tube than on the other. No doubt with carefully ground and polished surfaces these effects could be minimised, but even then the possibility of the presence of inhomogeneous films of gas or moisture would not be excluded. In our opinion, it is a matter of considerable difficulty to determine the mean height of a mercury meniscus with an accuracy much greater than 0·1 mm.

(*b*) Given a specimen of pure mercury of known density and surface tension in a truly cylindrical tube free from internal surface irregularities, the capillary depression and meniscus volume can be calculated from the general theory of capillarity for any meniscus height and tube diameter. Unfortunately, the calculation of the shape of a meniscus in a cylindrical tube is a matter of considerable complexity. Laplace's differential equaton for the equilibrium meridian of a meniscus of axial symmetry has proved impossible of solution in terms of known functions. It can, however, be integrated by numerical methods. This was done some fifty years ago by Bashforth and Adams,[8] but their results when calculated for the case of mercury apply only to tubes varying in diameter from 1·5 to 11·5 mm. For tubes greater in diameter than 22 mm., Rayleigh[9] has worked out an expression which gives a close approximation and is more accurate the wider the tube. The intermediate region is, however, the most important for high precision gas work. This gap has been bridged by Porter[10] who in a series of papers has shown how the three variables,

---

[7] Bakker, *Kapillarität und Oberflächenspannung* (Academische Verlagsgesellschaft. M.B.H. Leipzig 1928).

[8] Bashforth and Adams, *Capillary Action* (Camb. Univ. Press, 1883).

[9] Rayleigh, *Proc. Roy. Soc. A*, **92**, 184; *Collected Papers*, (VI), p. 350.

[10] Porter, *Phil. Mag.* 1934, **17**, 511; *ibid.*, 1932, **14**, 694; *Trans. Faraday Soc.*, 1933, **29**, 702; 1307.

capillary depression, meniscus volume and meniscus height can be determined by means of a relatively simple graphic interpolation. Quite recently, Blaisdell [11] in an elaborate computation has extended the results of numerical integration into the region in use in precise manometry and has published tables in a form easily applicable to practical experiment. His results when calculated for mercury apply to tube diameters varying from 11·5 to 23·6 mm. and hence cover many cases likely to arise in practice. Moreover, as he points out, his figures are of a greater accuracy than any hitherto published in this field. Both Porter's and Blaisdell's tables are in general form and apply to any liquid. To apply them to mercury meniscuses, they have to be transformed by means of the capillary constant for mercury which Porter defines as $\beta^2 = \frac{\sigma}{g(\rho^2 - \rho^1)}$, whilst Blaisdell uses $a^2 = \frac{2\sigma}{g(\rho^2 - \rho^1)}$. Blaisdell's conversion factor is hence $\sqrt{2}$ times that of Porter's. The capillary constant β^2 or a^2 then involves the surface tension σ, the gravitational constant g, and the difference in density $(\rho^2 - \rho^1)$ between mercury and the gas with which it is in contact. Unfortunately, there is a considerable variation in the published values for the surface tension, slight contamination seems to have a very marked effect, organic vapours and adsorbed gaseous films no doubt change the surface tension and hence the meniscus height and volume, so that unless the capillary constant is determined for the particular sample of mecury in use in a given apparatus, correction values calculated from theory may not be of the expected accuracy.

It might be thought that direct experiment would furnish more reliable data than theory on the relationship between meniscus height and meniscus volume, but such investigations have not been numerous. For meniscus volumes, the work of Scheele and Heuse [12] and of Palacios,[6] using different methods, are the most extensive and cover tube diameters ranging from 10 to 23 mm. The two sets of results differ somewhat from each other and exhibit a systematic divergence of about 3 %. As Blaisdell points out the values for wide tubes in the International Critical Tables are compiled from the average values of these two series giving data " which are not smooth to the desired accuracy ". Further, it should be noted that in both investigations the mercury meniscus was formed at the smooth orifice and not in the interior of cylindrical tubes. Moreover, Palacios used a steel cylinder and formed the meniscus at the periphery of steel rings of various sizes, so that both series of measurements were carried out under conditions differing somewhat from those which obtain in manometric practice. The only measurements of meniscus made directly in glass tubes are those published by Keesom, van der Horst and Taconis [15] and more recently by J. Kistemaker, who measured the silhouette of the meniscus by an X-ray shadow-graph method and so were able to compute its average height and volume directly *in situ*. Their results agree fairly well with those of Scheele and Heuse.

Systematic experimental measurements of capillary depression are also not numerous and for the purposes of manometry are restricted to those of Cawood and Patterson [13] and the earlier results of Heuse.[14] Cawood and Patterson in a comprehensive investigation measured the depression in soda-glass tubes ranging in diameter from 10 to 19 mm. A discussion of earlier work is given in their paper. They were the first to point out the importance of refraction errors in measuring meniscus heights and to show how they can be minimised. Their tables furnish results obtained under laboratory conditions which are of great value.

---

[11] Blaisdell, *J. Math. Physic*, 1940, **19**, 186.

[12] Scheele and Heuse, *Ann. Physik.*, 1910, **33**, 291.

[13] Cawood and Patterson, *Trans. Faraday Soc.*, 1933, **29**, 514.

[14] Heuse, *Z. Instr.*, 1927, **47**, 324.

The foregoing review of the data available in the literature for the correction of dead space volume with changing meniscus height shows that apart from theoretical calculations, the values of Keesom and his collaborators are the most directly applicable to practical manometric measurements. It seemed, however, desirable to make some experiments in actual dead spaces. Some years ago,[16] a differential apparatus was designed and constructed for the measurement of the compressibilities of gases in terms of the standard gas (oxygen), and results were obtained with it for hydrogen and silane, but although the individual values exhibited an agreement at least as good as any obtained previously the accuracy hoped for (a few parts in 100,000) was not reached. This was attributed (*a*) to a want of rigidity in the design of the apparatus, and (*b*) to uncertainty in the dead-space volumes on account of meniscus variation. Before this apparatus was set up, the two dead spaces were calibrated in the usual way and the procedure followed of measuring the meniscus height at each point setting. The correlation so obtained between dead space volume and meniscus height was not as close as had been expected, the points on plotting showing a divergence in the extreme of 10 c. mm. for the same meniscus height. Further the range of height was small varying from 1·38 to 1·63 mm. Since the setting-up of a more elaborate apparatus was planned, it was decided to carry out a preliminary investigation with a close attention to detail using fresh dead spaces.

Experimental.

In the attempt to reach a satisfactory correlation between dead space volume and meniscus height, three separate sets of experiments have been made : (1), (2) and (3). In (1), a dead space of Pyrex glass of conventional design, carrying a sealed-in glass point and provided with a capillary glass stopcock was used. This is shown in Fig. 1.

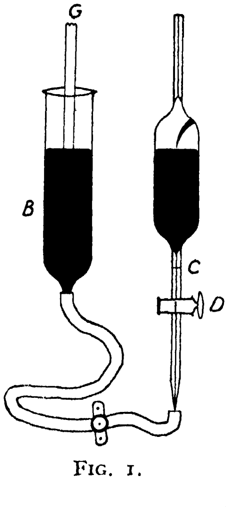

FIG. 1.

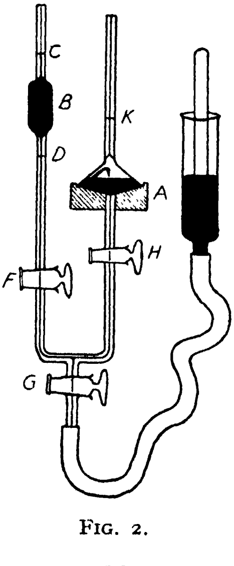

FIG. 2.

The height of the mercury meniscus was measured by means of a short focus telescope and micrometer reading to 0·001 mm. and special care was taken to illuminate the meniscus itself and its line of contact with the glass so as to obtain a true estimate of its height. Care was taken to subject the mercury to a

---

[15] Keesom, van der Horst, and Taconis, *Commun. Kamierlingh Onnes. Lab. Univ. Leiden*, 1937, 248*a*. Kistemaker, *Physica*, 1945, **9**.

[16] Addingley and Whytlaw-Gray, *Trans. Faraday Soc.*, 1928, **24**, 378.

very stringent purification and to clean and dry the interior glass surfaces. Dry air only was allowed to come in contact with the mercury in the experimental tube. The final setting of the mercury to the point in the dead space was made by means of the glass rod G which moved on a fine rackwork and raised the level of the mercury in B by small amounts.

The results are set out in Table I in which *h* is the meniscus height in mm. and *V* is the volume of the mercury in cc. in the tube from the glass point to the mark C.

TABLE I.—DIAMETER OF TUBE = 22·13 MM.

h =	1·25	1·28	1·40	1·43	1·46	1·50
V =	26·2190	26·2041	26·2164	26·2014	26·1896	26·1890
h =	1·52	1·56	1·65	1·68	1·68	1·93
V =	26·1989	26·1910	26·1727	26·1622	26·1878	26·1462

It will be noticed that the range in meniscus heights in these experiments is small. It was not found possible to obtain lower or higher meniscuses which were stable enough to allow of measurement. According to Porter's tables, these heights correspond approximately to contact angles varying from 30° to 55°.

On plotting meniscus heights against the volume of the mercury in the tube, the points are seen to be rather widely scattered, and it is impossible to tell whether the graph is strictly linear or has a slight curvature. Assuming linearity, the most probable straight line was calculated by the method of least squares giving the equation, $V = 26{\cdot}3474 - 0{\cdot}1015h$, where V is the volume of mercury in the tube in cc. for a meniscus height of h mm. and $V_0 = 26{\cdot}3474$, the volume when the meniscus is flat and $h = 0$.

A comparison of the values for the volumes of the tube from the point in the dead space to mark C on the capillary above the tap for different heights calculated in this way, with the actual experimental figures shows at once that the accuracy desired has not been reached and that the probable error of any one point is ± 7 c. mm. The values are little better than those obtained by Addingley and Whytlaw-Gray mentioned above.[16] They emphasise the difficulty of estimating the true volume of the meniscus by measuring its height in a cylindrical tube under the usual working conditions.

Since these deviations are far greater than any experimental error, either in setting the mercury to the point or in weighing the mercury, they can only be due to a variable line of contact between the mercury and the walls of the containing tube. If each time the mercury meniscus is set to the point the contact line is irregular or wavy or differs from a true circle by varying amounts, the meniscuses will be unsymmetrical and the apparent height will depend on the horizontal angle from which they are viewed. Direct measurement of the apparent height of the same meniscus from different angles in the same horizontal plane supports this explanation. In the many measurements of this kind that we have made, we have frequently observed differences in height amounting in some cases to as much as several tenths of a millimeter.

Especially is this noticeable when the mercury surface before measurement has been agitated or the tube tapped, a procedure adopted by some workers, which whilst ensuring that the meniscus assumes a more stable configuration, usually alters its symmetrical form and so renders the meniscus volume deduced from measured height of doubtful accuracy.

(2) In order to test this conclusion more stringently, another dead space was set up, the first one having been broken, and the greatest care was taken (*a*) to obtain symmetrical meniscuses, (*b*) to get reliable values for the mean height by measuring each meniscus in two directions at right angles to each other in the same horizontal plane. This was done by means of two short focus telescopes placed at right angles to each other and in the same horizontal plane as the fixed point.

The dead space tube, unlike the first one which was entirely of glass, consisted of a cylindrical tube, one end of which was sealed on to a capillary as before, but the other end was ground down and cemented into a steel block which carried a carefully sharpened steel point similar to that shown in Fig. 2. The advantage of this was that it allowed a more accurate centering of the point and that it obviated electrification effects which with glass points are liable to disturb the settings. The same rigid precautions were taken as before to ensure clean glass surfaces and pure mercury. The experimental figures are shown in Table II, where h is the arithmetic mean of the meniscus heights measured in two directions at right angles.

TABLE II.—VOLUME OF MERCURY IN TUBE FROM POINT TO MARK.

Tube diameter = 21·36 mm.

h Mean. (mm.)	Volume Exp. (cc.)	Volume Calc. (cc.)	Volume Exp. − Vol. Calc.
1·16	4·3636	4·3674	−0·0038
1·19	4·3663	4·3646	+0·0017
1·19	4·3672	4·3636	+0·0026
1·33	4·3585	4·3513	+0·0075
1·57	4·3330	4·3286	+0·0044
1·66	4·3187	4·3201	−0·0014
1·69	4·3148	4·3173	−0·0025
1·70	4·3130	4·3163	−0·0033
1·72	4·3138	4·3144	−0·0006
1·75	4·3110	4·3116	−0·0006
1·80	4·3033	4·3069	−0·0036
1·82	4·3081	4·3050	+0·0031
1·86	4·3090	4·3012	+0·0078
1·87	4·3086	4·3002	+0·0084

$$V = 4{\cdot}4772 - 0{\cdot}09465h.$$

Of these measurements, two differed by 0·11 mm., two by 0·07 and 0·09 mm., and the remaining 8 showed a variation of 0·05 mm. and less. It was clear that in spite of all precautions, the meniscuses were not perfectly symmetrical. As before, the points were averaged linearly by the least mean squares method and gave the equation, $V = 4{\cdot}4772 - 0{\cdot}09465h$, in which V is the volume of the mercury in cc. in the dead space tube for a meniscus of h mm. in height.

On comparing the calculated with the experimental volumes, the extreme variation is seen to be 12 c. mm. and the probable error of a single observation ± 3 c. mm. It is clear that for work of the precision required the errors are still too great.

Although, because of the difficulty of obtaining really symmetrical meniscuses in a cylindrical tube these results can make no claim to high accuracy, it is of some interest to compare them with the results obtained by Keesom and his co-workers by means of the X-ray shadowgraph procedure, the only experimental method published hitherto in which the measurements of meniscus were made in the interior of cylindrical tubes and which permitted the average height to be computed accurately. To do this, the meniscus co-volume was calculated from our least mean square line, i.e. $V_0 - V = \text{c}{\cdot}09465h$ and subtracted from the volume of a cylinder of the same height giving for the meniscus volume, $M = h(\pi r^2 - 0{\cdot}09465)$, or $M = 263{\cdot}7h$ c. mm.

From Keesom's results, the meniscus volumes for a tube of the same diameter as used here were obtained by interpolation. Further, for comparison are appended results (Table III) calculated theoretically from Blaisdell's tables assuming $\sigma = 459$ dynes/cm.^{2} for the surface tension of mercury.

From the table three points of interest emerge. (1) The satisfactory agreement between Keesom's experimental values and those in column 4 calculated from theory. Both sets of values over the range tabulated show nearly the same slope and nearly the same slight curvature towards the height axis. Our results for the lower meniscus heights differ appreciably because, on account of the wide scatter of the experimental points, only a linear extrapolation seemed justified when calculating the volume of tube for zero meniscus height. (2) For a tube of this diameter, the change in meniscus volume for a change in meniscus height of 0·1 mm. is about 27 c. mm., so that even if the mean height of the meniscus in a dead space could be measured to within 0·01 mm., the uncertainty in dead-space volume would not be less than 2 c. mm. (3) In spite of the agreement between the values in columns 3 and 4, there is an uncertainty of a few c. mm. for the volumes at large meniscus heights.

Although from these examples it is evident that the direct measurement of meniscus heights in tubes of a diameter suitable for accurate manometry does not allow the meniscus volume to be deduced with the accuracy desirable in high precision compressibility determinations, one further set of experiments may be quoted here.

It was thought that if a conical dead space with a vertex angle of 100° was used, the mercury would meet the walls at an angle close to the contact angle and that the variations in meniscus volume might be considerably reduced. Accordingly such a dead space was constructed, the two sides making an angle of 40° with the horizontal. Further, in order to eliminate the rather tedious operation of emptying the dead space and weighing the mercury after each setting, a pipette was made to have nearly the same volume as the dead space from the point to a mark on the capillary above. The pipette communicated with the dead space through a tap and capillary tubing which had been calibrated, and the position of the mercury in the capillary after filling the dead space from the pipette, gauged its volume with some accuracy. The arrangement is shown in Fig. 2 where A is the conical dead space, set in a steel block carrying a fine point. B is the pipette calibrated between the marks C and D. The capillary above and below the marks was also calibrated. Before the point setting was made, the pipette was filled with mercury to mark C, tap H being closed. Tap F was then closed, H opened and the mercury set to the point in the usual way. Tap G was then closed and the mercury from the pipette allowed to flow into the dead space by opening tap F and adjusted exactly to mark K using, if necessary, a slight air pressure. When this was done the position of the mercury in the capillary below D was an exact measure of the dead-space volume. This arrangement worked very satisfactorily and the volume could easily be measured to less than 1 c. mm.

TABLE III.—MENISCUS VOLUMES IN A TUBE OF 21·36 MM. INTERNAL DIAM.

Meniscus Height (mm.).	Meniscus volume (c. mm).		
	R. W.-G. and N. T.	Keesom.	Blaisdell. (σ = 459 dyne/cm.^{2}).
1·2	316	307	306
1·3	343	334	332
1·4	369	361	359
1·5	396	389	386
1·6	422	416	414
1·7	448	445	442
1·8	475	473	470
1·9	501	502	499
2·0	527	531	527

It was found, however, that even with very careful point settings and an apparently flat meniscus, the volume variation was considerable. After a preliminary set of readings had been made and the apparatus thoroughly tested out, the following values were obtained in 11 successive settings for the dead space volume: 6·4011, 6·3911, 6·3851, 6·3966, 6·3748, 6·3852, 6·4152, 6·4157, 6·4128, 6·3911 and 6·4239 cc. The extreme variation is 49 c. mm. and the variation on either side of the mean is 26 above and 23 c. mm. below. The diameter of the mercury surface when set to the point was close on 40 mm. Now Porter's tables show that the variation in meniscus volume to be expected in a tube of 37 mm. diam. for a change in meniscus height of 0·1 mm. is about 90 c. mm. whilst the capillary depression change is less than 0·0002 mm. The only advantage of the conical dead space would appear to be that the mercury around the edge is near its position of maximum stability and hence the variation in height which can occur is small. Nevertheless as these experiments clearly indicate, small variations in height do take place due no doubt to the peculiar clinging effect of mercury when moving over a glass surface. Hence the use of a wide diameter conical dead space does not sufficiently reduce the meniscus volume error, although it renders insignificant the error due to capillary depression.

Clearly, then, to reduce both errors to negligible proportions, it is only necessary to construct the apparatus of wide diameter tubing and measure directly the actual dead-space volume each time after setting the mercury to the point. This can readily be accomplished by using in the compressibility apparatus a slight modification of the pipette system just described. This modification of the usual type of compressibility apparatus is shown in Fig. 3, where A is the dead space, B the pipette, and C the upper chanber of the manometer.

The pipette is first filled with mercury from the reservoir J through stopcocks G and F, the stopcocks H and K remaining closed. On closing F and opening H and K, the mercury can be set to the point in the usual way. When equilibrium has been reached and a permanent setting achieved, K and G are gently closed, F opened and the mercury in the pipette transferred to the dead space and set to the mark M. From the position of the mercury in the calibrated capillary below the pipette, the exact volume of the dead space can be found.

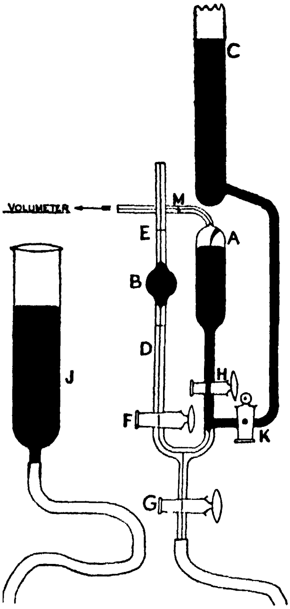

Fig. 3.

The pipette was adjusted beforehand so that its volume was slightly less than the smallest dead-space volume likely to be met with, so as to ensure that the reading after filling the dead space was always in the calibrated capillary. Another degree of freedom in adjustment can be provided by calibrating the capillary above the dead space. A convenient size for the capillary is a little over 1 mm. bore so that 1 mm. length corresponds to about 1 c. mm. For wide-diameter dead spaces in which the meniscus volume variation is large, the bore of the capillary can be increased and the position of the mercury read with a telescope.

The differential compressibility apparatus, mentioned earlier in this paper, has been constructed on the above plan, and a preliminary series of results has been obtained with it in which the mean deviation is 2 parts in 100,000. A full description of this apparatus will be published shortly.

This system by eliminating dead space errors allows the use of wide diameter tubing in the manometer and thus reduces capillary depression errors to a minimum. If the tubing is wide enough, it should be unnecessary to measure the meniscus height every time a pressure measurement is made. Thus, whilst in a tube of 14 mm. diam. the capillary depression may vary by 0·1 mm. for a change in meniscus height of 0·8 mm., the variation in a tube of diameter 37 mm. for the same height-change is only about 0·003 mm.

In order to take advantage of the greater accuracy in the dead-space volume entailed by this method, it is necessary to measure the pressure with corresponding precision. As has been indicated earlier in this paper, a multi-point gauge of the Rayleigh type is probably the best suited to achieve this. Such a point system was used first by Burt and Howarth [17] in their work on the compressibility of acetylene and an arrangement similar to the one they used, only constructed of tubing of diameter not less than 35 mm.[18] and provided with a pipette for the measurement of dead-space volume, would probably permit the measurement of low pressure compressibilities with an accuracy of a few parts in 100,000.

It should be remarked that the use of the pipette system with large diameter dead spaces necessitates a very rigid temperature control, for a larger fraction of the gas than usual is outside the volumeter. Although Howarth and Burt were working with a small dead space, their arrangement of surrounding volumeter, dead space, and manometer column with melting ice achieves this for

---

[17] Howorth and Burt, *Trans. Faraday Soc.*, 1925, **20**, 1.

[18] Stulla-Götz, *Physik. Z.*, 1934, **10**, 404.

0° c. A similar arrangement of having the whole apparatus in the same thermostat bath could be used for other temperatures. With the pipette, stopcocks protected from the action of water, and designed to be operated from outside, the bath would have to be used.

One of the authors (R. W.-G.) wishes to express his thanks to the Leverhulme Trustees for a grant from their Research Fund which enabled him to devote his time to the work.

Summary.

The variations in meniscus volume and in capillary depression in low pressure compressibility measurements are discussed and it is shown that very appreciable errors in high precision work are likely to arise unless these are taken into account.

Experiments are described in which the attempt was made to obtain an accurate correlation between meniscus height and meniscus volume in cylindrical tubes of sufficiently wide diameter to reduce the capillary depression errors to small values. In none of the three sets of experiments was the required accuracy attained. Recourse was made finally to a direct measurement of dead-space volume by means of a mercury pipette after each pressure reading. This device called the " dead-space pipette " enables dead-space volumes to be determined accurately and permits the use of manometric columns of such a diameter that capillary depression errors are negligible.

Chemistry Department,
The University,
Leeds.

A NEW CAUSE OF LOW-INTENSITY RECIPROCITY FAILURE.*

By W. F. Berg.

Received 24th November, 1947.

The inefficiency of formation of the latent-image silver speck in its first stages of growth has been recognised to cause reciprocity failure at low intensities ; once the first or sub-image stage has been overcome, the photolytic disintegration of silver halide by light appears to proceed at full efficiency.[1, 2, 3, 4] If this be accepted, a second possible cause of low-intensity reciprocity failure will be at once apparent. Imagine a photographic grain on which a latent-image silver speck has been produced fairly early in the course of the exposure under consideration, or one which carries a " fog speck " before the exposure began. An additional atom of silver will be produced for every quantum of light absorbed by the grain and a corresponding number of bromine atoms will be released. At low intensities a grain such as this may be very considerably " overexposed " before an appreciable number of other grains produce a latent image speck ; this grain during exposure constitutes a source of bromine. The bromine spreads to the neighbouring grains and destroys their sensitivity by attacking either the sensitivity specks, or recently formed, and therefore small, latent-image specks. After some time all the grains in the area being exposed will be completely desensitised. Only those grains which still carry a latent-image speck will develop; thus the maximum density is cut down and further exposure will not increase it. The purpose of this note is to present the evidence for the new cause of low-intensity reciprocity failure which the bromine effect visualised represents.

---

* Communication No. 1163H from the Kodak Research Laboratories, Harrow, Middlesex.

[1] Weinland, *J. Opt. Soc. Amer.*, 1927, **15**, 337 ; 1928, **16**, 295.

[2] Webb and Evans, *Photogr. J.*, 1940, **80**, 88.

[3] Berg, *Trans. Faraday Soc.*, 1943, **39**, 115.

[4] Burton and Berg, *Photogr. J.*, 1946, **86B**, 1.

Experimental.

Apparatus.—The apparatus used was designed for the investigation of reciprocity failure at intensities so low that a full exposure would take several days. The source of light is a piece of flashed opal glass, 0·05 in. diam., illuminated at a distance of 4 in. by a 100 w., 100 v. projector bulb, under-run at about half the normal voltage. The opal glass is situated at one end of a square-sectioned light-tight box, viz. a piece of air duct, 12 ft. long, which carries at its other end, the holder for the material to be exposed. The carrier for the sensitive material consists of 4 quarter-plate printing frames arranged in a square. A photographic density step wedge is placed in each frame, thus providing for an intensity scale of exposures in one direction. A pair of sliding shutters moves in the other direction at right-angles to the steps of the wedges, so that a time-scale of exposures can be given along each step of the wedges. The shutter consists of ¼-in.-thick sheets of Tufnol running in grooves and can be moved simultaneously from outside by means of an arrangement of wheels and cord of the type used to move curtains as illustrated in Fig. 1. The carrier for the sensitive material, and the back portion of the duct are sealed by a piece of glass to form a compartment separate from the rest of the apparatus, and can be kept at constant temperature by means of concealed electric heaters, a thermostat and a fan. A mercury-in-steel thermograph provides a continuous temperature record.

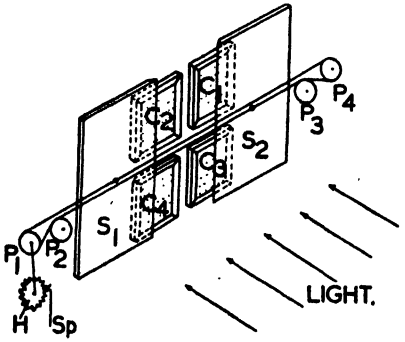

FIG. 1.—Diagrammatic lay-out of shutter and holder for the sensitive material. C_1, C_2, C_3 and C_4 are four printing-frames, with photographic density step-wedge in each. The steps are indicated by dotted lines. S_1 and S_2 are the two shutters which move simultaneously inward or outward by moving the cord. The whole mechanism is enclosed in a light-tight box, with only the hand-wheel H in the open. H is shaped as a click wheel, Sp being a flat spring.

Exposure times were controlled by withdrawing the shutters from the material under test, and were generally arranged to give a geometric series. Thus a long exposure would be given first, the neighbouring area being uncovered after some days, the exposure being continued in both areas, etc. The reason for this "uncovering" method was that it ensures all exposures to finish at the same moment; the "covering" method, however, in which the shutters move in the opposite direction, was also used occasionally.

On materials exposed by the uncovering method and processed in a normal way (4 min. in Elon hydroquinone developer, Kodak formula D. 16), bands of reduced density occurred along the edges of the more heavily exposed areas adjacent to areas which had been exposed previously for a longer time. Fig. 2 gives a reproduction of an exposed and processed film showing this effect. These white bands were first thought to be brought about by stray or infra-red light produced by the heaters, but were eventually traced down to processes occurring in the emulsion. The experiments to be described were all designed to ascertain the nature of these processes.

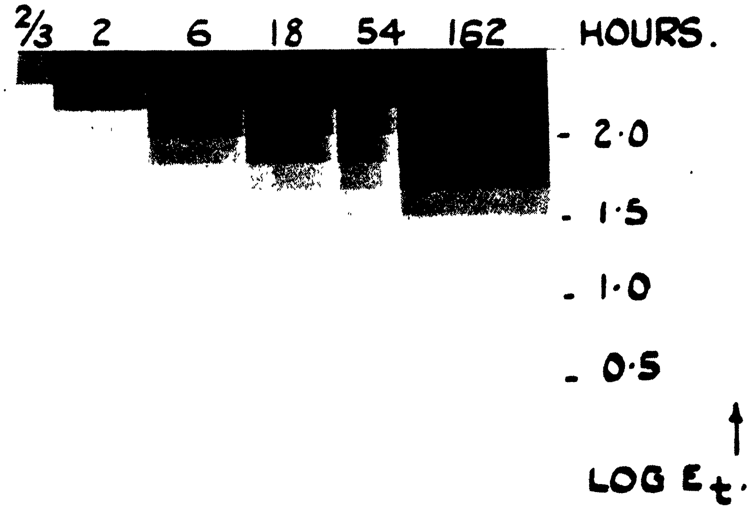

FIG. 2.—Reproduction of white-band effect.

[*To face page* 784.

(1) THE WHITE BANDS ARE DUE TO A DESENSITISATION. A piece of a slow, orthochromatic, line film (A) which exhibited the white band effect strongly, was exposed in the sensitometer through the step wedge for 7 days, the shutters being wide open. A second exposure was then applied in a time-scale sensitometer, the steps being at right-angles to the low-intensity scale steps. The times of the second exposure ranged from 1/300 sec. upwards, successive steps being in the ratio $1 : \sqrt{2}$. As a control, the order of the exposures was reversed for another piece of film. Fig. 3 shows some of the results, the density on processing in D. 16 for 4 min. at 68° F. in a dish being plotted against the logarithm of the intensity of the long-duration exposure. The different curves refer to different times of the short exposure. It will be seen that a long-duration first exposure desensitises the material towards the second exposure, whereas a long-duration second exposure builds up the density produced by a brief first exposure, an effect now well known as latent image intensification,[3, 4, 5] which need not be discussed here.

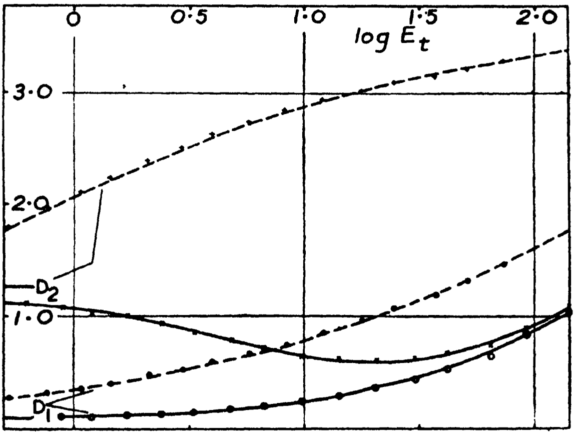

FIG. 3.—The density is plotted against the logarithm of the intensity-scale exposure of long duration, which is either preceded (dotted curves) or followed (solid curves) by uniform short exposures. These latter produce on their own uniform densities marked D_1 and D_2. Material used : line film A.

(2) THE WHITE BANDS ARE NOT RELATED TO SOLARISATION. This is already clear from the fact that the bands are produced by an effect which occurs in an area before it is actually exposed. It may be objected that light must diffuse from an area being exposed into the area still covered by the shutter. In order to see whether this light had any action on a latent image, exposures were made by running the shutter in the opposite direction, i.e. by the covering method. No white bands were ever obtained under these conditions.

(3) THE WHITE BANDS ARE NOT DUE TO CHANGES IN LATENT-IMAGE DISTRIBUTION. Experiments were made using our "surface developer,"[6] i.e. a developer which contains no silver halide solvents, and thus only reacts to latent-image specks situated on the surfaces of the grains. D. 16 was also tried for a wide range of developing times to see whether the white bands were perhaps caused by covering the silver bromide latent-image specks on the grain surfaces. Finally, tests were carried out using the method for developing the internal image only, in which the latent image specks on the surface of the grains are first bleached away, and the internal-image specks are then developed in a solution containing a silver halide solvent. It was found that the white bands appeared under all conditions of development, apparently equally strongly.

(4) THE WHITE BANDS DEPEND ON THE CONDITION OF THE EMULSION. The fact that the occurrence of white bands depends on the emulsion was first realised when different materials were found to differ considerably in their propensity to produce white bands. This may apply even to different batches of the same material. Of several batches of the same high-contrast line film, and also of a

---

[5] Moore, *Photogr. J.*, 1941, 81, 27.

[6] Berg, Marriage and Stevens, *ibid.*, 1941, 81, 413.

process film, some exhibited pronounced white bands and had a low maximum density and intensity-scale contrast, while others showed hardly any white bands on exposures of 7 days and a high maximum density and contrast. Fig. 4 shows the intensity-scale curves for two of these materials for exposure times of 7 days and 0·05 sec. These differences appeared to contain the clue to the explanation of the white-band effect and were thus studied in greater detail. In particular, attempts were made to impart the characteristics of one emulsion to the other by bathing treatments.

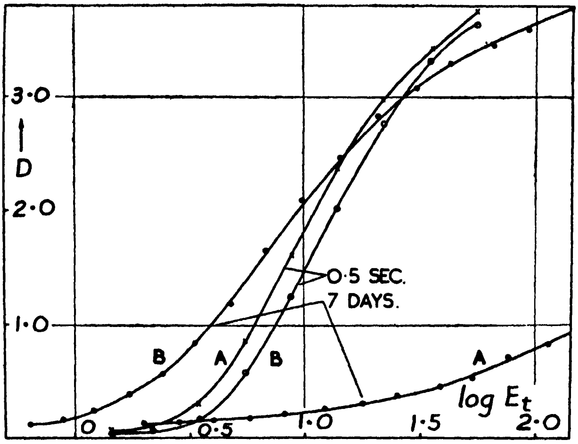

FIG. 4.—D-log E_t curves on two batches of the same material, for exposure times of 0·5 sec. and 7 days. Note that the absolute values of the scales for the 0·5 sec.-exposure are not comparable with those of the 7-day exposures. A and B refer to the two batches of the line film.

(5) THE WHITE BANDS ARE DUE TO BROMINE. It is obvious that the bands are due to something which diffuses from exposed to adjacent areas : this can hardly be anything but bromine. Further evidence is necessarily of an indirect nature. The bathing treatment designed to investigate the nature of the diffusing agent was carried out on the two batches of high-contrast line film mentioned and on a medium contrast process film.

All the baths used contained Teepol, a commercial wetting agent which is a mixture of sodium salts of long-chain alkyl sulphates of different lengths. It was necessary to use such an agent in order to achieve even wetting of the film ; without the presence of a wetting agent the results were very uneven. The other constituents of the various baths were either halogen acceptors in order to neutralise at once any bromine released, or potassium bromide in various concentrations, since washing in water will clearly remove some of the surplus bromide ions present in all emulsions. The baths consisted of : (*a*) Teepol 5 cc. water (dist.) 1000 cc. ; (*b*) Teepol 5 cc., $NaNO_2$ 0·5 g., water (dist.) 1000 cc. $(c)_1$ Teepol 5 cc., KBr 1·5 g., water (dist.) 1000 cc. ; $(c)_2$ as $(c)_1$ with KBr 0·3 g. $(c)_3$ as $(c)_1$ with KBr 0·06 g. ; (*d*) Teepol 5 cc., KBr 1·5 g., $NaNO_2$ 0·5 g., water (dist.) 1000 cc.

The film was immersed in the bath for 2 min. after which the solution was allowed to run off and the film was dried. Sheets of film, 4¾ by 6½ in., were treated and cut down to 3¼ by 4¼ in. before use.

Bath.	Line Film A.	Line Film B.	Process Film.
Untreated . . .	strong bands	no bands	strong bands
(*a*) H_2O . . .	bands almost gone	no bands	bands almost gone
(*b*) $NaNO_2$. . .	no bands		no bands
$(c)_1$ KBr 1·5 g./l. .	strong bands	no bands	strong bands
$(c)_2$ KBr 0·3 g./l. .	weak bands	no bands	
$(c)_3$ KBr 0·06 g./l. .	very weak bands	no bands	
(*d*) KBr + $NaNO_2$.	no bands		

The results obtained are summarised in the table, and are of some interest outside the scope of this investigation.

The addition of a halogen acceptor causes the white-band effect to disappear. Washing with water had almost the same effect. This was thought to be due to the washing out of bromide ions from the emulsion, an explanation which was thought to be very likely when it was found that adding bromide ions to the wash water caused the white bands to remain and the contrast and maximum density to drop. Fig. 5 shows characteristic curves (D-log I) for an exposure time of 18 hr. for the line film A treated with various concentrations of KBr, corresponding to baths, $(c)_1$, $(c)_2$ and $(c)_3$.

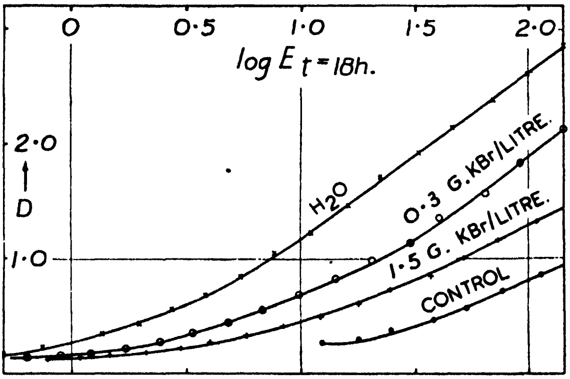

FIG. 5.—D-log E_t curves for t = 18 hr. and various bromide ion concentrations. Material used : line film A.

It is interesting to speculate as to the possible effect which the bromide ion concentration may have on the ease with which bromine atoms or molecules are bound by the medium surrounding the grains. There seem to be two possible explanations. The behaviour of gelatine towards bromine may alter with the bromide ion concentration, and the equilibrium of the reaction of bromine with water may also be affected, thus :

$$\begin{tikzcd} Br_2 + H_2O \arrow[r, shift left] & HOBr + HBr \arrow[l, shift left] \arrow[d, shift left] \\ & H^+ + Br^- \arrow[u, shift left] \end{tikzcd}$$

The presence of bromide ion will shift the equilibrium towards the bromine side, and the bromine will thus be forced to diffuse and attack sensitivity specks farther away from its source of origin, thus causing the desensitisation observed.

The finding that the line film B did not show the white bands was, at first, thought to be connected with the bromide ion concentration in the manufacturing process. Treating the film with different concentrations of bromide ions did not, however, affect its characteristics ; we conclude that there must be an efficient, insoluble, bromine acceptor already present in the emulsion. Presumably the differences between different emulsions are due to differences in the gelatine used.

(6) THE DESENSITISING EFFECT IS LARGELY REVERSIBLE. Expt. (1) was modified by the insertion of a bathing treatment in $NaNO_2$ solution (bath b) between the first long-duration and the second short-duration exposure, using the line film A and the process film. Some of the results for the process film are shown in Fig. 6 for the untreated (6a), and the nitrited material (6b), as plots of density against exposure time of the second exposure. It is clear that most of the desensitisation caused by the first exposure is removed by the nitrite treatment. It would be interesting to know whether the treatment has removed the desensitisation altogether. In (6b), most of the pre-exposed curves lie above the control, but they are not exactly parallel to it as they would be if the two exposures were strictly additive. Let us assume that, as the result of the first exposure, after nitriting treatment, we have some grains carrying a latent-image speck, the other grains not being affected in any way. The first exposure has probably used up the most sensitive grains, and we would therefore expect to find the control and the pre-exposed curves to come together at the higher densities. This is what we find in (6b), except for a cross-over at the high densities of curves 0 and 1, which is within the experimental errors. Most of the

desensitisation caused by the long exposure is therefore removed by the bathing treatment; whether any small permanent desensitisation results as well it is impossible to decide.

Conclusion.—All the evidence presented agrees with the supposition that the white bands observed are due to the bromine released by the grains, which have been most heavily exposed, desensitising the neighbouring grains before a latent image can form on them. Already in 1920 similar experiences have been reported,[7] although the effect did not manifest itself by reversal bands but merely by a reduction of the maximum density as the intensity of the exposing light decreased. If this effect is due to released bromine, an effect similar to solarisation might also be thought to occur. The incidence of solarisation is known to be favoured by exposing at high intensities,[8] when, with most emulsions, a considerable proportion of latent image is formed inside the grains. Solarisation occurs

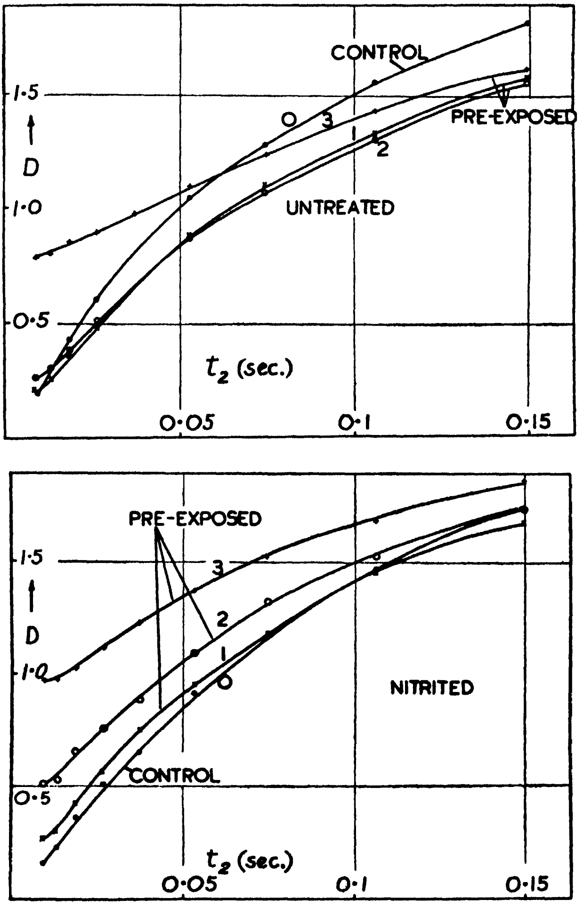

FIG. 6.—*D-t* curves for different long-duration pre-exposures, with and without sodium nitrite treatment between the two exposures. The control curves had no pre-exposure. Material used: process film.

---

[7] Channon, *Photogr. J.*, 1920, **60**, 164.

[8] See Meidinger, in Hay's *Handbuch der Photographie* (Wien 1932), vol. 5, pp. 293, 298.

only with the surface image[6] and has been accounted for by a re-bromination process which coats over, or completely destroys, the surface-image specks. The surplus of bromine necessary for this destruction comes from the internal latent image. If an exposure at high intensities were followed by one of very long duration at low intensities, the new silver formed by the second exposure would divide between surface and internal latent image specks. The bromine formed, however, would accumulate around the grain and eventually destroy the surface image. This effect has also been reported.[7] The effect here described is, however, thought to be well distinguished from solarisation, since with low-intensity exposures very little internal image is formed.

In investigating low-intensity exposures, the effect here ascribed to bromine is bound to play a decisive, and often a disturbing, part. The actual desensitisation obtained in any one small area will, amongst other causes, depend on the ease with which bromine can escape from the emulsion surface, since it diffuses inside the emulsion over distances of several millimetres. Thus, geometrical conditions, as, for example, intimacy of contact with a step wedge, will influence the sensitometric results profoundly. The reproducibility of low-intensity exposures is, in fact, decidedly poor, and good results cannot be obtained, unless the materials are treated with an efficient halogen acceptor. The realisation that the presence of a halogen acceptor is essential in order to obtain reasonable densities and contrast with low-intensity exposures may be of some practical value.

The mechanism of this cause of low-intensity reciprocity failure is indicated by experiment (6) to be an attack by the bromine on any new latent-image silver speck formed or being formed. The mechanism cannot be a destruction of sensitivity specks, since treatment with a bromine acceptor after a low-intensity exposure restores most of, if not all, the sensitivity. It is interesting to note that internal-image formation is also affected by the bromine. This might be taken to indicate that the presence of bromine outside the grains causes an equilibrium concentration of atomic bromine to be set up in the grain. Stasiw and Teltow[9] have shown this to occur with large crystals of silver halides. Alternatively, the desensitisation for the internal image may be due merely to the presence of adsorbed bromine which will combine with the electrons released by the light absorbed, thus decreasing the efficiency of both surface- and internal-image formation.

In conclusion, it is interesting to consider the actual amount of bromine which is released under conditions of low-intensity exposures and which has such drastic photographic effects. Assume that the density obtained is equal to 1·0 and that there are 10^9 grains/sq. cm. of coated emulsion surface. This density is then represented by approximately 3×10^8 grains. Normally, the number of quanta necessary to make a grain developable[10] is of the order of 100. Under our conditions, owing to the low-intensity reciprocity failure, exposure may be up to 100 times as heavy. The amount of bromine released is therefore at most 3×10^{12} bromine atoms per cm. square. This amount is far too small to be detected by any direct chemical analysis, but leads to practically complete desensitisation of the remaining grains in an emulsion.

Summary.

On very low-intensity time-scale exposures, bands of reduced density were found to occur along the edge of an area, adjacent to one which had received a longer exposure previously. On addition of a halogen acceptor before exposure, these bands disappeared, and at the same time the overall densities increased

---

[9] Stasiw and Teltow, *Nachr. Akad. Wiss., Göttingen ; Math. Physik. Kl.* (1944), p. 155.

[10] Sheppard, *Photogr. J.*, 1931, **71**, 331.

considerably. This and other results led to the conclusion that the bands were due to a desensitisation caused by bromine released from either fog grains, or grains in which a latent image was formed during the early stages of exposure, since exposure reduces such grains to silver and bromine at full quantum efficiency. At very low intensities of light this desensitisation is the most important cause of reciprocity failure.

Research Laboratory,
Kodak Limited,
The Works,
Wealdstone, Harrow,
Middlesex.

PYRIDINE COMPLEXES OF METALLIC PERCHLORATES.

PART II.—DISSOCIATION PRESSURES AND PRESSURE-COMPOSITION ISOTHERMALS OF COPPER PYRIDINE PERCHLORATES.

BY P. C. SINHA AND R. C. RAY.

Received 20th November, 1947.

In a previous paper[1] the methods of preparation and the general properties of the pyridine complexes of copper (ic), silver, magnesium, calcium, strontium, barium, cadmium, zinc, mercury (ic), manganese, nickel and cobalt have been described. The investigation was undertaken with the object of determining what parallelism existed between the pyridine and ammonia complexes of metallic salts, since it was to be expected that, as in both cases the complex formation took place through the lone pair of electrons of the N atom, a close similarity would be found between the two classes of compounds. In the present paper, the dissociation pressures of the copper pyridine perchlorates have been measured at different temperatures, and the number of copper pyridine perchlorates, which are definitely formed under laboratory conditions, have been determined by an isothermal study of the copper perchlorate-pyridine system at 30° c. and 50° c.

The ammonia complexes of metallic salts or metallic ammines have been investigated by a large number of workers. Measurements of dissociation pressures of ammines of various salts were made on a limited scope by Bonnefoi,[2] Baud[3] and Girardet.[4] The dissociation pressures of compounds of ammonia with the halides of silver and the chlorides of magnesium, calcium, zinc and mercury were determined by Isambert[5] and he also measured the heats of dissociation calorimetrically. Measurements of the hexammines of molybdate, tungstate, chromate, selenate and sulphate of nickel were made by Ephraim and Müller.[6] Later Ephraim made detailed investigation of the lower ammines and the higher, stable ammine complexes. Biltz and his co-workers made a more complete study of all the ammine complexes formed by each salt. The results were summarised and discussed by Biltz.[7] The relation of stability to heat of dissociation was discussed by Biltz, and Biltz and Grimm.[8] More recently,

---

[1] *J. Indian Chem. Soc.*, 1943, **20**, 32.
[2] *Ann. Chim. Phys.*, 1901, **23**, 317.
[3] *Compt. rend.*, 1901, **132**, 553.
[4] *Bull. Soc. Chim.*, 1910, **7**, 1028.
[5] *Compt. rend.*, 1868, **66**, 1259; 1876, **86**, 968.
[6] *Ber.*, 1921, **54**, 973.
[7] *Z. anorg. Chem.*, 1923, **130**, 93.
[8] *ibid.*, 1925, **145**, 63.

Hart and Partington[9] determined the dissociation pressures of the ammine and deuterammine systems of copper sulphate with varying temperatures and calculated the heats of dissociation from the slope of the linear graph of log p against $1/T$.

Experimental.

Determination of Dissociation Pressures.—The apparatus employed is shown diagrammatically in Fig. 1. It consisted of a close limb manometer M, the open end of which was sealed to a T piece, and the bulb containing the substance was sealed to the vertical limb of the T piece. To the other end of the T-piece, the U-tube S, about 80 cm. long, having two bulbs on the two arms, was sealed. At the bottom of the U-tube a small tube which was connected by means of pressure tubing to a reservoir of mercury which served as a levelling tube, was attached. The U-tube arrangement was inserted to avoid the use of a tap. The other end of the U-tube was connected to a rotary pump through the tap T and a wash-bottle containing H_2SO_4 and a tube fitted with P_2O_5 (not shown in Fig. 1) to absorb the pyridine. The whole apparatus except the tap T and the vacuum line was enclosed in a large electrically-operated air-thermostat provided with the heating lamp L, the heating coil H the thermo-regulator R and the fan F for agitating the air inside vigorously. The motor of the fan had to be kept outside the thermostat to prevent it from being unduly heated when measurements were made at high temperatures. Up to 50° C., a mercury-toluene regulator was used, but for higher temperatures a xylene-mercury regulator was employed. The temperature could be kept constant to ± 0·02°. It was necessary to keep the whole of the equilibrium system inside the thermostat, otherwise pyridine condensed in the cooler parts and the pressure recorded was not the equilibrium pressure at the desired temperature. The difference in the heights of mercury in the two arms of the manometer was read off by means of the cathetometer C which was provided with a vertical scale and vernier.

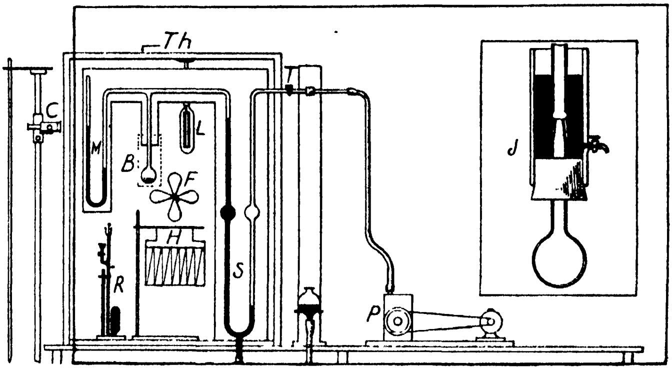

FIG. 1.

In carrying out a measurement, about 1 g. of the highest pyridine complex together with 1 cc. of pure pyridine was introduced into the bulb B which was then sealed on to the vertical arm of the T-piece. The thermostat was set at the desired temperature, the mercury reservoir was lowered until a clear passage was established through the U-tube S, and the excess of pyridine pumped off through the tap T. When the excess of pyridine was almost completely removed, the passage through the U-tube was closed by raising the mercury reservoir. The equilibrium pressure at the particular temperature was measured. It coincided with the vapour pressure of pure pyridine at that temperature, showing that the apparatus had been properly set up and that the pressure readings were correct. The lowering of the mercury reservoir and the pumping were repeated as long as the pressure values corresponded with the vapour pressure of pure pyridine. Gradually the pyridine complex became entirely free from the excess of pyridine, and finally the dissociation pressure of the

---

[9] *J. Chem. Soc.*, 1943, 104.

TABLE I.—TEMPERATURE-PRESSURE VALUES.

System : $Cu(ClO_4)_2 . 6/4\ C_5H_5N$.

t° C. . .	35	40	49·5	55·2	57·3	64	69	74·6	79·4	82·0	85·4	92·3
p (mm.) .	16·8	21·1	33·0	40·0	43·2	55·6	66·1	82·0	96·4	106·0	120·1	149·0
$10^6/T^\circ$ K. .	3247	3195	3101	3047	3027	2967	2924	2876	2838	2811	2790	2738
$Log_{10}\, p$.	1·225	1·324	1·518	1·602	1·636	1·745	1·820	1·914	1·984	2·025	2·079	2·173

Mean value of the heat of dissociation (calculated from graph) = 8,450 cal.

System : $Cu(ClO_4) . 4/0\ C_5H_5N$.

t° C. . .	35·0	44·0	50·0	55·0	60·0	65·2	70·2	75·0	80·1	85·1	90·1	95·0
p (mm.) .	6·6	11·7	16·0	21·3	28·6	36·8	46·0	58·6	73·5	96·7	119·0	150·5
$10^6/T^\circ$ K. .	3247	3155	3096	3049	3003	2958	2914	2874	2832	2792	2755	2717
$Log_{10}\, p$.	0·819	1·070	1·204	1·328	1·456	1·566	1·663	1·768	1·866	1·985	2·076	2·178

Mean value of the heat of dissociation (calculated from graph) = 11,640 cal.

complex was obtained. When the equilibrium pressure at a particular temperature was obtained, the equilibrium was disturbed by connecting the system with the pump line and the pressure was allowed to attain its original value. This process was repeated two or three times at each temperature and the final value was recorded. In this way the dissociation pressures were recorded with increasing temperatures. The dissociation pressures were then redetermined with falling temperatures, and the whole dissociation-pressure curves were determined, for both rising and falling temperatures. The experiments were repeated several times and reproducible results were obtained.

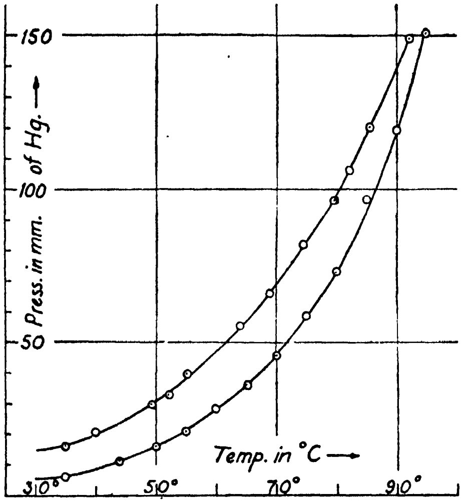

FIG. 2.

The results obtained are recorded in Table I and represented graphically in Fig. 2. The logarithms of pressures are also plotted against the reciprocals of the absolute temperature and the linear graphs obtained are shown in Fig. 3.

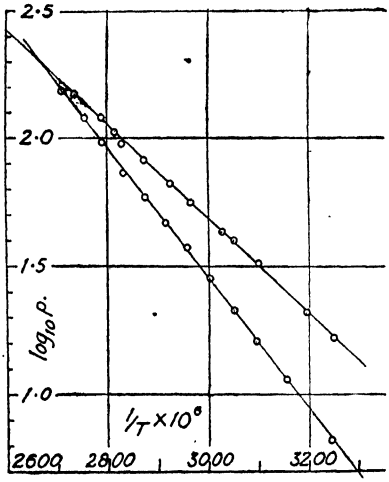

FIG. 3.

Determination of Isothermals.—The apparatus employed for this purpose was essentially the same as shown in Fig. 1 except that the bulb containing the pyridine complex was provided with a tightly-fitting ground-glass joint which was surrounded by a glass jacket J filled with mercury. The arrangement is shown in the inset of Fig. 1. The mercury seal was necessary as no lubricant could be used for the ground joint, since the bulb had to be disconnected from time to time and weighed.

The experiment consisted essentially of the determination of the loss of weight of pyridine with its gradual removal at a fixed temperature. For this purpose, approximately 1 g. of the pyridine complex was introduced in the bulb with about 1 cc. of freshly distilled, pure pyridine. The bulb was weighed and fitted into the ground-glass joint. Mercury was then poured into the jacket and the thermostat set at a fixed temperature and when the contents of the bulb attains that temperature, some pyridine was removed by pumping. The tap T was then closed and the bulb was left in the thermostat at the fixed temperature until the pressure reached its maximum value which was recorded. Air was then introduced into the apparatus, mercury was removed from the jacket J, the bulb detached, wiped clean and weighed. The process was repeated until no further change in the pressure could be noticed. A series of pressure values and the weights corresponding to each pressure were thus obtained. Isothermals were determined at 30° c. and 50° c. the room temperature being approximately 25° c. From the results the loss of the number of molecules of pyridine from the bulb and the number of molecules of pyridine that remained per molecule of the copper perchlorate were calculated. The results obtained are given in Fig. 4 where the pressures were plotted against the number of molecules of pyridine per molecule of copper perchlorate.

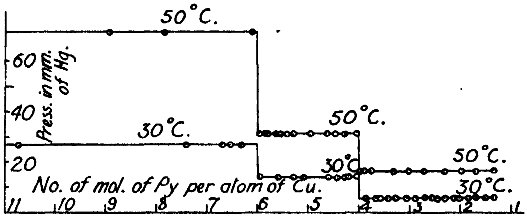

FIG. 4.

Discussion.

It is evident from the dissociation-pressure curves (Fig. 2 and 3) that in the solid phase only two stable complexes are formed between pyridine and copper perchlorates within the range of temperatures investigated. It should be mentioned, however, that indications of two other complexes —one possessing higher dissociation pressures than $Cu(ClO_4)_2 . 6C_5H_5N$, and one intermediate between the two stable complexes, $Cu(ClO_4)_2 . 6C_5H_5N$ and $Cu(ClO_4)_2 . 4C_5H_5N$—were obtained, but as the dissociation-pressure curves of these complexes were not reproducible, they have been left out. It is probable that loose absorption compounds are formed with the stable complexes under certain conditions. The isothermal curves (Fig. 4) leave no doubt, however, that in the solid state only two complexes $Cu(ClO_4)_2 . 6Pyr$ and $Cu(ClO_4)_2 . 4Pyr$ are formed.

The graphs (Fig. 3) obtained by plotting $\log_{10} p$ against $(1/T) \times 10^6$ are straight lines. The linear nature of the graphs is in agreement with previous results for heterogeneous systems as shown by Scheffer.[10] The dissociation pressure measurements can all be represented with sufficient accuracy by the equation, $\log p = A/T + B$, where A and B are constants. Thermodynamic consideration with approximations has been fully discussed by Schaffer (loc. cit.), who has shown that the equation may be written as $\log_{10} p = Q/4{\cdot}576T + B$, where Q is the heat of dissociation absorbed per molecule of pyridine. The value of Q can thus be calculated, the value of B being obtained from the slope of the linear graph of $\log_{10} p$ against $1/T$. The mean values of the heats of dissociation of the two complexes $Cu(ClO_4)_2 . 6Pyr$ and $Cu(ClO_4)_2 . 4Pyr$ are thus found to be 8450 cal./g. and 11,640 cal./g. respectively, showing that the 4-pyridine complex is much more stable than the hexapyridine copper perchlorate. Hart and Partington (loc. cit.) found that the heat of dissociation of tetramine copper sulphate is 15,270 cal./g. and that of tetradeuteramine copper sulphate 15,930 cal./g. It would therefore seem that the ammonia molecules are held more firmly by copper salts than pyridine molecules.

Dissociation pressures have been measured up to about 95°. The measurements could not be carried out at higher temperatures on account of experimental difficulties, and partly also for the fact that the thermostat could not be kept quite constant at these temperatures. If, however, the pressure-temperatures curves are extrapolated to higher temperatures (Fig. 3) they meet at 100·8° c. which may be regarded as the transition temperature of the hexapyridine complex into the tetrapyridine compound.

---

[10] *Proc. Acad. Sci. Amst.* 1917, **19**, 636.

According to the laws of heterogeneous equilibrium, every substance which give off a gaseous dissociation product has, at a given temperature, a perfectly definite dissociation pressure that is independent of the amount of the dissociating substance. It will be observed from the isothermal curves (Fig. 4) that as pyridine is progressively removed from the bulb containing the complex richest in pyridine in presence of excess of free pyridine, the pressure remains constant, 27 mm. at 30° c. and 71·5 mm. at 50° c., until the whole of the free pyridine is lost. These are the pressures of pure pyridine at these temperatures respectively, but as soon as the ratio of pyridine to copper perchlorate reaches the value of about 6/1, there is sudden fall of pressure, 14 mm. at 30° c. and 31·5 mm. at 50° c. which are the dissociation pressures of hexapyridine copper perchlorate at these two temperatures respectively. After this the pressure again remains constant until the whole of the hexapyridine complex is decomposed. When the ratio of copper perchlorate to pyridine attains the value of about 1/4, there is again a second fall of pressure, 6 mm. at 30° c. and 16·5 mm. at 50° c., the dissociation pressures of tetrapyridine copper perchlorates at these temperature. No further break in the graphs was found even when the ratio of the copper perchlorate to pyridine fell to 1/1·35. These results leave no doubt that only two complexes, hexapyridine and dipyridine complexes, are formed under the conditions of the experiments.

In their investigation on the formations of complex compounds of ammonia and deuterammonia with some metallic salts, Hart and Partington (loc. cit.) have found that, in the solid phase, the highest ammonia complex formed with copper sulphate is the pentamine and the corresponding deuteramine. They also obtained tetra-, di- and mono-amines and the corresponding deuteramines. With copper perchlorate, however, pyridine forms only two complexes, hexapyridine and tetrapyridine compounds. It would seem therefore that, as pointed out by Biltz, and Biltz and Grimm (loc. cit.), complex formation is closely connected with the nature of the crystal lattice and the lattice energy of the salt forming the complex.

Summary.

The dissociation pressures of the pyridine complexes of copper perchlorate have been measured at different temperatures and the isothermal curves showing pressures against number of molecules of pyridine per molecule of copper perchlorate have been determined at 30° c. and 50° c. From these results, it has been proved that in the solid phase only two stable complexes, namely $Cu(ClO_4)_2 . 6C_5H_5N$ and $Cu(ClO_4)_2 . 4C_5H_5N$ are formed. The heats of dissociation of the two complexes have been calculated from the $\log_{10} p$ against $1/T \times 10^6$ graphs and these values correspond to 8,450 and 11,640 cal. per g. respectively, indicating that the 4-pyridine is much stabler than the 6-pyridine complex.

Science College,
Patna.

A NOTE ON THE THEORY OF SURFACE DIFFUSION REACTIONS.

By F. Booth.

Received 24*th November*, 1947.

In this note we shall consider the theory of "tarnishing reactions". By "tarnishing reactions" we mean reactions in which a solid is attacked by either a gas or a liquid and a layer of the product forms between the two reactants. The reaction proceeds by the diffusion of either, or both, of the reactants through the product. This type of reaction is treated fully by Mott and Gurney;[1] examples of it are the oxidation of metals and the reaction between metals and halogens.

Let A denote the solid, B the gas or liquid phase, AB the solid product. For simplicity we shall assume that one mole of A is chemically equivalent to one mole of B. The modification of the analysis if this is not so, is trivial. In general the rate of reaction is determined by two factors.

(1) The rate of reaction between the diffusing material and the other reactant at the appropriate interface; for example, if B diffuses through AB it will be the rate of reaction at the A—AB interface.

(2) The rate of diffusion of either A or B through AB.

In what follows we shall consider process (2) only. We shall show later that the usual theory given for the rate of the reaction as determined by process (2), contains an invalid assumption; the condition for the assumption to be nearly valid is determined. We shall then present a more correct form of the theory.

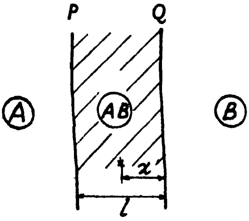

FIG. 1.

The usual derivation of the parabolic law for process (2) is as follows. For simplicity, suppose B diffuses through AB. Let n_1 and n_2 denote the concentrations of B at interfaces P and Q respectively, and n its concentration in AB. The mass of B moving to unit area of P in time dt is

$$-D\frac{\partial n}{\partial x}\bigg|_{x=l}\mathrm{d}t = \frac{M_B}{M_{AB}}\rho\,\mathrm{d}l \qquad . \quad . \quad . \quad . \quad (1)$$

where M_{AB} and M_B are the molecular weights of AB and B, ρ the density of the product AB, D the coefficient of diffusion and l the thickness of the layer AB; x is the distance measured from interface Q into AB. Assuming that the concentration gradient of B in AB is constant, we have

$$\frac{\partial n}{\partial x} = \frac{\partial n}{\partial x}\bigg|_{x=l} = -\frac{(n_2 - n_1)}{l} \qquad . \quad . \quad . \quad . \quad (2)$$

Hence from (1) and (2)

$$\frac{\mathrm{d}l}{\mathrm{d}t} = \frac{DM_{AB}(n_2 - n_1)}{M_B\rho}\cdot\frac{1}{l} \qquad . \quad . \quad . \quad . \quad . \quad (3)$$

or

$$l^2 = \frac{2DM_{AB}(n_2 - n_1)}{M_B\rho}t,$$

if t is the time from the beginning of the reaction. Hence the thickness of the product increases as $t^{\frac{1}{2}}$.

---

[1] *Electronic Processes in Ionic Crystals* (O.U.P. 1940), Ch. VIII.

But assumption (2), that the concentration gradient of B in AB is uniform, which is often regarded as self-evident (e.g. Mott and Gurney,[1] p. 252) is not correct. For from (2), it follows that

$$\frac{\partial^2 n}{\partial x^2} = 0. \qquad (4)$$

On the other hand, from (2) and the boundary conditions,

$$n = n_1 + (n_2 - n_1)\frac{(l - x)}{l} \qquad (5)$$

and so

$$\frac{\partial n}{\partial t} = (n_2 - n_1)\frac{x}{l^2} \cdot \frac{dl}{dt} \qquad (6)$$

since n_1 and n_2 are constant; we assume thermodynamic equilibrium at interfaces P and Q.

Thus $\partial n/\partial t$ is not zero unless x or dl/dt is zero. But $\partial n/\partial t$ and $\partial^2 n/\partial x^2$ should be related by Fick's law,

$$\frac{\partial n}{\partial t} = D\frac{\partial^2 n}{\partial x^2}. \qquad (7)$$

Hence (5) is not a solution of (7), and the gradient is not linear. Experimentally it is often found that (3) is followed quite well and it is therefore useful to find the condition that (2) should be nearly true. The simplest way of deriving this condition seems to be as follows.

Suppose the concentration gradient *is* uniform and therefore given by (2). From (6) and (7) we have

$$\frac{\partial^2 n}{\partial x^2} = \frac{(n_2 - n_1)}{D}\frac{x}{l^2} \cdot \frac{dl}{dt}. \qquad (8)$$

Integrating (8) twice with respect to x, and using the boundary conditions, $n = n_1$ at $x = l$, and $n = n_2$ at $x = 0$, we find

$$n = (n_2 - n_1)\left[\frac{l - x}{l} - \left(x - \frac{x^3}{l^2}\right)\frac{1}{6D} \cdot \frac{dl}{dt}\right] + n_1 \qquad (9)$$

and so

$$\frac{\partial n}{\partial x} = -(n_2 - n_1)\left[\frac{1}{l} + \left(1 - 3\frac{x^2}{l^2}\right)\frac{1}{6D} \cdot \frac{dl}{dt}\right]. \qquad (10)$$

Comparing (2) and (10) we see that they are only consistent provided

$$\frac{dl}{dt}\left|1 - 3\frac{x^2}{l^2}\right| \ll \frac{6D}{l} \qquad (11)$$

or

$$\frac{dl}{dt} \ll \frac{3D}{l} \qquad (12)$$

or, using (3)

$$n_2 - n_1 \ll \frac{\rho M_B}{M_{AB}}. \qquad (13)$$

Condition (13) is evidently the criterion for Fick's law (7) to be satisfied by a uniform concentration gradient.

Hence the concentration of the diffusing material must be small compared with the density of the product through which it diffuses. The experimental results on diffusion, if interpreted by the usual theory, give $(n_2 - n_1)D$ only; hence some independent method of finding $(n_2 - n_1)$ must be used to determine whether or not (13) is satisfied. Experimental evidence on this point seems scanty; there are some results, however, on the reaction between copper and gaseous oxygen. This is a tarnishing reaction in which the metal is coated by a film of cuprous oxide. Oxygen atoms are adsorbed in the oxide surface forming oxide and leaving unoccupied copper lattice points. The copper diffuses to the vacant lattice points. Hence, although the diffusing element is copper, the rate is determined by the concentration of oxygen in excess of the stoichiometric proportions. n_1 is effectively zero and n_2 has been measured by Wagner and Hammen.[2] They found $M_{AB}n_2/M_B\rho \sim 10^{-3}$ for temperatures of 1000° c. and O_2 pressure (p) 33 mm. Hg. The dependence of the concentration n_2 on the pressure was as $p^{1/5}$. In this particular example, therefore, it is evident that condition (13) is fulfilled.

Of course, with a physical mechanism of this type we should always expect the ratio $(n_2 - n_1)/\rho$ to be small, since otherwise there would be a large number of unoccupied lattice points and the lattice would break down. But there is no *a priori* reason for cases not to exist in which $(n_2 - n)/\rho$ is not very small and therefore it is of interest to enquire how (3) is modified if (13) is not satisfied. For example, is the form of the parabolic law modified and the rate of growth of product not inversely proportional to its thickness, or is the effect merely an alteration in the constant multiplying t in (3) ?

We require a solution of (7) so that $n = n_2$ at $x = 0$, and $n = n_1$ at the position $x = l$, l being determined by the integration of (1). Solutions of equations like (7) are well known but in this case we have the peculiar feature of a moving boundary—the motion being determined by the solution.

Assume that
$$n = \sum_0^\infty \alpha_r x^r \quad . \quad . \quad . \quad . \quad . \quad . \quad (14)$$

where the coefficients α_r are functions of t only.

Then, from the boundary conditions we have
$$n_2 = \alpha_0 \quad . \quad . \quad . \quad . \quad . \quad . \quad . \quad (15)$$

and
$$n_1 = \sum_0^\infty \alpha_r l^r. \quad . \quad . \quad . \quad . \quad . \quad . \quad (16)$$

From Fick's law (7) we find
$$D\sum_2^\infty r(r-1)\alpha_r x^{r-2} = \sum_0^\infty x^r \frac{d\alpha_r}{dt}. \quad . \quad . \quad . \quad (17)$$

Hence, equating coefficients of like powers of x in (17)
$$Dr(r-1)\alpha_r - \frac{d\alpha_{r-2}}{dt} \quad . \quad . \quad . \quad . \quad . \quad (18)$$

where r goes from 2 to infinity.

We have immediately $\alpha_2 = \alpha_4 = \alpha_{2r} = 0$ and the solution is
$$n = n_2 + \sum_0^\infty \frac{x^{2r+1}}{D^r(2r+1)!}\frac{d^r\alpha_1}{dt^r}. \quad . \quad . \quad . \quad (19)$$

Equation (16) gives
$$n_1 = n_2 + \sum_0^\infty \frac{l^{2r+1}}{D^r(2r+1)!}\frac{d^r\alpha_1}{dt^r}. \quad . \quad . \quad . \quad (20)$$

Now the function α_1 will be determined by the initial values of n, and the boundary conditions at $x = 0$ and $x = l$. If we assume that $t = 0$ when $l = 0$, we can change the independent variable t in α_1 to l and write
$$\alpha_1 = (n_2 - n_1)\sum_0^\infty a_r l^{-r} \quad . \quad . \quad . \quad . \quad (21)$$

where the a_r's are now constant.

---

[2] *Z. physik. Chem. B*, 1938, **40**, 197.

Now consider the moving boundary. From (1)

$$\frac{\mathrm{d}l}{\mathrm{d}t} = -\frac{M_{\mathrm{AB}}}{\rho M_{\mathrm{B}}}\sum_{0}^{\infty}\frac{l^{2r}}{D^{r-1}(2r)!}\,\frac{\mathrm{d}^r\alpha_1}{\mathrm{d}t^r}. \qquad (22)$$

But since $\mathrm{d}l/\mathrm{d}t \to 0$ as $l \to \infty$, we can write it in the form

$$\frac{\mathrm{d}l}{\mathrm{d}t} = \sum_{1}^{\infty}\frac{b_r}{\mathrm{e}^{-r}}. \qquad (23)$$

The method of solution is now clearly as follows. If we substitute α_1 of (21), in (20) and (22), and then use (23) for $\mathrm{d}l/\mathrm{d}t$ in both equations, by expanding both sides of each equation in powers of l we obtain ∞^2 equations for the ∞^2 coefficients

$$a_0,\ a_1,\ a_2\ \ldots \text{ and } b_1,\ b_2 \ldots .$$

Consider first the coefficients a_1 and b_1. The two equations to determine them are respectively

$$a_1\left(1 - \frac{b_1}{D3!} + \frac{3b_1^2}{D^2 5!} - \qquad\right) = -1 . \qquad (24)$$

and

$$a_1\left(1 - \frac{b_1}{D2!} + \frac{3b_1^2}{D^2 4!} - \qquad\right) = -\frac{\rho M_{\mathrm{B}} b_1}{D(n_2 - n_1)M_{\mathrm{AB}}}. \qquad (25)$$

Both series are readily summed :

$$\sum_{0}^{\infty}(-1)^n\frac{3\cdot 5\cdots(2n-1)}{(2n+1)!}\left(\frac{b_1}{D}\right)^n = \left(\frac{\pi D}{2b_1}\right)^{\frac{1}{2}}\operatorname{erf}\left(\frac{b_1}{2D}\right)^{\frac{1}{2}} \qquad (26)$$

where erf x is the error integral defined as $\operatorname{erf} x = \frac{2}{\sqrt{\pi}}\int_0^x \mathrm{e}^{-y^2}\mathrm{d}y$.

$$\sum_{0}^{\infty}(-1)^n\frac{3\cdot 5\cdots(2n-1)}{(2n)!}\left(\frac{b_1}{D}\right)^n = \mathrm{e}^{-b_1/2D}. \qquad (27)$$

Hence b_1 is obtained as the solution of

$$\frac{(n_2 - n_1)M_{\mathrm{AB}}}{\rho M_{\mathrm{B}}} = \left(\frac{b_1\pi}{2D}\right)^{\frac{1}{2}}\mathrm{e}^{b_1/2D}\operatorname{erf}\left(\frac{b_1}{2D}\right)^{\frac{1}{2}} \qquad (28)$$

and for a_1 we find

$$a_1 = -\left(\frac{2b_1}{\pi D}\right)^{\frac{1}{2}}\operatorname{erf}^{-1}\left(\frac{b_1}{2D}\right)^{\frac{1}{2}}. \qquad (29)$$

These equations are readily solved numerically ; the simplest procedure is to calculate $(n_2 - n_1)M_{\mathrm{AB}}/\rho M_{\mathrm{B}}$ for various values of $b_1/2D$ using (28). The value of b_1, for any given concentration difference $(n_2 - n_1)$ is then found by interpolation.

It is easily verified that when condition (13) is satisfied, b_1 has the value given by (3). For all the expressions on the right-hand side of (28) are increasing functions of b_1, and therefore (3) is satisfied for $b_1/2D \ll 1$. For this case, $\exp(b_1/2D) \to 1$, $\operatorname{erf}(b_1/2D)^{\frac{1}{2}} \to (2b_1/\pi D)^{\frac{1}{2}}$, and so

$$b_1 \to D(n_2 - n_1)M_{\mathrm{AB}}/M_{\mathrm{B}}\rho.$$

An alternative method of solution, suitable when (3) is approximately fulfilled, is to express both a_1 and b_1 as series of powers of τ where

$$\tau = \frac{(n_2 - n_1)M_{\mathrm{AB}}}{M_{\mathrm{B}}\rho} \qquad (30)$$

and then to substitute the series in (24) and (25). Comparing like powers of τ we determine the successive coefficients. If

$$a_1 = \sum_0^\infty a_{1n}\tau^n ; \quad b_1 = D\sum_0^\infty b_{1n}\tau^n$$

then

$$a_{10} = -1, \quad a_{11} = -\frac{1}{6}, \quad a_{12} = \frac{19}{360},$$

$$b_{10} = 0, \quad b_{11} = 1, \quad b_{12} = -\frac{1}{3}, \quad b_{13} = \frac{7}{45}.$$

Next consider a_2 and b_2; they are given by

$$a_2 - \frac{1}{3!\,D}(2a_2b_1 + a_1b_2) + \frac{1}{5!\,D^2}(8a_2b_1^2 + 7a_1b_1b_2) - \ldots = 0 \qquad (31)$$

$$b_2 + D\tau\left[a_2 - \frac{1}{2!\,D}(2a_2b_1 + a_1b_2) + \frac{1}{4!\,D^2}(8a_2b_1^2 + 7a_1b_1b_2)\ldots\right] = 0. \qquad (32)$$

Again writing a_2 and b_2 as expansions in powers of τ

$$a_2 = \sum_0^\infty a_{2n}\tau^n, \quad b_2 = \sum_0^\infty b_{2n}\tau^n,$$

we can solve (31) and (32) as we solved (24) and (25). From (31) we find $a_{20} = 0$; using this in (32) we find $b_{21} = 0$. Again from (31), $a_{21} = 0$; it is quite clear from the method of solution that all the a_{2n} and b_{2n} are zero, and so $a_2 = b_2 = 0$. The same result follows for all the higher coefficients $a_r, b_r (r > 1)$.

Hence we conclude that the rate of growth of product still follows a parabolic law but that the correct form of (3) is

$$\frac{dl}{dt} = D\tau f(\tau)\frac{1}{z} \qquad (33)$$

where for small τ

$$f(\tau) = 1 - \frac{1}{3}\tau + \frac{7}{45}\tau^2 -$$

or more generally, $f(\tau)$ is the solution of the equation

$$f = \frac{2\tau}{\pi} e^{-\tau f}\left[\operatorname{erf}\left\{\left(\frac{\tau f}{2}\right)^{\frac{1}{2}}\right\}\right]^{-2}. \qquad (34)$$

$f(\tau)$ calculated numerically from (34) is shown in Fig. 2.

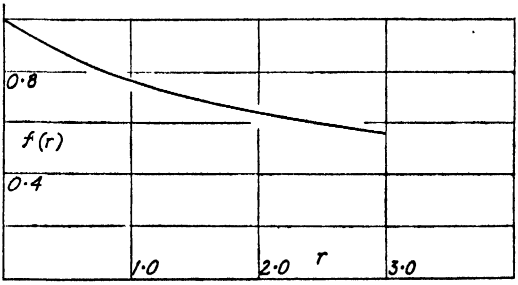

FIG. 2.—Dependence of $f(\tau)$ (eqn. (33)) on parameter $\tau = (n_2 - n_1)M_{AB}/\rho M_D$.

From (19)

$$n - n_1 = (n_2 - n_1)\,\frac{\operatorname{erf}\frac{x}{l}\left(\frac{b_1}{2D}\right)^{\frac{1}{2}}}{\operatorname{erf}\left(\frac{b_1}{2D}\right)^{\frac{1}{2}}}. \qquad (35)$$

Fig. 3 shows that the modification of the linear gradient is only marked for large τ.

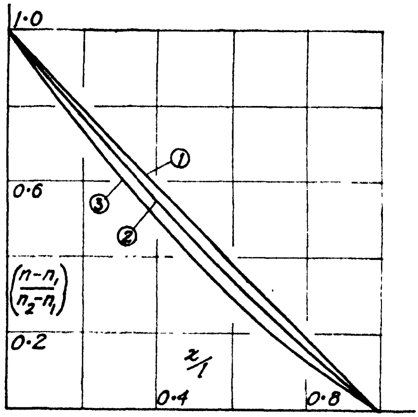

FIG. 3.—Dependence of concentration gradient upon parameter τ.
(1) $\tau = 0$. (2) $\tau = 1$. (3) $\tau = 3$.

Hence we see that the modification of the usual theory will only be noticeable in cases where the product can take up large quantities of the diffusing materials. Possibly, examples of interest may be found in the oxidation of some metals which form higher oxides; for example the oxidation of barium to barium oxide. The lattice structures of barium oxide and barium peroxide are so similar that it seems very likely that the oxide can acquire quite a high concentration of oxygen.

Summary.

An error is pointed out in the theory usually given for the rate of the reaction between a solid and a gas or liquid, in which the reaction proceeds by the diffusion of the reactants through a layer of the product formed on the surface of the solid. A condition for the applicability of the usual theory is given, and an exact solution derived. It is shown that the rate of growth of the product is inversely proportional to its thickness as in the simple theory, but that the constant of proportionality depends upon the density of the reactants in the product and the density of the product.

H. H. Wills Physical Laboratory,
The University,
Bristol.

THE EFFECT OF MOLECULAR INERTIA ON DIELECTRIC ABSORPTION.*

By J. G. Powles.

Received 4th December, 1947.

Recent developments in microwave radio technique have permitted an extension of dielectric investigation to wavelengths down to a few mm., where it would seem likely that molecular inertia may begin to exercise an effect on the motion of dipolar molecules in an applied alternating field and hence on the associated energy absorption. The effect may be expected to become appreciable when the kinetic energy of the orienting molecule becomes comparable with its thermal energy, and it may be noted that for a molecule having $I \doteq 500 \times 10^{-40}$ g. cm.^{2} and at a wavelength of 5 mm., $\frac{1}{2}I\omega^2$ is of the order of $0{\cdot}1\ kT$ at room temperature.

The possible importance of this effect has been recently referred to by Whiffen[1] and a partial analysis has been carried out by Rocard.[2] The present analysis seeks to extend this and, in particular, to consider the effect in relation to measurements of absorption in dilute solutions of a polar substance in a non-polar solvent.

Theoretical.

The theoretical treatment is essentially a modification of the existing Debye theory of dispersion in polar liquids at high frequencies.[3] In this theory the movement of the polar molecules is considered in two parts, denoted by Δ_1 and Δ_2, Δ_2 arising from Brownian or kinetic collisions with adjacent molecules and Δ_1 caused by the impressed alternating field. We shall assume that the Brownian motion of the molecules, i.e. Δ_2 is not affected by molecular inertia. The motion due to the impressed field is affected, and we shall deduce the necessary modification below.

The torque on a molecule of dipole moment μ at θ to the applied field $F = F_0 e^{i\omega t}$ is

$$M = -\mu F \sin \theta. \qquad (1)$$

Neglecting inertia, Debye writes

$$M = \zeta \frac{d\theta}{dt} \qquad (2)$$

and uses

$$\delta\theta = \frac{M}{\zeta}\,\delta t. \qquad (3)$$

where $\zeta = 2kT\tau$ and τ is a relaxation time, and from this he deduces that

$$\Delta_1 = -\frac{\partial}{\partial\theta}\left(2\pi f \frac{M}{\zeta}\delta t \sin\theta\right)\delta\theta. \qquad (4)$$

When inertia is included, (2) becomes

$$I\frac{d^2\theta}{dt^2} + \zeta\frac{d\theta}{dt} = M \qquad (5)$$

It may be noted that (5) is by no means the correct vibrational equation of motion of the polar molecule since although it accounts for the loss of energy of the oscillating molecule to the surrounding ones, it takes no account of the reverse process, namely the increase of the kinetic energy due to thermal fluctuations. This is demonstrated by taking the static case ($\omega = 0$) when (5) indicates that for a direct field all dipoles lie ultimately in the direction of the field. This is equally true of (2) and, as mentioned above, Debye allows for this by splitting the motion into two parts Δ_1 and Δ_2, a step which is justified to a certain extent by recent measurements.[4, 5, 6] It is proposed to neglect similarly the effect of thermal fluctuations in solving (5) to obtain a value for $\delta\theta$, the angle turned through by a polar molecule in time δt, which takes account of the inertia of the molecule.

---

* See additional note on p. 844.

[1] Whiffen, *Trans. Faraday Soc.*, 1946, **42***A*, 77.

[2] Rocard, *J. Physique Rad.*, 1933, **4**, 247.

[3] Debye, *Polar Molecules*, p. 77 *et seq.*

Solution of (5) shows that to a good approximation

$$\frac{d\theta}{dt} = \frac{M}{\zeta} \cdot \frac{1}{1 + \frac{i\omega I}{\zeta}} \quad . \quad . \quad . \quad . \quad . \quad (6)$$

The effect of inertia is thus to modify M or $\frac{1}{\zeta}$ in (3) by the factor $\frac{1}{1 + \frac{i\omega I}{\zeta}}$ and this leads to the differential equation for f, the distribution function for the polar molecules:

$$\frac{\partial f}{\partial t} = \frac{1}{\sin\theta} \frac{\partial}{\partial\theta}\left\{ \sin\theta\left[\frac{\bar{\theta}^2}{4\delta t} \frac{\partial f}{\partial\theta} - \frac{M}{\zeta} \frac{1}{1 + \frac{i\omega I}{\zeta}} \cdot f\right]\right\}^* . \quad . \quad (7)$$

Following Debye's procedure, $\frac{\bar{\theta}^2}{4\delta t}$ is derived from the steady-state condition given by $\frac{\partial f}{\partial t} = 0$ when $f = A\epsilon^{\frac{\mu F}{kT}\cos\theta}$. Thus

$$\frac{\bar{\theta}^2}{4\delta t} = \frac{kT}{\zeta} \frac{1}{1 + \frac{i\omega I}{\zeta}} \quad . \quad . \quad . \quad . \quad . \quad (8)$$

which reduces for $\omega = 0$, to the Debye form:

$$\frac{\bar{\theta}^2}{4\delta t} = \frac{kT}{\zeta} \quad . \quad . \quad . \quad . \quad . \quad . \quad (9)$$

Although (9) is certainly true at low frequencies, it seems probable that the value of $\frac{\bar{\theta}^2}{4\delta t}$ required for use in (7) at high frequencies needs modification for the effect of inertia. A suitable modification may be given by (8) but in view of the uncertainty we shall take the value of $\frac{\bar{\theta}^2}{4\delta t}$ given by

$$\frac{\bar{\theta}^2}{4\delta t} = \frac{kT}{\zeta} \cdot \frac{1}{1 + \alpha\frac{i\omega I}{\zeta}} \quad . \quad . \quad . \quad . \quad . \quad (10)$$

where $< 0 \quad \alpha < 1$ and we shall see later that the particular value of α chosen within this range makes little difference to the result where the expected deviation due to inertia is largest.

---

[4] Jackson and Powles, ref. 1, 101.

[5] Whiffen and Thompson, *ibid.*, 114.

[6] Sutherland and Cripwell, *ibid.*, 149.

[*] Compare with eqn. (46), p. 82, ref. 3.

Using (10) in (7) and solving by use of the trial solution,

$$f = A\left[1 + B\frac{\mu F}{kT}\cos\theta\right],$$

we find
$$B = \frac{1}{1 - x(\omega\tau)^2}\cdot\frac{1}{1 + i\omega\tau'}$$

where
$$\frac{\tau'}{\tau} = \frac{1 + (1 - \alpha)x}{1 - x(\omega\tau)^2},$$

using $\zeta = 2kT\tau$ and putting $x = \dfrac{I}{2kT\tau^2}$.

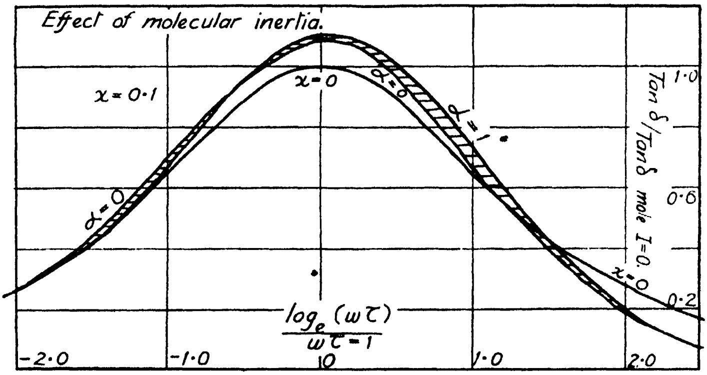

FIG. 1.

For liquids with a low dipolar concentration and dilute solutions of a polar substance in a non-polar solvent, this leads to the equation:

$$\tan\delta = C\frac{\omega\tau[1 + (1 - \alpha)x]}{[1 - x(\omega\tau)^2]^2 + (\omega\tau)^2[1 + (1 - \alpha)x]^2} \quad . \quad . \quad (11)$$

a relation which reduces to the Debye equation:

$$\tan\delta_{I=0} = C\frac{\omega\tau}{1 + (\omega\tau)^2} \quad . \quad . \quad . \quad . \quad . \quad (12)$$

for $I = 0$, $(x = 0)$.

The effect of molecular inertia is therefore given by the expression:

$$\frac{\tan\delta}{\tan\delta_{I=0}} = \frac{[1 + (1 - \alpha)x][1 + (\omega\tau)^2]}{[1 - x(\omega\tau)^2]^2 + (\omega\tau)^2[1 + (1 - \alpha)x]^2}.$$

For the purpose of illustration it is convenient to take $x = 0{\cdot}1$ and Fig. 1 shows the estimated effect of molecular inertia on the variation of tan δ with frequency for this value of x and for the limiting values 0 and 1 of α. It is seen that the deviation from the simple Debye curve is proportionally most marked for values of $\omega\tau > 4$.

Application to Dilute Solutions.

It is interesting to calculate the effect in the case of solutions of polar molecules in non-polar solvents, where it has been found that within the experimental error the relation (12) is obeyed for particular solutions.[4, 5, 6] It is therefore reasonable to assume that apart from the inertia effect the absorption depends on frequency in the manner given by (12) and to calculate the correction required. To do this, it is necessary to know the values of the moments of inertia for the polar molecules used. Since suitable figures are not available, estimates have been made by using atomic spacings as derived from infra-red and other measurements on simple molecules, and by use of ordinary mechanics. The resulting values are given in Table I.

TABLE I.

Polar Material.	$I \times 10^{40}$ g. × cm.^{2}	$\tau \times 10^{12}$ sec.	$\frac{\sqrt{I}}{\tau} \times 10^8$.
Benzophenone . .	1620	17·8	2·3
Nitrobenzene . .	793	12·8	2·2
Bromobenzene . .	912	12·0	2·5
Chloroform . . .	366	8·5	2·3
Acetone . . .	106	3·5	3·0

In most cases the value of the moment of inertia depends on the axis of rotation and the value of I to be used must be an average for all directions of the dipole relative to the field. It is, however, only necessary to average for small oscillations about all mean positions of the molecule in which the dipole is at right-angles to the field, since, for a mean position where the dipole is not at right-angles to the field, only the torque, and not the axis of oscillation is changed. Some care is required in the case of molecules where the moment of inertia varies greatly with the axis of oscillation. In spite of the approximate nature of the calculation we shall find that the figures for moments of inertia in Table I are sufficiently accurate for our purpose.

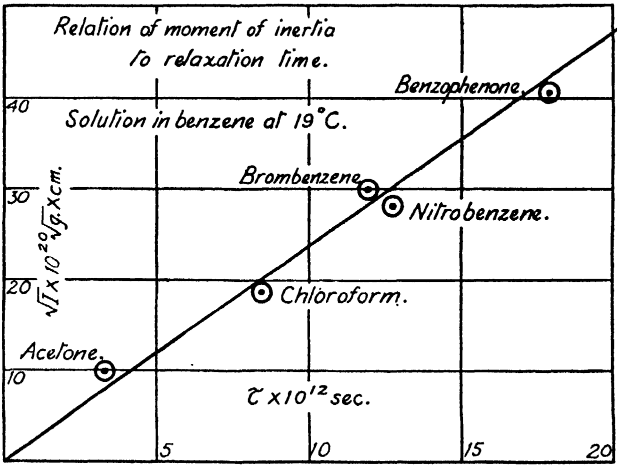

FIG. 2.

The values of relaxation time in benzene solution at 19° c. of the polar substances in question are given in the third column of Table I, and the derived values of $\sqrt{I}/\tau$ in the fourth column. It is seen that this ratio, and with it the value of $x = \frac{I}{2kT\tau^2}$, is substantially constant for the five solutions. This is illustrated by the plot of $\sqrt{I}$ against τ in Fig. 2. The linearity of this plot suggests that τ is proportional to some " mean radius " of the molecule and not to its volume as suggested by Debye (ref.[3], p. 85).

We are now in a position to assess the order of magnitude of the inertia effect on the premises of the preceding analysis. According to the data of Table I, x for these benzene solutions has the value 0·007, and by reference to Fig. 1 it is evident that the effect on the shape of the absorption curve is much less than could be distinguished by experiment with the present order of experimental error.

It is to be expected that the inertia effect will become more pronounced with decreasing solvent viscosity since the value of τ becomes smaller, for a given solute. For a solution of chloroform in heptane, Whiffen and Thompson [7] give $\tau = 3{\cdot}1 \times 10^{-12}$ sec. corresponding to which $x = 0{\cdot}047$, and it may be estimated that for solution in pentane, the hydrocarbon liquid with lowest viscosity available, $x \sim 0{\cdot}08$. These values are not sufficiently large for experimental assessment from measurements with values of $\omega\tau$ near unity and values of $\omega\tau > 2$ involve considerable difficulty at the present time. Thus for benzophenone in pentane measurements above a frequency of about 10^{11} c./sec. ($\omega\tau \approx 3$) would seem to be required for which oscillators are not yet available. The effect is not large enough to show promise as a method of estimating moment of inertia values of polar molecules.

The author wishes to record his thanks to Prof. Willis Jackson and Prof. H. Fröhlich for helpful discussions, and to the Department of Scientific and Industrial Research for a grant.

Summary.

It has been shown by an extension of Debye's analysis and with certain assumptions, that the effect of molecular inertia on the absorption in dilute solutions of polar substances in a non-polar solvent depends on the quantity $\frac{I}{2kT\tau^2}$, and that the greatest effect is to be expected with solvents of low viscosity rather than by the use of polar molecules with large moments of inertia. The effect is most marked for values of $\omega\tau \gg 1$ but departure from Debye's relation (12) might be noticeable in solvents of low viscosity for values of $\omega\tau$ near unity (see Fig. 1).

The present analysis shows that the effect of inertia is small for the frequencies at present available to measurement and it is unlikely that a complete analysis for this and other molecular models, including other possible causes of deviation from the Debye relation (12), could yet be checked effectively.

Electrical Engineering Department,
Imperial College,
London.

---

[7] Whiffen and Thompson, ref. 1, 167.

EMISSION BANDS FROM THE ELECTRODELESS DISCHARGE IN CARBON TETRABROMIDE VAPOUR.

By R. A. Durie and T. Iredale.

Received 8th December, 1947.

Band spectra of the radicals CCl, CBr, CI are not easy to obtain. In their study of an electric discharge in CCl_4 vapour at low pressures, Asundi and Karim [1] reported an emission spectrum consisting of continuous bands with maxima at 4600, 3348, 3070, 2580, 2430, 2300 A., also two other groups of bands in the short-wave ultra-violet region, one of which was practically coincident with a CO band-group. These authors have

---

[1] *Proc. Indian Acad. Sci. A*, 1937, **6**, 328.

into any vibrational scheme. The brown polymer, on analysis, gave the following results : C : 13·95 % ; Br : 85·76 % ; H : 0·20 %. The ratio of C to Br in this compound is therefore approximately 1 : 1, and it might conceivably be built up from CBr radicals. But it does not appear to be C_6Br_6. It is insoluble in ethyl alcohol and ether, and slightly soluble in warm benzene. It melts rather indefinitely about 160° c., and later decomposes, liberating Br_2.

The authors are indebted to Mr. R. C. Blake for carrying out some of the earlier experimental work.

Summary.

The spectrum of the electrodeless discharge in CBr_4 vapour has been photographed, and some new diffuse bands have been found in the ultra-violet region. They are provisionally attributed to CBr. A brown polymer was deposited on the walls of the discharge tube, consisting almost entirely of C and Br in the ratio 1 : 1.

Note added in proof.—Dr. Gaydon in a private communication has informed me that the band in the 2900 A. region is more likely due to Br_2, as he has obtained it from an electrodeless discharge in that gas. Long ago Strutt and Fowler (*Proc. Roy. Soc. A*, 1912, **86**, 109) obtained a similar band during their study of the reactivity of active nitrogen and bromine.

Physical Chemistry Laboratories,
University of Sydney,
Australia.

THE MECHANISM OF FORMATION OF DIETHYL ETHER USING THE HEAVY OXYGEN ISOTOPE ^{18}O AS A TRACER ELEMENT.

By I. Lauder and J. H. Green.

Received 16*th December*, 1947.

An etherification reaction between an ester of an inorganic oxy-acid and an alcohol must involve a fission of an alkyl-oxygen bond in one of the reactants. There is much indirect evidence that the bond in the ester is broken during reaction but, possibly, the most direct information on the process may be obtained by use of the heavy oxygen isotope, ^{18}O, as a tracer element. This method of approach has been used to investigate the mechanism of formation of diethyl ether by reaction between diethyl sulphate and ethyl alcohol.

This reaction occurs readily at 57° c.,[1] but more readily, even at room temperature, if an equivalent amount of alkali and a small amount of water are present.[2] As a first step, the reaction was investigated under the latter conditions. The procedure adopted was to allow "heavy-oxygen" ethyl alcohol to react with diethyl sulphate in the presence of sodium hydroxide and water, and the ^{18}O content of the ether formed was indirectly determined. The two possible mechanisms involved are represented by the equations :

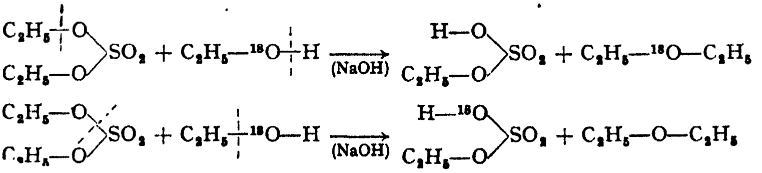

(1)

(2)

---

[1] Kremann, *Monatsh.*, 1906, **27**, 1265.

[2] Cade, *Chem. Met. Eng.*, 1923, **29**, 319.

If mechanism (1) is correct and no interfering reaction occurs, the ether formed should contain the oxygen originally present in the alcohol. On the other hand, if mechanism (2) is correct, the ether formed should contain " normal " oxygen. It is possible of course, that both mechanisms are involved, in which case the ^{18}O content of the ether would depend on the relative importance of the two reactions.

In a preliminary report on this investigation,[3] it was mentioned that the interpretation of the results was complicated by the occurrence of two side-reactions, namely, hydrolysis and alcoholysis. It is probable that both lead to the formation of " normal " ethyl alcohol, and so the measurement of the ^{18}O content of the ether isolated at the end of one fixed reaction-period does not reveal the exact nature of the etherification process. However, by varying the reaction period, the extrapolation of the curve obtained by plotting ^{18}O content of ether against time gives the desired result, viz. the ^{18}O content of the ether formed solely from the alcohol originally present in the mixture.

Experimental.

MATERIALS.—Diethyl sulphate was prepared and purified according to details given by Houben.[4]

Heavy oxygen alcohol was prepared by hydrolysis of ethyl bromide in excess heavy oxygen water made alkaline by magnesium hydroxide. As ethyl bromide and ethyl alcohol form an azeotropic mixture (7 mol. % C_2H_5OH ; b.p. 37·6° c.) it was found advisable to have slightly more magnesium hydroxide present than required for the hydrolysis of all the ethyl bromide to avoid loss of the desired product during the subsequent distillation process.

One g. magnesium oxide and 4 g. water were heated in a heavy-walled Pyrex glass tube for 24 hr. to establish isotopic equilibrium. A sample of water was then withdrawn for isotopic measurement and then 4·5 g. ethyl bromide were added. After removing the air, the tube was sealed and it was then heated at 110° c. with constant shaking for 3-7 days. After that period, the tube was cooled and the volatile products were pumped off while the temperature was gradually increased to 100° c. The product, aqueous alcohol containing usually a trace of ethyl bromide, was transferred to a small distillation vessel. On warming, any trace of ethyl bromide passed off (as the azeotropic mixture) and then the fraction distilling up to 100° c. was collected. This was redistilled and the distillate was collected until the ratio of water to ethyl alcohol had reached the desired value. The latter stage was judged by use of a small totally immersed " hydrometer " which had been adjusted to remain suspended at 0° c. in an alcohol-water mixture of the desired proportion. Both components were thus equally enriched in ^{18}O, viz. to about 0·4 %, the excess density of the water being 328 p.p.m. The excess density of the alcohol was not measured as such, since assay of the ^{18}O content is always made by conversion of the oxygen of alcohol, ether, etc., into water, the density of the latter being then measured.

Heavy oxygen water required for the above preparation was obtained by use of the thermal-diffusion apparatus described by one of the authors.[5]

PROCEDURE.—The reactants were mixed in the following proportion :

Diethyl sulphate	11·7 millimoles
Sodium hydroxide	8·95 ,,
Alcohol	8·95 ,,
Water	9·8 ,,

and, after removing the air, shaking was commenced. At the desired intervals, samples of ether were pumped off, while the reaction mixture was cooled to − 60° c. Only small traces of water and alcohol came off with the ether and these were removed from the sample by contact with sodium metal. The oxygen in the ether was then obtained in the form of water by a technique similar to that already described by Herbert and Lauder.[6] The excess density of the purified sample of water was determined by the micro-pyknometer method of Gilfillan and Polanyi.[7]

---

[3] Lauder and Green, *Nature*, 1946, **157**, 767.

[4] *Die Methoden der organischen Chemie* (Dr. Aufl.) **4**, 517.

[5] Lauder, *Trans. Faraday Soc.*, 1947, **43**.

[6] Herbert and Lauder, *Trans. Faraday Soc.*, 1938, **34**, 432.

[7] Gilfillan and Polanyi, *Z. physik. Chem.*, 1933, **166**, 254.

Results.

Duplicate density measurements on any sample of water agreed within the experimental error of ± 5 p.p.m. but the results obtained for corresponding periods from successive reaction mixtures showed a variation of ± 10 p.p.m. The results are shown graphically in Fig. 1 in which excess density has been plotted against reaction time. Each point represents the arithmetic mean of four determinations. The extrapolation of the curve, obtained by joining up the points for reaction times of 150, 31 and 16 min. respectively, cuts the excess density axis at a value approximately 320 ± 5 p.p.m. As the excess density of the water formed from oxygen present in the original "heavy-oxygen" alcohol was 328 p.p.m. it may be concluded that mechanism (1) is correct, i.e. the ether formed contains the oxygen originally present in the alcohol.

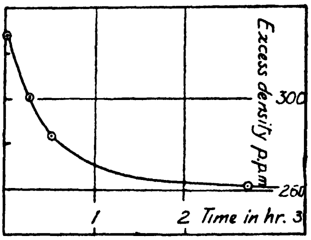

FIG. 1.

This investigation was financed by funds given to the University of Queensland by the Commonwealth Council for Scientific and Industrial Research.

Summary.

The mechanism of reaction between diethyl sulphate and ethyl alcohol has been investigated using the heavy-oxygen isotope as a tracer element. The results show that during reaction, the alkyl oxygen bond in the ester breaks, but not that in the alcohol.

Department of Chemistry,
University of Queensland,
Brisbane,
Australia.

THE VAPOUR PRESSURES OF SOME HIGH BOILING ESTERS.

BY P. A. SMALL, K. W. SMALL AND P. COWLEY.

Received 16*th December,* 1947.

In this paper we record measured values of the vapour pressures, between about 5×10^{-2} and 10^{-4} mm. Hg of a number of high boiling esters of molecular weight range 200-430, some of which are used in industry as plasticisers. As previously discussed,[1] a knowledge of the vapour pressure of a material is an important factor in assessing its serviceability as a plasticiser. From our results we can estimate an approximate value for the V.P. at 100° C. and also at other temperatures, by taking a calculated value for ΔH, for esters of known molecular weight, provided that they do not have a highly branched configuration, as found, for example, in the trialkyl phosphates. Values for dibutyl phthalate covering a much wider range are also given.

Experimental.

The vapour pressures of substances of low volatility have frequently been calculated from measurements of the rate of effusion of the vapour through small orifices or tubes, of diameter considerably less than the mean-free-path of the molecules. Many experimental methods have been described and our method resembled that of Ubbelohde [2] in many respects.

---

[1] Small, *J. Soc. Chem. Ind.*, 1947, **66**, 17.

[2] Ubbelohde, *Trans. Faraday Soc.*, 1938, **34**, 282.

In the apparatus (Fig. 1) used in the present work, the liquid to be investigated was placed in a spherical glass bucket (*a*) weighing about 0·75 g. and having a small circular sharp-edged hole. This hole was ground circular with fine carborundum powder and a steel needle, and the sharp edge was then made by grinding the outside of the bucket on a glass plate with carborundum. After the diameter of the orifice had been measured with a microscope, the handle was attached. This bucket was suspended on a calibrated steel spring (*b*—*c*) in a jacketed and lagged glass tube (*d*) connected through a trap to a three-stage oil diffusion pump. By circulating vapours of various liquids, boiling under atmospheric conditions in the jacket (*e*), temperatures up to 155° C. were obtained and maintained constant for the period of the experiments to within ± 0·1° C. in the tube. When temperature equilibrium was reached the system was evacuated and the residual gas pressure was reduced to 10^{-4} mm. Hg or less as indicated by a McLeod gauge. The rate of effusion of the vapour of the material in the bucket was followed with a cathetometer (*f*) reading to 0·001 cm. by recording the rate of contraction of the spring. The steel springs used extended by 5-7 cm./g. load and were calibrated at each temperature, the calibration being correct to one part in 200. The actual temperature of the glass bucket and its liquid contents at the time of evaporation differs slightly from that of the surrounding vacuum as read on the thermometer (*g*) suspended inside the jacket by factors depending on the effects due to (1) the change in external pressure on the thermometer which amounted for different thermometers to 0·5-1·0° C.; this effect was corrected for; (2) radiation to the cold, open end of the tube and (3) the cooling due to the evaporation of the liquid itself.

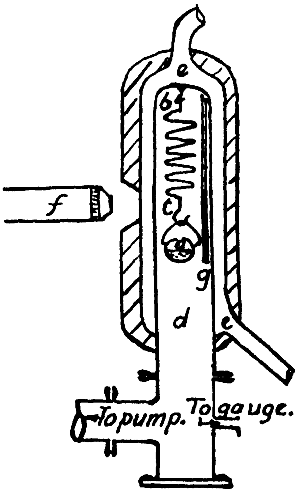

FIG. 1.—Apparatus for measuring rate of effusion of a vapour through an orifice.

From a consideration of the heat-balance between the bucket (assuming the emissivity of glass to be unity), and its surroundings, the effect of radiation to the end was estimated to lower the bucket temperature by an amount depending on the temperature of the outer tube, the maximum value of which was about 0·2° C. A correction was applied for this effect when it was significant.

The effect of the evaporation of the liquid was more serious. For butyl phthalate, a rate of evaporation of $1·5 \times 10^{-6}$ g./sec. was calculated to give an error of 1° C. By selecting orifices giving rates of evaporation not greater than this value, the correction could be estimated sufficiently exactly. The orifice diameters used were between 0·086 cm. and 0·627 cm., the hole being small with respect to the maximum section of the bucket, but not so small that it behaved as a tube rather than a hole in a very thin sheet. Hence in the system described, the space inside the bucket was assumed to be saturated with vapour which effused out into a region of effectively zero pressure, since for pressures of less than 10^{-4} mm. Hg the mean-free-path of the molecules is large compared with the dimensions of the orifice. In these circumstances the use of the kinetic formula for the rate of effusion μ through a small hole in a thin sheet is justified. That is

$$\mu^2 = \frac{p\rho}{2\pi} \quad (p \text{ in dyne cm.}^{-2},\ \rho, \text{ the gas density in g./cm.}^{-3}).$$

Hence, treating the vapour as a perfect gas,

$$p = 17·15\left(\frac{T}{M}\right)^{\frac{1}{2}}\mu$$

where p is the V.P. in mm. Hg of the substance with molecular weight M, at the temperature $T°$ K., and μ is in g. cm.$^{-2}$ sec.$^{-1}$.

In the case of dibutyl phthalate, one of the more volatile of the common plasticisers, V.P. measurements have been made up to temperatures approaching the boiling point, using an isoteniscope similar to that described by Smith and

Menzies,[3] and also by distillation at pressures controlled by a manostat. The results are not separately recorded but are given in Fig. 5.

Materials.—Commercial samples of good colour of dibutyl phthalate and sebacate were fractionated under reduced pressure to give colourless liquids of theoretical saponification values. In the case of tricresyl phosphate, measurements were made on a typical industrial sample (mixed isomers) of light brown colour, and also on a sample of tri-*m*-cresyl ester of good colour supplied by A. Boake Roberts & Co. which after distillation in the molecular still contained the theoretical amount of phosphate. The sample of butyl acetyl ricinoleate was from a laboratory preparation of A. Boake Roberts & Co. It was slightly yellow in colour and had a saponification value of 281 mg. KOH/g. and acid value 3·6 mg. KOH/g. No reasonably good sample of dioctyl phthalate was available but a pure sample was prepared by us from fractionated 2-ethyl hexanol and phthalic anhydride. The samples of pure *n*-methyl, ethyl, propyl and butyl phthalates were supplied by Dr. R. F. Tuckett. The *n*-amyl and *n*-hexyl phthalates, dioctyl and dibutoxyethyl sebacates, triphenyl, tributoxyethyl phosphates, tetrahydrofurfuryl oleate, and the nonyl esters were synthesised in I.C.I. laboratories. The Mesamoll IV[4] was of German origin, an ester allegedly of the formula $C_{15}H_{31}SO_3C_6H_5$. The ethyl abietate came from Finland. Both these materials are used as plasticisers for polyvinyl chloride in the countries of their origin.

Results.

The relation between V.P. and temperature has been expressed in the usual way by the relation

$$\log_{10} p = \frac{-A}{T} + B$$

or

$$\log_{10} p = \frac{-\Delta H}{2{\cdot}303\, RT} + \text{const.}$$

Plots of $\log_{10} p$ (V.P. in mm. Hg) against $1/T$ have been constructed from our experimental data and are shown in Fig. 2-5. Values of the constants A and B, and of ΔH, the latent heat of evaporation in kcal./g. mol. have been calculated from our results and are listed in Tables I-III together with some data already published. The temperature ranges for which the equations are valid are indicated on the graphs. In a few cases, the experimental values for the V.P. (expressed as $\log_{10} p$) at 100° C. are recorded, as data were not obtained at other temperatures.

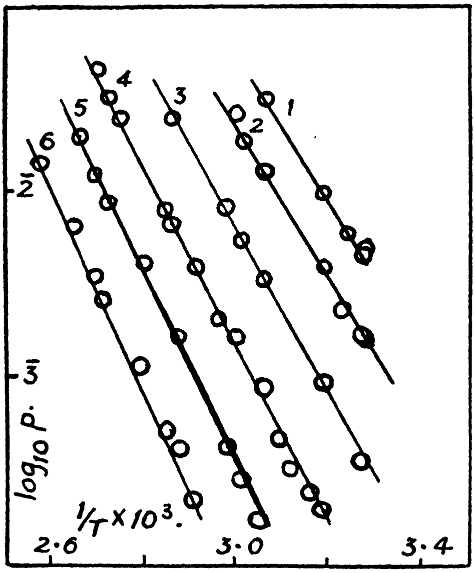

FIG. 2.—$\log_{10} p$ against $1/T$ for the normal phthalate esters.

Discussion.

No detailed analysis of the errors was made; the constants in the equation were obtained by the "zero-sum" method. Our method gave values of A, B and ΔH which are close to those of other workers for the few plasticisers for which V.P. data have been published. There is a good linear relation between ΔH and $\log_{10} p$ at 100° C. (calculated from the formula), as

---

[3] Smith and Menzies, *J. Amer. Chem. Soc.*, 1910, **32**, 1412.

[4] B.I.O.S. Final Report Na 440, Item No. 22.

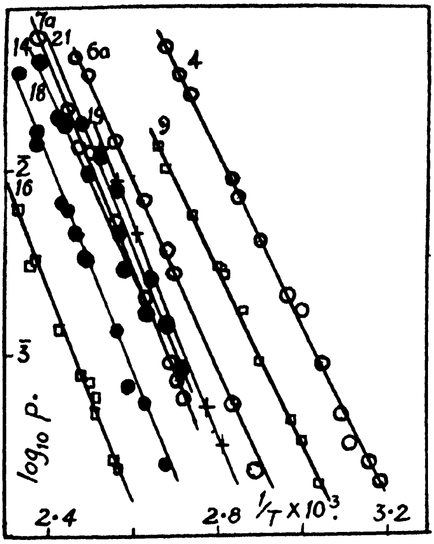

FIG. 3.—$\mathrm{Log}_{10}\,p$ against $1/T$ for some common plasticisers.

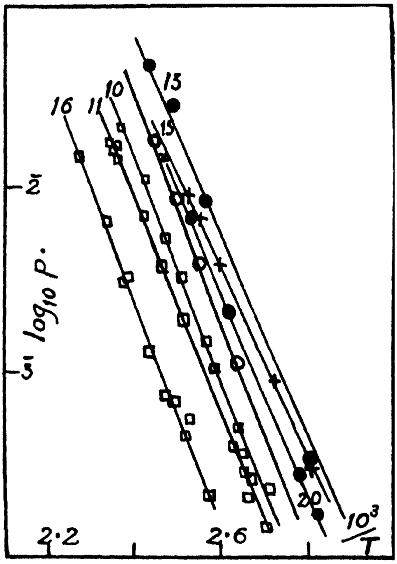

FIG. 4.—$\mathrm{Log}_{10}\,p$ against $1/T$ for various high boiling esters.

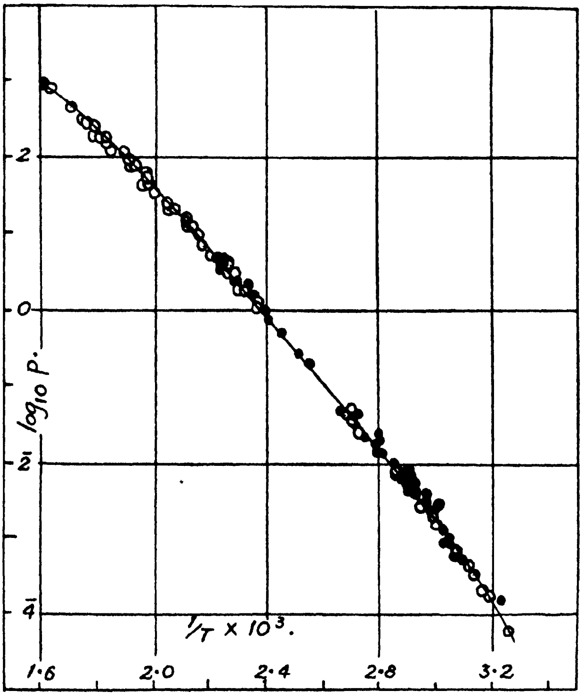

FIG. 5.—$\mathrm{Log}_{10}\,p$ against $1/T$ for dibutyl phthalate.

⊙ This paper. ○ Other published data.

shown in Fig. 6 despite the fact that the temperatures for which ΔH is estimated (the mid-points of the temperature ranges) are different. Thus approximately, $\Delta H = 19{\cdot}0 - 2{\cdot}4 \log_{10} p_{100}$. If this relation is extrapolated to lower molecular-weight esters, it does not fit very well and it is possible that a non-linear relation would hold better over a wider range. This relation is analogous to that found by Barclay and Butler[5] to hold between free energy and entropy of vaporisation from pure liquids and solutions.

There is also a fairly good relation in this series of compounds between molecular weight M and $\log_{10} p$ at 100° c. (Fig. 7). For the phthalates this relation is quite a good straight line ; the correlation chosen for the whole series is $\log_{10} p_{100} = 3{\cdot}34 - 0{\cdot}0167\,M$. It certainly applies only to a relatively restricted range of compounds.* As expected, esters containing branched alkyl chains give rather higher values for p than those calculated from this relation, which was deduced for normal straight-chain esters. However, this expression may prove useful in the prediction of approximate values of v.p.'s for other similar high-boiling esters ; in conjunction with the probably more general relation between ΔH and $\log_{10} p_{100}$, values of v.p. may be estimated at temperatures other than 100° c. It should not be used for phosphoric acid esters. The long-chain trialkyl phosphates, because of their much-branched configuration, have abnormally high v.p.'s and the triaryl phosphates, having a fairly rigid and bulky configuration, have abnormally low v.p.'s. It is of interest to note that among the ester plasticisers which have been investigated, those showing significant variation in physical properties such as v.p. and temperature gradient of viscosity from the average behaviour of the phthalate esters, when incorporated in polyvinyl chloride compositions have imparted rather extreme properties. In a study of the visco-elastic properties of plasticised vinylite VYNW, Aiken, Alfrey, Janssen

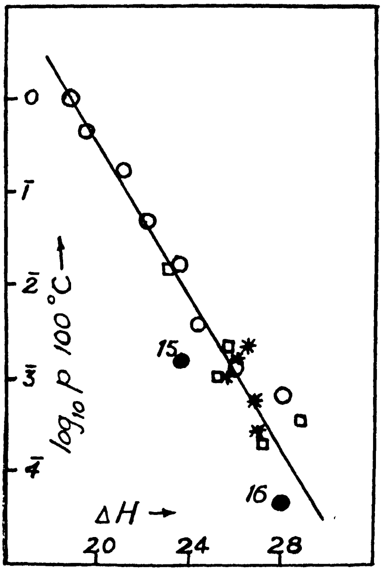

FIG. 6.—ΔH against $\log_{10} p_{100°\text{ c.}}$

● Cyclic compounds.
○ Phthalic esters.

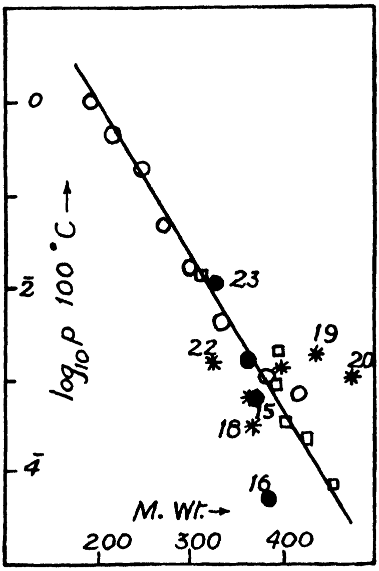

FIG. 7.—M. wt. against $\log_{10} p_{100°\text{ c.}}$

* Phosphates.
□ Aliphatic sebacates.

---

[5] Barclay and Butler, *Trans. Faraday Soc.*, 1938, **34**, 1445.
* This relation is probably only valid for di-esters.

and Mark[6] have observed marked differences in the two extreme cases of tricresyl and trioctyl phosphates, whilst dioctyl phthalate exhibits intermediate behaviour.

TABLE I.

VAPOUR PRESSURE-TEMPERATURE RELATIONS FOR THE PHTHALIC ESTERS.

Ester.	*A.*	*B.*	ΔH kcal./g. mol.	Graph Ref. No.
A. Normal esters.				
Dimethyl	4113	11·06	18·8	1
Diethyl	4308	11·26	19·7	2
Dipropyl	4634	11·66	21·2	3
Dibutyl	4871	11·75	22·3	4
Dibutyl (redist. techn.) .	4875	11·86	22·3	—
Dibutyl[5]	4680	11·21	21·4	—
Dibutyl[6]	5122	12·59	23·4	—
Diamyl	5191	12·04	23·7	5
Dihexyl	5381	11·98	24·6	6
B. Branched-chain esters.				
Di (*sec*-butyl) . . .	4899	12·15	22·4	4*a*
Di (2-ethyl hexyl)[5] . .	5590	12·12	25·6	—
Di (2-ethyl hexyl)[5] . .	5757	12·47	26·3	7*a*
Di (3 : 5 : 5-trimethyl hexyl) .	6175	13·36	28·3	8*a*

TABLE II.

VAPOUR PRESSURE-TEMPERATURE RELATIONS FOR LONG CHAIN ESTERS.

Ester.	*A.*	*B.*	ΔH kcal./g.mol.	$\log_{10} p_{100}$ (mm. Hg.)	Graph Ref. No.
A. Aliphatic.					
Adipate :					
Di (3 : 5 : 5-trimethyl hexyl)	5622	12·40	25·7	—	13
Sebacates :					
Dibutyl	5022	11·58	23·0	—	9
Dibutoxyethyl. . .	6287	13·34	28·7	—	10
Di (2-ethyl hexyl) . .	5934	12·25	27·1	—	11
Di (3 : 5 : 5-trimethyl hexyl)	—	—	—	$\bar{5}$·85	12
Butyl acetyl ricinoleate .	5497	11·71	25·1	—	14
B. Cyclic compounds with aliphatic chains.					
Tetrahydrofurfuryl oleate	5156	10·92	23·6	—	15
Mesamoll IV . . .	—	—	—	$\bar{4}$·78	17
Dibenzyl sebacate[5] . .	6320	12·78	28·9	—	—
Dibenzyl sebacate . .	6116	12·04	28·0	—	16
C. Diterpene derivative.					
Ethyl abietate . .	—	—	—	$\bar{2}$·03	23

DIBUTYL PHTHALATE.—V.P. data on this substance have been already published by Gardner and Brewer,[7] Verhoek and Marshall,[8] Hickman, Hecker and Embree,[9] and Burrows.[10] As these cover a wide pressure range and have been determined by a variety of methods, we have plotted

[6] Aiken, Alfrey, Janssen and Mark, *J. Polymer Sci.*, 1947, **2**, 178.
[7] Gardner and Brewer, *Ind. Eng. Chem.*, 1937, **29**, 179.
[8] Verhoek and Marshall, *J. Amer. Chem. Soc.*, 1939, **61**, 2737.
[9] Hickman, Hecker and Embree, *Ind. Eng. Chem.* (*Anal.*), 1937, **9**, 264.
[10] Burrows, *J. Soc. Chem. Ind.*, 1946, **65**, 360.

them together with our own, for comparison, on Fig. 5, with the exception of the data by Gardner and Brewer, for temperatures below 150° which are obviously unreliable. It was unfortunately necessary to take some of the values from graphs. The boiling point was found by us to be 338° C. at 753 mm., comparing with 340° (*I.C.T.*) and 339·2 (*Handbook of Chemistry and Physics* (Chemical Rubber Publishing Co.)).

TABLE III.

VAPOUR PRESSURE-TEMPERATURE RELATIONS FOR THE PHOSPHATES.

Ester.	*A.*	*B.*	ΔH kcal./ g. mol.	$\log_{10} p_{100}$ (mm. Hg.)	Graph Ref. No.
A. Trialkyl phosphates.					
Tri(2-ethyl hexyl) phosphate	5812	12·85	26·6	—	19
Tri(3 : 5 : 5-trimethyl hexyl) phosphate . . .	5607	11·98	25·6	—	20
Tri(butoxyethyl) phosphate .	5740	12·51	26·3	—	21
B. Triaryl phosphates.					
Triphenyl phosphate . .	—	—	—	$\bar{3}$·18	22
Tricresyl phosphate (techn.)	5925	12·69	27·1	—	18
Tri(*m*-cresyl) phosphate [4] .	6088	12·89	27·8	—	—
Tri(*m*-cresyl) phosphate [4] .	5373	10·98	24·6	—	—
Tri(*m*-cresyl) phosphate .	5895	12·22	27·0	—	18*m*
Tri(*p*-cresyl) phosphate [3] .	5926	12·22	27·1	—	—

The equation, $\log_{10} p = 7{\cdot}065 - \frac{1666}{T} - \frac{547700}{T^2}$ (p in mm.), fits the data fairly well. This form of equation appeared better than an Antoine equation, or one with a term in $\log_{10} T$. However, the results of Verhoek and Marshall, though obtained by several methods, seem systematically high compared with our own and those of Hickman, Hecker and Embree over the same pressure range.

Imperial Chemical Industries Ltd.,
(Plastics Division),
Black Fan Road,
Welwyn Garden City,
Herts.

A NOTE ON THE ULTRA-VIOLET ABSORPTION SPECTRUM OF FORMALDEHYDE.

BY A. J. EVERETT AND G. J. MINKOFF.

Received 18*th December*, 1947.

The ultra-violet absorption spectrum of formaldehyde has been reported as consisting of three main band systems; Henri and Schou [1] studied carefully the bands from 3700 A. to 2590 A., while Price [2] has investigated the bands at 1556 A. and at 1397 A.; the band systems all have vibrational structure, and the 3700-2590 A. system also shows rotational fine structure. In no case have bands been observed between 2590 A. and 1745 A. The purpose of this note is to record the detection of bands extending from 2590 A. to *ca.* 2310 A.; these are apparently of the same series as those between 3700 A. and 2590 A. The HCHO absorption spectrum is often used for following slow oxidations, and it is useful to have a complete knowledge of this spectrum, in order to be able to identify any other absorption bands appearing during oxidation. The detailed analysis of the bands from 3700 to 2590 A. was attempted by Henri and Schou (loc. cit.), and was modified by Herzberg [3]; the treatment failed for bands at wavelengths shorter than *ca.* 2900 A.; further discussions have thus been restricted to the bands at the longer wavelengths.[4] In view of the great difficulty of interpreting the absorption spectrum of HCHO, no attempt is made in this note to systematise the new bands, which were first observed during a study of the reactions of peroxides with aldehydes.[5]

---

[1] Henri and Schou, *J. Chim. Physique*, 1928, **25**, 665; 1929, **26**, 1.

[2] Price, *J. Chem. Physics*, 1935, **3**, 256.

TABLE I.

120 mm. of HCHO, at 180° C. Path length 200 cm. $LC = 5{\cdot}10 \times 10^{20}$ molecules.

Band Maxima (A.).	t_0 (sec.).	t (sec.).	$\log_{10}\frac{t_0}{t}$.	$\frac{1}{LC}\cdot\log_{10}\frac{t_0}{t}$. $\times 10^{20}$.
2563	240	7	1·534	0·299
2550	240	25	0·982	0·192
2543	240	48	0·699	0·137
2521	240	42	0·757	0·148
2493	240	48	0·699	0·137
2884	240	78	0·489	0·096
2470	240	130	0·265	0·052
2461	240	112	0·330	0·065
2456	240	108	0·346	0·068
2431	240	104	0·364	0·071

The experimental conditions differed slightly from those of previous workers; the path length of 200 cm. was twice that used by Henri and Schou, and the concentration of formaldehyde was up to ten times greater. The formaldehyde vapour was obtained from paraldehyde by six successive fractional distillations, the product being cooled at the temperatures of solid CO_2 and of liquid air.[6] In order to reduce fogging of the windows of the absorption tube by deposition of polymer, the absorption tube, connecting tubes, and mercury manometer were heated. It was shown that the temperature did not materially affect the absorption bands. The mercury manometer was disconnected after the pressure had been measured; enough mercury vapour remained in the absorption tube for the Hg line at 2537 A. to appear in absorption.

TABLE II.

Main Band Heads (A.).	Band Maxima (for weak bands) (A.).
2587	2395
2540	2371
2519	2338
2487	2325 ?
2483	2317 ?
2477	2303 ?
2453	
2424	
2421	
2416	

---

[3] Herzberg, *Trans. Faraday Soc.*, 1931, **27**, 378.

[4] Dieke and Kistiakowsky, *Physic. Rev.*, 1934, **45**, 4. Sponer and Teller, *Rev. Mod. Physics*, 1941, **13**, 113.

[5] Bunton, Everett, Halberstadt and Minkoff, *Nature* (in the course of publication).

[6] Spence and Wild, *J. Chem. Soc.*, 1935, 338.

A hydrogen discharge tube which gave light of constant intensity was used as a source of U.-V. radiation. The spectra were photographed on Ilford Zenith plates with a Hilger medium quartz spectroscope. Wavelengths were determined by comparison with an iron arc spectrum photographed on the same plate. In order to determine extinction coefficients, photometer deflections were measured at wavelengths corresponding to absorption maxima for different exposures of the hydrogen continuum on the same plate as the HCHO absorption spectra. The time of exposure t of the hydrogen continuum was then found which gave the same photometer deflection as a particular absorption peak. The approximate * extinction coefficient e was then calculated from the formula

$$e = \frac{1}{LC} \cdot \log_{10} \frac{t_0}{t},$$

where L is the path length, in cm.,
C is the number of molecules of HCHO per cm.,
and t_0 is the time of exposure of the HCHO spectrum.

Extinction coefficients were calculated for the main absorption bands, from spectra taken with a pressure of 120 mm. of HCHO. Photographs of the hydrogen continuum taken before the absorption tube had been filled with HCHO, and after it had been evacuated once more, showed that the windows had not become obscured (Table I). When a pressure of 250 mm. of HCHO was used, absorption bands were more clearly defined (see Plate I), but some fogging of the windows occurred, making it impossible to obtain correct values of the extinction coefficients. A scale has been superimposed on the photometer trace shown on Plate I, indicating the lengths of exposure (in sec.) of the hydrogen continuum to give the corresponding deflections (plotted linearly as ordinates). The positions of the main band heads are shown in Table II. A photograph of the absorption spectrum of HCHO at wavelengths greater than 2590 A. is also shown on the Plate; it was obtained with a pressure of 4 mm. of HCHO. As the pressure of HCHO was increased, absorption in this range became complete, and the new bands 2590-2310 A. appeared. For the sake of completeness, the positions of band maxima between 3700 A. and 2590 A. are shown in Table III, which is based on the data of Henri and Schou; these authors do not quote numerical values of the relative intensities of the bands.

TABLE III.—BAND MAXIMA FROM 2590 TO 3700 A.
(FROM HENRI AND SCHOU).

3700	3170	2952	2738
3531	3143	2935	2712
3431	3120	2906	2680
3386	3089	2884	2670
3295	3054	2807	2630
3260	3036	2792	2615
3238	3010	2756	2592
3203	2979	—	—

The authors wish to thank Prof. Sir Alfred C. Egerton and Dr. A. Gaydon for their interest and advice.

Department of Chemical Engineering and Applied Chemistry,
Imperial College of Science and Technology,
S.W.7.

---

[*] Since exposures, and not intensities, were used, the results are approximate.

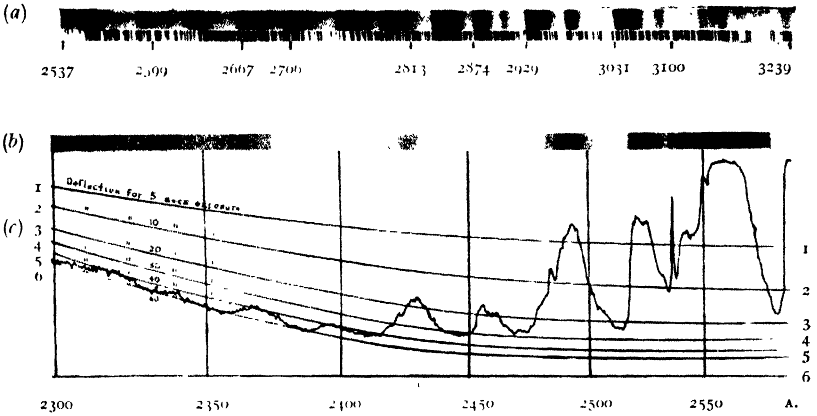

(*a*) Absorption spectrum of HCHO vapour. Path length 200 cm. Pressure 4 mm. Iron arc comparison spectrum.

(*b*) Absorption spectrum of HCHO vapour. Path length 200 cm. Pressure 250 mm.

(*c*) Microphotometer record of (*b*).

PLATE I.

[*To face page* 818.

EXPERIMENTS ON THE ELECTRODEPOSITION OF BRASS FROM CYANIDE SOLUTIONS.

BY TARAPADA BANERJEE AND A. J. ALLMAND.

Received 19th December, 1947.

Although many papers have appeared on the electrodeposition of alloys, with few exceptions their interest has been primarily a technical one. In no case have even the conditions for the deposition of the whole composition range of a binary alloy been determined in detail, nor have the internal structures of such a set of alloys been systematically examined. As a first step to further investigations, we chose the zinc-copper alloys for study, largely because, apart from their intrinsic interest, a good deal of valuable work, most of it semi-empirical, had already been done on that system. Using two major variables only, we have prepared alloys containing from 0·98 to 99·13 % Cu, and have examined their structures by X-ray analysis. Whilst the results are of interest from more than one point of view, it must be made clear at the outset that the paper has no direct bearing on the electroplater's problems ; some of the deposits were " burnt " and quite unsuitable for decorative or other commercial purposes. No attention indeed was paid to this aspect of the subject.

We employed the complex cyanide electrolyte used by the great majority of previous workers. In view of what has already been said, it seems unnecessary to refer in detail to earlier publications, of which the great bulk have been concerned with the deposition of yellow or α-brass. Some few authors have examined the crystal structure of their products. Nakamura [1] found that a deposit with 82·48 % Cu had the face-centred cubic structure of α-brass, the value of the a_0 lattice parameter being essentially identical with that of a thermal brass of the same composition. Kersten [2] obtained deposits which showed in one case an α-, in another an (α-β)-structure, while Kersten and Maas,[3] using electrolytes with varying high Zn/Cu ratios, prepared brasses with 11·4-21·4 % Cu, all of which had the ε-structure. The limits of the ε-brass field as given by the thermal diagram [4] for 200° C. are at 13·4 and 20·6 % Cu, and there is no reason to believe that these limits will appreciably differ at lower temperatures (Kersten and Maas worked at 50°). At each end, therefore, of its composition range, the ε-brass field had encroached on one of the adjacent heterogeneous (η-ε ; ε-γ) fields. A more elaborate study of this kind was carried out by Stillwell and others [5] on electrodeposited Ag-Cd alloys. Using relatively small volumes of unstirred complex cyanide electrolyte, and keeping the current density constant in any given experiment, they prepared about 20 alloys of compositions between 5-98 % Ag, varying bath composition, c.d. and temperature in their different experiments. The results of the structure determinations were exceedingly complex. Only in one case did the deposit consist of a single phase, and only in two cases of two adjacent or congruent phases. The great majority of the products were reported as containing 3, 4 or even 5 metallic phases, often including the pure metals ; in addition,

---

[1] *Sci. Papers Inst. Phys. Chem. Res., Tokyo,* 1925, **2**, 287.

[2] *Ind. Eng. Chem. (Anal.),* 1932, **4**, 178.

[3] *J. Physic. Chem.,* 1932, **36**, 2175.

[4] Raynor, *Annotated Equilibrium Diagram Series,* No. 3 (Institute of Metals, 1944).

[5] *J. Amer. Chem. Soc.,* 1932, **54**, 2583 ; 1933, **55**, 1864.

$Cd(OH)_2$ was sometimes present. In nearly every case the predominant metal phase in the electrodeposit was also present in a thermal alloy of the same composition.

From a general point of view it might be anticipated that, the more elaborate the state of order in the crystal, the less likely is this to be produced under the conditions of electrodeposition at low temperatures. A good example is furnished by electrolytic manganese ; α-Mn, stable at room temperature, has a complex cubic structure, the unit cell containing 58 atoms. Electrolytic manganese when first deposited has the tetragonal structure of γ-Mn, stable above 1191° c., and with the properties (softness, electrical conductivity) characteristic of a true metal.[6] On standing, however, it changes in the course of days to the stable α-form, and becomes brittle.[7] With such facts in mind, it seemed that similar circumstances might affect the electrolytic formation of γ-brass, with its 52 atoms per unit cell and a structure closely resembling that of α-Mn. This anticipation was, in fact, confirmed by our results.

Experimental.

All experiments were carried out at room temperature. The electrolyte was made up from cuprous, zinc and sodium cyanides, caustic soda (B.D.H. analytical reagents) and distilled water. Where the same electrolyte was used repeatedly in a series of runs, it was analysed for copper and zinc after each electrolysis, and its composition adjusted by the suitable addition of one or more of the constituents, including water. In all experiments a solid cylindrical cathode of Staybrite steel was used (height 6·35 cm., diam. 2·5 cm.) with an estimated effective surface area of 53 cm.^{2}. The deposit could be readily stripped from it, and it was not affected by the cyanide solution. The concentric annular anode (height 6·35 cm., internal diam. 6·1 cm.) was of copper, zinc or 60/40 brass, according to requirements. The first and second of these were conveniently used when the Cu/Zn ratio in the electrolyte was very high and very low respectively.

Current was supplied from storage cells, and measured on a 2-range (0-1, 0-10 amp.) Siemens ammeter. As, in the great majority of the experiments, the current strength varied with time, frequent readings were taken, and the area under the current-time curve measured with a planimeter, in order to obtain the total coulombs passed and the current efficiency. Cell voltages could be read to 0·05 v. on a Weston voltmeter. Cathode potentials were measured to 0·001 v. on a Cambridge vernier potentiometer. The reference electrode was amalgamated zinc in 0·0327 M. sodium zincate, connection being made by a Luggin capillary containing the same cyanide solution as in the bath. *p*H measurements were made by a glass electrode (Alki Electrode of the Cambridge Instrument Co.), combined with a T.F. 452 *p*H-meter (Marconi-Ekco Instruments, Ltd.). The latter was standardised by buffer solutions of *p*H 10 and *p*H 12.

In some few experiments, the potential of the deposited alloy was measured, as described, in the bath after the end of the run. Usually the electrode was removed from the bath immediately after interruption of the current, washed in distilled water, and its potential directly measured agaist zinc in 0·0327 M. zincate. It was then again washed successively with water and alcohol, dried in an exsiccator, weighed, and the deposited brass shaved off, avoiding the portions near the edges of the cylindrical cathode. Any residual metal was dissolved off with ammoniacal $(NH_4)_2S_2O_8$, and the electrode washed successively with distilled water, dil. HCl and distilled water, in preparation for the next run. The anodes were scratch-brushed after each experiment.

The analytical methods used for determining Cu and Zn in the electrolyte, which gave reproducible and concordant results, were founded on those employed by Meyer[8] and by Coats,[9] and will not be described in detail. After driving off the HCN, copper was determined electrolytically in acidic nitrate solution, using a rotating cylindrical gauze cathode, and zinc then estimated in the same

[6] Persson and Oehman, *Nature*, 1929, **124**, 333. Brunke, *Ann. Physik.* (v), 1934, **21**, 139.

[7] Bradley, *Phil. Mag.*, 1925, **50**, 1018. Westgren and Phragmen, *Z. Physik.*, 1925, **33**, 777. Brunke, (ref. 6).

[8] *Amer. Electroplaters' Soc.*, 1938, **25**, 180.

[9] *Trans. Electrochem. Soc.*, 1941, **80**, 445.

sample by titration at 80° with $K_4Fe(CN)_6$ in an acidified NH_4Cl solution, using uranium acetate as external indicator. The same methods were used for the analysis of the deposits, about 0·03-0·2 g., depending on the proportion of copper present, being used for the estimation. The results were so consistent that, as the work progressed, it became usual to determine the copper content of the deposit only.

The X-ray powder photographs were taken by means of a Metropolitan-Vickers set (9 cm. camera), using K_α copper radiation (0·019 mm. nickel filter). No attempt was made at this stage to get results of high precision,[10] as our main aim was the qualitative identification of the different phases of brass present in our deposits. In this, we were much helped by the British Non-Ferrous Metals Research Association, who prepared and placed at our disposal five thermally equilibrated specimens of cast brass (α, 76·68 % Cu ; β, 51·00 ; γ, 36·37 ; ε, 16·53 ; η, 0·54), covering all the single phases stable at room temperature, to serve as comparison X-ray standards. This greatly facilitated our work in its earlier stages.

Preliminary Experiments.

The first experiments were carried out using a small volume(250 cc.) of electrolyte, the current being constant during any given run and the cathode sometimes rotating, sometimes stationary. The significant results can be summarised as follows.

(1) In all but two experiments, the cathodic deposits contained either one or two (adjacent) brass phases only. The correspondence between the composition of an alloy and its phase attribution was, however, not the same as for thermal alloys ; in zinc-rich deposits, the η-phase seemed favoured at the expense of the ε-phase, and in alloys of intermediate compositions, both ε- and β-phases were favoured at the expense of the γ-phase.

(2) In two cases, the X-ray data showed the deposits to contain three different constituents (η-, ε- and γ-brasses), a result not possible for an alloy in thermal equilibrium. Subsequent experiments showed that one reason for this type of result was the *successive deposition* of different phases or mixtures of phases, due to changes in composition of electrolyte, which calculation had shown to be appreciable during the course of a single run.

(3) Such changes in nature of deposit at constant current were further shown to be bound up with changes in cathodic deposition potential. Thus, Fig. 1 shows the results of two experiments, E. 21 and E. 23 (cathode rotating and stationary respectively), in which the cathode potential was measured every 5 min. against a sheet of pure zinc in the bath itself, and the appearance of the deposit during the electrolysis continually noted. Deposition of alloy in each case commenced after about 1 hr., the first deposit having the pinkish-red appearance characteristic of β-brass,[11] and the polarisation at constant c.d. increasing. In

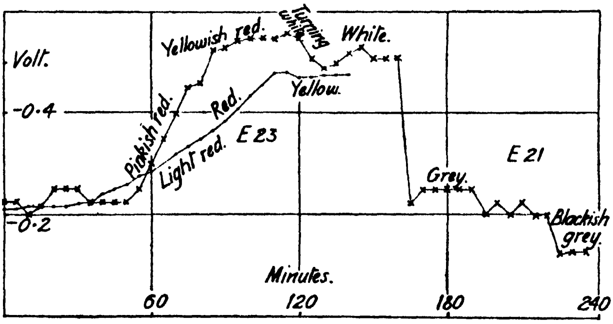

FIG. 1.

---

[10] It may be added at this point that we have not attempted to distinguish between the ordered and disordered forms of the β-phase.

[11] The nature of a brass electrodeposit can largely be gauged from its colour. α-Brasses rich in copper are red, and yellow at the zinc-rich end of their range. β-Brasses are pink, rather than a full red, γ-brasses silvery white, ε-brasses grey,

E. 23, this stage was succeeded by α-brass deposition (colour), but after 145 min., owing to the development of a poorly conducting layer on the anode, the experiment had to be concluded.

In E. 21, as will be seen, the formation of white γ-brass succeeded the production of the α-phase, whilst, at 160 min., there was an abrupt fall in cathode potential, with the appearance of a grey deposit, subsequently darkening in colour after another, smaller, potential drop. These last deposits doubtless contained ε- and probably η-brass. In this region exact control of the current was difficult, and led to potential fluctuations. Moreover, if at any time during the electrolysis the stirring were interrupted for a brief interval, the potential rose steadily to about — 0·48 v., and the colour of the deposit changed from whatever it happened to be, according to the sequence, grey → white → pink → yellow. On resuming the stirring, the original potential and colour were reverted to.

It may be added that, in these experiments, the copper content of the electrolyte *rose* steadily and considerably throughout the run, whilst that of the zinc rose slowly during the first 2 hr. and then remained almost constant. The " free " cyanide concentration (i.e. the concentration of NaCN in excess of that needed to form the ions $Cu(CN)_3''$ and $Zn(CN)_4''$) dropped rapidly throughout and soon became negative, whilst the OH′ concentration increased.

As the production of a particular phase of brass seemed to be associated with a particular cathode potential or cathodic potential range, experiments were carried out, on a small scale as before, in which, within each run, the current was no longer constant, but was continually adjusted in order to maintain the cathode potential, measured as described earlier against zinc in 0·0327 M. zincate, at a fixed and predetermined figure. Fifteen experiments were carried out. The molar electrolyte concentrations were as follows :

	CuCN.	$Zn(CN)_2$.	NaCN.
(1) E. 31-39	0·357	0·0681	0·90-1·14
(2) E. 40	0·0893	0·273	0·98
(3) E. 24, 28-30	0·0446	0·290	0·82
(4) E. 41	0·0223	0·324	0·82

In every case the NaOH was 0·0327 N.

The results are summarised in Table I. The second column in each case contains the cathode potential, referred to zinc in 0·0327 M. zincate. An X-ray structure designation enclosed in parenthesis denotes a constituent present in small proportion or as a trace as judged by the intensity of the relevant lines.

TABLE I.

Serial Number.	π.	% Cu.	Structure.	Serial Number.	π.	% Cu.	Structure.
E. 33	—0·355	69·4	α				
E. 34	—0·25	59·1	α, β	E. 40	—0·14	34·8	γ
E. 36	—0·22	52·1	β (α)				
E. 32	—0·182	51·2	β	E. 28	— 0·57	47·3	β γ
E. 37	—0·14	48·0	β, γ	E. 24	—0·65	34·0	γ
E. 31	—0·081	43·4	β, γ	E. 29	—0·177	30·5	γ, ε
E. 38	—0·080	35·2	γ	E. 30	—0·133	27·9	γ, ε
E. 39	—0·041	18·4	ε				
E. 35	—0·021	1·64	η	E. 41	—0·355	39·6	β, γ

The most striking features of Table I are that all the deposits consist of either one single or two adjacent phases, and that the structures agree in every case

sometimes with a blueish tinge, and η-brasses, also grey, are normally darker in colour than ε-brass. Mixtures have the colours to be anticipated from the above. Thus, (β-γ)-mixtures are light pink to pinkish-white, (γ-ε)-mixtures dull white or greyish-white, etc.

with the thermal structures ; it would seem that electrolysis at constant potential is the essential condition which has led to such results. It seems also definite that, at the same cathode potential, an increase in the Cu/Zn ratio in the electrolyte leads to a corresponding increase in the copper content of the deposit (cp. E. 41 and 33, E. 29 and 32 ; E. 30, 40 and 37). This is as would be expected and in accordance with general experience. In our case, however, it also leads to the conclusion that, by suitable variation of the two factors, cathode potential and Cu/Zn ratio in the electrolyte, it might be possible to deposit the whole range of electrolytic brasses in pure form.

It has been mentioned that the current was continually adjusted during electrolysis in order to keep the cathode potential constant. Whilst sometimes its value rose, frequently this procedure led to it dropping to very low figures at the end of the standard 2-hr. run, and one cause of this behaviour was certainly bound up with the changes in the composition of the electrolyte taking place during a run. Although it had been shown that a controlled cathode potential led to a deposit consisting of a definite phase or phases, it was therefore plainly desirable to use a large volume of circulating electrolyte in order to minimise concentration changes and thus to allow the use of reasonably high and constant c.d., whilst avoiding possible changes in composition of deposit occurring within the limits of existence of a single phase.

Main Experiments.

After an unsuccessful attempt with a cell through which a large volume of electrolyte was caused to circulate by gravity, the apparatus was redesigned, and all subsequent experiments were carried out with the cell shown in Fig. 2. C is the Staybrite cathode and A the anode. G is a Pyrex tube, having a side-tube at H. The rod S, to which are fixed four blades at P, curved in plan, rests on a pivot set in a disc of Perspex. These metal parts are all of stainless steel. The Perspex disc and the sides of the Pyrex tube have holes for the free passage of the electrolyte when the blades work. When the stirrer revolves, in our experiments at 700 r.p.m., the electrolyte is vigorously circulated up to, under and around the cathode, thus preventing any local changes in concentration due to electrolysis. The beaker (4·5 l. ; volume of electrolyte 4-4·5 l.) has an ebonite lid, with holes for the introduction of electrodes, the zincate auxiliary electrode at Z and the tightly fitting Pyrex tube. The design thus allows of vigorous stirring of the electrolyte, with the minimum of contact with air.

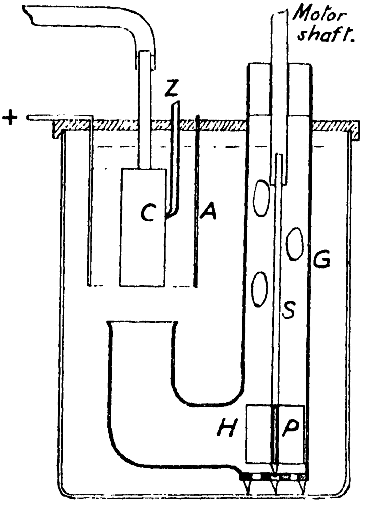

FIG. 2.

Seven series of experiments were carried out (Table II). The total molarity of CuCN and $Zn(CN)_2$ was kept constant at 0·500. The amount of NaCN present was determined empirically as that sufficient to keep the cyanides in solution and to permit of ready anodic solution of the anodes. No claim is made that the optimum concentrations required for those ends were used. In every case, the solution contained 0·0327 N. NaOH.

The figures in column 7 are calculated on the basis of the suggestion of Pan [12] that the complex zinc ion present in brass plating solutions is $Zn(CN)'_3$ and not $Zn(CN)''_4$; they are inserted because, if this is true, there then is little difference between the amounts of " free cyanide " present in the different series.

It can be stated at once that the results of the experiments fulfilled expectations. As in the earlier runs at constant cathode potential (Table I), all the deposits consisted either of a single or of two adjacent phases. Calculations made as before on the concentration changes during electrolysis, and confirmed by analyses of the electrolytes, showed negligible concentration changes to have taken place during a single run. Any changes in pH during electrolysis were trifling. In agreement with these facts, experiments carried out to see whether the composition of the deposit under given conditions was independent of time gave satisfactory results.

---

[12] *Trans. Electrochem. Soc.*, 1932, **62**, 63.

Changes in current during a run still took place, but usually only during the initial period of the electrolysis (for varying times up to perhaps 40 min.), and it was clear that they were essentially dependent on changes in the cathode surface during deposition, and were not a consequence of changes in the electrolyte.

TABLE II.

Series.	No. of Runs.	CuCN (M.).	$Zn(CN)_2$ (M.).	Total NaCN (M.).	Free NaCN.		pH.
					$Cu(CN)''_3$ $Zn(CN)''_4$.	$Cu(CN)''_3$ $Zn(CN)'_3$.	
A	2	0·499	0·001	1·50	0·50	0·501	11·12
Y	8	0·49	0·01	1·50	0·50	0·51	11·17
F	20	0·45	0·05	1·50	0·50	0·55	11·26
S	7	0·07	0·43	1·15	0·15	0·58	10·65
X	5	0·04	0·46	1·05	0·05	0·51	10·67
W	7	0·01	0·49	1·06	0·06	0·55	10·92
N	14	0·001	0·499	1·05	0·05	0·549	10·90

During our work we tabulated many observations, which need only be summarised here. In particular, data on c.d., time of electrolysis, coulombs passed, yield and current efficiency are not given in detail, in view of the varying degrees to which the non-typical conditions at the beginning of the electrolysis affected these results. The more-or-less constant c.d. observed in the later stages of electrolysis varied between the following limits in the different series. The second line contains the corresponding cathode potentials, in the great majority of cases also the limiting values.

	A.	Y.	F.	S.
Amp./dm.^{2} .	2·84 ; 0·15	1·51 ; 0·22	1·62 ; 0·16	0·83 ; 0·33
π (V.) . .	−0·5 ; −0·2	−0·5 ; −0·05	−0·3 ; −0·005	−0·4 ; −0·01

	X.	W.	N.
Amp./dm.^{2} . .	1·10 ; 0·64	2·84 ; 0·094	2·51 ; 0·12
π (V.)	−0·4 ; −0·05	−0·4 ; −0·0001	−0·25 ; −0·005

Increased polarisation naturally results in increased c.d. This effect is much more pronounced in those series where the ratio Cu/Zn in the electrolyte is either very high or very low than in others (cp. A and N with S and X).

Duration of electrolysis varied between 10-500 min. and total amp.min. passed between 12·0-67·0. Apart from one very exceptional case (F. 24 ; 0·04 g.), the weights of alloy deposited varied between 0·16-1·60 g.

Current Efficiencies.—Owing to differences in the rates of hydrogen evolution before and after the steel cathode is completely coated with brass, current efficiencies calculated from the planimetric ampere-min. results and the weights and analyses of deposits will not correspond exactly with those to be expected on long continued electrolysis. They are shown graphically in Fig. 3, the two points in Series A being plotted (broken curves) on diagram Y. For the actual % compositions of the deposits, reference should be made to Table III. F. 21, which gave an abnormal and unexplained result, is omitted and, where two or or more determinations were carried out under identical conditions, the mean value has been plotted. The two lower sets of curves represent the percentages of current employed in the deposition of copper and of zinc, whilst the upper set gives the total current efficiency of brass deposition or, read from above downwards, the percentages of current concerned with hydrogen evolution.

For reasons already given, the results only justify discussion in outline. Comparison between the different copper and zinc curves should, however, indicate the relative magnitudes of the factors affecting the ease of deposition of copper and of zinc ions, whilst the upper set of curves might be expected to link up with the nature of the surface as affecting hydrogen evolution. Following the sequence Y → F → S → X, the copper curves all rise, but less rapidly, with increasing polarisation, fall off at higher polarisations in W and, in the case of N, fall from the lowest cathode potential applied. Two factors would seem to be operative—increased rate of deposition of $Cu^{\bullet}$ ions as the cathode potential becomes more negative, and a superposed concentration polarisation due to the slow rate of dissociation of the complex cyanide ion. There is no abrupt change in the type of curve observed on passing from F to S, in spite of the large changes in both the copper content and the Cu/Zn ratio in the electrolyte. The deposition of zinc can be formally considered to be governed by the same factors, with the differences that the maximum rate of discharge of $Zn^{\bullet\bullet}$ ions, before concentration polarisation becomes effective, would seem to be reached at much lower

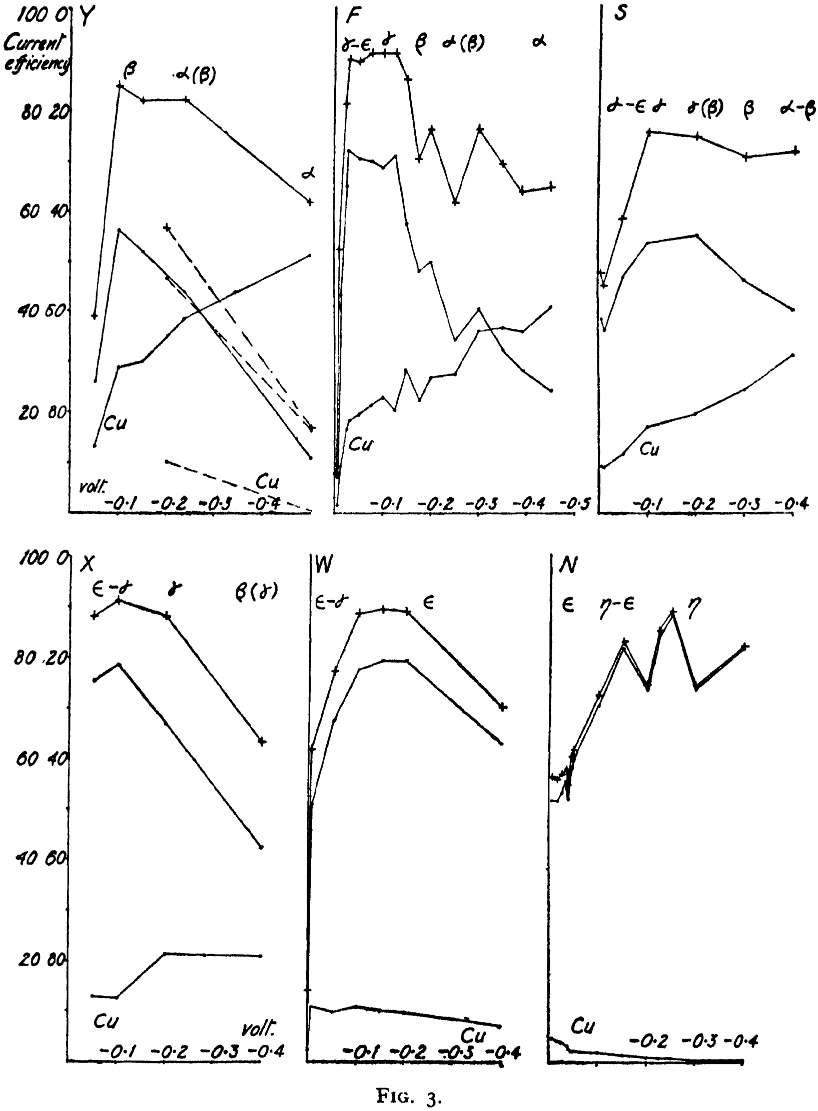

FIG. 3.

cathodic polarisations, and that the exhaustion effect comes in correspondingly early. This preferential discharge of zinc ions at low cathode potentials and the characteristic shape of the (current efficiency $-\pi$) curves when compared with those for copper, are perhaps best realised by comparing Y and W diagrams, where Cu/Zn and Zn/Cu ratios in the electrolyte are respectively identical (49/1). Only in diagram N does the zinc curve not fall markedly at high polarisations.

TABLE III.

Serial Number.	π.	% of Copper.	Structure.
SERIES A.			
A. 1	−0·5	99·1	α
A. 2	−0·2	90·1	α
SERIES Y.			
Y. 1	−0·5	90·3	α
Y. 4	−0·5	90·5	α
Y. 3	−0·5	90·0	α
Y. 7	−0·2375	62·7	α (β)
Y. 2	−0·15	52·9	β
Y. 6	−0·1	49·8	β
Y. 8	−0·1	49·5	β
Y. 5	−0·05	49·1	β
SERIES F.			
F. 9	−0·45	76·7	α
F. 17	−0·39	71·4	α
F. 8	−0·35	68·7	α
F. 23	−0·30	63·4	α
F. 5	−0·25	60·8	α (β)
F. 15	−0·20	50·8	β
F. 12	−0·175	47·5	β
F. 4	−0·15	49·0	β
F. 11	−0·125	35·2	γ
F. 19	−0·125	36·0	γ
F. 21	−0·125	53·3	β (α)
F. 6	−0·10	39·4	γ
F. 10	−0·10	39·0	γ
F. 13	−0·075	37·3	γ
F. 14	−0·075	37·1	γ
F. 16	−0·05	34·9	γ, ε
F. 18	−0·03	32·8	ε (γ)
F. 20	−0·025	32·8	γ, ε
F. 22	−0·125	29·6	ε (γ)
F. 24	−0·005	28·9	?
SERIES S.			
S. 6	−0·4	60·1	α, β
S. 7	−0·3	50·5	β
S. 1	−0·2	40·8	γ (β)
S. 2	−0·1	35·9	γ
S. 3	−0·05	32·6	γ, ε
S. 4	−0·01	32·6	ε (γ)
S. 5	−0·005	31·9	ε (γ)
SERIES X.			
X. 2	−0·4	48·6	β (γ)
X. 1	−0·2	38·0	γ
X. 3	−0·1	23·6	γ, ε
X. 5	−0·1	23·9	γ, ε
X. 4	−0·05	25·0	ε (γ)
SERIES W.			
W. 5	−0·4	18·1	ε
W. 4	−0·2	19·2	ε
W. 6	−0·15	19·7	ε
W. 7	−0·1	21·2	ε
W. 1	−0·05	22·2	ε (γ)
W. 2	−0·005	28·9	ε, γ
W. 3	−0·0001	27·9	ε, (γ)
SERIES N.			
N. 4	−0·4	0·98	η
N. 6	−0·3	1·19	η
N. 9	−0·25	1·55	η
N. 12	−0·225	2·02	η
N. 1	−0·2	2·42	η (ε)
N. 8	−0·15	3·28	η, ε
N. 2	−0·1	5·22	η, ε
N. 3	−0·05	6·42	η, ε
N. 13	−0·045	6·97	ε (η)
N. 14	−0·04	8·81	ε (η)
N. 11	−0·0375	9·67	ε
N. 10	−0·025	12·1	ε
N. 7	−0·015	14·1	ε
N. 5	−0·005	15·2	ε

The high $H^{\bullet}$ discharge at the lowest values of π (and of c.d.) can certainly largely be attributed to the relative importance of the initial period during which the steel cathode is being coated with brass. Apart from any differential effects of hydrogen overvoltage, all the conditions are present for local galvanic action resulting in re-solution of the deposited brass. The decrease in total metal current efficiency at high polarisations will certainly be partly due to the slow rate of regeneration of $Cu^{\bullet}$ and $Zn^{\bullet\bullet}$ ions by dissociation of the complex cyanide ions. Thompson[18] has, however, shown that, in our c.d. region, hydrogen overvoltage falls from its high value for η- and (η-ε)-brasses to a marked minimum at about 15-18 % Zn (ε-brass), rises again to a maximum in the γ-brass region, and then falls progressively through the β- and α-regions as the percentage of copper increases. This accords qualitatively with the course of the upper set of curves subsequent to the maximum in diagrams Y, F, S, X and W, and is in agreement with the shape of the corresponding curve in N.

---

[18] *Trans. Electrochem. Soc.*, 1931, **59**, 115.

With the exceptions of the ranges 90-100 % and 7-18 % Cu, brasses of all compositions were deposited, in one series or another of our experiments, at current efficiencies exceeding 60, and usually, 75 %. It is probable that, to deposit α-brasses rich in copper with high efficiency, electrolytes with a lower *p*H would be necessary, whilst the 50-60 % efficiencies found for the second group are probably connected with the low hydrogen overvoltage in this composition region. Differential overvoltage effects may also account for the nature of the current variations noticed at the beginning of the runs.

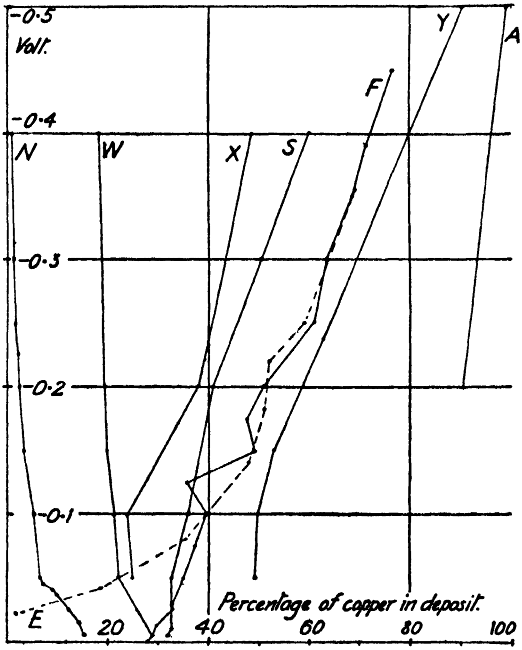

FIG. 4.

Currents which fell off with time, tending to a constant low figure, were always associated with the formation of α-, β- or γ-brass and their mixtures. On the other hand, initial currents which rose and tended to settle down at a higher figure were obtained when the deposits were two-phase, containing ε-brass as one constituent. Both these sets of results can be plausibly explained on the basis that α-, β- and γ-brasses have higher, and the (ε-γ)- and (ε-η)-mixtures lower, overvoltages than Staybrite steel, and the work of Thompson already alluded to,[13] and other experiments carried out by him with collaborators [14] on Fe-Cr and Fe-Ni alloys give general support to this view. Cases where the current passed through a maximum or minimum value are more difficult to explain, and in view of what is said later about probable changes in the nature of the deposit itself during or after deposition, no further discussion will be attempted.

Cathode Potential and Composition of Deposit.—The results are summarised in Table III.

One very obvious discrepancy is shown in F. 21, for which no satisfactory explanation can be given.

The data are plotted in Fig. 4, together with the figures for E. 31-39 (broken curves) obtained with a stationary electrolyte (Table I). Whilst the latter, at higher π values, lie close to those of Series F, to which the Cu/Zn ratio in the electrolyte most nearly corresponded, at low polarisations they diverge in the direction of deposits of lower copper content.

---

[14] *Trans. Electrochem. Soc.*, 1931, **60**, 229 ; 1934, **65**, 221.

Whereas in Series N and W, where the Zn/Cu ratio in the electrolyte is high, increasing values of π result in a brass of higher zinc content, this is the reverse in Series A, Y and F containing a preponderance of copper in the bath, and also in Series S and X, with a high Zn/Cu ratio, although lower than the values in N and W. One striking feature is the marked tendency for the curves to approach one another in the region of 30 % Cu in the deposit and at low values of π. Reference to Table III shows that, at the lowest polarisations worked at, (ϵ-γ)-mixtures are the product in all of the Series F-W. Variation in π is seen to have little effect on the composition of the deposits obtained in W, and similar variations have a rather greater effect of an opposed nature in X and S. This suggests that, for some electrolyte of Cu/Zn ratio intermediate between W and X, the dependence of composition of deposit on cathode potential would be reduced to a minimum. Graphs of % copper in the brass against log $\frac{[\mathrm{Cu}]}{[\mathrm{Zn}]}$ in the electrolyte for different applied cathode potentials give a sheaf of curves which intersect in the region corresponding to about 26 % Cu in the deposit and a Cu/Zn ratio in the electrolyte of about 0·017/0·483.

Comparison between the Phases of Electrolytic and Thermal Brasses.—As mentioned, all deposits formed at a constant cathode potential consist of one phase only or of two congruent adjacent phases. A detailed summary of the results is set out in Fig. 5, which also gives the limits of existence of the stable thermal alloys.[4] Five composition ranges of electrodeposits not covered by our experiments are indicated in black; the largest, at the junction of the ϵ- and (ϵ-γ)-fields, lies between 21·24 and 22·2 % Cu. There are also three composition ranges where the structure results are contradictory. At the (ϵ-γ)/γ-boundary, E. 24 and E. 40 show the γ-structure, whilst F. 16 is ϵ, γ; at the β/(β-γ)-boundary, F. 12 is β but E. 37 and X.2 are $\beta(\gamma)$; finally, at the (α-β)/β-boundary, E. 36 is $\beta(\alpha)$ and Y. 2 is β.

Certain points are obvious on a first inspection. The composition ranges of the α-, ϵ- and η-phases are all greater for the electrodeposits than for the thermal alloys. The reverse is true for the β- and γ-phases, if the definitely homogeneous one-phase fields are considered. Some of these conclusions are consistent with those already recorded in the preliminary experiments and with the observations of Kersten and Maas,[3] who prepared electrolytic ϵ-brasses containing both more and less copper than correspond to the thermal stability limits. If the disputed range at the junction of the (ϵ-γ)- and γ-phases is attributed to the γ-field (i.e. F. 16 becoming γ), then the lower limit of the γ-field will lie exactly at the point (32·8 % Cu) corresponding to thermal equilibrium, but the range of existence of γ-brass in the electrodeposits remains in any case less than that in thermal brass. In the case of β-brass, if the doubtful β/(β-γ)-range is attributed to the (β-γ)-field (i.e. F. 12 becoming (β-γ)) and the (α-β)/β-range to the β-field (i.e. E. 36 becoming β), then the existence ranges of electrolytic and thermal β-brasses (49·0-53·3 % Cu) will precisely coincide.

One further point should be noted. In Table III, the X-ray indications for (ϵ-γ)-mixtures are all of the ϵ-, γ- or $\epsilon(\gamma)$-types, and their distribution over the composition range is not as would be anticipated. In Fig. 5, the alloys described as $\epsilon(\gamma)$ are shown with an oblique upper tag. Instead of being concentrated at the zinc-rich end of the zone, they are scattered over the whole range. The different qualitative ascriptions assigned to three pairs of alloys of identical composition (F. 18 and 20; S. 3 and 4; E. 30 and W. 3) are striking in this connection. Moreover, in no case did the relative intensities of the lines in the X-ray diagrams suggest a high preponderance of γ with a small proportion of ϵ, i.e. $\gamma(\epsilon)$, a fact which is not explicable on the ground that the ϵ-lines are inherently stronger or more easy to detect. One similar anomaly is to be found in the (β-γ)-region, where S. 1 (40·8 % Cu) is classed as $\gamma(\beta)$, but E. 41 (39·6 % Cu), adjacent to the γ-field, as β, γ.

Mechanism of Formation of Electrolytic Brasses.

The explanation advanced for these results, and supported by a few additional facts mentioned later, is as follows. The first stage in the formation of electrolytic brasses, whatever their composition, from the primary amorphous deposit of zinc and copper atoms laid down by the current, is the appearance of an α or an η primary solution, i.e. of either a modified copper or a modified zinc lattice, depending on the conditions at the cathode during electrodeposition. These phases, if they contain less than 66·9 or more than 0·75 % Cu respectively, will be metastable, and the more so, the more they transgress these stability limits. They will therefore tend to transform spontaneously to a more stable, and finally, to the most stable form, following the law of successive states. These transitions should be facilitated by the disappearance of the primarily co-deposited hydrogen atoms as gaseous hydrogen, thus leaving vacant gaps in the rudimentary lattice. Further, it seems probable that a change from one pure phase to another of the same composition will take place more readily than the separation of a single phase into two congruent phases of different compositions.

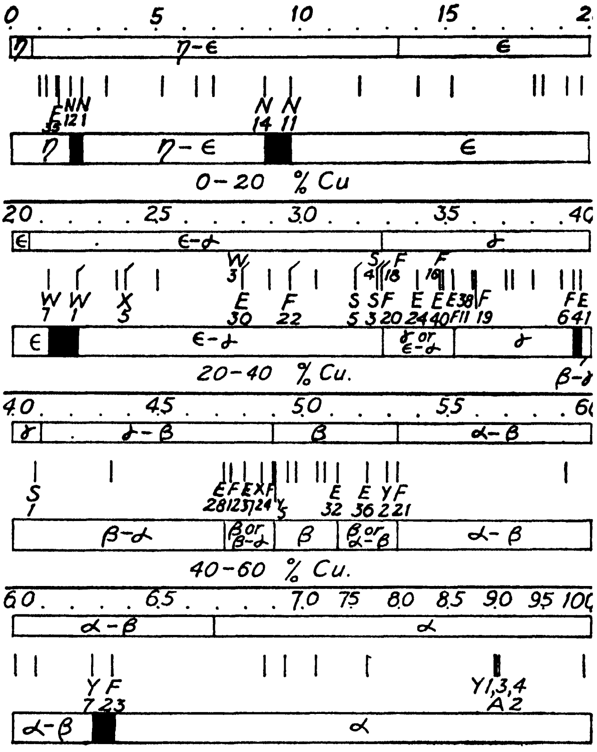

FIG. 5.—Relation between the percentage of copper in brass and the phase composition limits for thermal (upper shallow panels) and electrolytic (lower deeper panels) alloys. The vertical lines represent the experimental data.

Fig. 6, which is arbitrarily drawn so as to account formally for the experimental facts, illustrates the successive transformations possible on the above scheme, free energy being plotted against composition. The curves ABL, MCDO, EF, PGHR and SIJ represent the free energy-composition relations for the five single phases η, ϵ, γ, β and α respectively, the sections AB, CD, EF, GH and IJ corresponding to equilibrium conditions. The experimental facts do not require any extension of EF into metastable concentration regions. The linear portions BC, DE, FG and HI represent the free energies of equilibrium mixtures of (η-ϵ), (ϵ-γ)-, (γ-β)- and (β-α)-phases. The free energies of the lattices formed by primary organisation of the first amorphous deposits will therefore fall on one of the curves ABL and SIJ. All the primary lattices in Series A, Y, F and S are probably of the face-centred cubic copper type (SIJ) and in Series W and N of the close-packed hexagonal zinc type (ABL). In the case of Series X, where there is a marked change in composition between X. 1 (γ) and X. 3 (γ, ϵ) it seems likely that α-lattices are primarily formed at relatively high, and η-lattices at lower cathode potentials, and this would also be the case for the Series E experiments recorded in Table I, where α- and η-brasses were actually plated out from the same electrolyte. (γ-ϵ)-Brasses are thus regarded as derivable from either a primary α- or a primary η-brass.

The phase transformations required by the diagram are as follows :

Composition Range.	Predicted Transformations.	Phases actually Found.	Qualitative Evidence for Delayed Transformations.	Serial Number.
Primary η-lattice—				
AB 0-0·75 % Cu	None	(η)	—	—
BK 0·75-9	$\eta \to (\eta$-$\epsilon)$	η ; $(\eta$-$\epsilon)$	$\eta \to (\eta$-$\epsilon)$	(N. 4, 6, 9, 12 E. 35)
K*c* 9-13·4	$\eta \to \epsilon \to (\eta$-$\epsilon)$	ϵ	$\epsilon \to (\eta\epsilon$-$)$	(N. 11, 10)
cd 13·4-20·6	$\eta \to \epsilon$	ϵ	—	—
*d*L 20·6-29	$\eta \to \epsilon \to (\epsilon$-$\gamma)$	ϵ ; $(\epsilon$-$\gamma)$	$\epsilon \to (\epsilon$-$\gamma)$	(W. 7)
Primary α-lattice—				
JI 100-66·9 % Cu	None	α	—	—
IQ 66·9-58	$\alpha \to (\alpha$-$\beta)$	α ; $(\alpha$-$\beta)$	$\alpha \to (\alpha$-$\beta)$	(F. 23)
Q*h* 58-53·3	$\alpha \to \beta \to (\alpha$-$\beta)$	α-β	—	—
hg 53·3-49·0	$\alpha \to \beta$	β ; $(\alpha$-β	$\alpha \to \beta$	(E. 36)
gf 49·0-41	$\alpha \to \beta \to (\beta$-$\gamma)$	β ; $(\beta$-$\gamma)$	$\beta \to (\beta$-$\gamma)$	(F. 12)
fn 41-35	$\alpha \to \beta \to \gamma$	$(\beta$-$\gamma)$; γ	$\beta \to \gamma$	(S. 1 ; E. 41)
ne 35-32·8	$\alpha \to \epsilon \to \gamma$	γ ; $(\epsilon$-$\gamma)$	$\epsilon \to \gamma$	(F. 16)
*e*S 32·8-29	$\alpha \to \epsilon \to (\epsilon$-$\gamma)$	ϵ-γ	—	—

Additional evidence for delays in the postulated phase transformations is afforded (*a*) for the process $\epsilon \to (\epsilon$-$\gamma)$ by specimens described as $\epsilon(\gamma)$ where, from their compositions, the ascriptions ϵ, γ or $\gamma(\epsilon)$ would be expected (notably F. 18, S. 4, S. 5, F. 22, W. 3), and (*b*) for the process $\eta \to \epsilon$ and $\epsilon \to (\epsilon$-$\gamma)$ by three of the preliminary experiments (E. 13-15) where alloys with 24-25 % Cu were found to have an ϵ, η- instead of an ϵ, γ-structure.

Reviewing the evidence, it may be said to be strong for transformations of disproportionation type, where one phase breaks up into two adjacent phases of different compositions, i.e. in the cases of $\eta \to (\eta$-$\epsilon)$; $\epsilon \to (\eta$-$\epsilon)$; $\epsilon \to (\epsilon$-$\gamma)$; $\alpha \to (\alpha$-$\beta)$; $\beta \to (\beta$-$\gamma)$. Delays, even to the extent of complete inhibition under the conditions of experiment, are here inherently probable. It should be added that the experimental evidence hitherto available does not indicate whether the products in such cases are actually of equilibrium composition; precise X-ray measurements, not yet carried out would be necessary to settle this point.

The case for delayed transformation of the primary η- and α-lattices into ε- and β-lattices is less strong, as is also the probability of the delays in question. In the former case, there seems no reason to doubt the evidence afforded by E. 13-15. Two of these alloys were, in fact, further examined after annealing *in vacuo*. E. 14 was given 24 hr. at 150° after which time a marked ε, γ-structure had developed, the trace of η-phase still persisting. Another 24 hr. at 200° brought about a considerable reduction in the intensity of the η-lines, but not their complete disappearance. E. 13 was annealed successively for 12 hr. at each of the temperatures 200°, 150°, 100° and 50°. Its structure was then ε, γ-, the η-phase being indetectable. The case for delayed transformation of α- into β-brass depends solely on E. 36 (52·1 % Cu ; β(α)). Whilst there is no doubt about either its composition or its phase ascription, the experimental conditions were not as well defined in Series E as in the subsequent experiments, and it is not impossible that the trace of α-constituent found may have resulted from a minor change in electrolyte composition during the run or from a faulty adjustment of cathode potential at the beginning of the experiment. Rearrangements of the types β → γ and ε → γ are inherently more likely to be delayed on account of the complex structure of the γ-phase ; the latter transformation in particular involves a change from hexagonal to complex cubic symmetry.

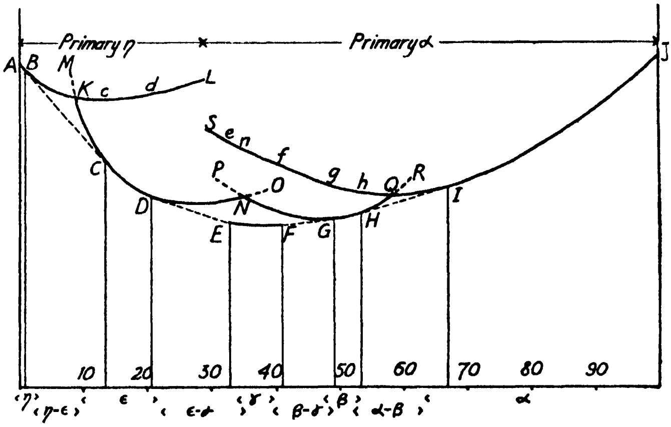

FIG. 6.—Percentage of copper in alloy.

Corroborative evidence, some of it very direct, supporting the idea of changes taking place in the deposited alloys immediately subsequent to their first formation, was noted during the work, in particular when γ-brass was a product. In a number of cases, persistent fluctuations in cathode potential or in current were noticed throughout a run, difficult to control and in no way dependent on the use of exceptionally high currents. Examples are E. 28 (β, γ), E. 29 (ε, γ), S. 1 (γ(β)), S. 3 (ε, γ) and, in particular, F. 11 (γ), F. 19 (γ) and F. 21 (β (α)), these last three all carried out at the same cathode potential. Further, it has been mentioned that the static potentials of the deposits were measured against a zincate electrode immediately after the conclusion of the runs. In the case of F. 11, after fluctuating between various shades of pinkish-white during electrolysis, the deposit was markedly pink when taken out of the bath, suggesting a β- or β(γ)-structure. Two minutes later, the first potential reading was taken, followed by others at 10-sec. intervals. The results (positive with respect to zinc) were as follows : 0·43, 0·51, 0·77, 0·815, 0·86, 0·88, 0·89 v. These changes in potential with time were much greater than those normally observed (of the order of 0·05-0·15 v., either positive or negative). At the conclusion of the readings, the colour of the deposit was a pale pinkish-white, and had become silver-white by the next day when the X-ray examination was made. A very similar set of potentials was noted in the case of E. 38 (also 35·2 % Cu ; γ)—0·32, 0·55, 0·70, 0·81, 0·838, 0·839, 0·844 v.—although in this case no parallel observations on change in colour are actually recorded. These rises in potential are just what would be expected (qualitatively) if they were the result of a metastable β-brass containing more than its equilibrium content of zinc changing spontaneously to stable γ-brass.

The general conclusions arrived at, therefore, are that transformations (i) of types $\alpha \rightarrow \beta$ and $\eta \rightarrow \epsilon$ normally take place readily (ii) of type $\beta \rightarrow \gamma$ may occur at an observable rate (iii) of type $\epsilon \rightarrow \gamma$ occur more slowly than $\beta \rightarrow \gamma$ (iv) of types $\epsilon \rightarrow \epsilon$-$\gamma$, $\alpha \rightarrow (\alpha$-$\beta)$, etc., take place still more slowly.

The arbitrary element in Fig. 6, more particularly in the (ϵ-γ)- and γ-regions, has already been implicitly recognised. It results in the following scheme for the formation of electrolytic brasses, where an asterisk denotes a phase which may, depending on its composition, be either stable or metastable.

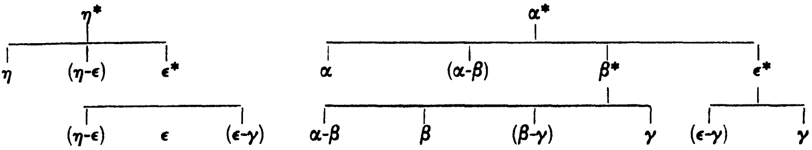

Pure γ-brass is thus derivable from α^*-brass only, whilst (ϵ-γ)-mixtures can result from either a primary α^*- or a primary η^*-lattice, the former path involving the transformation of a cubic close-packed (α^*) into a modified hexagonal close-packed (ϵ^*) structure. A more simple and symmetrical scheme would result if this last-mentioned transformation, with the subsequent changes $\epsilon^* \rightarrow (\epsilon$-$\gamma)$ and $\epsilon^* \rightarrow \gamma$, were not included, but γ-brass added as a possible product of the ϵ^*-phase derived from the η^*-phase. γ-Brass, not (ϵ-γ)-mixtures, would then be the final product derivable both from primary α- and from primary η-lattices, and the corresponding change in Fig. 6 would be a shift of points S and L to the right along their respective curves until they reach the composition corresponding to N (35 % Cu). Our decision to propose the less simple scheme is largely influenced by the fact that, whereas in Series W and N and in the last three runs in Series X, increased polarisation results in a brass containing a higher % Zn, this is the reverse in Series A, Y, F and S and in the first two experiments of X. We associate these types of behaviour with the primary production of a zinc (η-) and a copper (α-) lattice respectively and, not only is pure γ-brass not found as a product in the first group of experiments, but (ϵ-γ)-mixtures are formed at low polarisations both in F and in S.

The authors wish gratefully to acknowledge a grant from the Central Research Fund of the University of London, which enabled the X-ray equipment to be purchased, and to thank again the British Non-Ferrous Metals Research Association for its help in supplying authentic specimens of thermally-equilibrated brass phases. T. B. wishes to acknowledge the award of a State Scholarship by the Government of India, which enabled him to take part in this work.

Summary.

The heterogeneity of electrolytic brass, deposited at constant c.d., is primarily due to changes in cathode potential during electrolysis.

The composition of brass, deposited from an electrolyte of which the concentration remains essentially unchanged during the period of electrolysis, is

determined by the cathode potential employed and, if the latter is kept constant, remains unaffected by the duration of electrolysis.

Working at room temperature, with intensive circulation of electrolyte, with a total (Cu + Zn) content of 0·50 g.-atom/l., and with OH′ and free CN′ concentrations substantially the same in every case, brass of any required composition can be deposited by suitable variation of (*a*) Cu/Zn ratio in the electrolyte and (*b*) cathode potential. Such deposits contain either one pure phase or a mixture of two adjacent phases.

The composition limits of these phases do not correspond exactly to equilibrium conditions. The existence ranges of α-, η- and ϵ-brass are definitely enlarged, whilst that of the complex γ-phase is reduced.

Evidence suggests that the primarily formed brass lattices are either of the α- or of the η-type, depending on the conditions at the cathode during electrolysis, that the β- and ϵ-phases result from transformation of metastable forms of these primary lattices, and that γ-brass is a product of either metastable β-brass or of metastable ϵ-brass.

University of London,
King's College.

ON THE INTERACTION OF COLLOIDAL PARTICLES.

II.—DISCUSSION OF BASIS OF THEORY.

By S. Levine.

Received 3rd March, 1947; *as amended 1st January,* 1948.

I. Introduction.

In a preceding paper [1] (henceforth referred to as Part I), the author proposed a general method of determining the interaction of the double-layers of two colloidal particles. A difficulty was encountered when applying this method to infinite parallel plates, but no satisfactory solution was given.[2] Furthermore, our results differed from those reached by Verwey and Overbeek [3] in their theory of the forces between colloidal particles. Consequently, it seems necessary to examine the fundamental premises of the two theories. We have developed our method further and in this paper shall outline the main features of the mathematical arguments. Verwey and Overbeek derive their expression for the free energy in two different ways, which lead to the same result. We propose three different methods, two of which reduce to those of the above authors under certain special assumptions, in particular that the particle potential remains constant.

In the first method, we treat the density of ions (charge) on the surface of the particles as a thermodynamic variable, which we are free to choose. Then the condition that the free energy is a minimum fixes this density as a function of the particle separation. The familiar, fictitious charging-process employed by Debye and Hückel in their theory of electrolytes, is utilised here. This approach has been explained in Part I. In the second method, the surface density of ions on the particles is assumed to take on the equilibrium value at each stage of the charging process. This is essentially one of the starting points in the work of Verwey and Overbeek. We have already mentioned in Part I that the first and second methods are equivalent. The proof of this equivalence will be presented in a later paper. In the third method, we postulate that thermodynamic equilibrium can be attained for any surface density of ions by applying the appropriate external potential at the surface of the particles. This approach affords a deeper understanding of the relationships between the alternative methods of deriving the free-energy expressions. It can be shown that all three methods are completely equivalent provided that there exists such an external potential function producing equilibrium. In this paper we indicate how this method leads to a generalised Lippmann equation, which is the other starting point of Verwey and Overbeek.

---

[1] Levine, *Trans. Faraday Soc.*, 1946, **42B.**

[2] Discussion remarks by Overbeek and Levine, *ibid.*

[3] Verwey and Overbeek, *ibid.*; *Philips Res. Rep.*, 1945, 1, 33; *J. Physic. Chem.*, 1947, **51**, 631.

In § 2, the meaning of the potential difference between the particle surface and the interior of the solution is examined. The conclusion reached in Part I that, in general, this potential depends on the interparticle separation is confirmed. In § 3 the Lippmann equation is derived and in § 4 a comparison is made with the results of Verwey and Overbeek. In § 5, the application of our theory to spherical and cylindrical particle pairs, in very dilute sols, is discussed. A repulsion between the double layers is obtained when the mean potential at the particle surface is identified with the potential of the mean force. However, our expression for the mutual free energy is somewhat different from that of Verwey and Overbeek. The attraction obtained in Part I between two infinite, parallel plates is shown to be erroneous and a simple method of obtaining the repulsive force for this case is proposed.

The notation will be the same as in Part I and reference to the equations in Part I will have the additional designation I.

2. Formula for the Potential of the Mean Force.

Consider two parallel plates, each of area A, separated by a distance R and immersed in an aqueous electrolyte solution of volume V. The charge on the inner surface of each plate is assumed to arise from the adsorption of ν_1 ions of charge e_1 (type 1) per unit area. All the ions in the system are assumed to be carrying the fraction λ of the full charge, so that λ denotes the stage in the Debye-Hückel charging process. The density of adsorbed ions under equilibrium conditions is $\bar{\nu}_1(\lambda, R)$, a function of λ and R. In this section we assume the volume V is very large so that the asterisk superscript introduced in Part I is omitted from all formulæ. This means that the dependence on ν_1 and R of the chemical potential of an ion in the bulk of the solution is neglected. Also, the interaction energy of the two plates is independent of the volume V. Although these factors may be secondary in dilute sols, they should be quite important in concentrated sols. T is the temperature and k Boltzmann's constant.

Three separate potential functions have been introduced in the theories of the author and of Verwey and Overbeek; firstly, the mean potential at an adsorbed ion, which is due to the Coulomb forces exerted by the surrounding ions and which we denoted by $\bar{\psi}_1(\lambda, R/2)$ *; secondly, the corresponding potential of the mean force $\Phi_1(\lambda, R)$; finally the potential $\psi_0(\lambda) = \Delta\chi_1(\lambda)/\lambda e_1$ where $\Delta\chi_1(\lambda)$ is the change in the electrical self-energy of an ion of type 1, when it is adsorbed on the particle surface from the solution. This last quantity is introduced by Verwey and Overbeek and enters into their Lippmann equation. The first two potentials depend on the interparticle separation, whereas the third does not. We proceed to derive a relation between $\Phi_1(\lambda, R)$ and $\psi_0(\lambda)$, which was given without proof by equation (I, 21), namely,

$$\lambda e_1\psi_0(\lambda) = \Delta\chi_1(\lambda) = \left[\frac{\mathrm{d}f_0(\nu_1)}{\mathrm{d}\nu_1}\right]_{\nu=\bar{\nu}_1(\lambda, R)} + \lambda e_1\Phi_1(\lambda, R). \quad . \quad . \qquad (1)$$

---

* The factor $\frac{1}{2}$ appears in the function $\bar{\psi}_1(\lambda, R/2)$ simply because the median plane between the two plates marks the origin of x in the potential function $\bar{\psi}_1\lambda(, x)$.

Here $2A\mathrm{f}_0(\nu_1)$ denotes that part of the free energy $F_0(\nu_1)$ of the discharged system ($\lambda = 0$), which depends on the number ν_1 of discharged ions of type 1 per unit area of particle surface. The form of $\mathrm{f}_0(\nu_1)$ will depend on the particular sol under consideration. In Part I we chose a particular expression for $\mathrm{f}_0(\nu_1)$, based on the usual treatment of adsorbed molecules on surfaces.

To derive (1), a simple model is used to describe the statistical behaviour of the adsorbed ions. A classical partition function is used for these ions, which are imagined to be undergoing thermal motion over the plate area (including vibrations normal to the surface). To simplify matters, let each plate have unit area, $A = 1$. When ν_1 is varied, the density of adsorbed ions changes simultaneously on both particle surfaces. However, it is now convenient to distinguish between the densities, say ν_1' and ν_1'' on the two plates. Of course, the average densities will be the same, i.e. $\overline{\nu_1'} = \overline{\nu_1''} = \nu_1$.

An alternative form to that in Part I can be given for the electrical free energy which is associated with the ions of our system at stage λ and which we denote by $F(\lambda, \overline{\nu_1'}, \overline{\nu_1''}, R)$. For the completely discharged system this quantity becomes $F(0, \overline{\nu_1'}, \overline{\nu_1''})$ which is assumed independent of R. We make use of the usual relation from statistical mechanics for $F(\lambda, \overline{\nu_1'}, \overline{\nu_1''}, R)$ in terms of the configurational part of the classical Gibbs' phase integral, $\mathrm{I}(\lambda, \overline{\nu_1'}, \overline{\nu_1''}, R)$ say, which takes account of the Coulomb interaction of the ions. (The integral over momentum space need not be considered.) This relation reads

$$\exp[-\{F(\lambda, \overline{\nu_1'}, \overline{\nu_1''}, R) - F(0, \overline{\nu_1'}, \overline{\nu_1''}) - E_s(\lambda, \overline{\nu_1'}, \overline{\nu_1''})\}/kT] = \mathrm{I}(\lambda, \overline{\nu_1'}, \overline{\nu_1''}, R) \qquad (2)$$

where $E_s(\lambda, \overline{\nu_1'}, \overline{\nu_1''})$ is the electrical self-energy of all the ions. The increment in the latter quantity when $\overline{\nu_1'}$ is increased by 1 is $-\Delta\chi_1(\lambda)$. It can be shown that[4]

$$\frac{\mathrm{I}(\lambda, \overline{\nu_1'} + 1, \overline{\nu_1''}, R)}{\mathrm{I}(\lambda, \overline{\nu_1'}, \overline{\nu_1''}, R)} = \exp[-\lambda e_1 \Phi_1(\lambda, R)/kT]. \qquad (3)$$

We now write down the relation corresponding to (2) when $\overline{\nu_1'}$ is replaced by $\overline{\nu_1'} + 1$ and divide this by (2). Finally, use is made of (3) and of the fact that under equilibrium conditions, the free-energy change of the system is zero when $\overline{\nu_1'}$ is changed to $\overline{\nu_1'} + 1$. In this way, we obtain a relation which is equivalent to (1), but differs in form. The first term on the right-hand side of (1) is replaced by the change in the free energy $F(0, \overline{\nu_1'}, \overline{\nu_1''})$ when $\overline{\nu_1'}$ becomes $\overline{\nu_1'} + 1$.

The above analysis shows that the relation (1) is simply a form of the condition of thermodynamic equilibrium between the ions adsorbed on the particle surface and those in the solution. It follows that (1) must become identical with the equilibrium condition (I, 3*i*) when V is very large. This means that

$$\lambda e_1 \Phi_1(\lambda, R) = \left[\frac{\partial}{\partial \nu_1} \int_0^\lambda \frac{\overline{E}(\lambda, \nu_1, R)}{\lambda} d\lambda\right]_{\nu_1 = \overline{\nu_1}(\lambda, R)}, \qquad (4)$$

where $\overline{E}(\lambda, \nu_1, R)$ is the average electrostatic interaction-energy of the ions in the double-layers of the two particles at stage λ in the charging process.

We can interpret eqn. (4) in the following way. The electrostatic potential energy is the work done in charging the ions assuming that they are fixed in their average final positions. The free energy includes an extra entropy (or osmotic) term which represents the work done against the thermal motion resulting from the re-distribution of the ions during the charging process. In integrating with respect to λ on the right-hand side of (4), we charge with ν_1 constant and hence do no work against the thermal motion of the adsorbed ions on the particle surface. Thus we are really evaluating an electrostatic energy, and not a free energy for the surface ions. It follows that the right-hand side of (4) is the increase in energy associated with the Coulomb interaction of the ions in the double-layers of the two particles when an ion is transferred from the solution to one of the particle surfaces. It does not include the work done against the thermal motion of the surface ions. But the quantity $\lambda e_1 \Phi_1(\lambda, R)$ is the work required to overcome the Coulomb forces when bringing an ion to a given position on the surface, the thermal motion of the adsorbed ions again being ignored.

---

[4] See Fowler, *Statistical Mechanics* (Cambridge University Press, 1936), 261.

3. Derivation of the Lippmann Equation.

In relating our results to a Lippmann equation, we shall account for the dependence of the interaction energy of the two plates on the volume V. The formulæ in Part I which have the asterisk superscripts will now be considered. Thus, the change in electrical self-energy $\Delta\chi_1(\lambda)$ and the potential energy $\bar{E}(\lambda, \nu_1, R)$ are replaced by $\Delta\chi_1{}^*(\lambda)$ and $\bar{E}^*(\lambda, \nu_1, R)$ respectively. The latter quantities have additional terms which are due to the dependence on ν_1 and R of the chemical potential of an ion in the interior of the solution. Expressions for these terms in the case of dilute sols are given in Part I.

In the theory developed in Part I, ν_1 is treated as a thermodynamic quantity which can be varied at liberty. In experiments on electro-capillarity curves, this is done by applying an external potential difference between the surface (of mercury) and the interior of the solutions. This suggests the following assumption. Suppose that thermodynamic equilibrium of our system can be attained for any set of values of the parameters λ, ν_1 and R by imposing an appropriate external potential on the adsorbed ions of type 1. This potential will be a function of λ, ν_1 and R and will be denoted by $\psi_1{}^*(\lambda, \nu_1, R)$. For such a system, the free-energy expression (I, 2*ii*) is replaced by

$$F(\lambda, \nu_1, R) = \sum_{i=1}^{s} N_i \mu_i{}^0(\lambda) - 2A\nu_1\Delta\chi_1{}^*(\lambda) - 2A\lambda\nu_1 e_1 \psi_1{}^*(\lambda, \nu_1, R) + 2A\mathrm{f}_0(\nu_1) + 2A\int_0^\lambda \frac{\bar{E}^*(\lambda, \nu_1, R)}{\lambda}\,d\lambda. \qquad (5)$$

If we omit the additional term involving $\psi_1{}^*(\lambda, \nu_1, R)$, then the derivation of (5) has been outlined in Part I. The quantity $\mu_i{}^0(\lambda)$ has been defined by (I, 5*i*) and can be considered to be that part of the chemical potential of an ion of type i (there being s types in all) which is independent of ν_1 and R.

Keeping λ and R fixed, let us vary ν_1. Then we can introduce a new function $\Psi_1{}^*(\lambda, \nu_1, R)$ which satisfies a Lippmann equation in the form

$$\frac{\partial F}{\partial \nu_1} = -2A\lambda\nu_1 e_1 \frac{\partial \Psi_1{}^*(\lambda, \nu_1, R)}{\partial \nu_1}, \qquad . \quad . \quad . \quad . \quad (6)$$

provided

$$\lambda e_1 \Psi_1{}^*(\lambda, \nu_1, R) \equiv \Delta\chi_1{}^*(\lambda) + \lambda e_1 \psi_1{}^*(\lambda, \nu_1, R) \equiv \frac{d\mathrm{f}_0(\nu_1)}{d\nu_1} + \frac{\partial}{\partial \nu_1}\int_0^\lambda \frac{\bar{E}^*(\lambda, \nu_1, R)}{\lambda}\,d\lambda. \qquad (7)$$

When no external potential is applied, i.e. $\psi_1{}^*(\lambda, \nu_1, R) = 0$, then (7) reduces to the equilibrium condition (I, 3*i*) and hence defines the variation of surface density of adsorbed ions with λ and R, namely $\bar{\nu}_1(\lambda, R)$. Also, the expression (5) for the free energy becomes identical with the formula

(I, 2*ii*), given in Part I, with the difference that the general form for $f_0(\nu_1)$ is used. We observe that substitution of (4) into (1) yields the formula to which (7) reduces on putting $\psi_1^*(\lambda, \nu_1, R) = 0$ and omitting the asterisk superscripts.

The thermodynamic system considered in Part I is in equilibrium along the curve $\nu_1 = \bar{\nu}_1(\lambda, R)$ and its state is defined by the two variables λ and R. Here we have a hypothetical system in thermodynamic equilibrium, the state of which is defined by three variables λ, ν_1 and R. Keeping R fixed, let us choose an initial state A and a final state B on the curve $\nu_1 = \bar{\nu}_1(\lambda, R)$ in the (λ, ν_1) plane (see Fig. 1). The passage from the state A to the state B, which replaces the charging process described in Part I, can take place along any curve in the (λ, ν_1) plane, the end-points of which are at A and B. The change in the free energy of our thermodynamic system will depend only on the initial and final states. In particular, we can choose the path ACXB where ACX is any curve joining the points A and X. Integrating along this path and making use of (6), the free energy for state B can be written as

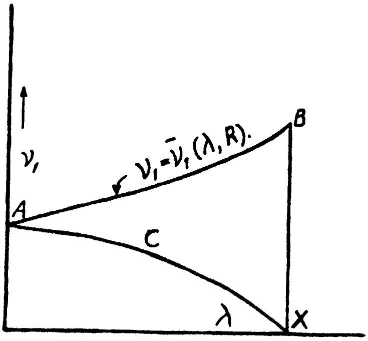

FIG. 1.

$$F(\lambda, \bar{\nu}_1(\lambda, R), R) = F(\lambda, 0, R) - 2A \int_{\Psi_1^*(\lambda, 0, R)}^{\psi_0^*(\lambda)} \sigma \, d\Psi_1^*, \qquad (8)$$

where $F(\lambda, 0, R)$ is the free energy of state X and we have introduced the surface charge-density $\sigma = \lambda \nu_1 e_1$, and the potential $\psi_0^*(\lambda) = \Delta\chi_1^*(\lambda)/\lambda e_1$. In this way the same formal integral as that given by Verwey and Overbeek is derived, with the difference that in general $\Psi_1^*(\lambda, 0, R)$ is different from zero (partly due to the image forces and partly to the " chemical " forces).

In the case of very large V (the asterisk superscript is dropped) a simple interpretation can be given to eqn. (7). The potential of the mean force $\Phi_1(\lambda, R)$ in eqn. (4) is defined for the equilibrium value $\nu_1 = \bar{\nu}_1(\lambda, R)$. However, when the density of adsorbed ions ν_1 is arbitrary, we can still define the potential of the mean force due to the Coulomb ionic interaction, acting on an adsorbed ion. This quantity will be denoted by $\Phi_1(\lambda, \nu_1, R)$ and is defined by (4) provided the right-hand side is evaluated for arbitrary ν_1 instead of $\bar{\nu}_1(\lambda, R)$. We can integrate this generalisation of eqn. (4) immediately and obtain

$$\int_0^\lambda \frac{\bar{E}(\lambda, \nu_1, R)}{\lambda} d\lambda = \lambda e_1 \int_0^{\nu_1} \Phi_1(\lambda, \nu_1, R) d\nu_1, \qquad (9)$$

provided image forces are neglected, so that $\Phi_1(\lambda, 0, R) = 0$. By using this relation, it is possible to avoid the evaluation of the volume integrals in the expression for $\bar{E}(\lambda, \nu_1, R)$ given in Part I. This property has been utilised by Derjaguin[5] and by Verwey and Overbeek. Finally the first equation in (7) simplifies to

$$\lambda e_1 \Psi_1(\lambda, \nu_1, R) \equiv \frac{df_0(\nu_1)}{d\nu_1} + \lambda e_1 \Phi_1(\lambda, \nu_1, R). \qquad (10)$$

The first term on the right-hand side of (10), which we designate the chemical term, includes the non-electrical part of the self-energy of an ion (short-range forces) and any entropy contribution associated with the possible arrangements of the adsorbed ions on the particle surface. The second term is the work done in bringing an ion to the surface against the interionic forces only.

---

[5] Derjaguin, *Acta Physicochim.*, 1939, **10**, 333 ; *Trans. Faraday Soc.*, 1940, **36**, 203.

4. Comparison with the Theory of Verwey and Overbeek.

The theory outlined above and in Part I becomes equivalent to that of Verwey and Overbeek when certain simplifications are introduced. We assume $f_0(\nu_1) = 0$ * and in this section consider again the case of an infinite volume of electrolyte. According to (10), the potential function $\Psi_1(\lambda, \nu_1, R)$ now becomes identical with the potential of the mean force $\Phi_1(\lambda, \nu_1, R)$ and if image forces are neglected, $\Phi_1(\lambda, 0, R) = 0$ and $F(\lambda, 0, R)$ is a function of λ only. Then the Lippmann equation (8) reduces to the result quoted by Verwey and Overbeek.

Let us now assume that the mean potential at an ion at position x between the plates is the same for the different types of ions. In Part I, this potential function $\overline{\psi}(\lambda, x)$ refers to an arbitrary value of ν_1 and we retain the same notation here. We also identify the potential of the mean force with the mean potential at an adsorbed ion. When all the above assumptions are made and we use (1), two conditions are obtained

$$\Delta\chi_1(\lambda) = \lambda e_1[\Phi_1(\lambda, \nu_1, R)]_{\nu_1=\overline{\nu}_1(\lambda, R)} = \lambda e_1[\overline{\psi}(\lambda, R/2)]_{\nu_1=\overline{\nu}_1(\lambda, R)}, \quad (11)$$

which is the equation (I, 20). Thus, under equilibrium conditions, the potential of the mean force at an adsorbed ion is assumed independent of the separation R.

We stated in the introduction that if the ions are charged in such a way that at each stage λ, ν_1 takes on its equilibrium value $\overline{\nu_1}(\lambda, R)$, then we derive the same free energy as obtained in the preceding section. If we introduce the potential function $\overline{\psi}(\lambda, R/2)$ and put $f_0(\nu_1) = 0$, then the free energy by this (second) method reads

$$F(\lambda, \overline{\nu_1}(\lambda, R), R) = \sum_{i=1}^{s} N_i\mu_i^0(\lambda) - 2A\int_0^\lambda d\lambda\, \overline{\nu_1}(\lambda, R)\left\{\frac{d\Delta\chi_1(\lambda)}{d\lambda} - \lambda e_1(\overline{\psi}(\lambda, R/2))_{\nu_1=\overline{\nu}_1(\lambda, R)}\right\}$$
$$+ 2A\int_0^\lambda \frac{d\lambda}{\lambda}\int_0^{R/2} [\overline{\psi}(\lambda, x)\overline{\rho}(\lambda, x)]_{\nu_1=\overline{\nu}_1(\lambda, R)}dx, \quad (12)$$

where $\overline{\rho}(\lambda, x)$ is the average charge density at position x. This formula can be obtained immediately from (I, 18). Now the model of Bernal and Fowler[6] for the hydration of an ion suggests that $\Delta\chi_1(\lambda)$ is roughly proportional to λ. In this case, it follows that $[\overline{\psi}(\lambda, R/2)]_{\nu_1=\overline{\nu}_1(\lambda, R)}$ is a constant, independent of λ and R and the second term on the right-hand side of (12) vanishes. This yields the first form for the free energy considered by Verwey and Overbeek. However, if we use the classical Born expression for the hydration energy of an ion, then we can expect $\Delta\chi_1(\lambda)$ to be proportional to λ^2, and the second term on the right of (12) is no longer zero.

Any approximations introduced in evaluating the free energy should satisfy the conditions that the three methods proposed in this paper be equivalent. When the linear Debye-Hückel equation is used to determine the function $\overline{\psi}(\lambda, x)$ and the condition (11) is introduced, it is shown in Part I that the second and third terms on the right-hand side of (12)

---

* In a private communication, Prof. Overbeek has pointed out that this condition should apply when the adsorbed ions are indistinguishable from one of the lattice ions which constitute the colloidal particles. However, there are many colloidal systems where this is not the case. If there is no entropy contribution to $f_0(\nu_1)$, then we can assume that $f_0(\nu_1) = \alpha\nu_1$ where α is a constant. However, since $df_0(\nu_1)/d\nu_1 = 0$ when the system is completely discharged, $\alpha = 0$.

[6] Bernal and Fowler, *J. Chem. Physics*, 1933, **1**, 515.

reduce to $-A\bar{\nu}_1(\lambda, R)\Delta\chi_1(\lambda)$ valid for any form of $\Delta\chi_1(\lambda)$. The same result is obtained by the first method referred to in the introduction and described in Part I, provided we again use (11) and also the formula (21) for the electrical free energy. However, in the general case where the Poisson-Boltzmann equation must be considered, Verwey and Overbeek apparently derive the same expression for the free energy both by their Lippmann equation and by their particular form of (12), only if condition (11) is used and in addition $\Delta\chi_1(\lambda)$ is proportional to λ. This also follows from our theory.

Thus Verwey and Overbeek assume (i) $f_0(\nu_1) = 0$, (ii) $\Delta\chi_1(\lambda)$ is proportional to λ, (iii) the mean potential at an adsorbed ion is equal to the potential of the mean force, (iv) the two plates are immersed in an infinite volume of electrolyte. The first two conditions may apply to some colloidal systems, but cannot be generally valid.* Further light on the third condition is obtained by the following considerations. We make use of the linear Debye-Hückel equation, valid for small potentials. Since the potential is the same for the different types of ions, there is no need to retain the subscript 1 to distinguish the adsorbed ions of type 1 from the others and we can refer to the potential at the surface.

Consider a single plane charged surface of charge density $\nu_1 e_1$ immersed in an electrolyte. The mean potential at distance x from the surface and at stage λ in the charging process is

$$\bar{\phi}(\lambda, \nu_1, x) = \frac{4\pi\nu_1 e_1}{D\kappa_0} e^{-\lambda\kappa_0 x} \quad . \quad . \quad . \quad (13)$$

where D is the dielectric constant of the dispersion medium and $1/\kappa_0$ is the familiar characteristic "thickness" of the diffuse outer layer, referred to $\lambda = 1$. The electrostatic potential energy of the double layer per unit plate area, $\bar{E}(\lambda, \nu_1)$ say, is readily obtained by integrating the energy density $(D/8\pi)[d\bar{\phi}(\lambda, \nu_1, x)/dx]^2$ over the double layer from $x = 0$ to $x = \infty$. We find that the mean potential at the particle surface $\bar{\phi}(\lambda, \nu_1, 0)$ can be identified with the potential of the mean force since †

$$\lambda e_1\bar{\phi}(\lambda, \nu_1, 0) = 2\frac{\partial}{\partial \nu_1}\int_0^\lambda \frac{\bar{E}(\lambda, \nu_1)}{\lambda}d\lambda. \quad . \quad . \quad . \quad (14)$$

Two other simple cases give the same result, namely a spherical and a cylindrical particle. If n_1 is the total number of adsorbed ions of charge e_1 on a spherical particle of radius a, then at stage λ, the mean potential in the diffuse layer at distance r from the centre of the particle is

$$\bar{\phi}(\lambda, n_1, r) = \frac{\lambda n_1 e_1 e^{\lambda\kappa_0 a}}{D(1 + \lambda\kappa_0 a)} \cdot \frac{e^{-\lambda\kappa_0 r}}{r}. \quad . \quad . \quad . \quad (15)$$

The electrostatic energy $\bar{E}(\lambda, n_1)$ is again obtained by integrating the energy density over the diffuse layer from $r = a$ to $r = \infty$. We readily derive that

$$\bar{\phi}(\lambda, n_1, a) = 2\frac{\partial}{\partial n_1}\int_0^\lambda \frac{\bar{E}(\lambda, n_1)}{\lambda}d\lambda, \quad . \quad . \quad . \quad (16)$$

which has the same form as (14).‡

---

* However, the second condition is not introduced in the Lippmann equation of these authors. Also (iv) should really be that the chemical potential of an ion in the bulk of the solution is independent of ν_1 and R. We shall show in a later paper that this implies the omission of an additional term in the free energy.

† The reason for a difference of factor 2 between the right-hand sides of eqn. (4) and (14) is that in the former case, where a particle pair is being considered, the density of ions changes simultaneously on both particles.

‡ In the case of a cylindrical particle of infinite length, the formula (16) is derived from the expression for the mean potential

$$\bar{\phi}(\lambda, n_1, r) = (2n_1 e_1/D\kappa_0 a)K_0(\lambda\kappa_0 r)/K_1(\lambda\kappa_0 a),$$

[*Footnote continued overleaf.*

The preceding analysis applies only to small surface potentials but it can readily be extended to larger potentials in the case of a single, plane, charged surface immersed in a binary symmetrical electrolyte. When the Poisson-Boltzmann equation is applied in this case, then we can show that (14) is again true. This is consistent with the result obtained by Casimir[7] that the Poisson-Boltzmann equation may be applied for large potentials as well as for small potentials. It would appear from the examples discussed above that in colloidal solutions, the use of the Poisson-Boltzmann equation and the identification of the mean potential with the potential of the mean force are good approximations.

5. Interaction Energy of Two Colloidal Particles:

We have not yet investigated how general is the validity of relations of the type (14) and (16).* In the case of two spherical particles and two parallel cylindrical particles, we can show that for large separations R and in the limiting case of small λ, such relations are valid. Since in general the mean potential will no longer be constant over the surface of each particle, we need to introduce some average, taken over each particle surface, of the mean potential. When the linear Debye-Hückel equation is used, the potential *distribution* on each particle surface will not depend on the total particle charge $\lambda n_1 e_1$. This suggests that in this case, the proper average is weighted in proportion to the density distribution of surface charge. In the general case, when the Poisson-Boltzmann equation must be used, the averaged potential will be obtained differently. We shall denote this potential simply by $\bar{\psi}_{\text{ave}}(\lambda, n_1, R)$.

In the linear case, the electrostatic energy of the double layers of the two particles, which we denote by $\bar{E}(\lambda, n_1, R)$ will have the form $n_1^2\bar{E}_0(\lambda_1 R)$. We now define the appropriate average of the potential of the mean force by

$$\lambda e_1 \Phi_{\text{ave}}(\lambda, n_1, R) = \frac{\partial}{\partial n_1}\int_0^\lambda \frac{\bar{E}(\lambda, n_1, R)}{\lambda}\,d\lambda = 2n_1\int_0^\lambda \frac{\bar{E}_0(\lambda, R)}{\lambda}\,d\lambda, \quad . \quad (17)$$

and assume that $\bar{\psi}_{\text{ave}}(\lambda, n_1, R)$ which has the form $n_1 g(\lambda, R)$, can be equated to $\Phi_{\text{ave}}(\lambda, n_1, R)$. Thus

$$\lambda e_1 g(\lambda, R) = 2\int_0^\lambda \frac{\bar{E}_0(\lambda, R)}{\lambda}\,d\lambda. \quad . \quad . \quad . \quad (18)$$

For both spherical and cylindrical particle pairs, the function $g(\lambda, R)$ increases as the distance R decreases. Investigations of the integral on the right-hand side of (18) indicates a similar behaviour and no minimum although $\bar{E}_0(\lambda, R)$ does have the latter property as a function of R.

However, the relation (18) is not satisfied for the model of two infinite parallel plates considered in Part I. In this case we find that the potential of the mean force at the surface is

$$\Phi_1(\lambda, \nu_1, R) = \frac{2\nu_1}{\lambda e_1}\int_0^\lambda \frac{\bar{E}_0(\lambda, R)}{\lambda}\,d\lambda = \frac{4\pi\nu_1 e_1}{D\kappa_0}\left(\coth \tfrac{1}{2}\lambda\kappa_0 R - \frac{2}{\lambda\kappa_0 R}\right), \quad (19)$$

which increases with R. On the other hand, the mean potential is given by

$$\bar{\psi}(\lambda, R/2) = \nu_1 g(\lambda, R) = \frac{4\pi\nu_1 e_1}{D\kappa_0}\coth \tfrac{1}{2}\lambda\kappa_0 R, \quad . \quad . \quad (20)$$

where n_1 is the number of adsorbed ions per unit length of particle, a is the radius of the circular cross-section, r is the distance from the axis of the cylinder perpendicular to it and K_0 and K_1 are Bessel functions of purely imaginary argument.

---

[7] Casimir, *Tweede Symposium over sterke Electrolyten en over de elektrische Dubellaag*, (The Hague, 1944), ed. Ned. Chem. Ver., 6.

* *Note added in proof*—A general proof of these relations has since been derived.

which decreases with R. Further, if $\lambda \to 0$ and ν_1 is kept fixed, $\Phi_1(\lambda, \nu_1, R) \to 0$ whereas the mean potential function $\bar{\psi}(\lambda, x)$ has the common limiting value $8\pi\nu_1 e_1/D\lambda\kappa_0^2 R$ (which tends to ∞ as $\lambda \to 0$) on the plates and in the region between the plates. Overbeek has pointed out that the erroneous result of an attraction between two infinite parallel plates, which we obtained in Part I, originates in this limiting infinite value. However, in the discussion remarks by Overbeek and the author, no satisfactory method of overcoming this difficulty was suggested.

In our theory it is assumed that the ions in the dispersion medium are uniformly distributed throughout this medium when they are all discharged. According to the Boltzmann distribution law, this means that the product $\lambda\bar{\psi}(\lambda, x) \to 0$ as $\lambda \to 0$. Suppose we have two finite parallel plates, and starting with the discharged system, we place a charge $e_i \mathrm{d}\lambda$ on each ion of type i. The charge on the plates will be $2A\nu_1 e_1 \mathrm{d}\lambda$ and the excess charge $-2A\nu_1 e_1 \mathrm{d}\lambda$ in the dispersion medium will be uniformly dispersed, so that only a very small fraction of it will lie between the plates. With each increment $\mathrm{d}\lambda$, there will be an infinitesimal distribution of ions in the dispersion medium, since the Debye charging process is a reversible one. This diffusion of ions will be in such a direction that the excess charge gradually shifts into the region between the plates. We can expect that most of the charge will have entered this region when the length $1/\lambda\kappa_0 \lessdot \sqrt{A}$. However, if the Debye-Hückel equation is applied to two infinite parallel plates, then the excess charge $-2A\nu_1 e_1 \mathrm{d}\lambda$ at the start of the charging process is all concentrated between the plates. This means that there has been an instantaneous re-distribution of ions throughout the dispersion medium, thereby involving an irreversible process. This anomaly is due to the infinite potential $\bar{\psi}(\lambda, x)$ when $\lambda = 0$, which implies that when the ions are completely discharged, the density of ions between the plates is different from that in the interior of the solution.

For two spherical or cylindrical particles, we find that for fixed R, the function $\bar{E}_0(\lambda, R) - \bar{E}_0(\lambda, \infty)$ is always positive for sufficiently small λ, although it becomes negative when R is large. The reason for the former behaviour is that the free energy of charging the ions includes the work done against the thermal motion during the diffusion of the excess charge into the region between the particles. Furthermore, if the interaction of two particles is to be repulsive, the integral in (18) must decrease as R increases. These properties should also apply to two parallel plates. The quantity $\bar{E}_0(\lambda, R) - \bar{E}_0(\lambda, \infty)$ cannot be negative for all R and λ (as our model in Part I yields), but must be positive in the vicinity of $\lambda = 0$. For parallel plates of area $A \gg R^2$, $\bar{E}_0(\lambda, R)$ will exhibit an extremely sharp maximum at some value of λ close to 0. This maximum arises from the relatively drastic re-distribution of ions which is required at the beginning of the charging process, in order to concentrate most of the excess charge in the dispersion medium between the plates. The work done against the osmotic forces in these initial stages would be quite large.

The additional term proposed by Overbeek in the discussion is absent provided the correct form for the function $\bar{E}_0(\lambda, R)$ in the vicinity of $\lambda = 0$ is used. *Thus our fundamental equations in Part I are sufficient and no term has been omitted.*

Although the model of two infinite parallel plates must therefore be discarded near $\lambda = 0$ in our theory, it can still be used provided $\lambda > 1/\kappa_0 A^{\frac{1}{2}}$. The analysis presented in this paper suggests that (18) should still be valid for two parallel plates when we identify the mean potential with the potential of the mean force and use the linear Debye-Hückel equation. Hence

$$2\int_0^{\lambda} \frac{\bar{E}(\lambda, \nu_1, R}{\lambda} \mathrm{d}\lambda = \lambda\nu_1 e_1 \bar{\psi}(\lambda, R/2), \quad . \quad . \quad . \quad (21)$$

remembering that $\bar{\psi}(\lambda, R/2)$ is evaluated for arbitrary ν_1. In the answer to Overbeek's criticisms of Part I, the author had already proposed this form. However, the remark was made that the objection to this solution is that it implies the free energy depends on R when $\lambda = 0$. The answer to this difficulty is that the particular form (20) for $\bar{\psi}(\lambda, R/2)$ cannot be used in the vicinity of $\lambda = 0$ since it tends to infinity as $1/\lambda$.* We shall substitute instead the appropriate average of the mean potential $\bar{\psi}_{ave}$ λ, ν_1, R) taken over the finite plates, such that $\lambda\bar{\psi}_{ave}(\lambda, \nu_1, R) \rightarrow 0$ as $\lambda \rightarrow 0$.

On the basis of the results outlined above and in Part I, the following method is proposed for determining the mutual free energy of two identical colloidal particles each having n_1 adsorbed ions of type 1 and surrounded by an infinite volume of electrolyte (e.g. spherical or parallel cylindrical or plate-like particles). The mean potential is equated to the potential of the mean force in the first part of equation (17) so that

$$\int_0^\lambda \frac{\bar{E}(\lambda, n_1, R)}{\lambda} d\lambda = \lambda e_1 \int_0^{n_1} \bar{\psi}_{ave}(\lambda, n_1, R) dn_1, \qquad (22)$$

which replaces (9). The function $\bar{\psi}_{ave}(\lambda, n_1, R)$ is obtained from the solution of the Poisson-Boltzmann equation. The mutual free energy at any stage λ is written as

$$-2n_1\Delta\chi_1(\lambda) + 2f_0(n_1) + 2\lambda e_1 \int_0^{n_1} \bar{\psi}_{ave}(\lambda, n_1, R)dn_1, \qquad (23)$$

and the equilibrium value $n_1 = \bar{n}_1(\lambda, R)$ is determined by the condition that (23) be a minimum with respect to variation in n_1, which yields

$$\lambda e_1 \bar{\psi}_{ave}(\lambda, n_1, R) = \Delta\chi_1(\lambda) - \frac{df_0(n_1)}{dn_1}. \qquad (24)$$

In Part I we proposed a general method of determining the force between two particles (eqn. (I, 39)). Application of this method yields the force

$$-2\lambda e_1 \left[\int_0^{n_1} \frac{\partial\bar{\psi}_{ave}(\lambda, n_1, R)}{\partial R} dn_1\right]_{n_1=\bar{n}_1(\lambda, R)} \qquad (25)$$

which is equivalent to the form given by Derjaguin in the particular case where n_1 is constant, independent of R. Since $\bar{\psi}_{ave}(\lambda, n_1, R)$ decreases as R increases, it follows from (25) that the force between two colloidal particles is repulsive, in agreement with the results of Verwey and Overbeek. However, our energy expression (23), subject to the condition (24) is more general than that of these authors, since it becomes equivalent to their Lippmann equation, which we write here as

$$-2\lambda e_1 \int_0^{\Delta\chi_1(\lambda)/\lambda e_1} n_1 d\bar{\psi}_{ave}(\lambda, n_1, R), \qquad (26)$$

on putting $f_0(n_1) = 0$.

Verwey and Overbeek conclude that the electrical interaction between the double-layers of colloidal particles always shows a repulsion and that the long-range attraction which is shown by tactoid formation (phase separation) must be attributed to van der Waals' forces. However, the above analysis only applies to dilute sols and preliminary investigations indicate that new features enter in concentrated colloids.

To derive (25) it is assumed that the characteristic quantity $\lambda\kappa_0$ (in electrolyte theory) is independent of n_1 and R. However, in concentrated sols, we have to deal with a function $\kappa(\lambda, n_1, R)$ and in § 3, this is taken into account in the case of two parallel plates. If we consider the particular case of a sol of plate-like particles, the interaction of which are neglected, then we need to replace $\lambda\kappa_0$ by a function $\kappa(\lambda, \nu_1)$ and also (14) by

---

* Reference was made in Part I to calculations made on tactoid formation of cylindrical particles which yielded an attraction. Here also the potential becomes infinite in the discharged state and hence this attraction cannot be correct.

$$\lambda e_1 \Phi_1{}^*(\lambda, \nu_1) = 2 \frac{\partial}{\partial \nu_1} \int_0^\lambda \frac{\overline{E}^*(\lambda, \nu_1)}{\lambda} d\lambda. \quad . \quad . \quad . \quad (27)$$

For small potentials, we can readily obtain expressions for $\kappa(\lambda, \nu_1)$ and $\overline{E}^*(\lambda, \nu_1)$ if we only retain terms up to the first power in the sol concentration.† Now, if $\Phi_1{}^*(\lambda, \nu_1)$ is the solution of the approximate Debye-Hückel equation, it should be obtained from $\overline{\phi}(\lambda, \nu_1, 0)$, which is defined in (13), simply by replacing $\lambda\kappa_0$ by $\kappa(\lambda, \nu_1)$. However, it is found that this expression for $\Phi_1{}^*(\lambda, \nu_1)$ does not satisfy (27), indicating that (25) cannot be used for the force between two particles in concentrated sols.

The author wishes to acknowledge the helpful correspondence with Prof. Overbeek on a number of points in this paper.

Summary.

In this paper we develop further our theory of the mutual free energy of two colloidal particles. It is shown how our results can be obtained from a form of the Lippmann equation, which reduces to the basic formula of Verwey and Overbeek on assuming that the surface potential is constant.

The model of two infinite parallel plates used in the earlier paper (I) yields the erroneous result of an attraction, because the edge effects are neglected. This leads to an infinite potential at the plates when the ions are discharged, assuming the number of adsorbed ions is fixed, and thereby introduces an irreversible process. A correct analysis of the influence of the finite size of the plates produces a repulsion.

Our theory does not omit any terms of an electrical nature, as suggested by Overbeek. It is more general than the theory developed by Verwey and Overbeek since it avoids the assumption of constant surface potential. A repulsion is obtained between the double layers of two colloidal particles in dilute sols, in agreement with the work of the above authors. Also, a good approximation is probably obtained by equating the mean potential to the potential of the mean force at the particle surface.

Birkbeck College,
Research Laboratory,
Torrington Square,
London, W.C.1.

---

† The quantity $\kappa(\lambda, \nu_1)$ is derived from (I, 10) and $\overline{E}^*(\lambda, \nu_1)$ from (I, 8*i*), (I, 12) and (I, 23) on putting $R = \infty$.

CORRIGENDA.

Page 351, Fig. 1(*b*). *For* structures *read* structure.

,, 352, l. 5. *For* indices (*hkl*) *read* indices (*hk*).

,, 352, 3rd para., l. 3-4. *For* liquid. . . . An oriented aggregate *read* liquid. In some experiments, an oriented aggregate.

,, 352, 3rd para., l. 6. *For* with the liquid, as follows. The mineral *read* with the liquid In most cases, however, a different method was used. The mineral.

,, 357, Table I. *Add to list of code letters.* *k* = treated with liquid at 200°.

,, 358, 2nd para., l. 8. *For* is *read* would be.

,, 360, last para., l. 18-19. *For* In contrast to *read* In contrast, with.

,, 363, legend to Fig. 5. *For* (*a*) glycol *read* (*a*) glycerol.
For (*e*) Cyclohexane *read* (*e*) Cyclohexanol.

,, 364, 2nd para. from foot of page is legend to Table II.

,, 366, l. 22. *For* suggests that the water *read* suggests that, in the vermiculites, the water.

,, 366, l. 36. *For* e.g. octophyllite *read* e.g. a particular sample of octophyllite.

Note on
The Effect of Molecular Inertia on Dielectric Absorption.

By J. G. Powles.

Received 8th September, 1948.

Since returning the proofs of my paper * on the above subject my attention has been drawn to a recent paper by Dmitriev and Gurevitch (*J. Expt. Theor. Physics, U.S.S.R.*, 1946, **16**, 937) which had escaped my notice.

The analysis given there is essentially similar to that in the first part of my paper except that the difficulty of the effect of inertia in the thermal agitation term is not considered. These authors do not, however, consider their work in the light of experiments now available † where it is known that a Debye relation is obeyed, at least to a good approximation. Before considering the effect of inertia in the case of large particles ($r > 10^{-6}$ cm.) in a non-polar medium it would appear necessary to confirm experimentally the Debye absorption peak, i.e. the rising part of their curve relating dipole conductivity and frequency. The approach by way of the dipole conductivity, obscures the fact that the greatest effect of inertia occurs when the measured quantity (tan δ) has a low value compared to that at the peak, and will therefore be difficult to measure accurately.

* This issue, p. 802.

† Ref. 4, 5 and 6 of my paper.

THE ENERGY OF CARBON BONDS—A RE-EXAMINATION OF THE FOX-MARTIN RULE.

By E. C. Baughan.

Received 19*th August*, 1947.

In theoretical organic chemistry the first approximation of great usefulness has always been to regard the behaviour of any compound as simply the sum of the behaviours, regarded as mutually independent, of its carbon skeleton and of its reactive groups. More detailed study shows discrepancies from this simple scheme as, for example, the problem of the stability of conjugated double-bonds, yet a tremendous amount of fact can be co-ordinated and predicted by means of it. Its equivalent translation in terms of energies implies that, for example, all C—C single bonds should have one single dissociation-energy, all C—H bonds another constant dissociation energy, and so on. Moreover, provided we are discussing only substitution energies, e.g. the *differences* between the R—H and R—Br dissociation energies of a given radical R, correct conclusions can be drawn even when the absolute value of either dissociation energy is unknown.

The estimation of carbon bond strengths at this level of first approximation gives, therefore, information of considerable value. Such tables of Average Bond Strengths have been in the past compiled in the following way : from the heat of vaporisation of carbon from its conventionally accepted thermochemical standard state of graphite to the monatomic vapour in its ground state, and the heats of combustion of graphite, methane and hydrogen we can obtain the average CH bond strength in methane by means of the well-established heat of dissociation of hydrogen into atoms. Assuming that the dissociation energy of methane into the methyl radical and a hydrogen atom is the same as this average bond strength, we can, from the heats of combustion of methane and ethane, obtain the value for the C single-bond energy, and such a scheme can be extended to any other bond on a carbon atom.

This simple " average bond-strength scheme " which was first put forward by Fajans,[1] and used for valuable discussion by several authors, particularly Sidgwick and Bowen,[2] and Pauling,[3] was until recently difficult to check. The value of the heat of vaporisation of carbon is not easily obtained with accuracy by direct experiment, and there was very little known about the absolute values of the energies of dissociation of any given carbon compounds into free radicals.

In the past few years, several lines of evidence have made clear that such schemes cannot be maintained for calculation of the absolute value of individual bond strengths without considerable modification. In the first place, more precise knowledge is becoming available on the heat of vaporisation of carbon by indirect methods, particularly from the molecule CO. The heats of combustion of CO and graphite are accurately known ; from these one could estimate the heat of vaporisation of carbon if one knew the dissociation energy of CO into carbon and oxygen atoms in their ground-states. Spectroscopic work on CO molecules has shown pre-dissociations which probably correspond to either 125 or 169 kcal.

---

[1] Fajans, *Ber.*, 1920, **53**, 643 ; 1922, **55**, 2836.

[2] Sidgwick and Bowen, *Ann. Reports*, 1931, 367 ; Sidgwick, *The Covalent Link in Chemistry* (Cornell University Press, 1933), Ch. IV.

[3] Pauling, *The Nature of the Chemical Bond* (Cornell University Press, 1939), Ch. II.

for the heat of vaporisation of carbon, this ambiguity being due to uncertainty as to the atomic states of the atoms produced.[4]

Secondly, the actual dissociation energies of some aliphatic molecules into free radicals are now established by several concordant methods. Thus the dissociation energy of methane into a methyl radical and hydrogen has been established at about 103 kcal. in the following ways—

(*a*) A great deal of work has been done, particularly by H. S. Taylor and his co-workers, on the activation energies of various reactions between hydrogen, methane and ethane.[5]

(*b*) The kinetics of thermal decomposition of alkyl iodides at very low pressures give activation energies,[6] identified with the C—I bond dissociation energies. From these values the corresponding carbon-hydrogen bond energies can be obtained from calorimetric data.[7]

(*c*) The interpretation of kinetic data on the photobromination of hydrocarbons.[8]

(*d*) The appearance potential data from electron bombardments.[9]

(*e*) Sidgwick and Springall[10] have pointed out that the *difference* between the CH_3—H and CH_3—Hg bonds can be obtained from calorimetric data; to explain the observed stability of $Hg(CH_3)_2$, a minimum value of the Hg—CH_3 bond must be postulated which, from this difference, implies a CH_3—H energy of 100 kcal. or more.

All these different methods agree that the dissociation energy of methane into methyl and hydrogen is about 103 kcal. which is weakened in the case of ethane giving ethyl and hydrogen to about 98 kcal. and further weakened for more complicated aliphatic hydrocarbons.

Thirdly, more precise calorimetric measurements have shown that the heats of substitution on a given aliphatic radical R are by no means as independent of the nature of R as had previously been supposed on the basis of less accurate work. This point has become particularly clear from the precise heats of combustion which have been determined in the last fifteen years by Rossini and his co-workers;[11] their values are confirmed by direct measurements on the heats of hydrogenation and bromination of olefines by Kistiakowsky and his school.[12]

---

[4] There are three main opinions on D, the energy of dissociation of CO into ground-state atoms, implying three corresponding values for L, the heat of vaporisation of carbon to the ^3P ground state:

(*a*) $D = 11{\cdot}11$ ev. ($L = 170$ kcal.),
(*b*) $D = 9{\cdot}14$ ev. ($L = 125$ kcal.),
(*c*) $D = 6{\cdot}92$ ev. ($L = 74$ kcal.).

(*a*) is the value used by Rossini and Bichowsky[39] on other grounds; it has since been defended on spectroscopic grounds by Kynch, Penney and Gaydon, cp. Gaydon, *Dissociation Energies* (Chapman and Hall, 1947), Ch. X, where the opposing views are clearly discussed and full references given; it is the value recommended by Baughan[13] and by Sidgwick and Springall.[10] (*b*) is the value recommended by Herzberg (*Chem. Rev.*, 1937, **20**, 145; *J. Chem. Physics*, 1942, **10**, 306), and by Long and Norrish,[15] and adopted by Pauling.[3] (*c*) which appears to be very low, can be made consistent by assuming that bond strengths really refer to the higher ^5S state of carbon; this argument is mainly due to Schmid and Gerö (for references, see Gaydon, *op. cit.*). Both these authors have since died—but their view has recently been defended by Valatin (*Nature*, 1946, **158**, 237; *Proc. Physic. Soc.*, 1947, **59**, 502).

Now that the dissociation energy of $(CN)_2$ into CN is approximately known,[36] the possibility of deriving L from the dissociation of the CN radical is open. So far the published discussions (Springall, *Trans. Faraday Soc.*, 1947, **43**, 177; Gaydon, *op. cit.*) favour (*a*) ($L = 170$ kcal.).

[5] For a review of this extensive work see Steacie, *Atomic and Free Radical Reactions* (Reinhold Co., New York, 1945), Ch. VI.

[6] Butler and Polanyi, *Nature*, 1940, **146**, 121; *Trans. Faraday Soc.*, 1943, **39**, 19.

[7] Baughan and Polanyi, *ibid.*, 1940, **146**, 685.

[8] Anderson, Kistiakowsky and van Artsdalen, *J. Chem. Physics*, 1942, **10**, 305, 653; 1943, **11**, 10.

[9] Stevenson, *J. Chem. Physics*, 1942, **10**, 291.

[10] Sidgwick and Springall, *Nature*, 1945, **156**, 599.

[11] *Bull. Bur. Stand. J. Res.*, from 1933 to date.

We now have, therefore, precise though ambiguous data for the heat of vaporisation of carbon, and agreed values for the dissociation energy of certain aliphatic bonds, and this increased knowledge has involved difficulties for the average bond-strength schemes. Thus it was pointed out some years ago [13] that the observed value of the dissociation energy of ethane into two methyl radicals agreed with the predictions of the average bond-strength systems, *provided* that (*a*) the four successive heats of hydrogenation of a carbon atom from monatomic vapour in the ground state to methane were all the same (the arguments defending this assumption are not, however, beyond criticism.[15]) (*b*) the higher value of 170 kcal. was correct for the heat of vaporisation of graphite, although at that time the lower spectroscopic value of 125 kcal. had been widely accepted. A considerable controversy has since been carried on as to the interpretation of the spectrum of CO.[1] It is not the object of this paper to attempt to review this controversy ; if, however, the lower value is correct then assumption (*a*) must be false. This latter conclusion is independently supported by evidence, based again on the observation of a pre-dissociation, that the dissociation energy of the CH molecule is perhaps as low as 80 kcal.,[14] 23 kcal. less than the dissociation energy of CH_4.

At present, therefore, the heat of vaporisation of carbon is still not finally established, but two isolated values are the most likely. Observed dissociation energies imply that, if the lower of these values be correct, then the calculation of average bond strengths will involve serious errors unless a detailed knowledge of the relative values of the four successive heats of hydrogenation of carbon atoms to methane is available.[15, 18] The energy of the last of these four steps may be regarded as definitely established, and there is some spectroscopic evidence on the first step. But values for the two intermediate steps are unknown, for the dissociation energies CH_3 and the CH_2 molecules have not yet been obtained. In a recent paper, Long and Norrish [15] have attempted to solve these problems by assuming that the dissociation energies of CH and CH_2 are equal, and that, following Mecke,[16] the dissociation energy of methyl into CH_2 + hydrogen would be the same as that of methane into CH_3 + hydrogen, except for a supposed change of the valence state of the carbon atom, by which the $CH_3 \rightarrow CH_2$ step would be assisted by the whole of the energy of the $^3P - {}^5S$ transition of carbon. These assumptions are open to some doubt : firstly, the energy of this transition is not yet definitely established, and independent evidence from the atomic spectra of carbon does not appear to support the value which Long and Norrish have had to assume.[17] Secondly, there are some theoretical reasons to believe that the whole of this transition energy should not appear in one single one of the four steps.[18] Thirdly, there is no conclusive reason to believe that the dissociation energies of the CH_2 and CH molecules are the same, or that those of the CH_4 and CH_3 molecules would be the same if it were not for the differing valence state of the carbon atom. Fourthly, the work of Rice and co-workers [19] on the chemical identification of the free radicals produced in the thermal decomposition of methane suggests that there is very little free methylene produced, and this fact is difficult to reconcile with Long and Norrish's [15] view which implies that the production of methylene from methyl should be particularly easy. If the Long and Norrish attempt is invalid it might alternatively be possible to calculate the relative energies of the four steps in atomisation of CH_4 from the detailed quantum treatment of the problem. The theoretical work that has so far been done on this problem is, however, probably not sufficiently precise, and there are indeed serious discrepancies between the results of the different treatments available.[18]

---

[12] Conn, Kistiakowsky and Smith, *J. Amer. Chem. Soc.*, 1938, **60**, 2764 ; Dolliver, Gresham, Kistiakowsky, Smith and Vaughan, *ibid.*, 1938, **60**, 440.

[13] Baughan, *Nature*, 1941, **147**, 542.

[14] Herzberg, *Molecular Spectrum and Molecular Structure—Diatomic Molecules* (Prentice-Hall, 1939). Shidei, *Japan. J. Physics*, 1936, **11**, 23.

[15] Long and Norrish, *Proc. Roy. Soc. A*, 1946, **187**, 337.

[16] Mecke, *Z. Elektrochem.*, 1930, **36**, 589.

[17] Edlen, *Nature*, 1947, **159**, 129.

[18] Goldfinger, Duchesne and Rosen, *Nature*, 1947, **159**, 130.

[19] Rice, *J. Amer. Chem. Soc.*, 1937, **56**, 488. Rice and Glasebrook, *ibid.*, 1934, **56**, 2381.

It would appear therefore that the older method of establishing bond strengths in any organic compounds must be considered unsatisfactory until more work, both theoretical and practical, is available on the dehydrogenation of methane, and until the heat of vaporisation of carbon is *independently* established beyond reasonable doubt. On the other hand, there have been definitely established some few dissociation energies of organic molecules. The object of this paper is therefore to try and see whether, on the basis of these energies, we can set up a table of carbon bond strengths in which the dissociation energies of bonds are related to some determinable equilibrium property of the same bond, the obvious choice being the equilibrium distance between the two atoms composing it. Other equilibrium properties which could be considered are the force constant and the ionisation potential of the bond. In this paper, the data on force constants provided by the work of Linnett [20] will be used primarily to show functional forms that may be expected between distance and dissociation energy; it is clear that these data provide a valuable basis for this discussion since differences in force constants are observed which show similar gradations to those inferred for the dissociation energies by Butler and Polanyi,[6] and by Baughan and Polanyi.[7] The ionisation potential, which affords a measure of the work of removal from the bond of the non-bonding electrons, is a quantity whose relation to the normal dissociation energy of the bond is at the moment difficult to understand theoretically except in certain simple cases; this paper will not therefore consider the remarkable correlations with ionisation potentials which have been established by Walsh.[21]

It is advisable at this point to discuss the complications in terminology which have inevitably been introduced by these modern refinements. As long as it was supposed that the average bond-strength scheme would give values to be identified with the directly observed dissociation energies for the split of an organic molecule into free radicals, the term " bond-strength " could be, and was, used indiscriminately for either. Now that it is clear that the situation is not so simple, a terminology is needed to keep these distinctions clear. In this paper from now onwards the energetic quantity observed in the actual process of the dissociation of a bond into free radicals will be called the " dissociation energy " of a bond; it is equivalent to the term " bond energy " in the earlier papers by Polanyi and his co-workers.[6, 7] The alternative energetic quantity which is essentially *defined* by the fact that the sum of such quantities for a molecule must equal the heat of atomisation of the molecule will be called the " bond strength "; it must be realised that estimates of this quantity may be in error through errors in energies of atomisation. These two quantities are unambiguously defined, but a second complication is introduced into the relation between them by the fact, insisted on particularly by Norrish,[22] that " energies of re-organisation " must be considered. As an example let us take the case of carbon tetrachloride.

---

[20] Linnett, *Trans. Faraday Soc.*, 1940, **36**, 1123; 1941, **37**, 469; 1942, **38**, 1; 1945, **41**, 223; *Quart. Rev.*, 1947, **1** (2).

[21] Walsh, *Trans. Faraday Soc.*, 1946, **42**, 56; 1947, **43**, 60, 158.

[22] Norrish, *ibid.*, 1934, **30**, 103; Long and Norrish, ref. [15].

It is known that the four C—Cl distances are equal, and therefore it is possible to define a bond strength in this system which has the interpretation that it is one-quarter of the total heat obtained by splitting off all four of the chlorine atoms. If, however, only *one* of the chlorine atoms is taken away, then the C—Cl distance in the CCl_3 radical will almost certainly change ; it is probable, for example, that in the series $CH_4 \rightarrow CCl_4$ the C—Cl distance becomes smaller as the number of chlorine atoms increases ; [23] hence there must be a rearrangement process in the CCl_3 radical during the dissociation, and to this process must correspond an appropriate energy of reorganisation, so that the dissociation energy $CCl_4 \rightarrow CCl_3 + Cl$ will *not* be equal to the bond strength defined above. A more extreme case of re-organisation energy would be in the process $CH_3 \rightarrow CH_2 + H$ on Long and Norrish's view [15] on which the whole of the ${}^5S$—${}^3P$ transition energy of carbon would appear as energy of re-organisation.

An attempt to compare observed dissociation energies with equilibrium distance may therefore be incorrect. The situation is thus far from simple, and the present paper can hardly do more than provide the first approximation, which may however be useful in our present knowledge, since the energy of re-organisation is a quantity of which we know very little. (As an example of the difficulties, it may be pointed out that the attempt of Long and Norrish [15] to estimate the energy of re-organisation terms in the dissociation of ethane is open to objection since it assumes that the C—H bond strengths in ethane are to be identified with the dissociation energy of ethane to ethyl + hydrogen.)

This paper proceeds, therefore, on the following lines : the discussion of force constants by Linnett [20] enables one to infer approximately the form of relation between the equilibrium distances and the dissociation energies in carbon-carbon bonds ; the functional form expected on these grounds is that suggested on the basis of average bond strengths several years ago by Fox and Martin.[24] As it is not possible to calculate exactly the energy of re-organisation terms, the attempted correlation must be confined to one between the observed energies of dissociation and observed equilibrium distances. It is recognised that this may involve an error due to energy of re-organisation, but it may be hoped that by taking sufficient points this uncertainty can be reduced to that of scatter of individual points about a common curve.

The investigations of Linnett [20] consider the problem: what simple general form of potential energy V as a function of interatomic distance r best gives the observed relations between force constants, distances, dissociation energies, etc., which have, from time to time, been recommended by various authors. For this he finds the reciprocal-exponential function,

$$V = a/r^m - be^{-nr},$$

where a, b, m, n, are constants, to be more satisfactory, for the calculation of the force constant, the anharmonicity constant, and the dissociation energy for several diatomic molecules than the other two functions, viz.,

$$V = a/r^m - b/r^n \text{ and } V = ae^{-mr} - be^{-nr}$$

(of which Morse's curve is a special case).[25] No doubt better agreement could be obtained with more complex forms ; but this simple reciprocal-exponential function predicts a relationship between force constant k

---

[23] Cp. Pirenne, *Diffraction of X-Rays and Electrons by Free Molecules* (Cambridge, 1946), p. 142.

[24] Fox and Martin, *J. Chem. Soc.*, 1938, 2106.

[25] Wu and Chang-Tsing Yang, *J. Physic. Chem.*, 1944, 48, 295, have considered the fourth case $a^{-mr} - b/r^n$, finding agreement with force constants about as good as Linnett's function adopted here. But calculation of dissociation energies from force constant and equilibrium distance is less accurate with this new variant. I am indebted to one of the referees of my paper for bringing this work to my attention.

and equilibrium distance r of the form, kr^{m+2} = constant, and Linnett finds, after reconsideration of the methylacetylene and dimethylacetylene cases, a close correlation (kr^6 = constant) for five molecules, ethane CH_3CN, ethylene, acetylene, and dimethylacetylene, the first four of which enter into Table I in this paper. And as the reciprocal-exponential function predicts that where an approximation kr^{m+2} is constant Dr^m should also be constant,* we may expect that for a carbon-carbon bond of dissociation energy D and equilibrium distance r, Dr^3 should be constant.

It is to be observed that this argument does not in any way involve the heat of vaporisation of carbon, and that the form predicted is precisely that found by Fox and Martin,[24] who used average bond strengths, although the average bond strength system involves different errors in C—C, C=C, C≡C bonds; this is probably due to the fact that these authors followed Sidgwick [2] in taking the heat of vaporisation of carbon at 150 kcal., which value would give average bond strengths in closer agreement with observed dissociation energies than the 124 kcal. adopted by Pauling.[3]

It remains therefore to recheck the Fox-Martin rule, whose soundness has been confirmed by Linnett's investigations, on the empirically obtained dissociation energy of carbon-carbon bonds. For this purpose, the basic experimental datum is the methyl-hydrogen dissociation energy in methane,[7] and its calorimetrically corresponding value for the $CH_3—CH_3$ energy in ethane, since, from these two energies we have, for any case for which we know the dissociation energy of any given R—C or R—H bond, the possibility of obtaining another experimental datum by replacing the carbon or hydrogen on R by a methyl radical; the energy of this replacement can be obtained from heats of combustion. This argument provides the dissociation energies for some of those interesting carbon-carbon single bonds which have been shown by Pauling, Springall, and Palmer [26] to be abnormally short because of their proximity to double or triple bond carbon atoms.

The following list gives therefore some directly determined dissociation heats and equilibrium distances; the dissociation heats are written in the notation: $D(R\overset{*}{-}R)$ implies the heat of dissociation of the R*—R molecule at the $R\overset{*}{-}R$ bond into two R radicals. Distances [27] are those found from (E.D) electron diffraction, (X) X-ray diffraction, (S) spectroscopic measurements, and are expressed in A.

(*a*) ETHANE. $D(CH_3\overset{*}{-}CH_3) = 89$ kcal.;[7] $r_0 = 1{\cdot}55$ (E.D). This value of D has already been discussed.

(*b*) ETHYLENE. $D(CH_2\overset{*}{=}CH_2) = 145$ kcal.;[7] this value is supported by the ultra-violet predissociation which gives $D \leqq 163$ kcal.;[28] $r_0 = 1{\cdot}353$[29] (S) or $1{\cdot}325$ (S).

By removal of one hydrogen from each of two ethylenes, and subsequent reuniting, we get butadiene.

$$CH_2{=}CH_2 + CH_2{=}CH_2 \rightarrow CH_2{=}CH{—}CH{=}CH_2 + H_2.$$

---

* To some extent, the argument is circular, since one of Linnett's reasons for adopting the reciprocal-exponential form was that it gave empirical equations of the form, Dr^x = constant; but examination of his actual evidence shows, however, that this was given comparatively minor weight compared with the force constant data.

In theory clearly we should refer a correlation of bond energy and distance to the bond energy at the absolute zero of temperature; in fact, the data are not in general available so that at present we must consider the heats of dissociation at constant pressure at room temperature. The errors so introduced are, however, small compared with the uncertainties in the two main quantities.

[26] Pauling, Springall and Palmer, *J. Amer. Chem. Soc.*, 1939, **61**, 927.

[27] All distances quoted in this paper come from the summary in Pauling's book, ref. [3], Ch. V, unless otherwise stated.

[28] Price, *Physic. Rev.*, 1944, **45**, 843; Hilgendorff, *Z. Physik*, **95**, 781.

[29] Galloway and Barker, *J. Chem. Physics*, 1942, **10**, 88.

The overall heat of reaction = − 5 kcal. (combustion heats). Taking the heat of removal of this one hydrogen as 106 kcal.,[21] we get

$$-2 \times 106 + D(\mathrm{CH_2{=}CH\overset{*}{-}CH{=}CH_2}) + 103 = -5,$$

hence

$$D = 104\ ;\ r_0 = 1{\cdot}46\ (\mathrm{E.D}).$$

(*c*) ACETYLENE. $D(\mathrm{HC\overset{*}{\equiv}CH})$. Price[30] estimates the energy of dissociation of this bond to be " slightly less than 187 kcal." Although this value is based on a predissociation, and the interpretation of predissociation of polyatomic molecules is not unambiguous, acetylene appears to be a very simple case. $r_0 = 1{\cdot}204$ (S).

Again, Cherton[31] has pointed out that in ultra-violet light (or in a high-frequency discharge) acetylene gives diacetylene, and gives reasons for supposing that the dissociation energy $D(\mathrm{CH{\equiv}C\overset{*}{-}H})$ must be about 121 kcal. The heat of reaction $\mathrm{CH_4 + HC{\equiv}CH \rightarrow H_2 + CH_3{-}C{\equiv}CH}$ is known[11] to be −6 kcal., whence from the dissociation energy of the methane molecule (− 103), the joining together of two hydrogens (+ 104) and the HC≡C—H value of 121, we obtain for methylacetylene

$$D(\mathrm{CH_3\overset{*}{-}C{\equiv}CH,}) = 114\ ;\ r_0 = 1{\cdot}462\ (\mathrm{S}).$$

(*d*) CYANOGEN. The dissociation energy $D(\mathrm{CN\overset{*}{-}CN})$ of this molecule has been determined from optical estimates of the temperature variation of the concentration of the CN radical in cyanogen. This experiment has given two estimates, 146 kcal. (White[32]), 77 kcal. (Kistiakowsky and Gershinowitz[33]) which differ enormously. The higher value is approximately supported by kinetic data,[34] and by observations on photochemical thresholds,[35] and the lower value depends on optical technique which can be shown to be inadequate. We shall therefore adopt here the value proposed by Evans and Walker,[36] after discussion of this evidence, i.e. $D = 130$ kcal. $r_0 = 1{\cdot}37$ (E.D).

From the values of $D(\mathrm{CH_3\overset{*}{-}H})$, $D(\mathrm{H\overset{*}{-}H})$ and $D(\mathrm{CN\overset{*}{-}CN})$, we can get $D(\mathrm{CH_3\overset{*}{-}CN})$ from the heat of the reaction

$$\mathrm{2CH_4 + (CN)_2 \rightarrow 2CH_3{-}CN + H_2}$$

from heat of combustion.

Unfortunately this calorimetric quantity is uncertain, since there is a discrepancy in recent values for the heat of combustion of cyanogen. Thus v. Wartenberg and Schutza[37] obtained 261·3 kcal. (I) for

$$\mathrm{C_2N_2}(g) + \mathrm{2O_2}(g) \rightarrow \mathrm{CO_2}(g) + \mathrm{N_2}(g)$$

but found 4 % of the nitrogen as oxides, for which correction had to be made. McMorris and Badger,[38] by a different technique, found no correction necessary (negligible proportion of oxides of nitrogen) and obtained 251·4 kcal. (II). Clearly this heat is not established ; the latter value is probably preferable since the reaction was more straightforward, but both points are plotted. From these data, and the heat of combustion of $\mathrm{CH_3CN}$ gas quoted by Bichowsky and Rossini[39] we obtain

$$D(\mathrm{CH_3\overset{*}{-}CN}) = 109\ (\mathrm{I})\ ;\ = 114\ (\mathrm{II})\ ;\ r_0 = 1{\cdot}49\ (\mathrm{E.D.}).$$

(*e*) BENZENE. An approximation can be obtained in the following way. In the absence of resonance energy the bond would be expected to be halfway between the C—C in ethane (89 kcal.) and the C—C in ethylene (145 kcal.) i.e. 117 kcal. But the benzene structure is known to be particularly stable by about 40 kcal.; splitting this 40 kcal. evenly between all the six C—C bonds we obtain 124 kcal. for each. (This treatment neglects the change in C—H bonds.) Here $r_0 = 1{\cdot}39$ (E.D and (X).

---

[30] Price, *Physic. Rev.*, 1945, **47**, 444.

[31] Cherton, *Bull. Soc. chim. Belg.* 1943, **52**, 26.

[32] White, *J. Chem. Physics*, 1940, **8**, 463.

[33] Kistiakowsky and Gershinowitz, *ibid.*, 1933, **1**, 432.

[34] Robertson and Pease, *ibid.*, 1942, **10**, 490.

[35] Hogness and T'sai, *J. Amer. Chem. Soc.*, 1932, **54**, 123.

[36] Evans and Walker, *Trans. Faraday Soc.*, 1944, **40**, 393.

[37] von Wartenberg and Schutza, *Z. physik. Chem. A*, 1933, **164**, 386.

[38] McMorris and Badger, *J. Amer. Chem. Soc.*, 1933, **55**, 1952.

[39] Bichowsky and Rossini, *Thermochemistry of Chemical Substances* (Reinhold, New York, 1937).

Hence we have Table I, arranged in order of *D*.

TABLE I.

Point No.	Bond.	*D*. (kcal.)	r_0. (A.)
1	$CH_3C\overset{*}{-}H_3$	89	1·55 (E.D)
2	$CH_2{=}CH\overset{*}{-}CH{=}CH_2$	104	1·46 (E.D)
3	$CH_3\overset{*}{-}CN$	109-114	1·49 (E.D)
4	$CH_3\overset{*}{-}C{\equiv}CH$	114	1·462 (S)
5	Benzene	124	1·39 (E.D, X)
6	$CN\overset{*}{-}CN$	130	1·37 (E.D)
7	$CH_2\overset{*}{=}CH_2$	145	1·353 (S) or 1·325 (S)
8	$CH\overset{*}{\equiv}CH$	187	1·204 (S)

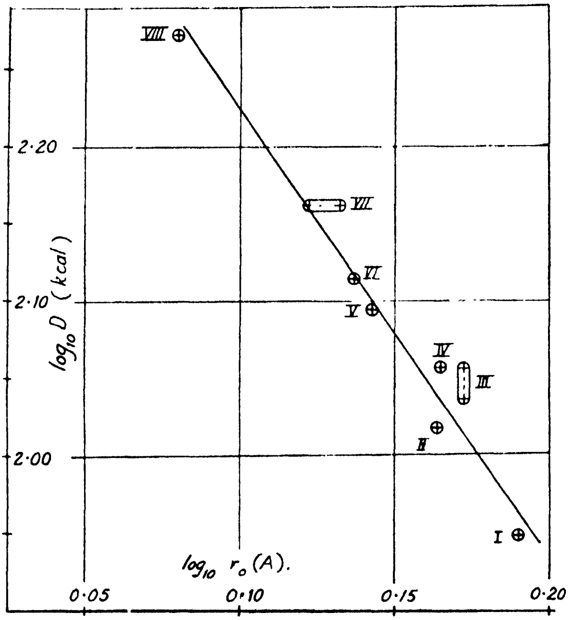

FIG. 1.

To check the Fox-Martin rule, Fig. 1 shows a plot of log *D* against log r_0 for the eight points given in Table I. It can be seen that a straight line of slope corresponding to $x = 3$ passes well through the points; the uncertainty in this slope is difficult to assess, since the data are not of equal merit. Fig. 2 shows this relation in another form, the relation, Dr_0^3 = constant, being the smooth curve drawn through the experimental points. The mean scatter of the individual points corresponds to ± 0·015A. to r_0, or to ± 4 kcal. in *D*, of the same order as the experimental errors. At this stage in the argument we may consider other equations which have been proposed as improvements on the Fox-Martin approximation. Here the important point arises that on average bond strength systems, errors in the basic assumptions do *not* enter as constants into a correlation of this kind. Thus an error x in the vaporisation heat of carbon on the average bond strength scheme involves an error of $\frac{1}{2}x$ in a C—C bond, or x in a C=C bond, or $3/2x$ in a C≡C bond. Since almost inevitably ethane, ethylene and acetylene become basic points for such schemes, there are therefore few empirical discussions of the Fox-Martin rule since their original paper in 1938 which add anything new ; an exception may be made of the interesting paper by Skinner,[40] in which for the first time the variation of the C—H bonds is explicitly considered, and the application of the distance—bond strength correlation is extended to several other types of bond.

TABLE II.—C—H BONDS

	D.	*r.*	Dr^4.	$D_{\text{calc.}}$
CH	80	1·120	(126)	93
CH_4	103	1·093	146	103
Ethylene . . .	106	1·071	140	111
Acetylene . . .	121	1·057	151 Mean 146	117

This relation may be further applied. For example, we may invert an argument of Fox and Martin [24] and consider diamond and graphite. Fox and Martin pointed out that since each carbon in graphite has three nearest neighbours while in diamond it has four, and since the heats of combustion show that the energies of formation of these two crystals from carbon vapour are very closely equal, then the C—C bond strength in graphite must be 4/3 times that in diamond. They used this argument to provide a point for their illustration of Dr_0^3 = constant. Assuming that Dr_0^3 is constant, this argument can be inverted to predict that the C—C spacing in the graphite crystal must be $\left(\frac{3}{4}\right)^{\frac{1}{3}}$ or 0·9085 times that in diamond. The observed value in diamond is 1·545 A, whence in graphite it should be 1·404, the observed value [41] being 1·421 A. The discrepancy corresponds only to about 4 kcal. per carbon atom, which is of the same order as the interlamellar van der Waals' forces in graphite which have been neglected.

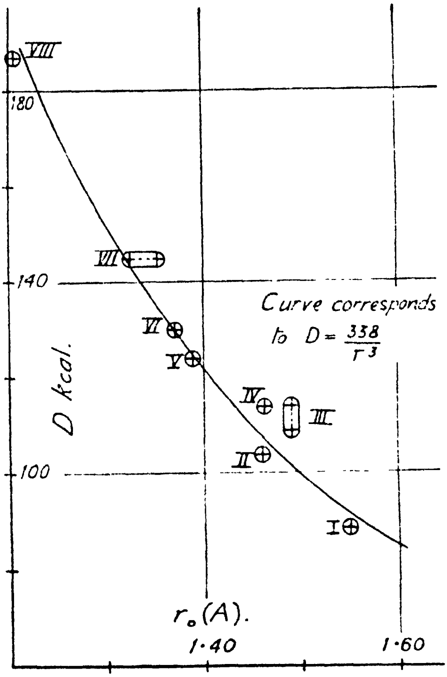

FIG. 2.

---

[40] Skinner, *Trans. Faraday Soc.*, 1945, **41**, 645.
[41] Observed values from Riley, quoted by Skinner, ref. [40]

Data for the detailed application of these ideas to other carbon bonds are still more inadequate. Thus for C—H bonds, we have only the spectroscopic method of estimating the distance. Linnett[20] pointed out that the relation, kr_0^6 = constant, held between force constant and distance for the three cases: CH, CH_4 and C_2H_2, implying Dr_0^4 constant. An attempt to check the functional form shows difficulty in relating to the other two the CH dissociation energy which is still only roughly known. It is probably better to take the last three points in Table II. (cp. Skinner[40]).

It can be seen that $Dr_0{}^4$ = constant fits the experimental points to within their probable error, but also that the range of variation is so small that almost any reasonable function would do—the simple linear dependence proposed by Skinner,[40] for example. A distinction might be reached if we knew the data for the CH molecule more accurately. For other bonds on carbon atoms the data are still more inadequate.

It is maintained, therefore, that the construction of a detailed carbon bond energy system on the basis of bond distance provides a useful approximation, in the light of which deviations from Fig. 2 may be considered as requiring special explanation; and this approximation may, if its range of validity be properly established, provide a method of estimating bond dissociation energies independent of the assumptions, at present very doubtful, inherent in average bond strength systems. More data are evidently required, but there is at any rate one exception already known where a bond of roughly normal length is weak due to resonance in the *radicals produced* by dissociation, which may be regarded as energy of re-organisation (Fig. 2 contains, of course, cases of bonds abnormally short and requiring abnormally high energies to dissociate them because of resonance in the *molecules before* dissociation.) This case is that of the central bond of bibenzyl, which can be dissociated into free radicals by about 50 kcal.[42] yet this length is 1·48 A. (X), corresponding to 104 kcal. from Fig. 2. It might appear therefore that the Fox-Martin rule in its revised form will take account of abnormal bonds in the original molecule, but not take account of bonds, otherwise normal, which can be unusually easily broken through resonance stability of the products. The C—C spacing in the simple aliphatic hydrocarbons is possibly an interesting case from this point of view, since the theory of Evans, Polanyi and the author[43] interprets the difference in dissociation energy in this series as mainly due to resonance stability of the radicals; on this interpretation one would *not* observe the lengthening by 0·03 A. from CH_3—CH_3 to *n*-butyl—CH_3 which would be predicted by taking the dissociation-energies[7] at their face value.

Finally, we may revert to the question of the heat of vaporisation of carbon and consider some implications of this new line of argument. If we consider a gaseous hydrocarbon C_mH_n, containing a carbon-carbon links of bond strengths A_1 . . . A_f, and n C—H links of bond strengths B . . . B_a, then clearly if H_f be the exothermic heat of formation of C_mH_n from graphite and hydrogen, and D the heat of the reaction, $H + H \rightarrow H_2$ (104·1 kcal.), we have

$$-mL - n/2D + \underset{a}{\Sigma}A + \underset{n}{\Sigma}B = H_f,$$

where L is the heat of vaporisation of carbon. Of these quantities, H_f, and D are well known. Supposing now we take $\underset{a}{\Sigma}A$ as given by the sum of the appropriate Fox-Martin predictions (an assumption true only if re-organisation energy be neglected) then

$$mL - \underset{n}{\Sigma}B = \underset{a}{\Sigma}A - n/2D - H_f \equiv Z,$$

the right-hand side of the equation being known. Let us call this quantity Z. We can now obtain L if $\underset{n}{\Sigma}B$ is known. It has already been pointed out that assumptions about this sum are inevitably made in the use of average bond strength systems ; what is not so generally realised is that, if L is to be ***chosen*** to give the best agreement with observed bond dissociation energies of C—C bonds, then different values of L are obtained from different assumptions about $\underset{n}{\Sigma}B$.

---

[42] Szwarc, *Faraday Soc. Discussions*, 1947, **2**.

[43] Baughan, Evans and Polanyi, *Trans. Faraday Soc.*, 1941, **37**, 377.

We may illustrate this point from the four molecules : C_2H_2, C_2H_4, CH_4 and C_2H_6. The H_f values are respectively $-$ 54, $-$ 13, + 18 and + 20 kcal.,[11] D is taken throughout at 104 kcal. Taking the C—C bond energies as given by $338/r_0^3$ (except that for ethane 89 is taken as standard), we have at this level of approximation the $\underset{a}{\Sigma}A$ values 194, 136, $\equiv 0$, 89, taking r_0 for ethylene [29] as 1·353 A.

Hence for the four hydrocarbons C_2H_2, C_2H_4, CH_4 and C_2H_6 we deduce the Z values, + 144, $-$ 59, $-$ 226, $-$ 243 kcal. (p, q, r, s). If we make the assumption that all C—H bonds are identical, then $\underset{n}{\Sigma}B = ny$, when y has a constant value ; this assumption is inherent in Pauling's treatment,[3] and although Sidgwick [2] makes a distinction between aliphatic and aromatic C—H bonds, he also assumes all aliphatic C—H bonds to be identical. By straightforward elimination of y between the four Z values we obtain six values for L : 173 (p, q), 171 (p, r), 169 (p, s), 167 (q, r), 155 (q, s), 192 (r, s) kcal. with a mean $L = 171 \pm 9$ kcal. This is essentially a more sophisticated form of the argument used by the author in 1941.[13] From $L = 171$, the four molecules give for y the values 99, 100, 99, 98 kcal., or 99 ± 1 kcal. for the mean C—H bond energy.

Let us now try another approximation : that in any one molecule, at any rate, all the C—H bonds are the same, and the energy can be obtained from the smoothed Fox-Martin values in Table II, taking the ethane value at 98 kcal. Hence the $\underset{n}{\Sigma}B$ values are respectively 2×117, 4×111, 4×103, 6×98, whence we deduce for the L values 189, 193, 186, 178 kcal., or a probable value of 188 kcal. This is a generalisation of the argument put forward by Cherton [31] for the special case of acetylene.

Suppose now we try the special case of methane CH_4. There are four steps :

$$\begin{aligned} C + H &\rightarrow CH + \alpha \text{ kcal.} \\ CH + H &\rightarrow CH_2 + \beta \text{ ,,} \\ CH_2 + H &\rightarrow CH_3 + \gamma \text{ ,,} \\ CH_3 + H &\rightarrow CH_4 + \delta \text{ ,,} \end{aligned}$$

and let us accept $\alpha = 80$, $\delta = 103$ kcal. If we take $\alpha = \beta$, $\gamma = \delta$, and equally if we assume a constant stepwise change from α through to δ . . . then $\underset{a}{\Sigma}A = 366$ and $L = 140$ kcal. Clearly yet further refinements would be possible if we knew the real ratios of α, β, γ, δ to one another.

These simple arguments show how the proper values for L in average bond strength systems depend on the assumptions made about the C—H bonds. Of the three different assumptions made, the first is almost certainly untrue, so is the second, and the third is without any independent justification. For application of average bond strength schemes to resonance energies, these uncertainties tend to cancel out ; for application to calculation of activation energies, we should choose the value which gives the best agreement with observed dissociation energies. This will depend on the assumptions made about the C—H bonds. But, as has been pointed out, the lengths of C—H bonds can only be determined for a very few particularly simple molecules. Hence in the actual application of average bond strength systems, one is practically forced to assume that all C—H bonds are the same. If this assumption is made, then $L = 170$ kcal. gives a consistently usable basis for such schemes which enable them to be applied to bond dissociation energies as a first approximation ; the use of the values 150, 124 kcal. assumed by Sidgwick [2] and Pauling [3] respectively, involves the *same* incorrect assumption, but has not this advantage. Any improvement in the basis of such systems must await the establishment of L from diatomic molecules (CO, CN),[4] or directly, and the definitive solution of the problem of the CH_4 molecule.

Chemistry Department,
Military College of Science,
Shrivenham,
Nr. Swindon, Wilts.

THE SECOND DISSOCIATION CONSTANT OF MAGNESIUM HYDROXIDE.

By D. I. Stock and C. W. Davies.

Received 23rd October, 1947.

Measurements of the hydrolysis of aqueous salt solutions are subject to numerous errors, of which the following have proved to be the most difficult to eliminate: (1) the salt used as starting material, either on account of hydrolysis during recrystallisation, or through contamination by mother liquor, may not contain precisely equivalent amounts of acid and base; (2) the *p*H of the unbuffered solution is very sensitive to impurities, of which the commonest is CO_2; (3) the liquid measured may contain insoluble products of hydrolysis, sometimes described as in colloidal solution; and (4) hydrolysis may proceed by stages, so that hydrolysis constants calculated from isolated measurements will be unreal.

We have studied the strength of magnesium hydroxide by a method involving the electrometric titration of $MgCl_2$ solutions with $Ba(OH)_2$, and believe that in this way we have avoided the errors enumerated. Magnesium chloride samples recrystallised from neutral and acid solutions were used in different runs, and the excess acid present in the latter case could be accurately allowed for by an analysis of the titration curve. Accurate allowance was also made for the CO_2 present, the amount of this being determined for each sample of conductivity water used in making up solutions, and the whole titration then being carried out without exposing the solutions to atmospheric contamination. Finally, the titration technique enabled the dissociation constant of the metal hydroxide to be calculated after each addition of $Ba(OH)_2$, that is, for gradually increasing concentrations of the hydrolysis products, and the constancy of the K values so obtained served as an indication that a homogeneous equilibrium was actually being studied; difficulties of the kind listed under (3) and (4) would have been exposed by a drift in the calculated K values.

Experimental.

Materials.—The "acid" magnesium chloride was prepared by dissolving A.R. magnesium chloride crystals in conductivity water and precipitating with gaseous HCl. After removing mother liquor by suction they were used without further treatment. The "neutral" sample was prepared from this by three recrystallisations from conductivity water in Pyrex apparatus. The $Ba(OH)_2$ solution, prepared in the usual way, was stored in a nickel container[1] and standardised, through HCl, against Na_2CO_3.

The water used never exceeded $0{\cdot}75 \times 10^{-6}$ ohm^{-1} cm.$^{-1}$ conductivity. The CO_2 content of each batch was calculated from its conductivity, using for the first dissociation stage of carbonic acid the values[2] $K_1 = 4{\cdot}45 \,.\, 10^{-7}$ and[3, 4] $\Lambda_0(H^{\bullet} + HCO_3{}') = 394{\cdot}4$. The procedure assumed that CO_2 was the only impurity present, and this assumption was confirmed by titrating a sample of water with baryta, in the way described in the next section, when the following results were obtained :

---

[1] Righellato, *Analyst*, 1934, **59**, 104.
[2] MacInnes and Belcher, *J. Amer. Chem. Soc.*, 1933, **55**, 2630.
[3] Shedlovsky and MacInnes, *ibid.*, 1935, **57**, 1705.
[4] Robinson and Davies, *J. Chem. Soc.*, 1937, 574.

370·2 g. water titrated with baryta containing 0·04654 equiv. $Ba(OH)_2$ per kg. solution. Specific conductivity of water 0·42 . 10^{-6} ohm^{-1} $cm.^{-1}$, giving total CO_2-content = 3·61 . 10^{-6} mol./l.

g. $Ba(OH)_2$.	0·063	0·129	0·237	0·373	0·710	1·352
$p\mathrm{H}_{\text{obs.}}$ . .	8·65	9·10	9·42	9·64	9·92	10·21
$p\mathrm{H}_{\text{calc.}}$ . .	8·63	9·10	9·41	9·62	9·92	10·20

The figures shown as $p\mathrm{H}_{\text{calc.}}$ were obtained by first calculating the amount of baryta used in reaction with CO_2 ; this correction can be obtained from the observed $p\mathrm{H}$ value in conjunction with the known dissociation constants of carbonic acid.[2] When this correction is deducted from the total weight of baryta added, the remainder gives the free alkali, and $p\mathrm{H}_{\text{calc.}}$ is the $p\mathrm{H}$ value that this will establish in the solution. The size of the CO_2-correction can be estimated from the fact that if it had not been applied the first $p\mathrm{H}_{\text{calc.}}$ value would have been 8·90. The good agreement of the calculated with the observed values shows that the conductivity of the water gives an adequate measure of its CO_2- content.

Apparatus and Procedure.—The glass electrode was a commercially made bulb which was filled with a solution 0·2 N. with respect to both HCl and KCl ; connection to this was made by a sealed-in silver-silver chloride electrode. The reference electrode consisted of another silver-silver chloride electrode sealed into a tube containing N. KCl. This terminated in a length of very fine-bore thermometer tubing carrying a ground-glass cap. It was flushed through with KCl before each run. The titration vessel was a seasoned Pyrex flask, the stopper of which carried, in addition to the electrodes, two inlet tubes with caps, through one of which the stem of the weight burette could be inserted whilst a stream of purified air entered the vessel through the other. The vessel was supported in a thermostat maintained at 25° C. ± 0·01° C., and all measurements were made at this temperature.

In carrying out a run, the stopper carrying the electrode system was transferred to a subsidiary vessel, and the electrode system standardised against a series of standard buffers.[5] The asymmetry potential was found to vary very slightly from day to day, though a linear relation between E.M.F. and $p\mathrm{H}$ was maintained. The electrode system was then washed with conductivity water, the KCl bridge and cap flushed out, the whole superficially dried and placed in the titration vessel and pure dry air passed. A suitable quantity of conductivity water was then weighed in, the sample of solid salt added, and, when this had completely dissolved, the $p\mathrm{H}$ was measured, and a sample of the solution was removed for analysis through a Pyrex siphon-tube. The $p\mathrm{H}$ was then checked, and the weight-titration against baryta begun. The filling and manipulation of the weight burette, like all other operations, were effected without exposing the solutions to unpurified air.

Results.

A titration run with the " neutral " sample of magnesium chloride gave the following results.

TABLE I.

Specific conductivity of water = 0·65 × 10^{-6} ohm^{-1} $cm.^{-1}$; hence CO_2 content of water = 7·77 . 10^{-6} mol./l. Initial weight of solution titrated = 354·4 g. ; initial concentration of $MgCl_2$ = 0·02959 mol./kg. Concentration of barium hydroxide = 0·04654 g.-equiv./kg.

g. $Ba(OH)_2$.	0	0·0305	0·0555	0·0800	0·1155	0·1440
$p\mathrm{H}$ . . .	6·32	7·18	7·64	7·90	8·06	8·20
$[MgOH^{\bullet}]$. 10^5	—	—	—	—	0·505	1·07
$p\mathrm{K}$ . . .	—	—	—	—	2·56	2·61

g. $Ba(OH)_2$.	0·2110	0·3015	0·6215	1·0030	1·530	
$p\mathrm{H}$ . . .	8·40	8·58	8·95	9·24	9·45	
$[MgOH^{\bullet}]$. 10^5	1·67	2·68	6·16	10·00	15·08	
$p\mathrm{K}$ . . .	2·67	2·69	2·69	2·61	2·54	

---

[5] Clark, *Determination of Hydrogen Ions*, 1928, p. 200.

The first two rows of figures give the experimental results. The extent of hydrolysis is calculated from these on the assumption that the first product of hydrolysis will be the $MgOH^\bullet$ ion. Any appearance of the species $Mg(OH)_2$ at the higher *p*H's will be shown by a drift in the calculated basic dissociation constants.

The first step is to calculate the amount of baryta used in reacting with CO_2. This is obtained from the dissociation constants :

$$\frac{f_1^2[H^\bullet][HCO_3']}{[H_2CO_3]} = K_1 = 4{\cdot}45 \times 10^{-7}, \text{ and } \frac{f_2[H^\bullet][CO_3'']}{[HCO_3']} = K_2 = 5{\cdot}7 \times 10^{-11} ;$$

f_1 and f_2 are ion activity coefficients for univalent and bivalent ions respectively, and were calculated from the equation :[6]

$$\log f_z = -\,0{\cdot}5\,.\,z^2\left(\frac{\sqrt{I}}{1+\sqrt{I}} - 0{\cdot}20I\right).$$

These equations may be combined to give :

$$[HCO_3']\left(1 + \frac{f_1^2[H^\bullet]}{K_1} + \frac{K_2}{f_2[H^\bullet]}\right) = [CO_2]_{\text{Total}},$$

and the concentration of the bicarbonate ion can be found by inserting in this equation the known concentration of CO_2, and the hydrogen ion concentration as given by the equation : $p\text{H}_{\text{obs.}} = -\log f_1[H^\bullet]$. The concentration of the carbonate ion can now be got from the K_2 equation.

If the magnesium ion had no acid properties, that is to say, if hydrolysis did not occur, the measured *p*H should correspond with the amount of barium hydroxide not used in this reaction with carbonic acid. Actually it is less, and the deficiency of hydroxide ion is attributed to the reaction :

$$OH' + Mg^{\bullet\bullet} \rightleftharpoons MgOH^\bullet.$$

The simplest starting point for calculating the extent of this reaction is the condition of electroneutrality of the solution, which gives :

$$2[Mg^{\bullet\bullet}] + [MgOH^\bullet] + 2[Ba^{\bullet\bullet}] + [H^\bullet] = [Cl'] + [OH'] + [HCO_3'] + 2[CO_3''].$$

Remembering that the magnesium and chloride radicles are present in equivalent amounts, i.e. :

$$[Cl'] = 2[Mg^{\bullet\bullet}] + 2[MgOH^\bullet],$$

this equation becomes

$$[MgOH^\bullet] = 2[Ba^{\bullet\bullet}] + [H^\bullet] - [OH'] - [HCO_3'] - 2[CO_3''],$$

in which all the terms on the right-hand side can be calculated.

The second dissociation constant of magnesium hydroxide is now calculated from the relation : $K = f_2\,.\,\frac{[Mg^{\bullet\bullet}][OH']}{[MgOH^\bullet]}$, and the negative logarithms of these calculated values are given in the last row of Table I. The titration was stopped at *p*H = 9·45 to prevent precipitation of magnesium hydroxide. In the range studied, which covers a 25-fold change in the concentration of the $MgOH^\bullet$ ion, the *p*K values remain reasonably constant, and it may therefore be concluded that the formation of $Mg(OH)_2$ does not occur to a significant extent.

Further measurements were made with higher concentrations of magnesium chloride. These are not reported here, as the ionic strengths of the solutions were too great for full reliance to be placed on the empirical activity-coefficient equation used. Within the limits of this uncertainty they confirmed the result given above. The " acid " magnesium chloride was next studied, and the results for a low concentration run are given in Table II.

The preparation clearly contained a considerable quantity of free HCl. The amount of this was determined by plotting the above figures as a differential titration curve, when a sharp endpoint was found at 8·240 ± 0·002 g. $Ba(OH)_2$ solution. Some of this baryta, however, had reacted with CO_2, and a further very small quantity had been utilised in forming $MgOH^\bullet$ ion ; these corrections could be calculated from the interpolated *p*H (6·60) at the endpoint, combined with the known dissociation constants of carbonic acid and the previously found constant for the $MgOH^\bullet$ ion ; they amounted in all to 0·052 g., and, deducting this correction, 8·188 g. baryta was found to be the equivalent of the free HCl in the original solution. 8·188 g. was therefore deducted from all the titration figures, and the calculation of [MgOH•] and of *p*K was then carried out exactly as before, with the results shown in the table. The mean *p*K is 2·57, and in view of the excellent constancy of the *p*K values in these acid solutions we give double weight to this figure, as compared with the mean value, 2·62, of the previous table, and derive the final value *p*K = 2·58, or $K = 2{\cdot}6 \,.\, 10^{-3}$ for the second dissociation constant of magnesium hydroxide.

---

[6] Davies, *J. Chem. Soc.*, 1938, 2093.

TABLE II.

Specific conductivity of water = $0{\cdot}75 \times 10^{-6}$ ohm^{-1} cm.$^{-1}$; CO_2 content of water = $10{\cdot}02 \,.\, 10^{-6}$ mol./l. Initial weight of solution titrated = 350·7 g.; concentration of $MgCl_2$ at free acid end-point = 0·02888 mol./kg. Concentration of barium hydroxide = 0·04654 g.-equiv./kg.

g. $Ba(OH)_2$.	0	1·202	5·717	7·628	7·934	8·0085
*p*H . . .	2·82	2·92	3·40	4·07	4·37	4·51
g. $Ba(OH)_2$.	8·0935	8·1455	8·170	8·1945	8·2255	8·249
*p*H . . .	4·76	5·02	5·19	5·43	6·03	6·91
g. $Ba(OH)_2$.	8·281	8·311	8·341	8·400	8·459	8·553
*p*H . . .	7·73	7·99	8·19	8·43	8·58	8·76
[MgOH•] . 10^5	—	0·493	0·804	1·40	2·01	2·96
*p*K . . .	--	2·56	2·57	2·57	2·58	2·57
g. $Ba(OH)_2$.	8·648	8·8015	9·410	9·922		
*p*H . . .	8·88	9·03	9·36	9·49		
[MgOH•] . 10^5	3·94	5·52	11·7	17·2		
*p*K . . .	2·57	2·57	2·57	2·60		

Earlier determinations of the constant have been made by Kolthoff[7] and Gjaldbaek.[8] Kolthoff used a colorimetric method and obtained values varying between $1{\cdot}6 \,.\, 10^{-3}$ and $5{\cdot}7 \,.\, 10^{-3}$; his mean value, $K = 0{\cdot}004 \pm 0{\cdot}001$ is in reasonable agreement with ours. Gjaldbaek titrated solutions of magnesium chloride saturated with magnesium hydroxide at 18° c. He adopted the value $K = 0{\cdot}008$, but his measurements in solutions of reasonably low ionic strength agree better with our results than this figure would indicate.

Summary.

The second dissociation constant of magnesium hydroxide has been determined by electrometric titrations of magnesium chloride solutions with barium hydroxide. The carbon dioxide content of the solutions was carefully controlled and allowed for in the calculations. The value $K = 2{\cdot}6 \,.\, 10^{-3}$ was obtained.

Battersea Polytechnic,
London, S.W.11.

Edward Davies Chemical Laboratories,
Aberystwyth, Wales.

---

[7] Kolthoff, *Rec. trav. chim.*, 1923, **42**, 977.

[8] Gjaldbaek, *Z. anorg. Chem.*, 1925, **144**, 283.

STUDIES IN ELECTROLYTIC POLARISATION.

PART V.—HYDROGEN OVERPOTENTIAL IN METHANOLIC SOLUTION.

BY J. O'M. BOCKRIS AND ROGER PARSONS.

Received 29th October, 1947.

The effect of the solvent on hydrogen overpotential has been the subject of little experimental work. In this work, until recently, single systems only have been studied. Thus, Swann and Edelmann[1] studied overpotential at a few cathodes with acetic acid as solvent. Lewina and Silberfarb[2] studied a Hg cathode with ethanol, Novoselski[3] a Hg cathode with ethanol and methanol, and Pleskov[4] Hg, Ni, and Pb cathodes with liquid ammonia as solvent. The work of Swann and Edelmann appears to be invalidated by neglect of precautions against resistance error in a system of very high resistance. The only valid result from Pleskov's work appears to be that for the nickel cathode * which is not directly comparable with work in aqueous solutions owing to the temperature (— 50° C.) at which these measurements were carried out. Hickling and Salt,[5] using an electronic interrupter, measured hydrogen overpotential at Hg, W, platinised Pt, Sn and Pb in N. HCl solutions in glycol, ethanol and cyclohexanol. Bockris,[6] and Bockris and Ignatowicz[7] have studied hydrogen overvoltage at the cathodes, Pb, Sn, Cu and Ni, in aqueous-non-aqueous mixtures as well as in the various solvents.

The work of Bockris[6, 7] has clearly shown that a marked solvent effect exists, and that it appears to depend on the cathode material. This apparent dependence is of considerable theoretical interest and has been investigated in the following work on the overpotential of a relatively large number of cathode materials in methanolic solutions of HCl.

Experimental.

It was decided to use the direct method of measurement at c.d.'s between 10^{-3} and 10^{-1} amp./cm.^{2} because at c.d.'s less than 10^{-1} amp./cm.^{2} the direct method is less open to criticism than the interrupter method, the resistance of N. HCl in water and methanol being relatively low. The lower limit of c.d. was chosen in order that extreme precautions to remove depolarisers were rendered unnecessary.[8] Hydrogen chloride was chosen as the electrolyte because, of the strong acids, it may be most readily purified and dried.

The choice of cathode material was limited to those available in suitable form and purity, and which are insoluble in normal aqueous and methanolic HCl. Those materials which it was found practicable to use were Ag, Au, Bi, C (in rod and filament form), Mo, Pd, Pt (smooth and platinised), Ta, Tl, and W. Ni, Pb and Cu were studied by Bockris and Ignatowicz.[6, 7] All the solid metals

---

* The results on Pb and Hg cathodes are vitiated by the presence of visible films of amalgam on the metal surface.

[1] Swann and Edelmann, *Trans. Amer. Electrochem. Soc.*, 1930, **58**, 75.

[2] Lewina and Silberfarb, *Acta Physicochim.*, 1936, **4**, 275.

[3] Novoselski, *J. Physic. Chem. Soc. Russ.*, 1938, **11**, 369; *Ber. Inst. physik. Chem. Acad. Wiss. Ukr.*, 1938, **11**, 125.

[4] Pleskov, *Acta Physicochim.*, 1939, **11**, 305.

[5] Hickling and Salt, *Trans. Faraday Soc.*, 1941, **37**, 224.

[6] Bockris, *Faraday Soc. Discussion*, 1947, **1**, 95.

[7] Bockris and Ignatowicz, *Trans. Faraday Soc.*, 1948, **44**, 519.

[8] Hickling and Salt, *ibid.*, 1941, **37**, 319; Azzam and Bockris (in press).

used were of the highest purity obtainable, usually Hilger Spectroscopic brand.
The choice of the solvent has been discussed by Bockris,[6] who stated five criteria for a solvent to be used in measuring hydrogen overpotential. These are completely satisfied only by the lower aliphatic alcohols, so that by considerations of availability in relatively large quantities the choice falls upon methanol or ethanol. Of these, methanol was chosen as being the more readily purified and dehydrated.

Apparatus and Technique of Measurements.—The cell and solution vessel used were in three sections of Pyrex glass construction so that, at no time, was the solution in contact with anything but Pyrex glass, platinum, the cathode * in use, and hydrogen (Fig. 1). The cell itself was in two parts connected by ground-glass joints. The smaller part was the anode compartment (A) while the larger consisted of the cathode compartment (B), the hydrogen electrode vessel (C), and the hydrogen distribution system (D). Diffusion of depolarisers from the anode was hindered by a plug of glass-wool at the base of the anode compartment (E). The hydrogen distribution system was arranged so that, from a single point of entry, hydrogen could be bubbled through the anode, cathode, and hydrogen electrode vessels and the solution vessel, and could be controlled by means of ungreased glass taps. The anode was a piece of Pt foil about 2 cm.^{2} in area supported by a Pt wire sealed into a vertical tube fused to the glass stopper. The cathode, which was renewed for each experiment, was supported in glass tubing (vide infra) which was passed through a wider tube sealed into the stopper and held outside the cell by a gas-tight rubber sleeve. The platinised Pt reference electrode was held in the stopper of the reference electrode compartment in the same way.

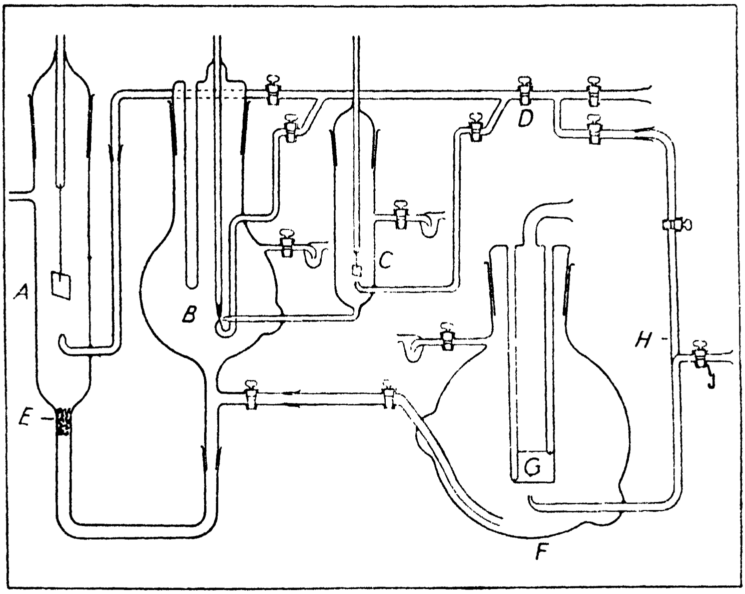

FIG. 1.

The third section of the apparatus was the solution preparation vessel (F) which was arranged so that it could be made the receiver in an all-glass distillation apparatus. The stopper was provided with two Pt wire electrodes (G) held a fixed distance apart for measurement of conductivity. This vessel had bubblers for the introduction of hydrogen (H) and HCl gas (J). It could be connected to the base of the cathode compartment by means of a ground-glass joint so that the prepared solution might be blown into the cell under hydrogen pressure

* The experimental details of this work have been described fully as it has become obvious that such details are necessary to assess the value of any work in this subject (cp. Levina and Sarinsky [23]).

without coming into contact with air. The four vessels were each fitted with an exit bubbler charged with the solvent to prevent diffusion of air into the apparatus.

HYDROGEN. Oxygen-free hydrogen from a cylinder was led through three Drechsel bottles (one with a sintered-glass bubbler) containing alkaline pyrogallol made up according to Haldane and McGill,[9] followed by one Drechsel bottle of distilled water. It was then dried by passing through three U-tubes packed with $CaCl_2$ (anhydrous), a Drechsel bottle containing A.R. conc. H_2SO_4 and three U-tubes packed with a mixture of P_2O_5 and powdered glass. It was finally passed through a bubbler containing a sample of the solvent in use. The joints between the glass apparatus were arranged so that as little rubber as possible came in contact with the hydrogen.

HYDROGEN CHLORIDE. The generator and drying train were of all-glass construction so that the HCl did not come into contact with rubber, because the reaction between HCl and rubber is appreciable. The HCl was generated by dropping H_2SO_4 on to NH_4Cl made into a sludge with conc. HCl, all reagents being of A.R. quality. It was then dried by passing through a tube 30 cm. long and 1 cm. diam. packed with anhydrous $CaCl_2$, two bubblers containing conc. H_2SO_4 and another tube, as above, packed with P_2O_5 and powdered glass. After passing through a trap it was introduced into the solution vessel by means of a bubbler. The concentration of the solution was determined by conductivity measurement, carried out by means of the electrode (G).

Preparation of Solvents.—WATER. Ordinary distilled water was redistilled from alkaline $KMnO_4$ solution and fractionally condensed in a block tin condenser of the type recommended by Vogel and Jeffery.[10] The resulting " equilibrium " water was distilled in a hydrogen atmosphere in an all-Pyrex glass apparatus using fragments of porous pot to prevent " bumping." The distillate was collected in the solution preparation vessel (vide supra).

METHANOL. Commercial " pure " methanol was subjected to a preliminary drying by refluxing for at least 10 hr. over 300 g. of freshly calcined $CaCl_2$ per l. of methanol and by distilling in an all-glass apparatus. The resulting alcohol which contained less than 1 % water was finally dried by the method of Lund and Bjerrum.[11] The methanol was then distilled in a hydrogen atmosphere into the solution preparation vessel using all Pyrex apparatus.

Hydrogen chloride was then passed into the solvent, which was stirred with hydrogen, until the conductivity of the solution showed it to be of normal concentration. The solution was forced by hydrogen pressure into the electrolysis cell which had previously been swept out with hydrogen.

Cleaning of Apparatus.—The cell and solution vessel were cleaned thoroughly between each experiment with chromic sulphuric acid followed by much streaming water. Before experiments using aqueous solutions the apparatus was rinsed with distilled water and finally with " equilibrium " water. Before experiments using methanolic solutions, the cell was rinsed with ethyl alcohol (absolute) and ether or acetone, and then dried by passing through it a current of filtered and dried air.

Preparation of Cathodes.—Three types of preparation were used.

(*a*) ELECTROPLATING.—The details are summarised in Table I.

TABLE I

Metal.	Electrolyte.	Current Density.	Time.	Substrate.	Notes.
Platinised platinum	H_2PtCl_4		5 min. each way	Pt	Ellis [12]
Palladium	$PdCl_2$	$3 \cdot 10^{-3}$ amp./cm.^{2}	2 hr.	Pt	Rough deposit
Gold	$KAu(CN)_2$	$3 \cdot 10^{-3}$ amp./cm.^{2}	3¾ hr.	Pt	Field and Weill [24]
Silver	$KAg(CN)_2$	$3 \cdot 10^{-3}$ amp./cm.^{2}	2 hr.	Cu and Pt	

---

[9] Haldane and McGill, *Analyst*, 1933, **58**, 378.
[10] Vogel and Jeffery, *J. Chem. Soc.*, 1931, 1201.
[11] Lund and Bjerrum, *Ber.*, 1931, **64**, 210.
[12] Ellis, *J. Amer. Chem. Soc.*, 1916, **38**, 737.

The platinised Pt and Pd electrodes were kept in " equilibrium " water until required. The Au and Ag electrodes were washed well and dried with filter-paper. Immediately before use they were wiped with filter-paper and washed with " equilibrium " water for a standard time (cp. Grant,[13] Hickling and Salt [14]).

(*b*) MELTING-IN.—This method was used for the lower melting metals. Hilger " spectroscopically standardised " metals were melted in a crucible and poured into Pyrex glass tubing to set. For Tl, the tube was L-shaped and was held so that the open end was closed by a porous porcelain plate. The molten metal was poured in, a Cu wire inserted, and the Tl allowed to solidify. The cathode consisted of a circular surface which was freshly cut with a hard steel knife immediately before the experiment. For Bi, some of the molten metal was drawn up into a straight tube, containing a Cu wire, and allowed to solidify. Part of the glass surrounding the metal was removed leaving a cylindrical cathode sealed into the remaining part of the glass tubing. These soft metal cathodes were scraped with a hard steel knife and wiped with filter-paper for a standard time immediately before use (vide supra).

(*c*) SEALING-IN.—Carbon rod and filament cathodes were sealed into glass tubing by means of a blowpipe and pre-treated before use in a similar manner to the soft metal cathodes.

A special method was developed for the hard metals, W, Mo, smooth Pt, and Ta. It was found that although these could be sealed into glass, a thin film of oxide was formed which vitiated results. Tungsten and Mo were therefore sealed into glass in a hydrogen atmosphere as follows. A piece of 5 mm. Pyrex tubing about 30 cm. long was gently heated about 8 cm. from one end and drawn so that a slight constriction was formed. When the glass had cooled, a piece of 2 mm. wire about 3 cm. long was placed in this constriction. Hydrogen was passed through the tube to sweep out the air. The end of the tube nearest the constriction was then sealed, the excess pressure being relieved through a mercury trap, and the metal wire sealed at the constriction for about 0·5 cm. of its length. Immediately before use, the short end of the tube was broken off just below the seal and the cathode put immediately into the solution. The cathode material should thus be completely freed from adsorbed matter except hydrogen, and is kept in a hydrogen atmosphere until immediately before use.*

For Ta, however, this method proved unsatisfactory, the metal becoming so brittle as to be unusable. A similar result would be expected using pure N_2 so that Ta, which was in the form of 0·2 mm. wire, was sealed into Pyrex tubing using a 99 % argon—1 % nitrogen mixture instead of hydrogen as in the above method.

REFERENCE ELECTRODE.—The reference electrode used was a hydrogen electrode prepared by the method of Ellis [12] which was chosen because no additives are present in the platinising solution. The reference electrode was checked between each experiment against a calomel electrode.

ELECTRICAL CIRCUIT.—The polarising current was derived from the 110 v. D.C. supply by means of two potential dividers, and was measured using a Cambridge Unipivot universal microammeter. The potential between the cathode and the reference electrode was measured by means of a Cambridge portable potentiometer.

General Procedure of Overvoltage Measurement.—After the solution had been forced into the cell, the stopper of the cathode compartment was momentarily removed and the electrode inserted. In work at high c.d.'s there is evidence to show that traces of oxygen, possibly introduced into the solution by this procedure, have inappreciable effects on the overvoltage.[8] The electrode was arranged so that it pressed firmly against the Luggin capillary. Hydrogen was bubbled through each compartment of the cell throughout the experiment. The potential of the electrode against the reference electrode was followed until it became " approximately constant " (vide infra). The electrode was then polarised negatively at a series of increasing c.d.'s with " rest " periods between each polarisation (cp. Part II). In both " rest " and polarisation periods the potential was followed until it became " approximately constant." The potential was taken as " approximately constant," following the convention of Hickling and Salt,[14] when it changed by less than 0·01 v. in 30 min. If, as occurred in a few experiments, the potential did not reach this degree of constancy within

---

* For a later development of this method, see Bockris and Conway.[36]

[13] Grant, *Trans. Faraday Soc.*, 1928, **24**, 226.

[14] Hickling and Salt, *ibid.*, 1940, **36**, 1226.

2 hr., the value accepted was that attained after 2 hr. The electrode and solution were completely renewed for each experiment. All experiments were carried out at room temperature of which the extremes recorded were 14° c. and 23° c., the temperature generally being between 17° c. and 20° c.

Results.

These are summarised in Table II.

TABLE II

Figures in parentheses refer to the total number of experiments performed on the given system including preliminary experiments made using different methods of preparing the electrode surface.

Cathode.	Solvent.	Overpotential in Volts at—				Mean Deviation from Mean.	No. of Experiments.
		10^{-3} amp./cm.^{2}.	10^{-2} amp./cm.^{2}.	$5 . 10^{-2}$ amp./cm.^{2}.	10^{-1} amp./cm.^{2}.		
Pt (platinised)	H_2O	0·01	0·02	0·03	0·04	± 0·00	2
	MeOH	0·01	0·02	0·02	0·03	± 0·00	2
Pd	H_2O	0·01	0·02	0·03	0·04	± 0·00	3
	MeOH	0·01	0·03	0·05	0·06	± 0·00	2
Au	H_2O	0·12	0·16	0·19	0·21	± 0·01	2
	MeOH	0·20	0·26	0·30	0·31	± 0·01	2
C (rod)	H_2O	0·15	0·20	0·22	0·25	± 0·01	2
	MeOH	0·30	0·32	0·33	0·33	± 0·01	2
C (fil.)	H_2O	0·21	0·27	—	0·37	± 0·05	5
	MeOH	0·38	0·43	—	0·51	± 0·04	3
Mo	H_2O	0·13	0·17	0·20	0·23	± 0·01	2
	MeOH	0·28	0·32	0·34	0·33	± 0·01	3
Ta	H_2O	0·20	0·28	0·39	0·44	± 0·06	4
	MeOH	0·36	0·41	0·48	0·52	± 0·02	2
W	H_2O	0·11	0·15	0·17	0·19	± 0·01	2
	MeOH	0·32	0·36	0·38	0·39	± 0·04	4
Ag	H_2O	0·59	0·71	0·93	0·61	± 0·03	2 (14)
	MeOH	0·21	0·25	0·27	0·28	± 0·00	2 (6)
Bi	H_2O	0·33	0·45	0·52	0·54	± 0·01	2
	MeOH	0·32	0·38	0·41	0·43	± 0·01	2
Tl	H_2O	0·61	0·72	1·12	1·15	± 0·03	3
	MeOH	0·44	0·54	0·60	0·62	± 0·01	2
Pt (smooth)	H_2O	0·27	0·49	0·57	0·62	± 0·07	3 (9)
	MeOH	0·19	0·24	0·30	0·33	± 0·02	2 (6)

Reproducibility.—The mean deviation from the mean over the whole series of the experiments is ± 0·02 v. For the experiments in aqueous solution it is ± 0·024 v., and in methanolic solutions it is ± 0·016 v. Details of the reproducibility in each system are recorded in Table II.

The Overpotential-log (Current Density) Relation.—The plot of overpotential against log (c.d.) is linear for Au, Bi, C, Pd, Pt (platinised), and W in both aqueous and methanolic solutions, for Ag, Pt (smooth) and Tl in methanolic solution, and for Mo in aqueous solution. The curves for Ta appear to curve upwards slightly in both solutions but the reproducibility of these results is not sufficient to justify consideration of this as a definite effect. It seems unlikely that this effect is due to ohmic overpotential, because the deviation from linearity is less in methanolic than in aqueous solution, whereas the resistance of methanolic HCl is greater than that of aqueous HCl. Pt (smooth) shows a slight deviation in the opposite direction but again the reproducibility is insufficient to establish a definite effect. The overpotential on Mo in methanolic solution tends to decrease with c.d. from $5 \cdot 10^{-2}$ to 10^{-1} amp./cm.^{2}. This seems to be a definite effect as the reproducibility is ± 0·01 v. Similarly, the curves for Tl and Ag cathodes in aqueous solution are sufficiently reproducible to define their shape. Tl shows a sharp increase of 0·4 v. in its overvoltage between 10^{-2} and $5 \cdot 10^{-2}$ amp./cm.^{2}. It is possible that at the lower c.d.'s dissolution of Tl took place. Silver shows a maximum in the curve at $5 \cdot 10^{-2}$ amp./cm.^{2}.* In spite of these few irregularities the solvent effect on these cathodes is quite definite.

The change of solvent appears to affect not only the absolute value of the overpotential, i.e. the constant *a* in the Tafel equation, but also the slope of the overpotential-log (c.d.) plot ; i.e. *b* in the Tafel equation. Considering the effect on both these quantities it appears that the cathodes studied may be divided into three groups.

A. Those for which there is no great change in either *a* or *b*, e.g. Pt (platinised) and Pd, and to a lesser extent Au (also Ni [6]) for which both *a* and *b* are slightly increased in methanolic solutions (Fig. 2).

B. Those for which *a* is increased in methanolic solutions by about 0·2 v. as compared with water, and for which *b* is decreased by approximately 0·02 v., e.g. C, Mo, Ta and W (Fig. 3).

C. Those for which both *a* and *b* are decreased in methanolic solutions, e.g. Ag, Bi, Pt (smooth) and Tl (also Pb, and Cu [6, 7]) (Fig. 3 and 4).

Rate of Growth of Overpotential.—The above classification seems to be supported by the study of the rate of attainment of a steady overvoltage. The time variation on metals of group A is very small. Thus, only on palladium at 10^{-3} amp./cm.^{2} at which an undervoltage is exhibited for a few minutes can any time variation be said to exist. The metals of group B show a striking similarity of behaviour in aqueous solution. At 10^{-3} amp./cm.^{2} when polarisation is commenced, the potential of the cathode is approximately 0·15 v. more negative than the final value. The potential becomes more positive with decreasing rapidity until it approaches the approximately steady state (vide infra for discussion). At the higher c.d.'s the final value is reached soon after the polarising current is switched on.

The metals of group C show two types of behaviour. The time variation on Bi and to a lesser extent Tl is small in aqueous solution, while for smooth Pt and Ag the overpotential rises considerably to more negative values. In methanolic solutions generally the time variation seems to be less, constant values being usually obtained within a few minutes of switching on the polarising current.

A general parallelism between the above classification of cathodes and properties such as melting-point of the metals may be noted.

Discussion.

Variation with Time.—The variation with time during the establishment of hydrogen overpotential is an aspect of overpotential which has received little attention by most previous authors. Hickling and Salt [15] have suggested that the variation is essentially due to the slow attainment of equilibrium of electromotively active atomic hydrogen at the cathode. This would occur more rapidly with the electro-deposited metals than others because of the probable co-deposition of hydrogen during the electrodeposition of the metal, in agreement with the results reported in the present paper. It is also in accord with the small time variation reported by Hickling and Salt [14] on W cathodes because in the process of manufacture of tungsten, this metal is repeatedly annealed in hydrogen. The present results do not support this contention, however, because both W and Mo cathodes were sealed into glass in a hydrogen atmosphere but still showed a considerable variation of overpotential with time during the first 2 hr. of polarisation at 10^{-3} amp./cm.^{2}. Further, for C, Mo, Ta and W, a decrease of overpotential with time after commencement of the polarising current has been observed ; although this might

---

* Recent work on solid silver cathodes has confirmed the above general shape of curve in solutions purified as in the work described in this paper, but tends to show that this maximum is eliminated on further purifying the solution by a preliminary electrolysis on an auxiliary silver cathode.

[15] Hickling and Salt, *Trans. Faraday Soc.*, 1942, **38**, 474.

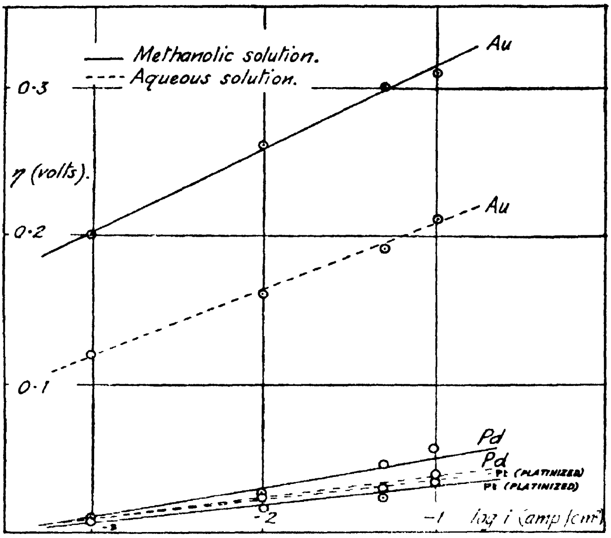

FIG. 2.

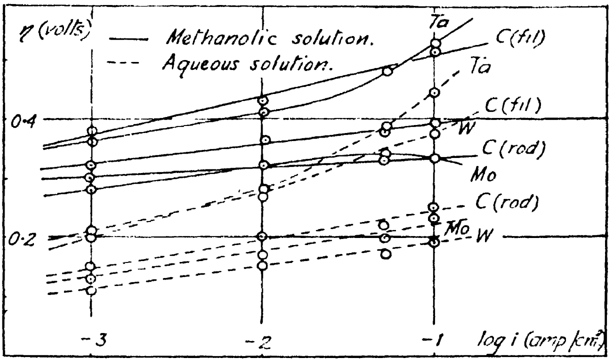

FIG. 3.

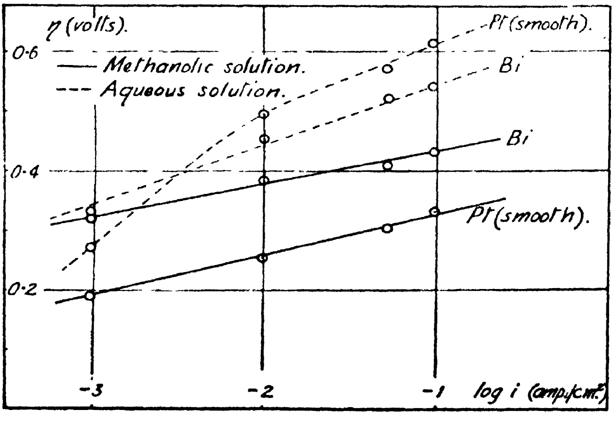

FIG. 4.

be regarded as an approach to equilibrium from a condition in which an excess of hydrogen existed in the electrode for the cathodes Mo and W, this suggestion cannot account for the almost identical behaviour of Ta which was sealed in an argon atmosphere and C which was sealed in air. The argon contained about 1 % N_2 so that it may be that the decrease with time for these cathodes is caused by the reduction of nitride and oxide films respectively (cp. Al cathode studied by Hickling and Salt [14]). It may also be noted here that Pt (smooth) although sealed in a hydrogen

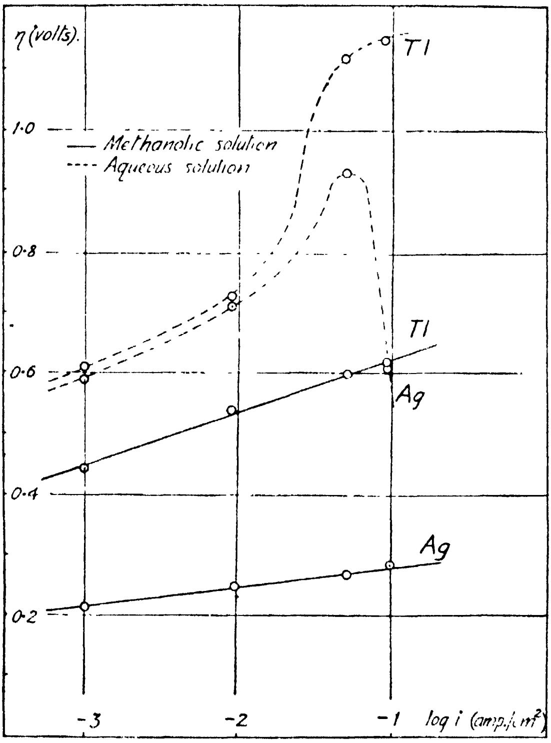

FIG. 5.

atmosphere by the same method shows an increase of overpotential with time at 10^{-3} amp./cm.^{2}. This would support the contention that the time variation is due to a specific property of the metal and does not arise primarily from the method of preparation.

Another possible explanation of the variation of hydrogen overpotential with time rests upon the supposition of a slow attainment of adsorption equilibrium with the anions in solution, but this is hardly admissible here, the chloride ion having poor properties of adsorption (cp. variation with time possibly caused by iodide ion adsorption, Jofa, *et al.*[16]).

Lastly, the possibility that the variations with time are due to the presence of impurities in the solution must be considered. The impurities which would be likely to cause such variation are oxygen and metal ions. Thus Bowden and Rideal[17] working at lower c.d.'s found that oxygen caused variation of overvoltage with time, but it seems unlikely that this effect would occur at the relatively high c.d.'s used in this work and with the precautions taken to exclude oxygen. Again, the presence of oxygen in the solution might explain an increase of overpotential with time but not a decrease (vide supra). Lewina, Lukowzew and Frumkin,[18] in their work on Ni cathodes consider the marked time variation observed to be due to the presence of an oxide film introduced during the heating of the cathode in moist hydrogen. Recent work in this laboratory has shown that this time variation occurs with cathodes that have been heated and sealed in a hydrogen atmosphere inside a glass envelope which is broken in the hydrogen-saturated solution. (The discrepancies between the results on W cathodes of Hickling and Salt and of the present authors were further investigated in subsidiary experiments. With a solution made by diluting a more concentrated stock solution (made from pure HCl and " equilibrium " water) with " equilibrium " water and saturating with hydrogen, very little time variation of the overpotential was observed (the absolute values were in close agreement with those obtained by Hickling and Salt [14]). With a solution prepared by the method described in this paper, however, the marked decrease of overpotential with time at 10^{-3} amp./cm.^{2} noted above, occurred; smaller variation was observed at other c.d.'s (the absolute values from this type of experiment, which are those quoted in this paper, are considerably lower for W cathodes than those obtained using the less pure stock solution)).

---

[16] Jofa *et al.*, *Acta Physicochim.*, 1939, **10**, 319.

[17] Bowden and Rideal, *Proc. Roy. Soc. A*, 192 18,**20**, 59.

The Effect of Change of Solvent.—The results reported in the present paper on the high overpotential metals, Bi and Tl, are in agreement with those reported by Levina and Silberfarb,[2] and by Novoselski [3] on mercury at low c.d.'s, for which metal a lowering effect was found to be caused by the substitution of ethanol or methanol for water as the solvent. The results are also in accord with those of Bockris [6] and Bockris and Ignatowicz [7] on Pb and Sn cathodes at high c.d.'s,* and the order of the change is about 0·1-0·2 v. for all these metals.

The principal result arising from the present work is the very clear emphasis of the dependence of the solvent effect upon the cathode material, namely that, in a general way, the overpotential in methanolic solution is lowered on the high overpotential metals, raised on the medium overpotential metals, and not greatly altered on the low overpotential metals, compared with the overpotential in aqueous solutions.

According to the theory of slow neutralisation as presented by Frumkin,[19] if approximate constancy of the gradient of the overpotential-log (c.d.) relation in the two solvents water and methanol is assumed, then change of solvent may affect the terms C and ζ in the equation,

$$\eta = C + \frac{RT}{\alpha F}\ln i - \frac{RT}{F}\ln a_{H^+} + \zeta,$$

The electrokinetic potential at sintered SiO_2-solvent interface in water and methanol was measured by Imai [21] who used the method of streaming potentials. This worker gives the value in water as − 0·045 v., and in methanol as − 0·079 v. These results would seem to indicate the direction, and possibly the order, of the effect to be expected from the change in electrokinetic potential, namely, a lowering of about 0·03 v.

The constant C is stated by Erdy-Gruz and Volmer [20] to contain rate constants which depend on the ability of the electron to escape from the metal lattice and neutralise the H^+ ion in the double layer. It appears probable that the solvation sheath of an adsorbed ion in the double layer is deformed and that the rate of electron escape to the adsorbed ion is largely independent of the ionic solvation in the bulk of the solution, and controlled by the adsorption energy level of the ion and the work function of the metal. Hence, the constant C would not on these grounds be expected to alter significantly with change of solvent, so that, having regard to the probably small effect of change of solvent on the electrokinetic potential, Frumkin's theory does not seem to yield an adequate explanation of the present results.

---

* The observations quoted are all in disagreement with those of Hickling and Salt [5] who found that the non-aqueous solvent tended to raise the overpotential on high overpotential metals. These results are rendered doubtful by the fact that Hickling and Salt used sealing wax as a support for cathodes. As sealing wax is appreciably soluble in alcohols a consistent poisoning of a working cathode might be expected.

[18] Lewina, Lukowzev and Frumkin, *Acta Physicochim.*, 1939, **11**, 21.

[19] Frumkin, *Z. physik. Chem.*, 1933, **164**, 121.

[20] Erdy-Gruz and Volmer, *ibid.*, 1930, **150**, 203.

[21] Imai, *Bull. Inst. Phys. Chem. Res. Tokyo*, 1934, **73**, 1351.

[22] Eyring, Glasstone and Laidler, *J. Chem. Physics*, 1939, **7**, 1053.

Butler[28] has given a general treatment of the energetics of the slow discharge of H_3O^+ ions, without reference to a detailed mechanism of the reaction. According to this, for discharge, the cathode potential, V, is given by

$$Ve < I - S - R - \phi, \quad . \quad . \quad . \quad . \quad (1)$$

where I is the ionisation energy of H^+, S the proton-solvent interaction energy, R the repulsive energy between the neutral H atoms and the solvent molecule, and ϕ is the work function of the cathode material; S depends upon the solvation energy of H^+ in methanol. It is possible to calculate the solvation energies of HCl in methanol from heat of solution measurements at great dilution. To obtain the heat of solvation of H^+ in methanol it is necessary to make some assumption regarding the distribution of the solvation heats between the H^+ and Cl^- ions. The calculations of Eley and Pepper[29] give a value of about 79 kcal./g. ion for the energy of solvation of Cl^- in methanol and acceptance of this figure and calculations from the heat of solution of HCl in methanol[31] gives the solvation energy of H^+ in methanol as approximately 257 kcal./g. ion, compared with 270 kcal./g. ion for H^+ in water. (Caution is necessary in applying any simpler method of approximate evaluation of solvation energies: e.g. the use of the Born equation with the macroscopic values of the dielectric constants of water and methanol obviously indicates a change in solvation energy in the other direction.)

Any calculation of R in methanolic solution is uncertain because it is based on equations applicable strictly only to symmetrical bodies. For this latter case, R is given by an equation of the form

$$R = k_1 + k_2r$$

where r is the distance of the internuclear separation of the atoms or molecules concerned. There seems to be no way of calculating any change in k_1 upon transition from water to methanol though there is some reason by analogy of the effect on k_1 of size in rare-gas repulsion-energy equations to consider that the change in k_1 will be very small. The distance r will be the same in the two systems to the first approximation as clearly r is a function of the hydrogen-oxygen bond length rather than the sum of the radius of the solvent molecule regarded as a sphere and that of the hydrogen atom. It can be considered, therefore, that the change in R on transition from water to methanol is somewhat uncertain and probably very small. This change will be assumed here to have a negligible effect on overpotential.

It follows that the change in the solvation energy of the proton on

---

[23] Levina and Sarinsky, *Acta Physicochim.*, 1936, **5**, 491.
[24] Field and Weill, *Electroplating.*
[25] Buckley and Hartley, *Phil. Mag.*, 1929, **8**, 320.
[26] Bockris and Conway, *J. Sci. Instr.* (in press).
[27] Bockris, *Trans. Faraday Soc.*, (in press).
[28] Butler, *Proc. Roy. Soc. A*, 1936, **157**, 423.
[29] Eley and Pepper, *Trans. Faraday Soc.*, 1941, **37**, 581.
[30] Gentile, *Z. Physik*, 1930, **63**, 795.
[31] Slansky, *J. Amer. Chem. Soc.*, 1940, **62**, 2430.

the transition water to methanol as solvent is mainly responsible for the change in cathode potential which, according to the above solvation energy value, should become about 0·56 v. more positive in methanol than in water. To evaluate from this the corresponding change in overpotential, the effect of the solvent upon the potential of the reversible hydrogen electrode must be considered. If A is the energy of adsorption of atomic hydrogen on the surface of an electrode then, for an electrode which adsorbs hydrogen, the condition for discharge is

$$Ve < I - S - R - \phi + A. \qquad (2)$$

It can be shown that the reversible potential is affected by the factors of eqn. (2). Three possibilities hence arise for the effect of the solvent on overpotential according to this treatment. Firstly, if the A term is not of importance for the working electrode (which is probably the case for high overpotential metals) and the A term for the reversible electrode is unaltered on change of solvent, no notable change will occur in overpotential because the solvation energy and other terms tend to annul each other at the working and stationary electrodes. This case does not accord with any observed result, overpotential being considerably reduced in methanol for the high overpotential metals. Secondly, the A term of the reversible electrode may be affected by the solvent but A may still be an unimportant term for the working electrode. It may be reasonably supposed that the adsorption energy A of hydrogen atoms on the reversible electrode in methanol is decreased, so that the reversible potential tends to become more negative. Hence, the overpotential would be lowered, and, as the cathode potential for the high overpotential metals according to this treatment is uniformly made more positive by the change in solvation energy from water to methanol, the lowering of overpotential indicated would be approximately constant as is so for Bi, Tl, Sn and Hg. In a third case, when the working electrode is a metal of low overpotential, the A term for this electrode becomes important and the solvent effect on overpotential would be expected to depend on the difference between the solvent effects on the A term for the working and reversible hydrogen electrodes. For platinised Pt and Pd which have similar properties to the reversible hydrogen electrodes, it is clear that only a very small solvent effect would be expected. For the group of metals which, according to the present work, are of intermediate overpotential properties and exhibit increased overpotentials in methanolic compared with aqueous solutions, it would be possible to postulate that the lowering of the energy of adsorption of hydrogen caused by the change of solvent to methanol is much more on the working cathode than that on the reversible electrode. The potential of the working electrode would hence become more negative relative to the reversible electrode so that the overpotential would increase. This latter interpretation involves, however, a purely *ad hoc*, and not very plausible, assumption.

In the theory of absolute reaction rates as applied to hydrogen overpotential,[22] it is assumed that the slow stage is the prototropic transfer of a hydrogen atom from a solvent molecule in the solution layer near the cathode to a solvent molecule in the layer of solvent molecules attached to the cathode. The equation relating the overpotential (η) to the current density (i) is :

$$i = C\left(\frac{kT}{h}\right)\frac{F}{N}\mathrm{e}^{\frac{-\Delta G^{\ddagger}}{RT}} \,.\, \mathrm{e}^{\frac{\alpha\eta F}{RT}},$$

or

$$\eta = \frac{RT}{\alpha F}\ln i - \frac{RT}{\alpha F}\ln C + \frac{\Delta G^{*}}{\alpha F} + \frac{RT}{\alpha F}\ln\left(\frac{hN}{kTF}\right),$$

where C is the surface concentration of the reaction species ; ΔG^{*} is the free energy of activation of the slow process, α is a proportionality factor and R, T, h, N, k, and F have their usual significance.

C can be calculated following the method of Eyring, Glasstone and Laidler from the known size of the methanol and water molecules. The change in *C* is found to lead to an increase of 0·02 v. of the overpotential in methanolic over that in aqueous solution (if α is assumed to be $\frac{1}{2}$). $\Delta G^{\ddagger}$ should be, as pointed out by Eyring, Glasstone and Laidler, analogous to the free-energy change (ΔG) for the reaction : $2ROH \rightleftharpoons ROH_2^+ + RO^-$.

Since the ionic products (k_s) of both water and methanol are recorded in the literature, it is possible to calculate ΔG from the reaction isotherm,

$$\Delta G = -RT \ln \left(\frac{k_s}{a^2_{ROH}}\right).^*$$

Therefore the absolute values of overpotential can be calculated from the above equation. At 25° C. it is found that at 10^{-3} amp./cm.^{2} the overpotential in aqueous solution should be $0{\cdot}44/\alpha$ and in methanolic solution $0{\cdot}58/\alpha$. Thus, if α remains constant at the usually quoted value of 0·5, the overpotential in methanolic solution is predicted to be 0·28 v. higher than in aqueous solution. This is in agreement with results in group B. To account for the experimental results of little change of overpotential on group A, an increase of α of about 50 % with change of solvent would be required. However, it seems probable that ΔG would vary with change of electrode material in a parallel manner in both solvents and that for low overpotential metals corresponding to low ΔG values a smaller change in α would therefore be required to produce similar absolute values in aqueous and methanolic solutions. For the metals in group C, however, an extremely large increase of α (i.e. decrease in *b*) would be required which is certainly not observed experimentally.

The above prediction of the solvent effect calculated quantitatively from the theory is in the opposite sense to that suggested qualitatively by Eyring, Glasstone and Laidler, but it may be emphasised here that the slow stage considered is $RO - H + ROH \rightleftharpoons RO^- + H_2O^+R$, which is the same as that considered by Eyring, Glasstone and Laidler.†

One of us has recently suggested that the slow combination theories of overpotential may be modified in a way to take into account specifically the solvent effect by assuming that there is a layer of solvent molecules attached to the cathode, either predominantly by long-range coulombic forces for the high overpotential metals, or predominantly by short-range adsorption forces for the lower overpotential metals of greater adsorbing power.[7, 27] The strength of attachment of the solvent to the latter (if the two solvents concerned have approximately the same order of ability to form hydrogen bonds, as have water and methanol) must be about the same and the slow combination reaction on the surface (for example, but not necessarily, the combination between hydrogen atoms) is not greatly affected, though tending to be raised in methanolic solutions owing to the larger size of the methanol molecule. Conversely, for the high overpotential metals, to which the solvent is attached predominantly by electrostatic means, the lesser polarisability of the methanol molecule presumably causes a less intense attachment of methanol molecules to the cathode surface ; so that, in accord with the results observed, the overpotential is lower in methanolic than in aqueous solutions. Thus, the solvent effect is considered to be primarily due to variations in the hindrance to the combination reaction on the cathode surface caused by the presence of solvent molecules.

---

* It must be observed that the ΔG used here is not the true $\Delta G^{\ddagger}$ for the slow reaction at the cathode-solution interface, as is clear from the fact that, were this so, it would imply a constant value of the overpotential on all metals. The method used (following Eyring, Glasstone and Laidler [22]) results in an order value for hydrogen overpotential in general. This value is connected to the true value of $\Delta G^{\ddagger}$ by a term involving the heat of adsorption of hydrogen atoms on the metal surface, i.e. the factor upon which, according to the absolute reaction rate theory, the effect of electrode material on hydrogen overpotential depends. However, this term may be regarded as approximately unaffected by the solvent, so that calculation of the difference of the overpotential on the same metal in two different solvents is not essentially altered by its neglect.

† Prototropic transfer from the H_3O^+ or ROH_2^+ complex is not considered here because, in following Eyring, Glasstone and Laidler, the same interpretation of the constancy of the *B* factor as given by these authors must be made and this precludes the possibility of discharge from the solvated ion. There is, of course, as yet no evidence that *B* is also constant or pseudo-constant in methanol, evidence concerning which matter must await work on the energy of activation and *p*H effects in non-aqueous solution.

Conclusions.—It can therefore be concluded that the present measurements are in consonance with the slow discharge mechanism for metals of high overpotential. The lack of a solvent effect on low overpotential metals could also be explained on this theory but the value of α for these metals cannot. The behaviour of metals of intermediate overpotential is also unexplained by this theory. The postulate of a solvent layer at the electrode surface which affects the velocity of combination of H atoms on it allows qualitative explanation of all the results. As, on other grounds, this theory is less probably applicable to metals of high overpotential, it probably forms a satisfactory interpretation only of the results on metals of intermediate and low overpotential. The reaction rate theory is not applicable to the results at the " high " and " low " groups of metals but applies to the " intermediate " group, so far as direction of change is concerned, but not in regard to the gradient of the η-log i lines, which should remain independent of solvent according to the theory (as α depends on the existence of a symmetrical distribution of solvent on the cathode and solution sides of the double layer and it appears that this should exist on the basis of the theory for methanol as well as for water).

Summary.

The hydrogen overpotential has been determined at the metals Bi, Tl, Ag, Ta, C (filament), C (rod), W, Mo, Au, Pt and Pd, in methanolic and aqueous acid solution over the c.d. range 10^{-3}-10^{-1} amp./cm.^{2}. The Tafel equation is generally applicable to the results except for those on Tl and Ag in aqueous solution. Some evidence is given that this lack of applicability is due to a poisoning effect.

The effect of change of solvent from methanol to water for the electrode materials, platinised Pt, Pd and, to a lesser extent, Au (also Ni[6]) is that little change occurs in either a or b of the Tafel equation ; on C, Mo, Ta, W, a is raised and b slightly decreased ; for Ag, Bi, Pt (smooth) and Tl (also Pb and Cu[6, 7]), a and b are decreased.

If the adsorption energy of a metal of low overpotential is less in methanolic than in aqueous solution, the results may be best interpreted by a slow discharge mechanism for the metals of high overpotential and by a slow combination mechanism for the metals of lower overpotential, assuming that adsorbed solvent molecules affect the rate of combination of hydrogen atoms.

Imperial College,
London, S.W.7.

MOLECULAR FORCE FIELDS.

PART III.—THE VIBRATION FREQUENCIES OF SOME PLANAR XY_3 MOLECULES.

BY D. F. HEATH AND J. W. LINNETT.

Received 21*st November*, 1947.

Previous work on molecular force fields has shown that the simple valency force field fails to account for the vibration frequencies of many molecules. Modification of this force field has been carried out mainly by the introduction of "cross-terms." This procedure has hardly been satisfactory, for only very rarely has it been possible either to predict which cross-terms should be important or to account for the importance of those which have been found empirically to be necessary.[1] In a previous paper, however, we showed that the vibration frequencies of the tetrahalides of Group IV elements could be correlated by adding to the simple valency force field a potential energy (P.E.) function, involving two constants, which represents a van der Waals' type of repulsion between the halogen atoms.[2] The field we then used was still not wholly satisfactory, for reasons discussed in our next paper, but there is no doubt that the addition of such a field between the non-bonded atoms will always be found necessary whenever the non-bonded atoms are crowded together.

In the present paper we have studied the vibration frequencies of six planar molecules and ions, BF_3, BCl_3, BBr_3, CO_3^-, NO_3^- and SO_3. It is well known that the simple valency force field is inapplicable to the out-of-plane vibrations of planar molecules and that, in the past, these have only been accounted for by the introduction of a separate angle bending-constant for the out-of-plane (A_2'') vibration.[3]

We find that, by means of a new field differing from the simple valency force field in its treatment of angular distortion, we can correlate satisfactorily all four fundamentals of these molecules using only one constant for angular distortion.

In order to derive this field, it is assumed that the bond-forming orbitals of an atom X are set at definite angles to each other, and that the most stable bond is produced when one of these orbitals overlaps the bond-forming orbital of the second atom Y to the maximum possible extent.[4] If Y is now displaced perpendicular to the bond a force will be set up tending to restore it to its most stable position. For the vibration to be simple harmonic the restoring force must be proportional to the perpendicular displacement of Y, and consequently to the angular displacement, $\Delta\beta$.

For the planar molecule XY_3 it is obvious that if the orbitals are symmetrical about their axes the restoring force for a given angular distortion in the plane is equal to the restoring force for the same displacement out of the plane. That is, the contribution to the potential energy of a distortion, $\Delta\beta_{ij}$, of the bond XY from the axis of the orbital ij is given by

$$2V = k'_\beta \Delta\beta_{ij}^2$$

in each case. We will call such a field the orbital valency force field.

---

[1] Linnett, *Quart. Rev.*, 1947 **1**, 73.

[2] Heath and Linnett, *Trans. Faraday Soc.*, 1948, **44**, 561.

[3] Anderson, Lassetre and Yost, *J. Chem. Physics*, 1936, **4**, 703.

[4] Pauling, *J. Amer. Chem. Soc.*, 1931, **53**, 1367.

The P.E. function for these molecules may now be written :

$$2V = 2B'\sum_{j}\Delta r_{ij} + k_1\sum_{j}\Delta r_{ij}^2 + k'_\beta\sum_{j}\Delta\beta_{ij}^2 - 2B\sum_{jk}\Delta R_{jk} + 2A\sum_{jk}\Delta R_{jk}^2, \quad (1)$$

where i represents the central atom and j, k, etc., the outer atoms ; Δr_{ij} is the increase in bond length r_{ij} and R_{jk} is the increase in the distance between the non-bonded atoms j and k ; $\Delta\beta$ is the angle defined above (cp. Fig. 1) ; B', k_1, k'_β, B and A are constants. The second and third terms are the orbital valency force field terms. The fourth and fifth are those which represent the repulsion between the non-bonded atoms expressed in the form (see Part II) :

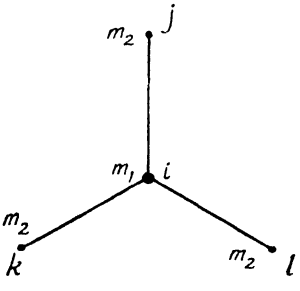

FIG. 1.

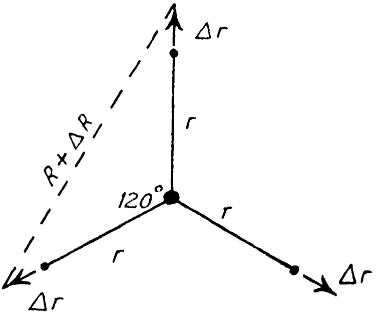

FIG. 2.

$$V = -B\,.\,\Delta R + A\,.\,\Delta R^2, \quad . \quad . \quad . \quad . \quad (2)$$

where $\quad B = -(\mathrm{d}V/\mathrm{d}R)$ and $A = \frac{1}{2}(\mathrm{d}^2V/\mathrm{d}R^2)$.

The P.E. function for this van der Waals' repulsion was assumed to be of the form :

$$V = a/R^{12}, \text{ where } a \text{ is a constant.}$$

This was assumed because it is the sort of repulsion law which might be expected to operate between the non-bonded atoms at short distances if they could be compared with the atoms of the inert gases,[5] and also because such a function has been justified from a study of the vibration frequencies of some Group IV tetrahalides (see next paper). This fixes the ratio of A to B/R such that

$$A : B/R = \tfrac{1}{2}(\mathrm{d}^2V/\mathrm{d}R^2) : -(\mathrm{d}V/\mathrm{d}R) = 6{\cdot}5 : 1.$$

The first term in (1) is included because a linear term $B'\sum_{j}\Delta r_{ij}$ is required to cancel the contribution of the linear terms in $B\sum_{jk}\Delta R_{jk}$, so that when Δr, $\Delta\beta$ and ΔR are all zero the energy is a minimum. From the symmetrical (A_1') vibration (see Fig. 2) :

$$3B'\Delta r = 3B\Delta R = 3\sqrt{3}B\Delta r,$$

whence $\quad B' = \sqrt{3}B. \quad . \quad . \quad . \quad . \quad . \quad . \quad (3)$

There are, therefore, three independent constants per molecule in terms of which four frequencies must be explained. However, both B/R_e (R_e is the equilibrium value of R) and A are left in the secular equations listed below so that they could be used when different assumptions were made about the repulsion between the non-bonded atoms.

The way in which the constant B' enters into the secular equations for the frequencies can be illustrated by working out the equation for the out-of-plane vibration. With reference to Fig. 3 it can be seen that

---

[5] Lennard-Jones, *Proc. Roy. Soc. A*, 1924, **106**, 463; Buckingham, *J. Amer. Chem. Soc.*, 1938, **168**, 264.

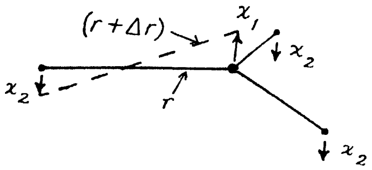

FIG. 3.

r is increased to $(r + \Delta r)$ by the displacements x_1 and x_2 perpendicular to the plane of the molecule. The relation between them is

$$(r + \Delta r)^2 = r^2 + (x_1 + x_2)^2,$$

from which

$$\Delta r = \frac{1}{2r}(x_1 + x_2)^2,$$

if powers of the displacement co-ordinates, x_1 and x_2, higher than the second are ignored. Then, since $\Delta\beta = (x_1 + x_2)/r_e$,

$$\begin{aligned}2V &= 3k'_\beta \Delta\beta^2 + 6B'\Delta r \\ &= 3(k_\beta + B'/r_e)(x_1 + x_2)^2 = 3(k_\beta + 3B/R_e)(x_1 + x_2)^2,\end{aligned}$$

where $k_\beta = k'_\beta/r_e^2$ and powers of the displacement co-ordinates higher than the second have been ignored. The third term in the P.E. function (1) only contributes terms in these higher powers. Combining the expression for the potential energy with that for the kinetic energy,

$$2T = 3m_2\dot{x}_2^2 + m_1\dot{x}_1^2,$$

we get, for the vibration frequency, n_4,

$$\lambda_4 = \left[k_\beta + 3\frac{B}{R_e}\right]\left[\frac{1}{m_2} + \frac{3}{m_1}\right],$$

where

$$\lambda_4 = 4\pi^2 n_4^2 c^2.$$

Similar terms involving B' (which is equivalent to B/R_e) arise whenever there is an angular distortion of the molecule.

The derivation of the quadratic equation for the degenerate vibrations illustrates an important consideration in the application of the orbital valency force field. The displacement co-ordinates we shall use are shown in Fig. 4. It is convenient to express the P.E. function in terms of the

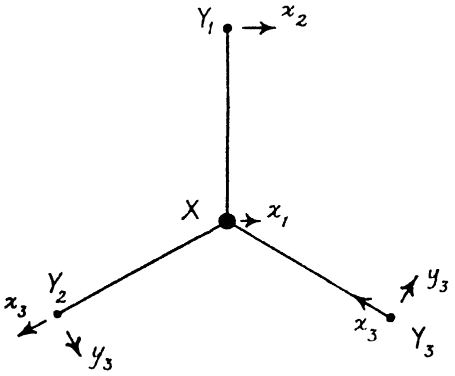

FIG. 4.

change of the angle, Y_1XY_2, which we will call $\Delta\alpha$. Then

$$r_e \, . \, \Delta\alpha = x_2 - \frac{3}{2}x_1 + y_3. \qquad (5)$$

Now, when there is a distortion of the molecule, the bond-forming orbitals of X will rotate about X to give the greatest overlap with the bond-forming orbitals of the three other atoms (Y_1, Y_2 and Y_3 in Fig. 4). This will happen at all stages of the vibration. Then the contribution of the angular part of the P.E. function (third term in (1)) is :

$$2V = k'_\beta[\Delta\beta^2_{XY_1} + \Delta\beta^2_{XY_2} + \Delta\beta^2_{XY_3}]$$
$$= k'_\beta\left[\left\{\left(\frac{x_2 - x_1}{r_e}\right) - \gamma\right\}^2 + 2\left\{\left(\frac{y_3 - \frac{1}{2}x_1}{r_e}\right) + \gamma\right\}^2\right], \quad . \quad (6)$$

where γ is the angle through which the bond-forming orbitals of X are rotated about an axis through X perpendicular to the plane of the molecule for these values of the displacement co-ordinates. When the overlap is the best possible, the potential energy must be a minimum. That is $dV/d\gamma = 0$.

Applying this to (6) gives

$$r_e\gamma = \tfrac{1}{3}(x_2 - x_1) - \tfrac{2}{3}(y_3 - \tfrac{1}{2}x_1). \quad . \quad . \quad . \quad (7)$$

Substitution of (7) into (6) followed by the application of (5) gives

$$2V = \tfrac{2}{3}k'_\beta\Delta\alpha^2.$$

The simple valency force field would give

$$2V = 2k_\alpha\Delta\alpha^2$$

where k_α is the simple valency force field angle bending constant.

The equations for the vibration frequencies are found to be :

(*a*) Totally symmetric valency vibration in Class A'_1 :

$$\lambda_1 = (k_1 + 6A)\frac{1}{m_2}.$$

(*b*) The two degenerate planar vibrations in Class E' :

$$\lambda_2 + \lambda_3 = \left(k_1 - \frac{3}{4}\frac{B}{R_e} + \frac{3}{2}A\right)\left(\frac{1}{m_2} + \frac{3}{2m_1}\right) + \left(k_\beta + \frac{9}{4}\frac{B}{R_e} + \frac{3}{2}A\right)\left(\frac{1}{m_2} + \frac{3}{2m_1}\right) - \left(2A - \frac{B}{R_e}\right)\frac{9}{4m_1},$$

$$\lambda_2 \,.\, \lambda_3 = \left\{\left(k_1 - \frac{3}{4}\frac{B}{R_e} + \frac{3}{2}A\right)\left(k_\beta + \frac{9}{4}\frac{B}{R_e} + \frac{3}{2}A\right) - \frac{9}{16}\left(2A - \frac{B}{R_e}\right)^2\right\}\left(\frac{1}{m_2{}^2} + \frac{3}{m_1m_2}\right).$$

(*c*) The out-of-plane vibration in Class A_2'' :

$$\lambda_4 = \left(k_\beta + 3\frac{B}{R_e}\right)\left(\frac{1}{m_2} + \frac{3}{m_1}\right),$$

where m_1 is the mass of the central atom and m_2 the mass of each outer atom.

The frequencies calculated using these equations are compared with the observed frequencies in Table I for the six molecules and ions under consideration. The three constants k_1, k_β and A were chosen separately for each molecule to give the best fit for the four frequencies. The values used are given in the table.

The average % deviation over all the frequencies is under 1 %. If the results for the nitrate ion are excluded, the average deviation is under 0·5 %. It is therefore clear that for the four molecules and the carbonate ion the orbital valency force field with the addition of terms for repulsion between the non-bonded atoms (this type of field will be referred to as O.V.F.F. from now on) provides a completely satisfactory explanation of the observed frequencies. It is moreover a field which accords much better than the simple valency force field plus repulsion terms (S.V.F.F.) with the generally accepted views of directed valency. Even for the nitrate ion the field is only slightly unsatisfactory. The deviations may arise because the basic assumption that the orbitals are cylindrically symmetrical about their axes is not justified in this case, or because large anharmonicity corrections need to be made to the observed frequencies to obtain the fundamentals.

It would be possible to explain the in-plane and out-of-plane bending vibrations of planar XY_3 molecules in terms of only one S.V.F.F. bending constant if it was supposed that, for the out-of-plane bending, the potential energy was a fourth power function of the displacements and depended on the small changes in the YXY angles during the out-of-plane motion.

TABLE I.—COMPARISON OF THE OBSERVED AND CALCULATED VIBRATION FREQUENCIES OF SOME PLANAR XY_3 MOLECULES. THE FORCE CONSTANTS ARE GIVEN IN DYNES PER CM. × 10^{-5} AND THE FREQUENCIES IN CM.$^{-1}$ (n_i).

Mol.	k_1.	k_β.	A.	B/R_e.	n_1.	n_2.	n_3.	n_4.	Av. % Deviation.
BF_3 .	Observed				888	1446	480	691	—
	5·98	0·646	0·475	0·073	888	1443	479	691	0·1
BCl_3 .	Observed				471	958	243	462	—
	3·10	0·305	0·215	0·033	462	974	245	455	1·45
BBr_3 .	Observed				279	806	151	372	—
	2·385	0·188	0·213	0·0327	279	815	151	372	0·25
$CO_3^{=}$.	Observed				1063	1415	680	879	—
	5·4	1·055	0·875	0·135	1063	1407	678	879	0·2
NO_3^{-} .	Observed				1050	1390	720	831	—
	5·4	1·10	0·925	0·1425	1078	1338	690	847	3·4
SO_3 .	Observed				1069	1330	532	652	—
	9·2	1·46	0·25	0·0385	1066	1337	535	647	0·55

This has been pointed out as a possibility by Bell.[8] We showed earlier that, for the in-plane vibrations k_β is equivalent to $3k_x$, so that for BF_3 we may assume that k_x is about 0·2 × 10^5 dynes/cm. Using Bell's formula this gives the frequency of the out-of-plane vibration as *ca.* 100 cm.$^{-1}$. This is of quite the wrong order of magnitude since it is 691 cm.$^{-1}$. So it seems that the in-plane and out-of-plane bending vibrations cannot be explained in terms of one S.V.F.F. constant. Moreover the isotope effect of substituting ^{10}B for ^{11}B is calculated to give a ratio of the frequencies for the out-of-plane vibrations of 1·02 if the P.E. is proportional to the fourth power of the displacement. If it is proportional to the second power, the ratio of the frequencies of the isotopic molecules is calculated to be 1·0405. This compares well with the observed ratio of 1·041. This evidence is strongly in favour of a quadratic P.E. function for the out-of-plane motion, and against a fourth power P.E. function. We therefore agree with Bell in the conclusion that for planar XY_3 molecules the out-of-plane motion is of the simple harmonic type.

The orbital valency force field therefore—(1) enables us to correlate the frequencies of six planar molecules to a mean accuracy of 1 %. In each case, choice of three constants leads to a satisfactory fit of four frequencies and physically reasonable repulsion fields ; (2) explains the out-of-plane vibration frequencies of these molecules in terms of the same constants as those used for the in-plane vibrations. If the S.V.F.F. is

---

[6] Born and Oppenheimer, *Ann. Physik*, 1927, **84**, 457.

[7] Herzberg, *Infra-red and Raman Spectra of Polyatomic Molecules* (Van Nostrand Co. Inc., 1945), 178.

[8] Bell, *Proc. Roy. Soc. A*, 1944, **183**, 328.

used it gives a very small value for the out-of-plane vibration frequency unless a special constant is introduced; (3) gives a picture of angular distortions in molecules which is much more in accordance with modern views on directed valency then does the S.V.F.F.

We wish to thank Imperial Chemical Industries for providing us with a calculating machine.

Summary.

The four frequencies per molecule of six planar XY_3 molecules and ions have been correlated with an average difference between calculated and observed frequencies of 1 % by a new force field, using three constants per molecule, which we have called the orbital valency force field. This field uses the same constant for both the angular distortion in the plane of the molecule and that out of the plane of the molecule, and is therefore preferable to the simple valency force field which is unable to explain the out-of-plane vibration frequencies without introducing a new constant for angular distortion.

Inorganic Chemistry Laboratory,
Oxford.

MOLECULAR FORCE FIELDS.

PART IV.—THE APPLICATION OF THE ORBITAL VALENCY FORCE FIELD TO TETRAHEDRAL HALIDES.

By D. F. Heath and J. W. Linnett.

Received 21*st November*, 1947.

In a previous paper[1] we have described the application to the tetrachlorides and tetrabromides of carbon, silicon, germanium and tin of the simple valency force field with the addition of a repulsion field between the non-bonded atoms represented by $V = a/R^n$. In that paper, a was supposed to have the same value for all halides of the same kind (e.g. all bromides) and n was given the value 4·5 throughout. Two valency constants were used per molecule, k_1 and k_α, for bond-stretching and -bending respectively. With these assumptions the 32 frequencies of these eight XY_4 molecules could be calculated with an average deviation from the observed values of only 0·6 % using 18 constants. This field, in spite of its success in correlating frequencies, is, however, unsatisfactory because it requires the introduction of $V = a/R^{4\frac{1}{2}}$ as the potential energy (P.E.) function for the interaction of the non-bonded atoms. There are two main objections to such a P.E. function.

(i) Lennard-Jones[2] has shown that a satisfactory P.E. function for the interaction of inert gas atoms is

$$V = \frac{a}{R^{12}} - \frac{b}{R} \quad . \quad . \quad . \quad . \quad . \quad (1)$$

It seems reasonable to suppose that the interaction between halogen atoms which are bonded to other atoms but not to one another might be similar to this in form. Now, in the final frequency formulæ there appear

$$A = \tfrac{1}{2}\mathrm{d}^2V/\mathrm{d}R^2 \text{ and } B/R = -(1/R)\mathrm{d}V/\mathrm{d}R.$$

Using the values of a and b obtained by Buckingham for argon atoms, which resemble bonded chlorine atoms electronically, we have when $R = 3{\cdot}33$ A. (cf. range of Cl—Cl distances in Table II) :

---

[1] Heath and Linnett, *Trans. Faraday Soc.*, 1948, **44**, 561.

[2] Lennard-Jones, *Proc. Roy. Soc. A*, 1924, **106**, 463.

$$A = 0{\cdot}0470 \times 10^5 \text{ and } B/R = 0{\cdot}0053 \times 10^5 \text{ dynes/cm.}$$

Thus A is much bigger than B/R and will outweigh the latter in its effect on the frequencies. In $A = 0{\cdot}0470 \times 10^5$, the contribution of the first repulsion term in (1) is $0{\cdot}0613 \times 10^5$ and of the second attraction term is $-0{\cdot}0143 \times 10^5$. Therefore, to a first approximation, we may omit the attraction term and represent the van der Waals' P.E. by $V = a/R^{12}$ only. On this basis the ratio of A to B/R must be 6½ to 1. The result of this assumption is, therefore, that it seems that we can represent in a reasonable manner the van der Waals' interaction of the non-bonded halogen atom by one constant, since, when A has been fixed, the value of B/R must be 2/13 of it. It may be pointed out that in the example given above, where $A = 0{\cdot}0470 \times 10^5$, $2/13 \times 0{\cdot}0470 \times 10^5 = 0{\cdot}0072 \times 10^5$ whereas the value of B/R according to the formula (1) is $0{\cdot}0053 \times 10^5$. This difference is very small as regards absolute magnitude and is a very small fraction of the other constants that have to be used in the vibration frequency formulæ. One general conclusion is, therefore, that $V = a/R^{12}$ is a satisfactory and reasonable function to use. Moreover, it has been used successfully with XY_4 molecules.[3] The function $V = a/R^{4\frac{1}{2}}$ is therefore quite unlike any that might be expected.

(ii) The value of the first differential of $V = a/R^{4\frac{1}{2}}$ derived from the actual constants used would produce a stretching of the C—Cl bond in carbon tetrachloride of about 0·4 A. over its value if no such repulsion existed as, for example, in methyl chloride. No determinations[4] of C—Cl bond lengths in these two molecules are consistent with a stretching of more than 0·1 A. The large stretching which would result if the $V = a/R^{4\frac{1}{2}}$ function were correct could not possibly have remained undetected.

It was therefore decided to attempt to calculate the observed frequencies using the simple valency force field (S.V.F.F.) and the orbital valency force field (O.V.F.F.) in turn, adding to each a P.E. function $V = a/R^{12}$ to represent the interaction of the non-bonded atoms, a being chosen independently for each molecule.

The equations for the frequencies derived from both the fields are given below.

S.V.F.F.

Class A_1.

$$\lambda_1 = \frac{1}{m_2}[k_1 + 8A],$$

Class F_2.

$$\lambda_2+\lambda_3 = \left[\frac{1}{m_2} + \frac{4}{3m_1}\right]\left[k_1 + \frac{8}{3}A - \frac{4}{3}\frac{B}{R}\right] + \left[\frac{1}{m_2} + \frac{8}{3m_1}\right]\left[2k_\alpha + \frac{4}{3}A + \frac{10}{3}\frac{B}{R}\right] - \frac{8}{3m_1}\left[\frac{8}{3}A - \frac{4}{3}\frac{B}{R}\right],$$

$$\lambda_2\lambda_3 = \left[\frac{1}{m_2^2} + \frac{4}{m_1m_2}\right]\left\{\left[k_1 + \frac{8}{3}A - \frac{4}{3}\frac{B}{R}\right]\left[2k_\alpha + \frac{4}{3}A + \frac{10}{3}\frac{B}{R}\right] - \frac{1}{2}\left[\frac{8}{3}A - \frac{4}{3}\frac{B}{R}\right]^2\right\}.$$

Class E.

$$\lambda_4 = \frac{1}{m_2}\left[3k_x + 2A + \frac{B}{R}\right].$$

---

[3] Heath and Linnett, *Trans. Faraday Soc.*, 1948, **44**, 873.

[4] Sutherland, *Trans. Faraday Soc.*, 1938, **34**, 325 ; *J. Chem. Physics*, 1939, **7**, 1066.

O.V.F.F.

Class A_1.

$$\lambda_1 = \frac{1}{m_2}[k_1 + 8A]$$

Class F_2.

$$\lambda_2 + \lambda_3 = \left[\frac{1}{m_2} + \frac{4}{3m_1}\right]\left[k_1 + \frac{8}{3}A - \frac{4}{3}\frac{B}{R}\right] + \left[\frac{1}{m_2} + \frac{8}{3m_1}\right]\left[k'_\alpha + \frac{4}{3}A + \frac{10}{3}\frac{B}{R}\right] - \frac{8}{3m_1}\left[\frac{8}{3}A - \frac{4}{3}\frac{B}{R}\right],$$

$$\lambda_2\lambda_3 = \left[\frac{1}{m_2^2} + \frac{4}{m_1m_2}\right]\left\{\left[k_1 + \frac{8}{3}A - \frac{4}{3}\frac{B}{R}\right]\left[k'_\alpha + \frac{4}{3}A + \frac{10}{3}\frac{B}{R}\right] - \frac{1}{2}\left[\frac{8}{3}A - \frac{4}{3}\frac{B}{R}\right]^2\right\}.$$

Class E.

$$\lambda_4 = \frac{1}{m_2}\left[k'_\alpha + 2A + \frac{B}{R}\right].$$

Here

$\lambda_i = 4\pi^2c^2n_i^2$,

n_i being the frequency in cm.$^{-1}$ of the ith vibration ;

m_1 = the mass of the central atom,

m_2 = the mass of the halogen atom,

k_1 = the bond-stretching constant of the X—Y bond,

r^2k_α = the angle bending constant on the S.V.F.F., i.e. of the YXY angle,

r^2k_α' = the angle bending constant on the O.V.F.F.,

r = the X—Y bond length ;

$-B$ and $2A$ are the first and second differentials, respectively, of the P.E. function representing the repulsion between the non-bonded atoms. That is, they are the constants in the expansion of V in terms of ΔR (the change in R from the value it has at the equilibrium configuration) :

$$\Delta V = V - V_0 = -B\Delta R + A\Delta R^2,$$

this being derived from $V = a/R^n$, by expanding to second powers.

In Table I the calculated and observed frequencies are compared. In assessing the % differences, no difference of 1 cm.$^{-1}$ has been considered significant. The reason for this is that the experimental error could certainly be 1 cm.$^{-1}$ and it seemed preferable to avoid giving a disproportionate weight to errors on small frequencies which may just as likely arise from errors in experiment.

The results bring out clearly the following facts.

(i) The orbital valency force field is clearly superior to the S.V.F.F. The average deviation for the O.V.F.F. of 0·45 % is probably within the experimental error in determining the frequencies. The average deviation for the S.V.F.F., however, is over 3 % and outside the range of either experimental error or the corrections which should be made to the frequencies to allow for anharmonicity.

(ii) The errors in Table I have been averaged separately over the pairs (n_1 and n_2) and (n_3 and n_4). The former are associated with vibrations which are mainly valency vibrations, while the latter are associated with deformation vibrations. It will be seen that the errors for the O.V.F.F. fall fairly evenly over all the frequencies. The differences of 0·6 % is easily attributable to the fact that n_3 and n_4 are smaller than n_1 and n_2 so that equal absolute errors correspond to greater % errors for the former pair. But the very large errors of the S.V.F.F. definitely seem to occur in n_3 and n_4. It would have been possible to reduce the disparity between the errors for the two pairs but only by considerably increasing the total error. It therefore seems to be a real effect that the main errors of the S.V.F.F. occur in n_3 and n_4. It can be shown, by determining the normal co-ordinates, that n_1 and n_2 correspond to vibrations involving almost entirely changes in bond length, and that n_3 and n_4 correspond to vibrations involving almost entirely changes in the valency angles. It therefore appears that the S.V.F.F. is particularly bad at correlating the frequencies of those vibrational modes involving angle changes ; that is, it fails precisely where it is expected to fail if it is based upon an incorrect P.E. function for angle changes.

TABLE I.—COMPARISON OF THE OBSERVED FREQUENCIES OF THE TETRAHEDRAL HALIDES WITH THOSE CALCULATED USING BOTH SIMPLE VALENCY AND ORBITAL FORCE FIELDS.

Mol. and Field.	Constants.				Vibr. Freq.				Percentage Error.	
	k_1	k_α, k'_α	A	B/R	n_1	n_2	n_3	n_4	n_1 and n_2.	n_3 and n_4.
	$\times 10^{-5}$ dynes per cm.				cm.$^{-1}$.					
CCl_4	Observed				459	780	313	217	—	—
OVFF	1·86	0·2992	0·31	0·0477	459	780	313	217	0	0
SVFF	1·90	0·1050	0·325	0·0500	467	767	309	222	1·7	1·8
$SiCl_4$	Observed				425	607	221	151	—	—
OVFF	2·58	0·1700	0·15	0·0231	428	607	219	154	0·35	1·44
SVFF	2·50	0·035	0·19	0·0292	442	593	214	158	3·15	3·9
$GeCl_4$	Observed				397	451	171	132	—	—
OVFF	2·44	0·147	0·10	0·0154	397	454	170	132	0·3	0
SVFF	2·30	0·037	0·13	0·0200	403	443	164	138	1·64	4·32
$SnCl_4$	Observed				366	404	134	104	—	—
OVFF	2·30	0·110	0·06	0·0092	367	403	130	108	0	3·35
SVFF	2·25	0·038	0·07	0·0108	369	399	125	113	1·13	7·31
CBr_4	Observed				265	667	183	123	—	—
OVFF	1·49	0·225	0·230	0·0354	266	666	182	124	0	0
SVFF	1·58	0·090	0·230	0·0354	270	668	178	127	0·94	3·0
$SiBr_4$	Observed				249	487	137	90	—	—
OVFF	2·03	0·150	0·110	0·0169	249	487	136	90	0	0
SVFF	2·075	0·060	0·110	0·0169	250	488	130	94	0	4·9
$GeBr_4$	Observed				234	328	111	78	—	—
OVFF	1·95	0·115	0·080	0·0123	234	331	110	78	0·5	0
SVFF	1·90	0·044	0·085	0·0131	234	326	106	82	0·3	5·0
$SnBr_4$	Observed				220	279	88	64	—	—
OVFF	1·85	0·080	0·053	0·0083	220	279	86	64	0	1·2
SVFF	1·89	0·040	0·050	0·0077	221	282	84	70	0·5	7·5
	Average for all the molecules :						OVFF		0·15	0·75
							SVFF		1·16	5·14
	Average over all the frequencies :							OVFF	0·45	
								SVFF	3·15	

(iii) It is possible to estimate from the value of B/R for a molecule XY_4 the stretching of the XY bond that is caused by repulsion between the non-bonded Y atoms.[5] This is done by equating the force between the non-bonded atoms to the force produced by stretching the bond against the bond force constant, k_1. It is found that, in CCl_4, the bond force constant, k_1, is low, being $1{\cdot}86 \times 10^5$ dynes per cm. The bond force constant of the CCl bond[6] in methyl chloride is $3{\cdot}37 \times 10^5$ dynes per cm., and in this molecule there is likely to be very little stretching due to repulsion between non-bonded atoms. By using a Morse function with reasonable constants it can be shown that d^2V/dR^2 (i.e. the force constant) might be expected to decrease from 3·37 to $1{\cdot}86 \times 10^5$ on stretching the bond 0·27 A. This calculation is necessarily very approximate. To calculate the stretching we shall assume that the stretching occurs against a force calculable from the average force constant,

---

[5] Badger, *J. Chem. Physics*, 1934, **2**, 128.

$$k'_1 = 2{\cdot}62 \times 10^5 \left(\frac{3{\cdot}37 + 1{\cdot}86}{2}\right).$$

Consideration of the form of the Morse function shows this to be reasonable. Then Δr, the stretching of the bond, will be given by

$$3B \cos \phi = k'_1 \Delta r,$$

where ϕ is the angle between the ClCl and CCl directions. Taking $B/R = 0{\cdot}0477 \times 10^5$ dynes per cm. (see Table I) it is found that $\Delta r = 0{\cdot}13$ A. Electron diffraction[7] shows that the bond length in CCl_4 is 1·755 A.[8] The bond length in methyl chloride is less certain. Electron diffraction determinations give 1·77 A. However, spectroscopic measurements give us that, if the bond angles remain close to the tetrahedral values, the CCl bond length is 1·66 A. Borge Bak has suggested that the electron diffraction and spectroscopic results could be made to agree if it is supposed that the interbond angles in methyl chloride are very different from the tetrahedral values.[9] Our calculations show that the repulsion between the non-bonded atoms is very considerable and would be expected to lead to a considerable stretching in CCl_4, namely 0·13 A. We are, therefore, inclined to favour Sutherland's interpretation of the data which suggests that the CCl bond is 0·1 A. longer in CCl_4 than in CH_3Cl (1·755 − 1·66), a difference which is in quite good agreement with the stretching our results have led us to expect. However, whatever the values of the bond lengths in these two molecules it is certain from our results that there exists in carbon tetrachloride a repulsion between the non-bonded atoms which will stretch the CCl bond considerably from the value it would have if no such repulsion existed. Very few considerations of the bond lengths in CCl_4 to be found in the literature seem to take this into account and treat the CCl bond as if no such large distorting factor were present.

(iv) It is reasonable to suppose that covalently combined chlorine atoms can be reasonably compared with argon atoms as regards the van der Waals' forces between them. It is, therefore, interesting to compare the values of A $(= \frac{1}{2}d^2V/dR^2)$ given in Table I (for O.V.F.F.) with the value of $\frac{1}{2}d^2V/dR^2$ calculated from $V = a/R^{12}$ using the value of a found by Buckingham for argon (1620×10^{-10} ergs. A^{12}) from measurements made on that gas.[10] The results of this comparison are given in Table II. The YY distances were calculated from the XY distances obtained by electron diffraction assuming the molecules to be tetrahedral.

The values of $A_{\text{calc.}}$ and A_{OVFF} are of the same order. This justifies the repulsion field that has been employed. It moreover supports the conclusions reached in section (iii). The ratio of the value of A obtained using the O.V.F.F. to that calculated increases as the molecules become more ionic, i.e. on passing from carbon to tin. This would be expected, for as the chlorine atoms tend to obtain greater electronic charges without their nuclear charge being affected, the electronic field will become more diffuse. Therefore, two chlorine atoms will be expected to exert a greater

[6] Linnett, *Quart. Rev.*, 1947, **1**, 73.
[7] Wierl, *Ann. Physik*, 1931, (5), **8**, 521.
[8] Brockway and Sutton, *J. Amer. Chem. Soc.*, 1935, **57**, 473.
[9] Borge Bak, *J. Chem. Physics*, 1946, **14**, 342.
[10] Buckingham, *Proc. Roy. Soc. A*, 1938, **168**, 264.

van der Waals' repulsion on each other the more negatively charged they become. We would therefore expect the ratio given in the last column of Table II to increase on passing from carbon to tin.

TABLE II.—COMPARISON OF THE VALUES OF A CALCULATED FROM BUCKINGHAM'S FIGURES FOR ARGON WITH THOSE GIVEN IN TABLE I, USING THE O.V.F.F.

Molecule.	YY Distance in A.	$A_{\text{calc.}}$ $\times 10^{-5}$.	A_{OVFF} $\times 10^{-5}$.	Ratio.
CCl_4 . .	2·87	0·494	0·31	0·63
$SiCl_4$ . .	3·27	0·079	0·15	1·9
$GeCl_4$.	3·40	0·046	0·10	2·2
$SnCl_4$ . .	3·76	0·011	0·06	5·5

(v) It is interesting to note the small values of the bond force constants. That for the CCl bond in CCl_4 is only just over half that of the CCl bond in methyl chloride. This decrease seems to be too large to be explained by the dissymmetry of the P.E. function as expressed by the Morse equation (see section (iii)). It is therefore likely that it is due to a real change in the CCl bonds in these two molecules. The values of the bond-stretching force constants were discussed in our previous paper.[1]

The following general conclusions may be drawn.

(*a*) The general superiority of the orbital valency force field over the simple valency force field, suggested by a previous paper,[3] is amply confirmed. The force field between the non-bonded atoms required by the O.V.F.F. if the frequencies are to be calculated satisfactorily produces a stretching of the bonds which is quite possible. But the force field required by the S.V.F.F. if satisfactory results are to be obtained would produce a very large stretching which would have, and has not, been observed.

(*b*) The force field between the non-bonded atoms in these molecules is similar to that existing between atoms of the inert gases.

We wish to thank Imperial Chemical Industries for providing us with a calculating machine.

Summary.

The orbital valency force field and the simple valency force field, each with the addition of a repulsion field represented by $V = a/R^{12}$ between the non-bonded atoms, were applied to the tetrachlorides and tetrabromides of carbon, silicon, germanium and tin. It was found that the orbital valency force field reproduced the observed vibrational frequencies very satisfactorily while the S.V.F.F. was definitely unsatisfactory.

The repulsion field used would be expected to give rise to a difference of about 0·13 A. between the C—Cl bond lengths in CCl_4 and CH_3Cl which compares satisfactorily with the 0·1 A. suggested by Sutherland. The repulsion is similar in type to that existing between the atoms of inert gases at small internuclear distances.

Inorganic Chemistry Laboratory,
Oxford.

MOLECULAR FORCE FIELDS.

PART V.—THE APPLICATION OF THE ORBITAL VALENCY FORCE FIELD TO SOME TETRAHEDRAL ANIONS.

By D. F. Heath and J. W. Linnett.

Received 21st November, 1947.

In this paper the equations for calculating the vibration frequencies of tetrahedral molecules given in Part IV [1] are applied to the anions ClO_4^-, SO_4^-, SeO_4^- and $PO_4^{\equiv}$. We have examined both the simple valency force field (S.V.F.F.) and the orbital valency force field (O.V.F.F., see Part III),[2] combining each with a repulsion field between the oxygen atoms which is represented by $V = a/R^{12}$ (see Part IV).[3] The observed frequencies are compared with the frequencies calculated by both fields in Table I. The figures in this table are those calculated so that the average error over all the frequencies for each molecule is a minimum.

It will be seen that, as before, the O.V.F.F. is considerably superior to the S.V.F.F., with an average error of only 1·6 % against an average error for the S.V.F.F. cf 4·2 %. It will be noted that, in every case, almost the whole error has been placed on n_3 and n_4 and that, for the S.V.F.F., almost the whole has been placed on n_3. It was found that, by doing this, the average % error was reduced to a minimum for each molecule, and that any attempt to even out the errors over all the frequencies increased the average error considerably. In addition, we also calculated the frequencies for which the sum of the squares of the errors was a minimum, this being another criterion of the "best fit." When this criterion was used it was found that the average error over all the sixteen frequencies, using S.V.F.F., was 5·8 %, the error on n_1 and n_2 being 3·3 % and that on n_3 and n_4 being 8·3 %. Therefore, using this criterion of "best fit" also the greatest errors fall on n_3 and n_4, the frequencies of the bending vibrations. With the O.V.F.F. also it was found that, whichever criterion was used, the greatest error fell on the frequencies of the bending vibrations. The average error for these bending vibration frequencies are 3·2 % using O.V.F.F. and 8·4 % using S.V.F.F. The O.V.F.F. is certainly much better than the S.V.F.F. but is not wholly satisfactory and apparently does not provide a complete explanation of the forces acting during the distortion of these ions.

The bonded oxygen atoms in these ions are electronically similar to neon atoms. Since the forces between the oxygen atoms are here supposed to be of the van der Waals' types, it is interesting to compare the value of A ($= \frac{1}{2}d^2V/dR^2$ for the repulsion potential energy) in Table I with the known values of this quantity for neon. The figures for neon have been obtained by Buckingham from observed P-V-T relationships for neon; a in the equation, $V = a/R^{12}$, was taken as $35{\cdot}5 \times 10^{-10}$ ergs A^{12} which is the value given by Buckingham.[5] The attraction term in the van der Waals' P.E. expression (b/R^6) may be omitted because we are concerned with relatively small interatomic distances at which the repulsion term far outweighs the attraction term. The comparison for each ion of A_{OVFF} (from Table I) with $\frac{1}{2}\mathrm{d}^2V/\mathrm{d}R^2$ calculated for neon atoms at the same interatomic distance (which we will call $A_{\text{calc.}}$) is shown in Table II. In the last column the ratio of $A_{\text{OVFF}}/A_{\text{calc.}}$ is given. It will be seen that, in all cases, A_{OVFF} is greater than $A_{\text{calc.}}$. This would be anticipated for, as the charge on the oxygen nucleus is less than that on the neon nucleus, the electron cloud round the bonded oxygen atom will be more diffuse than that round the neon atom. As the electron clouds round the oxygen atoms extend further, they will impinge on one another at greater internuclear distances and so the van der Waals' repulsion between bonded oxygen atoms will be greater than that between neon atoms at the same interatomic distance. And, if the repulsion P.E. expression is of the same form in the two cases, the second differential is likewise expected to be bigger also. In addition the increase in $A_{\text{OVFF}}/A_{\text{calc.}}$ on increasing the total charge on the ion is interesting. It would be expected that, as the negative charge on the ion increased, the electron cloud round the oxygen atoms would increase in density and size. This will mean that the van der Waals' repulsion between the bonded oxygen atoms should increase as the charge on the ion increases. The figures in the last column

---

[1] Heath and Linnett, *Trans. Faraday Soc.*, 1948, **44**, 878.

[2] Heath and Linnett, *ibid.*, 1948, **44**, 873.

[3] Lennard-Jones, *Proc. Roy. Soc. A*, 1924, **106**, 463.

[4] Kohlrausch, *Smekal-Raman Effekt* (Julius Springer, 1938).

[5] Buckingham, *Proc. Roy. Soc. A*, 1938, **168**, 264.

TABLE I.—COMPARISON OF THE OBSERVED VIBRATION FREQUENCIES OF FOUR OXYANIONS WITH THOSE CALCULATED USING THE O.V.F.F. AND THE S.V.F.F.[4]

Mol. and Field.	k_1	k_{α}	A	B/R	n_1	n_2	n_3	n_4	Average % Errors.			
	× 10⁻⁵ dynes per cm.				cm.⁻¹.				n_1 and n_2.	n_3 and n_4.	n_3.	All Freq.
ClO_4^-	Observed				935	1102	628	462				
OVFF	6·30	1·62	0·24	0·037	935	1104	606	476	0·1	3·3	3·6	1·7
SVFF	6·52	0·52	0·215	0·033	935	1101	513	463	0·05	9·3	18·33	4·7
$SO_4^=$	Observed				981	1104	613	451				
OVFF	6·05	1·20	0·38	0·059	981	1104	597	463	0	2·6	2·6	1·3
SVFF	6·27	0·39	0·35	0·054	981	1105	521	452	0·05	7·6	15·0	3·8
$SeO_4^=$	Observed				834	875	416	339				
OVFF	5·40	0·84	0·135	0·021	834	875	406	346	0	2·2	2·4	1·1
SVFF	5·40	0·26	0·15	0·023	837	875	347	342	0·2	8·7	16·6	4·5
$PO^{\equiv}_4$	Observed				980	1082	515	363				
OVFF	5·97	0·55	0·385	0·059	980	1085	493	382	0·15	4·8	4·3	2·5
SVFF	6·10	0·145	0·37	0·037	980	1087	433	363	0·25	8·0	15·9	4·1
	Orbital valency force field . . .								0·06	3·2	3·2	1·6
	Simple valency force field . . .								0·14	8·4	16·5	4·3

TABLE II.—COMPARISON OF $A_{\text{calc.}}$ FOR NEON WITH A_{OVFF} FOR BONDED OXYGEN ATOMS. A $\frac{1}{2}\mathrm{d}^2V/\mathrm{d}R^2$ FOR THE REPULSION POTENTIAL ENERGY.

Ion.	O—O Distance in A.	$A_{\text{calc.}}$ for Neon × 10⁻⁵ dynes per cm.	A_{OVFF} for Bonded Oxygen × 10⁻⁵ dynes per cm.	$\frac{A_{\text{OVFF}}}{A_{\text{calc.}}}$.
ClO_4^-	2·42	0·117	0·24	2·1
$SO_4^=$	2·465	0·091	0·38	4·2
$SeO_4^=$	2·63	0·037	0·135	3·6
$PO_4^{\equiv}$	2·53	0·063	0·385	6·1

of Table II show that a change in this sense does occur. The observations here are closely parallel to those described in Part IV where it was found that the repulsion between the chlorine atoms in the XCl_4 molecules increased as the XCl linkage became more ionic, i.e. the chlorine atom more negative.[1]

It is therefore concluded that (i) the O.V.F.F. is much superior to the S.V.F.F. in accounting for the vibration frequencies of these ions, (ii) the O.V.F.F. is not completely satisfactory for these ions, (iii) the values of A differ from the values calculated using the constants for neon in a way which follows closely the charge on the anion.

We wish to thank Imperial Chemical Industries for providing us with a calculating machine.

Summary.

The equations of Part IV were applied to the frequencies of four tetrahedral anions, XO_4^{n-}. It was found that the orbital valency force field was very much more satisfactory than the simple valency force field, repulsions between the non-bonded oxygen atoms being included in both cases. The orbital valency force field is not fully satisfactory. The O.V.F.F. gives a mean error of 3·1 % for the frequencies of vibrations involving primarily angular distortions.

Inorganic Chemistry Laboratory,
Oxford.

INHIBITION AND RETARDATION IN POLYMERISATION REACTIONS.

By H. W. Melville and W. F. Watson.

Received 8th December, 1947.

In conformity with the fact that polymerisation of ethylene derivatives proceeds by a chain mechanism, such reactions are subject to retardation or, in extreme cases, complete suppression by the addition of relatively small amounts of a great variety of substances. A survey of what literature exists on the subject shows a great diversity of effects and it would therefore now seem necessary to attempt some sort of codification with the important proviso that any classification into well-defined types is purely artificial, since it is inevitable that borderline cases will soon be discovered. However, it is important to specify extreme types in order that a more systematic approach may be made from the kinetic side.

The number of measurable quantities available for an analysis is fortunately considerable and the use of each one of them is, in principle, sufficient completely to specify the nature of the processes involved and also, in suitable cases, to specify quantitatively the magnitude of the corresponding velocity coefficients. These measurable quantities are :

(*a*) the correlation between rate of polymerisation and concentration of added substances ;
(*b*) the effect of the concentration of the added substance on the molecular weight of the polymer ;
(*c*) the time required for the growth of the polymer ;
(*d*) the effect of the rate of initiation of chain growth on kinetic chain length in presence of a large amount of retarder ;
(*e*) the rate of disappearance of the added substance.

In this connection it is convenient for the present to term inhibitors those substances that completely suppress polymer formation and retarders those substances that merely cut down the rate of polymerisation.

The range of phenomena really extends all the way from complete inhibition to copolymerisation—it is within this region that the present interest lies.

1. The simplest phenomenon is complete suppression.[1] Here there is no question that, if it is assumed that these reactions involve free radicals, the inhibitor reacts (*a*) with radicals produced from the monomer by radiation, (*b*) with radicals produced by sufficiently violent collisions between monomers, as in the thermal polymerisation of styrene, or (*c*) with radicals produced independently by thermal or photo-decomposition of suitable molecules. When the inhibitor is thus chemically removed, reaction should then at once proceed at normal speed, but this ideal behaviour is not always observed unless the velocity coefficient for the interaction of the inhibitor with the initiating radical is much greater than that of the monomer with the same radical. Such an ideal state of affairs is observed with the photopolymerisation of vinyl acetate and its polymerisation in presence of benzoquinone. If this criterion is not satisfied, there will be a period succeeding suppression of the polymer formation in which the rate will increase gradually as the inhibitor is removed.

2. This transitional type leads smoothly into a simple kind of retardation. In this case there is fair competition by the polymer free radical for the monomer or the retarder. When the retarder molecule adds to the radical, growth stops altogether. The detection of this kind of process is also comparatively easy for, besides the rate of polymerisation being cut down, there should be an exactly corresponding drop in molecular weight, provided transfer is absent. Similarly, the life-time of the reaction chain should exhibit a corresponding decrease if the growth coefficient does not alter much with radical size. Another measurable effect follows. In normal reactions the radicals interact and stop growth ; this has the effect that rate of polymerisation is proportional to the square root of the rate of starting—no matter how this is effected. If the retarder ends the growth by addition, this square-root dependence is replaced by a first-order dependence since only one radical is concerned in the process. There are many examples of this type, e.g. the photopolymerisation of methyl acrylate in the vapour phase with oxygen and butadiene ; vinyl acetate with benzoyl peroxide acting as retarder, etc. It is difficult to specify exactly the chemistry of this process, since if a free mono-radical reacts, say, with an unsaturated molecule or, in fact, any kind of molecule except a free mono-radical it is inevitable that some kind of free radical is produced. If the above criteria are satisfied, this can only mean that the radical so produced is itself so unreactive that it cannot continue polymerisation or even interact with polymer radicals. It must then eventually disappear by interaction with another of its kind.

3. Retardation may also occur by quite a different mechanism. This happens when the retarder specifically interferes with the initiation process but not to such an extent as to prevent polymerisation. The important distinction here is that once the chain has *started* growing the added substance has absolutely no effect on it. Such a mechanism of retardation gives rise to quite distinctive criteria from those mentioned above. If termination of growth occurs by mutual removal of free radicals, then this type of retardation will be characterised as follows :

(*a*) the square-root dependence still holds accurately ;
(*b*) the kinetic chain length increases (also the molecular weight, if there is no transfer).

This is the kind of behaviour that might occur if, for example, a retarder directly attacks the substance, e.g. a peroxide responsible for the provision of radicals for initiating polymerisation. The above criteria are therefore useful in looking for the possibility of the intervention of this mechanism. The only example so far recorded is the retarding effect of inert gases, He, A, H_2, on the photopolymerisation of vinyl acetate vapour when it appears that the photo-excited vinyl acetate molecules are simply deactivated by inert gases before they have time to grow further.*

---

[1] Foord, *J. Chem. Soc.*, 1940, 48.

4. There is another extension to type 2. There it has been assumed that the free radical finally produced by the interaction of the retarder molecule with the polymer radical takes no further part in the reaction. It is, however, possible in this chemistry of free radicals that such a radical might interact with a polymer radical but not with the monomer. This would therefore introduce an additional well-defined way in which radicals are used up.

This case has not previously been considered but is analysed below. The principal features of this mechanism are :

(*a*) the square-root dependence on starting still obtains ;
(*b*) the chain length is reduced ;
(*c*) there will be one molecule of retarder per two polymer molecules if there is disproportionation and a one-to-one ratio if combination occurs.

Examples of this kind of behaviour are given in the following experimental results.

5. The next gradual change from type 4 may arise in that the radical derived from the retarder is just sufficiently reactive to attack with difficulty the monomer. This means, of course, that the retarder really copolymerises with the vinyl derivative even though it cannot polymerise on its own. The criterion here is that although retardation is observed, more than one retarder molecule will be found in each polymer molecule.

The results, described in the pages on the polymerisation of methyl methacrylate and of styrene, throw some further light on the nature of retardation and inhibition and thereby illustrate some of the matters qualitatively outlined above.

Experimental.

For all kinetic work, the systems were contained in dilatometer reaction vessels of about 5 ml. capacity, under at most 10^{-4} mm. of non-condensable gas. These tubes had previously been thoroughly cleaned, and were flamed *in vacuo* just before use. Rather than adopt the usual method of having a large supply reservoir of monomer sealed to the vacuum line at some distance from the receiver, a graduated reservoir containing purified monomer was attached to a removable portion of the vacuum apparatus which was also sealed to the reaction vessel. In this way, the usual vacuum greases withstand the monomer vapour for the short time of evacuation and distillation into the receiver, and no mercury cut-offs were necessary. By calibration, the decrease in volume was found to be proportional to the extent of polymerisation and the extent of reaction could thus be followed accurately to less than 0·1 % by observing the decrease in meniscus level by a cathetometer reading to ± 0·01 mm.

Inhibition of the Thermal Polymerisation of Styrene by Quinones.

With styrene washed free from stabiliser and fractionally distilled twice *in vacuo*, a reproducible and strictly linear rate of polymerisation to within 15 % was noted between 60°-90° C.

In all cases where benzoquinone was added to the system, curves of the same form as those of Goldfinger [2] were obtained, including the lengthening of the transition period, between complete inhibition and the attainment of the thermal rate, with larger initial quinone concentrations. In order to demonstrate these complexities more clearly, considerably longer induction periods were produced than those obtained by the original authors. The dilatometer technique allows of a point-to-point following of the polymerisation curve, whereas by the precipitation method, a considerable extrapolation to zero extent of the reaction was required with the introduction of a large experimental error. In agreement with Goldfinger, the *approximate* relationship—

---

* See e.g. Tuckett and Melville, *J. Chem. Soc.* (in press).

[2] Goldfinger, Skeist and Mark, *J. Physic. Chem.*, 1943, **47**, 578.

length of inhibition period ~ initial inhibitor concentration, (*a*)

is found.

Fig. 1 shows three typical experiments on the inhibition of polymerisation

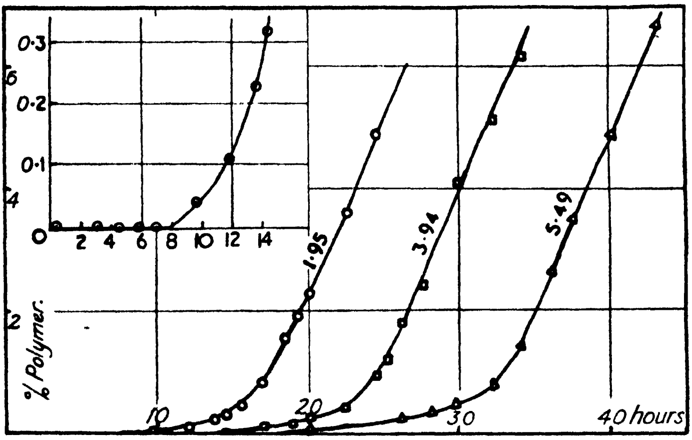

FIG. 1.—Effect of benzoquinone in mol./mol. monomer × 10⁴ on the thermal polymerisation of styrene (80° C.).

by different concentrations of quinone. As shown in the greatly magnified vertical scale in the insert, these curves are not asymptotic to the time axis but are definitely discontinuous within the considerable accuracy of the method of measurement. As can be seen from Table I, the above relationship (*a*) is only approximately observed, thus there is a definite trend of relative shortening of the inhibition period with higher quinone concentrations.

TABLE I.—EFFECT OF QUINONE ON THERMAL POLYMERISATION OF STYRENE AT 80° C.

Length of Inhibition Period, l (hr.).	Conc. of Inhibitor, c (mol./mol. monomer × 10^4).	$l/c \times 10^{-4}$.
8	1·95	4·12
14·5	3·94	3·7
18·5	5·49	3·4

The curves can be divided into three regions: (1) a period of complete inhibition, which is followed discontinuously by (2), a retardation stage, accelerating to (3), the normal thermal polymerisation curve. As these three regions are later treated as separate parts, it is necessary here to reinterpret the molecular-weight data of Goldfinger, who found that the molecular weight of the total polymer, precipitated after a considerable extent of thermal polymerisation had been allowed to proceed, decreased with increasing initial concentration of inhibitor. That this phenomenon is caused by increasing quantities of low molecular-weight material with larger quinone concentrations formed during the transition period (2), can be shown by correcting for the material formed in the thermal region. This is done to a first approximation—assuming Staudinger's viscosity rule—by the expression,

$$\eta_p = \frac{c_t\eta_t - c_i\eta_i}{c_p},$$

where η_p, η_t, η_i, are the intrinsic viscosities of the " thermal " polymer, " total " polymer, and "retarded" polymer of concentrations c_p, c_t, c_i respectively, as shown in Table II. Since the corrected molecular weights of polymer formed in the thermal portions of all polymerisations are practically constant, it has been accepted that in region (3) of the process, the conditions are identical with those of the uninhibited polymerisation.

TABLE II.

c_t.	c_p.	η_t.	η_p.
Conc. of low mol.-wt. polymer = 0·3 %.			
0·6	0·3	78	156
1·7	1·4	137	166
2·6	2·3	154	174
Conc. of low mol.-wt. polymer = 0·5 %.			
0·95	0·45	75	159
2·5	2·0	145	180
Conc. of low mol.-wt. polymer = 0·85 %.			
1·95	1·1	93	161

The effects of substituted quinones are of interest, for if Foord's mechanism is correct,[1] it is to be expected that the lengths of inhibition periods would be equal for equimolecular concentrations of the different quinones. Further, Foord obtained an anomalous result with chloranil, which proved twice as effective in inhibiting power as the parent compound.

Tetra-bromo- and tetra-iodo-quinone were prepared by the method of Jackson and Bolton.[3] Table III summarises the results using iodoanil. The same general characteristics are obtained as for benzoquinone, but there is a wide discrepancy in their equimolecular inhibiting power, iodoanil being 50 % more effective per molecule than benzoquinone from these figures. Similarly, with bromanil a typical series is shown in Fig. 2 and Table IV, the inhibiting power being approximately three times that of the unsubstituted quinone.

TABLE III.—IODOANIL AS INHIBITOR (80° C.).

Conc. of Inhibitor (mol./mol. Styrene $\times 10^4$).	Length of Induction Period (hr.).	$l/c \times 10^{-4}$.
0·432	2·75	6·36
0·619	3·75	6·05
0·925	4·75	5·12

TABLE IV.—EFFECT OF BROMANIL (80° C.).

Conc. of Inhibitor (mol./mol. Styrene $\times 10^4$).	Length of Induction Period (hr.).	$l/c \times 10^{-4}$.
0·425	5·0	11·9
0·447	5·5	12·3
0·685	8·0	11·6
1·750	15·0	8·5

The above experimental evidence confirms the occurrence of an inhibition and retardation period, but indicates that the simple theory of Foord requires modification, and that this correction may explain the anomalous quantitative results on number-average molecular weight. In all cases, there occurs a relative shortening of the inhibition period with increasing initial inhibitor concentration, not expected according to the approximate relationship (*a*). This is in harmony with the general statement of Church,[4] who unfortunately does not give any quantitative data.

---

[3] Jackson and Bolton, *J. Amer. Chem. Soc.*, 1914, **36**, 304.

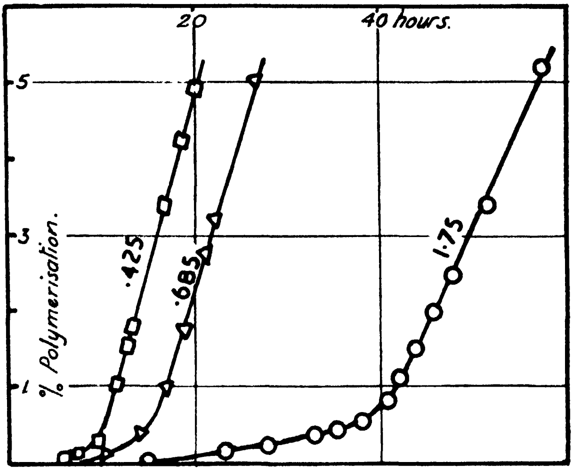

FIG. 2.—Inhibition of styrene polymerisation by bromanil at 80° C.

In view of considerable quantities of hydroquinone isolated on heating benzoquinone-styrene mixture *in vacuo* at 120° C.,[5] it is necessary, in eliminating possible reaction steps, to study the influence of hydroquinone on thermally polymerising styrene. Conflicting statements have been made on this subject,[4] but no experimental details have been given.

Hydroquinone is almost completely insoluble in benzene and styrene, and for this reason small quantities were weighed directly into reaction tubes. Table V gives the rate of polymerisation for two samples containing a wide variation in hydroquinone concentration, and for a control. It is seen at once that in concentrations much above that which could be produced in inhibition experiments, hydroquinone has no detectable influence on overall rate. Tube No. 3 contained an amount well above the saturation limit at 80° C., and on allowing polymerisation to proceed for several days to a high conversion, the undissolved hydro-

TABLE V.—INFLUENCE OF HYDROQUINONE ON THERMAL STYRENE POLYMERISATION (TEMP. 80° C.).

Tube No.	(1).	(2).	(3).
Wt. hydroquinone (g.) .	0	0·0008	0·0156
Wt. styrene (g.) . .	3·9	3·9	4·0
Time (min.).	**% Polymer.**	**% Polymer.**	**% Polymer.**
24	0·28	0·22	0·20
65	0·76	0·68	0·68
155	1·83	1·82	1·63
175	2·06	2·08	2·00

---

[4] Church, *Appl. Reports Progr. Chem. Ind.*, 1944.

[5] Breitenbach and Horeischy, *Ber. B*, 1941, **74**, 1386; Breitenbach and Breitenbach, *Z. Physik.*, 1941, **190**, 361; Breitenbach and Taglieber, *Ber. B*, 1943, **76**, 272.

quinone did not visibly diminish. Hence it is concluded that hydroquinone does not alter the rate of polymerisation by interfering with the initiation process, nor does it appear to enter into propagation or termination.

Production of Hydroquinone during the Inhibition of Styrene.

This occurrence of hydroquinone during the period of inhibition has given rise to opposing views of different authors.[2, 6] Thus, quantitative experiments, similar to those reported,[5] were performed. The solubility of hydroquinone in styrene at 0° C., is very low, and it is justifiable to measure the amount produced by weighing the precipitate formed on cooling the mixture.

A flask, sealed *in vacuo* and containing 0·86 g. benzoquinone in 51·2 g. styrene, was maintained at 120° C. After 6 hr., a considerable deposit of quinhydrone was detected, while after 24 hr. a white precipitate had formed and there was an increased viscosity and partial decolorisation. On diluting the mixture with toluene and filtering, the white deposit was shown by sublimation to be wholly hydroquinone. The amount produced was 0·122 g. These results confirm previous observations.[5] The yellow filtrate was vacuum-distilled to yield a colourless distillate and a bright-yellow, gummy residue. In a test experiment with the same intensity of a coloured solution of benzoquinone, an appreciable quantity of the volatile quinone distilled to give a markedly yellow condensate. It seems therefore that all the quinone had been consumed in the original experiment. If the reaction had followed Price's mechanism to give as final products hydroquinone and a long-chain mono-substituted quinone, the conversion of 50 % of the original quinone to hydroquinone by weight, would have been anticipated, a figure much in excess of that found.

Two flasks were heated at 80° C., one evacuated and the other with air present, each containing 0·895 g. benzoquinone in 43 g. styrene. After 72 hr., a dark green deposit collected on the walls on cooling, the yields being 0·308 g. in the evacuated and 0·304 g. in the unevacuated flask. This compound was identified as quinhydrone, while quinone was still present in the filtrate which had no noticeable increase in viscosity. Hence we find at least 0·15 g. hydroquinone is formed in 72 hr. at 80° C. From the third result of Table I and using relationship (*a*), it is readily calculated that the amount of benzoquinone expected for the inhibition is 0·095 g. This is much below the experimental yields; any experimental errors would have reduced the difference.

The facts provide definite evidence that (i) there is a shortening of inhibition period at higher concentrations and (ii) the reaction by which the hydroquinone is produced is of different origin from the initiation process. The efficiency of inhibition indicates that the rate-determining reaction is the production of chain nuclei, with the addition of quinone as a fast subsequent step. This mechanism is virtually independent of quinone concentration, whereas the hydroquinone production is markedly concentration-dependent. The view that the hydroquinone formation is a side reaction explains at once the deviations from relationship (*a*).

As a crucial test, a third flask containing concentrations close to those of the above two experiments was sealed up with 0·633 g. benzoyl peroxide in order to alter radically the rate of initiation. After 72 hr. at 80° C., 0·14 g. of a white precipitate of hydroquinone was isolated, i.e. almost half the yield of quinhydrone compared with that previously obtained. The formation of hydroquinone instead of quinhydrone is caused by the greater consumption of benzoquinone in the catalysed polymerisation.

Kern and Feuerstein [7] tested for the presence of phenyl acetylene, since they obtained only 0·05 g. hydroquinone, but the equivalent amount may have been undetectable. The filtrates of the above samples were fractionally distilled under a high reflux ratio, but no arrest was noted at its boiling point of 142° C. On testing the small 138°-142° C. fractions by the sensitive method of forming the mercury acetylide,[8] the results were negative.

Isolation of the Inhibition Product.—Since it is reasoned [2] that a substance is formed during inhibition which later acts as a retarder, and from the evidence in Table V, that this is not hydroquinone, a search was made for such a derivative. This work was carried out before access was gained to the results and

---

[6] Price, *Advancing Fronts of Chemistry*, 1945, p. 44.

[7] Kern and Feuerstein, *J. prackt. Chem.*, 1941, **158**, 186.

[8] Johnston and McEwen, *J. Amer. Chem. Soc.*, 1926, **48**, 469.

analytical methods of Kern and Feuerstein,[7] and it independently and qualitatively confirms their conclusions, though it does not explain their much greater yields of this derivative and the smallness of their hydroquinone formation compared with the present figures and those previously obtained.[5]

Two 250 ml. flasks containing (1) 3·26 g. benzoquinone and 200 ml. styrene, and (2) 3·64 g. benzoquinone and 50 ml. styrene, were sealed *in vacuo* and kept at 80° C. for 15 days. The reddish solutions became progressively decolorised for several days to a light yellow colour, which did not further diminish with time. On cooling, hydroquinone was filtered off and the styrene removed under vacuum. Deep-red resins which set to brittle red masses remained. Different separation methods were then employed.

Flask 1 : on addition of methyl alcohol to a concentrated benzene solution of the red resin, a flocculent white precipitate came down and coalesced after a few days to a viscous lower layer. This property and its solubility in acetone indicates a very low molecular-weight polystyrene. On decanting, filtering, and allowing to evaporate slowly, a crystalline yellow solid, which had a melting point considerably above that of benzoquinone separated first.

Flask 2 : the oil was dissolved in a small quantity of benzene, and on slow evaporation, a finely-divided solid again came out of solution first. This was recrystallised from methyl alcohol. Because of its solubility, this compound is clearly neither polystyrene nor benzoquinone. The melting point was indefinite but the substance remained unchanged at 220° C., 50° beyond the melting point of benzoquinone.

A C—H—O analysis[9] gave :

mg. Compound.	mg. CO_2.	mg. H_2O.	mg. Residue.
3·618	10·970	2·400	0·088

corresponding to the empirical formula $C_{14}H_{15}O$. Using Rast's method, the following data were obtained giving a molecular weight of 311 : m.pt. of camphor, 178·0° C. ; molar depression, using adipic acid and *p*-chloracetanilide, $35{\cdot}0 \times 10^{-3}$; 0·0043 g. substance in 0·0605 g. camphor has m.pt. of 170° C. The provisional formula is therefore $C_{28}H_{30}O_2$.

This corresponds approximately to a compound of two styrene molecules with one quinone, for which the molecular weight is 310 and molecular formula is $C_{22}H_{20}O_2$, which is in harmony with previous results.[7]

Polymerisation of Undistilled Styrene.—Several workers have observed that pure styrene, when exposed to the atmosphere at room temperature for an extended period, later polymerises *in vacuo* more rapidly than a freshly-distilled sample. In experiments with bromanil using styrene which has not been freshly distilled, an inhibition period was noted but of much shorter duration than expected, and the final rate of polymerisation was much higher. This indicates that exposure to air provides an increase in rate of initiation, probably by the formation of an unstable monomer peroxide. The length of inhibition period agrees with these deductions when related to the final rates as follows.

Let r_1 and r_2 = rates of polymerisation of styrene when exposed to air and freshly distilled respectively, and i_1 and i_2 = the rates of initiation. Then, assuming mutual termination, $\frac{r_1}{r_2} = \left(\frac{i_1}{i_2}\right)^{\frac{1}{2}}$. Since the inhibition period was reduced approximately four times, $r_1 = r_2(4)^{\frac{1}{2}} = 0{\cdot}92$ % per hour. The experimentally-observed final rate = 0·90 % per hour.

The Catalysed Polymerisation of Methyl Methacrylate.—Despite its extensive industrial application, little fundamental information has been published on the catalysed polymerisation of methyl methacrylate, except for the paper of Norrish and Brookman.[10] Their results can be re-interpreted so as to support the theory of mutual termination of growing chains. Table VI gives the values of $c^{\frac{1}{2}}/r$, where c is the catalyst concentration calculated from their Tables II, III, IV, showing clearly a square-root dependence of rate on catalyst concentration.

The results of the first column of Table VI agree closely with those of a series of experiments carried out at 80°, summarised in Table VII, where the rates of polymerisation in all cases were constant to the gel stage.[11]

---

[9] Weiler and Strauss, Micro-analytical Lab., Oxford.

[10] Norrish and Brookman, *Proc. Roy. Soc. A*, 1939, **171**, 147.

[11] Tromsdorff, *Colloquium* (1944), Freiberg B.I.O.S. Report, No. 363, Item 22.

TABLE VI.

From Norrish and Brookman's Table.

Catalyst.	II Benz. Perox. (× 10^3).	III Ozonide (× 10^{-2}).	IV Benz. Perox. (× 10^{-2}).
$c^{\frac{1}{2}}/r$	9·3	2·55	1·05
	9·97	2·51	1·05
	11·01	2·47	1·06
	9·70	2·54	1·07

TABLE VII.—Polymerisation of Methyl Methacrylate at 80° c.

Conc. of Benz. Peroxide (mol. % × 10^{-3}).	Rate (%/hr.).	$c^{\frac{1}{2}}/r \times 10^3$.
2·58	5·90	8·9
4·2	7·50	8·65
7·0	8·90	9·42
8·9	11·41	8·30

Influence of Benzoquinone on the Catalysed Polymerisation of Methyl Methacrylate.—When small quantities of benzoquinone are added to methyl methacrylate polymerising by catalysis at 80° c., its action is found to be fundamentally different from that on thermally-polymerising styrene. No trace of an inhibition or induction period is noted, the extent of polymerisation being linear with time up to at least 15-20 %. The rate in the presence of quinone is diminished, the degree of retardation increasing with increasing quinone concentration. A typical series of curves is shown in Fig. 3 for tubes containing a constant concentration of catalyst with varying concentrations of quinone.

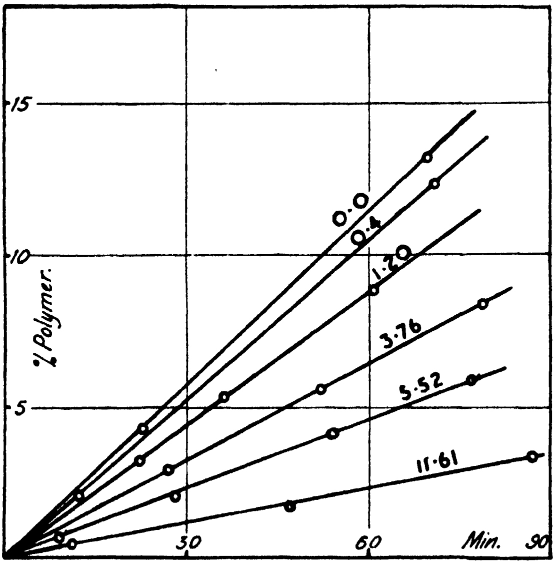

Fig. 3.—Effect of benzoquinone mol. per mol. monomer × 10^4 on the peroxide catalysed polymerisation ofmethyl methacrylate at 80° c.

In view of the strong inhibitory effect of quinone on the thermal polymerisation of styrene, it is of interest to compare the effect of quinone on peroxide-catalysed polymerisation of styrene. As Fig. 4 shows, quinone merely *retards* this reaction in exactly the same way as happens for methyl methacrylate (G. M. Burnett, unpublished experiments). The meaning of this discriminatory action of quinone is discussed at the end of the paper in relation to the question of determining whether mono-radicals or di-radicals are involved in a particular polymerisation process.

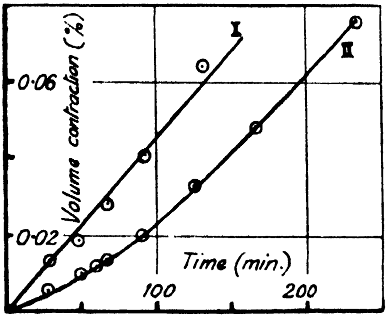

FIG. 4.—Quinone retardation of styrene (1·2 × 10^{-3} moles benzoyl peroxide per l.).
I. No quinone.
II. 9·76 × 10^{-4} moles quinone per l. (55° C.).

Mechanisms and Kinetics.

Retardation.—The retardation system, as exemplified by the action of quinone on methyl methacrylate, is the simpler and is thus considered first. The results derived are then of value in the more complicated case of inhibition and retardation consecutively occurring in the course of reaction.

It is well established that phenyl and benzoate radicals from the peroxide catalyse polymerisation by forming reactive mono-radicals which remain attached to the chain formed by covalent links.[12] From the known properties of quinones, the first step in retardation is probably the addition to the growing chain to produce a more stable radical.

Price[6] has suggested that this comparatively inert free radical does not grow further but reacts with a second quinone molecule in a tautomeric quinhydrone form. This scheme was primarily devised to explain hydroquinone production and is not confirmed by the present data.

Such a process pictures retardation as a chain-terminating process. This leads to the familiar difficulty of a simultaneously-operating first- and second-order termination with respect to radical concentration, thereby producing in the expression for free-radical concentration a quadratic equation which can only be solved by series of expansions and thus is limited greatly in application.[2] This radical must, however, eventually disappear and it is therefore of importance to take this fact into consideration. The following mechanism is suggested. It is capable of test by rigid kinetic derivation of the rate function. The stability of the free-radical formed by (ii) is, owing to resonance, much greater than the aliphatic radical, but it is assumed here that it behaves like a normal free radical in a polymerising system and there is a finite possibility that either a monomer molecule may add on (*c*), or another radical interacts, for example, by disproportionation (*d*):

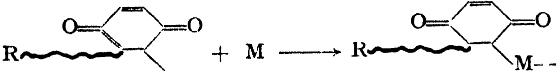

(*c*)

---

[12] Pfann, Williams and Mark, *J. Polymer Sci.*, 1946, **1**, 14.

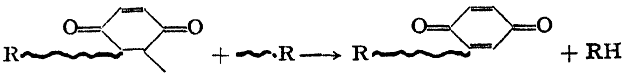
. (*d*)

It is important in the kinetics whether reaction (*c*) or (*d*) is dominant, for the above insoluble difficulty is removed by considering the *eventual* termination to be mutual.

This then transforms retardation into a special case of copolymerisation with unusually low values for certain of the velocity coefficients. The following gives Scheme (1) i.e.,

1. $A \rightarrow P_1$	Rate = Xa
2. $P_r + A \rightarrow P_{r+1}$	$k_{p_{aa}}$
3. $P_r + B \rightarrow Q_{r+1}$	$k_{p_{ab}}$
4. $Q_r + A \rightarrow P_{r+1}$	$k_{p_{ba}}$
5. $Q_r + B \rightarrow Q_{r+1}$	$k_{p_{bb}}$
6. $P_r + P_s \rightarrow A_r + A_s$	$k_{t_{aa}}$
7. $P_r + Q_s \rightarrow A_r + B_s$	$k_{t_{ab}}$
8. $Q_r + Q_s \rightarrow B_r + B_s$	$k_{t_{bb}}$

where A = molecule of monomer, B = molecule of retarder, P_r, Q_r = free radicals of length r units with A and B ends respectively, A_r, B_r = terminated chains with A and B ends respectively.

The contention of Price[13] that chloranil behaves as a chain-transfer agent is also included in Scheme (1), where Q_{r+1} then represents a chain A_r or B_r and a chain nucleus Q_1.

It is now necessary to deduce the relative magnitudes of the velocity coefficients, especially of propagation. Taking the criteria for a retarder that

(*a*) the great stability of Q_r arrests chain growth and

(*b*) a marked reduction in rate is caused by very small concentrations of retarder,

it is at once obtained from (*a*) that

$$k_{p_{ab}} \gg k_{p_{ba}}. \qquad (1)$$

The relative values of $k_{p_{aa}}$ and $k_{p_{ab}}$ are obtained from property (*b*). This is best illustrated by an example containing the orders of magnitude encountered in practice. For example, suppose the polymerisation of 1 g. mol. monomer is effectively retarded, i.e. retardation occurs in most chains, by 10^{-5} molecules of retarder and that the number average chain length is 10^5. Then one inhibitor molecule is used up per 10^5 molecules monomer when its concentration is 10^{-5} times smaller. That is, in practical cases, retarder and monomer are consumed in proportions comparable with their concentrations. This deduction appears to be confirmed by the linear form of the retardation curves in Fig. 4, where relative conditions are maintained for a considerable extent of reaction. Expressed kinetically,

$$\frac{k_{p_{ab}}(\Sigma P_r)(B)}{(B)} \approx \frac{k_{p_{aa}}(\Sigma P_r)(A)}{(A)},$$

i.e.

$$k_{p_{ab}} \approx k_{p_{aa}}. \qquad (2)$$

This example is merely to show that neither term can be neglected with respect to the other. For strong retarders obeying criterion (*a*),

---

[13] Price and Read, *J. Polymer Sci.*, 1946, **1**, 44.

$k_{p_{ab}}$ may be much less than $k_{p_{aa}}$. The various degrees of obedience to (*a*) provides a continuous change from retardation to copolymerisation. By analogy, it is probable that $k_{p_{ba}}$ and $k_{p_{bb}}$ for (Q_r) are comparable, although probability considerations makes the fifth step of Scheme (1) of very rare occurrence.

Summarising these relationships,

$$k_{p_{aa}} \text{ and } k_{p_{ab}} \gg k_{p_{ba}} \text{ and } k_{p_{bb}}. \qquad . \quad . \quad . \quad (3)$$

From copolymer theory, we have for mutual termination the general equation :

$$\frac{-\,\mathrm{d}(\mathrm{A})}{\mathrm{d}t} = \frac{(\mathrm{A})\{\sigma(\mathrm{A}) + (\mathrm{B})\}X_a^{\frac{1}{2}}}{\{\sigma^2\delta_a^2(\mathrm{A}) + 2\phi\sigma\mu\delta_a\delta_b(\mathrm{A})(\mathrm{B}) + \mu^2\delta_b^2(\mathrm{B})^2\}^{\frac{1}{2}}}, \qquad . \quad (4)$$

where $\sigma = \dfrac{k_{p_{aa}}}{k_{p_{ab}}}$, $\mu = \dfrac{k_{p_{bb}}}{k_{p_{ba}}}$, $\delta_a = \dfrac{k_{t_{aa}}^{\frac{1}{2}}}{k_{p_{aa}}}$, $\delta_b = \dfrac{k_{t_{bb}}^{\frac{1}{2}}}{k_{p_{bb}}}$, $\phi = \dfrac{k_{t_{ab}}^{\frac{1}{2}}k_{t_{ba}}^{\frac{1}{2}}}{k_{t_a}^{\frac{1}{2}}k_{t_b}^{\frac{1}{2}}}$,

i.e. $\sigma\delta_a = \dfrac{k_{t_a}^{\frac{1}{2}}}{k_{p_{ab}}}$, $\phi\sigma\mu\delta_a\delta_b = \dfrac{k_{t_{ab}}^{\frac{1}{2}}k_{t_{ba}}^{\frac{1}{2}}}{k_{p_{ab}}k_{p_{ba}}}$, $\mu\delta_b = \dfrac{k_{t_b}^{\frac{1}{2}}}{k_{p_{ba}}}$.

Since the concentration of (A) is in the initial stages almost that of the pure monomer (A_0) and, from criterion (*b*), (A) ≫ (B), (A) can be replaced by a constant (A_0) and σ(A) ≫ (B), as σ is comparable with unity by (2). Hence for the initial stages of polymerisation, (4) is of the form :

$$\frac{-\,\mathrm{d}(\mathrm{A})}{\mathrm{d}t} = \frac{k_1 X a^{\frac{1}{2}}}{\{k_2 + k_3(\mathrm{B}) + k_4(\mathrm{B})^2\}^{\frac{1}{2}}}. \qquad . \quad . \quad . \quad (5)$$

Relating rates to the unretarded rate expressed as

$$\frac{-\,\mathrm{d}(\mathrm{A})}{\mathrm{d}t_{s=0}} = 1, \qquad . \quad . \quad . \quad . \quad . \quad . \quad (6)$$

(5) becomes

$$\frac{-\,\mathrm{d}(\mathrm{A})}{\mathrm{d}t} = \frac{1}{\{1 + K_1(\mathrm{B}) + K_2(\mathrm{B})^2\}^{\frac{1}{2}}}. \qquad . \quad . \quad . \quad (7)$$

Using the simplifying assumption of copolymer theory that

$$k_{t_{ab}} = k_{t_{aa}}^{\frac{1}{2}} \,.\, k_{t_{bb}}^{\frac{1}{2}},$$

(4) is reduced to the form

$$\frac{-\,\mathrm{d}(\mathrm{A})}{\mathrm{d}t} = \frac{1}{1 + k(\mathrm{B})}. \qquad . \quad . \quad . \quad . \quad . \quad (8)$$

The experimental results of rate plotted against benzoquinone concentration for a constant catalyst concentration are shown in Fig. 5. Choice of k in an attempt to obtain a function of type (8) is shown by the broken line, where $k = 0{\cdot}233$. Similarly, the continuous curve shows the best fit for function (7), being expressed by the equation :

$$\text{Rate} = \{1 + 0{\cdot}24(\mathrm{B}) + 0{\cdot}11(\mathrm{B})^2\}^{-\frac{1}{2}}, \qquad . \quad . \quad . \quad (9)$$

where (B) is expressed in molecules × 10^4 per molecule of styrene.

The agreement of (9) with the experimental results is almost within the rather large experimental error, caused mainly by the volatility of quinone *in vacuo*. The deviation from the last experimental point is not unexpected, for the last term in the denominator increases very rapidly with (B), and a slight error in the constant has a much greater effect in this region.

Variation in catalyst concentration can be used as a better criterion of differentiation between the alternative mechanisms than the effect of retarder concentration. According to the proposal[6] that quinones and other retarders act as chain terminators, when retardation is the dominant terminating mechanism and no further account need be taken of the molecule produced, the kinetic derivation gives a first-order dependence on the rate of initiation.[14] This changes with reduction in retarder concentration to a square-root dependence when mutual termination becomes the more important. However, by (5), a square-root dependence on catalyst concentration is anticipated at all degrees of retardation.

To take fullest advantage of this difference, a constant quinone concentration in styrene, with varying catalyst concentrations such that the overall rate is always below 1/10 of the corresponding uninhibited reaction was employed. The former mechanism should thus give an almost first-order dependence of rate on amount of catalyst whereas, according to the above mechanism, the rate should depend on the square root of the concentration. The data for a series of experiments are given in Table VIII, and support closely the copolymer scheme

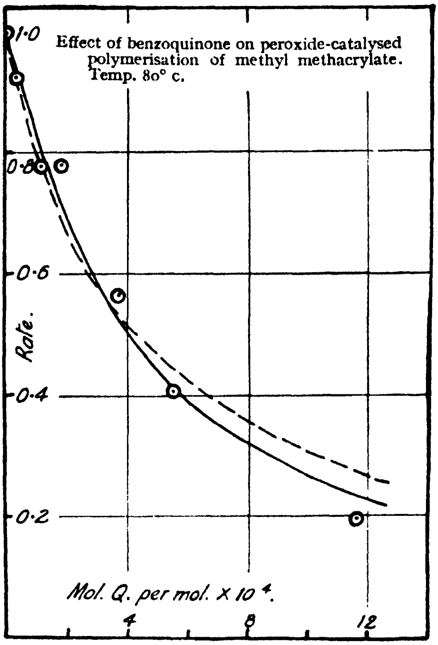

FIG. 5.

The function for the number-average chain length during the retarded polymerisation can be simply derived from the definition,

$$\bar{\nu}_n = \frac{-\,\mathrm{d(A + B)}/\mathrm{d}t}{X_a + X_b},$$

which reduces to :

$$\bar{\nu}_n = \bar{\nu}_0\{1 + K_1(\mathrm{B}) + K_2(\mathrm{B})^2\}^{-\frac{1}{2}} \quad (10)$$

in the case of constant initiation, where ν_0 is the degree of polymerisation of the polymer produced in the uninhibited reaction.

No accurate results for molecular weights have been obtained by absolute instruments, but the trend of decreasing molecular weight with increasing retarder concentration is shown in Table IX. This is an

TABLE VIII.—EFFECT OF VARIATION IN CATALYST CONC. ON QUINONE-RETARDED POLYMERISATION OF STYRENE AT 80° C.

Concentration of quinone 13·5 × 10⁻⁴ mol./mol. monomer.

Conc. of Catalyst (× 10⁴ mol./mol. mono.).	Rate (%/hr.).	$c^{\frac{1}{2}}/r$.	c/r.
2·92	0·98	1·75	2·97
1·46	0·65	1·86	2·24
0·97	0·51	1·93	1·90

---

[14] Gee and Melville, *Trans. Faraday Soc.*, 1944, **40**, 240.

important point since it might have been agreed that these retardation effects were due to a direct interaction between the peroxide of the radicals derived therefrom and the quinone. If this kind of reaction has been responsible, the molecular weight would have *increased* with increasing quinone concentration since fewer chains would have been started.

TABLE IX.—MOLECULAR WEIGHT OF POLYMER PRODUCED DURING RETARDATION.

Conc. of Catalyst (mol./mol. monomer $\times 10^4$).	Conc. of Quinone (mol./mol. monomer $\times 10^4$).	$[\eta]$.
0·95	0	1·2
0·95	0·4	0·70
0·95	1·2	0·38

The above results show that the scheme for retardation (1), considered as a special case of copolymerisation, agrees with the experimental values of change of overall rate affected by change of the two variables, catalyst and retarder, and is also supported qualitatively from molecular-weight determination by viscosity.

Thermal Polymerisation and its Inhibition.*

Kinetics of Thermal Polymerisation.—Evidence has been accumulating[7, 15, 16] in favour of a diradical initiation mechanism for thermal and photochemical polymerisation. The following kinetics for such a progress

$$\left.\begin{array}{lllll}
\text{Initiation} & \left\{\begin{array}{l} 2\mathrm{M} \\ h\nu + 2\mathrm{M}\ (\text{or M}) \end{array}\right. & \begin{array}{l} \longrightarrow \mathrm{P}_2 \\ \longrightarrow \mathrm{P}_2 \end{array} & \begin{array}{c} \dfrac{-\,\mathrm{d(M)}}{\mathrm{d}t} \\ ,, \end{array} & \begin{array}{l} = k_1(\mathrm{M})^2 \\ \quad 2AI \end{array} \\[3ex]
\text{Propagation} & \left\{\begin{array}{l} \mathrm{P}_r + \mathrm{M} \\ \mathrm{Q}_r + \mathrm{M} \end{array}\right. & \begin{array}{l} \xrightarrow{2k_2} \mathrm{P}_r + 1 \\ \xrightarrow{2k_2} \mathrm{Q}_r + 1 \end{array} & \begin{array}{c} ,, \\ ,, \end{array} & \begin{array}{l} \quad 2k_2(\mathrm{P}_r)(\mathrm{M}) \\ \quad k_2(\mathrm{Q}_r)(\mathrm{M}) \end{array} \\[3ex]
\text{Transfer} & \left\{\begin{array}{l} \mathrm{P}_r + \mathrm{M} \\ \mathrm{Q}_r + \mathrm{M} \end{array}\right. & \begin{array}{l} \xrightarrow{2k_3} \mathrm{Q}_r + \mathrm{Q}_1 \\ \xrightarrow{k_3} \mathrm{A}_r + \mathrm{Q}_1 \end{array} & \begin{array}{c} ,, \\ ,, \end{array} & \begin{array}{l} \quad 2k_3(\mathrm{P}_r)(\mathrm{M}) \\ \quad k_3(\mathrm{Q}_r)(\mathrm{M}) \end{array} \\[3ex]
\text{Termination} & \left\{\begin{array}{l} \mathrm{P}_r + \mathrm{P}_s \\ \mathrm{P}_r + \mathrm{Q}_s \\ \mathrm{Q}_r + \mathrm{Q}_s \end{array}\right. & \begin{array}{l} \xrightarrow{4k_4} \mathrm{Q}_r + \mathrm{Q}_s \\ \xrightarrow{2k_4} \mathrm{Q}_r + \mathrm{A}_s \\ \xrightarrow{k_4} \mathrm{A}_r + \mathrm{A}_s \end{array} & \begin{array}{c} \dfrac{-\,\mathrm{d}(\mathrm{P}_r)}{\mathrm{d}t} \\ ,, \\ \dfrac{-\,\mathrm{d}(\mathrm{Q}_r)}{\mathrm{d}t} \end{array} & \begin{array}{l} = 4k_4(\mathrm{P}_r)(\mathrm{P}_s) \\ \quad 2k_4(\mathrm{P}_r)(\mathrm{Q}_s) \\ = k_4(\mathrm{Q}_r)(\mathrm{Q}_s) \end{array}
\end{array}\right\} \quad (11)$$

where P_r = a diradical of chain length r,
Q_r = a monoradical of chain length r,
A_r = a terminated chain of length r.

give results identical with those of Dr. R. R. Smith,[17] but are somewhat simpler and more rigid in symbolism. No note has been made of our knowledge of the significant results of Lewis and co-workers in another field, the phosphorescence of dyes by radiation in the visible, where there is strong evidence of diradical formation by absorption of light quanta by ethylenic compounds.[18]

---

* Our treatment was carried out in 1944-46 and is contained in a Ph.D. Thesis presented to the University of Aberdeen at the end of 1946. Bamford and Dewar have treated the kinetics of diradical reactions in a similar sort of way (*Nature*, 1946, **158**, 380, and *Faraday Soc. Discussion*, 1947, **2**).

[15] Bamford and Dewar, *Nature*, 1946, **157**, 845.

[16] Burnett and Melville (in press).

[17] Dr. R. R. Smith (private communication).

In the above, Scheme (11), the velocity coefficient is defined as the rate of reaction of interaction of unit concentrations of mono-radicals. From simple probability considerations, the appropriate integral multiples are affixed.

Let
$$(\mathrm{P}) = \sum_{2}^{\infty} (\mathrm{P}_r) \quad \text{and} \quad (\mathrm{Q}) = \sum_{2}^{\infty} (\mathrm{Q}_r).$$

When a steady-state is reached,

$$d(\mathrm{P})/dt = 0 = \tfrac{1}{2}k_1(\mathrm{M})^2 + AI - 2(\mathrm{P})\{k_3(\mathrm{M}) + 2k_4(\mathrm{P}) + k_4(\mathrm{Q})\} \quad . \quad (12)$$

$$d(\mathrm{Q})/dt = 0 = 4k_3(\mathrm{P})(\mathrm{M}) + 4k_4(\mathrm{P})^2 - k_4(\mathrm{Q})^2. \quad . \quad . \quad . \quad (13)$$

Combining (12) and (13), and letting (T) = 2(P) + (Q), i.e. (T) represents the total concentration of free bonds in the system,

$$k_1(\mathrm{M})^2 + 2AI = k_4(\mathrm{T})^2. \quad . \quad . \quad . \quad . \quad (14)$$

From (12),
$$\tfrac{1}{2}k_4(\mathrm{T})^2 = 2(\mathrm{P})\{k_3(\mathrm{M}) + k_4(\mathrm{T})\}, \quad . \quad . \quad . \quad (15)$$

whence
$$(\mathrm{P}) = k_4(\mathrm{T})^2/\{4k_3(\mathrm{M}) + k_4(\mathrm{T})\}, \quad . \quad . \quad . \quad (16)$$

and
$$(\mathrm{Q}) = \frac{2k_3(\mathrm{M})(\mathrm{T}) + k_4(\mathrm{T})^2}{2\{k_3(\mathrm{M}) + k_4(\mathrm{T})\}}. \quad . \quad . \quad . \quad (17)$$

From (17), it is obvious that

$$\sum(\mathrm{Q}_r) \text{ formed by transfer} = k_3(\mathrm{M})(\mathrm{T})/\{k_3(\mathrm{M}) + k_4(\mathrm{T})\}, \quad . \quad (18)$$

and
$$\sum(\mathrm{Q}_r) \text{ formed by termination} = k_4(\mathrm{T})^2/2\,\{k_3(\mathrm{M}) + k_4(\mathrm{T})\}. \quad . \quad (19)$$

The *overall rate* is given by

$$-\,d(\mathrm{M})/dt = k_1(\mathrm{M}) - 2AI + (\mathrm{M})\{k_2 + k_3\}(\mathrm{T}), \quad . \quad . \quad (20)$$

which reduces to

$$-\,d(\mathrm{M})/dt = (\mathrm{M})^2\{k_1 + 2AI/(\mathrm{M})^2\}^{\frac{1}{2}}k_4^{-\frac{1}{2}}k_2, \quad . \quad . \quad (21)$$

since
$$k_2 \gg k_1 + 2AI \text{ and } k_3.$$

For thermal polymerisation alone, (21) gives

$$-\,d(\mathrm{M})/dt = k_1^{\frac{1}{2}}k_4^{-\frac{1}{2}}k_2(\mathrm{M})^2. \quad . \quad . \quad . \quad (22)$$

This is an expression identical with that for second-order initiation by monoradicals[14] if k_1 is substituted for the rate coefficient for the production of monoradicals, k_i. Hence the rate of the diradical initiation process is equal to 2½ times that of the corresponding monoradical initiation reaction. This fact greatly simplifies the scheme when retardation and copolymerisation are also involved. The mechanism can be treated as if monoradical initiation occurred and the results are very simply converted.

Number- and weight-average chain lengths are derived as follows :

$$\begin{aligned} d(\Sigma A_r)/dt &= k_3(\mathrm{Q})(\mathrm{M}) + 2k_4(\mathrm{P})(\mathrm{Q}) + k_4(\mathrm{Q})^2 \\ &= (\mathrm{Q})\{k_3(\mathrm{M}) + k_4(\mathrm{T})\}. \quad . \quad . \quad . \quad . \quad (23) \end{aligned}$$

$$\text{Instantaneous } \bar{\nu}_n = \frac{-\,d(\mathrm{M})/dt}{d(\Sigma A_r)/dt} = \frac{k_4(\mathrm{T})^2 + (k_2 + k_3)(\mathrm{M})(\mathrm{T})}{(\mathrm{Q})\{k_4(\mathrm{T}) + k_3(\mathrm{M})\}}.$$

---

[18] Lewis and Kasha, *J. Amer. Chem. Soc.*, 1944, **66**, 2100 ; 1945, **67**, 994.

From (17) and (14),

$$\bar{\nu}_n = 2k_2/\{2k_3 + k_2^{\frac{1}{2}}[k_1 + 2AI/(M)^2]\}^{\frac{1}{2}}. \quad . \quad . \quad (24)$$

For thermal polymerisation, (24) reduces to twice the chain length of the corresponding monoradical process as expected. From (24), the overall number-average chain length is constant with extent of reaction, and is always in value one-half of the overall weight average.

Inhibition and Retardation of Diradical Polymerisation.—The molecular weight and composition of the styrene-inhibitor complex strongly suggests the following simple Scheme (III) for the inhibition period.

$$\text{Initiation}: \quad 2M \rightarrow P_2, \qquad \text{Rate} = X_a \quad . \quad . \quad (25)$$

$$\text{Inhibition}: \quad P_2 + B \rightarrow P_2B \qquad = k_b(P_2)(B) \quad . \quad (26)$$

From the great efficiency of inhibition, reaction (25) is the slow step, and k_b is much greater than the propagation coefficient for the monomer.

Hence $$-\,d(B)/dt = X_a, \quad \text{or} \quad B_0 = X_a(t - t_{B-0}) \quad . \quad . \quad (27)$$

Eqn. (27) expresses the approximate relationship of Goldfinger[2] that the inhibition period, $(t - t_{B-0})$, is proportional to initial inhibitor concentration. However, as there occurs a side-reaction dependent on quinone concentration, the fraction consumed by it is larger for higher concentrations. This accounts for the experimentally observed relative shortening of the induction period. The nature of this side-reaction, by which hydroquinone is produced, is still unknown.

In view of the discontinuity at the end of the inhibition period, it is now convenient to shift the time origin for each curve to the origin of retarded polymerisation. At this point, the concentration of retarder, (X_0), is given by

$$(X_0) = (B_0) - (B_s) \quad . \quad . \quad . \quad . \quad (28)$$

where (B_s) = the amount of quinone used up in the side reaction.

The system is now exactly analogous to that for monoradical initiation given by Scheme (I). As has already been discussed, making a simple substitution of k_1 for k_i, we can utilise the kinetics already developed. If the diradical scheme (II) were separated to include the additional steps, it would become very cumbersome, involving seven different propagation and eight termination possibilities. We may apply eqn. (7) directly to the retardation range as the thermal initiation is constant for the initial stages of conversion here involved. In the previous case, the linear nature of the retarded rate curves justifies the neglect of variation in inhibitor concentration during reaction. With the thermal case, however, the retarded rate curve rapidly changes slope to reach the thermal rate, when (X) = 0. Hence, a variation of retarder from $(X)_0$ to (X) = 0 must be taken into account.

In copolymerisation theory, the values of the two components at any stage in the reaction are inextricably combined in the "copolymer composition" equation,[19] viz.,

$$\frac{d(M)}{d(X)} = \frac{(M)}{(X)} \cdot \frac{\sigma(M) + (X)}{(M) + \mu(X)}. \quad . \quad . \quad . \quad . \quad (29)$$

In general this does not give a simple integral, but for retardation we have the simplification that $(X) \ll (A)$. Assuming σ and μ are, say, within 10^2 and 10^{-2}, we obtain

$$\frac{d(M)}{d(X)} = \frac{\sigma(M)}{(X)}. \quad . \quad . \quad . \quad . \quad . \quad (30)$$

This equation is also gained by division of the following pair, which clearly apply

$$-\,d(M)/dt = k_{p_{aa}}(M)\Sigma(P_r) \quad . \quad . \quad . \quad (31)$$

and $$-\,d(X)/dt = k_{p_{ax}}(X)\Sigma(P_r).$$

[19] Mayo and Lewis, *ibid.*, 1944, **66**, 1594.

Integrating (30) and substituting in (7) gives the function which should fit the experimental curves :

$$-\,d(M)dt = 1/[1 + k_1X_0\{(M)/(M_0)\}^{1/\sigma} + k_2X_0^2\{(M)/(M_0)\}^{2/\sigma}]^{-1/2}. \quad (32)$$

The experimental data given in Fig. 1-3 do not allow of a rigid test of (32) since, besides k_1 and k_2 there are the undetermined quantities X_0 and σ. These curves have, however, a useful general property which is simply checked by experimental results. If all factors, other than retarder concentration, remain constant, then, no matter what retarder concentration is used initially, all the percentage polymer-time curves will be of the same shape. Thus, knowing the initial retarder concentration, the curves should be superposable by suitable adjustment of the origin of co-ordinates. It is found that tracings of these curves on a large scale do accurately fit the upper portions of those of the systems containing larger quantities of retarder.

The complications introduced by the term $(X_0)\{(M)/(M_0)\}^{1/\sigma}$ can in principle be overcome and (7) tested in its original form since the relative values of (X_0) for a series of curves are proportional to their inhibition periods. Hence a series of points of known values of (X) can be plotted on the most retarded curve, from which k_1 and k_2 can be determined from the slopes for any pair. Then a graph of $(X) - t$ can be constructed from the experimental results, and the value of (M) at any time read off from the integrated form of (7). The general shape of the retardation curves has been confirmed in this way, but the accuracy of the values of (X), determined from the end-point of the inhibition periods, is not sufficient to justify drawing curves of form (7) to fit the experimental values.

Discussion of the Mechanism of Inhibition and Retardation.

The above kinetic and analytical results are consistent with the hypothesis that quinones react with monoradicals and suitably spaced diradicals to give different products, in the first case a more stable free radical and in the latter a stable compound.

The proposed inhibition mechanism is at once observed to be closely similar to the Diels-Alder synthesis, as seen from the following examples.

D.A. reaction of acetylene carboxylic acids : [20]

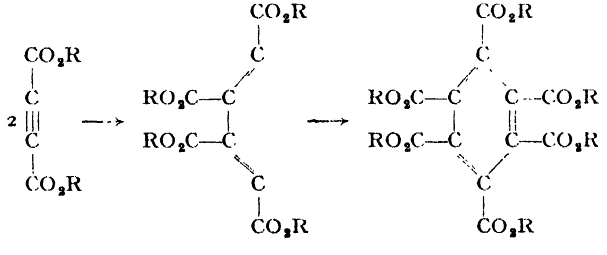

D.A. reaction of butadiene and quinone :

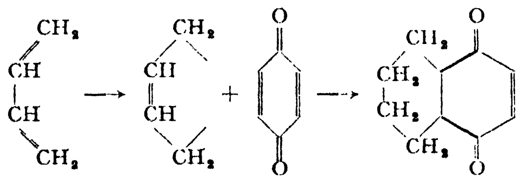

---

[20] Diels, *Ber. B*, 1942, **72**, 1452.

Initiation and inhibition of styrene polymerisation :

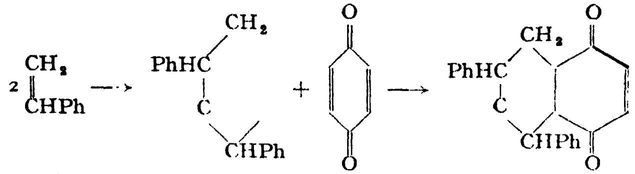

The assumption made here is that activation of the diene really consists in the production of a diradical.

The different nature of short-chain diradicals and monoradicals assists in clarifying otherwise puzzling results, a good example being the extensively studied polymerisation of cyclopentadiene. On heating the pure liquid the dimer is first formed, and later other condensed ring polymers up to the pentamer. This appears to be a simple diradical reaction :

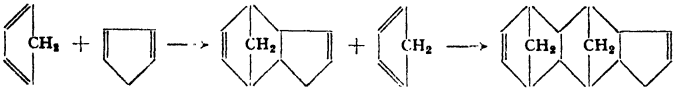

in which it might be said that cyclopentadiene is a good inhibitor of its own polymerisation.

The general applicability of the Diels-Alder reaction indicates that other ethylenic compounds containing the double bonds conjugated with carboxyl groups may be inhibitors of thermal polymerisation, e.g. maleic anhydride. On trial, however, the substance greatly accelerated the rate. Since this compound shows exceptional reactivity in heteropolymerisation, it is possible that it forms half of the original diradical in preference to a second styrene molecule, which diradical cannot attack another anhydride unit. As it structurally resembles quinone, it is thus expected that the latter will also not inhibit the reaction. In a test experiment, a quantity of quinone, which would have completely inhibited the same quantity of styrene present alone for 30 hr., produced a retarded polymerisation but no inhibition.

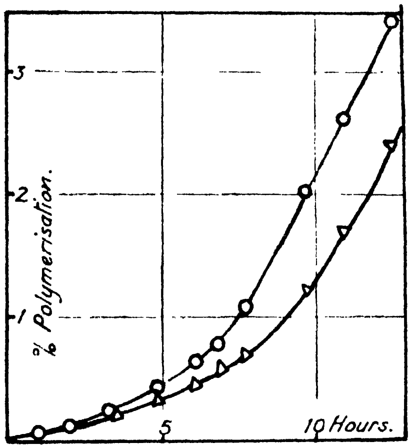

FIG. 6.—Effect of tetraphenyl hydrazine on thermal polymerisation of styrene.

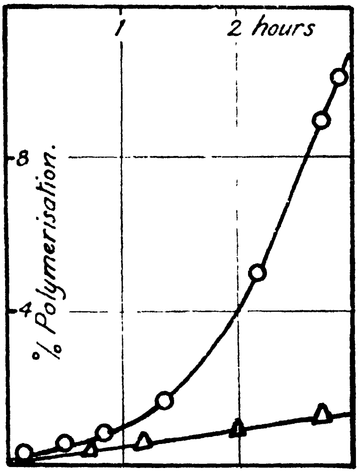

FIG. 7.—Effect of tetraphenyl hydrazine peroxide catalysed polymerisation of methyl methacrylate at 80°C.

It is of interest to study the action of a substance which is expected to reduce the overall rate solely by monoradical termination. In order to terminate a polymer chain without producing another free valency-bond, the substance required is another free radical which will not also initiate polymerisation. It was observed that tetraphenylhydrazine * has a retarding action on the polymerisation of methyl methacrylate and vinyl acetate. Since there is a ready dissociation to long-life free radicals, it appears that these are too stable to initiate polymerisation but capable of reaction with other free radicals, a process requiring less activation energy. On this view, such a chain-terminating substance will act in a similar manner, whether initiation is diradical or monoradical. Fig. 6 and 7 show the effect of tetraphenylhydrazine on the thermal polymerisation of styrene and the peroxide-catalysed polymerisation of methyl methacrylate. In both cases there is a marked retardation but no inhibition, in distinction to the action of quinones.

Mono- and Di-radical Reactions.

The mechanism of initiation of polymerisation is difficult to establish unambiguously from rate and molecular-weight data, e.g. the same results are obtained with the two combinations (*a*) monoradical initiation and termination by combination and (*b*) diradical initiation and disproportionation. The influence of quinones on overall rate gives a simple differentiation between mono- and di-radical chain nuclei in the cases studied. It may be that this method will prove of more general application.

Recent work has shown that the photopolymerisation of vinyl acetate and the uncatalysed photo-polymerisation of methyl methacrylate and styrene are inhibited by quinones, while the benzoyl peroxide-photosensitised polymerisation of vinyl acetate at room temperature is merely retarded. The facts suggest that thermal and photochemical polymerisations essentially involve diradicals and the catalysed reaction monoradicals in the inhibition process.

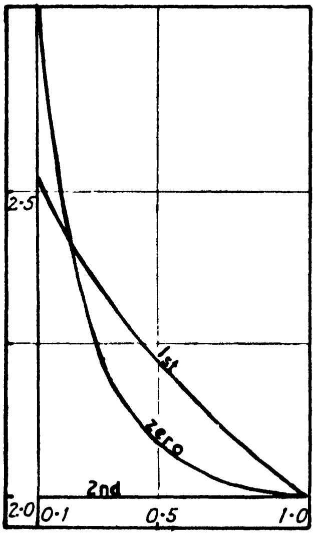

FIG. 8.—Fraction of monomer present. Ratio of overall weight-average to number-average molecular weight.

In photochemical and thermal polymerisation reactions, which are especially suitable for study of the fundamental reaction steps, it has still to be clarified whether the double-unit diradical chain is formed as the primary step by collection of two molecules with the required orientation and energy, or whether there is originally produced a single-unit diradical by accumulation of collisional energy and that inhibition occurs after the first propagation step.

This problem may be solved in a manner which has not so far been explicitly stated in the literature. It has been deduced for all cases that the ratio of the instantaneous weight- to number-average molecular weight is 2/1. However, the overall weight and number averages are not necessarily in this integral proportion. The three cases of zero-, first- and second-order initiation with mutual termination are plotted in Fig. 8. The ratio remains at the initial value of 2/1 for second-order reaction with or without transfer occurring, but the other orders of initiation give a continuous variation with extent of reaction. The osmotic method of measuring overall number-average molecular weights and the light-scattering means for weight average are now of sufficient accuracy to detect this difference of ratio between possible orders of reaction. Experiments are now proceeding with the object of studying the initiation mechanism by this technique.

---

* We are indebted to Mr. A. McLaren for a sample of this substance.

Summary.

An attempt is made to bring the phenomenon of inhibition, retardation and copolymerisation in polymer reactions into relationship with each other as a general aspect of free-radical reactions. Additional data with regard to the effect of retarders of the quinone type on thermal- and peroxide-catalysed polymerisation of styrene and the peroxide-catalysed polymerisation of methyl methacrylate is presented to illustrate some of the points brought forward in the general classification. Among other matters it is shown, in the case of styrene, that quinone completely suppresses the thermal polymerisation but only retards the peroxide-catalysed polymerisation. In the former reaction a product has been isolated during the period of inhibition corresponding approximately to two molecules of styrene and one of quinone. These results are best interpreted by supposing that in the thermal polymerisation the initial step is the creation of a diradical formed by the collision of two molecules of styrene, whereas in the peroxide reaction only mono-radicals are naturally produced.

Another new observation, also compatible with the general view-point is that in the quinone-retarded peroxide-catalysed polymerisation of methyl methacrylate the rate is proportional to the square root of peroxide concentration and not to the first power as might be expected. This observation is explicable on the assumption that the polymer radical attacks the quinone molecule forming an inactive radical which ultimately disappears by interaction with other radicals present in the system.

Chemistry Department,
University of Aberdeen.

THE HYDRATION OF ETHYLENE OXIDE.

By H. J. Lichtenstein and G. H. Twigg.

Received 16*th August*, 1947, *as revised* 22*nd December*, 1947.

The addition of water to ethylene oxide to form glycol has been studied by Brönsted, Kilpatrick and Kilpatrick[1] in neutral and acid solution. Values at 20° C. were obtained by these authors for the velocity constants of the uncatalysed and the hydrogen ion-catalysed reactions. These constants were measured by a dilatometric method and the authors report that " experiments in NaOH solutions up to 0·1 M. showed the effect of hydroxyl ion to be negligible."

However, in experiments which we have made on the production of ethylene oxide from ethylene chlorhydrin, the quantity of glycol found was in excess of that to be expected on the basis of an uncatalysed reaction alone. Further investigation, following the reaction analytically, has shown the existence of a hydroxyl ion-catalysed reaction between water and ethylene oxide to form glycol. A passing reference to this effect of hydroxyl ion has also been made in a recent paper by Porret.[2]

Experimental.

Reactions were carried out in stoppered conical flasks immersed in a thermostat bath. Samples were removed at frequent intervals and the ethylene oxide estimated by a modification of Lubatti's method.[3] The ethylene oxide which had reacted was periodically checked by determination of the glycol formed according to the periodate method (Voris, Ellis and Maynard [4]). It was found that ethylene glycol is the only product of the reaction within the limits of accuracy obtained in our experiments.

---

[1] Brönsted, Kilpatrick and Kilpatrick, *J. Amer. Chem. Soc.*, 1929, **51**, 428.
[2] Porret, *Helv. chim. Acta*, 1944, **27**, 1321.

The original method of Lubatti [3] is chiefly applicable to estimations of gaseous ethylene oxide, and for aqueous solutions the addition of solid magnesium chloride is recommended. In the present experiments, however, it was preferred to use as reagent a saturated solution of $MgCl_2$ acidified with 50 % H_2SO_4 to give a strength of 0·2 N. acid. A blank on the acidity was done periodically ; the acidity remained constant over a period of two months. Methyl orange was the indicator used. With this method, it was found on checking with weighed amounts of ethylene oxide that the estimates of ethylene oxide were low, and varied according to the size of the aqueous sample. By standardising the procedure and using a factor, reliable and reproducible results were obtained.

Mechanism of Lubatti's Method.

The explanation which has been given by Lubatti [3] for the mechanism of the reactions involved in this estimation is not satisfactory, particularly in regard to the failure of the reaction to estimate 100 % of the ethylene oxide. Lubatti regards the reaction as occurring between HCl and the oxide, and suggests that the salt may act " in two ways : first by increasing the effective concentration or activity of the acid ; secondly, by binding the water of solution and hindering hydrolysis."

Deckert [5] points out that the reactions

$$\begin{array}{lll}
\text{(I)} & (CH_2)_2O + H_2O & \longrightarrow (CH_2OH)_2 \\
\text{(II)} & (CH_2)_2O + H_2O + H_3O^+ & \longrightarrow (CH_2OH)_2 + H_3O^+ \\
\text{(III)} & (CH_2)_2O + H_2O + Cl' & \longrightarrow CH_2OH{-}CH_2Cl + OH' \\
\text{(IV)} & (CH_2)_2O + H_3O^+ + Cl' & \longrightarrow CH_2OH{-}CH_2Cl + H_2O
\end{array}$$

studied by Brönsted *et al.*[1] have a bearing on this question, but fails to draw any conclusions. Quantitative examination of Brönsted's results shows that under the conditions of estimation of ethylene oxide (i.e. high hydrogen ion concentration) reactions (I) and (III) are relatively too slow to be significant. Reaction (IV) is the reaction by which ethylene oxide is determined ; reaction (II) produces glycol and therefore causes the failure of the method to estimate 100 % of the ethylene oxide present.

A rough idea of the efficiency of this estimation can be obtained by using the velocity constants given by Brönsted *et al.* If c and g are the concentrations of ethylene chlorhydrin and glycol respectively formed at time t, and x is that of the ethylene oxide, the kinetic equations are

$$\frac{dg}{dt} = k_2 x [H^\bullet] \quad . \quad . \quad . \quad . \quad . \quad . \quad (1)$$

and

$$\frac{dc}{dt} = k_4 x [H^\bullet][Cl'] \quad . \quad . \quad . \quad . \quad . \quad (2)$$

hence

$$\frac{dg}{dc} = \frac{k_2}{k_4[Cl']}.$$

Since the chloride ion concentration does not change appreciably during the estimation this can be integrated and at the completion of the reaction the ratio of glycol to chlorhydrin G/C equals $k_2/k_4[Cl']$; the efficiency of estimation is

$$\frac{C}{G + C} = \frac{k_4[Cl']}{k_2 + k_4[Cl']}. \quad . \quad . \quad . \quad . \quad . \quad (3)$$

The values for k_2 and k_4 given by Brönsted *et al.* are at 20° C., $k_2 = 0{\cdot}32$ l. mole.$^{-1}$ min.$^{-1}$, and $k_4 = 1{\cdot}3$ l.^{2} mole.$^{-2}$ min.$^{-1}$. These values were determined in dilute solution and it is therefore not permissible simply to extrapolate them to the high concentrations used in the estimation of ethylene oxide. However, these figures give an indication of the order of efficiency to be expected, and eqn. (3) shows how the efficiency will fall off as the reagent is diluted.

---

[3] Lubatti, *J. Soc. Chem. Ind.*, 1932, **51**, *T*, 361.

[4] Voris, Ellis and Maynard, *J. Biol. Chem.*, 1930, **133**, 491.

[5] Deckert, *Z. anal. Chem.*, 1937, **109**, 166.

For example, with a saturated solution of $MgCl_2$ (46·7 g. $MgCl_2$/100 cc.), the efficiency should be 97·6 %; Lubatti [3] gives 98·9 % (experimentally determined). With a more dilute solution of chloride ions, e.g. 30·9 g. NaCl/100 cc. the efficiency is calculated to be 95·5 % and Lubatti finds 94·0 %.

The discrepancy between the calculated efficiencies and those determined by Lubatti is somewhat greater at the lower chloride ion concentrations, but the order of agreement is sufficient to confirm the view that the mechanism of the estimation of ethylene oxide is as stated here.

In the present experiments, the estimation was done by adding 2 cc. of the aqueous solution to 50 cc. of the reagent; the efficiency of estimation under these conditions was found, as a mean of three experiments, to be 96·8 % (in close agreement with calculations on the above basis) and the true concentration of ethylene oxide was calculated using this factor.

Results.

(A) The Uncatalysed Reaction.—The first-order velocity constants (k_0) were determined from the slope of the plots of the $\log_e$ [ethylene oxide] against time (Table I).

As this reaction is so much slower than the catalysed reactions (Brönsted *et al.* find a unimolecular constant of $2{\cdot}16 \times 10^{-5}$ at 20° c. corresponding to a half-time of 23 days), care has to be taken to keep the *p*H value at 7·0 to 8·0 throughout the reaction by the addition of a drop of dil. NaOH at the beginning of the reaction. The very slow reaction at 20° c. could not be carried very far, and accurate measurements of the velocity constant using this technique were not possible; discrepancies may be due to contamination by CO_2. However, the values found agree fairly well with Brönsted's value obtained by a dilatometric method.

TABLE I

T °c.	k_0 obs. (min.$^{-1}$).	
20·0	$2{\cdot}16 \times 10^{-5}$	(*a*)
20·0	$2{\cdot}5 \times 10^{-5}$	
30·2	$5{\cdot}45 \times 10^{-5}$	
48·0	$3{\cdot}55 \times 10^{-4}$	
70·3	$2{\cdot}68 \times 10^{-3}$	
113	$5{\cdot}1 \times 10^{-2}$	(*b*)
123	$1{\cdot}17 \times 10^{-1}$	
131	$1{\cdot}73 \times 10^{-1}$	

(*a*) Brönsted, Kilpatrick and Kilpatrick, *J. Amer. Chem. Soc.*, 1929, **51**, 428.

(*b*) H. M. Stanley and G. Minkoff (private communication); these experiments were carried out in a flow system under pressure.

Experiments were carried out at several temperatures and $\log_e k_0$ was plotted against the reciprocal of the absolute temperature. Also included are some values obtained by a different technique; all points were found to lie accurately on a straight line, from the slope of which the energy of activation for the catalysed reaction was found to be 19·0 ± 0·3 kcal.mole.$^{-1}$. The unimolecular velocity constant is then $3{\cdot}19 \times 10^9 e^{\frac{-19{,}000}{1{\cdot}99T}}$ min.$^{-1}$.

(B) The Hydroxyl Ion-Catalysed Reaction.—The conversion of ethylene oxide to glycol was carried out in the presence of NaOH; plots of $\log_e$ (ethylene oxide) against time were straight lines, showing that the reaction is first order with respect to ethylene oxide.

Effect of Ethylene Oxide Concentration.—The effect of ethylene oxide concentration is shown in Table II at a constant NaOH concentration of 1·010 M.

Although the experimental error is relatively large, the results show that, with increasing ethylene oxide concentration, there is no regular change in k_{OH}. The reaction is truly first order with respect to ethylene oxide.

Effect of Hydroxide Concentration.—The effect of the hydroxide concentration is given in Table III at an ethylene oxide concentration of 1·1 to 1·3 M.

k_{OH} is not constant here, but increases with the hydroxide concentration according to the equation, $10^3 k_{OH} = 3{\cdot}9 + 1{\cdot}0\,[OH']$ l. moles^{-1} min.$^{-1}$. This appears to be a primary salt effect of the type to be expected in reactions between an ion and an uncharged molecule. Owing to the high concentrations used, the effect observed is considerable, but it would amount to an increase in velocity constant of about 2·5 % in 0·1 N. NaOH, as compared with a 9 % increase at 0·1 N. salt concentration found by Brönsted *et al.* in the acid-catalysed reaction.

These experimental results show that besides the uncatalysed and the hydrogen ion-catalysed reactions, a hydroxyl ion-catalysed reaction exists. The general expression for the first-order velocity constant in this case is :

$$k = k_0 + k_H[H^{\bullet}] + k_{OH'}[OH'].$$

In comparison with other reactions in which there is a catalysis of this type, the value of k_{OH} is abnormally low. The ratio k_{OH}/k_H is about 10^{-2}, whereas in the case of the hydrolysis of esters and amides, it is generally about 10^4. Similarly, the ratio k_{OH}/k_{H_2O} (where $k_{H_2O} = k_0/55{\cdot}5$) is about 10^4 here in contrast to a number of examples [*] where the ratio is of the order of 10^{11}. On the other hand, the hydrolysis of ethers is not a reaction in which a hydroxyl ion catalysis has so far been observed. The relative smallness of k_{OH} accounts for the fact that at the lower concentrations investigated by previous workers the hydroxyl ion-catalysed reaction was overlooked.

TABLE II

k = observed first order constant ; k_0 = velocity constant of the uncatalysed reaction (Table I) ; k_{OH} = $(k - k_0)$ divided by the hydroxide concentration ; T = 20·0° C.

Expt. No.	C_2H_4O moles/l.	k (min.$^{-1}$).	$k-k_0$ (min.$^{-1}$).	k_{OH} (l. mol.$^{-1}$ min.$^{-1}$).
119D	0·135	$5{\cdot}47 \times 10^{-3}$	$5{\cdot}45 \times 10^{-3}$	$5{\cdot}40 \times 10^{-3}$
156C	0·221	$4{\cdot}36 \times 10^{-3}$	$4{\cdot}34 \times 10^{-3}$	$4{\cdot}30 \times 10^{-3}$
156B	0·299	$4{\cdot}46 \times 10^{-3}$	$4{\cdot}44 \times 10^{-3}$	$4{\cdot}40 \times 10^{-3}$
119C	0·309	$5{\cdot}02 \times 10^{-3}$	$5{\cdot}02 \times 10^{-2}$	$4{\cdot}96 \times 10^{-3}$
119B	0·543	$5{\cdot}40 \times 10^{-3}$	$5{\cdot}38 \times 10^{-3}$	$5{\cdot}33 \times 10^{-3}$
119A	0·861	$5{\cdot}21 \times 10^{-3}$	$5{\cdot}19 \times 10^{-3}$	$5{\cdot}14 \times 10^{-3}$
41	0·740	$4{\cdot}81 \times 10^{-3}$	$4{\cdot}79 \times 10^{-3}$	$4{\cdot}75 \times 10^{-3}$
71	1·092	$4{\cdot}93 \times 10^{-3}$	$4{\cdot}91 \times 10^{-3}$	$4{\cdot}86 \times 10^{-3}$
			Mean value	$4{\cdot}85 \times 10^{-3}$

TABLE III

T = 20·0° C.

Expt. No.	Molarity NaOH.	k (min.$^{-1}$).	$k-k_0$ (min.$^{-1}$).	k_{OH} (l. mol.$^{-1}$ min.$^{-1}$).
122E	0·257	$1{\cdot}04 \times 10^{-3}$	$1{\cdot}02 \times 10^{-3}$	$3{\cdot}97 \times 10^{-3}$
122D	0·511	$2{\cdot}32 \times 10^{-3}$	$2{\cdot}30 \times 10^{-3}$	$4{\cdot}51 \times 10^{-3}$
156D	1·010	$4{\cdot}93 \times 10^{-3}$	$4{\cdot}91 \times 10^{-3}$	$4{\cdot}86 \times 10^{-3}$
122C	1·030	$5{\cdot}46 \times 10^{-3}$	$5{\cdot}44 \times 10^{-3}$	$5{\cdot}28 \times 10^{-3}$
122B	1·540	$8{\cdot}69 \times 10^{-3}$	$8{\cdot}67 \times 10^{-3}$	$5{\cdot}63 \times 10^{-3}$
122A	2·020	$11{\cdot}68 \times 10^{-3}$	$11{\cdot}66 \times 10^{-3}$	$5{\cdot}77 \times 10^{-3}$

Activation Energy.—Values of $k_{OH'}$ were found at 3 temperatures (Table IV). Owing to the speed of the reaction at higher temperatures the hydroxide concentrations could not be made strictly comparable. The value at 20° C. was obtained by extrapolation of the results given in Table III to 0·1 M. hydroxide.

TABLE IV

Expt. No.	Molarity.		T (°C.).	$k_{OH'}$ (l. mol.$^{-1}$ min.$^{-1}$).
	NaOH.	C_2H_4O.		
Extrapolated	0·100	1·010	20·0	$3{\cdot}90 \times 10^{-3}$
44	0·100	1·050	48·0	$6{\cdot}40 \times 10^{-2}$
81	0·050	0·421	70·3	$3{\cdot}66 \times 10^{-1}$

---

[*] See Bell, *Acid-Base Catalysis* (Oxford, 1941), p. 92.

From the graph of log $k_{OH'}$ against $1/T$ the energy of activation is found to be 18·1 ± 1·0 kcal. mole^{-1}. The velocity constant for the catalysed reaction can be expressed as $1\cdot23 \times 10^{11}\, e^{\frac{-18,000}{1\cdot99T}}$ l. mole^{-1} min.$^{-1}$.

The authors wish to thank the Distillers' Company Limited for permission to publish these results.

Summary.

The hydration of ethylene oxide to ethylene glycol was studied in neutral and in alkaline solutions and at different temperatures and concentrations. In alkaline solution a hydroxyl ion-catalysed reaction, in addition to the uncatalysed reaction, occurs. The reaction is of the first order with respect to ethylene oxide and shows a small positive primary salt effect. The energies of activation for the uncatalysed and the hydroxyl ion-catalysed reactions were obtained.

The mechanism of Lubatti's method for estimating ethylene oxide is discussed.

The Distillers Company, Limited,
Research and Development Department,
Great Burgh,
Epsom, Surrey.

MONOLAYERS OF SOME DIESTERS.

By J. T. Davies.

Received 2nd February, 1948.

Many studies of monolayers of dibasic acids and esters have been made by Adam and co-workers,[1] using both potential and pressure measurements. The usual effect of adding a second polar group to a long hydrocarbon chain is to expand the film, and the diethyl ester with 11 CH_2 groups between the ester groups gives the most perfect gaseous films found, the product of the surface pressure, Π, in dynes cm.$^{-1}$, and the area in A.^{2} per molecule, being close to the theoretical value of 400, at the greatest areas. As the area is diminished there is a slight dip in the ΠA plot, attributed to the influence of lateral adhesions, but below 180 A.^{2} there is a steady and considerable rise in ΠA, undoubtedly due to the fact that the molecules, lying flat in the surface, occupy a large fraction of the area. The 16 CH_2 diester shows a second fall in ΠA, noticeable below 140 A.^{2}, due to the lateral adhesions between the molecules causing aggregation into the condensed state.

The film potentials of diesters were measured by Adam, Danielli and Harding,[2] using compounds in which the two polar groups were separated by 11 and 16 CH_2 groups. These authors found that the surface moments were constant at areas greater than 140 A.^{2}, being 1200 milli Debyes for the 11 CH_2 ester and 1120 mD. for the 16 CH_2 homologue. The value for one polar group, about 600 mD., is quite unusually large. At 140 A.^{2} the 16 CH_2 ester was found to start condensing ; and μ, the surface moment, decreased sharply, and fluctuated, showing the film to be inhomogeneous.

In the condensed state the molecules are considered to be oriented vertically, with one polar group in the surface and one away from it. Adam, Danielli and Harding [2] have studied the 20 and 32 CH_2 derivatives, which both give condensed films, and have found μ to be as low as 340 mD.

---

[1] Adam and Jessop, *Proc. Roy. Soc. A*, 1926, **112**, 376.
[2] Adam, Danielli and Harding, *ibid.*, 1934, **147**, 491.

The present investigation was undertaken to find the effect of changing the positions of the polar groups while the number of CH_2 groups in the molecule was kept constant. In the molecule $RO_2C . (CH_2)_n . CO_2R$, R is called the "end chain." The $(CH_2)_n$ is the "middle chain." As the carbonyl groups become closer together, the end chains will become freer, and, not necessarily lying in the surface, should permit compression of the film to a certain area corresponding to that part of the molecule held in the water surface by the attraction of the polar groups. Further compression will necessitate reorientation of the hydrocarbon part formerly lying in the interface, and the removal of one of the polar groups from the water. This process would be hindered by long end chains.

Experimental.

The usual surface balance and amplifying circuit were employed. Water was redistilled in an all-glass Pyrex apparatus.

The melting-points of the esters were :

Dilauryl oxalate : 38·7-38·9° C.
Didecyl adipate : 26·8-27·2° C.
Dioctyl sebacate : 18·2-18·4° C.
Dibutyl thapsate : 32·3-32·5° C.

Results.

In Fig. 1 are given the Π-A and μ-A curves for the various esters on N./100 HCl at 22° C. Those studied were dilauryl oxalate, didecyl adipate, dioctyl sebacate and dibutyl thapsate. The curves for $HO_2C . (CH_2)_{24} . CO_2H$ and $EtO_2C . (CH_2)_{20} . CO_2Et$ are also included from the results of Adam and Jessop,[1] and the potential of the latter substance from the work of Adam, Danielli and Harding.[2] These molecules all have a total number of carbon atoms of 26, except for dibutyl thapsate, which has 24. When the carboxyl groups in the molecule are brought closer together, in passing from dibutyl thapsate to dilauryl oxalate, the areas at a given pressure decrease regularly, and, in the case of didecyl adipate and dilauryl oxalate the film is no longer gaseous. The characteristic plot for a film obeying the ideal gas law is included for purposes of reference.

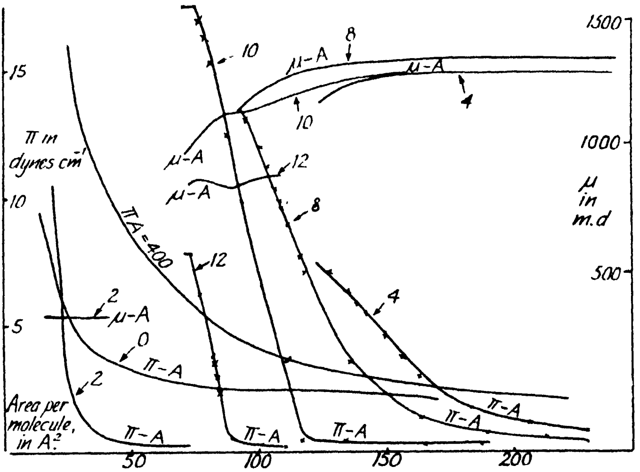

FIG. 1.—The numerals against the curves refer to numbers of carbon atoms in each end chain.

The diethyl ester gives a condensed film, with an area of about 20 Å.^{2} per molecule, and Adam and Jessop [1] found that films of the dibasic acid,

$$HO_2C . (CH_2)_{24} . CO_2H$$

gave gaseous characteristics, but that at 2 dynes, the area was about two-thirds that of the 16 CH_2 diethyl ester. They suggested that this greater cohesional correction was due to the enhanced attraction of the carboxyl groups between neighbouring molecules in the film. The acid film was rather unstable at higher pressures, and visible aggregates formed in the surface.

The potentials observed in the gaseous phase indicated a constant value of μ for the esters till about 140 A.^{2} per molecule, when a falling-off was observed, a phenomenon similar to that observed by Adam, Danielli and Harding.[2] The monolayers of didecyl adipate and dilauryl oxalate gave fluctuating potentials at areas greater than 165 A.^{2} and 110 A.^{2} respectively, indicating the formation of islands of material. The potential of dilauryl oxalate was much lower than that of the other esters at similar areas.

Plots of ΠA against Π (Fig. 2) showed a much greater deviation than those of Adam and Jessop,[1] from the theoretical value of 400 for ΠA, indicating that the esters used in the present work have a greater cohesional attraction than those studied by the former authors.

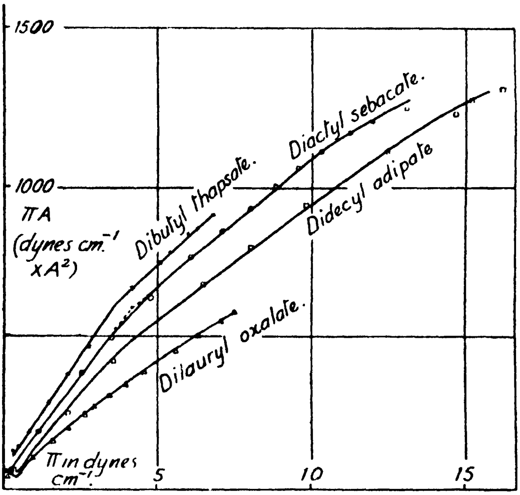

FIG. 2.

Discussion.

In Fig. 3 are plotted the moments at 2 and 7 dynes cm.$^{-1}$ for the various esters against the number of carbon atoms in each end chain. The number of CH_2 groups in the central portion of the molecule is 24, less twice the number in each end chain (except for dibutyl thapsate, which has two carbons fewer in the water surface). It is seen that the moments lie on a smooth curve, both at 2 and at 7 dynes cm.$^{-1}$. There is a maximum when there are six carbon atoms in each end chain, i.e. 12 carbon atoms in the middle portion and a total of 12 in the end chains. The maximum means that the polar groups can exert their greatest effect and any increase or decrease in the number of carbons in the end chains will lessen the contribution, due either to twisting the dipoles away from their positions of greatest vertical component, or by making possible a form which can more easily lose one polar group from the water surface.

The same figure shows the areas per molecule at 2 and 7 dynes cm.$^{-1}$. There is again a maximum at about the same point, indicating a maximum randomness when there is the same number of carbon atoms in the end chains as in the central portion of the molecule. The packing of the molecules in the surface is thus least dense at this point, evidently on account of lower van der Waals' forces between the hydrocarbon chains. A longer middle portion makes possible condensed films, and longer end chains also adhere together more strongly. When the change from the ethyl ester to the free acid is considered, there is not only the effect of increased van der Waals' forces between the middle chains, four carbons longer, but also the more powerful repulsion at small distances by the polar forces of the free carboxyl groups, previously esterified, which evidently exceeds the increased attraction, and an expansion results.

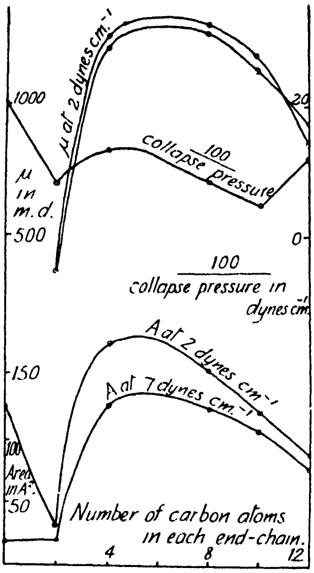

FIG .3.

In Fig. 3 are plotted also the reciprocals of the pressures at which the films collapse. Again the curve shows a maximum at the most "random" structure, which gives a monolayer less stable to pressure than one with long middle or end chains, both of which evidently facilitate adhesion, and give films less easily broken than the random structure. The increase in passing to the acid itself is seen in the graph, indicating that the repulsion between the carboxyl groups in the condensed state renders the film unstable to pressure.

There is also an interesting increase as the number of end chain carbon atoms increases from 10 to 12. The latter number is that of the dilauryl oxalate, and the two hydrocarbon chains joined to the contiguous polar groups interfere somewhat at this point unless extensive twisting occurs. This phenomenon opposes the van der Waals' attraction of the long chains, and a decreased stability to pressure results.

It is possible to correlate the areas with the distance apart of the polar groups in a different way, by making models of the molecules, and assuming that the polar groups hold the middle chain completely in the surface. The results are summarised in Table I.

The models were made from atoms built to scale, and the bond moments

TABLE I.—AREAS IN A.^{2}. MOMENTS IN MILLIDEBYES.

	Dibutyl Thapsate.	Dioctyl Sebacate.	Didecyl Adipate.	Dilauryl Oxalate.
Max. area of electrical homogeneity	∞	∞	165	110
Model area, molecule lying flat	157	163	167	160 (112)
Breaking area	124	93	73	74
Min. area from model	124	91	70	—
Area at which μ begins decreasing	155	135	140	(100)
Kink in Π-$A\Pi$ plot	154	133	—	—
μ at lowest pressure (observed)	1290	1330	1270	870
μ at lowest pressure (calculated)	1060	1060	1060	870
μ at break-point (observed)	1190	1150	1000	840
μ at break-point (calculated)	992	992	992	870
$\Delta\mu$ (observed)	100	180	270	30
$\Delta\mu$ (calculated)	68	68	68	0

of esters of Alexander and Schulman[3] were assumed to apply, and the moment results are compared with those observed in Table I. The differences between the values thus calculated and those found may be due to the dielectric constant of the surface being different from that in the case of monoesters, for which Alexander and Schulman worked out their ester bond moments. In the diester, since there is an even number of carbon atoms between the polar groups, a twist in the chain is necessary if both polar groups are to be oriented in the position of maximum vertical component. The minimum area corresponds to the end chains being vertically oriented with respect to the surface. There is, for these esters, no evidence that a polar group can be lifted out of the surface, such a process evidently being hindered by the long end chains.

It is interesting to note that the observed and calculated values of the moment agree closely for didecyl adipate in the compressed state, and for dilauryl oxalate, in both of which cases the arrangement of chains above the surface is similar to that in a compressed monoester film. In the case of dilauryl oxalate, the area of 112 A.^{2} corresponds to a V-shaped molecule, with the chains arranged regularly, and as far apart as possible.

The ΠA-Π plots shown in Fig. 2 for the four esters, dibutyl thapsate, dioctyl sebacate, didecyl adipate and dilauryl oxalate are not linear. If a van der Waals' equation held, i.e. the molecules were incompressible, the plot should be a straight line, with slope equal to the area occupied by a molecule in the surface. At higher pressures, this area is seen from the observed ΠA-Π plots to decrease, and, in the cases of dibutyl thapsate and dioctyl sebacate, there are discontinuities corresponding to areas of 154 A.^{2} and 133 A.^{2} respectively. There are no obvious kinks in the ΠA-Π plots of the other esters, but the slope decreases gradually. The slope at the lowest pressures give areas rather less than the maximum ones deduced from the models, and ΠA is very far from the ideal value of 400; even at 0·4 dyne it is 100 or less for the different ester molecules.

The author thanks sincerely Prof. E. K. Rideal, F.R.S., for continual help and encouragement. His thanks are also due to the Anglo-Iranian Oil Company for a gift of the esters, and the Council of Canterbury College, University of New Zealand, for an award of the Lord Rutherford Memorial Research Fellowship.

Summary.

Force-area and surface moment-area curves have been determined for four dibasic esters, dilauryl oxalate, didecyl adipate, dioctyl sebacate and dibutyl thapsate. As the ester linkages become more widely separated, the total number of carbon atoms remaining constant, the films expand.

A plot of areas at 2 and 7 dynes cm.$^{-1}$ against the number of carbon atoms in each end chain has been drawn, including the results of Adam and Jessop[1] for $HO_2C.(CH_2)_{24}.CO_2H$ and $EtO_2C.(CH_2)_{20}.CO_2Et$. Similar plots of μ and the reciprocal of the breaking pressure are also drawn, and in all cases a maximum is found close to the point where the number of carbon atoms in the end chains is equal to the number in the middle of the molecule.

Models of the various molecules have been constructed, and have been used to find the areas occupied in the surface when the end chains are vertical, and in the surface. The results agree well with experiment.

Davy Faraday Research Laboratory,
The Royal Institution,
21 Albemarle Street,
London, W.1.

---

[3] Alexander and Schulman, *Proc. Roy. Soc. A*, 1937, **161**, 115.

INTERMOLECULAR POTENTIALS IN NEON AND ARGON.

By J. Corner.

(*Communicated by* Sir John Lennard-Jones, F.R.S.)

Received 25th June, 1947, as revised 4th Febraury, 1948.

To determine intermolecular forces from a macroscopic property it is necessary that it be measurable experimentally with sufficient accuracy, and that there should be a secure theoretical foundation. The latter has been the limiting factor in the past, and explains why most work has been devoted to the analysis of equilibrium properties of gases at low densities; at first it was the second virial coefficient which was used for this purpose, but recently Hirschfelder, Ewell and Roebuck [1] have shown that the Joule-Thomson coefficient (extrapolated to zero density) can also be used. Recently, too, use has been made of experimental data on the solid state, by Herzfeld and Göppert-Mayer,[2] Kane [3] and Rice.[4] The theory of the liquid state is not yet so advanced that experimental data on liquids can be given great weight in such an analysis.

It has been necessary to have at least three arbitrary constants in the intermolecular potential, so it has been possible to reach a unique potential only when experimental data have been available for a wide range of temperature, and, moreover, when the data have covered as many properties as possible. For example, the intermolecular potential

$$E(r) = [6(r_0/r)^n - n(r_0/r)^6]\epsilon/(n-6), \quad . \quad . \quad . \quad (1)$$

where r is the distance between the centres of the molecules and r_0 the value of r at the minimum, leads to a second virial coefficient which has been expressed as a convergent series by Lennard-Jones,[5] and which can therefore easily be compared with experiment. There are three arbitrary constants in this potential, namely ϵ (the depth of the potential well), r_0 (the separation at which this minimum is attained) and n. It usually happens that for any n within the range of, say, 9 to 18, one can pick ϵ and r_0 to give a good fit to the observed second virial coefficient over a long temperature range. To fix the right n, it is essential to use some other property, such as the lattice distance or heat of sublimation, both taken at 0° K. to reduce uncertainties in the theory. The typical behaviour (cp. Fowler [6]) has been a disagreement in the values of n indicated by these two properties; it has been shown (Corner [7]) that this has been due partly to omission of the effect of the zero-point energy on the lattice distance. It will be made clear in the present paper that, at any rate for neon and argon, much of the remaining discrepancy arises from taking the most uncertain of the fitting processes at too early a stage.

Hirschfelder, Ewell and Roebuck [1] tried to fit the Joule-Thomson coefficient of argon with their theoretical expression derived from (1). It was not possible to get agreement for any values of the three arbitrary constants, and they concluded that this was probably due to the inadequacy of the form (1) for the intermolecular potential. They suggested that it might be possible to get agreement by using a repulsive potential of exponential type, $e^{-\alpha r}$, rather than an inverse power, r^{-n}.

---

[1] Hirschfelder, Ewell and Roebuck, *J. Chem. Physics*, 1938, **6**, 205.

[2] Herzfeld, and Göppert-Mayer, *Physic. Rev.*, 1934, **46**, 995.

[3] Kane, *J. Chem. Physics*, 1939, **7**, 603.

[4] Rice, *J. Amer. Chem. Soc.*, 1941, **63**, 8.

[5] Lennard-Jones, *Proc. Roy. Soc. A*, 1924, **106**, 463.

[6] Fowler, *Statistical Mechanics* (Cambridge, 1936), Ch. X.

[7] Corner, *Trans. Faraday Soc.*, 1939, **35**, 711.

There had been several indications that such an exponential repulsion would probably be more accurate than any inverse power (Born and Mayer,[8] Bleick and Mayer,[9] Huggins [10]). The objection to its use in this connection has been that to evaluate second virial or Joule-Thomson coefficients for this law of force it is necessary to use numerical integration. Buckingham [11] devised a less laborious, but approximate, method of finding the constants of an exponential repulsive potential by fitting to observed second virial data. In this process any changes in the data would make it necessary to repeat most of the work, and the accuracy of the derived potential is not easily determined. Buckingham's results were a pair of laws in non-overlapping regions, leaving some doubt as to the values in the intermediate region; with a smooth interpolation these potentials for neon and argon did, however, give good agreement with both lattice spacing and heat of sublimation at 0° K.

The present investigation was carried out to find the best potential, with repulsion of exponential type, that could be determined from data on neon and argon. These are certainly spherically symmetrical and not subject to large quantum corrections. Points to be cleared up were the accuracy of Buckingham's results, and the difficulties which Hirschfelder, Ewell and Roebuck had found in using the Joule-Thomson data for argon.

We use three types of data: (*a*) lattice distance, (*b*) heat of sublimation (both at 0° K.) and (*c*) second virial results at various temperatures; Joule-Thomson data, if available, are treated in the same fashion as second virial data. The first two are known or can easily be estimated for those substances for which second virial data are available, and moreover are likely to be more accurate than the last. We shall, therefore, impose on all our potentials the conditions that they reproduce the experimental lattice spacing and heat of sublimation at 0° K. This relates two of the three arbitrary parameters to the third, leaving this to be determined by fitting to the virial data. The theoretical virials can now be found from tables published recently by Buckingham and Corner.[12] The accuracy of fit to the experimental points is made obvious, particular values can be weighted if desired, and the use of new virial data means very little extra work. Changes of the accepted values of lattice spacing and heat of sublimation would involve rather more recalculation, but such changes are likely to be much smaller than alterations to the virial coefficients. This method leaves to the last the most uncertain process, which is the fitting to a set of usually rather scattered experimental points. Furthermore, this fitting is simplified by having at this stage only one parameter still arbitrary, instead of the two in the usual method.

A similar order of using the various data has been followed by Herzfeld and Göppert-Mayer [2] and Kane,[3] who worked with potentials which had exponential repulsion terms. Two relations between their three arbitrary constants were obtained from the observed lattice spacing and heat of sublimation at 0° K. Properties of the solid state were calculated as functions of the remaining parameter. These researches threw light on the theory of dense phases, but the methods are very laborious if one is merely trying to decide the best value of the third parameter. Rice [4] has shown how a potential energy curve can be found, without too much labour, from thermal and volumetric behaviour of the solid state, assisted by approximate integration of the second virial coefficient. The results are somewhat uncertain because of doubts about the effect of disorder in the solid.

---

[8] Born and Mayer, *Z. Physik*, 1932, **75**, 1.

[9] Bleick, and Mayer, *J. Chem. Physics*, 1934, **2**, 252.

[10] Huggins, *ibid.*, 1937, **5**, 143.

[11] Buckingham, *Proc. Roy. Soc. A*, 1938, **168**, 264.

[12] Buckingham and Corner, *ibid.*, 1947, **189**, 118.

Formulæ used.

(*a*) Equations for the Crystal.—We take the potential energy of a pair of molecules whose centres are a distance r apart to be

$$E = -\epsilon \mathrm{f}(\sigma), \quad . \quad . \quad . \quad . \quad . \qquad (2)$$

where

$$\sigma = r/r_0, \quad . \quad . \quad . \quad . \quad . \qquad (3)$$

and, if $\sigma > 1$,

$$\mathrm{f}(\sigma) = [\alpha(1+\beta) - 6 - 8\beta]^{-1}[\alpha\sigma^{-6}(1+\beta\sigma^{-2}) - (6+8\beta)\,\mathrm{e}^{-\alpha(\sigma-1)}], \qquad (4)$$

while, if $\sigma < 1$,

$$\mathrm{f}(\sigma) = [\alpha(1+\beta) - 6 - 8\beta]^{-1} \left[\alpha\sigma^{-6}(1+\beta\sigma^{-2})\,\mathrm{e}^{-4\left(\frac{1}{\sigma}-1\right)^3} - (6+8\beta)\mathrm{e}^{-\alpha(\sigma-1)}\right]. \qquad (5)$$

The notation is the same as in the paper of Buckingham and Corner.[12] The potential energy of this isolated pair of molecules has a minimum of $-\epsilon$ at $r = r_0$, where $\sigma = 1$, α is a measure of the steepness of the repulsion, and may be expected to lie in the neighbourhood of 12-15. The attractive potential consists of a term proportional to r^{-6}, the usual London dipole-dipole potential valid at large distances, and a dipole-quadrupole term proportional to r^{-8}. The relative importance of this term is determined by β, which is known from theory to be in the neighbourhood of 0·15 (Buckingham,[13] Margenau,[14] Orr[15]). The change in the function f in passing $\sigma = 1$ is only a discontinuity in the third and higher derivatives, and is introduced for convenience to prevent f from becoming infinite as σ tends to zero. In this section we shall be considering values of σ not less than 0·9, and it will be sufficiently accurate to use (4) throughout this section. The complete form, (4) and (5), was used in the preparation of the virial coefficients.

This form of potential energy can be applied only to molecules which are nearly spherically symmetrical. This restriction is more severe in the application to the crystal than in that to the gaseous state. It has been shown[15a] elsewhere that the form of the second virial coefficient as a function of temperature is not much altered by deviations from spherical symmetry.

Let R be the distance between the equilibrium positions of nearest neighbours in the face-centred cubic crystal at 0° K. Let R_i be the distance from the lattice point of a given molecule to the lattice point of its ith neighbour. Let $R/r_0 = \sigma$ and $R_i/r_0 = \sigma_i$. The potential energy of a molecule at a distance z from its equilibrium position, averaged over all orientations of this displacement, and with all other molecules at their lattice points, is

$$-\epsilon\{\alpha(1+\beta) - 6 - 8\beta\}^{-1}\sum_i [\alpha\sigma_i^{-6} + \alpha\beta\sigma_i^{-8} - (6+8\beta)\,\mathrm{e}^{-\alpha(\sigma_i-1)}] -$$

$$\alpha\epsilon(z^2/3r_0^2)\{\alpha(1+\beta) - 6 - 8\beta\}^{-1} \times$$

$$\sum_i [15\sigma_i^{-8} + 28\beta\sigma_i^{-10} - (6+8\beta)(\tfrac{1}{2}\alpha - \sigma_i^{-1})\,\mathrm{e}^{-\alpha(\sigma_i-1)}]. \qquad (6)$$

Now $\sum_i \sigma_i^{-n} = C_n\sigma^{-n}$, where C_n are numerical constants which have been computed by Lennard-Jones and Ingham.[16] The summation of the repulsive forces may be written as

---

[13] Buckingham, *ibid.*, 1937, **160**, 113.

[14] Margenau, *Rev. Mod. Physics*, 1939, **11**, 1.

[15] Orr, *Proc. Camb. Phil. Soc.*, 1942, **38**, 224.

[15a] Corner, *Proc. Roy. Soc. A*, 1948, **192**, 275.

$$\sum_i \mathrm{e}^{-\alpha(\sigma_i - 1)} = 12\theta(\alpha\sigma)\,\mathrm{e}^{-\alpha(\sigma - 1)}. \quad . \quad . \quad . \quad (7)$$

The contributions of non-nearest neighbours being small, θ is close to unity. We shall need also $d\theta/d(\alpha\sigma)$, abbreviated to θ' in later equations. Table I gives θ and $(\theta - \theta')$ over a range sufficient for applications of the present method, together with the summation factors C_6, C_8 and C_{10}.

TABLE I.—FUNCTIONS REQUIRED FOR APPLICATIONS TO CRYSTALS.

$\alpha\sigma$.	θ.	M''.	Δ'''.	$\theta - \theta'$.	M''.	Δ'''.
10·5	1·007408			1·010789		
		719	−93		1090	−144
11	5906			1·008567		
		557	−69		838	−108
11·5	4721			6824		
		434			648	−82
12	3783			5451		
		340			504	−62
12·5	3037			4365		
		268			394	
13	2443			3503		
		211			310	
13·5	1968			2816		
		167			245	
14	1587			2267		
		133			194	
14·5	1281			1828		
		106			154	
15	1·001036			1476		
		85			123	
15·5	1·000838			1·001193		
		69			99	
16	678			1·000965		

$C_6 = 14{\cdot}4539$; $C_8 = 12{\cdot}8019$; $C_{10} = 12{\cdot}3112$.

These tables are intended to be used with Bessel interpolation. M'' is the sum of adjacent second differences, modified to include the effect of the fourth difference. Third differences are tabulated as Δ''' where they need to be taken into account.

The term in (6) which depends on z^2 is needed only to give a small correction to the equilibrium lattice-spacing, and it is therefore possible to neglect in this term the repulsions from non-nearest neighbours. The potential energy of the molecule becomes

$$-\,\epsilon\{\alpha(1+\beta) - 6 - 8\beta\}^{-1}[\alpha C_6\sigma^{-6} + \alpha\beta C_8\sigma^{-8} - 12(6+8\beta)\theta\,\mathrm{e}^{-\alpha(\sigma-1)}] +$$
$$\alpha\epsilon(z^2/3r_0^2)\{\alpha(1+\beta) - 6 - 8\beta\}^{-1} \times$$
$$[12(6+8\beta)(\tfrac{1}{2}\alpha - \sigma^{-1})\,\mathrm{e}^{-\alpha(\sigma-1)} - 15C_8\sigma^{-8} - 28\beta C_{10}\sigma^{-10}]. \quad (8)$$

Let m be the mass of the molecule, and ν its frequency of vibration when all the others are held in their equilibrium positions. Then from (8),

$$\nu^2 = (6\pi^2 m r_0^2)^{-1}\alpha\epsilon\{\alpha(1+\beta) - 6 - 8\beta\}^{-1} \times$$
$$[12(6+8\beta)(\tfrac{1}{2}\alpha - \sigma^{-1})\,\mathrm{e}^{-\alpha(\sigma-1)} - 15C_8\sigma^{-8} - 28\beta C_{10}\sigma^{-10}]. \quad (9)$$

Let $\bar{\nu}$ be the mean frequency of the lattice vibrations. The total energy of a lattice of N molecules at 0° K., which we write as $N\Phi/2$, is equal to the potential energy of the molecules at their equilibrium positions, together with $3h\bar{\nu}N/2$, the zero-point energy of the lattice vibrations. The mean frequency $\bar{\nu}$ is related to our ν by a rather doubtful factor, which is, however, close to unity. We shall use the term $3h\bar{\nu}N/2$ only to estimate the effect of the zero-point energy on the lattice-spacing; this is about 0·05 A. for argon and 0·15 A. for neon. Thus we may replace * $\bar{\nu}$ by ν. Hence

---

[16] Lennard-Jones and Ingham, *Proc. Roy. Soc. A*, 1925, **107**, 636.

$$\Phi = -\epsilon\{\alpha(1+\beta) - 6 - 8\beta\}^{-1} [\alpha C_6\sigma^{-6} + \alpha\beta C_8\sigma^{-8} - 12(6+8\beta)\theta\,\mathrm{e}^{-\alpha(\sigma-1)}] + 3h\nu. \quad (10)$$

Under small pressures at 0° K., the value of σ is determined by the condition of minimum energy:

$$\frac{\partial\Phi}{\partial\sigma} = 0, \quad . \quad . \quad . \quad . \quad . \quad (11)$$

which from (9) and (10) reduces to

$$\chi \equiv 6C_6\sigma^{-7} + 8\beta C_8\sigma^{-9} - 12(6+8\beta)(\theta-\theta')\,\mathrm{e}^{-\alpha(\sigma-1)} + \{3h^2\{\alpha(1+\beta) - 6 - 8\beta\}/8\pi^2 m r_0^{\,2}\epsilon\alpha\}^{\frac{1}{2}} [12(6+8\beta)(\tfrac{1}{2}\alpha - \sigma^{-1})\,\mathrm{e}^{-\alpha(\sigma-1)} - 15C_8\sigma^{-8} - 28\beta C_{10}\sigma^{-10}] \times [120C_8\sigma^{-9} + 280\beta C_{10}\sigma^{-11} + 12(6+8\beta)(\sigma^{-2} + \alpha\sigma^{-1} - \tfrac{1}{2}\alpha^2)\,\mathrm{e}^{-\alpha(\sigma-1)}] = 0. \quad (12)$$

The theoretical energy of sublimation at 0° K. is

$$U_0 = (N\epsilon/2)\{\alpha(1+\beta) - 6 - 8\beta\}^{-1} \times [\alpha C_6\sigma^{-6} + \alpha\beta C_8\sigma^{-8} - 12(6+8\beta)\theta\,\mathrm{e}^{-\alpha(\sigma-1)}], \quad (13)$$

where σ is the solution of (12). The experimental value of U_0 is the observed heat of sublimation together with the zero-point energy $9Nk\Theta_D/8$, where Θ_D is the experimental low-temperature value of the Debye characteristic temperature.

U_0 and R being known, for any assumed values of α and β one can calculate ϵ from (13) as a function of σ, and χ can then be found from (12). Inverse interpolation shows the value of σ for which $\chi = 0$, and then the corresponding ϵ and r_0 are found. It is convenient to deduce ϵ and r_0 from assumed simple values of α and β because this simplifies interpolation in the tables of second virial and Joule-Thomson coefficients.

Although our rough calculation of $\bar{\nu}$ has been used in finding the effect of the zero-point energy on the lattice-spacing, the zero-point energy at the actual spacing is taken from the observed Θ_D. This simple way to correct lattice-spacings for zero-point energy was put forward in an earlier paper (Corner [7]), and Rice [4] has shown how this method can be refined to give the general equation of state of the solid, in a form which is still easy to use. Rigorous, but more laborious, methods of calculating $\bar{\nu}$ and the equation of state of the solid have been used by Herzfeld and Göppert-Mayer [2] and Kane.[3]

For substances forming a face-centred cubic or hexagonal close-packed lattice, the expansion of the nearest-neighbour distance at 0° K. by this effect is approximately $4(MT_c)^{-\frac{1}{2}}$ Ångstroms, where M is the molecular weight and T_c° K. is the critical temperature. The form of this comes from (12) and the fact that ϵ is proportional to T_c (Lennard-Jones and Devonshire [17]), while the constant is chosen to fit the results for neon.

The potential

$$f(\sigma) = (n\sigma^{-6} - 6\sigma^{-n})/(n-6)$$

is also important, and as we shall make some use of this form we give the equations which determine ϵ and r_0 when U_0 and R are known:

---

* This procedure would not be justifiable for helium or hydrogen, where the zero-point energy is a major contribution.

[17] Lennard-Jones and Devonshire, *Proc. Roy. Soc. A*, 1937, **163**, 53.

$$\chi \equiv C_6\sigma^{-7} - C_n\sigma^{-n-1} + [3h^2(\tfrac{1}{8} - 1/n)/16\pi^2 m\epsilon r_0^2]^{\frac{1}{2}}[40C_8\sigma^{-9} - (n-1)(n+2)C_{n+2}\sigma^{-n-3}] \times [(n+1)C_{n+2}\sigma^{-n-2} - 5C_8\sigma^{-8}] = 0 \quad . \quad . \quad . \quad . \quad . \quad (12\text{A})$$

$$U_0 = \tfrac{1}{2}N\epsilon[nC_6\sigma^{-6} - 6C_n\sigma^{-n}]/(n-6). \quad . \quad . \quad . \quad . \quad . \quad . \quad (13\text{A})$$

(*b*) The Second Virial and Low-pressure Joule-Thomson Coefficients.—The equation of state of a gas at low densities can be written as

$$pV = RT[1 + B/V + O(V^{-2})] \quad . \quad . \quad . \quad (14)$$

where V denotes molar volume and p and R have their usual meanings. The second virial coefficient B is a function of temperature only. B has the dimensions of a molar volume. It is usually measured in Amagat's unit of volume equal to the volume of one mole at N.T.P., namely 22·4 l. The variation of this unit from one gas to another is for our purposes negligible. We shall follow the practice of Fowler and of Buckingham,[11] taking B to be defined by (14), and given numerically in Amagat's units.

The second virial coefficient from the potential (2)-(5) may be written as

$$B = 2\pi n_0 r_0^3[\mathrm{F}_0(\epsilon/kT) + (\lambda/r_0)^2\mathrm{F}_1(\epsilon/kT)] \quad . \quad . \quad (15)$$

where F_0 and F_1 are functions of α, β and ϵ/kT which have been tabulated by Buckingham and Corner [12] and n_0 is Avogadro's number. Here λ is defined by

$$\lambda^2 = h^2/2\pi mkT. \quad . \quad . \quad . \quad . \quad (16)$$

The second term in (15) is a quantum correction, which arises because the probability of a configuration of potential energy E is not just proportional to exp $(-E/kT)$ as in classical statistical mechanics (cp. Slater,[18] Uhlenbeck and Gropper,[19], Wigner,[20] Kirkwood[21] and Uhlenbeck and Beth [22]). This is the only quantum correction which need be considered, except for helium at low temperatures.

The tables of F_0 and F_1 refer to $\beta = 0$ and 0·2, and cover α from 12·5 to 14·5 and ϵ/kT from 0·04 to 0·8. The latter range starts at about the critical temperature, and reaches the highest temperatures at which second virial coefficients have been measured for neon and argon.

Let μ_0 be the Joule-Thomson coefficient and $c_p{}^0$ the heat capacity per molecule, both extrapolated to zero density. From thermodynamics we have

$$c_p{}^0\mu_0 = T^2\frac{\mathrm{d}}{\mathrm{d}T}(B/n_0T). \quad . \quad . \quad . \quad . \quad (17)$$

For the intermolecular potential (2)-(5) this result can be written

$$c_p{}^0\mu_0 = 2\pi r_0{}^3[\mathrm{G}_0(\epsilon/kT) + (\lambda/r_0)^2\mathrm{G}_1(\epsilon/kT)] \quad . \quad . \quad (18)$$

where G_0 and G_1, which are functions of α, β and ϵ/kT, have been tabulated by Buckingham and Corner for the same ranges of the variables as were F_0 and F_1. The second term is the only quantum correction which need be included, except for helium.

Results for Neon.

Values of the fundamental constants were taken from Birge.[24] The distance between nearest neighbours in the neon lattice at 0° K. is 3·20 A. (de Smedt, Keesom and Mooy [25]) and the heat of sublimation at 0° K., corrected for zero-point energy, is 589 cal./mole (Keesom and Haantjes [26]). For second virial coefficients there are the observations of Holborn and Otto [27] from 65 to 673° K., and a set by Keesom and van Lammeren,[28] derived from measurements of velocity of sound, extending to as low as 30° K. We have used the former data. The latter set are about 10 % smaller in the 60-80° K. zone which is common to the two sets. This arises from the indirect virial coefficients having been fitted to the virial data of Cath and Onnes [29] at temperatures above 63° K.

---

[18] Slater, *Physic. Rev.*, 1931, **38**, 237.
[19] Uhlenbeck and Gropper, *ibid.*, 1932, **41**, 79.
[20] Wigner, *ibid.*, 1932, **40**, 749. [21] Kirkwood, *ibid.*, 1933, **44**, 31.
[22] Uhlenbeck, and Beth, *Physica*, 1936, **3**, 729.
[23] Whitelaw, *ibid.*, 1934, **1**, 749.
[24] Birge, *Rep. Progr. Physics*, 1941, **8**, 90 ; *Rev. Mod. Physics*, 1941, **13**, 233.
[25] de Smedt, Keesom and Mooy, *Leiden Comm.*, 203*e* (1930).

To find the best value of α we have minimised the root-mean-square deviation between theoretical and experimental values of R, taking these to have equal weight. The results are listed in Table II. It is possible to alter the " best " value of α by 0·1 or 0·2, for example, by giving equal weight to B/T instead of B as has sometimes been done. Thus differences of 0·1 in α are at present about the limit of significance in this subject.

TABLE II.—CONSTANTS OF EXPONENTIAL REPULSION FOR NEON.

β.	α.	$10^{15}\,\epsilon$ (ergs).	r_0 (A.).
0	13·6	5·12	3·16
0·2	13·2	5·18	3·16
0·15	13·3	5·16	3·16

The values of ϵ and r_0 vary so little with β that linear interpolation should be sufficiently accurate. Margenau [14] has estimated that $\beta = 0{\cdot}15$ for neon, and the corresponding parameters are given in Table II.

The residual differences between theoretical and experimental results are shown in Table III for the case $\beta = 0{\cdot}2$. Effectively the same fit is obtained for the other two potentials of Table II.

TABLE III.—COMPARISON OF THEORETICAL AND EXPERIMENTAL SECOND VIRIAL COEFFICIENTS FOR NEON.

T (°K.)	Obs. H. and O. $10^6\,B$ in Amagat Units.	Error from		
		$\beta = 0{\cdot}2$ Potential of Table II.	(20).	Buckingham (21)-(22).
65·1	−935	−30	−44	35
90·5	−365	2	− 5	39
173·2	288	−13	− 5	−13
223·2	406	2	15	− 7
273·2	475	8	26	− 8
373·2	529	32	56	10
473·2	582	14	42	−12
573·2	614	− 1	31	−30
673·2	612	8	43	−22
R.-m.-s. error . . .		16	34	23

The quantum correction to the second virial coefficient is largest at low temperatures and reaches 5 % at 65° K., the lowest temperature used in our comparison.

---

[26] Keesom and Haantjes, *Physica*, 1935, **2**, 460.
[27] Holborn and Otto, *Z. Physik*, 1925, **33**, 1.
[28] Keesom and van Lammeren, *Physica*, 1934, **1**, 1161.
[29] Cath and Onnes, *Leiden Comm.*, 156*a* (1923).

We have used also potentials of the type

$$E = -\epsilon f(\sigma)\,;\quad \sigma = r/r_0\,;\quad f(\sigma) = (n-6)^{-1}(n\sigma^{-6} - 6\sigma^{-n}) \quad . \quad (19)$$

where n need not be an integer. ϵ and r_0 can be evaluated from (12A) and (13A). The classical second virial coefficient can then be found from the analytical solution of Lennard-Jones.[5] We have carried out this process with $n = 9$, 12 and 15, adding the quantum correction tabulated by Buckingham and Corner for an exponential repulsion. By interpolation the most satisfactory index for the repulsive potential is $n = 12{\cdot}0$, and for this case

$$\epsilon = 5{\cdot}01 \times 10^{-15} \text{ ergs}\,;\quad r_0 = 3{\cdot}16 \text{ A.} \quad . \quad . \quad . \quad (20)$$

The deviations from experiment, shown in Table III, are larger than the residuals when an exponential repulsion is used. The form (19) with $n = 12$ has found many applications because of its mathematical convenience. The present results show that for neon it is also the best form with any inverse power to represent the repulsion, and that it is not greatly inferior to any potential with an exponential repulsion.

The best potentials with exponential repulsion (and $\beta = 0{\cdot}2$) and inverse-power repulsion are shown in Fig. 1, together with Buckingham's potential for neon, which is

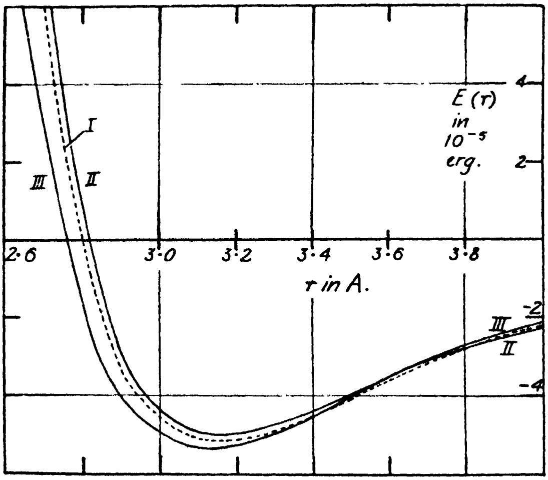

FIG. 1.—Interatomic potentials $E(r)$ for neon. I is the best potential with exponential repulsion and $\beta = 0{\cdot}2$; II is (20), the best potential with inverse-power repulsion ; III is Buckingham's result, (21)-(22).

$$E(r) = 2{\cdot}57 \times 10^{-9}\, e^{-r/0{\cdot}235} - 9 \times 10^{-12}\, r^{-6} \quad . \quad . \quad (21)$$

with E in ergs and r the distance in Ångstroms, for r between 2·6 and 3·0 A., and

$$E(r) = -6{\cdot}1 \times 10^{-12} r^{-6} - 8{\cdot}8 \times 10^{-12} r^{-8} \quad . \quad . \quad (22)$$

at distances equal to, or greater than, the distance of next-nearest neighbours in the crystal. The potential drawn consists of (21) up to $r = 4$ and (22) for r greater than 4·5 A. with a smooth interpolation between. This potential gives nearly the true interatomic distance and heat of sublimation at 0° K., and numerical integration has verified that there is good agreement with the observed virial coefficient (cp. Table III). This potential differs from those derived in the present paper by being smaller for distances greater than 3·8 A., and, to balance this, having a deeper minimum. The exponential repulsions have nearly the same slope.

The best potentials with $\beta = 0$ and $0{\cdot}2$ lie too close for both to be drawn on Fig. 1 without overcrowding.

Bleick and Mayer[9] have made a theoretical calculation of the repulsion between neon atoms at distances from 1·8 to 3·2 A. apart. The results could be represented by a potential $19 \times 10^{-9}\, e^{-r/0{\cdot}209}$ (r in A.). This is in fair agreement with the repulsive part of Buckingham's potential, or with closely similar results: for example, the potential given in Table II for $\beta = 0{\cdot}2$ has a repulsion term which agrees with the theoretical potential for distances near 3·4 A., and differs by a factor of two-thirds at 2·7 A.

Results for Argon.

Here R, the lattice spacing at 0° K., is 3·81 A. (Simon and von Simson;[30] de Smedt and Keesom[31]), and the heat of sublimation at 0° K., corrected for zero-point energy, is 2030 cal./mole (Born[32]). The best second virial coefficients at temperatures down to − 100° C. appear to be those of Holborn and Otto.[17] Roebuck and Osterberg[33] have measured the Joule-Thomson coefficient * from 300° C. to below − 100° C., over a pressure-range which allows an accurate extrapolation to zero density. There are other virial data at temperatures down to 80° K. (Cath and Onnes;[29] van Itterbeek and van Paemel[34]) to which we shall refer later. The tables of Buckingham and Corner end at $\epsilon/kT = 0{\cdot}8$, which for argon means a lower temperature limit of − 100° C. At lower temperatures it is necessary to do more numerical integration, and this is conveniently left till as much information as possible has been extracted from the data at higher temperatures.

Eqn. (17) has been used to test the consistency of the Joule-Thomson and second virial coefficient, by Whitelaw[23] and Hirschfelder, Ewell and Roebuck,[1] in the integrated form

$$B/n_0T = B(T_1)/n_0T_1 + \int_{T_1}^{T} c_p{}^0\mu_0 \mathrm{d}T/T^2 \qquad . \quad . \quad (23)$$

where T_1 is arbitrary. Neither (17) nor (23) provides a sensitive test. For in (17) there occurs a numerical differentiation of a curve represented by a set of experimental points, and the results of this process are not sufficiently reliable to show up other than gross errors in the Joule-Thomson coefficient. The uncertainty in (23) arises because the value of T_1 is at our disposal. The data of Roebuck and Osterberg have been used in (23), with $T_1 = 100°$ C., by Hirschfelder, Ewell and Roebuck,[1] and shown to give good agreement with the second virial coefficient from − 100° C. to 400° C. Difficulties in fitting theoretical curves have led us to repeat this test with a μ_0 increased by 7 % at − 100° C., unaltered at 0° C., with a smooth interpolation for the modification at intermediate temperatures. This actually improved the agreement between the two sides of (23).

As with neon, the results of the analysis are not sensitive to the value of β assumed. We take first the case $\beta = 0{\cdot}2$. The best fit to the virial data occurs for $\alpha = 13{\cdot}3$. The agreement is good (Table IV).

Table V shows the Joule-Thomson coefficient found by Roebuck and Osterberg, extrapolated to zero density, and the error in the theoretical values for $\alpha = 13{\cdot}5$. There is seen to be an increasing deviation at low temperatures. This occurs for all values of α and β, even for β increased several-fold over the expected value of 0·14 (Margenau[14]). This is precisely the behaviour reported by Hirschfelder, Ewell and Roebuck,[1] who

---

* A correction to these results has been published by Roebuck and Osterberg.[35]

[30] Simon and von Simson, *Z. Physik*, 1924, **25**, 160.

[31] de Smedt and Keesom, *Leiden Comm.*, 178*b* (1926).

[32] Born, *Ann. Physik*, 1922, **69**, 473.

[33] Roebuck and Osterberg, *Physic. Rev.*, 1934, **46**, 785.

[34] van Itterbeek and van Paemel, *Physica*, 1938, **5**, 845.

[35] Roebuck and Osterberg, *J. Chem. Physics*, 1940, **8**, 627.

used potentials of the form (19) with values of n between 9 and 15, without being able to reproduce the shape of the experimental curve. Our results show that the use of an exponential repulsion leads to little, if any, improvement and if this lack of agreement is still to be attributed to a bad

TABLE IV.—THEORETICAL AND OBSERVED SECOND VIRIAL COEFFICIENT ($10^6 B$) FOR ARGON.

T (°K.).	Obs., H. and O.	Error from				
		$\beta = 0{\cdot}2$, $\alpha = 13{\cdot}3$.	$\beta = 0{\cdot}2$, $\alpha = 13{\cdot}4$.	$\beta = 0$, $\alpha = 13{\cdot}9$.	(27).	Buckingham.
173·2	−2871	−51	−35	−27	−36	267
223·2	−1687	3	16	20	2	253
273·2	− 986	23	33	28	39	238
323·2	− 492	− 5	4	9	14	180
373·2	− 192	20	29	33	45	178
423·2	52	16	25	27	42	156
473·2	208	40	48	51	70	166
573·2	501	0	7	12	37	122
673·2	683	−15	− 9	− 2	26	99
	R.-m.-s. error	25	27	27	39	190

TABLE V.—THEORETICAL AND OBSERVED JOULE-THOMSON COEFFICIENTS AT LOW PRESSURE, FOR ARGON; IN 10^{-3} DEGREES/ATM.

T (°K.).	Obs., H. and O.	Error from				
		$\beta = 0{\cdot}2$, $\alpha = 13{\cdot}5$.	$\beta = 0{\cdot}2$, $\alpha = 13{\cdot}4$.	$\beta = 0$, $\alpha = 13{\cdot}9$.	(27).	Buckingham.
173·2	865	83	89	83	86	64
185·7	782	64	69	64	67	43
198·2	711	49	53	50	54	29
223·2	598	26	30	27	31	4
248·2	507	13	17	15	19	− 12
273·2	432	8	11	9	13	−19
298·2	372	3	5	5	8	−23
323·2	323	− 1	1	1	4	−26
348·2	279	− 2	1	0	3	−26
373·2	243	− 3	− 1	− 1	2	−26
398·2	211	− 3	− 1	− 1	1	−26
423·2	184	− 4	− 2	− 2	0	−26
473·2	138	− 4	− 2	− 3	− 1	−24
523·2	98	0	2	1	3	−19
573·2	64	5	7	6	8	−13

form for the intermolecular potential, then most extensive changes must be made in this form. Before accepting this conclusion, which has not been suggested by any other experimental data, we may examine other possible explanations.

The lattice-spacings at 0° K. may be wrong, or our correction for the effect of zero-point energy on lattice-spacing may be more crude than expected. These suggestions can be tested together by using a different spacing. The whole correction for zero-point energy is only 0·05 A.; the lattice distance itself was measured in two investigations (Simon and von Simson;[80] de Smedt and Keesom[81]), which are in good agreement; a change of lattice-spacing by 0·05 A. is as large a shift as could plausibly be made. Nevertheless, it makes only a small improvement in the curvature of the theoretical Joule-Thomson coefficient and gives a slightly worse fit for the second virial coefficient.

We have examined the effect of using $U_0 = 1700$ cal./mole, instead of 2030 cal./mole. This removes most of the surplus curvature from the theoretical Joule-Thomson coefficient, at the expense of a considerably worse fit to the virial. Moreover, this change in U_0 is much bigger than the possible experimental error.

Another possibility which has been considered is that the experimental values of the Joule-Thomson coefficient may be too low in the region from − 100 to 0° C. As we have mentioned, the second virial coefficient cannot detect the suspected errors of a few %. The greatest uncertainty in the experimental values of the Joule-Thomson coefficient occurs at temperatures below 0° C., where there were difficulties due to clogging of the porous plug and to the rapid variation of μ_0 with temperature. A systematic error in the Joule-Thomson coefficient, rising to a few % at − 100° C., appears to be possible, though this would be rather larger than expected.* We think, therefore, that the discrepancy between theoretical and observed Joule-Thomson coefficients is due mainly to the experimental results being a few % too small at the lowest temperatures.

Omitting results below 0° C., the best fit to the Joule-Thomson coefficient is given by $\alpha = 13{\cdot}5$. The best fit to second virial and Joule-Thomson data together occurs for $\alpha = 13{\cdot}4$. This is with $\beta = 0{\cdot}2$. The other parameters are then

$$\epsilon = 1{\cdot}72 \times 10^{-14} \text{ ergs}; \quad r_0 = 3{\cdot}87 \text{ A.} \qquad (24)$$

The corresponding results for $\beta = 0$ are

$$\alpha = 13{\cdot}9; \quad \epsilon = 1{\cdot}70 \times 10^{-14} \text{ ergs}; \quad r_0 = 3{\cdot}87 \text{ A.} \qquad (25)$$

The agreement with experiment is almost the same with both values of β, the relative magnitude of the dipole-quadrupole forces, and demonstrates that these observations are unlikely ever to determine β. With Margenau's estimate of 0·14 for argon, linear interpolation leads to

$$\alpha = 13{\cdot}5; \quad \epsilon = 1{\cdot}72 \times 10^{-14} \text{ ergs}; \quad r_0 = 3{\cdot}87 \text{ A.} \qquad (26)$$

It is of interest to carry out this programme also for potentials which have an inverse power to represent the repulsion. We have used (19) with $n = 9$, 12 and 15, taking the classical second virial coefficient from Lennard-Jones,[5] the Joule-Thomson coefficient from Hirschfelder, Ewell and Roebuck,[1] and the small quantum corrections from the computations with exponential repulsions. All the potentials were adjusted to give $R = 3{\cdot}81$ A. and $U_0 = 2030$ cal./mole. The best fit to the second virial and Joule-Thomson coefficients separately occurs for n about 12·1 and 12·5; the best potential therefore appears to have $n = 12{\cdot}3$, with

$$\epsilon = 1{\cdot}66 \times 10^{-14} \text{ ergs}; \quad r_0 = 3{\cdot}87 \text{ A.} \qquad (27)$$

The fit obtained is shown in Tables IV and V. Comparison with the best potentials with exponential repulsion shows that the latter is better than any inverse power, but the improvement is not very large. The inverse power has advantages of convenience in many applications, and our results show that in such cases it can be used without fear of any substantial loss of accuracy. The index, 12·3, is so close to 12 (which is an especially convenient figure) that the difference is hardly worth retention. The other constants of the interaction become, with $n = 12$

$$\epsilon = 1{\cdot}647 \times 10^{-14} \text{ ergs}; \quad r_0 = 3{\cdot}87 \text{ A.} \qquad (28)$$

---

* I am indebted to Prof. J. R. Roebuck for a helpful discussion of the possible errors.

The agreement between the values of α (or n) and β for neon and argon shows that these substances should obey the principle of corresponding states, except for quantum deviations due to the difference of atomic weight.

The second virial coefficient of argon has been measured to as low as 80° K. by Cath and Onnes [29] and van Itterbeek and van Paemel,[33] who used, respectively, the temperature scales of thermometers filled with argon and helium, and the velocity of sound in argon. The results are plotted in Fig. 2, together with three values computed from (24). Probably the best experimental curve is *I* of the diagram, which is furthest removed from the theoretical results. The sign of the difference shows that the potential (24) has too big an attraction at large distances, and the true energy must have a correspondingly deeper minimum. The experimental results at low temperatures were not used to fix the best potential because of the labour of computing the theoretical integrals at large values of ϵ/kT, which for argon is about 1·5 at 80° K. However, Fig. 2 makes it clear that even curve *I* would have made little difference to the best values of the parameters in the interatomic potential. Even as low as 80° K. the quantum correction does not rise above 1 %.

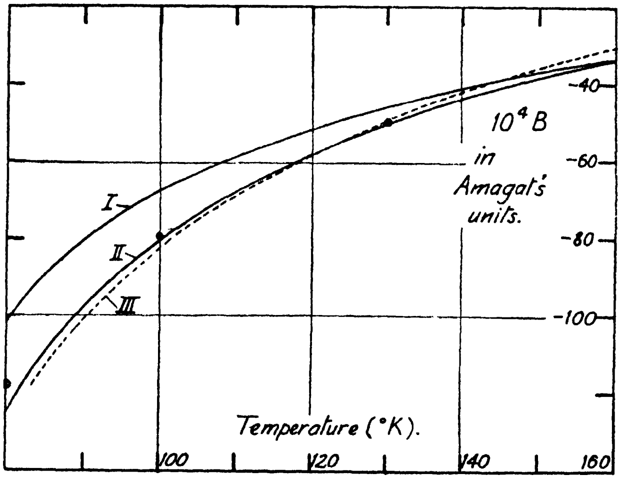

FIG. 2.—The second virial coefficient of argon at low temperatures. Curves *I* and *II* were found by van Itterbeek and van Paemel [34] from the velocity of sound,[27] the boundary conditions above 150° K. being taken from: *I*, Holborn and Otto; *II*, Onnes and Crommelin.[36] *III* is the experimental result of Cath and Onnes.[29] Theoretical values from the intermolecular potential (24) are shown as circles at 80, 100 and 130° K.

Fig. 3 shows two of the three potentials derived above: the best potential with exponential repulsion and $\beta = 0{\cdot}2$ (eqn. (24)) and the best potential with an inverse power repulsion (27). There are no large differences between these curves. The potential for $\beta = 0$ is too close to that for $\beta = 0{\cdot}2$ to be shown clearly.

In Fig. 4 are compared our result (24), the curves found by Rice [4] from properties of the solid state, and the potential obtained by Buckingham [11] from an analysis of the second virial coefficient:

$$E(r) = 1{\cdot}69 \times 10^{-8} e^{-r/0{\cdot}273} - 1{\cdot}02 \times 10^{-10} r^{-6} \text{ ergs}$$

(with distance in Ångstroms) for r between 3·4 and 3·6 A. We have drawn this potential up to $r = 4{\cdot}5$ A. Buckingham used his theoretical formulæ for the r^{-6} and r^{-8} potentials for second and more distant neighbours, that is, for r greater than 5·3 A.; we have followed this down to $r = 5$ A., with a smooth curve in the transition zone. This gives nearly the right

---

[36] Onnes and Crommelin, *Leiden Comm.*, 118*b* (1910).

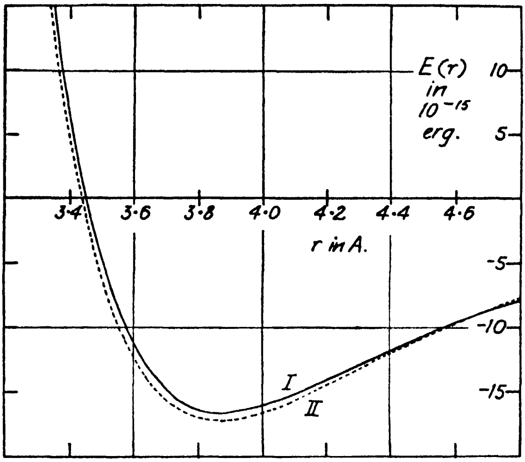

FIG. 3.—Interatomic potentials $E(r)$ for argon: *I* is (27), the best potential of the type (19) with the short-range repulsion represented by an inverse power of the distance; *II* is (24), the best with exponential repulsion and $\beta = 0·2$. Both these potentials give the observed lattice-spacing and heat of sublimation at 0° K.

heat of sublimation and lattice-spacing at 0° K. We have computed the second virial and Joule-Thomson coefficients for this potential (Tables IV and V). The large difference between theory and experiment arises

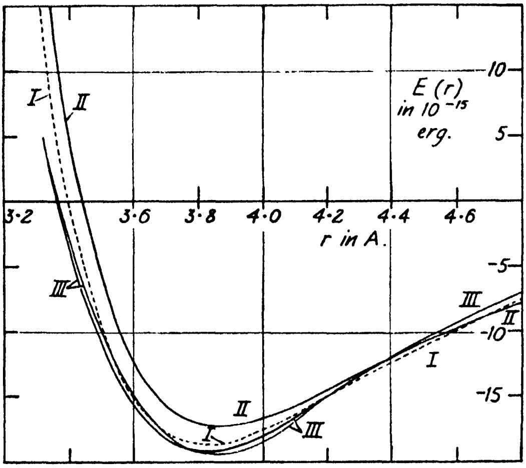

FIG. 4.—Interatomic potentials $E(r)$ for argon: *I* is Buckingham's potential with exponential repulsion; *II* is (24), our best potential with exponential repulsion and $\beta = 0·2$; *III* are potentials found by Rice.

from the use of the theoretical attraction down to $r = 5$ A., that is, into a region which has a considerable effect on the theoretical second virial coefficient. Buckingham's potential differs from our result (24) by being numerically smaller at large distances, with a deeper minimum at slightly smaller interatomic distance. These are changes in the same direction as indicated by the virial data at the lowest temperatures. It can be concluded that it is very unlikely that the true potential lies outside the zone bounded by curves *I* and *II* in Fig. 4.

Rice derived his potential from the heat capacity and equation of state of solid argon, assisted by an approximate integration of the second virial coefficient, and the potential is accordingly also a set of segments. The two potentials shown in Fig. 4 were obtained from different assumptions about disorder in the solid. Both curves differ considerably from our potentials, in the same way as do Buckingham's results but by a larger amount.

I am indebted to Prof. Sir John Lennard-Jones, F.R.S., for his encouragement of this work, to Prof. E. A. Guggenheim, F.R.S., for helpful criticism, and to the Chief Scientist, Ministry of Supply, for permission to publish this paper.

Summary.

The determination of intermolecular potentials from second virial and Joule-Thomson coefficients leads to unambiguous results only when supplemented by comparison with crystal properties. It is shown that there are advantages in using the latter properties from the start of the analysis. The process has been applied to neon and argon, with repulsive potentials represented by inverse powers and exponential functions of the distance between the molecular centres. The inclusion of a small attractive potential proportional to r^{-8} as an addition to the normal r^{-6} potential has very little effect on the shape of the best potential. The results have been compared with previous work on the properties of the solid and gaseous states of these substances.

Armament Research Department,
Ministry of Supply.

SOME PHYSICAL PROPERTIES OF URANIUM HEXAFLUORIDE

By C. B. Amphlett,* L. W. Mullinger (in part),
and L. F. Thomas (in part).

Received 1st April, 1948.

Very few physical data are available concerning UF_6, although this compound has been known for many years.[1] This is probably due to the experimental difficulties encountered in preparing and handling pure specimens of the material, which is highly corrosive in the presence of moisture and fluorinates many materials with the formation of the relatively inert tetrafluoride UF_4. However, UF_6, purified as described below, may be stored in evacuated glass vessels for long periods without deterioration and without attack on the glass, provided that the vessels have been evacuated to a pressure of the order of 10^{-5} mm. and thoroughly baked to remove moisture. The pure compound is easily handled by high-vacuum distillation in all-glass apparatus.

I. The Purification of UF_6.

Impurities likely to be present in samples of UF_6 prepared by the fluorination of uranium oxides or chlorides are HF, F_2 and SiF_4, the last arising from the action of HF upon glass vessels used for storage. In addition, samples containing moisture will be contaminated with uranyl fluoride, but as this is non-volatile it remains behind on vacuum distillation. Samples of UF_6 were obtained * in Pyrex vessels fitted with thin septa which could be broken by means of a magnetically-operated breaker. All manipulations were carried out in an apparatus of Pyrex glass which had been thoroughly degassed by flaming at a pressure of 10^{-5} mm. (measured on a McLeod gauge). Moisture must be rigidly excluded from the system, as the presence of the minutest trace leads to the rapid accumulation of impurities by the sequence of reactions shown below:

---

* Present address, A.E.R.E., Harwell, Berks.

[1] Ruff and Heinzelmann, *Ber.*, 1909, **42**, 495.

$$UF_6 + 2H_2O \rightarrow UO_2F_2 + 4HF$$
$$4HF + SiO_2 \text{ (glass)} \rightarrow SiF_4 + 2H_2O, \text{ etc.}$$

The sample vessel was opened at liquid-air temperature; fluorine was swept out with dry air and removed by evacuation through mercury traps, the mercury rapidly becoming coated with a fluoride layer. The sample was then distilled at room temperature and 10^{-5} mm. on to A.R. KF at liquid-air temperature and allowed to remain in contact with the reagent for several days at room temperature to remove HF; since KF is appreciably hygroscopic, thorough baking is necessary during evacuation to remove moisture and ensure that no decomposition of UF_6 occurs. If moisture is not completely removed, the reagent rapidly develops a yellow colour due to the formation of UO_2F_2. After removal of HF, the sample was distilled at room temperature from the KF to a second vessel cooled in a CO_2-alcohol bath to − 30° c., while connected to the pumps via a trap cooled in liquid air. The latter trap was found to contain, in addition to some UF_6, a white solid which volatilised completely at a very low temperature, and which contained both silicon and fluorine. Although this was not analysed, it appears reasonable to assume that it was SiF_4. Consideration of the vapour pressure curve for SiF_4 [2, 3] shows that the final distillation at − 30° c. should completely remove this impurity.

Samples of UF_6 purified by this method and sealed in glass containers consisted of lustrous, transparent crystals with a pale yellow tint in transmitted light. No attack on Pyrex glass was observed over very long periods, and the rate of attack on Apiezon greases was sufficiently slow for experiments to be carried out in apparatus containing greased stopcocks.

When distilling appreciable quantities of UF_6 (greater than 10 g.) it was found advantageous to use cooled vessels of the Dewar type, i.e. with the cooling liquid in an inner concentric finger, rather than the conventional type of concentric cold trap immersed in a cooling bath. With the latter type, the rapid expansion of solid UF_6 on warming up to room temperature is capable of breaking the trap, with release of toxic fumes and loss of the sample. With the type used, expansion merely causes the solid to break away from the cold finger and drop to the bottom of the vessel.

II. The Vapour Pressure and Vapour Density of UF_6.

The vapour pressure of solid UF_6 was determined at temperatures up to the sublimation point by a null method, the deflection produced in a quartz spiral manometer being balanced by the admission of dry air, the balancing pressure being read on a mercury manometer. Determinations of the vapour density were made by direct weighing of a known volume of vapour at a given temperature and pressure. In addition the density-pressure relationship of a sample of unsaturated vapour was investigated at a fixed temperature.

* Supplied by Messrs. I.C.I. Ltd., Widnes.

[2] Patnode and Papish, *J. Physic. Chem.*, 1930, **34**, 1494.

[3] Ruff and Ascher, *Z. anorg. Chem.*, 1931, **196**, 413.

Experimental.

Determinations were carried out in the apparatus shown in Fig. 1. A sample of purified UF_6 was distilled into the bulb C at − 50° c., after which the cooling liquid was run out from the annular space and the sample isolated by means of T_1 and T_3. This section of the apparatus was completely enclosed in a large, well-lagged water bath, which could be heated to 60° c. by immersion heaters. The bath was not thermostatically controlled, but by efficient stirring and careful control of the heaters it was found possible to maintain any temperature within the range 0-60° to within ± 0·5° c. over long periods. After opening T_1, the sample was allowed to exert its saturated vapour pressure at a series of temperatures up to the sublimation point, the temperature being maintained constant until the system was in equilibrium. The gauge G consisted of a quartz spiral fitted with a mirror and bifilar suspension, the movement being damped in Apiezon oil B. The gauge was used with a lamp and scale at distances of 340 cm. and 200 cm. respectively, and preliminary measurements indicated a sensitivity of 46 mm. deflection per mm. Hg excess pressure applied to one side of the gauge. The zero of the gauge remained constant over the whole pressure range, and was unaffected by the necessary manipulations, all parts of the apparatus being firmly clamped. When equilibrium had been attained and the light spot showed no further drift, dry air was admitted until the spot returned to the zero position; the time taken to reach equilibrium was usually about ½-1 hr. In practice, the light spot was always maintained slightly on the low-pressure side of the zero position by repeated addition of small volumes of air while the pressure in the system was increasing; the gauge was then never deflected far from its zero position, and errors due to permanent strains in the gauge were avoided. Using a mercury manometer of 12 mm. internal diameter, the values of the balancing pressure are considered to be correct to ± 0·5 mm. Hg.

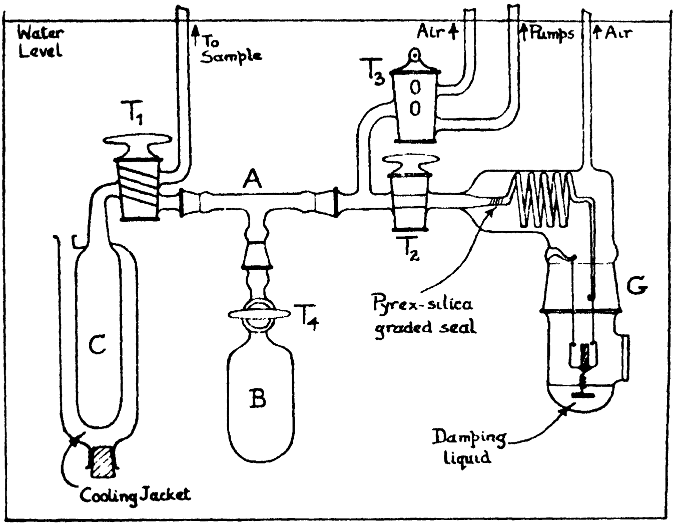

FIG. 1.—Diagram of apparatus used for determination of vapour density and vapour pressure of UF_6.

The vapour density was found by direct weighing in bulb B. After attainment of equilibrium at a chosen temperature, the pressure was measured and the sample isolated by closing T_4. UF_6 was then removed from the rest of the line, air was admitted and the bulb swung out of the bath by rotating A about a horizontal axis. B was then removed, cleaned and polished, and weighed against a counterpoise of approximately the same volume and dimensions, the evacuated bulb having been weighed previously. Preliminary experiments with the bulb evacuated showed that it was possible to carry out this sequence of operations several times in succession without appreciably affecting the recorded mass of the bulb. The volume of the bulb (including the bore of T_4)

was found by weighing it after evacuation and when filled with water at a known temperature, care being taken to remove all air-bubbles by evacuation.

The density of unsaturated vapour as a function of pressure at ~ 50° c. was found by the same method, except that while heating to 50° the sample in C was isolated at some suitable temperature below 50° by closing T_1, so that on further heating the vapour in the remainder of the system became unsaturated.

Two bulbs were used throughout this work, one of approximately 130 cc. capacity and the other of 270 cc. Standard procedures were adopted for cleaning and polishing the bulb and counterpoise; they were left in the balance case for 1 hr. before weighing, the difference in their masses attaining a constant value in this time. The masses of vapour recorded varied from 0·3 g. to 2 g., and were determined to 0·001 g. In the volume calibration, the mass of water was measured to 0·05 g., the actual masses being of the order of 150 g. and 300 g. for the two bulbs. With the masses and pressures involved it appears reasonable to claim an accuracy of ± 1 % for the vapour density figures at room temperature, and considerably better for those at 50° c.

Throughout this work, all stopcocks within the water-bath were lubricated with Apiezon grease L below 30° c. and with a special high-temperature grease, supplied by Messrs. W. Edwards, above 30° c. Apiezon L was used for all other stopcocks, the rate of attack by pure UF_6 being relatively slow.

Results.

The results are presented in Tables I-III and in Fig. 2 and 3. All pressures have been reduced to mm. Hg. at 0° c. The vapour pressure figures are single determinations made on a rising temperature scale.

TABLE I.—VAPOUR PRESSURE OF SOLID UF_6 FROM 12 TO 50° C.

T°K.	p, mm. Hg at 0°c.	$\text{Log}_{10}p$mm.	$10^3/T$°K.	$p_{\text{calc.}}$ (mm. Hg).
285·5	45·3	1·6561	3·502	45·9
287·3	52·0	1·7160	3·480	52·2
287·5	52·5	1·7202	3·477	53·2
287·7	53·6	1·7292	3·475	53·9
288·0	54·4	1·7356	3·472	54·8
290·6	66·1	1·8202	3·442	65·3
293·4	80·8	1·9074	3·408	80·4
298·1	113·5	2·0550	3·355	110·7
302·5	149·5	2·1747	3·306	147·9
308·3	216·8	2·3361	3·243	215·3
323·2	521·0	2·7168	3·094	521·2

TABLE II.—VAPOUR DENSITY OF UF_6.

t°c.	p, mm. Hg at 0°c.	Volume of Bulb, cc.	Mass of Vapour, g.	Density (H = 1.)	Molecular Weight (O = 16.)
14·1	52·0	271·0	0·279	176	355
14·8	54·4	271·0	0·293	178	357
17·4	66·1	270·8	0·347	174	352
29·7	157·5	126·4	0·369	174	352
50·0	521·0	270·8	2·488	176	355
50·0	419·0	270·8	1·987	175	353
50·0	392·1	270·8	1·854	174	352

TABLE III.—VARIATION OF DENSITY WITH PRESSURE AT 49·2° C.

p, mm. Hg at 0°C.	Volume of Bulb, cc.	Mass of Vapour, g.	$10^3\rho$, g./cc.	$10^{-5}P_{abs.}$, dyne/cm.^{2}
523·0	130·7	1·178	9·016	7·006
470·0	130·7	1·061	8·119	6·296
424·0	130·7	0·946	7·240	5·701
378·0	130·7	0·847	6·482	5·058
316·0	130·7	0·692	5·295	4·235
259·3	130·7	0·559	4·278	3·469
213·3	130·7	0·474	3·627	2·854
186·4	130·7	0·409	3·130	2·527

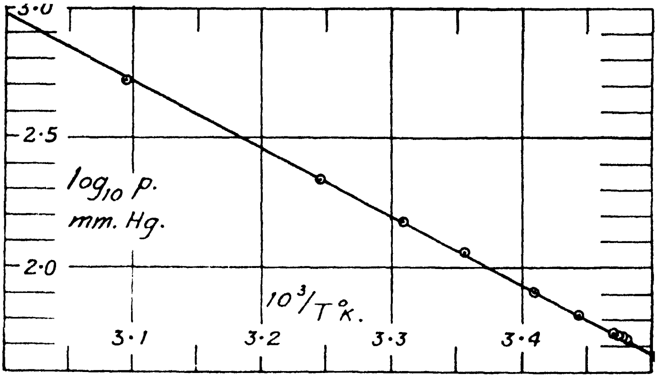

FIG. 2.—Vapour pressure of solid UF_6 from 12 to 56° C.

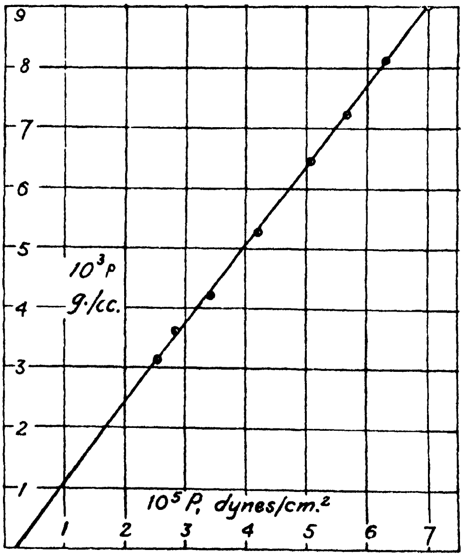

FIG. 3.—Pressure-density relationship for UF_6 vapour at 49·2° C.

Discussion.

The values of p and T quoted in Table I conform approximately to the linear relationship

$$\log_{10} p_{\text{mm.}} = 10{\cdot}74 - \frac{2592}{T}. \qquad \text{(Fig. 2)}$$

The values of $p_{\text{calc.}}$ quoted in the last column of Table I are obtained from this equation. The values of the latent heat of sublimation and of the sublimation temperature at atmospheric pressure obtained from this equation are :

$$L_s = 11{\cdot}82 \pm 0{\cdot}1 \text{ kcal. mole}^{-1},$$
$$t_s = 56{\cdot}7 \pm 0{\cdot}5^\circ \text{ C. at 760 mm. Hg.}$$

The justification for extrapolating the curve to the sublimation point is provided by earlier unquoted results[4] obtained with a Bourdon-type gauge which was subsequently found to possess a consistent error due to overstrain. Although the earlier figures themselves are not of any significance, a log p-$1/T$ plot shows that they obey a linear relationship over the range 0-56° C.

The arithmetic mean observed values of the molecular weight of the vapour at room temperature and at 50° C. are :

$$M = 355 \pm 3 \text{ at room temperature ;}$$
$$M = 353{\cdot}3 \pm 1 \text{ at } 50^\circ \text{ C. (theoretical } UF_6 = 352{\cdot}8).$$

The absolute values of ρ and P obey a linear relationship (Fig. 3), the slope of the line being given by

$$\left(\frac{\partial \rho}{\partial P}\right)_{49{\cdot}2^\circ \text{ C.}} = \left(1{\cdot}32 \pm 0{\cdot}01 \times 10^{-9}.\right)$$

The theoretical value of this quantity, assuming that the vapour obeys the simple gas laws, is $1{\cdot}313 \times 10^{-9}$.

The only published results on the vapour pressure and vapour density of UF_6 are those of Ruff and Heinzelmann,[5] who obtained five values for the former over the range 37-57° C., and two values of the vapour density at 448° C. From the log p-$1/T$ curve they derived extrapolated values of the vapour pressure at 0°, 20° and 56° C., and a mean value for L_s of 10·36 kcal. mole^{-1} ; a value of 338 was obtained for the molecular weight of the vapour. We consider that these results are open to doubt for the following reasons. Firstly, the methods used, viz. that of Smith and Menzies,[6] for the vapour pressure and that of Victor Meyer for the vapour density, do not readily lend themselves to determinations on a material which is highly reactive and sensitive to traces of moisture.

TABLE IV.

VAPOUR PRESSURE OF UF_6 ACCORDING TO RUFF AND HEINZELMANN.[5]

t°C.	p, mm. Hg.	$\log_{10} p_{\text{mm.}}$	$10^3/T$°K.
37	298·2	2·4745	3·223
41	406·1	2·6086	3·183
45	410·1	2·6129	3·143
48	521·2	2·7170	3·113
56·2	764·6	2·8834	3·032

---

[4] Amphlett, *Thesis* (Birmingham, 1944).

[5] Ruff and Heinzelmann, *Z. anorg. Chem.*, 1911, **72**, 63.

[6] Smith and Menzies, *J. Amer. Chem. Soc.*, 1910, **32**, 907.

Secondly, it is not clear that Ruff's material was free from HF. Finally, the agreement between the two vapour density figures is poor, these giving values of 327 and 349 for the molecular weight; in addition, the vapour pressures (which are quoted in Table IV) do not give a simple relationship between $\log_{10} p$ and $1/T°$ K. The extent to which the values of $\log_{10} p$ and $1/T$ deviate from a linear relationship may be seen from the figures quoted by the above authors for L_s over the above range, viz. 9·420 kcal. mole^{-1} (37-42° C.), 10·220 (42-47° C.), 10·330 (47-52° C.) and 10·550 (52-57° C.). No evidence was obtained in the present work of such a wide variation of L_s with temperature or of the existence of any transition point within the range 0-56° C.

We therefore conclude that the results quoted in this section are more reliable than the earlier figures and that they indicate that, within the range of these experiments, the behaviour of the vapour of UF_6 does not deviate appreciably from that predicted by the simple gas laws. The vapour density measurements appear to indicate that at ordinary temperatures the vapour consists of single, undissociated UF_6 molecules.

III. The Dielectric Constant of UF_6 Vapour.

The dielectric constant of UF_6 was measured by the heterodyne beat method, which has been developed for the study of dipole moments in the vapour phase.[7, 8, 9] By employing two oscillators of high frequency, a very small change in the frequency of one oscillator (produced by the change in capacity when the dielectric is withdrawn from a condenser within the tuned circuit) appears as a measurable change in the frequency of the beat produced when the outputs of the two oscillators are mixed. This capacity change may be balanced by the introduction of a known capacity into the variable oscillator until the beat frequency is restored to its original value. Variations in the beat frequency are detected by feeding the output to one pair of plates of a cathode ray tube, using the mains frequency of 50 c./sec. as a time-base to produce simple Lissajous figures, from which the frequency of the beat may be determined.

Experimental.

The condenser cell used to contain the dielectric was that described by Groves,[9] with suitable modifications to enable it to be sealed after filling with UF_6 vapour. The dielectric was removed from the cell by condensation in a side-tube cooled in liquid air, and the resulting capacity change was then balanced by adjustment of a precision variable condenser (Groves, loc. cit.) connected in parallel with the cell in the tuned circuit of one of the H.F. oscillators. The capacity change was then compared with that produced by the withdrawal of an equal pressure of pure, dry CO_2 gas, which was used as a standard. The figures obtained were corrected for the frequency drift of the oscillator during the period between the two readings (see below); a standardised procedure was adopted for making measurements so that this correction could be applied. From the ratio of the two capacity changes the dielectric constant of UF_6 can easily be found.

The cell was filled with UF_6 vapour at its saturated vapour pressure under room temperature conditions by connecting to a supply of pure UF_6 and allowing 48 hr. for equilibrium to be established before sealing off. Carbon dioxide was prepared by heating A.R. $NaHCO_3$ in an apparatus which had been evacuated and flushed several times with CO_2; the gas was dried over P_2O_5, condensed at − 180° C. and then vaporised at − 78° C. to remove the last traces of water. Results obtained at room temperature and at 207° C. with CO_2 prepared by this method were identical, indicating the absence of water vapour from the gas. Before filling either with CO_2 or with UF_6, the cell was evacuated to 10^{-5} mm. Hg while heated to 200° C.; the construction of the cell did not permit it to be heated to higher temperatures.

---

[7] Zahn, *Physic. Rev.*, 1924, **24**, 400.

[8] Watson, *et al.*, *Proc. Roy. Soc. A*, 1934, **143**, 558.

[9] Groves, *J. Chem. Soc.*, 1939, 1144.

The precision variable condenser described by Groves[9] was fitted with a micrometer head which could be read to 10^{-3} mm. The capacity variation was given as 0·1862 $\mu\mu$F./mm., so that capacity changes as low as 2×10^{-4} $\mu\mu$F. could be detected. Since ΔC is linearly proportional to the traverse on the condenser, the latter may be used as a measure of the capacity change (ΔC) in comparative methods of this kind.

The Beat Frequency Oscillator.—This consisted of two component oscillators of approximately 2 mc./sec. frequency, beating to produce a frequency of 50 c./sec., which was then fed to the cathode-ray tube. Modified Hartley oscillators were used ; the circuit design and construction are described in detail elsewhere.[4] The following precautions were taken to minimise various sources of instability which may arise in oscillator circuits.

(i) Mains fluctuations were smoothed through a constant voltage transformer unit.

(ii) Small thermal and vibration-induced capacity changes were reduced by adopting a very rigid construction, connections being made with the minimum length of stout wire, with ample support ; in many cases, connections were made with threaded rods.

(iii) Load on the oscillator valves due to external circuits was minimised by the use of electron-coupling to the mixing valve.[10]

(iv) Careful screening of the oscillators from one another and from the mixing circuit made it possible to obtain stable beats of frequencies as low as 3 c./sec. from 2 mc./sec. without forced oscillations.

(v) Temperature effects on the inductance and capacity of the tuned circuits were minimised by using high-grade silvered ceramic condensers and specially constructed coils. The ideal type of coil is one in which the metal winding is deposited in grooves cut into the coil former, since there can then be no differential thermal effects between the coil winding and former. Silica and ceramic formers have been used for this purpose,[11] but in these determinations a Pyrex former was used, using tubing free from flaws and air bubbles. A spiral groove was etched with HF, and the whole of the surface was then coated with several layers of a colloidal silver preparation * ; silver was then removed from the level surface of the tube, leaving a thin layer of silver in the groove. This was electroplated with copper, giving a coil to which connections could be soldered directly. The coils used had an inductance of ~ 30 μH. and a L.F. resistance of 2·5 Ω.

The stability of the beat was tested over long periods with both air and CO_2 in the cell, and also with the oscillator alone ; in these tests the frequency drift was followed by measuring the capacity change necessary to maintain the selected Lissajous figure on the screen. The circle was chosen as the standard figure, corresponding to an output frequency of 50 c./sec. This procedure was also followed during determinations for calculating the drift rates to be applied during the period when the dielectric was removed from the cell, the drift being measured over long periods before and after the removal. It was found that, once the oscillator had warmed up, the drift rate was small, fairly uniform, and always in the same direction. For example, the mean drift rate over a period of 3½ hr. was 0·005 mm./min. ; during most of this time the variation from the mean was no greater than ± 0·0005 mm./min., with a maximum variation of ± 0·002 mm./min. Observations were made at 2 min.-intervals over the entire period, with the screen under constant observation, so that any short-period fluctuations would have been observed. The mean drift of 0·005 mm./min. corresponds to a capacity change of $9{\cdot}31 \times 10^{-4}$ $\mu\mu$F./min., which is small compared with the capacity change when the dielectric is withdrawn.

Results.

If the mean traverses corrected to one atmosphere are respectively x and x' for CO_2 and for UF_6, allowing for the difference between the temperature of filling and that of the determination, then

$$\frac{\epsilon' - 1}{\epsilon - 1} = \frac{\Delta C'}{\Delta C} = \frac{x'}{x} = 4{\cdot}235.$$

---

* " Liquid Burnish Silver," supplied by Messrs. Johnson Matthey, Ltd.

[10] Dow, *Proc. Inst. Radio Eng.*, 1931, **19**, 2095.

[11] See, for example, H. A. Thomas, *Theory and Design of Valve Oscillators* (Chapman and Hall, 1939), ch. 6 and 9.

The dielectric constant of CO_2 has been repeatedly determined as an absolute measurement; following Le Fèvre and Russell[12] we take the mean of three relatively recent values[8, 13, 14] as $\epsilon = 1{\cdot}000905$ at 25° c. and 760 mm. Assuming that the temperature coefficient of ϵ may be neglected over the range 19-25° c., the value of ϵ' at 19·6° c. and 760 mm. is 1·0038. The error corresponding to a variation of ± 0·005 mm. in the traverse is ± 0·0001 unit, hence

TABLE V.—CELL FILLED WITH CO_2 AT 28° C. AND 570 mm. Hg.

t°c.	Traverse (mm.)	Drift Rate (mm./min.)	Time* (min.)	Corrected Traverse (mm.)
19	0·374	+ 0·002	1	0·376
	0·376	0·002	1	0·378
	0·375	0·002	1	0·377
	0·373	0·006	1	0·379
	0·375	0·003	1	0·378
	0·374	0·005	1	0·379
207	0·379	0·002	1½	0·382

* Time between last reading with dielectric in cell and first reading after freezing out.

Mean corrected traverse for 570 mm. CO_2 = 0·378 ± 0·001 mm.

TABLE VI.—CELL FILLED WITH UF_6 VAPOUR AT 16° C.; PRESSURE 58 mm.

t°c	Traverse (mm.)	Drift Rate (mm./min.)	Time (min.)	Corrected Traverse (mm.)
19·3	0·160	+ 0·006	1	0·166
19·5	0·158	0·005	1½	0·166
19·8	0·171	0·003	1	0·174
20·0	0·172	0·003	1	0·175

Mean corrected traverse for 58 mm. UF_6 = 0·170 ± 0·005 mm.

$$\epsilon_{UF_6} = 1{\cdot}0038 \pm 0{\cdot}0001 \text{ at } 19{\cdot}6° \text{ c. and } 760 \text{ mm.}$$

The total polarisation may be obtained from the Clausius-Mosotti relationship, viz.

$$_TP = \frac{\epsilon - 1}{\epsilon + 2} \cdot \frac{M}{\rho} = \frac{\epsilon - 1}{3} \cdot \frac{RT}{p} = 30{\cdot}7 \pm 1{\cdot}0 \text{ cc. at } 19{\cdot}6° \text{ c. and } 760 \text{ mm.}$$

TABLE VII.

Gas.	t°c.	$(\epsilon - 1) \times 10^3$.	$_TP$ cc.	Reference.
UF_6 . .	19·6	3·8	30·7	—
SF_6 . .	19·2	2·108	—	15
	25	2·049	16·51	8
	27·5	—	16·8	16
SeF_6 . .	20	2·481	—	15
TeF_6 . .	18·9	3·020	—	15
SiF_4 . .	25	1·702	13·78	8

---

[12] Le Fèvre and Russell, *Trans. Faraday Soc.*, 1947, **43**, 380.

[13] Stuart, *Z. Physik*, 1928, **47**, 457.

[14] McAlpine and Smyth, *J. Amer. Chem. Soc.*, 1933, **55**, 453.

[15] Linke, *Z. physik. Chem. B*, 1941, **48**, 193.

[16] Fuoss, *J. Amer. Chem. Soc.*, 1938, **60**, 1633.

There are no previously determined values for UF_6 with which to compare these figures ; $_TP$ is seen to be large, as is usually found in large molecules. A comparison with published data on other hexafluorides shows $(\epsilon - 1)$ to be of the same order, although $_TP$ is greater ; Table VII compares the values for UF_6 with those for the hexafluorides of the sulphur group, SiF_4 being also included. All values are at 760 mm.

It was intended to extend this work over a range of pressures and temperatures, but a serious accident to the gas cell and shortage of time prevented this aim from being realised. It appears unlikely, however, that UF_6 would possess a dipole moment, as the molecule would be expected to possess octahedral symmetry.

IV. The Ultra-Violet Absorption of UF_6 Vapour.

The experiments described below were made with a view to obtaining a qualitative picture of the absorption of UF_6 vapour between 2000 and 4000 A., and should be regarded as being of a preliminary nature.

Experimental.

Two cells were used, a 15 cm. Pyrex cell with silica windows and a 5 cm. cell of fused silica. A sample of pure UF_6 was contained in a small bulb attached to the cell by a T-piece ; by varying the temperature of the sample within this bulb the concentration of vapour in the cell could be varied. All subsequent references to temperature refer to this bulb. Exposures were made on a Hilger medium quartz spectrograph, with a hydrogen lamp as source and a copper arc for producing reference lines of known wavelengths. The hydrogen lamp has been described by Martin and Gull.[17] The slit dimensions were $2 \times 0{\cdot}025$ mm. Ilford Ordinary plates were used, and were developed for 3 min. in total darkness, using standard MQ developer.

Photometry of the spectra was carried out with the recording microphotometer and method described by Martin and Gull (loc. cit.). In this method, a series of blank exposures is made with the cell empty (by cooling the bulb in liquid air), the exposure times being calculated to correspond to a series of relative values of the extinction coefficient. If the latter quantity be represented by k, it can be shown that

$$kl \doteq p\,(\log t_1 - \log t_2),$$

where l is the length of the absorbing medium, p is a constant depending on the plate and method of development, and t_1 and t_2 are the exposures with the absorbing medium and with the empty cell respectively. Since l, t, and p remain constant, exposures corresponding to a series of relative values of k may be obtained by choosing suitable values of t_2. These are also recorded on the microphotometer, giving a series of lines crossing the absorption spectrum. The lines of the arc are also recorded, with the galvanometer shunted to reduce its swing.

Results.

Several plates were exposed, using both cells and varying the vapour concentration in the cell. The spectrum appears to be completely continuous, with no evidence of edges or other discontinuous structure. With concentrations of UF_6 vapour corresponding to its saturation vapour pressure at room temperature, absorption is complete below ~ 3100 A., but transmission may be extended to shorter wavelengths by reducing the pressure in the cell. Although the photometer records obtained with both cells were in good agreement when the vapour was at its room temperature concentration, at lower concentrations the spectrum extended towards much shorter wavelengths for the silica cell ; it was therefore concluded that at wavelengths below 3000 A. extraneous absorption occurred in the Pyrex cell, possibly due to the Canada balsam seals on the windows.

A typical microphotometer trace is shown in Fig. 4, which refers to the Pyrex cell containing UF_6 vapour at 91 mm. Approximate values of the extinction coefficients may be obtained by multiplying the relative figures by p/l, using the value of $p = 0{\cdot}91$ quoted by Martin and Gull for the plates and method of development used. Table VIII shows the effect of varying the concentration of UF_6 vapour on the wavelength at which complete extinction occurs, using the silica cell (l = 5 cm.).

---

[17] Martin and Gull, *J. Sci. Instr.*, 1935, **12**, 380.

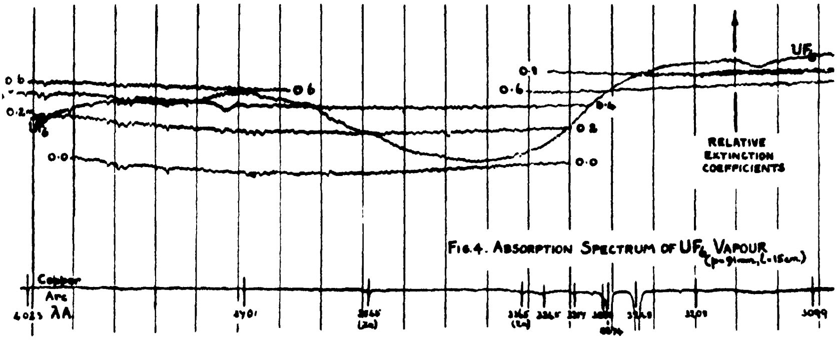

FIG. 4.

TABLE VIII

Bulb Temperature °C.	Pressure of UF_6 in Cell.* mm.	Concentration of UF_6 in moles/l.	Extinction Wavelength (A.)
17	64·3	$3{\cdot}48 \times 10^{-3}$	3100
−18	3·8	$2{\cdot}06 \times 10^{-4}$	2410
−48	$1{\cdot}7 \times 10^{-1}$	$\sim 1 \times 10^{-5}$	2270
−58	5×10^{-2}	$\sim 3 \times 10^{-6}$	2180
−77	3×10^{-3}	$\sim 2 \times 10^{-7}$	2130
−180	—	—	2130

* These values are extrapolated from the formula given in II; the low temperature values are approximate ones only.

It will be seen that, with a 5-cm. cell, pressures of vapour as low as 5×10^{-2} mm. still cause intense absorption below 2200 A.; below 2130 A. absorption by the optical system itself is complete. The question arises whether this intense absorption might be due to impurities such as HF or SiF_4, or to hydrogen diffusing into the cell when it is sealed off. HF is known [18] to show two bands in the ultra-violet, the second extending downwards from 2300 A. No reference could be found to the absorption of SiF_4 in this region, but consideration of the published figures for the vapours of the other silicon tetrahalides [19] suggests that continuous absorption by SiF_4 may commence in the far ultra-violet. The vapour-pressures of HF and of SiF_4 at − 77° C. are 4·6 mm.[20] and 3048 mm.[21] respectively, while at − 180° C. they are negligible. Consequently, if they were exhibiting absorption around 2100-2300 A. we should expect to find a difference in the extinction wavelengths recorded at − 77° C. and at − 180° C., contrary to observation. Furthermore, the final distillation at − 30° C. during purification should remove all traces of these impurities. The absence of hydrogen from the sample was demonstrated by exciting the emission spectrum of the vapour, using a Tesla discharge and external electrodes; no Balmer lines were observed

[18] Siga and Plumley, *Physic. Rev.*, 1935, **48**, 105.

[19] Deb, *Bull. Acad. Sci. United Provinces, India*, 1931-2, **1**, 92, gives the following values for the wavelengths at which continuous absorption begins: SiI_4, λ 3550 A.; $SiBr_4$, λ 2660 A.; $SiCl_4$, λ 2500 A.

[20] Extrapolated from the formula $\log_{10}p_{mm} = 7{\cdot}3739 - 1316{\cdot}79/T$ given by Claussen and Hildebrand, *J. Amer. Chem. Soc.*, 1934, **56**, 1820, for HF between 5-76 cm.

[21] Interpolated from the formula $\log_{10}p_{mm} = 8{\cdot}453 - 975{\cdot}0/T$ given by Patnode and Papish (ref.[3]) for liquid SiF_4.

when the spectrum was examined. It may reasonably be assumed, therefore, that the intense absorption at low wavelengths is due to UF_6 vapour, even at pressures as low as 10^{-2} mm. in a 5-cm. cell.

These investigations form part of a programme of work carried out at the University of Birmingham during the years 1941-43 for the Directorate of Tube Alloys (now the Directorate of Atomic Energy). The authors wish to express their appreciation of the interest shown in this work by Prof. Sir Norman Haworth ; thanks are also due to the staff of the Government Laboratory for facilities and helpful advice, and to the D.S.I.R. for a grant to one of us (C.B.A.) during the period of the work in London. We also wish to thank Sir John Cockcroft for permission to publish these results.

Summary.

Determination of the vapour pressure of carefully purified UF_6 from 12° c. to 50° c. gives the following equation :

$$\log_{10} p_{\text{mm.}} = 10{\cdot}74 - 2592/T,$$

from which the following values are obtained :

$$L_s = 11{\cdot}8 \pm 0{\cdot}1 \text{ kcal. mole}^{-1} ;$$
$$t_s = 56{\cdot}7 \pm 0{\cdot}5^\circ \text{ c. at 760 mm.}$$

The agreement between the observed and theoretical values for the molecular weight of the vapour at three different temperatures suggests that over this range the simple gas laws are obeyed within the limits of experimental error. This is supported by an investigation of the pressure-density relationship at a fixed temperature. Earlier results of Ruff and Heinzelmann are considered to be greatly in error.

The dielectric constant was measured by the heterodyne beat method relative to CO_2, the values obtained being

$$\left.\begin{array}{l} \epsilon = 1{\cdot}0038 \pm 0{\cdot}0001 \text{ relative to vacuum as unity} \\ {}_TP = 30{\cdot}7 \text{ cc.} \end{array}\right\} \begin{array}{l} \text{at } 20^\circ \text{ c. and} \\ 760 \text{ mm.} \end{array}$$

A preliminary examination of the ultra-violet absorption spectrum of the vapour showed continuous absorption at room temperature, with complete extinction below ~ 3100 A. in a 15-cm. cell filled with UF_6 vapour at 91 mm. Reasons are given for attributing this intense absorption to UF_6.

A detailed procedure for the purification of UF_6 is described.

Note added in proof.—Since this paper was prepared for publication there has appeared a paper by Weinstook and Crist (*J. Chem. Physics*, 1948, **16**, 436), giving the results of an independent determination of the vapour pressure of UF_6. The results are in good agreement with those quoted above, the vapour pressure equation for solid UF_6 being given (in the original declassified report MDDC-1295) as

$$\log_{10} p_{\text{mm.}} = 10{\cdot}8407 - 2623{\cdot}3/T.$$

A. E. Hills' Laboratories,
University of Birmingham.

The Government Laboratory,
Strand, W.C.2.

REVIEWS OF BOOKS.

Quarterly Reviews. Vol. II, No. 1. (London: The Chemical Society, 1948. Pp. 91. Price 8s.)

The Chemical Society's new publication, *Quarterly Reviews*, is now in its second year and the present is perhaps an appropriate time to take stock of the venture and attempt to assess its usefulness. It was planned as a means of countering a problem which is becoming increasingly difficult, namely that of keeping reasonably up to date on a broad front of chemical knowledge. Few chemists will wish to deny the existence of this problem, but the extent to which it can be met by the publication of review articles, which make up the contents of the new periodical, depends in a large measure on the way in which the articles are written. It is therefore a pleasure to be able to record the very general appreciation expressed for those which have appeared so far. The choice of subjects has been nicely balanced and the articles themselves have been readable and informative. The average number per volume is four, the titles for the present volume being:

" Disproportionation in inorganic compounds," by H. N. Wilson and J. G. M. Bremner.
" The chemistry of silicon polymers," by D. V. N. Hardy and N. J. L. Megson.
" Physiologically active unsaturated lactones," by L. J. Haynes.
" Far ultra-violet spectra, ionisation potentials and their significance in chemistry," by A. D. Walsh.

They differ from articles in the Society's Annual Reports in being much more general, and there seems to be place for the two publications provided their separate functions are borne in mind continually by the Society.

H. J. E.

Some Aspects of the Luminescence of Solids. By F. A. KRÖGER. Elsevier Publishing Co., Inc. (Cleaver-Hume Press Ltd., London, 1948. Pp. xi + 310. Price 30s).

This is neither a general survey nor a complete presentation of our knowledge of the phenomena of the luminescence of solids; it is a report of experimental work, hitherto unpublished, carried out in the laboratory of the N. V. Gloelampenfabrieken, Eindhoven, during the last five years, together with a theoretical discussion of certain aspects. Chapter I gives a discussion of the energy levels in pure and unperturbed crystals based mainly on energy diagrams; it is largely qualitative and could form an introduction to the subject for the general reader. The next four chapters are concerned almost entirely with the presentation of new results obtained with tungstates, molybdates and luminophors activated by manganese, titanium and uranium. The final chapter deals with the effect of temperature on the efficiency of luminescence from an experimental viewpoint and concludes with some qualitative theoretical considerations. An appendix of 45 pages has a brief account of applications and experimental methods and a Table including a full list of references, wherein luminescent systems are classified according to the activator.

The record of experimental data, published for the first time, and the attempt at classification will interest the specialist, but for the general reader the limitations imposed by confining the discussion to certain aspects of this wide subject may well give him a wrong impression of the present state of our knowledge. One is left in doubt whether the growing custom of publishing original results in book form is not an insidious practice which ought to be condemned, or whether by this method a partial solution of the difficulty of keeping in touch with a growing list of journals to be read by scientific workers might be found.

Isomerism and Isomerisation. By E. D. BERGMANN. (Interscience Publishers. New York, 1948. Price 21s.)

It is only when one comes across the writings of a contemporary to whom theories of organic chemistry *begin* with the doctrinaire acceptance of Pauling's extended theory of resonance that one realises the great extent to which the English outlook on mechanisms of organic reactions depends upon the pioneer work of Lapworth, who, over 40 years ago, made clear the ionic character of the majority of chemical changes, and thereby laid foundations for the logical interpretation, in the 1920's, of substitution, addition and isomerisation processes on an electro-dynamic basis.

Dr. E. D. Bergmann in his six lectures on *Isomerism and Isomerisation* touches upon many recent reactions of great interest, and tries to relate them to the structural features of resonating organic molecules, but it seems to the reviewer that his attempted correlations with the static structures of molecules frequently fail to explain facts which can be dealt with quite simply by the normal English approach to the electronic theory of valency. Dr. Bergmann does indeed talk about free cations, anions or neutral radicals, but he does not direct attention to their electrophilic or nucleophilic characteristics, and in discussing substitution processes he evidently does not realise the significance of the distinctions between the unimolecular and the bimolecular mechanisms, with the inevitable result that many important features of addition processes and molecular rearrangements are slurred over in a hasty, unco-ordinated fashion. In contrast, his sections dealing with the physics of molecular structure are both stimulating and useful.

In an introduction, Dr. H. Mark explains that these lectures were originally given to a research seminar at the Polytechnic Institute of Brooklyn. Undoubtedly they must have stimulated a very interesting discussion, and, to the outside reader, the value of the book would have been greatly enhanced if some of the points emerging from this discussion could have been printed also, in the manner of our own Discussions at Faraday Society meetings.

W. A. W.

CORRIGENDA.

P. 267. The legends of Fig. 1 and Fig. 2 should be interchanged.

P. 799. Eqn. (23). *For* e^{-r} *read* l^{-r}.

THE MECHANISM OF THE OXIDATION OF GLUCOSE BY PERIODATE.

By G. Hughes and T. P. Nevell.

Received 28th October, 1947.

It has been reported by Fleury and Lange [1] and by Malaprade [2] that periodic acid oxidises glucose quantitatively to formaldehyde and formic acid according to the following equation, in which the metaperiodate ion is represented as the oxidant:

$$C_6H_{12}O_6 + 5IO_4^- \rightarrow 5HCO_2H + HCHO + 5IO_3^-. \qquad (1)$$

The reaction conforms to the general type of periodate oxidations [3] and must, therefore, occur in a number of stages each of which consists of the oxidative fission of the carbon-carbon bond of an α-glycol, or potential α-glycol, group. The experiments to be described were undertaken to find an explanation for the fact that when glucose was oxidised with sodium periodate the reduction of the periodate appeared to be complete in quite a short time (1-2 hr.), whereas the production of formic acid occurred much more slowly,[4] the theoretical yield being attained only after several days.[5]

Experimental and Results.

The progress of reaction (1) is accompanied by increasing acidity of the system, and since the reaction rate might be dependent on *p*H the first experiments were made with buffered solutions. They were carried out at 0° C. and the concentration of periodate was measured at various times by allowing portions of the reaction mixture to react with standard arsenite in the presence of $NaHCO_3$ and KI, and back-titrating the excess of arsenite [6] with I_2. The results, illustrated in Fig. 1 and 2, show that the theoretical periodate consumption of 5 moles/mole glucose is attained rapidly in acid and neutral solutions but that the reaction is slower at *p*H 9·7. Whilst the reaction-rate curves for *p*H 4·6 and 6·9 are too complex for satisfactory analysis, the curve for *p*H 9·7 gives evidence of at least two stages in the reaction. First there is a very rapid initial reduction of one mole periodate/mole glucose and this is followed by a much slower reaction which is of zero order with respect to periodate over a considerable period of time.

During the course of the experiments at *p*H 9·7, it was observed that samples which had been back-titrated with I_2 after reacting with arsenite in the presence of $NaHCO_3$ and KI, slowly liberated considerable quantities of I_2 on standing; this reaction was complete in less than 1 hr. The amount of I_2 liberated was found to depend on the time elapsing between the back-titration with I_2 and the addition of the reaction sample to the mixture of standard arsenite, $NaHCO_3$ and KI. It also depended on the extent to which the reaction between periodate and glucose had proceeded, being greatest at the beginning and zero at the end. The effect appeared to be due, therefore, to the presence of partially oxidised intermediate products which act as oxidising agents towards I' ions. Although it was most marked in alkaline solutions it was also observed to a smaller extent in neutral and acid solutions. As a consequence of the effect the apparent amount of periodate reduced depends on the time elapsing before the back-titration with I_2 is carried out. These facts are illustrated by the results of two experiments recorded in Table I. In the first experiment the periodate was in excess but in the second there was 100 % excess of glucose so that the maximum theoretical consumption of periodate was only 2·5 moles/mole glucose.

---

[1] Fleury and Lange, *Compt. rend.*, 1932, **195**, 1395; *J. Pharm. Chim.*, 1933, **17**, 409.

[2] Malaprade, *Bull. Soc. chim.*, 1934, **1**, 833.

[3] Jackson, *Organic Reactions*, Vol. II (John Wiley and Sons, New York, 1944), Ch. 8.

[4] Private communication from T. G. Halsall and J. K. N. Jones, of Manchester University.

[5] Private communication from F. S. H. Head, of the Shirley Institute.

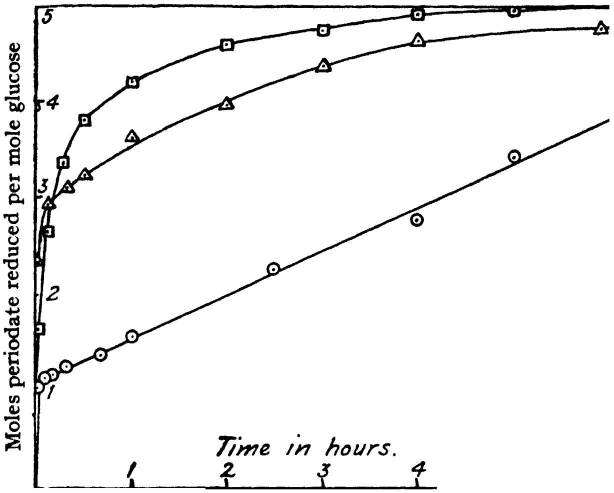

FIG. 1.—0·0025 M. glucose, 0·0175 M. periodate at 0° C.
△ *p*H 4·6, □ *p*H 6·9, ○ *p*H 9·7.

The evidence of the existence of intermediate products of oxidation was of obvious interest in relation to the delayed production of formic acid. Since the rate of formation of this acid could not be determined by alkali titrations in a buffered system, further experiments were made in unbuffered solutions. The apparent rate of reduction of periodate was measured by three methods each of which gave different results although they were all equally satisfactory for the estimation of periodate alone. The first method consisted of the procedure of Fleury and Lange [6] carried out exactly as described by them; $NaHCO_3$, standard arsenite and KI were added in that order to the reaction sample and the excess of arsenite was back-titrated with I_2 after 15 min. The second was a modifica-

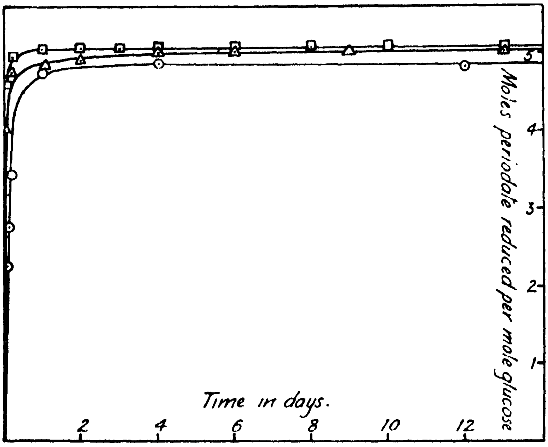

FIG. 2.—0·0025 M. glucose, 0·0175 M. periodate at 0° C.
△ *p*H 4·6, □ *p*H 6·9, ○ *p*H 9·7.

---

[6] Fleury and Lange, *J. Pharm. Chim.*, 1933, **17**, 107.

tion of the method of Fleury and Lange designed to permit greater precision in the measurement of reaction times. The reaction sample was run into a prepared mixture of standard arsenite, $NaHCO_3$ and KI, and the back-titration with I_2 was performed immediately. In the third method, the reaction sample was run into an excess of acidified KI solution and the I_2 liberated was titrated immediately with $Na_2S_2O_3$. Experiments were done at 20° C. and 0° C.

TABLE I.—OXIDATION OF GLUCOSE BY 0·0175 M. $NaIO_4$ AT pH 9·7

Concentration of Glucose (M.).	Approximate Reaction Time (min.).	Time before Back-titration with Iodine (min.).	Apparent Reduction of Periodate (moles/mole glucose).	Iodine Liberated after Completion of Titration (g. atom/mole glucose).
0·0025	3	5	0·96	0·67
,,	,,	15	0·71	0·24
,,	,,	30	0·61	0·03
,,	,,	60	0·60	0·00
,,	170	5	3·64	0·08
,,	,,	15	3·61	0·04
,,	,,	30	3·59	0·00
0·0070	3	5	0·97	0·43
,,	,,	15	0·87	0·11
,,	,,	60	0·79	0·00
,,	30	5	1·29	0·31
,,	,,	15	1·18	0·11
,,	,,	60	1·14	0·00
,,	180	5	2·12	0·14
,,	,,	15	2·07	0·02
,,	,,	60	2·04	0·00
,,	1 day	5	2·51	0·00

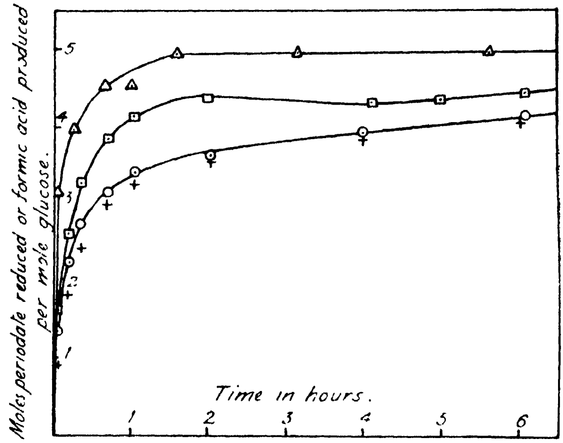

FIG. 3.—0·0125 M. glucose, 0·0875 M. periodate at 20° C.

Periodate by : Method of Fleury and Lange . . △
Modified method of Fleury and Lange ⊡
Thiosulphate method . . . ⊙
Formic acid by alkali titration . . . . . +

The results of the experiments at 20° C. are shown in Fig. 3 (for reaction times up to 6 hr.) and Table II (for reaction times up to 28 days). The production of formic acid is fairly slow, requiring several days to reach completion. The apparent amount of periodate reduced, as measured by the thiosulphate method, is identical with the yield of formic acid throughout the reaction except at the very beginning where it appears to be slightly greater. On the other hand, the method of Fleury and Lange indicates that the reduction of periodate is complete in less than 2 hr. The results obtained by the modified method of Fleury and Lange are intermediate between those obtained by the other two methods. At the end of the reaction, when no glucose remains, all three methods give substantially the same result. It may be noted that when the reaction is allowed to continue for a very long period (13 days and over), there is a slow progressive reduction of periodate beyond the theoretical value of 5 moles/mole glucose; this is accompanied by a corresponding decrease in the amount of formic acid present. This is no doubt due to the slow oxidation of formic acid and formaldehyde.[7] A qualitative test showed that the oxidation of formic acid by periodate leads to the liberation of I_2 and the presence of I_2 in the glucose-periodate reaction mixtures was clearly visible after about 20 days. This accounts for the serious discrepancy between the Fleury and Lange and the thiosulphate methods of estimating periodate at 28 days. In the former method, the whole of this iodine would be estimated as residual periodate but in the latter, only one quarter of it would be so estimated; hence the amount of periodate consumed would appear to be greater when measured by the thiosulphate method. The results of the experiments at 0° C. (Fig. 4 and Table III) are similar; the only effect of the reduction of temperature is a reduction in the speed of the reaction. In all these experiments the liberation of I_2 after the completion of

TABLE II.—OXIDATION OF 0·0125 M. GLUCOSE BY 0·0875 M. $NaIO_4$ AT 20° C.

Time.	Periodate reduced (moles/mole Glucose).			Formic Acid (moles/mole Glucose).
	Fleury and Lange Method.	Modified Fleury and Lange Method.	Thiosulphate Method.	
22 hr.	5·00	4·84	4·49	4·40
4 days	5·02	4·94	4·91	4·89
8 ,,	5·05	4·98	5·09	4·91
13 ,,	5·16	5·10	5·21	4·95
19 ,,	5·35	5·29	5·37	4·84
28 ,,	5·36	5·72	6·03	4·40

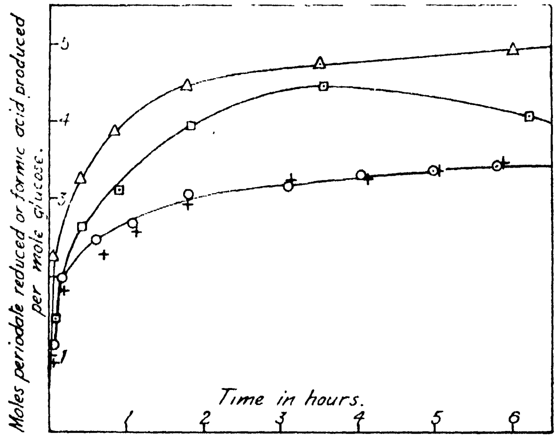

FIG. 4.—0·0125 M. glucose, 0·0875 M. periodate at 0° C.

Periodate by : Method of Fleury and Lange . . △
Modified method of Fleury and Lange ⊡
Thiosulphate method . . . ⊙
Formic acid by alkali titration . . . . . +

---

[7] Davidson, *J. Text. Inst.*, 1941, **32**, T109.

the Fleury and Lange titration was very marked in the early stages of the reaction, but it did not occur when the modified procedure was used. It will be observed from Fig. 3 and 4 that when the rate of reduction of periodate is measured by the modified method of Fleury and Lange the rate curve appears to pass through a maximum at a periodate consumption of about 4·5 moles/mole glucose. The region in which *apparent* re-oxidation of iodate took place was carefully examined in a separate experiment the results of which are shown in Fig. 5 and it is clear that in this region the modified method of Fleury and Lange for estimating periodate gives very erratic results; even the original method seems to be subject to somewhat greater variations than usual.

TABLE III.—OXIDATION OF 0·0125 M. GLUCOSE BY 0·0875 M. $NaIO_4$ AT 0° C.

Time.	Periodate reduced (moles/mole Glucose).			Formic Acid (moles/mole Glucose).
	Fleury and Lange Method.	Modified Fleury and Lange Method.	Thiosulphate Method.	
23 hr.	4·81	4·06	3·90	3·85
10 days	4·85	4·60	4·59	4·62
14 ,,	4·88	4·64	4·68	4·65
31 ,,	4·96	4·84	4·89	4·84

Experiments in Buffered Solution.—Sodium metaperiodate (0·0035 mole) was dissolved in water and sufficient buffer mixture to give a final concentration of 0·2 M. was added; the mixture was diluted to about 170 ml. and cooled to 0° C. The reaction was started by adding 0·02 M. glucose (25 ml.), cooled to 0° C., and making up to 200 ml. with water. The initial composition of the reaction mixtures was therefore 0·0175 M. with respect to periodate and 0·0025 M. with respect to glucose. The following buffer mixtures were used: (*a*) for *p*H 4·6, equimolar quantities of sodium acetate and acetic acid; (*b*) for *p*H 6·9, $(NH_4)_2HPO_4$ and $(NH_4)H_2PO_4$ in the molar ratio, 3/1; (*c*) for *p*H 9·7, equimolar quantities of K_2CO_3 and $KHCO_3$. The *p*H's were measured with a glass electrode in conjunction with a Cambridge *p*H-meter. The concentration of periodate was determined on 10 ml. portions of the reaction mixture withdrawn at suitable intervals, by the following modifications of the method of Fleury and Lange.•

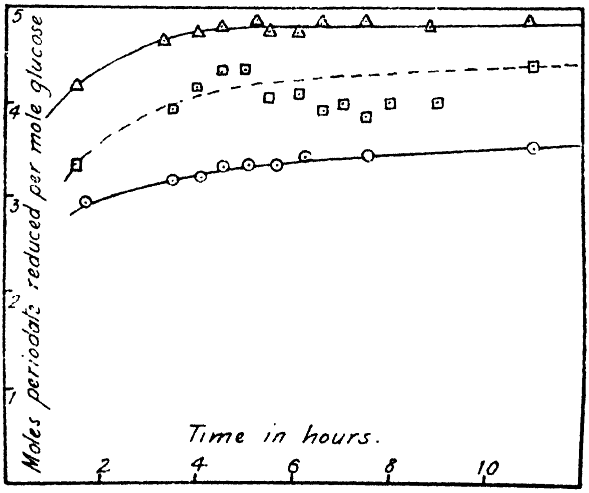

FIG. 5.—0·0125 M. glucose, 0·0875 M. periodate at 0° C.

Periodate by : Method of Fleury and Lange . . △
Modified method of Fleury and Lange ⊡
Thiosulphate method . . . ⊙

(*a*) At *p*H 4·6; the test portion was run into a mixture of 0·02 N. sodium arsenite (25 ml.), 10 % KI (2 ml.), saturated $NaHCO_3$ (10 ml.) and 0·1 N. NaOH (10 ml.), and titrated with 0·01 N. I_2 immediately.

(*b*) At *p*H 6·9; the procedure was the same as at *p*H 4·6 except that the 0·1 N. NaOH was omitted.

(*c*) At *p*H 9·7; the test portion and 0·1 N. H_2SO_4 (10 ml.) were run simultaneously into a mixture of 0·02 N. sodium arsenite (20 ml.), 20 % KI (5 ml.) and saturated $NaHCO_3$ (10 ml.) with vigorous shaking, and titrated with 0·04 N. I_2 immediately.

Liberation of Iodine after Completion of Titration.—The results shown in Table I were obtained from two experiments with 0·0175 M. sodium metaperiodate buffered at *p*H 9·7 by means of 0·1 M. K_2CO_3 and 0·1 M. $KHCO_3$; the initial concentrations of glucose were 0·0025 and 0·007 M. respectively. The periodate concentration was determined at suitable intervals by running test portions of the solution (10 ml.) and 0·1 N. H_2SO_4 (10 ml.) simultaneously into a mixture of 0·02 N. sodium arsenite (25 ml.), 10 % KI (5 ml.) and saturated $NaHCO_3$ (10 ml.); after standing for various times the mixtures were titrated with 0·01 N. I_2. After a further hour, the I_2 liberated was back-titrated with 0·01 N. sodium arsenite.

Experiments in Unbuffered Solutions.—Sodium metaperiodate (0·04375 mole) was dissolved in water (470 ml.) at 0° C. or 20° C., 0·25 M. glucose (25 ml.) at 0° C. or 20° C. was added, and the mixture was made up to 500 ml. with water. The initial composition of the reaction mixtures was therefore 0·0875 M. with respect to periodate and 0·0125 M. with respect to glucose. The concentrations of periodate and formic acid were determined on 10 ml. portions of the reaction mixture withdrawn at suitable intervals, by the following methods.

(*a*) METHOD OF FLEURY AND LANGE. To the test portion were added saturated $NaHCO_3$ (10 ml.), 0·1 N. sodium arsenite (25 ml.) and 20 % KI (5 ml.) in that order. After 15 min. the excess of arsenite was titrated with 0·1 N. I_2.

(*b*) MODIFIED METHOD OF FLEURY AND LANGE. The test portion was run into a mixture of 0·1 N. sodium arsenite (25 ml.), 20 % KI (5 ml.) and saturated $NaHCO_3$ (10 ml.), and titrated with 0·1 N. I_2 immediately.

(*c*) THIOSULPHATE METHOD. The test portion was run into a mixture of 20 % KI (8 ml.), 2 N. H_2SO_4 (5 ml.) and water (50 ml.); 0·25 N. $Na_2S_2O_3$ (20 ml.) was added immediately and the titration of the liberated I_2 was completed with 0·1 N. thiosulphate.

The three methods (*a*), (*b*) and (*c*) gave identical results when used for the analysis of pure periodate solutions.

(*d*) FORMIC ACID was determined by titration of the test portion with 0·05 N. NaOH after the destruction of the periodate present with ethylene glycol (5 ml. of a 10 % solution), phenolphthalein being used as indicator.[8]

Discussion.

The results reported above provide clear evidence that the oxidation of glucose by periodate proceeds by way of intermediate substances which are more stable in alkaline than in acid solutions, and which oxidise I′ ions more rapidly in acid than in alkaline solutions. In the interpretation of the results it is assumed that the main point of periodate attack is the potential α-glycol group in the 1 : 2-position of the glucose molecule, and that in the first stage of the reaction an intermediate substance is formed which decomposes into a pentose and formic acid. Later successive stages consist in the formation of similar intermediate substances from a pentose, tetrose, triose and biose, followed by their decomposition into formic acid and a tetrose, triose, biose and formaldehyde respectively. In the reaction at *p*H 9·7 (see Fig. 1) the rate-controlling process is the unimolecular decomposition of the intermediate substances. The first very rapid consumption of one mole of periodate per mole of glucose represents the production of the hexose intermediate which is then converted slowly into formic acid and a pentose. The pentose is rapidly attacked by periodate as soon as it is formed with the production of a pentose intermediate. The rate of this second reaction is therefore equal to the rate of decomposition of the hexose intermediate and is independent of the amount of periodate present, provided that there is an excess. In the same way the rate of decomposition of the pentose intermediate determines the rate at which periodate reacts with tetrose and so on. Hence the rate of oxidation is of zero order with respect to periodate.

---

[8] Brown, Dunstan, Halsall, Hirst and Jones, *Nature*, 1945, **156**, 785.

The discrepant analytical results obtained with unbuffered solutions may be explained in the following way. When the thiosulphate method is used to measure the apparent reduction of periodate the intermediate substances, as well as the residual periodate, react with the acidified KI, liberating I_2. Hence this method of analysis measures the rate of transformation of glucose into non-oxidising products and not the rate at which periodate is reduced to iodate. The substantial agreement between the rate of production of formic acid and the rate of oxidation measured by the thiosulphate method throughout the reaction is evidence that at every stage the principal attack of the periodate is directed at the potential α-glycol group in the 1 : 2-position of the aldose molecule. The small discrepancy at the beginning of the reaction may be attributed to a small amount of oxidation of α-glycol groups other than those in the 1 : 2-position ; such oxidation would not lead to the immediate production of formic acid.

When periodate consumptions are measured by the original method of Fleury and Lange, the intermediate substances do not oxidise I′ ions rapidly owing to the low H^+ ion concentration. Hence they contribute only slightly to the oxidation of the arsenite, which is due, in this case, mainly to the periodate present. The method gives, therefore, the closest approximation to the true rate of reduction of periodate, which is very rapid compared with the rate of production of formic acid. When the back-titration with I_2 has been completed the mixture in the titration flask still contains most of the intermediate substances and these continue to react slowly with the KI present causing the gradual liberation of I_2.

When the modified procedure of Fleury and Lange is adopted, the reaction samples are run into prepared mixtures of standard arsenite, $NaHCO_3$ and KI, and in these circumstances the intermediate substances have time to oxidise a considerable quantity of arsenite before being stabilised by the $NaHCO_3$. Hence results intermediate between those obtained by the other two methods are to be expected. Since there is no reason to suppose that the five possible intermediate substances (derived from hexose, pentose, tetrose, triose and biose) are all equally strong oxidising agents, a plausible explanation can be offered of the appearance of maxima in the curves obtained by the modified method (Fig. 3, 4 and 5). When the reaction has reached a certain stage, a small increase in the oxidising power of the intermediate substances would result in a greater proportion of them being estimated together with residual periodate. Thus an apparent decrease in the amount of periodate reduced would be observed.

The nature of the intermediate substances which have been detected is a matter for speculation. A recent paper,[9] which contains a review of the literature, shows that most previous workers have accepted the original suggestion of Criegee [10] that the fission of glycols by periodate proceeds by way of a cyclic diester, e.g.

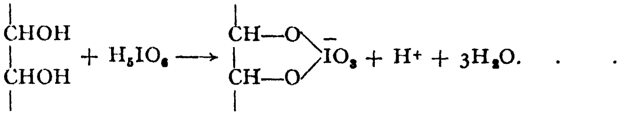

$$\begin{matrix} | \\ \text{CHOH} \\ | \\ \text{CHOH} \\ | \end{matrix} + H_5IO_6 \longrightarrow \begin{matrix} | \\ \text{CH—O} \\ | \\ \text{CH—O} \\ | \end{matrix}\!\!\!> IO_3^- + H^+ + 3H_2O. \quad . \quad . \quad (2)$$

The formation of such an ester would explain our results. The main objections are that our intermediate substances are produced under conditions not usually associated with ester formation and that they are

---

[9] Heidt, Gladding and Purves, *Paper Trade J.*, 1945, **121**, 81 (T.A.P.P.I.).

[10] Criegee, Kraft and Rank, *Annalen*, 1933, **507**, 159.

more stable in alkaline than in acid solutions. Such objections may be partly met by noting that the proposed ester is a cyclic one and that in all probability it carries a negative charge. It is possible to formulate a free-radical mechanism for the reaction (cp. Waters [11]) but it is difficult to believe that glycol free radicals could be sufficiently long-lived to account for the intermediate substances observed in the present work.

Summary.

The rate of reduction of unbuffered periodate solutions by glucose, and the rate of production of formic acid from the glucose, have been studied; the effect of pH on the rate of the reaction has also been investigated. The experimental results disclose the formation of intermediate products that are themselves oxidants and decompose into the final reaction products. It is suggested that these intermediate substances are cyclic diesters of periodic acid.

The British Cotton Industry Research Association,
Shirley Institute,
Didsbury,
Manchester.

[11] Waters, *Trans. Faraday Soc.*, 1946, **42**, 184.

THERMODYNAMICS OF MONOLAYERS.

BY C. KEMBALL, E. K. RIDEAL and E. A. GUGGENHEIM.

Received 7th November, 1947.

1. Introduction. — Surprisingly little work either experimental or theoretical has been applied to mixed adsorption. The present paper is devoted to a study of equations of state corresponding to the simplest possible kind of model for monolayers containing two kinds of adsorbed molecules. The formulæ will be compared with the simpler well-known formulæ for monolayers containing adsorbed molecules of only one kind, in particular the formulæ due to Volmer.[1] It will be shown that certain other formulæ which have been proposed are self-contradictory.

2. Monolayer as Two-Dimensional Gas.—It is well known that certain monolayers can profitably be regarded as the two-dimensional analogue of a gas. The close analogy between the formulæ for such a monolayer and those for a gas has been emphasised elsewhere.[2] In particular, we recall the form of the thermodynamic functions in the case of a single adsorbed species.

The free energy F^{ads} of the adsorbed monolayer is given by : [2]

$$\frac{F^{\mathrm{ads}}}{kT} = N \log \frac{jN}{A} - N + \frac{N^2 B}{A}, \quad . \quad . \quad . \quad (2.1)$$

where N denotes the number of molecules adsorbed on the area A at the absolute temperature T; k is Boltzmann's constant; j and B depend on the nature of the adsorbed molecules, on the nature of the surface and on the temperature, but are independent of N. The parameter B is the exact analogue of the second virial coefficient of a gas. If one chose to regard B as a co-volume, one might expect B to be independent of temperature, but there seems no point in introducing such a restriction on the nature of the virial coefficient

Formula (2.1) is the precise analogue of the formula for the free energy of a single, *slightly imperfect* gas. At high deviations from perfection, that is to say when NB/A is not small, one would need to introduce higher virial coefficients. We shall, however, not be concerned with such better approximations.

---

[1] Volmer, *Z. physik. Chem.*, 1925, **115**, 253.

[2] Fowler and Guggenheim, *Statistical Thermodynamics*, 1939. (Hereafter referred to as S.T.), § 1003.

By differentiation of (2.1) with respect to A we obtain for the two-dimensional spreading pressure ϕ

$$\frac{\phi}{kT} = \frac{N}{A} + \frac{N^2B}{A^2} = \Gamma + \Gamma^2B, \qquad (2.2)$$

where $\Gamma = N/A$.

By differentiation of (2.1) with respect to N, we obtain for the chemical potential μ,

$$\frac{\mu}{kT} = \log\frac{jN}{A} + \frac{2NB}{A} = \log j\Gamma + 2\Gamma B. \qquad (2.3)$$

By equating the chemical potential to that in the vapour phase, we obtain a relation between Γ and the partial vapour pressure p of the form

$$\log\frac{lp}{kT} = \log\,\Gamma + 2\Gamma B, \qquad (2.4)$$

where l, a quantity having the dimensions of a length, like j depends on T but is independent of Γ.

The extension of these formulæ to two adsorbed species by analogy with a mixture of two gases [3] is immediate. For the free energy of the adsorbed monolayer we have in place of (2.1)

$$\frac{F^{\text{ads}}}{kT} = N_1\log\frac{j_1N_1}{A} - N_1 + N_2\log\frac{j_2N_2}{A} - N_2 + \frac{(N_1+N_2)^2\overline{B}}{A}, \qquad (2.5)$$

where N_1, N_2 denote the number of molecules of the species, 1, 2 respectively adsorbed on the area A. j_1, j_2 depend on the temperature but not on N_1, N_2. The second virial coefficient denoted by $\overline{B}$, as well as depending on the temperature, depends on the relative values of N_1, N_2 according to

$$(N_1 + N_2)^2\overline{B} = N_1^2B_1 + 2N_1N_2B_{12} + N_2^2B_2, \qquad (2.6)$$

where B_1, B_2 and B_{12} depend on the temperature but are independent of N_1/N_2. It is convenient to define a quantity w by

$$w = B_{12} - \tfrac{1}{2}(B_1 + B_2), \qquad (2.7)$$

since for pairs of closely similar substances, such as two alcohols, it is plausible to assume that $w = 0$. Using (2.7) in (2.6) we obtain

$$(N_1 + N_2)^2\overline{B} = (N_1 + N_2)(N_1B_1 + N_2B_2) + 2N_1N_2w, \qquad (2.8)$$

or
$$B = \frac{\Gamma_1}{\Gamma_1 + \Gamma}B_1 + \frac{\Gamma_2}{\Gamma_1 + \Gamma_2}B_2 + \frac{2\Gamma_1\Gamma_2}{(\Gamma_1 + \Gamma_2)^2}w, \qquad (2.9)$$

where
$$\Gamma_1 = \frac{N_1}{A}, \text{ and } \Gamma_2 = \frac{N_2}{A}. \qquad (2.10)$$

Differentiating (2.5) with respect to A, we obtain for the spreading pressure ϕ

$$\frac{\phi}{kT} = \frac{N_1 + N_2}{A} + \frac{(N_1 + N_2)^2}{A^2}\overline{B} = \Gamma_1 + \Gamma_2 + (\Gamma_1 + \Gamma_2)^2\overline{B}. \qquad (2.11)$$

Differentiating (2.5) with respect to N_1, bearing in mind (2.8), we obtain for the chemical potential μ_1 of the species 1

$$\frac{\mu_1}{kT} = \log j_1\Gamma_1 + 2B_1\Gamma_1 + (B_1 + B_2 + 2w)\,\Gamma_2. \qquad (2.12)$$

Similarly
$$\frac{\mu_2}{kT} = \log j_2\Gamma_2 + 2B_2\Gamma_2 + (B_1 + B_2 + 2w)\,\Gamma_1. \qquad (2.13)$$

---

[3] S.T., formula (704.3).

By equating each chemical potential to that in the vapour phase, we obtain relations between Γ_1, Γ_2 and the partial vapour pressures p_1, p_2 of the two components

$$\log \frac{l_1 p_1}{kT} = \log \Gamma_1 + 2B_1\Gamma_1 + (B_1 + B_2 + 2w)\Gamma_2, \tag{2.14}$$

$$\log \frac{l_2 p_2}{kT} = \log \Gamma_2 + 2B_2\Gamma_2 + (B_1 + B_2 + 2w)\Gamma_1, \tag{2.15}$$

where l_1, l_2 are independent of Γ_1, Γ_2.

3. Alternative Forms.—Since formula (2.5) is correct only to the terms shown, further terms involving higher powers of N_1/A and N_2/A being neglected, we may if we choose without either gain or loss of accuracy, replace it by the alternative formula

$$\frac{F^{\text{ads}}}{kT} = N_1 \log \frac{j_1 N_1}{A - (N_1 + N_2)\overline{B}} - N_1 + N_2 \log \frac{j_2 N_2}{A - (N_1 + N_2)\overline{B}} - N_2, \tag{3.1}$$

where $\overline{B}$ is still defined by (2.6). We shall see that this particular choice is the natural extension of Volmer's [1] formulæ for monolayers containing molecules of only one kind. By using (3.1) instead of (2.5) we shall in the special case $w = 0$, without further mathematical approximations, be able to obtain a relation between p_1, p_2, ϕ not involving Γ_1, Γ_2.

Differentiating (3.1) with respect to A, we obtain for the spreading pressure ϕ

$$\frac{\phi}{kT} = \frac{N_1 + N_2}{A - (N_1 + N_2)\overline{B}} = \frac{1}{\overline{A} - \overline{B}}, \tag{3·2}$$

where

$$\overline{A} = A/(N_1 + N_2). \tag{3·3}$$

Differentiating (3.1) with respect to N_1, bearing in mind (2.8), we obtain

$$\frac{\mu_1}{kT} = \log \frac{j_1 \Gamma_1}{(\Gamma_1 + \Gamma_2)(\overline{A} - \overline{B})} + \frac{B_1 + 2\Gamma_2^2 w/(\Gamma_1 + \Gamma_2)^2}{\overline{A} - \overline{B}}, \tag{3·4}$$

$$\frac{\mu_2}{kT} = \log \frac{j_2 \Gamma_2}{(\Gamma_1 + \Gamma_2)(\overline{A} - \overline{B})} + \frac{B_2 + 2\Gamma_1^2 w/(\Gamma_1 + \Gamma_2)^2}{\overline{A} - \overline{B}}. \tag{3·5}$$

By equating each chemical potential to that in the vapour phase, we obtain relations between Γ_1, Γ_2 and the partial vapour pressures p_1, p_2 of the two components

$$\log \frac{l_1 p_1}{kT} = \log \frac{\Gamma_1}{(\Gamma_1 + \Gamma_2)(\overline{A} - \overline{B})} + \frac{B_1 + 2\Gamma_2^2 w/(\Gamma_1 + \Gamma_2)^2}{\overline{A} - \overline{B}}, \tag{3·6}$$

$$\log \frac{l_2 p_2}{kT} = \frac{\Gamma_2}{\log (\Gamma_1 + \Gamma_2)(\overline{A} - \overline{B})} + \frac{B_2 + 2\Gamma_1^2 w/(\Gamma_1 + \Gamma_2)^2}{\overline{A} - \overline{B}}, \tag{3·7}$$

where l_1, l_2 are independent of Γ_1, Γ_2.

By substitution from (3.2) we can rewrite (3.6), (3.7) in the forms

$$\log l_1 p_1 = \log \frac{\Gamma_1 \phi}{\Gamma_1 + \Gamma_2} + \left\{B_1 + \frac{2\Gamma_2^2 w}{(\Gamma_1 + \Gamma_2)^2}\right\}\frac{\phi}{kT}, \tag{3·8}$$

$$\log l_2 p_2 = \log \frac{\Gamma_2 \phi}{\Gamma_1 + \Gamma_2} + \left\{B_2 + \frac{2\Gamma_1^2 w}{(\Gamma_1 + \Gamma^2)}\right\}\frac{\phi}{kT}. \tag{3·9}$$

In the special case $w = 0$, relevant to a pair of very similar substances, (3.8) and (3.9) reduce to

$$\frac{\Gamma_1}{\Gamma_1 + \Gamma_2} = \frac{l_1 p_1}{\phi} e^{-B_1\phi/kT}, \tag{3.10}$$

$$\frac{\Gamma_2}{\Gamma_1 + \Gamma_2} = \frac{l_2 p_2}{\phi} e^{-B_2\phi/kT}. \tag{3.11}$$

It is interesting to note that in this special case we can by addition entirely eliminate Γ_1, Γ_2, obtaining the relation between ϕ, p_1, p_2,

$$l_1 p_1 \mathrm{e}^{-B_1\phi/kT} + l_2 p_2 \mathrm{e}^{-B_2\phi/kT} = \phi. \qquad (3.12)$$

4. Comparison with Volmer's Relations.—As already mentioned the formulæ of § 3 are neither more nor less accurate than those of § 2. Their chief claim to interest is their closer relationship to the formulæ given by Volmer for a single adsorbed species.

If we set $N_2 = 0$ in (3.1) and drop redundant subscripts and average signs, we obtain for a single adsorbed species

$$F^{\mathrm{ads}} = NkT \log \frac{jN}{A - NB}. \qquad (4.1)$$

At the same time (3.2) becomes

$$\frac{\phi}{kT} = \frac{N}{A - NB'} \qquad (4.2)$$

while (3.7) becomes, when we use $\Gamma\bar{A} = 1$

$$\frac{lp}{kT} = \frac{\Gamma}{1 - \Gamma B}\mathrm{e}^{\Gamma B/(1-\Gamma L)} \qquad (4.3)$$

Formulæ (4.2) and (4.3) are due to Volmer.

5. Gibbs' Absorption Formula.—The thermodynamic relation due to Gibbs between the spreading pressure ϕ and the partial vapour pressures may be written in the form[4] invariant with respect to Gibbs' geometrical surface

$$\frac{l}{kT}\mathrm{d}\phi = (\Gamma_1 - m_1\Gamma_0)\mathrm{d}\log p_1 + (\Gamma_2 + m_2\Gamma_0)\,\mathrm{d}\log p_2, \qquad (5.1)$$

where the subscript 0 refers to the solvent and m_1, m_2 denote the number of molecules of the solute species 1, 2 respectively per molecule of solvent. For dilute solutions, for which alone our formulæ are valid, we have $m_1 \ll 1$, $m_2 \ll 1$ and we may replace (5.1) by the simpler and better-known relation

$$\frac{1}{kT}\mathrm{d}\phi = \Gamma_1\mathrm{d}\log p_1 + \Gamma_2\mathrm{d}\log p_2. \qquad (5.2)$$

There is no difficulty in verifying that this relation is satisfied either by the formulæ of § 2 or by the formulæ of § 3, as it is indeed automatically satisfied by any set of formulæ derived either from a self-consistent model or from a consistently assumed form for the free energy of the adsorbed layer. It would not be necessary to mention this obvious truth, were it not that formulæ have been proposed which do not correspond to any model, which are not naturally consistent and which do not satisfy the thermodynamic criterion (5.2). We shall refer to such an example of impossible formulæ in § 6.

6. Ideal Localized Monolayer.—All the formulæ discussed hitherto relate to monolayers of the mobile kind. They are accordingly most suitable for application to adsorbed layers at the surface of a liquid. The opposite kind of monolayer, known as localized, corresponds more nearly to adsorbed layers at the surface of a crystal, though it may possibly also serve as a useful model in the case of adsorption at the surface of a liquid.

In the model of a localised monolayer it is assumed that the surface contains a definite number of sites arranged uniformly, each of which may either be occupied by an adsorbed molecule or be vacant. This model was introduced by Langmuir,[5] who at the same time derived, by kinetic arguments, formulæ relating the amounts adsorbed to the partial vapour pressures, in the simple case of no interaction between the adsorbed molecules. Such a localised monolayer is called ideal. These formulæ have subsequently been derived by statistical methods. Complete accounts are available elsewhere and there is no cause to reproduce such derivations. It will suffice to recall the formulæ for the equilibrium partial vapour pressure p_1, p_2 over a localized monolayer in which the fractions θ_1, θ_2 of the sites are occupied by molecules of the types 1, 2 respectively,[6]

---

[4] Guggenheim and Adam, *Proc. Roy. Soc. A*, 1933, **139**, 218.

[5] Langmuir, *J. Amer. Chem. Soc.*, 1918, **40**, 1361.

$$\frac{p_1}{p_{h_1}} = \frac{\theta_1}{1 - \theta_1 - \theta_2}, \quad . \quad . \quad . \quad . \quad (6.1)$$

$$\frac{p_2}{p_{h_2}} = \frac{\theta_2}{1 - \theta_1 - \theta_2}. \quad . \quad . \quad . \quad . \quad (6.2)$$

Here p_{h_1} denotes the value of p_1 when half the sites are occupied by molecules of type 1 and the other half are vacant, while p_{h_2} is defined similarly. We can solve (6.1), (6.2) for θ_1, θ_2 obtaining

$$\theta_1 = \frac{p_1/p_{h_1}}{1 + (p_1/p_{h_1}) + (p_2/p_{h_2})}, \quad . \quad . \quad . \quad (6.3)$$

$$\theta_2 = \frac{p_2/p_{h_2}}{1 + (p_1/p_{h_1}) + (p_2/p_{h_2})}. \quad . \quad . \quad . \quad (6.4)$$

If, as previously we denote by Γ_1, Γ_2 the number of molecules of the two kinds adsorbed per unit area, we can rewrite (6.3), (6.4) as

$$\Gamma_1 = \frac{p_1/p_{h_1}A_s}{1 + (p_1/p_{h_1}) + (p_2/p_{h_2})}, \quad . \quad . \quad . \quad (6.5)$$

$$\Gamma_2 = \frac{p_2/p_{h_2}A_s}{1 + (p_1/p_{h_1}) + (p_2/p_{h_2})}, \quad . \quad . \quad . \quad (6.6)$$

where A_s denotes the area per site. These formulæ correspond accurately to the model described. They are consequently mutually consistent and automatically satisfy the criterion of Gibbs' adsorption relation. We need say no more about them except to contrast them with a formula proposed by Butler and Ockrent[7]

$$\Gamma_2 = \frac{p_2/k_2}{1 + (A_1p_1)/k_1 + (A_2p_2)/k_2} \quad . \quad . \quad . \quad (6.7)$$

with a similar formula for Γ_1. In order to compare these with our formula we substitute

$$p_{h_1} = \frac{k_1}{A_1}, \quad p_{h_2} = \frac{k_2}{A_2}, \quad . \quad . \quad . \quad . \quad (6.8)$$

obtaining

$$\Gamma_1 = \frac{p_1/p_{h_1}A_1}{1 + (p_1/p_{h_1}) + (p_2/p_{h_2})}, \quad . \quad . \quad . \quad (6.9)$$

$$\Gamma_2 = \frac{p_2/p_{h_2}A_2}{1 + (p_1/p_{h_1}) + (p_2/p_{h_2})}. \quad . \quad . \quad . \quad (6.10)$$

This pair of formulæ differs from (6.4), (6.5) in the occurrence of two characteristic areas A_1, A_2 instead of the area per site A_s. These characteristic areas A_1, A_2 have not been precisely defined. The pair of formulæ containing them does not correspond to any well-defined model. They contradict Gibbs' adsorption formula. In short, they are impossible.

7. More than Two Adsorbed Species.—We have confined ourselves to two adsorbed species purely for the sake of brevity. All the formulæ may immediately be extended to three or more adsorbed species. In every case a set of formulæ, corresponding to a well-defined model or derived consistently from an assumed formula for the free energy of the monolayer, will automatically satisfy the criterion of Gibbs' adsorption relation. On the other hand a set of empirical formulæ such as (6.6) not derived in this manner is liable to be self-contradictory in not satisfying necessary thermodynamic relations.

---

[6] S.T., formula (1004,9).

[7] Butler and Ockrent, *J. Physic. Chem.*, 1930, **34**, 2842, formula (6).

8. Ideal Dilute Solutions.—When the solutions considered are sufficiently dilute so that Henry's law is obeyed by each of the adsorbed species, one can replace any formula involving partial vapour pressures by an analogous formula involving concentrations. In fact the formulæ of Butler and Ockrent referred to above were actually expressed in terms of concentrations, but this is quite irrelevant to our criticism of them.

In particular for ideally dilute solutions we may replace formulæ (3.10), (3.11), (3.12) by

$$\frac{\Gamma_1}{\Gamma_1 + \Gamma_2} = \frac{s_1 C_1}{\phi} e^{-B_1\phi/kT}, \qquad . \quad . \quad . \quad (8.1)$$

$$\frac{\Gamma_2}{\Gamma_1 + \Gamma_2} = \frac{s_2 C_2}{\phi} e^{-B_2\phi/kT}, \qquad . \quad . \quad . \quad (8.2)$$

$$s_1 C_1 e^{-B_1\phi/kT} + s_2 C_2 e^{-B_2\phi/kT} = \phi, \qquad . \quad . \quad . \quad (8.3)$$

where C_1, C_2 denote the concentrations of the species 1, 2 in the dilute solution while s_1, s_2 like l_1, l_2 are independent of the composition of the solution.

9. Comparison with Experiment.—As mentioned in § 1, experimental data on the spreading pressure of solutions with two solutes are sparse. Butler and Ockrent[6] have made measurements on aqueous solutions of ethyl alcohol and propyl alcohol and we hoped that these would supply an interesting test of the applicability of our formulæ. Unfortunately a cursory examination of the data reveals that within the experimental accuracy, not only $w = 0$ but also

$$B_1 = B_2 \qquad . \quad . \quad . \quad . \quad . \quad (9.1)$$

Considering the similarity of ethyl and propyl alcohols this is not surprising. The equality (9.1) does not prevent us from carrying out the comparison between the experimental data and the formulæ; it merely makes the comparison less interesting.

In view of (9.1) we may drop the subscript from B and write (8.3) as

$$\phi e^{B\phi/kT} = s_1 C_1 + s_2 C_2. \qquad . \quad . \quad . \quad . \quad (9.2)$$

In Table I we give Butler and Ockrent's experimental values of the

TABLE I.—VALUES OF SPREADING PRESSURE ϕ IN DYNE/CM. IN AQUEOUS SOLUTIONS OF ETHYL ALCOHOL AND PROPYL ALCOHOL AT 20° C.

Molarity of Ethyl Alcohol. / Molarity of Propyl Alcohol.	0.	0·5.	1·0.	2·0.
0	0	10·3	16·2	23·9
0·05	4·0	—	—	—
0·1	7·6	14·7	19·3	25·9
0·2	13·5	—	—	—
0·25	15·7	19·8	23·3	28·7
0·5	23·1	25·8	28·5	32·2

spreading pressure ϕ for several dilute aqueous solutions of ethyl alcohol and propyl alcohol. In Table II we give a comparison of values of the

TABLE II.

Test of formula $\phi e^{B\phi/kT} = s_1C_1 + s_2C_2$ with

$$B/kT = 0{\cdot}0400 \text{ cm.}^2/\text{erg}, \text{ or } B = 16{\cdot}2 \text{ Å}^2;$$

$$s_1 = 31{\cdot}1 \frac{\text{dyne}}{\text{cm.}} \frac{\text{l.}}{\text{mole}} \text{ for ethyl alcohol};$$

$$s_2 = 114{\cdot}0 \frac{\text{dyne}}{\text{cm.}} \frac{\text{l.}}{\text{mole}} \text{ for propyl alcohol.}$$

Molarity C_1 of Ethyl Alcohol.	0.		0·5.		1·0.		2·0.	
Molarity C_2 of Propyl Alcohol.	$\phi e^{B\phi/kT}$.	$s_1C_1 + s_2C_2$.	$\phi e^{B\phi/kT}$.	$s_1C_1 + s_2C_2$.	$\phi e^{B\phi/kT}$.	$s_1C_1 + s_2C_2$.	$\phi e^{B\phi/kT}$.	$s_1C_1 + s_2C_2$.
0	0	0	15·5	15·5	31·0	31·1	62·3	62·2
0·05	4·7	5·7	—		—		—	
0·1	10·3	11·4	26·5	26·9	41·8	42·5	73·0	73·6
0·2	23·2	22·8	—		—		—	
0·25	29·4	28·5	43·7	44·0	59·2	59·6	90·5	90·7
0·5	58·2	57·0	72·4	72·5	89·0	88·1	117·0	119·2

left and right sides of equation (9.2) calculated from the following assumed values of the parameters.

$$B/kT = 0{\cdot}0400 \text{ cm.}^2/\text{erg}, \quad \text{or} \quad B = 16{\cdot}2 \text{ Å}^2;$$

$$s_1 = 31{\cdot}1 \frac{\text{dyne}}{\text{cm.}} \frac{\text{l.}}{\text{mole}} \text{ for ethyl alcohol};$$

$$s_2 = 114{\cdot}0 \frac{\text{dyne}}{\text{cm.}} \frac{\text{l.}}{\text{mole}} \text{ for propyl alcohol.}$$

On the whole the agreement is remarkably good, in fact surprisingly so since $B\phi/kT$ is not small compared with 1, which means that $(\Gamma_1 + \Gamma_2)B$ is not small compared with 1.

It is interesting to compare the value of the virial coefficient B with the area occupied by closely packed —CH_2OH groups in long-chain alcohols, namely[8] 21·6 Å^2. If B were a co-volume, its value should be just twice this area, that is to say 43 Å^2. The fact that the actual value 16 Å^2 of B is much smaller shows that the mutual attraction between adsorbed molecules is by no means negligible.

Summary.

Well-known thermodynamic formulæ for monolayers containing adsorbed molecules of only one kind, in particular those of Volmer, are extended to monolayers containing adsorbed molecules of two or more kinds.

Dept. of Colloid Science, Cambridge University.
Royal Institution, London, W.1.
Dept. of Chemistry, Reading University.

---

[8] Adam, *Physics and Chemistry of Surfaces* (1941), p. 50.

SURFACE CONDUCTANCE AND CATAPHORESIS.

By F. Booth.

(*Communicated by* Prof. N. F. Mott, F.R.S.)

Received, 27th November, 1947.

1. Introduction.

The well-known formula due to Henry[1] for the rate U of cataphoresis of spherical particles of radius a in an electrolyte of viscosity η, where the field strength is E, may be written in the form

$$U = \frac{E\epsilon\zeta}{6\pi\eta}\{1 + \lambda F(b)\}. \quad . \quad . \quad . \quad . \qquad (1.1)$$

Here ζ is the electrokinetic potential, ϵ the dielectric constant of the electrolyte, and

$$F(b) = \frac{1}{8}b^2 - \frac{5}{24}b^3 - \frac{1}{48}b^4 + \frac{1}{48}b^5 + \frac{1}{4}b^4e^{b}E_i(b)\left(1 - \frac{b^2}{12}\right) \quad . \qquad (1.2)$$

where $$E_i(b) = \int_b^\infty \frac{e^{-x}}{x}\,dx.$$

The parameter b is defined by $b = \kappa a$, κ being given by

$$\kappa^2 = \frac{4\pi e^2}{\epsilon kT}\sum_{i=1}^{s} n_i z_i^2. \quad . \quad . \quad . \quad . \qquad (1.3)$$

n_i is the concentration of ions of type i in the electrolyte, z_i their valency, e is the electronic charge; k is Boltzmann's constant and T the absolute temperature. λ is defined as

$$\lambda = \frac{\sigma - \sigma_0}{2\sigma + \sigma_0}. \quad . \quad . \quad . \quad . \quad . \qquad (1.4)$$

where σ is the specific conductivity of the material forming the solid particles, and σ_0 that of the electrolyte. Henry's formula is a considerable improvement on Smoluchowski's work, but his treatment still contains various approximations; for example, he uses the Debye-Hückel approximation ($\zeta e/kT \leqslant 1$), neglects any distortion of the ionic atmosphere round the sphere, and drops the " inertia terms " in the equations of motion. The effect of not using these simplifications is to add to the right-hand side of eqn. (1.1) further terms containing ζ and E to higher powers than the first.[2, 3]

In the present paper, however, we shall not be concerned with these improvements of Henry's formula, but we shall carry out a refinement which may be of practical importance. Henry assumed in the derivation of eqn. (1.1), that the conductivity of the particle was *uniform*. For practically all materials except metals, this conductivity will almost certainly be zero in the interior, but *may* not vanish near the surface. For it may happen that the surface regions of the solid have a high conductivity. For example, if the surface charge is due to adsorbed ions, these ions may possess a high mobility and a high concentration.

---

[1] Henry, *Proc. Roy. Soc. A*, 1931, **133**, 106.
[2] Booth (to be published).
[3] Overbeek, *Sonderabruck Kolloid-Beiheften*, 1943, **54**, 287.

There is some experimental evidence indicating surface conductance in certain cases. Thus Rutgers[4] determined streaming potentials as a function of tube width and concentration of electrolyte for various electrolytes in glass capillaries. It was found that the potential-concentration curves differed for different tube widths, the potential exhibiting an apparent decrease with reduction of the capillary radius ; but the streaming potential should, of course, be independent of the radius of the capillary. A satisfactory explanation was obtained by assuming that part of the current set up by the streaming potential flowed through the surface of the capillary. Estimates were made of the surface conductance ; for solutions of KCl and HCl, for example, the surface conductance was nearly proportional to the concentration of electrolyte and reached values of 10^{-7} ohm^{-1}. Manegold and Solf[5] have also reported an apparent decrease of the electrokinetic potential with tube width in electrosmotic measurements. This is doubtless also due to surface conduction.

The importance of the surface conductance effect upon cataphoresis has been stressed by Bikerman,[6] but his quantitative results are not very useful since they only apply to particles in the form of long thin rods moving with their axes parallel to the direction of the field.

In the next paragraph we shall derive a modified form of eqn. (1.1) taking into account surface conductance. The concluding paragraph discusses the bearing of the results upon the experimental data.

2. Calculation of the Dependence of the Cataphoretic Velocity upon the Electrokinetic Potential.

Near the particle the electrostatic potential may be written as the sum of three terms,

$$\psi = \psi_1 + \psi_2 + \phi. \qquad (2.1)$$

ψ_1 denotes the potential in the equilibrium state, when no field is applied. ϕ represents the potential due to the external field if no charge were present on the particle and ψ_2 represents the distortion of ψ_1, produced by the external field.

First consider ϕ ; instead of examining the field near a sphere of conductivity σ immersed in an infinite medium of conductivity σ_0 (as in Henry's calculation) we must now find the field near a sphere of radius a, of conductivity σ surrounded by a concentric shell of conductivity σ' between radii a_2 and a_1, the sphere and shell being immersed in an infinite medium of conductivity σ_0. The appropriate potentials V_i, V_s, V_0 for the interior, shell and infinite medium, are respectively

$$\left.\begin{aligned} V_i &= -\frac{9\sigma_0\sigma' Er\cos\theta}{\Sigma(2\sigma'+\sigma)} \\ V_s &= -\frac{3\sigma_0 rE\cos\theta}{\Sigma}\left[1+\frac{a_1^3}{r^3}\left(\frac{\sigma'-\sigma}{2\sigma'+\sigma}\right)\right] \\ V_0 &= -rE\cos\theta\left[1-\frac{a_2^3}{r^3}\left(1-\frac{3\sigma_0}{\Sigma}\left\{1+\frac{a_1^3}{a_2^3}\left(\frac{\sigma'-\sigma}{2\sigma'+\sigma}\right)\right\}\right)\right] \end{aligned}\right\} \qquad (2.2)$$

where $$\Sigma = 2\sigma_0\left\{1+\frac{a_1^3}{a_2^3}\left(\frac{\sigma'-\sigma}{2\sigma'+\sigma}\right)\right\}+\sigma'\left\{1-\frac{2a_1^3}{a_2^3}\left(\frac{\sigma'-\sigma}{2\sigma'+\sigma}\right)\right\}. \qquad (2.3)$$

It is easily verified that the above expressions satisfy the boundary conditions at infinity and at $r = a_1$, and $r = a_2$. For example, at $r = a_2$ we have

$$V_s = V_0 \quad \text{and} \quad \sigma'\frac{\partial V_s}{\partial r}\bigg|_{a_2} = \sigma_0\frac{\partial V_0}{\partial r}\bigg|_{a_2}. \qquad (2.4)$$

---

[4] Rutgers, *Trans. Faraday Soc.*, 1940, **36**, 69.

[5] Manegold and Solf, *Kolloid-Z.*, 1931, **55**, 293.

[6] Kikerman, *Trans. Faraday Soc.*, 1940, **36**, 154.

Now evidently

$$\phi = \lim_{a_2 \to a_1 = a} V_0 \quad . \quad . \quad . \quad . \quad (2.5)$$

where we assume the quantity $\sigma'(a_2 - a_1)$ remains finite and equals the surface conductance σ_s.

We then find that

$$\phi = -Er\cos\theta\left[1 + \lambda_s\frac{a^3}{r^3}\right], \quad . \quad . \quad . \quad (2.6)$$

where

$$\lambda_s = \frac{a(\sigma_0 - \sigma) - 2\sigma_s}{a(\sigma + 2\sigma_0) + 2\sigma_s}. \quad . \quad . \quad . \quad . \quad (2.7)$$

Now let us consider the terms ψ_1 and ψ_2 of eqn. (2.1). It is easily shown [2] that

$$\psi_1 = \frac{\zeta a}{r}e^{(b - \kappa r)} + O(\zeta^2) \quad . \quad . \quad . \quad . \quad (2.8)$$

where $O(\zeta^2)$ denotes terms involving the square and higher powers of ζ.

The distortion of the field, ψ_2, can be shown to vary as ζ^2 and higher powers of ζ; we are now interested only in the dependence of U on the first power of ζ, and we shall accordingly not consider ψ_2 here.

Now Henry calculated the cataphoretic velocity assuming that the field due to the surface charge and double-layer remained spherically symmetrical. He assumed that the spheres had a *uniform* finite conductivity. Thus for the external field term ϕ, he used an expression identical in form with equation (2.6) but with λ_s replaced by the λ of eqn. (1.1). It follows that the results of his calculation can be carried over to find U in our case immediately. From eqn. (18) of his paper, we have

$$U = \frac{\epsilon E}{6\pi\eta}\left[\psi_1(b)(1 + \lambda_s) + 3a^3\lambda_s\left(2\int_a^\infty \frac{\psi_1(\kappa r)}{r^4}dr - 5a^2\int_a^\infty \frac{\psi_1(\kappa r)}{r^6}dr\right)\right]. \quad (2.9)$$

Substituting for ψ_1 from eqn. (2.8) and carrying through the integrations we finally have the formula,

$$U = \frac{E\epsilon\zeta}{6\pi\eta}(1 + \lambda_s F(b)) + O(\zeta^2) \quad . \quad . \quad . \quad (2.10)$$

where F(b) is defined in equations (1.2).

To find the dependence of U upon the higher powers of ζ in formula (2.10) we should require in the first place to add terms depending upon ζ^2 and higher powers in expression (2.8) for ψ_1. The effect of the distortion of the potential represented by the term ψ_2 of (2.1) would also have to be taken into account. The analysis of the latter effect has been developed by Overbeek [3] and the present writer [2] for the case of non-conducting particles. The calculations are very complicated however, and we shall not carry them through for our present problem. However, it seems likely that the additional terms in (2.10) are qualitatively very similar to the additional terms for the non-conducting particles. Thus we should expect the higher order terms to vanish for a very thin layer on a very thick double layer, and the correction to U due to these terms to reach its maximum value for a double-layer thickness about one-fifth of the radius. It is also easy to show that if the electrolyte is symmetrical —that is, has equal numbers of positive and negative ions—there are no terms of order ζ^2.

3. Discussion.

It is evident from relations (2.7) and (2.10) that the importance of the surface conductance effect in cataphoresis depends upon the relative magnitudes of the quantities σ_s, $a\sigma$ and $a\sigma_0$.

In the accompanying figure we have plotted the quantity $6\pi\eta U/E\epsilon\zeta$ (using expression (2.11) for U) as a function of $\log_e b$, for various values of the ratio $\sigma_s/\sigma_0 a$; the curves apply only to an insulating particle; that is, we have taken $\sigma = 0$. All the curves approach the value 1 as $b \rightarrow 0$; this is to be expected, for with a very extended double-layer the resistance to motion is given by the ordinary Stokes formula. As b increases, or as the thickness of the double-layer diminishes, the surface conductance effect becomes more and more important. Of course, in the expressions for U which we have used, the terms of order ζ^2 are dropped and therefore the curves drawn only apply in the limiting case of $\zeta e/kT$ small. From the results of our previous work on cataphoresis [2] we might expect that the curves would be modified appreciably for $\zeta e/kT \sim 1$.

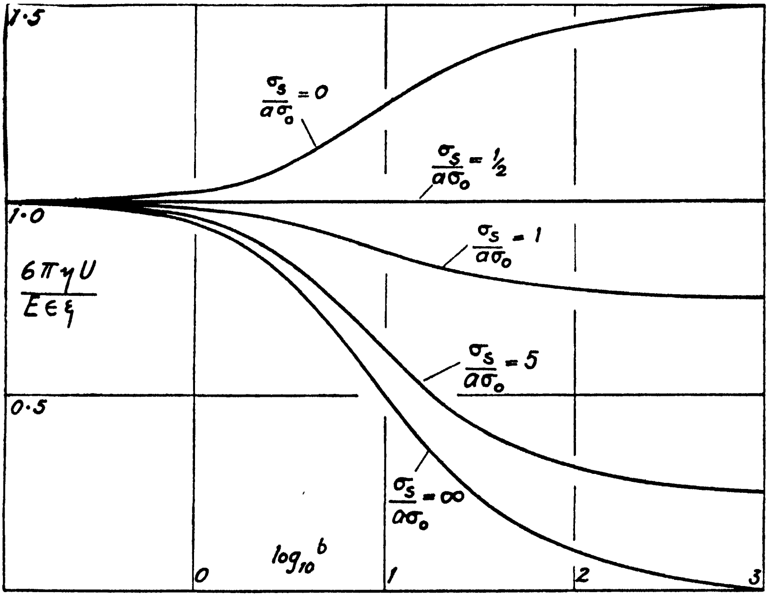

FIG. 1.—Dependence of cataphoretic velocity upon double-layer thickness and surface conductance for insulating particle.

Let us consider the limiting case of b large more closely. We have in the limit $b \rightarrow \infty$,

$$U = \frac{E\epsilon\zeta}{6\pi\eta}\,\frac{3a\sigma_0}{a(\sigma + 2\sigma_0) + 2\sigma_s}. \qquad (3.1)$$

If we let ζ_s denote the electrokinetic potential as calculated from the Smoluchowski formula

$$U = \frac{E\epsilon\zeta_s}{4\pi\eta}, \qquad (3.2)$$

then we see that

$$\zeta = \zeta_s\frac{a(\sigma + 2\sigma_0) + 2\sigma_s}{2a\sigma_0}. \qquad (3.3)$$

Now Rutgers found that σ_s for glass capillaries was very nearly proportional to the concentration of electrolyte; assuming σ_0 to be roughly proportional to the concentration, we can write

$$\sigma_s \simeq d\sigma_0 \qquad (3.4)$$

where the constant *d* has the dimensions of a length. For non-conducting particles eqn. (3.3) now becomes

$$\zeta \simeq \zeta_s\left(1 + \frac{d}{a}\right). \qquad . \quad . \quad . \quad . \quad (3.5)$$

For solutions of KCl, Rutgers found $d = 1{\cdot}1 \times 10^{-3}$ cm. hence from eqn. (4.5) we observe that the apparent electrokinetic potential as calculated from the Smoluckowski formula will begin to decrease rapidly as the particle radius is reduced below 10^{-3} cm. The sizes of some of the particles used in electrophoresis measurements are often considerably *less* than 10^{-3} cm. Some of the proteins, for example, are only 10^{-5} to 10^{-7} cm. diam.

A useful test of the above theory would be a determination of the rate of cataphoresis of particles of different radii; formula (3.1) would then give both ζ and σ_s for the concentration chosen. A measurement of streaming potentials by Rutgers' method using capillaries of the same material as the particles would then furnish an independent check of the values of ζ and σ_s. A complication in the cataphoresis measurements would be provided, of course, by the higher order terms in eqn. (2.10). Owing to their complexity it seems that the only course open is to choose *b* sufficiently large to allow them to be neglected. This, of course, sets a lower limit on the size of particles on which measurements could be made.

Summary.

The effect of surface conductance upon the rate of cataphoresis *U*, of spherical solid particles in an electrolyte, is investigated theoretically. A generalisation of Henry's formula for the relation between *U* and the electrokinetic potential ζ, taking into account surface conduction, is given. The importance of the effect on the interpretation of electrokinetic measurements is discussed, and suggestions made for experimental investigation.

H. H. Wills Physical Laboratory,
Bristol.

STUDIES ON QUENCHING OF FLUORESCENCE.

I. A CONTRIBUTION TO THE THEORY OF QUENCHING OF FLUORESCENCE.

BY K. WEBER AND M. LOKAR.

Received 22nd December, 1947.

The quenching of fluorescence in solutions by adding foreign matter is important from the theoretical point of view, besides having a certain practical significance. This is shown by the close theoretical relation which exists between quenching of fluorescence and inhibition of chemical reactions. Thus the problem of quenching of fluorescence becomes one of chemical kinetics.

The theories of quenching of fluorescence, so far established, can be divided into two groups.[1] To the first belong those in which the duration of the excited state of activated molecules (ions) has no influence on the amount of quenching because the molecules of the *quencher* (the foreign matter that quenches the fluorescence) are, certainly during the excitation and perhaps all the time, present in the sphere of action of the excited molecules. In this group belong those mechanisms of quenching postulated in the theories of polymerisation,[2] and of salting-out,[3] according to which the cause of quenching lies in the creation of molecular compounds between the quencher and the fluorescent matter.[4] These theories can be considered as *static theories* because according to these mechanisms the incapacity of the molecules of the fluorescent matter to re-emit absorbed light is due to a state of affairs existing before as well as after the exposure to light.

---

[1] See e.g. Wawilow, *Acta Physica Polonica*, 1936, **5**, 417; Bowen, *Trans. Faraday Soc.*, 1939, **35**, 15.

In the second group of theories belong the *theory of collisions of the second kind*[5] and the *theory of mutual reactions*.[6] In these, the life-time of the excited state of molecules activated by light plays an important role because it is necessarily assumed that the molecules (ions) of the quencher enter the sphere of action of the fluorescent matter only during irradiation. Such theories are called here *kinetic theories* and it has been shown that they apply successfully both the results and assumptions of the molecular kinetic theory as well as the theoretical interpretations of chemical macro-kinetics.

It is significant that none of the different theories is universally applicable, nor is able to explain all the known experimental data. Often, one or the other theory corresponds better with the experimental facts, depending on the system that is being examined and the conditions under which the experimental work is carried out. It might therefore be more correct to speak not of *theories* but of *effects*, e.g. of the polymerising effect, or the effect of collisions of the second kind, respectively.

In the present paper we have tried to find an experimental method that would make it possible to establish whether a kinetic or a static theory could be applied. We briefly present here the results of measurements which have been carried out for this purpose.

Experimental.

Fluorescence is predominantly a property of organic compounds (dyestuffs, alkaloids), that are more or less specifically adsorbed by different adsorbents. In this process, they generally preserve their fluorescent properties, and these may often be enhanced in the adsorbed state. If the adsorption is effected in a solution that contains in addition to a dyestuff, a quencher of certain concentration, it is expected that the dyestuff will always be adsorbed in the state in which it exists in the solution. In the case of a kinetic effect, the quenching takes place in a molecularly dispersed or ionised state ; in the case of a static effect, on the other hand, it forms either a polymer or a molecular compound with the quencher. In a kinetic effect the quencher will be adsorbed alone according to its own properties and more or less independently of the presence of dyestuff. If we now suppose that the molecules (ions) of the quencher are adsorbed to a greater or less extent than the molecules of the dyestuff, that is that the components of the system are adsorbed unequally, the adsorption will cause a change in the occurrence of quenching in these systems.

From the above, it follows that the behaviour of fluorescent systems (of dyestuffs and quenchers) adsorbed by some solid adsorbents, serves as an indication of whether the quenching has been caused by static or kinetic effects. With static effects, the dissolved system and the adsorbed system will show quantitatively the *same* dependence of the intensity of fluorescence on the concentration of the quencher. With kinetic effects, on the contrary, there will be a great difference in quenching between the two systems. In the latter case, a much greater effect of the quencher upon solutions than upon adsorbents can be generally expected. In our experiments we used as adsorbents filter-paper (*Schleicher-Schüll,* " White band," of 9 cm. diam.). They were immersed in a solution (10 cc.) of dyestuff and quencher of known concentration, taken out after several minutes, dried and their fluorescence measured under ultraviolet light. Simultaneously, the fluorescence of solutions of equal concentrations of the dyestuffs and quenchers was measured and the concentration of the quencher systematically altered, the intensity at each concentration being measured while the concentration of the quencher remained constant.

---

[2] Walter, *Wied. Ann.*, 1888, **34**, 316 ; Lewschin, *Z. Physik*, 1927, **43**, 230 ; 1931, **72**, 368, 382.

[3] Banow, *ibid.*, 1928, **58**, 811 ; *Z. physik. Chem. A*, 1933, **163**, 172.

[4] See Danckwortt and Eisenbrand, *Luminescenzanalyse* (Leipzig, 1940), p. 65.

[5] Wawilow, *Z. Physik.*, 1928, **50**, 52 ; 1929, **53**, 665. Frank and Wawilow, *ibid.*, 1931, **69**, 100. Perrin, *Compt. rend.*, 1924, **178**, 1978, 2252 ; 1927, **184**, 1121.

[6] Baur, *Z. physik. Chem. B*, 1932, **16**, 465. Franck and Lewi, *ibid.*, 1934, **27**, 409. Schneider, *ibid.*, 1935, **28**, 311. Weber, *ibid.*, 1935, **30**, 69.

The intensity of fluorescence of the dyestuff was measured in arbitrary units, i.e. as % of the intensity of the dyestuff with the quencher absent. A photo-electric fluorometer, the principle of which has been described earlier, was used.[7] A Philora Hg lamp (HPW), the glass of which was stained with nickel-oxide, served as the source of light, and filters used for the absorption of red- and ultraviolet light passing through the solutions of dyestuffs (Schott BG10 and (Schott GG 10) giving, therefore, mainly the 366 mμ line. The photoelectric apparatus was a selenium photo cell used in conjunction with a multiflex-galvanometer having a sensitivity of 1·9 × 10^{-9} amp. per scale unit. The experiments were carried out at room temperature.

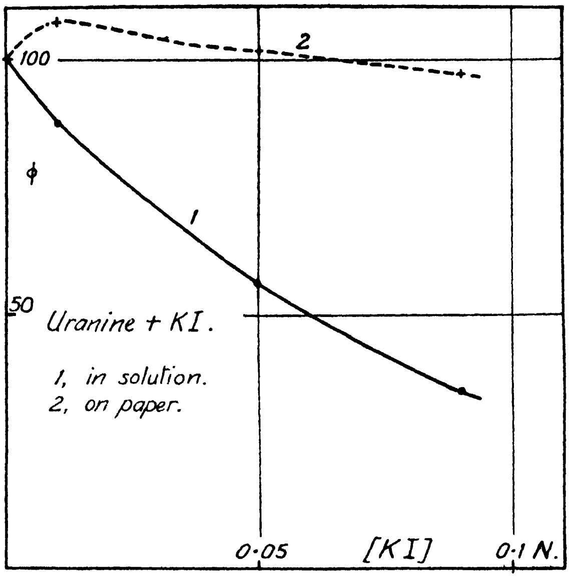

FIG. 1.

Uranine (1 × 10^{-3} mol./l.), quinoline red (1 × 10^{-4} mol./l.) and sodium-naphthionate (4·10^{-3} mol./l.) in aqueous solution were used as fluorescent substances. Their fluorescence was quenched by adding potassium halides and rhodanide and with organic compounds of mono-, or poly-phenols as well as aniline.

Fig 1 shows graphically the results obtained by quenching the fluorescence of uranine (the sodium salt of fluorescein) with potassium iodide. Curve 1 refers to the measurements in solutions, and curve 2 to the dyestuff adsorbed on paper. It is seen that KI vigorously represses the fluorescence of dissolved uranine but, on the contrary, has no effect upon the adsorbed dyestuff, thereby showing the *kinetic* effect of a free iodine-ion. The effect does not become manifest in the adsorbing paper because KI, or I^- respectively are considerably less adsorbed than uranine. The ions of other halogens as well as rhodanide ions also act in the same way upon the fluorescence of uranine. Of the organic quenchers used, phenol, *o*-cresol and aniline give also kinetic effects. Aniline vigorously quenches the fluorescence of dissolved uranine but has little effect if uranine is in the adsorbed state, although it was possible to detect a certain extinction in this state (Fig. 2).

Polyphenols, such as hydroquinone, pyrocatechol and pyrogallol quench to the same extent the fluorescence of uranine in the dissolved and adsorbed state. Fig. 3 shows the results obtained for the system uranine + pyrogallol.

---

[7] Weber, *loc. cit.*

We see that the curves have the same shape and differ very little. Similar results were obtained when quenching the fluorescence of uranine with the other polyphenols mentioned above. In these cases, the quenching is therefore due to static effects, consisting in the formation of *molecular* compounds between uranine and polyphenols. Such molecular compounds are not able to fluoresce and are adsorbed approximately to the same extent as uranine itself and therefore, as regards the aptitude for fluorescence, the same circumstances prevail on adsorbent paper as in solutions. The curves do not agree exactly probably because

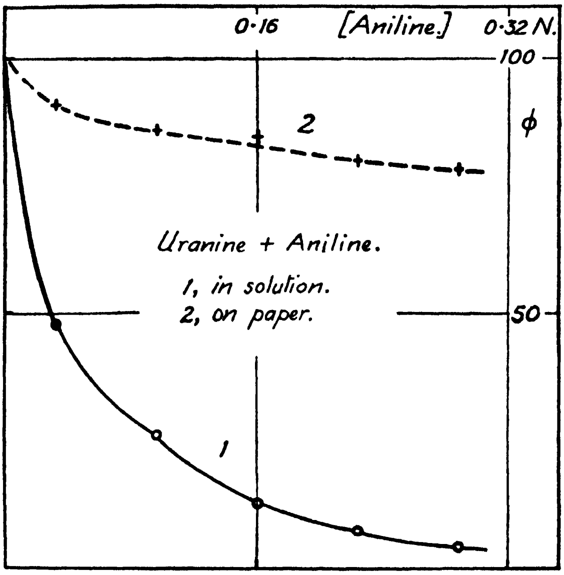

FIG. 2.

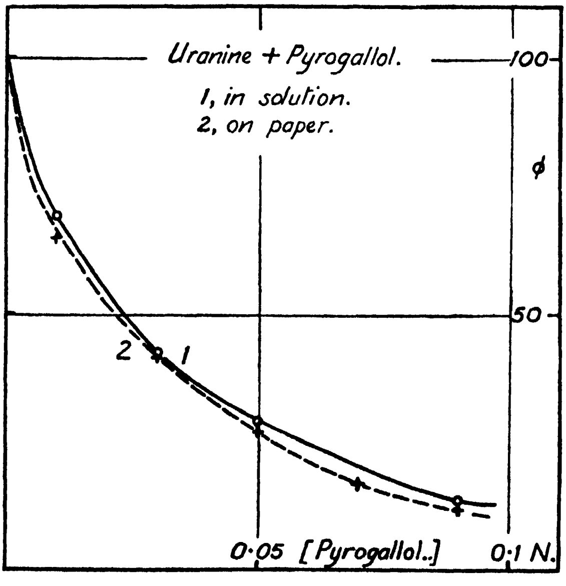

FIG. 3.

there is still a small difference between the adsorption of uranine and the molecular compound of uranine and the polyphenol.

In cases of the static effect, on comparing the concentration of uranine with concentrations of the quencher, it is seen that the latter in all cases are considerably *greater* than the concentration of the dyestuff. This is shown by the values in Table I, where the "semi-concentrations" of quenchers ($\bar{c}$), are given ; i.e. those molar concentrations of the quencher where the intensity of the fluorescence of uranine is reduced to half the value of that obtained in the absence of the quencher. These semi-concentrations are in all cases about 20-times greater than the concentration of uranine. That means that half the molecules of uranine form molecular compounds if the concentration of the quencher is 20-times greater or more. This, however, does not mean that so large a number of molecules of the quencher have combined with one molecule of uranine in these aggregates ; on the contrary it is much more probable that there exist simple stoichiometric relations in these molecular compounds. A large excess of one component (i.e. of the quencher) is necessary because the molecular compounds in the solution easily dissociate into their components and, with increase of concentration of the quencher, the formation of the molecular compound is favoured. The curves, representing the quenching of fluorescence are therefore dissociation curves of the molecular compound of uranine and quencher.

TABLE I.—URANINE : 1×10^{-3} MOL./L.

Quencher.	$\bar{c}$.	
	In Solution.	On Paper.
Hydroquinone .	0·021	0·018
Pyrocatechol .	0·023	0·021
Pyrogallol .	0·024	0·021

In connection with this, it is significant that the usual equation

$$\phi = \phi_0 \frac{1}{1 + \beta c} \quad . \quad . \quad . \quad . \quad . \quad (1)$$

(ϕ_0 = intensity of fluorescence in absence of quencher, ϕ = intensity of fluorescence with concentration c of the quencher, β = constant) that has been established both empirically and theoretically from the theory of collisions of the second kind,[8] as well as from the theory of mutual reactions,[9] can also be deduced from the general laws of chemical equilibrium.[10]

With the systems examined, this equation was always applicable in those cases where there was no question of the presence of a kinetic effect. This is shown by the numerical values of Table II for the systems, uranine + KBr and

TABLE II.—URANINE : 1×10^{-3} MOL./L.

Concentration of the Quencher mol./l.	KBr.		KCNS.	
	ϕ.	β.	ϕ.	β.
—	100	—	100	—
0·1	88·8	1·26	91·5	0·92
0·3	75·2	1·09	78·8	0·90
0·5	64·5	1·11	66·4	1·01
0·7	58·6	1·07	57·5	1·06
0·9	52·6	1·00	54·2	0·94

Mean : β = 1·10 β = 0·97.

---

[8] Wawilow, *loc. cit.*

[9] Ouellet, *Can. Chem. Metall.*, 1932, **16**, 168,. Weber, *loc. cit.*

[10] Katheder, *Kolloid-Z.*, 1940, **92**, 299 ; 1940, **93**, 28.

uranine + KCNS. For static effects of quenching in solutions and on paper, we have found that the equation is only approximately valid (Tables III and IV) because the " constant " in these cases, though small, steadily increases with increase in concentration of the quencher. The fact that equation (1) is not strictly valid in these cases, becomes understandable if it is noted that Katheder, in deriving the equation from the law of mass action, finally reached the general equation of quenching of fluorescence (1) only after carrying out considerable simplifications.

Using quinoline red we were unable to effect the quenching due to kinetic effects. Of halogen ions, only the iodide ion (KI) quenches the fluorescence of this dyestuff ; here the curves of quenching in solutions and on paper, though rather similar, still do not agree even approximately (Fig. 4). We consider this to be a static effect, due to salting out, since by adding larger quantities of KI, after standing for a longer time, a dark red sediment appears in the solution. This sediment can be " salted-out " dyestuff (perhaps a polymer, or the salt (iodide) of quinoline red). Even so, with weaker concentrations of iodide ions, *permanent* aggregates without the ability to fluoresce are formed in the solution.

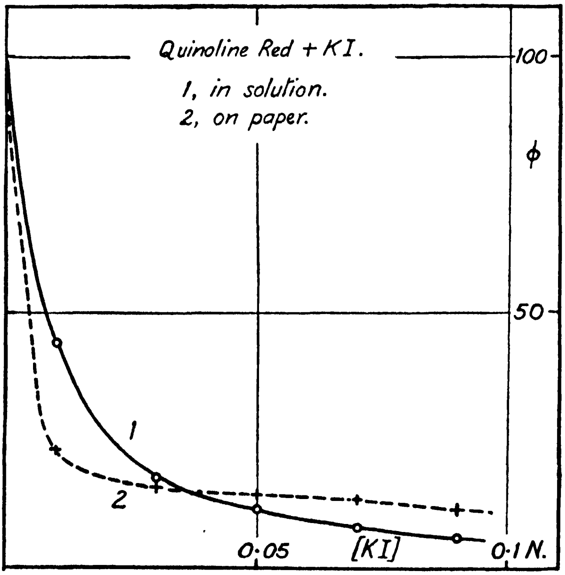

FIG. 4.

TABLE III.—URANINE : 1×10^{-3} MOL./L.

rocatechol mol./l.	ϕ.		β.	
	In Solution.	On Paper	In Solution.	On Paper.
—	100	100	—	—
0·01	70·4	67·0	42·0	49·2
0·03	43·5	39·5	43·3	51·0
0·05	29·5	28·0	47·8	51·4
0·07	21·5	21·5	52·1	53·7
0·09	16·0	15·2	58·3	61·9

We were able to confirm the effect of salting-out in other experiments, using water with the addition of 50 % methyl alcohol as solvent. Methyl alcohol was added in order to prevent the formation of any trace of sediment by the iodide. In these experiments, it was found that KI quenches the fluorescence of the quinoline red considerably less effectively in the presence of methyl alcohol than in solutions in pure water. Alcohol increases the solubility of the dyestuff and so lessens the salting-out effect. In addition we were able to show that equation (1) is only approximately valid (see Table V) because the values of the constant β decreased with the increase of the concentration of potassium iodide. The equation deduced by Banow,[11] in his theory of fluorescence as a consequence of salting-out, and experimentally proved for some systems,[11] viz.:

TABLE IV.—URANINE: 1×10^{-3} MOL./L.

Pyrogallol mol./l.	ϕ.		β.	
	In Solution.	On Paper.	In Solution.	On Paper.
—	100	100	—	—
0·01	69·3	64·8	44·3	57·9
0·03	42·3	41·5	45·4	46·8
0·05	29·5	25·2	47·4	59·3
0·07	21·2	16·7	53·1	71·1
0·09	16·0	11·7	58·3	83·8

$$\log \frac{\phi_0}{\phi} \quad k \,.\, \sqrt{[\mathrm{KI}]}, \qquad . \quad . \quad . \quad . \quad . \quad . \quad (2)$$

is in much better accord with the results.

TABLE V.—QUINOLINE RED IN WATER + 50 % CH_3OH.

KI mol./l.	ϕ.	β from eqn. (1).	k from eqn. (2).
—	100	—	—
0·03	77·0	9·93	0·655
0·05	68·5	9·20	0·735
0·10	56·4	7·73	0·786
0·15	48·6	7·05	0·809
0·20	44·4	6·26	0·788

Of organic quenchers, the effect of hydroquinone, pyrogallol and phenol on the fluorescence of quinoline red was examined. It was found that hydroquinone and pyrogallol quench the fluorescence in accordance with the static theories by formation of molecular compounds of the quencher and dyestuff. The curves of quenching in solution and on paper are practically identical and the semi-concentrations of quenching ($\bar{c}$) in order of size agree with the corresponding values of quenching of the fluorescence of uranine (see Table VI). The curves of quenching in solution and in the adsorbed state with phenol and quinoline red are different, but we cannot conclude with certainty that these are cases of quenching by kinetic effects.

TABLE VI.—QUINOLINE RED IN WATER: 1×10^{-4} MOL./L.

Quencher.	$\bar{c}$.	
	In Solution.	On Paper.
Hydroquinone . .	0·017	0·016
Pyrogallol . .	0·022	0·018

---

[11] Banow, *loc. cit.*

The fluorescence of sodium naphthionate was quenched with hydroquinone, pyrogallol and aniline. In all these cases we consider the quenching to be, without doubt, by kinetic effects. The curves of quenching in solution and in the adsorbed state are different (see Fig. 5) and in addition equation (1) is strictly valid for the solutions. That can be clearly seen in Table VII which shows the constancy of the value β for systems of sodium naphthionate with hydroquinone and aniline. It is significant that polyphenols, which quench other fluorescent matters by static effects, produce kinetic effects in this case. The cause of quenching is therefore in all cases a function of the physico-chemical properties of *both* components of the system, i.e. of the dyestuff and of the quencher.

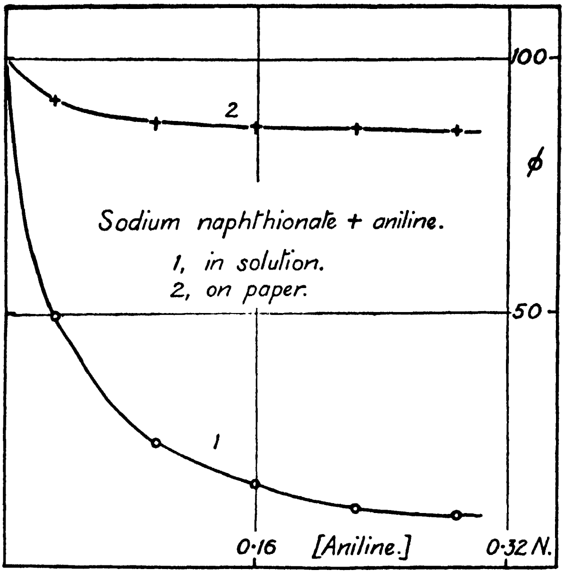

FIG. 5.

TABLE VII.—Sodium Naphthionate 4·0 × 10^{-3} mol./l.

Hydroquinone mol./l.	ϕ.	β.	Aniline mol./l.	ϕ.	β.
—	100	—	—	—	—
0·01	82·2	21·6	0·032	49·2	32·3
0·03	61·2	21·1	0·096	24·4	32·3
0·05	49·0	20·8	0·160	16·6	31·4
0·07	37·3	24·0	0·224	11·5	34·4
0·09	34·2	21·3	0·288	10·0	31·3

Mean : $\beta = 21·7$. $\beta = 32·3$.

Summary.

By parallel measurements of the quenching of fluorescence of dissolved systems and systems in the adsorbed state, it is possible to draw conclusions regarding the mechanism of quenching. With kinetic effects (collisions of the second kind, mutual reactions), the curves obtained for solutions and for adsorbed systems are different; with static effects (polymerisation, salting out, molecular compounds) the curves for the dependence of the intensity of fluorescence upon the concentration of the quencher are identical. With kinetic effects, the general equation of quenching is always strictly valid. With static effects this equation is only approximately valid, while in some cases Banow's equation, containing the square root of the concentration of the quencher, is valid. The mechanism of quenching is conditioned by physico-chemical properties of the fluorescent matter (dyestuff) as well as of the quencher.

Medical Faculty,
University of Zagreb,
Yugo-Slavia.

THE DEHYDROGENASE ACTIVITY OF *BACT. LACTIS AEROGENES.*

By A. M. James and C. N. Hinshelwood.

Received 2nd January, 1948.

The object of the experiments to be described is to investigate further the degree of correlation existing between growth of bacterial cells and their dehydrogenase activity. There is a quite well-defined parallelism between the dehydrogenase activity, estimated by the Thunberg Methylene Blue test, of *Bact. lactis aerogenes* towards various carbon sources and the adaptation of the bacteria to utilise these in growth, all the stages of training to utilise glycerol being, for example, reflected in the changes of the enzyme activity.[1] This work is now extended by a consideration of the following problems.

(1) When a culture of *Bact. lactis aerogenes* ages under various conditions, and the cells develop a lag on transfer to fresh medium, what connection exists between this lag and the previous decay of the dehydrogenase activity ? Conversely, when old cells pass through the lag phase in a new medium, at what stage does the dehydrogenase activity recover ?

(2) During the decay and recovery of enzyme activity, what degree of parallelism is there between the variations of different dehydrogenase functions of the same cells, for example, the activity towards glucose and that towards glycerol ?

(3) What action have growth-inhibiting drugs, such as sulphanilamide and proflavine, upon the dehydrogenase activity, and, where there is an inhibitory effect, is it removed by training of the cells to grow in presence of the drug ?

Experimental Results and Discussion.

Changes in Dehydrogenase Activity during the Ageing of Cells.—The method of working was as follows. A strain of *Bact. lactis aerogenes* of known history (explained later) was inoculated into a litre of test medium and allowed to grow, with aeration, at 40° C., samples being examined at intervals to ensure that the growth was following the normal course. When the culture was full-grown, and at suitable intervals afterwards during the process of ageing (for about 7 days), 75 ml. samples were removed and tested (at 40° C.) for dehydrogenase activity. For this purpose they were centrifuged, washed and re-centrifuged three times, and finally suspended in normal saline, the count being adjusted to $7{\cdot}5 \times 10^8$ cells/ml. At a standard time after the preparation of the suspension (though the results are insensitive to the precise value of this time) it was tested by the Thunberg method. Glucose and glycerol at a concentration of M./5 were normally employed as substrates and were buffered with a phosphate buffer to a *p*H of 7·12. The reciprocal of the time required for the Methylene Blue to be 90 % decolorised is adopted as a measure of dehydrogenase activity. In the actual test 1 ml. of the suspensions was mixed with 2 ml. phosphate buffer, 2 ml. M./2 glucose and 0·1 ml. Methylene Blue, 1 g./l., in hollow-stoppered Thunberg tubes previously evacuated and filled with nitrogen.

---

[1] Davies and Hinshelwood, *Trans. Faraday Soc.*, 1947, **43**, 257 ; Cooke and Hinshelwood, *ibid.*, 1947, **43**, 733 ; Postgate and Hinshelwood, *ibid.*, 1946, **42**, 45.

The experiments on the decay of the activity during ageing fall into several series according to the history of the cells and to the nature of the medium in which the ageing process is allowed to occur.

(*a*) In the first series the cells had been repeatedly grown in the usual phosphate-glucose-ammonium sulphate medium, and had not been trained to use glycerol. They were allowed to age in the growth medium itself. The glycerol activity was much smaller than the glucose activity but the two decayed from their respective maxima exactly in parallel. If the time is measured from the height of the activity, the decay is found to be exponential, as shown by the results in Table I. For both substrates the time of half-decay is 25 hr.

TABLE I.

Age of Cells (hr.).	T (hr.).	$(1/\Delta) \times 10^2$ Glucose		$(1/\Delta) \times 10^2$ Glycerol	
		Calc.	Obs.	Calc.	Obs.
10	0	7·5	7·5	1·0	1·0
20	10	5·6	5·5	0·75	0·78
30	20	4·2	4·2	0·56	0·60
40	30	3·1	3·0	0·42	0·45
50	40	2·3	2·0	0·31	0·30
60	50	1·7	1·2	0·23	0·20
100	90	0·5	0·3	0·07	0·10

If Δt is the Methylene Blue decoloration time (in min.), and T the age (in hr.) measured from maximum activity, then

$$1/\Delta t = A\,e^{-bT},$$

where $A = 7{\cdot}5 \times 10^{-2}$ for the glucose function
$A = 1{\cdot}0 \times 10^{-2}$ for the glycerol function,
but $b = 0{\cdot}029$ for *both* functions (see Table I).

(*b*) In the next series the cells had been previously trained by repeated subculture in a glycerol medium and the ageing occurred in this same medium. Once again the decay was exponential from a point soon after the maximum, i.e.

$$1/\Delta t = A\,e^{-bT},$$

where $A = 9{\cdot}0 \times 10^{-2}$ for glycerol and $4{\cdot}9 \times 10^{-2}$ for glucose,
$b = 0{\cdot}034$ for both.

(*c*) In the third series the cells had been grown repeatedly in the glucose medium, and, without previous adaptation to the glycerol medium, were cultured for the first time and allowed to age in it. At the height of their activity the cells in this experiment would be partially adapted to glycerol, but, as is known from previous experiments, the adaptation acquired in a single cycle of growth is unstable and easily lost. Correspondingly, the decay of the glucose and glycerol functions no longer keep pace with one another as in (*a*) and (*b*). The glycerol activity is initially greater than the glucose activity, but decays more rapidly, the two curves crossing at about 90 hr. The actual decay constants were initially 0·024 for glycerol, falling later, and a value, not accurately obtained but very considerably less for glucose. In this medium the *p*H remains in the region of 6·0. What is measured is, in effect, not a true decay, but a loss of the unstable initial glycerol adaptation.

(*d*) Various experiments were made on the effect of adding small amounts of a preparation of co-enzyme I, and of sterile filtrate from fully grown cultures of *Bact. lactis aerogenes*. None of these additions had any significant effect either on the test itself or on the rate of ageing of the culture, although corresponding additions quite markedly shortened the lag phase of inocula transferred to fresh media containing them.

(*e*) Cultures grown in the glucose medium acquire an acid *p*H, namely about 4·6. The value for those first subcultured in glycerol passes through a minimum of about 5·8 and finally rises to about 6·3. To find out the influence of *p*H on the ageing process, washed suspensions in various phosphate buffers were prepared and allowed to age, with tests over a period of about 14 days. (The samples for test were all re-centrifuged and suspended in the usual test medium.) The results are shown in Fig. 1. The time of half-decay is plotted against *p*H in Fig. 2. It is evident that the acid *p*H of cultures ageing in the parent medium is the main factor determining their rapid decay.

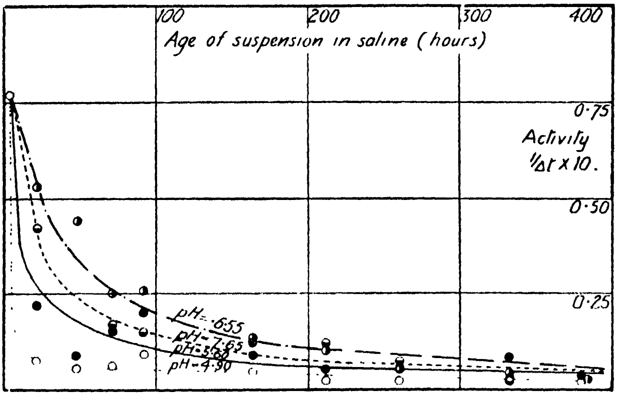

FIG. 1.—Decay of glucose dehydrogenase activity in buffered saline.
◑ *p*H, 6·55 ; ◒ *p*H, 7·65 ; ● *p*H, 5·60 ; ○ *p*H, 4·90.

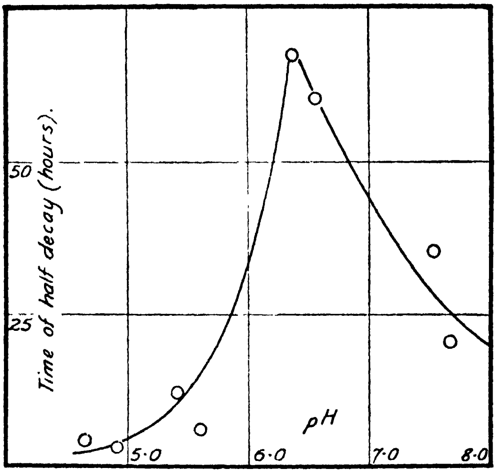

FIG. 2.—Time of half-decay in saline at different *p*H's.

Relation between Decay of Dehydrogenase Activity and the Development of Lag in Ageing Cultures.—In many of the experiments described in the previous section, inocula of 0·1 ml. were taken at intervals from the ageing cultures and transferred to fresh glucose medium, the lag being determined in the usual way. This lag could then be correlated with the state of the glucose dehydrogenase activity of the parent. As shown in Fig. 3, the lag, L, increases in a roughly linear manner over a considerable range of age, T. dL/dT is about 0·14 for the series referred to under (*a*) in the last section.

It might have been supposed that the lag represented the time required for the repair of the decayed dehydrogenase system, and it might further have been supposed that the latter would repair itself at the normal rate of cell growth.

Suppose an amount x_0 is needed before cell growth can start. After decay for a time, T, the amount left will be given by

$$x = x_0 e^{-bT},$$

where b is the decay constant. If repair occurs during the lag at a rate given by

$$x_0 = x e^{kL},$$

we shall have $bT = kL$

or $dL/dT = b/k =$ (mean generation time)/(time of half-decay) $= 0{\cdot}5/25 = 0{\cdot}02$.

Thus the lag develops about 7 times as rapidly as this simple view would suggest. The mechanism of development is in fact probably quite different, and depends more on the loss from the cell of essential intermediates than on actual enzyme decay. The former process can of course occur much more rapidly.

In the set of experiments where washed cells were allowed to age in a series of saline buffers, measurements were made of the lags of inocula transferred to fresh medium at various stages. Here again, there was a fairly rapid increase in lag during the early part of the ageing process—more rapid than could be accounted for by the decay of the dehydrogenase activity. This period was followed by a very long phase in which no further increase of lag occurred.

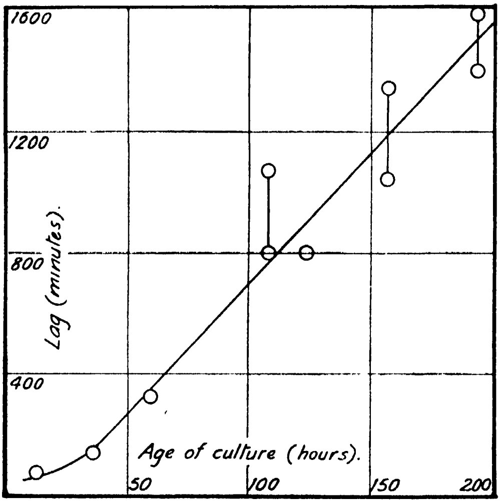

FIG. 3.—Lag-age curve of glucose-trained cells.

Recovery of Dehydrogenase Activity.—The principle of the next series of experiments was as follows. Cells were allowed to age until the dehydrogenase activity had fallen to a negligibly small value. They were then centrifuged and washed, and a large inoculum was transferred to a litre of fresh medium kept at 40° c., with gentle aeration. The cell count was fairly large, about $7{\cdot}5 \times 10^7$/ml., so that the Thunberg test could be carried out at intervals on 75 ml. samples after the usual centrifuging and washing. The course of the recovery of the dehydrogenase activity could thus be observed.

In the first set of measurements, cells previously cultured and aged in the glucose medium were transferred, in the way described, to a fresh supply of the same solution. The total time of lag was 15 hr. The glucose-dehydrogenase activity showed no detectable increase during this period. As soon as growth set in, however, it rose rapidly to a maximum, as shown in Fig. 4.

The initial viability of the culture, as determined by a method previously described [2] was 10-20 % only, and the question arises whether this fact weakens the conclusion that no important recovery of the dehydrogenases occurs during the lag phase. Actually it strengthens it as the following argument shows.

---

[2] Lodge and Hinshelwood, *J. Chem. Soc.*, 1943, 213.

Suppose, for example, that the initial count in arbitrary units is 99 for the dead cells and 1 for the living ones, and suppose that the limit of detection is 1 unit. Growth is recognised to have begun when the count reaches 101. Recovery of the enzyme activity is now just measurable for the first time, and, on the basis of total count, we conclude that it did not precede the onset of growth. If, however, the viability relations are taken into account, the detectable recovery is recognised to have required not the 1 % of cell increase from 100 to 101 but 100 % from 1 to 2, the only change in our conclusion being that for recovery even more growth is required than that estimated on the basis of the total count.

Various series of determinations were made on the recovery of glycerol dehydrogenase activity in cells which had been grown and aged in the glucose medium, and then allowed to recover in this same medium, always in the absence of glycerol. The general result was that the comparatively small glycerol activity did not necessarily recover to its original value until after several fresh subcultures. The imperfect recovery after long ageing is shown by the following numbers.

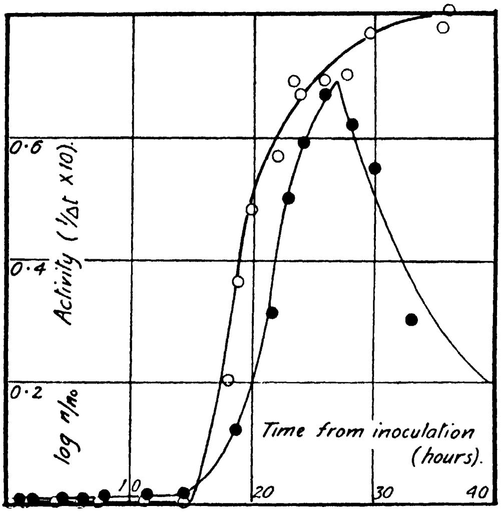

FIG. 4.—Recovery of the glucose function of the dehydrogenase activity of cells trained, aged and finally regrown in glucose.

○ Growth curve. ● Dehydrogenase activity.

History of Cells.	Maximum Activity ($1/\Delta t \times 10^2$).	
	Glucose.	Glycerol.
Original glucose-trained culture . . .	9·1	3·7
Aged for 113 hr. and then re-grown in glucose	8·1	3·0
Aged for 215 hr. and then re-grown in glucose	8·1	1·7

In the course of further subcultures in the glucose medium, the glycerol activity showed a slight upward trend with fluctuations.

The next series of measurements were made on a strain of cells grown in the glycerol medium after previous thorough training to it. The activity was allowed to decay, and a washed suspension transferred to fresh glycerol medium. No recovery of enzyme activity towards either glycerol or glucose occurred during the lag phase. After this the two activities increased in a more-or-less constant ratio (Fig. 5). The glycerol activity had regained its full value by the end of the logarithmic phase, but the glucose activity, although considerable at the end of the first subculture, only regained its full value at the end of a further growth cycle.

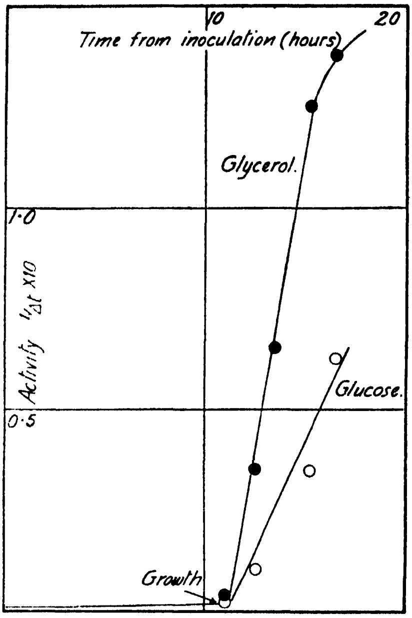

FIG. 5.—Recovery of glucose and glycerol dehydrogenases of cells trained, aged and regrown in glycerol.

Discussion of Experiments on Decay and Recovery.

The answers to the first two questions raised in the introduction seem now to be as follows.

(1) The initial development of lag as the culture ages is more rapid than the decay of the dehydrogenase enzymes. It appears to be associated with the loss of intermediates from the cells. With increasing age, cultures not infrequently show a rapid increase of lag, then a long period of more-or-less constant lag and finally a catastrophic increase ending in complete sterility. It is the latter phase which probably corresponds to destruction of enzymes. It was conceivable that the recovery of dehydrogenase activity constituted an essential operation to be completed during the lag phase in a new medium. This appears not to be so, since there is no appreciable recovery until after active growth has started.

(2) In stable cultures, that is, in cultures which have previously become fully adapted to the substrates in which they grow, glucose and glycerol activity vary in parallel, whichever carbon source is provided in the actual medium used. On the other hand, when the cells are not stably adapted, the two kinds of activity no longer keep in step, loss of adaptation being superposed on normal decay.

The tentative conclusion from this is that the glycerol function depends upon a modification imposed upon the enzyme responsible for the glucose function. When this modification is " ironed in " as it were, the enzyme activity decays and recovers as a whole. An unstable modification may be gained or lost independently.

Inhibition of the Dehydrogenase System by Drugs.

As a further means of examining the correlation between growth and dehydrogenase activity the inhibition of the latter by drugs was next studied. Here the situation is a little complicated by the fact that the inhibitory action of the drug is a function of the time for which it has been in contact with the cells.

In the first experiments, a known amount of the drug was added to the buffered glucose-Methylene Blue system in the longer arm of the Thunberg tube, the washed cell suspension was added from the side-arm after the tube had been filled with nitrogen, and the decoloration time observed in the usual way. High enough drug concentrations lengthened the time, but the results were irreproducible. The procedure was then modified. The contents of the longer arm of the Thunberg tube were : 2 ml. KH_2PO_4 solution (9 g./l.) buffered to pH = 7·12 ; x ml. drug solution, $(2 - x)$ ml. distilled water, 1 ml. washed cell suspension (9×10^8/ml.). The side-arm contained 1 ml. glucose solution to which the Methylene Blue had been added to a final concentration of 24 mg./l. The cell suspension, obtained from a culture at an age of 5·5 to 6 hr., was allowed to remain in contact with the drug at 40° c. for measured periods of time before the glucose and Methylene Blue were added. The decoloration time was then determined. The experimental results are best considered under the heading of the individual drugs.

Proflavine.—Fig. 6 shows a typical set of results obtained with a normal strain of *Bact. lactis aerogenes*. The reduction times, Δt, are plotted against the proflavine concentration in the test, m. The numbers beside the individual lines are the times of contact, T_c, of the cells with the drug before the start of the dehydrogenase test. For comparative measures of the inhibitory action, it is convenient to record the concentration of the drug required to reduce the dehydrogenase activity to one-fifth of its original value. Thus, if Δt is the reduction time of a control test without drug, then $m_{5\Delta t}$ is defined as the drug concentration corresponding to a reduction time of $5\Delta t$. Fig. 6 shows that with short times of contact a high concentration is necessary to produce the five-fold lengthening and that $m_{5\Delta t}$ falls rapidly with T_c. Numerical results are given in Table II.

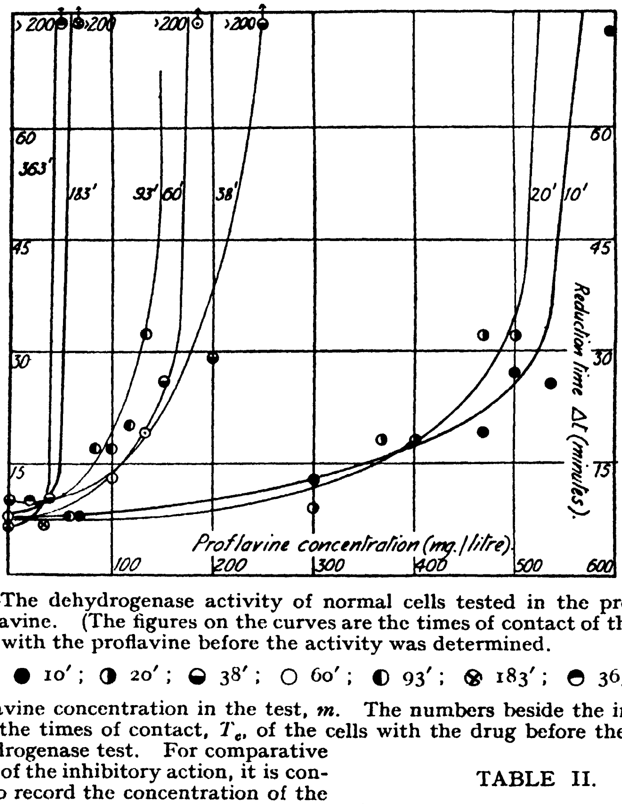

Fig. 6.—The dehydrogenase activity of normal cells tested in the presence of proflavine. (The figures on the curves are the times of contact of the resting cells with the proflavine before the activity was determined.

● 10′; ◑ 20′; ◒ 38′; ○ 60′; ◐ 93′; ⊗ 183′; ◓ 363′.)

TABLE II.

Time of Contact with the Drug (T_c) (min.).	$m_{5\Delta t}$ (mg./l.).
10	800
20	550
38	230
60	187
93	140
183	62
363	45
1175	20

The graph of $m_{5\Delta t}$ against $1/T_c$ is a straight line (Fig. 7), so that

$$m_{5\Delta t} = C/T_c. \qquad (1)$$

Repetition of the experiments with proflavine-trained cells gave curves similar to those of Fig. 6 but displaced along the axis of drug concentration. Eqn. (1) still held but the value of C increased with increasing values of $\bar{m}$ the concentration of drug at which the cells had been trained (Table III).

For a standard time of contact with the cells the concentration of proflavine necessary to cause the five-fold increase in reduction time increases with $\bar{m}$

(Table IV). Similarly, for the standard inhibition with a given concentration of proflavine, the time of contact increases with $\bar{m}$.

TABLE III.

Training Concentration $\bar{m}$ (mg./l.).	C.
0	10700
156	13300
313	25000
1540	25000

TABLE IV.

$\bar{m}$.	$m_{5\Delta t}$ (for 50 min. Contact Time).
0	220
156	280
312	500
1540	500

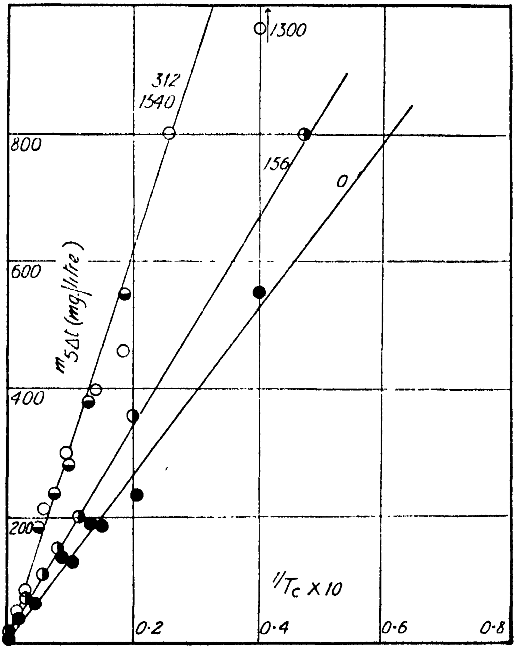

FIG. 7.—Curves showing $1/T_c$ plotted against $m_{5\Delta t}$ for strains trained to various proflavine concentrations. (The figures on the curves show the value of the proflavine training concentration.)

POTASSIUM TELLURITE.—The results found with this substance were generally similar to those found with proflavine (compare Fig. 8*d*). The values of the constant *C* of eqn. (1) are given in Table V.

TABLE V.

$\bar{m}$.	C.
0	9900
156	26200
312	36000

METHYLENE BLUE.—The cells were allowed to remain in contact with Methylene Blue before the test. For untrained cells the value of *C* was 3600 and for cells trained at 78 mg./l. it was 6600.

SULPHANILAMIDE. — Sulphanilamide at concentrations up to 1500 mg./l. had no effect on the dehydrogenase activity even after 20 hr. contact.

OTHER DRUGS.—A less detailed examination was made of certain other drugs, the time of contact being simply that of the test itself. The results are given in Table VI. Various other substances showed no inhibitory effect, under the conditions stated, up to the concentrations (mg./l.) given in brackets in the following list: chloroform (440), sodium azide (8300), *tert.*-butyl alcohol (8300), sodium nitrite (8300), hydroxylamine (270), capryl alcohol (170), quinine (1500), veronal (1000).

Table VI shows the concentration required (contact time confined to test itself) to reduce the dehydrogenase activity to zero, and, for comparison, an estimate of the concentration required to cause an infinite lag. The latter is seen to be much smaller.

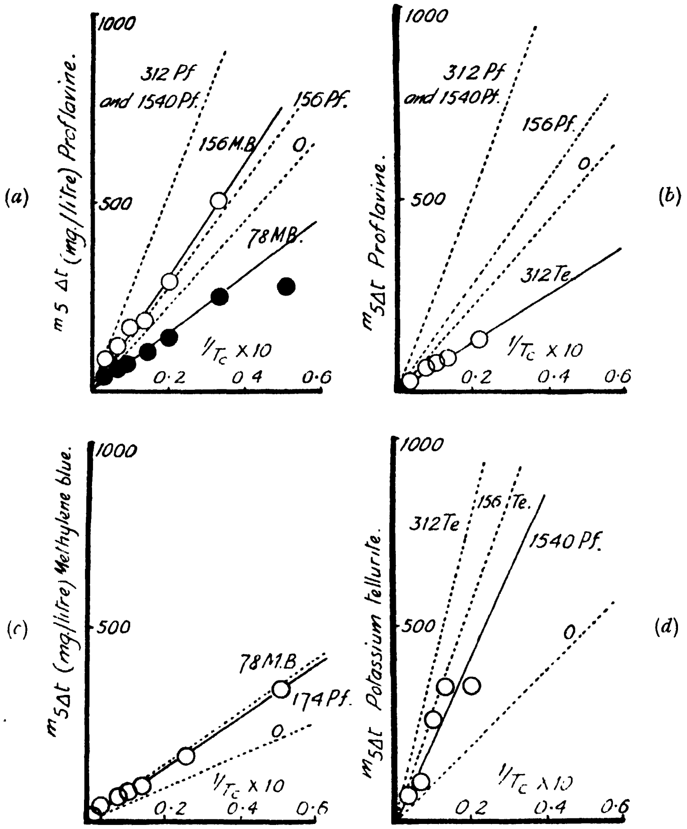

FIG. 8.—Cross training.

(*a*) Trained to Methylene Blue, tested in proflavine.
(*b*) Trained to potassium tellurite, tested in proflavine.
(*c*) Trained to proflavine, tested in Methylene Blue.
(*d*) Trained to proflavine, tested in potassium tellurite.

Cross Training.—Previous work has shown that *Bact. lactis aerogenes* trained to resist the action of amino acridines shows increased resistance to the antibacterial activity of Methylene Blue, but not to the action of sulphonamides. Training to sulphanilamide confers resistance to sulphaguanidine and vice versa, but sulphanilamide training does not confer resistance to proflavine. In this previous work the criteria of training were growth rates and lags. Experiments on " cross adaptation " have now been extended to include measurements on the dehydrogenase system.

Fig. 8*a* shows the results obtained for cells trained to Methylene Blue and tested in proflavine, the broken lines showing, for comparison, $m_{5\Delta t}^*$ against $1/T_c$ for cells trained (and tested) in proflavine. Cells trained to a low concentration of Methylene Blue exhibit little immunity to proflavine but those trained to higher concentrations do exhibit considerable cross adaptation. Similarly, cells trained to proflavine possess a considerable resistance to Methylene Blue (Fig. 8*c*).

Fig. 8*b* shows that cells fully trained to 312 mg./l. potassium tellurite are not trained at all to proflavine so far as the inhibition of the dehydrogenase system is taken as the criterion. On the other hand, Fig. 8*d* shows that training to 1540 mg./l. proflavine gives considerable resistance to potassium tellurite.

TABLE VI.

	Conc. required for Zero Dehydrogenase Activity.	Conc. required for Infinite Lag.
Proflavine	900	50
Methylene Blue	300	85
Potassium tellurite	260	9
m-Cresol	2500	800
Phenol	4500	1600
Sodium fluoride	1600	—
Mercuric chloride	1·0	0·4
Formaldehyde	1100	15

Discussion of Results on Drug Inhibition.

The answer to the last of the questions raised in the introduction may now be considered. It appears to be that there is a general parallelism between the action of drugs on dehydrogenase activity and their action on growth, but that there is nothing like a quantitative correspondence. The general shape of the curves representing reduction time as a function of proflavine concentration (Fig. 6) is quite similar to that of the lag concentration curves shown in previous papers,[3] but the concentration at which the reduction time and the lag respectively tend towards infinity differs widely for the two cases. Nor, in view of the pronounced time effect in the action of the drug on dehydrogenases, could any quantitative agreement be expected.

The response to training is similar for growth and for dehydrogenase activity, both functions easily becoming resistant to the action of such drugs as proflavine and potassium tellurite. Here again there are quantitative differences. In so far as dehydrogenase activity is concerned, there is a limit in the response to training, the results for $\bar{m} = 312$ being indistinguishable from those for $\bar{m} = 1540$. In respect of lag, marked increase of adaptation occurs over this range.[4]

A well-defined correlation between growth and dehydrogenase activity is evident in the experiments on cross adaptation. The reciprocal relations of proflavine and Methylene Blue correspond qualitatively to those found in the work on the lags.[5] In the present work, certain proflavine-trained strains showed resistance to potassium tellurite, but the tellurite strains showed no appreciable training to proflavine. The corresponding lag-concentration curves had not previously been determined, but special experiments showed that, here again, there was a qualitative correspondence.

Summary.

There is a general correlation between the dehydrogenase activity of *Bact. lactis aerogenes* towards glucose and glycerol and the growth of the cells in media

---

[3] Davies, Hinshelwood and Pryce, *Trans. Faraday Soc.*, 1945, **41**, 163.

[4] Davies, Hinshelwood and Pryce, *ibid.*, 1945, **41**, 778.

[5] Pryce, Davies and Hinshelwood, *ibid.*, 1945, **41**, 465.

containing these substances. The dehydrogenase activity decays as the culture ages, but the rate of decay is not great enough to account for the development of the lag, which must be attributed to other causes. During the lag phase of old cells there is no appreciable recovery of the enzyme activity which only becomes important during the period of active growth. In cultures fully adapted to a given growth medium, the dehydrogenase activity towards glucose and glycerol decay and recover in parallel, whichever substrate is provided in the medium actually used. With unstably adapted cells the two kinds of activity may not keep in step.

The effect of drugs on dehydrogenase activity is a function of the time of contact. For a given value of the latter the curve of Methylene Blue reduction time against drug concentration is similar in form to that of lag against concentration, but in general the drug concentrations needed to inhibit the enzyme activity are much higher than those which prevent growth. Training of the cells induces resistance to the action of the drugs on dehydrogenase activity as well as on growth. Cross adaptation phenomena are in evidence. The parallels, however, are qualitative rather than quantitative.

Physical Chemistry Laboratory,
Oxford University.

THE DECOMPOSITION, BOILING AND EXPLOSION OF TRINITROTOLUENE AT HIGH TEMPERATURES.

By A. J. B. Robertson.

Received 19th January, 1948.

The instability of 2 : 4 : 6-trinitrotoluene (TNT.) at high temperatures, as exemplified by its spontaneous explosion, is well known, but few detailed observations of the thermal decomposition and vaporisation preceding the explosion are to be found in the literature. Such data are, however, of some interest in the fundamental study of the thermal sensitiveness of explosives.

Experimental.

Material.—A commercial TNT., m.p. 80·5° c., containing approximately 99 % of α-TNT. was used for the decomposition and ignition experiments. α-TNT. was prepared from this by repeated recrystallisation from conc. H_2SO_4.

Measurement of Decomposition Rate.—The decomposition preceding explosion was examined in Pyrex glass reaction bulbs, nitrogen, hydrogen or air being present at atmospheric pressure to reduce distillation of the liquid from the hot zone. The methods for rapid heating of the sample of explosive and for recording rapid pressure changes were those described previously.[1]

Measurement of Boiling-point.—The induction period before the explosion of TNT. at its boiling point is sufficiently long (about 20 sec.) to enable a direct measurement of the b.p. to be made before the explosion. The sample of TNT. was introduced by an electromagnetic arrangement into a vertical Pyrex tube 1·5 cm. internal diam. immersed to a depth of 2-3 cm. in a bath of fused nitrates maintained at a temperature usually about 30° c. above that of the boiling point to be measured, and containing air or nitrogen at the required pressure. The hot junction of a platinum-platinum-rhodium thermocouple was fixed about 3 mm. above the surface of the TNT. to measure the temperature of the condensing vapour. This particular thermocouple has no catalytic effect on the decomposition of TNT. The E.M.F. was measured with a potentiometer and short-period galvanometer, the thermocouple being calibrated by direct immersion in a nitrate bath, and the resulting curve checked at four points by determining the boiling points of benzoic acid, phthalic anhydride, benzophenone and anthracene by the method used with the TNT., the values found being within 1½° c. of the accepted values. The b.p. of benzoic acid was also found at 12 cm. pressure and a value obtained in close agreement with the vapour pressure measurements of Kahlbaum.[2] The possibility of making the measurements in 15 sec. was established with these substances.

---

[1] Robertson, *Trans. Faraday Soc.*, 1948, **44**, 677.

A convenient quantity of TNT. was 50 mg., but the b.p. values remained unaltered on varying the quantity from 10-100 mg. The temperature of the heating bath could be varied from 15 to 60° c. above the b.p. without altering the readings. The accumulation of decomposition products in the TNT. did not appreciably alter the readings; thus at 267° c. the liquid could be steadily boiled for 15 min. without change of b.p. This was also the same in air and nitrogen.

Decomposition of TNT.

Pressure-time curves for the thermal decomposition of TNT. in a closed system showed first a rapid pressure rise due to partial vaporisation of the liquid, followed by a quiescent period in which no appreciable gas evolution occurred. This merged somewhat indefinitely into a period of accelerating gas evolution during which the TNT. gradually darkened, and above 275° c. (with 50 mg. TNT) the decomposition became sufficiently rapid after a time to give rise to an explosion. Above 350° c., however, no explosion occurred with this quantity of TNT. since the bulk of the material distilled from the hot zone leaving a dark residue. Larger quantities than 50 mg. were then required for explosion. The pressure (p) due to the decomposition of the TNT. after the quiescent period (that is the observed pressure increment minus the increment due to the vaporisation) followed the equation,

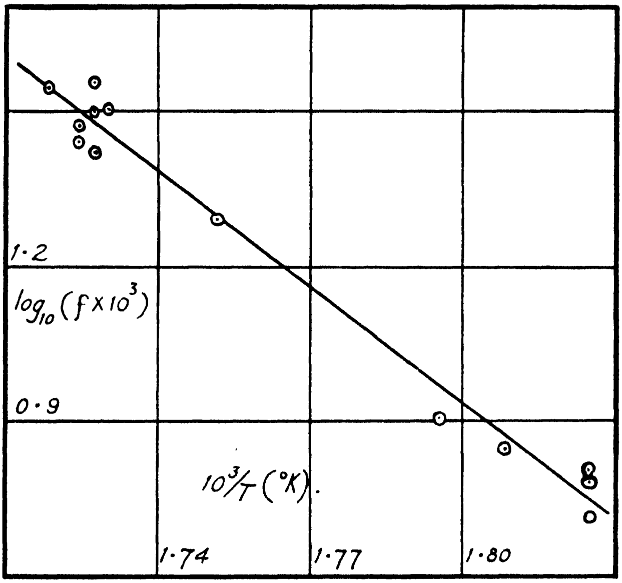

FIG. 1.—Decomposition of TNT.

$$\log_{10} p = ft + \text{constant},$$

where t is time and f a constant measuring the acceleration of the gas evolution. The temperature variation of f was given by the equation,

$$f\,(\text{sec.}^{-1}) = 10^{11 \cdot 4}\, e^{-34 \cdot 4\ \text{kcal.}/RT},$$

the experimental results for 50 mg. TNT. being shown in Fig. 1. The value for the apparent activation energy lies between that of 46 kcal./g. mol. which may be deduced from the temperature coefficient given by Robertson [3] for the very early stages of decomposition, and the value of 27 kcal./g. mol. given by

---

[2] Kahlbaum, *Z. physik. Chem.*, 1898, **26**, 577.

[3] Robertson, *J. Chem. Soc.*, 1921, 1.

Roginsky[4] from experiments in closed ampullæ, when autocatalysis is greatly facilitated.

Below the explosion temperature the rate of gas evolution, after attaining a maximum, finally diminished with time approximately in accordance with an exponential law. No difference in the pressure-time curves was observed with the different inert gases present. An increase in the quantity of TNT. used to over 100 mg. diminished both the quiescent period and the induction period before explosion, and increased *f*. This was considered to be due to self-heating and autocatalysis. The importance of autocatalysis in the decomposition could be shown by obtaining from the partially decomposed TNT. a strongly catalytic substance of low volatility. Addition of 10 % of this to TNT. completely removed the quiescent period and increased *f*. The quiescent period could also be removed by previous exposure of the sample to ultra-violet light (a quartz mercury lamp was used) for a few hours.

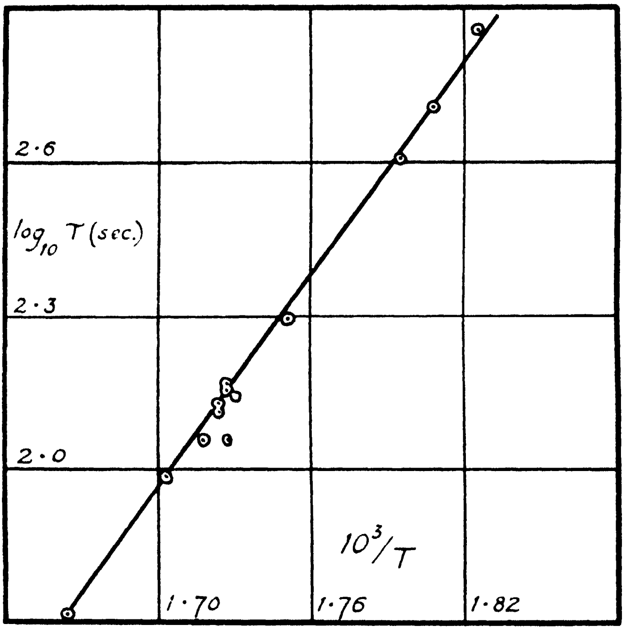

FIG. 2.—Induction period before explosion of TNT.

The induction period (τ) before explosion for 50 mg. TNT. was 12 min. at 275° C. and 50 sec. at 328° C. It followed the equation

$$\log_e \tau = E/RT + \text{constant},$$

E having a value of 32 kcal./g. mol. from the straight line shown in Fig. 2. The experimental error in the activation energies for *f* and τ was estimated as 2·5 kcal./g. mol., the small difference between them being considered insignificant.

Effect of Additions.—A considerable number of foreign substances when added to TNT. in small quantities increased *f* and diminished τ, but no substance was found which inhibited the decomposition to any large extent. Generally, the rise in *f* was in line with the fall in τ, as may be seen from Table I. With added explosives, two distinct types of behaviour were observed. The nitroamines and nitric esters decomposed first in solution in the TNT. leaving it to undergo its normal accelerative decomposition with some modification in *f* and τ. With added explosives containing the NO_2 group linked to carbon, the behaviour of the mixture was similar to that of TNT. alone. Ammonia present in the gas phase (with nitrogen to give a total pressure of 1 atm.) accelerated the decomposition of TNT. at 300° C. according to the equations,

$$\tau = \tau'(1 + 0{\cdot}11p)$$

and

$$f' = f(1 + 0{\cdot}06p),$$

---

[4] Roginsky, *Physik. Z. Sowjet.*, 1932, 1, 640.

where p is the partial pressure of ammonia (0·9 cm.) and τ' and f' are the modified constants which with ammonia present replace the normal ones τ and f.

TABLE I.—Effect of Additions on the Decomposition of TNT.

Addition.	%.	Temp. (°c.).	Increase in f.	Decrease in τ.
Ferric oxide	1·9	297	2·2	3·9
Manganese dioxide	12	298	16	17
Hopcalite	10	278	—	57
Hopcalite	1·9	297	2·8	2·3
Potassium permanganate	10	298	12	9·9
Benzophenone	11	300	5·0	3·1
Quinol	11·5	305	2·3	2·7
Triphenylcarbinol	9·5	299	—	8·0
Paraffin wax	7·5	284	4·1	5·1
α-Nitroso-β-naphthol	9	301	8·9	10
α-Nitroso-β-naphthol iron complex	11	276	—	45
Diphenylamine	9	287	10·5	14
p-Toluidine	10	297	7·0	6·1
m-Aminobenzoic acid	8	302	6·1	6·3
Thiocarbamide	10	301	—	7·5
m-Nitroaniline	9	302	2·8	2·8
p-Nitroaniline	11·5	299	3·8	4·0
Hexanitrodiphenylamine	9	299	2·0	1·1
Trinitroanisole	11·5	299	4·2	3·4
Trinitroxylene	10·5	301	0·86	0·71
Dinitrophenol	7	307	1·4	1·1
Cyclotrimethylenetrinitramine	13	301	5·1	4·3
Cyclotetramethylenetetranitramine	10	299	2·8	2·0
Tetryl	10·5	302	2·6	3·6
Pentaerythritol tetranitrate	11·5	302	3·1	1·4

The Boiling-point of TNT.

A knowledge of the boiling-point of TNT. is useful in interpreting the results of experiments on its behaviour at high temperatures. Belajev and Yusephovich [5] give the boiling-point at 2 mm. as 190° c. and at 50 mm. as 245-250° c., finding by extrapolation 300 ± 10° c. at atmospheric pressure. Extrapolation of the

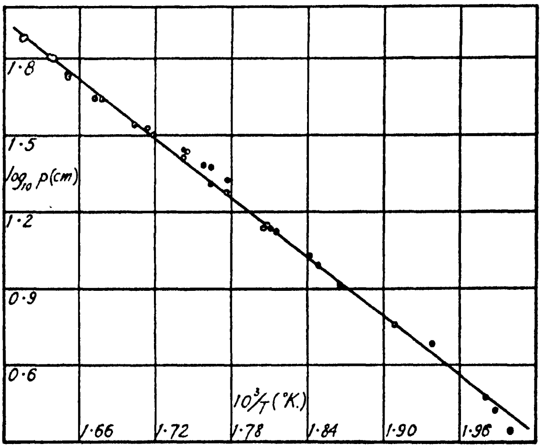

Fig. 3.—Vapour pressure of TNT.

---

[5] Belajev and Yusephovich, *Compt. rend., U.R.S.S.*, 1940, **27**, 133.

vapour pressure measurements of Menzies[6] for the range 82-102° c., using a value derived from his results of 12 kcal./g. mol. for the latent heat of vaporisation, and neglecting the temperature variation of this quantity, gives for the b.p. 530° c. To clarify this discrepancy, a direct measurement of the temperature of condensation of α-TNT. vapour was made at various pressures. At 76 cm. pressure this was 345° ± 2° c., and at 3 cm. 232° c. Identical results were obtained with the commercial sample and α-TNT. On representing the b.p. results by plotting the logarithm of the vapour pressure (p) against $1/T$ the points shown in Fig. 3 were obtained, the equation for the vapour pressure from the straight line shown being

$$\log_{10} p \text{ (cm.)} = 8{\cdot}11 - 3850/T^\circ \text{ K.}$$

This gives a latent heat of vaporisation of 17,500 cal./g. mol. with an error estimated at 1000 cal./g. mol. The results are not sufficiently accurate to justify the addition to the equation of another term allowing for the difference in specific heat between the liquid and the vapour. Menzies gives the vapour pressure at 100° c. as $1{\cdot}06 \times 10^{-2}$ cm. whereas the value calculated from the equation, above is $0{\cdot}62 \times 10^{-2}$ cm. The discrepancy could arise from the presence of volatile impurity in the sample used by Menzies.

The Explosion of TNT.

The Vapour.—The vapour alone exploded less readily than the liquid, for it was heated in bulbs of 2 cm. diam. up to 357° c. without explosion, although extensive decomposition was noted, this being less subject to autocatalysis than that of the liquid. Mixtures of the vapour with air, nitrogen or hydrogen propagated a flame readily once this was initiated, but the necessary concentration of vapour was not determined. These flames could be initiated by exposing the vapour to cold ferric oxide, when a reaction occurred and some of the oxide particles became incandescent. Thus if TNT. was heated rapidly in a test tube and iron oxide brought to the mouth of the tube a flame was initiated at the oxide which passed down the tube and ignited the liquid TNT. At lower temperatures flames could be produced in the vapour which did not suffice to ignite the liquid: thus, cold TNT. brought into contact with iron oxide at 200° c. produced almost immediately a small flame confined to the vapour, the bulk of the liquid TNT. exploding many seconds later after accelerative decomposition.

The Liquid.—The lowest temperature at which liquid TNT. in equilibrium with vapour exploded spontaneously after thermal decomposition depended on the quantity of liquid present, being lower for larger quantities. The lowest ignition temperature for a given initial quantity of TNT. could, therefore, be raised by increasing the proportion vaporising by altering the volume available to the vapour or by diminishing the inert gas pressure. An apparent upper temperature limit of explosion was observed if all the liquid disappeared from the hot zone by vaporisation or boiling before the thermal decomposition accelerated to explosion. The upper temperature limit of 380° c. for deflagration of TNT. reported by Andreew[7] can probably be interpreted in this way.

Observations of the explosion of TNT. after the induction period revealed that the liquid attained a bright red heat and a flame was propagated through the vapour above it, considerable quantities of carbon being deposited. The survival without damage of the glass bulb used showed clearly that no detonation occurred under the conditions used. The rate of decomposition of the liquid before ignition was greater at higher temperatures, and also greater in the presence of the more efficient accelerators of reaction: the results, in general, led to the conclusion that the condition satisfied before ignition was the attainment of a certain extent of decomposition (such that the pressure had risen to about half the final non-explosive thermal decomposition value) and not the attainment of a certain rate of gas evolution. This was also true in general for TNT. containing up to 10 % of foreign substances such as metallic salts and oxides, organic compounds, other explosives and various waxes. The four substances, hopcalite, ammonium dichromate, ferric oxide and barium hydroxide, however, present to the extent of 10 % in TNT. caused ignition at 300° c. with no perceptible prior decomposition, probably as a result of vigorous exothermic reaction between the TNT. and the added substance. Catalytic substances which could be isolated from partially decomposed TNT. also greatly facilitated the ignition of fresh samples of TNT. One may also note in this connection the well-known effect of alkalis in increasing the ease of ignitability of TNT.

---

[6] Menzies, *J. Amer. Chem. Soc.*, 1920, **42**, 2218.

[7] Andreew, *Acta Physicochim.*, 1935, **3**, 119.

Discussion.

Although the acceleration of the decomposition of TNT. with time proceeds in accordance with the mathematical formulation for branching-chain reactions, there is as yet no clear evidence for the actual existence of reaction chains : in fact, the acceleration of the reaction by quinol, benzoquinone and diphenylamine might be considered to point to the absence of free-radical chains. Furthermore, if the final stages of the TNT. decomposition below the explosion temperature are treated somewhat arbitrarily as a first-order reaction of activation energy 34 kcal., the actual rate of reaction can then be represented by an Arrhenius equation $B\,e^{-E/RT}$ with a value for B of about 10^{11} sec.$^{-1}$. The view of Semenoff [8] that chain reactions in TNT. lead to an abnormally large value for B is not supported. It seems probable that the primary reactions lead to the formation of substances of higher molecular weight which catalyse subsequent decomposition and may be involved in bimolecular reactions.

To a first approximation, the normal behaviour of TNT. with respect to spontaneous explosion may be represented by assuming the condition for explosion to be the attainment of a critical concentration of autocatalyst in the liquid phase, so that explosion occurs after a certain definite degree of decomposition. If the TNT. is at a temperature $T°$ K. and the reaction rate constant k for the formation of autocatalyst is given by $k = B\,e^{-E/RT}$, then if the amount of catalyst formed is small, the condition for explosion may be written

$$k\tau = C,$$

where C is the critical ratio, catalyst/TNT., for explosion and τ is the induction period. This equation assumes the catalyst to be formed at a constant rate and neglects the quantity of TNT. decomposed and lost by vaporisation. From this equation the temperature variation of the induction period arises from the temperature variation of k and is given by

$$\log_e \tau = E/RT + \log_e (C/B). \quad . \quad . \quad . \quad (1)$$

An equation of this type with E of 32,000 cal./g. mol. is applicable to TNT. According to Urbanski and Rychter [9] this equation also applies in the temperature range 390-450° C., that is above the boiling point, but E is only 14 kcal./g. mol. Edwards [10] has also observed a diminution of E above the boiling point. This is explicable by the evaporation of the TNT. during the induction period. The volatility of the catalyst formed in the decomposition is much less than that of TNT., and its evaporation during the induction period may be neglected in comparison with that of TNT. If the temperature of the reaction vessel, with an area A in contact with TNT., is T, and the boiling point of TNT. is T_B, the quantity (q) of TNT. evaporated during the induction period τ is given by

$$qL = hA(T - T_B)\tau, \quad . \quad . \quad . \quad . \quad (2)$$

where L is the latent heat of vaporisation cf TNT. and h is the appropriate heat transfer coefficient. The explosion condition, neglecting the quantity of TNT. converted into catalyst, becomes

$$(Q - \tfrac{1}{2}q)k_B\tau/(Q - q) = C, \quad . \quad . \quad . \quad . \quad (3)$$

where Q is the original quantity of TNT. and k_B is the value of k at T_B. When the vessel temperature is just equal to the boiling point, the explosion condition becomes

$$k_B\tau_B = C, \quad . \quad . \quad . \quad . \quad . \quad . \quad (4)$$

---

[8] Semenoff, *Chemical Kinetics and Chain Reactions* (Oxford Univ. Press, 1935), Ch. 17.

[9] Urbanski and Rychter, *Compt. rend.*, 1939, **208**, 900.

[10] G. E. Edwards (private communication).

where τ_B is the induction period under these conditions. Eqn. (2), (3) and (4) give

$$\tau = \tau_B + \frac{QL}{hA(T - T_B)} - \sqrt{\tau_B^2 + \frac{Q^2L^2}{h^2A^2(T - T_B)^2}}. \quad . \quad . \quad (5)$$

In Table II some induction periods calculated with (5) for α-TNT. at 15 lb./sq. in. air pressure when $T_B = 346°$ c. are compared with experimental figures kindly given by Dr. G. E. Edwards, the only quantity not determined by the experiments, hA/QL, being taken as 0·00065 sec.$^{-1}$ degree^{-1}. It is clear that these results are well represented by (5). Thus a value for E obtained from experiments above the boiling point with (1) cannot be interpreted as an activation energy of a chemical process. These considerations may also be of interest in the interpretation of high temperature measurements of induction periods carried out with other volatile explosives.

TABLE II.—INDUCTION PERIODS OF TNT.

Temperature (°c.).	τ (Observed) (sec.).	τ (Calculated) (sec.).
346	42·5	42·5
350	40	40·5
360	34	34·5
370	29	29·5
380	25·5	25·7
390	22·0	22·5
400	19·5	19·9
410	17·5	17·7
420	16·0	16·0
430	14·5	14·6

The author has much pleasure in thanking Prof. E. K. Rideal for his interest and encouragement. This work forms part of a programme carried out at the Dept. of Colloid Science, Cambridge, jointly with the Dept. of Chemistry at Bristol and the Royal Technical College, Glasgow, and the author thanks Mr. L. A. Wiseman and Dr. G. E. Edwards for many discussions. This paper is published by permission of the Chief Scientist, Ministry of Supply.

Summary.

The thermal decomposition of TNT. is markedly autocatalytic and can lead to spontaneous explosion after an induction period. An overall activation energy of 32-34 kcal. is obtained for the processes prior to explosion. Numerous foreign substances accelerate the decomposition. The boiling point of TNT. is 345° c. and the latent heat of vaporisation 17,500 cal./g. mol. Liquid TNT. explodes when a certain extent of decomposition is attained. The effect of boiling on the induction period before explosion can be treated quantitatively.

Davy Faraday Laboratory,
The Royal Institution,
Albemarle St., London W.1.

A QUANTUM-MECHANICAL INVESTIGATION OF THE AZULENE MOLECULE.

PART I.

By R. D. Brown.

Received 3rd February, 1948.

The azulene molecule offers a unique opportunity for testing the accuracy of approximate quantum-mechanical calculations of the position of attack by chemical reagents. The orientation of substituents in aromatic substitution has been predicted from calculations of electron densities or of polarisation energies; hitherto the molecules so treated have been substituted benzenes, naphthalene,[1, 2] and the simpler heterocyclic molecules.[1, 2, 3] In the case of naphthalene the theoretical prediction of substitution in the α-position obtains without appealing to experimental results. This is not so in the case of molecules containing atoms other than carbon and hydrogen; in such instances two or more arbitrary parameters must be introduced. In many cases the point of attack is determined merely by the sign of a parameter, about which there is usually no doubt. Nevertheless naphthalene remains the only molecule whose treatment is independent of arbitrary constants. However, in naphthalene the theory need only distinguish between two possible positions whereas in azulene, whose treatment similarly does not entail any empirical parameters, there are five possible positions of attack. Clearly then, azulene provides a good test of the theory.

Previous computations have been based upon two extreme points of view. Wheland and Pauling,[1] and Longuet-Higgins and Coulson,[3] calculated electron densities at the various positions in the molecule and then, in common with other more qualitative treatments of the problem, assumed that electrophilic attack would occur at positions of highest electron density, nucleophilic attack at points of lowest electron density. Wheland [2] pointed out that this procedure completely ignores the contributions of equally important covalent structures to the activated complex hybrid, and set out a method for calculating certain polarisation energies which is equivalent to the other extreme of considering these covalent structures only. He carried out the calculations of these polarisation energies for various molecules, at the same time drawing attention to the need for examining both extremes separately. In the present instance both electron densities and polarisation energies have been used to predict the course of substitution in azulene.

Outline of Method.

The well-known LCAO molecular orbital treatment was utilised. In this the effect of the σ-electrons is assumed to be constant and so is neglected. The π-electrons are considered to occupy molecular orbitals which, as an approximation, are written:

$$\Psi = c_1\psi_1 + c_2\psi_2 + \ldots + c_n\psi_n.$$

---

[1] Wheland and Pauling, *J. Amer. Chem. Soc.*, 1935, **57**, 2086.

[2] Wheland, *ibid.*, 1942, **64**, 900.

[3] Longuet-Higgins and Coulson, *Trans. Faraday Soc.*, 1947, **43**, 87.

In the case of azulene n, which represents the number of carbon atoms in the conjugated system, is 10 ; ψ_a represents the $2p$ atomic orbital of carbon atom a and the c's are constants whose values are determined by the variation method. This leads to the secular equations and the secular determinant of azulene :

$$\begin{vmatrix} y & 1 & 0 & 0 & 0 & 0 & 0 & 0 & 1 & 0 \\ 1 & y & 1 & 0 & 0 & 0 & 0 & 0 & 0 & 0 \\ 0 & 1 & y & 0 & 0 & 0 & 0 & 0 & 0 & 1 \\ 0 & 0 & 0 & y & 1 & 0 & 0 & 0 & 0 & 1 \\ 0 & 0 & 0 & 1 & y & 1 & 0 & 0 & 0 & 0 \\ 0 & 0 & 0 & 0 & 1 & y & 1 & 0 & 0 & 0 \\ 0 & 0 & 0 & 0 & 0 & 1 & y & 1 & 0 & 0 \\ 0 & 0 & 0 & 0 & 0 & 0 & 1 & y & 1 & 0 \\ 1 & 0 & 0 & 0 & 0 & 0 & 0 & 1 & y & 1 \\ 0 & 0 & 1 & 1 & 0 & 0 & 0 & 0 & 1 & y \end{vmatrix} = 0$$

The lower energy levels of the molecule are obtained by inserting the roots of the secular determinant in the equation :

$$E = \alpha - \frac{y}{1 - S_0 y}\beta_0$$

in which α is the coulomb integral and $\beta_0 = \gamma_0 - S_0\alpha$ where γ_0 is the exchange integral. S_0 is the so-called " overlap " integral :

$$S_0 = \int \psi_n \psi_m d\tau$$

where n and m are adjacent carbon atoms. For the calculation of polarisation energies a value of 0·25 was employed as an approximation to Mulliken's computed value of 0·27 for C=C.[4] The value of S_0 has no effect upon the π-electron density and bond-order results and in this part of the work it was assumed to be zero, following the habit of previous workers.

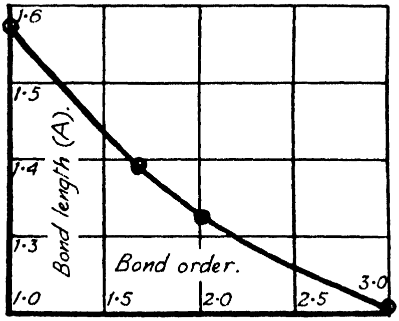

FIG. 1.—Relation between bond order and bond length.

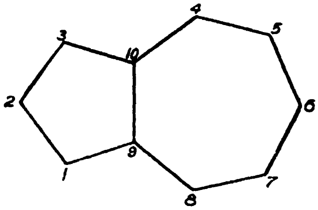

FIG. 2.—Numbering system employed.

The procedure set out by Wheland [2] was followed in the calculations of polarisation energies, and the π-electron densities and bond orders were computed by a method developed by Coulson (e.g. Longuet-Higgins and Coulson, loc. cit.).

The bond lengths were obtained from the computed bond orders by means of the graph given in Fig. 1. For the latter the bond lengths of the carbon to carbon linkages in ethane, ethylene, and acetylene were taken as 1·573, 1·353 and 1·207 A. respectively.[5] The corresponding bond orders employed were 1, 2, 3 (strictly these should be 1·12, 2·12, 3 if the effect of hyperconjugation is considered [6]). Benzene was assumed to have a bond length of 1·390 A. and a bond order of 1·667.

---

[4] Mulliken, *J. Chem. Physics*, 1939, **7**, 20.

[5] Herzberg, *Infra-red and Raman Spectra of Polyatomic Molecules* (1945), p. 440.

Results.

Polarisation Energies.—The energies required to polarise azulene at each of the five possible positions in a manner appropriate for electrophilic, nucleophilic, and radical substitution are listed in Table I. The energies are expressed in units of $-\beta_0$ which is approximately 38 kcal./mol. The positions have been numbered as shown in Fig. 2 ; this agrees with the numbering used in the American Chemical Abstracts.

TABLE I.

Position Attacked.	W_e.	W_n.	W_r.
1	1·352	2·090	1·721
2	1·728	1·728	1·728
4	1·808	1·231	1·520
5	1·655	1·655	1·655
6	1·959	1·280	1·620

The symbols W_e, W_n, W_r represent polarisation energies for electrophilic, nucleophilic, and radical substitution respectively. From the table it is apparent that electrophilic attack will occur in position 1, nucleophilic and radical attack both at position 4. For the case of electrophilic substitution especially the energy for position 1 is much lower than for any other position.

π-Electron Densities and Bond Lengths.—The results of calculations of π-electron densities and bond orders are shown in Fig. 3 and calculated bond lengths are indicated in Fig. 4. It is significant that carbon atom 1 has the highest π-electron density and carbon atom 4 the lowest π-electron density, thus completely confirming the predictions of the polarisation-energy computations. It is also interesting that the bond orders are all close to the value 1·667 for benzene except the bond joining atoms 9 and 10. This is somewhat in contrast to the bond orders in naphthalene for example ; the results for this mole-

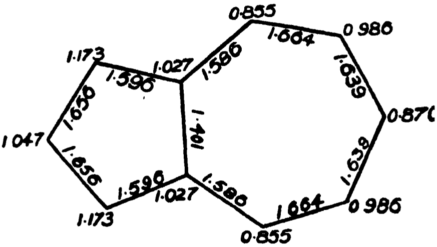

FIG. 3.—Electron densities and bond orders.

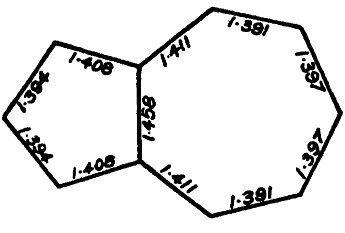

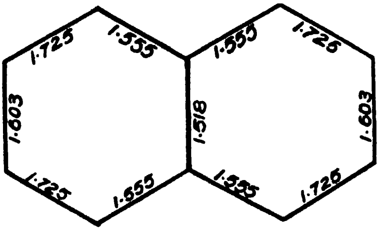

FIG. 4.—Bond lengths. FIG. 5.—Bond orders in naphthalene.

---

[6] Mulliken, Rieke and Brown, *J. Amer. Chem. Soc.*, 1941, 63, 54.

cule [7] are shown in Fig. 5. (The π-electron densities are all 1 for naphthalene.) These results are not unexpected because consideration of the most important structures contributing to the azulene hybrid (Fig. 6) shows that all bonds have approximately half double-bond *character* (as distinct from *order*) except the bond common to both rings which has predominantly single-bond character. In benzene similarly all bonds have approximately half double-bond character

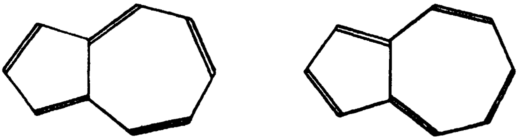

FIG. 6.

due to equal contribution to the hybrid by the two Kékulé structures. From similar considerations for naphthalene (Fig. 7) it can be seen that all bonds have 1/3 double-bond character except the four α-β bonds which have 2/3 double-bond character.

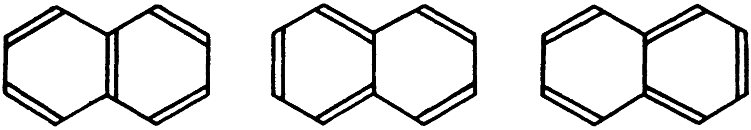

FIG. 7.

As a consequence the bonds of azulene are all similar in length to those of benzene except that the 9-10 bond is somewhat longer. The increased length of this latter could probably be detected by X-ray measurements.

The experimental determination of the course of substitution in azulene is now being undertaken.

I would like to thank Dr. F. N. Lahey for his interest in this work.

Summary.

Approximate quantum-mechanical calculations of polarisation energies and π-electron densities both indicate that electrophilic substitution will take place at position 1 while nucleophilic substitution will occur at position 4. Polarisation energy calculations show that radical substitution will occur at position 4 also. No arbitrary parameters were required in the computations.

Bond orders and bond lengths have also been calculated. It is suggested that the increased length of the bond joining atoms 9 and 10 could be detected by X-ray diffraction experiments.

Chemistry Department,
University of Melbourne,
Australia.

---

[7] Lennard-Jones and Coulson, *Trans. Faraday Soc.*, 1939, **35**, 820.

BONDS IN THE PHOSPHORUS MOLECULE, P_4.

BY W. E. MOFFITT.

Received 16*th February*, 1948.

On the basis of new experimental evidence, the energy to be associated with bonds between a pair of phosphorus atoms has recently been recalculated, first by Skinner [1] and then by Dainton.[2] Accepting Dainton's scheme,

$$P_4(g) \rightarrow 2P_2(g) - 30 \text{ kcal./mole,}$$
$$P_2(g) \rightarrow 2P(g) - 116{\cdot}9 \text{ kcal./mole,}$$

---

[1] Skinner, *Trans. Faraday Soc.*, 1945, **41**, 645.

[2] Dainton, *ibid.*, 1947, **43**, 244.

the bond energy to be associated with a P—P bond in P_4 is 47·5 kcal./mole. The importance of these bond energies for the kinetic study of the oxidation of phosphorus, prompts a closer examination of the conditions of bonding in P_4 and, in particular, a calculation of the " strain " energy to be associated with the bonds in this molecule.

Preliminary Analysis.

It is clear that the bonding orbitals of trivalent phosphorus in unstrained molecules like PH_3 or PF_3 are predominantly $3p$ in type. The internuclear separations in these molecules lead to a covalent radius for phosphorus of $\sim$ 1·1 A. Since the P—P distance in P_4 is 2·21 A., we suppose that the atomic bonding orbitals are also essentially $3p$ here.

Arnold[9] has recently suggested that the valence state of phosphorus in P_4 is $(3p)(3d)^2$, but this seems unlikely. The promotion of two electrons without a compensating increase in the phosphorus valence is not very plausible on energetic grounds, and was probably only suggested in the premature belief that the stability of P_4 was incompatible with the normal $(3p)^3$ valence state. Further, whereas one would expect the $3d$ radius of phosphorus to be rather greater than that of $3p$, the P—P separations in P_4 are apparently normal.

Accepting Pauling's concept of bond strength,[3] which associates the strength of a bond with the value of the bond eigenfunction (orbital) in the bond direction, Skinner[1] has derived the formula,

$$E_{90} = \sec^2 \theta \,.\, E_{(90-2\theta)}.$$

This relates the energy E_{90} of an unstrained P—P bond with the energy $E_{(90-2\theta)}$ of a bond whose bond eigenfunctions are directed at an angle θ to the bond direction. Skinner has put $2\theta = (90\text{-}60)^\circ = 30^\circ$ for the P—P bonds in tetrahedral P_4 and this leads to a strain energy of 3·5 kcal. on the basis $E_{(90-2\theta)} = 47{\cdot}5$. A closer examination (vide infra) of the geometry involved shows, however, that $2\theta \approx 39^\circ$ and not 30° as assumed by Skinner. The strain energy now becomes 6 kcal. so that a considerable error is incurred in his treatment. Pauling's postulate therefore leads to an unstrained P—P bond energy of 53·5 kcal./mole.

A more fundamental calculation will now be undertaken formalising the concept of bent bonds[4] as applied to the P_4 molecule and calculating the degree of delocalisation to be associated with these bonds. It will be shown that the unstrained P—P bond energy is indeed near 54 kcal. In this way, although Pauling's concept of bond strength lacks a theoretical basis, it appears to be justified empirically.

The Pure Valence State (PVS) Approximation.

For purposes of clarity, the P_4 tetrahedron is inscribed in a cube with centre O. At each phosphorus atom P_a, a right-handed system of rectangular co-ordinate axes $P_a x_a y_a z_a$ is set up so that the vector $\overrightarrow{P_aO}$ has direction cosines $\left(\frac{1}{\sqrt{3}}, \frac{1}{\sqrt{3}}, \frac{1}{\sqrt{3}}\right)$ with respect to it. Further, the system is so oriented about $\overrightarrow{P_aO}$ that $\overrightarrow{P_ax_a}$, $\overrightarrow{P_aO}$ and $\overrightarrow{P_aP_b}$ are coplanar ; it follows that $\overrightarrow{P_ay_a}$, $\overrightarrow{P_aO}$ and $\overrightarrow{P_aP_c}$ are coplanar, as are $\overrightarrow{P_az_a}$, $\overrightarrow{P_aO}$ and $\overrightarrow{P_aP_d}$. Here, as in what follows, a, b, c, d are all different.

The $3p$ atomic orbitals of phosphorus are now chosen so that they each have zero component of angular momentum referred to one of the atomic axes so constructed. In virtue of the coplanarity of $\overrightarrow{P_a x_a}$, $\overrightarrow{P_a O}$ and $\overrightarrow{P_a P_b}$, we abbreviate $\psi_a(3p\sigma_x)$ to τ_a^b; the twelve $3p$ orbitals

---

[3] Pauling, *J. Amer. Chem. Soc.*, 1931, **53**, 1367.
[4] Coulson and Moffitt, *J. Chem. Physics*, 1947, **15**, 151.

$$\tau_a^b(a, b = 1, \ldots, 4;\ a \neq b)$$

are now fully defined. If we write $\eta = P_b\widehat{P_a}O$ and $\xi = x_a\widehat{P_a}O$, it is readily shown by geometry that $\eta = \sin^{-1}\frac{1}{\sqrt{3}}$; $\xi = \cos^{-1}\frac{1}{\sqrt{3}}$; so that the angle between the direction of the $3p$ orbital τ_a^b and the bond direction $\overrightarrow{P_a P_b}$ is $\xi - \eta = \sin^{-1}\frac{1}{3} \approx 19\frac{1}{2}^\circ$. That is, the angle of "bending" is $19\frac{1}{2}^\circ$ and not 15° as supposed by Skinner.

Clearly, that perfectly paired structure which approximates most closely to the actual electronic state of the ground state of the P_4 mole-

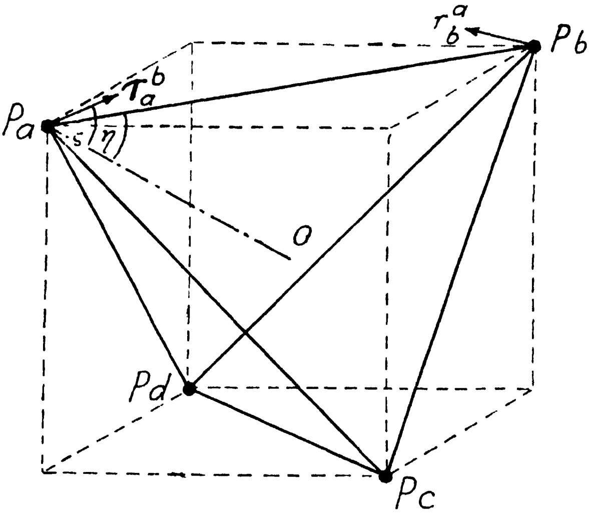

FIG. 1.

cule, is defined by the property that the spins of the electrons associated with every pair of orbitals τ_a^b, τ_b^a are fully coupled or anti-parallel in these pairs. We denote this by writing for each bent bond[4] of this type the symbol $(\tau_a^b : \tau_b^a)$. The six bonds thus obtained account for all twelve electrons to which binding is attributed. In the pure valence state (PVS) approximation, therefore, we use the wave function $\Psi(P) \supset (\tau_a^b : \tau_b^a)$ for all pairs a, b.

As a final extension of the notation. we write

$$(\tau_a^b/\tau_{a'}^{b'}) = \iint \tau_a(i)\tau_{a'}^{b'}(j)\mathcal{H}\tau_{a'}^{b'}(i)\tau_a^b(j)dv_i dv_j,$$

as the exchange integral between τ_a^b and $\tau_{a'}^{b'}$.

The exchange energy associated with any one P—P bond in P_4, apart from a constant term which is independent of the spin orientations, is now[5]

$$\tfrac{3}{2}(\tau_a^b/\tau_b^a).$$

It is easily shown that, with neglect of $\sigma\pi$-type bonding, the exchange

---

[5] Penney, *Proc. Roy. Soc. A*, 1934, **146**, 223.

integral which occurs here may be expended in terms of the more usual integrals,[5] *as follows :*

$$(\tau_a^b/\tau_b^a) = \cos^4(\xi - \eta) \,.\, P_{\sigma\sigma\sigma\sigma} + \sin^4(\xi - \eta) \,.\, P_{\pi\pi\pi\pi}.$$

A comparison is made between the (physical) overlap of the phosphorus $3p\sigma$ and $3p\pi$ orbitals at a nuclear separation of 2·21 A. and the analogous overlap of the carbon $2p\sigma$ and $2p\pi$ orbitals (1·54 A.) using simplified atomic functions.[6] By these means the following values are assigned to the $\sigma\sigma$ and $\pi\pi$ exchange integrals of phosphorus, on the basis of the corresponding figures for carbon,

$$P_{\sigma\sigma\sigma\sigma} = -2{\cdot}5 \text{ ev.} \quad \text{and} \quad P_{\pi\pi\pi\pi} = -1{\cdot}0 \text{ ev.}$$

For a " straight " unstrained pure $3p$-type P—P bond, the exchange energy is

$$\text{const.} + \tfrac{3}{2}P_{\sigma\sigma\sigma\sigma}.$$

Thus, neglecting Coulomb terms and any effects arising from possible differences in internuclear distance, the strain energy to be associated with each P—P bond in P_4 is

$$\tfrac{3}{2}\,|\, P_{\sigma\sigma\sigma\sigma}\{1 - \cos^4(\xi - \eta)\} - \sin^4(\xi - \eta) \,.\, P_{\pi\pi\pi\pi} \,|\,, \quad \text{or} \quad \sim 0{\cdot}77 \text{ ev.}$$

The Energy of Delocalisation in P_4.

In any geometrically constrained system, such as cyclopropane or the P_4 molecule, the approximation of perfect pairing is expected to be less accurate than for the related molecules whose bonds, being unstrained, may be regarded as straight. For example any $3p$ orbital of a phosphorus atom in P_4 may be at least formally coupled with as many as nine bonding orbitals belonging to nearest neighbours of that atom. Accordingly we investigate the resonance energy of delocalisation of the twelve bonding electrons in P_4.

A complete solution of this problem would necessitate the group-theoretical reduction of a representation with 132 dimensions and the subsequent solution of the resulting irreducible secular problem. A fair approximation to this treatment may, however, be obtained by considering only those excited structures which retain four of the normal pairs of coupled orbitals of the PVS structure ; and these structures are easily shown to fall into three classes :

(i) structures involving monovalent phosphorous which are neglected ;
(ii) structures characterised by pairs of adjacent sides of the P_4 tetrahedron ;
(iii) structures characterised by pairs of skew sides of this tetrahedron.

Explicitly the members of the last two classes may be defined by means of the sets of functions $\Psi(abc)$, $\Psi(ab)$ respectively ; $\Psi(abc)$ is associated with the sides $\overrightarrow{P_aP_b}$, $\overrightarrow{P_bP_c}$ in the sense that its two " formal " bonds are coupled according to the scheme $(\tau_a^b : \tau_b^c)(\tau_b^a : \tau_c^b)$. It follows that

$$\Psi(abc) = \Psi(cba),$$

and that the set contains twelve members.

$\Psi(ab)$ is similarly associated with the skew lines $\overrightarrow{P_aP_b}$, $\overrightarrow{P_cP_d}$ by means of $(\tau_b^a : \tau_d^c)(\tau_a^b : \tau_c^d)$. Here, however, $\Psi(ab) \neq \Psi(ba)$ and c, d must be ordered according to some rule, say $c > d$. It is then easily shown that there are six such structures, but that the manifold subtended by these and the pure valence state structure $\Psi(P)$, is of four dimensions only —i.e. only three of the $\Psi(ab)$ are independent in any set containing also

---

[6] Slater, *Physic. Rev.*, 1930, **36**, 56.

Ψ(P). For definiteness, let us choose those three structures $\Psi(ab)$ for which $a > b$ and $c > d$.

Since we are interested in the ground state of the P_4 molecule, whose wave function is supposed to belong to the identical representation A_1 of the cubic point group T_d, Ψ has the form

$$r\Psi(\mathrm{P}) + s\Sigma\Psi(abc) + t\Sigma\Psi(ab).$$

This may easily be verified by means of group theory, and shows that the secular equation is now only of the third degree.

In order to set up this secular cubic, it is necessary to evaluate all the elements

$$(A/B) \equiv \int \Psi(A)\mathscr{H}\Psi(B)\mathrm{d}V$$

of the energy matrix, where $\Psi(A)$, $\Psi(B)$ represent any two structures. The $(1 + 3 + 12)^2 = 256$ elements which arise are, however, easily classified by virtue of the isomorphism that exists between the set of structures and the corresponding set of geometrical elements :

1 like (P/P), 3 like (ab/ab), 12 like (abc/abc)
6 like (P/ab), 6 like (ab/ac), 24 like (P/abc)
24 like $(ab/abc + abd)$, 24 like $(ab/acb + adb)$
12 like (abc/adc), 24 like (abc/bac), 24 like (abc/abd)
24 like (abc/bad), 24 like (abc/adb), 24 like (abc/cad).

We may express these (A/B) elements linearly in terms of five primitive integrals, viz. the four interatomic integrals

$$\alpha = (\tau_b^a/\tau_a^b), \quad \beta = (\tau_b^a/\tau_a^c), \quad \gamma = (\tau_b^a/\tau_c^a), \quad \delta = (\tau_b^a/\tau_d^c)$$

and the intra-atomic integral

$$\epsilon = (\tau_b^a/\tau_b^c).$$

The evaluation of α, β, γ and δ is perfectly straight-forward, since they are all linear combinations of $\mathrm{P}_{\sigma\sigma\sigma\sigma}$ and $\mathrm{P}_{\pi\pi\pi\pi}$ when $\sigma\pi$-type bonding is neglected. In virtue of Beardsley's successful calculations of the intra-atomic integrals for carbon,[7] ϵ was calculated *ab initio* using Slater functions [6] for phosphorus of the form

$$\psi(3p\sigma) = S_1^0 \, . \, \mathrm{f}(r), \quad S_1^0 = \left(\frac{3}{4\pi}\right)^{\frac{1}{2}} \cos\theta,$$

$$\psi(3p\pi) = S_1^1 \, . \, \mathrm{f}(r), \quad S_1^1 = \left(\frac{3}{2\pi}\right)^{\frac{1}{2}} \sin\theta\cos\phi,$$

where the normalised harmonics S_n^m satisfy

$$S_1^0 \, . \, S_1^1 = \left(\frac{3}{10\pi}\right)^{\frac{1}{2}} S_2^1.$$

After using Legendre's expansion for $1/r_{12}$, the addition theorem for zonal harmonics and orthogonality,[8] the integration is elementary and leads to the value

$$\epsilon = 1{\cdot}420 \text{ ev.}$$

The secular equation may be reduced to the simple form

$$\begin{vmatrix} x & 3x & 3(2x-u) \\ 3x & 3(6x-v) & 6(3x-u) \\ 3(2x-u) & 6(3x-u) & 3(15x-w-11u) \end{vmatrix} = 9 \begin{vmatrix} x & 0 & -3u \\ 0 & 3x-v & u \\ -u & u & 3x-w+u \end{vmatrix} = 0,$$

where

$$u = 4\beta - 2\gamma - 2\epsilon = -2{\cdot}62, \quad v = 8\delta - 8\alpha = 12{\cdot}26, \quad w = 8\beta - 8\alpha = 14{\cdot}52 \text{ ev.}$$

---

[7] Beardsley, *ibid.*, 1932, **39**, 913.
[8] Hobson, *Spherical and Ellipsoidal Harmonics*, (C.U.P., 1931).
[9] Arnold, *J. Chem. Physics*, 1946, **14**, 351.

and $-3x = E - Q - 9\alpha$ is the resonance energy of delocalisation. It is found that the additional stabilisation of the P_4 molecule thereby attained, accounts for some 0·26 ev. per P—P bond.

It is reasonable to suppose that the error incurred in our treatment using only a restricted representation for the energy matrix, is of the same order as that associated with the PVS approximation as applied to unstrained molecules. Accordingly the strain energy per P—P bond is now only 0·77-0·26 $\sim$ 0·5 ev. In order to include $\sigma\pi$-type bonding which we have previously neglected and the absence of non-adjacent repulsions in P_4, we allow for an extra stabilisation of some 0·2 ev. This figure is obtained by an appropriate adaptation to P_4 of the discrepancy between the empirical and similarly calculated strain energy for cyclopropane.[4] A final estimate of the strain energy to be associated with calculations based on the bond additivity assumption, is therefore

$$\sim 0{\cdot}3 \text{ ev.}, \quad \text{or} \quad \sim 7 \text{ kcal. per P—P bond.}$$

Using Dainton's value for the bond energy in P_4, this gives an unstrained pure $3p$ $\sigma\sigma$-type P—P bond an energy of

$$54{\cdot}5 \text{ kcal./mole}$$

—which is very close to the value predicted on the basis of Pauling's postulate. Our calculation is probably reliable to within ± 0·5 kcal. ; the error should certainly not exceed 1 kcal.

The writer would like to thank Prof. C. A. Coulson for suggesting this problem and the Board of the British Rubber Producers' Research Association for a grant.

Summary.

An examination of P—P bonding in the P_4 tetrahedron has been undertaken by means of the HLSP method. It leads us to associate a strain energy of 7 kcal./mole and an energy of delocalisation of 6 kcal./mole with each P—P bond. On the basis of Dainton's figure of 47·5 kcal. for these P—P bond energies, a bond energy of approximately 54·5 kcal. is assigned to an unstrained P—P bond.

New College,
Oxford.

THE FREE AND TOTAL ENERGIES OF INTERACTION OF COALS WITH METHYL ALCOHOL.

BY EVA M. DRESEL, M. GRIFFITH AND W. HIRST.

Received 18*th February*, 1948.

It is possible, in principle, to calculate the heat of immersion of a solid in a liquid from adsorption data. Thus, for reversible adsorption of an insoluble vapour, the free-energy lowering ΔG of the adsorbent is given by the integrated form of the Gibbs-Duhem equation,[1]

$$\Delta G = \frac{RT}{M}\int_{p_1}^{p_2} m \, \mathrm{d} \log_e f, \quad . \quad . \quad . \quad . \quad (1)$$

where p_1, p_2 are the initial and final pressures of the vapour, m is the quantity in grams of vapour adsorbed at a pressure p (or fugacity f), and M is the molecular weight of the adsorbate. This equation holds whatever the mechanism of interaction : e.g. whether the adsorbed phase is mobile or static, and whether the solid is rigid or expands during the adsorption. If p_1 is zero and p_2 is the saturation vapour pressure p_0, it is convenient to denote the value of ΔG by ΔG_V. The free-energy lowering ΔG_L, when the pure solid is wetted by liquid, is not in general identical with ΔG_V ; if, for example, the process of immersion represents merely the wetting of an area Σ of an adsorbed film,

---

[1] Bangham, *Nature*, 1944, **154**, 837.

$$\Delta G_L = \Delta G_V + \Sigma\gamma_{LV}\cos\theta, \quad . \quad . \quad . \quad . \quad (2)$$

where γ_{LV} is the surface tension of the liquid when in contact with its saturated vapour and θ the contact angle.*[2] The change in total energy ΔH associated with a free-energy lowering ΔG is given by the Gibbs-Helmholtz equation, so that the heats of saturation and of wetting of the adsorbent are :

$$\Delta H_V = \Delta G_V - T\frac{\partial(\Delta G_V)}{\partial T}, \quad . \quad . \quad . \quad . \quad (3)$$

$$\Delta H_L = \Delta G_L - T\frac{\partial(\Delta G_L)}{\partial T}. \quad . \quad . \quad . \quad . \quad (4)$$

The heat evolved when the pure solid is exposed to saturated vapour can, therefore, be evaluated directly from a pair of adsorption isotherms at different temperatures (eqn. (1) and (3)) ; to calculate the heat of wetting, ΔH_L, information must be available concerning the processes which take place when, after exposure to saturated vapour, the solid is immersed in the liquid.

The adsorption method sometimes has advantages over the direct calorimetric measurement. For example, when some of the heat is liberated slowly it may be hidden by the cooling losses of the calorimeter, and the apparent heat of wetting may be far lower than the real value. The isotherms, however, can be determined under such conditions that each point represents an equilibrium measurement ; the calculated heat changes, ΔH_V, are therefore correct. Since the difference between ΔH_V and ΔH_L is usually fairly small,† the method is useful when there is a suspicion of large errors in the calorimetric results.

In an earlier investigation,[3] it was concluded from calorimetric evidence that the greater part of the heat of wetting of coals by methyl alcohol is liberated rapidly. Subsequent measurements [4] of the densities of coals in a number of liquids showed that the pores in coals are not uniform in diameter along their length but contain constrictions no more than a few Ångström units in diameter. Furthermore, the apparent densities sometimes drifted slowly with time towards higher values suggesting that several hours were required to achieve complete penetration. This result reopened the question whether some part of the heat of wetting might be liberated too slowly to be detected in the calorimeters which were available, and it was decided to use the adsorption method as a check.

Certain difficulties have to be overcome. King and Wilkins [5] have found that the adsorption isotherms of water on coals show hysteresis, and Maggs [6] also found hysteresis when using methyl alcohol as adsorbate. The isotherms therefore do not satisfy the thermodynamic condition of reversibility assumed in eqn. (1) above, and the appropriate method of calculating the free-energy lowering has to be found. The second difficulty arises from the peculiar mechanical properties of coals. King and Wilkins,[6] and Dunningham[7] have shown that when freshly mined coal is dried and subsequently exposed to water vapour, the amount of water adsorbed is less than the original moisture content of the coal; the effect has been attributed to an irreversible shrinkage of the coal material when it is first dried. In addition, Dunningham[7] attributed the hysteresis in the adsorption isotherms to irreversibility of the mechanical properties, and Maggs[8] has shown for several coals that the stress-strain relationships are only partly reversible. Lawall and Holland[9] also observed hysteresis in the stress-strain curves of West Virginia coals.

---

* If the adsorbent saturated with vapour expands on immersion, the expression for ΔG_L is more complicated and includes a term to represent the work of expansion. On the other hand, when there is capillary condensation $\Delta G_V = \Delta G_L$. For further details, see ref. [13].

† For the adsorbent used here (coal), there is insufficient knowledge to enable the difference between ΔH_V and ΔH_L to be calculated as suggested in the preceding paragraph.

[2] Bangham and Razouk, *Trans. Faraday Soc.*, 1937, **33**, 1459.

[3] Griffith and Hirst, *Proc. Conf., Ultrafine Structure of Coals and Cokes, B.C.U.R.A.* (London, 1944), p. 80.

[4] Franklin, *Trans. Faraday Soc.* (in press).

[5] King and Wilkins, ref. 3, p. 46.

[6] Maggs, *ibid.*, p. 95.

The mechanical instability makes it difficult to determine the temperature dependence of the sorption isotherm in order to derive the quantity $\frac{\partial(\Delta G_V)}{\partial T}$ (eqn. (3)). The difficulty arises in the following way. Bangham and Maggs[10] have found evidence showing that the swelling of coal which accompanies adsorption is primarily due to the pressure of the adsorbed film. If the temperature is raised, the film pressure increases and the solid swells further. On lowering the temperature, the solid may not then revert to its original condition. Thus, if the vapour pressure is measured at T_1, then at a higher temperature T_2, and finally at T_1 once more, the two measured pressures at T_1 may be different. It is therefore necessary to ensure that the experimental observations used to calculate the temperature dependence are properly chosen.

In the presentation which follows, the results of preliminary experiments are described to illustrate the characteristic features of the sorption isotherms of methanol on coal and the phenomena associated with the measurement of the temperature dependence. These experiments are discussed in the light of existing knowledge of the structure and physical properties of coals. The method, which then emerges, for obtaining the heat changes from the sorption isotherms is used to derive the numerical values of the heats of wetting of three coals.

Experimental.

Apparatus.—The volumetric method was used for determining the sorption isotherms. A diagram of the glass apparatus is shown in Fig. 1. The mercury cut-offs also served as pressure gauges which were read by a vernier cathetometer. The quantities adsorbed on the coal were calculated assuming that the vapour obeyed Boyle's law. The whole system was connected to a mercury-vapour diffusion pump backed by a rotary oil pump. Prior to adsorption measurements, coal samples were evacuated first in the cold and then, for several hours, at 110° C. to a final pressure of 10^{-5} mm. Hg.

Materials.—METHYL ALCOHOL. Pure methyl alcohol, as supplied by James Burrough Ltd., was freed from dissolved gases and submitted to vacuum distillation in the adsorption line. The middle fraction was used for measurements.

COALS. Three bituminous coals were investigated: a Northumberland coal K, a Yorkshire coal H, and a South Wales coal F. The analyses are given in Table I. For the heat of wetting and sorption measurements the samples were ground to pass a 240 B.S. sieve.

Description of the Sorption Isotherms.—The main features of the methanol sorption isotherms are summarised below.

(1) The isotherms on coals K and H are sigmoid in shape, whereas that on coal F is similar to the Langmuir isotherm showing no point of inflexion (Fig. 2).

(2) The area of the hysteresis loop increases with the sorption capacity of the coal. Thus coal F, which at saturation adsorbs 5 % of methanol by weight,

[7] Dunningham, *ibid.*, p. 57.

[8] Maggs, *Trans. Faraday Soc.*, 1946, **42B**, 284.

[9] Lawall and Holland, *Eng. Exp. Station, Res. Bull. No.* 17 (West Virginia University).

[10] Bangham and Maggs, ref. 3, p. 118.

shows only a small hysteresis loop confined to a limited pressure range ; whereas with coals K and H, which adsorb 26 % and 18 % respectively, the hysteresis loops cover the whole pressure range, and the adsorption and desorption curves are further apart (Fig. 2)

(3) The desorption curves can be traced back to the origin, i.e. the adsorbed vapour can be removed completely. This is true no matter whether the coal has previously been exposed to methanol vapour or not.

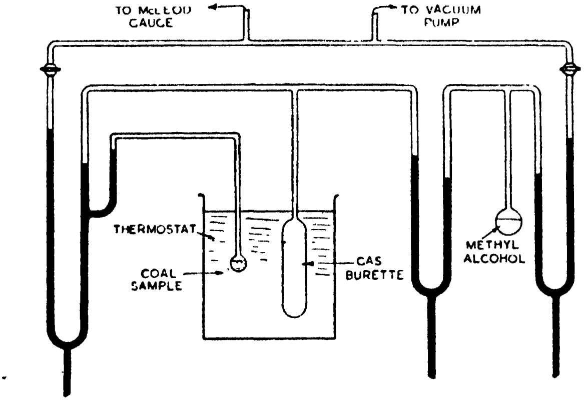

FIG. 1.

(4) If successive isotherms are determined on a fresh sample of coal, the amount adsorbed at a particular pressure on the second adsorption may exceed the corresponding quantity on the first.

(5) If the coal is flushed with methanol vapour prior to the determination of the isotherm, the *adsorption* curve may be reproduced.

(6) When there is hysteresis, the *desorption* curve has no unique position but depends on how far the adsorption has been taken (Fig. 3).

Phenomena Associated with the Determination of the Temperature Dependence.—The first attempts to determine the temperature dependence of the isotherms were made on the desorption part of the cycle. When the equilibrium pressure obtained after desorbing a quantity of vapour at a temperature T_1 had been determined, the temperature was raised to T_2 and the new pressure was measured after allowing about 16 hr. to attain equilibrium. On returning to the original temperature the pressure was higher than before, the difference between the two pressures at T_1 being about 50 % of the difference between the later pressure at T_1 and the pressure at T_2.

TABLE I.

	Coal K.	Coal H.	Coal F.
Ultimate Analysis			
% D.m.f. (Parr's basis)			
Carbon . . .	82·5	83·1	90·0
Hydrogen . . .	5·3	5·3	5·0
Nitrogen . . .	2·1	2·0	1·7
Oxygen . . .	10·1	9·6	3·3
Volatile matter, d.m.f..	38·2	35·5	24·3
B.S. Swelling number .	1½	2½	9

Subsidiary experiments were carried out to investigate the effect in more detail and the following general observations were made.

(1) When the temperature dependence was observed on the *adsorption* part of the cycle, the pressure changes were reversible.

(2) After ***desorption*** at T_1, attaining equilibrium, and raising the temperature to T_2, the pressure drifted to higher values. The drift at T_2 was observed even when the pressure at T_1 had been steady for two days.

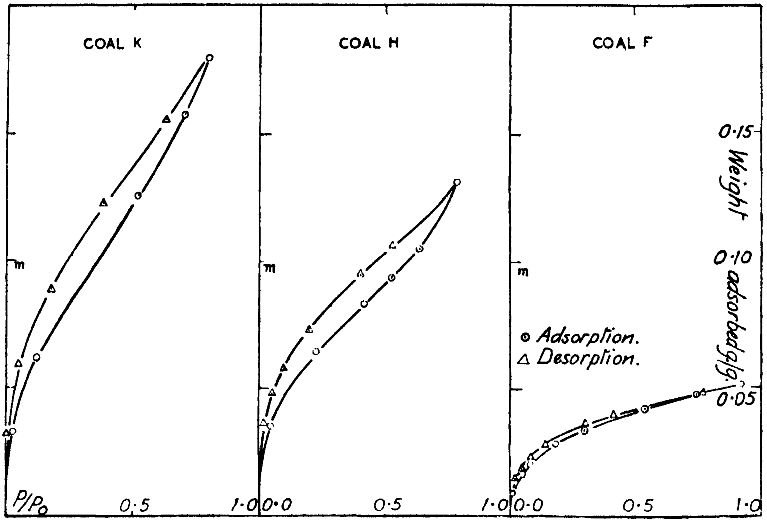

FIG. 2.—Equilibrium relative pressure.

(3) If the temperature was then lowered to the original value T_1 a steady pressure was reached in about 15 min. and no change in pressure was observed during the subsequent 24 hr.

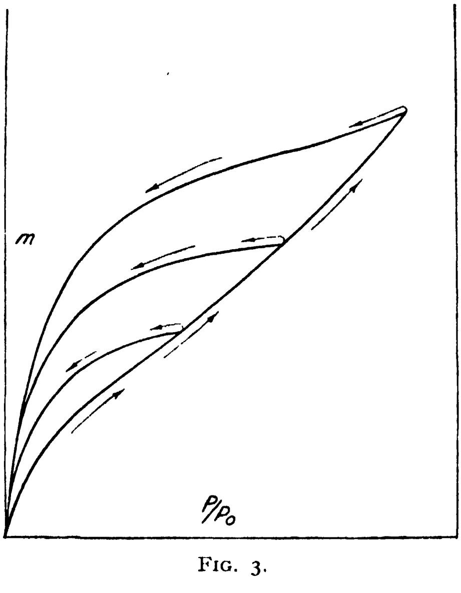

FIG. 3.

(4) If the temperature was raised temporarily above T_2, the drift at T_2 was accelerated.

(5) On the logarithmic scale, the difference between the original and final pressures at the lower temperatures was equal (within experimental error) to the drift which occurred at the higher temperature.

(6) The drifts were greatest in the region of greatest hysteresis.

(7) If desorption was effected at T_2 (the higher temperature) instead of at T_1, the pressure change on going to T_1 was reversible.

These observations strongly suggest that the peculiar behaviour of the system is due to the superposition of two effects, one which is reversible to within experimental error, the other an irreversible effect which sets in when the temperature is raised. The irreversible effect causes a gradual drift of the vapour pressure to higher values. In general, the magnitude of the reversible effect may be obtained from the pressure at the higher temperature and the value of the pressure *subsequently* observed at the lower temperature.

Discussion.

I. Sorption Isotherms on Coals.

The main features of the isotherms are consistent with, and lend support to, a model for the structure of lower rank coals proposed by Bangham, Franklin, Hirst and Maggs.[11] The model was put forward as being the simplest representation of the structure of coal in accord with the essential features of the known experimental facts. The model is, of course, idealised. It is supposed that in an early stage of coalification, micelles of preferred size are formed and that throughout the subsequent history these tend to retain their individuality. A low rank coal is likened to an assembly of close-packed spherical micelles of equal size (about 200 A. diam.). From the physical standpoint, coalification is regarded as a process whereby the contact regions of the micelles flatten so that the contact areas increase and the whole assembly consolidates. The coals used in the present investigation are three of those on which the experimental measurements leading to the model were made, and it may be stated that the Northumberland coal K would be represented as a close-packed spherical aggregate with little flattening in the contact regions, the Yorkshire coal H would have rather larger contacts and the Welsh coal F would have very large contact regions between the micelles (Fig. 4).

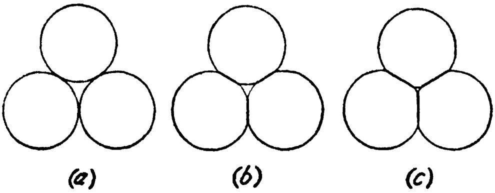

FIG. 4.

Assemblies of this kind owe their cohesion in part to the strength of the actual contacts and in part to the surface forces which act across the narrow gaps around the contacts. As the contacts increase in size one would expect the relative contribution of the surface forces to diminish. This contribution should therefore be greatest for the Northumberland coal, less for the Yorkshire coal and least for the Welsh coal.

The swelling of solids which occurs on adsorption of vapours has been discussed by Bangham,[12] and one of the present authors [13] has extended Bangham's theory to cover the case when surface forces contribute appreciably to the cohesion. In this extension of the theory, it is supposed that in the course of adsorption the constituent units of the solid tend to be forced apart * by the spreading force of the adsorbed film. Since surface forces fall off as an inverse power of the distance over which they act, the forces tending to cause the swollen solid to revert to its original condition are weaker than those which initially opposed swelling. It follows that on lowering the vapour pressure the solid does not revert to its original condition and the isotherms exhibit hysteresis. It may be noted that the observed sizes of the hysteresis loops are in the order which this theory would predict from the coal models. It should further be noted that according to the theory the following primary meaning is attached to the hysteresis loops: the large initial resistance to swelling prevents the solid from expanding sufficiently to adsorb the quantity of vapour consistent with the minimum free energy of the adsorbent for the vapour pressure. It follows that the free-energy lowering of the adsorbent must be calculated by using eqn. (1) in conjunction with the *desorption* curve.†

---

[11] Bangham, Franklin, Hirst and Maggs (in preparation).

[12] Bangham, Fakhoury and Mohamed, *Proc. Roy. Soc. A*, 1934, **147**, 152. Bangham, ref. 3, p. 26.

[13] Hirst, *Faraday Soc. Discussion*, 1948, **3**.

The above ideas on the structure of coals and the mechanism of swelling suggest an explanation of the phenomena encountered when attempting to measure the temperature dependence of the isotherms. The pore system in an assembly of spheres contains constrictions whenever neighbouring spheres are in contact, and during swelling and shrinking these small holes will expand and contract. During desorption, the narrowing constrictions may trap some of the adsorbate. Helped by the increase in film pressure when the temperature is raised, the trapped adsorbate might force its way out, thus increasing the vapour pressure. This would explain very simply why the pressure changes should be reversible when desorption is carried out at the higher temperature. It is perhaps significant that, when the sorption isotherms were retraced to the origin, the adsorbate could not be removed by pumping only. It was always necessary to raise the temperature to remove the last traces.

To sum up, it appears from the preliminary experiments that the heat of saturation of coal by methyl alcohol may be calculated from the isotherms as follows:

(1) by using the *desorption* isotherm to derive the free-energy lowering;
(2) by assessing the temperature dependence from the vapour pressures at two temperatures, when the temperature is changed from a higher to a lower value.

II. Numerical Results.

The Heat of Saturation and the Heat of Wetting.—The sorption isotherms were extrapolated to saturation pressure p_0, and the numerical values for the free-energy lowerings per gram of solid when exposed to saturated vapour, were derived by applying eqn. (1) to (*a*) the desorption curve and (*b*) the adsorption curve. From the reversible temperature dependence of the isotherms determined on desorption, the temperature derivatives of the free-energy lowerings were evaluated and hence the heats of saturation, ΔH_V, by applying eqn. (3). The results obtained for the three coals investigated are shown in Table II. Table II also gives the heats of wetting measured directly, on identical samples, in a calorimeter (the " routine " calorimeter described in an earlier paper [3]).

---

* There is experimental evidence that on adsorption of vapours the constituent units of coal do, in fact, tend to separate. First, the volume of methyl alcohol adsorbed at saturation pressure exceeds the original pore volume by the order of 100 %, even when allowance is made for the compression of the liquid in the adsorbed phase. (It is assumed throughout that methyl alcohol is adsorbed on coal as an insoluble surface film.) Second, Maggs [14] has demonstrated for one coal that the material is more deformable in the swollen condition.

† It is shown elsewhere [13] that if the work of expansion is appreciable the free-energy lowerings calculated from the desorption isotherms may be too great. No reliable measurements of the work of expansion are yet available, but it is believed that the corrections would not be large.

[14] Maggs (unpublished).

Discussion.—From Table II it appears that the heats of wetting determined experimentally are *higher* than the values calculated from the isotherms.[*] The measured calorimetric values could exceed the heat of wetting if the physical process were accompanied by a chemical reaction. It is, however, found experimentally that the calorimetric heat liberations are not lowered by repeated measurements on the same sample, so that the possibility of irreversible chemisorption may be ruled out. It is therefore concluded that the experimental values are not greater than the real heats of wetting, and hence that the calculated heats of saturation, ΔH_V, are less than the heats of wetting.

TABLE II.

Coal.	$-\frac{\partial(\Delta G_V)}{\partial T}$. (cal./degree)	Desorption.		Adsorption.		Calorimetric.
		ΔG_V.	ΔH_V.	ΔG_V.	ΔH_V.	ΔH_L.
		(cal./g.).		(cal./g.).		(cal./g.).
K . .	0·19	8·4	13·2	7·1	11·1	17·6
H . .	0·17	6·3	9·5	5·4	8·1	12·2
F . .	0·24	2·5	4·2	2·1	3·8	4·7

Two possible explanations of this result suggest themselves.

1. As mentioned above, ΔH_V and ΔH_L are not necessarily identical. For example, Bangham and Razouk [15] have shown experimentally that there is a real difference between the free-energy lowerings accompanying the saturation and wetting of charcoal by methanol. If the assumption is made that the ratio $\Delta H_L/\Delta H_V$ (= 1·25) calculated from their data [15] for the charcoal-methanol systems holds also for the coal-methanol system, one obtains the values for ΔH_L shown in columns (4) and (5) of Table III. It will be seen that for coals K and H there still remains an appreciable difference between ΔH_L calculated from the *adsorption* data (4) and the experimental values (6). The observation supports the hypothesis that the free-energy change should be calculated from the *desorption*

TABLE III.

Coal.	ΔH_V (cal./g.).			ΔH_L (cal./g.).		
	Calculated from Isotherms –			Calculated from Isotherms using $\Delta H_L/\Delta H_V$ for Charcoal.		Experimental (calorimetric).
	as Observed.		Corrected.			
	Adsorption (1).	Desorption (2).	Desorption (3).	Adsorption (4).	Desorption (5).	(6).
K .	11·1	13·2	15·8	13·9	16·5	17·6
H .	8·1	9·5	11·5	10·1	11·9	12·2
F .	3·8	4·2	4·7	4·7	5·3	4·7

---

[*] The reverse might have been expected, had the calorimetric results been subject to errors due to slow heat evolution (cp. p. 2).

[15] Bangham and Razouk, *Proc. Roy. Soc. A*, 1938, **166**, 572.

isotherm and the good agreement between columns (5) and (6) will be noted.

2. The free-energy lowerings, ΔG_V, calculated from the desorption isotherms of coals K and H (which show marked hysteresis) may be too low. This is because the position of the desorption curve depends on how far the adsorption is taken (Fig. 3) and the true curve can only be obtained after allowing the solid to reach adsorption equilibrium at saturation vapour pressure. Unfortunately,* with the apparatus used, it was difficult, without loss of experimental accuracy, to take the isotherm further than 0·85 saturation pressure. The observed desorption curves may therefore lie below the true curves. An attempt has been made to set a limit to the resulting error † in the calculated values ΔH_V column (2), and the corrected values so obtained are shown in column (3) of Table III. These are in much closer agreement with the experimental heats of wetting. It should be noted that there is no corresponding correction which would raise the experimental *adsorption* curve so that the discrepancy between the values in columns (1) and (6) still remains.

When the desorption isotherms are used as the basis for calculation, the two suggested methods of correction (perhaps taken together) are adequate to account for the discrepancy between the calculated and experimental heats : i.e. there is no evidence to show that a significant difference exists between these values. It is concluded, therefore, that the experimental heats of wetting are approximately correct, and that no large part of the heat is liberated too slowly to be detected by the calorimeter. It should be emphasised, however, that this result was obtained using samples of coal of a particular size grading (—240 B.S.S.). The effect of particle size on the apparent heat of wetting and the structural changes which occur when coals are ground, form the subject-matter of a later paper.

Note on the Differential Heats of Adsorption.—From the measured temperature dependence of the equilibrium vapour pressure,† the differential heats of adsorption of methyl alcohol on the three coals have been calculated using the Clapeyron-Clausius equation. The net heats (i.e. the difference between the total energy of adsorption and the latent heat of condensation—9,200 cal./mole—of methanol) derived at various points on the isotherms are shown in Table IV. (The estimated accuracy is ± 200 cal./mole.) The results may be summarised as follows.

(1) All the net heat values exceed zero by an appreciable amount.

(2) Over the course of the isotherm the net heat of adsorption drops from 3,500-4,000 cal./mole to about 1,000 cal./mole for coals K and H, and from 3,000 cal./mole to about 1,500 cal./mole for coal F. The larger drop suggests that in the case of the first two coals the adsorbed films are thicker. This is also suggested by the difference in the shape of the isotherms and would be in accord with the predictions of the theory underlying the model concerning the relative pore sizes of the coals.

---

* The theoretical argument (see p. 997 and ref. [13]), that the desorption isotherm should be used for calculating the free-energy lowering, developed from consideration of the experimental results given in the present paper. These were sufficient to show that there was no *large* error in the calorimetric heats of wetting and the primary object of the investigation had thus been achieved. To determine the exact position of the desorption isotherm further experimental work, using more suitably designed apparatus, will clearly be necessary. For the present purpose the magnitude of the correction was estimated roughly as follows. The extrapolation of the desorption isotherm to saturation pressure gives a smaller saturation capacity than is obtained by extrapolating the adsorption curve. If we assume that, at any pressure, the ratio of sorption capacities corresponding to the true and observed desorption curves, respectively, is equal to the ratio of the saturation capacities obtained by the two methods of extrapolation, then the true and apparent free-energy lowerings would show the same relative difference. For coals K and H this difference is of the order of 20 %.

† The reversible temperature dependence determined as suggested on p. 997.

(3) The low-pressure values for the net heats are about 4,000 cal./mole. for coals K and H, and 3,000 cal./mole for coal F. A small increase in the methanol heat of adsorption with the oxygen content of the coal is therefore indicated.

TABLE IV.—DIFFERENTIAL HEATS OF ADSORPTION.

	Coal K				
p/p_0	0·02	0·15	0·41	0·52	0·69
$m \times 10^2$ (g./g.) . . .	4·1	7·6	11·5	12·5	14·9
Net diff. heat (cal./mole) .	3,600	2,500	1,600	1,200	900
	Coal H				
p/p_0	0·02	0·10	0·20	0·51	0·79
$m \times 10^2$ (g./g.) . . .	3·6	5·8	7·2	10·3	12·9
Net diff. heat (cal./mole) .	4,300	3,000	2,300	1,500	900
	Coal F				
p/p_0	0·02	0·14	0·42	0·70	0·87
$m \times 10^2$ (g./g.) . . .	1·2	2·6	3·9	4·7	5·0
Net diff. heat (cal./mole) .	3,100	2,500	2,000	1,700	1,500

(4) The low-pressure value for the methanol heat of adsorption on coal F is in good agreement with the value obtained by Razouk [16] for methanol on charcoal (3,200 cal./mole). The latter figure was found to remain constant up to saturation pressure.

The authors wish to record their gratitude to Dr. D. H. Bangham, Director of B.C.U.R.A. Research Laboratories, for his interest and advice in connection with this work.

Summary.

Pairs of sorption isotherms at different temperatures enable the free and total energies at saturation to be calculated by the method of integration. Sorption hysteresis, where present, introduces an element of uncertainty into the calculation, but an attempt is made to overcome this difficulty and to explain the cause of the hysteresis effects encountered. The calculated values of the heats of saturation are compared with the heats of immersional wetting in the liquid as determined calorimetrically.

Values for the differential heats of adsorption are deduced at several points of the isotherm.

B.C.U.R.A.,
13 *Grosvenor Gardens, S.W.*1.

---

[16] Razouk, *J. Physic. Chem.*, 1941, **45**, 190.

THE MERCURY-CHABAZITE SYSTEM.

BY R. M. BARRER AND M. WOODHEAD.

Received 19*th February,* 1948.

Among observations by Grandjean [1] on the sorption of inorganic vapours by zeolites was the discovery that chabazite would take up 27 % of its own weight of mercury. Wyart [2] later found that as much as 60 % by weight of mercury could be occluded, and his X-ray study suggested a regular array of mercury atoms in interstitial positions within the crystal. Measurements of sorption by chabazite and other zeolites are nearly always made using mercury as manometric fluid, so that it is important to study quantitatively the sorption kinetics and equilibria of mercury in chabazite, not only for themselves, but also to find to what extent mercury vapour may interfere with equilibria involving other vapours. There are few quantitative investigations of uptake of mercury vapour on any sorbent, an exception being a study by Coolidge[8] of the mercury-charcoal system. Coolidge was able to establish that mercury vapour would not interfere appreciably with other charcoal-vapour equilibria, and that the sorption of *liquid* mercury by charcoal occurs endothermally.

---

[1] Grandjean, *Bull. Soc. franc. Miner.*, 1910, **33**, 5.
[2] Wyart, *ibid.*, 1933, **56**, 81 and 142.

Experimental.

Neither Grandjean nor Wyart made any attempt to exclude air from the mercury-chabazite system. In the present study, high-vacuum conditions were used for many measurements, by modifying the McBain-Bakr silica spring sorption balance to operate up to 400° c. Coarsely powdered chabazite was suspended in a small glass bucket, in a sealed Pyrex tube. This Pyrex " balance-case " was surrounded by a tubular electrically heated furnace, well lagged but with a narrow unlagged slit at the front and back. The slit served as a window for measurement by cathetometer of the length of the spring. The balance case was joined at its lower end to a small reservoir of carefully purified mercury, independently heated. Manual control of both reservoir and balance case gave an accuracy of 1° c. in each temperature. The silica spring was calibrated at three different temperatures covering the range of the measurements. Reliable interpolation to other temperatures within this range was then possible. After it had been outgassed *in situ* in the balance case for 20 hr. at 380° to 400° c., the chabazite was exposed in the sealed case to mercury vapour at various pressures and temperatures, and isotherms measured. The pressure, p, of mercury vapour, was obtained for any temperature, T, from $p-T$ data.* The sensitivity of the spring was 4·904 cm./g. at 17° c., and 4·730 cm./g. at 363° c.; extensions could be read to 0·002 cm., corresponding to an accuracy of 0·4 mg. The weight of the chabazite being 0·3622 g., this corresponds to about 1 mg./g. of chabazite. A small correction was made for the buoyancy of the bucket, chabazite and spring itself, at varying pressures of mercury vapour, but this was never more than 0·3 mg.

Results.

On exposing the chabazite to mercury vapour at a temperature of 320° c., a substantial sorption was noted, but when the mercury vapour pressure was made negligible (by cooling the mercury) desorption was only partial. In successive cycles of exposure to mercury (up to 120 mm. pressure) and removal of vapour, there was a progressive *irreversible* uptake of mercury † (Fig. 1). Simultaneously the chabazite developed a deep bronze colour. On breaking open the seal into the system it was found that about 3 cm. pressure of gas

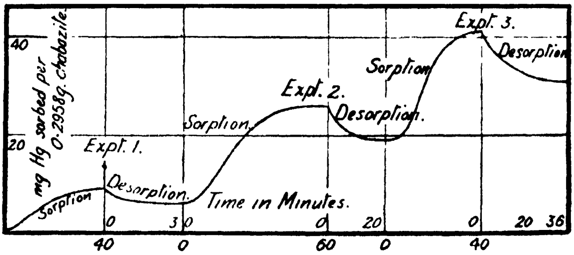

FIG. 1.—Irreversible uptake of mercury in presence of air.

---

[8] Coolidge, *J. Amer. Chem. Soc.*, 1927, **49**, 1949.

* *Inter. Crit. Tables.*

† The time scale in Fig. 1 does not represent the true rate of sorption or desorption but is believed to be that for heating or cooling of the mercury.

had collected, due to slow leak or to desorption from the Pyrex under the influence of hot mercury vapour. When the bronze product was exposed to (moist) air, the colour darkened rapidly, becoming a lustrous jet black within 20 min. The amount of mercury taken up irreversibly was about 11 % by weight of the chabazite, as estimated by weighings on the McBain-Bakr balance, by weighing the product and comparing with the original weight of chabazite, and through density determinations (by flotation in benzene and ethylene dibromide for natural chabazite and in ethylene dibromide and bromoform for the black product).*

This behaviour in imperfect vacuum suggested that the irreversible sorption may be associated with the presence of air or other gases. The colour changes were, moreover, rather similar to those observed by Grandjean and Wyart, who, as already noted, did not exclude air. Proof of this is provided by experiments given on p. 1005. In order that the vacuum could be checked periodically, the sorption system was modified so that the balance case could be isolated by a mercury cut-off rather than by sealing off. In high vacuum, sorption of mercury vapour was now found to be fully reversible, and equilibrium was established extremely rapidly. Moreover this reversible sorption was very much smaller than that previously observed [1, 2] in presence of air, e.g. at 245° C. the total uptake of mercury at the highest pressure used was 3·5 mg. Isotherms at five temperatures are shown in Fig. 2. The experimental points make it clear that in all cases the sorption is proportional to the pressure, and the full lines are drawn by the method of least squares. The temperature coefficient in the

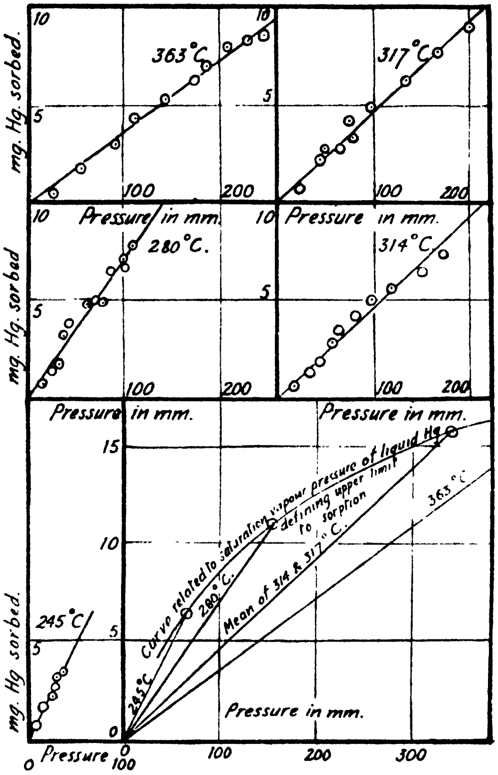

FIG. 2.—Sorption isotherms for Hg on chabazite under high-vacuum conditions (0·3622 g. of chabazite in each case).

---

* Allowing here for water which entered the chabazite on exposure to moist air. None of the liquids used in density determinations are themselves occluded by chabazite.

isotherms is not great, and to avoid confusion in presentation the isotherms are given separately. The heat of sorption ΔH can be calculated from the relation

$$\left(\frac{\partial \ln p}{\partial T}\right)_x = \frac{\Delta H}{RT^2}$$

p being the equilibrium pressure for a fixed sorption, x, of mercury. The slope of the curve in which $\ln p$ is plotted against $1/T$ is then $-\Delta H/R$ (provided ΔH does not change in the temperature interval considered). The experimental points so plotted did fall nearly on a straight line (see Fig. 3) and the best line

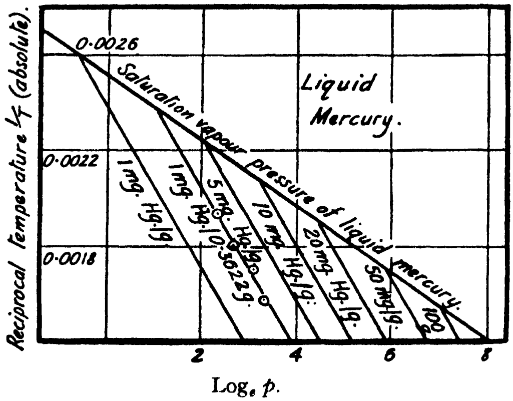

FIG. 3.—Isosteres for sorption of Hg by chabazite.

drawn by the method of least squares gave $\Delta H = -5{,}800$ cal./g.-atom of mercury. This heat is less than the initial sorption heat of nitrogen in chabazite, about the same as that for argon, and greater than that for hydrogen. As separated atoms therefore, mercury behaves very like the permanent gases, and does not show towards its environment a great polarisability, α, or van der Waals' cohesive constant, a, such as characterises it in the liquid state. The isotherms were unavoidably in the dilute range ; whether a dense interstitial population of mercury atoms would develop any metallic properties could not therefore be tested.

The heat of sorption is also considerably smaller than the latent heat of condensation, $\Delta H_c = -13{,}600$ cal./g.-atom. Thus the transfer of mercury from liquid mercury to chabazite will be an endothermal process, favoured by high temperatures. It is important to find the maximum sorption values at each temperature, and to attempt an extrapolation to the low temperature end so as to show how much, if any, mercury will interfere with sorption equilibria involving other gases. From the isotherms, one may derive the isostere corresponding to an uptake of 1 mg. of mercury by 0·3622 g. chabazite, and plot this in the form $\ln p$ against $1/T$. Assuming that Henry's law continues to describe the sorption equilibria, parallel isosteres corresponding to 1, 5, 10, 20, 50 and 100 mg. Hg/g. chabazite can be drawn (Fig. 3). In Fig. 3 is also shown the saturation vapour pressure of liquid mercury, the plot of which (as $\ln p$ against $1/T$) intersects the isosteres. The points of intersection set an upper limit to the maximum possible sorption at each temperature, since if $\ln p$ passes to the right of the saturation pressure line, liquid mercury will appear.* Table I shows the maximum sorptions possible at different temperatures.

TABLE I.—MAXIMUM SORPTION OF MERCURY VAPOUR.

Temperature in °C.	Maximum Wt. of Hg sorbed in g/.100 g. Chabazite.
100	<0·1
200	0·8
250	1·9
300	3·9
350	7·0
400	11·6
450	19·0

---

* A similar procedure has been used by Coolidge[3] to obtain the maximum sorptions possible in charcoal.

These data show clearly that mercury is sorbed only to a negligible extent at room temperatures or below, and is quite suitable as manometric fluid in sorption studies involving chabazite. Likewise the data indicate that the 27 % increase in weight of chabazite heated with mercury in air at 320° c. observed by Grandjean, and the 40-60 % increase at 360° c. of Wyart far exceed the theoretically possible reversible sorption limit. Moreover the sorption we have studied above produced none of the vivid colour changes noted by these workers, and by ourselves, for the *irreversible* uptake noted earlier. Experiments were accordingly made to demonstrate conclusively that oxygen was occluded with the mercury in an irreversible interstitial reaction.

The Mercury-Oxygen-Chabazite System.

The method finally adopted to demonstrate simultaneous uptake of oxygen and mercury was as follows. Chabazite (~ 2·2 g.) outgassed at 380° c. was heated in a bulb containing pure oxygen.* The bulb was joined to a manometer, and except for small sections of capillary tubing at room temperature, the temperature was controlled to within 0·1° c. by water or liquid paraffin baths. A graph was constructed showing the pressure registered as a function of temperature, over the range room temperature to 150° c. (Fig. 4, Curve 1). A small appendage to the main bulb contained mercury which during the heating was at room temperature. By tilting the apparatus, however, the mercury was run into the main bulb into contact with the chabazite, and the mercury-oxygen-chabazite system heated at 300° c. for 1 hr. The initially high oxygen pressure at 300° c. was actually observed falling as the chemisorption proceeded, and the chabazite developed the characteristic colour already noted (golden yellow deepening to bronze). After this period of 1 hr. at 300° c. a pressure-temperature curve was again obtained over the interval room temperature to 150° c. This second curve lay far below the first one (Fig. 4, Curve 2). From the known dimensions of the apparatus it was calculated from the pressures at 150° c. that ~ 18·6 ml. oxygen at N.T.P. had been chemisorbed.† Assuming as a reasonable estimate that one atom of mercury is chemisorbed for each atom of oxygen, this corresponds to a 15 % increase in weight during uptake of mercury and oxygen.

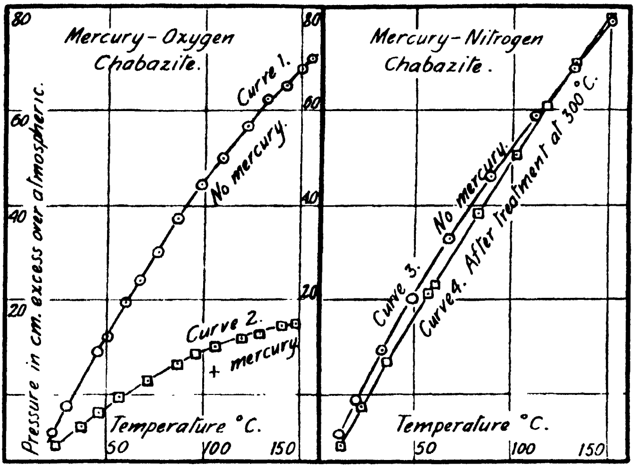

FIG. 4.—Mercury-oxygen-chabazite and mercury-nitrogen-chabazite behaviour.

---

* Obtained from outgassed $KMnO_4$ by heating in vacuum, and dried over P_2O_5.

† The approximation sign is used because there may be a slight van der Waals' sorption at 150° c. both before and after chemisorption, and the degree of convergence of the graphs in Fig. 4 towards the lower temperatures, shows that the sorptive power for oxygen of the mercury-containing chabazite is less than that of the mercury-free chabazite, so that the figure of 18·6 ml. at N.T.P is a lower limit to the amount chemisorbed.

As a final test, an exactly comparable experiment was made using nitrogen. As expected (Fig. 4, Curves 3 and 4) the curves before and after heating with mercury nearly coincide, and there is no evidence of chemisorption in the mercury-nitrogen-chabazite system. There was no colour formation whilst the chabazite was hot, although on cooling a faint grey tint developed, ascribed to desorption of mercury as tiny liquid droplets on cooling, as would have occurred under vacuum conditions.

Colour Changes in the Mercury-Oxygen-Chabazite System.—It has been noted, in agreement with Grandjean,[1] that on heating the mercury-oxygen-chabazite system, the chabazite is coloured first yellow then bronze, and that this product sorbs water to give shining black crystals of sorbent. Also, on heating, the black product becomes orange, yellow and finally white, water being evolved before mercury. It was then further demonstrated that other carefully dried polar gases also gave characteristic colour changes with the bronze or yellow crystals, as summarised in Table II.

TABLE II.—COLOUR OF CRYSTALS BEFORE TREATMENT, PALE YELLOWISH-BROWN.

Gas.	How Dried.	Colour Developed in Crystals after Treatment.
H_2S	Over phosphoric oxide, prolonged treatment	Dark grey, lustrous, resembling lump graphite
SO_2	As above	Lustrous black with brownish tendency
NH_3	Over freshly ignited quicklime	Silvery grey, not so dark as with H_2S, resembling galena

Thus nearly neutral (H_2O), acidic (H_2S, SO_2) and basic (NH_3) molecules may give these colour changes. It is perhaps significant that all may donate electrons and form co-ordinate links.

The colour changes in the mercury-oxygen-chabazite system are themselves complex and need further study. The product described as bronze is a deep orange brown when hot, but becomes paler and duller on cooling. If sufficient mercury and oxygen are chemisorbed it is possible to obtain a product which fails to blacken on exposure to moisture, possibly because the interstitial channels are fully occupied by mercury and oxygen and there is no room for water to enter. Wyart [2] mentions a product formed at 360° C. which is shining black but which turns brick red on exposing to moist air. This phenomenon, which we have not observed, would be a colour change in the reverse sense to the normally found sequence.

Discussion.

The present paper forms an introduction to a chemistry of interstitially-distributed atoms. Whatever the nature of the mercury-oxygen complex within the chabazite, it cannot be distributed spatially with the lattice characteristic of any bulk oxide of mercury. Rather, it must form a rarefied lattice—possibly as linear arrays of mercury and oxygen ions—supported by the framework of the zeolite. The complex series of colour changes with polar gases suggest interactions of a chemical nature which do not recall known reactions of bulk mercury oxides. The behaviour suggests a field of study in which interstitial reactions between occluded molecules may be examined and compared with those in gaseous and bulk phases. Such pairs of molecules may have to react in special orientations and in strongly perturbing force fields due to the zeolitic lattice.

Summary.

In high-vacuum conditions, mercury vapour is sorbed reversibly and exothermally by chabazite, according to Henry's law. The sorption heat is less than the initial sorption heat of nitrogen and about the same as that of argon,

and the mercury atoms in their interstitial environment, evidently show between themselves or with the chabazite, little of the strong adhesion which characterises them in liquid mercury. This results in sorption of *liquid* mercury by chabazite being strongly endothermic, the amounts then occluded being negligible except at elevated temperatures (> 200° c.). Mercury is therefore suitable as a manometric fluid in studying other sorptive equilibria in chabazite.

In the presence of air or oxygen, mercury and oxygen at high temperatures together undergo an irreversible intracrystalline chemisorption. This chemisorption is often accompanied by vivid colour changes. No less vivid additional colour changes are shown when H_2O, NH_3, H_2S or SO_2 are contacted with the interstitial mercury-oxygen complex.

The Chemistry Department,
Bedford College (Univ. of London),
Regent's Park, N.W. 1.

The Chemical Laboratories,
The Technical College,
Bradford, Yorks.

STATISTICAL THERMODYNAMICS OF CO-OPERATIVE SYSTEMS (A GENERALIZATION OF THE QUASI-CHEMICAL METHOD).

By E. A. Guggenheim.

Received 19th February, 1948.

1. Introduction.

The exact application of statistical thermodynamics to co-operative systems leads to insuperable mathematical complications. To make useful headway some kind of approximation is necessary. One approximate method of approach, which has proved useful, is that called the *quasi-chemical method.* This method of approximation was first applied to a model of a regular solution [1] in which each molecule is supposed to occupy one site of a lattice. The same method was later applied to a superlattice [2] in a solid alloy. Finally the method was extended to a mixture of any number of kinds of molecules differing among themselves in the number of sites occupied by one molecule.[3] At the same time it was shown that an apparently different method of approach, generally known as *Bethe's method,* in fact implicitly uses the same approximation as the quasi-chemical method and consequently must lead, by more devious routes, to identical results.

The conditions of quasi-chemical equilibrium and all the thermodynamic formulæ derived from them, contain parameters w closely related to the heats of mixing. It is the object of the present paper to examine more carefully than hitherto the physical definition of w and to show that the assumption hitherto made that w is independent of temperature is unnecessarily restrictive.

It will be necessary to begin by summarizing the notation, definitions, assumptions and conclusions of a previous paper [3] before proceeding to discuss and generalize them. For the sake of brevity the discussion will be confined to the simple case of a mixture containing only two kinds of molecules. The conclusion reached is, however, *mutatis mutandis* valid for mixtures of any number of kinds of molecules and also to superlattices in crystalline alloys.

---

[1] Guggenheim, *Proc. Roy. Soc. A*, 1935, **148**, 304. Rushbrooke, *Proc. Roy. Soc. A*, 1938, **166**, 296.

[2] Fowler and Guggenheim, *Proc. Roy. Soc. A*, 1940, **174**, 189.

[3] Guggenheim, *Proc. Roy. Soc. A*, 1944, **183**, 213.

2. Notation and Counting Operations.

Let N_A, N_B denote the number of molecules of types A, B respectively. Let each molecule A occupy r_A sites and each molecule B occupy r_B sites. Let the number of sites which are neighbours of any one site be z. It will be assumed that the structure of both kinds of molecules are such that the elements which occupy a single site are interconnected in the molecule as a simple chain or a branched chain, but that there are no closed rings in the molecule. Parameters q_A, q_B are defined by

$$z(r_A - q_A) = 2(r_A - 1), \qquad (2.1)$$

$$z(r_B - q_B) = 2(r_B - 1). \qquad (2.2)$$

The physical meaning of q_A is that zq_A is the number of sites neighbours of the r_A sites occupied by a molecule A, excluding those neighbours of each site occupied by the next element of the same molecule. The physical meaning of q_B is similar.

Let f_A, f_B denote the partition functions of molecules of types A, B respectively attached to a given set of sites ; f_A, f_B are assumed independent of the choice of the given sites. This assumption is accurate provided each possible internal rotation in a molecule is either unrestricted or completely restricted.

It is assumed that in any given configuration of the system the intermolecular potential energy U consists of a sum of terms, each pair of neighbouring sites occupied by elements of different molecules contributing one term. Let u_{AA}, u_{BB}, u_{AB} denote the contribution to U by a pair of sites according as both sites are occupied by A molecules or both by B molecules or one site by each type of molecule.

Let the number of pairs of neighbouring sites occupied one by a molecule A, the other by a molecule B be denoted by zX. Then from the definitions of q_A, q_B it follows that the number of pairs of neighbouring sites both occupied by molecules A is

$$\tfrac{1}{2}z(q_A N_A - X), \qquad (2.3)$$

and the number of pairs of neighbouring sites both occupied by molecules B is

$$\tfrac{1}{2}z(q_B N_B - X). \qquad (2.4)$$

The total intermolecular potential energy U of the system is then given by

$$\begin{aligned} U &= \tfrac{1}{2}z(q_A N_A - X)u_{AA} + zXu_{AB} + \tfrac{1}{2}z(q_B N_B - X)u_{BB} \\ &= \tfrac{1}{2}zq_A N_A u_{AA} + \tfrac{1}{2}zq_B N_B u_{BB} + zXu, \end{aligned} \qquad (2.5)$$

where u is defined by

$$u = u_{AB} - \tfrac{1}{2}u_{AA} - \tfrac{1}{2}u_{BB}. \qquad (2.6)$$

It is convenient to include in the partition functions f_A and f_B factors $\exp(-\tfrac{1}{2}zq_A u_{AA}/kT)$ and $\exp(-\tfrac{1}{2}zq_B u_{BB}/kT)$ respectively. If we do this we shall not need to pay any further attention to the first two terms in (2.5). We need consider only ΔU, the excess of U in the mixture over its value for the two components A and B before mixing. We accordingly replace (2.5) by

$$\Delta U = zXu. \qquad (2.7)$$

The quantities here denoted by U, u have previously been denoted by W, w respectively. The change in notation is deliberate and the reason for it will appear shortly.

3. Quasi-Chemical Method.

We must now recall and summarize as briefly as possible the fundamental principles of the quasi-chemical method taken directly from a previous paper [3] but confining ourselves for the sake of brevity to mixtures of only two species of molecules.

The partition function Q of the system is written in the form

$$Q = \Sigma_X \, g(N_A, N_B, X) \exp(-zXw/kT), \qquad . \quad . \quad (3.1)$$

where $g(N_A, N_B, X)$ denotes the number of distinguishable configurations of all the N_A molecules A and N_B molecules B for a given value of X. This combinatory factor $g(N_A, N_B, X)$ is expressible as an explicit function of N_A, N_B, X involving as parameters z, r_A, r_B, q_A, q_B. The summation in (3.1) extends over all possible values of X.

The quantity w occurring in (3.1) may be roughly described as the free energy of formation of a single contact between a molecule A and a molecule B. The precise physical nature of w will be discussed in § 5, where we shall find that w is closely related to but not identical with u.

As usual for any macroscopic system we may without any sensible loss of accuracy replace the sum (3.1) by its maximum term in which X is determined by

$$\left(\frac{\partial Q}{\partial X}\right)_{N_A, N_B} = 0. \qquad . \quad . \quad . \quad . \quad (3.2)$$

When we insert the complete expression for $g(N_A, N_B, X)$ into Q, eqn. (3.2) becomes

$$\frac{X^2}{(q_A N_A - X)(q_B N_B - X)} = e^{-2w/kT}, \qquad . \quad . \quad . \quad (3.3)$$

which is called the condition of *quasi-chemical equilibrium* because of its formal similarity to the condition of equilibrium for the chemical reaction

$$\mathrm{AA} + \mathrm{BB} \rightleftharpoons 2\mathrm{AB}. \qquad . \quad . \quad . \quad . \quad (3.4)$$

It is convenient to define a fraction θ by

$$\theta = \frac{q_A N_A}{q_A N_A + q_B N_B}, \qquad 1 - \theta = \frac{q_B N_B}{q_A N_A + q_B N_B}, \qquad . \quad (3.5)$$

and a quantity β by

$$\beta = \{(1 - 2\theta)^2 + 4\theta(1 - \theta) e^{2w/kT}\}^{\frac{1}{2}}. \qquad . \quad . \quad (3.6)$$

The solution of the quadratic equation (3.3) for X may then be written in the form

$$\frac{X}{q_A N_A + q_B N_B} = \frac{2\theta(1 - \theta)}{\beta + 1}. \qquad . \quad . \quad . \quad . \quad (3.7)$$

If we replace β by 1 in (3.7) we obtain the zeroth approximation referred to in Section 7.

4. Free Energy of Mixing.

The free energy F is related to the partition function Q by

$$F = kT \log Q, \qquad . \quad . \quad . \quad . \quad (4.1)$$

where Q may be replaced by its maximum term identified by (3.7). We are in fact interested mainly in the excess ΔF, called the *free energy of mixing*, by which F of the mixture exceeds F of the two components unmixed. We obtain eventually

$$\Delta F = \Delta F_1 + \Delta F_2, \qquad . \quad . \quad . \quad . \quad (4.2)$$

where

$$\frac{\Delta F_1}{kT} = \log \frac{(r_A N_A)!\,(r_B N_B)!}{(r_A N_A + r_B N_B)!} + \tfrac{1}{2} z \log \frac{(q_A N_A)!\,(q_B N_B)!\,(r_A N_A + r_B N_B)!}{(r_A N_A)!\,(r_B N_B)!\,(q_A N_A + q_B N_B)!}, \quad . \quad (4.3)$$

$$\frac{\Delta F_2}{kT} = \tfrac{1}{2} z (q_A N_A + q_B N_B) \left\{ \theta \log \frac{\beta - 1 + 2\theta}{\theta(\beta + 1)} + (1 - \theta) \log \frac{\beta + 1 - 2\theta}{(1 - \theta)(\beta + 1)} \right\}. \quad (4.4)$$

Whereas ΔF_1 is independent of w, ΔF_2 vanishes with w. We may therefore regard ΔF_2 as the part of the free energy due to w differing from zero.

For full details of this derivation the reader is referred to the previous publication.[3]

5. Nature of w.

We now come to the main point of the present paper, which is to examine the physical meaning and thermodynamic properties of the quantity w. In order to do this, let us discard all previous definitions of w and consider whether we may not regard the fundamental equation (3.1) of the quasi-chemical method as defining w. There obviously must be some quantity w having the dimensions of a molecular energy such that, if we assign to it a suitable value, formula (3.3) which follows directly from formula (3.1) will give the right value for X. The w so defined is in fact a rather complicated average energy. Consider a given pair of sites both occupied by A molecules and another given pair both occupied by B molecules and let W_1 denote the intermolecular energy of the whole system when the two given pairs of sites are occupied as described while all other sites are occupied in all conceivable ways and one averages over all physically possible configurations attaching the exact appropriate Boltzmann factor to each configuration. Now suppose each of the given pairs of sites to be occupied by two molecules one A, the other B, and let W_2 denote the intermolecular energy of the whole system averaged in a manner similar to that used to define W_1. Then the difference $W_2 - W_1$ is equal to the quantity $2w$ which will make equation (3.1) accurate. We may loosely describe $2w$ as the average work required to change the manner of occupation of the two pairs of sites quasi-statically and isothermally or still more loosely as the increase in the intermolecular free energy when the manner of occupation of the two pairs of sites is changed as described.

Whatever definition we choose of w in (3.1) and (3.3) the two following points are clear.

(*a*) It is essential for the usefulness of the equation of quasi-chemical equilibrium to regard w as independent of the composition of the mixture. This is, in fact, the fundamental approximation in this treatment.

(*b*) The whole argument, including the definitions and the formulation of the condition of quasi-chemical equilibrium, is isothermal. Everything which has been said may be regarded as applying to a given temperature. Nothing in the argument requires that w, any more than f_A, should be independent of the temperature.

We shall accordingly proceed as hitherto to regard w as independent of composition, but in contrast to our previous attitude we shall no longer regard w as independent of temperature.

6. Total Energy of Mixing.

From the free energy F we can derive the total energy E according to usual thermodynamic procedure by differentiating F/T with respect to $1/T$. Since $\Delta F_1/T$ is independent of T, it contributes nothing to the energy of mixing, which is due entirely to $\Delta F_2/T$ and is given by

$$\Delta E = \frac{d(\Delta F_2/T)}{d\beta} \cdot \frac{d\beta}{d(w/T)} \cdot \frac{d(w/T)}{d(1/T)}. \qquad (6.1)$$

By straightforward, if lengthy, algebra it is found that

$$\frac{d(\Delta F_2/T)}{d\beta} = \tfrac{1}{2}zk(q_A N_A + q_B N_B)\frac{4\theta(1-\theta)\beta}{\{\beta^2 - (1-2\theta)^2\}\{\beta + 1\}}, \qquad (6.2)$$

$$\frac{d\beta}{d(w/T)} = \frac{\beta^2 - (1-2\theta)^2}{k\beta}, \qquad (6.3)$$

$$\frac{d(w/T)}{d(1/T)} = w - T\frac{dw}{dT}. \qquad (6.4)$$

Substituting the last three relations into (6.1), we obtain

$$\Delta E = z(q_A N_A + q_B N_B)\frac{2\theta(1-\theta)}{\beta + 1}\left(w - T\frac{dw}{dT}\right). \qquad (6.5)$$

This formula differs from the formula previously obtained by the extra term $-T dw/dT$. There will be a corresponding extra term in dw/dT

in the formula for the entropy of mixing, since there is no change in the formula for the free energy.

Comparing (6.5) with (3.7) we observe that

$$\Delta E = z\bar{X}\left(w - T\frac{\mathrm{d}w}{\mathrm{d}T}\right), \quad . \quad . \quad . \quad . \quad (6.6)$$

where $\bar{X}$ denotes the average or equilibrium value of X corresponding to the maximum term in the partition function Q. But with this interpretation of X, it follows from (2·7) and it is in fact physically obvious that

$$\Delta E = z\bar{X}u. \quad . \quad . \quad . \quad . \quad . \quad (6.7)$$

Comparison of (6.6) with (6.7) reveals that

$$u = w - T\frac{\mathrm{d}w}{\mathrm{d}T}. \quad . \quad . \quad . \quad . \quad . \quad (6.8)$$

It is accordingly reasonable to call w the *free energy of formation of a single AB contact* and to call u the *total energy of formation of a single AB contact.* In the previous treatment it was assumed that w was independent of temperature, in which case the distinction between u and w disappears.

7. Zeroth Approximation.

The zeroth approximation is obtained by expanding β in powers of w/kT and neglecting terms of the order $(w/kT)^2$. We accordingly replace (3.6) by

$$\beta = 1 + 4\theta(1 - \theta)w/kT.. \quad . \quad . \quad . \quad (7.1)$$

Using this in (4.3) we obtain correct to terms of the first degree in w/kT

$$\Delta F_2 = z(q_A N_A + q_B N_B)\theta(1 - \theta)w = \frac{q_A N_A \, . \, q_B N_B}{q_A N_A + q_B N_B} zw, \quad . \quad (7.2)$$

in place of (4.3). Formula (4.2) is unaffected by the approximation.

The formula for the energy of mixing ΔE follows immediately from (7.2), namely

$$\Delta E = \frac{q_A N_A \, . \, q_B N_B}{q_A N_A + q_B N_B} z \left(w - T\frac{\mathrm{d}w}{\mathrm{d}T}\right). \quad . \quad . \quad . \quad (7.3)$$

This differs from the previously obtained formula by the inclusion of the term $-T\mathrm{d}w/\mathrm{d}T$. There will be a corresponding term in $\mathrm{d}w/\mathrm{d}T$ in the entropy of mixing.

8. Flory's Approximation.

The zeroth approximation outlined in the previous section relates to ΔF_2, but does not affect ΔF_1. A different approximation affecting ΔF_1 can be obtained as follows. We begin by using Stirling's formula for the factorials in (4.3) and at the same time use (2.1) and (2.2). We thus obtain

$$\begin{aligned}
\frac{\Delta F_1}{kT} &= -(\tfrac{1}{2}z - 1)r_A N_A \log \frac{r_A N_A}{r_A N_A + r_B N_B} - (\tfrac{1}{2}z - 1)r_B N_B \log \frac{r_B N_B}{r_A N_A + r_B N_B} \\
&\qquad + \tfrac{1}{2}zq_A N_A \log \frac{q_A N_A}{q_A N_A + q_B N_B} + \tfrac{1}{2}zq_B N_B \log \frac{q_B N_B}{q_A N_A + q_B N_B} \\
&= N_A \log \frac{r_A N_A}{r_A N_A + r_B N_B} + N_B \log \frac{r_B N_B}{r_A N_A + r_B N_B} \\
&\quad - \tfrac{1}{2}zq_A N_A \log \left\{1 + \frac{(r_A q_B - q_A r_B)N_B}{q_A(r_A N_A + r_B N_B)}\right\} - \tfrac{1}{2}zq_B N_B \log \left\{1 + \frac{(q_A r_B - r_A q_B)N_A}{q_B(r_A N_A + r_B N_B)}\right\} \\
&= N_A \log \frac{r_A N_A}{r_A N_A + r_B N_B} + N_B \log \frac{r_B N_B}{r_A N_A + r_B N_B} \\
&\quad - \tfrac{1}{2}zq_A N_A \log \left\{1 + \frac{(r_A - r_B)N_B}{\tfrac{1}{2}zq_A(r_A N_A + r_B N_B)}\right\} - \tfrac{1}{2}zq_B N_B \log \left\{1 + \frac{(r_B - r_A)N_A}{\tfrac{1}{2}zq_B(r_A N_A + r_B N_B)}\right\}.
\end{aligned}$$

$$(8.1)$$

Formula (8.1) is as accurate as the original formula (4.3). We now assume that

$$\tfrac{1}{2}zq_Aq_B \gg |r_A - r_B|, \quad . \quad . \quad . \quad . \quad (8.2)$$

so that we may expand the last two logarithms in (8.1) and replace each by its leading term. When we do this we find that these two terms cancel, so that (8.1) reduces to

$$\frac{\Delta F_1}{kT} = N_1 \log \frac{r_AN_A}{r_AN_A + r_BN_B} + N_B \log \frac{r_BN_B}{r_AN_A + r_BN_B}. \quad . \quad (8.3)$$

This approximate formula was first obtained by Flory.[4] I had previously shown [2] that this approximation can be obtained using the assumption

$$\tfrac{1}{2}z \gg 1, \quad . \quad . \quad . \quad . \quad . \quad (8.4)$$

which does not correspond closely to reality, since the maximum value of $\tfrac{1}{2}z$, corresponding to close packing, is 6. I am indebted to Dr. G. Gee for pointing out that (8.4) may be replaced by a less restrictive condition such as (8.2).

The condition (8.2) would of course be satisfied if (8.4) were satisfied. It is also obviously satisfied when $r_A = r_B$, in which case ΔF_1 takes the same form as ΔF for ideal mixtures. A more interesting case is when

$$\tfrac{1}{2}zq_A \gg 1, \quad \tfrac{1}{2}zq_B \gg 1, \quad . \quad . \quad . \quad . \quad (8.5)$$

so that, *a fortiori*,

$$\tfrac{1}{2}zr_A \gg 1, \quad \tfrac{1}{2}zr_B \gg 1. \quad . \quad . \quad . \quad . \quad (8.6)$$

9. Conclusion.

We have seen that it is allowable to remove the restriction that w be regarded as independent of temperature. There remains the question whether it is useful to do so. It seems quite likely that it can be useful for the following reason. It has been shown by Gee [5] that for solutions of rubber in various solvents there is satisfactory agreement between theory and experiment as regards the free energy of mixing but not as regards the energy nor the entropy of mixing. Gee has suggested that the agreement as regards the free energy may be due to a fortuitous cancelling of errors. I prefer to believe that the agreement as regards the free energy is not fortuitous, but suggest that the disagreement as regards the energy and the entropy may be due to the omission of the terms in $\mathrm{d}w/\mathrm{d}T$.

Summary.

The quasi-chemical method of approximating to the thermodynamic functions of a co-operative system is analysed more deeply than previously and is generalized by removing the restriction of treating the parameter w as independent of the temperature. This quantity w may be regarded as the free energy of formation of a single contact between two molecules of different types. The corresponding total energy of formation of each such contact is $w - T\mathrm{d}w/\mathrm{d}T$.

Chemistry Department,
Reading University.

---

[4] Flory, *J. Chem. Physics*, 1942, **10**, 51.
[5] Gee, *J. Chim. Physique*, 1947, **44**, 66.

THE ADDITIVITY OF T_c^3 FOR SOME NON-LINEAR MOLECULES.

BY L. GRUNBERG AND A. H. NISSAN.

Received 8*th March*, 1948.

Recently[1] we derived from the theory of viscosity at the critical point that the cube of the critical temperature, T_c^3, should be proportional to the molecular weight for the *n*-paraffins C_3 to C_8. Agreement was found between the prediction and the experimental results, as can be seen from Fig. 1. Since the molecular weight is an additive property, we deduced that T_c^3 is an additive property for these compounds. We investigated a number of other substances with respect to the additivity of T_c^3.

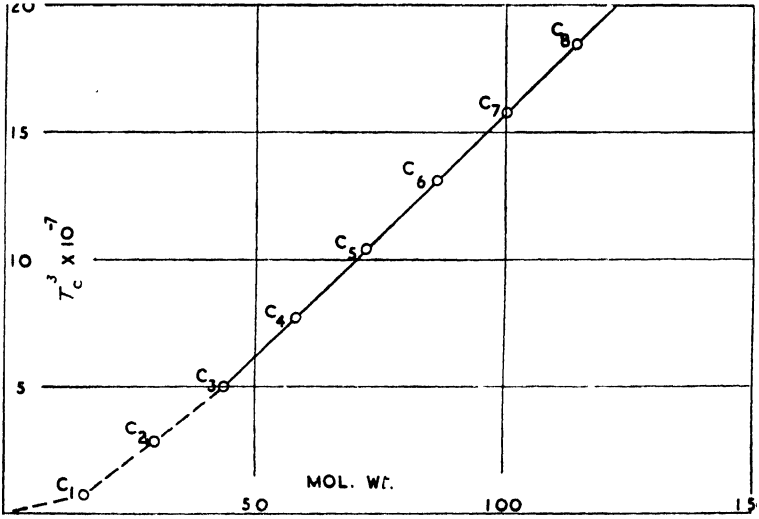

FIG. 1.

The results of our investigations showed that the additivity of T_c^3 seems to be characteristic of many classes of substances. Expressing

$$T_c^3 = \sum \Delta T_c^3,$$

one can attribute to every atomic grouping a characteristic value of ΔT_c^3 so that the sum of the ΔT_c^3 values equals to T_c^3. Quite generally we found that—

(*a*) The additivity rule is restricted to non-linear polyatomic molecules. For example, the ΔT_c^3 value for chlorine, obtained from aliphatic or aromatic chlorine compounds, cannot be used to compute the critical temperature of chlorine itself.

(*b*) An atomic grouping, introduced into a molecule in such a way as to reduce internal rotation, increases the value of ΔT_c^3. Thus the presence of several methyl groups on the same carbon atom or on adjacent carbon atoms increases the ΔT_c^3 values.

---

[1] Grunberg and Nissan, *Nature*, 1948, **161**, 170.

(c) Externally hindered rotation, such as hydrogen-bond formation increases the ΔT_c^3 values. In a homologous series the ΔT_c^3 value of the hydrogen bond-forming group decreases as we ascend the series, due to steric shielding by the non-polar part of the molecule.

In the following part of the paper the additivity rule of T_c^3, as applicable to various classes of compounds, will be investigated. The units of T_c^3 used throughout are in 10^7 (degrees).^{3}

Investigation of Additivity Rule.

n-Paraffins.

Table I gives the values of the critical temperature and T_c^3 for the *n*-paraffins C_1 to C_{13}. The values of ΔT_c^3 for the —CH_2— group were obtained by subtracting the values of T_c^3 of successive members of the homologous series. From C_3 to C_{13}, the value ΔT_c^3 for —CH_2— equals, on the average, 2·68. Using this value we found the value of ΔT_c^3 for an end-methyl group to be 1·20 on the average.

TABLE I

Hydrocarbon.	T_c, °c. (Obs.).	T_c^3 (× 10^7).	ΔT_c^3, —CH_2—.	ΔT_c^3, —CH_3.	T_c, °c. (Calc.).
CH_4	−82·5	0·694	—	—	—
C_2H_6	32·1	2·84	2·15	—	—
C_3H_8	95·6	5·02	2·18	—	—
C_4H_{10}	153·0	7·75	2·73	1·195	153·1
C_5H_{12}	197·2	10·42	2·67	1·190	197·9
C_6H_{14}	234·8	13·12	2·70	1·200	234·8
C_7H_{16}	266·8	15·77	2·65	1·185	267·3
C_8H_{18}	296·0	18·45	2·68	1·185	296·3
C_9H_{20}	322·8	21·20	2·65	1·220	322·3
$C_{10}H_{22}$	330·4	22·00	0·80*	—	346·8
$C_{11}H_{24}$	369·4	26·52	4·52*	1·200	369·0
$C_{12}H_{26}$	390·4	29·25	2·73	1·225	390·3
$C_{13}H_{28}$	410·0	31·90	2·65	1·210	409·9

* The value of (ΔT_c^3, —CH_2—) calculated from the difference ($C_{11} - C_9$) is 2·66.

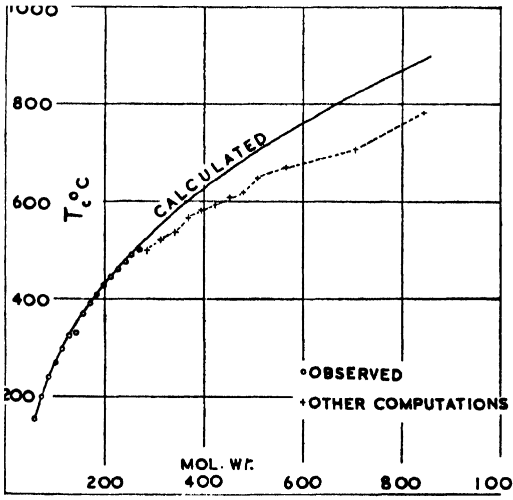

FIG. 2.

A certain number of data in Table I do not conform to the general rule. The difference in T_c^3 between C_2 and C_1 is 2·15 and between C_3 and C_2 is 2·18. This value is considerably lower than that found for $—CH_2—$ in the higher paraffins.

We shall now proceed to investigate the correctness of a number of data reported in the literature. One example is the critical temperature of *n*-decane, which is given as 330° C. If this value is correct we obtain for $—CH_2—$ from $C_{10} - C_9$ a value of 0·80 and from $C_{11} - C_{10}$ a value of 4·52. The value of $—CH_2—$ calculated from $\frac{C_{11} - C_9}{2}$ is 2·66. It appears probable that the value of the critical temperature of *n*-decane reported in the literature is incorrect. From the additivity rule we calculated a value of 346·8° C. for its critical temperature.

Fig. 2 shows the calculated critical temperature of the *n*-paraffins up to C_{60}. The values reported in the literature are indicated on the graph by points. Up to a molecular weight of 270 (C_{19}), the correspondence of the calculated and observed values is acceptable. An exception is C_{10}. The experimental value does not fall on a smooth curve with the results for the other paraffins.

For C_{20} and higher paraffins we can compare our values with those obtained by other means.[2] The calculated values for these hydrocarbons may represent only a " theoretical critical temperature " which could not be realised in practice due to the tendency of these substances to " crack " to substances of lower molecular weight on reaching high temperatures.

Iso-Paraffins.

TABLE II

2-Methyl paraffins ;

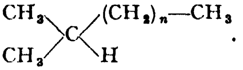

$$\begin{matrix} CH_3 \\ CH_3 \end{matrix}\!\!>\!C\!<\!\!\begin{matrix} (CH_2)_n—CH_3 \\ H \end{matrix}$$.

n.	0.	1.	2.	3.	4.	5.
T_c^3, ($\times 10^7$)	6·76	9·80	12·68	15·00	17·47	20·30
ΔT_c^3 $n CH_2 + CH_3$	1·20	3·88	6·56	9·24	11·92	14·60
ΔT_c^3 $\begin{matrix} CH_3 \\ CH_3 \end{matrix}\!\!>\!C\!<\!H$	5·56	5·92	6·12	5·76	5·55	5·70
T_c, °K. (obs.)	407·2	461·0	502·2	531·1	558·7	587·6
T_c, °K. (calc.)	411·3	458·5	497·8	531·3	561·0	588·0
Calc.-obs.(T_c)	+4·1	−2·5	−4·4	+0·2	+2·3	+0·4

TABLE III

3-Methyl paraffins ;

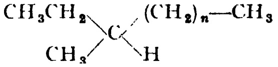

$$\begin{matrix} CH_3CH_2 \\ CH_3 \end{matrix}\!\!>\!C\!<\!\!\begin{matrix} (CH_2)_n—CH_3 \\ H \end{matrix}$$

n.	0.	1.	2.	3.	4.
T_c^3, ($\times 10^7$)	9·80	12·53	15·37	17·82	20·53
ΔT_c^3 $n CH_2 + CH_3$	1·20	3·88	6·56	9·24	11·92
ΔT_c^3 $\begin{matrix} CH_3CH_2 \\ CH_3 \end{matrix}\!\!>\!C\!<\!H$	8·60	8·65	8·81	8·58	8·61
T_c, °K. (obs.)	461·0	500·2	535·6	562·6	589·8
T_c, °K (calc.)	461·8	500·2	533·7	563·3	590·0
Calc.-obs.(T_c)	+0·8	0	−1·9	+0·7	+0·2

The results of our calculations for the 2 : methyl-, the 3 : methyl- and 4 : methyl-paraffins are given in Tables II-IV. It appears that the group values of ΔT_c^3 given in Table V fit the data.

[2] Wilson and Bahlke, *Ind. Eng. Chem.*, 1924, **16**, 115 ; Doss, *Physical Constants of the Principal Hydrocarbons*, (The Texas Co., 1939).

The difference between these values is 2·88 and 2·86, corresponding to a —CH_2— group in a short side-chain, compared with 2·68 for —CH_2— in a longer main chain. Thus ΔT_c^3 in a short side-chain attached to a tertiary carbon atom is increased by 0·20, probably due to restricted internal rotation.

TABLE IV

4-Methyl paraffins ;

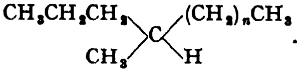
$CH_3CH_2CH_2(CH_3)CH(CH_2)_nCH_3$.

n.	0.	1.	2.	3.
T_c^3, (× 10^7) . . .	12·68	15·37	18·19	20·72
ΔT_c^3 $nCH_2 + CH_3$ . .	1·20	3·88	6·56	9·24
ΔT_c^3 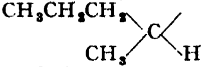 $CH_3CH_2CH_2(CH_3)C(H)\!<$.	11·48	11·49	11·63	11·48
T_c, °K. (obs.) . . .	502·2	535·6	566·5	591·5
T_c, °K. (calc.) . . .	502·5	535·8	565·2	591·8
Calc.-obs.(T_c) . . .	+0·3	+0·2	−1·3	+0·3

TABLE V

ΔT_c^3, 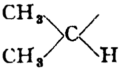 $CH_3(CH_3)C(H)\!<$ . .	5·77
ΔT_c^3, 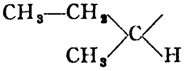 $CH_3{-}CH_2(CH_3)C(H)\!<$.	8·65
ΔT_c^3, 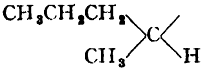 $CH_3CH_2CH_2(CH_3)C(H)\!<$	11·51

TABLE VI

Compound.	ΔT_c^3, 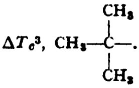 $CH_3{-}\overset{CH_3}{\underset{CH_3}{C}}{-}$.
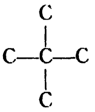 $C{-}\overset{C}{\underset{C}{C}}{-}C$ . . .	8·37
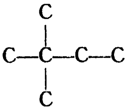 $C{-}\overset{C}{\underset{C}{C}}{-}C{-}C$ . .	7·59
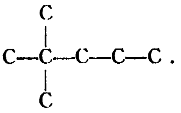 $C{-}\overset{C}{\underset{C}{C}}{-}C{-}C{-}C$ . .	7·61
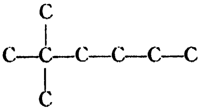 $C{-}\overset{C}{\underset{C}{C}}{-}C{-}C{-}C{-}C$.	7·40
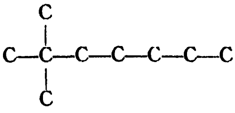 $C{-}\overset{C}{\underset{C}{C}}{-}C{-}C{-}C{-}C{-}C$	7·10

Similar conclusions can be reached from the examination of the results obtained with 2 : 2-dimethyl paraffins. The value of ΔT_c^3 for $CH_3{-}\overset{CH_3}{\underset{CH_3}{C}}{-}$ in $(CH_3)_3 . C . (CH_2)_n . CH_3$ increases from 7·10 to 8·37 as the value of *n* decreases from 4 to 0 (Table VI).

These values were obtained on the assumption that the values of 2·68 for —CH_2— and 1·20 for —CH_3 are unaffected by the three substituted methyl groups. It is, however, likely that ΔT_c^3 for —CH_2— and ΔT_c^3 for —CH_3 will be slightly affected and that a value of about 7·0 represents the true value of ΔT_c^3 for $(CH_3)_3C$—.

Table V contains a number of group values of ΔT_c^3. Using these values and 2·68 for —CH_2— and 1·20 for —CH_3 we calculated the critical temperature of the hydrocarbons shown in Tables II-IV. The values are given in the respective tables. Of fifteen values, two show an error of the order of 4°, three of the order of 2°, whilst ten of the order of 1° or less.

In Table VII again a number of calculated and observed values are compared. For the compounds 1, 2, 3, 4 agreement within 1-3° exists between the calculated and the observed values. For the compounds 5, 6, 7, with substitution on adjacent carbon atoms, the calculated values are too low. This is probably due to the increased steric hindrance in these compounds.

TABLE VII

Compound.	No.	T_c, °K. (Obs.).	T_c, °K. (Calc.).	Calc.-Obs. (T_c).
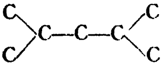	1	520·3	521·8	+ 1·5
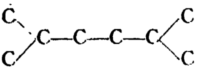	2	550·0	552·5	+ 2·5
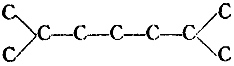	3	579·2	580·8	+ 1·6
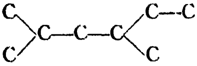	4	553·8	554·5	+ 0·7
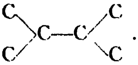	5	500·1	486·8	− 13·3
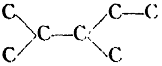	6	537·8	524·2	− 13·6
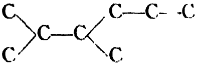	7	562·2	556·6	− 6·6

Cyclo-paraffins.

The critical temperature of cyclohexane is 280·9° c., corresponding to a T_c^3 value of 17·00 × 10^7. If we consider the molecule to be built up of six —CH_2— groups, we obtain a value of ΔT_c^3 for —CH_2— = 2·83, showing that the hindrance to rotation of a —CH_2— group is equivalent to an increase of 0·15 in ΔT_c^3, —CH_2— for this cyclic compound as compared with the *n*-paraffins.

Methyl-cyclohexane (T_c = 301·5° c.) can be considered to be made up of five CH_2 groups, one CH_3 and a tertiary carbon-hydrogen group ≡CH. The ΔT_c^3 value of this group, calculated on the assumption, ΔT_c^3 for —CH_2— = 2·83 and ΔT_c^3 for —CH_3 = 1·20, is found to be 3·65. This value compares well with the values of ΔT_c^3 for ≡CH, obtained from the *iso*-paraffins, assuming that ΔT_c^3 for —CH_2— = 2·68 and ΔT_c^3 for −CH_3 = 1·20 as shown in Table VIII.

TABLE VIII

Group.	ΔT_c^3, ≡ CH.
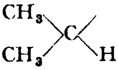	3·37
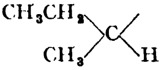	3·57
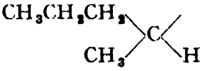	3·75

Aromatic Hydrocarbons.

Using ΔT_c^3 values obtained from the investigation of the *n*- and the *iso*-paraffins we calculated the ΔT_c^3 value for a monosubstituted benzene ring,

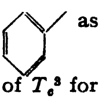

as shown in Table IX. The average value of ΔT_c^3 is 19·67. The value of T_c^3 for benzene itself is only 17·73 units. Steric hindrance again is probably the reason for the increase in the value of ΔT_c^3.

TABLE IX.—MONOSUBSTITUTED BENZENES

Substituent Group.	$—CH_3$.	$—CH_2CH_3$.	$—CH_2CH_2CH_3$.	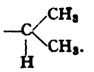 $—\underset{H}{C}\langle^{CH_3}_{CH_3}$.	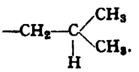 $—CH_2—\underset{H}{C}\langle^{CH_3}_{CH_3}$.
T_c, °C.	320·6	346·0	365·6	362·7	377·7
T_c^3, (× 10^7)	20·95	23·80	26·12	25·75	27·62
ΔT_c^3 substituent	1·20	3·88	6·56	5·77	8·45
ΔT_c^3 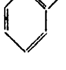	19·75	19·92	19·56	19·98	19·17

This effect is still better illustrated if we examine the di-substituted benzenes such as the xylenes. We may expect

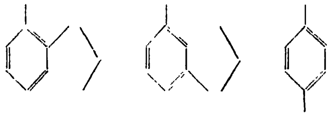

Indeed we find values for the benzene nucleus of 23·80 for *o*-xylene, 22·35 for *m*-xylene and 21·20 for *p*-xylene. The values of ΔT_c^3 for the benzene nucleus in polysubstituted benzenes fall in line with the principles outlined above, as is shown in Table X.

TABLE X.—POLY-SUBSTITUTED BENZENES

Compound.	ΔT_c^3 Benzene Nucleus.
1 : 2 : 4-Trimethyl benzene	24·45
1 : 3 : 5-Trimethyl benzene	22·67
1 : 2 : 3 : 5-Tetramethyl benzene	24·27
1 : 2 : 4 : 5-Tetramethyl benzene	26·05
Pentamethyl benzene	27·05

Molecules with Externally-Hindered Rotation.

Molecules containing a polar group or able to form hydrogen bonds show externally-hindered rotation. Let us consider the way in which certain atomic groupings will influence the critical temperature of molecules. If the grouping is accessible, i.e. placed on an exposed part of the molecule, we may expect a stronger interaction than if the grouping is shielded by non-polar portions of the molecule. Thus for any one polar grouping the ΔT_c^3 value may now be expected to decrease as the length of the hydrocarbon chains in the molecule increases. The ΔT_c^3 value will decrease to an asymptotic value, corresponding to the contribution of the grouping to T_c^3 in absence of external hindrance. Several classes of compounds will now be discussed from this point of view.

Alcohols.

Table XI and Fig. 3 show that the value of ΔT_c^3 for —OH in the primary alcohols decreases from 12·33 for methanol to an asymptotic value of approximately 8·5 as the length of the hydrocarbon chain increases. From *iso*butyl and *iso*amyl alcohol we obtained 8·46 and 8·30 for ΔT_c^3 for —OH, corresponding to slightly greater shielding of the —OH group.

TABLE XI

Primary alcohols; $CH_3 . (CH_2)_n . OH$

n.	0.	1.	2.	3.	6.	7.
T_c, °K. (obs.) . .	513·2	516·3	536·9	560·9	638·2	658·2
T_c^3, ($\times 10^7$) . .	13·53	13·79	15·51	17·57	26·02	28·55
ΔT_c^3, $(CH_2)_nCH_3$.	1·20	3·88	6·56	9·24	17·28	19·96
ΔT_c^3, —OH . .	12·33	9·91	8·95	8·33	8·74	8·59

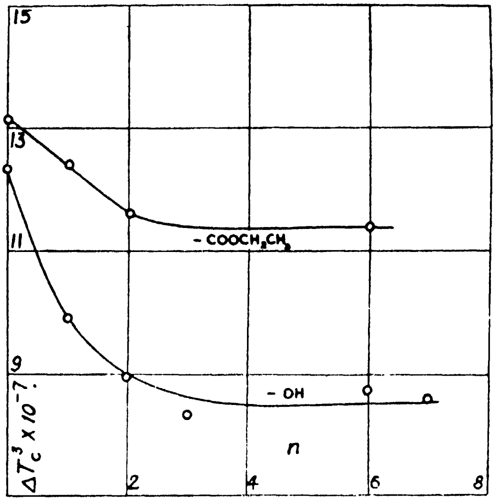

FIG. 3.

Acids.

As can be seen from Table XII, ΔT_c^3 for —COOH decreases from 19·85 in acetic acid to about 18·5 in higher acids.

TABLE XII

Monobasic acids; $CH_3 . (CH_2)_n . COOH$

n.	0.	1.	2.	3.
T_c, °K. (obs.) . .	594·8	612·7	628·2	652·2
T_c^3, ($\times 10^7$) . .	21·05	23·05	24·82	27·75
ΔT_c^3, $(CH_2)_nCH_3$.	1·20	3·88	6·56	9·24
ΔT_c^3, —COOH . .	19·85	19·17	18·26	18·51

Esters.

Table XIII shows the values of ΔT_c^3 for different esters. The general trend of the figures is similar to that observed with alcohols and acids. As the size of R increases, the value of ΔT_c^3 decreases. Fig. 3 shows the variation of ΔT_c^3 for —COOR for the ethyl esters. The asymptotic value for this group of compounds is approximately 11·4. From this value and from ΔT_c^3 for CH_3CH_2—

the value of ΔT_c^3 for —COO— was calculated to be 7·5. The last column in Table XIII gives calculated asymptotic values for ΔT_c^3 for —COOR, using ΔT_c^3 for —COO— = 7·5.

TABLE XIII

Esters ; $\mathrm{CH_3} . (\mathrm{CH_2})_n . \mathrm{COOR}$

n.	0.	1.	2.	3.	6.	Asymptotic Value (Calc.).
R	ΔT_c^3 for —COOR					
$\mathrm{CH_3}$—	11·84	11·07	10·50	9·03	—	8·7
$\mathrm{CH_3 . CH_2}$— . .	13·13	12·42	11·62	—	11·37	11·4
$\mathrm{CH_3 . CH_2 . CH_2}$— .	15·95	15·47	15·09	—	—	14·1
$\mathrm{(CH_3)_2 . CH . CH_2}$— .	17·12	16·92	16·29	—	—	16·0

Chlorine Compounds.

Table XIV indicates that ΔT_c^3 for —Cl has a value of about 5·6. Similar values can be obtained from other chlorine compounds. The critical temperature of 1 : 2-dichloroethane is 556·2° K., corresponding to $T_c^3 = 17·25$ units.

TABLE XIV

Chlorine compounds ; $\mathrm{CH_3} . (\mathrm{CH_2})_n . \mathrm{Cl}$

n.	0.	1.	2.
T_c, °K. (obs.)	416·3	456·1	494·2
T_c^3, (× 10^7)	7·22	9·50	12·08
ΔT_c^3, $(\mathrm{CH_2})_n\mathrm{CH_3}$	1·20	3·88	6·56
ΔT_c^3, —Cl	6·02	5·62	5·52

Subtracting $2\Delta T_c^3$ —$\mathrm{CH_2}$ = 5·36 we obtain $2\Delta T_c^3$ (Cl) = 11·89, or ΔT_c^3 for Cl = 5·95. For chlorobenzene, T_c = 632·2° K. and T_c^3 = 25·30. Subtracting ΔT_c^3 for —$\mathrm{C_6H_5}$ = 19·67, we obtain ΔT_c^3 for —Cl = 5·63.

As mentioned in the introduction this value of ΔT_c^3 cannot be used for the calculation of the critical temperature of chlorine. The value for $2\Delta T_c^3$ equals 11·26, yet T_c^3 for $\mathrm{Cl_2}$ is 7·27 × 10^7 (T_c = 417·2° K.).

Amines.

TABLE XV

n.	0.	1.	2.
Primary amines ; $\mathrm{CH_3} . (\mathrm{CH_2})_n . \mathrm{NH_2}$			
T_c, °K. (obs.)	430·1	456·7	491·2
T_c^3, (× 10^7)	7·97	9·53	11·87
ΔT_c^3, $(\mathrm{CH_2})_n\mathrm{CH_3}$	1·20	3·88	6·56
ΔT_c^3, —$\mathrm{NH_2}$	6·17	5·65	5·31
Secondary amines ; $\mathrm{CH_3} . (\mathrm{CH_2})_{n2} . \mathrm{NH}$			
T_c, °K. (obs.)	437·8	496·7	550·2
T_c^3, (× 10^7)	8·41	12·25	16·65
$2\Delta T_c^3$, —$(\mathrm{CH_2})_n\mathrm{CH_3}$ . . .	2·40	7·76	13·12
ΔT_c^3, =NH	6·01	4·49	3·53

Further values which must be considered are T_c^3 for $\mathrm{NH_3}$ = 6·68 units and ΔT_c^3 for NH (in trimethylamine) = 4·59.

The tendency of these compounds to hydrogen-bond formation and the shielding effect of hydrocarbon radicals can be seen from Fig. 4, where ΔT_c^3 for $—NH_2$, $=NH$ and $\equiv N$ is shown as a function of the size and number of hydrocarbon radicals.

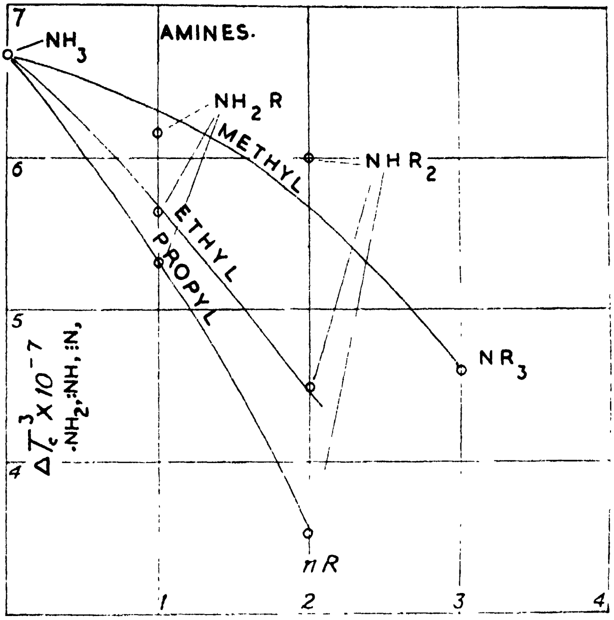

FIG. 4.

Summary.

It is shown that for some non-linear molecules the cube of the critical temperature is essentially an additive property. Restricted internal rotation and externally-hindered rotation increase the value of T_c^3. Numerical values for the increments ΔT_c^3 of various atomic groupings are calculated and given in tabular form.

Bowater Paper Corporation, Ltd.,
Northfleet,
Gravesend.

THE ELECTROPHORESIS OF SUSPENDED PARTICLES.

IV. THE SURFACE CONDUCTIVITY EFFECT.

BY D. C. HENRY.

Received 9th March, 1948.

1. The Equation of Electrophoresis.

In Part I of this series[1] Smoluchowski's electrophoresis equation for suspended particles of radius large in comparison with the effective thickness of the electrical double-layer was extended to apply to particles of any size. For spherical particles the resulting equation was

---

[1] Henry, *Proc. Roy. Soc. A*, 1931, **133**, 106.

$$U = \frac{DX}{6\pi\eta}\left\{\psi_a(1 + \lambda) + 3\lambda a^3\left(5a^2\int_{\infty}^{a}\frac{\psi}{r^6}\mathrm{d}r - 2\int_{\infty}^{a}\frac{\psi}{r^4}\mathrm{d}r\right)\right\}, \quad . \quad (1)$$

where $\lambda = (\mu_0 - \mu')/(2\mu_0 + \mu')$.

For particles of large radius of insulating material, this reduces, independently of any assumptions about the constitution of the electrical double-layer, to Smoluchowski's equation,

$$U = DX\zeta/4\pi\eta. \quad . \quad . \quad . \quad . \quad . \quad (2)$$

If the electrical double-layer is constituted in conformity with the Debye-Hückel distribution

$$\psi = \psi_a(a/r)\,\mathrm{e}^{-\kappa(r-a)}, \quad . \quad . \quad . \quad . \quad . \quad (3)$$

the right-hand side of (1) can be evaluated without size restriction and for insulating particles was presented in the form

$$U = DX\zeta\,.\,\mathrm{f}(\kappa a)/4\pi\eta \quad . \quad . \quad . \quad . \quad (4)$$

and a graph of f(κa) against log κa was printed, which for convenient reference is repeated here.

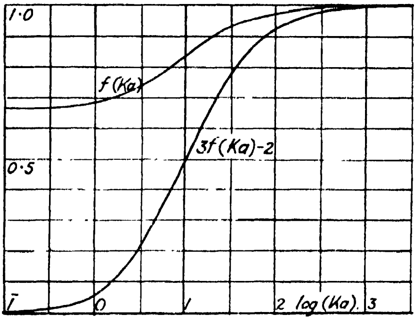

FIG. 1.—f(κa) and 3f(κa) − 2 plotted against log (κa).

Symbols.—U is the electrophoretic velocity under an applied field X of a spherical particle of radius a and specific conductivity μ' suspended in a liquid of dielectric constant D, viscosity η and specific conductivity μ_0. ψ is the electrostatic potential of the electrical double-layer at distance r from the centre of the sphere and ψ_a its value at the surface; if ψ is taken as zero at places remote from the particle, $\psi_a = \zeta$, the "electrokinetic potential" of the particle. κ is the Debye-Hückel constant

$$= (4\pi e^2 \sum_i n_i z_i^2/DkT)^{\frac{1}{2}}$$

where e is the electronic unit of charge, k Boltzmann's constant, T the absolute temperature and z_i, n_i are respectively the valency and concentration (ions/cc.) of the ion of species i.

In addition to certain hydrodynamic assumptions which are probably valid under normal experimental conditions, the extension of Smoluchowski's theory, like the original, rests on an assumption (explicitly stated by Smoluchowski and the author) which is certainly not valid, namely that the applied field and the field of the electrical double-layer may be simply superimposed without mutual distortion. Any such distortion will affect the electrophoresis equation in two ways: (1) the field of the electrical double-layer will cease to have spherical symmetry, being distorted in such a sense that it slows the electrophoretic motion. This so-called "relaxation effect" has been considered, among others, by Komagata[2] and Hermans,[3] but has proved mathematically difficult so that only a first approximation to the solution has been obtained, which, however, shows that large uncertainties (perhaps as large as 100 %) may be introduced by its neglect[*]; (2) the applied field will be modified in the neighbourhood of the particle by the abnormal electrical conductivity in the electrical double-layer. This effect was anticipated by Smoluchowski himself and has been discussed by many subsequent writers,[4] while the existence of a measurable surface conductivity is well established experimentally.

---

[2] *Res. Electrotech. Lab., Tokyo,* 1935, No. 387.

[3] *Trans. Faraday Soc.,* 1940, **36**, 133.

It is the object of this paper to extend the Smoluchowski-Henry electrophoresis equation for spherical particles to take account of the surface-conductivity effect.

2. Preliminary Considerations.

The surface conductance due to the electrical double-layer arises in reality from a conductivity which varies in a continuous manner over a small but finite distance outside the surface of the particle; in common with other surface properties it is, however, most conveniently treated as an excess conductance associated with unit area of the interface, in a shell of infinitesimal thickness, superimposed on the normal conductance of the medium. This is the point of view to be adopted here, but since it is not self-evident that the thin-shell model which is equivalent to the real distribution from the point of view of conductance measurements will also be equivalent in its effect on the electrophoretic velocity of the particle, we shall first attempt to justify this mode of attack.

Surface conductance will modify the electrophoretic velocity in two ways: (1) it will alter the form of the potential distribution ϕ of the applied field in the liquid as a whole, and (2) by altering the field, and hence the fluid motion, within the electrical double-layer, it will modify the stresses exerted on the particle by the fluid in immediate contact with it.[†]

In the neighbourhood of a small element of surface, take co-ordinate axes n normal to the surface and s tangentially in the surface along the direction, at the point in question, of the applied field. The local hydrodynamic flow is given by

$$\eta \frac{d^2v}{dn^2} = \frac{dp}{ds} - \rho \frac{d\phi}{ds}, \qquad . \quad . \quad . \quad . \quad . \quad (5)$$

where v, p, ϕ and ρ are the local values of the tangential fluid velocity, hydrostatic pressure, potential of the applied field and electric charge density. Considering the case where all the ions present are univalent and treating, as would seem likely to be the case, the local tangential current density as substantially independent of the local value of the specific conductivity μ,

$$\text{then } d\phi/ds \propto 1/\mu \text{ and } \mu \propto u_+ e^{-\epsilon\psi/kT} + u_- e^{\epsilon\psi/kT},$$

where u_+, u_- are the absolute mobilities of cation and anion; the exponential terms arise from the variation in the ionic concentrations as determined by Boltzmann's law. Suppose ψ to be positive, then to a close approximation

$$\mu \propto e^{\epsilon\psi/kT} \text{ and } d\phi/ds \propto e^{-\epsilon\psi/kT}.$$

---

[*] *Added in Proof*—Overbeek (*Philips Res. Reports*, 1946, **1**, 315) has given reasons for supposing that the error will be negligibly small when the thickness of the donble-layer is small in comparison with the dimensions of the particle (Smoluchowski's case); for $\kappa a \sim 100$ he estimates the error as a few per cent, for $\kappa a \sim 1000$ as less than 1 % (see also Overbeek, *Kolloidchem. Beih.*, 1943, **54**, 287).

[†] Ref. [1], p. 115.

[4] See, for example, Bikerman, *Z. physik. Chem. A*, 1934, **171**, 209; McBain, and Foster, *J. Physic. Chem.*, 1935, **39**, 331; Rutgers and De Smet, *Trans. Faraday Soc.*, 1947, **43**, 102; White, Monaghan and Urban, *J. Physic. Chem.*, 1936, **40**, 207; in all of which articles, references to earlier publications are given.

At the same spot,

$$\rho \propto e^{-\epsilon\psi/kT} - e^{\epsilon\psi/kT}$$

or numerically to a similar approximation $\rho \propto e^{\epsilon\psi/kT}$. Hence $\rho \,.\, d\phi/ds$ is to the same approximation independent of ψ, that is, of the position in the electrical double-layer. The right-hand side of eqn. (5) does not therefore vary significantly over the finite thickness of the double-layer and the surface stresses will be sensibly the same as if the *exterior* applied field defined by ϕ extended right up to the surface. We are therefore justified in considering that our thin-shell model is a satisfactory equivalent to the real distribution.

3. Calculation of the Surface-Conductivity Correction.

To determine the distribution of the field potential ϕ as modified by surface conductance, we first consider a sphere (radius a, specific conductivity μ') surrounded by a shell (thickness t, specific conductivity μ'') immersed in a fluid of specific conductivity μ_0.

Set $$\phi = -X\cos\theta\left(r + \frac{A}{r^2}\right) \text{ in the fluid,}$$

$$\phi'' = -X\cos\theta\left(Br + \frac{C}{r^2}\right) \text{ in the shell,}$$

and $$\phi' = -X\cos\theta \,.\, Dr \text{ within the sphere.}$$

Applying the conditions of continuity of ϕ and of electric flux at the boundaries $r = a$ and $r = a + t$, a straightforward calculation shows that

$$\frac{A}{(a+t)^3} = \frac{(a+t)^3(\mu_0 - \mu'')(2\mu'' + \mu') + a^3(\mu'' - \mu')(\mu_0 + 2\mu'')}{(a+t)^3(2\mu'' + \mu')(2\mu_0 + \mu'') + 2a^3(\mu_0 - \mu'')(\mu'' - \mu')}.$$

If $t \rightarrow 0$ and the product $\mu''t$ is identified with the surface conductivity μ_s, we find

$$\frac{A}{a^3} = \frac{\mu_0 - \mu' - 2\mu_s/a}{2\mu_0 + \mu' + 2\mu_s/a} = \lambda' \text{ (say)} \quad . \quad . \quad (6)$$

so that $$\phi = -X\cos\theta(r + \lambda' a^3/r^2).$$

This is of the same form as the corresponding equation of the paper referred to as Part I,[1] with λ' substituted for λ. The solution of the problem is thus clearly given by eqn. (1) of the present paper with the same substitution. Evaluating the right-hand side as before and introducing the author's function $f(\kappa a)$, this reduces to

$$U = \frac{DX\zeta}{6\pi\eta}\{1 + \lambda'(3f(\kappa a) - 2)\}. \quad . \quad . \quad . \quad (7)$$

For an insulating particle, $\mu' = 0$ and

$$\lambda' = (\mu_0 - 2\mu_s/a)/2(\mu + \mu_s/a). \quad . \quad . \quad . \quad (8)$$

If the particle is large in comparison with the thickness of the electrical double-layer, $f(\kappa a) = 1$ and we obtain

$$U = \frac{DX\zeta}{4\pi\eta}\,\frac{\mu_0}{\mu_0 + \mu_s/a} \quad . \quad . \quad . \quad . \quad . \quad (9)$$

which shows the correction which must be applied to Smoluchowski's equation for large insulating particles. That this correction is by no means negligible may be demonstrated by an example.

Fricke and Curtis[5] experimented on glass particles of about 10^{-4} cm. radius and found $\mu_s \sim 10^{-9}$ ohm^{-1} in a solution for which $\mu_0 \sim 10^{-5}$ ohm^{-1} cm.$^{-1}$. The correcting factor in eqn. (9) may thus be of the order 0·5, so

[5] *J. Physic. Chem.*, 1936, 40, 715.

that the use of Smoluchowski's equation uncorrected leads to a value of ζ which is too small by a factor of 2 on this account; it must be remembered that the error due to neglect of the relaxation effect is still present.

In view of the experimental observation (especially of Abramson[6]) that particles having the same surface but widely differing shapes show the same electrophoretic mobility, the question arises, to what extent the conductivity correction for large insulating particles may, like Smoluchowski's equation itself, be independent of the particle shape, provided a suitable interpretation is given to the parameter a. In default of a general demonstration, the calculations of this section were repeated for cylindrical particles set broadside on to the applied field[*]—not because such particles are likely to be met with in practice (but see Sumner and Henry[7]), but because the calculation for this case happens to be feasible. Eqn. (9) was again obtained, lending some support to the speculation put forward. Against this, however, must be set Bikerman's calculation (loc. cit.) for cylindrical particles of length l and radius a ($l \gg a$) set axially to the applied field which leads to a correction factor $\dfrac{\mu_0}{\mu_0 + 2\mu_s/(l - a)}$. In view of the present uncertainty of the allowance to be made for the relaxation effect, it would seem not unreasonable to employ equations (7) and (9) even for particles which have decided asymmetry, if a is interpreted as the "mean equivalent radius" as determined, for example, by the use of Stokes' law.

4. Measurement of Surface Conductivity.

In view of the magnitude of the correction introduced by surface conductivity, it is of importance to develop a reliable method of measuring this quantity in suspensions. Direct measurement in a slit or capillary tube, as employed by McBain, White and Urban, and Rutgers[4] is clearly not applicable and the only suitable method so far proposed would appear to be that of Fricke and Curtis[5] who make use of an expression deduced by Clark Maxwell[8] for the conductivity of a suspension of equal spheres, each carrying a surface shell of different material. For insulating particles of surface conductivity μ_s suspended in a medium of specific conductivity μ_0 this expression reduces to

$$\frac{\mu}{\mu_0} = \frac{2(\mu_s/a)(1 + 2\gamma) + 2\mu_0(1 - \gamma)}{2(\mu_s/a)(1 - \gamma) + \mu_0(2 + \gamma)}, \quad . \quad . \quad . \quad (10)$$

where μ is the specific conductivity of a suspension of volume concentration γ.

This deduction ignores the contribution to the conductivity of the charge carried by the electrophoretically moving spheres, a contribution which the following calculations show is not by any means generally negligible. Denoting it by μ_p, we have

$$\mu_p = n \,.\, (U/X) \,.\, 4\pi a^2 \sigma,$$

where n is the number of particles per cc., U/X their electrophoretic mobility under unit potential gradient and σ the surface charge-density. Setting

$$U = DX\zeta \,.\, \mathrm{f}(\kappa a)/4\pi\eta, \quad \sigma = D\zeta(1 + \kappa a)/(4\pi a) \quad \text{and} \quad n = 3\gamma/4\pi a^3, \quad (11)$$

we have $\mu_p = 3D^2\zeta^2\gamma \,.\, \mathrm{f}(\kappa a) \,.\, (1 + \kappa a)/16\pi^2 a^2 \eta.$

Inserting numerical values of constants and conversion factors, this becomes

$$\mu_p = 1{\cdot}5 \times 10^{-13}\gamma\zeta^2 \,.\, \mathrm{f}(\kappa a) \,.\, (1 + \kappa a)/a^2 \ \text{ohm}^{-1}\ \text{cm.}^{-1}, \quad . \quad (12)$$

where ζ is measured in volts.

---

[*] Cp. ref. [1], section 3.

[6] *J. Physic. Chem.*, 1931, **35**, 291.

[7] *Proc. Roy. Soc. A*, 1931, **133**, 130.

[8] *Electricity and Magnetism*, Vol. I, p. 133.

It is evident that μ of eqn. (10) should be interpreted as $\mu_{obs.} - \mu_p$, where $\mu_{obs.}$ is the observed specific conductivity of the suspension. Current estimates of the magnitude of surface conductivity are somewhat diverse, but, taking as a representative measurement Fricke's experiment with glass spheres in which $\mu_0 \sim 10^{-5}$ and $\mu_s \sim 10^{-9}$, we obtain the figures of the following table for suspensions, of volume concentration 0·1, of spheres of various sizes in (say) a solution of KCl of about 10^{-4} M.

a (cm.).	$\frac{\mu - \mu_0}{\mu_0}$ (Eqn. 10).	$\frac{\mu_p}{\mu_0}$ (Eqn. 12)—	
		for ζ = 0·015 v.	for ζ = 0·050 v.
10^{-4}	0·08	0·00	0·01
10^{-5}	0·28	0·01	0·11
10^{-6}	0·33	0·30	3·4

(The figures in the last column should be regarded as indications only, since eqn. (11) depend on the first approximation solution for the Debye-Hückel equation which is only valid for small ζ, although Hartley[9] has given reasons for supposing it may not be seriously in error outside its true range of validity.)

It is evident that, especially for small particles and high ζ-potentials, the contribution of the particle to the conductivity of the suspension cannot be neglected. The argument is not much affected if we assume higher values of μ_s (as, for example, those found by Rutgers, which are some 10 times larger than those assumed above) since for the smaller particles the value of $(\mu - \mu_0)/\mu_0$ is already approaching the limiting value $3\gamma/(1 - \gamma)$ which it assumes for $\mu_s/a \gg \mu_0$. The assumption of lower values of μ_s such as those deduced theoretically by Bikerman would merely emphasise still more the relative importance of μ_p.

Since μ_s is not known until ζ has been determined and this in turn requires a knowledge of μ_s, it will evidently be necessary to proceed by successive approximations.

It is, once more, difficult to predict to what extent the equations of this section may fairly be applied to suspensions of varying particle size and shape. An experimental study has been started in this laboratory which it is hoped may throw light on this question ; in the meanwhile provisional use will be made of the equations developed.

Summary.

The effect of surface conductivity on electrophoresis is discussed, and the Smoluchowski-Henry equation for the electrophoretic velocity of particles of any size is extended by introducing a correcting factor to take account of this effect. The method of Fricke and Curtis for the measurement of surface conductivity in suspensions is amended by the inclusion of a term representing the conductivity arising from the motion of the charged particles.

The Thomas Graham Colloid Research Laboratory,
The Victoria University of Manchester.

[9] *Trans. Faraday Soc.*, 1935, **31**, 31.

THE DIFFUSION OF DYES THROUGH CELLOPHANE—THE ANOMALOUS SALT EFFECT.

By S. M. Neale.

Received 9th March, 1948.

Crank[1] has recently carried out a far-reaching mathematical analysis of the available data relating to this problem. He has, however, in order to explain the observed effects, been compelled to make assumptions which are incompatible with the generally accepted theories of equilibrium dyeing. In particular, his treatment assumes that his factor R, which describes the equilibrium between adsorbed dye anions and free dye anions in *the same equipotential region*, varies with the salt concentration. It cannot, therefore, be concluded that a satisfactory explanation of the principal effects of added salts, upon the dyeing process, is yet available.

The object of this paper is to summarise the present state of knowledge and to offer a tentative suggestion as to a possible cause of the anomalous salt effect. This effect can be outlined as follows.

The rate of diffusion $\frac{\partial S}{\partial t}$ at any point x, is, according to Fick's equation given by *

$$\frac{\partial S}{\partial t} = - D\frac{\partial c}{\partial x}$$

where c is the concentration, and D the diffusion coefficient. For dyes in aqueous solution, D decreases with addition of salt.[2] In pure water, the mobile Na^+ ions proceed ahead of the much larger colour ions and set up a potential gradient along the axis of x so that the movement of the colour anions is accelerated. In presence of excess NaCl the Cl^- ions reduce the potential gradient towards zero, and the dye anions therefore diffuse more slowly when added salt is present. In diffusion through cellulose, on the other hand, D increases rapidly with the salt concentration S.

In considering the diffusion of dyes through cellulose we may regard either $\frac{\partial c}{\partial x}$ or $\frac{\partial A}{\partial x}$ as the concentration gradient, where A = concentration of adsorbed dyestuff, and c = corresponding concentration of equilibrium solution. $\frac{\partial A}{\partial x}$ was used by Neale and Stringfellow[3] to deduce their "apparent diffusion" coefficient from the rate of increase of total absorption with time.

Diffusion through Cellulose at Constant Salt Concentration, and Varying Dye Concentration.—Here it was found by Garvie and Neale,[4] when c and consequently A are varied (the equilibrium relation being approximately $A \propto c^{\frac{1}{2}}$) that $\frac{\partial S}{\partial t}$ increases less rapidly than $\frac{\partial c}{\partial x}$, but more rapidly than $\frac{\partial A}{\partial x}$ (see Fig. 1).

---

* To conform with standard nomenclature, the diffusion coefficient is here represented by D and not by k as in ref. 4; this necessitates changing D (concentration of absorbed dye) in that paper to A.

[1] Crank, *J. Soc. Dyers Col.*, 1947, **63**, 412.

[2] Hartley and Robinson, *Proc. Roy. Soc., A*, 1931, **134**, 20.

[3] Neale and Stringfellow, *Trans. Faraday Soc.*, 1933, **29**, 1167.

[4] Garvie and Neale, *Trans. Faraday Soc.*, 1938, **34**, 335.

Since $c \propto A^3$ approx.,

$$\frac{\partial c}{\partial x} \propto A^2 \frac{\partial A}{\partial x}.$$

This behaviour could be explained by supposing that diffusion occurs partly in capillary spaces equipotential with the external solution, and partly on the internal " surfaces " (i.e. without desorption), or in layers of solution closely adjacent to those surfaces, i.e.

$$\frac{\partial S}{\partial t} = \mathrm{f}\left(\frac{\partial c}{\partial x}, \frac{\partial A}{\partial x}\right).$$

Diffusion through Cellulose when the Dye Concentration in Solution is Constant and the Salt Solution is Varied.—Here it is found that $\frac{\partial S}{\partial t}$ increases even more rapidly than $\frac{\partial A}{\partial x}$, at constant c, with the salt concentration * (see Fig. 2). The same effect has also been found with Chlorazol Fast Red K, Benzopurpurin 4B, and Heliotrope 2B. No dye tested has failed to show this anomalous salt effect. The supposition that diffusion occurs partly in solution and partly on the surface is evidently incapable of explaining this fact, since $\frac{\partial c}{\partial x}$ is independent of the salt concentration.

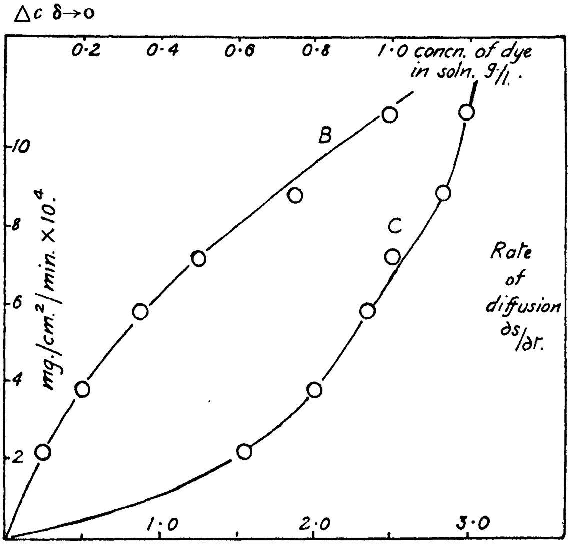

Fig. 1.

Curve B : $\partial S/\partial t$ against Δc
C : $\partial S/\partial t$ against ΔA.

We may suppose that the cellulose surface is, owing to the adsorption of the dye anions, negatively charged, and that the relatively long-range electrostatic forces set up a diffuse layer in which the electrical potential ψ gradually falls off with distance from the surface. At the surface the negative potential ψ_0 is given by the expression

$$\psi_0 = \frac{RT}{zF} \ln c_e/c_s,$$

---

* Neale and co-workers, *Trans. Faraday Soc.*, 1933, **29**, 1167; 1934, **30**, 71, 386 and 905.

where c_0 is the concentration of *free* dyestuff anions of valency z in the surface layer, and c_s their concentration in the bulk solution. According to the treatment of Hanson, Neale and Stringfellow,[5] c_0 is proportional to A, the surface concentration of *adsorbed* dye.

At a distance y from the surface, the potential is $\psi = \beta\psi_0$, where β is less than unity, and

$$\psi = \frac{RT}{zF} \ln c/c_s = \frac{RT}{F} \ln \lambda$$

where λ is the ion concentration ratio for a monovalent ion.

If we now imagine the channel between the adjacent cellulose surfaces to vary in width, then at any point where the channel narrows to $2y$, the dyestuff ions diffusing along the x direction in the middle of the channel will have to cross an electrical potential barrier of height ψ, and, since these ions carry a charge zF per g. mol. their rate of diffusion will decrease in the ratio

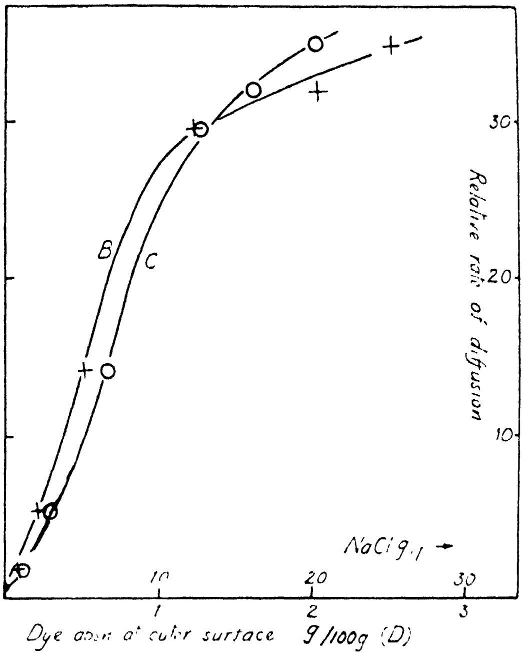

FIG. 2.
Curve B : $(\partial S/\partial t)$ against [NaCl]
C : $(\partial S/\partial t)$ against A.

$$e^{-\frac{z\psi F}{RT}} = \lambda^n.$$

Since λ increases towards unity as the salt concentration increases, $\frac{\partial S}{\partial t}$ will therefore increase. However, the height ψ of the potential barrier cannot well be greater than ψ_0, the surface potential, hence the rate of increase of $\frac{\partial S}{\partial t}$ with salt concentration cannot be greater than the rate of increase of λ_0^n with salt concentration, i.e. than the rate of increase of A with salt concentration, since, on the present assumptions,

---

[5] Hanson, Neale and Stringfellow, *Trans. Faraday Soc.*, 1931, **31**, 1718.

$$A \propto c_0 = \lambda_0^n c_s.$$

Fig. 2 shows, however, that $\frac{\partial S}{\partial t}$ increases at first more rapidly than A, when the concentration of salt increases.

The hypothesis that diffusion proceeds in solution is therefore incapable of explaining the facts, even if one also allows for the variation in thickness of the diffuse layer with salt concentration, since the electrical potential barrier to diffusion in solution cannot exceed that for approach to the surface.

Migration along a Non-equipotential Surface.—One might, on the other hand, suppose that diffusion occurs mainly in the adsorbed layer. In this case $\frac{\partial S}{\partial t}$ should be $\propto \frac{\partial A}{\partial x}$, or $\frac{\partial x}{\partial A} \cdot \frac{\partial S}{\partial t} = \text{const.}$ Now to explain the fact that $\frac{\partial x}{\partial A} \cdot \frac{\partial S}{\partial t}$ increases with A, we might suppose that the dye diffusing in the " surface " layer under the concentration gradient $\frac{\partial A}{\partial x}$ has to surmount hypothetical electrical potential barriers whose height decreases with A when c is constant, i.e. as the salt concentration increases. These barriers may arise from the presence of ionised carboxylic acid groups in the cellulose. The height and range of the negative potential barriers arising from them will decrease with electrolyte concentration, and so the surface diffusion will increase more rapidly with salt concentration than does A itself. The experimental fact would therefore be explained on this hypothesis.

There is a difficulty in reconciling the idea of diffusion within the " surface " layer with the very high temperature coefficient of diffusion of dyes in cellophane,[6] which indicates an activation energy of the order 14 kcal. mole^{-1} and suggests that desorption must precede diffusion. This activation energy, however, may be simply the energy required to open up the necessary " holes " in the amorphous parts of the cellulose, and this idea is supported by the apparent constancy of the value for various dyestuffs.

If the suggestion that the carboxyl groups play an important role in impeding diffusion of large multivalent anions is sound, then one should not find the anomalous salt effect in diffusion of dyes through cellulose free from carboxylic acid groups. No data are yet available to check this.

The idea that the suppression of electrical repulsion lies at the root of the anomalous salt effect is, however, strongly supported by the observation of a reversed effect for cationic dyes in Cellophane.[7]

College of Technology,
Manchester 7.

---

[6] Garvie, Griffiths and Neale, *Trans. Faraday Soc.*, 1934, **30**, 271.

[7] Neale, *Trans. Faraday Soc.*, 1947, **43**, 338.

ACID SALTS OF MONOCARBOXYLIC ACIDS AS *p*H STANDARDS; POTASSIUM-HYDROGEN BENZOATE AND PHENYLACETATE.

By Neville Smith and J. C. Speakman.

Received 23rd March, 1948.

Acid salts of mono-basic organic acids have been known for more than a century.[1] A survey of the literature shows that these compounds are formed by most simple acids, and that they are often more easily obtained than the expected neutral salts because they are less soluble in water. Such acid salts may be formed with all the alkali metals, with the alkaline earths, and with many others. The sodium and potassium compounds are best known; and, since the latter more often conform to the 1 : 1 type and are usually not hydrated, our attention has been confined to potassium salts.

As has been pointed out,[2] such acid salts are convenient materials for the preparation of buffer solutions. During the neutralisation of a weak acid by a strong base, maximum buffering capacity obtains at the half-neutralisation point, where the *p*H is approximately equal to *p*K ($= - \log K$, where K is the acid dissociation constant). Since the relative amounts of acid and salt are guaranteed by the stoichiometric composition of the substance itself, a single, relatively rough weighing of the solid will enable an accurately reliable buffer solution to be prepared.

The chief disadvantages are that suitable acids do not cover a very wide variety of strengths, so that the range of *p*H values accessible is limited; that otherwise suitable acids are often not very soluble in water so that the effective solubility of the acid salt is usually restricted; and that some of the more soluble salts (such as potassium hydrogen acetate) are unstable, losing free acid on exposure to the air. Nevertheless it is possible to specify a number of useful buffer solutions, capable of being used as *p*H standards. This paper describes work done to test the suitability of potassium hydrogen benzoate and potassium hydrogen phenylacetate. The work falls into three sections: (*a*) preparations (*b*) solubilities which are somewhat complicated and were studied by reference to the ternary solubility diagrams for the systems, acid-salt-water, and (*c*) the *p*H values of suitable solutions on a standardised scale.

Experimental.

Preparation.—Many of these acid salts can be easily prepared by dissolving an equivalent of the acid and half an equivalent of KOH, or K_2CO_3, in hot alcohol, and collecting the solid that crystallises out on cooling. In other cases it may be more convenient to add aqueous K_2CO_3 to a hot acetone solution of the acid. Potassium hydrogen benzoate[3] was obtained by dissolving 2·8 g. KOH and 12·0 g. benzoic acid in 250 cc. of hot alcohol. The solid which separated on cooling was recrystallised from alcohol, giving thin plates, which had no satisfactory melting-point. The substance was analysed by determination of the equivalent (279, 283) and of % K (13·71), the values calculated for $C_6H_5COOK \cdot C_6H_5COOH$ being 282 and 13·86 respectively.

---

[1] e.g. Berzelius, *Lehrbuch der Chemie*, 1847, iv, 314; Gmelin, *Handbook of Chemistry* (4th edn.), 1853, viii. 299.

[2] *Nature*, 1945, **155**, 698.

[3] Gerhardt, *Annalen*, 1853, **87**, 150; Farmer, *J. Chem. Soc.*, 1903, **83T**, 1442.

Potassium hydrogen phenylacetate, which was first described by Bakunin and Vitale,[4] was prepared in a similar way. It separates as monoclinic needles, melting at 142°. Analysis gave an equivalent of 307 and the potassium content as 12·31 % compared with 310 and 12·58 % calculated for $C_7H_7COOK \cdot C_7H_7COOH$. Both of these substances can be kept for long periods in a stoppered tube without undergoing detectable change.

Solubility Relationships.—Both compounds belong to the class of double salts that are said to be decomposed by water. Examination of the isothermal solubility diagrams for the ternary systems, acid-neutral salt-water, was therefore relevant to the present purpose.

Two of the separate binary pairs in the system benzoic acid-potassium benzoate-water have been examined by various workers,[5] and Landrieu[6] has reported two points in the ternary systems at about 16°. Our measurements were made at 20·0°. The benzoic acid was of A.R. quality; the potassium benzoate (trihydrate) was a commercial sample, it having first been shown that a recrystallisation did not affect the results. Various mixtures of acid and salt were stirred with water for at least 12 hr., a time found sufficient to ensure equilibrium. After filtration through sintered glass, the solutions were analysed for free acid by titration with CO_3''-free NaOH to the calculated *p*H (usually about 9·2) with thymol blue, and for potassium by evaporation and conversion of the residue to K_2SO_4. In some experiments the wet solid was also analysed. High accuracy was not easily attainable because of the great disparity between the solubilities of acid and salt; it was generally necessary to estimate a small amount of acid in presence of a large amount of salt, so that the end-point in a titration was not sharp.

For the same reason it was not convenient to plot our results on the usual triangular diagram. Using orthogonal axes, Fig. 1 represents average results based on over 60 individual determinations; AB shows the solubility of benzoic acid in presence of increasing concentrations of the salt; BC that of the acid salt, as was confirmed by analyses of the wet solids; and CD, which was difficult to fix accurately, the solubility of potassium benzoate trihydrate in presence of excess acid. The line OE indicates the direction of the 1 : 1 acid salt. Although this compound is more soluble in water containing an excess of benzoate, in the absence of any such excess, benzoic acid is liable to separate out if the concentration exceeds 0·024 M. at 20° (point F). This concentration may be regarded as the *effective solubility* of the acid salt. Its value, which will not differ considerably from the solubility of benzoic acid in pure water, has been determined for several temperatures as shown in Table I.

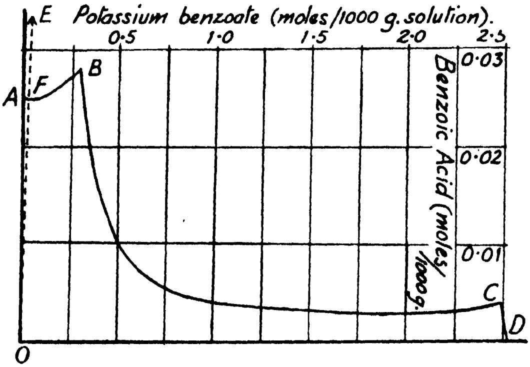

FIG. 1.

---

[4] Bakunin and Vitale, *Gazz. chim. ital.*, 1935, **65**, 593.

[5] Benzoic acid-water: e.g. Bourgoin, *Ann. chim. phys.* (5), 1878, **15**, 171; Alexejew, *Ann. Physik*, 1886, **28**, 305; Hoffmann and Langbeck, *Z. physik. Chem.*, 1905, **51**, 393; Sidgwick and Ewbank, *J. Chem. Soc.*, 1921, **119**, 979; Wright, *J. Chem. Soc.*, 1927, 1336; Ward and Cooper, *J. Physic. Chem.*, 1930, **34**, 1448. Potassium benzoate-water: Pajetta, *Gazz. chim. ital.*, 1906, **36** (ii), 67; Sidgwick and Ewbank, *J. Chem. Soc.*, 1922, **121**, 1844.

[6] *Compt. rend.*, 1920, **170**, 1450; 1920, **171**, 1066; see also Larsson, *Z. physik. Chem.*, 1930, **148** *A*, 148.

The ternary system, phenylacetic acid—potassium phenylacetate—water, has not been examined hitherto. Previous work has been confined to two of the constituent binary systems.[7] Our results (based on nearly 100 individual points) at 20·0° are represented by Fig. 2, the experimental details being essentially the same as those described above and the accuracy rather better. Allowing for the different scale of ordinates the diagram follows the pattern of Fig. 1 except for a notable difference in the neighbourhood of point B. Although it was difficult to obtain accurately reproducible results in this region, it is certain that a great increase in solubility occurs.

TABLE I

EFFECTIVE SOLUBILITIES OF ACID SALTS AT VARIOUS TEMPERATURES

Temp. (°c.).		15.	20.	25.	30.
Solubility (moles/1000 g. of solution)	Benzoate	0·021*	0·024	0·029*	0·037
	Phenylacetate	—	0·116	0·135	0·168

* Estimated from solubility-temp. curve for free acid.

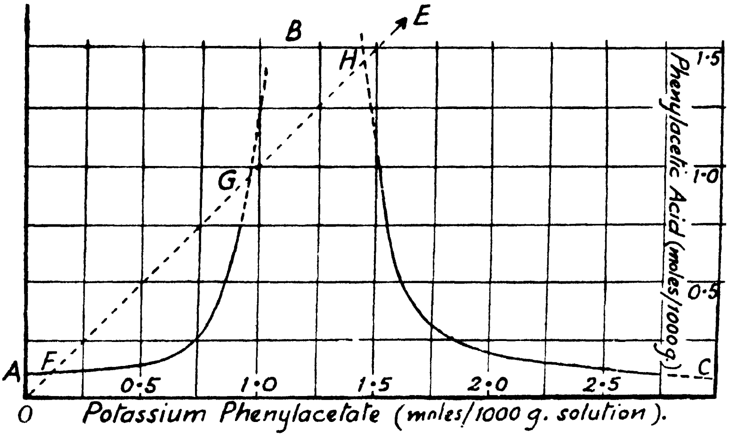

FIG. 2.

A consequence of this anomaly is that the acid salt (indicated by the direction OE) can exist in presence of its own solution provided that the concentration is high (between G and H); but that, on dilution past the point G, it is decomposed by water. A solution containing 1·0 g. of acid salt and 1·2 cc. of water appears to be quite stable at room temperature, but on adding a small amount of water a copious precipitate of the acid at once appears. This phenomenon of the precipitation of a solute (not a hydrolysis product) on dilution is unusual. An essentially similar effect was described by Schreinemakers[8] in binary systems which may have their freezing-points *raised* by addition of a third component that does not form solid solutions. In the present instance, it implies that the fugacity of the acid remains constant along curve GB although the acid and salt are being added to the liquid in relative proportions exceeding those corresponding to the (1 : 1) acid salt. This seems likely to occur only if there is a sharp tendency for complex ions or micelles of the type $[(A^-(HA)_n)_m]$ to be formed.

[7] Phenylacetic acid-water: Timofeiew, *Dissertation* (Kharkov), 1894; Knox and Richards, *J. Chem. Soc.*, 1919, **115**, 508; Hammett and Chapman, *J. Amer. Chem. Soc.*, 1934, **56**, 1282; Sidgwick and Ewbank, *loc. cit.* 1921. Phenylacetic acid-potassium phenylacetate: Bakunin and Vitale, *loc. cit.*

[8] Roozeboom, *Die Heterogenen Gleichgewichte*, iii (part 1), 144.

Two items of evidence seem to support this conclusion. First, Sidgwick[9] has observed a similar, but more marked, enhancement of the solubility of β-phenylpropionic acid in presence of its salt (together with the appearance of a second liquid phase). Although no marked solubility increase obtains with benzoic acid, Kolthoff and Bosch[10] have suggested that acid anions, HA_2^-, begin to be formed at high concentrations of salt. Any tendency towards soap formation will increase with ascent of the homologous series, and the phenomena observed with phenylacetic acid seem to fall into place in the sequence. Secondly, we have noticed a decided rise in viscosity of the solutions in this region, the concentrated solution of potassium hydrogen phenylacetate mentioned above having a viscosity more than four times that of water.

Effective solubilities of potassium hydrogen phenylacetate are shown in Table I. On the basis of the solubility data, 0·015 and 0·033 M. are respectively suggested as suitable concentrations for benzoate and phenylacetate buffer solutions.

***p*H Values.**—*p*H was originally defined with reference to the hydrogen-ion *concentration* of the solution. If it is referred to the hydrogen-ion *activity*, as is the common practice now,[11] an arbitrary standardisation of the *p*H scale is necessary, since an individual ion activity cannot be rigorously measured or defined. The convention suggested by Cohn, Heyroth and Menkin,[12] and used by Hitchcock and Taylor,[13] defines the scale in such a way that the correct thermodynamic dissociation constant (K) or a weak acid (HA) results when the hydrogen-ion activity thus derived is introduced into the equation,

$$K = \frac{a_{\mathrm{H}^+}[\mathrm{A}^-]\,.\,f_1}{[\mathrm{HA}]\,.\,f_0},$$

where f_0 is the activity coefficient of the neutral molecule HA, and where f_1, that of the anion A^-, is derived from the Debye-Hückel equation. Arbitrary assumptions about individual ion activities enter the equation twice over, and it may be hoped that errors will cancel out, provided that the liquid junction potential (which is always involved in *p*H measurements) remains constant and reproducible.

Accepting this method of standardisation, the *p*H of a new buffer solution can be found in two ways : (*a*) from the dissociation constant of the acid concerned, with due allowance for f_0 and f_1 ; or preferably (*b*) by experimentally comparing the unknown *p*H with those of certain of the standard buffer solutions recommended by previous workers.[14]

(*a*) The Debye-Hückel limiting law $(-\log f_1 = 0{\cdot}5\sqrt{I})$ is hardly applicable at values of the ionic strength (I) so high as 0·015 and 0·033 M. But, using the (approximate) extended form of the Debye-Hückel equation, $-\log f_1 = \dfrac{0{\cdot}5\sqrt{I}}{1 + \sqrt{I}}$, and taking pK $= 4{\cdot}20$ for benzoic acid at 25°,[15, 16] and pK $= 4{\cdot}31$ for phenylacetic acid,[15] we obtain 4·15 and 4·23 as approximate *p*H values for the corresponding buffer solutions. (*b*) All our *p*H measurements have been based on the standard buffers of Hitchcock and Taylor, who give *p*H values for 25° and 38°. For work at 20° we estimated values from theirs by a short extrapolation. During the past four years we have carried out many *p*H determinations on the benzoate and phenylacetate buffer solutions using the glass electrode at 20°. The average *p*H values found were 4·16 and 4·24 respectively, with a probable error of less than ± 0·01 unit.

For a more rigorous comparison we have made use of the quinhydrone electrode. The hydrogen electrode is apt to behave irregularly with some aromatic acids,[17] and we placed more reliance on the quinhydrone, which was used with a platinum electrode in presence of a slow stream of purified N_2. Liquid junctions between buffer solutions and saturated KCl were formed in a special way described later. Using the cell,

---

[9] Sidgwick, *J. Chem. Soc.*, 1910, **26P.**, 60.

[10] Kolthoff and Bosch, *J. Physic. Chem.*, 1932, **36**, 1689.

[11] Bates, *Chem. Rev.*, 1948, **42**, 1.

[12] *J. Amer. Chem. Soc.*, 1928, **50**, 696.

[13] *Ibid.*, 1937, **59**, 1812 ; 1938, **60**, 2710.

[14] Hitchcock and Taylor, *loc. cit.* ; McInnes, Belcher and Shedlovsky, *ibid.*, 1938, **60**, 1094 ; Manov, De Lollis and Acree, *Bur. Stand. J. Res.*, 1945, **34**, 115.

[15] Dippy and Williams, *J. Chem. Soc.*, 1934, **161**, 1888.

[16] Rule and La Mer, *J. Amer. Chem. Soc.*, 1938, **60**, 1981.

[17] Hamer and Acree, *Bur. Stand. J. Res.*, 1943, **33**, 87, mention phthalate solutions. (We also found difficulty in attaining constant potentials in benzoate solutions.)

$$\mathrm{Pt} \mid \text{Quinhydrone } (s) \mid \text{Buffer solution} \mid \text{Saturated KCl} \mid Hg_2Cl_2\ (s) \mid \mathrm{Hg},$$

the E.M.F.'s given by our own buffer solutions were compared with those given by 0·05M. potassium hydrogen phthalate and by 0·1 M. acetic acid + 0·1 M. sodium acetate. Results are shown in Table II. The *p*H values were found by interpolation between those (in parenthesis) attributed to the accepted standards. It is believed that the values stated for the benzoate and phenylacetate buffer solutions are correct to within 0·01 unit, which is probably the limit of validity of any system of *p*H standardisation. Portions of these solutions have been in use for periods of six months without undergoing any appreciable change of *p*H. They do not seem to be liable to become contaminated with moulds, as is the phthalate solution.

TABLE II.—E.M.F. MEASUREMENTS.

Molality of free acid equal to molality of neutral salt throughout.

Buffer Solution.	E.M.F. (V.).		*p*H Value.	
	20·0°.	25·0°.	20·0°.	25·0°.
0·05 M. Phthalate	0·2227	0·2184	(4·000)	(4·005)
0·015 M. Benzoate	0·2132	0·2090	4·16	4·16
0·033 M. Phenylacetate	0·2093	0·2040	4·24	4·25
0·1 M. Acetate	0·1860	0·1810	(4·643)	(4·643)

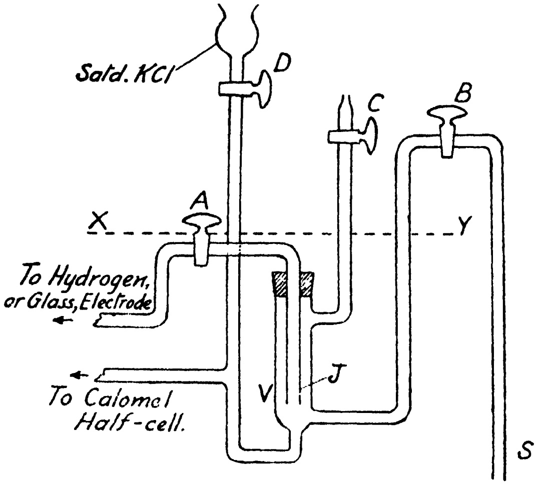

FIG. 3.

Liquid Junctions.—To procure a reproducible junction of the free diffusion type, Guggenheim [18] recommends that it be formed under conditions of cylindrical symmetry. The apparatus shown in Fig. 3 was found to be convenient for this purpose. It was constructed mainly out of semi-capillary tubing, and it was so designed that all important parts of the cell could be kept below the surface (XY) of the constant temperature bath. The aim is to produce an initially sharp boundary between the buffer solution (above) and the saturated KCl (below) within the tube J and about 1-2 mm. from its lower end. Opening taps A and B allowed the solution in the electrode vessel to flush out J and leave it filled to its lower end, excess liquid running to waste via the siphon tube S.

[18] *J. Amer. Chem. Soc.*, 1930, **52**, 1315.

With A closed and C open to the air, the outer part of the junction vessel V could next be emptied by use of B. With B closed and C still open, tap D allowed saturated KCl from the reservoir to rise slowly in the junction vessel and make contact with the buffer solution in J. C was then closed and D re-opened momentarily so as slightly to compress the air trapped in the upper part of V. It was possible to carry out the foregoing operations in such a way that, on opening A, the compressed air caused the junction to rise 1-2 mm. inside J. The junction formed in this manner is not extremely sharp; rather it will correspond to conditions in an initially sharp boundary that has aged, which is not necessarily a disadvantage. In any case a reproducible E.M.F. was at once attained. During measurement the tap A may be closed if desired, the film of electrolyte round the barrel of the tap usually conferring sufficient conductivity. At any time the old junction can be washed away through the waste outlet, and a new one formed if desired.

The arrangement suggested by Coates[19] requires only two taps, though one of them has to be of the three-way type. The system described above is considered to be more convenient in that it allows all liquid columns to be immersed in the thermostatic liquid, whilst at the same time allowing all tap handles to be clear of it, and in that (by keeping tap A closed) it can readily be used with electrodes around which a gas is being bubbled.

This work was carried out in the University of Sheffield, and we wish to thank the West Riding County Council for financial aid which enabled one of us (N. S.) to take part in it.

Summary.

Potassium hydrogen benzoate, $KH(C_6H_5COO)_2$, and potassium hydrogen phenylacetate, $KH(C_7H_7COO)_2$, have been investigated as materials for the preparation of standard buffer solutions. Their solubility relationships have been examined by reference to the ternary isothermal diagrams for the system, acid-salt-water. The phenylacetate system shows a very large "salting-in" effect. The *p*H values (expressed on a standardised scale) of 0·015 M. benzoate and of 0·033 M. phenylacetate have been determined at 20° and 25° C. A convenient apparatus for forming the liquid junction between a buffer solution and saturated potassium chloride is described.

The Technical College,
Derby.

Chemistry Department,
The University,
Glasgow, W.2.

[19] *J. Chem. Soc.*, 1945, 489.

THE CALCULATION OF SURFACE TENSION FROM INTERMOLECULAR FORCES.

II. NUMERICAL RESULTS.

BY J. CORNER.

(*Communicated by* SIR JOHN LENNARD-JONES, F.R.S.)

Received 26th June, 1947, *as revised 18th May,* 1948.

1. Introduction.

In an earlier paper Lennard-Jones and Corner[1] showed how surface tension could be calculated, in principle, from a "cell" model of the liquid state. The general relations between the intermolecular forces and the characteristics of the surface tension, including in particular the parachor, were also discussed. The paper did not include the detailed numerical consequences of the cell model, since these had not been completed; it was obvious that some time would elapse before the authors were able to return to this subject. Lately it has become possible to complete the computations, which are reported in the present paper.

---

[1] Lennard-Jones and Corner, *Trans. Faraday Soc.*, 1940, **36**, 1156.

After a résumé of the formulæ needed from the first paper, and their relation to work which has appeared since that time, the theoretical results are compared with experiment. The mathematical details are discussed in Sections 4 and 5.

2. The Relation between Surface Tension and Intermolecular Forces.

The surface tension, σ, of a liquid is, in the notation of the paper of Lennard-Jones and Corner,[1]

$$\sigma = \Psi_0 - \Phi_0 + N_s kT \ln (V_f^*/V_s^*) \quad . \quad . \quad . \quad (1)$$

where $\Psi_0 - \Phi_0$ is the increase in the potential energy, per unit total area of interface, when two semi-infinite blocks of liquid with plane faces are moved from zero to infinite separation in a reversible isothermal process; N_s is the number of molecules on unit area of the face exposed. The quantities V_s^* and V_f^* are the free volumes of a molecule at a site on the exposed face and in the bulk liquid respectively. In deriving (1) it is assumed that the density of the vapour is negligible compared with the density of the liquid.

Let V be the volume of a mole of the liquid of N molecules. It is convenient to introduce at this point the intermolecular potential which we shall use—

$$E = \phi[(r_0/r)^{12} - 2(r_0/r)^6)] \quad . \quad . \quad . \quad . \quad (2)$$

where ϕ is the maximum depth of the potential, attained at a separation r_0.

The empirical relation (Eötvos' law [2])

$$\sigma V^{\frac{2}{3}} = K(T_0 - T) \quad . \quad . \quad . \quad . \quad (3)$$

in which K and T_0 are independent of the temperature, was derived from (1) by Madelung [3] and Born and Courant.[4] For this, one neglects the temperature-dependence of the ratio of the free volumes and uses the fact that N_s is proportional to $V^{-\frac{2}{3}}$. If, further, one assumes that $\Psi_0 - \Phi_0$ is proportional to the surface density of molecules, that is, to $V^{-\frac{2}{3}}$, and is independent of temperature, eqn. (3) is obtained. This was the course followed by Madelung, who took a plausible approximation for the change in the free volume caused by the change in the number of neighbours, and obtained K near the correct value. Born and Courant [4] treated the motion of the surface molecules as the vibrations of an elastic system, in much the same way as in Debye's theory of specific heats, and arrived at a formula for K which agreed with experiment to within a few per cent. A very similar calculation was made by Brillouin.[5] In all these treatments $\Psi_0 - \Phi_0$ was not calculated, and it was assumed that it gave the constant term KT_0 in Eötvos' law. We shall show in Section 3 that in fact the two terms in (1) do not correspond to the two terms in Eötvos' law, nor indeed is the division of σ into the two terms of (1) completely unique.

Belton and Evans [6] have calculated surface tensions from a cell model of a liquid, and have shown that the potential energy contribution to the surface tension is sufficient to account for most of the observed temperature-dependence. They explained the remainder as arising from a surface

[2] Eötvos, *Wied. Ann.*, 1886, **27**, 456.
[3] Madelung, *Physik. Z.*, 1913, **14**, 729.
[4] Born and Courant, *ibid.*, 731.
[5] Brillouin, *Compt. rend.*, 1925, **180**, 1248.
[6] Belton and Evans, *Trans. Faraday Soc.*, 1941, **37**, 1.

free volume not equal to that of a molecule in the bulk phase. They did not calculate the preferred face or the surface free volume, and their assumed intermolecular potential differs from that which we use.

The surface energy per unit area is

$$U_s = \sigma - T\mathrm{d}\sigma/\mathrm{d}T = \Psi_0 - \Phi_0 - T(\mathrm{d}V/\mathrm{d}T)\mathrm{d}(\Psi_0 - \Phi_0)/\mathrm{d}V \\ - N_s kT^2 \partial \ln (V_j^*/V_s^*)/\partial T - NkT^2(\mathrm{d}V/\mathrm{d}T)\partial \ln (V_j^*/V_s^*)/\partial V \quad . \quad (4)$$

Of these terms we may neglect that involving $\partial \ln (V_j^*/V_s^*)/\partial T$. For $kT^2 \partial \ln V_j^*/\partial T$ is the part of the mean potential energy of an interior molecule due to its motion around its equilibrium position. It is, for example, $3kT/2$ when the motion is that of a three-dimensional harmonic oscillator. It is nearly the same for a surface molecule as for one in the interior of the liquid, so that we may take $\ln (V_j^*/V_s^*)$ to be nearly independent of the temperature (at constant density). Moreover, calculation shows (cf. Section 5) that the ratio of the free volumes varies only slowly with the density of the liquid, so that the last term in (4) is only about 10 % of $\Psi_0 - \Phi_0$. On the other hand the term involving $\mathrm{d}(\Psi_0 - \Phi_0)/\mathrm{d}V$ is comparable to $\Psi_0 - \Phi_0$ itself. It follows that surface energies cannot be calculated from the term $\Psi_0 - \Phi_0$ evaluated at one temperature, though if this be calculated as a function of temperature the surface energy can be obtained with an error of about 10 %.

Harasima[7] has obtained $\Psi_0 - \Phi_0$ for a face-centred cubic lattice of molecules with intermolecular potential (2). He assumed that the exposed surface of the lattice was a (100) plane. With force-constants from second virial analysis, the surface energies calculated from $\Psi_0 - \Phi_0$ were in good agreement with experimental values extrapolated to 0° K. Harasima did not calculate the free volumes at the surface or in the interior, and hence did not obtain the surface tension.

3. Theoretical Calculation of Surface Tension and Comparison with Experiment.

We proceed now to more detailed calculations. Following Lennard-Jones and Devonshire,[8] we assume that the equilibrium positions of the molecules form a face-centred cubic lattice. The first question to be settled is which of the crystal faces will be exposed at the surface The answer is, of course, the face of lowest free energy per unit area, that is, with the lowest surface tension. Of the three densely-occupied planes of the face-centred cubic, namely the (100), (110) and (111) planes, one can be excluded immediately by the following considerations.

Table I shows the salient features of the three faces. The potential energy contribution $\Psi_0 - \Phi_0$ to the surface tension is only partly due to the loss of nearest-neighbour bonds, but it is clear that (110) and (111) will give smaller values than (100). As a matter of fact, an accurate calculation shows that the (111) face does give a smaller contribution than the (110) face, as indicated in Table I, though the difference is smaller than the limit of reliability of such an approximate calculation.

The free energy of the surface is less than the potential energy contribution by a term proportional to the surface density of the molecules, and proportional to the temperature. This term depends also on the free volume of a surface molecule, which may be somewhat different for the three faces. It is therefore not possible to say immediately which of the (110) and (111) faces will have the lower surface tension. This can determined only by more accurate calculations. It will be shown in Section 5 that the (111) face has the lower surface tension, by about 10 %. From this point, therefore, all theoretical results quoted will be those for the (111) face.

[7] Harasima, *Proc. Phys.-Math. Soc. Japan*, 1940, **22**, 825.

[8] Lennard-Jones and Devonshire, *Proc. Roy. Soc. A*, 1938, **165**, 1.

The computed surface tension depends explicitly on both density and temperature, and before a comparison with experiment can be made one must choose some relation between liquid density and temperature. The theoretical results of Lennard-Jones and Devonshire [8, 9, 10] for the equation of state of simple liquids give a fair representation of the empirical results, but the inaccuracy is sufficient to obscure the error in the surface tension due to the imperfections of this model as regards the surface phase.

TABLE I.—GEOMETRICAL PROPERTIES OF SURFACES OF FACE-CENTRED CUBIC LATTICES.

The distance between nearest neighbours is a.

Face.	(100).	(110).	(111).
Number of nearest neighbours of a surface molecule . . .	8	7	9
Number of nearest neighbour bonds broken, per surface molecule .	4	5	3
Area per molecule . . .	a^2	$\sqrt{2}a^2$	$\sqrt{3}a^2/2$
Number of nearest neighbour bonds broken, per area a^2 . . .	4	3·54	3·46

In short, the inaccuracy of the equation of state from the model of Lennard-Jones and Devonshire is well-known; if we wish to find how well this model reproduces surface properties it is clearer to use an empirical equation of state.

Guggenheim [11] has shown that the density of simple liquids (Ne, A, N_2 and O_2) is closely represented by

$$V_c/V = 1 + 0{\cdot}75(1 - T/T_c) + 1{\cdot}75\,(1 - T/T_c)^{\frac{1}{3}} \quad . \quad . \quad (5)$$

with errors of, for example, 0·2 % for argon throughout the whole range of the liquid phase. Here V_c is the critical molar volume. To use this relation in our computation of surface tension we must connect ϕ and r_0 with T_c and V_c. A relation between ϕ and T_c was first obtained by Lennard-Jones and Devonshire,[12] whose theory of critical phenomena gave $kT_c/\phi = 4/3$. This is close to the empirical results, for which an average for Ne, A, N_2 and CH_4 is (cf. Appendix)

$$kT_c/\phi = 1{\cdot}29 \quad . \quad . \quad . \quad . \quad . \quad (6)$$

The theoretical result for V_c/r_c^3 was not very successful; as shown in Appendix, an empirical mean (Ne, A, Xe, CO, CH_4 and N_2) is

$$V_c/V_0 = 3{\cdot}05 \quad . \quad . \quad . \quad . \quad . \quad (7)$$

where

$$V_0 = Nr_0^3/\sqrt{2} \quad . \quad . \quad . \quad . \quad (8)$$

We have used the equation of state (5), relating T_c and V_c to the force-constants ϕ and r_0 by (6) and (7), and have computed the surface tension at two temperatures near the lower part of the liquid range; two temperatures well below the triple point have also been studied to verify that no unreasonable results appear outside the liquid range. The theoretical surface tension and its constituent parts are given in Table II. The contribution of the potential energy term is written as $\phi S/2$ per molecule, and there is also a term $kT \ln (V_s^*/V_f^*)$. By (1), their difference is the

---

[9] Lennard-Jones and Devonshire, *ibid.*, 1939, **169**, 317.

[10] Lennard-Jones and Devonshire, *ibid.*, 1939, **170**, 464.

[11] Guggenheim, *J. Chem. Physics*, 1945, **13**, 253.

[12] Lennard-Jones and Devonshire, *Proc. Roy. Soc. A*, 1937, **163**, 53.

surface free energy per molecule, and by converting to the free energy per unit area we reach the surface tension, σ.

It will be noticed that the free volume available to a surface molecule is, for $(V_0/V)^2 = 0{\cdot}7$, only slightly greater than the free volume of a molecule in the interior. Under certain conditions the surface free volume can even be less than the free volume in the liquid. This result is surprising at first sight, since it means that the removal of half the lattice, including three of the nearest neighbours, actually decreases the free volume available to a molecule. The explanation is that the molecule takes up a new equilibrium position closer towards the bulk of the liquid, and in this position it can, under certain conditions, be in a potential well which is both deeper and steeper than before. This lower potential energy will be calculated (Section 4) in our discussion of the potential energy contribution to the surface tension. We might prefer to calculate the potential energy and free volume terms on the basis of the original equilibrium position. It can be shown that the surface free volume would be increased and the surface free energy reduced thereby, but that this would be exactly counterbalanced by an increase in the potential energy $\Psi_0 - \Phi_0$. Thus the division of the surface tension into terms arising from potential energy and free volume changes is not unique.

TABLE II.—THEORETICAL SURFACE TENSION, USING GUGGENHEIM'S EQUATION OF STATE

$(V_0/V)^2$.	T/T_c.	ϕ/kT.	$S/2$.	$(kT/\phi) \times \ln (V_s^*/V_f^*)$.	$\sigma/r_0^2\phi$.
0·7	0·620	1·2495	1·905	0·007	1·946
0·8	0·521	1·4871	2·338	0·103	2·396
0·9	0·421	1·8432	2·686	0·160	2·817
1·0	0·319	2·4280	2·950	0·176	3·203

Guggenheim[11] has shown that the experimental data on surface tension can be accurately represented by

$$\sigma = \sigma_0(1 - T/T_c)^r \quad . \quad . \quad . \quad . \quad (9)$$

where $r = 11/9$ and σ_0 is a constant such that $\sigma_0 V_c^{2/3}/T_c$ has almost the same value, 4·4 erg degree^{-1} mole$^{-2/3}$ for the simpler molecules. A relation of form (9) can be fitted to our theoretical results, using (6) and (7), and the points lie within ½ % of a single curve. Since, however, only the two highest temperatures are really applicable to the liquid state, it is perhaps more significant to use only these; we then find $r = 0{\cdot}897$ and $\sigma_0 V_c^{2/3}/T_c = 5{\cdot}91$ erg degree^{-1} mole$^{-2/3}$. The deviations are therefore about 30 % for both parameters. A factor which may account for most of this difference is the high co-ordination number, 12, of the face-centred cubic lattice assumed here; co-ordination numbers around 10 have been derived from X-ray observations on liquids.[13]

4. Calculation of the Surface Tension of a (111) Face.

To obtain the potential energy contribution to the surface energy we must first calculate the position of the outermost layer of molecules. This will not be at the same distance from its neighbours that would occur in an infinite lattice. To calculate the equilibrium distance we minimise the potential energy of the system. The displacement from the normal distance is small, amounting to about 6 % of the nearest-neighbour separation, when the molar volume of the liquid is $1{\cdot}1\ V_0$. At this density the motion of the outermost layer decreases the potential energy contribution to the surface tension by about 5 %; at the boiling-point the effect is to reduce the surface tension by roughly 10 %.*

---

[13] For a typical monatomic liquid, cf. Lark-Horovitz and Miller, *Nature*, 1940, **146**, 460.

We take rectangular Cartesian axes, Ox, Oy, Oz, and write a as the distance between the lattice-points of the face-centred cubic. Then the lattice-points of the unit cell are at (000), $(110)a/\sqrt{2}$, $(101)a/\sqrt{2}$, and $(011)a/\sqrt{2}$, and all points of the lattice can be obtained by a translation $(p, q, r)a\sqrt{2}$ (where p, q and r are integers or zero), applied to the four lattice-points in the unit cell. We consider a semi-infinite lattice bounded by a (111) plane through the origin, so that only those lattice-points are occupied which satisfy the condition $x + y + z \geqslant 0$. In the summations over lattice-points we have used the 428 points which are not more than $5a$ from the origin, and have extrapolated to all lattice-points as explained later.

Let the face molecules be moved a distance $na\sqrt{3/2}$ perpendicular to the (111) face. The molecule at the origin is moved to $(111)na/\sqrt{2}$. Let its potential energy in this position be written $-\phi\chi(n)$; χ is a function of the specific volume of the lattice, but it is not necessary to make explicit reference to this parameter. The potential energy of a pair of molecules with a distance d between centres is

$$\phi[(V_0/V)^4(a/d)^{12} - 2(V_0/V)^2(a/d)^6]$$

since V is the molar volume of the lattice, namely $Na^3/\sqrt{2}$, and V_0 is related to the parameter r_0 in the intermolecular potential (2) by the definition $V_0 = Nr_0^3/\sqrt{2}$. To calculate $\chi(n)$, we sum $(a/d)^6$ and $(a/d)^{12}$ over all the neighbours of the central molecule, remembering that all the face molecules have received the same displacement as the central molecule. $\Sigma(a/d)^{12}$ presents no difficulty, since the successive terms diminish rapidly. For $\Sigma(a/d)^6$ some form of extrapolation is necessary, since there is a substantial contribution from neighbours which are more than $5a$ away. We have used the following method.

Let ν be the number of neighbours whose distance from the origin is not more than a certain arbitrary distance μa. Let ma be the radius of the hemisphere which would be occupied by these molecules at the average density $\sqrt{2}/a^3$, so that $m^3 = 3\nu/2\sqrt{2}\pi$. We replace the neighbours not included in these ν by a continuous distribution of density $\sqrt{2}/a^3$, and approximate to the sum $\Sigma(a/d)^6$ over these outer neighbours by the integral of $(a/d)^6$ over the continuous distribution, giving, as an approximation for $\Sigma(a/d)^6$,

$$\sum(a/d)^6 \simeq \sum(\nu) \equiv \sum_1^\nu(a/d)^6 + (8\pi^2/9\nu)(1 + (3/2)^{5/2}n/m).$$

By plotting $\Sigma(\nu)$ against $1/\nu$ one can extrapolate to infinite ν. By using the values $\nu = 301$, 355 and 428, it is possible to obtain $\Sigma(a/d)^6$ to an accuracy of about 1 in 10,000, and this can be improved by a process explained later.

In this way $\Sigma(a/d)^6$ and $\Sigma(a/d)^{12}$ were computed, to 4 and 5 decimal places respectively, for $n = -0{\cdot}5\ (0{\cdot}025)\ 0{\cdot}1$, and χ was calculated for these values of n at $(V_0/V)^2 = 0{\cdot}7$, $0{\cdot}8$, $0{\cdot}9$, $0{\cdot}95$ and 1. From these results was obtained the value of n, namely, n_m, which makes χ a minimum, and the minimum χ was located with an error of less than 1 in 10^5. In Table III are given n_m, $\chi(n_m)$ and, for comparison, $\chi(0)$.

We turn now to the calculation of the complete potential energy term $\Psi_0 - \Phi_0$ in the formula (1) for the surface tension. This term is a function of n, and the face molecules will take up the value of n which minimises $\Psi_0 - \Phi_0$. This is the energy of the bonds broken in the formation of unit surface area. Let $-\phi\zeta(V_0/V)$ be the potential energy of a molecule in an infinite face-centred cubic lattice, so that the potential energy of the lattice is $-\phi\zeta/2$ per molecule. The values of $\Sigma(a/d)^6$ and $\Sigma(a/d)^{12}$ for an infinite lattice have been obtained by Lennard-Jones and Ingham,[14] and lead to

---

* Harasima[7] neglected this motion of the outer layer in his calculations of surface energy.

TABLE III.—MOTION OF AN EXPOSED (111) FACE

$(V_0/V)^2$.	n_m.	$\chi(n_m)$.	$\chi(0)$.
0·7	0·075	10·6524	10·1361
0·8	0·054	11·1648	10·8585
0·9	0·036	11·5496	11·3994
0·95	0·027	11·6947	11·6019
1·0	0·020	11·8077	11·7589

$$\zeta = 12{\cdot}13188\,(V_0/V)^4 - 28{\cdot}90784\,(V_0/V)^2. \quad . \quad . \quad (10)$$

The potential energy of a face molecule is (algebraically) greater than its potential in a complete lattice, by the amount $\phi[\zeta - \chi(n)]$. Let $-\phi\Omega_2(n)$ be the potential energy of a face molecule at n, by its interactions with the molecules in the second layer. Then a molecule in the second layer has a potential $-\phi\chi(0)$ from the third and all succeeding layers, while it has also a potential energy $-\phi\Omega_2(n)$ from interaction with the face molecules. The gain of potential energy of such a second-layer molecule when the face is formed is therefore $\phi[\zeta - \chi(0) - \Omega_2(n)]$. Similarly, the gain of energy of a molecule in the third layer is

$$\phi[\zeta - \chi(0) - \Omega_2(0) - \Omega_3(n)].$$

The potential energy, per molecule, associated with the surface is $\phi S(n)$, with

$$S(n) = [\zeta - \chi(n)] + [\zeta - \chi(0) - \Omega_2(n)] + [\zeta - \chi(0) - \Omega_2(0) - \Omega_3(n)] + \ldots \quad (11)$$

In a (111) face the area per molecule is $\sqrt{3}a^2/2$. The potential energy $\phi S(n)$ is a consequence of the formation of two such areas, and the potential energy per unit area is

$$\phi S(n)/a^2\sqrt{3} = (\phi/r_0^2)(V_0/V)^{\frac{2}{3}}S(n)/\sqrt{3} \quad . \quad . \quad . \quad (12)$$

This is the term which in Section 2 was denoted by $(\Psi_0 - \Phi_0)/N_s$.

The calculation of such terms as $\Omega_2(n)$ reduces to summations over the molecules in one layer; the summations are therefore less laborious and extrapolation is easier. To find $\Sigma(a/d)^6$ we proceed in a manner analogous to that followed in the calculation of the space-summation. The (111) face has a surface density $2/a^2\sqrt{3}$ and therefore ν sites, distributed with this density, fill a circle of radius ma, where $m^2 = \sqrt{3}\nu/2\pi$. Let the layer considered be the $(p + 1)$th, namely $x + y + z = pa/\sqrt{2}$. Then an integration over the smoothed-out distribution of molecules outside a radius ma leads to the approximation

$$\sum(a/d)^6 \simeq \sum(\nu) \equiv \sum_1^{\nu}(a/d)^6 + 9\pi/4\sqrt{3}(p^2 + 3\sqrt{3}\nu/4\pi)^2 \quad . \quad (13)$$

The convergence of $\Sigma(\nu)$ is very rapid for these layer summations and a result correct to four decimal places can be obtained by using the value where the part by accurate summation extends to $5a$ from the origin.

---

[14] Lennard-Jones and Ingham, *Proc. Roy. Soc. A*, 1925, **107**, 636.

In this way were computed $\Sigma(a/d)^6$ and $\Sigma(a/d)^{12}$, to 4 and 5 decimals respectively for the first 13 layers, for the values n_m in Table III, and also for $n = 0$.

The minimum value of $S(n)$ occurs at that n which makes $\chi(n)$ a maximum; this makes it sufficient to compute $S(n_m)$ alone and not the general function $S(n)$.

With these values can be performed two checks which verify the accuracy of our enumeration of the lattice sites, the extrapolations, and the numerical working. In the first place, the sum of the layer summations of $(a/d)^6$ or $(a/d)^{12}$ must equal the direct summation over the semi-infinite lattice. For $(a/d)^{12}$ this is merely a test of the numerical working. For $n = 0$ the observed difference of 1 part in 150,000 was traced to an accumulation of rounding-off.

The corresponding test on $\Sigma(a/d)^6$ is also a check on the methods of extrapolation. It is necessary to carry out an extrapolation over the layers beyond the 13th. Putting $\nu = 0$ in (11), we find the contribution from the $(p + 1)$th layer to be $9\pi/4p^4\sqrt{3}$, if p is more than 7, say. The sum of $(a/d)^6$ over the whole space $x + y + z > p_0 a/\sqrt{2}$ is therefore $\pi\sqrt{3}/4p_0^3$. Using this with $p_0 = 12{\cdot}5$, the sum of the layer summations (for $n = 0$) was found to differ by only two in the last place from the extrapolation of the space-summation.

There is a second check on the enumeration of the lattice-points and also on the extrapolated value of $\Sigma(a/d)^6$ over the semi-infinite lattice. The potential energy of a molecule in a complete lattice is equal to twice the potential energy when it is in the face of a half-lattice, minus the potential energy to the other face molecules. This equality holds for the separate summations of $(a/d)^6$ and $(a/d)^{12}$. Using the values for the complete lattice found by Lennard-Jones and Ingham,[14] exact agreement was found for $\Sigma(a/d)^{12}$ to the five decimals kept throughout the calculation of the individual terms. If for $\Sigma(a/d)^6$, summed over the half-lattice, we use the sum of the layer-summations, then the check is satisfied to the four decimals kept in the computations of $(a/d)^6$. This is a sensitive test.

We return now to the function $S(n)$, formed from the layer sums whose calculation and checking we have just described. The summation in S requires yet another extrapolation, treated in the same manner as before, and which in this case amounts to only a few units in the fourth decimal place. Table IV shows the final results. It is to be noted that $S(n_m)$ is not independent of density; this contradicts the assumption made by Madelung, and by Born and Courant, in their derivation of Eötvos' law.

TABLE IV.—POTENTIAL ENERGY CONTRIBUTION TO THE SURFACE TENSION; (111) FACE

$(V_0/V)^2$.	$(V_0/V)^{2/3} S(n_m)/\sqrt{3}$.	$S(n_m)$.
0·7	1·953	3·809
0·8	2·507	4·677
0·9	2·995	5·373
0·95	3·211	5·657
1	3·406	5·899

To complete the derivation of the surface tension, it remains to calculate the free volume of a molecule in the interior and at the (111) face. The former has been reduced by Lennard-Jones and Devonshire[12] to the computation of an integral over one variable. At the surface the molecule is in a much less symmetrical field, and the computation is more laborious. It amounts to the numerical calculation of a double integral, in the case of the (111) face, and to the calculation of a triple integral for the (110) surface. We sketch here the method used for the former.

The position of the other molecules in the surface does not affect, except to a minor extent, the free volume available to the central molecule considered. It will make little difference if we assume that the other surface molecules lie in the plane $x + y + z = 0$, instead of being at their equilibrium positions in the plane $x + y + z = 3n_m a/\sqrt{2}$, where n_m is given in Table III. We write $-\phi\chi'(n)$ for the potential energy of the molecule when it is at $x = y = z = na/\sqrt{2}$ and the other surface molecules lie in $x + y + z = 0$. The function $\chi'(n)$ can be computed by the methods used for $\chi(n)$. Let n'_m be the value of n which makes χ' a maximum; n'_m is close to n_m.

Consider any position of the central molecule. This position can be specified by quoting the values of n, ξ and θ, where the position lies in the plane $x + y + z = 3na/\sqrt{2}$, at a distance ξa from $x = y = z = na/\sqrt{2}$, the line to which makes an angle θ with some fixed reference line. Let $-\phi P(n, \xi, \theta)$ be the potential energy in this position. We have to calculate the free volume of a surface molecule

$$V_s^* = (3/2)^{\frac{1}{2}}a^3\int_{-\infty}^{\infty}\mathrm{d}n\int_0^{\infty}\xi\mathrm{d}\xi\int_0^{2\pi}\exp[\phi\{(P - \chi'(n'_m))\}/kT]\mathrm{d}\theta.$$

The surface molecules are in hexagonal close-packed array. This highly symmetrical arrangement allows us to replace the averaging of $\exp(\phi P/kT)$ with respect to θ by the simpler averaging of P itself, so that

$$V_s^* = \pi\sqrt{6}a^3\int_{-\infty}^{\infty}\mathrm{d}n\int_0^{\infty}\exp[\phi\{\bar{P}(n, \xi) - \chi'(n'_m)\}/kT]\xi\mathrm{d}\xi.$$

For the calculation of $\bar{P}(n, \xi)$ we divide it into two parts; the value at $\xi = 0$ is just $\chi'(n)$, and this we compute accurately; the change in potential energy in moving from $\xi = 0$ to ξ, staying in the plane n, is approximated by considering only interactions with 24 of the nearest neighbours, namely the 9 nearest, the 3 next-nearest, and 6 from each of the next two shells. This should give a close approximation to the free area in each plane.

The formulæ for potential energies averaged with respect to θ are easily derived. Consider a ring of c molecules in a plane $x + y + z =$ constant, all at a distance R from the foot of the normal from the origin. Let the plane $x + y + z = 3na/\sqrt{2}$, in which the central molecule is moving, be at a perpendicular distance l from the plane of the c molecules. When these are arranged symmetrically at an angular spacing of $2\pi/c$, the mean potential on the circle $\xi =$ constant is c times the mean potential when only one is present, and this can be computed from the means of the inverse sixth and twelfth powers of the separation. The first of these is

$$\frac{(R^2 + l^2)^2 + (2l^2 + 4R^2)(\xi a)^2 + (\xi a)^4}{[(R^2 + l^2)^2 + 2(l^2 - R^2)(\xi a)^2 + (\xi a)^4]^{5/2}}$$

and the second is

$$\frac{(R^2 + l^2 + (\xi a)^2)[(R^2 + l^2)^4 + 4(R^2 + l^2)^2(6R^2 + l^2)(\xi a)^2 + (76R^4 + 52R^2l^2 + 67^4)(\xi a)^4 + 4(6R^2 + l^2)(\xi a)^6 + (\xi a)^8]}{[(R^2 + l^2)^2 + 2(l^2 - R^2)(\xi a)^2 + (\xi a)^{11/2}]}$$

As a check we may put $l = 0$, when the formulæ reduce to those given by Devonshire.[15]

For the neighbours of a (111) molecule we use the first three rings of neighbours in the face and the first two rings in the second layer of molecules in the lattice. With these formulæ we can calculate $\bar{P}(n, \xi) - \chi'(n)$ as a function of n and ξ for any value of the specific volume V/V_0. If,

---

[15] Devonshire *Proc. Roy. Soc. A*, 1937, **163**, 132.

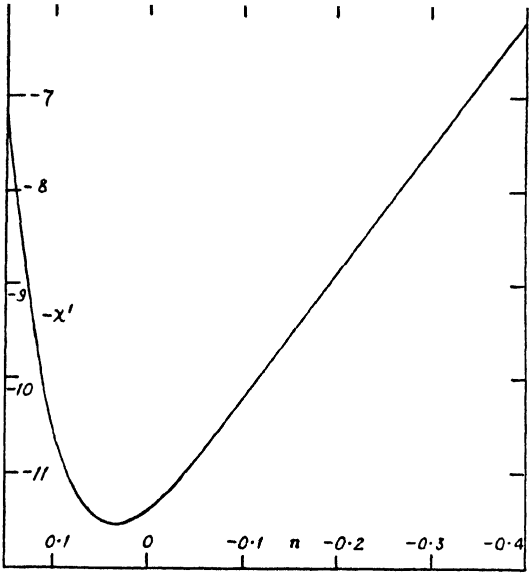

FIG. 1.—The potential energy $-\phi\chi'$ of a face molecule at $x = y = z = na/\sqrt{2}$, interacting with the face-centred cubic half-lattice $x + y + z > 0$. The other molecules of the (111) face are in their normal positions. $(V_0/V)^2 = 0{\cdot}9$.

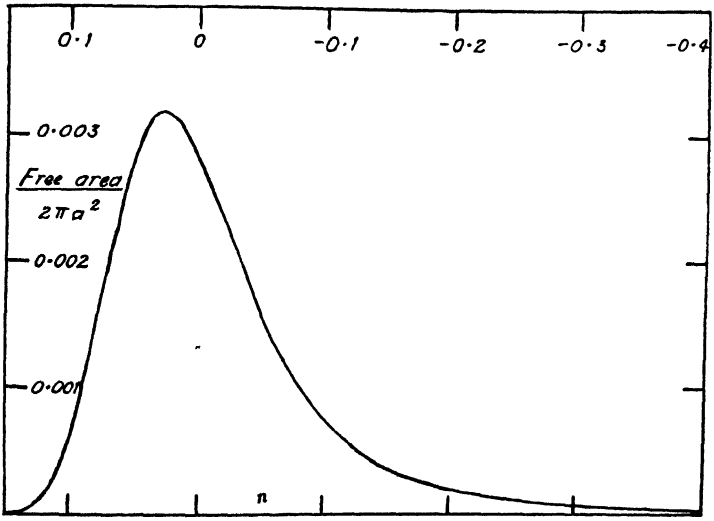

FIG. 2.—Free area available in plane $x + y + z = 3na/\sqrt{2}$ for a molecule of the (111) face. $(V_0/V)^2 = 0{\cdot}9$; $\phi/kT = 1{\cdot}317$.

further, we know ϕ/kT corresponding to this specific volume, we can compute

$$\int_0^\infty \xi \exp\,[\phi\{\bar{P}(n,\xi) - \chi'(n)\}/kT]\mathrm{d}\xi \qquad . \quad . \quad (14)$$

and then by a repetition with other values of n we obtain finally the free volume per molecule

$$V_s^* = \pi\sqrt{6}a^3\int_{-\infty}^{\infty}\exp[\phi\{\chi'(n) - \chi'(n_m)\}/kT]\ \mathrm{d}n\int_0^\infty \xi\,\exp[\phi\{\bar{P}(n,\xi) - \chi'(n)\}/kT]\mathrm{d}\xi \quad (15)$$

Our computation of (15) was carried out for

$$n = -\,0{\cdot}4\ (0{\cdot}1)\ -0{\cdot}1\ (0{\cdot}05)\ 0{\cdot}15$$

and additional values were interpolated. Nine sets of $(V/V_0,\ \phi/kT)$ were used. The function $\chi'(n)$ was computed for

$$n = -\ 0{\cdot}4\ (0{\cdot}1)\ -0{\cdot}1,\ -0{\cdot}5\ (0{\cdot}025)\ 0{\cdot}1,\ 0{\cdot}15 \text{ and } 0{\cdot}2,$$

and additional values were interpolated. Fig. 1 shows a typical $\chi'(n)$, this particular curve corresponding to rather more than the normal liquid density. Finally the surface free volume was computed from (15).

In Fig. 2 is shown the contribution of various planes to the surface free volume for $(V_0/V)^2 = 0{\cdot}9$; $\phi/kT = 1{\cdot}317$.

5. Calculation of the Surface Tension of a (110) Face.

Little need be said about the potential energy terms for this face, since the methods of calculation are precisely the same as have already been sketched for the (111) face. In particular, it is possible to verify the accuracy of large parts of the work by simple checks. The calculation of the surface free volume is, however, much more troublesome, owing to the low symmetry of the restraining field in which the molecule is moving ; another difficulty is the weakness of this field, so that the molecule can make embarrassingly large excursions from its equilibrium position. It is clearly insufficient to average the potential around a circle with centre at the equilibrium position, and one must compute a triple integral instead of the double integral sufficient for the (111) face. It would not be justified to go into the details of this computation, since it is found in the end that the surface tension would be higher than for the (111) face, and hence only the latter has physical significance. The difference in surface tensions is shown in Table V. The calculations were carried out for four values of the density of the lattice, with corresponding values of kT/ϕ from the paper by Lennard-Jones and Devonshire[8] on the vapour pressure of a liquid. The surface tensions depend on the free volume available to an internal molecule, and this dependence does not disappear completely when we consider the difference of the surface tensions. The

TABLE V.—COMPARISON OF PROPERTIES OF (111) AND (110) FACES OF THE FACE-CENTRED CUBIC

$(V_0/V)^2$.	ϕ/kT.	Difference of Surface Tensions.	V_s^*/V_f^* for (110).	(111).
0·8	1·067	0·1 ϕ/r_0^2	2·49	1·34
0·9	1·317	0·2 ,,	2·37	1·46
0·95	1·500	0·2 ,,	2·40	1·52
1·0	1·750	0·3 ,,	2·38	1·60

values of the internal free volume V_f^* were computed from the formulæ of Lennard-Jones and Devonshire (loc. cit.). The variation in V_s^*/V_f^* for the (110) face, shown in Table V, is less than the possible error of the computation, which must be expected to rise to a few per cent. at the end of the rather elaborate series of interpolations and integrations carried out. The sign of the difference of surface tensions is, however, clearly shown by computations even of this accuracy.

I am indebted to Prof. Sir John Lennard-Jones, F.R.S., for his continued encouragement of this work, to Prof. E. A. Guggenheim, F.R.S., for his helpful suggestions, and to the Chief Scientist, Ministry of Supply, for permission to publish this paper.

Summary.

Theoretical expressions for the surface tension of a liquid whose structure is approximately close-packed have been published by Lennard-Jones and Corner. In the present paper these formulæ are evaluated numerically and compared with experimental results for normal liquids. The theoretical surface tension is about 30 % too large and its temperature-dependence is in error by roughly the same amount. It seems probable that at least the former of these differences is due to the assumption of a close-packed liquid structure, which leads to an overestimate of the binding energy of the bulk liquid phase.

Appendix: The Values of kT_c/ϕ and V_c/V_0.

This survey is restricted to the substances with simple molecules and only small quantum corrections to the translational motion. The experimental data in Tables VI and VII are well known, and therefore references are made only to the sources of ϕ and V_0. The mean value of kT_c/ϕ is 1·29. The value of V_c/V_0 for krypton seems to be well out of line, and we neglect it in forming the mean, which is $V_c/V_0 = 3{\cdot}05$.

TABLE VI.—VALUES OF kT_c/ϕ

	Ne.	A.	N_2.	CH_4.
ϕ, in 10^{-14} ergs . .	0·501^a	1·647^a	1·307^b	1·95^c
T_c, °K.	44·7	150·7	126·0	190·7
kT_c/ϕ	1·23	1·26	1·33	1·35

TABLE VII.—VALUES OF V_c/V_0

	Ne.	A.	Kr.	Xe.	CO.	CH_4.	N_2.
V_c, cc./mole. .	41·7	75·25	92·1	114	93	98·6	90
V_0, cc./mole. .	13·4^a	24·7^a	28·0^d	37·5^d	30·3^d	32·7^c	29·6^b
V_c/V_0 . . .	3·11	3·05	3·29	3·04	3·07	3·02	3·04

SOURCES OF DATA—

a: derived from an analysis of second virial and low-pressure Joule-Thomson coefficients (Corner, *Trans. Faraday Soc.* (in press)).

b: Corner, *Trans. Faraday Soc.*, 1940, **36**, 780.

c: computed from gas isotherms of Kvalnes and Gaddy, *J. Amer. Chem. Soc.*, 1931, **53**, 394, and Joule-Thomson data of Budenholzer, Sage and Lacey, *Ind. Eng. Chem.*, 1939, **31**, 369.

d: derived from experimental lattice-spacing at low temperatures.

Armament Research Establishment,
Ministry of Supply.

REVIEWS OF BOOKS.

Newer Methods of Preparative Organic Chemistry. Translated and Revised from the German. (Interscience Publishers, Inc., New York, 1948). Pp. xiii + 657. Price 51s.

Most organic chemists knew *Neuere Methoden der präparativen organischen Chemie* which appeared in 1942, being reprinted in 1944, and which itself was a collection of articles published somewhat earlier in *Die Chemie.* The present work is rather more than a mere translation of the original work. It consists of revised translations of thirteen out of the seventeen original articles together with excellent compound and subject indexes.

Though the individual chapters have been the responsibility of different American translators, the quality of the resulting text is remarkably uniform and high, and successfully avoids giving the impression of a mere compilation. The level of present usefulness of these articles is, inevitably perhaps, less even ; they range from essays such as those on Raney Nickel Catalysts (R. Schröter), Hydrogen Fluoride in Organic Reactions (K. Wiechert) and Syntheses with Diazomethane (B. Eistert) which engage at least the interest, if not the practice, of all organic chemists, to articles such as that on Biochemical Oxidations and Reductions (F. G. Fischer) which are of more limited attraction. In respect of detail, the text appears to be satisfyingly free from errors, the few that have been noted, like " acenaphthene (XVIII) " for " acenaphthene (XVII) " (p. 7) being typographical and unlikely to lead to misunderstanding. The revision mostly consists of the addition of selected and mainly American references, and the opportunity might have been taken to bring the text more nearly and more completely up to date. The valuable method of desulphurisation by means of Raney nickel, for example, appears to have been awarded only one early reference and not a single example is cited. On the other hand the revision in, for example, the chapter on Boron Fluoride as Catalyst (D. Kastner) seems very satisfactory in its extent. The shortcomings of this book are, however, truly minor ones when considered together with more than six hundred pages tightly packed with so much information of preparative importance which is not to be found in the older texts ; matter which is so obvious and constant a feature of modern organic chemistry that its ready reference becomes the cause of some bewilderment. Well and durably produced as this book is, it is regrettably costly when it is recalled how rapid and continuous has been the development of " newer methods of preparative organic chemistry," and how that development is likely to be maintained in the coming years.

A. H. C.

Mechanical Behaviour of High Polymers. By TURNER ALFREY, Jr. (Interscience Publishers Inc. New York, 1948). Pp. xvi + 581. Price 57s.

The publication of Dr. Alfrey's book on mechanical properties of large polymers has been awaited with interest since its preparation was announced some time ago. This subject is probably the most difficult in high-polymer chemistry for it includes not only chemistry but much fundamental physics and even engineering. While a number of books have discussed the subject in relation to the more general problem of the strength and mechanical properties of materials, none has been devoted wholly to high-polymers. The subject is of vital importance for, in the end, the practical use of a high-polymer is governed far more by its physical than by its chemical properties. Yet the chemical properties determine the physical properties and consequently it is of the first importance to try and achieve as complete a correlation as possible. The problem is much more difficult than that in metallurgy, for the variety of physical behaviour exhibited by high-polymers is wider than that displayed by metals. The accumulation of data on high-polymers has now mounted to such an extent that even though inadequately complete, it is sufficient to justify a thorough discussion and appraisal by one who has been intimately concerned with both chemical and physical sides of the problems involved.

In the main design of the book the detailed chemistry of high-polymers has been wisely omitted for it is dealt with in other volumes of the series and, what is more important, this detail is not of predominant importance in the present discussion. The book is divided into five major sections, together with a discussion on the ultimate strength of high-polymers, a number of appendices describing the mathematical technique for dealing with stresses and strains and a short section on the methods of, but not the machines for, mechanical testing.

The first major section deals with those properties of matter particularly relevant to those belonging to high-polymers. It opens with a thorough discussion of the mathematics of elasticity ; it deals with the flow of Newtonian and non-Newtonian fluids. The behaviour of substances neither solid or liquid so characteristic of many high-polymers completes the section. With this preparation the systematic treatment follows and is based on the *general* structural characteristics of high-polymers rather than chemical constitution. Hence section two is devoted solely to the behaviour exhibited by amorphous linear high-polymers. Here there is comprehensive discussion of mechanical properties partly on the basis of springs and dashpots as the only presently available method of dealing with that kind of matter lying between solid and liquid phases. Once again the emphasis is on behaviour, illustrative examples being drawn from high-polymers of a number of types. Having dealt with the behaviour of assemblages of chains, section three is concerned with three-dimensional net-works not only of the compact type in which the number of cross-links is large, as in phenol-formaldehyde resins, but also of the vulcanised rubber type. In order to make this section reasonably complete some short account of the various methods of synthesising cross-linked polymers is given. The crystallisation of high-polymers and the mechanical behaviour of anisotropic material is discussed in section four, where particular emphasis is laid on fibre behaviour. Section five is shorter than the others. It deals on the one hand with the behaviour of plasticised high-polymer systems, and on the other, with the viscous properties of buffet high-polymer solutions. The thermodynamic approach to the problem is rightly excluded in view of the general thesis of the volume. Finally there is section five, a discussion of the vexed question of the ultimate strength of high-polymers, but again, mainly from the method of measuring the ultimate strength and less from its general discussion in relation to the strength of matter as a whole.

In a review with such a tremendous field to cover the author is beset by numerous difficulties. The volume of material is so large that it is extremely difficult to be critical and remain unbiased. When Dr. Alfrey realises this he does the only fair thing, and quotes verbatim from the author. The reader is then left to judge for himself. The book reveals only too well the wide gaps in knowledge in this division of science. There is, however, little doubt that the varieties of behaviour are now well recognised and it is plainly a task for the future to try and settle outstanding points by study of existing systems rather than multiply the number of systems simply for the sake of multiplication.

H. W. M.

Radioactive Tracers in Biology. An Introduction to Tracer Methodology. By MARTIN D. KAMEN. (New York: Academic Press, Inc., 1947). Price $5.80.

According to its title, Professor Kamen's book is meant for the instruction of those who want to use radioactive tracers in biological work; but this does not mean that biologists only can profit from it. Such research is usually carried out by teams which comprise, as collaborators of the biologists, chemists and physicists, and it seems that the book will be particularly useful for these scientific helpers in the common work; for it is written not so much from the point of view of the biological problems as of the technique to be applied in radioactive tracer work, whether biological or not. The introductory chapters on radioactivity, on the production of tracers, and on their measurement—which in parts do not differ much from other U.S. publications—will be found very helpful by any research worker who is new to the subject; the biological bias of Prof. Kamen's book becomes obvious only in the selection of his examples of tracer application many of which he could take from his own well-known research work.

The valuable book contains very few mistakes. As the author has already appended a brief list of Errata, the following additions to it may be found useful. Page 21, line 7 from bottom: the fission products of uranium extend from element 30 to 64; page 27, line 7 from bottom: the words "proton" and "neutron" should be interchanged; page 92, line 3 from top: the uncertainty of the curie is hardly half the value given; page 177, line 9 from top: the activity of a millicurie requires $1{\cdot}7 \times 10^{15}$ T atoms.

F. A. P.

The Chemistry of Acetylene and Related Compounds. By E. D. BERGMANN. (Interscience Publishers.) Pp. 108. Price 18s.

The book under review is based on three lectures delivered by Dr. Bergmann at the Polytechnic Institute of Brooklyn in the autumn of 1946. Its object is to provide an introduction to acetylene chemistry and to serve as an incentive to further study.

A brief account of the more important reactions of the simple acetylenic compounds is given, due emphasis being placed on recent developments.

Certain aspects of the subject are discussed at some length and the topics for such treatment are well selected. Thus a large section is devoted to the processes developed in recent years for the condensation of aldehydes and ketones with acetylene, and some of the applications of the products are described. The polymerisation of acetylene to vinylacetylene and cyclo-octatetraene, and an account of the more important reactions of these compounds, are also included. In fact, in the small space available, the author has succeeded in covering a surprisingly large amount of a very extensive field. This feature should render the book of value to those who require a short and readily assimilable account of the salient reactions and applications of acetylene.

An attempt is also made to indicate the theoretical aspects of some of the reactions described and to relate the chemical behaviour of acetylene " to its molecular structure as determined by the methods of physical chemistry." However, the present reviewer finds some of these sections to contain statements and conclusions with which he is unable to concur, and occasionally to lack the lucidity characteristic of the remainder of the text. Thus in the account of the anionotropic rearrangement of ethylenic acetylenic carbinols (p. 88), it is asserted both that " ethinyl alcohols . . . lead to carbonyl compounds," which is incomprehensible in this connection, and also that the ethinyl carbinols rearrange more rapidly than the corresponding vinyl compounds, which is incorrect (cf. Braude and Jones, *J. Chem. Soc.*, 1946, 128). Further it should be remembered that some of the reaction mechanisms suggested have little experimental verification, though, of course, they may be of value in indicating the directions in which further investigation may profitably be undertaken.

The reader will, however, find this book and the numerous references which it contains to the original literature, a useful introduction to the field of acetylene chemistry.

B. C. L. W.

Chemical and Electroplated Finishes. By H. SILMAN. (Chapman and Hall, London, 1948). Pp. xiii + 414. Price 30s. net.

In this book the author starts by describing clearly the effect of corrosion of the commoner metals and shows why the processes he describes are necessary. He then describes the processes of polishing, pickling, and cleaning in considerable detail, after which metal colouring and electroplating are dealt with. The section on electroplating covers most of the industrial processes and also deals with modern automatic plant. There is a chapter on finishing light alloys.

This book is clearly written and may be read by those with no special knowledge of the subject. It should appeal particularly to engineers, designers and executives who wish to decide on the most suitable methods to apply to their products.

A chapter on testing deposits is included, although it is felt that this is not as full as it might be, and it is hoped that the author may be able to expand this in a later edition.

The book contains some 400 pages, is fully illustrated and should prove of great interest to all who are concerned with metal finishing.

E. A. O.

Selected Values of Properties of Hydrocarbons. Circular C 461 of National Bureau of Standards, 1947. By F. D. Rossini, K. S. Pitzer and Others. (U.S. Government Printing Office, Washington, D.C.) Pp. 483. Price $2.75.

The review of the above book written by me was published in the May number of the *Transactions*. I have subsequently received a letter from Doctor Rossini in which he writes, "This is to thank you very much for sending me a copy of your review of our volume on *Selected Values of Properties of Hydrocarbons*, which is N.B.S. Circular 461. We are particularly glad to learn that your 'only criticisms relate to details of presentation.' As I see it, most of your points would have been taken care of if we had had time to prepare for the bound volume an appropriate list of definitions of the several symbols and terms used. What happened was that we had to meet a deadline date after which the funds for printing the bound volume would no longer have been available. Accordingly, we decided to concentrate on having all of the numerical data as nearly free of errors as possible and to forego the definitions."

Had this information been available at the time I wrote the review, I should not have included the remark, "All these small defects in the presentation suggest that the actual preparation of the tables may have been left too much in the hands of mere computers rather than experienced physical chemists."

E. A. G.

Proceedings of the Third International Electrodeposition Conference. (London : The Electrodepositors' Technical Society, 1948.) Pp. 219. Price 50s.

The Third International Electrodeposition Conference organised by the Electrodepositors' Technical Society, was held in London in 1947, and the present volume gives an account of the conference together with the papers presented and the accompanying discussions. It provides a useful cross-section of current interests and techniques in the electrolytic treatment of metals, and is particularly valuable inasmuch as the previous Conference was held in 1939 and the intervening war years have hindered the ready exchange of information. Of the twenty-four papers which are printed, four deal with the methods and applications of electrolytic polishing, and in this rapidly developing subject these authoritative articles—including one by Jacquet, the discoverer of the method—are especially welcome ; the discussion reveals the imperative need for further fundamental work on the scientific basis of the process. Some seven papers are concerned with the structure and properties of electrodeposited metals and show the steady, if slow, progress which is being made in this difficult field. Four papers deal with new plating processes and solutions, and these include a very full account of the electrodeposition of tungsten alloys. The remaining papers consist of descriptions of particular technical processes, surveys of plating practice in different countries, and an interesting account of the organisation of research projects sponsored by the American Electroplaters' Society. The Electrodepositors' Technical Society is to be congratulated on producing a useful and attractive record of a successful meeting.

A. H.

Transactions of the Faraday Society.

SUBJECT INDEX—VOLUME XLIV, 1948.

PAGE

Absorption and Fluorescence Spectra of Bivalent Samarium, Europium and Ytterbium. F. D. S. Butement 617
—— Cell, Wave-guide, Operating in the H_{01} Mode, Measurement of Absorption in Liquids at 1·2 cm. and 0·8 cm. Wavelength using a. J. G. Powles 537
—— Dielectric, The Effect of Molecular Inertia on. J. G. Powles . . . 802
—— in Liquids at 1·2 cm. and 0·8 cm. Wavelength using a Wave-guide Absorption Cell Operating in the H_{01} Mode, Measurement of. J. G. Powles 537
—— of Organic Vapours by Thin Films of Polystyrene, The. E. C. Baughan 495
—— Spectra of Butane undergoing Slow Combustion, The. Part II of: Observations on the Slow Combustion of Hydrocarbons. Sir Alfred Egerton and G. H. S. Young 750
—— Spectra of Peroxides, The. Part I of: Observations on the Slow Combustion of Hydrocarbons. Sir Alfred Egerton, E. J. Harris and G. H. S. Young 745
—— Spectra of Phenylated Anthracenes, The. Y. Hirshberg. . . . 285
—— Spectrum, Infra-Red, and Structure of Trioxane. D. A. Ramsay . . 289
—— Spectrum, Ultra-Violet, of Formaldehyde, A Note on the. A. J. Everett and G. J. Minkhoff 816
Acetaldehyde-Methyl Alcohol, The System. Part II of: Studies on Hemi-acetal Formation. I. Lauder 734
—— -Water, The System. Part I of: Studies on Hemi-acetal Formation. I. Lauder 729
Acetic Acid and Acetic Anhydride, Solvents, Kinetic Studies in the. Part I. Properties of the Solvo-system. H. A. E. Mackenzie and E. R. S. Winter 159
—— and Acetic Anhydride, Solvents, Kinetic Studies in the. Part II. The Thiele Acetylation of Benzoquinone and Toluquinone (Experimental). H. A. E. Mackenzie and E. R. S. Winter 171
—— and Acetic Anhydride, Solvents, Kinetic Studies in the. Part III. The Thiele Acetylation of Benzoquinone and Toluquinone (Theoretical). H. A. E. Mackenzie and E. R. S. Winter 243
Acetic Anhydride, Kinetic Studies in the Solvents Acetic Acid and. Part I. Properties of the Solvo-system. H. A. E. Mackenzie and E. R. S. Winter 159
—— Kinetic Studies in the Solvents Acetic Acid and. Part II. The Thiele Acetylation of Benzoquinone and Toluquinone (Experimental). H. A. E. Mackenzie and E. R. S. Winter 171
—— Kinetic Studies in the Solvents Acetic Acid and. Part III. The Thiele Acetylation of Benzoquinone and Toluquinone (Theoretical). H. A. E. Mackenzie and E. R. S. Winter 243
—— The Hydrolysis of. V. Gold 506
Acetylation, Thiele, of Benzoquinone and Toluquinone, The (Experimental) Part II of: Kinetic Studies in the Solvents Acetic Acid and Acetic Anhydride. H. A. E. Mackenzie and E. R. S. Winter . . . 171
—— Thiele, of Benzoquinone and Toluquinone, The (Theoretical). Part III of: Kinetic Studies in the Solvents Acetic Acid and Acetic Anhydride. H. A. E. Mackenzie and E. R. S. Winter 243
Acid Salts of Monocarboxylic Acids as *p*H Standards; Potassium Hydrogen Benzoate and Phenylacetate. N. Smith and J. C. Speakman . 1031
Adiabatic Systems, Reaction Kinetics of. M. Gordon. 196
Adsorption of Gases SO_2, NH_3, CO_2 and N_2O on BaF_2 Crystals, The. V. A. Crawford and F. C. Tompkins 698
—— Theory of Brunauer, Emmett and Teller, and Brunauer, Deming, Deming and Teller, An Examination of the. S. J. Gregg and J. Jacobs . 574
Aldehydes and Ketones, The Ionisation of Simple. Part II of: The Ionisation Potentials of Polyatomic Molecules. T. M. Sugden and W. C. Price 116
Alkyl Sulphates, Sodium, and Related Compounds, A New Method for the Rapid Titrimetric Analysis of. S. R. Epton. 226
Alloys, Magnesium-Indium, in the Region 20 to 50 Atomic per cent. of Indium, The Constitution of. G. V. Raynor 15

PAGE

Aluminium-Magnesium-Zinc, Equilibrium between $Al_2Mg_3Zn_3$ and the Primary Solid Solution in the System. G. V. Raynor and W. Hume-Rothery . . . 29

Ammonia, Carbon Dioxide, Nitrous Oxide and Sulphur Dioxide on BaF_2 Crystals, The Adsorption of the Gases. V. A. Crawford and F. C. Tompkins . . . 698

—— Metal-, Solutions, The Nature of. Part II. A. J. Birch and D. K. C. MacDonald . . . 735

Ammonium Nitrate, Interaction between Trinitrotoluene and. Part I of: Physico-Chemical Processes occurring at High Pressures and Temperatures. John L. Copp and A. R. Ubbelohde . . . 646

Amphiphilic Properties, Effect of Constitution on. Part VIII of: Hydrotropy, Solubilisation and Related Emulsification Processes. P. A. Winsor . . . 463

Amplifier for Use with Conductance Bridges, An. D. J. G. Ives and R. W. Pittman . . . 644

Analysis, Rapid Titrimetric, of Sodium Alkyl Sulphates and Related Compounds, A New Method for the. S. R. Epton . . . 226

Anions, Tetrahedral, The Application of the Orbital Valency Force Field to some. Part V of: Molecular Force Fields. D. F. Heath and J. W. Linnett . . . 884

Anodic Behaviour of Metals, The. Part V. Copper. A. Hickling and D. Taylor . . . 262

Anthracenes, Phenylated, The Absorption Spectra of. Y. Hirshberg. . . 285

Apparatus for the Measurement of Diffusion Rates, A Simple. A. H. W. Aten, Jun. and J. v. Dreve . . . 202

***d*-Arabinose,** *Bact. Lactis Aerogenes* and. The Training of Bacteria to New Carbon Sources. S. Jackson and C. N. Hinshelwood . . . 568

Argon, Intermolecular Forces in Neon and. J. Corner . . . 914

Arsenic Trichloride, Monophenylchlorarsine, Diphenylchlorarsine and Triphenylarsine, An Investigation of the Chemical Equilibria involving the Molecules. Alwyn G. Evans and Ernest Warhurst . . . 189

Atomic Positions from X-Ray Data, A New "Averaging" Method for the Location of. A. D. Booth . . . 282

Azulene Molecule, A Quantum Mechanical Investigation of the. Part I. R. D. Brown . . . 984

Bacterial Cells, Penetration of Proflavine into. S. Jackson and C. N. Hinshelwood . . . 527

Bact. Lactis, Aerogenes, and *d*-Arabinose. The Training of Bacteria to New Carbon Sources. S. Jackson and C. N. Hinshelwood . . . 568

—— The Dehydrogenase Activity of. A. M. James and C. N. Hinshelwood . 967

Barium Fluoride Crystals, The Adsorption of Gases SO_2, NH_3, CO_2 and N_2O on. V. A. Crawford and F. C. Tompkins . . . 698

Benzene and Ethylene Dichloride, The Use of Dilute Solutions of Thiophene in Benzene as Test Mixtures and a Comparison with Mixtures of. Part II of: Fractional Distillation. E. A. Coulson, J. L. Hales and E. F. G. Herington . . . 636

—— Molybdenum Oxide Catalysts for the Reduction of Phenol to. L. A. Woodward and A. T. Glover . . . 608

Benzoquinone and Toluquinone, The Thiele Acetylation of (Experimental). Part II of: Kinetic Studies in the Solvents Acetic Acid and Acetic Anhydride. H. A. E. Mackenzie and E. R. S. Winter. . . 171

—— and Toluquinone, The Thiele Acetylation of (Theoretical). Part III of: Kinetic Studies in the Solvents Acetic Acid and Acetic Anhydride. H. A. E. Mackenzie and E. R. S. Winter. . . 243

Benzoyl Peroxide—Catalysed Oxidation of Ethyl Linoleate, The. Part VI of: Kinetic Studies in the Chemistry of Rubber and Related Materials. J. L. Bolland . . . 669

Bonds, Carbon, The Energy of—A Re-examination of the Fox-Martin Rule. E. C. Baughan . . . 845

—— in the Phosphorus Molecule P_4. W. E. Moffitt . . . 987

Brass from Cyanide Solutions, Experiments on the Electrodeposition of. T. Banerjee and A. J. Allmand . . . 819

Butane, The Effect of Diluents and other Substances on the Slow Combustion of. Part III of: Observations on the Slow Combustion of Hydrocarbons. Sir Alfred Egerton and G. H. S. Young. . . 755

PAGE
Butane, Undergoing Slow Combustion, The Absorption Spectra of. Part II of: Observations on the Slow Combustion of Hydrocarbons. Sir Alfred Egerton and G. H. S. Young 750
Calcium Sulphate, Thermodynamics of the Conversion KCl $\rightarrow$ K_2SO_4 with the aid of. E. Abel and J. M. Fanto 97
Carbon Bonds, The Energy of—A Re-examination of the Fox-Martin Rule. E. C. Baughan 845
—— Dioxide, Nitrous Oxide, Sulphur Dioxide and Ammonia on BaF_2 Crystals, The Adsorption of the Gases. V. A. Crawford and F. C. Tompkins 698
—— Monoxide-Oxygen Mixtures. Part II of: The Mechanism of Spark Ignition. W. E. Frost and J. M. Linnett 416
—— Sources, The Training of Bacteria to New. *Bact. Lactis Aerogenes* and *d*-Arabinose. S. Jackson and C. N. Hinshelwood . . . 568
—— Tetrabromide Vapour, Emission Bands from the Electrodeless Discharge in. R. A. Durie and T. Iredale 806
Catalysts—Catalysed, Benzoyl Peroxide-, Oxidation of Ethyl Linoleate, The. Part VI of: Kinetic Studies in the Chemistry of Rubber and Related Materials. J. L. Bolland. 669
—— Metallic, The Absolute Rate of Conversion of Parahydrogen by. D. D. Eley 216
—— Molybdenum Oxide, for the Reduction of Phenol to Benzene. L. A. Woodward and A. T. Glover 608
Cataphoresis, Surface Conductance and. F. Booth 955
Cathode, Dropping-Mercury, The Reduction of Nitrocompounds at the. Part I, The Nitrobenzenes and Nitrotoluenes. J. Pearson . . 683
—— -Ray Polarograph, A. J. E. B. Randles 322
—— -Ray Polarograph, A. Part II. The Current-Voltage Curves. J. E. B. Randles 327
Cell for the Measurement of Diffusion in Aqueous Solution, A. J. C. Gage . 253
Cellophane, The Diffusion of Dyes through: The Anomalous Salt Effect. S. M. Neale 1027
Cells, Bacterial, Penetration of Proflavine into. S. Jackson and C. N. Hinshelwood 527
Cellulose and on Electrokinetic Equations, Notes on the Electrokinetic Potential of. A. S. Buchanan and E. Heymann. . . . 318
Chabazite, Mercury-, System, The. R. M. Barrer and M. Woodhead . . 1001
Changes of State in Films adsorbed at the Gas-Solid Interface, Detection of. S. J. Gregg and F. A. P. Maggs 123
β-Chloro-β′-Hydroxy Diethyl Sulphide, The Isolation of. The Replacement Reactions of β-β′-Dichlorodiethyl Sulphide and of Some Analogues in Aqueous Solution. A. G. Ogston, with (in part) E. R. Holiday, J. St. L. Philpot and L. A. Stocken . . . 45
Chlorsulphonic Acid, The Total Vapour Pressure of Mixtures of Sulphur Trioxide and. Part IV of: Studies in Vapour Pressure Measurement. E. W. Balson and N. K. Adam 412
Clays with Organic Compounds, Complexes of. Part I. Complex Formation between Montmorillonite and Halloysite and Certain Organic Liquids. D. M. C. MacEwan 349
—— with Organic Compounds, Complexes of. Part II. Investigation of the Ethylene Glycol-Water-Montmorillonite System using the Karl Fischer Reagent. R. C. Mackenzie 368
Coals with Methyl Alcohol, The Free and Total Energies of Interaction of. E. Dresel, M. Griffith and W. Hirst 992
Collagen Fibre, A Contribution to the Theory of the Structure of Protein Fibres with Special Reference to the so-called Thermal Shrinkage of the. (The late) Dorothy Jordan Lloyd and Marjorie Garrod . 441
Colloids, Colloidal Particles, On the Interaction of. Part II. Discussion of Basis of Theory. S. Levine 833
Combustion, Slow, of Hydrocarbons, A Note on the Decomposition of Hydrogen Peroxide and its Formation during the. E. J. Harris . . . 764
—— Slow, of Hydrocarbons Observations on the. Part I. The Absorption Spectra of Peroxides. Sir Alfred Egerton, E. J. Harris and G. H. S. Young 745
—— Slow, of Hydrocarbons, Observations on the. Part II. The Absorption Spectra of Butane undergoing Slow Combustion. Sir Alfred Egerton and G. H. S. Young 750

PAGE

Combustion, Slow, of Hydrocarbons, Observations on the. Part III. The Effect of Diluents and other Substances on the Slow Combustion of Butane. Sir Alfred Egerton and G. H. S. Young 755
—— Slow, Processes, The Oxidation of Sulphur Dioxide in. G. Whittingham 141
Complexes of Clays with Organic Compounds. Part I. Complex Formation between Montmorillonite and Halloysite and Certain Organic Liquids. D. C. M. MacEwan 349
—— of Clays with Organic Compounds. Part II. Investigation of the Ethylene Glycol-Water-Montmorillonite System using the Karl Fischer Reagent. R. C. Mackenzie 368
—— Pyridine, of Metallic Perchlorates. Part II. Dissociation Pressures and Pressure-Composition Isothermals of Copper Pyridine Perchlorates. P. C. Sinha and R. C. Ray 790
—— Starch-Iodine. Part I. G. A. Gilbert and J. V. R. Marriott. . . 84
Complex Formation between Montmorillonite and Halloysite and Certain Organic Liquids. Part I of: Complexes of Clays with Organic Compounds. D. M. C. MacEwan 349
— Formation, The Quenching of Fluorescence in Liquids by. Determination of the Mean Life of the Complex. G. Weber 185
— Ion Formation in Zinc Halide Solutions. Part XVI of: A Thermodynamic Study of Bivalent Metal Halides in Aqueous Solution. R. H. Stokes 137
Composition, Pressure-, Isothermals of Copper Pyridine Perchlorates, Dissociation Pressures and. Part II of: Pyridine Complexes of Metallic Perchlorates. P. C. Sinha and R. C. Ray 790
Conductance Bridges, An Amplifier for Use with. D. J. G. Ives and R. W. Pittman 644
—— Surface, and Cataphoresis. F. Booth. 955
Conductivity, Electrical, of Foam, The. N. O. Clark 13
—— Surface, Effect, The. Part IV of: The Electrophoresis of Suspended Particles. D. C. Henry 1021
—— Thermal, of Organic Materials near the Melting Point, The. J. H. Read and D. M. G. Lloyd 721
Co-operative Systems, Statistical Thermodynamics of. (A Generalisation of the Quasi-Chemical Method.) E. A. Guggenheim . . . 1007
Copper. Part V of: The Anodic Behaviour of Metals. A. Hickling and D. Taylor 262
—— -Pyridine Perchlorates, Dissociation Pressures and Pressure-Composition Isothermals of. Part II of: Pyridine Complexes of Metallic Perchlorates. P. C. Sinha and R. C. Ray 790
Critical Temperature Factor, T_c^3 for some Non-Linear Molecules, The Additivity of the. L. Grunberg and A. H. Nissan 1013
Crystals, BaF_2, The Adsorption of Gases SO_2, NH_3, CO_2 and N_2O on. V. A. Crawford and F. C. Tompkins 698
Crystalline Materials, Distribution Functions and. A. D. Booth . . . 37
Cyanide Solutions, Experiments on the Electrodeposition of Brass from. T. Banerjee and A. J. Allmand 719
Cyclobutane, Application to: Thermodynamic Functions of the Quartic Oscillator. T. L. Cottrell 716
Cyclo-Octatetraene in Relation to Structure, On Some Properties of. R. C. Pink and A. R. Ubbelohde. 708
Decomposition, Boiling and Explosion of Trinitrotoluene at High Temperatures, The. A. J. B. Robertson 977
—— of Hydrogen Peroxide and the Possibility of its Formation during the Slow Combustion of Hydrocarbons, A Note on the. E. J. Harris . . 764
—— Thermal, of Disilane and Trisilane, The. K. Stokland 545
—— Thermal, of Explosives, The. Part I. Ethylenedinitramine and Tetryl. A. J. B. Robertson 677
—— Thermal, of Silver Oxalate. F. C. Tompkins 206
Degradation of Long-chain Molecules, On the. Part II. H. H. G. Jellinek 345
Dehydrogenase Activity of *Bact. Lactis Aerogenes*, The. A. M. James and C. N. Hinshelwood 967
Detonation, The Effect of " Inert " Components on. Part II of: Physico-Chemical Processes occurring at High Pressures and Temperatures. John L. Copp and A. R. Ubbelohde. 658
β-β′-Dichlorodiethyl Sulphide and of Some Analogues in Aqueous Solution, The Replacement Reactions of: the Isolation of β-Chloro-β′-Hydroxy Diethyl Sulphide. A. G. Ogston, with (in part) E. R. Holiday, J. St. L. Philpot and L. A. Stocken 45

PAGE

Dielectric Absorption, The Effect of Molecular Inertia on. J. G. Powles. 802

—— Constant, Static, General Theory of the. H. Fröhlich. 238

—— Constant, The Salting-out Effect and. J. O'M. Bockris and Harold Egan 151

Diesters, Monolayers of Some. J. T. Davies 909

Diethyl Ether using the Heavy Oxygen Isotope as a Tracer Element, The Mechanism of Formation of. I. Lauder and J. H. Green 808

Differential Analyser to a Problem in Chemical Kinetics, The Application of the. A. M. Wood, J. Crank and G. H. Twigg. 256

Diffusion in Aqueous Solution, A Cell for the Measurement of. J. C. Gage 253

—— of Dyes through Cellophane, The: The Anomalous Salt Effect. S. M. Neale 1027

—— Rates, A Simple Apparatus for the Measurement of. A. H. W. Aten, Jun. and J. v. Dreve 202

—— Reactions, Surface, A Note on the Theory of. F. Booth 796

Diphenylchlorarsine, Triphenylarsine, Arsenic Trichloride and Monophenylchlorarsine, An Investigation of the Chemical Equilibria involving the Molecules. Alwyn G. Evans and Ernest Warhurst 189

Discharge, Electrodeless, in Carbon Tetrabromide Vapour, Emission Bands from the. R. A. Durie and T. Iredale 806

Disilane and Trisilane, The Thermal Decomposition of. K. Stokland. 545

Dispersion of the Gas Phase in Foam, The Degree of. N. O. Clark and M. Blackman 1

Dissociation Constant, Second, of Magnesium Hydroxide, The. D. I. Stock and C. W. Davies 856

—— Pressures and Pressure-Composition Isothermals of Copper Pyridine Perchlorates. Part II of: Pyridine Complexes of Metallic Perchlorates. P. C. Sinha and R. C. Ray 790

Distribution Functions and Crystalline Materials. A. D. Booth 37

Dropping-Mercury Cathode, The Reduction of Nitrocompounds at the. Part I. The Nitrobenzenes and Nitrotoluenes. J. Pearson 683

Dust and Smoke, The Action and Design of Mechanical Filters for. E. A. B. Birse and (the late) J. K. Roberts 273

Dyes through Cellophane, The Diffusion of: The Anomalous Salt Effect. S. M. Neale 1027

Electrodeless Discharge in Carbon Tetrabromide Vapour, Emission Bands from the. R. A Durie and T. Iredale 806

Electrodeposition of Brass from Cyanide Solutions, Experiments on the. T. Banerjee and A. J. Allmand 819

Electrokinetic Equations, Notes on the Electrokinetic Potential of Cellulose and on. A. S. Buchanan and E. Heymann 318

—— Potential of Cellulose and on Electrokinetic Equations, Notes on the. A. S. Buchanan and E. Heymann 318

Electrolytes, 2 : 1 and 1 : 2, at 25°, and Discussion of Results, Revision of Data for all. Part XVII of: A Thermodynamic Study of Bivalent Metal Halides in Aqueous Solution. R. H. Stokes 295

Electron Diffraction and Rectification from Silicon and Pyrite Surfaces. J. M. Cowley and J. L. Symonds 53

—— by Fatty Acid Layers on Metal Surfaces. J. M. Cowley 60

Electrophoresis of Suspended Particles, The. Part IV. The Surface Conductivity Effect. D. C. Henry 1021

Emission Bands from the Electrodeless Discharge in Carbon Tetrabromide Vapour. R. A. Durie and T. Iredale 806

Emulsification Processes, Hydrotropy, Solubilisation and Related. Parts I-IV. P. A. Winsor 376

—— Processes, Hydrotropy, Solubilisation and Related. Part V. Solubilisation in Ethylene Glycol. P. A. Winsor 451

—— Processes, Hydrotopy, Solubilisation and Related. Part VI. Effect of Temperature on the Solubilisation of Liquids. P. A. Winsor. 455

—— Processes, Hydrotropy, Solubilisation and Related. Part VII. Solubilisation of Solids, Freezing Point Depression Effects in Solubilised Systems. P. A. Winsor 459

—— Processes, Hydrotropy, Solubilisation and Related. Part VIII. Effect of Constitution on Amphiphilic Properties. P. A. Winsor 463

Energy, Energies of Interaction, Free and Total, of Coals with Methyl Alcohol, The. E. Dresel, M. Griffith and W. Hirst 992

—— of Carbon Bonds, The—A Re-examination of the Fox-Martin Rule. E. C. Baughan 845

PAGE

Equilibria, Chemical, involving the Molecules Arsenic Trichloride, Monophenylchlorarsine, Diphenylchlorarsine and Triphenylarsine, An Investigation of the. Alwyn G. Evans and Ernest Warhurst . . 189

Equilibrium between $Al_2Mg_3Zn_3$ and the Primary Solid Solution in the System Aluminium-Magnesium-Zinc. G. V. Raynor and W. Hume-Rothery 29

Esters, Some High Boiling, The Vapour Pressure of. P. A. Small, K. W. Small and P. Cowley 810

Ethylene Dichloride, The Use of Dilute Solutions of Thiophene in Benzene as Test Mixtures and a Comparison with Mixtures of Benzene and. Part II of: Fractional Distillation. E. A. Coulson, J. L. Hales and E. F. G. Herington 636

—— -dinitramine and Tetryl. Part I of: The Thermal Decomposition of Explosives. A. J. B. Robertson 677

—— Glycol, Solubilisation in. Part V of: Hydrotropy, Solubilisation and Related Emulsification Processes. P. A. Winsor 451

—— Glycol-Water-Montmorillonite System using the Karl Fischer Reagent, Investigation of the. Part II of: Complexes of Clays with Organic Compounds. R. C. Mackenzie 368

—— Oxide, The Hydration of. H. J. Lichtenstein and G. H. Twigg . . 905

Ethyl Linoleate, The Benzoyl Peroxide-Catalysed Oxidation of. Part VI of: Kinetic Studies in the Chemistry of Rubber and Related Materials. J. L. Bolland 669

Europium, Ytterbium and Samarium, Absorption and Fluorescence Spectra of Bivalent. F. D. S. Butement 617

Explosives Explosion of Trinitrotoluene at High Temperatures, The Decomposition, Boiling and. A. J. B. Robertson 977

—— The Thermal Decomposition of. Part I. Ethylenedinitramine and Tetryl. A. J. B. Robertson 677

Fatty Acid Layers on Metal Surfaces, Electron Diffraction by. J. M. Cowley 60

Fibres, Protein, with Special Reference to the so-called Thermal Shrinkage of the Collagen Fibre, A Contribution to the Theory of the Structure of. (The late) Dorothy Jordan Lloyd and Marjorie Garrod. . . . 441

Fibre, Wool, On the Cause of the Frictional Difference of the. K. Rachel Makinson 279

Films adsorbed at the Gas-Solid Interface, Detection of Changes of State in. S. J. Gregg and F. A. P. Maggs 123

—— Thin, of Polystyrene, The Absorption of Organic Vapours by. E. C. Baughan 495

Filters, Mechanical, for Smoke and Dust, The Action and Design of. E. A. B. Birse and (the late) J. K. Roberts. 273

Flame Speeds in Gaseous Mixtures, The Determination of. S. Sherratt and J. W. Linnett 596

—— Transient, The Measurement of Ionisation in a. E. R. Andrew, D. W. E. Axford and T. M. Sugden 427

Fluorescence in Liquids by Complex Formation, The Quenching of. Determination of the Mean Life of the Complex. G. Weber . . . 185

—— Spectra of Bivalent Samarium, Europium and Ytterbium, Absorption and. F. D. S. Butement 617

—— Studies on Quenching of. Part I. A Contribution to the Theory of Quenching of Fluorescence. K. Weber and M. Lokar. . . . 959

Foam, The Degree of Dispersion of the Gas Phase in. N. O. Clark and M. Blackman 1

—— The Electrical Conductivity of. N. O. Clark. 13

—— The Transmission of Light through. N. O. Clark and M. Blackman . 7

—— under Shear, On the Transformation of "Solid" Foam to a "Fluid." M. Blackman 205

Force Constants of Some OH and NH Links, The. R. E. Richards . . 40

—— Fields, Molecular. Part I. The Structure of the Water Molecule. D. F. Heath and J. W. Linnett 556

—— Fields, Molecular. Part II. The Force Fields of the Tetrahalides of the Group IV Elements. D. F. Heath and J. W. Linnett 561

—— Fields, Molecular. Part III. The Vibration Frequencies of some Planar XY Molecules. D. F. Heath and J. W. Linnett 873

—— Fields, Molecular. Part IV. The Application of the Orbital Valency Force-Field to Tetrahedral Halides. D. F. Heath and J. W. Linnett 878

—— Fields, Molecular. Part V. The Application of the Orbital Valency Force Field to some Tetrahedral Anions. D. F. Heath and J. W. Linnett 884

PAGE

Formaldehyde, A Note on the Ultra-Violet Absorption Spectrum of. A. J. Everett and G. J. Minkoff 816
Fox-Martin Rule, The Energy of Carbon Bonds—A Re-examination of the. E. C. Baughan 845
Fractionation, Fractional Distillation. Part I. The Selection of Test Mixtures for Estimating the Efficiency of Fractionating Columns. E. A. Coulson and E. F. G. Herington 629
—— Fractional Distillation. Part II. The Use of Dilute Solutions of Thiophene in Benzene as Test Mixtures and a Comparison with Mixtures of Benzene and Ethylene Dichloride. E. A. Coulson, J. L. Hales and E. F. G. Herington 636
—— Fractionating Columns, The Selection of Test Mixtures for Estimating the Efficiency of. Part I of: Fractional Distillation. E. A. Coulson and E. F. G. Herington 629
Free and Total Energies of Interaction of Coals with Methyl Alcohol, The. E. Dresel, M. Griffith and W. Hirst 992
—— Energies of Formation, Standard, of Gaseous Compounds, The: A Group Method of Summation. J. G. M. Bremner and G. D. Thomas . 230
—— Radicals $CH_2(CH)_{2m-1}CH_2$, The. W. E. Moffitt and C. A. Coulson . 81
Freezing Point Depression Effects in Solubilised Systems, Solubilisation of Solids. Part VII of: Hydrotropy, Solubilisation and Related Emulsification Processes. P. A. Winsor 459
Frictional Difference of the Wool Fibre, On the Cause of the. K. Rachel Makinson 279
Gases—Gaseous Mixtures, The Determination of Flame Speeds in. S. Sherratt and J. W. Linnett 596
—— Gaseous Organic Compounds, The Standard Free Energies of: A Group Method of Summation. J. G. M. Bremner and G. D. Thomas . 230
—— SO_2, NH_3, CO_2 and N_2O on BaF_2 Crystals, The Adsorption of. V. A. Crawford and F. C. Tompkins 698
—— The Mercury Meniscus in Precision Measurements on. R. Whytlaw-Gray and N. Teich 774
Gas-Phase in Foam, The Degree of Dispersion of the. N. O. Clark and M. Blackman 1
Gas-Solid Interface, Detection of Changes of State in Films adsorbed at the. S. J. Gregg and F. A. P. Maggs 123
Gilfillan-Polanyi Micropyknometer, Some Notes on the. I. Lauder . . 78
Glucose by Periodate, The Mechanism of the Oxidation of. G. Hughes and T. P. Nevell 941
Group IV Elements, The Force Fields of the Tetrahalides of the. Part II of: Molecular Force Fields. D. F. Heath and J. W. Linnett . . 561
—— Method of Summation, The Standard Free Energies of Formation of Gaseous Organic Compounds: A. J. G. M. Bremner and G. D. Thomas . 230
Halides, Tetrahedral, The Application of the Orbital Valency Force Field to. Part IV of: Molecular Force Fields. D. F. Heath and J. W. Linnett 878
Halloysite and Certain Organic Liquids, Complex Formation between Montmorillonite and. Part I of: Complexes of Clays with Organic Compounds. D. M. MacEwan 349
Heavy Oxygen Isotope ^{18}O as a Tracer Element, The Mechanism of Formation of Diethyl Ether using the. I. Lauder and J. H. Green . . 808
Hemiacetal Formation, Studies on. Part I. The System Acetaldehyde-Water. I. Lauder 729
—— Formation, Studies on. Part II. The System Acetaldehyde-Methyl Alcohol. I. Lauder 734
H_{01} **Mode,** Measurement of Absorption in Liquids at 1·2 cm. and 0·8 cm. Wave-length using a Wave-guide Absorption Cell Operating in the. J. G. Powles 537
Hydration of Ethylene Oxide, The. H. J. Lichtenstein and G. H. Twigg . 905
Hydrocarbons, A Note on the Decomposition of Hydrogen Peroxide and the Possibility of its Formation during the Slow Combustion of. E. J. Harris 764
—— Observations on the Slow Combustion of. Part I. The Absorption Spectra of Peroxides. Sir Alfred Egerton, E. J. Harris and G. H. S. Young 745
—— Observations on the Slow Combustion of. Part II. The Absorption Spectra of Butane undergoing Slow Combustion. Sir Alfred Egerton and G. H. S. Young 750

PAGE

Hydrocarbons, Observations on the Slow Combustion of. Part III. The Effect of Diluents and other Substances on the Slow Combustion of Butane. Sir Alfred Egerton and G. H. S. Young 755

Hydrogen Overpotential in Methanolic Solution. Part V of: Studies in Electrolytic Polarisation. J. O'M. Bockris and R. Parsons . . 860

—— Overpotential, The Effect of the Solvent on the. Part IV (ii) of: Studies in Electrolytic Polarisation. J. O'M. Bockris and S. Ignatowicz . 519

—— -Oxygen Mixtures, Effect of Adding Organic Vapours to. Part III of: The Mechanism of Spark Ignition. W. E. Frost and J. W. Linnett 421

—— Peroxide and the Possibility of its Formation during the Slow Combustion of Hydrocarbons, A Note on the Decomposition of. E. J. Harris 764

—— Peroxide in Aqueous Solution, The Photo-reaction between Iodine and. J. G. Bennett and R. O. Griffith 471

—— Sulphide, Introduction and the Ionisation Potentials of Water and. Part I of: The Ionisation Potentials of Polyatomic Molecules. W. C. Price and T. M. Sugden 108

Hydrolysis of Acetic Anhydride, The. V. Gold 506

Hydrotropy, Solubilisation and Related Emulsification Processes. Parts I-IV. P. A. Winsor 376

—— Solubilisation and Related Emulsification Processes. Part V. Solubilisation in Ethylene Glycol. P. A. Winsor 451

—— Solubilisation and Related Emulsification Processes. Part VI. Effect of Temperature on the Solubilisation of Liquids. P. A. Winsor. . 455

—— Solubilisation and Related Emulsification Processes. Part VII. Solubilisation of Solids, Freezing Point Depression Effects in Solubilised Systems. P. A. Winsor 459

—— Solubilisation and Related Emulsification Processes. Part VIII. Effect of Constitution on Amphiphilic Properties. P. A. Winsor . . 463

Indium, The Constitution of the Magnesium-Indium Alloys in the Region of 20 to 50 Atomic per cent. of. G. V. Raynor 15

Inertia, Molecular, on Dielectric Absorption, The Effect of. J. G. Powles . 802

Infra-Red Absorption Spectrum and Structure of Trioxane. D. A. Ramsay 289

—— Frequencies, Characteristic, and Chemical Properties of Molecules. M. St. C. Flett 767

Inhibition and Retardation in Polymerisation Reactions. H. W. Melville and W. F. Watson 886

Interface, Gas-Solid, Detection of Changes of State in Films adsorbed at the. S. J. Gregg and F. A. P. Maggs 123

Intermolecular Forces, The Calculation of Surface Tension from. Part II. Numerical Results. J. Corner 1036

—— Potentials in Neon and Argon. J. Corner 914

Iodine and Hydrogen Peroxide in Aqueous Solution, The Photo-reaction between. J. G. Bennett and R. O. Griffith 471

—— Starch-, Complexes. Part I. G. A. Gilbert and J. V. R. Marriott . . 84

Ionisation in a Transient Flame, The Measurement of. E. R. Andrew, D. W. E. Axford and T. M. Sugden 427

—— Potentials of Polyatomic Molecules, The. Part I. Introduction and the Ionisation Potentials of H_2O and H_2S. W. C. Price and T. M. Sugden 108

—— Potentials of Polyatomic Molecules, The. Part II. The Ionisation of Simple Aldehydes and Ketones. T. M. Sugden and W. C. Price 116

Isothermals, Pressure-Composition, of Copper Pyridine Perchlorates, Dissociation Pressures and. Part II of: Pyridine Complexes of Metallic Perchlorates. P. C. Sinha and R. C. Ray 790

Isotope ^{18}O as a Tracer Element, The Mechanism of Formation of Diethyl Ether using the Heavy Oxygen. I. Lauder and J. H. Green. . 808

Karl Fischer Reagent, Investigation of the Ethylene Glycol-Water-Montmorillonite System using the. Part II of: Complexes of Clays with Organic Compounds. R. C. Mackenzie 368

Ketones, The Ionisation of Simple Aldehydes and. Part II of: The Ionisation Potentials of Polyatomic Molecules. T. M. Sugden and W. C. Price 116

Kinetics, Chemical, The Application of the Differential Analyser to a Problem in. A. M. Wood, J. Crank and G. H. Twigg 256

—— of Open Reaction Systems, The. K. G. Denbigh, Margaret Hicks and F. M. Page 479

PAGE

Kinetics, Reaction, of Adiabatic Systems. M. Gordon 196
Kinetic Studies in the Chemistry of Rubber and Related Materials. Part VI. The Benzoyl Peroxide-Catalysed Oxidation of Ethyl Linoleate. J. L. Bolland 669
—— Studies in the Solvents Acetic Acid and Acetic Anhydride. Part I. Properties of the Solvo-system. H. A. E. Mackenzie and E. R. S. Winter 159
—— Studies in the Solvents Acetic Acid and Acetic Anhydride. Part II. The Thiele Acetylation of Benzoquinone and Toluquinone (Experimental). H. A. E. Mackenzie and E. R. S. Winter 171
—— Studies in the Solvents Acetic Acid and Acetic Anhydride. Part III. The Thiele Acetylation of Benzoquinone and Toluquinone (Theoretical). H. A. E. Mackenzie and E. R. S. Winter 243
Layers, Fatty Acid, on Metal Surfaces, Electron Diffraction by. J. M. Cowley 60
Light through Foam, The Transmission of. N. O. Clark and M. Blackman. 7
Liquids, An Interpretation of the Viscosity of. R. C. L. Bosworth. . . . 308
Magnesium Hydroxide, The Second Dissociation Constant of. D. I. Stock and C. W. Davies 856
—— Indium Alloys in the Region 20 to 50 Atomic per cent. of Indium, The Constitution of. G. V. Raynor 15
—— -Zinc, Aluminium-, Equilibrium between $Al_2Mg_3Zn_3$ and the Primary Solid Solution in the System. G. V. Raynor and W. Hume-Rothery 29
Mean Life of the Complex, Determination of the. The Quenching of Fluorescence in Liquids by Complex Formation. G. Weber. . . . 185
Melting Point, The Thermal Conductivity of Organic Materials near the. J. H. Read and D. M. G. Lloyd 721
Meniscus, Mercury, in Precision Measurements on Gases, The. R. Whytlaw-Gray and N. Teich 774
Mercury-Chabazite System, The. R. M. Barrer and M. Woodhead . . . 1001
—— Meniscus in Precision Measurements on Gases, The. R. Whytlaw-Gray and N. Teich 774
Metal-Ammonia Solutions, The Nature of. Part II. A. J. Birch and D. K. C. MacDonald 735
—— Bivalent, Halides in Aqueous Solution, A Thermodynamic Study of. Part XVI. Complex Ion Formation in Zinc Halide Solutions. R. H. Stokes 137
—— Bivalent, Halides in Aqueous Solution, A Thermodynamic Study of. Part XVII. Revision of Data for all 2 : 1 and 1 : 2 Electrolytes at 25°, and Discussion of Results. R. H. Stokes 295
—— Surfaces, Electron Diffraction by Fatty Acid Layers on. J. M. Cowley 60
Metallic Catalysts, The Absolute Rate of Conversion of Parahydrogen by. D. E. Eley. 216
—— Perchlorates, Pyridine Complexes of. Part II. Dissociation Pressures and Pressure-Composition Isothermals of Copper Pyridine Perchlorates. P. C. Sinha and R. C. Ray 790
Metals, The Anodic Behaviour of. Part V. Copper. A. Hickling and D. Taylor 262
Methyl Alcohol, Methanolic Solution, Hydrogen Overpotential in. Part V of: Studies in Electrolytic Polarisation. J. O'M. Bockris and R. Parsons 860
—— Acetaldehyde-, The System. Part II of: Studies on Hemiacetal Formation. I. Lauder 734
—— The Free and Total Energies of Interaction of Coals with. E. Dresel, M. Griffith and W. Hirst 992
Micropyknometer, Gilfillan-Polanyi, Some Notes on the. I. Lauder . . 78
Molecular Distillation and Sublimation. P. C. Carman 529
—— Force Fields. Part I. The Structure of the Water Molecule. D. F. Heath and J. W. Linnett 556
—— Force Fields. Part II. The Force Fields of the Tetrahalides of the Group IV Elements. D. F. Heath and J. W. Linnett 561
—— Force Fields. Part III. The Vibration Frequencies of some Planar XY Molecules. D. F. Heath and J. W. Linnett 873
—— Force Fields. Part IV. The Application of the Orbital Valency Force Field to Tetrahedral Halides. D. F. Heath and J. W. Linnett . 878
—— Force Fields. Part V. The Application of the Orbital Valency Force Field to some Tetrahedral Anions. D. F. Heath and J. W. Linnett. . 884

PAGE

Molybdenum Oxide Catalysts for the Reduction of Phenol to Benzene. L. A. Woodward and A. T. Glover 608
Monocarboxylic Acids, Acid Salts of, as *p*H Standards; Potassium Hydrogen Benzoate and Phenylacetate. N. Smith and J. C. Speakman. . 1031
Monolayers of Some Diesters. J. T. Davies 909
—— Thermodynamics of. C. Kemball, E. K. Rideal and E. A. Guggenheim. 948
Monophenylchlorarsine, Diphenylchlorarsine, Triphenylarsine and Arsenic Trichloride, An Investigation of the Chemical Equilibria involving the Molecules. Alwyn G. Evans and Ernest Warhurst. . . 189
Montmorillonite and Halloysite and Certain Organic Liquids, Complex Formation between. Part I of: Complexes of Clays with Organic Compounds. D. M. C. MacEwan 349
—— Ethylene Glycol-Water-, System using the Karl Fischer Reagent, Investigation of the. Part II of: Complexes of Clays with Organic Compounds. R. C. Mackenzie 368
Neon and Argon, Intermolecular Forces in. J. Corner. 914
NH Links, The Force Constants of Some OH and. R. E. Richards . . 40
Orbital Valency Force Field to some Tetrahedral Anions, The Application of the. Part V of: Molecular Force Fields. D. F. Heath and J. W. Linnett 884
—— Force Fields to Tetrahedral Halides, The Application of the. Part IV of: Molecular Force Fields. D. F. Heath and J. W. Linnett . . 878
Organic Compounds, Complexes of Clays with. Part I. Complex Formation between Montmorillonite and Halloysite and Certain Organic Liquids. D. M. C. MacEwan 349
—— Compounds, Complexes of Clays with. Part II. Investigation of the Ethylene Glycol-Water-Montmorillonite System using the Karl Fischer Reagent. R. C. Mackenzie. 368
—— Compounds, Gaseous, The Standard Free Energies of Formation of: A Group Method of Summation. J. G. M. Bremner and G. D. Thomas 230
—— Materials near the Melting Point, The Thermal Conductivity of. J. H. Read and D. M. G. Lloyd 721
—— Vapours by Thin Films of Polystyrene, The Absorption of. E. C. Baughan 495
—— Vapours to Hydrogen-Oxygen Mixtures, Effect of adding. Part III of: The Mechanism of Spark Ignition. W. E. Frost and J. W. Linnett 421
Overpotential, Hydrogen, in Methanolic Solution. Part V of: Studies in Electrolytic Polarisation. J. O'M. Bockris and R. Parsons . . 860
—— Hydrogen, The Effect of the Solvent on the. Part IV (ii) of: Studies in Electrolytic Polarisation. J. O'M. Bokris and S. Ignatowicz. . 519
Oxidation of Glucose by Periodate, The Mechanism of the. G. Hughes and T. P. Nevell 941
—— of Sulphur Dioxide in Slow Combustion Processes, The. G. Whittingham 141
—— -Reduction Potentials, A Feedback Potentiometer for the Measurement of *p*H Values and. C. Morton 588
Oxygen, Carbon Monoxide-, Mixtures. Part II of: The Mechanism of Spark Ignition. W. E. Frost and J. W. Linnett 416
—— Heavy, Isotope ^{18}O as a Tracer Element, The Mechanism of Formation of Diethyl Ether using the. I. Lauder and J. H. Green . . . 808
—— Hydrogen-, Mixtures, Effect of adding Organic Vapours to. Part III of: The Mechanism of Spark Ignition. W. E. Frost and J. W. Linnett 421
Parahydrogen by Metallic Catalysts, The Absolute Rate of Conversion of. D. D. Eley. 216
Perchlorates, Metallic, Pyridine Complexes of. Part II. Dissociation Pressures and Pressure-Composition Isothermals of Copper Pyridine Perchlorates. P. C. Sinha and R. C. Ray 790
Periodate, The Mechanism of the Oxidation of Glucose by. G. Hughes and T. P. Nevell 941
Peroxides, The Absorption Spectra of. Part I of: Observations on the Slow Combustion of Hydrocarbons. Sir Alfred Egerton, E. J. Harris and G. H. S. Young 745
Phenol to Benzene, Molybdenum Oxide Catalysts for the Reduction of. L. A. Woodward and A. T. Glover 608
Phenyl Acetate, Acid Salts, of Monocarboxylic Acids as *p*H Standards; Potassium Hydrogen Benzoate and. N. Smith and J. C. Speakman . 1031

PAGE

Phenylated Anthracenes, The Absorption Spectra of. Y. Hirshberg . . 285

Phosphorus Molecule P_4, Bonds in the. W. E. Moffitt. 987

Photo-reactions between Iodine and Hydrogen Peroxide in Aqueous Solution, The. J. G. Bennett and R. O. Griffith 471

pH Standards, Acid Salts of Monocarboxylic Acids as; Potassium Hydrogen Benzoate and Phenylacetate. N. Smith and J. C. Speakman. . 1031

—— Values and Oxidation-Reduction Potentials, A Feedback Potentiometer for the Measurement of. C. Morton 588

Polarisation, Electrolytic, Studies in. Part IV (ii). The Effect of the Solvent on the Hydrogen Overpotential. J. O'M. Bockris and S. Ignatowicz 519

—— Electrolytic, Studies in. Part V. Hydrogen Overpotential in Methanolic Solution. J. O'M. Bockris and R. Parsons. 860

Polarograph, A Cathode Ray. J. E. B. Randles. 322

—— A Cathode Ray. Part II. The Current-Voltage Curves. J. E. B. Randles 327

Polymerisation Reactions, Inhibition and Retardation in. H. W. Melville and W. F. Watson 886

Polystyrene, The Absorption of Organic Vapours by Thin Films of. E. C. Baughan 495

Potassium Chloride to Potassium Sulphate with the aid of $CaSO_4$, Thermodynamics of the Conversion of. E. Abel and J. M. Fanto . . 97

—— Hydrogen Benzoate and Phenylacetate, Acid Salts of Monocarboxylic Acids as *p*H Standards. N. Smith and J. C. Speakman. . . 1031

—— Sulphate with the aid of $CaSO_4$, Thermodynamics of the Conversion Potassium Chloride to. E. Abel and J. M. Fanto . . . 97

Potentials, Intermolecular, in Neon and Argon. J. Corner 914

Potentiometer, Feedback, for the Measurement of *p*H Values and Oxidation-Reduction Potentials, A. C. Morton 588

Pressure-Composition Isothermals of Copper Pyridine Perchlorates, Dissociation Pressures and. Part II of: Pyridine Complexes of Metallic Perchlorates. P. C. Sinha and R. C. Ray . . . 790

Proflavine into Bacterial Cells, Penetration of. S. Jackson and C. N. Hinshelwood 527

Protein Fibres with Special Reference to the so-called Thermal Shrinkage of the Collagen Fibre, A Contribution to the Theory of the Structure of. (The late) Dorothy Jordan Lloyd and Marjorie Garrod . . . 441

Pyridine Complexes of Metallic Perchlorates. Part II. Dissociation Pressures and Pressure-Composition Isothermals of Copper Pyridine Perchlorates. P. C. Sinha and R. C. Ray 790

Pyrite Surfaces, Electron Diffraction and Rectification from Silicon and. J. M. Cowley and J. L. Symonds. 53

Quantum Mechanical Investigation of the Azulene Molecule, A. Part I. R. D. Brown 984

Quartic Oscillator, Thermodynamic Functions of the: Application to Cyclobutane. T. L. Cottrell 716

Quenching of Fluorescence, Studies on. Part I. A Contribution to the Theory of Quenching of Fluorescence. K. Weber and M. Lokar . 959

Rate Constants of "Unimolecular" Reactions, A Note on. R. M. Barrer . 399

—— of Conversion, Absolute, of Parahydrogen by Metallic Catalysts, The. D. D. Eley 216

Reactions in Closed Systems, A Refractometric Method for following. H. W. Melville and W. F. Watson 68

—— "Unimolecular," A Note on Rate Constants of. R. M. Barrer . . 399

Reaction Systems, Open, The Kinetics of. K. G. Denbigh, Margaret Hicks and F. M. Page 476

Reciprocity Failure, Low-Intensity, A New Cause of. W. Berg . . . 783

Rectification from Silicon and Pyrite Surfaces, Electron Diffraction and. J. M. Cowley and J. L. Symonds 53

Refractometric Method for following Reactions in Closed Systems, A. H. W. Melville and W. F. Watson 68

Replacement Reactions of β-β′-Dichlorodiethyl Sulphide and of Some Analogues in Aqueous Solution: the Isolation of β-Chloro-β′-Hydroxy Diethyl Sulphide, The. A. G. Ogston, with (in part) E. R. Holiday, J. St. L. Philpot and L. A. Stocken. 45

Resonance Energies from Thermal Data, The Calculation of. J. G. M. Bremner and G. D. Thomas 338

PAGE

Retardation in Polymerisation Reactions, Inhibition and. H. W. Melville and W. F. Watson 886

Rubber and Related Materials, Kinetic Studies in the Chemistry of. Part VI. The Benzoyl Peroxide-Catalysed Oxidation of Ethyl Linoleate. J. L. Bolland 669

Salt Effect, Anomalous, The Diffusion of Dyes through Cellophane: The. S. M. Neale 1027

Salting-out Effect, and Dielectric Constant, The. J. O.M. Bockris and Harold Egan 151

Salts, Acid, of Monocarboxylic Acids as *p*H Standards; Potassium Hydrogen Benzoate and Phenylacetate. N. Smith and J. C. Speakman. . 1031

Samarium, Europium and Ytterbium, Absorption and Fluorescence Spectra of Bivalent. F. D. S. Butement 617

Shear, On the Transformation of " Solid " Foam to a " Fluid " Foam under. M. Blackman 205

Shrinkage, Thermal, of the Collagen Fibre, A Contribution to the Theory of the Structure of Protein Fibres with Special Reference to the so-called. (The late) Dorothy Jordan Lloyd and Marjorie Garrod . . . 441

Silicon and Pyrite Surfaces, Electron Diffraction and Rectification from. J. M. Cowley and J. L. Symonds 53

Silver Oxalate, The Thermal Decomposition of. F. C. Tompkins . . . 206

Smoke, The Action and Design of Mechanical Filters for Dust and. E. A. B. Birse and (the late) J. K. Roberts 273

Sodium Alkyl Sulphates and Related Compounds, A New Method for the Rapid Titrimetric Analysis of. S. R. Epton 226

Solid, Gas-, Interface, Detection of Changes of State of Films adsorbed at the. S. J. Gregg and F. A. P. Maggs 123

—— Solution, Primary, in the System Aluminium-Magnesium-Zinc, Equilibrium between $Al_2Mg_3Zn_3$ and the. G. V. Raynor and W. Hume-Rothery 29

Solubilisation, Hydrotropy and Related Emulsification Processes. Parts I-IV. P. A. Winsor 376

—— Hydrotropy and Related Emulsification Processes. Part V. Solubilisation in Ethylene Glycol. P. A. Winsor 451

—— Hydrotropy and Related Emulsification Processes. Part VI. Effect of Temperature on the Solubilisation of Liquids. P. A. Winsor. . 455

—— Hydrotropy and Related Emulsification Processes. Part VII. Solubilisation of Solids, Freezing Point Depression Effects in Solubilised Systems. P. A. Winsor 459

—— Hydrotropy and Related Emulsification Processes. Part VIII. Effect of Constitution on Amphiphilic Properties. P. A. Winsor . . 463

Solution, Regular, Surface Tension of a. I. Prigogine 626

Solvents Acetic Acid and Acetic Anhydride, Kinetic Studies in the. Part I. Properties of the Solvo-system. H. A. E. Mackenzie and E. R. S. Winter 159

—— Acetic Acid and Acetic Anhydride, Kinetic Studies in the. Part II. The Thiele Acetylation of Benzoquinone and Toluquinone (Experimental). . H. A. E. Mackenzie and E. R. S. Winter 171

—— Acetic Acid and Acetic Anhydride, Kinetic Studies on the. Part III. The Thiele Acetylation of Benzoquinone and Toluquinone (Theoretical). H. A. E. Mackenzie and E. R. S. Winter 243

Solvent on the Hydrogen Overpotential, The Effect of. Part IV (ii) of: Studies in Electrolytic Polarisation. J. O'M. Bockris and S. Ignatowicz 519

Spark Ignition, The Mechanism of. Part II. Carbon Monoxide-Oxygen Mixtures. W. E. Frost and J. W. Linnett 416

—— The Mechanism of. Part III. Effect of adding Organic Vapours to Hydrogen-Oxygen Mixtures. W. E. Frost and J. W. Linnett. . 421

Starch-Iodine Complexes. Part I. G. A. Gilbert and J. V. R. Marriott . 84

Statistical Thermodynamics of Co-operative Systems (A Generalization of the Quasi-Chemical Method). E. A. Guggenheim . . . 1007

Sublimation, Molecular Distillation and. P. C. Carman 529

Sulphur Dioxide, Ammonia, Carbon Dioxide and Nitrous Oxide on BaF_2 Crystals, The Adsorption of the Gases. V. A. Crawford and F. C. Tompkins 698

PAGE

Sulphur Dioxide in Slow Combustion Processes, The Oxidation of. G. Whittingham 141
—— Trioxide and Chlorsulphonic Acid, The Total Vapour Pressure of Mixtures of. Part IV of: Studies in Vapour Pressure Measurement. E. W. Balson and N. K. Adam 412
Summation, The Standard Free Energies of Formation of Gaseous Organic Compounds: A Group Method of. J. G. M. Bremner and G. D. Thomas 230
Surface Conductance and Cataphoresis. F. Booth 955
—— Conductivity Effect, The. Part IV of: The Electrophoresis of Suspended Particles. D. C. Henry 1021
—— Diffusion Reactions, A Note on the Theory of. F. Booth . . . 796
—— Tension from Intermolecular Forces, The Calculation of. Part II. Numerical Results. J. Corner 1036
—— Tension of a Regular Solution. I. Prigogine 626
Surfaces, Metal, Electron Diffraction by Fatty Acid Layers on. J. M. Cowley 60
—— Silicon and Pyrite, Electron Diffraction and Rectification from. J. M. Cowley and J. L. Symonds 53
Suspensions—Suspended Particles, The Electrophoresis of. Part IV. The Surface Conductivity Effect. D. C. Henry 1021
Tetrahalides of the Group IV Elements, The Force Fields of the. Part II of: Molecular Force Fields. D. F. Heath and J. W. Linnett . . 561
Tetrahedral Anions, The Application of the Orbital Valency Force Field to some. Part V of: Molecular Force Fields. D. F. Heath and J. W. Linnett 884
—— Halides, The Application of the Orbital Valency Force Field to. Part IV of: Molecular Force Fields. D. F. Heath and J. W. Linnett . 878
Tetryl, Ethylenedinitramine and. Part I of: The Thermal Decomposition of Explosives. A. J. B. Robertson 677
Thermal Data, The Calculation of Resonance Energies from. J. G. M. Bremner and G. D. Thomas 338
—— Decomposition of Disilane and Trisilane, The. K. Stokland. . . 545
—— Decomposition of Explosives, The. Part I. Ethylenedinitramine and Tetryl. A. J. B. Robertson 677
—— Decomposition of Silver Oxalate, The. F. C. Tompkins . . . 206
—— Shrinkage of the Collagen Fibre, A Contribution to the Theory of the Structure of Protein Fibres with Special Reference to the so-called. (The late) Dorothy Jordan Lloyd and Marjorie Garrod . . 441
Thermodynamics, Functions of the Quartic Oscillator: Application to Cyclobutane. T. L. Cottrell 716
—— of Monolayers. C. Kemball, E. K. Rideal and E. A. Guggenheim. . 948
—— of the Conversion KCl → K_2SO_4, with the aid of $CaSO_4$. E.Abel and J. M. Fanto 97
—— Statistical, of Co-operative Systems (A Generalisation of the Quasi-Chemical Method). E. A. Guggenheim 1007
—— Study of Bivalent Metal Halides in Aqueous Solution, A. Part XVI. Complex Ion Formation in Zinc Halide Solutions. R. H. Stokes . 137
—— Study of Bivalent Metal Halides in Aqueous Solution, A. Part XVII. Revision of Data for all 2 : 1 and 1 : 2 Electrolytes at 25°, and Discussion of Results. R. H. Stokes. 295
Thiele Acetylation of Benzoquinone and Toluquinone, The (Experimental). Part II of: Kinetic Studies in the Solvents Acetic Acid and Acetic Anhydride. H. A. E. Mackenzie and E. R. S. Winter. . . . 171
—— Acetylation of Benzoquinone and Toluquinone, The (Theoretical). Part III of: Kinetic Studies in the Solvents Acetic Acid and Acetic Anhydride. H. A. E. Mackenzie and E. R. S. Winter. . . . 243
Thiophene in Benzene as Test Mixtures and a Comparison with Mixtures of Benzene and Ethylene Dichloride, The Use of Dilute Solutions of. Part II of: Fractional Distillation. E. A. Coulson, J. L. Hales and E. F. G. Herington 636
Toluquinone, The Thiele Acetylation of Benzoquinone and. (Experimental.) Part II of: Kinetic Studies in the Solvents Acetic Acid and Acetic Anhydride. H. A. E. Mackenzie and E. R. S. Winter. . . . 171
—— The Thiele Acetylation of Benzoquinone and. (Theoretical.) Part III of: Kinetic Studies in the Solvents Acetic Acid and Acetic Anhydride. H. A. E. Mackenzie and E. R. S. Winter 243

PAGE

Tracer Element, The Mechanism of Formation of Diethyl Ether using the Heavy Oxygen Isotope O as a. I. Lauder and J. H. Green . . 808
Trinitrotoluene and Ammonium Nitrate, Interaction between. Part I of: Physico-Chemical Processes occurring at High Temperatures and Pressures. John L. Copp and A. R. Ubbelohde . . . 646
—— at High Temperatures, The Decomposition, Boiling and Explosion of. A. J. B. Robertson 977
Trioxane, Infra-Red Absorption Spectrum and Structure of. A. D. Ramsay. 289
Triphenylarsine, Arsenic Trichloride, Monophenylchlorarsine and Diphenylchlorarsine, An Investigation of the Chemical Equilibria involving the Molecules. Alwyn G. Evans and Ernest Warhurst . . . 189
Trisilane, The Thermal Decomposition of Disilane and. K. Stokland. . 545
Ultra-Violet Absorption Spectrum of Formaldehyde, A Note on the. A. J. Everett and G. J. Minkoff 816
" **Unimolecular** " Reactions, A Note on Rate Constants of. R. M. Barrer . 399
Vapour, Carbon Tetrabromide, Emission Bands from the Electrodeless Discharge in. R. A. Durie and T. Iredale. 806
—— Pressure Measurement, Studies in. Part IV. The Total Vapour Pressure of Mixtures of Sulphur Trioxide and Chlorsulphonic Acid. E. W. Balson and N. K. Adam 412
—— Pressure of some High Boiling Esters, The. P. A. Small, K. W. Small and P. Cowley 810
—— Pressure, Total, of Mixtures of Sulphur Trioxide and Chlorsulphonic Acid, The. Part IV of: Studies in Vapour Pressure Measurement. E. W. Balson and N. K. Adam 412
Vapours, Organic, by Thin Films of Polystyrene, The Absorption of. E. C. Baughan 495
—— Organic to Hydrogen-Oxygen Mixtures, Effect of adding. Part II of: The Mechanism of Spark Ignition. W. E. Frost and J. W. Linnett 421
Vibration Frequencies of some Planar XY Molecules, The. Part III of: Molecular Force Fields. D. F. Heath and J. W. Linnett . . 873
Viscosity of Liquids, An Interpretation of the. R. C. L. Bosworth . . 308
Water, Acetaldehyde-, The System. Part I of: Studies on Hemiacetal Formation. I. Lauder 729
—— and Hydrogen Sulphide, Introduction and the Ionisation Potentials of. Part I of: The Ionisation Potentials of Polyatomic Molecules. W. C. Price and T. M. Sugden 108
—— Molecule, The Structure of the. Part I of: Molecular Force Fields. D. F. Heath and J. W. Linnett 556
Wave-guide Absorption Cell Operating in the H_{01} Mode, Measurement of Absorption in Liquids at 1·2 cm. and 0·8 cm. Wavelength using a. J. G. Powles 537
Wool Fibre, On the Cause of the Frictional Difference of the. K. Rachel Makinson 279
X-Ray Data, A New " Averaging " Method for the Location of Atomic Positions from. A. D. Booth 282
Ytterbium, Samarium and Europium, Absorption and Fluorescence Spectra of Bivalent. F. D. S. Butement 617
Zinc, Aluminium-Magnesium-, Equilibrium between $Al_2Mg_3Zn_3$ and the Primary Solid Solution in the System. G. V. Raynor and W. Hume-Rothery 29
—— Halide Solutions, Complex Ion Formation in. Part XVI of: A Thermodynamic Study of Bivalent Metal Halides in Aqueous Solution. R. H. Stokes 137

AUTHOR INDEX—VOLUME XLIV, 1948.

PAGE

Abel, E., and **Fanto, J. M.** Thermodynamics of the conversion $KCl \rightarrow K_2SO_4$ with the aid of $CaSO_4$ 97

Adam, N. K. See *Balson, E. W.*, and

Allmand, A. J. See *Banerjee, T.*, and

Amphlett, C. B., **Mullinger, L. W.**, and **Thomas, L. F.** Some physical properties of uranium hexafluoride 927

Andrew, E. R., **Axford, D.W. E.**, and **Sugden, T. M.** The measurement of ionisation in a transient flame 427

Aten, A. H.W., Jun., and **Dreven, J. v.** A simple apparatus for the measurement of diffusion rates 202

Axford, D. W. E. See *Andrew, E. R.*, *Axford, D. W. E.*, and *Sugden, T. M.*

Balson, E. W., and **Adam, N. K.** Studies in vapour pressure measurement. Part IV: The total vapour pressure of mixtures of sulphur trioxide and chlorsulphonic acid 412

Banerjee, T., and **Allmand, A. J.** Experiments on the electrodeposition of brass from cyanide solutions 819

Barrer, R. M. A note on rate constants of " unimolecular " reactions . . 399

—— and **Woodhead, M.** The mercury-chabazite system 1001

Baughan, E. C. The absorption of organic vapours by thin films of polystyrene 495

—— The energy of carbon bonds—a re-examination of the Fox-Martin rule 845

Bennett, J. G., and **Griffith, R. O.** The photo-reaction between iodine and hydrogen peroxide in aqueous solution 471

Berg, W. F. A new cause of low intensity reciprocity failure . . . 783

Birch, A. J., and **MacDonald, D. K. C.** The nature of metal-ammonia solutions. Part II 735

Birse, E A. A., and **Roberts, J. K.** The action and design of mechanical filters for dust and smoke 273

Blackman, M. On the transformation of " solid " foam to a " fluid " foam under shear 205

—— See *Clark, N. O.*, and

Bockris, J. O'M., and **Egan, H.** The salting-out effect and dielectric constant 151

—— and **Ignatowicz, S.** Studies in electrolytic polarisation IV: The effect of the solvent on the hydrogen overpotential (ii) 519

—— and **Parsons, R.** Part V: Hydrogen overpotential in methanolic solution 860

Bolland, J. L. Kinetic studies in the chemistry of rubber and related materials. Part VI: The benzoyl peroxide-catalysed oxidation of ethyl linoleate 669

Booth, A. D. Distribution functions and crystalline materials . . . 37

—— A new " averaging " method for the location of atomic positions from X-ray data. 282

Booth, F. A note on the theory of surface diffusion reactions . . . 796

—— Surface conductance and cataphoresis 955

Bosworth, R. C. L. An interpretation of the viscosity of liquids . . . 308

Bremner, J. G. M., and **Thomas, G. D.** The standard free energies of formation of gaseous organic compounds. A group method of summation 230

—— The calculation of resonance energies from thermal data . . . 338

Brown, R. D. A quantum mechanical investigation of the azulene molecule. Part I 984

Buchanan, A. S., and **Heymann, E.** Notes on the electrokinetic potential of cellulose and on electrokinetic equations 318

Butement, F. D. S. Absorption and fluorescence spectra of bivalent samarium, europium and ytterbium 617

Carman, P. C. Molecular distillation and sublimation 529

Clark, N. O. The electrical conductivity of foam 13

—— and **Blackman, M.** The degree of dispersion of the gas phase in foam . 1

—— The transmission of light through foam 7

PAGE

Copp. J. L., and **Ubbelohde, A. R.** Physico-chemical processes occurring at high pressures and temperatures. Part I: Interaction between trinitrotoluene and ammonium nitrate 646
—— Part II: The effect of " inert " components on detonation . . . 658
Corner, J. Intermolecular potentials in neon and argon 914
—— The calculation of surface tension from intermolecular forces. II: Numerical results 1036
Cottrell, T. L. Thermodynamic functions of the quartic oscillator: Application to cyclobutane 716
Coulson, C. A. See *Moffitt, W. E.*, and
Coulson, E. A., and **Herington, E. F. G.** Fractional distillation. Part I: The selection of test mixtures for estimating the efficiency of fractionating columns. 629
—— **Hales, J. L.**, and **Herington, E. F. G.** Part II: The use of dilute solutions of thiophene in benzene as test mixtures, and a comparison with mixtures of benzene and ethylene dichloride 636
Cowley, J. M. Electron diffraction by fatty acid layers on metal surfaces . 60
—— and **Symonds, J. L.** Electron diffraction and rectification from silicon and pyrite surfaces 53
Cowley, P. See *Small, P. A.*, *Small, K. W.*, and
Crank, J. See *Wood, A. M.*, *Crank, J.*, and *Twigg, G. H.*
Crawford, V. A., and **Tompkins, F. C.** The adsorption of SO_2, NH_3, CO_2 and N_2O on BaF_2 crystals 698
Davies, C. W. See *Stock, D. I.*, and
Davies, J. T. Monolayers of some diesters 909
Denbigh, K. G., **Hicks, M. J.**, and **Page, F. M.** The kinetics of open reaction systems 479
Dresel, E., **Griffith, M.**, and **Hirst, W.** The free and total energies of interaction of coals with methyl alcohol 992
Dreven, J. v. See *Aten, A. H. W., Jun.*, and
Durie, R. A., and **Iredale, T.** Emission bands from the electrodeless discharge in carbon tetrabromide vapour 806
Egan, H. See *Bockris, J. O'M.*, and
Egerton, A., **Harris, E. J.**, and **Young, G. H. S.** Observations on the slow combustion of hydrocarbons. Part I: The absorption spectra of peroxides 745
—— and **Young, G. H. S.** Part II: The absorption spectra of butane undergoing slow combustion 750
—— Part III: The effect of diluents and other substances on the slow combustion of butane 755
Eley, D. D. The absolute rate of conversion of parahydrogen by metallic catalysts 216
Epton, S. R. A new method for the rapid titrimetric analysis of sodium alkyl sulphates and related compounds 226
Evans, A. G., and **Warhurst, E.** An investigation of the chemical equilibria involving the molecules arsenic trichloride monophenylchlorarsine diphenylchlorarsine and triphenylarsine . . . . . [illegible]
Everett, A. J., and **Minkoff, G. J.** A note on the ultra-violet absorpti spectrum of formaldehyde . . . . [illegible]
Fanto, J. M. See *Abel, E.*, and
Flett, M. St. C. Characteristic infra-red frequencies and chemical properties of molecules 767
Fröhlich, H. General theory of the static dielectric constant 238
Frost, W. E., and **Linnett, J. W.** The mechanism of spark ignition. Part II: Carbon monoxide-oxygen mixtures 416
—— Part III: Effect of adding organic vapours to hydrogen-oxygen mixtures 421
Gage, J. C. A cell for the measurement of diffusion in aqueous solution . 253
Garrod, M. See *Lloyd, D. Jordan*, and
Gilbert, G. A., and **Marriott, J. V. R.** Starch-iodine complexes. Part I . 84
Glover, A. T. See *Woodward, L. A.*, and
Gold, V. The hydrolysis of acetic anhydride 506
Gordon, M. Reaction kinetics of adiabatic systems 196
Green, J. H. See *Lauder, I.*, and
Gregg, S. J., and **Jacobs, J.** An examination of adsorption theory of Brunauer, Emmett and Teller, and Brunauer, Deming, Deming and Teller 574

PAGE

Gregg, S. J. and **Maggs, F. A. P.** Detection of changes of state in films adsorbed at the gas-solid interface 123

Griffith, M. See *Dresel, Eva M., Griffith, M.*, and *Hirst, W.*

Griffith, R. O. See *Bennett, J. G.*, and

Grunberg, L., and **Nissan, A. H.** The additivity of $T_c{}^3$ for some non-linear molecules 1013

Guggenheim, E. A. Statistical thermodynamics of co-operative systems (A generalization of the quasi-chemical method) 1007

—— See *Kemball, C., Rideal, E. K.*, and

Hales, J. L. See *Coulson, E. A., Hales, J. L.*, and *Herington, E. F. G.*

Harris, E. J. A note on the decomposition of hydrogen peroxide and the possibility of its formation during the slow combustion of hydrocarbons 764

—— See *Egerton, A., Harris, E. J.*, and *Young, G. H. S.*

Heath, D. F., and **Linnett, J. W.** Molecular force fields. Part I: The structure of the water molecule 556

—— Part II: The force fields of the tetrahalides of the group IV elements . 561

—— Part III: The vibration frequencies of some planar XY_3 molecules . 873

—— Part IV: The application of the orbital valency force field to tetrahedral halides 878

—— Part V: The application of the orbital valency force field to some tetrahedral anions 884

Henry, D. C. The electrophoresis of suspended particles. Part IV: The surface conductivity effect 1021

Herington, E. F. G. See *Coulson, E. A.*, and

Heymann. E. See *Buchanan, A. S.*, and

Hickling, A., and **Taylor, D.** The anodic behaviour of metals. Part V: Copper 262

Hicks, M. J. See *Denbigh, K. G., Hicks, M. J.*, and *Page, F. M.*

Hinshelwood, C. N. See *Jackson, S.*, and

—— See *James, A. M.*, and

Hirschberg, Y. The absorption spectra of phenylated anthracenes . . 285

Hirst, W. See *Dresel, Eva M., Griffith, M.*, and

Holiday, E. R. See *Ogston, A. G., Holiday, E. R., Philpot, J. St. L.*, and *Stocken, L. A.*

Hughes, G., and **Nevell, T. P.** The mechanism of the oxidation of glucose by periodate 941

Hume-Rothery, W. See *Raynor, G. V.*, and

Ignatowicz, S. See *Bockris, J. O'M.*, and

Iredale, T. See *Durie, R. A.*, and

Ives, D. J. G., and **Pittman, R. W.** An amplifier for use with conductance bridges 644

Jackson, S., and **Hinshelwood, C. N.** Penetration of proflavine into bacterial cells 527

—— The training of bacteria to new carbon sources *Bact. Lactis Aerogenes* and *d*-Arabinose 568

acobs, J. See *Gregg, S. J.*, and

mes, A. M., and **Hinshelwood, C. N.** The dehydrogenase activity of *Bact. Lactis Aerogenes* 967

Jellinek, H. H. G. On the degradation of long-chain molecules. Part II . 345

Kemball, C., Rideal, E. K., and **Guggenheim, E. A.** Thermodynamics of monolayers 948

Lauder, I. Some notes on the Gilfillan-Polanyi micropyknometer . . 78

—— Studies on hemiacetal formation. Part I: The system acetaldehyde-water 729

—— Part II: The system acetaldehyde-methyl alcohol 734

—— and **Green, J. H.** The mechanism of formation of diethyl ether, using the heavy oxygen isotope ^{18}O as a tracer element 808

Levine, S. On the interaction of colloidal particles. Part II: Discussion of basis of theory 833

Lichtenstein, H. J., and **Twigg, G. H.** The hydration of ethylene oxide . 905

Linnett, J. W. See *Frost, W. E.*, and

—— See *Heath, D. F.*, and

—— See *Sherratt, S.*, and

Lloyd, Dorothy Jordan-, and **Garrod, M.** A Contribution to the theory of the structure of protein fibres, with special reference to the so-called "thermal shrinkage" of the collagen fibre 441

PAGE

Lloyd, D. M. G. See *Read, J. H.*, and
Lokar, M. See *Weber, K.*, and
Maggs, F. A. P. See *Gregg, S. J.*, and
Makinson, Mrs. K. Rachel. On the cause of the frictional difference of the wool fibre 279
Marriott, J. V. R. See *Gilbert, G. A.*, and
Melville, H. W., and **Watson, W. F.** A refractometric method for following reactions in closed systems 68
—— Inhibition and retardation in polymerisation reactions 886
Minkoff, G. J. See *Everett, A. J.*, and
Moffitt, W. E. Bonds in the phosphorus molecule, P_4 987
—— and **Coulson, C. A.** The free radicals $CH_2(CH)_{2m-1}CH_2$ 81
Morton, C. A feedback potentiometer for the measurement of pH values and oxidation-reduction potentials 588
Mullinger, L. W. See *Amphlett, C. B.*, *Mullinger, L. W.*, and *Thomas, L. F.*
MacDonald, D. K. C. See *Birch, A. J.*, and
Mackenzie, H. A. E., and **Winter, E. R. S.** Kinetic studies in the solvent acetic acid and acetic anhydride. Part I: Properties of the solvo-system . 159
—— Part II: The Thiele acetylation of benzoquinone and toluquinone (Experimental) 171
—— Part III: The Thiele acetylation of benzoquinone and toluquinone (Theoretical) 243
MacEwan, D. M. C. Complexes of clays with organic compounds. Part I: Complex formation between montmorillonite and halloysite and certain organic liquids 349
Mackenzie, R. C. Complexes of clays with organic compounds. Part II: Investigation of the ethylene glycol-water-montmorillonite system using the Karl Fischer reagent 368
Neale, S. M. The diffusion of dyes through cellophane. The anomalous salt effect 1027
Nevell, T. P. See *Hughes, G.*, and
Nissan, A. H. See *Grunberg, L.*, and
Ogston, A. G., **Holiday, E. R.**, **Philpot, J. St. L.**, and **Stocken, L. A.** The replacement reactions of β-β'-dichlorodiethyl sulphide and of some analogues in aqueous solution: the isolation of β-chloro-β'hydroxy diethyl sulphide 45
Page, F. M. See *Denbigh, K. G.*, *Hicks, M. J.*, and *Page, F. M.*
Parsons, R. See *Bockris, J. O'M.*, and
Pearson, J. The reduction of nitrocompounds at the dropping-mercury cathode. Part I: The nitrobenzenes and nitrotoluenes . . . 683
Philpot, J. St. L. See *Ogston, A. G.*, *Holiday, E. R.*, *Philpot, J. St. L.*, and *Stocken, L. A.*
Pink, R C., and **Ubbelohde, A. R.** On some properties of cyclo-octatetraene in relation to structure 708
Pittman, R. W. See *Ives, D. J. G.*, and
Powles, J. G. The effect of molecular inertia on dielectric absorption . . 802
—— Measurement of absorption in liquids at 1·2 cm. and 0·8 cm. wavelength using a waveguide absorption cell operating in the H_{01} mode . . 537
Price W. C. See Sugden, T. M., and
—— and **Sugden, T. M.** The ionisation potentials of polyatomic molecules. Part I: Introduction and the ionisation potentials of H_2O and H_2S 108
Prigogine, I. Surface tension of a regular solution 626
Ramsay, D. A. Infra-red absorption spectrum and structure of trioxane . 289
Randles, J. E. B. A cathode ray polarograph. Part I 322
—— Part II: The current-voltage curves 327
Ray, R. C. See *Sinha, P. C.*, and
Raynor, G. V. The constitution of the magnesium-indium alloys, in the region 20 to 50 atomic per cent. of indium 15
—— and **Hume-Rothery, W.** Equilibrium between $Al_2Mg_3Zn_3$ and the primary solid solution in the system aluminium-magnesium-zinc . 29
Read, J. H., and **Lloyd, D. M. G.** The thermal conductivity of organic materials near the melting point 721
Richards, R. E. The force constants of some OH and NH links . . . 40
Rideal, E. K. See *Kemball, C.*, *Rideal, E. K.*, and *Guggenheim, E. A.*
Roberts, J. K. See *Birse, E. A. B.*, and
Robertson, A. J. B. The thermal decomposition of explosives. Part I: Ethylenedinitramine and tetryl 677
—— The decomposition, boiling and explosion of trinitrotoluene at high temperatures 977

PAGE

Sherratt, S., and **Linnett, J. W.** The determination of flame speeds in gaseous mixtures 596
Sinha, P. C., and **Ray, R. C.** Pyridine complexes of metallic perchlorates. Part II: Dissociation pressures and pressure-composition isothermals of copper pyride perchlorates 790
Small, K. W. See *Small, P. A., Small, K. W.*, and *Cowley, P.*
Small, P. A., Small, K. W., and **Cowley, P.** The vapour pressures of some high boiling esters 810
Smith, N., and **Speakman, J. C.** Acid salts of monocarboxylic acids as *p*H standards; potassium hydrogen benzoate and phenylacetate 1031
Speakman, J. C. See *Smith, N.*, and
Stock, D. T., and **Davies, C. W.** The second dissociation constant of magnesium hydroxide. 856
Stocken, L. A. See *Ogston, A. G., Holiday, E. R., Philpot, J. St. L.*, and
Stokes, R. H. A thermodynamic study of bivalent metal halides in aqueous solution. Part XVI: Complex ion formation in zinc halide solutions 137
—— Part XVII: Revision of data for all 2 : 1 and 1 : 2 electrolytes at 25°, and discussion of results 295
Stokland, K. The thermal decomposition of disilane and trisilane. . . . 545
Sugden, T. M. See *Andrew, E. R., Axford, D. W. E.*, and *Sugden, T. M.*
—— and **Price, W. C.** The ionisation potentials of polyatomic molecules. II: The ionisation of simple aldehydes and ketones . . . 116
—— See *Price, W. C.*, and
Symonds, J. L. See *Cowley, J. M.*, and
Taylor, D. See *Hickling, A.*, and
Teich, N. See *Whytlaw-Gray, R.*, and
Thomas, G. D. See *Bremner, J. G. M.*, and
Thomas, L. F. See *Amphlett, C. B., Mullinger, L. W.*, and
Tompkins, F. C. The thermal decomposition of silver oxalate . . 206
—— see *Crawford, V. A.*, and
Twigg, G. H. See *Lichtenstein, H. J.*, and
—— See *Wood, A. M., Crank, J.*, and *Twigg, G. H.*
Ubbelohde, A. R. See *Copp, J. L.*, and
—— See *Pink, R. C.*, and
Warhurst, E. See *Evans, A. G.*, and
Watson, W. F. See *Melville, H. W.*, and
Weber, G. The quenching of fluorescence in liquids by complex formation. Determination of the mean life of the complex 185
Weber, K., and **Lokar, M.** Studies on quenching of fluorescence. Part I: A contribution to the theory of quenching of fluorescence . . 959
Whittingham, G. The oxidation of sulphur dioxide in slow combustion processes 141
Whytlaw-Gray, R., and **Teich, N.** The mercury meniscus in precision measurements on gases 774
Winsor, P. A. Hydrotropy, solubilisation and related emulsification processes. Part I 370
—— Part II: The solubilisation of petroleum ether with sodium secondary C_{10}-C_{18} alkyl sulphates 382
—— Part III: (*a*) The solubilisation of miscellaneous organic liquids with sodium secondary C_{10}-C_{18} alkyl sulphates 387
(*b*) The effect of dilution on solubilisation 389
—— Part IV: Solubilisation with miscellaneous amphiphiles 390
—— Part V: Solubilisation in ethylene glycol 451
—— Part VI: Effect of temperature on the solubilisation of liquids. . . 455
—— Part VII: Solubilisation of solids, freezing point depression effects in solubilised systems 459
—— Part VIII: Effect of constitution on amphiphilic properties . . . 463
Winter, E. R. S. See *Mackenzie, H. A. E.*, and
Wood, A. M., Crank, J., and **Twigg, G. H.** The application of the differential analyser to a problem in chemical kinetics 256
Woodhead, M. See *Barrer, R. M.*, and
Woodward, L. A., and **Glover, A. T.** Molybdenum oxide catalysts for the reduction of phenol to benzene 608
Young, G. H. S. See *Egerton, A.*, and
—— See *Egerton, A., Harris, E. J.*, and

INDEX TO REVIEWS—VOLUME XLIV, 1948.

PAGE

Advances in enzymology and related subjects of biochemistry. Volume VII. Edited by F. F. Nord 95
Alfrey, T. Mechanical behaviour of high polymers 1048
Bergmann, E. D. Isomerism and isomerisation 940
—— The chemistry of acetylene and related compounds 1050
Bikerman, J. J. Surface chemistry for industrial research 269
Chemical architecture. Frontiers in chemistry, Volume V. Edited by R. E. Burk and O. Grummitt 270
Chemical Society. Quarterly Reviews, Volume II, No. 1 939
De Mille, J. B. Strategic minerals 94
Electrodepositors' Technical Society. Proceedings of the Third International Electrodeposition Conference 1052
Encyclopedia of chemical technology. Volume I. Edited by R. Kirk and D. Othner 184
Fifty years of progress. The story of the Castner-Kellner Alkali Company (1895-1945) 272
"Heat-Treater." Fundamental principles and applications of induction heating 344
Journal of the Electrodepositors' Technical Society, Volume XXI (1945-1946) 272
Kamen, M. D. Radioactive tracers 1050
Kaye, G. W. C., and Laby, T. H. Tables of physical and chemical constants (10th Edition) 744
Kennard, E. H. See *Richtmeyer, F. K.*, and
Kolthoff, I. M., and Stenger, V. A. Volumetric analysis. Volume II: Titration methods 181
Kröger, F. A. Some aspects of the luminescence of solids 939
Kuhn, Werner. Physikalische chemie 183
Laby, T. H. See *Kaye, G. W. C.*, and
Newer methods of preparative organic chemistry 1048
Overbeek, J. Th. G. See *Verwey, E. J. W.*, and
Richtmeyer, F. K., and Kennard, E. H. Introduction to modern physics (4th Edition) 183
Silman, H. Chemical and electro-plated finishes 1050
Snoek, J. L. New developments in ferromagnetic materials 269
Statistical methods in research and production. Edited by Owen L. Davies 438
Stenger, V. A. See *Kolthoff, I. M.*, and
Szent-Györgi, A. Chemistry of muscular contraction 437
Theilheimer, W. Synthetic methods of organic chemistry. Volume I (1942-1944) 743
U.S. National Bureau of Standards. Selected values of properties of hydro-carbons 342 and 1052
Verwey, E. J. W., and Overbeek, J. Th. G. Theory of the stability of lyophobic colloids 439
Vogel, A. I. A text book of practical organic chemistry 343

MINUTES OF THE 42ND ANNUAL GENERAL MEETING

Held on FRIDAY, 24th September, 1948, at Ashorne Hill, Leamington Spa, Warwickshire.

The President, Prof. A. J. Allmand, F.R.S., was in the Chair.

1. The Minutes of the 41st Annual General Meeting were taken as read and were confirmed.

2. In presenting the Annual Report for the year 1947 (Session 1947-48), the President mentioned that henceforward the reports of the General Discussions would be called "Discussions of the Faraday Society," the first two volumes of the new series being reports of the Discussions held in 1947.

   During the year the arrears of papers awaiting publication had been cleared off.

   The membership showed a gratifying increase, and was now double that of 1938.

   MR. MARLOW. A warm personal tribute to the late Secretary had appeared in the April issue of the *Transactions*, but the President said he would like to remind members of what they already knew, the extraordinary debt which the Society owed to Mr. Marlow.

   Dr. Tompkins, who had taken over from Mr. Marlow the position of Editor, was now taking over also that of Secretary.

   FINANCE. In presenting the Accounts for 1947, the Hon. Treasurer said that there had been a small loss, due to the abnormal expenditure on printing, caused by the accumulation of papers and the increased cost of printing. The Society was applying to the Chemical Council for assistance in meeting this expenditure. It was not intended at present to increase the annual membership subscription.

   The Report was unanimously adopted.

3. The Officers and Members of Council were elected to take office on the 1st of October as follows :—

President

PROF. SIR JOHN LENNARD-JONES, K.B.E., D.SC., F.R.S.

Vice-Presidents who have held the Office of President

PROF. N. V. SIDGWICK, SC.D., D.SC., F.R.S.
PROF. M. W. TRAVERS, D.SC., F.R.S.
PROF. E. K. RIDEAL, M.B.E., D.SC., F.R.S.
PROF. W. E. GARNER, C.B.E., D.SC., F.R.S.
PROF. A. J. ALLMAND, D.SC., F.R.S.

Vice-Presidents

R. P. Bell, M.A., F.R.S.
G. M. Bennett, C.B., M.A., Sc.D., F.R.S.
Prof. H. J. Emeléus, D.Sc., F.R.S.
Prof. M. G. Evans, D.Sc., F.R.S.
Prof. Sir Cyril Hinshelwood, Sc.D., F.R.S.
G. S. Hartley, D.Sc.
Prof. H. W. Melville, Ph.D., F.R.S.

Honorary Treasurer

R. E. Slade, D.Sc.

Chairman of the Publications Committee

Prof. E. A. Guggenheim, M.A., Sc.D., F.R.S.

Ordinary Members of Council

Dr. A. E. Alexander, M.A., Ph.D.
Prof. C. E. H. Bawn, Ph.D.
J. Ferguson, Ph.D.
G. Gee, Sc.D.
Sir Charles Goodeve, O.B.E., D.Sc., F.R.S.
R. Lessing, Ph.D.
W. G. Penney, O.B.E., D.Sc., F.R.S.
Prof. J. T. Randall, D.Sc., F.Inst.P., F.R.S.
Sir Robert Robertson, K.B.E., D.Sc., F.R.S.
G. B. B. M. Sutherland, M.A., Ph.D.

4. The Society's Auditors, Messrs. Knox Cropper & Co., were re-appointed.
5. The thanks of the Society were accorded with acclamation to the retiring Officers and Members of Council.

This concluded the business of the meeting.

CORRIGENDA

Vol. 43, 1947:

Plate facing page 396. The three patterns shown as (*h*), (*a*) and (*b*) of Fig. 1 should be (*c*), (*f*) and (*g*) of Fig. 4, and vice versa.

Vol. 44, 1948:

Page 192, Fig. 1. *The legend should read* Disproportionation of ϕ_2AsCl.

At 252° c. —○— ϕ_2AsCl$_2$ —△— ϕAsCl$_2$ —Y— ϕ_3As.

At 304° c. --○-- ϕ_2AsCl$_2$ --△-- ϕAsCl$_2$ --Y-- ϕ_3As.

,, 193, Fig. 2. *Add to legend* - - ○ - - ϕ_2AsCl$_2$ uncatalysed reaction.

Fig. 3. *The legend should read* Disproportionation of ϕAsCl$_2$.

At 256° c. —△— ϕAsCl$_2$ —○— ϕ_2AsCl —□— AsCl$_3$.

At 304° c. --△-- ϕAsCl$_2$.

,, 267. The legends of Fig. 1 and Fig. 2 should be interchanged.

,, 345, l. 4. *Delete* as finally revised 17th March, 1947.

,, 346, eqn. (1). *For* $\left(\frac{m}{a}\right)$ *read* $\binom{m}{a}$.

,, 351, Fig. 1(*b*). *For* structures *read* structure.

,, 352, l. 5. *For* indices (*hkl*) *read* indices (*hk*).

,, 352, 3rd para., l. 3-4. *For* liquid. . . . An oriented aggregate *read* liquid. In some experiments, an oriented aggregate.

,, 352, 3rd para., l. 6. *For* with the liquid, as follows. The mineral *read* with the liquid. In most cases, however, a different method was used. The mineral.

,, 357, Table I. *Add to list of code letters.* *k* = treated with liquid at 200°.

,, 358, 2nd para., l. 8. *For* is *read* would be.

,, 360, last para., l. 18-19. *For* In contrast to *read* In contrast, with.

,, 363, legend to Fig. 5. *For* (*a*) glycol *read* (*a*) glycerol.
For (*e*) Cyclohexane *read* (*e*) Cyclohexanol.

,, 364, 2nd para. from foot of page is legend to Table II.

,, 366, l. 22. *For* suggests that the water *read* suggests that, in the vermiculites, the water.

,, 366, l. 36. *For* e.g. octophyllite *read* e.g. a particular sample of octophyllite.

,, 396, Table VIII, columns 1 and 3. The numbers within chain brackets refer to G, G + S$_2$ and S$_2$ respectively in vertically descending order. Column 5. *Delete* gel G.

,, 397, Table IX, column 3. Type to be moved one line up.

,, 403, eqn. (20). *For* E$_1$ read E.

,, 799, eqn. (23). *For* e^{-r} *read* l^{-r}.

I.A.R.I. 75

INDIAN AGRICULTURAL RESEARCH INSTITUTE LIBRARY, NEW DELHI

Date of Issue	Date of Issue	Date of Issue
28-3-58		
16-1-59		
18.10.60		
[illegible]		
29.1.68.		

GIPNLK—H-40 I.A.R.I.—29-4- 5—15,000